

SPRINGER
REFERENCE

Ernesto Fattorusso
William H. Gerwick
Orazio Tagliatela-Scafati
Editors

VOLUME 1

Handbook of Marine Natural Products

 Springer

Contents

VOLUME 1

Part 1	Natural Product Trends in Different Groups of Marine Life	1
1	Taxonomy and Marine Natural Products Research	3
	John Blunt, John Buckingham, and Murray Munro	
2	The Chemistry of Marine Algae and Cyanobacteria	55
	Hyukjae Choi, Alban R. Pereira, and William H. Gerwick	
3	The Chemistry of Marine Bacteria	153
	Brian T. Murphy, Paul R. Jensen, and William Fenical	
4	The Chemistry of Marine Sponges	191
	Sherif S. Ebada and Peter Proksch	
5	The Chemistry of Marine Tunicates	295
	Marialuisa Menna and Anna Aiello	
Part 2	Structure Elucidation of Marine Natural Products	387
6	The Role of Databases in Marine Natural Products Research	389
	John Blunt, Murray Munro, and Meg Upjohn	
7	Contemporary Strategies in Natural Products Structure Elucidation	423
	Jaime Rodríguez, Phillip Crews, and Marcel Jaspars	
8	Strategies for Structural Assignment of Marine Natural Products Through Advanced NMR-based Techniques	519
	Alfonso Mangoni	
9	NMR Methods for Stereochemical Assignments	547
	Kirk R. Gustafson	

10 Quantum Chemical Calculation of Chemical Shifts in the Stereochemical Determination of Organic Compounds: A Practical Approach	571
Simone Di Micco, Maria Giovanna Chini, Raffaele Riccio, and Giuseppe Bifulco	
11 Marine Natural Products Synthesis	601
Victoria L. Wilde, Jonathan C. Morris, and Andrew J. Phillips	

VOLUME 2

Part 3 Marine Natural Products and Chemical Ecology	675
12 Antipredatory Defensive Roles of Natural Products from Marine Invertebrates	677
Joseph R. Pawlik	
13 Antipredatory Defensive Role of Planktonic Marine Natural Products	711
Adrianna Ianora, Antonio Miralto, and Giovanna Romano	
14 Antifouling Activity of Marine Natural Products	749
Pei-Yuan Qian and Sharon Ying Xu	
15 Chemically Mediated Competition and Host–Pathogen Interactions Among Marine Organisms	823
Marc Slattery and Deborah J. Gochfeld	
16 Marine Metabolites and Metal Ion Chelation	861
Stephen H. Wright, Andrea Raab, Jörg Feldmann, Eva Krupp, and Marcel Jaspars	
Part 4 Biosynthesis of Marine Natural Products	893
17 Biosynthetic Studies Through Feeding Experiments in Marine Organisms	895
Angelo Fontana, Emiliano Manzo, M. Letizia Ciavatta, Adele Cutignano, Margherita Gavagnin, and Guido Cimino	
18 Biosynthetic Principles in Marine Natural Product Systems	947
David H. Sherman, Christopher M. Rath, Jon Mortison, Jamie B. Scaglione, and Jeffrey D. Kittendorf	
19 Mechanisms of Halogenation of Marine Secondary Metabolites	977
Claudia Wagner and Gabriele M. König	

Part 5 Biomedical Potential of Marine Natural Products	1025
20 Marine Natural Products That Target Microtubules	1027
Raymond J. Andersen, Dehai Li, Matt Nodwell, Michel Roberge, Wendy Strangman, and David E. Williams	
21 Marine Natural Products Active Against Protozoan Parasites	1075
Ernesto Fattorusso and Orazio Taglialatela-Scafati	
22 Mechanism-based Screening for Cancer Therapeutics with Examples from the Discovery of Marine Natural Product-based HIF-1 Inhibitors	1111
Dale G. Nagle and Yu-Dong Zhou	
23 Enzyme Inhibitors from Marine Invertebrates	1145
Yoichi Nakao and Nobuhiro Fusetani	
24 Fluorescent Proteins from the Oceans: Marine Macromolecules as Advanced Imaging Tools for Biomedical Research	1231
Edward G. Smith, Cecilia D'Angelo, Franz Oswald, G. Ulrich Nienhaus, and J. Wiedenmann	
25 From Biosilica of Sponges (Demospongiae and Hexactinellida) to Fabricated Biomedical Materials	1259
Xiaohong Wang, Heinz C. Schröder, Matthias Wiens, Lu Gan, Wolfgang Tremel, and Werner E. G. Müller	
26 Meeting the Supply Needs of Marine Natural Products	1285
David J. Newman and Gordon M. Cragg	
27 Legal and Ethical Issues Involving Marine Biodiscovery and Development	1315
Gordon M. Cragg, Flora Katz, David J. Newman, and Joshua Rosenthal	
Part 6 Marine Toxins: A Problem for Public Health and Seafood Resources	1343
28 Seafood Toxins: Classes, Sources, and Toxicology	1345
Patrizia Ciminiello, Martino Forino, and Carmela Dell'Aversano	
29 Marine Protein Toxins	1389
Hiroshi Nagai	
30 Marine Natural Products into the Future	1421
William H. Gerwick	
Index	1429

Introduction

Ernesto Fattorusso, Willam H. Gerwick, and Orazio
Tagliatalata-Scafati

The use of both terrestrial and marine natural products (MNPs) as treatments for different ailments has accompanied humanity from its earliest civilizations. Nature represents an endless arsenal of new bioactive compounds and the study of these metabolites has historically proven to be of immense benefit in the drug discovery process.

The chemical investigation of terrestrial natural products can be dated back to the beginning of the nineteenth century, when organic molecules started to be studied with scientific rigour. Much younger is the chemical investigation of marine natural products (MNPs), now about 65 years old. Although approximately 70% of the earth's biosphere is made up by oceans, a unique environment that hosts a wealth of plants, animals, and microorganisms, a variety of reasons have hampered the development of MNP chemistry in the nineteenth and at the beginning of twentieth century. These are mainly related to technical constraints resulting from difficulties in the collection of marine organisms from the sea and, related to this, the relatively small amount of organisms that could be collected. As a result, this situation inevitably resulted in a very limited quantity of metabolites obtained from the extraction and purification processes.

Due to impressive progress in collection techniques (with the introduction of SCUBA), purification, and, above all, in structural studies through improvements in spectroscopic technologies, the last 40 years have witnessed an explosion of research focused on the immense biodiversity of the marine environment. This has resulted in a multidisciplinary endeavor involving natural product chemists, marine ecologists, pharmacologists and biochemists. The number of novel MNPs discovered to date has been recently estimated to be about 30,000, and their incredible diversity can be well appreciated by consulting the precious reviews published by the late D. J. Faulkner in *Natural Products Reports*, a series now continued by Blunt, Munro, and others. These annual reviews report all the new marine natural products emerging in the scientific literature and also give a fine idea of the relative prolificacy of the different organisms. Marine invertebrates (sponges, tunicates, soft corals, gorgonians, molluscs, echinoderms) are by far the most prolific producers of secondary metabolites, compared to fish and other vertebrates. This observation can have at least two possible explanations: (1) Their sessile and soft-bodied forms, combined with their consequent lack of mechanical or morphological weapons to be used as protection, force them to rely largely on a chemical

arsenal to deter predation from other reef organisms. Since the production of secondary metabolites has been selected by these organisms as a strategy for their survival, the greater is the number of secondary metabolites produced by an organism the greater are its chances in winning the evolutionary competition. (2) These marine invertebrates harbor in their tissue, in extra- and intracellular spaces, a great number of symbiotic and associated microorganisms and, thus, their biosynthetic potential is indirectly increased by the contribution of the biosynthetic machinery of the different symbiotic cells.

Thus, it is not surprising that one of the most recent trends in MNP chemistry, the direct chemical investigation of marine microbes (e.g., bacteria collected in the sediments and cyanobacteria), has revealed an incredible richness of interesting secondary metabolites. Moreover, some classes of marine microorganisms are actually responsible for the production of the toxic metabolites found in marine invertebrates, and several have been demonstrated to cause human intoxications of various levels of seriousness. The study of marine toxins was initiated at the very beginning of the MNP era, reaching milestones such as the isolation and structure elucidation of maitotoxin, the largest nonproteinaceous toxin known to date, and characterized by a skeleton of 164 carbon atoms.

With this wealth and variety of topics in mind, we decided to structure the present handbook with the aim of representing the different aspects of MNP science (i.e., ecology and pharmacology of bioactive compounds; recent advances in isolation, biosynthesis, and structural elucidation) in a volume which should provide representative examples of recent results as well as of the future outlook of this multidisciplinary branch of science. Obviously, this handbook is not intended as a comprehensive coverage of the entire field of MNP research, but we feel that through the diversity of topics treated, it can provide a good idea of its variety and richness. Thus, this handbook should be useful to a mixture of scientists and students in academia as well as industry that are interested in the most recent developments in this area. In addition, we have asked the authors to present their topics in a clear and didactic way, making a frequent use of examples and connections to their practical utility. Thus, we believe that this handbook will also serve as an excellent textbook for Ph.D. and postdoctoral students in several courses within the marine sciences. The study questions included at the end of each chapter are intended to be thought provoking stimuli to further deepen student knowledge and interest in the subject matter.

The handbook includes 30 chapters grouped into six sections. Section I provides an overall idea of the production and diversity of MNPs within some representative groups of marine organisms. Of course, the five chapters in this section do not aim at reporting all of the molecules isolated from each group, but rather, they describe the characteristics as well as unique carbon and heterocyclic skeletons and assorted functional groups. The astounding variety (and often complexity) of the chemical structures of MNP poses challenging problems to the chemists engaged in their stereostructural elucidation, which is also made more difficult by the small amounts commonly obtained from natural sources. In Sect. II, the reader will find described different aspects of the structural elucidation process with special attention given to

NMR spectroscopy. Recent advancements in NMR spectroscopy have allowed modern MNP laboratories to routinely solve structures on submicrogram quantities, and have undoubtedly fostered the recent explosion of novel marine compounds appearing in the literature. In the same section, a chapter by Blunt and Munro describes the importance of databases in the structural elucidation process while the chapter by Phillips et al. illustrates the elegance of several total syntheses of MNPs, highlighting also the role that these syntheses can play in confirming or revising the chemical structures assigned to marine compounds.

Section III illustrates the role of MNPs in chemical ecology, investigating the real purpose driving the production of MNPs and explaining how the coexistence and the interaction of an enormous number of species in the marine environment greatly rely on chemical signaling processes. Section IV is inherently connected to the previous one because it describes the biosynthetic origins of these metabolites, or how they can be acquired from dietary sources and/or symbiotic-associated organisms. A rapidly expanding number of MNP scientists have been investigating the molecular biology and genetics of marine secondary metabolite biosynthesis with the goal of understanding and manipulating their biosynthetic pathways (particularly polyketide and non-ribosomal peptide syntheses). If the development of this subdiscipline is able to attain its long-term goal, then the fermentation and cultivation of microbes could offer a practical solution to the problems of short supply of materials, a fundamental and significant issue which has long delayed and stalled the full development of MNP science.

Section V illustrates one of the most important applications of the MNP science, namely, the biomedical potential of small molecule natural products. Since Bergman's discovery of the antiviral and antitumor arabinose-containing nucleosides "spongothymidine" and "spongouridine" from *Cryptotethia crypta* in 1955, the potential of marine organisms in pharmaceutical applications has been the driving force of many of these scientific investigations. At the moment, five marine-derived drugs have been approved by the FDA or EMA (the EU agency), namely, two nucleosides (cytarabine and vidarabine), a polypeptide (ziconotide), the complex alkaloid trabectedin (ET-743), and the fantastically complicated synthetic derivative, Halaven, of the sponge metabolite halichondrin. Moreover, a further 15 compounds are in different phases of clinical trial and several hundred promising compounds are in preclinical stages. The eight chapters of Section V illustrate different aspects of the biomedical potential of MNPs, highlighting how this "natural library" can contain lead compounds to be used as an inspiration to design and develop new useful therapeutic agents, or to gain initial information about the pharmacophore and structure-activity relationships. ► [Chapters 20](#), ► [21](#), and ► [23](#) describe some specific pharmacological activities of small marine organic molecules, while ► [Chaps. 24](#) and ► [25](#) are focused on the potential use of marine macromolecules, fluorescent proteins, and biologically formed polymers of silica, respectively. The last two chapters of Section V discuss the long-standing and perplexing problem of compound supply, an inherent feature of working in the marine environment, and the legal and ethical issues connected to the exploitation of this environment. With the growing number of commercial

applications of MNPs, it is critical for practitioners of this field to possess a deep knowledge of intellectual property protection and constraints on public disclosure. Finally, Sect. VI includes two chapters reporting on marine toxins, one of the oldest fields of MNP chemistry but one still very active and interesting for its toxicological, pharmacological, and economic implications.

We cannot conclude this introductory chapter without thanking the friendly contributions of all of the colleagues that accepted the task of providing their invaluable expert knowledge through the preparation of the different chapters. We hope that this handbook on MNPs will succeed in further stimulating enthusiasm and interest in this relatively young but extremely dynamic and rapidly evolving discipline.

Part 1

Natural Product Trends in Different Groups of Marine Life

Taxonomy and Marine Natural Products Research

1

John Blunt, John Buckingham, and Murray Munro

Contents

1.1	Introduction	4
1.2	How Many Species on Earth?	4
1.3	Marine Natural Products Chemistry	7
1.3.1	Historical	7
1.3.2	The Marine Resource	11
1.4	Marine Taxonomy and Natural Products Chemistry	33
1.5	The Results Achieved	39
1.6	Macro or Micro: Which is the Producer?	40
1.7	Marine Biodiversity: Into the Future	43
1.8	The “Neglected Phyla” and Marine Natural Products in the Future	44
1.9	Study Questions	46
	References	46

Abstract

A taxonomic overview of the marine environment is presented along with specifics on the key phyla. This is accompanied by a brief history of marine natural products research, the aspirations in this field of research, and an analysis, on a taxonomic basis, of the results of the past 60 years of marine natural products research. In the final sections of the chapter, conclusions are drawn from the work as to the phyla that might be of interest for future research.

J. Blunt (✉) • M. Munro

Department of Chemistry, University of Canterbury, Christchurch, New Zealand
e-mail: john.blunt@canterbury.ac.nz, murray.munro@canterbury.ac.nz

J. Buckingham

Dictionary of Natural Products, CRC Press/Informa, 1-4 Singer St., 4th Floor, London, UK
e-mail: johnbuckingham@blueyonder.co.uk

1.1 Introduction

“Is it from pride, humour or irony that man has given the name “earth” to his own planet?” [1]

It was undoubtedly pride, not humor or irony, as Earth is the only planet of the Solar System not named from Greek or Roman mythology. Earth probably originates from the Middle English word, *erthe*, which can be traced back through Old English, Old High German, Greek to the Hebrew word *erez*, meaning ground [2]. It is however ironic and indeed humorous when Earth is viewed from space. The land masses our forbears took pride in are simply islands floating in enormous oceans. The 71% of the Earth’s surface that is the oceans is strikingly illustrated by the “Blue Marble” photo of earth taken from Apollo 17 [3] (Fig. 1.1). The oceans are a critical component of the Earth’s biosphere, unique in the Solar System and most probably among the several hundred other planetary systems throughout the Universe that have been identified in recent years.

The essential nonliving components of the biosphere are the atmosphere with its oxygen richness, the hydrosphere, predominantly saline, to an average depth of 3,800 m, and the land mass with its average height of 840 m [4]. In combination, these features support an amazing diversity of life forms.

1.2 How Many Species on Earth?

Systematics attempts to categorize this biological diversity on Earth and sort the various life forms into congruent groups, but there is no one single definition of what constitutes a species. Systematics has been influenced by the influx of new data and new methodology, particularly at the molecular level. As a consequence, taxonomy and recognition of groupings at the species level are constantly evolving. Taxonomists have attempted to impose a classification scheme on the whole of creation during an era of rapidly evolving knowledge. In the opinion of some, genomics will soon be capable of imposing an informatically robust relationship tree on all organisms. Most taxonomists beg to differ, claiming that changes and similarities are expressed through the phenotype not the genotype, and the genomic view disregards the possibility of convergent evolutionary pathways. What is true, however, is that in recent years there have been some major realignments of taxonomic groups based on genomic studies, even in such intensively studied and well-known groups as the higher plants.

The nineteenth-century high-level classification of organisms into plant and animal kingdoms has been abandoned since about the 1960s with the development of cladistic analysis. Since then it has become increasingly clear that certain groups of organisms, some of them previously little studied, such as the cyanobacteria or cyanophytes (so-called blue-green algae; more closely related to bacteria), the chromista (including the brown algae), and the archaeobacteria or archaea, show greater differences in both fundamental biochemistry and genetics from each other and from the so-called higher organisms than higher plants and animals show from each other. It was Whittaker



Fig. 1.1 A view of the earth taken from Apollo 17, December 7, 1972

in 1959 who proposed that the most fundamental division should be between the prokaryotes and the eukaryotes [5], a classification that has now been generally accepted but subsequently modified to include the discovery of the archaea in the 1970s [6].

Major projects are in place worldwide to collate information from available datasets and document the Earth's biodiversity. These include the *Global Biodiversity Information Facility* [7] and the *Species 2000/Integrated Taxonomic Information System* [8] responsible for the *Catalogue of Life*. In the 9th edition (2009), their Annual Checklist, with 1,160,711 distinct species being listed, was estimated to contain just more than one half of the known species [9]. The goal ultimately is to list every distinct species in each group of organisms. At present, some groups are globally complete, some are nearing completion, and others are partial only. At the top level of the taxonomic hierarchy *The Catalogue of Life* lists organisms, based on contemporary perspectives, as the prokaryotic Archaea and Bacteria and the eukaryotes organized as Animalia, Chromista, Fungi, Plantae, and Protozoa. This whole topic has been thoughtfully discussed by Gordon [10] as a management hierarchy or classification system for the *Catalogue of Life*. The partially rooted relationships between these groupings can be depicted diagrammatically in a phylogenetic tree of life [11] (Fig. 1.2).

Based on the known organisms there appears to be consensus [12–15] that the number of known species on Earth is 1.75–1.9 million. These numbers have modest certainty when dealing with the larger organisms or distinctive taxonomic groups, but there is considerable uncertainty when dealing with groups that are harder to classify,

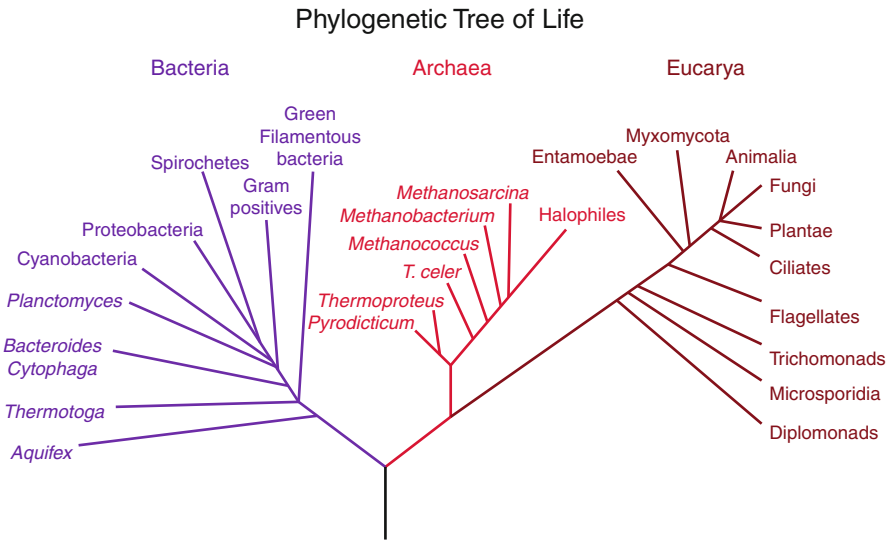


Fig. 1.2 A partially rooted phylogenetic tree of life

Table 1.1 Compilation of species numbers based on higher-order taxonomic groupings

	Total species			Marine species		
	Catalogue of Life [9]	Chapman [13] (World accepted)	Chapman [13] (World estimate)	WoRMS (2009) [16]	Bouchet (2006) [17]	Groombridge and Jenkins (2002) [4]
Archaea	281	–	–	0	0	?
Bacteria	9,773	10,307	~1,000,000	629	5,800	?
Fungi	44,669	98,998	1,500,000	1054	500	500
Protozoa ^a	6,866	28,871	>1,000,000	6,852	>14,800	12,500
Chromista ^a	7,901	~25,044	~200,500	4,098	7,600	1,500
Plantae	211,249	~310,129	~390,800	8,329	8,750	11,000
Animalia	953,661	1,424,153	~6,836,000	139,359	192,667	~205,000
	1,234,500	1,897,502	>10,900,000	160,319	>230,117	~250,000

^aFor comparative purposes the unicellular eukaryotic species have been partitioned between Chromista and Protozoa based on the systematics used by the *Catalogue of Life*. This should be considered speculative as not all databases or authors use these groupings, preferring instead Protocista. The *Catalogue of Life* places the Bacillariophyceae at a phylum level in the Plantae, but acknowledges this as a problem [10]

are microscopic, or are not economically important. It is likely to be many years before definitive answers emerge, but the total number of species will increase. Again estimates vary from 3–5 million [12] to 10–14 million [13, 15], or to 50 [14] to perhaps as many as 100 million species [15]. The breakdown of defined species in the *Catalogue of Life*, as of November 2009, is shown in Table 1.1. These numbers can

be contrasted with the 2009 compilation of world species by Chapman [13] who drew on information from systematists, the taxonomic literature, and previous compilations to arrive at an accepted number of species (~1.9 million) as well as providing an estimate of the total number of species on Earth (~11 million).

The contribution from the marine environment to the total species on Earth is relatively modest. At present the *World Register of Marine Species* (WoRMS) [16] lists 160,829 valid species (Table 1.1), 243,356 species names including synonyms, and 302,955 species to phyla. This data bank aims to capture all of the estimated 230,000 marine species by 2010. Two other sources [4, 17] have data on the estimated number of marine species (Table 1.1). Of the two sources, the data from Bouchet [17], who lists some 230,000 species, is the more definitive and thoughtful. Just as Chapman [13] extrapolated from the accepted number of world species to estimated world species and concluded that there were millions of Arthropod, Bacteria, Chromista, and Protozoa species yet to be characterized, Bouchet carried out a similar exercise for the marine world and speculated on the potential for greater numbers among the microbes and symbionts and the potential for the deep sea to produce a wide array of new species. There is clear evidence based on close field observations and culture-independent molecular techniques that the true number of marine species is considerably greater than that listed in Table 1.1.

The apparent lower species diversity between the terrestrial and hydrospheres (1.67 vs. 0.23 million) is a consequence of the overwhelming number of terrestrial arthropods (~1 million) for which there is no marine equivalent. In the marine world, species from Animalia are totally dominant accounting for 84% of the defined species (see Table 1.2 and Fig. 1.3).

All but one of the Animalia phyla have marine representation; the phylum Onychophora is the sole exception. The other notable feature is that the bulk of the Animalia phyla are exclusively, or nearly exclusively, marine, for example, Porifera, Echinodermata, and Bryozoa. Using data derived by May [14] on the relative numbers and distribution of the Animalia phyla this marine preference can be effectively depicted (Fig. 1.4). The aquatic and marine habitats are provided in the chart.

1.3 Marine Natural Products Chemistry

1.3.1 Historical

Rather surprisingly the natural products chemistry associated with marine species – marine natural products (MNP) – has only emerged over the past 75 years. This is in distinct contrast to the history of terrestrial natural products chemistry, which can readily be traced back to the earliest exponents of natural products chemistry at the start of the nineteenth century. For example, morphine was extracted and subsequently purified from the opium poppy plant about 1804 in Germany [18, 19]. However, the use of extracts from both terrestrial and marine sources as medicines, narcotics, or poisons stretches back to the earliest civilizations and is well documented in der Marderosian's 1969 review on marine pharmaceuticals [20].

Table 1.2 Suggested numbers for the marine phyla

Distribution of the marine phyla (Bouchet [17])			
Archaea	>0	Arthropoda (Chelicerata)	2,267
Archaea	–	Arthropoda (Crustacea)	44,950
		Brachiopoda	550
Bacteria	5,800	Cephalorhyncha (Priapulida; Loricifera; Kinorhyncha)	156
Cyanophyta	1,000	Chaetognatha	121
Bacteria	4,800	Chordata (Ascidiaceae)	4,900
		Chordata (Cephalochordata)	32
Fungi	500	Chordata (Mammalia)	110
Fungi	500	Chordata (Actinopterygi)	16,475
		Cnidaria	9,795
Protozoa	>14,800	Ctenophora	166
Ciliophora	?	Cycliophora	1
Sporozoa	?	Echinodermata	7,000
Euglenophyta	250	Echiura	176
Dinophyta (Dinomastigota)	4,000	Ectoprocta/Bryozoa	5,700
Radiolaria	550	Entoprocta/Kamptozoa	170
Foraminifera	10,000	Gastrotricha	395
		Gnathostomulida	97
Chromista	7,600	Hemichordata	106
Ochrophyta (Phaeophyceae)	1,600	Mesozoa (Rhombozoa; Orthonectida)	106
Ochrophyta (Chrysophyceae)	500	Mollusca	52,525
Haptophyta ^a	500	Nematoda	12,000
“Bacillariophyta”	5,000	Nematomorpha	5
		Nemertea	1200
Plantae	8,750	Onychophora	0
Chlorophyta	2,500	Phoronida	10
Magnoliophyta ^b	50	Placozoa	–
Rhodophyta	6,200	Platyhelminthes	15,000
		Porifera	5,500
Animalia	192,667	Rotifera	50
Acanthocephala	600	Sipuncula	144
Annelida	12,000	Tardigrada	212
Annelida (Pogonophora)	148		

^aFigure extracted from the *Catalogue of Life* [9]

^bBouchet had not included any members of the Magnoliophyta (mangroves, saltmarsh plants) in his estimates. The estimated figure for the Magnoliophyta from Groombridge and Jenkins [4] has been included

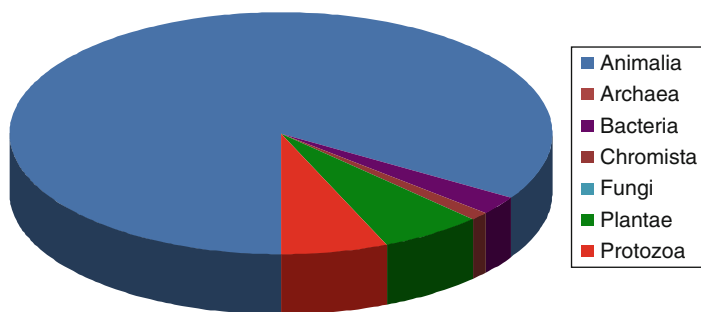


Fig. 1.3 Distribution of marine species by higher-order taxonomic grouping

This review is interesting as it surveyed this new and developing field from a taxonomic perspective. Of course at that stage relatively few compounds had been characterized and the emphasis was very much on toxins, pharmacology, and the biomedical potential for marine natural products. This emphasis was natural following on from Bergman's 1950s discovery of the non-ribose nucleosides spongthymidine and spongouridine from the West Indian sponge *Cryptotethia crypta* [21–25]. The subsequent evaluation of the biomedical potential of these arabinose-based nucleosides undoubtedly stimulated tremendous interest in the potential for pharmaceutical discoveries from the oceans. Bergman's first publication on marine organisms was in 1933 [26] while his 50th and last marine paper *Marine Products L, Phospholipides of Sponges* was in 1961 [27]. Over that 28-year period, Bergman studied sponges, sea anemones (cnidarians), and algae with a structural, not a biomedical, focus. In the 1950s, Nigrelli, Burkholder, and Ciereszko worked and commented specifically on biomedical aspects of marine natural products, for example, the neurotoxic effects of saponins from sea cucumbers, the antibiotic properties of sponge constituents and gorgonians, and antitumor activities associated with molluscs, echinoderms, and annelids [28–33]. In the meantime, work on toxins from marine vertebrates and invertebrates was initiated by Hirata, Scheuer, and Moore [34–38]. The first systematic study of a range of marine animals, both invertebrates as well as vertebrates, was reported in 1970 by Pettit who had collected from broad geographical areas [39]. This early systematic study was expanded by Rinehart with his bioassay-directed collections and onboard screening in the areas of Baja California (1974) and the Caribbean (1978) [40]. By the 1970s, species from across the marine phyla had been collected and were being studied. It was Faulkner, another early leader in the field, who commented that by 1975 there were already three parallel fields of study in marine natural products: marine toxins, MNP chemistry, and marine chemical ecology [41]. The distinct tracks, recognized over 30 years ago, continue today with systematic studies directed toward a particular phylum, toward a particular class of compounds, or following a particular bioactivity in the field of natural products chemistry. The study of marine toxins is still a dynamic aspect of the field and the role of MNPs in ecological studies has flourished. The major development of the past 20 years has

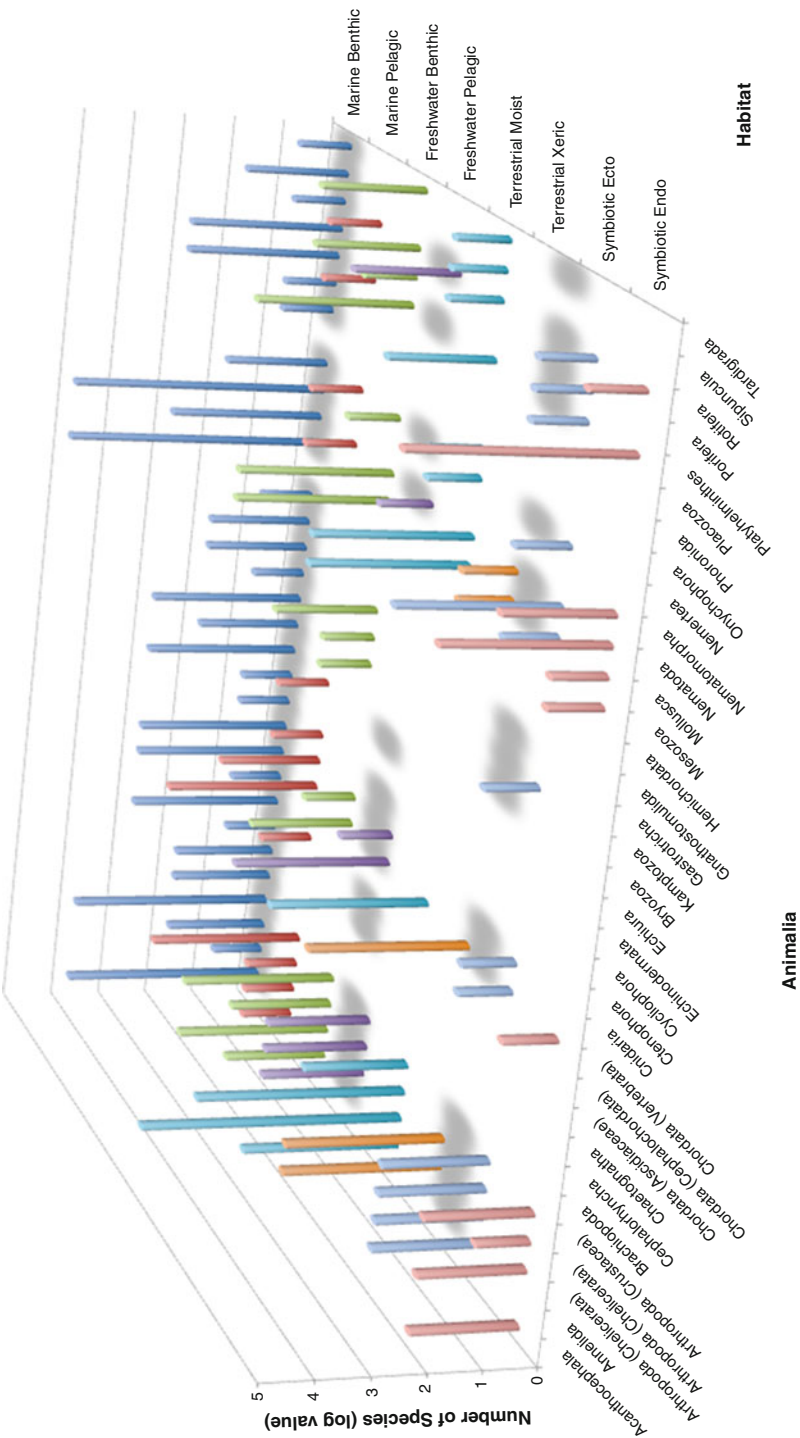


Fig. 1.4 Distribution (log scale) of Animalia species by phyla and habitat

been the discovery and realization of the importance of marine-associated and marine-derived microorganisms. Led by Fenical, the study of marine microorganisms has rapidly become a major focus for a rapidly rising number of researchers [42]. Any survey would also have to note the rapid rise, since 2000, of studies associated with mangroves, whose habitats are right at the marine–terrestrial interface [43].

That study of just a few phyla by Bergman in the 1930s and 1940s was followed by a systematic exploration of the marine environment that has established the marine environment as a rich source of novel, bioactive compounds.

1.3.2 The Marine Resource

The marine environment is an extremely complex one, showing immense biodiversity. It is now clear that, while many marine natural products are located in the tissues of the larger marine animals and plants, and are thus genuine natural products of those organisms, many others are produced by associated endo- or epibiotic microorganisms. Most marine microorganisms have not yet been successfully cultured, and definitive proof of origin is in most cases currently lacking making it extremely difficult to distinguish between commensalism, saprophytism, symbiosis, or parasitism. These products produced by symbiotic, commensal, or epiphytic microorganisms appear in many cases to play a role in chemical defense mechanisms.

To better understand the depth of the marine resource, each of the major divisions/phyla is briefly described. The following descriptions of the characteristic features of each marine phylum have been condensed from the very full descriptions contained in the *Dictionary of Marine Natural Products* (DMNP) [44] which should be referred to for more detail. The DMNP descriptions also include more numerous examples of representative natural products from each phylum, and further surveys of the chemistry of some of the phyla are contained in subsequent chapters of this Handbook. Another particularly useful reference source is *Substances Naturelles d'Origine Marine* by Kornprobst [45].

Alternative taxonomic views are possible. In some groups of organism (e.g., molluscs) there is reasonable agreement among taxonomists about the major subdivisions of the phylum, but in others (e.g., Protozoa and Chromista) there are huge differences between alternative taxonomic schemes. For example, the Annual Checklist of the *Catalogue of Life* has an inconsistent treatment of diatoms and needs correcting. The diatoms appear in three places and it appears that two classification systems are in simultaneous use such that two diatom classes – Coscinodiscophyceae and Fragilariophyceae – are listed under phylum Ochrophyta in kingdom Chromista, whereas class Bacillariophyceae is listed as a phylum-rank entry under kingdom Plantae [10]. In this review of taxonomy and chemistry, the *Catalogue of Life*'s higher taxa are used and in general the *Catalogue*'s system of assigning phyla adhered to.

1.3.2.1 Archaea

The archaea are prokaryotic organisms inhabiting extreme environments, both marine and terrestrial, such as hydrothermal vents, and also highly saline regions.

There are three generally recognized groups: thermophiles (heat-tolerant), halophiles (tolerant of highly saline media such as in the Dead Sea; some species are also extremely alkali tolerant, growing in media up to pH 12), and methanogens (some species of which are also highly thermotolerant). It is also convenient to recognize a group of “psychrophiles” tolerant of cold Arctic and Antarctic conditions. Although only discovered in the 1970s [6], it now appears that the archaea are in fact the most abundant bacteria in the marine environment [46]. They show major differences from other prokaryotes in their genome, and these are carried through into fundamental differences in membrane structure and biochemistry. Their cell walls do not contain the glycopeptides found in the Bacteria. Stabilization of the membrane structure is effected by esters of glycerol with characteristic branched-chain terpenoid fatty acids, a role that in prokaryotes is performed by carotenoids and/or hopanoids and in eukaryotes by sterols.

1.3.2.2 Bacteria

The Bacteria are characterized by a cell wall structure based on a glycoprotein formed by (1 → 4) linked *N*-acetylglucosamine and *N*-acetylmuramic acid cross-linked by peptide side chains containing unusual amino acids which render different bacterial strains biochemically and immunologically distinct. In Gram-positive bacteria, the glycoprotein coat forms the outermost layer; in Gram-negative bacteria there is an outer membrane coat that prevents this layer being stained by the reagent. Bacteria may be photosynthetic or non-photosynthetic, and the photosynthetic bacteria may be anaerobic (sulfur bacteria) or aerobic (which includes the cyanobacteria). The former group utilizes the bacteriochlorophylls as photosynthetic pigments. Further major subdivisions such as alpha-, beta-, gamma-, and delta-proteobacteria have been delineated according to various schemes, but the overall picture is complex [47–49]. The majority of secondary metabolites are produced by the cyanobacteria and by the actinobacteria, which are described separately in the following sections.

Cyanobacteria

The older term blue-green algae is now considered a misnomer, and the cyanobacteria are considered a subdivision of the photosynthetic Bacteria. They are unicellular organisms that are both marine and terrestrial; some marine species also inhabit fresh water. Some are truly monocellular, but when found unassociated with other organisms, many species adhere via their mucilaginous coats into filaments or tufts visible to the naked eye. Cyanobacteria are among the earliest known organisms. Schemes for the subclassification of the cyanobacteria are based on their mode and degree of such association, or alternatively by the type of spores formed. Attempts have also been made to classify them chemotaxonomically. About 1,000 species have currently been described. Cyanobacteria are responsible for frequent algal blooms, the toxicity of which is associated with their high level of secondary metabolites [50, 51]. Cyanobacteria are present in the tissues of many sponges, often as a major component of the biomass. The most characteristic secondary metabolites are peptidic and are also characterized by a high degree of halogenation.

Actinobacteria

The Actinobacteria are a particular class of the Gram-positive Bacteria showing filamentous growth, and some similarities to fungi. (In the past they have often been classified as filamentous fungi and are sometimes called “higher bacteria.”) They also merit special treatment biochemically speaking because of their vast production of different types of natural products, many of them with strong antibiotic or other pharmacological activity. The most important genera, in terms of natural products, are *Streptomyces* and *Actinomyces*. Actinobacteria occur in marine sediments, and probably as endophytes in many marine organisms. The recent discovery of three marine genera is notable and already significant, and novel chemistry has come from these discoveries (*vide infra*) [52–56]. As a group they tolerate a wide range of salinities.

1.3.2.3 Protozoa

The term “protozoa” is difficult to define taxonomically and is subject to ongoing modification in the light of biochemical studies, which are leading to the reclassification of many groups. It was formerly used as a blanket term to describe almost any kind of unicellular organism, but it is now known that the dinoflagellates are more closely related to the brown algae (Chromista: Ochrophyta; Phaeophyceae) than to other unicellular organisms. The ciliate organisms, for example, *Paramecium*, can be placed here, although it now appears that they are biochemically closest to the dinoflagellates. It is convenient to recognize four subdivisions: flagellates, amoebae, sporozoans (Apicomplexa), and ciliates based on their modes of locomotion, but the reservations expressed above concerning their fundamental dissimilarities must be borne in mind, and a proper classification remains premature.

Dinophyta (Dinoflagellates)

These monocellular organisms are economically important as the causative agents of toxic “red tides.” Biochemical and other studies have shown clearly that they are more closely related to the ciliates and to certain other groups than they are to other flagellate organisms. About 4,000 species are known (Table 1.2). Only just over half are photosynthetic; some are carnivorous. Their main anatomical characteristic is the possession of two flagellae, one equatorial and one longitudinal. Most are unicellular but some are filamentous. They participate in a range of symbiotic associations, especially with corals and with molluscs. Those organisms which are photosynthetic contain chlorophylls *a* and *c*. They contain a range of xanthophylls. The characteristic steroids are a range of 4 α -methyl derivatives representing an intermediate stage between the tetracyclic triterpenoids and the cholestane/ergostane type predominant in the phaeophyta and relatives.

Many shellfish toxins are now known to be dinoflagellate metabolites but may not currently have been specifically described as such in the literature. The known toxins of dinoflagellates fall into two main groups, though the exact type of toxin produced is genus specific. The first main group is polyketide-derived, either long-chain with some cyclic ether formation (e.g., amphidinols [57, 58]) or with multiple ether rings (“polyether ladders”) (e.g., *brevetoxins* (see Fig. 1.5) [59, 60]).

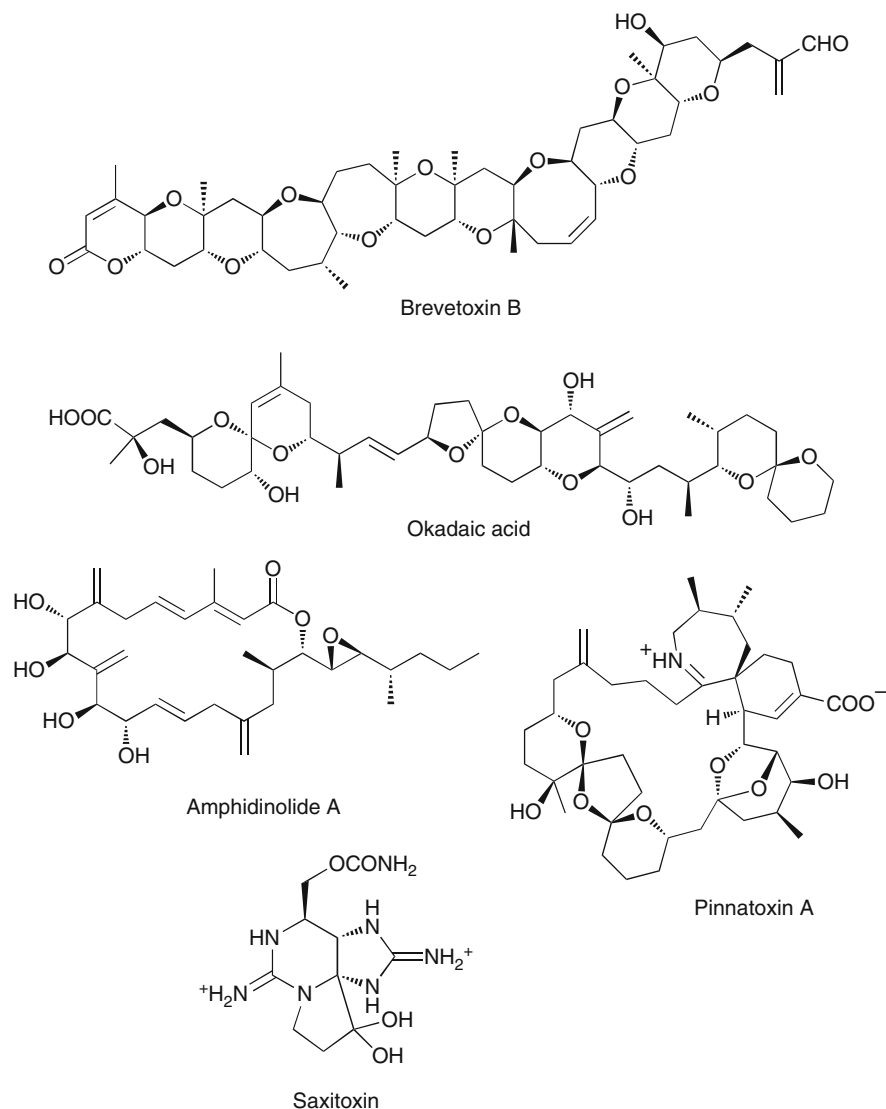


Fig. 1.5 Metabolites from protozoa

Another structural subtype is shown by *okadaic acid* [61], while other polyketides are macrolides such as the *amphidinolides* [62, 63]. Alicyclic nitrogenous polyketides, such as the *pinnatoxins* [64, 65] which have been isolated from shellfish are known to be dinoflagellate produced. It is notable that in known cases the biosynthesis of polyketides in dinoflagellates is by a totally different pathway from that in other organisms. The other main class is composed of nitrogenous guanidinoid toxins of which *saxitoxin* is the prototype [66].

Ciliophora (Ciliates)

Genera studied chemically include *Euplotes*, *Tetrahymena*, *Litonotus*, and *Pseudokeronopsis*. The ciliates are non-photosynthetic organisms but can often harbor photosynthetic algae as symbionts. Chemical studies have been fairly limited, but a range of sesquiterpenoids, and some highly unusual triterpenes, have been isolated.

1.3.2.4 Chromista

The term Chromista was first introduced in 1981 as a higher-order taxon and includes all algae whose chloroplasts contain chlorophylls *a* and *c* [67]. Previously, the photosynthetic chromists had been classified as plants, while non-photosynthetic chromists were classified with the fungi or animals with the close relationship among chromists not appreciated until the advent of ultrastructural and molecular studies. Chlorophyll *c* and a number of other pigments found in the Chromista are not found in any plant group, and it is these pigments which give them their characteristic brown or golden color. Within the Chromista, the phylum that has been of greatest interest to marine natural product chemists is the Ochrophyta which encompasses the class Phaeophyceae, or the “brown algae.”

Ochrophyta: Phaeophyceae (Brown Algae)

About 1,600 species of brown alga are known, almost exclusively marine. The term “phaeophyta” is to be preferred, even if it is depicted as being at a phylum level. Modern studies have shown that the phaeophyta are only very distantly related to the other algae and the term “brown alga” is therefore a misnomer, although it remains in widespread use. Together with the diatoms and the chrysophytes, they constitute what has been described as the Stramenopiles. Whereas the other two subgroups are entirely monocellular, the vast majority of brown algae are multicellular and macroscopic, sometimes attaining very large size. Most species inhabit cold and temperate, often rough, seas and are sessile, demonstrating a well-defined differentiation into a foot (holdfast), stem (stipe), and frond and growing in surface or relatively shallow waters. The exception is the brown algae of the Sargasso Sea, which are two free-floating *Sargassum* species inhabiting tropical waters. The photosynthetic pigments of all species within the Stramenopiles are chlorophylls *a*, *c*₁, and *c*₂ (characteristic absence of chlorophyll *b*). The carotenoid content is limited to fucoxanthin and lesser amounts of violaxanthin. Both the structural and the storage carbohydrates of the phaeophytes differ from those present in other classes of algae.

The range of sterols found is limited and mostly based on minor modifications of the fucosterol structure, which is the major steroid. There is a wide range of unusual oxylipins, for example, bridged epoxy compounds and prostanoid-like cyclopentanoids.

Brown algae contain a wide range of terpenoids, phenolics, and meroterpenoids, but a striking and somewhat unexpected feature is the paucity of halogenated compounds, and those that are found in small amounts are bromo- and iodo- rather than chloro-substituted. They are unique in their ability to concentrate iodine (and also arsenic) to concentrations of up to 1% dry weight, and although 99% of

the iodine in the tissues is inorganic, the other 1% finds its way into thyroxine and other iodinated tyrosines and a small number of miscellaneous phenolics. The major secondary metabolite content of brown algae is represented by phenols and phenolic meroterpenoids, many of them sulfated and/or halogenated. The content of these in the tissues may reach 20% by weight and they may play a role in the prevention of larval fixation by marine animals and for protection against bacteria. A major series is represented by the phlorotannins, which are radical-induced oligomers of phlorotannin containing C–C or C–O–C linkages. The genus *Cytoseira* has been much investigated and has yielded a large range of structurally diverse meroterpenoids.

Haptophyta and Ochrophyta: Bacillariophyceae (“Bacillariophyta”; Diatoms), Chrysophyceae (Golden Algae)

It was this grouping of unicellular organisms together with the phaeophyta that constituted the Stramenopiles. The term “algae” formerly applied to some of these groups is now considered in biochemical and sub-microstructural studies to be a misnomer (cf. phaeophyta). Although these organism types are linked together in the classification scheme used here, this is a tentative assignment. These organisms have been relatively little studied chemically by comparison with the phaeophyta. The diatoms and haptophytes secrete hard exoskeletons of aluminosilicates and calcium salts respectively, while the golden algae do not, though they may contain silica microspicules. There are ~500 known species of marine golden algae and ~500 haptophytes. The number of marine diatom species, recognized to be 5,000, may be as high as 50,000, constituting the bulk of the phytoplankton at certain times of the year, and therefore of crucial importance to marine ecosystems.

The storage polysaccharide of diatoms and golden algae is chrysolaminarin. Photosynthetic pigments resemble those of the brown algae, with no phycobilins but with chlorophylls *c* and the more recently discovered chlorophyll *c*₃. There have been extensive studies on their lipids on account of their biotechnological importance (cf. algae). The content of sulfur glycerides, especially 1,2-diacylglycerol 6-sulfoquinovosides [68] (also found in other classes of organism), is relatively high. The range of known steroids resembles that of the phaeophyta in being based on limited side-chain modification of the cholestane skeleton, with some sulfation. The prymnesins are toxic polyethers produced by a haptophyte [69]. The range of terpenoids isolated is very narrow and limited so far to simple phytanes. It is noteworthy that in two studied diatom species, the biosynthesis of these (in the chloroplasts) is by a non-mevalonate pathway while the steroids, produced in the cytoplasm, are mevalonate derived. Nitrogenous compounds are similarly few in number, but the toxic pyrrolidine *domoic acid* (see Fig. 1.6), also found in red algae, was isolated as a shellfish toxin resulting from *Nitzschia* infection [70].

1.3.2.5 Plantae

The algae, considered in their totality, can be described as lower, mostly multicellular plants of a simple body plan, lacking well-defined differentiation

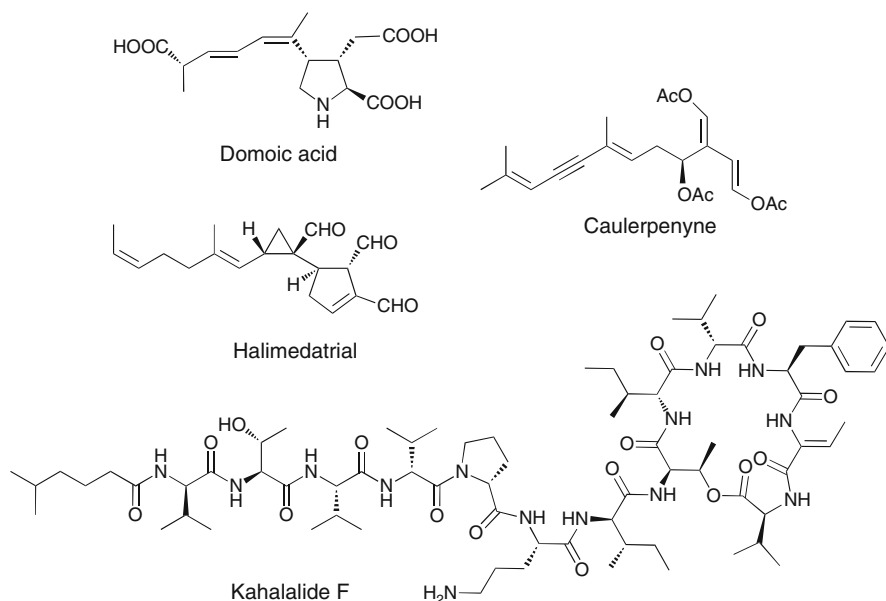


Fig. 1.6 Metabolites from “Bacillariophyta” and Chlorophyta

into roots, stems, and leaves. The higher plants, which show such differentiation, are virtually absent from the oceans, although some species (mangroves; several different spp. of higher plant) are important components of the estuarine saltmarsh environment and have currently become of considerable interest. The classification of algae has undergone a number of changes in recent decades and there is no definitive overall plan that takes care of every subgroup. The most fundamental division is between the brown algal branch, now better described as the phaeophyta as a grouping within the Chromista, and the green algal branch: two groupings which show large biochemical differences one from the other. The “green” branch comprises not only the green algae proper (Chlorophyta), but also the red algae (Rhodophyta), which are now considered more closely related to the green algae than either are to the phaeophyta and relatives.

Chlorophyta (Green Algae)

About 2,500 species are recognized inhabiting mostly surface waters of the calmer seas. Of these, about 20% have so far been investigated chemically, principally in the orders Bryopsidophyceae and Ulvophyceae. In their fundamental biochemistry (photosynthetic pigments, storage polysaccharides, etc.) the Chlorophyta resemble the higher plants. Some members are unicellular, sometimes as endophytes in other species of green algae. Green algae photosynthesize using the common carotenoids α - and β -carotenes, and contain a range of relatively common xanthophylls such as lutein. The most common storage polysaccharides are amylose and amylopectin, and the most common structural polysaccharide is cellulose, although

some groups also secrete β -1,3-xylan and β -1,4-mannan. The most widespread sterols are cholesterol, brassicasterol, sitosterol, and close relatives, although some rarer sterols have been characterized. Studies have not always distinguished between sterols involved in the algal membrane structure and those present in the cytoplasm.

The known secondary metabolites of the green algae are rather limited in structural range and are mostly confined to terpenoids of relatively common skeleton, and a range of aromatics including meroterpenoids. Halogenation is uncommon, and the terpenoids are so far limited to sesqui- and diterpenes and a few triterpenes. Many of the terpenoids contain enoloid functionality, for example, *caulerpenyne*, [71] and/or furan rings formed biogenetically by the cyclization of the related unsaturated aldehydes. Some of these metabolites have also been isolated from species that feed on green algae, such as molluscs. *Halimedatriol* is the only terpenoid so far isolated from green algae containing a carbon skeleton that has not been found elsewhere [72]. Nitrogenous compounds found in green algae tend to be low-molecular-weight amines related to aminoacids, or peptides and modified peptides such as the *kahalalides* [73].

Rhodophyta (Red Algae)

The red algae are characterized by a unique and complex reproductive cycle involving three alternating generations. The great majority of the 6,200 species known are marine, sometimes inhabiting deep water. They may be mono- or multicellular with a complete absence of flagellae. The chloroplasts have a double membrane similar to those of cyanobacteria and presumably arose by endosymbiosis with these organisms. There is no general agreement about the subclassification of red algae. An important biochemical similarity between the red algae and the cyanobacteria is the presence of the phycobilins, phycocyanobilin (blue-green), and phycoerythrobilin (red). It is the latter that is responsible for the red color of the tissues, but the color may be modified or masked by the presence of phycocyanobilin and/or chlorophylls. The red algae contain chlorophyll *a* and the characteristic pigment chlorophyll *d*.

The secondary metabolites of the red algae are characterized by a high proportion of halogenated terpenoids and aromatics, particularly in the intensively studied genus *Laurencia*. The terpene skeletons are strongly weighted toward the lower MW members of the series (especially sesquiterpenes), and there are many representatives of unique terpene skeletons not found in higher plants or elsewhere in the algae. The sesquiterpenes of *Laurencia* are based on more than 20 different carbon skeletons, some of them “traditional” and found also in terrestrial organisms, others novel. Many of these have also been isolated from molluscs and other animals that feed on red algae. There is also a wide range of halogenated (mostly brominated) diterpenes, many derived from the common (marine and terrestrial) skeleton labdane and other skeletons closely related to it. The parguerane skeleton, as found in *parguerene* (see Fig. 1.7) and related compounds, is however unique to marine organisms [74]. Certain *Laurencia* and *Chondria* species have also yielded a series of triterpenoid polyethers derived from squalene, for example, *thyrseferol* [75]. The most characteristic class of natural product isolated from these genera,

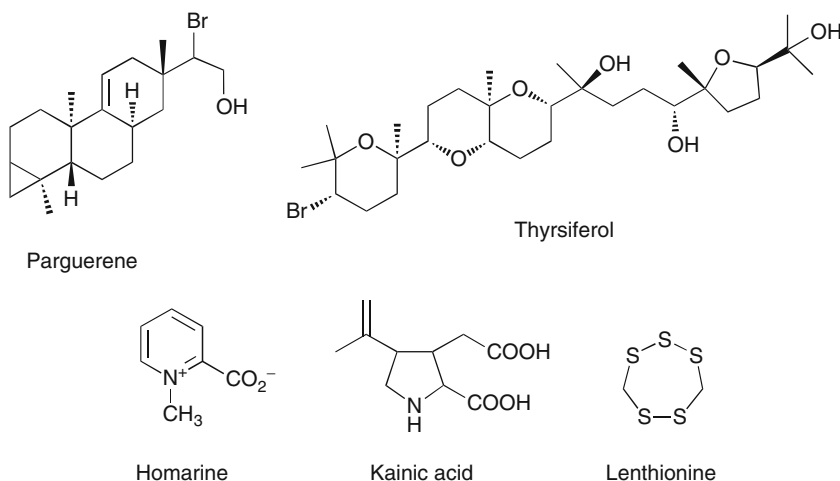


Fig. 1.7 Metabolites from Rhodophyta

however, is the extensive series of mostly halogenated compounds based on a linear C_{15} skeleton, the first of which to be discovered was laurencin in 1968 [76, 77]. A wide variety of structures based on ether formations are found on this basic skeleton (e.g., obtusenyne [78]), which probably arise by loss of a C_1 fragment from a C_{16} precursor. The Ceramiales also contain a range of halogenated phenolics. Nitrogenous natural products are relatively scarce in the majority of red algae, and mostly limited to widely distributed small molecules such as *homarine* [79, 80]. A range of simple halogenated indoles were isolated from *Rhodophyllis membranacea*. Once again, it is the Ceramiales that show a much greater range. A characteristic aminoacid is *kainic acid* [81] and other analogs. The chemo-taxonomic unpredictability of this group of organisms is shown by studies of *Chondria californica*, which yielded a range of polysulfur compounds such as *lenthionine* [82]. These were unaccompanied by terpenes, and were not found in apparently closely related species.

1.3.2.6 Fungi

Fungi, part of the Eukaryota, are characterized by the lack of a photosynthetic mechanism and a mode of life which is saprophytic, parasitic, or symbiotic [83]. Another major biochemical difference from algae lies in their cell wall structure usually based on chitin rather than cellulose. Fungi are found throughout a wide range of terrestrial and marine environments and it is not possible to produce a meaningful definition of “marine fungi,” only to refer to a range of halotolerance among the various fungal species that are widely distributed. Thus marine sediments and marine invertebrate tissues yield fungal species from genera also found terrestrially, but which have developed a preference for growing in saline environments. Of the approximately 100,000 fungal species so far described, about

500 have been found in marine environments, but this figure is certain to increase in the light of further research. The majority of fungi fall into the category of higher fungi or Eumycetes having typical fungal biochemistry, and which can be subdivided into the four main classes of Zygomycetes, Ascomycetes, Basidiomycetes, and Deuteromycetes. These groups are distinguished by their method of spore formation (zygospores, asci, and basidia, respectively, for the first three groups). The Deuteromycetes are an ill-defined group roughly corresponding with the term fungi imperfecti (the terms Mycelia sterilia and Hyphomycetes are also found according to various schemes). These are fungi in which no reproduction is observable and which are therefore extremely difficult to identify. The Ascomycetes and the Deuteromycetes are the most represented in the marine environment and have been the most investigated chemically [84, 85].

The great majority of fungal secondary metabolites have been isolated from fungi associated with other organisms. Marine algae (green, red, and phaeophyta), like higher plants, harbor a wide variety of endophytic fungal species; for example, 116 different fungal strains were cultivated from a single specimen of *Fucus serratus* [86]. It is not in general known whether any particular relationship should be considered as symbiotic, benign, or pathogenic. There are usually strong structural similarities between the natural products from these epiphytic marine fungi and their terrestrial equivalents.

Fungal mycelia are also found in marine animal tissues. Evidence for their presence is based entirely on culturing experiments and as yet there is no evidence from direct microscopic examination or other techniques. Their role is unknown. In general, compounds produced by fungi associated with marine animals are structurally related to other fungal metabolites and are distinct from natural products produced by the organisms themselves. It does not appear that fungi are the biogenetic source of natural products isolated from marine invertebrates, unlike the situation found with bacteria. The most characteristic sterols of all fungi are ergosterol and related ergostanes. Reports of 5,7-dienic steroids from other marine species are suggestive of fungal contamination. There are very few reports of the incorporation of halogens. Most fungal secondary metabolites are based on a polyketide biogenesis, but some terpenoids are found, for example, the unusual nitrobenzoyl esters of 6,14-dihydroxy-7-drimen-12,11-olide (see Fig. 1.8) [87].

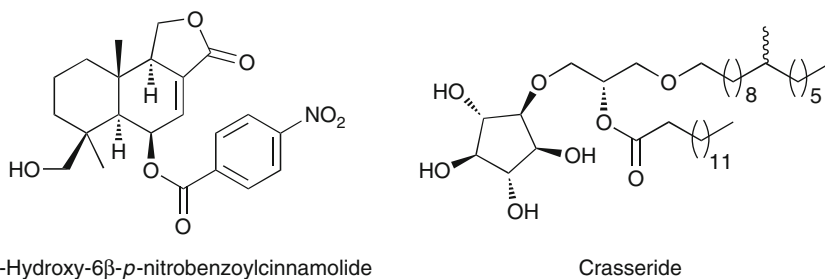


Fig. 1.8 Metabolites from fungi and Porifera

The alkaloids obtained from marine fungi are dominated by diketopiperazines/indoles, as is the case with terrestrial fungi. Very few biosynthetic studies have been reported for natural products specifically from marine fungi.

1.3.2.7 Animalia

All animals are members of the Animalia which range in size from no more than a few cells to organisms weighing many tons. Based on their body plans they are grouped into 30–33 different phyla of which the Arthropoda contains the greatest number of species (~1 million). All members of the Animalia are multicellular eukaryotes, a feature that separates them from bacteria and most protists, and they can be distinguished from plants, algae, and fungi by a lack of rigid cell walls. All members of the Animalia are heterotrophs and so rely directly or indirectly on other organisms for their nourishment. Most ingest food and digest it in an internal cavity with one or two entrances. The bodies of most animals, except the sponges (Phylum Porifera), are made up of cells organized into specialized tissues. Other distinguishing characteristics include a sexual mode of reproduction, at least at some point in the life cycle, and employ differentiated eggs and sperm.

Porifera

The sponges are considered as the most primitive of the multicellular organisms, providing an evolutionary bridge between the monocellular eukaryotes and the rest of the animal kingdom. They are multicellular organisms lacking all organ differentiation (including gonads) and some can uniquely reconstitute themselves after passing through a sieve. They are almost exclusively marine. Sponges are found at all marine depths but the proportion of calcareous sponges diminishes with depth owing to the physicochemical effect of pressure on the ability of the organisms to secrete calcium. The taxonomy of sponges is particularly difficult owing to the paucity of well-marked morphological feature by which they can be distinguished [88]. Many species have been synonymized and genera renamed (e.g., *Aplysina* = *Verongia*), and there are numerous views on their classification at higher levels; a recent multivolume treatise [89] proposes many changes. Three main subdivisions have been generally recognized, depending on the nature of the skeletons that they secrete; calcareous, siliceous, or askeletal. The largest group is the demosponges, about 95% of known species, in which the skeleton is of spongine, a proteinaceous polymer similar to keratin. The Hexactinellida sponges, characterized by silica spicules of sixfold symmetry, are found only at great depth and have been little studied chemically.

Sponges participate in a wide range of symbiotic/commensal relationships, and a large number of the isolations of natural products earlier reported from them are in fact owing to the presence of cyanophytes in particular. Given the extent of these associations, it is not surprising that the diversity of natural products reported from sponges and sponge aggregates covers the whole range of known types. Other natural products reported may be true metabolites of the symbionts [90]. A wide variety of cell membrane components have been isolated, not only extensive series

of both straight-chain, branched, and methylenic (cyclopropanoid) fatty acids but alkylglycerols and hopanoids as well as a vast range of steroids. There are also numerous brominated and α -hydroxyacids. Associated with the membrane structure is a wide variety of glycolipids, many of them of unique structural type [91]. The simpler *N*-containing parents are the sphingosines, the *N*-acyl derivatives collectively known as ceramides, and the glycosides, known as glycosphingolipids or cerebro-sides. The nitrogen-free glycolipid content also includes some structural types not found elsewhere, such as the *crasserides* [92], which as a class have been suggested to be uniquely diagnostic of the Porifera and found in all species examined.

Among calcareous sponges the most investigated genera are *Clathrina* and *Leucetta*. These genera have yielded in particular long-chain unsaturated aminoalcohols, a range of imidazole and other alkaloids, and cyclic peptides. By far the most studied have been the demosponges, reflecting their numerical preponderance and shallow-water accessibility. Demosponges contain a very wide range of steroids, which encompasses not only the conservatively modified structures biogenetically not far removed from cholesterol found in the algae, but also a large number showing more profound modification. These include 19-norsteroids and a range of A-ring abeosteroids (3-hydroxymethyl-A-norsteroids). The most common type of modification however is further side-chain methylation which leads to an extensive series of steroids having various branching patterns up to C₃₂. Side-chain cyclopropasterols occur in the range C₂₇–C₃₁, and there are also a large number of secosterols with fission at 5,6, 8,9, 8,14, and 9,11. There are also many polyhydroxylated and sulfated sterols of the type found in many other marine organisms, and many steroidal glycosides. Halogenated steroids and steroidal alkaloids are rare.

Demosponges of the genera *Plakortis* and *Plakinastrella* (order Homosclerophorida) contain a wide range of oxylipins, including many cyclic peroxides. Another group of unusual natural products found in sponges are the terpenic isocyanides together with their related isothiocyanates, isocyanates, and formamides. A wide range of alkaloids and terpenoids are found in demosponges. Indole alkaloids range from simple halogenated indoles such as the plakohypaphorines to polycyclics such as the pentacyclic pyridoacridines. Demosponges are the most prolific of all marine organisms in terms of the secondary metabolites that have been isolated from (but not necessarily produced by) them.

Cnidaria (Jellyfish, Sea Anemones, Gorgonians, and Corals)

This class of organisms represents the first major development in body plan over the undifferentiated sponges, showing cellular differentiation into cells with different functions, but in general no well-defined organs. The term Cnidarian replaces the older "Coelenterate." This is a class of organisms typified by a carnivorous lifestyle, the presence of specialized stinging cells (cnidocytes) used in the capture of prey and for defense, and a digestive system consisting of a sac with only one opening. They have a basically radial body plan, which may be modified either in the direction of a fixed polyp with a central gastric cavity (hydras) or a free-swimming medusa form (jellyfish) in which the gastric cavity is underneath. Reproduction is sexual, producing a free-swimming larval planula which develops into a free-swimming followed by a

polyp form, although in some species only one of these is formed. About 10,000 species are documented. The sea anemones, gorgonians, and corals have no free-floating phase and have a skeletal structure consisting either of secreted calcareous minerals or of proteinaceous material (gorgonine, analogous to the spongine found in the sponges). They are divided into two groups depending on their symmetry – eightfold in the octacorals (alcyonians or soft corals and gorgonians) and sixfold or a multiple of sixfold (hexacorals, including the sea-anemones and hard corals) [93] – and have been the most studied group of the cnidarians chemically.

In general, relatively few nitrogenous secondary metabolites have been isolated. The proportion of halogenated metabolites is also relatively low, except from *Briareum* spp. Octacorals are rich in prostanoids, steroids, terpenoids (but only sesqui- and diterpenes), and aromatics. The prostanoids include a number identical with those found in higher organisms of the prostaglandin series (A, B, E, and F), but also halogenated prostanoids containing Cl, Br, and I, especially from *Clavularia*. Further oxylipins are now being found in other cnidarians and it appears that their presence may be ubiquitous. The hexacorals also contain a range of polyunsaturated long-chain acids.

Like the sponges, cnidarians contain a wide range of sterols, both typical cholesterol related and those with modified side-chains. An important class are the side-chain cyclopropanoid steroids although it has been shown that these are produced by symbiotic dinoflagellates. There are many polyhydroxylated steroids, often showing side-chain epoxidation and a considerable number of secosteroids. Also encountered are pregnane glycosides, but in contrast to the sponges, *O*-sulfation is absent. The hexacorals produce polyhydroxylated ecdysteroids which are thought to protect the organism against crustacean larvae. The sesqui- and diterpenes found in the octacorals are diverse and include some skeletons unique to them that in most cases are unique to certain families. In contrast, terpenoids are almost absent from the hexacorals. The sesquiterpene hydrocarbon content of octacoral tissues may be exceptionally high and they are thought to play an ecological role as predator and larval implantation repellents. An important feature is the frequent occurrence of common terpenoids enantiomeric to those familiar from terrestrial plants. The hexacorals have yielded only a few sesquiterpenes; there is a complete absence of the isocyanides characteristic of the sponges and only a limited range of terpenoid alkaloids. The octacorals are very rich in diterpenoids, with over 1,900 belonging to 50 isolated skeletal types. As with the sesquiterpenes, some skeletons are widespread throughout the phylum, while others are restricted to a single family and can be considered as chemotaxonomic markers. Particularly widespread skeletons include cembranes, xenicanes, lobanes, briaranes, cladiellanes, dolabellanes, and amphilectanes. As with the sponges, many skeletons are prenylogues of widespread sesquiterpenoid skeletons. Some diterpene alkaloids have been found such as the *sarcodictyins* (see Fig. 1.9) [94]. The hexacorals produce a range of ceramides, often containing unusual sphingosines, and other acyclic amides. Their range of cyclic alkaloids is restricted, but includes the unique class of fluorescent pigments based on the cycloheptadiimidazole skeletons of parazoanthoxanthin A and *pseudozoanthoxanthin* A [95].

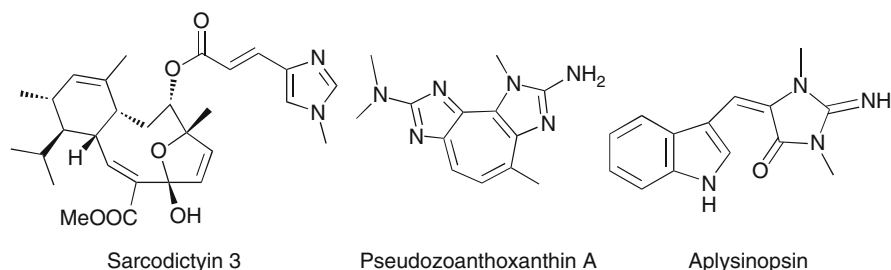


Fig. 1.9 Metabolites from Cnidaria

Hexacorals of the order Zoantharia (genus *Zoanthus*) have yielded a range of polyketide alkaloids. Chemically and pharmacologically, the most significant natural product isolated from cnidarians is probably palytoxin [35, 96]. Hexacorals inhabiting surface waters also contain a range of mycosporins which are closely related to analogs found in fungi and appear to perform a photoprotective function. They also contain a range of small nitrogenous betaines and other amines, some purines, and some simple indole-imidazole alkaloids centered on *aplysinopsin* [97].

Other classes of the cnidarians include the Cubozoa (box jellies), Hydrozoa (hydras), and Scyphozoa (true jellyfish). Chemical studies have been mostly confined to their venoms, which are peptides. One difficulty associated with studying their secondary metabolites is the large amount of water in the tissues, which can reach 98%. Some steroids have been identified, plus a small range of polyketides and simple alkaloids. There are also the nitrogenous compounds associated with the bioluminescence of some species such as *Cypridina*.

Platyhelminthes (Flukes, Tapeworms, and Free-Living Flatworms)

These are the flatworms, characterized by a bilateral body plan and the complete absence of a digestive cavity with about 15,000 species known. They may be terrestrial, freshwater, or marine and many belong to orders which are exclusively parasitic (e.g., flukes). The majority of marine species belong to the class of planarians (turbellarians). These are mobile, carnivorous animals having no physical means of defense and relying entirely on substances absorbed or modified from the diet, or produced by symbiotic organisms, as chemical antifeedants. The most studied genus is *Amphiscolops*. These worms are protected by amphidinolides produced by symbiotic dinoflagellates and other dinoflagellate metabolites [62, 63]. Other planarians feeding on ascidians have yielded alkaloids.

Annelida (True Worms)

These are the segmented worms, having an alimentary canal. They include the polychaetes, oligochaetes (earthworms; mostly terrestrial), hirudineans (leeches; mostly freshwater), echiurians, and Vestimentifera. They locomote by means of bristles which can be irritant or venomous. The best-known genus among the echiurians is the spoonworm *Bonellia viridis*, most studied on account

of its tetrapyrrole pigment bonellin which also plays a role in inducing sexual differentiation in the larva [98]. The Vestimentifera include the recently discovered giant hydrothermal vent dwellers *Riftia* which coexist with sulfur bacteria and store elemental sulfur in the tissues. So far there has been little study of lipid or steroid content. The carotenoid pigments appear to be mainstream components and are derived dietetically. Other annelid pigments are anthracene and anthraquinone based. Annelids also contain brominated phenols and derived aromatics which protect them against bacteria. Certain annelids exhibit bioluminescence and in *Odontosyllis* spp. this is based on pteridines such as 6-propionyllumazine. Nereistoxin is a simple aminodithiolane with powerful cytotoxic properties produced by *Lumbriconereis* sp. [99].

Nemertea and Phoronida

The ribbon-worms or nemerteans have yielded the powerful nicotinic receptor agonist anabaseine, used as a venom by the worm, together with several related oligopyridines. Toxins of the tetrodotoxin series are also found in the tissues, and also some peptide toxins. The unsegmented phoronidian worms *Phoronopsis* have yielded antibacterial bromophenols like those obtained from the annelids.

Bryozoa

These colonial organisms are entirely aquatic and mostly marine. They are distinguished by their unique form of gastric cavity, which is surrounded by tentacles forming an organ called the lophophore. The colonies are produced by budding and therefore consist of genetically identical individuals, each of which is surrounded by a bilayered exoskeleton, the inner layer calcareous (not always continuous) and the outer layer chitinous. They are suspension feeders, feeding on plankton and bacteria, and are found at all depths. Bryozoans have so far been less studied than the number of known species (5,700) would justify given the range of interesting natural products already isolated from them. This is probably a consequence of the difficulty of harvesting them.

Terpenoids and steroids have been little studied. The single diterpenoid murrayanolide isolated has a unique skeleton which implies that many more unusual terpenoids may exist in other bryozoans. The similarly limited studies of steroid content have yielded only relatively common types based on cholestane methylated in the side chain and/or hydroxylated. One or two anthraquinone pigments have been characterized, of which the most unusual is bryoanthrathiophene. The most numerous metabolites from bryozoans are defense chemicals, which comprise numerous alkaloids, and the *bryostatins* (see Fig. 1.10) [100], an important series of polyether polyketide toxins with anticancer properties, some of which have also been found in other marine organisms. The ultimate source of these may be a *Candidatus* bacterium [101]. The range of alkaloids is extensive taking into account the limited amount of work that has so far been done. There are simple halogenated phenethylamines, pyrroles, and pyrrolidines. The indoles found are mostly brominated simple indoles, but *Flustra foliacea* yielded a series of alkaloids of the physostigmine type unique in the marine environment [102]. The securamines, chartellines, and chartellamides

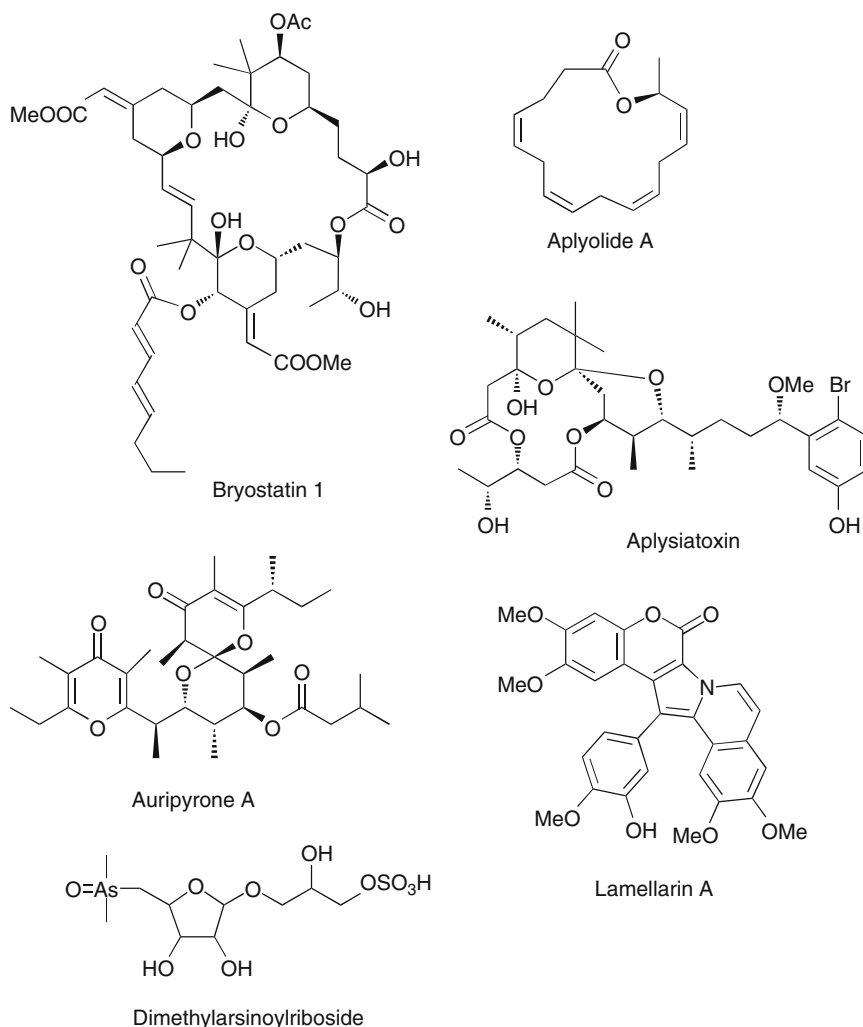


Fig. 1.10 Metabolites from Bryozoa and Mollusca

represent a further elaboration of this structural type up to a maximum of seven rings [103–105]. There are also a number of quinolinequinones, halogenated or bearing thioether substituents. The presence of nitro groups in a few alkaloids is notable.

Mollusca

This is a diverse and widely distributed phylum of organisms [106]. The body plan is basically non-segmented and bilateral, although in some molluscs (the gastropods) it is often modified by torsion into a spiral surrounded by a shell. There are well-developed organs inside a more or less thickened outer layer, the mantle,

which secretes a shell formed of calcareous matter and protein. This shell may be external, as in the gastropods, internal as in squids, or may be totally lacking (octopuses and nudibranchs). There is generally a muscular foot and a cephalic region which may be highly developed into tentacles and other organs, as in the cephalopods. The alimentary canal is well developed and furnished with a rasping radula used in feeding. Different classes of molluscs show variation in this general body plan, for example, the bivalves have a hinged shell, no cephalic region and no radula, and some of them also lack the foot. Many species of mollusc are known, present in marine, freshwater, and terrestrial environments, ranging in size from microscopic to very large. They show a wide range of dietary behavior (carnivores, herbivores, filter feeders, and detritus feeders) and undergo a wide range of symbiotic relationships. In particular, in some molluscs the mantle incorporates symbiotic algae providing toxic antipredator substances. The phylum is usually divided taxonomically into seven unequal classes, but of these four (including Chitons) are numerically limited and have been studied chemically little or not at all [107]. The most important classes both in terms of number of species, economic importance, and chemical studies are the gastropods, the bivalves, and the cephalopods. However, the bivalves, with their well-developed physical protective mechanism of the double shell, appear to have less need for chemical defense mechanisms and their secondary metabolites are less profuse. They have mostly been studied in terms of their economically important shellfish toxins, which are in fact microbial/dinoflagellate products. The cephalopods too have been rather little studied; their most characteristic metabolites are adenochromines [108]. The most studied organisms chemically have been various types of gastropod which have little or no physical defense and rely almost entirely on chemical defense against predators. The numerous gastropods are sometimes further divided into three subclasses: the Prosobranchia, the Opisthobranchia, and the Pulmonata. This division is not recognized by the *Catalogue of Life*, but since it is a convenient subdivision of a large group of natural product-producing organisms, it is followed here.

Terpenoids are numerous. The genus *Planaxis* (Gastropoda, Prosobranchia) has provided a series of cembranoids. Among the opisthobranchs, the sea hares or aplysians, which are herbivorous, feed on cyanobacteria and algae, and their digestive systems and mantles contain a wide variety of unchanged and metabolized secondary metabolites which perform an antifeedant function. These alimentary chains are complex and have been much studied. The two most studied genera are *Aplysia* and *Dolabella*; the former feed mostly on red algae and contain many halogenated and nonhalogenated terpenoids, cyclic halogenated ethers, lactones, and both peptide and nonpeptidal alkaloids. *Dolabella* spp. feed on brown algae, and in accordance with the terpenoid profile shown by these, contain mostly nonhalogenated diterpenoids as well as lactones, peptides (notably the extensive range of highly cytotoxic dolastatins, from cyanobacterial symbiosis), and alkaloids. A few *Aplysia* spp. feed on brown algae and also contain nonhalogenated diterpenes. Other products isolated from this type of mollusc appear to derive from symbiotic/commensal green algae, *aplyolides* [109], and even fungi, *aplysiatoxin* [110, 111].

The shell-less nudibranchs can incorporate cnidocysts obtained from cnidarians into their mantle, and also rely heavily on compounds, especially terpenes, ingested in the diet as a means of defense. A wide range of skeletal types have been isolated, and include sponge-derived terpenoid isocyanides and compounds derived metabolically from them. However, nudibranchs also synthesize terpenoids *de novo* via the mevalonate pathway. Many terpenoids are present as glyceryl esters. In general it is possible to predict with a fair degree of accuracy what types of compounds (though not necessarily the exact compounds) will be isolable from nudibranch tissues by studying the prey of the different species. The sacoglossan gastropods also contain a range of terpenoids, but these animals are herbivorous and the terpenoids derive from commensal green algae entering into the tissues. Nudibranchs contain a narrow range of carotenoids and steroids. Other defense allomones include quinonoid and related meroterpenoids, and macrocyclic lactones. Also noteworthy is the isolation of prostanoid lactones from *Tethys fimbria*.

The distribution of polyketides in molluscs is patchy. They are found only in some classes of the gastropods, for example, the *auripyrone*s (strictly, polypropionates) from *Dolabella* [112]. Pulmonarians have also afforded a number of polypropionates. Long chain aromatic and heteroaromatic metabolites, which do not appear to be derived from the diet, are found in *Navanax* spp., *Haminoea* spp., and other genera. Peptides, especially cyclic oligopeptides often containing unusual amino acid residues, are probably widely distributed and show structural resemblances to similar compounds found further down the food chain, for example, the kahalalides [73]. Among other nitrogenous metabolites, the best-known from gastropods is the dye-stuff 6,6'-dibromoindigotin, known since ancient times. The genus *Lamellaria* (Gastropoda; Prosobranchia) yielded a wide range of the pyrrole alkaloids, the *lamellarins* [113].

Carnivorous gastropods of the genus *Conus* produce a vast series (there appear to be tens of thousands of chemically distinct compounds) of highly toxic peptides the conotoxins [114], which are delivered to the prey by means of a highly specialized injecting organ. The bivalve toxins (e.g., pinnatoxins [64, 65]) responsible for various kinds of shellfish poisoning are mostly produced by commensal dinoflagellates and have been mentioned above. There are differences in the distribution of different members of the saxitoxin series between the tissues of the bivalves and the originating dinoflagellates [115].

The kidneys of the giant clam *Tridacna maxima* concentrate up to 0.1% of arsenic, the function of which is unknown. It is stored as various *dimethylarsinoyl-ribosides* [116].

Echinodermata (Crinoids, Starfish, Sea Urchins, Sea Cucumbers, Brittle-Star, etc.)

These organisms are characterized by a radially symmetrical body plan (which is acquired in the adult stage, the larvae being bilaterally symmetrical) and a unique system of respiration through water-filled tube feet which also provide locomotion. There is a calcareous endoskeleton. This is the largest phylum of exclusively marine animals, with about 7,000 species known. They may be herbivores,

suspensivores, detritivores, carnivores, or necrophages, and the carnivorous species may prey, for example, on corals or other echinoderms. There are many examples of commensalism and parasitism between echinoderms and other organisms. Although various classification schemes for echinoderms differ in detail, five main groups are generally recognized. The most primitive, widely represented in the fossil record, are the Crinoids in which the mouth and anus are on the same surface. They have a planktonic larval form followed by an adult form that may be sessile (sea lilies) or mobile (feather stars). The other four groups, in which the mouth and anus are on opposing faces, are the starfish (Asterozoa), sea urchins (Echinozoa), sea cucumbers (Holourozoa) [117], and Ophiurozoa.

The presence of steroidal saponins of different types in the starfish and in the sea urchins is unique in the animal kingdom, and serves to delineate them from the other echinoderms and from each other. Other characteristic markers are the dominance of 3α -hydroxylated steroids in the ophiurians, and of quinonoid pigments of different types in the crinoids and in the sea urchins. The various types of echinoderm produce a variety of specialized polysaccharides, the study of which is still in its infancy. One that has been characterized is frondecside [118]. The lipid content of sea urchins and ophiurians is high in polyunsaturates. The starfish have been relatively little investigated but appear to follow the same pattern, with some prostanoid precursors. A high proportion of branched-chain acids have been isolated from sea cucumbers, but these are probably of bacterial origin. Phospholipids and glycosphingolipids appear to be universally present in echinoderms and a wide range of structural types of ceramides and cerebrosides have been isolated from starfish and holothuroids. Throughout the echinoderms, halogenation is rare and found only in a few anthraquinone pigments such as the *gymnochromes* (see Fig. 1.11) (from crinoids) [119]. There are also few alkaloids of greater complexity than a range of aliphatic amines. The few exceptions to this generalization are most probably derived from organisms such as dinoflagellates present in the food chain.

The type and extent of steroid content is a major distinguishing feature of different types of echinoderm. The crinoids and echinoids have been little studied, but appear to contain exclusively “classical” steroid types closely related

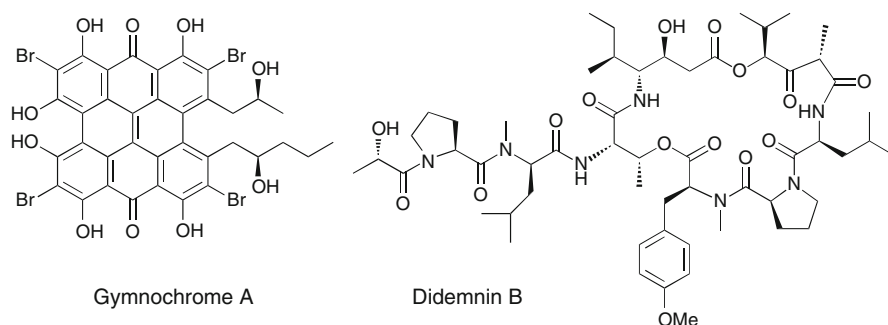


Fig. 1.11 Metabolites from Echinodermata and Ascidiaceae

structurally to cholesterol. The ophiurians, which in some respects are intermediate between the primitive crinoids and the more highly evolved echinoderms, contain many 3α -hydroxysteroids with only one or two glycosides. In the starfish, the range of glycosides and steroid sulfates is extensive, derived from a wide range of side-chain-modified parent steroids, which, however, are mostly 3β -hydroxylated. The side chain may be degraded or cyclopropanated. Polyhydroxylation/*O*-sulfation of the steroid nucleus, which is widespread in marine organisms, is at its most extensive here. The glycosides, such as the asterosaponins play a role in chemical defense through their surface-active properties. Both pentose and hexose residues are found. The holothurians contain many steroids, some biosynthesized *de novo* from acetate via lanostane triterpenes, others apparently derived from the diet. In *Holothuria*, it has been shown that two biosynthetic routes operate, one via lanosterol and the other via parkeol. The chief distinguishing feature of the holothurians, however, is the exclusive occurrence of specialized triterpenoid glycosides of the holostane type. Examples of the anthraquinonoid pigments are readily extracted from crinoids. Some of these are *O*-sulfates. The sea urchin pigments however are exclusively naphthoquinonoid. The number of alkaloid-like compounds isolated from echinoderms is extremely limited.

Arthropoda (Crustaceans)

The crustaceans, including the decapods, are the only type of animals in the vast arthropod phylum that occur to any extent in the sea. In the past the crustaceans have been considered a separate phylum, but it should be noted that the majority of taxonomists, including the *Catalogue of Life*, now assign the crustacea as a major subphylum of the arthropoda rather than as a separate phylum as they have in common the hard chitinous exoskeleton and the body divided into head, thorax, and abdomen. About 45,000 species are known, some of them (ostracods, e.g., *Cypridina*, and copepods, e.g., *Calanus*) very small planktonic organisms. The best known large species are the decapods (crabs and lobsters). Chitin, derived industrially from crab shells, is an important industrial material.

Chemical studies on crustaceans have been fragmentary and are mostly confined to their carotenoid pigments, some of which have also been obtained from other marine organisms but which were originally characterized as crustacean products. The molting hormones of crustaceans are terpenoid (methyl farnesate) and steroidal. Steroid studies have been fragmentary and have indicated a preponderance of cholesterol and closely related compounds.

Hemichordata

This is a numerically limited class of animal (about 100 species recorded), consisting of two surviving types of organisms; the acorn worms (Enteropneusts) inhabiting temperate and tropical waters, and the pterobranchs, colonial animals inhabiting chitinous tube galleries and found in polar waters. There is differentiation of the body into three well-defined zones, and they have some, but not all, of the morphological characters that define the chordates. Two types of natural products have been identified from them. The first is a range of toxic cyclohexanes,

halogenated phenols, and halogenated indoles isolated from *Ptychodera*, *Balanoglossus*, and *Glossobalanus* spp. These are used by the worms as defense chemicals and are of environmental significance. Of greater biochemical interest are the highly cytotoxic disteroidal metabolites the cephalostatins from *Cephalodiscus gilchristi* [120]. Owing to the difficulty of culturing hemichordate species, there is no information currently available concerning their possible distribution elsewhere in the phylum, or on their biosynthesis.

Chordata; Ascidiaceae (Ascidians, Tunicates)

These simplest chordate animals, also known as the protochordata, are generally divided into two unequal groups the urochordates (which include the ascidians or tunicates) and the cephalochordates which are free-swimming bilaterally symmetrical animals (*Branchiostoma*). Protochordates are the most developed of the invertebrates and have a notochord that is the evolutionary precursor of the spinal column characteristic of the vertebrates. They are exclusively marine. The larger group of urochordates is divided into three classes. Of these, two, including the free-floating salps, have been little investigated. Most chemical studies have been on the third group, the sessile ascidians [121]. These are filter feeders, often harboring commensal cyanobacteria and other organisms that may be the true source of some of the reported natural products. Their chemistry is dominated by the presence of an extraordinary range of mostly biologically potent nitrogen compounds. The ascidians also famously accumulate vanadium to a very high concentration in specialized cells, and some have highly acidic tissues (down to pH 1). The epidermis of ascidians contains a range of sulfated glycans, including some unusual residues such as L-iduronic acid, and the unusual polysulfated polymannose kakelokelose [122]. The membrane lipids have been little studied, and presumably are close to those of other higher organisms in structure. A few oxylipins have been isolated, along with ceramides and cerebrosides. These appear to be widespread as in the echinoderms, with some unusual types such as didemniserinolipids isolated [123]. Ascidians contain a range of carotenoids, both common ones and some rarer examples probably derived from metabolic alteration of more common carotenoids present in the filtered plankton. The steroids so far identified lack the wide structural range shown by the echinoderms and are mostly straightforward cholestanes and ergostanes, with some 5,8-epidioxysteroids and secosteroids. Nonnitrogenous secondary metabolites are few in number and terpenoids are rare. Several series of meroterpenoids have been isolated, especially from the Polyclinidae. The ritterazines from *Ritterella* have disteroid structures linked by a central pyrazine ring [124], showing close structural similarity to the cephalostatins from hemichordates [125].

Among the nitrogenous metabolites, many of which doubtless also spring from commensal organisms, there is a very wide range of structure including some with, and some without, analogies in other phyla. Firstly, there is an extensive range of modified peptides and depsipeptides. Several series of these are macrocyclic thiazoles and oxazoles, for example, the patellamides [125, 126]. Other cyclic depsipeptides are more strictly peptide related, although containing a range of unusual aminoacids.

The most studied have been the *didemnins* and their relatives [127, 128]. Heterocyclic alkaloids are numerous and include the extensive range of pyrroloisoquinolines, the lamellarins which were first isolated from molluscs (*vide supra*), but which are the products of ascidians on which they prey, or possibly of a symbiotic association involving sponges [113, 129]. Quinoline alkaloids are represented and the basic quinoline ring system is further elaborated into pyridoacridines. These too are also found in other marine organism classes. In the ascidians they fulfill the role of pigmentation and are also mostly cytotoxic. Indole alkaloids are also numerous, again known mostly as polycyclic condensed systems. Ascidians also contain a wide range of sulfur compounds, both sulfur-heterocycles and polysulfides.

Chordata; Actinopterygi (Fish)

The fish represent the most numerous of marine vertebrates. They are well studied taxonomically and extensively documented in the online database *Fishbase* (a contributor database to the *Catalogue of Life*). They can be divided into cartilaginous fishes (e.g., sharks), and the larger category of bony fishes, considered more highly evolved.

The cartilaginous fishes contain a wide range of polyhydroxylated nitrogenous and nonnitrogenous sterols based on 5 β -cholestane and include the important drug lead *squalamine* (see Fig. 1.12) [130]. The difference in the color of fish is due to the presence of various carotenoids and xanthophylls.

The fish products that have received the most chemical attention, apart from the lipids, are the toxins produced by various species. These may be steroidal, peptide, or alkaloid like, such as the much studied *tetrodotoxin* and its relatives from

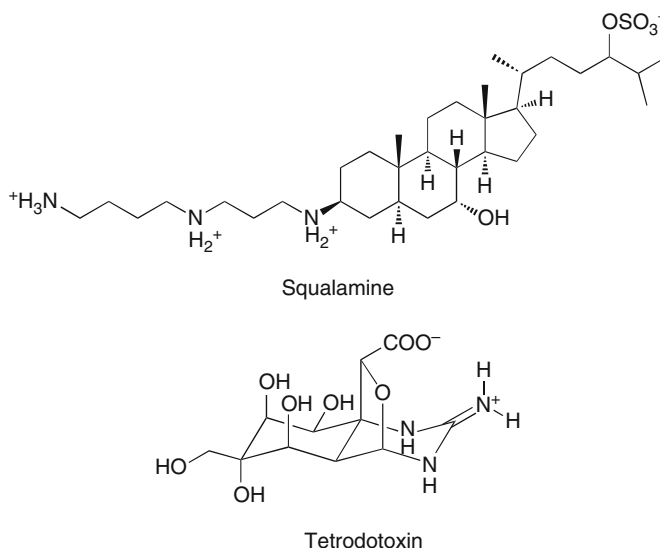


Fig. 1.12 Metabolites from Actinopterygi (fish)

fugu fish (various species of the Tetraodontidae) [131]. The latter, however, are metabolites of *Pseudomonas* bacteria or dinoflagellates in the fish, and are also found in other marine organisms and even terrestrial ones. Some fish secrete peptide venoms in specialized spines to deter prey.

1.4 Marine Taxonomy and Natural Products Chemistry

Biodiversity at the higher taxonomic levels (phyla and classes) is greater in the marine phyla. Of the 76+ phyla recognized by the *Catalogue of Life* across the Eukaryota, about 60 have marine representation compared with around 40 for terrestrial and freshwater environments. This comparison is even more extreme for the Animalia with all but one phylum out of the 30+ recognized having marine representatives (see Fig. 1.4). In contrast, species diversity is lower in the sea with just 250,000 species recognized against the >1.5 million terrestrial and freshwater species.

In looking back over the modern history of marine natural products, definite trends and preferences in the selection of phyla are discernible. To analyze these trends the database MarinLit [132] was used. This is a database of the marine natural products literature. In addition to the usual bibliographic data, the database contains an extensive collection of keywords, trivial names, compound information including structures, formulae, molecular mass, numbers of various functional groups, and UV data. All of these items can be searched for either individually or in various logical combinations. Taxonomic data are also included, permitting the exploration of relationships at various levels from genus up to phylum. The taxonomic descriptors used in MarinLit are aligned with the *Catalogue of Life*, thus avoiding the circumspection associated with alternative taxonomic schemes (cladification vs classification) and the use of pseudonyms. The data extracted from MarinLit were compared in the first instance against Bouchet's modified list of marine species [17] at the higher taxa level. The comparisons are shown in Tables 1.3 and 1.4. The criteria used were the total number of species studied in each taxon, the percentage this represented of that taxon, and the number of papers

Table 1.3 Comparative data for species studied from the higher-order taxonomic levels

Higher taxa	Number of marine species (Bouchet 17))	% of marine higher taxa	Species studied	% coverage of marine higher taxa	Number of papers by taxa	% of papers published
Archaea	>0	>0%	5	-	4	0.02%
Bacteria	5,800	2.5%	504	8.7%	1,622	8.0%
Fungi	500	0.2%	289	57.8%	612	3.0%
Protozoa	>14,800	~6.4%	192	~1.3%	929	4.6%
Chromista	7,600	3.3%	639	8.4%	1,3489	6.6%
Plantae	8,700	3.8%	1,062	12.2%	2,202	10.9%
Animalia	192,667	83.9%	4,071	2.1%	13,596	66.9%
	>230,117		6,762	~2.9%	20,314	

Table 1.4 Comparative data for marine natural products from the higher-order taxonomic levels

Higher taxa	Number of marine species (Bouchet [17])	% of marine taxa	Species producing new compounds (number, %)	Number (%) of compounds isolated	Number (%) of papers on new compounds
Archaea	>0	>0%	2 (?%) ^a	24 (0.1%) ^b	2 (0.03%) ^c
Bacteria	5,800	2.5%	201 (3.5%)	1,178 (5.9%)	545 (7.0%)
Fungi	500	0.2%	196 (39.2%)	969 (4.8%)	369 (4.7%)
Protozoa	>14,800	6.4%	60 (0.4%)	308 (1.5%)	193 (2.5%)
Chromista	7,600	3.3%	182 (2.4%)	1,231 (6.1%)	467 (6.0%)
Plantae	8,700	3.8%	282 (2.1%)	1,975 (9.9%)	798 (10.3%)
Animalia	192,667	83.9%	1,941 (1.0%)	14,372 (71.7%)	5421 (69.6%)
	>230,117		2,864 (~1.25%)	20,057	7,795

published along with the relative percentage contribution to the overall output of papers. Some 84% of all marine species belong to the Animalia. The observation that 4,071 of the 6,762 marine species studied belong to the Animalia is in keeping with this dominance of the Animalia among the marine species. The actual number of species studied is probably higher than this as many of the samples studied were identified to the genus level only. The 129 citations of *Laurencia* sp. or the 132 citations of *Streptomyces* sp. have each been counted as only one in the list of species studied, even though they might represent many different species. However, this will be offset as many will be identical to samples fully identified to the species level. The number of papers published by taxon is generally in step with the relative numbers of species/taxon with 13,596 of the 20,314 papers published up to early 2009 having an Animalia focus. Despite the focus on the phyla of the Animalia, the relative percentage coverage of this taxon (2.1%) is noticeably lower than for most of the other taxa, except the Archaea.

Many aspects of MNPs are covered in MarinLit. These include first syntheses of MNPs, assignment or correction of stereochemistry, environmental studies, as well as the isolation of new natural products, and these are the data covered in Table 1.3. The isolation of new natural products is the focus of Table 1.4. Studies on 2,864 species resulted in the isolation of 20,057 compounds reported in 7,795 papers. These are the data to early 2009. Again the actual number of species is not totally reliable as many samples were reported to the genus level only. Not surprisingly the major focus has once again been on the Animalia as the prime source of new compounds (14,372). There is a good correlation between the papers published and the numbers of compounds isolated. Despite the focus on Animalia the overall percentage of species in this taxon yielding new compounds is only 1%.

The data outlined in the Tables shows the output and general emphasis over the past 75 years in MNP chemistry, but to get to the detail it is necessary to examine the data at a phylum level. These data are portrayed in Tables 1.5 and 1.6. For some taxa, Bouchet's breakdown [17] was not detailed enough and the added phyla are shown in italics as, for example, in Table 1.5, Actinobacteria, etc.

Table 1.5 Comparative isolation and publication data for the Archaea, Bacteria, Fungi, Protozoa, Chromista, and Plantae taxa

Taxa	Marine species	Species with new compounds	Species studied	Compounds isolated	Papers with new compounds	Total papers
<i>Archaea</i>						
Euryarchaeota	–	2	3	24	2	4
	>0	2	3	24	2	4
<i>Bacteria</i>						
Bacteria	4,800	128	295	571	283	699
<i>Actinobacteria</i>		59	116	348	167	357
<i>Bacteroidetes</i>		8	15	16	8	25
<i>Firmicutes</i>		8	13	51	25	60
<i>Proteobacteria</i>		53	151	156	83	257
Cyanophyta	1,000	73	209	607	262	923
	5,800	201	504	1,178	545	1622
<i>Fungi</i>						
Fungi	500					
<i>Ascomycota</i>		195	278	968	368	605
<i>Basidiomycota</i>		1	5	1		4
<i>Zygomycota</i>			6		1	3
	500	196	289	969	369	612
<i>Protozoa</i>						
Ciliophora	?	7	11	27	10	18
Sporozoa						
Phylum not assigned	?					
Class Sporozoa						
Dinophyta (Dinomastigota)	4,000	52	177	278	182	905
Euglenozoa	250	1	3	2	1	5
Radiolaria		–	–	–	–	–
Phylum not assigned	550					
Class Sarcomastigophora						
Foraminifera		–	–	–	–	–
Phylum not assigned	10,000					
Class Granuloreticulosea						
	>14,800	60	191	307	193	928
<i>Chromista</i>						
Ochrophyta	1,600	161	456	1166	437	1120
Class Phaeophyceae						

(continued)

Table 1.5 (continued)

Taxa	Marine species	Species with new compounds	Species studied	Compounds isolated	Papers with new compounds	Total papers
Ochrophyta	500	18	174	57	27	222
Class						
Chrysophyceae						
<i>Labyrinthista</i>		1	3	3	1	2
<i>Oomycota</i>		–	2	–	–	2
Haptophyta	500	1	1	3	1	1
“Bacillariophyta”	5,000	1	3	2	1	2
	7,600	182	639	1,231	467	1,349
<i>Plantae</i>						
Chlorophyta	2,500	60	305	275	113	541
Magnoliophyta	50	26	73	125	43	98
Rhodophyta	6,200	195	682	1,574	641	1,562
	8,750	281	1,060	1,974	798	2,201
Totals	37,450	922	2,683	5,683	2,371	6,712

For the taxa from Archaea through to Plantae, shown in Table 1.5, there are 37,450 species of which 2,683 have been studied at one level or another, some 5,683 compounds have been isolated, 2,371 compound structural papers published, and a total of 6,712 papers refer to these species in one way or another. These seven taxa represent just over 16% of the known/recognized marine species, but just over 7% of these recognized species have been examined with the bulk of this work having been accomplished over the past two decades.

The taxon Animalia, covered in Table 1.6, portrays a somewhat different picture.

This one higher taxon, the Animalia, represents 84% of the established marine species and comprises 30 phyla (Table 1.6), although the actual number of phyla is variable from 30 to 33 depending on the taxonomic authority consulted. Of the 29 phyla with recognized marine representatives, only 13 have been sampled over the years by natural product chemists (Table 1.6). In all 4,071 species out of a total of 192,667 (2.1%) of the Animalia have been examined. Of these 1,554, or 38%, have come from the Porifera alone, another 806 (20%) from Cnidaria, 587 (14%) from Mollusca, and 407 (10%) from Echinodermata. So, 82% of the Animalia species examined have come from just four phyla. Furthermore, about half of the compounds isolated from the Animalia have been of Porifera origin (7,024 out of 14,372) and the phylum accounts for one third of all publications across all branches of marine natural products chemistry. As only 5,683 compounds came from all the other higher taxa combined, this one phylum, the Porifera with an estimated 5,500 species, has been the origin of about 30% of all of the MNP chemistry. In keeping with the isolation and publication rate, the percentage

Table 1.6 Comparative isolation and publication data for the Animalia

<i>Taxa</i>	Marine species	Species with new compounds	Species studied	Compounds isolated	Papers on new compounds	Total papers
Animalia						
Acanthocephala	600	—	—	—	—	
Annelida	12,148	14	52	48	25	90
Arthropoda	47,217	9	77	11	10	88
Brachiopoda	550	—	2	—	—	2
Bryozoa	5,700	28	77	172	75	334
Cephalorhyncha	156	—	—	—	—	
Chaetognatha	121	—	—	—	—	
Chordata	21,517	184	475	957	396	1,513
Cnidaria	9,795	415	806	3,909	1,307	2,545
Ctenophora	166	—	—	—	—	
Cycliophora	1	—	—	—	—	
Echinodermata	7,000	205	407	1,172	446	852
Echiura	176	—	—	—	—	
Gastrotricha	395	—	—	—	—	
Gnathostomulida	97	—	—	—	—	
Hemichordata	106	3	18	29	12	68
Kamptozoa	170	—	—	—	—	
Mesozoa	106	—	—	—	—	
Mollusca	52,525	201	587	1,046	459	1,729
Nematoda	12,000	2	7	2	3	9
Nematomorpha	5	—	—	—	—	
Nemertea	1200	—	1	—	—	7
Onychophora	0	—	—	—	—	
Phoronida	10	—	—	—	—	
Placozoa	—	—	—	—	—	
Platyhelminthes	15,000	2	8	2	2	63
Porifera	5,500	878	1,554	7,024	2,686	6,296
Rotifera	50	—	—	—	—	
Sipuncula	144	—	—	—	—	
Tardigrada	212	—	—	—	—	
Totals	192,667	1,941	4,071	14,372	5,421	13,596

coverage of that phylum for chemistry has been very high with 878 out of the estimated 5,500 species having been examined for chemistry and a further 676 species implicated in environmental studies, reviews, and the like. This equates to a 28% overall coverage of that phylum.

When the outputs and the foci of MNP chemistry are examined, it is obvious that right from Bergman's first papers [21–27] MNP chemistry has been *Porifera-centric*. Is there an anthropomorphic bias to these results? Undoubtedly! There was no doubting the enormous academic and medicinal chemistry interest in

Bergman's discovery of the arabino-pentosyl nucleosides. It was from this discovery that the development of the nucleoside-based drugs ara-A, ara-C, and AZT could be traced, and this development has been well documented [133, 134]. The 1967 symposium held in Rhode Island with the ambitious title *Drugs from the Sea* [135] promoted greater interest in the field and raised the promise for other potential pharmaceuticals. Perhaps the mindset was that the Porifera must hold further secrets? Certainly the phylum Porifera has fascinated and held the interest of researchers from the 1950s onward. Every year 25–30% of all MNP publications refer to this phylum. This same Porifera-centric selection showed up in the marine component of the collections of the Natural Products Branch of the NCI's Developmental Therapeutics Program undertaken between 1986 and 2004. From the 9,945 individual organisms tested no less than 4,600 were sponges [136]. Again, this is a figure that is out of all proportion to the species-abundance of this phylum and strongly supportive of anthropomorphic bias in the collection process. This is not surprising as sponges are well represented in depths readily accessible by snorkeling or SCUBA diving, are often colorful and easily spotted underwater, quite varied in structure, and range in size from thin encrusting films (not usually collected) through a very convenient size range for collection in enormous vases and cups.

There have been different foci of interest at different points in time and this too was possibly a result of different collection techniques as well as advances in separation technologies. For example, during the 1960s and 1970s there was about as much interest in the red algae (Rhodophycota) as there was in the sponges. In the semi-decade 1974–1978, publications on red algae ran at about the 20% mark compared with 25% for sponges [132]. This then steadily dropped down over the years to the current level of about 5%. Interest in the brown algae (Ochrophyta) shows a similar pattern (10% decaying to about 4%). Both the red and the brown algae are easily accessible by shore-wading and not reliant on snorkeling or SCUBA diving, so early focus on red algae can probably in part be ascribed to ease of collection as chemists first started to explore the marine environment. Another readily collected phylum is the Mollusca which has featured in around 7% of all publications each year since the early 1960s [132].

The type of chemistry that has been published through the years also shows definite influences. The metabolites published in the early years tended to be nonpolar, lower molecular weight compounds, in keeping with the chromatographic practices of the 1960s and 1970s, for example, halogenated monoterpenes and sesquiterpenes from red alga. In Faulkner's first review of marine natural products chemistry covering the period 1974–1976 [137], >90% compounds covered were nonnitrogenous and nonpolar in character. This percentage rapidly decreased with the advent of new chromatographic techniques and chromatographic phases in the 1970s and 1980s that were better suited to dealing with polar compounds. Simultaneously, greater emphasis was being placed on biological activity. In keeping with Lipinski's rules [138] such compounds are polar molecules, so the range and type of metabolites sought, isolated, and characterized was changing from less polar to more polar metabolites.

Another advantage of shore-wading had been the ability to collect large samples relatively easily. Initially snorkeling and then SCUBA diving markedly expanded the range of species available, but necessarily limited the scale at which collections could be made. But, introduction of new techniques such as ESMS and progressive changes in NMR techniques and field strengths saw marked reductions in the amount of compound required and significant increases in the complexity of the molecules that could be successfully studied. This effectively allowed work on much smaller field samples, perhaps at the 10 g scale rather than a kg scale with a marked expansion of collection options as very small samples only needed to be collected. For example, effective sampling from the myriad of thin, encrusting invertebrates that compete for space on a cliff face. Other, more recent advances in NMR technologies has seen the introduction of capillary probes [139] and small diameter cryoprobes [140] leading to NMR spectroscopy on the nanomole scale [141]. This has effectively reduced the field sample requirement to 50 mg or less [142]. These sources of bias need to be borne in mind when considering how the field of MNP chemistry developed and why it evolved as it has.

1.5 The Results Achieved

Terrestrial natural products chemistry has traditionally been the source of the modern pharmacopeia: the expectations for the marine counterpart were not dissimilar. Despite that amazing start provided by Bergman, the realization of the potential of marine natural products has been a long time in coming. Through the years many other potentially bioactive compounds have been identified. Few have been developed, but many are serving useful roles as biomolecular probes. The first marine natural product to be marketed as a drug was ω -conotoxin MVIIA, in 2004 under the trade name Prialt, for the treatment of intractable pain. ω -Conotoxin MVIIA had originally been isolated from the Pacific marine snail *Conus magus* [114]. This development was followed in 2007 by the approval of Yondelis for soft tissue sarcomas. Yondelis, or ET-743, is a fused tris-isoquinoline isolated from the Caribbean tunicate *Ecteinascidia turbinata* [143, 144]. Until about 12 years ago the bioactivity most sought after was anticancer. Since then a much wider range of selective bioassays have been deployed and more often than not the natural products chemists have been working in collaboration with pharmacologists to achieve these results. Recent reviews have highlighted marine natural products of biological relevance [145–148]. Of particular interest is the source organism for these compounds. The largest collection and screening effort on marine organisms has been that carried out by the NCI [136]. Approximately 12,000 marine samples were collected from the Caribbean and the Indo-Pacific, and extracts from 9,945 individual organisms were tested in the NCI human cancer one dose/60-cell-line prescreen. Close to 50% of these samples were from the phylum Porifera. From this assembly, 620 organisms across 12 phyla were considered active with 407 being of sponge origin. When the data were reduced to a percentage “hit-rate,” eliminating the Porifera-centric character of the collection strategy, other marine phyla with

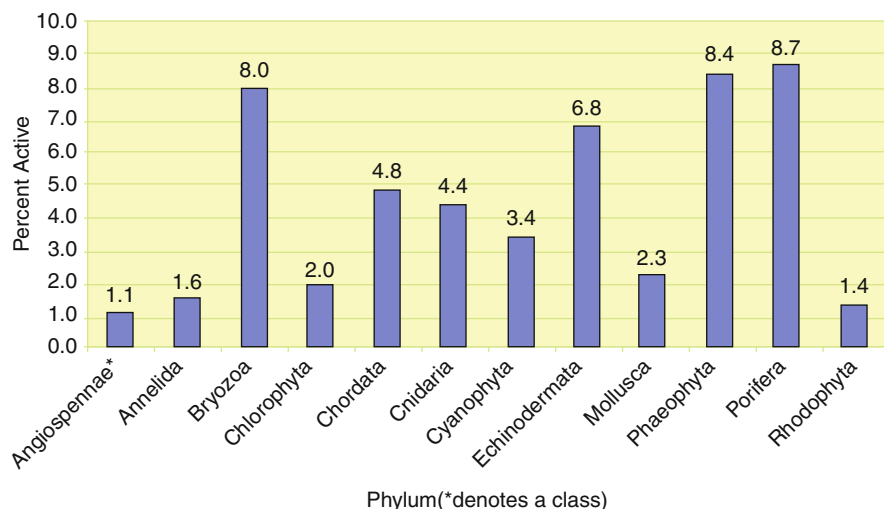


Fig. 1.13 Number of antileukemia “active” marine specimen extracts from marine phyla expressed as a percentage of the total number tested (Reproduced, with permission, from [136])

biological potential were revealed (see Fig. 1.13), suggesting that collection strategies in the future should be modified so as to be better balanced and include a wider range of marine phyla.

Over the past 30 years, many bioactive compounds have been isolated from marine organisms and a number have undergone extensive biological assessment and some are currently progressing through phase trials. These are potential candidates to join Prialt and Yondelis as drugs of marine origin. Others have been tested and for one reason or another were not suitable for advancement. A list of 40 bioactives and their biological origins has been compiled [73, 149–187] (Table 1.7 and Figs. 1.13 and 1.14) and serves to highlight the importance of marine phyla other than Porifera, if bioactivity is a consideration.

1.6 Macro or Micro: Which is the Producer?

Although isolated from macroorganisms such as sponges, bryozoans, or ascidians, it is by no means always certain that the parent organism is the producer of the (bioactive) compounds. Much progress has recently been made in assigning a definite microbial origin to many natural products. Take the case of swinholide A: originally isolated from the sponge *Theonella swinhoei*, centrifugation of macerated cell samples from the sponge showed that the macrolide was located within heterotrophic unicellular bacterial cells, but was absent from the sponge cells themselves and the co-occurring cyanobacterium *Aphanocapsa feldmanni* [188]. More recently, however, swinholide A has been found in field collections of

Table 1.7 A selection of bioactive marine compounds and their source phyla

Name	Phylum
Marinomycins [149]	Actinobacteria
Saliniketal A/B [150]	Actinobacteria
Salinosporamide A [151]	Actinobacteria
Thiocoraline [152]	Actinobacteria
Bryostatin 1 [100]	Bryozoa
Ascididemin [153]	Chordata
Aplidine [128]	Chordata
Diazonamide A [154]	Chordata
Didemnins B [127]	Chordata
<i>Yondelis</i> [143, 144]	Chordata
Meridianins [155]	Chordata
Vitilevuamide [156]	Chordata
Squalamine [157]	Chordata
Eleutherobin [158]	Cnidaria
Pseudopterosin [159]	Cnidaria
Apratoxin E [160]	Cyanophyta
Coibamide A [161]	Cyanophyta
Cryptophycins [162, 163]	Cyanophyta
Curacin A [164]	Cyanophyta
Largazole [165]	Cyanophyta
Symplostatin 1 [166]	Cyanophyta
Dolastatin 10 [167]	Mollusca
Indirubins [168]	Mollusca
Kahalalide F [73]	Mollusca
<i>Prialt</i> [114]	Mollusca
Spisulosine [169]	Mollusca
Bengamide [170, 171]	Porifera
Dictyodendrin [172]	Porifera
Dictyostatin [173]	Porifera
Discodermolide [174, 175]	Porifera
Dysidiolide [176]	Porifera
Halichondrin B [177]	Porifera
Hemiasterlin [178]	Porifera
Jaspamide [179, 180]	Porifera
Laulimalide [181]	Porifera
Nakijiquinone [182]	Porifera
Peloruside [183]	Porifera
Phorboxazole [184]	Porifera
Salicylhalamide A [185, 186]	Porifera
Variolin [187]	Porifera

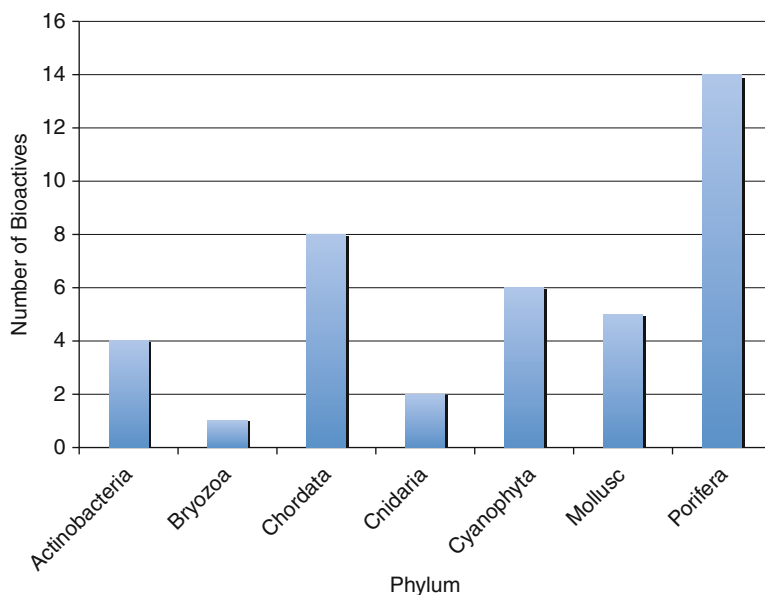


Fig. 1.14 The source phyla for a range of 40 bioactive marine metabolites

cyanobacteria [189], and it has been speculated that it may be produced by one component of this symbiont system, and stored by another [51, 189]. A comparable suggestion came from work on the phorboxazoles and the phorbosides with the comment that “they may actually be produced by cyanobacteria that either live within the host, or expressed from microbial genes that have been integrated into the host sponge.” [145]. Molecular genetics techniques were used to convincingly show that the patellamides A and C are biosynthesized by *Prochloron didemni*, the cyanobacterial symbiont that is hosted by the sponge *Lissoclinum patella* [190]. Molecular techniques also established that the bryostatins are likely produced by an unculturable endosymbiotic γ -proteobacterium “*Candidatus Endobugula sertula*” that is transmitted vertically between generations [101].

Natural products isolated from the higher marine organisms can also have a dietary origin. A good example would be dolastatin 10, isolated originally from an Indian Ocean sea hare (Mollusca) with a microbial origin suspected. The subsequent isolation of simplotatin, differing from dolastatin by a methyl group, from a cyanophyte suggested a possible Cyanophyta origin, which was subsequently confirmed by the isolation of dolastatin 10 from a *Symploca* species [166, 167, 191].

In some cases definite de novo biosynthesis of some natural products has been demonstrated, but it may also be true that although a particular metabolite isolated from a higher animal has not yet been found among the lower forms such as cyanophytes in the same ecosystem, this is merely an accident of the search process.

From a bioprospecting perspective the parent organism will remain the object of primary interest, but for development of a potential lead, the matter of supply is a vital question that must be answered right at the outset. It is at that point that questions on symbiont versus host-cell origin need to be answered, not during the search of the marine environment for new (bioactive) compounds.

1.7 Marine Biodiversity: Into the Future

The currently accepted number of marine species is of the order of 230,000–275,000 species and there are about 1,300–1,750 new species being added to that inventory each year, but these are mainly in the area of the Mollusca and Crustacea (Arthropoda). There is an enormous gulf between that accepted value and the estimated number of species which runs as high as 100 million depending on the authority consulted. Chapman has suggested a total of 11 million with dramatic rises in the invertebrates, most notably the arthropods, the fungi, bacteria, chromista, and protozoa with estimates in some of these taxa rising by several orders of magnitude [13]. Knowledge of the potential species remaining to be described is increasingly dependent on culture-independent molecular techniques. Although applied primarily to explore the diversity of Archaea and Bacteria assemblages, these techniques have not been restricted to prokaryote domains. The suggested 99,000 species of fungi [13] (described 45,000 [9]) is likely to rise to 1.5 million, an estimate considered “accurate” within a factor of 5 with the increase in described species likely to arise from ectoparasites and non-mycorrhizal endophytic species [192]. What proportion of these are marine is conjecture only, but Bouchet’s number of just 500 marine fungi seems very conservative.

Chromista and Protozoa diversities present uncertainties with only about 7,000 species in each taxon described (*Catalogue of Life*), but the numbers of projected species counts are listed in hundreds of thousands. Taking account of the large geographical areas still to be explored from a phycological perspective and the morphological similarities that mask genetic diversity, these suggested figures are not unreasonable. Culture-independent molecular techniques are also being widely used in studying protistan diversity [192].

Moving beyond the microbial world to the Animalia there are again important questions to ask on species biodiversity. A large part of the marine biodiversity is that of the symbionts – the commensals, associates, and parasites. How many copepods are there? How many marine helminthes? Reasoned answers suggest figures way beyond the currently accepted numbers. For example, the marine helminthes might number between 100 and 200,000 [17]. No comment has yet been made about the deep sea and what that area contributes to marine biodiversity. The deep sea was traditionally seen as a harsh environment inhabited only by those few and cosmopolitan species capable of living in the dark under enormous pressures and near freezing temperatures. But, following Grassle and Maciolo’s 1992 seminal paper [193] on deep sea biodiversity, opinions have been markedly changed leading to comments such as “a riot of species in an environmental calm” [17] to describe the deep ocean and its accompanying biodiversity. Grassle and

Maciolo found 798 mainly new species of polychaetes and isopods in 233 box cores of 30×30 cm taken on a 176 km transect along a 2,100 m depth contour off the North Eastern coast of the USA. As there is 3×10^8 km² of ocean floor deeper than 1,000 m, it sparked a vigorous debate as to the actual numbers of species contributed by the deep sea ranging from 100 million downward. Until deepwater basins in the other oceans of the world are explored no consensus can be reached as to the contribution of the deep seas to overall marine biodiversity.

1.8 The “Neglected Phyla” and Marine Natural Products in the Future

Regardless of the actual numbers of marine species available, some conclusions can be reached based on the efforts over the past 75 years. Research on the phylum Porifera has dominated the effort and the subsequent chemistry. This focus has been productive and the chemistry novel and fascinating. It is not difficult to reach a conclusion for this fixation as succeeding generations of natural product chemists will naturally focus on areas that have proven successful in the past, and sponges are relatively easy to collect in good mass (>100 g), even for the inexperienced diver. This focus on sponges has led to a rather unequal coverage of the other major taxa and phyla. Some comparative data based on compounds isolated, papers published, and relative coverage of the major *macroorganisms*, which includes 12 of the phyla from Animalia, are presented in Table 1.8. The Cyanophyta have been included in this comparison as they too can be collected in bulk from the wild. Also included are the origins of 35 of the 40 compounds of interest listed in Table 1.7. Four of the remaining were of Bacteria origin and the fifth was isolated from a higher chordate (shark). Studies on the macrophyta have produced $>90\%$ of the marine natural products from just 1.4% of the accepted number of species in these phyla. These data, when coupled with the NCI’s study [136] (Fig. 1.13), suggest that studies that include Bryozoa, Cnidaria, Chordata (Ascidiaceae), Mollusca, Ochrophyta (Phaeophyceae), and Cyanophyta should be productive, particularly if the search for bioactivity is the objective. These phyla have been *neglected*. Furthermore, as no work has been reported on the other 18–21 phyla of the Animalia, one may be forgiven for coming to the conclusion that these are “forgotten” phyla.

Most of the biodiversity yet to be classified in the marine environment resides in the microscopic world of the Archaea, Bacteria, and the multicellular, but still microscopic members of the Eukaryota belonging to the Chromista and Protozoa taxa. The projected numbers of species still to be defined is estimated to be in the millions [13, 17, 52]. Despite the inherent difficulties of working with organisms from the Protozoa and Chromista, a significant body of work is evolving on the chemistry of the Ciliphora, Dinophyta, Euglenozoa, and from the Chrysophyceae (Ochrophyta), but as yet little or nothing has appeared on the chemistry of species in the Bacillariophyta, Radiolaria, and Foraminifera (Table 1.5). The chemistry of obligate marine, or at least marine-derived, fungi is of rapidly growing interest within the MNP community and already 289 species have been examined for new

Table 1.8 Comparative data for marine natural products from the macroorganisms

<i>Taxa</i>	Marine species	Species with new compounds	Coverage of phylum (%)	Compounds (% total)	Bioactive papers ^a (%)	Compounds of interest
Animalia						
Annelida	12,148	14	0.12	0.24	100	–
Arthropoda (Crustacea)	44,950	9	0.02	0.05	11	–
Brachiopoda	550	0	0.91	0	0	–
Bryozoa	5,700	28	0.49	0.86	14.1	1
Chordata (Ascidiaeae)	4,900	184	3.76	4.77	65.4	7
Cnidaria	9,795	415	4.24	19.49	22.5	2
Echinodermata	7,000	205	2.9	5.84	18.8	–
Hemichordata	106	3	2.77	0.14	17.6	–
Mollusca	52,525	201	0.38	5.22	12.2	5
Nematoda	12,000	2	0.017	0.01	0	–
Platyhelminthes	15,000	2	0.013	0.01	0	–
Porifera	5,500	878	15.96	35.03	63.4	14
Chromista						
Ochrophyta (Phaeophyceae)	1,600	161	10.1	5.81%	13.1	–
Plantae						
Chlorophyta	2,500	60	2.4	1.37%	11.5	–
Magnoliophyta	50	26	52.0	0.62%	27.6	–
Rhodophyta	6,200	195	3.10	7.85%	11.0	–
Bacteria						
Cyanophyta	1,000	73	0.73	3.03%	64.9	6
	181,524	2,456		90.34%		35

^aNumber of papers reporting bioactive compounds as percentage of all papers reporting compounds for each phylum

chemistry (Table 1.5). This interest seems destined to continue, and with the predicted burgeoning of the fungal species to 1.5 million, [13] there will be enormous scope in this aspect of marine natural products. Soil bacteria, especially members of the *Streptomyces* and *Micromonospora* genera of the Actinobacteria, have been the source of over 50% of the clinically useful microbial antibiotics. The first marine actinomycete was discovered in 1984 [53]. Since then at least three marine genera have been described [54–56]. These include the genus *Salinispora* [56] which has an obligate requirement for sodium ions. This discovery by Fenical and Jensen of the first *Salinispora* sp. has been followed by the identification of at least six actinomycete families [52] including marine-derived species related to the genus *Streptomyces*. The chemistry associated with these obligate marine actinomycetes has also been remarkable with discoveries of compounds such as salinosporamide, which is currently in Phase 1 trials as a 20S-proteasome

inhibitor [194]. These metabolites being isolated from the obligate marine actinomycetes show a high degree of halogenation, a feature considered desirable for induction of biological activity [195], and in the case of salinosporamide an essential feature of the mechanism of action [196, 197].

Every milliliter of seawater contains 10^6 microorganisms with marine sediment being even richer (10^9) [52]. This is a resource beyond comprehension. The terrestrial actinomycetes have been chemically prolific. There is every reason to believe that the marine counterparts will be equally prolific. Using a combination of metagenomics, genome analysis, and selective culture techniques, the potential for discovering other genera and new chemical entities from the microscopic world is enormous. If this is coupled with a fuller exploration of the “neglected” macroorganism phyla, the future viability, stability, and promise of marine natural products chemistry is assured.

1.9 Study Questions

1. Taking a particular organism group (e.g., molluscs) make a brief study of the differing taxonomic classifications that have been proposed for this group by taxonomists.
2. Could the differing taxonomic views for such a group have had an impact on the statistics of natural product occurrence in the group?
3. For a particular organism, or a small group of organisms, ascertain what is known about the dietary regime and predation pattern and determine if that coincides with what is known about the characterized constituents.
4. (a) As an ambitious young starting academic in the field of marine natural products, what considerations should you give to the selection of organisms (phylum, class, order, family, or genus) to study that would optimize your chances of finding new compounds and thus gaining publications?
(b) Suggest the collecting resources that you would need to access to effectively pursue your organisms of choice.
(c) Besides collecting resources, list the other resources or collaborations you think would be necessary in order to be successful.

References

1. Doak W (1979) The cliff dwellers: an undersea community. Hodder and Stoughton, New Zealand
2. <http://answers.yahoo.com/question/index?qid=20080413091945AA> VikPT. Accessed 10 Nov 2009
3. http://nssdc.gsfc.nasa.gov/imgcat/html/object_page/a17_h_148_22727.html. Accessed 10 Nov 2009
4. Groombridge B, Jenkins MD (2002) World atlas of biodiversity. University of California Press, Berkeley
5. Whittaker RH (1959) On the broad classification of organisms. *Quart Rev Biol* 34:21–26

6. Woese C, Fox G (1977) Phylogenetic structure of the prokaryotic domain: the primary kingdoms. *Proc Natl Acad Sci USA* 74:5088–5090
7. Global Biodiversity Information Facility (2009) <http://www.gbif.org/>. Accessed 10 Nov 2009
8. Bisby FA, Roskov YR, Orrell TM et al (eds) (2009) Species 2000 and ITIS catalogue of life. <http://www.catalogueoflife.org>. Accessed 10 Nov 2009
9. 2009 Annual checklist. <http://www.catalogueoflife.org/annual-checklist/2009/>. Accessed 10 Nov 2009
10. Gordon DP (2009) Towards a management hierarchy (classification) for the catalogue of life: draft discussion document. In: Bisby FA, Roskov YR, Orrell TM et al (eds) Species 2000 and ITIS catalogue of life: 2009 annual checklist. CD-ROM. Species 2000, Reading
11. http://upload.wikimedia.org/wikipedia/commons/7/70/Phylogenetic_tree.svg. Accessed 10 Nov 2009
12. Hawksworth DL, Kalin-Arroyo MT (1995) Magnitude and distribution of biodiversity. In: Heywood V (ed) Global biodiversity assessment. Cambridge University Press, Cambridge
13. Chapman AD (2009) Numbers of living species in Australia and the World, 2nd edn. Australian Biological Resources Study, Canberra. ISBN (printed): 978 0 642 56860 1. ISBN (online): 978 0 642568618. <http://www.environment.gov.au/biodiversity/abrs/publications/other/species-numbers/2009/index.html>. Accessed 10 Nov 2009
14. May RM (1998) How many species are there on earth? *Science* 241:1441–1449
15. Tangley L (1997) How many species are there? *US News and World Report* Aug 18, 1997. http://www.usnews.com/usnews/culture/articles/970818/archive_007681.htm. Accessed 10 Nov 2009
16. SMEBD (2009) The world register of marine species. <http://www.marinespecies.org>. Accessed 17 Jan 2010
17. Bouchet P (2006) The magnitude of marine biodiversity. In: Duarte CM (ed) The exploration of marine biodiversity. Scientific and technological challenges. Fundacion BBVA, Bilbao
18. Sertürner F (1805) *Journal der Pharmacie fuer Aerzte und Apotheker* 13:229–243
19. Sertürner F (1817) Ueber das Morphinum, eine neue salzfähige Grundlage, und die Mekonsäure, als Hauptbestandtheile des Opiums. *Ann Phys* 55:56–89
20. der Marderosian AJ (1969) Marine pharmaceuticals. *Pharm Sci* 58:1–33
21. Bergmann W, Feeney RJ (1950) Isolation of a new thymine pentoside from sponges. *J Am Chem Soc* 72:2809–2810
22. Bergmann W, Feeney RJ (1951) Contributions to the study of marine products XXXII. The nucleosides of sponges. I. *J Org Chem* 16:981–987
23. Bergmann W, Burke DC (1955) Contributions to the study of marine products XXXIX. The nucleosides of sponges. III. Spongthymidine and spongouridine. *J Org Chem* 20:1501–1507
24. Bergmann W, Burke DC (1956) Contributions to the study of marine products XL. The nucleosides of sponges. IV. Spongosine. *J Org Chem* 21:226–228
25. Bergmann W, Watkins JC, Stempien MF et al (1957) Contributions to the study of marine products. XLV. Sponge nucleic acids. *J Org Chem* 22:1308–1313
26. Bergmann W, Johnson TB (1933) The chemistry of marine animals I. The sponge *Microciona pralifera*. *Z Physiol Chem* 222:220–226
27. Landowne RA, Bergmann W (1961) Contributions to the study of marine products L. Phospholipides of sponges. *J Org Chem* 26:1256–1261
28. Friess SL, Standaert FG, Whitcomb ER et al (1959) Some pharmacologic properties of holothurin, an active neurotoxin from the sea cucumber. *J Pharm Exp Ther* 126:323–329
29. Jakowska S, Nigrelli RF (1960) Antimicrobial substances from sponges. *Ann NY Acad Sci* 90:913–916
30. Burkholder PR, Burkholder LM (1956) Microbiological assay of vitamin B12 in marine solids. *Science* 123:1071–1073
31. Sharma GM, Burkholder PR (1967) Antimicrobial substances of sponges. I. Isolation, purification, and properties of a new bromine-containing anti-bacterial substance. *J Antibiot Ser A* 20:200–203

32. Ciereszko LS (1962) Chemistry of coelenterates III. Occurrence of antimicrobial terpenoid compounds in the zooxanthellae of alcyonarians. *Trans NY Acad Sci* 24:502–503
33. Nigrelli RF, Stempien MF Jr, Ruggieri GD et al (1967) Substances of potential biomedical importance from marine organisms. *Fed Proc* 26:1197–1205
34. Goto T, Kishi Y, Takahashi S et al (1965) Tetrodotoxin. *Tetrahedron* 21:2059–2088
35. Moore RE, Scheuer PJ (1971) Palytoxin: new marine toxin from a coelenterate. *Science* 172:495–498
36. Scheuer PJ (1977) Marine toxins. *Acc Chem Res* 10:33–39
37. Moore RE, Bartolini G (1981) Structure of palytoxin. *J Am Chem Soc* 103:2491–2494
38. Moore RE, Bartolini G, Barchi J et al (1982) Absolute stereochemistry of palytoxin. *J Am Chem Soc* 104:3776–3779
39. Pettit GR, Day JF, Hartwell JL et al (1970) Antineoplastic components of marine animals. *Nature* 227:962–963
40. Rinehart KL Jr, Shaw PD, Shield LS et al (1981) Marine natural products as sources of antiviral, antimicrobial, and antineoplastic agents. *Pure Appl Chem* 53:795–817
41. Faulkner DJ (2000) Highlights of marine natural products chemistry (1972–1999). *Nat Prod Rep* 17:1–6
42. Blunt JW, Copp BR, Hu W-P et al (2009) Marine natural products. *Nat Prod Rep* 26:170–244
43. Blunt JW, Copp BR, Munro MHG et al (2010) Marine natural products. *Nat Prod Rep* 27:165–237
44. Blunt JW, Munro MHG (eds) (2008) Dictionary of marine natural products. Chapman & Hall/CRC, Boca Raton
45. Kornprobst J-M (2005) Substances Naturelles d'Origine Marine. Lavoisier, Paris
46. DeLong EF (1998) Everything in moderation: archaea as 'non-extremophiles'. *Curr Opin Genet Dev* 8:649–654
47. Lepage SP, Sneath PHA, Lessel EF et al (1992) International code of nomenclature of bacteria, 1990 revision, bacteriological code. American Society for Microbiology, Washington, DC
48. Piel J (2004) Metabolites from symbiotic bacteria. *Nat Prod Rep* 21:519–538
49. Garrity GM et al (ed in chief) (2001) *Bergey's manual of systematic bacteriology*, vols 1–2. De Vos P et al (ed in chief) (2009) *Bergey's manual of systematic bacteriology*, vol 3. *Bergey's Manual Trust*, Springer, New York
50. Austin B (2002) Novel pharmaceutical compounds from marine bacteria. *Rec Adv Mar Biotech* 6:1–28
51. König GM, Kehraus S, Seibert SF et al (2006) Natural products from marine organisms and their associated microbes. *Chembiochem* 7:229–238
52. Fenical W, Jensen PR (2006) Developing a new resource for drug discovery: marine actinomycete bacteria. *Nat Chem Biol* 2:666–673
53. Helmke E, Weyland H (1984) *Rhodococcus marinonascens* sp. nov., an actinomycete from the sea. *Int J Syst Bacteriol* 34:127–138
54. Han SK, Nedashkovskaya OI, Mikhailov VV et al (2003) *Salinibacterium amurkyense* gen. nov., sp. nov., a novel genus of the family *Microbacteriaceae* from the marine environment. *Int J Syst Evol Microbiol* 53:2061–2066
55. Yi H, Schumann P, Sohn K et al (2004) *Serinicoccus marinus* gen. nov., sp. nov., a novel actinomycete with L-ornithine and L-serine in the peptidoglycan. *Int J Syst Evol Microbiol* 54:1585–1589
56. Maldonado LA, Fenical W, Jensen PR et al (2005) *Salinispora* gen nov., a home for obligate marine actinomycetes belonging to the family *Micromonosporaceae*. *Int J Sys Evol Microbiol* 55:1759–1766
57. Paul GK, Matsumori N, Konoki K et al (1997) Chemical structures of amphidinols 5 and 6 isolated from marine dinoflagellate *Amphidinium klebsii* and their cholesterol-dependent membrane disruption. *J Mar Biotech* 5:124–128

58. Oishi T, Kanemoto M, Swasono R et al (2008) Combinatorial synthesis of the 1,5-polyol system based on cross metathesis: structure revision of amphidinol 3. *Org Lett* 10:5203–5206
59. Lin Y-Y, Risk M, Ray SM et al (1981) Isolation and structure of brevetoxin B from the 'Red Tide' dinoflagellate *Ptychodiscus brevis* (*Gymnodium breve*). *J Am Chem Soc* 103:6773–6775
60. Shimizu Y, Bando H, Chou H-N et al (1986) Absolute configuration of brevetoxins. *J Chem Soc Chem Commun* 1656–1658
61. Tachibana K, Scheuer PJ, Tsukitani Y et al (1981) Okadaic acid; a cytotoxic polyether from two marine sponges of the genus *Halichondria*. *J Am Chem Soc* 103:2469–2471
62. Kobayashi J, Ishibashi M, Nakamura H et al (1986) Amphidinolide-A; an antineoplastic macrolide from the marine dinoflagellate *Amphidinium* sp. *Tetrahedron Lett* 27:5755–5758
63. Trost BM, Harrington PE (2004) Structure elucidation of (+)-amphidinolide A by total synthesis and NMR chemical shift analysis. *J Am Chem Soc* 126:5028–5029
64. Uemura D, Chou T, Haino T et al (1995) Pinnatoxin A: a toxic amphoteric macrocycle from the Okinawan bivalve *Pinna muricata*. *J Am Chem Soc* 117:1155–1156
65. Chou T, Kamo O, Uemura D (1996) Relative stereochemistry of pinnatoxin A, a potent shellfish poison from *Pinna muricata*. *Tetrahedron Lett* 37:4023–4026
66. Schantz EJ, Ghazarossian VE, Schnoes HK et al (1975) The structure of saxitoxin. *J Am Chem Soc* 97:1238–1239
67. Cavalier-Smith T (1981) Eukaryote kingdoms: seven or nine? *Biosystems* 14:461–481
68. Kitagawa I, Hamamoto Y, Kobayashi M (1979) Sulfonoglycolipid from the sea urchin *Anthocidaris crassispina* A. Agassiz. *Chem Pharm Bull* 27:1394–1397
69. Igarashi T, Satake M, Yasumoto T (1999) Structures and partial stereochemical assignments for prymnesin-1 and prymnesin-2: potent hemolytic and ichthyotoxic glycosides isolated from the red tide alga *Prymnesium parvum*. *J Am Chem Soc* 121:8499–8511
70. Walter JA, Falk M, Wright JLC (1994) Chemistry of the shellfish toxin domoic acid: characterization of related compounds. *Can J Chem* 72:430–436
71. Amico V, Oriente G, Piattelli M et al (1978) Caulerpenyne; an unusual sesquiterpenoid from the green alga *Caulerpa prolifera*. *Tetrahedron Lett* 3593–3596
72. Paul VJ, Fenical W (1984) Novel bioactive diterpenoid metabolites from tropical marine algae of genus *Halimeda* (Chlorophyta). *Tetrahedron* 40:3053–3062
73. Hamann MT, Scheuer PJ (1993) Kahalalide F: a bioactive depsipeptide from the sacoglossan mollusk *Elysia rufescens* and the green alga *Bryopsis* sp. *J Am Chem Soc* 115:5825–5826
74. Rochfort SJ, Capon RJ (1996) Parguerenes revisited: new brominated diterpenes from the southern Australian marine red alga *Laurencia filiformis*. *Aust J Chem* 49:19–26
75. Blunt JW, Hartshorn MP, McLennan TJ et al (1978) Thyrsiferol; a squalene-derived metabolite of *Laurencia thyrsifera*. *Tetrahedron Lett* 19:69–72
76. Irie T, Suzuki M, Masamune T (1965) Laurencin; a constituent from *Laurencia* species. *Tetrahedron Lett* 1091–1099
77. Forbes Cameron A, Cheung KK, Ferguson G et al (1969) *Laurencia* natural products: crystal structure and absolute stereochemistry of laurencin. *J Chem Soc B* 559–564
78. King TJ, Imre S, Oztunc A et al (1979) Obtusenyne, a new acetylenic nine-membered cyclic ether from *Laurencia obtusa*. *Tetrahedron Lett* 1453–1454
79. Ackermann D (1953) The occurrence of homarine, trigonelline, and a new base, anemonine, in the sea anemone *Anemonia sulcata*. *Hoppe Seyler's Z Physiol Chem* 295:1–9
80. McClintock JB, Baker BJ, Hamann MT et al (1994) Homarine as a feeding deterrent in common shallow water Antarctic lamellarian gastropod *Marseniopsis mollis*: rare example of chemical defense in marine prosobranch. *J Chem Ecol* 20:2539–2549
81. Nitta I, Watase H, Tomiie Y (1958) Structure of kainic acid and its isomer, allokainic acid. *Nature* 181:761–762
82. Wratten SJ, Faulkner DJ (1976) Cyclic polysulfides from the red alga *Chondria californica*. *J Org Chem* 41:2465–2467

83. Kirk PM, Cannon PF, David JC et al (eds) (2001) Dictionary of the fungi, 9th edn. CABI, Wallingford
84. Jensen PR, Fenical W (2002) Secondary metabolites from marine fungi. In: Hyde KD (ed) Fungi in marine environments. Fungal Diversity Press, Hong Kong
85. Bugni TS, Ireland CM (2004) Marine-derived fungi: a chemically and biologically diverse group of microorganisms. *Nat Prod Rep* 21:143–163
86. Zuccaro A, Schoch CL, Spatafora JW et al (2008) Detection and identification of fungi intimately associated with the brown seaweed *Fucus serratus*. *Appl Environ Micro* 74: 931–941
87. Belofsky GN, Jensen PR, Renner MK et al (1998) New cytotoxic sesquiterpenoid nitrobenzoyl esters from a marine isolate of the fungus *Aspergillus versicolor*. *Tetrahedron* 54:1715–1724
88. Watanabe Y, Fusetani N (eds) (1998) Sponge sciences: multidisciplinary perspectives. Springer, Tokyo
89. Hooper JNA, van Soest RWM (eds) (2002) Systema Porifera: a guide to the classification of sponges. Kluwer/Plenum, New York
90. Faulkner DJ, Unson MD, Bewley CA (1994) The chemistry of some sponges and their symbionts. *Pure Appl Chem* 66:1983–1990
91. Fattorusso E, Magnoni A (1997) Marine glycolipids. *Prog Chem Org Nat Prod* 72:215–301
92. Costantino V, Fattorusso E, Mangoni A (1994) The stereochemistry of crasserides. *J Nat Prod* 57:1726–1730
93. Anderluh G, Macek P (2002) Cytolytic peptide and protein toxins from sea anemones (Anthozoa: Actiniaria). *Toxicon* 40:111–124
94. D'Ambrosio M, Guerriero A, Pietra F (1988) Isolation from coral *Sarcodictyon roseum* of sarcodictyin C, D, E, and F, novel diterpenoidic alcohols esterified by (*E*)- or (*Z*)-*N*-(1)-methylurocanic acid. *Helv Chim Acta* 71:964–976
95. Schwartz RE, Yunker MB, Scheuer PJ et al (1978) Constituents of bathyal marine organisms: a new zoanthoxanthin from a coelenterate. *Tetrahedron Lett* 2235–2238
96. Cha JK, Christ WJ, Finan JM et al (1982) Stereochemistry of palytoxin. 4. Complete structure. *J Am Chem Soc* 104:7369–7371
97. Kazlauskas R, Murphy PT, Quinn RJ et al (1977) Aplysinopsin, a tryptophan derivative from a sponge (*Aplysinopsis* or *Thorecta* genus). *Tetrahedron Lett* 61–64
98. Ballantine JA, Psaila AF, Pelter A et al (1980) The structure of bonellin and its derivatives. Unique physiologically active chlorins from the marine echinurian *Bonellia viridis*. *J Chem Soc (Perkin) 1*:1972–1999
99. Okaichi T, Hashimoto Y (1962) The structure of nereistoxin. *Agric Biol Chem* 26:224–227
100. Pettit GR, Herald CL, Doubek DL et al (1982) Isolation and structure of bryostatin 1. *J Am Chem Soc* 104:6846–6848
101. Sudek S, Lopanik NB, Waggoner LE et al (2007) Identification of the putative bryostatin polyketide synthase gene cluster from “*Candidatus* Endobugula sertula”, the uncultivated microbial symbiont of the marine bryozoan *Bugula neritina*. *J Nat Prod* 70:67–74
102. Carle JS, Christophersen C (1979) Bromo-substituted physostigmine alkaloids from a marine bryozoa *Flustra foliacea*. *J Am Chem Soc* 101:4012–4013
103. Rahbaek L, Anthoni U, Christophersen C et al (1996) Marine alkaloids. 18. Securamines and securines, halogenated indole-imidazole alkaloids from the marine bryozoan *Securiflustra securifrons*. *J Org Chem* 61:887–889
104. Anthoni U, Chevolut L, Larsen C et al (1987) Marine alkaloids. 12. Chartellines, halogenated β -lactam alkaloids from the marine bryozoan *Chartella papyracea*. *J Org Chem* 52:4709–4712
105. Anthoni U, Bock K, Chevolut L et al (1987) Marine alkaloids. 13. Chartellamide A and B, halogenated β -lactam indole-imidazole alkaloids from the marine bryozoan *Chartella papyracea*. *J Org Chem* 52:5638–5639
106. Cimino G, Gavagnin M (eds) (2006) Molluscs: from chemico-ecological study to biotechnological application. Progress in molecular and subcellular biology, vol 43. Springer, Berlin

107. Cimino G, Fontana A, Gavagnin M (1999) Marine opisthobranch molluscs: chemistry and ecology in sacoglossans and dorids. *Curr Org Chem* 3:327–372
108. Ito S, Nardi G, Palumbo A et al (1979) Isolation and characterization of adenochrome, a unique iron(III)-binding peptide from *Octopus vulgaris*. *J Chem Soc (Perkin)* 1:2617–2623
109. Spinella A, Zubia E, Martinez E et al (1997) Structure and stereochemistry of aplyolides A-E, lactonized dihydroxy fatty acids from the skin of the marine mollusk *Aplysia depilans*. *J Org Chem* 62:5471–5475
110. Kato Y, Scheuer PJ (1974) Aplysiatoxin and debromoaplysiatoxin; constituents of the marine mollusk *Stylocheilus longicauda*. *J Am Chem Soc* 96:2245–2246
111. Moore RE, Blackman AJ, Cheuk CE et al (1984) Absolute stereochemistries of the aplysiatoxins and oscillatoxin A. *J Org Chem* 49:2484–2489
112. Suenaga K, Kigoshi H, Yamada K (1996) Auripyrone A and B, cytotoxic polypropionates from the sea hare *Dolabella auricularia*: isolation and structures. *Tetrahedron Lett* 37:5151–5154
113. Andersen RJ, Faulkner DJ, He CH et al (1985) Metabolites of the marine prosobranch mollusk *Lamellaria* sp. *J Am Chem Soc* 107:5492–5495
114. Olivera BM, Gray WR, Zeikus R et al (1985) Peptide neurotoxins from fish-hunting cone snails. *Science* 230:1338–1343
115. Choi MC, Hsieh DPH, Lam PKS et al (2003) Field depuration and biotransformation of paralytic shellfish toxins in scallop *Chlamys nobilis* and green-lipped mussel *Perna viridis*. *Mar Biol* 143:927–934
116. Edmonds JS, Francesconi KA, Healy PC et al (1982) Isolation and crystal structure of an arsenic-containing sugar sulfate from the kidney of the giant clam, *Tridacna maxima*. X-ray crystal structure of (2S)-3-[5-deoxy-5-(dimethylarsinoyl)- β -D-ribofuranosyloxy]-2-hydroxypropyl hydrogen sulfate. *J Chem Soc (Perkin)* 1:2989–2993
117. Stonik VA, Kalinin VI, Avilov SA (1999) Toxins from sea cucumbers (holothuroids): chemical structures, properties, taxonomic distribution, biosynthesis and evolution. *J Nat Toxins* 8:235–248
118. Findlay JA, Yayli N, Radics L (1992) Novel sulfated oligosaccharides from the sea cucumber *Cucumaria frondosa*. *J Nat Prod* 55:93–101
119. De Riccardis F, Iorizzi M, Minale L et al (1991) The gymnochromes: novel marine brominated pheanthroperylenequinone pigments from the stalked crinoid *Gymnocrinus richeri*. *J Org Chem* 56:6781–6787
120. Pettit GR, Inoue M, Kamano Y et al (1988) Isolation and structure of the powerful cell growth inhibitor cephalostatin I. *J Am Chem Soc* 110:2006–2007
121. Davidson BS (1993) Ascidians: producers of amino acid-derived metabolites. *Chem Rev* 93:1771–1791
122. Riccio R, Kinnel RB, Bifulco G et al (1996) Kakelokelose, a sulfated mannose polysaccharide with anti-HIV activity from the Pacific tunicate *Didemnum molle*. *Tetrahedron Lett* 37:1979–1982
123. Kiyota H, Dixon DJ, Luscombe CK et al (2002) Synthesis, structure revision, and absolute configuration of (+)-didemnerinolipid B, a serinol marine natural product from a tunicate *Didemnum* sp. *Org Lett* 4:3223–3226
124. Fukuzawa S, Matsunaga S, Fusetani N (1994) Ritterazine A, a highly cytotoxic dimeric steroidal alkaloid, from the tunicate *Ritterella tokioka*. *J Org Chem* 59:6164–6166
125. Ireland CM, Durso AR, Newman RA et al (1982) Antineoplastic cyclic peptides from the tunicate *Lissoclinum patella*. *J Org Chem* 47:1807–1811
126. Hamada Y, Shibata M, Shioiri T (1985) New methods and reagents in organic synthesis. 56. Total syntheses of patellamides B and C, cytotoxic cyclic peptides from a tunicate. 2. Their real structures have been determined by their syntheses. *Tetrahedron Lett* 26:5159–5162
127. Rinehart KL, Kobayashi J, Harbour GC et al (1981) Structures of the didemnins, antiviral and cytotoxic depsipeptides from a Caribbean tunicate. *J Am Chem Soc* 103:1857–1859
128. Rinehart KL, Lithgow-Bertelloni AM (1991) Dehydrodidemnin B. WO9104985 (A1)

129. Krishnaiah P, Reddy VLN, Venkataramana G et al (2004) New lamellarin alkaloids from the Indian ascidian *Didemnum obscurum* and their antioxidant properties. *J Nat Prod* 67:1168–1171
130. Moore KS, Wehrli S, Roder H et al (1993) Squalamine: an aminosterol antibiotic from the shark. *Proc Natl Acad Sci USA* 90:1354–1358
131. Nakamura M, Yasumoto T (1985) Tetrodotoxin derivatives in puffer fish. *Toxicon* 23:271–276
132. <http://www.chem.canterbury.ac.nz/marinlit/marinlit.shtml>. Accessed 10 Nov 2009
133. Suckling CJ (1991) Chemical approaches to the discovery of new drugs. *Sci Prog* 75:323–359
134. Newman DJ, Cragg GM, Snader KM (2000) The influence of natural products upon drug discovery. *Nat Prod Rep* 17:215–234
135. Freudenthal HD (1968) Transactions of the drugs from the sea symposium, University of Rhode Island, 27–29 Aug 1967. Marine Technology Society, Washington, DC, pp 1–297
136. Cragg GM, Newman DJ, Yang SS (2006) Natural product extracts of plant and marine origin having antileukemia potential. The NCI experience. *J Nat Prod* 69:488–498
137. Faulkner DJ (1977) Interesting aspects of marine natural products chemistry. *Tetrahedron* 33:1421–1443
138. Lipinski CA, Lombardo F, Dominy BW et al (1997) Experimental and computational approaches to estimate solubility and permeability in drug discovery and development settings. *Adv Drug Del Rev* 23:3–25
139. <http://www.micronmr.com/>. Accessed 20 Nov 2009
140. http://www.bruker-biospin.com/cryoprobe_micro.html. Accessed 20 Nov 2009
141. Dalisay DS, Molinski TF (2009) NMR quantitation of natural products at the nanomole scale. *J Nat Prod* 72:739–744
142. Lang G, Mayhudin NA, Mitova MI et al (2008) Evolving trends in the dereplication of natural product extracts: new methodology for rapid, small-scale investigation of natural product extracts. *J Nat Prod* 71:1595–1599
143. Wright AE, Forleo DA, Gunawardana GP et al (1990) Antitumor tetrahydroisoquinoline alkaloids from the colonial ascidian *Ecteinascidia turbinata*. *J Org Chem* 55:4508–4512
144. Rinehart KL, Holt TG, Fregeau NL et al (1990) Ecteinascidins 729, 743, 745, 759A, 759B, and 770: potent antitumor agents from the Caribbean tunicate *Ecteinascidia turbinata*. *J Org Chem* 55:4512–4515
145. Molinski TF, Dalisay DS, Lievens SL et al (2009) Drug development from marine natural products. *Nat Rev Drug Disc* 8:69–85
146. Newman DJ, Cragg GM (2004) Marine natural products and related compounds in clinical and advanced preclinical trials. *J Nat Prod* 67:1216–1238
147. Cragg GM, Newman DJ (2009) Nature: a vital source of leads for anticancer drug development. *Phyt Rev* 8:313–331
148. Cragg GM, Grothaus PG, Newman DJ (2009) Impact of natural products on developing new anti-cancer agents. *Chem Rev* 109:3012–3043
149. Kwon HC, Kauffman CA, Jensen PR et al (2006) Marinomycins A–D, antitumor-antibiotics of a new structure class from a marine actinomycete of the recently discovered genus *Marinispora*. *J Am Chem Soc* 128:1622–1632
150. Williams PG, Asolkar RN, Kondratyuk T et al (2007) Saliniketals A and B, bicyclic polyketides from the marine actinomycete *Salinispora arenicola*. *J Nat Prod* 70:83–88
151. Feling RH, Buchanan GO, Mincer TJ et al (2003) Salinosporamide A: a highly cytotoxic proteasome inhibitor from a novel microbial source, a marine bacterium of the new genus *Salinispora*. *Angew Chem Int Ed* 42:355–358
152. Perez Baz J, Canedo LM, Fernandez Puentes JL et al (1997) Thiocoraline, a novel depsipeptide with antitumor activity produced by a marine *Micromonospora*. II. Physico-chemical properties and structure determination. *J Antibiot* 50:738–741
153. Kobayashi J, Cheng J, Nakamura H et al (1988) Ascidiemin, a novel pentacyclic aromatic alkaloid with antileukemic activity from Okinawan tunicate *Didemnum* sp. *Tetrahedron Lett* 29:1177–1180

154. Lindquist N, Fenical W, Van Duyne GD et al (1991) Isolation and structure determination of diazonamides A and B, unusual cytotoxic metabolites from the marine ascidian *Diazona chinensis*. *J Am Chem Soc* 113:2303–2304
155. Franco LH, Joffe EBD, Puricelli L et al (1998) Indole alkaloids from the tunicate *Aplidium meridianum*. *J Nat Prod* 61:1130–1132
156. Fernandez AF, He H-Y, McDonald LA et al (1998) Structural studies of marine peptides. *Pure Appl Chem* 70:2130–2138
157. Moore KS, Wehrli S, Roder H et al (1993) Squalamine: an aminosterol antibiotic from the shark. *Proc Nat Acad Sci USA* 90:1354–1358
158. Lindel T, Jensen PR, Fenical W et al (1997) Eleutherobin, a new cytotoxin that mimics paclitaxel (taxol) by stabilizing microtubules. *J Am Chem Soc* 119:8744–8755
159. Look SA, Fenical W, Matsumoto GK et al (1986) The pseudoptererosins: a new class of antiinflammatory and analgesic diterpene pentosides from the marine sea whip *Pseudopterogorgia elisabethae* (Octocorallia). *J Org Chem* 51:5140–5145
160. Matthew S, Schupp PJ, Luesch H (2008) Apratoxin E, a cytotoxic peptolide from a Guamanian collection of the marine cyanobacterium *Lyngbya bouillonii*. *J Nat Prod* 71:1113–1116
161. Medina RA, Goeger DE, Hills P et al (2008) Coibamide A, a potent antiproliferative cyclic depsipeptide from the Panamanian marine cyanobacterium *Leptolyngbya* sp. *J Am Chem Soc* 130:6324–6325
162. Schwartz RE, Hirsch CF, Sesin DF et al (1990) Pharmaceuticals from cultured algae. *J Indust Microbiol* 5:113–124
163. Trimurtulu G, Ohtani I, Patterson GML et al (1994) Total structures of cryptophycins, potent antitumor depsipeptides from the blue-green-alga *Nostoc* sp strain GSV-224. *J Am Chem Soc* 116:4729–4737
164. Nagle DG, Geraldts RS, Yoo HD et al (1995) Absolute configuration of curacin A, a novel antimetabolic agent from the tropical marine cyanobacterium *Lyngbya majuscula*. *Tetrahedron Lett* 36:1189–1192
165. Taori K, Paul VJ, Luesch H (2008) Structure and activity of largazole, a potent antiproliferative agent from the Floridian marine cyanobacterium *Symploca* sp. *J Am Chem Soc* 130:1806
166. Harrigan GG, Luesch H, Yoshida WY et al (1998) Symplostatin 1: a dolastatin 10 analog from the marine cyanobacterium *Symploca hydnoides*. *J Nat Prod* 61:1075–1077
167. Pettit GR, Kamano Y, Herald CL et al (1987) The isolation and structure of a remarkable marine animal antineoplastic constituent – dolastatin 10. *J Am Chem Soc* 109:6883–6885
168. Bloxam WP, Perkin AG (1910) Indirubin. *J Chem Soc* 1460–1475
169. Rinehart KL, Fregeau NL, Warwick RA et al (1999) Spisulosine compounds having antitumor activity. *PCT Int Appl WO 9952521 A1* 19991021 73 pp
170. Quiñoà E, Adamczeski M, Crews P et al (1986) Bengamides; heterocyclic anthelmintics from a Jaspidae marine sponge. *J Org Chem* 51:4494–4497
171. Adamczeski M, Quiñoà E, Crews P (1990) Novel sponge-derived amino acids. 11. The entire absolute stereochemistry of the bengamides. *J Org Chem* 55:240–242
172. Warabi K, Matsunaga S, van Soest RWM et al (2003) Dictyodendrins A–E, the first telomerase-inhibitory marine natural products from the sponge *Dictyodendrilla verongiformis*. *J Org Chem* 68:2765–2770
173. Pettit GR, Cichacz ZA, Gao F et al (1994) Isolation and structure of the cancer cell growth inhibitor dictyostatin 1. *J Chem Soc Chem Commun* 1111–1112
174. Gunasekera SP, Gunasekera M, Longley RE et al (1990) Discodermolide: a new bioactive polyhydroxylated lactone from the marine sponge *Discodermia dissoluta*. *J Org Chem* 55:4912–4915
175. Gunasekera SP, Gunasekera M, Longley RE et al (1991) Discodermolide: a new bioactive polyhydroxylated lactone from the marine sponge *Discodermia dissoluta*. *J Org Chem* 56:1346

176. Gunasekera SP, McCarthy PJ, Kelly-Borges M et al (1996) Dysidiolide: a novel protein phosphatase inhibitor from the Caribbean sponge *Dysidea etheria* de Laubenfels. *J Am Chem Soc* 118:8759–8760
177. Hirata Y, Uemura D (1986) Halichondrins – antitumor polyether macrolides from a marine sponge. *Pure App Chem* 58:701–710
178. Talpir R, Benayahu Y, Kashman Y et al (1994) Hemiasterlin and geodiamolide TA: two new cytotoxic peptides from the marine sponge *Hemiasterella minor* (Kirkpatrick). *Tetrahedron Lett* 35:4453–4456
179. Zabriskie TM, Klocke JA, Ireland CM et al (1986) Jaspamide, a modified peptide from a *Jaspis* sponge, with insecticidal and antifungal activity. *J Am Chem Soc* 108:3123–3124
180. Crews P, Manes LV, Boehler M (1986) Jasplakinolide; a cyclodepsipeptide from the marine sponge; *Jaspis* sp. *Tetrahedron Lett* 27:2797–2800
181. Corley DG, Herb R, Moore RE et al (1988) Laulimalides: new cytotoxic macrolides from marine sponge (*Hyatella* sp) and nudibranch predator (*Chromodoris lochi*). *J Org Chem* 53:3644–3646
182. Shigemori H, Madono T, Sasaki T et al (1994) Nakijiquinones A and B, new antifungal sesquiterpenoid quinones with an amino acid residue from an Okinawan marine sponge. *Tetrahedron* 50:8347–8354
183. West LM, Northcote PT, Battershill CN (2000) Peloruside A: a potent cytotoxic macrolide isolated from the New Zealand marine sponge *Mycale* sp. *J Org Chem* 65:445–449
184. Searle PA, Molinski TF (1995) Phorboxozoles A and B: potent cytostatic macrolides from marine sponge Phorbas species. *J Am Chem Soc* 117:8126–8131
185. Erickson KL, Beutler JA, Cardellina JH et al (1997) Salicylihalamides A and B, novel cytotoxic macrolides from the marine sponge *Haliclona* sp. *J Org Chem* 62:8188–8192
186. Erickson KL, Beutler JA, Cardellina JH et al (2001) Salicylihalamides A and B, novel cytotoxic macrolides from the marine sponge *Haliclona* sp. *J Org Chem* 66:1532–1532
187. Trimurtulu G, Faulkner DJ, Perry NB et al (1994) Alkaloids from the Antarctic sponge *Kirkpatrickia varialosa* Part 2: Variolin A and N(3')-methyl tetrahydrovariolin B. *Tetrahedron* 50:3993–4000
188. Bewley CA, Holland ND, Faulkner DJ (1996) Two classes of metabolites from *Theonella swinhoei* are localized in distinct populations of bacterial symbionts. *Experientia* 52:716–722
189. Andrianasolo EH, Gross H, Goeger D et al (2005) Isolation of swinholide A and related glycosylated derivatives from two field collections of marine cyanobacteria. *Org Lett* 7:1375–1378
190. Schmidt EW, Nelson JT, Rasko DA et al (2005) Patellamide A and C biosynthesis by a microcin-like pathway in *Prochloron didemni*, the cyanobacterial symbiont of *Lissoclinum patella*. *Proc Natl Acad Sci USA* 102:7315–7320
191. Luesch H, Moore RE, Paul VJ et al (2001) Isolation of dolastatin 10 from the marine cyanobacterium *Symploca* species VP642 and total stereochemistry and biological evaluation of its analogue symplostatin 1. *J Nat Prod* 64:907–910
192. Bull AT, Ward AC, Goodfellow M (2000) Search and discovery strategies for biotechnology: the paradigm shift. *Micro Mol Biol Rev* 64:573–606
193. Grassle JF, Maciolek NJ (1992) Deep-sea species richness: regional and local diversity estimates from quantitative bottom samples. *Am Nat* 139:313–341
194. Feling RH, Buchanan GO, Mincer TJ et al (2003) Salinosporamide A: a highly cytotoxic proteasome inhibitor from a novel microbial source, a marine bacterium of the new genus *Salinispora*. *Angew Chem Int Ed* 42:355–357
195. Naumann K (1999) Influence of chlorine substituents on biological activity of chemicals. *J Prakt Chem* 341:417–435
196. Macherla VR, Mitchell SS, Manam RR et al (2005) Structure-activity relationship studies of salinosporamide A (NPI-0052), a novel marine derived proteasome inhibitor. *J Med Chem* 48:3684–3687
197. Williams PG, Buchanan GO, Feling RH et al (2005) New cytotoxic salinosporamides from the marine actinomycete *Salinispora tropica*. *J Org Chem* 70:6196–6203

Hyukjae Choi, Alban R. Pereira, and William H. Gerwick

Contents

2.1	Introduction	56
2.2	Marine Cyanobacteria	57
2.2.1	Overview of the Biology of Cyanobacteria	57
2.2.2	Overview of the Trends in Secondary Metabolism in Marine Cyanobacteria	59
2.2.3	Overview in Pharmacological Trends	59
2.2.4	Carbohydrate-based Metabolites	60
2.2.5	Terpenoids	60
2.2.6	Fatty Acids	62
2.2.7	Polyketides	62
2.2.8	Polypeptides	64
2.2.9	Lipopeptides	67
2.2.10	Conclusions on Cyanobacterial Natural Products	75
2.3	Marine Microalgae	76
2.3.1	General Introduction to Marine Microalgae	76
2.3.2	Dinoflagellates	76
2.3.3	Diatoms	86
2.3.4	Chrysophytes	92
2.3.5	Prymnesiophytes	96
2.4	Marine Macroalgae	96
2.4.1	General Introduction to Marine Macroalgae	96
2.4.2	Chlorophyta	98
2.4.3	Rhodophyta	105
2.4.4	Phaeophyceae	120
2.5	Conclusions	130
2.6	Study Questions	131
	References	132

H. Choi (✉) • A.R. Pereira • W.H. Gerwick

Scripps Institution of Oceanography, Skaggs School of Pharmacy and Pharmaceutical Sciences,
University of California, San Diego, CA, USA

e-mail: h5choi@ucsd.edu, alpereinabadilla@ucsd.edu, wgerwick@ucsd.edu

Abstract

This chapter reviews the major metabolic themes that are characteristic of the prominent groups of marine algae and cyanobacteria. The taxonomic organization of the chapter facilitates an appreciation of the uniqueness of each of these groups in their capacity to elaborate specific classes of secondary metabolites. For each compound discussed, which are chosen as representatives of chemical themes, a brief story is presented which describes the natural history of the organism, the isolation of the natural product, its structure elucidation, and as appropriate, the pharmacology, chemical ecology, and biosynthesis of the isolated metabolite. Many unanswered questions remain in understanding these diverse algal chemistries, and numerous areas for future exploration are suggested throughout the chapter.

2.1 Introduction

Some of the earliest efforts in exploring the organic chemistry of the marine environment involved study of the chemistry of marine algae, and thus this topic has a more mature and well-developed nature relative to other areas of marine natural products. Pioneering work in Japan and the United States first examined intertidal red algae for their unique constituents and quickly established that they had a spectacular capacity to produce halogenated organic compounds of unusual structure. Moreover, in Japan there was a developed ethnological use of some seaweeds for their medicinal qualities, and this was another focus of early work; for example, the red alga *Digenia simplex* had been used to eliminate intestinal parasites, and an early investigation of the chemical basis for this property revealed kainic acid. Kainic acid owes its anthelmintic properties to its activity at the kainate receptor and, as the naming would suggest, has become an important tool in neurobiology. Subsequently, over the period 1970–2000, various research groups explored one or another group of algae for their unique constituents, and over time, a picture has emerged of distinctive chemical trends in each of the various algal groups. Articulation and description of these trends are the goals of this chapter.

The groups of algae to be examined in this chapter include both the eukaryotic algae of macroscopic as well as microscopic size and the prokaryotic algae (blue-green algae = cyanobacteria), which also are of both an easily visible as well as microscopic character. In this regard, we hold to the definition of “algae” as aquatic photosynthetic organisms with plant-like qualities [1]. It should be noted that some controversy exists over this definition of “algae”; however, the main point of contention, the cyanobacteria, is currently classified using both the botanical and microbiological coding systems. From this perspective, as well as the ecological and environmental perspective of how these exist in nature, they are appropriately covered in this chapter.

Many review perspectives have been written on various specialized aspects of algal and cyanobacterial secondary metabolites, and a few of the most recent

ones are given here [2–4]. To the student of marine natural products chemistry, a extraordinarily wide range of natural product themes are present in the algae, and imbedded in these structures are diverse stories of organic chemistry, biosynthesis, chemical ecology, pharmacology, and drug development. It is the intention of this chapter to retell some of these accounts using the natural product structures as entry points.

2.2 Marine Cyanobacteria

2.2.1 Overview of the Biology of Cyanobacteria

The cyanobacteria, or blue-green algae, are photosynthetic chlorophyll *a*-containing bacteria which occur both as single cells, colonies of single cells, unbranched filaments, and even branched filaments [5]. Thus, they range in size from single cells of a micron in diameter (*Microcystis* species) to large mats and tufts that may be picked up by hand and weigh kilograms in mass. Several of the tuft-forming species of the genus *Lyngbya* are readily visible by snorkeling or SCUBA as finely divided filaments that wave back in forth in the currents and swell, looking much like human hair growing up off the seafloor; hence, the nickname “mermaid’s hair.” These wonderfully diverse groups of bacteria are ancient inhabitants of our planet, with specimens being identified in the geological record going back some 2.5 billion years. They have had many eons over which to diversify, occupy many specialized ecological niches, and evolve different routes of metabolism. As a result, they are among the most exciting groups of marine organisms for their production of structurally unique and biologically active secondary metabolites.

The taxonomy of the cyanobacteria is in a state of flux as the field is currently transitioning from using morphological and growth characteristics to assign taxonomy to a system of using 16S rRNA gene phylogeny. A major problem in our current taxonomic understanding results from the fact that many radiations of the cyanobacteria have separately evolved similar morphological features, such as filaments composed of short barrel-shaped cells, and thus, this traditional system has given an imprecise and oftentimes incorrect perception of their relationships. As we apply 16S rRNA gene sequences, or even more powerfully, a multitude of genes and gene types, as in multilocus sequence typing (MLST), we are finding that they are much more diverse than ever realized [6]. In the not-very-distant future, we will look back on our current efforts as quite primitive and lacking in power, as with new DNA sequencing approaches on the horizon that are estimated to provide 1-megabase of sequence for \$1.00, we will be soon performing genome-based phylogenies that more accurately and precisely delineate the relationships between these organisms. Nevertheless, the current understanding of the taxonomy of cyanobacteria derives in parallel from their consideration in both bacterial and botanical classifications, with a fair concordance between the two, which both divide these organisms into five

subcategories (bacteriological, five subsections groups I to V; botanical, five families Chroococcales, Pleurocapsales, Oscillatoriales, Nostocales, Stigonematales, respectively) [7].

Marine cyanobacteria occupy essentially all regions of the sea where there is sufficient light energy to drive photosynthesis, from pelagic to nearshore to benthic. In the tropics, they can become dominant members of shallow water environments, overgrowing many other organisms as thin veils or even dense mats (e.g., *Phormidium* and *Lyngbya* spp.); the latter are capable of smothering and killing subtending organisms such as corals. Cyanobacteria play a critical role in nitrogen cycling on coral reefs, habitats renowned for being limited in nitrogen and phosphorous, because of their capacity to fix atmospheric nitrogen into organic forms. Additionally, in areas of high nutrient input, such as from rivers and human activities, cyanobacteria abound and often form a dominant cover.

Cyanobacteria participate in numerous symbiotic relationships, growing in specialized tissue arrangements especially within tunicates (hemichordates) and sponges. Within these symbioses, the products of photosynthesis as well as secondary metabolism are exchanged between the cyanobacterium and the host [8]. Cyanobacteria are a favored food of some types of invertebrate mollusks, such as *Dolabella* and *Stylocheilus* sea slugs. These organisms are capable of chemolocation of cyanobacteria, often a *Lyngbya* or *Symploca* species, and consume it for both nutrition as well as assimilation of its natural products. It is generally regarded that these fleshy animals derive benefit from sequestration of the antipredatory natural products of their cyanobacterial diet. In summary of the above discussion, many marine natural products ascribed to sponges, tunicates, and sea hares have subsequently been shown, or are strongly implicated, to derive from the associated or consumed cyanobacteria.

As prokaryotes, cyanobacteria have distinctive metabolic and anatomical features [5]. The cells of different species range from spherical (e.g., unicells) 1–10 μm in diameter to flattened pancake-like shapes (e.g., in filaments) with cells only 1–2 μm long yet possessing a width of up to 60–80 μm . Cyanobacteria of filamentous construction are often covered with a sheath of extracellular material, and in some cases, this can become quite massive, resulting in individual filaments 10–20 cm in length and roughly the thickness of a human hair (overall width up to 100 μm). As prokaryotes, they lack cellular organelles; however, their photosynthetic apparatus is organized onto thylakoids, as in chloroplasts in plants and other algae (indeed, the latter represent ancient endosymbiotic incorporations of cyanobacteria!). Light is harvested by elaborate photoreceptor structures, known as phycobilisomes, which are arranged on the thylakoids and organize a complement of chlorophyll *a* and accessory pigments including phycoerythrin, phycocyanin, and allophycocyanin, as well as carotenoids. As a result, these “blue-green algae” can take on colors in nature ranging from brown to red to mossy green or blue green, depending on the organism and the available light quality and quantity.

2.2.2 Overview of the Trends in Secondary Metabolism in Marine Cyanobacteria

The major group contributing to the rich secondary metabolite chemistry of the cyanobacteria (773 metabolites reported as of 2011) is predominately the Oscillatoriales (58% of reported metabolites, group III), followed by the Nostocales (24%), Chroococcales (10%), and Stigonematales (8%) [9]. Metabolites from the fifth cyanobacterial group, the Pleurocapsales, have only rarely been reported, although the biosynthetic genes necessary for making nonribosomal peptides have been detected [10]. The most important marine group to contribute to this rich chemistry is the Oscillatoriales and is dominated by the genus *Lyngbya* (43% of all cyanobacterial metabolites, 336 compounds). However, as noted above, cyanobacterial taxonomy is both imprecise and in need of revision, and likely, a multitude of diverse organisms have been lumped into the *Lyngbya* group.

The molecular weights of cyanobacterial metabolites (excluding proteins and biopolymers) distribute into a skewed bell-shaped curve extending from as little as 100 to a maximum of 1801 Da. The majority of reported compounds are between 200 and 1100 molecular weight with an average of 645 Da and a mean of 604. Different classes of secondary metabolites predominate in these weight classes; for example, natural products greater than 700 Da are almost exclusively of a nonribosomal peptide synthetase (NRPS) origin, although oftentimes combined with some polyketide synthase (PKS)-derived sections. In fact, from an overview perspective, the dominant theme in the secondary metabolites of marine cyanobacterial natural products is the integration of these two biosynthetic classes, NRPSs and PKSs, to form ketopeptides (PKS to NRPS biosynthetic origin) and peptoketides (NRPS to PKS biosynthetic origin). However, pure peptides or polyketides are also common, as are alkaloids which are more distantly derived from peptides. Relatively few terpenoids, fatty acids, or other molecular classes have been described from these organisms to date [11].

The dominant amino acid classes used in cyanobacterial natural products are aliphatic and polar, dominated in the former by leucine, isoleucine, alanine, valine, phenylalanine, and proline and in the later by threonine, serine, cysteine, tyrosine, and glycine. Very often, these amino acids are modified by methylation (*N*-methyl or *O*-methyl), epimerization to the *D*-isomer, extended by a ketide section, heterocyclized to the carbonyl of an adjacent amino acid, or otherwise modified such as by halogenation. A number of reviews and perspectives have appeared over the past decade on the chemistry [11–13], biosynthesis [14], and biological properties [3] of marine cyanobacterial natural products.

2.2.3 Overview in Pharmacological Trends

With nearly 800 reported metabolites, the biological properties of the cyanobacterial natural products are highly diverse, and many or most are not described or known.

Nevertheless, a few trends can be discerned; many have potent cell toxicity by virtue of their ability to interfere with polymerization of either tubulin or actin, two well-validated targets of cytotoxins. Additionally, a number of fresh water cyanobacterial metabolites are known to exert neurotoxic activity, many through interactions at the voltage-gated sodium channel (VGSC) of neurons. Relatively recently, this pharmacological theme has also been observed in marine metabolites with a growing number of both VGSC blockers and activators being reported [15]. One way to advance the discovery of marine cyanobacterial metabolites into more meaningful scientific arenas is to develop a molecular level understanding of their pharmacology; this type of research should be given higher priority in the future.

2.2.4 Carbohydrate-based Metabolites

While a number of peptide and polyketide metabolites of marine cyanobacteria have been found as glycosides, usually with various methylated pentose or hexose sugars, pure sugar or oligosaccharide metabolites have only rarely been isolated (Fig. 2.1), and these have been exclusively reported from freshwater specimens. In part, this lack of reported pure carbohydrate-based metabolites may result from the bias of most natural product programs being away from water soluble materials. An example of a polyketide appended with a methylated pentose sugar is given by lyngbyalioside (**1**), isolated from *Lyngbya bouillonii* [16]. This 16-membered macrolide shows several interesting features which are typical of cyanobacterial polyketides, including a vinyl bromide, tetrahydropyran ring, and methyl groups attached to C-1 positions of the polyketide (e.g., so-called β -branches). The hexopyranose sugar (a trimethyldeoxymannose derivative) is α -linked, possesses methoxy groups at the 2-, 3-, and 4-positions, and is deoxygenated at the 6-position. Another example, a complex ketopeptolide with an attached methylated sugar, is given by malyngamide J (**2**), isolated from a Curaçao collection of *Lyngbya majuscula* [17]. In this case, the sugar is a dimethoxyxylose residue with an α -linkage to the polyketide cyclohexenone section. Malyngamide J shows modest toxicity to brine shrimp and fish, and thus may function as an antifeedant. Other highly bioactive polyketides with related methylated sugar residues have been reported from red algae, such as polycavernoside A (**3**), a metabolite which caused several fatal human poisonings in Guam [18]. However, structural precedents for both the aglycone and sugar portions strongly suggest a cyanobacterial source for polycavernoside A, and thus, it is likely that a fine turf of the producing cyanobacterium grows on the surface of this red alga.

2.2.5 Terpenoids

Cyanobacteria utilize the terpene biosynthetic pathway only to a limited extent, with the most common examples being to produce primary metabolites (essential to the basic life processes) rather than secondary metabolites (compounds with

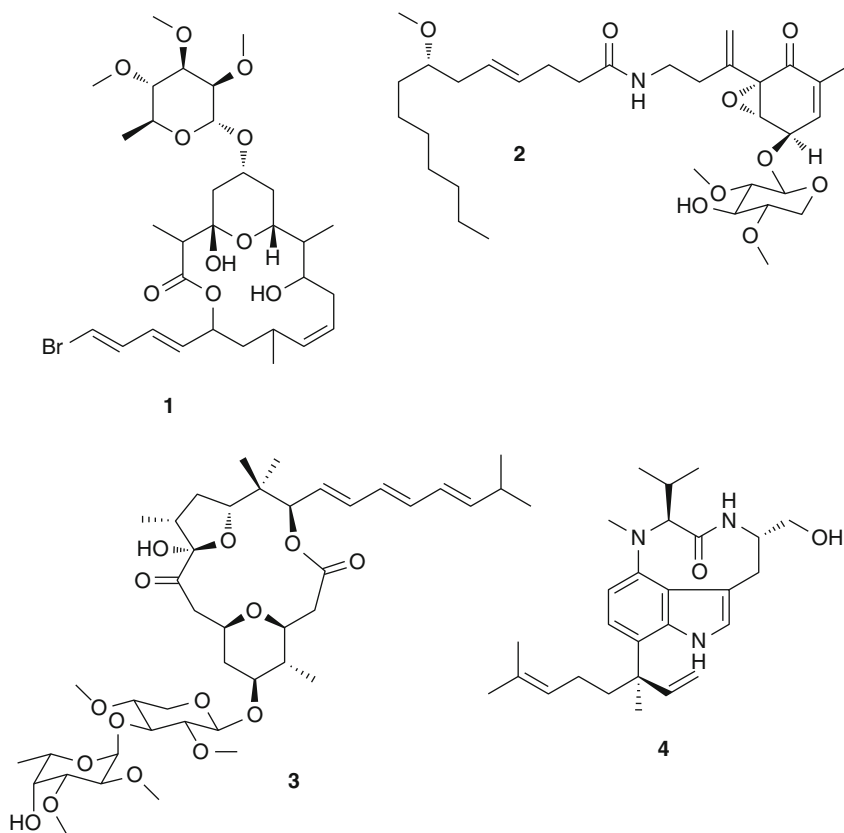


Fig. 2.1 Carbohydrate-based metabolites and terpenoids from marine cyanobacteria

adaptive functions). Examples of cyanobacterial terpenes falling into the primary metabolite class include carotenoid pigments (accessory pigments employed to harvest light and funnel its energy to photosynthesis) and steroid equivalents known as “hopanoids” which contribute to membrane structure [19].

An example of a cyanobacterial terpene-containing secondary metabolite is given by the lyngbyatoxins (e.g., lyngbyatoxin A, **4**) [20]. Following stormy periods around Waikiki, Hawaii, small tufts of the benthic cyanobacterium *Lyngbya majuscula* become dislodged from substrate and are frequently found floating in the nearshore surf zones. Swimmers coming in contact with these tufts, especially on areas of sensitive skin, develop rashes and occasionally ulcerations, giving rise to the common name for this occurrence as “swimmer’s itch.” The responsible secondary metabolite causing this irritation was investigated by the laboratory of the University of Hawaii pioneer of cyanobacterial natural products, Richard E. Moore, and resulted in characterization of a terpene section fused to a novel dipeptide derivative [20]. This metabolite, named lyngbyatoxin A (**4**), was shown to be a potent protein kinase C (PKC) activator, and thus has proinflammatory

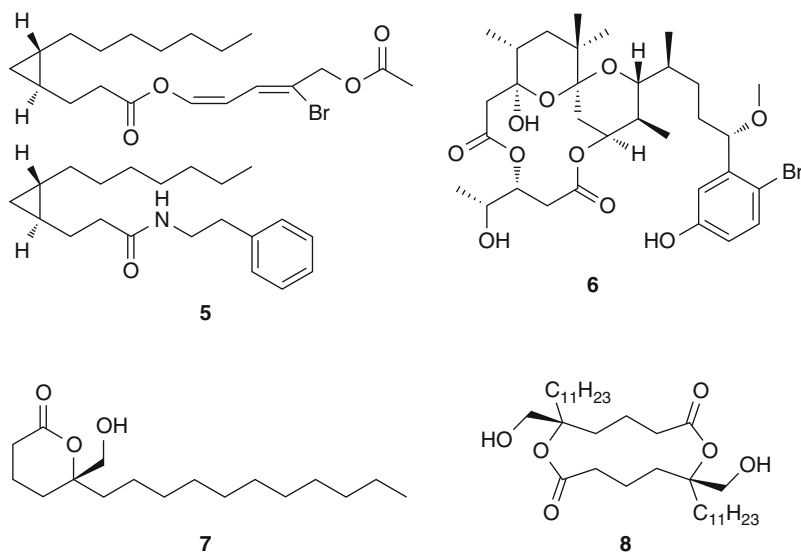


Fig. 2.2 Fatty acids and polyketides from marine cyanobacteria

activity. The biosynthesis of lyngbyatoxin A has been explored using a molecular genetics approach [21] and shown to possess several novel steps, including a reductive offloading of a dipeptide from a NRPS assembly system, a novel aromatic substitution reaction, and an interesting reverse prenylation of the core indole.

2.2.6 Fatty Acids

The common fatty acids of cyanobacteria, such as those present in membrane lipids, are typically of 16- and 18-carbon chain length, of variable degree of unsaturation, and remarkably, are present as complex lipid species quite similar to those found in higher plant chloroplast membranes (e.g., glycolipids) [22]. In the secondary metabolism of cyanobacteria, fatty acid metabolites have a number of interesting structural features, such as unusual pendant carbon atoms, isonitrile functionalities, and various patterns of oxidation to form oxylipins [11]. For example, collections of the cyanobacterium *Lyngbya majuscula* from Grenada in the Southeastern Caribbean Sea yielded a series of metabolites with cyclopropyl ring-containing fatty acids in amide or ester linkage with smaller functionalized moieties (e.g., **5**) [23] (Fig. 2.2).

2.2.7 Polyketides

Predominately, the polyketide natural products found in marine cyanobacteria are present in combination with amino acid-derived sections, the latter almost certainly

incorporated by nonribosomal peptide synthetases. These mixed biosynthesis compounds, which constitute the dominant secondary metabolite biosynthetic theme of marine cyanobacteria, are considered in a separate section below. However, a few cyanobacterial metabolites are predicted to derive exclusively from the PKS pathway, and these show some interesting secondary modifications, including ring formation containing oxygen atoms, juncture of multiple PKS fragments by ester bonds, including dimerization, halogenations, and unique patterns of methylation. Two examples illustrating some of these biosynthetic themes are presented below.

As noted above, some strains of *L. majuscula* can cause skin irritation and ulceration in swimmers that come in contact with dislodged tufts of the cyanobacterium. This phenomenon of “swimmer’s itch” may be caused either by the presence of the lyngbyatoxins discussed above [20] or pure polyketides of the aplysiatoxin family (e.g., **6**) [24]. The latter class of dermatotoxin was first described from the intestines of the cyanobacterial-feeding sea hare *Stylocheilus longicauda*, but was subsequently described as a metabolic product of the cyanobacterium *L. majuscula*, and is particularly abundant strains occurring in Hawaii, Australia, and Madagascar. Indeed, some bays of Australia are overgrown by aplysiatoxin-producing strains which render their waters unsuitable for human recreation [25]. In the authors’ experience, large accumulations of floating mats of *L. majuscula* were found in nearshore waters off the northwest coast of Madagascar, and upon collection by hand, rendered our skin tingling with a menthol-like coolness which lasted for several hours; subsequently, debromoaplysiatoxin was found as the major metabolite of this extract. Structure elucidation of the aplysiatoxins, and the related oscillatoxins, was initially accomplished by NMR and MS analysis to give planar structures with relative stereochemistry, and subsequently, CD analysis was used to assign absolute configurations [24]. Biosynthetically, it appears that a benzoic acid derivative may initiate assembly of the main PKS chain. Seven rounds of PKS extension are predicted along with several methylation events from *S*-adenosylmethionine (SAM) to introduce the five pendant methyl groups. The mechanism of formation of the two spiro-connected tetrahydropyran rings is currently unknown, but will certainly reveal new biochemical steps when studied. Similarly, the molecular logic by which the lower pentanoic acid chain is incorporated is unknown at present, but may involve a unique NRPS-like mechanism utilizing the β -hydroxy group of 3,4-dihydroxypentanoic acid. Due to the substitution pattern in those aplysiatoxins possessing an aromatic halogen atom, bromine incorporation likely involves a bromoperoxidase, an enzyme reported from other strains of cyanobacteria [26]. The potent biological effects of the aplysiatoxins have been studied in some detail [27], and these metabolites are also activators of protein kinase C (PKC), thereby possessing proinflammatory effects as well as promoting tumor formation. As such, they have become useful tool molecules in studying cell and animal physiology.

Another polyketide example is provided by the isolation of tanikolide (**7**) [28] and its dimeric form, tanikolide dimer (**8**) [29]. Collections of *L. majuscula* from near Tanikely Island, Madagascar first yielded the monomeric polyketide, and its

structure was elucidated by normal methods with absolute stereochemistry from a modified Mosher ester method. Tanikolide displayed both antifungal effects and brine shrimp toxicity at low microgram levels [28]. Subsequently, a dimeric form of tanikolide was isolated from this collection, and while the planar structure was readily apparent, determining the absolute configuration of both halves was significantly more involved. Initial data suggested that the metabolite was composed of one *R*-enantiomer and one *S*-enantiomer of tanikolide; however, subsequent chemical synthesis of all three possible tanikolide dimers and comparison by NMR and GCMS revealed tanikolide dimer to be formed from two monomeric *R*-enantiomers (**8**) [29]. Interestingly, all three of the synthetic tanikolide dimer pairs were equally active in inhibiting an enzyme involved in mammalian gene regulation, namely SIRT2, a member of the histone deacetylase (HDAC) family, with an $IC_{50} = 176$ nM in one assay format and 2.4 μ M in another. This was especially interesting because tanikolide dimer lacks a recognizable analog of the pharmacophore present in other known HDAC inhibitors (e.g., an alkyl chain with a zinc binding functional group at the terminus).

2.2.8 Polypeptides

As noted above, peptide-based metabolites are extremely common in marine cyanobacteria, although most contain sections of lipids, as described in the next section on lipopeptides. Nevertheless, pure peptides are well represented and, in general, are formed by amino acids with aliphatic and polar neutral amino acids. Alternately described, marine cyanobacterial peptides rarely contain charged amino acids (e.g., acidic residues such as glutamic or aspartic acid, or basic ones such as lysine or arginine); interestingly, this is a point of difference with the metabolites of freshwater cyanobacteria which tend to possess such charged amino acids more commonly.

In only the last few years, it has been revealed that peptide metabolites from marine cyanobacteria have two fundamentally different biosynthetic origins. On the one hand, they are synthesized by the nonribosomal peptide synthetase enzyme machinery which uses an assembly-line molecular logic and a discrete set of dedicated enzymes for the incorporation of each residue [30]. Alternatively, the ribosomal machinery of cyanobacteria has more recently been revealed to produce propeptides (small proteins), short sections of which are then modified, cleaved out, and usually cyclized to form a class of compound that has come to be known as the “cyanobactins” [31]. Examples of these two classes of peptide-based metabolites are described below (Fig. 2.3).

2.2.8.1 Nonribosomally Encoded Peptides and Their Biosynthesis

One of the more prevalent groups of pure peptides to be encoded by a cyanobacterial NRPS are the so-called cyanopeptolins, classified as such by their overall cyclic structure and presence of an aminohydroxypipicolinic (Ahp) acid unit. Characteristically, the overall cyclic structure is created by an ester

to a branching threonine residue, and this usually extends to an acyclic section with one or more modified amino acid residues. Cyanopeptolin metabolites have been isolated from diverse cyanobacteria, both freshwater and marine, and from taxonomic groups as varied as type I (Chroococcales) to type III (Oscillatoriales).

For example, from different marine collections of *Lyngbya* sp., somamide A (**9**) was isolated; its structure was determined by standard methods, including degradation to amino acid fragments and chiral analysis, and it was found to be a selective low nanomolar inhibitor of elastase [17, 32]. Thus, these cyanopeptolin metabolites are especially interesting for their biological properties in that they represent some of the most potent protease inhibitors known, with various showing selectivity for chymotrypsin, others for trypsin, and still others such as somamide A for elastase. Another example is given by investigations of a *Symploca* sp. from Papua New Guinea which led to the isolation of symplocamide A (**10**), an exceptionally potent cancer cell cytotoxin which also inhibits serine proteases with a 200-fold greater inhibition of chymotrypsin over trypsin [33]. The presence of several unusual structural features in symplocamide A provided new insights into the pharmacophore model for protease selectivity in this drug class, and its potent chymotrypsin inhibiting activity may underlie the exceptional cytotoxicity of this compound to H-460 human lung cancer cells ($IC_{50} = 40$ nM) as well as neuro-2a murine neuroblastoma cells ($IC_{50} = 29$ nM) [34].

The biosynthesis of members of this class has been studied at the molecular genetic level; however, these studies have employed freshwater strains such as *Anabaena*, *Planktothrix*, and *Microcystis* [35]. The beginning of each of these clusters is initiated in an interesting fashion, involving either the activation of a hydroxy acid (e.g., glyceric acid or phenylpyruvic acid) with its subsequent sulfation or phosphorylation, or activation of a polar amino acid (e.g., glutamine) and its *N*-formylation. Subsequent addition of amino acids occurs via regular NRPS mechanisms, and in each case, terminates with incorporation of a threonine residue that is involved in macrocyclization. One of the sequenced clusters was for a chlorinated metabolite (anabaenopeptilide 90B), and the cluster showed the presence a bacterial halogenase as expected. Symplocamide A (**10**), with its brominated tyrosine residue, would be expected to be produced by a highly analogous set of genes and enzymes. However, from analysis of the published gene clusters encoding for the biosynthesis of cyanopeptolin natural products, it is uncertain if these gene clusters are undergoing frequent exchange by horizontal gene transfer (HGT) events or if an ancient gene transfer event has been subject to parallel coevolutionary pressures in the various cyanobacterial strains.

2.2.8.2 Ribosomally Encoded Peptides (Cyanobactins) and Their Biosynthesis

The discovery that a large number of highly modified cyclic peptides, known as cyanobactins, are produced in cyanobacteria from ribosomally encoded peptide precursors was highly unexpected and only occurred quite recently (2005). Taking two complementary approaches, one by genome shotgun cloning and the other by genome sequencing, two groups simultaneously discovered this new pathway

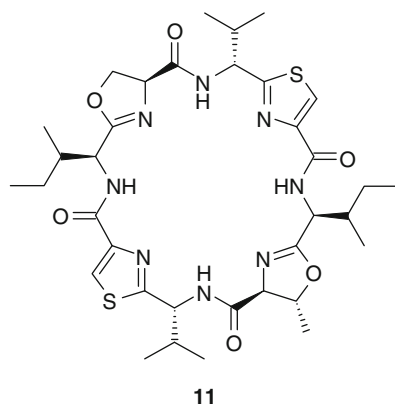
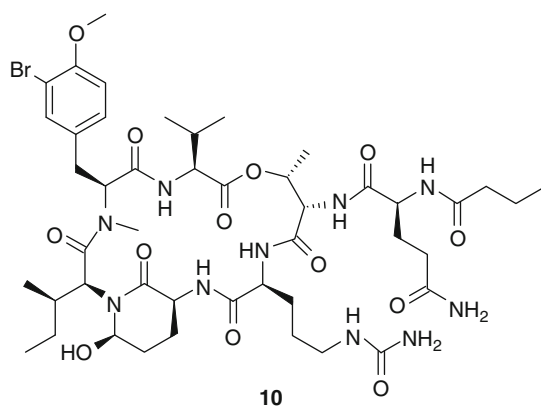
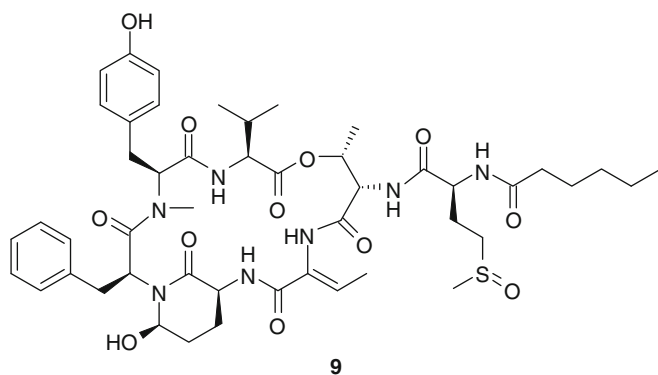


Fig. 2.3 Cyanobacterial polypeptides

to cyanobacterial peptides in the complex symbiotic relationship of a tropical South Pacific tunicate, *Lissoclinum patella*, and a cyanobacterium of the genus *Prochloron* [36, 37]. Indeed, emerald green veins identify channels within the translucent tunicate body where *Prochloron* cells are segregated and presumably, nurtured as a source of photosynthetic nutrients. The isolated metabolites from this symbiotic pair are a series of structurally distinctive cyclic peptides, the patellamides (e.g., **11**) and related substances, which, in general, have quite potent cancer cell toxicity properties [38].

Characteristic of these cyanobactin natural products is their overall cyclic structure, alternation of polar (cys, thr, or ser) and aliphatic residues (val, ala, ile, leu, phe), conversion of polar residues to oxazole/oxazoline or thiazole/thiazoline rings, or occasionally, prenylation of the polar residues. A growing understanding of the biosynthesis of the cyanobactins has revealed that the propeptides that give rise to the final structures are preceded by a short leader sequence which “programs” other enzymes encoded by nearby genes (thus forming a gene cluster) to proteolytically cleave out the final oligopeptide, convert the polar residues to their corresponding heterocycles (or engage in prenylation), and produce the macrocycle [39]. As such, this system is ideally suited for genetic manipulation and engineering to produce structurally diverse libraries that can be probed for their biological properties [14]. Subsequently, marine cyanobacteria have been identified by genetic and mass spectrometric methods to utilize ribosomal processes along with catalytically promiscuous enzymes to produce a vast array of intriguing molecular structures [40].

2.2.9 Lipopeptides

The dominant and distinctive theme in marine cyanobacterial metabolites is the production of lipopeptide-type natural products which merge sections deriving from polyketide or fatty acid origin with those coming from the NRPS pathway [11–13]. Some representatives of this complex class of natural products are among the most bioactive compounds known from cyanobacteria, and several have promising biomedical utility. The relative orientation of lipid and peptide sections varies, with the lipid section sometimes biosynthetically preceding the peptide section, other times following the peptide section, or quite often, both of these orientations are observed within a single metabolite. To distinguish them, the terms “ketopeptide,” “peptoketide,” and “complex ketopeptide” have been coined to refer to the above orientations, respectively, and are useful for discussing these various biosynthetic classes. Below are examples of each of these mixed biosynthetic classes of metabolites, and furthermore, these occur in both linear and cyclic forms.

2.2.9.1 Linear Lipopeptides

Linear ketopeptides are a familiar and common motif in cyanobacterial natural products (Fig. 2.4). While there are many examples, a notable example is given by

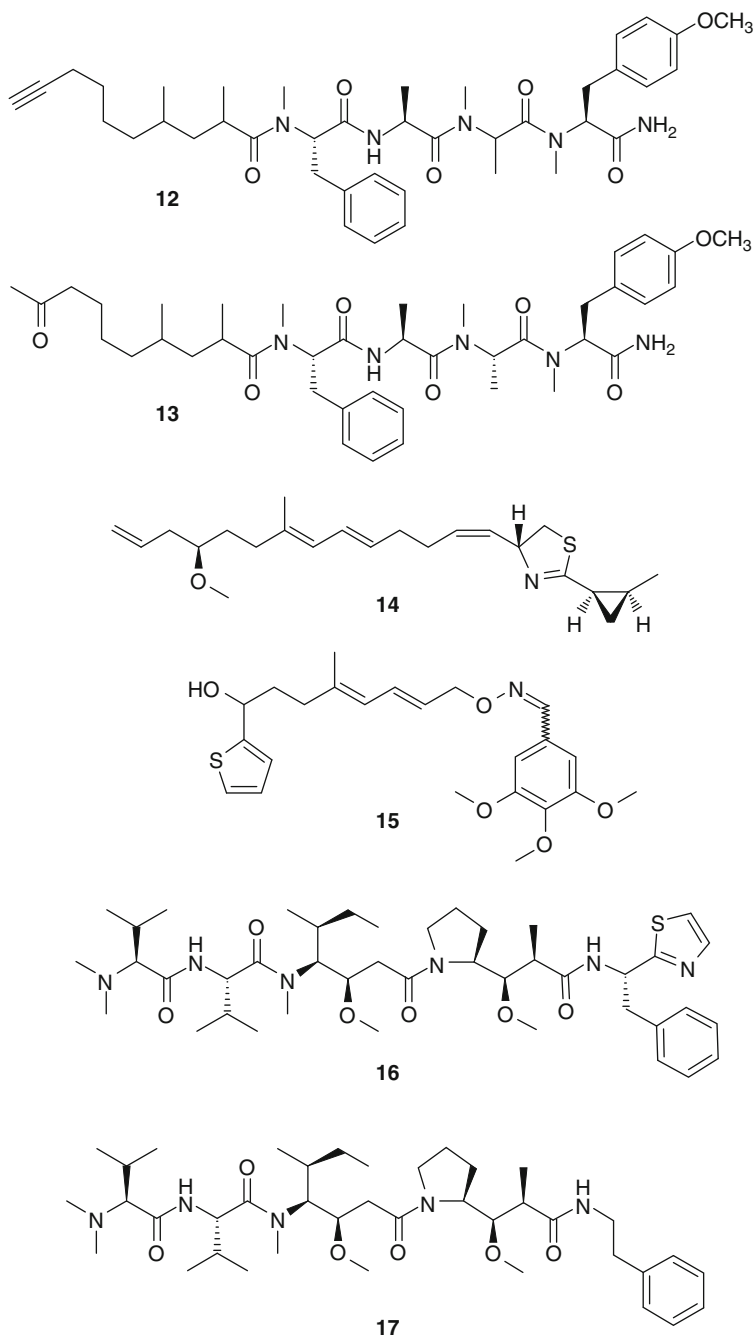


Fig. 2.4 Cyanobacterial linear lipopeptides

the carmabins (**12**, **13**) [41]. Carmabins A and B were reported from a Curaçao collection of the marine cyanobacterium *Lyngbya majuscula* and were isolated from relatively polar fractions in response to cancer cell cytotoxicity associated with this crude material. Unfortunately, the assays were no longer available by the time compound isolation was accomplished, and characterization of the carmabins in further cancer models has not occurred, although carmabin A has been reported to possess antimalarial-type properties [42]. Nevertheless, these are fascinating molecules with carmabin A possessing a 10-carbon chain with a terminal acetylene functionality and secondary methyl groups at the C-2 and C-4 position, whereas in carmabin B, the acetylene group is replaced by a methyl ketone. Attached to either of these acyl chains is a tetrapeptide composed of *N*-methyl Phe, Ala, *N*-methyl Ala, and *N,O*-dimethyl Tyr as its primary amide. Configurations at the six stereocenters have not yet been determined. A partial gene sequence encoding for the carmabins has been deduced and suggests that its biosynthesis is initiated by the incorporation of a hexanoic acid precursor, possibly 5-hexenoic acid. This is followed by a desaturase that presumably forms the acetylene bond, followed by two PKS modules with C-methylation domains (for incorporation of the two secondary methyl groups). A series of NRPS modules follow for incorporation of the four amino acids, three of which also have *N*-methyltransferase domains. The cluster terminates in an unexpected way with no clear type I thioesterase domain; it will be intriguing to study the biochemistry of this novel aspect of the pathway which is believed to be responsible for forming the unusual primary amide functionality.

A second linear and complex ketopeptide example is given by curacin A (**14**), a potent antiproliferative agent to cancer cells, also isolated from a *Lyngbya majuscula* collection from Curaçao [43]. Curacin A possesses a structure mainly composed of polyketide origin; however, a single cysteine unit intervenes and is cyclized and dehydrated to form the thiazoline ring. Curacin A was shown to possess low nanomolar to high picomolar antiproliferative activity in various cancer cell lines and to exert this powerful cytostatic activity via inhibition of tubulin polymerization through action at the colchicine binding site [44]. Because of these potentially useful biological properties as an anticancer agent, the National Cancer Institute performed advanced evaluations of this agent, and while it showed some slight activity in vivo, it was not nearly as efficacious as hoped. This result along with other clues helped to identify that the molecule was unstable in vivo and very difficult to formulate due to its high hydrophobicity. Hence, medicinal chemical efforts to synthesize analogs with improved pharmaceutical properties were undertaken, and an improved analog (**15**) with greater stability and water solubility was produced and showed equal in vitro potency to cancer cells [45]. However, for reasons unreported in the literature, this analog has also failed to advance into clinical trials.

Nevertheless, there has been intense interest into the biosynthesis of this deceptively simple marine cyanobacterial metabolite. These latter investigations were enabled by initial isotope-labeled precursor feeding experiments using cultures of the producing cyanobacterium [46]. This mapped out the fundamental units involved in creating curacin A, and revealed a very interesting initiation of the

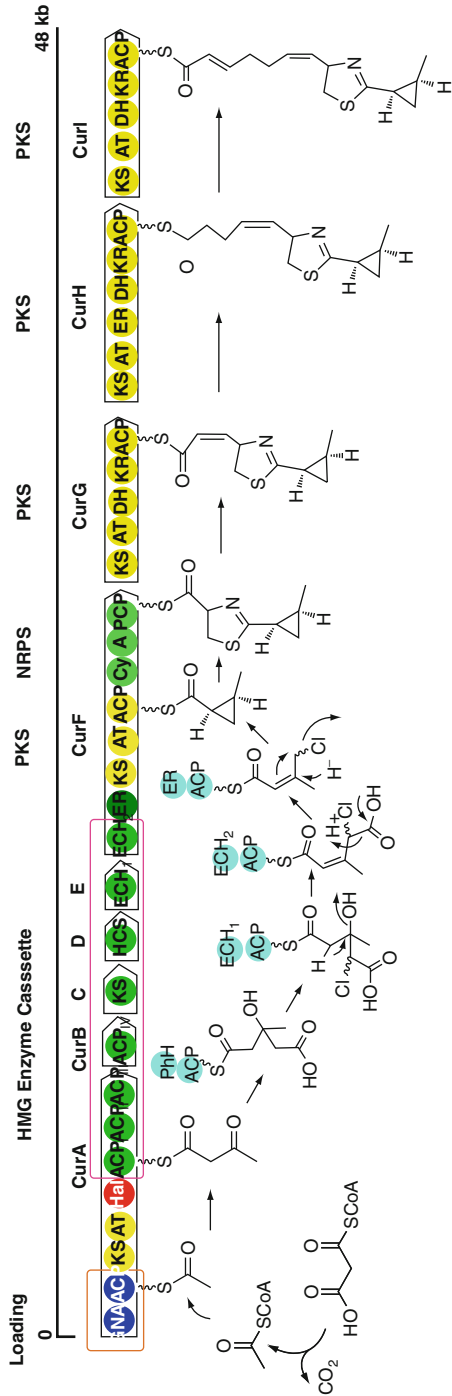


Fig. 2.5 (continued)

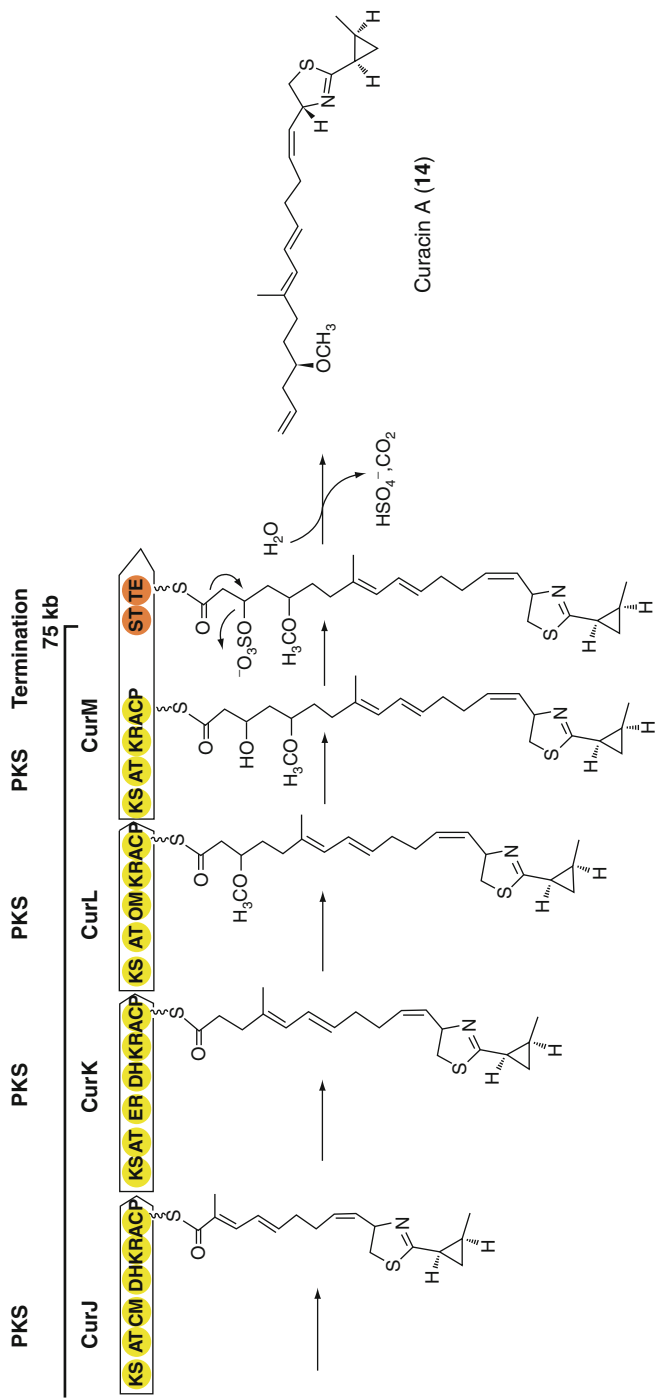


Fig. 2.5 Biosynthetic pathway and gene cluster of curacin A (14)

pathway to create the cyclopropyl ring, and an equally intriguing termination to produce the terminal olefinic bond. Ensuing, a gene cluster was identified for curacin A biosynthesis which gave powerful insight into the process of biosynthesis, especially these most unusual assembly steps [14] (Fig. 2.5). Expression of the biosynthetic enzymes and study of their catalytic properties *in vitro* have revealed that the cyclopropyl ring is formed by a variant of the terpene biosynthetic pathway and includes a cryptic chlorination reaction to activate a methyl group for cyclopropyl ring formation [47]. The chlorinating enzyme in this pathway, and many others of marine cyanobacterial metabolites, utilizes a novel mechanism involving very high energy chlorine radical species so as to halogenate at unactivated carbon centers [48]. The carbon branches that are produced in these terpene-like reactions, so-called β -branch reactions, are now realized to be of frequent occurrence in cyanobacterial metabolites, as well as other microbial natural products, and result in diverse functional groups such as secondary methyl groups, hydroxymethyl groups, exo-olefins with and without attached chlorine atoms, and cyclopropyl rings. At the other end of the curacin A molecule, an equally unusual set of reactions occur to activate the system for a terminal decarboxylation reaction as a novel mode of release from the biosynthetic enzyme manifold. Sulfation of the β -hydroxy group activates this group for departure coincident with decarboxylation, thus yielding a terminal olefin group as the enzyme-released product [49].

In 1972, the Pettit group in Arizona collected a large number of *Dolabella auricularia* sea hares from the Indian Ocean; biological evaluation at the National Cancer Institute showed their organic extract to increase life span in the P388 lymphocytic leukemia mouse model by 100%. Sea slugs are slow moving marine gastropods that lack obvious means of defense; however, in general, the extracts or secretions of the skin and organs of sea hares are highly toxic and have played a nefarious role in ancient history as poisons. The molecular basis for the more recently detected anticancer activity was not characterized until 1987 after some 15 years of intense effort because the active materials were present in vanishingly small quantities. This resulted in the identification of a group of potent toxins known as the “dolastatins” [50]. Dolastatin 10 (**16**) and its analogs generated much excitement due to their potent *in vivo* anticancer properties. Dolastatin 10 has been shown to act via disruption of cancer cell microtubule networks, thus disturbing normal cell division and the ordered separation of chromosomes. Although this natural product progressed into Phase II clinical trials, it was ultimately dropped as a single agent due to undesired peripheral toxicity. Chemical modification efforts to reduce toxicity resulted in the synthesis of TZT-1027 (**17**, Auristatin, Soblidotin), which more recently completed a Phase II clinical trial in patients with advanced or metastatic soft-tissue sarcomas [51]. The authors of this latter study indicated that “TZT-1027 was found to be safe and well tolerated.” Subsequently, dolastatin 10 (**16**) was isolated directly from the benthic cyanobacterium *Symploca* sp. [52], thus explaining the very low yield from the cyanobacterial-feeding sea hares.

2.2.9.2 Cyclic Lipopeptides

Throughout the Western and South Pacific, one may observe thin red veils covering small openings in the reef which are actually networks of the cyanobacterium *Lyngbya bouillonii*. However, laboratory cultures of this cyanobacterium do not grow with this morphology; rather, they grow as a flask of dispersed filaments. The key to this mystery is revealed when one collects this veil-like growth; suddenly, from behind the *L. bouillonii* comes a small shrimp with a massive single claw nearly the size of the animal's body. The claw is proportionately extremely powerful and makes an audible clicking noise underwater as it attempts to defend this covering to its home. Indeed, the shrimp is responsible for weaving the veil of cyanobacterial filaments and stitching this to the reef, deriving both visual and chemical protection against predation.

Initial efforts on the secondary metabolites of this cyanobacterium occurred from collections in Guam, but subsequently, efforts have involved samples obtained from Papua New Guinea and Palmyra Atoll as well. The initial work with Guam collections yielded a single major component with exquisitely potent cancer cell cytotoxicity, and was named apratoxin A (**18**) after these initial collections from Apra Harbor [53] (Fig. 2.6). The complete planar and stereostructure was deduced in these early efforts, but the molecule was inactive in an in vivo mouse model of cancer. The mechanism of action of apratoxin A has been studied by two laboratories, and while not completely defined yet, appears to involve inhibition of STAT phosphorylation, down-regulation of an IL-6 transducer and several cancer specific receptor tyrosine kinases, with subsequent prevention of the translocation of several proteins involved in the secretory pathway [54]. However, there is also a report that apratoxin A interacts with heat shock protein 90 (HSP90) [55]. A reinvestigation of the in vivo potential of apratoxin A, using synthetic materials [56], led to an understanding that the drug had to be administered as a daily injection rather than a single bolus, and under these conditions, in vivo anticancer effects were observed. Subsequently, apratoxins B, C, and E have been reported from Guam, D from Papua New Guinea, and F and G from Palmyra Atoll collections [57]. From these diverse molecular structures, some initial structure-activity relationships (SAR) have been deduced which begin to define the Eastern and Northern regions as being of critical importance, whereas the Western and Southern sections are more tolerant of modification [57].

The biosynthesis of apratoxin A (**18**) has been studied in some detail using an innovative gene cloning approach that depended on a partial genome sequence from DNA obtained from single cells [58]. This revealed a roughly 56 kB gene cluster with deduced proteins that exactly match the order and nature of the enzymes needed to construct apratoxin A by a combined NRPS and PKS logic. The pathway begins with the large Eastern PKS section of the molecule, and appears to involve an acetate moiety which is methylated three times to produce the tertiary butyl group. Following two additional rounds of PKS extension, a β -branch is produced, in this case with full reduction to a secondary methyl group. Additional PKS extensions are followed by an NRPS-incorporating cysteine and heterocyclization

to form a thiazoline ring. Fairly standard extensions with a PKS unit and then four NRPS-encoded amino acids follow, terminating with a proline unit. Interestingly, the final section of the gene cluster shows not the expected thioesterase (TE) which normally cleaves the growing lipopeptide from the enzyme assembly, but rather, the truncated condensation domain of yet another NRPS unit. While highly speculative at this point, it is attractive to propose that the condensation domain of this final module is responsible for catalyzing release of apratoxin A with coincident cyclization.

A Florida collection of the marine cyanobacterium *Symploca* sp. yielded a cytotoxic extract that was progressively fractionated to yield a novel cancer cell-selective cytotoxin named largazole (**19**) [59] (Fig. 2.6). The planar structure of largazole was determined by standard NMR and MS–MS methods, and its chirality was established by a reaction sequence involving ozonolysis, oxidative workup, acid hydrolysis, and chiral HPLC in comparison with chemical standards. Largazole possesses several highly unusual structural elements, including two polyketide sections connected through a thioester, a condensed cysteine-alanyl unit which forms a thiazole ring, and a 4-methyl thiazoline ring formed from a second cysteine residue. While this latter modification has been seen previously in cyanobacterial metabolites (e.g., in didehydromirabazole) [60], this was the first thioester linkage to be observed in a cyanobacterial natural product. Largazole (**19**) shows exceptional antiproliferative activity with GI₅₀ values to cancer cell lines in the low nanomolar range. Interestingly, non-transformed cells were much less sensitive to the effects of the drug, suggesting a drug target unique to cancerous cells. Recent work on the molecular mechanism of action of largazole has identified histone deacetylases, and it is tempting to suggest that the unusual thioester-containing side chain plays a role in this activity.

A final cyclic lipopeptide example is given by antillatoxin (**20**), another *Lyngbya majuscula* metabolite from the island country of Curaçao; however, this one shows remarkable neuromodulatory properties through interaction at VGSC [61] (Fig. 2.6). The extracts of collections of this cyanobacterium were highly toxic to goldfish in a matter of seconds, and this assay was then used to direct the isolation of two classes of fish toxic metabolites, the more potent of which was antillatoxin [62]. Antillatoxin is approximately as potent a fish toxin as brevetoxin B, a dinoflagellate polyether “red tide toxin” which annually kills thousands of fish along the Florida coastlines. The pharmacology of antillatoxin has been studied in some detail, and like brevetoxin, it activates VGSCs to increase passage of sodium into cells, an event which ultimately activates ligand gated calcium channels to increase calcium influx, a lethal event to neurons. However, antillatoxin promotes this channel activation at a novel pharmacological position on the channel, and thus defines a new drug binding site. The consequences of this are still under exploration; however, antillatoxin has already shown different pharmacological properties from other VGSC activators such as the brevetoxins and veratridine, and thus represents a new tool for pharmacological investigations [63]. Indeed, both marine and fresh water cyanobacteria, in general, have been a rich source of new tool compounds in the field of neuropharmacology [15]. Structurally, antillatoxin (**20**)

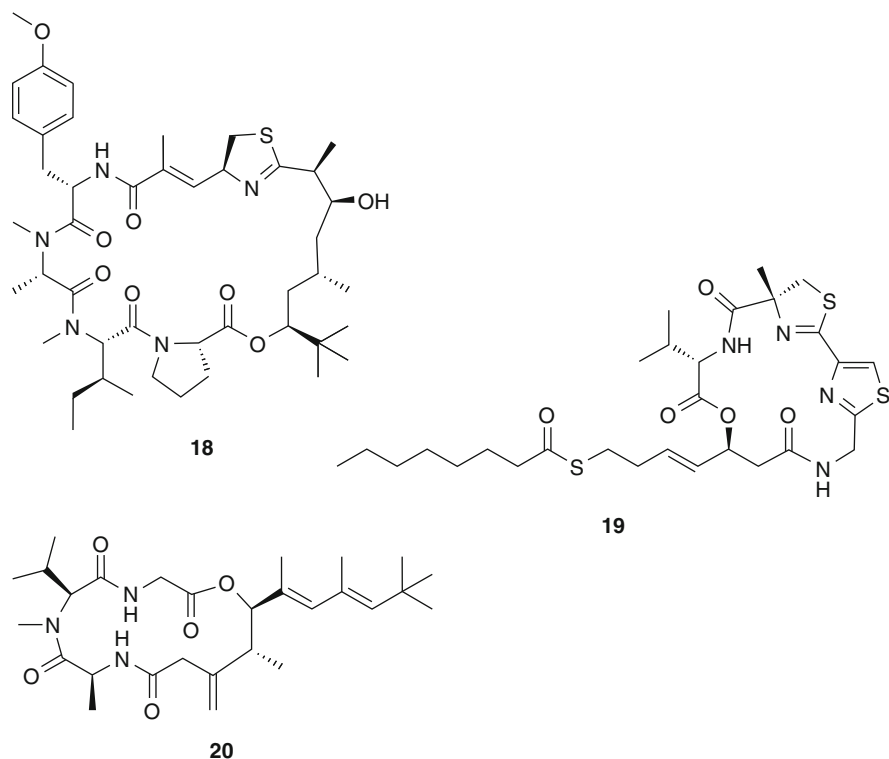


Fig. 2.6 Cyanobacterial cyclic lipopeptides

contains a tertiary butyl group at one end, a highly methyl-substituted polyketide chain, and a tripeptide section which also contains a high level of methylation (e.g., *N*-methylated aliphatic amino acids). The biosynthesis of antillatoxin has not been studied, but it seems reasonable that the pathway begins similarly to that of apratoxin (**18**), that almost all of the acetate units are *C*-methylated at C-2 positions of the acetate units from SAM, and that there is one β -branch at a C-1 position of acetate near the terminus of the polyketide ([Fig. 2.6](#)).

2.2.10 Conclusions on Cyanobacterial Natural Products

Summarizing on the natural products chemistry of marine cyanobacteria, they clearly constitute an extremely diverse source of nitrogen-rich lipids, largely constructed of segments introduced by NRPS and PKS biosynthetic assembly systems. Many of these are exquisitely bioactive in cellular systems, and in the few cases studied, they serve natural antipredatory roles for the producing cyanobacteria [64]. At the same time, these diverse and bioactive natural products represent a treasure trove of molecular scaffolds for drug discovery efforts. Indeed, marine cyanobacteria have

been identified as one of the most promising resources of bioactive compounds for pharmaceutical screening. As genomic and biosynthetic information has become more available in the past decade for these organisms, it appears that nearly every separate population has its own unique capacity to produce unique secondary metabolites, and thus, the opportunities for continued study are immense.

2.3 Marine Microalgae

2.3.1 General Introduction to Marine Microalgae

Marine microalgae are generally free-living eukaryotes and constitute the most important primary producers in the marine environment. Sometimes, populations of these microscopic algae increase rapidly and profoundly, and this causes algal blooms known as “red tides.” Marine microalgae are well-known producers of various natural products including polycyclic ethers, alkaloids, and polyhydroxylated compounds. Many of these marine microalgal metabolites are highly toxic to oceanic and terrestrial animals, including humans; thus, many marine microalgal toxic events have been reported. This section will describe selected secondary metabolites of the following groups of marine microalgae: dinoflagellates, diatoms, chrysophytes, and prymnesiophytes.

2.3.2 Dinoflagellates

2.3.2.1 General Introduction to Dinoflagellates

The dinoflagellates are unicellular microalgae which are mostly found in the marine environment, although some are also found in freshwater. While classified as eukaryotes, dinoflagellates are also considered as mesokaryotes due to their very low content of histones and nucleosomes as well as the presence of condensed chromosomes during mitosis. However, dinoflagellates do contain golgi, mitochondria, and chloroplasts which are typical organelles of eukaryotes.

Currently, nearly 2,000 species in 125 genera of dinoflagellates have been described. However, somewhat reminiscent of the cyanobacteria, dinoflagellates taxonomy is confusing as they were independently classified by both the zoological and botanical codes; only very recently have the disciplines converged to a single taxonomic system. Dinoflagellates characteristically have two flagella known as the longitudinal flagellum and the transverse flagellum. The longitudinal flagellum provides most of the motive force propelling the cell forward, whereas the transverse flagellum acts as a rudder. As a result, dinoflagellates have considerable motility as free-swimming organisms. However, some species of dinoflagellates are benthic or closely associated with other organisms (e.g., as the symbiotic zooxanthellae of corals).

Photosynthetic dinoflagellates, constituting about one half of all known dinoflagellates, have important roles in aquatic ecosystems as primary producers. They have chloroplasts containing chlorophyll *a* and *c* and either peridinin or fucoxanthin

as accessory pigments. The peridinin-containing plastid which is very abundant in photosynthetic dinoflagellates derives evolutionarily as a result of the endosymbiosis of a red alga. Nonpigmented dinoflagellates are general grazers of other protozoa. As noted above, many dinoflagellates live symbiotically with invertebrates and play critical roles in tropical reef ecosystems. For example, members of the genus *Symbiodinium* spp. live in association with corals and produce a number of interesting natural products. Members of another dinoflagellate genus, *Amphidinium*, live symbiotically in marine flat worms, and in isolated form as pure cultures, produce a series of macrolides with exceptionally potent cancer cell toxicities. Alternatively, some free-swimming dinoflagellates form blooms which discolor the ocean surface to produce “red tides”; many of these latter dinoflagellates produce potent toxins that are responsible for devastating toxic events. For further details on these toxins, the reader can see ► [Chap. 28](#).

2.3.2.2 Polyether Toxins

Okadaic Acid

A toxic event which occurred in Japan during 1976 was associated with the ingestion of contaminated shellfish. The typical symptom of intoxication was severe diarrhea, and thus, the event was termed as “diarrhetic shellfish poisoning” (DSP). Subsequently, the complex polyether metabolite, okadaic acid (**21**), was revealed as the toxin responsible for DSP [65] ([Fig. 2.7](#)). Interestingly, okadaic acid was named from the sponge *Halichondria okadai*, the original source from which the toxin was isolated. It was subsequently found to be produced by the dinoflagellates *Prorocentrum* spp. and *Dinophysis* spp. and then accumulates in filter feeders such as sponges and shellfish [66, 67]. Okadaic acid is a very potent cell toxin with an EC₅₀ value of 1.7 nM against the P388 cell line. It has also been shown to promote tumor formation as a result of its potent and specific inhibition of protein phosphatases 2A and 1 [68, 69].

Brevetoxins

The dinoflagellate *Karenia brevis* (formerly known as *Gymnodinium breve* or *Ptychodiscus brevis*) is common in the Gulf of Mexico, and it is responsible for red tides along the Florida coast [70]. Blooms of *K. brevis* cause massive fish kills, mollusk poisonings, and human food intoxications termed “neurotoxic shellfish poisoning” (NSP) [70]. The causative agents were first isolated from cultured *K. brevis* and thus named the “brevetoxins” [71]. Subsequently, they have also been found in other dinoflagellate species such as *Chattonella marina*, *Chattonella antiqua*, *Fibrocapsa japonica*, and *Heterosigma akashiwo* [72–74].

Structurally, the brevetoxins are ladder-like polycyclic ethers of fascinating molecular architecture. Brevetoxins A (**22**) and B (**23**) were first reported in 1975 as undefined compounds with the names GB-1 and GB-2 [75], but in 1981, the structure of brevetoxin B (= GB-2 and PbTx-2) was elucidated by X-ray crystallography [71]. The structure of brevetoxin A (= GB-1 and PbTx-1) was more challenging to determine, but following chemical modifications, Shimizu and coworkers were able to form a crystal that could also be analyzed by X-ray crystallography [76].

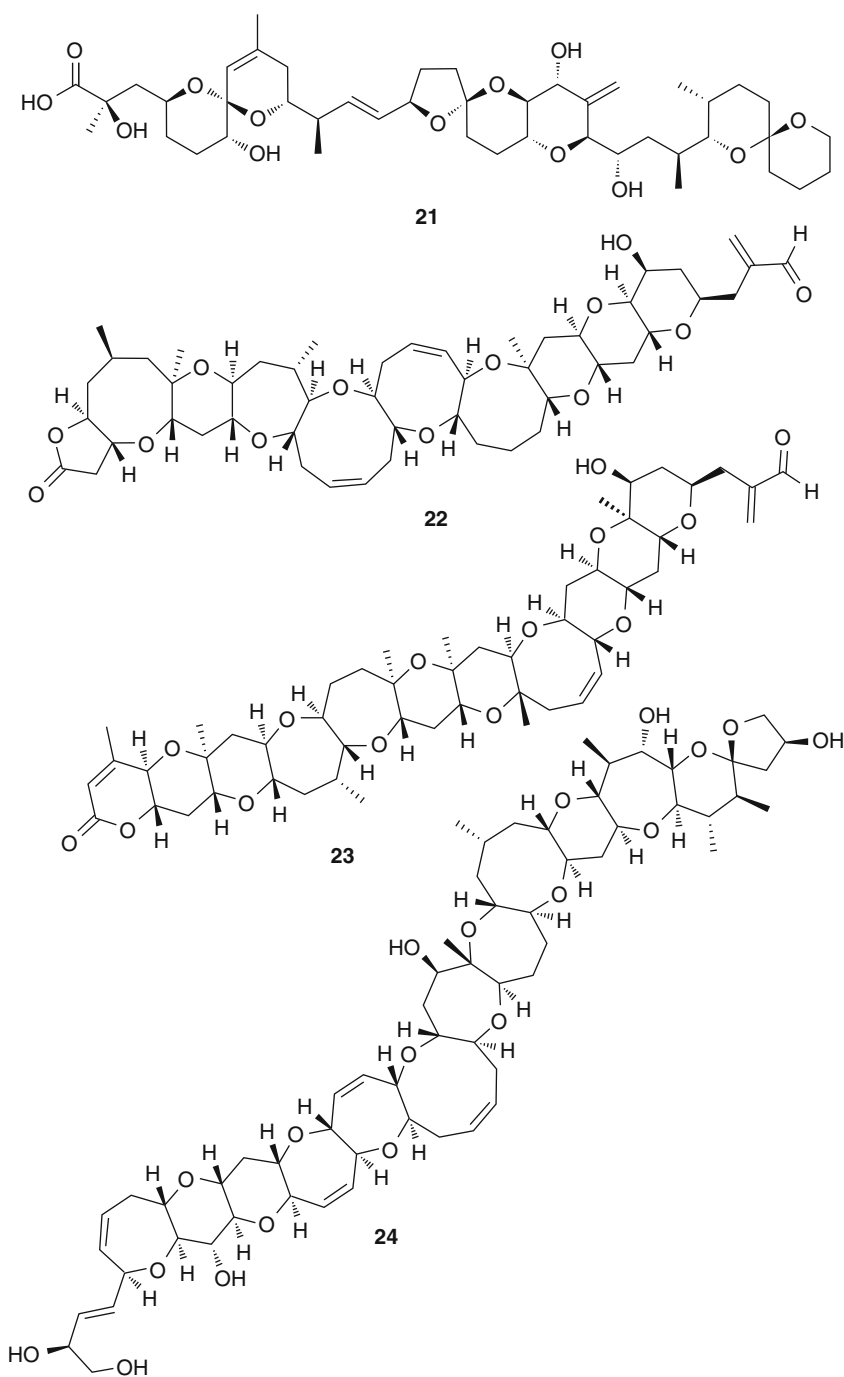


Fig. 2.7 Polyether toxins from dinoflagellates

Interestingly, brevetoxin A possesses 5-, 6-, 7-, 8-, and 9-membered rings, which have fascinated and challenged the synthetic organic chemistry community. However, due to the complexity of brevetoxin A, it was not until 1997 that the first total synthesis was accomplished by K. C. Nicolaou [77]. Although BTX A and B have two different carbon skeletons, they each consist of a single carbon chain (Fig. 2.8). This suggests that BTX A and B may derive from polyketide biosynthetic pathways. Further labeling experiments using sodium [1- ^{13}C]- and [2- ^{13}C]acetate and [methyl- ^{13}C] methionine have demonstrated that the citric acid cycle is involved in their biosynthesis. The brevetoxins bind to site 5 of VGSC, thus maintaining the channel in an open configuration and leading to uncontrolled sodium influx into cells [78]. As a result, the brevetoxins are extremely potent toxins to fish (lethal dose to guppies at 4 ng/mL) as well as mammals (lethal oral dose to mice of 520 $\mu\text{g/kg}$ body weight) [76, 79]. The symptoms of sublethal NSP are gastroenteritis along with nausea, peripheral tingling and numbness, loss of motor control, and severe muscle pain [80, 81]. The brevetoxins can be transferred from contaminated water to air as aerosols, and inhalation of these has resulted in respiratory illnesses in coastal populations [82].

Ciguatoxin

Ciguatera fish poisoning (CFP) was first described by a surgeon's mate, John Anderson, on the crew of HMS Resolution in 1774 [83]. CFP is one of the most commonly reported seafood poisonings in the world. Annually, 25,000 people are intoxicated by the consumption of toxin-contaminated coral reef fish [84]. Ciguatoxin (CTX) (24), the causative toxin of CFP, was first isolated in 1980, and its structure was elucidated in 1989 [85, 86] (Fig. 2.7). To elucidate its structure, 0.35 mg of CTX was obtained from 4,000 kg of moray eel (*Gymnothorax javanicus*) collected in French Polynesian waters. This very limited quantity of CTX was insufficient to record a ^{13}C NMR spectrum, and thus, its structure was elucidated entirely by ^1H NMR-based experiments. Absolute configuration of CTX was determined by Yasumoto and coworkers in 1997 via chemical degradation and chiral HPLC in combination with CD spectroscopy [87]. The dinoflagellate origin of CTX and its congeners was subsequently identified as *Gambierdiscus toxicus*, which is also the producer of maitotoxin, another exceedingly complex polyether toxin.

CTX-4B, a less oxygenated precursor of CTX, was reported from *G. toxicus* collected in the Gambier Islands [88]. It is first transferred to herbivorous fish by ingestion and subsequently to carnivorous fish via the food chain [89]. In fish, the precursor CTX-4B appears to be transformed into the more oxygenated form, CTX. Currently, more than twenty CTX congeners have been reported from *G. toxicus* or coral reef fish [90]. Similar to brevetoxins, CTX selectively binds to site 5 on α -subunits of the VGSC and permanently activates the channel at nanomolar to picomolar concentrations [91]. The binding affinity of CTX to site 5 is 30 times higher than brevetoxins. In mice, CTX is lethal when injected intraperitoneally at a dose of only 0.25 $\mu\text{g/kg}$ [92]. CTX is very heat-resistant such that ciguatoxin-contaminated fish cannot be detoxified by conventional cooking [93]. The characteristic symptoms of CFP are severe neurologic disturbance and a reversal of thermal sensation (e.g., cold items are perceived as hot, and vice versa) [84, 91].

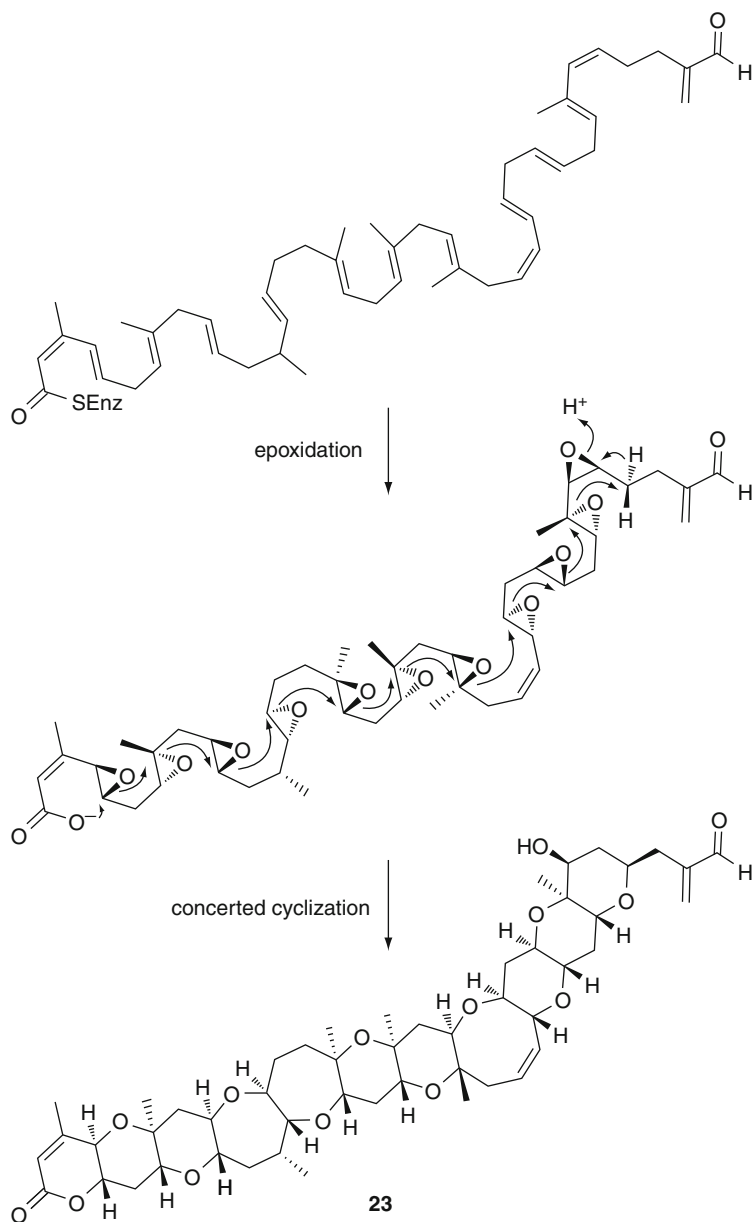


Fig. 2.8 Proposed biosynthesis of brevetoxin B (**23**) from a polyunsaturated fatty acid by epoxidation of double bonds and a concerted sequence of epoxide ring openings leading to the extended polyether structure of *trans*-fused rings

Palytoxin

In Hawaiian folklore, it was described that a poisonous reddish “moss” grown in a pond close to the ocean, in Muolea, in the district of Hana. The “moss” was coated on spear points to make them poisonous and was called “Limu make o hana” (Seaweed of Death from Hana). In 1971, its toxic component, palytoxin (PTX) (**25**), was first isolated from the seaweed-like soft coral *Palythoa toxica* [94]. The chemical structure of PTX was independently elucidated by two different groups in 1981 [95, 96] (Fig. 2.9). PTX is a very large and complex molecule with a long polyhydroxylated aliphatic chain containing 64 chiral centers. PTX has the longest chain of continuous carbon atoms of any known natural products. Remarkably, the total synthesis of PTX was accomplished by the Kishi laboratory in 1994 [97, 98]. PTX was originally isolated from colonial zoanthids; however, PTX and its analogs have since been isolated from a variety of marine organisms including the red alga *Chondria crispus* and the benthic dinoflagellate *Ostreopsis siamensis* [99, 100]. Symbiotic bacteria found in association with several of these organisms have been studied as a possible source of PTX production. PTX hemolytic activity has been observed in the extracts of several bacteria including *Pseudomonas*, *Brevibacterium*, and *Acinetobacter* [101, 102]. However, by enzyme-linked immunosorbent assay (ELISA), the Gram-negative bacteria *Vibrio* sp. and *Aeromonas* sp. were identified as potential producers of PTX or its congeners [103]. Indeed, the presence of PTX and its congeners in a variety of marine organisms suggests a bacterial origin for PTX production [102, 104].

PTX is regarded as one of the most potent toxins found in nature. Its pharmacological target has been identified as the extracellular portion of the Na^+/K^+ -ATPase with the result that Na^+ and K^+ transport is inhibited [105]. PTX shows an LD_{50} of 0.025 $\mu\text{g}/\text{kg}$ in rabbits and 0.45 $\mu\text{g}/\text{kg}$ in mice 24 h following intravenous injection [95]. Human fatalities by consumption of PTX-contaminated seafood have been reported in the Philippines (crabs), Brazil (sea urchins), and in Japan (fish) [106–110]. Recently, human intoxication in Germany and the USA occurred following dermal exposure to zoanthid corals being kept as home aquarium specimens [111, 112]. In Italy, a sea aerosol generated during an *Ostreopsis ovata* bloom caused human intoxications that involved respiratory illness [113]. Typical symptoms reported include bitter taste sensation, abdominal cramps, nausea, vomiting, diarrhea, cyanosis, and respiratory distress.

2.3.2.3 Alkaloids

Saxitoxin

Saxitoxin (STX) (**26**) is the most potent of the paralytic shellfish poisoning (PSP)-related toxins and is generally caused by the consumption of contaminated shellfish [114]. A toxic event occurring in 1927 in the San Francisco Bay is the earliest PSP-related report, the result of which sickened over 100 people and 6 died [115]. This toxic event was apparently caused by ingestion of sea mussels which had accumulated STX from the dinoflagellate *Alexandrium catenella*. STX was first isolated in pure form from the Alaskan butter clam *Saxidomus giganteus* in 1957

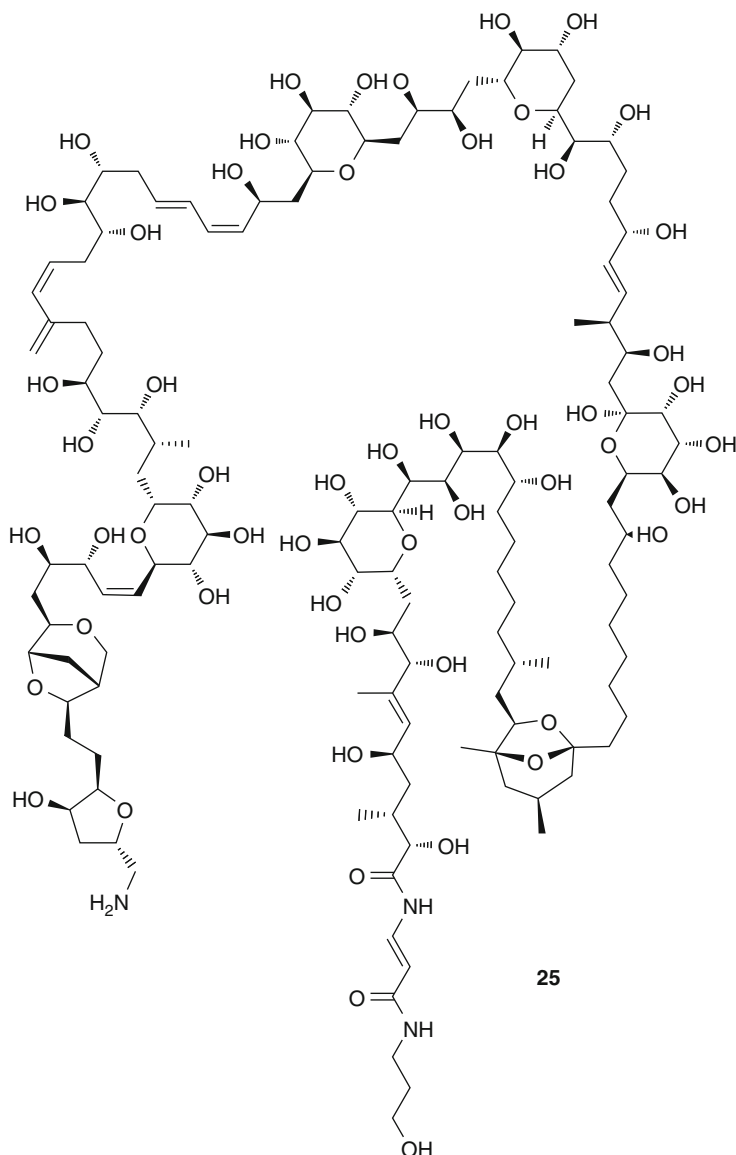


Fig. 2.9 Structure of palytoxin (25)

[116], and its structure subsequently elucidated by X-ray crystallography [117]. Notable features of the structure of STX are the presence of a carbamate and a 3,4-propinoperhydropurine tricyclic ring. The presence of two guanidine groups makes STX water soluble. Since the first total synthesis of racemic STX, accomplished in 1977 by the Kishi group [118], a number of syntheses have been developed by other groups [119, 120], and in 2006, the DuBois laboratory synthesized chiral

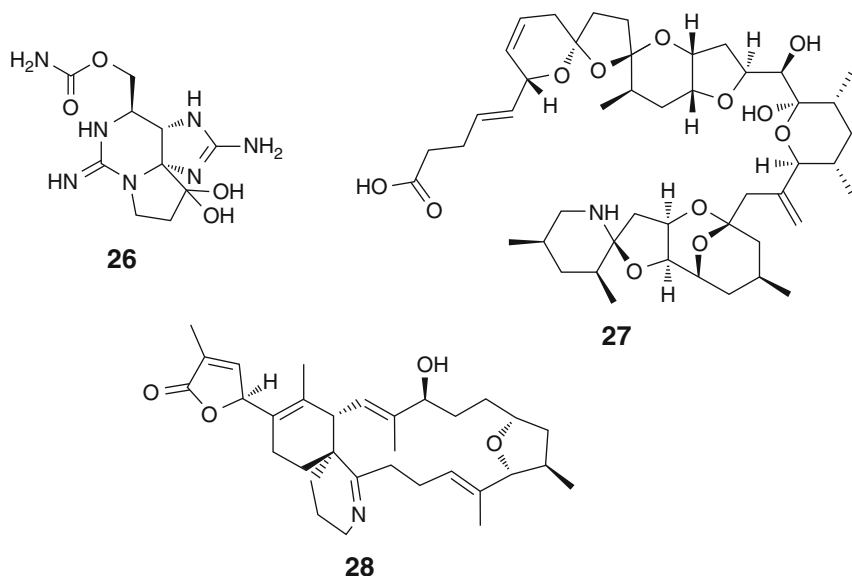


Fig. 2.10 Alkaloids from dinoflagellates

STX by selective oxidation of a nine-membered ring guanidine intermediate followed by dehydrative cyclization [120, 121]. Shimizu and coworkers performed an isotope-labeled precursor feeding study in 1984 and proposed the biosynthesis of STX analogs as produced in cyanobacteria [122]. In 2008, Kellmann revised the proposed biosynthetic pathway from *in silico* deduced functional inferences based on the STX biosynthetic gene cluster and complemented this with an LC–MS/MS analysis of biosynthetic intermediates [123].

Continued study has revealed that STX is present in diverse life forms, including dinoflagellates of the genera *Alexandrium*, *Gymnodinium*, and *Pyrodinium* [124], various cyanobacteria [125], marine pufferfish, and Brazilian freshwater tilapia [126]. Thus, it seems logical that STX is produced by symbiotic bacteria; however, the experimental evidence is not conclusive on this point. Pharmacologically, STX binds to neurotoxin site 1 of the VGSC, thereby blocking the ion channel pore and inhibiting sodium influx [127]. The LD_{50} of orally administered STX was 3–10 $\mu\text{g}/\text{kg}$ body weight in mice and 5.7 $\mu\text{g}/\text{kg}$ for humans. The symptoms of intoxication include initially a tickling sensation of the mouth and tongue, followed by difficulty in breathing, respiratory arrest, and cardiovascular shock [128]. Because STX and its analogs are exceptionally toxic, their manufacture, use, transfer, and reuse are strictly regulated by the Organization for the Prohibition of Chemical Weapons (Fig. 2.10).

Azaspiracid

Azaspiracid (AZA) (27) is an alkaloidal polyether-type toxin that accumulates in shellfish and is associated with gastrointestinal intoxications. Since the first report

from the Netherlands in 1995, AZA has been found in shellfish from the coastal areas of Europe (Netherlands, Ireland, France, UK, and Norway) and Africa (Morocco) [129–136]. In 2004, the EU established a regulatory limit of AZA (160 µg AZA/kg shellfish in flesh) to protect public health [137]. The structure of AZA was elucidated in 1998 [129], and the name of AZA was based on its unusual structural features of a cyclic amine (aza group), a trispiro ring assembly and a carboxylic acid. However, the original structure reported in 1998 was found to be incorrect by total synthesis, and a structure revision was accomplished by extensive study of the NMR spectra in 2004 [138–141]. While originally isolated from shellfish, the polyether structure of AZA suggested a dinoflagellate origin, and subsequently, the heterotrophic dinoflagellate *Protoperidinium crassipes* has been identified as the likely producer of AZA [129, 142, 143]. A variety of analogs of AZA have been detected by LC–MS/MS from the extract of individually isolated *P. crassipes* [144, 145]; however, large scale culture or bulk sampling of this dinoflagellate for the presence of the toxin has been unsuccessful. The symptom of AZA intoxication is similar to that of okadaic acid in that it causes nausea, vomiting, severe diarrhea, and stomach cramps. Partially purified AZA was lethal to mice with an intraperitoneal injection of 150 µg/kg [146] and induced organ damage in stomach, liver, thymus, and spleen tissues [147]. Little is known about the molecular pharmacology of AZA, and its molecular target has not yet been identified. However, the pathology of AZA is unique among other marine toxins.

Gymnodimine

Gymnodimine (**28**) was first isolated as a phycotoxin from New Zealand oysters and the dinoflagellate *Gymnodinium* sp. [148, 149]. Subsequent research has shown that this phycotoxin, found in such shellfish as the greenshell mussel, blue mussel, scallop, and abalone, is produced by the dinoflagellate *Karenia selliformis* (formerly named *Gymnodinium selliforme*) [150–152]. The structure of gymnodimine was elucidated by NMR spectroscopy and X-ray crystallography [148, 153]. Gymnodimine possesses several unusual structural features such as a 2,4-disubstituted butenolide, a spirocyclic imine ring, and a trisubstituted tetrahydrofuran embedded in a 16-membered macrocyclic ring. Gymnodimine was first suggested to act on VGSCs, but subsequently shown to target muscular and neuronal nicotinic acetylcholine receptors with high affinity [149, 154].

2.3.2.4 Macrolides

Marine dinoflagellates are rich producers of macrolides as well as polycyclic ethers (Figs. 2.11 and 2.12). A series of macrolides named the “amphidinolides” was obtained from the dinoflagellate *Amphidinium* sp., which lives symbiotically with Okinawan marine flatworms of the genus *Amphiscolops* sp. In turn, flatworms are typically found living on algae or seaweeds in coral reef environments [155]. Among the previously reported 42 analogs, amphidinolide N (**29**) is the most toxic compound with IC₅₀ values of 0.00005 µg/mL to murine lymphoma L1210 cells and 0.00006 µg/mL to human epidermoid carcinoma KB cells [156]. The structure of amphidinolide N was elucidated as a 26-membered macrolide

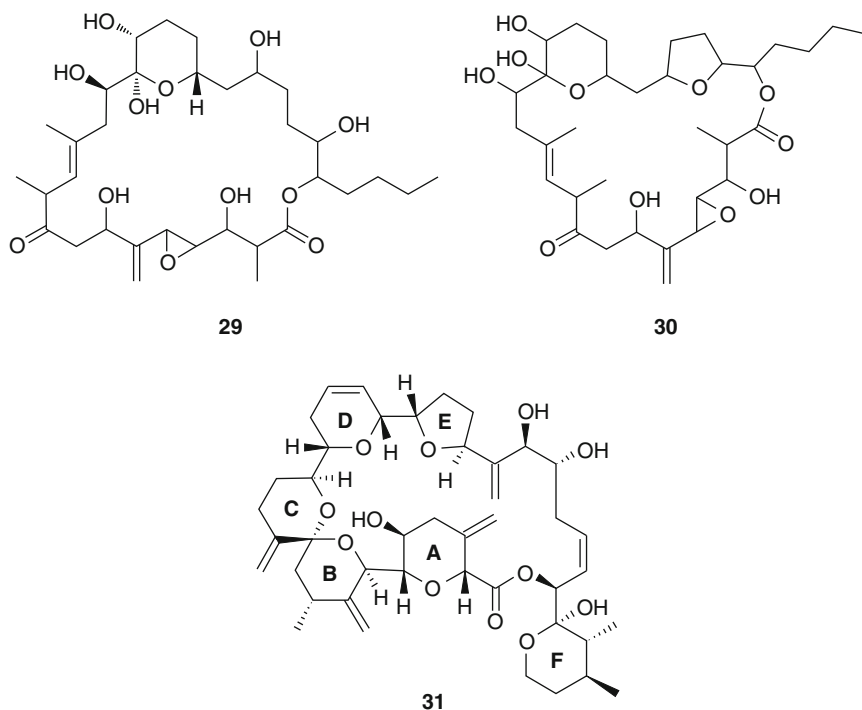


Fig. 2.11 Macrolides from dinoflagellates

containing a 6-membered hemiacetal ring, an epoxide, a ketone, four C1 branches, and seven hydroxy groups [156] (Fig. 2.11). The absolute stereochemistry at C-13 has not yet been determined.

Caribenolide I (**30**), having the same skeleton as amphidinolide N but with derivatization of the 1,4-diol to a furan ring, was isolated from a free-swimming dinoflagellate *Amphidinium operculatum* var nov *Gibbosum* by Shimizu and coworkers in 1995 [157] (Fig. 2.11). Caribenolide I was reported to show potent cytotoxicity with IC_{50} values of 0.001 $\mu\text{g/mL}$ against both drug sensitive and resistant HCT116 human colon tumor cell lines. In addition, caribenolide I showed in vivo activity against murine P388 tumors ($T/C = 150$ at 0.03 mg/kg).

In 1968, an antifungal agent named goniodomin was isolated from the dinoflagellate *Goniodoma* sp. by Sharma and coworkers; however, a structure was not reported in this initial report [158]. In 1988, Murakami and coworkers reported the structure of a goniodomin-related compound, goniodomin A (**31**), isolated from *Alexandrium hiranoi* (formerly known as *Goniodoma pseudogoniaulax*) [159]. Goniodomin A is a polyether macrolide with a spiroacetal ring (B/C-ring), four additional oxacycles (A, D, E, and F rings), and 17 stereogenic centers embedded within a 36-carbon chain (Fig. 2.11). Goniodomin A showed inhibitory activity against *Mortierella ramannianus* and *Candida albicans* at a concentration of 0.5 $\mu\text{g/mL}$.

The dinoflagellate *Symbiodinium* sp., classified as a zooxanthella because of its common symbiotic relationship with corals and other marine invertebrates, is reported as a rich producer of “super carbon-chain compounds” (SCC) [160–162]. For example, in 1995, zooxanthellatoxin A (**32**) was isolated from *Symbiodinium* sp. collected from the flatworm *Amphiscolops* sp. [163]. Zooxanthellatoxin A is a polyol macrolide with 15 double bonds, 42 hydroxy groups, one sulfate, five tetrahydropyran rings, and a 62-membered ring, the largest lactone ring yet observed among natural products (Fig. 2.12). Zooxanthellatoxin A shows potent vasoconstrictive activity in rat blood vessels [164].

In 2007, symbiodinolide (**33**), a congener of zooxanthellatoxin A, was isolated from cultures of the symbiotic dinoflagellate *Symbiodinium* sp. collected from the Okinawan flatworm *Amphiscolops* sp. [165] (Fig. 2.12). Symbiodinolide showed a potent voltage-dependent *N*-type Ca^{2+} channel-opening activity and increased intracellular concentrations of free Ca^{2+} . In addition, symbiodinolide caused rapid rupturing of the tissue surface of host flatworm cells, and thus, this impressive natural product may constitute a defense against digestion by the host.

Dinoflagellates of the genus *Amphidinium* are rich producers of antifungal and hemolytic polyhydroxy secondary metabolites as well as cytotoxic macrolides. In 1991, amphidinol-1 (**34**) was described by Yasumoto and coworkers from cultures of field collected *A. klebsii* [166]. Amphidinol-1 is a polyhydroxypolyene compound with a conjugated triene, an exomethylene and two tetrahydropyran rings (Fig. 2.12). The bioactivities of amphidinol are associated with the membrane permeability of the molecule. It was proposed that the polyene region, two of the hydrophilic tetrahydropyran rings, and the polyhydroxy chain play key roles in binding to lipid bilayers, stabilizing the binding, and pore forming properties of these molecules in the cell membrane [167].

2.3.3 Diatoms

2.3.3.1 General Introduction to Diatoms

Diatoms are unicellular microalgae, also known as “golden-yellow algae,” due to their characteristic color resulting from chlorophyll *a* and *b* plus a number of carotenoids and are classified with the stramenopiles [5]. Some forms of diatoms can form pseudofilaments and aggregations which can give them a macroscopic appearance. They are ubiquitous in aquatic distribution, both in fresh and marine water, and comprise approximately 200 genera that are divided into two orders, the Pennales (pennate shaped) and the Centrales (centrosymmetric). Interestingly, pennate diatoms but not centric ones are capable of movement; the mechanism for this movement, which is sometimes coordinated between individuals, is not well understood; however, they do leave behind slime trails. The chloroplasts of diatoms derive from an ancient endosymbiosis of a red alga, and diatom cells are contained within a very characteristic frustule composed of two overlapping halves of silica, much like a petri dish for the centrate diatoms. This unique cell wall construction is accessed when trying to rid algal cultures of diatom contaminants. Addition

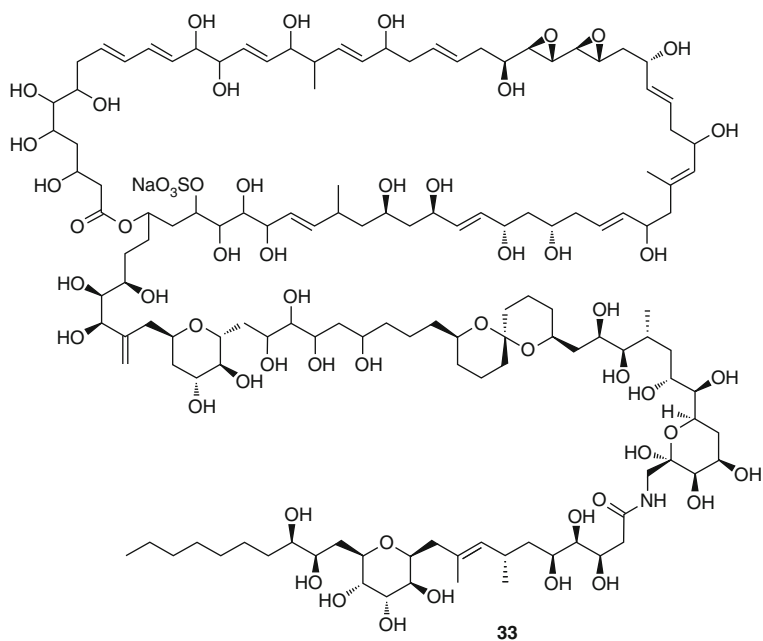
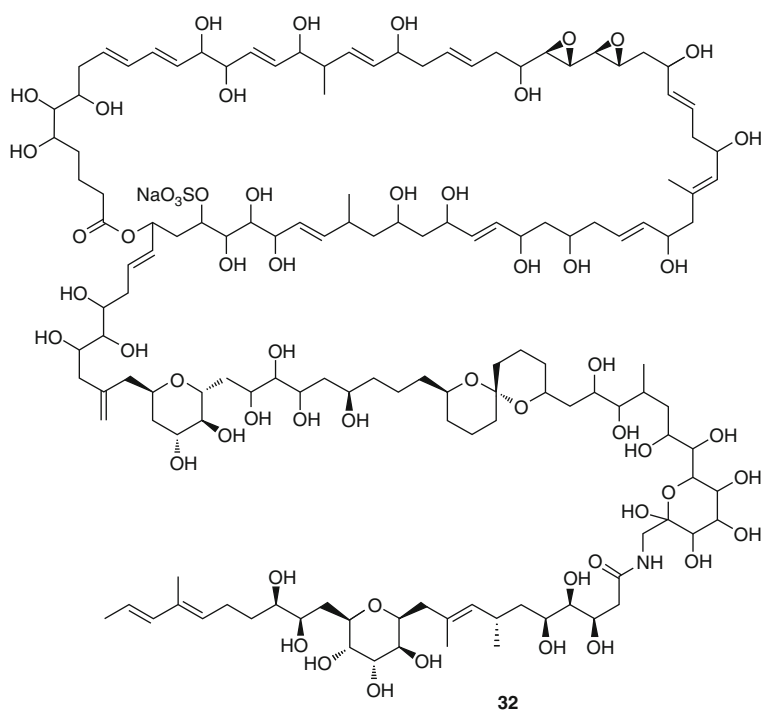


Fig. 2.12 (continued)

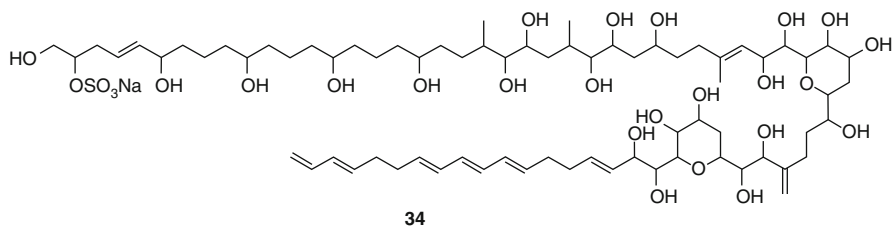


Fig. 2.12 Macrolides from dinoflagellates

of GeO_2 to contaminated cultures is selectively toxic to diatoms as it interferes with the biochemical machinery responsible for frustule formation. The accumulation of diatom outer cells walls over geological time scales has given rise to sedimentary deposits of diatomaceous earth. These deposits have been used as important components of water filters, paints, toothpastes, and many other common household products. Additionally, the frustules of diatoms are intricately created with many fine pores and other surface features, produced with great precision and fidelity by a set of enzymes known as silicases. The industrial value of silicases is being explored in various nanotechnology applications. Diatoms have the characteristic of storing oils rather than starches as a reserve energy source, and thus are leading candidates for algal biofuel production. In a couple of cases, draft genomes of diatoms have been deduced (e.g., *Thalassiosira pseudonana*), and they appear to be roughly of 32.4 MB [168, 169]. Finally, diatoms are capable of both sexual as well as vegetative reproduction. However, when reproducing vegetatively, the cell size becomes progressively smaller, ultimately terminating due to physical constraints of the solid silica cell wall.

2.3.3.2 The Natural Products of Diatoms

The natural products of diatoms have been studied to a fairly limited degree, and there is clearly much refinement and further exploration needed; this may well occur as a result of their being top candidates for algal biofuels. A first major trend in the secondary metabolism of diatoms is the capacity of some pennate diatoms to produce simple analogs of the amino acid glutamate, such as domoic acid (**35**), which function as powerful glutamate receptor agonists. When these build up in the food chain, they cause a well-described environmental toxicity to humans and marine mammals known as “amnesic shellfish poisoning.” A second very important natural product class is derived from polyunsaturated fatty acids that become oxidized and then undergo various ensuing reactions, such as carbocyclization, carbon-chain cleavage, and further oxidations; oxidized lipids of this type are known as “oxylipins.” A third major trend in diatom metabolism is a group of terpenoid hydrocarbons which are curious for their uniquely branched carbon framework.

Domoic Acid

In 1987, a cluster of symptoms emerged from individuals eating shellfish in Nova Scotia, Canada which were unlike any known shellfish intoxication, and involved

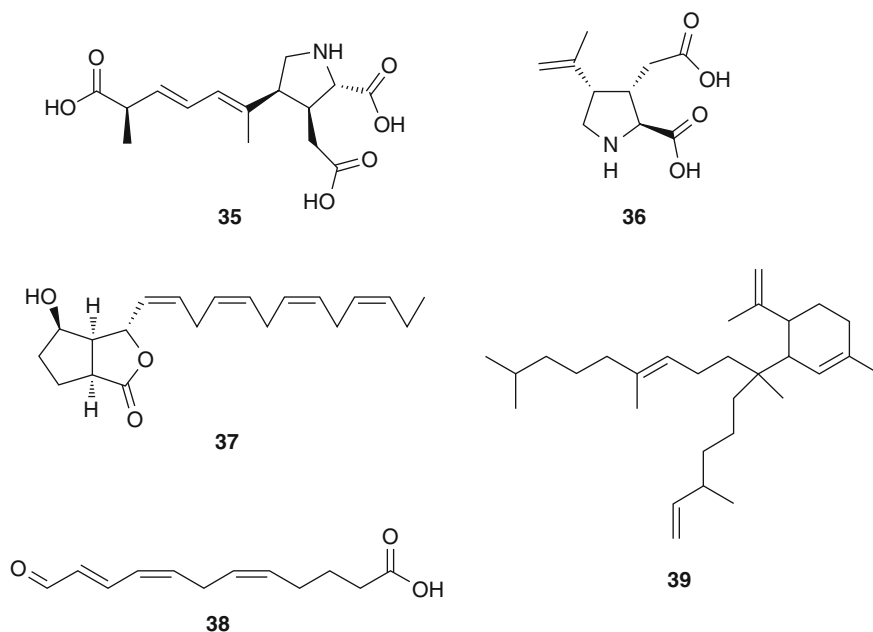


Fig. 2.13 Secondary metabolites of diatoms

gastrointestinal effects, extreme headache, and permanent short-term memory loss in strongly affected individuals, ultimately becoming known as “amnesic shellfish poisoning” [170]. A frantic effort to identify the responsible toxins and toxin sources ensued and ultimately traced this to the pennate diatom *Pseudo-nitzschia*. An investigation remarkable for its speed and efficiency identified the toxin as the known metabolite “domoic acid” (35), a natural product which had been earlier characterized as a product of the Japanese macrophytic red alga *Chondria armata* [171]. This and another red alga, *Digenia simplex*, were historically known in Japan for their ability to treat parasitic worm infections, and structural characterizations of the active compounds, named domoic acid after the Japanese name “doumoi” and kainic acid (36) after the name “Kainin-sou,” were two of the early discoveries in the field of marine natural products chemistry.

The structures of these two compounds are highly similar with the difference being an extra five-carbon “prenyl” group present in domoic acid (35) relative to kainic acid (36) (Fig. 2.13). It may be that the increased lipophilicity imparted by this modification enhances the neurotoxic effect of this agent when ingested. Imbedded in both structures is a “glutamate” residue, which for domoic acid is modified by the attachment of a ten-carbon terpenoid chain, presumably from geraniol. Investigations with isotope-labeled precursors provided evidence for the biosynthetic condensation of α -ketoglutarate with geraniol; however, because feeding studies to the diatom with $[2-^{13}\text{C}, ^2\text{H}_3]\text{acetate}$ resulted in a complete absence of deuterium incorporation, it appears that the isoprenoid chain may be

synthesized by a novel pathway [172]. Pharmacologically, domoic acid activates AMPA, kainite, as well as NMDA neurochemical receptors by mimicking glutamate, thereby causing an influx of calcium and ensuing neurotoxicity [170]. The hippocampus and amygdaloid nucleus regions of the brain are especially prone to domoic acid-induced neurotoxicity which results in memory loss, seizures, and in extreme cases, death, both in humans and marine mammals.

Oxylipins

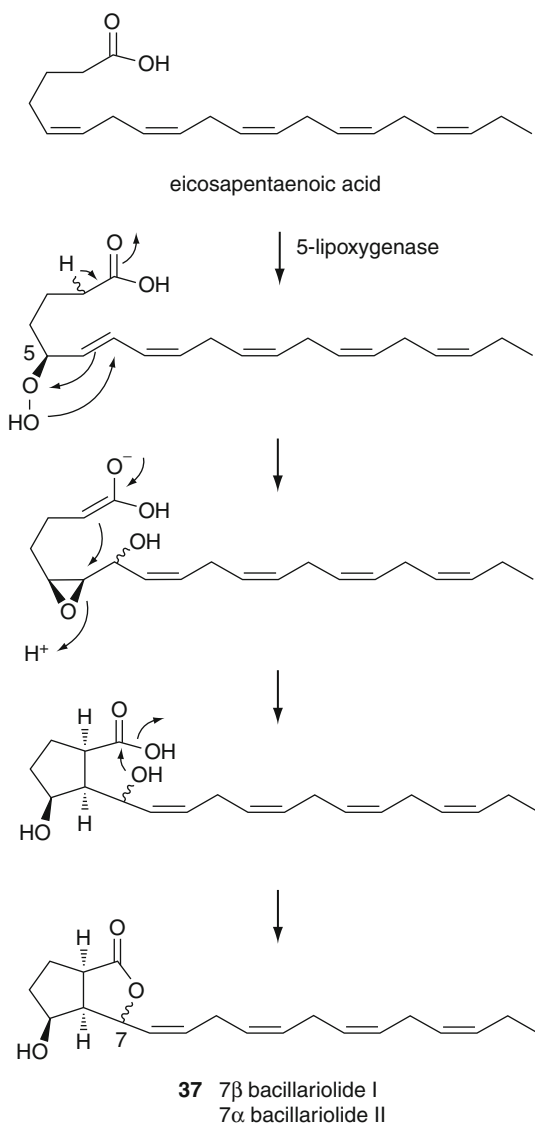
Oxylipins, defined as polyunsaturated fatty acids which are modified by molecular oxygen-dependent oxidations [173], are broadly present in various classes of marine photosynthetic organisms, including the diatoms. One of the earliest characterizations of an oxylipin from a diatom was by the Shimizu group during their independent investigations of the causative agent for amnesiac shellfish poisoning [174]. Their work, which focused on the pennate diatom *Nitzschia pungens*, led to the isolation and complete characterization of two epimeric oxylipins, named bacillariolide I (37) and II, which are unique for possessing a carbocycle involving C2 and C6 to form a five-membered ring. The presence of an adjacent C5 alcohol is tantalizing for the mechanistic suggestion that a 5-lipoxygenase initiates the biosynthetic pathway, followed by epoxide ring formation and then ring formation from a C2 anion equivalent [175]. Additionally, these metabolites contain a lactone ring which involves ester formation between the C1 carboxylic acid and a C7 carbocation, yielding a γ -lactone (see Fig. 2.14). The biological properties of the bacillariolides have not been reported, so it is uncertain to what extent they may contribute to some of the symptoms of amnesic shellfish poisoning.

Since these earliest reports of diatom oxylipins, it has been found that natural blooms of these photosynthetic unicellular algae, as well as laboratory cultures, are very active in producing simple oxidized derivatives which decrease the reproductive success in planktonic micrograzers such as copepods [176]. Mechanistically, this appears to occur largely from the oxidative cleavage of polyunsaturated fatty acids to polyunsaturated aldehydes by action of a hydroperoxide lyase, and these induce apoptosis and teratogenesis in copepod nauplii [177]. In addition to aldehydes (e.g., 38), other classes of oxylipins are produced by diatoms which uniquely derive from eicosapentaenoic acid or variously unsaturated hexadecenoic acids, and possess hydroxy, ketone, or epoxyalcohol functional groups. In fact, various species of diatoms have unique “signatures” of oxylipin metabolites, and this can vary as a function of environmental parameters [178]. Characterization of the oxylipins of diatoms is an area of active investigation in several laboratories, notably the Ianora and Fontana laboratories in Italy and the Pohnert laboratory in Germany, and it is quite certain that new appreciation of the functional roles of oxylipin synthesis in diatoms will emerge from these continuing efforts.

Triterpenes

The final class of diatom natural products to be discussed is a series of curious C-30 triterpene hydrocarbons, unique for their irregular pattern of isoprene units (e.g., 39). Biosynthetic experiments utilizing [2-¹³C] acetate led to hydrocarbons labeled

Fig. 2.14 Proposed biogenesis of the bacillariolides (**37**) from eicosapentaenoic acid in the marine diatom *Nitzschia pungens*



at positions consistent with the mevalonate pathway and provided an overall perspective of the connection between separate diterpene and monoterpene components [179]. Related hydrocarbons have been detected in marine sediments and utilized as geochemical markers of planktonic diatoms of the genus *Pleurosigma* [180].

2.3.4 Chrysophytes

Chrysophytes or golden algae are common microscopic inhabitants of primarily freshwater bodies (e.g., *Ochromonas* and *Poterioochromonas*), although some species, particularly within the Sardinochrysidales and Chrysomeridales, occur in brackish, marine, or terrestrial environments. Some species are colorless, but the vast majority are photosynthetic. In addition to chlorophyll, they also contain the pigment fucoxanthin which gives them their characteristic yellow-brown color. There are more than a thousand described species of golden algae, and although the genera included within the chrysophytes are still in a state of flux, they are currently placed in the Heterokontophyta (Stramenopiles) within the Chromalveolates. Chrysophytes are morphologically diverse and occur as unicellular flagellates, colonial flagellates, filaments, and thalloids. Most chrysophytes are planktonic, but some are benthic, epibiotic, or neustonic.

Chlorosulfolipids, styrylchromones, and dimeric diarylbutene macrolides comprise the three natural product scaffolds reported thus far from chrysophytes, collected in both freshwater and marine habitats. Their intriguing structures and potent biological activities have made them the focus of multiple stereochemical studies and total syntheses, as well as novel target validation investigations.

2.3.4.1 Chlorosulfolipids

Chlorosulfolipids represent an unusual and fascinating class of natural product that was first reported in the late 1960s [181]. These compounds contain up to 11 chlorine atoms and 2 sulfate groups and have been isolated from the ubiquitous fresh water algae *Ochromonas danica* (40–46) [181–185] and *Poterioochromonas malhamensis* (47) [186–188], as well as from digestive glands of contaminated shellfish *Mytilus galloprovincialis* (48–50) along the Adriatic coast of Italy [189–193], and the Formosan octocoral *Dendronephthya griffini* (48) [194] (Fig. 2.15). The apparent localization of sulfolipids 40–46 in the cellular and flagellar membranes of *O. danica*, their substantial presence (91 mol% of the polar lipids in the flagellar membrane) [195], and the lack of significant quantities of phospholipids led to speculation that these unusual compounds might play a structural role within cell membranes. The planar structures of these lipids were initially elucidated by mass spectrometric analysis and chemical degradation studies [181–185], and just recently, assignments made for their relative and absolute configurations using a combination of *J*-based configuration, modified Mosher's analyses and chemical synthesis [196]. The extent of chlorination appears to be influenced by the concentration of chloride ion in the environment [181]. Chlorination likely occurs one halogen at a time at unactivated carbons, possibly via a radical mechanism, and the lipids are apparently formed as single stereoisomers [184]. Danicalipin A (46), which has been identified as the most abundant of all *O. danica* sulfolipids, displayed moderate toxicity to brine shrimp larvae (LC₅₀ 2.2 µg/mL) [196].

Malhamensilipin A (47) is the main component of extracts derived from laboratory cultured *P. malhamensis* [186–188]. Besides exhibiting antiviral and

antimicrobial activity, compound **47** displayed moderate inhibition of tyrosine kinase (IC_{50} 35 μ M); overactivated tyrosine kinases contribute to the initiation or progression of cancer [186]. The structure of **47** suggests that it might share a common biosynthetic origin with the lipids of *O. danica*, and this is further supported by the close taxonomic relationship of these two algal species.

Although their isolation and structural elucidation were first described from toxic mussels [189–193], based on their close structural relationship to the above chlorosulfolipids, compounds **48–50** are likely produced by microalgae. These compounds displayed modest cytotoxic activity and thus fueled a renewed interest by synthetic chemists into this class of natural products due to their possible involvement in Diarrhetic Shellfish Poisoning [190–193]. This aspect stimulated efforts toward their total synthesis and has resulted in the development of new stereoselective chlorination methodologies [197–200], a new procedure to produce (*E*)-chlorovinyl sulfate moieties [188], comprehensive configurational studies [201], and the total syntheses of **48** [200], **46** [202], and **47** [188].

2.3.4.2 Hormothamnione Styrylchromones

Hormothamnione (**51**) and 6-desmethoxyhormothamnione (**52**) constitute the two members of this unique class of chrysophyte-derived natural product, both isolated from *Chrysophaeum taylori* collected from the north coast of Puerto Rico [203, 204] (Fig. 2.16). These compounds constituted the first naturally occurring styrylchromones and were named after the marine cyanophyte *Hormothamnion enteromorphoides* which was the initially reported source organism for **51**, but later revised as *C. taylori* upon light microscopy experiments of fresh and preserved material, culture work, and comparison with original taxonomic descriptions [204, 205]. The structure of **51**, unprecedented in the natural products field at the time of its isolation, was solved using X-ray diffraction data obtained from the corresponding triacetylated derivative [203]. Classical heteronuclear long-range 2D NMR experiments were used to determine the substitution pattern of proton, hydroxy, and methoxy groups on the chromone ring of **52** [204]. Biosynthetically, it is equally plausible for hormothamnione to derive from acetate or shikimate pathways, although some of the sites of oxidation are inconsistent with the expected patterns resulting from either biogenetic sequence.

Hormothamnione (**51**) was found to be a potent cytotoxic agent to P388 lymphocytic leukemia (IC_{50} 11.5 nM) and HL-60 human promyelocytic leukemia (IC_{50} 250 pM) cell lines [203], whereas analog **52** showed significant toxicity to KB carcinoma cells (LD_{50} \sim 2.5 μ M) [204]. Further pharmacological characterization attributed antioxidant [206] and anti-inflammatory [207] activities to the semisynthetic diacetate **53** (Fig. 2.16). Both **51** and **52** have been the subject of multiple total syntheses [208–211], given the potent and diverse biological activities measured for these metabolites.

2.3.4.3 Chrysophaentins A–H

Chrysophaeum taylori, this time collected from Round Bay on the Island of St. John (US Virgin Islands), was found to produce a suite of eight symmetrical and

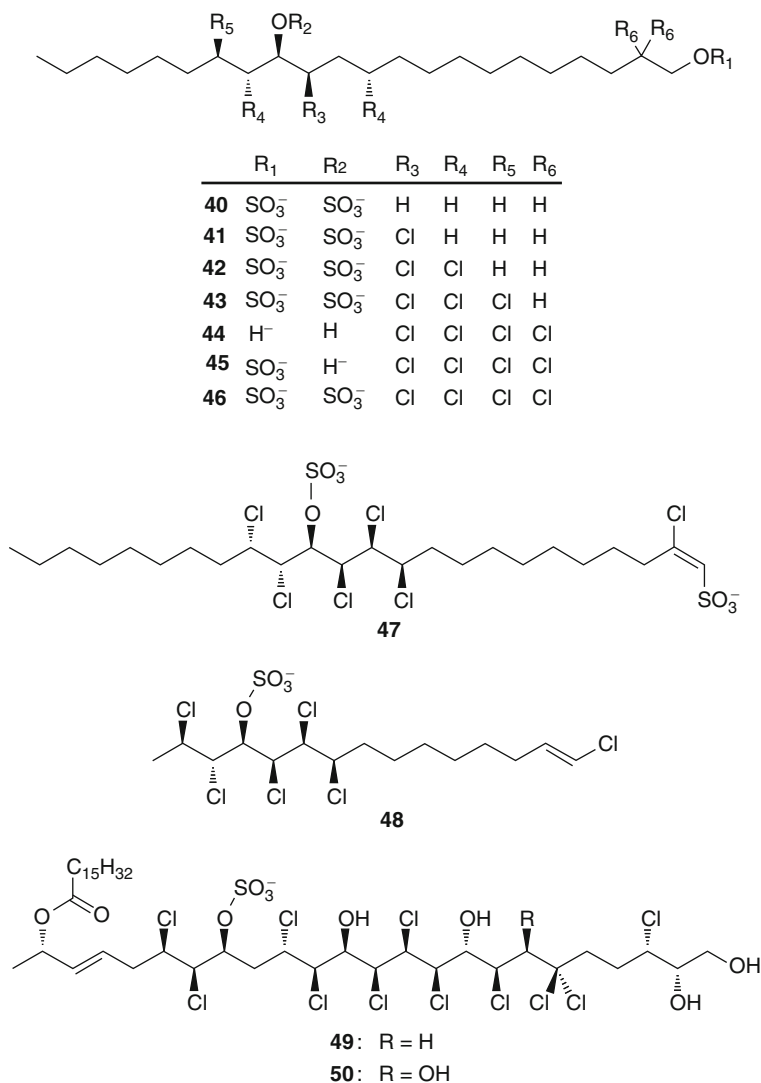


Fig. 2.15 Structures of chlorosulfolipids from chrysophytes

asymmetrical macrocycles comprised of two polyhydroxylated, polyhalogenated ω,ω' -diarylbutene units connected through two ether bonds [212]. Termed chrysophaentins A–H (**54–61**) (Fig. 2.16), these compounds represented a new natural product scaffold in nature. Hormothamnione (**51**) was also found in these latter collections of *C. taylori* [212]. The most potent of these new antibiotics, chrysophaentin A (**54**), inhibited the growth of clinically relevant Gram-positive

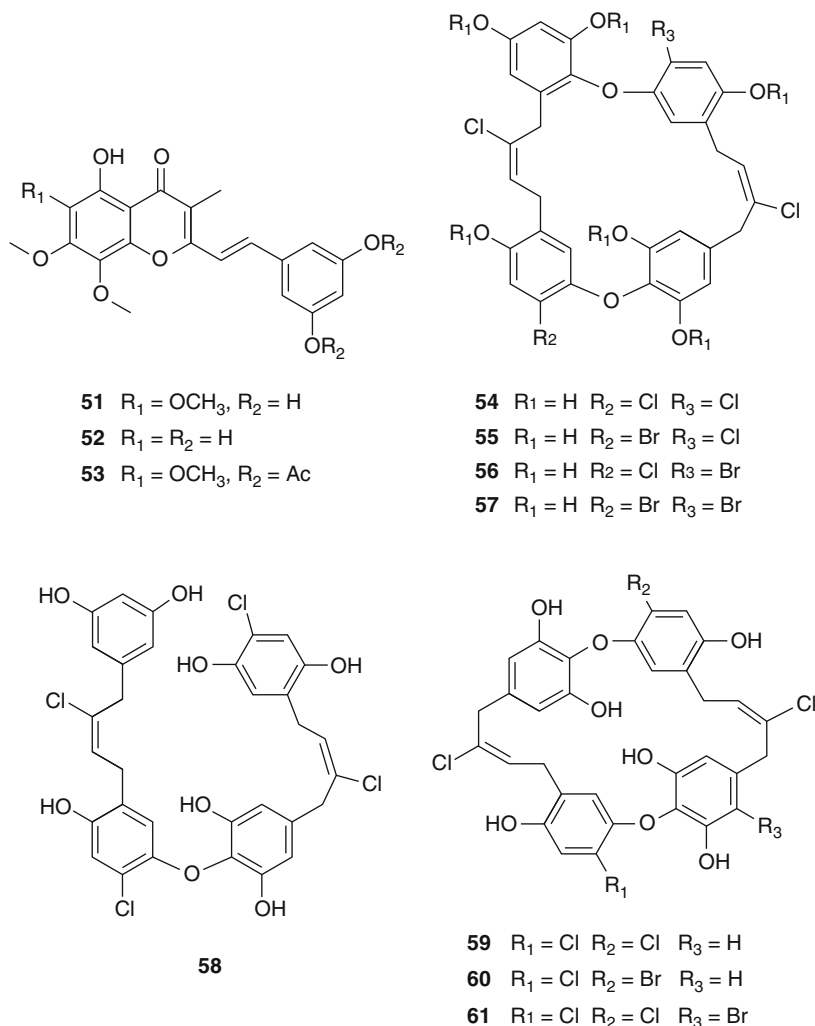


Fig. 2.16 Secondary metabolites of chrysophytes

bacteria including methicillin-resistant *Staphylococcus aureus* (MIC_{50} 1.5 ± 0.7 $\mu\text{g/mL}$), multidrug-resistant *S. aureus* (1.3 ± 0.4 $\mu\text{g/mL}$), and vancomycin-resistant *Enterococcus faecium* (2.9 ± 0.8 $\mu\text{g/mL}$). Additionally, in vitro enzyme assays, transmission electron microscopy, and saturation transfer difference (STD) NMR showed **54** to inhibit GTPase activity and polymerization of the bacterial cytoskeletal protein FtsZ (IC_{50} of 6.7 ± 1.7 $\mu\text{g/mL}$), a relatively new target in antimicrobial drug discovery due to its essential role in cell division and high degree of conservancy among almost all bacteria [213].

2.3.5 Prymnesiophytes

Over the past century, numerous toxic blooms of the red tide phytoflagellate *Prymnesium parvum* in low-salinity water have had devastating effects on coastal ecology by killing massive populations of fish, shellfish, mollusks, and virtually all benthic animals and algae [214–218]. This global phenomenon seems to have increased in both frequency and geographical distribution as a result of eutrophication of coastal waters, and these harmful algal blooms cause enormous economic damage to fish farming and the entire aquaculture industry [219, 220].

The toxicity of *P. parvum* was attributed for more than 30 years to a collection of compounds exhibiting potent cytotoxic, hemolytic, neurotoxic, and ichthyotoxic effects, known as the “prymnesins” [221–224]. However, the chemical nature of these toxins remained unknown until 1996, when the structure of the major component, prymnesin-2 (**63**), was elucidated via extensive 2D NMR and mass spectrometry analyses [219, 220, 225]. Both prymnesin-1 (**62**) and prymnesin-2 (**63**) have been shown to consist of a polycyclic ether moiety bearing polyhydroxy and polyenyn side chains, featuring a straight chain of 90 carbons with one branching methyl group, a fused polycyclic ether ring system (A–E), four distinct 1,6-dioxadecalin units (FG, HI, JK, and LM), multiple conjugated double and triple bonds, three chlorine atoms, and one amino group, as well as a variety of glycosidic residues. The relative stereochemistry of the fused A–E polycyclic ether ring domain and four 1,6-dioxadecalin units was determined by extensive NMR analysis and verified by NMR comparison with synthetic models [220, 226–228]. Degradation and derivatization studies established *S* absolute configuration for both the amino group-bearing C14 and the chlorinated C85 stereocenters in **63** [229]. The configuration of the C76–C85 acyclic portion remains undetermined (Fig. 2.17).

2.4 Marine Macroalgae

2.4.1 General Introduction to Marine Macroalgae

Marine macroalgae produce an impressive variety of secondary metabolites ranging from linear acyclic entities to complex polycyclic molecules. A significant portion of these natural products are halogenated, reflecting the availability of chloride and bromide ions in seawater. Interestingly, although chloride occurs in higher concentrations in seawater than any other halogen, bromide is more frequently integrated by algae for organohalogen compound production.

Thus, a major focus of macroalgae chemical research has been the discovery and characterization of new halogenated natural products, along with a remarkable effort toward the evaluation of their possible biomedical and biotechnological applications. Among all marine macroalgae, red algae are the main producers of chlorinated and brominated terpenes, with the genus *Laurencia* (Rhodophyceae)

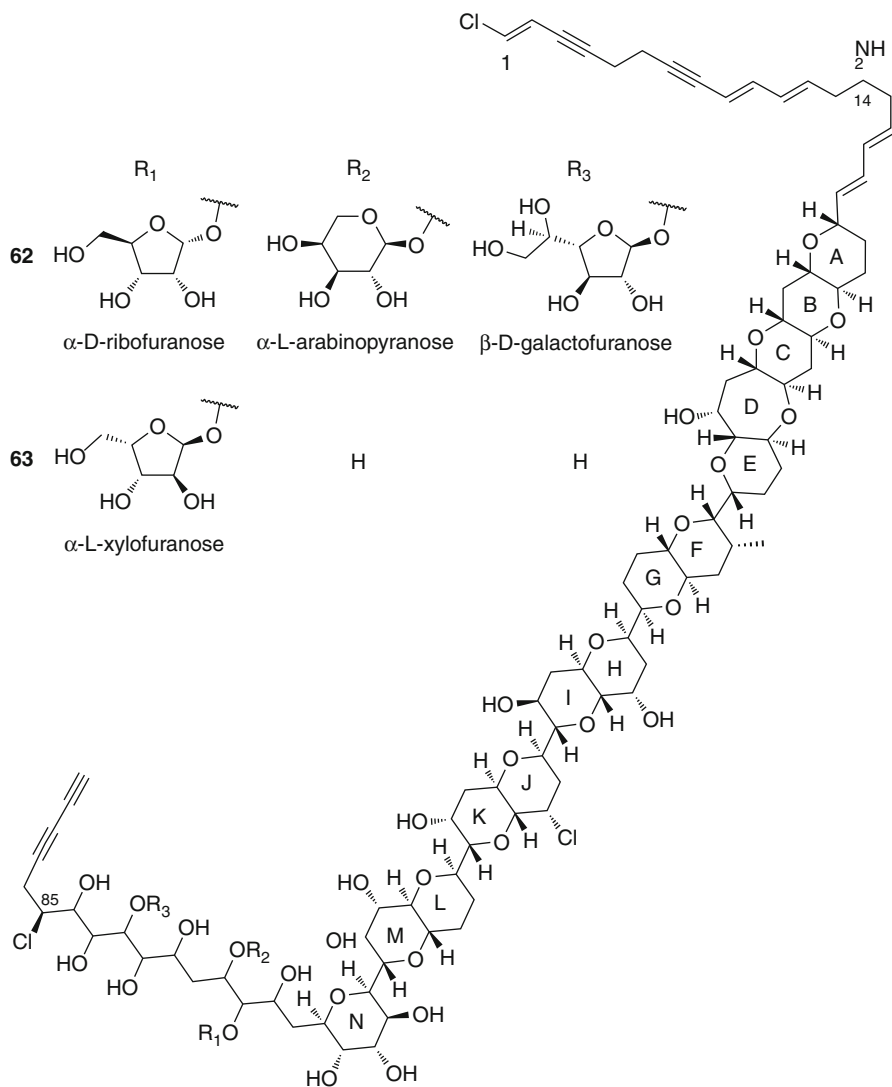


Fig. 2.17 Structures of prymnesins-1 (**62**) and -2 (**63**)

being the most prolific. Although incorporation of iodine and fluorine is quite unusual, some orders of brown algae, such as the Laminariales, accumulate and use iodine in halogenation processes. In fact, iodination is more frequent in brown algae than in red and green algae metabolites. The ecological role of most of these metabolites has not been experimentally investigated, although a few metabolites have been shown to have critical roles in reproduction and defense.

2.4.2 Chlorophyta

The Chlorophyta are major inhabitants of shallow marine, fresh, and brackish waters. Most of the known species are unicellular, benthic, or planktonic, and some are free-living while others are colonial or multicellular. One group, the Caulerpales are coenocytic in that cell walls are not created following nuclear division. The name “Chlorophyta” derives from the Greek words *chloros* and *phyton*, which mean “green plant.” Similar to terrestrial higher plants, members of the Chlorophyta contain chlorophyll *a* and *b*, carotenoids, and xanthophylls. They produce starch as a by-product of excess photosynthesis and store it in pyrenoids that are present in the chloroplasts. Most Chlorophyta undergo sexual reproduction, which is isogamous, anisogamous, or oogamous; however, asexual reproduction by fission, budding, fragmentation, or zoospores is also possible. The Chlorophyta have been classified into 15 orders, all within the class of Chlorophyceae. Marine representatives are found in the Cladophorales, Acrosiphonales, Ulvales, Dasycladales, Siphonocladales, and Caulerpales. Various classes of bioactive natural products reported from the Chlorophyta include terpenoids, halogenated meroterpenes, bisindoles, coumarin derivatives, bromophenols, and oxylipins, as described below.

2.4.2.1 Terpenoids

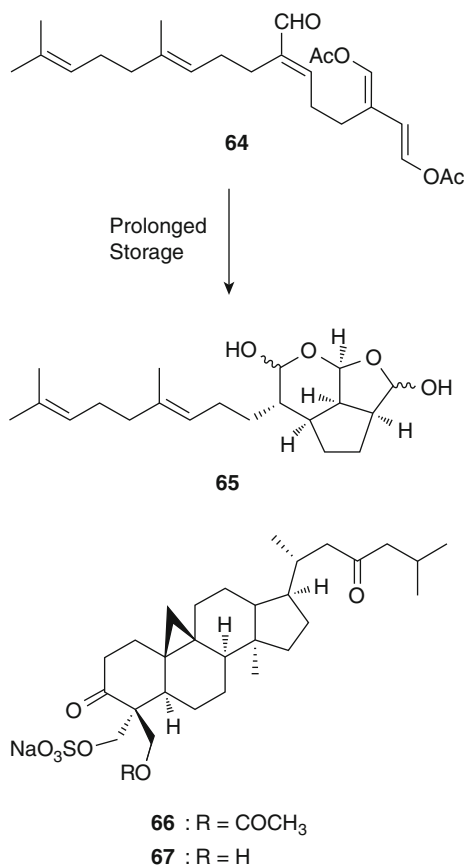
Udoteal

The calcareous green alga *Udotea flabellum* is very common in sandy environments of shallow tropical waters. *U. flabellum* produces several fish feeding-deterrent natural products, presumably aiding its survival in these intense herbivore environments. The major component of *U. flabellum* was found to be udoteal (**64**), a diterpenoid with 1,4-diacetoxybutadiene functionality. This protected 1,4-dialdehyde derivative is quite common among the chemical defense agents of other green algae, such as *Caulerpa*, *Chlorodesmus*, and *Rhipocephalus* [230]. Udoteal produces significant feeding avoidance by the herbivorous fish *Pomacentrus coeruleus*. Prolonged storage of udoteal (**64**) in ethanol promoted conversion into hydrates of udoteatrial (**65**) which, in turn, showed antimicrobial activity against *Staphylococcus aureus* and *Candida albicans* [231] (Fig. 2.18).

Capisterones

Marine benthic organisms are constantly exposed to the threats of water-borne marine pathogens. The green alga *Penicillus capitatus*, abundant in shallow water of the tropical Atlantic Ocean, was found to produce triterpene sulfate esters, capisterones A (**66**) and B (**67**), which are potent antifungal compounds against the marine algal pathogen *Lindra thallasiae*. Capisterones A and B inhibited the growth of *L. thallasiae* with LD₅₀ values equal to 0.03 and 0.94 µg/mL, respectively [232]. In biomedical testing, they enhanced the activity of the antifungal drug fluconazole against a strain of *Saccharomyces cerevisiae* which overexpresses a drug efflux pump of *Candida albicans*. However, they showed no inherent antifungal activity against several opportunistic pathogens and no cytotoxicity to

Fig. 2.18 Terpenoids from Chlorophyta



human cancer and noncancer cell lines [233]. Therefore, capisterones A and B may have potential in combination therapies of fungal infections caused by clinically relevant azole-resistant strains (Fig. 2.18).

2.4.2.2 Cymopols

Until the mid-1970s, halogenated natural products had been mostly reported from the Rhodophyta and Phaeophyta. However, two prenylated bromohydroquinones, cymopol (68) and cyclocymopol (69), were found from *Cymopolia barbata* in 1976, and since, a number of cymopol-related compounds have been reported from this alga [234]. Cymopol (68) exhibited potent antioxidant activity and inhibited bee venom-derived phospholipase A₂ function and cell adhesion of HL-60 cells to CHO-ICAM-1 cells [206, 207, 235]. A mixture of cyclocymopol diastereomers were isolated from the extract of *C. barbata* and found to inhibit sea urchin feeding [236, 237]. Subsequently, cymobarbatol (70) and 4-isocymobarbatol (71)

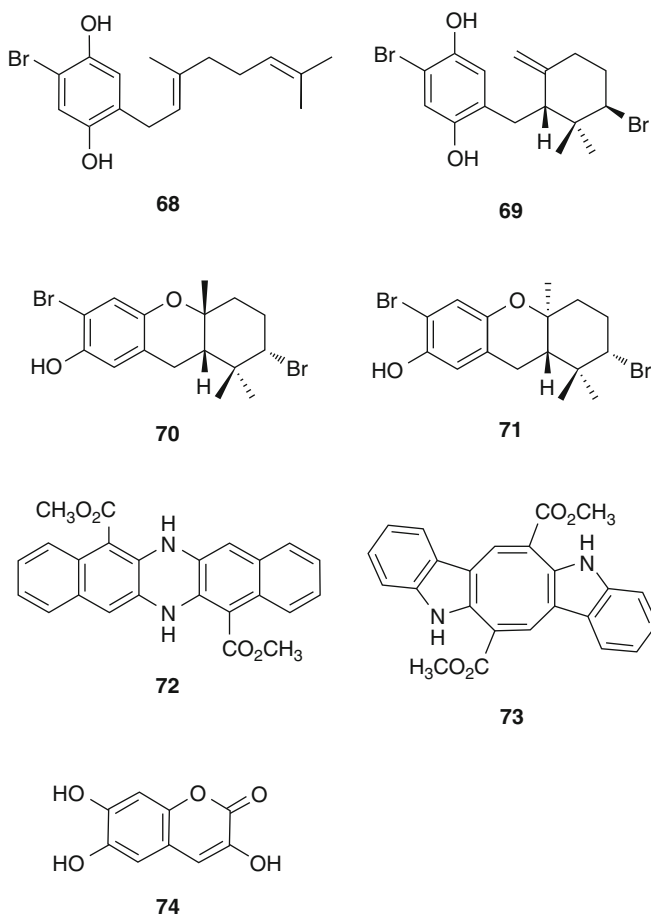


Fig. 2.19 Various secondary metabolites of Chlorophyta

were discovered and found to have antimutagenic properties [238]. The natural occurrence of the diastereomers of cyclocymopol and cymobarbatol support enzymatic conversion of cymopol to a *Z*-olefinic isomer followed by a bromonium ion-induced cyclization in their biosynthetic mechanism (Figs. 2.19, 2.20).

2.4.2.3 Bisindoles (Caulerpin)

Several species in the genus *Caulerpa* are edible and have been consumed for many years in the Philippines and other tropical Pacific regions. However, some of these consumed species are not eaten in the rainy season because they develop an extremely peppery taste. Aguilar-Santos and Doty investigated the toxic constituents of *Caulerpa* and found an orange-red pigment, designated as “caulerpin,” as one of the common components of this genus [239]. Caulerpin was first isolated from three species of *Caulerpa* in the Philippines: *C. racemosa* var. *clavifera*, *C. sertularioides*, and *C. serrulata*. The chemical structure of caulerpin was first

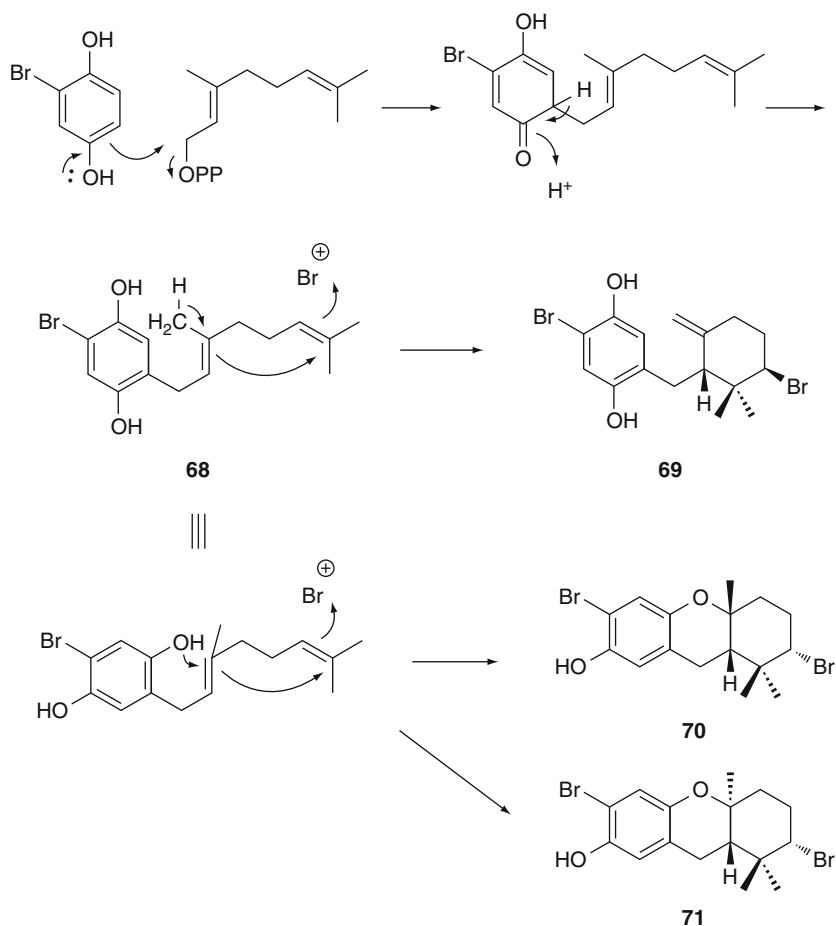


Fig. 2.20 Proposed biosynthesis of cymopol (**68**), cyclocymopol (**69**), cymobarbatol (**70**), and isocymobarbatol (**71**) by the green alga *Cymopolia barbata* involving bromonium ion-induced cyclization

reported as a dihydrodibenzo[b,i]phenazine (**72**) in 1970 [240]; however, this was later revised to the *bis*-indolyl structure **73** by Maiti and Thomson who used a combination of chemical degradation and synthesis techniques [241] (Fig. 2.19). Caulerpin, a dimer of indole-3-acrylic acid, promotes plant root growth similarly to its monomeric counterpart as well as indole-3-acetic acid (auxin) [242].

The diverse pharmacological activities of caulerpin have been studied over the intervening years. It has been shown to inhibit hypoxia-inducible factor-1 (HIF-1), an important molecular target for anticancer drug discovery, through inhibition of mitochondrial respiration [243]. It also has antinociceptive and anti-inflammatory activity in the mouse writhing and hot plate tests, the formalin-induced pain test,

the capsaicin-induced ear edema, and the carrageenan-induced peritonitis in mice [244]. Recently, it has been reported to possess insecticidal activity against the mosquito *Culex pipiens* [245].

2.4.2.4 3,6,7-Trihydroxycoumarin

Dasycladus vermicularis, a member of the siphonaceous green algae, is abundant in the North Atlantic and Mediterranean. In order to cope with a wide range of UV light intensities, *D. vermicularis* accumulates and excretes the UV-absorbing metabolite 3,6,7-trihydroxycoumarin (THC, **74**) [246, 247] (Fig. 2.19). Coumarins in the Dascladaceae, including THC, have been reported with diverse antimicrobial, antioxidant, and wound-healing properties [247–249]. Subsequently, the antioxidant role of THC under diverse environmental stressors was reported.

2.4.2.5 Brominated Phenols (Avrainvilleol)

Before avrainvilleol (**75**) was isolated from the green alga *Avrainvillea longicaulis* in 1983 [250], most bromophenolic natural products had been reported from marine annelids [251] and red algae [252, 253]. Avrainvilleol is a brominated diphenylmethane which appears to result from dimerization of a precursor bromo-*p*-hydroxybenzyl alcohol (Fig. 2.21). In 1987, another brominated diphenyl methane, 5'-hydroxyisovrainvilleol (**76**), was isolated from *A. nigricans* along with avrainvilleol and 3-bromo-4,5-dihydroxybenzyl alcohol (**77**), the presumed monomer of 5'-hydroxyavrainvilleol [254]. Subsequently, rawsonol (**78**) [255] and isorawsonol were described from *A. rawsonii* (**79**) [256]; these metabolites appear to form from condensation of two molecules of avrainvilleol (**75**) (Fig. 2.22). As revealed by this series of metabolites, these types of bromophenols have a chemical and biochemical propensity for condensation to form higher order oligomers [255].

Avrainvilleol was first reported for its antibacterial activity against *Vibrio anguillarum* as well as its fish toxicity and fish-feeding deterrence properties [250]. Subsequently, avrainvilleol was found to inhibit inosine 5'-monophosphate dehydrogenase (IMPDH) [256] and LFA-1/ICAM-1-mediated cell adhesion [207], as well as show potent antioxidant activities [206] (Figs. 2.21, 2.22).

2.4.2.6 Oxylipins Nigriganoside A

Monogalactosyldiacylglycerol derivatives are major constituents of membrane lipids in higher plants and cyanobacteria. In 2007, nigriganosides A (**80**) and B (**81**), unprecedented antimitotic glycolipids, were reported from *Avrainvillea nigricans* collected in Dominica [257]. The extract of *A. nigricans* showed extremely potent antimitotic activity. However, only trace quantities of the bioactive molecules were obtained, and this was insufficient for structure elucidation. As a result of an 8-year effort to collect enough material (28 kg wet wt of *A. nigricans*) for structural analysis of the bioactive compounds, the methyl esters of nigriganosides A (800 µg, 0.000003% wet wt) and B (400 µg, 0.0000015% wet wt) were obtained, and their planar structures elucidated (Fig. 2.23). Nigriganosides A and B contain a glycosidic linkage between galactose and C-1 of glycerol, a common structural feature

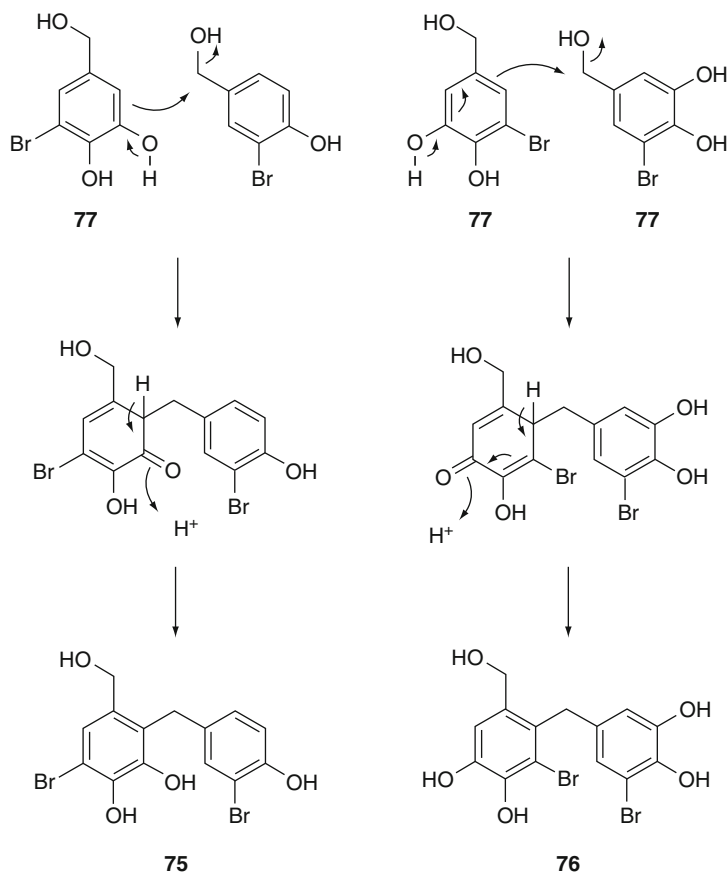


Fig. 2.21 Proposed biosynthesis of avrainvilleol (**75**) and 5'-hydroxyisoavrainvilleol (**76**) from 3-bromo-4,5-dihydroxybenzyl alcohol (**77**) by the green algae *Avrainvillea longicaulis* and *A. nigricans*

of glycolipids. However, two oxygen-containing fatty acid chains were linked together via an ether linkage, and one was further connected to the galactose residue; two other fatty acids were linked as normal esters to the glycerol backbone. Nigricanoside A dimethyl ester arrested cell mitosis in human breast cancer cells and promoted tubulin polymerization in human breast cancer and colon cancer cells. Methylation of the crude fractions, which was performed to facilitate the isolation process, diminished the potency of this material, and hence, the free dicarboxylic acids are thought to be the bioactive natural products.

Oxylipins from *Acrosiphonia coalita*

Although oxylipins are abundantly found in red algae [258] and other marine macroalgae [259], the first series of oxylipins to be isolated from a marine chlorophyte came from the Oregon coastal chlorophyte *Acrosiphonia coalita* [260]

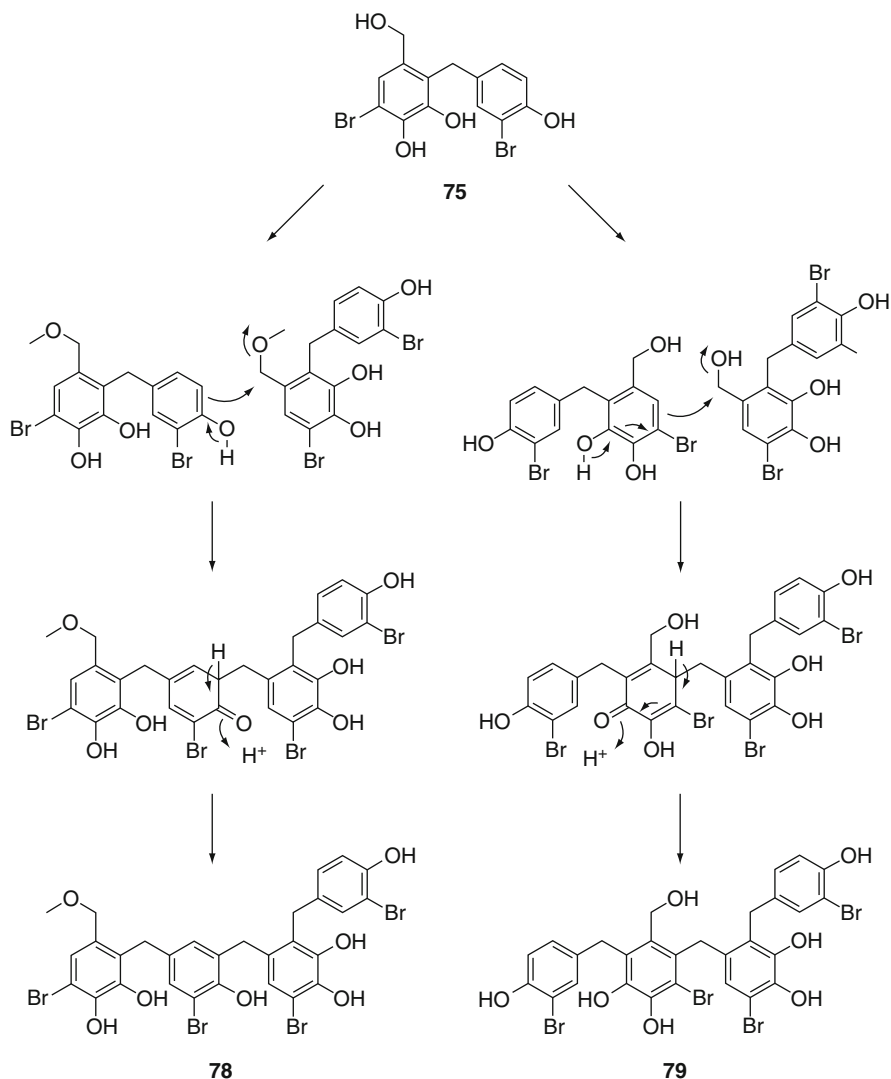


Fig. 2.22 Proposed biosynthesis of rawsonol (**78**) and isorawsonol (**79**) from avrainvilleol (**75**) by the green alga *A. rawsonii*

(Fig. 2.24). A ten-carbon conjugated trienal, named coalital (**82**), showed strong antimicrobial activity against *Candida albicans*. Related to coalital were three novel branched-chain conjugated trienal oxylipins (e.g., **83**, **84**) in which the aldehyde was present as a branching carbon on a 17-carbon fatty acid chain. Additionally, two novel conjugated unbranched trienone octadecanoids (**85**, **86**) were also isolated and characterized. It has been proposed that these trienals and trienones derive from α -linolenic acid or stearidonic acid by 9- and 16-lipoxygenase directed oxidation

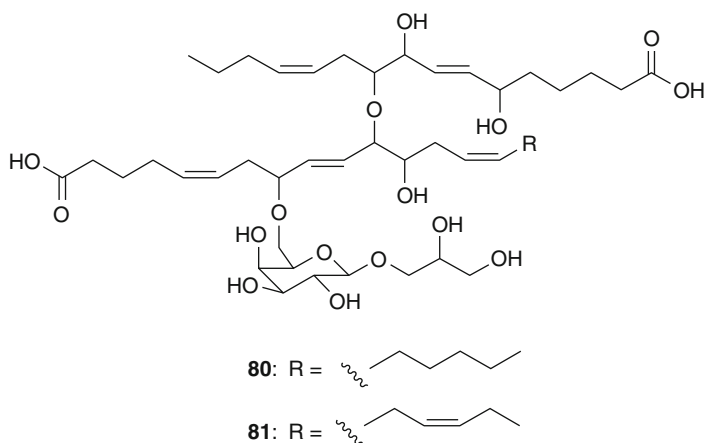


Fig. 2.23 Structures of nigricanosides A (**80**) and B (**81**)

reactions. A family of related epoxy-alcohols (**87–89**) was also obtained from *A. coalita*. As shown in the soybean lipoxygenase system, oxidation of linoleic or linolenic acids at either C-9 or C-13 by lipoxygenases is often followed by an oxygen-rebound reaction leading to the formation of epoxy-alcohols [261]. However, the mechanism of branched chain aldehyde formation in these green algae remains unknown at present.

2.4.3 Rhodophyta

2.4.3.1 General Biology of the Rhodophyta

The Rhodophyta, or red algae, are some of the more conspicuous inhabitants of the temperate intertidal environment, although there are many known from tropical, arctic, and subtidal locations as well. Overall, there are more than 5,000 species of red algae (possibly as many as 10,000), and they exist mainly as macroscopic plant-like algae, although a few unicellular or filamentous species do exist. In the larger multicellular species, their algal body is typically composed of holdfast, stipe and blade components which roughly accord to the root, stem, and leaf of higher plants [5].

The Rhodophyta are unique among all algae in that there is no flagellated stage in their life history. Also, they have unique accessory pigments, namely phycoerythrin, phycocyanin, allophycocyanin which are present as protein complexes known as phycobilisomes. The phycobilisomes are arranged on membranes within the chloroplasts known as thylakoids, and serve to harvest a broader range of light wavelengths than the normal complement of chlorophyll *a* and *d* present in these organisms. Floridean starch, which is similar to amylopectin, is used as a food reserve and is found with the cytoplasm. Reproduction and life histories are very complex in this group of algae, and much of the taxonomy of the Rhodophyta is based on reproductive appendages and processes. For example, they have quite

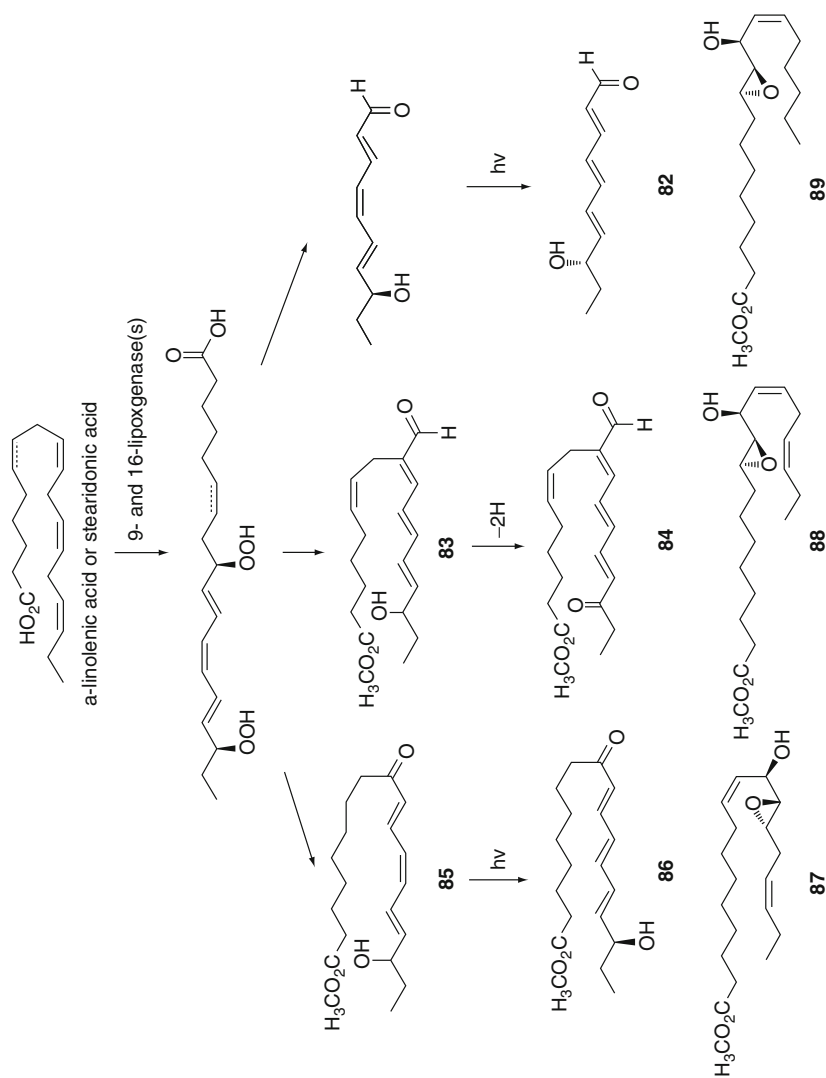


Fig. 2.24 Oxylipins from Chlorophyta (*Acrosiphonia coalita*)

specialized cells and organs for reproduction, including carpogonia for female cells and spermatagia for male cells. Some species have both male and female individuals, whereas others have both within the same individual. Additionally, in some species, the 1n and 2n phases of the organism have the same morphology (isomorphic), whereas in others have different morphologies (heteromorphic).

The cell walls of Rhodophyte algae are composed of an amorphous matrix formed mainly by sulfated galactans, and resulting in extracted products known as agar and carrageenan. Calcium carbonate deposition occurs into the cell wall of many species, particularly in the Corallinaceae, either as calcite or aragonite, and contributes substantially to coral reef building in the tropics. Some multicellular red algae have specialized secretory or gland cells, particularly in the family Bonnemaisoniaceae, and this is the cellular site of halogenated natural product production and storage in these species.

As noted elsewhere in this chapter, the taxonomy of the algae is in a state flux as new insights into the relationships of organisms are generated from genome sequence data. However, the Rhodophyta are traditionally composed of two subclasses, although recent taxonomic treatments organize this group of algae differently. Natural products have been reported from the more advanced subclass, the Florideophycidae, and within this group, several notable families, such as the Bonnemaisoniaceae, Ceramiaceae, and Rhodomelaceae, are especially rich in secondary metabolites.

Perhaps because the Rhodophyta, as a group, are some of the more conspicuous members of the intertidal, and certainly as a result of the large number of species and their propensity to elaborate natural products, this taxonomic group was one of the first to be actively investigated for new and bioactive metabolites. Much of the early work occurred in Japan, with Toshi Irie being one of the true pioneers of this field [262], but soon afterward, numerous groups from the USA, Canada, Europe, and Australia focused their investigations on the red algae as well. Hence, several thousand natural products are now known from this group of algae, with the majority falling into the categories of metabolites discussed below. One of the dominant metabolic features, which is present in many of these natural product classes described below, is the covalent incorporation of halogen atoms (chlorine, bromine, and even iodine) [263–265], and it was this unique aspect that drew so many pioneering marine natural products chemists to first investigate this algal group.

2.4.3.2 Chemistry of the Rhodophyta

Simple and Complex Bromophenols

One of the first natural product classes described from red algae were simple bromophenols from such temperate and cold water species (e.g., Nova Scotia) of red algae as *Odonthalia dentata*, *Polysiphonia lanosa*, and *Rhodomela confervoides* [266]. A common and well-described member of this class is known as lanosol (**90**), a seven-carbon metabolite with two phenolic and one primary hydroxy group, and two bromine atoms. Often, one or more of the phenolic hydroxy groups are present as sulfate esters, and these are known to be quite hydrolytically unstable, ultimately

giving rise to a large number of presumed degradation products. Additionally, the benzylic alcohol is prone to oxidation (to the aldehyde or carboxylic acid) or ether formation with the extraction solvent (ethanol). Biologically, red algal bromophenols are believed to confer protection against microbial pathogens as well as epiphytes and herbivores [267], and their distribution within algal thalli is quite variable [268]. Surprisingly, the precise mechanism of bromine incorporation into lanosol has not been completely established, but is believed to involve an uncharacterized bromoperoxidase enzyme.

The essential bromophenolic unit of lanosol is a conceptual precursor to a wide number of other red algal metabolites. For example, a collection of *Polysiphonia ferulacea* from Senegal yielded an interesting dimeric metabolite (**91**) wherein two new carbon–carbon bonds link the subunits [269]. As a result of the new carbon linkages, and the large bromine substituent *ortho* to the direct biphenyl linkage, the molecule exists in a single conformation and thus exhibits atropisomerism. Its structure including absolute stereochemistry was established by a combination of spectroscopic methods complemented by molecular mechanic calculations.

Another interesting example of a likely product deriving from lanosol was obtained from the Rhodophyte *Vidalia obtusiloba* collected from Martinique in the Southeastern Caribbean [270]. Shipboard testing of its extract at the time of collection showed it potently inhibited PLA₂, a key enzyme involved in arachidonic acid release and ensuing inflammation in mammals. The major brominated metabolite, vidalol A (**92**), was found to be composed of one C₇ lanosol-type unit linked via a carbon–carbon bond to a second six-carbon bromophenol unit. Vidalol B was simply the next iteration of such an assembly with two lanosol units fused to a central C₆ core. These *ortho*-catechol metabolites were found to have antifungal and antibiotic properties, to inhibit feeding by herbivorous fish, and to inhibit inflammation and edema in the ears of mice topically stimulated with phorbol esters (PMA).

A final example in this class is given by a metabolite (**93**) found in another species of *Vidalia* from Australia, *V. spiralis* [271]. Unfortunately, while the CH₂Cl₂ extract possessed antihypertensive effects, the isolated bromophenol-type metabolite was inactive in this assay (the active antihypertensive agent remains unknown or unreported!). The relationship of vicinal bromine atoms and vicinol diol functionality is identical to that observed for lanosol, and thus, it appears that the aromaticity of the ring has been disrupted through an apparent ring contraction and carbon loss from a lanosol precursor. Intriguingly, the molecule was chiral ($[\alpha]_D +124^\circ$) with the two hydroxy groups oriented *trans* to one another; however, absolute configuration has not yet been assigned in this molecule (Fig. 2.25).

Halogenated Ketones and Quorum Sensing

Several species of the genus *Bonnemaisonia* have yielded halogenated alkanes and alkenes with a variety of oxygen functional groups, including ketones, alcohols, epoxides, and acids [272]. It appears that these derive from an initially formed methyl ketone which is polyhalogenated at the reactive alpha-positions (e.g., to produce 1,1,3,3-tetrabromoheptanone, **94**). The methyl ketone is believed to form

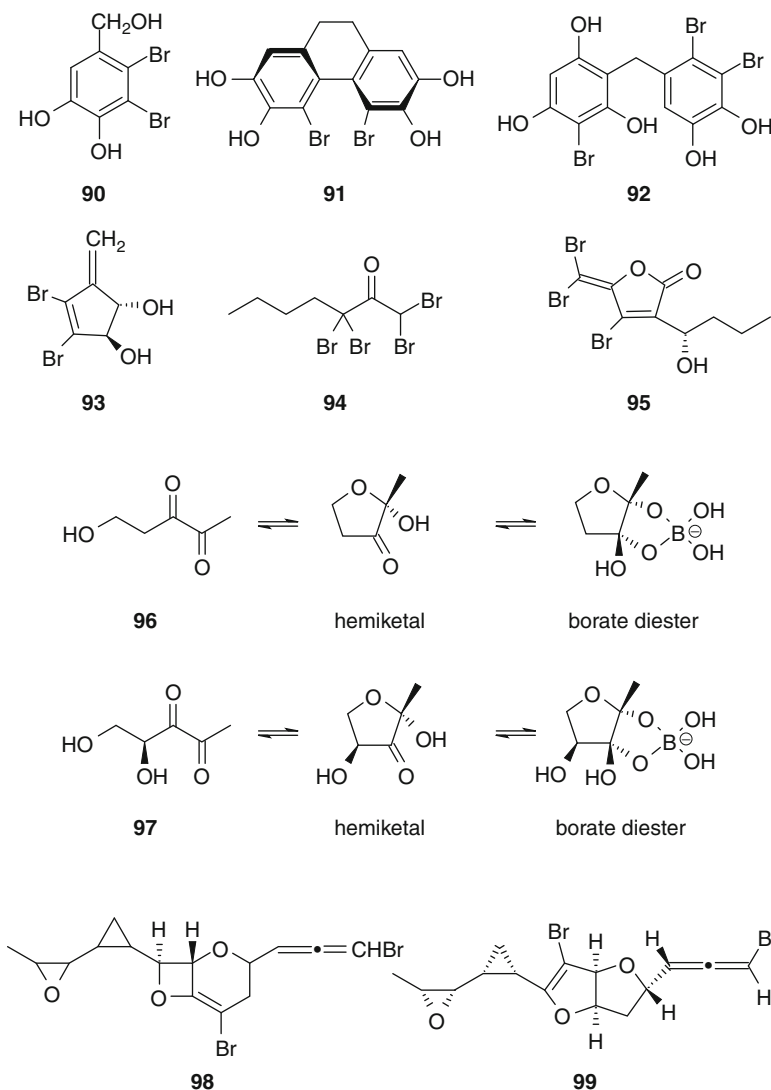


Fig. 2.25 Various secondary metabolites of Rhodophyta

from β -keto acids which undergo facile decarboxylation. The halogenated methyl ketones are then prone to various reactions, including Favorskii-type rearrangements, and this is believed to occur *in vivo* as even very gentle methods of extraction (e.g., a brief dipping in pentane or hexane) yield chain-rearranged alkanolic acids. These halogenated ketones are stored, and perhaps synthesized, in specialized gland cells that are characteristically present on the surface of the algal thalli in this genus. Early studies on these highly halogenated compounds found that some had powerful antibiotic activity, and more recent investigations have shown

that substances such as 1,1,3,3-tetrabromoheptanone exert potent antibiotic effects to bacteria occurring in these shallow water environments [273], and thus result in a reduced number of bacteria as well as an altered species composition on the surfaces of *Bonnemaisonia* [274].

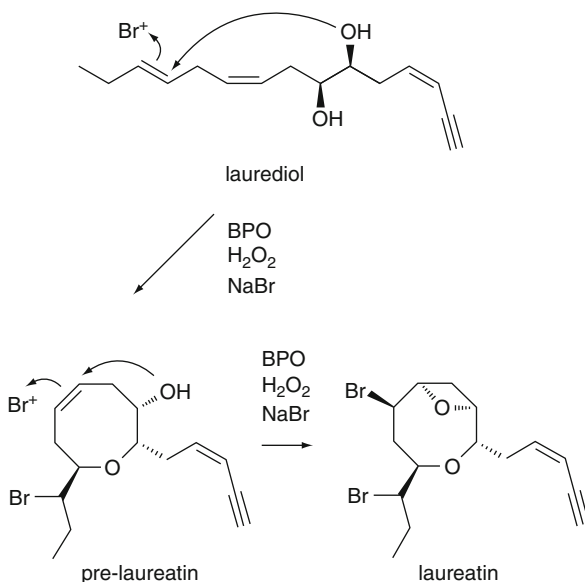
Similarly, on the south Australian coast, a subtidal species of red algae, *Delisea pulchra*, grows abundantly with a flat leaf-like morphology. Remarkably, this algal surface, continuously bathed in warm nutrient-laden seawater with high bacterial and spore counts, remains essentially free of bacterial biofilms or the downstream colonization by encrusting invertebrates or epiphytes. In this case, the answer to this mystery was found to be a small halogenated ketone, similar in biosynthetic origin to the above *Bonnemaisonia* compounds, and actually deriving from a carbon-chain-rearranged Favorskii reaction [275]. The natural products, known as “fimbrolides” (95), as well as various synthetic derivatives, have been actively pursued as potential additives to marine paints that could inhibit fouling in an environmentally benign fashion. Because organotin or organocopper-based paints have been or are in the process of removal from the market [276], there is a huge unmet need for antifouling marine paints, and this has motivated many in the marine natural product community to have antifouling screens in their portfolio of biological assays. In this case, several of the fimbrolides have been studied in considerable detail and shown to inhibit bacterial quorum sensing through antagonist activity at the luxR receptor, a component of the homoserine lactone quorum sensing system in Gram-negative bacteria [277].

When first isolated from the Oregon intertidal seaweed *Laurencia spectabilis*, laurencione (96) was more of a chemical curiosity with its simple five-carbon structure containing two carbonyls and one primary hydroxy group [278]. It was insightful at the time in revealing that this small metabolite was prone to oxidative dimerization or trimerization and hence, that several other reported “metabolites” were in fact isolation artifacts [279]. However, several years later, the crystal structure of a protein involved in bacterial signaling was found to have its cognate ligand bound, named autoinducer-2 (AI-2, 97), which was a borate diester of a metabolite very similar in structure to laurencione (the difference is that AI-2 has one more hydroxy group than laurencione) [280]. As a result, laurencione became a target of several chemical syntheses and bacterial quorum sensing programs, and its borate diester was characterized to have agonist activity as a quorum sensor, although less potent than AI-2 [281]. While it is tantalizing to envision that laurencione may function to maintain the algal surface free from biofilms and the resulting colonization by epiphytes, this interesting chemical ecological dimension remains unstudied to date.

C-15 Acetogenins

A large number of oxidized and halogenated C-15 polyketide or fatty acid-derived compounds have been isolated from various species of the genus *Laurencia*, and these represent one of the more intriguing biosynthetic classes from the Rhodophyta. Early on, it was envisioned that a simplified precursor, presumably arising by decarboxylation and oxidation of fatty acid precursors,

Fig. 2.26 Biosynthesis of laureatin from laurediol involving bromonium ion-induced oxycyclizations



was functionalized by a series of bromoperoxidases to result in several related metabolites that apparently arise from bromonium ion-induced oxycyclizations. Some of the ultimate precursors and intermediates to these diverse C-15 acetogenins have also been characterized, and a picture of the metabolic pathway is emerging. Embedded in these pathways are a range of interesting reactions, such as decarboxylations, halogenations, isomerizations, and carbon–carbon bond formations; the enzymological and mechanistic details of these remain unstudied. A proposed pathway involving some of these precursors and intermediates is shown in Fig. 2.26.

As an example of this metabolic class, the molecule known as okamurallene (originally **98**) provides a particularly fascinating illustration because of its dense functionalization and the complexities experienced in its structure elucidation [282]. Collected from the southwest coast of Hokkaido, Japan, the species *Laurencia okamurai* was found to contain a rich complement of natural products, both terpenoids and C-15 acetogenins. Okamurallene was isolated and analyzed by a number of 1D NMR techniques prevalent at the time of its isolation (1981), and a most unusual structure was proposed with sequential functional groups including an epoxide, cyclopropyl ring, four-membered oxetane fused to a vinyl bromide containing dihydropyran ring, and an allene with terminal vinyl bromide (this may represent a record in terms of density of functional groups on a 15-carbon skeleton!). Ultimately however, continued study revealed an error in the structure elucidation, and this was revised first by 2D NMR and then confirmed with X-ray crystallographic information, the latter also providing absolute configuration [283]. The corrected structure (**99**) alters the relative bond connections of the central

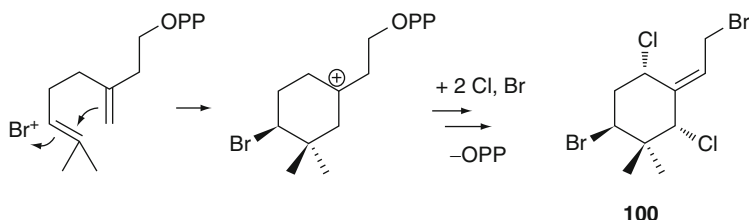


Fig. 2.27 Predicted early steps in the biosynthesis of ochtodene (**100**) involving bromonium ion-induced carbocyclization

bicyclo section, resulting in a fused dihydropyran–tetrahydropyran ring system with an embedded vinyl bromide. As is the case with so many natural products, structural characterization results in more questions than answers, and in this case, there are an abundance concerning the biosynthesis of such an amazing molecule.

Terpenoids

Another dominant theme in the secondary metabolism of red algae is the elaboration of various metabolites deriving from the terpene biosynthetic pathway. The size class of the terpene produced (e.g., C-10, C-15, or C-20) is relatively characteristic of the genus and species of organism, with some possessing exclusively monoterpenes, others sesquiterpenes, and still others di- or triterpenes. Many of the terpenes of the red algae are functionalized with either oxygen or halogen atoms, mostly bromine and chlorine, and logically derive from cyclization events involving halonium ion-induced events. The enzymology of electrophillic halogenations has been studied, and involves unique haloperoxidases that possess either vanadium or iron as the active site metal, and the intermediate production of a “Br⁺” species, possibly as HOBr, Br₂, Br₃, or Enz-Br [284].

The tropical red alga *Ochtodes osmundaceae* is a notable member of shallow wave swept environments in that it has a delicate appearance seemingly at odds with its preferred habitat, and further, it displays a colorful iridescence from its surface. Freshly collected specimens have a pungent “insecticidal” odor that reveals a rich suite of highly halogenated monoterpenes. Such a collection by the Fenical group and isolation by silica chromatography yielded a major component, named ochtodene (**100**), that possessed a cyclohexane-containing monoterpene skeleton with two bromine and two chlorine atoms [285]. A combination of chemical reactivity, mass spectrometry, and NMR spectroscopy was used to determine the planar structure and relative configuration of ochtodene (**100**). Biosynthetically, it is logical to again speculate on the involvement of a bromonium ion-induced cyclization in forming the skeleton of ochtodene and related halogenated monoterpenes (Fig. 2.27). Other red algal genera characteristically producing halogenated monoterpenes of a related nature are *Chondrococcus* and *Plocamium*, inhabitants of colder waters such as Southern Australia, South Africa, and Northern California/Oregon. The natural role of these monoterpenes has been characterized to some extent, and they generally

appear to deter potential predators from feeding upon their soft algal tissues. Interestingly, it seems that different terpenes have antifeedant activity against different classes of predators (e.g., octodene was effective against fish predation, whereas a mixture of other halogenated monoterpenes were selective in inhibiting copepod grazing) [286]. Nevertheless, specialist herbivores such as sea hares (e.g., *Stylocheilus longicauda* and *Dolabella auricularia*) selectively prey upon these and other natural product rich seaweeds, and while they sequester and store these algal natural products, this occurs only in the digestive gland, and thus, it is uncertain if this is involved in chemical defense [287]. Bioengineering efforts have used microplatelets of *Ochtodes* as a model organism for measuring the production of a natural product (e.g., octodene) as a function of bioreactor conditions and growth [288].

The genus *Laurencia* is extraordinarily rich in sesquiterpene-derived compounds, many of which also contain multiple bromine and chlorine atoms. An example of this structure class is given by the widespread bicyclic sesquiterpene elatol (**101**), originally isolated from *L. elata* in the Caribbean, but subsequently isolated from strains of this alga from many parts of the world. Its structure was developed from NMR features and ultimately solidified with absolute configuration from an X-ray diffraction study [289]. The bicyclic ring system, known as a “chamigrene,” is quite common among the sesquiterpenes of *Laurencia* and appears to form as a result of halonium-induced cyclization events as noted above (Fig. 2.28). Curiously, both enantiomers of elatol have been reported in the literature [290], suggesting that either (a) the biosynthetic events creating the stereocenters can occur from either face in the nascent terpene, or (b) these occur outside of a chiral environment (e.g., after release from the active site of the enzyme). The physical location of the rich suite of sesquiterpenes, such as elatol, in *Laurencia* tissues has been investigated by several techniques, including X-ray microanalysis and fluorescence microscopy, and these substances are generally found in distinctive intracellular compartments known by the French term *corps en cerise* (cherry bodies) due to their characteristic shape [291]. Elatol and other stored sesquiterpenoids are then released upon injury, or possibly through vesicle release, to prevent biofouling, inhibit bacterial infections, and deter predation [292]. However and as noted above, in some cases, specialist predators, such as *Aplysia dactylomela*, target these terpene-rich red algae for consumption and then sequester these substances both within the digestive gland and, in this case, the mantle as well; the presence of noxious halogenated terpenoids like elatol (**101**) in the latter tissues may protect against potential predators of these soft-bodied animals [293]. Purified elatol has been reported to possess cancer cell cytotoxicity, antimicrobial properties, and antileishmanial activities [294].

Diterpene-derived natural products are also abundant in red algae with more than 100 such metabolites reported from a few genera (e.g., *Laurencia*, *Sphaerococcus*, *Callophycus*) [295] and organisms which feed upon red algae (e.g., *Aplysia*). Because of their interesting structures and biological activities, and more recent discovery, a few of the metabolites of *Callophycus* will be used to illustrate the trends in this group. Actually, the *Callophycus* metabolites are all found attached

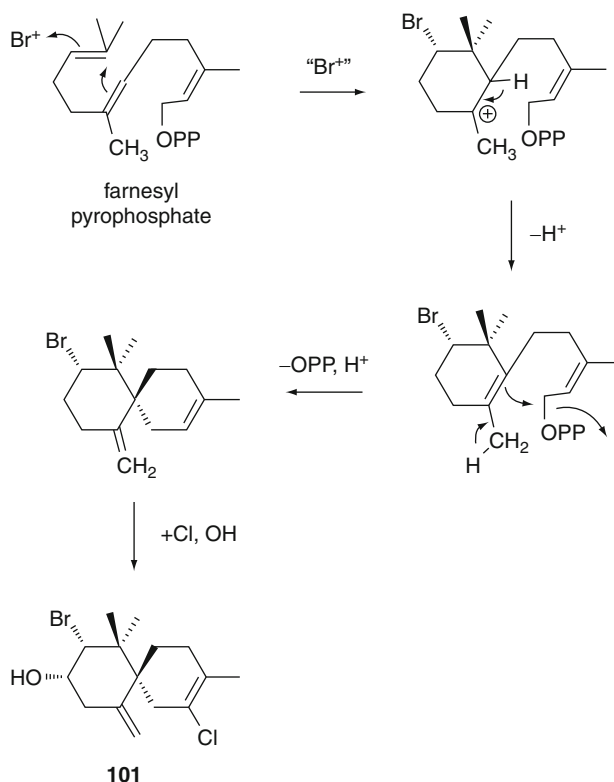


Fig. 2.28 Proposed bromonium ion-induced carbocyclization and ensuing reactions to form the sesquiterpene elatol (**101**)

by a carbon–carbon bond to a benzoic acid moiety, formally making these meroditerpenes (interestingly, meroditerpenes are also characteristic metabolites of the brown algal family Dictyotaceae). Another striking feature of these *Callophycus* metabolites is their abundance of covalent bromine atoms.

Callophycus serratus is a relatively abundant red alga in shallow waters around the Fijian Islands, appearing as finely divided bushy plants of pink to rose color. An investigation motivated by drug discovery efforts associated with the International Cooperative Biodiversity Group (ICBG) program in Fiji resulted in the initial characterization of a series of meroditerpenes, most of which contained several bromine atoms [296]. A combination of classical NMR-based approaches complemented by an X-ray diffraction analysis was used to define these as a series of macrolides formed by the closure of a benzoic acid residue to the terminal olefin of a tethered diterpene. As illustrated below (Fig. 2.29), the proposed biosynthesis of the major metabolite, bromophycolide A (**102**), involves three separate additions of electrophilic bromine to the carbon chain, two which produce bromohydrin-related structures and one apparently inducing cyclohexyl ring formation. Subsequently, a large series of related meroditerpenes were

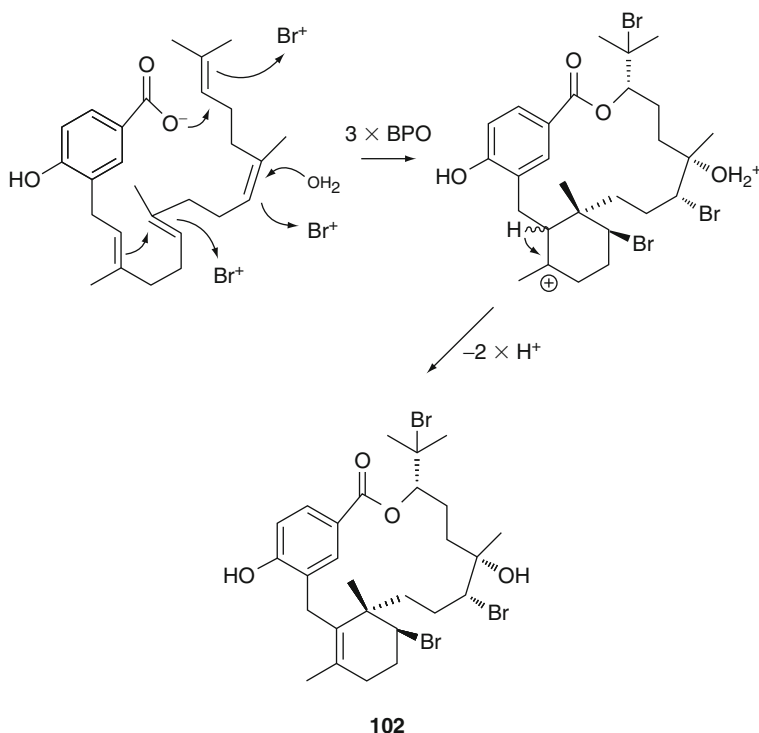
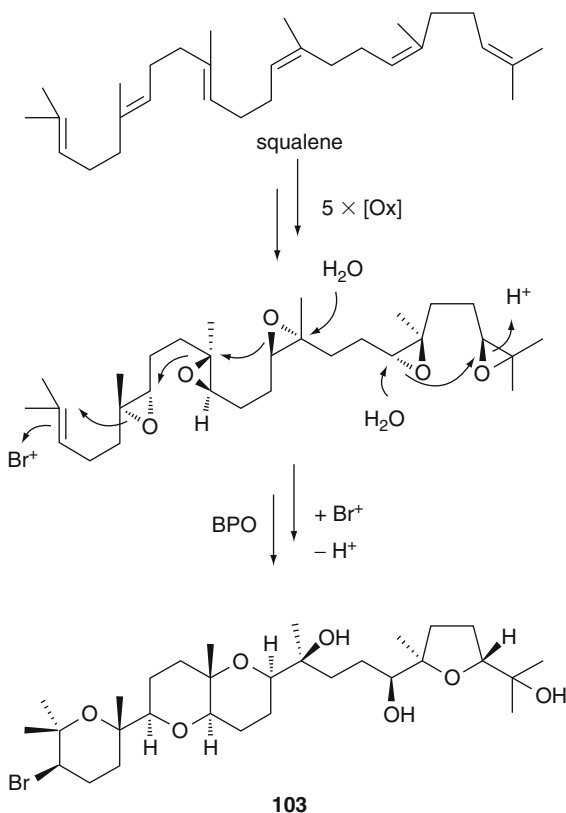


Fig. 2.29 Proposed biosynthesis of bromophycolide A (**102**) by the red alga *Callophycus serratus* involving multiple bromonium ion additions to a complex terpenoid precursor. BPO = bromoperoxidase

reported with alternate halogenations patterns, both on the diterpene skeleton and the aromatic ring. Again, the positions of bromine atoms, and in two cases chlorine, are consistent with their addition to positions of unsaturation in the terpenoid precursor, in some cases inducing further rearrangements of the terpene skeleton and forming diverse ring structures. All of these halogen additions suggest the involvement of a bromoperoxidase forming an electrophilic Br^+ like species. Indeed, a potential meroditerpene precursor containing only unsaturations and vicinal diol but no bromine atoms has recently been reported. Subsequent phylogenetic analysis suggests that there are two clades of *C. serratus* which alternately produce these different classes of meroditerpenoids [297]. While initial reports on these various structures revealed cancer cell toxicity and antimalarial properties (the latter submicromolar for some members) [298], a potential natural function for these substances was revealed when they were shown to possess potent antifungal activity to the pathogenic marine fungus, *Lindra thalassia*. An innovative use of DESI-mass spectrometry was able to localize these antifungal natural products to specific discolored patches on the algal thallus [299]. One suggestion given to explain this observation was that the alga secretes antifungal brominated meroditerpenoids into areas of the thallus that are injured by mechanical damage,

Fig. 2.30 Proposed biosynthesis of thysiferol (**103**) from squalene by the red alga *Laurencia thysifera* involving a polyepoxide intermediate followed by two separate cascades of electrons and one bromonium ion addition. BPO = bromoperoxidase



and thus would be prone to pathogen attack. Overall, the emerging picture of the chemistry and pharmacology of this tropical red alga is a nice illustration of a number of principals in the biosynthesis and chemical ecology of red algal diterpene natural products.

The New Zealand red alga *Laurencia thysifera* was investigated for its antimicrobial products early on in the development of marine natural products chemistry by the group of Monroe and Blunt and found to contain a unique triterpene, named thysiferol (**103**) [300] of which the relative configuration was assigned by X-ray crystallography. Subsequently, this and related compounds such as laurenmariannol have been isolated from other *Laurencia* species collected in diverse regions of the world, such as the Canary Islands and the South China Sea [301, 302]. Importantly, these later efforts revealed that compounds of this series have quite potent cancer cell toxicity, and thus combined with their intriguing polyether structure, they have been targets of multiple total synthesis investigations [303]. The relationship of ether rings and functional groups in thysiferol has spawned considerable speculation on their biogenesis, which is envisioned as deriving from a polyepoxy precursor that undergoes a cascade of electron shifts to yield the final polyether system (Fig. 2.30).

Oxylipins

One of the more surprising yet pervasive chemical classes to be discovered in red algae is “oxylipins,” oxygenated fatty acid derivatives [304]. Some of the earliest work in this area occurred as a result of a poisoning syndrome known as “Ogonori poisoning” (nausea, vomiting, and hypotension, in some cases, lethal) observed in Japan after eating the red alga *Gracilaria verrucosa* [305]. An active compound was isolated and structurally defined as the known prostaglandin, PGE₂. Interestingly, coral prostaglandin derivatives of similar structure were studied as to their ecological role and appear to induce avoidance in potential consumers through an induced emesis [306]; indeed, prostaglandins taken orally by people have a similar effect. It may be that the *G. verrucosa* prostaglandins serve a similar avoidance role and when consumed by humans, produce such a toxic effect. The biosynthetic pathway to these *Gracilaria* prostaglandins has not been studied; however, because red algae have subsequently been found to be a very rich source of lipoxygenase products [304], their prostaglandins are speculated to involve lipoxygenase-mediated routes similar to those found in corals, rather than the cyclooxygenase pathways found in mammals.

As an example of a red algal metabolite clearly deriving from lipoxygenase metabolism, several red algae from the Oregon coast, including *Farlowia mollis* and *Gracilariopsis lemaneiformis*, were found to produce 12*R*,13 *S*-dihydroyeicosapentaenoic acid (12*R*,13 *S*-diHEPE, **104**) [307]. This metabolite, found both as a free acid and as a component of complex monogalactosyl diacylglycerol derivatives which are characteristic of chloroplast membranes, had the interesting property of interfering with luteal function in ewes (sheep), perhaps in part by altering luteal response to luteinizing hormone [308]. A study of its biosynthesis showed that it is initiated by a unique sodium-dependant lipoxygenase that stereospecifically incorporates dioxygen to the 12 *S* position in an eicosapentaenoic acid (EPA) precursor. Subsequently, the distal oxygen is used to oxygenate the adjacent C-13 position in an oxygen-rebound mechanism [309].

Continued study of oxylipins from red algae has revealed many chemical structures with inherently interesting and partially characterized biosynthetic pathways; curiously however, their biological properties remain poorly characterized, and this represents an enormous opportunity in both the biomedical and ecological arenas! For example, *Laurencia hybrida* from Great Britain yielded hybridalactone (**105**), a fascinating polycyclic oxylipin [310]. A combination of synthetic studies and mechanistic proposals suggests that this metabolite also derives from a 12 *S*-lipoxygenase-initiated metabolism and that a fascinating cascade of electron shifts occurs to ultimately lead to its complex structure (Fig. 2.31 and 2.32) [311]. A similar investigation of the wine glass-shaped red alga, *Constantinea simplex* from the Oregon coast, resulted in the constanolactones (e.g., **106**), and once again, a mixture of experiments and speculation strongly implicate a 12 *S*-lipoxygenase-initiated metabolism with an ensuing series of electron rearrangements [312]. As a unifying biosynthetic theme, many of the unique carbocyclic oxylipins of red algae appear to involve an epoxy allylic carbocation as a strategic biosynthetic intermediate [313].

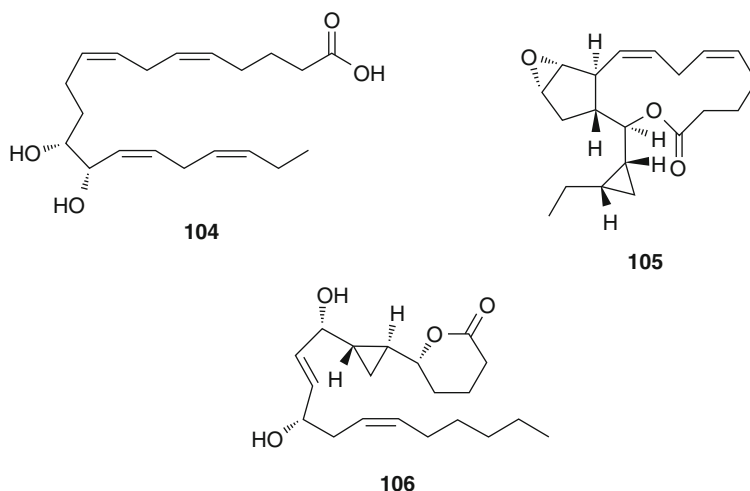


Fig. 2.31 Oxylipins from Rhodophyta

Future biosynthetic investigations of these oxylipin structures are certain to be rewarded with a wealth of enzymes possessing unique specificities and reactivities! (Fig. 2.32).

2.4.3.3 Conclusions on the Rhodophyta

In summary, the natural products of the Rhodophyta have been relatively well studied as a result of being the subject of continuing efforts since the beginning of marine natural products investigations in the 1960s. In general, red algae tend to produce non-nitrogenous metabolites (there are exceptions!) that derive from the shikimate, terpene, and fatty acid biosynthetic pathways. Secondary to these themes, they prolifically decorate carbon scaffolds with halogen atoms, primarily bromine and chlorine, which are incorporated via electrophilic halogenation mechanisms [284]. Many of these metabolites possess biological properties of utility in drug discovery, notably cytotoxicity with application to treating cancer, and antibiotic properties with applications in infectious and parasitic diseases. Remarkably, with new technologies in organic structure analysis, primarily soft ionization MS techniques and NMR able to investigate at the nanomole level [314], we are now able to reach more deeply into the secondary metabolomes of these organisms and find new metabolites with surprising structural features. Some of these recent discoveries, such as the bromophycolides described above (e.g., **102**), possess very interesting biological properties and thus could be useful in treating human diseases, such as malaria, that are currently untreated or poorly treated. Thus, there are still opportunities for fundamental discoveries in the natural products chemistry of red algae, and as presented in this section, natural product discoveries stimulate ensuing questions into biosynthesis, pharmacology, and chemical ecology, most of which remain poorly studied to date.

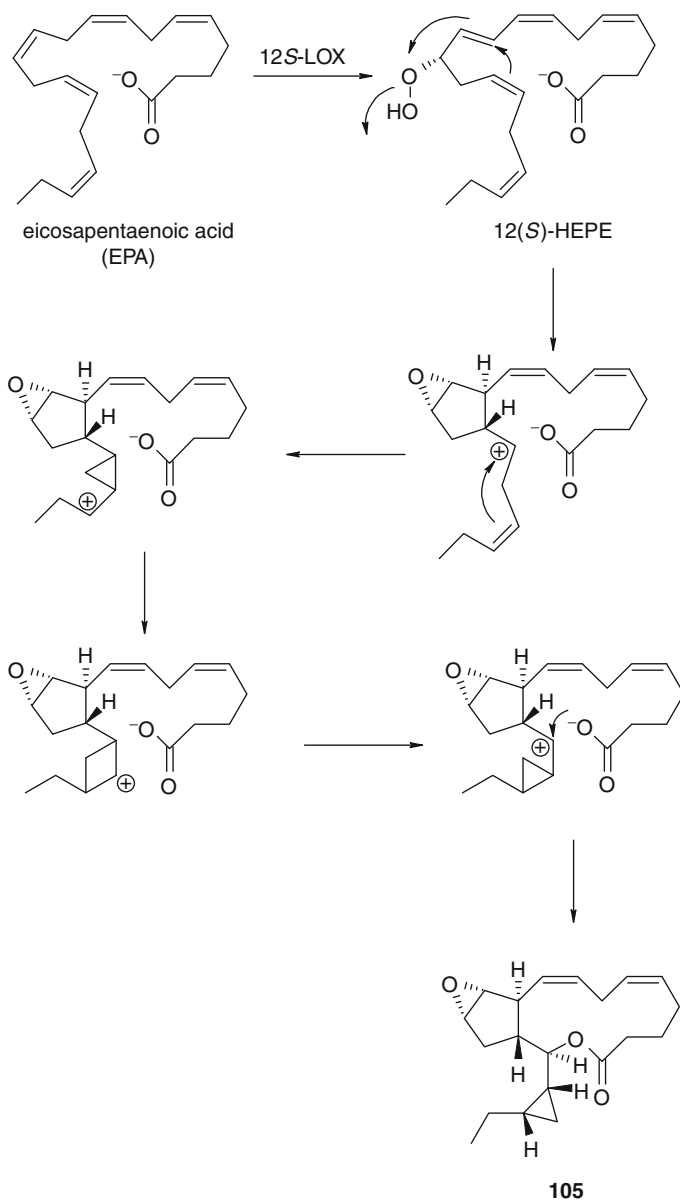


Fig. 2.32 Proposed biosynthesis of hybridalactone (**105**) from eicosapentaenoic acid by the red alga *Laurencia hybrida*, initiated by a 12S-lipoxygenase followed by multiple electron migrations including a cyclopropylcarbinyll-cyclobutyl-cyclopropylcarbinyll cation manifold, and ultimately quenched by the carboxylate anion

2.4.4 Phaeophyceae

Found almost exclusively in the marine environment, there are around 1,500–2,000 species of brown algae (Phaeophyceae) worldwide, varying in size from microscopic to the largest algae in the sea (e.g., the kelp *Macrocystis* grows up to 60 m in length) [315]. Some simple forms of brown seaweeds can be filamentous or have intertwined filaments, whereas more complex forms have differentiated cell types and complex morphologies, on par with higher plants [315–317]. Their cell wall is comprised of two layers, an inner one made of cellulose and an outer of alginic acid [315, 318–322]. The latter polysaccharide consists of a mixture of β -D-mannuronic and α -L-guluronic acids linked covalently in a 1–4 fashion. Alginic acid is used industrially as an additive in antacids, foods, microbiology encapsulation, and paper [318–322]. Brown algae employ another polysaccharide, the glucose-based laminaran, as their main food reserve [323, 324]. Their pigments include chlorophyll *a* and *c*, β -carotene, violaxanthin, and fucoxanthin; this latter one is responsible for their characteristic brown coloration [315, 325]. Sexual reproduction in the brown algae involves motile gametes [326, 327].

Brown algae produce a great variety of secondary metabolites possessing many different skeletal types and biological activities, including aliphatic hydrocarbons, resorcinols, and other polyphenolics, terpenes (sesquiterpenes, diterpenes, meroditerpenoids), and oxylipins. The biological properties of these diverse substances include antibacterial, antifungal, antiviral, anti-inflammatory, antiproliferative, antifouling, antifeedant, cytotoxic, ichthyotoxic, and insecticidal [328–331].

2.4.4.1 Aliphatic Pheromones

A variety of unsaturated but otherwise nonfunctionalized acyclic or cyclic C11 olefins are released as chemical signals by female gametes of marine brown algae in order to attract the corresponding motile male gametes [332]. These molecules constitute blends of pheromones containing various configurational isomers and enantiomeric mixtures which exhibit threshold concentrations for release and attraction generally in the range of 1–1000 picomoles using a water drop assay [332].

One representative example of a brown alga pheromone is the C8 hydrocarbon (3*E*,5*Z*)-octa-1,3,5-triene (fucoserratene, **107**), identified from *Fucus serratus* [333, 334]. Biosynthetically, **107** was found to derive from (5*Z*,8*Z*,11*Z*,14*Z*,17*Z*)-eicosapentaenoic acid (**108**) via oxidative cleavage of the corresponding 12-hydroperoxy intermediate **109** by a hydroperoxide lyase, to yield fucoserratene (**107**) and the polar fragment 12-oxododeca-5,8,10-trienoic acid (**110**) [335–338]. The involvement of a 12-lipoxygenase was supported by inhibition experiments in which the formation of **108** was suppressed under anaerobic conditions, and reactivated by addition of molecular oxygen [338]. A defensive role has also been suggested for compound **110** [336]. In turn, the biosynthesis of ectocarpene (**111**) in the cosmopolitan brown alga *Ectocarpus siliculosus* involves a presumed functionalization of **108** by a 9-lipoxygenase, yielding hydroperoxide **112** [339–341]. This intermediate is proposed to undergo rearrangement to the Hock-oxycarbenium ion **113** before cleavage into the labile C11

divinylcyclopropane **114** and the highly water soluble C9 by product **115**. Finally, spontaneous Cope rearrangement of **114** in principle yields the expected algal pheromone **111** [339–341] (Fig. 2.33).

Additional pheromone hydrocarbons isolated from *E. siliculosus* include dictyotene (**116**), multifidene (**117**), hormosirene (**118**), and finavarrene (**119**) [342] (Fig. 2.34). Biosynthetic studies using ^2H -labeled natural eicosanoids and shortened unnatural fatty acids revealed that dictyotene (**116**) is derived from (5Z,8Z,11Z,14Z)-eicosatetraenoic acid (arachidonic acid), whereas the remaining metabolites are produced from eicosapentaenoic acid (EPA) (**108**) [343, 344].

2.4.4.2 Resorcinols

Resorcinols comprised of phloroglucinol with an attached C-20 acyl side chain are characteristic metabolites of the brown algae genus *Zonaria* [345] (Fig. 2.35). Compound **120** has been isolated from several *Zonaria* specimens [346–349], accompanied by numerous analogs displaying different methylation and acetylation patterns on the phloroglucinol substructure, as well as different degrees of unsaturation and oxidation on the acyl side chain. In general, they show antibacterial activity and toxicity against shrimp (*Artemia salina*, *Macrobrachium lanchesteri*), fish (*Poecilia reticulata*), and diatoms (*Chaetoceros gracilis*) [350]. Such effects suggest a possible role as chemical defenses against herbivores as well as reduction of biofouling by epiphytic algae and larvae.

2.4.4.3 Polyphenolics

Polyphenolic compounds have been reported from almost all brown algal orders and can be grouped into a single structural class known as the phlorotannins [351]. These metabolites are formed by the polymerization of 1,3,5-trihydroxybenzene (phloroglucinol, **121**) and biosynthesized via the acetate-malonate pathway [351, 352]. They present a wide range of molecular sizes (126–650 kDa) and can be considered counterparts to the terrestrial tannins produced by vascular plants [351, 353]. Brown algal cells store these phenolic secondary metabolites in vesicles called “physodes” [351, 354, 355], and they have been assigned a defensive role against natural enemies due to their function as herbivore deterrents, digestion inhibitors (e.g., reducing the nutritive value of the algal tissue), and antibacterial agents [351, 353, 356–359]. Additionally, phlorotannins protect algal cells from harmful UV radiation (280–320 nm) and may be involved in the chelation of metal ions [351, 360].

Based on the type of structural linkages that result from polymerization of phloroglucinol and also on the number of hydroxyl groups, phlorotannins are divided into six categories: fucols, phlorethols, fucophlorethols, fuhalols, isofuhalols, and eckols (compounds **122–127**) [351, 361, 362]. Eckol (**127**), a trimeric phlorotannin isolated from the cold water kelp *Eisenia arborea* collected near Vancouver Island, Canada, has been shown to be a potent and specific antiplasmin inhibitor as well as a possible lead compound for the development of antithrombotic agents [363–365]. The compound also inhibits α -2 macroglobulin, tyrosinase, human aldose reductase, hyaluronidases, HIV-1 reverse transcriptase

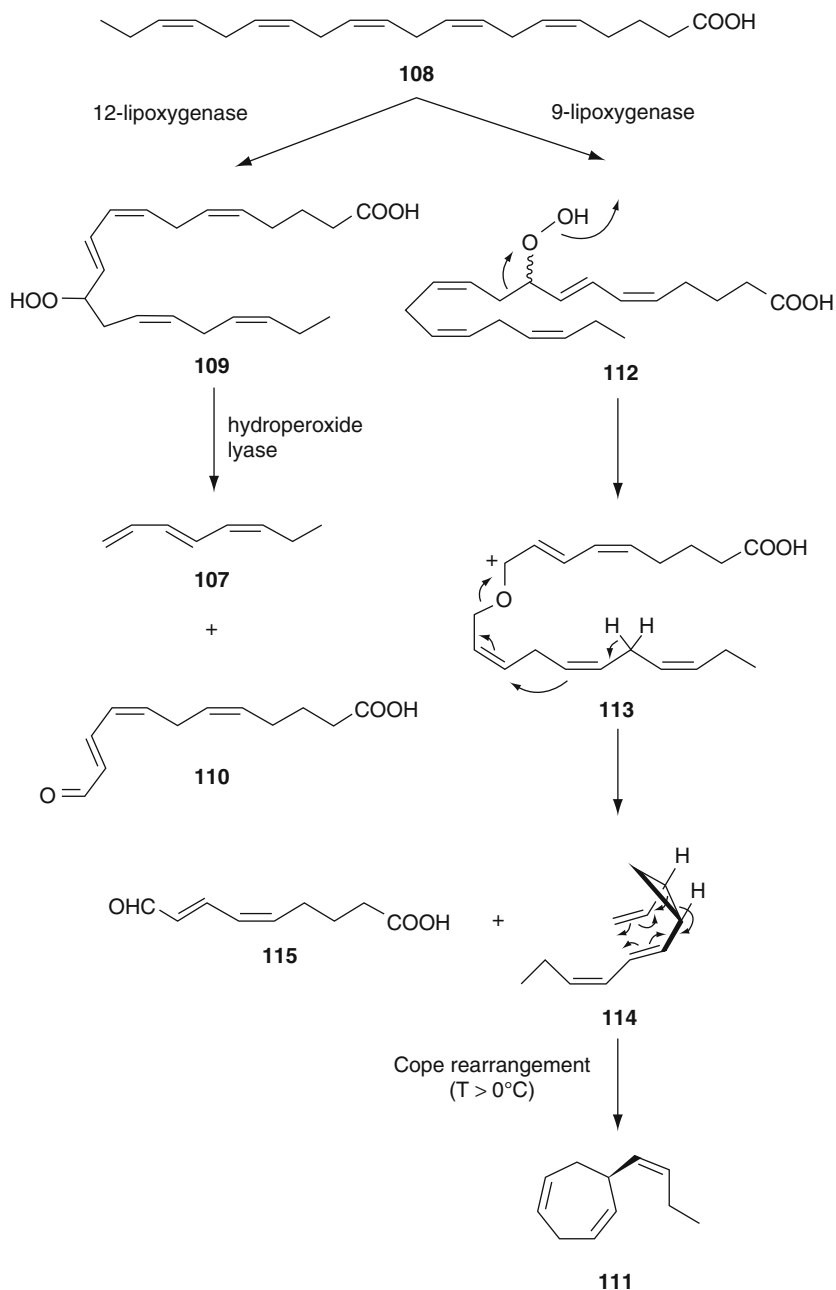
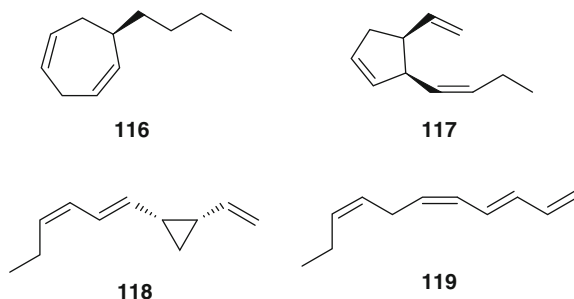


Fig. 2.33 Proposed biosynthesis of brown algal pheromone from (5Z,8Z,11Z,14Z,17Z)-eicosapentaenoic acid involving lipoxygenases

Fig. 2.34 Pheromone hydrocarbons isolated from *E. siliculosus*



and protease, among other therapeutically relevant enzymes [366–370], and exhibits potent antioxidant, bactericidal and algicidal activities [371–374].

2.4.4.4 Terpenes

Among the diterpenes produced by Phaeophyceae (Fig. 2.36, 2.37), pachydictyol A (**128**) was first reported from *Pachydictyon coriaceum*, found along the Pacific coast of California, from Santa Barbara to Baja California [375]. Its structure was determined by NMR and X-ray analyses. Later, specimens of *Dictyota dichotoma*, collected intertidally at Overton on the Bristol Channel (UK), afforded **128** accompanied by three closely related structural analogs [376]. Interestingly, *Dictyota* metabolites have been found to possess high inhibitory activity toward fish predation [377]. Pachydictyol A (**128**) is no exception, and inclusion of this metabolite as 1.0% of an algal dry mass diet led to a 48% reduction in the growth of commonly co-occurring fish (*Diplodus holbrooki*) [377]. After a few days, the fish came to “recognize” the presence of compound **128** and began avoiding algal diets containing pachydictyol A. Thus, fish predation on populations of *Dictyota* is reduced, and consequently, the seaweed becomes a “sanctuary” for smaller animals [378]. Although initially reported as a mild antibiotic, pachydictyol A and several of its analogs were subsequently shown to possess cytotoxic properties [379, 380]. Specifically, **128** has been shown to be cytotoxic against murine fibroblast KA3IT ($IC_{50} < 10 \mu\text{g/mL}$) [381], HeLa, SNU G4, and THP-1 cell lines ($IC_{50} < 100 \mu\text{M}$) [382].

Another representative terpenoid produced by a Phaeophyceae alga is dictyodial (**129**), a major diterpene isolated from the brown algae *Dictyota crenulata* and multiple *Dictyota* collections from other geographically diverse areas (e.g., Oahu, Hawaii; Sonora, Mexico; Aegean Sea, Greece; Oualidia lagoon, Morocco) [383–386]. The compound was initially isolated together with dictyodiol (**130**) and dictyolactone (**131**), and their structures were determined by a combination of NMR and X-ray diffraction experiments [383]. Dictyodial (**129**) and pachydictyol (**128**), among others, are components of an exceptional chemical defense strategy produced by the brown seaweeds *D. ciliata*, *D. menstrualis*, and *D. ciliolata* [387, 388]. These antifouling agents were found responsible for high levels of larval mortality, abnormal development, and reduced growth rates for 3 species of co-occurring invertebrates [388]. Dictyodial (**129**) showed good antibiotic activity against *Staphylococcus aureus* and *Bacillus subtilis*, as well as

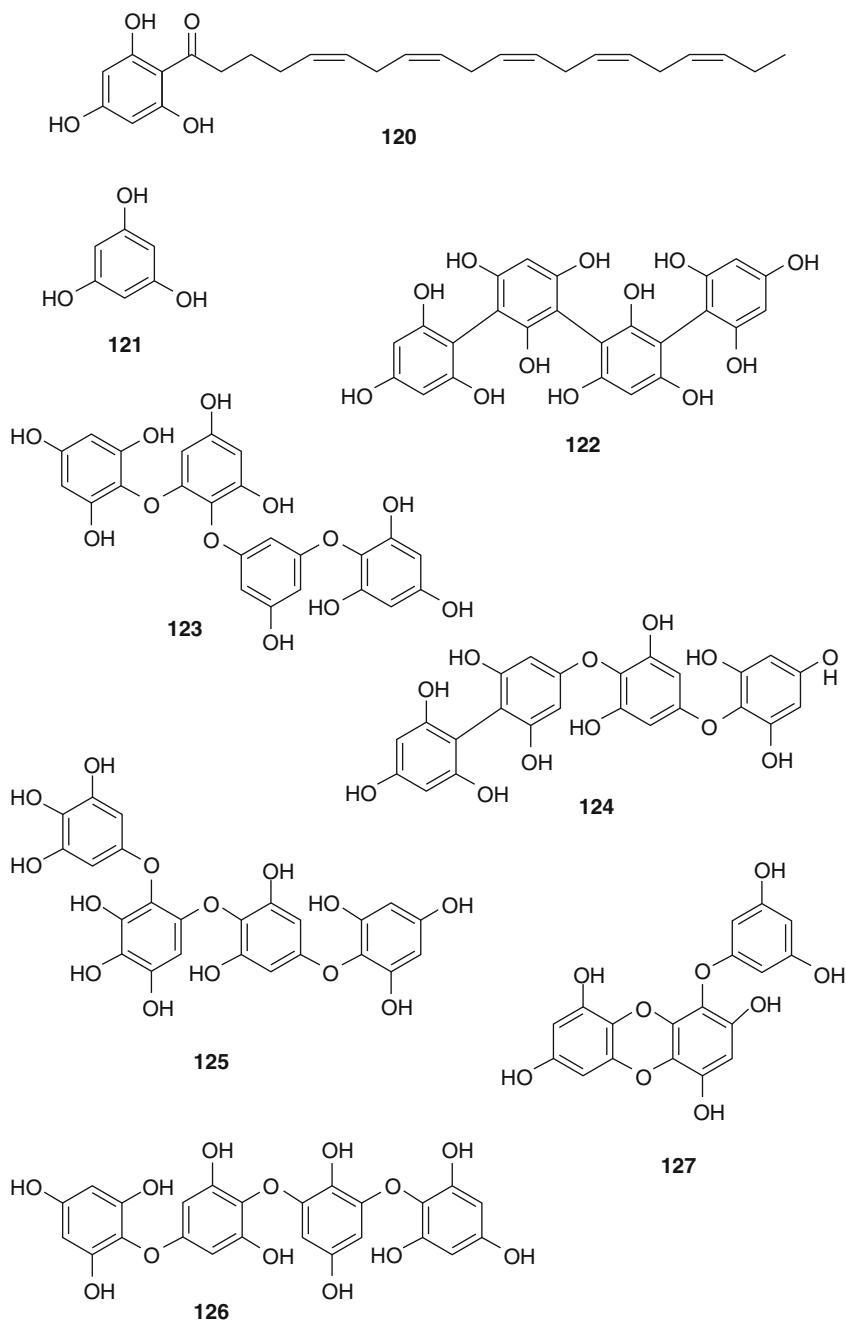


Fig. 2.35 Resorcinol and polyphenols from Phaeophyceae: resorcinol (**120**), phloroglucinol (**121**), tetraphulcinol A (**122**), tetraphloretol B (**123**), fucodiphloretol A (**124**), tetrafulhalol (**125**), tetrafulhalol (**126**), and eckol (**127**)

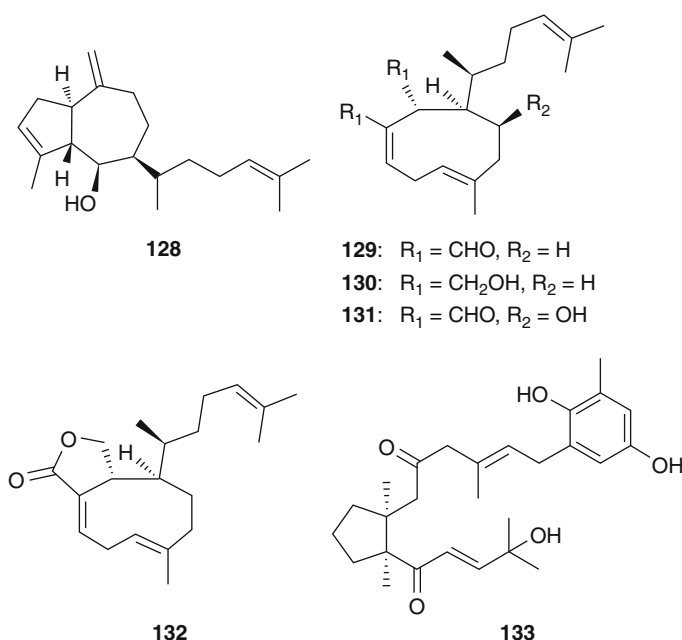


Fig. 2.36 Terpenes from Phaeophyceae

antifungal activity against *Candida albicans* [383]. Furthermore, compound **129** and the closely related 4-hydroxy analog (**132**) inhibited HIV-1 reverse transcriptase with IC_{50} values of 9.2 and 4.3 $\mu\text{g/mL}$, respectively [389].

The meroterpenoid bifurcarenone (**133**), the major biologically active metabolite isolated from the brown seaweed *Bifurcaria galapagensis* (Cystoseiraceae) obtained from the Galapagos Islands, was the first marine natural product to exhibit a monocyclic diterpenoid moiety in combination with a hydroquinone unit [390]. Its planar structure was initially derived via chemical and NMR-based spectroscopic studies, and the compound displayed inhibition of mitotic cell division and moderate antibacterial activity [390]. Total synthesis of the natural product and its enantiomer led to a structural revision and allowed assignment of relative and absolute configurations [391, 392]. Subsequently, a number of bifurcarenone (**133**) structural analogs have been reported from diverse *Cystoseira* species collected around the globe [393].

The tropical brown algae genus *Stypodium* is also a well-known source of polycyclic meroditerpenoids [394–398]. Interestingly, the specific components within a given species vary depending on collection, location, and season [397, 399, 400]. Several of these meroditerpenoids display potent biological activities which may be of biomedical and pharmacological utility.

For example, stypolactone (**134**) [400] and atomaric acid (**135**) [395, 396] are cytotoxic to human lung and colon carcinoma cells, while stypoldione (**136**) and 14-keto stypodiol diacetate are inhibitors of microtubule assembly [401–403]. Stypoldione (**136**) [394], epistypodiol (**137**), stypodiol (**138**), stypotriol (**139**), and

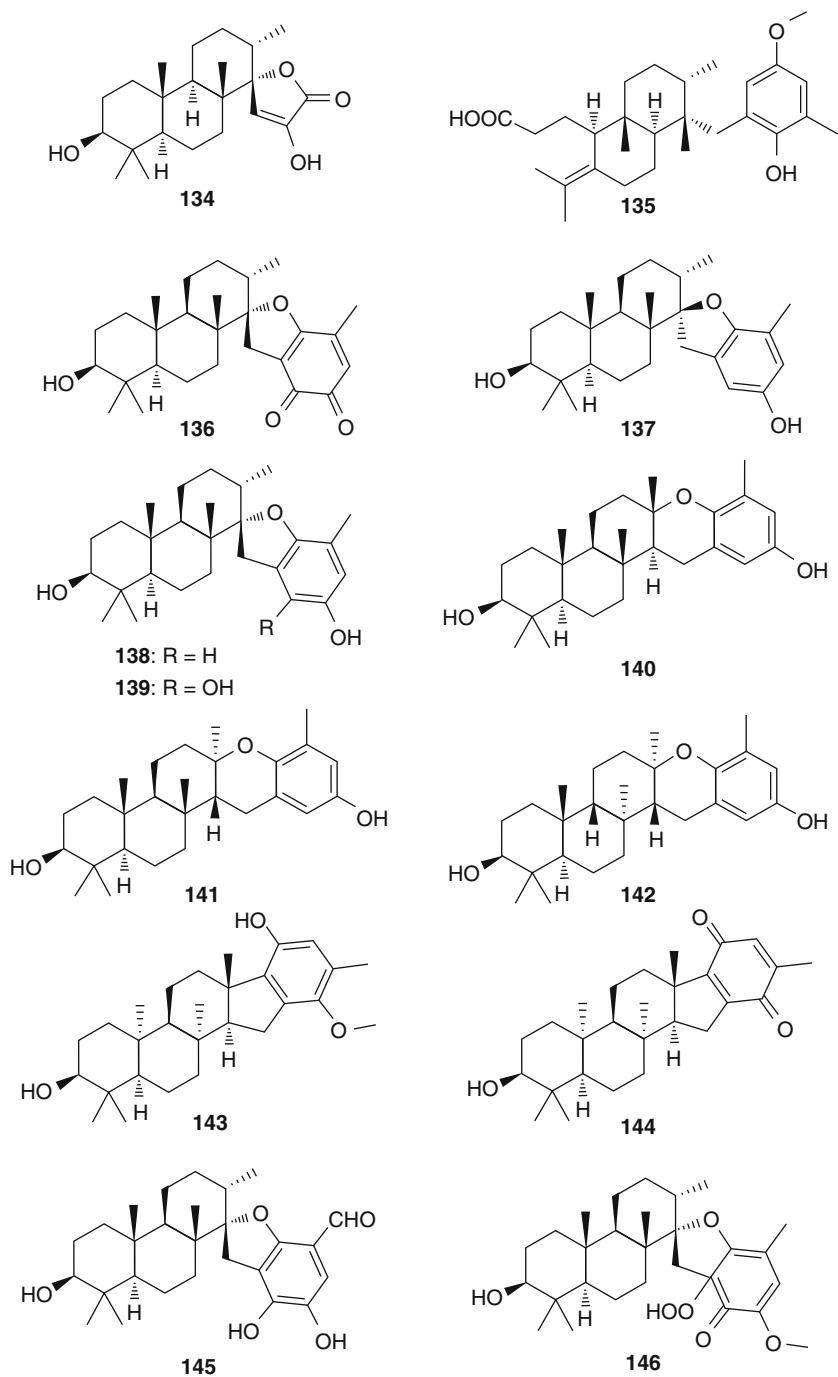
taondiol (**140**) are ichthyotoxic [395, 396]; diacetylepitaondiol has a negative inotropic effect on isolated rat atrium [404]; and stypoquinonic acid and atomaric acid inhibit tyrosine kinase [405]. Isoepitaondiol (**141**) is reported to have insecticidal activity [406]. In the case of 2 β ,3 α -epitaondiol (**142**), flabellinol (**143**), flabellinone (**144**), stypotriolaldehyde (**145**), and stypohydroperoxide (**146**), isolated from *Stypopodium flabelliforme* collected in Papua New Guinea, it has been suggested that their ichthyotoxic and cytotoxic activities are at least in part due to a blockade of the voltage-gated sodium channel (VGSC) [407] (Fig. 2.37).

The biosyntheses of these metabolites may occur via the cyclization of 2-(2,3-epoxygeranylgeranyl)-6-methylhydroquinone (**147**), in a manner reminiscent of sterol cyclizations [408]. For example, to produce 2 β ,3 α -epitaondiol (**142**), the terpene chain must be prefolded into a chair-boat-chair conformation with attack by the ortho-positioned phenolic hydroxy group occurring from the Re face (see Fig. 2.38). To produce flabellinol (**143**) and flabellinone (**144**), the terpene chain is predicted to be prefolded into a chair conformation for rings A and C and a twist boat for ring B. The five-membered carbocycle is proposed to be formed by electron shifts initiated from the *meta*-phenolic hydroxyl function, extending through the *ortho*-unsubstituted position and attacking the Si face of the C-2/C-3 double bond (see Fig. 2.38). Formation of the hydroperoxide in **146** would logically occur through the addition of singlet oxygen to stypotriol (**139**). In general, acyclic terpene folding patterns should be flexible during the biosynthesis so as to give metabolites in both the taondiol and epitaondiol stereochemical classes [407]. Additionally, quenching of the carbocations produced at the termini of terpene cyclizations can occur through direct interaction of the phenol functionality, producing benzofuran or benzopyran rings. Alternatively, quenching may occur through electron shifts emanating from the phenol function but involving formation of a five-membered carbocyclic ring. Finally, further oxidation of the aromatic ring leads to biologically reactive functionalities, such as aldehydes and hydroperoxides [407].

2.4.4.5 Oxylipins

Several members of the brown algae order Laminariaceae produce a suite of cyclopentane-containing oxylipins presumably via lipoxygenase-initiated biosynthetic routes (see below). The first reported family of such brown algal oxylipins, named the ecklonialactones, was isolated from *Ecklonia stolonifera* collected in Tsuruoka, Japan [409, 410]. Their structures were determined by spectral and chemical methods, as well as X-ray crystallography. Ecklonialactone A (**151**) showed weak feeding-deterrent activity against species of abalone of the genus *Haliotis* [409].

Subsequently, egregiachlorides A (**153**), B (**154**), and olefin analog **155** were identified via NMR and mass spectrometric methods from extracts of the Oregon kelp, *Egregia menziesii*, together with ecklonialactones A (**151**) and B (**152**), among others [411, 412]. The co-occurrence of these two families of oxylipins and their similar structural features suggest a common biogenetic origin, analogous to prostaglandin biosynthesis but presumably initiated by a lipoxygenase showing ω 6 specificity on stearidonic acid (**148**) [412] (Fig. 2.39). Subsequent formation of

**Fig. 2.37** Meroterpenes from Phaeophyceae

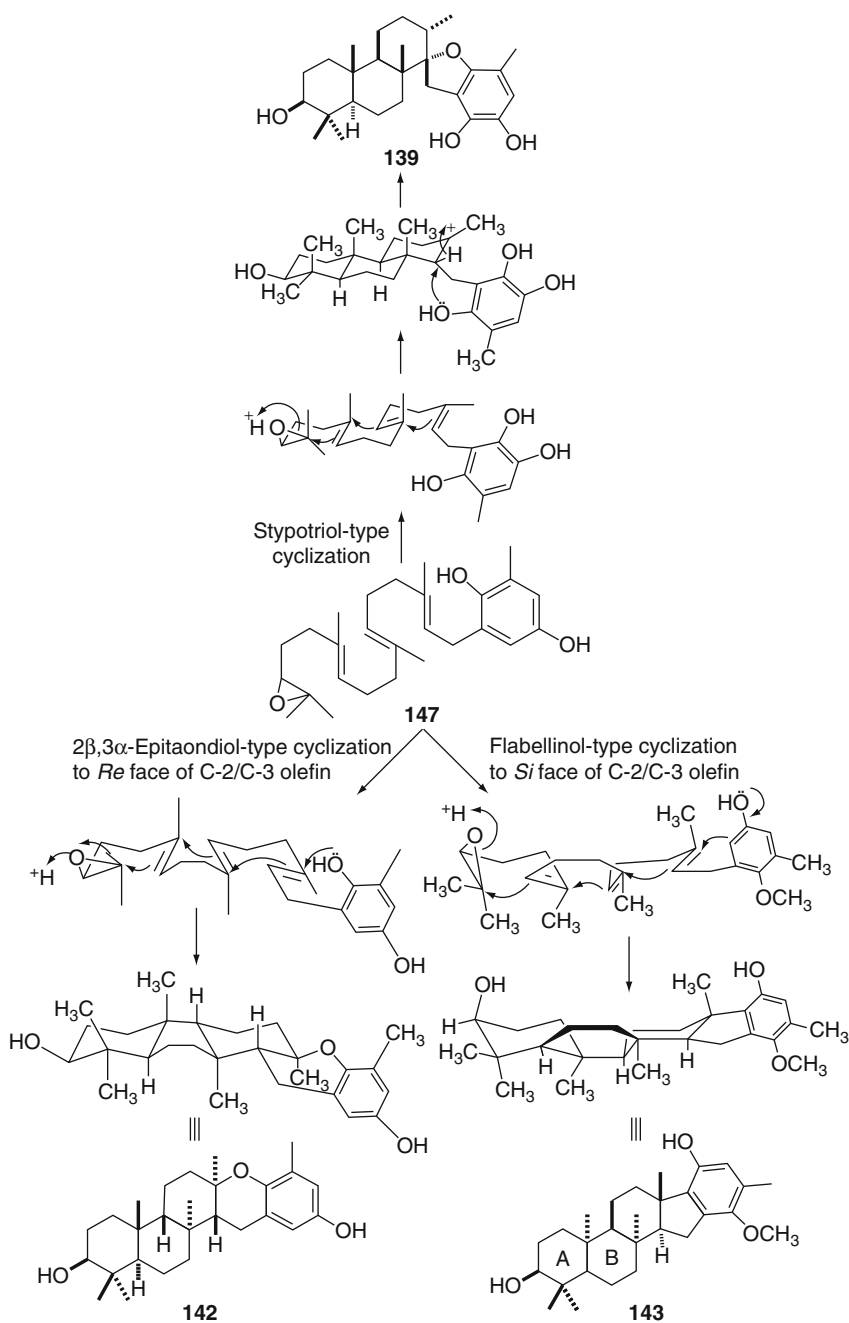


Fig. 2.38 Proposed biosynthesis of brown algal terpenes, stypotriol (**139**), 2β,3α-epitaondiol (**142**), and flabellinol (**143**) from 2-(2,3-epoxygeranylgeranyl)-6-methylhydroquinone (**147**) involving various cyclizations

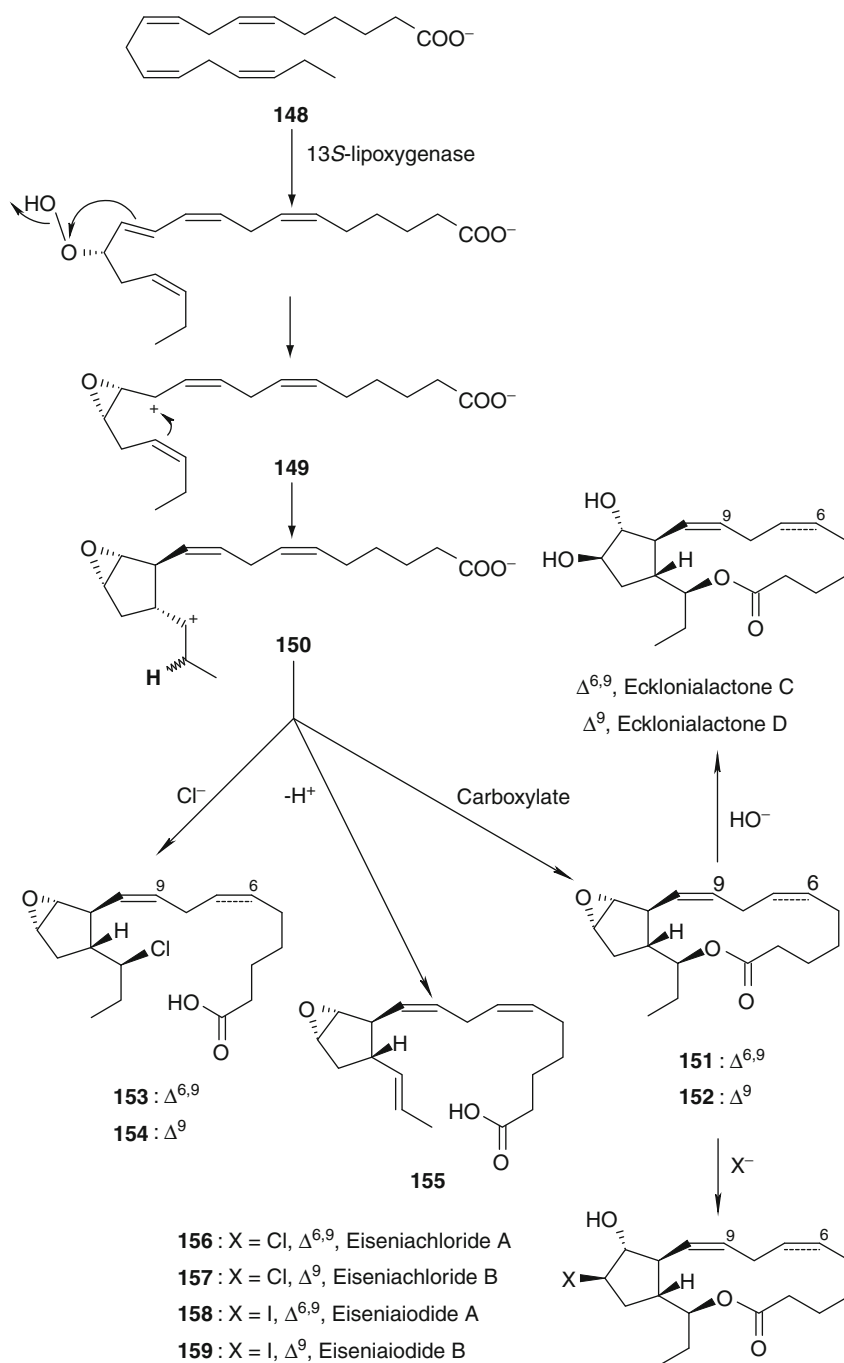


Fig. 2.39 Proposed biogenesis of various brown algal oxylipins from stearidonic acid (148)

Fig. 2.40 Structure of marine sediment-derived triterpene hydrocarbon

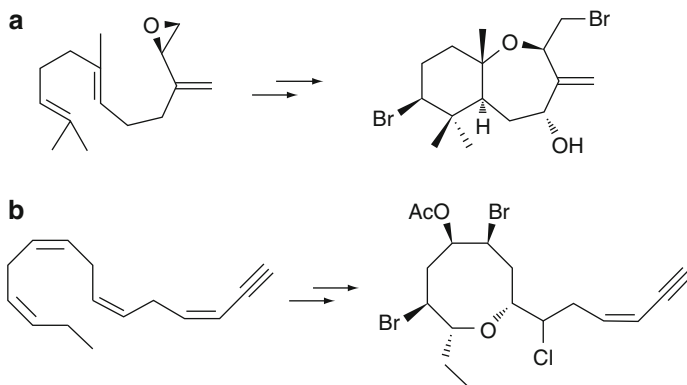
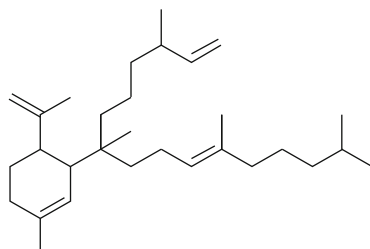


Fig. 2.41 Red algal metabolites and their biosynthetic precursors

a pivotal epoxy cation intermediate (**149**) could lead to a secondary cyclopentyl cation (**150**). Trapping of this latter intermediate could occur either with chloride or carboxylate addition, or by the loss of a proton. Further modification at the 3-membered epoxide ring leads to additional ecklonialactones and to a series of halogenated macrolactones, the most recent members of this oxylipin class. This latter family of oxylipins was reported from the brown seaweed *Eisenia bicyclis*, often visible around the coasts of Japan [413] (Fig. 2.39). In addition to the new eiseniachlorides and eiseniaiodides, the alga was found to contain two new olefin analogs as well as several ecklonialactones and egregiachloriades A–C, further supporting their common biogenesis. Compounds **156–159** showed weak antibacterial activity [413].

2.5 Conclusions

The natural products of marine algae and cyanobacteria are wonderfully diverse, essentially representing all molecular classes such as terpenes, fatty acids, alkaloids, peptides, polyketides, and polyphenolics. Moreover, many of these scaffolds are decorated by the producing organisms with unique functional groups, and most remarkably, many possess covalently attached halogen atoms such as bromine and

chlorine. A necessary consequence of this broad chemical diversity is that the biological properties of marine algal and cyanobacterial metabolites are in many different arenas, both in terms of their natural function as well as their potential biomedical application. For example, while many of the above discussed metabolites have been shown or are predicted to have antipredatory roles, a function that seems understandable in light of the benthic and non-motile life history of most of these organisms, other natural products have protective and defensive functions against microbial life forms, whereas others have been shown to have roles in intraspecies or interspecies communication phenomena. Thus, while much has been learned about the organic chemistry of marine algal and cyanobacterial natural products, and in some isolated cases, knowledge developed of their natural role, biomedical properties, and biosynthesis, many more questions have been raised in these studies, and there are many exciting frontiers in the areas of molecular pharmacology and ecology, marine biotechnology, and development of genomic level understanding of these organisms, their evolution and their interactions with one another.

2.6 Study Questions

1. *Cyanobacteria* Cyanobacteria, along with heterotrophic bacteria and fungi, are commonly associated with sponges. For example, the filamentous cyanobacterium *Oscillatoria spongellae* is abundant in tissues of the sponge *Dysidea herbacea*, and cyanobacterial-like compounds have been isolated from field collections of the sponge. Outline five (5) conceptual approaches you might use to demonstrate the biosynthesis of a natural product in a microbial subpopulation that is present in a complex community such as a sponge.
2. *Dinoflagellates* Propose a chemically rationale mechanism for the biosynthesis of brevetoxin A.
3. *Diatoms* Propose a chemically rationale mechanism for the biosynthesis of the marine sediment-derived triterpene hydrocarbon shown below (Fig. 2.40).
4. *Chrysophytes* The chrysophyte alga *Chrysosphaerum taylori* has been found to produce both the chrysosphaerins and hormothamnione. Are these metabolites biogenetically related? If so, propose a plausible biogenetic pathway for these compounds.
5. *Prymnesiophytes* Both prymnesin-1 and -2 possess structural motifs similar to those found in dinoflagellate natural products. What are the structural differences? Which biosynthetic pathways are behind those differences? Do they provide a sense of evolutionary divergence between prymnesiophytes and dinoflagellates?
6. *Chlorophyta* Udoteal, a fish feeding-deterrent terpenoid produced by *Udotea flabellum*, was chemically converted into udoteatrial under ethanol preservation. Propose a rationale mechanism for this chemical conversion.
7. *Rhodophyta* Propose a biogenetic pathway from the precursors shown in each case to the products formed. Show all electron and atom migrations as distinct

steps. Oxidations with molecular oxygen may be involved. In each case, outline a possible biosynthesis of the precursor as well (Fig. 2.41).

8. *Phaeophytes* Which class of brown algal metabolites is considered to be the counterpart to tannins produced by vascular plants? Why and for what purpose?

References

1. Leflaive J, Ten-Hage L (2007) Algal and cyanobacterial secondary metabolites in freshwaters: a comparison of allelopathic compounds and toxins. *Freshwater Biol* 52:199–214
2. Jones AC, Gu L, Sorrels CM, Sherman DH, Gerwick WH (2009) New tricks from ancient algae: natural products biosynthesis in marine cyanobacteria. *Curr Opin Chem Biol* 13:216–223
3. Tan LT (2010) Filamentous tropical marine cyanobacteria: a rich source of natural products for anticancer drug discovery. *J Appl Phycol* 22:659–676
4. Blunt JW, Copp BR, Munro MHG, Northcote PT, Prinsep MR (2011) Marine natural products. *Nat Prod Rep* 28:196–268
5. Bold HC, Wynne MJ (1978) Introduction to the algae; structure and reproduction. Prentice-Hall, Englewood Cliffs
6. Engene N, Coates RC, Gerwick WH (2010) 16S rRNA Gene heterogeneity in the filamentous marine cyanobacterial genus *Lyngbya*. *J Phycology* 46:591–601
7. Castenholz RW, Rippka R, Herdman M (2001) Phylum BX cyanobacteria. In: Garrity GM, Boone DR, Castenholz RW (eds) *Bergey's manual of systematic bacteriology*, Vol 1. Springer, New York
8. Erwin PM, Thacker RW (2008) Phototrophic nutrition and symbiont diversity of two Caribbean sponge-cyanobacteria symbioses. *Mar Ecol Prog Ser* 362:139–147
9. MarinLit Database. Department of Chemistry, University of Canterbury. <http://www.chem.canterbury.ac.nz/marinlit/marinlit.shtml>. Accessed 17 Nov 2011
10. Ishida T, Watanabe MM, Sugiyama J, Yokota A (2001) Evidence for polyphyletic origin of the members of the orders of Oscillatoriales and Pleurocapsales as determined by 16S rDNA analysis. *FEMS Microbiol Lett* 201:79–82
11. Tidgewell K, Clark BT, Gerwick WH (2010) The natural products chemistry of cyanobacteria. In: Moore B, Crews P (eds) *Comprehensive natural products chemistry*, 2nd edn. Elsevier, Oxford
12. Tan LT (2007) Bioactive natural products from marine cyanobacteria for drug discovery. *Phytochem* 68:954–979
13. van Wagoner RM, Drummond AK, Wright JLC (2007) Biogenetic diversity of cyanobacterial metabolites. *Adv Appl Microbiol* 61:89–217
14. Jones AC, Monroe EA, Eisman EB, Gerwick L, Sherman DH, Gerwick WH (2010) The unique mechanistic transformations involved in the biosynthesis of modular natural products from marine cyanobacteria. *Nat Prod Rep* 27:1048–1065
15. Grindberg RV, Shuman CF, Sorrels CM, Wingerd J, Gerwick WH (2008) Neurotoxic alkaloids from cyanobacteria. In: Fattorusso E, Tagliatela-Scafati O (eds) *Modern alkaloids, structure, isolation, synthesis and biology*. Wiley-VCH Verlag GmbH & Co, Weinheim
16. Klein D, Braekman JC, Daloze D, Hoffmann L, Demoulin V (1997) Lyngbyaloside, a novel 2,3,4-tri-*O*-methyl-6-deoxy- α -mannopyranoside macrolide from *Lyngbya bouillonii* (cyanobacteria). *J Nat Prod* 60:1057–1059
17. Wu M, Milligan KE, Gerwick WH (1997) Three new malyngamides from the marine cyanobacterium *Lyngbya majuscula*. *Tetrahedron* 53:15983–15990
18. Paquette LA, Yotsu-Yamashita M (2007) Polycavernosides. In: Botana LM (ed) *Phycotoxins: chemistry and biochemistry*. Blackwell, Ames

19. Simonin P, Juergens UJ, Rohmer M (1992) 35-O-beta-6-Amino-6-deoxyglucopyranosyl bacteriohopanetetrol, a novel triterpenoid of the hopane series from the cyanobacterium *Synechocystis* sp. PCC 6714. *Tetrahedron Lett* 33:3629–3632
20. Cardellina JH II, Marner FJ, Moore RE (1979) Seaweed dermatitis: structure of lyngbyatoxin A. *Science* 204:193–195
21. Edwards DJ, Gerwick WH (2004) Lyngbyatoxin biosynthesis: sequence of biosynthetic gene cluster and identification of a novel aromatic prenyltransferase. *J Am Chem Soc* 126:11432–11433
22. Sato N, Wada H (2009) Lipid biosynthesis and its regulation in cyanobacteria. In: Wada H, Murata N (eds) *Advances in photosynthesis and respiration*, 30 (Lipids in photosynthesis essential and regulatory function). Springer, Dordrecht
23. Sitachitta N, Gerwick WH (1998) Grenadadiene and grenadamide, cyclopropyl-containing fatty acid metabolites from the marine cyanobacterium *Lyngbya majuscula*. *J Nat Prod* 61:681–684
24. Moore RE, Blackman AJ, Cheuk CE, Mynderse JS, Matsumoto GK, Clardy J, Woodard RW, Craig JC (1984) Absolute stereochemistries of the aplysiatoxins and oscillatoxin A. *J Org Chem* 49:2484–2489
25. Osborne NJ, Shaw GR, Webb PM (2007) Health effects of recreational exposure to Moreton Bay, Australia waters during a *Lyngbya majuscula* bloom. *Environ Int* 33:309–314
26. Palenik B, Ren Q, Dupont CL, Myers GS, Heidelberg JF, Badger JH, Madupu R, Nelson WC, Brinkac LM, Dodson RJ, Durkin AS, Daugherty SC, Sullivan SA, Khouri H, Mohamoud Y, Halpin R, Paulsen IT (2006) Genome sequence of *Synechococcus* CC9311: insights into adaptation to a coastal environment. *Proc Natl Acad Sci USA* 103:13555–13559
27. Kishi Y, Rando RR (1998) Structural basis of protein kinase C activation by tumor promoters. *Acc Chem Res* 31:163–172
28. Singh IP, Milligan KE, Gerwick WH (1999) Tanikolide, a toxic and antifungal lactone from the marine cyanobacterium *Lyngbya majuscula*. *J Nat Prod* 62:1333–1335
29. Gutiérrez M, Andrianasolo EH, Shin WK, Goeger DE, Yokochi A, Schemies J, Jung M, France D, Cornell-Kennon S, Lee E, Gerwick WH (2009) Structural and synthetic investigations of tanikolide dimer, a SIRT2 selective inhibitor, and tanikolide seco acid from the madagascar marine cyanobacterium *Lyngbya majuscula*. *J Org Chem* 74:5267–5275
30. Gruenewald J, Marahiel MA (2006) Chemoenzymatic and template-directed synthesis of bioactive macrocyclic peptides. *Microbiol Mol Biol Rev* 70:121–146
31. Donia MS, Ravel J, Schmidt EW (2008) A global assembly line for cyanobactins. *Nat Chem Biol* 4:341–343
32. Taori K, Paul VJ, Luesch H (2008) Kempopeptins A and B, serine protease inhibitors with different selectivity profiles from a marine cyanobacterium, *Lyngbya* sp. *J Nat Prod* 71:1625–1629
33. Linington RG, Edwards DJ SCF, McPhail KL, Matainaho T, Gerwick WH (2008) Symplocamide A, a potent cytotoxin and chymotrypsin inhibitor from the marine cyanobacterium *Symploca* sp. *J Nat Prod* 71:22–27
34. Ersmark K, Del Valle JR, Hanessian S (2008) Chemistry and biology of the aeruginosin family of serine protease inhibitors. *Angew Chem Int Ed* 47:1202–1223
35. Rouhiainen L, Paulin L, Suomalainen S, Hyytiäinen H, Buikema W, Haselkorn R, Sivonen K (2000) Genes encoding synthetases of cyclic depsipeptides, anabaenopeptilides, in *Anabaena* strain 90. *Mol Microbiol* 37:156–167
36. Long PF, Dunlap WC, Battershill CN, Jaspars M (2005) Shotgun cloning and heterologous expression of the patellamide gene cluster as a strategy to achieving sustained metabolite production. *ChemBioChem* 6:1760–1765
37. Schmidt EW, Nelson JT, Rasko DA, Sudek S, Eisen JA, Haygood MG, Ravel J (2005) Patellamide A and C biosynthesis by a microcin-like pathway in *Prochloron didemni*, the cyanobacterial symbiont of *Lissoclinum patella*. *Proc Natl Acad Sci USA* 102:7315–7320

38. Rashid MA, Gustafson KR, Cardellina JH II, Boyd MR (1995) Patellamide F, a new cytotoxic cyclic peptide from the colonial ascidian *Lissoclinum patella*. *J Nat Prod* 58:594–597
39. McIntosh JA, Schmidt EW (2010) Marine molecular machines: heterocyclization in cyanobactin biosynthesis. *ChemBioChem* 11:1413–1421
40. Li B, Sher D, Kelly L, Shi Y, Huang K, Knerr PJ, Joewono I, Rusch D, Chisholm SW, van der Donk W (2010) Catalytic promiscuity in the biosynthesis of cyclic peptide secondary metabolites in planktonic marine cyanobacteria. *Proc Nat Acad Sci USA* 107:10430–10435
41. Hooper GJ, Orjala J, Schatzman RC, Gerwick WH (1998) Carmabin A and B, new lipopeptides from the Caribbean cyanobacterium *Lyngbya majuscula*. *J Nat Prod* 61:529–533
42. McPhail KL, Correa J, Linington RG, Gonzalez J, Ortega-Barria E, Capson TL, Gerwick WH (2007) Antimalarial linear lipopeptides from a Panamanian strain of the marine cyanobacterium *Lyngbya majuscula*. *J Nat Prod* 70:984–988
43. Gerwick WH, Proteau PJ, Nagle DG, Hamel E, Blokhin A, Slate D (1994) Structure of curacin A, a novel antimitotic, antiproliferative, and brine shrimp toxic natural product from the marine cyanobacterium *Lyngbya majuscula*. *J Org Chem* 59:1243–1245
44. Blokhin AV, Yoo H-D, Geraldts RS, Nagle DG, Gerwick WH, Hamel E (1995) Characterization of the interaction of the marine cyanobacterial natural product curacin A with the colchicine site of tubulin and initial structure-activity studies with analogs. *Mol Pharmacol* 48:523–531
45. Wipf P, Reeves JT, Balachandran R, Day BW (2002) Synthesis and biological evaluation of structurally highly modified analogues of the antimitotic natural product curacin A. *J Med Chem* 45:1901–1917
46. Chang Z, Sitachitta N, Rossi JV, Roberts MA, Flatt PM, Jia J, Sherman DH, Gerwick WH (2004) Biosynthetic pathway and gene cluster analysis of curacin A, an anti-tubulin natural product from the tropical marine cyanobacterium *Lyngbya majuscula*. *J Nat Prod* 67:1356–1367
47. Gu L, Wang B, Kulkarni A, Geders TW, Grindberg RV, Gerwick L, Håkansson K, Wipf P, Smith JL, Gerwick WH, Sherman DH (2009) Metamorphic enzyme assembly in polyketide diversification. *Nature* 459:731–735
48. Neumann CS, Fujimori DG, Walsh CT (2008) Halogenation strategies in natural product biosynthesis. *Chem Biol* 15:99–109
49. Gu L, Wang B, Kulkarni A, Gehret JJ, Lloyd KR, Gerwick L, Gerwick WH, Wipf P, Hakansson K, Smith JL, Sherman DH (2009) Polyketide decarboxylative chain termination preceded by O-sulfonation in curacin A biosynthesis. *J Am Chem Soc* 131:16033–16035
50. Pettit GR, Day JF, Hartwell JL, Wood HB (1970) Antineoplastic components of marine animals. *Nature* 227:962–963
51. Patel S, Keohan ML, Saif MW, Rushing D, Baez L, Feit K, DeJager R, Anderson S (2006) Phase II study of intravenous TZT-1027 in patients with advanced or metastatic soft-tissue sarcomas with prior exposure to anthracycline-based chemotherapy. *Cancer* 107:2881–2887
52. Luesch H, Moore RE, Paul VJ, Mooberry SL, Corbett TH (2001) Isolation of dolastatin 10 from the marine cyanobacterium *Symploca* species VP642 and total stereochemistry and biological evaluation of its analogue symplostatin 1. *J Nat Prod* 64:907–910
53. Luesch H, Yoshida WY, Moore RE, Paul VJ, Corbett TH (2001) Total structure determination of apratoxin A, a potent novel cytotoxin from the marine cyanobacterium *Lyngbya majuscula*. *J Am Chem Soc* 123:5418–5423
54. Liu Y, Law BK, Luesch H (2009) Apratoxin A reversibly inhibits the secretory pathway by preventing cotranslational translocation. *Mol Pharmacol* 76:91–104
55. Shen S, Zhang P, Lovchik MA, Li Y, Tang L, Chen Z, Zeng R, Ma D, Yuan J, Yu Q (2009) Cyclodepsipeptide toxin promotes the degradation of Hsp90 client proteins through chaperone-mediated autophagy. *J Cell Biol* 185:629–639

56. Doi T, Numajiri Y, Munakata A, Takahashi T (2006) Total synthesis of apratoxin A. *Org Lett* 8:531–534
57. Tidgewell K, Engene N, Byrum T, Media J, Valeriote FA, Gerwick WH (2010) Diversification of a modular natural product pathway: production of apratoxins F and G, two cytotoxic cyclic depsipeptides from a Palmyra collection of *Lyngbya bouillonii*. *ChemBioChem* 11:1458–1466
58. Grindberg RV, Ishoey T, Brinza D, Esquenazi E, Coates RC, Liu W, Gerwick L, Dorrestein PC, Pevzner P, Lasken R, Gerwick WH (2011) Single cell genome amplification accelerates natural product pathway characterization from complex microbial assemblages. *PLoS One* 6(4):e18565
59. Kanchan T, Paul VJ, Luesch H (2008) Structure and activity of largazole, a potent antiproliferative agent from the Floridian marine cyanobacterium *Symploca* sp. *J Am Chem Soc* 130:1806–1807
60. Carmeli S, Moore RE, Patterson GML (1991) Mirabazoles, minor tantazole-related cytotoxins from the terrestrial blue-green alga *Scytonema mirabile*. *Tetrahedron Lett* 32:2593–2596
61. Li WI, Berman FW, Okino T, Yokokawa F, Shioiri T, Gerwick WH, Murray TF (2001) Antillatoxin is a marine cyanobacterial toxin that potently activates voltage-gated sodium channels. *Proc Natl Acad Sci USA* 98:7599–7604
62. Orjala J, Nagle DG, Hsu V, Gerwick WH (1995) Antillatoxin, an exceptionally ichthyotoxic cyclic lipopeptide from the tropical cyanobacterium *Lyngbya majuscula*. *J Am Chem Soc* 117:8281–8282
63. Cao Z, Gerwick WH, Murray TF (2010) Antillatoxin is a sodium channel activator that displays unique efficacy in heterologously expressed rNav1.2, rNav1.4 and rNav1.5 alpha subunits. *BMC Neurosci* 11:154
64. Nagle DG, Paul VJ (1999) Production of secondary metabolites by filamentous tropical marine cyanobacteria: ecological functions of the compounds. *J Phycol* 35:1412–1421
65. Tachibana K, Scheuer PJ, Tsukitani Y, Kikuchi H, Engen DV, Clardy J, Gopichand Y, Schmitz FJ (1981) Okadaic acid, a cytotoxic polyether from two marine sponges of the genus *Halichondria*. *J Am Chem Soc* 103:2469–2471
66. Murakami M, Oshima Y, Yasumoto T (1982) Identification of okadaic acid as a toxic component of a marine dinoflagellate *Prorocentrum lima*. *B Jpn Soc Sci Fish* 48:69–72
67. Yasumoto T, Oshima Y, Sugawara W, Fukuyo Y, Oguri H, Igarashi T, Fujita N (1980) Identification of *Dinophysis fortii* as the causative organisms of diarrhetic shellfish poisoning. *Nippon Suisan Gakk* 46:1405–1411
68. Bialojan C, Takai A (1988) Inhibitory effect of a marine-sponge toxin, okadaic acid, on protein phosphatases. *Biochem J* 256:283–290
69. Haystead TAJ, Sim ATR, Carling D, Honnor RC, Tsukitani Y, Cohen P, Hardie DG (1989) Effects of the tumour promoter okadaic acid on intracellular protein phosphorylation and metabolism. *Nature* 337:78–81
70. Shimizu Y (1978) Dinoflagellate toxins. In: Scheuer PJ (ed) *Marine natural products*. Academic, New York
71. Lin YY, Risk M, Ray SM, van Engen D, Clardy J, Golik J, James JC, Nakanishi K (1981) Isolation and structure of brevetoxin B from the “red tide” dinoflagellate *Ptychodiscus brevis* (*Gymnodinium breve*). *J Am Chem Soc* 103:6773–6775
72. Sagir Ahmed MD, Arakawa O, Onoue Y (1995) Toxicity of cultured *Chattonella marina*. In: Lassus P, Arzul G, Erhard E, Gentien P, Marcaillou C (eds) *Harmful marine algal blooms*. Lavoisier, Paris
73. Khan S, Arakawa O, Onoue Y (1997) Neurotoxins in a toxic red tide of *Heterosigma akashiwo* (Raphidophyceae) in Kagoshima Bay, Japan. *Aquac Res* 28:9–14
74. Hallegraeff GM, Munday BL, Baden DG, Whitney PL (1998) *Chattonella marina* raphidophyte bloom associated with mortality of cultured bluefin tuna (*Thunnus accoyii*) in south Australia. In: Reguera B, Blanco J, Fernandez M, Wyatt T (eds) *Harmful algae*,

- Proceedings of the VIII international conference on harmful algae. Xunta de Galicia/IOC of UNESCO, Vigo, Spain
75. Alam M, Trieff NM, Ray SM, Hudson JE (1975) Isolation and partial characterization of toxins from the dinoflagellate *Gymnodinium breve* Davis. *J Pharm Sci* 64:865–867
 76. Shimizu Y, Chou HN, Bando H, van Duyn GD, Clardy J (1986) Structure of brevetoxin A (GB-1 toxin), the most potent toxin in the Florida red tide organism *Gymnodinium breve* (*Ptychodiscus brevis*). *J Am Chem Soc* 108:514–515
 77. Nicolaou KC, Yang Z, Shi G-Q, Gunzner JL, Agrios KA, Gärtner P (1998) Total synthesis of brevetoxin A. *Nature* 392:264–269
 78. Baden DG (1983) Marine food-born dinoflagellate toxins. *Int Rev Cytol* 82:99–150
 79. Kirkpatrick B, Fleming LE, Squicciarini D, Backer LC, Clark R, Abraham W, Benson J, Cheng YS, Johnson D, Pierce R, Zaias J, Bossart GD, Baden DG (2004) Literature review of Florida red tide: implications for human health effects. *Harmful Algae* 3:99–115
 80. Morris PD, Campbell DS, Taylor TJ, Freeman JJ (1991) Clinical and epidemiological features of neurotoxic shellfish poisoning in North Carolina. *Am J Public Health* 81:471–474
 81. Baden DG, Adams DJ (2000) Brevetoxins: chemistry, mechanism of action, and methods of detection. In: Botana LM (ed) *Seafood and freshwater toxins: pharmacology, physiology and detection*. Marcel Dekker, New York
 82. Cheng YS, Zhou Y, Irvin CM, Pierce RH, Naar J, Backer LC, Fleming LE, Kirkpatrick B, Baden DG (2005) Characterization of marine aerosol for assessment of human exposure to brevetoxins. *Environ Health Perspect* 113:638–643
 83. Sandler L (2010) Fish tale. *New York Times*. April 9, 2010
 84. Terao K (2000) Ciguatera toxins: toxicology. In: Botana LM (ed) *Seafood and freshwater toxins: pharmacology, physiology and detection*. Marcel Dekker, New York
 85. Murata M, Legrand AM, Ishibashi Y, Yasumoto T (1989) Structures of ciguatoxin and its congener. *J Am Chem Soc* 111:8929–8931
 86. Murata M, Legrand AM, Ishibashi Y, Fukui M, Yasumoto T (1990) Structures and configurations of ciguatoxin from the moray eel *Gymnothorax javanicus* and its likely precursor from the dinoflagellate *Gambierdiscus toxicus*. *J Am Chem Soc* 112:4380–4386
 87. Satake M, Morohashi A, Oguri H, Oishi T, Hirama M, Harada N, Yasumoto T (1997) The absolute configuration of ciguatoxin. *J Am Chem Soc* 119:11325–11326
 88. Yasumoto T, Nakajima I, Bagnis R, Adachi R (1977) Finding of a dinoflagellate as a likely culprit of ciguatera. *B Jpn Soc Sci Fish* 43:1021–1026
 89. Legrand AM (1999) Ciguatera toxins: origin, transfer through the food chain and toxicity to humans. In: Reguera B, Blanco J, Fernandez M, Wyatt T (eds) *Harmful algae, Proceedings of the VIII international conference on harmful algae*. Xunta de Galicia/IOC of UNESCO, Vigo, Spain
 90. Guzman-Perez SE, Park DL (2000) Ciguatera toxins: chemistry and diction. In: Botana LM (ed) *Seafood and freshwater toxins: pharmacology, physiology and detection*. Marcel Dekker, New York
 91. Lewis RJ, Molgo J, Adams DJ (2000) Pharmacology of toxins involved in ciguatera and related fish poisonings. In: Botana LM (ed) *Seafood and freshwater toxins: pharmacology, physiology and detection*. Marcel Dekker, New York
 92. Lewis RJ, Sellin M, Poli MA, Norton RS, MacLeod JK, Sheil MM (1991) Purification and characterization of ciguatoxins from moray eel (*Lycodontis javanicus*, Muraenidae). *Toxicon* 29:1115–1127
 93. Scheuer PJ, Takahashi W, Tsutsumi J, Yoshida T (1967) Ciguatoxin: isolation and chemical nature. *Science* 155:1267–1268
 94. Moore RE, Scheuer PJ (1971) Palytoxin-new marine toxin from a coelenterate. *Science* 172:495–498
 95. Moore RE, Bartolini G (1981) Structure of palytoxin. *J Am Chem Soc* 103:2491–2494
 96. Uemura D, Ueda K, Hirata Y, Naoki H, Iwashita T (1981) Further-studies on palytoxin II. Structure of palytoxin. *Tetrahedron Lett* 22:2781–2784

97. Armstrong RW, Beau JM, Cheon SH, Christ WJ, Fujioka H, Ham W-H, Hawkins LD, Jin H, Kang SH, Kishi Y, Martinelli MJ, McWhorter WW Jr, Mizuno M, Nakata M, Stutz AE, Talamas FX, Taniguchi M, Tino JA, Ueda K, Uenishi J, White JB, Yonaga M (1989) Total synthesis of palytoxin carboxylic acid and palytoxin amide. *J Am Chem Soc* 111:7530–7533
98. Suh EM, Kishi Y (1994) Synthesis of palytoxin from palytoxin carboxylic acid. *J Am Chem Soc* 116:11205–11206
99. Maeda M, Kodama R, Tanaka T, Yohizumi H, Nomyoto K, Takemoto T, Fujita M (1985) Structures of insecticidal substances isolated from a red alga, *Chondria armata*. In: Symposium Organizing Committee (eds) Proceedings of the 27th symposium on the chemistry of natural products, Hiroshima, Japan
100. Usami M, Satake M, Ishida S, Inoue A, Kan Y, Yasumoto T (1995) Palytoxin analogs from the dinoflagellate *Ostreopsis siamensis*. *J Am Chem Soc* 117:5389–5390
101. Carballeira NM, Emiliano A, Sostre A, Restituyo JA, González IM, Colón GM, Tosteson CG, Tosteson TR (1998) Fatty acid composition of bacteria associated with the toxic dinoflagellate *Ostreopsis lenticularis* and with Caribbean *Palythoa* species. *Lipids* 33:627–632
102. Seemann P, Gernert C, Schmitt S, Mebs D, Hentschel U (2009) Detection of hemolytic bacteria from *Palythoa caribaeorum* (Cnidaria, Zoantharia) using a novel palytoxin-screening assay. *Antonie van Leeuwenhoek* 96:405–411
103. Frolova GM, Kuznetsova TA, Mikhailov VV, Elyakov GB (2000) An enzyme linked immunosorbent assay for detecting palytoxin-producing bacteria. *Russ J Bioorg Chem* 26:285–289
104. Piel J (2009) Metabolites from symbiotic bacteria. *Nat Prod Rep* 26:338–362
105. Bottinger H, Beress L, Habermann E (1986) Involvement of (Na^+ , K^+ -ATPase) in binding and actions of palytoxin on human erythrocytes. *Biochim Biophys Acta* 861:164–176
106. Alcalá AC, Alcalá LC, Garth JS, Yasumura D, Yasumoto T (1998) Human fatality due to ingestion of the crab *Demania reynaudii* contained a palytoxin-like toxin. *Toxicon* 26:105–107
107. Granéli E, Ferreira CEL, Yasumoto T, Rodrigues E, Neves MHB (2002) Sea urchins poisoning by the benthic dinoflagellate *Ostreopsis ovata* on the Brazilian coast. *The Xth International Conference on Harmful Algae*, 21–25 October, Florida, USA
108. Fukui M, Murata M, Inoue A, Gawel M, Yasumoto T (1987) Occurrence of palytoxin in the trigger fish *Melichthys vidua*. *Toxicon* 25:1121–1124
109. Onuma Y, Satake M, Ukena T, Roux J, Chanteau S, Rasolofonirina N, Ratsimaloto N, Naoki H, Yasumoto T (1999) Identification of putative palytoxin as the cause of clupeotoxism. *Toxicon* 37:55–65
110. Taniyama S, Arakawa O, Terada M, Nishio S, Takatani T, Mahmud Y, Noguchi T (2003) *Ostreopsis* sp., a possible origin of palytoxin (PTX) in parrotfish *Scarus oviifrons*. *Toxicon* 42:29–33
111. Hoffmann K, Hermanns-Clausen M, Buhl C, Buchler MW, Schemmer P, Mebs D, Kaufenstein S (2008) A case of palytoxin poisoning due to contact with zoanthid corals through a skin injury. *Toxicon* 51:1535–1537
112. Deeds JR, Schwartz MD (2009) Human risk associated with palytoxin exposure. *Toxicon* 56:150–162
113. Ciminiello P, Dell'Aversano C, Fattorusso E, Forino M, Magno GS, Tartaglione L, Grillo C, Melchiorre N (2006) The Genoa 2005 outbreak. Determination of putative palytoxin in Mediterranean *Ostreopsis ovata* by a new liquid chromatography tandem mass spectrometry method. *Anal Chem* 78:6153–6159
114. Kodama M (2000) Ecology, classification, and origin. In: Botana LM (ed) *Seafood and freshwater toxins: pharmacology, physiology and detection*. Marcel Dekker, New York
115. Sommer H, Meyer KF (1937) Paralytic shellfish poisoning. *Arch Pathol* 24:560–598
116. Schantz EJ, Mold JD, Stanger DW, Shavel J, Riel FJ, Bowden JP, Lynch JM, Wyler RS, Riegel B, Sommer H (1957) Paralytic shellfish poison. VI. A procedure for the isolation and purification of the poison from toxic clam and mussel tissues. *J Am Chem Soc* 79:5230–5235

117. Schantz EJ, Ghazarossian VE, Schnoes HK, Strong FM, Springer JP, Pezzanite JO, Clardy J (1975) Structure of saxitoxin. *J Am Chem Soc* 97:1238–1239
118. Tanito H, Nakata T, Kaneko T, Kishi Y (1977) A stereospecific total synthesis of d/l-saxitoxin. *J Am Chem Soc* 99:2818–2819
119. Jacobi PA, Martinelli MJ, Polanc S (1984) Total synthesis of (+/–)-saxitoxin. *J Am Chem Soc* 106:5594–5598
120. Fleming JJ, Fiori KW, Du Bois J (2003) Novel iminium ion equivalents prepared through C – H oxidation for the stereocontrolled synthesis of functionalized propargylic amine derivatives. *J Am Chem Soc* 125:2028–2029
121. Fleming JJ, Du Bois J (2006) A synthesis of (+)-saxitoxin. *J Am Chem Soc* 128:3926–3927
122. Shimizu Y, Norte M, Hori A, Genenah A, Kobayashi M (1984) Biosynthesis of saxitoxin analogues: the unexpected pathway. *J Am Chem Soc* 106:6433–6434
123. Kellmann R, Mihali TK, Jeon YJ, Pickford R, Pomati F, Neilan BA (2008) Biosynthetic intermediate analysis and functional homology reveal a saxitoxin gene cluster in cyanobacteria. *Appl Environ Microbiol* 74:4044–4053
124. Shumway SE (1990) A review of the effects of algal blooms on shellfish and aquaculture. *J World Aquacult Soc* 21:65–104
125. Carmichael WW, Evans WR, Yin QQ, Bell P, Moczydlowski E (1997) Evidence for paralytic shellfish poisons in the freshwater cyanobacterium *Lyngbya wollei* (Farlow ex Gomont) comb. nov. *Appl Environ Microbiol* 63:3104–3110
126. Galvão JA, Oetterer M, Bittencourt-Oliveira MC, Barros SG, Hiller S, Erler K, Luckas B, Pinto E, Kujbida P (2009) Saxitoxins accumulation by freshwater tilapia (*Oreochromis niloticus*) for human consumption. *Toxicon* 54:891–894
127. Arias HR (2006) Marine toxins targeting ion channels. *Mar Drugs* 4:37–69
128. Lagos N, Andrinolo D (2000) Paralytic shellfish poisoning (PSP): toxicology and kinetics. In: Botana LM (ed) *Seafood and freshwater toxins: pharmacology, physiology and detection*. Marcel Dekker, New York
129. Satake M, Ofuji K, Naoki H, James KJ, Furey A, McMahon T, Silke J, Yasumoto T (1998) Azaspiracid, a new marine toxin having unique spiro ring assemblies, isolated from Irish mussels, *Mytilus edulis*. *J Am Chem Soc* 120:9967–9968
130. James KJ, Fidalgo Saez MJ, Furey A, Lehane M (2003) Azaspiracid poisoning, the food-borne illness associated with shellfish consumption. *Food Addit Contam* 21:879–892
131. Hess P, McMahon T, Slattery D, Swords D, Dowling G, McCarron M, Clarke D, Gibbons W, Silke J, O' Cinneide M (2003) Use of LC-MS testing to identify lipophilic toxins, to establish local trends and interspecies differences and to test the comparability of LC-MS testing with the mouse bioassay: an example from the Irish biotoxin monitoring programme 2001. In: Villalba A, Reguera B, Romalde JL, Beiras R (eds) *Molluscan shellfish safety*. Proceedings of the 4th international conference on molluscan shellfish safety. Consellería de Pesca e Asuntos Marítimos da Xunta de Galicia and Intergovernmental Oceanographic Commission of UNESCO, Santiago de Compostela, Spain
132. Braña Magdalena A, Lehane M, Krysz S, Fernandez ML, Furey A, James KJ (2003) The first identification of azaspiracids in shellfish from France and Spain. *Toxicon* 42:105–108
133. James KJ, Furey A, Lehane M, Ramstad H, Aune T, Hovgaard P, Morris S, Higman W, Satake M, Yasumoto T (2002) First evidence of an extensive northern European distribution of azaspiracid poisoning (AZP) toxins in shellfish. *Toxicon* 40:909–915
134. Aasen JAB, Torgersen T, Dahl E, Naustvoll L-J, Aune T (2006) Confirmation of azaspiracids in mussels in Norwegian coastal areas, and full profile at one location. In: Henshilwood K, Deegan B, McMahon T, Cusack C, Keaveney S, Silke J, O' Cinneide M, Lyons D, Hess P (eds) *Proceedings of the 5th international conference on molluscan shellfish safety*, Galway, Ireland, June 14–18 2004, The Marine Institute, Rinville, Oranmore, Galway, Ireland
135. Torgersen T, Bruun Bremmes N, Rundberget T, Aune T (2008) Structural confirmation and occurrence of azaspiracids in Scandinavian brown crabs (*Cancer pagurus*). *Toxicon* 51:93–101

136. Taleb H, Vale P, Amanhir R, Benhadouch A, Sagou R, Chafik A (2006) First detection of azaspiracids in mussels in north west Africa. *J Shellfish Res* 25:1067–1070
137. Anonymity (2004) Regulation (EC) No 853/2004 of 29 April 2004 laying down specific hygiene rules for the hygiene of foodstuffs. *Off J Eur Commun* L139, 55ff
138. Nicolaou KC, Li Y, Uesaka N, Koftis TV, Vyskocil S, Ling T, Govindasamy M, Qian W, Bernal F, Chen D (2003) Total synthesis of the proposed azaspiracid-1 structure, Part 1: Construction of the enantiomerically pure C1-C20, C21-C27, and C28-C40 fragments. *Angew Chem* 42:3643–3648
139. Nicolaou KC, Chen D, Li Y, Quan W, Ling T, Vyskocil S, Koftis TV, Govindasamy M, Uesaka N (2003) Total synthesis of the proposed azaspiracid-1 structure, Part 2: Coupling of the C1-C20, C21-C27, and C28-C40 fragments and completion of the synthesis. *Angew Chem* 42:3649–3653
140. Nicolaou KC, Vyskocil S, Koftis TV, Yamada TMA, Ling T, Chen DYK, Tang W, Petrovic G, Frederick MO (2004) Structural revision and total synthesis of azaspiracid-1, Part 1: Intelligence gathering and tentative proposal. *Angew Chem* 116:2–8
141. Nicolaou KC, Koftis TV, Vyskocil S, Petrovic G, Ling T, Yamada TMA, Tang W, Frederick MO (2004) Structural revision and total synthesis of azaspiracid-1, Part 2: Definition of the ABCD domain and total synthesis. *Angew Chem Int Ed* 43:4318–4324
142. Yasumoto T (2001) The chemistry and biological function of natural marine toxins. *Chem Record* 1:228–242
143. Ito E, Satake M, Ofuji K, Kurita N, McMahon T, James K, Yasumoto T (2000) Multiple organ damage caused by a new toxin Azaspiracid, isolated from mussels produced in Ireland. *Toxicon* 38:917–930
144. James KJ, Moroney C, Roden C, Satake M, Yasumoto T, Lehane M, Furey A (2003) Ubiquitous ‘benign’ alga emerges as the cause of shellfish contamination responsible for the human toxic syndrome, azaspiracid poisoning. *Toxicon* 41:145–151
145. James KJ, Sierra MD, Lehane M, Braña Magdalena A, Moroney C, Furey A (2004) Azaspiracid poisoning: Aetiology, toxin dynamics and bioconversion in shellfish. In: Steidinger K, Landsberg J, Tomas CR, Vargo GA (eds) *Harmful algae 2002*, Florida Fish and Wildlife Conservation Commission, Florida Institute of Oceanography, and Intergovernmental Oceanographic Commission of UNESCO
146. Satake M, Ofuji K, James KJ, Furey A, Yasumoto T (1998) New toxic event caused by Irish mussels. In: Reguera B, Blanco J, Fernandez M, Wyatt T (eds) *Harmful algae*, Proceedings of the VIII international conference on harmful algae. Xunta de Galicia/IOC of UNESCO, Vigo, Spain
147. Ito E, Terao K, McMahon T, Silke J, Yasumoto T (1998) Acute pathological changes in mice caused by crude extracts of novel toxins isolated from Irish mussels. In: Reguera B, Blanco J, Fernandez M, Wyatt T (eds) *Harmful algae*, Proceedings of the VIII international conference on harmful algae. Xunta de Galicia/IOC of UNESCO, Vigo, Spain
148. Seki T, Satake M, Mackenzie L, Kaspar HF, Yasumoto T (1995) Gymnodimine, a new marine toxin of unprecedented structure isolated from New Zealand oysters and the dinoflagellate *Gymnodinium* sp. *Tetrahedron Lett* 36:7093–7096
149. Seki T, Satake M, MacKenzie L, Kaspar HF, Yasumoto T (1996) Gymnodimine, a novel toxic imine isolated from the Foveaux strait oysters and *Gymnodinium* sp. In: Yasumoto T, Oshima Y, Fukuyo Y (eds) *Harmful and toxic algal blooms*. Intergovernmental Oceanographic Commission of UNESCO, Paris
150. Mackenzie L, Haywood A, Adamson J, Truman P, Till D, Seki T, Satake M, Yasumoto T (1996) Gymnodimine contamination of shellfish in New Zealand. In: Yasumoto T, Oshima Y, Fukuyo Y (eds) *Harmful and toxic algal blooms*. Intergovernmental Oceanographic Commission of UNESCO, Paris
151. Stirling DJ (2001) Survey of historical New Zealand shellfish samples for accumulation of gymnodimine. *New Zeal J Mar Fresh* 35:851–857
152. Haywood AJ, Steidinger KA, Truby EW, Bergquist PR, Bergquist PL, Adamson J, Mackenzie L (2004) Comparative morphology and molecular phylogenetic analysis

- of three new species of the genus *Karenia* (Dinophyceae) from New Zealand. *J Phycol* 40:165–179
153. Stewart M, Blunt JW, Munro MHG, Robinson WT, Hannah DJ (1997) The absolute stereochemistry of the New Zealand shellfish toxin gymnodimine. *Tetrahedron Lett* 38:4889–4890
154. Kharrat R, Servent D, Girard E, Ouanounou G, Amar M, Marrouchi R, Benoit E, Molgo J (2008) The marine phycotoxin gymnodimine targets muscular and neuronal nicotinic acetylcholine receptor subtypes with high affinity. *J neurochem* 107:952–963
155. Provasoli L (1968) Media and prospects for the cultivation of marine algae. In: Watanabe A, Hattori A (eds) *Culture and collection of algae*. Japanese Society of Plant Physiology, Tokyo, Japan
156. Ishibashi M, Yamaguchi N, Sasaki T, Kobayashi J (1994) Amphidinolide N, a novel 26-membered macrolide with remarkably potent cytotoxicity from the cultured marine dinoflagellate *Amphidinium* sp. *J Chem Soc Chem Comm* 12:1455–1456
157. Bauer J, Maranda L, Young KA, Shimizu Y, Fairchild C, Cornell L, MacBeth J, Huang S (1995) Isolation and structure of caribenolide I, a highly potent antitumor macrolide from a cultured free-swimming Caribbean dinoflagellate, *Amphidinium* sp. S1-36-5. *J Org Chem* 60:1084–1086
158. Sharma GM, Michaels L, Burkholder PR (1968) Goniodomin, a new antibiotic from a dinoflagellate. *J Antibiot* 21:659–664
159. Murakami M, Makabe K, Yamaguchi K, Konosu S, Walchli MR (1988) Goniodomin A, a novel polyether macrolide from the dinoflagellate *Goniodoma pseudogoniaulax*. *Tetrahedron Lett* 29:1149–1152
160. Trench RK (1981) Cellular and molecular interactions in symbioses between dinoflagellates and marine invertebrates. *Pure Appl Chem* 53:819–835
161. Blank RJ, Trench RK (1985) Speciation and symbiotic dinoflagellates. *Science* 229:656–658
162. Rowan R, Powers DA (1991) A molecular genetic classification of zooxanthellae and the evolution of animal-algal symbioses. *Science* 251:1348–1351
163. Nakamura H, Asari T, Murai A, Kan Y, Kondo T, Yoshida K, Ohizumi Y (1995) Zooxanthellatoxin-A, a potent vasoconstrictive 62-membered lactone from a symbiotic dinoflagellate. *J Am Chem Society* 117:550–551
164. Rho MC, Nakahata N, Nakamura H, Murai A, Ohizumi Y (1995) Activation of rabbit platelets by Ca^{2+} influx and thromboxane A₂ release in an external Ca^{2+} -dependent manner by zooxanthellatoxin-A, a novel polyol. *Brit J Pharmacol* 115:433–440
165. Kita M, Ohishi N, Konishi K, Kondo M, Koyama T, Kitamura M, Yamada K, Uemura D (2007) Symbiodinolide, a novel polyol macrolide that activates N-type Ca^{2+} channel, from the symbiotic marine dinoflagellate *Symbiodinium* sp. *Tetrahedron* 63:6241–6251
166. Satake M, Murata M, Yasumoto T, Fujita T, Naoki H (1991) Amphidinol, a polyhydroxypolyene antifungal agent with an unprecedented structure, from a marine dinoflagellate, *Amphidinium klebsii*. *J Am Chem Soc* 113:9859–9861
167. Houdai T, Matsuoka S, Morsy N, Matsumori N, Satake M, Murata M (2005) Hairpin conformation of amphidinols possibly accounting for potent membrane permeabilizing activities. *Tetrahedron* 61:2795–2802
168. Armbrust EV, Berges JA, Bowler C et al (2004) The genome of the diatom *Thalassiosira pseudonana*: Ecology, evolution, and metabolism. *Science* 306:79–86
169. Bowler C, Allen AE, Badger JH et al (2008) The Phaeodactylum genome reveals the evolutionary history of diatom genomes. *Nature* 456:239–244
170. Lefebvre KA, Robertson A (2010) Domoic acid and human exposure risks: a review. *Toxicol* 56:218–230
171. Wright JLC, Boyd RK, De Freitas ASW, Falk M, Foxall RA, Jamieson WD, Laycock MV, McCulloch AW, McInnes AG et al (1989) Identification of domoic acid, a neuroexcitatory amino acid, in toxic mussels from eastern Prince Edward Island. *Can J Chem* 67:481–90

172. Ramsey UP, Douglas DJ, Walter JA, Wright JLC (1998) Biosynthesis of domoic acid by the diatom *Pseudo-nitzschia multiseries*. *Nat Toxins* 6:137–146
173. Gerwick WH, Moghaddam MF, Hamberg M (1991) Oxylipin metabolism in the red alga *Gracilariopsis lemaneiformis*: Mechanism of formation of vicinal dihydroxy fatty acids. *Arch Biochem Biophys* 290:436–444
174. Wang R, Shimizu Y (1990) Bacillarolides I and II, a new type of cyclopentane eicosanoids from the diatom *Nitzschia pungens*. *J Chem Soc Chem Comm* 5:413–14
175. Wang R, Shimizu Y, Steiner JR, Clardy J (1993) The absolute configuration of bacillarolides I and II, a new type of cyclopentane icosanoids from a marine diatom. *J Chem Soc Chem Comm* 4:379–81
176. Ianora A, Miralto A (2010) Toxicogenic effects of diatoms on grazers, phytoplankton and other microbes: a review. *Ecotoxicology* 19:493–511
177. Pohnert G (2005) Diatom/copepod interactions in plankton: the indirect chemical defense of unicellular algae. *ChemBioChem* 6:946–959
178. Fontana A, d'Ippolito G, Cutignano A, Miralto A, Lanora A, Romano G, Cimino G (2007) Chemistry of oxylipin pathways in marine diatoms. *Pure Appl Chem* 79:481–490
179. Masse G, Belt ST, Rowland SJ (2004) Biosynthesis of unusual monocyclic alkenes by the diatom *Rhizosolenia setigera* (Brightwell). *Phytochem* 65:1101–1106
180. Simon TB, Guillaume Massé WGA, Jean-Michel R, Steven JR (2001) C25 highly branched isoprenoid alkenes in planktonic diatoms of the *Pleurosigma* genus. *Org Geochem* 32:1271–1275
181. Elovson J, Vagelos PR (1969) A new class of lipids: chlorosulfolipids. *Proc Natl Acad Sci USA* 62:957–963
182. Haines TH, Pousada M, Stern B, Mayers GL (1969) Microbial sulpholipids: (R)-13-Chloro-1-(R)-14-docosanediol disulphate and polychlorosulpholipids in *Ochromonas danica*. *Biochem J* 113:565–566
183. Elovson J, Vagelos PR (1970) Structure of the major species of chlorosulfolipid from *Ochromonas danica*. 2,2,11,13,15,16-Hexachloro-n-docosane-1,4-disulfate. *Biochemistry* 9:3110–3126
184. Haines TH (1973) Sulfolipids and halosulfolipids. In: Erwin JA (ed) *Lipids and biomembranes of eukaryotic microorganisms*. Academic, New York
185. Haines TH (1973) Halogen- and sulfur-containing lipids of *Ochromonas*. *Annu Rev Microbiol* 27:403–412
186. Chen JL, Proteau PJ, Roberts MA, Gerwick WH, Slate DL, Lee RH (1994) Structure of malhamensilipin A, an inhibitor of protein tyrosine kinase, from the cultured chrysophyte *Poterioochromonas malhamensis*. *J Nat Prod* 57:524–527
187. Pereira AR, Byrum T, Shibuya GM, Vanderwal CD, Gerwick WH (2010) Structure revision and absolute configuration of malhamensilipin A from the freshwater chrysophyte *Poterioochromonas malhamensis*. *J Nat Prod* 73:279–283
188. Bedke DK, Shibuya GM, Pereira AR, Gerwick WH, Vanderwal CD (2010) A concise enantioselective synthesis of the chlorosulfolipid malhamensilipin A. *J Am Chem Soc* 132:2542–2543
189. Ciminiello P, Fattorusso E, Forino M, Magno S, Di Rosa M, Ianaro A, Poletti R (2001) Structural elucidation of a new cytotoxin isolated from mussels of the Adriatic Sea. *J Org Chem* 66:578–582
190. Ciminiello P, Dell'Aversano C, Fattorusso E, Forino M, Di Rosa M, Ianaro A, Poletti R (2002) Structure and stereochemistry of a new cytotoxic polychlorinated sulfolipid from Adriatic shellfish. *J Am Chem Soc* 124:13114–13120
191. Ciminiello P, Dell'Aversano C, Fattorusso E, Forino M, Magno S (2003) Toxins from Adriatic blue mussels. A decade of studies. *Pure Appl Chem* 75:325–336
192. Ciminiello P, Dell'Aversano C, Fattorusso E, Forino M, Magno S, Di Meglio P, Ianaro A, Poletti R (2004) A new cytotoxic polychlorinated sulfolipid from contaminated Adriatic mussels. *Tetrahedron* 60:7093–7098

193. Ciminiello P, Fattorusso E (2004) Shellfish toxins – Chemical studies on northern Adriatic mussels. *Eur J Org Chem* 12:2533–2551
194. Chao CH, Huang HC, Wang GH, Wen ZH, Wang WH, Chen IM, Sheu JH (2010) Chlorosulfolipids and the corresponding alcohols from the octocoral *Dendronephthya griffini*. *Chem Pharm Bull* 58:944–946
195. Chen LL, Pousada M, Haines TH (1976) The flagellar membrane of *Ochromonas danica*. *J Biol Chem* 251:1835–1842
196. Kawahara T, Kumaki Y, Kamada T, Ishii T, Okino T (2009) Absolute configuration of chlorosulfolipids from the chrysophyta *Ochromonas danica*. *J Org Chem* 74:6016–6025
197. Shibuya GM, Kanady JS, Vanderwal CD (2008) Stereoselective dichlorination of allylic alcohol derivatives to access key stereochemical arrays of the chlorosulfolipids. *J Am Chem Soc* 130:12514–12518
198. Kanady JS, Nguyen JD, Ziller JW, Vanderwal CD (2009) Synthesis and characterization of all four diastereomers of 3,4-dichloro-2-pentanol, motifs relevant to the chlorosulfolipids. *J Org Chem* 74:2175–2178
199. Yoshimitsu T, Fukumoto N, Tanaka T (2009) Enantiocontrolled synthesis of polychlorinated hydrocarbon motifs: a nucleophilic multiple chlorination process revisited. *J Org Chem* 74:696–702
200. Nilewski C, Geisser RW, Carreira EM (2009) Total synthesis of a chlorosulpholipid cytotoxin associated with seafood poisoning. *Nature* 457:573–576
201. Nilewski C, Geisser RW, Ebert MO, Carreira EM (2009) Conformational and configurational analysis in the study and synthesis of chlorinated natural products. *J Am Chem Soc* 131:15866–15876
202. Bedke DK, Shibuya GM, Pereira A, Gerwick WH, Haines TH, Vanderwal CD (2009) Relative stereochemistry determination and synthesis of the major chlorosulfolipid from *Ochromonas danica*. *J Am Chem Soc* 131:7570–7572
203. Gerwick WH, Lopez A, Van Duyne GD, Clardy J, Ortiz W, Baez A (1986) Hormothamnione, a novel cytotoxic styrylchromone from the marine cyanophyte *Hormothamnion enteromorphoides* Grunow. *Tetrahedron Lett* 27:1979–1982
204. Gerwick WH (1989) 6-Desmethoxyhormothamnione, a new cytotoxic styrylchromone from the marine Chrysophyte *Chrysosphaera taylori*. *J Nat Prod* 52:252–256
205. Lewis IF, Bryan HF (1941) A new protophyte from the dry tortugas. *Am J Bot* 28:343–348
206. Takamatsu S, Hodges TW, Rajbhandari I, Gerwick WH, Hamann MT, Nagle DG (2003) Marine natural products as novel antioxidant prototypes. *J Nat Prod* 66:605–608
207. Takamatsu S, Nagle DG, Gerwick WH (2004) Secondary metabolites from marine cyanobacteria and algae inhibit LFA-1/ICAM-1 mediated cell adhesion. *Planta Med* 70:127–131
208. Alonso R, Brossi A (1988) Synthesis of hormothamnione. *Tetrahedron Lett* 29:735–738
209. Ayyangar NR, Khan RA, Deshpande VH (1988) Synthesis of hormothamnione. *Tetrahedron Lett* 29:2347–2348
210. McGarry LW, Detty MR (1990) Synthesis of highly functionalized flavones and chromones using cycloacylation reactions and C-3 functionalization. A total synthesis of hormothamnione. *J Org Chem* 55:4349–4356
211. Niveta J, Gambhir G, Krishnamurthy HG (2001) Synthesis of hormothamnione and 6-desmethoxyhormothamnione. *Indian J Chem* 40B:278–283
212. Plaza A, Keffer JL, Bifulco G, Lloyd JR, Bewley CA (2010) Chrysosphaentins A-H, antibacterial bisdiarylbutene macrocycles that inhibit the bacterial cell division protein FtsZ. *J Am Chem Soc* 132:9069–9077
213. Lock RL, Harry EJ (2008) Cell-division inhibitors: new insights for future antibiotics. *Nat Rev Drug Discovery* 7:324–338
214. Otterstrøm CV, Steemann-Nielsen E (1940) Two cases of extensive mortality in fishes caused by the flagellate *Prymnesium parvum* Carter. *Rep Dan Biol Sta* 44:1–24

215. Shilo M, Aschner M (1953) Factors governing the toxicity of cultures containing phytoflagellate *Prymnesium parvum* Carter. J Gen Microbiol 8:333–343
216. Lindholm T, Virtanen T (1992) A Bloom of *Prymnesium parvum* Carter in a small coastal inlet in Dragsfjord, Southwestern Finland. Environ Toxic Water Qual 7:165–170
217. Guo MX, Harrison PJ, Taylor FJR (1996) Fish kills related to *Prymnesium parvum* N. Carter (Haptophyta) in the people's Republic of China. J Appl Phycol 8:111–117
218. Watson S (2001) Literature review of the microalga *Prymnesium parvum* and its associated toxicity. Prepared for the Texas Parks and Wildlife Department. <http://www.tpwd.state.tx.us/landwater/water/environconcerns/hab/ga/literature/>. Accessed 22 March 2011
219. Manning SR, La Claire JW (2010) Prymnesins: toxic metabolites of the golden alga, *Prymnesium parvum* Carter (Haptophyta). Mar Drugs 8:678–704
220. Igarashi T, Satake M, Yasumoto T (1999) Structures and partial stereochemical assignments for Prymnesin-1 and Prymnesin-2: potent hemolytic and ichthyotoxic glycosides isolated from the red tide alga *Prymnesium parvum*. J Am Chem Soc 121:8499–8511
221. Shilo M, Rosenberger M (1960) Studies on the toxic principles formed by the chrysomonad *Prymnesium parvum* Carter. Ann NY Acad Sci 90:866–876
222. Yariv J, Hestrin S (1961) Toxicity of the extracellular phase of *Prymnesium parvum* cultures. J Gen Microbiol 24:165–175
223. Ulitzur S, Shilo M (1970) Procedure for purification and separation of *Prymnesium parvum* toxins. Biochim Biophys Acta 201:350–363
224. Kozakai H, Oshima Y, Yasumoto T (1982) Isolation and structural elucidation of hemolysin from the phytoflagellate *Prymnesium parvum*. Agric Biol Chem 46:233–236
225. Igarashi T, Satake M, Yasumoto T (1996) Prymnesin-2: a potent ichthyotoxic and hemolytic glycoside isolated from the red tide alga *Prymnesium parvum*. J Am Chem Soc 118:479–480
226. Sasaki M, Shida T, Tachibana K (2001) Synthesis and stereochemical confirmation of the HI/JK ring system of prymnesins, potent hemolytic and ichthyotoxic glycoside toxins isolated from the red tide alga. Tetrahedron Lett 42:5725–5728
227. Sasaki M, Ebine M, Takagi H, Takakura H, Shida T, Satake M, Oshima Y, Igarashi T, Yasumoto T (2004) Synthesis of the CDE/FG ring models of prymnesins: reassignment of the relative configuration of the E/F ring juncture. Org Lett 6:1501–1504
228. Sasaki M, Takeda N, Fuwa H, Watanabe R, Satake M, Oshima Y (2006) Synthesis of the JK/LM-ring model of prymnesins, potent hemolytic and ichthyotoxic polycyclic ethers isolated from the red tide alga *Prymnesium parvum*: confirmation of the relative configuration of the K/L-ring juncture. Tetrahedron Lett 47:5687–5691
229. Morohashi A, Satake M, Oshima Y, Igarashi T, Yasumoto T (2001) Absolute configuration at C14 and C85 in Prymnesin-2, a potent hemolytic and ichthyotoxic glycoside isolated from the red tide alga *Prymnesium parvum*. Chirality 13:601–605
230. Paul VJ, Sun HH, Fenical W (1982) Udoteal, a linear diterpenoid feeding deterrent from tropical green alga *Udotea flabellum*. Phytochem 21:468–469
231. Nakatsu T, Ravi BN, Faulkner DJ (1981) Antimicrobial constituents of *Udotea flabellum*. J Org Chem 46:2435–2538
232. Puglisi MP, Tan LT, Jensen P, Fenical W (2004) Capisterones A and B from the tropical green alga *Penicillus capitatus*: unexpected anti-fungal defenses targeting the marine pathogen *Lindra thalassiae*. Tetrahedron 60:7035–7039
233. Li X-C, Jacob MR, Ding Y, Agarwal AK, Smillie TJ, Khan SI, Nagle DG, Ferreira D, Clark AM (2006) Capisterones A and B, which enhance fluconazole activity in *Saccharomyces cerevisiae*, from the marine green alga *Penicillus capitatus*. J Nat Prod 69:542–546
234. Hogberg HE, Thomason RH, King TJ (1976) The cymopols, a group of prenylated bromohydroquinones from the green calcareous alga *Cymopolia barbata*. J Chem Soc Per Trans 1(16):1696–1701
235. Mayer AMS, Paul VJ, Fenical W, Norris JN, de Carvalho MS, Jacobs RS (1993) Phospholipase A2 inhibitors from marine algae. Hydrobiologia 260–261:521–529

236. McConnell OJ, Hughes PA, Targett NM (1982) Diastereoisomers of cyclocymopol and cyclocymopol monomethyl ether from *Cymopolia barbata*. *Phytochem* 21:2139–2141
237. McConnell OJ, Hughes PA, Targett NM, Daley J (1982) Effects of secondary metabolites from marine algae on feeding by the sea urchin, *Lytechinus variegatus*. *J Chem Ecol* 8:1437–1453
238. Wall ME, Wani MC, Manikumar G, Taylor H, Hughes TJ, Gaetano K, Gerwick WH, McPhail AT, McPhail DR (1989) Plant antimutagenic agents, 7. Structure and antimutagenic properties of cymobarbatol and 4-isocymobarbatol, new cymopols from green alga (*Cymopolia barbata*). *J Nat Prod* 52:1092–1099
239. Aguilar-Santos G, Doty MS (1968) Chemical studies on three species of the marine algal genus *Caulerpa*. In: Freudenthal HD (ed) *Drugs from the sea*. Marine Technology Society, Washington, DC
240. Aguilar-Santos G (1970) Caulerpin, a new red pigment from green algae of the genus *Caulerpa*. *J Chem Soc (C)* 6:842–843
241. Maiti BC, Thomson RH, Mahendran M (1978) The structure of caulerpin, a pigment from *Caulerpa* algae. *J Chem Res Synop* 4:126–127
242. Raub MF, Cardellina JH II, Schwede JG (1987) The green algal pigment caulerpin as a plant growth regulator. *Phytochem* 26:619–620
243. Liu Y, Morgan JB, Coothankandaswamy V, Liu R, Jekabsons MB, Mahdi F, Nagle DG, Zhou Y-D (2009) The *Caulerpa* pigment caulerpin inhibits HIF-1 activation and mitochondrial respiration. *J Nat Prod* 72:2104–2109
244. de Souza ET, de Lira DP, de Queiroz AC, da Silva DJC, de Aquino AB, Mella EAC, Lorenzo VP, de Miranda GEC, de Araujo-Junior JX, Chaves MCO, Barbosa-Filho JM, de Athayde-Filho PF, Santos BVO, Alexandre-Moreira MS (2009) The antinociceptive and anti-inflammatory activities of caulerpin, a bisindole alkaloid isolated from seaweeds of the genus *Caulerpa*. *Mar Drugs* 7:689–704
245. Alarif WM, Abou-Elnaga ZS, Ayyad SN, Al-lihaibi SS (2010) Insecticidal metabolites from the green alga *Caulerpa racemosa*. *Clean: Soil, Air, Water* 38:548–557
246. Perez-Rodriguez E, Gomez I, Karsten U, Figueroa FL (1998) Effects of UV radiation on Photosynthesis and excretion of UV-absorbing compounds of *Dasycladus vermicularis* (Dasycladales, Chlorophyta) from Southern Spain. *Phycologia* 37:379–387
247. Menzel D, Kazlauskas R, Reichelt J (1983) Coumarins in the siphonacean green algal family Dasycladaceae Kützting (Chlorophyceae). *Bot Mar* 29:23–29
248. Baily F, Maurin C, Teissier E, Vezin H, Cotel P (2004) Antioxidant properties of 3-hydroxycoumarin derivatives. *Bioorg Med Chem* 12:5611–5618
249. Ross C, Kupper FC, Vreeland V, Waite JH, Jacobs RS (2005) Evidence of a latent oxidative burst in relation to wound repair in the giant unicellular Chlorophyte *Dasycladus vermicularis*. *J Phycol* 41:531–541
250. Sun HH, Paul VJ, Fenical W (1983) Avrainvilleol, a brominated diphenylmethane derivative with feeding deterrent properties from the tropical green alga *Avrainvillea longicaulis*. *Phytochem* 22:743–745
251. Higa T, Scheuer PJ (1975) Constituents of the marine annelid *Thelepus setosus*. *Tetrahedron* 31:2379–2381
252. Pedersen M (1978) Bromochlorophenols and brominated diphenylmethane in red algae *Marianne Pedersen*. *Phytochem* 17:291–293
253. Chevolut-Magueur A, Cave A, Potier P, Teste J, Chiaroni A, Riche C (1976) Composés bromés de *Rytiphlea tinctoria* (Rhodophyceae). *Phytochem* 15:767–771
254. Colon M, Guevara P, Gerwick WH, Ballantine D (1987) 5'-Hydroxyisovrainvilleol, a new diphenylmethane derivative from the tropical green alga *Avrainvillea nigricans*. *J Nat Prod* 50:368–374
255. Carte BK, Troupe N, Chan JA, Westley JW, Faulkner J (1989) Rawsonol, an inhibitor of HMG-CoA Reductase from the tropical green alga *Avrainvillea Rawsonii*. *Phytochem* 28:3917–2919

256. Chen JL, Gerwick WH, Schatzman R, Laney M (1994) Isorawsonol and related IMP dehydrogenase inhibitors from the tropical green alga *Avrainvillea rawsonii*. *J Nat Prod* 57:947–952
257. Williams DE, Sturgeon CM, Roberge M, Andersen RJ (2007) Nigricanosides A and B, antimicrobial glycolipids isolated from the green alga *Avrainvillea nigricans* collected in Dominica. *J Am Chem Soc* 129:5822–5823
258. Gerwick WH, Bernart MW, Moghaddam MF, Jiang JD, Solem ML, Nagle DG (1990) Eicosanoids from the Rhodophyta: a new metabolism in the alga. *Hydrobiologia* 204(205):621–628
259. Gerwick WH, Bernart MW (1992) Eicosanoids and related compounds from marine algae. In: Zabonky OR, Attaway DH (eds) *Marine biotechnology*, Vol I, Pharmaceutical and bioactive natural products. Plenum, New York
260. Bernart W, Whatley GG, Gerwick WH (1993) Unprecedented oxylipins from the marine green alga *Acrosiphonia coalita*. *J Nat Prod* 56:245–259
261. Gardner HW (1989) Soybean lipoxygenase-1 enzymically forms both (9 S)- and (13 S)-hydroperoxides from linoleic acid by a pH-dependent mechanism. *Biochim Biophys Acta* 1001:274–281
262. Irie T, Suzuki T, Yasunari Y, Kurosawa E, Masamune T (1969) Laurene, a sesquiterpene hydrocarbon from *Laurencia* species. *Tetrahedron* 25:459–68
263. Fenical W (1975) Halogenation in the Rhodophyta. *J Phycol* 11:245–259
264. Gribble GW (2008) Structure and biosynthesis of halogenated alkaloids. In: Fattorusso E, Tagliatella-Scafati O (eds) *Modern alkaloids, structure, isolation, synthesis and biology*. Wiley-VCH Verlag GmbH & Co, Weinheim
265. Wagner C, El Omari M, Koenig GM (2009) Biohalogenation: nature's way to synthesize halogenated metabolites. *J Nat Prod* 72:540–553
266. Craigie JS, Gruenig DE (1967) Bromophenols from red algae. *Science* 157:1058–1059
267. Phillips DW, Towers GHN (1982) Chemical ecology of red algal bromophenols. I. Temporal, interpopulational and within-thallus measurements of lanosol levels in *Rhodomela larix* (Turner) C. Agardh. *J Exp Mar Biol Ecol* 58:285–293
268. Carlson DJ, Lubchenco J, Sparrow MA, Trowbridge CD (1989) Fine-scale variability of lanosol and its disulfate ester in the temperate red alga *Neorhodomela larix*. *J Chem Ecol* 15:1321–1333
269. Aknin M, Samb A, Mirailles J, Costantino V, Fattorusso E, Mangoni A (1992) Polysiphenol, a new brominated 9,10-dihydrophenanthrene from the Senegalese red alga *Polysiphonia ferulacea*. *Tetrahedron Lett* 33:555–558
270. Wiemer DF, Idler DD, Fenical W (1991) Vidalols A and B, new anti-inflammatory bromophenols from the Caribbean marine red alga *Vidalia obtusiloba*. *Experientia* 47:851–853
271. Kazlauskas R, Murphy PT, Wells RJ (1982) A brominated metabolite from the red alga *Vidalia spiralis*. *Australian J Chem* 35:219–220
272. McConnell OJ, Fenical W (1980) Halogen chemistry of the red alga *Bonnemaisonia*. *Phytochem* 19:233–247
273. Nylund GM, Cervin G, Persson F, Hermansson M, Steinberg PD, Pavia H (2008) Seaweed defence against bacteria: a poly-brominated 2-heptanone from the red alga *Bonnemaisonia hamifera* inhibits bacterial colonisation. *Mar Ecol* 369:39–50
274. Nylund GM, Persson F, Lindegarth M, Cervin G, Hermansson M, Pavia H (2010) The red alga *Bonnemaisonia asparagoides* regulates epiphytic bacterial abundance and community composition by chemical defense. *FEMS Microbiol Ecol* 71:84–93
275. de Nys R, Givskov M, Kumar N, Kjelleberg S, Steinberg PD (2006) Furanones. *Progr Mol Subcell Biol* 42:55–86
276. Kugler M (2005) Booster biocides for antifouling products: stricter environmental demands change the market. *Chim Oggi* 23:10–12
277. Koch B, Liljefors T, Persson T, Nielsen J, Kjelleberg S, Givskov M (2005) The LuxR receptor: the sites of interaction with quorum-sensing signals and inhibitors. *Microbiol* 151:3589–3602

278. Bernart MW, Gerwick WH, Corcoran EE, Lee AY, Clardy J (1992) Laurencione, a heterocycle from the red alga *Laurencia spectabilis*. *Phytochem* 31:1273–1276
279. San-Martin A, Rovirosa J, Xu C, Lu HSM, Clardy J (1987) Further structural studies on the 2-methyl-3(2 H)-furanone derived metabolites of the marine alga *Laurencia chilensis*. *Tetrahedron Lett* 28:6013–6014
280. Galloway WRJD, Hodgkinson JT, Bowden SD, Welch M, Spring DR (2011) Quorum sensing in gram-negative bacteria: small molecule modulation of AHL and AI-2 quorum sensing pathways. *Chem Rev* 111:28–67
281. Lowery CA, McKenzie KM, Qi L, Meijler MM, Janda KD (2005) Quorum sensing in *Vibrio harveyi*: probing the specificity of the LuxP binding site. *Bioorg Med Chem Lett* 15:2395–2398
282. Suzuki M, Kurosawa E (1981) Constituents of marine plants. Part 46. Okamurallene, a novel halogenated C15 metabolite from the red alga *Laurencia okamurai* Yamada. *Tetrahedron Lett* 22:3853–3856
283. Suzuki M, Kondo H, Tanaka I (1991) Constituents of marine plants. 79. The absolute stereochemistry of okamurallene and its congeners, halogenated C15 nonterpenoids from the red alga *Laurencia intricata*. *Chem Lett* 1:33–34
284. Carter-Franklin JN, Butler A (2004) Vanadium bromoperoxidase-catalyzed biosynthesis of halogenated marine natural products. *J Am Chem Soc* 126:15060–15066
285. McConnell OJ, Fenical W (1978) Ochtodene and ohtodiol: novel polyhalogenated cyclic monoterpenes from the red seaweed *Ochtodes secundiramea*. *J Org Chem* 43:4238–4241
286. Paul VJ, Hay ME, Duffy JE, Fenical W, Gustafson K (1988) Chemical defense in the seaweed *Ochtodes secundiramea*. Effects of its monoterpenoid components upon diverse coral-reef herbivores. *J Exp Mar Biol Ecol* 114:249–260
287. Pennings SC, Paul VJ (1993) Sequestration of dietary secondary metabolites by three species of sea hares: location, specificity and dynamics. *Mar Biol* 117:535–546
288. Polzin JJ, Rorrer GL, Cheney DP (2003) Metabolic flux analysis of halogenated monoterpene biosynthesis in microplantlets of the macrophytic red alga *Ochtodes secundiramea*. *Biomol Eng* 20:205–215
289. Sims JJ, Lin GHY, Wing RM (1974) Marine natural products. X. Elatol, a halogenated sesquiterpene alcohol from the red alga *Laurencia elata*. *Tetrahedron Lett* 39:3487–3490
290. Brennan MR, Erickson KL, Minott DA, Pascoe KO (1987) Chamigrane metabolites from a Jamaican variety of *Laurencia obtusa*. *Phytochem* 26:1053–1057
291. Salgado LT, Viana NB, Andrade LR, Leal RN, da Gama BAP, Attias M, Pereira RC, Amado Filho GM (2008) Intra-cellular storage, transport and exocytosis of halogenated compounds in marine red alga *Laurencia obtusa*. *J Struct Biol* 162:345–355
292. Vairappan CS, Anangdan SP, Tan KL, Matsunaga S (2010) Role of secondary metabolites as defense chemicals against ice-ice disease bacteria in biofouler at carrageenophyte farms. *J Appl Phycol* 22:305–311
293. Dias T, Brito I, Moujir L, Paiz N, Darias J, Cueto M (2005) Cytotoxic sesquiterpenes from *Aplysia dactylomela*. *J Nat Prod* 68:1677–1679
294. Oliveira dos Santos A, Veiga-Santos P, Ueda-Nakamura T, Dias Filho BP, Sudatti DB, Bianco EM, Rerespo P, Nakamura CV (2010) Effect of elatol, isolated from red seaweed *Laurencia dendroidea*, on *Leishmania amazonensis*. *Mar Drugs* 8:2733–2743
295. Kornprobst JM, Al-Easa HS (2003) Brominated diterpenes of marine origin. *Curr Org Chem* 7:1181–1229
296. Kubanek J, Prusak AC, Snell TW, Giese RA, Hardcastle KI, Fairchild CR, Aalbersberg W, Raventos-Suarez C, Hay ME (2005) Antineoplastic diterpene-benzoate macrolides from the Fijian red alga *Callophycus serratus*. *Org Lett* 7:5261–5264
297. Lane AL, Stout EP, Hay ME, Prusak AC, Hardcastle K, Fairchild CR, Franzblau SG, Le Roch K, Prudhomme J, Aalbersberg W, Kubanek J (2007) Callophycoic acids and callophycols from the Fijian red alga *Callophycus serratus*. *J Org Chem* 72:7343–7351

298. Stout EP, Prudhomme J, Le Roch K, Fairchild CR, Franzblau SG, Aalbersberg W, Hay ME, Kubanek J (2010) Unusual antimalarial meroditerpenes from tropical red macroalgae. *Bioorg Med Chem Lett* 20:5662–5665
299. Lane AL, Nyadong L, Galhena AS, Shearer TL, Stout EP, Parry RM, Kwasnik M, Wang MD, Hay ME, Fernandez FM, Kubanek J (2009) Desorption electrospray ionization mass spectrometry reveals surface-mediated antifungal chemical defense of a tropical seaweed. *Proc Nat Acad Sci USA* 106:7314–7319
300. Blunt JW, Hartshorn MP, McLennan TJ, Munro MHG, Robinson WT, Yorke SC (1978) Thysiferol: a squalene-derived metabolite of *Laurencia thysifera*. *Tetrahedron Lett* 1:69–72
301. Gonzalez AG, Arteaga JM, Fernandez JJ, Martin JD, Norte M, Ruano JZ (1984) Marine natural products from the Atlantic zone. 39. Terpenoids of the red alga *Laurencia pinnatifida*. *Tetrahedron* 40:2751–2755
302. Ji NY, Li XM, Xie H, Ding J, Li K, Ding LP, Wang BG (2008) Highly oxygenated triterpenoids from the marine red alga *Laurencia mariannensis* (rhodomelaceae). *Helvetica Chim Acta* 91:1940–1946
303. Little RD, Nishiguchi GA (2008) Synthetic efforts toward, and biological activity of, thysiferol and structurally-related analogues. *Stud Nat Prod Chem* 35:3–56
304. Gerwick WH, Singh IP (2002) Structural diversity of marine oxylipins. In: Kuo TM, Gardner HW (eds) *Lipid biotechnology*. Marcel Dekker, New York
305. Noguchi T, Matsui T, Miyazawa K, Asakawa M, Iijima N, Shida Y, Fuse M, Hosaka Y, Kirigaya C et al (1994) Poisoning by the red alga ‘Ogonori’ (*Gracilaria verrucosa*) on the Nojima Coast, Yokohama, Kanagawa Prefecture, Japan. *Toxicon* 32:1533–1538
306. Gerhart DJ (1984) Prostaglandin A2: an agent of chemical defense in the Caribbean gorgonian *Plexaura homomalla*. *Mar Ecol Prog Ser* 19:181–187
307. Solem ML, Jiang ZD, Gerwick WH (1989) Three new and bioactive icosanoids from the temperate red marine alga *Farlowia mollis*. *Lipids* 24:256–260
308. Orwig KE, Leers-Sucheta S, Moghaddam MF, Jiang ZD, Gerwick WH, Stormshak F (1992) Unique metabolites of eicosapentaenoic acid interfere with corpus luteum function in the ewe. *Prostaglandins* 44:519–530
309. Hamberg M, Gerwick WH (1993) Biosynthesis of vicinal dihydroxy fatty acids in the red alga *Gracilariopsis lemaneiformis*: Identification of a sodium-dependant 12-lipoxygenase and a hydroperoxide isomerase. *Arch Biochem Biophys* 305:115–122
310. Higgs MD, Mulheirn LJ (1981) Hybridolactone, an unusual fatty acid metabolite from the red alga *Laurencia hybrida* (Rhodophyta, Rhodomelaceae). *Tetrahedron* 37: 4259–4262
311. Corey EJ, De B, Ponder JW, Berg JM (1984) The stereochemistry and biosynthesis of hybridolactone, an eicosanoid from *Laurencia hybrida*. *Tetrahedron Lett* 25:1015–1018
312. Nagle DG, Gerwick WH (1990) Constanolactones A and B, novel cyclopropyl hydroxy eicosanoids from the temperate red alga *Constantinea simplex*. *Tetrahedron Lett* 31:2995–2998
313. Gerwick WH (1993) Carbocyclic oxylipins of marine origin. *Chem Rev* 93:1807–1823
314. Molinski TF (2010) Microscale methodology for structure elucidation of natural products. *Curr Opin Biotechnol* 21:819–826
315. van den Hoek C, Mann DG, Jahns HM (1995) *Algae: an introduction to phycology*. Cambridge University Press, Cambridge
316. Katsaros C, Karyophyllis D, Galatis B (2006) Cytoskeleton and morphogenesis in brown algae. *Ann Bot* 97:679–693
317. Charrier B, Coelho SM, Le Bail A, Tonon T, Michel G, Potin P, Kloareg B, Boyen C, Peters AF, Cock JM (2008) Development and physiology of the brown alga *Ectocarpus siliculosus*: two centuries of research. *New Phytol* 177:319–332
318. Cathell MD, Szweczyk JC, Schauer CL (2010) Organic modification of the polysaccharide alginate. *Mini-Rev Org Chem* 7:61–67

319. Hunt NC, Grover LM (2010) Cell encapsulation using biopolymer gels for regenerative medicine. *Biotech Lett* 32:733–742
320. Qin Y (2010) Functional alginate fibers. *Chem Fibers Int* 60:32–33
321. Hara M (1986) Use of alginic acid. Properties and mannuronic acid/guluronic acid ratio of alginic acid. *New Food Ind* 28:10–14
322. Ashton WR (1975) Alginates in the food industry. *Afinidad* 32:653–658
323. Rioux LE, Turgeon SL, Beaulieu M (2010) Structural characterization of laminaran and galactofucan extracted from the brown seaweed *Saccharina longicruris*. *Phytochem* 71:1586–1595
324. Maeda M, Nishizawa K (1968) Fine structure of laminaran of *Eisenia bicyclis*. *J Biochem* 63:199–206
325. Strain HH, Sherma J (1972) Chloroplast pigments of higher plants, green algae, and brown algae and their influence upon the invention, modifications, and applications of Tswett's chromatographic method. *J Chromatogr* 7:371–397
326. Maier I (1995) Brown algal pheromones. *Prog Phycol Res* 11:51–102
327. Jaenicke L (1977) Sex and sex attraction in seaweed. *Trends Biochem Sci* 7:152–155
328. Blunt JW, Copp BR, Munro MHG, Northcote PT, Prinsep MR (2010) Marine natural products. *Nat Prod Rep* 27:165–237
329. Blunt JW, Copp BR, Hu WP, Munro MHG, Northcote PT, Prinsep MR (2009) Marine natural products. *Nat Prod Rep* 26:170–244
330. Cabrita MT, Vale C, Rauter AP (2010) Halogenated compounds from marine algae. *Mar Drugs* 8:2301–2317
331. Abad MJ, Bedoya LM, Bermejo P (2008) Natural marine anti-inflammatory products. *Mini-Rev Med Chem* 8:740–754
332. Boland W (1995) The chemistry of gamete attraction: chemical structures, biosynthesis, and biotic degradation of algal pheromones. *Proc Natl Acad Sci USA* 92:37–43
333. Mueller DG, Jaenicke L (1973) Fucoserraten, the female sex attractant of *Fucus serratus* (Phaeophyta). *FEBS Lett* 30:137–138
334. Mueller DG, Gassmann G (1985) Sexual reproduction and the role of sperm attractants in monoecious species of the brown algae order Fucales (*Fucus*, *Hesperophycus*, *Pelvetia*, and *Pelvetiopsis*). *J Plant Physiol* 118:401–408
335. Moore BS (1999) Biosynthesis of marine natural products: microorganisms and macroalgae. *Nat Prod Rep* 16:653–674
336. Hombeck M, Boland W (1998) Biosynthesis of the algal pheromone fucoserratene by the freshwater diatom *Asterionella formosa* (Bacillariophyceae). *Tetrahedron* 54:11033–11042
337. Juettner F, Mueller H (1979) Excretion of octadiene and octatrienes by a freshwater diatom. *Naturwissenschaften* 66:363–364
338. Wendel T, Juettner F (1996) Lipxygenase-mediated formation of hydrocarbons and unsaturated aldehydes in freshwater diatoms. *Phytochem* 41:1445–1449
339. Pohnert G, Boland W (1997) Pericyclic reactions in nature: synthesis and Cope rearrangement of thermolabile bis-alkenylcyclopropanes from female gametes of marine brown algae (Phaeophyceae). *Tetrahedron* 53:13681–13694
340. Pohnert G, Boland W (1996) Biosynthesis of the algal pheromone hormosirene by the freshwater diatom *Gomphonema parvulum* (Bacillariophyceae). *Tetrahedron* 52:10073–10082
341. Boland W, Pohnert G, Maier I (1995) Biosynthesis of algae pheromones. 4. Pericyclic reactions in nature: spontaneous Cope rearrangement inactivates algae pheromones. *Angew Chem Int Ed Engl* 34:1602–1604
342. Mueller DG, Schmid CE (1988) Qualitative and quantitative determination of pheromone secretion in female gametes of *Ectocarpus siliculosus* (Phaeophyceae). *Biol Chem Hoppe-Seyler* 369:647–653
343. Stratmann K, Boland W, Mueller DG (1993) Biosynthesis of pheromones in female gametes of marine brown algae (Phaeophyceae). *Tetrahedron* 49:3755–3766

344. Stratmann K, Boland W, Mueller DG (1992) Pheromones of marine brown algae: a new branch of eicosanoid metabolism. *Angew Chem Int Ed Engl* 31:1246–1248
345. Faulkner DJ (1987) Marine natural products. *Nat Prod Rep* 4:540–576
346. Amico V, Currenti R, Oriente G, Piattelli M, Tringali C (1981) A phloroglucinol derivative from the brown alga *Zonaria tournefortii*. *Phytochem* 20:1451–1453
347. Gerwick W, Fenical W (1982) Phenolic lipids from related marine algae of the order Dictyotales. *Phytochem* 21:633–637
348. Blackman AJ, Rogers GI, Volkman JK (1988) Phloroglucinol derivatives from three Australian marine algae of the genus *Zonaria*. *J Nat Prod* 51:158–160
349. Munakata T, Ooi T, Kusumi T (1997) A simple preparation of 17 (*R*)-hydroxyeicosatetraenoic acid and eicosapentaenoic acid from the eicosanoyl phloroglucinols, components of the brown alga, *Zonaria diesingiana*. *Tetrahedron Lett* 38:249–250
350. Wisesongpand P, Kuniyoshi M (2003) Bioactive phloroglucinols from the brown alga *Zonaria diesingiana*. *J Appl Phycol* 15:225–228
351. Ragan MA, Glombitza KW (1986) Phlorotannins, brown algal polyphenols. *Prog Phycol Res* 4:130–241
352. Herbert RB (1989) The biosynthesis of secondary metabolites, 2nd edn. Chapman and Hall, London
353. Hay ME, Fenical W (1988) Marine plant–herbivore interactions: the ecology of chemical defense. *Annu Rev Ecol Syst* 19:111–145
354. Ragan MA (1976) Physodes and the phenolic compounds of brown algae. Composition and significance of physodes in vivo. *Bot Mar* 19:145–154
355. Kaur I, Vijayaraghavan MR (1992) Physode distribution and genesis in *Sargassum vulgare* (C. Agardh) and *Sargassum johnstonii* Setchell and Gardner. *Aquat Bot* 45:375–384
356. Rosenthal GA, Janzen DH (1979) Herbivores, their interaction with secondary plant metabolites. Academic, New York
357. Norris JN, Fenical W (1982) Chemical defenses in tropical marine algae. In: Rutzler K, Macintyre IG (eds) The Atlantic barrier reef ecosystem at Carrie Bow Cay, Belize. Smithsonian Contribution to the Marine Sciences. Smithsonian Institution Press, Washington, DC
358. Bernays EA, Cooper-Driver G, Bilgener M (1989) Herbivores and plant tannins. *Adv Ecol Res* 19:263–302
359. Steinberg PD (1992) Geographical variation in the interaction between marine herbivores and brown algal secondary metabolites. In: Paul VJ (ed) Marine chemical ecology. Cornell, New York
360. Pavia H, Cervin G, Lindgren A, Aberg P (1997) Effects of UV-B radiation and simulated herbivory on phlorotannins in the brown alga *Ascophyllum nodosum*. *Mar Ecol Prog Ser* 157:139–146
361. Higa T (1981) Phenolic substances. In: Scheuer PJ (ed) Marine natural products, chemical and biological perspective, vol 4. Academic, London
362. Fukuyama Y, Kodama M, Miura I, Kinzyo Z, Mori H, Nakayama Y, Takahashi M (1990) Anti-plasmin inhibitor. VI. Structure of phlorofucofuroeckol A, a novel phlorotannin with both dibenzo-1,4-dioxin and dibenzofuran elements, from *Ecklonia kurome* Okamura. *Chem Pharm Bull* 38:133–135
363. Glombitza KW, Gerstberger G (1985) Antibiotics from algae. Part 31. Phlorotannins with dibenzodioxin structural elements from the brown alga *Eisenia arborea*. *Phytochem* 24:543–551
364. Fukuyama Y, Kodama M, Miura I, Kinzyo Z, Kido M, Mori H, Nakayama Y, Takahashi M (1989) Anti-plasmin inhibitor. Part III. Structure of an anti-plasmin inhibitor, eckol, isolated from the brown alga *Ecklonia kurome* Okamura and inhibitory activities of its derivatives on plasma plasmin inhibitors. *Chem Pharm Bull* 37:349–353
365. Nakayama Y, Takahashi M, Fukuyama Y, Kinzyo Z (1989) Anti-plasmin inhibitor. Part IV. An anti-plasmin inhibitor, eckol, isolated from the brown alga *Ecklonia kurome* Okamura. *Agric Biol Chem* 53:3025–3030

366. Fukuyama Y, Miura I, Kinzyo Z, Mori H, Kido M, Nakayama Y, Takahashi M, Ochi M (1985) Eckols, novel phlorotannins with a dibenzo-p-dioxin skeleton possessing inhibitory effects on α -2-macroglobulin from the brown alga *Ecklonia kurome* Okamura. *Chem Lett* 6:739–742
367. Mitani Y, Sakai S (1992) Eckols as tyrosinase inhibitors. Japan Patent 04235110 A 19920824
368. Shibata T, Nagayama K, Tanaka R, Yamaguchi K, Nakamura T (2003) Inhibitory effects of brown algal phlorotannins on secretory phospholipase A2s, lipoyxygenases and cyclooxygenases. *J Appl Phycol* 15:61–66
369. Shibata T, Fujimoto K, Nagayama K, Yamaguchi K, Nakamura T (2002) Inhibitory activity of brown algal phlorotannins against hyaluronidase. *Int J Food Sci Tech* 37:703–709
370. Ahn MJ, Yoon KD, Min SY, Lee JS, Kim JH, Kim TG, Kim SH, Kim NG, Huh H, Kim J (2004) Inhibition of HIV-1 reverse transcriptase and protease by phlorotannins from the brown alga *Ecklonia cava*. *Biol Pharm Bull* 27:544–547
371. Nakamura T, Nagayama K, Uchida K, Tanaka R (1996) Antioxidant activity of phlorotannins isolated from the brown alga *Eisenia bicyclis*. *Fisheries Sci* 62:923–926
372. Kim KC, Kang KA, Zhang R, Piao MJ, Kim GY, Kang MY, Lee SJ, Lee NH, Surh YJ, Hyun JW (2010) Up-regulation of Nrf2-mediated heme oxygenase-1 expression by eckol, a phlorotannin compound, through activation of Erk and PI3K/Akt. *Int J Biochem Cell Biol* 42:297–305
373. Glombitza KW, Vogels HP (1985) Antibiotics from algae. XXXV. Phlorotannins from *Ecklonia maxima*. *Planta Med* 4:308–312
374. Nagayama K, Iwamura Y, Shibata T, Hirayama I, Nakamura T (2002) Bactericidal activity of phlorotannins from the brown alga *Ecklonia kurome*. *J Antimicrob Chemother* 50:889–893
375. Hirschfeld DR, Fenical W, Lin GHY, Wing RM, Radlick P, Sims JJ (1973) Marine natural products. VIII. Pachydictyol A, an exceptional diterpene alcohol from the brown alga, *Pachydictyon coriaceum*. *J Am Chem Soc* 95:4049–4050
376. Faulker DJ, Ravi BN, Finer J, Clardy J (1977) Diterpenes from *Dictyota dichotoma*. *Phytochem* 16:991–993
377. Hay ME, Duffy JE, Pfister CA (1987) Chemical defense against different marine herbivores: are amphipods insect equivalents? *Ecology* 68:1567–1580
378. Duffy JE, Hay ME (1990) Seaweed adaptations to herbivory. *BioScience* 40:368–375
379. Gedara SR, Abdel-Halim OB, El-Sharkawy SH, Salama OM, Shier TW, Halim AF (2003) Cytotoxic hydroazulene diterpenes from the brown alga *Dictyota dichotoma*. *Z Naturforsch* 58c:17–22
380. Folmer F, Jaspars M, Dicato M, Diederich M (2010) Photosynthetic marine organisms as a source of anticancer compounds. *Phytochem Rev* 9:557–579
381. Ayyad SEN, Abdel-Halim OB, Shier WT, Hoye TR (2003) Cytotoxic hydroazulene diterpenes from the brown alga *Cystoseira myrica*. *Z Naturforsch* 58c:33–38
382. Zubia M, Fabre MS, Kerjean V, Lann KL, Stiger-Pouvreau V, Fauchon M, Deslandes E (2009) Antioxidant and antitumoural activities of some Phaeophyta from Brittany coasts. *Food Chem* 116:693–701
383. Finer J, Clardy J, Fenical W, Minale L, Riccio R, Battaile J, Kirkup M, Moore RE (1979) Structures of dictyodial and dictyolactone, unusual marine diterpenes. *J Org Chem* 44:2044–2047
384. Kirkup MP, Moore RE (1983) Two minor diterpenes related to dictyodial A from the brown alga *Dictyota crenulata*. *Phytochem* 22:2539–2541
385. Siamopoulou P, Bimplakis A, Iliopoulou D, Vagias C, Cos P, Berghe DV, Roussis V (2004) Diterpenes from the brown algae *Dictyota dichotoma* and *Dictyota linearis*. *Phytochem* 65:2025–2030
386. Manzo E, Ciavatta ML, Bakkas S, Villani G, Varcamonti M, Zanfardino A, Gavagnin M (2009) Diterpene content of the alga *Dictyota ciliolata* from a Moroccan lagoon. *Phytochem Lett* 2:211–215

387. Cronin G, Hay ME (1996) Chemical defenses, protein content, and susceptibility to herbivory of diploid vs. haploid stages of the isomorphic brown alga *Dictyota ciliata* (Phaeophyta). *Bot Mar* 39:395–399
388. Schmitt TM, Lindquist N, Hay ME (1998) Seaweed secondary metabolites as antifoulants. Effects of *Dictyota* spp. diterpenes on survivorship, settlement, and development of marine invertebrate larvae. *Chemoecology* 8:125–131
389. Ninomya M, Matsuka S, Kawakubo A, Bito N (1995) HIV-1 reverse transcriptase inhibitors containing hydroxydictydial or dictydial. Japan Patent 07285877 A 19951031
390. Sun HH, Ferrara NM, McConnell OJ, Fenical W (1980) Bifurcarenone, an inhibitor of mitotic cell division from the brown alga *Bifurcaria galapagensis*. *Tetrahedron Lett* 21:3123–3126
391. Mori K, Uno T (1989) Synthesis and structure revision of bifurcarenone, a unique monocyclic diterpene in combination with hydroquinone C7 unit as an inhibitor of mitotic cell division. *Tetrahedron* 45:1945–1958
392. Mori K, Uno T, Kido M (1990) Determination of the absolute configuration of bifurcarenone by the synthesis of its (1'R,2'R)-isomer. *Tetrahedron* 46:4193–4204
393. Amico A (1995) Marine brown algae of family Cystoseiraceae: chemistry and chemotaxonomy. *Phytochem* 39:1257–1279
394. Faulkner DJ (2002) Marine natural products. *Nat Prod Rep* 19:1–48 and references therein
395. Gerwick WH, Fenical W, Fritsch N, Clardy J (1979) Stypotriol and stypoldione-ichthyotoxins of mixed biogenesis from the marine alga *Stypopodium zonale*. *Tetrahedron Lett* 2:145–148
396. Gerwick WH, Fenical W (1981) Ichthyotoxic and cytotoxic metabolites of the tropical brown alga *Stypopodium zonale* (Lamouroux) Papenfuss. *J Org Chem* 46:22–27
397. Gerwick WH, Fenical W, Norris JN (1985) Chemical variation in the tropical seaweed *Stypopodium zonale* (Dictyotaceae). *Phytochem* 24:1279–1283
398. Sampli P, Tsitsimpikou C, Vagias C, Harvala C, Roussis V (2000) Schimperiol, a new meroterpenoid from the brown alga *Stypopodium schimperi*. *Nat Prod Lett* 14:365–372
399. Dorta E, Diaz-Marrero AR, Cueto M, Darias J (2003) On the relative stereochemistry of atomaric acid and related compounds. *Tetrahedron* 59:2059–2062
400. Dorta E, Cueto M, Diaz-Marrero AR, Darias J (2002) Stypolactone, an interesting diterpenoid from the brown alga *Stypopodium zonale*. *Tetrahedron Lett* 43:9043–9046
401. Depix MS, Martinez J, Santibanez F, Roviroso J, San Martin A, Maccioni RB (1998) The compound 14-keto-stypodiol diacetate from the algae *Stypopodium flabelliforme* inhibits microtubules and cell proliferation in DU-145 human prostatic cells. *Mol Cell Biochem* 187:191–199
402. O'Brien ET, White S, Jacobs RS, Boder GB, Wilson L (1984) Pharmacological properties of a marine natural product, stypoldione, obtained from the brown alga *Stypopodium zonale*. *Hydrobiologia* 116–117:141–145
403. White SJ, Jacobs RS (1983) Effect of stypoldione on cell-cycle progression, DNA and protein synthesis, and cell division in cultured sea-urchin embryos. *Mol Pharmacol* 24:500–508
404. Martinez JL, Sepulveda SP, Roviroso J, San Martin A (1997) Effects in rat isolated aortic ring and atrium of diacetyl epitaondiol, diterpenoid from *Stypopodium flabelliforme* algae. *An Asoc Quim Argent* 85:69–75
405. Wessels M, Koenig GM, Wright AD (1999) A new tyrosine kinase inhibitor from the marine brown alga *Stypopodium zonale*. *J Nat Prod* 62:927–930
406. Roviroso J, Sepulveda M, Quezada E, San-Martin A (1992) Isoepitaondiol, a diterpenoid of *Stypopodium flabelliforme* and the insecticidal activity of stypotriol, epitaondiol and derivatives. *Phytochem* 31:2679–2681
407. Sabry OMM, Andrews S, McPhail KL, Goeger DE, Yokochi A, LePage KT, Murray TF, Gerwick WH (2005) Neurotoxic meroditerpenoids from the tropical marine brown alga *Stypopodium flabelliforme*. *J Nat Prod* 68:1022–1030

408. Sanchez-Ferrando F, San-Martin A (1995) Epitaondiol: the first polycyclic meroditerpenoid containing two fused six-membered rings forced into the twist-boat conformation. *J Org Chem* 60:1475–1478
409. Kurata K, Taniguchi K, Shiraishi K, Hayama N, Tanaka I, Suzuki M (1989) Ecklonialactone A and B, two unusual metabolites from the brown alga *Ecklonia stolonifera* Okamura. *Chem Lett* 2:267–270
410. Kurata K, Taniguchi K, Shiraishi K, Suzuki M (1993) Ecklonialactones C-F from the brown alga *Ecklonia stolonifera*. *Phytochem* 33:155–159
411. Todd JS, Proteau PJ, Gerwick WH (1994) The absolute configuration of ecklonialactones A, B, and E, novel oxylipins from brown algae of the genera *Eckonia* and *Egregia*. *J Nat Prod* 57:171–174
412. Todd JS, Proteau PJ, Gerwick WH (1993) Egregiachlorides A-C: new chlorinated oxylipins from the marine brown alga *Egregia menziesii*. *Tetrahedron Lett* 34:7689–7692
413. Kousaka K, Ogi N, Akazawa Y, Fujieda M, Yamamoto Y, Takada Y, Kimura J (2003) Novel oxylipin metabolites from the brown alga *Eisenia bicyclis*. *J Nat Prod* 66:1318–1323

Brian T. Murphy, Paul R. Jensen, and William Fenical

Contents

3.1	Introduction	154
3.2	Secondary Metabolites from Gram-Negative Marine Bacteria	155
3.2.1	Proteobacteria	155
3.2.2	Bacteroidetes	160
3.2.3	Chloroflexi	163
3.2.4	Verrucomicrobia	163
3.2.5	Aquificae	163
3.2.6	Undescribed Gram-Negative Marine Bacteria	164
3.3	Secondary Metabolites from Gram-Positive Marine Bacteria	164
3.3.1	Firmicutes	164
3.3.2	Actinobacteria (Actinomycetes)	166
3.4	Conclusions	183
3.5	Study Questions	183
	References	184

Abstract

The world's oceans harbor extensive levels of bacterial diversity. Although much of this diversity remains uncharacterized, cultured representatives from a broad range of taxonomic groups are proving to be an important source of novel secondary metabolites. These metabolites include new carbon skeletons as well as compounds with a high degree of halogenation, a relatively common feature of marine-derived secondary metabolites. The bacteria being cultured from marine sources include new taxa, which are proving to be a particularly important source of new chemical entities. This chapter will provide the reader with a brief, though not comprehensive history of the secondary metabolites that

B.T. Murphy (✉) • P.R. Jensen • W. Fenical
 Center for Marine Biotechnology and Biomedicine, Scripps Institution of Oceanography,
 University of California, San Diego, CA, USA
 e-mail: btmurphy@uic.edu, pjensen@ucsd.edu, wfenical@ucsd.edu

have been isolated from marine bacteria. The focus is on the taxonomic distribution of the producing strains and interesting structural features and biological activities of the compounds that are being discovered from marine bacteria.

3.1 Introduction

The marine environment is composed of a myriad of ecologically distinct habitats. Thus, it is not surprising that bacteria adapted to life in the marine environment are both diverse, phylogenetically distinct, and maintain survival adaptations that differ from bacteria that occur on land. One of the earliest physiological differences identified among marine-derived bacteria was the requirement of seawater, or more specifically sodium, for growth. Historically, bacteria demonstrating this physiological requirement were defined as obligate marine. However, there is no *a priori* reason to presume that bacteria lacking this specific marine adaptation should not be considered as part of the autochthonous marine bacterial community. It is common to culture bacteria from marine samples that grow equally well in media prepared with seawater or deionized water. Conversely, bacteria capable of growth on media prepared with salt concentrations equivalent to that of seawater can be readily cultured from nonmarine samples. These strains, it can be presumed, have the potential to grow in both environments. Studies of secondary metabolites from marine-derived bacteria have included strains that appear highly adapted to life in the ocean as well as more cosmopolitan taxa that occur both in the sea and on land. Both groups of bacteria are yielding interesting new secondary metabolites. The following sections highlight select secondary metabolites produced by various taxonomic groups of marine-derived bacteria.

After Alexander Fleming's discovery of penicillin in 1929, terrestrial microorganisms became the focal point for one of the most prolific drug discovery efforts in history. The discoveries of penicillin and later actinomycin (1940) led to the "Great Antibiotic Era" which yielded more than 120 drugs for the treatment of infectious diseases, cancer, elevated cholesterol, immunomodulation, and others. Some of the most important of these discoveries came from studies of the filamentous actinomycete bacteria, which because of their growth forms, were at one time considered to be fungi (hence the suffix "mycetes"). The actinomycetes are responsible for the majority of the antibiotics in clinical use today. From the period 1950 to 1990, most of the pharmaceutical companies invested heavily in microorganism-based drug discovery with financial commitments that reached in the vicinity of \$10 B per year. The intensity of these explorations led to discoveries of new microorganisms from virtually all accessible terrestrial environments, from arctic and cold temperate regions to tropical environments. Interestingly, although the world's oceans occupy more than 70% of the surface of the Earth, this massive resource remained unexplored.

It is now clear that bacteria use small organic molecules, or secondary metabolites, for many important adaptive functions including communication and antagonism. The unique environmental conditions experienced by marine bacteria afford

opportunities for the selective production of secondary metabolites that are not observed outside of the marine environment. One clear example of this is the high level of halogenation observed among the secondary metabolites of marine bacterial origin.

This chapter highlights some of the structurally interesting secondary metabolites that have been isolated from cultured marine bacteria. It is beyond its scope to provide a comprehensive review of all metabolites produced by marine bacteria or to report on cyanobacterial metabolites, which will be addressed in another chapter. Instead, an overview of the metabolites produced by various taxonomic groups of heterotrophic marine bacteria is offered, with a few compounds highlighted for each group. For further information on specific topics, the reader is referred to review articles cited in the Bibliography [1–16]. With a few exceptions, articles published after June 2010 are not included.

This chapter begins with unicellular Gram-negative bacteria and ends with filamentous Gram-positive actinomycetes. It is written with a focus on chemistry and includes details about compound biological activity and the environmental source of the producing strains. We chose to organize this chapter following the framework used in *Bergey's Manual of Determinative Bacteriology* and "The Prokaryotes – A Handbook on the Biology of Bacteria" [17].

3.2 Secondary Metabolites from Gram-Negative Marine Bacteria

Gram-negative bacteria are ubiquitous in marine environments. They are more abundant than their Gram-positive counterparts and are the best studied of the marine bacteria from a taxonomic, ecological, and phylogenetic perspective. In terms of secondary metabolite discovery, fewer compounds have been discovered from Gram-negative marine bacteria, possibly because these bacteria have not been studied as intensively with this goal in mind or that they do not maintain genes involved in secondary metabolism as commonly as Gram-positive forms.

3.2.1 Proteobacteria

The Proteobacteria, formerly known as purple bacteria, constitute the largest and most physiologically diverse bacterial phylum. Indicative of this diversity, the phylum was named after the Greek god Proteus, son of Poseidon, who had the ability to assume different shapes. This phylum comprises the majority of medically and agriculturally significant Gram-negative bacteria. Found within the β -, δ -, and γ -divisions of the Proteobacteria are bacteria that maintain gliding motility. These include a large group of chemically prolific gliding bacteria called the myxobacteria, many of which form fruiting bodies under low-nutrient conditions. In the following two sections, proteobacterial secondary metabolites are organized by class.

3.2.1.1 α - and δ -Proteobacteria

Categorized within the phylum Proteobacteria are the classes α - and δ -Proteobacteria. The mitochondria, found in the eukaryotic cell, are believed to have originated from α -Proteobacteria, a class that is crucial to the regulation of Earth's carbon, sulfur, and nitrogen cycles. The majority of the α -Proteobacteria are rod-shaped. This class includes prokaryotic predators (*Bdellovibrio*), strains that have the ability to glide (myxobacteria), and those that can reduce sulfur. To date, relatively few secondary metabolites have been identified from marine representatives within these classes.

From the cells of an undescribed species of the unicellular marine α -proteobacterium *Agrobacterium*, agrochelin A (**1**), a cytotoxic thiazole alkaloid was isolated [18, 19]. This strain was cultivated from a tunicate collected in the Mediterranean Sea off the east coast of Spain. It displayed inhibitory activity against a panel of tumor cell lines and was shown to form a complex with Zn^{2+} ions. In the search for endothelin-converting enzyme (ECE) inhibitors, B-90063 (**2**), a dimeric oxazole–pyridone analog was isolated from an undescribed species of the marine α -proteobacterium *Blastobacter* [20]. This strain was isolated from the water column on the coast of Ojika Peninsula, Japan, and required seawater for growth. It exhibited antagonistic activities toward endothelins, peptides responsible for the constriction of blood vessels. In addition to the two aforementioned metabolites from α -Proteobacteria, two polyketide-derived metabolites were discovered from two marine-derived myxobacterial strains. An ethylated polyene-substituted pyrone metabolite (phenylnannolone A, **3**) was isolated from the marine δ -proteobacterium *Nannocystis exedens* [21]. Although polyene pyrones have been reported from various terrestrial sources, the presence of an ethyl group on the polyene chain represented a novel deviation from this class of molecules. Biosynthetic studies suggested unprecedented biochemical reactions are employed to form phenylnannolone A. In a program designed to isolate marine myxobacteria, the δ -proteobacterium *Haliangium luteum* was isolated from a marine alga collected in Kanagawa, Japan. This myxobacterium required approximately 2–3% NaCl for growth and the production of the metabolite haliangicin (**4**) [22, 23]. Compound **4** was found to display antifungal activity toward a number of fungi, including the pathogenic strain *Phytophthora capsici* (Fig. 3.1).

3.2.1.2 γ -Proteobacteria

The γ -Proteobacteria consist of over 180 genera and more than 750 species (as of 2007) and are the largest class within the phylum Proteobacteria. This class contains several human and animal pathogens including *Escherichia coli*, *Salmonella typhi* (typhoid fever), *Yersinia pestis* (plague), *Vibrio cholerae* (cholera), *Pseudomonas aeruginosa*, and *Acinetobacter baumannii*. Of all Gram-negative marine bacteria, the γ -Proteobacteria harbor the greatest number of secondary metabolites published in the literature, and these metabolites subsequently exhibit the most structural and functional diversity. Four families within this class, namely, Vibrionaceae, Alteromonadaceae, Pseudoalteromonadaceae, and

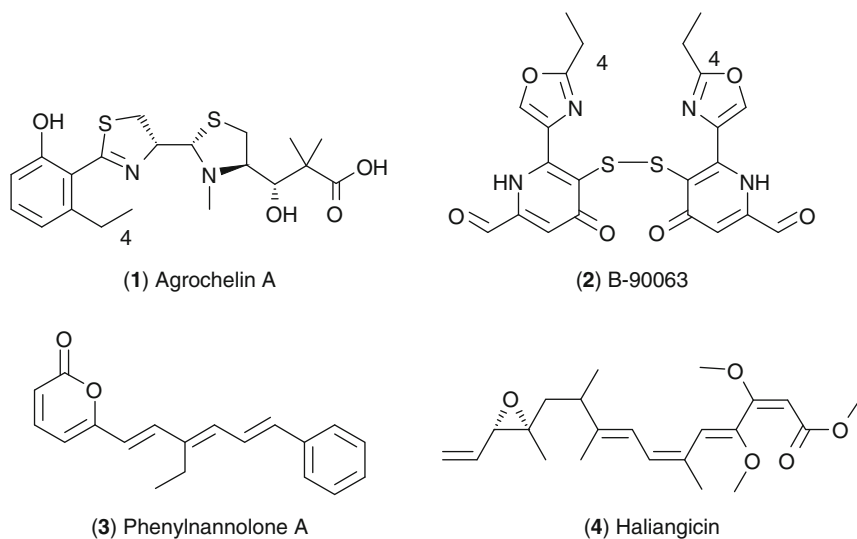


Fig. 3.1 Secondary metabolites from marine α - and δ -Proteobacteria

Pseudomonadaceae, contain genera responsible for the production of the majority of molecules from the Proteobacteria.

Members of the family Vibrionaceae are typically rod-shaped, facultative anaerobes and include several human pathogens such as *V. cholerae*. In the following few examples, indole natural products were isolated from two diverse marine environments. First, an undescribed species of *Vibrio* was isolated from an Okinawan sponge, *Hyrtios altum*. This bacterium produced an unusual indole trimer, trisindoline (**5**) [24]. Similarly, the toxic mucus of the boxfish *Ostracion cubicus* was found to harbor the microbial strain *V. parahaemolyticus*. This fish excretes mucus in response to stress. A structurally similar bis-indole (vibrindole A, **6**) was isolated from this strain and exhibited antibacterial activity against a number of pathogenic bacteria [25]. Also isolated from a *Vibrio* sp. colonizing the surface of the soft coral *Sinularia polydactyla* in the Red Sea (Aquaba, Jordan) was aqabamycin E (**7**) [26].

In a program designed to discover bioactive metabolites from poorly studied taxa, the antibacterial cyclic depsipeptide unnarmicin A (**8**) was isolated from cultures of a bacterium of the genus *Photobacterium*, family Vibrionaceae [27]. The strain was isolated from the water column near Okinawa, Japan. Unnarmicin A exhibited inhibitory activity toward a few α -Proteobacterial strains of the genus *Pseudovibrio* that are common culturable strains from the marine environment. Antimicrobial activity against Gram-positive bacteria (*Bacillus subtilis*) and microalgae (*Prorocentrum micans*) was discovered in association with the unusual magnesium-containing metabolite magnesidin A (**9**) [28, 29]. Magnesidin A is produced by *Vibrio gazogenes*, a pink-colored bacterium isolated from the marine

alga *Caulerpa peltata*, though it originally appeared several years earlier as an impure mixture from a marine *Pseudomonas* sp.

One final example of a natural product isolated from the family Vibrionaceae is that of a rare boron-containing small molecule involved in cell-to-cell bacterial communication known as quorum sensing. AI-2 (**10**) is a fused, bicyclic boronic acid anion that acts as an autoinducer, or an extracellular signaling molecule. AI-2 was first identified in the marine bacterium *Vibrio harveyi*, but its structure eluded the scientific community until it was cocrystallized with its sensor protein target LuxP [30]. AI-2 was found to be one of two molecules that regulate bioluminescence in *V. harveyi* and is one of a growing number of signaling molecules isolated from marine microorganisms. It is now accepted that communication among microbes via secondary metabolites is essential to a variety of processes from bioluminescence to biofilm formation, and even secondary metabolite production (Fig. 3.2).

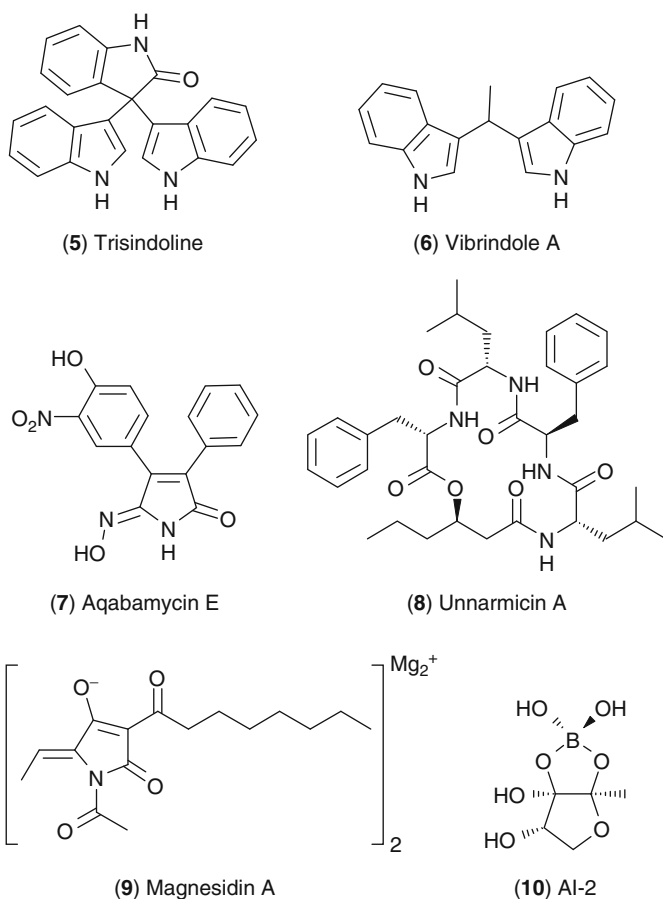


Fig. 3.2 Secondary metabolites from marine γ -Proteobacteria (Vibrionaceae)

As of 2007, the family Pseudomonadaceae contained approximately 15 genera characterized by straight or curved rods. It was from a marine strain of *Pseudomonas bromoutilis* that the first marine microbial natural product, pentabromopseudilin (**11**), was identified in 1966 [31]. This antibiotic contains an unusual framework, possessing a small carbon skeleton while the majority of its molecular mass is derived from bromine. Pentabromopseudilin was known to possess biological activity; however, it was not until 2009 that its specific mechanism of action was identified. It was shown to potently inhibit myosin, a motor protein that facilitates the transport of other important proteins such as tubulin [32]. The potential therapeutic applications of selective myosin inhibitors include the treatment of cancer, heart failure, and malaria.

Within the family Alteromonadaceae is the genus *Alteromonas*, which was originally described in 1972 in order to encompass a number of Gram-negative *Pseudomonas*-like strains isolated from the marine environment. A tripeptide-derived metabolite, **12**, with a novel β -aminopimelic acid component was isolated from a partly classified bacterium falling within the genera *Pseudomonas*/*Alteromonas* [33]. This bacterium was found associated with the common black sea sponge *Dysidea fragilis*. Another sponge associate, an undescribed species of *Alteromonas*, was shown to produce the macrocyclic lactam alteramide A (**13**) [34]. This bacterium was isolated from a sample of the sponge *Halichondria okadai* collected in Kanagawa, Japan, and the resulting metabolite displayed cytotoxicity toward a number of cancer cell lines. An additional *Alteromonas* species that has yet to undergo complete taxonomic identification is *Alteromonas* cf. *rava*. Isolated from seawater, this bacterium produced thiomarinol B (**14**), which displayed antibacterial activity against various Gram-negative and Gram-positive bacteria [35]. This metabolite is a hybrid structure of two previously known antibiotic classes: the pseudomonic acids and the pyrrothines. Finally, an undescribed species of *Alteromonas* was found to colonize the surface of shrimp embryos (*Palaemon macrodactylus*). This bacterium was found to produce a small molecule (isatin, **15**) that chemically defended the embryos from the common crustacean fungal pathogen *Lagenidium callinectes* [36]. This remains a rare example of the functional elucidation of a secondary metabolite within the ecological niche of its producing microorganism.

Within the family Pseudoalteromonadaceae is the genus *Pseudoalteromonas*, which is the source of a large number of marine natural products. Among them is a brominated korormicin derivative (**16**) isolated from a *Pseudoalteromonas* strain collected from the surface of an undescribed species of the macroalga *Halimeda* from the Palauan Sea [37]. The original metabolite korormicin inhibited Na⁺-translocating NADH-quinone reductase, a process of Na⁺ ion translocation that is prevalent in Gram-negative bacteria [38]. This property suggested that korormicin may be useful as an antibiotic against any bacterial strain requiring a sodium pump for survival. The marine strain *Pseudoalteromonas maricaloris*, which was isolated as an epibiont of the Australian sponge *Fascaplysinopsis reticulata*, produced a brominated cyclic peptide (bromoalterochromide A', **17**) that possessed a unique peptidic chromophore [39]. This, and related peptides, exhibited cytotoxicity

toward developing eggs of the sea urchin *Strongylocentrotus intermedius*, thus suggesting a possible ecological role for the metabolites.

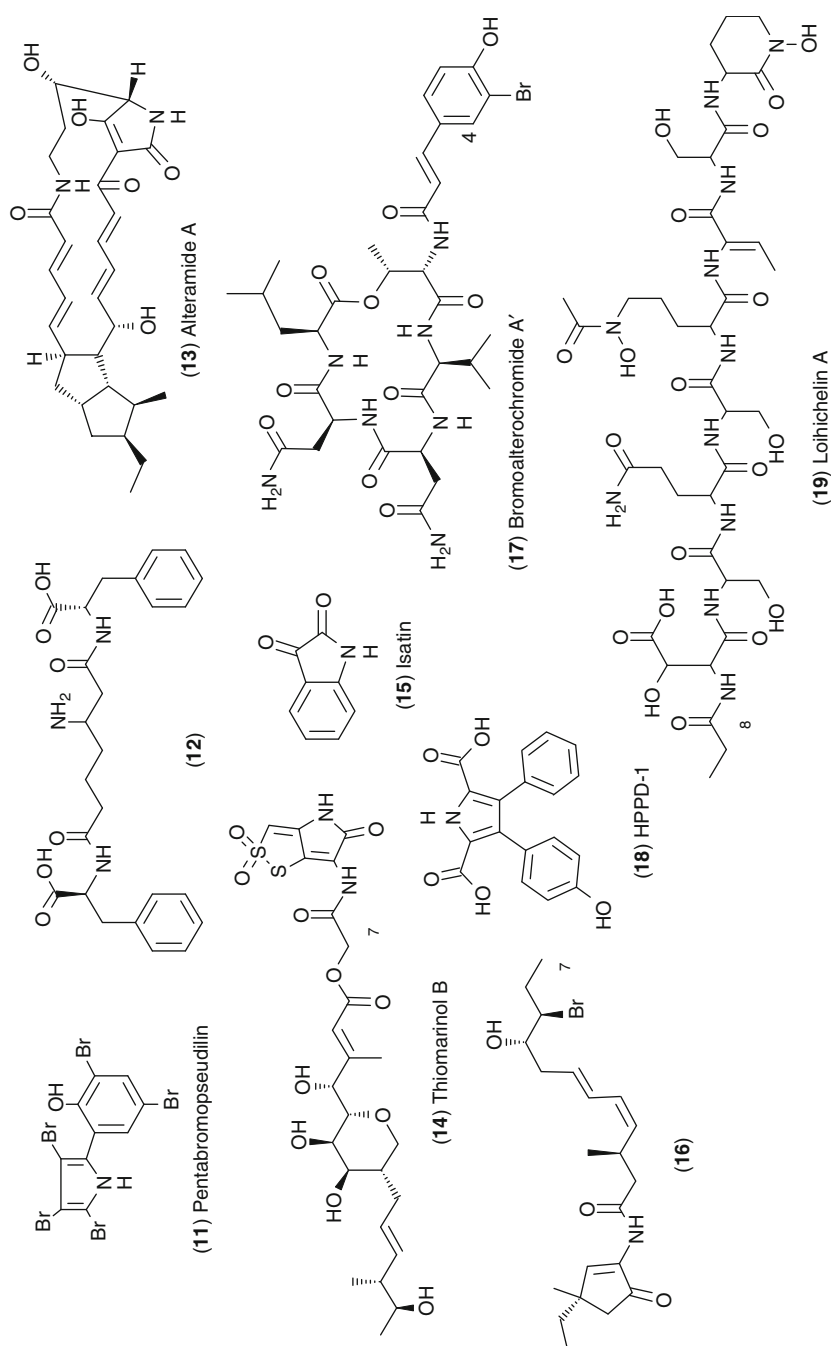
An unidentified species of *Halomonas* from the family Pseudomonadaceae, collected from a water sample in the East Frisian Wadden Sea, Germany, produces the metabolite HPPD-1 (**18**) [40]. It is a diarylpyrrole that exhibited chemopreventive properties. This study provided a nice example of the optimization of growth conditions to boost production of target metabolites. Since laboratory culture conditions do not perfectly represent the environment in which the bacterium previously existed, experimenting with different culture conditions may greatly alter the ability of a microorganism to produce secondary metabolites. One final example of a natural product from a *Halomonas* sp. is the amphiphilic siderophore loihichelin A (**19**) [41]. The producing strain was studied as part of an effort to explore reduced Fe-, Mn-, or S-requiring microorganisms from basaltic rocks. The strain was isolated at approximately 1,700 m from partially weathered surfaces of submarine basalts at the Loihi Seamount, an active Hawaiian volcano laden with Fe(II)-rich hydrothermal fluids. The loihichelins differ from other peptidic siderophores by an increased hydrophilicity due to their longer peptide and shorter fatty acid chains. Their role in nutrient acquisition and interactions with basaltic rock is the topic of ongoing studies (Fig. 3.3).

3.2.2 Bacteroidetes

The phylum Bacteroidetes contains some bacteria that are also considered gliding bacteria. They are typically chemoheterotrophs, found in a diversity of environments, and play important roles in the breakdown of high-molecular-weight dissolved organic matter. There are relatively few studies involving the isolation of natural products from genera within the phylum Bacteroidetes; a few examples are presented below.

Although some bacteria contain terpenoid biosynthetic pathways for the production of carotenoid pigments, bacteria only rarely produce terpenoid secondary metabolites. There are a couple of notable exceptions. From the gliding bacterium *Saprospira grandis* (Saprospiraceae), which captures and digests other bacteria, four diterpenoids of the neoverrucosane class, Fig. 3.4 (**20**), were isolated [42]. From an undescribed species of *Rapidithrix* (family Flammeovirgaceae), which also maintains gliding motility, a new linear hybrid NRPS–PKS peptide antibiotic called ariakemicin A (**21**) was isolated [43]. This compound exhibited selective antibiotic activity against Gram-positive bacteria and was especially potent against the pathogen *Staphylococcus aureus*.

The unusual metabolites **22–25** have also been isolated from two strains of *Cytophaga* (BIO137 and BIO138) within the family Flexibacteriaceae [44]. Strains BIO137 and BIO138 were isolated from biofilms in the North Sea. These new naturally occurring polysulfides were the result of an effort to identify volatile molecules that are typically overlooked in natural product studies. The investigators used gas chromatography coupled with mass

**Fig. 3.3** Secondary metabolites from marine γ -Proteobacteria

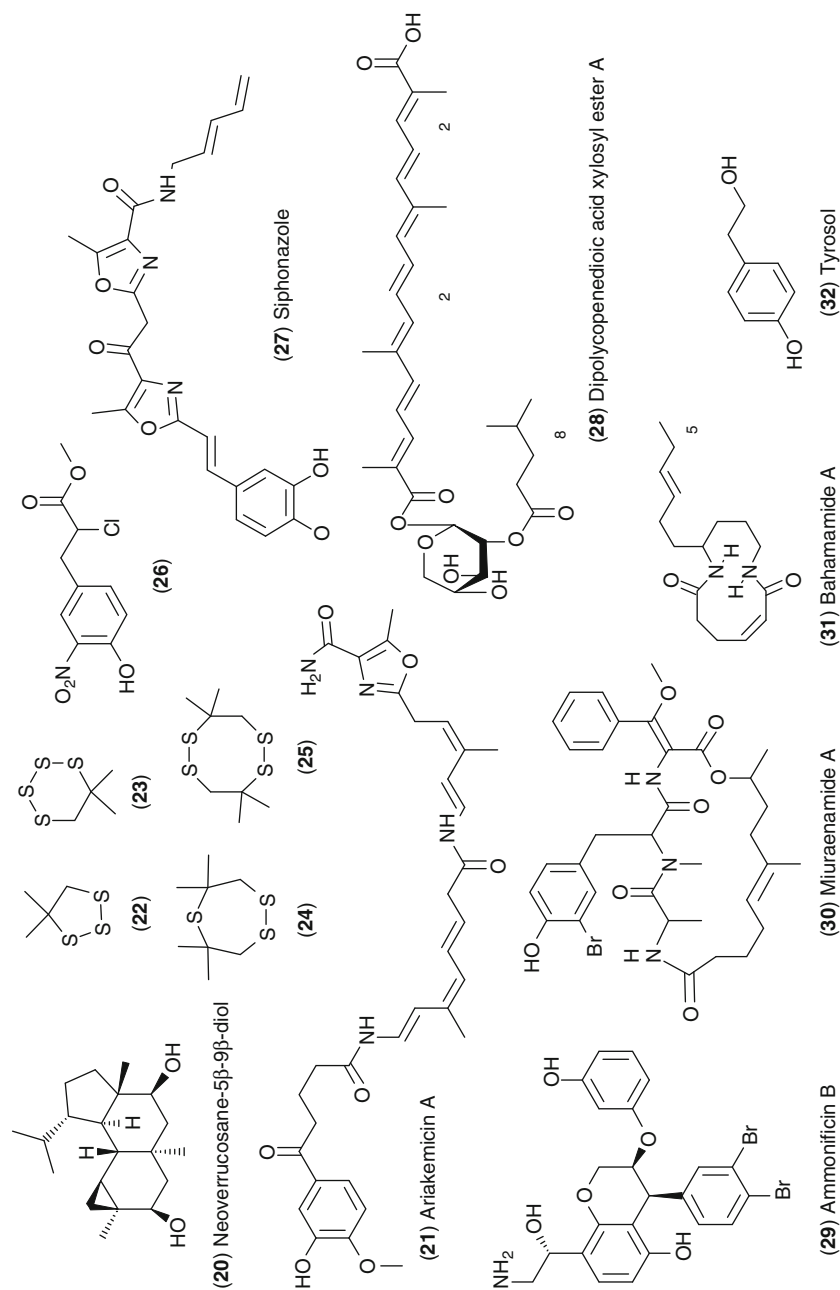


Fig. 3.4 Secondary metabolites from remaining marine Gram-negative bacteria

spectrometry to analyze the volatile components of these strains, and the result was the identification of seven unique thiacycloalkanes, four of which are presented here. Additional metabolites from this family include 25 aromatic nitro derivatives isolated in small yields from the psychrotolerant (ability to survive in cold temperatures) bacterium *Salegentibacter* sp., one of which is presented here (**26**) [45]. These were isolated as a result of efforts to explore secondary metabolite production by marine microorganisms in Arctic and Antarctic habitats.

3.2.3 Chloroflexi

The phylum Chloroflexi is highly diverse and can be divided into five major subdivisions. It is predominantly represented by Gram-negative, filamentous strains with unusual cell envelopes containing either no or little peptidoglycan in their cell walls. It is also the only phylum that consists entirely of bacteria that possess gliding motility. In an effort to expand upon what little is known about the capacity of strains from this phylum to produce secondary metabolites, siphonazole (**27**), a new class of natural products containing both oxazole and aromatic moieties, was isolated from a *Herpetosiphon* sp. [46].

3.2.4 Verrucomicrobia

The phylum Verrucomicrobia, which was established in 2001, is composed of strains that exhibit coccoid or rod-shaped morphologies. They have been observed in environments ranging from the cold sediment of the Arctic Ocean to the tissues of the giant tubeworm *Riftia pachyptila*, an organism found near deep-sea hydrothermal vents. A novel glycosylated polyene named dipolycopenedioic acid xylosyl ester A (**28**) was isolated from the strain *Rubritalea squalenifaciens* within the family Verrucomicrobiaceae [47]. This strain was isolated from the marine sponge *Halichondra okadai*. This molecule was isolated as part of a search for rare carotenoid-like molecules from pigmented marine bacteria.

3.2.5 Aquificae

Within the phylum Aquificae is the order *Aquificales*, members of which are chemolithoautotrophic thermophiles. The bacterium *Thermovibrio ammonificans*, within the family Desulfurobacteriaceae, was isolated from a deep-sea hydrothermal vent on the East Pacific Rise. *T. ammonificans* is a thermophilic, anaerobic strain that produced the dibrominated hydroxyethylamine chroman derivative ammonificin B (**29**) [48]. To date, this is the only known secondary metabolite isolated from this group of bacterial extremophiles.

3.2.6 Undescribed Gram-Negative Marine Bacteria

Taxonomic information has not always been provided from bacterial strains from which natural products have been reported, although there is a movement underway to at least require the deposition of a partial 16 S rRNA gene sequence in association with the report of a bacterial natural product. The following three examples are of metabolites isolated from undescribed Gram-negative marine bacteria. From a slightly halophilic myxobacterial strain (SMH-27-4) isolated from a shallow water sediment collected off the Miura Peninsula, Japan, the antibiotic depsipeptide miuraenamides **30** was isolated [49]. This was part of ongoing attempts to explore the secondary metabolite potential of slow-growing marine-derived strains. Compound **30** exhibited selective inhibition of the phytopathogenic fungus *Phytophthora* sp. and most likely targeted the electron transfer system of the mitochondrial respiratory chain. Bahamamide A (**31**), a 12-membered ring bis-amide that is not commonly observed in nature, was isolated from strain CNE-852 [50]. This strain was isolated from a sediment sample collected in the Bahamas. In an unusual example of symbiosis, embryo surfaces of the American lobster (*Homarus americanus*) were colonized almost entirely by a rod-shaped Gram-negative epibiotic bacterial strain, SGT-76. This strain produced the simple antifungal molecule tyrosol (**32**), which inhibited the growth of the common crustacean pathogenic fungus *Lagenidium callinectes*, thus suggesting a potential ecological function for the natural product and its producing bacterium [51] (Fig. 3.4).

3.3 Secondary Metabolites from Gram-Positive Marine Bacteria

Marine Gram-positive bacteria have been poorly studied by marine microbiologists relative to their Gram-negative counterparts. This may in part be due to the general observation that they are numerically less abundant in most marine habitats. Like terrestrial Gram-positive bacteria, however, marine strains have proven to be a rich source of secondary metabolites. In fact, the majority of natural products that have been characterized from marine bacteria are from Gram-positive strains. Representative compounds and producing organisms are described below.

3.3.1 Firmicutes

The name Firmicutes is derived from the Latin words “firmus” and “cutis,” which mean “strong” and “skin,” respectively. These bacteria are generally unicellular and contain a low G + C content. Within the phylum Firmicutes is the family Bacillaceae, which is typically comprised of rod-shaped cells capable of producing endospores. This family produces the majority of the secondary metabolites reported from the phylum, predominantly because of the chemical capacity of the

genus *Bacillus*. *Bacillus* is one of just under 40 genera in the family Bacillaceae and includes pathogenic strains such as *B. anthracis*, the causative agent of anthrax. Terrestrial bacilli are well-known producers of antibiotics as evidenced by bacitracin, polymyxin, tyrocidin, and gramicidin. As might be expected, marine-derived *Bacillus* strains are also proving to be a rich source of novel secondary metabolites.

From an undescribed deep-sea sediment bacterium (later isolated from a marine strain of *Bacillus amyloliquefaciens*), a novel 24-membered lactone (macrolactin A, **33**) representing a new class of macrolides was isolated [52, 53]. Macrolactin A exhibited considerable antibacterial activity and also antiviral activity against *Herpes simplex*. To date, there have been at least 18 macrolactins isolated, and nearly all have been produced by marine *Bacillus* strains (*B. marinus*, *B. subtilis*, *B. polyfermenticus*, *B. amyloliquefaciens*, and *Bacillus* spp.) [54].

A *Bacillus cereus* strain isolated from the Japanese sponge *Halichondria japonica* was found to produce a cyclic peptide (YM-266183, **34**) composed of a pyridine ring, six thiazole rings, and a number of unusual amino acids [55]. This peptide displayed antibacterial activity selective against a number of Gram-positive drug-resistant strains. Another *B. cereus* strain, isolated from the sea snail *Littorina* sp., was found to produce the potently cytotoxic cyclic peptide homocereulide (**35**) [56], while a strain of *B. silvestris* isolated from a crab collected off Chile was found to produce the antibacterial cyclic peptide bacillistatin 1 (**36**) [57]. Cyclic peptides were also isolated from two undescribed *Bacillus* strains, one sediment-derived strain produced the cyclic heptapeptide halobacillin (**37**), and one collected in Papua New Guinea produced the antibiotic cyclic decapeptide loloin A (**38**) [58].

Another undescribed *Bacillus* species, isolated from the tissues of a tube worm collected in waters off Papua New Guinea, produced the unique nonribosomal peptide bogorol A (**39**) [59]. This linear, cationic peptide is thought to kill bacteria quickly by physically disrupting the cell membrane, and this structural class was proclaimed as a new template for cationic peptide antibiotics. Using the bogorol family of antibiotics, methods for determining the amino acid sequence of cationic peptides was subsequently described [60].

In a feeding study, an undescribed *Bacillus* sp. produced the antibiotic selenohomocysteine (**40**) when grown in a medium containing seleno-DL-methionine [61]. Compound **40** was antibacterial against the Gram-positive bacterial strain *Micrococcus luteus*. In another study, *B. subtilis* was isolated from the intestines of a sardine (*S. melanosticta*) collected off Japan and shown to produce the isocoumarin metabolite bacilosarcin A (**41**) [62]. Although no antibiotic activity was observed, it did contain an unprecedented bicyclic ring system combined with an otherwise common terrestrial metabolite.

In general, marine bacilli have been implicated in the production of cyclic peptides or polyketide-derived macrolides that possess antibacterial activity. The occurrence of macrolactins is, to this date, highly conserved among the genus *Bacillus*.

Of the non-*Bacillus* strains of the family Bacillaceae, a strain of *Halobacillus halophilus* produced the novel C₃₀ carotenoid (**42**) in a study aimed at isolating

carotenoids from pigmented bacteria [63]. *Halobacillus salinus* was shown to produce secondary metabolites that inhibit quorum-sensing-controlled phenotypes in Gram-negative bacteria [64]. This strain was isolated from a sea grass sample collected off the coast of Rhode Island. In cocultivation experiments, the bacterium was found to excrete a metabolite that inhibited bioluminescence in *Vibrio harveyi*. Subsequently, the phenethylamide derivative *N*-(2'-phenylethyl)-isobutyramide (43) was isolated and hypothesized to competitively inhibit typical Gram-negative bacterial signaling molecules (*N*-acyl homoserine lactones) and thereby act as bacterial quorum-sensing agonists.

An additional family within the phylum Firmicutes is the Thermoactinomycetaceae. All members of this taxon contain *meso*-diaminopimelic acid (*meso*-A_{2pm}) in their cell wall and are generally classified as aerobic, chemoorganotrophic microorganisms. From an undescribed species of the genus *Thermoactinomyces*, the potent antitumor thiopeptide mechercharmycin A (44) was discovered [65]. The producing strain was isolated from sea mud collected from Mercherchar in the Republic of Palau. In later studies, this molecule along with its analogs were shown to induce apoptosis in certain cancer cells [66] (Fig. 3.5a, b).

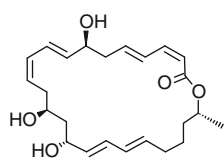
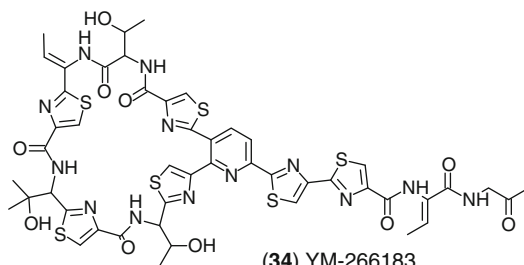
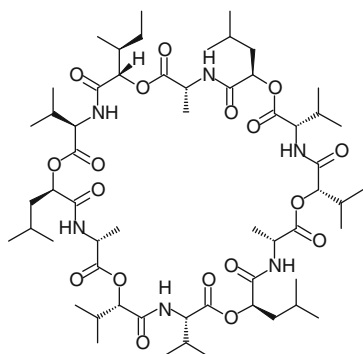
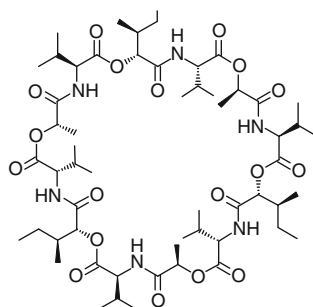
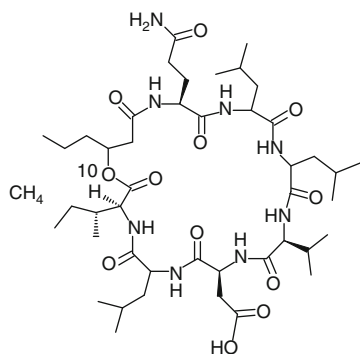
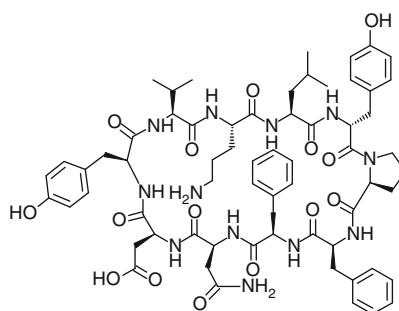
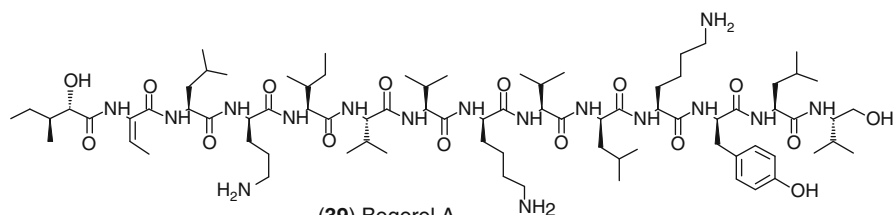
3.3.2 Actinobacteria (Actinomycetes)

In 1875, the first actinomycete genus *Streptothrix* was described, although because of its filamentous morphology, it was originally reported to be a fungus. To differentiate actinomycetes from fungi, the order Actinomycetales was proposed in 1917. Actinomycetes are high G + C content Gram-positive bacteria and are physiologically and morphologically quite diverse. A majority of these bacteria produce branching filaments and form mycelia. There are approximately 50 families containing 195 validated genera (as of 2007) within the phylum Actinobacteria, although only a few families account for more than half of microbial antibiotics discovered to this date, most of which are produced by the genus *Streptomyces*.

3.3.2.1 Streptomycetaceae

Within the family Streptomycetaceae, members of the genus *Streptomyces* are the source of the majority of secondary metabolites isolated from marine-derived bacteria. Although the genus *Streptomyces* is common in terrestrial soils, recent studies have revealed that phylogenetically distinct marine groups can be resolved within this highly diverse genus. The following section presents a compilation of unique structures that may be either of rare occurrence or completely unprecedented from terrestrial bacteria. Descriptions of their chemical and biological properties will be brief, as the focus is intended to be on the diversity of the structures isolated. Additional metabolites discovered from marine-derived *Streptomyces* sp. can be found in Table 3.1 and Figs. 3.6 and 3.7 [67–85].

An undescribed *Streptomyces* species (Merv8102) isolated from a sediment sample collected in the Mediterranean Sea along the Egyptian coastline produced

a**(33)** Macrolactin A**(34)** YM-266183**(35)** Homocereulide**(36)** Bacillistatin 1**(37)** Halobacillin**(38)** Loloatin A**(39)** Bogorol A**Fig. 3.5** (continued)

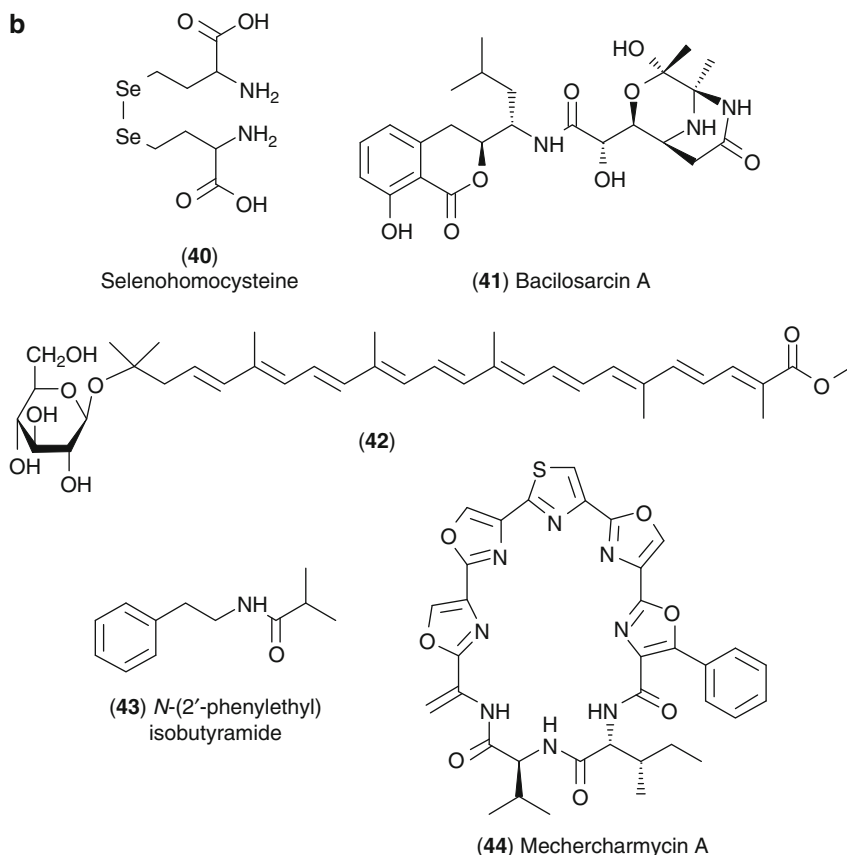


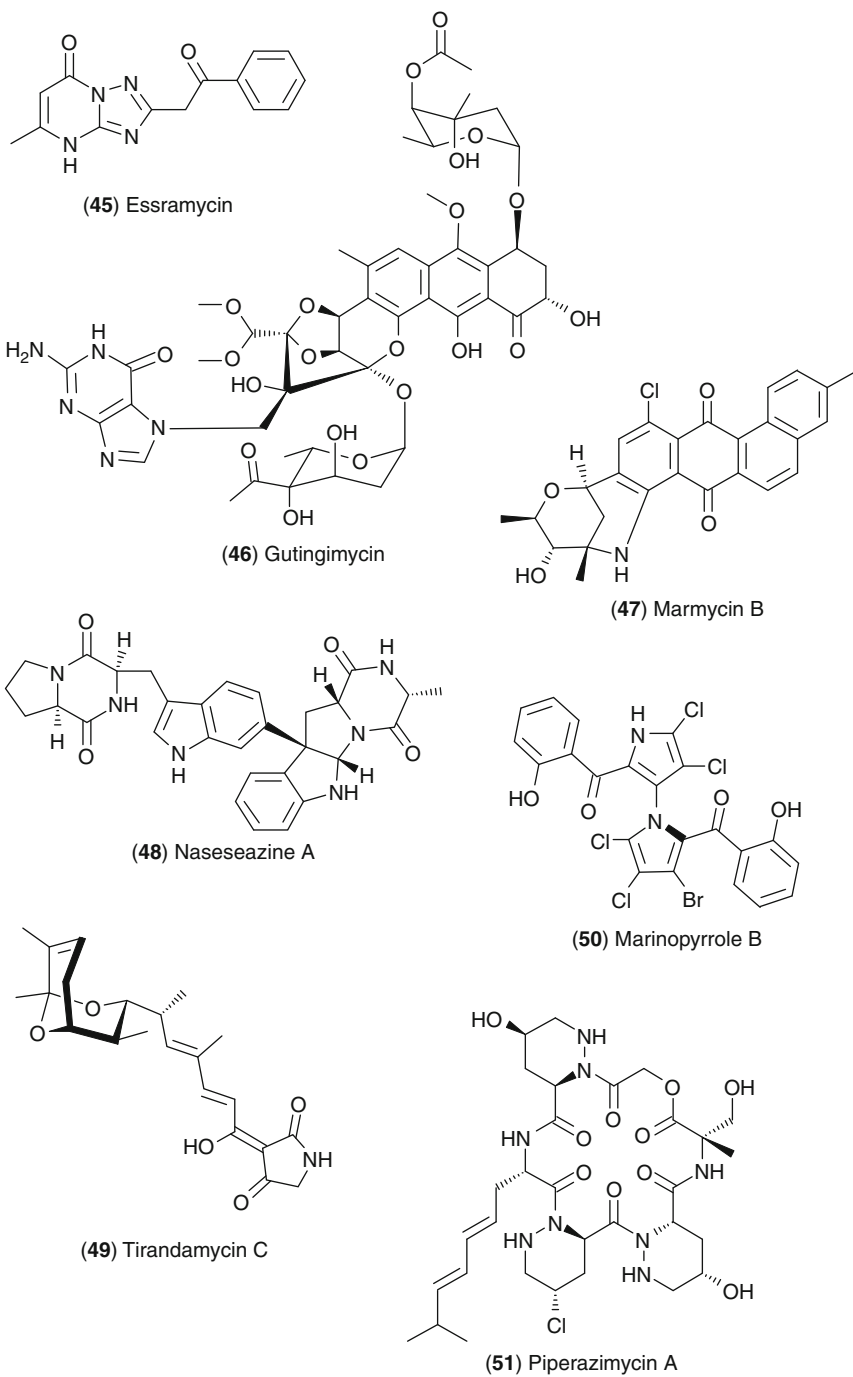
Fig. 3.5 Secondary metabolites from marine Bacillaceae

the first reported naturally occurring triazolopyrimidine antibiotic (essramycin, **45**) [86]. Gutingimycin (**46**), a complex guanine/trioxacarcin A conjugate, was also isolated from an undescribed *Streptomyces* species [87]. The compound was cytotoxic and showed antibacterial activity against a variety of Gram-positive and Gram-negative strains. The biological activity of this complex metabolite was hypothesized to be the result of nucleophilic attack on bacterial DNA resulting in strand cleavage thus offering a potential explanation for its potent cytotoxicity.

Another new structure was obtained from a *Streptomyces* strain cultured from a sediment sample collected in the Sea of Cortez, Baja California Sur, Mexico. Culture of this organism produced the angucycline-like cytotoxic quinone marmycin B (**47**) [88]. This was the first report of an angucycline with both C- and N-glycoside linkages, which resulted in a novel hexacyclic skeleton. From subunits of a common metabolite, new members of a novel chemical scaffold were

Table 3.1 Additional secondary metabolites produced by marine *Streptomyces* spp.

Compound	Source	Properties	Reference
(56) Aburatubolactam A	<i>Streptomyces</i> sp.	Polycyclic macrolactam exhibiting diverse bioactivity	Bae et al. [67]
(57) Altemicidin	<i>Streptomyces</i> sp.	Monoterpene alkaloid with rare azaindene skeleton	Takahashi et al. [68]
(58) Aureoverticillactam	<i>S. aureoverticillactus</i>	22-Membered cytotoxic macrocyclic lactam	Mitchell et al. [69]
(59) Bioxalomycin α 1	<i>Streptomyces</i> sp.	Complex aromatic, polycyclic alkaloid	Bernan et al. [70]
(60) Caboxamycin	<i>Streptomyces</i> sp.	A deep-sea benzoxazole antibiotic active against <i>B. Subtilis</i>	Hohmann et al. [71]
(61) Chinikomycin A	<i>Streptomyces</i> sp.	Chlorinated, aromatic manumycin derivatives; antitumor activity	Li et al. [72]
(62) Daryamide A	<i>Streptomyces</i> sp.	Cytotoxic and weak antifungal metabolite	Asolkar et al. [73]
(63) Glaciapyrrole A	<i>Streptomyces</i> sp.	Rare pyrrole-sesquiterpene metabolite	Macherla et al. [74]
(64) Halawanone A	<i>Streptomyces</i> sp.	Of the isochromane class of quinone antibiotics	Ford et al. [75]
(65) Halichomycin	<i>S. hygroscopicus</i>	16-Membered macrolactam isolated from fish; cytotoxic agent	Takahashi et al. [76]
(66) JBIR-34	<i>Streptomyces</i> sp.	Strain was selected on the basis of a screen for unique NRPS genes	Motohashi et al. [77]
(67) Lajollamycin	<i>S. nodosus</i>	Rare spiro- β -lactone- γ -lactam unit; antitumor and antibiotic activity	Manam et al. [78]
(68) Mansouramycin D	<i>Streptomyces</i> sp.	Compound class showed cytotoxicity toward a panel of tumor cells	Hawas et al. [79]
(69) Marineosin A	<i>Streptomyces</i> sp.	Cytotoxic; hypothesized to derive from novel prodigiosin pathway	Boonlarpradab et al. [80]
(70) Salinamide A	<i>Streptomyces</i> sp.	Complex bicyclic hexadepsipeptide; anti-inflammatory activity	Trischman et al. [81]
(71) Splenosin A	<i>Streptomyces</i> sp.	Inhibitor of pro-inflammatory cytokine production (antiasthma)	Strangman et al. [82]
(72) SS-228Y	<i>Chainia purpurogena</i> (e.g., <i>Streptomyces</i>)	Antibiotic; one of the earliest bioactive molecules isolated from a marine actinomycete	Okazaki et al. [83]
(73) Streptokordin	<i>Streptomyces</i> sp.	Cytotoxic metabolite of the methylpyridine class	Jeong et al. [84]
(74) Teleocidin A ₁	<i>Streptomyces</i> sp.	Isolated from marine-obligate <i>Streptomyces</i> , a sponge colonizer	Izumikawa et al. [85]

**Fig. 3.6** (continued)

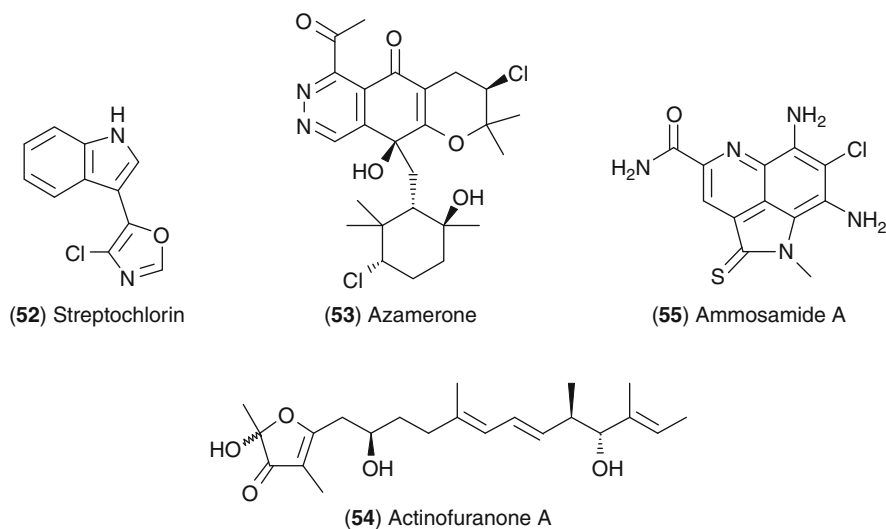
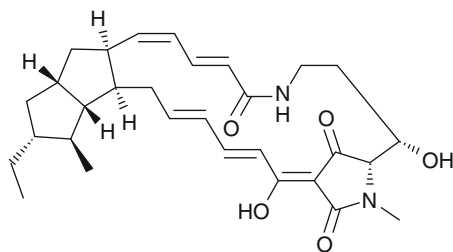


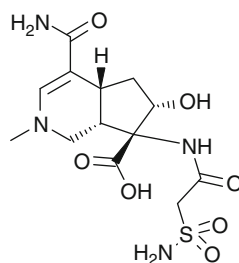
Fig. 3.6 Structures of secondary metabolites from marine *Streptomyces*

observed from a *Streptomyces* strain cultured from a Fijian marine sediment [89]. Nasezeazine A (**48**) and two other classes of dimeric diketopiperazines (asperazines and pestalazines, produced by fungi; not shown here) were hypothesized to result from indole resonance from which nucleophilic attack yielded differing regioselective substitution patterns around the nucleophile's aromatic ring [89]. In a study that afforded the known antibiotic tirandamycin C (**49**), the authors employed a method commonly used to isolate unstable secondary metabolites [90]. Mesh bags of sterilized organic XAD resin were added directly to the microbial fermentation in order to capture metabolites as they were produced. This served to prevent compound degradation or enzymatic conversion within the broth and facilitate the extraction process. Tirandamycin C is a tetramic acid derivative with a 2,4-pyrrolidinedione and is predicted to be produced by hybrid polyketide-nonribosomal peptide biosynthetic machinery [91].

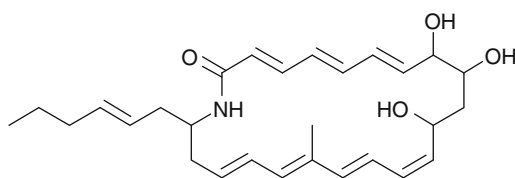
From a marine-derived *Streptomyces* strain that required seawater for growth, marinopyrrole B (**50**) was isolated [92]. This was the first report of a natural product bearing a *N*-, C-2-linked bispyrrole structure. In addition to cytotoxic activity, the marinopyrrole class of molecules displayed significant inhibition against MRSA and with further development may represent a novel pharmacophore for the treatment of this drug-resistant pathogen [93]. The marinopyrroles were also used to develop a streamlined approach toward cellular target elucidation of bioactive natural products [94]. Such an approach serves to increase the efficiency of drug discovery by elucidating the target of a potential drug candidate early in the discovery process; this is especially relevant for metabolites that interact with undesirable targets. In this study, an acyl dye transfer protocol enabled transfer of



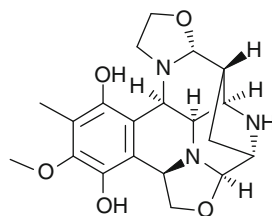
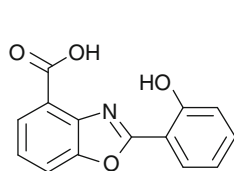
(56) Aburatubolactam A



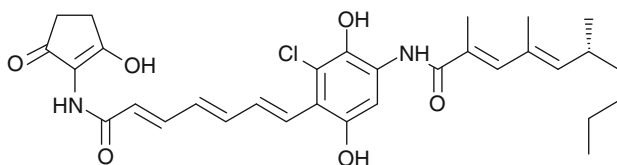
(57) Alternemicidin



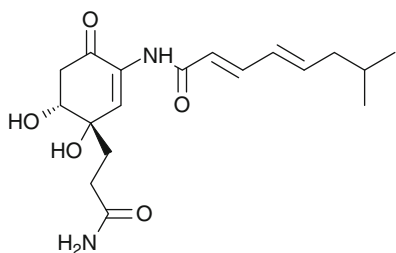
(58) Aureoverticillactam

(59) Bioxalomycin α_1 

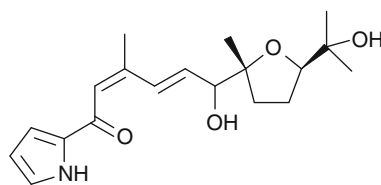
(60) Caboxamycin



(61) Chinikomycin A

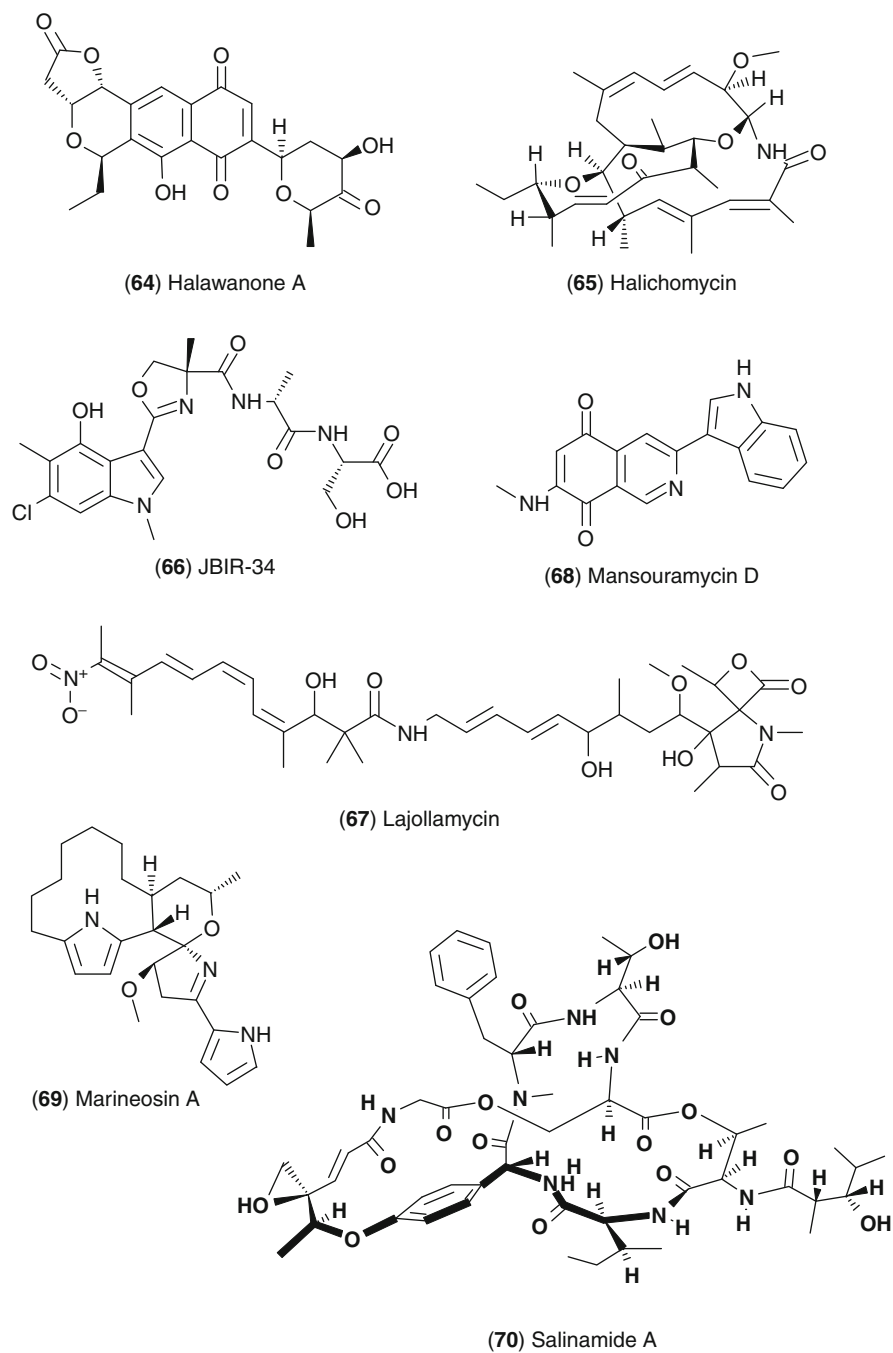


(62) Daryamide A



(63) Glaciapyrrole A

Fig. 3.7 (continued)

**Fig. 3.7** (continued)

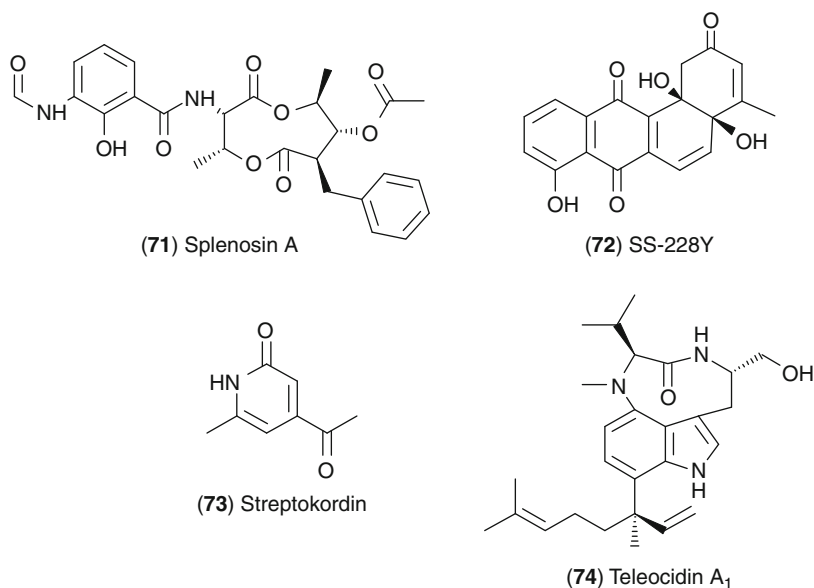


Fig. 3.7 Additional secondary metabolites from marine *Streptomyces*

an immunoaffinity fluorescent tag from the natural product to the protein target. After immunoprecipitation and mass spectral analyses, the protein target of the marinopyrrole class of natural products was determined to be actin.

A sediment-derived *Streptomyces* sp. collected in Guam produced the cyclic hexadepsipeptide piperazimycin A (**51**) [95]. The compound includes a number of rare amino acids. Screening of this molecule against the National Cancer Institute's (NCI) 60-cancer cell line panel revealed that it displayed broad, nanomolar-level cytotoxicity. Sediment from Ayajin Bay, East Sea, Korea, afforded an undescribed species of *Streptomyces*. This strain produced the small molecule streptochlorin (**52**), an indole-substituted chlorinated oxazole [96]. Streptochlorin was found to exhibit antiangiogenic properties through the inhibition of NF κ B, a transcription factor implicated in the progression of certain cancers [97]. Azamerone (**53**) was isolated from a strain that is believed to belong to a new marine species within the genus *Streptomyces* [98]. Azamerone was found to have an unprecedented chloropyranophthalazinone core. This was the first report of a phthalazinone ring system in a natural product. Compound **53** is of mixed polyketide–terpene biosynthetic origin and belongs to the class of metabolites known as meroterpenoids. Thus far, the production of this class of compounds appears to be a trait that is a characteristic of a new group of marine-derived *Streptomyces*, which has tentatively been called MAR4. Also isolated from a related strain was actinofuranone A (**54**), a molecule of polyketide origin [99].

A final example of *Streptomyces* metabolites, the ammosamides, were produced by an undescribed *Streptomyces* species cultured from a deep-sea sediment (1,618 m)

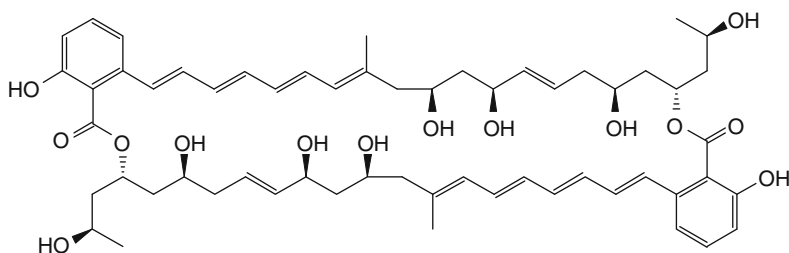
collected in the Bahamas [100]. The cytotoxic agent ammosamide A (**55**) resembled a few other microbial and sponge-derived metabolites, but it was the first natural product to contain a thio- γ -lactam moiety. Using fluorescent labeling techniques, it was determined that the ammosamides target the cytoskeletal protein myosin, an entity involved in cell cycle progression that is of particular interest in the treatment of cancer [101].

A number of new marine lineages have been observed closely related to the genus *Streptomyces* based on 16 S rRNA sequence analysis. Among these is a deeply rooted clade that was originally called MAR2 and subsequently given the informal genus name “*Marinispora*.” The first chemical study of a member of the genus “*Marinispora*” resulted in the isolation of the marinomycins, 44-membered ring macrolides with an unusual substitution pattern of polyol and polyene functionalities when compared to typical polyene macrolides such as amphotericin. Marinomycin A (**75**) showed selective cytotoxicity toward eight melanoma cell lines in the NCI 60 cell line panel and also displayed strong antibacterial activity toward a few drug-resistant bacterial pathogens [102]. Similarly, a study of a “*Marinispora*” strain collected from a sediment sample collected at a depth of 51 m off the coast of La Jolla, California, resulted in the isolation of several 34-membered ring macrolides called the marinisporolides [103]. Marinisporolide A (**76**) contains a bicyclic spiro-bis-tetrahydropyran ketal unit, the only examples of spiroketal-polyenol-polyol macrolides isolated from nature. Like the marinomycins, the marinisporolides are photoreactive and photoisomerize in sunlight to yield olefin isomers. From a sediment sample collected from Cocos Lagoon, Guam, three oxazolidinones were isolated (lipoxazolidinone A–C) from a member of the marine taxon “*Marinispora*” [104]. Lipoxazolidinone A (**77**) exhibited broad-spectrum antibiotic activity, and it was suggested that the oxazolidinone ring system was essential for their bioactivity. Also exhibiting broad-spectrum antibiotic activity were the lynamycins (lynamicin A, **78**), isolated from a “*Marinispora*” sp. cultured from a sediment sample collected from Mission Bay in San Diego, California [105]. These are novel, chlorinated *bis*-indole pyrroles that most importantly show activity against MRSA and vancomycin-resistant *Enterococcus faecium* (VREF) (Fig. 3.8).

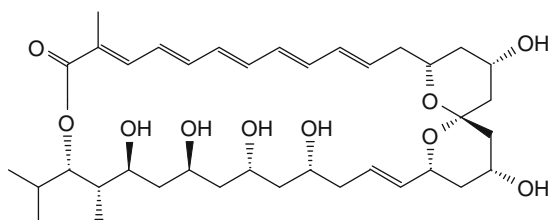
3.3.2.2 Micromonosporaceae

Described in 1938, the Micromonosporaceae is an actinomycete family comprised of more than 20 genera. Within this family are two genera, *Micromonospora* and *Salinispora*, which exemplify the capacity of marine bacteria to produce structurally intriguing secondary metabolites. The genus *Salinispora* is unique among the true marine actinomycete genera described to date in that strains fail to grow when seawater is replaced with deionized water in the culture medium. The genus is currently composed of three species: *S. arenicola*, *S. tropica*, and “*S. pacifica*” (proposed name).

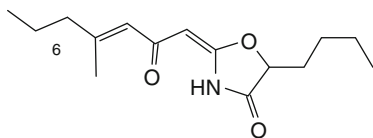
Salinosporamide A (**79**) is undoubtedly the most significant natural product to be isolated from a *Salinispora* species (*S. tropica*) [106]. The producing strain was isolated from a sediment sample collected in the Bahamas. The compound is



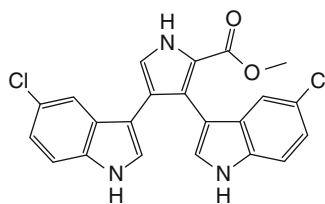
(75) Marinomycin A



(76) Marinisporolide A



(77) Lipoxazolidinone A



(78) Lynamycin A

Fig. 3.8 Secondary metabolites from “*Marinispora*”

structurally similar to the β -lactone omuralide. However, the conspicuous halogenation of the ethyl side chain provides an essential structural element that is required for the potent, irreversible binding to the 20 S proteasome, a validated target in cancer chemotherapy. This natural product is currently in Phase I clinical trials for the treatment of various cancers. Interestingly, it is the natural product itself, not any of the synthetic and semisynthetic analogs that were considered during preclinical development, that was taken into the clinic, further emphasizing “the beauty and power of a selection process offered only by nature [107].” In order to produce quantities sufficient for clinical development and commercialization, several steps of the bacterial fermentation process were optimized to increase production of **79** from a few mg/L (original laboratory conditions) to 450 mg/L [108–110]. This represented the first manufacture of a substance in clinical trials by saline fermentation and emphasized the advantages and flexibility of producing a drug candidate through microbial fermentation.

The discovery of salinosporamide A has also inspired molecular engineering of the pathway in an effort to produce new derivatives. One such example is the

engineered production of fluorosalinisporamide A (**80**) by *S. tropica* [111]. Though fluorinated natural products are rare, they account for 15% of pharmaceutical products on the market. To create the fluorinated version of the compound, a *S. tropica* mutant was generated in which the fluorination gene *flA*, taken from *Streptomyces cattleya*, was used to replace the *salL* chlorinase gene normally found in *S. tropica*. This mutant produced **80** in the presence of inorganic fluoride, thus emphasizing an avenue by which a host organism may be genetically engineered to produce novel analogs of a biomedically important secondary metabolite.

Other secondary metabolites from *S. tropica* include salinilactam (**81**) and the polycyclic macrolide sporolide A (**82**) [112, 113]. The biosynthetic pathway for salinilactam production was originally identified during the analysis of the *S. tropica* strain CNB-440 genome sequence. Bioinformatic analysis played a key role in assigning the final structure of this compound, thus illustrating the value of combining genomic analyses with natural product isolation and identification. Sporolide A is a remarkable polycyclic chlorinated macrolide that is composed of a highly oxidized carbon skeleton (23 out of its 24 carbons are oxygenated or sp² hybridized). The majority of this skeleton has never been reported in any chemical or biological study. The chlorinated cyclopenta[*a*]indene ring was shown to emerge from an unstable nine-membered enediyne precursor via the nucleophilic addition of chloride, a process that has been verified in laboratory experiments [114]. Sequence analysis of the *S. tropica* genome uncovered two biosynthetic loci that encoded for enediyne polyketide synthases (PKSEs), one of which strongly correlated with the formation of the proposed sporolide precursor. This biosynthetic study highlights the breadth of information available when genomic analyses are coupled with traditional drug discovery efforts.

Three cyclic heptapeptides (cyclomarins A-C) were found to be produced by *S. arenicola* (and earlier from a *Streptomyces* species) [115, 116]. Cyclomarin A (**83**), the major metabolite, was composed of four unusual amino acids and displayed in vitro and in vivo anti-inflammatory activity. An *S. arenicola* strain from a Fijian sediment collection was shown to produce the cyclohexadepsipeptide arenamide A (**84**) [117]. This metabolite displayed chemopreventive properties, inhibiting NFκB and nitric oxide production. From another *S. arenicola* strain, a 26-membered macrolide (arenicolide A, **85**) in addition to the unusual polyketide saliniketal (**86**) was isolated [118, 119]. Saliniketal contains a novel bicyclic ring system and was shown to inhibit ornithine decarboxylase induction, an important target for cancer chemoprevention. Both metabolites **85** and **86** were isolated from an *S. arenicola* strain cultured from sediment samples collected from the coastal waters off Guam. Arenimycin (**87**) was isolated from an *S. arenicola* strain found in association with the ascidian *Ecteinascidia turbinata*, collected from a mangrove channel at Sweetings Cay, Grand Bahama Island [120]. This program focused on the screening of actinomycetes against a rifampin-resistant strain of the pathogen MRSA. Arenimycin exhibited strong inhibition of this pathogen, although potent cytotoxicity prevented further exploration of its antibiotic activities.

From a strain of “*S. pacifica*” isolated from a sediment sample collected in the waters off Palau, the simple polyketide salinipyron A (**88**) was isolated [121].

This metabolite is thought to be derived from a mixed precursor polyketide biosynthesis involving acetate, propionate, and butyrate building blocks. Also produced by a “*S. pacifica*” strain isolated from a sediment sample collected at a depth of 500 m off Palau is cyanosporaside A (**89**) [122]. The cyano-containing halogenated aglycone was found to possess a novel 3-keto-pyranohexose sugar. Like sporolide A (**82**), cyanosporaside A is thought to be the cyclization product of an enediyne precursor (Fig. 3.9).

A *Micromonospora* strain cultured from the ascidian *Didemnum proliferum* produced diazepinomicin (**90**), whose unique dibenzodiazepine skeleton was the first to be reported in the peer-reviewed literature [123]. This metabolite was discovered as a result of a program designed to screen microbes for cytotoxic agents that can be linked to monoclonal antibodies targeting tumor-specific antigens. A halophilic strain of the same genus, *Micromonospora lomaivitiensis*, was isolated from the ascidian *Polysyncraton lithostrotum*. This bacterium produced two dimeric diazobenzofluorene glycosides (lomaivitins A (**91**) and B) that exhibited potent cytotoxicity [124]. The structural architecture of the lomaivitins is somewhat similar to the kinamycin antibiotics, although they are unique in the sense of their greater complexity. The antitumor agent thiocoraline (**92**) was isolated from a culture of *Micromonospora marina*, isolated from a soft coral from the Indian Ocean [125]. Thiocoraline A is a symmetric, octadepsipeptide that resembles the quinoxaline antibiotics echinomycin and triostin A, although thiocoraline contains a thioester in its backbone and two glycine residues in place of alanine residues. The latter trait has been proposed to afford improved DNA intercalation [126, 127]. A *Micromonospora* sp., isolated from an Indian Ocean coral, was found to produce the spiroketal-containing macrolide IB-96212 (**93**), which displayed cytotoxic properties [128].

The genus *Verrucosispora* within the family Micromonosporaceae has also proven to be chemically prolific. *Verrucosispora maris*, isolated from a sediment sample from the Sea of Japan (depth 289 m), produced the abyssomicins (abyssomicin C, **94**) and proximicins, the latter of which are characterized by 4-amino-furan-2-carboxylic acid cores [129, 130]. Abyssomicin C was the first natural product found to inhibit *p*-aminobenzoic acid biosynthesis (*p*ABA), a new target for antibiotic drug discovery. Its bioactivity, unique structure, and novel mechanism of action serve as an example of the potential for marine taxa to produce interesting, biomedically significant molecules. This discovery was the result of a program designed to screen microorganisms for inhibitors of the *p*ABA pathway. Proximicin A (**95**) was found to contain a previously unknown γ -amino acid and displayed cytotoxicity toward a few tumor cell lines.

A strain of *Verrucosispora gifthornensis* cultured from an unidentified ascidian collected off Hiroshima, Japan, was found to produce the terpenoid gifthornelone A (**96**) [131]. This isopimaradiene derivative was the result of a program specifically designed to discover novel terpenoids from actinomycetes; its structural similarity to known steroidal androgen antagonists such as dihydrotestosterone led to the discovery of antagonistic activity against an androgen receptor.

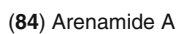


Fig. 3.9 (continued)

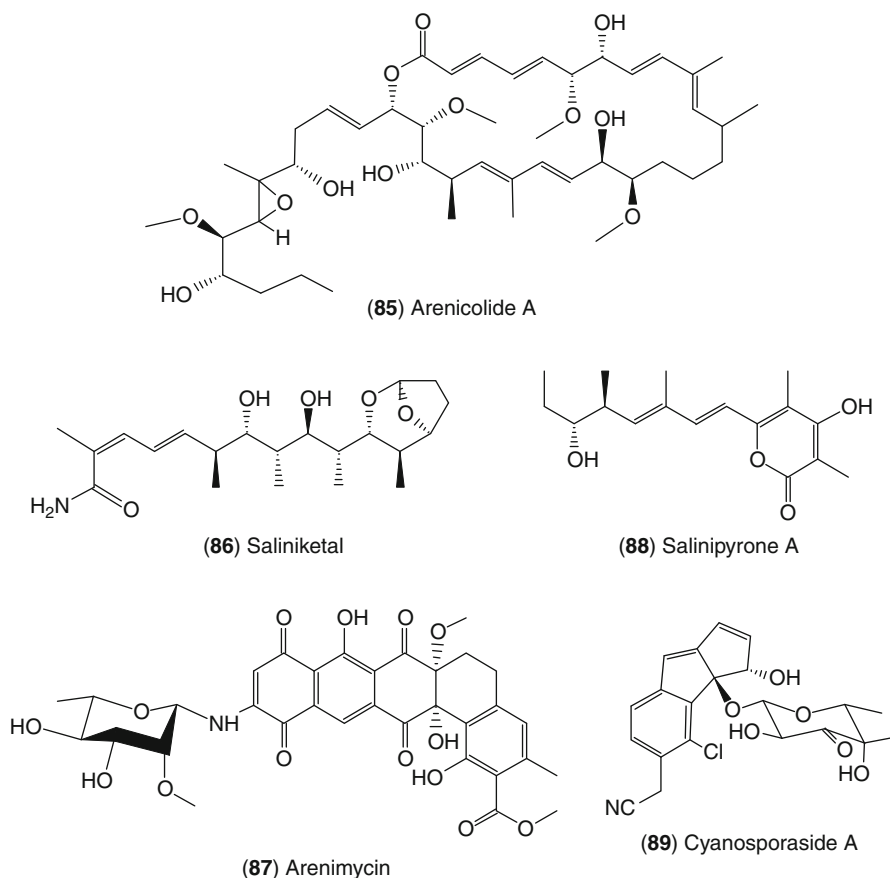
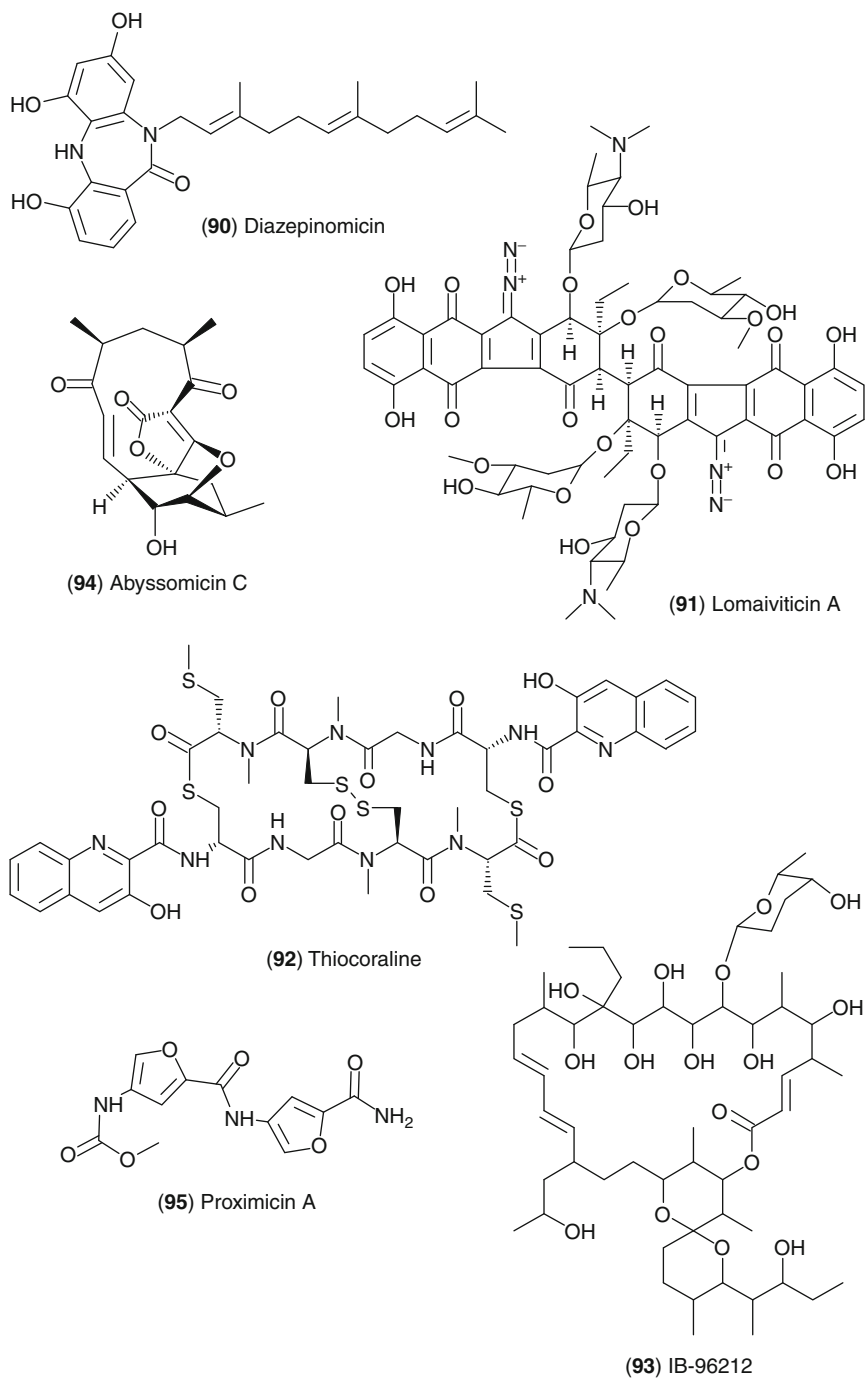


Fig. 3.9 Secondary metabolites from *Salinispora*

3.3.2.3 Additional Families of Actinobacteria

The family Nocardiopepsaceae was created in 1996 in order to accommodate a number of phylogenetically related strains of *Nocardiopepsis*. Two peptides, MKN-349A (97) and lucentamycin A (98), were reported from marine-derived strains of *Nocardiopepsis* [132, 133]. Lucentamycin A is a cytotoxic substance isolated from *Nocardiopepsis lucentensis*, cultured from a strain isolated from a shallow saline pond in the Bahamas. It was the first report of a ethylenepiprole amino acid unit in nature. Kahakamide A (99) is a rare *N*-glycosyl indole antibiotic isolated from *N. dassonvillei* cultured from a marine sediment collected from Kauai, Hawaii [134]. It displayed antibacterial activity against *B. subtilis*.

The family Pseudonocardiaceae is composed of fewer than 20 genera. Within this family is the genus *Saccharopolyspora*. A *Saccharopolyspora* strain was cultured from a sample of the sponge *Haliclona* sp. and found to produce

**Fig. 3.10** (continued)

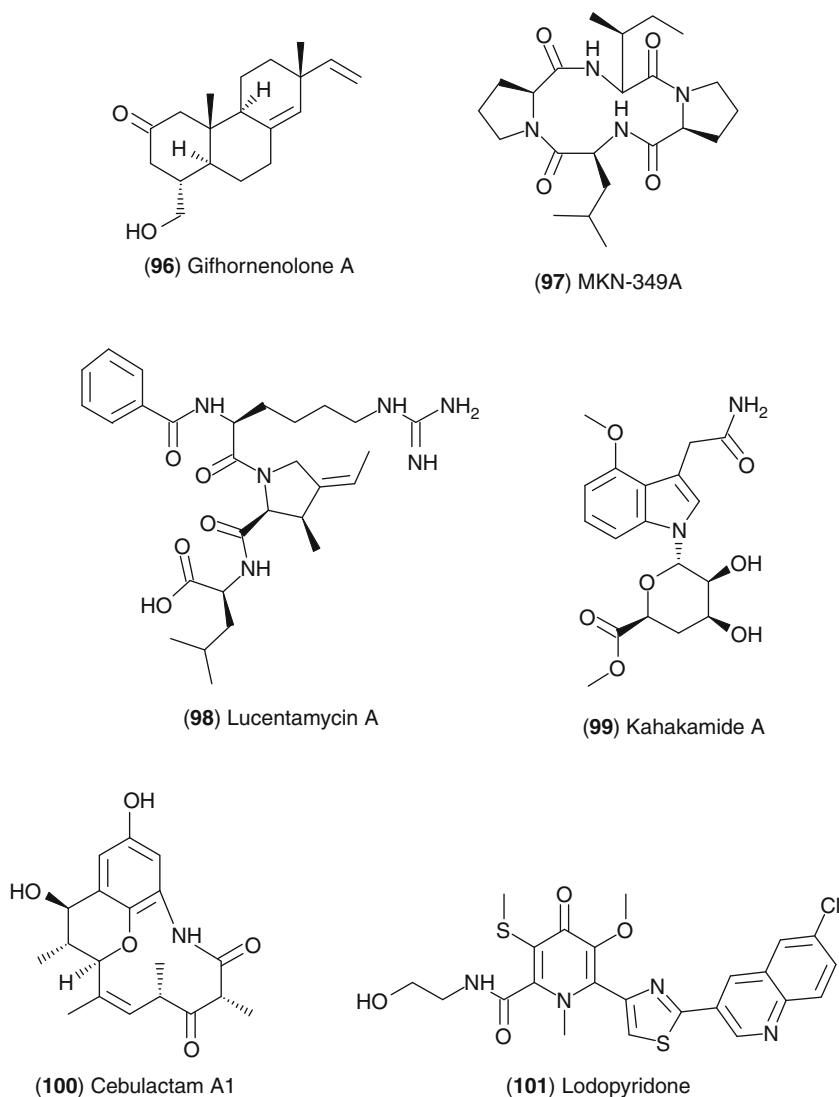


Fig. 3.10 Secondary metabolites from marine *Micromonosporaceae*

cebulactam A1 (**100**) [135]. This study included the first report of an obligate marine *Saccharopolyspora*. Another actinomycete that was reported to have an obligate requirement of seawater for growth was the *Saccharomonospora* strain CNQ-490. This strain was isolated at a depth of 45 m from a sediment sample collected in the La Jolla Canyon off San Diego, CA. In culture, this strain produced lodopyridone (**101**), a quinoline alkaloid of an unprecedented carbon skeleton

whose combination of heterocyclic units (oxygenated 4-pyridone, thiazole, and chlorinated quinoline) is unlike any secondary metabolite observed to this date [136] (Fig. 3.10).

3.4 Conclusions

Bacteria produce small molecules that are not essential for survival but that may enhance fitness or provide survival advantage. These secondary metabolites not only serve as both initiators and regulators of diverse ecological processes, but they can also be used to treat or probe the causes of human disease. Modern medicine has long relied on microbial natural products to treat infectious disease, cancer, and other recalcitrant ailments. However, the arsenal of small molecule drug candidates has shrunk in part due to a paradigm shift by the pharmaceutical industry away from microbial natural products in favor of other drug discovery platforms. There is now however an ongoing resurgence of interest in natural product drug discovery. This interest is fueled by the availability of new and more precise techniques in analytical chemistry and the recognition that nature remains the best resource for the types of new small molecule organic scaffolds around which pharmaceutical agents have historically been developed. Included among current natural product discovery efforts are studies of new populations of bacteria, including those that reside in the marine environment. Marine-derived bacteria include new taxonomy groups as well as species that also occur on land. Collectively, these bacteria are yielding a wealth of new structures including agents that are advancing through various stages of clinical development, solidifying the importance of exploring new habitats and resources in the search for novel bacterial secondary metabolites.

3.5 Study Questions

1. Although often similar in appearance, how are bacteria different from fungi?
2. What family of bacteria is recognized as the most prolific producers of bioactive compounds? What is the most important genus?
3. What is the fundamental difference between Gram-positive and Gram-negative bacteria?
4. What was the first truly marine genus of bacteria to be described?
5. When and by whom was penicillin discovered?
6. The ocean comprises what percentage of the Earth's surface?
7. Which bacterial group, Gram-positive or Gram-negative, produces the most antibiotics?

Acknowledgments The authors thank the National Institutes of Health (Grant # RO1 GM85770 to PRJ), and in particular the National Cancer Institute (Grant # R37 CA044848 to WF), for their support in developing the field of marine microbial natural products chemistry.

References

1. Blunt JW, Copp BR, Hu WP et al (2008) Marine natural products. *Nat Prod Rep* 25:35–94
2. Bull AT, Stach JE (2007) Marine actinobacteria: new opportunities for natural product search and discovery. *Trends Microbiol* 15:491–499
3. Clardy J (2005) Using genomics to deliver natural products from symbiotic bacteria. *Genome Biol* 6:232
4. Cragg GM, Grothaus PG, Newman DJ (2009) Impact of natural products on developing new anti-cancer agents. *Chem Rev* 109:3012–3043
5. Dobretsov S, Teplitski M, Paul V (2009) Mini-review: quorum sensing in the marine environment and its relationship to biofouling. *Biofouling* 25:413–427
6. Fenical W, Jensen PR (2006) Developing a new resource for drug discovery: marine actinomycete bacteria. *Nat Chem Biol* 2:666–673
7. Fenical W (1993) Chemical studies of marine bacteria. *Chem Rev* 93:1673–1683
8. Lam KS (2006) Discovery of novel metabolites from marine actinomycetes. *Curr Opin Microbiol* 9:245–251
9. Miller MB, Bassler BL (2001) Quorum sensing in bacteria. *Annu Rev Microbiol* 55:165–199
10. Molinski TF, Dalisay DS, Lievens SL et al (2009) Drug development from marine natural products. *Nat Rev Drug Discov* 8:69–85
11. Moore BS (2005) Biosynthesis of marine natural products: microorganisms (Part A). *Nat Prod Rep* 22:580–593
12. Nett M, König GM (2007) The chemistry of gliding bacteria. *Nat Prod Rep* 24:1245–1261
13. Olano C, Mendez C, Salas JA (2009) Antitumor compounds from marine actinomycetes. *Mar Drugs* 7:210–248
14. Ward AC, Bora N (2006) Diversity and biogeography of marine actinobacteria. *Curr Opin Microbiol* 9:279–286
15. Williams PG (2009) Panning for chemical gold: marine bacteria as a source of new therapeutics. *Trends Biotechnol* 27:45–52
16. Laatsch H (2006) Marine bacterial metabolites. In: Proksch P, Müller WEG (eds) *Frontiers in marine biotechnology*. Horizon Bioscience, Norfolk, pp 225–288
17. Dworkin M, Falkow S (2006) *The prokaryotes: a handbook on the biology of bacteria*. Springer, New York
18. Acebal C, Canedo LM, Puentes JL et al (1999) Agrochelin, a new cytotoxic antibiotic from a marine *Agrobacterium*. Taxonomy, fermentation, isolation, physico-chemical properties and biological activity. *J Antibiot* 52:983–987
19. Canedo LM, de la Fuente JA, Gesto C et al (1999) Agrochelin, a new cytotoxic alkaloid from the marine bacteria *Agrobacterium* sp. *Tetrahedron Lett* 40:6841–6844
20. Takaishi S, Tuchiya N, Sato A et al (1998) B-90063, a novel endothelin converting enzyme inhibitor isolated from a new marine bacterium, *Blastobacter* sp. SANK 71894. *J Antibiot* 51:805–815
21. Ohlendorf B, Leyers S, Krick A et al (2008) Phenylannolones A–C: biosynthesis of new secondary metabolites from the myxobacterium *Nannocystis exedens*. *Chembiochem* 9:2997–3003
22. Fudou R, Iizuka T, Sato S et al (2001) Haliangicin, a novel antifungal metabolite produced by a marine myxobacterium. 2. Isolation and structural elucidation. *J Antibiot* 54:153–156
23. Kundim BA, Ito Y, Sakagami Y et al (2003) New haliangicin isomers, potent antifungal metabolites produced by a marine myxobacterium. *J Antibiot* 56:630–638
24. Kobayashi M, Aoki S, Gato K et al (1994) Marine natural products. XXXIV. Trisindoline, a new antibiotic indole trimer, produced by a bacterium of *Vibrio* sp. separated from the marine sponge *Hyrtios altum*. *Chem Pharm Bull (Tokyo)* 42:2449–2451
25. Bell R, Carmeli S, Sar N (1994) Vibrindole A, a metabolite of the marine bacterium, *Vibrio parahaemolyticus*, isolated from the toxic mucus of the boxfish *Ostracion cubicus*. *J Nat Prod* 57:1587–1590

26. Fotso Fondja Yao CB, Zereini WA, Fotso S et al (2010) Aqabamycins A-G: novel nitro maleimides from a marine *Vibrio* species: II. Structure elucidation. *J Antibiot* 63:297–301
27. Oku N, Kawabata K, Adachi K et al (2008) Unnarmicins A and C, new antibacterial depsipeptides produced by marine bacterium *Photobacterium* sp. MBIC06485. *J Antibiot* 61:11–17
28. Gandhi NM, Nazareth J, Divekar PV et al (1973) Letter: magnesidin, a novel magnesium-containing antibiotic. *J Antibiot* 26:797–798
29. Imamura N, Adachi K, Sano H (1994) Magnesidin A, a component of marine antibiotic magnesidin, produced by *Vibrio gazogenes* ATCC29988. *J Antibiot* 47:257–261
30. Chen X, Schauder S, Potier N et al (2002) Structural identification of a bacterial quorum-sensing signal containing boron. *Nature* 415:545–549
31. Burkholder PR, Pfister RM, Leitz FH (1966) Production of a pyrrole antibiotic by a marine bacterium. *Appl Microbiol* 14:649–653
32. Fedorov R, Bohl M, Tsiavaliaris G et al (2009) The mechanism of pentabromopseudilin inhibition of myosin motor activity. *Nat Struct Mol Biol* 16:80–88
33. De Rosa S, De Giulio A, Tommonaro G et al (2000) A beta-amino acid containing tripeptide from a *Pseudomonas-alteromonas* bacterium associated with a black sea sponge. *J Nat Prod* 63:1454–1455
34. Shigemori H, Bae M-A, Yazawa K et al (1992) Alteramide A, a new tetracyclic alkaloid from a bacterium *Alteromonas* sp. associated with the marine sponge *Halichondria okadai*. *J Org Chem* 57:4317–4320
35. Shiozawa H, Kagasaki T, Torikata A et al (1995) Thiomarinols B and C, new antimicrobial antibiotics produced by a marine bacterium. *J Antibiot* 48:907–909
36. Gil-Turnes MS, Hay ME, Fenical W (1989) Symbiotic marine bacteria chemically defend crustacean embryos from a pathogenic fungus. *Science* 246:116–118
37. Yoshikawa K, Adachi K, Nishida F et al (2003) Planar structure and antibacterial activity of korormicin derivatives isolated from *Pseudoalteromonas* sp. F-420. *J Antibiot* 56:866–870
38. Yoshikawa K, Nakayama Y, Hayashi M et al (1999) Korormicin, an antibiotic specific for gram-negative marine bacteria, strongly inhibits the respiratory chain-linked Na⁺-translocating NADH: quinone reductase from the marine *Vibrio alginolyticus*. *J Antibiot* 52:182–185
39. Speitling M, Smetanina OF, Kuznetsova TA et al (2007) Bromoalterochromides A and A', unprecedented chromopeptides from a marine *Pseudoalteromonas maricaloris* strain KMM 636 T. *J Antibiot* 60:36–42
40. Wang L, Grosse T, Stevens H et al (2006) Bioactive hydroxyphenylpyrrole-dicarboxylic acids from a new marine *Halomonas* sp.: production and structure elucidation. *Appl Microbiol Biotechnol* 72:816–822
41. Homann VV, Sandy M, Tincu JA et al (2009) Loihichelins A-F, a suite of amphiphilic siderophores produced by the marine bacterium *Halomonas* LOB-5. *J Nat Prod* 72:884–888
42. Spyere A, Rowley DC, Jensen PR et al (2003) New neoverrucosane diterpenoids produced by the marine gliding bacterium *Saprospira grandis*. *J Nat Prod* 66:818–822
43. Oku N, Adachi K, Matsuda S et al (2008) Ariakemicins A and B, novel polyketide-peptide antibiotics from a marine gliding bacterium of the genus *Rapidithrix*. *Org Lett* 10:2481–2484
44. Sobik P, Grunenberg J, Boroczky K et al (2007) Identification, synthesis, and conformation of tri- and tetrathiacycloalkanes from marine bacteria. *J Org Chem* 72:3776–3782
45. Schuhmann I, Yao CB, Al-Zereini W et al (2009) Nitro derivatives from the Arctic ice bacterium *Salegentibacter* sp. isolate T436. *J Antibiot* 62:453–460
46. Nett M, Erol O, Kehraus S et al (2006) Siphonazole, an unusual metabolite from *Herpetosiphon* sp. *Angew Chem Int Ed Engl* 45:3863–3867
47. Shindo K, Asagi E, Sano A et al (2008) Diapolycopenedioic acid xylosyl esters A, B, and C, novel antioxidative glyco-C30-carotenoic acids produced by a new marine bacterium *Rubritalea squalenifaciens*. *J Antibiot* 61:185–191

48. Andrianasolo EH, Haramaty L, Rosario-Passapera R et al (2009) Ammonificins A and B, hydroxyethylamine chroman derivatives from a cultured marine hydrothermal vent bacterium, *Thermovibrio ammonificans*. J Nat Prod 72:1216–1219
49. Iizuka T, Fudor R, Jojima Y et al (2006) Miuraenamides A and B, novel antimicrobial cyclic depsipeptides from a new slightly halophilic myxobacterium: taxonomy, production, and biological properties. J Antibiot 59:385–391
50. Boehler M, Jensen PR, Fenical W (1997) Bahamamide, an unusual cyclic bis-amide produced by an undescribed marine bacterium. Nat Prod Lett 10:75–78
51. Gil-Turnes MS, Fenical W (1992) Embryos of *Homarus americanus* are protected by epibiotic bacteria. Biol Bull 182:105–108
52. Gustafson K, Roman M, Fenical W (1989) The macrolactins, a novel class of antiviral and cytotoxic macrolides from a deep-sea marine bacterium. J Am Chem Soc 111:7519–7524
53. Rychnovsky SD, Skalitzy DJ, Pathirana C et al (1992) Stereochemistry of the macrolactins. J Am Chem Soc 114:671–677
54. Lu XL, Xu QZ, Liu XY et al (2008) Marine drugs – macrolactins. Chem Biodivers 5:1669–1674
55. Suzumura K, Yokoi T, Funatsu M et al (2003) YM-266183 and YM-266184, novel thiopeptide antibiotics produced by *Bacillus cereus* isolated from a marine sponge II. Structure elucidation. J Antibiot 56:129–134
56. Wang G-Y-S, Kuramoto M, Yamada K et al (1995) Homocereulide, an extremely potent cytotoxic depsipeptide from the marine bacterium *Bacillus cereus*. Chem Lett 791–792
57. Pettit GR, Knight JC, Herald DL et al (2009) Antineoplastic Agents. 570. Isolation and Structure Elucidation of Bacillistatins 1 and 2 from a Marine *Bacillus silvestris*. J Nat Prod 72(3):366–371
58. Gerard JM, Haden P, Kelly MT et al (1999) Loloatins A-D, cyclic decapeptide antibiotics produced in culture by a tropical marine bacterium. J Nat Prod 62:80–85
59. Barsby T, Kelly MT, Gagne SM et al (2001) Bogorol A produced in culture by a marine *Bacillus* sp. reveals a novel template for cationic peptide antibiotics. Org Lett 3:437–440
60. Barsby T, Warabi K, Sorensen D et al (2006) The Bogorol family of antibiotics: template-based structure elucidation and a new approach to positioning enantiomeric pairs of amino acids. J Org Chem 71:6031–6037
61. Imada C, Okami Y, Hotta K (2002) Production of selenohomocystine as an antibiotic by a marine *Bacillus* sp. no. 14 with selenomethionine resistance. J Antibiot 55:223–226
62. Azumi M, K-i O, Fujita T et al (2008) Bacilosarins A and B, novel bioactive isocoumarins with unusual heterocyclic cores from the marine-derived bacterium *Bacillus subtilis*. Tetrahedron 64:6420–6425
63. Osawa A, Ishii Y, Sasamura N et al (2010) Hydroxy-3,4-dehydro-apo-8'-lycopene and methyl hydroxy-3,4-dehydro-apo-8'-lycopenoate, novel C(30) carotenoids produced by a mutant of marine bacterium *Halobacillus halophilus*. J Antibiot. doi:10.1038/ja.2010.33:1-5
64. Teasdale ME, Liu J, Wallace J et al (2009) Secondary metabolites produced by the marine bacterium *Halobacillus salinus* that inhibit quorum sensing-controlled phenotypes in gram-negative bacteria. Appl Environ Microbiol 75:567–572
65. Kanoh K, Matsuo Y, Adachi K et al (2005) Mechercharmucins A and B, cytotoxic substances from marine-derived *Thermoactinomyces* sp. YM3-251. J Antibiot 58:289–292
66. Hernandez D, Altuna M, Cuevas C et al (2008) Synthesis and antitumor activity of mechercharmucins A analogues. J Med Chem 51:5722–5730
67. Bae M-A, Yamada K, Ijuin Y et al (1996) Aburatubolactam A, a novel inhibitor of superoxide anion generation from a marine microorganism. Heterocycl Commun 2:315–318
68. Takahashi A, Ikeda D, Nakamura H et al (1989) Altemicidin, a new acaricidal and antitumor substance II. Structure determination. J Antibiot 42:1562–1566

69. Mitchell SS, Nicholson B, Teisan S et al (2004) Aureoverticillactam, a novel 22-atom macrocyclic lactam from the marine actinomycete *Streptomyces aureoverticillatus*. J Nat Prod 67:1400–1402
70. Bernan VS, Montenegro DA, Korshalla JD et al (1994) Bioxalomycins, new antibiotics produced by the marine *Streptomyces* sp. LL-31 F508: taxonomy and fermentation. J Antibiot 47:1417–1424
71. Hohmann C, Schneider K, Bruntner C et al (2009) Caboxamycin, a new antibiotic of the benzoxazole family produced by the deep-sea strain *Streptomyces* sp. NTK 937. J Antibiot 62:99–104
72. Li F, Maskey RP, Qin S et al (2005) Chinikomycins A and B: isolation, structure elucidation, and biological activity of novel antibiotics from a marine *Streptomyces* sp. isolate M045. J Nat Prod 68:349–353
73. Asolkar RN, Jensen PR, Kauffman CA et al (2006) Daryamides A-C, weakly cytotoxic polyketides from a marine-derived actinomycete of the genus *Streptomyces* strain CNQ-085. J Nat Prod 69:1756–1759
74. Macherla VR, Liu J, Bellows C et al (2005) Glaciapyrroles A, B, and C, pyrrolosequiterpenes from a *Streptomyces* sp. isolated from an Alaskan marine sediment. J Nat Prod 68:780–783
75. Ford PW, Gadepalli M, Davidson BS (1998) Halawanones A-D, new polycyclic quinones from a marine-derived streptomycete. J Nat Prod 61:1232–1236
76. Takahashi C, Takada T, Yamada T et al (1994) Halichomycin, a new class of potent cytotoxic macrolide produced by an actinomycete from a marine fish. Tetrahedron Lett 35:5013–5014
77. Motohashi K, Takagi M, Shin-Ya K (2010) Tetrapeptides possessing a unique skeleton, JBIR-34 and JBIR-35, isolated from a sponge-derived actinomycete, *Streptomyces* sp. Sp080513GE-23. J Nat Prod 73:226–228
78. Manam RR, Teisan S, White DJ et al (2005) Lajollamycin, a nitro-tetraene spiro-beta-lactone-gamma-lactam antibiotic from the marine actinomycete *Streptomyces nodosus*. J Nat Prod 68:240–243
79. Hawas UW, Shaaban M, Shaaban KA et al (2009) Mansouramycins A-D, cytotoxic isoquinolinequinones from a marine streptomycete. J Nat Prod 72:2120–2124
80. Boonlarpapradab C, Kauffman CA, Jensen PR et al (2008) Marineosins A and B, cytotoxic spiroaminals from a marine-derived actinomycete. Org Lett 10:5505–5508
81. Trischman JA, Tapiolas DM, Jensen PR et al (1994) Salinamides A and B: anti-inflammatory depsipeptides from a marine streptomycete. J Am Chem Soc 116:757–758
82. Strangman WK, Kwon HC, Broide D et al (2009) Potent inhibitors of pro-inflammatory cytokine production produced by a marine-derived bacterium. J Med Chem 52:2317–2327
83. Okazaki T, Kitahara T, Okami Y (1975) Studies on marine microorganisms. IV. A new antibiotic SS-228 Y produced by *Chainia* isolated from shallow sea mud. J Antibiot 28:176–184
84. Jeong SY, Shin HJ, Kim TS et al (2006) Streptokordin, a new cytotoxic compound of the methylpyridine class from a marine-derived *Streptomyces* sp. KORDI-3238. J Antibiot 59:234–240
85. Izumikawa M, Khan ST, Komaki H et al (2010) JBIR-31, a new teleocidin analog, produced by salt-requiring *Streptomyces* sp. NBRC 105896 isolated from a marine sponge. J Antibiot 63:33–36
86. El-Gendy MM, Shaaban M, Shaaban KA et al (2008) Essramycin: a first triazolopyrimidine antibiotic isolated from nature. J Antibiot 61:149–157
87. Maskey RP, Sevvana M, Usón I et al (2004) Gutingimycin: a highly complex metabolite from a marine streptomycete. Angew Chem Int Ed Engl 43:1281–1283
88. Martin GD, Tan LT, Jensen PR et al (2007) Marmycins A and B, cytotoxic pentacyclic C-glycosides from a marine sediment-derived actinomycete related to the genus *Streptomyces*. J Nat Prod 70:1406–1409

89. Raju R, Piggott AM, Conte M et al (2009) Naseseazines A and B: a new dimeric diketopiperazine framework from a marine-derived actinomycete, *Streptomyces* sp. *Org Lett* 11:3862–3865
90. Carlson JC, Li S, Burr DA et al (2009) Isolation and characterization of tirandamycins from a marine-derived *Streptomyces* sp. *J Nat Prod* 72:2076–2079
91. Carlson JC, Fortman JL, Anzai Y et al (2010) Identification of the tirandamycin biosynthetic gene cluster from *Streptomyces* sp. 307–9. *Chembiochem* 11:564–572
92. Hughes CC, Prieto-Davo A, Jensen PR et al (2008) The marinopyrroles, antibiotics of an unprecedented structure class from a marine *Streptomyces* sp. *Org Lett* 10:629–631
93. Hughes CC, Kauffman CA, Jensen PR et al (2010) Structures, reactivities, and antibiotic properties of the marinopyrroles A–F. *J Org Chem* 75:3240–3250
94. Hughes CC, Yang YL, Liu WT et al (2009) Marinopyrrole a target elucidation by acyl dye transfer. *J Am Chem Soc* 131:12094–12096
95. Miller ED, Kauffman CA, Jensen PR et al (2007) Piperazimycins: cytotoxic hexadepsipeptides from a marine-derived bacterium of the genus *Streptomyces*. *J Org Chem* 72:323–330
96. Shin HJ, Jeong HS, Lee HS et al (2007) Isolation and structure determination of streptochlorin, an antiproliferative agent from a marine-derived *Streptomyces* sp. 04DH110. *J Microbiol Biotechnol* 17:1403–1406
97. Choi IK, Shin HJ, Lee HS et al (2007) Streptochlorin, a marine natural product, inhibits NF-kappaB activation and suppresses angiogenesis in vitro. *J Microbiol Biotechnol* 17:1338–1343
98. Cho JY, Kwon HC, Williams PG et al (2006) Azamerone, a terpenoid phthalazinone from a marine-derived bacterium related to the genus *Streptomyces* (Actinomycetales). *Org Lett* 8:2471–2474
99. Cho JY, Kwon HC, Williams PG et al (2006) Actinofuranones A and B, polyketides from a marine-derived bacterium related to the genus *Streptomyces* (actinomycetales). *J Nat Prod* 69:425–428
100. Hughes CC, MacMillan JB, Gaudencio SP et al (2009) The ammosamides: structures of cell cycle modulators from a marine-derived *Streptomyces* species. *Angew Chem Int Ed Engl* 48:725–727
101. Hughes CC, MacMillan JB, Gaudencio SP et al (2009) Ammosamides A and B target myosin. *Angew Chem Int Ed Engl* 48:728–732
102. Kwon HC, Kauffman CA, Jensen PR et al (2006) Marinomycins A–D, antitumor-antibiotics of a new structure class from a marine actinomycete of the recently discovered genus “*Marinispora*”. *J Am Chem Soc* 128:1622–1632
103. Kwon HC, Kauffman CA, Jensen PR et al (2009) Marinisporolides, polyene-polyol macrolides from a marine actinomycete of the new genus *Marinispora*. *J Org Chem* 74:675–684
104. Macherla VR, Liu J, Sunga M et al (2007) Lipoxazolidinones A, B, and C: antibacterial 4-oxazolidinones from a marine actinomycete isolated from a Guam marine sediment. *J Nat Prod* 70:1454–1457
105. McArthur KA, Mitchell SS, Tsueng G et al (2008) Lynamicins A–E, chlorinated bisindole pyrrole antibiotics from a novel marine actinomycete. *J Nat Prod* 71:1732–1737
106. Feling RH, Buchanan GO, Mincer TJ et al (2003) Salinosporamide A: a highly cytotoxic proteasome inhibitor from a novel microbial source, a marine bacterium of the new genus *Salinispora*. *Angew Chem Int Ed* 42:355–357
107. Fenical W, Jensen PR, Palladino MA et al (2009) Discovery and development of the anticancer agent salinosporamide A (NPI-0052). *Bioorg Med Chem* 17:2175–2180
108. Tsueng G, Lam KS (2007) Stabilization effect of resin on the production of potent proteasome inhibitor NPI-0052 during submerged fermentation of *Salinispora tropica*. *J Antibiot* 60:469–472
109. Lam KS, Tsueng G, McArthur KA et al (2007) Effects of halogens on the production of salinosporamides by the obligate marine actinomycete *Salinispora tropica*. *J Antibiot* 60:13–19

110. Denora N, Potts BC, Stella VJ (2007) A mechanistic and kinetic study of the beta-lactone hydrolysis of Salinosporamide A (NPI-0052), a novel proteasome inhibitor. *J Pharm Sci* 96:2037–2047
111. Eustaquio AS, O'Hagan D, Moore BS (2010) Engineering fluorometabolite production: fluorinase expression in *Salinispora tropica* yields fluorosalinosporamide. *J Nat Prod* 73:378–382
112. Buchanan GO, Williams PG, Feling RH et al (2005) Sporolides A and B: structurally unprecedented halogenated macrolides from the marine actinomycete *Salinispora tropica*. *Org Lett* 7:2731–2734
113. Udvary DW, Zeigler L, Asolkar RN et al (2007) Genome sequencing reveals complex secondary metabolome in the marine actinomycete *Salinispora tropica*. *Proc Natl Acad Sci USA* 104:10376–10381
114. Perrin CL, Rodgers BL, O'Connor JM (2007) Nucleophilic addition to a p-benzynes derived from an enediyne: a new mechanism for halide incorporation into biomolecules. *J Am Chem Soc* 129:4795–4799
115. Renner MK, Shen Y-C, Cheng X-C et al (1999) Cyclomarins A-C, New Antiinflammatory Cyclic Peptides Produced by a Marine Bacterium (*Streptomyces* sp.). *J Am Chem Soc* 121:11273–11276
116. Schultz AW, Oh DC, Carney JR et al (2008) Biosynthesis and structures of cyclomarins and cyclomazones, prenylated cyclic peptides of marine actinobacterial origin. *J Am Chem Soc* 130:4507–4516
117. Asolkar RN, Freel KC, Jensen PR et al (2008) Arenamides A-C, Cytotoxic NFκB Inhibitors from the Marine Actinomycete *Salinispora arenicola*. *J Nat Prod* 72:396–402
118. Williams PG, Miller ED, Asolkar RN et al (2007) Arenicolides A-C, 26-membered ring macrolides from the marine actinomycete *Salinispora arenicola*. *J Org Chem* 72:5025–5034
119. Williams PG, Asolkar RN, Kondratyuk T et al (2007) Saliniketals A and B, bicyclic polyketides from the marine actinomycete *Salinispora arenicola*. *J Nat Prod* 70:83–88
120. Asolkar RN, Kirkland TN, Jensen PR et al (2010) Arenimycin, an antibiotic effective against rifampin- and methicillin-resistant *Staphylococcus aureus* from the marine actinomycete *Salinispora arenicola*. *J Antibiot* 63:37–39
121. Oh DC, Gontang EA, Kauffman CA et al (2008) Salinipyrones and pacificanones, mixed-precursor polyketides from the marine actinomycete *Salinispora pacifica*. *J Nat Prod* 71:570–575
122. Oh DC, Williams PG, Kauffman CA et al (2006) Cyanosporasides A and B, chloro- and cyano-cyclopenta[a]indene glycosides from the marine actinomycete "*Salinispora pacifica*". *Org Lett* 8:1021–1024
123. Charan RD, Schlingmann G, Janso J et al (2004) Diazepinomicin, a new antimicrobial alkaloid from a marine *Micromonospora* sp. *J Nat Prod* 67:1431–1433
124. He H, Ding WD, Bernan VS et al (2001) Lomaivitins A and B, potent antitumor antibiotics from *Micromonospora lomaivitiensis*. *J Am Chem Soc* 123:5362–5363
125. Perez Baz J, Canedo LM, Fernandez Puentes JL et al (1997) Thiocoraline, a novel depsipeptide with antitumor activity produced by a marine *Micromonospora*. II. Physico-chemical properties and structure determination. *J Antibiot* 50:738–741
126. Erba E, Bergamaschi D, Ronzoni S et al (1999) Mode of action of thiocoraline, a natural marine compound with anti-tumour activity. *Br J Cancer* 80:971–980
127. Negri A, Marco E, Garcia-Hernandez V et al (2007) Antitumor activity, X-ray crystal structure, and DNA binding properties of thiocoraline A, a natural bisintercalating thiodepsipeptide. *J Med Chem* 50:3322–3333
128. Canedo LM, Fernandez-Puentes JL, Baz JP (2000) IB-96212, a novel cytotoxic macrolide produced by a marine *Micromonospora*. II. Physico-chemical properties and structure determination. *J Antibiot* 53:479–483

129. Riedlinger J, Reicke A, Zahner H et al (2004) Abyssomicins, inhibitors of the para-aminobenzoic acid pathway produced by the marine *Verrucosisspora* strain AB-18-032. *J Antibiot* 57:271–279
130. Fiedler HP, Bruntner C, Riedlinger J et al (2008) Proximicin A, B and C, novel aminofuran antibiotic and anticancer compounds isolated from marine strains of the actinomycete *Verrucosisspora*. *J Antibiot* 61:158–163
131. Shirai M, Okuda M, Motohashi K et al (2010) Terpenoids produced by actinomycetes: isolation, structural elucidation and biosynthesis of new diterpenes, gifhornenolones A and B from *Verrucosisspora gifhornensis* YM28-088. *J Antibiot* 63:245–250
132. Shin J, Seo Y, Lee HS et al (2003) A new cyclic peptide from a marine-derived bacterium of the genus *Nocardiopsis*. *J Nat Prod* 66:883–884
133. Cho JY, Williams PG, Kwon HC et al (2007) Lucentamycins A-D, cytotoxic peptides from the marine-derived actinomycete *Nocardiopsis lucentensis*. *J Nat Prod* 70:1321–1328
134. Schumacher RW, Harrigan BL, Davidson BS (2001) Kahakamides A and B, new neosidomycin metabolites from a marine-derived actinomycete. *Tetrahedron Lett* 42:5133–5135
135. Pimentel-Elardo SM, Gulder TAM, Hentschel U et al (2008) Cebulactams A1 and A2, new macrolactams isolated from *Saccharopolyspora cebuensis*, the first obligate marine strain of the genus *Saccharopolyspora*. *Tetrahedron Lett* 49:6889–6892
136. Maloney KN, Macmillan JB, Kauffman CA et al (2009) Lodopyridone, a structurally unprecedented alkaloid from a marine actinomycete. *Org Lett* 11:5422–5424

Sherif S. Ebada and Peter Proksch

Contents

4.1	Introduction	192
4.2	Alkaloids	193
4.2.1	Manzamine Alkaloids	193
4.2.2	Bromopyrrole Alkaloids	196
4.2.3	Bromotyrosine Derivatives	208
4.3	Peptides	217
4.4	Terpenes	240
4.4.1	Sesterterpenes (C ₂₅)	241
4.4.2	Triterpenes (C ₃₀)	250
4.5	Concluding Remarks	268
4.6	Study Questions	269
	References	270

Abstract

Marine sponges continue to attract wide attention from marine natural product chemists and pharmacologists alike due to their remarkable diversity of bioactive compounds. Since the early days of marine natural products research in

*The section on sponge-derived “terpenes” is from a review article published in *Marine Drugs* 8: 313–346 (2010) and is reproduced here by permission of the journal.

S.S. Ebada (✉)

Institute of Pharmaceutical Biology and Biotechnology, Heinrich-Heine University,
Universitätsstrasse 1, Duesseldorf, Germany
and

Department of Pharmacognosy and Phytochemistry, Faculty of Pharmacy, Ain-Shams University,
Organization of African Unity, Street 1, Cairo, Egypt

e-mail: sherif.Elsayed@uni-duesseldorf.de, sherif_elsayed@pharm.asu.edu.eg

P. Proksch

Institute of Pharmaceutical Biology and Biotechnology, Heinrich-Heine University,
Universitätsstrasse 1, Duesseldorf, Germany

e-mail: proksch@uni-duesseldorf.de

the 1960s, sponges have notoriously yielded the largest number of new metabolites reported per year compared to any other plant or animal phylum known from the marine environment. This not only reflects the remarkable productivity of sponges with regard to biosynthesis and accumulation of structurally diverse compounds but also highlights the continued interest of marine natural product researchers in this fascinating group of marine invertebrates.

Among the numerous classes of natural products reported from marine sponges over the years, alkaloids, peptides, and terpenoids have attracted particularly wide attention due to their unprecedented structural features as well as their pronounced pharmacological activities which make several of these metabolites interesting candidates for drug discovery. This chapter consequently highlights several important groups of sponge-derived alkaloids, peptides, and terpenoids and describes their biological and/or pharmacological properties.

4.1 Introduction

The true chemical and biological diversity of the marine environment is far from being understood today, and the oceans continue to be unique resources for bioprospecting providing a diverse array of natural products that are encountered in each group of marine organisms from prokaryotic bacteria and cyanobacteria to the top predators of the food chain such as sharks [1]. Nevertheless, the largest numbers of natural products reported since the early days of marine natural product research in the 1960s until today originate from marine invertebrates, with sponges being clearly at the top [2]. More than 5,300 different natural products are known from sponges, and more than 200 additional new metabolites from sponges are reported each year [3]. It is widely accepted today that the rich chemical diversity of sponges provides an effective chemical defense to these sedentary and soft-bodied organisms against environmental threats such as predation, overgrowth by fouling organisms, or microbial infections [4].

Numerous sponge-derived natural products such as the halichondrins, discodermolide, hemiasterlins, and arenastatin A exhibit also pronounced activities in pharmacologically driven screening programs and have been identified as lead compounds for the treatment of tumors, inflammation, and other diseases [5]. On the other hand, evidence is mounting that not all sponge-derived natural products are necessarily biosynthesized by sponges but may rather trace back to bacteria and other microorganisms that either reside within sponges or are inhaled by filter feeding [6, 7]. Examples of metabolites originally isolated from sponges that are in fact biosynthetic products of microorganisms include okadaic acid, a phosphatase inhibitor obtained from *Halichondria* sponges [8] that was shown later to be produced by dinoflagellates of the genus *Prorocentrum* [9]. Other examples include manzamine A and its 8-hydroxy derivative, antimalarial compounds first obtained from marine sponge of the genus *Haliclona*, that were isolated from a *Micromonospora* strain from the sponge *Acanthostrongylophora* sp. [7]. For many other compounds originally reported from sponges, a microbial origin is

likewise suspected even though clear evidence apart from obvious structural analogies with known microbial compounds is still lacking.

In this chapter, we will survey prominent groups of secondary metabolites derived from marine sponges and will focus on alkaloids, peptides, and terpenes which continue to attract wide attention of marine natural product researchers around the globe.

4.2 Alkaloids

Alkaloids are one of the most important classes of natural products providing drugs since ancient times. During the last decades, marine-derived alkaloids proved to be particularly important for drug discovery as exemplified by the new antitumor drug Yondelis[®] (ET-743). Marine alkaloids represent about one quarter of the more than 25,000 marine natural products reported to date, and a little more than half of them were obtained from sponges [2]. The present review will focus on three typical and major classes of sponge-derived alkaloids which include manzamine alkaloids, bromopyrrole alkaloids, and bromotyrosine-derived compounds.

4.2.1 Manzamine Alkaloids

The manzamines are polycyclic β -carboline-derived alkaloids. Manzamine A (**1**) (Fig. 4.1), the prototype of this group of compounds, was first isolated (as hydrochloride salt) in 1986 from an Okinawan sponge of the genus *Haliclona* and exhibited significant in vitro cytotoxicity against P388 murine leukemia cells with an IC_{50} of 0.07 $\mu\text{g/mL}$ (0.13 μM) [10].

Since the first report of **1**, more than 50 further manzamine-type alkaloids have been identified from nine other different sponge genera belonging to four different taxonomic orders [11–14]. These compounds are characterized by featuring a fused and bridged tetra- or pentacyclic ring system, which is linked to a β -carboline moiety through an apparent Pictet-Splenger reaction involving an aldehyde known as ircinal A (**2**) as shown in Scheme 4.1 [15]. This proposed biogenetic pathway was supported

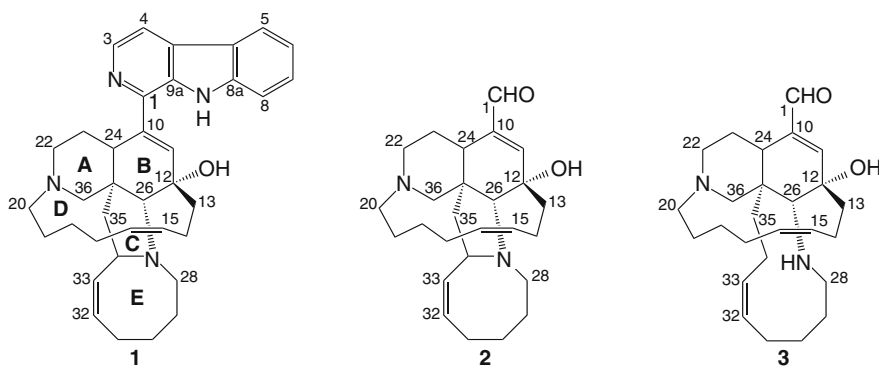
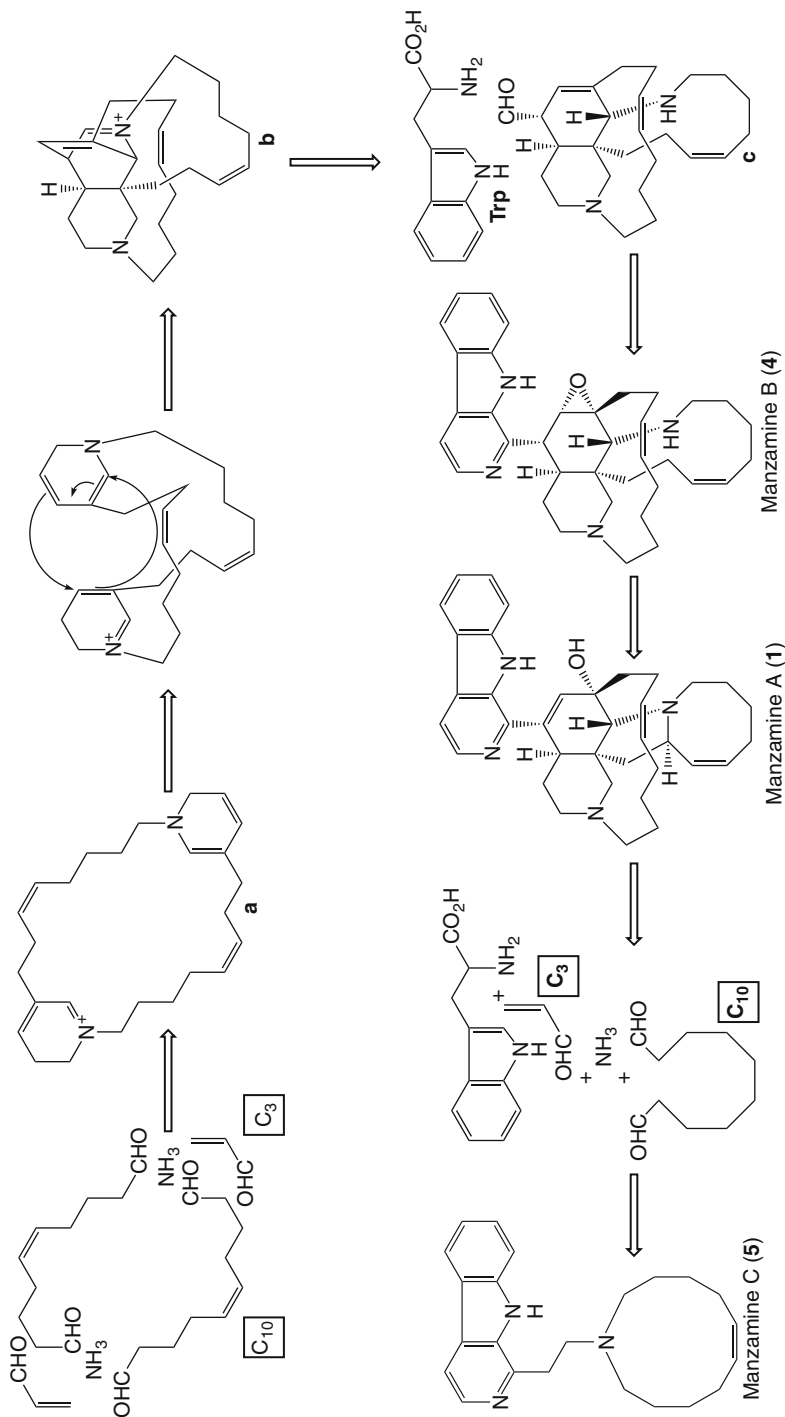


Fig. 4.1 Structures of manzamine A (**1**), ircinals A (**2**), and B (**3**)



Scheme 4.1 Plausible biogenetic pathway of manzamines A–C proposed by Baldwin and Whitehead [15]

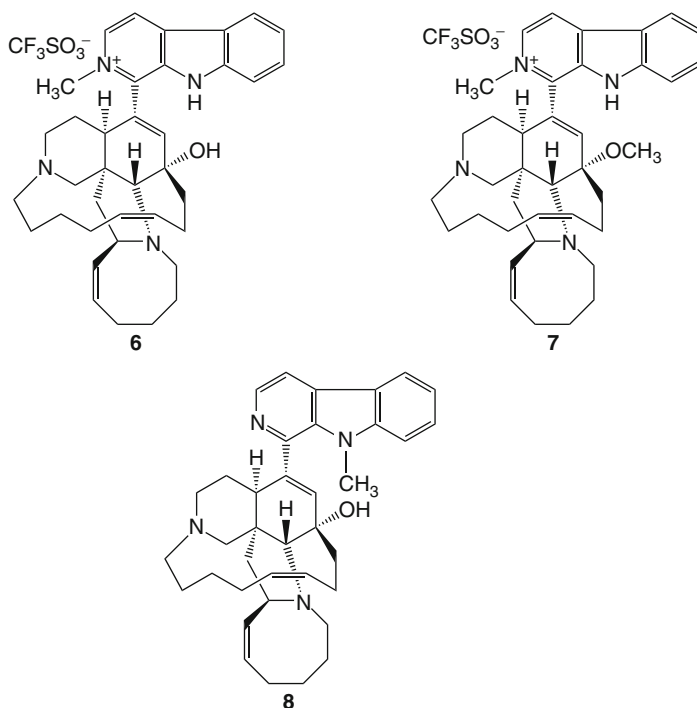


Fig. 4.2 Structures of synthetic mono- and dimethylated quaternary carbonilium cations (6–8) of manzamine A

by isolation of ircinals A (**2**) and B (**3**) (Fig. 4.1) from the Okinawan marine sponge *Ircinia* sp. [16]. Two further alkaloids isolated from a sponge of the genus *Amphimedon* which were designated as ircinols A and B were depicted to have opposite absolute configurations compared to **2** and **3**, respectively [17] (Fig. 4.1).

In addition to ircinols A and B, Kobayashi et al. in 1994 isolated a further β -carboline alkaloid, keramaphidin B, that was considered as a plausible biogenetic precursor of ircinals A (**2**) and B (**3**) and manzamine alkaloids as well [18, 19] (Scheme 4.1).

The broad range of bioactivities exhibited by manzamine alkaloids includes cytotoxicity [10], insecticidal [20], and antibacterial [21] as well as the interesting in vivo curative activity against malaria in animal models [22, 23]. These findings increasingly stimulated research efforts to synthesize manzamine alkaloids and their derivatives as well to conduct structure-activity relationship (SAR) studies [24–26].

In 2008, Ibrahim et al. performed a SAR study on the 2-*N*-methyl modifications of manzamine A [27]. In this study, mono- and dimethylated quaternary carbolinium cations of manzamine A (**1**) were synthesized (6–8) (Fig. 4.2) and evaluated for their in vitro antiplasmodial and antimicrobial activities, cytotoxicity, and also for their potential as inhibitors of glycogen synthase kinase (GSK-3 β) activity using molecular docking studies. Among the synthesized analogues,

2-*N*-methylmanzamine A (6) exhibited in vitro antiplasmodial activity (IC₅₀ 0.7–1.0 μ M) but was less potent than manzamine A (1) (IC₅₀ 0.017–0.02 μ M). However, 6 was less cytotoxic to mammalian kidney fibroblasts (Vero cells), and hence, the selectivity index was in the same range as for manzamine A (Fig. 4.2).

A new group of manzamine-related compounds includes nakadomarin A (9) [28], ma'eganedin A (10) [29], manadomanzamines A (11) and B (12) [30], and zamamidines A–C (13–15) [31, 32] which were isolated from different specimens of the sponge *Amphimedon* collected from Kerawa and Seragaki Islands, Okinawa, along with the unprecedented manzamine dimer, *neo*-kauluamine (16), from the common Indo-Pacific sponge genus *Acanthostrongylophora* [33, 34].

Zamamidines A–C (13–15) as well as manzamine A revealed inhibitory activities against *Trypanosoma brucei brucei*, the parasite causing sleeping sickness, (IC₅₀ values: 1.4, 1.4, 0.4, and 0.07 μ M) and against *Plasmodium falciparum* (IC₅₀: 9.6, 16.3, 0.8, and 1.8 μ M, respectively) [32]. In vitro analysis of several manzamine analogues against *Toxoplasma gondii* indicated significant activity. Manzamine A (1) displayed 70% inhibition of the parasite at 0.1 μ M concentrations without displaying host cell toxicity. The activity significantly increased at concentrations of 1 and 10 μ M even though it was accompanied by an increase in host-cell toxicity. As a result, manzamine A was selected for in vivo analysis. A daily intraperitoneal (i.p.) dose of 8 mg/kg of manzamine A, given for 8 consecutive days, beginning on day 1 following the infection, prolonged the survival of SW mice to 20 days, as compared to 16 days for untreated controls [35]. Additional information on the antiprotozoan activity of manzamines can be found in ► Chap. 21 (Fig. 4.3).

SAR studies and optimized dosing will probably further improve the in vivo efficacy of the manzamines against *T. gondii*. All new and known manzamines, with the exception of *neo*-kauluamine (16), induced 98–99% inhibition of *Mycobacterium tuberculosis* (H37Rv) with an MIC < 12.5 μ g/mL. Manzamine A, E, and 8-hydroxymanzamine A exhibited MIC endpoints of 2.8, 5.5, and 5.5 μ M, respectively [35].

In conclusion, manzamine alkaloids are valuable candidates for further investigation and possibly even development as promising leads against malaria and other serious infectious diseases. The need for developing antimalarials derived from novel structural classes and with unique mechanisms of action is important for the long-term and sustainable control of drug resistant *Plasmodium* strains.

The occurrence of manzamine alkaloids in seemingly unrelated sponge genera has raised speculations about a possible microbial origin of these compounds [36].

4.2.2 Bromopyrrole Alkaloids

Bromopyrrole alkaloids constitute a class of marine compounds found exclusively in marine sponges. Oroidin (17) (Fig. 4.4) was the prototype of this group and was first isolated from the marine sponge *Agelas oroides* in 1971 [37]. Oroidin (17) is considered as the key precursor for this group of compounds since many

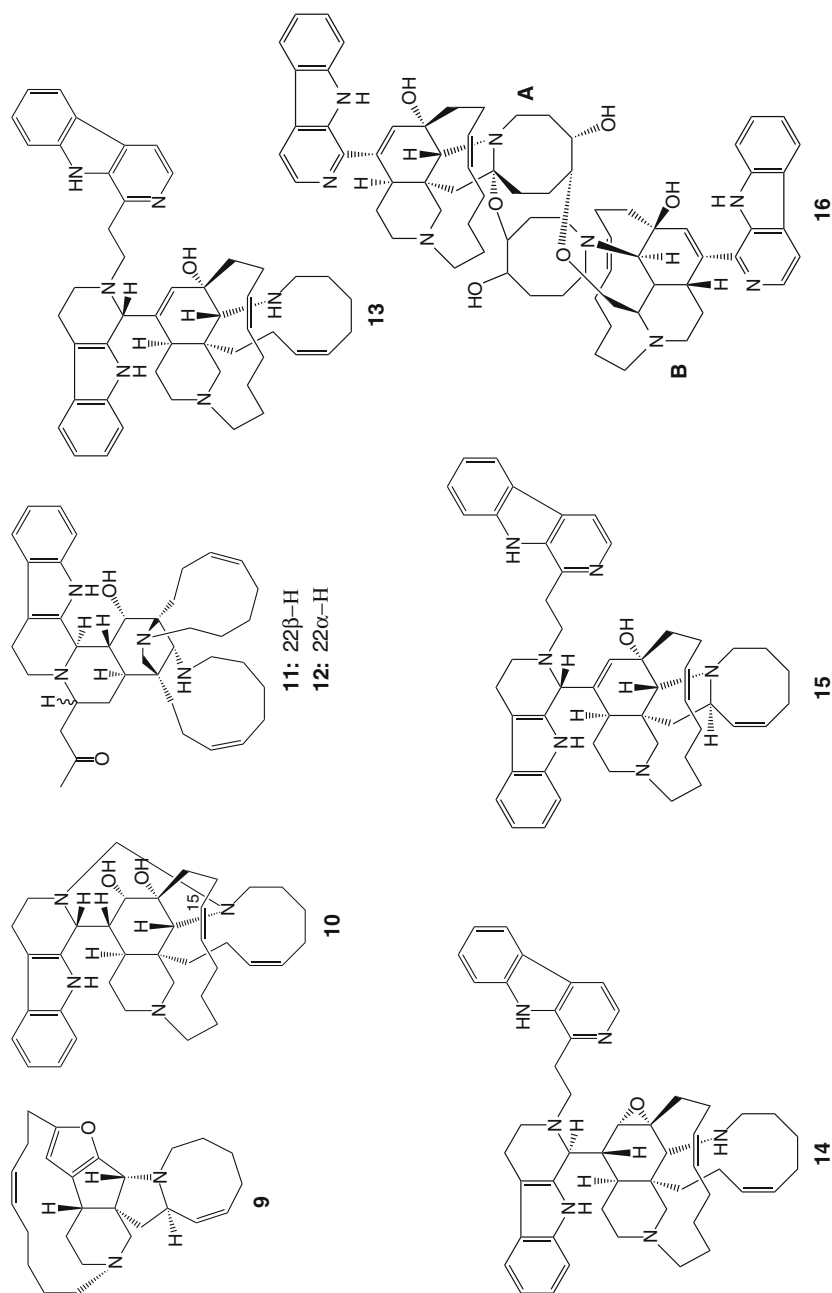
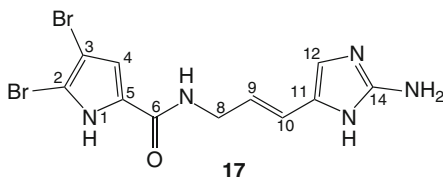
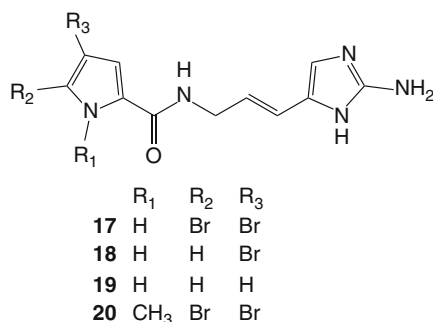
**Fig. 4.3** Structures of manzamine-related alkaloids (9–16)

Fig. 4.4 Oroidin, the prototype precursor of bromopyrrole alkaloids

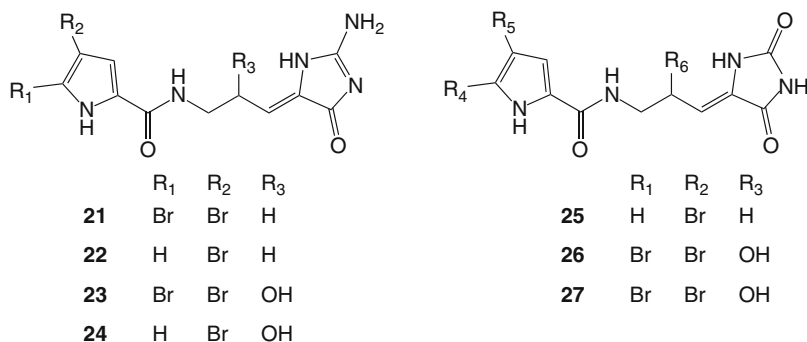


bromopyrrole alkaloids constituting a pyrrole-imidazole unit can be considered as metabolic derivatives of the $C_{11}N_5$ skeleton of oroidin.

Since the discovery of oroidin, more than 150 derivatives, with a wide variety of structures and interesting bioactivities, have been isolated from more than 20 different sponge taxa from different genera belonging mainly to the families Agelasidae, Axinellidae, and Halichondridae [38]. Their deterrent activity against predators is of ecological significance as shown for Caribbean reef sponges of the genus *Agelas* [39, 40]. Bromopyrrole alkaloids are also of interest due to their pronounced pharmacological activities including cytotoxicity, antimicrobial, and immunosuppressive activities which have driven the research interest of natural product chemists toward their total syntheses primarily during the last decade. These synthetic efforts lead to successful total syntheses of many bromopyrrole alkaloids such as dimeric pyrrole-imidazole alkaloids including sceptrin, oxysceptrin, and ageliferin [41]; nagelamides D [42] and E [41]; and hymenialdisine analogues [72].

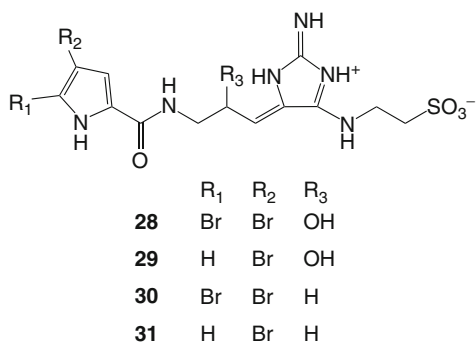


Hymenidin (2-debromooroidin) (18), clathrocin (2,3-debromooroidin) (19), and sventrin (pyrrole *N*-methyloroidin) (20) were isolated from an unspecified Okinawan marine sponge of the genus *Hymeniacidon* [43] and from the Caribbean sponges *Agelas clathrodes* [44], and *A. sventres* [45], respectively. The biological activities of these compounds were found to be linked to the bromination pattern of the pyrrole moiety. For example, in a feeding assay, hymenidin exhibited lower deterrence against fishes as compared to oroidin [46]. *N*-methylation of pyrrole moiety in sventrin (20) likewise reduced fish feeding deterency [45]. The reduction of voltage-dependent calcium elevation in PC12 cells was found to be directly proportional to the number of bromine atoms associated with the pyrrole ring in oroidin and hymenidin [47]. Oroidin, hymenidin, and clathrocin furthermore revealed pronounced anticholinergic and antiserotonergic activities [43, 45].

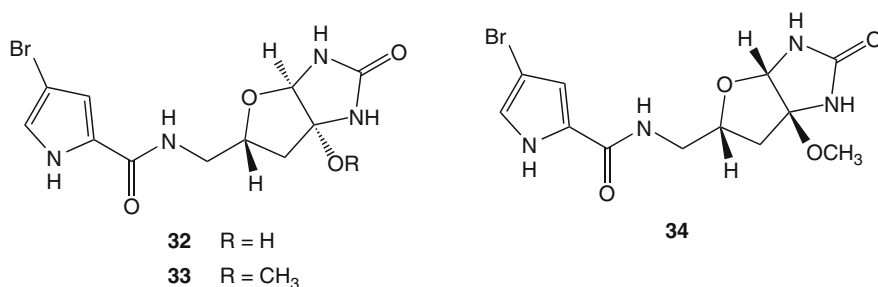


Dispacamides A–D (21–24) were isolated from four different species of the genus *Agelas* namely, *A. conifer*, *A. longissima*, *A. clathrodes*, and *A. dispar* [48, 49], in which the 2-aminoimidazole moiety was oxidized to an alkylidene glycoyamidine. Dispacamide A (21) and B (22) differ from oroidin (17) and hymenidin (18), respectively, both with regard to the position of the double bond in the amine side chain and with regard to the presence of an aminoimidazolone moiety. Compounds (21) and (22) were found inactive with regard to anticholinergic and antiserotonergic activities. On the contrary, all dispacamides exhibited a remarkable antihistaminic activity on the guinea pig ileum through a reversible noncompetitive binding to histamine receptors, with dispacamide A (21) being the most active derivative [48]. Dispacamide C (23) and D (24) showed only mild activity in comparison which indicated the importance of the hydroxyl group in the side chain and also implicated that its orientation resulted in a notable reduction of antihistaminic activity [49]. Recently, debromodispacamides B and D were reported from *Agelas mauritiana* collected off the Solomon Islands [50].

Mukanadin A (= dispacamide D) (24) and B (25) have been isolated from the Okinawan sponge *Agelas nakamurai* [51]. Mukanadin D (26) was obtained from the Jamaican sponge *Didiscus oleata* [52]. In mukanadin B (25), D (26), and compound (27), isolated from *Axinella verrucosa* [53], the 2-aminoimidazole unit of dispacamides is replaced by a hydantoin moiety.



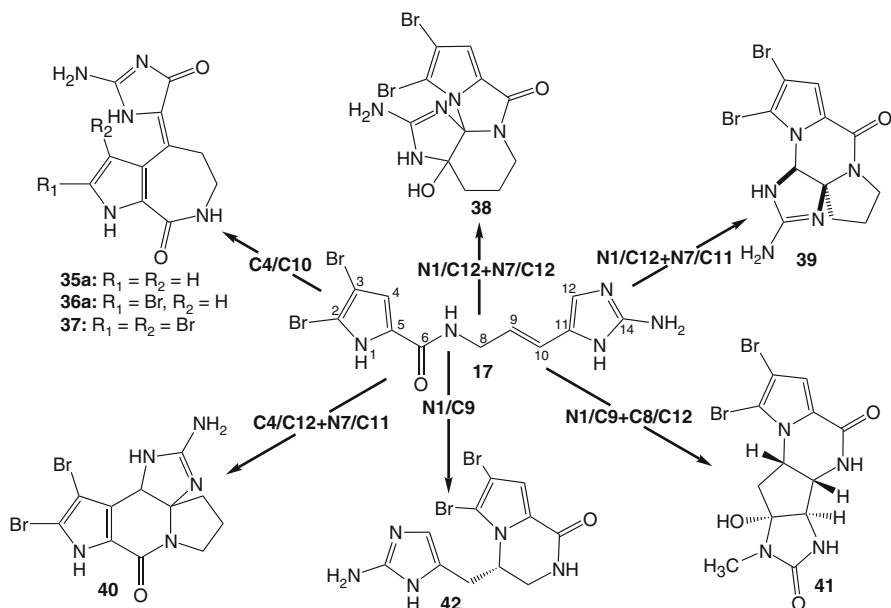
Mauritamide A, isolated from the Fijian sponge *Agelas mauritiana*, was the first bromopyrrole alkaloid featuring a rare taurine moiety [54]. Taurine moieties are also present in tauroacidin A (28) and B (29), isolated from an Okinawan *Hymeniacidon* sp. [55]; in taurodispacamide (30), isolated from the Mediterranean sponge *Agelas oroides* [56]; and in its debromo derivative (31), isolated from *Axinella verrucosa* [53]. Interestingly, various pharmacological activities have been reported for these four compounds (28–31). Tauroacidins A (28) and B (29) inhibited EGF receptor kinase and *c-erbB*-2 kinase activities ($IC_{50} = 20 \mu\text{g/mL}$) [55]. Taurodispacamide (30) showed significant antihistaminic activity [56], while its debromo derivative (31) showed potent neuroprotection through acting as glutamate and serotonin antagonist [53].



Slagenins A–C (32–34) were isolated from the Okinawan marine sponge *Agelas nakamurai* [57]. They are characterized by an additional cyclization step in comparison to oroidin (17), the key precursor for this class. Both slagenins B (33) and C (34) were proven to be cytotoxic against murine leukemia L1210 cells in vitro with IC_{50} values of 21 and $19.5 \mu\text{M}$, respectively, although slagenin A (32) proved to be inactive [57].

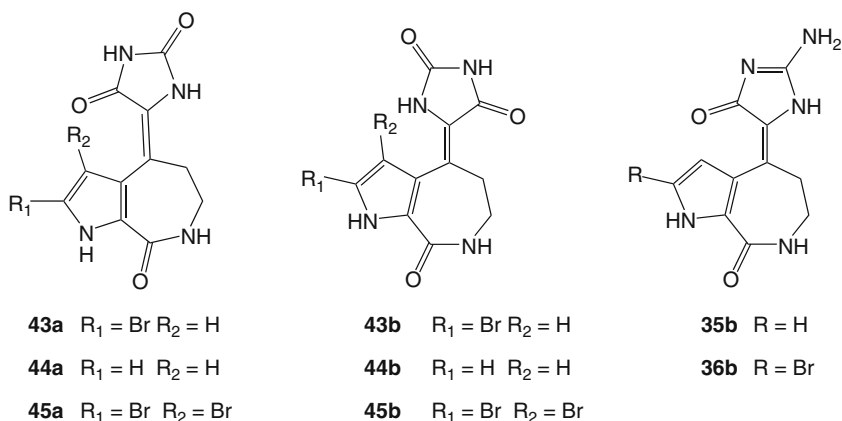
Polycyclic bromopyrrole alkaloids are thought to be derived from oroidin, the parent compound, through formation of one (or more) C–C or C–N bonds. Polycyclic bromopyrrole alkaloids can be divided into five major classes based on the oroidin atoms involved in the cyclization (Scheme 4.2) [56].

Debromohymenialdisine (35a), hymenialdisine (36a), and 3-bromohymenialdisine (37) (Scheme 4.2) represent the first cyclization mode of oroidin which occurs between C4 and C10. Debromohymenialdisine (35a) was first isolated from the Great Barrier Reef sponge *Phakellia* sp. in 1980 [58], while hymenialdisine (36a) was reported 2 years later from different sponge genera including *Acanthella*, *Axinella*, and *Hymeniacidon* [59–61]. 3-Bromohymenialdisine (37) was first isolated from the tropical marine sponge *Axinella carteri* [62]. All compounds (35a, 36a, and 37) were tested for cytotoxicity and insecticidal activity. In a cytotoxicity assay, debromohymenialdisine (35a) was the most active compound against mouse lymphoma L5178Y cells with IC_{50} value of $1.8 \mu\text{g/mL}$ ($4.1 \mu\text{M}$) [62], while hymenialdisine (36a) and 3-bromohymenialdisine (37) were essentially



Scheme 4.2 An overview of cyclization modes of the oroidin skeleton [56]

equitoxic with $IC_{50} = 3.9 \mu g/mL$ for both. Both **35a** and **36a** exhibited insecticidal activity toward larvae of the pest insect *Spodoptera littoralis* (LD_{50} values of 88 and 125 ppm, respectively), whereas **37** proved to be inactive in this assay [62].

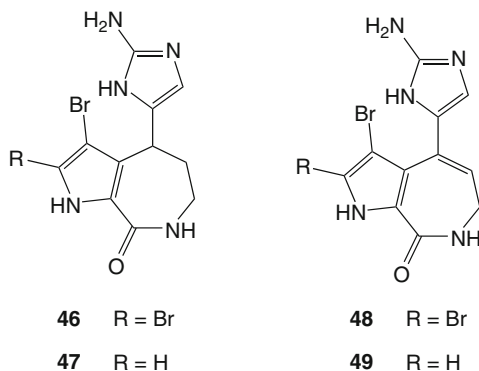


Axinohydantoin (43–45) feature the same fused pyrroloazepine ring as present in hymenialdisine (**36a**). However, instead of a glycoyamidine ring, a pyrroloazepine ring is linked to a hydantoin ring via either (*E*) or (*Z*) double bond. (*E*)-axinohydantoin (**43a**) was isolated in 1990 from the sponge *Axinella* sp., and its structure was proven

by X-ray crystallography [63]. (Z)-Axinohydantoin (**43b**) as well as the bromine derivatives (**44b**, **45b**) were reported in 1997 [64] and 1998 [65], respectively. As for the axinohydantoin, the (*E*) isomers of debromohymenialdisine (**35b**) and hymenialdisine (**36b**) have also been isolated [66].

Hymenin (**46**) is an α -adrenoceptor antagonist isolated from *Hymeniacidon* sp. and furthermore exhibits antibacterial activity against *Bacillus subtilis* and *Escherichia coli* [67]. Another hymenin analogue differing in the presence of a double bond between C9 and C10 was isolated from *Pseudaxynissa cantharella* [68], and it was named stevensine (= odiline) (**48**). 2-Debrominated derivatives of both hymenin (**47**) and stevensine (**49**) were isolated from the Indo-Pacific sponge *Stylissa carteri* [69]. Stevensine (**48**) has been demonstrated to play a major role in the chemical defense of the reef sponge *Axinella corrugata* against predators [70].

Hymenialdisine and its analogues are of interest due to their strong inhibitory activity against several protein kinases, such as CDKs, GSK-3 β , CK1, and Chk1, which are involved in regulating vital cellular functions such as gene expression, cellular proliferation, membrane transport, and apoptosis [71, 74]. Targeting these kinases has been appealing for the treatment of diseases like Alzheimer's disease, type II diabetes, and cancer [72, 73] thereby providing a rationale for medication. In addition, hymenialdisines inhibited formation of several proinflammatory cytokines (IL-1, IL-2, IL-6, and NO) through inhibition of the NF- κ B signaling pathway [71] which is potentially valuable for treatment of serious inflammatory diseases such as rheumatoid arthritis and osteoarthritis or for treatment of cancer.



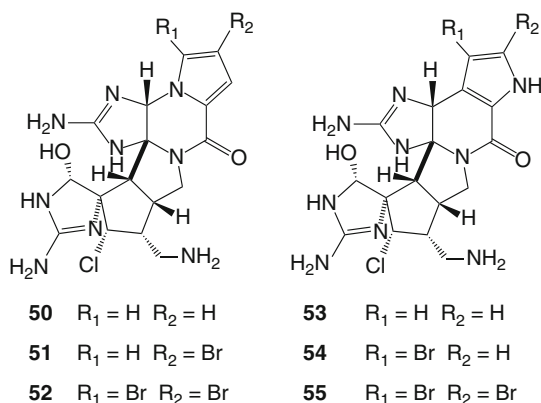
In 2009, an elegant review summarized all known hymenialdisines and provided a summary of their protein kinase inhibitory activities [75]. It came to the conclusion that (1) halogenation at R₁ and R₂ of the pyrrole ring does not significantly increase or decrease the activity of these compounds, (2) pyrrole derivatives appear to be more potent inhibitors than indole analogues which resulted in up to a fourfold reduction in activity, (3) a change in the geometry of the double bond (either (*E*) or (*Z*)) does not influence the activity, and (4) the existence of an aminoimidazolone ring, in particular the guanidine moiety, is crucial for the activity. Modifying the amino group dramatically decreased

activity possibly due to steric hindrance and loss of hydrogen bonding and hymenin (46), which features an aminoimidazole ring, proved to have much lower kinase inhibitory activity than hymenialdisine analogues [75].

The second cyclization mode, occurring between both N1 and N7 with C12, is exemplified, to the best of our knowledge, only in dibromoagelospongins (38) - (Scheme 4.2) which was isolated from the marine sponge *Agelas* sp. collected off the Tanzanian coasts [76]. Dibromoagelospongins (38) is closely related to dibromophakellins (39) (Scheme 4.2) in which N7 is bonded to C11 instead. The latter was first isolated in 1971 by Sharma et al. [77]. Later, several other phakellins have been reported from *Pseudaxynissa cantharella* [68] and *Agelas* sp. [78]. In 1997, a further derivative, phakellistatin, which differs from 39 in having a urea-type carbonyl instead of amino group present in the guanidine moiety, was isolated from the Indian Ocean sponge *Phakellia mauritiana* [79]. Phakellistatin exhibited potent antiproliferative activity against a variety of human cancer cell lines (IC₅₀ values from 0.3 to 0.4 μ M) [79].

The next cyclization mode of oroidin involving N7/C11 and C4/C12 affords a class of compounds called isophakellins, from which dibromoisophakellin (40) was the first derivative reported [80]. The compounds of this class are isomeric compared to the phakellins with the only difference in the linkage of imidazole C12 with C4 instead of N1.

The group of phakellins and isophakellins includes structurally complex metabolites known as palau'amines (50–52) or styloguanidines (53–55), respectively. In each of these compounds, the corresponding basic skeleton of phakellin or isophakellin is conjugated with an aminoimidazolyl propene unit.



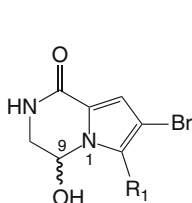
Palau'amines (50–52) were reported from *Stylotella agminata* [81] and from *Stylotella aurantium* [82]. They revealed potent cytotoxicity against several cancer cell lines with IC₅₀ values from 0.1 to 10 μ g/mL along with antibacterial, antifungal, and immunosuppressive activities [81, 82]. Styloguanidines (53–55) were obtained together with palau'amines from the sponge *Stylotella aurantium* collected in the Yap Sea and exhibited potent inhibition of chitinase, a key enzyme involved, e.g., in the ecdysis of insects and crustaceans. The inhibition of this

enzyme affects the settlement of barnacles and hence could be a potential target for antifouling agents [83].

Agelastatin A (**41**) (Scheme 4.2) was the first reported member of the N1/C9 and C8/C12 cyclization series and was isolated from *Agelas dendromorpha* [84]. Other derivatives were later reported from the same sponge [85] as well as from *Cymbastela* sp. [86]. Agelastatins are potent antiproliferative agents against several cancer cell lines [85]. Moreover, agelastatin A (**41**) inhibited glycogen synthase kinase (GSK-3 β), which could be useful for treatment of serious diseases including Alzheimer's disease, cancer, and type II diabetes [71].

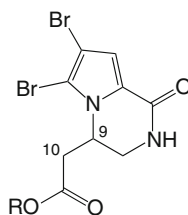
The last proposed cyclization mode of oroidin (**17**) occurring between N1 and C9, as shown in Scheme 4.2, affords cyclooroidin (**42**), first reported in the year 2000 from the Mediterranean sponge *Agelas oroides* [56]. Other members of this class of compounds include agesamides, isolated from an Okinawan sponge *Agelas* sp. [87], which differ from **42** in featuring a hydantoin ring instead of a glycohydantoin ring. Oxycyclostylidol, another compound of this class was the first pyrrole-imidazole alkaloid, reported containing an oxidized pyrrole moiety [88].

Cyclooroidin (**42**) can be considered as a biosynthetic precursor of the nonimidazole bromopyrrole alkaloids including longamides (**56–60**) and aldinses (**61–64**).



56 R = Br

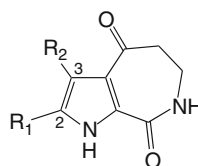
57 R = H



58 R = H

59 R = C₂H₅

60 R = CH₃



61 R₁ = H R₂ = H

62 R₁ = Br R₂ = H

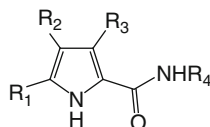
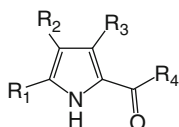
63 R₁ = H R₂ = Br

64 R₁ = Br R₂ = Br

Longamide A (**56**) was identified as a novel unusual pyrrolo-piperazine alkaloid and was isolated as (9*S*) isomer from the Caribbean sponge *Agelas longissima* [89]. The 2-debromo derivative (= mukonadin A) (**57**) was obtained from the sponge *Axinella carteri* [90] together with 2-bromoaldisine (**62**), while aldisine (**61**) was reported from the sponge *Hymeniacidon aldis* [91]. 3-Bromoaldisine (**63**) and 2,3-dibromoaldisine (**64**) were isolated from *Axinella damicornis* and *Stylissa flabelliformis* [92]. Longamide B (**58**) has been isolated as a racemate from the Caribbean sponge *Agelas dispar* [93]. Hanishin, longamide B ethyl ester (**59**) was named after the Hanish Islands (Red Sea) where the sponge *Acanthella carteri* was collected [94].

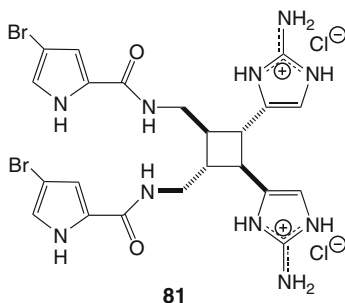
Other smaller bromopyrrole alkaloids (**65–73**), which are considered as building blocks leading to oroidin (**17**), have been isolated from *Agelas oroides* (**65**) [36], *Agelas flabelliformis* (**66**) [96], *Acanthella carteri* (**67**, **68**) [94], *Axinella damicornis* (**69**, **70**) [92], *Agelas nakamurai* (**71**, **74**) [97], *Acanthostylotella* sp.

(**72**, **73**) [98], *Homaxinella* sp. (**75**) [95], and *Axinella verrucosa* (**76**) [53]. Acanthamides A–D (**77**–**80**) were isolated from an Indonesian marine sponge *Acanthostylotella* sp. [98]. Antipredatory activity seems to be the main ecological function for these small bromopyrroles [36, 92, 94].



	R ₁	R ₂	R ₃	R ₄		R ₁	R ₂	R ₃	R ₄
65	Br	Br	H	OH	74	Br	H	H	CH ₂ OCH ₃
66	Br	Br	H	OCH ₃	75	Br	Br	H	CH ₂ OCH ₃
67	Br	Br	H	NH ₂	76	H	Br	H	CH ₂ OCH ₃
68	Br	H	H	NH ₂	77	H	Br	Br	(CH ₂) ₃ OCH ₃
69	H	Br	Br	NH ₂	78	H	Br	Br	(CH ₂) ₃ OC ₂ H ₅
70	H	Br	Br	OH	79	H	Br	Br	(CH ₂) ₂ OCH ₃
71	Br	H	H	NH ₂	80	H	Br	Br	(CH ₂) ₂ OC ₂ H ₅
72	H	Br	Br	OCH ₃					
73	Br	H	Br	OH					

In 1981, dimeric bromopyrrole alkaloids have been reported for the first time from the Caribbean sponge *Agelas sceptrum* which gave the name sceptrin to one of the metabolites isolated (**81**) [99]. Historically, **81** is considered as the parent compound of this group and represents a symmetrical dimer of 2-debromooroidin. Sceptrin (**81**) displayed a broad spectrum of bioactivities such as antimicrobial activity against different bacterial and fungal pathogens [99]. In addition, it exhibited antiviral [100], antimuscarinic [45], and antihistaminic properties [49].

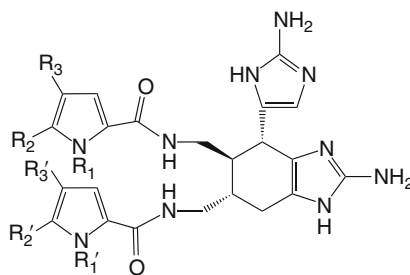


Later, dimeric bromopyrrole alkaloids were also reported from other genera of marine sponges including *Stylissa* [101, 102], *Axinella* [103], *Hymeniacidon* [104], and most frequently from *Agelas*. Among this group of

dimeric alkaloids, two series can be identified which include agelifेरins and nagelamides.

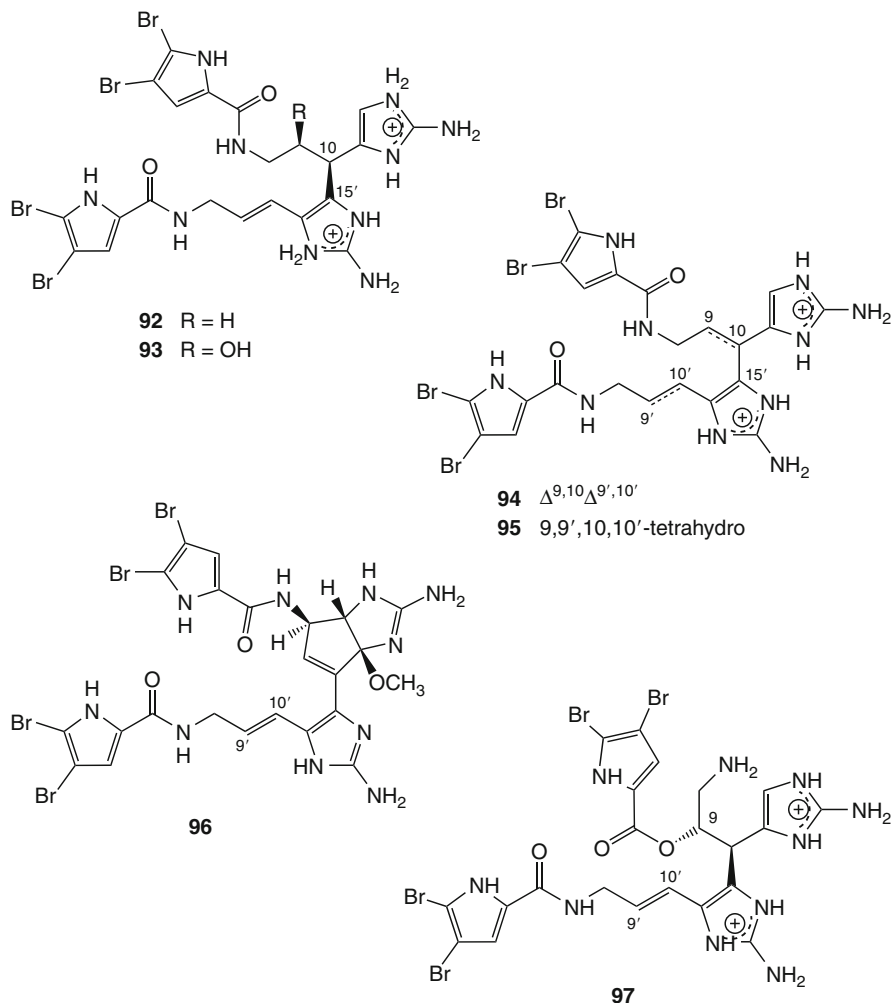
Ageliferin (**82**), bromoageliferin (**83**), and dibromoageliferin (**84**) were first isolated from *Agelas conifera* and *A. cf. mauritiana* in 1989 by Rinehart [105]. Afterward, their detailed structural elucidation and stereochemistry were reported in 1990 by Kobayashi et al. [106]. Both **83** and **84** reduced voltage-dependent calcium entry in PC12 cells which leads to vasorelaxation [107].

Seven further ageliferin derivatives (**85–91**), methylated at one or at several of the pyrrole nitrogens, together with the formerly isolated bromo- (**83**) and dibromoageliferin (**84**) were obtained from the calcareous sponge *Astrosclera willeyana* collected off Ant Atoll, Pohnpei, Micronesia [108].

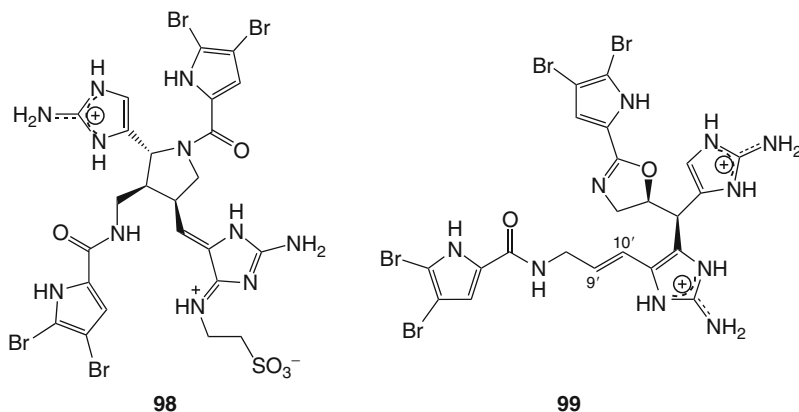


	R ₁	R ₂	R ₃	R ₁ '	R ₂ '	R ₃ '
82	H	H	Br	H	H	Br
83	H	Br	Br	H	H	Br
84	H	Br	Br	H	Br	Br
85	H	H	Br	CH ₃	H	Br
86	CH ₃	H	Br	CH ₃	H	Br
87	H	H	Br	CH ₃	Br	H
88	CH ₃	H	Br	CH ₃	Br	H
89	H	Br	Br	CH ₃	H	Br
90	H	H	Br	CH ₃	Br	Br
91	H	Br	Br	CH ₃	Br	Br

Nagelamides comprise 15 dimeric bromopyrrole derivatives including nagelamides A–H [109], J–L [110, 111], and O–R [112, 113]. All of them were reported by Kobayashi et al. from different collections of an unspecified Okinawan sponge of the genus *Agelas* collected off Seragaki beach.



Nagelamides A–D (**92–95**) are connected via a C–C bond between C10 and C15'. Nagelamides E–G were proven to be diastereomers of ageliferin (**82**), bromoageliferin (**83**), and dibromoageliferin (**84**), respectively. Nagelamide J (**96**) is the first bromopyrrole alkaloid possessing a cyclopentane ring fused to an aminoimidazole ring [110]. In addition, nagelamide L (**97**) was identified as a unique dimeric bromopyrrole alkaloid containing an ester linkage [111].



Nagelamide Q (**98**) is a rare dimeric bromopyrrole alkaloid possessing a pyrrolidine ring, while nagelamide R (**99**) was the first bromopyrrole alkaloid featuring an oxazoline ring [113]. Nagelamides have been tested for antimicrobial activity against a vast array of bacterial and fungal pathogens including *Bacillus subtilis*, *Escherichia coli*, *Micrococcus luteus*, *Staphylococcus aureus*, *Trichophyton mentagrophytes*, *Cryptococcus neoformans*, *Candida albicans*, and *Aspergillus niger*. Most of the nagelamides showed antimicrobial activity with MIC values between 7.7 and 38.4 μM [109–113]. Nagelamides A, G, and H showed also inhibitory activity against protein phosphatase 2A, a major serine/threonine protein phosphatase involved in cellular growth and potentially in cancer development, with IC_{50} values of 48, 13, and 46 μM , respectively [109].

4.2.3 Bromotyrosine Derivatives

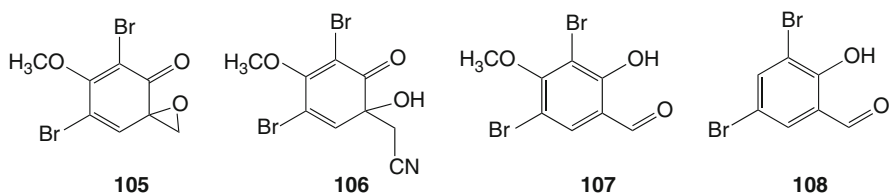
(+)-Aerplysinin-1 (**100**, Scheme 4.3) was the first reported member of this group of alkaloids. It was obtained from marine sponges belonging to the order Verongida. In 1970, Fattorusso et al. isolated **100** from *Verongia aerophoba* collected off the Bay of Naples (Italy) [114]. Later, it was also reported from other marine sponges from different geographic locations including *Psammoposilla purpurea* (Marshall Islands) [115], *Aplysina laevis* (Australia) [116], and *Aplysia caissara* (Brazil) [117]. Its (–)-isomer was first isolated from *Ianthella ardis* [118].

Aerplysinin-1 (**100**) proved to be antiproliferative in small micromolar doses against various cancer cell lines such as Hela (human cervical carcinoma) and L5178Y (mouse lymphoma) in addition to human mammary and colon carcinoma cell lines [119–121]. In 2002, Rodríguez-Nieto et al. reported that **100** inhibited the growth of BAECs (bovine aortic endothelial cells) and induced apoptotic cell death [122]. Aerplysinin-1 inhibits the endothelial cell migration and capillary tube formation in matrigel through inhibition of matrix-metalloproteinase 2 and urokinase in endothelial cell conditioned medium [119]. The same study reported in vivo inhibition of

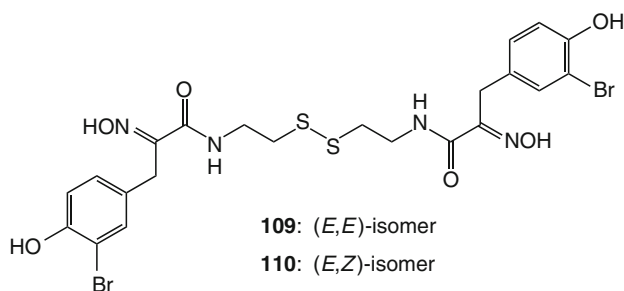
aerplysinin-1 (**100**) and a dienone analogue (**101**) (Scheme 4.3) [120, 123–127] (Scheme 4.3).

Receptor tyrosine kinases (RTKs), such as the epidermal growth factor receptor (EGFR) and the platelet-derived growth factor receptor (PDGFR), are critically involved in the transduction of mitogenic signals across the plasma membrane and therefore in the regulation of cell growth and proliferation. Enhanced RTK activity is associated with proliferative diseases such as cancer, psoriasis, and atherosclerosis, while decreased function may be associated, for instance, with diabetes [128]. Aerplysinin-1 inhibited tyrosine kinase activity of EGFR in vitro and blocked ligand-induced endocytosis of the EGF receptor and PDGF receptor in vitro [129]. Hence, a proposed EGFR-dependent mechanism of action was depicted; however, the compound showed no activity when tested in a whole-cell assay system [129].

Therefore, a series of aerplysinin-1 analogues was synthesized and evaluated as RTK inhibitors to enhance membrane permeability in cell-based assays with retained tendency for nucleophilic covalent binding to the enzyme-binding site [128]. Four synthetic analogues (**105–108**) exhibited promising inhibitory activity against EGFR and PDGFR tyrosine kinases in cellular assays with IC_{50} values in the low micromolar range, but none of them have yet been assessed for antiangiogenesis.



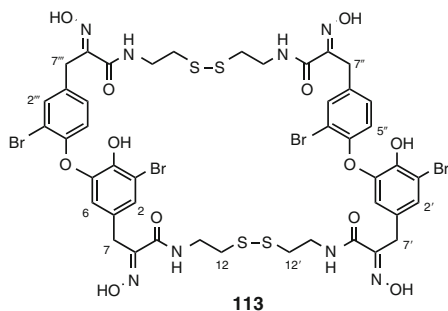
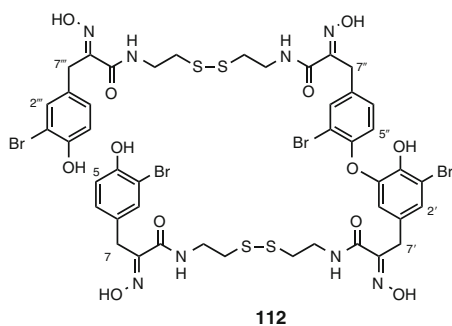
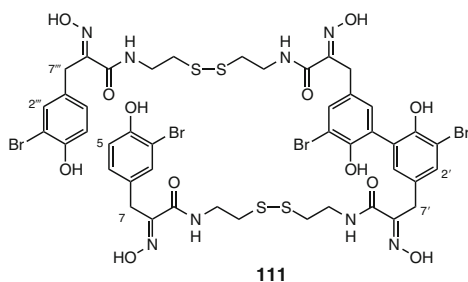
Psammaplin A is a symmetrical brominated tyrosine metabolite containing a disulfide linkage and is usually obtained as a mixture of isomers, [(*E,E*)-isomer (**109**) and (*E,Z*)-isomer (**110**)] which differ in the configuration of their oxime groups.



In 1987, psammaplin A was reported simultaneously by Quin   and Crews [130] and Rodr  guez et al. [131] from *Psammaplysilla purpurea* and *Thorectopsamma xana* sponges, both belonging to the order Verongida. Psammaplin A was also obtained from *Aplysinella rhax* [132] and *Pseudoceratina purpurea* [133] in addition to two Korean non-Verongid sponges of the genera *Jaspis* and *Poecillastra*

[134, 135]. Later, a vast diversity of psammaplins have been reported, including 13 monomeric psammaplins (A–M) isolated from the Indo-Pacific sponge *Pseudoceratina purpurea* [133], the Fijian sponge *Aplysinella rhax* (thought to be synonymous with *Pseudoceratina purpurea*) [136] and from two-sponge associations of *Jaspis* sp. And *Poecillastra* sp. collected from Korean waters [135].

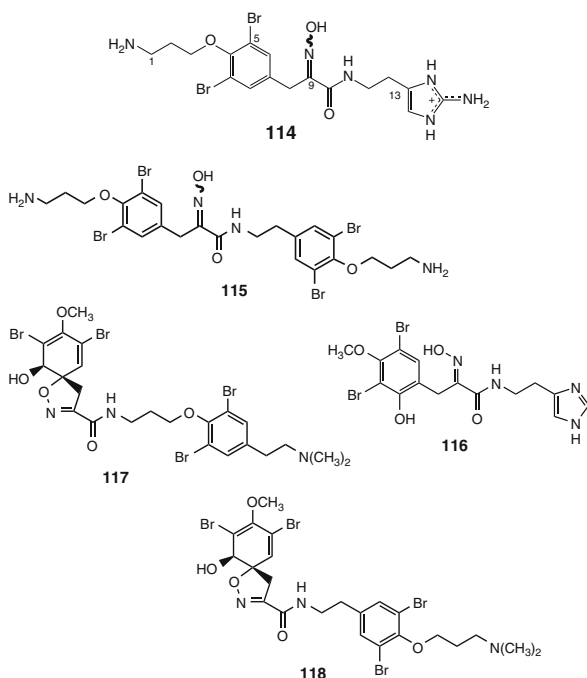
In addition, dimeric psammaplin derivatives were obtained which occur either in an opened form such as bisaprasin A (**111**) and bispsammaplin A (**112**) or in a cyclized form represented by cyclobispsammaplin A (**113**). All of these compounds were reported from different Korean collections of sponges of the genera *Jaspis* and *Poecillastra* [134, 135]. Moreover, 11'-sulfate derivatives of **109** and **111** were isolated from the sponge *Aplysinella rhax* collected from Queensland (Australia) [132].



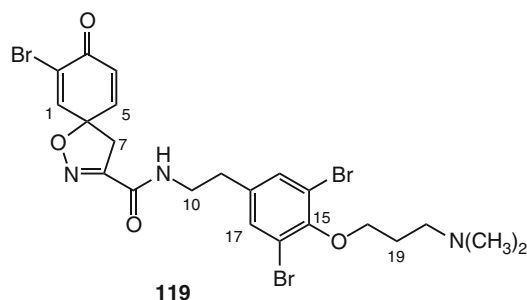
The cytotoxicity of psammaplin A (PsA, **109**) toward a vast array of human cancer cells was studied by numerous groups [134, 135, 137–139]. PsA inhibits the

proliferation of BAECs [139]. It furthermore inhibits DNA synthesis and DNA gyrase [140], farnesyl protein transferase and leucine aminopeptidase [137], chitinase B from *Serratia mercrescens* [136], in vitro replication of SV40 DNA through α -primase targeting [138], activation of peroxisome proliferator-activated receptor gamma [141], and histone deacetylases (HDACs) in cell-based assays, the latter having been highlighted as one of the key enzymes involved in both oncogenesis and angiogenesis, inducing cell cycle arrest and apoptosis [143–145]. PsA also inhibited DNA methyltransferase activity in vitro [142]. However, the lack of in vivo inhibition of DNA methylation suggests that this enzyme is not a major cellular target. Furthermore, it inhibited aminopeptidase N (APN), a Zn-dependent metalloproteinase that has been implicated in tumor invasion and angiogenesis [139]. Both homodimers and heterodimers were further assayed for antibacterial activity against methicillin-resistant *Staphylococcus aureus* and structure refinement of promising lead compounds through parallel synthesis afforded a series of antibacterial agents significantly more active than the natural product [140, 146].

Purealidin A (**114**) represents the prototype of a group of bromotyrosine-derived alkaloids that includes 17 additional purealidins (B–H and J–S) [147–153]. All compounds were isolated from different collections of the Okinawan sponge *Psammaphysilla porea* except for purealidins J and S that were obtained from the Fijian sponge *Druinella* sp. [153].

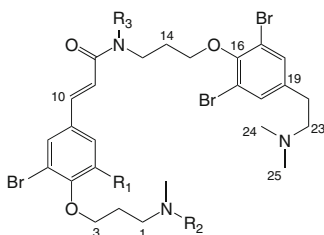


Purealidin A (**114**) exhibited cytotoxic activity against murine leukemia L1210 cells in vitro with IC_{50} value of $2.1 \mu M$ [147], while purealidins C (**115**), N (**116**), P (**117**), and Q (**118**) showed cytotoxicity against human epidermoid carcinoma KB cells (IC_{50} : 4.3, 0.16, 10.2, and $1.6 \mu M$, respectively) and murine lymphoma L1210 cells (IC_{50} : 3.2, 0.15, 3.8, and $1.3 \mu M$, respectively) [148, 152]. In both cell lines, purealidin N (**116**) was found to be the most potent analogue followed by purealidin Q (**118**). Furthermore, purealidin C (**115**) proved antifungal and antibacterial [148] while purealidins P (**117**) and Q (**118**) revealed inhibitory activity against EGF receptor kinase with IC_{50} values of 24.2 and $14.8 \mu M$, respectively [152]. Eight purpurealidins (A–H) were isolated from the Indian sponge *Psammaplysilla purpurea* [154].



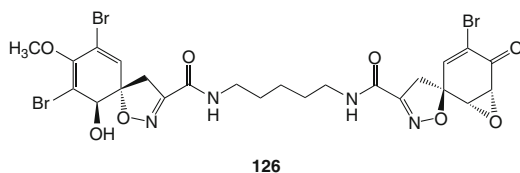
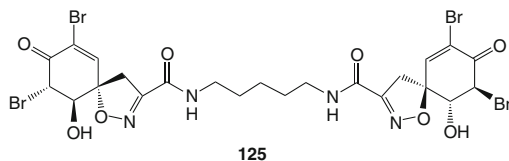
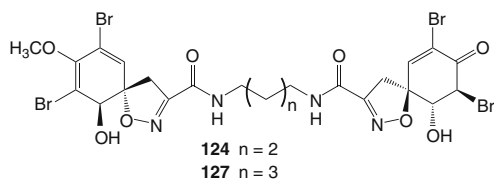
All purpurealidins were screened for antibacterial and antifungal activities. Only purpurealidin B (**119**) showed moderate activity against *Staphylococcus aureus*, *Escherichia coli*, and *Vibrio cholerae* and weak activity against *Shigella flexneri* with MIC values of 10, >12, 25, and $100 \mu g/mL$, respectively [154]. Suggested ecological roles for these bromotyrosine compounds are mainly feeding deterrents [121].

Psammaplysenes A–D (**120–123**) represent a group of bromotyrosine-derived alkaloids which have been obtained from *Psammaplysilla* sp. collected in the Indian Ocean [155] and from the Australian sponge *Psammoclemma* sp. [156]. Psammaplysene A (**120**) compensated for the loss of PTEN tumor suppressor by relocating the transcription factor FOXO1a to the nucleus ($IC_{50} = 5 \mu M$) compared to psammaplysene B (**121**) ($IC_{50} = 20 \mu M$) [155]. The growth-inhibiting PTEN phosphatase proved important for regulation of the growth-promoting PI3-kinase signal. Hence, loss of functional mutations in PTEN can result in an inappropriate increase in stimulatory signals, and such mutations have been linked with Cowden's disease, a hereditary disease with a predisposition to breast, thyroid, and other cancers [155]. Both psammaplysene C (**122**) and D (**123**) showed cytotoxicity ($IC_{50} = 7 \mu M$). Hence, their bioactivity in both P2X₇ and hemolysin specificity assays was attributed to cytotoxicity against the premonocytic cell line THP-1, which expresses the P2X₇ receptor [156]. In 2005, Georgiades and Clardy synthesized **120** and **121** by a flexible efficient route using 4-iodophenol as a common starting substrate [157].

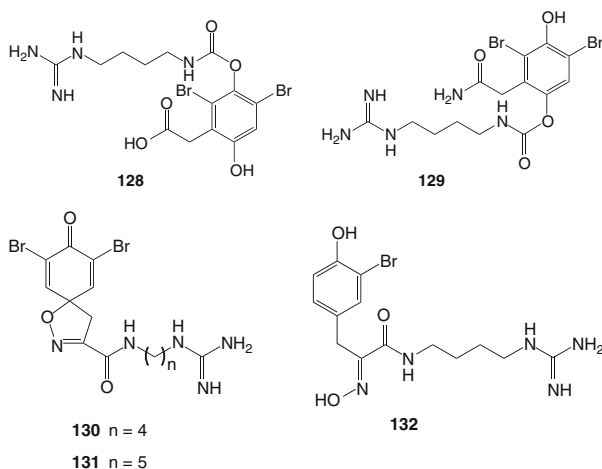


- 120** $R_1 = \text{Br}$ $R_2 = \text{CH}_3$ $R_3 = \text{H}$
121 $R_1 = \text{Br}$ $R_2 = \text{H}$ $R_3 = \text{H}$
122 $R_1 = \text{H}$ $R_2 = \text{CH}_3$ $R_3 = \text{CH}_3$
123 $R_1 = \text{Br}$ $R_2 = \text{CH}_3$ $R_3 = \text{CH}_3$

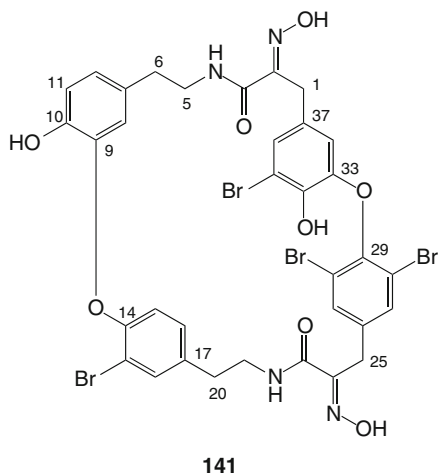
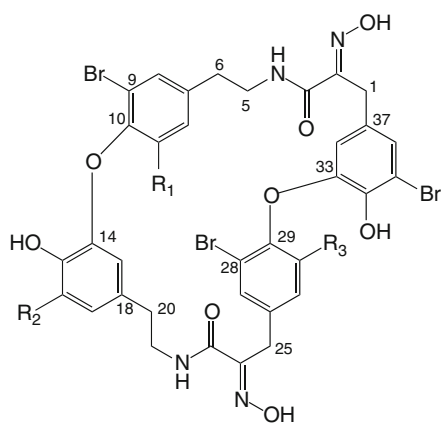
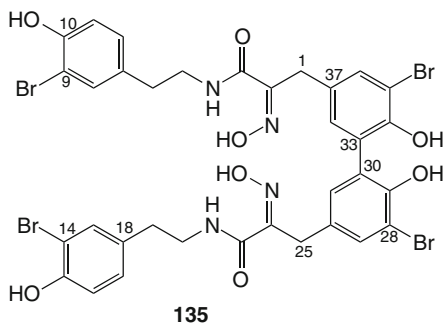
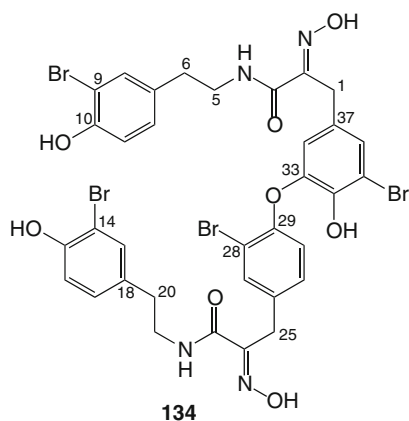
The sponge *Aplysina gerardogreeni* collected at the Gulf of California yielded four cytotoxic dibromotyrosine-derived metabolites, aplysinones A–D (**124**–**127**) [158]. Cytotoxicity of aplysinones (A–D) was evaluated against three human tumor cell lines MDA-MB-231 (breast adenocarcinoma), A-549 (lung carcinoma), and HT-29 (colon adenocarcinoma) [158]. Against MDA-MB-231 cells, all aplysinones showed cytotoxicity with IC_{50} values between 3.0 and 7.6 μM , whereas only aplysinone B (**125**) showed cytotoxicity against lung carcinoma A-549 cells with an IC_{50} value of 4.1 μM . Furthermore, aplysinones A (**124**), B (**125**), and D (**127**) proved cytotoxic against colon adenocarcinoma HT-29 cells with IC_{50} values of 9.1, 3.0, and 11.3 μM , respectively [158].



Antithrombotics (= anticoagulants) are crucial therapeutic agents for a number of thrombotic disorders such as myocardial infarction, angina, pulmonary embolism, and cerebrovascular incidences. The conventional antithrombotic therapy is performed by intravenous administration of heparin followed by oral treatment with warfarin. Besides being indirect and nonspecific inhibitors of coagulation serine proteases, both heparin and warfarin require very careful and costly monitoring to ensure safe therapeutic drug levels over treatment duration due to the high risk of bleeding. Therefore, enormous efforts focused on new plausible drug candidates with an improved efficacy-to-safety index compared to heparin and warfarin. Factor XIa (FXIa) is a trypsin-like serine protease that plays a major role in the amplification phase of the coagulation cascade and in maintaining clot integrity. FXIa is a unique target as its specific inhibitors might inhibit thrombosis without intimate interruption of normal hemostasis and thus might prevent or minimize the risks of hemostatic complications. In an attempt to achieve this target, Buchanan et al. isolated a series of bromotyrosine-derived alkaloids from two different collections of the Australian Verongid sponge *Suberea clavata*, trivially named as clavatadine A–E (**128**–**132**) [159, 160]. All clavatadines were tested for their inhibitory activities against factor Xla. Only clavatadines A (**128**) and B (**129**) inhibited selectively FXIa with IC₅₀ values of 1.3 and 27 μ M, respectively [159], while other clavatadines showed only weak inhibitory activity (17–37%) against FXIa at concentrations up to 222 μ M [160]. The crystal structure and molecular docking of **128** enabled understanding of SARs. Conclusively, they revealed that clavatadine A (**128**) can approach/bind in the S1–S1' pocket of FXIa by favorable interactions with Asp189 at its guanidine group on one end and the free carboxylate to either Arg37D or Lys192 of the other. This would result in a close contact between the side chain of Ser195 and the carbamate group of **128**, which eventually leads to the covalent binding with FXIa. Clavatadine B (**129**) is more than one order of magnitude less potent than **128**, presumably due to weaker interactions between its amide group and either Arg37D or Lys192, compared to the carboxylate moiety in **128** [159].



Bastadins are heterodimers biogenetically derived from oxidative coupling of two brominated tyrosine-tyramine amides. To date, a total of 24 bastadin analogues have been isolated from the Indo-Pacific Verongid sponges *Ianthella basta* [161–171], *Ianthella quadrangulata* [172, 173], *Ianthella* sp. [174], and *Psammaphysilla purpurea* [175, 176] in addition to the Dendroceratid sponge *Dendrilla cactos* [177].



	R ₁	R ₂	R ₃
136	H	Br, EA ^{5,6}	H
137	Br	Br	H
138	H	H	H
139	Br	H	H
140	Br	Br	Br

Bastadins are structurally classified into three groups, according to the proposed biosynthetic pathway by Jaspars et al. [166] (Scheme 4.4), depending upon the degree and position of the phenolic couplings linking the monomeric units such as hemibastadin (**133**) (Scheme 4.4) [165, 178]. The linear (= acyclic) bastadins contain a single ether or biaryl linkage like in bastadin 1 (**134**) and bastadin 3 (**135**), while the macrocyclic members of the series possess either the bastarane skeleton (Scheme 4.4) including bastadin 4 (**136**), 6 (**137**), 9 (**138**), 16 (**139**), and 24 (**140**) in which the hemibastadin units are linked by phenolic ethers from C10 to C14 and from C29 to C33, or the isobastarane skeleton (Scheme 4.4) such as bastadin 13 (**141**), in which ethers link C9 to C14 and C29 to C33 (Scheme 4.4).

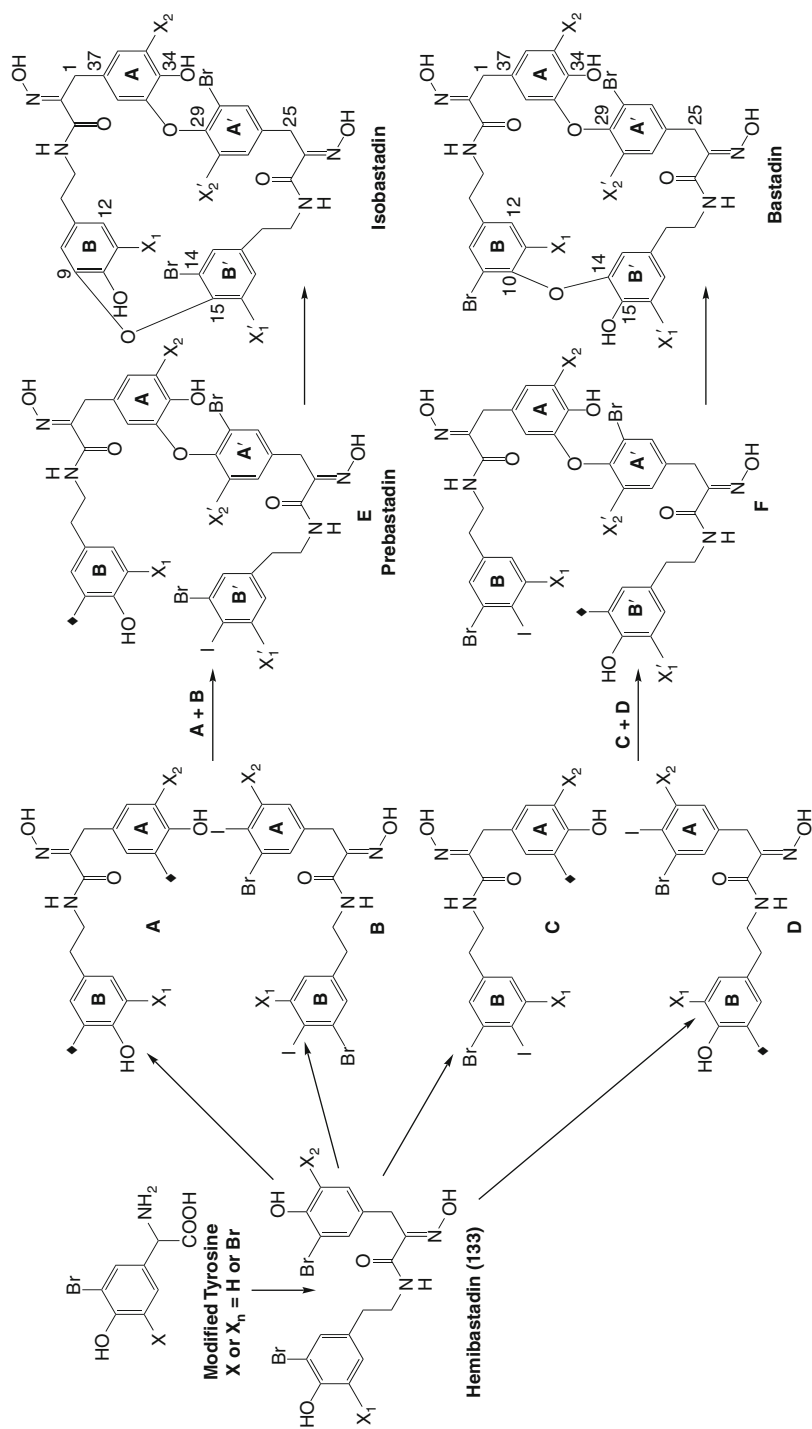
Bastadins were first isolated from the Australian sponge *lanthella basta* and revealed potent in vitro antimicrobial activity against Gram-positive bacteria [161, 162]. Since then, bastadins have demonstrated a vast array of biological activities including cytotoxicity [163, 164, 173, 175, 177, 179], anti-inflammatory activity [163], inhibitory activity of topoisomerase II, dehydrofolate reductase, inosine 5'-phosphate dehydrogenase, 12- and 15-human lipoxigenases [166, 175, 180], and agonistic activity toward the sarcoplasmic reticulum Ca^{2+} channel through modulation of the Ry_1R FKBP12 receptor complex [168, 181, 182]. In addition, the antiangiogenic activity of the bastadins has been reported by Kobayashi et al. [169, 170]. Furthermore, Proksch et al. investigated the antifouling activity of selected sponge metabolites on settling of barnacle larvae, or cyprids, of *Balanus improvisus* [171].

The study included selected sponge-derived natural products displaying pronounced activity in other bioassays such as ageliferin (**82**), isofistularin-3 (**102**) (Scheme 4.3), and sceptrin (**81**) which are known to be fish deterrents [183, 184] and hymenidin (**18**) and **81** inhibit serotonin being involved in cyprid settling behavior [106] in addition to psammaphin A (**109**), hemibastadin (**133**), bastadins 3 (**135**), 4 (**136**), 9 (**138**), and 16 (**139**). In this study, only bastadins and psammaphin A inhibited the settlement of the cyprids in a dose-dependent manner in a range of 0.1–10 μM [171].

However, hemibastadin (**133**) and psammaphin A (**109**) proved to be toxic to *B. improvisus* when tested at a dose of 10 μM . The antifouling activity of the active compounds is linked to the oxime moiety as a uniting structural feature. In order to justify this hypothesis, two synthetic products including debromohemibastadin-1 and L-tyrosinyltyramine, differing only in the presence of an oxime vs. amino function, were investigated. Although L-tyrosinyltyramine proved to be completely inactive even at a concentration of 100 μM , the oxime-bearing debromohemibastadin inhibited barnacle settlement at almost similar concentrations as the brominated derivatives thus corroborating the importance of the oxime function [171].

4.3 Peptides

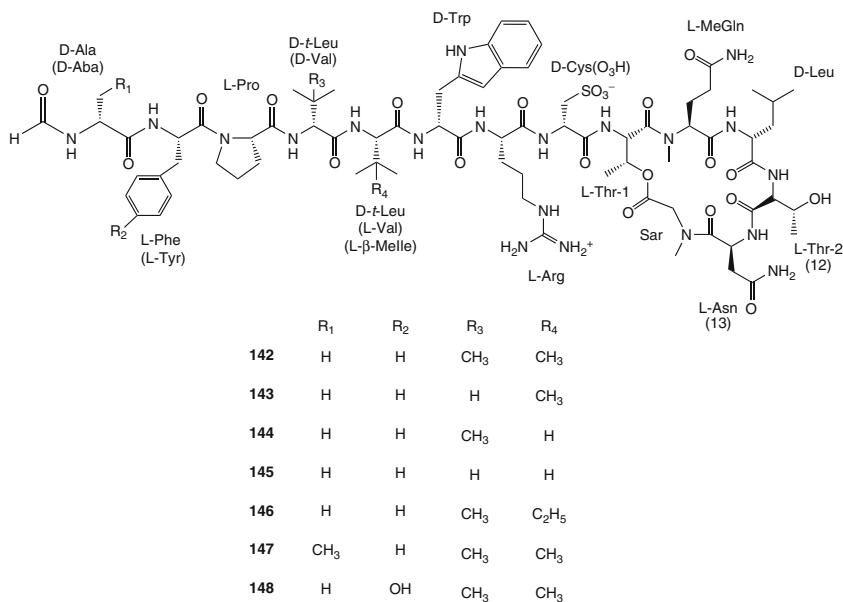
Bioactive peptides from marine sponges are receiving considerable interest by natural product chemists and pharmacologists alike and represent

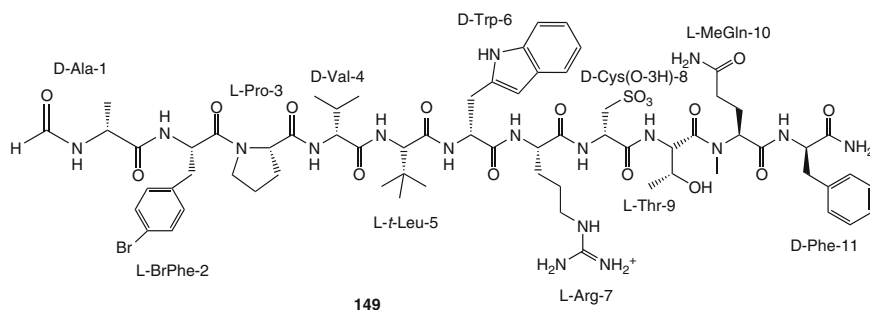


Scheme 4.4 Biosynthetic pathway of bastadins as proposed by Jaspars et al. [166]. Donor site = ● (phenolic oxygen) Acceptor site = ◆ (aryl bromine)

a well-established sector of marine natural products research. Most bioactive peptides from marine sponges comprise unique structures in comparison with those from other sources. For example, marine peptides are often cyclic or linear peptides containing unusual amino acids which are either rare or even absent in terrestrial and microbial peptides. In addition they frequently contain uncommon linkages between amino acids such as kapakahines isolated from a Pohnpei sponge *Cribrochalina olemda* [185–187].

Discodermin A (**142**) was the first bioactive peptide isolated from the marine sponge *Discodermia kiiensis* collected at Shikine Island (Japan) [188, 189]. Further chemical investigation of the extract of the same sponge resulted in the isolation of three additional discodermins B–D (**143–145**) [190], whereas bioassay-guided fractionation of the extract of *D. kiiensis* collected off Atami in the Gulf of Sagami (Japan) led to the isolation of discodermin E [191]. Structural study of discodermin E revealed the presence of a D-kynurenine residue replacing a D-Trp residue and a reversed sequence of the 12th and 13th residues from the *N*-terminus compared to discodermin A (**142**) [191]. In addition to discodermin E, three further congeners including discodermins F–H (**146–148**) were obtained from the latter sponge [192]. Discodermins A–H and the structurally related discobahamins A and B [193], polydiscamides A–D [194, 195], and halicylindramides A–E [196, 197] have been obtained from marine sponges of the genera *Discodermia*, *Iricina* and *Halichondria*, respectively. They represent a group of bioactive peptides containing 13 to 14 known as well as rare amino acid residues with a macrocyclic ring formed by lactonization of a threonine moiety with the carboxy terminal of the peptide chain. Halicylindramide E (**149**) is an exception as it is a linear peptide composed of 11 amino acids.

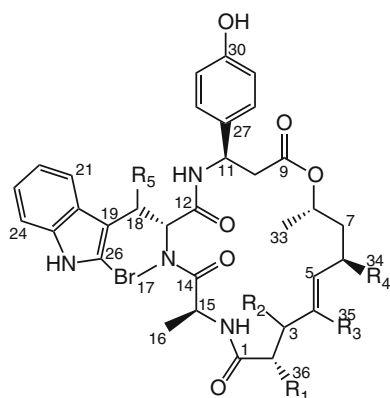




Discodermins A–D (**142–145**) revealed *in vitro* antibacterial activity [188–191]. They were later found to be potent inhibitors of phospholipase A₂ (PLA₂) and **142** inhibited the tumor promotion activity of okadaic acid [191]. In addition, discodermins F–H (**146–148**) were cytotoxic against P388 murine leukemia cells with IC₅₀ values of 0.6, 0.23, and 0.6 μ M, respectively [192]. Discobahamins A and B exhibited weak antifungal activity against *Candida albicans* [193]. Polydiscamide A inhibited the proliferation of human lung cancer A549 cell line (IC₅₀ = 0.4 μ M) *in vitro* and the growth of *Bacillus subtilis* (MIC of 1.8 μ M) [194]. Interestingly, polydiscamides B–D acted as pain modulators by activating the sensory neuron-specific G protein coupled receptors (SNSRs), which are expressed solely in dorsal root ganglia [198]. Previous studies showed that SNSRs are key players in both acute and persistent pain [199]. Due to the highly restricted distribution of SNSRs in the body, ligands that interact with these receptors may potentially modulate pain with very few side effects [195]. Polydiscamides B–D showed potent agonist activity against human SNSR with EC₅₀ values of 1.26, 3.57, and 2.80 μ M [195], and they were the first examples of nonendogenous compounds with human SNSR agonist activity. Therefore, they could potentially be modified for therapeutic use as pain modulators.

Halicylindramides A–D, featuring D-Phe and L-BrPhe instead of D-Leu and L-Phe (or L-Tyr) in discodermins, respectively, exhibited antifungal activity against *Mortierella ramanniana* at 7.5 μ g/disk as well as cytotoxic activity against P388 murine leukemia cells with IC₅₀ values of 0.3, 0.1, 0.01, and 1.2 μ M, respectively [196, 197].

Two families of closely related cyclic depsipeptides, the jaspamides and the geodiamolides, have been isolated from a variety of tropical marine sponges. Jaspamide (jasplakinolide) (**150**), obtained independently from *Jaspis* sp. collected off Palau [200] and Fiji [201] in 1986, was the first member of this group of depsipeptides to be reported. Thereafter, several reports on the presence of jaspamide in other sponge genera, including *Auleta* cf. *constricta* [202] and *Hemiassterella minor* [203] were published. Geodiamolides A (**154**) and B (**155**) were isolated from the Caribbean sponge *Geodia* sp. [204].



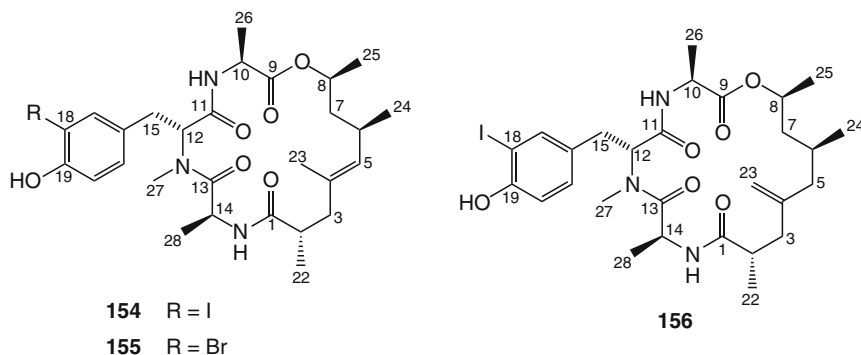
	R ₁	R ₂	R ₃	R ₄	R ₅
150	CH ₃	H	CH ₃	CH ₃	H
151	H	H	CH ₃	CH ₃	H
152	CH ₃	H	CH ₃	H	H
153	CH ₃	H	CH ₃	CH ₃	OH

After the discovery of jaspamide (**150**) and its pronounced biological activities which include antifungal [205], anthelmintic, insecticidal [200, 201], and cytotoxic activity [206], sponges of the genus *Jaspis* have received considerable attention. Sixteen additional jaspamide derivatives (B–H and J–R) have been isolated from different collections of the marine sponge *Jaspis splendens* [207–211]. All jaspamide derivatives exhibited a consistent antiproliferative activity with IC₅₀ values ranging from 0.01 to 10 μ M [210, 211] when tested against MCF-7 human breast adenocarcinoma, HT-29 colon carcinoma, or L5178Y mouse lymphoma cell lines.

The antimicrofilament activity was measured and paralleled the observed in vitro cytotoxicity. A thorough structural analysis indicated that the sole invariable residue in all jaspamides is β -tyrosine whereas a wide variability of the alkylation and oxidation pattern of the polypropionate subunit as well as of the identity of the first two amino acids, namely, alanine and abrine (*N*-methyltryptophan), of the tripeptide portion was observed. Therefore, the β -tyrosine residue appeared to be the only strict common feature essential for biological activity in the tested tumor cell lines, mainly assuring a β -turn motif for the folding of the entire molecule [210]. Moreover, the modifications of the abrine residue, claimed as essential for the observed biological activity [212], appeared to have little influence on the observed antiproliferative effect with the exception of jaspamide N (**153**), where the β -hydroxylation of tryptophan unit causes a diminution of the biological activity. As suggested by Maier [213], the 1,3 methyl groups of the polypropionate subunit, imposing to the macrocycle conformational constraints through *syn* pentane

interactions, play a significant role in assuring a correct folding of the entire molecule as suggested by the drop of activity for jaspamides F (**151**) and H (**152**).

Geodiamolides A (**154**) and B (**155**) were first isolated from the Caribbean sponge *Geodia* sp. [204]. Geodiamolides C–F [214] and geodiamolide G (**156**) [215] have been reported from a *Cymbastela* sp. collected in Papua New Guinea. Geodiamolides H and I have been reported from the marine sponge *Geodia* sp. collected off Macqueripe Bay (Trinidad) [216]. Geodiamolide TA was isolated from the South African sponge *Hemiassterella minor* [203], while the structurally related neosiphoniamolide A has been obtained from the New Caledonian sponge *Neosiphonia superstes* [217]. In addition, geodiamolides J–P and R were isolated from the marine sponge *Cymbastela* sp. collected in Papua New Guinea [218].

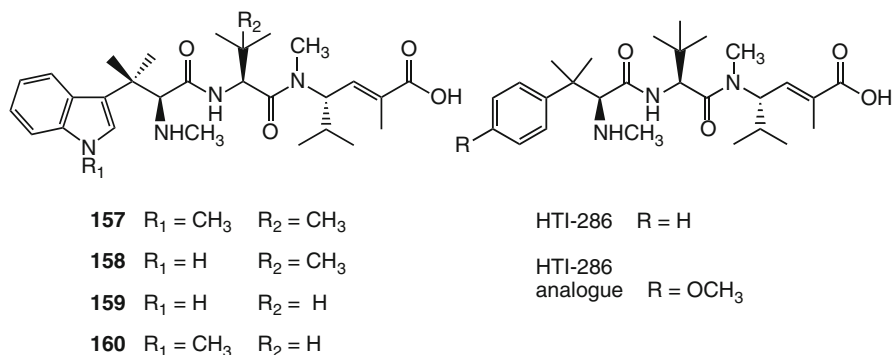


There are now, to the best of our knowledge, 19 known members of the geodiamolide family of cyclodepsipeptides. Variations have been observed in all three amino acid positions and also in the polyketide portion of the molecule. However, comparison of their cytotoxicities showed that significant variation in the three amino acid residues causes only minor changes in the levels of cytotoxicity exhibited by this class of compounds. In contrast, geodiamolide G (**156**) (in vitro human glioblastoma/astrocytoma U373, IC_{50} 12 μ M; in vitro inhibition of human ovarian carcinoma HEY, IC_{50} 13.4 μ M) [215], with its modified polyketide fragment, is significantly less toxic than the analogous geodiamolide A (**154**) (in vitro inhibition of human glioblastoma/astrocytoma U373, IC_{50} 0.02 μ M; in vitro inhibition of human ovarian carcinoma HEY, IC_{50} 0.07 μ M) [218].

The jaspamide/geodiamolide family of metabolites occurs across taxonomically distant groups of sponge species [200–218]. It has been suggested that microorganisms associated with the respective sponges may be responsible for the production of these metabolites [203]. The isolation of chondramides, which are jaspamide analogues, from cultures of various strains of *Chondromyces crocatus* [219] strongly supported the hypothesis of a microbial origin for the jaspamides/geodiamolides.

Hemiassterlin (**157**) is a prototype of a group of antimitotic tripeptides which was first isolated together with geodiamolide TA in 1994 from the marine sponge *Hemiassterella minor* [203]. It revealed significant cytotoxicity against P388 leukemia cell line with IC_{50} value of \sim 0.02 μ M [203]. The related isomers hemiassterlins

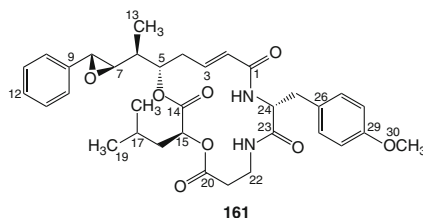
A (**158**) and B (**159**) were obtained from sponges of the genus *Auleta* and *Cymbastella* in 1995 [215], whereas a fourth analogue, hemiasterlin C (**160**) was isolated from the marine sponge *Siphonochalina* sp. collected off the coast of Papua New Guinea in 1999 [220]. In 1996, an X-ray crystal structure analysis of the hemiasterlin methyl ester confirmed its linear structure and unusual amino acids existence [221]. All hemiasterlins (**157–160**) exhibited pronounced in vitro cytotoxicity against a variety of human and murine cell lines with IC_{50} values in the nanomolar range [215]. The potent antiproliferative activity of hemiasterlins was found to be due to the induction of mitotic arrest in metaphase with cellular dynamics similar to those of known tubulin binders, such as the chemotherapeutics paclitaxel or vinblastine, at ED_{50} values ranged from 0.5 nM (hemiasterlin) to 28 nM (hemiasterlin B) [222].



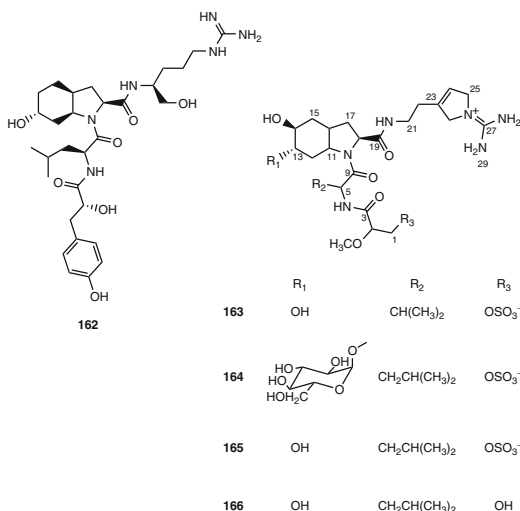
Extensive SAR studies demonstrated that HTI-286, a simpler synthetic analogue of hemiasterlin (**157**) with a phenyl substituent replacing the *N*-methyltryptophan, is more potent than **157** [221], whereas an analogue of HTI-286 with a *para*-methoxyl substituent on the benzene ring was even more potent [220]. Other structural elements, including the geminal β,β -dimethyl group and the *N*-methyl on the first amino acid residue (N terminus), the isopropyl and an olefin in the homologated γ -amino acid (C terminus) including a terminal carboxylic acid or methyl ester, were essential for activity. The aryl side chain on the N terminus could be replaced synthetically by alkyl groups (e.g., *tert*-butyl) while still retaining potent activity [223–226]. Preclinical studies showed that HTI-286 causes tumor regression and growth inhibition of human xenografts in mice [227]. An open-label phase I clinical trial of HTI-286 was completed in patients with advanced solid tumors; however, there were no objective responses and common toxicities observed including neutropenia, nausea, alopecia and pain [228]. Therefore, phase II trials have been halted. Nevertheless, there is still interest in HTI-286 according to recent results including high antitumor activity in androgen-dependent and androgen-independent mouse models of refractory prostate cancer and in a newly established in vitro taxane-resistant prostate PC-3 cell line [229].

Arenastatin A (**161**) is another example of cytotoxic cyclic depsipeptides that was isolated from the Okinawan marine sponge *Dysidea arenaria* [230]. Arenastatin A exhibited potent cytotoxicity against KB human epidermoid

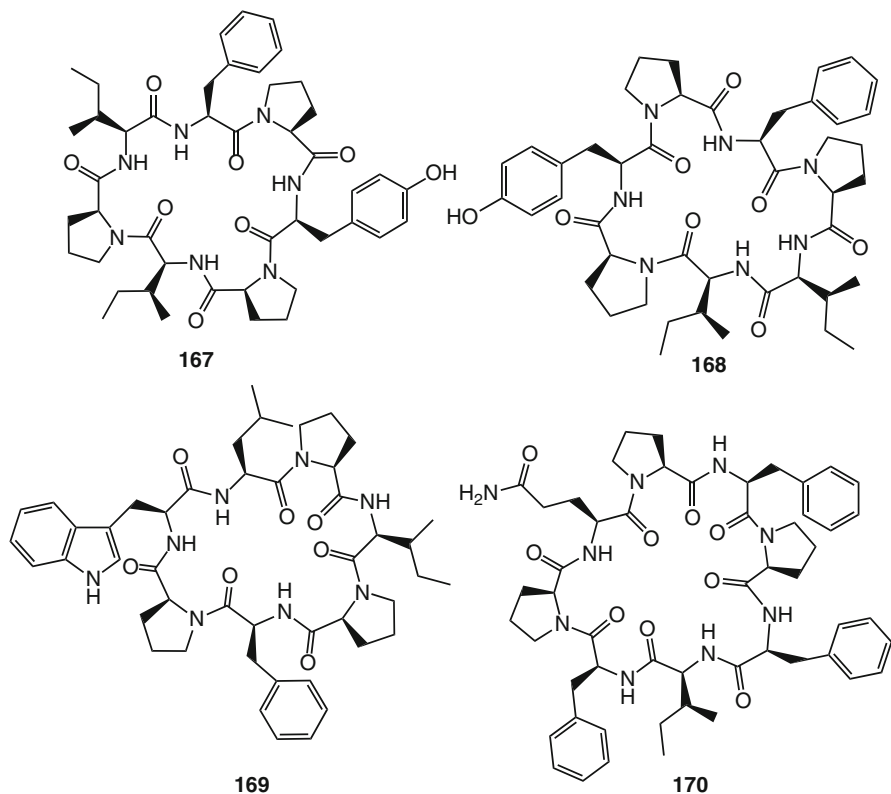
carcinoma cells with IC_{50} value of 8.3 pM [230]. Its absolute configuration [231] and its total synthesis [232] were reported.



From the family Dysideidae, dysynosins A–D (**163–166**) have been reported [233, 234]. Dysynosin A (**163**) was isolated from a new genus of sponges found near Lizard Island (Australia) [233]. Afterward, it was reisolated together with the other three dysynosins B–D from the Australian marine sponge *Lamellodysidea chlorea* [234]. Dysynosins are structurally related to the cyanobacterial metabolites aeruginosins [235–237]. Aeruginosin 98-A (**162**) was reported in 1994 as a thrombin and trypsin inhibitor from the cyanobacterium *Microcystis aeruginosa* [235]. Not surprisingly, dysynosins A–D also exhibited inhibitory activity against thrombin (IC_{50} values of 0.17–> 5.1 μ M) and factor VIIa (IC_{50} values of 0.09–1.32 μ M) [233, 234]. Dysynosins A–D (**163–166**) were further investigated to assess their SARs. The X-ray structural analysis of dysynosin A (**163**) revealed a hydrogen bonding network forming the dysynosin-A-thrombin complex [233]. The introduction of a sugar unit at C-13 in dysynosin B (**164**) gave a slight increase in inhibition of factor VIIa compared to both dysynosins A (**163**) and C (**165**) (0.09 μ M compared to 0.108 and 0.124 μ M, respectively), while selectivity relative to thrombin decreased to 1.9 compared to 4.2 and 4.4, respectively [234]. Desulfated dysynosin D (**166**) was found to be ten times less potent against both factor VIIa and thrombin compared to other sulfated dysynosins, indicating the importance of the sulfate group [234].



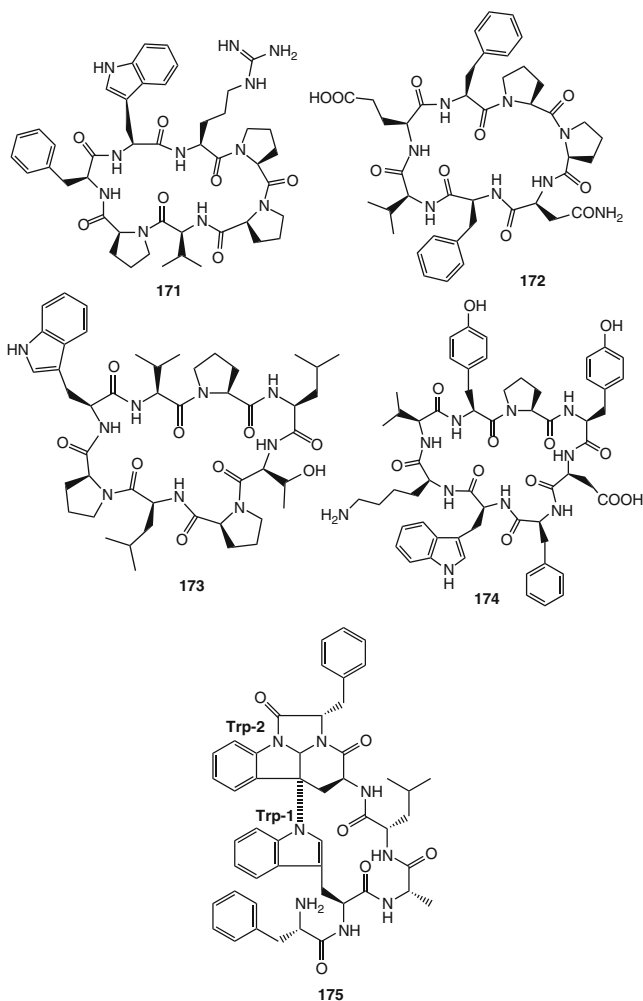
Phakellistatins and hymenamides are two groups of proline-rich cyclopeptides. They were isolated mainly from different species of the marine sponge genera *Phakellia* and *Hymeniacidon*, respectively. However, phakellistatins 1–14 and isophakellin 3 were isolated from different species of the genus *Phakellia* [238–247], and two conformers of phakellistatin 2 have been reported from the Fijian marine sponge *Stylotella aurantium* [248]. Phakellistatin 1 (**167**) was the first reported congener from the Indo-Pacific (Truk Archipelago) marine sponge *Phakellia costata* [238]. Phakellistatin 1 revealed moderate cytotoxicity against P388 cells ($IC_{50} = 9.0 \mu M$) [238]. Amongst the reported phakellistatins to date, phakellistatins 2 (**168**) [239], 6 (**169**) [242], and 11 (**170**) [244] exhibited the most potent antiproliferative activity against P388 murine leukemia cell line with IC_{50} values of 0.4, 0.2, and 0.2 μM , respectively. Moreover, phakellistatin 6 (**169**) was more active than phakellistatin 2 (**168**) against a panel of six human cancer cell lines, namely, ovarian (OVCAR-3), brain (SF-295), renal (A498), lung (NCI-H460), colon (KM20L2), and melanoma (SK-MEL-5) cell lines, with GI_{50} ranges of 0.02–0.09 μM [242] and 1.2–3.6 μM [239], respectively.



Hymenamides (A–K) have been isolated from the Okinawan marine sponge *Hymeniacidon* sp. [249–252]. Hymenamides A (**171**) and B (**172**) were reported in 1994, and only the latter exhibited cytotoxicity against L1210 and KB tumor cell lines

with IC_{50} values of 3.8 and 7.2 μM , respectively [249]. In addition to hymenamide B, only hymenamide J (**174**) showed cytotoxicity against L1210 and KB tumor cell lines (IC_{50} values of 2.4 and 0.7 μM , respectively), while hymenamide H (**173**) exhibited cytotoxicity only against L1210 cells ($IC_{50} = 7.0 \mu M$) [252].

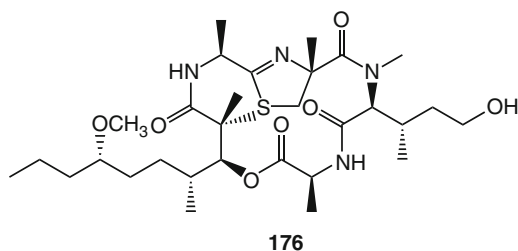
Beside hymenamides, hymenistatin 1, a proline-rich cyclo-octa peptide, was also purified from the marine sponge *Hymeniacidon* sp. collected in Palau [253]. Hymenistatin 1 was active against the P388 murine leukemia cell line (IC_{50} 3.9 μM) [253]. In addition, it was found to exert an immunosuppressive effect (both in the humoral and cellular immune responses) comparable to that of the well-known immunosuppressive agent cyclosporin [254].



From other sponges of the same order Halichondrida, axinastatins [255, 256], axinellins A–C [257, 258], and stylissamides A–D [259] have been reported

from different species of the marine sponge genus *Axinella*, the Fijian marine sponge *Stylotella aurantium* and *Stylissa caribica*, respectively. They all exhibited mild to moderate antiproliferative activity. However, from a Jamaican collection of *Stylissa caribica*, two proline-rich cyclic heptapeptides, stylisins 1 and 2, have been isolated. In contrast to other peptides, stylisins 1 and 2 proved inactive in antimicrobial, antimalarial, anticancer, anti-HIV-1, anti-Mtb, and anti-inflammatory assays [260]. Kapakahines A–G are also proline-containing cyclic peptides isolated from a Pohnpei sponge *Cribrochalina olemda* (order Haplosclerida) [185–187]. They share a unique structural feature: two tryptophan residues (Trp-1 and Trp-2) are not linked by an amide bond but by a N–C bond from the indole nitrogen of Trp-1 to the β -indole carbon of Trp-2. Kapakahine B (**175**) was the first reported congener, and it exhibited moderate cytotoxicity against P388 cells ($IC_{50} = 5.9 \mu M$) [185]. All other kapakahine derivatives exhibited moderate to weak cytotoxic activity [186, 187]. Their structures, however, were found to be unique and of biogenetic interest.

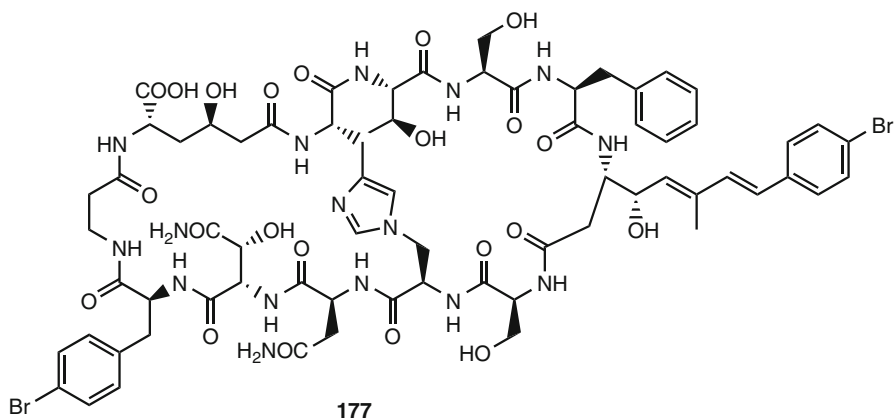
Haligramides A and B were also identified as proline-rich cyclopeptides from the marine sponge *Haliclona nigra* collected from the northern coast of Papua New Guinea [261]. The cyclic depsipeptides, halipeptins (A–D), were isolated from another species of the genus *Haliclona* collected in Vanuatu [262, 263]. Although, haligramides A and B exhibited moderate activity in the cytotoxicity assay against four human tumor cell lines [261], halipeptin A (**176**) revealed no significant results in either cytotoxicity, antifungal, antiviral, or antimicrobial assays [262].



Interestingly, halipeptin A (**176**) was found to possess potent *in vivo* anti-inflammatory activity, causing about 60 % inhibition of edema in mice at the dose of 0.3 mg/kg (i.p.) compared to indomethacin and naproxen (ED_{50} of 12 and 40 mg/kg, respectively) [262].

Recently, euryjanicins (A–D) have been reported from the Caribbean marine sponge *Prosuberites laughlini* [264, 265]. They are cycloheptapeptides containing two or three prolines, an array of apolar residues, and one or two aromatic residues. Euryjanicins A, C, and D each contain a serine residue, whereas euryjanicin B possesses one threonine unit. When tested against the National Cancer Institute 60 tumor cell line panel, all euryjanicins displayed weak cytotoxicity [265].

Theonellamides (A–F) are a group of cytotoxic peptides with novel amino acid residues and complex bicyclic macrocyclic rings isolated from the marine sponge *Theonella* sp. collected off Hachijo-jima Island (Japan) [266, 267].

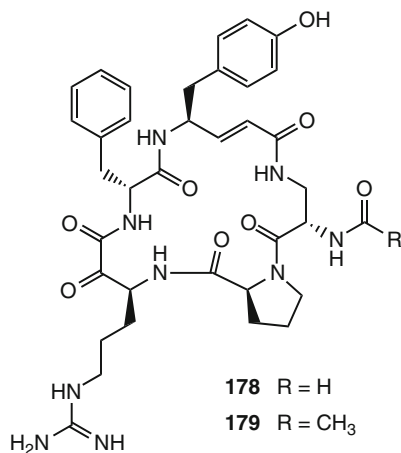


Theonellamide F (**177**) was the first reported congener exhibiting antifungal activity against pathogenic fungi *Candida* sp., *Trichophyton* sp., and *Aspergillus* sp. at MIC values between 1.8 and 7.3 μM . It is also cytotoxic against L1210 and P388 leukemia cells with IC_{50} values of 1.9 and 1.6 μM , respectively [266]. In addition, all other theonellamides (A–E) were cytotoxic against P388 cells (IC_{50} 's between 0.5 and 2.8 μM) [267].

Polytheonamides (A–C) are polypeptides consisting of 20 amino acid residues with unprecedented structural features. They were reported from the marine sponge *Theonella swinhoei* (Hachijo-jima Island, Japan) [268, 269]. Polytheonamides exhibited potent cytotoxic activity against P388 cells (IC_{50} = 13.5–15.5 pM) [269].

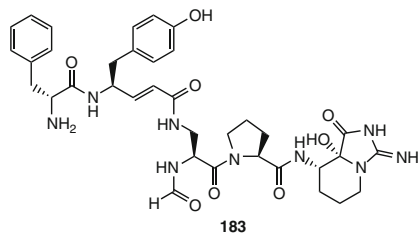
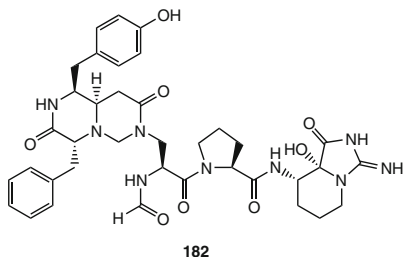
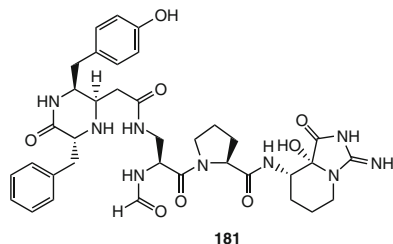
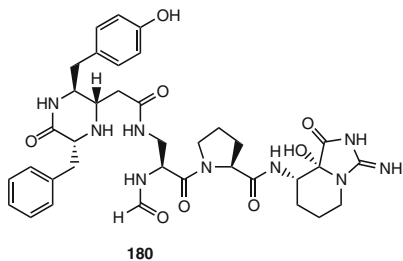
Cyclotheonamides A (**178**) and B (**179**) are cyclic peptides containing unusual amino acid residues, i.e., vinylogous tyrosine (V-Tyr), α -ketohomoarginine (K-Arg), and β -linked-diaminopropionic acid (Dpr). They were isolated from the marine sponge *Theonella swinhoei* (Japan) [270] together with two additional congeners C and D [271], whereas cyclotheonamide E was isolated from a morphologically different specimen of *Theonella swinhoei* [271]. Chemical investigation of the marine sponge *Theonella* sp. collected off Tanegashima Island led to the isolation of cyclotheonamides E2 and E3 [272], while cyclotheonamides E4 and E5 were obtained from the Okinawan marine sponge *Ircinia* sp. [273]. Cyclotheonamides (A–E) and (E2–E5) were found to possess potent inhibitory activity against serine proteases including thrombin, trypsin, and plasmin [270–273]. Their mode of action was elucidated by X-ray crystallography of the complex between cyclotheonamide A (**178**) and human α -thrombin which disclosed that (1) the binding of **178** to the catalytic triad of the enzyme is achieved through forming a network of hydrogen bonds between the α -keto group of the K-Arg residue and the hydroxyl group of Ser195 of the enzyme, (2) V-Tyr residue proved to be involved in the bonding mechanism, and (3) cyclotheonamide D which

possesses D-Leu instead of D-Phe in **178** showed comparable activity against thrombin; thus, a further hydrophobic amino acid can replace D-Phe [271].

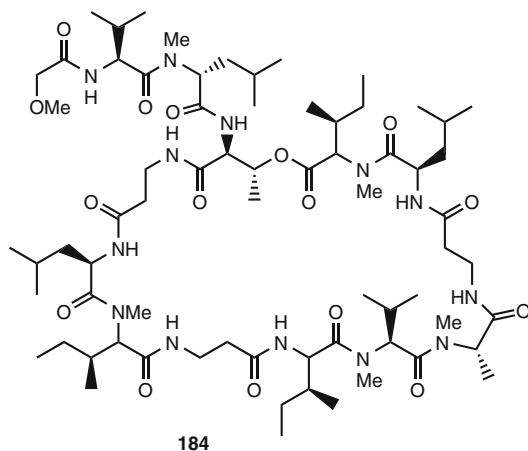


However, a comparative X-ray study against either human α -thrombin or bovine β -trypsin revealed that cyclotheonamide A (**178**) inhibited trypsin stronger than thrombin (IC_{50} = 16 and 23 nM, respectively) [272]. These results were substantiated to the more favorable (1) aromatic interaction of the D-Phe in **178** with Tyr39 and Phe41 in trypsin than with Glu39 and Leu41 in thrombin and (2) interaction of *N*-formyl Dpr residue with Gly174 and Gln175 in trypsin than Ile174 and Arg175 in thrombin [272]. Since the cyclotheonamides exhibited potent inhibitory activity against serine proteases, the marine sponge *T. swinhoei* has been thoroughly investigated. From a specimen collected off Hachijo-jima Island in 1993, pseudotheonamides A₁, A₂, B₂, C, D, and dihydrocyclotheonamide A were isolated [273].

Pseudotheonamides A₁ (**180**), A₂ (**181**), and B₂ (**182**) are linear pentapeptides embracing the rare piperazinone and piperidinoiminoimidazolone ring systems, while pseudotheonamide C (**183**) contains V-Tyr instead of a piperazinone ring. Pseudotheonamide D, a tetrapeptide lacking a C-terminal K-Arg unit and dihydrocyclotheonamide A, is a reduction product of cyclotheonamide A (**178**). Peptides **180–183** and dihydrocyclotheonamide A inhibited thrombin with IC_{50} values of 1.0, 3.0, 1.3, 0.19, 1.4, and 0.33 μ M, respectively, whereas they inhibited trypsin with IC_{50} values of 4.5, >10, 6.2, 3.8, >10, and 6.7 μ M, respectively [274]. As revealed by a SAR study of cyclotheonamides, potent inhibition of serine proteases is associated with the presence of the α -keto group of K-Arg residue [270–273]. Therefore, it was not surprising that pseudotheonamides, in which the α -keto group was either modified or missing, showed only moderate activity [274]. Thus, cyclotheonamides and pseudotheonamides inhibited serine proteases including trypsin and thrombin. These results suggested that cyclotheonamides and pseudotheonamides may be useful for treatment of asthma and other disorders associated with inflammation of the respiratory tract in addition to coagulatory disorders [273].



Theonellapeptolides are a group of tridecapeptide lactones characterized by the presence of high proportions of D-amino acids, *N*-methyl amino acids and β -amino acids. Theonellapeptolide Id (**184**) was the first reported congener from the Okinawan marine sponge *Theonella swinhoei* [275]. From the same specimen, theonella-peptolides (Ia–Ic, Ie, and Iid) have also been purified [276–280], whereas theonella-peptolide Iie was isolated from an Indonesian specimen of *T. swinhoei* collected using SCUBA in Baranglombo Island [281]. From the same Indonesian specimen, four cyclic depsipeptides named barangamides (A–D) have been reported [281, 282].

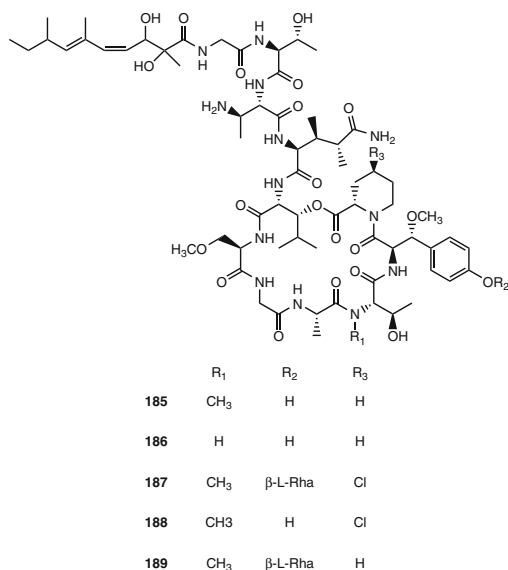


Biological activity of theonellapeptolides include cytotoxicity, ion-transport activity for Na^+ , K^+ , and Ca^{2+} ions [278], Na^+ , K^+ -ATPase inhibitory activity [283], and mild immunosuppressive activity [281]. However, other theonellapeptolide

(III series) exhibiting in vitro cytotoxicity against the P388 cell line ($IC_{50} = 5.2 \mu M$) have also been reported from a New Zealand deep-water sponge, *Lamellomorpha strongylata*, belonging to a different order compared to *T. swinhoei* [284].

The cyclic depsipeptides, papuamides (A–D), were isolated from two-sponge associations of *Theonella mirabilis* and *T. swinhoei* collected in Papua New Guinea [285]. They contain a number of unusual amino acids including 3,4-dimethylglutamine, β -methoxytyrosine, 3-methoxylanine, and 2,3-diaminobutanoic acid or 2-amino-2-butenic acid residues. Papuamides also contain a previously undescribed 2,3-dihydroxy-2,6,8-trimethyldeca-(4*Z*,6*E*)-dienic acid moiety linked to a terminal glycine residue. In addition, they were the first marine-derived peptides reported to contain 3-hydroxyleucine and homoproline residues [285]. Papuamides A (**185**) and B (**186**) inhibited the infection of human T-lymphoblastoid cells by HIV-1_{RF} in vitro with an EC_{50} of approximately 2.6 nM [285]. Papuamide A (**185**) was also cytotoxic against a panel of human cancer cell lines with a mean IC_{50} of 0.05 μM [285].

Mirabamides (A–D) are cyclic depsipeptides structurally related to papuamides. However, mirabamides were isolated from an aqueous extract of the marine sponge *Siliquariaspongia mirabilis* (Chuuk Lagoon, Micronesia), and they differ from papuamides in either being chlorinated (4-chlorohomoproline) and/or glycosylated (β -methoxytyrosine 4'-*O*- α -L-rhamnopyranoside) derivatives [286]. A comparative study to determine the effects of mirabamides on HIV-1 infection was performed using two different viral strains, namely, HXB2 (T-cell-tropic virus) and SF162 (macrophage-tropic virus) in HIV-1 neutralization assay. In addition, HIV-1 envelope-mediated cell fusion assay was also carried out to determine whether the compounds act at early stages of infection, i.e., viral entry.

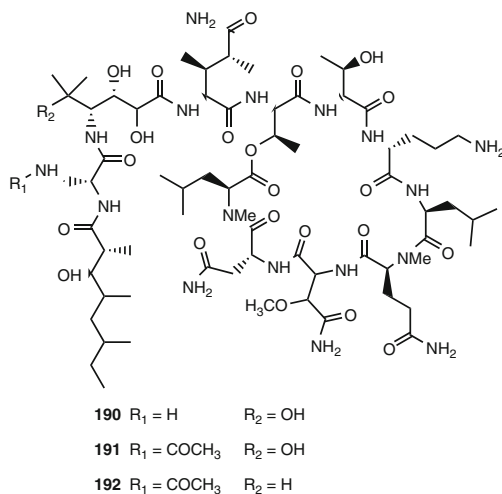


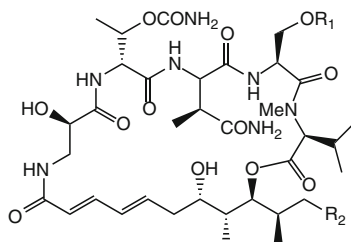
Results of testing mirabamides (A–D) and papuamide A revealed that mirabamides A (**187**), C (**188**), and D (**189**), as well as papuamide A (**185**) inhibit

HIV-1 envelope-mediated fusion with activities comparable to those observed in the neutralization assays [286]. Mirabamide A (**187**) and papuamide A (**185**) were found to be the most potent inhibitors in the fusion assay, with respective IC_{50} values of 41 and 73 nM, while mirabamides C (**188**) and D (**189**) inhibited fusion at lower micromolar concentrations (IC_{50} 's between 0.14 and 3.9 μ M) [286]. Mirabamide B is the only mirabamide containing a 2,3-dehydro-2-aminobutanoic acid residue instead of the 2,3-diaminobutanoic acid residue (Dab) that is present in other mirabamides as well as in papuamides A (**185**) and B (**186**). Interestingly, mirabamide B was consistently found to be less potent than other mirabamides (**187**–**189**) in both neutralization and fusion assays. Thus, the Dab residue in this class of peptides appeared to be important for anti-HIV activity [286].

As for the role of β -methoxytyrosine residue (β -OMe Tyr), mirabamide A (**187**), with rhamnosylated β -Tyr residue, was found to be the most potent analogue among the four mirabamides. This indicates that Tyr residues bearing substitutions at the 4' position can be tolerated with no deleterious effect on antiviral activity and that the presence of a free 4' hydroxyl on the Tyr unit is not essential [286]. In summary, the reported results disclosed that mirabamide A (**187**) is equipotent to papuamide A (**185**) (which also contains a β -OMe Tyr residue), whereas theopapuamide A (**190**), which was isolated from a Papua New Guinea lithistid sponge *Theonella swinhoei* and lacks a β -OMe Tyr residue, was inactive [287]. One hypothesis that would be consistent with these results is that the β -OMe Tyr residue imparts a specific conformation required for binding to target protein(s) involved in HIV-1 entry [286]. However, neither 4-chlorohomoproline nor β -methoxytyrosine 4'-*O*- α -L-rhamnopyranoside that are present in mirabamides affected their anti-HIV activities [286].

Celebesides A–C (**193**–**195**) and theopapuamides (B–D) together with **190** were isolated from the marine sponge *Siliquariaspongia mirabilis* (Sulawesi Island, Indonesia) [288].





193 $R_1 = \text{PO}_3\text{H}_2$ $R_2 = \text{C}_2\text{H}_5$

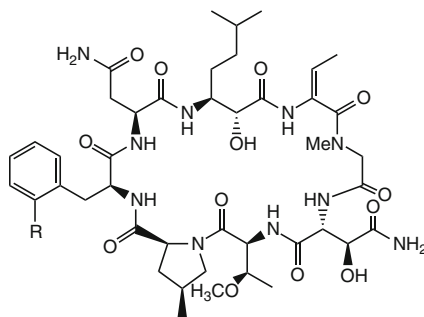
194 $R_1 = \text{PO}_3\text{H}_2$ $R_2 = \text{CH}_3$

195 $R_1 = \text{H}$ $R_2 = \text{C}_2\text{H}_5$

Celebesides are unusual cyclic depsipeptides that comprise a polyketide moiety established as 7,9-dihydroxy-8,10-dimethyltrideca-2,4-dienoic acid (Dtd) and five amino acid residues including an uncommon 3-carbamoyl threonine and a phosphoserine residue in celebesides A (**193**) and B (**194**). Celebeside A (**193**) neutralized HIV-1 in a single-round infectivity assay with an IC_{50} value of $2.1 \mu\text{M}$, while its nonphosphorylated analogue, celebeside C (**195**), was inactive at concentrations as high as $60 \mu\text{M}$ [288]. This correlates the observed anti-HIV activity of celebesides to the presence of phosphoserine in the molecule.

Theopapuamides A–C (**190–192**) showed cytotoxicity against HCT-116 human colon carcinoma cells in vitro with IC_{50} values between 1.3 and $2.5 \mu\text{M}$, and they also exhibited strong antifungal activity against wild-type and amphotericin B-resistant strains of *Candida albicans* at loads of 1 – $5 \mu\text{g/disk}$ [288]. However, celebesides (A–C) displayed neither antibacterial nor antifungal activities against the tested microorganisms at concentrations up to $50 \mu\text{g/disk}$ [288].

Perthamides (B–D) are further examples of cyclic depsipeptides isolated from two different collections of the lithistid sponge *Theonella swinhoei* [289, 290]. Perthamide B was identified as a cytotoxic peptide [289], while perthamides C (**196**) and D (**197**) lacked antiproliferative activity on KB cell line up to a dose of $10 \mu\text{g/mL}$ [290].

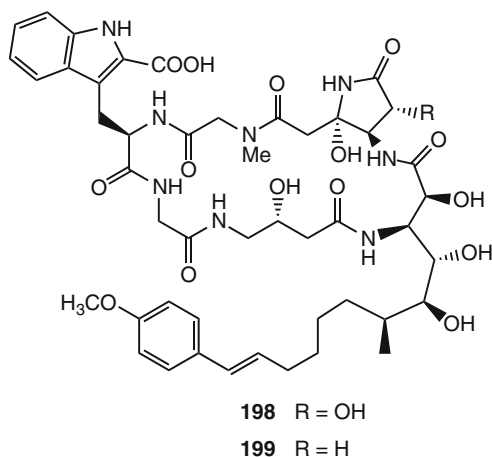


196 $R = \text{OH}$

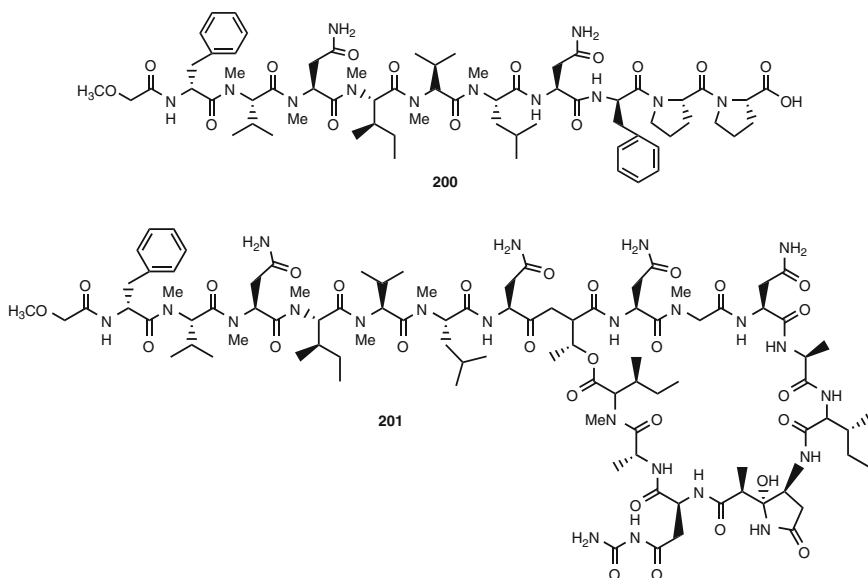
197 $R = \text{H}$

Interestingly, perthamides C (**196**) and D (**197**) reduced carrageenan-induced mouse paw edema significantly in vivo causing 60% and 46% reduction of edema at a dose of 300 $\mu\text{g/kg}$ (i.p.) similar to haliptin A (**176**) [290]. These data compare well with the most common NSAID sold in the pharmaceutical market, naproxen ($\text{ED}_{50} = 40 \text{ mg/kg}$), and clearly indicate that perthamides C and D in addition to haliptin A are about 100 times more potent. Furthermore, the observed in vivo activity implies that these compounds are able to access the site of inflammation [262, 290].

The microsclerodermins (A–I) are a family of antifungal cyclic hexapeptides which have been isolated from different collections of the lithistid sponges *Theonella* sp. and *Microscleroderma* sp. [291–293]. Microsclerodermins A (**198**) and B (**199**) were the first reported members of this family from the New Caledonian lithistid sponge *Microscleroderma* sp. [291]. Both of them, together with microsclerodermin F, showed potent antifungal properties by inhibiting the growth of *C. albicans* at 2.5 and 1.5 $\mu\text{g/disk}$, respectively [291–293]. In addition, microsclerodermins F–I showed nearly similar in vitro cytotoxic activity against HCT-116 cell line (IC_{50} 's of 1.0–2.5 μM) [293].

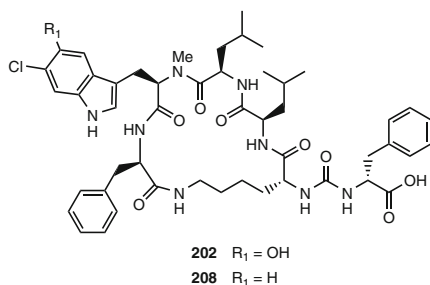


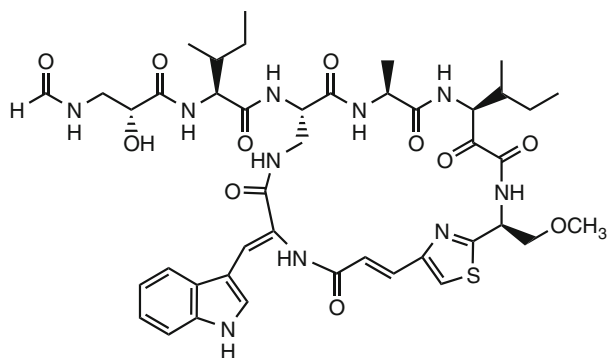
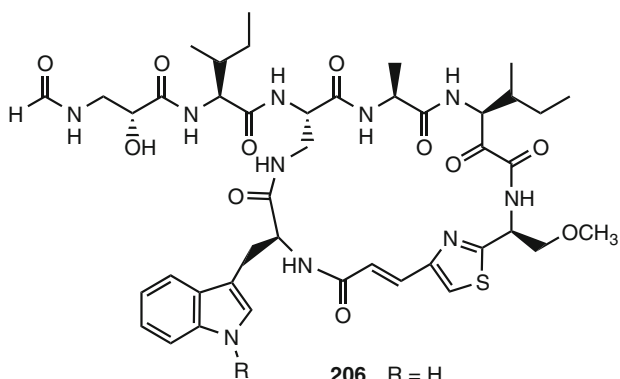
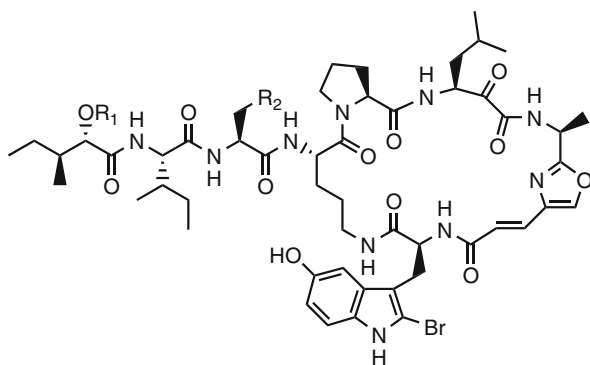
Koshikamide A₁ (**200**) and A₂ are linear peptides that were isolated from the sponge *Theonella* sp. collected off the Koshiki-jima Island (Japan) [294, 295]. Koshikamide B (**201**) was isolated from two separate collections of the marine sponge *Theonella* sp. [296]. Koshikamide B (**201**) is a 17-residue peptide lactone composed of six proteinogenic amino acids, two D-isomers of proteinogenic amino acids, seven *N*-methylated amino acids, and two unusual amino acid residues, namely, *N*^δ-carbamoylasparagine and 2-(3-amino-2-hydroxy-5-oxopyrrolidin-2-yl) propionic acid. Koshikamides A₁ (**200**), A₂ and B (**201**) exhibited cytotoxicity against P388 murine leukemia cells in vitro with IC_{50} values of 1.7, 4.6, and 0.2 μM , respectively [294–296].



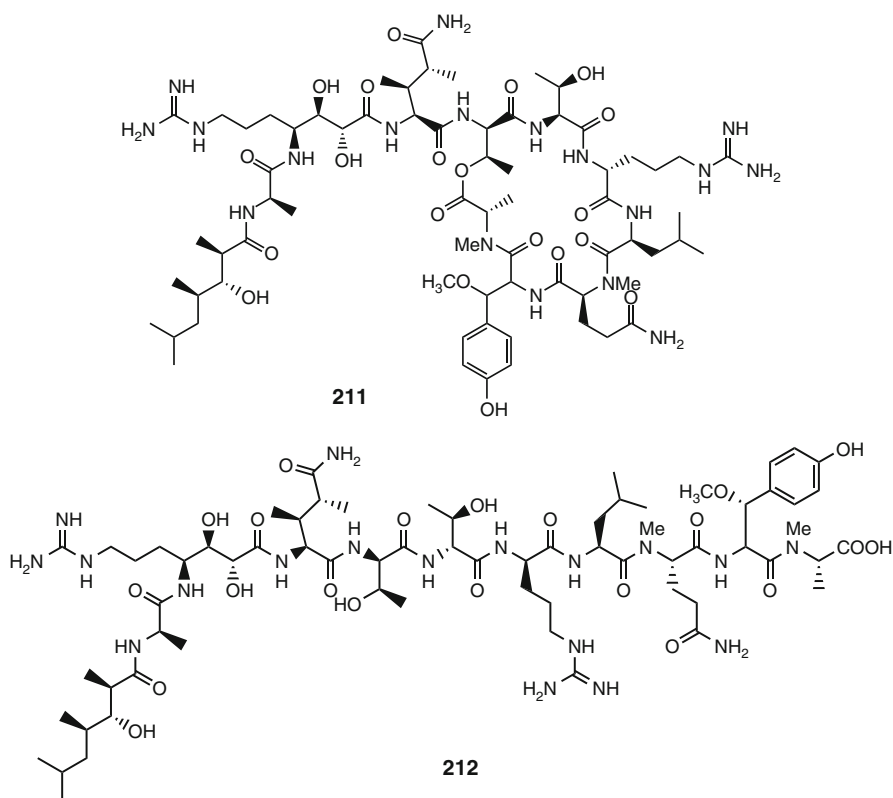
Keramamides (A–J and K–N) are a group of cyclic peptides isolated from different collections of the Okinawan marine sponge *Theonella* sp. [297–302]. They were named after the location of the first collection of the sponge which was Kerama Island, Okinawa. Keramamides A (**202**) and L (**208**) are characterized by having an ureido bond and a 6-chloro-*N*-methyltryptophan residue. Keramamides B (**203**) and (C–E) contain an oxazole ring as a structural feature, while keramamides (F–H) and (J–K) share the presence of a thiazole ring. Keramamides M (**209**) and N (**210**) are sulfate esters of keramamides D (**204**) and E (**205**), respectively.

Most of the known keramamides feature *in vitro* cytotoxic activity when tested against L1210 murine lymphoma (IC_{50} 's between 0.5 and 2.3 μ M) and KB human epidermoid carcinoma (IC_{50} 's between 0.45 and 6.2 μ M) cell lines [299–302]. Among the tested congeners, keramamides K (**207**) and L (**208**) were the most potent derivatives with IC_{50} values of 0.77 and 0.5 μ M against L1210 cells and 0.45 and 0.97 μ M against KB cells, respectively [301].



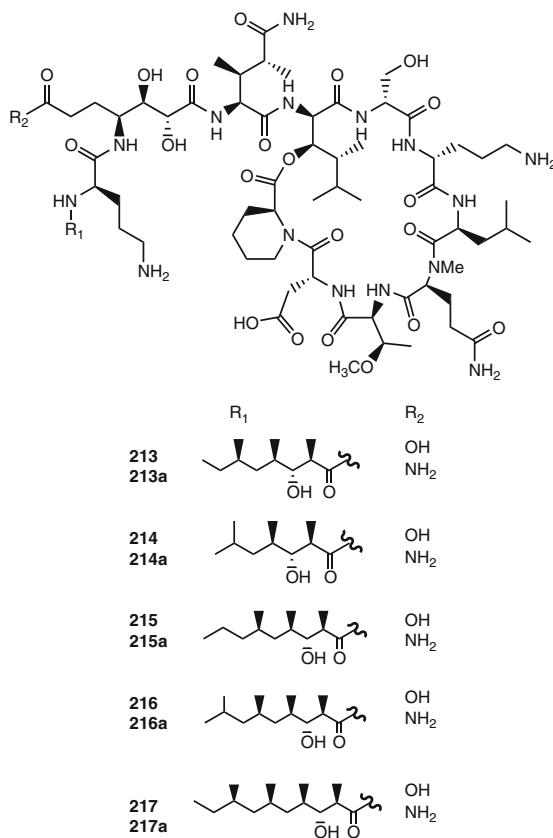
**203****206** R = H**207** R = CH₃**204** R₁ = H R₂ = CH₃**205** R₁ = H R₂ = C₂H₅**209** R₁ = SO₃H R₂ = CH₃**210** R₁ = SO₃H R₂ = C₂H₅

Callipeltins are a group of marine peptides with unusual structural features and remarkable biological activities isolated from the marine sponges *Callipelta* sp. [303, 304] and *Latrunculia* sp. [305–307]. Callipeltin A (**211**) is the parent compound of this family which comprises 12 further congeners (B–M). Apart from the cyclic congeners, callipeltins A and B, all the other callipeltins are linear derivatives structurally related to callipeltin C (**212**) which, in turn, represents the acyclic counterpart of callipeltin A (**211**). Structurally, the most distinctive feature of callipeltins is the presence of several nonproteinogenic units while from a biological point of view, callipeltin A displays a broad range of bioactivities, including antiviral, antifungal, and cytotoxicity against several human tumor cell lines and regulatory activity of the myocardial force of contractions [303–309]. The unusual structural features of callipeltins and the interesting biological activities have aroused considerable interest among the synthetic chemistry community.



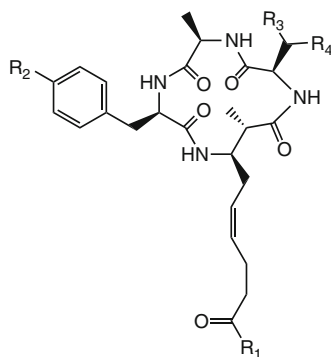
As a result, all nonproteinogenic units in this group of metabolites, namely, (3*S*,4*R*)-3,4-dimethyl-L-pyrroglutamic acid (the N-terminus unit in callipeltin B) [310], (2*R*,3*R*,4*S*)-4-amino-7-guanidino-2,3-dihydroxyheptanoic acid [311], (2*R*,3*R*,4*R*)-3-hydroxy-2,4,6-trimethylheptanoic acid [312] linked to the N-terminus of callipeltins A, C, D, and F–I; and (*R*)- β -methoxy-D-tyrosine were obtained in a stereoselective manner [313].

Homophymine A (**213**) was isolated as the principal active constituent of the New Caledonian lithistid sponge *Homophymia* sp. [314]. Homophymine A is a cyclic depsiundecapeptide structurally related to other aforementioned marine peptides isolated from the order Lithistida such as callipeltin A, papuamides, theopapuamides, and mirabamides which are well known for their potent HIV-inhibitory activity. In addition to the common structural features, homophymine A (**213**) contains two hitherto unprecedented residues, i.e., the 4-amino-2,3-dihydroxy-1,7-heptandioic acid and 2-amino-3-hydroxy-4,5-dimethylhexanoic acid. Homophymine A exhibited cytoprotective activity against HIV-1 infection with an IC_{50} of 75 nM [314]. Recently, nine additional homophymines, namely, B–E (**214–217**) and A1–E1 (**213a–217a**) have been isolated from the same sponge [315]. From the structural point of view, homophymines (A1–E1) feature the 4-amino-6-carbamoyl-2,3-dihydroxyhexanoic acid residue compared to the corresponding (A–E) possessing the same residue in its carboxyl form.



All homophymines were subjected to an antiproliferative activity assay against a wide panel of cell lines including human and simian cancer and noncancer cells and displayed potent cytotoxicity (IC_{50} values between 2 and 100 nM) [315]. A comparison of activities against different tumor cell lines showed a moderate selectivity toward PC3 human prostate and OV3 ovarian carcinoma cell lines. However, when the sensitive and their resistant counterpart cell lines were compared (MCF7/MCF7R, HCT116/HCT15, HLC60/HL60R), no significant difference was observed [315]. Homophymine A1–E1 (**213a**–**217a**) exert stronger biological activity compared to the corresponding congeners A–E (**213**–**217**) [315]. Further extensive biological investigations were carried out to distinguish whether the homophymines possess antiproliferative and/or acute toxic activity. The results strongly suggested that the toxic effect of homophymines was due to an acute and a nonspecific toxicity toward various tested human cell lines [315].

Azumamides A–E (**218**–**222**), isolated from the Japanese marine sponge *Mycale izuensis*, are five cyclic tetrapeptides that exhibit potent histone deacetylase (HDAC) inhibitory activity (IC_{50} 's of 0.045–1.3 μ M) [316]. Furthermore, azumamide A (**218**) at a concentration of 19 μ M significantly inhibited angiogenesis [316]. Only few examples of marine HDAC inhibitors are known up to date such as psammaplin A (PsA, **109**) (see Section 4.2.3) obtained from marine sponge *Pseudoceratina purpurea* [133], whereas azumamides A–E (**218**–**222**) were the first examples of cyclic peptides with HDAC inhibitory activity isolated from marine organisms.



	R ₁	R ₂	R ₃ = R ₄	IC ₅₀ (μ M) (HDAC)
218	NH ₂	H	CH ₃	0.045
219	NH ₂	OH	CH ₃	0.11
220	OH	OH	CH ₃	0.11
221	NH ₂	H	H	1.3
222	OH	H	CH ₃	0.064

After the crystal structure of the complex between a HDAC-like protein and the HDAC inhibitor, trichostatin A (TSA) [317], had been solved, interesting insights into the binding modes of HDAC inhibitors were disclosed [318]. According to the TSA structure, a plausible binding mode to the enzyme is by inserting the long aliphatic chain of TSA into the hydrophobic pocket of the enzyme. Then, the terminal hydroxymic group coordinates with a zinc ion at the polar bottom of the pocket while the aromatic dimethylaminophenyl portion of TSA makes contact with the pocket entrance and an adjacent surface group thereby capping the pocket. Trapoxin A [319] and apicidin [320] are the parent congeners of two classes of HDAC inhibitory cyclic tetrapeptides containing groups that may be analogous to the aliphatic side chain of TSA. Trapoxins possess a 2-amino-8-oxo-9,10-epoxy-decanoic acid, in which the epoxide moiety is thought to bind irreversibly to the enzyme [317], while the apicidins comprise a 2-amino-8-oxo-decanoic acid, with the keto group being responsible for zinc chelation [321].

The corresponding terminal function for azumamides is probably the amide or the carboxylate group. Despite that the affinity of an amide group to zinc is much weaker than that of a carboxylic acid, azumamides A (218) and B (219) with an amide end showed equivalent levels of HDAC inhibitory activity as C (220) and E (222) congeners, which have carboxylate functionality [316].

In conclusion, many peptides from marine sponges showed potent activities such as antitumoral, antiviral, immunosuppressive, antifungal as well as cardiac stimulant properties. However, these bioactivities cannot clearly explain their *in situ* role inside the marine sponges. Interestingly, the most striking feature of this class of metabolites is the preponderance of nonproteinogenic amino acids suggesting that these metabolites are the result of the NRPS/PKS pathways of microorganisms, proposing that symbiotic microorganisms, including cyanobacteria, are the real producers of these metabolites. Therefore, the symbiotic associations within sponges and other marine invertebrates need further intensive research which will ultimately unravel the innate sources of these bioactive metabolites.

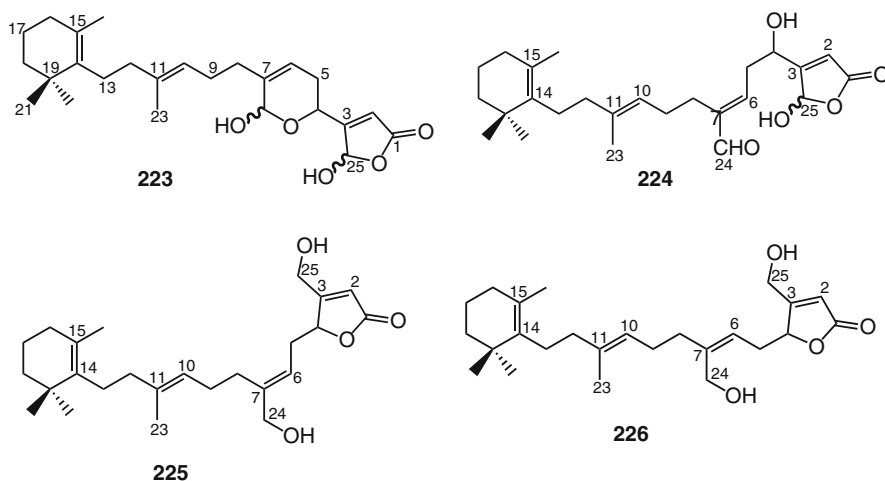
4.4 Terpenes

Terpenes include primary and secondary metabolites, all biosynthesized from the five carbon isoprene building units [322]. Structural modification of these isoprene units leads a massively diverse range of derivatives with a wide array of chemical structures and biological properties.

Steroidal terpenoids were the first marine isoprenes to be discovered by Bergmann during the 1930s–1940s, particularly sterols that were obtained from various marine macroorganisms [323]. Since then, a huge number of terpenoidal secondary metabolites have been obtained from marine resources. In addition to our recent review on this topic [324], we will survey two major classes of marine isoprenes from sponges, namely, the sesterterpenoids (C_{25}) and triterpenoids (C_{30}) with particular attention of their biological activities.

4.4.1 Sesterterpenes (C_{25})

Manoalide (**223**) is the parent compound of a series of marine sponge metabolites belonging to the sesterterpene class. Manoalide was first reported in 1980 by Scheuer from the marine sponge *Luffariella variabilis* (class Demospongiae; order Dictyoceratida; family Thorectidae) collected in Palau [325] with activity as an antibiotic against *Streptomyces pyogenes* and *Staphylococcus aureus*. One year later, Scheuer reported three additional related metabolites from the same Palauan sponge, namely, secomanalide (**224**), (*E*)-neomanalide (**225**), and (*Z*)-neomanalide (**226**) [326].



All three compounds, as well as the parent compound (**223**), displayed antibacterial activity against Gram positive bacteria (*Staphylococcus aureus* and *Bacillus subtilis*) but were inactive against *Escherichia coli*, *Pseudomonas aeruginosa* and *Candida albicans* [326].

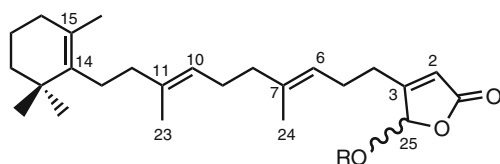
Later, marine sponges belonging to the family Thorectidae, including species of the genera *Luffariella* [327–339], *Hyrtios* [340, 341], *Thorectandra* [342], *Cacospongia* [343, 344], *Fasciospongia* [345–348], *Acanthodendrilla* [349], and *Aplysinopsis* [350], were also found to be rich sources of novel bioactive sesterterpenoids related to manoalide.

Manoalide was further investigated and found to be a potent inhibitor of phospholipase A_2 (PLA $_2$) [351–358]. Subsequently, many structurally related metabolites with PLA $_2$ inhibitory activity were also reported [328, 359–365]. PLA $_2$ is an enzyme that specifically catalyzes the hydrolysis of phospholipids at the S_N -2 position to produce a lysophospholipid and arachidonic acid, which in turn provides the substrate for proinflammatory mediators such as leukotrienes, prostaglandins, and thromboxanes, collectively known as the eicosanoids [361]. Since manoalide revealed an irreversible inhibition of phospholipase A_2 (PLA $_2$) [353], the structure-activity relationships (SAR) of this compound attracted scientific interests to study

and to understand both PLA₂ function and mechanism of action in the whole cell. Therefore, several studies were successfully performed to determine the contributions of the various functional groups incorporated in **223** and its analogues, such as the γ -hydroxybutenolide, α -hydroxydihydropyran, and trimethylcyclohexenyl ring systems, to the efficacy as PLA₂ inhibitors [356, 361, 365]. These studies indicated that (1) the existence of the hemiacetal in the α -hydroxydihydropyran ring is crucial for irreversible binding, (2) the γ -hydroxybutenolide ring is involved in the initial interaction with PLA₂, and (3) the hydrophobic nature of the trimethylcyclohexenyl ring system allows nonbonded interactions with the enzyme that enhances the potency of these analogues. These studies suggested that the closed ring form of manoalide is the predominant molecular moiety that accounts for the selective and potent inhibition of PLA₂ [356].

Manoalide analogues also exhibited other bioactivities including molluscicidal [330], cytotoxicity [333, 334, 336, 340, 343, 346, 349, 350, 367–369], inhibitory activity of Cdc25 phosphatase [366], nicotinic antagonistic activity [332], and fish deterrent properties [346, 369]. Therefore, chemical synthesis and derivatization of manoalide attracted much interest leading to a better understanding of the structure-activity relationships (SAR) and/or for the plausible mechanism of action [355, 358–360, 363, 364, 370, 371]. Manoalide (**223**) was licensed to Allergan Pharmaceuticals and reached phase II clinical trials as a topical antipsoriatic. Its development was, however, discontinued due to formulation problems. The compound is now commercially available as a biochemical standard tool to block the action of PLA₂ [372].

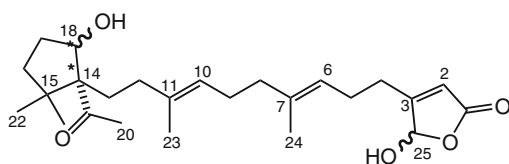
Luffariellolide (**227**) is a sesterterpenoid analogue of secomanalide (**224**), which was first reported from a Palauan sponge *Luffariella* sp. [328]. Structurally, luffariellolide differed in having C-24 as methyl group instead of an aldehyde functionality as in secomanalide, and it was obtained as the (Z) isomer as well.



227 R = H

228 R = CH₃

229 R = CH₂CH₃

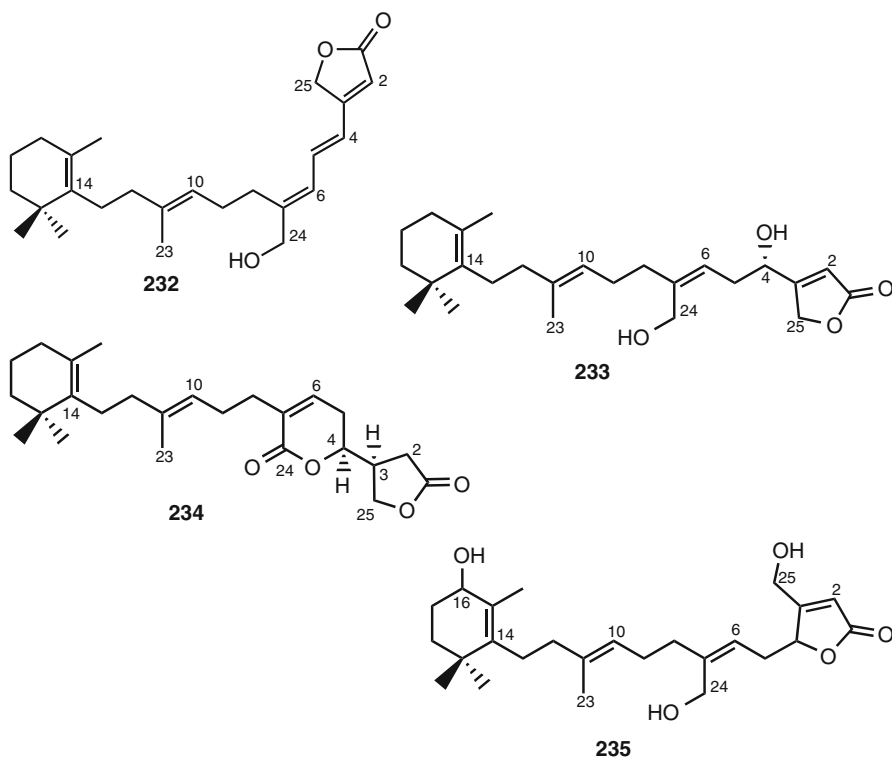


230 18- β -(OH)

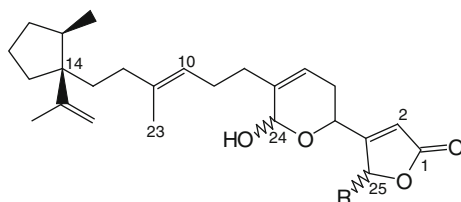
231 18- α -(OH)

In contrast to the irreversible inhibitory action of manoalide (**223**) toward PLA₂, luffariellolide (**227**) is a slightly less potent but a partially reversible inhibitor. This meant that **227** became a more preferable anti-inflammatory agent for potential pharmacological investigation [328]. In addition to luffariellolide (**227**), its 25-*O*-methyl (**228**) and 25-*O*-ethyl derivatives (**229**), five related sesterterpenes, acantholides (A–E), were obtained from the Indonesian sponge *Acanthodendrilla* sp. [349]. Acantholide D (**230**) and E (**231**) represent rare variants for the C₁₄–C₂₀ segment in this type of linear sesterterpenes in which they have the 1-acetylcyclopentan-5-ol moiety replacing the trimethylcyclohexenyl ring. Luffariellolide (**227**) and its 25-*O*-methyl congener (**228**), as well as acantholide E (**231**), were cytotoxic against the mouse lymphoma L5178Y cell line with IC₅₀ values of 8.5, 1.8, and 16.8 μ M, respectively. Interestingly, these results suggest that the 25-*O*-methyl group in **228** and the stereochemistry of 1-acetylcyclopentan-5-ol in **231** play an important role [349]. Luffariolides (A–J) represent a related group of sesterterpenoidal analogues, which have been obtained from different collections of the Okinawan marine sponge *Luffariella* sp. [333, 334, 336].

All luffariolides exhibited significant cytotoxicity against murine lymphoma L1210 cells with IC₅₀ values ranging between 2.9–19.3 μ M. Among them, luffariolides A (**232**, IC₅₀ 2.9 μ M), B (**233**, IC₅₀ 3.23 μ M), E (**234**, IC₅₀ 3.0 μ M), and F (**235**, IC₅₀ 3.8 μ M) were the most active ones [333, 334, 336].



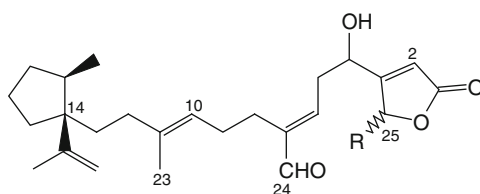
Luffariellins A (**236**) and B (**237**) [327] together with their respective 25-acetoxy derivatives (**240** and **241**) [338] were isolated from the marine sponge *Luffariella variabilis* collected off different locations in Palau and in Australia, whereas luffariellins C (**238**) and D (**239**) were obtained from the shell-less marine mollusc *Chromodoris funerea* collected from the Kaibakku lake shores in Palau [373].



236 R = OH

238 R = H

240 R = OAc



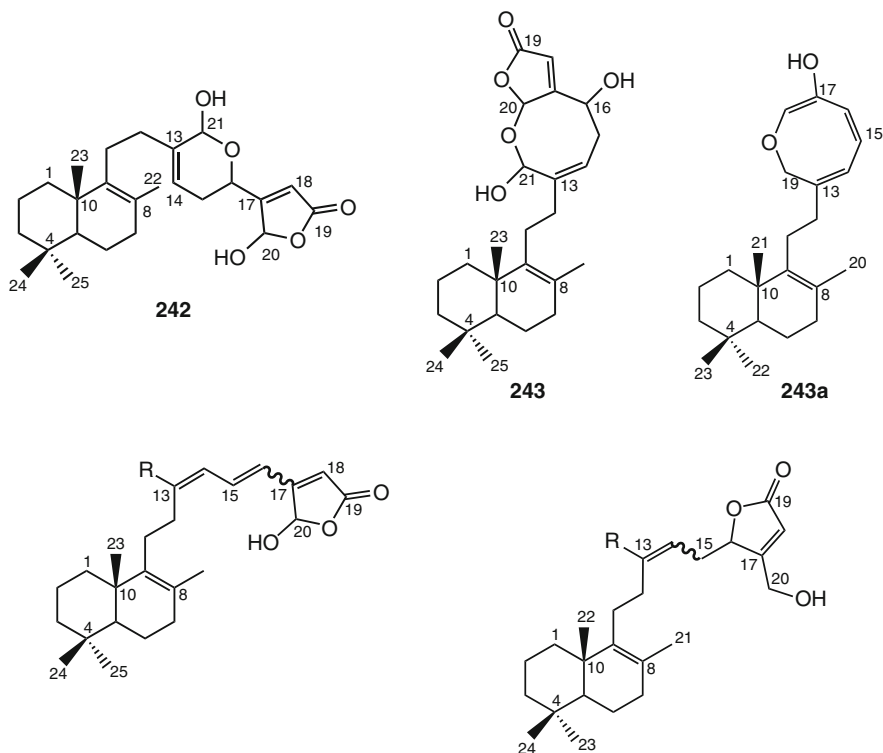
237 R = OH

239 R = H

241 R = OAc

Luffariellins (**236–241**) are all characterized by the 1-isoproprenyl-2-methylcyclopentane ring system replacing the trimethylcyclohexenyl moiety in other manoalide analogues. Despite this discrepancy in chemical structure, luffariellins A (**236**) and B (**237**) retain identical functional groups as present in manoalide (**223**) and secomanoalide (**224**), respectively. Therefore, not surprisingly, each respective pair was shown to have similar anti-inflammatory properties to **223** and **224** [327]. Luffarin metabolites comprise another group of compounds represented by 28 derivatives. Twenty-six of them, luffarins (A–Z), have been reported from the Australian marine sponge *Luffariella geometrica* [332], while the other two were obtained from the Adriatic Sea sponge *Fasciospongia cavernosa* [348]. Based on the chemical structures, luffarins have been classified into 14 bicyclic sesterterpenes, luffarins (A–N); one bicyclic bisnorsesterterpene, luffarin O; one monocyclic sesterterpene, luffarin P; and six acyclic sesterterpenes, luffarin (Q–V), in addition to four diterpenoid derivatives, luffarin (W–Z) [332]. All luffarins were tested for antimicrobial activity against *Staphylococcus aureus*, *Micrococcus* sp., and *Saccharomyces cerevisiae*. Only luffarins C–F (**244–247**), K (**248**), and L (**249**) showed activity against both *S. aureus* and *Micrococcus* sp. [332], whereas luffarins

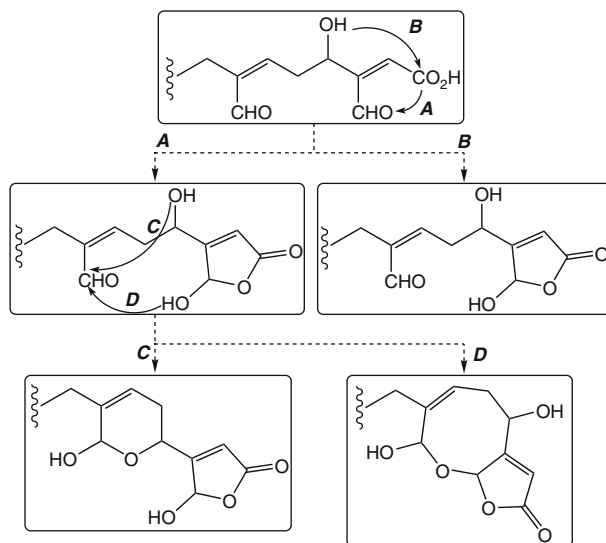
A (**242**) and M (**250**) revealed only mild activity against the latter. Moreover, some luffarins were also found to be effective inhibitors of nicotinic receptors [332].



244	R = CHO	15(16)-trans	248	R = CH ₂ OH	13(14)-trans
245	R = CH(OCH ₃) ₂	15(16)-trans	249	R = CH ₂ OH	13(14)-cis
246	R = CH ₂ OH	15(16)-trans	250	R = CHO	13(14)-trans
247	R = CH ₂ OH	15(16)-cis			

Biosynthetically, a relationship could be recognized between the various luffarins as illustrated in Scheme 4.5. Luffarins appear to belong to the same enantiomeric series as reported for manoalide-type marine natural products. It is also curious to note that no acyclic luffarins incorporated the hydroxylated butenolide functionality. Perhaps the most interesting luffarins from a biosynthetic point of view are luffarins B (**243**) and O (**243a**), which were the first examples of a hitherto unknown cyclization pattern in compounds of this class [332].

Another example of bicyclic sesterterpenes are thorectandrols A–E (**253–257**) that were isolated from a Palauan collection of the marine sponge *Thorectandra* sp. [367, 368] together with the parent compounds of this group palauolide (**251**) and



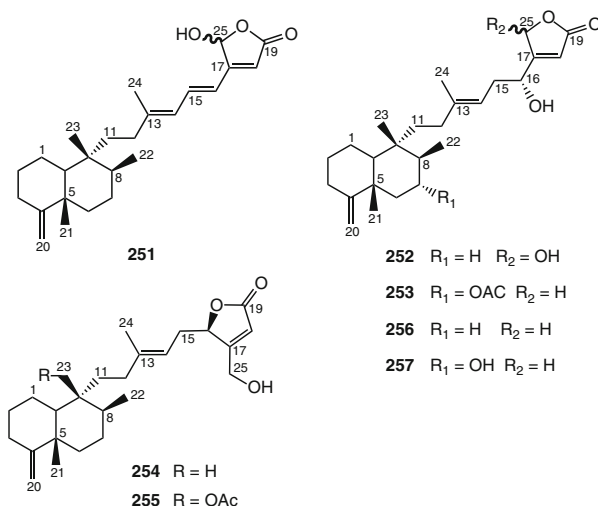
Scheme 4.5 Postulated biosynthetic relationship between all known *Luffariella* metabolites [332]

palauolol (**252**). Palauolide (**251**) was obtained first as an antimicrobial sesterterpene from a three-sponge association collected in Palau [374], while palauolol (**252**) was identified as an anti-inflammatory sesterterpene from the Palauan sponge *Fascaplysinopsis* sp., and chemically, it was recognized as being a secondary alcohol that upon dehydration yields **251** [375].

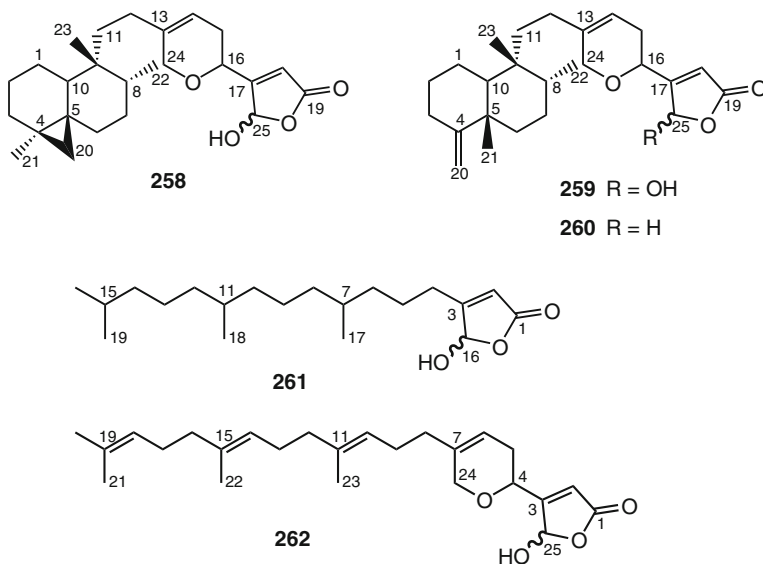
All thorectandrols (**253–257**) in addition to palauolide (**251**) and palauolol (**252**) were tested for antiproliferative activity against 6 to 12 human tumor cell lines depending on sample availability [368]. Palauolol (**252**) was active against all tested cell lines except A549 (non-small cell lung cancer), with IC_{50} values in the range 1.2–1.7 μ M, while palauolide (**251**) showed a diminished activity. On the other hand, thorectandrols (A–E) revealed only weak to no cytotoxicity against the tested cell lines (IC_{50} 's 70–100 μ M). While firm deductions on the structural requirements for activity were not possible, it appeared that the presence of both the hemiacetal lactone functionality and the 16-hydroxyl group in palauolol (**252**) enhanced cytotoxicity compared to palauolide (**251**) and other thorectandrols [368].

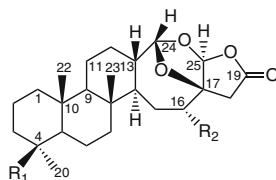
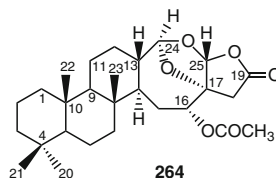
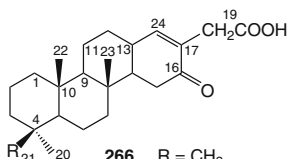
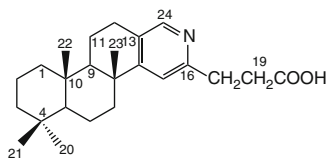
Cacospongionolides (**258–262**) were isolated from different collections of the marine sponge *Fasciospongia cavernosa* (= *Cacospongia mollior*) collected from the Mediterranean Sea [343, 346, 369, 376]. Cacospongionolides A (**258**), B (**259**), and its 25-deoxy derivative (**260**) revealed a bicyclic sesterterpenoidal skeleton, resembling luffarins and thorectandrols, with the addition of a γ -hydroxybutenolide moiety. The other cacospongionolides C (**261**) and D (**262**) are acyclic diterpenoidal derivatives. Despite the structural relation with luffarins and thorectandrols, cacospongionolides (**258–260**) together with cacospongionolide D (**262**) exhibited significant cytotoxicity [343, 346, 369, 376]. This notion

suggested a possible relation between the presence of the γ -hydroxybutenolide moiety and the cytotoxicity.

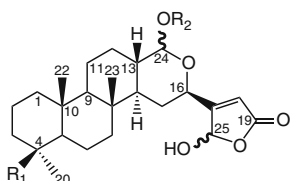
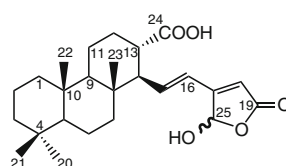


Petrosaspongiolides A (**263**) and B (**264**) were the first cheilantane sesterterpene lactones to be isolated from a New Caledonian sponge incorrectly assigned to the genus *Dactylospongia* [377] and then reassigned as a new genus and a new species: *Petrosaspongia nigra* (Bergquist 1995 sp. nov., class Demospongiae; order Dictyoceratida; family Spongidae) [378]. From another New Caledonian collection of the same sponge, 15 additional petrosaspongiolide congeners (C–R) were isolated [379, 380].

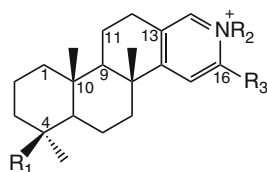


**263** $R_1 = \text{CH}_3$ $R_2 = \text{OAc}$ **265** $R_1 = \text{CH}_2\text{OAc}$ $R_2 = \text{OAc}$ **264****266** $R = \text{CH}_3$ **266a** $R = \text{CH}_2\text{OH}$ **267**

From the chloroform extract of another Dictyoceratida sponge of the genus *Spongia*, 21-hydroxy derivatives of petrosaspongiolides K (**266a**) and P (**270a**) were isolated in addition to four other pyridinium alkaloids named spongidines A–D (**273–276**) [381]. Spongidines were found to be structurally related to petrosaspongiolide L (**267**) particularly in the presence of pyridine ring. Petrosaspongiolides (A–L) were subjected to in vitro cytotoxicity assay against the human bronchopulmonary NSCLC-N6 carcinoma cell line. They revealed IC_{50} values ranging between 1.0–32.2 μM [379]. Petrosaspongiolides C (**265**) and K (**266**) exhibited the highest potency with IC_{50} values of 1.0 and 3.5 μM , respectively. However, petrosaspongiolides A (**263**) and B (**264**) were the least cytotoxic congeners in vitro with IC_{50} values of 28.0 and 32.2 μM , respectively; **263** inhibited tumoral proliferation in vivo at 20 mg/kg without significant toxicity when tested on immunosuppressed rats carrying a bronchopulmonary tumor (NSCLC-N6) [379].

**268** $R_1 = \text{CH}_3$ $R_2 = \text{OAc}$ **269** $R_1 = \text{CH}_2\text{OAc}$ $R_2 = \text{OAc}$ **270** $R_1 = \text{CH}_3$ $R_2 = \text{H}$ **270a** $R_1 = \text{CH}_2\text{OH}$ $R_2 = \text{H}$ **271** $R_1 = \text{CH}_2\text{OAc}$ $R_2 = \text{H}$ **272**

Petrosaspongiolides M–R (**268–272**) revealed the presence of a γ -hydroxybutenolide moiety and a hemiacetal function. Due to these structural similarities to manoalide (**223**), petrosaspongiolides (M–R) have received special attention from the scientific community to study their inhibitory activity against PLA₂ from different resources to point out their specificity. Two main groups of PLA₂ enzymes have been reported [382], the secretory PLA₂ (sPLA₂ groups I, II, III, V, IX, and X with relatively small molecular weights) and the cytosolic PLA₂ (cPLA₂ groups IV, VI, VII, and VIII with higher molecular weights). Inhibition of specific PLA₂ constitutes a potentially useful approach for treating a wide variety of inflammatory disorders such as septic shock, adult respiratory distress syndrome, arthritis, and acute pancreatitis [381]. Petrosaspongiolides M–R (**268–272**) together with 21-hydroxy derivatives of petrosaspongiolides K (**266a**) and P (**270a**), and spongidines A–D (**273–276**) were tested on five different sPLA₂s belonging to the groups I (*Naja naja* venom and porcine pancreatic enzymes), II (human synovial recombinant and rat air-pouch secretory enzymes), and III (bee venom enzyme) [380, 381].



273	$R_1 = \text{CH}_3$	$R_2 = \text{CH}_2\text{COOH}$	$R_3 = \text{H}$
274	$R_1 = \text{CH}_2\text{OAc}$	$R_2 = \text{CH}_2\text{COOH}$	$R_3 = \text{H}$
275	$R_1 = \text{CH}_3$	$R_2 = \text{CH}_2\text{COOH}$	$R_3 = \text{CH}_2\text{CH}_2\text{COOH}$
276	$R_1 = \text{CH}_3$	$R_2 = \text{CH}_2\text{CH}_2\text{SO}_3\text{H}$	$R_3 = \text{H}$

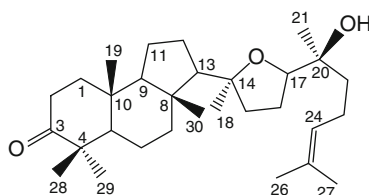
Among petrosaspongiolide derivatives, **268** and **270a** inhibited mainly human synovial PLA₂ with IC₅₀ values of 1.6 and 5.8 μM , respectively, compared to manoalide (**223**) (IC₅₀ = 3.9 μM) [380, 381]. Petrosaspongiolide M (**268**) also inhibited bee venom PLA₂ enzyme with IC₅₀ of 0.6 μM , compared to **223** (IC₅₀ of 7.5 μM) [380]. The mechanism of action of petrosaspongiolides M–R (**268–272**) as anti-inflammatory marine metabolites has been the topic for many research articles [383–388]. The covalent binding of **268** to bee venom PLA₂ has been investigated by mass spectrometry and molecular modeling. The mass increment observed was consistent with the formation of a Schiff base by reaction of a PLA₂ amino group with the hemiacetal function at the C-25 atom of the petrosaspongiolide M γ -hydroxybutenolide ring [383]. The molecular mechanism of inactivating the bee venom and the human type IIA secretory PLA₂s by petrosaspongiolides R (**272**) [387] and M (**268**) [388], respectively, has been investigated. In both cases, either covalent (imine formation) and/or noncovalent (van der Waals) interactions contributed to the inhibitory activity against PLA₂ enzymes [387, 388]. Due to potent anti-inflammatory properties of petrosaspongiolides, their chemical synthesis has been investigated. Recently, the first enantioselective synthesis of petrosaspongiolide R (**272**) has been successfully performed [389].

4.4.2 Triterpenes (C₃₀)

Steroidal triterpenes were the first marine isoprenes to be discovered in the 1930s. Scientific interest has been driven toward these metabolites due to the isolation of biosynthetically unprecedented derivatives possessing a broad spectrum of bioactivity (ies). Marine triterpenoids have been reported from various marine macroorganisms. In this section, we survey two examples of triterpenoidal metabolites, namely, isomalabaricane triterpenes and steroidal saponins obtained from marine sponges, with particular attention being drawn to their pharmacological significance.

4.4.2.1 Isomalabaricane Triterpenes

Malabaricol (**277**) is the chief triterpene constituent of a yellow pigment obtained from the wood of the terrestrial plant *Ailanthus malabarica* (family Simaroubaceae), after which the whole group of related compounds was named [390–392]. Malabaricane, the trivial name of this group of compounds, was given to the hydrocarbon system (3*S**,3*aR**,5*aS**,9*aS**,9*bS**)-3*a*,6,6,9*a*-tetramethyl-3-(1,5,9-trimethyldecyl)perhydryl-obenz[*e*]indene, where the tricyclic nucleus has a *trans-anti-trans* ring junction [391, 392].

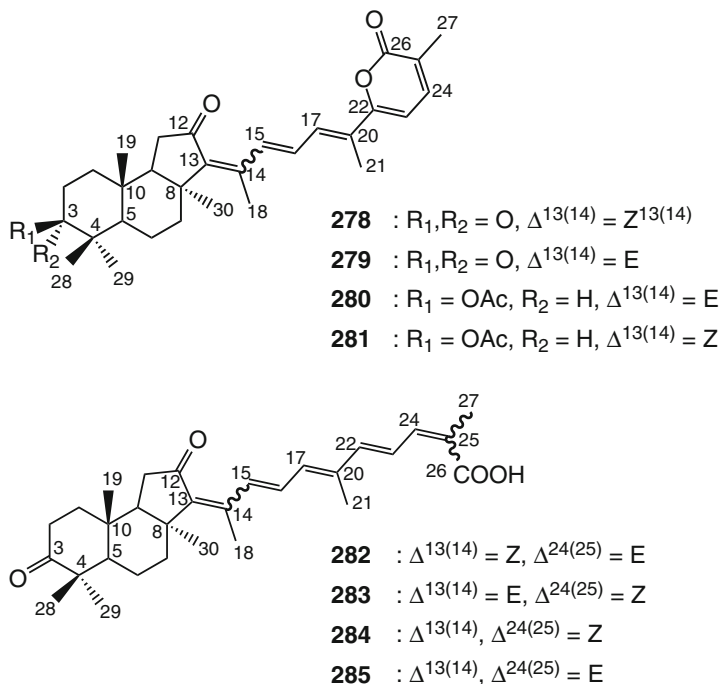


277

The malabaricanes are structurally characterized by a tricyclic triterpenoid core and a conjugated polyene side chain [390–392], whereas the isomalabaricane skeleton is embedded in a 4,4,8,10-tetramethyl-perhydrobenz[*e*]indene with a *trans-syn-trans* ring junction, that leads to an unfavorable twist-boat conformation for the central ring [393, 394]. Isomalabaricane triterpenes were first reported from a Fijian collection of the sponge *Jaspis stellifera* [393] and the Somalian marine sponge *Stelletta* sp. [394]. Since then, they have been isolated from several genera of marine sponges belonging to the order Astrophorida including members of the genera *Rhabdastrella* [395, 400, 402, 406, 413, 414, 416, 420], *Stelletta* [397–399, 405, 408, 412], *Jaspis* [401, 407, 409, 418, 419, 421, 422], and *Geodia* [403, 410, 415]. Isomalabaricane triterpenoids having polyene conjugated functionality can be classified into three groups: (1) stelletins principally possessing the γ -pyrone functionality, which could be ring-opened in some of its congeners yielding the side chain with terminal free carboxylic acid and methyl moieties, (2) stelliferins oxygenated at C-22, and (3) globostellatic acids whose main feature is a carboxyl group at C-4. In addition to triterpenoids, the isomalabaricane core has also been recognized in some sesqui- and/or sesterterpenes. The isomalabaricane terpenoids were sometimes trivially named according to their sponge origin. Upon light exposure, the isomalabaricane-type terpenes readily isomerize at the C-13 position.

Therefore, during isolation and characterization processes, they rapidly equilibrate into a 1:1 mixture of the 13*E* and 13*Z* isomers [398–400, 408, 409, 418, 419]. Nevertheless, these compounds continue to gain a great deal of attention because of their significant cytotoxic activity [399, 409], whereas the nature of the natural isomer, either 13*E* or 13*Z* or both, is still unresolved. Recently it was reported that the ^1H NMR spectrum of a crude extract obtained from the fresh sponge *Rhabdastrella* aff. *distinca* (Hainan, the South China Sea) revealed that it mostly contained isomalabaricanes with the 13*E*-configuration (H-15 of most derivatives appeared around 7.0 ppm). Thus, the 13*Z* isomers were suggested in this case to be formed through isomerization during the isolation and analytical procedures [406].

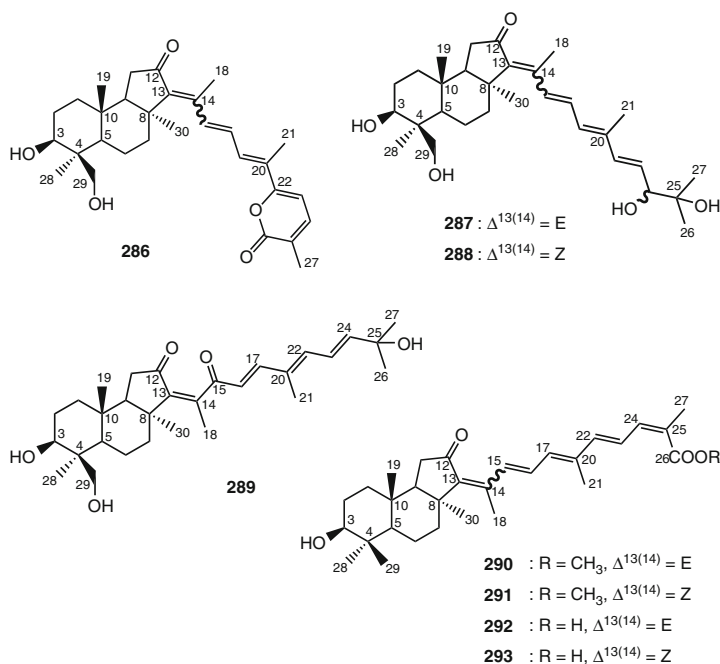
Stelletins comprise the first group of isomalabaricane-type triterpenoids. Stelletin A (**278**) was recognized in 1981 as a yellow triterpenoidal pigment from the Fijian marine sponge *Jaspis stellifera* [393]. Later, it was obtained together with its *E* isomer, stelletin B (**279**), from the marine sponge *Stelletta tenuis* collected off Hainan Island, China [397]. Stelletin A (**278**) revealed significant cytotoxicity against murine leukemia P388 cell line with IC_{50} of 2.1 nM [397].



Stelletin G (**284**), with an opened γ -pyrone and featuring terminal $-\text{COOH}$ and $-\text{CH}_3$ functionalities, was isolated together with **278** from *J. stellifera* [393]. Later, stelletins G (**284**) was reported from the Australian marine sponge *Stelletta* sp. together with stelletins E (**282**) and F (**283**) [398]. The *E* isomer of stelletin G (**284**) was isolated from the marine sponge *Rhabdastrella globostellata* collected from the South China Sea, and it was given the trivial name rhabdastrellic acid-A (**285**)

[395, 396]. Research interests have been intensively driven toward this group of triterpenoidal derivatives, which led to the isolation of eight further stelletins C, D, and H–M [398–400, 402, 405] in addition to 22,23-dihydrostellatin D [401].

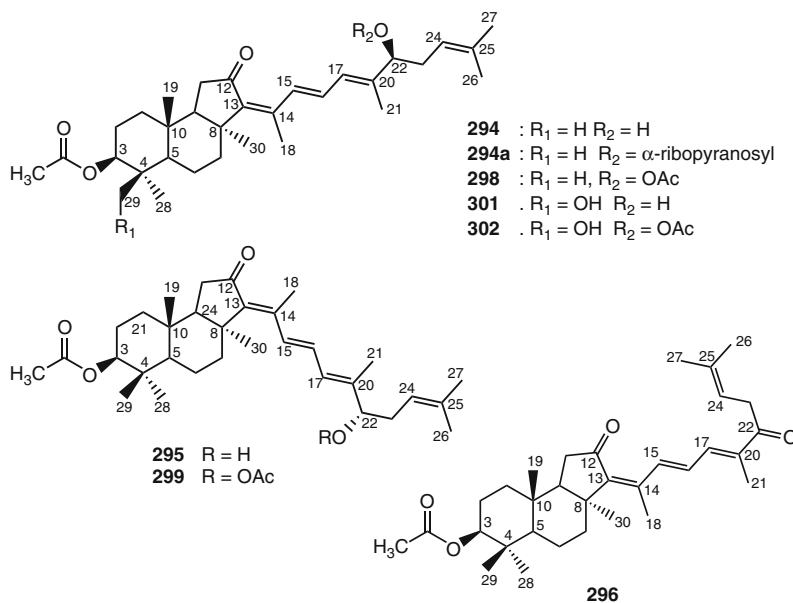
Rhabdastrellins A–F (286–291), along with stelletins L (292) and M (293), were obtained from the marine sponge *Rhabdastrella* aff. *distinca* collected from a coral reef off Hainan in the South China Sea [406]. Four of the rhabdastrellins (286–289) exhibited a primary alcohol moiety at C-29 instead of a methyl group as for the stelletins and the other two rhabdastrellins E (290) and F (291). All rhabdastrellins and stelletins L and M share a hydroxyl group at C-3 instead of a carbonyl group as in other stelletins [406]. The antiproliferative profile of stelletins A–F (278–283) has been examined at the National Cancer Institute (NCI, Australia) against 60 cell lines. Due to the rapid isomerization upon light exposure, stelletins were tested as isomeric pairs. Stelletin C(280)/D(281) pair was the most potent derivative with a mean panel GI₅₀ of 0.09 μ M. The stelletin E(282)/F(283) pair was approximately ten times less potent (mean GI₅₀ of 0.98 μ M) [399]. Apoptotic cell death is a stress response of cells to cytotoxic agents that might be executed either through a receptor-mediated pathway that activates caspase-8 or through a receptor-independent pathway that involves the cyclin-kinase inhibitors p53/p21. Both pathways lead to a translocation of proapoptotic Bax protein to the mitochondria, thereby resulting in a dissipation of mitochondrial membrane potential, activation of caspase-3, and execution of the apoptotic machinery [404].

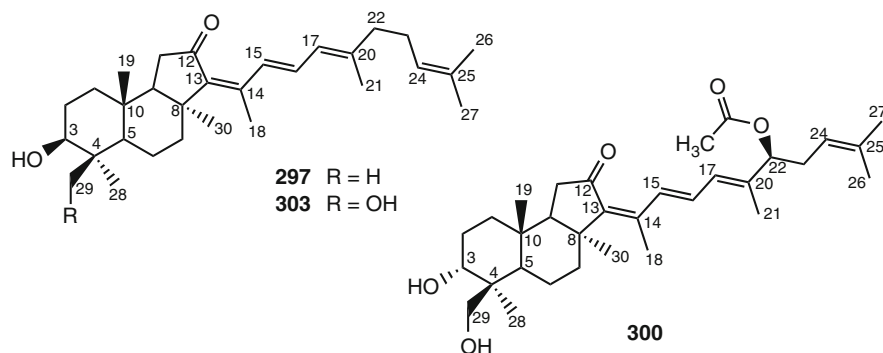


Stelletin A (**278**) demonstrated a differential cytotoxicity against human leukemia HL-60 cells (IC_{50} 0.9 μM) compared to human prostate cancer LNCaP cells (IC_{50} 260 μM) by activation of NADPH oxidase, which induces oxidative cell death through a FasL-caspase-3-apoptotic pathway [403]. Stelletins B (**279**) and E (**282**) revealed selective cytotoxicity toward p21-deficient human colon tumor HCT-116 cells with IC_{50} values of 0.043 and 0.039 μM , respectively [400]. Stelletins L (**292**) and M (**293**) exhibited selective cytotoxicity against stomach cancer AGS cells with IC_{50} values of 3.9 and 2.1 μM , respectively [405]. Rhabdastrellic acid-A (**285**) also inhibited proliferation of human leukemia HL-60 cells with an IC_{50} value of 1.5 μM through inhibition of the PI3K/Akt pathway and induction of caspase-3-dependent apoptosis [396]. Only rhabdastrellin A (**286**) possessed moderate inhibitory activity toward human leukemia HL-60 cells (IC_{50} = 8.7 μM) while other rhabdastrellins were inactive (IC_{50} > 20 μM) [406].

Stelliferins are the second group of isomalabaricane triterpenes. To the best of our knowledge, 13 compounds belonging to this group have been reported. In addition to stelliferins A–F (**294**–**299**), which have been isolated from the Okinawan marine sponge *Jaspis stellifera* [407], stelliferin G (**300**) and 29-hydroxy derivatives of stelliferins A (**301**) and E (**302**) have been isolated from an unidentified species of the genus *Jaspis* collected near Tonga [409].

The 29-hydroxy derivative of stelliferin D (**303**) together with 3-epimeric isomers of **301** and **302** were reported from the marine sponge *Stelletta globostellata* collected by SCUBA off Mage-jima Island, Japan [408], whereas stelliferin riboside (**294a**), the first example of a glycosylated stelliferin, was isolated from the Fijian sponge *Geodia globostellata* [410].





Stelliferins A–F (**294–299**) exhibited potent *in vitro* antineoplastic activities against murine lymphoma L1210 cells (IC_{50} of 1.1–5.0 μM) and human epidermoid carcinoma KB cells (IC_{50} of 2.8–13.0 μM) [407], while the isomeric mixture of stelliferin G (**300**) and 29-hydroxystelliferin A (**301**) showed the highest inhibitory activity against the melanoma MALME-3 M cell line with IC_{50} values of 0.2 and 0.4 μM , respectively [409]. Stelliferin riboside (**294a**) displayed moderate cytotoxicity against ovarian A2780 cancer cells (IC_{50} = 60 μM) [410].

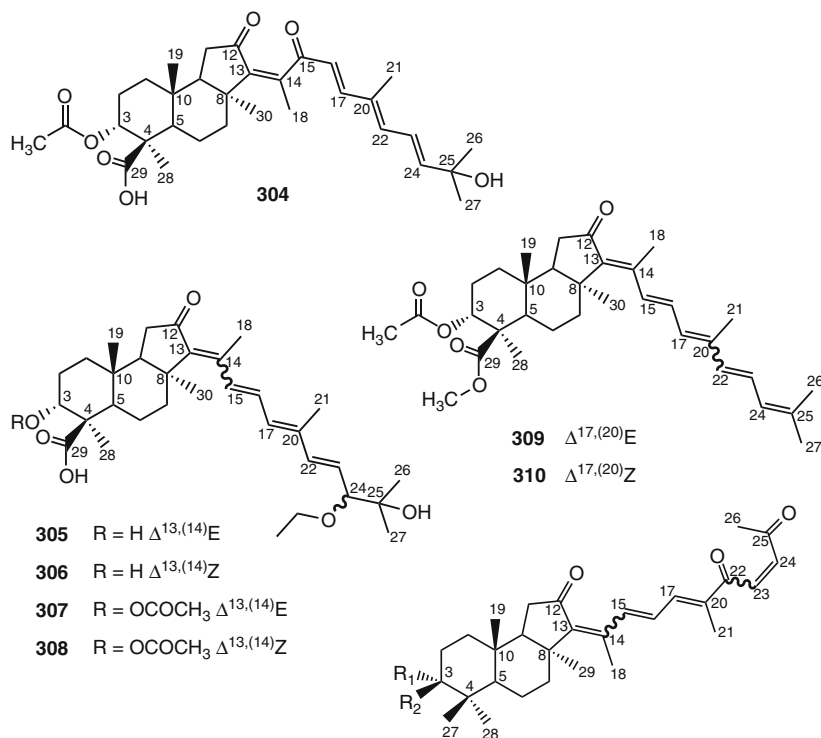
Due to the significant antiproliferative activity exhibited by stelletins and stelliferins, research efforts have been directed toward their chemical synthesis. In 1999, Raeppl et al. successfully synthesized the common *trans-syn-trans* perhydrobenz[e]indene moiety in the isomalabaricane-type terpenoids, which enabled the chemical synthesis of stelletins and stelliferins [411].

Globostellatic acid (**304**) is the prototype of the third group of isomalabaricane-type triterpenoids sharing carboxylation at C-4. It was first isolated together with three other derivatives, globostellatic acids (B–D), from the marine sponge *Stelletta globostellata* collected off Mage Island near Kagoshima, Japan [412]. Other globostellatic acid congeners, (F–M), and X methyl esters, have been reported from different collections of the Indonesian marine sponge *Rhabdastrella globostellata* [413, 414]. Globostellatic acids revealed potent cytotoxicity similar to the stelletins and stelliferins. Globostellatic acids (A–D) demonstrated significant cytotoxicity against murine leukemia P388 cells with IC_{50} values of 0.2–0.8 μM [412]. For cytotoxicity toward mouse lymphoma L5178Y cells, the 3-*O*-deacetyl congeners, globostellatic acids H/I (**305/306**) were the most active with an IC_{50} of 0.31 nM. However, acetylation of the C-3 hydroxyl group decreases its bioactivity abruptly, as in globostellatic acids J/K (**307/308**), with an IC_{50} of 8.28 nM. The reverse was found for the 13*Z* isomer of stelliferin riboside (**294a**) that revealed higher activity than its 3-*O*-deacetyl congener with IC_{50} values of 0.22 and 2.40 nM, respectively [413].

On the other hand, globostellatic acids showed only moderate or no cytotoxicity against either human cervix carcinoma HeLa or rat pheochromocytoma PC-12 cell lines [413]. Two globostellatic acid X methyl esters (**309** and **310**), possessing the 13*E*-geometry, inhibited proliferation of human umbilical vein endothelial cells

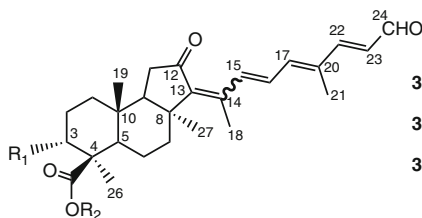
(HUVECs), 80- to 250-fold greater in comparison to several other cell lines and hence inhibited angiogenesis which, if pathologically uncontrolled, accompanies several diseases such as atherosclerosis, arthritis, diabetic retinopathy, and cancer. 13*E*,17*E*-Globostellatic acid X methyl ester (**309**) also inhibited basic fibroblast growth factor (bFGF)-induced tubular formation and vascular endothelial growth factor (VEGF)-induced migration of HUVECs. In addition, **309** induced apoptosis of HUVECs without affecting their VEGF-induced phosphorylation of ERK1/2 kinases [414].

Geoditins, which are stelliferin-related isomalabaricane triterpenoids, are mainly oxygenated at both C-22 and C-25. Five geoditins (**311–315**) were obtained from the marine sponges *Geodia japonica* [415] and *Rhabdastrella* aff. *distinca* [416] collected at different locations in the South China Sea.



Geoditins (**311–315**) were submitted for bioassays against several human tumor cell lines including HL-60 (promyelocytic leukemia), PC-3MIE8 (prostate carcinoma), BGC-823 (gastric carcinoma), MDA-MB-423 (breast carcinoma), Bel-7402 (hepatocellular carcinoma), and HeLa (cervical carcinoma) cells. Isogeoditin A (**313**) showed significant cytotoxicity toward the former three cell lines with IC_{50} values of 0.3, 0.2, and 1.0 μM , respectively. 13*E*-isogeoditin A (**314**) revealed no cytotoxic activity, implying that the *Z*-geometry at C-13 enhances antiproliferative activity compared to the *E*-form [416]. Geoditin A (**311**) proved to be cytotoxic against HL-60 cells (IC_{50} = 6.7 μM), while geoditin B (**312**) exhibited relatively weak cytotoxicity. Mechanistically, geoditin A (**311**) markedly induced reactive oxygen species (ROS), decreased mitochondrial membrane potential, and mediated a caspase-3 apoptosis pathway [417].

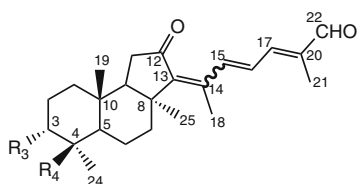
Jaspiferals (**316–325**) and aurorals (**326–329**) are isomalabaricane-type terpenoids differentiated into nortriterpenoids, norsesterterpenoids, and norditerpenes possessing a 3 α -hydroxy group. Jaspiferals A–G (**316–322**) were purified from the Okinawan marine sponge *Jaspis stellifera* [418], while the 3-*O*-acetyl and methyl ester derivatives of jaspiferals B (**323**), D (**324**), and E (**325**) were obtained from a new species of *Jaspis* collected at the Vanuatu Islands [419]. Aurorals (**326–329**) have been isolated from the New Caledonian marine sponge *Rhabdastrella globostellata* [420]. Jaspiferals A–G (**316–322**) exhibited in vitro cytotoxicity against murine lymphoma L1210 cells with IC_{50} values of 1.6–10.4 μM , whereas only jaspiferals E–G (**320–322**) revealed antineoplastic activity against human epidermoid carcinoma KB cells (IC_{50} of 5.2–14.7 μM) [418]. Jaspiferal G (**322**) exhibited antifungal activity against *Cryptococcus neoformans* (MIC, 144 μM) and *Trichophyton mentagrophytes* (MIC, 36 μM) and antibacterial activity against *Sarcina lutea* (MIC, 144 μM), while the mixture of jaspiferals E (**320**) and F (**321**) showed antifungal activity against *T. mentagrophytes* (MIC, 134 μM) [418]. On the other hand, the 3-*O*-acetyl, methyl ester derivatives of jaspiferals B (**323**), D (**324**), and E (**325**) revealed weak cytotoxicity against L1220 cells (IC_{50} > 8.8 μM) [419].



316: $R_1 = OH$ $R_2 = H$, $\Delta^{13(14)} = Z$

317: $R_1 = OH$ $R_2 = H$, $\Delta^{13(14)} = E$

323: $R_1 = OAc$ $R_2 = CH_3$, $\Delta^{13(14)} = E$



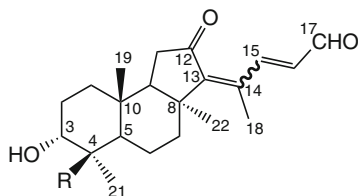
318: $R_1 = OH$ $R_2 = COOH$, $\Delta^{13(14)} = Z$

319: $R_1 = OH$ $R_2 = COOH$, $\Delta^{13(14)} = E$

324: $R_1 = OAc$ $R_2 = COOCH_3$, $\Delta^{13(14)} = E$

326: $R_1 = OH$ $R_2 = CH_2OH$, $\Delta^{13(14)} = Z$

327: $R_1 = OH$ $R_2 = CH_2OH$, $\Delta^{13(14)} = E$

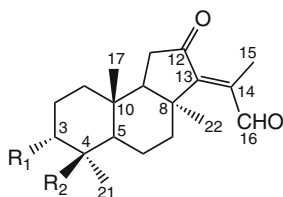


320: R = COOH, $\Delta^{13(14)} = Z$

321: R = COOH, $\Delta^{13(14)} = E$

328: R = CH₂OH, $\Delta^{13(14)} = Z$

329: R = CH₂OH, $\Delta^{13(14)} = E$



322: R₁ = OH R₂ = COOH

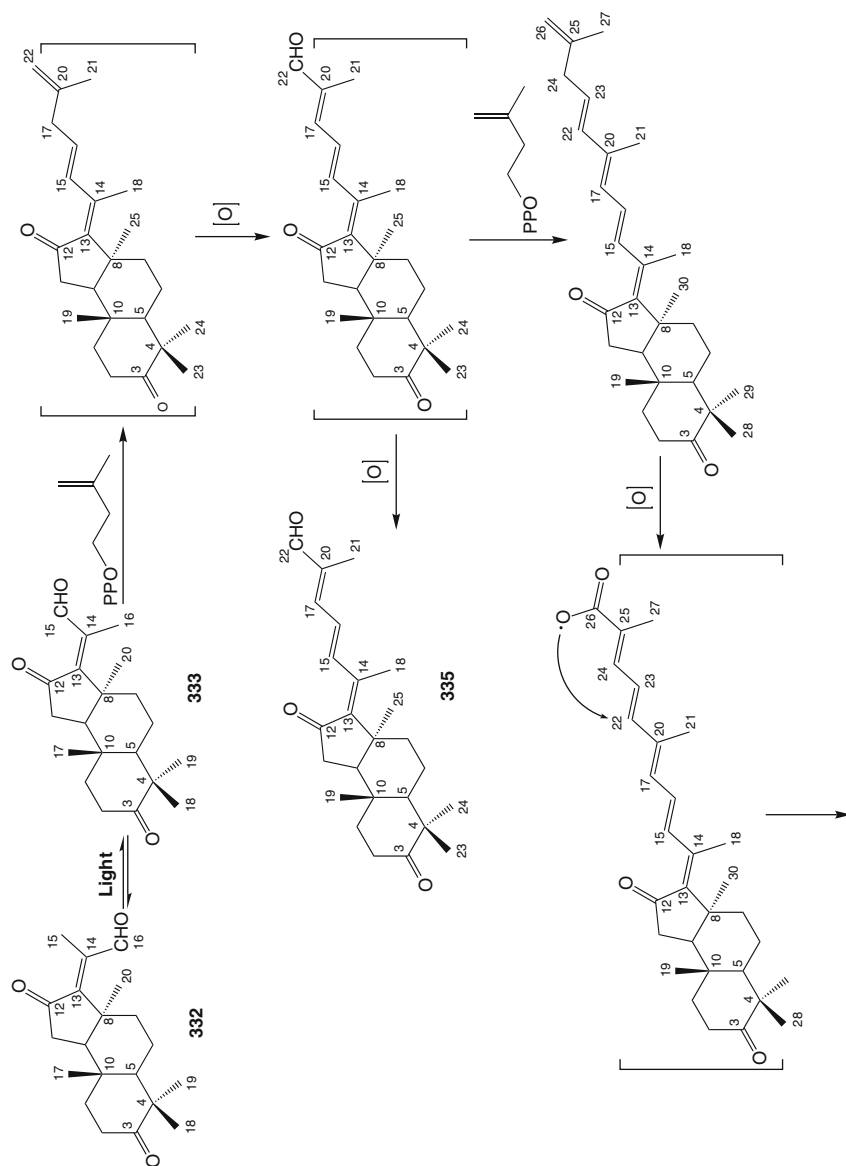
325: R₁ = OAc R₂ = COOCH₃

Aurorals (**326–329**), which differ from jaspiferals C–F (**318–321**) by the presence of a primary alcohol group at the C-4 position, exhibited stronger cytotoxicity against KB cells. The isomeric mixtures of aurorals (**326/327**), (**328/329**), and jaspiferals C/D (**318/319**) showed IC₅₀ values of 0.5, 22.2, and 13.3 μ M, respectively, while jaspiferals E/F (**320/321**) were inactive up to 27 μ M [420].

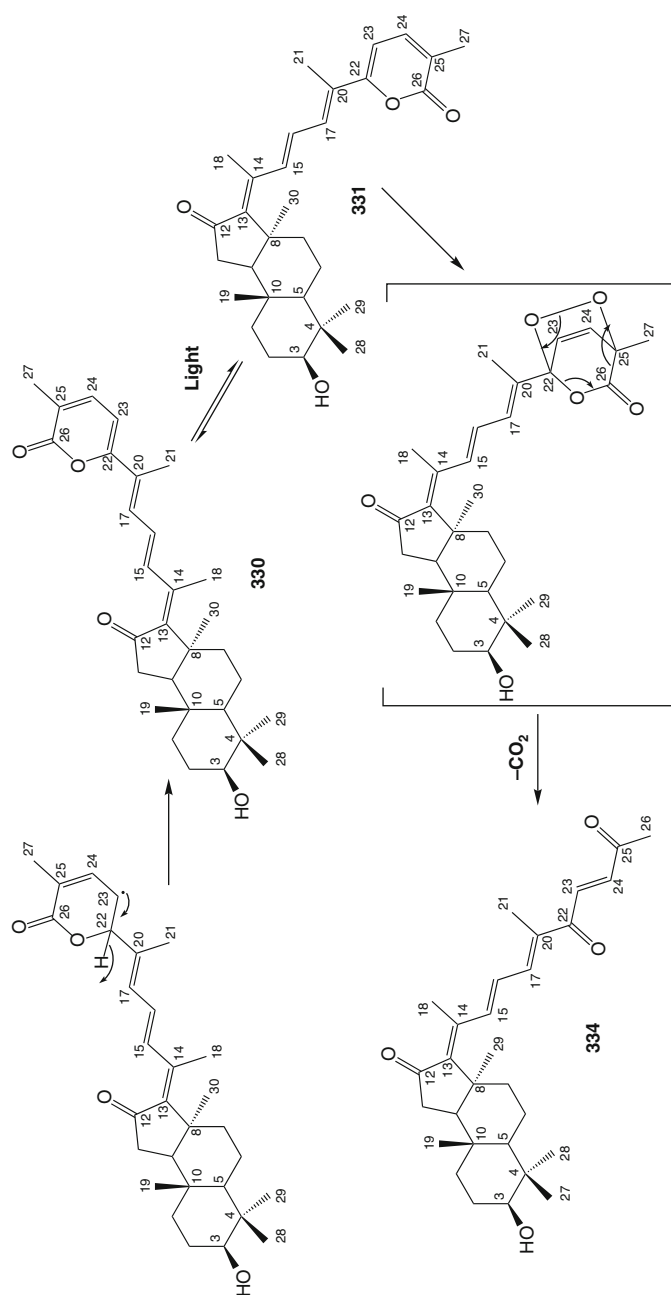
Jaspolides represent another example of isomalabaricane-type terpenoids of either monomeric or dimeric congeners. Monomeric congeners of jaspolides could be classified into triterpenes, jaspolides A (**330**) and B (**331**); sesterterpene, jaspolide F (**335**); diterpenes, jaspolides C (**332**) and D (**333**); and nortriterpene, jaspolide E (**334**) which were all isolated from the marine sponge *Jaspis* sp. collected from the South China Sea [421]. A presumable biogenetic transformation scheme of jaspolides A–F (**330–335**) (Scheme 4.6) revealed that light-induced isomerization is responsible for the jaspolides A/B (**330/331**) and C/D (**332/333**) isomeric pairs. In addition, it substantiated jaspolide D (**333**) as a precursor to jaspolide F (**335**), formed through condensation with an isoprenyl pyrophosphate (IPP) followed by oxidation at a terminal methyl group [421]. Jaspolides G (**336**) and H (**337**) are dimeric isomalabaricane congeners which were isolated from the same Chinese sponge *Jaspis* sp., and their proposed biogenetic pathway (Scheme 4.7) suggested that they were derived from stelletin A (**278**) yielding the left moiety and the nortriterpene, geoditin A (**311**) yielding the right moiety [422].

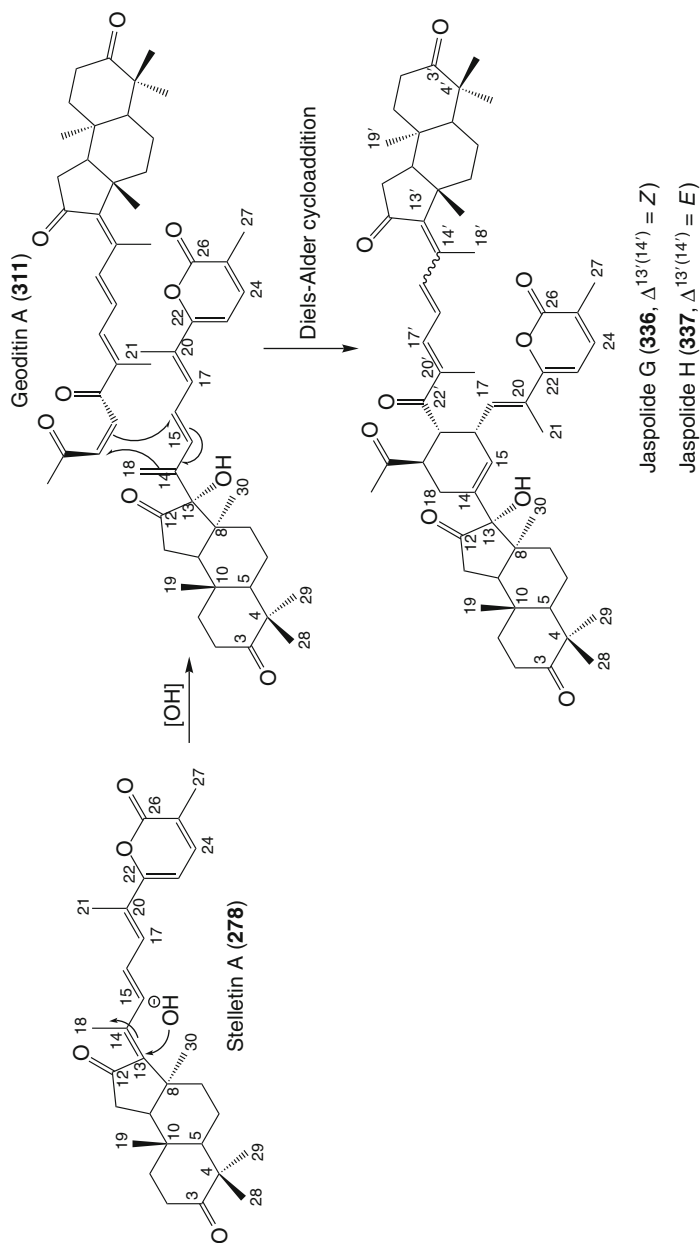
Jaspolide B (**331**) arrested HL-60 cells in the G₂/M phase of the cell cycle and induced apoptosis in a dose- and time-dependent manner. Jaspolide B with an IC₅₀ value of 0.61 μ M exhibited a comparable efficacy to that of paclitaxel (IC₅₀ = 0.78 μ M). These results suggested **331** to be a promising anticancer agent for chemotherapy of leukemia by prohibiting cell cycle progression at the G₂/M phase and triggering apoptosis [423].

In a further study with human hepatoma cells, jaspolide B (**331**) inhibited the growth of Bel-7402 and HepG2 cells with IC₅₀ values of 29.1 and 29.5 μ M, respectively. Incubation with 0.5 μ M of **331** caused time-dependent induction of



Scheme 4.6 (continued)

**Scheme 4.6** Proposed biogenetic transformation of jaspolides (A-F) [421]



Scheme 4.7 Postulated biogenetic pathway of jaspolidides G and H [422]

apoptosis in Bel-7402 as confirmed by the enhancement of mitochondrial masses, cell membrane permeability, and nuclear condensation. In conclusion, the anticancer effect of jaspolid B involves multiple mechanisms including apoptosis induction, cell cycle arrest, and microtubule disassembly, but these were weaker than observed for colchicine, a well-known microtubule-disassembly agent [424]. These multiple mechanisms of jaspolid B, especially the apoptosis induction, pose interesting perspectives for further exploration of the isomalabaricane-type terpenes as potential anticancer agents.

Since the class of isomalabaricane terpenoidal metabolites has been reported in the literature from different sponge species of the genera *Rhabdastrella*, *Stelletta*, *Jaspis*, and *Geodia* as shown above, the identity of these sponges has been questioned and reevaluated. Interestingly, the taxonomic reevaluation of these sponges revealed that they all might be reassigned to *Rhabdastrella globostellata* (class Demospongiae; order Astrophorida; family Ancorinidae) [400]. However, this could not be ascertained for the isomalabaricane producing *Stelletta* sp. from Somalia [394] and *Stelletta tenuis* from China [397]. The latter, collected from an identical location (Hainan Island), was taxonomically recognized as *R. globostellata* [395].

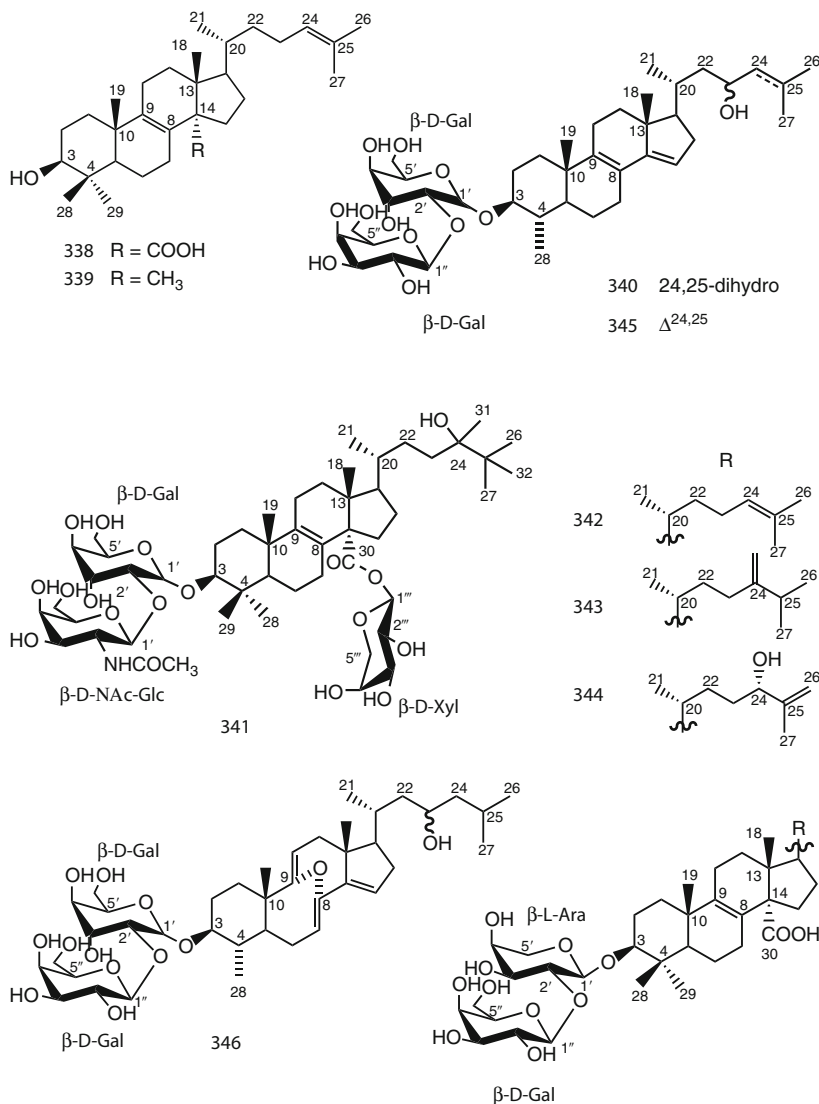
4.4.2.2 Steroidal Saponins

In the Kingdom Animalia, steroidal and triterpene glycosides are predominant metabolites of starfishes and sea cucumbers, respectively [427]. In addition, these types of glycosides have also been isolated from marine sponges. To the best of our knowledge, around 80 triterpenoidal sponge glycosides have been reported to date, including erylosides [427–434], formosides [435, 436], nobiloside [437], and sokodosides [438] from different sponge species of the genus *Erylus*; sarasinoids from the marine sponges *Asteropus sarasinus* [440–443], *Melophylus isis* [444], and *M. sarassinorum* [445]; mycalosides from *Mycale laxissima* [446–448]; ectyoplasides and feroxosides from the Caribbean marine sponge *Ectyoplasia ferox* [449, 450]; ulososides from *Ulosa* sp. [451, 452]; wondosterols from a two-sponge association [453]; and pachastrelloside A from a marine sponge of the genus *Pachastrella* [454]. The majority of these glycosides belong to norlanostane-triterpenoidal saponins, derived from lanosterol or related triterpenes as a result of oxidative elimination of one or two methyl groups.

Penasterol (338), an acidic steroidal metabolite closely related to lanosterol (339) and possessing potent antileukemic activity, was originally isolated from the Okinawan marine sponge *Penares* sp. in 1988 [425]. Penasterol together with its analogues penasterone and acetylpenasterol, isolated from the Okinawan marine sponge *Penares incrustans*, inhibit IgE-dependent histamine release from rat mast cells [426].

Eryloside A (340) was the first eryloside congener isolated from the Red Sea sponge *Erylus lendenfeldi* (class Demospongiae; order Choristida; family Geodiidae) [427]. Twenty-eight additional erylosides (A–F, F₁–F₇, G–V) have been reported from different species of the genus *Erylus* including *E. goffrilleri* [429, 434], *E. formosus* [430, 433], *E. nobilis* [431] in addition to another collection

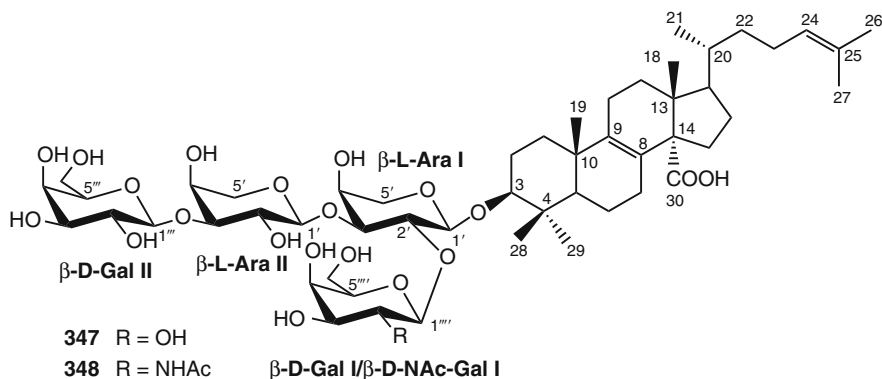
of *E. lendenfeldi* [432]. For eryloside A (**340**), antitumor activity against murine leukemia P388 cells with an $IC_{50} = 5.7 \mu M$ and antifungal activity against *Candida albicans* ($MIC = 21.1 \mu M$) have been reported [427]. Eryloside E (**341**), glycosylated at C-30 through an ester linkage with the rare *t*-butyl substitution of the side chain, was isolated from an Atlantic sponge *Erylus goffrilleri* [429]. It revealed immunosuppressive activity with an EC_{50} of $1.8 \mu M$ and a therapeutic index (TI) of 9.5, which indicated that the immunosuppressive effect is specific and is not due to a general cytotoxic effect [429].

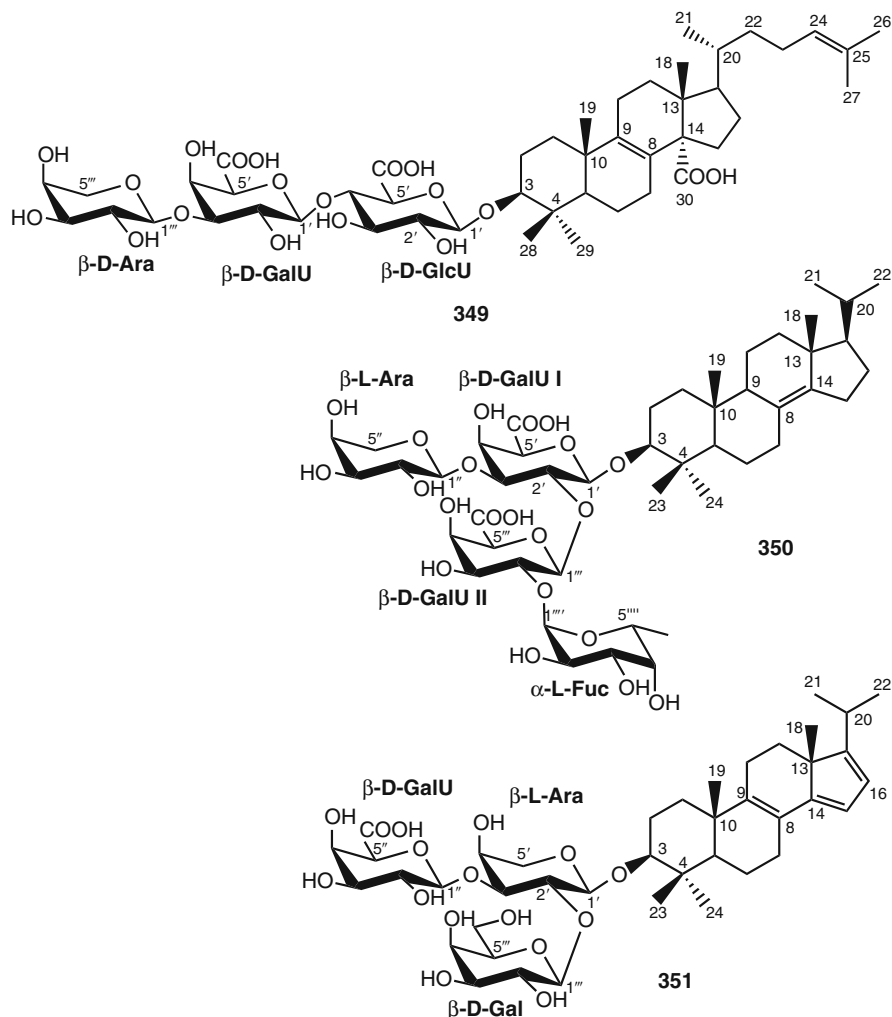


Eryloside F (**342**) was reported from two collections of the marine sponge *E. formosus* [430] and exhibited potent thrombin receptor antagonistic activity. Furthermore, it inhibited platelet aggregation in vitro. Against hepatocyte HepG2 cells, **342** possessed little activity [430]. Erylosides F₁ (**343**) and F₃ (**344**) were isolated along with nine other congeners from the Caribbean sponge *E. formosus* [433]. In contrast to its 24-epimer, eryloside F₃ (**344**) induced early apoptosis in Ehrlich carcinoma cells at 130 μ M, while erylosides F (**342**) and F₁ (**343**) activated the Ca²⁺ influx into mouse splenocytes at the same doses [433].

Erylosides K (**345**) and L (**346**) have been obtained together with **340** from another collection of the Red Sea marine sponge *Erylus lendenfeldi* [432]. While **345** was identified as the 24,25-didehydro congener of eryloside A, eryloside L (**346**) incorporated a naturally unprecedented 8 α ,9 α -epoxy-4 α -methyl-8,9-secocholesta-7,9(11),14-triene skeleton [432]. Erylosides A (**340**) and K (**345**) led to a 50% mortality rate in the brine shrimp assay at a concentration of 0.14 mM. Eryloside L (**346**) was inactive at the same concentration [432]. In addition to erylosides, the marine sponges *E. formosus* and *E. nobilis* produced other steroidal saponins identified as formosides A (**347**) [435] and B (**348**) [436] and nobiloside (**349**) [437], respectively, whilst sokodosides A (**350**) and B (**351**) have been obtained from the marine sponge *Erylus placenta* [438]. A convergent synthesis of the trisaccharides of **351** has been successfully performed [439]. Formoside A (**347**) was first reported by Jaspars and Crews in 1994 from the Caribbean marine sponge *Erylus formosus* [435]. Later, it was isolated together with formoside B (**348**) from another collection of the same sponge from the Bahamas [436]. Formoside A (**347**) and its *N*-acetyl galactosamine derivative, formoside B (**348**) possess deterrent properties against predatory fish. Therefore, they were suggested to have important ecological functions, resembling those ascribed to similar compounds present in sea stars, sea cucumbers, and terrestrial plants [436].

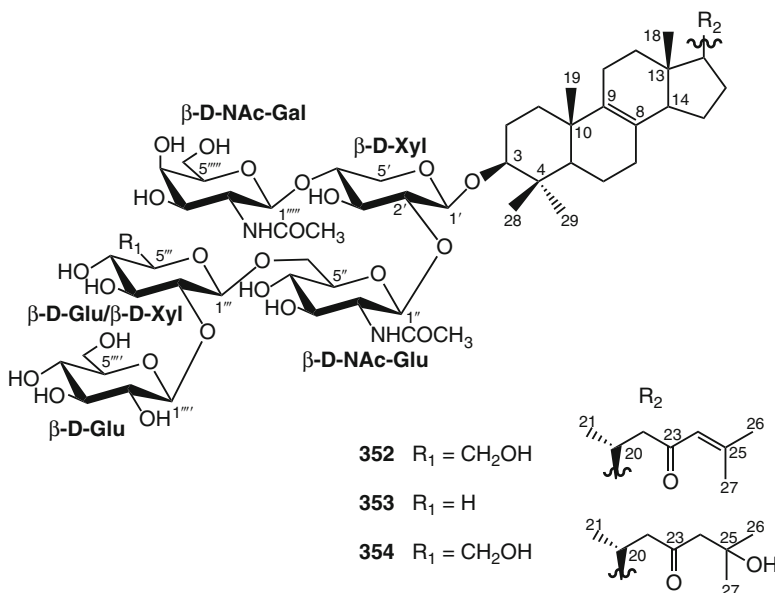
Nobiloside (**349**), a penasterol saponin, was reported from the marine sponge *E. nobilis* collected off Shikine-jima Island, Japan [437], and revealed the presence of a carboxylic group at C-30 in addition to uronic acid moieties. Nobiloside (**349**) inhibited neuraminidase from the bacterium *Clostridium perfringens* with an IC₅₀ of 0.5 μ M [437].





Sokodosides A (**350**) and B (**351**) were obtained from the marine sponge *E. placenta* collected off Hachijo Island, Japan [438]. They possessed a novel carbon skeleton as characterized by the presence of a combination of an isopropyl side chain and the 4,4-dimethyl steroid nucleus. Moreover, sokodoside B (**351**) exhibited double bonds at unusual positions $\Delta^{8(9),14(15),16(17)}$.

Both sokodosides displayed moderate antifungal activity against the fungus *Mortierella ramanniana* and the yeast *Saccharomyces cerevisiae* but no antibacterial activity was found. Additionally, sokodosides A (**350**) and B (**351**) exhibited cytotoxic activity against P388 cells with IC_{50} values of 103 and 62 μ M, respectively [438].



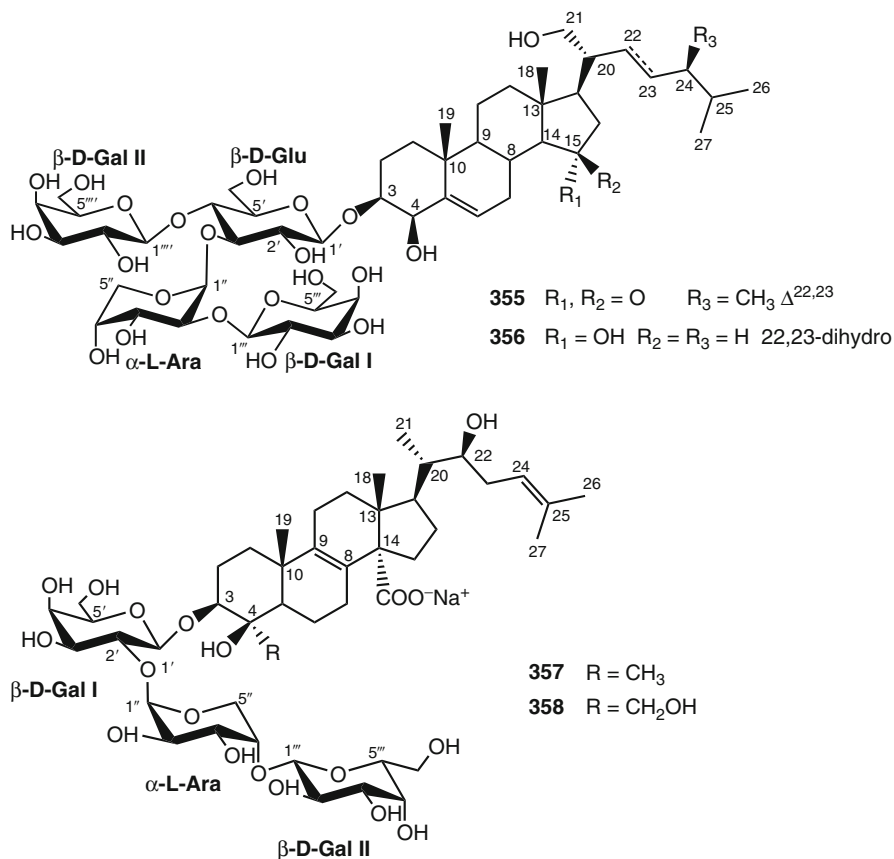
Sarasinosides follow erylosides in the number of isolated metabolites. To date, 21 sarasinoside congeners have been reported, which all feature a carbonyl group at C-23 position. Sarasinoside A₁ (**352**) was the first steroidal saponin reported in the literature, even before eryloside A (**340**), from the Palauan marine sponge *Asteropus sarasinum*, together with other eight new congeners that had been described [440–442]. Then, from the same sponge collected in the Solomon Islands, four additional sarasinosides (D–G) were reported [443]. From each of the marine sponges *Melophylus isis* (Guam) [444] and *M. sarassinorum* (Indonesia) [445], four sarasinoside congeners were isolated. Among the sarasinoside congeners known to date, sarasinoside A₁ (**352**) and B₁ (**353**) exhibited piscicidal activity against *Poecilia reticulata* with LD₅₀ values (48 h) of 0.3 and 0.6 μM , respectively [440, 442]. Sarasinoside A₁ is known to possess moderate cytotoxicity in vitro against leukemia P388 [441] and K562 [444] cell lines with IC₅₀ values of 2.2 and 5.0 μM , respectively. Sarasinoside A₃, which differs from A₁ (**352**) in having $\Delta^{8(9),14(15)}$ instead of $\Delta^{8(9)}$ unsaturation, exhibited mild cytotoxic activity with an IC₅₀ of 13.3 μM [444]. In the agar diffusion antimicrobial assay (10 $\mu\text{g}/\text{disk}$), sarasinoside A₁ showed strong and selective activity against the yeast *S. cerevisiae* but was inactive against *B. subtilis* and *E. coli*. On the other hand, sarasinoside J (**354**) was active against *S. cerevisiae* and showed moderate antibacterial activity against *B. subtilis* and *E. coli* [445].

Mycalosides include 11 steroidal saponin congeners that were isolated from the Caribbean marine sponge *Mycale laxissima* (class Demospongiae; order Poecilosclerida; family Mycalidae) collected near San Felipe Island,

Cuba [446–448]. They were all characterized by having oxygenated C-4, C-15, and C-21 positions.

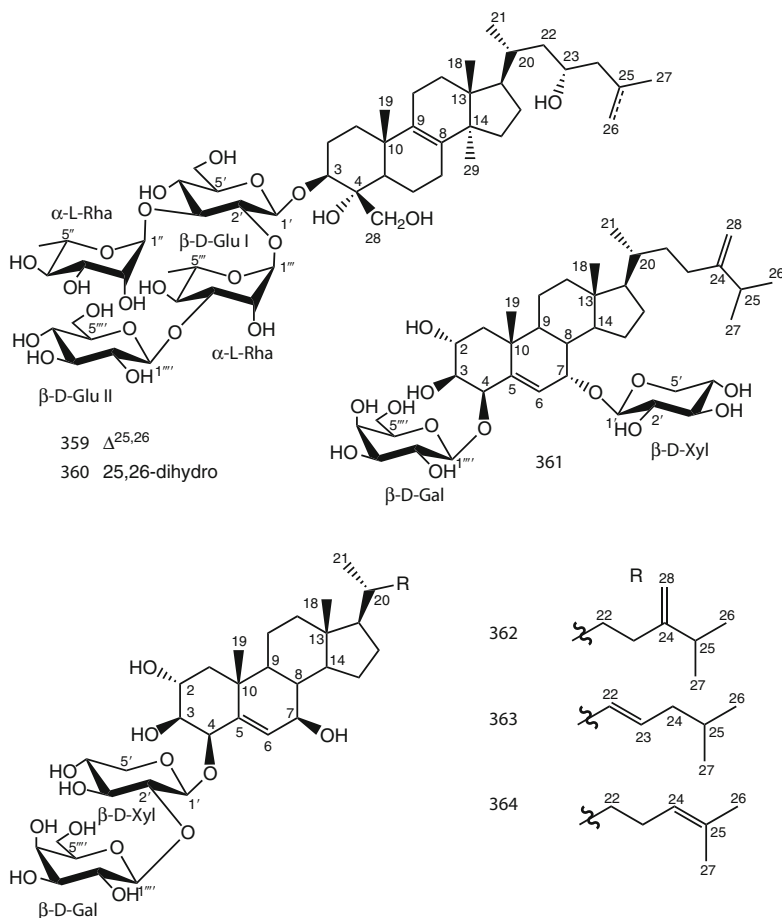
Mycaloside A (355) and G (356) as well as the total glycoside fraction did not influence nonfertilized eggs and the developing embryo up to the 8-blastomere stage at concentrations of up to 94.6 μM . However, these compounds were effective as spermatostatics when preincubated for 15 min with sea urchin sperm with an EC_{50} of 3.04 μM . The total glycoside fraction generated a less toxic effect ($\text{EC}_{50} = 7.03 \mu\text{g/mL}$) [447].

Ectyoplasides A (357) and B (358) were first isolated from the Caribbean sponge *E. ferox* (class Demospongiae; order Axinellida; family Raspaliidae) collected along the coasts of San Salvador Island, Bahamas [449]. The compounds are C-4 norpenasterol triterpenoidal derivatives. Later, ectyoplasides were reisolated together with feroxosides A (359) and B (360) from the same sponge collected along the coasts of Grand Bahama Island [450]. Feroxosides have been shown to be unusual C-4 norlanostane triterpenes glycosylated with a rhamnose-containing tetrasaccharide chain.



Against murine fibrosarcoma WEHI164, murine leukemia P388, and murine monocyte-macrophage J774 cell lines, both ectyoplasides (**357** and **358**) exhibited moderate in vitro cytotoxic activity with IC_{50} values ranging from 9.0 to 11.4 μM [449], while against the latter cell line, feroxosides (**359** and **360**) were mildly cytotoxic ($IC_{50} = 17.6 \mu M$) [450].

Pachastrelloside A (**361**) was obtained from the marine sponge *Pachastrella* sp. (Kagami Bay, Japan) and revealed the presence of a cholest-5,24-diene- $2\alpha,3\beta,4\beta,7\alpha$ -tetraol aglycone that was glycosylated at the C-4 and C-7 positions with β -D-xylopyranose and β -D-galactopyranose moieties, respectively [454]. A Korean sponge association composed of *Poecillastra wondoensis* and *Jaspis wondoensis* resulted in the isolation of wondosterols A–C (**362–364**), which are structurally related to **361** [443]. Wondosterols were shown to have a β -OH group at C-7, and they were all diglycosylated at C-3 with β -D-xylopyranose connected to β -D-galactopyranose.



Wondosterols A–C (**362–364**) were weakly cytotoxic against P388 cells ($IC_{50} = 63 \mu M$), and at a concentration of $10 \mu g/disk$, only **362** and **364** showed antibacterial activities against *P. aeruginosa* and *E. coli* [453]. Pachastrelloside A (**361**) inhibited cell division of fertilized starfish (*Asterina pectinifera*) eggs at $35 \mu M$ [454].

4.5 Concluding Remarks

The enormous diversity of marine natural products combined with improved global concerns to find new therapeutic agents for the treatment of different ailments provide the stimulus to evaluate marine natural products in clinical trials. Marine drug discovery faces many obstacles including a sufficient supply and the low concentrations of some compounds that may account for less than $10^{-6}\%$ of the wet weight [6]. However, there have been substantial advances, suggesting that sustainable sourcing could be achievable. Since the continuous and exhaustive harvesting of terrestrial drug lead resources proved to be unreliable and resulted in the frequent re-isolation of known compounds, researchers from academia and from pharmaceutical companies alike are now turning their focus to the sea in search for new lead structures from nature. Nevertheless, the large-scale production of marine natural products for clinical use is a real challenge, and, therefore, environmentally sound and economically feasible alternatives are required.

Chemical synthesis is among the first strategies to be explored, but unfortunately, the structural complexity of marine metabolites with novel mechanisms of action and high selectivity has resulted in only a few successful examples of this strategy such as the conus toxin ziconotide [455]. A second strategy, but also as labor-intensive, is to study the pharmacological significance of marine natural product pharmacophores and then attempt to define the critical pharmacophore that can result in practical drugs based on a marine prototype via chemical synthesis, degradation, modification, or a combination of these.

Aquaculture of the source organisms, including sponges, tunicates, and bryozoans, with an aim at securing a sustainable supply of the active constituent(s), has progressed notably in cancer applications. However, in most cases, the biomass currently generated is still far from that required should a marine-based drug finally enter the pharmaceutical market [456]. Furthermore, the cultivation of invertebrates in their natural environment is subject to several hazards and threats, such as destruction by storms or diseases. An intriguing strategy has been to identify the true producers of bioactive compounds and to explore whether or not they are of microbial origin including bacteria, cyanobacteria, or fungi that are known to thrive within the tissues of marine invertebrates.

If bacterial or other associated microorganisms prove to produce the compounds of interest, a careful design of special culture media would be crucial for large-scale fermentation, e.g., ET-743 production. Currently, only 5% or less of the symbiotic bacteria present in marine specimens can be cultivated under standard

conditions [457]. Consequently, molecular approaches offer particularly promising alternatives through the transfer of biosynthetic gene clusters to a vector suitable for large-scale fermentation, thereby avoiding the obstacles in culturing symbiotic bacteria. Oceans will play a potential role in the future to control and relieve the global disease burden. In spite of the substantial development that has been achieved in disclosing novel drug leads from marine resources, more efforts are still required for more chemical entities to reach to clinical applications.

4.6 Study Questions

1. Considering that oroidin is believed to be the precursor of most of the spongal bromopyrrole alkaloids, delineate a plausible biogenetic pathway connecting oroidin with other bromopyrrole alkaloids.
2. What are the main molecular targets of hymenialdisine and analogues, and what are the structural requirements that are responsible for the biological activities of these compounds?
3. Depict the biogenetic relationships between the sponge-derived alkaloids aerophysinin-1, aerophobin-2, and isofistularin-3. What is the amino acid precursor for these alkaloids? Depict the wound-induced biotransformation of brominated isoxazoline alkaloids in *Aplysina* sponges.
4. The bastadins are important bromotyrosine-derived sponge metabolites. Depict a plausible biogenetic scheme that explains the formation of bastadins in sponges. What are the most important biological activities of bastadin derivatives?
5. The jaspamides are important sponge-derived depsipeptides. What are the most promising biological activities of these compounds? Do they bear structural resemblances to other natural products that might support the notion that some sponge metabolites are derived from microorganisms?
6. Azumamides are the first cyclic peptides with histone deacetylase (HDAC) inhibitory activity isolated from marine organisms. Briefly discuss the structural resemblance between azumamides and trichostatin A (TSA) and their relevance for HDAC inhibitory activity.
7. To which group of terpenes does manoalide belong? What are the most prominent biological activity and mode of action of manoalide?
8. Isomalabaricane triterpenes comprise a group of marine sponge natural products with polyene conjugated functionality. Briefly enumerate with examples the different classes of isomalabaricane triterpenes.
9. Jaspolidides represent an example of isomalabaricane-type terpenoids including both monomeric and dimeric congeners. Classify different jaspolidides based on their chemical structures and depict a plausible biogenetic pathway of the dimeric jaspolidide congeners.

Acknowledgment Continuous support by BMBF to P.P. is gratefully acknowledged. A predoctoral fellowship granted and financed by the Egyptian government (Ministry of High Education) to S.S.E. is acknowledged.

References

1. Proksch P, Edrada-Ebel RA, Ebel R (2003) Drugs from the sea - opportunities and obstacles. *Mar Drugs* 1:5–17
2. Blunt JW, Copp BR, Munro MHG, Northcote PT, Prinsep MR (2010) Marine natural products. *Nat Prod Rep* 27:165–237
3. Laport MS, Santos OCS, Muricy G (2009) Marine sponges: potential sources of new antimicrobial drugs. *Curr Pharm Biotech* 10:86–105
4. Paul VJ, Ritson-Williams R (2008) Marine chemical ecology. *Nat Prod Rep* 25:662–695
5. Molinski TF, Dalisay DS, Lievens SL, Saludes JP (2009) Drug development from marine natural products. *Nat Rev Drug Discov* 8:69–85
6. Proksch P, Edrada RA, Ebel R (2002) Drugs from the seas-current status and microbiological implications. *Appl Microbiol Biotechnol* 59:125–134
7. Piel J (2009) Metabolites from symbiotic bacteria. *Nat Prod Rep* 26:338–362
8. Tachibana K, Scheuer PJ, Tsukitani Y, Kikuchi H, van Engen D, Clardy J, Gopichand Y, Schmitz FJ (1981) Okadaic acid, a cytotoxic polyether from two marine sponges of the genus *Halichondria*. *J Am Chem Soc* 103:2469–2471
9. Murakami Y, Oshima Y, Yasumoto T (1982) Identification of okadaic acid as a toxic component of a marine dinoflagellate *Prorocentrum lima*. *Bull Jap Soc Fish Sci* 48:69–72
10. Sakai R, Higa T (1986) Manzamine A, a novel antitumor alkaloid from a sponge. *J Am Chem Soc* 108:6404–6405
11. Magnier E, Langlois Y (1998) Manzamine alkaloids, syntheses and synthetic approaches. *Tetrahedron* 54:6201–6258
12. Tsuda M, Kobayashi J (1997) Structures and biogenesis of manzamines and related alkaloids. *Heterocycles* 46:765–794
13. Rao KV, Donia MS, Peng J, Garcia-Palomero E, Alonso D, Martinez A, Medina M, Franzblau SG, Tekwani BL, Khan SI, Wahyuono S, Willet KL, Hamann MT (2006) Manzamine B and E and Ircinal A related alkaloids from an Indonesian *Acanthostrongylophora* sponge and their activity against infectious, tropical parasitic, and Alzheimer's diseases. *J Nat Prod* 69:1034–1040
14. Zhang B, Higuchi R, Miyamoto T, van Soest RWM (2008) Neuritogenic activity-guided isolation of a free base form manzamine A from a marine sponge, *Acanthostrongylophora* aff. *ingens* (Thiele, 1899). *Chem Pharm Bull* 56:866–869
15. Baldwin JE, Whitehead RC (1992) On the biosynthesis of manzamines. *Tetrahedron Lett* 33:2059–2062
16. Kondo K, Shigemori H, Kikuchi Y, Ishibashi M, Sasaki T, Kobayashi J (1992) Ircinals A and B from the Okinawan marine sponge *Ircinia* sp.: plausible biogenetic precursors of manzamine alkaloids. *J Org Chem* 57:2480–2483
17. Tsuda M, Kawasaki N, Kobayashi J (1994) Ircinols A and B, first antipodes of manzamine-related alkaloids from an Okinawan marine sponge. *Tetrahedron* 50:7957–7960
18. Kobayashi J, Tsuda M, Kawasaki N, Matsumoto K, Adachi T (1994) Keramaphidin B, a novel pentacyclic alkaloid from a marine sponge *Amphimedon* sp.: a plausible biogenetic precursors of manzamine alkaloids. *Tetrahedron Lett* 35:4383–4386
19. Tsuda M, Inaba K, Kawasaki N, Honma K, Kobayashi J (1996) Chiral resolution of (±)-keramaphidin B and isolation of manzamine L, a new β -carboline alkaloid from a sponge *Amphimedon* sp. *Tetrahedron* 52:2319–2324
20. Edrada RA, Proksch P, Wray V, Witte L, Mueller WEG, van Soest RWM (1996) Four new bioactive manzamine-type alkaloids from the Philippine marine sponge *Xestospongia ashmorica*. *J Nat Prod* 59:1056–1060
21. Nakamura H, Deng S, Kobayashi J, Ohizumi Y, Tomotake Y, Matsuzaki T (1987) Keramamine A and B, novel antimicrobial alkaloids from the Okinawan marine sponge *Pellina* sp. *Tetrahedron Lett* 28:621–624

22. Ang KKH, Holmes MJ, Higa T, Hamann MT, Kara UAK (2000) *In vivo* antimalarial activity of the beta-carboline alkaloid manzamine A. *Antimicrob Agents Chemother* 44:1645–1649
23. El Sayed KA, Kelly M, Kara UAK, Ang KKH, Katsuyama I, Dunbar DC, Khan AA, Hamann MT (2001) New manzamine alkaloids with potent activity against infectious diseases. *J Am Chem Soc* 123:1804–1808
24. Martin SF, Humphrey JM, Ali A, Hillier MC (1999) Enantioselective total syntheses of ircinal A and related manzamine alkaloids. *J Am Chem Soc* 121:866–867
25. Coldham I, Crapnell KM, Fernández JC, Moseley JD, Rabot R (2002) Synthesis of the ABC ring system of manzamine A. *J Org Chem* 67:6181–6187
26. El Sayed KA, Khalil AA, Yousaf M, Labadie G, Kumar GM, Franzblau SG, Mayer AMS, Avery MA, Hamann MT (2008) Semisynthetic studies on the manzamine alkaloids. *J Nat Prod* 71:300–308
27. Ibrahim MA, Shilabin AG, Prasanna S, Jacob M, Khan SI, Doerksen RJ, Hamann MT (2008) 2-N-methyl modifications and SAR studies of manzamine A. *Bioorg Med Chem* 16:6702–6706
28. Kobayashi J, Watanabe D, Kawasaki N, Tsuda M (1997) Nakadomarin A, a novel hexacyclic manzamine-related alkaloid from *Amphimedon* sponge. *J Org Chem* 62:9236–9239
29. Tsuda M, Watanabe D, Kobayashi J (1998) Ma'eganedin A, a new manzamine alkaloid from *Amphimedon* sponge. *Tetrahedron Lett* 39:1207–1210
30. Peng J, Hu JF, Kazi AB, Li Z, Avery M, Peraud O, Hill RT, Franzblau SG, Zhang F, Schinazi RF, Wirtz SS, Tharnish P, Kelly M, Wahyuono S, Hamann MT (2003) Manadomanzamines A and B: a novel alkaloid ring system with potent activity against Mycobacteria and HIV-1. *J Am Chem Soc* 125:13382–13386
31. Takahashi Y, Kubota T, Fromont J, Kobayashi J (2009) Zamamidines A and B, new manzamine alkaloids from the sponge *Amphimedon* sp. *Org Lett* 11:21–24
32. Yamada M, Takahashi Y, Kubota T, Fromont J, Ishiyama A, Otoguro K, Yamada H, Omura S, Kobayashi J (2009) Zamamidine C, 3,4-dihydro-6-hydroxy-10,11-epoxymanzamine A, and 3,4-dihydromanzamine J N-oxide, new manzamine alkaloids from sponge *Amphimedon* sp. *Tetrahedron* 65:2313–2317
33. Rao KV, Kasanah N, Wahyuono S, Tekwani BL, Schinazi RF, Hamann MT (2004) New manzamine alkaloids from a common Indonesian sponge and their activity against infectious and tropical parasitic diseases. *J Nat Prod* 67:1314–1318
34. Rao KC, Santarsiero BD, Mesecar AD, Schinazi RF, Tekwani BL, Hamann MT (2003) New manzamine alkaloids with activity against infectious tropical parasitic diseases from an Indonesian sponge. *J Nat Prod* 66:823–828
35. Hamann MT (2007) The manzamines as an example of the unique structural classes available for the discovery and optimization of infectious disease controls based on marine natural products. *Curr Pharm Design* 13:653–660
36. Koenig GM, Kehraus S, Seibert SF, Abdel-Lateff A, Mueller D (2006) Natural products from marine organisms and their associated microbes. *ChemBioChem* 7:229–238
37. Forenza S, Minale L, Riccio R, Fattorusso E (1971) New bromo-pyrrole derivatives from the sponge *Agelas oroides*. *J Chem Soc, D Chem Commun* 1971:1129–1130
38. Braeckman JC, Daloze Q, Stoller C, van Soest RW (1992) Chemotaxonomy of *Agelas* (Porifera: Demospongiae). *Biochem Syst Ecol* 20:417–430
39. Wilson DM, Puyama M, Fenical W, Pawlik JR (1999) Chemical defense of the Caribbean reef sponge *Axinella corrugata* against predatory fishes. *J Chem Ecol* 25:2811–2823
40. Lindel T, Hoffmann H, Hochguertel M, Pawlik JR (2000) Structure-activity relationship of inhibition of fish feeding by sponge-derived and pyrrole-imidazole alkaloids. *J Chem Ecol* 26:1477–1496
41. O'Malley DP, Li K, Maue M, Zografos AL, Baran PS (2007) Total synthesis of dimeric pyrrole-imidazole alkaloids: sceptrin, ageliferin, nagelamide E, oxysceptrin, nakamuric acid, and the axinellamine carbon skeleton. *J Am Chem Soc* 129:4762–4775

42. Bhandari MR, Sivappa R, Lovely CJ (2009) Total synthesis of the putative structure of nagelamide D. *Org Lett* 11:1535–1538
43. Kobayashi J, Ohizumi Y, Nakamura H, Hirata Y (1986) A novel antagonist of serotonergic receptors, hymenidin, isolated from the Okinawan marine sponge *Hymeniacidon* sp. *Experientia* 42:1176–1177
44. Morales JJ, Rodriguez AD (1991) The structure of clathrodin, a novel alkaloid isolated from the Caribbean Sea sponge *Agelas clathrodes*. *J Nat Prod* 54:629–631
45. Rosa R, Silva W, de Motta GE, Rodriguez AD, Morales JJ, Ortiz M (1992) Anti-muscarinic activity of a family of C₁₁N₅ compounds isolated from *Agelas* sponges. *Experientia* 48:885–887
46. Assmann M, Zea S, Koeck M (2001) Sventrin, a new bromopyrrole alkaloid from the Caribbean sponge *Agelas sventres*. *J Nat Prod* 64:1593–1595
47. Bickmeyer U, Drechsler C, Koeck M, Assmann M (2004) Brominated pyrrole alkaloids from marine *Agelas* sponges reduce depolarization-induced cellular calcium elevation. *Toxicon* 44:45–51
48. Cafieri F, Fattorusso E, Mangoni A, Taglialatela-Scafati O (1996) Dispacamides, anti-histamine alkaloids from Caribbean *Agelas* sponges. *Tetrahedron Lett* 7:3587–3590
49. Cafieri F, Carnuccio R, Fattorusso E, Taglialatela-Scafati O, Vallefucio T (1997) Anti-histaminic activity of bromopyrrole alkaloids isolated from Caribbean *Agelas* sponges. *Bioorg Med Chem Lett* 7:2283–2288
50. Vergne C, Appenzeller J, Ratinaud C, Martin MT, Debitus C, Zaparucha A, Al-Mourabit A (2008) Debromodispacamides B and D: isolation from the marine sponge *Agelas mauritiana* and stereoselective synthesis using a biomimetic proline route. *Org Lett* 10:493–496
51. Uemoto H, Tsuda M, Kobayashi J (1999) Mukanadins A–C, new bromopyrrole alkaloids from marine sponge *Agelas nakamurai*. *J Nat Prod* 62:1581–1583
52. Hu JF, Peng J, Kazi AB, Kelly M, Hamann MT (2005) Bromopyrrole alkaloids from the Jamaican sponge *Didiscus oxeata*. *J Chem Res* 7:427–428
53. Aiello A, D'Esposito M, Fattorusso E, Menna M, Mueller WEG, Pervoic-Ottstadt S, Schroeder HC (2006) Novel bioactive bromopyrrole alkaloids from the Mediterranean sponge *Axinella verrucosa*. *Bioorg Med Chem* 14:17–24
54. Jimenez C, Crews P (1994) Mauritamide A and accompanying oroidin alkaloids from the sponge *Agelas mauritiana*. *Tetrahedron Lett* 35:1375–1378
55. Kobayashi J, Inaba K, Tsuda M (1997) Tauroacidins A and B, new bromopyrrole alkaloids possessing a taurine residue from *Hymeniacidon* sponge. *Tetrahedron* 53:16679–16682
56. Fattorusso E, Taglialatela-Scafati O (2000) Two novel pyrrole-imidazole alkaloids from the Mediterranean sponge *Agelas oroides*. *Tetrahedron Lett* 41:9917–9922
57. Tsuda M, Uemoto H, Kobayashi J (1999) Slagenins A–C, novel bromopyrrole alkaloids from marine sponge *Agelas nakamurai*. *Tetrahedron Lett* 40:5709–5712
58. Sharma GM, Buyer JS, Pomerantz MW (1980) Characterization of a yellow compound isolated from the marine sponge *Phakellia flabellate*. *J Chem Soc, Chem Commun* 10:435–436
59. Mattia CA, Mazzarella L, Puliti R (1982) 4-(2-Amino-4-oxo-2-imidazolin-5-ylidene)-2-bromo-4,5,6,7-tetrahydropyrrolo-[2,3-C] azepine –8-one Methanol solvate—a new bromo compound from the sponge *Acanthella aurantiaca*. *Acta Crystallogr, Sec B, Struct Sci* 38:2513–2515
60. Cimino G, De Rosa S, De Stefano S, Mazzarella L, Puliti R, Sodano G (1982) Isolation and X-ray crystal structure of a novel bromo compound from two marine sponges. *Tetrahedron Lett* 23:767–768
61. Kitagawa I, Kobayashi J, Kitanaka K, Kido M, Kyogoku Y (1983) Marine natural products. XII. On the chemical constituents of the Okinawan marine sponge *Hymeniacidon aldii*. *Chem Pharm Bull* 3:2321–2328

62. Supriyono A, Schwarz B, Wray V, Witte L, Mueller WEG, van Soest R, Sumaryono W, Proksch P (1995) Bioactive alkaloids from the tropical marine sponge *Axinella carteri*. *Z Naturforsch* 50c:669–674
63. Pettit GR, Herald CL, Leet JE, Gupta R, Schaufelberger DE, Bates RB, Clewlow PJ, Doubek DL, Manfredi KP, Rutzler K, Schmidt JM, Tackett LP, Ward FB, Bruck M, Camou F (1990) Antineoplastic agents. 168. Isolation and structure of axinohydantoin. *Can J Chem* 68:1621–1624
64. Patil AD, Freyer AJ, Killmer L, Hofmann G, Randall K (1997) Z-axinohydantoin and debromo-Z-axinohydantoin from the sponge *Stylotella aurantium*: inhibitors of protein kinase C. *Nat Prod Lett* 9:201–207
65. Inaba K, Sato H, Tsuda M, Kobayashi J (1998) Spongiacidins A–D, new bromopyrrole alkaloids from *Hymeniacidon* sponge. *J Nat Prod* 61:693–695
66. Williams DH, Faulkner DJ (1996) Isomers and tautomers of hymenialdisine and debromohymenialdisine. *Nat Prod Lett* 9:57–64
67. Kobayashi J, Ohizumi Y, Nakamura H, Hirata Y, Wakamatsu K, Miyazawa T (1986) Hymenin, an α -adrenoceptor blocking agent from the Okinawan marine sponge *Hymeniacidon* sp. *Experientia* 42:1064–1065
68. De Nanteuil G, Ahond A, Guilhem J, Poupat C, Tran Huu Dau E, Potier P, Pusset M, Pusset J, Laboute P (1985) Marine invertebrate of Neo-Caledonian V. Isolation and identification of the metabolites of the new Caledonian sponge *Pseudaxinyssa cantharella*. *Tetrahedron* 41:6019–6033
69. Eder C, Proksch P, Wray V, Steube K, Bringmann G, van Soest RWM, Sudarsono FE, Pattisina LA, Wiryowidagdo S, Moka W (1999) New alkaloids from the Indopacific sponge *Stylissa carteri*. *J Nat Prod* 62:184–187
70. Wilson DM, Puyana M, Fenical W, Pawlik JR (1999) Chemical defense of the Caribbean reef sponge *Axinella corrugata* against predatory fishes. *J Chem Ecol* 25:2811–2823
71. Meijer L, Thunnissen AMWH, White AW, Garnier M, Nikolic M, Tsai LH, Walter J, Cleverley KE, Salinas PC, Wu YZ, Biernat J, Mandelkow EM, Kim SH, Pettit GR (2000) Inhibition of cyclin-dependent kinases, GSK-3 beta and CK1 by hymenialdisine, a marine sponge constituent. *Chem Biol* 7:51–63
72. Nikoulina SE, Ciaraldi TP, Mudaliar S, Mohideen P, Carter L, Henry RR (2000) Potential role of glycogen synthase kinase-3 in skeletal muscle insulin resistance of type 2 diabetes. *Diabetes* 49:263–271
73. Martinez A, Castro A, Dorronsoro I, Alonso M (2002) Glycogen synthase kinase (GSK-3) inhibitors as new promising drugs for diabetes, neurodegeneration, cancer and inflammation. *Med Res Rev* 22:373–384
74. Sharma V, Lansdell TA, Jin G, Tepe JJ (2004) Inhibition of cytokine production by hymenialdisine derivatives. *J Med Chem* 47:3700–3703
75. Nguyen TNT, Tepe JJ (2009) Preparation of hymenialdisine, analogues and their evaluation as kinase inhibitors. *Curr Med Chem* 16:3122–3143
76. Fedoreyev SA, Ilyin SG, Utkina NK, Maximov OB, Reshetnyak MV, Antipin MY, Struchkov YT (1989) The structure of dibromoagelospongins – a novel bromine-containing guanidine derivative from the marine sponge *Agelas* sp. *Tetrahedron* 45:3487–3492
77. Sharma GM, Burkholder PR (1971) Structure of dibromophakellin, a new bromine-containing alkaloid from the marine sponge *Phakellia flabellate*. *J Chem Soc D Chem Commun* 3:151–152
78. Gautschi JT, Whitman S, Holman TR, Crews P (2004) An analysis of phakellin and oroidin structure stimulated by further study of an *Agelas* sponge. *J Nat Prod* 67:1256–1261
79. Pettit GR, McNulty J, Herald DL, Doubek DL, Chapuis JC, Schmidt JM, Tackett LP, Boyd MR (1997) Antineoplastic agents. 362. Isolation and X-ray crystal structure of dibromophakellistatin from the Indian Ocean sponge *Phakellia mauritiana*. *J Nat Prod* 60:180–183

80. Fedoreyev SA, Utkina NK, Ilyin SG, Reshetnyak MV, Maximov OB (1986) The structure of dibromoisophakellin from the marine sponge *Acanthella carteri*. *Tetrahedron Lett* 27:3177–3180
81. Kinnel RB, Gehrken HP, Scheuer PJ (1993) Palau'amine: a cytotoxic and immunosuppressive hexacyclic bisguanidine antibiotic from the sponge *Stylotella agminata*. *J Am Chem Soc* 115:3376–3377
82. Kinnel RB, Gehrken HP, Swali R, Skoropowski G, Scheuer PJ (1998) Palau'amine and its congeners: a family of bioactive bisguanidines from the marine sponge *Stylotella aurantium*. *J Org Chem* 63:3281–3286
83. Kato T, Shizuri Y, Izumida H, Yokoyama A, Endo M (1995) Styloguanidines, new chitinase inhibitors from the marine sponge *Stylotella aurantium*. *Tetrahedron Lett* 36:2133–2136
84. D'Ambrosio M, Guerriero A, Debitus C, Ribes O, Pusset J, Leroy S, Pietra F (1993) Agelastatin A, a new skeleton cytotoxic alkaloid of the oroidin family. Isolation from the Axinellid sponge *Agelas dendromorpha* of the Coral Sea. *J Chem Soc Chem Commun* 16:1305–1306
85. D'Ambrosio M, Guerriero A, Ripamonti M, Debitus C, Waikede J, Pietra F (1996) 65. The active centers of agelastatin A, a strongly cytotoxic alkaloid of the Coral Sea Axinellid sponge *Agelas dendromorpha*, as determined by comparative bioassays with semisynthetic derivatives. *Helv Chim Acta* 79:727–735
86. Hong TW, Jimenez DR, Molinski TF (1998) Agelastatins C and D, new pentacyclic bromopyrroles from the sponge *Cymbastela* sp., and potent anthrhopod toxicity of (–)-agelastatin A. *J Nat Prod* 61:158–161
87. Tsuda M, Yasuda T, Fukushi E, Kawabata J, Sekiguchi M, Fromont J, Kobayashi J (2006) Agesamides A and B, bromopyrrole alkaloids from sponge *Agelas* species: application of DOSY for chemical screening of new metabolites. *Org Lett* 8:4235–4238
88. Grube A, Koeck M (2006) Oxocyclostylidol, an intramolecular cyclized oroidin derivative from the marine sponge *Stylissa caribica*. *J Nat Prod* 69:1212–1214
89. Cafieri F, Fattorusso E, Mangoni A, Taglialatela-Scafati O (1995) Longamide and 3,7-dimethylisoguanine, two novel alkaloids from the marine sponge *Agelas longissima*. *Tetrahedron Lett* 36:7893–7896
90. Li CJ, Schmitz FJ, Kelly-Borges M (1998) A new lysine derivative and new 3-bromopyrrole carboxylic acid derivative from two marine sponges. *J Nat Prod* 61:387–289
91. Schmitz FJ, Gunasekera SP, Lakshmi V, Tillekeratne LMV (1985) Marine natural products: pyrrololactams from several sponges. *J Nat Prod* 48:47–53
92. Hassan W, Elkhayat E, Edrada R, Ebel R, Proksch P (2007) New bromopyrrole alkaloids from the marine sponges *Axinella damicornis* and *Stylissa flabelliformis*. *Nat Prod Commun* 2:1–6
93. Cafieri F, Fattorusso E, Taglialatela-Scafati O (1998) Novel bromopyrrole alkaloids from the sponge *Agelas dispar*. *J Nat Prod* 61:122–125
94. Mancini I, Guella G, Amade P, Roussakis C, Pietra F (1997) Hanishin, a semiracemic, bioactive C₉ alkaloid of the Axinellid sponge *Acanthella carteri* from the Hanish Islands. A shunt metabolite? *Tetrahedron Lett* 38:6271–6274
95. Umeyama A, Ito S, Yuasa E, Arihara S, Yamada T (1998) A new bromopyrrole alkaloid and the optical resolution of the racemate from the marine sponge *Homaxinella* sp. *J Nat Prod* 61:1433–1434
96. Gunasekera SP, Cranick S, Longley RE (1989) Immunosuppressive compounds from a deep water marine sponge, *Agelas flabelliformis*. *J Nat Prod* 52:757–761
97. Iwagawa T, Kaneko M, Okamura H, Nakatani M, van Soest RWM (1998) New alkaloids from the Papua New Guinean sponge *Agelas nakamurai*. *J Nat Prod* 61:1310–1312
98. Ebada SS, Edrada-Ebel RA, de Voogd NJ, Wray V, Proksch P (2009) Dibromopyrrole alkaloids from the marine sponge *Acanthostylotella* sp. *Nat Prod Commun* 4:47–52
99. Walker RP, Faulkner DJ (1981) Sceptrin, an antimicrobial agent from the sponge *Agelas sceptrum*. *J Am Chem Soc* 103:6772–6773

100. Keifer PA, Schwartz RE, Koker MES, Hughes RG Jr, Rittschof D, Rinehart KL (1991) Bioactive bromopyrrole metabolites from the Caribbean sponge *Agelas conifera*. *J Org Chem* 56:2965–2975
101. Nishimura S, Matsunaga S, Shibazaki M, Suzuki K, Furihata K, van Soest RWM, Fusetani N (2003) Massadine, a novel geranylgeranyl transferase type I inhibitor from the marine sponge *Stylissa* aff. *massa*. *Org Lett* 5:2255–2257
102. Grube A, Koeck M (2006) Stylissadines A and B: the first tetrameric pyrrole-imidazole alkaloids. *Org Lett* 8:4675–4678
103. Urban S, de Almedia LP, Carroll AR, Fechner GA, Smith J, Hooper JNA, Quinn RJ (1999) Axinellamines A–D, novel imidazo-azolo-imidazole alkaloids from the Australian marine sponge *Axinella* sp. *J Org Chem* 64:731–735
104. Kobayashi J, Suzuki M, Tsuda M (1997) Konbu'acidin A, a new bromopyrrole alkaloid with cdk4 inhibitory activity from *Hymeniacidon* sponge. *Tetrahedron* 53:15681–15684
105. Rinehart KL (1989) Biologically active marine natural products. *Pure Appl Chem* 61:525–528
106. Kobayashi J, Tsuda M, Murayama T, Nakamura H, Ohizumi Y, Ishibashi M, Iwamura M, Ohta T, Nozoe S (1990) Ageliferins, potent actomyosin ATPase activators from the Okinawan marine sponge *Agelas* sp. *Tetrahedron* 46:5579–5586
107. Bickmeyer U (2005) Bromoageliferin and dibromoageliferin, secondary metabolites from the marine sponge *Agelas conifera*, inhibit voltage-operated, but not store-operated calcium entry in PC12 cells. *Toxicol* 45:627–632
108. Williams DH, Faulkner DJ (1996) *N*-methylated ageliferins from the sponge *Astrosclera willeyana* from Pohnepi. *Tetrahedron* 52:5381–5390
109. Endo T, Tsuda M, Okada T, Mitsunashi S, Shima H, Kikuchi K, Mikami Y, Fromont J, Kobayashi J (2004) Nagelamides A–H, new dimeric bromopyrrole alkaloids from marine sponge *Agelas* species. *J Nat Prod* 67:1262–1267
110. Araki A, Tsuda M, Kubota T, Mikami Y, Fromont J, Kobayashi J (2007) Nagelamide J, a novel dimeric bromopyrrole alkaloid from a sponge *Agelas* species. *Org Lett* 9:2369–2371
111. Araki A, Kubota T, Tsuda M, Mikami Y, Fromont J, Kobayashi J (2008) Nagelamides K and L, dimeric bromopyrrole alkaloids from sponge *Agelas* species. *Org Lett* 10:2099–2102
112. Yasuda T, Araki A, Kubota T, Ito J, Mikami Y, Fromont J, Kobayashi J (2009) Bromopyrrole alkaloids from marine sponge of the genus *Agelas*. *J Nat Prod* 72:488–491
113. Araki A, Kubota T, Aoyama K, Mikami Y, Fromont J, Kobayashi J (2009) Nagelamides Q and R, novel dimeric bromopyrrole alkaloids from sponges *Agelas* sp. *Org Lett* 11:1785–1788
114. Fattorusso E, Minale L, Sodano G (1970) Aerplysinin-1, a new bromo-compound from *Aplysina aerophoba*. *Chem Commun* 12:751–752
115. Chang CWJ, Weinheimer AJ (1977) 2-Hydroxy, 3,5-dibromo, 4-methoxyphenylacetamide. A dibromotyrosine metabolite from *Psammoposilla purpurea*. *Tetrahedron Lett* 18:4005–4008
116. Capon RJ, Macleod JK (1987) Two epimeric dibromo nitriles from the Australian sponge *Aplysina laevis*. *Austr J Chem* 40:341–346
117. Saeki BM, Granato AC, Berlinck RGS, Magalhães A, Schefer AB, Ferreira AG, Pinheiro US, Hajdu E (2002) Two unprecedented dibromotyrosine-derived alkaloids from the Brazilian endemic marine sponge *Aplysina caissara*. *J Nat Prod* 65:796–799
118. Fulmor W, van Lear GE, Morton GO, Mills RD (1970) Isolation and absolute configuration of the aeroplysinin-1 enantiomeric pair from *Ianthella ardis*. *Tetrahedron Lett* 11:4551–4552
119. Kreuter MH, Bernd A, Holzmann H, Mueller-Klieser W, Maidhof A, Weissmann N, Kljajić Z, Batel R, Schroeder HC, Mueller WEG (1989) Cytostatic activity of aeroplysinin-1 against lymphoma and epithelioma cells. *Z Naturforsch* 44c:680–688
120. Teeyapant R, Woerdenbag HJ, Kreis P, Hacker J, Wray V, Witte L, Proksch P (1993) Antibiotic and cytotoxic activity of brominated compounds from the marine sponge *Verongia aerophoba*. *Z Naturforsch* 48c:939–945

121. Koulman A, Proksch P, Ebel R, Beekman AC, van Uden W, Konings AWT, Pedersen JA, Pras N, Woerdenbag HJ (1996) Cytotoxicity and mode of action of aeroplysinin-1 and a related dienone from the sponge *Aplysina aerophoba*. *J Nat Prod* 59:591–594
122. Rodríguez-Nieto S, González-Iriarte M, Carmona R, Muñoz-Chápuli R, Medina MA, Quesada AR (2002) Antiangiogenic activity of aerplysinin-1, a brominated compound isolated from a marine sponge. *FASEB J* 16:261–263
123. Teeyapant R, Proksch P (1993) Biotransformation of brominated compounds in the marine sponge *Verongia aerophoba* – Evidence for an induced chemical defense? *Naturwissenschaften* 80:369–370
124. Weiss B, Ebel R, Elbraechter M, Kirchner M, Proksch P (1996) Defense metabolites from the marine sponge *Verongia aerophoba*. *Biochem Syst Ecol* 24:1–7
125. Ebel R, Brenzinger M, Kunze A, Gross HJ, Proksch P (1997) Wound activation of protoxins in marine sponge *Aplysina aerophoba*. *J Chem Ecol* 23:1451–1462
126. Thoms C, Ebel R, Proksch P (2006) Activated chemical defense in *Aplysina* sponges revisited. *J Chem Ecol* 32:97–123
127. Putz A, Kloeppel A, Pfannkuchen M, Bruemmer F, Proksch P (2009) Depth-related alkaloid variation in Mediterranean *Aplysina* sponges. *Z Naturforsch* 64c:279–287
128. Hinterding K, Knebel A, Herrlich P, Waldmann H (1998) Synthesis and biological evaluation of aeroplysinin analogues: a new class of receptor tyrosine kinase inhibitors. *Bioorg Med Chem* 6:1153–1162
129. Kreuter MH, Leake RE, Rinaldi F, Mueller-Klieser W, Maidhof A, Mueller WEG, Schroeder HC (1990) Inhibition of intrinsic protein tyrosine kinase activity of EGF-receptor kinase complex from human breast cancer cells by the marine sponge metabolite (+)-aeroplysinin-1. *Comp Biochem Physiol* 97B:151–158
130. Quiñoà E, Crews P (1987) Phenolic constituents of *Psammaphysilla*. *Tetrahedron Lett* 28:3229–3232
131. Rodríguez AD, Akee RK, Scheuer PJ (1987) Two bromotyrosine-cysteine derived metabolites from a sponge. *Tetrahedron Lett* 28:4989–4992
132. Pham NB, Butler MS, Quinn RJ (2000) Isolation of psammaphin A 11'-sulfate and bisaprasin 11'-sulfate from the marine sponge *Aplysinella rhax*. *J Nat Prod* 63:393–395
133. Piña IC, Gautschi JT, Wang GYS, Sanders ML, Schmitz FJ, France D, Cornell-Kennon S, Sambucetti LC, Remiszewski SW, Perez LB, Bair KW, Crews P (2003) Psammaphins from the sponge *Pseudoceratina purpurea*: inhibition of both histone deacetylase and DNA methyltransferase. *J Org Chem* 68:3866–3873
134. Park Y, Liu Y, Hong J, Lee CO, Cho H, Kim DK, Im KS, Jung JH (2003) New bromotyrosine derivatives from an association of two sponges, *Jaspis wondoensis* and *Poecillastra wondoensis*. *J Nat Prod* 66:1495–1498
135. Shinde PB, Lee YM, Dang HT, Hong J, Lee CO, Jung JH (2008) Cytotoxic bromotyrosine derivatives from a two-sponge association of *Jaspis* sp. and *Poecillastra* sp. *Bioorg Med Chem Lett* 18:6414–6418
136. Tabudravu JN, Eijssink VGH, Gooday GW, Jaspars M, Komander D, Legg M, Synstad B, van Aalten DMF (2002) Psammaphin A, a chitinase inhibitor isolated from the Fijian marine sponge *Aplysinella rhax*. *Bioorg Med Chem* 10:1123–1128
137. Shin J, Lee HS, Seo Y, Rho JR, Cho KW, Paul VJ (2000) New bromotyrosine metabolites from the sponge *Aplysinella rhax*. *Tetrahedron* 56:9071–9077
138. Jiang Y, Ahn EY, Ryu SH, Kim DK, Park JS, Yoon HJ, You S, Lee BJ, Lee DS, Jung JH (2004) Cytotoxicity of psammaphin A from a two-sponge association may correlate with the inhibition of DNA replication. *BMC Cancer* 4:70
139. Shim JS, Lee HS, Shin J, Kwon HJ (2004) Psammaphin A, a marine natural product, inhibits aminopeptidase N and suppresses angiogenesis *in vitro*. *Cancer Lett* 203:163–169
140. Kim D, Lee IS, Jung JH, Yang SI (1999) Psammaphin A, a natural bromotyrosine derivative from a sponge, possesses the antibacterial activity against methicillin-resistant *Staphylococcus aureus* and the DNA gyrase-inhibitory activity. *Arch Pharm Res* 22:25–29

141. Mora FD, Jones DK, Desai PV, Patny A, Avery MA, Feller DR, Smillie T, Zhou YD, Nagle DG (2006) Bioassay for the identification of natural product-based activators of peroxisome proliferator-activated receptor- γ (PPAR γ): The marine sponge metabolite psammaplin A activates PPAR γ and induces apoptosis in human breast tumor cells. *J Nat Prod* 69:547–552
142. Godert AM, Angelino N, Woloszynska-Read A, Morey SR, James SR, Karpf AR, Sufrin JR (2006) An improved synthesis of psammaplin A. *Bioorg Med Chem Lett* 16:3330–3333
143. Kim DH, Shin J, Kwon HJ (2007) Psammaplin A is a natural prodrug that inhibits class I histone deacetylase. *Exp Mol Med* 39:47–55
144. Ahn MY, Jung JH, Na YJ, Kim HS (2008) A natural histone deacetylase inhibitor, psammaplin A, induces cell cycle arrest and apoptosis in human endometrial cancer cells. *Gynecol Oncol* 108:27–33
145. McCulloch MWB, Coombs GS, Banerjee N, Bugni TS, Cannon KM, Harper MK, Veltri CA, Virshup DM, Ireland CM (2009) Psammaplin A as a general activator of cell-based signaling assays via HDAC inhibition and studies on some bromotyrosine derivatives. *Bioorg Med Chem* 17:2189–2198
146. Nicolaou KC, Hughes R, Pfefferkorn JA, Barluenga S (2001) Optimization and mechanistic studies of psammaplin A type antibacterial agents active against methicillin-resistant *Staphylococcus aureus* (MRSA). *Chem Eur J* 7:4296–4310
147. Ishibashi M, Tsuda M, Ohizumi Y, Sasaki T, Kobayashi J (1991) Puralidin A, a new cytotoxic bromotyrosine-derived alkaloid from the Okinawan marine sponge *Psammaphysilla purea*. *Experientia* 47:299–300
148. Kobayashi J, Tsuda M, Agemi K, Shigemori H, Ishibashi M, Sasaki T, Mikami Y (1991) Puralidins B and C, new bromotyrosine alkaloids from the Okinawan marine sponge *Psammaphysilla purea*. *Tetrahedron* 47:6617–6622
149. Tsuda M, Shigemori H, Ishibashi M, Kobayashi J (1992) Puralidin D, a new pyridine alkaloid from the Okinawan marine sponge *Psammaphysilla purea*. *Tetrahedron Lett* 33:2597–2598
150. Tsuda M, Shigemori H, Ishibashi M, Kobayashi J (1992) Puralidins E–G, new bromotyrosine alkaloids from the Okinawan marine sponge *Psammaphysilla purea*. *J Nat Prod* 55:1325–1327
151. Kobayashi J, Honma K, Tsuda M, Kosaka T (1995) Lipopuralidins D and E and puralidin H, new bromotyrosine alkaloids from the Okinawan marine sponge *Psammaphysilla purea*. *J Nat Prod* 58:467–470
152. Kobayashi J, Honma H, Sasaki T, Tsuda M (1995) Puralidins J–R, new bromotyrosine alkaloids from the Okinawan marine sponge *Psammaphysilla purea*. *Chem Pharm Bull* 43:403–407
153. Tabudravu JN, Jaspars M (2002) Puralidin S and purpuramine J, bromotyrosine alkaloids from the Fijian marine sponge *Druinella* sp. *J Nat Prod* 65:1798–1801
154. Tilvi S, Rodrigues C, Naik CG, Parameswaran PS, Wahidhulla S (2004) New bromotyrosine alkaloids from the marine sponge *Psammaphysilla purpurea*. *Tetrahedron* 60:10207–10215
155. Schroeder FC, Kau TR, Silver PA, Clardy J (2005) The psammaplysenes, specific inhibitors of FOXO1a nuclear export. *J Nat Prod* 68:574–576
156. Buchanan MS, Carroll AR, Addepalli R, Avery VM, Hooper JNA, Quinn RJ (2007) Psammaplysenes C and D, cytotoxic alkaloids from *Psammoclema* sp. *J Nat Prod* 70:1827–1829
157. Georgiades SN, Clardy J (2005) Total synthesis of psammaplysenes A and B, naturally occurring inhibitors of FOXO1a nuclear export. *Org Lett* 7:4091–4094
158. Hernández-Guerrero CJ, Zubía E, Ortega MJ, Carballo JL (2007) Cytotoxic dibromotyrosine-derived metabolites from the sponge *Aplysina gerardogreeni*. *Bioorg Med Chem* 15:5275–5282
159. Buchanan MS, Carroll AR, Wessling D, Jobling M, Avery VM, Davis RA, Feng Y, Xue Y, Oester L, Fex T, Deinum J, Hooper JNA, Quinn RJ (2008) Clavatadine A, a natural product

- with selective recognition and irreversible inhibition of Factor XIa. *J Med Chem* 51:3583–3587
160. Buchanan MS, Carroll AR, Wessling D, Jobling M, Avery VM, Davis RA, Feng Y, Hooper JNA, Quinn RJ (2009) Clavatadines C–E, guanidine alkaloids from the Australian sponge *Suberea clavata*. *J Nat Prod* 72:973–975
161. Kazlauskas R, Lidgard RO, Murphy PT, Wells RJ (1980) Brominated tyrosine-derived metabolites from the sponge *Ianthella basta*. *Tetrahedron Lett* 21:2277–2280
162. Kazlauskas R, Lidgard RO, Murphy PT, Wells RJ, Blount JF (1981) Brominated tyrosine-derived metabolites from the sponge *Ianthella basta*. *Aust J Chem* 34:765–786
163. Pordesimo EO, Schmitz FJ (1990) New bastadins from the sponge *Ianthella basta*. *J Org Chem* 55:4704–4709
164. Miao S, Andersen RJ, Allen TM (1990) Cytotoxic metabolites from the sponge *Ianthella basta* collected in Papua New Guinea. *J Nat Prod* 53:1441–1446
165. Butler MS, Lim TK, Capon RJ, Hammond LS (1991) The bastadins revisited: new chemistry from the Australian marine sponge *Ianthella basta*. *Aust J Chem* 44:287–296
166. Jaspars M, Rali T, Laney M, Schatzman RC, Diaz MC, Schmitz FJ, Pordesimo EO, Crews P (1994) The search for inosine 5'-phosphate dehydrogenase (IMPDH) inhibitors from marine sponges. Evaluation of the bastadin alkaloids. *Tetrahedron* 50:7367–7374
167. Park SK, Jurek J, Carney JR, Scheuer PJ (1994) Two more bastadins, 16 and 17, from an Indonesian sponge *Ianthella basta*. *J Nat Prod* 57:407–410
168. Franklin MA, Penn SG, Lebrilla CB, Lam TH, Pessah IN, Molinski TF (1996) Bastadin 20 and bastadin *O*-sulfate esters from *Ianthella basta*: novel modulators of the $R_{y1}R$ FKBP12 receptor complex. *J Nat Prod* 59:1121–1127
169. Aoki S, Cho S, Hiramatsu A, Kotoku N, Kobayashi M (2006) Bastadins, cyclic tetramers of brominated-tyrosine derivatives, selectively inhibit the proliferation of endothelial cells. *J Nat Med* 60:231–235
170. Aoki S, Cho S, Ono M, Kuwano T, Nakao S, Kuwano M, Nakagawa S, Gao JQ, Mayumi T, Shibuya M, Kobayashi M (2006) Bastadin 6, a spongean brominated tyrosine derivative, inhibits tumor angiogenesis by inducing selective apoptosis to endothelial cells. *Anticancer Drugs* 17:269–278
171. Ortlepp S, Sjoegren M, Dahlstroem M, Weber H, Ebel R, Edrada RA, Thoms C, Schupp P, Bohlin L, Proksch P (2007) Antifouling activity of bromotyrosine-derived sponge metabolites and synthetic analogues. *Marine Biotechnol* 9:776–785
172. Coll JC, Kearns PS, Rideout JA, Sankar V (2002) Bastadin 21, a novel isobastarane metabolite from the Great Barrier Reef marine sponge *Ianthella quadrangulata*. *J Nat Prod* 65:753–756
173. Greve H, Kehraus S, Krick A, Kelter G, Maier A, Fiebig HH, Wright AD, Koenig GM (2008) Cytotoxic bastadin 24 from the Australian sponge *Ianthella quadrangulata*. *J Nat Prod* 71:309–312
174. Dexter AF, Garson MJ, Hemling ME (1993) Isolation of a novel bastadin from the temperate marine sponge *Ianthella* sp. *J Nat Prod* 56:782–786
175. Carney JR, Scheuer PJ, Kelly-Borges M (1993) A new bastadin from the sponge *Psammaphysilla purpurea*. *J Nat Prod* 56:153–157
176. Venkateswarlu Y, Venkatesham U, Rao MR (1999) Novel bromine-containing constituents of the sponge *Psammaphysilla purpurea*. *J Nat Prod* 62:893–894
177. Reddy AV, Ravinder K, Narasimhulu M, Sridevi A, Satyanarayana N, Kondapi AK, Venkateswarlu Y (2006) New anticancer bastadin alkaloids from the sponge *Dendrilla cactos*. *Bioorg Med Chem* 14:4452–4457
178. Pettit GR, Butler MS, Williams MD, Filiatrault MJ, Pettit RK (1996) Isolation and structure of hemibastadinols 1–3 from the Papua New Guinea marine sponge *Ianthella basta*. *J Nat Prod* 59:927–934
179. Pettit GR, Butler MS, Bass CG, Doubek DL, Williams MD, Schmidt JM, Pettit RK, Hooper JNA, Tackett LP, Filiatrault MJ (1995) Antineoplastic agents, 326. The stereochemistry of

- bastadins 8, 10, and 12 from the Bismarck Archipelago marine sponge *Ianthella basta*. J Nat Prod 58:680–688
180. Segraves EN, Shah RR, Segraves NL, Johnson TA, Whitman S, Sui JK, Kenyon VA, Cichewicz RH, Crews P, Holman TR (2004) Probing the activity differences of simple and complex brominated aryl compounds against 15-soyabean, 15-human, and 12-human lipoxygenase. J Med Chem 47:4060–4065
181. Mack MM, Molinski TF, Buck ED, Pessah IN (1994) Novel modulators of skeletal muscle FKBP12/calcium channel complex from *Ianthella basta*. J Biol Chem 269:23236–23249
182. Chen L, Molinski TF, Pessah IN (1999) Bastadin 10 stabilizes the open conformation of the ryanodine-sensitive Ca^{2+} channel in an FKBP12-dependent manner. J Biol Chem 274:32603–32612
183. Assmann M, Lichte E, Pawlik JR, Koeck M (2000) Chemical defenses of the Caribbean sponges *Agelas wiedenmayeri* and *Agelas conifera*. Mar Ecol Prog Ser 207:255–262
184. Thoms C, Wolff M, Padmakumar K, Ebel R, Proksch P (2004) Chemical defense of Mediterranean *Aplysina cavernicola* and *Aplysina aerophoba*. Z Naturforsch 59c:113–122
185. Nakao Y, Yeung BKS, Yoshida WY, Scheuer PJ (1995) Kapakahine B: a cyclic hexapeptide with an α -carboline ring system from the marine sponge *Cribrochalina olemda*. J Am Chem Soc 117:8271–8272
186. Yeung BKS, Nakao Y, Kinnel RB, Carney JR, Yoshida WY, Scheuer PJ, Kelly-Borges M (1996) The kapakahines, cyclic peptides from the marine sponge *Cribrochalina olemda*. J Org Chem 61:7168–7173
187. Nakao Y, Kuo J, Yoshida WY, Kelly M, Scheuer PJ (2003) More kapakahines from the marine sponge *Cribrochalina olemda*. Org Lett 5:1387–1390
188. Matsunaga S, Fusetani N, Konosu S (1984) Bioactive marine metabolites VI. Structure elucidation of discodermin A, and antimicrobial peptide from the marine sponge *Discodermia kiiensis*. Tetrahedron Lett 25:5165–5168
189. Matsunaga S, Fusetani N, Konosu S (1985) Bioactive marine metabolites IV. Isolation and the amino acid composition of discodermin A, an antimicrobial peptide, from the marine sponge *Discodermia kiiensis*. J Nat Prod 48:236–241
190. Matsunaga S, Fusetani N, Konosu S (1985) Bioactive marine metabolites VII. Structures of discodermins B, C, and D, antimicrobial peptides from the marine sponge *Discodermia kiiensis*. Tetrahedron Lett 26:855–856
191. Ryu G, Matsunaga S, Fusetani N (1994) Discodermin E, a cytotoxic and antimicrobial tetradecapeptide, from the marine sponge *Discodermia kiiensis*. Tetrahedron Lett 35:8251–8254
192. Ryu G, Matsunaga S, Fusetani N (1994) Discodermins F–H, cytotoxic and antimicrobial tetradecapeptides, from the marine sponge *Discodermia kiiensis*: structure revision of discodermins A–D. Tetrahedron 50:13409–13416
193. Gunasekera SP, Pomponi SA, McCarthy PJ (1994) Discobahamins A and B, new peptides from the Bahamian deep water marine sponge *Discodermia* sp. J Nat Prod 57:79–83
194. Gulavita NK, Gunasekera SP, Pomponi SA, Robinson EV (1992) Polydiscamide A: a new bioactive depsipeptide from the marine sponge *Discodermia* sp. J Org Chem 57:1767–1772
195. Feng Y, Carroll AR, Pass DM, Archbold JK, Avery VM, Quinn RJ (2008) Polydiscamides B–D from a marine sponge *Ircinia* sp. as potent human sensory neuron-specific G protein coupled receptor agonists. J Nat Prod 71:8–11
196. Li H, Matsunaga S, Fusetani N (1995) Halicyclindramides A–C, antifungal and cytotoxic depsipeptides from the marine sponge *Halichondria cylindrata*. J Med Chem 38:338–343
197. Li H, Matsunaga S, Fusetani N (1996) Halicyclindramides D and E, antifungal peptides from the marine sponge *Halichondria cylindrata*. J Nat Prod 59:163–166
198. Dong X, Han S, Zylka MJ, Simon MI, Anderson DJ (2001) A diverse family of GPCRs expressed in specific subsets of nociceptive sensory neurons. Cell 106:619–632
199. Simonin F, Kieffer BL (2002) Two faces for an opioid peptide—and more receptors for pain research. Nat Neurosci 5:185–186

200. Zabriskie TM, Klocke JA, Ireland CM, Marcus AH, Molinski TF, Faulkner DJ, Xu C, Clardy J (1986) Jaspamide, a modified peptide from a *Jaspis* sponge, with insecticidal and antifungal activity. *J Am Chem Soc* 108:3123–3124
201. Crews P, Manes LV, Boehler M (1986) Jaspaklinolide, a cyclodepsipeptide from the marine sponge, *Jaspis* sp. *Tetrahedron Lett* 27:2797–2800
202. Crews P, Farias JJ, Emrich R, Keifer PA (1994) Milnamide A, an unusual cytotoxic tripeptide from the marine sponge *Auletta* cf. *constricta*. *J Org Chem* 59:2932–2934
203. Talpir R, Benayahu Y, Kashman Y, Pannell L, Schleyer M (1994) Hemiasterlin and geodiamolide TA; two new cytotoxic peptides from the marine sponge *Hemiasterella minor* (Kirkpatrick). *Tetrahedron Lett* 35:4453–4456
204. Chan WR, Tinto WF, Manchand PS, Todaro LJ (1987) Stereostructures of geodiamolides A and B, novel cyclodepsipeptides from the marine sponge *Geodia* sp. *J Org Chem* 52:3091–3093
205. Scott VR, Boehme R, Matthews TR (1998) New class of antifungal agents: jaspaklinolide, a cyclodepsipeptide from the marine sponge, *Jaspis* species. *Antimicrob Agents Chemother* 32:1154–1157
206. Inman W, Crews P (1989) Novel marine sponge derived amino acids, 8. conformational analysis of jaspaklinolide. *J Am Chem Soc* 111:2822–2829
207. Zampella A, Giannini C, Debitus C, Roussakis C, D'Auria MV (1999) New jaspamide derivatives from the marine sponge *Jaspis splendens* collected in Vanuatu. *J Nat Prod* 62:332–334
208. Gala F, D'Auria MV, De Marino S, Zollo F, Smith CD, Copper JE, Zampella A (2007) New jaspamide derivatives with antimicrofilament activity from the sponge *Jaspis splendens*. *Tetrahedron* 63:5212–5219
209. Gala F, D'Auria MV, De Marino S, Sepe V, Zollo F, Smith CD, Copper JE, Zampella A (2008) Jaspamides H–L, new actin-targeting depsipeptides from the sponge *Jaspis splendens*. *Tetrahedron* 64:7127–7130
210. Gala F, D'Auria MV, De Marino S, Sepe V, Zollo F, Smith CD, Keller SN, Zampella A (2009) Jaspamides M–P: new tryptophan modified jaspamide derivatives from the sponge *Jaspis splendens*. *Tetrahedron* 65:51–56
211. Ebada SS, Wray V, de Voogd NJ, Deng Z, Lin W, Proksch P (2009) Two new jaspamide derivatives from the marine sponge *Jaspis splendens*. *Mar Drugs* 7:435–444
212. Kahn M, Nakanishi H, Su T, Lee JH, Johnson M (1991) Design and synthesis of nonpeptide mimetics of jaspamide. *Int J Pept Protein Res* 38:324–334
213. Marimganti S, Wieneke R, Geyer A, Maier ME (2007) Synthesis and conformational analysis of geodiamolide analogues. *Eur J Org Chem* 2007:2779–2790
214. de Silva ED, Andersen RJ, Allen TM (1990) Geodiamolides C to F, new cytotoxic cyclodepsipeptides from the marine sponge *Pseudaxinyssa* sp. *Tetrahedron Lett* 31:489–492
215. Coleman JE, de Silva ED, Kong F, Andersen RJ (1995) Cytotoxic peptides from the marine sponge *Cymbastela* sp. *Tetrahedron* 51:10653–10662
216. Tinto WF, Lough AJ, McLean S, Reynolds WF, Yu M, Chan WR (1998) Geodiamolides H and I, further cyclodepsipeptides from the marine sponge *Geodia* sp. *Tetrahedron* 54:4451–4458
217. D'Auria MV, Paloma LG, Minale L, Zampella A, Debitus C, Perez J (1995) Neosiphoniamolide A, a novel cyclodepsipeptide with antifungal activity from the marine sponge *Neosiphonia superstes*. *J Nat Prod* 58:121–123
218. Coleman JE, van Soest R, Andersen RJ (1999) New geodiamolides from the sponge *Cymbastela* sp. collected in Papua New Guinea. *J Nat Prod* 62:1137–1141
219. Kunze B, Jansen R, Sasse F, Hoefle G, Reichenbach H (1995) Chondramides A–D, new antifungal and cytostatic depsipeptides from *Chondromyces crocatus* (Myxobacteria) Production, physico-chemical and biological properties. *J Antibiot* 48:1262–1266
220. Gamble WR, Durso NA, Fuller RW, Westergaard CK, Johnson TR, Sackett DL, Hamel E, Cardellina JH II, Boyd MR (1999) Cytotoxic and tubulin-interactive hemiasterlins from *Auletta* sp. and *Siphonochalina* sp. sponges. *Bioorg Med Chem* 7:1611–1615

221. Coleman JE, Patrick BO, Andersen RJ, Rettig SJ (1996) Hemiasterlin methyl ester. *Acta Cryst Sec C* C52:1525–1527
222. Anderson HJ, Coleman JE, Andersen RJ, Roberge M (1997) Cytotoxic peptides hemiasterlin, hemiasterlin A and hemiasterlin B induce mitotic arrest and abnormal spindle formation. *Cancer Chemother Pharmacol* 39:223–226
223. Nieman JA, Coleman JE, Wallace DJ, Piers E, Lim LY, Roberge M, Andersen RJ (2003) Synthesis and antimitotic/cytotoxic activity of hemiasterlin analogues. *J Nat Prod* 66:183–199
224. Zask A, Birnberg G, Cheung K, Kaplan J, Niu C, Norton E, Suayan R, Yamashita A, Cole D, Tang Z, Krishnamurthy G, Williamson R, Khafizova G, Musto S, Hernandez R, Annable T, Yang X, Discafani C, Beyer C, Greenberger LM, Loganzo F, Ayral-Kaloustian S (2004) Synthesis and biological activity of analogues of the antimicrotubule agent N, β , β -trimethyl-L-phenylalanyl-N1-[(1 S,2E)-3-carboxy-1-isopropylbut-2-enyl]-N1,3-dimethyl-L-valinamide (HTI-286). *J Med Chem* 47:4774–4786
225. Zask A, Birnberg G, Cheung K, Kaplan J, Niu C, Norton E, Yamashita A, Beyer C, Krishnamurthy G, Greenberger LM, Loganzo F, Ayral-Kaloustian S (2004) D-piece modifications of the hemiasterlin analogue HTI-286 produce potent tubulin inhibitors. *Bioorg Med Chem Lett* 14:4353–4358
226. Yamashita A, Norton EB, Kaplan JA, Niu C, Loganzo F, Hernandez R, Beyer CF, Annable T, Musto S, Discafani C, Zask A, Ayral-Kaloustian S (2004) Synthesis and activity of novel analogues of hemiasterlin as inhibitors of tubulin polymerization modification of the A segment. *Bioorg Med Chem Lett* 14:5317–5322
227. Loganzo F, Discafani CM, Annable T, Beyer C, Musto S, Hari M, Tan X, Hardy C, Hernandez R, Baxter M, Singanallore T, Khafizova G, Poruchynsky MS, Fojo T, Nieman JA, Ayral-Kaloustian S, Zask A, Andersen RJ, Greenberger LM (2003) Antimicrotubule agent that circumvents P-glycoprotein-mediated resistance *in vitro* and *in vivo*. *Cancer Res* 63:1838–1845
228. Ratain MJ, Undevia S, Janisch L, Roman S, Mayer P, Buckwalter M, Foss D, Hamilton BL, Fischer J, Bukowski RM (2003) Phase 1 and pharmacological study of HTI-286, a novel antimicrotubule agent: correlation of neutropenia with time above a threshold serum concentration. *Proc Am Soc Clin Oncol* 22:516
229. Hadaschik BA, Ettinger S, Sowery RD, Zoubeidi A, Andersen RJ, Roberge M, Gleave ME (2008) Targeting prostate cancer with HTI-286, a synthetic analogue of the marine sponge product hemiasterlin. *Int J Cancer* 122:2368–2376
230. Kobayashi M, Aoki S, Ohyabu N, Kurosu M, Wang W, Kitagawa I (1994) Arenastatin A, a potent cytotoxic depsipeptide from the Okinawan marine sponge *Dysidea arenaria*. *Tetrahedron Lett* 35:7969–7972
231. Kobayashi M, Kurosu M, Ohyabu N, Wang W, Fujii S, Kitagawa I (1994) The absolute stereostructure of arenastatin A, a potent cytotoxic depsipeptide from the Okinawan marine sponge *Dysidea arenaria*. *Chem Pharm Bull* 42:2196–2198
232. Kobayashi M, Kurosu M, Wang W, Kitagawa I (1994) A total synthesis of arenastatin A, an extremely potent cytotoxic depsipeptide, from the Okinawan marine sponge *Dysidea arenaria*. *Chem Pharm Bull* 42:2394–2396
233. Carroll AR, Pierens GK, Fechner G, de Almeida LP, Ngo A, Simpson M, Hyde E, Hooper JNA, Bostroem SL, Musil D, Quinn RJ (2002) Dysinosin A: a novel inhibitor of factor VIIa and thrombin from a new genus and species of Australian sponge of the family Dysideidae. *J Am Chem Soc* 124:13340–13341
234. Carroll AR, Buchanan MS, Edser A, Hyde E, Simpson M, Quinn RJ (2004) Dysinosins B–D, inhibitors of factor VIIa and thrombin from the Australian sponge *Lamellodysidea chlorea*. *J Nat Prod* 67:1291–1294
235. Ishida K, Okita Y, Matsuda H, Okino T, Murakami M (1999) Aeruginosins, protease inhibitors from the cyanobacterium *Microcystis aeruginosa*. *Tetrahedron* 55:10971–10988

236. Matsuda H, Okino T, Murakami M, Yamaguchi K (1996) Aeruginosins 102-A and B, new thrombin inhibitors from the cyanobacterium *Microcystis viridis* (NIES-102). *Tetrahedron* 52:14501–14506
237. Murakami M, Ishida K, Okino T, Okita Y, Matsuda H, Yamaguchi K (1995) Aeruginosins 98-A and B, trypsin inhibitors from the blue-green alga *Microcystis aeruginosa* (NIES-98). *Tetrahedron Lett* 36:2785–2788
238. Pettit GR, Cichacz Z, Barkoczy J, Dorsaz A, Herald DL, Williams MD, Doubek DL, Schmidt JM, Tackett LP, Brune DC, Cerny RL, Hooper JNA, Bakus GJ (1993) Isolation and structure of the marine sponge cell growth inhibitory cyclic peptide phakellistatin 1. *J Nat Prod* 56:260–267
239. Pettit GR, Tan R, Williams MD, Tackett L, Schmidt JM, Cerny RL, Hooper JNA (1993) Isolation and structure of phakellistatin 2 from the Eastern Indian Ocean marine sponge *Phakellia carteri*. *Bioorg Med Chem Lett* 3:2869–2874
240. Pettit GR, Tan R, Herald DL, Cerny RL, Williams MD (1994) Antineoplastic agents. 277. Isolation and structure of phakellistatin 3 and isophakellistatin 3 from a Republic of Comoros marine sponge. *J Org Chem* 59:1593–1595
241. Pettit GR, Xu J, Cichacz ZA, Williams MD, Dorsaz A, Brune DC, Boyd MR, Cerny RL (1994) Antineoplastic agents 315. Isolation and structure of the marine sponge cancer cell growth inhibitor phakellistatin 5. *Bioorg Med Chem Lett* 4:2091–2096
242. Pettit GR, Xu J, Cichacz ZA, Williams MD, Chapuis J, Cerny RL (1994) Antineoplastic agents 323. Isolation and structure of phakellistatin 6 from a Chuuk Archipelago marine sponge. *Bioorg Med Chem Lett* 4:2677–2682
243. Pettit GR, Xu J, Dorsaz A, Williams MD, Boyd MR, Cerny RL (1995) Isolation and structure of the human cancer cell growth inhibitory cyclic decapeptides phakellistatins 7, 8 and 9. *Bioorg Med Chem Lett* 5:1339–1344
244. Pettit GR, Tan R, Ichihara Y, Williams MD, Doubek DL, Tackett LP, Schmidt JM, Cerny RL, Boyd MR, Hooper JNA (1995) Antineoplastic agents, 325. Isolation and structure of the human cancer cell growth inhibitory cyclic octapeptides phakellistatin 10 and 11 from *Phakellia* sp. *J Nat Prod* 58:961–965
245. Pettit GR, Tan R (2003) Antineoplastic agents 390. Isolation and structure of phakellistatin 12 from a Chuuk Archipelago marine sponge. *Bioorg Med Chem Lett* 13:685–688
246. Li W, Yi Y, Wu H, Xu Q, Tang H, Zhou D, Lin H, Wang Z (2003) Isolation and structure of the cytotoxic cycloheptapeptide phakellistatin 13. *J Nat Prod* 66:146–148
247. Pettit GR, Tan R (2005) Isolation and structure of phakellistatin 14 from the Western Pacific marine sponge *Phakellia* sp. *J Nat Prod* 68:60–63
248. Tabudravu JN, Jaspars M, Morris LA, Kettenes-van den Bosch JJ, Smith N (2002) Two distinct conformers of the cyclic heptapeptide phakellistatin 2 isolated from the Fijian marine sponge *Stylotella aurantium*. *J Org Chem* 67:8593–8601
249. Kobayashi J, Tsuda M, Nakamura T, Mikami Y, Shigemori H (1993) Hymenamides A and B, new proline-rich cyclic heptapeptides from the Okinawan marine sponge *Hymeniacidon* sp. *Tetrahedron* 49:2391–2402
250. Tsuda M, Shigemori H, Mikami Y, Kobayashi J (1993) Hymenamides C–E, new cyclic heptapeptides with two proline residues from the Okinawan marine sponge *Hymeniacidon* sp. *Tetrahedron* 49:6785–6796
251. Kobayashi J, Nakamura T, Tsuda M (1996) Hymenamide F, new cyclic heptapeptide from marine sponge *Hymeniacidon* sp. *Tetrahedron* 52:6355–6360
252. Tsuda M, Sasaki T, Kobayashi J (1994) Hymenamides G, H, J, and K, four new cyclid octapeptides from the Okinawan marine sponge *Hymeniacidon* sp. *Tetrahedron* 50:4667–4680
253. Pettit GR, Clewlow PJ, Dufresne C, Doubek DL, Cerny RL, Ruetzler K (1990) Antineoplastic agents. 193. Isolation and structure of the cyclic peptide hymenistatin 1. *Can J Chem* 68:708–711

254. Cebrat M, Wieczorek Z, Siemion IZ (1996) Immunosuppressive activity of hymenistatin I. *Peptides* 17:191–196
255. Pettit GR, Gao F, Cerny RL, Doubek DL, Tackett LP, Schmidt JM, Chapuis J (1994) Antineoplastic agents. 278. Isolation and structure of axinastatins 2 and 3 from a Western Caroline Island marine sponge. *J Med Chem* 37:1165–1168
256. Pettit GR, Gao F, Schmidt JM, Chapuis J (1994) Isolation and structure of axinastatin 5 from a Republic of Comoros marine sponge. *Bioorg Med Chem Lett* 4:2935–2940
257. Randazzo A, Dal Piaz F, Orrù S, Debitus C, Roussakis C, Pucci P, Gomez-Paloma L (1998) Axinellins A and B: new proline-containing antiproliferative cyclopeptides from the Vanuatu sponge *Axinella carteri*. *Eur J Org Chem* 1998:2659–2665
258. Tabudravu JN, Morris LA, Kettenes-van den Bosch JJ, Jaspars M (2002) Axinellin C, a proline-rich cyclic octapeptide isolated from the Fijian marine sponge *Stylotella aurantium*. *Tetrahedron* 58:7863–7868
259. Schmidt G, Grube A, Koeck M (2007) Styliissamides A–D – new proline-containing cyclic heptapeptides from the marine sponge *Stylissa caribica*. *Eur J Org Chem* 2007:4103–4110
260. Mohammed R, Peng J, Kelly M, Hamann MT (2006) Cyclic heptapeptides from the Jamaican sponge *Stylissa caribica*. *J Nat Prod* 69:1739–1744
261. Rashid MA, Gustafson KR, Boswell JL, Boyd MR (2000) Haligramides A and B, two new cytotoxic hexapeptides from the marine sponge *Haliclona nigra*. *J Nat Prod* 63:956–959
262. Randazzo A, Bifulco G, Giannini C, Bucci M, Debitus C, Cirino G, Gomez-Paloma L (2001) Halipeptins A and B: two novel potent anti-inflammatory cyclic depsipeptides from the Vanuatu marine sponge *Haliclona* sp. *J Am Chem Soc* 123:10870–10876
263. Nicolaou KC, Schlawe D, Kim DW, Longbottom DA, de Noronha RG, Lizos DE, Manam RR, Faulkner DJ (2005) Total synthesis of halipeptins: isolation of halipeptin D and synthesis of oxazoline halipeptin analogues. *Chem Eur J* 11:6197–6211
264. Vicente J, Vera B, Rodríguez AD, Rodríguez-Escudero I, Raptis RG (2009) Euryjanicin A: a new cycloheptapeptide from the Caribbean marine sponge *Prosuberites laughlini*. *Tetrahedron Lett* 50:4571–4574
265. Vera B, Vicente J, Rodríguez AD (2009) Isolation and structural elucidation of euryjanicins B–D, proline-containing cycloheptapeptides from the Caribbean marine sponge *Prosuberites laughlini*. *J Nat Prod* 72:1555–1562
266. Matsunaga S, Fusetani N, Hashimoto K, Waelchli M (1989) Theonellamide F. A novel antifungal bicyclic peptide from a marine sponge *Theonella* sp. *J Am Chem Soc* 111:2582–2588
267. Matsunaga S, Fusetani N (1995) Theonellamides A–E, cytotoxic bicyclic peptides, from a marine sponge *Theonella* sp. *J Org Chem* 60:1177–1181
268. Hamada T, Sugawara T, Matsunaga S, Fusetani N (1994) Polytheonamides, unprecedented highly cytotoxic polypeptides, from the marine sponge *Theonella swinhoei* 1. Isolation and component amino acids. *Tetrahedron Lett* 35:719–720
269. Hamada T, Matsunaga S, Yano G, Fusetani N (2005) Polytheonamides A and B, highly cytotoxic, linear polypeptides with unprecedented structural features, from the marine sponge, *Theonella swinhoei*. *J Am Chem Soc* 127:110–118
270. Fusetani N, Matsunaga S (1990) Cyclotheonamides, potent thrombin inhibitors, from a marine sponge *Theonella* sp. *J Am Chem Soc* 112:7053–7054
271. Nakao Y, Matsunaga S, Fusetani N (1995) Three more cyclotheonamides, C, D, and E, potent thrombin inhibitors from the marine sponge *Theonella swinhoei*. *Bioorg Med Chem* 3:1115–1122
272. Nakao Y, Oku N, Matsunaga S, Fusetani N (1998) Cyclotheonamides E2 and E3, new potent serine protease inhibitors from the marine sponge of the genus *Theonella*. *J Nat Prod* 61:667–670
273. Murakami Y, Takei M, Shindo K, Kitazume C, Tanaka J, Higa T, Fukamachi H (2002) Cyclotheonamides E4 and E5, new potent tryptase inhibitors from an *Ircinia* species of sponge. *J Nat Prod* 65:259–261

274. Nakao Y, Masuda A, Matsunaga S, Fusetani N (1999) Pseudotheonamides, serine protease inhibitors from the marine sponge *Theonella swinhoei*. *J Am Chem Soc* 121:2425–2431
275. Kitagawa I, Kobayashi M, Lee NK, Shibuya H, Kawata Y, Sakiyama F (1986) Structure of theonellapeptolide Id, a new bioactive peptolide from an Okinawan marine sponge, *Theonella* sp. *Chem Pharm Bull* 34:2664–2667
276. Kitagawa I, Lee NK, Kobayashi M, Shibuya H (1987) Structure of theonellapeptolide Ie, a new tridecapeptide lactone from an Okinawan marine sponge, *Theonella* sp. (Theonellidae). *Chem Pharm Bull* 35:2129–2132
277. Kitagawa I, Lee NK, Kobayashi M, Shibuya H (1991) Marine natural products. XXV. Biologically active tridecapeptide lactones from the Okinawan marine sponge *Theonella swinhoei* (Theonellidae) (1). Structure of theonellapeptolide Id. *Tetrahedron* 47:2169–2180
278. Kobayashi M, Lee NK, Shibuya H, Momose T, Kitagawa I (1991) Marine natural products. XXVL. Biologically active tridecapeptide lactones from the Okinawan marine sponge *Theonella swinhoei* (Theonellidae). (2). Structures of theonellapeptolides Ia, Ib, Ic, and Ie. *Chem Pharm Bull* 39:1177–1184
279. Tsuda M, Shimbo K, Kubota T, Mikami Y, Kobayashi J (1999) Two theonellapeptolide congeners from marine sponge *Theonella* sp. *Tetrahedron* 55:10305–10314
280. Kobayashi M, Kanzaki K, Katayama S, Ohashi K, Okada H, Ikegami S, Kitagawa I (1994) Marine natural products. XXXIII. Theonellapeptolide IId, a new tridecapeptide lactone from the Okinawan marine sponge *Theonella swinhoei*. *Chem Pharm Bull* 42:1410–1415
281. Roy MC, Ohtani II, Ichiba T, Tanaka J, Satari R, Higa T (2000) New cyclic peptides from the Indonesian sponge *Theonella swinhoei*. *Tetrahedron* 56:9079–9092
282. Roy MC, Ohtani II, Tanaka J, Higa T, Satari R (1999) Barangamide A, a new cyclic peptide from the Indonesian sponge *Theonella swinhoei*. *Tetrahedron Lett* 40:5373–5376
283. Nakamura H, Kobayashi J, Nakamura Y, Ohizumi Y, Kondo T, Hirata Y (1986) Theonellamine B, a novel peptidal Na⁺, K⁺-ATPase inhibitor from an Okinawan marine sponge of the genus *Theonella*. *Tetrahedron Lett* 27:4319–4322
284. Li S, Dumdei EJ, Blunt JW, Munro MHG, Robinson WT, Pannell LK (1998) Theonella-peptolide IIIe, a new cyclic peptolide from the New Zealand deep water sponge *Lamellomorpha strongylata*. *J Nat Prod* 61:724–728
285. Ford PW, Gustafson KR, McKee MC, Shigematsu N, Maurizi LK, Pannell LK, Williams DE, de Silva D, Lassota P, Allen TM, van Soest R, Andersen RJ, Boyd MR (1999) Papuamides A–D, HIV-inhibitory and cytotoxic depsipeptides from the sponges *Theonella mirabilis* and *Theonella swinhoei* collected in Papua New Guinea. *J Am Chem Soc* 121:5899–5909
286. Plaza A, Gustchina E, Baker HL, Kelly M, Bewley CA (2007) Mirabamides A–D, depsipeptides from the sponge *Siliquariaspongia mirabilis* that inhibit HIV-1 fusion. *J Nat Prod* 70:1753–1760
287. Ratnayake AS, Bugni TS, Feng X, Harper MK, Skalicky JJ, Mohammed KA, Andjelic CD, Barrows LR, Ireland CM (2006) Theonpauamide, a cyclic depsipeptide from a Papua New Guinea lithistid sponge *Theonella swinhoei*. *J Nat Prod* 69:1582–1586
288. Plaza A, Bifulco G, Keffer JL, Lloyd JR, Baker HL, Bewley CA (2009) Celebesides A–C and theonpauamides B–D, depsipeptides from an Indonesian sponge that inhibit HIV-1 entry. *J Org Chem* 74:504–512
289. Gulavita NK, Pomponi SA, Wright AE, Yarwood D, Silis MA (1994) Isolation and structure elucidation of perthamide B, a novel peptide from the sponge *Theonella* sp. *Tetrahedron Lett* 35:6815–6818
290. Festa C, de Marino S, Sepe V, Monti MC, Luciano P, D'Auria MV, Débitus C, Bucci M, Vellecco V, Zampella A (2009) Perthamides C and D, two new potent anti-inflammatory cyclopeptides from a Solomon lithistid sponge *Theonella swinhoei*. *Tetrahedron* 65:10424–10429
291. Bewley CA, Debitus C, Faulkner DJ (1994) Microsclerodermins A and B. Antifungal cyclic peptides from the lithistid sponge *Microscleroderma* sp. *J Am Chem Soc* 116:7631–7636

292. Schmidt EW, Faulkner DJ (1998) Microsclerodermins C–E, antifungal cyclic peptides from the lithistid marine sponges *Theonella* sp. and *Microscleroderma* sp. *Tetrahedron* 54:3043–3056
293. Qureshi A, Colin PL, Faulkner DJ (2000) Microsclerodermins F–I, antitumor and antifungal cyclic peptides from the lithistid sponge *Microscleroderma* sp. *Tetrahedron* 56:3679–3685
294. Fusetani N, Warabi K, Nogata Y, Nakao Y, Matsunaga S, van Soest RRM (1999) Koshikamide A₁, a new cytotoxic linear peptide isolated from a marine sponge, *Theonella* sp. *Tetrahedron Lett* 40:4687–4690
295. Araki T, Matsunaga S, Fusetani N (2005) Koshikamide A₂, a cytotoxic linear undecapeptide isolated from a marine sponge of *Theonella* sp. *Biosci Biotechnol Biochem* 69:1318–1322
296. Araki T, Matsunaga S, Nakao Y, Furihata K, West L, Faulkner DJ, Fusetani N (2008) Koshikamide B, a cytotoxic peptide lactone from a marine sponge *Theonella* sp. *J Org Chem* 73:7889–7894
297. Kobayashi J, Sato M, Ishibashi M, Shigemori H, Nakamura T, Ohizumi Y (1991) Keramamide A, a novel peptide from the Okinawan marine sponge *Theonella* sp. *J Chem Soc Perkin Trans 1*:2609–2611
298. Kobayashi J, Itagaki F, Shigemori H, Ishibashi M, Takahashi K, Ogura M, Nagasawa S, Nakamura T, Hirota H, Ohta T, Nozoe S (1991) Keramamides B–D: novel peptides from the Okinawan marine sponge *Theonella* sp. *J Am Chem Soc* 113:7812–7813
299. Itagaki F, Shigemori H, Ishibashi M, Nakamura T, Sasaki T, Kobayashi J (1992) Keramamide F, a new thiazole-containing peptide from the Okinawan marine sponge *Theonella* sp. *J Org Chem* 57:5540–5542
300. Kobayashi J, Itagaki F, Shigemori H, Takao T, Shimonishi Y (1995) Keramamides E, G, H, and J, new cyclic peptides containing an oxazole or a thiazole ring from a *Theonella* sponge. *Tetrahedron* 51:2525–2532
301. Uemoto H, Yahiro Y, Shigemori H, Tsuda M, Takao T, Shimonishi Y, Kobayashi J (1998) Keramamides K and L, new cyclic peptides containing unusual tryptophan residue from *Theonella* sponge. *Tetrahedron* 54:6719–6724
302. Tsuda M, Ishiyama H, Masuko K, Takao T, Shimonishi Y, Kobayashi J (1999) Keramamides M and N, two new cyclic peptides with a sulfate ester from *Theonella* sponge. *Tetrahedron* 55:12543–12548
303. Zampella A, D'Auria MV, Paloma LG, Casapullo A, Minale L, Debitus C, Henin Y (1996) Callipeltin A, an anti-HIV cyclic depsipeptide from the New Caledonian Lithistida sponge *Callipelta* sp. *J Am Chem Soc* 118:6202–6209
304. D'Auria MV, Zampella A, Paloma LG, Minale L, Debitus C, Roussakis C, Le Bert V (1996) Callipeltins B and C; bioactive peptides from a marine Lithistida sponge *Callipelta* sp. *Tetrahedron* 52:9589–9596
305. Zampella A, Randazzo A, Borbone N, Luciani S, Trevisi L, Debitus C, D'Auria MV (2002) Isolation of callipeltins A–C and of two new open-chain derivatives of callipeltin A from the marine sponge *Latrunculia* sp. A revision of the stereostructure of callipeltins. *Tetrahedron Lett* 43:6163–6166
306. Sepe V, D'Orsi R, Borbone N, D'Auria MV, Bifulco G, Monti MC, Catania A, Zampella A (2006) Callipeltins F–I: new antifungal peptides from the marine sponge *Latrunculia* sp. *Tetrahedron* 62:833–840
307. D'Auria MV, Sepe V, D'Orsi R, Bellotta F, Debitus C, Zampella A (2007) Isolation and structural elucidation of callipeltins J–M: antifungal peptides from the marine sponge *Latrunculia* sp. *Tetrahedron* 63:131–140
308. Trevisi L, Bova S, Cargnelli G, Danieli-Betto D, Floreani M, Germinario E, D'Auria MV, Luciani S (2000) Callipeltin A, a cyclic depsipeptide inhibitor of the cardiac sodium-calcium exchanger and positive inotropic agent. *Biochem Biophys Res Commun* 279:219–222
309. Trevisi L, Cargnelli G, Ceolotto G, Papparella I, Semplicini A, Zampella A, D'Auria MV, Luciani S (2004) Callipeltin A: sodium ionophore effect and tension development in vascular smooth muscle. *Biochem Pharmacol* 68:1331–1338

310. Acevedo CM, Kogut EF, Lipton MA (2001) Synthesis and analysis of the sterically constrained L-glutamine analogues (3 *S*,4*R*)-3,4-dimethyl-L-glutamine and (3 *S*,4*R*)-3,4-dimethyl-L-pyroglutamic acid. *Tetrahedron* 57:6353–6359
311. Chandrasekhar S, Ramachandar T, Venkateswara Rao B (2001) Chiron approach to callipeltin A: first synthesis of fully protected (2*R*,3*R*,4 *S*)-4,7-diamino-2,3-dihydroxyheptanoic acid. *Tetrahedron: Assymetry* 12:2315–2321
312. Guerlavais V, Carroll PJ, Joullié MM (2002) Progress towards the total synthesis of callipeltin A. *Asymmetric synthesis of (2*R*,3*R*,4 *S*)-3-hydroxy-2,4,6-trimethylheptanoic acid*. *Tetrahedron: Assymetry* 13:675–680
313. Okamoto N, Hara O, Makino K, Hamada Y (2002) Diastereoselective synthesis of all stereoisomers of β -methoxytyrosine, a component of papuamides. *J Org Chem* 67:9210–9215
314. Zampella A, Sepe V, Luciano P, Bellotta F, Monti MC, D'Auria MV, Jepsen T, Petek S, Adeline M, Laprêve O, Aubertin A, Debitus C, Poupat C, Ahond A (2008) Homophymine A, an anti-HIV cyclodepsipeptide from the sponge *Homophymia* sp. *J Org Chem* 73:5319–5327
315. Zampella A, Sepe V, Bellotta F, Luciano P, D'Auria MV, Cresteil T, Debitus C, Petek S, Poupat C, Ahond A (2009) Homophymines B–E and A1–E1, a family of bioactive cyclodepsipeptides from the sponge *Homophymia* sp. *Org Biomol Chem* 7:4037–4044
316. Nakao Y, Yoshida S, Matsunaga S, Shindoh N, Terada Y, Nagai K, Yamashita JK, Ganesan A, van Soest RWM, Fusetani N (2006) Azumamides A–E: histone deacetylase inhibitory cyclic tetrapeptides from the marine sponge *Mycale izuensis*. *Angew Chem Int Ed* 45:7553–7557
317. Yoshida M, Kijima M, Akita M, Beppu T (1990) Potent and specific inhibition of mammalian histone deacetylase both *in vivo* and *in vitro* by trichostatin A. *J Biol Chem* 265:17174–17179
318. Finnin MS, Donigian JR, Cohen A, Richon VM, Rifkind RA, Marks PA, Breslow R, Pavletich NP (1999) Structures of a histone deacetylase homologue bound to the TSA and SAHA inhibitors. *Nature* 401:188–193
319. Itazaki H, Nagashima K, Sugita K, Yoshida H, Kawamura Y, Yasuda Y, Matsumoto K, Ishii K, Uotani N, Nakai H, Terui A, Yoshimatsu S, Ikenishi Y, Nakagawa Y (1990) Isolation and structural elucidation of new cyclotetrapeptides, trapoxins A and B, having detransformation activities as antitumor agents. *J Antibiotics* 43:1524–1532
320. Singh SB, Zink DL, Polishook JD, Dombrowski AW, Darkin-Rattray SJ, Schmatz DM, Goetz MA (1996) Apicidins: novel cyclic tetrapeptides as coccidiostats and antimalarial agents from *Fusarium pallidroseum*. *Tetrahedron Lett* 37:8077–8080
321. Colletti SL, Myers RW, Darkin-Rattray SJ, Gurnett AM, Dulski PM, Galuska S, Allocco JJ, Ayer MB, Li C, Lim J, Crumley TM, Cannova C, Schmatz DM, Wyratt MJ, Fisher MH, Meinke PT (2001) Broad spectrum antiprotozoal agents that inhibit histone deacetylase: structure–activity relationships of apicidin. Part 1. *Bioorg Med Chem Lett* 11:107–111
322. Ruzicka ZL (1953) The isoprene rule and the biogenesis of terpenic compounds. *Experientia* 9:357–367
323. Bergmann W, Johnson TB (1933) The chemistry of marine animals. I. The sponge *Microciona prolifera*. *Z Physiol Chem* 222:220–226
324. Ebada SS, Lin W, Proksch P (2010) Bioactive sesterterpenes and triterpenes from marine sponges: occurrence and pharmacological significance. *Mar Drugs* 8:313–346
325. De Silva ED, Scheuer PJ (1980) Manoalide, an antibiotic sesterterpenoid from the marine sponge *Luffariella variabilis* (Polejaeff). *Tetrahedron Lett* 21:1611–1614
326. De Silva ED, Scheuer PJ (1981) Three new sesterterpenoid antibiotics from the marine sponge *Luffariella variabilis* (Polejaeff). *Tetrahedron Lett* 22:3147–3150
327. Kernan MR, Faulkner DJ, Jacobs RS (1987) The luffariellins, novel anti-inflammatory sesterterpenes of chemotaxonomic importance from the marine sponge *Luffariella variabilis*. *J Org Chem* 52:3081–3083

328. Albizzati KF, Holman T, Faulkner DJ, Glaser KB, Jacobs RS (1987) Luffariellolide, an anti-inflammatory sesterterpene from the marine sponge *Luffariella* sp. *Experientia* 43:949–950
329. Kernan MR, Faulkner DJ, Parkanyi L, Clardy J, de Carvalho MS, Jacobs RS (1989) Luffolide, a novel anti-inflammatory terpene from the sponge *Luffariella* sp. *Experientia* 45:388–390
330. Koenig GM, Wright AD, Sticher O (1992) Four new antibacterial sesterterpenes from a marine sponge of the genus *Luffariella*. *J Nat Prod* 55:174–178
331. Potts BCM, Capon RJ, Faulkner DJ (1992) Luffalactone and (4*E*,6*E*)-dehydromanoalide from the sponge *Luffariella variabilis*. *J Org Chem* 57:2965–2967
332. Butler MS, Capon RJ (1992) The luffarins (A–Z), novel terpenes from an Australian marine sponge, *Luffariella geometrica*. *Aust J Chem* 45:1705–1743
333. Tsuda M, Shigemori H, Ishibashi M, Sasaki T, Kobayashi J (1992) Luffariolides A–E, new cytotoxic sesterterpenes from the Okinawan marine sponge *Luffariella* sp. *J Org Chem* 57:3503–3507
334. Kobayashi J, Zeng CM, Ishibashi M, Sasaki T (1993) Luffariolides F and G, new manoalide derivatives from the Okinawan marine sponge *Luffariella* sp. *J Nat Prod* 56:436–439
335. Reddy MVR, Harper MK, Faulkner DJ (1997) Luffasterols A–C, 9,11-secoosterols from the Palauan sponge *Luffariella* sp. *J Nat Prod* 60:41–43
336. Tsuda M, Endo T, Mikami Y, Fromont J, Kobayashi J (2002) Luffariolides H and J, new sesterterpenes from a marine sponge *Luffariella*. *J Nat Prod* 65:1507–1508
337. Namikoshi M, Suzuki S, Meguro S, Nagai H, Koike Y, Kitazawa A, Kobayashi H, Oda T, Yamada J (2004) Manoalide derivatives from a marine sponge *Luffariella* sp. collected in Palau. *Fish Sci* 70:152–158
338. Ettinger-Epstein P, Motti CA, de Nys R, Wright AD, Battershill CN, Tapiolas DM (2007) Acetylated sesterterpenes from the Great Barrier Reef sponge *Luffariella variabilis*. *J Nat Prod* 70:648–651
339. Gauvin-Bialecki A, Aknin M, Smadja J (2008) 24-*O*-Ethylmanoalide, a manoalide-related sesterterpene from the marine sponge *Luffariella* cf. *variabilis*. *Molecules* 13:3184–3191
340. Kobayashi M, Okamoto T, Hayashi K, Yokoyama N, Sasaki T, Kitagawa I (1994) Marine natural products. XXXII. Absolute configurations of C-4 of the manoalide family, biologically active sesterterpenes from the marine sponge *Hyrtios erecta*. *Chem Pharm Bull* 42:265–270
341. Bourguet-Kondracki ML, Debitus C, Guyot M (1996) Biologically active sesterterpenes from a new Caledonian marine sponge *Hyrtios* sp. *J Chem Res* 1996:192–193
342. Cambie RC, Craw PA, Bergquist PR, Karuso P (1988) Chemistry of sponges, III. Manoalide monoacetate and thorectolide monoacetate, two new sesterterpenoids from *Thorectandra excavatus*. *J Nat Prod* 51:331–334
343. De Rosa S, de Stefano S, Zavodnik N (1988) Cacospongionolide: a new antitumoral sesterterpene, from the marine sponge *Cacospongia mollior*. *J Org Chem* 53:5020–5023
344. Tasdemir D, Concepción GP, Mangalindan GC, Harper MK, Hajdu E, Ireland CM (2000) New terpenoids from a *Cacospongia* sp. from the Philippines. *Tetrahedron* 56:9025–9030
345. Montagnac A, País M, Debitus C (1994) Fasciospongides A, B and C, new manoalide derivatives from the sponge *Fasciospongia* sp. *J Nat Prod* 57:186–190
346. De Rosa S, Crispino A, de Giulio A, Iodice C, Pronzato R, Zavodnik N (1995) Cacospongionolide B, a new sesterterpene from the sponge *Fasciospongia cavernosa*. *J Nat Prod* 58:1776–1780
347. De Rosa S, Crispino A, de Giulio A, Iodice C, Tommonaro G (1997) Cavernosolide, a new sesterterpene from a Tyrrhenian sponge. *J Nat Prod* 60:844–846
348. De Rosa S, Carbonelli S (2006) Two new luffarin derivatives from the Adriatic Sea sponge *Fasciospongia cavernosa*. *Tetrahedron* 62:2845–2849

349. Elkhayat E, Edrada RA, Ebel R, Wray V, van Soest R, Wiryowidagdo S, Mohamed MH, Mueller WEG, Proksch P (2004) New luffariellolide derivatives from the Indonesian sponge *Acanthodendrilla* sp. *J Nat Prod* 67:1809–1817
350. Ueoka R, Nakao Y, Fujii S, van Soest RWM, Matsunaga S (2008) Aplysinoiplides A–C, cytotoxic sesterterpenes from the marine sponge *Aplysinopsis digitata*. *J Nat Prod* 71:1089–1091
351. De Freitas JC, Blankemeier LA, Jacobs RS (1984) *In vitro* inactivation of the neurotoxic action of β -bungarotoxin by the marine natural product, manoalide. *Experientia* 40:864–865
352. Lombardo D, Dennis EA (1985) Cobra venom phospholipase A_2 inhibition by manoalide. A novel type of phospholipase inhibitor. *J Biol Chem* 260:7234–7240
353. Glaser KB, Jacobs RS (1986) Molecular pharmacology of manoalide. Inactivation of bee venom phospholipase A_2 . *Biochem Pharmacol* 35:449–453
354. Glaser KB, Jacobs RS (1987) Inactivation of bee venom phospholipase A_2 by manoalide. A model based on the reactivity of manoalide with amino acids and peptide sequences. *Biochem Pharmacol* 36:2079–2086
355. Bennett CF, Mong S, Clarke MA, Kruse LI, Crooke ST (1987) Differential effects of manoalide on secreted and intracellular phospholipases. *Biochem Pharmacol* 36:733–740
356. Glaser KB, de Carvalho MS, Jacobs RS, Kernan MR, Faulkner DJ (1989) Manoalide: structure-activity studies and definition of the pharmacophore for phospholipase A_2 inactivation. *Mol Pharmacol* 36:782–788
357. Jacobson PB, Marshall LA, Sung A, Jacobs RS (1990) Inactivation of human synovial fluid phospholipase A_2 by the marine natural product, manoalide. *Biochem Pharmacol* 39:1557–1564
358. Ortiz AR, Pisabarro MT, Gago F (1993) Molecular model of the interaction of bee venom phospholipase A_2 with manoalide. *J Med Chem* 36:1866–1879
359. Deems RA, Lombardo D, Morgan BP, Mihelich ED, Dennis EA (1987) The inhibition of phospholipase A_2 by manoalide and manoalide analogues. *Biochim Biophys Acta* 917:258–268
360. Reynolds LJ, Morgan BP, Hite GA, Mihelich ED, Dennis EA (1988) Phospholipase A_2 inhibition and modification by manoalogue. *J Am Chem Soc* 110:5172–5177
361. Potts BCM, Faulkner DJ, Jacobs RS (1992) Phospholipase A_2 inhibitors from marine organisms. *J Nat Prod* 55:1701–1717
362. Reynolds LJ, Mihelich ED, Dennis EA (1991) Inhibition of venom phospholipase A_2 by manoalide and manologue. *J Biol Chem* 266:16512–16517
363. Potts BCM, Faulkner DJ, de Carvalho MS, Jacobs RS (1992) Chemical mechanism of inactivation of bee venom phospholipase A_2 by the marine natural products manoalide, luffariellolide, and scalaradial. *J Am Chem Soc* 114:5093–5100
364. De Rosa M, Giordano S, Scettri A, Sodano G, Soriente A, Pastor PG, Alcaraz MJ, Payá M (1998) Synthesis and comparison of the anti-inflammatory activity of manoalide and cacospongionolide B analogues. *J Med Chem* 41:3232–3238
365. Mann J (1992) Sponges to wipe away pain. *Nature* 358:540
366. Blanchard JL, Epstein DM, Boisclair MD, Rudolph J, Pal K (1999) Dysidiolide and related γ -hydroxybutenolide compounds as inhibitors of the protein tyrosine phosphatase, CDC25. *Bioorg Med Chem Lett* 9:2537–2538
367. Charan RD, McKee TC, Boyd MR (2001) Thorectandrols A and B, new cytotoxic sesterterpenes from the marine sponge *Thorectandra* species. *J Nat Prod* 64:661–663
368. Charan RD, McKee TC, Boyd MR (2002) Thorectandrols C, D, and E, new sesterterpenes from the marine sponge *Thorectandra* sp. *J Nat Prod* 65:492–495
369. De Rosa S, de Giulio A, Crispino A, Iodice C, Tommonaro G (1997) Further bioactive sesterterpenes from the Tyrrhenian sponge *Fasciospongia cavernosa*. *Nat Prod Res* 10:267–274
370. Barrero AF, Alvarez-Manzaneda EJ, Chahboun R, Cuerva JM, Segovia A (2000) Synthetic applications of the thermal rearrangement of ozonides: first enantiospecific synthesis of marine metabolite Luffarin W. *Synlett* 9:1269–1272

371. Boukouvalas J, Robichaud J, Maltais F (2006) A unified strategy for the regiospecific assembly of homoallyl-substituted butenolides and γ -hydroxybutenolides: first synthesis of luffariellolide. *Synlett* 16:2480–2482
372. Gross H, Koenig GM (2006) Terpenoids from marine organisms: unique structures and their pharmacological potential. *Phytochemistry Rev* 5:115–141
373. Kernan MR, Barrabee EB, Faulkner DJ (1988) Variation of the metabolites of *Chromodoris funerea*: comparison of specimen from a Palauan marine lake with those from adjacent waters. *Comp Biochem Physiol* 89B:275–278
374. Sullivan B, Faulkner DJ (1982) An antimicrobial sesterterpene from a Palauan sponge. *Tetrahedron Lett* 23:907–910
375. Schmidt EW, Faulkner DJ (1996) Palauolol, a new anti-inflammatory sesterterpene from the sponge *Fascaplysinopsis* sp. from Palau. *Tetrahedron Lett* 37:3951–3954
376. De Rosa S, Puliti R, Crispino A, de Giulio A, de Sena C, Iodice C, Mattia CA (1995) 25-Deoxycacospongionolide B and cacospongionolide C, two new terpenoids from the sponge *Fasciospongia cavernosa*. *Tetrahedron* 51:10731–10736
377. Lal AR, Cambie RC, Rickard CEF, Bergquist PR (1994) Sesterterpene lactones from a sponge species of the genus *Dactylospongia*. *Tetrahedron Lett* 35:2603–2606
378. Cambie CR, Lal AR, Rickard CEF (1996) A sesterterpene lactone from *Petrosaspongia nigra* sp. nov. *Acta Cryst C* 52:709–711
379. Gomez-Paloma L, Randazzo A, Minale L, Debitus C, Roussakis C (1997) New cytotoxic sesterterpenes from the New Caledonian marine sponge *Petrosaspongia nigra* (Bergquist). *Tetrahedron* 53:10451–10458
380. Randazzo A, Debitus C, Minale L, Pastor PG, Alcaraz MJ, Payá M, Gomez-Paloma L (1998) Petrosaspongiolides M–R: new potent and selective phospholipase A₂ inhibitors from the New Caledonian marine sponge *Petrosaspongia nigra*. *J Nat Prod* 61:571–575
381. De Marino S, Iorizzi M, Zollo F, Debitus C, Menou JL, Ospina LF, Alcaraz MJ, Payá M (2000) New pyridinium alkaloids from a marine sponge of the genus *Spongia* with a human phospholipase A₂ inhibitor profile. *J Nat Prod* 63:322–326
382. Balsinde J, Balboa MA, Insel PA, Dennis EA (1999) Regulation and inhibition of phospholipase A₂. *Ann Rev Pharmacol Toxicol* 39:175–189
383. Dal Piaz FD, Casapullo A, Randazzo A, Riccio R, Pucci P, Marino G, Gomez-Paloma L (2002) Molecular basis of phospholipase A₂ inhibition by petrosaspongiolide M. *ChemBioChem* 3:664–671
384. Monti MC, Casapullo A, Riccio R, Gomez-Paloma L (2004) Further insights on the structural aspects of PLA₂ inhibition by γ -hydroxybutenolide-containing natural products: a comparative study of petrosaspongiolides M–R. *Bioorg Med Chem* 12:1467–1474
385. Monti MC, Casapullo A, Riccio R, Gomez-Paloma L (2004) PLA₂-mediated catalytic activation of its inhibitor 25-acetyl-petrosaspongiolide M: serendipitous identification of a new PLA₂ suicide inhibitor. *FEBS Lett* 578:269–274
386. Gomez-Paloma L, Monti MC, Terracciano S, Casapullo A, Riccio R (2005) Chemistry and biology of anti-inflammatory marine natural products. Phospholipase A₂ inhibitors. *Curr Org Chem* 9:1419–1427
387. Monti MC, Riccio R, Casapullo A (2009) Effects of petrosaspongiolide R on the surface topology of bee venom PLA₂: a limited proteolysis and mass spectrometry analysis. *Bioorg Chem* 37:6–10
388. Monti MC, Casapullo A, Cavasotto CN, Tosco A, Dal Piaz F, Ziemys A, Margarucci L, Riccio R (2009) The binding mode of petrosaspongiolide M to the human group IIA phospholipase A₂: exploring the role of covalent and noncovalent interactions in the inhibition process. *Chem Eur J* 15:1155–1163
389. Ferreira-Mederos L, Lanners S, Henchiri H, Fekih A, Hanquet G (2009) Hemisynthesis of two marine cheilantane sesterterpenes from (–)-sclareol: first enantioselective synthesis of petrosaspongiolide R. *Nat Prod Res* 23:256–263

390. Chawla A, Dev S (1967) A new class of triterpenoids from *Ailanthus malabarica* DC. Derivatives of malabaricane. *Tetrahedron Lett* 8:4837–4843
391. Sobti RR, Dev S (1968) A direct correlation of (+)-malabaricol with (+)-ambreinolide. *Tetrahedron Lett* 9:2215–2217
392. Paton WF, Paul IC, Bajaj AG, Dev S (1979) The structure of malabaricol. *Tetrahedron Lett* 20:4153–4154
393. Ravi BN, Wells RJ, Croft KD (1981) Malabaricane triterpenes from a Fijian collection of the sponge *Jaspis stellifera*. *J Org Chem* 46:1998–2001
394. McCabe T, Clardy J, Minale L, Pizza C, Zollo F, Riccio R (1982) A triterpenoid pigment with the isomalabaricane skeleton from the marine sponge *Stelletta* sp. *Tetrahedron Lett* 23:3307–3310
395. Rao Z, Deng S, Wu H, Jiang S (1997) Rhabdastrellic acid–A, a novel triterpenoid from the marine sponge *Rhabdastrella globostellata*. *J Nat Prod* 60:1163–1164
396. Guo JF, Zhou JM, Zhang Y, Deng R, Liu JN, Feng GK, Liu ZC, Xiao DJ, Deng SZ, Zhu XF (2008) Rhabdastrellic acid–A inhibited PI3K/Akt pathway and induced apoptosis in human leukemia HL–60 cells. *Cell Biol Int* 32:48–54
397. Su JY, Meng YH, Zeng LM, Fu X, Schmitz FJ (1994) Stellettin A, a new triterpenoid pigment from the marine sponge *Stelletta tenuis*. *J Nat Prod* 57:1450–1451
398. McCormick JL, McKee TC, Cardellina JH II, Leid M, Boyd MR (1996) Cytotoxic triterpenes from a marine sponge, *Stelletta* sp. *J Nat Prod* 59:1047–1050
399. McKee TC, Bokesch HR, McCormick JL, Rashid MA, Spielvogel D, Gustafson KR, Alavanja MM, Cardellina JH II, Boyd MR (1997) Isolation and characterization of new anti-HIV and cytotoxic leads from plants, marine, and microbial organisms. *J Nat Prod* 60:431–438
400. Tasdemir D, Mangalindan GC, Concepción GP, Verbitski SM, Rabindran S, Miranda M, Greenstein M, Hooper JNA, Harper MK, Ireland CM (2002) Bioactive isomalabaricane triterpenes from the marine sponge *Rhabdastrella globostellata*. *J Nat Prod* 65:210–214
401. Tang SA, Deng ZW, Li J, Fu HZ, Pei YH, Zhang S, Lin WH (2005) A new isomalabaricane triterpenoid from sponge *Jaspis* sp. *Chin Chem Lett* 16:353–355
402. Clement JA, Li M, Hecht SM, Kingston DGI (2006) Bioactive isomalabaricane triterpenoids from *Rhabdastrella globostellata* that stabilize the binding of DNA polymerase β to DNA. *J Nat Prod* 69:373–376
403. Liu WK, Cheung FWK, Che CT (2006) Stellettin A induces oxidative stress and apoptosis in HL–60 human leukemia and LNCaP prostate cancer cell lines. *J Nat Prod* 69:934–937
404. Krysko DV, Roels F, Leybaert L, D’Herde K (2001) Mitochondrial transmembrane potential changes support the concept of mitochondrial heterogeneity during apoptosis. *J Histochem Cytochem* 49:1277–1284
405. Lin HW, Wang ZL, Wu JH, Shi N, Zhang HJ, Chen WS, Morris-Natschke SL, Lin AS (2007) Stellettins L and M, cytotoxic isomalabaricane-type triterpenes, and sterols from the marine sponge *Stelletta tenuis*. *J Nat Prod* 70:1114–1117
406. Lv F, Xu M, Deng Z, de Voogd NJ, van Soest RWM, Proksch P, Lin WH (2008) Rhabdastrellins A–F, isomalabaricane triterpenes from the marine sponge *Rhabdastrella* aff. *distinca*. *J Nat Prod* 71:1738–1741
407. Tsuda M, Ishibashi M, Agemi K, Sasaki T, Kobayashi J (1991) Stelliferins A–F, new antineoplastic isomalabaricane triterpenes from the Okinawan marine sponge *Jaspis stellifera*. *Tetrahedron* 47:2181–2194
408. Oku N, Matsunaga S, Wada SI, Watabe S, Fusetani N (2000) New isomalabaricane triterpenes from the marine sponge *Stelletta globostellata* that induce morphological changes in rat fibroblasts. *J Nat Prod* 63:205–209
409. Meragelman KM, McKee TC, Boyd MR (2001) New cytotoxic isomalabaricane triterpenes from the sponge *Jaspis* species. *J Nat Prod* 64:389–392
410. Tabudravu JN, Jaspars M (2001) Stelliferin riboside, a triterpene monosaccharide isolated from the Fijian sponge *Geodia globostellifera*. *J Nat Prod* 64:813–815

411. Raeppe F, Weibel JM, Heissler D (1999) Synthesis of the *trans-syn-trans* perhydrobenz[e] indene moiety of the stelletins and the stelliferins. *Tetrahedron Lett* 40:6377–6381
412. Ryu G, Matsunaga S, Fusetani N (1996) Globostellatic acids A–D, new cytotoxic isomalabaricane triterpenes from the marine sponge *Stelletta globostellata*. *J Nat Prod* 59:512–514
413. Fouad M, Edrada RA, Ebel R, Wray V, Mueller WEG, Lin WH, Proksch P (2006) Cytotoxic isomalabaricane triterpenes from the marine sponge *Rhabdastrella globostellata*. *J Nat Prod* 69:211–218
414. Aoki S, Sanagawa M, Watanabe Y, Setiawan A, Arai M, Kobayashi M (2007) Novel isomalabaricane triterpenes, exhibiting selective anti-proliferative activity against vascular endothelial cells, from marine sponge *Rhabdastrella globostellata*. *Bioorg Med Chem* 15:4818–4828
415. Zhang WH, Che CT (2001) Isomalabaricane-type nortriterpenoids and other constituents of the marine sponge *Geodia japonica*. *J Nat Prod* 64:1489–1492
416. Lv F, Deng Z, Li J, Fu H, van Soest RWM, Proksch P, Lin WH (2004) Isomalabaricane-type compounds from the marine sponge *Rhabdastrella* aff. *distinca*. *J Nat Prod* 67:2033–2036
417. Liu WK, Ho JCK, Che CT (2005) Apoptotic activity of isomalabaricane triterpenes on human promyelocytic leukemia HL-60 cells. *Cancer Lett* 230:102–110
418. Kobayashi J, Yuasa K, Kobayashi T, Sasaki T, Tsuda M (1996) Jaspiferals A–G, new cytotoxic isomalabaricane-type nortriterpenoids from Okinawan marine sponge *Jaspis stellifera*. *Tetrahedron* 52:5745–5750
419. Zampella A, D'Auria MV, Debitus C, Menou JL (2000) New isomalabaricane derivatives from a new species of *Jaspis* sponge collected at the Vanuatu Islands. *J Nat Prod* 63:943–946
420. Bourguet-Kondracki ML, Longeon A, Debitus C, Guyot M (2000) New cytotoxic isomalabaricane-type sesterterpenes from the new Caledonian marine sponge *Rhabdastrella globostellata*. *Tetrahedron Lett* 41:3087–3090
421. Tang S, Pei Y, Fu H, Deng Z, Li J, Proksch P, Lin WH (2006) Jaspolides A–F, six new isomalabaricane-type terpenoids from the sponge *Jaspis* sp. *Chem Pharm Bull* 54:4–8
422. Tang S, Deng Z, Proksch P, Lin WH (2007) Jaspolides G and H, unique bisomalabaricanes from the Chinese marine sponge *Jaspis* sp. *Tetrahedron Lett* 48:5443–5447
423. Li M, Wei SY, Tang SA, Lin WH, Cui JR (2008) Antileukemic activity of jaspolide B, an isomalabaricane-type triterpene from marine sponge *Jaspis* sp. on human promyelocytic leukemia HL-60 cells. *J Ch Pharm Sci* 17:11–15
424. Wei SY, Li M, Tang SA, Sun W, Xu B, Cui JR, Lin WH (2008) Induction of apoptosis accompanying with G₁ phase arrest and microtubule disassembly in human hepatoma cells by jaspolide B, a new isomalabaricane-type triterpene. *Cancer Lett* 262:114–122
425. Cheng JF, Kobayashi J, Nakamura H, Ohizumi Y, Hirata Y, Sasaki T (1988) Penasterol, a novel antileukemic sterol from the Okinawan marine sponge *Penares* sp. *J Chem Soc Perkin Trans I* 8:2403–2406
426. Shoji N, Umeyama A, Motoki S, Arihara S, Ishida T, Nomoto K, Kobayashi J, Takei M (1992) Potent inhibitors of histamine release, two novel triterpenoids from the Okinawan marine sponge *Penares incrustans*. *J Nat Prod* 55:1682–1685
427. D'Auria MV, Paloma LG, Minale L, Riccio R, Debitus C (1992) Structure characterization by two-dimensional NMR spectroscopy, of two marine triterpene oligosaccharides from a Pacific sponge of the genus *Erylus*. *Tetrahedron* 48:491–498
428. Carmely S, Roll M, Loya Y, Kashman Y (1989) The structure of eryloside A, a new antitumor and antifungal 4-methylated steroidal glycoside from the sponge *Erylus lendenfeldi*. *J Nat Prod* 52:167–170
429. Gulavita NK, Wright AE, Kelly-Borges M, Longley RE, Yarwood D, Sills MA (1994) Eryloside E from an Atlantic sponge *Erylus goffrilleri*. *Tetrahedron Lett* 35:4299–4302
430. Stead P, Hiscox S, Robinson PS, Pike NB, Sidebottom PJ, Roberts AD, Taylor NL, Wright AE, Pomponi SA, Langely D (2000) Eryloside F, a novel penasterol disaccharide possessing potent thrombin receptor antagonist activity. *Bioorg Med Chem Lett* 10:661–664

431. Shin J, Lee HS, Woo L, Rho JR, Seo Y, Cho KW, Sim CJ (2001) New triterpenoid saponins from the sponge *Erylus nobilis*. J Nat Prod 64:767–771
432. Fouad M, Al-Trabeen K, Badran M, Wray V, Edrada R, Proksch P, Ebel R (2004) New steroidal saponins from the sponge *Erylus lendenfeldi*. ARKIVOC xiii:17–27
433. Antonov AS, Kalinovskiy AI, Stonik VA, Afiyatulloev SS, Aminin DL, Dmitrenok PS, Molloy E, Cimino G (2007) Isolation and structures of erylosides from the Caribbean sponge *Erylus formosus*. J Nat Prod 70:169–178
434. Afiyatulloev SS, Kalinovskiy AI, Antonov AS, Ponomarenko LP, Dmitrenok PS, Aminin DL, Krasokhin VB, Nosova VM, Kisin AV (2007) Isolation and structures of erylosides from the Caribbean sponge *Erylus goffrilleri*. J Nat Prod 70:1871–1877
435. Jaspars M, Crews P (1994) A triterpene tetrasaccharide, formoside, from the Caribbean Choristida sponge *Erylus formosus*. Tetrahedron Lett 35:7501–7504
436. Kubanek J, Pawlik JR, Eve TM, Fenical W (2000) Triterpene glycosides defend the Caribbean reef sponge *Erylus formosus* from predatory fishes. Mar Ecol Prog Ser 207:69–77
437. Takada K, Nakao Y, Matsunaga S, van Soest RWM, Fusetani N (2002) Nobiloside, a new neuraminidase inhibitory triterpenoidal saponin from the marine sponge *Erylus nobilis*. J Nat Prod 65:411–413
438. Okada Y, Matsunaga S, van Soest RWM, Fusetani N (2006) Sokodosides, steroid glycosides with an isopropyl side chain, from the marine sponge *Erylus placenta*. J Org Chem 71:4884–4888
439. Dasgupta S, Pramanik K, Mukhopadhyay B (2007) Oligosaccharides through reactivity tuning: convergent synthesis of the trisaccharides of the steroid glycoside sokodoside B isolated from marine sponge *Erylus placenta*. Tetrahedron 63:12310–12316
440. Kitagawa I, Kobayashi M, Okamoto Y, Yoshikawa M, Hamamoto Y (1987) Structures of sarasinoids A₁, B₁, and C₁; new norlanostane-triterpenoid oligosaccharides from the Palauan marine sponge *Asteropus sarasinusum*. Chem Pharm Bull 35:5036–5039
441. Schmitz FJ, Ksebati MB, Gunasekera SP, Agarwal S (1988) Sarasinoid A₁: a saponin containing amino sugars isolated from a sponge. J Org Chem 53:5941–5947
442. Kobayashi M, Okamoto Y, Kitagawa I (1991) Marine natural products. XXVIII. The structures of sarasinoids A₁, A₂, A₃, B₁, B₂, B₃, C₁, C₂, and C₃, nine new norlanostane-triterpenoid oligosaccharides from the Palauan marine sponge *Asteropus sarasinusum*. Chem Pharm Bull 39:2867–2877
443. Espada A, Jiménez C, Rodríguez J, Crews P, Riguera R (1992) Sarasinoids D–G: four new triterpenoid saponins from the sponge *Asteropus sarasinusum*. Tetrahedron 48:8685–8696
444. Lee HS, Seo Y, Cho KW, Rho JR, Shin J, Paul VJ (2000) New triterpenoid saponins from the sponge *Melophlus isis*. J Nat Prod 63:915–919
445. Dai HF, Edrada RA, Ebel R, Nimtz M, Wray V, Proksch P (2005) Norlanostane triterpenoidal saponins from the marine sponge *Melophlus sarassinorum*. J Nat Prod 68:1231–1237
446. Kalinovskiy AI, Antonov AS, Afiyatulloev SS, Dmitrenok PS, Evtuschenko EV, Stonik VA (2002) Mycaloside A, a new steroid oligoglycoside with an unprecedented structure from the Caribbean sponge *Mycale laxissima*. Tetrahedron Lett 43:523–525
447. Antonov AS, Afiyatulloev SS, Kalinovskiy AI, Ponomarenko LP, Dmitrenok PS, Aminin DL, Agafonova IG, Stonik VA (2003) Mycalosides B–I, eight new spermostatic steroid oligoglycosides from the sponge *Mycale laxissima*. J Nat Prod 66:1082–1088
448. Afiyatulloev SS, Antonov AS, Kalinovskiy AI, Dmitrenok PS (2008) Two new steroid oligoglycosides from the Caribbean sponge *Mycale laxissima*. Nat Prod Commun 3:1581–1586
449. Cafieri F, Fattorusso E, Tagliatalata-Scafati O (1999) Ectyoplasides A–B – unique triterpene oligoglycosides from the Caribbean sponge *Ectyoplasia ferox*. Eur J Org Chem 1999:231–238
450. Campagnuolo C, Fattorusso E, Tagliatalata-Scafati O (2001) Feroxosides A–B, two norlanostane tetraglycosides from the Caribbean sponge *Ectyoplasia ferox*. Tetrahedron 57:4049–4055

451. Antonov AS, Kalinovskiy AI, Stonik VA (1998) Ulososide B, a new unusual norlanostane-triterpene glycoside and its genuine aglycone from the Madagascar sponge *Ulosa* sp. *Tetrahedron Lett* 39:3807–3808
452. Antonov AS, Kalinovskii AI, Dmitrenok PS, Stonik VA (2002) New triterpene glycosides from *Ulosa* sp. sponge. *Russ J Bioorg Chem* 28:183–188
453. Ryu G, Choi BW, Lee BH, Hwang KH, Lee UC, Jeong DS, Lee NH (1999) Wondosterols A–C, three steroidal glycosides from a Korean marine two-sponge association. *Tetrahedron* 55:13171–13178
454. Hirota H, Takayama S, Miyashiro S, Ozaki Y, Ikegami S (1990) Structure of a novel steroidal saponin, pachastrelloside A, obtained from a marine sponge of the genus *Pachastrella*. *Tetrahedron Lett* 31:3321–3324
455. Olivera BM (2000) ω -Conotoxin MVIIA: from marine snail venom to analgesic drug. In: Fusetani N (ed) *Drugs from the sea*. Basel, Switzerland
456. Mendola D (2000) Aquacultural production of bryostatin 1 and ecteinascidin 743. In: Fusetani N (ed) *Drugs from the Sea*. Basel, Switzerland
457. Fenical W (1993) Chemical studies of marine bacteria: developing a new resource. *Chem Rev* 93:1673–1683

Marialuisa Menna and Anna Aiello

Contents

5.1	Introduction	296
5.2	Alkaloids	297
5.2.1	Polycyclic Aromatic Alkaloids with Pyridoacridine-Based Nucleus	297
5.2.2	Polycyclic Aromatic Alkaloids with Carboline-Based Nucleus	302
5.2.3	Indole-Based Alkaloids	307
5.2.4	Tyrosine- and Phenylalanine-Derived Alkaloids	312
5.2.5	Lysine-Derived Alkaloids	321
5.2.6	Protoalkaloids	324
5.3	Peptides	327
5.3.1	Tunichromes and Related Compounds	327
5.3.2	Cyclic Peptides	329
5.3.3	Depsipeptides	336
5.3.4	Linear Peptides	340
5.4	Meroterpenes	341
5.5	Macrolides	348
5.6	Other Nonnitrogenous Compounds	352
5.6.1	Spiroketal-Containing Products	352
5.6.2	Nonnitrogenous Phenylalanine- or Tyrosine-Derived Metabolites	354
5.6.3	Stolonoxides and Stoloniac Acids	355
5.7	Sulfur-Containing Metabolites	357
5.8	Study Questions	364
	References	365

M. Menna (✉) • A. Aiello

Dipartimento di Chimica delle Sostanze Naturali, Università degli Studi di Napoli "Federico II",
Via D. Montesano 49, Naples, Italy

e-mail: mlmenna@unina.it, aiello@unina.it

Abstract

The chapter illustrates the chemistry which has been generated through the investigation of marine ascidians in the last 30 years, highlighting the structural diversity of the compounds produced by these organisms. About 600 structures are here discussed in terms of their occurrence, structural type, and reported pharmacological activity. The chemistry of ascidians is presented in an order based on the general compound type of the metabolites and/or their likely biosynthetic origin.

5.1 Introduction

The tunicates include a wide variety of invertebrates that are classified within the Phylum Chordata based on the presence of a larval notochord during their early development. They are about 3% of the 45,000 or so species of chordates and contain about 3,000 species, usually divided into Ascidiacea (Aplousobranchia, Phlebobranchia, Stolidobranchia), Thaliacea (Pyrosomida, Doliolida, Salpida), Appendicularia (Larvacea), and Sorberacea classes. The great majority are benthic sac-like filter feeders (Ascidiacea and Sorberacea); they live on the ocean floor and filter water by a variety of mechanisms to extract fine planktonic food particles. Those within the two much smaller classes (Thaliacea and Appendicularia) have abandoned the benthic existence in favor of a holoplanktonic lifestyle, that is they live in the pelagic zone as adults.

Despite their simple appearance, they are closely related to vertebrates, and therefore, they represent the most highly evolved group of animals commonly investigated by marine natural products chemists. Most chemical studies have been performed on Ascidiacea (commonly known as the ascidians). An interest in ascidians' chemistry was kindled as early as 1847, when unusual color changes in ascidian blood from yellow-green to deep blue were observed upon exposure to air [1]. A German physiologist discovered that the blue coloring was due to relatively large amounts of vanadium and sulfuric acid, along with an uncharacterized nitrogenous metabolite. Early researchers proposed that the pigmentation was due to oxygen-carrying proteins called hemovanadins. This postulate has proven wrong, but the conquest to understand the role of vanadium in ascidian blood has led to a huge amount of chemical and biological studies [2]. The possible mode of complexation of vanadium was proposed to be by very unstable hydroquinoid compounds, called tunichromes, isolated from the blood cells of several species of ascidians; however, the biological function of these pigments as well as the functional role of the vanadium to the ascidians remains still unclear [3, 4].

Then, attention has focused on ascidians because of their biologically active metabolites, and it has been stimulated by the frequent discovery of antineoplastic agents. Although the birth of the field of marine natural products is generally credited to Bergmann, who in 1950 isolated several modified arabino-nucleosides from a *Tedania* sponge, it was not until 1974 that Fenical isolated the first ascidian metabolite, the geranylhydroquinone, from *Aplidium* sp. [5]. This compound

exhibited chemopreventive activity against some forms of leukemia, Rous sarcoma, and mammary carcinoma in test animals. The occurrence of an anticancer compound in a marine organism, coupled with the general absence of neoplasms in ascidians, provided a powerful incentive to further expand research on these organisms. Since that time, ascidians have been the source of numerous natural products, many with interesting biological activities. The chemistry of ascidians has become one of the most active fields of marine natural products; it has been amply demonstrated that these sea creatures are prolific producers of unusual structures with significant bioactivities [6, 7]. Most of these products fall within the area of cancer therapy, and a significant number of ascidian-derived compounds have entered into preclinical and clinical trials as antitumor agents [8, 9].

The overall goal of this review is not to numerate all the known ascidians metabolites; its primary focus is rather to illustrate the chemistry which has been generated through the investigation of marine ascidians in the last 30 years, highlighting the structural diversity of the compounds produced by these organisms. The metabolites discussed in this review are presented in an order based on their general structural type or on a plausible biosynthetic origin (amino acid origin). As it will be evident, ascidians' chemistry is dominated by the presence of nitrogenous metabolites, among which there is a large variety of structures. There is an extensive range of modified peptides and depsipeptides, sometimes containing unusual amino acids. Heterocyclic alkaloids are also numerous and include pyridoacridines, tryptophan-derived alkaloids (i.e., β -carboline-, and indole-based alkaloids), alkaloids derived from phenylalanine and tyrosine (i.e., isoquinolines), and lysine-derived alkaloids. Nonnitrogenous secondary metabolites are few in number. However, apart from few examples of carotenoids (both common ones and some rarer ones, probably derived from metabolic alteration of commoner carotenoids present in the filtered plankton), steroids (mostly straightforward cholestanes and ergostanes, with some 5,8-epidioxysteroids and secosteroids), and terpenoids, a significant number of acetogenins have been described, including families of macrocyclic lactones, polyethers, cyclic peroxides, and simple alkyl sulfates. Ascidians have also proved to be the source of a sizeable number of terpene-quinone derivatives (meroterpenes), compounds of mixed biogenesis, as well as of a broad spectrum of sulfur-containing metabolites, with fascinating structures and different biological activity.

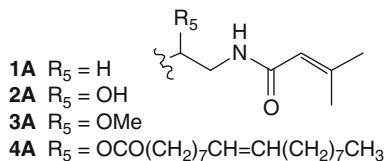
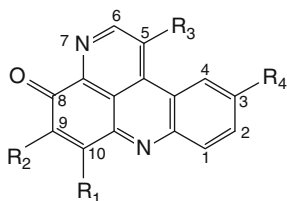
5.2 Alkaloids

5.2.1 Polycyclic Aromatic Alkaloids with Pyridoacridine-Based Nucleus

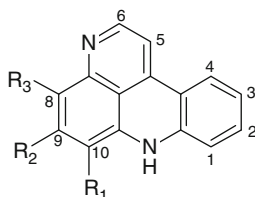
Pyridoacridine alkaloids isolated from ascidians are typically fused tetra- or pentacycle aromatic alkaloids based on the pyrido [*k,l*] acridine skeleton, usually possessing a functionalized alkylamine side chain; more complex polycyclic

pyridoacridines have been reported, too. There has been considerable interest on the biological activity of these compounds, mainly on their potential as antitumor agents [10, 11]. Almost all natural pyridoacridines have been reported to possess significant cytotoxic activity against tumor cells, in part due to their capacity to intercalate into DNA [10]. However, the most intriguing property of the pyridoacridine compounds is their capacity to interfere with the catalytic functions of topoisomerase (TOPO) II; the great chemical diversity in this family of alkaloids provided a large set of tools to manipulate the activity of this enzyme, either stimulating cleavage of DNA through stabilization of covalent TOPO II-DNA complexes or promoting the catenation of DNA [12]. During the past 25 years, both natural pyridoacridines and their analogues have constituted excellent targets for synthetic works [11], confirming that this family of alkaloids as a whole is of interest as a source of new lead structures for drug development.

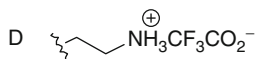
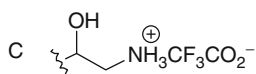
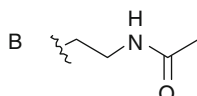
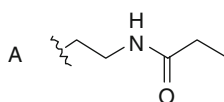
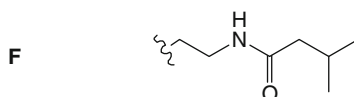
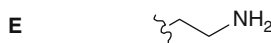
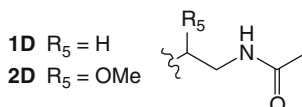
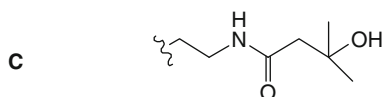
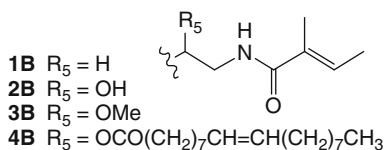
The known tetracyclic pyridoacridine alkaloids from marine sources are dominated by those isolated from ascidians. They show an oxygen function at C-8, which can be a carbonyl group, a hydroxyl, or an ether moiety. Pantherinine (**1**), a cytotoxic brominated alkaloid isolated from *Aplidium pantherinum* [13], can be considered the simplest member of the immiquinone series, which include also cystodytins A–K (**2–12**), a large family of strongly cytotoxic molecules [14–17]. Cystodytins A–C, isolated from an Okinawan *Cystodytes dellechiaiei*, were shown to possess, in addition to a potent cytotoxic activity, powerful Ca^{2+} -releasing activity in the sarcoplasmic reticulum [14]. Diplamine A (**13**), isolated from a *Diplosoma* sp. [18], possesses a thio-methyl functionality on the aromatic nucleus at C-9, like its deacetyl analogue diplamine B (**14**), isolated from *Lissoclinum* cf. *badium* [19]. The S-methyl group seems to be important for cytotoxicity; furthermore, movement of this function from C-9 to C-5 in isodiplamine (**15**), isolated from *L. notti* [17] reduces cytotoxicity. Lissoclins A and B (**16** and **17**), isolated from an Australian collection of *Lissoclinum* sp. [20], are strictly related to diplamine, but no cytotoxic activity data have been reported for these two alkaloids. Nor-segoline (**18**) possesses the 11H-pyrido [4,3,2-*m,n*] acridine nucleus; it was isolated from a purple tunicate from the Red Sea, *Eudistoma* sp. [21, 22], and exhibited potent antileukemic properties [23]. The same aromatic skeleton has been found again in varamines A and B (**19** and **20**), cytotoxic thioalkaloids isolated from a Fijian collection of *L. vareau* [24], and in styelsamines A–D (**21–24**), isolated from an Indonesian collection of *Eusynstyela latericius* [25].



	R ₁	R ₂	R ₃	R ₄
1	H	NH ₂	H	Br
2	1A	H	H	H
3	1B	H	H	H
4	C	H	H	H
5	2A	H	H	H
6	2B	H	H	H
7	3A	H	H	H
8	3B	H	H	H
9	4A	H	H	H
10	4B	H	H	H
11	1D	H	H	H
12	2D	H	H	H
13	1D	SCH ₃	H	H
14	E	SCH ₃	H	H
15	1D	H	SCH ₃	H
16	F	SCH ₃	H	H
17	1B	SCH ₃	H	H

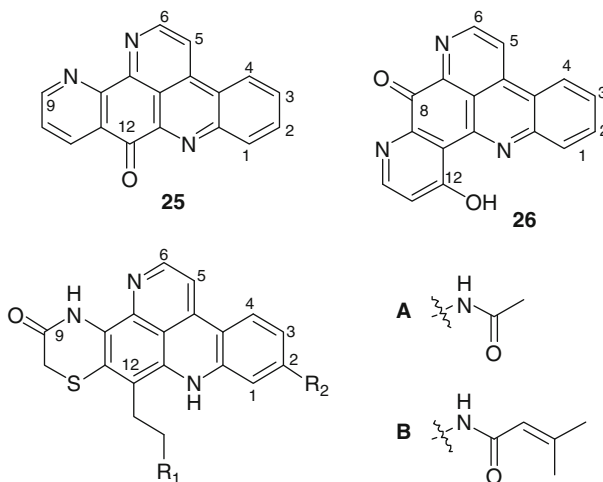


	R ₁	R ₂	R ₃
18	COOMe	H	OMe
19	A	SCH ₃	OMe
20	B	SCH ₃	OMe
21	C	H	OH
22	B	H	OH
23	CHO	H	OH
24	D	H	OH



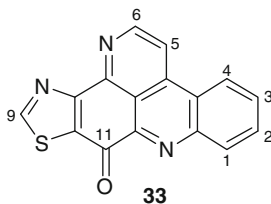
Pentacyclic pyridoacridine alkaloids isolated from ascidians possess an additional ring of various kind, generally fused at C9,10 or at C8,9 of the acridine ring C. Examples are the highly cytotoxic alkaloids ascididemin (**25**), from a *Didemnum* sp. [26], and meridine (**26**) [27], from *Amphicarpa meridiana*, both containing a further pyridine moiety. The shermilamines (**27–32**), isolated from a purple

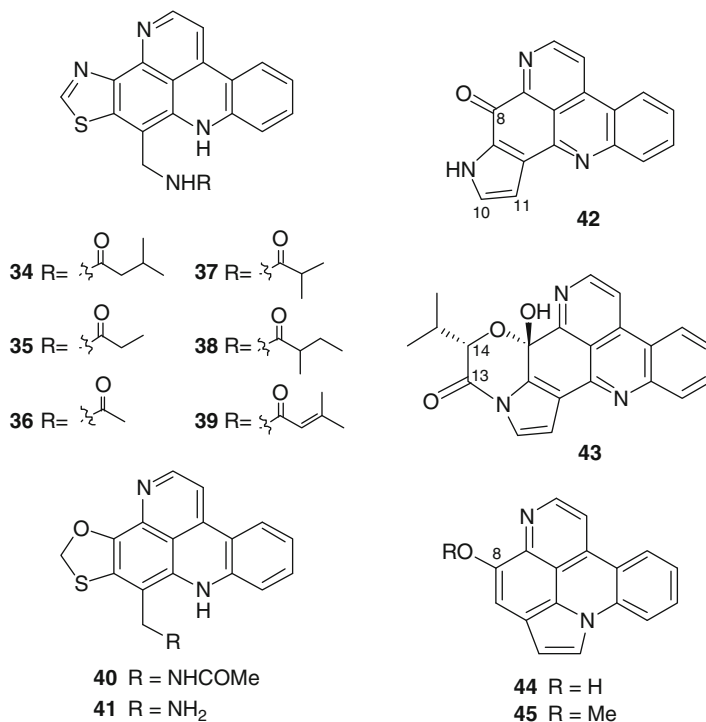
tunicate *Trididemnum* sp., collected in Guam, are thiazinone-containing pentacyclic alkaloids differing in their C-12 side chain [28–31].



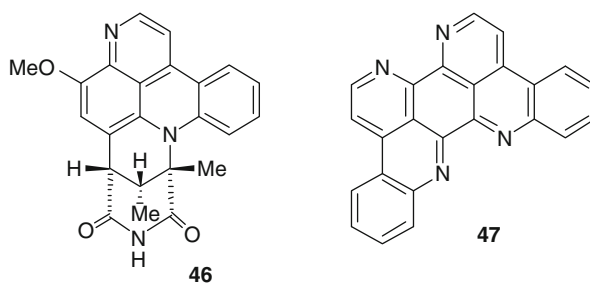
	R ₁	R ₂	R ₃	R ₄
27	A	Br	H	Br
28	A	H	H	H
29	B	H	H	H
30	NMe ₂	H	H	H
31	N(O)Me ₂	H	H	H
32	NH ₂	H	H	H

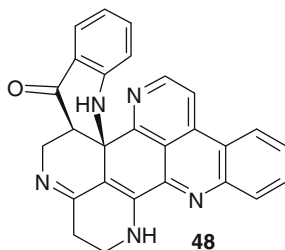
A series of thiazole-containing compounds, kuanoniamines A–F (33–39), was isolated from both an unidentified Micronesian ascidian and the Lamellariidae mollusk *Chelynotus semperi*, believed to be a predator of the ascidian [32, 33]. The structure of kuanoniamine A contains the same tetracyclic iminoquinone-containing pyridoacridine ring system found in ascididemin (25), while the remaining kuanoniamines differ in their acylated phenethylamine side chains. Lissoclinidines (40, 41), isolated from ascidians of *Lissoclinum* genus [17, 19], feature a benzoxathiole moiety, while both sebastianines (42 and 43), from a Brazilian collection of *Cystodites dellechiaiei* [34], and arnoamines (44 and 45), from a *Cystodites* sp. [35], contain a pyrrole ring.





Among the more complex pyridoacridines from ascidians, segolines (**46**, segoline A), possessing a benzo-1,6-diazaphenanthroline ring system, eilatin (**47**), having an unusual symmetrical heptacyclic structure, and eudistones (**48**, eudistone A), can be mentioned. All these alkaloids have been isolated from *Eudistoma* ascidians [20, 21, 36–38]; they have been shown to be potent regulators of cellular growth and differentiation and affect cAMP-mediated processes [39].

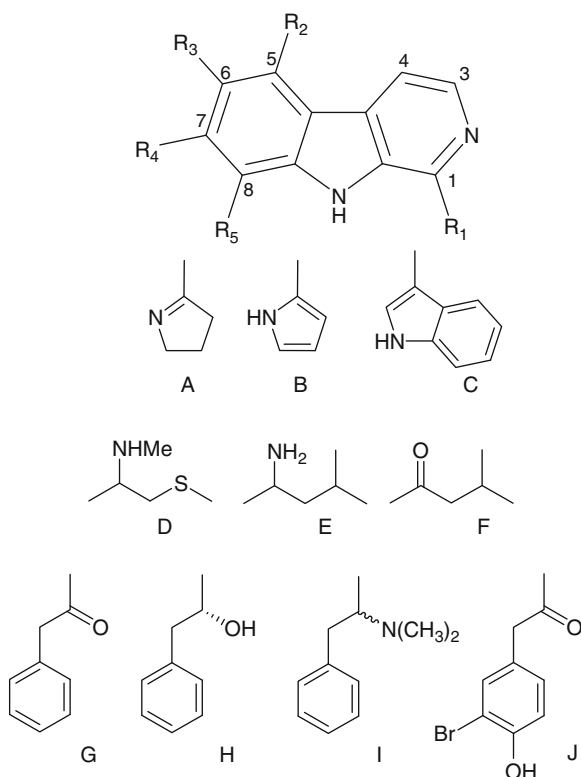




5.2.2 Polycyclic Aromatic Alkaloids with Carboline-Based Nucleus

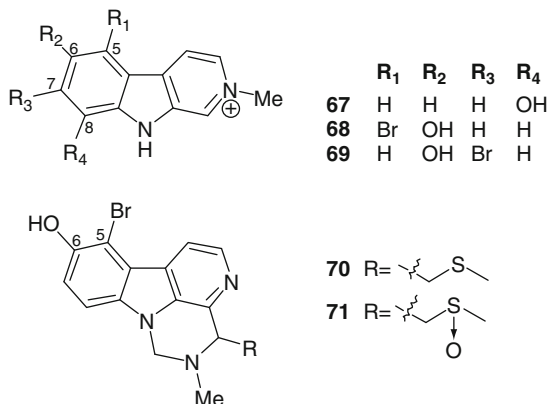
Polysubstituted β -carbolines, as well as dihydro-, and tetrahydro- β -carbolines form a large group of tryptophan-derived ascidian metabolites. The majority of these alkaloids have been isolated from tunicates belonging to the genus *Eudistoma*; they include most of the large group of eudistomins, **49–62** [40–44] and **91–95** [45], eudistomidins (**64**, **65**, **70–72**, **83–84**) [46–49], eudistalbins (**65** and **66**) [50], the N-methyl β -carbolinium derivatives **68** and **69** [51], woodinine (**85**) [52], and the tryptargine derivatives **87** and **100** [53]. Alkaloids based on a β -carboline ring system have also been reported from other tunicate genera, such as *Ritterella* [54, 55], *Pseudodistoma* [56–68], *Didemnum* [59–63], *Synoicum* [64], and *Lissoclinum* [20, 65]. Almost all the reported compounds are hydroxylated and/or brominated at C5, C6, C7, and C8; apart from few members of the group, which are unsubstituted at C1, they show different substituents at this position, such as pyrrole, pyrroline, or indole rings, as well as hydroxylated, carboxylated, or thiomethylated alkyl residues. Actually, all of the β -carboline metabolites isolated thus far are related biosynthetically; the production of these metabolites is generally believed to involve the coupling of tryptophan with a second amino acid, whose nature clearly affects C1 substitution. For example, eudistomins A (**54**) and M (**55**), as well as G (**50**) and P (**52**), may be considered to be derived from tryptophan and glutamine [40], while the 2-phenylacetyl- β -carbolines, eudistomines R (**56**) and T (**57**), are, in addition to tryptophan, made up of phenylalanine or phenylpyruvic acid. Similarly, the unusual amino acids, *p*-methylphenyl-L-alanine and S-methyl-D-cysteine have been supposed to be involved in the production of eudistomidins B (**83**) and C (**64**) [47], respectively. A proline-derived precursor is evident in eudistomins G, I, P (**50–52**), A (**54**), and M (**55**); eudistomidin A (**63**); and woodinine (**85**). In vivo studies with *E. olivaceum* confirmed that tryptophan and proline are the primary precursors of eudistomin I (**51**) [66]. Some of the most intriguing members of these alkaloids are those bearing an oxathiazepine ring (eudistomins C, E, F, K, and L, **91–95**) which apparently originate from condensation of tryptophan with cysteine [45]. Eudistalbins A (**65**) and B (**66**) likely derive from leucine.

Examples of simple β -carboline alkaloids are the eudistomins **49–62** [40–44], eudistomidins A (**63**) and C (**64**) [46, 47], and eudistalbins (**65** and **66**) [50].

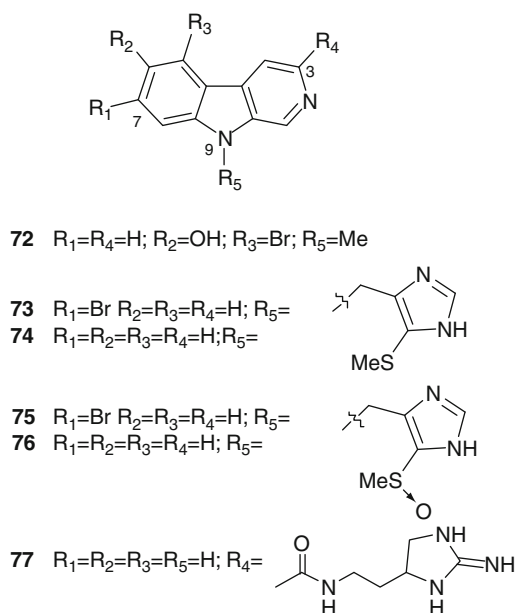


name		R1	R2	R3	R4	R5
Eudistomin J	49	H	H	OH	Br	H
Eudistomin G	50	A	H	H	Br	H
Eudistomin I	51	A	H	H	H	H
Eudistomin P	52	A	H	OH	Br	H
Eudistomin V	53	A	H	Br	Br	H
Eudistomin A	54	B	H	OH	Br	H
Eudistomin M	55	B	H	OH	H	H
Eudistomin R	56	G	H	H	Br	H
Eudistomin T	57	G	H	H	H	H
Eudistomin U	58	C	H	H	H	H
Eudistomin W	59	H	H	OH	H	H
Eudistomin X	60	I	H	OH	H	H
Eudistomin D	61	H	Br	OH	H	H
Eudistomin Y4	62	J	H	Br	H	H
Eudistomidin A	63	A	H	Br	H	OH
Eudistomidin C	64	D	Br	OH	H	H
Eudistalbin A	65	E	H	H	Br	H
Eudistalbin B	66	F	H	H	Br	H

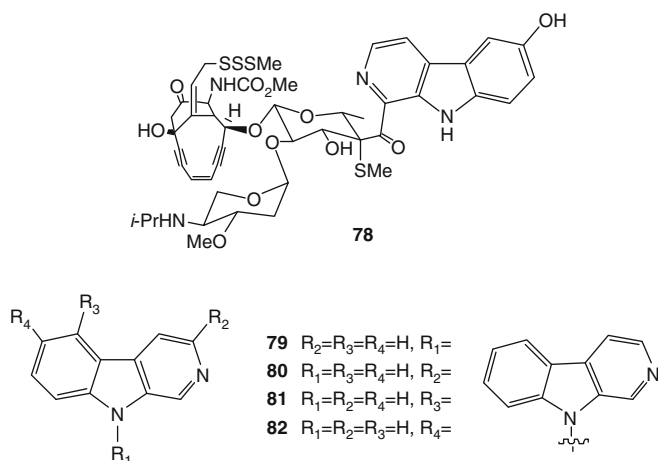
Pseudodistamine (**67**) [58] as well as 2-methyleudistomins D (**68**) and J (**69**) [51] are rare examples of N-methyl β -carboline derivatives described from marine sources, while eudistomidins E (**70**) and F (**71**) are structurally unique, with a tetrahydropyrimidine ring fused to the β -carboline skeleton [48].



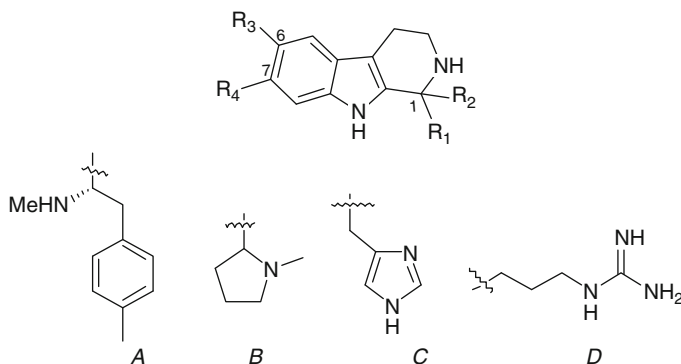
Eudistomidin D (**72**) as well as didemnolines A–D (**73–76**) differ from the other ascidian β -carboline metabolites in that they are substituted at the N9 position of the β -carboline ring, rather than at the C1 position [47, 59]. Tiruchanduramine (**77**) is a β -carboline guanidine alkaloid, and it is the sole 3-substituted β -carboline isolated to date from ascidians [64].



Shishijimicins (shishijimicin A, **78**) are perhaps the most complex β -carbolines from ascidians; they belong to the enediyne class of antibiotics, which are also potent antitumor agents [60]. Both symmetrical and nonsymmetrical β -carboline dimers (**79–82**) have been reported from *Didemnum* sp., and their structures were confirmed by synthesis [61, 62].



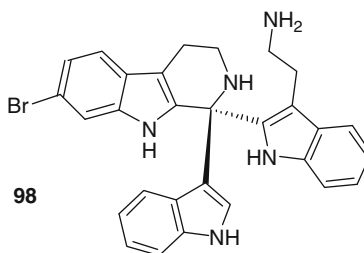
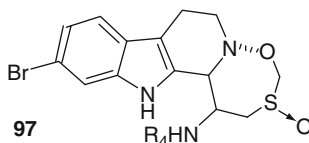
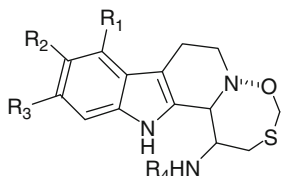
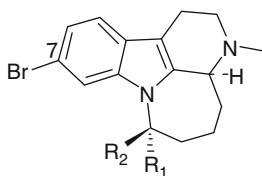
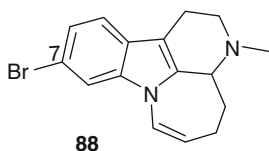
A number of tetrahydro- β -carbolines with various substituents at C1 have been reported; they include eudistomidins B (**83**) and G (**84**) [47, 49], woodinine (**85**) [52], lissoclin C (**86**) [20], and compound **87** the 1-carboxyl analogue of tryptargine, a tetrahydro- β -carboline previously isolated from the skin of the African frog *Kassina senegalensis* [53].



	R_1	R_2	R_3	R_4
83	A	H	Br	H
84	A	H	H	Br
85	B	H	Br	H
86	C	H	H	Br
87	D	CO ₂ H	H	H

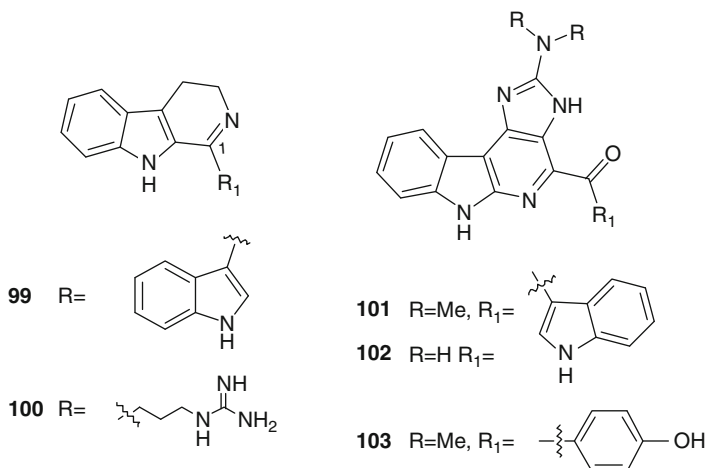
Arborescidines B–D (**88–90**) [57]; eudistomins C, E, F, K, L (**91–95**) [45]; K-sulfoxide (**97**) [54]; and debromoeudistomin K (**96**) [55] contain a 7-membered additional ring attached to the tetrahydro β -carboline moiety which, in the case of the eudistomins, is an oxathiazepine ring. Bengacarboline (**98**) is

a tetrahydro- β -carboline with two indole units attached to C1 of the carboline nucleus; it resulted cytotoxic toward a 26 cell line human tumor panel in vitro and inhibited the catalytic activity of TOPO II [63].



The eudistomins display a variety of biological activities, including a broad spectrum of antibiotic activity and cytotoxicity, but they are notable for the strong antiviral properties displayed by some members of the family [67, 68]. The tetrahydro- β -carboline generally exhibited higher levels of biological activity than their fully aromatic relatives; the oxathiazepino-eudistomins **88–94**, for example, exhibit the highest level of antiviral activity and were also endowed with antimicrobial activity. Eudistomin K (**91**) is significantly active against *Herpes simplex* Type I (HSV-1) and *Polio* virus, while the sulfoxide (**94**) and debromo (**90**) derivatives are active against both virus but less potent. Enhancement of antiviral activity correlates to bromination at C7. Eudistomidin A (**66**) and C (**67**) display calmodulin antagonistic activity, while eudistomidin B (**81**) activates rabbit heart muscle actomyosin ATPase [69].

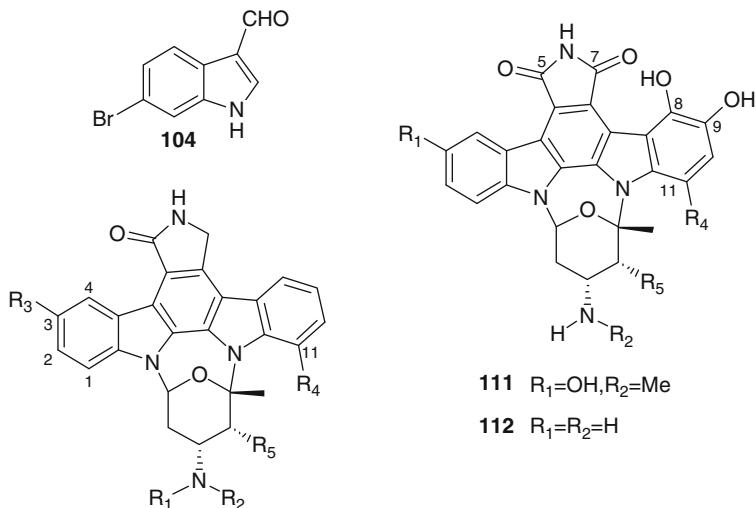
There are only few reported examples of dihydro- β -carboline from ascidians. The first was isoeudistomin U (**99**) which was initially reported to be a 4-substituted dihydro- α -carboline derivative [65], but whose structure was revised after total synthesis to 3,4-dihydroeudistomin U [70]; the bioactivity of isoeudistomin U was reported to be similar to that of the related eudistomin U (**59**). A 1,2-dehydro analogue of tryptargine, named tryptargimine (**100**), has been reported from a previously undescribed *Eudistoma* sp. [53].



Also α -carbolines are not common ascidian metabolites. The grossularines (**101–103**) from *Dendrodia grossularia* are the sole representatives of this structural class and are the first α -carbolines to be isolated from a natural source. The initial structure reported for grossularine (=grossularine-1) [71] was incorrect, and it was revised when data for both grossularine-1 (**101**) and -2 (**103**) were reported [72]. Both grossularines are cytotoxic and cause accumulation of cells in the G1-phase; grossularine-2 appears to act on DNA as a mono-intercalating agent. N,N-didesmethylgrossularine-1 (**102**) has been reported from *Polycarpa aurata*, but no activity data were presented [73].

5.2.3 Indole-Based Alkaloids

The structures of indole-based alkaloids isolated from ascidians span a wide range of complexity, spreading from the simple 6-bromoindole-3-carbaldehyde (**104**), isolated from *Pyura sacciformis* [74] which was previously found in a marine pseudomonad [75] to the complex indolocarbazoles of the staurosporine type (**105–112**) isolated from some Polycitoridae species [76–81]. Staurosporine and its derivatives have been isolated from various actinomycete strains as well as from some marine organisms, including ascidians [82]. These alkaloids were shown to be strong inhibitors of several kinases, in particular protein kinase C (PKC); other activities include inhibition of platelet aggregation and smooth muscle contraction, induction of cell cycle arrest and apoptosis, and the reversal of multidrug resistance in some cancer cell lines. The potential of these derivatives as anticancer agents is supported by the example of 7-hydroxystaurosporine which is in clinical phase I trials at the NCI [79].



105 $R_1=H$, $R_2=Me$, $R_3=H$, $R_4=OH$, $R_5=OMe$

106 $R_1=H$, $R_2=Me$, $R_3=OH$, $R_4=H$, $R_5=OH$

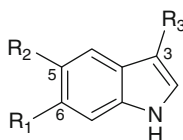
107 $R_1=H$, $R_2=H$, $R_3=H$, $R_4=OH$, $R_5=OMe$

108 $R_1=Me$, $R_2=Me$, $R_3=OH$, $R_4=H$, $R_5=OMe$

109 $R_1=H$, $R_2=H$, $R_3=OH$, $R_4=H$, $R_5=OMe$

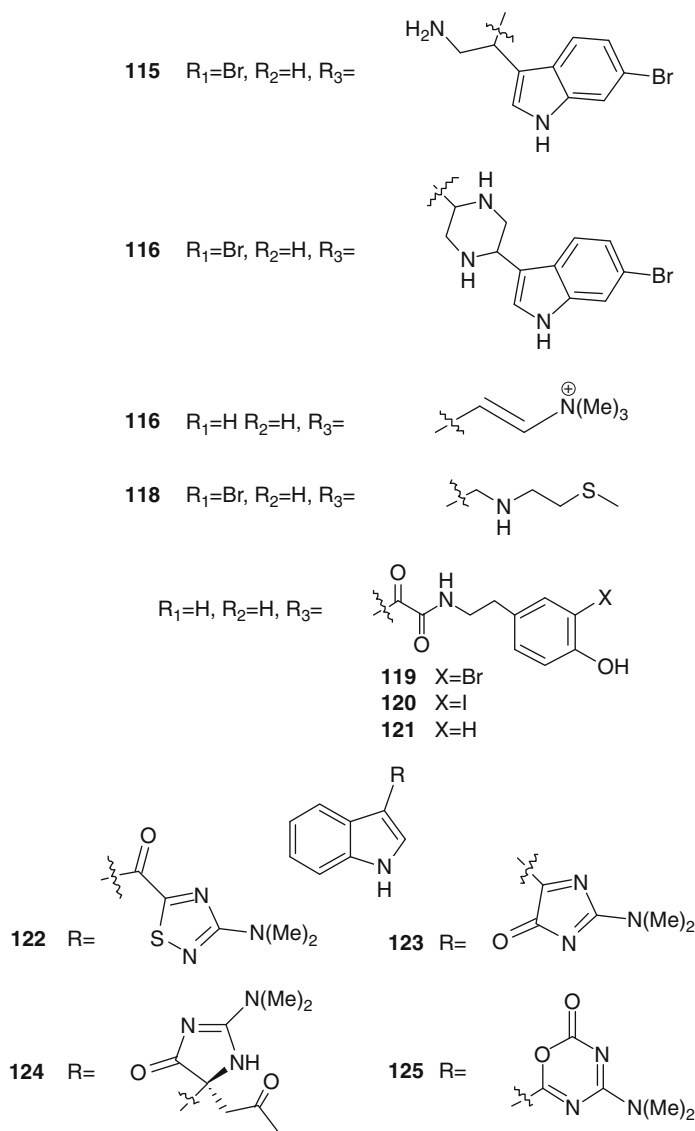
110 $R_1=H$, $R_2=H$, $R_3=H$, $R_4=H$, $R_5=OH$

A number of 3-substituted indoles have been isolated from ascidians. Examples are 6-bromotryptamine (**113**) and its derivatives (**114–116**), isolated from *Didemnum candidum* [83], conicamin (**117**), from *Aplidium conicum*, with histamine-antagonistic activity [84], citorellamine (**118**), from *Polycitorella mariae*, the first indole disulfide dihydrochloride from a marine organism [85, 86], and the indolyl-3-glyoxylic acid derivatives polyandrocarpamides A–C (**119–121**) [87]. *Dendrodoa grossularia* was the source of several indole alkaloids with different heterocyclic moieties linked at three position (compounds **122–125**) [88–91]. Among them, alboinon (**125**) contained an oxadiazinone system, found in nature for the first time [90].



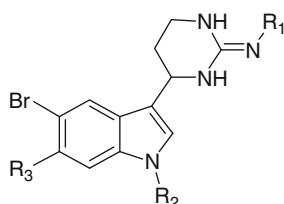
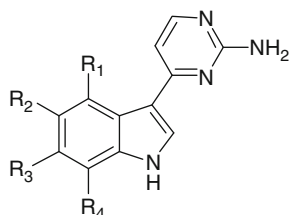
113 $R_1=Br$, $R_2=H$, $R_3=-CH_2CH_2NH_2$

114 $R_1=H$, $R_2=Br$, $R_3=-CH_2CH_2N(Me)_2$



Meridianins are brominated and/or hydroxylated 3-(2-aminopyrimidine)-indoles which have been isolated from *Aplidium meridianum* [92, 93]. Seven meridianins A–G (**126–132**) have been discovered so far, differing in the bromine and/or hydroxyl substitution. They constitute a new family of protein kinase inhibitors, inhibiting various protein kinases such as cyclin-dependent kinases, glycogen synthase kinase-3, cyclic nucleotide-dependent kinases, and casein kinase 1; they also prevent proliferation and induce apoptosis probably due to their ability to enter

cells and to interfere with the activity of kinases important for cell division and death [94]. Structurally related to meridianins are aplicyanins A–F (**133–138**), isolated from *Aplidium cyaneum* and containing a 6-tetrahydropyrimidine substituent at C-3; these alkaloids can be considered reduced forms of the relevant meridianins and, thus, their biogenetic precursors [95].



126 $R_1=OH$; $R_2=R_3=R_4=H$

127 $R_1=OH$; $R_2=R_4=H$; $R_3=Br$

128 $R_1=R_3=R_4=H$; $R_2=Br$

129 $R_1=R_2=R_4=H$; $R_3=Br$

130 $R_1=OH$; $R_2=R_3=H$; $R_4=Br$

131 $R_1=R_4=H$; $R_2=R_3=Br$

132 $R_1=R_2=R_3=R_4=H$

133 $R_1=R_2=R_3=H$

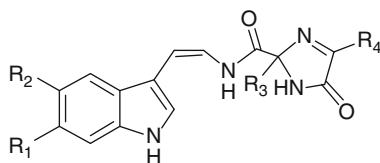
134 $R_1=Ac$; $R_2=R_3=H$

135 $R_1=R_3=H$; $R_2=OMe$

136 $R_1=Ac$; $R_2=OMe$; $R_3=H$

137 $R_1=H$; $R_2=OMe$; $R_3=Br$

138 $R_1=Ac$; $R_2=OMe$; $R_3=Br$

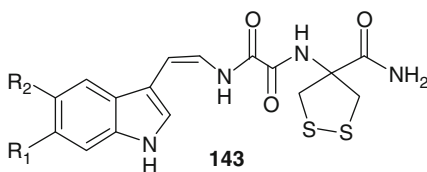


139 $R_1=R_2=Br$; $R_3=2\text{-propyl}$; $R_4=2\text{-butyl}$

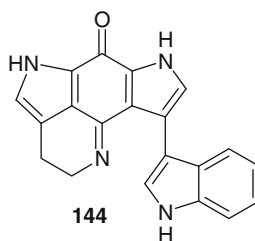
140 $R_1=Br$; $R_2=H$; $R_3=2\text{-propyl}$; $R_4=2\text{-butyl}$

141 $R_1=H$; $R_2=Br$; $R_3=2\text{-propyl}$; $R_4=2\text{-butyl}$

142 $R_1=R_2=Br$; $R_3=2\text{-Butyl}$; $R_4=Methyl$



143

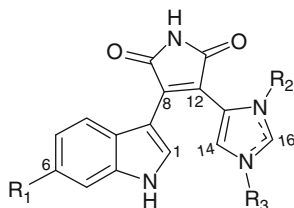


144

Kottamides (**139–142**) have been isolated from a New Zealand collection *Pycnoclavella kottae* [96, 97]; kottamides A–D (**139–142**) are imidazol-4-one containing alkaloids; their biogenesis could involve stereospecific imidazolone ring formation from modified Trp-Val-Ile and Trp-Ile-Ala tripeptide precursors [96]. Kottamide E (**143**) represents the first report of a natural product bearing

a 4-amino-1,2-dithiolane-4-carboxylic acid residue [97]. Wakayin (**144**), from *Clavelina* sp., provides the first example of a pyrroloiminoquinone alkaloid to be isolated from an ascidian. It is also one of the first camptothecin (CPT)-like TOPO I inhibitors isolated from a marine organism, the indole ring linked to the bispyrrole iminoquinone core playing a significant role in this activity [98].

Four predator-deterrent alkaloids possessing a novel indole–maleimide–imidazole carbon skeleton, didemnimides A–D (**145–148**), were isolated from a Caribbean collection of *Didemnum conchylitum* [99]. They were the first examples of a new alkaloid structural class and add to a relatively small group of naturally occurring maleimides. Successively, didemnimide E (**149**) was isolated from *Didemnum granulatum* collected in Brazil together with a less polar and deep purple cyclized didemnimide alkaloid, isogranulatimide (**150**) [100]. Almost at the same time, Fenical's group independently obtained this compound from *D. conchylitum* [101]. Compound **150** is the cyclization product of didemnimide A (**145**) formed via a C-2 indole condensation with the imidazole nitrogen and represented the first alkaloid to be isolated with this cyclized indole–maleimide–imidazole structure. Isogranulatimide (**150**) and its isomer granulatimide (**151**) could be biomimetically synthesized involving the photocyclization of **145**. Subsequently, **151** and its 6-bromo derivative **152** were obtained as naturally occurring compounds from a new collection of Brazilian *D. granulatum* [102]. Isogranulatimide **150** was reported as the first noncytotoxic, specific G2 cell cycle checkpoint inhibitor, and the mechanism of this antitumor action was elucidated at molecular level [100, 103].



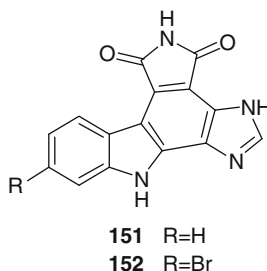
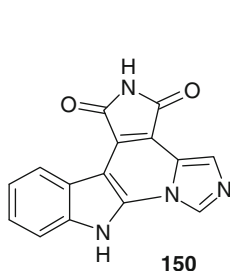
145 $R_1=R_2=H$

146 $R_1=Br; R_2=H$

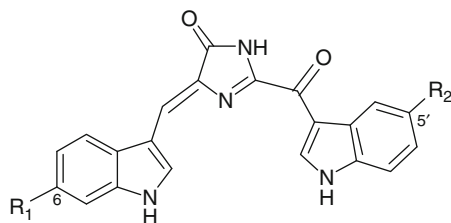
147 $R_1=H; R_2=Me$

148 $R_1=Br; R_2=Me$

149 $R_1=H; R_3=Me$



Apart from the above mentioned staurosporine derivatives **105–112**, other examples of bisindole alkaloids are rhopaladins (**153–156**), from *Rhopalaea* sp., possessing an imidazolinone moiety [104], and iheyamines A (**157**) and B (**158**), from a *Polycytorella* sp., with a new heteroaromatic skeleton composed of an azocine unit fused onto a bisindole system [105]. The 12H-pyrido[1,2-a:3,4-b]diindole ring system forms the framework of the red pigment fascaplysin (**159**), which was isolated in 1988 from the sponge *Fascaplysinopsis Bergquist* and successively found in other Thorectidae sponges; this compound, together with its 3-bromo derivative (**160**), has been found in some *Didemnum* collections [63, 106, 107]. Fascaplysin and its derivatives exhibit a broad range of bioactivities including antibacterial, antifungal, antiviral, HIV-1-RT, p56 tyrosine kinase, antimalarial, cytotoxicity against numerous cancer cell lines, specific inhibition of Cdk 4, and DNA intercalation, demonstrating a huge potential for therapeutic assays [108].

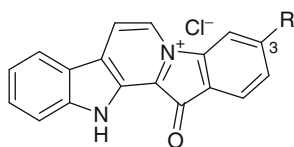


153 $R_1=OH$; $R_2=Br$

154 $R_1=OH$; $R_2=H$

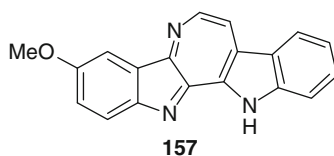
155 $R_1=H$; $R_2=Br$

156 $R_1=R_2=H$

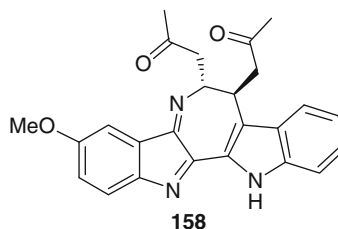


159 $R=H$

160 $R=Br$



157

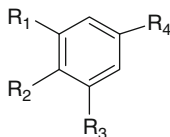


158

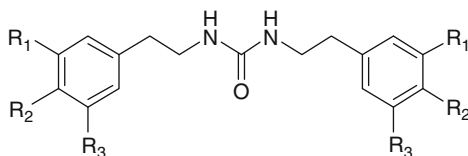
5.2.4 Tyrosine- and Phenylalanine-Derived Alkaloids

Tyrosine is the precursor of a wide number of alkaloids whose structures are characterized by possessing the $Ar-C_2-N$ subunit derived from Tyr, commonly via dopamine; often, additional $Ar-C_1$ and $Ar-C_2$ moieties are present, derived from a partial degradation of the amino acids Phe or Tyr. Furthermore, the aromatic ring of all these subunits is usually oxygenated at 4-, 3,4-, or

3,4,5-positions. The amino acid DOPA [2-amino,3-(3',4'-dihydroxyphenyl) propionic acid] in particular, appears to play an important role in the metabolism of ascidians, serving as the apparent precursors not only of peptide products but also of several alkaloid metabolites. In this group fall simple aromatic alkaloids, derived directly or indirectly from phenylalanine, tyrosine, phenylethylamine, tyramine, or dopamine, as well as complex highly condensed structures. Phenylethylamine itself (**161**) and its urea derivative (**162**) have been found in a *Lissoclinum* sp. and in *Didemnum ternatanum*, respectively [20, 109]. Iodinated and/or brominated tyramine derivatives, such as compounds **163–172**, are often found within ascidians metabolites [53, 110–114]. The guanidine derivatives tubastrine (**173**) and its saturated analogue **174** have been found in a New Zealand collection of *Aplidium orthyum* [115]; an Australian collection of *Polycarpa aurata* contained the three *p*-methoxybenzoyl derivatives **175–177** [116].



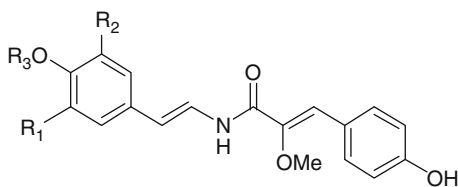
- 161** $R_1=R_2=R_3=H$; $R_4=-CH_2CH_2NH_2$
163 $R_1=I$; $R_2=OMe$; $R_3=I$; $R_4=-CH_2CH_2NH_2$
165 $R_1=I$; $R_2=OMe$; $R_3=I$; $R_4=-CH_2CONH_2$
166 $R_1=I$; $R_2=OMe$; $R_3=I$; $R_4=-CH_2CH_2NHCOH$
167 $R_1=I$; $R_2=OMe$; $R_3=I$; $R_4=-CH_2CH_2NHCOPhe$
168 $R_1=I$; $R_2=OH$; $R_3=H$; $R_4=-CH_2CH_2NH_2$
169 $R_1=I$; $R_2=OH$; $R_3=H$; $R_4=-CH_2CH_2N(Me)_3+$
170 $R_1=Br$; $R_2=OH$; $R_3=H$; $R_4=-CH_2CH_2NH_2$
171 $R_1=Br$; $R_2=OH$; $R_3=Br$; $R_4=-CH_2CH_2NH_2$
172 $R_1=Br$; $R_2=OH$; $R_3=H$; $R_4=-CH_2CH_2N(Me)_3+$
173 $R_1=OH$; $R_2=OH$; $R_3=H$; $R_4=-CH=CHNHCNHNH_2$
174 $R_1=OH$; $R_2=OH$; $R_3=H$; $R_4=-CH_2CH_2NHCNHNH_2$
175 $R_1=H$; $R_2=OMe$; $R_3=H$; $R_4=-CONHCNHNH_2$
176 $R_1=H$; $R_2=OMe$; $R_3=H$; $R_4=-COCOO(CH_2)_3CH_3$
177 $R_1=H$; $R_2=OMe$; $R_3=H$; $R_4=-COCONHCH_3$



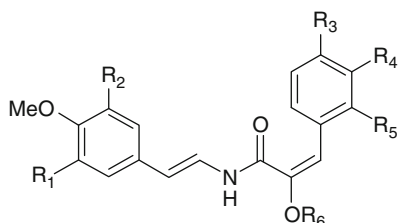
- 162** $R_1=R_2=R_3=H$
164 $R_1=I$; $R_2=OMe$; $R_3=I$

Botryllamides (A–J, **178–187**) are a series of brominated tyrosine derivatives isolated from several *Botryllus* species [117–120]; they form a new class of

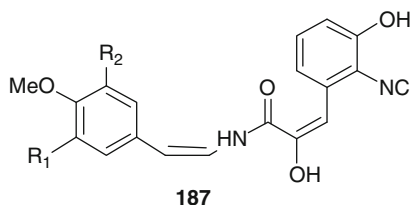
selective inhibitors of ABCG2, a human ATP-binding cassette (ABC) transporter gene usually associated with multidrug resistance in cancer [119, 121].



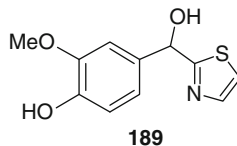
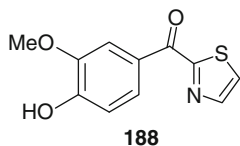
- 178** $R_1=R_2=Br$; $R_3=Me$
180 $R_1=Br$; $R_2=H$; $R_3=Me$
182 $R_1=R_2=H$; $R_3=Me$
183 $R_1=R_2=H$; $R_3=H$
184 $R_1=R_2=Br$; $R_3=H$

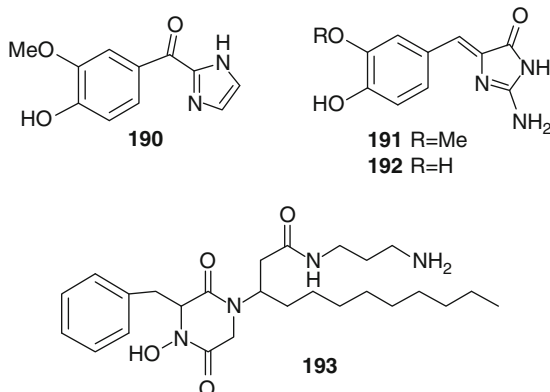


- 179** $R_1=R_2=Br$; $R_3=OH$; $R_4=R_5=H$; $R_6=Me$
181 $R_1=Br$; $R_2=H$; $R_3=OH$; $R_4=R_5=H$; $R_6=Me$
185 $R_1=R_2=R_3=H$; $R_4=OH$; $R_5=NC$; $R_6=H$
186 $R_1=R_2=H$; $R_3=OH$; $R_4=R_5=H$; $R_6=Me$

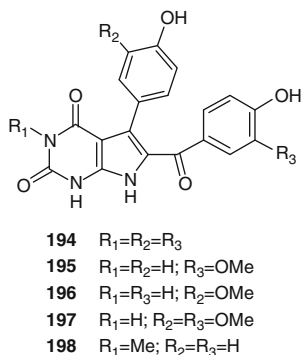


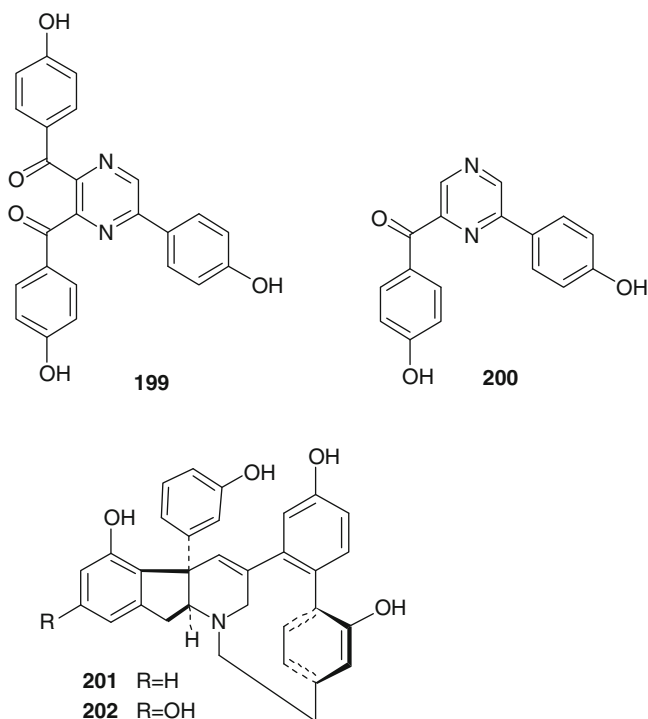
In some metabolites, the amino group of what initially was the amino acid residue has ended up as a part of a heteroaromatic ring. Examples are the thiazole and imidazole metabolites **188–190** isolated from *Aplidium pliciferum* [122] as well as the polyandrocarpamines A and B (**191** and **192**), from a Fijian *Polyandrocarpa* sp. possessing a 2-aminoimidazolone moiety [123]. A condensation between phenylalanine and glycine is expected to form the 1,4-diketopiperazine unit present in etzionin (**193**), an unusual antifungal metabolite isolated from an unidentified Red Sea tunicate [124].





Rigidin (**194**), isolated from the Okinawan tunicate *Eudistoma cf. rigida*, was the first pyrrolopyrimidine alkaloid to be isolated from a marine source; it exhibited calmodulin antagonistic activity for inhibition of calmodulin-activated brain phosphodiesterase [125]. Four rigidin congeners, rigidins B–E (**195**–**198**), have been successively isolated from *Cystodites* and *Eudistoma* species [126, 127]. Botryllazines A and B (**199** and **200**) have been isolated from *Botryllus leachi*; the structure of botryllazine A is unprecedented since three tyrosine precursors are involved in the formation of a pyrazine nucleus. It has been proposed that the biogenetic pathway leading to botryllazine B from two tyrosine units involves amide formation and, subsequently, cyclization *via* imine formation [128]. Haouamines A and B (**201** and **202**), isolated from *Aplidium haouarianum* [129], demonstrate intriguing stereochemical features; in solution, each haouamine exists as an inseparable mixture of two interconverting isomers derived by the presence of a highly strained 3-aza-[7]-paracyclophane moiety in their structures. Even if one Ar–C2–N and three Ar–C2 subunits can be readily identified in the structures of haouamines, the oxygenation pattern of all these units, hydroxylated at the meta position with respect to the C2 chain, does not allow establishing a relationship between these alkaloids and the amino acid tyrosine. Thus, the biosynthesis of these alkaloids should imply either an unusual loss of the C4 hydroxyl group of tyrosine along the biosynthetic pathway or the involvement of an undescribed natural amino acid precursor exclusively meta hydroxylated [129].





The lamellarins form a group of more than 50 highly condensed DOPA- and TOPA-derived pyrrole alkaloids; they were first isolated from the proso-branch mollusk *Lamellaria* sp. in 1985 [130] and, since then, they have been reported from diverse marine organisms, mainly but not exclusively ascidians and sponges, which suggests a potential microbial link to their biosynthesis [131].

The lamellarins fall into two structural groups, depending on whether the central pyrrole ring is fused (group I) or unfused (group II) to adjacent aromatic rings (Fig. 5.1). Group I could be further divided into two subgroups, Ia, including compounds with an olefin at C5/C6, and Ib, with compounds in which this olefin is saturated. The family also includes sulfated members. Most of lamellarins have shown a wide range of bioactivities, such as antibiotic activity, HIV-1 integrase inhibition, immunomodulation, antioxidant activity; a considerable number of lamellarins have been found to be cytotoxic and, more interestingly, some of them were reported to act as nontoxic inhibitors of acquired multidrug resistance (MDR) in various cancer cell lines. In light of their fascinating novel structures and intriguing biological properties, lamellarins have got to be a particularly important subject for synthetic as well

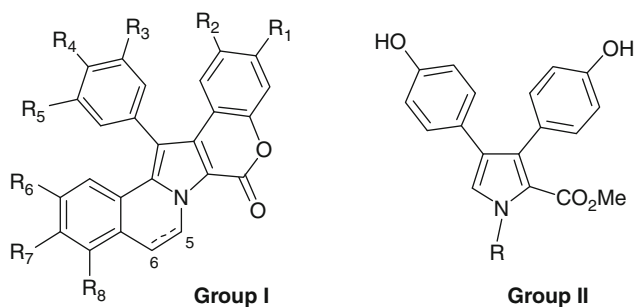
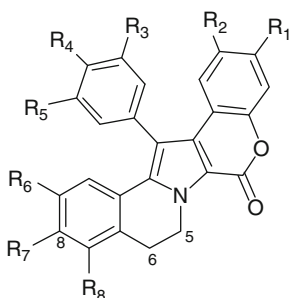
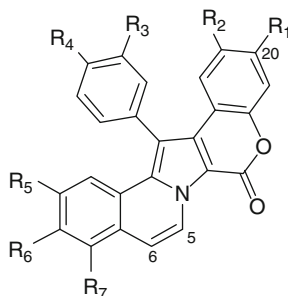


Fig. 5.1 Core structures of lamellarins

as SAR studies [131, 132]. A number of lamellarins have been isolated from ascidians belonging to *Didemnum* genus, all with the hexacyclic skeleton of group I; examples are lamellarins E–M (203–211) [133, 134], Z (212) [135], α , ε , ζ , η , and ϕ (213–217) [136, 137]; triacetate of lamellarin N (218) [134]; lamellarin G 8-sulfate (219) [135]; the 20-sulfate derivatives of lamellarins B, C, L, and α (220–223) [135, 138].

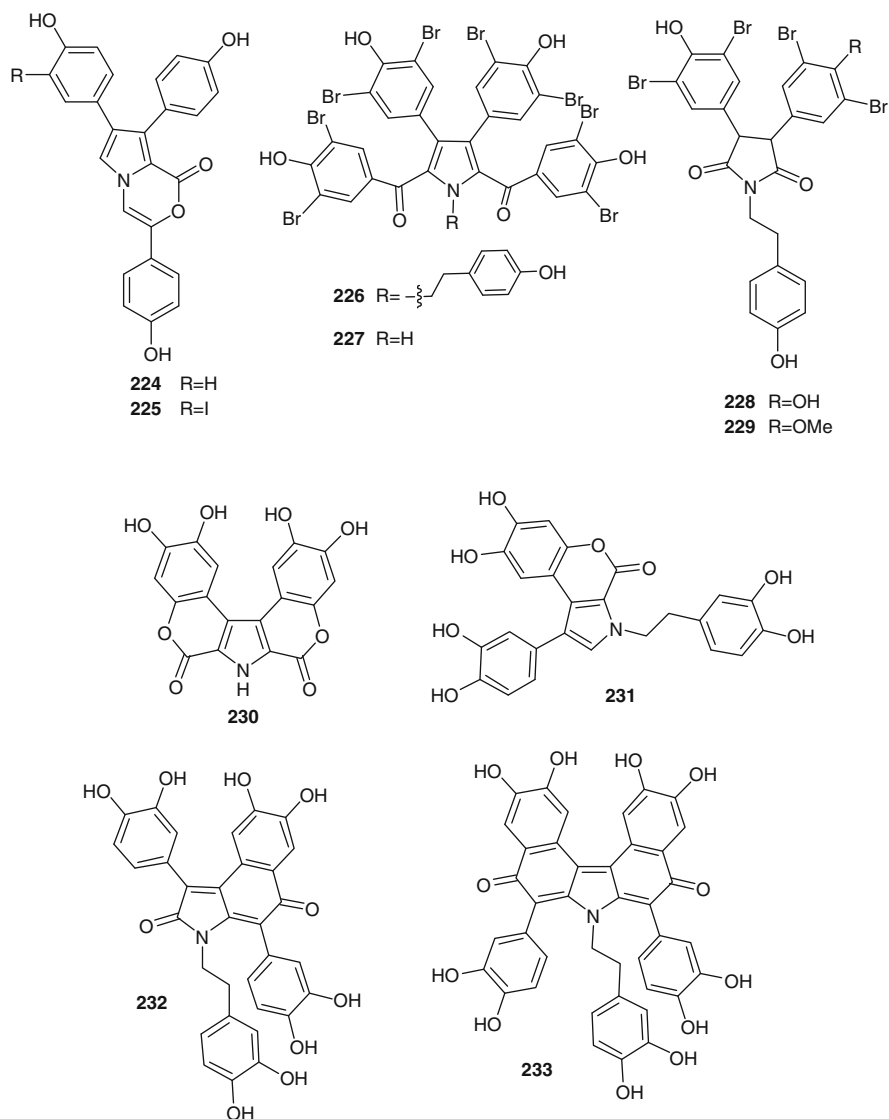


Lamellarin E	203	$R_1=R_8=OH$; $R_2=R_4=R_5=R_6=R_7=OMe$; $R_3=H$
Lamellarin F	204	$R_1=R_5=R_8=OH$; $R_2=R_4=R_6=R_7=OMe$; $R_3=H$
Lamellarin G	205	$R_1=R_4=R_6=OMe$; $R_2=R_5=R_7=OH$; $R_3=R_8=H$
Lamellarin I	207	$R_1=OH$; $R_2=R_4=R_5=R_6=R_7=R_8=OMe$; $R_3=H$
Lamellarin J	208	$R_1=R_7=OH$; $R_2=R_4=R_5=R_6=OMe$; $R_3=H$
Lamellarin K	209	$R_1=R_4=R_8=OH$; $R_2=R_5=R_6=R_7=OMe$; $R_3=H$
Lamellarin l	210	$R_1=R_5=R_7=OH$; $R_2=R_4=R_6=OMe$; $R_3=R_8=H$
Lamellarin α	213	$R_1=R_6=OMe$; $R_2=R_4=R_5=R_7=OH$; $R_3=R_8=H$
Lamellarin ζ	215	$R_1=OSO_3^-$; $R_2=R_5=R_6=R_7=R_8=OMe$; $R_4=OH$; $R_3=H$
Lamellarin η	216	$R_1=OSO_3^-$; $R_2=R_4=R_6=OMe$; $R_5=R_7=OH$; $R_3=R_8=H$
Lamellarin ϕ	217	$R_1=R_4=R_6=OMe$; $R_2=R_5=OH$; $R_7=OSO_3^-$; $R_3=R_8=H$



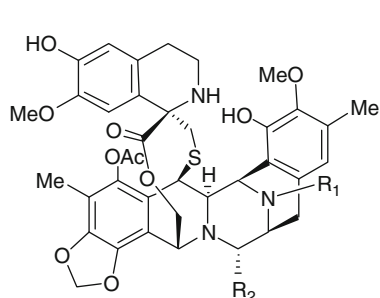
Lamellarin H	206	$R_1=R_2=R_3=R_4=R_5=R_6=OH$; $R_7=H$
Lamellarin M	211	$R_1=R_3=R_7=OH$; $R_2=R_4=R_5=R_6=OMe$;
Lamellarin Z	212	$R_1=R_4=R_6=OAc$; $R_2=R_3=R_5=OMe$; $R_7=H$
Lamellarin ϵ	214	$R_1=OSO_3^-$; $R_2=R_4=R_5=R_6=R_7=OMe$; $R_3=OH$
Lamellarin N triacetate	218	$R_1=OSO_3Na$; $R_2=R_3=R_5=R_6=OMe$; $R_4=OH$; $R_7=H$
Lamellarin G 8-sulfate	219	$R_1=R_4=OH$; $R_2=R_3=R_5=R_6=OMe$; $R_7=H$
Lamellarin B 20-sulfate	220	$R_1=R_7=OH$; $R_2=R_3=R_4=R_5=R_6=OMe$
Lamellarin C 20-sulfate	221	$R_1=OH$; $R_2=R_3=R_4=R_5=R_6=R_7=OMe$
Lamellarin L 20-sulfate	222	$R_1=OH$; $R_2=R_3=R_4=R_5=R_6=OMe$; $R_7=H$
Lamellarin α 20-sulfate	223	$R_1=R_3=R_5=OAc$; $R_2=R_4=R_6=R_7=OMe$

Pyrrole-derived alkaloids related to lamellarin include lukianols (**224–225**) [139], polycitones (**226–227**) [140, 141], polycitrins (**228–229**) [140], and ningalins (**230–233**) [142]. The structures of the lukianols A and B, isolated from an unidentified Pacific tunicate, contained a pyrrolooxazinone moiety; they appear to arise by the same biogenetic pathways leading to lamellarin O and P isolated from the marine sponge *Dendrilla cactus*. Lukianol A (**224**) inhibited DNA synthesis in L1210 lymphocytic leukemia cell lines with less effect on RNA and protein synthesis, demonstrating a therapeutic profile very similar to current clinically used anticancer agents [139]. Polycitone A (**226**) was isolated from a *Polycitor* sp., together with polycitrins A and B (**228** and **229**), containing a maleimide unit; polycitone B (**227**) was successively isolated from *Polycitor africanus*. Ningalins A–D (**230–233**) are condensed aromatic systems with the unifying theme that all appear derived from the condensation of two, three, four, and five DOPA precursors, respectively. Although a potential role for these alkaloids in metal sequestration has not been demonstrated, they are structurally related to other metal binding ascidian-derived *o*-catechols; it is thus conceivable that they too participate in the metal chelating phenomena characteristic of this class of marine invertebrates [131, 139].

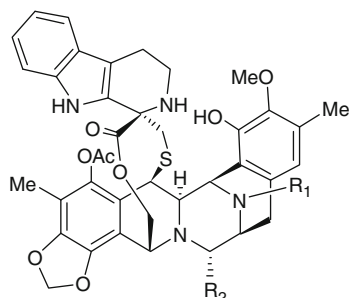


Tetrahydroisoquinoline alkaloids are uncommon in ascidians, but the sole representatives of this class, ecteinascidins, mainly from the Caribbean ascidian *Ecteinascidia turbinata*, are probably the most useful anticancer agents found to date in marine source. Their lead compound, Yondelis[®] (trabectedin, ET-743), is the first marine anticancer agent approved in the European Union for patients with soft tissue sarcoma (STS). Positive results of a large randomized phase III clinical trial in ovarian cancer have recently been presented [143]. The first description and structural

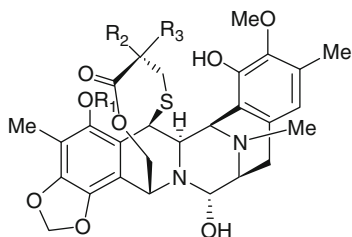
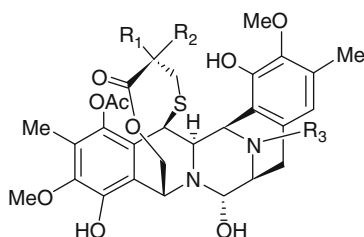
characterization of six new chemical entities called ET 729 (**234**), ET 743 (**235**), ET 745 (**236**), ET 759A (**237**), ET 759B (**238**), and ET 770 (**239**) was reported by the Rinehart group in 1990 of which ET-743 was the most abundant representative [144]. Simultaneously, Wright and coworkers described compounds **234** and **235** [145], but the unequivocal assignment of the absolute stereochemistry was achieved only when the X-ray crystal structures of the natural N¹²-oxide of ET-743 (**240**) and a synthetic O-methyl analogue of N¹²-formyl ET-729 (**241**) were solved [146]. Successively, a number of additional new members of this class of molecules have been isolated, such as compounds **242** and **243** [147], **244–247** [148], **248** [149], **249–252** [150].



ET 729	234	R ₁ =H; R ₂ =OH
ET 743	235	R ₁ =Me; R ₂ =OH
ET 745	236	R ₁ =Me; R ₂ =H
ET 759 A	237	R ₁ =Me; R ₂ =O(lactam)
ET 759 B	238	R ₁ =Me; R ₂ =OH, S-oxide
ET 770	239	R ₁ =Me; R ₂ =CN
ET 743 N ¹² -oxide	240	R ₁ =Me; R ₂ =OH, N-oxide
ET 729 N ¹² -formyl	241	R ₁ =CHO; R ₂ =OH
ET 815	245	R ₁ =Me; R ₂ =CH(CHO) ₂
ET 731	246	R ₁ =R ₂ =H
ET 745 B	247	R ₁ =H; R ₂ =OH, S-oxide
ET 786	248	R ₁ =Me; R ₂ =CN, S-oxide



ET 722	242	R ₁ =H; R ₂ =OH
ET 736	243	R ₁ =Me; R ₂ =OH
ET 808	244	R ₁ =Me; R ₂ =CH(CHO) ₂

ET 594 **249**

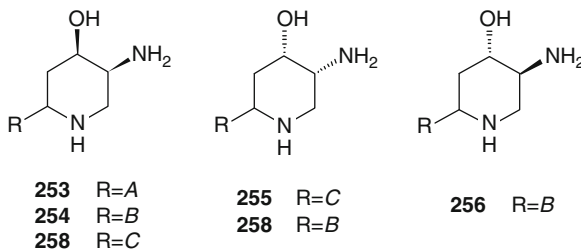
ET 583	250	R ₁ =H; R ₂ =NH ₂ ; R ₃ =H
ET 597	251	R ₁ =H; R ₂ =NH ₂ ; R ₃ =Me
ET 596	252	R ₁ =R ₂ =O; R ₃ =Me

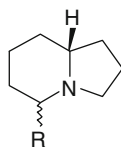
The interesting biological properties as well as the extraordinary three-dimensional molecular architecture of these compounds have made them a fascinating target for the synthetic organic chemist, allowing a number of original synthetic and semisynthetic methodologies for the preparation of a wide variety of ecteinascidins to be discovered [151]. The unique structure of ecteinascidins consists of a monobridged pentacyclic skeleton composed of two fused tetrahydroisoquinoline rings (subunits A and B) linked to a 10-membered lactone bridge through a benzylic sulfide linkage. Most ecteinascidins have an additional tetrahydroisoquinoline or tetrahydro- β -carboline ring (subunit C) attached to the rest of the structure through a spiro-ring. As for the biogenesis of the ecteinascidins, it has been proposed that A–B units could be formed by condensation of two DOPA-derived building blocks, and the tetrahydroisoquinoline ring in unit B is closed by condensation with a serine- (or glycine)-derived aldehyde as in the case of the related saframycins. S-Adenosylmethionine is the likely source of methyl groups at C-6, O-7, C-16, O-17, and N-12 [150].

5.2.5 Lysine-Derived Alkaloids

Alkaloids based on a 2-amino-3-hydroxyoctadecane moiety, generally referred to as lysine-derived metabolites, have been found in several genera of ascidians. Monocyclic examples are the piperidine alkaloids, which are among the most abundant metabolites of terrestrial plants, but there are relatively few examples isolated from marine organisms.

Pseudodistomins A (253) and B (254), isolated from the Okinawan ascidian *Pseudodistoma kanoko*, represent the first piperidine alkaloids obtained from marine sources [152]. The structure of the side chains of 253 and 254 has been revised after the first disclosure of the molecules [153, 154], while the stereostructure of the piperidine nucleus has been established by synthesis of their tetrahydroacetyl derivatives [155, 156]. Other members of the group have been successively isolated, from other *Pseudodistoma* species, including pseudodistomin C (255), with the absolute configuration at C-4 and C-5 opposite to those found in 253 and 254 [157], and pseudodistomins D–F (256–258) [158]. Pseudodistomins A and B exhibited cytotoxic activity with calmodulin antagonistic activity; pseudodistomins B–F were found to be active in a cell-based assay for DNA damage induction. Uoamines A (259) and B (260) also are monocyclic piperidine alkaloids isolated from *Aplidium uouo*; in these compounds, the 3-hydroxyl group present on the piperidine nucleus is esterified by (*E*)- or (*Z*)-3-thiomethylacrylic acid, respectively [159].



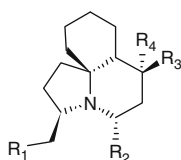


264 $R = \text{CH}_2\text{CH}=\text{CH}(\text{CH}_2)_6\text{CH}_3$

265 $R = \text{CH}=\text{CHCH}=\text{CH}(\text{CH}_2)_5\text{CH}_3$

266 $R = \text{CH}=\text{CHCH}=\text{CHCH}=\text{CH}(\text{CH}_2)_3\text{CH}_3$

Tasmanian collections of *C. cylindrica* yielded the tricyclic alkaloids cylindricines A–K (**267–277**) [163–165]; cylindricine B (**268**) represented the first example of the new perhydropyrido[2,1-*j*]quinoline ring system, while cylindricine A (**269**) is the first perhydropyrrolo[2,1-*j*]quinoline known from nature. The skeleton of cylindricines A (**267**), C–I (**269–275**), and K (**277**) is closely related to the indolizidine system of piclavines by having an extra 6-membered carbocyclic fused ring. In the same way, structures of cylindricines B (**268**) and J (**276**) are related to the quinolizidine system of the clavicipitines and pictamines. Cylindricines F (**272**) and G (**273**) are the first thiocyanates from an ascidian. Closely related to cylindricines A and B are polycitorols A (**278**) and B (**279**), isolated from a marine ascidian of the family Polycitoridae [166]; they lack C-4 oxygenation found in cylindricines and have a OH group instead of a chlorine atom at C-13 and a butyl instead of a hexyl appendage at C-2. Other analogous metabolites are lepadiformines A–C (**280–282**) isolated from *C. lepadiformis* and *C. moluccensis* [167, 168] and fascicularin (**283**) from *Nephteis fascicularis* [169]. The initially reported structure of lepadiformine A was revised through its total synthesis; in the same study fascicularin (**283**) was also synthesized, allowing its absolute configuration to be assigned [170]. Early biological experiments on fascicularin suggested that its cytotoxic properties may stem from its ability to damage cellular DNA [169]. Successive studies revealed fascicularin as the first natural product found to generate a DNA-alkylating aziridinium ion via a mechanism analogous to the clinically used anticancer drugs mechlorethamine, melphalan, and chlorambucil [171]. Biological studies on lepadiformines showed that they have marked effects on the cardiovascular system when tested on frog atrial myocytes, the potency varying with the alkaloid structure [168].



267 $R_1 = \text{Cl}; R_2 = \text{C}_6\text{H}_{13}; R_3, R_4 = \text{O}$

269 $R_1 = \text{OH}; R_2 = \text{C}_6\text{H}_{13}; R_3, R_4 = \text{O}$

270 $R_1 = \text{OMe}; R_2 = \text{C}_6\text{H}_{13}; R_3, R_4 = \text{O}$

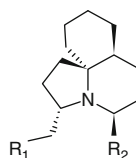
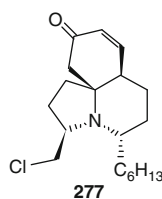
271 $R_1 = \text{OAc}; R_2 = \text{C}_6\text{H}_{13}; R_3, R_4 = \text{O}$

272 $R_1 = \text{SCN}; R_2 = \text{C}_6\text{H}_{13}; R_3, R_4 = \text{O}$

274 $R_1 = \text{SCN}; R_2 = \text{C}_4\text{H}_9; R_3 = \text{H}; R_4 = \text{OAc}$

275 $R_1 = \text{NCS}; R_2 = \text{C}_4\text{H}_9; R_3 = \text{H}; R_4 = \text{OAc}$

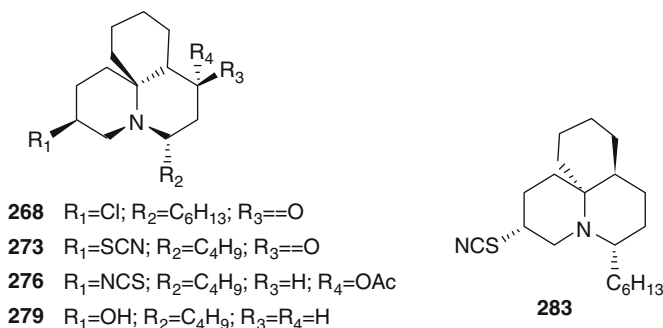
278 $R_1 = \text{OH}; R_2 = \text{C}_4\text{H}_9; R_3 = R_4 = \text{H}$



280 $R_1 = \text{OH}; R_2 = \text{C}_6\text{H}_{13}$

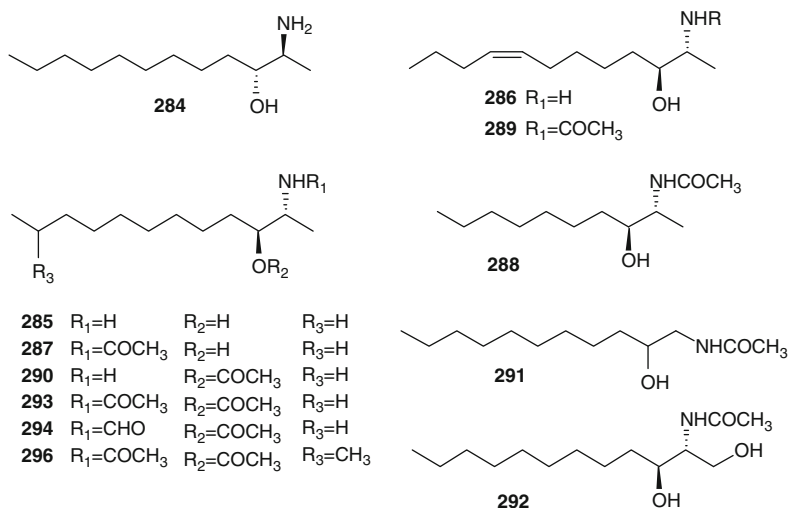
281 $R_1 = \text{OH}; R_2 = \text{C}_4\text{H}_9$

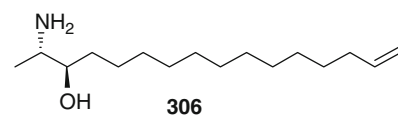
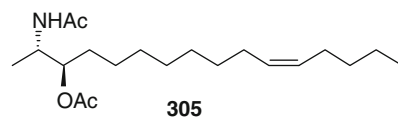
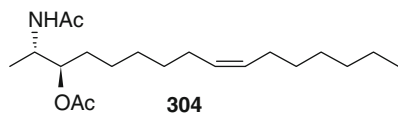
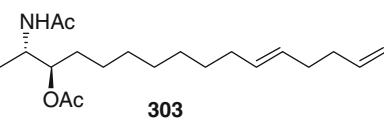
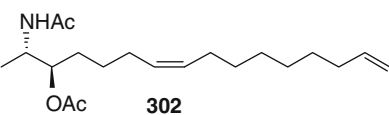
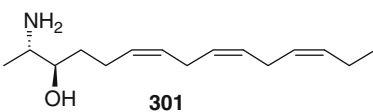
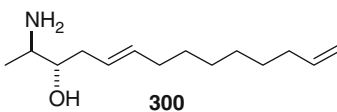
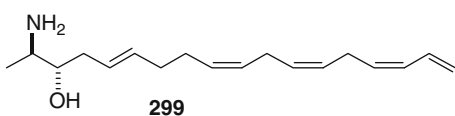
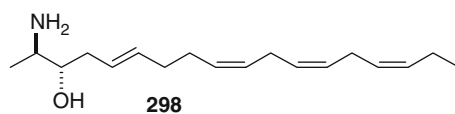
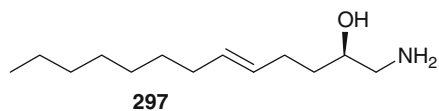
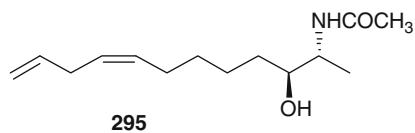
282 $R_1 = \text{H}; R_2 = \text{C}_4\text{H}_9$



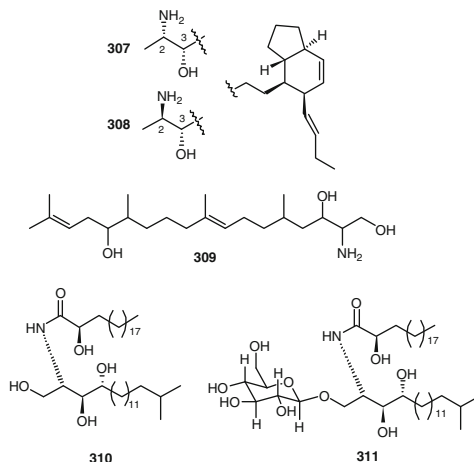
5.2.6 Protoalkaloids

Ascidians have been also the source of protoalkaloids, simple amines in which the nitrogen is not in a heterocyclic ring. *Clavelina* and *Pseudodistoma* genera have been prolific in the production of linear 2-amino-alkanols and their unsaturated and/or acetylated derivatives. Structurally, these compounds are related to the sphingosine derivatives, which are central structural elements of sphingolipids and important constituents of the lipid portion of cell membranes in living organisms. The carbon chain length of these sphingolipid derivatives vary from C12 to C18 amino alcohols. Examples are the C12 saturated amino alcohol (2S,3R)-2-aminododecanol-3-ol (**284**) isolated from *C. oblonga* [172], the clavaminols A–N (**285–296**), twelve saturated and unsaturated cytotoxic sphingoids isolated from the Mediterranean *C. phlegraea* [173, 174], and the antifungal 2-amino alcohol **297** isolated from an Australian *Didemnum* sp. [175]. Crucigasterins 277, 275, and 225 (**298–300**) and A–E, and obscuraminols A–F (**301–306**) are examples of polyunsaturated 2-amino-3-alkanols; they have been isolated as their diacetyl derivative from *P. crucigaster* and *P. obscurum*, respectively [176, 177].

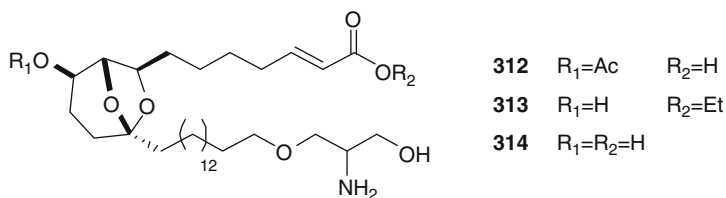


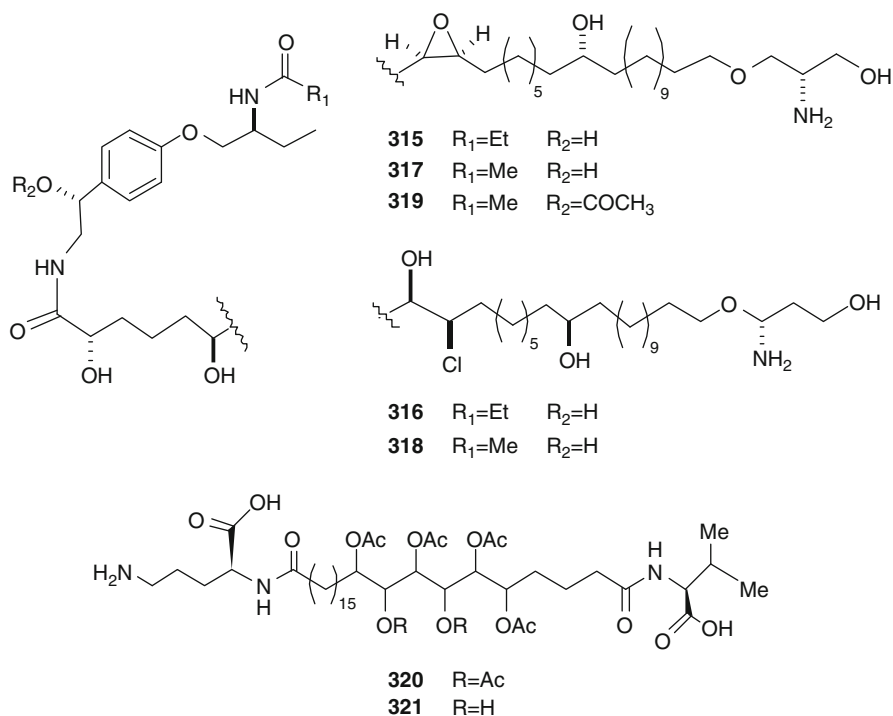


Two bicyclic amino alcohols, amaminols A e B (**307–308**) have been isolated from an unidentified tunicate of the family Polyclinidae [178]. Total synthesis of amaminol A (**307**) allowed to establish its absolute stereochemistry [179]. Other sphingosine-related compounds are apolidiasphingosine (**309**), and the two lipids (**310–311**) isolated from *Cystodytes* cf. *dellechiajei* as PLA2 inhibitors [180, 181].



Didemniserinolipids A–C (**312–314**) are unprecedented serinolipids, compounds containing a unique serinol component and a 6,8-dioxabicyclo[3.2.1]octane core, isolated as antibacterial constituents of a tunicate of the family Didemnidae [182]. En route to proving the absolute and relative stereochemistry, through synthesis, of (+)-didemniserinolipid B (**313**), it was discovered that the isolated natural product was in fact its 31-sulfate configured $8R,9R,10R,13S,30S$. This structural reassignment was only possible after the development of a microwave-assisted method for the sulfation of unreactive hydroxyl groups [183]. Further serinolipid derivatives, shishididemniols A–E (**315–319**) have been isolated as antibacterial constituents of a tunicate of the family Didemnidae [184, 185]; they are complex lipids with tyramine-derived tether and two serinol units. An unidentified tunicate from Pohnpei Micronesia yielded sagittamides A (**320**) and B (**321**), with a C26 dicarboxylic acid that acylates terminal L-valine and L-ornithine groups [186]; the structures contain an unprecedented internal *O*-hexacetyl-1,2,3,4,5,6-hexaol moiety. The stereochemistry of sagittamide A has been extensively investigated; its absolute configuration has been established through a detailed ^1H NMR analysis of the two remote diastereomers, followed by doping experiments of them with the authentic natural product [187].



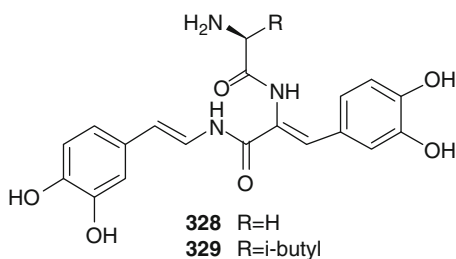
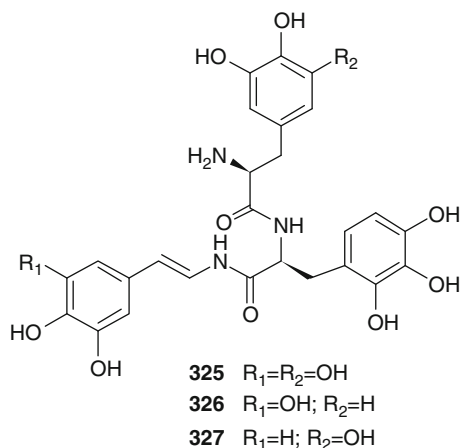
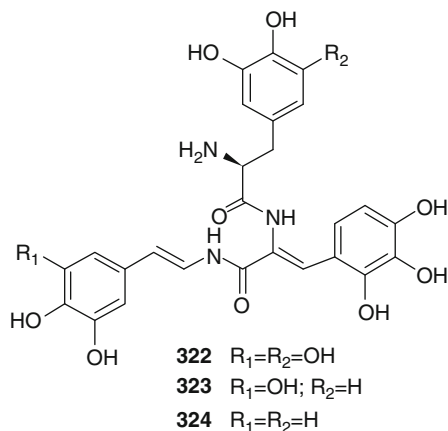


5.3 Peptides

5.3.1 Tunichromes and Related Compounds

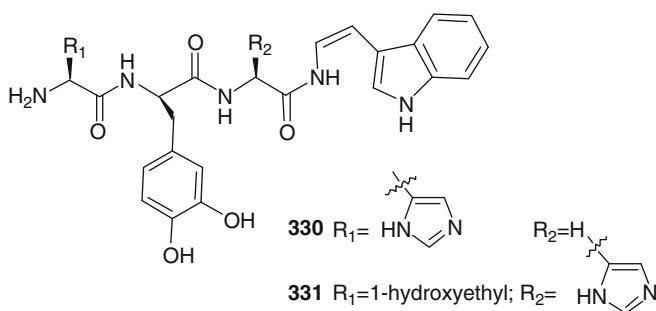
While the vast majority of ascidian metabolites have been isolated from whole-body extractions, several investigations have concentrated on compounds isolated from specific tissues or physiological fluids. A series of very unstable compounds, called the tunichromes, was isolated from the blood of several species of ascidians. Tunichromes are small modified peptides containing one or more DOPA (3,4-dihydroxyphenylalanine) or TOPA (3,4,5-trihydroxyphenylalanine) residues or their unsaturated derivatives; they have been isolated from *Ascidia*, *Phallusia*, *Molgula* and *Styela* genera. The biological function of these pigments remains unclear; they appear to be involved in the vanadium and, to a lesser extent, iron accumulation and storage in ascidian blood cells [3, 4, 188]. Because these compounds are extremely sensitive to air and water, the original isolation was carried out under totally anaerobic and anhydrous conditions. Synthetic studies have yielded a breakthrough in the isolation methodology which involves protection of the hydroxyl groups as their tert-butyldimethylsilyl ethers and free amino groups as their tert-butyloxycarbonyl derivatives. In addition to allowing the straightforward

separation of individual tunichromes, the protecting groups may be subsequently removed, providing native tunichromes for further biological studies [189].



The first isolated member of the series was tunichrome B-1, which is now referred to as *An*-1 (**322**), since it was isolated from *A. nigra* [190]. Its structure consisted of a modified tripeptide of three DOPA-derived fragments. Later, the structures of *An*-2 (**323**) and *An*-3 (**324**) were determined, differing only in the degree of

hydroxylation [191]. More recently, three tunichromes, *Pm*-1, *Pm*-2, and *Pm*-3 (325–327), have been identified from the blood cells of *P. mamillata* [192]; the structural difference between these tunichromes and those from *A. nigra* is that *Pm* tunichromes are saturated at the C11–C12 bond. A third group of tunichromes, *Mm*-1 (328) and *Mm*-2 (329) have been isolated from the iron-accumulating ascidian *M. manhattensis* [191]; they bear only two DOPA residues linked to a glycine (Mn-1, 328) or a leucine (Mn-2, 329) residue. Recently, a modified pentapeptide has been isolated from *S. plicata* [193]; it was designated as a tunichrome (tunichrome *Sp*-1) since (1) it was a linear low molecular weight peptide, (2) it was recovered in the ascidian hemocytes, and (3) it has an oxidatively decarboxylated C-terminus derived from a hydroxylated aromatic amino acid residue and two hydroxylated amino acid in its sequence. Related to the tunichromes are halocyamines A and B (330 and 331) isolated from the hemocytes of the solitary ascidian *Halocynthia roretzi* [194]; they are tetrapeptides which contain a DOPA residue which showed antimicrobial as well as cytotoxic properties.

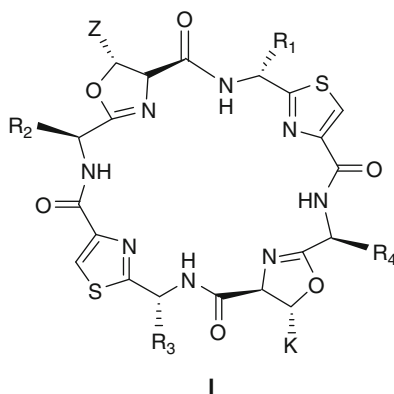


5.3.2 Cyclic Peptides

A variety of cyclic peptides have been isolated from ascidians and have shown to exhibit moderate to high cytotoxicity. Structure elucidation of these compounds has been fraught with difficulty and minor or major revisions have been made for a number of the originally proposed structures. Ascidians of the genus *Lissoclinum* are a prolific source of unusual cyclic peptides containing both D- and L-amino acids, many modified in the form of thiazole, oxazole, thiazoline, or oxazoline rings. The cyclic peptides that have been isolated from *L. patella* belong to two general families of compounds, the octapeptide patellamide family, **I**, and the heptapeptide lissoclinamide family, **II**, according to the number of amino acids and inclusion of thiazole (Thz), thiazoline (Thn), and oxazoline (Oxn) rings within their structure [195].

Compounds of the patellamide family, (**I**: 332–340) [196–203], are characterized by thiazole alternating with oxazoline rings, and some of their structures have been confirmed by synthesis [204–211]. Structure-activity studies of the sets 332–334 and 338–339 and related synthetic or semisynthetic compounds have revealed that the oxazoline ring is vital for the cytotoxic activity of these compounds and that the bridging disulfide unit in 339 greatly enhances cytotoxicity [212]. Studies of the

conformation of azole-based marine cyclic peptides, both in solution and in solid state, have provided valuable insights into the factors which may affect the reactivity and the biology of these metabolites [213–219]. An X-ray crystal structure determination of the C₂-symmetric ascidiacyclamide (**338**), for example, showed that it has a “square” (also sometimes referred to as “saddle-shaped”) conformation with its thiazole and oxazoline rings occupying the corners of a rectangle with all of the NH bonds directed to the interior of the macrocyclic ring [213, 220–222]. Patellamide A (**332**) has a similar rectangular shape in the solid state [216, 223], but, by contrast, X-ray analysis of the closely related patellamide D (**335**) shows that it assumes a “twisted figure of eight” conformation stabilized by intramolecular hydrogen bond and by π -stacking between its thiazole rings [214].

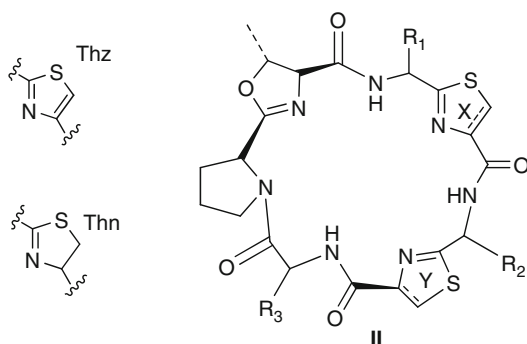


name	Z	K	R ₁	R ₂	R ₃	R ₄
patellamide A	332	H	Me	D-Val	L-Ile	D-Val
patellamide B	333	Me	Me	D-Ala	L-Leu	D-Phe
patellamide C	334	Me	Me	D-Ala	L-Val	D-Phe
patellamide D	335	Me	Me	D-Ala	L-Ile	D-Phe
patellamide E	336	Me	Me	D-Val	L-Val	D-Phe
patellamide F	337	Me	H	D-Ala	L-Val	D-Phe
ascidiacyclamide	338	Me	Me	D-Val	L-Ile	D-Val
ulithiacyclamide	339	Me	Me	D-Leu	L-1/2Cys	D-Leu
ulithiacyclamideB	340	Me	Me	D-Phe	L-1/2Cys	D-Leu

There is now a substantial literature which demonstrates that these marine metabolites have a high propensity to chelate metal ions [224–229]. A large number of analytical and spectroscopic methods have been used to study the metal complexation behavior of *Lissoclinum* peptides. Thus, it was established that although patellamides A (**332**), B (**333**), and E (**336**) could bind comfortably to Zn²⁺ and Cu²⁺, they showed no affinity for binding to such metals as Mg²⁺ and Ca²⁺ [230]. There is no doubt that copper is the preferred metal for the patellamide family of cyclic peptides in ascidians that adopt a “square” conformation [231, 232].

Peptides of lissoclinamide family, (II: **341–351**) [197, 201, 214, 233–235], show structures which feature an oxazoline ring together with one or more thiazole and/or thiazoline units, derived from unusual amino acids residues,

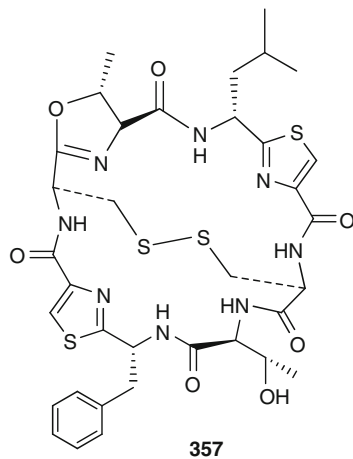
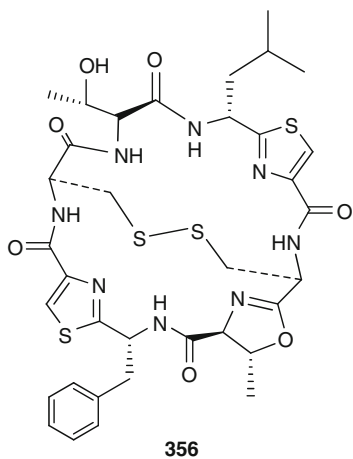
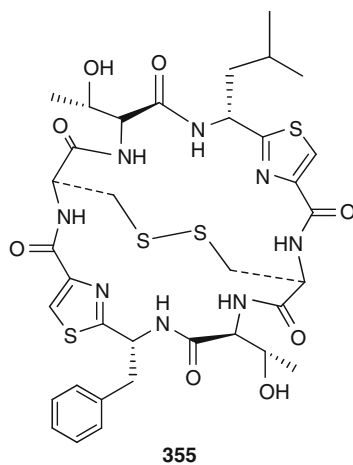
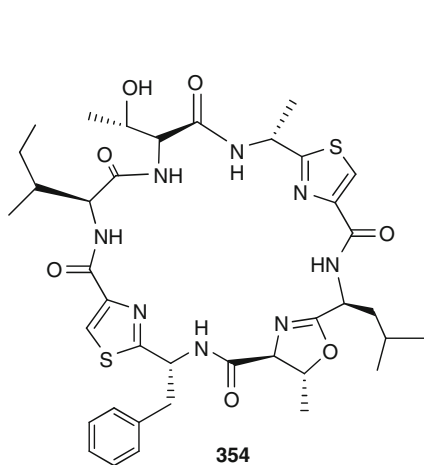
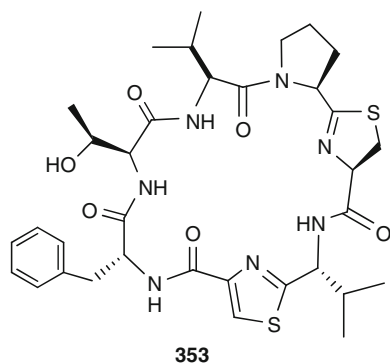
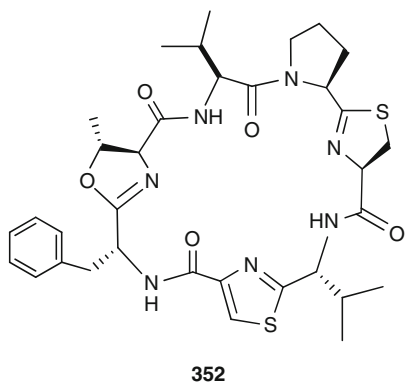
incorporated in a cyclic heptapeptide, e.g., lissoclinamide 4 (**344**), lissoclinamide 5 (**345**), and lissoclinamide 7 (**347**). The lissoclinamides 1–8 (**341**–**348**) and the ulicyclamide (**351**) [236] are all derived from a cyclic heptapeptide in which a threonine has been cyclized to an oxazoline and two cysteines have been cyclized to give a thiazole or thiazoline [235]. The correct assignment of the chiral centers adjacent to the thiazole, and especially the thiazoline rings in lissoclinamide 4, 5, and 7 was particularly problematic since these centers are prone to undergo epimerization during the usual methods of cyclopeptide hydrolytic degradation and during their synthesis [234, 237]. Based on a total synthesis, the stereochemistries published for natural lissoclinamide 4 and lissoclinamide 5 [194] were re-assigned as **344** and **345**, respectively [238, 239]. The cytotoxicity of the lissoclinamides was tested in vitro using transitional bladder carcinoma cells (T24), SV40-transformed fibroblasts (MRC5CV1), and normal peripheral blood lymphocytes. Lissoclinamide 7 (**347**) is by far the most cytotoxic with an IC_{50} value of 0.04 $\mu\text{g/mL}$ for a 1 h exposure against MRC5CV1 cell line [234].



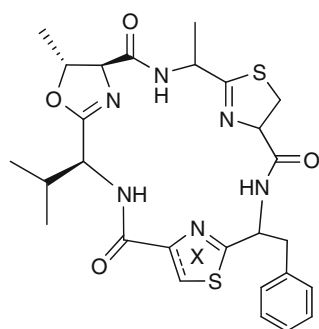
name		X	Y	R ₁	R ₂	R ₃
lissoclinamide 1	341	Thz	Thz	L-Val	D-Ile	L-Phe
lissoclinamide 2	342	Thn	Thz	D-Ile	D-Ala	L-Phe
lissoclinamide 3	343	Thn	Thz	D-Ile	L-Ala	L-Phe
lissoclinamide 4	344	Thn	Thz	L-Val	L-Phe	L-Phe
lissoclinamide 5	345	Thz	Thz	L-Val	L-Phe	L-Phe
lissoclinamide 6	346	Thn	Thz	D-Val	D-Phe	L-Phe
lissoclinamide 7	347	Thn	Thn	D-Val	D-Phe	L-Phe
lissoclinamide 8	348	Thn	Thz	Val	Phe	L-Phe
lissoclinamide 9	349	Thn	Thz	L-Ile	D-Val	D-Phe
lissoclinamide 10	350	Thn	Thn	L-Ile	L-Ile	D-Phe
ulicyclamide	351	Thz	Thz	L-Ile	D-Ala	L-Phe

The heptapeptide cyclodidemnamide (**352**), isolated from *Didemnum molle* collected in the Philippine Islands, possesses both oxazoline and thiazole rings together with a thiazoline-proline unit [240]. The stereochemistry of **352** has been revised through a synthetic work [241–243]. The stereochemical structure of cyclodidemnamide B (**353**), isolated from the same species collected in Mozambique, has been established on the basis of its total synthesis [244]. A feature common to the four cyclic peptides patellamide G (**354**) and ulithiacyclamides

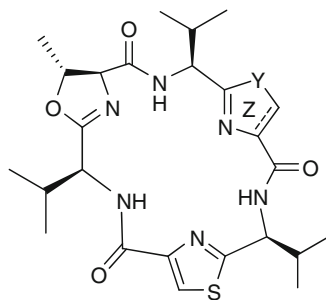
E–G (355–357), isolated from *L. patella* collected in Micronesia, is that one or more of the threonine units is not cyclized to an oxazoline ring [245].



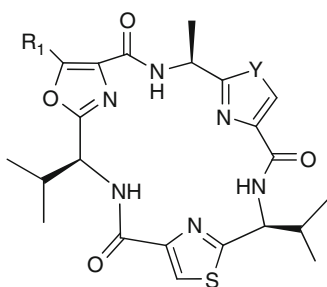
The cyclic hexapeptides bistratamides A (**358**) B (**359**), D (**361**), E (**362**), and F (**363**), isolated from *L. bistratum* collected in Australia and Philippines, possess the modified amino acid residues methyloxazoline (mOxn), thiazole (Thz), thiazoline (Thn), oxazole (Oxz), and oxazoline (Oxn) [246–248]. From the same species collected in Philippines, bistratamide C (**360**) and bistratamides G–J (**364–367**) were also isolated [247, 248]. The total synthesis of **360**, **361**, and **363–366** has been performed [249–251]. Bistratamide D (**361**) showed depressant effects when introduced directly into the central nervous system of mice by intracerebral injection [252]; at a 65 μg dose, mice exhibited decreased motor activity, sluggishness, and sedation relative to control [247]. Bistratamides E–J showed weak to moderate activity against human colon tumor (HCT-116) cell line; the compounds **365** and **367**, containing two thiazole rings, are more active than those containing a thiazole ring and an oxazole ring (**364** and **366**) [248].



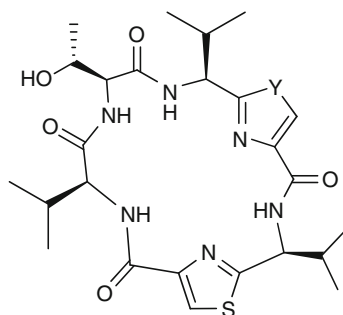
358 X=Thn
359 X=Thz



361 Y=O Z=Oxz
362 Y=S Z=Thz
363 Y=O Z=Oxn



	Y	R ₁
360	S	H
364	O	Me
365	S	Me

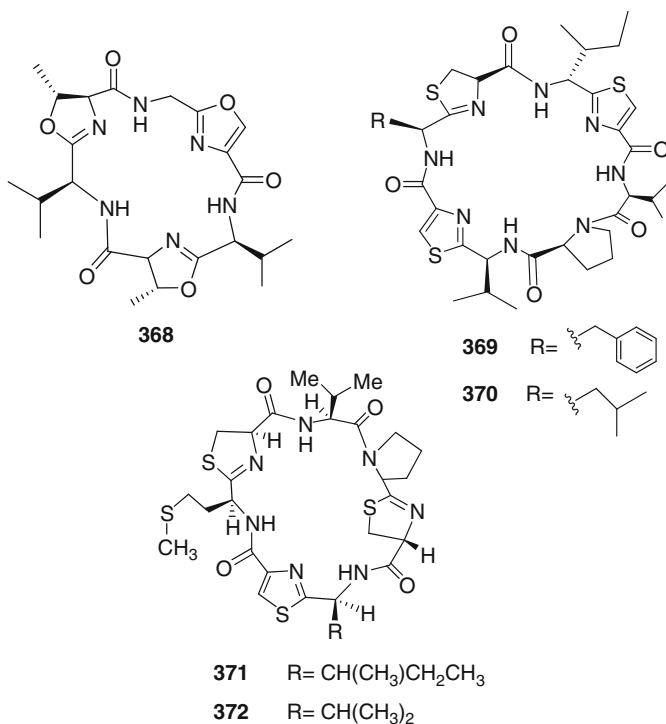


366 Y=O
367 Y=S

Two cyclic hexapeptides, didmolamide A and B, strictly related to bistratamides, were isolated from *D. molle* collected in Madagascar [253]. The total synthesis of didmolamides has been reported [254]. In addition, a quite similar hexapeptide **368**

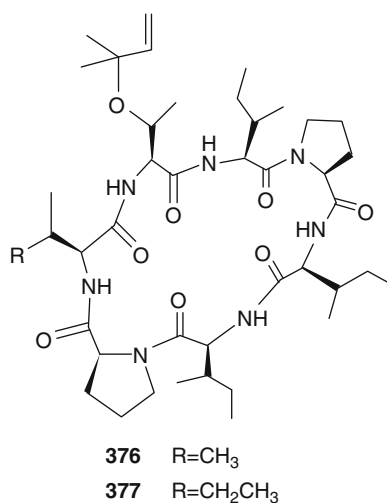
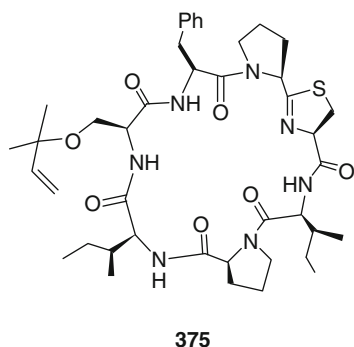
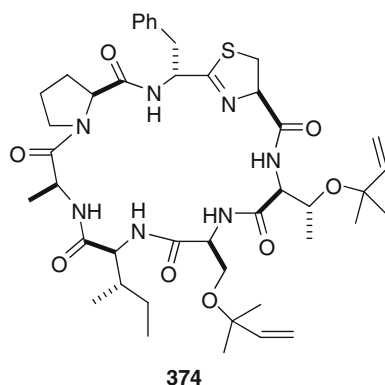
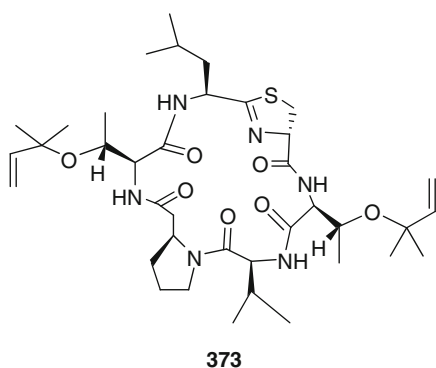
has been reported under two different names from both *L. bistratum* (cycloxazoline) [255] and the terrestrial cyanobacteria, *Westialloopsis prolifica* (westiellamide) [256], which led to the suggestion that the peptides were produced by symbiotic cyanobacteria. This hypothesis has not yet been confirmed. On the other hand, Faulkner et al. found that the peptides are not stored in cyanobacterial cells and are instead present in significant quantities throughout the ascidian tunic. The best approach to this problem would be to determine the cellular location of the peptides using an antibody to a specific peptide or to determine the location of the biosynthetic genes, both of which are technically difficult procedures [203]. The copper (II) coordination chemistry of westiellamide as well as of three synthetic analogues has been investigated [257]. Because cyclic peptides with oxazole building block in the cyclic backbone have been proposed to be useful structures for the construction of molecular receptors, the structural investigation of westiellamide analogues has been performed [258].

Tawicyclamides A (369) and B (370), isolated from *L. patella* collected in the Philippine Islands [259], and mayotamides A (371) and B (372), isolated from *D. molle* collected in the North-West of Madagascar [260], belong to another set of cytotoxic cyclic peptides, possessing thiazole- and thiazoline-amino acids but lacking the oxazoline ring characteristic of patellamide (I) and lissoclinamide (II) families. A characteristic feature of mayotamides A–B is the presence of a methionine unit.



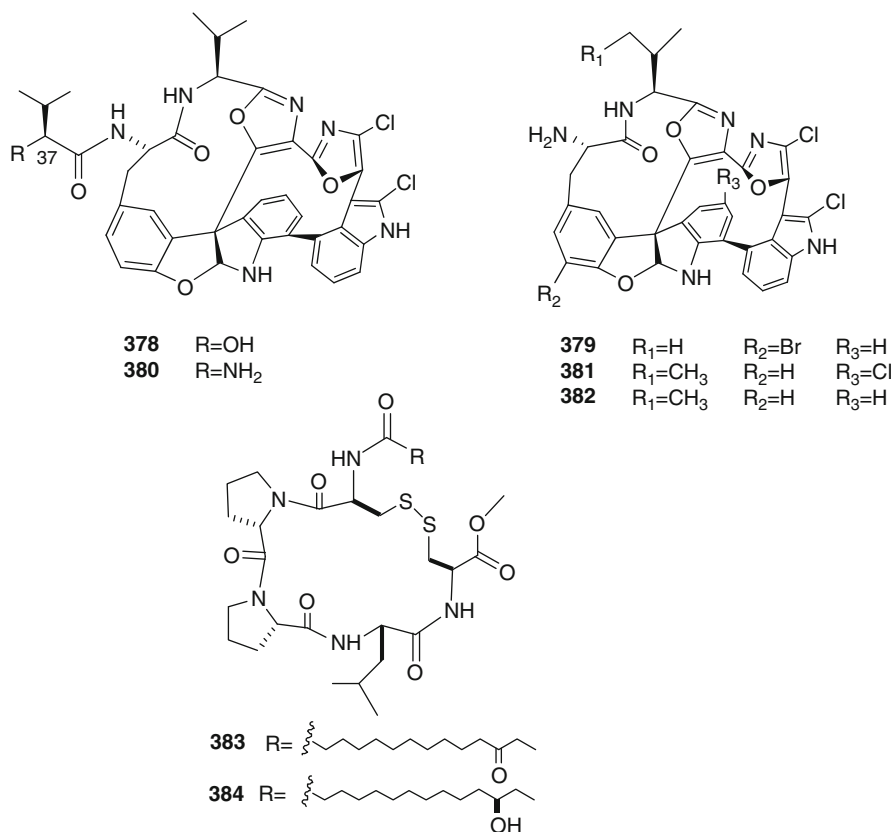
Several cyclopeptides isolated from ascidians of the genera *Lissoclinum* and *Didemnum*, patellins 1–6 [261], trunkamide A (374) [261], mollamide (375)

[262, 263], mollamides B–C [264], as well as hexamollamide [265] and comoramides A–B [260], are structurally uniquely characterized by the presence of a single thiazoline heterocycle in the peptide backbone, as well as of threonine and serine residues whose side chains have been modified as dimethylallyl (reverse prenylated) ethers. Patellin 2 (**373**), containing a thiazoline and two threonine residues modified as dimethylallyl ethers, was shown to exist in different conformations in solution and in the crystal on the basis of X-ray crystallography, NMR spectroscopy, and molecular modeling [266]. The structure of trunkamide A (**374**) initially suggested was incorrect in terms of the configuration of the Phe residue. The total synthesis performed by Wipf showed that the correct configuration was D by comparison of the synthetic and natural products [267]. Nairaiamides A (**376**) and B (**377**), two heptapeptides isolated from a Fijian *L. bistratum*, possess two proline residues, several isoleucines and a dimethylallylthreonine (daT); **376** possesses a Val residue in place of an Ile in **377** [268].



The diazonamides (**378–382**) [269, 270] are a family of halogenated cyclic peptides isolated from *Diaza angulata* (originally misidentified as *D. chinensis*). The first structural proposal for diazonamides A–B (**378–379**) [269] was later revised, and the final structures of diazonamides A (**378**) and B (**379**) have been established after reinterpretation of the NMR and X-ray data and total synthesis of diazonamide A [271–273]. The cytotoxic activity of diazonamides A–E (**378–382**) has been evaluated against a panel of three human tumor cell lines, including lung (A549), colon (HT29), and breast (MDA-MB-231). The potent activity, with values in the low nanomolar range, observed for diazonamide A suggested that the hydroxyl group at C-37 must play a key role in the cytotoxicity of these metabolites [269, 270].

The lipopeptides eudistomides A (**383**) and B (**384**) have been isolated from the Fijian ascidian *Eudistoma* sp. They are the first ascidian-derived peptides cyclized solely by a disulfide bridge [274].

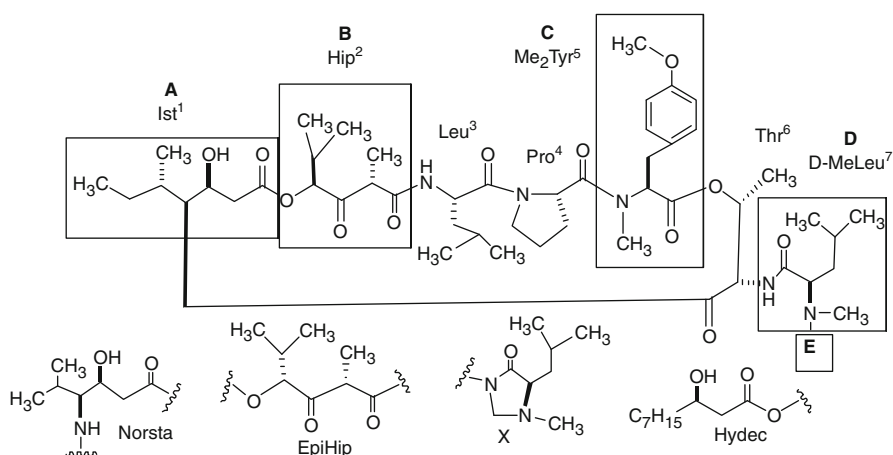


5.3.3 Depsipeptides

Depsipeptides are natural metabolites, having sequences of amino and hydroxy carboxylic acid residue, in which one or more of the amide (–CONHR–) bonds

are replaced by ester (COOR) bonds; in cyclodepsipeptides, the residues are connected in a ring.

In 1981, a new class of cyclic depsipeptides, the didemnins A–C, was isolated from a Caribbean tunicate of the genus *Trididemnum* by K.L. Rinehart et al. [275, 276]. Later, *Trididemnum solidum* and *T. cyanophorum* both have been reported to contain didemnins [277, 278]. Additional cyclic depsipeptides, didemnins D (388), E (389), nordidemnins A and B (395–396), and the formaldehyde adduct methylenedidemnin A (398), as well as didemnin G (390), were also reported [279]. *T. cyanophorum* ether extract was shown to contain didemnin H (=M) (391) [280]. Seven didemnins – didemnin M (=H) (391), N (392), X (393), and Y (394), nordidemnin N (397), and epididemnin A₁ (399), as well as a ring-opened form of didemnin A, acyclodidemnin A (400) – were isolated by Sakai et al. from an extract of the Caribbean tunicate *T. solidum* [281].



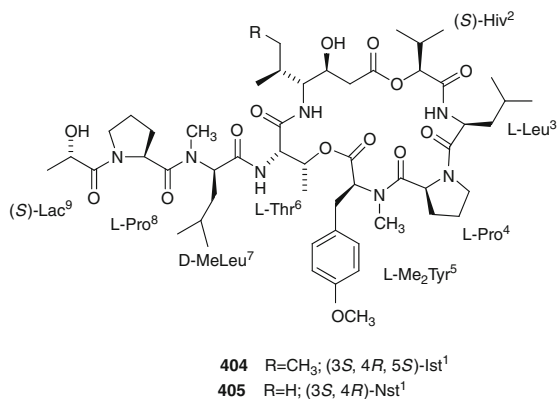
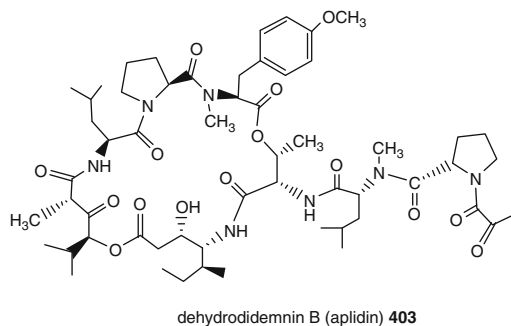
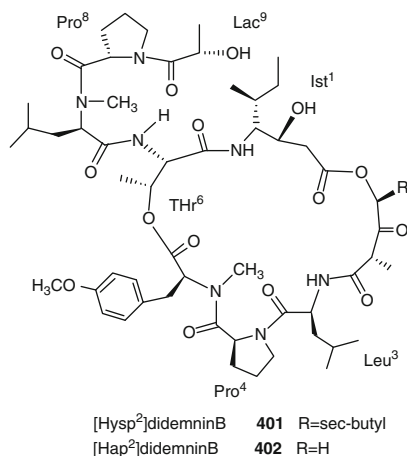
name		A	B	C	D	E
didemnin A	385	Ist	Hip	Me ₂ Tyr	D-MeLeu	-H
didemnin B	386	Ist	Hip	Me ₂ Tyr	D-MeLeu	-Pro-Lac
didemnin C	387	Ist	Hip	Me ₂ Tyr	D-MeLeu	-Lac
didemnin D	388	Ist	Hip	Me ₂ Tyr	D-MeLeu	-Pro-Lac-Gln-Gln-Gln-pGlu
didemnin E	389	Ist	Hip	Me ₂ Tyr	D-MeLeu	-Pro-Lac-Gln-Gln-pGlu
didemnin G	390	Ist	Hip	Me ₂ Tyr	D-MeLeu	-CHO
didemnin H (=M)	391	Ist	Hip	Me ₂ Tyr	D-MeLeu	-Pro-Lac-Gln-pGlu
didemnin N	392	Ist	Hip	Tyr	D-MeLeu	-Pro-Lac
didemnin X	393	Ist	Hip	Me ₂ Tyr	D-MeLeu	-Pro-Lac-Gln-Gln-Gln-Hydec
didemnin Y	394	Ist	Hip	Me ₂ Tyr	D-MeLeu	-Pro-Lac-Gln-Gln-Gln-Gln-Hydec
nordidemnin A	395	Norsta	Hip	Me ₂ Tyr	D-MeLeu	-H
nordidemnin B	396	Norsta	Hip	Me ₂ Tyr	D-MeLeu	-Pro-Lac
nordidemnin N	397	Norsta	Hip	Tyr	D-MeLeu	-Pro-Lac
methylenedidemnin A	398	Ist	Hip	Me ₂ Tyr	X	-H
epididemnin A ₁	399	Ist	epiHip	Me ₂ Tyr	D-MeLeu	-H
acyclodidemnin A	400	Ist	Hip	Me ₂ TyrOH	D-MeLeu	-H

The originally reported suggestion for the structure of didemnin B (**386**) [277] has been revised several times: (1) The configuration of the N-methyl-leucine in the side chain has been identified as *R* [282]. (2) M. Joullie et al. established the 2*S*,4*S*-configuration for the hydroxyisovalerylpropionic acid [= (2*S*,4*S*)-4-hydroxy-2,5-dimethyl-3-oxohexanoic acid; Hip] [283]. (3) By means of NMR investigations, B. Castro et al. demonstrated that isostatin [= (3*S*,4*R*,5*S*)-4-amino-3-hydroxy-5-methyleptanoic acid; Ist] and not statine is a ring building block [284]. A reliable elucidation of the structure has been achieved by X-ray crystallography and total synthesis [285, 286]. Didemnins A–C were efficiently prepared in a stereocontrolled manner, producing the common macrocycle and introducing the substituents on the amino group of L-threonine as optically pure units [287].

All didemnins (**385–400**) contain the same basic structure consisting of a 23-membered macrocycle, with an attached side chain. The macrocycle is made up of six subunits, (*S*)-Leu, (*S*)-Pro, (1*S*2*R*)-Thr, (*S*)-N(Me)-O(Me)-Tyr, (3*S*,4*R*,5*S*)-isostatine, and (2*S* 4*S*)-HIP. The side chain, whose first amino acid is always (*R*)-N(Me)-Leu, is joined to the threonine of the macrocycle, and its structure differentiates the various didemnins: In the simplest member of the family, didemnin A (**385**), it consists only of (*R*)-N(Me)-Leu, whereas in other cases, it can be appreciably more complex. Certain didemnins exhibit significant antiproliferative and immunosuppressive activity. Didemnin B (**386**) exhibited strong antiviral, immunosuppressive, and cytotoxic activities. Didemnin B inhibited DNA viruses *Herpes simplex* types I and II in vitro at 0.05 μ M concentrations, and it has demonstrated in vivo anticancer activity in mice against P388 murine leukemia (T/C 199 at 1.0 mg/kg) and B16 melanoma (T/C 160 at 1.0 mg/kg). Didemnin B was tested against a number of tumors in a human tumor stem-cell assay, and significant activity was observed after 1 h of exposure at concentrations as low as 0.1 μ g/mL in ovarian, sarcoma, kidney, and breast cells [288]. Phase I and phase II clinical and pharmacological studies indicated that didemnin B had little or no significant antitumor activity in some of the common carcinomas and showed significant toxic side effects such as nausea, vomiting, and neuromuscular toxicity [289]. Despite the limited clinical promise of didemnin B as anticancer agent, there was widespread interest in didemnins. In order to understand the marked difference of the biological activity of didemnins, conformational analysis of them has been performed [290].

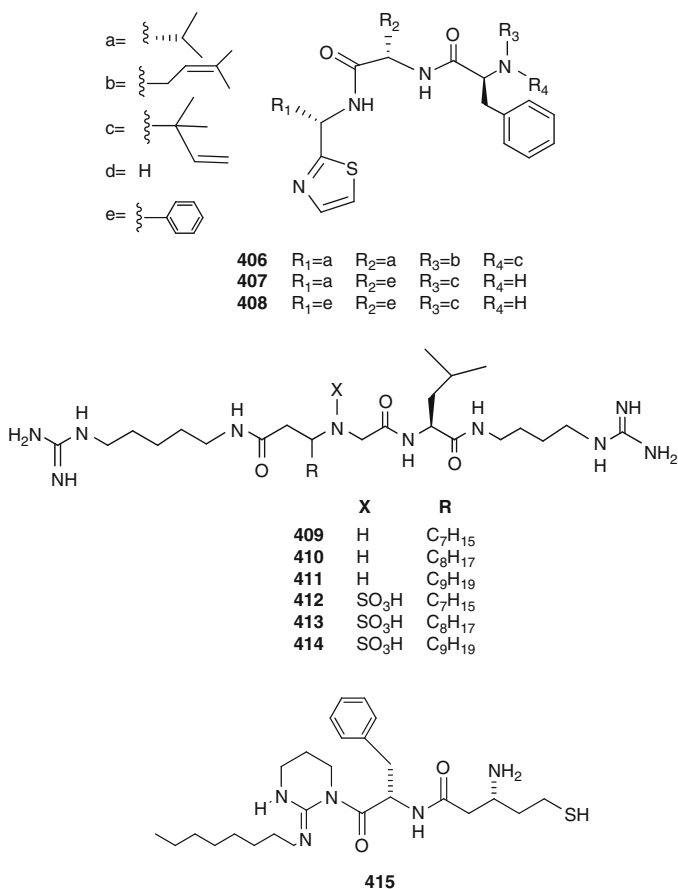
[Pyruvyl]⁹ didemnin B was discovered in a Mediterranean tunicate *Aplidium albicans* [291], whereas [Tyr⁵]didemnin B (described by Sakai as didemnin N) and [D-Pro⁴]didemnin B were reported by E. Abou-Monsour et al. [292]. Later, the structure elucidation of [Hysp²] (**401**) and [Hap²]didemnin B (**402**), two[His²]-modified didemnin B isolated from the tunicate *T. cyanophorum*, have been reported [293]. In 1990, a new member of this family was isolated from the Mediterranean tunicate *A. albicans* (application PCT/GB 90/01495) [294–296]; this depsipeptide was named dehydrodidemnin B (**403**); it has a piruvoyl-proline residue instead of the lactyl-proline residue found in the linear peptide moiety of didemnin B. Dehydrodidemnin B (=aplidine) was shown to possess higher antineoplastic activity than didemnin B both in vitro and in vivo [297]. Total synthesis of dehydrodidemnin B was performed [298].

Two cytotoxic depsipeptides, tamandarin A (**404**) and B (**405**), were isolated from an unidentified Brazilian marine ascidian of the family Didemnidae [299]. Tamandarin A (**404**), similar in structure to didemnin B (**386**), was shown to be somewhat more active *in vitro* than **386** against pancreatic carcinoma with an ED_{50} value 1.5–2 ng/mL. Total syntheses and biological evaluation of tamandarins A and B and of their respective analogues have been reported [300–302].

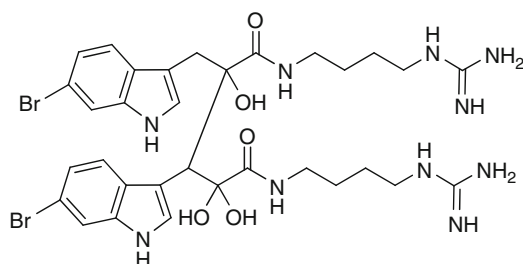


5.3.4 Linear Peptides

Three linear cytotoxic peptides, virenamides A–C (**406–408**) have been isolated from *Diplosoma virens* collected on the Great Barrier Reef, Australia. Virenamides A–C showed modest cytotoxicity toward a panel of cultured cells; virenamide A also exhibited TOPO II inhibitory activity (IC₅₀ of 2.5 µg/mL) [303–305]. Six peptide guanine derivatives, named minalemines A–F (**409–414**), have been isolated from *Didemnum rodriguezii* [306, 307]. These compounds incorporate one agmantine (Agma) and one homoagmantine (Hagma) terminal unit with their guanidine groups free and the primary amino groups linked through a peptidic bond to L-Leu and a very rare β-*N*-carboxymethyl amino acid (Ncma) bearing a saturated long chain. Minalemines D–F are the sulfamic acid derivatives of minalemines A–C and constitute the first examples of such a functional group in a marine organism. From the same ascidian, caledonin (**415**) was also isolated; this linear peptide possesses a unique β-amino acid residue and a cycloguanidine group. It exhibited strong metal-complexing properties [308].



A highly modified dimer peptide, eusynstyelamide (**416**), was the major component of an aqueous extract of *Eusynstyela misakiensis*. It is a modified tryptophan–arginine dipeptide dimer [309].



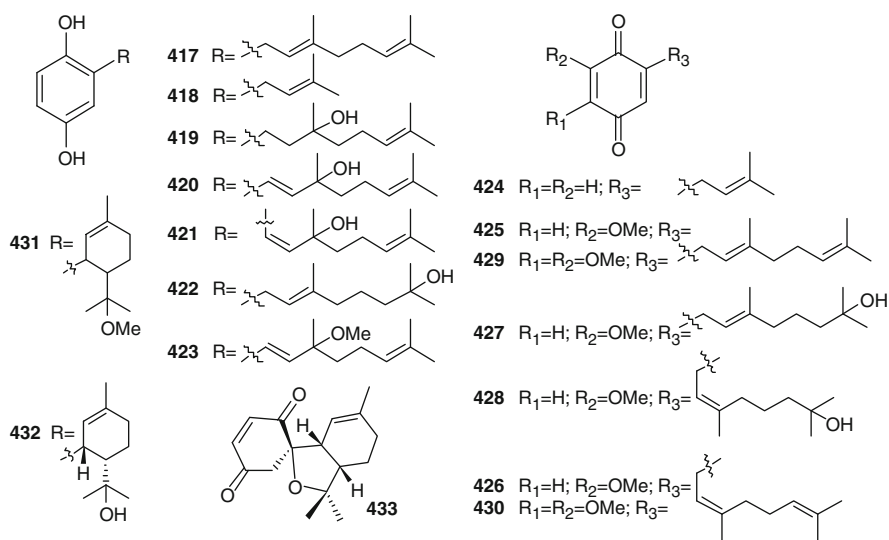
416

5.4 Meroterpenes

Meroterpenes are compounds of mixed biosynthesis, mostly quinones or hydroquinones bonded with a terpenoid portion ranging in size from one to nine isoprene units. In the marine environment, these secondary metabolites are isolated mainly from brown algae, but other sources include microorganisms, soft corals, and invertebrates [310]. Among marine ascidians, they have been found almost exclusively in species belonging to the genus *Aplidium*, which have been the source of a vast array of prenyl-quinone, -hydroquinone, -chromene, and/or -chromane derivatives, either linear or cyclic, originated from intra- and intermolecular cyclizations and/or rearrangements, thus giving macrocyclic or polycyclic skeletons, often linked to amino acids or taurine residues [311].

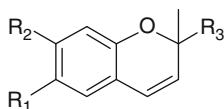
The first biologically active tunicate metabolite, geranylhydroquinone (**417**), was isolated from an *Aplidium* sp. and, successively, found in many others *Aplidium* species; it was shown to offer protection against leukemia and tumor development in test animals [5]. Several isoprenoid hydroquinones have been then reported, such as compounds **419** and **420** from *A. multiplicatum* [312], **421** from *A. savignyi* [313], **422** and **423** from *A. conicum* [314]. *A. californicum* has been the source of the simple monoprenyl hydroquinone **418** and the relevant quinone **424** [315]. An *Aplidium* sp. collected in French Atlantic waters was shown to contain verapliquinone **B** (**426**) and **D** (**428**) as the first examples of linear diprenylquinones of the neryl type, besides their respective isomers verapliquinones A (**425**) and C (**427**) of the geranyl type [316]. Glabruquinone B (**429**), isolated from *A. glabrum* together with its isomer glabruquinone A (desmethylobiquinone Q₂, **430**) is a further but rare example of neryl derivative, the majority of natural prenyl benzoquinones possessing a linear side chain of the geranyl type [317]. Compound **430** is closely related to the ubiquinones, although lacking the methyl group in the quinoid moiety; it is not a cytotoxin but demonstrated good cancer-preventive activity on JB6 Cl 41 cells

transformation activated by epidermal growth factor (EGF). Structure-activity relationships studies on its synthetic analogues demonstrated that this activity depend on the length of the side chain and on the position of the methoxyl groups in the quinone part of the molecule [318]. In vivo anticancer properties of **430** and its analogues as well as the molecular mechanism of its action against tumor cells have been examined; it was shown to inhibit the growth of the solid Ehrlich carcinoma in mice and to induce apoptosis in various human tumor cell lines [319]. Cycloidioprenyl hydroquinones/quinones have been isolated from *A. aff. densum* (methoxyconidiol, **431**) [320] and from *A. conicum* (conitriol, **432** and conidione, **433**) [315]. Methoxyconidiol (**431**) displayed an antimitotic action on the first division of sea urchin embryos, disrupting M-phase progression and completely blocking cytokinesis without having any effect on DNA replication [321].



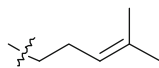
The occurrence of chromenols has been reported in *A. californicum* (**434**) [315], *A. costellatum* (**435**) [322], *A. multiplicatum* (**436**) [312], and *A. solidum* (**437** and **438**) [323]. The chromane derivative **439** has been isolated from *Synoicum castellatum* [324], a species closely allied to the genus *Aplidium*, and successively found in *A. conicum* together with its C-1' epimer, conicol (**440**) [314]. Didehydroconicol (**441**) has been isolated from *A. aff. densum* [320]. Chromene derivatives clearly arise from the relevant prenylated para-quinones via tautomerization/electrocyclization [325]. The formation of cyclized compounds such as **431–433** and **439–441** from the relevant quinones/hydroquinones can be easily rationalized through a sequence of acid-catalyzed cyclizations. With the data available, it is not possible to argue whether the above mentioned transformations

occur in the organism, either enzymatically or not, prior to its extraction, or they take place during isolation and/or chromatographic purification.

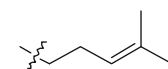


434 $R_1=OH$; $R_2=H$; $R_3=Me$

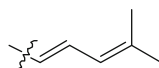
435 $R_1=OH$; $R_2=H$; $R_3=$



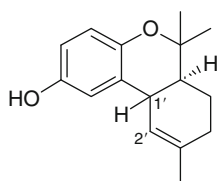
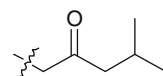
436 $R_1=OH$; $R_2=OMe$; $R_3=$



437 $R_1=OH$; $R_2=H$; $R_3=$

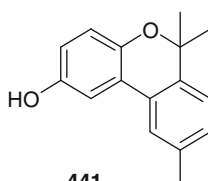


438 $R_1=OH$; $R_2=H$; $R_3=$



439 H-1' a

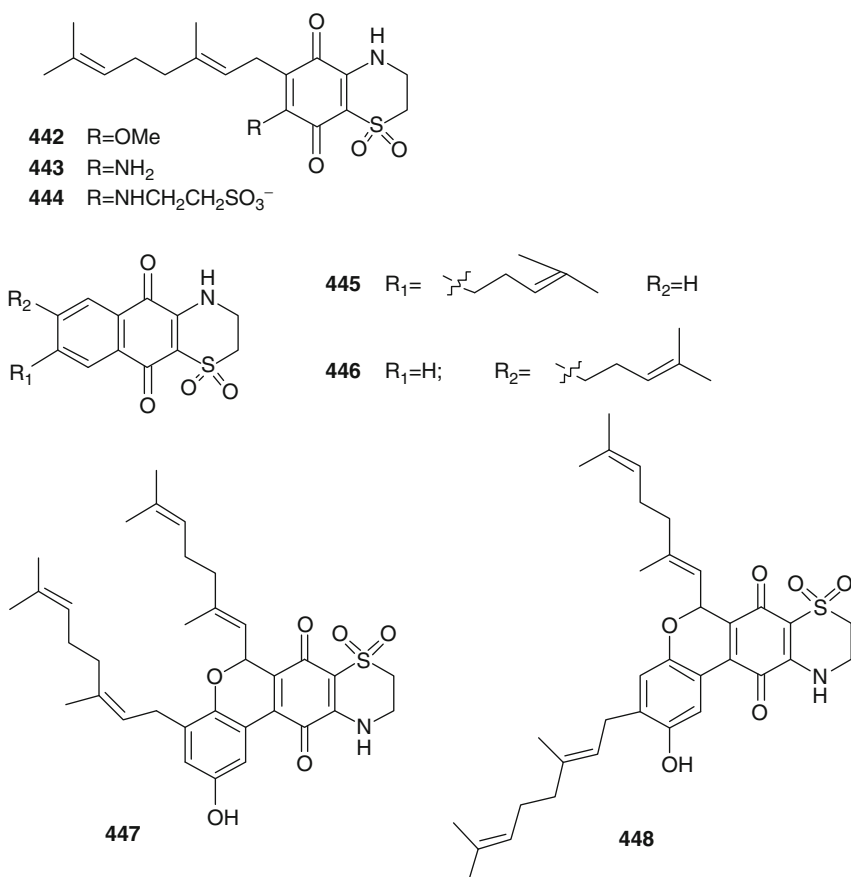
440 H-1' b



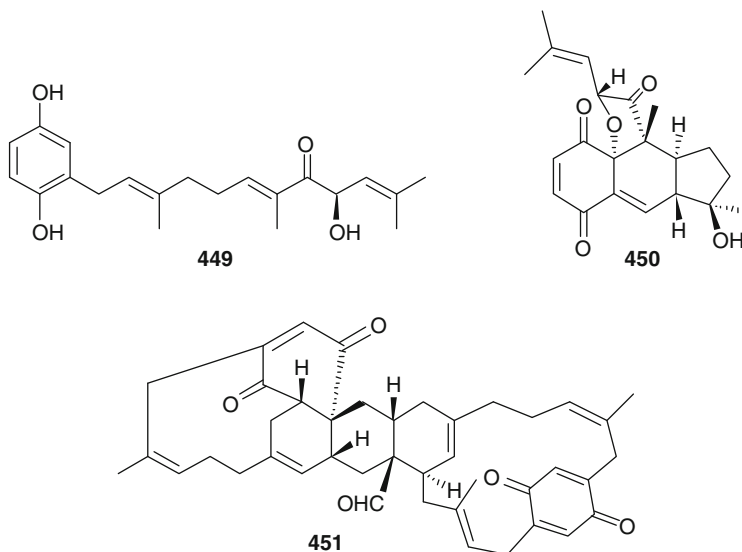
441

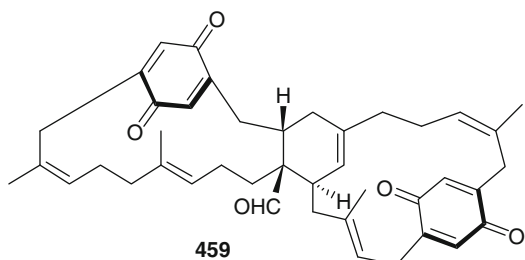
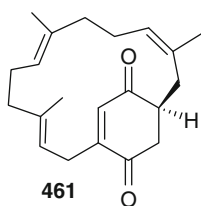
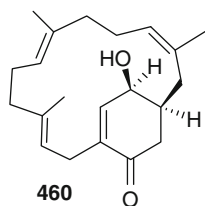
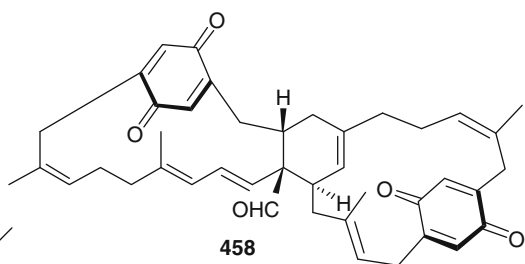
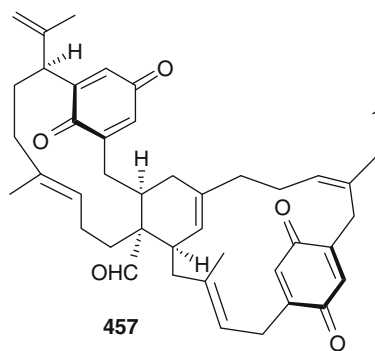
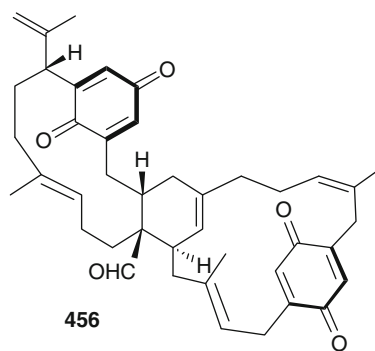
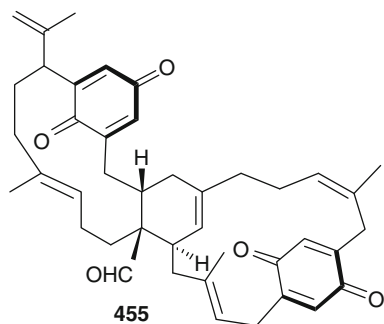
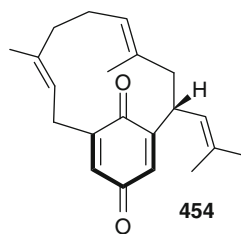
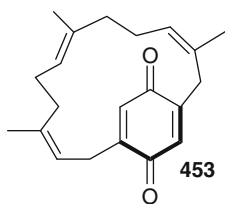
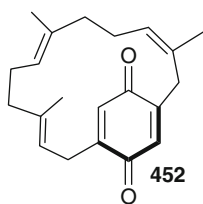
Interestingly, *A. conicum* showed a metabolic content that is different depending on the geographical place of collection. Apart from the meroterpenes **417**, **419**, **422**, **423**, **432**, **433**, **435**, **439**, and **440** above reported, isolated from a Spanish collection of the ascidian, a sample of *A. conicum* collected along Sardinia coasts gave rise to the isolation of a large group of unique meroterpenes, compounds **442–448**, whose structures all feature an unusual 1,1-dioxo-1,4-thiazine ring fused with the quinone portion [326–328]. Aplidinones A–C (**442–444**) and conicaquinones A and B (**445** and **446**) possess a benzoquinones and a naphthoquinone moiety, respectively; thiaplidiaquinones A and B (**447** and **448**) possess an unprecedented tetracyclic core and visibly are composed of two geranylated benzoquinones that have fused together. Both conicaquinones A and B showed marked and selective cytotoxic effects on rat glioma cells [326]; thiaplidiaquinones were strongly cytotoxic against Jurkat cell line, derived from a human T lymphoma, inducing cell death by apoptosis. The pro-apoptotic mechanism of thiaplidiaquinones involves the induction of a strong production of intracellular reactive oxygen species (ROS) in the

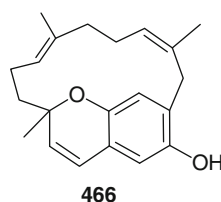
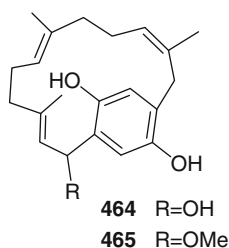
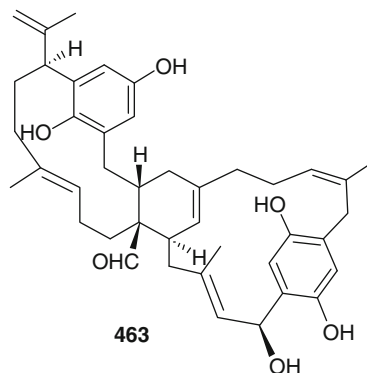
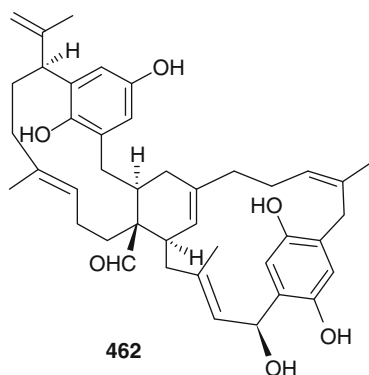
cells, likely due to the inhibition of the plasma membrane NADH-oxidoreductase (PMOR) system, an important target for anticancer drugs, through interference with the coenzyme Q-binding site [328]. In order to validate the structural assignment made for aplidinones by theoretical means, a synthetic approach has been undertaken which yielded some synthetic analogues of aplidinone A in which the geranyl chain is replaced by other alkyl chains; these compounds as well as the natural metabolite **442** were subjected to cytotoxicity assays and preliminary structure-activity relationships (SAR) studies. Both aplidinone A and its synthetic analogues were shown to possess interesting cytotoxic effects; SAR studies revealed that cytotoxic activity depends on the nature and the length of side chain linked to the benzoquinone ring and, mainly, on its position with respect to the dioxothiazine ring. The study evidenced also one of the synthetic analogues as a potent cytotoxic and pro-apoptotic agent against several tumor cell lines which also inhibits the TNF α -induced NF- κ B activation in a human leukemia T cell line [329].



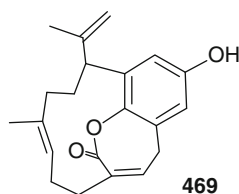
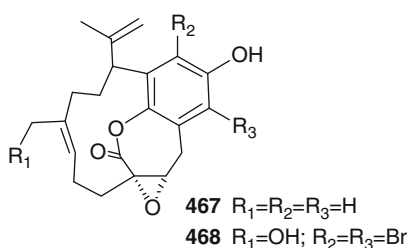
Rossinones A (**449**) and B (**450**) are triprenylated (farnesyl) hydroquinone and quinone, respectively. They have been isolated from an Antarctic *Aplidium* species and exhibited anti-inflammatory, antiviral, and antiproliferative activities [330]. *A. longithorax* has been the source of longithorones A–K (**451–461**) and longithorols A–E (**462–466**), a unique class of macrocyclic C_{21} or C_{42} prenylated quinone/hydroquinone derivatives featuring unprecedented carbocyclic skeletons formed by an unusual cyclization of the farnesyl chain with the hydroquinone unit to give [9] and [10]metacyclophane, as well as [12]paracyclophane structures [331–335]. Longithorones A (**451**) and E–I (**455–459**) are dimeric compounds; it has been speculated that they may arise by Diels–Alder reactions of suitable unsaturated precursors, and the discovery of the monomers longithorones B–D (**452–454**), J (**460**), and K (**461**) supports this suggestion. The stereochemistry of the central carbocyclic rings in **451** and **455–459** is consistent with such a fusion [332]. Longithorones A–I have restricted rotations in their macrocyclic rings, resulting in atropisomerism; longithorone J is the first example of a γ -hydroxy-cyclohexenone in this class of compounds. Longithorols (**462–466**) are hydroquinone derivatives; longithorols A (**462**) and B (**463**) were isolated as their pentaacetates because of their rapid decomposition occurring under purification conditions [334]. Longithorol E (**466**), a macrocyclic chromenol, is possibly an artifact of the isolation process as it can be envisaged that longithorol C (**464**) could undergo an intramolecular cyclization followed by dehydration to yield **466** [335]. To date, the only biological activity reported for longithorones/longithorols class of marine metabolites pertains to longithorone A (**451**), which was shown to display cytotoxicity against P388 murine leukemia cells.





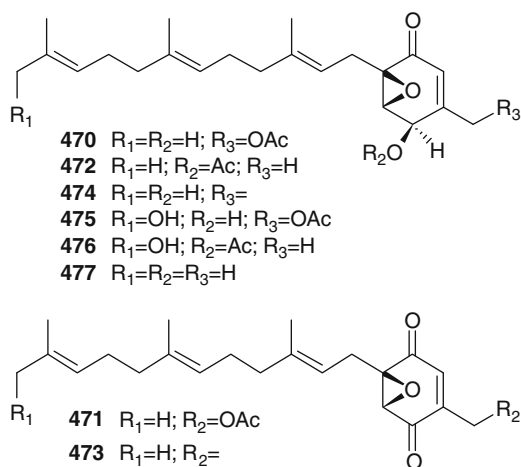


Floresolides A–C (**467–469**) are three further cyclofarnesylated hydroquinones cytotoxic against KB cells isolated from an Indonesian *Aplidium* sp.; they are unique relatives of longithorols, possessing an endocyclic ϵ -lactone bridging the aromatic ring and a [10]metacyclophane moiety [336].



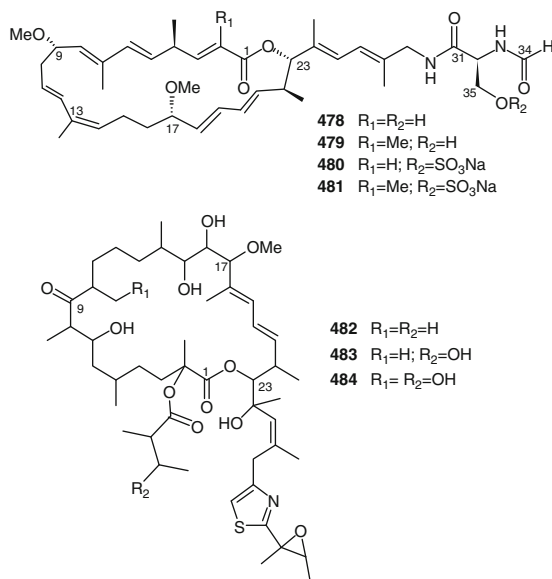
Eight bioactive farnesylated epoxy cyclohexenones closely related to some of the above reported meroterpenes, yanuthones A–E (**470–474**), 1-hydroxyyanuthones A (**475**) and C (**476**), and 22-deacetylanuthone A (**477**) have been reported from an *Aspergillus niger* isolate obtained from tissue homogenates of an *Aplidium* ascidian [337]. The structural similarities between yanuthones and the meroterpenes isolated

from ascidians raise some question about the origin of the latter compounds; the possibility exists that they or, at least, a portion of their structure could be a microbial product.

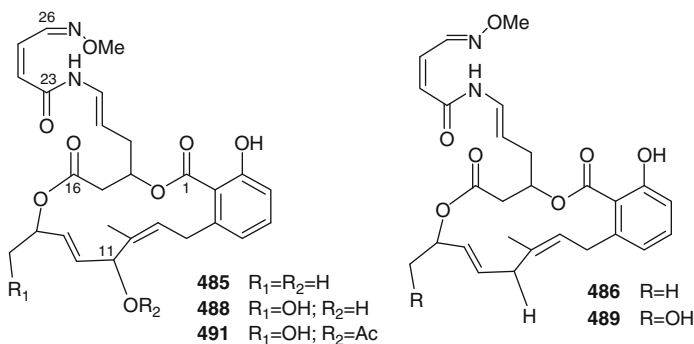


5.5 Macrolides

A significant number of large macrocyclic lactones (macrolides) have been found in ascidians; they constitute another family of ascidians metabolites which have attracted great interest because of their potent antineoplastic properties, thus becoming one of the challenging targets for total synthesis or as candidate of new antitumor drugs. Iejimalides (**478–481**) are a group of 24-membered macrolides isolated from *Eudistoma* cf. *rigida* [338, 339] and from *Cystodites* sp. [340]; they exhibited strong cytotoxic properties in vitro and antitumor activity in vivo. Iejimalides A (**478**) and B (**479**) represent the first macrocyclic lactones isolated from a tunicate; a rare *N*-formyl-L-serine unit (C-31–C-35) is included in their side chains. Iejimalides C (**480**) and D (**481**) are the C-35 sulfates of **478** and **479**, respectively. *Lissoclinum patella* has been the source of patellazoles (A–C, **482–484**), a family of cytotoxic and antifungal 24-membered macrolides having a pendant thiazole-epoxy group [341, 342]. Although patellazoles appear predominantly polyketide-derived, the thiazole moiety probably originates from an amino acid. The patellazoles are potent cytotoxins; they are extremely cytotoxic toward HCT 116 human colon tumor cells; treatment with nanomolar amounts of these compounds results in immediate inhibition of protein synthesis and cell cycle arrest at the G1 and S phase. The opening of the epoxide ring does not greatly affect the bioactivity although the cellular toxicity is generally decreased [343].



Lobatamides A–F (**485–490**) are a group of macrocyclic lactones which have been isolated from three different shallow water Australian collections of *Aplidium lobatum* [344], from a deep water collection of an *Aplidium* sp. [345], and from an unidentified Philippine ascidian [345]. The overall structures of the lobatamides are unique, due primarily to the unusual enamide-oxime methyl ether moiety which terminates the side chain of the macrolide. Lobatamides A, B, D, and E have been shown to be the same compounds as those previously isolated from an Australian *Aplidium* sp. and named aplidites A, B, C, and D, respectively, whose structures were incorrectly assigned [346]. The Australian authors also reported the isolation of further aplidites, E–G; the earlier reported structures and nomenclature of these compounds have been revised to those for lobatamides G–I (**491–493**) [345].



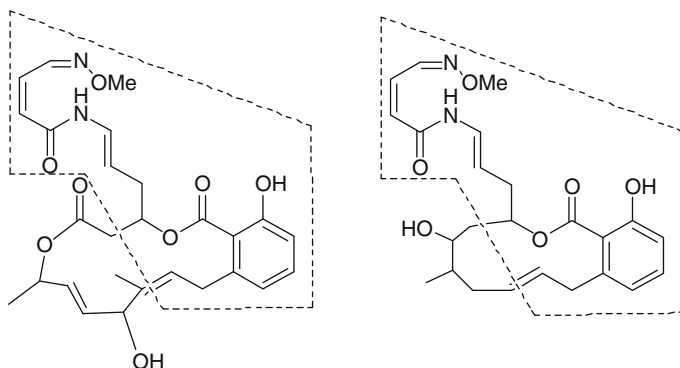
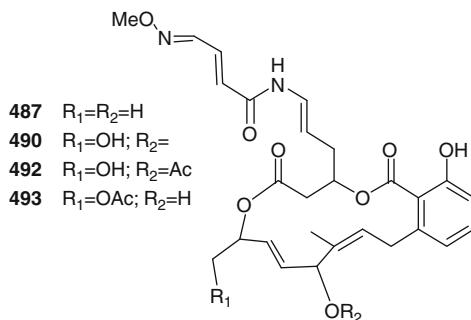
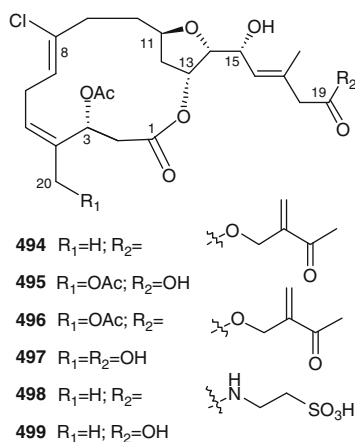


Fig. 5.2 Common core structural component shared by the lobatamides (*left*, lobatamide A9) and the salicylihalamides (*right*, salicylihalamide A)

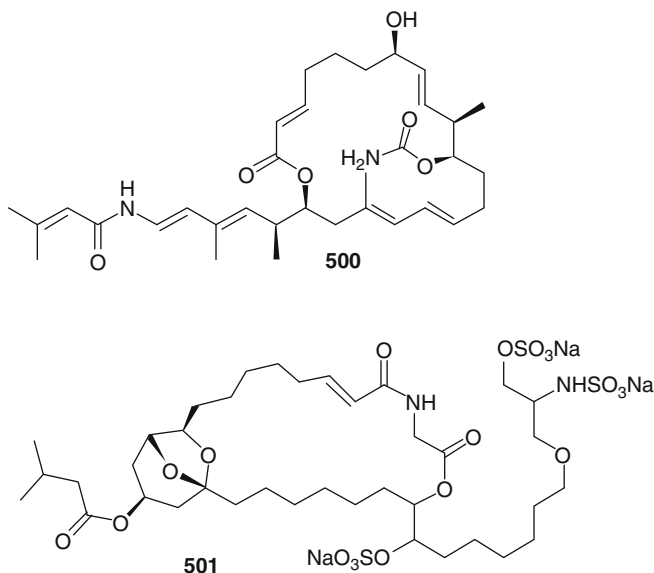


Lobatamides are related to salicylihalamides (Fig. 5.2) isolated from a sponge *Haliclona* sp.; while the size of the macrolide ring differs (12 for salicylihalamides and 15 for lobatamides), both families contain the common core structure depicted in Fig. 5.2. Lobatamides and salicylihalamides are member of the salicylate enamide macrolides class, an emerging group of antitumor natural products that have attracted considerable interest especially due to their mechanism of action [347]. Like the salicylihalamides, the lobatamides display high potency against tumor cell lines [345] which may be derived from their ability to inhibit vacuolar-ATPase (V-ATPase), largely responsible for cellular and organellar pH regulation but also implicated in cancer treatment [347].

Haterumalide B (**494**) and biselides A–D (**495–498**) are rare examples of halogenated marine macrolides. Haterumalide B is a chlorinated 14-membered ring macrolide and has been found in an Okinawan *Lissoclinum* sp. [348]; biselides A–D are haterumalide B close analogues and have been recovered in the organic extract of an Okinawan Didemnidae sp., together with the structurally related haterumalide NA (**499**) previously isolated from an Okinawan sponge [349, 350].



Palmerolide A (**500**) is a 20-membered macrolide decorated with a polyunsaturated N-acyl dienamine side chain distinct from the N-acyl enamine found in lobatamides. It has been isolated from a sample of *Synoicum adareanum* collected in Antarctica, one of the most inaccessible areas of the world [351]. Its earlier reported structure was successively revised to a diastereomer of that previously proposed [352]. Palmerolide A is a potent and selective inhibitor of melanoma cell growth; it also targets transmembrane proton pump, the V-ATPase, for which it is a potent inhibitor. Cyclodidemniserinol trisulfate (**501**), isolated from the Palauan ascidian *Didemnum guttatum*, is an inhibitor of HIV-1 integrase, which is an attractive target for anti-retroviral chemotherapy [353].

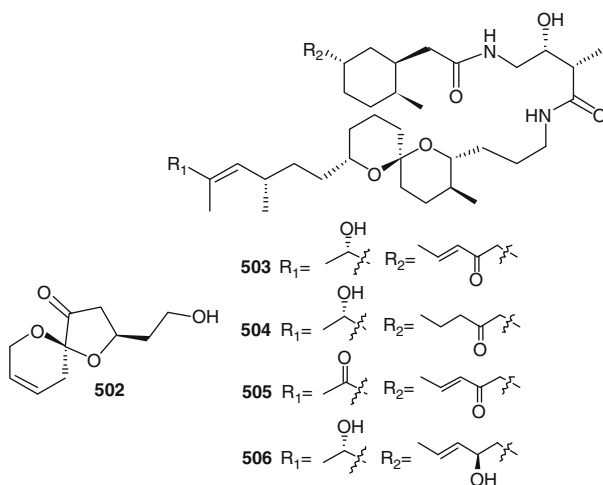


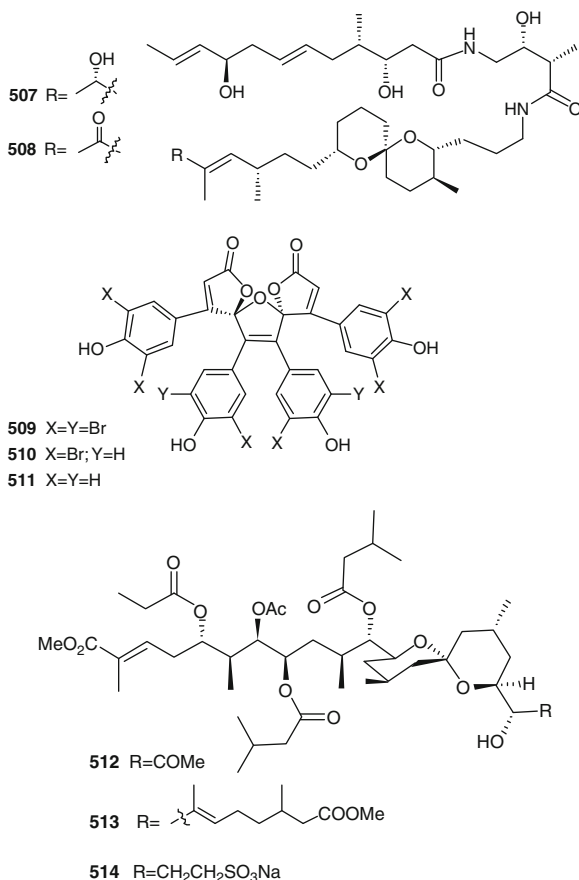
The question about the real producers of marine natural products is today an open question; macrolides such as those found in ascidians have been isolated from many other marine microorganisms (sponges, nudibranch eggs, and bryozoans). Lobatamide A (**485**) is identical to the structure of YM-75518 reported from a terrestrial *Pseudomonas* sp. cultured from an Indonesian soil sample [354]. The occurrence of identical and/or biosynthetically related compounds in collections of different tunicates from distinct geographical locations (e.g., iejimalides and lobatamides), in different organisms (e.g., haterumalides, salicylihalamides), and in terrestrial source suggests the possibility of their biosynthesis by associated microorganisms or of accumulation through dietary intake.

5.6 Other Nonnitrogenous Compounds

5.6.1 Spiroketal-Containing Products

Most marine natural products, especially polyketides, possess polyhydroxy and polyoxy substituents in their structures. A number of bicyclic (bridged ring) and/or spirocyclic acetals have been isolated from marine organisms [355], these motifs being the result of intramolecular dehydration of their hydroxy ketone precursors. In addition to the previously mentioned didemniserinolipids A–C (**312–314**, see Sect. 5.2.6) from *Didemnum* sp., spiroketal-containing metabolites isolated from ascidians include small molecules like lissoketal (**502**), isolated from *Lissoclinum voeltzkowi* and endowed with a 1,6-dioxaspiro[4,5]dec-8-en-4-one moiety [356] as well as families of complex molecules, biosynthetically unrelated, such as bistranides (**503–508**), prunolides (**509–511**), and didemnaketals (**512–514**).





Bistramides are a family of polyether toxins possessing a 1,7-dioxaspiro [5] undecane spiroketal unit. The first of the series, bistratene A (bistratene A, **503**) was isolated from *Lissoclinum bistratum* [246, 357]; additional bistramides (B–D and K, **504–507**) were later recovered also from *L. bistratum* [358], while the only report of these compounds from another source is 39-oxobistramide K (**508**) from *Trididemnum cyclops* [359]. The bistramides have been shown to display diverse bioactivities, including immunomodulating and weak antimalarian activity, but their most notable trait is their antitumor properties. Bistratene A (**503**) promises to become a useful agent with which to dissect the complex processes controlling cell growth, differentiation, and death [360, 361]. Unfortunately, high toxicity prevents them from therapeutic use; among bistramides, compounds **506** and **507** are less toxic but far less abundant in nature.

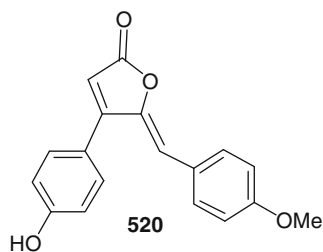
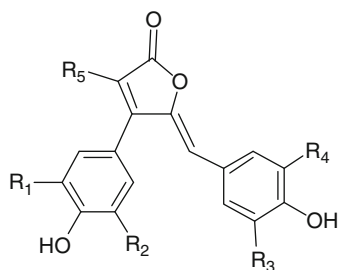
Prunolides A–C (**509–511**) are tetraphenolic bis-spiroketal containing a unique 1,6,8-trioxadispiro[4.1.4.2]trideca-3,10,12-triene-2,9-dione carbon

skeleton which have been isolated from an Australian collection of *Synoicum prunum* [362]. They represent a structurally novel family of ascidian metabolites; they have been frequently co-isolated with rubrolides (515–529, see Sect. 5.6.2), suggesting that they probably arise from an oxidative dimerization of a rubrolide precursor. The prunolides also bear some resemblance to the alkaloids polycitone A (226) and polycitrins A and B (228–229), and they probably share a common biogenesis.

In 1991, Potts et al. reported that an unidentified Palauan ascidian of the genus *Didemnum* contained two polyisoprenoid, didemnaketal A and B (512–513) containing a 1,7-dioxaspiro [5]undecane spiroketal unit; both of them inhibited the activity of HIV-1 protease [363]. A reinvestigation of the same organisms yielded as the major secondary metabolite: the isoethonic ester 514, didemnaketal C [364]. It was therefore assumed that compounds 512 and 513 had been produced from didemnaketal C during prolonged storage in methanol by mechanisms involving oxidation and methanolysis, respectively. Unfortunately, didemnaketal C (514) did not inhibit HIV-1 in a peptidolysis assay.

5.6.2 Nonnitrogenous Phenylalanine- or Tyrosine-Derived Metabolites

The rubrolides (515–529) are a structurally unique family of biologically active ascidians metabolites. Rubrolides A–H (515–522) were first described as antibacterial, phosphatase-inhibiting metabolites of *Ritterella rubra* [365], followed by the discovery of six new members of the family, rubrolides I–N (523–528) in *Synoicum blochmani* with rubrolides I, K, L, and M exhibiting significant cytotoxicity [366]. A New Zealand *Synoicum* n. sp. contained rubrolide O (529) which, unlike the others rubrolides reported solely as the Z isomers, exists as a mixture of E/Z isomers; moreover, it is the first anti-inflammatory rubrolide reported [367]. A related biogenesis from either phenylalanine or tyrosine appears most likely for rubrolides; therefore, even though they are part of the very small minority of tunicate metabolites that do not contain nitrogen, rubrolides probably share an amino acid biogenetic origin with the majority of the other tunicate metabolites. Rubrolides B (516), H (522), I (523), and K–O (525–529) are rare examples of chlorinated tunicate metabolites; rubrolide N (528) displays an unprecedented halogenation pattern among the rubrolides since it contains an α -bromo- β -lactone ring and a chlorinated aromatic substituent. Rubrolide A (515) has also been detected in the Australian *S. prunum*, from which were isolated the related prunolides (509–511, see Sect. 5.7) [362], and from an ascidian of the genus *Botryllus*, which also yielded the cadiolides (530–531) [368], other furanone metabolites structurally related to the rubrolides but possessing a novel carbon skeleton probably originated from three molecules of phenylalanine.



515 $R_1=R_2=R_3=R_4=Br$; $R_5=H$

516 $R_1=R_2=R_3=R_4=Br$; $R_5=Cl$

517 $R_1=R_2=R_5=H$; $R_3=R_4=Br$

518 $R_1=R_2=Br$; $R_3=R_4=R_5=H$

519 $R_1=R_2=R_3=R_4=R_5=H$

523 $R_1=H$; $R_2=R_3=R_4=Br$; $R_5=Cl$

524 $R_1=H$; $R_2=R_3=R_4=Br$; $R_5=H$

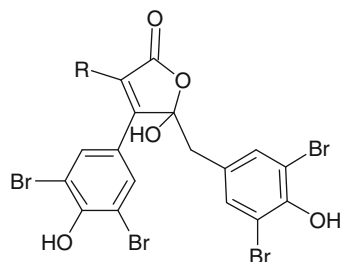
525 $R_1=R_3=H$; $R_2=R_4=Br$; $R_5=Cl$

526 $R_1=R_2=H$; $R_3=R_4=Br$; $R_5=Cl$

527 $R_1=R_2=R_3=H$; $R_4=Br$; $R_5=Cl$

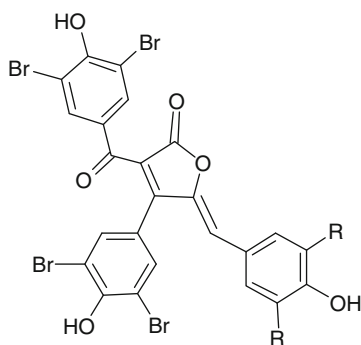
528 $R_1=R_3=H$; $R_2=Cl$; $R_4=R_5=Br$

529 $R_1=R_2=R_3=Br$; $R_4=H$; $R_5=Cl$ (mixture of E/Z isomers)



521 $R=H$

522 $R=Cl$

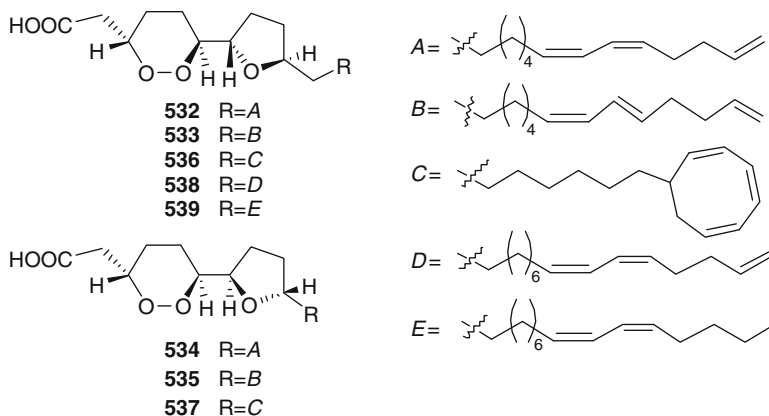


530 $R=H$

531 $R=Br$

5.6.3 Stolonoxides and Stolonic Acids

Linear and cyclic peroxides have been encountered in marine organisms, but they are mainly confined to sponges of the genera *Chondrilla*, *Plakortis*, and *Xestospongia*. However, *Stolonica* ascidians have been showed to be an additional source of fatty acid-derived cyclic peroxides, like stolonoxides and stolonic acids (**532–539**) which constitute a family of aliphatic endoperoxides with an unprecedented molecular arrangement.



Differently from other known peroxides, stolonoxides display an unusual structure with a 1,2-dioxane ring directly linked to a tetrahydrofuranyl (THF) moiety. Stolonoxide A (**532**), the first member of the series, has been isolated as its methyl ester from *Stolonica socialis* [369]; compound **532**, together with three new analogues, stolonoxides B–D (**533–535**), were independently isolated from another sample of the same species [370]. Two further stolonoxides, E and F (**536**, **537**), have been recently isolated also from *S. socialis* [371]; while being members of the stolonoxide family, they incorporate a 1,3,5-octatriene ring in their molecules, an element of structural novelty with only one precedent in marine natural products. This ring seems to originate from an unstable tetraene at the end of the aliphatic chain of a potential precursor. There is also the probability that 1,3,5-octatriene ring could be formed during the process of extraction and purification of the compounds [371]. Stolononic acids A and B (**538**, **539**), possessing a longer aliphatic chain, have been isolated from an undescribed *Stolonica* species collected in the Indian Ocean [372]. Both stolononic acids and stolonoxides were strongly cytotoxic against several mammalian tumor cell lines; interestingly, the activity displayed by stolonoxides E (**536**) and F (**537**) was weaker than that measured for their analogues stolonoxides A–D (**532–535**) and for stolononic acids (**538** and **539**). This suggests that the presence of the diene and the vinyl terminal group in these latter compounds plays a key role in the cytotoxic activity displayed by members of this family [371]. The molecular arrangement of compounds **532–539** resembles the adjacent bis-THF group of Annonaceous acetogenins, a class of antitumor and pesticidal compounds whose main mode of action is the inhibition of the mitochondrial respiratory chain, the fundamental process that drives the ATP synthesis under anaerobic metabolism in cells. Based on this structural analogy, stolonoxides A (**532**) and C (**534**) were tested in beef heart submitochondrial particles (SMP) and were found to be inhibitors of the mitochondrial respiratory chain, affecting specifically the functionality of complex II (succinate:ubiquinone oxidoreductase) and complex II (ubiquinol:cytochrome *c* oxidoreductase) in mammalian cells [373].

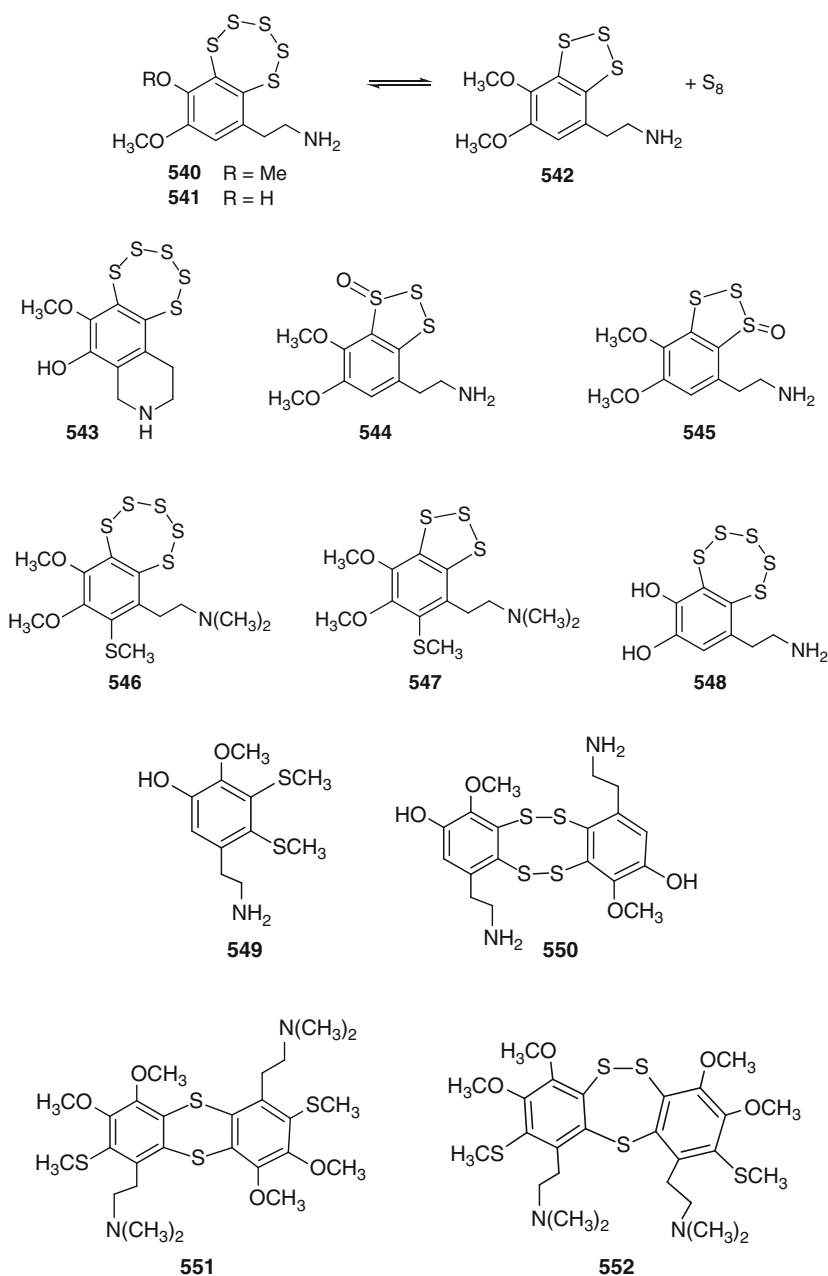
5.7 Sulfur-Containing Metabolites

Sulfur-containing compounds, although relatively unusual, occur in marine organisms. Ascidians have been an extremely rich source of sulfur-containing molecules; they include sulfides/polysulfides, sulfur-heterocycles, sulfoxides, and alkyl sulfates. Some of these compounds (mostly molecules with sulfur-heterocycle, methyl sulfide, and sulfoxide moieties) have been already showed in the previous sections since they flatly fell into one of the main structural groups identified. Here described are essentially sulfides, polysulfides, and simple alkyl sulfates.

A number of unique cyclic polysulfides derived from dopamine have been reported from ascidians of the genera *Lissoclinum*, *Polycitor*, and *Eudistoma* [17, 374–378]; they have received considerable attention both for their unique chemical structures and for their often significant biological activities. Varacin (**540**), the first naturally occurring benzopentathiepin, has been isolated from *L. vareau*, a lavender-colored encrusting species collected in the Fiji Islands [375]. Compound **540** has been synthesized from vanillin providing unambiguous confirmation of the structure proposed [379, 380]. Similar compounds, lissoclinotoxin A (**541**), originally reported to have a cyclic trithiane structure [381], and lissoclinotoxin B (**542**) [376], have been isolated from *L. perforatum* collected in northern Brittany. Evidences have been provided indicating that unsymmetrically substituted benzopentathiepins, such as varacin and lissoclinotoxin A, are chiral because of a high activation barrier to interconversion of the low energy chair conformations of the polysulfide ring [382]. In addition to having unique structures, varacin and lissoclinotoxin A exhibit significant biological activities. Varacin was originally reported to have antifungal activity against *Candida albicans* (14-mm zone of inhibition of 2 µg of varacin/disk) as well as cytotoxicity toward human colon tumor cell line HCT 116 (IC₉₀ 0.05 µg/mL) [375], while lissoclinotoxin A was reported to have antimicrobial and antifungal activity (*S. aureus*, Ø inhibition: 15 mm/300 µg) [381]. Furthermore, a differential cytotoxicity toward the CHO cell lines EM9 (chlorodeoxyuridine sensitive) versus BR1 (BCNU resistant) indicated that varacin's mechanism of action may involve the formation of single-stranded DNA breaks [375, 383]. It has been reported that some aromatic fused benzopentathiepins are capable of decomposing into sulfur and the corresponding benzotrithioles in solution [384]. Examination of varacin (**540**) as well as varacin A (**543**) by ¹H NMR and MS revealed that both of these compounds readily equilibrate to a mixture of **540** and **543**. In fact, the reaction “**540** = **543** + S₈” was observed to occur in CHCl₃, MeOH and pyridine [383]. Varacin B e C (**544 e 545**), isolated from *Polycitor* sp. [380] are the 3'-S-oxide and the 1'-S-oxide, respectively, of varacin A.

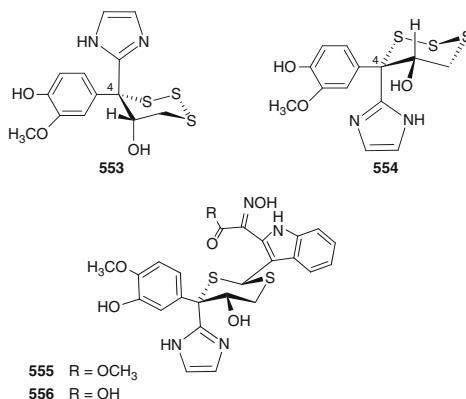
Compagnone et al. reported the isolation and protein kinase C inhibitory activity of N,N-dimethyl-5-(methylthio)varacin (**546**) and the corresponding trithiane **547** from a Palauan collection of *Lissoclinum japonicum* and 3,4-desmethylvaracin (**548**) from *Eudistoma* sp. from Pohnpei [374]. Lissoclinotoxin C (**549**) and the dimeric lissoclinotoxin D (**550**) have been isolated from *Lissoclinum* sp. collected from the Great Reef, Australia [20], while lissoclinotoxins E and F (**551, 552**) have been found

in a Philippine didemnid ascidian. Montecarlo conformational searching using MM2 force field suggested that the *N*-alkyl chains about the tricyclic systems of lissocli-notoxins E and F had *trans* and *cis* orientations, respectively [385].

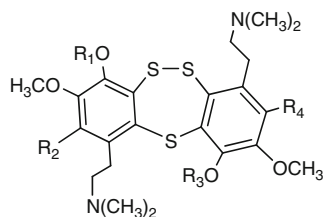
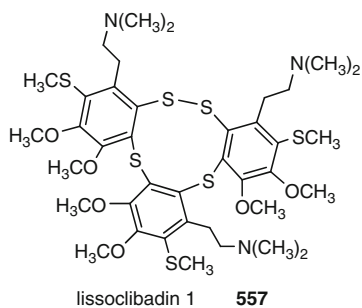


Another trithiane derivative (**553**) was isolated from the New Zealand ascidian *Aplidium* sp. [386]. Compound **553** was observed to be unstable in slightly alkaline solutions or even in neutral CD₃OD, giving a mixture of two new components, one of which was shown to be the diastereomer **554** bearing the opposite configuration at the central chiral carbon (C-4). Both trithiane derivatives **553** and **554** exhibited modest cytotoxic activity against P388 murine leukemia with IC₅₀ values of 13 and 12 µg/mL, respectively, in addition to inhibiting the growth of *Bacillus subtilis* and *Candida albicans* (–20 µg/disk) [386].

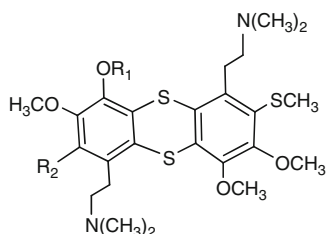
Enantiomeric marine natural products are uncommon, and it is rare to find enantiomers with two or more chiral centers. The (–)-**553** enantiomer of compound (+)-**554** was isolated from the delicate pink stalked ascidian *Hypsistozoa fasmeriana* collected at Tutukaka, North Island, New Zealand [387]. Another collection of *H. fasmeriana* collected at Leigh Harbor, Northland, New Zealand afforded (–)-**553** and two dithiane metabolites **555** and **556** named fasmerianamine A and B, respectively [387].



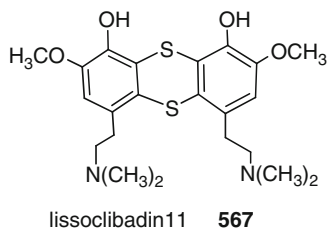
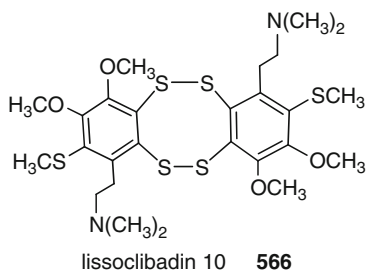
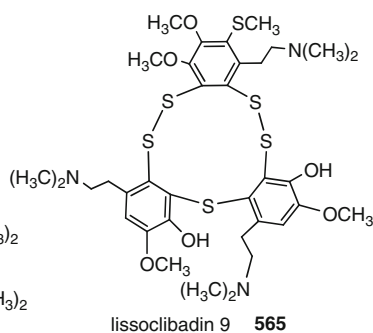
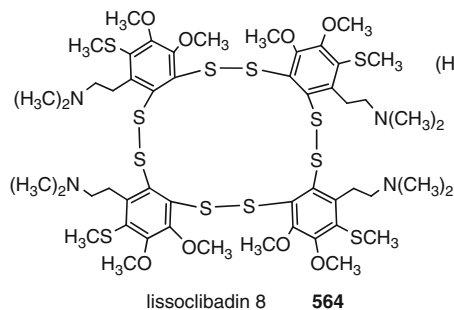
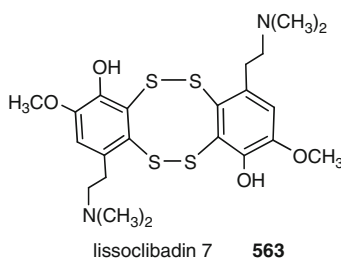
Fourteen polysulfur dopamine-derived compounds lissoclibadin 1–14 (**557**–**570**) have been isolated from *Lissoclinum* cf. *badium*, collected in Indonesia [388–391]. Lissoclibadins 1 and 2 (**557** and **558**) and lissoclinotoxin F (**552**) showed a very strong activity against human solid tumor cell lines and are more potent than the anticancer drug cisplatin. Lissoclibadin 2 (**558**) was the most interesting compound possessing potent inhibitory activity against colon cancer cell lines (DLD-1 and HCT116), breast (MDA-MB-231), renal (ACHN), and non-small-cell lung (NCI-H460) cancer cell lines and showing no toxicity following a 50 mg/kg single treatment to mice, and preferable stability in rat plasma. Therefore, the activities of compounds possessing a dimeric or trimeric structure with a disulfide bond are stronger than those of the dimeric compound with two sulfide bonds (**559**) and monomeric compounds (**546**, **547**) [392].

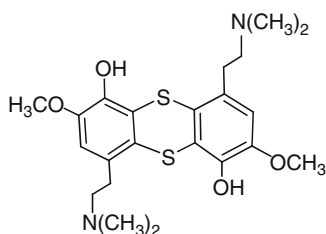
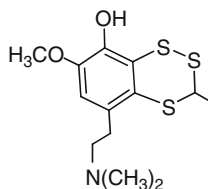
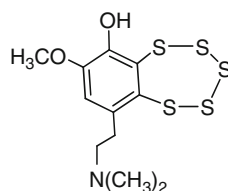


		R ₁	R ₂	R ₃	R ₄
lissoclibadin 2	558	Me	SMe	Me	SMe
lissoclibadin 4	560	H	H	H	H
lissoclibadin 5	561	H	H	Me	SMe

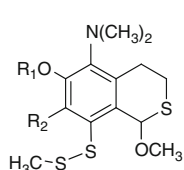


		R ₁	R ₂
lissoclibadin 3	559	Me	SMe
lissoclibadin 6	562	H	H

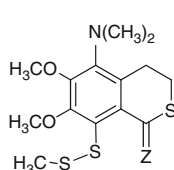


lissoclibadin 12 **568**lissoclibadin 13 **569**lissoclibadin 14 **570**

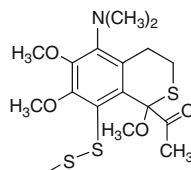
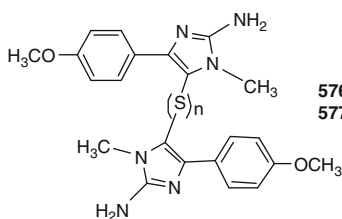
Several disulfides compounds have been isolated from ascidians of the genus *Polycarpa*. They include polycarpamines A–E (**571**–**575**), found in *P. auzata* [393], and polycarpine (**576**), a cytotoxic metabolite isolated from several collections of *P. aurata* and subsequently reported from *P. clavata* [73, 394, 395]. Polycarpamines as well as polycarpine presented various biological activities, such as antifungal activity [393], cytotoxicity [394], inhibition of inosine monophosphate dehydrogenase (IMPDH) [396], and induction of apoptosis in JB6 cells through p53- and caspase 3-dependent pathways [397]. From a sample of *P. aurata* collected in the Lembeh Strait, Indonesia, in addition to polycarpine (**576**), polycarparines A (**577**), B (**578**), and C (**579**) have been isolated [398].



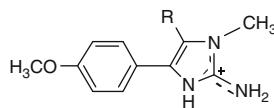
571 $R_1=CH_3$ $R_2=OCH_3$
575 $R_1=H$ $R_2=H$



572 $Z=O$
573 $Z=S$

**574**

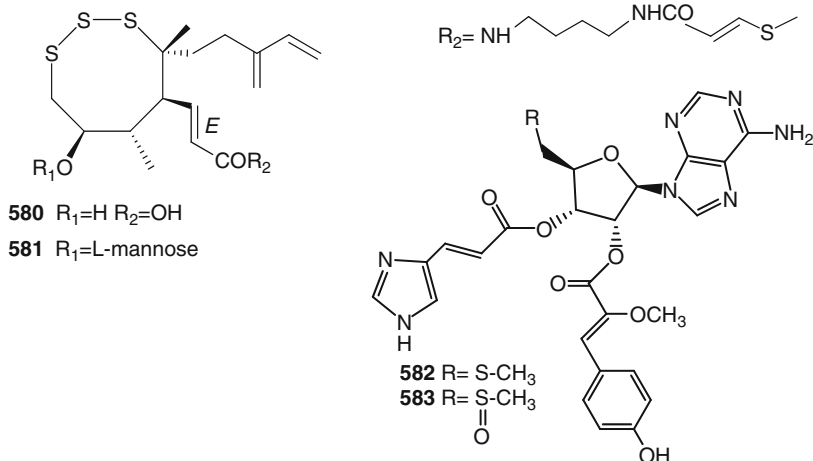
576 $n=2$
577 $n=1$



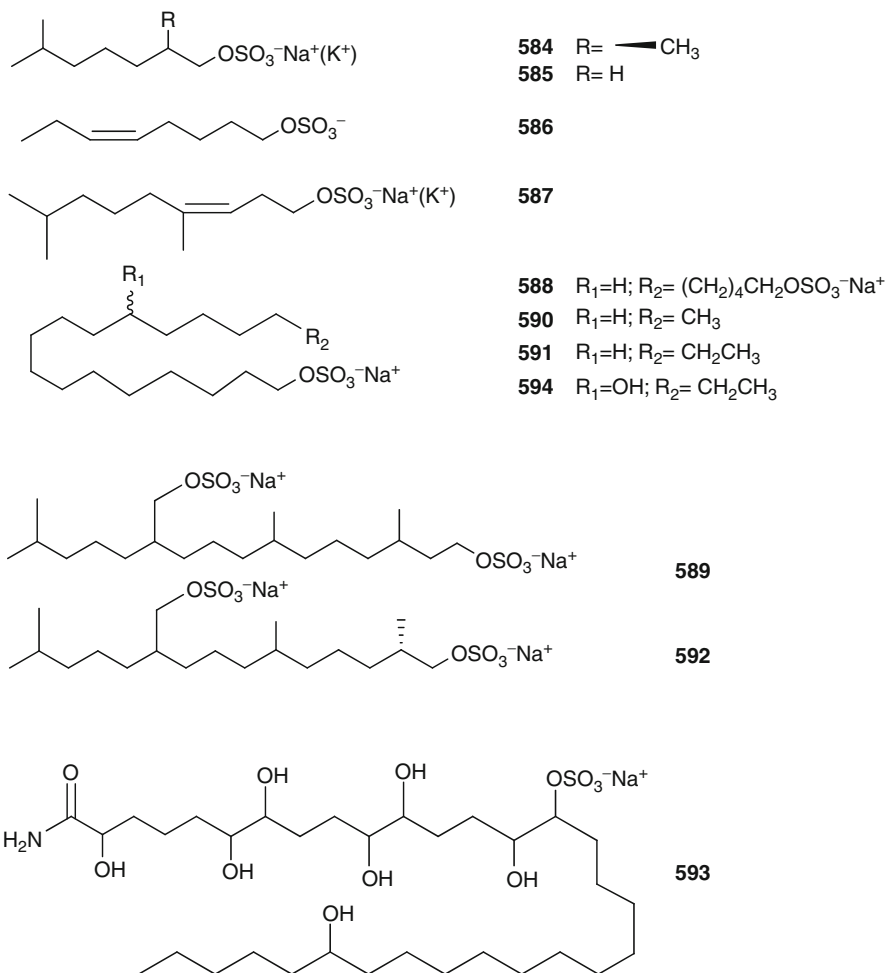
578 $R=SO_3^-$
579 $R=S-SO_3^-$

Two sulfur derivatives, **580** and **581**, the latter of which is a glycoside, containing substituted 1,2,3-trithiocane cycles have been isolated from *Perophora viridis* collected off the Atlantic of North Carolina [399].

Two complex nucleosides, (**582**–**583**) containing the rare methylthioadenosine and methylsulfinyladenosine moieties, were found in *Atrium robustum*. Compound **582** inhibits cAMP accumulation in Chinese hamster ovary (CHO) cell membranes recombinantly expressing the human A_3 adenosine receptor, thus indicating that the adenosine derivative also acted as a partial agonist at A_3 ARs [400].

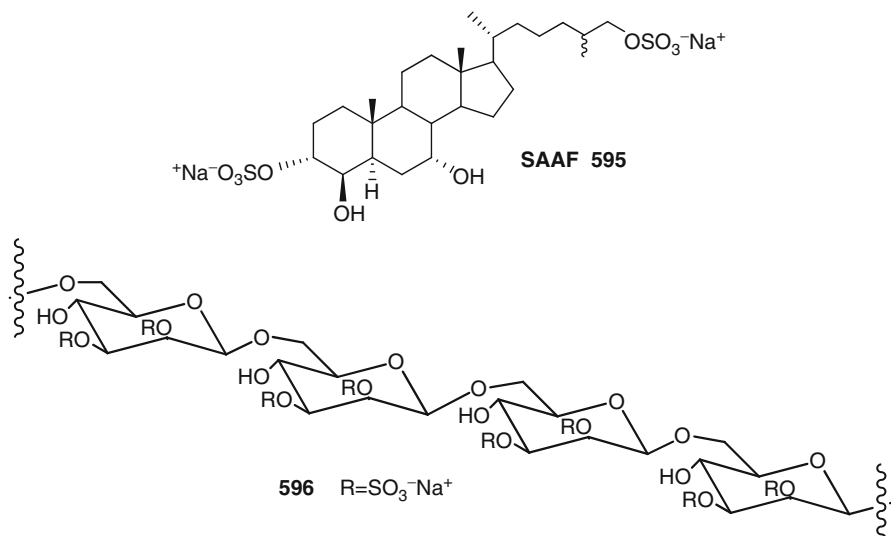


Only a few examples of sulfated alkanes/alkene have been reported from marine sources. Although the isolation of some alkane/alkene sulfate esters from two Japanese ascidians have been reported [401, 402], a series of these metabolites have been isolated from Mediterranean tunicates. Most of these compounds, often having quite simple structures, are cytotoxic or antimicrobial. The first report of a sulfated hydrocarbon from a tunicate was the finding of sodium (or potassium) 2,6-dimethylheptyl sulfate (**584**) from *Policitor adriaticus* in 1994 [403, 404]; it was also isolated, as a racemate, from the hepatopancreas of *Halocynthia roretzi* [401] and from *H. papillosa* together with compounds **585–586** [405]. Further cytotoxic and antiproliferative analogues have been isolated from other Mediterranean ascidians, such as compound **587** from *Microcosmus vulgaris* [406] and **588–589** from *Ascidia mentula* [407]. A selective cytotoxic agent, named turbinamide (**593**) [408] has been isolated from the Mediterranean tunicate *Sidnyum turbinatum* together with three sulfated alkanes **590–592** [409]. Turbinamide (**593**) showed a potent and selective cytotoxic effect against neuronal rather than immune system cells; C6 rat glioma cells were shown to be very sensible to this metabolite. Gliomas are also considered among the most malignant forms of cancer whose therapeutic treatment is up to now only palliative. Studies on the cellular effects of turbinamide have been performed, and it is demonstrated that turbinamide-induced cytotoxicity in C6 cells is due to apoptosis: The activity of caspase-3 is enhanced in a concentration-dependent manner by this compound, having no effect on J774 cells [410]. Compound **594**, structurally related to the alkyl sulfates isolated from *A. mentula* and *S. turbinatum*, has been isolated from a marine tunicate of the family Polyclinidae as a matrix metalloproteinase 2 (MMP2) inhibitor with an IC_{50} value of 9.0 $\mu\text{g/mL}$ [402].



Sperm chemotaxis toward eggs before fertilization has been demonstrated in many animals and plant, and several peptides and small organic compounds acting as chemoattractants have been identified [411]. An endogenous non-peptidic sperm-activating and sperm-attracting factor, SAAF **595**, was isolated from the eggs of *Ciona intestinalis* and *C. savignyi* [412]; the synthesis of **595** allowed to define completely the structure and to provide further biological studies [413]. Spermatozoa of the ascidian *C. intestinalis* are slightly motile when suspended in seawater. However, when an unfertilized egg is set in the sperm suspension, the spermatozoa near the egg are intensely activated and being to show chemotactic behavior toward the egg. A method was established for quantitative analysis of sperm chemotaxis and clearly showed that the chemotactic

behavior of *Ciona* sperm is controlled by the “chemotactic turn” associated with decrease in concentration of SAAF [412]. Kakelokelose (**596**), an unusual sulfated mannose polysaccharide with anti-HIV activity in vitro has been found in *D. molle* [414].



5.8 Study Questions

1. Which structural features of pyridoacridine alkaloids could be principally related to their capacity of intercalate into DNA and cleave the DNA double helix or inhibit the action of topoisomerase II?
2. All complex β -carboline alkaloids isolated from tunicates have been considered to be biogenetically related, being derived from tryptophan and a second amino acid. Which amino acid, in addition to the primary biosynthetic precursor tryptophan, could be involved in a plausible pathway leading to eudistomin Y4 (**62**)?
3. Propose a plausible biogenetic pathway for clavaminols A (**285**), G (**291**), and H (**293**), respectively.
4. Explain why the structural features of tunichromes and the related halocyamines could be strongly indicative of their role in vanadium accumulation and reduction in ascidian blood cells.
5. Explain why the occurrence of identical and/or biosynthetically related compounds in collections of different organisms raises a question about the real producer of the metabolites.

References

1. Bruening RC, Oh EM, Furukawa J, Nakanishi K, Kuetin K (1986) Isolation of Tunichrome B-1, a reducing blood pigment of the sea squirt, *Ascidia nigra*. *J Nat Prod* 49:193–204
2. Davidson BS (1993) Ascidians: producers of amino acid derived metabolites. *Chem Rev* 93:1771–1791
3. Martoja R, Gouzerh P, Monniot F (1994) Cytochemical studies of vanadium, tunichromes and related substances in ascidians, possible biological significance. *Oceanogr Mari Biol Ann Rev* 32:531–556
4. Hamada T, Asanuma M, Ueki T, Hayashi F, Kobayashi N, Yokoyama S, Michibata H, Hirota H (2005) Solution structure of vanabin2, a vanadium(IV)-binding protein from the vanadium rich ascidian, *Ascidia sydneiensis samea*. *J Am Chem Soc* 127:4216–4222
5. Fenical W (1976) Geranyl hydroquinone, a cancer-protective agent from the tunicate *Aplidium* species. *Food-Drugs Sea Proc* 4:388–394
6. Faulkner DJ (2002) Marine natural products: metabolites of marine invertebrates. *Nat Prod Rep* 19:1–48 and earlier reports in the series
7. Blunt JW, Copp BR, Munro MHG, Northcote PT, Prinsep MR (2010) Marine natural products. *Nat Prod Rep* 27:165–237 and earlier reports in the series
8. Menna M (2009) Antitumor potential of natural products from Mediterranean ascidians. *Phytochem Rev* 8:461–472
9. Mayer AMS, Glaser KB, Cuevas C, Jacobs RS, Kem W, Little RD, McIntosh JM, Newman DJ, Potts BC, Shuster DE (2010) The odyssey of marine pharmaceuticals: a current pipeline perspective. *Trends Pharmacol Sci* 31:255–265
10. Ding Q, Chichak K, Lown JW (1999) Pyrroloquinoline and pyridoacridine alkaloids from marine sources. *Curr Med Chem* 6:1–27
11. Delfourne E, Bastide J (2003) Marine pyridoacridine alkaloids and synthetic analogues as antitumour agents. *Med Res Rev* 23:234–252
12. Dias N, Vezin H, Lansiaux A, Bailly C (2005) Topoisomerase inhibitors of marine origin and their potential use as anticancer agents. *Top Curr Chem* 253:89–108
13. Kim J, Pordesimo EO, Toth SI, Schmitz FJ (1993) Pantherinine, a cytotoxic aromatic alkaloid, and 7-deazainosine from the ascidian *Aplidium pantherinum*. *J Nat Prod* 56:1813–1816
14. Kobayashi J, Cheng J, Walchli MR, Nakamura H, Hirata Y, Sasaki T, Ohizumi Y (1988) Cystodytins A, B, and C, novel tetracyclic aromatic alkaloids with potent antineoplastic activity from the Okinawan tunicate *Cystodytes dellechiaiei*. *J Org Chem* 53:1800–1804
15. Kobayashi J, Tsuda M, Tanabe A, Ishibashi M, Cheng JF, Yamamura S, Sasaki T (1991) Cystodytins D-I, new cytotoxic tetracyclic aromatic alkaloids from the Okinawan marine tunicate *Cystodytes dellechiaiei*. *J Nat Prod* 54:1634–1638
16. McDonald LA, Eldredge GS, Barrows LR, Ireland CM (1994) Inhibition of Topoisomerase II catalytic activity by pyridoacridine alkaloids from a *Cystodytes* sp. ascidian: a mechanism for the apparent intercalator-induced inhibition of Topoisomerase II. *J Med Chem* 37:3819–3827
17. Appleton DR, Pearce AN, Lambert G, Babcock RC, Copp BR (2002) Isodiplamine, cystodytin K and lissoclinidine: novel bioactive alkaloids from the New Zealand ascidian *Lissoclinum notti*. *Tetrahedron* 58:9779–9783
18. Charyulu GA, McKee TC, Ireland CM (1989) Diplamine, a cytotoxic polyaromatic alkaloid from the tunicate *Diplosoma* sp. *Tetrahedron Lett* 30:4201–4202
19. Clement JA, Kitagaki J, Yang Y, Saucedo CJ, O’Keefe BR, Weissman AM, McKee TC, McMahon JB (2008) Discovery of new pyridoacridine alkaloids from *Lissoclinum* cf. *badium* that inhibit the ubiquitin ligase activity of Hdm2 and stabilize p53. *Bioorg Med Chem* 16:10022–10028

20. Searle PA, Molinski TF (1994) Five new alkaloids from the tropical ascidian, *Lissoclinum* sp. lissoclinotoxin A is chiral. *J Org Chem* 59:6600–6605
21. Rudi A, Benayahu Y, Goldberg I, Kashman Y (1988) Alkaloid metabolites of the marine tunicate *Eudistoma* sp.: segoline A, isosegoline A and norsegoline. *Tetrahedron Lett* 29:3861–3862
22. Rudi A, Kashman Y (1989) Six new alkaloids from the purple Red Sea tunicate *Eudistoma* sp. *J Org Chem* 54:5331–5337
23. Einat M, Nagler A, Lishner M, Amiel A, Yarkoni S, Rudi A, Gellerman G, Kashman Y, Fabian I (1995) Potent antileukemic activity of the novel agents norsegoline and dibezine. *Clin Cancer Res* 1:823–829
24. Molinski TF, Ireland CM (1989) Varamines A and B, new cytotoxic thioalkaloids from *Lissoclinum vareau*. *J Org Chem* 54:4256–4259
25. Copp BR, Jompa J, Tahir A, Ireland CM (1998) Styelsamines A-D: new tetracyclic pyridoacridine alkaloids from the Indonesian ascidian *Eusynstyela latericius*. *J Org Chem* 63:8024–8026
26. Kobayashi J, Cheng JF, Nakamura H, Ohizumi Y, Hirata Y, Sasaki T, Ohta T, Nozoe S (1988) Ascidiademin, a novel pentacyclic aromatic alkaloid with potent antileukemic activity from the Okinawan tunicate *Didemnum* sp. *Tetrahedron Lett* 29:1177–1180
27. Schmitz FJ, DeGuzman FS, Hossain MB, Van der Helm D (1991) Cytotoxic aromatic alkaloids from the ascidian *Amphicarpa meridiana* and *Leptoclinides* sp.: meridine and 11-hydroxyascidiademin. *J Org Chem* 56:804–808
28. Cooray NM, Scheuer PJ, Parkanyi L, Clardy J (1988) Shermilamine A: a pentacyclic alkaloid from a tunicate. *J Org Chem* 53:4619–4620
29. Carroll AR, Cooray NM, Poiner A, Scheuer PJ (1989) A second shermilamine alkaloid from a tunicate *Trididemnum* sp. *J Org Chem* 54:4231–4232
30. Koren-Goldshlager G, Aknin M, Gaydou EM, Kashman Y (1998) Three new alkaloids from the marine tunicate *Cystodytes violatinctus*. *J Org Chem* 63:4601–4603
31. Lopez-Legentil S, Dieckmann R, Bontemps-Subielos N, Turon X, Banaigs B (2005) Qualitative analysis of alkaloids in color morphs of *Cystodites* (Ascidacea). *Biochem Syst Ecol* 33:1107–1119
32. Carroll AR, Scheuer PJ (1990) Kuanoniamines A, B, C, and D: pentacyclic alkaloids from a tunicate and its prosobranch mollusk predator *Chelynotus semperi*. *J Org Chem* 55:4426–4431
33. Nilar PJS, Carté BK, Butler MS (2002) Three new pyridoacridine type alkaloids from a Singaporean ascidian. *J Nat Prod* 65:1198–1200
34. Torres YR, Bugni TS, Berlinck RGS, Ireland CM, Magalhaes A, Ferreira AG, Moreira da Rocha R (2002) Sebastianines A and B, novel biologically active pyridoacridine alkaloids from the Brazilian ascidian *Cystodytes dellechiaiei*. *J Org Chem* 67:5429–5432
35. Plubrukarn A, Davidson BS (1998) Arnoamines A and B, new cytotoxic pentacyclic pyridoacridine alkaloids from the ascidian *Cystodytes* sp. *J Org Chem* 63:1657–1659
36. Viracaoundin I, Faure R, Gaydou EM, Aknin M (2001) A new alkaloid from the purple Indian Ocean tunicate *Eudistoma bituminis*. *Tetrahedron Lett* 42:2669–2671
37. He HY, Faulkner DJ (1991) Eudistones A and B: two novel octacyclic alkaloids from a seychelles tunicate *Eudistoma* sp. *J Org Chem* 56:5369–5371
38. Rudi A, Benayahu Y, Goldberg I, Kashman Y (1988) Eilatins, a novel alkaloid from the marine tunicate *Eudistoma* sp. *Tetrahedron Lett* 29:6655–6656
39. Shochet NR, Rudi A, Kashman Y, Hod Y, El-Maghrabi MR, Spector I (1993) Novel marine alkaloids from the tunicate *Eudistoma* sp. are potent regulators of cellular growth and differentiation and affect cAMP-mediated processes. *J Cell Physiol* 157:481–492
40. Kobayashi J, Harbour GC, Gilmore J, Rinehart KL Jr (1984) Eudistomins A, D, G, H, I, J, M, N, O, P, and Q, bromo, hydroxy, pyrrolyl and iminoazepino β -carbolines from the antiviral Caribbean tunicate *Eudistoma olivaceum*. *J Am Chem Soc* 106:1526–1528

41. Rinehart KL Jr, Kobayashi J, Harbour GC, Gilmore J, Mascal M, Holt TG, Shield LS, Lafargue F (1987) Eudistomins A-Q, β -carboline alkaloids from the antiviral Caribbean tunicate *Eudistoma olivaceum*. *J Am Chem Soc* 109:3378–3387
42. Kinzer KF, Cardellina II JH (1987) Three new β -carboline alkaloids from the Bermudian tunicate *Eudistoma olivaceum*. *Tetrahedron Lett* 28:925–926
43. Schupp P, Poehner T, Edrada R, Ebel R, Berg A, Wray V, Proksch P (2003) Eudistomins W and X, two new β -carboline alkaloids from the Micronesian tunicate *Eudistoma* sp. *J Nat Prod* 66:272–275
44. Wang W, Nam S, Lee B, Kang H (2008) β -Carboline alkaloids from a Korean Tunicate *Eudistoma* sp. *J Nat Prod* 71:163–166
45. Rinehart KL, Kobayashi J, Harbour GC, Hughes RG Jr, Mizsak SA, Scahill TA (1984) Eudistomins C, E, K, and L, potent antiviral compounds containing a novel oxathiazepine ring from the Caribbean tunicate *Eudistoma olivaceum*. *J Am Chem Soc* 106:1524–1526
46. Kobayashi J, Nakamura H, Ohizumi Y, Hirata Y (1986) Eudistomidin A, a novel calmodulin antagonist from the Okinawan tunicate *Eudistoma glaucus*. *Tetrahedron Lett* 27:1191–1194
47. Kobayashi J, Cheng JF, Ohta T, Nozoe S, Ohizumi Y, Sasaki T (1990) Eudistomidins B, C, and D: novel antileukemic alkaloids from the Okinawan marine tunicate *Eudistoma glaucus*. *J Org Chem* 55:3666–3670
48. Murata O, Shigemori H, Ishibashi M, Sugama K, Hayashi K, Kobayashi J (1991) Eudistomidins E and F, new β -carboline alkaloids from the Okinawan marine tunicate *Eudistoma glaucus*. *Tetrahedron Lett* 32:3539–3542
49. Takahashi Y, Ishiyama H, Kubota T, Kobayashi J (2010) Eudistomidin G, a new β -carboline alkaloid from the Okinawan marine tunicate *Eudistoma glaucus* and structure revision of eudistomidin B. *Bioorg Med Chem Lett* 20:4100–4103
50. Adesanya SA, Chbani M, Pais M, Debitus C (1992) Brominated β -carboline alkaloids from the marine tunicate *Eudistoma album*. *J Nat Prod* 55:525–527
51. Rashid MA, Gustafson KR, Boyd MR (2001) New cytotoxic N-methylated β -carboline alkaloids from the marine ascidian *Eudistoma gilboverde*. *J Nat Prod* 4:1454–1456
52. Debitus C, Laurent D, Pais M (1988) Alkaloids from an ascidian of New Caledonia, *Eudistoma fragum*. *J Nat Prod* 51:99–801
53. Van Wagoner RM, Jompa J, Tahir A, Ireland CM (1999) Trypargine alkaloids from a previously undescribed *Eudistoma* sp. ascidian. *J Nat Prod* 62:794–797
54. Lake RJ, Brennan MM, Blunt JW, Munro MHG, Pannell LK (1988) Eudistomin K sulfoxide. An antiviral sulfoxide from the New Zealand ascidian *Ritterella sigillinoides*. *Tetrahedron Lett* 29:2255–2256
55. Lake RJ, Blunt JW, Munro MHG (1989) Eudistomins from the New Zealand ascidian *Ritterella sigillinoides*. *Aust J Chem* 42:1201–1206
56. Davis RA, Carroll AR, Quinn RJ (1998) Eudistomin V, a New β -Carboline from the Australian ascidian *Pseudodistoma aureum*. *J Nat Prod* 61:959–960
57. Chbani M, Pais M, Delauneux JM, Debitus C (1993) Brominated indole alkaloids from the marine tunicate *Pseudodistoma arborescens*. *J Nat Prod* 56:99–104
58. Rashid MA, Gustafson KR, Cartner LK, Pannell LK, Boyd MR (2001) New nitrogenous constituents from the South African marine Ascidian *Pseudodistoma* sp. *Tetrahedron* 57:5751–5755
59. Schumacher RW, Davidson BS (1995) Didemnolines-D, new N9-substituted β -carboline alkaloids from the marine ascidian *Didemnum* sp. *Tetrahedron* 51:10125–10130
60. Oku N, Matsunaga S, Fusetani N (2003) Shishijimicins A-C, novel enediyne antitumor antibiotics from the ascidian *Didemnum proliferum*. *J Am Chem Soc* 125:2044–2045
61. Kearns PS, Coll JC, Rideout JA (1995) A β -carboline dimer from an ascidian, *Didemnum* sp. *J Nat Prod* 58:1075–1076

62. Kearns PS, Rideout JA (2008) Nonsymmetrical β -carboline dimers from an ascidian, *Didemnum* sp. J Nat Prod 71:1280–1282
63. Foderaro TA, Barrows LR, Lassota P, Ireland CM (1997) Bengacarboline, a new β -carboline from a marine ascidian *Didemnum* sp. J Org Chem 62:6064–6065
64. Ravinder K, Reddy AV, Krishnaiah P, Ramesh P, Ramakrishna S, Laatsch H, Venkateswarlu Y (2005) Isolation and synthesis of a novel β -carboline guanidine derivative tiruchanduramine from the Indian ascidian *Synoicum macroglossum*. Tetrahedron Lett 46:5475–5478
65. Badre A, Boulanger A, Abou-Mansour E, Banaigs B, Combaut G, Francisco C (1994) Eudistomin U and isoeudistomin U, new alkaloids from the Caribbean ascidian *Lissoclinum fragile*. J Nat Prod 57:528–533
66. Shen GQ, Baker BJ (1994) Biosynthetic studies of the eudistomins in the tunicate *Eudistoma olivaceum*. Tetrahedron Lett 35:1141–1144
67. Che CT (1991) Marine products as a source of antiviral drug leads. Drug Dev Res 23:201–218
68. Van Maameveen JH, Hermkens PHH, De Clercq E, Balzarini J, Scheeren HW, Kruse CG (1992) Antiviral and antitumor structure-activity relationship studies on tetracyclic eudistomines. J Med Chem 35:3223–3230
69. Baker BJ (1996) β -Carboline and isoquinoline alkaloids from marine organisms (chap. 4). In: Pelletier SW (ed) Alkaloids: chemical and biological perspectives, vol 10. Pergamon Press, New York, pp 357–407
70. Massiot G, Nazabadioko S, Bliard C (1995) Structural revision of isoeudistomin U by total synthesis. J Nat Prod 58:1636–1639
71. Moquin C, Guyot M (1984) Grossularine, a novel indole derivative from the marine tunicate, *Dendrodoa grossularia*. Tetrahedron Lett 25:5047–5048
72. Moquin-Pathey C, Guyot M (1989) Grossularine-1 and grossularine-2, cytotoxic α -carbolines from the tunicate *Dendrodoa grossularia*. Tetrahedron 45:3445–3450
73. Abas SA, Hossain MB, van der Helm D, Schmitz FJ, Laney M, Cabuslay R, Schatzman RC (1996) Alkaloids from the tunicate *Polycarpa aurata* from Chuuk Atoll. J Org Chem 61:2709–2712
74. Niwa H, Yoshida Y, Yamada K (1988) A brominated quinazolinedione from the marine tunicate *Pyura sacciformis*. J Nat Prod 51:343–344
75. Wratten SJ, Wolfe MS, Andersen RJ, Faulkner DJ (1977) Antibiotic metabolites from a marine pseudomonad. Antimicrob Agents Chemother 11:411–414
76. Kinnel RB, Scheuer PJ (1992) 11-Hydroxystaurosporine: a highly cytotoxic, powerful protein kinase C inhibitor from a tunicate. J Org Chem 57:6327–6329
77. Horton PA, Longley RE, Mc Connell OJ, Ballas LM (1994) Staurosporine aglycon (K252-c) and arcyliaflavin A from the marine ascidian, *Eudistoma* sp. Experientia 50:843–845
78. Schupp P, Eder C, Proksch P, Wray V, Schneider B, Herderich M, Paul V (1999) Staurosporine derivatives from the ascidian *Eudistoma toalensis* and its predatory flatworm *Pseudoceros* sp. J Nat Prod 62:959–962
79. Schupp P, Steube K, Meyer C, Proksch P (2001) Anti-proliferative effects of new staurosporine derivatives isolated from a marine ascidian and its predatory flatworm. Cancer Lett 174:165–172
80. Schupp P, Proksch P, Wray V (2002) Further new staurosporine derivatives from the ascidian *Eudistoma toalensis* and its predatory flatworm *Pseudoceros* sp. J Nat Prod 65:295–298
81. Reyes F, Fernandez R, Rodriguez A, Bueno S, de Eguilior C, Francesch A, Cuevas C (2008) Cytotoxic staurosporines from the marine ascidian *Cystodytes solitus*. J Nat Prod 71:1046–1048
82. Omura S, Sasaki Y, Iwai Y, Takeshima H (1995) Staurosporine, a potentially important gift from a microorganism. J Antibiot 48:535–548
83. Fahy E, Potts BCM, Faulkner DJ, Smith K (1991) 6-Bromotryptamine derivatives from the Gulf of California tunicate *Didemnum candidum*. J Nat Prod 54:564–569

84. Aiello A, Borrelli F, Capasso R, Fattorusso E, Luciano P, Menna M (2003) Conicamin, a novel histamine antagonist from the Mediterranean tunicate *Aplidium conicum*. *Bioorg Med Chem Lett* 13:4481–4483
85. Roll DM, Ireland CM (1985) Citorellamine, a new bromindole derivative from *Polycitrella mariae*. *Tetrahedron Lett* 26:4303–4306
86. Moriarty RM, Roll DM, Ku YY, Nelson C, Ireland CM (1987) A revised structure for the marine bromindole derivative citorellamine. *Tetrahedron Lett* 28:749–752
87. Lindquist N, Fenical W (1990) Polyandrocarpamides A–D, novel metabolites from the marine ascidian *Polyandrocarpa* sp. *Tetrahedron Lett* 31:2521–2524
88. Heitz S, Durgeat M, Guyot M, Brassy C, Bachet B (1980) New indolic derivative of 1,2,4-thiadiazole, isolated from a tunicate (*Dendrodoa grossularia*). *Tetrahedron Lett* 21:1457–1458
89. Guyot M, Meyer M (1986) An 3-indolyl-4H-imidazol-4-one from the tunicate *Dendrodoa grossularia*. *Tetrahedron Lett* 27:2621–2622
90. Bergmann T, Schories D, Steffan B (1997) Alboinon, an oxadiazinone alkaloid from the ascidian *Dendrodoa grossularia*. *Tetrahedron* 53:2055–2060
91. Loukaci A, Guyot M, Chiaroni A, Riche C (1998) A new indole alkaloid from the marine tunicate *Dendrodoa grossularia*. *J Nat Prod* 61:519–522
92. Franco LH, Joffe EB, Puricelli L, Tatian M, Seldes AM, Palermo JA (1998) Indole alkaloids from the tunicate *Aplidium meridianum*. *J Nat Prod* 61:1130–1132
93. Seldes AM, Brasco MFR, Franco LH, Palermo JA (2007) Identification of two meridianins from the crude extract of the tunicate *Aplidium meridianum* by tandem mass spectrometry. *Nat Prod Res* 2:555–563
94. Gompel M, Leost M, De Kier JEB, Puricelli L, Franco LH, Palermo J, Meijer L (2004) Meridianins, a new family of protein kinase inhibitors isolated from the ascidian *Aplidium meridianum*. *Bioorg Med Chem Lett* 14:1703–1707
95. Reyes F, Fernandez R, Rodriguez A, Francesch A, Taboada S, Avila C, Cuevas C (2008) Aplicyanins A–F, new cytotoxic bromindole derivatives from the marine tunicate *Aplidium cyaneum*. *Tetrahedron* 64:5119–5123
96. Appleton DR, Page MJ, Lambert G, Berridge MV, Copp BR (2002) Kottamides A–D: novel bioactive imidazolone-containing alkaloids from the New Zealand ascidian *Pycnoclavella kottae*. *J Org Chem* 67:5402–5404
97. Appleton DR, Copp BR (2003) Kottamide E, the first example of a natural product bearing the amino acid 4-amino-1,2-dithiolane-4-carboxylic acid (Adt). *Tetrahedron Lett* 44:8963–8965
98. Copp BR, Ireland CM, Barrows LR (1991) Wakayin: a novel cytotoxic pyrroloiminoquinone alkaloid from the ascidian *Clavelina* species. *J Org Chem* 56:4596–4597
99. Vervoort HC, Richards-Gross SE, Fenical W, Lee AY, Clardy J (1997) Didemnimides A–D: novel predator-deterrent alkaloids from the Caribbean mangrove ascidian *Didemnum conchyliatum*. *J Org Chem* 62:1486–1490
100. Berlinck RGS, Britton R, Piers E, Lim L, Roberge M, Moreira da Rocha R, Andersen RJ (1998) Granulatimide and Isogranulatimide, Aromatic Alkaloids with G2 Checkpoint Inhibition Activity Isolated from the Brazilian Ascidian *Didemnum granulatum*: Structure Elucidation and Synthesis. *J Org Chem* 63:9850–9856
101. Vervoort HC, Fenical W, Keifer PA (1999) A cyclized didemnimide alkaloid from the Caribbean Ascidian *Didemnum conchyliatum*. *J Nat Prod* 62:389–391
102. Britton R, de Oliveira JHHL, Andersen RJ, Berlinck RGS (2001) Granulatimide and 6-bromogranulatimide, minor alkaloids of the Brazilian ascidian *Didemnum granulatum*. *J Nat Prod* 64:254–255
103. Henon H, Messaoudi S, Anizon F, Aboab B, Kucharczyk N, Leonce S, Golsteyn RM, Pfeiffer B, Prudhomme M (2007) Bis-imide granulatimide analogues as potent checkpoint 1 kinase inhibitors. *Eur J Pharmacol* 554:106–112

104. Sato H, Tsuda M, Watanabe K, Kobayashi J (1998) Rhopaladins A-D, new indole alkaloids, from marine tunicate *Rhopalaea* sp. *Tetrahedron* 54:8687–8690
105. Sasaki T, Ohtani II, Tanaka J, Higa T (1999) Iheyamines, new cytotoxic bisindole pigments from a colonial ascidian, *Polycitorella* sp. *Tetrahedron Lett* 40:303–306
106. Segraves NL, Lopez S, Johnson TA, Said SA, Fu X, Schmitz FJ, Pietraszkiewicz H, Valeriote FA, Crews P (2003) Structures and cytotoxicities of faspaplysins and related alkaloids from two marine phyla-*Faspaplysinsopsis* sponges and *Didemnum* tunicates. *Tetrahedron Lett* 4:3471–3475
107. Segraves NL, Robinson SJ, Garcia D, Said SA, Fu X, Schmitz FJ, Pietraszkiewicz H, Valeriote FA, Crews P (2004) Comparison of faspaplysins and related alkaloids: a study of structures, cytotoxicities, and sources. *J Nat Prod* 67:783–792
108. Zhidkov ME, Baranova OV, Balaneva NN, Fedorov SN, Radchenko OS, Dubovitskii SV (2007) The first syntheses of 3-bromofaspaplysin, 10-bromofaspaplysin and 3,10-dibromofaspaplysin-marine alkaloids from *Faspaplysinsopsis reticulata* and *Didemnum* sp. by application of a simple and effective approach to the pyrido[1,2-a:3,4-b']diindole system. *Tetrahedron Lett* 48:7998–8000
109. Ireland CM, Durso AR Jr (1981) N, N¹ Diphenethylurea, a metabolite from the marine ascidian *Didemnum ternatanum*. *J Nat Prod* 44:360–361
110. Ford PW, Davidson BS (1997) Plakinidine D, a new pyrroloacridine alkaloid from the ascidian *Didemnum rubeum*. *J Nat Prod* 60:1051–1053
111. Smith CJ, Venables DA, Hopmann C, Salomon CE, Jompa J, Tahir A, Faulkner DJ, Ireland CM (1997) Plakinidine D, a new pyrroloacridine alkaloid from two ascidians of the genus *Didemnum*. *J Nat Prod* 60(104):8–1050
112. Lindsay BS, Battershill CN, Copp BR (1998) Isolation of 2-(3¹-bromo-4¹-hydroxyphenol) ethanamine from the New Zealand ascidian *Cnemidocarpa bicornuta*. *J Nat Prod* 61: 857–858
113. Aiello A, Fattorusso E, Imperatore C, Menna M, Müller WEG (2010) Iodocionin, a cytotoxic iodinated metabolite from the mediterranean ascidian *Ciona edwardsii*. *Mar Drugs* 8: 285–291
114. Solano G, Motti CA, Jaspars M (2009) New iodotyramine derivatives from *Didemnum rubeum*. *Tetrahedron* 65:7482–7486
115. Pearce AN, Chia EW, Berridge MV, Maas EW, Page MJ, Harper JL, Webb VL, Copp BR (2008) Orthidines A-E, tubastrine, 3,4-dimethoxyphenethyl-β-guanidine, and 1,14-sperminedihomovanillamide: potential anti-inflammatory alkaloids isolated from the New Zealand ascidian *Aplidium orthium* that act as inhibitors of neutrophil respiratory burst. *Tetrahedron* 64:5748–5755
116. Wessels M, König GM, Wright AD (2001) New 4-methoxybenzoyl derivatives from the ascidian *Polycarpa aurata*. *J Nat Prod* 64:1556–1558
117. McDonald LA, Swersey JC, Ireland CM, Carroll AR, Coll JC, Bowden BF, Fairchild CR, Cornell L (1995) Botryllamides A-D, new brominated tyrosine derivatives from styelid ascidians of the genus *Botryllus*. *Tetrahedron* 51:5237–5244
118. Rao MR, Faulkner DJ (2004) Botryllamides E-H, four new Tyrosine derivatives from the ascidian *Botrylloides tyreum*. *J Nat Prod* 67:1064–1066
119. Henrich CJ, Robey RW, Takada K, Bokesch HR, Bates SE, Shukla S, Ambudkar SV, McMahon JB, Gustafson KR (2009) Botryllamides: natural product inhibitors of ABCG2. *Chem Biol* 4:637–647
120. Yin S, Cullinane C, Carroll AR, Quinn RJ, Davis RA (2010) Botryllamides K and L, new tyrosine derivatives from the Australian ascidian *Aplidium altarium*. *Tetrahedron Lett* 51:3403–3405
121. Takada K, Inamura N, Gustafson KR, Henrich CJ (2010) Synthesis and structure-activity relationship of botryllamides that block the ABCG2 multidrug transporter. *Bioorg Med Chem Lett* 20:330–333

122. Arabshahi L, Schmitz FJ (1988) Thiazole and imidazole metabolites from the ascidian *Aplydium pliciferum*. *Tetr Lett* 29:1099–1102
123. Davis RA, Aalbersberg W, Meo S, Moreira da Rocha R, Ireland CM (2002) The isolation and synthesis of polyandrocarpamines A and B. Two new 2-aminoimidazolone compounds from the Fijian ascidian, *Polyandrocarpa* sp. *Thetr* 58:3263–3269
124. Hirsch S, Miroz A, McCarthy P, Kashman Y (1989) Etzionin, a new antifungal metabolite from a red sea tunicate. *Tetrahedron Lett* 30:4291–4294
125. Kobayashi J, Cheng J, Kikuchi Y, Ishibashi M, Yamamura S, Ohizumi Y, Ohta T, Nozoe S (1990) Rigidin, a novel alkaloid with calmodulin antagonistic activity from the Okinawan marine tunicate *Eudistoma rigida*. *Tetrahedron Lett* 31:4617–4620
126. Tsuda M, Nozawa K, Shimbo K, Kobayashi J (2003) Rigidins B-D, new pyrrolopyrimidine alkaloids from a tunicate *Cystodytes* species. *J Nat Prod* 66:292–294
127. Davis RA, Christensen LV, Richardson AD, Moreira da Rocha R, Ireland CM (2003) Rigidin E, a new pyrrolopyrimidine alkaloids from a Papua New Guinea tunicate *Eudistoma* species. *Mar Drugs* 1:27–33
128. Durán R, Zubía E, Ortega MG, Naranjo S, Salvá J (1999) Novel alkaloids from the red ascidian *Botryllus leachi*. *Tetrahedron* 55:13225–13232
129. Garrido L, Zubía E, Ortega MG, Salvá J (2003) Haouamines A and B: a new class f alkaloids from the ascidian *Aplidium haouarianum*. *J Org Chem* 68:293–299
130. Andersen RJ, Faulkner DJ, Cun-heng H, Van Duyne GD, Clardy J (1985) Metabolites of the marine prosobranch mollusc *Lamellaria* sp. *J Am Chem Soc* 107:5492–5495
131. Fan H, Peng J, Hamann MT, Hu JF (2008) Lamellarins and related pyrrole-derived alkaloids from marine organisms. *Chem Rev* 108:264–287
132. Bailly C (2004) Lamellarins, from A to Z: a family of anticancer marine pyrrole alkaloids. *Curr Med Chem: Anti-Cancer Agents* 4:363–378
133. Lindquist N, Fenical W, Van Duyne GD, Clardy J (1988) New alkaloids of the Lamellarin class from the marine ascidian *Didemnum chartaceum*. *J Org Chem* 53:4570–4574
134. Carroll AR, Bowden BF, Coll JC (1993) Studies of Australian ascidians. I. Six new lamellarin-class alkaloids from a colonial ascidian, *Didemnum* sp. *Aust J Chem* 46:489–501
135. Davis RA, Carroll AR, Pierens GK, Quinn RJ (1999) New lamellarin alkaloids from the Australian ascidian *Didemnum chartaceum*. *J Nat Prod* 62:419–424
136. Reddy MVR, Rao MR, Rhodes D, Hansen MST, Rubins K, Bushman FD, Venkateswarlu Y, Faulkner DJ (1999) Lamellarin α -20 sulfate, an inhibitor of HIV-1 integrase active against HIV-1 virus in cell culture. *J Med Chem* 42:1901–1907
137. Krishnaiah P, Reddy VLN, Venkataramana G, Ravinder K, Srinivasulu M, Raju TV, Ravikumar K, Chandrasekar D, Ramakrishna S, Venkateswarlu Y (2004) New lamellarin alkaloids from the Indian ascidian *Didemnum obscurum* and their antioxidant properties. *J Nat Prod* 67:1168–1171
138. Reddy SM, Srinivasulu M, Satyanarayana N, Kondapi AK, Venkateswarlu Y (2005) New potent cytotoxic lamellarin alkaloids from Indian ascidian *Didemnum obscurum*. *Tetrahedron* 61:9242–9247
139. Yoshida WY, Lee KK, Carroll AR, Scheuer PJ (1992) A complex pyrrolo-oxazinone and its iodo derivative isolated from a tunicate. *Helv Chim Acta* 75:1721–1725
140. Rudi A, Goldberg I, Stein Z, Frolow F, Benayahu SM, Kashman Y (1994) Polycitone A and Polycitrins A and B: new alkaloids from the marine ascidian *Polycitor* sp. *J Org Chem* 59:999–1003
141. Rudi A, Evan T, Akinin M, Kashman Y (2000) Polycitone B and Prepolycitrin A: two novel alkaloids from the marine ascidian *Polycitor africanus*. *J Nat Prod* 63:832–833
142. Kang H, Fenical W (1997) Ningalins A-D: novel aromatic alkaloids from a western Australian ascidian of the genus *Didemnum*. *J Org Chem* 62:3254–3262
143. Cuevas C, Francesch A (2009) Development of Yondelis[®] (trabectedin, ET-743). A semisynthetic process solves the supply problem. *Nat Prod Rep* 26:322–337

144. Rinehart KL, Holt TG, Fregeau NL, Stroh JG, Keifer PA, Sun F, Li LH, Martin DG (1990) Ecteinascidins 729, 743, 745, 759A, 759B, and 770: potent antitumor agents from the Caribbean tunicate *Ecteinascidia turbinata*. *J Org Chem* 55:4512–4515
145. Wright AE, Forleo DA, Gunawardana GP, Gunasekera SP, Koehn FE, McConnell OJ (1990) Antitumor tetrahydroisoquinoline alkaloids from the colonial ascidian *Ecteinascidia turbinata*. *J Org Chem* 55:4508–4512
146. Guan Y, Sakai R, Rinehart KL, Wang AHJ (1993) Molecular and crystal structures of ecteinascidins: potent antitumor compounds from the Caribbean tunicate *Ecteinascidia turbinata*. *J Biomol Struct Dyn* 10:793–818
147. Sakai R, Rinehart KL, Guan Y, Wang AHJ (1992) Additional antitumor ecteinascidins from a Caribbean tunicate: crystal structures and activities in vivo. *Proc Natl Acad Sci USA* 89:11456–11460
148. Rinehart KL, Sakai R (2004) Isolation, structure elucidation, and bioactivities of novel ecteinascidins from *Ecteinascidia turbinata*. US Patent Application Publication 0059112
149. Suwanborirux K, Charupant K, Amnuoyopol S, Pummangura S, Kubo A, Saito N (2002) Ecteinascidins 770 and 786 from the Thai Tunicate *Ecteinascidia thurstoni*. *J Nat Prod* 65:935–937
150. Sakai R, Jares-Erijman EA, Manzanares I, Silva Elipe MV, Rinehart KL (1996) Ecteinascidins: putative biosynthetic precursors and absolute stereochemistry. *J Am Chem Soc* 118:9017–9023
151. Menchaca R, Martínez V, Rodríguez A, Rodríguez N, Flores M, Gallego P, Manzanares I, Cuevas C (2003) Synthesis of Natural Ecteinascidins (ET-729, ET-745, ET-759B, ET-736, ET-637, ET-594) from Cyanosafrafin B. *J Org Chem* 68:8859–8866
152. Ishibashi M, Ohizumi Y, Sasaki T, Nakamura H, Hirata Y, Kobayashi J (1987) Pseudodistomins A and B, novel antineoplastic piperidine alkaloids with calmodulin antagonistic activity from the Okinawan tunicate *Pseudodistoma kanoko*. *J Org Chem* 52:450–453
153. Kiguchi T, Yuamoto Y, Ninomiya I, Naito T, Deki K, Ishibashi M, Kobayashi J (1992) Pseudodistomin B: revised structure and first total synthesis. *Tetrahedron Lett* 33:7389–7390
154. Ishibashi M, Deki K, Kobayashi J (1995) Revised structure of pseudodistomin A, a piperidine alkaloid isolated from the Okinawan tunicate *Pseudodistoma kanoko*. *J Nat Prod* 58:804–806
155. Knapp S, Hale J (1993) Synthesis of (+)-tetrahydropseudodistomin. *J Org Chem* 58:2650–2651
156. Naito T, Yuamoto Y, Ninomiya I, Kiguchi T (1992) First total synthesis of pseudodistomin tetrahydroacetate. *Tetrahedron Lett* 33:4033–4036
157. Kobayashi J, Naitoh K, Doi Y, Deki K, Ishibashi M (1995) Pseudodistomin C, a new piperidine alkaloid with unusual absolute configuration from the Okinawan tunicate *Pseudodistoma kanoko*. *J Org Chem* 60:6941–6945
158. Freyer AJ, Patil AD, Killmer L, Troupe N, Mentzer M, Carte B, Faucette L, Johnson LK (1997) Three new pseudodistomins, piperidine alkaloids from the ascidian *Pseudodistoma megalarva*. *J Nat Prod* 60:986–990
159. Mc Coy MC, Faulkner DJ (2001) Uoamines A and B, piperidine alkaloids from the ascidian *Aplidium uouo*. *J Nat Prod* 64:1087–1089
160. Raub MF, Cardellina II JH, Choudhary MI, Ni CZ, Clardy J, Alley MC (1991) Clavepictines A and B: cytotoxic quinolizidines from the tunicate *Clavelina picta*. *J Am Chem Soc* 113:3178–3180
161. Kong F, Faulkner DJ (1991) Pictamine, a quinolizidine alkaloid from the tunicate *Clavelina picta*. *Tetrahedron Lett* 32:3667–3668
162. Raub MF, Cardellina II JH (1992) The piclavines, antimicrobial indolizidines from the tunicate *Clavelina picta*. *Tetrahedron Lett* 33:2257–2260

163. Blackman AJ, Li CP, Hockless DCR, Skelton BW, White AH (1993) Cylindricines A and B, novel alkaloids from the ascidian *Clavelina cylindrica*. *Tetrahedron* 49:8645–8656
164. Li CP, Blackman AJ (1994) Cylindricines C-G, perhydropyrrolo[2,1-j]quinolin-7-one alkaloids from the ascidian *Clavelina cylindrica*. *Aust J Chem* 47:1355–1361
165. Li CP, Blackman AJ (1995) Cylindricines H-K, novel alkaloids from the ascidian *Clavelina cylindrica*. *Aust J Chem* 48:955–965
166. Issa HH, Tanaka J, Rachmat R, Setiawan A, Trianto A, Higa T (2005) Polycitorols A and B, new tricyclic alkaloids from an ascidian. *Mar Drugs* 3:78–83
167. Biard JF, Guyot S, Roussakis C, Verbist JF, Vercauteren J, Weber JF, Boukef K (1994) Lepadiformine, a new marine cytotoxic alkaloid from *Clavelina lepadiformis*. *Tetrahedron Lett* 4:2691–2694
168. Sauviat MP, Vercauteren J, Grimaud N, Jugé M, Nabil M, Petit JY, Biard JF (2006) Sensitivity of cardiac background inward rectifying K⁺ outward current (IK1) to the alkaloids lepadiformines A, B, and C. *J Nat Prod* 69:558–562
169. Patil AD, Freyer AJ, Reichwein R, Carte B, Killmer LB, Faucette L, Johnson LK, Faulkner DJ (1997) Fascicularin, a novel tricyclic alkaloid from the ascidian *Nephtheis fascicularis* with selective activity against a DNA repair-deficient organism. *Tetrahedron Lett* 38:363–364
170. Abe H, Aoyagi S, Kibayashi C (2000) First total synthesis of the marine alkaloid (±)-fascicularin and (±)-lepadiformine based on stereocontrolled intramolecular Acylnitroso-Diels-Alder-Reaction. *J Am Chem Soc* 122:4583–4592
171. Dutta S, Abe H, Aoyagi S, Kibayashi C, Gates KS (2005) DNA damage by fascicularin. *J Am Chem Soc* 127:15004–15005
172. Kossuga MH, MacMillan JB, Rogers EW, Molinski TF, Nascimento GG, Rocha RM, Berlinck RG (2004) (2S,3R)-2-aminododecan-3-ol, a new antifungal agent from the ascidian *Clavelina oblonga*. *J Nat Prod* 67:1879–1881
173. Aiello A, Fattorusso E, Giordano A, Menna M, Navarrete C, Muñoz E (2007) Clavaminols A–F, novel cytotoxic 2-amino-3-alkanols from the ascidian *Clavelina phlegraea*. *Bioorg Med Chem* 15:2920–2926
174. Aiello A, Fattorusso E, Giordano A, Menna M, Navarrete C, Muñoz E (2009) Clavaminols G–N, six new marine sphingoids from the Mediterranean ascidian *Clavelina phlegraea*. *Tetrahedron* 65:4384–4388
175. Searle PA, Molinski TF (1993) Structure and absolute configuration of (R)-(E)-1-amino-tridec-5-en-2-ol, an antifungal amino alcohol from the ascidian *Didemnum* sp. *J Org Chem* 58:7578–7580
176. Jares-Erijman EA, Bapat CP, Lithgow-Bertelloni A, Rinehart KL, Sakai R (1993) Crucigasterins, new polyunsaturated amino alcohols from the mediterranean tunicate *Pseudodistoma crucigaster*. *J Org Chem* 58:5732–5737
177. Garrido L, Zubía E, Ortega MJ, Naranjo S, Salvá J (2001) Obscuraminols, new unsaturated amino alcohols from the tunicate *Pseudodistoma obscurum*: structure and absolute configuration. *Tetrahedron* 57:4579–4588
178. Sata NU, Fusetani N (2000) Amaminols A and B, new bicyclic amino alcohols from an unidentified tunicate of the family Polyclinidae. *Tetrahedron Lett* 41:489–492
179. Kumpulainen ETT, Koskinen AMP, Rissanen K (2007) Total synthesis of amaminol A: establishment of the absolute stereochemistry. *Org Lett* 9:5043–5045
180. Carter G, Rinehart KL (1978) Aplidiasphingosine, an antimicrobial and antitumor terpenoid from an *Aplidium* sp. (marine tunicate). *J Am Chem Soc* 100:7441–7442
181. Loukaci A, Bultel-Poncé V, Longeon A, Guyot M (2000) New lipids from the tunicate *Cystodytes* cf. *dellechiaiei* as PLA2 inhibitors. *J Nat Prod* 63:799–802
182. González N, Rodríguez J, Jiménez C (1999) Didemniserinolipids A–C, Unprecedented Serinolipids from the tunicate *Didemnum* sp. *J Org Chem* 64:5705–5707

183. Kiyota H, Dixon DJ, Luscombe CK, Hettstedt S, Ley SV (2002) Synthesis, structure revision, and absolute configuration of (+)-didemniserinolipid B, a serinol marine natural product from a tunicate *Didemnum* sp. *Org Lett* 4:3223–3226
184. Kobayashi H, Ohashi J, Fujita T, Iwashita T, Nakao Y, Matsunaga S, Fusetani N (2007) Complete structure elucidation of shishididemniols, complex lipids with tyramine-derived tether and two serinol units, from a marine tunicate of the family Didemnidae. *J Org Chem* 72:1218–1225
185. Kobayashi H, Miyata Y, Okada K, Fujita T, Iwashita T, Nakao Y, Fusetani N, Matsunaga S (2007) The structures of three new shishididemniols from a tunicate of the family Didemnidae. *Tetrahedron* 63:6748–6754
186. Lievens SC, Molinski TF (2005) Sagittamides A and B. Polyacetoxo long-chain acyl amino acids from a didemnid ascidian. *Org Lett* 7:281–2284
187. Seike H, Ghosh I, Kishi Y (2006) Stereochemistry of sagittamide A: prediction and confirmation. *Org Lett* 8:3865–3868
188. Taylor SW, Kammerer B, Bayer E (1997) New perspectives in the chemistry and biochemistry of the tunichromes and related compounds. *Chem Rev* 97:333–346
189. Kim D, Li Y, Nakanishi K (1991) Isolation of unstable tunichromes from tunicate blood via protection-deprotection. *J Chem Soc Chem Commun* 1:9–10
190. Bruening RC, Oltz EM, Furukawa J, Nakanishi K (1985) Isolation and structure of tunichrome B-1, a reducing blood pigment from the tunicate *Ascidia nigra* L. *J Am Chem Soc* 107:5298–5300
191. Oltz EM, Bruening RC, Smith MJ, Kustin K, Nakanishi K (1988) The tunichromes. A class of reducing blood pigment from sea squirts: isolation, structures, and vanadium chemistry. *J Am Chem Soc* 110:6162–6172
192. Bayer E, Schiefer G, Waidelich D, Scippa S, de Vincentiis M (1992) Structure of the tunichrome of tunicates and their role in vanadium enrichment. *Angew Chem Int Ed Engl* 31:52–54
193. Tincu JA, Taylor SW (2002) Tunichrome Sp-1: new pentapeptide tunichrome from the hemocytes of *Styela plicata*. *J Nat Prod* 65:377–378
194. Azumi K, Yokosawa H, Ishii S (1990) Halocyamines: novel antimicrobial tetrapeptide-like substances isolated from the hemocytes of the solitary ascidian *Halocynthia roretzi*. *Biochemistry* 29:159–165
195. Sesin DF, Gaskell SJ, Ireland CM (1986) The chemistry of *Lissoclinum patella*. *Bull Soc Chim Belg* 95:853–867
196. Ireland CM, Durso AR Jr, Newman RA, Hacker MP (1982) Antineoplastic cyclic peptides from the marine tunicate *Lissoclinum patella*. *J Org Chem* 47:1807–1811
197. Degnan BM, Hawkins CJ, Lavin MF, McCaffrey EJ, Parry DL, van den Brenk AL, Watters DJ (1989) New cyclic peptides with cytotoxic activity from the ascidian *Lissoclinum patella*. *J Med Chem* 32:1349–1354
198. Mc Donald L, Ireland CM (1992) Patellamide E: a new cyclic peptide from the ascidian *Lissoclinum patella*. *J Nat Prod* 55:376–379
199. Rashid MA, Gustafson KR, Cardellina II JH, Boyd MR (1995) Patellamide F: a new cytotoxic cyclic peptide from the colonial ascidian *Lissoclinum patella*. *J Nat Prod* 58:594–597
200. Yamamoto Y, Endo M, Nakagawa M, Nakanishi T, Mizukawa K (1983) A new cyclic peptide, ascidiacyclamide, isolated from ascidian. *J Chem Soc Chem Commun* 323–324
201. Ireland C, Scheuer PJ (1980) Ulicyclamide and Ulithiacyclamide, two new small peptides from a marine tunicate. *J Am Chem Soc* 102:5688–5691
202. Williams DE, Moore RE (1989) The structure of ulithiacyclamide B. Antitumor evaluation of cyclic peptides and macrolides from *Lissoclinum patella*. *J Nat Prod* 52:732–739
203. Salomon CE, Faulkner J (2002) Localization studies of bioactive cyclic peptides in the ascidian *Lissoclinum patella*. *J Nat Prod* 65:689–692

204. Hamada Y, Kato S, Shioiri T (1985) New methods and reagents in organic synthesis. 51. A synthesis of ascidiacyclamide, a cytotoxic cyclic peptide from ascidian. Determination of its absolute configuration. *Tetrahedron Lett* 26:3223–3226
205. Schmidt U, Utz R, Gleich P (1985) What is the structure of the patellamides? *Tetrahedron Lett* 26:4367–4370
206. Hamada Y, Shibata M, Shioiri T (1985) New methods and reagents in organic synthesis. 55. Total synthesis of patellamides B and C, cytotoxic cyclic peptides from a tunicate 1. Their proposed structures should be corrected. *Tetrahedron Lett* 26:5155–5158
207. Hamada Y, Shibata M, Shioiri T (1985) New methods and reagents in organic synthesis. 56. Total synthesis of patellamides B and C, cytotoxic cyclic peptides from a tunicate 2. Their real structures have been determined by their synthesis. *Tetrahedron Lett* 26: 5159–5162
208. Hamada Y, Shibata M, Shioiri T (1985) New methods and reagents in organic synthesis. 58. A synthesis of patellamide A, a cytotoxic cyclic peptide from a tunicate. Revision of its proposed structure. *Tetrahedron Lett* 26:6501–6504
209. Schmidt U, Griesser H (1986) Total synthesis and structure determination of patellamide B. *Tetrahedron Lett* 27:163–166
210. Kato S, Hamada Y, Shibata M, Shioiri T (1986) Total synthesis of ulithiacyclamide, a strong cytotoxic cyclic peptide from marine tunicates. *Tetrahedron Lett* 27:2653–2656
211. Schmidt U, Weller D (1986) Total synthesis of ulithiacyclamide. *Tetrahedron Lett* 27:3495–3496
212. Shioiri T, Hamada Y, Kato S, Shibata M, Kondo Y, Nakagawa H, Kohda K (1987) Cytotoxic activity of cyclic peptides of marine origin and their derivatives: importance of oxazoline functions. *Biochem Pharmacol* 36:4181–4185
213. Ishida T, Inoue M, Hamada Y, Kato S, Shioiri T (1987) X-ray crystal structure of ascidiacyclamide, a cytotoxic cyclic peptide from ascidian. *J Chem Soc Chem Commun* 5:370–371
214. Schmitz FJ, Ksebat MB, Chang JS, Wang JL, Hossain MB, van der Helm D, Engel MH, Serban A, Silber JA (1989) Cyclic peptides from the ascidian *Lissoclinum patella*: conformational analysis of patellamide D by X-ray analysis and molecular modeling. *J Org Chem* 54:3463–3472
215. Ishida T, Ohishi H, Inoue M, Kamigauchi M, Sugiura M, Takao N, Kato S, Hamada Y, Shioiri T (1989) Conformational properties of ulithiacyclamide, a strong cytotoxic cyclic peptide from a marine tunicate, determined by ^1H nuclear magnetic resonance and energy minimization calculations. *J Org Chem* 54:5337–5343
216. In Y, Doi M, Inoue M, Ishida T (1994) Patellamide A a cytotoxic cyclic peptide from the ascidian *Lissoclinum patella*. *Acta Cryst C* 50:432–434
217. Ishida T, In Y, Shinozaki F, Doi M, Yamamoto D, Hamada Y, Shioiri T, Kamigauchi M, Sugiura M (1995) Solution conformations of patellamides B and C, cytotoxic cyclic hexapeptides from marine tunicate, determined by NMR spectroscopy and molecular dynamics. *J Org Chem* 60:3944–3952
218. Asano A, Yamada T, Numata A, Katsuya Y, Sasaki M, Taniguchi T, Doi M (2002) A flat squared conformation of an ascidiacyclamide derivative caused by chiral modification of an oxazoline residue. *Biochem Biophys Res Commun* 297:143–147
219. Asano A, Yamada T, Numata A, Doi M (2003) Cyclo (–Cha–Oxz–D–Val–Thz–Ile–Oxz–D–Val–Thz–) N, N-dimethyl-acetamide dihydrate: a square form of cyclohexylalanine-incorporated ascidiacyclamide having the strongest cytotoxicity. *Acta Cryst C* 59:o488–o490
220. Ishida T, Tanaka M, Nabae M, Inoue M, Kato Y, Hamada Y, Shioiri T (1998) Solution and solid-state conformations of ascidiacyclamide, a cytotoxic cyclic peptide from ascidian. *J Org Chem* 53:107–112
221. Ishida T, In Y, Doi M, Inoue M, Hamada Y, Shioiri T (1992) Molecular conformation of ascidiacyclamide, a cytotoxic cyclic peptide from Ascidian: x-ray analyses of its free form and solvate crystals. *Biopolymers* 32:131–143

222. Asano A, Minoura K, Yamada T, Numata A, Ishida T, Katsuya Y, Mezaki Y, Sasaki M, Tanigauchi T, Nakai M, Hasegawa H, Doi M (2002) Effect of asymmetric modification on the conformation of ascidiacyclamides analogs. *J Peptide Res* 60
223. In Y, Doi M, Inoue M, Ishida T, Hamada Y, Shioiri T (1993) Molecular conformation of patellamide A, a cytotoxic cyclic peptide from the ascidian *Lissoclinum patella*, by x-ray crystal analysis. *Chem Pharm Bull* 41:1686–1690
224. Bertram A, Pattenden G (2007) Marine metabolites: metal binding and metal complexes ofazole-based cyclic peptides of marine origin. *Nat Prod Rep* 24:18–30
225. van den Brenk AL, Fairlie DP, Hanson GR, Gahan LR, Hawkins CJ, Jones A (1994) Binding of copper(II) to the cyclic octapeptide patellamide D. *Inorg Chem* 33:2280–2289
226. van den Brenk AL, Byriel KA, Fairlie DP, Gahan LR, Hanson GR, Hawkins CJ, Jones A, Kennard CHL, Moubaraki B, Murray KS (1994) Crystal structure and electrospray ionization mass spectrometry, electron paramagnetic resonance, and magnetic susceptibility study of $[\text{Cu}_2(\text{ascidH}_2)(1,2\text{-}\mu\text{-CO}_3)(\text{H}_2\text{O})_2]\cdot 2\text{H}_2\text{O}$, the Bis(copper(II)) complex of ascidiacyclamide (ascidH4), a Cyclic peptide isolated from the ascidian *Lissoclinum patella*. *Inorg Chem* 33:3549–3557
227. Grondahl L, Gahan LR, Fairlie DP, Hanson GR, Sokolenko N, Abbenante G (1999) Interaction of zinc(II) with the cyclic octapeptides, cyclo[Ile(Oxn)-D-Val(Thz)]₂ and ascidiacyclamide, a cyclic peptide from *Lissoclinum patella*. *J Chem Soc Dalton Trans* 8:1227–1234
228. Cusack RM, Grondahl L, Abbenante G, Fairlie DP, Gahan LR, Hanson GR, Hambley TW (2000) Conformations of cyclic octapeptides and the influence of heterocyclic ring constraints upon calcium binding. *J Chem Soc Perkin Trans 2*:323–331
229. Cusack RM, G Grondahl L, Fairlie DP, Gahan LR, Hanson GR (2002) Cyclic octapeptides containing thiazole. Effect of stereochemistry and degree of flexibility on calcium binding properties. *J Chem Soc Perkin Trans 2* 3:556–563
230. Freeman DJ, Pattenden G, Drake AF, Siligardi G (1998) Marine metabolites and metal ion chelation. Circular dichroism studies of metal binding to *Lissoclinum* cyclopeptides. *J Chem Soc Perkin Trans 2* 1:129–136
231. Morris LA, Milne BF, Jaspars M, Versluis K, Heck JR, Kelly SM, Price NC (2001) Metal binding of *Lissoclinum patella* metabolites. Part 2: *Lissoclinamides* 9 and 10. *Tetrahedron* 57:3199–3207
232. Morris LA, Milne BF, Thompson GS, Jaspars M (2002) Conformational change in the thiazole and oxazoline containing cyclic octapeptides, the patellamides. Part 1. Cu^{2+} and Zn^{2+} induced conformational change. *J Chem Soc Perkin Trans 2* 6:1072–1075
233. Wasyluk JM, Biskupiak JE, Costello CE, Ireland CM (1983) Cyclic peptide structures from the Tunicate *Lissoclinum patella* by FAB Mass Spectrometry. *J Org Chem* 48:4445–4449
234. Hawkins CJ, Lavin MF, Marshall KA, van den Brenk AL, Watters DJ (1990) Structure-activity relationships of the *lissoclinamides*: cytotoxic cyclic peptides from the ascidian *Lissoclinum patella*. *J Med Chem* 33:1634–1638
235. Morris LA, Kettenes-van den Bosch JJ, Verluis K, Thompson GS, Jaspars M (2000) - Structure determination and MS n analysis of two new *lissoclinamides* isolated from the Indo-Pacific ascidian *Lissoclinum patella*: NOE restrained molecular dynamics confirms the absolute stereochemistry derived by degradative methods. *Tetrahedron* 56: 8345–8353
236. Sugiura T, Hamada Y, Shioiri T (1987) A facile synthesis of ulicyclamide. *Tetrahedron Lett* 28:2251–2254
237. Wipf P, Fritch PC (1996) Total synthesis and assignment of configuration of *lissoclinamide* 7. *J Am Chem Soc* 118:12358–12367
238. Boden CDJ, Pattenden G (1995) Cyclopeptides from ascidians. Total synthesis of *lissoclinamide* 4, and a general strategy for the synthesis of chiral thiazoline-containing macrocyclic peptides. *Tetrahedron Lett* 36:6153–6156
239. Boden C, Pattenden G (1994) Total synthesis of *lissoclinamide* 5, a cytotoxic cyclic peptide from the tunicate *Lissoclinum patella*. *Tetrahedron Lett* 35:8271–8274

240. Toske SG, Fenical W (1995) Cyclodidemnamide: a new cyclic heptapeptide from the marine ascidian *Didemnum molle*. *Tetrahedron Lett* 36:8355–8358
241. Boden CDJ, Norley MC, Pattenden G (1996) Total synthesis of the thiazoline-based cyclopeptide cyclodidemnamide. *Tetrahedron Lett* 37:9111–9114
242. Norley MC, Pattenden G (1998) Total synthesis and revision of stereochemistry of cyclodidemnamide, a novel cyclopeptide from the marine ascidian *Didemnum molle*. *Tetrahedron Lett* 39:3087–3090
243. Boden CDJ, Norley MC, Pattenden G (2000) Total synthesis and assignment of configuration of the thiazoline-based cyclopeptide cyclodidemnamide isolated from the sea squirt *Didemnum molle*. *J Chem Soc Perkin Trans I* 6:883–888
244. Arrault A, Witzak-Legrand A, Gonzales P, Bontemps-Subielos N, Banaigs B (2002) Structure and total synthesis of cyclodidemnamide B, a cycloheptapeptide from the ascidian *Didemnum molle*. *Tetrahedron Lett* 43:4041–4044
245. Fu X, Do T, Schmitz FJ, Andrushevich V, Engel MH (1998) New cyclic peptides from the ascidian *Lissoclinum patella*. *J Nat Prod* 61:1547–1551
246. Degnan BM, Hawkins CJ, Lavin MF, McCaffrey EJ, Parry DL, Watters DJ (1989) Novel cytotoxic compounds from the ascidian *Lissoclinum bistratum*. *J Med Chem* 32:1354–1359
247. Foster MP, Concepcion GP, Caraan GB, Ireland CM (1992) Bistratamides C and D. Two new oxazole-containing cyclic hexapeptides isolated from a Philippine *Lissoclinum bistratum*. *J Org Chem* 57:6671–6675
248. Perez LJ, Faulkner DJ (2003) Bistratamides E–J, modified cyclic hexapeptides from the Philippine ascidian *Lissoclinum bistratum*. *J Nat Prod* 66:247–250
249. Anguilar E, Meyers AI (1994) Total synthesis of (–)-Bistratamide C. *Tetrahedron Lett* 35:2477–2480
250. Downing SV, Anguilar E, Meyers AI (1999) Total synthesis of Bistratamide D. *J Org Chem* 64:826–831
251. You SL, Kelly JW (2005) The total synthesis of bistratamides F–I. *Tetrahedron* 61:241–249
252. Clark C, Olivera BM, Cruz L (1981) A toxin from the venom of the marine snail *Conus geographus* which acts on the vertebrate central nervous system. *Toxicol* 19:691–699
253. Rudi A, Chill L, Aknin M, Kashman Y (2003) Didmolamide A and B, two new cyclic hexapeptides from the marine ascidian *Didemnum molle*. *J Nat Prod* 66:575–577
254. You SL, Kelly JW (2005) The total synthesis of didmolamides A and B. *Tetrahedron Lett* 46:2547–2570
255. Hambley TW, Hawkins CJ, Lavin MF, van den Brenk A, Watters DJ (1992) Cycloxazoline: a cytotoxic cyclic hexapeptide from the ascidian *Lissoclinum bistratum*. *Tetrahedron Lett* 48:341–348
256. Prinsep MR, Moore RE, Levine IA, Patterson GML (1992) Westiellamide, a bistramide-related cyclic peptide from the blue-green alga *Westiellopsis prolifica*. *J Nat Prod* 55:140–142
257. Comba P, Gahan LR, Haberhauer G, Hanson GR, Noble CJ, Seibold B, van den Brenk A (2008) Copper (II) coordination chemistry of westiellamide and its imidazole, oxazole and thiazole analogues. *Chem Eur J* 14:4393–4403
258. Haberhauer G, Drosdow E, Oeser T, Rominger F (2008) Structural investigation of westiellamide analogues. *Tetrahedron* 64:1835–1859
259. McDonald LA, Foster MP, Phillips DR, Ireland CM, Lee AY, Clardy J (1992) Tawicyclamides A and B, new cyclic peptides from the ascidian *Lissoclinum patella*: studies on the solution-solid-state conformations. *J Org Chem* 57:4616–4624
260. Rudi A, Aknin M, Gaydou EM, Kashman Y (1998) Four new cytotoxic hexa- and heptapeptides from the marine ascidian *Didemnum molle*. *Tetrahedron* 54:13203–13210
261. Carroll AR, Coll JC, Bourne DJ, MacLeod JK, Zabriskie TM, Ireland CM, Bowden BF (1996) Patellins 1–6 and trunkamide A: novel cyclic hexa-, hepta- and octa-peptides from colonial ascidians, *Lissoclinum* sp. *Aust J Chem* 49:659–667

262. Bowden BF, Carroll AR, Coll JC, Hockless DCR, Skelton BW, White AH (1994) Studies of Australian Ascidians. IV. Mollamide, a cytotoxic cyclic heptapeptide from the compound ascidian *Didemnum molle*. *Aust J Chem* 47:61–69
263. McKeever B, Pattenden G (2003) Total synthesis of the cytotoxic cyclopeptide mollamide, isolated from the sea squirt *Didemnum molle*. *Tetrahedron* 59:2701–2712
264. Donia MS, Wang B, Dunbar DC, Desai PV, Patny A, Avery M, Hamann MT (2008) Mollamides B and C, cyclic hexapeptides from the Indonesian tunicate *Didemnum molle*. *J Nat Prod* 71:941–945
265. Teruya T, Sasaki H, Suenaga K (2008) Hexamollamide, a hexapeptide from an Okinawan ascidian *Didemnum molle*. *Tetrahedron Lett* 49:5297–5299
266. Zabriskie TM, Foster MP, Stout TJ, Clardy J, Ireland CM (1990) Studies on the solution- and solid-state structure of patellin 2. *J Am Chem Soc* 112:8080–8084
267. Wipf P, Uto Y (2000) Total synthesis and revision of stereochemistry of the marine metabolite trunkamide A. *J Org Chem* 65:1037–1049
268. Foster MP, Ireland CM (1993) Nairaiamides A and B. Two novel di-proline heptapeptides isolated from a Fijian *Lissoclinum bistratum* ascidian. *Tetrahedron Lett* 34:2871–2874
269. Linquist N, Fenical W (1991) Isolation and structure determination of diazonamides A and B, unusual cytotoxic metabolites from the marine ascidian *Diazona chinensis*. *J Am Chem Soc* 113:20303–22304
270. Fernandez R, Martin MJ, Rodriguez-Acebes R, Reyes F, Francesch A, Cuevas C (2008) Diazonamides C-E, new cytotoxic metabolites from the ascidian *Diazona* sp. *Tetrahedron Lett* 49:2283–2285
271. Li J, Jeong S, Esser L, Harran PG (2001) Total synthesis of nominal diazonamides. Part: convergent preparation of the structure proposed for (–)-diazonamide A. *Angew Chem Int Ed* 40:4765–4770
272. Li J, Burgett AWG, Esser L, Amezcua C, Harran PG (2001) Total synthesis of nominal diazonamides. Part 2: on the true structure and origin of natural isolates. *Angew Chem Int Ed* 40:4770–4773
273. Nicolau KC, Chen DYK, Huang X, Ling T, Bella M, Snyder SA (2004) Chemistry and biology of diazonamide A: first total synthesis and confirmation of the true structure. *J Am Chem Soc* 126:12897–12906
274. Whitson EL, Ratnayake AS, Bugni TS, Harper MK, Ireland CM (2009) Isolation, structure elucidation, and synthesis of eudistomides A and B, lipopeptides from a Fijian ascidian *Eudistoma* sp. *J Org Chem* 74:1156–1162
275. Rinehart KL Jr, Gloer JB, Hughes RG Jr, Renis HE, McGroven JP, Swynenberg EB, Strigfellow DA, Kuentzel SL, Li LH (1981) Didemnins: antiviral and antitumor from a Caribbean tunicate. *Science* 212:933–935
276. Rinehart KL Jr, Gloer JB, Cook JC Jr, Mizesak SA, Scaphill TA (1981) Structures of the didemnins, antiviral and cytotoxic depsipetiteds from a Caribbean tunicate. *J Am Chem Soc* 103:1857–1859
277. Banaigs B, Jeanty G, Francisco C, Jouin P, Poncet J, Heitz A, Cave A, Jc P, Wahl M, Lafargue F (1989) Didemnin B: comparative study and conformational approach in solution. *Tetrahedron* 45:181–190
278. Guyot M, Davoust D, Morel EC (1987) Isodidemnine-1, a cytotoxic cyclodepsipeptide isolated from a tunicate, *Trididemnum cyanophorum* (Didemnidae). *C R Acad Sci Ser* 305:681–686
279. (a) Gloer JB (1983) PhD thesis, University Of Illinois, Urbana; (1983) *Chem Abstr* 103:122692 b; (1983) *Diss Abstr Int B* 45:188–189. (b) Gutowsky REMS (1984) Thesis, University Of Illinois, Urbana
280. Boulanger A, Abou-Mansour E, Badre A, Banaigs B, Combaut G, Francisco C (1994) The complete spectral assignment of didemnin H, a new constituent of the tunicate *Trididemnum cyanophorum*. *Tetrahedron Lett* 35:4345–4348

281. Sakai R, Stroth JG, Sullins DW, Rinehart KL (1995) Seven new didemnins from the marine tunicate *Trididemnum solidum*. *J Am Chem Soc* 117:3734–3748
282. Rinehart KL Jr (1985) Applications of fast atom bombardment mass spectrometry. *Anal Chem Sym Ser* 24:119–148
283. Ewing WR, Bhat KL, Joullie MM (1986) Synthetic studies of didemnins. I. Revision of the stereochemistry of the hydroxyisovalerylpropionyl (HIP) unit. *Tetrahedron* 42:5863–5868
284. Castro B, Jouin P, Cave A, Dufour M, Banaigs B, Francisco C (1988) Structure elucidation of the major cytotoxic component of *Trididemnum cyanophorum*. *Pept Chem Biol Proc Am Pept Symp* 10th (Meeting Date 1987) 656–657
285. Hossain MB, Van der Helm D, Antel J, Sheldrick GM, Sanduja SK, Weinheimer AJ (1988) Crystal and molecular structure of didemnin B, an antiviral and cytotoxic depsipeptide. *Proc Natl Acad Sci USA* 85:4118–4122
286. Rinehart KL Jr, Kishore V, Nagarajan S, Lake RJ, Gloer JB, Bozich FA, Li KM, Maleczka RE Jr, Todsén WL, Munro MHG, Sullins DW, Sakai R (1987) Total synthesis of Didemnins A, B, and C. *J Am Chem Soc* 109:6846–6848
287. Li WR, Ewing WR, Harris BD, Joullie MM (1990) Total synthesis and structural investigations of didemnins A, B, and C. *J Am Chem Soc* 112:7659–7672 and ref. cited therein
288. Jiang TL, Liu RH, Salmon SE (1983) Antitumor activity of didemnin B in the human tumor stem cell assay. *Cancer Chemother Pharmacol* 11:1–4
289. Shin DM, Holoye PY, Forman A, Winn R, Perez-Soler R, Dakhil S, Rosenthal J, Raber MN, Hong WK (1994) Phase II clinical trial of didemnin B in previously treated small cell lung cancer. *Invest New Drugs* 12:243–249
290. Kessler H, Will M, Antel J, Beck H, Sheldrick GM (1989) Conformational analysis of didemnins. A multidisciplinary approach by means of X-ray, NMR, molecular-dynamics, and molecular-mechanism techniques. *Helv Chim Acta* 72:530–555
291. (a) Rinehart KL, US Patent Application P-82, 663, 13 Dec 1990 and British Patent Application 8922026.3 filed 29 Sept 1989; (b) Rinehart KL, Bertelloni-Lithgow AM PCT International Patent Application WO 91.04985, 18 Apr 1991
292. Abou-Mansour E, Boulanger A, Badre A, Bonnard I, Banaigs B, Combaut G, Francisco C (1995) [Tyr⁵]didemnin B and [D-pro⁴]didemnin B; two new natural didemnins with a modified macrocycle. *Tetrahedron* 51:12591–12600
293. Banaigs B, Abou-Mansour E, Bonnard I, Boulanger A, Francisco C (1999) [Hyp²] and [Hap²]didemnin B, two new [Hip²]-modified didemnin B from the tunicate *Trididemnum cyanophorum*. *Tetrahedron* 55:9559–9574
294. Rinehart KL (1994) US Patent 5,294,603, pp 1–25
295. Schmitz FJ, Yasumoto T (1991) The 1990 United States-Japan seminar on bioorganic marine chemistry, meeting report. *J Nat Prod* 54:1469–1490
296. Sakai R, Rinehart KL, Kundu B, Faircloth G, Gloer JB, Carney JR, Namikoshi M, Sun F, Hughes RG, Gravalos DG, de Quesada TG, Wilson GR, Heid RM (1996) Structure-activity relationships of the didemnins. *J Med Chem* 39:2819–2834
297. Urdiales JL, Morata P, De Castro IN, Jimenez-Sanchez F (1996) Antiproliferative effect of dehydrodimerin B (DDB), a depsipeptide isolated from Mediterranean tunicate. *Cancer Lett* 102:31–37
298. Jou G, Gonzales I, Alberici F, Lloyd-Williams P, Giralt E (1997) Total synthesis of dehydrodimerin B. Use of uranium and phosphonium salt coupling reagents in peptide synthesis in solution. *J Org Chem* 62:354–366
299. Vervoort H, Fenical W, RdeA E (2000) Tamandarins A and B: new cytotoxic depsipeptides from a Brazilian ascidian of the family Didemnidae. *J Org Chem* 65:782–792
300. Joullie MM, Portonovo P, Liang B, Richard DJ (2000) Total synthesis of (–)-tamandarin B. *Tetrahedron Lett* 41:9373–9376
301. Liang B, Richard DJ, Portonovo PS, Joullie MM (2001) Total syntheses and biological investigations of tamandarins A and B and tamandarin A analogs. *J Am Chem Soc* 123:4469–4474

302. Adrio J, Cuevas C, Manzanares I, Joullie MM (2007) Total synthesis and biological evaluation of tamandarin B analogues. *J Org Chem* 72:5129–5138
303. Carroll AR, Feng Y, Bowden BF (1996) Studies of Australian ascidians. 5. Virenarnides A-C, new cytotoxic linear peptides from the colonial didemnid ascidian *Diplosoma virens*. *J Org Chem* 61:4059–4061
304. Feng Y, Bowden BF (1997) Studies of Australian ascidians. VI. Virenarnides D and E, linear peptides from the colonial didemnid ascidian *Diplosoma virens*. *Aust J Chem* 50:337–339
305. Moody CJ, Hunt JCA (1999) Synthesis of virenarnide B, acytotoxic thiazole-containing peptide. *J Org Chem* 64:8715–8717
306. Exposito MA, Lopez B, Fernandez R, Vazquez M, Debitus C, Iglesias T, Jimenez C, Quinoa E, Riguera R (1998) Minalarnines A-F: sulfarnic acid peptide guanidine derivatives isolated from the marine tunicate *Didemnum rodriguessi*. *Tetrahedron* 54:7539–7550
307. Exposito MA, Fernandez-Suarez M, Vazquez M, Iglesias T, Munoz L, Riguera R (1998) Total synthesis and absolute configuration of Minalarnine A, a guanidine peptide the marine tunicate *Didemnum rodriguessi*. *J Org Chem* 66:4206–4213
308. Vazquez MJ, Quinoa E, Riguera R, Ocampo A, Iglesias T, Debitus C (1995) Caledonin, a natural peptide bolaphile with Zn^{II} and Cu^I complexing properties from the tunicate *Didemnum rodriguessi*. *Tetrahedron Lett* 36(48):8853–8856
309. Swersey JC, Ireland CM (1994) Eusynstyelarnide, a highly modified dimer peptide from the ascidian *Eusynstyela misakiensis*. *J Nat Prod* 57:842–845
310. Simon-Levert A, Menniti C, Souler L, Barthomeuf C, Banaigs B, Witczak A (2010) Marine natural meroterpenes: synthesis and antiproliferative activity. *Mar Drugs* 8:347–358
311. Zubia E, Ortega M, Salvá J (2005) Natural products chemistry in marine ascidians of the genus *Aplidium*. *Mini-Rev Org Chem* 2:546–564
312. Sato A, Shindo T, Kasanuki N, Hasegawa K (1989) Antioxidant metabolites from the tunicate *Amaroucium multiplicatum*. *J Nat Prod* 52:975–981
313. Akin M, Dayan TLA, Rudi A, Kashman Y, Gaydou EM (1999) Hydroquinone antioxidants from the Indian Ocean tunicate *Aplidium savignyi*. *J Agric Food Chem* 47:4175–4177
314. Garrido L, Zubia E, Ortega MJ, Salvá J (2002) New meroterpenoids from the ascidian *Aplidium conicum*. *J Nat Prod* 65:1328–1331
315. Howard BM, Clarkson K (1979) Simple prenylated hydroquinone derivatives from the marine urochordate *Aplidium californicum* natural anticancer and antimutagenic agents. *Tetrahedron Lett* 46:4449–4452
316. Guella G, Mancini I, Pietra F (1987) Verapliquinones: novel diprenylquinones from an *Aplidium* sp. (Ascidacea) of Ile-Verte waters, Brittany. *Helv Chim Acta* 70:621–626
317. Shubina LK, Fedorov SN, Radchenko OS, Balaneva NN, Kolesnikova SA, Dmitrenok PS, Bode A, Dong Z, Stonik VA (2005) Desmethylubiquinone Q2 from the far-eastern ascidian *Aplidium glabrum*: structure and synthesis. *Tetrahedron Lett* 46:559–562
318. Fedorov SN, Radchenko OS, Shubina LK, Balaneva NN, Bode AM, Stonik VA, Dong Z (2006) Evaluation of cancer-preventive activity and structure-activity relationship of 3-demethylubiquinone Q2, isolated from the ascidian *Aplidium glabrum* and its synthetic analogs. *Pharm Res* 23:70–81
319. Fedorov SN, Radchenko OS, Shubina LK, Balaneva NN, Agafonova IG, Bode AM, Jin JO, Kwak JY, Dong Z, Stonik V (2008) Anticancer activity of 3-demethylubiquinone Q2. In vivo experiments and probable mechanism of action. *Anticancer Res* 28:927–932
320. Levert AS, Arrault A, Subielos NB, Canal C, Banaigs B (2005) Meroterpenes from the ascidian *Aplidium* aff. *densum*. *J Nat Prod* 68:1412–1415
321. Levert AS, Azec A, Subielos NB, Banaigs B, Genevière AM (2007) Antimitotic activity of methoxyconidiol, a meroterpene isolated from an ascidian. *Chem-Bio Int* 168:106–116
322. Targett NM, Keeran WS (1984) A terpenehydroquinone from the marine ascidian *Aplidium constellatum*. *J Nat Prod* 47:556–557

323. Rochfort SJ, Metzger R, Hobbs L, Capon RJ (1996) New chromenols from a southern Australian tunicate *Aplidium solidum*. *Aust J Chem* 49:1217–1219
324. Carrol AR, Bowden BF, Coll JC (1993) Studies of Australian ascidians. III. A new tetrahydrocannabinol derivative from the ascidian *Synoicum costellatum*. *Austr J Chem* 46:1079–1083
325. Lumb JP, Trauner D (2005) Pericyclic reactions of prenylated naphthoquinones: biomimetic syntheses of mollugin and microphyllaquinone. *Org Lett* 7:5865–5868
326. Aiello A, Fattorusso E, Luciano P, Manna ML, Esposito G, Iuvone T, Pala D (2003) Conicaquinones A and B, two novel Cytotoxic terpene quinones from the Mediterranean ascidian *Aplidium conicum*. *Eur J Org Chem* 2003:898–900
327. Aiello A, Fattorusso E, Luciano P, Mangoni A, Menna ML (2005) Isolation and structure determination of aplidinones A–C from the Mediterranean ascidian *Aplidium conicum*: a successful regiochemistry assignment by quantum mechanical C NMR chemical shift calculations. *Eur J Org Chem* 2005:5024–5030
328. Aiello A, Fattorusso E, Luciano P, Macho A, Menna ML, Muñoz E (2005) Antitumor effects of two novel naturally occurring terpene quinones isolated from the Mediterranean ascidian *Aplidium conicum*. *J Med Chem* 48:3410–3416
329. Aiello A, Fattorusso E, Luciano P, Menna ML, Calzado MA, Muñoz E, Bonadies F, Guiso M, Sanasi MF, Cocco G, Nicoletti R (2010) Synthesis of structurally simplified analogues of aplidinone A, a pro-apoptotic marine thiazinoquinone. *Bio Med Chem* 18:719–727
330. Appleton DR, Chuen CS, Berridge MV, Webb VL, Copp BR (2009) Rossinones A and B, biologically active meroterpenoids from the Antarctic ascidian, *Aplidium* species. *J Org Chem* 74:9195–9198
331. Fu X, Hossain MB, van der Helm D, Schmitz FJ (1994) Longithorone A: unprecedented dimeric prenylated quinone from the Tunicate *Aplidium longithorax*. *J Am Chem Soc* 116:12125–12126
332. Fu X, Hossain MB, Schmitz FJ, van der Helm D (1997) Longithorones, unique prenylated para- and metacyclophane type quinones from the Tunicate *Aplidium longithorax*. *J Org Chem* 62:3810–3819
333. Davis RA, Carroll AR, Quinn RJ (1999) Longithorones J and K, two new cyclofarnesylated quinone derived metabolites from the Australian ascidian *Aplidium longithorax*. *J Nat Prod* 62:158–160
334. Fu X, Ferreira MLG, Schmitz FJ (1999) Longithorols A and B, novel prenylated paracyclophane- and metacyclophane-type hydroquinones from the Tunicate *Aplidium longithorax*. *J Nat Prod* 62:1306–1310
335. Davis RA, Carroll AR, Quinn RJ (1999) Longithorols C–E: three new macrocyclic sesquiterpene hydroquinone metabolites from the Australian ascidian *Aplidium longithorax*. *J Nat Prod* 62:1405–1409
336. Issa HH, Tanaka J, Rachmat R, Higa T (2003) Floresolides, new metacyclophane hydroquinone lactones from an ascidian, *Aplidium* sp. *Tetrahedron Lett* 44:1243–1245
337. Bugni TS, Abbanat D, Bernan VS, Malese WM, Greenstein M, Van Wagoner R, Ireland CM (2000) Yanuthones; novel metabolites from a marine isolate of *Aspergillus niger*. *J Org Chem* 65:7195–7200
338. Kobayashi J, Cheng J, Ohta T, Nozoe S, Hirata Y, Ohizumi Y, Sasaki T (1998) Iejimalides A and B, novel 24-membered with potent antileukemic activity from the Okinawan tunicate *Eudistoma cf. rigida*. *J Org Chem* 53:6147–6150
339. Kikuchi Y, Ishibashi M, Sasaki T, Kobayashi J (1991) Iejimalides C and D, new antineoplastic 24-membered macrolide sulfates from the Okinawan marine tunicate *Eudistoma cf. rigida*. *Tetrahedron Lett* 32:797–798
340. Nozawa K, Tsuda M, Ishiyama H, Sasaki T, Tsuruo T, Kobayashi J (2006) Absolute stereochemistry and antitumor activity of iejimalides. *Biol Med Chem* 14:1063–1067

341. Corley DG, Moor DR (1988) Patellazole B: a novel cytotoxic thiazole-containing macrolide from the marine tunicate *Lissoclinum patella*. *J Am Chem Soc* 110:7920–7922
342. Zabriskie TM, Mayne CL, Ireland CM (1988) Patellazole C: a novel cytotoxic macrolide from *Lissoclinum patella*. *J Am Chem Soc* 110:7920–7922
343. Richardson AD, Aalbersberg W, Ireland CM (2005) The patellazoles inhibit protein synthesis at nanomolar concentrations in human colon tumor cells. *Anti-Cancer Drugs* 16: 533–541
344. Galinis DL, McKee TC, Pannell LK, Cardellina II JH, Boyd MR (1997) Lobatamides A and B, novel cytotoxic macrolides from the tunicate *Aplidium lobatum*. *J Org Chem* 62:8968–8969
345. McKee TC, Galinis DL, Pannell LK, Cardellina II JH, Laakso J, Ireland CM, Murray L, Capon RJ, Boyd MR (1998) The lobatamides, novel cytotoxic macrolides from Southwestern Pacific tunicates. *J Org Chem* 63:7805–7810
346. Murray L, Lim TK, Currie G, Capon RJ (1995) Aplidites (A–G): macrocyclic orthonitrites from an Australian tunicate, *Aplidium* sp. *Aust J Chem* 48:1253–1266
347. Shen R, Ting Ling C, Porco JA Jr (2002) Total synthesis and stereochemical assignment of the salicylate antitumor macrolide Lobatamide C. *J Am Chem Soc* 124:5650–5651
348. Ueda K, Hu Y (1999) Haterumalide B, a new cytotoxic macrolide from a Okinawan ascidian *Lissoclinum* sp. *Tetrahedron Lett* 40:6305–6308
349. Teruya T, Shimogawa H, Suenaga K, Kigoshi H (2004) Biselides A and B, novel macrolides from the Okinawan ascidian *Didemnidae* sp. *Chem Soc Jap* 33:1184–1185
350. Teruya T, Suenaga K, Maruyama S, Kurotaki M, Kigoshi H (2005) Biselides A–E: novel polyketides from the Okinawan ascidian *Didemnidae* sp. *Tetr* 61:6561–6567
351. Diyabalanage T, Amsler CD, McClintock JB, Bake BJ (2006) Palmerolide A, a cytotoxic macrolide from the antarctic tunicate *Synoicum adareanum*. *J Am Chem Soc* 128:5630–5631
352. Jiang X, Liu B, Lebreton S, De Brabander JK (2007) Total synthesis and structure revision of the marine metabolite palmerolide A. *J Am Chem Soc* 129:6386–6387
353. Mitchell SS, Rhodes D, Bushman FD, Faulkner DJ (2000) Cyclodidemniserinol trisulfate, a sulfated serinolipid from the Palauan ascidian *Didemnum guttatum* that inhibits HIV-1 integrase. *Org Lett* 2:1605–1607
354. Suzumura K, Takahashi I, Matsumoto H, Nagai K, Setiawan B, Rantiatmodjo RM, Suzuki K, Nagano N (1997) Structural elucidation of YM-75518, a novel antifungal antibiotic isolated from *Pseudomonas* sp. Q38009. *Tetrahedron Lett* 38:7573–7576
355. Kiyota H (2006) Synthesis of marine natural products with bicyclic and/or spirocyclic acetals. *Top Heterocycl Chem* 5:65–95
356. Hopmann C, Faulkner DJ (1997) Lissoketal, a spiroketal from the Palauan ascidian *Lissoclinum voeltzkowi*. *Tetrahedron Lett* 38:169–170
357. Foster MP, Mayne CL, Dunkel R, Pugmire RJ, Grant DM, Kornprobst JM, Verbist JF, Biard JF, Ireland CM (1992) Revised structure of bistramide A (bistratene A): application of a new program for the automated analysis of 2D INADEQUATE spectra. *J Am Chem Soc* 114:1110–1111
358. Biard J, Roussakis C, Kornprobst J, Gouiffes-Barbin D, Verbist J, Cotellet P, Foster MP, Ireland CM, Debitus C (1994) Bistramides A, B, C, D, and K: a new class of bioactive cyclic polyethers from *Lissoclinum bistratum*. *J Nat Prod* 57:1336–1345
359. Murphy BT, Cao S, Brodie P, Maharavo J, Andriamanantoanina H, Ravelonandro P, Kingston DGI (2009) Antiproliferative bistramides from *Trididemnum cyclops* from Madagascar. *J Nat Prod* 72:1338–1340
360. Watters D, Marshall K, Hamilton S, Michael J, McArthur M, Seymour G, Hawkins C, Gardiner R, Lavin M (1990) The bistratenes: new cytotoxic marine macrolides which induce some properties indicative of differentiation in HL-60 cells. *Biochem Pharmacol* 39:1609–1614

361. Watters DJ, Michael J, Hemphill JE, Hamilton SE, Lavin MF, Pettit GR (1992) Bistratene A: a novel compound causing changes in protein phosphorylation patterns in human leukemia cells. *J Cell Biochem* 49:417–424
362. Carroll AR, Healy PC, Quinn RJ, Tranter CJ (1999) Prunolides A, B, and C: novel tetraphenolic bis-spiroketal from the Australian ascidian *Synoicum prunum*. *J Org Chem* 64:2680–2682
363. Potts BCM, Faulkner DJ, Chan JA, Simolike GC, Offen P, Hemling ME, Francis TA (1991) Didemnaketals A and B, HIV-1 protease inhibitors from the ascidian *Didemnum* sp. *J Am Chem Soc* 113:6321–6322
364. Salomon CE, Williams DH, Lobkovsky E, Clardy JC, Faulkner DJ (2002) Relative and absolute stereochemistry of the didemnaketals, metabolites of a Palauan ascidian, *Didemnum* sp. *Org Lett* 4:1699–1702
365. Miao S, Andersen RJ (1991) Rubrolides A-H, metabolites of the colonial tunicate *Ritterella rubra*. *J Org Chem* 56:6275–6280
366. Ortega MJ, Zubía E, Ocaña JM, Naranjo S, Salvá J (2000) New rubrolides from the ascidian *Synoicum blochmanni*. *Tetrahedron* 56:3963–3967
367. Pearce N, Chia EW, Berridge MV, Maas EW, Page MJ, Webb VL, Harper JL, Copp BR (2007) E/Z-Rubrolide O, an anti-inflammatory halogenated furanone from the New Zealand ascidian *Synoicum* n. sp. *J Nat Prod* 70:111–113
368. Smith CJ, Hettich RL, Jompa J, Tahir A, Buchanan MV, Ireland CM (1998) Cadiolides A and B, new metabolites from an ascidian of the genus *Botryllus*. *J Org Chem* 63:4147–4150
369. Fontana A, González MC, Gavagnin M, Templado J, Cimino G (2000) Structure and absolute stereochemistry of stolonoxide A, a novel cyclic peroxide from the marine tunicate *Stolonica socialis*. *Tetrahedron Lett* 41:429–432
370. Durán R, Zubía E, Ortega MJ, Naranjo S, Salvá J (2000) Minor metabolites from the ascidian *Stolonica socialis* and cytotoxicity of Stolonoxides. *Tetrahedron* 56:6031–6037
371. Reyes F, Rodríguez-Acebes R, Fernandez R, Bueno S, Francesch CC (2010) Stolonoxides E and F, Cytotoxic Metabolites from the Marine Ascidian *Stolonica socialis*. *J Nat Prod* 73:83–85
372. Davies-Coleman MT, Gustafson KR, Cantrell CL, Beutler JA, Pannell LK, Boyd MR (2000) Stolonix acids A and B, new cytotoxic cyclic peroxides from an Indian Ocean ascidian *Stolonica* species. *J Nat Prod* 63:1411–1413
373. Fontana A, Cimino G, Gavagnin M, González MC, Estornell E (2001) Novel inhibitors of mitochondrial respiratory chain: endoperoxides from the marine tunicate *Stolonica socialis*. *J Med Chem* 44:2362–2365
374. Compagnone RS, Faulkner DJ, Carté BK, Chan G, Freyer A, Hemling ME, Hofmann GA, Mattern MR (1994) Pentathiepins and trithianes from two *Lissoclinum* species and a *Eudistoma* sp.: inhibitors of protein kinase C. *Tetrahedron* 50:12785–12792
375. Davidson BS, Molinski TF, Barrows LR, Ireland CM (1991) Varacin: a novel benzopentathiepin from *Lissoclinum vareau* that is cytotoxic toward a human colon tumor. *J Am Chem Soc* 113:4709–4710
376. Litaudon M, Tringalo F, Martin M-T, Frappier F, Guyot M (1994) Lissoclinotoxins: antibiotic polysulfur derivatives from the tunicate *Lissoclinum perforatum*. Revised structure of lissoclinotoxin A. *Tetrahedron* 50:5323–5334
377. Patil AD, Freyer AJ, Killmer L, Zuber G, Carté B, Jurewicz AJ, Johnson RK (1997) Lissoclin disulfide, a novel dimeric alkaloid from the ascidian *Lissoclinum* sp. Inhibitor of interleukin-8 receptors. *Nat Prod Lett* 10:225–229
378. Makarieva TN, Stonik VA, Dmitrenok AS, Grebnev BB, Isakov VV, Rebachyk NM (1995) Varacin and three new marine antimicrobial polysulfides from the far-eastern ascidian *Polycitor* sp. *J Nat Prod* 58:254–258
379. Ford PW, Davidson BS (1993) Synthesis of varacin, a cytotoxic naturally occurring benzopentathiepin isolated from a marine ascidian. *J Org Chem* 58:4522–4523

380. Ford PW, Narbut MR, Belli J, Davidson BS (1994) Synthesis and structural properties of the benzopentathiepins varacin and isolissoclinotoxin A. *J Org Chem* 59:5955–5960
381. Litaudon M, Guyot M (1991) Lissoclinotoxins, an antibiotic 1,2,3-trithiane derivative from the tunicate *Lissoclinum perforatum*. *Tetrahedron* 32:911–914
382. Davidson BS, Ford PW, Wahlan M (1994) Chirality in unsymmetrically substituted benzopentathiepins: the result of a high barrier to ring inversion. *Tetrahedron Lett* 35:7185–7188
383. Barrows LR, Paxton MB, Kennedy KA, Thompson LH (1991) Characterization of revertants of the CHO EM9 mutant arising during DNA transfection. *Carcinogenesis* 12:805–811
384. Chenard BL, Harlow RL, Johnson AL, Vladuchik SA (1985) Synthesis, structure, and properties of pentathiepins. *J Am Chem Soc* 107:3871–3879
385. Davis RA, Sandoval IT, Concepcion GP, Moreira da Rocha R, Ireland CM (2003) Lissoclinotoxins E and F, novel cytotoxic alkaloids from a Philippine didemnid ascidian. *Tetrahedron* 59:2855–2859
386. Copp BR, Blunt JW, Munro HG, Pannell LK (1989) A biologically active 1,2,3-trithiane derivative from the New Zealand ascidian *Aplidium* sp. *D Tetrahedron Lett* 30:3703–3706
387. Pearce AN, Babcock RC, Battershill CN, Lambert G, Copp BR (2001) Enantiomeric 1,2,3-trithiane-containing alkaloids and two new 1,3-dithiane alkaloids from New Zealand ascidians. *J Org Chem* 66:8257–8259
388. Liu H, Pratasik SB, Nishikawa T, Shida T, Tachibana K, Fujiwara T, Nagai H, Kobayashi H, Namikoshi M (2004) Lissoclibadin 1, a novel trimeric sulfur-bridged dopamine derivative, from the tropical ascidian *Lissoclinum cf. badium*. *Tetrahedron Lett* 45:7015–7017
389. Liu H, Fujiwara T, Mishima Y, Nagai H, Shida T, Tachibana K, Kobayashi H, Mangindaan REP, Namikoshi M (2005) Lissoclibadins 1–3, three new polysulfur alkaloids, from the ascidian *Lissoclinum cf. badium*. *Tetrahedron* 61:8611–8615
390. Nakazawa T, Xu J, Nishikawa T, Oda T, Fujita A, Ukai K, Mangindaan REP, Rotinsulu H, Kobayashi H, Namikoshi M (2007) Lissoclibadins 4–7, polysulfur aromatic alkaloids, from the Indonesian ascidian *Lissoclinum cf. badium*. *J Nat Prod* 70:439–442
391. Wang W, Takahashi O, Oda T, Nakazawa T, Ukai K, Mangindaan REP, Rotinsulu H, Wewengkang DS, Kobayashi H, Tsukamoto S, Namikoshi M (2009) Lissoclibadins 8–14, polysulfur dopamine-derived alkaloids from the colonial ascidian *Lissoclinum cf. badium*. *Tetrahedron* 65:9598–9603
392. Oda T, Kamoshita K, Maruyama S, Masuda K, Nishimoto M, Xu J, Ukai K, Mangindaan REP, Namikoshi M (2007) Cytotoxicity of lissoclibadins and lissoclinotoxins, isolated from a tropical ascidian *Lissoclinum cf. badium*, against human solid-tumor-derived cell lines. *Biol Pharm Bull* 30:385–387
393. Linquist N, Fenical W (1990) Polycarpamines A-E, antifungal disulfides from the marine ascidian *Polycarpa ausata*. *Tetrahedron Lett* 31:2389–2392
394. Fedoreyev SA, Radchenko OS, Novikov VL, Isakov VV, Ilyin SG, Popov AM, Elyakov GB, Murphy PT, Willis RH, Baker JT (1995) In: Proceedings of the 8th international symposium on marine natural products, Santa Cruz de Tenerife, Canary Islands, pp 196–197
395. Kang H, Fenical W (1996) Polycarpine dihydrochloride: a cytotoxic dimeric disulfide alkaloid from the Indian Ocean ascidian *Polycarpa clavata*. *Tetrahedron Lett* 37:2369–2372
396. Radchenko OS, Novikov VL, Willis RH, Murphy PT, Elyakov GB (1997) Synthesis of polycarpine, a cytotoxic sulfur-containing alkaloid from the ascidian *Polycarpa aurata*, and related compounds. *Tetrahedron Lett* 38:3581–3584
397. Fedorov SN, Bode AM, Stonik VA, Gorshkova IA, Schmid PC, Radchenko OS, Berdyshev EV, Dong Z (2004) Marine alkaloid polycarpine and its synthetic derivative dimethylcarpine induce apoptosis in JB6 cells through p53- and caspase 3-dependent pathways. *Pharm Res* 21:2307–2319

398. Wang W, Oda T, Fujita A, Mangindaan REP, Nakazawa T, Ukai K, Kobayashi H, Namikoshi M (2007) Three new sulfur-containing alkaloids, polycarpaurines A, B, and C, from an Indonesian ascidian *Polycarpa aurata*. *Tetrahedron* 63:409–412
399. Rezanka T, Dembitsky VM (2002) Eight-membered cyclic 1,2,3-trithiocane derivatives from *Perophora viridis* an Atlantic tunicate. *Eur J Org Chem* 2002:2400–2404
400. Kehraus S, Gorzalka S, Hallmen C, Iqbal J, Muller CE, Wright AD, Wiese M, König GM (2004) Novel amino acid derived natural products from the ascidian *Atriolum robustum*: identification and pharmacological characterization of a unique adenosine derivative. *J Med Chem* 47:2243–2255
401. Tsukamoto S, Kato H, Hirota H, Fusetani N (1994) Antibacterial and antifungal sulfated alkane and alkenes from the hepatopancreas of the ascidian *Halocynthia roretzi*. *J Nat Prod* 57:1606–1609
402. Fujita M, Nakao Y, Matsunaga S, Nishikawa T, Fusetani N (2002) Sodium 1-(12-hydroxy) octadecanoyl sulfate, an MMP2 Inhibitor, isolated from a tunicate of the family Polyclinidae. *J Nat Prod* 65:1936–1938
403. Crispino A, De Giulio A, De Rosa S, De Stefano S, Milone A, Zavodnik N (1994) A sulfated normonoterpenoid from the ascidian *Polycitor adriaticus*. *J Nat Prod* 57:1936–1938
404. De Rosa S, Milone A, Crispino A, Jaklin A, De Giulio A (1997) Absolute configuration of 2,6-dimethylheptyl sulfate and its distribution in Ascidiacea. *J Nat Prod* 60:462–463
405. Aiello A, Carbonelli S, Esposito G, Fattorusso E, Iuvone T, Menna M (2000) Novel bioactive sulfated alkene and alkanes from the Mediterranean ascidian *Halocynthia papillosa*. *J Nat Prod* 63:1590–1592
406. Aiello A, Fattorusso E, Menna M, Carnuccio R, Iuvone T (1997) A new antiproliferative sulfated alkene from the Mediterranean tunicate *Microcosmus vulgaris*. *Tetrahedron* 53:11489–11492
407. Aiello A, Fattorusso E, Menna M, Carnuccio R, D'Acquisto F (1997) Novel antiproliferative alkyl sulfates from the Mediterranean tunicate *Ascidia mentula*. *Tetrahedron* 53:5877–5882
408. Aiello A, Carbonelli S, Esposito G, Fattorusso E, Iuvone T, Menna M (2001) Turbinamide, a new selective cytotoxic agent from the Mediterranean tunicate *Sidnyum turbinatum*. *Org Lett* 3:2941–2944
409. Aiello A, Carbonelli S, Fattorusso E, Iuvone T, Menna M (2001) New bioactive sulfated metabolites from the Mediterranean tunicate *Sidnyum turbinatum*. *J Nat Prod* 64:219–221
410. Esposito G, Aiello A, Carbonelli S, Fattorusso E, Menna M, Iuvone T (2002) Mechanism of cytotoxicity of turbinamide in vitro. *Anticancer Res* 22:2827–2832
411. Cosson MP (1990) Sperm chemotaxis. In: Cagnon C (ed) *Controls of sperm motility: biological and clinical aspects*. CRC Press, Boca Raton, pp 104–135
412. Yoshida M, Murata M, Inaba K, Morisawa M (2002) A chemoattractant for ascidian spermatozoa is a sulfated steroid. *Proc Natl Acad Sci USA* 99:14831–14836
413. Oishi T, Tsuchikawa H, Murata M, Yoshida M, Morisawa M (2003) Synthesis of Endogenous sperm-activating and attracting factor isolated from ascidian *Ciona intestinalis*. *Tetrahedron Lett* 44:6387–6389
414. Riccio R, Kinnel RB, Bifulco G, Scheuer PJ (1996) Kakelokelose, a sulfated mannose polysaccharide with anti-HIV activity from the Pacific tunicate *Didemnum molle*. *Tetrahedron Lett* 37:1979–1982

Part 2

Structure Elucidation of Marine Natural Products

The Role of Databases in Marine Natural Products Research

6

John Blunt, Murray Munro, and Meg Upjohn

Contents

6.1	Dereplication	390
6.2	Natural Products Databases	390
6.3	Commercial Databases	392
6.3.1	CAS REGISTRY and CAPLUS	392
6.3.2	REAXYS	393
6.3.3	DICTIONARY OF NATURAL PRODUCTS AND DICTIONARY OF MARINE NATURAL PRODUCTS	393
6.3.4	ANTIBASE	394
6.3.5	MARINLIT	394
6.3.6	ANTIMARIN	395
6.3.7	Spectroscopic Databases	395
6.4	Free Access Databases	396
6.4.1	PUBCHEM	397
6.4.2	CSLS	397
6.4.3	CHEMSPIDER	398
6.5	Approaches to Dereplication	398
6.5.1	Selection of Database	399
6.5.2	Dereplication Based on Molecular Mass/Molecular Formula	401
6.5.3	Dereplication Based on UV Data	402
6.5.4	NMR-Based Approaches to Dereplication	406
6.6	Examples of Dereplication	410
6.6.1	Compound Isolated from a Cnidarian	410
6.6.2	Dereplication of a <i>Suberites</i> sp. Extract	412
6.6.3	Dereplication of an <i>Aspergillus</i> sp. Extract	414
6.7	Commentary on Approaches to Dereplication	415
6.8	Dereplication at the Nanomole Level	418

J. Blunt (✉) • M. Munro

Department of Chemistry, University of Canterbury, Christchurch, New Zealand
e-mail: john.blunt@canterbury.ac.nz, murray.munro@canterbury.ac.nz

M. Upjohn

Physical Sciences Library, University of Canterbury, Christchurch, New Zealand
e-mail: m.upjohn@gmail.com

6.9 Relative Costs of the Databases	419
6.10 Study Questions	419
References	420

Abstract

Access to suitable databases is essential for the rapid dereplication (assessment of novelty) of crude extracts in natural product research. The efficiency of this dereplication process relies heavily on the interpretation of molecular mass, molecular formula, UV, and NMR spectral data. In this chapter, the availability and the suitability of the available databases for dereplication is critically examined. The chapter concludes with examples of dereplication strategy based on available natural product databases.

6.1 Dereplication

One definition of dereplication is the *differentiation of novel metabolites from known compounds in a natural products extract*. The task of dereplication then is one of instituting approaches that achieve this differentiation as quickly and as efficiently as possible. An added bonus is if the process can be achieved on as small a scale as practical. How difficult a task is this? As of June 2011, the DICTIONARY OF NATURAL PRODUCTS [1] listed 159,670 unique naturally occurring compounds. In November 2009, the suggested number of natural products in the CAS database [2] was 250,000 while in REAXYS [3] the number was 170,000. While a definitive figure is not possible, it is not unreasonable to assume that there are most probably 175,000 natural products that have been isolated and characterized to date. Thus, the probability that a crude natural products extract will contain new compounds is not high. The history of marine natural products does not extend back as far as that of their terrestrial counterpart, but there are at least 22,000 marine natural products, again offering high odds against the discovery of new compounds. To effectively undertake dereplication of a crude natural product extract, it is first necessary to obtain definitive information about each component of interest in the extract and then compare those data against appropriate chemical and natural product-based databases. The efficiency of this process is very much a function of the quality and accessibility of the relevant data in the available databases. This chapter is focused on surveying the available databases and examining the requirements for dereplication.

6.2 Natural Products Databases

Access to appropriate databases is essential for the efficient study of (marine) natural products whether the aims be the discovery of new compounds, the synthesis of known compounds or analogues, analysis of data relating to taxonomy and distribution of

Table 6.1 A compiled list of databases dealing with natural products

Public domain	Private domain	Commercial
CHEMSPIDER [19]	ALL PHARMA	CAS REGISTRY [2, 4–6]
CSLS [18]	GVK BIOSCIENCES NPD [40]	SPECINFO [11]
PUBCHEM [17]	UC UV DB [24]	REAXYS [3]
NMRSHIFT DB [25]	DTU UV DB [22]	ACD/LABS [13]
NAPROC-13 [26]	MARINE NP DB [41]	NAPRALERT [20]
SUPERNATURAL [27]	INTERMED UV DB [42]	DICTIONARY OF NATURAL PRODUCTS [1]
SDBS [28]	INTERMED NMR DB[42]	DICTIONARY OF MARINE NATURAL PRODUCTS [8]
	NOVARTIS IR DB [43]	ANTIBASE [10]
	NATIONAL CENTRE PLANT METABOLISM [44]	MARINLIT [12]
	CH-NMR-NP [45]	ANTIMARIN [14]

compounds and source organisms, or studies on bioactivities to name but a few. There are specialized databases of chemical literature, X-ray crystal structure data, NMR spectra, reactions, physicochemical, and bioactivity data. Private domain, free access, and commercial databases abound with an array of different content, coverage and access restrictions. A selection of those considered most relevant is depicted in Table 6.1.

Recent developments in open access and open source resources have generated a rapid increase in the amount of publically available chemical information and the development of sophisticated, free tools to extract these data. Research funded by the US National Institutes of Health (NIH), the Wellcome Trust (British), the Italian National Institute of Health (ISS), the European Research Council, and many other research institutes and universities is required to be made available through a publically accessible repository after acceptance for publication. Freely available data from sources like these provide the core content of other open access databases with specialized search capabilities.

Private Domain databases are those that have been commented on or alluded to in the primary literature. Undoubtedly, there are many more Private Domain databases than those listed in Table 6.1. For dereplication, it is unfortunate that these sources are not generally available as they would be invaluable and would give access to collections of data not otherwise available. The classic examples of this sort of resource are those databases that have been generated by the pharmaceutical companies. Pharmaceutical companies maintain their own extensive libraries of resources, but these are strictly private and inaccessible to other researchers. None of the Private Domain databases will be surveyed here.

There are commercial databases available that contain sufficient substances, data about them, and search capabilities to serve the needs of natural products dereplication, but there is enormous variation in accessibility and fee structure

for access to these resources. Most are very expensive, but academic discounts are often available and pricing options are sometimes offered, catering to occasional users or to those who only need access to a portion of the data. The more expensive of these databases have very broad coverage and contain bibliographic entries and substance information of interest to a wide range of users other than natural products chemists or biologists. The less expensive databases are naturally smaller and more specialized, but among these are resources that provide access to the most comprehensive publically available collections of natural products and they are particularly suited to the process of natural products dereplication.

The challenge is to select a database that returns the best quality and quantity of return for the time and money involved in extracting the needed data. For a commentary on relative costs, see [Sect. 6.9](#). The following discussion describes some of the attributes of the more significant of these commercial and open access databases.

6.3 Commercial Databases

6.3.1 CAS REGISTRY and CAPLUS

Undoubtedly, the most comprehensive compilation of information on natural product substances is the Chemical Abstracts Service CAS REGISTRY database in which each substance is identified by a unique CAS Registry Number (RN). Included are chemical structures, trade names, systematic names, synonyms, molecular formula, and calculated and experimental property data. The companion CAPLUS database contains patent and journal article references with abstracts. CAS REGISTRY contains over 63 million organic and inorganic substances, and it is estimated that more than 250,000 of them are natural products [4]. There are a number of options for gaining access to these databases.

6.3.1.1 STN

STN [5] is an online service that provides a single platform for access to over 200 of the most significant science, technology, and patent databases from different suppliers throughout the world, including CAS REGISTRY and CAPLUS. Various means of access include STN Express which permits desktop access to all STN databases. It uses a powerful but complex STN command-language interface that is intended for experienced online searchers. Similar interaction with the selected databases is also provided through a web interface, STN on the Web. For occasional and novice searchers, an easier search interface that uses keywords and Boolean operators (no special command-language is required) is available via web access with STN Easy. An option for one-off search needs is a mediated search to the user's requirements that will be carried out on STN databases by experts who will send the results to the user. This service is available through the FIZ Karlsruhe's search service.

6.3.1.2 SciFINDER

The other major access pathway to the CAS REGISTRY and CAPLUS files is through SciFINDER [6], a database produced by the American Chemical Society. SciFINDER provides a single, graphical interface to access the CAS REGISTRY and CAPLUS databases, as well as CASREACT (a reaction database), CHEMCATS (chemical supplier listings), CHEMLIST (regulated chemical information), MARPAT (Markush structures of organic and organometallic molecules from patents), and MEDLINE (the National Library of Medicine database). SciFINDER is available on subscription as a web-based and/or client-based system.

Access to the CAS REGISTRY database is mandatory in any MNP investigation that produces a supposedly new compound to ensure that what is being claimed as new is indeed the case. The SciFINDER interface is very versatile, permitting searches in various ways to establish the previous occurrence or novelty of a compound, or its similarity to other known compounds. One of the first pieces of experimental information that is often obtained for a compound under investigation is its molecular mass. Somewhat surprisingly, in SciFINDER it is not possible to search directly for all substances with a particular mass, but this result can be achieved by first carrying out a substructure search for all compounds containing C and then refining the search based on mass.

The CAS REGISTRY and CAPLUS files are updated on a daily basis, with data usually being current to within only a few months from publication.

6.3.2 REAXYS

REAXYS [3] contains an extensive repository of experimentally validated data including structures, reactions (including multistep reactions), and physical properties. These data are derived from CrossFire Beilstein, CrossFire Gmelin, and Patent Chemistry Database. While this combined database is primarily designed to meet the needs of synthetic chemists, the easy-to-use web interface is well-suited to the needs of natural products chemists, providing flexible access to information on an estimated 170,000 natural products. The actual number of MNPs in this database is not readily discernable, but is estimated to be quite significant. REAXYS would be particularly valuable to those researchers interested in the synthesis of natural products.

The REAXYS database is updated monthly with data extracted from over 150 journals and from patent offices (US, WO, EP, class C07). The average time from receipt of an article to its inclusion in the database is 6 weeks.

6.3.3 DICTIONARY OF NATURAL PRODUCTS AND DICTIONARY OF MARINE NATURAL PRODUCTS

The Chapman & Hall/CRC Press DICTIONARY OF NATURAL PRODUCTS (DNP) [1] is a structured database holding information on chemical substances including descriptive and numerical data on chemical, physical, and biological properties of compounds, systematic and common names of compounds, literature references,

and structure diagrams and their associated connection tables. DNP is available by annual subscription with desktop data and supporting software on DVD, or access can be obtained through the web-based CHEMnetBASE [7]. Version 20:1 (June 2011) of DNP contained 220,470 entries, of which 159,670 were ascribed to isolated natural products. The additional 60,800 entries were for derivatives of the actual natural products. THE DICTIONARY OF MARINE NATURAL PRODUCTS (DMNP) [8] is a subset of data from DNP based on the biological source of the compounds. DMNP is available as a book with CD-ROM for a desktop version, and also from the web-based CHEMnetBASE. The web version (November 2009) contains 34,685 entries, of which 22,664 are for isolated MNPs, with the balance being for derivatives. The number of isolated MNPs contains a significant number of compounds that were first isolated from terrestrial sources but were subsequently also found in marine organisms. Both the desktop and web-based versions of DNP and DMNP permit flexible searching and reporting options, including substructure searches. Structure results for many compounds do not show stereochemistry in the diagrams. Only the parent compound in a series of related compounds is represented by a stereodiagram, while the related compounds can be viewed as planar diagrams with text descriptions of the variations in configurations. Linear peptides are shown as sequences rather than as diagrams. A recent reviewer of DMNP found issue with a number of the offered features of the electronic dictionary [9]. Updated DVD and CHEMnetBASE versions of DNP are released every 6 months, while the CHEMnetBASE version of DMNP is updated annually. Each release has data current to within 6–12 months of publication.

6.3.4 ANTiBASE

ANTiBASE 2011 [10] is a comprehensive desktop database of 36,000 natural compounds from microorganisms and higher fungi. ANTiBASE includes descriptive data (molecular formula and mass, elemental composition, CAS registry number), physicochemical data (melting point, optical rotation), some spectroscopic data (UV, ^{13}C - and ^1H -NMR, IR, and mass spectra), biological data (pharmacological activity, toxicity), information on origin and isolation, and a summary of literature sources. A feature of ANTiBASE is the use of predicted ^{13}C -NMR spectra (SPECINFO [11]) for those compounds where no measured spectra are available. This database is becoming increasingly important for MNP investigations as more MNPs are discovered from microorganisms where the overlap between “marine” microorganisms and “terrestrial” microorganisms can be difficult to determine. Having knowledge of the chemistry of terrestrial microorganisms is therefore highly desirable. ANTiBASE is updated annually with data current to within only a few months of publication.

6.3.5 MARiNLiT

With the exception of CAplus, all of the databases described above are compound-centric. MARiNLiT [12] is a desktop database comprising records relating to

publications covering all aspects of MNP research. Thus, not all entries contain information on newly isolated MNP structures, but they may cover aspects of synthesis, biosynthesis, ecological studies, bioactivity investigations, reisolation of known compounds, and also reviews. MARINLIT currently has 24,000 records of publications, of which 8,500 describe 22,000 structures for compounds isolated for the first time from marine sources. All records contain the usual bibliographic information, an extensive list of keywords, and where appropriate, taxonomy, structures, MW, formulae, UV data, and calculated (ACD/Labs [13]) ^1H and ^{13}C NMR chemical shifts. Very flexible searching and reporting options are available for combinations from all of these data fields including substructure searching. A unique feature in MARINLIT (and ANTIMARIN – see below) is the inclusion of searchable data fields containing the numbers of each structural feature (^1H -SF) that can be determined from inspection of the ^1H -NMR spectrum of a compound. These features include the numbers of methyl groups of various types – singlets, doublets, triplets, or -OMe, -NMe, -SMe, etc., types of substituted benzene rings, and numbers of $\text{sp}^2\text{-H}$, $\text{sp}^3\text{-CH}$ or $\text{sp}^3\text{-CH}_2$ groups to name a few. The value of this feature for MNP dereplication and discovery investigations will be described later in this chapter. MARINLIT updates are released twice each year with the data being current to within 1–2 months of publication.

6.3.6 ANTIMARIN

ANTIMARIN [14] is available to current subscribers to both ANTIbase and MARINLIT. It is a compound-centric desktop database containing data for 53,000 compounds from ANTIbase and MARINLIT. The compound data from each database is enhanced by the inclusion of searchable data fields containing the numbers of each structural feature that can be determined from inspection of the ^1H -NMR spectrum of a compound, as described above for MARINLIT. This combined database with the structural features data included provides a valuable tool for the process of dereplication, as described later in this chapter. ANTIMARIN is updated annually with data current to within a few months of publication.

6.3.7 Spectroscopic Databases

While the previously described databases contain some spectroscopic data for compounds, or at least reference to the source of experimental spectroscopic data for a compound, there are other databases dedicated to the cataloging and/or calculation of spectroscopic properties. Access to these data can be particularly helpful in the investigation of MNPs, either to establish that the experimental data obtained in an investigation is the same as that previously found for a proposed structure, or to determine if the observed data for a new proposed structure is reasonable. The following descriptions do not include packages that attempt to generate a structure from experimentally obtained data.

6.3.7.1 SPECINFO

SPECINFO [11] is a spectroscopic database whose primary aim is to assist with spectral interpretation and structure elucidation. These functions are supported by facilities for searching the database for compounds with NMR and/or IR spectra, or fragments of spectra, matching the experimental data. Additionally, compounds can be searched for using structures or substructures or other structurally related information such as CAS numbers. NMR spectrum prediction for a proposed structure is also an integral part of SPECINFO. These capabilities are supported by a knowledge base of 359,000 ^{13}C NMR spectra, 130,000 ^1H NMR spectra, 90,000 heteroatom (^{15}N , ^{17}O , ^{19}F , ^{11}B and ^{31}P) NMR spectra, 139,000 mass spectra, and 21,000 IR spectra.

6.3.7.2 ACD/Labs

ACD/Labs [13] provide a collection of software packages directed principally at the handling and processing of experimental data, mostly spectroscopic. For the natural products chemists, the packages of most interest would be the HNMR and CNMR Predictors. These permit the calculation of ^1H and ^{13}C NMR spectra from user-inputted structures. These Predictors utilize algorithms based on more than 1.7 million assigned ^1H chemical shifts from more than 210,000 chemical structures and 2.5 million assigned ^{13}C chemical shifts from about 200,000 chemical structures. Use of these Predictors can be very helpful for comparing the calculated spectra for a proposed structure with the experimental data to assess the feasibility of a proposed structure. Further tools are available in ACD/NMR Workbook for more direct comparisons of calculated 2D spectra with the experimental spectra, again assisting with the verification of a proposed structure. Of particular relevance to MNP chemists are the internal databases in the Predictor packages. These contain the published chemical shift data for $\sim 240,000$ compounds. These data are only entered into the internal databases after a rigorous analysis of the data to establish that the assignments as published are consistent with those arrived at by calculation. Presently, over half of the marine natural products have their data included in the internal databases, and these data are being added to on a regular basis so that the proportion of MNPs contained in the internal databases will eventually be much higher. Currently, the ACD/Labs-calculated ^1H and ^{13}C NMR chemical shift data for all MNPs are accessible from within MARINLIT, as described earlier. Additional useful data in the internal databases are the original references, solvents, frequency, NMR techniques, molecular formulae, molecular masses, IUPAC names, and trivial names, all of which can be searched, viewed, and printed.

6.4 Free Access Databases

There are now over 50 databases with free access to chemical structures from various sources [15, 16]. However, of more use to natural products chemists are

those databases containing compound data collected from a wide range of other open access or proprietary databases. In general, these combined databases contain the chemical structures and a limited amount of other associated data but do not refer to the source of the compounds. They do, however, provide links to the source database from which the data were compiled, and thus allowing the user to make their own arrangements for access to the complete information relating to a compound. A particularly valuable feature of these combined databases is that they allow the user to determine if a structure may have been previously characterized, although this will not be a complete substitute for verifying novelty of a compound as necessary through the use of the CAS REGISTRY. In general, these databases do not provide comprehensive classification of compounds that might be natural products. It is not possible to describe all of the databases that are available, and the following descriptions are for those that are likely to be the most generally useful for natural products studies.

6.4.1 PubCHEM

PubCHEM [17] includes substance information, compound structures, and bioactivity data in three primary databases: PC Substance, PC Compound, and PCBioAssay, respectively, with data collated from over 80 other databases. PC Compound contains more than 25 million unique structures.

6.4.2 CSLS

The Chemical Structure Lookup Service (CSLS) [18] can be regarded as an address book for chemical structures. It has two major modes of operation: The first mode permits the submission of one or more chemical structures in the form of an SD file, as SMILES strings, or in one of more than 20 other molecular structure formats that CSLS understands. The service will determine whether the submitted structures are present in any of the databases that are currently indexed in CSLS. The second mode allows the submission of a document, from which CSLS will attempt to extract all possible chemical information that this document might contain – InChI string, InChIKey, SMILES string, molecular formula, or NCI/CADD Structure Identifiers (uuuuu, FICuS, or FICTS). It then conducts a search with these extracted chemical data. There are 74 million entries in CSLS collated from about 100 databases, representing 46 million unique structures. In the classification section of CSLS, there is a check box for natural products. However, this refers to about 124,000 entries from the NCI Frederick NP database, of which only about one third are actual natural products. An additional 8,000 natural product structures from the CHMIS-C database are included in this section.

6.4.3 CHEMSPIDER

CHEMSPIDER [19] is a compound-centric search engine and database, now being developed under the auspices of the Royal Society of Chemistry, which is aggregating and indexing chemical structures and their associated information into a single searchable repository. This database aims to capture and manage chemical structures from online resources, from commercial databases, and from users of the CHEMSPIDER platform who have the ability to submit their own data. Users can access the open access data immediately and where possible, the CHEMSPIDER search engine also provides links to commercial resources that contain information matching the users' query. Many additional properties have been added to each of the chemical structures thus enhancing the value of the collection. These include spectral data, links to publications, reaction synthesis details, and various experimental properties. For MNP researchers, perhaps the greatest value will be to determine if there is any information available about a compound of interest. Access to CHEMSPIDER is without charge. Of particular value is the ability to search by substructure, a feature that is not available in CSLS. Currently (2011), there are in excess of 26 million unique entries in CHEMSPIDER from over 300 data sources. There are numerous cases of the same natural product in the database with various levels of partial to complete stereochemistry as provided by a number of the depositors. Members of the CHEMSPIDER team are focused on curating the structure collection. The information in CHEMSPIDER is updated daily as a result of new compound depositions and curation activities, but the currency and accuracy of the data is only as good as that of the databases from which the data is sourced.

6.5 Approaches to Dereplication

In a dereplication exercise, a minimal set of must-know data would include the molecular masses (and molecular formulas) of the components of the mixture, relevant UV data and, if possible, ^1H NMR spectra. The taxonomy of the organism, although very useful, is not an absolute requirement.

The molecular mass and UV data can be generated from an LC/MS analysis of an aliquot of the crude extract using Diode Array Detection (DAD) in combination with electrospray mass spectrometric analysis (ESMS). Under high-resolution conditions (LC/HRESMS), the individual molecular formulas of the components can be obtained. With access to a CapNMR probe or small-tube cryoprobe, it is now possible to obtain a good ^1H NMR spectrum of individual components from the same LC run (see Sect. 6.8). The ideal situation would be to use this minimal set of data, perhaps in combination with taxonomic data if it is available, and make a definitive identification of the compound as either new or known. Of course, there are other ways that

this minimal data set could be generated, for example, by chromatography on the crude extract followed by MS or HRMS, ^1H NMR, and UV measurements on the isolated individual components. Taxonomic identification of marine organisms can be fraught with difficulties, but this knowledge undoubtedly can be of assistance.

6.5.1 Selection of Database

Not all of the natural product databases suggested (Table 6.1) can give definitive answers using part, or even all of this suggested data set. In Table 6.2, a “filtered” list of databases has been provided listing the attributes and the data that can be extracted readily.

In Table 6.2, the databases are arranged from the largest (CAS REGISTRY) to the smallest (MARINLIT). The smaller databases, from NAPRALERT [20] downward, are the dedicated natural product databases. The number of natural products in each database has been listed. In the larger databases such as SciFINDER and REAXYS this is an estimate only. With the exception of NAPRALERT all of the databases are kept current, or within a few months of current. NAPRALERT’s coverage of MNPs since 2004 has been sporadic only and for this reason has not been covered in this chapter. Within the range of databases in Table 6.2, molecular formula-based searches are possible and, with the exception of CSLS, it is possible to search on a molecular mass range, although doing so within SciFINDER is not obvious as it is first necessary to have generated a subset from SciFINDER that contains all compounds containing C and then to initiate a search using the molecular mass range of interest as a filter. All of the databases except NAPRALERT are capable of carrying out substructure searching. This is a particularly helpful feature for using recognizable fragments in searches. These fragments can arise from interpretation of NMR and/or MS data. As well, taxonomic and biological activity data can be searched in most of the databases listed. The distinction between the utility of the various databases comes when the availability of actual UV and NMR data is considered. For UV data (λ and ϵ), the two DICTIONARIES and MARINLIT contain this data with partial coverage included in NAPRALERT, ANTIMARIN and ANTIBASE. For NMR data within this group of databases, δ_{C} values are searchable within MARINLIT. The only databases available that can provide spectral data are MARINLIT and ANTIBASE. Through an arrangement with ACD/Labs, *calculated* ^1H , ^{13}C chemical shift data and HSQC/DEPT spectra are accessible in MARINLIT. This is a facility that is particularly useful for comparing actual data from a potential new compound against data that have been generated for known compounds. The last NMR feature listed in this figure is ^1H NMR Structural Features (^1H -SF). This is a unique aspect for searching ^1H NMR data for matching features and is only available using the MARINLIT or ANTIMARIN databases. As noted earlier, these two databases include searchable data fields containing the actual numbers of each

Table 6.2 A “filtered” list of databases that are of potential use for the derperplication of (marine) natural product extracts

Number of compounds ^a													NMR data ^b		
DATABASE	Total	Natural products	Current up to	MW	MF	UV ^c λ	SSS ^d	Tax. ^e	Biol. ^f	δ	Spectra	¹ H-SF	HSQC/DEPT		
CAS REGISTRY	6.3 × 10 ⁷	~250,000	Current	+ ^g	+	—	+	+	+	—	—	—	—		
CSLS	4.6 × 10 ⁷	?	Current	—	+	—	+	—	?	—	—	—	—		
CHEMSPIDER	2.6 × 10 ⁷	?	Current	+	+	—	+	—	—	—	—	—	—		
PUBCHEM	3.7 × 10 ⁷	?	Current	+	+	—	+	—	+	—	—	—	—		
REAXYS	>10 ⁷	170,000	Current	+	+	—	+	+	?	—	—	—	—		
NAPRALERT		>150,261	~2004	+	+	+ ^h	—	+	+	—	—	—	—		
DICTIONARY OF NATURAL PRODUCTS		159,670	2011	+	+	+	+	+	+	—	—	—	—		
ANTIMARIN		43,000	2010	+	+	+ ^h	+	+	+ ^h	—	—	+	—		
ANTIBASE		36,000	2010	+	+	+ ^h	+	+	+	+ ^h	—	—	—		
DICTIONARY OF MARINE NATURAL PRODUCTS		22,691	2006	+	+	+	+	+	+	—	—	—	—		
MARINLIT		22,000	2011	+	+	+	+	+	+ ^h	+	+	+	+		

^aWhere possible an estimate is given for the number of natural products in the database

^bFour options for NMR data: the δ values (calculated or actual), spectra, ¹H NMR structural features (¹H-SF) or calculated HSQC/DEPT spectra

^cActual λ(ε) values for UV data as opposed to a reference to the data

^dSub-structure searching capability

^eTaxonomic data

^fBiological activity data

^gIn the current version of SciFinder the extraction of molecular mass data is not straightforward

^hPartial data only

structural feature that can be deduced from the ^1H NMR spectrum of a compound. For example, the numbers of methyl groups of various types – singlets, doublets, triplets, or -OMe, -NMe, -SMe, etc. This unique feature, in combination with mass and perhaps UV data, is very effective in discriminating between alternative structures in the dereplication process, as will be described in Sect. 6.6.

6.5.2 Dereplication Based on Molecular Mass/Molecular Formula

An early step in dereplication is to obtain the MS of compounds isolated by chromatography of the crude extract or by running an LC/MS experiment on the crude sample. Depending on the resolution and/or mode of the MS or LC/MS, two outcomes are possible. If the MS, typically ESMS, has been run under low resolution conditions ($<1:5,000$) then unit mass differentiation is possible. That is the distinction between say m/z 490 and 491. Under higher resolution conditions, the actual molecular formula can be obtained. For example, $\text{C}_{30}\text{H}_{50}\text{O}_5$ which has $m/z = 490.3658$. Either or both of these outcomes can be searched in databases. The results of such a search are shown in Table 6.3. Even for the more specialized databases, the number of “hits” recorded is often too great even when searching for a molecular formula. Sometimes molecular mass data is all that is available, but that alone is not a good discriminator. Ideally, less than ten hits is an acceptable number.

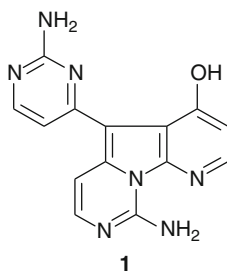
If a new compound that has an unusual or a unique molecular formula, obtaining the molecular formula may be all that is necessary to identify it as a new compound. That was the case with variolin B, a bioactive alkaloid isolated from the Antarctic sponge *Kirkpatrickia variolosa* [21]. Variolin B (**1**) had a molecular formula of $\text{C}_{14}\text{H}_{11}\text{N}_7\text{O}$. At the time a search of the specialist natural product databases gave zero hits thus establishing that this was a new compound. Nearly 20 years later,

Table 6.3 Search of relevant databases from both free access and commercial sources for molecular mass and molecular formula data

Database	m/z 490–491	$\text{C}_{30}\text{H}_{50}\text{O}_5$ (m/z 490.3658)
CHEMSPIDER	58,938	173
CAS REGISTRY	171,904	2,366
CSLS	na ^a	250 (81NP's)
DICTIONARY OF NATURAL PRODUCTS	653	292
DICTIONARY OF MARINE NATURAL PRODUCTS	94	44
MARINLIT	78	35
ANTIMARIN	118	43

^aIt is not possible, at this stage of development, to search CSLS for molecular mass information. Molecular formula searches can be carried out and 250 matches found with 81 of these in the Natural Product section of the database

MARINLIT still records variolin B as the only compound with that molecular formula while in SciFinder there are 79 compounds recorded with that molecular formula. However, it is usually necessary to have more than just molecular mass/molecular formula data for the dereplication process.



When dealing with natural product extracts, there can be problems and uncertainty in obtaining reliable molecular mass/molecular formula data. This could arise because:

- the mass spectrometry sample is only one or two fractionation steps removed from the crude extract, and there are multiple candidates for the supposed molecular ion from impurities;
- such impurities could dominate the ionization giving misleading results;
- there can be ionization suppression problems from traces of TFA (often used as a polar modifier in HPLC);
- of ready fragmentation, even under ESMS conditions;
- of formation of adduct ions (MNa^+ , MNH_4^+ , etc.).

Some of these problems have been very nicely addressed by a group at the Danish Technical University group who, in the area of mycotoxins and fungal metabolites, compiled a database of 474 compounds using standardized HPLC/UV/MS methodology [22] (see Table 6.1).

6.5.3 Dereplication Based on UV Data

UV profiles or maxima are readily acquired using a Diode Array Detector (DAD) as part of the LC or LC/MS examination of a crude extract. That the data are semiquantitative at best is not relevant. What is important are the actual profiles, or the maxima (λ_{\max}), as the chromophores that lead to these spectral properties are distinctive and can be searched for. The UV spectra and λ_{\max} are indicative of a *chromophore* within a structure, not necessarily the structure itself and therefore offers clues as to potential substructures that can be searched for, for example, the 1,2,3,5-tetrasubstituted aromatic system characteristically found in compounds of polyketide origin. Compounds containing this chromophore have a characteristic UV profile with

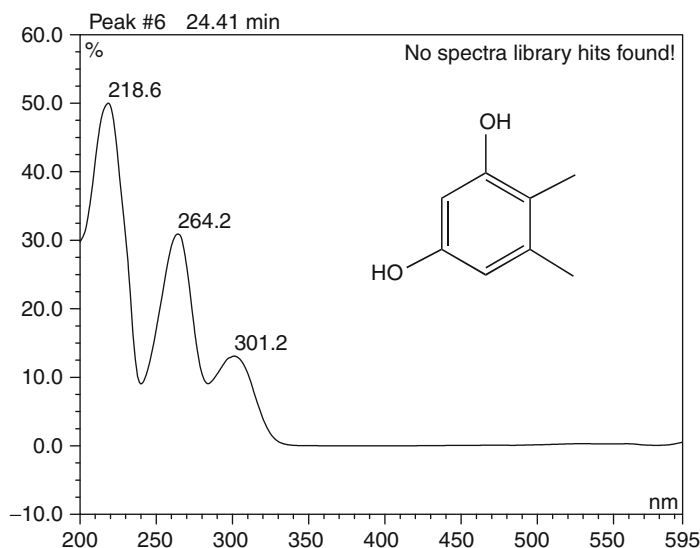


Fig. 6.1 The characteristic UV profile of a 1,2,3,5-tetrasubstituted aromatic system

λ_{\max} at around 220, 265, and 300 nm (see Fig. 6.1) that is easily recognizable. Using UV data with mass data is a powerful and cheap method of dereplication. The one major drawback to this approach is that not all compounds contain UV chromophores.

6.5.3.1 UV λ_{\max} Data

Among the natural product databases, a number contains searchable UV λ_{\max} data, though in some cases this is partial coverage only (see Table 6.2). An example of this approach to dereplication is work that was carried out on a bioactive extract obtained from the deep-water sponge *Lamellomorpha strongylata* [23]. All of the bioactivity associated with this extract eluted in the early fractions from an LH-20 column (higher molecular mass compounds) and the two components in these early fractions each had identical and characteristic chromophores (see Fig. 6.2).

A search was made in MARINLIT using the following search profile: Phylum = Porifera; Mass range 750–2,000; UV = 340 (see Fig. 6.3). The database returned 16 matches from 22,000 possible compounds. Within MARINLIT it is possible to select a second UV maxima and refine the search. This was done using the second maxima at 226 nm and resulted in just nine compounds that matched. All but one of these compounds were calyculin derivatives. Based

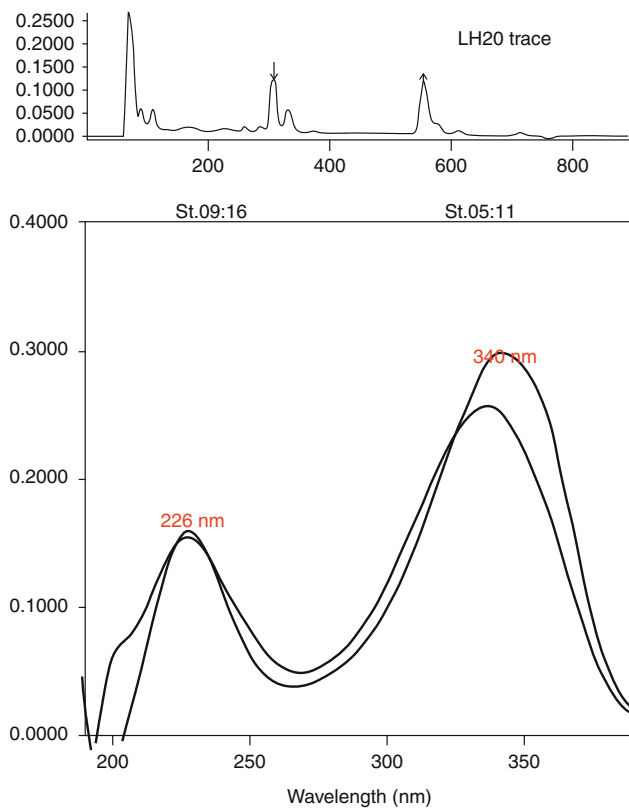


Fig. 6.2 HPLC trace (detection at 340 nm) and extracted UV data for the peaks at 320 and 550 s from an LH-20 column (Fraction 1)

on these data, the two bioactive compounds from *Lamellomorpha strongylata* were rapidly identified as calyculin A and a new, but related compound, calyculinamide A (**2**).

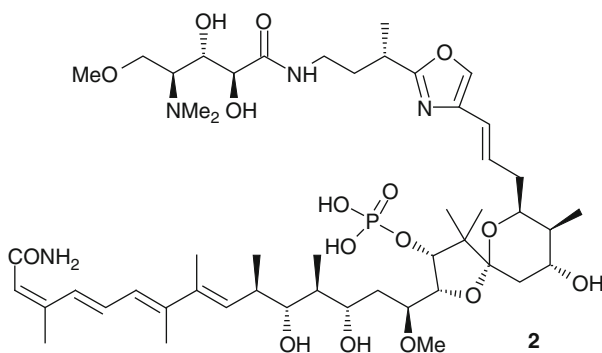


Fig. 6.3 Search profile in MarinLit

The screenshot shows a 'Search Profile' window with the following sections:

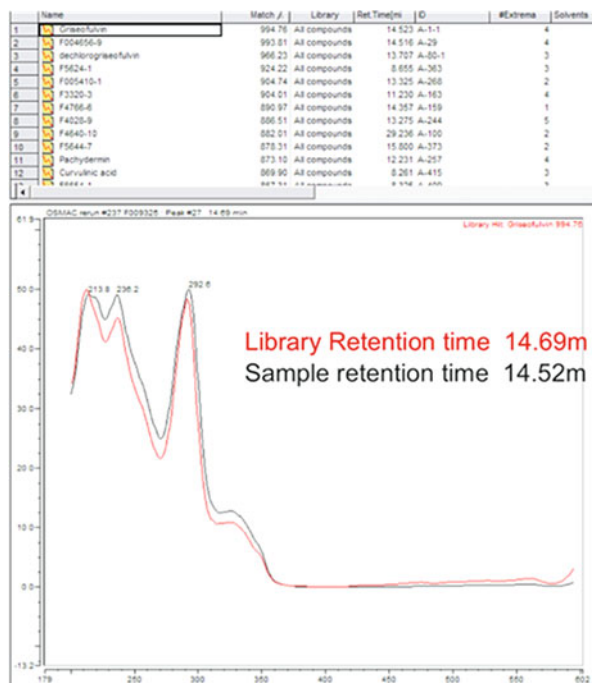
- BIBLIOGRAPHIC DATA**: An empty text box.
- AND**: A connector between sections.
- COMPOUND DATA**: A text box containing 'Mass FROM 750 TO 2000 AND UV max = 340e5'. Below it, in smaller text, is '(AND operations only)'.
- AND**: A connector between sections.
- TAXONOMY DATA**: A text box containing 'Phylum IS Porifera'. Below it, in smaller text, is '(OR operations only)'.
- AND**: A connector between sections.
- SUBSTRUCTURE**: A section with instructions: 'Enter substructure in ChemDraw window, select, use command c to put structure on clipboard, then double click on Gen' and 'Paste substructure into Subs.pct window, and then close Subs.pct window.' There is a 'Gen' button.

On the right side of the window, there are three buttons: 'clear all', 'do search', and 'home screen'.

6.5.3.2 UV Spectra

There is considerably more information contained in the UV spectrum than just the λ_{max} data. Matching spectra is a superior and more definitive approach to the use of UV spectra in the dereplication exercise. Such approaches have been commented on in the primary literature, and it can be assumed that all pharma carrying out natural product research and quite a number of other natural product laboratories have in-house UV spectral databases. Unfortunately, no UV spectral databases that also contain other information essential to the dereplication process are available. Apart from privacy and IP issues, a major difficulty is the platform to be used for comparing the spectra. Most modern HPLCs have the necessary software for capturing and comparing UV acquired spectral data, but not for comparing that data with spectra acquired on other HPLCs. For the past 10 years in the Marine Group at the University of Canterbury, all UV data from all extracts is archived in a searchable library (All Compounds). Once the identity of compound is established, the UV profile is added to a second library (Known Compounds). As all HPLC runs have been carried out using the same solvents, column manufacturer, and gradient profile the retention times as well as the UV profiles of unknowns can be run against the library and, frequently, unknowns can be identified by UV/retention time correlations only [24]. An example illustrates just how useful this approach can be for compounds with distinctive UV chromophores. By this approach, griseofulvin was identified as a metabolite from a marine fungus (see Fig. 6.4). Note the close match between the retention times of the unknown and the reference sample as well as the comparable UV spectra. The library provides a score, out of 1,000, for the closeness of the spectral match – the griseofulvin score was 994. As appropriate, the retention time window can be widened or eliminated altogether in order to match against the UV spectrum only.

Fig. 6.4 DAD UV spectrum of griseofulvin compared with that stored in the known compounds library



6.5.4 NMR-Based Approaches to Dereplication

^1H NMR spectra are rich in structural information, which in combination with 2D homo- and heteronuclear experiments, molecular mass, molecular formula, and UV data lead to structural assignments. Inherently, there are two drawbacks to the routine use of NMR techniques for dereplication purposes where a rapid answer to the question of novelty is required. The first of these is sensitivity. Of the spectroscopic techniques routinely used in organic structure determination, NMR spectroscopy is by far and away the least sensitive. The limit of detection for routine mass spectrometers is in the 1–10 pg range (10^{-12} g), that for UV spectroscopy 100–1,000 pg, while for most routine NMR spectrometers, 500–1,000 μg are required for ^1H NMR measurements and about five times that for ^{13}C NMR spectroscopy. In recent years, the limit of detection for ^1H NMR has dropped to 1 μg using specialist probes (see Sect. 6.8). This is still 10^6 times less sensitive than mass spectrometry. The implications are that it is possible to obtain excellent LC/MS and associated UV data by the analysis of micrograms of crude extract, but to get NMR data on the components of a crude extract, it is necessary to process mgs or even grams of crude extract.

The second drawback is that of complexity. In order to derive substructures for database searching, interpretation of the 1D and 2D NMR data is required.

Depending on the complexity of the molecule this can sometimes be a complex process, but the derived substructures can then be searched for in any of the natural product databases (Table 6.2). There are also spectral databases available, such as ACD/Labs and SPECINFO, which can be searched to find a match based on molecular formula comparisons. And in the Public Domain arena (Table 6.1), there are other spectral sources that can be searched. These are the likes of NMRSHIFT DB, NAPROC-13, SUPERNATURAL and SDBS [25–28]. From the natural product databases listed in Table 6.1, only ANTIbase and MARINLIT have searchable NMR data. MARINLIT, in an arrangement with ACD/Labs, can provide calculated ^1H and ^{13}C chemical shift data for any of the individual compounds in the database along with ^{13}C and HSQC/DEPT spectra based on the ACD predictors (see Sect. 6.3.7.2), allowing the ready checking of actual NMR data against that stored for individual compounds in MARINLIT identified using other parameters. MARINLIT also allows for the direct searching of the database for individual or a series of ^{13}C chemical shifts. ANTIbase provides partial lists of actual or calculated ^1H and/or ^{13}C NMR data which are also searchable.

ANTIMARIN is a combination of parts of the MARINLIT and ANTIbase databases. Both this combined database and MARINLIT have a search capability that is not readily available in any other database. This is the capability of searching for the actual numbers of functional groups contained within a molecule. Certain features in a ^1H NMR spectrum are immediately obvious and do not need any interpretation to know what they are. The number and types of methyl groups in a molecule would be a good example. Within these two databases, the number and type of methyl group, alkenes, carbinol protons, acetal, formyl, acetyl, amide, imine, aromatic substitution patterns, sp^3 methines, and methylenes and sp^2H have been extracted and placed in searchable fields. A simple inspection of a ^1H NMR spectrum and integrals immediately allows the identification of many of the classes of functional group listed above, but *with no consideration* of any relative connectivity. Entry of the relevant numbers for each functional group, along with other relevant data such as taxonomy, molecular mass, molecular formula, provides a very effective method for the dereplication of natural products extracts as the ^1H structural features (^1H -SF) aspect built into ANTIMARIN and MARINLIT is very discriminating.

6.5.4.1 Why ^1H -SF is Discriminatory

^1H structural features (^1H -SF) allows the examination of combinations of structural features in a molecule. The probability of compounds having identical combinations of ^1H NMR features is low, and if these data are also taken in combination with molecular mass, molecular formula and UV data unique search patterns are generated which can quickly establish the novelty of an isolated compound. The page for each compound in ANTIMARIN displays the relevant UV, MS, and ^1H -SF features for that compound. This is displayed in Fig. 6.5 which highlights features such as the Me groups and the 1,4-disubstituted benzene. The search data are entered via a simple graphical interface comparable to that shown in the figure.

Two simple examples will serve to demonstrate this selectivity. In the first instance, the simple act of counting the number of methyl groups in a compound

The screenshot displays the ANTIMARIN database interface. On the left, a chemical structure of Kodastatin-A is shown with various functional groups highlighted by colored circles: a red circle around a carboxylic acid group, a green circle around a double bond, a blue circle around a triple bond, and a yellow circle around a phenol group. Below the structure, the following data is provided:

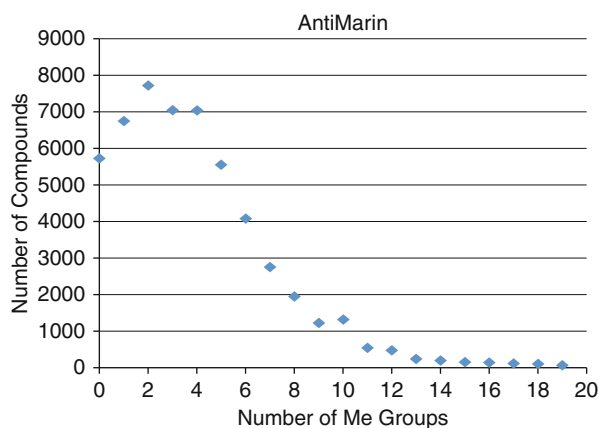
ID Number	23683	formula	C ₃₅ H ₃₄ O ₁₁	molecular weight	630.638
HRMS	630.209595	HRMSP	631.217407	HRMSN	629.202891
				HRMSNa	653.199402
Name	Kodastatin-A				
Source	Aspergillus terreus Thom DSM 11847				

On the right, a grid of searchable fields is shown, each with a numerical value:

UV_Neutral	MeOH (292, 45500) (333sh,)		
All CH3	Singlet CH3	Doublet CH3	Triplet CH3
4	2	1	1
sp3_methylene	sp3_methine	all_alkene	vinyl
2	2	5	0
trisub_alkene	all_single_co	pi_single_co	sec_single_co
2	7	0	1
tert_acetal	all_carbonyl	aldehyde	acetyl
0	4	0	1
amide	B1	B12	B13
0	0	0	0
B135	B1234	B1235	B1245
0	0	0	1
Py4	Py23	Py24	Py25
0	0	0	0
Py234	Py235	Py236	Py245
0	0	0	0

Fig. 6.5 ANTIMARIN showing a range of the data in searchable fields

Fig. 6.6 Distribution of compounds containing methyl groups in the ANTIMARIN database



is informative. Figure 6.6 shows the distribution of the ~52,000 compounds containing methyl groups in the ANTIMARIN database. Of particular relevance is the large number of compounds (~6,000) with zero methyl groups. The second example focuses on the types of methyl group recognized in the MARINLIT and ANTIMARIN databases. There are eight types in all (singlet Me, doublet Me, triplet Me, -OMe, -SMe, -NMe, vinyl Me, and acetyl Me). For compounds that contain any two methyl

Table 6.4 The distribution of combinations of any two methyl groups in the *ANTIMARIN* database

	Singlet	Doublet	Triplet	Vinyl	Acetyl	-OMe	-NMe	-SMe
Singlet	1,000							
Doublet	268	1011						
Triplet	153	589	813					
Vinyl	279	385	151	400				
Acetyl	72	168	244	77	93			
OMe	509	435	401	217	148	490		
NMe	78	77	50	30	18	132	223	
SMe	0	4	2	6	5	17	16	91

4 × Me groups (any type) 7,674 hits, or
 1 × formyl group 2,578 hits, or
 1 × 1,4-disubstituted benzene 2,201 hits, or
 1 × 1,2,4-trisubstituted benzene 2,425 hits, or
 1 × 1,2,3,5-tetrasubstituted benzene 3,090 hits

But

4 × Me (any type) + 1 × formyl 358 hits, or
 2 × Me(s) + 2 × Me(d) + 1 × formyl 43 hits, or
 2 × Me(s) + 2 × Me(d) + 1 × 1,4-disubstituted benzene 13 hits, or
 2 × Me(s) + 2 × Me(d) + 1 × 1,2,4-disubstituted benzene 8 hits, or
 2 × Me(s) + 2 × Me(d) + 1 × 1,2,3,5-tetrasubstituted benzene 3 hits

Fig. 6.7 Results from searching on easily recognized functional groups or combinations

groups, 8,385 in the database, there are 36 possible combinations. The distribution from searching all 36 combinations is shown in Table 6.4 and illustrates just how discriminating this approach to dereplication is with all possible combinations of two methyl groups out of eight types being populated to one level or another. That was just using methyl groups as the discriminator. If other easily recognized groups such as formyl, 1,4-disubstituted-, 1,2,4-trisubstituted-, and 1,2,3,5-tetrasubstituted benzenes are now added into the mix, the level of discrimination rises. This is shown in Fig. 6.7. Quite large numbers of possible hits are obtained by searching on individual groups, but by looking at combinations, the number of possible hits is rapidly narrowed (Table 6.4 and Fig. 6.7).

Take the example of the search based on a ^1H NMR spectrum that contained two singlet and two doublet methyl groups and a 1,2,3,5-tetrasubstituted benzene. Using the ^1H NMR data alone, as detailed in Fig. 6.7, the search was narrowed to just three possibilities from 53,000 compounds (see Fig. 6.8) and if low resolution mass data was then added (ESMS: MH^+ $m/z = 321$), the unknown could be tentatively identified as debromohamigeran E (that was originally isolated from the sponge *Hamigera taragensis*) [29]. To confirm that assignment, the original literature would now be consulted and direct comparisons made with the NMR and other relevant spectral data.

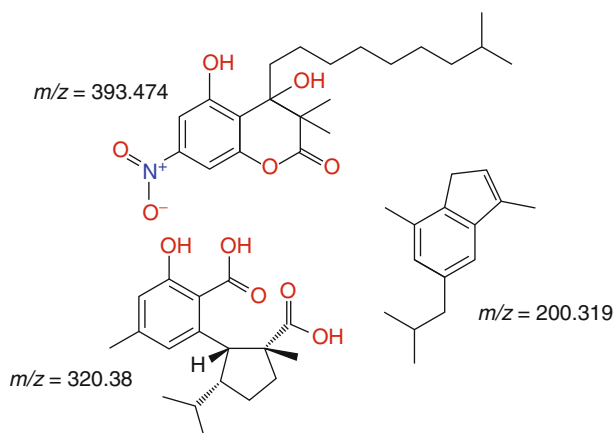


Fig. 6.8 Candidates from search on 2xMe(d) + 2xMe(s) + 1,2,3,5-tetrasubstituted benzene

6.6 Examples of Dereplication

Very seldom is it possible to dereplicate a crude extract without accessing several pieces of information about the components in the extract. Most often these data would be combinations of the source taxonomy, molecular mass/molecular formula, UV, and NMR data. With access to appropriate natural product databases, it is then possible to verify the novelty or not of the components of the extract. In the sections that follow, several worked examples will show how this can be achieved.

6.6.1 Compound Isolated from a Cnidarian

Several compounds were isolated from the crude extract of a cnidarian, possibly a *Minabea* sp. The compound of interest had a low resolution molecular mass of 470, had a UV λ_{max} at 240 nm, and a ^1H NMR spectrum which contained a number of easily recognizable features (see Fig. 6.9).

6.6.1.1 Taxonomy Approach

A search in MARINLIT using Phylum = Cnidaria gave a total of 2,807 articles containing 4,491 compounds. This clearly is not sufficiently discriminating, but if the cnidarian was indeed a *Minabea* sp., the search is narrowed down to just five articles and 21 known compounds. When the mass data of the compound of interest

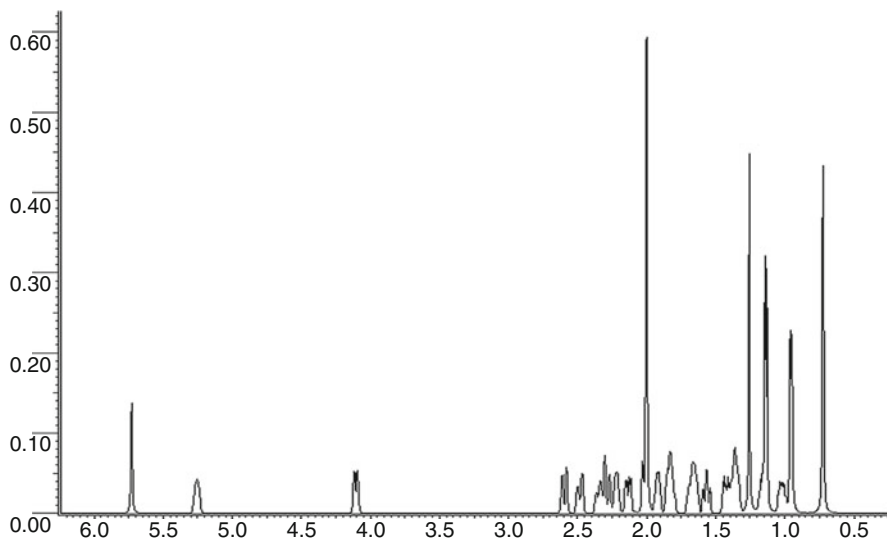
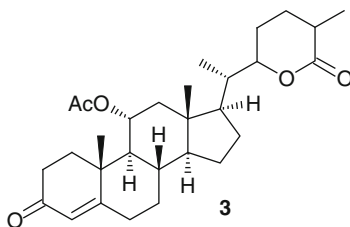


Fig. 6.9 ^1H NMR spectrum of compound isolated from a cnidarian

was searched against the database, four compounds matched and all had the molecular formula $\text{C}_{29}\text{H}_{42}\text{O}_5$. If the UV data, indicative of an $\alpha\beta$ -unsaturated ketone, is added into the profile, only one compound, minabeolide-8 (**3**), matched. This process would have effectively dereplicated the compound of interest in that extract.



6.6.1.2 Alternative Approaches

If the taxonomic data that in combination with the mass and UV data allowed assignment of structure had not been available, what alternative approaches could have been made? There are several possibilities. Examination of the ^1H NMR data suggests that the compound contains five methyl groups of which three are singlets and two are doublets. Of the singlets, one of these ($\delta = 2.05$) could readily

be assigned as an *-OAc*. Using search profiles in MARINLIT gives the following results:

Cnidaria	2,807 articles/4,491 compounds
Cnidaria + $\lambda_{\text{max}} = 240 \text{ nm}$	198 articles/355 compounds
Cnidaria + UV + $m/z = 470\text{--}471$	5 articles/5 compounds
Cnidaria + UV + $m/z = 470\text{--}471 + 5 \times \text{Me groups}$	1 article/1 compound

giving the same answer as before.

An alternative search profile based initially on ^1H NMR data could be

$5 \times \text{Me groups}$	1,774 articles/3,166 compounds
$5 \times \text{Me groups} + 3x \text{ singlet}/2x \text{ doublet}$	264 articles/424 compounds
$5 \times \text{Me groups} + 3x \text{ singlet}/2x \text{ doublet} + 1x\text{-OAc}$	64 articles/77 compounds

If the source phylum is now entered, the number of articles is 42 articles/33 compounds and, finally with the mass data, the numbers drop to 1 article/1 compound.

What if only NMR data were used? There are other resonances that can be used from the ^1H NMR spectrum. For instance, the 1-H resonances at δ 4.2, 5.25, and 5.75 can readily be assigned as $2x\text{-CH-O-}$ and $1x > \text{C} = \text{CH-}$. Using these data produces the following:

$5 \times \text{Me groups} + 3x \text{ singlet}/2x \text{ doublet} + 1x\text{-OAc}$	64 articles/77 compounds
$5 \times \text{Me groups} + 3xs/2xd + 1x\text{-OAc} + 1x > \text{C} = \text{CH-}$	24 articles/26 compounds

If the alternative argument had been used the answer would have been

$5 \times \text{Me groups} + 3xs/2xd + 1x\text{-OAc} + 2x \text{-CH-O-}$	17 articles/19 compounds
--	--------------------------

Using just ^1H NMR data, it was still possible to reduce the number of possible candidates to acceptable levels. Addition of the mass data (m/z 470–471) brought the selection down to one compound from one article.

6.6.2 Dereplication of a *Suberites* sp. Extract

The extract from an Antarctic *Suberites* sp. of sponge collected by SCUBA at 40 m was bioactive against the P388 cell line. The bioactive compound was isolated and partially characterized. The molecular mass was 220.04691 Da ($\text{C}_{10}\text{H}_8\text{N}_2\text{O}_4$), the λ_{max} was 348, and from the ^1H NMR spectrum, a 1,2,4-trisubstituted benzene

system (doublet, doublet, singlet) and a trisubstituted alkene were recognizable. Notable was the lack of methyl groups in the compound. A search using m/z 220–221 Da in MARINLIT returned 106 matches, but a search with $C_{10}H_8N_2O_4$ gave zero matches and established the possible novelty of the compound. To gain clues as to a possible structural type, the balance of the preliminary structural data was incorporated into a search profile:

λ_{\max} 348	249 matches
λ_{\max} + 0x Me groups	63 matches
λ_{\max} + 0x Me + 1x 1,2,4-trisub. bz	11 matches
λ_{\max} + 0x Me + 1x 1,2,4-trisub. bz + 1x > C = CH–	4 matches
λ_{\max} + 0x Me + 1x 1,2,4-trisub. bz + 1x > C = CH– + m/z 220–221	0 matches

There were matches in the database right up to the point where the mass was entered. If the four matches are now examined (see Fig. 6.10), three can be quickly eliminated on the basis of disparity in mass, leaving one compound that differed by just 1 Da from a known compound: $C_{10}H_8N_2O_4$ (m/z 220) compared with $C_{10}H_9N_3O_3$ (m/z 219) for polyandrocarpamine previously isolated from the Fijian ascidian *Polyandrocarpa* sp. [30] With this structural clue, a hydantoin

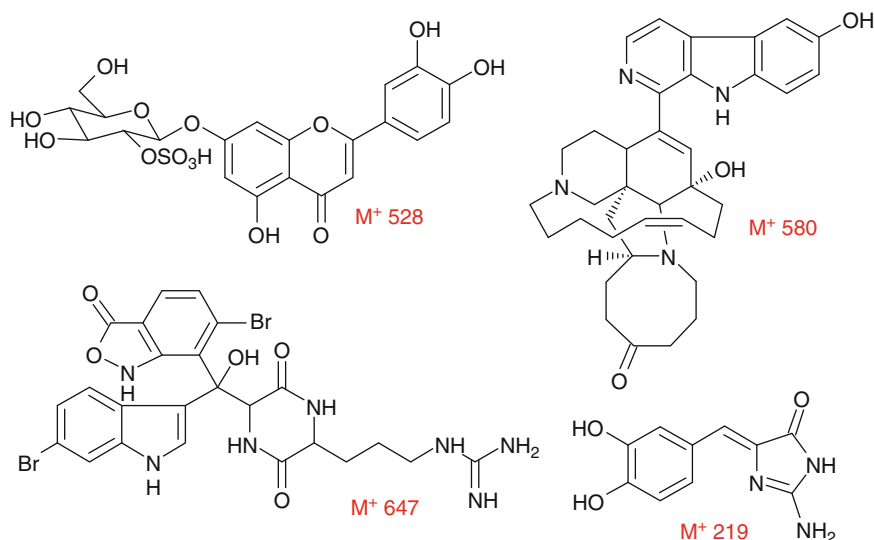
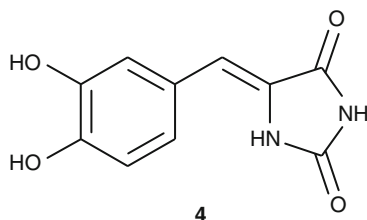


Fig. 6.10 Possible structures matching UV and NMR data from an Antarctic *Suberites* sp.

structure (4) was quickly established for the bioactive compound from the *Suberites* sp.: it was a new compound [31].

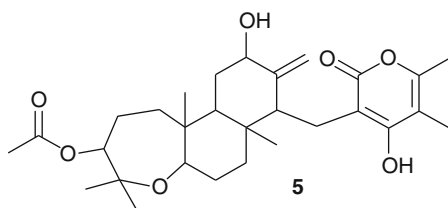


In this instance, just using molecular formula data was sufficient to establish that a new compound had been isolated, but interrogation of the database using other preliminary data gave essential clues as to the identity of the new compound.

6.6.3 Dereplication of an *Aspergillus* sp. Extract

Although not isolated from a marine source, the dereplication of this extract is a good example of the power of the ^1H -SF approach to solving problems. The ^1H NMR spectrum of a bioactive component isolated from the extract of an *Aspergillus* sp. isolated as an endophyte from *Garcinia scortechnii*, a Malaysian medicinal plant, contained seven singlet methyl groups (see Fig. 6.11). As the compound was isolated from a microorganism, the ANTIMARIN database was consulted returning just 387 possible hits out of 53,000 compounds in the database. Consideration of the chemical shift data suggested that of the seven singlet methyl groups, two were vinyl methyls and one an acetoxyl group. This refined search reduced the number of hits to five only. If the low resolution mass data (502 Da) was now added, one hit only was returned. Comparison of the ^1H NMR data with published data for this compound (5) [32] established that they were identical and completed the dereplication. The structural elucidation of three further isomers was then trivial based on the established core structure of this unusual triterpene-pyrone [33].

Alternative approaches would have used the low resolution mass data first. That would have given 91 hits reducing to just two if seven singlet methyls were included in the profile of which only one would have matched the ^1H NMR data obtained.



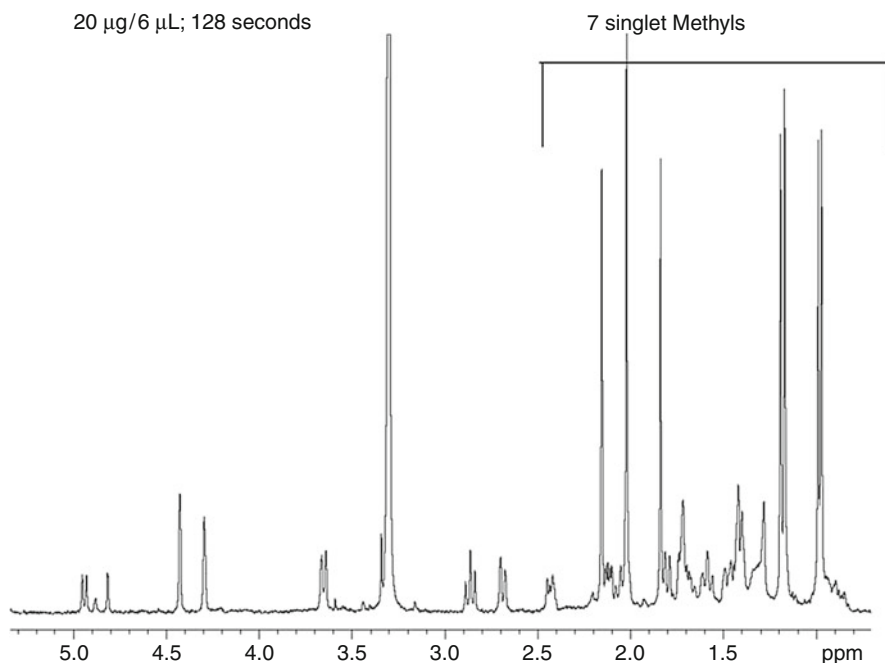


Fig. 6.11 ^1H NMR spectrum for a triterpene pyrone isolated from an *Aspergillus* sp. endophyte

6.7 Commentary on Approaches to Dereplication

In the section above, various approaches to achieving resolution in the dereplication process were considered. The obvious starting point is normally the molecular mass and the molecular formula, but with over 160,000 known natural products, this is not often discriminatory. Adding in taxonomic data can help narrow the dereplication to a class of compound. UV spectral data is a powerful tool in the dereplication process but is not discriminatory as it is the recognition of the chromophore, not the molecule that is occurring, and not all compounds contain chromophores. Fragmentation patterns from mass spectrometry also provide a powerful approach but require experience and skill in interpretation. The MS approach, like that of UV spectroscopy, suffers from a lack of appropriate searchable databases. The ultimate goal in dereplication is full structure determination, but to accomplish that for each and every compound in a crude extract is not a satisfactory approach and requires acquisition and interpretation of full sets of 1D and 2D NMR data in addition to relevant mass and UV data. Such a conventional approach to dereplication is shown diagrammatically in Fig. 6.12a. The alternative approach, as outlined above, is to more productively use a *minimal* set of data that helps define a structure. The recognition that a search

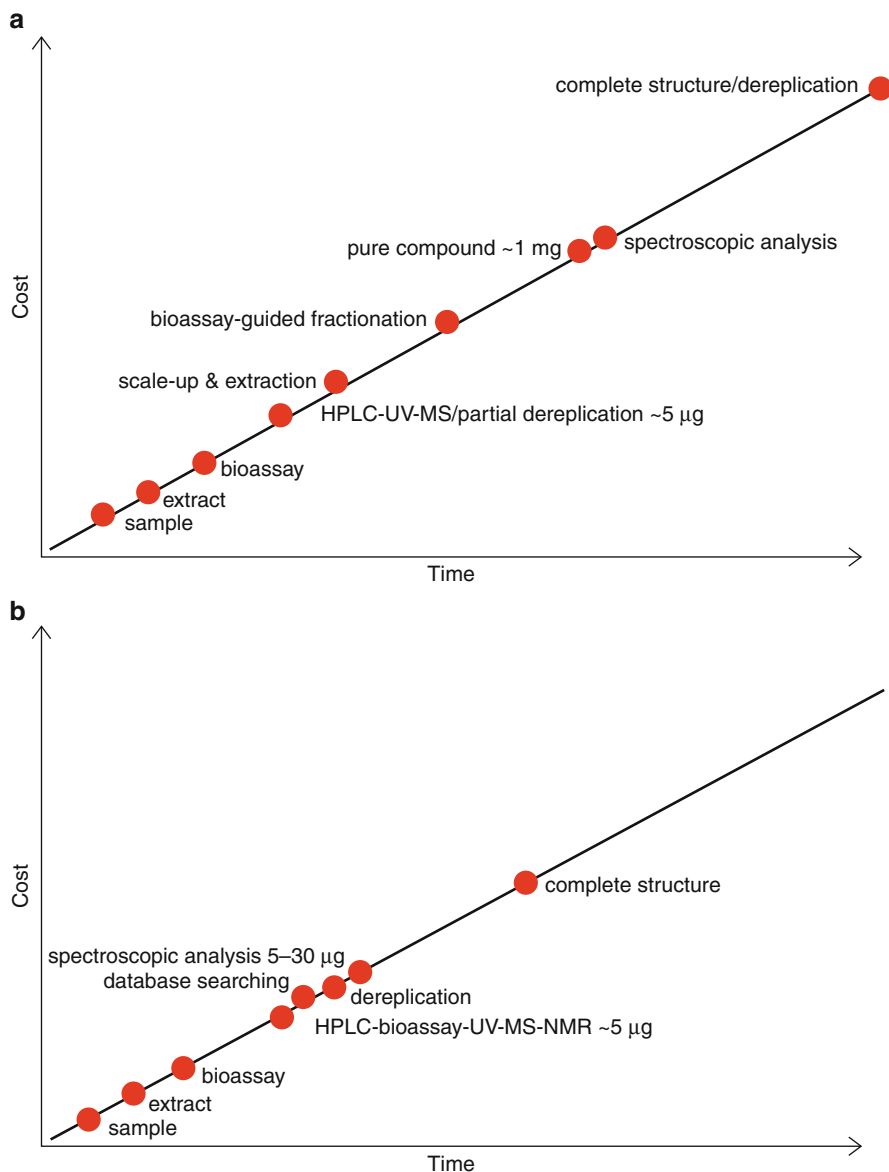


Fig. 6.12 (a) Conventional approach to dereplication; (b) Dereplication based on ^1H -SF approach and nanomole-scale NMR determinations

based on the numbers of functional groups easily recognizable by ^1H NMR spectroscopy was a powerful method for discriminating between alternative structures was the starting point for the development of the ^1H structural features aspect of MARINLIT and subsequently ANTIMARIN. These are the only two databases that have such functionality. This approach allows dereplication to be accomplished and

novelty established shortly after the ^1H NMR spectrum has been obtained and before a full interpretation of the data (see Fig. 6.12b).

This ^1H -SF-based approach to dereplication is well illustrated in one last example. Two isomeric compounds of molecular mass 490.3658 Da, corresponding to the molecular formula $\text{C}_{30}\text{H}_{50}\text{O}_5$ were isolated from a soft coral. Use of the various databases to look for possible structures based on this mass data has already been commented on in Table. 6.3. The ^1H NMR data and interpretation for one of the isomers is shown in Fig. 6.13. Without reference to mass data and simply relying on methyl group count and type, the number of possible hits in MarinLit was reduced to 43. If other information was then used, such as the four 1-H carbinol protons (δ 3.5–4.9) and the trisubstituted alkene (1-H; δ 6.35), the hits were progressively reduced to three and then two hits which corresponded to the 11-acetoxy and 12-acetoxy isomers shown in Fig. 6.13, which were first isolated from the soft coral *Capnella lacertiliensis* in 2003 [34].

If mass data had been used with the NMR interpretation, the same definitive result would have been achieved but with less NMR interpretation ($\text{C}_{30}\text{H}_{50}\text{O}_5$ gave 35 hits; $\text{C}_{30}\text{H}_{50}\text{O}_5 + 3 \times \text{Me}$ singlets + $4 \times \text{Me}$ doublets gave 7 hits). Either approach would have lead to a full and definitive answer as to whether these were new compounds or not. The actual assignment of structure to the isomers would then be by comparison against the original data. So as with the other cases examined, dereplication has

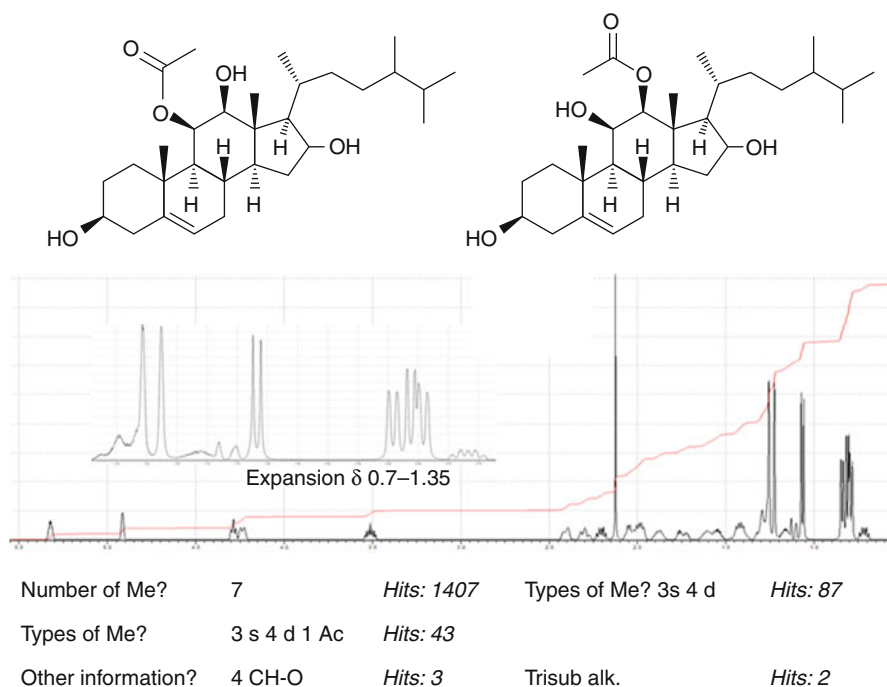


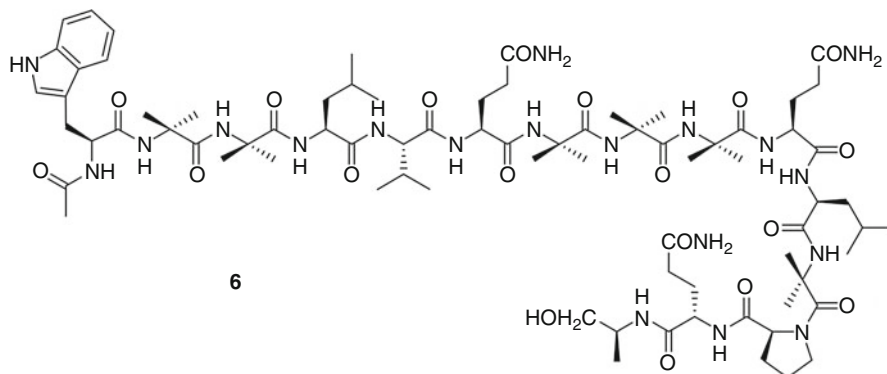
Fig. 6.13 NMR-based dereplication strategy for compounds isolated from a soft coral

been carried through quickly and efficiently and did not rely on a full structural assignment.

6.8 Dereplication at the Nanomole Level

The recent advances in NMR probe design has led to cryoprobes [35] and capillary flow probes [36] that yield 1D and 2D NMR spectra with excellent signal/noise ratios on just 2–20 μg of sample in a matter of minutes for a ^1H NMR spectrum to an hour or so for the likes of a COSY NMR to several hours only for an HMBC spectrum. An example of such a ^1H NMR spectrum is shown above in Fig. 6.11. This spectrum was obtained on 20 μg of material in 6 μL of CD_3OD in less than 2 min. This enormous advance in the relative sensitivity of the NMR experiment quickly led to numerous papers on compounds isolated at the μg level and has led to the description of a microtiter plate-based dereplication built around a Protasis CapNMR probe [37] and the MARINLIT/ANTI-MARIN databases [12, 14]. Essentially, 200–500 μg of extract are injected onto a RP-18 analytical HPLC column using an acetonitrile/water gradient (10–70% acetonitrile over 22 min) with the effluent from the column collected into 88 wells (250 μL /well) after UV and ELSD monitoring. Two daughter plates are prepared by removing 5 μL /well for biological testing and mass spectrometry. The master plate is dried and after bioassay of the daughter plate the MS and ^1H NMR spectra of the bioactive well(s) are obtained. These data can be immediately searched in databases and dereplication achieved. If a new compound has been detected, then further NMR data as necessary can be collected while the sample is still in the probe which meets the optimal pathway suggested in Fig. 6.12b. If a known compound had been detected, the work could be halted at that juncture.

An example of this approach would be the isolation, characterization, and structural elucidation of a new peptaibol, chrysaibol (**6**) from an extract of the fungus *Sepedonium chrysospermum* [38]. This work was carried out with an estimated 30 μg of chrysaibol isolated during HPLC analysis into the microtiter plate. This included obtaining 2D NMR data. Dereplication on the nanomole scale is possible and practicable using the database-assisted processes described in this chapter.



6.9 Relative Costs of the Databases

The cost of database searching is a real consideration. The larger databases such as REAXYS or the various version of CAS, such as SciFinder, are particularly expensive with the actual cost calculated based on factors such as the number of licenses and location. Such databases are usually paid for by central libraries at institutions rather than by individual groups. The specialized natural product databases cost considerably less and, in the main, are initially more useful for the natural product chemist. Estimates of the relative costs of the relevant databases are given in Table 6.5. Gaining access to relevant databases is not cheap, but efficient dereplication procedures can save considerable time and circumvent wasted effort leading to the more efficient throughput of samples by the researchers which is a money saver. Figure 6.12a and b attempt to depict this aspect of efficient dereplication in terms of a time/cost exercise. In Corley's 1994 paper on the strategies for database dereplication, he estimated that "in our laboratory that for each natural product dereplicated, at an average cost of \$300 of online time (using STN databases), a savings of \$50,000 is incurred in isolation and identification time." [39] If that was a true cost/benefit analysis in 1994, imagine the benefits in 2012 and into the future? Databases play an essential role in the dereplication of natural product extracts (Table 6.5).

6.10 Study Questions

1. What are the advantages and disadvantages of using a specialist database to extract specific data in a narrow field such as marine natural products as opposed to using a generalist, all encompassing database such as CAS Registry?

Table 6.5 Relative costings of the databases useful in natural products research

DATABASE	Cost	Number of compounds	
		Total	Natural products
SciFINDER	>US\$50,000	6.3×10^7	~260,000
CSLS	free	4.6×10^7	extracts
CHEMSPIDER	free	2.6×10^7	?
PUBCHEM	free	3.7×10^7	?
REAXYS	>US\$40,000	$>10^7$	170,000
NAPRALERT	US\$0.5/citation		>150,261
DICTIONARY OF NATURAL PRODUCTS	US\$6,600		159,670
ANTIMARIN ^a	\$0		53,000
ANTIBASE	US\$3,500		36,000
DICTIONARY OF MARINE NATURAL PRODUCTS	US\$625		22,691
MARINLIT	US\$1,850		22,000

^aTo obtain a copy of ANTIMARIN it is first necessary to be a current subscriber to the ANTiBASE and MARINLIT databases

2. In the dereplication of a natural product extract, suggest a minimal data set that would establish the uniqueness of each compound isolated.
3. What are the pitfalls that may be encountered when using taxonomic data in a dereplication exercise?
4. Outline the problems that would be encountered if molecular mass or molecular formulae only were used in a dereplication exercise?
5. Suggest reasons why a database that includes NMR characteristics for each compound is more likely to be discriminating than any based on other spectral and physical properties such as mass, molecular formulae, UV, MS fragmentation, or IR.

References

1. Buckingham J (ed) (2011) Dictionary of natural products on DVD. Chapman & Hall/CRC, Boca Raton
2. CAS, www.cas.org. Accessed 18 Nov 2011
3. Reaxys, <https://www.reaxys.com/info/>. Accessed 18 Nov 2011
4. CAS Registry, www.cas.org/expertise/cascontent/registry/index.html. Accessed 18 Nov 2011
5. STN, <http://www.stn-international.de/index.php?id=123>. Accessed 18 Nov 2011
6. SciFinder, <http://www.cas.org/products/scifinder/>. Accessed 18 Nov 2011
7. ChemNetBase, <http://www.chemnetbase.com/>. Accessed 18 Nov 2011
8. Blunt JW, Munro MHG (eds) (2008) Dictionary of marine natural products. Chapman & Hall/CRC, Boca Raton
9. Jaspars M (2008) Underwater chemistry. Chem World 5(Jan). <http://www.rsc.org/chemistryworld/Issues/2008/January/Reviews.asp>. Accessed 18 Nov 2011
10. AntiBase, <http://www.wiley-vch.de/publish/dt/books/forthcomingTitles/LS00/3-527-32827-0/?sID=fdd57124490d0f87cfd550f72e2684d5>. Accessed 18 Nov 2011
11. SpecInfo, <http://cds.dl.ac.uk/cds/datasets/spec/specinfo/specinfo.html>. Accessed 18 Nov 2011
12. MarinLit, <http://www.chem.canterbury.ac.nz/marinlit/marinlit.shtml>. Accessed 18 Nov 2011
13. ACD/Labs, <http://www.acdlabs.com>. Accessed 18 Nov 2011
14. AntiMarin: a combination database formed from AntiBase and MarinLit. <http://www.wiley-vch.de/publish/dt/books/forthcomingTitles/LS00/3-527-32827-0/?sID=fdd57124490d0f87cfd550f72e2684d5> and <http://www.chem.canterbury.ac.nz/marinlit/marinlit.shtml>. Accessed 18 Nov 2011
15. <http://depth-first.com/articles/2011/10/12/sixty-four-free-chemistry-databases/>. Accessed 18 Nov 2011
16. Williams AJ (2008) Public chemical compound databases. Current Opin Drug Discov Develop 11:393–404
17. PubChem, <http://pubchem.ncbi.nlm.nih.gov/>. Accessed 18 Nov 2011
18. CCLS, <http://cactus.nci.nih.gov/lookup/>. Accessed 18 Nov 2011
19. ChemSpider, <http://www.chemspider.com/>. Accessed 18 Nov 2011
20. NaprAlert, <http://www.napralert.org/>. Accessed 18 Nov 2011
21. Perry NB, Ettouati L, Litaudon M et al (1994) Alkaloids from the Antarctic sponge *Kirkpatrickia variolosa* Part 1: Variolin B, a new antitumor and antiviral compound. Tetrahedron 50:3987–3992
22. Nielsen KF, Smedsgaard J (2003) Fungal metabolite screening: database of 474 mycotoxins and fungal metabolites for dereplication by standardized liquid chromatography-UV-mass spectrometry methodology. J Chrom A 1002:111–136

23. Dumdei EJ, Blunt JW, Munro MHG et al (1997) Isolation of the calyculins, calyculinamides and swinholid H from the New Zealand deep water sponge *Lamellomorpha strongylata*. *J Org Chem* 62:2636–2639
24. The Marine Group, University of Canterbury's UV data was acquired on a Dionex HPLC using Chromeleon software. The library of known compounds is available on application to murray.munro@canterbury.ac.nz or john.blunt@canterbury.ac.nz
25. NMR Shift DB, <http://nmrshiftdb.nmr.uni-koeln.de/>. Accessed 18 Nov 2011
26. Naproc-13, <http://c13.usal.es/c13/usuario/views/inicio.jsp?lang=en&country=EN>. Accessed 18 Nov 2011
27. SuperNatural, <http://bioinformatics.charite.de/supernatural/>. Accessed 18 Nov 2011
28. SDBS (Spectral Database for Organic Compounds), http://riodb01.ibase.aist.go.jp/sdbs/cgi-bin/cre_index.cgi?lang=eng. Accessed 18 Nov 2011
29. Wellington KD, Cambie RC, Rutledge PS et al (2000) Chemistry of sponges 19. Novel bioactive metabolites from *Hamigera taragensis*. *J Nat Prod* 63:79–85
30. Davis RA, Aalbersberg W, Meo S et al (2002) The isolation and synthesis of polyandrocarpamines A and B. Two new 2-aminoimidazolone compounds from the Fijian ascidian, *Polyandrocarpa* sp. *Tetrahedron* 58:3263–3269
31. MacLean WJ (2005) Unpublished results. PhD thesis. University of Canterbury, Christchurch
32. Suzuki K, Kuwahara A, Nishikiori T et al (1997) NF00659A1, A2, A3, B1 and B2, novel antitumor antibiotics produced by *Aspergillus* sp. NF 00659. II. Structural elucidation. *J Antibiot* 50:318–324
33. Sun Lin (2009) Unpublished work. PhD thesis. University of Canterbury, Christchurch
34. Wright AD, Goclik E, König GM (2003) Oxygenated analogues of gorgosterol and ergosterol from the soft coral *Capnella lacertiliensis*. *J Nat Prod* 66:157–160
35. See for example <http://www.bruker-biospin.com/cryoprobes.html>, or http://www.varianinc.com/cgi-bin/nav?products/nmr/probes/liquids/cold_probes/index&cid=LNMJOLHKFI. Accessed 18 Nov 2011
36. <http://www.protasis.com/OMNMR/index.htm>. Accessed 18 Nov 2011
37. Lang G, Mayhudin NA, Mitova MI et al (2008) Evolving trends in the dereplication of natural product extracts: new methodology for rapid, small-scale investigation of natural product extracts. *J Nat Prod* 71:1595–1599
38. Mitova MI, Murphy AC, Lang G et al (2008) Evolving trends in the dereplication of natural product extracts. 2. The isolation of chrysaibol, an antibiotic peptaibol from a New Zealand sample of the mycoparasitic fungus *Sepedonium chrysospermum*. *J Nat Prod* 71:1600–1603
39. Coreley DG, Durley RC (1994) Strategies for database dereplication of natural products. *J Nat Prod* 57:1484–1490
40. GVK Biosciences Natural Product DB, http://www.gvkbio.com/db_products.html. Accessed 18 Nov 2011
41. Lei J, Zhou J (2002) A marine natural product database. *J Chem Info Comput Sci* 42:742–748
42. Bitzer J, Kopcke B, Stadler M et al (2007) Accelerated dereplication of natural products, supported by reference libraries. *Chimia* 61:332–338
43. Moss S, Bovermann G, Denay R et al (2007) Efficient structure elucidation of natural products in the pharmaceutical industry. *Chimia* 61:346–349
44. The National Centre for Plant and Microbial Metabolomics, <http://www.metabolomics.bbsrc.ac.uk/currentactivities.htm>. Accessed 18 Nov 2011
45. CH-NMR-NP, <http://www.las.jp/english/software/chnmnp.html>. Accessed 18 Nov 2011

Jaime Rodríguez, Phillip Crews, and Marcel Jaspars

Contents

7.1	Methods in Common Use in Structure Elucidation Analysis	424
7.2	Steps in Establishing a Molecular Structure	431
7.3	Looking for the Molecular Formula (MF) and the Unsaturation Number (UN): Mass Spectrometry	433
7.3.1	Different Ways of Producing Ions: Ionization Techniques	434
7.3.2	The Search of the Molecular Formula Through Mass Spectrometry	443
7.3.3	Ion Analyzers and Mass Accuracy	447
7.3.4	Terms in Mass Spectrometry	449
7.4	Substructures, Working Structures, and Final Structures: Nuclear Magnetic Resonance (NMR)	454
7.4.1	Chemical Shifts and Peak Areas	455
7.4.2	Factors that Determine Chemical Shifts	456
7.4.3	Chemical Shift Positions of $^1\text{H}/^{13}\text{C}$ Attached to Common Functional Groups	457
7.4.4	Discovering Substructures from NMR: Scalar Coupling	461
7.4.5	The Nuclear Overhauser Effect	475
7.4.6	Multipulse NMR	477
7.5	Complementary Spectroscopic Techniques: IR and UV	492
7.5.1	Confirming Functional Groups: Infrared Spectroscopy	492
7.5.2	Confirming Functional Groups: UV Spectroscopy	496

J. Rodríguez (✉)

Departamento de Química Fundamental, Campus da Zapateira. Universidade da Coruña,
A Coruña, Spain

e-mail: jaime.rodriguez@udc.es

P. Crews

Department of Chemistry and Biochemistry, University of California, Santa Cruz, CA, USA

e-mail: crews@chemistry.ucsc.edu

M. Jaspars

Department of Chemistry, Marine Biodiscovery Centre, University of Aberdeen, Aberdeen, UK

e-mail: m.jaspars@abdn.ac.uk

7.6	Limitations of Spectroscopic Data in Structure Analysis	500
7.7	Study Questions	504
	References	514

Abstract

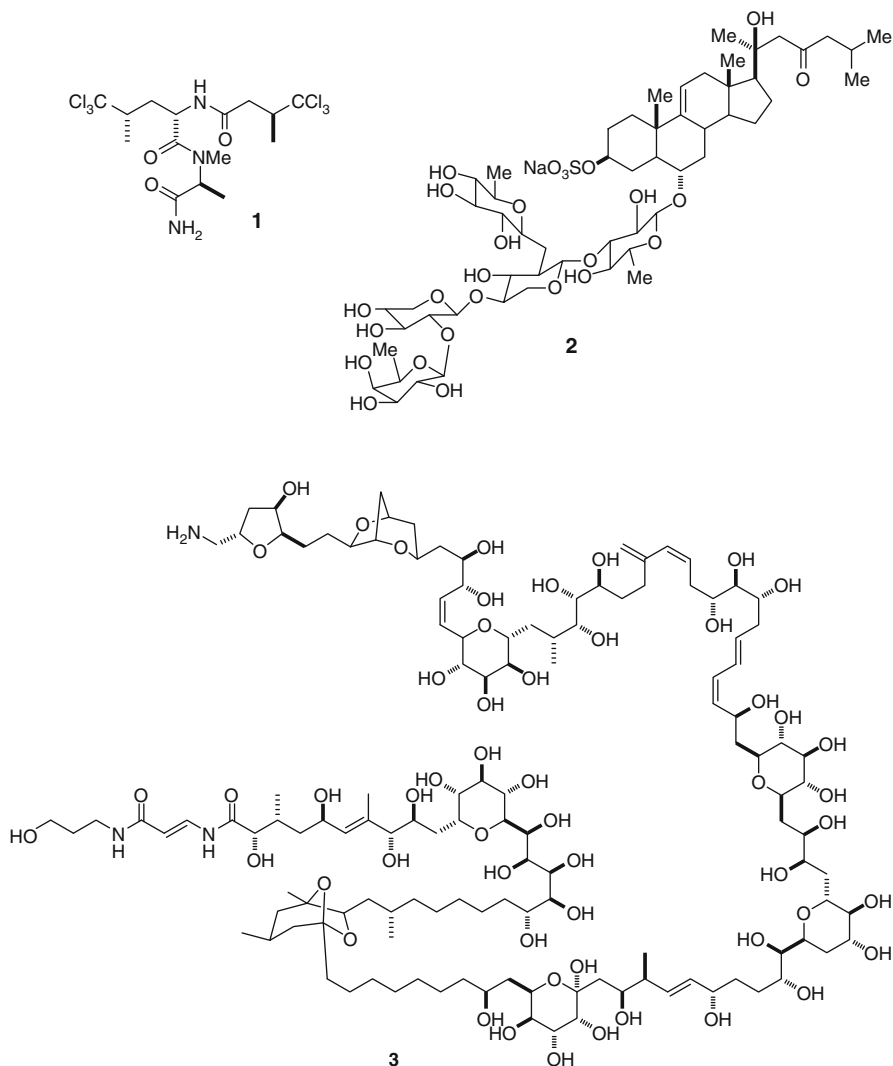
This chapter will describe the four primary spectroscopic techniques utilized for organic structure analysis: *nuclear magnetic resonance* (NMR), *infrared* (IR), *ultraviolet–visible* (UV–VIS), and *mass spectrometry* (MS). Each of these methods is used on a daily basis by most organic chemists in the course of structure elucidation analysis, requiring a very small amount of material in a generally nondestructive approach.

7.1 Methods in Common Use in Structure Elucidation Analysis

Four primary spectroscopic techniques for organic structure analysis have been in use since the early 1960s [1]. They are *Nuclear Magnetic Resonance* (NMR), *Infrared* (IR), *Ultraviolet–visible* (UV–VIS), and *Mass Spectrometry* (MS) [2]. Each of these methods is used on a daily basis by most organic chemists in the course of structure elucidation analysis, requiring a very small amount of material in a generally nondestructive approach. The use of NMR, IR, UV–VIS, and MS should be supplemented by another well-known, powerful tool, *X-ray crystallography*. However to use this technique typically requires well-formed crystals, and liquids or powders are not suitable for analysis.

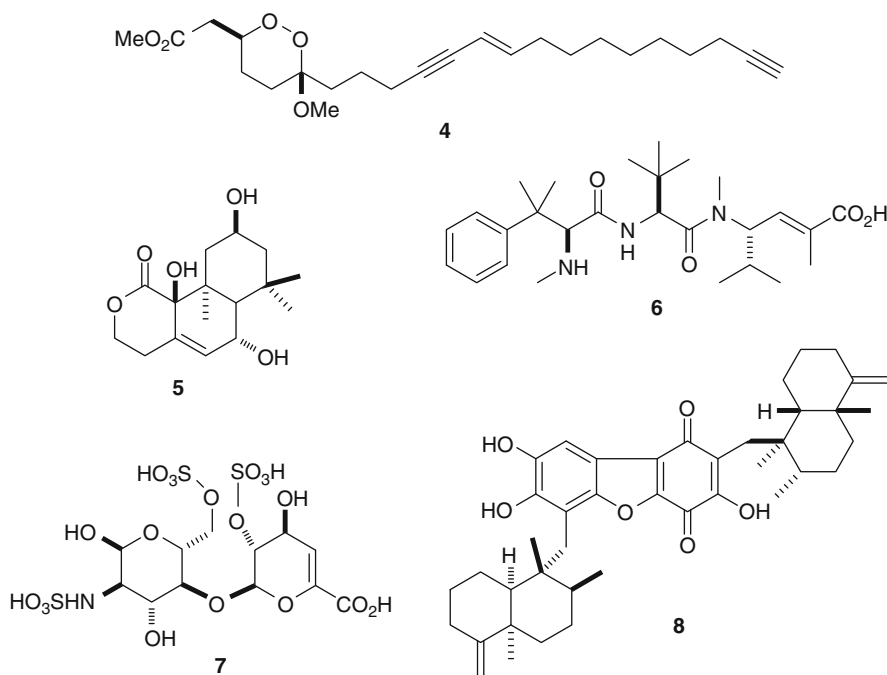
Compounds with molecular weights of less than $\sim 1,500$ amu are excellent candidates for study by the methods of organic spectroscopy, and this is the case for more than 95% of marine natural products. It is generally believed that the unequivocal structure analysis of such small organic compounds by spectroscopic methods is now a routine task. Powerful tools, widely available, consisting of multidimensional NMR, ultrahigh resolution mass spectrometry, tandem mass spectrometry, and chiroptical measurements should all be used in combination. As an illustration, collecting one or more pieces of such data allows a scientist to rapidly recognize the presence of the hexachlorinated dysidenamide (**1**) (504.98 amu, $C_{15}H_{23}Cl_6N_3O_3$), produced from the symbiotic association of the sponge *Dysidea herbacea* with the filamentous cyanobacterium *Oscillatoria spongeliae* [3]. A data set consisting of a mass spectrum alongside a 1H NMR spectrum would help distinguish this structure from other polychlorinated analogs, which are also ubiquitous in the sponge-bacterium association. A synergistic approach of using MS, 1H NMR, and ^{13}C NMR data provides immense power especially in the characterization of substances rich in H atoms and methyl groups. For example, utilizing such data makes it possible to completely assemble the structure of glycoside-steroids such as ophidianoside F (**2**) (1234.54 amu, $C_{56}H_{91}SO_{26}Na$) a sea star derived toxin [4].

Representative of more complex structures that can be solved using one or more of these tools, NMR, IR, UV–VIS, and MS, includes descriptions of the molecular architecture of exceedingly atom rich natural products. Perhaps at the top of the list is the intricate structure of the polyether marine product palytoxin (**3**) of mass 2679.48 amu and molecular formula $C_{129}H_{223}N_3O_{54}$. Its seemingly “never ending” structure was initially proposed based on spectroscopic data. But the process of collecting the appropriate data, making unambiguous interpretations, and reevaluating the data, including that obtained from total synthesis, took some 20 years.



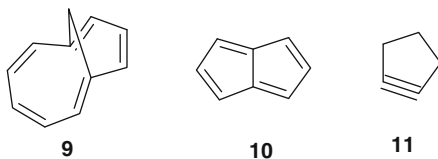
Using multiple pieces of analytical data is the best recipe to efficiently establish or validate an important molecular structure. A brief review of selected examples

from several compound classes provides some useful lessons. The peroxyacarnic methyl ester (**4**) (404.26 amu, $C_{24}H_{36}O_5$), a marine polyketide, whose signature functional groups are identified by NMR, IR and UV data, its molecular formula was determined by the election of the right ionization technique. Laying out the complete list of the functional groups of strobilactone (**5**) (296.16 amu, $C_{16}H_{24}O_5$), a sesquiterpene of marine origin with inhibitory activity against cultured COLO 201 cells, was challenging because no heteroatom protons were visible in the 1H NMR spectrum. The peptide HTI-286 (**6**) (473.32 amu, $C_{27}H_{43}N_3O_4$), a synthetic hemiasterlin-like antitumor agent, is rich in methyl and carbonyl residues [5]. Great atom diversity is present in the major disaccharide heparin-like **7** (576.97 amu, $C_{12}H_{19}NO_{19}S_3$) obtained from the marine mollusk *Callista chione* [6]. Not to be overlooked is that in recent years, advances in NMR and MS instrumentation and in experimental techniques have even made it possible to tackle the structure elucidation of very complex compounds, made up of nonrepeating biosynthetic subunits. However, connoisseurs of this subject recognize that even when all of these tools are applied, errors can be made and other considerations including organic synthesis may be needed. To be discussed later in this chapter are several cases taken from the literature where difficulties were encountered in deriving correct molecular structures.



To be successful in the task of structure elucidation analysis, especially when an exotic compound is in hand, requires several attributes. In addition to chemical common sense [7], five other aspects are important:

- A general knowledge of principles of organic structures is essential. You should also have an understanding of common functional groups. Being able to pick out the quinone alkaloid substructure present in popolophuanone E (**8**), a potent inhibitor of the topoisomerase II [8], provides a simple illustration about dealing with functional groups. It is important to have facility for conceptualizing structures that are especially stable, such as homoazulene (**9**) (a nonbenzenoid aromatic); exceedingly unstable, for instance pentalene (**10**) (a planar $4n$ π -electron system); or immensely strained, such as cyclopentyne (**11**).
- Using an organized and systematic approach (see Figs. 7.1 and 7.2).
- A good understanding of how to interpret spectroscopic information is essential (see Table 7.1).
- An appreciation of the dangers of using negative or unreliable data to make positive conclusions about a molecular structural feature is important (see Table 7.8).
- An ability to maintain a proper perspective in situations where conflicting data sets seem to be in hand. When this occurs, it is helpful to draw on experience gained from past successes in problem solving. Finally, to simultaneously use data from NMR, IR, UV–VIS, and MS and to look repeatedly for multiple pieces of data to support individual conclusions should be considered as an ultimate goal. Taking time to reevaluate a conclusion will also help to avoid mistakes. This can be accomplished by defending the logic of how a structure was elucidated before a critical audience (e.g., the practice of peer review).



Determining a complete organic molecular structure begins with the isolation or synthesis of a *pure* compound. Spectroscopic data is then obtained to derive the following information: (a) molecular formula, (b) identities of functional groups, (c) carbon connectivities, (d) positions of substituents and functional groups on the carbon framework, and (e) stereochemical properties including static and dynamic aspects. The overall flow of information processing is summarized in Fig. 7.1.

The step-by-step approach actually used in organic structure determination will vary greatly as a function of several variables, such as the source of the material under study. In the case of new compounds, an extensive data set must be obtained for a newly isolated natural product when its structure is presumed to be unknown. Undertaking a complete analysis of *all* the data from each of the four spectroscopic methods is not always the most effective way to proceed. An infrared or a mass spectrum can contain more information than can be correlated with specific elements of organic structure, so only a portion of the data obtained is useful. Also, data from the four spectroscopic techniques are not equivalent in the extent to which they will aid the identification of various organic structural elements.

Fig. 7.1 Steps in establishing a molecular structure

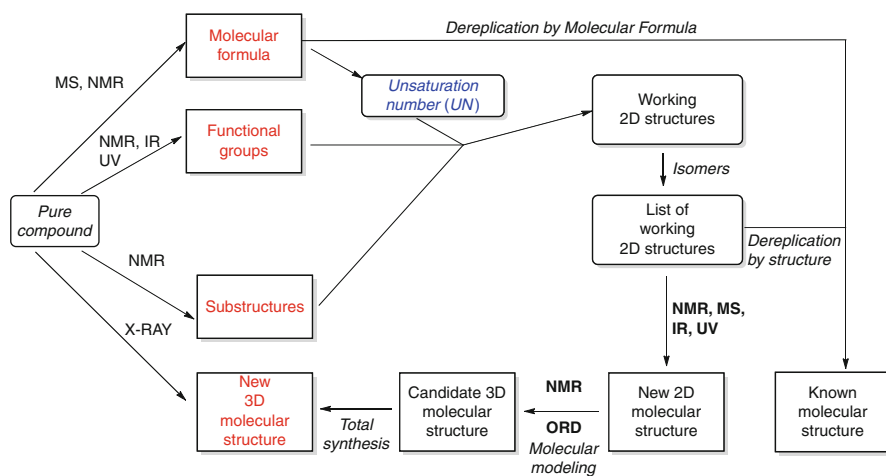
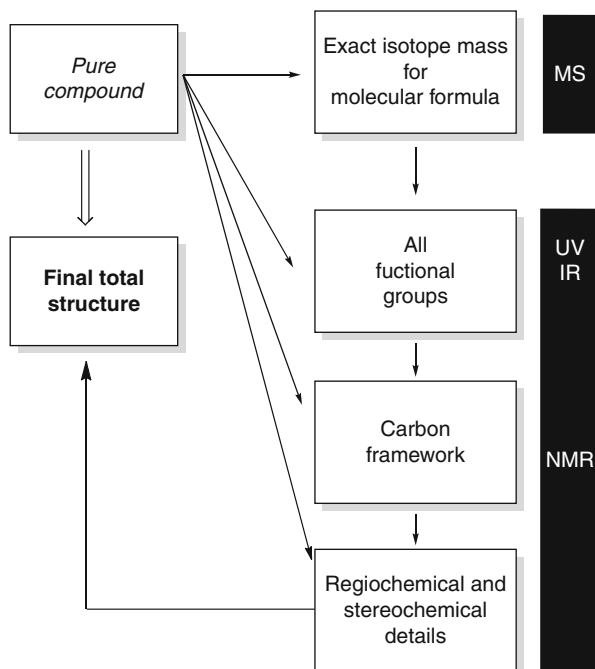
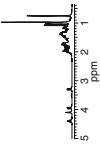
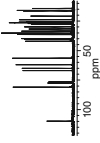

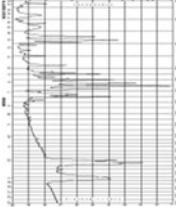
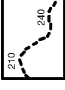

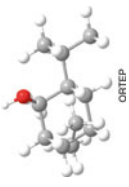


Fig. 7.2 The road map to organic structure analysis

Table 7.1 Characteristics of important spectrometric methods in common use

	¹ H NMR	¹³ C NMR	MS	IR/RAMAN	UV-VIS	ORD/CD	X-RAY
Spectral scale	0–15 ppm	0–220 ppm	50–4,000 amu	400–4,000 cm ^{–1}	200–800 nm	185–600 nm	Not relevant
Average sample	≈1 mg	≈5 mg	<1 mg	<1 mg	<1 mg	<1 mg	Single crystal
Molecular formula	Partial	Partial	Yes	No	No	No	Yes
Functional groups	Yes	Yes	Limited	Yes	Very limited	Very limited	Yes
Substructures	Yes	Limited	Yes	Limited	Limited	No	Yes
Carbon connectivity	Yes	Yes	No	No	No	No	Yes
Substituent regiochemistry	Yes	Yes	No	Limited	No	No	Yes
Substituent stereochemistry	Yes	Yes	No	Limited	No	No	Yes
Analysis of isomer mixtures	Yes	Yes	Yes	Yes	No	No	Yes (if separate)
Purity information	Yes	Yes	Yes	Yes	Limited	Limited	Limited
What is measured	Peak areas	Chemical shifts	Singly or multiple charged ions	Vibrational transitions	Electronic transitions	[α]	Relative atom positions
Chemical shifts							R/S absolute stereochemistry
Coupling		Coupling					
Relaxation		Relaxation					
Typical units	δ (ppm)	δ (ppm)	m/z	cm ^{–1}	nm	nm	–
Typical representations							

It is useful to focus on specific characteristics of the major spectroscopic methods. Summarized in Table 7.1 are properties of nuclear magnetic resonance (NMR), infrared (IR), ultraviolet–visible (UV–VIS), optical rotatory dispersion–circular dichroism (ORD–CD), mass spectrometry (MS), and X-ray crystallography. Take a moment to scan this table, compare the data collected, and become familiar with the limitations of each technique in structure elucidation analysis.

A characteristic of each of these methods, except MS, is that a compound is subjected to irradiation by photons from different regions of the electromagnetic spectrum. It is the electromagnetic waves or photons which initiate the various molecular processes such as nuclear, vibrational, or electronic transitions that result in the various NMR, IR, or UV–VIS “peaks.” In the X-ray method, the very high electromagnetic energy is diffracted by the crystal lattice and a complex pattern results.

Both neutral and charged species can be investigated by NMR, IR, and UV–VIS. As indicated in Table 7.1, the spectral scale in each of these methods is in frequency units. Also, sharp peaks are typically observed in NMR; some regions of the IR spectrum have sharp peaks, while UV–VIS and ORD/CD spectra usually contain very broad peaks. Long-lived radical ions, cations, or anions are generated during MS determinations, but only charged species can be observed by this technique. Some of these ions have the same mass as the original material, but they can also associate to form clusters of higher mass or fragment to species of lower mass. The scale in MS is in units of atomic mass (amu) to charge, or m/z . Overall, it is possible to observe a large number of sharp MS peaks.

Fortunately, both liquid and solid compounds can be easily examined in NMR, IR, and UV–VIS. In addition, no more than just a few mg of a compound are needed for any of these techniques. As a final point, two of the other methods in Table 7.1 have very special sample requirements. A chiral or scalemic compound is needed for ORD/CD, while a crystalline solid is requisite for X-ray analysis.

Nuclear Magnetic Resonance. Many consider NMR to be the most powerful tool in organic structure analysis because it provides direct insight into the backbone of an organic molecule. An NMR spectrum arises from transitions between nuclear spin states, and the ^1H and ^{13}C isotopes are the most common targets although ^{15}N is becoming more common. If one to tens of milligrams of a pure sample is available, then a ^{13}C NMR spectrum or the combination of HSQC/HMBC spectra can be rapidly obtained to provide an analysis of carbon and hydrogen content as accurate as that from either MS or classical combustion analysis [9]. Similarly, ^1H NMR data can also be used to assess hydrogen content, and this can be done on submilligram samples. The identity of various functional groups can often be established entirely by NMR, but this requires careful comparison to data of model compounds from databases or theoretical calculations. Many HC–CH connectivity relationships can be established by two-dimensional homonuclear ^1H – ^1H COSY (correlation spectroscopy) and heteronuclear ^1H – ^{13}C correlation spectra. Finally, nuclear Overhauser enhancement (NOE) data, along with chemical

shift and/or coupling constant data from ^1H and ^{13}C NMR data, can provide stereochemical insights. The use of pulsed field gradients and inverse detection is essential for sample limited situations.

Mass spectrometry is often considered to be second priority in importance for structure elucidation. It involves generating an ionic species of an organic molecule followed by mass analysis with an electric or magnetic field. The data obtained by this process are invaluable for deriving molecular formulas (or partial formulas), and different techniques have been developed to facilitate obtaining a MS peak containing the molecular formula information.

There are several types of *optical spectroscopic methods* in use. Overall, as we saw previously (Table 7.1), their value in organic structure analysis is not as high as data from NMR or MS. These methods are distinguished by the energy of the molecular transition that is examined. Thus, infrared irradiation causes bond vibrational changes, and UV–VIS irradiation causes transitions of the bonding or nonbonding electrons. In general, IR spectroscopy is an excellent tool for identifying certain functional groups, but UV–VIS data can only be applied to molecules with conjugated multiple bonds. The technique of optical rotatory dispersion (ORD) or circular dichroism (CD) is restricted to optically pure (chiral), or enriched (scalemic) compounds, which are subjected to an elliptically polarized source of UV–VIS irradiation. It is the positive or negative nature of ORD or CD spectral peaks which can be used to establish the absolute stereochemistry. This can occur empirically by reference to empirically derived correlation rules, reference spectra, or the results of theoretical calculations.

A lengthy discussion here of X-ray crystallography is not justified, and more information can be obtained from specialized texts [10]. It should be noted that when a suitable crystal is obtained and dereplication efforts have shown that a new compound is in hand, then an X-ray diffraction study ought to be initiated. A major limitation is that many compounds, or their heavy atom derivatives (e.g., *p*-bromobenzoates), are either not crystalline or do not give suitable crystals and thus cannot be subjected to X-ray crystallography.

It is extremely useful to compare data from a sample under study with data of structurally analogous compounds (i.e., standards). Correlation tables serve as an excellent device and are included in many reference sources. One indispensable source of such data is the book by Pretsch et al. *Tables of Spectral Data for Structure Determination of Organic Compounds* [11]. There are many websites emerging that also have such data. Also invaluable are catalogs on paper or online of actual spectra for the major spectroscopic methods.

7.2 Steps in Establishing a Molecular Structure

The process by which a pure compound can be analyzed to establish its molecular structure is outlined in Fig. 7.2. The most direct route would be to obtain a crystal of suitable quality and then subject it to X-ray diffraction analysis. However, this does not represent a practical route for compounds that are resistant to being

crystallized. Thus, for our purposes, the ideal starting point is to obtain the molecular formula (MF). As will be introduced in the next section, an MF can be derived by several methods, and high-resolution mass spectrometry provides the most unambiguous data. The determination of an unequivocal MF is often complicated, so many efforts to establish a molecular structure begin without this information being firmly in hand.

Once obtained the MF is used to calculate the unsaturation number (UN) – the number of multiple bonds and rings. Two other pieces of primary information must also be obtained which include making a list of all functional groups, and conceptualizing the substructures – the frameworks of all carbon/hydrogen containing moieties. It is important to recheck the final list of functional groups and substructures for agreement with the atoms present in the molecular formula. Some common functional groups are easy to pinpoint, such as alkene moieties, aromatic residues, six-membered rings, three-membered carbocyclics, various types of carbonyl groups, alcohol groups, and amines. Alternatively, there are some that can be considered to be harder to recognize. These are headed by cumulenes, ethers and epoxides, thioethers, thiocarbonyls, guanidine groups, isonitriles, imines, and nitro groups.

Combining three elements – the UN, the functional groups, and the substructures – provides the first milestone, creating a *working 2D structure*. This stage in the process is most often reached when there is agreement between the MF, functional groups, and substructures but that does not guarantee that any of these are absolutely correct! The next step is to use the concepts present in the *working 2D structure* to generate a larger list of possible structures. This process will be further illustrated below. Sometimes a compound suspected to be new has already been described in the literature. To check for this possibility, it is wise to engage in a process called “dereplication” [12]. For example, molecular formula searches can be carried out using commercial or proprietary databases. The most comprehensive is the ACS SciFinder, but others such as the Dictionary of Organic Compounds, Chemspider [13], MarinLit [14], and even the Merck Index are useful. The next step involves assessing the properties of the literature “hits” versus those of the compound under investigation. Similar searches can be done using the various *working 2D structures* or *substructures*.

The next hurdle in a structure determination effort is to prune the list of *working 2D structures*. This can also be a difficult task to accomplish and sometimes requires the use of both spectroscopic and chemical data. Assuming that the dereplication efforts have been completed, the compound can be designated as having a *new 2D molecular structure*. To establish the total structure with details of relative stereochemistry (e.g., *R**, *S** designations) and then the absolute stereochemistry (e.g., *R*, *S* designations) represents additional steps in this process [15]. Final tests for the overall structure and stereochemistry relationships might include forming a chiral derivative followed by NMR analysis, additional attempts to obtain crystals for X-ray study, a chiral total synthesis of the proposed structure, and/or theoretical study by molecular mechanics or electronic structure calculations.

7.3 Looking for the Molecular Formula (MF) and the Unsaturation Number (UN): Mass Spectrometry

A compound cannot be considered as characterized until its molecular formula has been established [16]. The classical way to obtain this information is from combustion microanalysis on a carefully dried compound [17]. Elemental analysis data (e.g., % C, H, N) can be used to calculate an empirical formula and is still generally required by many chemical journals before the publication of a new compound [18]. However, it is also recognized that such data only provides a proof of purity, because many molecular formulas can be derived from a single empirical formula. In practice, molecular formula information is obtained in another way: by mass spectrometry (MS).

Once the molecular formula has been secured, it is immediately used to calculate another piece of fundamental information, the *unsaturation number* (UN, degree of unsaturation, or double bond equivalent). The UN is important because it is the sum of the number of multiple bonds and rings present, and as such provides information about the relative complexity of a compound. Equation 7.1 shown below can be used to calculate the UN for any type of compound comprised of carbon, hydrogen, nitrogen, oxygen, sulfur, and halogens. Equation 7.1 is based on comparing the known molecular formula to the theoretical formula expected for a completely saturated molecule, which is C_nH_{2n+2} . Thus, stable ionic species (i.e., $(CH_3)_4N^+$) or radical species (i.e., $R_2NO\cdot$) cannot be directly treated by this Eq. 7.1.

Calculating an unsaturation number (UN)

$$\text{For a compound of } C_aH_bO_cN_dX_e; \quad UN = \frac{[(2a+2)-(b-d+e)]}{2} \quad (7.1)$$

The unsaturation number can be used to compute the number of rings present. This is accomplished by taking the total count of multiple bonds and subtracting it from the unsaturation number. Quantitative hydrogenation is the classical way to determine a count of multiple bonds, but such data must be carefully interpreted because a cyclopropane can also take up H_2 under mild catalytic conditions.

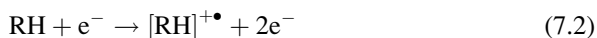
The technique of mass spectrometry does not entail absorption or emission of electromagnetic radiation (review Table 7.1). Rather, it involves visualizing ions of different mass. The essential principle of mass spectrometry is to produce ions from either organic, inorganic, or biomolecules by any suitable methodology, to separate these ions by their *mass-to-charge ratio* (m/z , “m divided by z”), and finally to identify them by their particular m/z values and abundance [19]. Traditionally, the most common technique for producing ions involved electron impact mass spectrometry (EIMS), although electrospray ionization (ESI) has become the most commonly employed technique in the last decade.

7.3.1 Different Ways of Producing Ions: Ionization Techniques

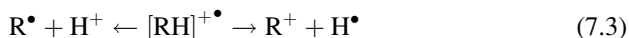
As noted above, the classical way to generate MS ions is by electron impact (EI). However, there are three additional contemporary techniques commonly used for forming ions in mass spectrometry. These are ion molecule reactions, laser desorption, and spray techniques. For the most part, the ionization involves a process that converts analyte molecules into gas-phase ionic species. With so many choices, maximizing the information obtainable from MS depends on matching the compound type to both a particular ionization and an ion detection method.

7.3.1.1 Electron Impact

EIMS analysis involves vaporizing a compound in an evacuated chamber (ca. 10^{-6} – 10^{-5} torr) and then bombarding it with electrons having 25–80 eV (2.4–7.6 MJ/mol) of energy. The high energy electron stream causes a valence electron to be ejected from the compound (symbolized below by RH) under analysis, which generates a radical-cation molecular ion $[RH]^{+\bullet}$ shown below. Since the $[RH]^{+\bullet}$ formed has a great deal of excess energy, this MS method is often referred to as a *hard ionization* process:



In a typical positive ion EIMS, the molecular ion peak is accompanied by numerous additional lower mass fragmentation peaks. However, as is observed in Fig. 7.3 for two C_6H_{14} isomers, in some cases the $[M]^{+\bullet}$ peak can be the base peak and different ionization methods are needed to optimize this situation. The simplest fragmentation of a molecular ion species can occur by a one-bond homolysis or heterolysis, but the former is more common. Each nonequivalent bond in a molecule represents a potential site for such fragmentation, and this can contribute a multitude of distinct species including neutrals, radicals, or ions:



Fragmentation, either by rupture of a bond between two directly connected atoms or by rupture of multiple bonds, will generate many species of discrete mass. Still other new species can arise through molecular rearrangements occurring either before or after a fragmentation event. As might be expected when the number of bonds involved in a fragmentation process increases, the possible combinations of the fragment ion masses will also increase.

The EI mode of ionization is very easy to use and provides library-searchable spectra for a large range of organic compounds. However, a very serious limitation of EI is that many compounds are not stable under these conditions. Another limitation of EI is the requirement that analytes must be in the gas phase prior to ionization. This constraint makes thermally labile and nonvolatile compounds

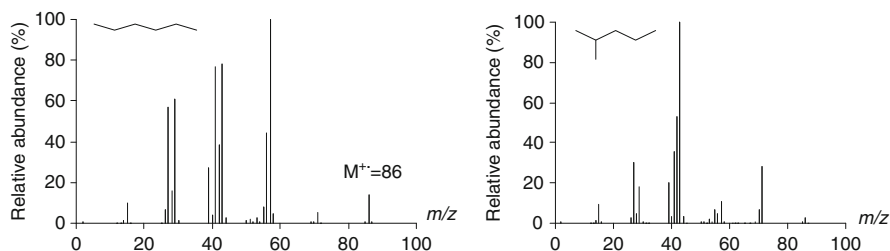


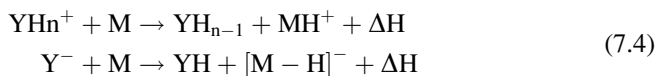
Fig. 7.3 Low-resolution EIMS of two C_6H_{14} (MW 86) isomers

inaccessible to EI, making the determination of the molecular mass challenging. Extensive fragmentation may also make the interpretation of a mass spectrum difficult. Also, there is lack of a causal link between precursor and fragments. A useful mass range for compounds that are amenable to EI is rather low (ca. <1,000 amu).

Alternatively, there are a host of *soft ionization processes* such as chemical ionization and spray ionization techniques that provide an extra approach to obtain MS data. In general, soft ionization results in spectra where the molecular ion dominates [20].

7.3.1.2 Chemical Ionization (CI)

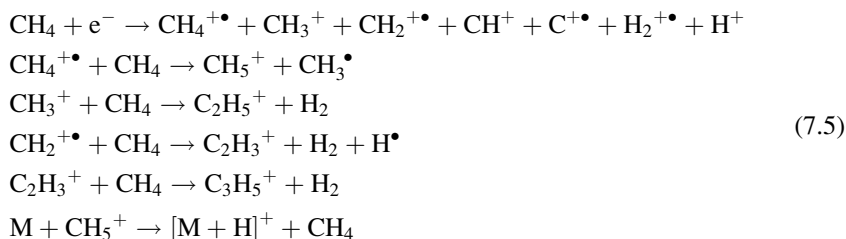
The purpose of CI is to use an *ion-molecule reaction* to maximize the intensity of molecular ions while diminishing that of fragment ions [21]. Relatively high pressures (0.5–1.5 torr) are used, and a substrate is ionized by reaction with the reagent gas (YH) which has been pre-ionized by the electron beam. The ionized reagent gas YH^+ or Y^- can interact with a substrate via proton or charge exchange reactions. Many such reactions are possible, and they are exemplified by those generating positive or negatively charged molecular ions, respectively:



Ion transfer in CI requires a positive ΔH (exothermic reaction). In this context, the ΔH for the reaction that generates the MH^+ is the difference of the proton affinity (PA) of the conjugate base of reagent gas YH minus the PA of the substrate M. In positive CI, the usual choices are ammonia, methane, and hydrogen.

A series of reactions occur to produce the reactive reagent ions. Methane serves as an interesting example because several cation species are formed. The major ones responsible for ion exchange in positive CI are shown in bold below. The process is begun by electron impact reaction with the reagent gas (e.g., CH_4),

followed by a series of ion-molecule reactions according to the following equations:



Clearly, it is important to know what major ions are produced as a function of the reagent gas employed in positive CI. In general, most analytes accessible to EI can be analyzed by CI; however, a major benefit of CI vs. EI is to provide molecular mass information. Another useful feature of CI is selectivity in ionization. The extent of fragmentation can be controlled by the correct choice of a reagent gas. On the other hand, CI has major drawbacks: (a) nonvolatile compounds cannot be studied, and (b) many compounds with polar functional groups are excluded from analysis. The CI data are dependent on experimental conditions, making results from this technique not useful for library-searching of databases. As with EI the mass range for compounds that are amenable to CI is also low (ca. <1,000 amu).

7.3.1.3 Spray Techniques

Spray ionization techniques such as electrospray (ESI), thermospray (TSI), or photospray (APPI) employ the strategy of rapid vaporization [22]. These methods have gained in popularity since 1995 because they are effective for most samples including those unresponsive or unsuited to EI or CI. Currently, ESI is the spray method of choice. Although the concept of electrospray was first conceived by Malcolm Dole in 1968, the development of ESI-MS is attributed to John Fenn, who was awarded the 2002 Nobel Prize in Chemistry for that contribution. The original stimulus for its development was to analyze high molecular weight, nonvolatile materials.

A process analogous to that employed by a perfume atomizer is the basis of spray ionization. A liquid aerosol containing finely dispersed droplets at atmospheric pressure is dispersed from a capillary. During the evaporation of the ionizing solvent by a drying gas such as nitrogen, multiply charged ions are expelled and are extracted by an electric potential difference into the mass analyzer vacuum region of the MS. Thermospray ionization (TSI) was one of the first applications of this process; it is based on passing the droplets through a small heated capillary. The method of ESI involves placing an electric field at the tip of the capillary, which facilitates the process of dispersing charged species from the aerosol. Samples dispersed in aqueous methanolic solution can be directly ionized by ESI, as shown in Fig. 7.4.

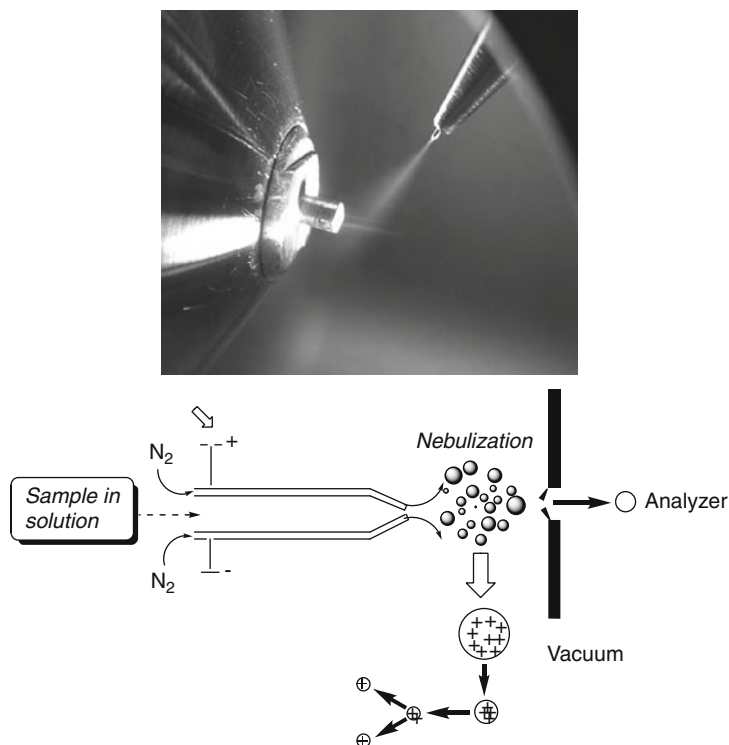


Fig. 7.4 How does electrospray ionization mass spectrometry work?

Electrospray ionization is achieved by passing the sample, in solution, through a metal capillary which is held at a high voltage. As the sample exits the capillary, it is nebulized by a flow of nitrogen gas to produce a fine aerosol of charged droplets. By the use of a flow of nitrogen gas and gentle heating, the droplets evaporate. As the droplets decrease in size, the sample ions in the droplet are forced together until repulsion causes them to be ejected from the surface (ion evaporation followed by a Coulomb explosion). The ions are then extracted through a small orifice into the mass spectrometer vacuum.

An illustration of the type of results obtainable on nonvolatile organic compounds of medium molecular weight is shown in Fig. 7.5a for the HCl salt of the sponge-derived compound manzamine A (**12**) (MW 548). Under positive-ion conditions, an intense $[M + H]^+$ peak occurs at m/z 549.3 for **12**, accompanied by a smaller signal for the $[M + 2H]^{2+}$ peak at m/z 275.2. A singly charged $[M - H]^-$ peak is observed in the negative-ion spectrum of marine-derived steroid **13** at m/z 575.4, as shown in Fig. 7.5b.

It is useful to discuss the strategies for recognizing multiply charged ESI peaks as well as some of the complications that accompany the analysis of high molecular weight substances. A characteristic of some ESI spectra is that clusters of multiply

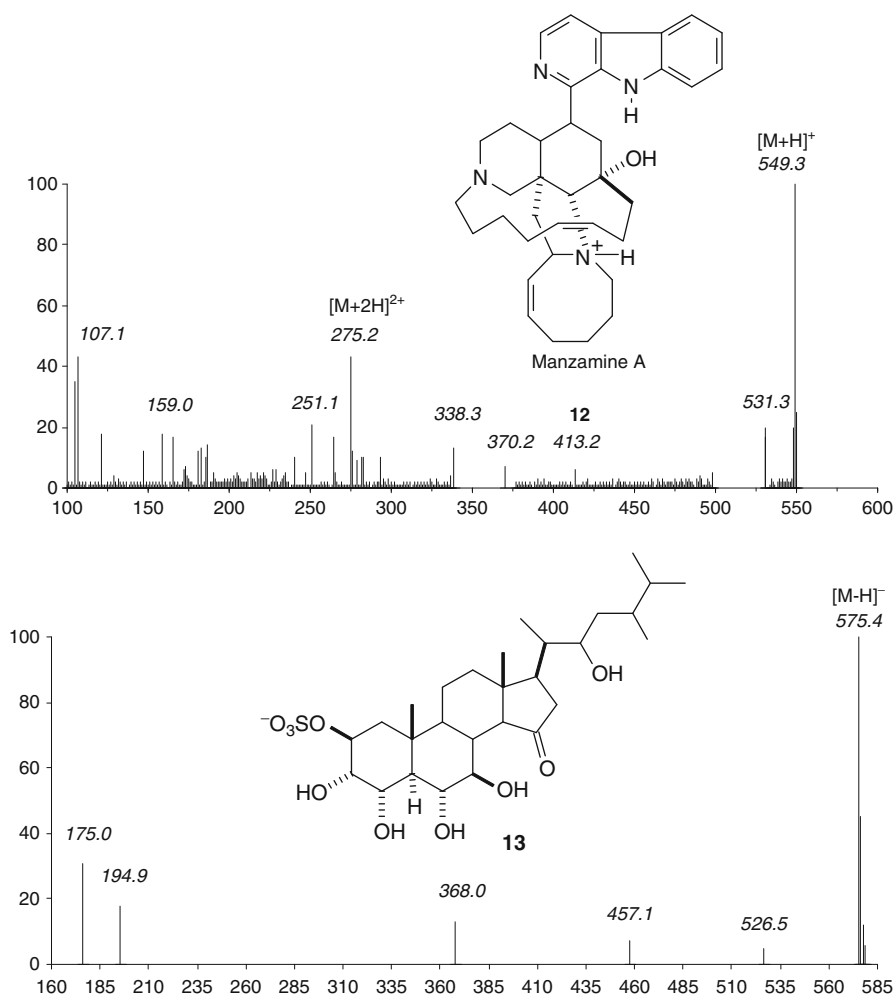


Fig. 7.5 (a) ESI (positive ion) of manzamine A (**12**) ($C_{36}H_{44}N_4O$, MW 548). (b) ESI (negative ion) of a sulfated steroid (**13**) ($C_{28}H_{48}SO_{10}$, MW 576)

charged peaks are observed in either positive mode, $[M + nH]^{n+}$, or negative mode, $[M - nH]^{n-}$, where n may vary from 1 to greater than 15. When a series of multiply charged molecular ion peaks are observed, each peak differs from the neighboring peak by one charge for the positive-ion ESIMS of myoglobin (**14**) (MW 16951.5), as illustrated in Fig. 7.6. A high-resolution scan on any one of the molecular ion peaks of myoglobin will show additional fine structure diagnostic of the number of charges present for that ion.

The isotopic relationships also dictate the appearance of the $[M + 2H]^{2+}$ ion, which has a diagnostic appearance in that the peaks are separated by 0.5 amu; similarly a $[M + 3H]^{3+}$ ion has peaks separated by 0.33 amu. So the actual charge

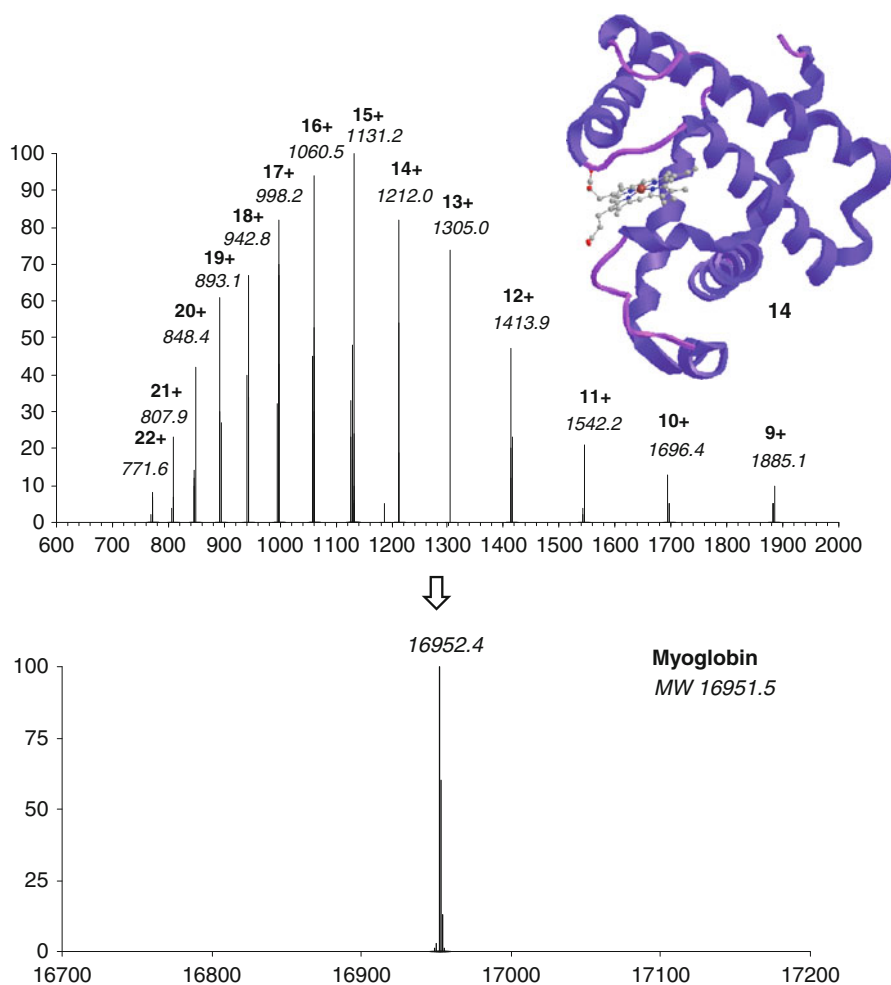


Fig. 7.6 Positive ion ESI spectrum of myoglobin (**14**) (MW 16951.5) in aqueous solution

count can be made by tallying the peaks within a 1 amu region or by using the simple equation: amu distance between peaks = $1/n$, where n equals the charge count. There is deconvolution software where both charge separation, isotope pattern and the m/z base peak of the cluster are taken in consideration in order to easily calculate the MF of an unknown.

7.3.1.4 Atmospheric Pressure Ionization (API)

In atmospheric pressure ionization (API), ions are formed under acidic conditions at ambient pressures followed by introduction into the source region. The sample ions together with solvent vapor and the ambient gas (usually nitrogen) are all held in the

ion source. There are three forms of ionization used in API, which can be applied for either direct insertion of compounds or as a detector for liquid chromatography–MS. These are heated nebulizer with a corona discharge, electrospray ionization (ESI), and thermospray ionization (TSI). The most common form of API consists of the vaporization of solvent and the substrate which is then directed into the ion formation region of the mass spectrometer where chemical ionization at atmospheric pressure (APCI) occurs using the vaporized solvent as the reagent gas. Overall, the technique of APCI is complimentary to ESI. It is used for compounds that do not have appropriate functionality (e.g., alkenes, aromatics) to be easily responsive to ESI.

An important modification of this form of API was introduced in 2005, and it is known as DART (direct analysis in real time) ionization, where the analyte is introduced in an open source. This atmospheric pressure ionization method uses a hot stream of excited-state helium atoms to excite clusters of water molecules in the atmosphere, which in turn transfer protons to the molecules of interest, thus creating the organic ions. Producing a spectrum requires only that the sample be held momentarily in a gas stream. Thin layer chromatography linked to high-resolution mass spectrometry can be carrying out with this innovative methodology [23].

7.3.1.5 Secondary Ion Mass Spectrometry (SIMS) and Fast Atom Bombardment (FAB)

FAB is useful for compounds, especially polar molecules, unresponsive to either EI or CI mass spectrometry. Excellent spectra are obtained with intense molecular ion peaks accompanied by few fragment ion signals. Chronologically, secondary ionization mass spectrometry (SIMS) was the forerunner of the FAB method. In SIMS, the sample is bombarded with a beam of high energy ions, resulting in the formation of secondary ions. A sample is usually placed as a thin monolayer from which the collision of the ion beam of heavy ions radiates secondary ions. Beams of low ion-current density must be employed, resulting in poor yields of ions, making the detection sensitivity a real problem. Also in SIMS, the secondary ion current lasts only for a brief period. Consequently, FAB is a better technique because it overcomes these problems. Fast atom bombardment (FAB) enables both nonvolatile and high molecular weight compounds (up to 20,000 amu) to be analyzed. Reasonably intense parent ions can be observed for both nonpolar and polar compounds including salts. In this technique, a sample is dissolved or dispersed in a polar and relatively nonvolatile liquid matrix, introduced into the source on a copper probe tip. Next, this matrix is bombarded with a beam of atoms of ~ 8 keV energy. FAB uses a beam of neutral gas (Ar or Xe atoms), and both positive- and negative-ion FAB spectra can be obtained. Molecular ions appear as positive-ion $[M + H]^+$ or negative-ion $[M - H]^-$ species (see behavior of compound **15** in Fig. 7.7). Often alkali metal ions, specifically Na^+ and K^+ , substitute for H^+ in the molecular ion, inducing the formation of positive ions like $(M + Na)^+$ or $(M + K)^+$. If the substrate has basic sites, species such as $[M - H + 2Na]^+$ or $[M - H + 2K]^+$ (or $[M - nH + \{(n + 1) \text{ Metal}\}]^+$) will be observed.

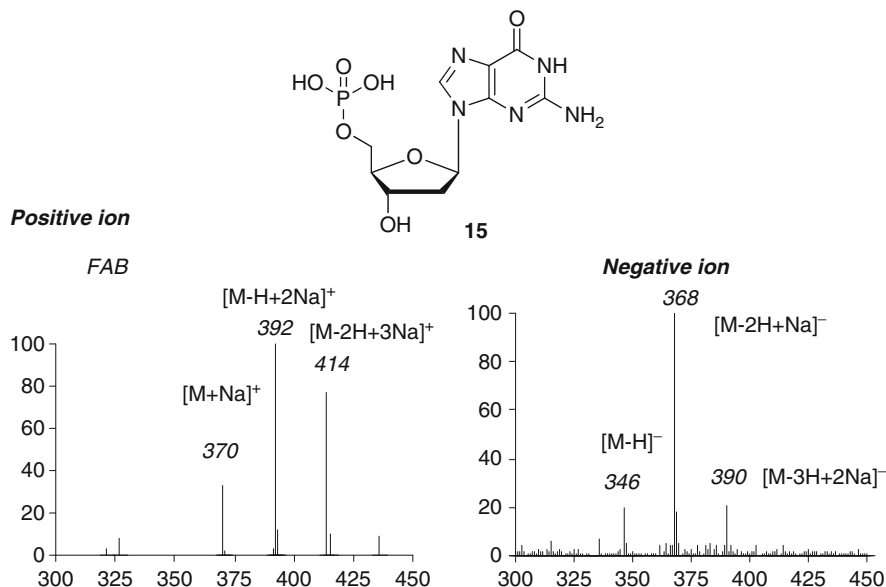


Fig. 7.7 FAB (Xe) spectra of 5'-deoxyguanosine monophosphate (**15**) (MW 347)

It is important to take note of the interfering peaks from the matrix, which must be reasonably viscous, chemically inert, and nonvolatile. In addition, it must possess good solvent and electrolytic properties. Glycerol and α -thioglycerol are two reagents frequently used. Other standard matrices which have been used for many years include the mixture of dithiothreitol and dithioerythritol (5:1) also known as *magic bullet*, 3-nitrobenzyl alcohol (NBA), polyethylene glycol, diethanolamine, and triethanolamine. The proper choice of a liquid matrix is a very crucial step in obtaining a high-quality FAB mass spectrum. For an intense $[M + H]^+$ ion signal, the matrix should be more acidic than the sample molecule, and for good $[M - H]^-$ ion production, the matrix must be more basic.

The molecular mass measurement and structural characterization of a wide range of organic, inorganic, and biochemical compounds (e.g., glycosides, peptides, antibiotics, lipids, carbohydrates, nucleotides, and nucleic acids) are major advantages of FAB. In general, FAB and liquid SIMS will give excellent molecular mass information in the range of m/z 100–2,000. Above this value, the abundance of molecular ions tends to diminish until, in the region of m/z 4,000–5,000, they become either absent or very difficult to discern against the background. It can be useful to collect both positive and negative ion data, as shown by the results of compound **15**.

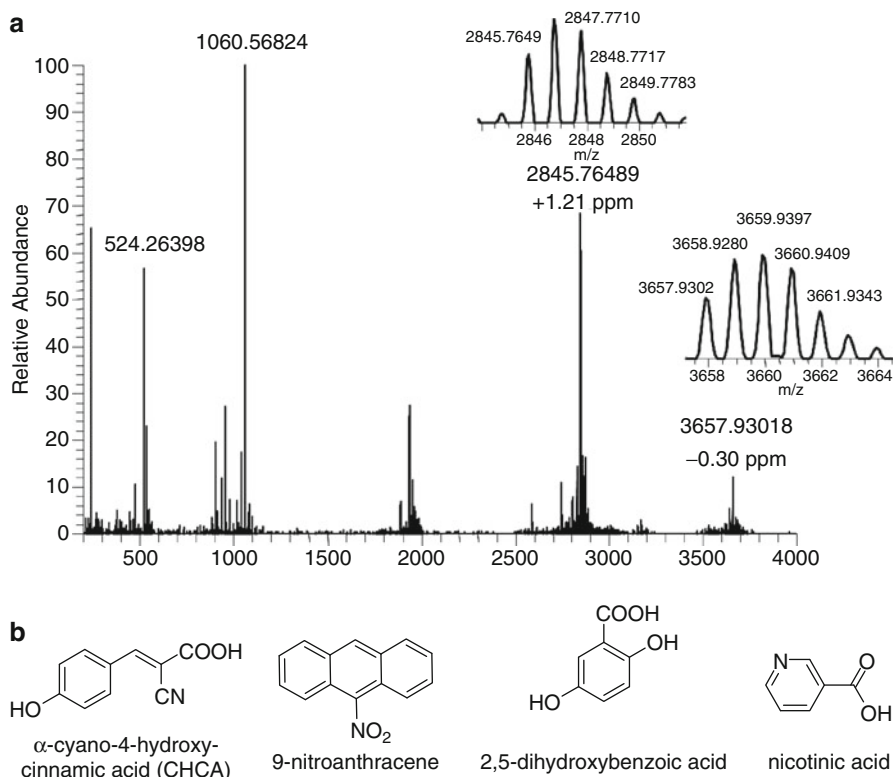


Fig. 7.8 (a) MALDI spectrum of mellitin (amino acid sequence *GIGAVLKVLTTGLPALIS-WIKRKRQQ* (MF $C_{131}H_{230}N_{39}O_{31}$, $[MH]^+$: 2845.761447)). Detected with an LTQ-Orbitrap, provided by Thermo Fisher. (b) Some solid matrices used in MALDI

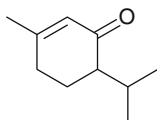
7.3.1.6 Matrix-Assisted Laser Desorption Ionization (MALDI)

Another important method for ion generation by rapid desorption involves irradiation of a sample by a strong laser beam [24]. Compounds of high molecular weight are successfully ionized by this method, called laser desorption ionization (LDI). An important modification of LDI involves using a solid matrix to absorb energy to minimize decomposition of the substrate under analysis. The purpose of the matrix is to absorb the large amount of energy produced by the laser and in a controlled fashion to transfer some of this energy to the substrate. This technique, referred to as MALDI, enables ionization of very large ions of up to m/z 1,000,000. Singly charged ions are produced by MALDI, in contrast to the multiply charged ions commonly observed in ESI, see Fig. 7.8. The obvious disadvantage of MALDI in the analysis of low molecular weight compounds is that some of the matrices used in MALDI completely obscure the region between 100 and 500 amu.

7.3.2 The Search of the Molecular Formula Through Mass Spectrometry

7.3.2.1 Isotopes

Mass spectrometry is based upon the separation of charged ionic species by their m/z ratio. We can calculate the molecular mass of 3-methyl-6-*i*-propylcyclohex-2-ene-1-one (piperitone, **16**) to $152.23 \text{ g mol}^{-1}$ using the average atomic masses of the elements. Since the mass spectrometer does not separate by elements but by isotopic mass, no signal at m/z 152.23 will be observed in the mass spectrum. Instead, a major peak at m/z 152.12 is present accompanied by a minor one at m/z 153.12. In order to fully understand a mass spectrum, we have to know about the different isotopes present for an element, their abundances, and *isotopic patterns*.



16

Chemical Formula: $\text{C}_{10}\text{H}_{16}\text{O}$

Exact Mass: 152.12

Molecular Weight: 152.23

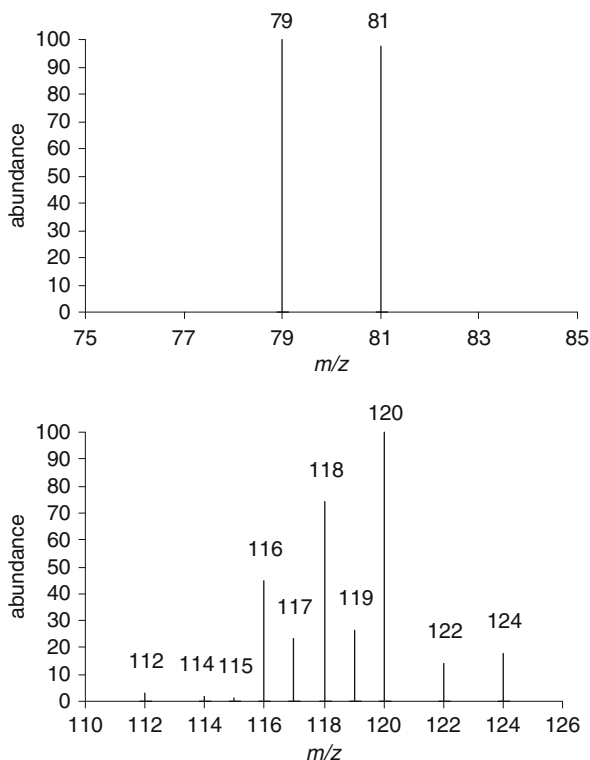
Atoms with nuclei having identical atomic number but differing in the number of neutrons are described as *isotopes*. One differs from another of the same element in that it possesses a different number of neutrons, and therefore a different *mass number*. This number is the sum of the total number of neutrons and protons in an atom, molecule, or ion. The mass number of an isotope is represented by a superscript in the elemental symbol, e.g., ^1H .

Depending upon the number of stable isotopes, elements can be monoisotopic (e.g., ^9Be , ^{19}F , ^{23}Na , ^{27}Al , ^{31}P , or ^{127}I), di-isotopics (e.g., $^1\text{H}/^2\text{H}$, $^6\text{Li}/^7\text{Li}$, $^{10}\text{B}/^{11}\text{B}$, $^{12}\text{C}/^{13}\text{C}$, $^{14}\text{N}/^{15}\text{N}$, $^{35}\text{Cl}/^{37}\text{Cl}$), and polyisotopics (e.g., $^{16}\text{O}/^{17}\text{O}/^{18}\text{O}$, $^{28}\text{Si}/^{29}\text{Si}/^{30}\text{Si}$, $^{32}\text{S}/^{33}\text{S}/^{34}\text{S}/^{36}\text{S}$, or 9 isotopes of Xe). The relative abundance of each isotope of an element must be considered when evaluating the peaks in a mass spectrum. Bar graph representations (histograms) are a great mode to visualize the isotopic composition (see Fig. 7.9), and they depend on the abundance of each isotope.

According to McLafferty's scheme [19b], another type of classification is dividing the elements into three general categories: "*A elements*" with only one natural isotope in abundance; "*A + 1 elements*" those that have two isotopes, the second of which is one mass unit heavier than the most abundant isotope; and "*A + 2 elements*" that have an isotope that is two mass units heavier than the most abundant isotope.

Examples of *A elements* are fluorine, phosphorus, and iodine. Hydrogen can also be included in this class because the abundance of its *A + 1* isotope, deuterium, is very small. Nitrogen and carbon are considered *A + 1 elements* since their second

Fig. 7.9 Isotopic patterns of bromine and tin



isotope is not insignificant and it is one amu higher than the most abundant isotope. $A + 2$ elements are the easiest to distinguish and the first to look for. Oxygen, sulfur, chlorine, and bromine are the most common examples. The presence of these elements in an ion is easily recognized from their isotopic distributions or *cluster*. Chlorine and bromine are very easy to pinpoint by MS. Having two major natural isotopes, they exhibit peaks in a ratio approximately 3:1 and 1:1, respectively.

Since few elements are monoisotopic, it is usually the most abundant species which is considered, especially when evaluating the parent ion M^{+} . For a compound $C_aH_bO_cN_dSi_eS_f$ under analysis, the molecular ion as well as most of the fragment ion peaks would be evaluated by considering only the major isotopes of $^{12}C^{1}H^{16}O^{14}N^{28}Si^{32}S$.

However, the existence of satellite peaks in a mass spectrum has to be considered because they can be useful information in order to deduce the molecular formula of an unknown. These peaks are isotopically shifted lines that emerge at masses one or more units higher than the most important peak M . The satellite peaks, nominated as $M + 1$, $M + 2$, and so on, reproduce the variation in the natural abundances of the isotopes. From the elemental composition of a molecular ion or

fragment ion, the abundances of its satellite peaks (the isotopic pattern or cluster) can be predicted as follows:

E.g., compound MF: $C_aH_bO_cN_dSi_eS_f$;

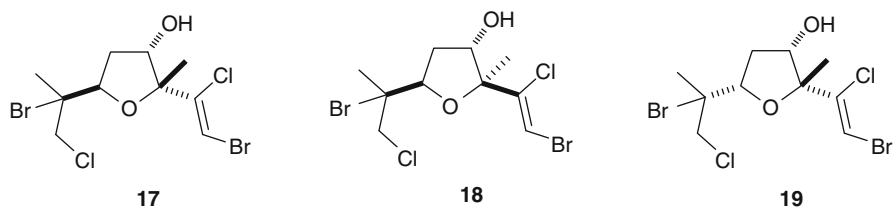
If $[M] = 100\%$, then

$$\%[M + 1] = a(1.08)^* + b(0.011)^* + c(0.038)^* + d(0.369)^* + e(5.0778)^* + f(0.80)^*$$

*Abundances for ^{13}C , 2H , ^{17}O , ^{15}N , ^{29}Si , ^{33}S , respectively

As briefly discussed above, the incidence of $A + 2$ elements is more noticeable for Cl and Br because the $A + 2$ isotopes are highly abundant. The contribution of one chlorine atom to the abundance of the $M + 2$ peak is 31.96%, and that of one bromine atom is 97.28%. In the case that one compound contains one chlorine atom, its $[M + 2]$ will be approximately one-third of $[M]$.

The contribution of more than one $A + 2$ element is calculated from expansion of the binomial $(a + b)^n$, where a is the natural abundance of the light isotope, b that of the heavy isotope, and n the number of atoms of that element present. If two different $A + 2$ elements are present (e.g., Br and Cl), the isotopic pattern is calculated by the expansion of the product given in $(a + b)^n (c + d)^m$, where c and d are natural abundances of the light and heavy isotopes of the second element and m is the number of that element. Using the clusters of peaks (separated by 2 amu) and their intensities as guide enables making a direct count of the number of Br and/or Cl atoms that might be present. Since the contribution of each isotope can be computed by different mathematical approaches, there are several software tools or web pages available to calculate the isotope distribution for an ion of a specific elemental composition and known isotopic abundances [25]. Thus, the structures of the furoplocamioids A-C (17–19), three pantofuranoids isolated from the Antarctic algae *Pantoneura plocamioides*, were determined on the basis of these types of clusters [26].



As we will see in electronic impact mass spectrometry (EIMS), compounds containing C, H, O, and with any type of charge *always* have an even molecular weight, an even number of H atoms, and display an even amu $[M]^{+*}$ as an odd electron ion. Compounds having a halogen atom (X) follow the same pattern because the difference in mass between H and X is even. This is a consequence that the most abundant isotope of all elements has either even mass and even

valence, or both are odd, apart from nitrogen, which has even mass but odd valence. This fortunate coincidence leads to what is known as the *nitrogen rule*. Compounds containing a single nitrogen atom are treated by reversing all of the above rules. For example, a $C_nH_mO_yN_1$ compound would have an odd molecular weight, an odd number of H atoms, and possess an odd amu $[M]^{+*}$ as an odd electron ion.

For multiple numbers of nitrogen atoms, the preceding rules apply when the total count is odd and they are reversed when the count is even. The only exception is quaternary ammonium salts (R_4N^+) which have an even molecular weight and H count. Keep in mind that an obvious possibility for error arises when the molecular ion of a compound without nitrogen is not visible, which makes the largest observed m/z odd due to a fragmentation process.

There are several approaches to calculating a molecular formula once a molecular ion peak has been identified. The M^{+*} cluster can be used by comparing either the measured to calculated M^{+*} , $[M + 1]^{+*}$, and $[M + 2]^{+*}$ peak intensities or the candidate molecular formulas obtained from the M^{+*} by the *Rule of 13* to the count of C and H obtained by NMR (see next sections). One of the most effective procedures is to use the NMR CH count along with high-resolution M^{+*} data.

There is a simple strategy to derive candidate molecular formulas systematically from any m/z peak [8]. It is based on the assumption that C_nH_n and its amu equivalent, 13 for $n = 1$, is present in all molecular and fragment ion formulas. Thus, dividing an M^{+*} mass by 13 gives the value of n , and any remainder represents a count of additional hydrogens. As an example, benzene has an $M^{+*} = 78$, and its molecular formula is easily derived. The molecular formula of toluene with an $M^{+*} = 92$ is similarly obtained taking into account the remainder as hydrogen atom ($92/13 = 7$, $\rightarrow R = 1 \rightarrow C_7H_8$). To consider heteroatoms, the hypothetical C_nH_m formula must first be derived by using the procedure just given. Next the formula is modified by using a series of C_nH_m equivalents deduced by applying the rule of 13 to the mass of such heteroatom. For example, ^{16}O is equivalent to CH_4 , and ^{14}N is equivalent to CH_2 .

Any isotope aX

$$\begin{aligned} a/13 &= b \rightarrow R = c; \\ \text{CH equivalent} &= \\ C_bH_{b+c} \end{aligned}$$

Examples

$$^{16}O \ 16/13 = 1 \rightarrow R = 3; CH + H_3 = CH_4$$

$$^{35}Cl \ 35/13 = 2 \rightarrow R = 9, C_2H_{2+9} = C_2H_{11}$$

The procedure for handling heteroatoms is exemplified by the calculation of candidate molecular formulas for anisole with an $M^{+*} = 108$: $C_8H_{12} - (CH_4) + O = C_7H_8O$. When an odd amu M^{+*} is encountered, the first heteroatom to consider is nitrogen (or odd multiples). Thus, aniline with an $M^{+*} = 93$ has candidate molecular formulas ($93/13 = 7$, $R = 2 \rightarrow C_7H_9$; $N = CH_2$; $C_7H_9 - CH_2 + N = C_6H_7N$, $C_7H_9 - 2(CH_2) + 2N = C_5H_5N_2$, $C_7H_9 - 3(CH_2) + 3N = C_4H_3N_3$, $C_7H_9 - (CH_2) - (CH_4) + N + O = C_5H_3NO$, etc.)

7.3.3 Ion Analyzers and Mass Accuracy

In order to calculate the approximate mass of a molecule, we must sum the integer masses of all elements present. For a molecule with formula CH_4 , we calculate what is called the *nominal mass* by adding $12 \text{ amu} + 4 \text{ amu} = 16 \text{ amu}$. The concept is widely used by spectrometrists and is defined as the integer mass of the most abundant naturally occurring stable isotope of an element, and those values represent the low-resolution mass spectrometry (LRMS). This mode in collecting mass spectrometry data is achieved with a single-stage type mass analyzer such as a magnetic or quadrupole sector. In this manner, only integral m/z values are resolved (distinct peaks appear for ions 1 amu apart).

The masses of isotopes can be measured with great accuracy, better than parts per billion, e.g., ^{23}Na : $22.98976928 \pm 0.00000002 \text{ amu}$. This accuracy is reached by the use of mass spectrometers analyzing the ions in the so-called high-resolution mass spectrometry mode (HRMS). In mass spectrometry, the term *mass accuracy* is defined as the difference between experimentally measured mass and calculated exact mass. The mass accuracy can be measured as absolute units of amu (or *milliamu* = mmu) or as relative mass accuracy in ppm.

Good mass accuracy is obtained from adequately sharp and regularly shaped peaks that are well separated from each other. The capability of a mass spectrometer to achieve such separation is called *resolving power*, and it is the function of the *resolution* (R) of such instrument. R is described as the ratio of the mass of interest (m) to the difference in mass (Δm), as defined by the width of a peak at a specific fraction of the peak height.

By definition, it is assumed that two peaks are well separated when the valley separating their maxima has decreased to 10% of their intensity. A larger R means that smaller mass differences can be resolved. Especially useful for spectrometer manufacturers is the definition of FWHM (full width at half maximum) where the peaks separated by a 50% valley are considered as resolved.

The accuracy in mass spectrometry is highly dependent on the type of technique used for analyzing the ions. The separation of ions capitalizes on the inherent differences in the ratio of mass to charge for each ion species. These distinct ions will behave differently in an electric or magnetic field, which provides a convenient way to effect their separation.

An extremely effective way to analyze MS ions after they are formed from electron impact involves passing them through a magnetic field. The radius of curvature for the path of an ion is proportional to m/z . This allows a distinction between heavy ions, which have a less curved trajectory, and the lightest ions, whose trajectory will be more curved.

A relatively simple way to separate ions involves passing them through a quadrupole mass filter [27]. It consists of four parallel rods arranged symmetrically around an ion flight path. Each opposite pair of rods is electrically connected and an electric field is created from a dc voltage overlaid with an RF potential. The ions that pass through the central region are influenced by the dc and RF voltages. Most ions are deflected onto the rods, but those of an

appropriate m/z are modulated in a helical path and enter the detector. Quadrupole detection is very attractive because it is relatively inexpensive and the instruments require less expertise to tune and operate. This analyzer is widely used in GC/MS, LC/MS, and tandem MS instruments.

There is a mass filter which has many features in common with a quadrupole analyzer. In fact, it is popularly known as a *quadrupole ion trap* (QIT), and it was introduced in 1958 by Wolfgang Paul, a contribution that was recognized by the awarding of the 1989 Nobel Prize in Physics [28]. A QIT analyzer consists of three doughnut-shaped central ring electrodes with two end caps. Both an RF and dc potential are applied to generate a stable trajectory for the various ions. The ion trap has a very compact design and, because of its extremely low cost, is widely used as a detector in GC-MS and HPLC-MS applications. Newer instruments merge electrospray ionization with an ion trap analyzer. Additional features too complex to discuss here are incorporated to carry out tandem MS-type experiments. A problem with the ion trap detector is that relatively poor accuracy is achieved at large m/z , but advances in technology are overcoming this limitation. Very recently, *linear ion traps* (LITs) or two-dimensional ion traps have gained interest either as stand alone or as an element of more complex mass analyzers (hybrids). An LIT is similar to a quadrupole formed by four circular or hyperbolic rods placed symmetrically. In a linear ion trap, the ions are confined radially by a two-dimensional RF field.

In a *time-of-flight* (TOF) mass spectrometer analyzer, ions are separated according to their velocities and hence the mass-to-charge ratio. Ions are generated in a short burst and then accelerated. The time taken to traverse a specified path, usually up to 2.5 m, to the detector depends on the mass of the ion; consequently, the velocities of ions are an inverse function of the square root of their m/z values, and therefore, lighter ions travel more rapidly to the detector. TOF mass analyzers can be used in *reflectron mode*, an energy-correcting electrostatic mirror that can minimize undesired effects of initial spatial and energy spreads. With the reflectron, the flight path is increased without changing the physical size of the instrument, resulting in an increase in the mass resolving power.

In FTMS, gas phase ions are introduced into a cubic cell located within the solenoid of a magnet. Contemporary FTMS instruments use high-field superconducting magnets (7T is typical). The phenomenon behind FTMS is that the trapped ions move in a circular path (the cyclotron orbit) at different frequencies due to the strength of B and the mass-to-charge ratio. Detection of the different ions occurs from an RF excitation pulse that accelerates them into a resonant cyclotron orbit. Subsequently, a distinct RF signal is emitted and can be detected as a *time-domain* pattern. This type of signal can be amplified, digitized, and converted by a Fourier transform into the familiar plot of m/z vs. intensity. Overall, the FTMS technique is very different from those described previously. Among its advantages is that the FT approach provides very high resolution and a way to greatly improve signal-to-noise ratio for high mass ions.

An innovative type of mass analyzer, known as the *orbitrap*, has recently been introduced [29]. It works on the principle of an orbital trapping of ions around an axial central electrode with a purely electrostatic field. Since its appearance, the orbitrap mass analyzer has been considered as a potential alternative for FT-ICR because of its high resolution (approximately 150,000 FWHM) and good mass accuracy (better than 3 ppm without internal reference), large space-charge capacity, good sensitivity, and an m/z range up to 6,000.

Ion Mobility: (IM) coupled with mass spectrometry has evolved into a powerful analytical technique for investigating the gas-phase structures of biomolecules [30]. An ion mobility spectrometer uses gas-phase mobility rather than the m/z ratio as a criterion to separate ions. The mobility of ions is measured under the influence of an electrical field gradient and cross-flow of a buffer gas, and depends on ion's collision cross section and net charge. A more accurate mass analysis is obtained when the IMS is coupled to a quadrupole or TOF mass analyzer. Such systems can be engaged for the studies of mixtures of proteins or tryptic digests of peptides and proteins.

Mass spectrometers may be built by combining different types of mass analyzers in a single so-called *hybrid instrument*. The expansion of hybrid instruments started from magnetic sector–quadrupole hybrids, combining the advantageous properties of each mass analyzer. Special nomenclature is used to describe each hybrid spectrometer: symbols Q (quadrupole), q (collision cell-quadrupole), B (magnetic sector), and E (ESA, electrostatic analyzer), along with the previously described terms QIT, LIT, TOF, and ICR are combined to illustrate the different geometries of commercial spectrometers. BqQ, QqQ, Qq-TOF, QIT-TOF, and Q-LIT (or Q-TRAP) are examples that carry the advantage of powerful and affordable machines for tandem MS as will be explained later. Qq-TOF and QqQ systems can be regarded as the commercially most successful hybrids, whereas the next level of performance will be achieved with Qq-FT-ICR spectrometers.

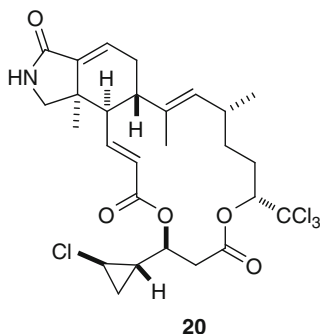
7.3.4 Terms in Mass Spectrometry

7.3.4.1 Exact Mass

Data from HRMS are essential for unambiguous determination of a molecular formula, and its *exact mass* is defined as the mass combination of the most abundant isotopes. HRMS data are obtained at an accuracy better than 0.0001 amu (0.1 mmu), and consequently, this permits a distinction between species of the same unit mass such as $[\text{CO}]^+$ (exact mass: 27.99437 amu) vs. $[\text{C}_2\text{H}_4]^+$ (exact mass: 28.03130 amu).

Care has to be taken when we want to calculate the exact mass of a neutral or charged species, where the mass of an electron ($m_e = 0.000548$ amu) has to be considered. This is the case for muironolide A (**20**), a tetrachloro polyketide isoindolone isolated from the marine sponge *Phorbas* sp. at the nanomole scale,

when its molecular formula was calculated with high precision by Fourier transformation mass spectrometry [31].



The *exact ionic mass* of a positive ion species produced by the removal of one or more electrons from a molecule is equivalent to its monoisotopic mass minus the mass of the electron. Consequently, for negative ions, the electron mass has to be added.

7.3.4.2 Mass Defect

Comparing the exact mass to the unit (or nominal) mass for each element generates an estimate of the *mass defect* or *mass sufficiency*. Its value can be either positive or negative. For example, notice that ¹H, with nominal mass of 1 amu and exact mass of 1.00783 amu, has a slightly positive mass defect, whereas for ¹⁶O, of nominal mass 16 and exact mass 15.9949, the defect is slightly negative.

Obtaining experimental *m/z* data with a tenth of a mass unit accuracy (or better) can provide the overall estimate of the mass defect for a compound under study. Taking note of the direction of this mass defect can be helpful in many situations. Knowledge about mass defects is essential for correct analysis of low-resolution MS data for compounds of MW near 1,000 Da (or greater), and it can also be helpful in studying unknowns. As an example, low molecular weight compounds with two or more sulfur atoms will have negative mass defects.

7.3.4.3 Hyphenated Mass Spectrometry

Typically, MS is coupled or combined with separation methods such as gas chromatography (GC) or high-pressure liquid chromatography (LC) [32]. For many years GC–MS has been the method of choice in the analysis of complex nonpolar and low MW mixtures, including those from natural product extracts, human body fluids, toxic waste mixtures, industrial processes, and so on. It has been estimated that during the 1980s, about 2,000 papers were published each year in the GC–MS field. In GC–MS, spectra of acceptable quality are obtainable for every component that is separated by gas chromatography, even though the components may be present in nanogram quantities and eluted over periods of only a few seconds. A plot of total ion current vs. time provides a visualization of the retention time and the quantities of individual components eluted from the

GC or LC column. Valuable alternative views of such GC data can be obtained from reconstruction of the GC trace using selected ions such as those characteristic of a particular fragmentation process. Another important tactic involves comparison of the full MS of each GC peak to those within libraries of spectra; this facilitates the rapid identification of known compounds. Thus, GC–MS and LC–MS are widely used as important analytical tools.

7.3.4.4 Tandem Mass Spectrometry (MS–MS)

This technique has grown very rapidly as a tool in biochemical research during the last 5 years [33]. It also has great potential value in organic structure analysis, but it has been somewhat ignored by contemporary researchers engaged in structure elucidation and identification of organic compounds. Tandem mass spectrometry includes several techniques where mass chosen ions are subjected to a second mass spectrometric analysis. MS–MS takes advantage of fragmentations that occur in the field-free regions of magnetic sector instruments or in a collision region of a multiple quadrupole apparatus.

The strategy of collisionally activated decomposition (CAD), also known as collision-induced dissociation (CID), is an important adjunct to the soft ionization techniques discussed. Recall that for soft ionization, the level of fragmentation is relatively low, yielding little or no structural information. The purpose of CAD is to regenerate a fragment ion pattern by subjecting a selected ion to collision with energetically rich species.

As noted above, one method employs collision of the ions with high-energy atoms of an inert gas (e.g., He or Ar) while another uses RF to activate the ions for fragmentation. Triple quadrupole instruments use low-energy (10–100 eV) RF collisions in the central quadrupole to initiate this process. If high energies are desired (~100 eV), then magnetic sector instruments must be used. Two other types of instruments utilizing the concept of MS–MS are ion traps and FT-ICR. Both employ the CAD process, which is then followed by ion detection. In addition, the CAD method has been extended to the analysis of multiply charged ions generated by ESI.

The greatest advantage of MS–MS is that it provides a way to establish an unequivocal relationship between a set of precursor and product ions. With such information in hand, it is possible to prove that a particular fragmentation mechanism is operating, which can be useful in pinpointing substructures or functional groups when diagnostic sets of ions are located. MS–MS can also distinguish between isomeric compounds expected to have different but predictable fragmentation patterns.

Depending on which analyzers are used, four main scan modes for tandem MS–MS can be distinguished (see Fig. 7.10):

- The *product-ion scan* mode is the most familiar mode of MS/MS operation and is very useful for the structure elucidation of an unknown. To obtain this spectrum, the first mass analyzer is set to transmit only the precursor ion chosen, and the second mass spectrometer is scanned over a desired m/z range.

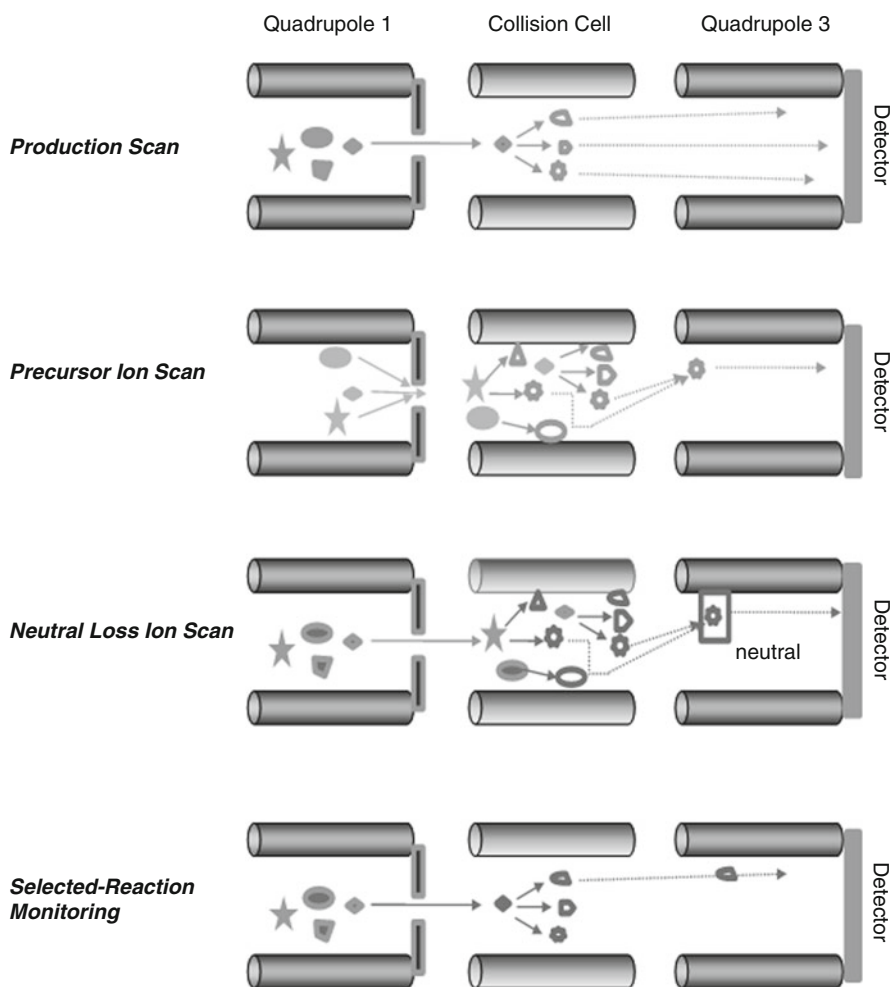


Fig. 7.10 Scan modes in tandem MS-MS

- The *precursor-ion scan* provides in the second analyzer a spectrum of all precursor ions that might fragment to a common, diagnostic product ion. This scan mode is useful for the identification of a closely related class of compounds in a mixture.
- In the *neutral-loss scan*, all precursors that suffer the loss of a particular common neutral fragment are examined. To acquire this information, both mass analyzers are scanned at the same time, but with a mass offset that links with the mass of the specified neutral (e.g., H_2O , CO_2 , CO , N_2). This scan mode is similar to the precursor ion scan, being useful in the selective identification of closely related class of compounds in a mixture.
- *Selected reaction monitoring (SRM)* is similar to the product-ion scan. However, instead of scanning the second mass spectrometer in a broad mass range, the two

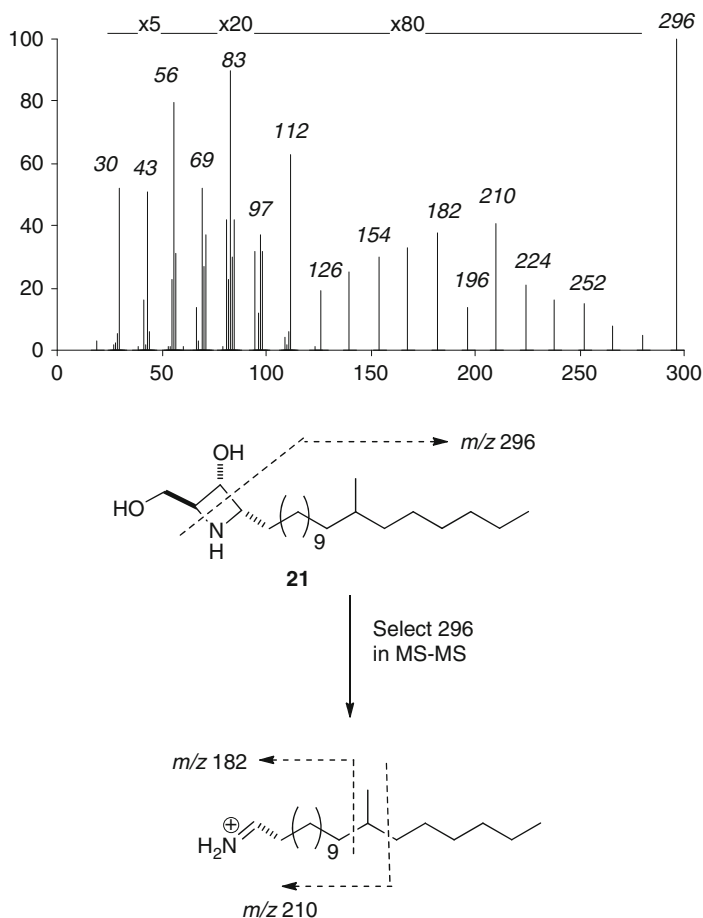


Fig. 7.11 Penazetidine (**21**) (MW 369): assignment of Me side chain by FABMS-MS

mass analyzers are adjusted to monitor one or more chosen precursor–product pairs. This technique is useful in quantitative measurements of analytes present in complex mixtures. When more than one reaction is monitored, the scan mode is termed *multiple reaction monitoring* (MRM).

A good example of product-ion scan mode is the location of the methyl group on the C18 side chain of penazetidine A (**21**) (MW 369) was established by FAB MS–MS data). The lack of dispersion in the 1D and 2D NMR spectrum of **21** meant that NMR data were not useful in addressing this issue. However, MS data were extremely valuable, and the first task was to select the positive fragment ion at m/z 296, not shown but detected by the first mass analyzer. The m/z 296 ion was then subjected to CAD which generated the spectrum shown in Fig. 7.11. This two-step process focuses the fragmentation on that typical of an alkane, so the reduced

intensity of the peak at m/z 196 could be used to specify the location where the methyl group was attached.

One of the most common applications of MS–MS is in the sequencing of peptides [34] which are first ionized by ESI or MALDI. In general, MH^+ species are selected for further CAD to produce a complex pattern of fragment ions.

7.4 Substructures, Working Structures, and Final Structures: Nuclear Magnetic Resonance (NMR)

More information about an unknown compound can be developed by obtaining NMR data for both protons and carbons [35]. Certain isotopes of these nuclei have magnetic properties, which is the characteristic required to generate NMR peaks. It is known that a spinning charge has an associated magnetic field, and much can be learned by briefly reviewing the magnetic characteristics of an electron before looking further at atomic nuclei. Two electrons occupying the same orbital can be distinguished because (by the Pauli exclusion principal) they must be spin paired. A single electron can have two possible spin “orientations”. Magnetic spin properties are further characterized by a fundamental parameter, the spin quantum number I , and its value provides a guide when writing out all possible quantized spin and energy states. The electron has $I = 1/2$, and the labels of $+1/2$ and $-1/2$ designate both its energy and spin states. Like an electron, some atomic nuclei have a spin, but, more importantly, there is a greater range of possible I values. As one example, the two isotopes of hydrogen have different I values. The most important 1H isotope (protium, 99.98% abundance) has $I = 1/2$, so its magnetic properties, especially spin and energy states, are analogous to those of an electron. The 2H isotope (deuterium, 0.02% abundance) has $I = 1$, and, as will be discussed later, its properties are somewhat different. Finally, one of the isotopes of carbon, ^{13}C (1.1% natural abundance), also has $I = 1/2$.

There are a large number of nuclides present in natural products which would be of interest for NMR. However, not many meet the strict criterion to be included in our final list of “commonly studied species.” Recall that those having $I = 1/2$ represent the optimal types. Two additional factors are a reasonable natural abundance and a general presence in organic compounds. Only 1H , ^{13}C , ^{19}F , and ^{31}P meet these requirements, but it is just 1H and ^{13}C that are common to *all* organic compounds. Consequently, these two nuclides will be the major focus of our attention here. There is a second list of nuclei that are growing in popularity, and this includes ^{15}N , 2H , ^{11}B , and ^{29}Si . A species of high relative abundance, ^{14}N , that is not on this list also influences the appearance of NMR spectra. Thus, it will be important to consider how each of these nuclides affects the appearance of 1H and ^{13}C spectra.

In order to get information out of NMR, different parameters can be computed. These include peak areas (integrals), chemical shifts (δ), coupling constants (J), and relaxation effects (especially nuclear Overhauser enhancement, NOE).

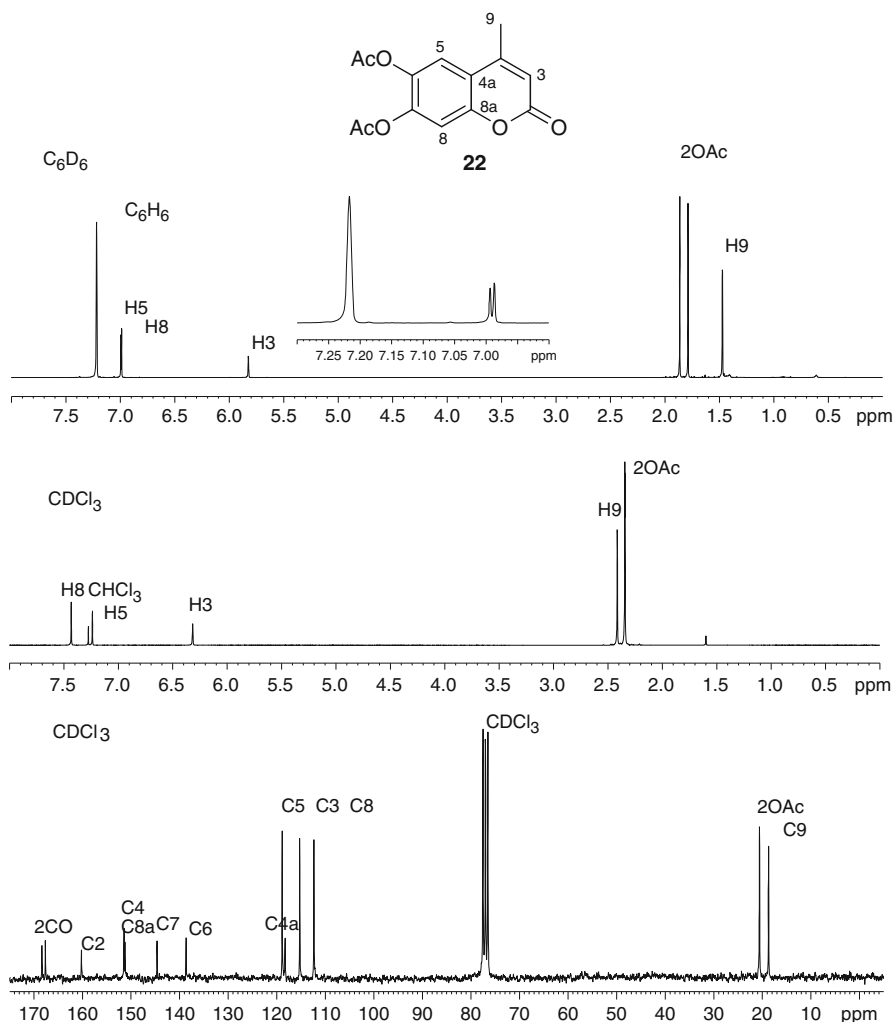


Fig. 7.12 ^1H (500MHz) and ^{13}C (62.3MHz) NMR spectra of 6,7-diacetoxy-4-methylcoumarin (**22**)

7.4.1 Chemical Shifts and Peak Areas

Since chemical shifts and peak areas are some of the first data employed in the analysis of organic structures, it is appropriate to examine briefly how such information is used. Let us inspect the ^{13}C and ^1H NMR spectra of 6,7-diacetoxy-4-methylcoumarin (**22**, $\text{C}_{14}\text{H}_{12}\text{O}_6$) shown in Fig. 7.12. Its ^{13}C NMR spectrum at 125 MHz contains single peaks for each carbon. It was obtained by the procedure of broadband proton decoupling to eliminate all proton J coupling effects. Twelve, rather than fourteen, peaks are observed in the ^{13}C NMR spectrum because

resonances accidentally overlap for the two OAc methyls and for C4a and C8a. At first glance, the ^1H NMR spectrum (500 MHz, CDCl_3 ; the tiny peak at δ 1.6 is due to H_2O) is also a bit confusing – the intense signal at δ 2.36 corresponds to two nonequivalent methyl groups. The ^1H NMR spectrum in benzene- d_6 (500 MHz) is more straightforward (the miniscule H_2O peak at δ 0.6 is closer to TMS) because there are six singlets that are resolved and the peak areas show three methyls, one vinyl H, and two aromatic Hs. Comparison of the ^{13}C NMR carbon count to that in the molecular formula indicates that the molecule is devoid of symmetry. The 11 carbon signals between δ 110 and 170 are due to four double bonds (the ^1H NMR suggests three trisubstituted double bonds) plus three ester groups. Collectively, these features make up seven of the nine unsaturations (calculated from the MF). Also, a tetrasubstituted benzenoid ring is evident from the two protons at δ 7.2–7.5 (CDCl_3); the methyl group δ_{H} 2.2 (CDCl_3) indicates that it is adjacent to an sp^2 center. Notice that the intensities of the ^{13}C NMR resonances in Fig. 7.12 are quite varied. Some peaks with a higher than expected intensity are due to the superposition of two carbons, but there is another factor which explains the low intensity peaks. Quaternary carbons often exhibit smaller peaks, and this can be helpful because it is therefore easier to identify them.

7.4.2 Factors that Determine Chemical Shifts

Early NMR spectrometers operated in a “field sweep” mode in which the magnetic field (B_0) was varied to bring each nucleus into resonance separately [36]. Second generation instruments incorporated a “frequency sweep” design to accomplish this same task, but the pulse Fourier transform technique is now the method of choice. Interestingly, many of the words used to describe relative chemical shifts (δ s) of peaks were derived from the original spectrometer design, and the NMR spectra were plotted with B_0 increasing from left to right. Thus, peaks close to TMS are said to be “upfield,” and those that are far away are “downfield.” Comparing the $^1\text{H}/^{13}\text{C}$ chemical shifts of tetramethylmethane at δ 0.89/ δ 27 to those of tetramethylsilane at δ 0.0/ δ 0.0 illustrates how increased electron density at the proton and carbon in TMS requires a higher B_0 for resonance (hence, “high field”). The greater electron density at the silicon atom of TMS generates a larger induced magnetic field B_0 , resulting in diamagnetic shielding (or an upfield shift) for its attached protons and carbon.

The chemical shifts evident in the NMR spectrum of 6,7-diacetoxy-4-methylcoumarin (Fig. 7.12) arise because the local magnetic fields experienced by protons and carbons in different parts of an organic molecule are not the same. Thus, chemical shifts represent alterations of B_{net} at individual nuclei, so the practice of reporting δ values as differences relative to a standard such as TMS is quite logical [37].

A major factor in ^1H NMR chemical shifts is the effect produced by the circulation of 1s hydrogen electrons, as well as the effects created by neighbors with π -orbitals. The effect arising from the electronic shielding of a nucleus

diminishes in proportion to the inverse of the distance between the nucleus and the valence electrons. Electronegativity greatly influences proton chemical shifts and provides a simple way to look at this effect.

The position of ^{13}C shifts is well known to be dominated by effects of electronic asymmetry. This effect increases proportionally to the sum of multiple bond contributions and the number of p -electrons. However, this dominant effect in heavy nuclei decreases proportionally to the average product of the electronic excitation energy, and the cube of the distance r between a p -electron and the nucleus.

7.4.3 Chemical Shift Positions of $^1\text{H}/^{13}\text{C}$ Attached to Common Functional Groups

A summary of the characteristic positions of various proton and carbon types appears in Tables 7.2 and 7.3, respectively. They provide important background information needed to begin to correlate functionality with chemical shift ranges. For example, comparison between the ^1H shifts in Table 7.2 and the ^{13}C shifts in Table 7.3 shows that carbons or hydrogens at sp^3 , sp^2 , or sp hybridized sites have the same relative chemical shift positions. This is also true for a variety of functional groups; alkyl groups attached to an aliphatic chain occur at highest field, whereas those attached to oxygen or halogen are in the middle. The CH resonances at sp^2 centers occur near the center when no heteroatoms are present, but the addition of O or N results in shifts to the left, and the aldehyde and ketone resonances are found to the far left.

It is important to become familiar with the chemical shift regions in both the ^{13}C and ^1H NMR where the most common groups resonate. Also note the differences of ^{13}C vs. ^1H chemical shifts. For example, the ^{13}C shifts of a polyene and a benzene ring occur in nearly the same region, whereas their ^1H shifts are distinctly separated. Aldehydes can be directly observed by ^1H NMR; other carbonyls cannot. As we will see, ^{13}C NMR represents a convenient tool for observing carbonyl groups because many of the various substructures have distinctive shifts.

The overall complexity of a molecular structure will determine the number of distinct chemical shifts observable in an NMR spectrum. Alternatively, there are circumstances where the tally of individual chemical shifts can be difficult to correlate to features of organic structure, especially in an unknown. For example, compounds possessing elements of symmetry or chirality represent one type of challenge. Another troublesome situation occurs for acyclic or cyclic compounds undergoing dynamic processes such as chemical exchange, intramolecular rearrangements associated with tautomeric equilibria, or conformational interconversions. Fundamental insights gained from a brief tour through principles of static and dynamic stereochemistry can be useful and should help in demystifying such situations [15].

There are two elements of symmetry to look for when examining a molecular structure. They are a rotational axis (C_n) and a mirror plane (σ) (a σ is equivalent to

Table 7.2 Proton chemical shifts of different functional groups

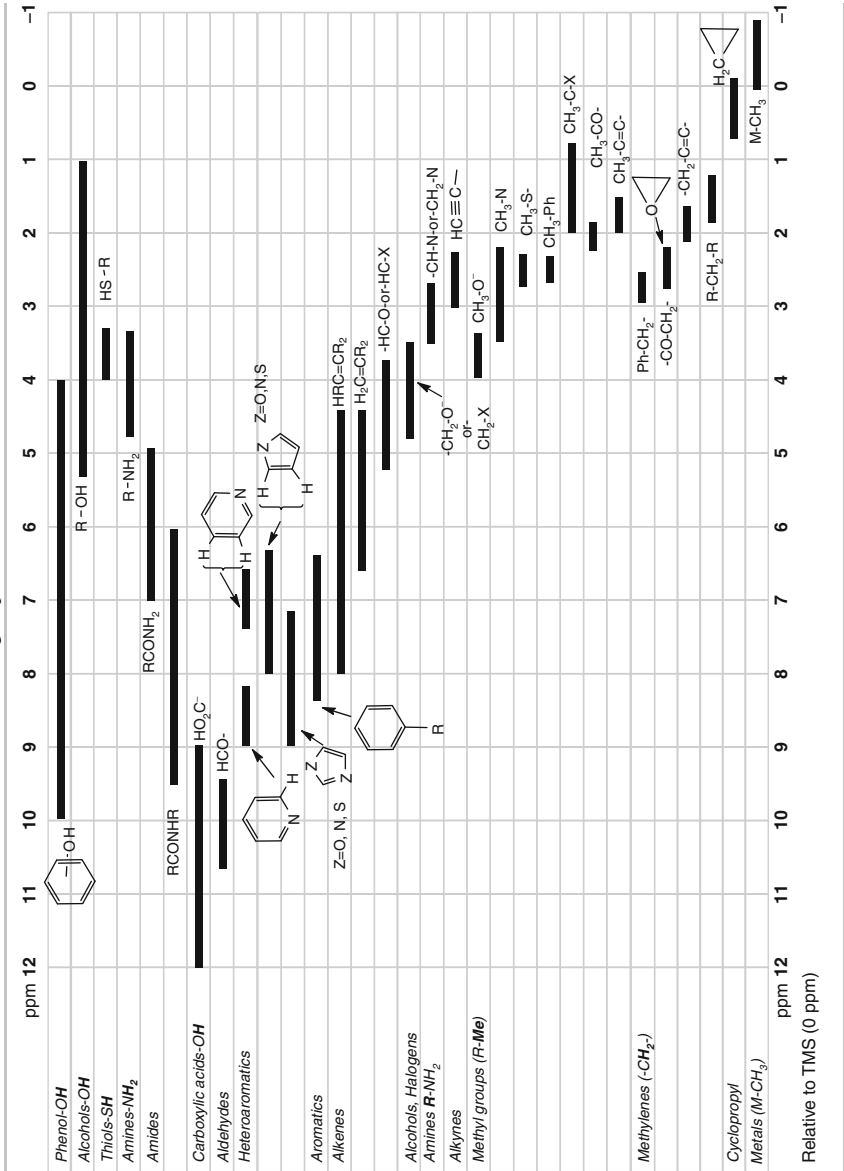
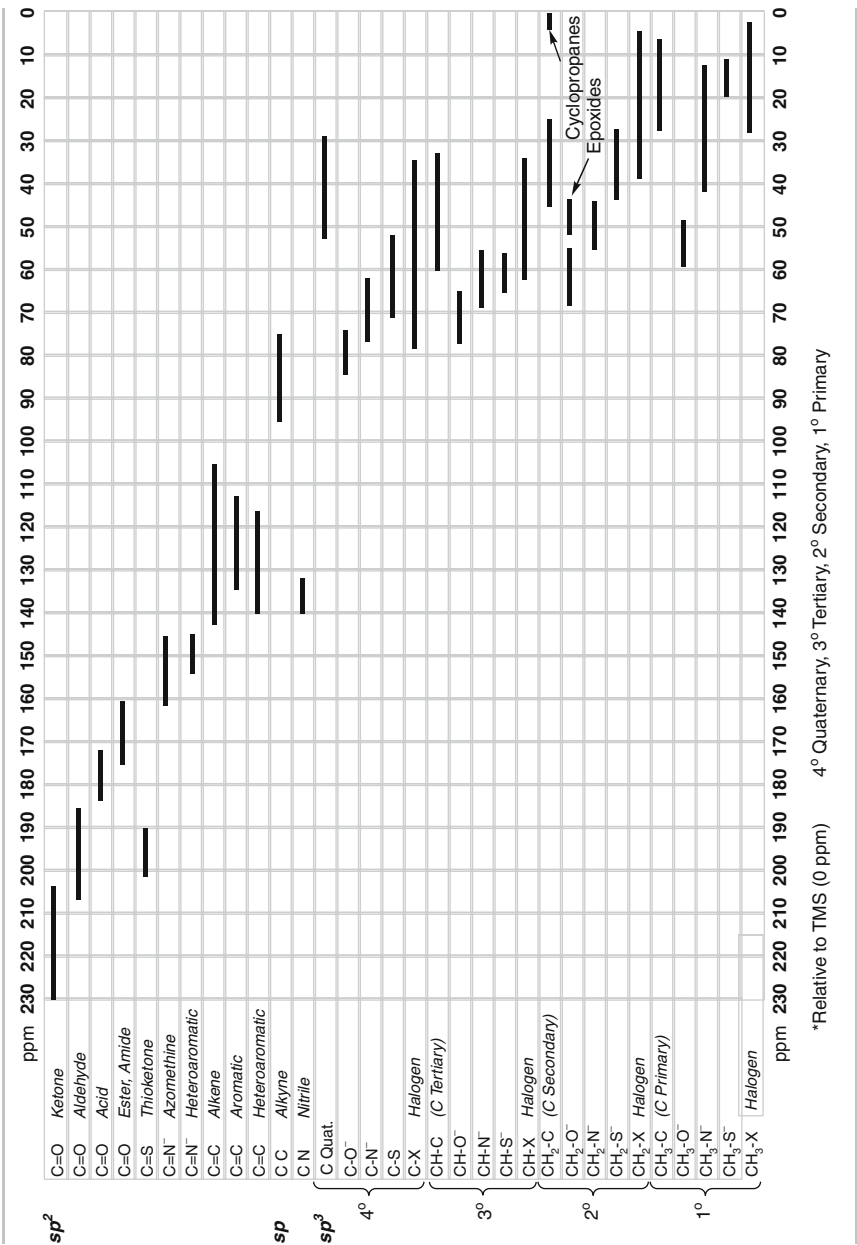


Table 7.3 Carbon chemical shifts of different functional groups



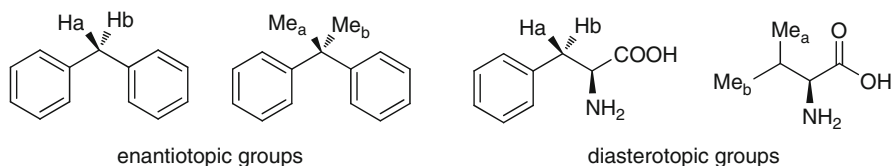
a rotation–reflection axis, S_n). When present, symmetry will allow absolute predictions to be made about the identical (*isochronous*) or nonidentical (*anisochronous*) chemical shifts expected for groups being compared. The best way to identify symmetry in a molecule is to be systematic. First look for a rotational axis (C_n); next search for a mirror plane (σ). The two symmetry elements can be used to relate groups that are either within the same molecule (i.e., an intramolecular comparison) or in different molecules (i.e., an intermolecular comparison).

Several widely used terms ending in “topic,” first coined by Professor Kurt Mislow at Princeton University in the 1960s, describe symmetry relationships between nuclei or groups using the C_n and σ symmetry operations. When two atoms or groups of atoms in the same molecule can be related by a C_n , they are called *homotopic* and will always have identical chemical shifts. Examples of homotopic protons are H_a and H_b in diphenyl methane and homotopic groups Me_a and Me_b in 2,2-diphenylpropane. When two groups can be related only by a σ , they are termed *enantiotopic* and will also have identical chemical shifts in normal solvents. Examples are enantiotopic protons H_a and H_b in benzyl alcohol and enantiotopic groups Me_a and Me_b in 2-phenylpropan-2-ol. Groups in an identical two-dimensional environment (e.g., same connectivity relationships) but not related by either a C_n or σ operation are termed *diastereotopic* and should have nonidentical chemical shifts in normal NMR solvents. Examples of diastereotopic protons and diastereotopic groups: the benzyl substructure bearing a chiral substituent (G^*) or a 2-phenylpropane substituted at C2 with G^* . Be sure that you understand the relationships present in this last example. It should also be apparent that when groups (or protons) being compared are in different structural environments, they should have nonidentical chemical shifts; these are sometimes called *heterotopic*.

Correctly identifying enantiotopic or diastereotopic groups in acyclic molecules can sometimes be troublesome. Also, predicting their NMR behavior in situations of dynamic motion can be difficult. Another point to be mindful of is that very often groups that are nonidentical are observed at the same chemical shift position. This is referred to as *accidental isochrony*, and it can occur in both ^{13}C and ^1H NMR for nuclei or groups that are heterotopic or diastereotopic (or enantiotopic being examined in a chiral solvent). The best way to resolve an inherent shift difference that seemingly cannot be observed is either to change the solvent (Fig. 7.12) or increase the magnetic field strength, or perhaps lower the temperature of the sample to slow down fluxional processes. It is useful to consider further how to identify enantiotopic or diastereotopic groups rapidly as well as recognizing dynamic processes that will unexpectedly simplify an NMR spectrum.

As an important rule of thumb, the presence of a single chiral (or stereogenic center) in either an acyclic or cyclic molecule is all that is needed to generate diastereotopic relationships. This often happens in compounds containing ethyl and isopropyl subunits. At this point, you should be able to recognize the enantiotopic relationships present for the methylene protons of ethanol and for the gem methyl groups of isopropanol. As noted previously, the presence of chiral substituents (G^*)

will make identical geminal groups diastereotopic and will resolve these species as separate NMR signals. The *i*-propyl moiety is considered to be an NMR “chiral reporter group,” and many researchers have used it to examine processes where chirality is created (e.g., by the introduction or presence of chiral centers, axes, or planes).



It is also important to highlight groups that are “symmetrical tops.” The most common are a methyl and a *t*-butyl, and they normally exhibit equivalent NMR signals. The protons of a methyl group and the methyl carbons and protons of a *t*-butyl group are homotopic under all circumstances where rapid rotation can occur. For a methyl in a compound that also contains a chiral center, there are three nonequivalent Hs present in each rotamer, but all three will be averaged to one type (e.g., they become equivalent) when interconversion between rotamers is rapid. The C–C bond rotational barrier is small (about 12 kJ/mol or 3 Kcal/mol), so the room temperature spectra of protons of a methyl *always* appear at the same chemical shift. An identical situation exists for the methyl groups in a *t*-butyl group. Namely, they are equivalent and occur at the same chemical shift in either ^{13}C or ^1H NMR, owing to rapid rotamer interconversion. Alternatively, if restricted rotation about the C–C bond to the *t*-butyl quaternary carbon occurs, then three distinct methyl signals would be expected; this has been reported in the literature for some sterically hindered compounds.

7.4.4 Discovering Substructures from NMR: Scalar Coupling

The phenomenon of scalar coupling is prominently represented in most ^1H NMR spectra and often results in a large number of peaks being observed. Nuclei in close proximity with $I \neq 0$ having a small or zero electric quadrupole moment might exhibit the phenomena of “coupling,” which is unique to NMR. It arises from a nuclear spin–spin interaction transmitted by the bonding electrons of proximal atoms.

It is important to be able to distinguish between two different circumstances responsible for the closely spaced ^1H NMR peaks often less than 20 Hz apart. These can arise from spin–spin (J) coupled nonequivalent nuclei or isolated nonequivalent nuclei without any direct magnetic interaction. The *coupling constant* is the absolute separation (in Hz) between two or more peaks arising from coupling, and it is reported as a J value. The multiplets from $I = 1/2$ nuclei can sometimes be interpreted by the familiar rule: number of peaks = $n + 1$ (n is the count of neighbors).

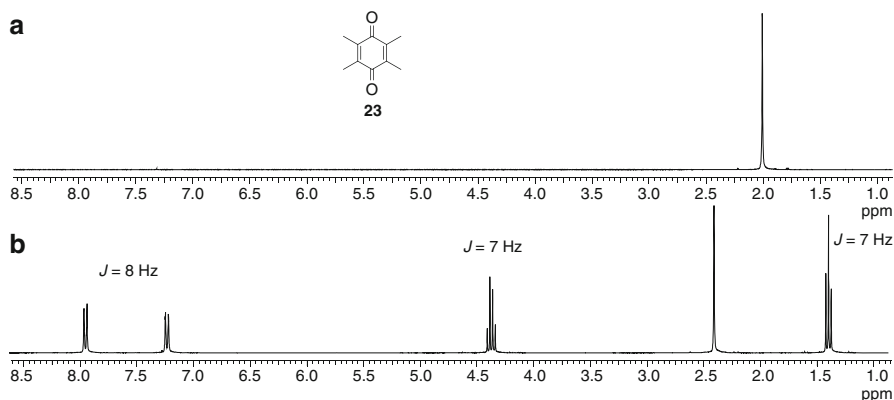


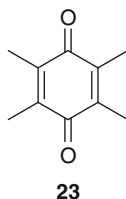
Fig. 7.13 ^1H NMR spectra of $\text{C}_{10}\text{H}_{12}\text{O}_2$ isomers (300MHz, CDCl_3)

It has been argued that the NMR J value is one of the most valuable parameters employed in the analysis of organic compounds. The process of establishing chains of $-\text{CH}_n-\text{CH}_m-$ moieties is greatly simplified by using J value information. Furthermore, having this data assists in the task of defining the conformations of flexible molecules and in establishing relative stereochemistry between pairs of substituents. Other features of the molecular structure can be decided by careful analysis of coupling patterns including carbon hybridization type, number of heteroatoms attached at CH_n , ring size, symmetry relationships, or the presence of dynamic processes.

Proficiency in translating multiplets into substructures and working structure is important in analyzing spectra of organic compounds. A simple example will be presented now to give a sampling of conclusions derived from analyzing multiplet patterns and coupling constant data. Consider the possible structures for two compounds of formula $\text{C}_{10}\text{H}_{12}\text{O}_2$, whose ^1H NMR spectra are shown in Fig. 7.13.

The ^1H NMR spectrum of one isomer (compound **23** in Fig. 7.13) displays just a singlet at δ_{H} 2.0, which is a mixed blessing. Observing multiplets that can be explained by the familiar $n + 1$ rule (recall that n is the number of neighbor protons) is the first step in piecing together carbon-carbon subunits. In general, singlet peaks indicate the lack of nearby protons but little else. In this case, the δ_{H} 2.0 chemical shift of the singlet resonance indicates the presence of sp^3 -type proton(s). In view of the molecular formula, four methyl groups are most likely attached to sp^2 carbons and related by symmetry. The $n + 1$ rule multiplets observable for the second isomer in Fig. 7.13b are informative, but the most important inferences again pertain to the chemical shifts, which can be measured and ascribed to three features as follows. The signals that resemble doublets ($J \approx 8$ Hz) at δ_{H} 7–8 are due to a 1,4-disubstituted benzene ring, the quartet-triplet pattern ($J \approx 7$ Hz) at δ_{H} 4.4 and 1.4 indicates an OCH_2CH_3 group, the singlet at δ_{H} 2.4 is characteristic of a methyl group attached to an sp^2 carbon, and the remaining atoms, from the molecular formula of $\text{C}_{10}\text{H}_{12}\text{O}_2$, must be a carbonyl group. These various subunits can be

straightforwardly combined to define either *p*-methoxyphenyl methyl ketone or ethyl 4-methylbenzoate. Returning to the compound in Fig. 7.13a and after much pondering, we can clearly see that a simple benzenoid ring will not fit the scant data. Once a tetramethyl quinone ring is visualized, then progress can be made, and only one possibility, the 1,4 quinone **23**, can be drawn.



The take home message illustrated by analysis of the data in Fig. 7.13 is that a worthwhile approach to structure analysis can take place for NMR spectra containing either single lines or many multiplets. Invaluable structural information will be derived by considering complex first-order multiplets, and it will be important to develop strategies to analyze these as well as non-first-order multiplets. We have briefly seen that NMR spectra comprised of mostly singlets can be problematic, and the lack of *J* value data may result in a protracted analysis process. As another complication, even after all of the *J*s have been analyzed, additional data are often needed to distinguish between a set of working structures. In such situations, more advanced NMR experiments are often undertaken to indirectly provide coupling constant data.

7.4.4.1 First-Order Spectra and the $n + 1$ Rule

There are a number of conditions that must be met for a multiplet cluster derived from spin–spin coupling to be considered as a *simple first-order* pattern. The most important is that all coupled spins have a ratio between the chemical shift difference in Hz and the spin coupling magnitude *J* of greater than 6 (expressed as $\Delta\nu/J > 6$) [38]. Another consideration is that when chemically equivalent protons (e.g., homotopic or enantiotopic) are present, they will be magnetically equivalent to one another. The intensities of first-order multiplet peaks will be the greatest at the center of the pattern, and approximately equal intensities should be observed for pairs of peaks equidistant from the midpoint of the multiplet cluster. Finally, peaks observed due to spin–spin coupling should correspond to the expression: $2nI + 1$ (*n* is a total count of neighboring nuclei that have the same *J* to the nucleus under consideration). In contrast to the preceding situation, a *complex first-order* pattern will not have peak intensity and peak counts that fit the relationships just described.

All simple first-order multiplets will have characteristic intensity patterns. The relative peak height will correspond to the coefficients obtained from the polynomial expression $(a + b)^n$. These can also be derived from Pascal's triangle where intensities are calculated by adding the numbers from the top down, as shown for multiplets in Fig. 7.14.

			1						<i>Singlet</i>	(s)
			1		1				<i>Doublet</i>	(d)
			1		2		1		<i>Triplet</i>	(t)
		1		3		3		1	<i>Quartet</i>	(q)
	1		4		6		4		<i>Pentet</i>	(p)
	1	5		10		10		5	<i>Sextet</i>	(sx)
1		6	15		20		15	6	<i>Septet</i>	(sp)

Fig. 7.14 Intensity profile for basic multiplicities

To be more specific, a first-order multiplet will be observed for two protons coupled by $J = 7$ Hz with a chemical shift difference of greater than 42 Hz at 300 MHz, or 0.14 ppm. The advantage of obtaining proton NMR spectra at high fields is now obvious! At 600 MHz, protons coupled by $J = 7$ Hz need only be separated by 0.07 ppm to give a first-order spectrum, and this will be true for many spin systems.

There are three situations in which simple first-order multiplets will not be observed. The first case involves unequal coupling from two or more neighbors and results in *complex first-order multiplets* [39]. The second circumstance occurs when $\Delta\nu/J \leq 6$, and this produces convoluted patterns called *non-first-order multiplets*. The third situation involves coupling between sets of chemically equivalent (e.g., enantiotopic) but *magnetically nonequivalent nuclei*, and this also produces non-first-order multiplets. It is possible by simple inspection to measure J s in spectra containing complex first-order multiplets. By contrast, very few J s can be easily extracted from non-first-order multiplets. Usually such J s can only be obtained by using spectral simulation computer programs that provide an exact match of an experimental and calculated spectrum when the proper coupling constants and chemical shifts are entered.

7.4.4.2 Using Coupling Constants to Understand the Appearance of Spectra

The task of making ^1H and ^{13}C NMR spectral assignments can be accelerated when insights are applied from J value analysis. It is important to consider another fundamental issue pertaining to measuring J values for magnetically equivalent nuclei. Recall that *no* J multiplets will be seen between two protons having identical chemical shifts, either because of chemical equivalence or accidental isochrony between nonequivalent species.

Measuring proton vicinal couplings or $^3J_{\text{HH}}$ can be very important because useful structural information can be derived from the J value. The major determinants of $^3J_{\text{HH}}$ include the HCCH angle, the HCC angle, the C–C bond length, and the presence of electronegative atoms along the coupling path. When these factors

can be isolated, they provide a powerful application of J values to probe structural features. For example, the well-known Karplus equation ($^3J_{HH} = A + B(\cos\Psi) + C(\cos 2\Psi)$) [40] is invaluable in analyzing vicinal couplings in rigid aliphatic systems. The correlation between angle HCCH (obtained from a Newman projection) and J (shown in the left panel of Fig. 7.15), or the relationship between bond order to J (not shown here), is often used to analyze saturated and unsaturated bonds, respectively. Shortly we will consider examples of how $^3J_{HH}$ values can be employed to make relative configuration assignments.

Two other couplings, $^3J_{HC}$ and $^2J_{HC}$, are sensitive to configuration and conformation, and it is often rewarding to measure them. The heteronuclear 3J values follow a Karplus-type pattern (see middle panel of Fig. 7.15) and provide angular relationship information. Obviously the value of $^2J_{HC}$ does not directly depend on a vicinal angular relationship, but there is an important twist. All $^2J_{HC}$ values are sensitive to the dihedral angle between a proton and an electronegative atom three bonds away, as shown in Fig. 7.15 (right panel), and this can be used to extract configuration information.

7.4.4.3 Coupling Constant Values for Different Carbon and Proton Types

Coupling constants can be measured between two nonequivalent ^1H s, ^{13}C s, or a ^1H and a ^{13}C . In principle J s can be quantified between any other pair of $I \neq 0$ nuclei in close proximity [41]. Such data provide a powerful means to assess functionality, exact connectivity, symmetry, stereochemistry, or other parameters of molecular structure. Unlike chemical shifts, coupling constants are invariant at different magnetic field strengths, and they can be determined to an accuracy of ± 0.1 Hz.

To use J values effectively in organic structure analysis requires an understanding of the factors that influence their magnitudes. Empirical and theoretical work shows that the value of H–H or C–H couplings is influenced by the number of intervening bonds, electron density changes, angular relationships, bond hybridization, or electronegativity of atoms along the coupling path. The J values can be “+” or “–” as a function of alignment of nuclear spins. For a ^{13}C – ^1H , the most stable orientation is both spins parallel to each other, which represents a positive coupling sign. The alternative where the two spins are antiparallel yields a negative coupling sign, but only absolute values are actually measured from an NMR trace. Theory predicts that normally 1J s are “+,” 2J s are “–,” and 3J s are “+,” but a negative magnetic moment (μ) species engaged in coupling will have “–” couplings. Both ^{15}N and ^{29}Si have a negative μ , so all of the ^{15}N – ^1H and ^{29}Si – ^1H J s will be negative.

There are some important problems connected with obtaining coupling constant data. Recall that only first-order or complex first-order spectra can be analyzed by sight to afford J data. Two nuclei can actually be coupled, but this may not be reflected in the spectrum. Keep in mind that different nuclei having the same chemical shift are sometimes referred to as isochronous. Protons with different δ s are referred to as anisochronous and multiplets will always be observed if they are proximate. Nevertheless, nonequivalent nuclei that are accidentally isochronous (same δ) will give singlet peaks!

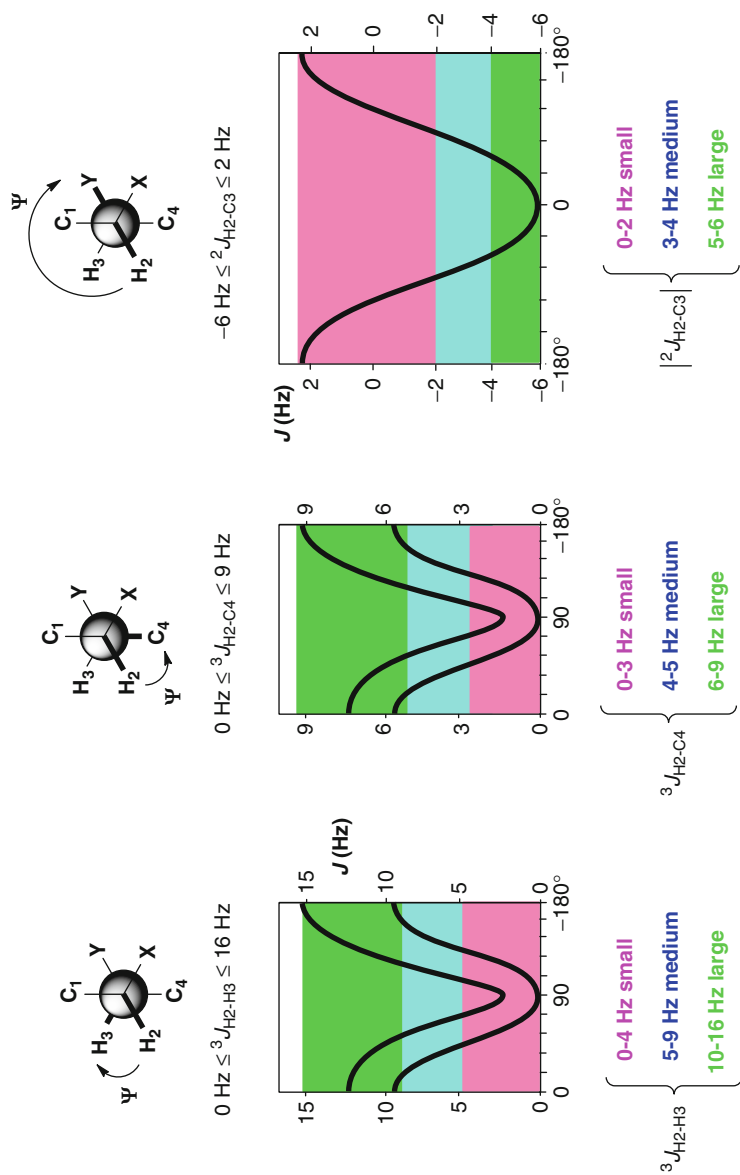
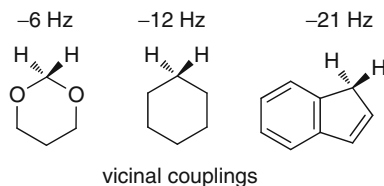


Fig. 7.15 Relationship between coupling constants (${}^3J_{\text{HH}}$, ${}^3J_{\text{HC}}$, ${}^2J_{\text{HC}}$) and dihedral angle (ψ); *upper curves* – carbon frameworks without heteroatoms, *lower curves* – carbon frameworks with heteroatoms

One Bond Js. $^1J_{CH}$, $^1J_{CC}$. A linear relationship exists between the percent CH s character and the $^1J_{CH}$ magnitude according to the following equation: $\%s = (0.2)(^1J_{CH})$. The $^1J_{CH}$ coupling values range from 125 Hz for aliphatic, sp^3 (25% s), 157 Hz for vinyl, sp^2 to 250 Hz for alkyne, sp (50% s) carbons. While this correlation is only of minimal diagnostic value, the regular increase in the $^1J_{CH}$ magnitude with increasing electronegativity of substituents is highly useful as illustrated by the $^1J_{CHs}$ in the series CHZ, Z: Li (98 Hz), C (125–129 Hz), NR (131–134 Hz), OR (140 Hz). Typical values for $^1J_{CC}$ are 30–50 Hz, and these are easiest to measure in ^{13}C -labeled compounds.

Two Bond Js. $^2J_{CCH}$, $^2J_{HCH}$, $^2J_{CCC}$. A variety of 2J values can be observed for both homonuclear and heteronuclear interactions. Values of J_{HH} range from +3 Hz for CH_2 to –14 Hz for CH_2 , while the $^2J_{HC}$ vary from –6 Hz for HCC, +5 Hz for $\text{HC}=\text{C}$, +1–2 for benzenoid $\text{HC}=\text{C}$, to +50 for $\text{HC}\equiv\text{C}$; by contrast, the $^2J_{CC} \approx 0$. The large differences observed for $^2J_{HH}$ across an sp^2 vs. an sp^3 carbon are especially noteworthy. Diagnostic changes occur for aliphatic proton J s when at least two electronegative substituents are present, or for rigidly oriented adjacent π -bonds. These trends are illustrated by 2J s in this series: cyclohexane (–12 Hz), 1,3-dioxane (–6 Hz), and indene (–21 Hz). Molecular orbital calculations have been able to simulate the direction rather than the real value of these trends.

The trends in $^2J_{CH}$ range from –5 to +50 Hz, parallel to those observed for $^2J_{HH}$. The orientation of adjacent electronegative groups can increase the coupling magnitude; this has been useful in conformational analysis studies of carbohydrates. Larger values are observed when the coupling path includes an sp^2 carbon, but this does not apply to benzenoid aromatics. This can be seen by comparing the $^2J_{CH}$ data for benzene (1 Hz) to that of furan (5–7 Hz).

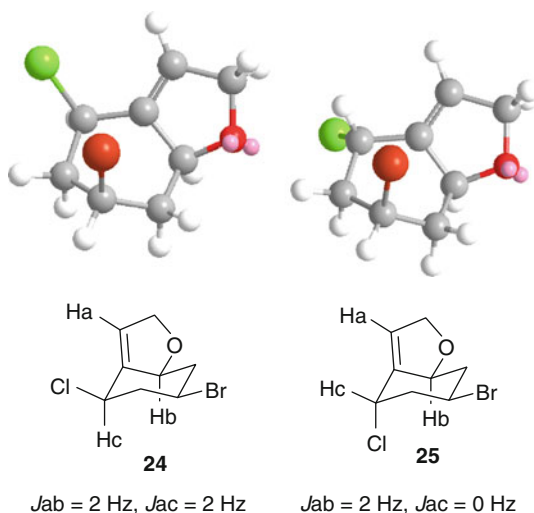


Three Bond Js. $^3J_{HCCCH}$, $^3J_{HCCC}$, $^3J_{CCCC}$. Vicinal couplings are routinely employed in structure analysis. Vicinal 3J values for ethane are typified by $^3J_{HH} = +7$ Hz, $^3J_{CH} = +6$ Hz, and $^3J_{CC} = +4$ Hz (propane). A similar trend is observed for this series across double bonds. Collectively these data illustrate that substitution of a proton by a carbon reduces the coupling magnitude by a factor of approximately 0.6–0.8 given by the following relationship: $^3J_{CC} = (a)(^3J_{CH})$ and $^3J_{CH} = (a)(^3J_{HH})$, where $a = 0.6$ –0.8.

Four Bond Js. $^4J_{HCCCCH}$. Couplings between protons separated by four or more bonds (sometimes called long-range couplings) generally need not be included when applying the $n + 1$ rule. A $^4J_{HH} \approx 0$ is normal when the coupling path consists entirely of sp^3 bonds in an acyclic array. A series of exceptions to this are represented by some cases but are usually 2–3 Hz. An interesting situation is presented by rigid cyclic systems and exceptional among these are bicyclopentane

with a ${}^4J_{\text{HH}} = 18$ Hz and bicyclo (3.1.1) heptane with ${}^4J = 5.5$ Hz. The best opportunity to observe ${}^4J_{\text{HH}}$ is when the coupling path includes one or more sp^2 Cs, and J s from 2–4 Hz often occur. An important example is the benzene ring *meta* coupling of up to 3 Hz.

Both empirical results and theory show ${}^4J_{\text{HH}}$ is maximized when the coupling path atoms are in a “W” coplanar geometry. Only a single 4J from the “W” path is observed for bicyclohexane, even though there are several routes possible for this coupling. Values between 1 and 3 Hz can be observed when the coplanar Cs vary from all sp^3 to all sp^2 . The appearance of a ${}^4J_{\text{HH}}$ can be used to solve stereochemistry problems. For example, the 4J s in the halogenated natural products chondrocole A (**24**) and chondrocole B (**25**) allowed the determination of the stereochemistry of both H_b and H_c by the “W” couplings observed to H_a (build molecular models to verify these relationships).

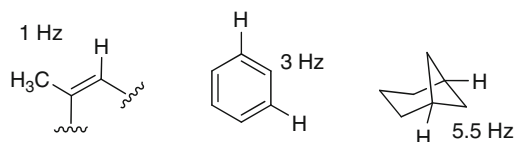


The Karplus relationship, shown previously in Fig. 7.15, is extremely useful because it provides a way to estimate stereochemistry from the J values of aliphatic systems. A graph of its parameters predicts the following correspondence between ${}^3J_{\text{HH}}$ and proton dihedral angle (ψ): $\psi = 0^\circ$ $J = 11.5$; $\psi = 90^\circ$ $J = 0$; $\psi = 180^\circ$ $J = 13$. The subsequent modifications incorporated by the Altona equation [42] provide data for electronegative substituents in the coupling path, and a slight lowering in the magnitude of J is observed. The steep slope of the curve from 180° to 90° is what makes J data so effective in the stereochemical analysis of both acyclic and cyclic C–C chains. Parallel curves are observed for ${}^3J_{\text{CH}}$ and ${}^3J_{\text{CC}}$, and these couplings compared to those of ${}^3J_{\text{HH}}$ will allow you to estimate additional J s.

Assignment of axial or equatorial stereochemistry in a cyclohexane ring is a straightforward example of how to use the J vs. angular relationship in stereochemical analysis. The way ${}^3J_{\text{HH}}$ varies in a cyclohexane ring is illustrated by the appearance of the axial protons. Note that two vicinal diaxial cyclohexane ring Hs with a dihedral angle of 180° have a ${}^3J_{\text{ax-ax}} = 12$ Hz, whereas vicinal

axial–equatorial (or equatorial–equatorial) Hs with a dihedral angle of 60° have a $^3J_{\text{ax-eq}} = ^3J_{\text{eq-eq}} = 4 \text{ Hz}$.

Obtaining vicinal couplings for vinyl protons can be beneficial. The stereochemistry of a 1,2-disubstituted double bond can be quickly assigned via the angular variation of 3J s. The coupling constants for vinyl protons are *cis* = 11 Hz and *trans* = 17 Hz, and these data can be used to assign double bond geometry. The variation in J for an $\text{HC}=\text{CH}$ with ring size change illustrates the influence of the angle HCC. This angle decreases in going from a cyclopropane to a larger ring while the J value increases, but the dihedral angle HCCH is constant and the change in J is as follows: cyclopropene (2 Hz), cyclobutene (5 Hz), cyclopentene (6 Hz), cyclohexene (10 Hz), and cycloheptene (11 Hz).



some long range proton-proton couplings

The presence of electronegative groups along the coupling path slightly reduces the magnitude of $^3J_{\text{HH}}$. It is reassuring that 3J s are still sensitive to stereochemical changes even when several electronegative groups are present. Be aware that variations of J s in accordance with the Karplus equation can also be seen in heterocyclic rings, for example, in the tetrahydropyran rings of carbohydrates.

An evaluation of the ^1H NMR spectrum for the marine compound cartilagineal (**26**) $\text{C}_{10}\text{H}_{11}\text{OCl}_3$ shows signals including multiplets for eight individual protons plus an intense methyl singlet. The ^{13}C NMR spectrum shown (Fig. 7.16b) has eight intense singlet peaks and two weaker signals. This spectrum was acquired with accompanying broadband proton decoupling to eliminate all J_{CH} multiplets which results in singlet peaks for each carbon.

Before real progress can be made in the assignment of the resonances of cartilagineal (**26**), it is essential to have ^{13}C NMR data showing multiplet information from $^1J_{\text{CH}}$. Rather than examining such a spectrum now, let us focus just on the results. This important multiplicity information is indicated in Fig. 7.16b by letters above each peak representing the count of attached protons such as S, D, T, and Q to indicate a C (singlet), a CH (doublet), a CH_2 (triplet), or a CH_3 -type residue (quartet), respectively. Observe that one or more of these carbon types are present in cartilagineal and are noted in the spectrum. There are two singlet carbons with the characteristic smaller intensities due to the absence of NOE that arises for a carbon with directly attached protons. Chemical shift differences expected for sp^2 and sp^3 carbons allow assignment of the quaternary signals such as: C2 (δ 143.7) and C6 (δ 65). These characteristic chemical shifts plus α -substituent effects enable three of the six doublet carbons to be denoted as: C9 (δ 187), C1 (δ 143.9), and C5 (δ 70). A provisional assignment of C7 (δ 136) could be based on β -additivity effects which leaves C3 and C4 associated with the remaining two doublet carbons (δ 134 and 131). The last two carbons are a triplet C8 (δ 116) and a quartet (δ 24).

Turning now to the ^1H NMR resonances of cartilaginal (26), we find that each one can be definitively assigned. The intense upfield singlet resonance (δ 1.71) is associated with a methyl group, while the intense low field singlet peak (δ 7.05) is due to H1. The lowest field proton H9 (δ 9.04) is a d, $J = 2.0$ Hz, reflecting a 4J coupling by a “W” path to H3 (δ 6.49) a ddd, $J = 15.3, 2.0, 1.0$ Hz. This proton is in turn coupled to H4 (δ 7.05) a dd, $J = 15.3, 8.5$ Hz. In addition, the coupling to this

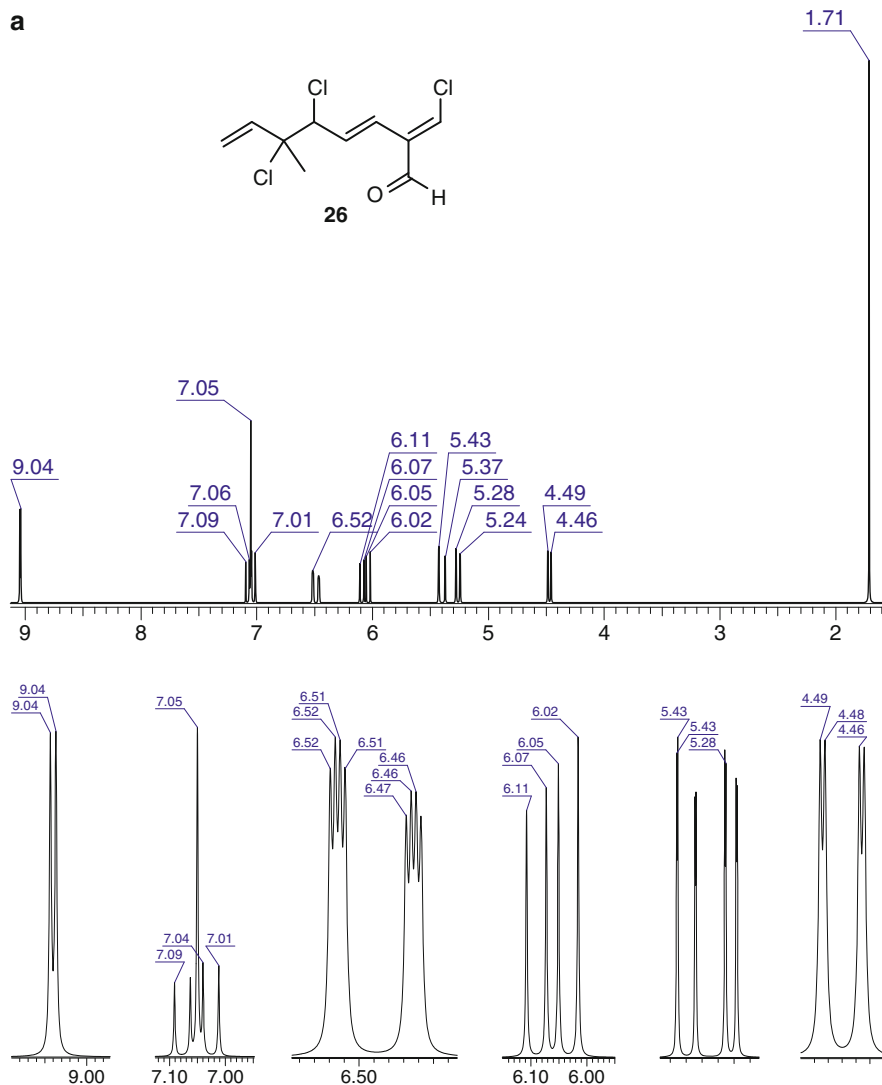


Fig. 7.16 (continued)

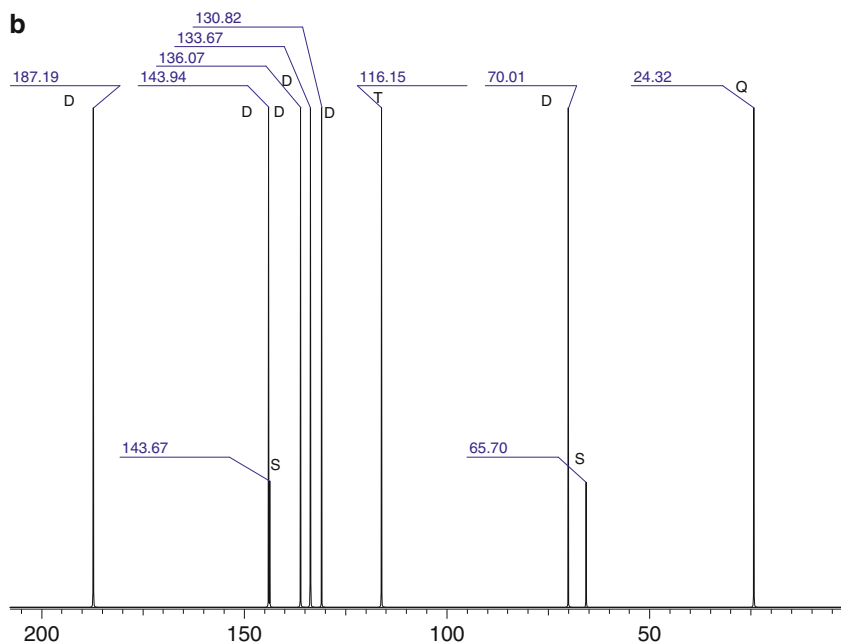


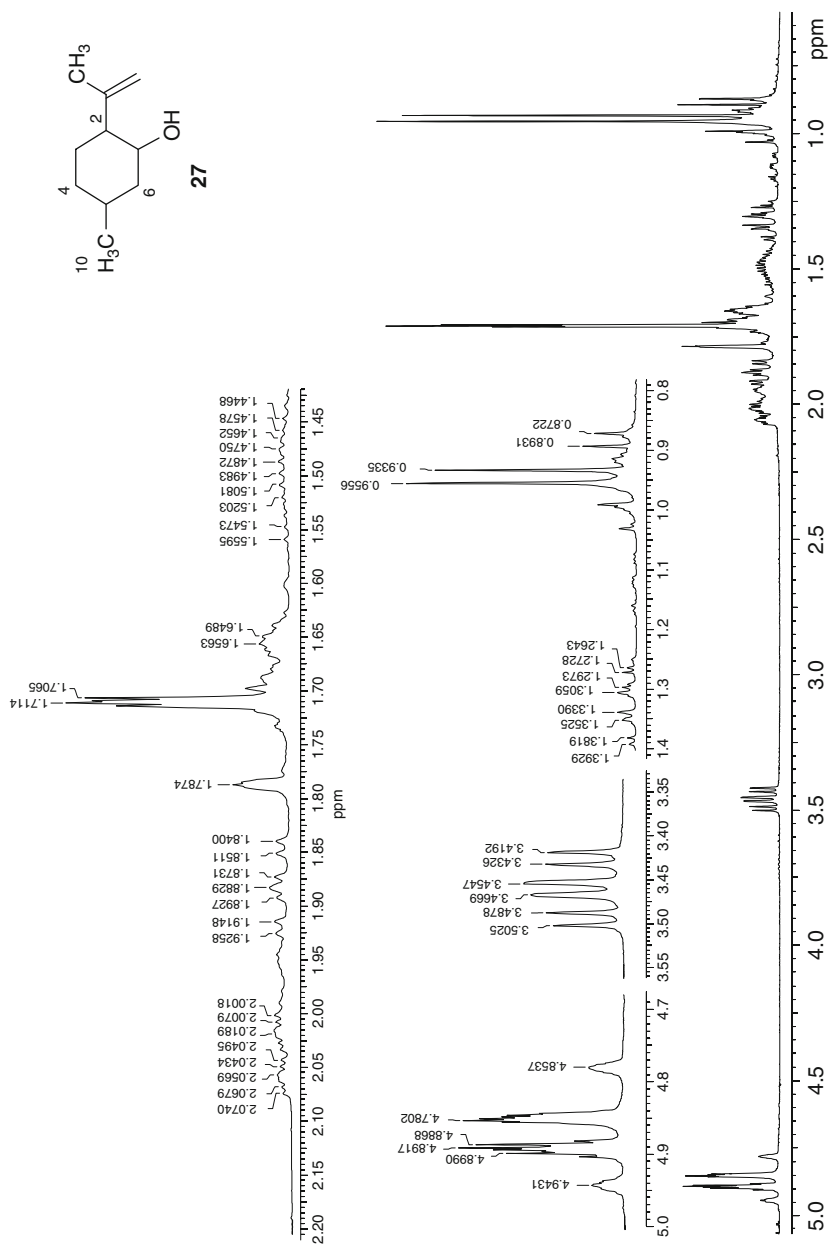
Fig. 7.16 (a) ^1H NMR spectra (CDCl_3 300MHz) of cartilagineal (**26**). (b) ^{13}C NMR spectra (CDCl_3 75MHz) of cartilagineal (**26**)

latter proton allows assignment of H5 (δ 4.47) a dd, $J = 8.5, 1.0$ Hz. The three remaining protons display the characteristic pattern of an isolated vinyl group: H8 (δ 5.26) a dd, $J = 10.5, 1.0$ Hz; H8 (δ 5.40) a dd, $J = 17.0, 1.0$ Hz; and H7 (δ 6.06) a dd, $J = 17.0, 10.5$ Hz.

7.4.4.4 Using Coupling Constants to Make Configurational Assignments

Let us now consider how a J value can be used to define geometrical relationships between substituents on varying molecular frameworks. Our focus will be on adjacent (1,2) or alternate (1,3) configurational centers along a carbon chain. An important element of the process involves cataloging relationships visualized by using Newman projections. Take a moment to revisit how changes in 3J and 2J data depend on dihedral angles (ψ), as indicated in Fig. 7.15. As will be further discussed next, the absolute J values shown are further summarized by a statement about the relative size (small, medium, or large), also defined below as $J_{\text{magnitude}}$.

Take a moment to examine the ^1H NMR spectrum (300 MHz, CDCl_3) of isopulegol (**27**) ($\text{C}_{10}\text{H}_{18}$) shown in Fig. 7.17. Try to assign as many protons as possible to the many multiplets observed. Even though the shapes of the multiplets can be assessed using the $n + 1$ rule, most of them are actually complex first order.

**Fig. 7.17** ¹H NMR of isopulegol (CDCl₃, 300 MHz)

With this first inspection completed, it should now be possible to make a list of the J data for the Hs which will provide information to determine the ring conformation of **27** and establish the configuration of its substituents.

The major steps in translating the ^1H NMR data of isopulegol (**27**) into three-dimensional assignments are made using arguments already discussed. The first action, to define the conformation of the ring, is based on locating the J 's diagnostic for Hs at axial or equatorial positions. In this case, a rigid chair form can be confidently proposed for **27** based on observing large J 's diagnostic of bis-axial related protons. For example, the carbinol carbon H1 at δ_{H} 3.45 is a dt $J = 4, 10$ Hz with the large magnitude for the triplet arising from mutual coupling from axial Hs at positions 2 and 6. So the OH group can be concluded to be equatorial, and the propenyl group must also be equatorial. Further confirmation of the latter conclusion comes from looking at the allylic ring proton at position 2. It is expected to be at relatively low field and can be assigned to the ddd multiplet cluster centered at δ_{H} 1.88, $J = 3.3, 9.9, 12.9$ Hz (from two large axial–axial and one smaller axial–equatorial couplings). Clearly H2 is axial verifying that the geminal propenyl group is equatorial. Assessing the geometry at CH_3 10 cannot be decided based on H5, because this proton at δ_{H} 1.49 has a “forest” of peaks. Alternatively evaluating the couplings to axial H6 provides an unambiguous way to set the geometry of this methyl group. However, locating the resonance of axial H6 requires ingenuity because it is obscured by the doublet $J = 6.6$ resonance of CH_3 –10 at δ_{H} 0.94. The H6 axial multiplet appears as a 1:3:3:1 quartet, $J = 12.2$ Hz consisting of the following four transitions at δ_{H} 0.9960, 0.9556, 0.9336, and 0.8931 – but notice that two of these peaks overlap those of CH_3 –10! This quartet pattern is based on one $J_{\text{gem}} = 12.2$ and two $J_{\text{vic}} = 12.2$ Hz couplings. With the assignment completed, the presence of axial–axial coupling between H5 and H6 is now fully documented, making it possible to assign CH_3 –10 as equatorial. No more data analysis is needed to finalize the full configuration assignment of isopulegol (**28**).

Another strategy, which was introduced in 1999 and extends the power of using J s for configurational analysis of polysubstituted acyclic carbon frameworks, is the commonly called the “Murata J -based method” [43]. This is outlined in Fig. 7.18 and involves the evaluation of carbon chain fragment rotamers. The essence of the strategy is to draw Newman projections for the *syn* (threo) or *anti* (erythro) relative configurations of a four-carbon fragment and then use Karplus-type curves to translate the observed dihedral angles into J values. The approach is comprehensive in that it uses three sets of coupling constants: $^3J_{\text{HH}}$, $^3J_{\text{HC}}$, and $^2J_{\text{HC}}$. A series of rotamers drawn for each coupling reflect the three ranges of J s expected (see Fig. 7.18), and these are the basis for the nine rotamers shown in Fig. 7.18. In practice, only the staggered gauche and antirotamers represent NMR-relevant conformations, reducing the total to six. The several important requirements and assumptions connected with the use of the “Murata J -based method” are as follows:

(a) The carbon framework should be conformationally mobile. (b) The $^3J_{\text{HH}}$, $^3J_{\text{HC}}$ values must follow the Karplus relationship and arise from the anti and/or gauche conformations. (c) The substituents are limited to Y, Z = CH_3 , OH, OCH_3 , Cl, or Br. (d) Absolute J values can be used but must be accurately measured

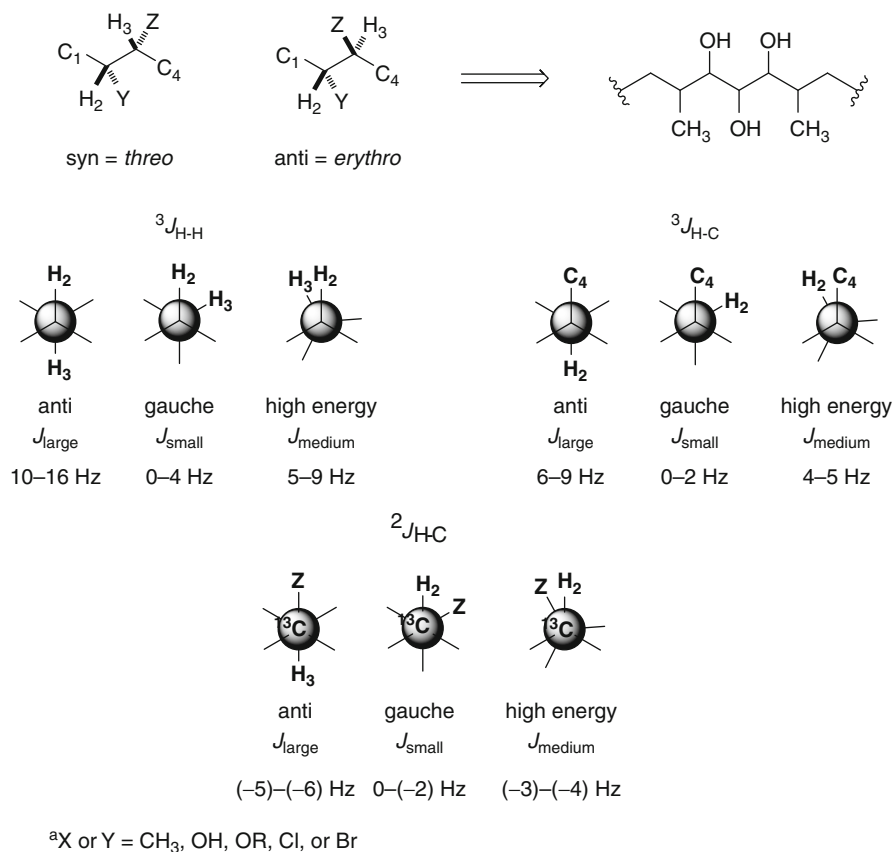


Fig. 7.18 The Murata J -based method to determine relative configurations in acyclic systems

($^3J_{HH}$ to 0.1 Hz; $^2J_{HC}$ and $^3J_{HC}$ to 1 Hz). (e) The conclusion about *syn* vs. *anti* configuration is based on the relative large vs. small J value which varies for each J type, as shown in Fig. 7.19.

The process for implementing the “Murata J -based method” involves obtaining the actual J value followed by substituting these data into a conclusion framework. The analysis is based on a review of six major rotamer forms shown in Fig. 7.18 – three (T1, T2, and T3) for the threo (*syn*) configuration, and three (E1, E2, and E3) for the erythro (*anti*) configuration. The key $J_{magnitudes}$ results shown are for 42 different possibilities for a chain of four carbons containing the allowed Y and Z substituents. Do not forget that the $J_{magnitudes}$ indicated by “small” or “large” are relevant as indicated by the data in Fig. 7.19. Be aware that the J -based method cannot be employed when “medium” magnitudes are observed including $^3J_{HH} = 5$ to 9 Hz, $^3J_{HC} = 4$ to 5 Hz, and $^2J_{HC} = (-3)$ to (-4) Hz.

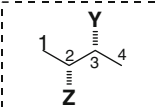
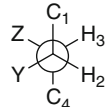
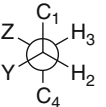
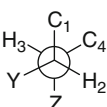
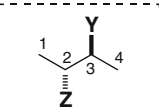
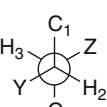
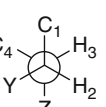
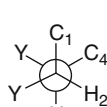
				
1,2 threo=syn		gauche (T1)		
			gauche (T2)	anti (T3)
	$^3J_{H2-H3}$	small	small	large
	$^3J_{H2-C4}$	small	large	small
	$^3J_{C1-H3}$	small	large	small
X=Me	$^3J_{CY-H3}$	large	small	small
Y=OR	$^2J_{C3-H2}$	small	large	large
X=OR	$^2J_{C2-H3}$	small	large	large
Y=OR	$^2J_{C3-H2}$	small	large	large
				
1,2 erythro=anti		gauche (E1)		
			gauche (E2)	anti (E3)
	$^3J_{H2-H3}$	large	small	small
	$^3J_{H2-C4}$	small	large	small
	$^3J_{C1-H3}$	small	small	large
X=Me	$^3J_{CY-H3}$	small	large	small
Y=OR	$^2J_{C3-H2}$	large	large	small
X=OR	$^2J_{C2-H3}$	large	small	large
Y=OR	$^2J_{C3-H2}$	large	large	small

Fig. 7.19 The logic network based on $J_{\text{magnitudes}}$ for use in the Murata J -based method to determine relative configurations

7.4.5 The Nuclear Overhauser Effect

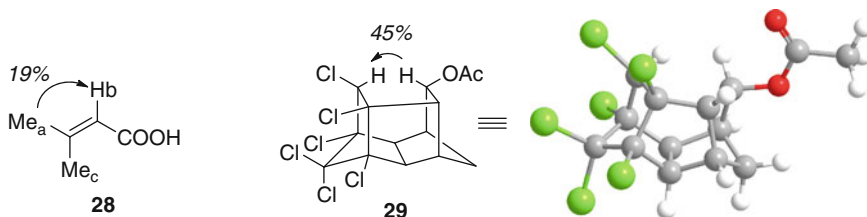
Under certain experimental conditions, unexpected increases or decreases can be observed in the integrated intensities of an NMR absorption. The first application of this phenomenon involved monitoring the intensity of one spin during low-power spin decoupling at a second. This provides what is now commonly called the nuclear Overhauser enhancement (NOE). Currently, there are a variety of situations where NOE data are used, and second generation approaches (often termed nuclear Overhauser effect) do not involve peak integration [44]. A very common application of the NOE is in ^1H decoupling routinely used in acquiring ^{13}C NMR spectra. Such decoupling not only generates ^{13}C NMR singlets but it also provides nuclear Overhauser enhancements at carbon of up to 200%. Similarly, in homonuclear ^1H NMR, a NOE of up to 50% is possible. The maximum percentage enhancement can

be predicted by the following Eq. 7.6, which is based on ratios of γ' (gyromagnetic ratio).

$$\% \text{ NOE epeak increase} = (100)\gamma'_A/2\gamma'_X \quad (7.6)$$

(A is the peak saturated; X is the peak observed)

In practice, small effects are actually observed in homonuclear ^1H NMR experiments. For example, 3-methyl-2-butenic acid (**28**) often serves as a standard to ensure a proton NOE experiment is being properly performed. Irradiation of Me_b yields a 19% enhancement in the integrated area of H_a , while irradiation of Me_c results in a 2% decrease in the integrated area of H_a . Even more striking is an NOE observation for the “half-caged” compound **29**, because irradiation of H_a causes a 45% increase in the signal of H_b . Notice in these ^1H NMR examples the use of a concise convention, shown in the drawings of **28** and **29**, in which a curved arrow points from the irradiated proton toward the one experiencing the NOE.



Homonuclear ^1H NOE data are especially useful for making relative stereochemical assignments or in setting distance constraints for molecular modeling calculations. This is possible because the NOE offers an *indirect* measurement of dipolar coupling occurring between nuclei that are in close proximity. Such nuclei can interact by a through-space dipole–dipole relaxation mechanism. A rule of thumb states that the magnitude of an NOE is proportional to the inverse of the sixth power of the distance between two nuclei. However, this relationship must be applied cautiously because the dipole–dipole relaxation pathways that determine NOE magnitudes can be quite varied. Furthermore, molecular motion dynamics which also contribute to an NOE can be both random and variable in different parts of the same molecule. In spite of these potential complications, it is often stated that short, medium, or long-range NOEs are defined as H–H distances of up to 2.8 Å, 3.4 Å, or 4.2 Å, respectively. A further subdivision of the NOE intensities correlated to distance constraints includes [% intensity // distance in Å] strong = 6.1–14%/1.8–2.8 Å; medium = 4.1–6.0%/2.8–3.4 Å; and weak = 1.0–4.0%/3.4–5.0 Å. Finally, it is further assumed that interproton distances of greater than 5–6 Å cannot give a detectable NOE.

It is useful to briefly visit the origin of the nuclear Overhauser effect. Recall that the NOE is the signal intensity change of a first nucleus when the resonance (or transition) of a second nucleus is perturbed. A set of two $I = 1/2$ nuclei whose

distance is less than 5 Å which are interacting by dipole–dipole relaxation (sometimes called coupling) has six pathways for the relaxation mechanism. It is the dominance of one path over another which ultimately influences the type of NOE to be observed: positive, nil, or negative. In this regard, random molecular motions denoted as τ_c (rotational correlation time) occurring within the compound dictate which dipole–dipole relaxation pathway will prevail. Molecular size and molecular shape influences the magnitude of τ_c : Small molecules have short correlation times ($\tau_c \approx 10^{-12}$), and macromolecules have long correlation times ($\tau_c \approx 10^{-8}$). When τ_c is short, then a positive NOE will be observed, and when τ_c is long, then a negative NOE might be observed.

In summary, the technique of NOE difference spectroscopy is widely used and is certainly effective in homonuclear ^1H applications. However, there are two-dimensional methods such as NOESY (*nuclear Overhauser effect spectroscopy*) which are more attractive and are being increasingly applied to obtain NOE data.

7.4.6 Multipulse NMR

Success in using NMR data to assemble partial or total molecular structures depends on the accurate interpretation of just four parameters: chemical shifts, coupling constants, peak areas, and relaxation effects. Up to this point, we have been evaluating one-dimensional (1D) NMR spectra obtained by the “single-pulse” FT NMR method. Often 1D NMR data obtained at the highest available magnetic field do not provide enough information to complete a structure analysis or to assign the resonances in a complex spectrum. Two impediments are common, especially in ^1H NMR. The first involves spectra having many coincident resonances (overlap), and the second includes spectra where mostly proton singlets are observed. In both situations, the obstacle to further progress is the lack of interpretable J and/or δ values.

The only way to obtain accurate J and δ parameters in these cases is by 2D NMR spectroscopy. Some 2D NMR experiments simultaneously reveal all spin–spin couplings. Such data can be used to derive firm conclusions about connectivities between proton–proton, proton–carbon, and carbon–carbon subunits.

A large number of multidimensional NMR methods are available for routine use today. The acronyms for both 1D and 2D NMR techniques seem unusual, for example: COSY, NOESY, HOHAHA, DEPT, INADEQUATE, TOCSY, and HMBC (see [Tables 7.4](#) and [7.5](#) for more information about these and others). In this chapter, we will not consider all of the 1D and 2D NMR methods known. Instead, our focus will be on the principal strategies that provide useful information for molecular structure analysis.

Usually the first types of 2D NMR experiments performed are NMR, ^1H – ^1H COSY and ^1H – ^{13}C correlation spectroscopy (\approx HSQC or HMQC). These are valuable because all spin–spin couplings are simultaneously revealed between magnetically nonequivalent species of the same element (homonuclear) or between different elements (heteronuclear). Most of these techniques are concerned with

Table 7.4 One-dimensional NMR experiments useful for molecular structural studies

Information desired	Experiment	Nucleus	Results
Proton–proton connectivity	Homonuclear decoupling	^1H	^1H multiplets collapse
Proton–proton connectivity	1D-TOCSY	^1H	All protons within a J -coupled spin system appear upon selective excitation of one proton in the spin system
Number of protons attached to a carbon	DEPT	^{13}C	^{13}C – ^1H coupling revealed by positive intensity singlets for CH_3 and CH and negative singlets for CH_2 's with C's nulled DEPT
Spatial relationships	NOE	^1H	Changes in peak intensities that can be measured by difference spectroscopy Modern variant is a selective NOE experiment in which selective excitation of one proton leads to appearance of peaks in spectrum which are close in space
Exchange reaction mechanisms	DNMR	^{13}C , ^1H	Narrow lines at separate δ 's broaden and eventually merge by varying the temperature
Proton–carbon connectivity	SIMBA	^{13}C	Selective excitation at one carbon reveals coupled protons up to three bonds removed

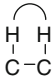
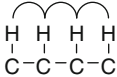
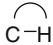
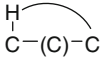
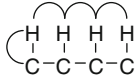
^1H and ^{13}C , but with small modifications, they can also be applied to other $I = 1/2$ nuclei common in organic molecules such as ^{31}P and ^{15}N .

7.4.6.1 One-Dimensional Multipulse NMR Techniques

A useful method to determine the multiplicity type of the carbon you are dealing with is the *distortionless enhancement by polarization transfer* (DEPT) experiment. The DEPT-135 spectrum displays CHs and CH_3 s as positive singlet peaks and CH_2 s as negative singlet peaks with the quaternary Cs nulled (Fig. 7.20). DEPT-45 gives all protonated carbons as positive peaks, while quaternary carbons are nulled. The DEPT-90 gives CH peaks positive with all other carbon peaks nulled. Automated editing (by addition and subtraction) of these three types of DEPT spectra taken can be used to obtain spectra which display only one carbon type. However, in practice, completely “clean” (e.g., CH_3 s only) edited spectra are difficult to obtain. Overall, the DEPT-135 is used most often as it gives the most information because a distinction can be made between CHs and CH_3 s, since peaks at lower chemical shifts ($< \delta$ 20) can be assigned to methyls (except CHs in cyclopropyl rings) and peaks at shifts greater than δ 30 to CHs (except *O*-methyls at δ 60 and *N*-methyls at δ 30–40). The major purpose of this experiment is to provide an unambiguous way to assign carbon types. Taken one step further, this data provides a count of carbons and protons that can be used to determine a partial molecular formula. We will see later how the same information can be obtained from edited ^1H – ^{13}C correlation experiments (edited HSQC).

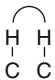
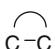
The development of frequency selective, low power, “shaped” pulses has allowed a large number of new 1D pulse sequences to be developed. These are extremely useful, especially when there is a high degree of overlap in the

Table 7.5 Two Dimensional NMR experiments useful for molecular structural studies

Information desired		Experiment	Nucleus	Results
Proton–proton couplings (vicinal proton connectivities)		^1H – ^1H COSY	^1H	Auto-correlated spectrum with frequencies along each axis and the diagonal. Off-diagonal contours, those that can be connected by a line perpendicular to the diagonal, show ^1H – ^1H spin-couplings
Long-range proton–proton couplings (all protons in one spin system)		^1H – ^1H TOCSY	^1H	Auto correlated spectrum like ^1H – ^1H COSY, showing geminal, vicinal and longer range couplings simultaneously depending on mixing time used. The intensity of the contour is independent of the coupling between the protons
Direct proton to carbon couplings (proton to carbon connectivities)		HMQC, HSQC	^{13}C , ^1H	Cross-correlated spectrum with proton frequencies along one axis and carbon frequencies along the second axis. Cross-peaks show one bond ^1H – ^{13}C couplings = 140 Hz
Long range proton–carbon couplings via a H–C–C or H–C–C–C coupling pathway		HMBC	^{13}C , ^1H	Cross-correlated spectrum with proton frequencies along one axis and carbon frequencies along the other. Intersection contours show ^1H – ^{13}C long range couplings = 5–10 Hz. Two or three bond correlations across quaternary C or heteroatoms possible
Long range proton–carbon couplings via a H–H–C coupling pathway (proton to carbon connectivities within one spin system)		HMQC-TOCSY, HSQC-TOCSY	^{13}C , ^1H	Cross-correlated spectrum with proton frequencies along one axis and carbon frequencies along the other. Shows direct responses (one bond) and multiple bond correlations (up to seven bonds depending on mixing time) on the same plot. Gives ^1H – ^1H connectivities equivalent to TOCSY spectrum, sorted by carbon chemical shifts Correlations across

(continued)

Table 7.5 (continued)

Information desired	Experiment	Nucleus	Results
Spatial relationships between protons	 ^1H – ^1H NOESY ^1H – ^1H ROESY	^1H	quaternary C or unprotonated heteroatoms not possible Auto-correlated spectrum with frequencies along each axis and the diagonal. Off-diagonal contours, those that can be connected by a line at 90° to the diagonal, show ^1H – ^1H spin-couplings or NOE's
Carbon–carbon connectivities	 INADEQUATE	^{13}C	Double quantum spectrum with carbons as pairs of doublets for C–C units connected by a horizontal line ending at the f_2 value corresponding to the carbon chemical shift. The horizontal lines are separated along the f_1 frequency axis

corresponding area of the 1D spectrum. A selective pulse is shaped so that only one resonance in the NMR spectrum is excited, and it is possible to obtain a spectrum of that resonance alone, although this would be of little value in a structure elucidation process. The key is translating the information from the frequency domain (the chemical shift of the resonance to be excited) via an “inverse Fourier transform” into a shaped pulse in the time domain so that no other resonances are excited.

One of the most useful applications of selective pulses is in the selective 1D TOCSY spectrum, which is a one-dimensional variant of the ^1H – ^1H TOCSY. The pulse sequence is extremely simple. The selective $(90^\circ)_x$ pulse centered on the resonance of interest is followed by a spin-lock mixing period which is of variable length. During this period, transfer of magnetization occurs between the excited proton and adjacent protons within the spin system. The nature of the TOCSY mixing process means that protons in the spin system are excited in strict sequence, which makes this a powerful technique to simplify complex overlapping spectra and assign resonances to structural features very quickly as in the antibiotic amikacin (**30**). In this example $\text{H}_2 = 3.53$ ppm, $\text{H}_3 = 3.65$ ppm, $\text{H}_4 = 3.23$ ppm, $\text{H}_5 = 3.88$ ppm, and $\text{H}_6/6' = 3.32/3.01$ ppm. In modular structures such as saccharides and peptides, exciting the easily identified anomeric protons or α -protons, respectively, permits the rapid assignment of all resonances and relative configurations of some of the chiral carbons (Fig. 7.21).

A second powerful experiment which relies on selective excitation by shaped pulses is the selective 1D NOE experiment in which a single resonance is excited and its through-space coupling partners identified. An example is given in Fig. 7.22

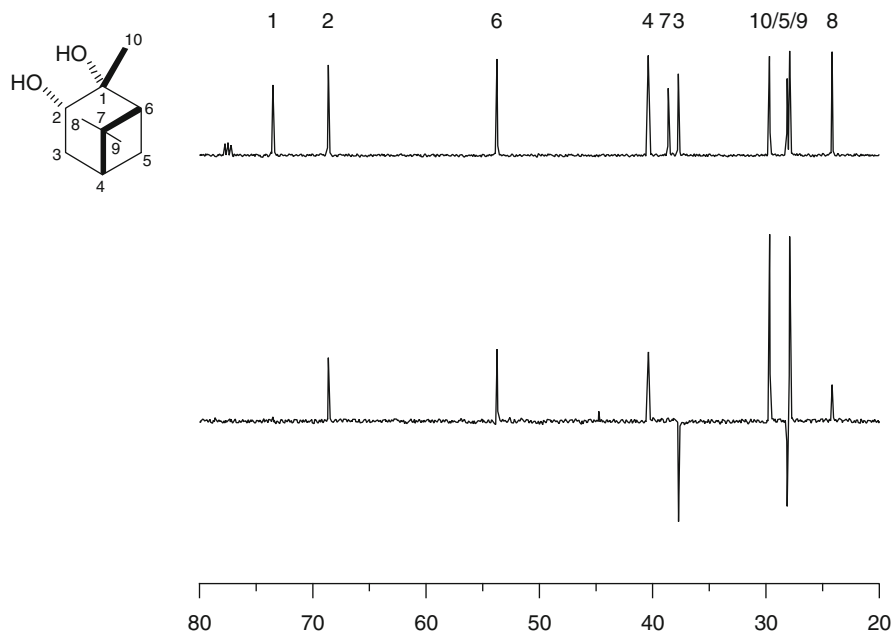


Fig. 7.20 ^{13}C NMR and DEPT-135 of (+)-pinane-1,2-diol (CDCl_3 , 125MHz). Signals have been phased so that CH_3 and CH are up, CH_2 is down, and C is nulled

for 2-chloro-dodec-2,11-dien-1-ol which contains a trisubstituted double bond, and for this reason, the stereochemistry cannot be determined using coupling constants. The *E* and *Z* configurations would give different NOEs for H1 (Fig. 7.22); for *E* we would expect H1–H4 and for *Z* we would expect H1–H3. For the *Z* configuration shown, H1 and H3 are in close proximity, whereas for the *E* geometry, H1 and H4 would be close in space. In this experiment, H1 was selectively excited and an NOE to H3 observed indicating that the *Z* geometry shown is correct. Note that the phase of the NOE peak is opposite to that of the excited peak, and that the spectrum contains very few artifacts compared to a typical NOE difference spectrum. Very weak NOEs can be detected using this pulse sequence, down to 1–2% in magnitude.

7.4.6.2 Two-Dimensional NMR Techniques

The groundwork for two-dimensional NMR experiments can be traced back to theoretical descriptions appearing during the mid-1970s. It took almost a decade of further development before such procedures became routine, work for which Richard Ernst received the Nobel Prize in 1991 [45]. The most important benefit of these methods is that individual chemical shifts and all coupling constants can be measured unequivocally even when multiplets are overlapping. Many 2D

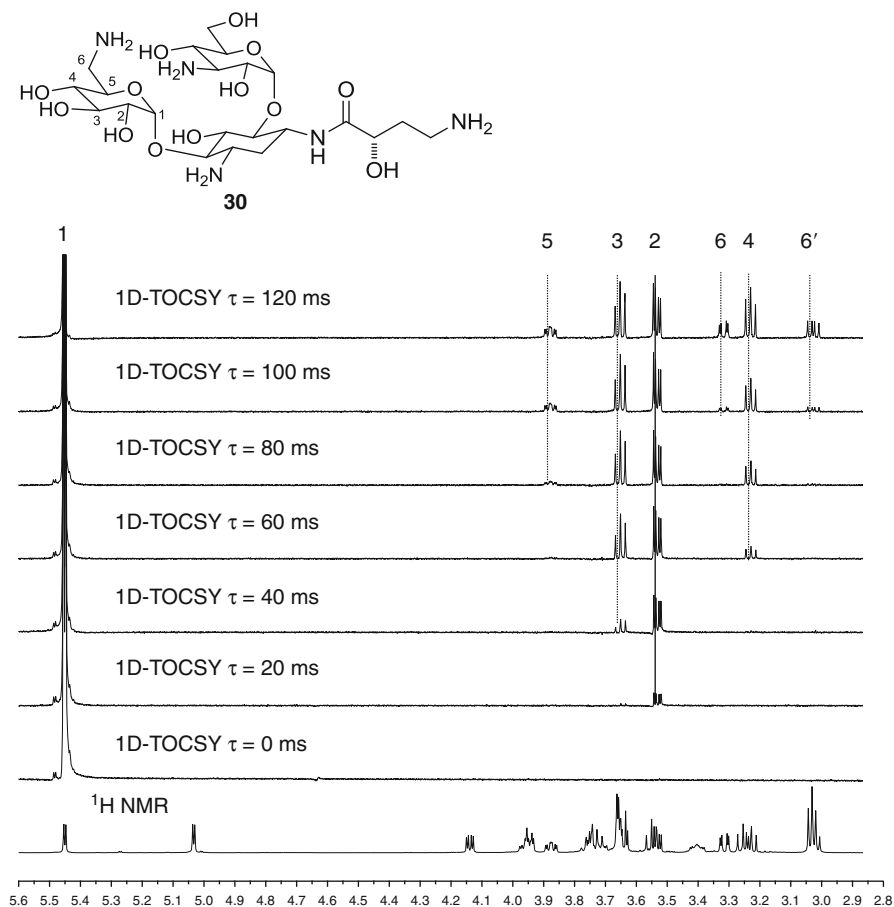


Fig. 7.21 The effect of increasing mixing times in the selective 1D-TOCSY pulse sequence carried out on amikacin (30). Irradiation at 5.45 ppm (H1)

experiments are made up of five basic “building blocks”: spin echo, polarization transfer (DEPT), COSY, TOCSY, and HMQC. Thus, an enormous number of 2D NMR procedures can be conceptualized by combining these building blocks, some of which will be discussed later.

Two-dimensional spectra are obtained by a modification of the approach used to obtain 1D multipulse spectra. The major difference is that the time domain 1D FIDs are further manipulated by incrementing the evolution time t_1 for each successive FID (n “increments”). A second FT converts the time dependence of the evolution into a second frequency, yielding a 2D spectrum where both axes are in frequency units; the f_2 axis is associated with the FID (the normal 1D spectrum), and the new axis f_1 is obtained as a result of the evolution period.

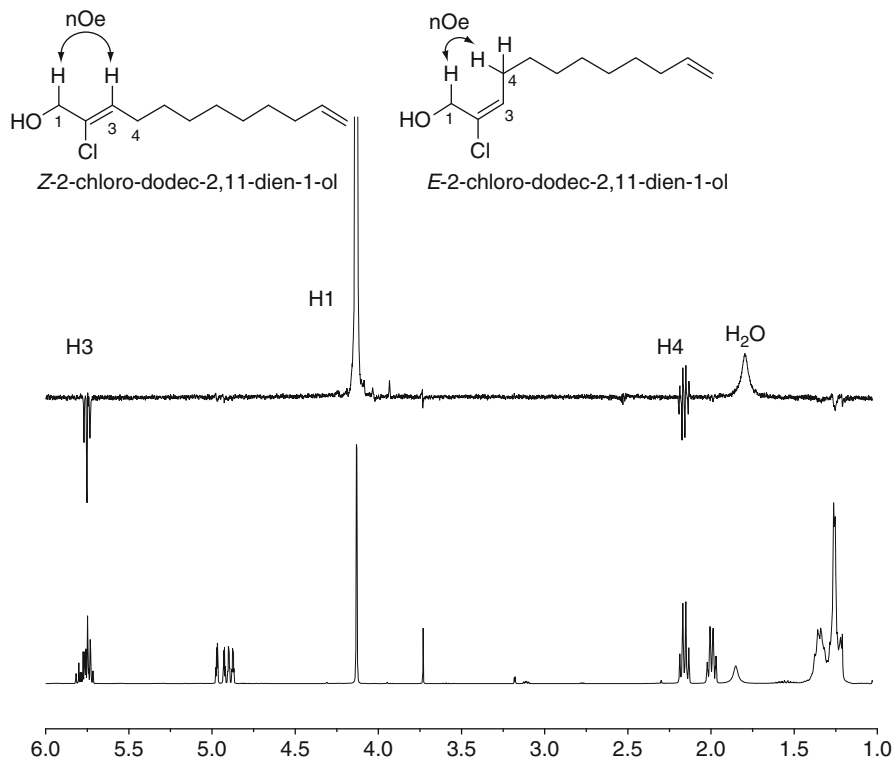


Fig. 7.22 The use of a selective 1D NOE experiment ($\tau = 800$ ms) to determine the stereochemistry of a trisubstituted double bond in 2-chloro-dodec-2,11-dien-1-ol

Most 2D experiments can be divided into auto-correlated or cross-correlated types. Multipulse procedures in which a magnetization (or coherence) transfer occurs within a homonuclear spin system represent auto-correlated experiments, and they produce what are called *off-diagonal* correlation peaks. Two commonly used auto-correlated experiments are the ^1H – ^1H COSY (proton–proton correlated spectroscopy) where homonuclear spin coupling serves to correlate protons along one axis to protons along a second and the 2D NOE (termed NOESY) where correlations between axes occur via homonuclear dipole–dipole interactions. In cross-correlated experiments, the magnetization of one nucleus is modulated by the coupling effects of heteronuclei. The 2D peaks appear at the intersection of f_1 and f_2 ; examples of this technique include ^1H – ^{13}C correlation spectroscopy experiments such as HMQC, HSQC, and HMBC.

Both auto-correlated and cross-correlated experiments are used to obtain data to link different NMR parameters that could not previously be observed easily in the same 1D NMR spectrum. For example, two-dimensional J spectra correlate ^1H chemical shifts on the f_2 axis to ^1H – ^1H spin coupling constants on the f_1 axis

(auto-correlated). Data from an often employed 2D NMR experiment, ^1H - ^1H COSY, have completely changed the approach to identifying protons that are mutually coupled with selective decoupling no longer being very common. Likewise, ^1H - ^{13}C correlation experiments provide invaluable 2D data, since overlapping protons can be resolved by the larger chemical shifts inherent in ^{13}C .

Inverse detection probes are available on most NMR instruments and allow observation of the ^1H FIDs after a pulse sequence has been applied at ^1H and ^{13}C . This approach was developed to deal with limited sample situations where low sensitivity of ^{13}C often gives unacceptable results. This technology takes advantage of the larger γ for ^1H , and it required both a change in probe design as well as the creation of quantum coherences during the experiment. These experiments cannot be described by the vector approach, but extensive explanations of them are in advanced monographs [46]. The key experiments which yield ^1H - ^{13}C correlation information are the HMQC (*heteronuclear multiple quantum coherence*) experiment and its equivalent HSQC (*heteronuclear single quantum coherence*) which give 1-bond H-C correlations and the HMBC (*heteronuclear multiple bond correlation*) experiment which gives 2-3 bond H-C information. In addition to inverse detected NMR methods, a major advance has been the routine application of pulsed field gradients (PFG) to allow the rapid acquisition of nearly artifact-free 2D NMR spectra through coherence pathway selection. Pulsed field gradients form the basis of magnetic resonance imaging, but their application to multidimensional NMR has increased what is possible by a large extent. In previous pulse sequences, "phase cycling" was necessary to remove artifacts, and sometimes these required up to 64 FIDs to be collected for each increment. The application of PFGs on suitable samples permits the acquisition of a single FID per increment, drastically reducing the time needed to acquire 2D NMR spectra. Most NMR instruments now employ PFGs in their pulse sequences to improve performance, and their implementation does not require operator input beyond the initial setting up of the parameters when the pulse sequence is first employed.

7.4.6.3 Strategies for Structure Determination Using 2D NMR

We have considered several multipulse 1D and 2D NMR experiments. These are extremely powerful in solving the connectivities and stereochemistry of the carbon skeleton of a compound under study. Summarized in Table 7.5 are the various proton-proton and proton-carbon connectivities that can be investigated using the most common 2D NMR experiments. A large number of acronyms are used to describe multipulse NMR experiments. These are spread throughout the chemical literature and are in common usage among many NMR spectroscopists. It is useful to review the various types of multipulse NMR spectra that can be employed in solving molecular structure and spectral assignment problems.

Different types of data can be derived from the 2D NMR spectra giving information on C-C (INADEQUATE), C-H (HSQC, HMBC), and H-H (COSY) connectivities. The most unambiguous of these are C-C correlations, but these can also be indirectly obtained from ^{13}C - ^1H and ^1H - ^1H data. Two strategies can be

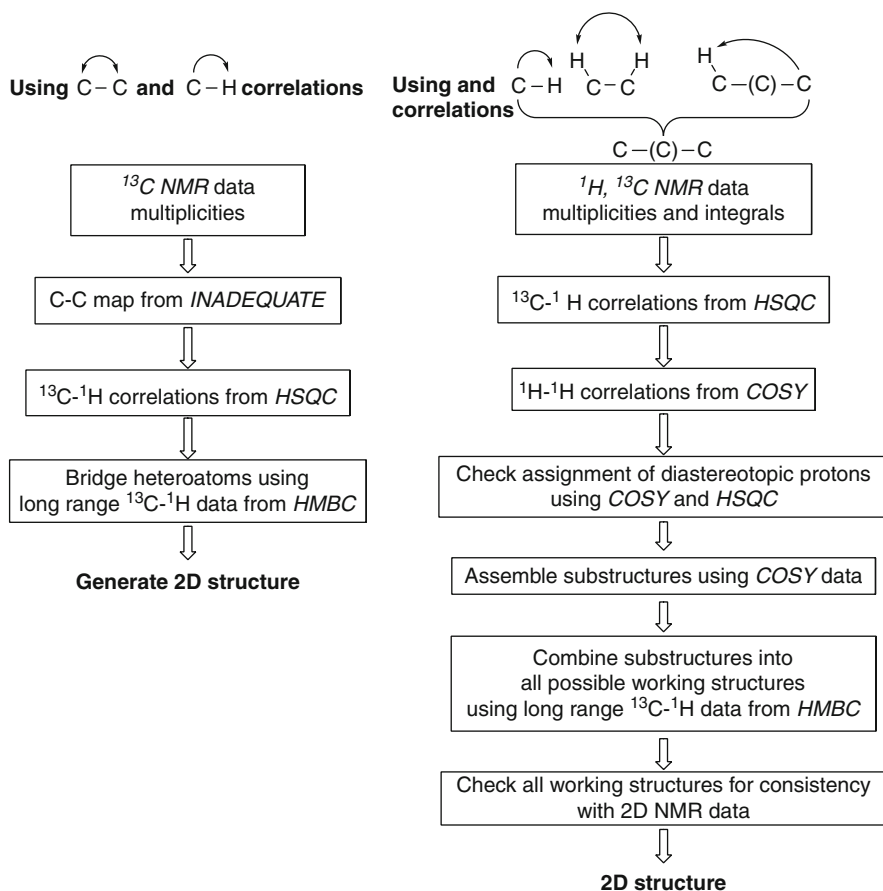


Fig. 7.23 Two possible structure elucidation strategies

envisaged to lead to a 2D structure (Fig. 7.23). The first relies on the use of the INADEQUATE experiment to directly obtain C-C correlations (Table 7.5), and this is complemented by the use of HMQC/HSQC data to obtain direct ^{13}C - ^1H information. This strategy would appear ideal as it gives rise to the carbon skeleton and proton assignments in two steps. For structures whose skeletons are interrupted by heteroatoms, the data have to be supplemented by the use of long-range ^{13}C - ^1H (HMBC) or through-space (NOE) data to bridge the gaps created by the heteroatoms. The alternative and more common strategy is one in which the direct ^{13}C - ^1H (HMQC/HSQC) correlations are used to assign protons to specific carbons, followed by the assembly of substructures using ^1H - ^1H (COSY) data. These substructures are then combined, and quaternary carbons included, using long-range ^{13}C - ^1H (HMBC) data (Fig. 7.23) to give a number of working structures which are confirmed using additional NMR experiments and comparison to literature data. The disadvantage of this strategy is that the HMBC technique gives both C-C-H

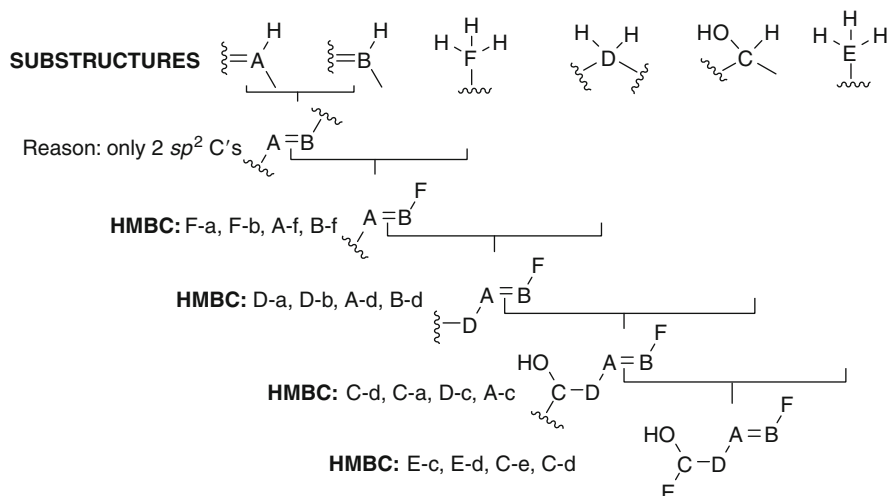


Fig. 7.24 Stepwise use of long-range data to assemble substructures into a secure 2D structure

(2-bond) and C–C–C–H (3-bond) correlations. Specialized pulse sequences such as the 1,1-ADEQUATE can be used to obtain 2-bond correlations only, which may assist in difficult structure determinations.

A simplified example of how such a process is completed using the second strategy is shown in Fig. 7.24. Obvious structural features such as double bonds should be assembled first, followed by the addition of substructures to satisfy the long-range correlations. In principle, two substructures are combined and assessed to determine whether the long-range correlations are satisfied. An iterative process leading to the correct structure then results in each step of the structure elucidation increasing the number of correlations that are satisfied. At the end of the process, the proposed 2D structure must satisfy *all* long-range correlations. The alternative, to assemble all possible structures from the substructures and then assessing these to see if they fit the long-range correlations, would lead to a very large number of possible structures (24 in this case, but far larger numbers for more complex structures) which would be difficult to achieve; hence, the strategy in Fig. 7.24 is inherently more sensible.

Table 7.6 summarizes the sample and time requirements for the two different approaches using standard 5-mm inverse detected probes. A concentrated sample and long acquisition time are necessary to execute the strategy depending on the INADEQUATE sequence. This is a “double quantum” method which involves suppressing the normal carbon singlet signals while enhancing the signals from pairs of adjacent carbons. The use of low volume probes, for mass-limited samples with high solubilities, or cryoprobe technology, means that INADEQUATE data can now be acquired on much smaller samples than previously possible.

Cryoprobes tuned for ^{13}C and ^{15}N are now available to obtain useful data in cases where the previous approach is unsuccessful and can yield a fourfold

Table 7.6 Comparison of typical sample and time requirements for two possible structure elucidation strategies

C–C strategy		C–H strategy	
Experiment	Time	Experiment	Time
^1H NMR	<1 min	^1H NMR	1 min
^{13}C NMR	<1 min	^{13}C NMR	1–4 h
DEPT-135	<1 min	DEPT-135	1–4 h
HSQC nt = 1, ni = 256	15 min	HSQC nt = 4, ni = 256	1 h
HMBC nt = 1, ni = 512	15 min	HMBC nt = 4, ni = 512	1 h
NOESY nt = 4, ni = 256	1 h	NOESY nt = 4, ni = 256	1 h
INADEQUATE	24 h	COSY nt = 1, ni = 256	15 min
Total time	~26 h		6–12 h
Sample conc	6 M		10–100 mM

nt number of transients (FIDs for each increment), ni number of increments

sensitivity advantage. More recently, parallel recording of different data types (^{13}C , C–C, direct and long-range C–H correlations) in a single experiment using such a probe allowed for the very fast structure determination of a small molecule. These techniques offer the possibility to revolutionize the elucidation of 2D structures, but are still at an early stage of application [47].

7.4.6.4 Use of NOESY and ROESY to Determine Relative Stereochemistry and Conformations

As it has been shown, the nuclear Overhauser enhancement (NOE) is critical in determining a molecule's relative stereochemistry. The two-dimensional equivalents of the NOE difference or selective 1D NOE experiments are the NOESY (*n*uclear *O*verhauser *e*nhancement *s*pectroscopy) and ROESY (*r*otating *O*verhauser *e*nhancement *s*pectroscopy) which are used under different circumstances. The appearance of a NOESY or ROESY spectrum is very similar to a COSY spectrum, but the cross peaks are due to dipole–dipole interactions through space rather than through-bond correlations as is the case for a COSY spectrum. An example of a NOESY spectrum is given in Fig. 7.25. Note that true NOE peaks are the opposite phase to the diagonal, and this fact can be used to differentiate them from artifact peaks (COSY peaks, which are positive). The mixing time is field dependent and should be set to the average T_1 for the protons in the ^1H NMR spectrum. The T_1 values can be determined using the inversion-recovery pulse sequence, but rather than a full calculation, a rule of thumb is to set the mixing time τ to the t_1 which results in a ^1H NMR spectrum with half the peaks pointing up and the other half pointing down.

The size of the NOE effect is proportional to the product of the Larmor frequency (ω_0 , which is proportional to the field strength) and the rotational correlation time τ_c (also known as the tumbling rate). The rotational correlation time is long for large molecules and short for small molecules. Small molecules have a maximum enhancement of 50%, whereas very large molecules have an enhancement of 100% in the opposite direction. However, for mid-sized molecules

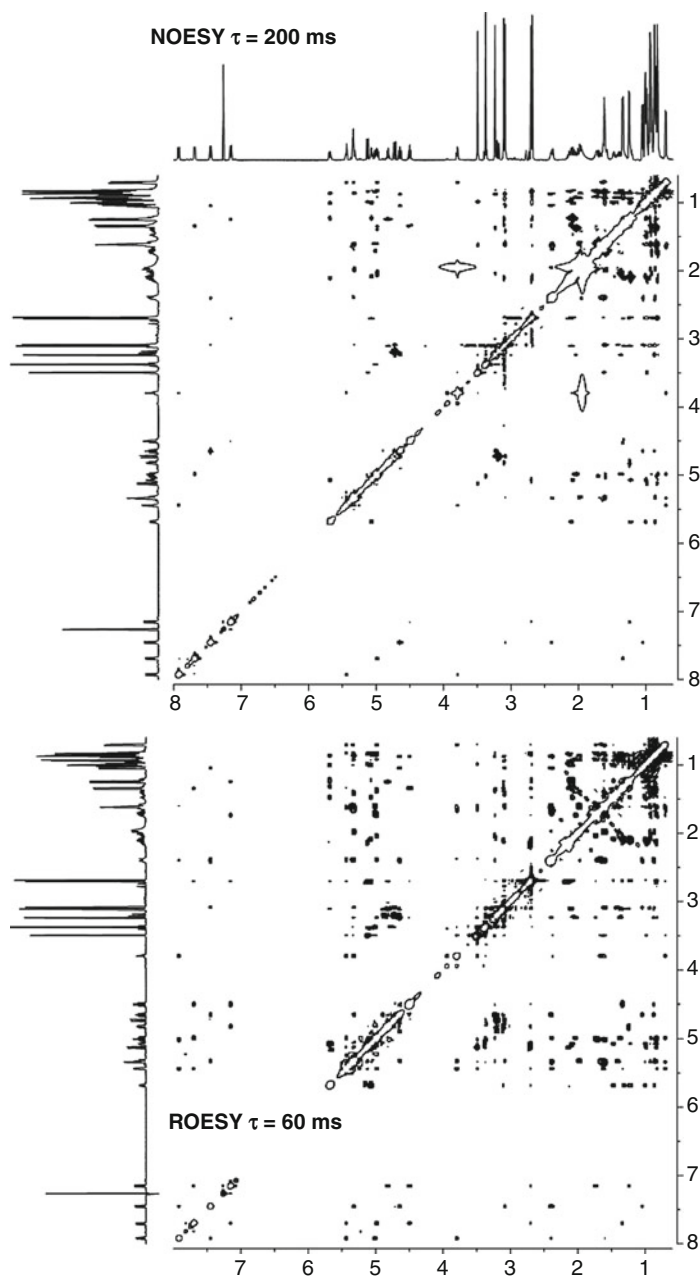


Fig. 7.25 A comparison of the NOESY ($\tau = 200$ ms) and ROESY ($\tau = 60$ ms) of the cyclic undecapeptide immunosuppressant cyclosporine (MW 1202) at 500 MHz. Multiple contours are negative and single contours are positive

(500–1,500 amu depending on their shape) $\omega_0\tau_c = 1$ and the NOE = 0, meaning that it is very difficult to obtain useful NOE data using a standard NOESY pulse sequence. For this size range, the ROESY experiment is ideal as the NOE is always positive and never crosses zero giving useful cross peaks for mid-sized molecules. Artifacts (TOCSY peaks) appear as antiphase peaks. The mixing time for a ROESY should be set to half the average T_1 determined as described above. A comparison of a NOESY and ROESY for a mid-sized molecule (cyclosporine A, MW = 1202) is shown in Fig. 7.25. Despite the longer mixing time in the NOESY, only very weak correlations are visible, whereas the ROESY taken with a short mixing time shows excellent correlations with greater intensity. This greater intensity in the ROESY also means that a larger number of correlations will be visible, and therefore, this is the preferred experiments when a NOESY experiment yields little data (e.g., when the molecular size and field strength multiply to give $\omega_0\tau_c = 1$).

NOE data can be very powerful when applied to solving the relative stereochemistry of complex molecules, particularly in conjunction with coupling constant-derived dihedral angles. It can be used for instance to make diastereotopic assignments or to determine if certain protons are on the same face of the molecule. The use of molecular modeling to determine relative stereochemistry when used together with NOE data can allow you to distinguish between different diastereomers. All possible stereoisomers can be subjected to a conformational search to determine their global energy minimum. Measurement of key distances can then be made to determine if they are consistent with the NOE data, remembering that the maximum possible distance for the NOE effect is 5 Å, but in practice, this is often much less. Be careful as in some cases a small NOE does not necessarily mean the two protons are not close in space as other effects may be involved. The possible structure that satisfies all of the NOE data is then a good candidate for the correct relative stereochemistry of the molecule under study.

7.4.6.5 Specialized Pulse Sequences

There are many 2D NMR pulse sequences that might be applied to solving a chemical structure, and the main ones in everyday use have been discussed in the previous sections and are listed in Table 7.5. There are a number of other more specialized sequences that you will need to be aware of that may be very useful in certain instances to solve complex problems. In addition to this, there are many, many more sequences that you will find in the current NMR literature that will not be discussed here [48].

We will begin with the discussion of a sequence that combines the features of the ^1H – ^{13}C correlation spectrum (HSQC) with the advantages of a DEPT-135. The edited HSQC gives both types of data simultaneously, thus obviating the need to obtain a separate DEPT-135 which saves time and can be a challenging experiment on dilute NMR samples. The use of inverse detected techniques brings with it an inherent sensitivity gain, and this is employed to great advantage here. The 1-bond correlations in the edited HSQC can be easily separated into CH/CH₃ and CH₂ using the phase of the correlation with the former being positive and the latter

negative. As discussed for DEPT, you can use chemical shift information as well as integrals of ^1H peaks to separate CH and CH_3 .

The task of establishing connectivities between protons separated by four or more bonds and between protons and carbons separated by two or more bonds is important. These constitute long-range relationships, and 2D NMR methods provide a way to interrelate such *pairs* of unconnected nuclei. There are three additional 2D techniques that can be used alongside the ^1H – ^1H COSY and HMBC (^1H – ^{13}C correlation, $J = 9$ Hz) to interrelate three or more nuclei at a time. All mutually coupled proton spins can be grouped from the cross peaks present in a TOCSY (*total correlation spectroscopy*) or its near equivalent, a HOHAHA (*homonuclear Hartmann-Hahn*) spectrum. The HMQC-TOCSY or HSQC-TOCSY experiment links together two 2D NMR procedures and provides a way to analyze crowded ^1H NMR spectra because additional resolution is provided along the ^{13}C chemical shifts.

Other sequences exist (e.g., ACCORDION) which allow acquisition of HMBC spectra with ranges of mixing times set from 2 to 25 Hz so that all possible $^{2,3}J_{\text{CH}}$ and some $^4J_{\text{CH}}$ are observed in one spectrum. Other variants of the HMBC sequence (e.g., HSQMBC or *J*-HMBC) are useful to obtain accurate $^{2,3}J_{\text{CH}}$ values to apply Murata's method of configurational analysis.

In many cases, it would be desirable to distinguish between $^2J_{\text{CH}}$ and $^3J_{\text{CH}}$ in an HMBC spectrum to aid the structure elucidation process. One experiment that makes this possible is the 1,1-ADEQUATE which reports only the $^2J_{\text{CH}}$ correlations and by comparison with the HMBC, which gives $^{2,3}J_{\text{CH}}$, allows the $^3J_{\text{CH}}$ to be distinguished. Despite this apparent usefulness, the experiment still requires more time than an HMBC, so it is often not used until a strict distinction between two and three bond C–H correlations is needed. Other variants of this experiment exist, and these are powerful in situations where there are quaternary carbons in a molecule which are more than three bonds from the nearest proton, and hence show no correlations in an HMBC. These experiments, called n,n-ADEQUATE, can give up to six-bond correlations and should be considered when you suspect such a situation may be at hand [49].

The TOCSY (\approx HOHAHA) technique identifies all mutually coupled protons, whereas the HMQC-TOCSY or HSQC-TOCSY method reveals connectivities between a CH and all other protons in the same spin system. The HMQC-TOCSY or HSQC-TOCSY spectrum is regarded as the most powerful among this trio because it can be applied in cases where a proton NMR spectrum is severely congested.

7.4.6.6 Experimental Measurement of $^{2,3}J_{\text{CH}}$ Couplings

Despite yielding valuable structural information, the low sensitivity of ^{13}C has meant that the measurement of heteronuclear coupling constants was very difficult until quite recently. In the last 10 years, spectroscopists have developed a large number of experiments to implement these measurements. There is no generally accepted method, and all have advantages and disadvantages. These experiments can be classified in two groups: HSQC-TOCSY and HMBC type.

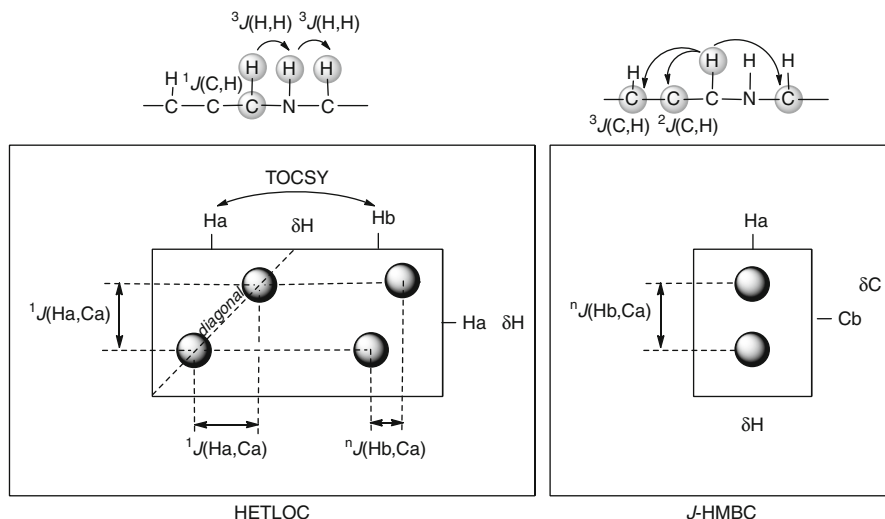


Fig. 7.26 Direct measurement of $^{2,3}J(\text{CH})$ coupling constants through analysis of HETLOC cross peaks and J -HMBC

The original methods used by Murata were called 2D hetero half-filtered TOCSY (HETLOC) and a phase-sensitive heteronuclear multiple bond correlation (PS-HMBC). HETLOC is a two-dimensional homonuclear correlation experiment in which the usual TOCSY-type peaks are complemented in both dimensions by heteronuclear couplings (see Fig. 7.26). In particular, a correlation in the spectrum corresponding to long-range coupling between two protons (Ha and Hb) shows a diagonal displacement due to the heteronuclear direct coupling between Ha and Ca ($^1J_{\text{CaHb}}$). These two correlations also display a very valuable splitting in the second dimension due to the heteronuclear long-range coupling between Ha and Cb ($^2J_{\text{CaHb}}$ or $^3J_{\text{CaHb}}$). The major drawback in the HETLOC method lies in the intrinsic nature of the peaks: the two protons must belong to the same spin system and must exhibit a TOCSY correlation peak. For this reason, it is impossible to use this experiment to measure coupling constants between a proton and a quaternary carbon or a proton and a carbon belonging to a different spin system. To obtain these latter values, methods based on HMBC pulse sequences provide information on long-range couplings between protons and carbons separated by two or three bonds. Among others the J -HMBC experiment can be used to quantitatively analyze the proton–carbon coupling constants by observation of the splitting of HMBC correlations in the ^{13}C dimension. Also, an HMBC-type experiment is the HSQMBC which allows the measurement of long-range heteronuclear coupling constants from protonated carbons to quaternary carbons.

7.4.6.7 Computer-Assisted Structure Elucidation

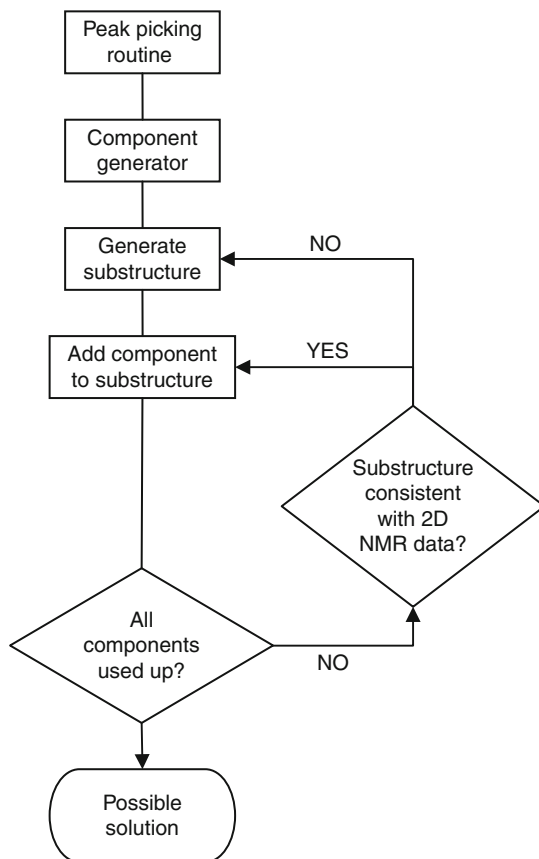
Many of the processes described in this chapter to derive a 2D molecular structure can be automated. Sophisticated computer programs now exist that can analyze 1D and 2D NMR data and, given a molecular formula or accurate mass, propose structures consistent with all the data. This is referred to as computer-assisted structure elucidation (CASE) [50], and their mode of operation is very similar to the human thought process, as depicted in Figs. 7.23 and 7.24. In all cases, a trained human operator is necessary to obtain reliable results from these programs. A simplified flow chart of CASE is shown in Fig. 7.26, and this is similar to the process depicted in Fig. 7.23 for the method using C–H and H–H information. The first step is peak picking which can either be done by the operator, or by the program, but the latter must be checked by the operator to ensure that noise peaks are not assigned as correlations. The use of pulsed-field gradients in 2D NMR pulse sequences means that noise levels are reduced and false peak picking is less likely. Typically the HSQC spectrum is assessed for correlations to protons at the 1D ^{13}C NMR resonance frequencies to give the direct C–H correlations. After this the COSY and HMBC spectra are analyzed for two and three bond correlations producing a number of data tables which are used to generate a number of components. These are then assembled as in Fig. 7.24, and after each stage, the substructure produced is checked to see if it satisfies the long-range correlations. If it does, then an additional component is added and the process repeated. If it does not satisfy the long-range correlation, then the component is removed and another added in its place and the new substructure assessed to see if it fits the long-range correlations. This cycle is repeated until all components are used up giving a possible solution to the problem, which should then be inspected by the human operator to see if it is chemically sensible and to check the ^{13}C NMR shifts against literature values (Fig. 7.27).

7.5 Complementary Spectroscopic Techniques: IR and UV

7.5.1 Confirming Functional Groups: Infrared Spectroscopy

All organic molecules absorb light in the infrared region of the electromagnetic spectrum due to vibrational changes in the chemical bonds between atoms [51]. The collection of vibration responses, called an IR spectrum, is distinct for every organic compound because the frequencies of these absorptions are sensitive to molecular structure. Prior to the widespread use of NMR data, infrared spectroscopy (IR) was considered the most important tool used to characterize an organic compound. Instrumentation for IR is relatively inexpensive and it is commonplace. Collecting an IR spectrum continues to be useful because it can provide invaluable information to identify functional groups. Very often IR spectra are also employed in analyses to compare samples suspected of being identical. A serious limitation is that specific information about atom connectivities or stereochemical features

Fig. 7.27 Simplified flowchart for the decision processes used by computer-assisted structure elucidation (CASE) programs



cannot usually be deduced by this method. As another important development, new generation IR spectrometers are being used in food science and technology applications to detect common organic substances. Such automated analyses provide quantitative estimates of important components of foods and beverages ranging from estimates of sugar compositions to the measurement of alcohol levels and beyond.

The IR wavelengths are typically divided into three subregions. These are the near IR ($4,000\text{--}13,000\text{ cm}^{-1}$, $2.5\text{--}0.8\text{ }\mu\text{m}$), the mid IR ($400\text{--}4,000\text{ cm}^{-1}$, $25\text{--}2.5\text{ }\mu\text{m}$), and the far IR ($400\text{--}40\text{ cm}^{-1}$, $250\text{--}25\text{ }\mu\text{m}$). It must be noted that the units most commonly used in IR spectroscopy are wavenumbers ν' in $\text{cm}^{-1} = 10,000/\mu\text{m}$. Only the mid-IR is of direct use in organic structure analysis because this is where the observed stretching vibrations occur that can be correlated to molecular structural features. Thus, the data sought from an IR trace are absorption band

positions and shapes, as well as semiquantitative peak intensities. Specific functional groups have “characteristic group frequencies,” and these are used to determine the functionality present in the molecule under investigation (see Fig. 7.28). This area of an IR spectrum, from 4,000 to 1,500 cm^{-1} , is usually referred to as the “functional group region.” In all cases an IR spectrum shows many more bands than can be easily correlated to structural features. Often only a few of the bands corresponding to particular functional groups are interpreted, whereas the rest are used only for detailed molecular comparisons. The so-called “fingerprint region” appears on the right hand side of an IR spectrum from 1,500 to 500 cm^{-1} . The peaks seen here arise from very complicated absorptions usually ascribed to all possible mechanisms of bending vibrations.

Introductory organic chemical texts usually point out that IR spectra taken under the same conditions for identical compounds must be the same. Also no two compounds (except enantiomers) will have identical IR “fingerprint” regions. It would therefore seem safe to assume that the IR of two identical samples ought to be identical, but care must be taken to compare data obtained under similar conditions. In fact, slight changes in band positions or shapes can be observed for the same compound in a solution as compared to a neat film or a KBr pellet. Also a spectrum of a compound in the crystalline state may contain more absorptions compared to that of a melt or of a sample in solution. Polymorphic crystals of the same compound can occasionally display nonidentical absorption bands.

The task of deciding which IR peaks confirm the presence or absence of a particular functional group is greatly simplified by the use of correlation charts or tables. The first place to begin this process is to note that Fig. 7.28 summarizes characteristic frequencies for a core group of substructures. Encyclopedic tables and discussions of small variations of frequencies for different functional groups can be found in a specialized text such as that by Socrates [52] or Colthup [53] or in compilations of IR spectra [54]. Be mindful that structural conclusions drawn from IR analysis can be readily correlated to that from ^{13}C NMR data, and this should be done whenever possible.

Using correlation charts does not involve matching each peak to a molecular structural feature. Instead, general regions of an IR spectrum are analyzed, and the three regions which should be initially scrutinized are the Z–H stretch region from 3,100 to 3,700 cm^{-1} , the C–H stretch region from 2,700 to 3,100 cm^{-1} , and the C = O/C = C stretch region from 1,600 to 1,850 cm^{-1} . Relative intensity of peaks should be noted, and a comparison might be considered for a spectrum run on a sample prepared as a mull or in a solvent such as CHCl_3 . Reference to correlation charts, tables, or data memorized from past experience is drawn on to identify the presence or absence of various functional groups.

To summarize, analysis of an IR spectrum will normally consist of the following steps:

- (a) Examine the functional group region to determine the presence or absence of peaks characteristic of common structural features such as: OH, NH, carbon types (sp^3 , sp^2 , sp carbons), C = O, C = C, and $\text{C}\equiv\text{N}$.

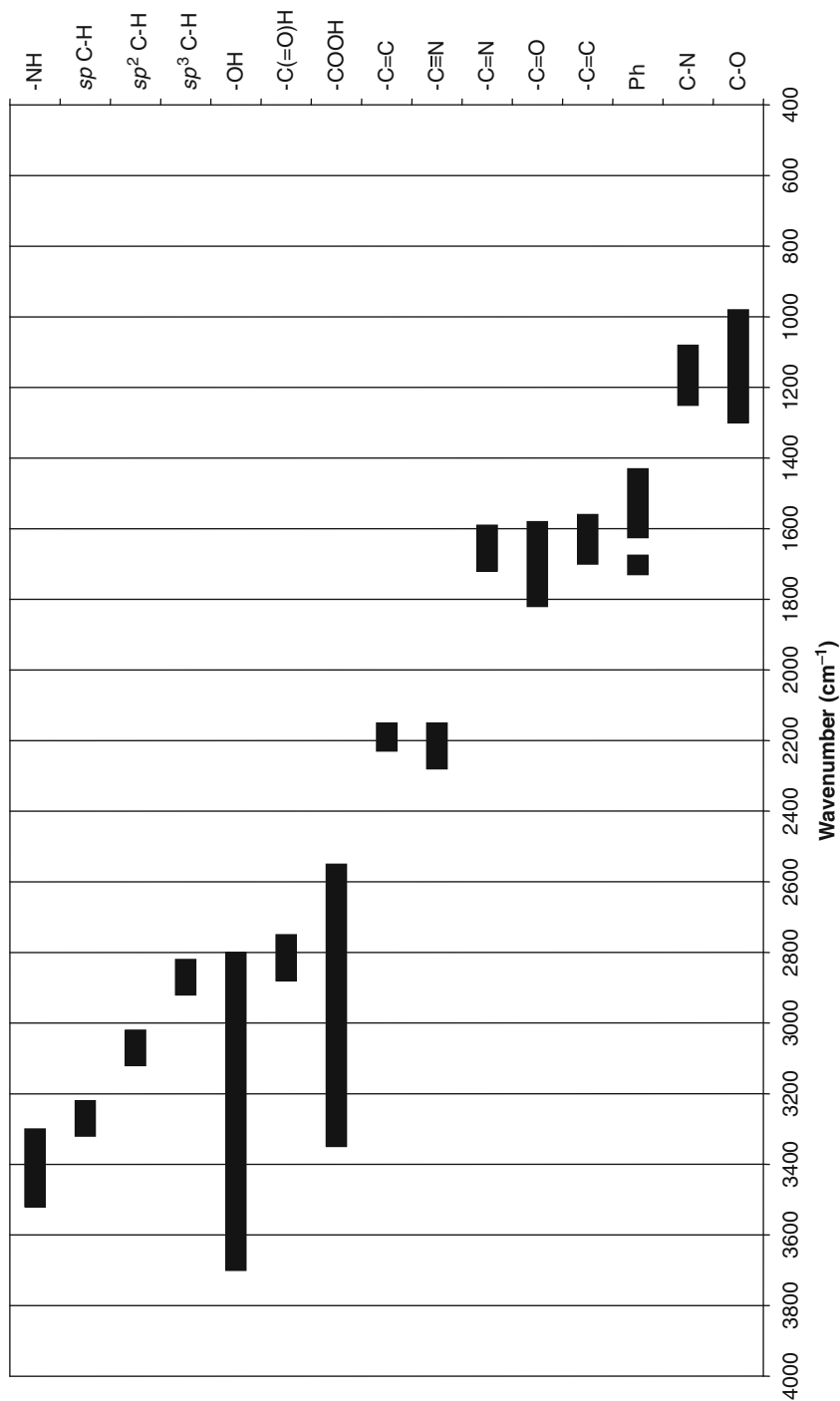


Fig. 7.28 A summary of IR bands for common functional groups

- (b) Confirm the presence of a particular structural feature by searching for bands which are complementary to the major functional group bands. As an example, the C–O stretch at $\approx 1,100\text{ cm}^{-1}$ would be expected to accompany an OH stretch at $3,300\text{ cm}^{-1}$, or an sp^2 C–H stretch at $2,720\text{ cm}^{-1}$ should accompany a C = O stretch at $1,720\text{ cm}^{-1}$ for an aldehyde.
- (c) Use ^{13}C NMR data to confirm inferences about a particular structural feature or to resolve ambiguities of a range of functional groups assignable to a particular band.
- (d) Use the “fingerprint” region to establish a positive identity for a known compound by comparison to spectral libraries. Two obvious difficulties to be expected are that water impurities or C = O overtones might be mistaken for an alcohol group, and many IR spectra are insensitive to stereochemical or isomeric structural variations.

7.5.2 Confirming Functional Groups: UV Spectroscopy

All organic compounds absorb ultraviolet (UV) light. However, the absorption frequencies of the C–C or C–H bonds of an organic molecule, as well as those of isolated functional groups such as a C = C, cannot be observed in the easily accessible region of the UV spectrum. The value of UV is based in examining compounds with groups such as $\text{R}_2\text{C} = \text{O}$, $-\text{O}(\text{R})\text{C} = \text{O}$, $-\text{NH}(\text{R})\text{C} = \text{O}$, or polyunsaturated compounds with conjugated multiple bonds. At one point UV spectroscopy was the only physical method available for the analysis of organic compounds. Nowadays, due to the limitations noted above, few organic chemists rely on UV as a primary tool for structural elucidation.

UV represents a method similar to IR for structure analysis, and like IR, this technique utilizes electromagnetic radiation that can be absorbed by a compound. The light frequencies that are employed span the ultraviolet (200–400 nm) and the visible (400–800 nm) regions of the electromagnetic spectrum. UV wavelengths below 200 nm are strongly absorbed by air (oxygen and carbon dioxide), or solvents commonly used in UV spectroscopy, so vacuum techniques are required to observe transitions in this range. Vacuum UV data in the region between 200 and 10 nm are not often obtained because few commercial instruments are designed to scan these wavelengths.

How much specific structural information can be obtained from a UV λ_{max} value? Inferences about the presence or absence of conjugated multiple bonds can be made from a UV spectrum. Obviously, when no absorptions are observed in a UV spectrum, this indicates the absence of conjugated multiple bonds. It should be emphasized that in most situations, UV data are used to reaffirm a conclusion about the presence or absence of a chromophore previously identified by NMR or IR. The most common situations in which specific conclusions about functionality can be obtained from UV data are summarized in [Table 7.7](#).

Also with recent improvements in theoretical chemistry software and increases in computing power, it is now possible to calculate the UV spectra of

Table 7.7 Summary of UV λ_{\max} and transition types for simple chromophores

Chromophore	Compound	Transition	λ_{\max} (nm)	ϵ
C–H	CH ₄	$\sigma \rightarrow \sigma^*$	122	
C–C	C ₂ H ₆	$\sigma \rightarrow \sigma^*$	135	
C = C	C ₂ H ₄	$\pi \rightarrow \pi^*$	103	15,000
			174	5,500
C = C = C	C ₃ H ₄	$\pi \rightarrow \pi^*$	170	4,000
			227	630
C \equiv C	R–C \equiv C–R'	$\pi \rightarrow \pi^*$	178	10,000
			196	2,000
			223	160
C–O	R–O–R	$n \rightarrow \sigma^*$	180	500
C–O	R–O–R'	$n \rightarrow \sigma^*$	180	3,000
C–N	Amino	$n \rightarrow \sigma^*$	190–200	2,500–4,000
C–S	R–S–H	$n \rightarrow \sigma^*$	195	1,800
C–S	R–S–R	$n \rightarrow \sigma^*$	235	180
C = O	Aldehyde/Ketone	$n \rightarrow \sigma^*$	166	16,000
		$\pi \rightarrow \pi^*$	189	900
		$n \rightarrow \pi^*$	270	10–20
C = O	Carboxylic acid	$n \rightarrow \pi^*$	200	50
C = O	Carboxylate	$n \rightarrow \pi^*$	210	150
C = O	Ester	$n \rightarrow \pi^*$	210	50
C = O	Amide	$n \rightarrow \pi^*$	205	200
C = N	(NH ₂) ₂ C = NH	$n \rightarrow \pi^*$	265	15
C \equiv N	CH ₃ C \equiv N	$\pi \rightarrow \pi^*$	<170	
N = N	Me–N = N–Me	$n \rightarrow \pi^*$	350–370	15
N = O	Me ₃ NO	$n \rightarrow \pi^*$	300	100
			665	120
N = O	Me ₃ NO ₂	$n \rightarrow \pi^*$	276	27
C = C = O	Et ₂ C = C = O	$\pi \rightarrow \pi^*$	227	360
		$n \rightarrow \pi^*$	375	20
C–Cl		$n \rightarrow \sigma^*$	173	200
C–Br		$n \rightarrow \sigma^*$	208	300
C–I		$n \rightarrow \sigma^*$	259	400

small to medium sized molecules, although expert knowledge is required to achieve the best results. For very small molecules such as ethene, which has a gas phase $\lambda_{\max} = 171$ nm, it is possible to calculate the energies and oscillator strengths of electronic excitations using quantum chemical methods based on advanced molecular orbital calculations which can then be converted into absorbance maxima. Using different variations of this approach, the theoretically calculated λ_{\max} is found to range from 162 to 179 nm, the best being a prediction of 172 nm.

As another consideration, the theoretical approach is computationally very expensive. Most theoretical UV predictions for molecules of a chemically interesting size use electronic structure calculations at the density functional theory (DFT) level to achieve excellent results in a reasonable time. The major limitations are that solvent, concentration, and temperature effects on the λ_{max} generally cannot easily be incorporated yet, although improvements are constantly being made to allow theory to reliably match with experimental data. In brief, the geometry of the molecule under study is optimized at some suitable level of theory, after which time-dependent DFT (TDDFT) is used to calculate the UV spectrum. The most commonly used form of TDDFT in spectroscopic applications such as calculations of UV/Vis spectra does not involve the calculation of excitation energies directly as differences between the ground state and excited state configurations. Instead, the linear response of the ground state density to an applied electric field is calculated using perturbation theory.

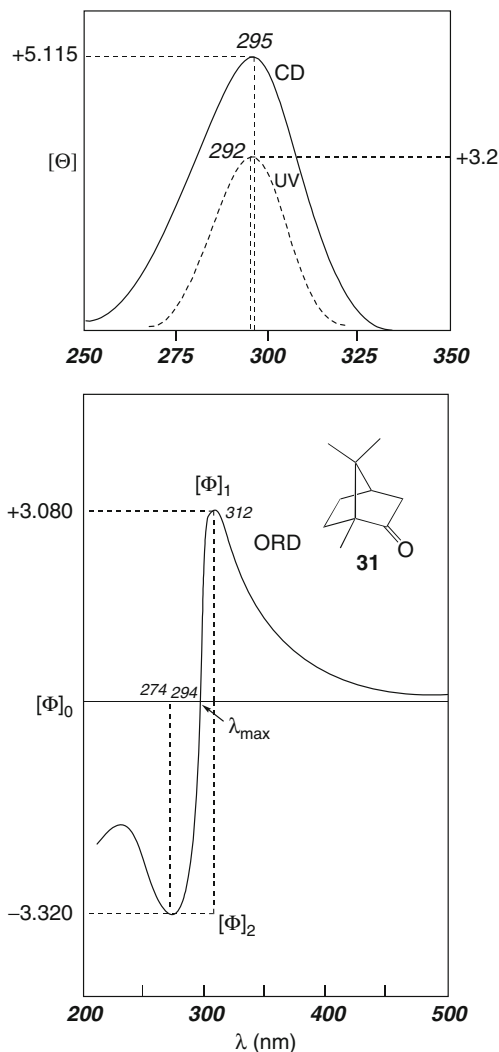
7.5.2.1 The Behavior of Chiral Chromophores ORD–CD

Chiral molecules can rotate the plane of polarized light, and this property is the basis of optical activity. Optical rotation data are reported as a specific rotation, $[\alpha]$, measured at a particular temperature, concentration, and wavelength of light, usually at 589 nm, the sodium D line. The $[\alpha]$ value can be calculated from the experimentally obtained rotation, α : $[\alpha] = 100\alpha/lc$, where c is the concentration of the solute in g/100 ml and l is the path length in decimeters. Molar rotations $[\Phi]$ are also sometimes reported when rotatory power is being compared on a quantitative basis: $[\Phi] = [\alpha] \text{ (MW/100)}$.

A useful approach to stereochemical analysis is the measurement of a series of $[\alpha]$ or $[\Phi]$ values for an enantiomerically pure compound over a range of polarized light wavelengths. The resultant is referred to as an optical rotatory dispersion (ORD) plot [55]. Plane polarized light can be viewed as a superposition of equal quantities of left- and right-handed circularly polarized light. These are differentially absorbed by a chiral compound and yield elliptically polarized light, with molar ellipticity $[\theta]$. The difference between the molar extinction coefficients, $\delta\epsilon$, of the left- and right-handed circularly polarized light can be measured. For small values of $[\theta]$, the molar ellipticity and molar extinction coefficients are related by $[\theta] = 3,300\delta\epsilon$. A plot of $\delta\epsilon$ or $[\theta]$ vs. wavelength is a circular dichroism (CD) plot [56]. The availability of commercial instruments makes it possible to routinely obtain both ORD and CD traces.

Chiral compounds containing a UV chromophore can give anomalous CD or ORD curves, known as the Cotton effect. An ORD spectrum in which the peak is at higher λ than the trough is said to have a positive Cotton effect, and the opposite situation with the peak at lower λ than the trough has a negative Cotton effect. Optically pure enantiomers always display opposite Cotton effect ORD curves of identical magnitude. Another feature of the ORD plot is that the zero crossover point between the peak and trough closely corresponds to the normal UV λ_{max} .

Fig. 7.29 ORD, CD, and UV of camphor (**31**)



The appearance of CD plots is rather simple in that they are Gaussian rather than S-shaped. The positive or negative nature of the CD curve is given by the sign of $\delta\epsilon$ or $[\theta]$ and corresponds to the sign of the Cotton effect. A comparison of the CD, ORD, and UV spectra of camphor (**31**) is shown in Fig. 7.29. Akin to ORD, CD peaks occur only in the vicinity of a UV absorption band, and the maximum absorption in a CD spectrum occurs at approximately the UV λ_{\max} . In situations where more than one Cotton effect is observed, a CD spectrum with its simpler absorption peaks is often more straightforward to interpret than ORD displaying overlapping S-shaped peaks.

Interpreting Cotton effect curves for carbonyl-containing compounds is the most important application of ORD–CD data in organic structure analysis. In spite of the low ϵ for the $C=O$ $n \rightarrow \pi^*$ transition, occurring at approximately 280 nm, it can easily be observed by ORD–CD on dilute samples (10^{-2} – 10^{-6} M). A set of semiempirical rules has been developed to allow conclusions to be made about $C=O$ location, ring conformational properties, and absolute stereochemistry. Using these rules, either the constitution, conformation, or configuration of a molecule can be determined, provided two such features are known. This involves use of the octant rule to translate the sign of a $C=O$ Cotton effect peak into a conclusion about molecular structure. It was developed from the study of rigid cyclohexanones and has been extended to a large number of compound classes [57].

7.5.2.2 The Exciton Chirality Method

Most circular dichroic spectra are the result of one chromophore per molecule interacting with the electromagnetic field of light. In this case, the interaction with the chromophores in neighboring molecules is negligible. However, if two UV chromophores are present in one molecule, exciton coupling is observed. Simply put, exciton coupling is the delocalization of the excited state between two chromophores, resulting in the splitting of the excited state (exciton coupling or Davydov splitting) [58]. Excitations to the two split energy levels generate Cotton effects of mutually opposite signs. This effect is manifested in the CD spectrum as two bands of opposite sign, and the maximum and minimum are separated by $\Delta\lambda$ (Davydov splitting). The signs of the first (greater λ) and second (smaller λ) Cotton Effect can be used to determine the spatial disposition of the chromophores. Sugars can be derivatized as benzoates, and the absolute sense of the twist between two of these groups can be determined using the exciton chirality rules previously mentioned. This method has been used to determine the absolute stereochemistry of both small natural products as well as large natural products such as brevetoxin B [58].

7.6 Limitations of Spectroscopic Data in Structure Analysis

Even seasoned investigators sometimes experience difficulties in analyzing the structures of organic compounds. At times, problems occur in interpreting NMR, IR, UV–VIS, or MS data, or in applying the strategies outlined in Fig. 7.1, or both. Also, ambiguities can arise if extraneous signals are present from impurities. When this happens, reconsidering the conclusions by an iterative process will sometimes resolve the difficulty. In some cases, additional efforts are needed including obtaining additional data from a simple derivative, examining degradation products, or carrying out total synthesis of the putative structure or a model compound. Success in using spectra for organic structure analysis requires the careful comparison of data and conclusions derived from the four techniques. Of course, whenever possible, two or more arguments based on

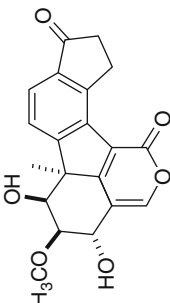
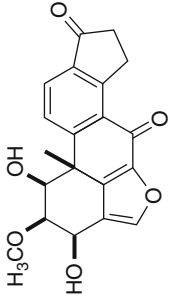
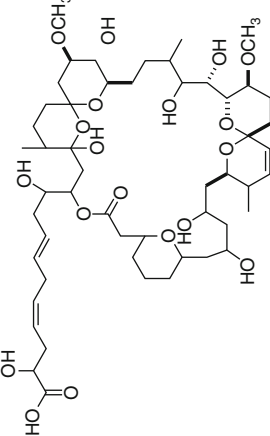
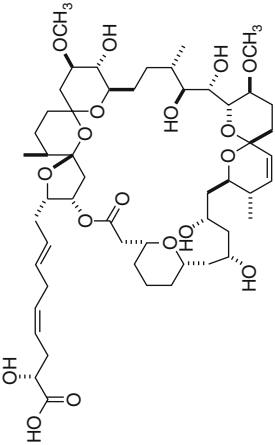
spectroscopic or chemical data should be used to generate a conclusion about a particular structural element. It is important to learn from past success and failures in organic structure analysis. However, what usually attracts much attention is when something goes wrong. There are hundreds of cases in the chemical literature where revisions have been made to a published structure [59]. Some of the most common types of difficulties where a (published) *reasonable 2D or 3D molecular structure* did not endure the test of time are represented in three examples shown in Table 7.8. These compounds are all natural products ranging from terpenoids, polyketides, to alkaloids, and all are in the mass range of 250–1,100 amu in molecular weight. The “original structures” for these compounds were based on a great deal of supporting data within the papers listed by each of these structures. However, the second literature citation accompanying each entry contains another viewpoint based on new experimental information – either from the original investigators or from others – leading to a “revised structure.”

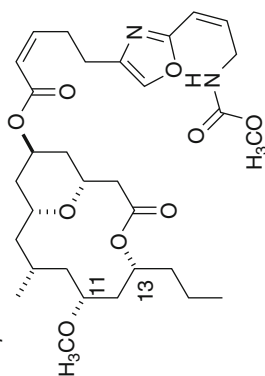
Failure to propose correct functional groups, even when the molecular formula was known, has caused problems. The characterization of the polycyclic polyketide TAEMC161 was sidetracked because not enough possibilities were considered for the substructure containing three fused rings comprised of two six-sided and one five-sided system. The ^{13}C NMR chemical shifts were seemingly in accord with the initial structure. However, further evaluation of the carbon shifts predicted by density functional theory revealed that the structure represented by viridiol provided a better fit. The total synthesis of this structure provided additional data to confirm the revision.

A faux pas in establishing an appropriate molecular formula can be devastating. When this happens, the list of substructures and functional groups will always be incorrectly assembled into a final *2D structure*. It took a surprisingly short time to amend the originally proposed rendering for spirastrellolide. It heads a family of compounds of greater than 1,000 amu having a polyether polyketide framework and possesses 21 chiral centers. Advanced NMR data were used to substantiate the ten units of unsaturation as a carboxylic acid, a macrocyclic lactone, a homoconjugated diene, one dihydropyran ring, and three pyran groups. The myriad of remaining oxygen atoms were considered to be present as 2 OCH_3 and 8 OH residues. Subsequent peracetylation of spirastrellolide methyl ester gave only a pentaacetate product, indicating a serious inconsistency. Reevaluation of the molecular formula by ultrahigh-resolution mass spectrometry indicated a first problem, that the count of hetero atoms was O_{17}Cl and not O_{19} . A substantial additional effort carried out over a 4-year period provided the final corrected structure by isolating analogs, obtaining degradation products, and total synthesis of key fragments.

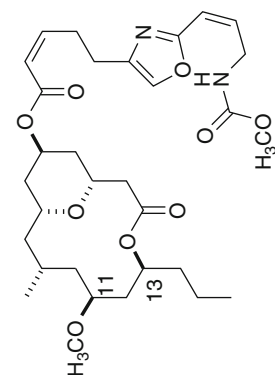
The complete 3D structure of (+)-neopeltolide was quickly challenged after its publication. In this case, the spectroscopic data of the natural product did not match that of material prepared by enantioselective synthesis. This example provides an unexpected outcome in the process shown in Fig. 7.2 – transforming a *reasonable 3D molecular structure* into a *very secure 3D molecular structure*.

Table 7.8 Some marine organic structure analyses gone bad

Original structure	Revised structure	Features
<p>TAEMC161</p>  <p><i>J. Nat. Prod.</i> 2000, 63, 1677</p>	<p>Viridiol</p>  <p><i>J. Nat. Prod.</i> 2003, 66, 716</p>	<p>TAEMC161 = Viridiol</p> <p>This cytotoxic compound was isolated from a tunicate. The entire carbon chain structure was revised by automated analysis of the ^{13}C-^{13}C Correlation (2D INADEQUATE)</p>
<p>Spirasterellolide</p>  <p><i>J. Am. Chem. Soc.</i> 2003, 125, 5296</p>	 <p><i>Org. Lett.</i> 2004, 6, 2607</p>	<p>A sponge derived polyketide of isotopic mass = 1026.5. The original MF $\text{C}_{53}\text{H}_{86}\text{O}_{19}$ was corrected to $\text{C}_{53}\text{H}_{83}\text{O}_{17}\text{Cl}$. An inconsistency was the methyl ester formed a pentaacetate. Synthesis of fragments and degradations on other analogs supported the revised structure and absolute stereochemical assignments shown</p>

(+)-Neopeltolide

J. Nat Prod. 2007, 70, 412



J. Am. Chem. Soc. 2008, 130, 804

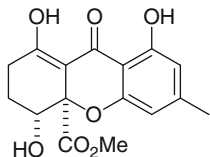
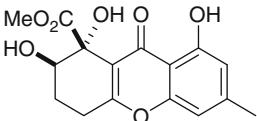
This deep-water sponge metabolite is a powerful cytotoxin. Extensive use of advanced NMR methods was used to identify parallel features to that of leucascandrolide. The original 11*R*, 13*R* assignment was revised to 11*S*, 13*S* after examination of the NMR properties of diastereomers

Many additional attempts were undertaken to decipher the stereochemistry at the six chiral centers of neopeltolide. All of them involved the synthesis of other logical diastereomers (e.g., *working stereo structures*). Eventually, a revised structure was published based on a side-by-side comparison of the synthetic isomers to the natural sample.

The preceding discussion, as well as the compilation of Table 7.8, raises an important question. Can the process of organic structure analysis ever produce an *absolutely secure 3D molecular structure*? Some would argue that the answer is – rarely! Recall the steps in establishing a molecular structure discussed earlier in this chapter (e.g., Fig. 7.1). One important milestone in the process involves pruning a broad list of possible *working 2D structures* to obtain a single candidate which after further analysis can be designated as a *reasonable 3D molecular structure*. Collecting and recollecting data are what it usually takes to substantiate that a *very secure 3D molecular structure* has been proposed. But when does this process stop? Is a combination of spectroscopic data, the results of total synthesis, or even data from X-ray crystallography the minimum needed in support of the designation as a *very secure* or even *absolutely secure 3D molecular structure*? Seldom would a compound be subject to such intense scrutiny. With experience gained in applying the concepts outlined in this chapter along with acquiring skill in solving complex structure elucidation problems, you will be able to formulate a conclusion on this issue. The next step might involve spending month or years solving such problems. We suggest that you now embark on such a journey!

7.7 Study Questions

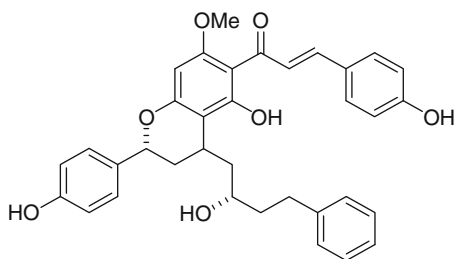
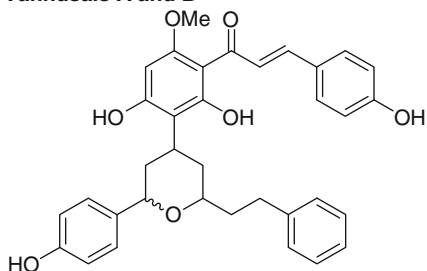
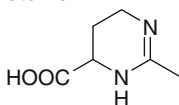
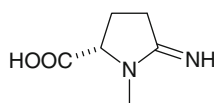
1. The ^{13}C NMR spectrum of CDCl_3 shows a triplet (intensities 1:1:1) separated by 31.9 Hz. Explain.
2. The structure for three marine products was wrongly assigned and later revised based on synthetic models. Propose the structural features which were responsible for these three mistakes!

Originally reported structure	Revised structure
<p>Diversolic acids</p> 	

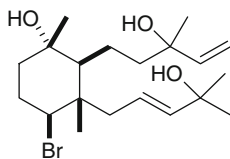
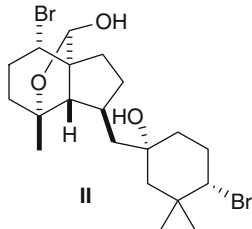
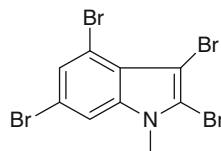
(continued)

Originally reported structure

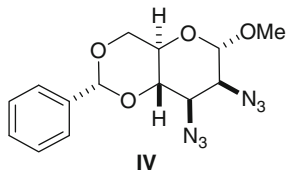
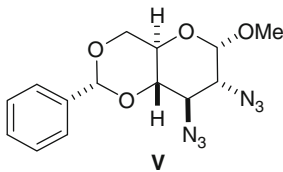
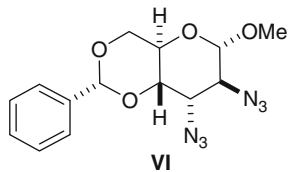
Revised structure

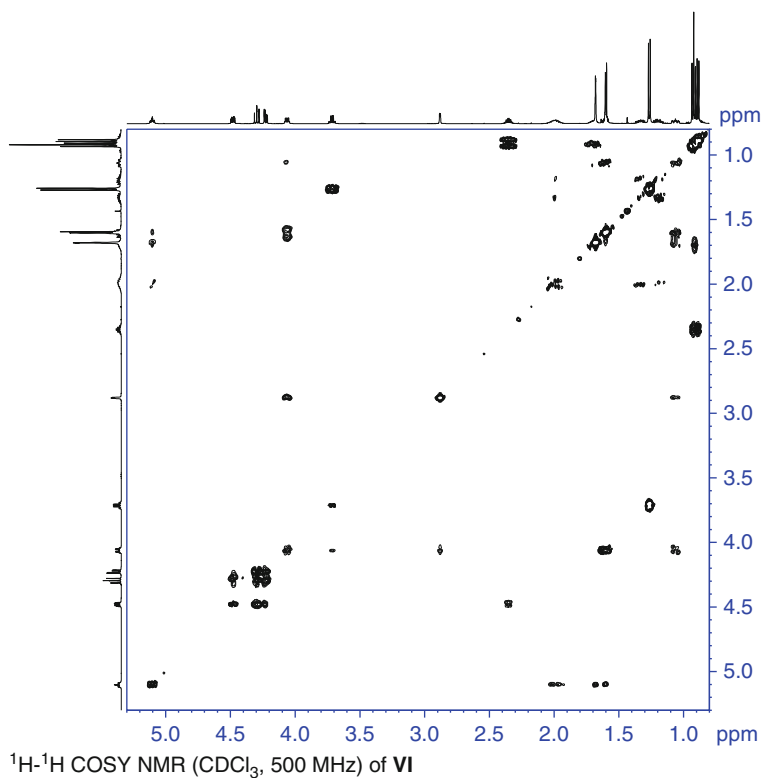
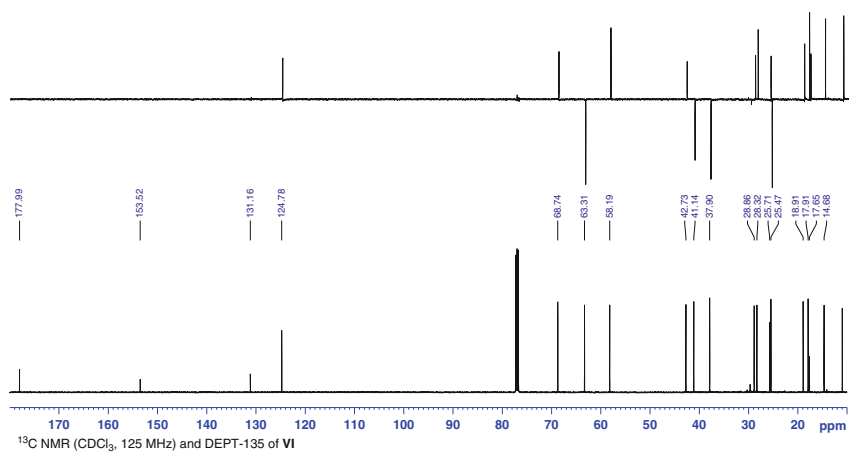
Vannusals A and B**Ectoine****2-imino-1-methylpyrrolidine-5-carboxylic acid.**

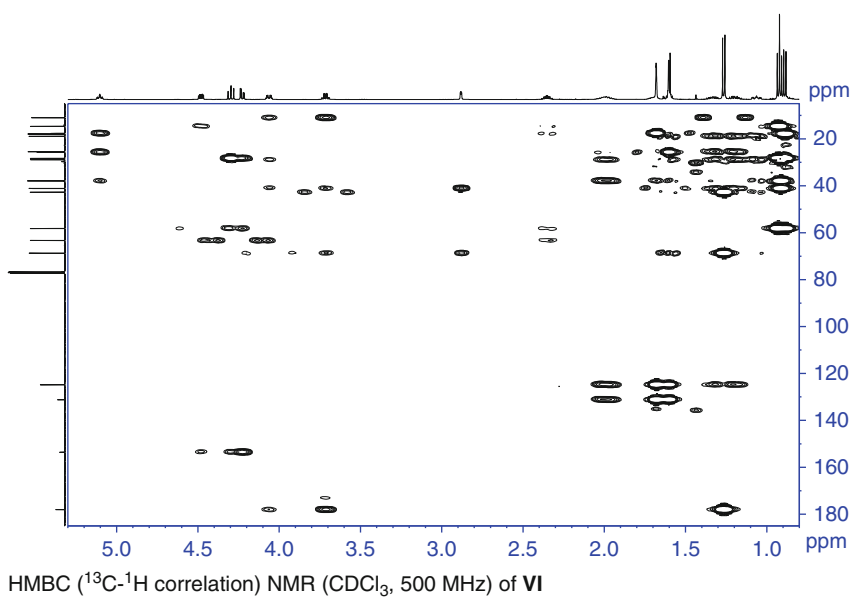
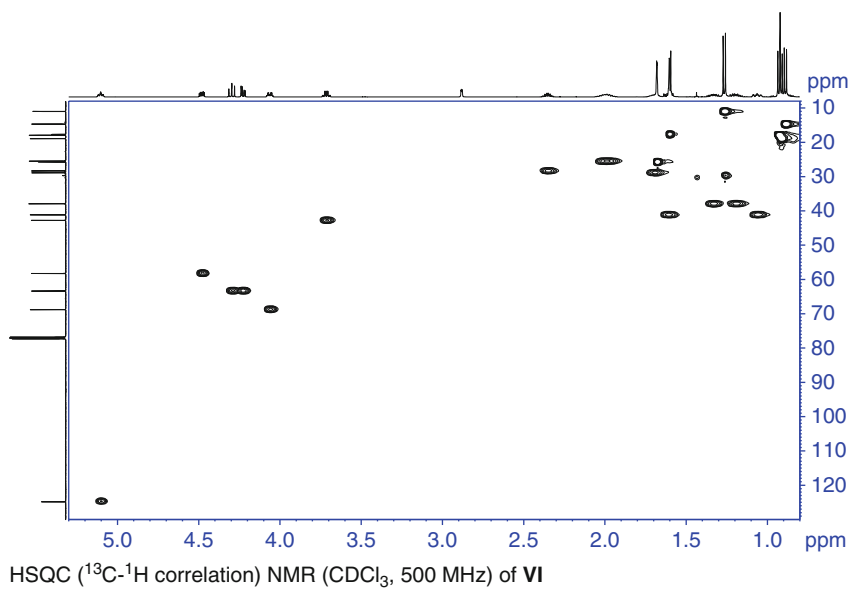
3. Three marine natural compounds isolated from marine red alga *Laurencia decumbens* were analyzed by MS means. Describe the expected cluster patterns for the (+)-ESIMS of **I**, **II** and **III**.

**I****II****III**

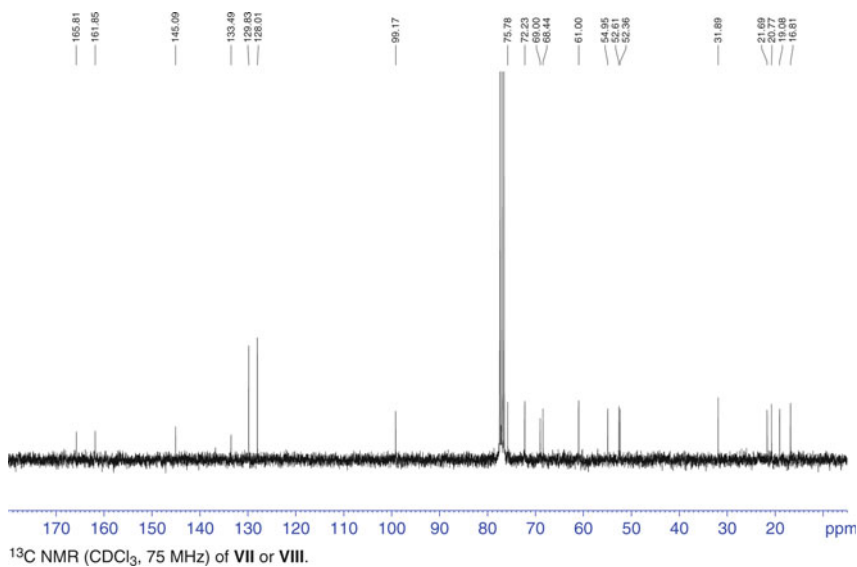
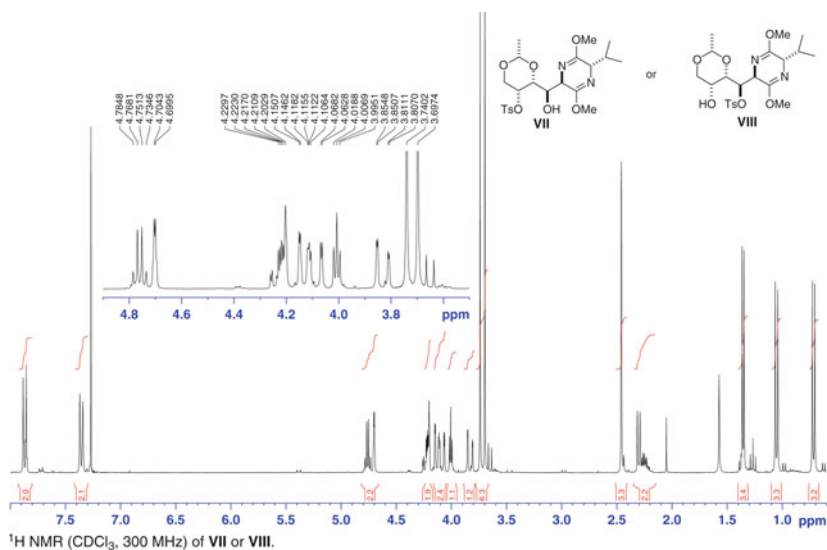
4. Distinguish between the three alternative structures **IV**, **V** and **VI** based on the analysis of the following ^1H NMR data: δ_{H} 7.51 (m, 2H), 7.39 (m, 3H), 5.67 (s, 1H), 4.73 (d, 1H, $J = 1.7\text{Hz}$); 4.29 (dd, 1H, $J = 10.7$ and 15.8Hz); 4.16 (dd, 1H, $J = 3.7$ and 10.3Hz); 4.07 (t, $J = 10.3\text{Hz}$); 3.91 (dd, 1H, $J = 1.5$ and 3.7Hz), 3.85 (m, 2H), 3.42 (s, 3H).

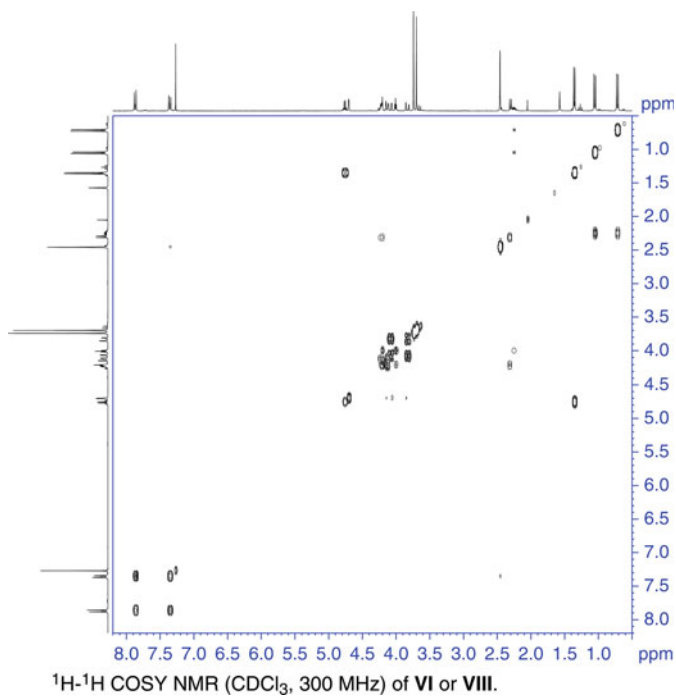
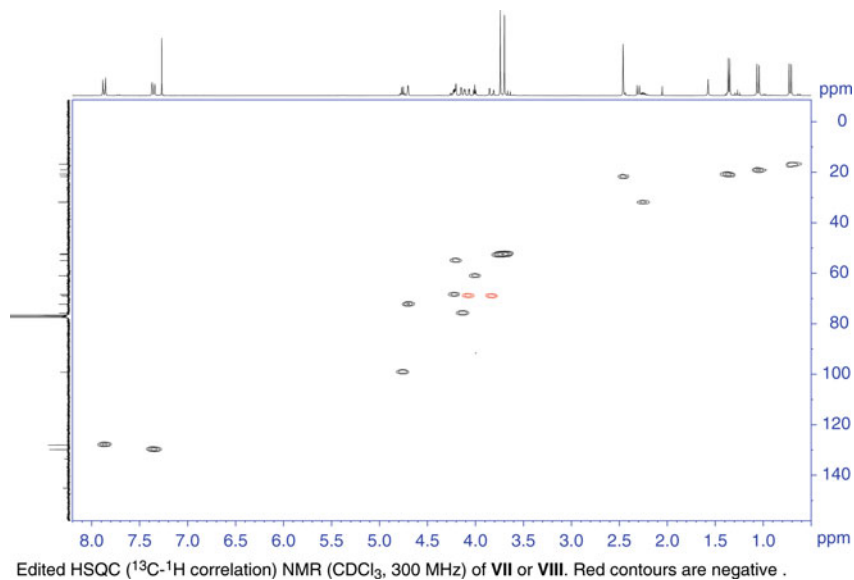
**IV****V****VI**

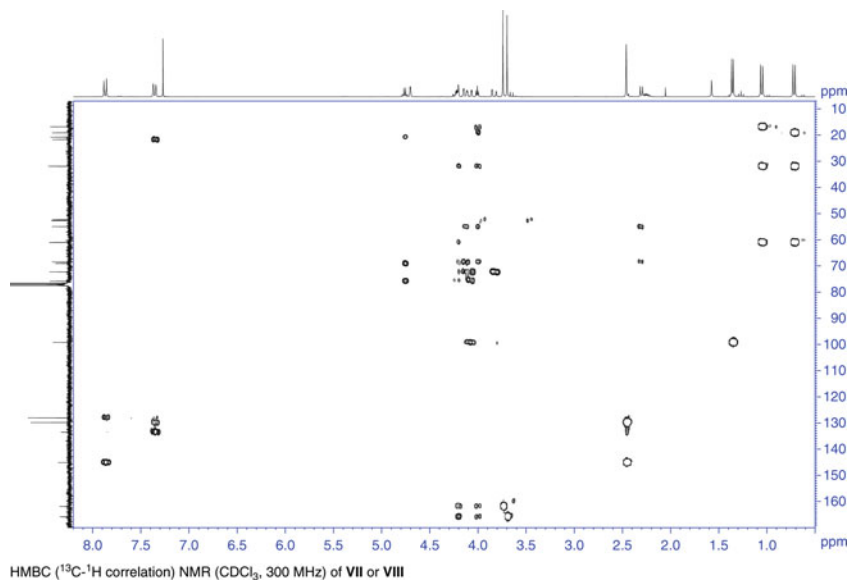




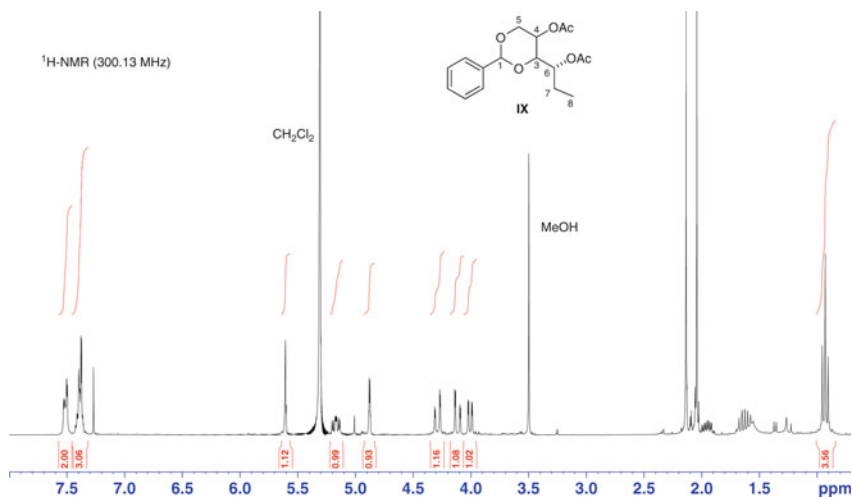
8. The tosylation of a diol gave an intermediate which the NMR data can be assigned to either **VII** or **VIII**. What is it?

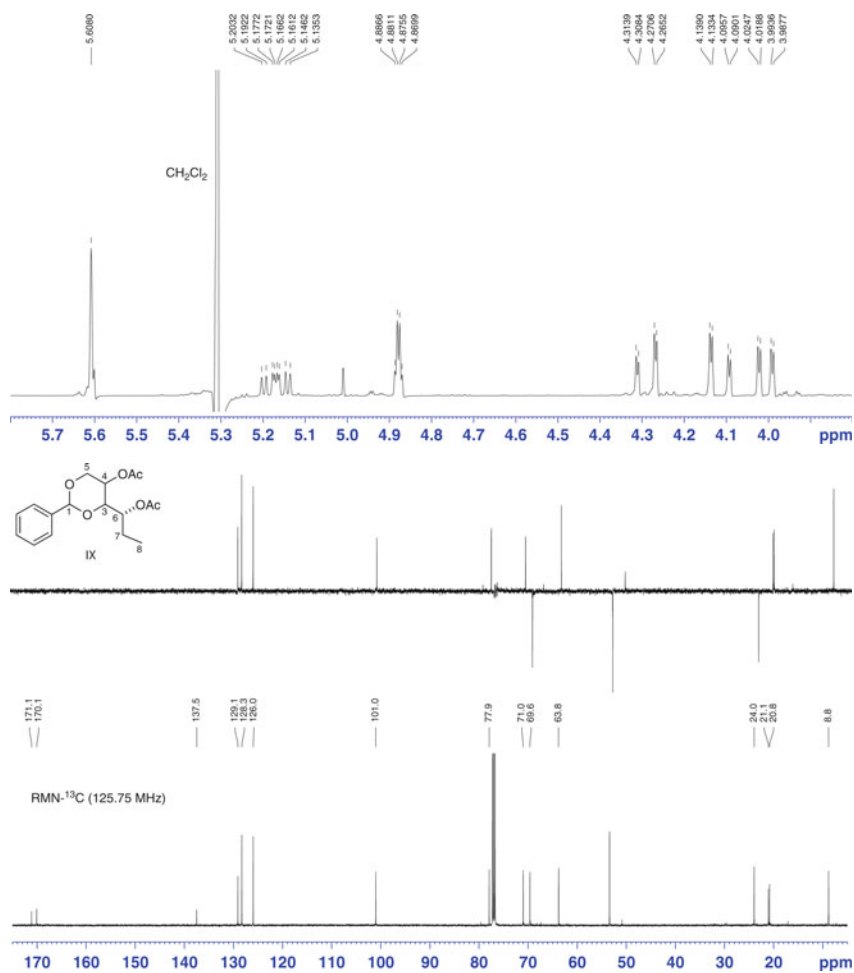


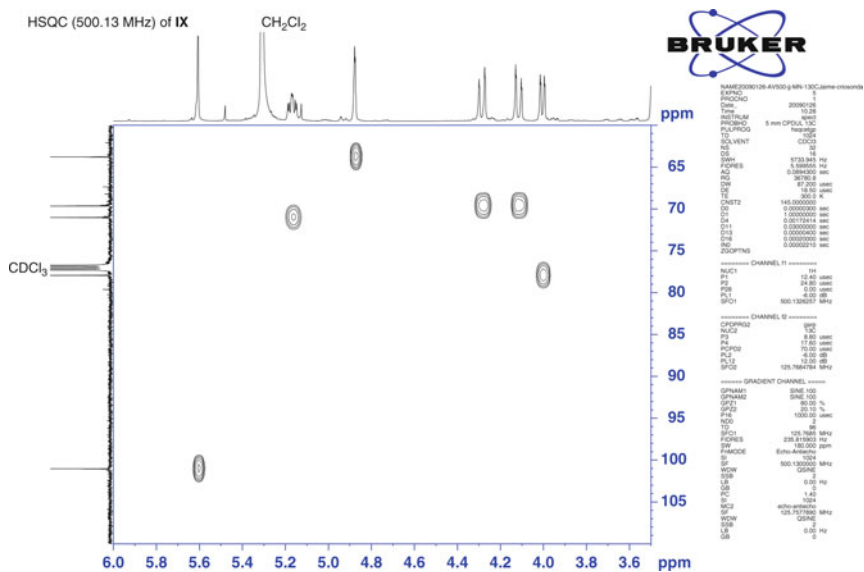


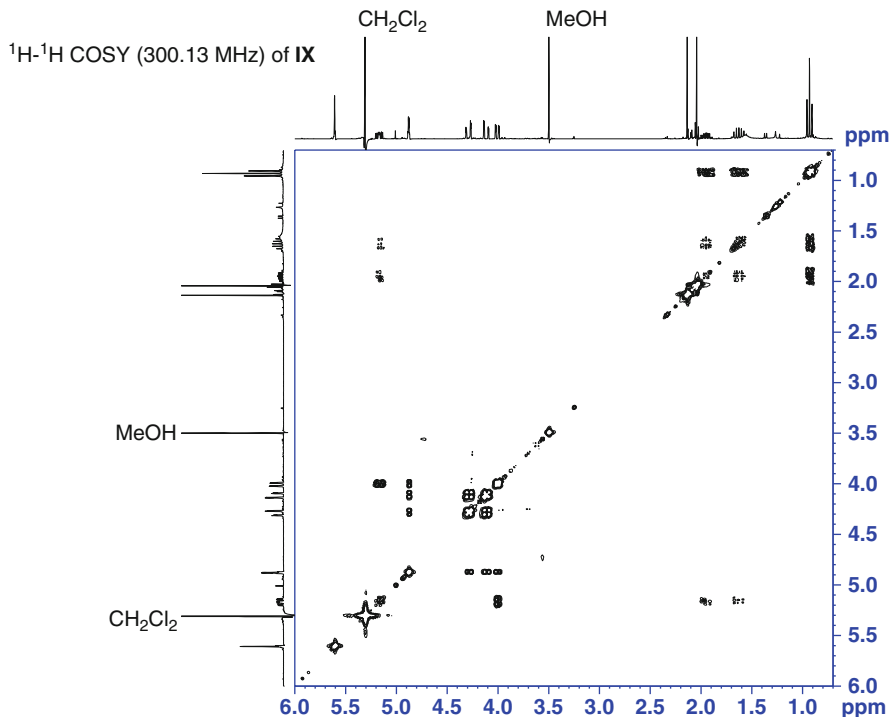


9. **IX** is a key synthetic intermediate in the total synthesis of a marine natural compound. Using NMR data, deduce the stereochemistry at positions 1, 3, and 4.









Acknowledgments Thanks to the Spanish Ministerio de Ciencia e Innovación for grant CTQ2008-04024/BQU. Also thanks to professors Maria Ruiz-Pita Romero, Montserrat Martinez Cebeiro, Jose Pérez Sestelo, and Vicente Ojea Cao for providing NMR spectra for the study questions.

References

1. Crews P, Rodríguez J, Jaspars M (2010) Organic structure analysis, Chapter 1, 2nd edn. Oxford University Press, New York
2. (a) Vogel AI, Tatchell AR, Furnis BS, Hannaford AJ, Smith, PWG (1996) Vogel's textbook of practical organic chemistry, 5th edn. Prentice Hall, New York; (b) McMurry J (2007) Organic chemistry, 7th edn. Brooks/Cole, Pacific Grove; (c) Vollhardt PC, Shore NE (2005) Organic chemistry structure and function, 5th edn. W. H. Freeman, San Francisco
3. Jiménez JI, Scheuer PJ (2001) New lipopeptides from the Caribbean cyanobacterium *Lyngbya majuscula*. J Nat Prod 64:200–203
4. Iorizzi M, Bifulco G, De Riccardis F, Minale L, Riccio R, Zollo F (1995) Starfish saponins, part 53. A reinvestigation of the polar steroids from the starfish *Oreaster reticulatus*: isolation of sixteen steroidal oligoglycosides and six polyhydroxysteroids. J Nat Prod 58:10–25
5. Niu C, Ho DM, Zask A, Ayral-Kaloustian S (2010) Absolute configurations of tubulin inhibitors taltobulin (HTI-286) and HTI-042 characterized by X-ray diffraction analysis and NMR studies. Bioorg Med Chem Lett 20:1535–1538

6. Luppi L, Cesaretti M, Volpi N (2005) Purification and characterization of heparin from the Italian clam *Callista chione*. *Biomacromolecules* 6:1672–1678
7. Smith MB, March J (2006) March's advanced organic chemistry, 6th edn. Wiley, Hoboken
8. Ueki Y, Itoh M, Katoh T, Terashima S (1996) Synthesis of various model compounds for the central tricyclic ring system of popolophuanone E. *Tetrahedron Lett* 37:5719–5772
9. Shriner RL, Hermann CKF, Morrill TC, Curtin DY, Fuson RYC (2003) Systematic identification of organic compounds, 8th edn. Wiley, Hoboken
10. Main P, Clegg W, Blake AJ, Gould RO (2002) Crystal structure analysis. Principles and practice. Oxford University Press, New York
11. Pretsch E, Bühlmann P, Badertscher M (2009) Tables of spectral data for structure determination of organic compounds, 4th edn. Springer, Berlin
12. Bobzin SC, Yang S, Kasten TP (2000) LC-NMR: a new tool to expedite the dereplication and identification of natural products. *J Ind Microbiol Biotechnol* 25:342–345
13. Chemspider a free text and structure searching tool at www.chemspider.com
14. MarinLit: a comprehensive database of the literature for marine natural products. Version February 2011. <http://www.chem.canterbury.ac.nz/marinlit/marinlit.shtml>. Accessed 21 Nov 2011
15. Eliel EL (2004) Stereochemistry of organic compounds. Wiley, New York
16. Crews P, Rodríguez J, Jaspars M (2010) Organic structure analysis, Chapter 6, 2nd edn. Oxford University Press, New York
17. (a) Ma TS, Rittner RC (1979) Modern organic elemental analysis. Taylor & Francis, Marcel Dekker Inc., New York; (b) Bance S (1980) Handbook of practical organic microanalysis recommended methods for determining elements and groups. Ellis Horwood Limited, Chichester
18. "Guidelines for authors" ACS Paragon Plus Web Site: pubs.ACS.org/paragonplus. Accessed 21 Nov 2011
19. (a) Budzikiewicz H, Djerassi C, Williams DH (1967) Mass spectrometry of organic compounds. Holden Day, San Francisco; (b) McLafferty, FW, Turecek F (1993) Interpretation of mass spectra, 4th edn. University Science Books, Mill Valley; (c) Howe I, Williams, DH, Brown RD (1981) Mass spectrometry: principles and applications, 2nd edn. McGraw-Hill, New York; (d) Watson JT, Sparkman OD (2007) Introduction to mass spectrometry, 4th edn. John Wiley & Sons Ltd., West Sussex
20. (a) Chapman JR (1995) Practical organic mass spectrometry 2nd edn. Wiley, New York; (b) Desiderio DM (1992) Practical organic mass spectrometry. Modern analytical chemistry series, vol I. Plenum, New York
21. Harrison AG (1992) Chemical ionization mass spectrometry, 2nd edn. CRC Press, Boca Raton
22. (a) Cole RB (1997) Electrospray mass spectrometry. Wiley, New York; (b) Pramanik BN, Gross ML (2002) Applied electrospray mass spectrometry. Marcel Dekker, New York
23. (a) Cody RB, Laramée JA, Durst HD (2005) Versatile new ion source for the analysis of materials in open air under Ambient conditions. *Anal Chem* 77:2297–2302; (b) Smith NJ, Domin MA, Scott LT (2008) HRMS directly from TLC slides. A powerful tool for rapid analysis of organic mixtures. *Org Lett* 10:3493–3496
24. (a) Karas M, Bahr U, Giessman U (1991) Matrix-assisted laser desorption ionization mass spectrometry. *Mass Spec Rev* 10:335–357; (b) Hillenkamp F, Katalinic JP (2007) MALDI MS: a practical guide to instrumentation, methods and applications. Wiley, Weinheim
25. (a) Hsu CS (1984) Diophantine approach to isotopic abundance calculations. *Anal Chem* 56:1356–1361; (b) <http://www.sisweb.com/mstools.htm>. (c) MS tools to calculate isotopic distributions. <http://www.shef.ac.uk/~chem/chemuter/isotopes.html>; (d) Rockwood AL, Van Orden SL (1996) Ultrahigh-speed calculation of isotope distributions. *Anal Chem* 68:2027–2030
26. Darias J, Rovirosa J, San Martín A, Díaz A, Dorta E, Cueto M (2001) Furoplacamidioids A-C, novel polyhalogenated furanoid monoterpenes from *Plocamium cartilagineum*. *J Nat Prod* 64:1383–1387

27. (a) Dawson PH (1976) Quadrupole mass spectrometry. Elsevier, Amsterdam; (b) Dawson PH (1997) Quadrupole mass spectrometry and its applications. AVS classics in vacuum science and technology. American Inst. of Physics
28. March RE (2005) Quadrupole ion trap mass spectroscopy. John Wiley & Sons, Hoboken
29. Makarov A (2000) Electrostatic axially harmonic orbital trapping: high-performance technique of mass analysis. *Anal Chem* 72:1156–1162
30. Clemmer DE, Jarrold MF (1997) Ion mobility measurements and their applications to clusters and biomolecules. *J Mass Spectrom* 32:577
31. Dalisay DS, Morinaka BI, Skepper CK, Molinski TF (2009) A tetrachloro polyketide hexahydro-1H-isoidolone, muironolide A, from the marine sponge *Phorbas* sp. Natural products at the nanomole scale. *J Am Chem Soc* 131:7552–7553
32. (a) McMaster, MC (2005) LC/MS: a practical user's guide. Wiley, Hoboken, New Jersey; (b) Robert EA (2003) Liquid chromatography-mass spectrometry: an introduction. Wiley, Hoboken, New Jersey
33. (a) Newton RP (1992) Mass spectrometry in the biological sciences: a tutorial, Chapters 2, 3, and 26. Kluwer, Dordrecht (b) Yates, JR, Eng JK, McCormack AL, Schieltz D (1995) Direct analysis of protein mixtures by tandem mass spectrometry. *Anal Chem* 67:1426–1436
34. Chapman JR (2006) Mass spectrometry of proteins and peptides in methods in molecular biology. Humana Press, Totowa
35. Crews P, Rodríguez J, Jaspars M (2010) Organic structure analysis, Chapter 3, 4 and 5, 2nd edn. Oxford University Press, New York
36. Bovey FA (1968) NMR spectroscopy. Academic, New York
37. (a) Stothers JB (1972) Carbon-13. In: NMR spectroscopy. Academic Press, New York; (b) Breitmaier E, Voelter, W (1987) Carbon-13. In: NMR spectroscopy, 3rd edn. VCH, Weinheim
38. (a) Becker ED (1980) High resolution NMR theory and chemical applications, 2nd edn. Academic, New York. pp 202–206 of this book give an excellent description of many first- and second-order splitting patterns; (b) Bible RH (1963) Interpretation of NMR: an empirical approach. Plenum, New York
39. Hoyer TR, Hanson PR, Vyvyan JR (1994) A practical guide to first-order multiplet analysis in 1H NMR spectroscopy. *J Org Chem* 59:4096–4103
40. Gutowsky HS, Karplus M, Grant DM (1959) Angular dependence of electron-coupled proton interactions in CH₂ groups. *J Chem Phys* 31:1278–1289
41. (a) Breitmaier E, Voelter W (1987) C-13 NMR spectroscopy, 3rd edn. VCH, Weinheim; (b) Marshall JH (1983) Carbon-carbon and carbon-proton NMR couplings: application to stereochemistry and conformational analysis. Verlag Chemie International, Deerfield Beach; (c) Pretsch E, Buhlmann P, Affolter C (2000) Structure determination of organic compounds: tables of spectral data. Springer, New York
42. Haasnoot CAG, de Leeuw FAAM, Altona CA (1980) The relationship between proton-proton NMR coupling constants and substituent electronegativities—I: An empirical generalization of the Karplus equation 7. *Tetrahedron* 36:2783–2792
43. Matsumori N, Kaneno D, Murata M, Nakamura H, Tachibana K (1999) Stereochemical determination of acyclic structures based on carbon – proton spin-coupling constants. A method of configuration analysis for natural products. *J Org Chem* 64:866–876
44. (a) Noggle JH, Schirmer RE (1971) The nuclear Overhauser effect. Academic, New York; (b) Friebolin H (2005) Basic one and two dimensional NMR spectroscopy 4th edn. VCH, Weinheim; (c) Derome AE (1987) Modern NMR techniques for chemistry research. Pergamon, New York; (d) Sanders JKM, Hunter BK (1993) Modern NMR spectroscopy, 2nd edn. Oxford University Press, Oxford
45. (a) Ernst RR, Bodenhausen G, Wokaun A (1987) Principles of NMR in one and two dimensions. Clarendon Press, Oxford; (b) Freeman R (1999) Spin choreography - Basic steps in high resolution NMR. Oxford University Press, Sausalito (CA)

46. (a) Claridge TDW (2008) High-resolution NMR techniques in organic chemistry. Elsevier Science, Burlington; (b) Sanders JKM, Hunter BK (1993) Modern NMR spectroscopy, 2nd edn. Oxford University Press, Oxford
47. Kupce E, Freeman R (2008) Molecular structure from a single NMR experiment. *J Am Chem Soc* 130:10788–10792
48. Reynolds WF, Enriquez RG (2002) Choosing the best pulse sequences, acquisition parameters, postacquisition processing strategies, and probes for natural product structure elucidation by NMR spectroscopy. *J Nat Prod* 65:221–244; Berger S, Braun S (2004) 200 and more NMR experiments - A practical course. VCH, Weinheim
49. Reiff B, Kock M, Kerssebaum R, Kang H, Fenical W, Griesinger C (1996) ADEQUATE, a new set of experiments to determine the constitution of small molecules at natural abundance. *J Mag Reson A* 118:282–285
50. Elyashberg M, Williams AJ, Blinov K (2010) Structural revisions of natural products by Computer-Assisted Structure Elucidation (CASE) systems. *Nat Prod Rep* 27:1296–1328
51. Based on Chapters 9, and 10 of Crews P, Rodríguez J, Jaspars M (2010) Organic structure analysis, 2nd edn. Oxford University Press, New York
52. Socrates GIR (1994) Characteristic group frequencies, 2nd edn. Wiley, New York
53. Lin-Vien D, Colthup NB, Fateley WG, Grasselli JG (1991) Infrared and Raman characteristic frequencies of organic molecules. Academic, New York
54. Pouchert CJ, Behnke C (eds) (1985) Aldrich library of FT-IR spectra, 1st edn. Aldrich Chemical Company, Milwaukee. Also available on CD-ROM. Many IR spectra are now provided for compounds sold on the Aldrich website: www.sigmaaldrich.com
55. Rodger A, Nordén B (1997) Circular dichroism and linear dichroism. Oxford University Press, Oxford
56. Berova N, Nakanishi K, Woody RW (eds) (2000) Circular dichroism, principles and applications. VCH, Weinheim
57. Lightner DA, Gurst JE (2000) Organic conformational analysis and stereochemistry from circular dichroism spectroscopy. Wiley, New York
58. Zhao N, Kumar K, Neuenschwander K, Nakanishi K, Berova N (1995) Quaternary ammonium salts as chromophores for exciton-coupled circular dichroism: absolute configuration of hypocholesterolemic quinuclidines. *J Am Chem Soc* 117:7844–7845
59. Nicolaou KC, Zinder SA (2005) Chasing molecules that were never there: misassigned natural products and the role of chemical synthesis in modern structure elucidation. *Angew Chem Int Ed* 44:1012–1044

Strategies for Structural Assignment of Marine Natural Products Through Advanced NMR-based Techniques

8

Alfonso Mangoni

Contents

8.1	Introduction	520
8.2	Basic 2D NMR Experiments	521
8.2.1	^1H – ^1H Connectivity	521
8.2.2	^1H – ^{13}C Connectivity	527
8.2.3	^{13}C – ^{13}C Connectivity	531
8.3	Real-Life Examples	531
8.3.1	Starting from HMBC	532
8.3.2	HMBC and “False HSQC” Peaks	533
8.3.3	Dealing with Alkyl Chains	534
8.3.4	Dealing with Non-first-order Multiplets: Spectral Simulation	536
8.3.5	Dealing with Non-first-order Multiplets: ^{13}C -Coupled HSQC	538
8.3.6	Coupling Constants and Furanose Sugars	540
8.4	Future Perspectives	541
8.5	Study Questions	543
	References	544

Abstract

This chapter surveys the standard 2D NMR techniques (COSY, TOCSY, NOESY and ROESY, HSQC and HMQC, HMBC, and INADEQUATE) including also some suggestion about the most suitable experimental parameters to be utilized in the different cases. In addition, an entire section describes some tricks and techniques that can be used in difficult cases of structural elucidation.

A. Mangoni

Dipartimento di Chimica delle Sostanze Naturali, Università di Napoli Federico II, Via D. Montesano 49, Naples, Italy
e-mail: mangoni@unina.it

8.1 Introduction

In spite of the increasing interest in the biological activity, ecology, and biogenesis of natural compounds, structure elucidation remains the central part of the study of natural products. Since its introduction in late 1970s, two-dimensional NMR (2D NMR) spectroscopy has represented by far the most valuable technique for the elucidation of the structure of unknown organic compounds. After the molecular formula of an unknown compound has been determined from mass spectrometry, its structure (even a complex one) can be often determined using NMR alone.

The wide availability of highly automated spectrometers has made 2D NMR spectra routinely available to nonspecialists, and most organic chemists are involved in their interpretation on an everyday basis. In most cases, the 1D ^1H and ^{13}C spectra and three standard 2D experiments (COSY, HSQC, and HMBC) lead easily to an unambiguous structure, as far as stereochemistry is not concerned. We assume that the reader has at least some familiarity with these basic 2D experiments. More or less standard strategies for structure elucidation can then be used, which are widely discussed in reviews [1] and textbooks [2]. In more difficult cases, however, less common experiments and/or more sophisticated interpretation strategies are required. Barring exceptionally complex molecules (such as some polyether toxins), complexity itself is seldom the problem. More often, difficulties can arise from:

- Overlapped signals (particularly overlapped coupled protons, i.e., strongly coupled systems)
- Proton-poor molecules or molecular moieties (such as aromatic compounds and heterocycles)
- Unusually large long-range proton–proton couplings (like in bridged polycyclic compounds)
- Molecules experiencing conformational equilibria.

In such cases, additional experiments may be needed, but the choice of the most appropriate experiment to perform among the myriad of pulse sequences available in the literature (and provided by the manufacturers along with any NMR spectrometer) is not trivial. Alternatively, the use of standard sequences with a rational modification of the acquisition parameters or of the experimental conditions (solvent, temperature, sample concentration) may be the easiest way to get to the structure. Finally, spectral simulation can be a useful aid to extract NMR parameters (particularly coupling constants) which cannot be measured directly from strongly coupled or overlapped multiplets.

The present chapter contains a section surveying the standard 2D NMR techniques, with some suggestion about the most suitable experimental parameters, followed by a section describing some tricks and techniques that can be used in difficult cases of structural elucidation. Methods specifically directed to the determination of relative and absolute configurations will not be treated because they are covered by another chapter of this book.

8.2 Basic 2D NMR Experiments

The general goal of all NMR experiments is to make available the NMR parameters of the nuclei present in a molecule, which are then translated into structural information. Chemical shift provides information of the chemical environment of a given nucleus, and dipolar coupling (which is not directly observable in isotropic solution but can be detected indirectly through the nuclear Overhauser effect, NOE, and the rotating-frame Overhauser effect, ROE) provides information on distances between nuclei. Scalar coupling is by far the most informative phenomenon. The *presence* (or absence) of a coupling is essential to determine connectivities between atoms; the *magnitude* of a coupling constant may provide useful information about relative configurations, especially for cyclic or conformationally biased systems, through the well-known Karplus relationship [3] or more sophisticated empirical [4] or quantum-mechanical approaches (► Chap. 10 of this book). In this respect, the work of Murata [5] has recently extended to proton–carbon couplings what had been done for years with proton–proton couplings.

If *all* the chemical shifts and couplings of all the nuclei in a molecule are known, the structure of this molecule is always unequivocally determined (except for stereochemistry). This goal can rarely be achieved completely. The work of the NMR spectroscopist is to find a way to determine as many NMR parameters as possible, and the experiments described below are by far the most useful tools to this end.

8.2.1 ^1H – ^1H Connectivity

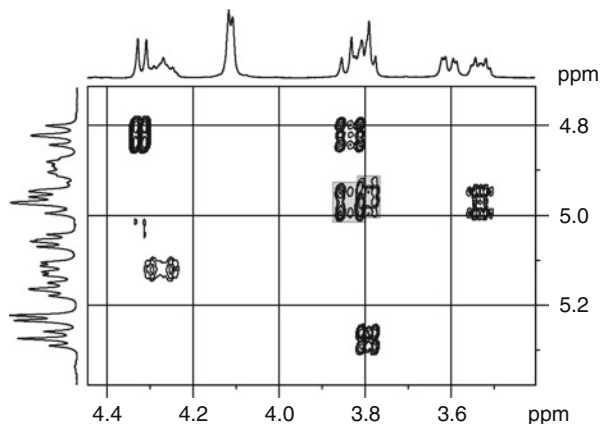
8.2.1.1 COSY

The COSY experiment is the first introduced [6] and most frequently acquired 2D NMR experiment. The simple and sensitive basic COSY sequence (sometimes called COSY-90) can be run even on the oldest spectrometers. Several improved COSY sequences have been proposed which find a significant use in structure elucidation work. Long-range COSY enhances small coupling constants; double-quantum filtered COSY (DQF-COSY) [7] shows less pronounced diagonal peaks, which moreover assume the same phase of cross peaks, allowing phase-sensitive acquisition. E-COSY [8] simplifies the multiplet pattern of COSY cross peaks, making the measurement of coupling constants easier.

In addition, the gradient-enhanced versions of all the above sequences exist. They are slightly less sensitive than their nongradient counterparts, but require shorter phase cycles (even 1 scan per t_1 increment) and therefore shorter acquisition times, and are useful for concentrated samples where sensitivity is not an issue (as it is often the case with the sensitive COSY sequence). For more diluted samples, requiring more than 8 scans per t_1 increment, the nongradient COSY sequences usually produce better spectra.

In spite of all the improved COSY sequences, when dealing with an unknown compound, the original, magnitude-mode COSY-90 sequence (or its

Fig. 8.1 Two partially overlapped peaks (*gray squares*) are easily discerned in a COSY-90 spectrum



gradient-enhanced version for concentrated samples) remains the sequence of choice. In fact, thanks to the clear rectangular shape of the cross peak which is characteristic of this experiment, it is very easy to discern partially overlapped cross peaks and follow the correct connectivity pathway even in very crowded spectra (Fig. 8.1).

To fully exploit this advantage, it is important to acquire an adequately large number of points in the F1 dimension, usually at least 512, corresponding to an F1 acquisition time of about 100 ms for a typical 4,000-Hz spectral width. Such a long F1 acquisition time cannot be replaced by F1 linear prediction, which is not useful for COSY spectra, because the antiphase COSY cross peaks start with zero intensity. While using a relatively long F1 acquisition time, an enhancement of cross peaks arising from small couplings is also observed, limiting the need of a dedicated long-range COSY experiment to very special situations.

It is often argued that the more sophisticated double-quantum filtered COSY (DQF-COSY) experiment should always be preferred to the original COSY sequences. DQF-COSY allows phase correction to give pure-absorption multiplets, so as to distinguish between active (i.e., the one generating the cross peak) and passive couplings in a multiplet. This advantage is rarely exploited in practice, because the active couplings give antiphase components, making phase correction tedious and analysis of fine structure difficult for complex multiplets, and the majority of published COSY spectra are recorded and transformed in magnitude mode. If the spectrum has to be transformed in magnitude mode, then it is better to use the original COSY-90 sequence, which is more sensitive and requires a shorter phase cycle. If, on the other hand, one intends to use DQF-COSY for a detailed analysis of fine structure of cross peaks, then a higher digital resolution is required (typically, F2 acquisition time of at least 500 ms, corresponding to 2,048 complex points for a 4,000-Hz spectral width).

In summary, use COSY-90 and at least 512 points in the F1 dimension. Leave the other parameters to their default values. Do not use F1 linear prediction.

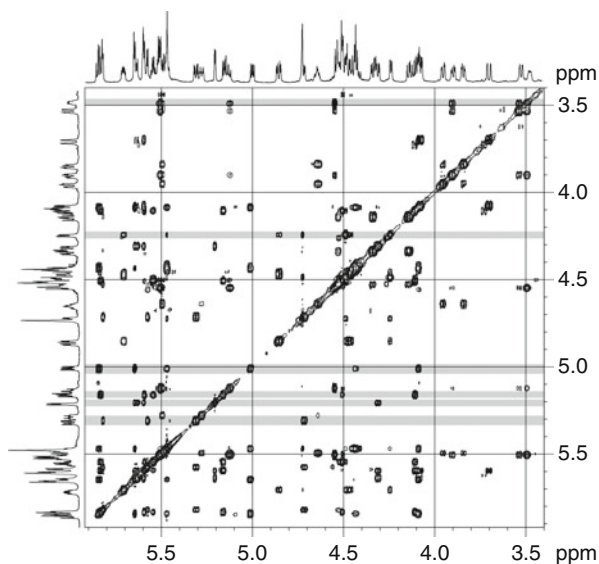
8.2.1.2 TOCSY

In the TOCSY experiment [9], cross peaks are generated between all protons belonging to a coupled spin network (spin system). The inphase coherence transfer occurs during the isotropic mixing, and its extent is related to the duration of the coherence transfer period (mixing time). In case of large spin systems, the coherence transfer is limited to 4–5 couplings when the standard 80–100-ms mixing time is used (see Sect. 8.3.3 below); in addition, the coherence transfer is blocked by very small couplings. As long as the signal of at least one proton of a certain spin system is not overlapped to other signals, all the protons belonging to the spin system can be easily identified (Fig. 8.2). Therefore, TOCSY is typically used for compounds composed of many isolated spin systems, such as peptides and oligosaccharides.

However, TOCSY is by no means limited to these classes of compounds but may find a very general use in structural elucidation of any kind of compounds. The inphase coherence transfer, characteristic of the TOCSY experiment, fully preserves the fine structure of multiplets. When suitable acquisition parameters are used, a trace extracted from a 2D TOCSY spectrum is a subspectrum containing only signals from a particular spin system, with multiplicities as distinct as in a 1D proton spectrum (Fig. 8.3). TOCSY can therefore allow the direct measurement of coupling constants from multiplets even in crowded spectra.

If TOCSY has to be used in this way, some care must be taken in selecting the correct sequence and acquisition parameters. Because the measurement of coupling constants requires a good lineshape, a filtered TOCSY sequence that takes advantage of the zero-quantum filter recently proposed by Thrippleton and Keeler [10] (zTOCSY) should be used. In this filter, zero-quantum coherence is suppressed by applying simultaneously a 180° adiabatic pulse and a gradient, leading to

Fig. 8.2 The zTOCSY spectrum of the peracetylated glycosphingolipid vesparioside B, a glycosphingolipid from the marine sponge *Spheciospongia vesparia*. The correlation peaks on each gray line identify protons belonging to the same sugar



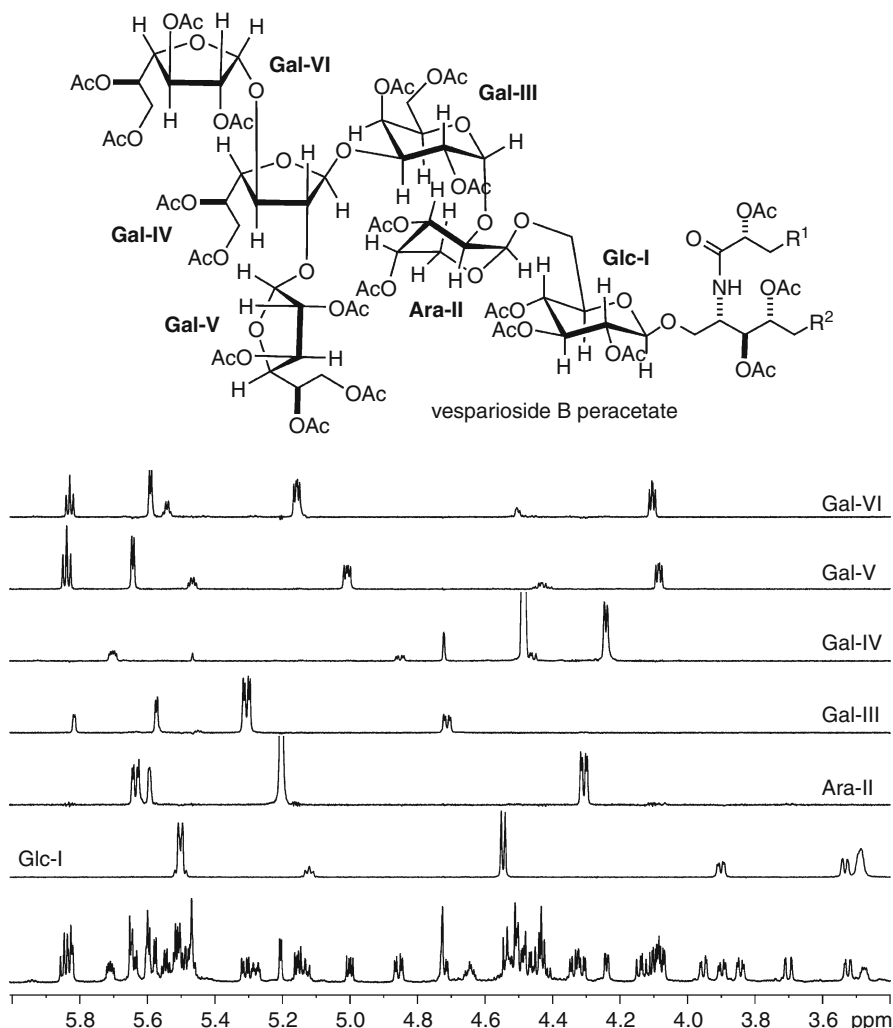
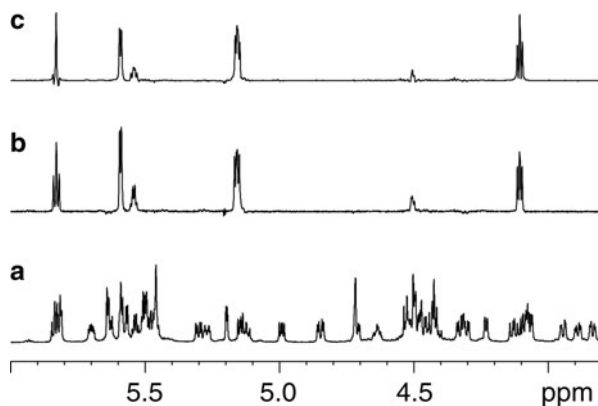


Fig. 8.3 Sections of the zTOCSY spectrum in Fig. 8.2 showing separate subspectra for each of the six sugars of vesparioside B. The spectrum was acquired with 8,192 complex points and transformed at 16,000 points in the direct dimension. Multiplet resolution was comparable with that of the 1D proton spectrum

pure-absorption inphase multiplets. Figure 8.4 compares a trace from the zTOCSY spectrum (a) and the nonfiltered TOCSY spectrum (b) of peracetylated vesparioside B, a glycosphingolipid from the marine sponge *Spheciospongia vesparia*: [11] in the latter spectrum, lineshape distortion from zero-quantum coherence is apparent. This sequence is available from all the NMR manufacturers and is preinstalled in the most recent spectrometers; if the spectrometer supports it, there is no reason to prefer standard TOCSY over zTOCSY.

Fig. 8.4 (a) The ^1H NMR spectrum of peracetylated vesparioside B. (b) A section of the zTOCSY spectrum. The pure absorption in-phase multiples preserved the lineshape of the proton spectrum. (c) A section of the standard TOCSY experiment. The multiplets are distorted by zero-quantum coherence effects (see in particular the triplet at δ 5.32)



In addition, a long t_2 acquisition time should be selected to achieve an adequate digital resolution, much longer than the usual few hundred microseconds used in 2D experiments. An acquisition time of about 2 s is suggested, corresponding to a 0.5-Hz digital resolution or 8,192 complex points in F2 for a typical spectral width of 4,000 Hz. After such a long acquisition, the relaxation delay can be set to 0 or to a few ms, taking care to disable or delete from the sequence the gradient and/or rf pulses sometimes used to suppress the residual magnetization from the previous scan. During processing, a generous fourfold zero filling in the F2 dimension will allow an easier comprehension of the structure of complex multiplets as well as an accurate measurement of coupling constants.

As for the F1 dimension, 256 t_1 increments are enough if one plans to use the 2D spectrum in the structure elucidation work (linear prediction works fine with TOCSY), while 128 increments may be sufficient if one is only interested in extracting the 1D traces. More t_1 increments can be considered only if correlation peaks from two sharp and very close signals need to be distinguished.

If a molecule contains very extended spin systems (like, e.g., in many polycyclic terpenoids), the TOCSY spectrum may contain many overlapped correlation peaks, nullifying most of the advantages discussed above. It may then be helpful to use a very short mixing time (10–15 ms) so that coherence transfer is limited to one or two couplings. The spectrum is then greatly simplified (it indeed becomes similar to a COSY spectrum), but the multiplets are still inphase and can be easily analyzed.

In summary, use zTOCSY if your hardware supports it, 4,000 or 8,000 points in the F2 dimension (they come at almost no cost and can be cut during processing if not needed), and a 100-ms mixing time. Use F1 linear prediction if needed.

8.2.1.3 NOESY and ROESY

The NOESY [12] and ROESY [13] experiments are mainly used for configurational assignment but are also useful to determine the atom connectivity, especially in proton-poor compounds such as heteroaromatics. While the information they

provide is similar, i.e., spatial proximity between protons, there are some important differences that need to be discussed. The NOESY experiment relies on the conventional nuclear Overhauser effect and therefore on T_1 (longitudinal) relaxation. The sign of NOE depends on the molecular tumbling rate, and fast-tumbling small molecules show positive NOE, which results in cross peaks opposite in sign to diagonal peaks in the 2D NOESY spectrum, while macromolecules show negative NOE. Midsize molecules, like many complex natural products, fall between these two regimes and can show little or no NOE.

In contrast, ROESY relies on rotating-frame NOE, which occurs when magnetization vectors are locked in the transverse plane (spin-lock) either by a continuous low-power rf field or by a suitable pulse train, and rotating-frame relaxation ($T_{1\rho}$ relaxation) develops. The rotating-frame NOE is always positive (cross peaks are opposite in sign to diagonal peaks), irrespective of the size of the molecule, and this is the reason why ROESY is used more often than NOESY in the structure elucidation of natural products.

Interpretation of ROESY is often complicated by the presence in the spectrum of cross peaks arising from TOCSY coherence transfer that also occurs during spin-lock. In ROESY experiments, TOCSY coherence transfer is suppressed, keeping the rf power for spin-lock lower (2,000–4,000 Hz) than in TOCSY experiments; in addition, a spin-lock pulse train has been developed to reduce TOCSY transfers [14]. The experiment using it is called transverse ROESY (abbreviated as tr-ROESY, T-ROESY, or TROESY). Even so, TOCSY-type cross peaks between protons sharing large coupling constants (e.g., geminal protons) are invariably present in ROESY spectra. Actually, the TOCSY-type cross peaks cannot be confused with ROESY cross peaks because they are opposite in sign (TOCSY peaks have the same phase as diagonal peaks), but they can hide potentially useful ROESY peaks between coupled protons. Another source of artifacts in ROESY spectra is zero-quantum coherence: it produces weak cross peaks, which can be easily recognized because they are antiphase peaks, but may hide useful information.

The most important experimental parameter of a ROESY spectrum is the mixing time τ_m , i.e., the duration of the spin-lock, during which the ROESY transfer takes place. The maximum intensity of ROESY cross peaks is observed when τ_m is close to the rotating-frame relaxation time $T_{1\rho}$, which in turn is close to T_1 for small molecules. Because T_1 is different for different protons within the molecule, τ_m will be necessarily a compromise value. As a rule of thumb, mixing times between 200 and 500 ms can be used, with mixing times at the low end of this range for large natural products and at the high end for very small ones. There is no particular requirement regarding digital resolution in ROESY experiments, so even a matrix of 512×256 complex points can be enough in the absence of very close resonances.

If the molecule under study is a small natural product, and is therefore definitely in the positive NOE regime, then the NOESY experiment should be considered, because the TOCSY artifacts are not present in NOESY. In addition, the zero-quantum filter described above [10] for zTOCSY can be applied to the NOESY

sequence. The resulting zNOESY experiment is devoid of the weak antiphase cross peaks which are originated by zero-quantum coherence. The optimal mixing time for NOESY is chosen in the same way as for ROESY. For small natural products, zNOESY can give better results than ROESY because of the clean spectra it produces. Like zTOCSY, zNOESY is preinstalled in recent spectrometers.

ROESY and NOESY spectra can also be used to study chemical exchange processes with a rate constant comparable, or a little faster, than $1/\tau_m$ (faster exchange rates lead to broadening and eventually coalescence of the exchanging signals). Exchange cross peaks can be easily identified because they have the same phase as diagonal peaks and therefore opposite phase compared to ROESY and NOESY cross peaks (however, they can be confused with the TOCSY artifacts present in the ROESY spectra).

In summary, use ROESY with a mixing time of 200–500 ms but beware of TOCSY artifacts. For small natural products, which are certainly in the positive NOE regime, zNOESY is a cleaner alternative.

8.2.2 ^1H – ^{13}C Connectivity

8.2.2.1 HSQC and HMQC

Once considered a demanding experiment, the proton-detected one-bond ^1H – ^{13}C correlation experiment HSQC [15] is now easily performed by any recent spectrometer. It has been constantly improved along the years (phase-sensitive acquisition, gradient selection, echo–antiecho acquisition, DEPT-like multiplicity editing, adiabatic inversion pulses), but these features are mostly transparent to the user, who just need to use the most recent sequence available on the spectrometer. However, because it contains several 180° pulses, the HSQC sequence is quite sensitive to pulse miscalibration. Sometimes the alternative HMQC sequence [16] is used instead of HSQC. It produces very similar results, but it is characterized by a lower ^{13}C resolution and is less suitable to F1 linear prediction, [17] so HSQC is always the experiment of choice.

The most important parameter that may need to be optimized is the evolution delay used to create antiphase proton magnetization. This is usually adjusted for an average $^1J_{\text{CH}}$ of 145 Hz, which is adequate for most compounds. When sensitivity is really an issue, a smaller value should be used for fully aliphatic compounds, reflecting the typical 125-Hz coupling constant between protons and sp^3 carbon atoms, while a larger value is preferable for aromatic and heterocyclic compounds, for which proton–carbon coupling constants are around 160–170 Hz. This optimization is not critical, except for compounds with very large coupling constants, like those observed in terminal alkynes (about 250 Hz) and some heterocycles (e.g., 206 Hz for C-2 of imidazole).

The DEPT-like multiplicity editing (giving cross peaks of CH_2 groups with opposite phase compared to CH and CH_3 groups) is a very useful aid in the interpretation of HSQC spectra. However, the multiplicity-edited HSQC

sequence is much more sensitive than standard HSQC to $^1J_{\text{CH}}$ coupling constants significantly different from that for which the experiment is optimized. Multiplicity editing is the most likely cause of failure in detecting HSQC peaks (particularly those of CH_2 groups) for compounds with a wide spread of $^1J_{\text{CH}}$ values and should not be used for such compounds. Alternatively, two multiplicity-edited HSQC spectra optimized for different coupling constants can be acquired.

The HSQC experiments are more sensitive than the 1D ^{13}C NMR spectrum, and many researchers prefer to determine ^{13}C chemical shift indirectly from HSQC and, for nonprotonated carbons, HMBC experiments. If this is the case, it is advisable to use a higher number of t_1 increments than the default (at least 256, better 512) together with linear prediction to achieve a reasonable accuracy.

The HSQC cross peaks preserve the fine structure of the proton signals and could in principle be used to access the multiplicity of overlapped proton signals in the same way as TOCSY. However, the ^{13}C broadband decoupling used in the HSQC experiment is very demanding for the probe, and therefore HSQC acquisition time is usually limited to 150–200 ms, corresponding to a digital resolution of 5–7 Hz. As a consequence, small couplings are not resolved, and large couplings cannot be measured accurately. In addition, often the sensitivity of the HSQC sequence is high enough to detect the presence of a peak, but not to discern its multiplicity. In spite of these limits, analysis of multiplicity of HSQC correlation peaks can be sometimes useful to detect the gross features of an overlapped multiplet, for example, to distinguish between an axial and an equatorial proton in a six-membered ring (Fig. 8.5).

It is also possible to turn off ^{13}C decoupling and acquire a ^{13}C -coupled HSQC spectrum. In this spectrum, each correlation peak is split by the large coupling constant, making interpretation less easy, but the acquisition time, and therefore the digital resolution, may be as long as desired (in addition, the side bands introduced by the ^{13}C decoupling are not present). An acquisition time around 1 s corresponds to a digital resolution of about 1 Hz, so that even small coupling constants can be measured. The sensitivity of the HSQC experiment, however, is further lowered when long acquisition times are used, and therefore, this technique requires a quite concentrated sample. Another use of the ^{13}C -coupled HSQC spectrum will be discussed later (Sect. 8.3.5).

In summary, use multiplicity-edited HSQC with default parameters and linear prediction. Try not to use multiplicity editing when some correlation peaks appear missing because of anomalous $^1J_{\text{CH}}$ coupling constants. Use ^{13}C -coupled HSQC if a high digital resolution is required.

8.2.2.2 HMBC and Related Experiments

The HMBC experiment [18], which detects couplings between proton and carbons across two or three bonds, is extremely useful in structure elucidation because it may extend the connectivity network across nonprotonated carbon atoms and heteroatoms. It is also one of the most frequent reasons for structural misassignments because of its inherent inability to discern between $^2J_{\text{CH}}$ and $^3J_{\text{CH}}$. Like HSQC, also, the HMBC sequence has been improved over the years,

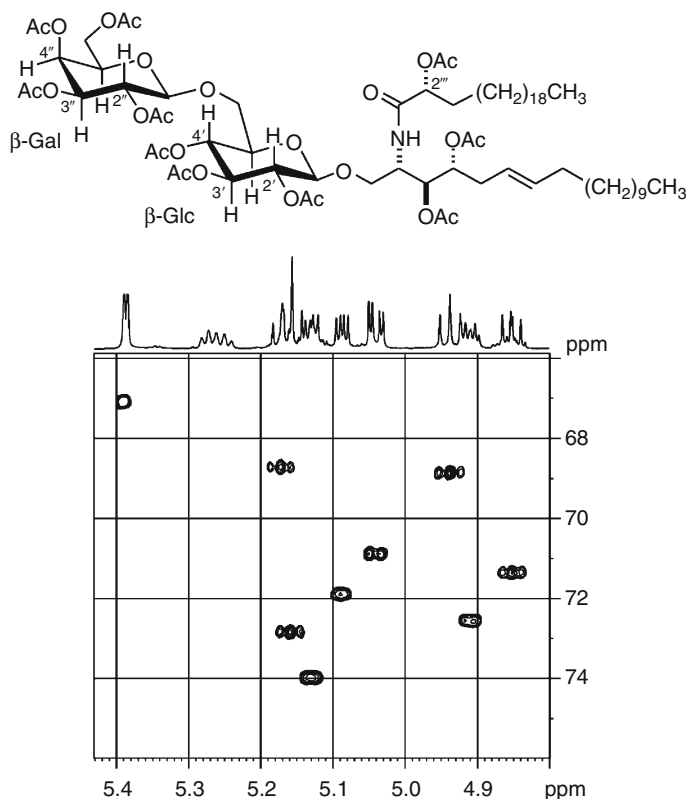


Fig. 8.5 Partial plot of the HSQC spectrum of peracetylated ampicramide B. In spite of the low digital resolution, the two large coupling constants of the two partially overlapped signals at δ 5.16 (the axial proton H-2'') and 5.17 (the axial proton H-3') are apparent. In contrast, resolution is not sufficient to discern the multiplicity of the signal at δ 5.13 (H-2')

with gradient selection, adiabatic carbon pulses, and experiments with pure-absorption lineshape in F1.

Both the $^2J_{CH}$ and the $^3J_{CH}$ coupling constants vary over a wide range of values (0–12 Hz), but the experiment can be optimized only for a single value, usually a compromise 7–8 Hz. If the J_{CH} is much smaller than this, the relevant correlation peak may be weak or absent. In addition, *homonuclear* coupling constants also evolve during the evolution delay, and this may also lead to the complete cancellation of a correlation peak. As a result, in most HMBC spectra, not all the theoretical correlation peaks are present, or, in other words, the *absence* of an HMBC peak is not diagnostic. To maximize the number of observed correlation peaks, it is a good idea to acquire a series of two or more HMBC experiments, optimized for different $^2J_{CH}$ couplings, for example, 8 and 5 Hz.

While the HMBC experiment relies on $^2J_{CH}$ and $^3J_{CH}$ couplings, it is not the first-choice experiment when one wishes to measure the value of such coupling

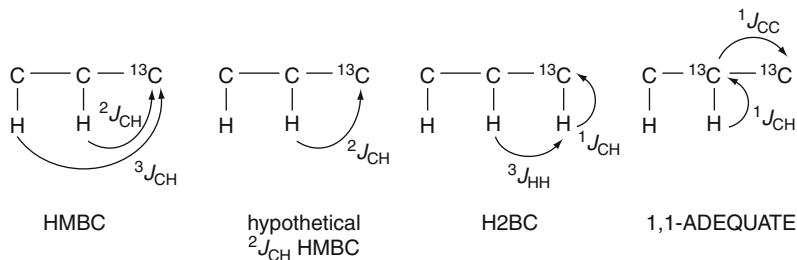


Fig. 8.6 Coherence transfer scheme in HMBC, a hypothetical $^2J_{\text{CH}}$ -selective HMBC, H2BC, and 1,1-ADEQUATE experiments

constants (this usually happens when a relative configuration needs to be determined using the Murata method) [5]. In fact, the presence of homonuclear couplings results in phase-modulated cross peaks which are difficult to analyze. Specific experiments (HETLOC, HSQMBC) may be used to this end, which will not be discussed here because they are extensively treated in ► Chap. 9 of this book.

Interpretation of HMBC spectra is hampered by the fact that a correlation peak may mean that the proton is either two bonds or three bonds away from the carbon. An HMBC experiment which can discern between $^2J_{\text{CH}}$ and $^3J_{\text{CH}}$ would be highly desirable, but this is impossible in principle because the very phenomenon on which HMBC relies, long-range coupling between ^1H and ^{13}C , has similar magnitude across two and three bonds. However, several experiments have been proposed providing similar information as a hypothetical $^2J_{\text{CH}}$ -selective HMBC but using different coherence transfer schemes (Fig. 8.6).

The H2BC sequence [19] can be described as an HSQC/COSY experiment, so that correlation peaks rely on $^1J_{\text{CH}}$ and $^3J_{\text{HH}}$ couplings. Therefore, only correlation peaks across two bonds are present. However, no correlations are observed for nonprotonated carbon atoms, vanishing one of the main advantages of HMBC. This experiment may be useful in complex spectra, where analysis of proton–proton couplings is difficult, and has indeed been used in the analysis of complex carbohydrates [20].

The 1,1-ADEQUATE sequence [21], as well as its improved version ACCORD-ADEQUATE [22], is comparable to an HSQC-INADEQUATE experiment. Proton coherence is transferred first to the directly bound carbon atom through $^1J_{\text{CH}}$ and then to the next carbon atom through $^1J_{\text{CC}}$. Therefore, the information provided by the experiment is fully equivalent to that of a “true” $^2J_{\text{CH}}$ HMBC, with the subtle difference that correlations of protons bound to heteroatoms are missing. An additional advantage is that small $^2J_{\text{CH}}$ couplings, causing missing correlations in the standard HMBC experiments, do not affect the 1,1-ADEQUATE spectrum. The main disadvantage of 1,1-ADEQUATE is the low sensitivity (at least for natural abundance samples) that it shares with all the experiments which rely on $^1J_{\text{CC}}$ couplings. 1,1-ADEQUATE is at least one order of magnitude less sensitive than HMBC but, being both proton-excited and proton-detected, is still much more

sensitive than the ^{13}C – ^{13}C INADEQUATE experiment (see below). To date, 1,1-ADEQUATE and ACCORD-ADEQUATE have found only occasional use in structure elucidation (see, e.g., Refs. [23, 24]) but, with the increase in sensitivity provided by cryogenic probes and improved instrument design, are expected to become more and more used.

In summary, use standard HMBC optimized for ^{13}C – ^1H coupling of 8 Hz. A second experiment optimized for 5 Hz may show additional correlation peaks. If sensitivity is not a problem, 1,1-ADEQUATE can make structure elucidation much easier.

8.2.3 ^{13}C – ^{13}C Connectivity

8.2.3.1 INADEQUATE

The homonuclear ^{13}C – ^{13}C correlation experiment INADEQUATE [25, 26] is potentially very useful to structure elucidation of natural compounds, allowing a direct access to the carbon skeleton of the molecule even for molecules or molecular portions devoid of protons. In spite of this theoretical advantage, it has only a limited use in practice (see, e.g., Refs. [27, 28]) because of its very low sensitivity when used on natural abundance samples. Only in one molecule out of about 10,000 ^{13}C is present at both ends of a given bond, and this adds up to the inherent lower sensitivity of ^{13}C -detected experiments. When the metabolite of interest is produced by a cultured microorganism, this problem can be strongly alleviated using a ^{13}C -enriched medium to obtain a ^{13}C -enriched sample [29, 30]. It is quite surprising that, in spite of the increasing diffusion of sensitive ^{13}C cold probes, the INADEQUATE experiment is not gaining popularity. A possible reason may be that in most situations, ^1H – ^{13}C correlation experiments are sufficient to solve a structure.

In summary, if enough sample is available, and the other 2D experiments did not solve the structure, INADEQUATE should be definitely tried.

8.3 Real-Life Examples

Structure elucidation based on the experiments described in the previous sections (and, of course, on molecular formula deduced by mass spectrometry) is straightforward for many compounds. There are still situations, however, where NMR data cannot unambiguously solve a structure, especially when only little amounts of sample are available and the less sensitive experiments such as INADEQUATE and 1,1-ADEQUATE are not possible. What do we do in these situations? Before trying to crystallize the compound for X-ray diffraction studies, one should consider that NMR experiments contain, or can provide, more information than is commonly used. The knowledge and the intelligent use of *all* the information NMR can provide can lead to solve structures that appear irresolvable by NMR at first sight. In this section, several examples will be given, mostly taken from my own real-life

structure elucidation work. They have been selected to draw attention to some less common aspects of structural elucidation that are not usually treated in general reviews or textbooks. Emphasis is not placed on theoretical aspects but rather on the nonstandard interpretation of standard experiments or in the use of standard experiments with unusual parameters.

8.3.1 Starting from HMBC

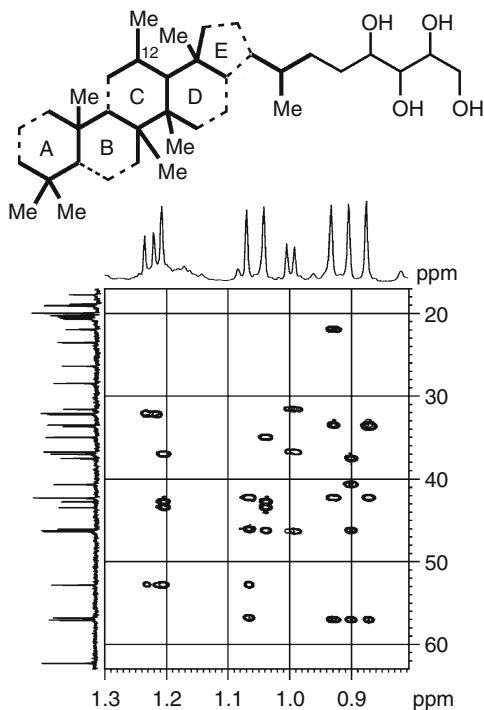
In the classical structure elucidation flow, the HMBC experiment is used to connect partial structures which have been previously determined from the analysis of the COSY, HSQC, and maybe TOCSY experiments. When dealing with some classes of compounds, most typically polycyclic terpenes, this may not be the best strategy because the analysis of COSY spectrum is made difficult by the extensive overlapping between aliphatic proton signals and the significant chance to observe large long-range W couplings. A valuable alternative strategy starts the analysis from the HMBC spectrum and, in particular, from the correlation peaks of the methyl protons.

We have mentioned before that in a typical HMBC spectrum, many expected correlation peaks are missing. This problem is not present when correlations of methyl protons are concerned. The free rotation about the C–CH₃ bonds guarantees that $^2J_{\text{CH}}$ and $^3J_{\text{CH}}$ do not vary much, being around 4.5 and 6 Hz, respectively [31, 32]; homonuclear coupling evolution is absent for methyl singlets, while for methyl doublets, the single 7-Hz homonuclear coupling does not affect much the intensity of the correlation peaks; finally, the methyl resonances are strong and narrow and produce correspondingly strong HMBC correlations peaks.

As a result, *all* the expected HMBC peaks of methyl protons (which are four for a methyl on a quaternary carbon, three for a methyl on a tertiary carbon, and two for an ethyl group) are invariably present in the spectrum. These peaks are still visible when the sample is so diluted that all the other correlation peaks are obscured by noise; if one is only interested in the correlations of methyl protons, the acquisition time for an HMBC experiment can be considerably shorter than that for a good HSQC. In favorable cases, it is possible to assign most skeletal carbon atoms of a polycyclic terpene just looking at the HMBC correlations of methyl groups.

An example of this strategy is found in the structural elucidation of 12-methylbacteriohopanetetrol [33]. The pentacyclic skeleton was devoid of functional groups, and most proton signals were severely overlapping. All the methyl groups (six singlets and two doublets) were well discernible in the spectrum, and each showed all the expected correlation peaks in the HMBC spectrum. In addition, identification of two-bond correlations for the six singlet methyl protons was easy because the relevant carbon atoms were necessarily quaternary carbon atoms. Overall, 27 out of the 31 carbon atoms in the pentacyclic hopane skeleton were assigned unequivocally, and 23 of them were connected into a single framework (Fig. 8.7).

Fig. 8.7 The HMBC spectrum of 12-methylhopanetetrol (only the correlation peaks of methyl groups are visible) and partial structure determined by long-range proton–carbon couplings of methyl protons



Starting from this carbon framework, completion of the structure elucidation was straightforward: the relevant protons were identified using the HSQC spectrum, and the remaining connections were determined from COSY and/or other HMBC correlation peaks.

8.3.2 HMBC and “False HSQC” Peaks

While the HMBC experiment is designed to detect two- and three-bond couplings between protons and carbons, correlation peaks originating from one-bond couplings are also present in the spectrum. These one-bond correlation peaks are easily recognizable: because no ¹³C decoupling is used in the HMBC experiment, these signals appear as wide doublets in F2 due to the large ¹J_{CH} coupling constant, while the true HMBC peaks are not visibly split by the small two- and three-bond couplings. These signals are generally unwanted and are suppressed by a pulse sequence element called “low pass filter,” but even so, they are occasionally present in the HMBC spectrum.

In some compounds, however, a regular correlation peak (not a doublet), identical to the peak present in the ¹³C-decoupled HSQC spectrum, can be observed at the chemical shift of directly linked proton and carbon atoms (the peak may appear in the middle of the doublet from one-bond correlation, if the latter is present). These “false HSQC” peaks may appear puzzling at first sight (directly linked

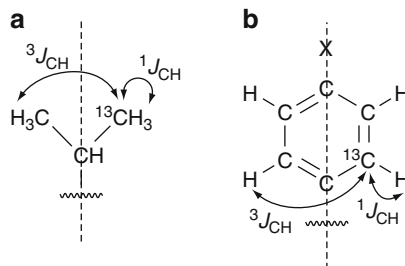


Fig. 8.8 (a) A ^{13}C nucleus in the methyl of an isopropyl group is coupled with the protons of the other methyl. A “false HSQC” correlation between methyl protons and methyl carbons is present in the HMBC spectrum. (b) In a *para*-substituted benzene, the ^{13}C nucleus is coupled through one and three bonds, respectively, with two protons with the same chemical shift, and a “false HSQC” correlation appears in the HMBC spectrum

protons and carbons appear to be long-range coupled) but are absolutely obvious when the structure is drawn.

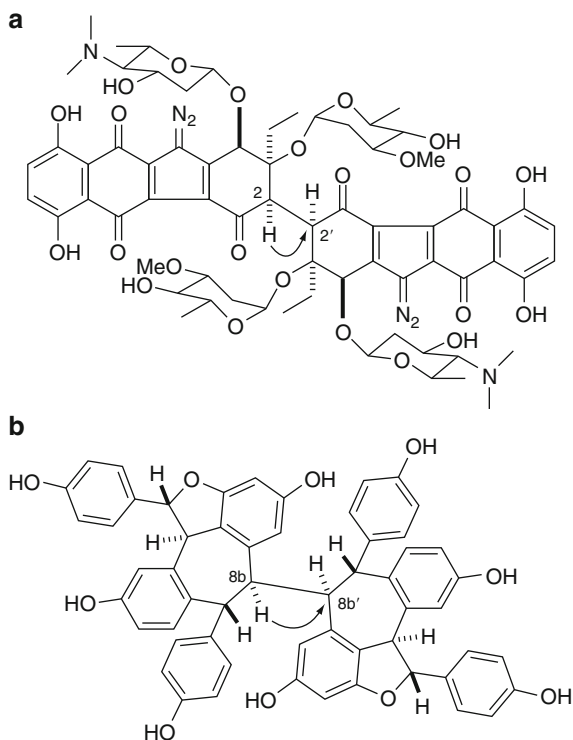
The most common (although not the most useful) example of this is seen in isopropyl groups. A ^{13}C nucleus in the methyl group of an isopropyl is long-range coupled with the protons of the other methyl group, which are equivalent to the protons directly linked to the ^{13}C nucleus (Fig. 8.8a). As a consequence, an HMBC correlation peak will appear between the methyl protons and carbon signals, exactly where the HSQC peak would appear. Similar peaks can be observed in *para*-disubstituted and monosubstituted benzene rings (Fig. 8.8b).

These “false HSQC” correlation peaks have been used sporadically in structural elucidation of complex molecules, such as lomaiviticin A, an antibiotic from the ascidian *Micromonospora lomaivitiensis*. [34] The connection between the two symmetric halves of lomaiviticin A was demonstrated by the HMBC correlation peak between H2/H2' and the relevant carbons C2/C2' (Fig. 8.9a). The connection between the two halves of hopeaphenol, a tetrastilbene from the plant *Carex pumila* [35], was demonstrated similarly (Fig. 8.9b). Other than for solving complex structures like the ones shown, the “false HSQC” peaks are indeed very useful in the early steps of structure elucidation because they are only observed in symmetric structures or partial structures and are a clear hint for them.

8.3.3 Dealing with Alkyl Chains

Nonfunctionalized alkyl chains are a common source of problems in NMR-based structure elucidation. In such structures, proton chemical shifts heavily overlap even at high fields, preventing to follow the connectivity pathway using the standard experiment triad COSY/HSQC/HMBC. A means to overcome this problem is the TOCSY experiment, in which the coherence transfer is effective also for protons with coincident chemical shifts. This makes it possible to relate neighboring functional groups connected through alkyl chains.

Fig. 8.9 Structures of lomaiviticin A (**a**) and hopeaphenol (**b**). The linkage between the two couples of equivalent atoms C2/C2' and C8b/C8b' was established from “false HSQC” correlation peaks



A significant example of how the TOCSY spectrum can be used in this context is the determination of location of methyl branches in either of the two alkyl chains of clathroside B (Fig. 8.10), an atypical glycolipid isolated from the marine sponge *Agelas clathrodes* [36]. This required correlation of the terminal methyl groups of the alkyl chains with protons at C-3 or C-3', but the presence of a large number of overlapped methylene signals made a sequential assignment impossible. The only way to correlate these protons was a TOCSY experiment. Coherence had to be transferred through as many as 13 vicinal couplings for the experiment to be successful, which are much more than the 5–6 coherence transfers that occur in the standard 80–120-ms mixing time. A very long mixing time (600 ms) was therefore used, which turned out to be the best compromise between the increased coherence transfer obtained as the mixing time increases and the overall loss of sensitivity due to relaxation during the mixing time. In addition, the 1D version of TOCSY was used to maximize the sensitivity. In a first experiment, selective excitation of the allylic proton H-3a (δ 2.21) was performed, and only the methyl triplet of the unbranched chain (δ 0.88) appeared in the spectrum (Fig. 8.10b); in contrast, when H-3'a (δ 1.65) was excited, only the methyl signals of the anteiso chain appeared in the spectrum (Fig. 8.10c). Therefore, the additional methyl group was in the “southern” chain, i.e., linked to C-13'.

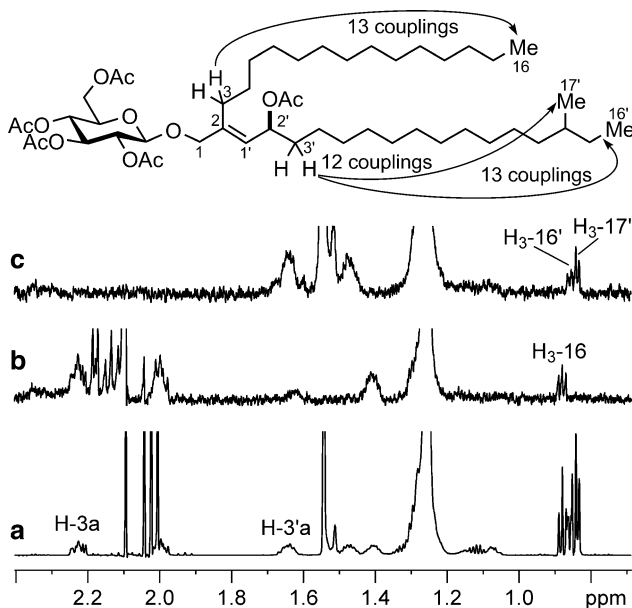


Fig. 8.10 (a) The ^1H NMR spectrum of peracetylated clathroside B. (b) 1D TOCSY, mixing time 600 ms, selective excitation at δ 2.21, H-3a; the terminal methyl triplet of the unbranched chain is clearly visible. (c) 1D TOCSY, mixing time 600 ms, selective excitation at δ 1.65, H-3'a; only the branched chain methyl protons are visible

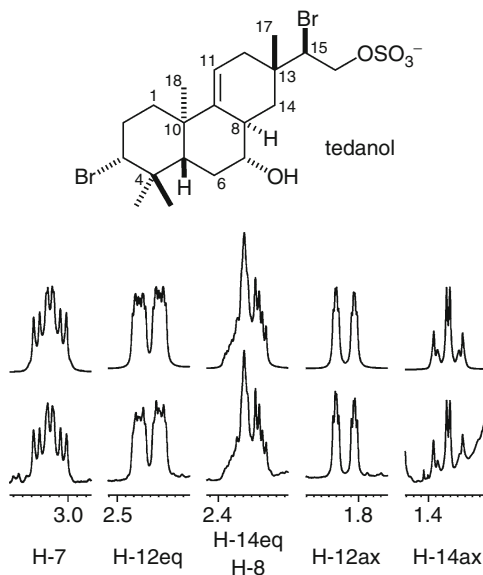
This work also illustrated an important limit of the TOCSY spectrum, i.e., that it does not allow to measure the number of coherence transfer steps which give rise to a correlation peak, or, in other words, how far apart are the protons connected by a TOCSY correlation peak. This information would have made it possible to determine the length of the two alkyl chains of clathrosides, which instead had to be determined by chemical degradation.

8.3.4 Dealing with Non-first-order Multiplets: Spectral Simulation

In a ^1H NMR spectrum, non-first-order multiplets appear when coupled protons have close chemical shifts. Chemically equivalent protons which are not magnetically equivalent may also give rise to non-first-order multiplets. The common approach of the natural product chemist toward non-first-order multiplets is to report them as *m* in the NMR characterization and give up from the beginning any attempt to get information from their lineshape.

As a matter of fact, the theoretical tools to predict the lineshape of a non-first-order multiplet have been known for a long time, and the necessary computational efforts are not a problem for modern computers for spin systems up to 10–12 protons.

Fig. 8.11 Selected signals of the simulated spectrum of the spin system of H-5 through H-14 (*upper trace*) of tedanol compared to the experimental spectrum (*lower trace*). The lineshapes of the non-first-order multiplets of H8/H14eq and H-14ax are accurately reproduced



A comparison of the predicted and experimental lineshapes makes it possible to determine all the NMR parameters of the spin system under examination. Therefore, if spectral simulation is used, even an apparently hopeless bump can provide the same coupling constant information as a clear first-order multiplet.

The reasons why spectral simulation is not as popular as it should be among natural product chemists can be identified in the need to obtain and learn specific software for a technique that is useful only in some particular situations and, in the quite lengthy process, required to extract the NMR parameters. (A very good simulation program, NMR-SIM, is included in the commercial Bruker's TopSpin suite. Unfortunately, no automated fitting procedure is present in this program, so that the optimization has to be performed manually. A free alternative, which also allows some automatic optimization, is Spin Works, <http://www.umanitoba.ca/chemistry/nmr/spinworks/index.html>). This use of spectral simulation first requires an intelligent guess of the initial parameters, followed by their optimization for the best possible fit of experimental and simulated signals. In spite of the lengthy process, whenever the comprehension of the fine structure of a multiplet is important for structure elucidation, spectral simulation represents an important tool to use.

For example, spectral simulation has been used in structure elucidation of the brominated and sulfated diterpene tedanol from the marine sponge *Tedania ignis* [37]. The key connection between H-8 and the two protons at C-14 could not be evinced from the COSY spectrum because the chemical shifts of H-8 and H-14eq were almost identical, leading to non-first-order multiplets. However, this coupling could be demonstrated by spectral simulation. The subspectrum of the 10-proton spin system comprising all protons on rings B and C was calculated (Fig. 8.11), optimizing

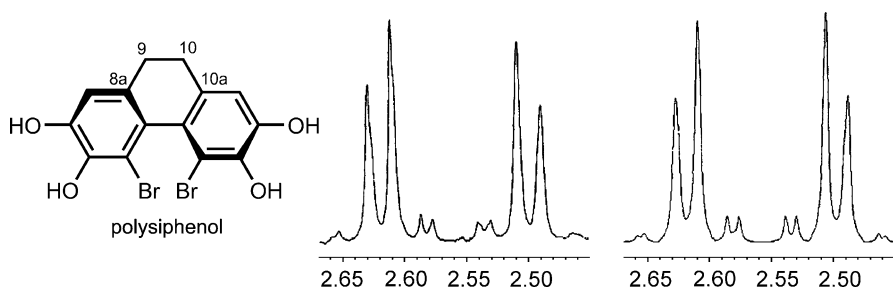


Fig. 8.12 The experimental (*left*) and simulated (*right*) ^1H NMR spectrum of methylene protons of polysiphenol

the unknown NMR parameters until the simulated multiplets reproduced accurately the experimental ones. The simulation also evidenced an otherwise undetectable W coupling (3.1 Hz) between H-12eq and H-14eq.

In an older example [38], the AA'BB' system originating from the methylene protons of polysiphenol, a conformationally blocked 9,10-dihydrophenanthrene, was studied using spectral simulation (Fig. 8.12). The coupling constants determined in this way were used to calculate, by a generalized Karplus equation [4], the torsion angle C8a–C9–C10–C10a; this torsion angle was a necessary information to determine the absolute configuration of the molecule from CD data.

8.3.5 Dealing with Non-first-order Multiplets: ^{13}C -Coupled HSQC

An alternative approach to deal with non-first-order multiplets is to acquire a ^{13}C -coupled HSQC spectrum. Let us consider two coupled protons, H_A and H_B , with very close chemical shifts. In a ^{13}C -coupled HSQC experiment, the correlation peak of H_A is split into two correlation peaks along the ^1H dimension by the large (125–170 Hz) $^1J_{\text{CH}}$ coupling constant with C_A (the two peaks are actually branches of the same multiplet but can be safely considered as separate peaks in the following discussion). These peaks now resonate at a frequency which is no longer overlapped with H_B (the correlation peak only originates from the molecules having a ^{13}C nucleus at C_A ; in these molecules, proton B experiences only a small $^2J_{\text{CH}}$ coupling with C_A , and its resonance frequency is unchanged). Therefore, the two peaks now appear as first-order multiplets along the ^1H dimension, and their coupling constants can be easily measured. Of course, the same applies also to the correlation peak of H_B . While using this method, it is essential to use a long acquisition time, to achieve an enough digital resolution (see Sect. 8.2.2 above) to resolve small couplings.

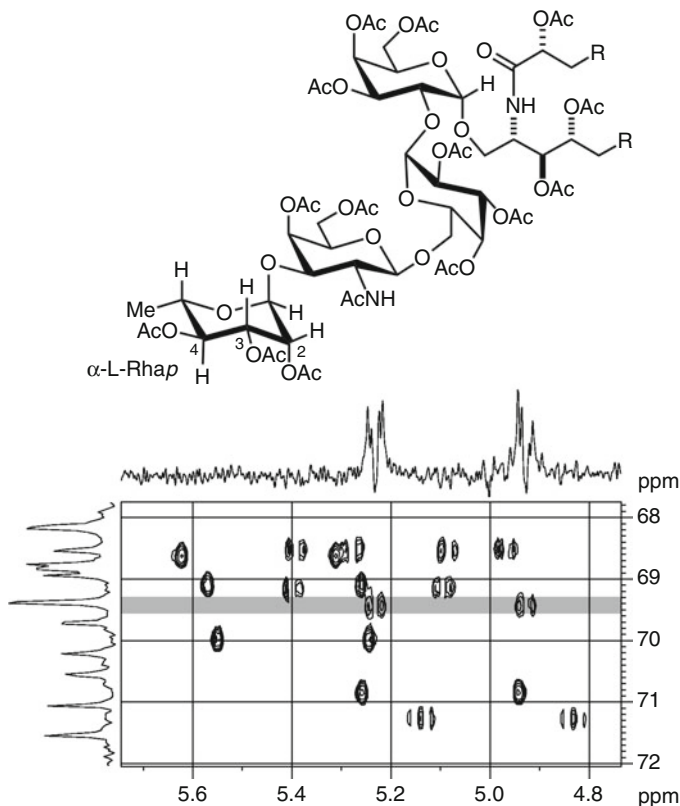


Fig. 8.13 Partial plot of the ^{13}C -coupled HMQC spectrum of clarhamnoside peracetate (**1b**). The top trace is the section of the spectrum at δ 69.4, which was used to measure coupling constants of H-3

This method has been used in the structure elucidation of clarhamnoside, a glycosphingolipid isolated from the marine sponge *Agelas clathrodes* [39]. Coupling constants are routinely used to determine relative configuration of sugars, but for the rhamnose IV of clarhamnoside, the nearly coincident chemical shifts of H-2 and H-3 prevented the measurement of their coupling constants. Instead, in the ^{13}C -coupled HMQC spectrum (in this work, HMQC was used instead of the almost equivalent HSQC), the signal of H-3 appeared as a well-defined first-order multiplet, with only one large axial–axial coupling constant (Fig. 8.13). Because H-4 was known to be axial, the orientation of H-2 was determined as equatorial, and the 6-deoxysugar was established to be a rhamnose.

This approach has also been used to measure coupling constants between equivalent protons, for example, to distinguish between *cis* and *trans* symmetric stilbenes [40].

8.3.6 Coupling Constants and Furanose Sugars

Today, the structure of a pyranose sugar is routinely determined by 2D NMR methods because *J*-coupling analysis provides an easy means for addressing stereochemical issues in a six-membered ring. The successful use of coupling constant information for stereochemical assignment in pyranosides is based on the conformationally rigid six-membered ring they contain. This is not the case for furanosides, where the flexibility of the five-membered ring (leading to the so-called pseudorotation) causes large variations in coupling constants between conformers, which prevent such an easy correlation between coupling constant values and relative configuration of adjacent carbon atoms. Therefore, when the sugar is in the furanose form, proton–proton coupling constants are considered to be of little use.

As a matter of fact, some correlation between vicinal couplings and relative configuration of furanosides is present in the literature. As early as in 1963, in a paper reporting the proton NMR spectra of all methyl pentofuranosides [41], it was clearly recognized that a small vicinal coupling in a furanoside implies that the coupled protons are *trans*-oriented. However, this principle has been used in the subsequent structure elucidation work only sporadically, partly because the threshold below which a coupling constant can be considered “small” had not been defined.

An in-depth computational study of coupling constants of furanosides as a function of the pseudorotation angle of the furanose ring was recently performed [11]. The dependence of the vicinal proton–proton coupling constants on the pseudorotation angle was calculated for each of the eight diastereomeric pentofuranosides (the presence of the additional CH₂OH of hexoses has a negligible influence on the conformation of the five-membered ring) using quantum-mechanical DFT methods (mPW1PW91/6-31G+).

The results (Fig. 8.14) showed that, when for *cis*-oriented pairs of protons, no conformation exists in which the calculated coupling is lower than 2.5 Hz for the H-1/H-2 pair, 4.0 Hz for the H-2/H-3 pair, and 2.5 Hz for the H-3/H-4 pair. Therefore, even allowing for some error in the calculation, whenever a furanoside vicinal coupling constant is <2 Hz (for H-1/H-2 or H-3/H-4) or <3.5 Hz (for H-2/H-3), the relevant protons must be *trans*-oriented. Of course, this rule does not work the other way round, and a coupling above the threshold does not provide any information about the stereochemistry of the coupled protons. This principle was used to define the relative configuration of one furanose sugar of the complex glycosphingolipid vesparioside B. The small coupling constants of the H-1/H-2 and H-2/H-3 pairs demonstrated the *trans* relationship of these pairs of protons (Fig. 8.15).

It must be noted that this is *not* an empirical rule because it does not rely on a particular conformation of the furanoside, but is based on the geometrical behavior of five-membered rings, in which the dihedral angle between the *cis*-oriented pair of protons cannot reach the values close to 90° that would lead to small coupling constants. For the same reason, the rule can most likely be extended to cover five-membered carbocycles.

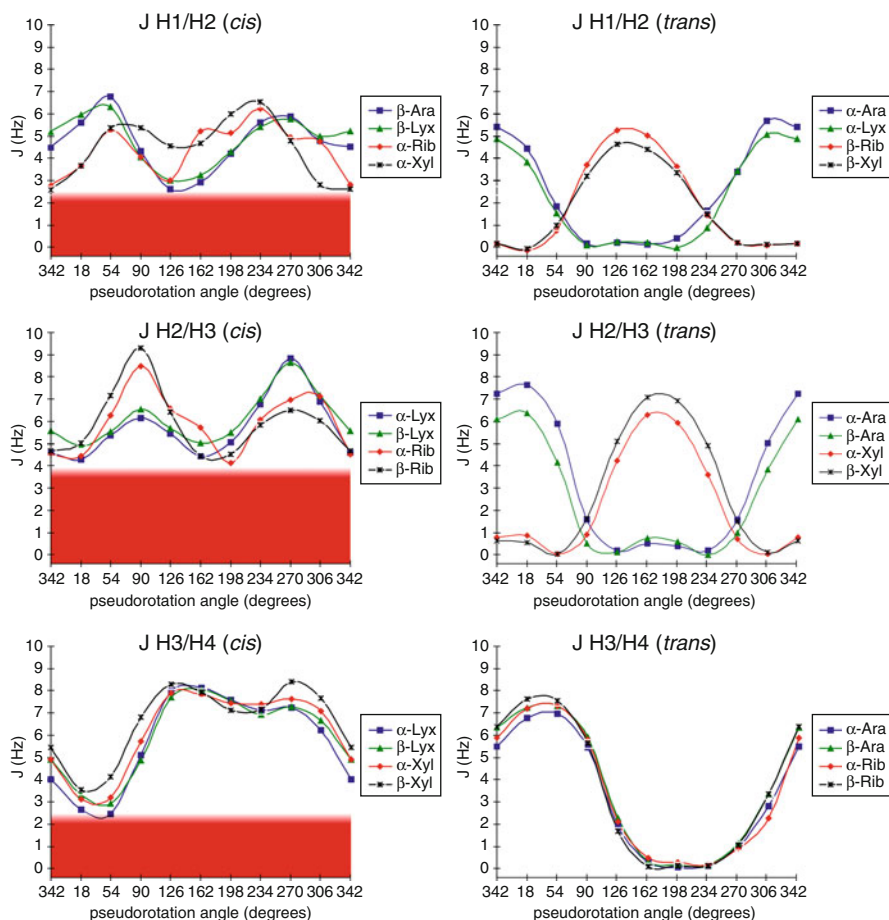
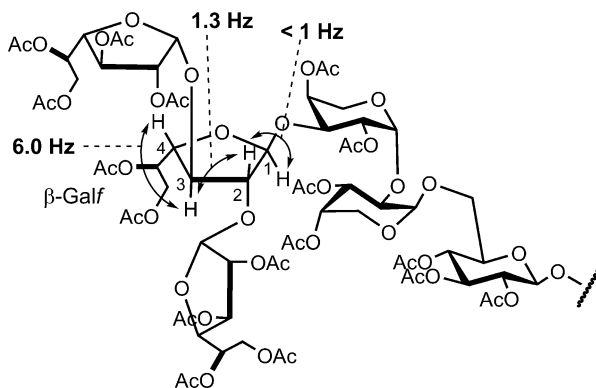


Fig. 8.14 Coupling constant of vicinal proton pairs in the eight pentofuranosides as a function of the pseudorotational angles of the furanose ring. The coupling constants were calculated using quantum-mechanical DFT methods. It is apparent that, in spite of the flexibility of five-membered rings, small coupling constants between *cis* vicinal protons are not possible in any conformation of the furanose ring. Therefore, a small coupling constant points to the *trans* relationship between vicinal protons. The threshold value is higher (3.5 Hz) for the H-2/H-3 pair and lower (2 Hz) for the H-1/H-2 and H-3/H-4 pairs

8.4 Future Perspectives

Structure determination by NMR is a well-established practice that in most cases leads smoothly to the desired results. However, as shown in the previous sections, there are still some unresolved problems and therefore a need for improvements in several areas.

Fig. 8.15 The saccharide chain of peracetylated vesparioside B. In the central galactofuranose, the small coupling constants between H-1 and H-2 and between H-2 and H-3 are a proof of the *trans* relationship of the two pairs of protons. On the contrary, the 6.0-Hz coupling constant between H-3 and H-4 does not provide any information about the relative configuration of C-3 and C-4



Many innovations in structure elucidation have been driven by the technical development of NMR spectrometers, so it is interesting to see what is going on in this respect. The race toward higher magnetic fields has currently come to a stop because the current technology based on niobium wires is close to its limits. The highest field available for NMR magnets was 400 MHz in 1980, 600 MHz in 1990, and 900 MHz in 2000, but only this year, after more than 10 years, a 1000 MHz magnet has become available. Only a drastic change in the superconducting material will allow a significant further increase in magnet fields. Much more significant is the dramatic enhancement of sensitivity (one order of magnitude and more) of NMR spectrometers that occurred in the last 10 years, following the introduction of the new micro and cold probes. This now makes possible structure elucidation of samples available in microgram amounts. Probe design is still susceptible to improvements, and further gains in sensitivity are expected.

A new frontier is the development of spectrometers with multiple receivers for the parallel acquisition of different 2D NMR experiments, which promises a further improvement in the speed of data acquisition. Specific experiments (e.g., PANACEA [42]) that allow to combine without interference the excitation schemes of two or more different homo- and heteronuclear 2D NMR experiments have been proposed, leading to shorter acquisition times and higher consistency between experiments (because the experiments are acquired in parallel, there is no risk of physical changes of the sample or of the instrument). Higher sensitivity and shorter acquisition times are of course extremely useful to the work of natural product chemists, but do not affect significantly the general strategy and the methods used for structure elucidation.

Some efforts are being devoted to the automated structure elucidation from raw spectroscopic data. One program has been proposed at the end of the 1990s [43] and is not being developed anymore, another one is commercially available, [44] but these tools have never come into common practice. While such programs can potentially be valuable for scientists involved in structure elucidation only occasionally, it appears unlikely that in the near future they will be a standard work tool for natural product chemists as they are becoming for protein chemists. On one hand, the amount of data to be handled is much lower, making it easily manageable

on paper; on the other hand, the workflow of structure elucidation of a natural product is much less defined than in protein chemistry, making its implementation into an algorithm more challenging. However, because these programs are not biased by the expectations of the researcher about the “most likely” structure, they could maybe find a role in the validation of new structures and therefore lower the rate of incorrect structures in the literature.

The major issue in structure elucidation remains the determination of stereochemistry, for which no general NMR method exists, particularly when stereocenters are located on conformationally flexible molecules and/or involve nonprotonated carbon atoms. Progress in this respect is coming from quantum-mechanical prediction of chemical shifts and coupling constants combined with conformational analysis of the molecule under study. However, in spite of some interesting attempts on specific targets [45], determination by NMR of the relative configuration of remote stereocenters is still an unsolved problem. Some help could come from the use of residual dipolar couplings [46, 47], especially if simpler methods for inducing molecule alignment will be developed. Although undoubtedly useful, these methods are not expected to be as revolutionary as 2D NMR has been, so it is likely that many unassigned configurations will continue to appear in the literature.

Finally, it must be mentioned that, as most chemists involved in the study of natural products may have experienced, there are many compounds which still elude NMR analysis. They typically show spectra with very broad and unresolved signals and are unsuitable for any 2D technique. They are sometimes polymeric compounds, but there may be many reasons why small molecules may behave this way, including complexation with paramagnetic ions, conformational or tautomeric equilibria, or aggregation phenomena. These intractable compounds are usually simply ignored by natural product chemists who, like anyone else, move along the line of least resistance. However, in a time when dereplication is becoming an increasingly important task for natural product chemists, there is room for some creative efforts toward these compounds.

8.5 Study Questions

1. One of the common artifacts present in the ROESY and NOESY spectra are peaks from zero-quantum coherence (Sect. 8.2.1.3). Look in the literature and NMR textbooks for a definition of zero-quantum coherence and the reason why it can affect cross-relaxation experiments like ROESY and NOESY.
2. ^{13}C decoupling in proton-detected experiments (such as HSQC) is a much more demanding technique than proton decoupling in ^{13}C -detected experiments (such as the 1D ^{13}C and DEPT experiments). Why?
3. Consider a mid-sized molecule, dissolved in CDCl_3 , which shows a very weak NOE because it falls between the positive and negative NOE regimes. What happens to NOE if the same compound is dissolved in a high-viscosity solvent such as DMSO?

References

1. Kwan EE, Huang SG (2008) Structural elucidation with NMR spectroscopy: practical strategies for organic chemists. *Eur J Org Chem* 2008:2671–2688
2. Crews P, Rodriguez J, Jaspars M (2009) *Organic structure analysis*, 2nd edn. Oxford University Press, New York
3. Karplus M (1963) Vicinal proton coupling in nuclear magnetic resonance. *J Am Chem Soc* 85:2870–2871
4. Haasnoot CAG, DeLeeuw FAAM, Altona C (1980) The relationship between proton-proton NMR coupling constants and substituent electronegativities—I: an empirical generalization of the Karplus equation. *Tetrahedron* 36:2783–2792
5. Matsumori N, Kaneno D, Murata M, Nakamura H, Tachibana K (1999) Stereochemical determination of acyclic structures based on carbon-proton spin-coupling constants. A method of configuration analysis for natural products. *J Org Chem* 64:866–876
6. Bax A, Freeman R (1981) Investigation of complex networks of spin-spin coupling by two-dimensional NMR. *J Magn Reson* 44:542–561
7. Rance M, Sørensen OW, Bodenhausen G, Wagner G, Ernst RR, Wüthrich K (1983) Improved spectral resolution in COSY ^1H NMR spectra of proteins via double quantum filtering. *Biochem Biophys Res Commun* 117:479–485
8. Griesinger C, Sørensen OW, Ernst RR (1985) Two-dimensional correlation of connected NMR transitions. *J Am Chem Soc* 107:6394–6396
9. Braunschweiler L, Ernst RR (1983) Coherence transfer by isotropic mixing: application to proton correlation spectroscopy. *J Magn Reson* 53:521–528; Bax A, Davis DG (1985) MLEV-17-based two-dimensional homonuclear magnetization transfer spectroscopy. *J Magn Reson* 65:355–360
10. Thrippleton MJ, Keeler J (2003) Elimination of zero-quantum interference in two-dimensional NMR spectra. *Angew Chem Int Ed* 42:3938–3941
11. Costantino V, Fattorusso E, Imperatore C, Mangoni A (2008) J-coupling analysis for stereochemical assignments in furanositides: structure elucidation of vesparioside B, a glycosphingolipid from the marine sponge *Spheciospongia vesparia*. *J Org Chem* 73:6158–6165
12. Jeener J, Meier BH, Bachmann P, Ernst RR (1979) Investigation of exchange processes by two-dimensional NMR spectroscopy. *J Chem Phys* 71:4546–4553
13. Bothner-By AA, Stephens RL, Lee JM, Warren CD, Jeanholz RW (1984) Structure determination of a tetrasaccharide: transient nuclear Overhauser effects in the rotating frame. *J Am Chem Soc* 106:811–813. Bax A, Davis DGJ (1985) Practical aspects of two-dimensional transverse NOE spectroscopy. *J Magn Reson* 63:207–213
14. Hwang TL, Shaka AJ (1992) Cross relaxation without TOCSY: transverse rotating-frame Overhauser effect spectroscopy. *J Am Chem Soc* 114:3157–3159
15. Bax A, Ikura M, Kay LE, Torchia DA, Tschudin R (1990) Comparison of different modes of two-dimensional reverse-correlation NMR for the study of proteins. *J Magn Reson* 86:304–318
16. Bendall MR, Pegg DT, Doddrell DM (1983) Pulse sequences utilizing the correlated motion of coupled heteronuclei in the transverse plane of the doubly rotating frame. *J Magn Reson* 52:81–117
17. Reynolds WF, McLean S, Tay LL, Yu M, Enriquez RG, Estwick DM, Pascoe KO (1997) Comparison of ^{13}C resolution and sensitivity of HSQC and HMQC sequences and application of HSQC-based sequences to the total ^1H and ^{13}C spectral assignment for clinasterol. *Magn Reson Chem* 35:455–462
18. Bax A, Summers MF (1986) Proton and carbon-13 assignments from sensitivity-enhanced detection of heteronuclear multiple-bond connectivity by 2D multiple quantum NMR. *J Am Chem Soc* 108:2093–2094
19. Nyberg NT, Duus JØ, Sørensen OW (2005) Heteronuclear two-bond correlation: suppressing heteronuclear three-bond or higher NMR correlations while enhancing two-bond correlations even for vanishing $^2J_{\text{CH}}$. *J Am Chem Soc* 127:6154–6155

20. Petersen BO, Vinogradov E, Kay W, Würtz P, Nyberg NT, Duusa JØ, Sørensen OW (2006) H2BC: a new technique for NMR analysis of complex carbohydrates. *Carbohydr Res* 341:550–556
21. Kock M, Reif B, Fenical W, Griesinger C (1996) Differentiation of HMBC two- and three-bond correlations: a method to simplify the structure determination of natural products. *Tetrahedron Lett* 37:363–366
22. Williamson RT, Marquez BL, Gerwick WH, Koehn FE (2001) ACCORD-ADEQUATE: an improved technique for the acquisition of inverse-detected INADEQUATE data. *Magn Reson Chem* 39:544–548
23. He H, Janso JE, Williamson RT, Yang HY, Carter GT (2003) Cytosporacin, a highly unsaturated polyketide: application of the ACCORD-ADEQUATE experiment to the structural determination of natural products. *J Org Chem* 68:6079–6082
24. Wright AD, Nielson JL, Tapiolas DM, Motti CA, Ovenden SPB, Kearns PS, Liptrot CH (2003) Detailed NMR, including 1,1-ADEQUATE, and anticancer studies of compounds from the echinoderm *Colobometra perspinosa*. *Mar Drugs* 7:565–575
25. Bax A, Freeman R, Kempell SP (1980) Natural abundance carbon-13-carbon-13 coupling observed via double-quantum coherence. *J Am Chem Soc* 102:4849–4851
26. Levitt MH, Ernst RR (1983) Improvement of pulse performance in NMR coherence transfer experiments. A compensated INADEQUATE experiment. *Mol Phys* 50:1109–1124
27. Bugni TS, Bernan VS, Greenstein M, Janso JE, Maiese WM, Mayne CL, Ireland CM (2003) Brocaenols A-C: novel polyketides from a marine-derived *Penicillium brocae*. *J Org Chem* 68:2014–2017
28. Fujita Y, Kasuya A, Matsushita Y, Suga M, Kizuka M, Iijima Y, Ogita T (2005) Structural elucidation of A-74528, an inhibitor for 20,50-phosphodiesterase isolated from *Streptomyces* sp. *Bioorg Med Chem Lett* 15:4317–4321
29. Williamson RT, Boulanger A, Vulpanovici A, Roberts MA, Gerwick WH (2002) Structure and absolute stereochemistry of phormidolide, a new toxic metabolite from the marine cyanobacterium *Phormidium* sp. *J Org Chem* 67:7927–7936
30. Doi Y, Ishibashi M, Nakamichi H, Kosaka T, Ishikawa T, Kobayashi J (1997) Luteophanol A, a new polyhydroxyl compound from symbiotic marine dinoflagellate *Amphidinium* sp. *J Org Chem* 62:3820–3823
31. Marshall JL (1983) Carbon-carbon and carbon-proton NMR couplings: applications to organic stereochemistry and conformational analysis, vol 2, *Methods in Stereochemical Analysis*. VCH, New York
32. Pretsch E, Bühlmann P, Badertscher M (2009) *Structure determination of organic compounds*, 4th edn. Springer, Berlin, p 81
33. Costantino V, Fattorusso E, Imperatore C, Mangoni A (2000) The first 12-methylhopanoid: 12-methylbacteriohopanetetrol from the marine sponge *Plakortis simplex*. *Tetrahedron* 56:3781–3784
34. He H, Ding WD, Bernan VS, Richardson AD, Ireland CM, Greenstein M, Ellestad GA, Carter GT (2001) Lomaiviticins A and B, potent antitumor antibiotics from micromonospora lomaivitiensis. *J Am Chem Soc* 123:5362–5363
35. Kawabata J, Fukushi E, Hara M, Mizutani J (1992) Detection of connectivity between equivalent carbons in a C2 molecule using isotopomeric asymmetry: identification of hopeaphenol in *Carex pumila*. *Magn Reson Chem* 30:6–10
36. Costantino V, Fattorusso E, Imperatore C, Mangoni A (2006) Clathrosides and isoclathrosides, unique glycolipids from the Caribbean Sponge *Agelas clathrodes*. *J Nat Prod* 69:73–78
37. Costantino V, Fattorusso E, Mangoni A, Perinu C, Cirino G, De Gruttola L, Roviezzo F (2009) Tedanol: a potent anti-inflammatory ent-pimarane diterpene from the Caribbean Sponge *Tedania ignis*. *Bioorg Med Chem* 17:7542–7547
38. Akin M, Samb A, Mirailles J, Costantino V, Fattorusso E, Mangoni A (1992) Polysiphenol, a new brominated 9,10-dihydrophenantrene from the Senegalese Red Alga *Polysiphonia ferulacea*. *Tetrahedron Lett* 33:555–558

39. Costantino V, Fattorusso E, Imperatore C, Mangoni A (2004) Clarhamnoside, the first rhamnose-containing α -glycosyl ceramide from the Marine Sponge *Agelas clathrodes*. *J Org Chem* 69:1174–1179
40. Mucci A, Parenti F, Schenetti L (2002) On the Recovery of $^3J_{\text{H,H}}$ and the Reduction of Molecular Symmetry by Simple NMR Inverse Detection Experiments. *Eur J Org Chem* 2002:938–940
41. Rinehart KL, Chilton WS, Hitchens M, Von Phillipsborn W (1963) Chemistry of the neomycins. XI. NMR assignment of the glycosidic linkages. *J Am Chem Soc* 84:3216–3218
42. Kupce E, Freeman R (2008) Molecular structure from a single NMR experiment. *J Am Chem Soc* 130:10788–10792
43. Lindel T, Junker J, Köck M (1997) Cocon: from NMR correlation data to molecular constitutions. *J Mol Model* 3:364–368
44. ACD/Structure Elucidator, Advanced Chemistry Development
45. Ohtaki T, Akasaka K, Kabuto C, Ohrai H (2005) Chiral discrimination of secondary alcohols by both ^1H -NMR and HPLC after labeling with a chiral derivatization reagent, 2-(2,3-anthracenedicarboximide)cyclohexane carboxylic acid. *Chirality* 17(Suppl):S171–176
46. Gil RR, Gayathri C, Tsarevsky NV, Matyjaszewski K (2008) Stretched poly(methyl methacrylate) gel aligns small organic molecules in chloroform. Stereochemical analysis and diastereotopic proton NMR assignment in ludartin using residual dipolar couplings and ^3J coupling constant analysis. *J Org Chem* 73:840–848
47. Kummerlöwe G, Crone B, Kretschmer M, Kirsch SF, Luy B (2011) Residual dipolar couplings as a powerful tool for constitutional analysis: the unexpected formation of tricyclic compounds. *Angew Chem Intl Ed* 50:2643–2645

NMR Methods for Stereochemical Assignments

9

Kirk R. Gustafson

Contents

9.1 Assignment of Absolute Configuration Using Chiral Anisotropic Reagents	548
9.2 <i>J</i> -Based Determination of Relative Configurations	556
9.3 Measurement of <i>J</i> Values	563
9.4 Concluding Remarks	565
9.5 Study Questions	566
References	568

Abstract

Various NMR techniques have been developed that allow assignment of the relative and absolute configuration of many of the stereogenic carbons that occur in marine natural products. The application of chiral anisotropic reagents in conjunction with NMR analyses has been particularly useful for determining the absolute configuration of secondary alcohols, α -substituted primary amines, and α -substituted carboxylic acids. Derivatization of these functional groups with appropriate chiral reagents (e.g., MTPA) provides diastereomeric products that have diagnostic differences in their ^1H chemical shifts. A recently developed technique known as *J*-based configurational analysis uses proton–proton couplings and 2- and 3-bond carbon–proton couplings ($^2,^3J_{\text{CH}}$) to assign the relative configuration of adjacent (1, 2) stereogenic carbons in conformationally flexible molecules. The *J*-based method involves comparing experimentally measured scalar couplings and NOE interactions with those predicted from this model to assign the relative configuration of the chiral methines. This technique is also applicable to oxygenated systems since there is a dihedral angle dependence for $^2J_{\text{CH}}$ couplings between a proton and an adjacent carbon that bears an

K.R. Gustafson

Molecular Targets Laboratory, Center for Cancer Research, National Cancer Institute-Frederick, Frederick, MD, USA

e-mail: gustafki@mail.nih.gov

electronegative oxygen substituent. Strategies have also been developed to utilize *J*-based configurational analysis when there is a methylene separating the two stereogenic methine carbons, and even when conformational interconversion results in the coexistence of two major conformers.

9.1 Assignment of Absolute Configuration Using Chiral Anisotropic Reagents

Marine natural products are often comprised of complex molecular architectures that incorporate one or more stereogenic carbon atom. Assignment of the absolute configuration of these chiral carbons is crucial to define the three-dimensional structure of a molecule, and this can be a significant challenge in the structural elucidation of new metabolites. A variety of chemical and spectroscopic methodologies (e.g., X-ray crystallography, circular dichroism) have been developed to address questions concerning absolute stereochemistry, but each technique has quite specific requirements and limitations that can restrict their utility. While there are no universal approaches for assigning absolute configuration that are applicable to all compounds of interest, NMR techniques based on chiral anisotropic reagents have been widely used in the structural determination of new marine natural products.

These NMR-based methods are useful for characterizing chiral secondary alcohols, α -substituted primary amines, and α -substituted carboxylic acids, and they are based on the shielding effect of a benzene ring (or other aryl group) in a chiral auxiliary that is appended to the molecule of interest. This methodology generally entails derivatization of the natural product with the two enantiomers of a chiral anisotropic reagent and comparison of the ^1H NMR chemical shifts of the resulting diastereomers. Characteristic changes in the chemical shifts of protons in the two diastereomeric derivatives can be explained by the ring current effect of an aryl group that occurs in the applied magnetic field of an NMR spectrometer. When π -electrons circulate at right angles to an applied magnetic field, they induce their own secondary magnetic field that can perturb nearby nuclei. Protons that reside where the magnetic lines of force for the induced magnetic field oppose the applied field experience a shielding effect, while protons situated where the induced magnetic field complements the applied field are deshielded. For a benzene ring, protons located directly above or below the center of the ring are shielded and shifted upfield, while protons lateral to the ring are deshielded and shifted downfield (Fig. 9.1). This kind of spatial variation of magnetic field is referred to as diamagnetic anisotropy.

In 1973, the Mosher laboratory in Stanford described an empirical correlation between the configuration of a chiral alcohol and the NMR chemical shifts of the diastereomeric products that result from reaction with specific chiral esterification reagents [1, 2]. All of these reagents contained an aryl substituent that caused characteristic changes in the chemical shifts of neighboring protons due to the anisotropic effect of the aromatic ring current. The most useful diastereomers for these NMR studies were the α -methoxy- α -trifluoromethylphenylacetic acid

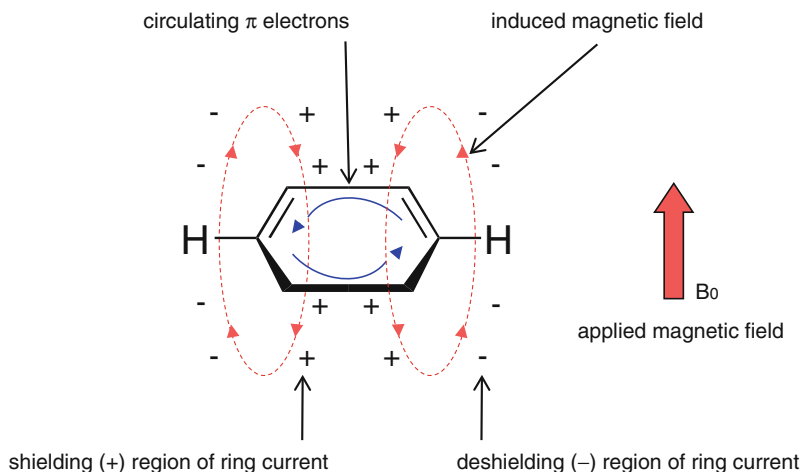


Fig. 9.1 Diamagnetic shielding and deshielding effects of the benzene ring current

(MTPA) ester derivatives of the chiral alcohols. A model was developed to rationalize the correlation between NMR chemical shift changes and the configuration of the stereogenic carbinol carbon. The model proposed that MTPA ester derivatives adopt a predominant conformation in which the original carbinol proton, the ester carbonyl, and the trifluoromethyl group all lie in the same plane (Fig. 9.2). This conformational hypothesis has been supported by X-ray crystal studies and computational analyses, and the plane defined by these three substituents is commonly referred to as the MTPA plane.

As illustrated in Fig. 9.2, R_1 and R_2 represent the substituents or faces of the original secondary alcohol that are located on opposite sides of the MTPA plane. When viewed in this manner, R_1 is oriented behind or to the right of the MTPA plane, while R_2 is in front of or to the left of the plane. In the case of the (*S*)-MTPA ester, R_1 is on the same side of the plane as the MTPA methoxy group, while in the (*R*)-MTPA ester, it is on the same side of the plane as the MTPA phenyl ring. The most significant diamagnetic impact of this phenyl substituent on neighboring protons in spatial proximity to its ring current is a shielding effect. It therefore stands to reason that proton resonances for R_1 in the (*S*)-MTPA ester, which do not experience this shielding, will be downfield relative to the corresponding R_1 protons in the (*R*)-MTPA ester.

This correlation between NMR shifts and the configuration of the MTPA ester was later refined and elaborated into the advanced Mosher's method [3, 4], which took advantage of more recent advances in high field NMR that allowed assignment of virtually all of the proton resonances in complex molecules. In this modified method, the difference in chemical shift between the (*S*)- and (*R*)-MTPA esters was experimentally determined for all of the proton signals that could be resolved and assigned. This increased the reliability of the methodology because it utilized numerous data points that could be analyzed for their internal consistency and

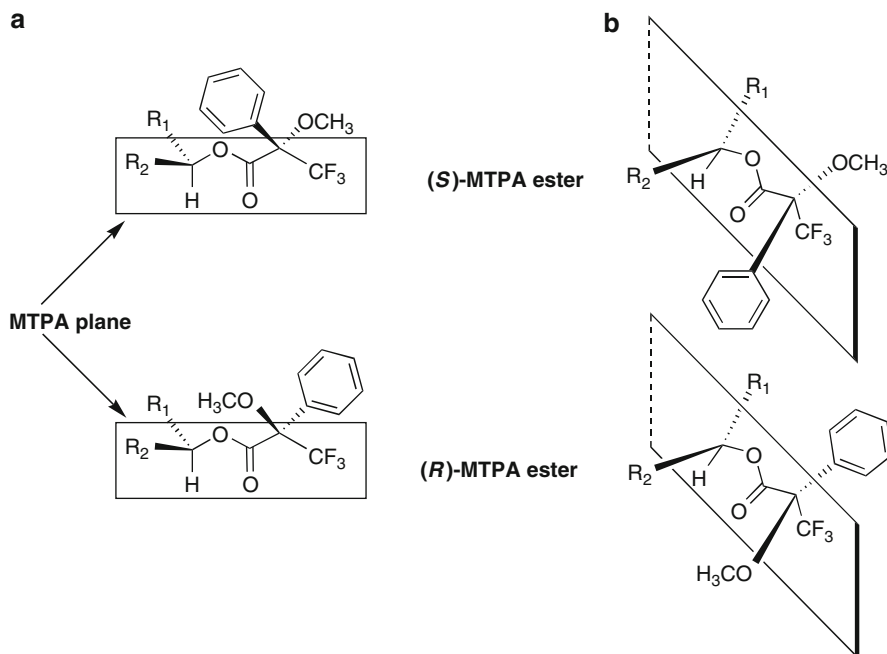


Fig. 9.2 Two alternative views, (a) and (b), of the ideal conformation of the MTPA ester and the resulting MTPA plane

regularity of distribution. The advanced Mosher's method has proven to be a reliable, effective, and easy to implement procedure for assigning the absolute configuration of secondary alcohols, and it has been successfully applied to a wide variety of marine natural products.

Assignments are made by preparing both the (*S*)- and (*R*)-MPTA ester derivatives of a natural product which contains a chiral secondary alcohol, and then determining the precise NMR chemical shifts of all of the protons that are in spatial proximity to the stereogenic carbon. The chemical shift of each proton in the (*R*)-MPTA ester (δ_R) is then subtracted from the chemical shift of its counterpart in the (*S*)-MPTA ester (δ_S) to give the difference in chemical shift ($\Delta\delta$) for that position in the molecule ($\Delta\delta^{S-R} = \delta_S - \delta_R$). There should be a systematic distribution of positive and negative $\Delta\delta$ values on either side of the MTPA plane. When the chiral carbon is viewed in the same plane as the β and β' carbons, and with the -OMTPA group and the carbinyl proton oriented as illustrated in Fig. 9.3, then the $\Delta\delta^{S-R}$ values for protons on substituent R₁ will be positive and those on R₂ will be negative.

The absolute magnitude of the $\Delta\delta^{S-R}$ values are inversely proportional to the distance between the proton and the MTPA group, and protons with $\Delta\delta^{S-R} = 0$ are either too far from the MTPA moiety to experience the anisotropic effect of the aryl ring or they lie on the MTPA plane. The value of $\Delta\delta^{S-R}$ for the carbinyl proton should be zero in the ideal conformation; however, deviation of the MTPA ester

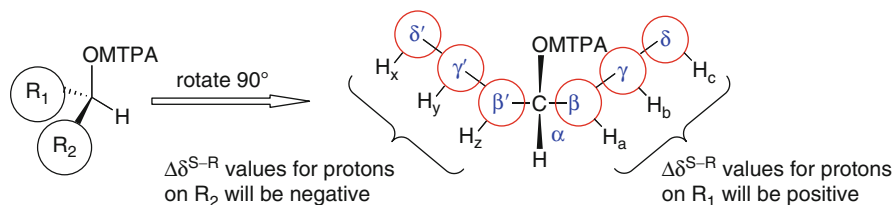


Fig. 9.3 Application of the modified Mosher's method. When the MTPA ester is viewed as illustrated, protons with $\Delta\delta^{S-R}$ values > 0 are assigned to R_1 , and those with $\Delta\delta^{S-R}$ values < 0 are assigned to R_2 . If there is a consistent pattern of positive and negative $\Delta\delta^{S-R}$ values about the MTPA plane, then the absolute configuration can be assigned

from the ideal conformation can cause $\Delta\delta^{S-R}$ for this proton to be non-zero. Anisotropic effects of the nearby ester carbonyl can also impact the carbinyl proton so $\Delta\delta^{S-R}$ values at this position are unreliable and should not be considered when making a configurational assignment. In certain instances, steric factors can cause the -OMTPA group to adopt a conformation that deviates significantly from the MTPA model. In these instances, the $\Delta\delta$ values of the MTPA derivatives will have an irregular distribution that deviates from the rules. If the $\Delta\delta$ values are irregularly arranged across the MTPA plane rather than systematically distributed as predicted, then the modified Mosher's method cannot be used for that particular configurational assignment. Another instance where this technique is inadequate for making an unambiguous assignment is when $\Delta\delta$ values can only be determined for protons on one of the substituents but not the other. This situation can occur when extensive signal overlap in the NMR spectrum prevents precise measurement of the pertinent proton resonances or when one of the substituents has no protons in the vicinity of the original secondary alcohol group [5].

It should be noted that the literature covering the use of chiral anisotropic reagents can be somewhat confusing. The original work by Mosher utilized $\Delta\delta^{R-S}$ values in which $\Delta\delta = \delta^R - \delta^S$, and an extensive body of work with chiral anisotropic reagents from the Rigüera laboratory adopted this same convention [6, 7]. However, the advanced Mosher's method employed $\Delta\delta^{S-R}$ values in which $\Delta\delta = \Delta\delta^S - \Delta\delta^R$. There was no inconsistency with regard to the stereochemical conclusions that resulted from using these two contrasting definitions of $\Delta\delta$ because different models were used for placement of the substituents with positive $\Delta\delta$ values versus substituents with negative $\Delta\delta$ values (R_1 and R_2 in Fig. 9.3). When the configuration of an unknown is being determined, it is imperative that the configurational model used to make the assignment is consistent with how $\Delta\delta$ is calculated. Most of the literature data on MTPA derivatives of marine natural products utilizes the $\Delta\delta^{S-R}$ convention, so that is the format used in this chapter.

The most common approach for preparing MTPA esters is to treat the natural product containing a secondary alcohol with MTPA chloride in the presence of a mild base, such as triethylamine or pyridine. An acylation catalyst such as 4-dimethylaminopyridine can also be used to speed the reaction. Both the (*R*)- and (*S*)-MTPA chlorides are commercially available. However, it is important to note

that due to IUPAC rules for nomenclature and functional group priorities, (*R*)-MTPA chloride will produce the (*S*)-MTPA ester, while (*S*)-MTPA chloride will generate the (*R*)-MTPA ester. MTPA ester formation is generally performed at room temperature for 1–15 h. The course of the esterification reaction can be monitored by TLC, and it should be worked up when the starting material is gone or decomposition becomes apparent. HPLC purification of the MTPA esters is usually required to facilitate unambiguous NMR analyses. Use of aromatic NMR solvents such as benzene-*d*₆ and pyridine-*d*₅ for analyzing the MTPA esters should be avoided due to the potential for spurious results. The concentration of the (*S*)- and (*R*)-MTPA esters for NMR analyses should be the same and each spectra should be carefully referenced to an internal standard such as the residual deuterated solvent signal. The data from a combination of ¹H NMR, COSY (or TOCSY), and HSQC experiments is generally sufficient to make all of the necessary proton assignments and chemical shift measurements for the MTPA esters. These are relatively sensitive NMR experiments, so complete MTPA ester characterizations have routinely been accomplished on sub-milligram samples using NMR spectrometers equipped with conventional room temperature probes and on samples weighing 10–100 μg with cryogenically cooled probes. An application of the Mosher's ester methodology is illustrated below (Fig. 9.4) for assignment of the absolute configuration of a secondary alcohol in enigmazole A (**1**), a marine sponge-derived phosphomacrolide [8].

If the chemical shift differences of the diastereomeric MTPA esters are so small that they are within experimental error, then a variety of other chiral anisotropic reagents are available that have been reported to produce larger proton NMR shift differences [9–11]. Use of methoxyphenylacetic acid (MPA) as a chiral auxiliary has been recommended by the Rigüera laboratory for a variety of reasons [5–7], including the fact that $\Delta\delta$ values for diastereomeric MPA esters can be increased simply by acquiring their ¹H NMR spectra at lower temperature (Fig. 9.5).

The modified Mosher's method is also applicable to chiral methine carbons bearing a primary amine group. In this case, diastereomeric (*S*)- and (*R*)-MTPA amides are prepared and analyzed by NMR in a manner directly analogous to MTPA esters. NMR data for the pair of amide derivatives is collected and analyzed, and $\Delta\delta^{S-R}$ values are calculated and assigned to R₁ and R₂ as illustrated in Fig. 9.6. MTPA amides generally produce larger $\Delta\delta$ values than MTPA esters.

Chiral anisotropic reagents such as phenylglycine methyl ester (PGME) are also available for elucidating the configuration of stereogenic methine carbons that are α to a carboxylic acid [12]. In this case, the (*R*)- and (*S*)-enantiomers of PGME are condensed with the carboxylic acid to generate a pair of diastereomeric PGME amides. The ¹H NMR spectra of these amides are assigned, $\Delta\delta^{S-R}$ values are calculated, and the R₁ and R₂ substituents are defined as illustrated in Fig. 9.7. The ideal conformation of the PGME amide has the original stereogenic carbon, the new amide carbonyl, and the nitrogen, α -carbon, and carbonyl carbon of PGME all coplanar. In this conformation, the PGME phenyl group exerts a diamagnetic shielding effect on protons in R₁ and R₂ similar to that seen with MTPA esters. Thus, protons on R₁ have $\Delta\delta^{S-R}$ values > 0, while protons on R₂ have $\Delta\delta^{S-R}$ values < 0.

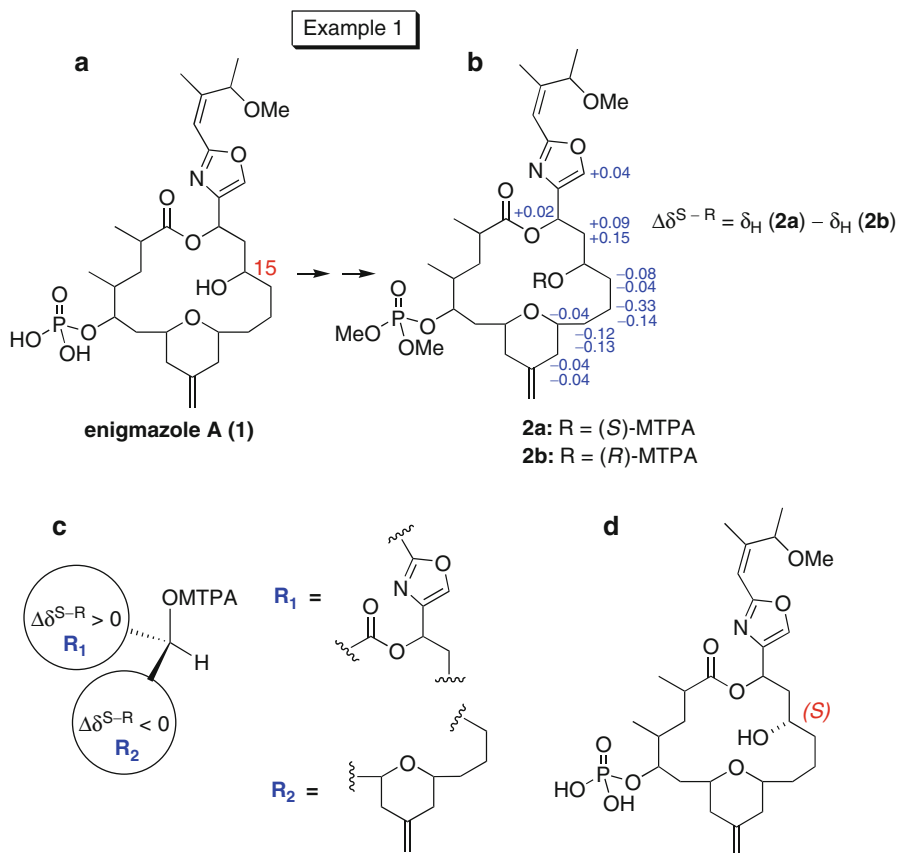


Fig. 9.4 Example 1: Assignment of the absolute configuration at C-15 of enigmazole A. (a) The phosphate group was protected by methylation, and then treatment with (*R*)- or (*S*)-MTPA chloride provided the (*S*)- and (*R*)-MTPA esters, respectively. (b) The $\Delta\delta$ values were calculated, and they showed a systematic distribution of positive and negative values. (c) When the MTPA ester was modeled as shown above, the R_1 and R_2 substructures could be identified. This established the absolute configuration at C-15 as *S*. (d) The structure of enigmazole A with *S*-configuration at C-15

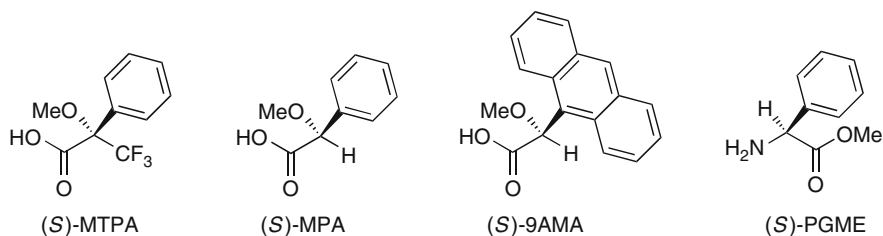


Fig. 9.5 Structures of some of the more commonly utilized chiral anisotropic reagents: MTPA (methoxytrifluoromethylphenylacetic acid), MPA (methoxyphenylacetic acid), 9-AMA (9-anthrylmethoxyacetic acid), and PGME (phenylglycine methyl ester)

Fig. 9.6 Distribution of $\Delta\delta^{S-R}$ values when the MTPA amide is viewed as illustrated

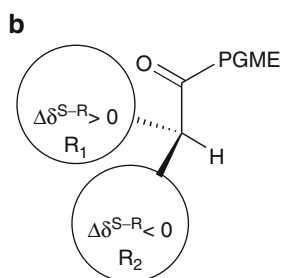
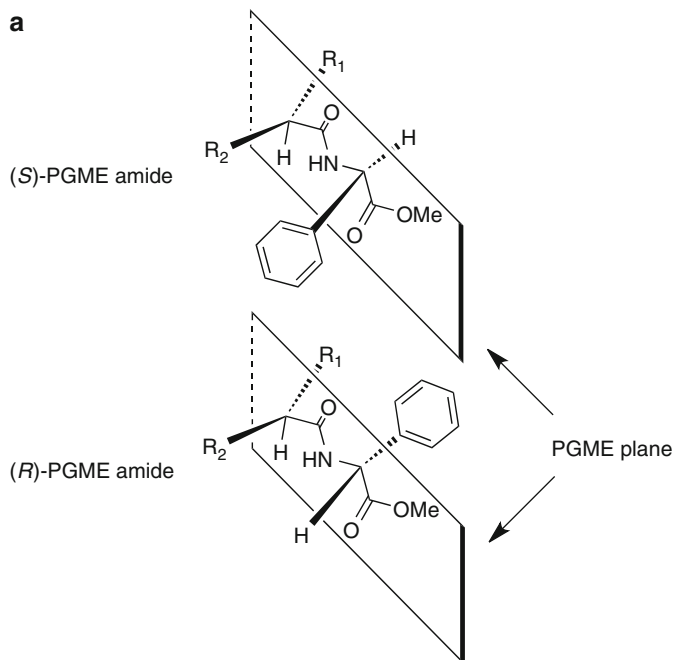
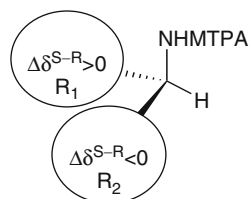


Fig. 9.7 Conformation of the PGME amide (**a**) and distribution of the $\Delta\delta^{S-R}$ values for assigning the absolute configuration (**b**)

In practice, PGME is condensed with the carboxylic acid in the presence of base (triethylamine), a peptide coupling reagent (PyBOP[®]), and a racemization suppressor (HOBt) at room temperature for 1–4 h. Both enantiomers of PGME are commercially available, and this reagent has been successfully used with a variety of structurally complex natural products. Phenylglycine dimethylamide (PGDA) and a variety of other chiral auxiliary reagents have also been used to determine the configuration of α -chiral carboxylic acids [12, 13]. The use of PGME to assign the absolute configuration at C-2 of enigmazole A (**1**) is illustrated in Fig. 9.8 [10]. In this case, the macrocyclic ester functionality in compound **1** was hydrolyzed to generate a linear carboxylic acid-containing product, which could then be derivatized with PGME to give the desired diastereomeric PGME amides.

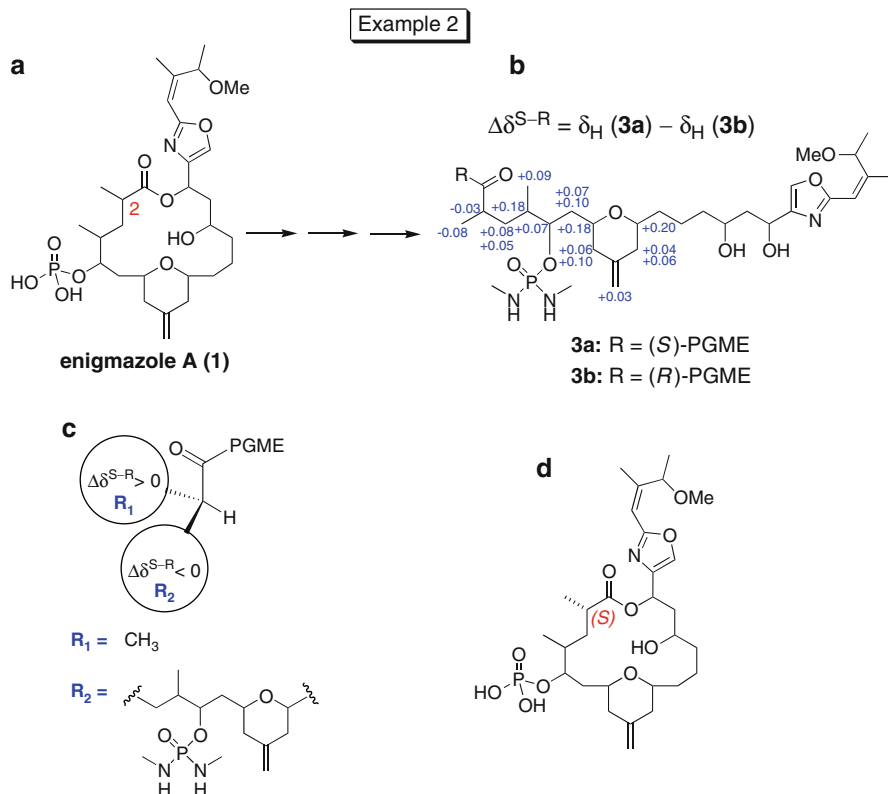


Fig. 9.8 Example 2: Assignment of the absolute configuration at C-2 of enigmazole A. (a) The phosphate group was protected as an *N,N*-dimethylphosphorodiamidate, and then the macrocyclic ring was hydrolyzed. The linear, carboxylic acid-containing product was condensed with (*S*)- or (*R*)-PGME to give the (*S*)- and (*R*)-PGME amides, respectively. (b) The $\Delta\delta$ values were calculated, and they showed a systematic distribution of positive and negative values. (c) The R_1 and R_2 substituents were assigned based on the PGME amide model. This established the absolute configuration at C-2 as *S*. (d) The structure of enigmazole A with *S*-configuration at C-15

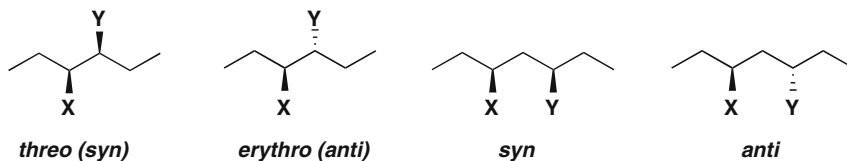


Fig. 9.9 Relative configuration of 1,2-methine diastereomers and 1,3-methine diastereomers

9.2 *J*-Based Determination of Relative Configurations

A seminal paper by Murata and coworkers in 1999 described a method to assign the relative configuration of stereogenic methine carbons based on analysis of long-range (2- and 3-bond) carbon–proton coupling constants, 3-bond proton–proton coupling constants, and nuclear Overhauser effect (NOE or ROE) interactions [14]. This technique is often referred to as *J*-based configurational analysis or as the Murata method, and it can be applied to acyclic compounds and to larger macrocyclic structures that are conformationally flexible. Advances in NMR hardware, probe design, and pulse sequences have made measurement of $^{2,3}J_{\text{CH}}$ coupling constants feasible for mass-limited samples, and this has greatly facilitated further development and application of this method. The utility of *J*-based configurational analysis for making stereochemical assignments has now been demonstrated in a large number of structurally diverse marine natural products.

Before describing details of the Murata method, it is useful to clarify some of the terms used to define stereochemical arrangements. The relative configuration of two adjacent chiral methine carbons can be described as *threo* or *erythro*. This nomenclature is derived from Fischer projections used in carbohydrate chemistry, but in the present discussion, it is most useful to look at its application with structures drawn in an extended zigzag projection (staggered formation). The main carbon chain defines a plane, and the substituents project behind the plane or in front of the plane. When two chiral centers are adjacent, if the two substituents with highest priority are on the same side of the plane, then the relative stereochemistry is *threo* or *syn*. If they are on opposite sides of the plane, then the diastereomer is *erythro* or *anti*. When chiral centers are not adjacent, the *syn* and *anti* nomenclature should be used to describe the relative configuration (Fig. 9.9).

For acyclic structures and other flexible systems, the relative conformation of adjacent stereogenic centers can be represented by six staggered rotamers. Newman projections for the three possible *threo* rotamers and the three *erythro* rotamers of a 1,2-methine system are shown in Fig. 9.10. For each configuration, the chiral methine protons have an *anti* orientation in one rotamer and *gauche* orientations in the other two rotamers.

If this system adopts one main conformer (> 85% of the total), then analysis of selected homonuclear and heteronuclear coupling constants associated with the methine protons can be informative. The magnitude of vicinal ^1H – ^1H couplings ($^3J_{\text{HH}}$) and vicinal ^1H – ^{13}C couplings ($^3J_{\text{CH}}$) are dihedral angle dependent, and they

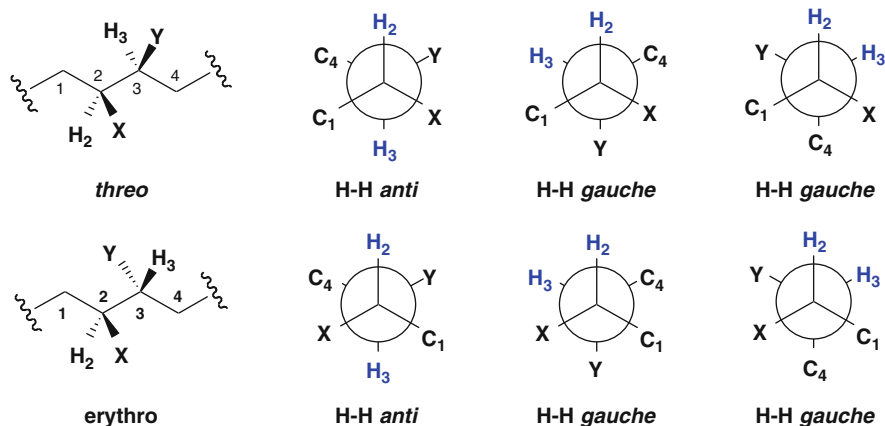


Fig. 9.10 Staggered rotamers of *threo* and *erythro* diastereomers

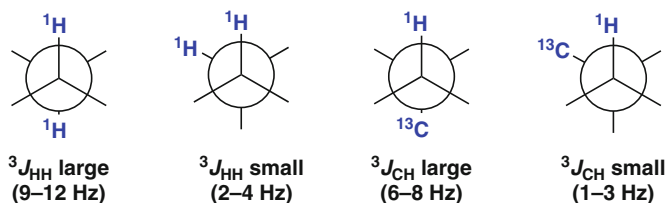


Fig. 9.11 Vicinal (3J) ^1H – ^1H and ^1H – ^{13}C coupling constants. J values adapted from Matsumori et al. [14]

can be described by the Karplus equation [15]. The range of expected 3-bond coupling values for *anti* (180° dihedral angle) and *gauche* (60° dihedral angle) orientations are shown in Fig. 9.11.

The J -based configurational method involves conceptually breaking a larger, more complex molecule into a series of adjacent (1,2) or alternating (1,3) asymmetric centers, and then assigning the relative configuration of the two chiral carbons in that structural fragment. All of the relevant ^1H – ^1H and ^1H – ^{13}C scalar coupling constants are experimentally determined, and then these values are compared with the predicted values (large or small) for the three staggered rotamers that arise from each diastereomer. Theoretical coupling values for a 1,2-methine fragment are illustrated in Fig. 9.12. It can be seen that there is a unique distribution of large and small coupling values for each of the four rotamers where H_2 and H_3 are *gauche*. So when the methine protons in the dominant conformer are *gauche*, it should be possible to identify the rotamer that best fits the experimental coupling data, and thus assign the relative configuration as *threo* or *erythro*. The two rotamers in which H_2 and H_3 are *anti* have identical distributions of large and

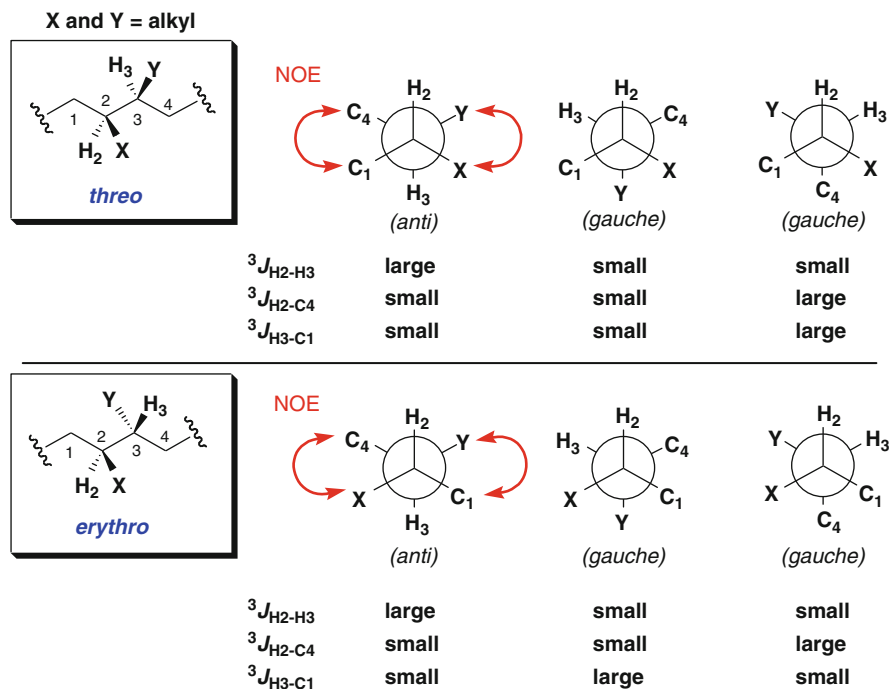


Fig. 9.12 $^3J_{HH}$ and $^3J_{CH}$ coupling values for the rotamers of a 1,2-methine system when substituents X and Y are alkyl

small couplings, and thus they cannot be distinguished by this type of analysis alone. However, when the chiral methine protons are *anti*, then C_1 and C_4 are *gauche* in the *threo* diastereomer, and NOE interactions between their respective protons (H_1 and H_4) should be possible. For the *erythro* diastereomer, when H_2 and H_3 are *anti*, then C_1 and C_4 are also *anti*, and no NOE interactions between H_1 and H_4 are possible. In this case, if substituents X or Y are protonated, then H_1-H_Y or H_4-H_X NOE interactions might be observable. Diagnostic NOE interactions can often be used to distinguish between the two different *anti* rotamers, and they can also help verify the identity of *gauche* rotamers that were assigned on the basis of coupling constant analyses (Fig. 9.12).

When X or Y is an electronegative substituent such as oxygen (OH or OR), then geminal C–H couplings ($^2J_{CH}$) can also be diagnostic. Unlike $^3J_{CH}$ values which are positive, the sign of these 2-bond couplings is generally negative. While $^2J_{CH}$ values do not show a direct C–H dihedral angle dependence (the carbon and proton do not constitute a dihedral angle), they are related to the dihedral angle between the proton and the electronegative substituent bound to the coupled carbon (Fig. 9.13). When an oxygenated functionality is oriented *anti* to the neighboring methine proton, then the absolute value of the 2-bond heteronuclear coupling between that proton and the oxygen-bearing carbon is small. Conversely, when the oxygen substituent is *gauche*, the geminal C–H coupling is large.

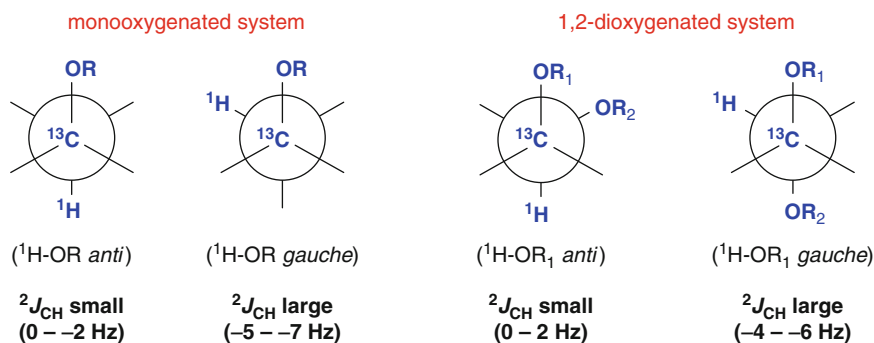


Fig. 9.13 Dihedral angle dependence for $^2J_{\text{CH}}$ coupling between a proton and an adjacent coupled carbon that bears an electronegative substituent such as oxygen (R = H or alkyl)

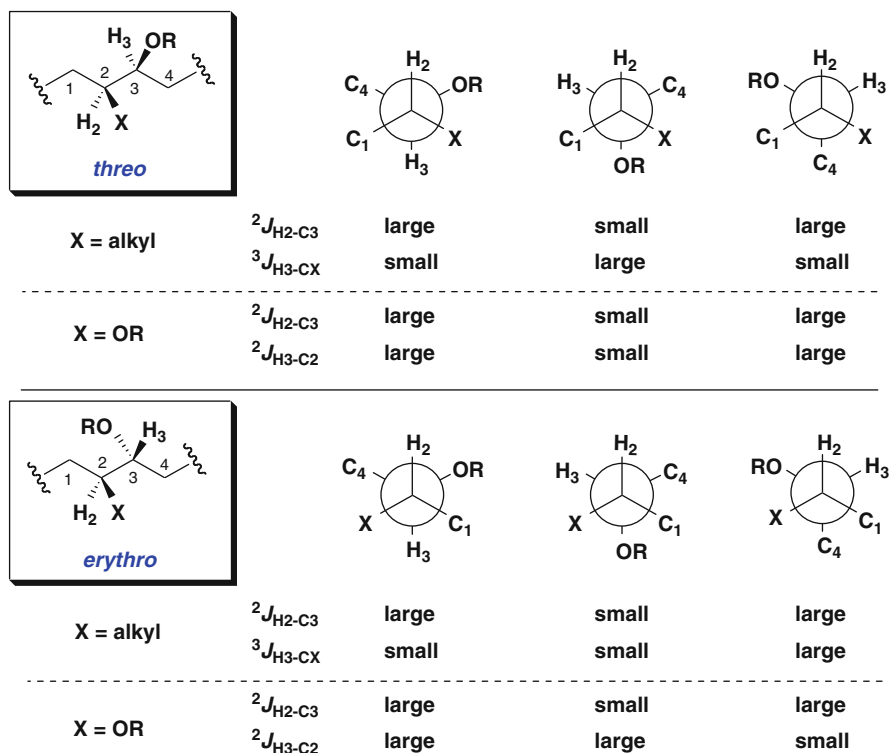


Fig. 9.14 $^2J_{\text{CH}}$ coupling patterns for the rotamers of oxygenated 1,2-methines

When assigning the relative configuration of 1,2-monooxygenated or 1,2-dioxygenated chiral fragments, the $^2J_{\text{CH}}$ values show a diagnostic pattern and they can be used in conjunction with 3J homonuclear and heteronuclear couplings. It should be noted that the distribution of large and small $^3J_{\text{HH}}$ and $^3J_{\text{CH}}$ couplings in

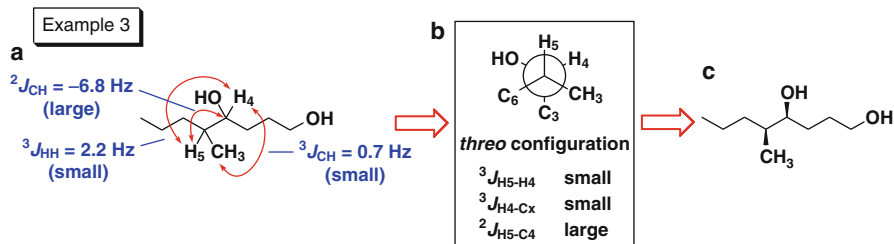


Fig. 9.15 Example 3: Assignment of the relative configuration of 4-hydroxy-5-methyloctanol. (a) Experimentally measured J values are classified as large or small in accordance with the scheme in Fig. 9.3. (b) H_4 and H_5 must be *gauche* due to their small vicinal coupling. Similarly, H_4 and the CH_3 group (C_x) have a small vicinal coupling, and they must also be *gauche*. H_5 has a large geminal coupling to C_4 , which requires a *gauche* orientation with the hydroxyl group. Comparison of the distribution of large and small couplings observed for the compound under study with the coupling patterns for the six possible staggered rotamers in Fig. 9.6 confirms that the configuration at C_4 and C_5 is *threo*. (c) The relative configuration of 4-hydroxy-5-methyloctanol illustrated in an extended (zigzag) structure. (Note: The J values used in this exercise are for illustrative purposes only; they do not represent actual measured values)

these oxygenated systems is the same as those for alkyl-substituted 1,2-methines. However, the magnitude of these 3-bond vicinal couplings can be somewhat reduced [14, 16]. The characteristic distribution of $^2J_{\text{CH}}$ values for mono- and dioxygenated systems, which can help define the configuration of adjacent methines, are illustrated in Fig. 9.14. Even with these additional 2-bond couplings, the *threo* and *erythro* diastereomers cannot be distinguished by J measurements alone when H_2 and H_3 are *anti*. In this case, additional NOE experiments are needed to assign the relative configuration.

The characteristic influence of oxygen substitution on $^2J_{\text{CH}}$ values is also observed with other electronegative substituents, such as nitrogen or halogens. These elements also result in $^2J_{\text{CH}}$ couplings that are dependent on the dihedral angle between the proton in question and the electronegative substituent bound to the coupled carbon. While the overall pattern of large and small J_{CH} values that is observed with these other substituents is identical to the distribution described for oxygen, the range of J_{CH} couplings can vary. Experimentally determined ranges of large and small J_{CH} values for various electronegative substituents have been described, and these should be consulted when J -based configurational analysis is done with these systems [16, 17] (Fig. 9.15).

When two diastereomeric methines are separated by a methylene, both methylene protons must be assigned in a stereospecific manner with respect to the adjacent methines. This requires that the methylene protons resonate at sufficiently different chemical shifts that accurate coupling constant measurements can be made. This type of 1,3-methine system can conceptually be broken into two overlapping two-carbon fragments which are separately analyzed. First, the methylene protons are stereospecifically assigned relative to the first methine based on the unique pattern of $^3J_{\text{H,H}}$ and $^{2,3}J_{\text{C,H}}$ values for the six possible rotamers (Fig. 9.16). Once this stereospecific relationship is established, the methylene

a			
$^3J_{H2-H3a}$ $^3J_{H2-H3b}$ $^3J_{H2-C4}$ $^3J_{H3a-C1}$ $^3J_{H3b-C1}$	large small small small large	small large small small small	small small large large small
X = alkyl $^3J_{H3a-CX}$ $^3J_{H3b-CX}$	small small	large small	small large
X = OR $^2J_{H3a-C2}$ $^2J_{H3b-C2}$	large large	small large	large small
b			
$^3J_{H3a-H4}$ $^3J_{H3b-H4}$ $^3J_{H3a-C5}$ $^3J_{H3b-C5}$ $^3J_{H4-C2}$	small large small small small	large small small large small	small small large small large
Y = alkyl $^3J_{H3a-CY}$ $^3J_{H3b-CY}$	large small	small small	small large
Y = OR $^2J_{H3a-C4}$ $^2J_{H3b-C4}$	small large	large large	large small
c			
$^3J_{H3a-H4}$ $^3J_{H3b-H4}$ $^3J_{H3a-C5}$ $^3J_{H3b-C5}$ $^3J_{H4-C2}$	large small small small small	small small small large large	small large large small small
Y = alkyl $^3J_{H3a-CY}$ $^3J_{H3b-CY}$	small large	large small	small small
Y = OR $^2J_{H3a-C4}$ $^2J_{H3b-C4}$	large small	small large	large large

Fig. 9.16 Configurational analysis of 1,3-methine systems when X = alkyl or -OR, and Y = alkyl. (a) The *erythro* or *threo* orientation, relative to H₂, of the diastereotopic methylene protons H_{3a} and H_{3b} can be assigned based on the pattern of their respective *J* values. (b and c) Next, the configuration of H₄ relative to H_{3a} and H_{3b} can be established in a similar manner. This process correlates the stereochemical orientation of both H₂ and H₄ with the two diastereotopic methylene protons, and thus the relative configuration at C₂ and C₄ can be assigned as *syn* or *anti*

Example 4

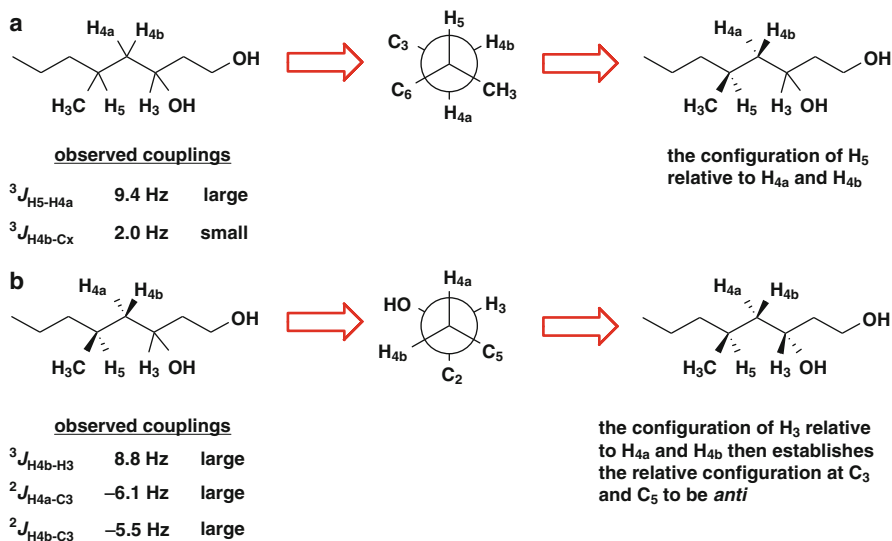


Fig. 9.17 Example 4: Assignment of the relative configuration of 3-hydroxy-5-methyloctanol. (a) The configuration of H_5 relative to the diastereotopic methylene protons H_{4a} and H_{4b} is established by selecting the appropriate rotamer that fits the experimental J values. In this case, two key couplings were sufficient. The large vicinal coupling between H_5 and H_{4a} defines an *anti* orientation for these two protons, while the small vicinal coupling between H_{4b} and the CH_3 group (C_x) requires a *gauche* orientation for these two substituents. Thus, H_{4a} has a *threo* relationship to H_5 , and H_{4b} is *erythro*. (b) Once the stereospecific orientation of H_{4a} and H_{4b} has been defined, their configuration relative to H_3 can be established. H_3 and H_{4b} must be *anti* due to the large vicinal coupling. Large geminal couplings for H_{4a} and H_{4b} with C_3 require them both to be *gauche* to the hydroxyl group, which then defines the appropriate rotamer. This establishes an *erythro* relationship between H_{4a} and H_3 , which means the relative configuration of C_3 and C_5 is *anti*. Note: The J values used in this example are for illustrative purposes only; they do not represent actual measured values

protons are correlated with the second methine using the same J -based analysis. In this manner, the configurational relationship of the 1,3-methines can be unambiguously assigned via the intervening diastereotopic methylene protons. The configuration of two methines separated by two intervening methylenes can be correlated in a similar fashion, if all the resonances of the diastereotopic methylene protons are sufficiently resolved (Fig. 9.17).

For some acyclic or highly flexible molecules, conformational interconversion results in the coexistence of two or three different rotamers. When multiple conformers do exist, if any one conformer accounts for over 85% of the population, then J -based configurational analysis of only the dominant conformer is still valid. However, if $^3J_{HH}$ couplings have intermediate values between those expected for either the H-H *anti* or *gauche* rotamers, then the presence of two major conformers needs to be considered. It is often valid to view these systems as two interconverting

staggered rotamers. In these instances, the ^1H – ^1H and ^1H – ^{13}C couplings represent a weighted average of the values for each conformer, and the observed coupling values can be large (when two large couplings are averaged), small (when two small couplings are averaged), or medium (when a large and a small coupling are averaged). For a 1,2-methine system, there are four possible pairs of rotamers where one alternating conformer has H-H *anti* and the other has H-H *gauche*. These pairs of alternating rotamers can be distinguished based on their unique distribution of $^3J_{\text{HH}}$ and $^{2,3}J_{\text{CH}}$ values, and thus the configuration can be assigned as illustrated in Fig. 9.18. When both interconverting conformers have H-H *gauche*, then analysis of coupling values alone is not sufficient to assign the relative configuration. *J*-based analysis also breaks down when there are significant contributions from three different rotamers since this causes all of the *J* values to be averaged. When multiple conformers exist, it may be possible to reduce conformational interconversion and enhance the percentage of a single conformer by acquiring the NMR data at low temperature.

9.3 Measurement of *J* Values

The ability to accurately determine both ^1H – ^1H and ^1H – ^{13}C coupling constants is crucial for successfully employing *J*-based configurational analysis in structure elucidation studies. Vicinal ^1H – ^1H couplings can often be measured directly from standard ^1H NMR spectra when the resonances are adequately resolved. For overlapped resonances, selective pulse sequences such as 1D TOCSY, 1D NOESY, or 1D ROESY may eliminate the other overlapping signals and allow direct measurement of ^1H – ^1H coupling constants [18, 19]. Phase-sensitive 2D COSY experiments such as DQF-COSY and E-COSY [20] can often be effective for overlapped or extensively coupled resonances. While the determination of ^1H – ^1H coupling values is relatively straightforward, there are inherent problems associated with the measurement of long-range ^1H – ^{13}C couplings, such as low signal-to-noise and digital resolution limitations. A variety of 2D NMR experiments have been described for determining $^{2,3}J_{\text{CH}}$ coupling constants, but they all have some practical limitations or experimental challenges associated with their routine use [21]. Three of the more common pulse sequences that have been successfully applied in natural products studies are the HETLOC [22], *J*-HMBC [23], and HSQMBC [24] experiments. HETLOC (hetero half-filtered TOCSY) is similar to a ^1H – ^1H TOCSY experiment except the correlations have E-COSY-type splitting patterns, with 1-bond $^1J_{\text{CH}}$ coupling in F_1 and the long-range $^{2,3}J_{\text{CH}}$ coupling as an offset in F_2 . Heteronuclear coupling values can be read directly from the HETLOC spectrum, but this experiment relies on TOCSY-like correlations so its application is limited to protonated carbons within a given proton–proton spin system. J_{CH} couplings cannot be measured for quaternary carbons or for protonated carbons outside of the ^1H spin system. The *J*-HMBC pulse sequence provides spectra similar to HMBC, but the correlation peaks are split in the F_1 dimension by a multiple of the heteronuclear coupling constant and a *J*-scaling

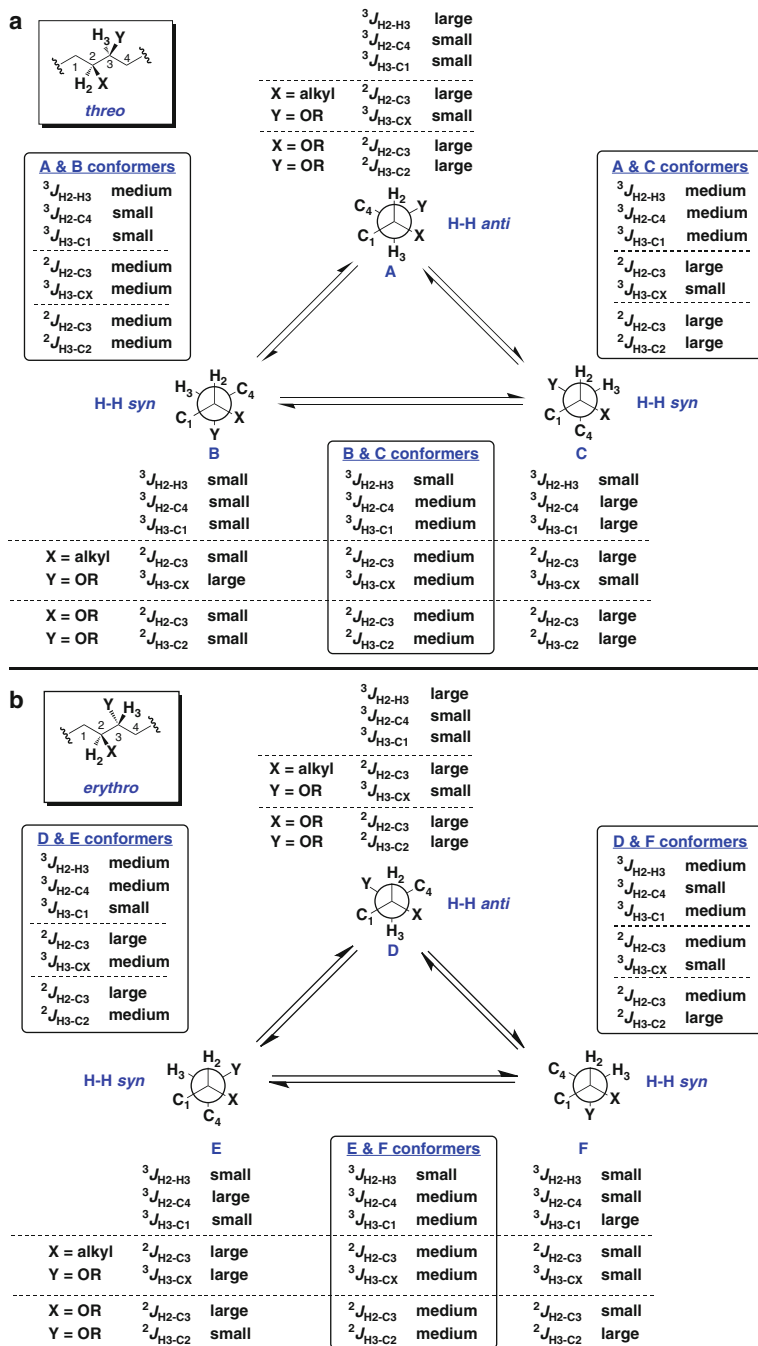


Fig. 9.18 (continued)

factor (observed F_1 splitting = $^{2,3}J_{\text{CH}}$ x J -scaling factor). The J -scaling factor can be controlled by changing the variable delay periods in the pulse sequence. The actual $^{2,3}J_{\text{CH}}$ values in a J -HMBC data set are obtained by applying a mathematical correction to the measured F_1 splittings. Low signal-to-noise due to the length of the pulse sequence can be an inherent problem with J -HMBC, but this experiment can provide heteronuclear coupling constants for quaternary carbons and for couplings that encompass components from different ^1H spin systems. The HSQMBC experiment employs a modified HSQC-type pulse sequence for the evolution of long-range ^1H – ^{13}C couplings. It does not rely on ^1H – ^1H coupling, so it can be used to measure long-range couplings with quaternary carbons or couplings between systems that are separated by a heteroatom or quaternary carbon. Extraction of $^{2,3}J_{\text{CH}}$ coupling constants from HSQMBC data is relatively straightforward for systems with simple ^1H – ^1H coupling patterns, but it can be more challenging for systems with complex ^1H – ^1H couplings. When there are complex ^1H multiplets, a peak-fitting protocol may be required to match the 1D ^1H resonance with the dispersive coupling pattern of a 1D slice through its HSQMBC correlation peak. This latter process can be complicated by nonuniform phase effects in the data.

It is anticipated that the continued evolution and improvement of these and other NMR pulse sequences will enhance our ability to accurately determine $^{2,3}J_{\text{CH}}$ coupling constants, and thus expand the utility of the J -based methods for making configurational assignments. In addition to these experimental NMR approaches for measuring long-range heteronuclear couplings, computational methods have recently been developed to predict homonuclear and heteronuclear spin–spin couplings [16, 25]. Quantum mechanical density functional theory calculations of J -coupling values can now be exploited to predict coupling constants for all of the staggered rotamers and compare these computed values with the experimentally determined ones. This computational approach has already been employed in the structural assignment of natural products, and its utility and application is likely to increase in the future.

9.4 Concluding Remarks

The utilization of NMR methods to successfully make both relative and absolute configurational assignments has significantly increased the utility of this



Fig. 9.18 Interconverting pairs of rotamers for *threo* (a) and *erythro* (b) configurations. The averaged J values for the alternating conformers have a unique distribution when there is interconversion between H-H *anti* and H-H *gauche* rotamers. Thus, the *threo* conformer pairs A and B and A and C can be distinguished from their *erythro* counterparts, D and E and D and F, and the configuration can be unambiguously assigned when any of these conformer pairs coexist. The averaged J values for an equilibrium mixture of the *threo* conformers B and C (both H-H *gauche*) cannot be distinguished from the corresponding mixture of conformers (E and F) for the *erythro* configuration, so a stereochemical assignment is not possible for these conformer pairs

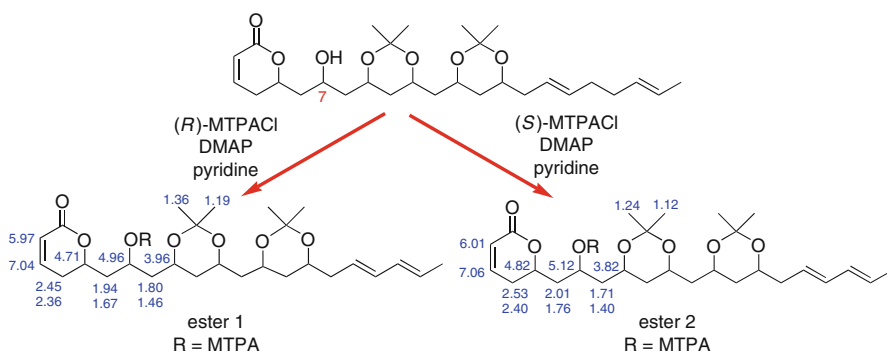
spectroscopic technique in the structural elucidation of natural products. While NMR has long been paramount in determining the planar structures of new metabolites, its utility for establishing stereochemical features of complex organic compounds was often quite limited. The development and validation of new NMR methodologies such as those employing chiral anisotropic reagents, or the *J*-based configurational approach illustrate the continuing evolution and expansion of NMR applications. These advancements have been possible due to a multitude of factors, including improvements in both NMR hardware and pulse sequences. The availability of NMR spectrometers with higher magnet field strengths has increased both the sensitivity and resolution of individual resonances, while the advent of cryogenically cooled probes provided dramatic signal-to-noise improvements. The development and refinement of new pulse sequences now allow the fairly “routine” measurement of long-range $^2,3J_{\text{CH}}$ coupling constants and ^1H – ^1H couplings of heavily overlapped proton resonances. While these pulse sequences are now available from the pulse sequence libraries NMR vendors provide with their current software, care must be taken in selecting appropriate experimental parameters. Unambiguous interpretation of the coupling data can also be problematic at times, so it is highly recommended that these types of experiments be performed initially on standards with known coupling values. One should be wary of using these experiments with unknowns until the coupling data has been successfully acquired and analyzed for a standard compound.

Improvements in NMR technologies themselves have only set the stage for the current and future applications of NMR to solve stereochemical challenges. The real credit goes to those individuals who have observed reproducible patterns in the NMR data they acquired with chiral compounds, and then conceptually developed the models to explain these patterns. These were the fundamental contributions that allowed the NMR techniques to develop. Recognition of the potential of chiral anisotropic reagents and *J*-based analysis in the stereochemical elucidation of new natural product structures was also essential for the now widespread use of these techniques. The continued refinement of these current approaches, and the development of new NMR methods for configurational analysis, will undoubtedly continue in the future. It is imperative that those involved in contemporary natural products structural studies develop confidence and expertise in the application of these experiments.

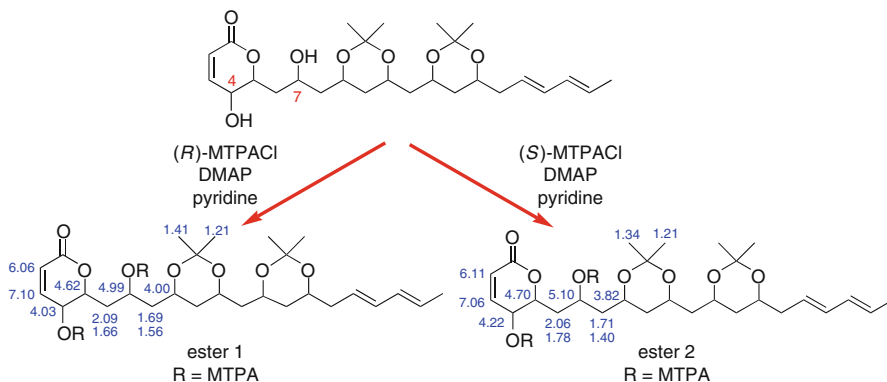
9.5 Study Questions

1. The bis-acetonide derivative of a polyol natural product was treated with MTPA-Cl, and ^1H NMR data for the two resulting MTPA esters is shown

below. From this data, determine the absolute configuration of the hydroxy methine carbon at C-7

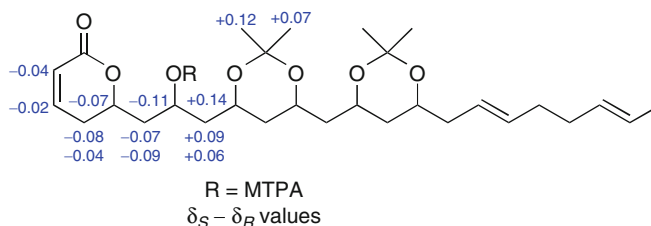


2. A hydroxylated analogue was also treated with MTPA-Cl, and NMR data for the bis-MTPA esters was acquired. From this data, can the Mosher's method be used to assign the configuration of the C-4 and C-7 hydroxy methine carbons? If so, what is the absolute configuration at C-4 and at C-7?

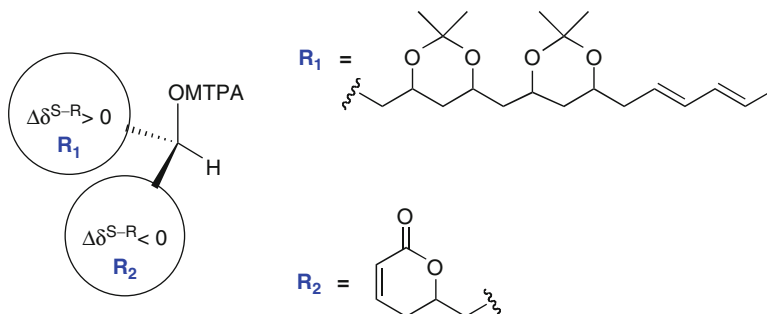


Answer 1

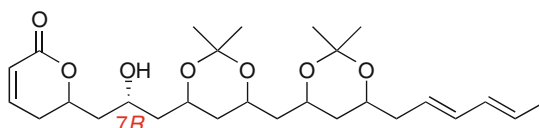
Calculate the $\delta_S - \delta_R$ values.



There is a consistent distribution pattern of $\Delta\delta^{S-R}$ values, so the Mosher's method is applicable in this case. Model the MTPA ester as shown, and assign R_1 and R_2 .

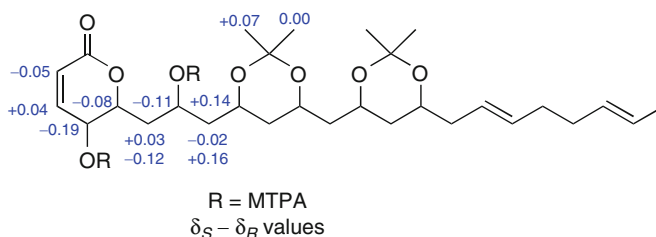


When R_1 and R_2 have been assigned, use the Cahn–Ingold–Prelog priority rules to establish the absolute configuration of the hydroxy methine carbon in the natural product.



Answer 2

Calculate the $\delta_S - \delta_R$ values.



The sum of the shielding and deshielding effects of two MTPA esters in close proximity resulted in a random distribution of positive and negative $\Delta\delta^{S-R}$ values. Assignment of the absolute configuration at C-4 and C-7 by the Mosher's method is not possible in this case.

References

1. Dale JA, Mosher HS (1973) Nuclear magnetic resonance enantiomer reagents. Configurations *via* nuclear magnetic resonance chemical shifts of diastereomeric mandelate, *O*-methylmandelate, and α -methoxy- α -trifluoromethylphenylacetate (TPA) esters. *J Am Chem Soc* 95:512–519
2. Sullivan GR, Dale JA, Mosher HS (1973) Correlation of configuration and ^{19}F chemical shifts of α -methoxy- α -trifluoromethylphenylacetate derivatives. *J Org Chem* 38:2143–2147

3. Ohtani I, Kusumi T, Kashman Y, Kakisawa H (1991) High-field FT NMR applications of Mosher's method. The absolute configurations of marine terpenoids. *J Am Chem Soc* 113:4092–4096
4. Kusumi T, Ohtani I (1999) Determination of the absolute configuration of biologically active compounds by the modified Mosher's method. In: Cooper R, Snyder JK (eds) *The biology chemistry interface*. Marcel Dekker, New York, pp 103–137
5. Seco JM, Quiñoá E, Riguera R (2000) The assignment of absolute configurations by NMR of arylmethoxyacetate derivatives: is this methodology being correctly used? *Tetrahedron Asymmetry* 11:2781–2791
6. Seco JM, Quiñoá E, Riguera R (2001) A practical guide for the assignment of the absolute configuration of alcohols, amines and carboxylic acids by NMR. *Tetrahedron Asymmetry* 12:2915–2925
7. Seco JM, Quiñoá E, Riguera R (2004) The assignment of absolute configuration by NMR. *Chem Rev* 104:17–117
8. Oku N, Takada K, Fuller RW, Wilson JA, Peach ML, Pannell LK, McMahon JB, Gustafson KR (2010) Isolation, structural elucidation, and absolute stereochemistry of enigmazole A, a cytotoxic phosphomacrolide from the Papua New Guinea marine sponge *Cinachyrella enigmatica*. *J Am Chem Soc* 132:10278–10285
9. Seco JM, Latypov S, Quiñoá E, Riguera R (1994) New chirality recognizing reagents for the determination of absolute stereochemistry and enantiomeric purity by NMR. *Tetrahedron Lett* 35:2921–2924
10. Kusumi T, Takahashi H, Xu P, Fukushima T, Asakawa Y, Hashimoto T, Kan Y, Inouye Y (1994) New chiral anisotropic reagents, NMR tools to elucidate the absolute configurations of long-chain organic compounds. *Tetrahedron Lett* 35:4397–4400
11. Williamson RT, Barrios Sosa AC, Mitra A, Seaton PJ, Weibel DB, Schroeder FC, Meinwald J, Koehn FE (2003) New silyl ether reagents for the absolute stereochemical determination of secondary alcohols. *Org Lett* 5:1745–1748
12. Nagai Y, Kusumi T (1995) New chiral anisotropic reagents for determining the absolute configuration of carboxylic acids. *Tetrahedron Lett* 36:1853–1856
13. Ferreiro MJ, Latypov SK, Quiñoá E, Riguera R (2000) Assignment of the absolute configuration of α -chiral carboxylic acids by ^1H NMR spectroscopy. *J Org Chem* 65:2658–2666
14. Matsumori N, Kaneno D, Murata M, Nakamura H, Tachibana K (1999) Stereochemical determination of acyclic structures based on carbon-proton spin-coupling constants. A method of configuration analysis for natural products. *J Org Chem* 64:866–876
15. Minch MJ (1994) Orientational dependence of vicinal proton-proton NMR coupling constants: the Karplus relationship. *Concepts Magn Reson* 6:41–56
16. Bifulco G, Dambruoso P, Gomez-Paloma L, Riccio R (2007) Determination of relative configuration in organic compounds by NMR spectroscopy and computational methods. *Chem Rev* 107:3744–3779
17. Nilewski C, Geisser RW, Ebert M-O, Carreira EM (2009) Conformational and configurational analysis in the study and synthesis of chlorinated natural products. *J Am Chem Soc* 131:15866–15876
18. Dalvit C, Bovermann G (1995) Pulsed field gradient one-dimensional NMR selective ROE and TOCSY experiments. *Magn Reson Chem* 33:156–159
19. Scott K, Keeler J, Van QN, Shaka AJ (1997) One-dimensional NOE experiments using pulsed field gradients. *J Magn Reson* 125:320–324
20. Griesinger C, Sørensen OW, Ernst RR (1986) Correlation of connected transitions by two-dimensional NMR spectroscopy. *J Chem Phys* 85:6837–6852
21. Márquez B, Gerwick WH, Williamson RT (2001) Survey of NMR experiments for the determination of nJ (C, H) heteronuclear coupling constants in small molecules. *Magn Reson Chem* 39:499–530

22. Uhrín D, Batta G, Hruby VJ, Barlow PN, Kövér KE (1998) Sensitivity- and gradient-enhanced hetero (ω_1) half-filtered TOCSY experiment for measuring long-range heteronuclear coupling constants. *J Magn Reson* 130:155–161
23. Meissner A, Sørensen OW (2001) Measurement of $J(\text{HH})$ and long-range $J(\text{X}, \text{H})$ coupling constants in small molecules. Broadband XLOC and J-HMBC. *Magn Reson Chem* 39:49–52
24. Williamson RT, Márquez BL, Gerwick WH, Kövér KE (2000) One- and two-dimensional gradient-selective HSQMBC NMR experiments for the efficient analysis of long-range heteronuclear coupling constants. *Magn Reson Chem* 38:265–273
25. Bifulco G, Bassarello C, Riccio R, Gomez-Paloma L (2004) Quantum mechanical calculations of NMR J coupling values in the determination of relative configuration in organic compounds. *Org Lett* 6:1025–1028

Quantum Chemical Calculation of Chemical Shifts in the Stereochemical Determination of Organic Compounds: A Practical Approach

10

Simone Di Micco, Maria Giovanna Chini, Raffaele Riccio, and Giuseppe Bifulco

Contents

10.1	Introduction	572
10.2	Calculation Protocol for Molecular Frameworks	572
10.2.1	First Step: Building the Molecules	573
10.2.2	Second Step: Conformational Search	574
10.2.3	Final Energy and Geometry Optimization	581
10.2.4	^{13}C NMR Chemical Shifts Calculation	585
10.2.5	J Coupling Constants Calculation	589
10.2.6	Solvent Effects	593
10.3	Conclusions	594
10.4	Study Questions	595
	References	595

Abstract

In this chapter, we report an integrated approach of NMR and quantum mechanical calculation for the determination of the relative configuration of natural products. The entire protocol is described starting from building the investigated compound to the calculation of NMR properties at quantum theory level and the interpretation of the results. Each step of the protocol is described, and the main applied methods are reported. We report, as case studies, the determination of the relative configuration of two natural products: bonannione B isolated from *Bonannia graeca*, and callipeltin A isolated from the sponges *Callipelta* sp. and *Latrunculia* sp. Through the analysis of these natural products, we show the use of ^{13}C chemical shift and homo and hetero J coupling constants, respectively, as

S. Di Micco • M.G. Chini • R. Riccio (✉) • G. Bifulco (✉)

Department of Pharmaceutical and Biomedical Sciences, University of Salerno, Via Ponte Don Melillo, Fisciano (Salerno), Italy

e-mail: sdimicco@unisa.it, mchini@unisa.it, riccio@unisa.it, bifulco@unisa.it

an important tool in the interpretation of the experimental data for the determination of the relative configuration of organic compounds.

10.1 Introduction

In the last decade, quantum chemical approaches have shown their potential in solving chemical problems. This has been mostly due to the ever increasing computational capabilities at a relatively affordable cost and to a parallel development of user-friendly software. While many aspects of molecular structure and dynamics may be solved with the use of classical methods based on empirical force fields, quantum chemistry allows the comprehension of many problems related to the electronic density distribution. In particular, quantum chemistry methods can be applied for calculating the spectroscopic properties of molecules, and the efficient prediction of UV, IR, CD, and NMR spectra have been extensively reported in the last 15 years. NMR chemical shift calculation by quantum mechanical methods has attracted the interest not only of the theoretical chemists but also of the experimental NMR spectroscopists. In fact, this kind of approach has been used by our and other research groups as a contribution to the structure elucidation of natural products. We have presented two original methodologies, based on GIAO (gauge including atomic orbitals) quantum mechanical ^{13}C chemical shift calculations, that have been efficiently employed as a support in the analysis of the NMR data of organic molecules. The first methodology regards the structure validation of natural products by means of GIAO ^{13}C chemical shift calculations, while the second one, based on the same methodology, has been directed to the determination of the relative configuration of flexible compounds. For the interested readers, the most significant applications of quantum chemical calculations of NMR parameters in the resolution of stereochemical problems have been recently reported by us in two reviews. On the other hand, the scope of this chapter is to present a step-by-step guide for the NMR parameter calculation of organic compounds in the determination of their relative configuration.

10.2 Calculation Protocol for Molecular Frameworks

Different experimental approaches have been proposed for the determination of the configuration of organic compounds [1, 2]. One of the most used is the total synthesis, which is highly demanding in terms of human and economical resources. On the other side, there are analytical methods, such as nuclear magnetic resonance (NMR), X-ray crystallography, circular dichroism (CD), and mass spectrometry, which allow also to preserve the investigated compound. For the stereostructural determination of natural products, it is possible to apply a protocol based on the calculation of ^1H and/or ^{13}C of chemical shifts as a support in the experimental data analysis (Fig. 10.1) [3, 4]. Such a protocol consists of up to six fundamental steps: (a) building the molecules by dedicated software; (b) conformational search at the empirical theory level [5, 6], generally through molecular dynamics (MD) or by Monte Carlo multiple minimum

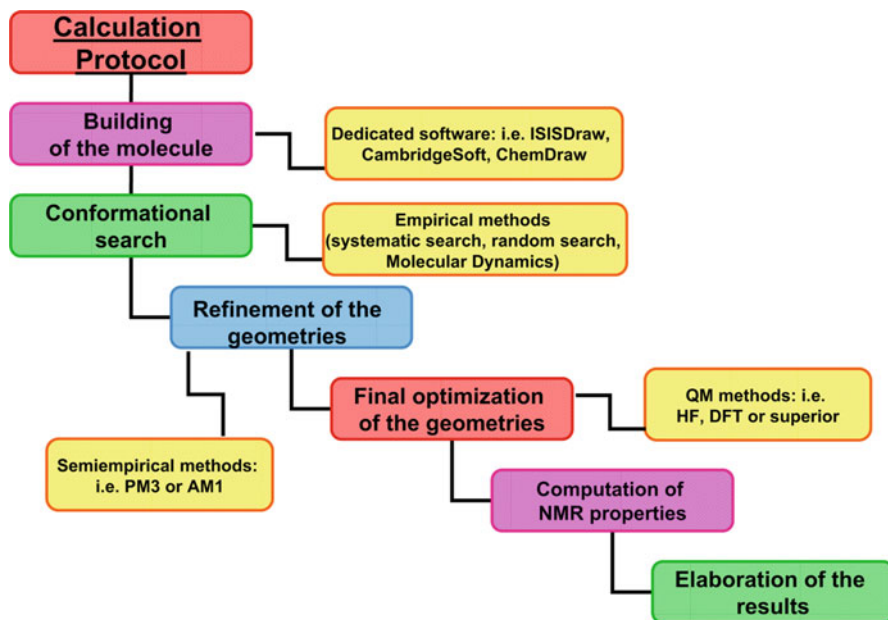


Fig. 10.1 General protocol used for the determination of the relative configuration of organic compounds

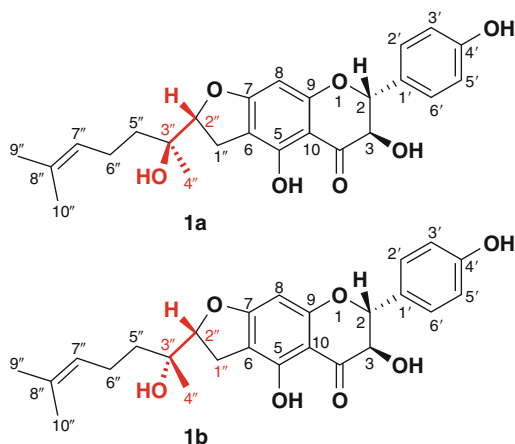
methods (MCM) [7]; (c) preliminary geometry optimization at semiempirical level (e.g., AM1 [8], PM3 [9]) of all the significantly populated conformers of each stereoisomer; (d) final geometry optimization of all the species at the quantum mechanical (QM) level; (e) GIAO (gauge including atomic orbital) ^{13}C and/or ^1H NMR calculations of all the structures obtained by the optimization at QM level of all diastereomers, taking into account the Boltzmann distribution; and (f) elaboration of the results comparing the Boltzmann-averaged NMR parameters calculated for each stereoisomer with those experimentally measured for the compound under examination. In order to facilitate the understanding of the protocol, we will show an application of the QM/NMR methodology to a real case: the assignment of the relative configuration of the bonannione B (**1**, Fig. 10.2), a flavanone isolated as minor compounds from the aerial parts of *Bonannia graeca* (*Umbelliferae*) [10].

The example of the flavonoid bonannione B (**1**, Fig. 10.2) represents a straightforward application of ^{13}C NMR chemical shift calculation, since the configuration of stereopair (C-2'' and C-3'') under investigation could not be deduced by simple analysis of the 2D ROESY spectra, and the small amount of the isolated compound was not sufficient to apply Mosher's method [11].

10.2.1 First Step: Building the Molecules

The generation of the molecule model represents the starting point for any computational chemistry study. The tridimensional model (3D) defines the relative

Fig. 10.2 Molecular structure of two possible diastereoisomers of bonannione B (**1a** and **1b**)



position of the atoms in the space through a set of Cartesian coordinates obtained from several sources. The X-ray crystallographic database [12], the building from a preexisting fragment library, the conversion of 2D structural data (e.g., .cdx, .skc, .sk2, and smiles files) into 3D form (e.g., .mol, .pdb, .mol2, .mae, and .gif files) with a dedicated software – ACD/ChemSketch [13], ISISDraw [14], and ChemDraw [15] – represent some examples for the achievement of the model. In the illustrated case of bonannione B (Fig. 10.3), it is possible to build the 2D structure with a molecular editor software, for example, by using the ChemOffice package, and then converting it into a file containing the Cartesian coordinates (Fig. 10.4).

The choice of method to adopt depends on the case and the resources of the user, but in any case, a reasonable and reliable initial geometry is essential for the quality of the following investigation.

10.2.2 Second Step: Conformational Search

The QM calculation of properties belonging to the investigated compound, such as energy, UV, NMR parameters, must be performed on models that better represent the real conformations of the molecule: the minima of the potential energy surface. In fact, differently from rigid molecular systems, flexible molecules may exist in more than a single conformation. The changing among the conformers, derived from the variation of dihedral angles around single bonds, corresponds to different points in the potential energy surface. The diverse energy points, coinciding with local minima, may represent the different conformations adopted at the thermal equilibrium by the molecule. As the spectroscopic properties strictly depend on the compound geometry, their calculation needs to take into account all the possible representative local minima in equilibrium because each conformer will have a specific weight in the global spectroscopic properties. (These concepts can be better understood analyzing the different conformation of ethane and n-butane.

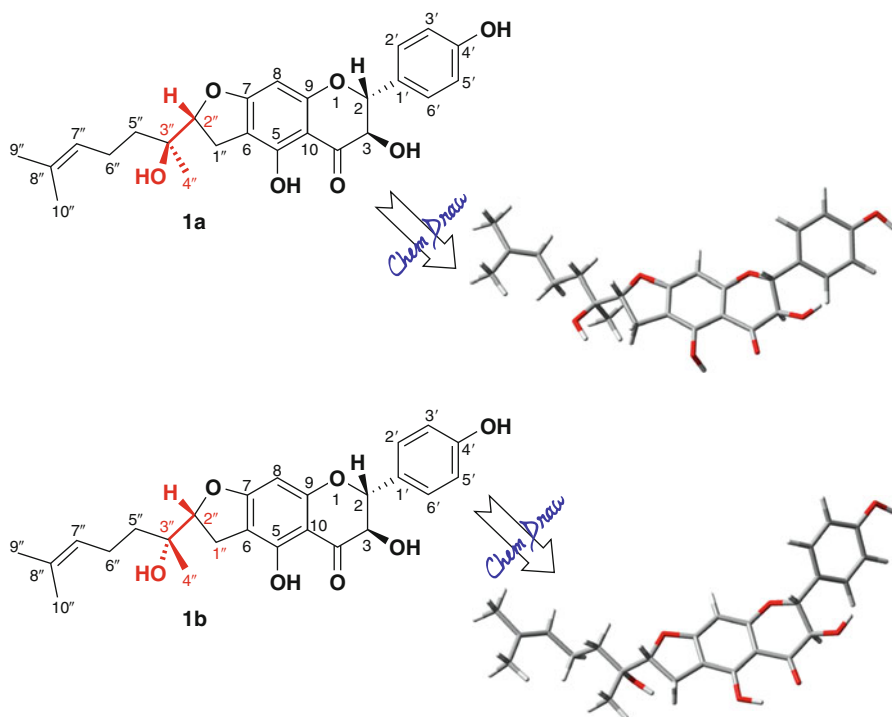


Fig. 10.3 Conversion of 2D structure into a 3D model of bonannione B

Increments of 60° for torsion angle around the C–C bond in ethane translate in two extreme cases: three eclipsed conformations at 0° , 120° , and 240° (global maxima), and three staggered conformations at 60° , 180° , and 300° (global minima), and so for the study of its physical and chemical properties, only the staggered arrangements must be considered (Fig. 10.5). Even if the rotation around carbon–carbon bond is not completely free owing to the energy difference between the two conformer families, in the case of ethane, the difference of 2.8 kcal/mol is small enough to be overcome, and thus, the conformers are interconvertible at room temperature. In the case of n-butane, increments of 60° for torsion angle around the bond C2–C3 give rise to one maximum global at 0° (eclipsed form), two local minima at 60° and 300° (*gauche* form), two local maxima at 120° and 240° , and one global minimum at 180° (*anti* form). At room temperature, the *gauche* and *anti* rotamers (energy difference of 0.9 kcal/mol) are in conformational equilibrium accounting for a 30:70 ratio, respectively, and so, both the conformations must be considered when the physical and chemical properties are studied.)

```

                                Cartesian Coordinates
                                {
COMPND  bonannione.PDB
ATOM    1  C          0   -0.313   0.595   1.218   C
ATOM    2  C          0   -0.200  -0.052   2.477   C
ATOM    3  C          0    1.067  -0.513   2.927   C
ATOM    4  C          0    2.219  -0.326   2.118   C
ATOM   21  O          0   -1.655   0.986   0.966   O
ATOM   23  C          0   -1.532  -0.153   3.151   C
ATOM   31  C          0   -3.398  -1.214   1.128   C
ATOM   32  O          0   -4.363  -0.075   3.074   O
ATOM   33  H          0    0.750   1.275  -0.570   H
CONNECT  1    2    6   21
CONNECT  2    1    3   23
CONNECT  3    2    4   19
CONNECT  4    3    5    7
ENDMDL
END
                                } Atom types
                                {
                                Connection between atoms

```

Fig. 10.4 The PDB file representation of the bonannione B

Consequently, the conformational search and the analysis of relative stability of different conformers are mandatory to obtain significative results after the QM calculation of NMR parameters.

This fundamental step for the search of the most representative rotamers can be performed in several ways (systematic search or grid search, random search or Monte Carlo methods, and molecular dynamics) by different dedicated softwares (Discover [16], Insight Package [17, 18], Gromacs [19, 20], Spartan [21], Macromodel [22], etc.).

10.2.2.1 Conformational Analysis Methods

The systematic search (grid search) consists in the step-by-step changes for the all possible dihedral angles of the entire and/or a part of molecule for all 360° , taking in account all the possible combinations between them. Each generated conformation must be subsequently minimized. One simple example of this conformational search through this algorithm can be the analysis of the poly-L-alanine peptide (Fig. 10.6).

Considering planar and in *trans* conformation the amide bonds, and the bonds' angles and distances fixed, the only two variables that regulate the different conformations are represented by φ and ψ angles (Fig. 10.6). The systematic increments of $15\text{--}30^\circ$ for both the dihedral angles in the region between 180° and -180° result in changes of the conformation and energy of the peptide. The variation of the energy as function of φ and ψ , in fact, can be visualized in the Ramachandran plot (Fig. 10.7), where the systematic angle changes are equivalent to examine all the significant points of a grid.

In the case of poly-L-alanine peptide, in the grid, few minima points are identifiable and so the most of conformations, after a minimization step, often converge toward the same rotamer. The main inconvenience of the systematic

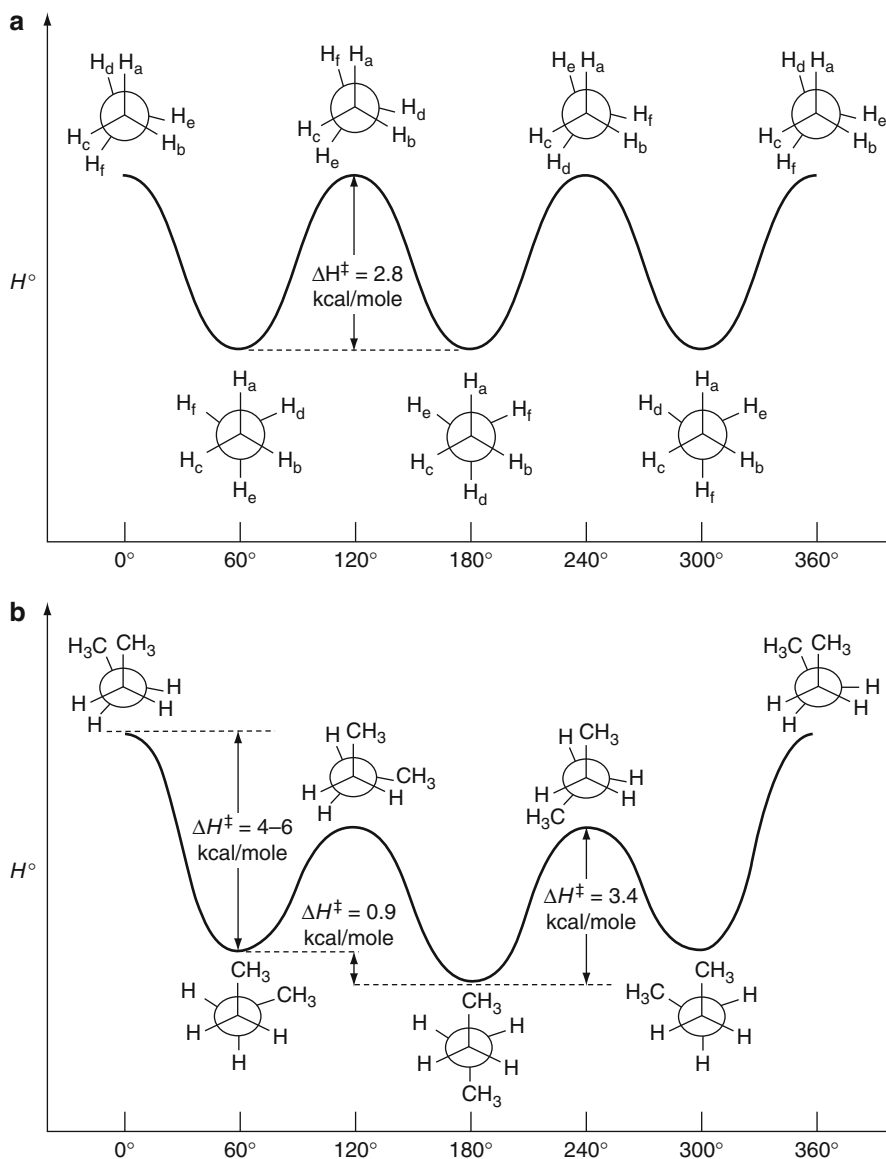


Fig. 10.5 Variation of energy for ethane (a) and n-butane (b) as function of dihedral angle

search is represented by the number of the generated conformations that exponentially increase with the number of rotatable bonds. This method is also difficult to apply to cyclic compounds where the dihedral angles are not independent between each other. On the other hand, the application of the grid search provides a comprehensive exploration of the conformational space, differently from the methods that will be discussed further.

Fig. 10.6 Molecular structure of poly-L-alanine peptide

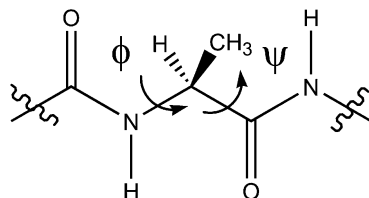
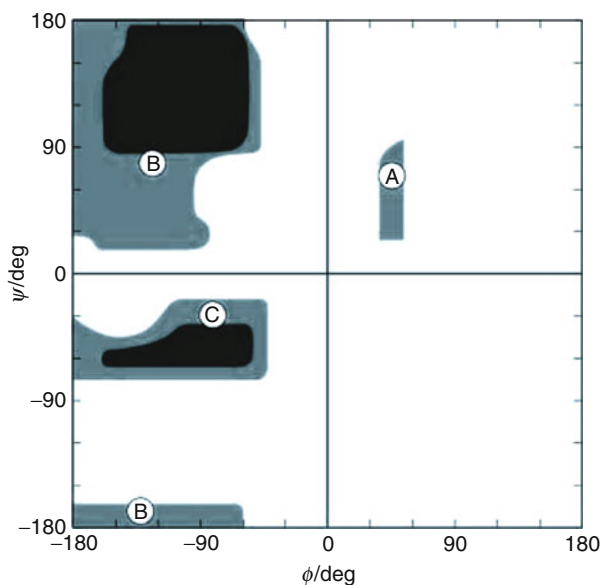


Fig. 10.7 A Ramachandran plot for poly-L-alanine peptide. The *black-and-gray* areas (numbered **a–c**) represent the allowed conformations; the white regions represent the forbidden rotamers



Differently from the systematic search described above, by the Monte Carlo method, the conformational space is explored in a random mode. The conformations are achieved by varying randomly the torsional angles, and then minimizing the so-obtained casual conformations. In particular, the new conformation is generated in two possible ways: varying or the Cartesian coordinates of each atom, or the dihedral angles of random amount. The resulting conformation is minimized, and its energy is compared against those of all structures previously found, and, if unique, it is stored (criterion based on an energy cut off). After this cycle, another conformation is chosen, and the proceeding is resumed. In order to compensate intrinsic limits of the random search, it is appropriate to perform several parallel runs starting from diverse rotamers. In addition to the casual choice, different approaches exist to select the starting structure, and one of these methods consists in using the local minimum found for each search. The main advantage for the Monte Carlo method is the possibility to sample cyclic systems that are difficult to treat by systematic methods. Another advantage is the potential treatment of molecular systems of any size, even though very large and flexible molecules may not provide converging results due to their wide conformational space.

The molecular dynamics (MD) represents another efficient method for the exploration of the molecular conformational space. It may be used for linear compounds with multiple torsions, when both the systematic and the random search are unadvisable, or for cyclic compounds, when the conformational analysis by the random search is complicated by the required computational time. The fundamental aim of the MD is the reproduction of the real behavior of the molecule, mimicking the time-dependent motions of the atoms. The generation of the new structure represents the principal difference of this approach with respect to the other two described above because the molecular dynamics is a deterministic approach, where the new generated structure is causally determined by previous conformer. In particular, given a set of initial coordinates and velocities with a force (F_i), the evolution of the system, all atoms will be moved to new positions following the Newton's second law (Eq. 10.1)

$$F_i(t) = m_i a_i(t) \quad (10.1)$$

where F is the force on atom i at time t , m_i is the mass of atom i , and a_i is the acceleration of atom i at time t . The so obtained conformation will be used as starting point for a new step, the cycle will be repeated for a predefined number of times, and the conformers will be collected (conformational ensemble). In particular, since significant conformational changes do not always happen at room temperature, especially when more atoms are involved, the MD simulations are performed at different increasing temperatures for supplying a sufficient kinetic energy to overcome the energetic barriers between the possible rotamers. During the MD simulations, in order to increase the probability to explore the entire conformational space, it is convenient to vary some fundamental parameters during the calculation as for example the simulation temperature, the time step, the equilibration, and the simulation time. However, if converged results are desired, different parallel MD simulations must be performed starting from different conformations, at diverse temperature – it is preferable to use a gradient of temperature from 450 to 650/700 K – and long time simulations should be used. Thanks to the kinetic energy of molecules it is possible that some collected conformers represent the local and/or global maximum points, and so, after the MD simulation, a minimization process of this ensemble of rotamers is always necessary.

A particular MD simulation is represented by simulated annealing. This methodology consists in a molecular dynamics at high temperature where temperature is gradually decreased to 0 K. During the simulation at high temperature, the molecules are able to explore conformations very different among each other, and thanks to the temperature dropping the molecule may converge in a local minimum. In order to obtain a collection of low energy conformations, the cycle will be repeated several times. The main advantage of simulated annealing with respect to the classic MD approach is represented by the possibility to avoid the minimization step since the resulting structures represent energy minima.

For all the above considerations, the choice of the method is exclusively dictated by the molecule under study, e.g., if it is linear, or cyclic, how many torsions are

present, if some experimental data are available, etc. In conclusion, it should be kept in mind that each method has its advantages and/or limitations.

In addition to the exploration method, the efficiency of the conformational search depends on a series of other factors such as the force fields and the algorithms of minimization.

In the molecular mechanics, the calculation of the energy is obtained through the force fields, functions that approximate the electronic potential surface using the specific parameters and mathematical equations of classic physics. The most simple force field equation is described in Eq. 10.2:

$$E_{\text{total}} = E_{\text{tors}} + E_{\text{vdw}} + E_{\text{elec}} + E_{\text{Hbond}} + E_{\text{oop}} \dots \quad (10.2)$$

where the total energy (E_{total}) of the molecule is obtained by the sum of energy terms associated with the internal coordinates. E_{vdw} , for example, represents the energy related to the van der Waals interactions between atoms, and it is described by the Leonard–Jones equation (Eq. 10.3):

$$E_{\text{vdw}} = \varepsilon \left[\left(\frac{r_0}{r} \right)^{12} - 2 \left(\frac{r_0}{r} \right)^6 \right] \quad (10.3)$$

The electrostatic term (E_{elec}) is calculated by Coulomb's law; E_{tors} is a cosine periodic function (Eq. 10.4), etc.

$$E_{\text{tors}} = k\omega(1 - \cos 3\omega) \quad (10.4)$$

The parameter sets of the force field, e.g., the length and angles of the bonds, the hybridization of the atoms, the charges of the atoms, derive from the experimental data, and so the different force fields are tailored for a particular molecular system and are not able to describe all types of structures under investigation. For example, MM2 [23] is parameterized for the organic molecules, MM3 [24] for conjugated systems, AMBER [25, 26] for the peptides and nucleic acids, and OPLS* [27, 28] for peptides.

In this context, it is clear that the obtained geometries by specific method of conformational search must be minimized. Also in this step, different methods exist for the minimization process, but the most used algorithms are the steepest descent, conjugate gradient, and Newton–Raphson. These utilize the first and second derivative values of energy function in order to choose the direction to undertake. The steepest descent algorithm uses the first derivative value to move the atoms toward the local minimum; this algorithm works very well with conformation far from the equilibrium, but it is less efficient in the conformations close to the energy minimum. The steepest descent direction is also considered in the conjugate gradient algorithm, but in this case, the new direction is dependent from the previous; this permits a dramatic improvement of the efficiency of the method in proximity to the local minima points. The Newton–Raphson algorithm is able to discern between the minima and the maxima points, considering also the value of the second derivative.

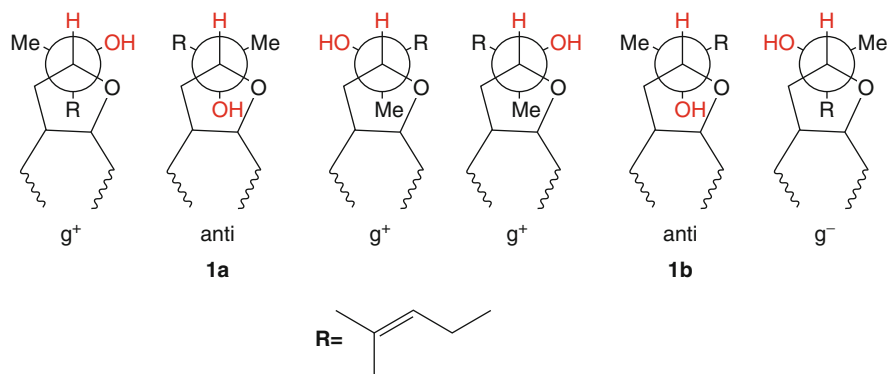


Fig. 10.8 The gauche (g^+ and g^-) and anti rotamers around C-2''-C-3'' for compounds **1a** and **1b**. The gauche and anti positions are referred to the -OH group

Moreover, in addition to the gradient, the curvature of the function allows to identify the search direction. The only disadvantage of this method is represented by the computational resource required (N^2 for N internal coordinates), but it is efficient enough in the conformation close to the minima points. On consequence, for small/medium molecules far from the minimum, it is preferable to apply as first the steepest descent and then the Newton-Raphson method; on the other hand, for biggest molecules, the Newton-Raphson method can be replaced by the conjugate gradient.

Taking into account the above-reported arguments, in the real illustrated example of bonannione B (**1a** and **1b**, Fig. 10.2), the several free molecular dynamics calculations are performed using the MMFFs [29] force field at different temperatures (between 400 K and 650 K) for 10 ns (simulation time), with a time step and an equilibration time of 1.5 fs and 1.0 ps, respectively (MacroModel software package) [22]. All the structures so obtained (numbering 100) are minimized by using the Polak-Ribier conjugate gradient algorithm [30] (PRCG, 1,000 steps, maximum derivative less than 0.05 kcal/mol). This approach leads to the selection of the lowest energy minimum rotamers (g^+ , *anti* and g^-) around the C-2''/C-3'' bond for each diastereoisomers (Fig. 10.8) that can be submitted to the next step: the final energy and geometry optimization.

10.2.3 Final Energy and Geometry Optimization

Following the scheme of the protocol reported in Fig. 10.1, after the conformational search and the preliminary geometry optimization of all found conformers, a further refinement of the three-dimensional coordinates is performed by using a more sophisticated theoretical level. As described above, the force fields are based on classical mechanics laws, and they include, in the description of a given chemical system, parameters derived from experiments or from quantum mechanical calculations. Molecular mechanics methods do not explicitly model the electrons in the

description of a molecular system, but the electrons are treated in the force field by parameterization. This approximation renders the molecular mechanics approaches faster than other more sophisticated theories and allows its application to very large systems. For a well-parameterized general force field, many molecular properties, such as geometry and relative conformational energies, can be calculated with high accuracy for a broad chemical space. Otherwise, where a force field is not able to describe well certain chemical species, the use of more sophisticated theories, such as quantum mechanics, is needed. It is noteworthy that the prediction of molecular properties, where the electron effects are predominant, such as transition state, the formation or breaking of a bond, and spectroscopic parameters, cannot be afforded by molecular mechanics. The quantum mechanics explicitly model the electron system of a molecule, and thus it can be used to study chemical issues.

The geometry optimization is a crucial step to study chemical problems, such as transition state, or to predict spectroscopic properties, such as NMR parameters, IR, and so on. In our case, the aim is to predict chemical shifts or coupling constants for the relative configuration assignment of organic compounds [1, 2, 31]. Moreover, the treatment of the investigated structure by quantum mechanical theory allows to get more accurate energy values for each considered conformers. These energy values are useful to calculate the Boltzmann distribution, which is a function of the energy (Eq. 10.11, see below). Taking into account the Boltzmann distribution is important to forecast molecular properties of flexible chemical systems because the predicted values result from the energy-weighted contribution of each conformer in solution.

Following the general protocol, the conformers' geometry obtained and optimized by using molecular mechanics force fields should be refined through semiempirical methods [32] before the application of quantum theory. The semiempirical methods differ from molecular mechanics because their theory combines the Schrödinger equation and some experimental derived parameters to simplify the computation. The most popular methods applied to organic compounds are AM1 [8] and PM3 [9]. The semiempirical methods present the advantage of being faster than quantum chemical methods, but it is not always that they can correctly predict a molecular property. This is due to the fact that the experimental derived parameters are not representative of all chemical systems. Compared to the quantum mechanical calculation of NMR parameters, the geometry optimization is more time-consuming. Thus, the aim to run a geometry optimization by semiempirical methods is to speed up the following computation at more time-consuming quantum mechanical theory level. Nowadays, thanks to the development of more potent computers this step is not necessary. Indeed, also by a desktop computer, it is possible to optimize the geometry with a modest theoretical level in a reasonable time.

The quantum mechanics is not based on classical mechanics laws and on the use of experimental parameters; indeed, the molecular properties are calculated by solving the Schrödinger equation:

$$\hat{H}\Psi = \hat{H}E \quad (10.5)$$

where \hat{H} is the Hamiltonian operator, Ψ is the wave function, and E is the energy. The wave function Ψ is a mathematical function of the electron and nuclear positions, and it represents a probabilistic description of electron behavior. In details, it can describe the probability of electrons being in certain locations, but it cannot predict exactly where electrons are located. As the quantum mechanics can describe mathematically the correct behavior of the electrons, it is possible to predict chemical properties of molecular systems, by applying relative mathematical operator corresponding to a particular chemical physical observable. For example, in Eq. 10.5, the Hamiltonian operator allows to calculate the energy of the electron, whereas the application of the spin-Hamiltonian can predict NMR parameters. (In order to obtain a physically relevant solution of the Schrödinger equation, the wave function must be continuous, single-valued, normalizable, and antisymmetric with respect to the interchange of electrons.

The Hamiltonian operator \hat{H} is, in general,

$$\hat{H} = - \sum_i^{\text{particles}} \frac{\nabla_i^2}{2m_i} + \sum_{i < j}^{\text{particles}} \sum \frac{q_i q_j}{r_{ij}} \quad (10.6)$$

where ∇_i^2 is the Laplacian operator acting on particle i . Particles indicate electrons and nuclei. The symbols m_i and q_i are the mass and charge of particle i , and r_{ij} is the distance between particles. The first term represents the kinetic energy of the particle, and the second term is the energy due to Coulomb interactions of particles. This formulation is the time-independent, nonrelativistic Schrödinger equation. Additional terms can appear in the Hamiltonian when relativity or interactions with electromagnetic radiation or fields are taken into account.)

Only in few simple cases the Schrödinger equation can be exactly solved, such as particle in the box, harmonic oscillator. The solution of this fundamental equation requires the use of mathematical approximations, and different quantum theories have been developed to this aim. The starting point of all quantum mechanical methods is the Born–Oppenheimer approximation (Eq. 10.6). This approximation treats the electrons and nuclei motions as separated and considers the nuclei fixed, thus neglecting the kinetic contribution of the nuclei.

$$\hat{H} = - \sum_i^{\text{electrons}} \frac{\nabla_i^2}{2} - \sum_i^{\text{nuclei}} \sum_j^{\text{electrons}} \frac{Z_i}{r_{ij}} + \sum_{i > j}^{\text{electrons}} \sum \frac{1}{r_{ij}} \quad (10.7)$$

Here, the first term is the kinetic energy of the electrons only, the second one is the attraction of electrons to nuclei, and the third term is the repulsion between electrons called correlation. The repulsion between nuclei is added onto the energy at the end of the calculation. The motion of nuclei can be described by considering this entire formulation to be a potential energy surface on which nuclei move.

One of the most applied theories is the Hartree–Fock (HF) [32], which is based on the central field approximation. It considers the Coulomb repulsion between two electrons by integrating the repulsion term. This approximation does not give

the exact effect of the electrons repulsion (correlation) but only an average of this repulsive interaction, and it represents an important limitation of HF application. This effect is important because including correlation generally improves the accuracy of computed energies and molecular geometries, as well as NMR parameters [1, 2, 31]. The wave function results from a linear combination of atomic orbitals, which are described by a set of functions called basis set.

One of the most used post-HF methods is the Møller–Plesset [33], which accounts the correlation by adding to the Hartree–Fock wave function the perturbation term. Different Møller–Plesset methods have been developed and the mostly used is the second order (MP2) [34]. Compared to HF theory, the Møller–Plesset methods are more accurate but very computationally expensive; thus, their application is limited to small molecular systems.

In the last years, the density functional theory (DFT) [35, 36] has been gaining a great success due to the lower demanding computational costs but with results accuracy similar to the post-HF methods, such as Møller–Plesset. DFT considers that the energy of a molecule can be determined from the electron density instead of the wave function. The electron density is expressed as a linear combination of basis functions similar in mathematical form to HF orbitals. In particular, a determinant is then formed from these functions, obtaining the Kohn–Sham orbitals. From the electron density of these orbitals, the energy is calculated applying a density functional. Different functionals [37, 38] have been developed, and between them, the most used is B3LYP in the geometry optimization of investigated compounds. The MPW1PW91 [35, 36] has shown to produce adequate structural geometry, and many application of this functional are reported in literature [1, 2, 31]. Recently, new promising functionals have been introduced: M05 [39] and M05-2X [40, 41]. The DFT takes into account the electron correlation, giving better results than the HF-based methods [1, 2, 31].

It is noteworthy that independently from the QM theory applied, the choice of the basis set is important in the prediction of the molecular properties. The basis set should be large enough, for example, to take into account the electron correlation effects or to describe the molecular charge distribution. At the same time, the basis set should be small enough to be applied to the investigated molecule, especially for larger chemical systems. In our contribution, where different methods have been compared in the prediction of chemical shift of organic compounds, we observed that the 6–31 G with DFT is the right trade-off between accuracy and rapidity of calculation [31].

Different softwares dedicated to the quantum mechanical (QM) calculation of molecular properties are available: Gaussian [42], HyperChem [43], Jaguar [44], and Spartan [21]. These softwares allow the application of different theoretical methods to carry out the forecast of different molecular properties.

Let us continue with the case study of the determination of the relative configuration of bonannione B (**1**), to show the application of QM approach for geometry refinement and the prediction of ^{13}C NMR chemical shift (Sect. 10.2.4). From the conformational search, three main conformers are found for two considered stereoisomeric hypothesis, and all of them have to be treated by the software

Gaussian 03 [45]. For all six staggered rotamers, six input files are prepared. Each file contains the coordinates derived from molecular mechanics level and the instruction for the optimization of the geometry.

In this case, the geometry refinement is performed by applying the DFT theory, the B3LYP as functional, and 6–31 G(d) basis set. After the calculation, a new geometry for each staggered rotamer of **1a** and **1b** is obtained, and it is used for the calculation of the chemical shifts (Sect. 10.2.4). Besides the new spatial arrangements of the conformers, associated energy values are achieved by the computation. This value is expressed in Hartree, and it can be converted in kJ: one Hartree is 2625.5 kJ mol⁻¹.

10.2.4 ¹³C NMR Chemical Shifts Calculation

The nuclear magnetic resonance (NMR) has been playing a crucial role in solving molecular structural aspects thanks to the ability of some NMR parameters (coupling constant, chemical shift) to provide fundamental information on the configurational and conformational arrangement of organic molecules. The configuration of cyclic compounds with three- to six-membered rings, and of compounds with predictable conformational behavior, can be easily determined by analyzing NMR parameters, such as proton–proton *J* coupling values, chemical shifts, and/or nuclear Overhauser effect intensities. The relative configurational assignment of flexible systems, such as polysubstituted open chains and macrocycles, is more difficult to study, due to geometrical uncertainty associated with these types of molecules.

In the last years, great advances have been made in developing quantum mechanical (QM) methods of chemical interest able to predict molecular properties [1, 2, 32]. In particular, quantum mechanical calculation of NMR parameters has been used as an emerging strategy for the assignment of the relative configuration of flexible organic molecules on the basis of the high accuracy in the reproduction of the experimental NMR properties also achieved at a low level of theory [1, 2, 31, 46].

The final step of the protocol described in this chapter is the calculation of an NMR parameter: ¹H, ¹³C, ^{2,3}*J*_{H-H}, and ^{2,3}*J*_{C-H}.

Different approaches have been devised to calculate the chemical shift, such as IGLO [47], LORG [48], and CSGT [49], but the most popular is GIAO (gauge including atomic orbital) [50, 51], which is based on the perturbation theory, resulting suitable for HF or DFT theories. In particular, GIAO has shown to provide more reliable results compared with other methods at the same basis set [1, 2, 31, 32, 50, 51]. The electron correlation effect is not negligible in the chemical shift calculation, especially for ¹³C; in fact, DFT or MP theories have shown to give more accurate results than HF approach [31, 52]. In this field, DFT is successfully emerging due to its accuracy in NMR properties prediction and its ability to handle large molecular systems not easily treatable by post-HF methods [1, 2, 52]. For this reason, DFT is widely used in the calculation of NMR parameters

[1, 2]. The most popular functionals applied in the calculations of NMR parameters are B3LYP, MPW1PW91, and PBE1PBE [53, 54].

It is also important that sufficiently large basis sets are used [31]. Of course, the choice of the basis set to use is based on the accuracy and on the size of the molecule under study. The 6-31 G (d) basis set should be considered the absolute minimum for reliable results, but better outcomes are obtained by using 6-31 G(d,p) [31]. The choice of the basis set, thus, depends both on the accuracy and on the size of the molecule and also on the number of the chemical species to take into account.

Continuing with the reported case study, all conformers for both the diastereoisomers under investigation have been optimized by using DFT/B3LYP approach. The new coordinates, derived by quantum mechanical optimization, are now used to calculate the ^{13}C chemical shifts by GIAO method. Thus, six input files are set up, indicating the instruction for the chemical shift calculation. The theory level to apply is the same of that one used in the geometry optimization (DFT/B3LYP), but the basis set is 6-31 G(d,p).

In particular, the quantum mechanical methods calculate the shielding tensor and not directly the chemical shift. One of the mostly used methods to obtain the chemical shift is to subtract the isotropic shielding value of TMS from the shielding tensor of the conformer. This can be easily done by collecting the data in a spreadsheet and subtracting the isotropic shielding tensors of the conformer and TMS in absolute value. Of course, the shielding tensor of TMS has to be calculated at the chosen theoretical level for the investigated compound. We observed for sp^3 carbons referenced to TMS a good fitting between experimental and calculated, whereas for the sp^2 carbons, this agreement is lower [31]. For this reason, the sp^2 carbons could not be considered in the comparison with the experimental chemical shifts. Recently, the multi-standard approach (MSTD) has been reported [55] which is demonstrated to perform better than the application of TMS as reference compound. The MSTD consists on the use of two different reference compounds and calculates the chemical shift through the following equation:

$$\delta_{\text{calc}}^i = \sigma_{\text{ref}} + \sigma_i + \delta_{\text{exp}}^{\text{ref}} \quad (10.8)$$

where σ_{ref} and σ_i are the shielding tensors of atom i and the reference compound, respectively, and the $\delta_{\text{exp}}^{\text{ref}}$ is the experimental value of the reference. In particular, the calculation of sp^3 carbon atoms is referenced to methanol, whereas the chemical shifts of sp^2 and sp carbon are calculated from benzene.

Another method is based on linear regression analysis. In particular, calculated chemical shift of a collection of organic compounds is plotted against their experimental values. The intercept and the slope of the obtained straight line can be used to scale the calculated values:

$$\delta_{\text{scaled}} = \frac{\delta_{\text{calc}} - \text{intercept}}{\text{slope}} \quad (10.9)$$

In the reported case study, the chemical shifts are referenced to TMS. It is important to keep in mind that the experimental chemical shift is a weighted value from the contribution of conformers in equilibrium among them:

$$\delta_{\text{exp}} = \delta_i p_i + \delta_j p_j + \dots \quad (10.10)$$

where p_i is the population fraction of N_i molecules in a determined conformation and δ_i the associated chemical shift. The same is for the number of molecules j and all other conformers in solution. The number of molecules in a specific three-dimensional arrangement depends on the energy of that conformation. The ratio of the number of conformers N_i with energy E_i , to the number of molecules in state j is given by the Boltzmann distribution:

$$\frac{N_i}{N_j} = e^{-(E_i - E_j)/k_B T} \quad (10.11)$$

where k_B is the Boltzmann constant (1.38066×10^{-23} J/K) and T the temperature. Following the Eq. 10.11, two conformers differing for 3 kcal/mol (≈ 10 kJ/mol) in energy present a ratio of 99:1. Thus, each conformation differing from the global minimum by \geq of 3 kcal/mol does not effectively contribute to the averaged chemical shift and can be neglected in the calculation. From the computed energy values for each conformer at quantum theory level, it is possible to calculate the population fractions contributing to the weighted chemical shift, by using the following equation:

$$\delta = \sum_i \left[\delta_i \exp(-E_i/RT) / \sum_i \exp(-E_i/RT) \right] \quad (10.12)$$

where δ_i is the chemical shift of conformer i , R is the molar gas constant (8.3145 J K^{-1} mol^{-1}), T is the temperature (298 K), and E_i is the calculated energy of conformer i relative to the energy of the global minimum.

In the output file, along with isotropic shielding tensors, an energy value at the basis set 6-31 G(d,p) is obtained and is taken into account in the Boltzmann distribution calculation.

From the calculated energies, it is obtained for isomer **1a** that the *anti* and g^+ conformers represent 70% and 28% of the total population, respectively, due to the hydrogen bond between the OH group and the oxygen atom of the ring for both these rotamers. The remaining 2% is attributed to the g^- conformer. A similar trend of the energies and the population distribution is observed for **1b**, where the *anti* rotamer accounts for 71% and the g^+ rotamer for 28%, and 1% is represented by the rotamer g^- (Table 10.1)

The calculated chemical shifts, according to the Boltzmann distribution, are compared with the experimental ones in order to find which of the two considered diastereoisomers (**1a** and **1b**) presents the best fitting with the experimental set of

Table 10.1 Comparison of calculated for stereoisomers **1a** and **1b** vs. experimental ^{13}C NMR chemical shifts in CDCl_3

Carbons	1a	1b	Experimental
2	81.4	81.5	79.0
3	46.2	46.1	42.7
4	187.5	187.5	196.3
5	155.4	155.4	158.3
6	103.2	103.2	105.8
7	161.7	161.7	169.5
8	86.3	86.4	90.5
9	158.4	158.4	163.6
10	101.9	101.9	103.1
1'	127.2	127.2	129.6
2'	122.4	122.5	127.6
3'	107.4	107.4	115.8
4'	150.5	150.5	156.8
5'	111.0	110.9	115.8
6'	123.2	123.3	127.6
1''	29.1	29.5	25.9
2''	94.0	94.0	91.3
3''	73.9	73.9	73.8
4''	23.1	19.7	22.4
5''	37.3	40.6	36.6
6''	24.8	25.0	21.8
7''	122.1	122.5	123.7
8''	128.7	128.0	132.0
9''	26.5	26.4	25.4
10''	17.5	17.6	17.5

resonances. The comparison is made, calculating the difference between the predicted and experimental values (Table 10.1). Other parameters could be taken into consideration to understand which hypothesized structure best reproduce the experimental. The mean absolute error is a statistical parameter obtained from the following equation:

$$\text{MAE} = \sum [|(\delta_{\text{exp}} - \delta_{\text{calcd}})|] / n \quad (10.13)$$

where δ_{exp} – δ_{calcd} are respectively the experimental and calculated chemical shifts, and n is the total number of considered resonances. A variant of the MAE is the corrected mean absolute error (CMAE), where the calculated values are scaled with the experimental chemical shifts. In detail, the predicted set of resonances are plotted in function of the experimental values, and the intercept and the slope obtained by linear regression are used to correct the forecast chemical shifts, by using Eq. 10.9. From the scaled values, the MAE is calculated obtaining the CMAE.

$$\text{CMAE} = \sum [|(\delta_{\text{exp}} - \delta_{\text{scaled}})|] / n \quad (10.14)$$

The correlation coefficient, r , is also used as parameter to compare calculated and experimental chemical shifts. Recently, Smith and Goodman have introduced the DP4 probability which performs better than the mean absolute error and correlation coefficient [56].

It is possible to observe that the resonances of almost all carbon atoms for both diastereoisomers (**1a** and **1b**) are very similar to the experimental chemical shift, differing by a maximum of 0.2 ppm. Large differences are found around the couple of stereocenters under study, in particular, for the C-4'' and C-5'', which are bound to C-3'' (Table 10.1). The predicted values of C-4'' are 23.1 ppm and 19.7 ppm for **1a** and **1b**, respectively. Concerning the C-5'', the **1a** resonance is predicted at $\delta = 37.3$ ppm and at $\delta = 40.6$ ppm for **1b** (Table 10.1). Isomer **1a** shows a variation from the experimental of 0.7 ppm for C-4'' and C-5'', whereas for **1b** larger $\Delta\delta$ values are found: 2.7 ppm and 4.0 ppm for C-4'' and C-5'', respectively. It is noteworthy that the obtained discrepancies reflect the different magnetic environment of the methyl group in the 4''-position and the methylene group in the 5''-position in **1a** and **1b** due to the different configuration of C-3''. Thus, the ^{13}C chemical shift calculation is a useful tool to probe the different 3D spatial arrangement of stereogenic carbon substituents, suggesting the correct relative configuration of the investigated compound. The relative configuration of bonannione B can be assigned as **1a**.

10.2.5 J Coupling Constants Calculation

In the previous section, it has been shown that ^{13}C NMR chemical shifts have been predicted by quantum mechanics method to assign the relative configuration of the compound under study. The chemical shift is not the only NMR parameter that can be calculated by QM approach and used in the stereostructure analysis. Homo and heteronuclear coupling constants can be predicted, and they could be integrated with experimental values to shed light on the relative configuration. The relative configuration assignment of the natural product callipeltin A (**2**, Fig. 10.9), isolated from the sponges *Callipelta* sp. and *Latrunculia* sp. [57], is reported here as an example. In particular, the compound is a peptide (Fig. 10.9) constituted by nine amino acids, but only the following portion has been determined by QM- J method: the two units (named AGDHE_{2,3} and AGDHE_{3,4}) contained in the AGDHE fragment, the two threonine residues (named D- α Thr1 and D- α Thr2), and the β -OMeTyr amino acid.

Behind the use of J coupling constants to assign the relative configuration, through this case study, it is shown how to afford the analysis of large molecule presenting more than one couple of stereocenters. In detail, the strategy consists in dividing the entire molecule in small C_2 fragments, following a rational building: at least two heavy groups (carbon, oxygen atoms) substitute the main chain, and every branched chain is replaced by at least one heavy atom [58]. For each C_2 fragment,

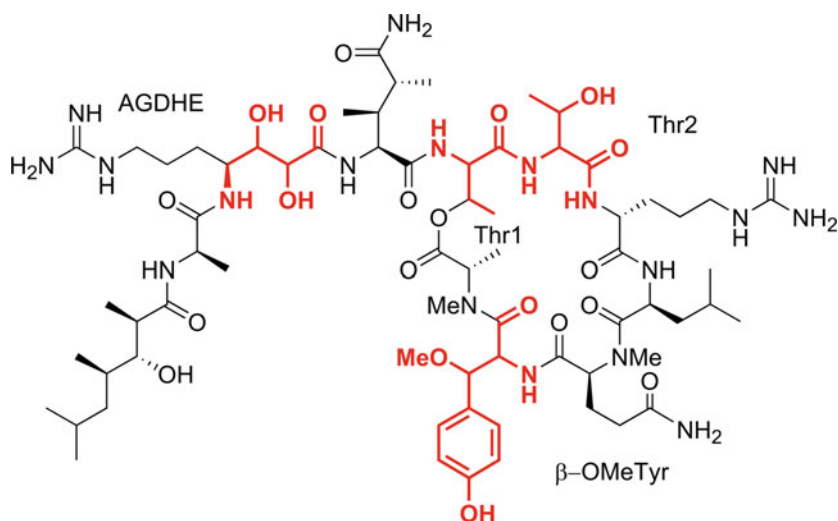


Fig. 10.9 Callipeltin A (**2**) with amino acid residues still stereochemically undetermined represented in red

the *erythro* and *threo* configuration are considered, and for each diastereoisomer, three main staggered rotamers are built (*anti*, g^+ and g^-) (Fig. 10.10).

As the analysis is based on simple molecular fragments derived from the whole molecule, directly the main three staggered rotamers are built and considered in the calculations. The basic idea to simplify the entire structure with more than one couple of stereocenters is to limit the number of conformers to analyze at the quantum mechanical level. Indeed, the number of combinations of all staggered conformers from C_2 arrangements is $N_r = 6^n$, where n is the number of pairs of stereocenters [58]. The simplification is possible because local atomic environment mainly affects the coupling constants. Usually, further than two atoms away from the nuclei involved in the scalar coupling, the effects are negligible [58].

Let us apply this strategy to the callipeltin A. The following C_2 fragments are built and investigated (Fig. 10.11):

For sake of simplicity, only the analysis of D-aThr1 fragment is described, but the approach is repeated for all the investigated simplified systems. The *anti* and two *gauche* rotamers are built for *erythro* and *threo*, and the geometry optimization is performed at DFT theory level by using the functional MPW1PW91 and the basis set 6-31 G(d). The calculations are performed by taking into account the contributions of the following interactions: Fermi contact (FC), paramagnetic spin-orbit (PSO), diamagnetic spin-orbit (DSO), and spin-dipole (SD). As made for the bonannione B (see previous section), on the optimized geometry at quantum mechanics level, the calculation of the NMR parameter is performed. In this case, the prediction concerns the $^{2,3}J_{C-H}$ and $^{2,3}J_{H-H}$ through the same functional of the optimization step (MPW1PW91) and by the 6-31 G(d,p) basis set. Both the quantum mechanical calculation steps (optimization and NMR property prediction)

Fig. 10.10 Main staggered rotamers (*anti*, g^+ , and g^-) for each relative stereochemical arrangement *erythro* and *threo*

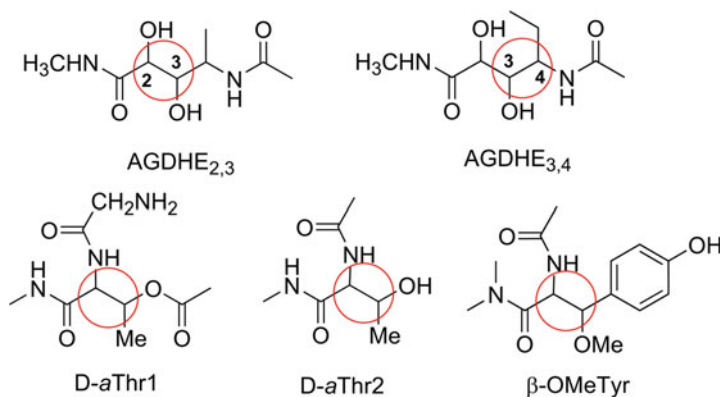
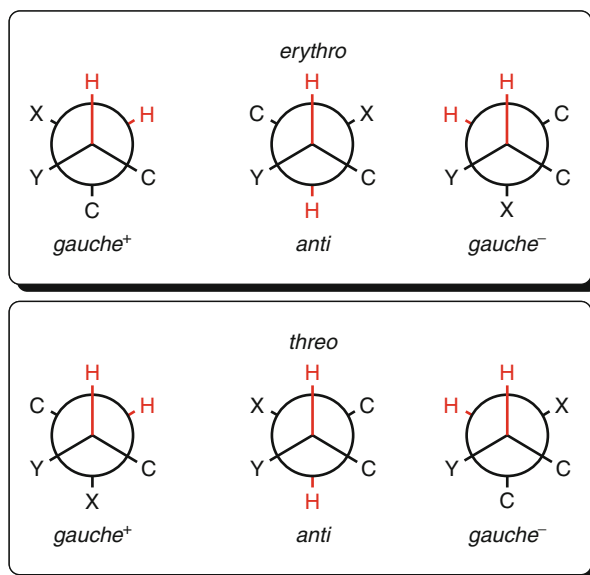


Fig. 10.11 Molecular structures of C_2 fragments from callipeltin A, considered in the QM calculations. The couples of the investigated stereocenters are indicated by red circles

are made by using the IEF-PCM solvent continuum model, to mimic the presence of the methanol. The choice to use the solvent is due to the presence of hydrogen donors and acceptors, which influence the conformational arrangement in absence of the solvent and could cause misleading information for the assignment of relative configuration.

The set of calculated coupling constants for all staggered rotamers of *erythro* and *threo* is compared with the experimental one (Table 10.2). The comparison is made through the total absolute deviation (TAD) values: $\sum |J_{\text{calc}} - J_{\text{expl}}|$. The conformer

Table 10.2 Calculated J values for the six conformational arrangements belonging to *erythro* and *threo* series of C₂ fragments from callipeltin A, in comparison with the experimental data: single deviations and TAD ($\Sigma|J_{\text{calc}} - J_{\text{exp}}|$) values are reported

	Calc						Exp
	<i>Erythro</i>			<i>Threo</i>			
	g^+	<i>Anti</i>	g^-	g^+	<i>Anti</i>	g^-	
D-aThr1							
$^3J_{\text{H2-H3}}$	3.7	8.6	2.6	4.5	9.2	1.3	2.8
$^2J_{\text{H2-C3}}$	0.9	−4.4	−4.9	−4.5	−4.2	0.6	−5.7
$^3J_{\text{H2-Me}}$	0.7	2.3	4.0	0.3	2.7	1.9	5.0
$^2J_{\text{H3-C2}}$	−1.4	−2.2	0.3	−0.6	−1.8	0.6	−1.4
$^3J_{\text{H3-C=O}}$	7.2	2.4	1.4	7.4	1.0	2.1	2.0
TAD	17.0	11.0	4.3	13.8	11.6	13.0	
AGDHE_{2,3}							
$^3J_{\text{H2-H3}}$	4.6	8.0	3.2	1.8	5.9	6.6	9.0
$^2J_{\text{H2-C3}}$	−3.0	−3.7	−0.3	2.2	−2.7	−3.0	−4.0
$^3J_{\text{H2-C4}}$	6.7	2.3	0.3	0.4	4.6	5.3	2.6
$^2J_{\text{H3-C2}}$	1.9	−0.8	−1.3	3.8	0.3	−2.4	−3.5
$^3J_{\text{H3-C=O}}$	0.1	1.8	6.6	0.2	4.0	7.1	1.2
TAD	16.0	4.9	19.4	23.9	13	13.1	
AGDHE_{3,4}							
$^3J_{\text{H3-H4}}$	3.3	8.7	3.1	4.0	5.0	0.9	1.7
$^3J_{\text{H3-C5}}$	0.4	1.5	4.9	3.8	0.0	2.6	1.7
$^2J_{\text{H4-C3}}$	−4.3	−4.4	0.5	−3.9	−5.3	0.7	1.2
$^3J_{\text{H4-C2}}$	6.2	4.0	0.6	5.9	0.1	2.5	1.2
TAD	13.4	15.6	5.9	14.2	12.6	3.5	
D-aThr2							
$^3J_{\text{H2-H3}}$	3.7	8.6	2.8	4.6	7.7	1.7	3.5
$^2J_{\text{H2-C3}}$	−0.4	−4.9	−4.9	−4.2	−3.6	−1.5	−4.1
$^3J_{\text{H2-Me}}$	0.5	1.9	4.1	4.3	4.4	1.6	1.1
$^2J_{\text{H3-C2}}$	−1.6	−0.3	2.4	−1.2	1.1	0.9	−2.8
$^3J_{\text{H3-C=O}}$	7.3	3.2	0.7	7.0	1.5	2.0	7.3
TAD	5.7	13.2	16.2	6.2	17.6	13.8	
β-OMeTyr							
$^3J_{\text{H2-H3}}$	1.5	8.7	3.9	8.3	10.7	3.7	9.1
$^2J_{\text{H2-C3}}$	−5.4	−3.2	0.0	−3.4	−4.3	−3.4	−3.9
$^3J_{\text{H2-Ph}}$	3.8	2.5	0.7	5.6	1.8	1.1	1.3
$^2J_{\text{H3-C2}}$	−0.8	−2.6	−2.7	−1.2	−2.3	0.4	−3.2
$^3J_{\text{H3-C=O}}$	1.4	2.0	6.4	6.6	1.6	1.5	1.7
TAD	14.3	3.2	14.9	12.5	3.5	9.1	

showing the lowest difference with the experimental values represents the right relative configuration. Concerning the D-aThr1 residue, the lowest sum of absolute errors (4.3 Hz) is observed for g^- *erythro* arrangement, whereas the TAD for all other conformers ranges between 11 and 17 Hz (Table 10.2).

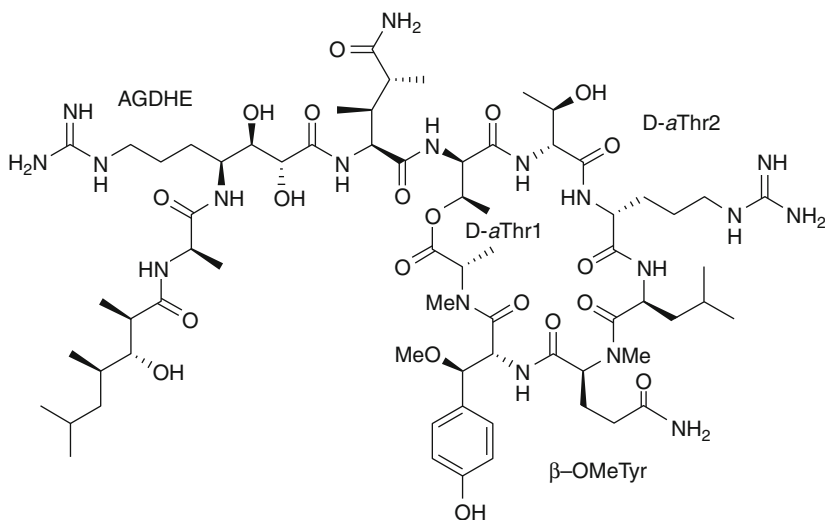


Fig. 10.12 Molecular structure of callipeltin A, with all residues stereostructurally determined

The same analysis is made for the other considered C_2 fragments. In particular, for the residue AGDHE_{3,4}, the best agreement between calculated and experimental is found for the g^- *threo* arrangement, characterized by a total deviation of only 3.5 Hz (compared to TAD values of 5.9–15.6 Hz for the reminder conformers). Also, for the AGDHE_{2,3} fragment, the *anti erythro* model displays the lowest TAD value of 4.9 Hz, much below the other deviations (13.0–23.9 Hz). The analysis of D-aThr2 and β-OMeTyr residues is more complicated because two possible conformers present similar TAD values. For the D-aThr2, the g^+ of *erythro* presents a deviation of 5.7 vs. 6.2 Hz of g^+ of *threo*. For the β-OMeTyr residue, the *anti* arrangements of *erythro* and *threo* show comparable TAD values: 3.2 and 3.5 Hz, respectively. Thus, for these residues, the investigation is integrated by an analysis of ROESY spectra, which confirms the QM-based results. In details, a strong ROE effect between the H-2 proton and the methyl group confirms the g^+ *erythro* arrangement for the D-aThr2. This observation is also consistent with the small $^3J_{H-2,Me}$ value and, consequently, with a *gauche* relationship between these groups. Concerning the β-OMeTyr residue, the observed ROE cross-peak between the aromatic and amide protons suggests the *erythro* configuration as representative arrangement. By using the presented strategy, the fully stereostructural determination of callipeltin A has been carried out (Fig. 10.12).

10.2.6 Solvent Effects

Many of the organic compounds are soluble in nonpolar solvents, and the prediction of NMR parameters can be fairly well conducted in vacuum [1–4, 31, 41]. However, NMR parameters are very sensitive to the surrounding environment. Thus, solvents

are not negligible in the calculations, especially for the polar ones [59]. The solvation affects the solute geometry and the electronic structure, which along with solute–solvent interactions induces variation in the NMR properties [60–62].

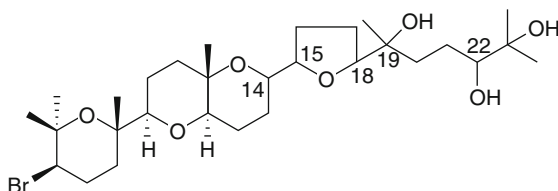
In general, the methods to model the solvent fall in two main categories: the implicit and explicit solvent models. The first model represents the solvent as continuous medium with a uniform dielectric constant, surrounding the solute molecular cavity. The most commonly used methods are the polarized continuum model (PCM) [63], the conductor-like screening model (COSMO) [64], and the generalized born surface area (GBSA) [65]. The explicit model treats the solvent molecules as discrete entities, and it is mostly applied in molecular dynamics. Both methods present advantages and shortcomings, but they could improve the prediction of NMR parameters where solvent effects are not negligible. As reported in literature [60–62], the solvent effects limited to conformational changes of the investigated chemical system are well described by using continuum models. Where the solute–solvent interactions play a crucial role, the use of explicit solvent molecules give better predictions. One strategy to model the discrete solvent molecules around the solute is to run molecular dynamics or Monte Carlo simulations, in order to obtain different configurations of the investigated compound and the surrounding solvent molecules. On the obtained arrangements, the NMR calculation at quantum mechanical levels is performed. However, it is not trivial to model the orientation and the number of solvent molecules around solute counterparts and not always perform well in prediction of NMR properties. This method, based on molecular mechanics to model compound embedded by the solvent, is not feasible for the configurational assignment due to the large number of chemical systems to treat at quantum mechanical level. To date, there is not a well-defined strategy to account the effects of the solute–solvent interactions in the stereostructural studies.

10.3 Conclusions

The protocol described in this chapter shows how the calculation of NMR parameters at the QM theoretical level is a useful tool for conformational and configurational analysis of natural products. The great success of QM prediction of molecular properties is due to its ability to reproduce the experimental data at affordable computational expense.

In particular, two case studies have been reported regarding the determination of the relative configuration of two natural products: bonannione B isolated from *Bonannia graeca*, and callipeltin A isolated from the sponges *Callipelta* sp. and *Latrunculia* sp. With these two examples, we respectively show the use of ^{13}C , $^2,3J_{\text{H-H}}$, and $^2,3J_{\text{C-H}}$ values calculation as a tool for the determination of the relative configuration of organic molecules. It is noteworthy that both calculated NMR properties at QM theory level can be combined for the stereostructural investigation depending on the organic compound under examination. Moreover, besides the use of QM calculation of NMR parameters in the conformational and

Fig. 10.13 Molecular structure of aplysiol B



configuration analysis, the fast and convenient quantum chemical approach can be applied to lead the total synthesis of complex natural compounds toward the correct stereoisomers, saving time and resources.

It should be highlighted that QM methods have been shown to accurately reproduce experimental molecular properties in vacuum, especially in cases where non-polar solvents are used for acquiring the experimental spectra. On the other hand, solvent effects limited to conformational changes of the solute can be taken into account by continuum solvent models; in cases where the solute–solvent interactions have a significant weight, an explicit solvent treatment should be applied.

10.4 Study Questions

1. What are the molecular features to be considered in the choice of the force field for the conformational search?
2. Why are quantum mechanical methods required to study chemical problems, such as transition state, or to predict spectroscopic properties?
3. Why DFT or MP may be more accurate than HF in the prediction of NMR parameters?
4. In which cases is DFT approach preferred to MP methods?
5. Try to establish a protocol to determine the relative configuration of the stereocenters C-14, C-15, C-18, C-19, and C-22 of aplysiol B isolated from *Aplysia dactylomela* [66] (Fig. 10.13).
6. What are the main features of implicit and explicit solvent models?
7. What are the criteria to select the appropriate solvent model?
8. Why is it important to get an accurate energy value for each conformer?
9. What is a basis set?

References

1. Di Micco S, Chini MG, Riccio R, Bifulco G (2010) Quantum mechanical calculation of NMR parameters in the stereostructural determination of natural products. *Eur J Org Chem* 8:1411–1434. doi:10.1002/ejoc.200901255
2. Bifulco G, Dambruoso P, Gomez-Paloma L, Riccio R (2007) Determination of relative configuration in organic compounds by NMR spectroscopy and computational methods. *Chem Rev* 107:3744–3779. doi:10.1021/cr030733c
3. Barone G, Gomez-Paloma L, Duca D, Silvestri A, Riccio R, Bifulco G (2002) Structure validation of natural products by quantum-mechanical GIAO calculations of ^{13}C NMR

- chemical shifts. *Chem Eur J* 8:3233–3239. doi:10.1002/1521-3765(20020715)8:14 < 3233::AID-CHEM3233 > 3.0.CO;2-0/abstract/
4. Barone G, Duca D, Silvestri A, Gomez-Paloma L, Riccio R, Bifulco G (2002) Determination of the relative stereochemistry of flexible organic compounds by ab initio methods: conformational analysis and Boltzmann-averaged GIAO ^{13}C NMR chemical shifts. *Chem Eur J* 8:3240–3245. doi:10.1002/1521-3765(20020715)8:14 < 3240::AID-CHEM3240 > 3.0.CO;2-G/abstract
 5. van Gunsteren WF, Berendsen HJC (1990) Computer simulation of molecular dynamics: methodology, applications, and perspectives in chemistry. *Angew Chem Int Ed* 29:992–1023. doi:10.1002/anie.199009921
 6. Höltje HD, Sippl W, Folkers G (2003) Molecular modeling basic principles and applications. Wiley-VCH, Weinheim
 7. Chang G, Guida WC, Still WC (1989) An internal-coordinate Monte Carlo method for searching conformational space. *J Am Chem Soc* 111:4379–4386. doi:10.1021/ja00194a035
 8. Dewar MJS, Zoebisch EG, Healy EF, Stewart JJP (1985) Development and use of quantum mechanical molecular models. 76. AM1: a new general purpose quantum mechanical molecular model. *J Am Chem Soc* 107:3902–3909. doi:10.1021/ja00299a024
 9. Stewart JJP (1989) Optimization of parameters for semiempirical methods I. Method. *J Comput Chem* 10:209–220. doi:10.1002/jcc.540100208
 10. Rosselli S, Bruno M, Maggio A, Bellone G, Formisano C, Mattia CA, Di Micco S, Bifulco G (2007) Two new Flavonoids from *Bonannia graeca*: a DFT-NMR combined approach in solving structures. *Eur J Org Chem* 15:2504–2510. doi:10.1002/ejoc.200600969
 11. Dale JA, Mosher HS (1973) Nuclear magnetic resonance enantiomer reagents. Configurational correlations via nuclear magnetic resonance chemical shifts of diastereomeric mandelate, O-methylmandelate, and α -methoxy- α -(trifluoromethyl)phenylacetate (MTPA) esters. *J Am Chem Soc* 95:512–519. doi:10.1021/ja00783a034
 12. (a) Protein Data Bank (PDB) See <http://www.rcsb.org/pdb/home/home.do>; (b) Nucleic Acid Databank (NDB) See <http://ndbserver.rutgers.edu/>; (c) Cambridge Structural Database (CSD) See <http://www.ccdc.cam.ac.uk/products/csd/>; (d) Crystallography Open Database (COD) See <http://www.crystallography.net/>. Accessed 04 Nov 2011
 13. http://www.acdlabs.com/products/draw_nom/draw/chemsketch/. Accessed 04 Nov 2011
 14. MDL Information Systems, Inc. (MDL ISISTM) <http://mdl-isis-draw.software.informer.com/>. Accessed 04 Nov 2011
 15. <http://www.cambridgesoft.com/software/ChemDraw/>. Accessed 04 Nov 2011
 16. Discover molecular modeling software (1993) Biosym Technologies Inc., San Diego, CA
 17. Insight INSIGHT II molecular modeling package (2000) Accelrys, San Diego, CA
 18. <http://accelrys.com/>. Accessed 04 Nov 2011
 19. Van Der Spoel D, Lindahl E, Hess B, Groenhof G, Mark AE, Berendsen HJC (2005) GROMACS: fast, flexible, and free. *J Comput Chem* 26:1701–1718. doi:10.1002/jcc.20291
 20. <http://www.gromacs.org/>. Accessed 04 Nov 2011
 21. Wavefunction, Inc., Irvine. <http://www.wavefun.com/products/spartan.html>. Accessed 04 Nov 2011
 22. Mohamadi F, Richard NGJ, Guida WC, Liskamp R, Lipton M, Caufield C, Chang G, Hendrickson T, Still WC (1990) MacroModel – an integrated software system for modeling organic and bioorganic molecules using molecular mechanics. *J Comput Chem* 11:440–467. doi:10.1002/jcc.540110405
 23. Allinger NL (1977) Conformational analysis. 130. MM2. A hydrocarbon force field utilizing V_1 and V_2 torsional terms. *J Am Chem Soc* 99:8127–8134. doi:10.1021/ja00467a001
 24. Allinger NL, Yuh YH, Lii JH (1989) Molecular mechanics. The MM3 force field for hydrocarbons. 1. *J Am Chem Soc* 111:8551–8566. doi:10.1021/ja00205a001
 25. Weiner SJ, Kollman PA, Case D, Singh UC, Alagona G, Profeta S, Weiner P (1984) A new force field for molecular mechanical simulation of nucleic acids and proteins. *J Am Chem Soc* 106:765–784. doi:10.1021/ja00315a051

26. Weiner SJ, Kollman PA, Nguyen NT, Case DA (1986) An all atom force-field for simulations of proteins and nucleic-acids. *J Comput Chem* 7:230–252. doi:10.1002/jcc.540070216
27. Jorgensen WL, Tirado-Rives J (1988) The OPLS [optimized potentials for liquid simulations] potential functions for proteins, energy minimizations for crystals of cyclic peptides and crambin. *J Am Chem Soc* 110:1657–1666. doi:10.1021/ja00214a001
28. Jorgensen L, Chandrasekhar J, Madura JD, Impey RW, Klein ML (1983) Comparison of simple potential functions for simulating liquid water. *J Chem Phys* 79:926–935. doi:10.1063/1.445869
29. Halgren TA (1999) MMFF VI. MMFF94s option for energy minimization studies. *J Comput Chem* 20:720–729. doi:10.1002/(SICI)1096-987X(199905)20:7<720::AID-JCC7>3.0.CO;2-X/abstract
30. Polak E, Ribiere G (1969) Note sur la convergence de methods de directions conjuguées. *Revue Française Informat Recherche Operationnelle* 16:35–43
31. Cimino P, Gomez-Paloma L, Duca D, Riccio R, Bifulco G (2004) Comparison of different theory models and basis sets in the calculation of ^{13}C NMR chemical shifts of natural products. *Magn Reson Chem* 42:S26–S33. doi:10.1002/mrc.1410
32. Young DC (2001) *Computational chemistry*. Wiley, New York
33. Møller C, Plesset MS (1934) Note on an approximation treatment for many-electron systems. *Phys Rev* 46:618–622. doi:10.1103/PhysRev.46.618
34. Head-Gordon M, Pople JA, Frisch MJ (1988) MP2 energy evaluation by direct methods. *Chem Phys Lett* 153:503–506. doi:10.1016/0009-2614(88)85250-3
35. Hohenberg P, Kohn W (1964) Inhomogeneous electron gas. *Phys Rev B* 136:B864–B871. doi:10.1103/PhysRev.136.B864
36. Kohn W, Sham LJ (1965) Self-consistent equations including exchange and correlation effects. *Phys Rev A* 140:A1133–A1138. doi:10.1103/PhysRev.140.A1133
37. Adamo C, Barone V (1998) Exchange functionals with improved long-range behavior and adiabatic connection methods without adjustable parameters: the mPW and mPW1PW models. *J Chem Phys* 108:664–675. doi:10.1063/1.475428
38. Adamo C, Barone V (1999) Toward reliable density functional methods without adjustable parameters: the PBE0 model. *J Chem Phys* 110:6158–6170. doi:10.1063/1.478522
39. Zhao Y, Schultz NE, Truhlar DG (2005) Exchange-correlation functionals with broad accuracy for metallic and nonmetallic compounds, kinetics, and noncovalent interactions. *J Chem Phys* 123:161103-1–161103-4. doi:10.1063/1.2126975
40. Zhao Y, Schultz NE, Truhlar DG (2006) Design of density functionals by combining the method of constraint satisfaction with parametrization for thermochemistry, thermochemical kinetics, and noncovalent interactions. *J Chem Theory Comput* 2:364–382. doi:10.1021/ct0502763
41. Zhao Y, Truhlar DG (2008) Density functionals with broad applicability in chemistry. *Acc Chem Res* 41:157–167. doi:10.1021/ar700111a
42. www.gaussian.com. Accessed 04 Nov 2011
43. www.hyper.com. Accessed 04 Nov 2011
44. <http://www.schrodinger.com/>. Accessed 04 Nov 2011
45. Frisch MJ, Trucks GW, Schlegel HB, Scuseria GE, Robb MA, Cheeseman JR, Montgomery Jr JA, Vreven T, Kudin KN, Burant JC, Millam JM, Iyengar SS, Tomasi J, Barone V, Mennucci B, Cossi M, Scalmani G, Rega N, Petersson GA, Nakatsuji H, Hada M, Ehara M, Toyota K, Fukuda R, Hasegawa J, Ishida M, Nakajima T, Honda Y, Kitao O, Nakai H, Klene M, Li X, Knox JE, Hratchian HP, Cross JB, Bakken V, Adamo C, Jaramillo J, Gomperts R, Stratmann RE, Yazyev O, Austin AJ, Came R, Pomelli C, Ochterski JW, Ayala PY, Morokuma K, Voth GA, Salvador P, Dannenberg JJ, Zakrzewski VG, Dapprich S, Daniels AD, Strain MC, Farkas O, Malick DK, Rabuck AD, Raghavachari K, Foresman JB, Ortiz JV, Cui Q, Baboul AG, Clifford S, Cioslowski J, Stefanov BB, Liu G, Liashenko A, Piskorz P, Komaromi I, Martin RL, Fox DJ, Keith T, Al-Laham MA, Peng C Y, Nanayakkara A, Challacombe M, Gill PMW, Johnson B, Chen W, Wong MW, Gonzalez C, Pople JA (2004) Gaussian 03, Revision E.01. Gaussian, Inc., Wallingford CT

46. Cheeseman JR, Trucks GW, Keith TA, Frisch MJ (1996) A comparison of models for calculating nuclear magnetic resonance shielding tensors. *J Chem Phys* 104:5497–5509. doi:10.1063/1.471789
47. (a) Kutzelnigg W (1980) Theory of magnetic susceptibilities and NMR chemical shifts in terms of localized quantities. *Isr J Chem* 19:193–200; (b) Schindler M, Kutzelnigg W (1982) Theory of magnetic susceptibilities and NMR chemical shifts in terms of localized quantities. II. Application to some simple molecules. *J Chem Phys* 76:1919–1933. doi:10.1063/1.443165
48. Hansen AE, Bouman TD (1985) Localized orbital/local origin method for calculation and analysis of NMR shieldings. Applications to ^{13}C shielding tensors. *J Chem Phys* 82:5035–5047. doi:10.1063/1.448625
49. Keith TA, Bader RFW (1993) Calculation of magnetic response properties using a continuous set of gauge transformations. *Chem Phys Lett* 210:223–231. doi:10.1016/0009-2614(93)89127-4
50. Ditchfield RJ (1972) Molecular orbital theory of magnetic shielding and magnetic susceptibility. *J Chem Phys* 56:5688–5691. doi:10.1063/1.1677088
51. Wolinski K, Hinton JF, Pulay P (1990) Efficient implementation of the gauge-independent atomic orbital method for NMR chemical shift calculations. *J Am Chem Soc* 112:8251–8260. doi:10.1021/ja00179a005
52. Helgaker T, Jaszunski M, Ruud K (1999) Ab initio methods for the calculation of NMR shielding and indirect spin – spin coupling constants. *Chem Rev* 99:293–352. doi:10.1021/cr960017t
53. Ernzerhof M, Perdew JP, Burke K (1997) Coupling-constant dependence of atomization energies. *Int J Quantum Chem* 64:285–295. doi:10.1002/(SICI)1097-461X(1997)64:3<285::AID-QUA2>3.0.CO;2-S/abstract
54. Ernzerhof M, Scuseria GE (1999) Assessment of the Perdew–Burke–Ernzerhof exchange–correlation functional. *J Chem Phys* 110:5029–5036. doi:10.1063/1.478401
55. Sarotti AM, Pellegrinet SC (2009) A multi-standard approach for GIAO ^{13}C NMR calculations. *J Org Chem* 74:7254–7260. doi:10.1021/jo901234h
56. Smith SG, Goodman JM (2010) Assigning stereochemistry to single diastereoisomers by GIAO NMR calculation: The DP4 probability. *J Am Chem Soc* 132:12946–12959. doi:10.1021/ja105035r
57. Bassarello C, Zampella A, Monti MC, Gomez-Paloma L, D’Auria MV, Riccio R, Bifulco G (2006) Quantum mechanical calculation of coupling constants in the configurational analysis of flexible systems: determination of the configuration of callipeltin A. *Eur J Org Chem* 604–609. doi:10.1002/ejoc.200500740
58. Bifulco G, Bassarello C, Riccio R, Gomez-Paloma L (2004) Quantum mechanical calculations of NMR J coupling values in the determination of relative configuration in organic compounds. *Org Lett* 6:1025–1028. doi:10.1021/ol049913e
59. Cramer CJ (2004) *Essentials of computational chemistry*. Wiley, Chichester
60. Bagno A, Rastrelli F, Saielli G (2005) NMR techniques for the investigation of solvation phenomena and non-covalent interactions. *Prog Nucl Magn Reson Spectrosc* 47:41–93. doi:10.1016/j.pnmrs.2005.08.001
61. Aidas K, Møgelhøj A, Kjør K, Nielsen CB, Mikkelsen KV, Ruud K, Christiansen O, Kongsted J (2007) Solvent effects on NMR isotropic shielding constants. A comparison between explicit polarizable discrete and continuum approaches. *J Phys Chem A* 111: 4199–4210. doi:10.1021/jp068693e
62. Dračinský M, Bouř P (2010) Computational analysis of solvent effects in NMR spectroscopy. *J Chem Theory Comput* 6:288–299. doi:10.1021/ct900498b
63. Tomasi J, Mennucci B, Came R (2005) Quantum mechanical continuum solvation models. *Chem Rev* 105:2999–3093. doi:10.1021/cr9904009
64. Klamt A, Schüürmann G (1993) COSMO: a new approach to dielectric screening in solvents with explicit expressions for the screening energy and its gradient. *J Chem Soc Perkin Trans* 2:799–805. doi:10.1039/P29930000799

-
65. Qiu D, Shenkin PS, Hollinger FP, Still WC (1997) The GB/SA continuum model for solvation. A fast analytical method for the calculation of approximate born radii. *J Phys Chem A* 101:3005–3014. doi:10.1021/jp961992r
 66. Manzo E, Gavagnin M, Bifulco G, Cimino P, Di Micco S, Ciavatta ML, Guoc YW, Cimino G (2007) Aplysiols A and B, squalene-derived polyethers from the mantle of the sea hare *Aplysia dactylomela*. *Tetrahedron* 63:9970–9978. doi:10.1016/j.tet.2007.07.055

Victoria L. Wilde, Jonathan C. Morris, and Andrew J. Phillips

Contents

11.1	Some Beginnings: <i>Cypridina hilgendorfi</i> Luciferin and Tetrodotoxin	602
11.2	The Continuing Role of Synthesis in Structure Elucidation, Confirmation, and Correction: Palmerolide A, Diazonamide A, Azaspiracid-1, and Palau'amine	607
11.2.1	Palmerolide A	608
11.2.2	Diazonamide A	611
11.2.3	Azaspiracid-1	619
11.2.4	Palau'amine	622
11.3	In Pursuit of Nature's Perfection: Biosynthetic Principles and the Synthesis of Hemibrevetoxin B, Methyl Sarcophytoate, Longithorone, and 11,11'- Dideoxyverticillin	622
11.3.1	Hemibrevetoxin B	622
11.3.2	Methyl Sarcophytoate and Longithorone A	630
11.3.3	(+)-11,11'-Dideoxyverticillin A	632
11.4	New Reactions and New Strategies: Azaspiracid-1, Amphidinolide A1, Bryostatin 16, Ningalin B, and Cyanthiwigins U and F	632
11.4.1	Azaspiracid-1	632
11.4.2	Amphidinolide A1	637
11.4.3	Bryostatin 16	641
11.4.4	Ningalin D	643
11.4.5	Cyanthiwigins U and F	643
11.5	At the Edges of the Known Universe of Molecular Complexity	646
11.6	Gram-Scale Synthesis: Moving Toward Realistic Supply of Compounds for Preclinical Evaluation	649
11.7	Supply by Synthesis: The Arrival of Halaven [®] and Yondelis [®] in the Clinic	655

V.L. Wilde • A.J. Phillips (✉)

Department of Chemistry, Yale University, New Haven, CT, USA

e-mail: Victoria.wilde@yale.edu, andrew.phillips@yale.edu

J.C. Morris

School of Chemistry, University of New South Wales, Sydney, Australia

e-mail: jonathan.morris@unsw.edu.au

E. Fattorusso, W. H. Gerwick, O. Tagliatela-Scafati (eds.),

Handbook of Marine Natural Products, DOI 10.1007/978-90-481-3834-0_11,

© Springer Science+Business Media B.V. 2012

11.8	Conclusions and Future Perspectives	664
11.9	Study Questions	664
	References	664

Abstract

Synthetic chemistry has played a significant role in the development of natural products chemistry, and the histories of the two fields are inextricably intertwined. Biology, isolation, structure elucidation, and synthesis are central to marine natural products chemistry and many advancements in the past 40 years have come in response to the challenges presented by compounds from the oceans. In this chapter we present an overview of marine natural products synthesis through a looking glass that focuses on some selected total syntheses from the past 40 odd years. In this light we can only provide a snapshot of where the field currently stands and the road that has led here. The vectors that define the size of the field and the constraints of this forum unfortunately do not cross, and as such it is not possible to be comprehensive. We direct the reader to recent reviews that cover the field in greater detail.

11.1 Some Beginnings: *Cypridina hilgendorffii* Luciferin and Tetrodotoxin

Synthetic chemistry has played a significant role in the development of natural products chemistry, and the histories of the two fields are inextricably intertwined [1]. Biology, isolation, structure elucidation, and synthesis are central to marine natural products chemistry, and many advancements in the past 40 years have come in response to the challenges presented by compounds from the oceans. This chapter presents an overview of marine natural products synthesis through a looking glass that focuses on some selected total syntheses from the past 40 odd years. In this light we can only provide a snapshot of where the field currently stands and the road that has led here. The vectors that define the size of the field and the constraints of this forum unfortunately do not cross, and as such it is not possible to be comprehensive. We direct the reader to recent reviews that cover the field in greater detail [2].

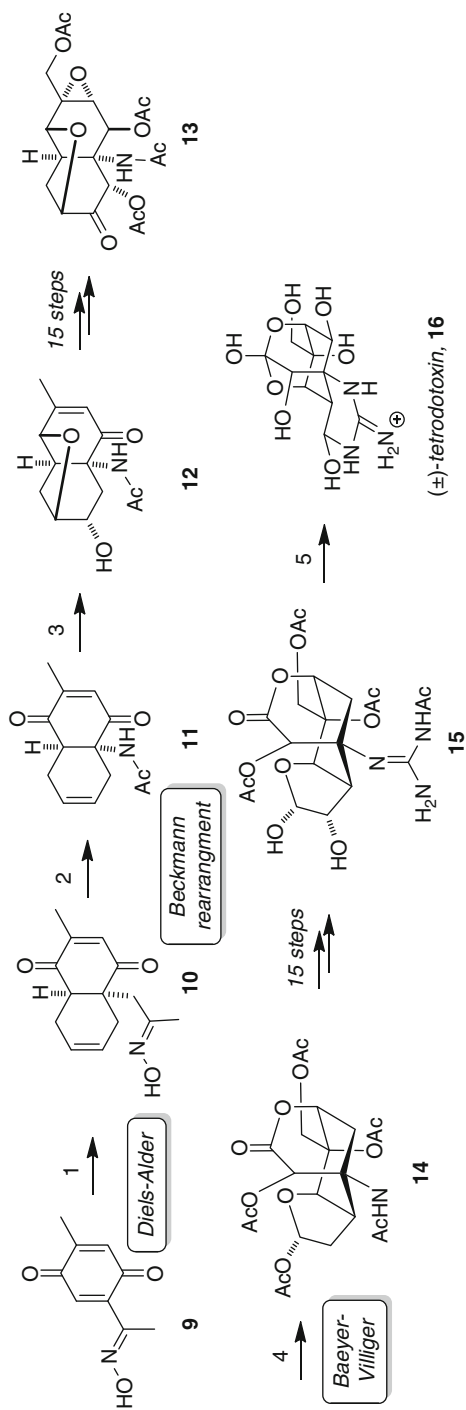
The papers that founded the science of marine natural products chemistry are difficult to identify, although there is little doubt that contemporaneous efforts by scientists in the United States and Japan in the period of 1955–1965 were responsible for the birth of the field. Notable research in this light includes early work by Paul Scheuer at the University of Hawaii into the causative agent of ciguatera poisoning [3], which later led to the structure of palytoxin [4], and by Yoshimasa Hirata at Nagoya University into the structure of the luciferin from the sea firefly *Cypridina hilgendorffii* (now *Vargula hilgendorffii*). It is instructive to consider some of the early work from Nagoya as it provides an illustration of the challenges in structure elucidation at the time and historical significance of total synthesis in structure confirmation.

Heroic efforts to secure crystalline luciferin from *Cypridina hilgendorfi* by Osamu Shinomura (Nobel Laureate in 2008 for the discovery of green fluorescent protein) (see ► [Chap. 24](#)) in the laboratory of Yoshimasa Hirata in the period of 1955–1960 produced material [5] that ultimately culminated in a structure proposal that was published in 1966 as part of a series of three papers [6]. The structure elucidation, which was predicated on careful degradative studies and comparisons to known compounds, suggested luciferin to be **7** ([Scheme 11.1](#)). Oxidation would lead to oxyluciferin, **8**, which was known to be degraded to etioluciferin and α -keto- β -methylglutaric acid by acid hydrolysis. In an accompanying paper, Yoshito Kishi confirmed the structure by total synthesis ([Scheme 11.2](#)) and ushered in the beginnings of an important role for synthesis in marine natural products chemistry: structure confirmation when limited amounts of natural material were available [6, 7].

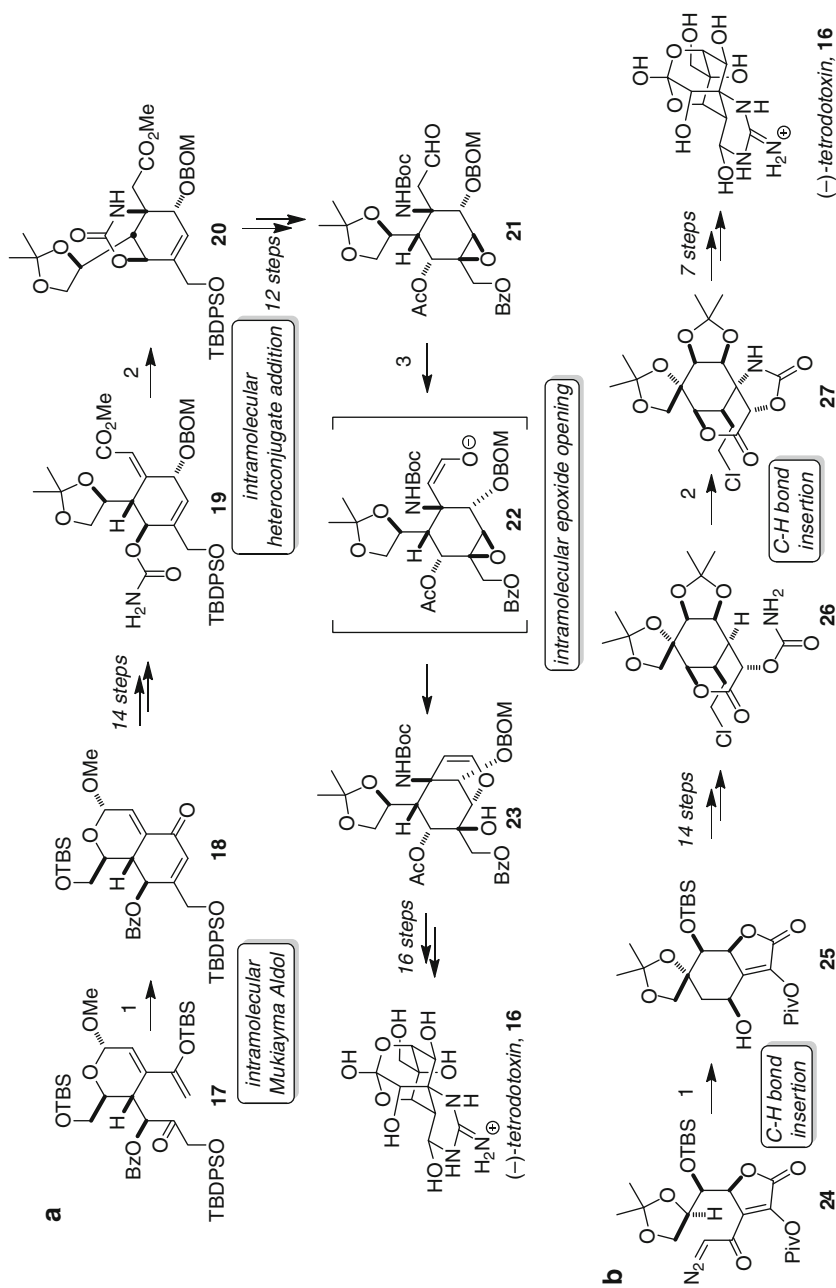
The structure of tetrodotoxin was arrived at almost simultaneously by three groups – Hirata-Goto, Tsuda, and Woodward – and involved an extensive process of degradation and painstaking spectroscopic analysis [8, 9]. The absolute stereochemistry was secured in 1972 by X-ray analysis, and was followed only 2 years later by Kishi's remarkable total synthesis. The Kishi synthesis commenced with oxime-substituted *p*-benzoquinone **9**, which could be subjected to a sequence of SnCl_4 -catalyzed Diels–Alder reaction with butadiene and Beckmann rearrangement to give **11**. Selective reduction of the C5 ketone with sodium borohydride and epoxidation of the di-substituted olefin led to tricycle **12**. A sequence of 15 steps transformed enone **12** into tetraacetate **13**. Baeyer–Villiger oxidation broke open the decalin ring system and formed bridged tricycle **14**. A series of modifications installed the remaining oxidation functionalities to give diol **15**. Diol cleavage with periodic acid followed by treatment with base closed the final two rings to give tetrodotoxin, **16**.

Almost 30 years after Kishi's synthesis of racemic tetrodotoxin [10], the first asymmetric syntheses of this molecule were reported by the groups of Isobe [11] and Du Bois [12]. The intervening three decades had provided a wealth of new methods that could be brought to bear on the synthesis problems posed by tetrodotoxin and both syntheses leveraged these advances. However, in a similar vein to the Kishi work, strategic aspects of the two syntheses were also focused on the functionalization of the cyclohexane core of the molecule.

Key steps for the functionalization of the cyclohexane core of tetrodotoxin from Isobe's synthesis are shown in [Scheme 11.3a](#). Silyl enol ether **17** (derived from 2-acetoxy-tri-*O*-acetyl-D-glucal in 23 steps) was subjected to an intramolecular aldol reaction mediated by TBAF, and subsequent elimination with trichloroacetylchloride-pyridine provided enone **18** in >70% yield. Further manipulations advanced **18** to **19**, and upon treatment with potassium *tert*-butoxide in THF, the primary carbamate underwent heteroconjugate addition to produce oxazolidinone **20** in 90% yield. The final key functionalization of the cyclohexane was achieved by an interesting intramolecular *O*-alkylation of enolate **22** by the epoxide to give **23**. With **23** in hand, the first asymmetric synthesis of tetrodotoxin (**16**) was completed by a 15-step sequence consisting of largely straightforward transformations.



Scheme 11.2 Reagents and conditions: (1) butadiene, SnCl_4 ; (2) (a) MsCl , Et_3N ; (b) H_2O , heat, 50% (three steps); (3) (a) NaBH_4 ; (b) $m\text{CPBA}$, CSA, 72% (two steps); (4) (a) KOAc , HOAc , 98% (two steps); (5) (a) HIO_4 ; (b) NH_4OH , $\text{MeOH}/\text{H}_2\text{O}$, 15% (two steps)



In a distinctly different approach, Du Bois and Hinman relied on their newly developed CH bond insertion reaction methodology [13] as the cornerstone of their efforts to functionalize the central cyclohexane ring (Scheme 11.3b). Treatment of diazoketone **24** (available in nine steps from D-isoascorbic acid) with 1.5 mol% $\text{Rh}_2(\text{HNCOCPh}_3)_4$ in CCl_4 results in a CH insertion reaction to give a cyclohexanone that is subsequently reduced with $\text{NH}_3\cdot\text{BH}_3$ to give alcohol **25** in 75% yield over the two steps. Advancement of **25** to carbamate **26** was achieved by a 14-step sequence, and set the stage for the second CH bond insertion. Subjecting this carbamate to conditions related to earlier methods developed in the Du Bois laboratories resulted in CH bond insertion of the carbamate to form oxazolidinone **27** in 77% yield. Given the structural complexity of the substrate, the yield for this reaction is truly remarkable, and nicely underscores the utility of this reaction in a target-oriented setting. A sequence of seven steps led to tetrodotoxin (**16**).

The challenges to synthesis presented by tetrodotoxin's structure were met by employing distinctly different strategies over the course of three decades. The Kishi synthesis employed a classic Diels–Alder reaction with substrate-based stereocontrol for reactions that further functionalized the core of the molecule. Isobe's synthesis relied on an intramolecular aldol reaction and conjugate addition to form two key bonds on a highly functionalized intermediate and the Du Bois synthesis showcases strategic avenues opened by advances in CH insertion reactions on highly functionalized compounds (Fig. 11.1).

11.2 The Continuing Role of Synthesis in Structure Elucidation, Confirmation, and Correction: Palmerolide A, Diazonamide A, Azaspiracid-1, and Palau'amine

The rise of modern spectroscopic methods such as NMR that began in the 1960s resulted in significant numbers of new structures being determined each year, and with increasing ease. Indeed, a survey of the structures recorded in MarinLit by the decade of their initial description shows that the 1960s produced 12 structures; the 1970s, 310 structures; the 1980s, 873; the 1990s, 1,459; and the period 2000–2009 produced 4,781 new structures [14]. In this section we consider a number of contemporary examples where synthesis has played roles in structure elucidation, structure confirmation, or structure corrections. Synthesis remains particularly important in the context of questions of stereochemistry, especially when the amounts of material isolated are small enough to permit connectivity to be established.



Scheme 11.3 (a) Key cyclohexane functionalization reactions from Isobe's synthesis of (-)-tetrodotoxin. Reagents and conditions: (1) TBAF, THF- H_2O then Cl_3CCOCl , DMAP, pyridine, >70%; (2) $t\text{-BuOK}$, THF, 90%; (3) DBU, *o*-dichlorobenzene, 130°C, >68%. (b) Du Bois's synthesis of (-)-tetrodotoxin. Reagents and conditions: (1) (a) 1.5 mol% $\text{Rh}_2(\text{HNCOCPh}_3)_4$, CCl_4 , (b) $\text{NH}_3\cdot\text{BH}_3$, $\text{CH}_2\text{Cl}_2\text{-MeOH}$, 75% (two steps); (2) 10 mol% $\text{Rh}_2(\text{HNCOCF}_3)_4$, $\text{PhI}(\text{OAc})_2$, MgO , PhH , 65°C, 77%

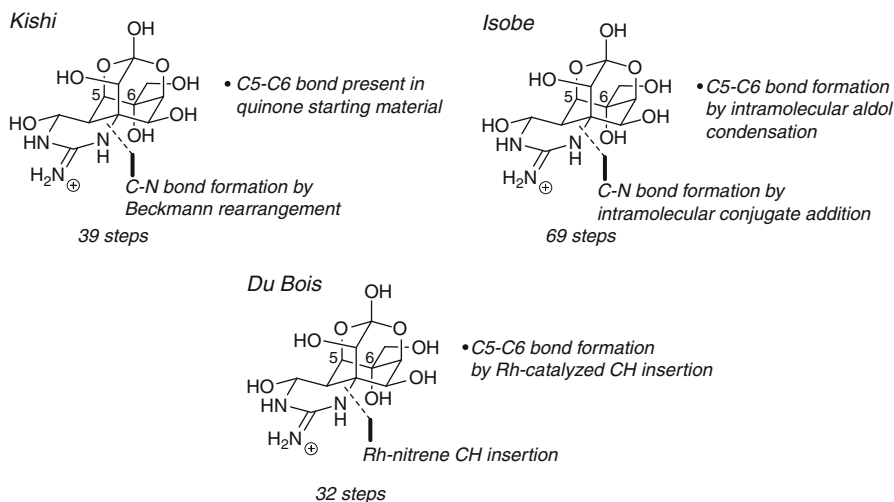
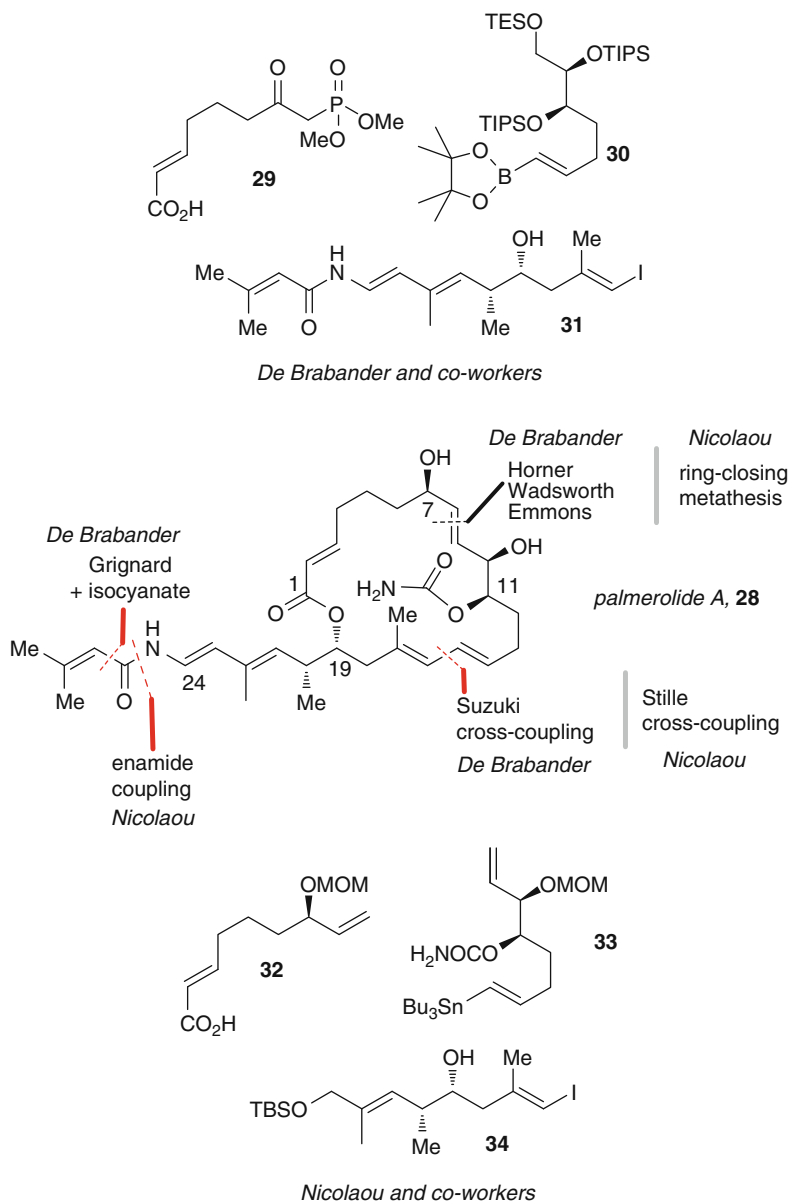


Fig. 11.1 A comparison of key reactions in the Kishi, Isobe, and Du Bois tetrodotoxin syntheses

11.2.1 Palmerolide A

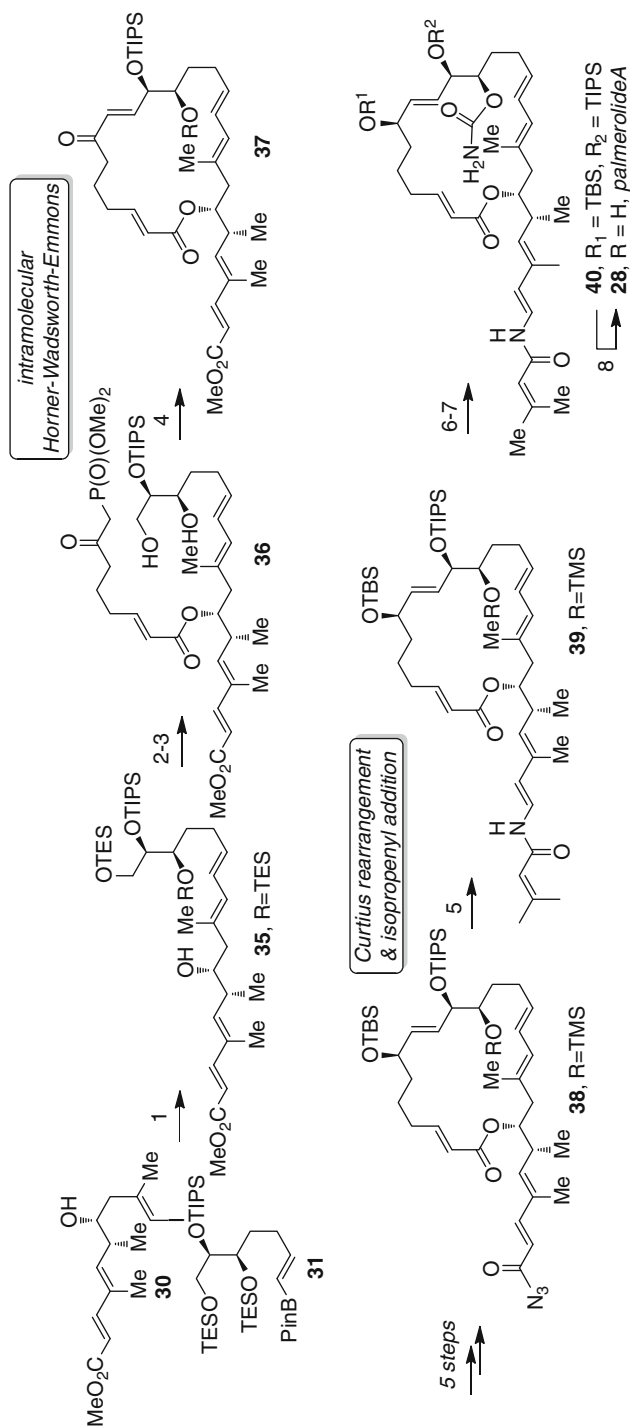
Palmerolide A (**28**) is a complex 20-membered macrolide isolated from an Antarctic tunicate *Synoicum adareanum* [15]. The original structure was described in 2006, and underpinned by the reported potent and selective cytotoxicity toward melanoma cells (UACC-62 LC₅₀ = 18 nM), there was an immediate flurry of activity that resulted in the first total syntheses by the De Brabander [16] and Nicolaou [17] groups (Scheme 11.4). These two total syntheses are instructive because they illustrate (1) the balance of new methods and well-used reactions in the context of a complex macrolide synthesis, (2) the speed with which contemporary total synthesis can provide structural information, and (3) the application of retrosynthetic analysis in the context of macrolide synthesis.

A key step in the De Brabander synthesis was a Suzuki cross coupling of vinyl iodide **31** with pinacolboronate **30**, which proceeded smoothly in the presence of Pd(PPh₃)₄ with TiCl₂CO₃ as base to yield **35** (79%) (Scheme 11.5). Acylation of the alcohol with **29** using Yamaguchi conditions (69%), followed by removal of the TES ethers with PPTS in MeOH, led to **36** in 95% yield. The key Horner–Wadsworth–Emmons macrocyclization was achieved by a two-step protocol consisting of selective primary alcohol oxidation with PhI(OAc)₂/TEMPO to yield the aldehyde, and subsequent treatment with K₂CO₃ and 18-crown-6 in toluene at room temperature to provide **37** in 70% yield over these two steps. Enone **37** was then converted to acyl azide **38** in five steps (92%). Upon heating under reflux in benzene, Curtius rearrangement occurred to give an intermediate isocyanate that was intercepted with 2-methyl-1-propenylmagnesium bromide at –78°C to install the *N*-acyl enamine and give **39** in 76% yield over these two steps. Removal of the

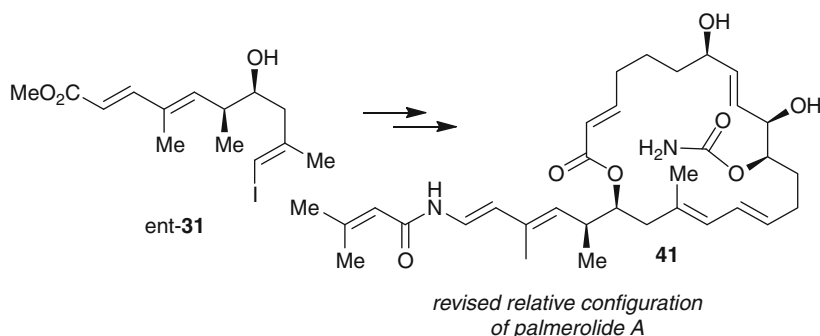


Scheme 11.4 Palmerolide A; a comparison of strategies

TMS ether with $\text{HF}\cdot\text{pyr}$ buffered with pyridine (95%) and introduction of the carbamate with $\text{Cl}_3\text{CC}(\text{O})\text{NCO}$ gave **40** (95%) and all that was required at this juncture to complete the synthesis was removal of the TBS and TIPS ethers. This was achieved with TBAF in THF at 0°C to give palmerolide A (**28**) in 41% yield.



Scheme 11.5 De Brabander's synthesis of palmerolide A. Reagents and conditions: (1) cat. Pd(PPh₃)₄, TiCl₄, THF, H₂O, rt, 79%; (2) **29**, 2,4,6-trichlorobenzoyl chloride, Et₃N, DMAP, PhMe, rt, 69%; (3) PPTS, MeOH, 0°C, 95%; (4) (a) PhI(OAc)₂, TEMPO, CH₂Cl₂, H₂O, room temp; (b) K₂CO₃, 18-C-6, PhMe, 60°C, 70% (two steps); (5) PhH, reflux then 2-methyl-1-propenylmagnesium bromide, -78°C, 76% (two steps); (6) HF-pyr, pyr, THF, rt, 95%; (7) Cl₃CC(O)NCO, CH₂Cl₂, 0°C, Al₂O₃, room temp, 95%; (8) TBAF, THF, 0°C, 41%



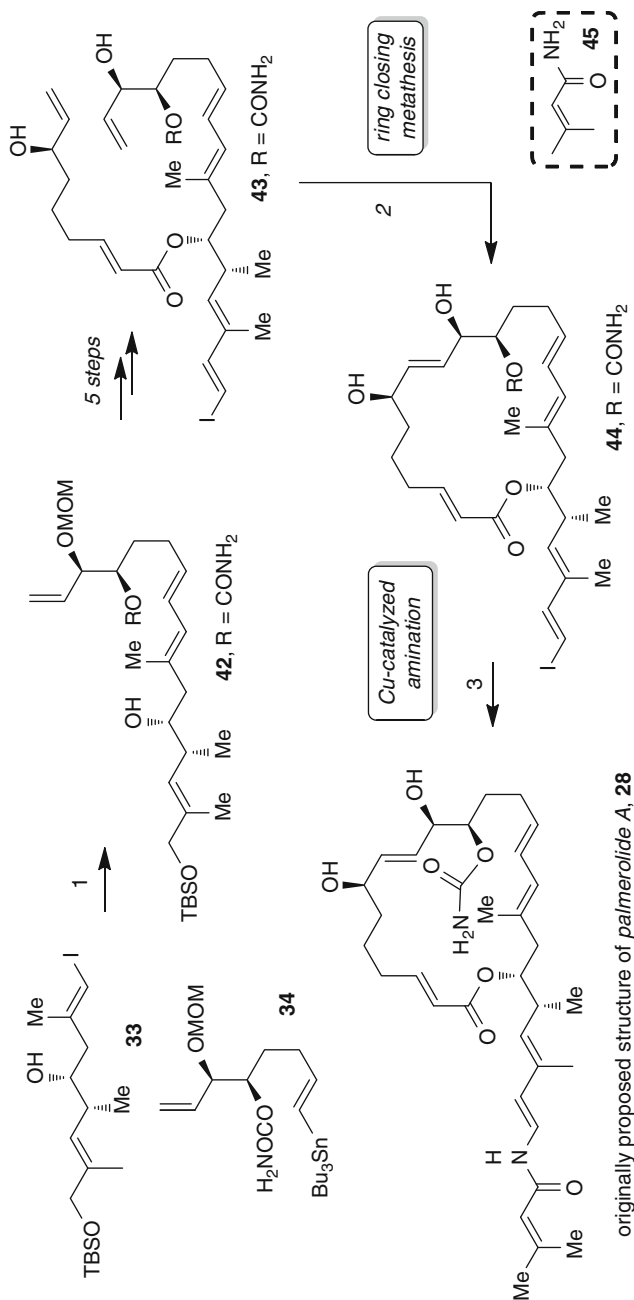
Scheme 11.6 Structure revision of palmerolide by synthesis

Unfortunately, the spectroscopic data for synthetic palmerolide A (**28**) was not consistent with that reported for the natural product, and after careful analysis of both the stereochemical assignments for the synthetic material and the natural product, De Brabander and coworkers concluded that the C19 and C20 stereochemistry was likely enantiomeric to that originally proposed by Baker. Synthesis of the proposed structure was achieved from *ent*-**31** (Scheme 11.6), and this provided material **41** that was identical to palmerolide A with the exception of the sign of optical rotation. As such the structure of palmerolide A was reassigned by synthesis to be the enantiomer of **41**. Contemporaneous with the work, the Baker group also published a reassignment based on degradative studies [18].

The Nicolaou synthesis of the originally proposed structure for palmerolide A involved Stille cross-coupling of **33** and **34** to produce **42** in 67% yield. Acylation with the mixed anhydride derived from **42** under Yamaguchi conditions followed by a four-step sequence gave the ring-closing metathesis precursor **43** [19], which was then treated with 20 mol% of the second generation Grubbs catalyst, and smooth cyclization at room temperature occurred to give **44** in 76% yield. The synthesis was completed by Pd-catalyzed amidation [20] of the vinyl iodide **44** with **45** to yield **28**. As was the case in the De Brabander studies, Nicolaou and co-workers concluded that the correct structure was **41**, and a synthesis of this compound was also completed by the same strategy as delineated in Scheme 11.7. The Nicolaou group has continued to study palmerolide A's chemistry and biology, and palmerolide A also continues to stimulate substantial synthesis activity from other groups [21].

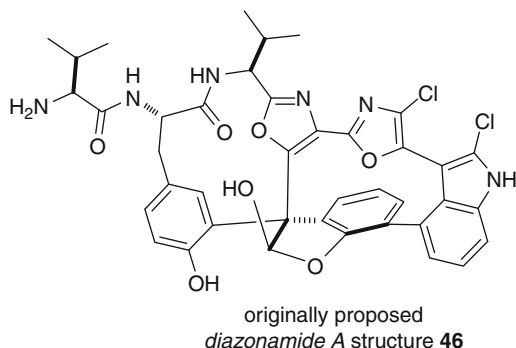
11.2.2 Diazonamide A

The intricate architecture of diazonamide A **46**, isolated from *Diazona angulata*, was first described by Lindquist, Fenical, and Clardy in 1991 (Fig. 11.2) [22]. The initial structure was secured by X-ray crystallography of the related diazonamide B, and synthesis efforts, driven in part by interest in the impressive anti-mitotic activity, quickly followed [23].



Scheme 11.7 Nicolaou's synthesis of the originally proposed structure for palmerolide A. Reagents and conditions: (1) 25 mol% Pd(dba)₂ Ph₃As, LiCl, NMP, 23°C, 67%; (2) 20 mol% Grubbs II cat., CH₂Cl₂, 23°C, 76%; (3) 45, CuI, Cs₂CO₃, *N,N'*-dimethylethylenediamine, DMF, 23°C, 44% based on 36% recovered starting material

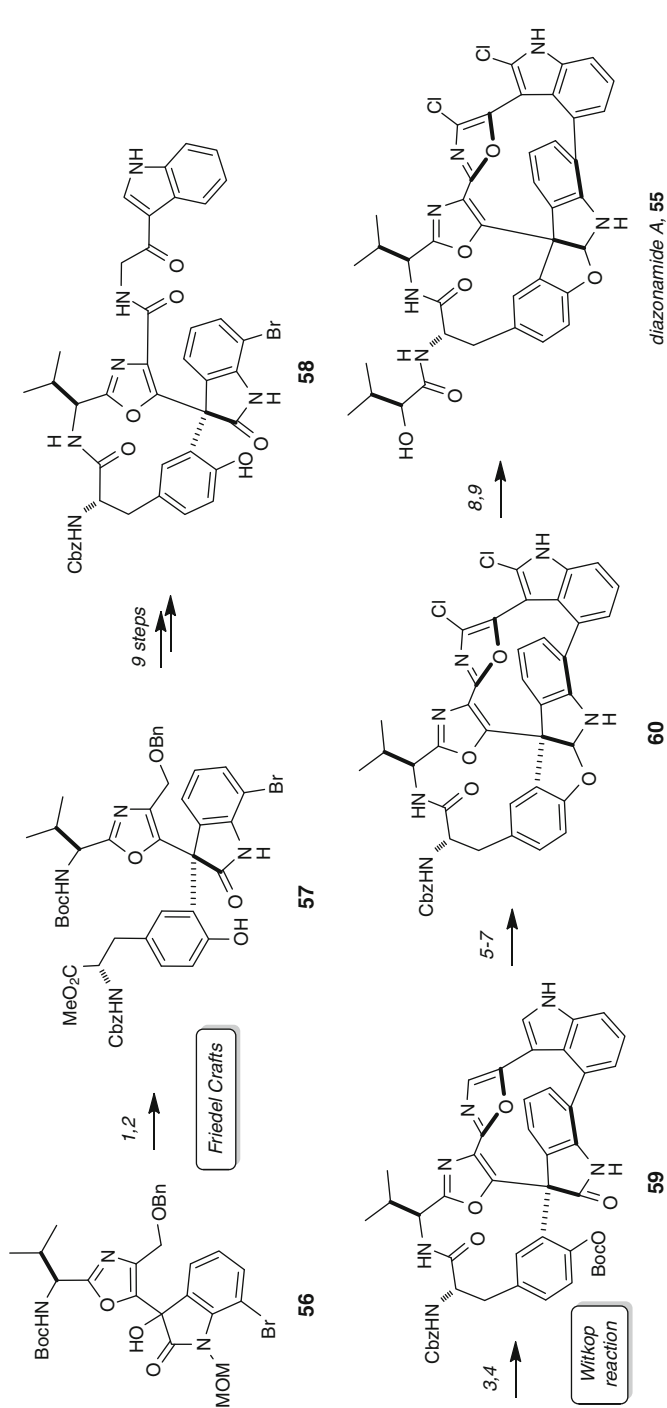
Fig. 11.2 The originally proposed diazonamide A structure



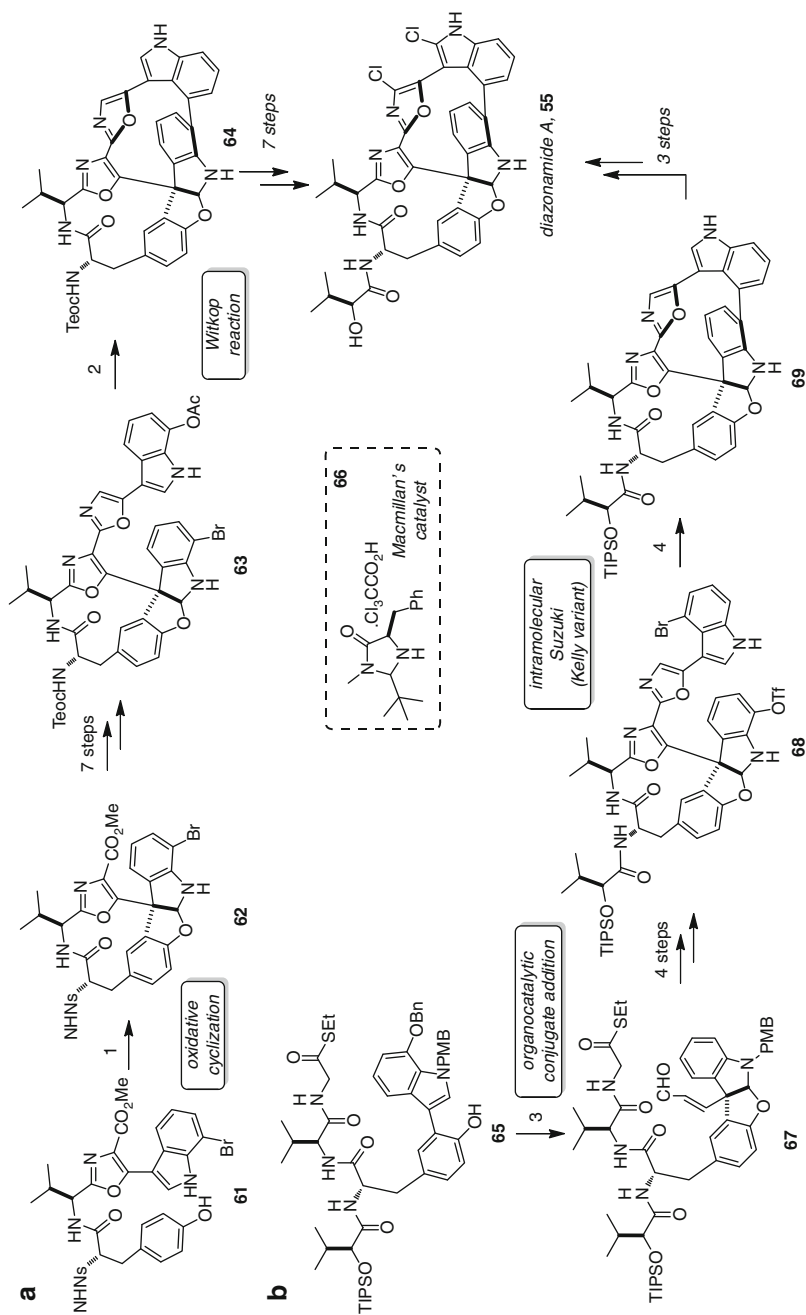
A landmark paper by the Harran group disclosed the synthesis of diazonamide A in 2001 [24]. The synthesis, shown in [Scheme 11.8](#), involved an initial macrocyclization of iodide **47** by Heck reaction to produce **48**. Protection of the phenol and stoichiometric dihydroxylation using **49** gave diol **50**, which underwent pinacol rearrangement upon exposure to *p*-TsOH to produce aldehyde **51** as a single diastereomer. A 12-step sequence led to **52**, and the second macrocycle was formed by a photochemical Witkop reaction to yield **53** as a single atropisomer. Chlorination of the indole and the proximal oxazole produced **54**, and a further four steps led to diazonamide A (**46**). At this juncture it became immediately apparent that the synthesized structure was not the same as natural diazonamide A, especially by comparison of ^1H NMR data. On the basis of synthetic work and reinterpretation of the X-ray crystallographic data, Harran proposed that the structure of diazonamide A be revised to **55**.

The newly revised structure of diazonamide A, **55**, was ratified by total synthesis in the Nicolaou laboratories only 1 year later ([Scheme 11.9](#)) [25]. The synthesis commenced with a Friedel–Crafts alkylation of Cbz-tyrosine methyl ester with **56** to give **57** (after reintroduction of the Boc carbamate). A nine-step sequence led to macrocycle **58**, which was then exposed to Gabriel–Robinson cyclodehydration conditions and radical cyclization to give macrocycle **59**. Installation of the chlorines followed by selective BOC deprotection and DIBAL-H- initiated ring closure led to intermediate **60**. Hydrogenolysis of the Cbz- protecting group and installation of the peptide side chain completed the synthesis of diazonamide A, **55**.

With the structure of diazonamide A secured by the combined efforts of Harran in pursuit of the originally proposed connectivity and Nicolaou in providing the confirmation of structure by synthesis, more recent efforts have focused on diazonamide as a vehicle for methods development and investigations of the underlying biology. Four further total, or formal, syntheses, have been completed. Key elements of the Harran total synthesis of diazonamide A are shown in [Scheme 11.10](#) [26]. Oxidative cyclization produced **62** in a very direct fashion from compound **61**, which was transformed, via a seven-step sequence, to macrocycle **63**. The second macrocycle was then formed via Witkop reaction



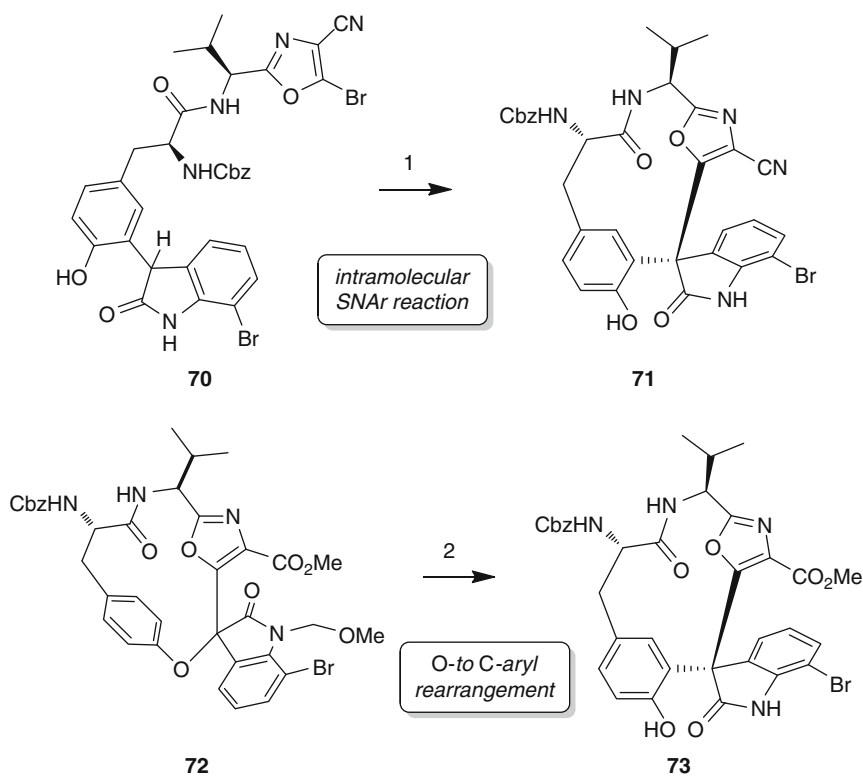
Scheme 11.9 Nicolaou's synthesis of diazonamide A. Reagents and conditions: (1) CbzTyrOMe, *p*-TsOH, 1,2-DCE; (2) (Boc)₂O, aqueous NaHCO₃/dioxane, 21% (two steps); (3) POCl₃, pyridine; (4) hv, epichlorohydrin, LiOAc, MeCN/H₂O, 16% (two steps); (5) NCS, CCl₄/THF; (6) TFA; (7) DIBAL-H, THF, 29% (three steps); (8) H₂, Pd(OH)₂/C, EtOH, (9) EDC, HOBt, NaHCO₃, DMF, 82% (two steps)



Scheme 11.10 (a) Harran's synthesis of diazonamide A, and (b) The MacMillan synthesis of diazonamide A. Reagents and conditions: (1) $\text{PhI}(\text{OAc})_2$, LiOAc , 2,2,2-trifluoroethanol, 25%; (2) hv (300 nm), CH_3CN , H_2O , LiOH ; (3) propynal, 85%, >20:1 dr; (4) $\text{Pd}(\text{PPh}_3)_4$, $(\text{BPin})_2$, KF , MW, 50%

to give bis-macrocyclic **64** which was then taken on to diazonamide A via a seven-step sequence. MacMillan completed a total synthesis of diazonamide A in 2011 via use of an organocatalytic conjugate addition of thioester **65** with catalyst **66** to give enal **67** [27]. Enal **67** was then taken through a four-step sequence to give macrocycle **68**, which underwent a Kelly-type intramolecular Suzuki coupling to give bis-macrocyclic **69**. The total synthesis was then completed via addition of the chlorine residues and deprotection to afford diazonamide A.

Both Sammakia and Magnus have completed formal total syntheses that employ interesting and elegant approaches to the C10 quaternary center (Scheme 11.11) [28]. In the case of the Sammakia synthesis, an intramolecular nucleophilic aromatic substitution reaction was used to form the quaternary center at the same time as closing one of the macrocycles (**70** \rightarrow **71**). In light of strategic considerations that balance the importance of formation of the macrocycles against the challenges inherent in the diastereoselective formation of the C10 center, this is the most direct solution to date. The Magnus synthesis was highlighted by the rearrangement of **72**–**73**, a process that is formally a Friedel–Crafts reaction.



Scheme 11.11 The Sammakia and Magnus syntheses of the quaternary center. Reagents and conditions: (1) Na_2CO_3 , DMF, 65°C , 20 h, 56%; (2) CHCl_3 , reflux, 70%

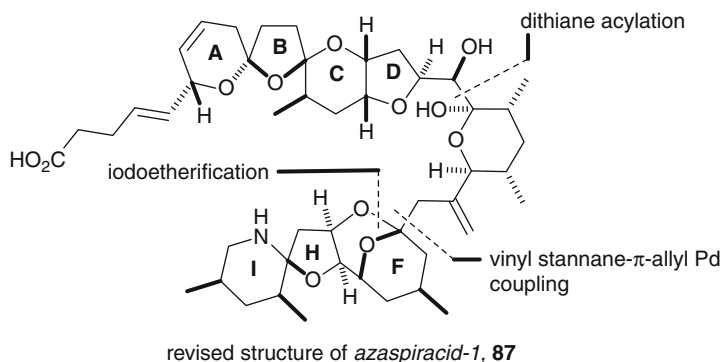


Fig. 11.3 Key carbon–carbon bond forming reactions in the Nicolaou azaspiracid-1 synthesis

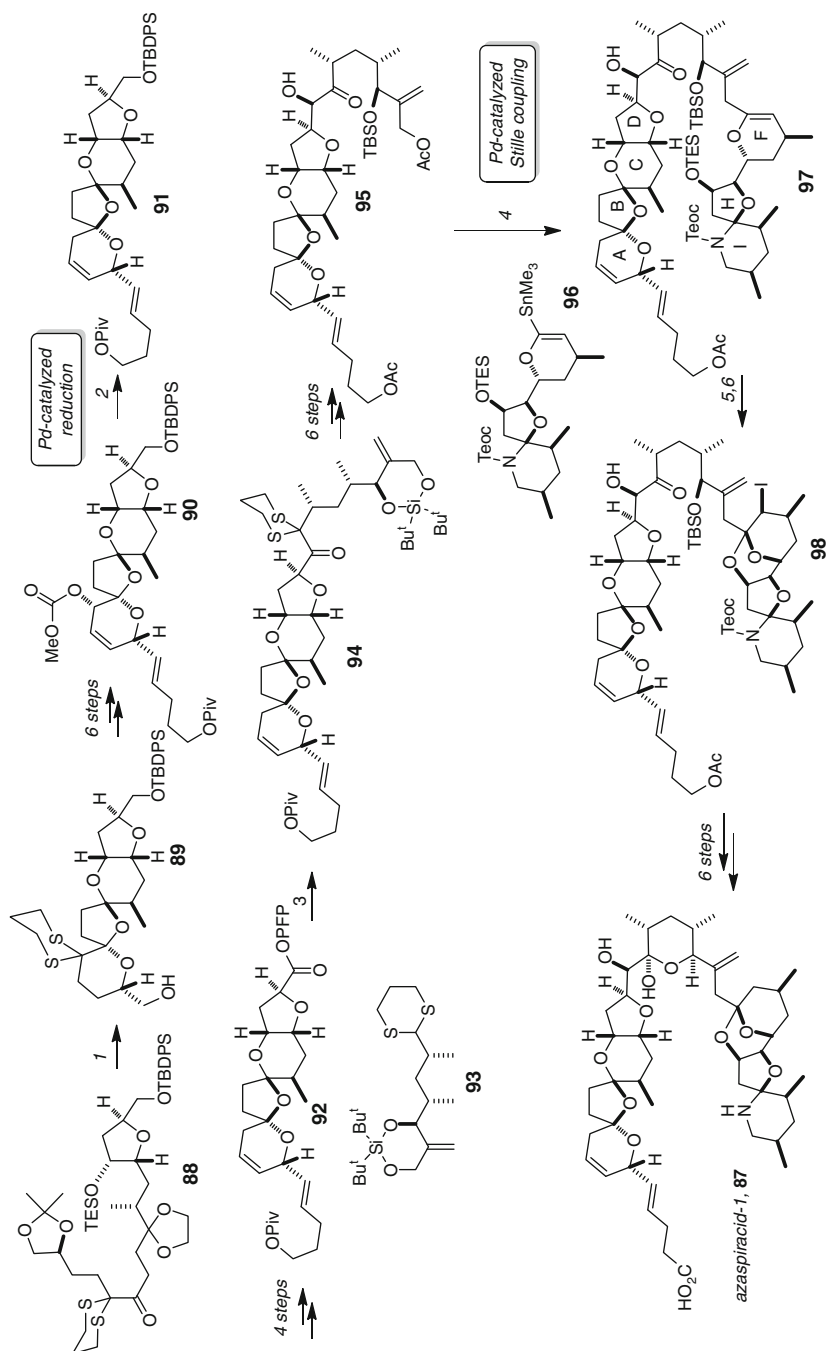
11.2.3 Azaspiracid-1

A more complex example of the role of total synthesis in structure correction comes from Nicolaou's synthesis of azaspiracid-1, a complex alkaloidal polyether first described in 1998 by Takeshi Yasumoto and coworkers [29]. In 2003, Nicolaou and co-workers established by total synthesis [30, 31] that the initially proposed structure for azaspiracid-1 was incorrect (**74**, Scheme 11.12). Subsequent degradative studies and synthesis were required to revise the structure of azaspiracid-1 [32]. In work described in 2003, upon realizing that there were structural questions remaining to be resolved, the first path was to degrade natural azaspiracid-1 to smaller fragments and then locate the positions of error by synthesis. This approach was also expected to allow the determination of the relative stereochemistry between the ABCDE and FGHI domains. To this end, an authentic sample of azaspiracid was reacted with TMSCHN_2 and the methyl ester obtained was treated with NaIO_4 , which resulted in cleavage of the C20–C21 bond. This provided lactone **75** and aldehyde **76**, which were subjected to short sequences of common transformations to yield alcohol **77** (the stereochemistry shown for this compound corresponds to that originally proposed).

Synthetic materials for comparison with structures **76** → **77** were prepared by coupling of **78** and **79** by a Pd(0)-mediated Stille coupling to give dihydropyran **80**. Removal of the TES ether with HF-pyridine, followed by treatment with *N*-iodosuccinimide to induce iodoetherification, produced iodoether **81** in 38%



Scheme 11.12 Chemical degradation and derivatization of azaspiracid-1 (originally proposed structure) to C1–C20 alcohol **77** and C21–C40 lactone **75**. Reagents and conditions: (1) TMSCHN_2 , MeOH, 25°C; (2) NaIO_4 , MeOH/H₂O (4:1), 25°C, ~100% over two steps; (3) NaBH_4 , MeOH, 25°C, ~90%; (4) **78**, 90 mol% $[\text{Pd}_2\text{dba}_3]$, LiCl, AsPh₃, DIPEA, syringe pump addition of stannane; (5) HF-pyr, THF-pyr; (6) NIS, NaHCO₃, THF, 38% (three steps); (7) TBAF, THF, 88%



Scheme 11.13 (continued)

yield (for the three steps). Two further steps gave **82** and comparison of the spectral data for this compound with compound **75** showed them to be the same. This established that the structure of the compound obtained by degradation is in fact diastereomeric in terms of the stereochemistry around the E ring to that which was originally proposed. A synthesis of the compound in which the FGHI rings were enantiomeric was also completed by this route, but it did not match the data for **83**. These, and related, synthetic studies established the absolute stereochemistry for this domain. The availability of synthetic materials also allowed questions regarding the connectivity and stereochemistry of the ABCD ring-containing domain to be answered. Desilylation of previously synthesized compound **83** to give **84** allowed for a comparison with degradation product **77**. The spectroscopic data for these two samples differed substantially, particularly in the A ring. Progress towards a corrected structure was assisted by comparison of NMR data with a related compound, lissoketal (**85**) [33]. Based on this comparison, a new structure for **77** in which the A-ring double bond has been relocated was proposed; however, final resolution of the problem did not come until the synthesis of several closely related structures had been completed. Based on this work, the stereochemistry and connectivity shown in compound **86** was secured as being correct.

Armed with the information gleaned from these studies, and the earlier synthesis, plans could be laid to complete a total synthesis of the revised structure **87**, by employing the key couplings shown in Fig. 11.3.

Key steps of the synthesis are shown in Scheme 11.13. Malic acid-derived tetrahydrofuran **88** was treated with TMSOTf in CH_2Cl_2 at low temperature to induce the desired deprotection–spirocyclization sequence to give **89** in 89% yield as a single stereoisomer. A sequence of six steps led to allylic carbonate **90**, and deoxygenation of this compound to give **91** was achieved by employing a modification of an earlier-described Pd-catalyzed method [34] which produced the desired compound in 82% yield (with 7:1 selectivity for the $\Delta^{7,8}$ olefin). After advancement to pentafluorophenyl ester **92**, introduction of the C21–C27 domain involved acylation of the dithiane anion derived from **93** to give **94** in 50% yield. Six further steps provided compound **95** which served as the key precursor to the A \rightarrow E domain for the final steps of the synthesis. The crucial coupling of the ABCD and FHI subunits occurred by Pd-mediated Stille-type reaction between allylic acetate **95** and dihydropyranyl stannane **96** to give **97** in 55% yield. Removal of the C34 TES ether (TBAF, 80%) and iodoetherification with N-iodosuccinimide produced **98** in an impressive 62% yield given the complexity of the substrate. The synthesis was then completed by a short sequence of six steps that consisted of redox chemistry and protecting group manipulations. Material obtained by this route matched all characterization data for the natural product.



Scheme 11.13 Synthesis of the revised structure of azaspiracid-1 **87**. Reagents and conditions: (1) **93**, *n*-BuLi–*n*-Bu₂Mg, THF, 0°C \rightarrow 25°C; then –90°C; then **92**, 50%; (2) **95**, 30 mol% Pd₂dba₃, 30 mol% AsPh₃, LiCl, DIPEA; then **96**, NMP, 40°C, 55%; (3) TBAF, THF, 0°C, 80%; (4) NIS, NaHCO₃, THF, 0°C, 62%

11.2.4 Palau'amine

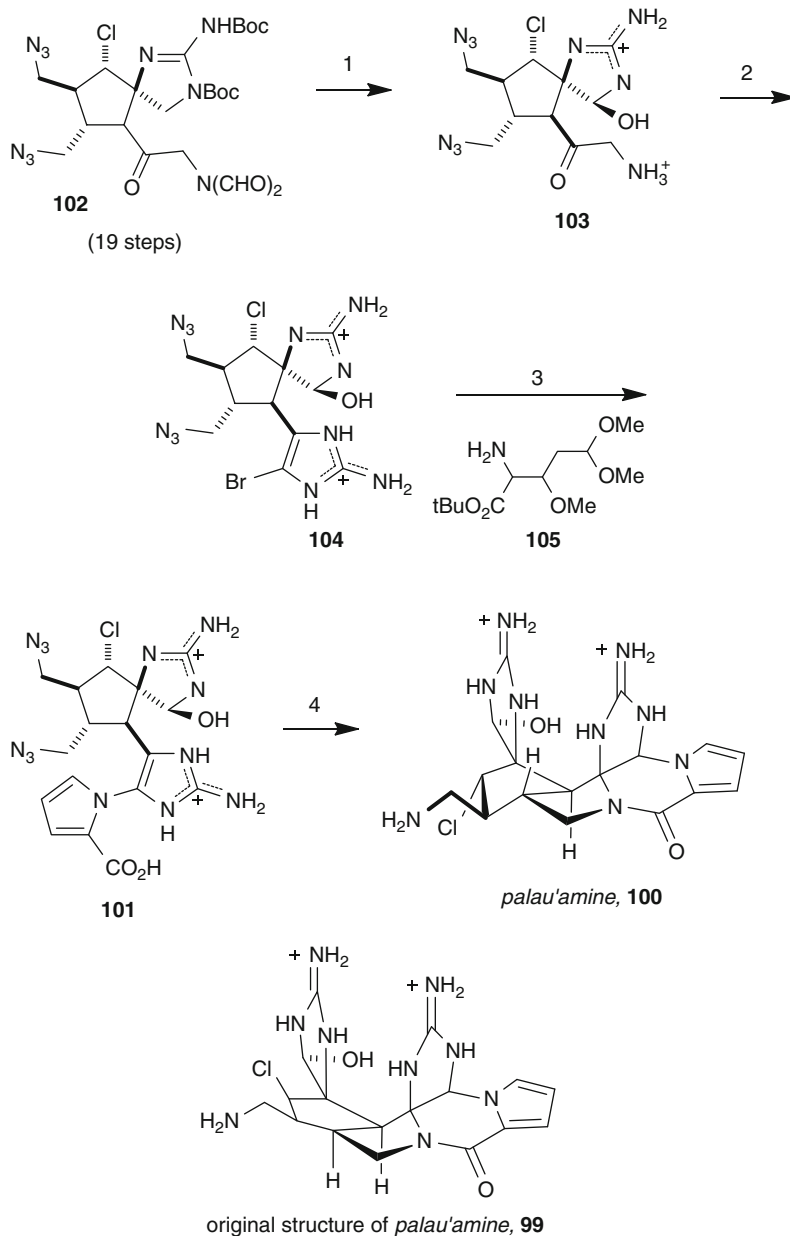
The complex hexacyclic architecture of palau'amine (**99**) has long stood as one of the major challenges of organic synthesis [35]. In 2007, the geometry of the azabicyclo [3.3.0] octane core was determined to be *trans* **100**, rather than the proposed *cis* [36]. Using this information, Baran and coworkers were able to successfully complete a total synthesis of palau'amine [37]. The synthetic strategy was based on the premise that a “macro palau'amine” could be generated from **101** and an irreversible transannular cyclization would yield the desired target (Scheme 11.14). To prepare **101**, Baran converted the cyclopentane core **102** (available in 19 steps) to the hemiaminal **103** in 64% yield, using a selective silver(II)-oxidation protocol. Conversion to the 2-aminoimidazole was achieved by reaction of **103** with cyanamide, and this compound was brominated (Br₂, TFA, TFAA) to afford the bromide **104** in 35% yield for the two steps. After initial efforts to introduce an intact pyrrole failed, the key pyrrole **101** was prepared in 44% yield by reacting bromide **104** with amino ester **105** (AcOH, THF), then heating in TFA. Reduction of the azide groups was achieved by reaction with hydrogen gas and palladium acetate, and this was then followed by reaction with EDC to form the macrocycle. Without isolating the material, TFA was added and the solution heated at 70°C to trigger the critical transannular cyclization and generate palau'amine **100** in 17% yield (from **101**).

A comprehensive coverage of other examples of the role of synthesis in structure reassignment is not possible here, but some further examples are highlighted in Fig. 11.4. The reader is directed to an excellent review by Snyder and Nicolaou that covers in detail this topic [38].

11.3 In Pursuit of Nature's Perfection: Biosynthetic Principles and the Synthesis of Hemibrevetoxin B, Methyl Sarcophytoate, Longithorone, and 11,11'-Dideoxyverticillin

11.3.1 Hemibrevetoxin B

Much has been made of the proposed biosynthesis of the ladder polyether class via cascade epoxide cyclizations (for a review that also details the alternative Townsend oxidative cyclization process see: [39]), as exemplified for brevetoxin B (**113**) below in Scheme 11.15. Early work in the field of polyethers took guidance from these ideas, and Nicolaou provided a solution to the problem of the preference for so-called 5-exo vs. 6-endo cyclization manifolds for the cyclization of hydroxy epoxides by incorporation of a proximal alkene (Scheme 11.16a, **114** → **115**) [40]. This approach has seen broad application, however more recent results from Jamison have demonstrated the possibility for direct cyclization of hydroxy-poly epoxides **121** and **122** to tris-pyran **123** and tetra-pyran **124** (Scheme 11.16b). These reactions are uniquely possible in H₂O as solvent [41].



Scheme 11.14 The final stages of Baran's palau'amine synthesis. Reagents and conditions: (1) 50% TFA/H₂O then 10% TFA, silver(II)-picolinate, H₂O, 64%; (2) (a) H₂NCN, brine; (b) TFAA/TFA; Br₂, 35% (two steps); (3) **105**.AcOH, THF; TFA/CH₂Cl₂, 44%; (4) Pd (OAc)₂, H₂, TFA/H₂O then EDCI, HOBt, DMF; TFA, 17%

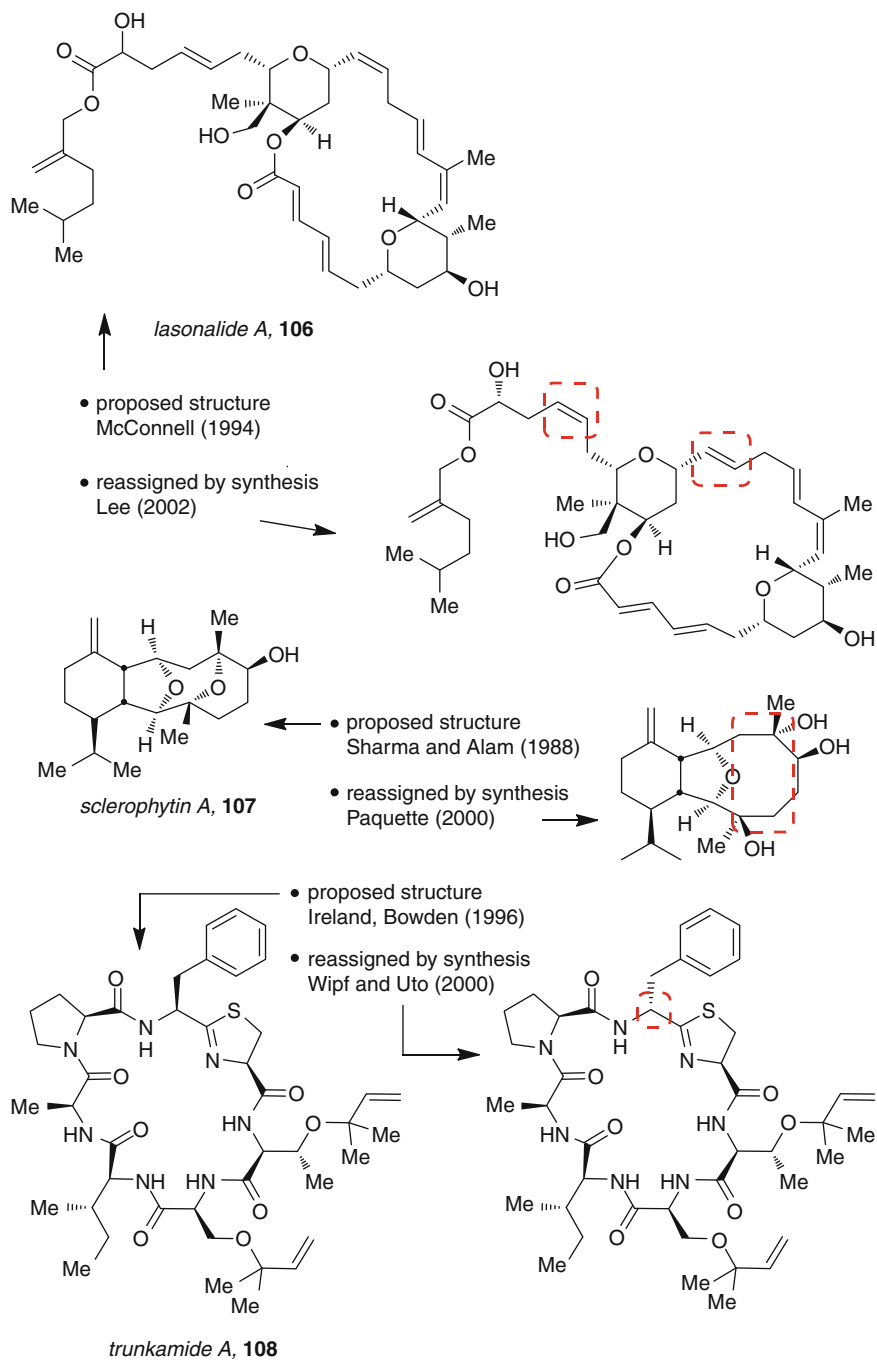
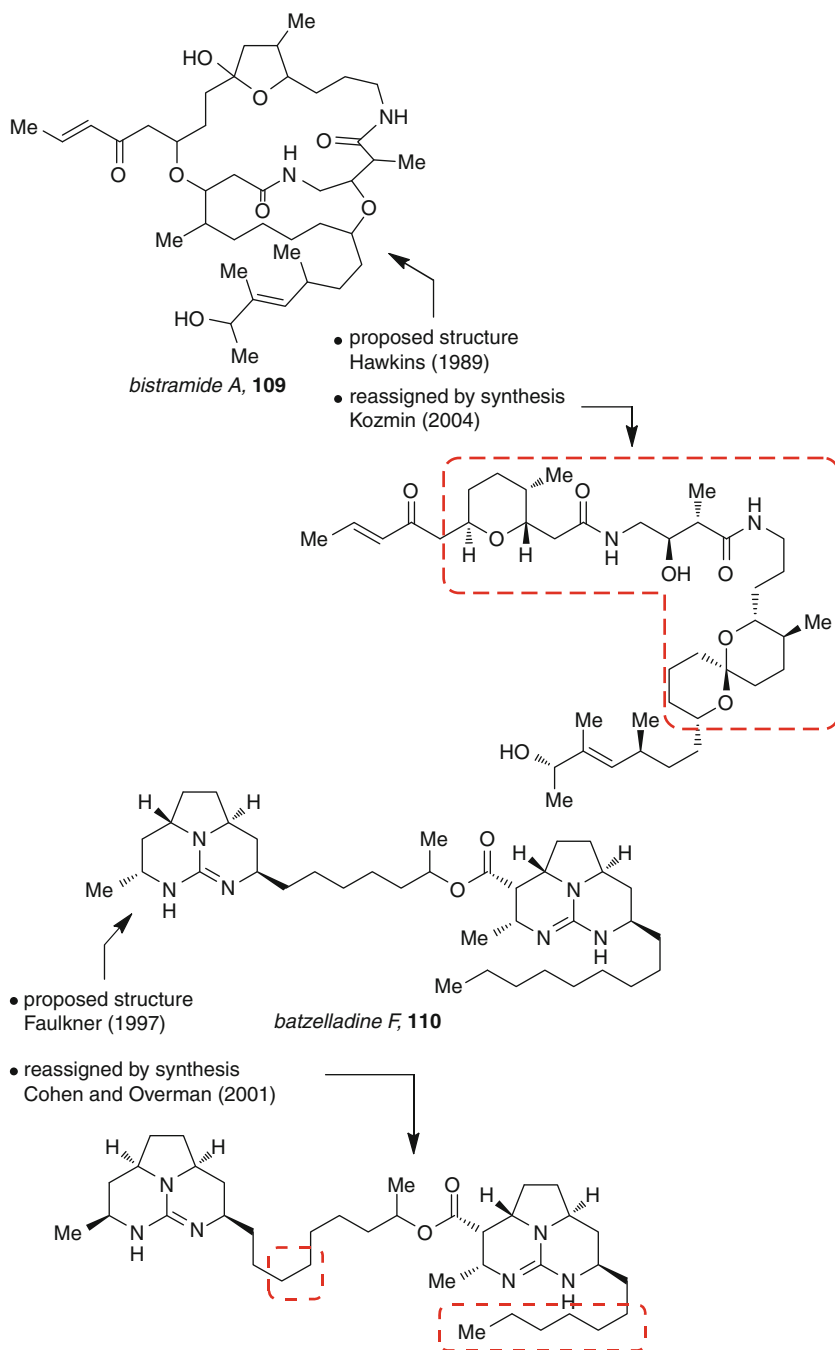


Fig. 11.4 (continued)

**Fig. 11.4** (continued)

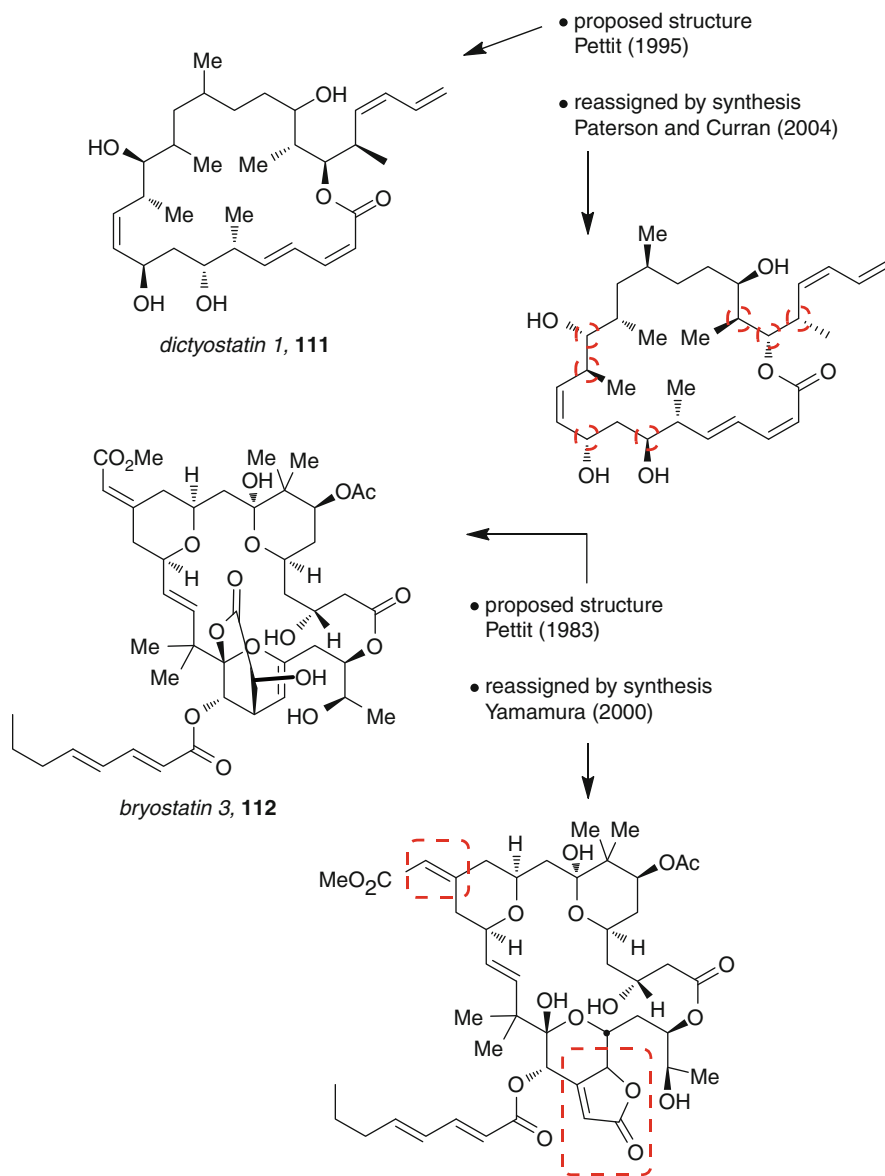
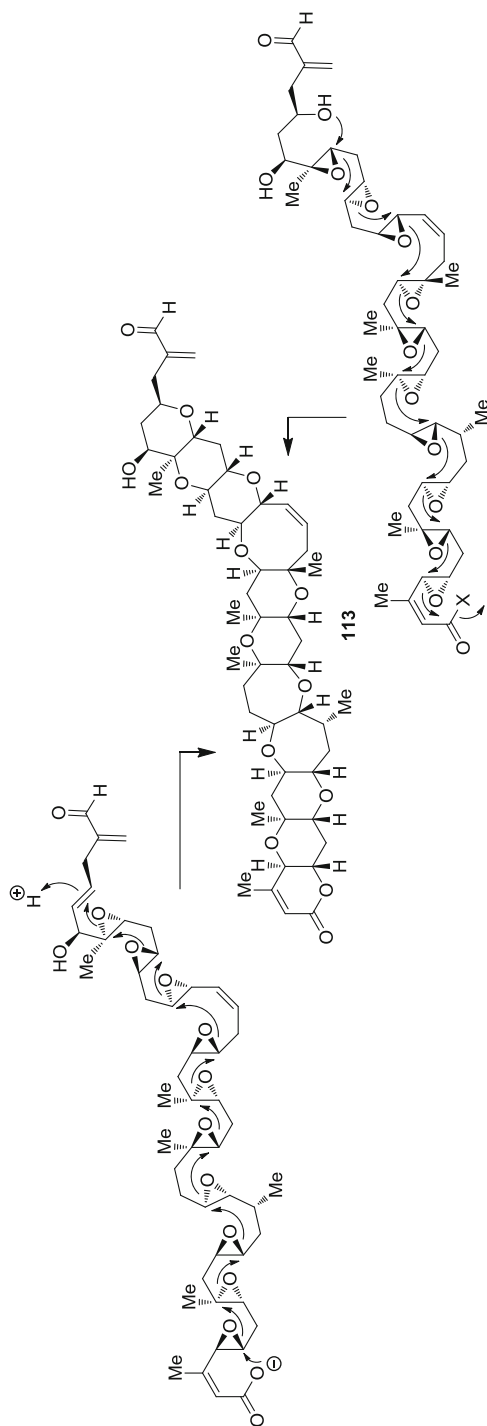
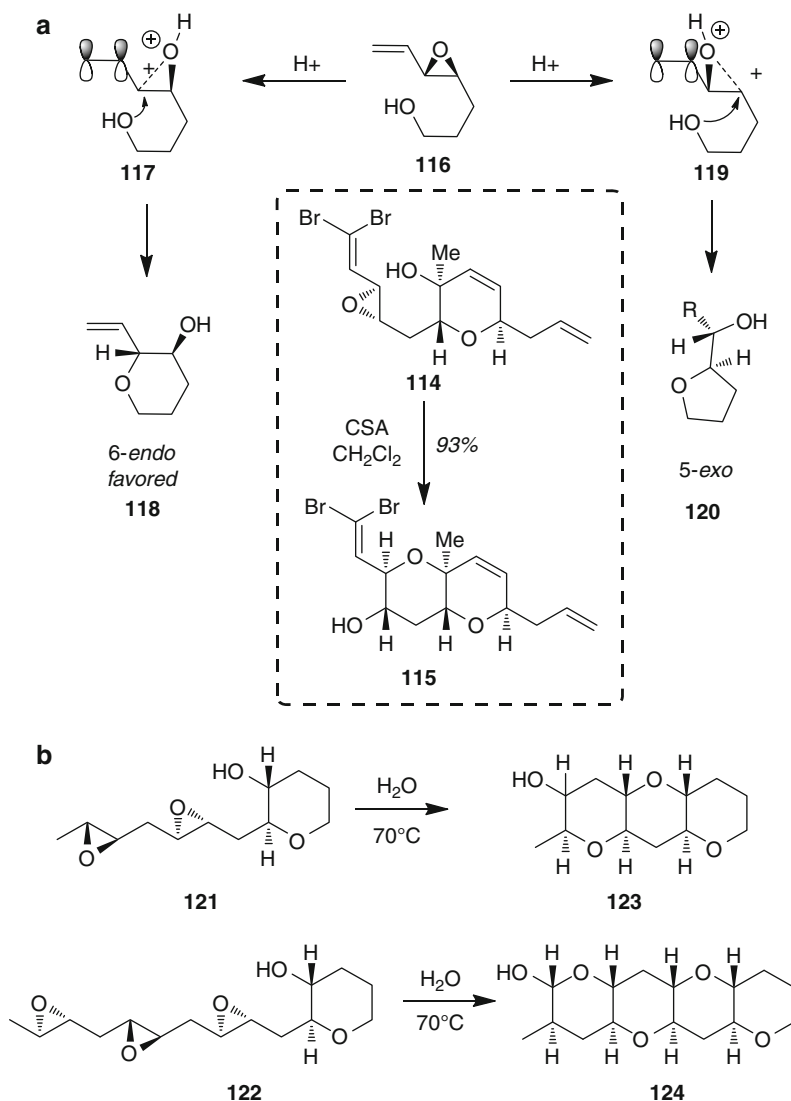


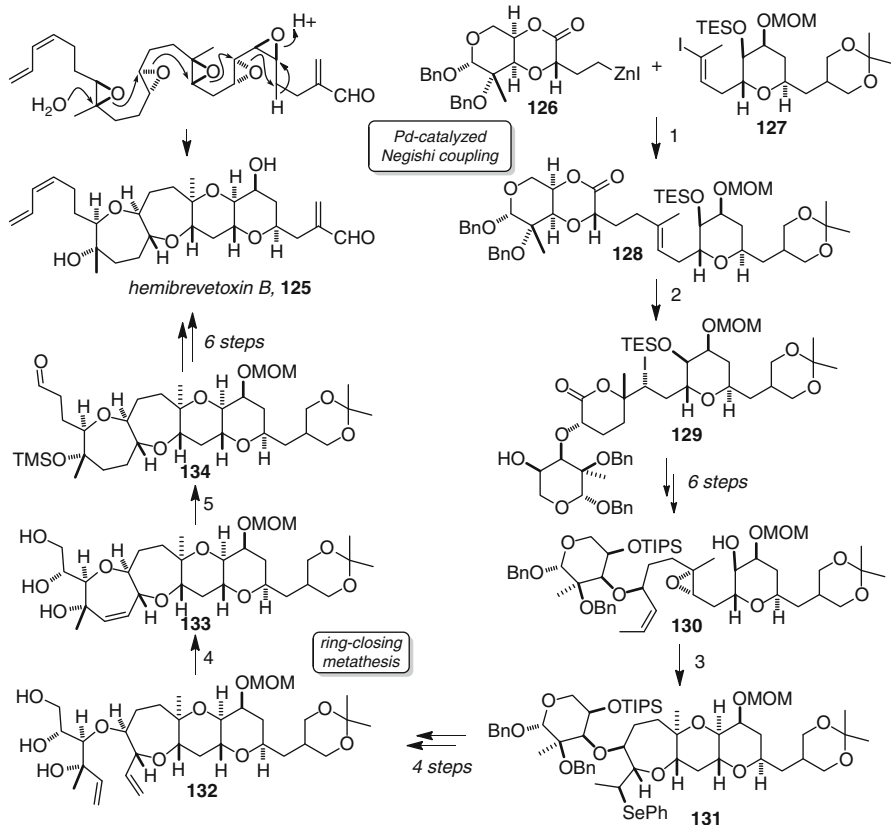
Fig. 11.4 Some initially misassigned structures where synthesis has played a key role in structure reassignment and confirmation: lasonolide (**106**) [111], sclerophytin A (**107**) [112], trunkamide (**108**) [113], bistramide (**109**) [114], batzelladine (**110**) [115], dictyostatin (**111**) [116], and bryostatin (**112**) [117]

**Scheme 11.15** Nakanishi–Nicolaou hypothesis [110]



Scheme 11.16 (a) Nicolaou's original approach to pyran formation from epoxy alcohols and (b) Jamison's discovery of the importance of H₂O as solvent

Holton's synthesis of hemibrevetoxin B125 [42] is based partly on these principles and is shown in [Scheme 11.17](#) [43]. The first key union of subunits involved a Negishi coupling between organozinc **126** ([Scheme 11.17](#), prepared from the corresponding iodide, which was in turn prepared from benzyl β-D-arabinopyranoside in 12 steps) and iodide **127** (prepared from tri-O-acetyl-D-glucal



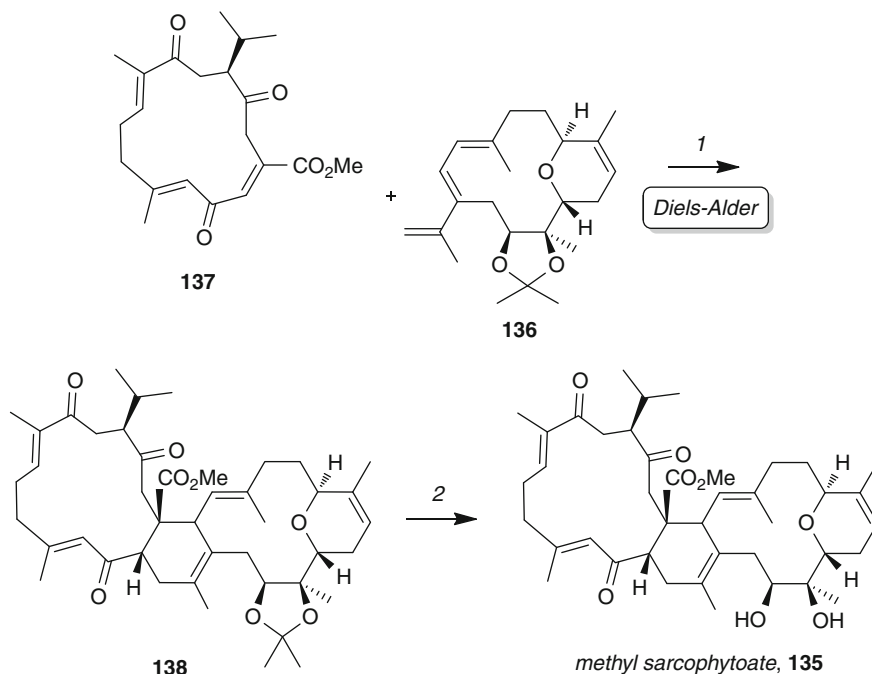
Scheme 11.17 Cascade epoxide cyclization-based biosynthesis of polyethers such as hemibrevetoxin B. Reagents and conditions: (1) 3 mol% $\text{PdCl}_2(\text{dppf})$, THF, rt, 76%; (2) (a) LiOH, THF– H_2O , 0°C ; (b) NIS, 2,6-lutidine, -10°C , 75%; (3) *N*-(phenylseleno)phthalimide, $(\text{CF}_3)_2\text{CHOH}$, 0°C , 83%; (4) 10 mol% Grubbs II catalyst, PhH, 80°C , 85%; (5) (a) NaIO_4 , $\text{Et}_2\text{O}/t\text{BuOH}/\text{H}_2\text{O}$; (b) $(\text{EtO})_2\text{P}(\text{O})\text{CH}_2\text{C}(\text{O})\text{N}(\text{Me})\text{OMe}$, NaH, THF; (c) H_2 , 20% $\text{Pd}(\text{OH})_2/\text{C}$, EtOAc; (d) TMSCl, Et_3N , CH_2Cl_2 ; (e) DIBAL-H, THF, -78°C , 79% (five steps)

via a 13-step sequence), which provided **128** in 75% yield. Lactone hydrolysis with lithium hydroxide, followed by iodolactonization with *N*-iodosuccinimide, produced iodolactone **130** (75%). A sequence of six steps converted **129** to epoxide **130**, which upon treatment with *N*-(phenylseleno)phthalimide underwent cyclization to give polycycle **131** as a single diastereoisomer in 83% yield. This sequence presumably is initiated by electrophilic selenation of the double bond, subsequent epoxonium ion formation, and termination by trapping by the free alcohol. Routine manipulations converted **131** to **132** via a sequence of four steps, and set the stage for formation of the oxepane ring by ring-closing metathesis (Scheme 11.17).

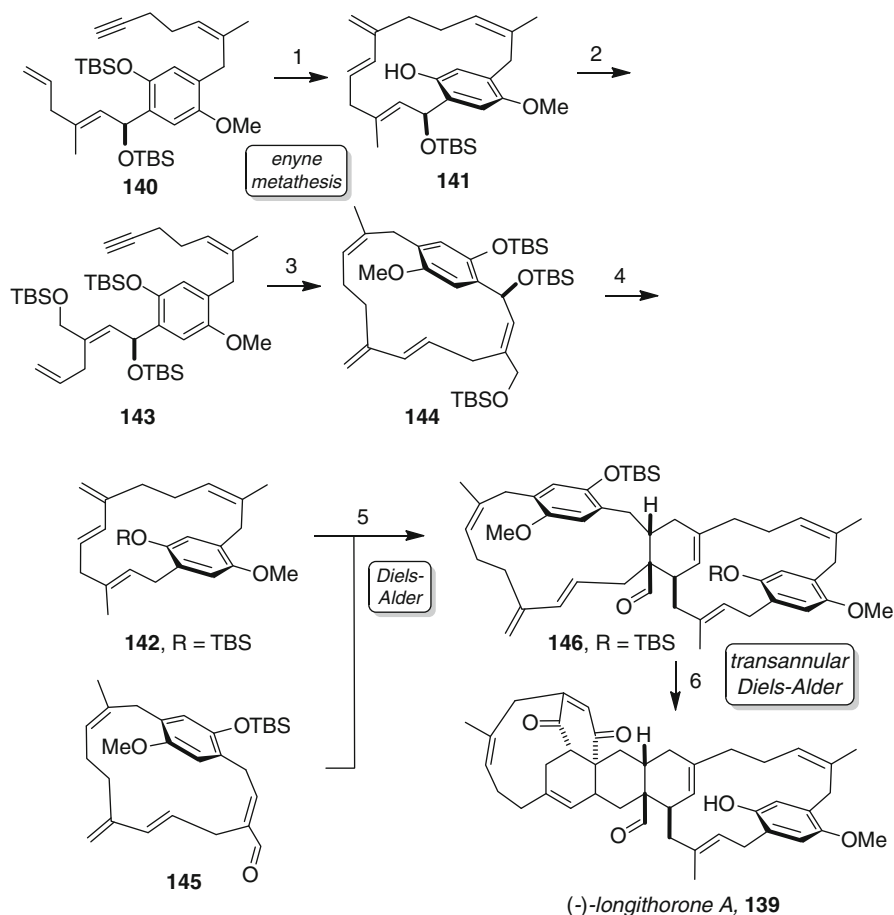
Upon exposure of **132** to Grubbs' second-generation catalyst, in benzene at reflux, ring-closure to yield **133** occurred in 85% yield. A sequence of 11 steps was used to convert **133** to hemibrevetoxin B, **125**.

11.3.2 Methyl Sarcophytoate and Longithorone A

Diels–Alder reactions have repeatedly proven their worth in the area of complex molecule synthesis, and in the cases of some natural products, the application of the Diels–Alder reaction after consideration of potential biosynthetic pathways can lead to the rapid assembly of molecules. Two recent examples are considered here. The synthesis of biscembranoid methyl sarcophytoate (**135**), which was developed by Nakata and coworkers [44], employs a Diels–Alder reaction between methyl sarcoate and another complex cembrane as the key step (Scheme 11.18). When **136** was heated with **137** in PhMe at 100°C for 1.5 days, the desired adduct **138** was obtained in 22% yield. Removal of the acetonide by treatment with aqueous AcOH completed the synthesis (50% for the final step). Notwithstanding the exact sequencing to reactions (and the use of protecting groups in the case of the laboratory synthesis), it seems likely that this process mimics the likely biogenesis.



Scheme 11.18 Synthesis of methyl sarcophytoate. Reagents and conditions: (1) PhMe, 100°C, 22%; (2) AcOH–H₂O, 50°C, 50%



Scheme 11.19 Shair's total synthesis of (-)-longithorone A. Reagents and conditions: (1) (a) 30–50 mol% Grubbs I, ethylene, 45°C, >20:1 atropisomer ratio; (b) TBAF, THF, 0°C, 31% (two steps); (2) (a) NaCNBH₃, TFA, CH₂Cl₂, 69% (b) TBSOTf, *i*Pr₂NEt, 0°C, 75%; (3) 0.5 eq Grubbs I, ethylene, 31%; (4) (a) TFA, Et₃SiH, CH₂Cl₂, (b) PPTS, EtOH 45°C, 46% (two steps), (c) Dess–Martin periodinane, CH₂Cl₂, 99%; (5) Me₂AlCl, CH₂Cl₂, –20°C, 70%; (6) (a) TBAF, THF, 0°C, (b) PhI(O), MeCN–H₂O, 0°C → 25°C, 90% (two steps)

The key elements of the Schmidt hypothesis for the biosynthesis of the longithorones were borne out in Shair's total synthesis of longithorone A (**139**) [45]. The synthesis highlights the strategic power of “biomimetic” Diels–Alder reactions and the utility of enyne metathesis reactions for the assembly of complex dienes. The key steps of the synthesis are shown in Scheme 11.19.

Enyne **140** underwent enyne metathesis followed by TBS deprotection to give cyclophane **141** with excellent selectivity for the desired atropisomer. Deoxygenation and protection led to diene **142**. Alkyne **143** was treated with Grubbs' catalyst to give diene **144**. Ionic hydrogenation, followed by deprotection

and oxidation, afforded aldehyde **145**. An intermolecular Diels–Alder reaction between diene **142** and enal **145** gave cyclohexene **146**. Deprotection followed by transannular Diels–Alder cycloaddition completed Shair’s total synthesis of (-)-longithorone A, **139**.

11.3.3 (+)-11,11'-Dideoxyverticillin A

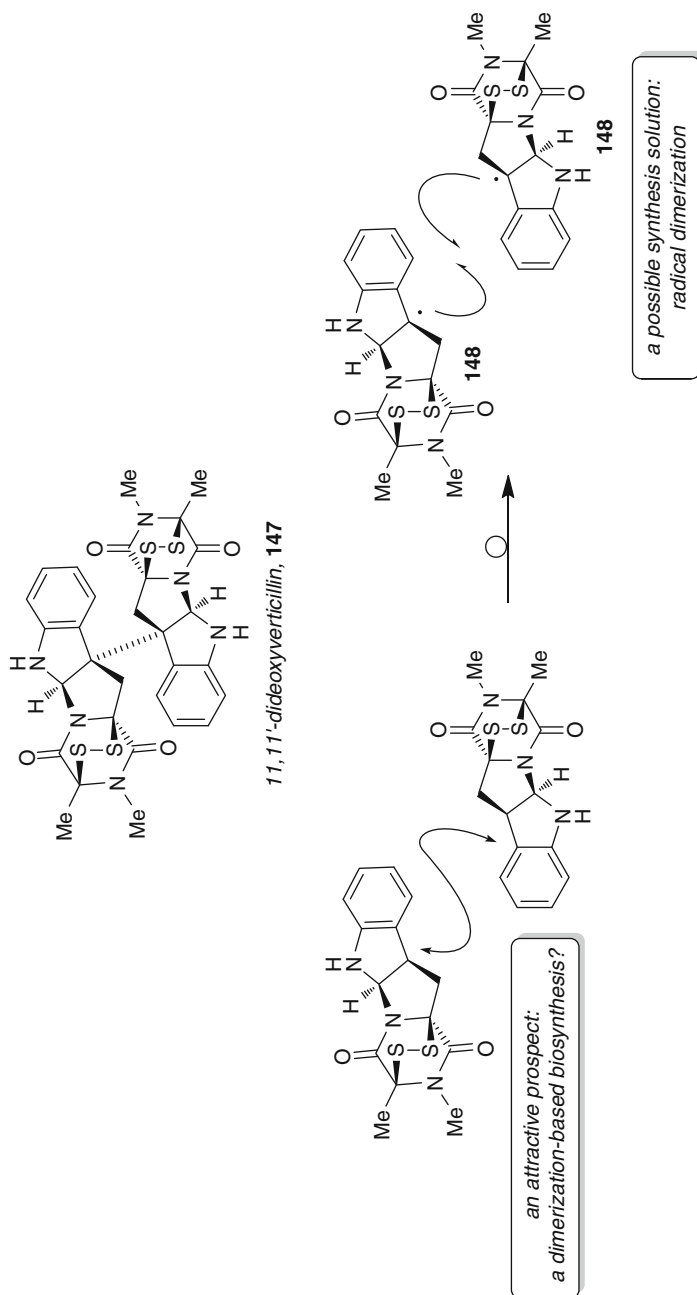
The dimeric epidithiodiketopiperazine alkaloids, as represented by (+)-11,11'-dideoxyverticillin A (**147**), are challenging synthetic targets that can be unraveled quickly by consideration of biosynthetic principles. Such an analysis led Movassaghi to a synthesis plan that was based on exploiting the dimerization of radicals **148** (Schemes 11.20) [46].

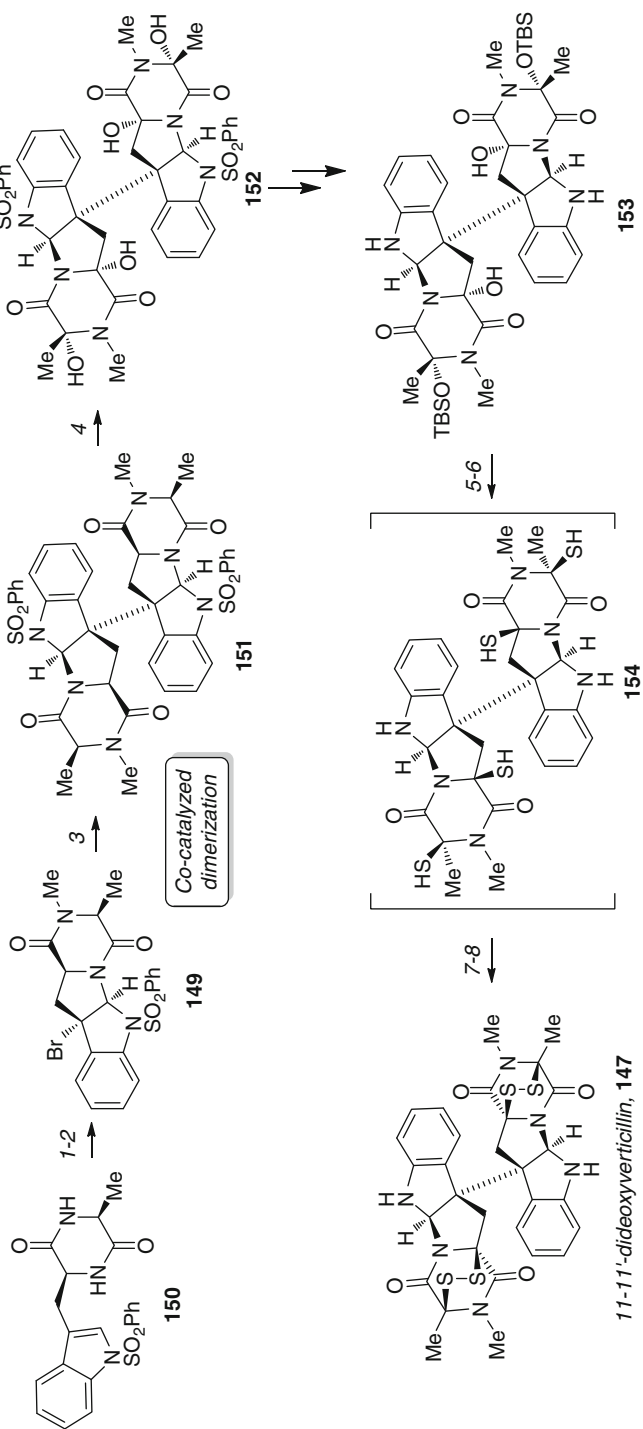
The dimerization precursor **149** was readily prepared in 58% yield by first reacting diketopiperazine **150** with bromine (MeCN, 0°C), then methylation with methyl iodide and potassium carbonate (Scheme 11.21). Reductive dimerization of **149** with tris(triphenylphosphine)cobalt (I) chloride in acetone gave the dimer **151** in 46% yield. After much experimentation, it was determined that the desired tetraol **152** could be prepared by oxidation with 4.8 equivalents of bis(pyridine) silver(I) permanganate in dichloromethane. This provided the tetraol **152** as a single diastereomer in an impressive 63% yield. However, it was found that **152** was highly acid and base sensitive, and while it could be transformed into the target molecule, it was a low-yielding process. It was discovered that these difficulties could be overcome by conversion to the diol **153**. This was prepared in 55% yield by selective protection using *t*-butyldimethylsilyl chloride and 5 mol% of Fu’s PPY catalyst [47]. Reaction with potassium trithiocarbonate and trifluoroacetic acid, followed by addition of ethanolamine gave a tetrathiol **154**, which could be readily converted to the target molecule by reaction with potassium triiodide. This impressive sequence proceeded in 35% overall yield. Clearly, the success of this strategy suggests that the proposed biosynthetic sequence is plausible.

11.4 New Reactions and New Strategies: Azaspiracid-1, Amphidinolide A1, Bryostatin 16, Ningalin B, and Cynathiwigins U and F

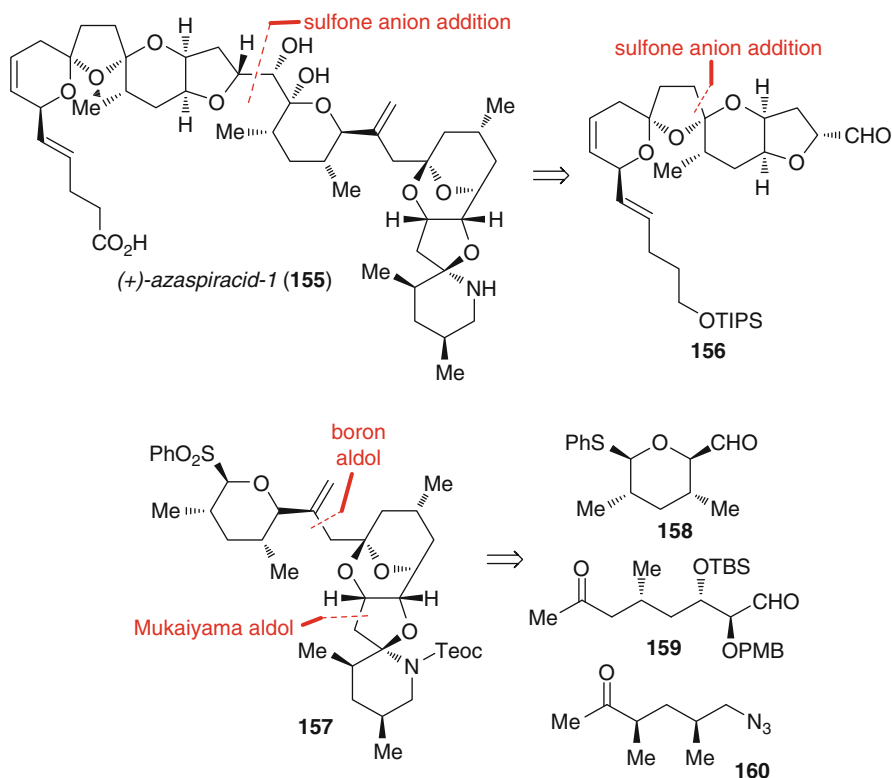
11.4.1 Azaspiracid-1

Complex natural products such as the azaspiracids have also served as excellent vehicles for the development and application of new synthetic methods. Subsequent to the Nicolaou synthesis, Evans reported a total synthesis of (+)-azaspiracid-1 (**155** the enantiomer of the natural product) [48]. An overview of the synthesis plan is shown in Scheme 11.22, and ultimately the key building blocks can be traced to compounds **158**, **159**, and **160**. This plan called for the preparation of these

**Scheme 11.20** Strategic analysis of 11,11'-dideoxyverticillin through the eyes of biomimetic synthesis planning



Scheme 11.21 Movassaghi's synthesis of (+)-11,11'-dideoxyverticillin. Reagents and conditions: (1) Br_2 , MeCN , 0°C , 76%; (2) MeI , K_2CO_3 , acetone, rt, 77%; (3) $\text{CoCl}(\text{PPh}_3)_3$, acetone, rt, 46%; (4) $\text{Py}_2\text{AgMnO}_4$, CH_2Cl_2 , rt, 63%; (5) TBSCl , 5 mol% PPY , NEt_3 , DMF , rt, 55%; (6) 5% $\text{Na}(\text{Hg})$, NaH_2PO_4 , MeOH , rt, 87%; (7) K_2CS_3 , TFA , CH_2Cl_2 , rt, 56%; (8) $\text{HOCH}_2\text{CH}_2\text{NH}_2$, acetone, rt, then KI_3 , pyridine, CH_2Cl_2 , rt, 62%



Scheme 11.22 An overview of Evans' analysis of (+)-azaspiracid-1 and the building blocks envisaged as being derived from asymmetric catalysis

compounds by Sn(II)- and Cu(II)-catalyzed asymmetric reactions that are part of a suite of powerful methods developed in the Evans group in the period 1990–2010, and azaspiracid-1 was expected to provide a worthy testing ground for the utility of these reactions in complex molecule synthesis.

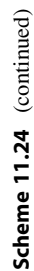
Access to the ketone **161** was achieved in 13 linear steps, starting with an asymmetric Mukaiyama aldol reaction of (silyloxy)furan **162** with *N*-phenyl glyoxamide (**163**), in the presence of 10 mol% of chiral Sn²⁺ complex **164** (Scheme 11.23). This reaction afforded the lactone **165** in 67% yield and >99% *ee* after recrystallization, and was followed by reduction of the double bond using Crabtree's catalyst [49] to give **166**. Transformation of this material to the required aldehyde **161** was achieved in a further 12 steps. Ketone **167** and aldehyde **168** could be accessed from the same intermediate, chiral tetrahydropyran **165**. The initial step of the sequence used to prepare **170** was the hetero Diels–Alder cycloaddition between **171** and **172** in the presence of Cu²⁺ complex **173** to give **174** in 84% yield and with excellent control of enantio- and diastereoselectivity. Simple reduction over Pd/C with H₂ gave **170**, and access to the E-ring fragment

167 from **170** was achieved by firstly forming the lactol thioether **175**, then epimerization of the ester substituent with potassium *t*-butoxide. This epimerization provides a tetrahydropyran with all four substituents equatorial. Reduction of the ester group with DIBAL-H afforded the aldehyde **168**. To access the third fragment required for the synthesis of EFGHI sulfone, the chiral tetrahydropyran **170** was transformed to the tosylate **169** via a four-step sequence as detailed in [Scheme 11.26](#). The tosylate was then converted to the desired HI-ring fragment **167** by Wacker oxidation and azide displacement.

With access to all the required fragments, attention was focused on fragment assembly by a series of aldol couplings ([Scheme 11.24](#)). First, ketone **167** and aldehyde **161** were coupled together using a chelate-controlled Mukaiyama aldol addition of enolsilane **176** with the aldehyde **161** in the presence of freshly prepared $\text{MgBr}_2 \cdot \text{OEt}_2$ to give the desired compound **177** as a single diastereomer in 93% yield. The second aldol coupling employed a boron-mediated aldol reaction between **172** and aldehyde **168** to give aldol adduct **178** as an inconsequential 60:40 mixture of diastereomers. Removal of the TBS ethers by aqueous HF in acetonitrile also resulted in cyclization to afford the FG bicyclic ketal as mixture of diastereomers. This mixture was oxidized with Dess–Martin periodinane to afford ketone **179**. At this juncture removal of the PMB ether with DDQ and reduction of the azide led to formation of the HI spiroaminal system **180** in 77% yield for the two steps. This ketone **180** was transformed to the desired EFGHI sulfone **181** and was methylenated using Tebbe's reagent in the presence of pyridine. Oxidation of the sulfide was carried out in the presence of pyridine to ensure that the sulfur group was not lost. With the assembly of the EFGHI sulfone **181**, the synthesis of azaspiracid-1 was almost complete. Coupling of the two major fragments was achieved by deprotonation of the sulfone **181** with *n*-BuLi, then addition of the aldehyde **182**. Quenching at -78°C with pH5 buffer afforded a near 1:1 mixture of lactol diastereomers, **183** and **184**, in 50% overall yield. Fortunately, the diastereomers are separable by chromatography and the undesired alcohol **183** could be transformed to the desired material **184** by oxidation under Swern conditions and diastereoselective reduction. Removal of the silyl protecting groups and a two-step oxidation of the C1 terminus provided (+)-azaspiracid-1 (**155**). The convergent approach allows the synthesis to proceed in just 26 linear steps, providing a nice example of complex molecule synthesis underpinned by powerful new asymmetric methods for the preparation of building blocks.

11.4.2 Amphidinolide A1

The amphidinolides have proven themselves a fertile environment for the development of new methods and strategies and, at the same time, have provided many instances of where synthesis has been able to assist in the structure assignment. This has always been a challenging task for this class in large part due to the minute amounts of material that are often initially isolated. The story of (+)-amphidinolide A1 [50] is noteworthy in this context as an example of the



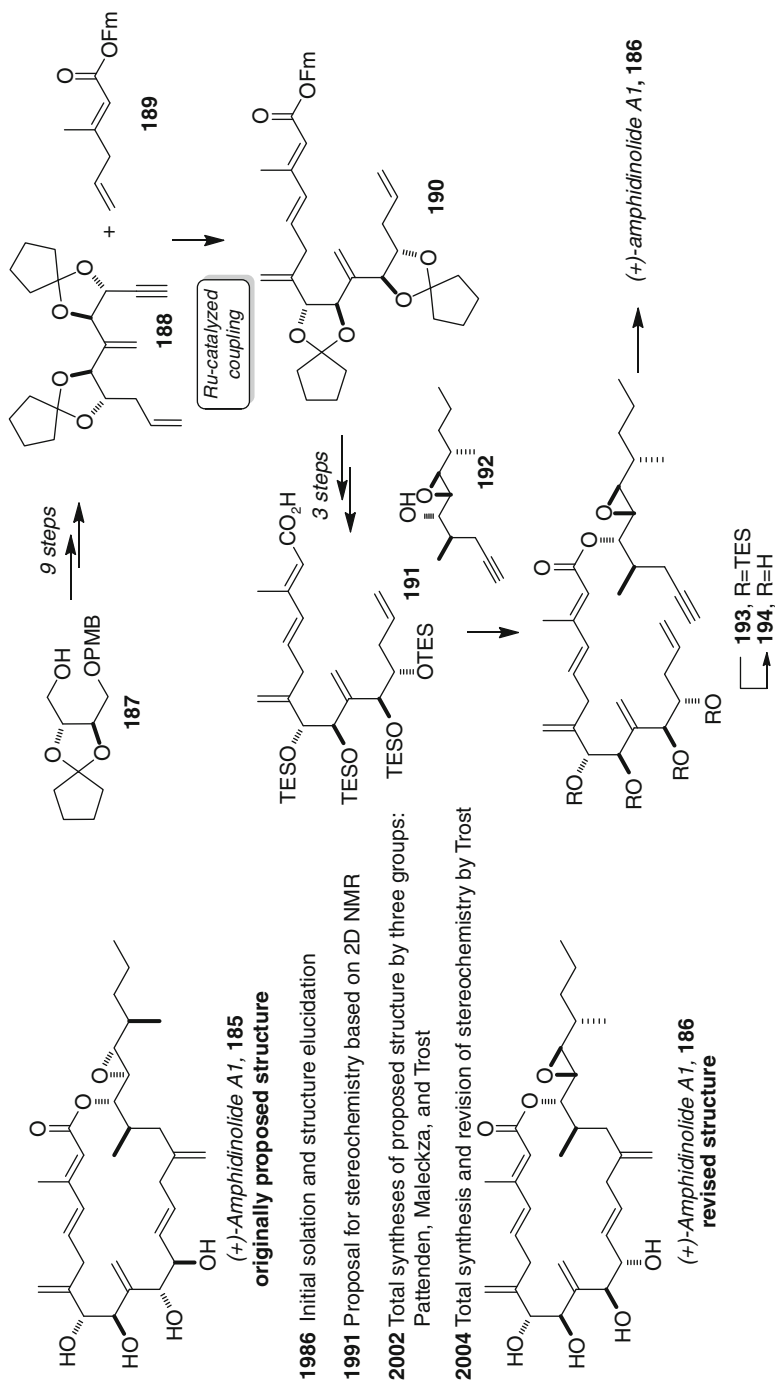
value of synthesis to the structure elucidation of complex marine natural products (Scheme 11.25). Kobayashi's initially proposed structure **185** was synthesized in 2002 in independent efforts by the groups of Trost [51], Pattenden [52], and Maleczka [53]. None of these efforts however produced material that matched the reported data which suggested that there were questions regarding the stereochemistry of the molecule remaining to be answered. This puzzle was solved in 2004 by Trost and Harrington when they described the structure elucidation of (+)-amphidinolide A1 (**186**) by a combination of total synthesis and NMR analysis [54] (Scheme 11.25).

The synthesis highlights Trost's new methodology for the construction of 1,4-dienes by the Ru-catalyzed coupling of alkenes and alkynes (Scheme 11.25) [55]. The first subunit coupling was achieved by reaction of **188** with **189** in the presence of $\text{Cp}^*\text{Ru}(\text{MeCN})_3\text{PF}_6$ as catalyst was employed. This catalyst provided the branched product **190** in 23% yield (39% yield based on recovered starting material). A straightforward sequence of three steps provided acid **191** which was coupled to the potentially sensitive epoxy alcohol **192** under Kita's conditions [56] to give ester **193** in 51% yield. After removal of the triethylsilyl ethers with TBAF–AcOH, $[\text{Cp}^*\text{Ru}(\text{MeCN})_3]\text{PF}_6$ -catalyzed macrocyclization of **194** provided amphidinolide A1, **186**. Although the yield may seem modest (33% or 38% based on recovered starting material), this is an impressive example of the remarkable selectivity of the Ru-catalyzed alkene–alkyne addition. The spectral data for synthetic material matched very well to the natural product with only two protons deviating from that reported by greater than 0.01 ppm (the two deviations were by 0.03 ppm and by 0.02 ppm), the ^{13}C NMR spectrum deviated by 0.1 ppm or less in CDCl_3 , J values in three solvents were also in agreement, and the optical rotation was also consistent with reported data (synthetic $[\alpha]_{\text{D}}^{24} +56^\circ$ (c 0.05, CHCl_3) cf. reported $[\alpha]_{\text{D}}^{24} +46^\circ$ (c 1.0, CHCl_3)). Even with these excellent comparisons, in the absence of authentic material for comparison, Trost and Harrington conclude their paper with guarded comments:

In conclusion, we have employed a combination of synthesis and NMR spectroscopy as tools to determine the correct structure of amphidinolide A1. Although the lack of a sample of the natural product prevents a definitive comparison, the excellent correlation [of our synthetic compound] strongly suggests it is (+)-amphidinolide A1.



Scheme 11.24 Evans' synthesis of the EFGHI sulfone fragment of (+)-azaspiracid-1 and completion of the synthesis. Reagents and conditions: (1) LiHMDS, TMSCl, Et_3N , THF, -78°C , 89%; (2) $\text{MgBr}_2 \cdot \text{OEt}_2$, CH_2Cl_2 , 0°C , 93%; (3) Cy_2BCl , $i\text{Pr}_2\text{NEt}$, CH_2Cl_2 , -78°C , then **168**, $-78^\circ\text{C} \rightarrow 0^\circ\text{C}$; (4) HF, H_2O , CH_3CN , 0°C , 92% (two steps); (5) Dess–Martin periodinane, pyr., CH_2Cl_2 , 85%; (6) DDQ, pH 7 buffer, CH_2Cl_2 , 0°C ; (7) H_2 , Pd/C, THF, 77% (two steps); (8) **181**, $n\text{-BuLi}$, -78°C , then **182**, NaOAc/AcOH buffer, $-78^\circ\text{C} \rightarrow \text{rt}$, 27% of **183** and 23% of **184**; (9) $(\text{COCl})_2$, DMSO, Et_3N , CH_2Cl_2 , $-78^\circ\text{C} \rightarrow -20^\circ\text{C}$, 60%; (10) LiBH_4 , CH_2Cl_2 , -40°C , 56%

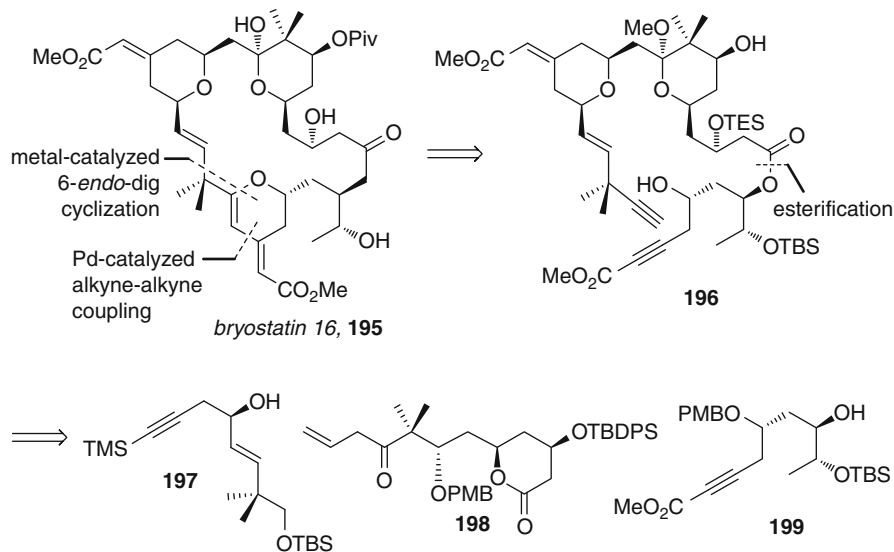


Scheme 11.25 Trost's synthesis of amphidinolide A1. Reagents and conditions: (1) **189**, $[\text{Cp}^*\text{Ru}(\text{MeCN})_3]\text{PF}_6$, 23%; (2) piperidine, 88%; (3) $\text{AcOH}/\text{H}_2\text{O}$ (3:1); (4) TESOTf , $i\text{-Pr}_2\text{NEt}$, 83% (two steps); (5) (1) $[\text{RuCl}_2(p\text{-cymene})]_2$, ethoxyacetylene; (2) **192**, CSA, 51%; (6) TBAF, AcOH , 79%; (7) $[\text{Cp}^*\text{Ru}(\text{MeCN})_3]\text{PF}_6$, 33%

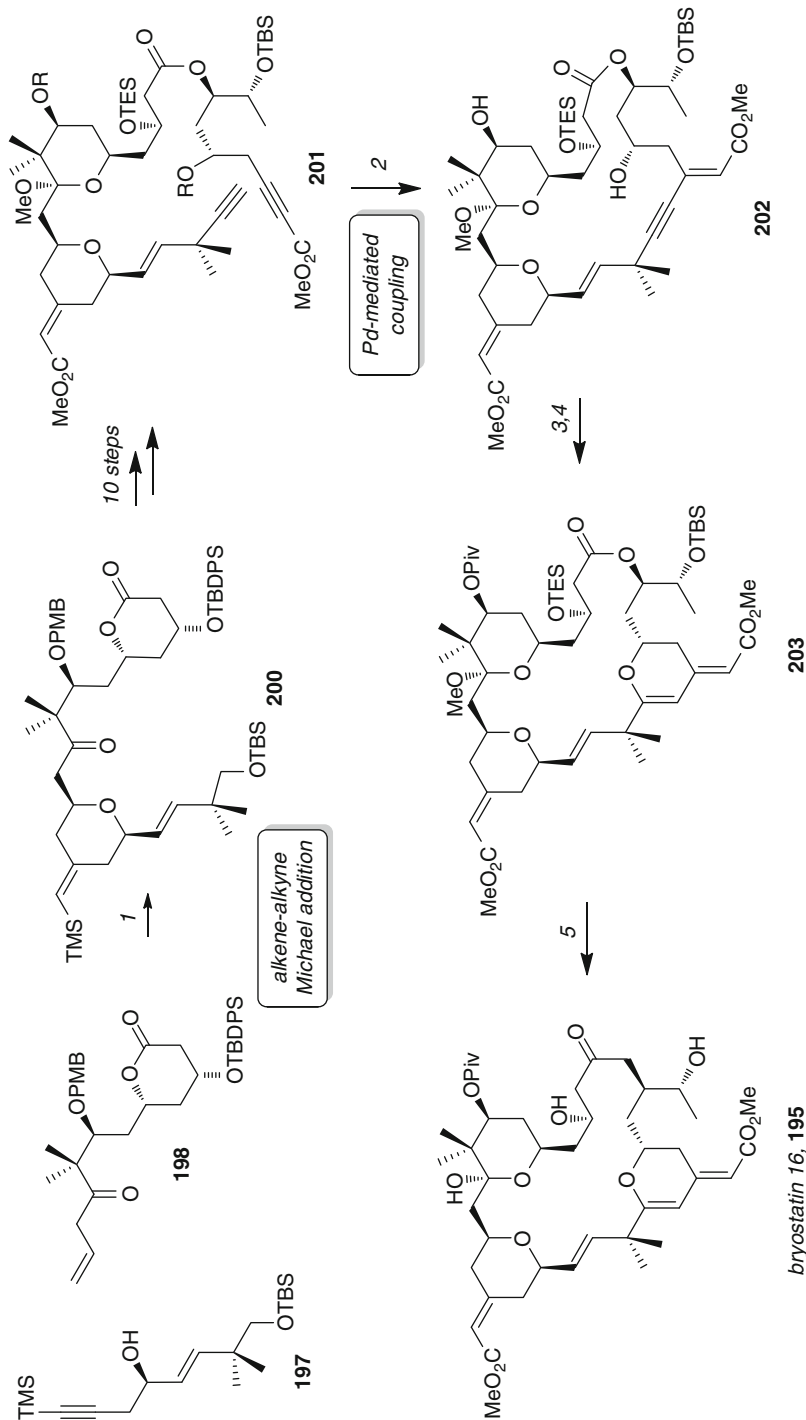
11.4.3 Bryostatin 16

The bryostatin family of macrolides have attracted significant attention over the years since the initial description of bryostatin 1 by Pettit and Clardy [57]. Synthetic highlights include five total syntheses [58], the development of a detailed pharmacophore model [59], and the preparation of much simplified functional analogs [60]. Here we highlight the total synthesis of bryostatin 16 (**195**) by Trost and Dong [39], which employs a number of new(er) transition metal-catalyzed reactions and underscores the value of new reactions in the arena of target synthesis: the longest linear sequence is only 26 steps. As detailed in [Scheme 11.26](#), it was envisaged that the macrocycle could be formed from **196** using a palladium-catalyzed alkyne-alkyne coupling, followed by a metal-catalyzed 6-*endo-dig* cyclization. The key substrate **196** would be assembled from the fragments **197**, **198**, and **199**.

A chemoselective ruthenium-catalyzed tandem alkene-alkyne coupling/Michael addition (13 mol% $\text{CpRu}(\text{MeCN})_3\text{PF}_6$, DCM) was used to form the *cis*-tetrahydropyran **200** in 34% yield (80% based on recovered starting material) ([Scheme 11.27](#)). Although modest in its conversion, the strategic power of this reaction for subunit assembly is impressive. The macrocycle **202** was generated in 56% yield by reaction of **201** with 12 mol% of palladium acetate and 15 mol% tris (2,6-dimethoxyphenyl)phosphine in PhMe at room temperature. It was found that the reaction had to be run at low concentration (0.002 M) and that the choice of solvent and the ligand/palladium ratio were critical to the success of the reaction. Treatment of the resulting alcohol **202** with a cationic gold catalyst ($\text{Au}(\text{PPh}_3)\text{SbF}_6$, NaHCO_3) initiated a 6-*endo-dig* cyclization and afforded the desired ring system in



Scheme 11.26 An overview of the Trost synthesis plan for bryostatin 16



Scheme 11.27 Trost and Dong's synthesis of bryostatin 16. Reagents and conditions: (1) $\text{CpRu}(\text{MeCN})_3\text{PF}_6$, CH_2Cl_2 , 34%; (2) $\text{Pd}(\text{OAc})_2$ (12 mol%), TDMPP (15 mol%), PhMe , 56%; (3) $\text{AuCl}(\text{PPh}_3)_2$, AgSbF_6 , NaHCO_3 , DCM/MeCN , 0°C to rt, 73%; (4) Piv_2O , DMAP, 73%; (5) TBAF, 52%

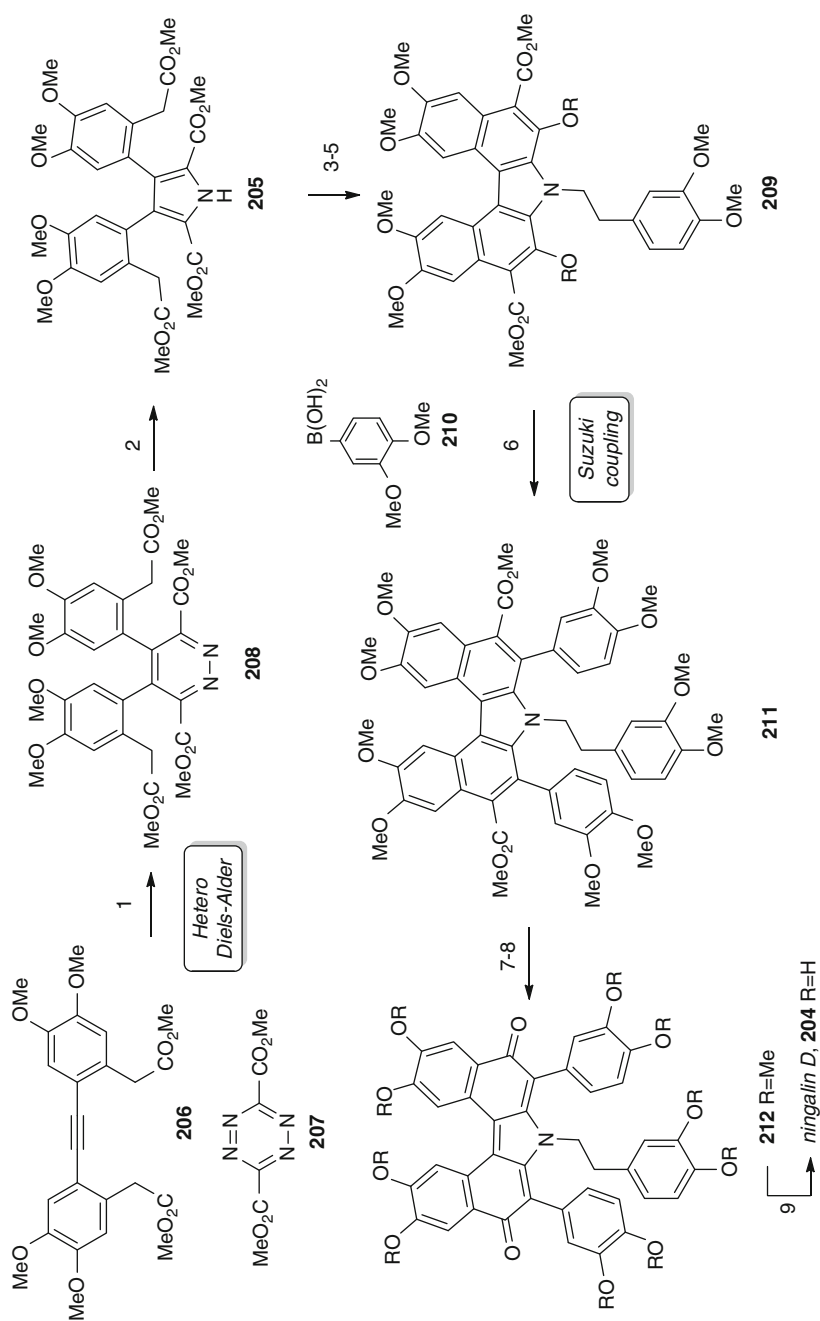
73% yield. After pivalation of the secondary alcohol to give macrocycle **203**, efforts focused on the global deprotection to afford bryostatin 16. After some experimentation, it was found that treatment of **203** with five equivalents of tetrabutylammonium fluoride gave bryostatin 16, **195**, in 52% yield.

11.4.4 Ningalin D

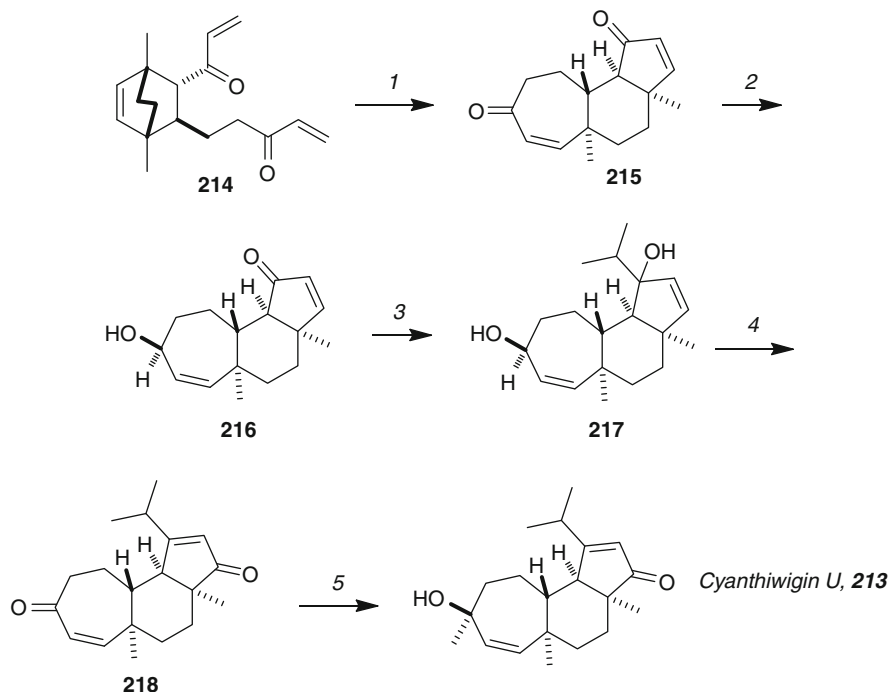
Complex alkaloids such as ningalin D (**204**) present substantial challenges for synthesis, and although cross-coupling chemistry is a dominant strategy for polyaromatic compounds, Boger has showcased the utility of alternative methods to produce an essentially ideal synthesis. In this case he completed a nine-step synthesis of ningalin D (**204**), which proceeds in 19% overall yield [61] (Scheme 11.28). The tetrasubstituted pyrrole **205** was rapidly assembled by firstly utilizing an inverse electron demand heterocyclic azadiene Diels–Alder reaction between symmetrical alkyne **206** and readily available tetrazine **207** to give symmetrical 1,2-diazine **208** in 87% yield. Reaction with 30 equivalents of zinc in trifluoroacetic acid at room temperature leads to cleavage of the diazine ring, followed by in situ cyclization to generate the pyrrole **205** in 64% yield. After alkylation of **205**, the aryl C and D rings were formed by double Dieckmann condensation by reaction with NaH in DMF at room temperature. The resulting diphenol **209** was triflated, and the F and G aryl rings were attached via a double Suzuki coupling with boronic acid **210**. Efforts to convert **211** into ningalin D were hampered by the steric congestion of the esters. However, hydrolysis of **211** with anhydrous hydroxide, followed by a modified Curtius rearrangement, afforded permethylated ningalin D **212** in a remarkable 70% yield. Clearly, the expected diamine was oxidized in situ and the resulting imines were hydrolyzed upon workup to generate the desired biphenylene quinone methide system. The ten methyl ethers were removed by reaction of **212** with 15 equivalents of BBr₃ to provide ningalin D, **204**, in 96% yield.

11.4.5 Cyanthiwigins U and F

The cyanthiwigin family of diterpenoids have stimulated the development of new methods and strategies (for a review see, [62]). For example, the Phillips–Pfeiffer synthesis of cyanthiwigin U (**213**) employed an efficient tandem metathesis reaction to convert bridged bicycle **214** into fused tricycle **215** in >43% yield (Scheme 11.29) [63]. Reduction of the more electrophilic carbonyl group with LAH gave **216**, and addition of isopropyllithium to the other carbonyl group gave bis-allylic alcohol **217**. Pyridinium chlorochromate oxidation resulted in formation of the cycloheptenone and, at the same time, gave Dauben oxidative transposition of the cyclopentenol to provide **218**. Simple addition of methyllithium completed the synthesis.



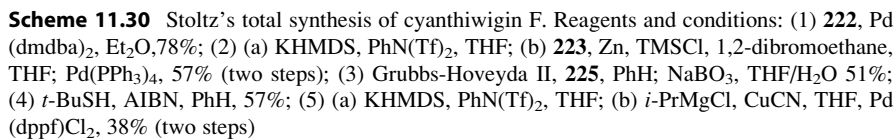
Scheme 11.28 (continued)



Scheme 11.29 Phillips and Pfeiffer's synthesis of cyanthiwigin U. Reagents and conditions: (1) 20 mol% Grubbs II, ethylene, PhMe, >43%; (2) LAH, THF, 92%; (3) *i*-PrLi, CeCl₃ THF; (4) PCC, CH₂Cl₂, 90% (two steps); (5) MeLi, THF, quantitative (*dr* = 9:1)

In a similar vein, Stoltz and Enquist completed a total synthesis of cyanthiwigin F (**219**) that was underpinned by reaction development (Scheme 11.30) [64]. Earlier studies into the asymmetric Tsuji decarboxylative allylation reaction [65] had provided a method for the conversion of **220** into **221** by treatment with catalytic Pd(0) in the presence of phosphino-oxazoline **222**. Subsequent enol-triflation and cross-coupling with the organozinc derived from iodide **223** gave **224** and set the stage for a ring-closing metathesis with Grubbs–Hoveyda catalyst (second generation) and simultaneous cross metathesis of the other olefin with vinylboronate **225**. An oxidative workup gave aldehyde **226** in 51% yield. Radical cyclization proceeded smoothly to produce tricyclic compound **227**, which could be advanced to cyanthiwigin F (**219**) by conversion of the cyclopentanone ring to the enol triflate and cross coupling with *i*-propylmagnesium chloride.

Scheme 11.28 The Boger synthesis of ningalin B, **204**. Reagents and conditions: (1) toluene, 110°C, 87%; (2) Zn, TFA, rt, 64%; (3) 3,4-dimethoxyphenyl ethyl iodide, CsCO₃, DMF, 60°C, 92%; (4) NaH, DMF, 25°C, 81%; (5) Tf₂O, pyridine-CH₂Cl₂, 0°C → 5°C, 92%; (6) (PPh₃)₄Pd, LiCl, 1 M aq. K₂CO₃-DME, 80°C, 88%; (7) *t*-BuOK, H₂O, DMSO, 80°C, 84%; (8) DPPA, *i*Pr₂NEt, CH₂Cl₂, 25°C; then H₂O, THF, air, reflux, 70%; (9) BBr₃, CH₂Cl₂, -78°C → rt, 96%



The marine environment produces some remarkably complex structures, and these compounds have in turn stimulated tremendous efforts in total synthesis. In this section we briefly highlight the synthesis of ladder polyethers, but in

advance of doing so we present four molecules that represent substantial complexity in Fig. 11.5. All of these molecules are accessible by synthesis: ciguatoxin CTX3C (**227**) was made by Hirama and Inoue in 2001 [66]; palytoxin (**228**) by Kishi and Suh in 1994 [67]; norhalichondrin B (**229**) by Kishi (1992) [68] and Phillips (2009) [69]; and phorboxazole A (**230**) by Forsyth (1999) [70], Smith (2001) [71], Williams (2003) [72], Pattenden (2003) [73], and White (2006) [74].

The Nicolaou group was one of the first to engage in synthetic studies directed toward the ladder polyethers, and among the many total syntheses from the group in this area there has been a significant amount of reaction discovery and development, which we briefly highlight here (Scheme 11.31). For example, the formation of cyclic ethers by thiohemiacetal formation (**231** \rightarrow **233**) and reductive removal of the sulfur to give structures of type **234** has seen widespread use by many groups. An especially creative solution to the formation of bis-oxepane rings is the reductive cyclization of dithionolactones (**235** \rightarrow **236**) and their subsequent conversion to **238** by desulfurization and hydrogenation [75].

Elements of the methods described above were employed in Nicolaou's first total synthesis of brevetoxin B (**113**), the closing steps of which are shown in Scheme 11.32 [76]. Subunit coupling by Wittig reaction between phosphonium salt **239** and aldehyde **240** gave **241** after removal of the TMS ether. Reductive etherification by the two-step approach outlined above gave **242** in an impressive 85% yield, and the synthesis was completed in five further steps.

More recently, Sasaki and coworkers have completed a synthesis [77] of gymnocin A (**243**), a polyether toxin from the red tide dinoflagellate *Karenia mikimotoi* [78]. The total synthesis employed some daring applications of their earlier-developed method for polyether synthesis based on a β -alkyl Suzuki–Miyaura coupling followed by hydroboration and reductive etherification as the key strategy for subunit couplings. The key steps involved in the assembly of the complete A \rightarrow N ring system are summarized in Scheme 11.33. Hydroboration of complex enol ether **244** with 9-BBN to give borane **245** is followed by cross-coupling with nonacyclic enol triflate **246** in the presence of Pd(PPh₃)₄ to give **247**. Given the very high complexity of the substrates, the yield for this reaction is a remarkable 81%, and should serve to underscore the power of contemporary cross-coupling reactions in complex settings. Conversion of **247** to the precursor for acetal formation was achieved by a four-step sequence: (a) hydroboration-oxidation, (b) protection as the triethylsilyl ether, (c) removal of the p-methoxybenzyl ether, and (d) oxidation to produce ketone **248** (56% overall yield for four steps). Treatment of **249** with ethanethiol in the presence of Zn (OTf)₂ provided the desired thioacetal **250** in 40% yield along with 38% of thioacetal **251** in which one of the tert-butyldimethylsilyl ethers had been removed. This compound was readily resilylated to produce **250**. Reductive desulfurization under radical conditions with AIBN and triphenylstannane converted the thioacetal into the desired ether **252** in an impressive 98% yield. Compound **252**, which contains the complete A \rightarrow N ring system, was converted to gymnocin A, **243**, by an eight-step sequence.

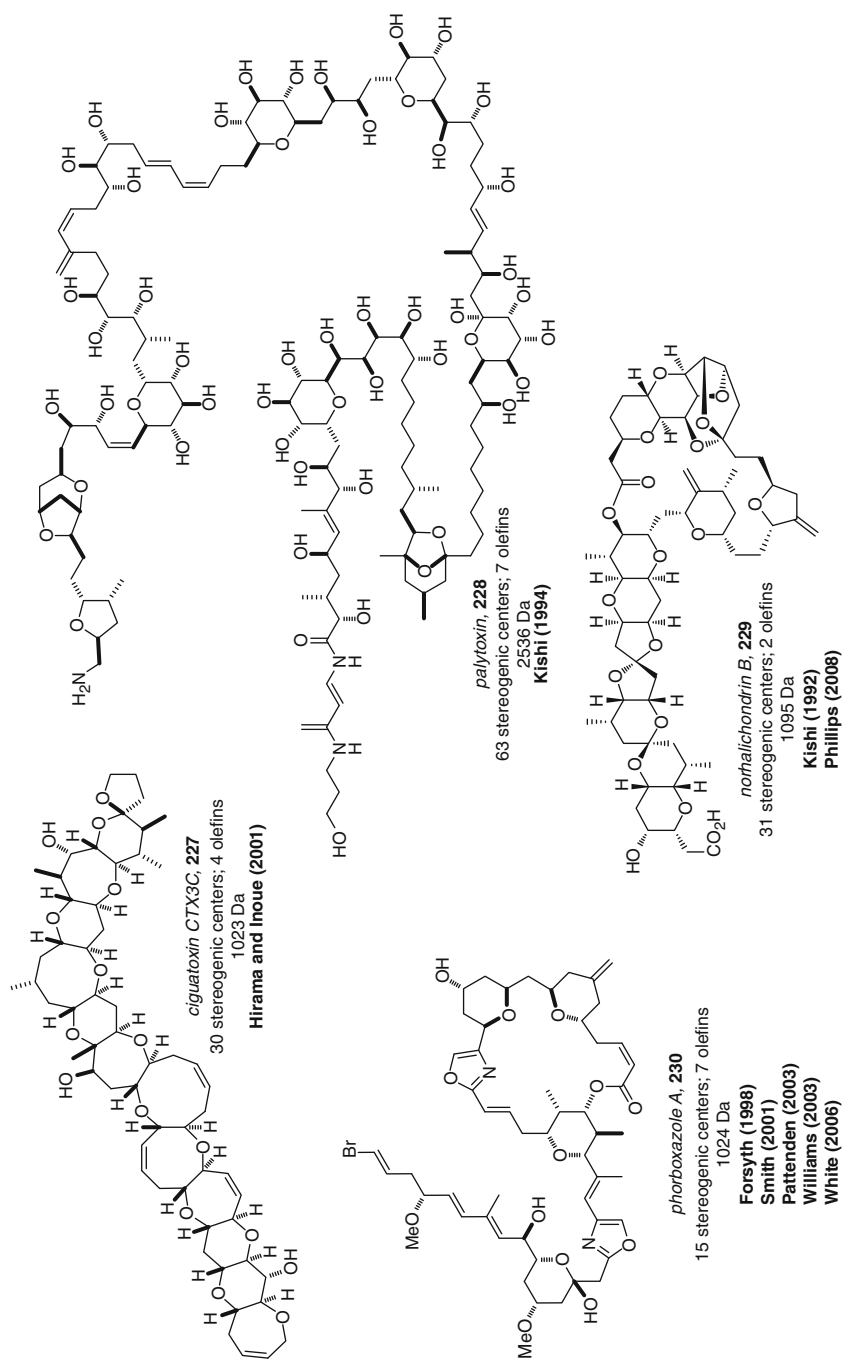
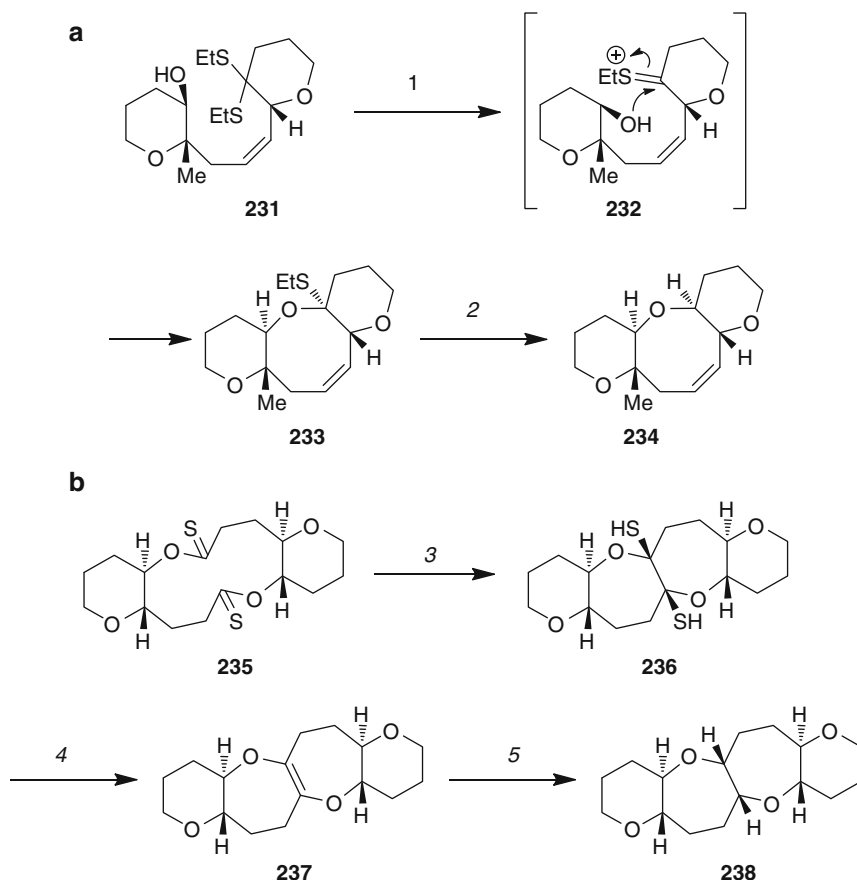


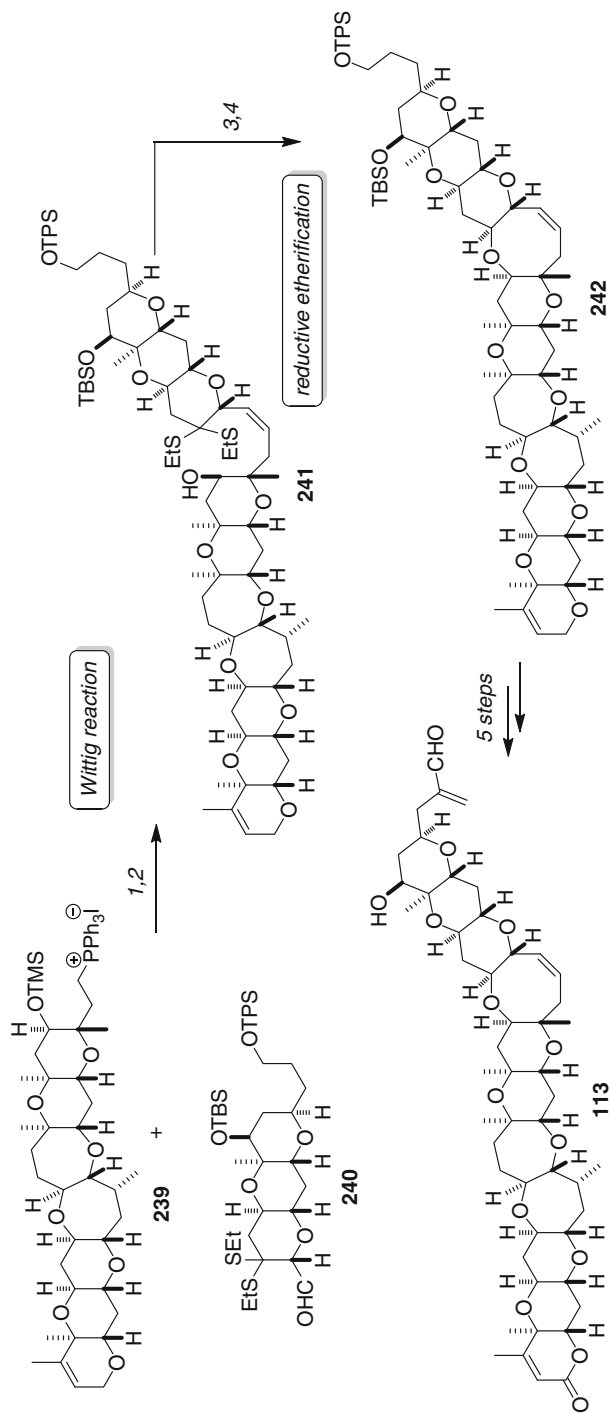
Fig. 11.5 Examples of the level of molecular complexity that can be attained by modern organic synthesis



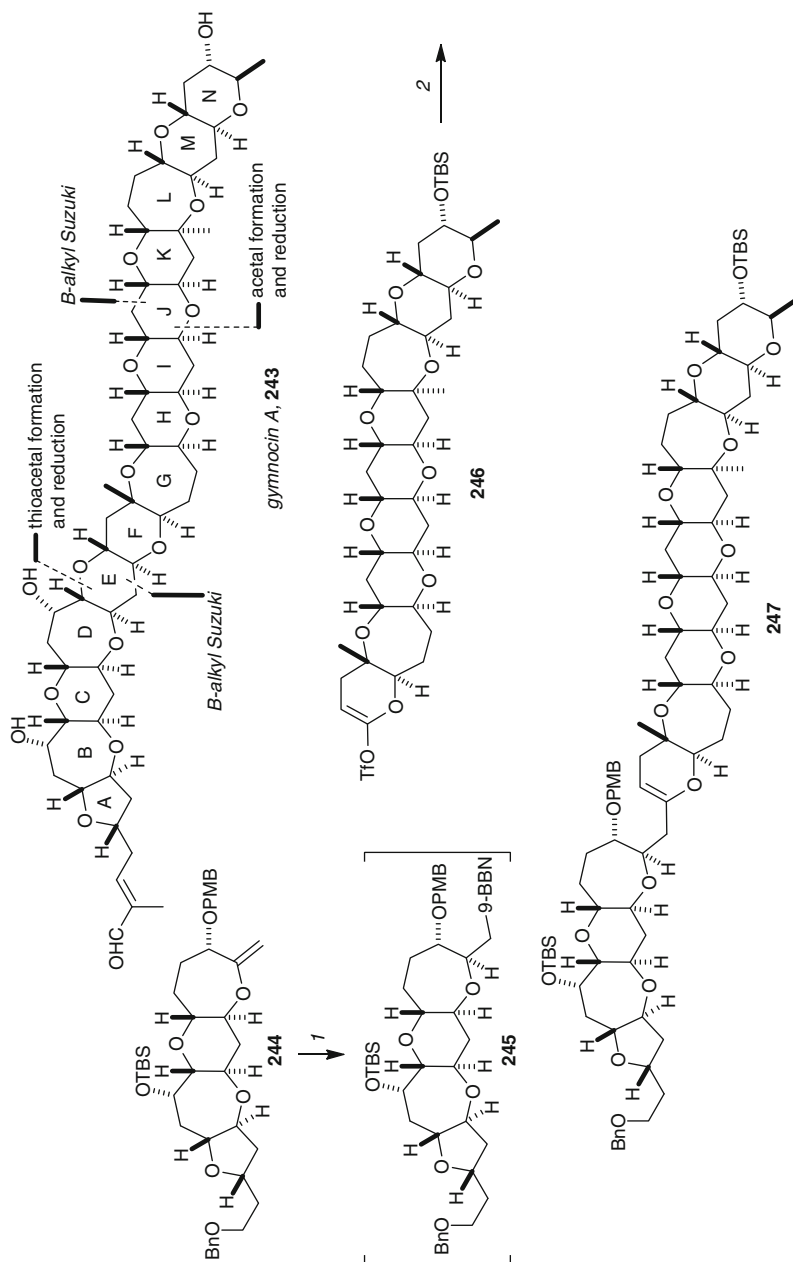
Scheme 11.31 Early technologies from Nicolaou for complex ladder polyether synthesis. **(a)** Reductive etherifications, and **(b)** formation of bis-oxepanes by reductive coupling of dithionolactones. Reagents and conditions: (1) AgNO_3 , NCS, SiO_2 , 2,6-lutidine, CH_3CN , 3 Å MS, 92%; (2) Ph_3SnH , AIBN, PhCH_3 , 110°C , 95%; (3) sodium naphthalenide, THF, -78°C ; MeI, 80%; (4) $n\text{Bu}_3\text{SnH}$, AIBN, PhCH_3 , heat, 99%; (5) H_2 , $\text{Pd}(\text{OH})_2$, EtOAc, 70%

11.6 Gram-Scale Synthesis: Moving Toward Realistic Supply of Compounds for Preclinical Evaluation

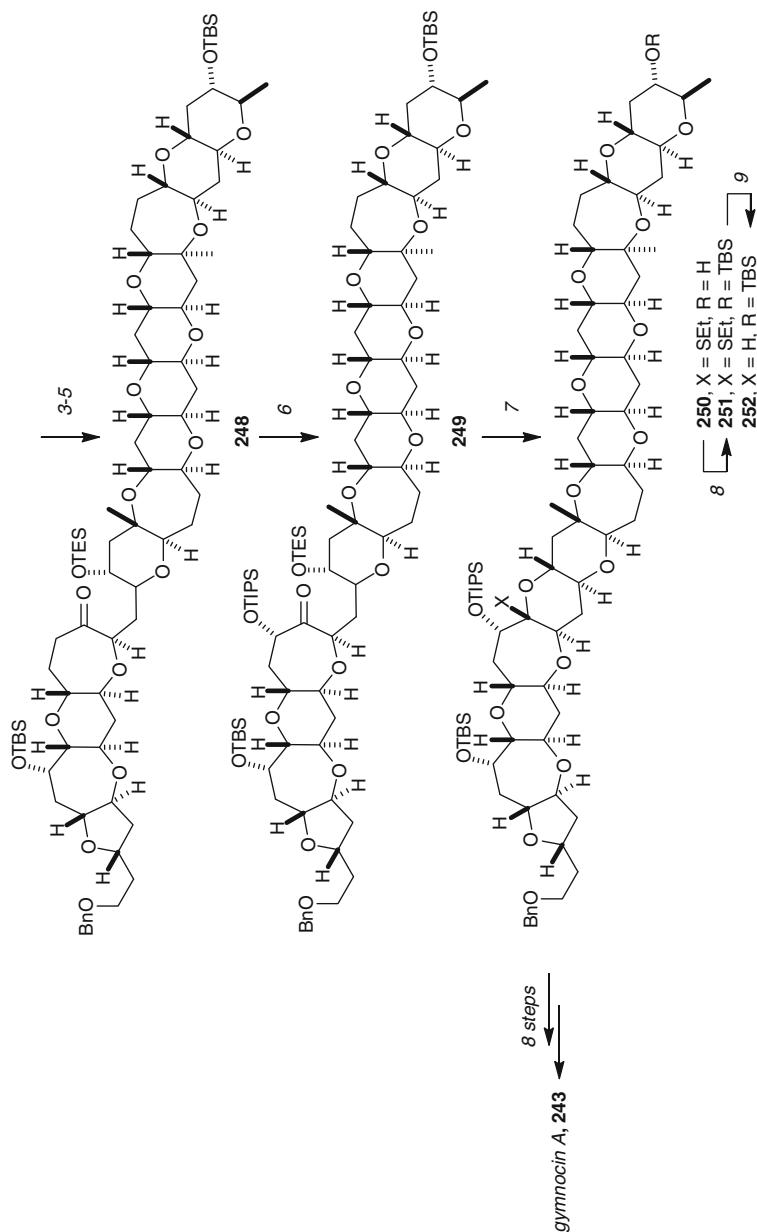
One of the major challenges of marine natural products is the limited supplies available from the natural source, which often stymies further investigation into the biological properties. Many marine natural products cannot be evaluated as clinical agents due to these limited supplies, and the development of a practical synthetic route is absolutely critical to the further development of such compounds.



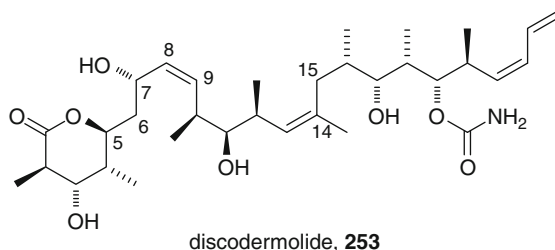
Scheme 11.32 Subunit couplings and completion of Nicolaou's pioneering synthesis of brevetoxin B. Reagents and conditions: (1) *n*-BuLi, HMPA; (2) PPTS, MeOH, 25°C, 75% (two steps); (3) AgClO₄, NaHCO₃, SiO₂, 4 Å MS, MeNO₂, 25°C; (4) Ph₃SnH, AIBN, 110°C, 85% (two steps)



Scheme 11.33 (continued)



Scheme 11.33 Closing steps of Sasaki's total synthesis of gymnocin A. Reagents and conditions: (1) 9-BBN, THF, rt; (2) **245**+**246**, 3 M Cs₂CO₃, Pd(PPh₃)₄, DMF, rt, 81%; (3) BH₃·SMe₂, THF, 0°C → rt then NaOH, H₂O₂, 75%; (4) (a) TESOTf, 2,6-lutidine, CH₂Cl₂, rt, (b) DDQ, CH₂Cl₂, pH 7 phosphate buffer, 0°C, 79% (two steps); (5) TPAP, NMO, 4 Å MS, CH₂Cl₂, rt, 95%; (6) (a) LiHMDS, TMSCl, Et₃N, THF, -78°C, (b) OsO₄, NMO, THF-H₂O, rt, (c) TIPSOt, 2,6-lutidine, CH₂Cl₂, rt, 85% (three steps); (7) EtSH, Zn(OTf)₂, MeNO₂, 0°C → rt, 40% **252**, 38% **251**; (8) TBSOTf, 2,6-lutidine, CH₂Cl₂, rt, 71%; (9) Ph₃SnH, AIBN, PhMe, 110°C, 98%

**Schreiber (1993)**

4.3% overall yield, 24 steps LLS

Key fragments

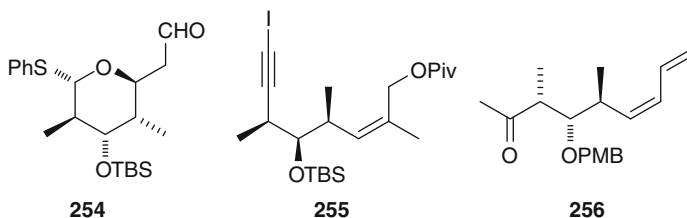


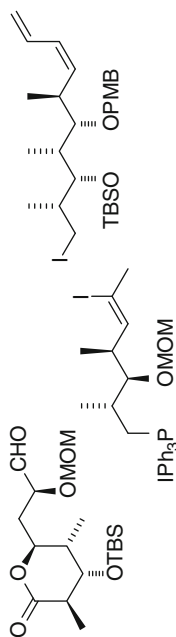
Fig. 11.6 The structure of discodermolide, and the main building blocks for Schreiber's initial total synthesis

One of the best examples of the value of total synthesis in providing realistic supplies of a natural product is discodermolide, **253**, which is a biologically active polyketide isolated in just 0.002 wt.% from the marine sponge *Discodermia dissoluta* [79]. The potent biological activity, coupled with the scarce supply from its natural source, has triggered intense activity in the total synthesis community [80]. Schreiber's group reported the first total synthesis, which confirmed the relative stereochemistry and established the absolute configuration [81]. As summarized in Fig. 11.6, his retrosynthetic analysis gave three key fragments, **254**, **255**, and **256**, with a Nozaki–Kishi coupling and an enolate alkylation being the critical bond-forming steps.

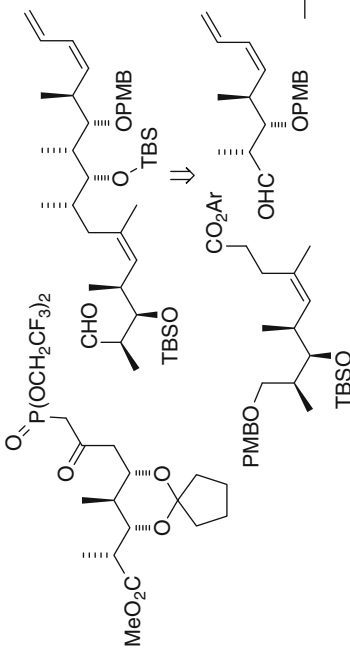
Since this work, a further 11 total syntheses have been reported from the academic groups of Smith [82], Paterson [83], Myles [84], Marshall [85], Panek [86], and Ardisson [87]. Of these syntheses, the groups of Smith and Paterson having refined their initial efforts and have reported fourth and third generation syntheses, respectively. As illustrated in Scheme 11.34, Smith's group utilized a Wittig reaction (C8–C9) and a Negishi cross-coupling (C14–C15) to assemble his key fragments, which allowed the generation of discodermolide in 9% overall yield and 17 steps for the longest linear sequence. While Paterson's initial syntheses had used boron aldol couplings, the difficulties of scale-up led his group to develop a third-generation synthesis where a Still–Gennari olefination was utilized. This resulted in an improved overall yield of 11.1%.

Smith (1995, 1999, 2003, 2005)

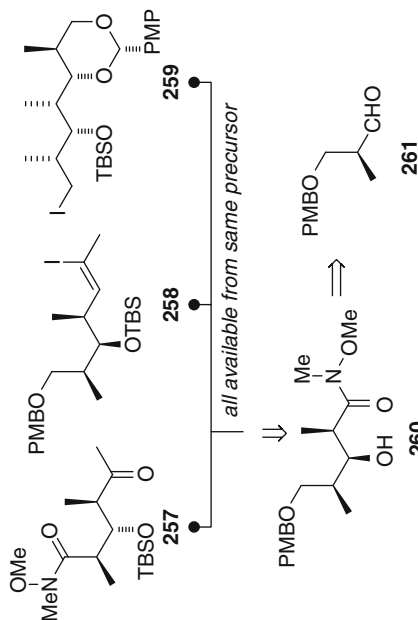
Fourth generation: 9% overall yield, 17 steps LLS
Key fragments

**Paterson (2000, 2003, 2004)**

Third generation: 11.1% overall yield, 21 steps LLS
Key fragments

**Novartis (2004)**

1.1% overall yield, 25 steps LLS



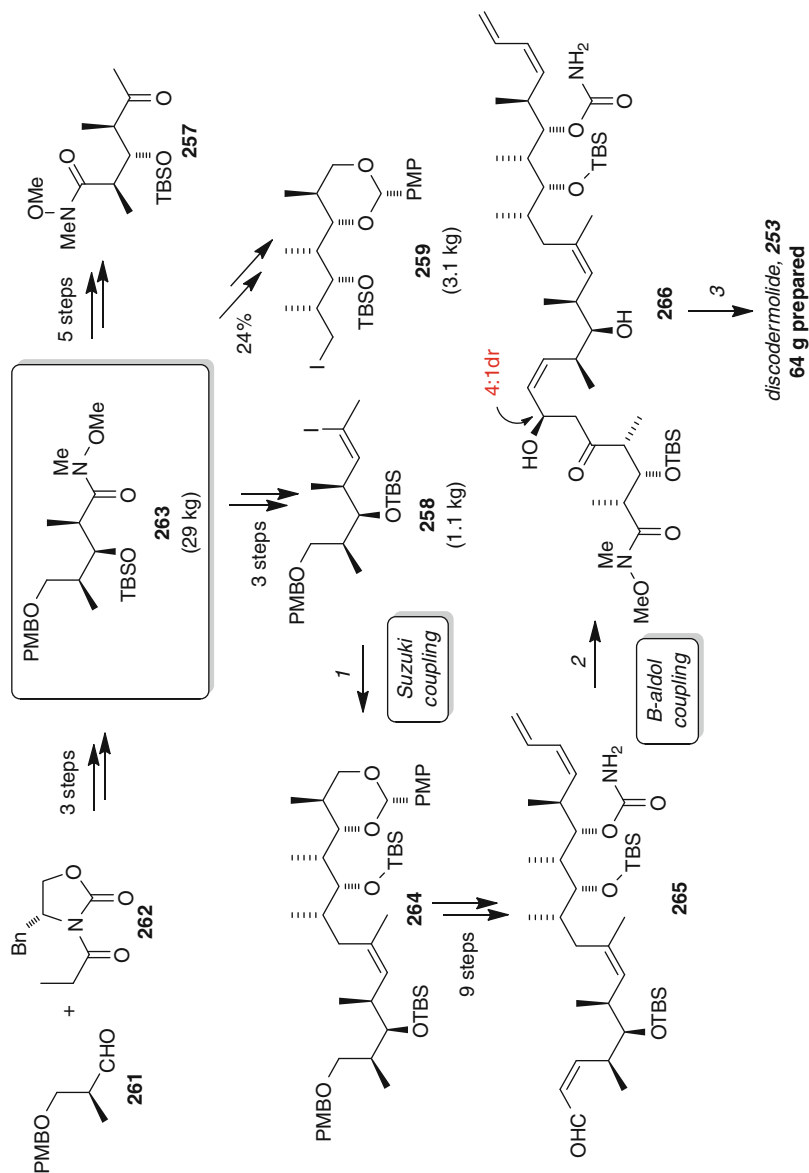
Scheme 11.34 Discodermolide synthesis: the foundational work for the Novartis synthesis

The advances made by these academic syntheses, in particular the efforts by the groups of Smith and Paterson, led Novartis to proceed with a total synthesis that could be carried out on an industrial scale so that over 60 g of discodermolide could be prepared [88]. This synthesis can be viewed as a hybrid of Smith and Paterson's routes, using the Paterson β -aldol disconnection at C6–C7 and the Smith–Marshall cross-coupling at C14–C15 as the key assembly steps. The three key fragments (**257**, **258**, **259**) are generated from the common precursor, **260**, originally reported by Smith. The synthesis proceeded in 25 steps (longest linear sequence) and 1.1% overall yield (Scheme 11.35). The common precursor **260** was prepared in three steps from the readily available aldehyde **261** and propionimide **262** and allowed the generation of 29 kg of material. As summarized in Scheme 11.35, **263** can be transformed into each of the key fragments (**257**, **258**, **259**), using routes related to Smith's syntheses. While Smith had used a Negishi cross-coupling to generate **264** from iodides **258** and **259**, the Novartis group chose to use a Suzuki cross-coupling, as originally reported by Marshall. Thus, iodide **259** was converted to the borane and coupled with iodide **258** using $\text{Pd}(\text{dppf})_2\text{Cl}_2$ as the catalyst. This key reaction proceeded in 73% yield on kilogram scale. To complete the synthesis, the Novartis group decided to utilize the endgame developed by Paterson. Accordingly, **264** was transformed into enal **265** in a nine-step sequence, with only two chromatographic separations required. After extensive experimentation, a reagent-controlled boron aldol coupling of aldehyde **265** and ketone **257**, using (+)- Ipc_2BCl , gave 67 g of the aldol product **266** (50–55% yield). An Evans-Saksena reduction ($\text{Me}_4\text{NBH}(\text{OAc})_3$, 73% yield) generated the C5-stereocenter stereoselectively and treatment with 3 N HCl was used to achieve global deprotection and lactonization and afforded discodermolide (**253**). This remarkable synthesis allowed the generation of 64 g of discodermolide, which allowed Novartis to initiate clinical trials. Unfortunately, toxicity issues have meant that these trials were discontinued [89].

Other complex marine natural products where “gram-scale” synthesis has provided materials for further evaluation include spongistatin (**267**) [90–96], kapakahines(**268**),(**269**)[97, 98],and iejimalide B (**270**) [99] (Fig. 11.7).

11.7 Supply by Synthesis: The Arrival of Halaven[®] and Yondelis[®] in the Clinic

In 2007, trabectedin (or ET-743, **271**), under the brand name Yondelis[®], was approved in the European Union for the treatment of soft tissue sarcoma, becoming the first marine natural product to be used in the treatment of cancer. It was originally isolated from the colonial ascidian *Ecteinascidia turbinata* and biological investigations revealed that it was a potent anti-cancer agent [100]. While aquaculture was initially used by PharmaMar to generate quantities of the compound for pre-clinical evaluation, the low yield, just 1 g being obtained from 1 t of ascidian,



Scheme 11.35 Synthetic strategy of the Novartis scale-up synthesis. Reagents and conditions: (1) **259**, (+)-Ipc₂BCl, NEt₃, 63%; (3) (a) MeN₄BH(OAc)₃, 73% (b) 3 N HCl, 61% (2) **257**, (+)-Ipc₂BCl, NEt₃, 63%; (3) (a) MeN₄BH(OAc)₃, 73% (b) 3 N HCl, 61%

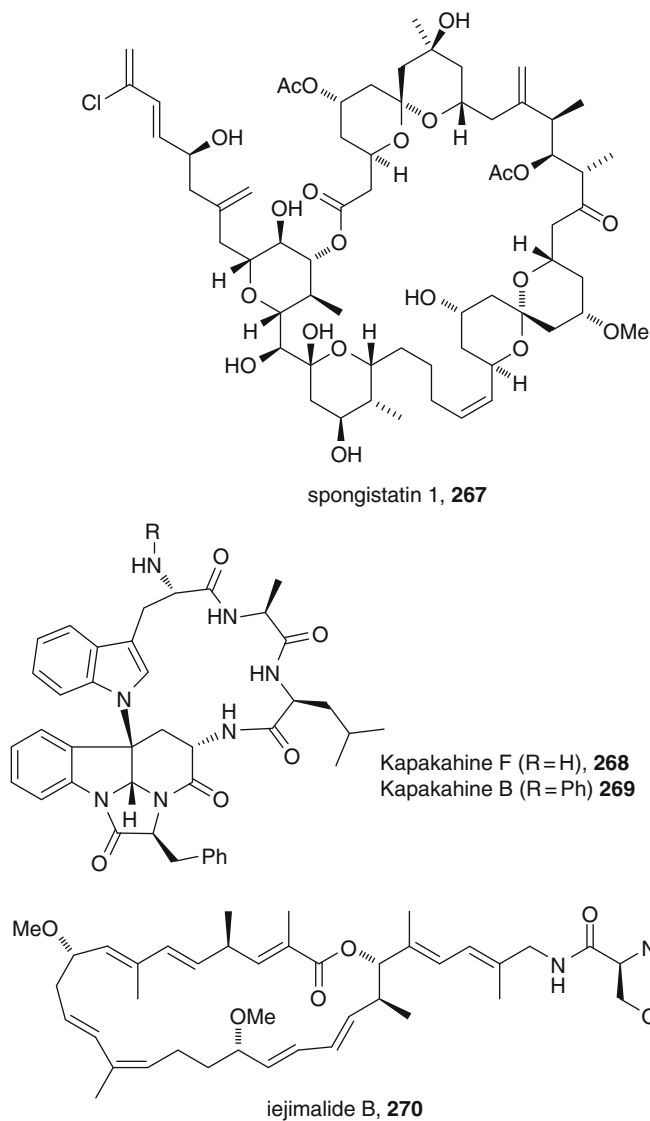


Fig. 11.7 Complex marine natural products available in appreciable amounts by synthesis

meant that this strategy would not be viable economically [101]. Thus, it was realized that an efficient, practical synthesis was the only realistic way that trabectedin could be supplied to the clinic.

The first total synthesis was developed by Corey and coworkers in 1996 and involved generation of the ten-membered lactone **272** via the trapping

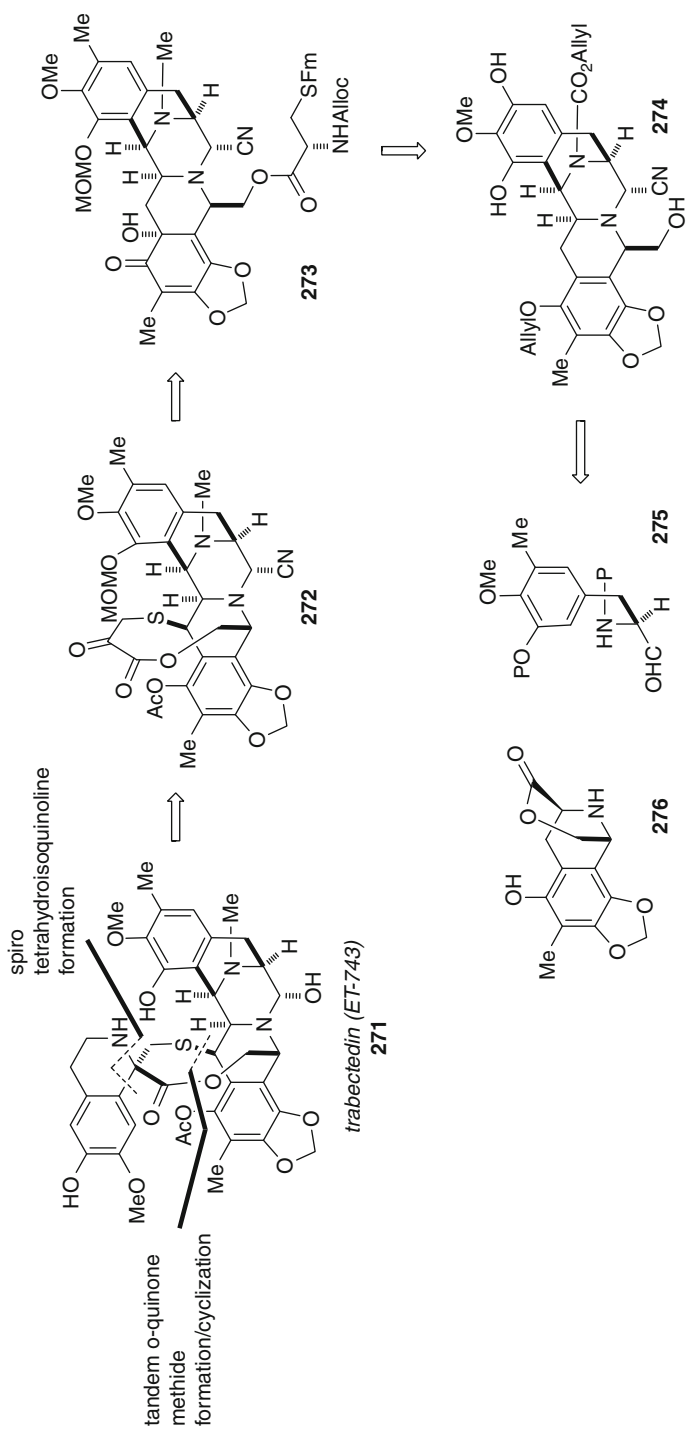
of a quinone methide intermediate as a key step (Scheme 11.36) [102]. Overall, the synthesis proceeded in 36 steps with a yield of 0.72%. Further work by Corey's group led to an enhancement in the overall yield (2.04%) but no reduction in the step count [103].

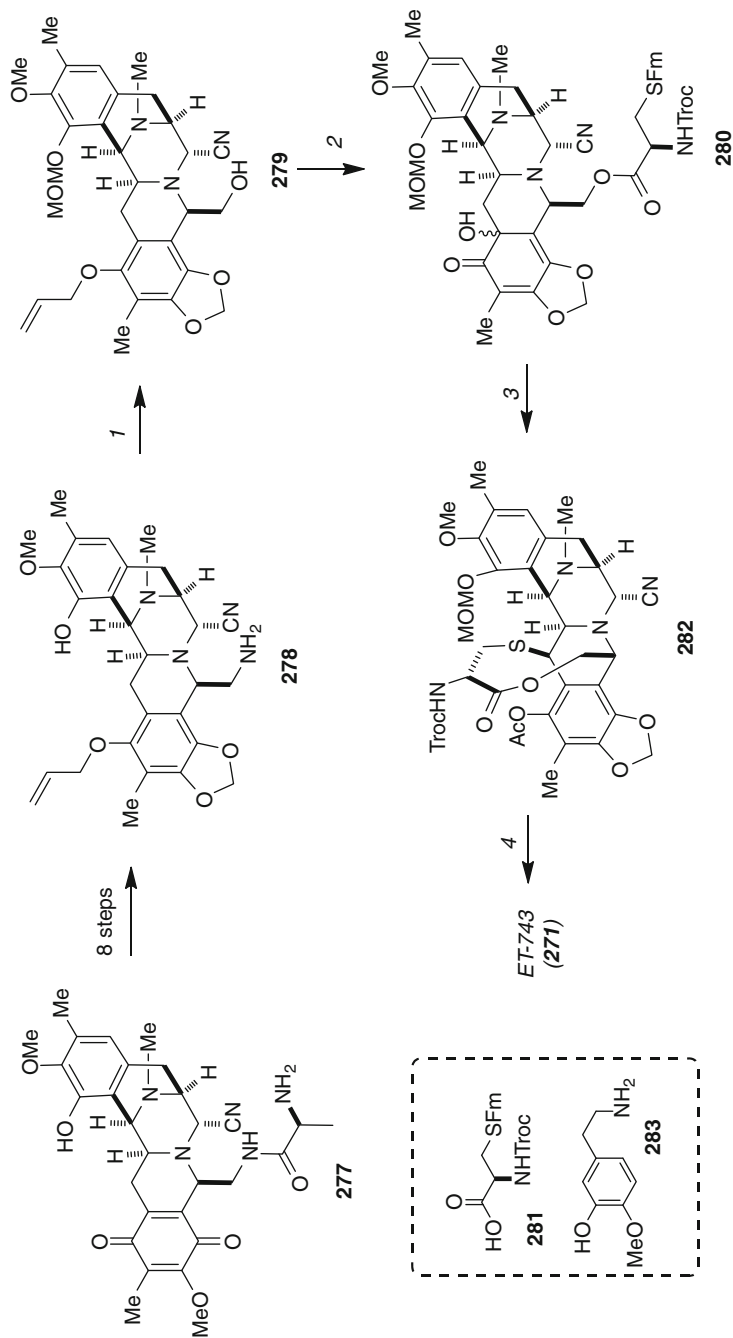
The synthesis provided an avenue for the generation of more material, but it was recognized by PharmaMar that the scale-up of this synthesis would be difficult. Using the key design principles of the Corey synthesis, they developed an efficient semi-synthesis from cyanosafracin B (**277**), which is readily available from fermentation from the bacteria *Pseudomonas fluorescens* [104]. As illustrated in Scheme 11.37, they were able to transform cyanosafracin B (**277**) into the alcohol **279** in 12 steps and 6% overall yield. Alcohol **279** can then be transformed into the quinone methide precursor **280** in three steps, using the protocols developed by Corey. The end game of the semi-synthesis was based on Corey's work, with some key changes in the protecting groups used and the ordering of the steps. Conversion to ten-membered lactone **282** was achieved in 58% yield, using the one-pot protocol developed by Corey. In contrast to Corey, the MOM and Troc protecting groups were removed first. The required α -keto lactone was generated in 57% yield using Corey's transamination protocol (4-methylpyridinium-4-carboxaldehyde iodide, DBU, $(\text{CO}_2\text{H})_2$). To complete the synthesis, the final tetrahydroisoquinoline system was introduced using a diastereoselective Pictet–Spengler condensation with 5-(2-aminoethyl)-2-methoxyphenol (**283**) in the presence of silica gel in 90% yield, and then, the nitrile group was substituted using silver nitrate in acetonitrile and water to afford trabectedin (**271**) in 90% yield. Overall, the semisynthesis requires 21 steps and proceeds in 0.96% overall yield. More importantly, it can be carried out on an industrial scale and is being used to provide the clinical supply of Yondelis[®].

Other groups have been active in the area, with the groups of Fukuyama [105] and Zhu [106] each reporting total syntheses. Danishefsky [107] and Williams [108] have also reported formal syntheses, intersecting with key intermediates in the Fukuyama synthesis.

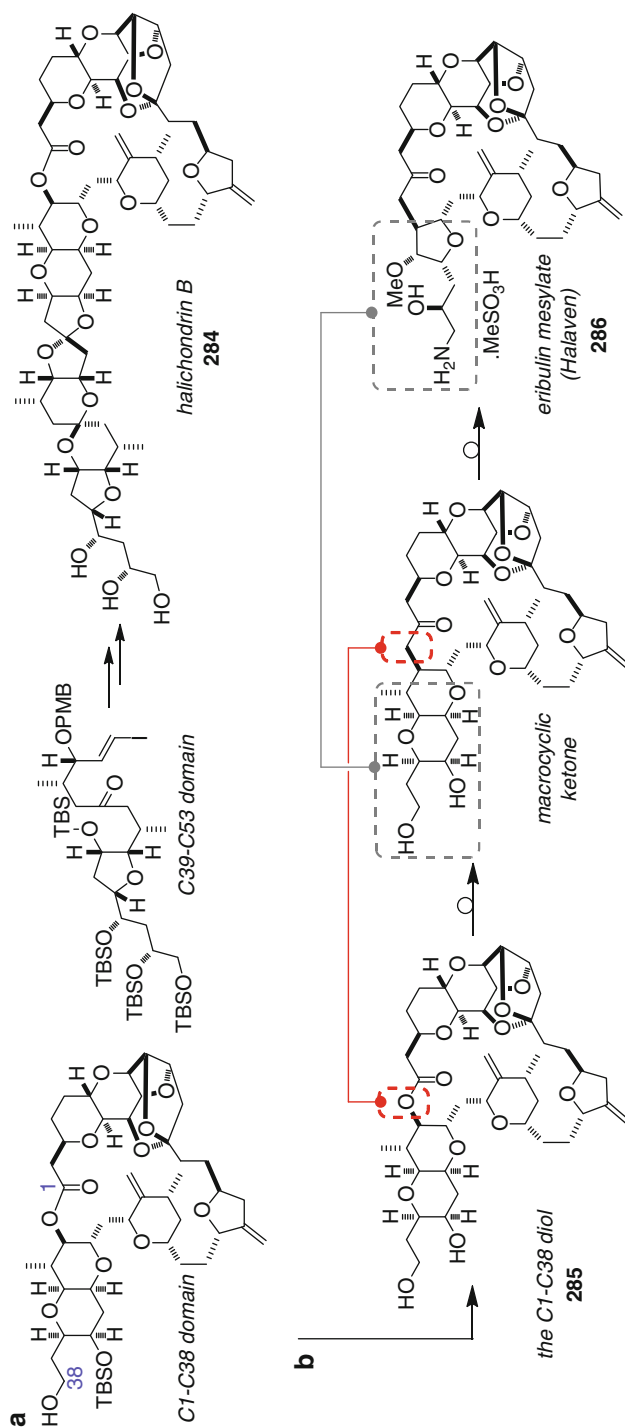
In 1992, samples of synthetic halichondrin B (**284**) and several intermediates were provided by the Kishi group to the Eisai Research Institute (Andover, MA) with a goal of evaluating in vitro and in vivo activity. In a significant discovery, the C1–C38 diol **285** was found to have a substantial fraction of the activity observed for the parent halichondrin B (Scheme 11.38) [109]. Evolution of this compounds ultimately produced E7389, eribulin mesylate (**286**), which was approved as a treatment for refractory breast cancer in November 2010 by the United States FDA.

The Eisai synthesis of eribulin mesylate (**286**) employs much of the technology laid down in Kishi's studies on norhalichondrin B and halichondrin B (for a review see [110]). We pick up the synthesis here at the point of subunit couplings: Nozaki–Hiyama–Kishi coupling of aldehyde **287** with vinyl iodide **288** and subsequent base-induced cyclization provided a 3:1 mixture of C27 diastereomers favoring the desired product (Scheme 11.39). The PMB ether was then removed to yield **289**, at which point the diastereomers were separable. Alcohol **289** was converted to sulfone **290** in four steps. Deprotonation of **290** with *n*-BuLi, followed by addition to aldehyde **291** and oxidation gave **292**. Removal of the sulfone group with

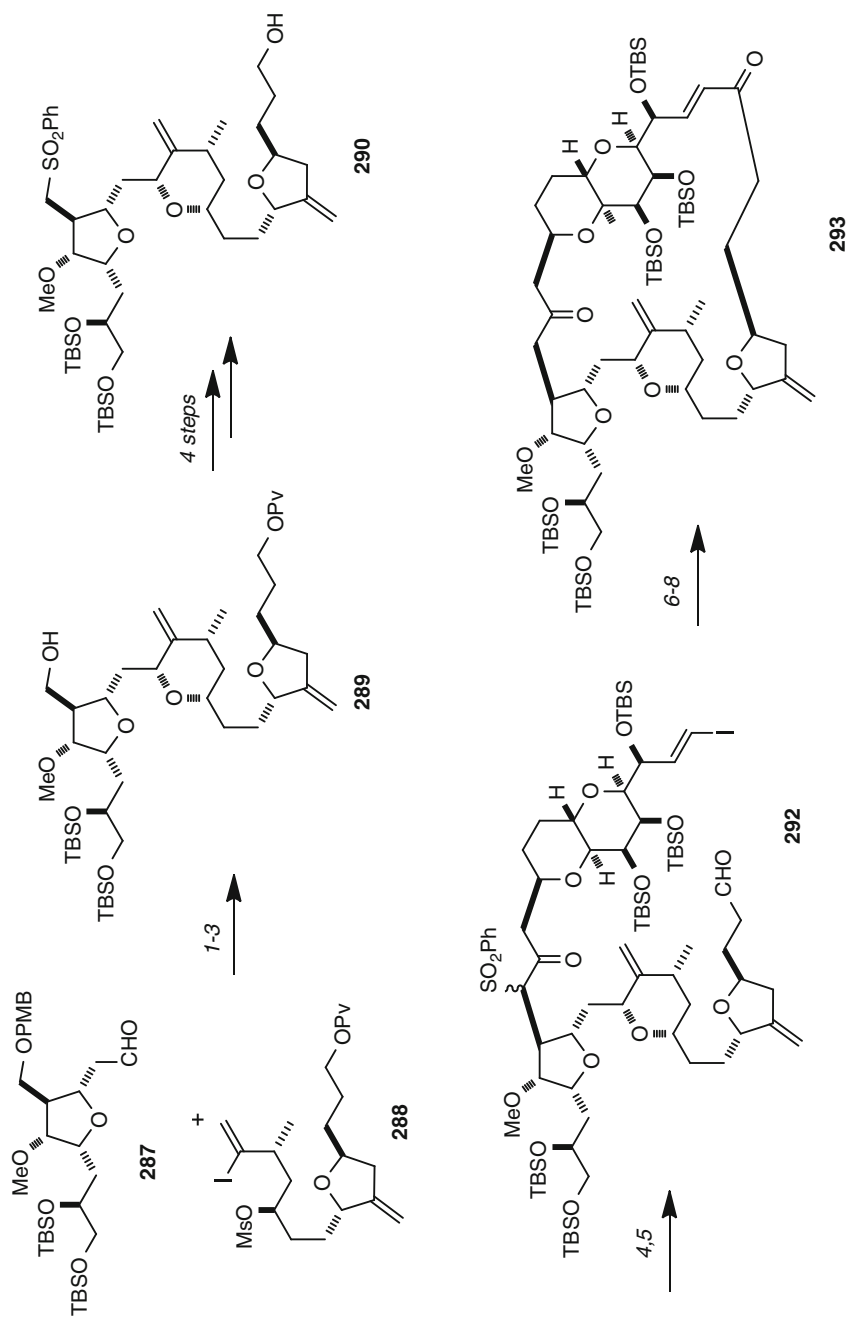
**Scheme 11.36** The Corey retrosynthetic analysis for trabectedin

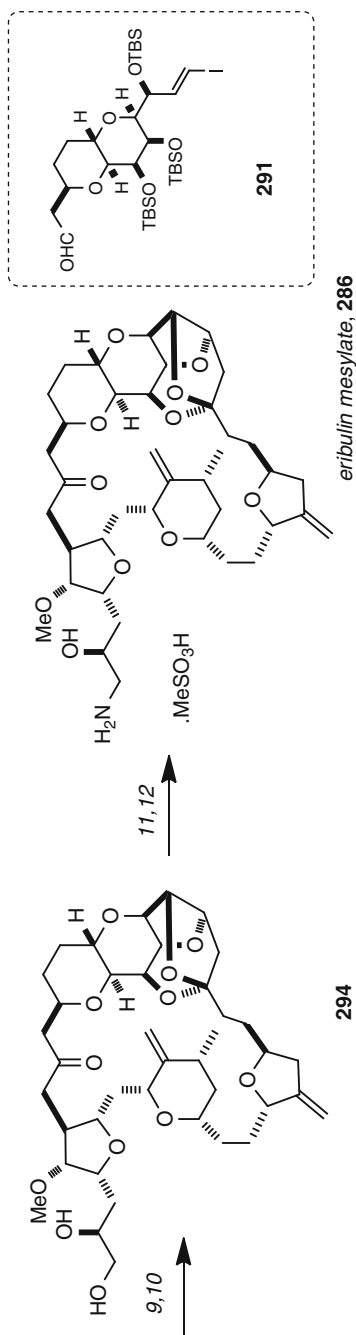


Scheme 11.37 The PharmaMar semi-synthesis of trabectedin (Yondelis[®]). Reagents and conditions: (1) (a) TrocCl, pyridine, CH_2Cl_2 ; (b) MOMBr, $i\text{-Pr}_2\text{NEt}$, DMAP, CH_3CN ; (c) Zn, aq AcOH; (d) NaNO_2 , AcOH, THF, H_2O , 36% (four steps); (2) (a) **281**, EDC.HCl, DMAP, CH_2Cl_2 ; (b) Bu_3SnH , $(\text{PPh}_3)_2\text{PdCl}_2$, AcOH, CH_2Cl_2 ; (c) $(\text{PhSeO})_2\text{O}$, CH_2Cl_2 ; 78% (three steps); (3) DMSO, TiF_2 , O , CH_2Cl_2 ; $i\text{-Pr}_2\text{NEt}$; $t\text{-BuOH}$; $(\text{Me}_2\text{N})_2\text{C} = \text{N-}t\text{-Bu}$; Ac_2O , 58%; (4) (a) TMSCl, NaI, CH_2Cl_2 , CH_3CN ; (b) Zn, aq AcOH; (c) [N-methylpyridinium-4-carboxaldehyde]I, DBU, $(\text{CO}_2\text{H})_2$; (d) **283**, silica gel, EtOH; (e) AgNO_3 , CH_3CN , H_2O , 36% (five steps)



Scheme 11.38 (a) The two key advanced building blocks of the Kishi total synthesis of halichondrin B, and (b) the evolution of the Cl-C38 diol into a macrocyclic ketone and then into Halaven®

**Scheme 11.39** (continued)



Scheme 11.39 The Eisai synthesis of eribulin mesylate (Halaven[®]). Reagents and conditions: (1) 0.5% $\text{NiCl}_2/\text{CrCl}_2$, 4:1 THF-DMF; (2) KHMDS, THF; (3) DDQ, CH_2Cl_2 , aqueous buffer, 44% (three steps); (4) $n\text{-BuLi}$, then **291**; (5) Dess-Martin periodinane, 82% (two steps); (6) SmI_2 , THF-MeOH; (7) 1% $\text{NiCl}_2/\text{CrCl}_2$, 4:1 THF-DMF; (8) Dess-Martin periodinane, 60% (three steps); (9) TBAF, imidazole.HCl; (10) PPTS, CH_2Cl_2 , 90% (two steps); (11) MsCl , collidine, 90%; (12) EtOH saturated with NH_3 , MsOH (five equiv), 93%

samarium (II) iodide, Nozaki–Hiyama–Kishi macrocyclization, and allylic alcohol oxidation gave enone **293**. Exposure of **293** to TBAF buffered with imidazole hydrochloride, followed by PPTS in CH_2Cl_2 , installed the polycyclic ketal domain, and the product **294** could be converted to eribulin mesylate by selective mesylation of the terminal alcohol and then aminolysis with NH_3 in EtOH. While current demand for clinical supply of Halaven is unknown, it is clear that Eisai's route has the capacity to provide multi-hundred-gram batches of API. Subsequent to regulatory approval by the FDA, Halaven has been approved for use in Singapore, Japan, and the European Union.

11.8 Conclusions and Future Perspectives

In this chapter, we have provided an overview of marine natural products synthesis that highlights some of the long-held rationales for the endeavor as well as the interplay between methods and strategy development in the context of challenging structures. These agendas will remain central to the science of synthesis, but the development of “gram-scale” syntheses and the arrival of Yondelis[®] and Halaven[®] in the clinic have ushered in an era in which synthesis may well be able to provide material that can address problems in human health.

11.9 Study Questions

1. In [Scheme 11.2](#), Kishi uses a series of stereoselective processes to prepare tetrodotoxin. Provide a stereochemical rationalization of the following reactions: (a) The conversion of **9** to **10** and (b) The conversion of **11** to **12**.
2. The Witkop reaction has been used by researchers to prepare the macrocycle of the diazonamide structure. Provide a mechanism for this reaction.
3. In Baran's synthesis of palau'amine, he generates the pyrrole **101** by reaction of bromide **104** and amino ester **105**. Provide a mechanism for this transformation.
4. Phillips' synthesis of cyanthiwigin U involves the conversion of bicyclic compound **214** to tricyclic compound **215**. Provide a mechanism.
5. Provide a mechanism for the intramolecular enyne metathesis that converts **140** to **141** in Shair's synthesis of longithorone A.
6. Evans uses a chelate-controlled Mukiyama aldol reaction to generate **177**. Provide a stereochemical rationale for the formation of **177** as a single diastereomer.
7. Boger's synthesis of ningalin D generates a tetra-substituted pyrrole **208** in two steps, from **206** to **207**. Provide a mechanistic rationale for each synthetic step.

References

1. (a) Corey EJ, X-M Cheng (1995) The logic of chemical synthesis. Wiley-Interscience, New York; (b) Nicolaou KC, Sorensen EJ (1996) Classics in total synthesis: targets,

- strategies, methods. Wiley-VCH, Weinheim; (c) Nicolaou KC, Snyder SA (2003) Classics in total synthesis II: more targets, strategies, methods. Wiley-VCH, Weinheim; (d) Nicolaou KC, Chen JS (2011) Classics in total synthesis III: further targets, strategies, methods. Wiley-VCH, Weinheim
2. (a) Morris JC, Nicholas GM, Phillips AJ (2007) Marine natural products: synthetic aspects. *Nat Prod Rep* 24:87–108; (b) Morris JC, Phillips AJ (2008) Marine natural products: synthetic aspects. *Nat Prod Rep* 25:95–117; (c) Morris JC, Phillips AJ (2009) Marine natural products: synthetic aspects. *Nat Prod Rep* 26:245–265; (d) Morris JC, Phillips AJ (2010) Marine natural products: synthetic aspects. *Nat Prod Rep* 27:1186–1203; (e) Morris JC, Phillips AJ (2011) Marine natural products: synthetic aspects. *Nat Prod Rep* 28:269–289; (f) Nicholas GM, Phillips AJ (2006) Marine natural products: synthetic aspects. *Nat Prod Rep* 23:79–99
 3. Scheuer PJ (1994) Tetrahedron perspective number 2: ciguatera and its off-shoots – chance encounters en route to a molecular structures. *Tetrahedron* 50:3–18
 4. Moore RE, Scheuer PJ (1971) Palytoxin: a new marine toxin from a coelenterate. *Science* 172:495–498
 5. Shimomura O, Goto T, Hirata Y (1957) Crystalline *Cypridina luciferin*. *Bull Chem Soc Jpn* 30:929–933
 6. (a) Kishi Y, Goto T, Hirata Y, Shimomura O, Johnson FH (1966) *Cypridina* bioluminescence I: structure of *Cypridina luciferin*. *Tetrahedron Lett* 3427–3436; (b) Kishi Y, Goto T, Eguchi S, Hirata Y, Watanabe E, Aoyama T (1966) *Cypridina* bioluminescence II structural studies of *Cypridina luciferin* by means of a high resolution mass spectrometer and an amino acid analyzer. *Tetrahedron Lett* 7:3437–3444; (c) Kishi Y, Goto T, Inoue S, Sugiura S, Kishimoto H (1966) *Cypridina* bioluminescence III total synthesis of *Cypridina luciferin*. *Tetrahedron Lett* 7:3445–3450
 7. White EH, Karpetsky TP (1971) Unambiguous synthesis of *Cypridina etioluciferamine*. Application of titanium tetrachloride to the synthesis of pyrazine N-oxides. *J Am Chem Soc* 93:2333–2335
 8. (a) Goto T, Kishi Y, Takahashi S, Hirata Y (1965) Tetrodotoxin. *Tetrahedron* 21:2059–2088; (b) Tsuda K, Ikuma S, Kawamura M, Tachikawa R, Sakai K, Tamura C (1964) Tetrodotoxin. VII. On the structures of tetrodotoxin and its derivatives. *Chem Pharm Bull* 12:1357–1374; (c) Woodward RB (1964) The structure of tetrodotoxin. *Pure Appl Chem* 9:49–74
 9. American Chemical Society (1964) Tetrodotoxin has hemilactal structure: Japanese and U.S. scientists find independently that the potent neurotoxin in pufferfish is identical to tarichatoxin. *Chem Eng News* 42(23):42–43
 10. Kishi Y, Fukuyama T, Aratani M, Nakatsubo F, Goto T, Inoue S, Tanino H, Sugiura S, Kakoi H (1972) Synthetic studies on tetrodotoxin and related compounds. IV. Stereospecific total synthesis of DL-tetrodotoxin. *J Am Chem Soc* 94:9219–9221
 11. Ohyabu N, Nishikawa T, Isobe M (2003) First asymmetric total synthesis of tetrodotoxin. *J Am Chem Soc* 125:8798–8805
 12. Hinman A, Du Bois J (2003) A stereoselective synthesis of (–)-tetrodotoxin. *J Am Chem Soc* 125:11510–11511
 13. Espino CG, Du Bois JJ (2001) A Rh-catalyzed C-H insertion reaction for the oxidative conversion of carbamates to oxazolidinones. *Angew Chem Int Ed* 40:598–600
 14. (a) MarinLit database, Department of Chemistry, University of Canterbury, Christchurch, New Zealand. <http://www.chem.canterbury.ac.nz/marinlit/marinlit.shtml>. (b) Blunt JW, Personal communication
 15. Diyabalange T, Amsler CD, McClintock JB, Baker BJ (2006) Palmerolide A, a cytotoxic macrolide from the antarctic tunicate *Synoicum adareanum*. *J Am Chem Soc* 128:5630–5631
 16. Jiang X, Liu B, Lebreton S, De Brabander JK (2007) Total synthesis and structure revision of the marine metabolite palmerolide A. *J Am Chem Soc* 129:6386–6387

17. Nicolaou KC, Guduru R, Sun Y-P, Banerji B, Chen DY-K (2007) Total synthesis of the originally proposed and revised structures of palmerolide A. *Angew Chem Int Ed* 46:5896–5900
18. Lebar M, Baker BJ (2007) On the stereochemistry of palmerolide A. *Tetrahedron Lett* 48:8009–8010
19. Nicolaou KC, Bulger PG, Sarlah D (2005) Metathesis reactions in total synthesis. *Angew Chem Int Ed* 44:3281–3284
20. Shen R, Porco JA Jr (2000) Synthesis of enamides related to the salicylate antitumor macrolides using copper-mediated vinylic substitution. *Org Lett* 2:1333–1336
21. (a) Chandrasekhar S, Vijeender K, Chandrasekhar G, Reddy CC (2007) Towards the synthesis of palmerolide A: asymmetric synthesis of C1–C14 fragment. *Tetrahedron: Asymm* 18:2473–2478; (b) Penner M, Rauniyar V, Kaspar LT, Hall DG (2009) Catalytic asymmetric synthesis of palmerolide A via organoboron methodology. *J Am Chem Soc* 131:14216–14217; (c) Cantagrel G, Meker C, Cossy J (2007) Synthetic studies towards the marine natural product palmerolide A: synthesis of the C3–C15 and C16–C23 fragments. *Synlett* 19:2983–2986
22. Lindquist N, Fenical W, Van Duyne GD, Clardy J (1991) Isolation and structure determination of diazonamides A and B, unusual cytotoxin metabolites from the marine ascidian *Diazona chinensis*. *J Am Chem Soc* 113:2303–2304
23. Lachia M, Moody C (2008) The synthetic challenge of diazonamide A, a macrocyclic indole bis-oxazole marine natural product. *Nat Prod Rep* 25:227–253
24. (a) Li J, Jeong S, Esser L, Harran PG (2001) Total synthesis of nominal diazonamides – part 1: convergent preparation of the structure proposed for (–)-diazonamide A. *Angew Chem Int Ed* 40:4765–4769; (b) Li J, Burgett AWG, Esser L, Amezcua C, Harran PG (2001) Total synthesis of nominal diazonamides – part 2: on the true structure and original of natural isolates. *Angew Chem Int Ed* 40:4770–4773
25. Nicolaou KC, Bella M, Chen DY-K, Huang X, Ling T, Snyder SA (2002) Total synthesis of diazonamide A. *Angew Chem Int Ed* 41:3495–3499
26. Burgett AWG, Li Q, Wei Q, Harran PG (2003) A concise and flexible total synthesis of (–)-diazonamide A. *Angew Chem Int Ed* 42:4961–4966
27. Knowles RR, Carpenter J, Blakey SB, Kayano A, Mangion IK, Sinz CJ, MacMillan DWC (2011) Total synthesis of diazonamide A. *Chem Sci* 2:308–311
28. (a) Mai CM, Sammons MF, Sammakia T (2010) A concise formal synthesis of diazonamide A by the stereoselective construction of the C10 quaternary center. *Angew Chem Int Ed* 49:2397–2400; (b) Cheung CM, Goldberg FW, Magnus P, Russell CJ, Turnbull R, Lynch V (2007) An expedient formal total synthesis of (–)-diazonamide A via a powerful, stereoselective O-Aryl to C-Aryl migration to form the C10 quaternary center. *J Am Chem Soc* 129:12320–12327
29. Satake M, Ofuji K, Naoki H, James KJ, Furey A, McMahon T, Silke J, Yasumoto T (1998) Azaspiracid, a new marine toxin having unique spiro ring assemblies, isolated from Irish mussels, *Mytilus edulis*. *J Am Chem Soc* 120:9967–9968
30. Nicolaou KC, Li Y, Uesaka N, Koftis TV, Vyskocil S, Ling T, Govindasamy M, Qian W, Bernal F, Chen DYK (2003) Total synthesis of the proposed azaspiracid-1 structure, part 1: construction of the enantiomerically pure C1–C20, C21–C27 and C28–C40 fragments. *Angew Chem Int Ed* 42:3643–3648
31. Nicolaou KC, Chen DYK, Li Y, Qian W, Ling T, Vyskocil S, Koftis TV, Govindasamy M, Uesaka N (2003) Total synthesis of the proposed azaspiracid-1 structure, part 2: coupling of the C1–C20, C21–C27 and C28–C40 fragments and completion of the synthesis. *Angew Chem Int Ed* 42:3649–3653
32. (a) Nicolaou KC, Vyskocil S, Koftis TV, Yamada YMA, Ling T, Chen DYK, Tang W, Petrovic G, Frederick MO, Li Y, Satake M (2004) Structural revision and total synthesis of azaspiracid-1, part 1: intelligence gathering and tentative proposal. *Angew Chem Int Ed* 43:4312–4318; (b) Nicolaou KC, Koftis TV, Vyskocil S, Petrovic G, Ling T, Yamada

- YMA, Tang W, Frederick MO (2004) Structural revision and total synthesis of azaspiracid-1, part 2: definition of the ABCD domain and total synthesis. *Angew Chem Int Ed* 43:4318–4324
33. Hopmann C, Faulkner DJ (1997) Lissoketal, a spiroketal from the Palauan ascidian *Lissoclinum voeltzkowi*. *Tetrahedron Lett* 38:169–170
34. Nakamura H, Ono M, Shida Y, Akita H (2002) New total syntheses of (+)-macrosphelides C, F and G. *Tetrahedron: Asymm* 13:705–713
35. Kinnel RB, Henning PG, Scheuer PJ (1993) Palau'amine: a cytotoxin and immunosuppressive hexacyclic bisguanidine antibiotic from the sponge *Stylotella agminata*. *J Am Chem Soc* 115:3376–3377
36. (a) Kobayashi H, Kitamura K, Nagai K, Nakao Y, Fusetani N, van Soest RWM, Matsunaga S (2007) Carteramine A, an inhibitor of neutrophil chemotaxis, from the marine sponge *Stylissa carteri*. *Tetrahedron Lett* 48:2127–2129; (b) Buchanan MS, Carroll AR, Addepalli R, Avery VM, Hooper JNA, Quinn RJ (2007) Natural products, stylissadines A and B, specific antagonists of the P2X₇ receptor, an important inflammatory target. *J Org Chem* 72:2309–2317; (c) Grube A, Köck M (2007) Structural assignment of tetrabromostylodiguanidine: does the relative configuration of the Palau-amines need revision? *Angew Chem Int Ed* 46:2320–2324
37. Seiple IB, Su S, Young IS, Lewis CA, Yamaguchi J, Baran PS (2009) Total synthesis of palau-amine. *Angew Chem Int Ed* 122:1113–1116
38. Nicolaou KC, Snyder SA (2005) Chasing molecules that were never there: misassigned natural products and the role of chemical synthesis in modern structure elucidation. *Angew Chem Int Ed* 44:1012–1044
39. Koert U (1995) Oxidative polycyclization versus the “polyepoxide cascade”: new pathways in polyether (bio)synthesis? *Angew Chem Int Ed Engl* 34:298–300
40. Nicolaou KC, Duggan ME, Hwang C-K, Somers PK (1985) Activation of 6-endo over 5-exo epoxide openings. Ring-selective formation of tetrahydropyran systems and stereocontrolled synthesis of the ABC ring framework of brevetoxin B. *J Chem Soc Chem Commun* 1359–1362
41. Vilotijevic I, Jamison TF (2007) Epoxide-opening cascades promoted by water. *Science* 317:1189–1192
42. Prasad AVK, Shimizu Y (1989) The structure of hemibrevetoxin-B: a new type of toxin in the Gulf of Mexico red tide organism. *J Am Chem Soc* 111:6476–6477
43. Zakarian A, Batch A, Holton RA (2003) A convergent total synthesis of hemibrevetoxin B. *J Am Chem Soc* 125:7822–7824
44. Ichige T, Okano Y, Kanoh N, Nakata M (2007) Total synthesis of methyl sarcophytoate. *J Am Chem Soc* 129:9862–9863
45. (a) Layton ME, Morales CA, Shair, MD (2001) Biomimetic Synthesis of (-)-longithorone. *J Am Chem Soc* 124:773–775; (b) Morales CA, Layton ME, Shair MD (2004) Synthesis of (-)-longithorone A: using organic synthesis to probe a proposed biosynthesis. *Proc Natl Assoc Soc* 101:12036–12041
46. Kim J, Ashenhurst J, Movassaghi M (2009) Total synthesis of (+)-11,11'-dideoxyverticillin A. *Science* 324:238–241
47. Hodous B, Fu GC (2002) Enantioselective synthesis of quaternary stereocenters via intermolecular C acylation of silyl ketene acetals: dual activation of the electrophile and the nucleophile. *J Am Chem Soc* 125:4050–4051
48. (a) Evans DA, Kværnø L, Mulder JA, Raymer B, Dunn TB, Beauchemin A, Olhava EJ, Juhl M, Kagechika K (2007) Total synthesis of (+)-azaspiracid-1. Part 1: synthesis of the fully elaborated ABCD aldehyde. *Angew Chem Int Ed* 46:4693–4697; (b) Evans DA, Dunn TB, Kværnø L, Beauchemin A, Raymer B, Olhava EJ, Mulder JA, Juhl M, Kagechika K, Favor DA (2007) Total synthesis of (+)-azaspiracid-1. Part 2: synthesis of the EFGHI sulfone and the completion of the synthesis. *Angew Chem Int Ed Engl* 46:4698–4703

49. Crabtree RH, Davis MW (1986) Directing effects in homogeneous hydrogenation with [Ir(cod)(PCy₃)(py)]PF₆. *J Org Chem* 51:2655–2661
50. (a) Kobayashi J, Ishibashi M, Nakamura H, Ohizumi Y, Yamasu T, Sasaki T, Hirata Y (1986) Amphidinolide A, a novel antineoplastic macrolide from the marine dinoflagellate *amphidinium* sp. *Tetrahedron Lett* 27:5755–5758; (b) Kobayashi J, Ishibashi M, Hirota H (1991) ¹H- and ¹³C-nmr Spectral investigation on amphidinolide, an antileukemic marine macrolide. *J Nat Prod* 54:1435–1439
51. Trost BM, Chisholm JD, Wrobleksi ST, Jung M (2002) Ruthenium-catalyzed alkene-alkyne coupling: synthesis of the proposed structure of amphidinolide A. *J Am Chem Soc* 124:12420–12421
52. Lam HW, Pattenden G (2002) Total synthesis of the presumed amphidinolide. *Angew Chem Int Ed* 41:508–511
53. Maleczka RE Jr, Terrell LR, Geng F, Ward JS III (2002) Total synthesis of proposed amphidinolide A via a highly selective ring-closing metathesis. *Org Lett* 4:2841–2844
54. Trost BM, Harrington PE (2004) Structure elucidation of (+)-amphidinolide A by total synthesis and NMR chemical shift analysis. *J Am Chem Soc* 126:5028–5029
55. (a) Trost BM, Indolese A (1993) Ruthenium-catalyzed addition of alkenes to acetylenes. *J Am Chem Soc* 115:4361–4362; (b) Trost BM, Indolese AF, Mueller TJJ, Treptow B (1995) A Ru catalyzed addition of alkenes to alkynes. *J Am Chem Soc* 117:615–623; (c) Trost BM, Toste FD (1999) A new Ru catalyst for alkene-alkyne coupling. *Tetrahedron Lett* 40:7739–7743; (d) Trost BM, Toste FD (2000) Ruthenium-catalyzed cycloisomerizations of 1,6- and 1,7-enynes. *J Am Chem Soc* 122:714–715; (e) Schnaderbeck M (1998) The Ruthenium Catalyzed Alder-Ene Reaction. Ph.D. Thesis, Stanford University, 1998; (f) Sundermann MI (2000) The Ruthenium Catalyzed Alder-Ene Reaction: Macrocyclization and Studies of Alternate Catalysts. PhD thesis, Stanford University, 2000
56. Kita Y, Maeda Y, Omori K, Okuno T, Tamura Y (1993) A novel efficient synthesis of 1-ethoxvinyl esters and their use in acylation of amines and alcohols synthesis of water-soluble oxanomyacin derivatives. *Synlett* 4:273–275
57. Pettit GR, Herald CL, Doubek DL, Herald DL, Arnold E, Clardy J (1982) Isolation and structure of bryostatin 1. *J Am Chem Soc* 104:6846–6848
58. (a) Evans DA, Carter PH et al (1998) Asymmetric synthesis of bryostatin 2. *Angew Chem Int Ed* 37:2354–2359; (b) Kageyama MT, Tamura T, Nantz MH, Roberts JC, Somfai P, Whritenour DC, Masamune S (1990) Synthesis of bryostatin 7. *J Am Chem Soc* 112(20):7407–7408; (c) Keck GE, Poudel YB, Cummins TJ, Rudra A, Covell JA (2011) Total Synthesis of Bryostatin 1. *J Am Chem Soc* 133:744–747; (d) Ohmori KY, Ogawa Y, Obitsu T, Ishikawa Y, Nishiyama S, Yamamura S (2000) Total synthesis of bryostatin 3. *Angew Chem Int Ed* 39:2290–2294; (e) Trost BM, Dong G (2008) Total synthesis of bryostatin 16 using atom-economical and chemoselective approaches. *Nature (London)* 456:485–488
59. Wender PA, Cribbs CM, Koehler KF, Sharkey NA, Herald CL, Kamano Y, Pettit GR, Blumberg PM (1998) Modeling of the bryostatins to the phorbol ester pharmacophore on protein kinase C. *Proc Natl Assoc Soc* 85:7197–7201
60. (a) Wender PA, De Brabander J, Harran PG, Jimenez J-M, Koehler MFT, Lippa B, Park C-M, Shiozaki M (1998) Synthesis of the first members of a new class of biologically active bryostatin analogs. *J Am Chem Soc* 120:4534–4535; (b) Wender PA, De Brabander J, Harran PG, Jimenez J-M, Koehler MFT, Lipp B, Park C-M, Siedenbiedel C, Pettit GR (1998) The design, computer modeling, solution structure, and biological evaluation of synthetic analogs of bryostatin 1. *Proc Natl Assoc Soc* 95:6624–6629; (c) Wender PA, Hilinski MK, Mayweg AVW (2005) late-stage intermolecular CH activation for lead diversification: a highly chemoselective oxyfunctionalization of the C-9 position of potent bryostatin analogues. *Org Lett* 7:79–82; (d) Wender PA, DeChristopher BA, Schrier AJ (2008) Efficient synthetic access to a new family of highly potent bryostatin analogues via a prins-driven macrocyclization strategy. *J Am Chem Soc* 130:6658–6659

61. Hamasaki A, Zimpleman JM, Hwang I, Boger DL (2005) Total synthesis of ningalin D. *J Am Chem Soc* 127:10767–10770
62. Enquist JA Jr, Stoltz BM (2009) Synthetic efforts toward cyathane diterpenoid natural products. *Nat Prod Rep* 26:661–680
63. Pfeiffer MWB, Phillips AJ (2005) Total synthesis of (+)-cyanthiwigin U. *J Am Chem Soc* 127:5334–5335
64. Enquist JA Jr, Stoltz BM (2008) The total synthesis of (-)-cyanthiwigin F by means of double catalytic enantioselective alkylation. *Nature* 453:1228–1231
65. (a) Behenna DC, Stoltz BM (2004) The enantioselective Tsuji allylation. *J Am Chem Soc* 126:15044–15045; (b) Mohr JT, Behenna DC, Harned AM, Stoltz BM (2005) Deracemization of quaternary stereocenters by Pd-catalyzed enantioconvergent decarboxylative allylation of racemic β -ketoesters. *Angew Chem Int Edn Engl* 44:6924–6927
66. Hirama M, Oishi T, Uehara H, Inoue M, Maruyama M, Oguri H, Satake M (2001) Total synthesis of ciguatoxin CTX 3 C. *Science* 294:1904–1907
67. Suh EM, Kishi Y (1994) Synthesis of palytoxin from palytoxin carboxylic acid. *J Am Chem Soc* 116:11205–11206
68. Aicher TD, Buszek KR, Fang FG, Forsyth CJ, Jung SH, Kishi Y, Metelich MC, Scola PM, Spero DM, Yoon SK (1992) Total synthesis of halichondrin B and norhalichondrin B. *J Am Chem Soc* 114:3162–3164
69. Jackson KL, Henderson JA, Motoyoshi H, Phillips AJ (2009) A total synthesis of norhalichondrin B. *Angew Chem Int Ed* 48:2346–2350
70. Forsyth CJ, Ahmed F, Cink RD, Lee CS (1998) Total synthesis of phorboxazole A. *J Am Chem Soc* 120:5597–5598
71. Smith AB III, Verhoest PR, Minbiole KP, Schelhass M (2001) Total synthesis of (+)- phorboxazole A. *J Am Chem Soc* 123:4834–4836
72. Williams DR, Kiryanov AA, Emde U, Clark MO, Berliner MA, Reeves JT (2003) Total synthesis of phorboxazole A. *Angew Chem Int Ed* 42:1258–1262
73. Gonzalez MA, Pattenden G (2003) A convergent total synthesis of phorboxazole A. *Angew Chem Int Ed* 42:1255–1258
74. White JD, Lee TH, Kuntiyong P (2006) Total synthesis of phorboxazole A. 2. Assembly of subunits and completion of the synthesis. *Org Lett* 8:6043–6046
75. Nicolaou KC, Hwang C-K, Duggan ME, Nugiel DA, Abe Y, Bal Reddy K, DeFrees SA, Reddy DR, Awartani RA (1995) Total synthesis of brevetoxin B. 1. First generation strategies and new approaches to oxepane systems. *J Am Chem Soc* 117:10227–10238
76. Nicolaou KC, Yang Z, Shi G-Q, Gunzner JL, Agrios KA, Gartner P (1998) Total synthesis of brevetoxin A. *Nature* 392:264–269
77. (a) Tsukano C, Sasaki M (2003) Total synthesis of gymnocin-A. *J Am Chem Soc* 125:14294–14295; (b) Sasaki M, Tsukano C, Tachibana K (2003) Synthetic entry to the ABCD ring fragment of gymnocin-A, a cytotoxic marine polyether. *Tetrahedron Lett* 44:4351–4354
78. Satake M, Shoji M, Oshima Y, Naoki H, Fujita T, Yasumoto T (2002) Gymnocin-A, a cytotoxic polyether from the notorious red tide dinoflagellate, *Gymnodinium mikimotoi*. *Tetrahedron Lett* 43:5829–5832
79. Gunasekera SP, Gunasekera M, Longley RE (1990) Discodermolide: a new bioactive polyhydroxylated lactone from the marine sponge *Discodermia dissoluta*. *J Org Chem* 55:4912–4915
80. (a) Florence GF, Gardner NM, Paterson I (2008) Development of practical syntheses of the marine anticancer agents discodermolide and dictyostatin. *Nat Prod Rep* 25:342–375; (b) Paterson I, Florence GF (2009) The chemical synthesis of discodermolide. *Top Curr Chem* 286:73–119
81. (a) Nerenberg JB, Hung DT, Somers PK, Schreiber SL (1993) Total synthesis of the immunosuppressive agent (-)-discodermolide. *J Am Chem Soc* 115:12621–12622;

- (b) Hung DT, Nerenberg JB, Schreiber SL (1996) Synthesis of discodermolides useful for investigating microtubule binding and stabilization. *J Am Chem Soc* 118:11054–11080
82. (a) Smith III AB, Qiu YP, Jones DR, Kobayashi K (1995) Total synthesis of (-)-discodermolide. *J Am Chem Soc* 117:12011–12012; (b) Smith III AB, Kaufman MD, Beauchamp TJ, LaMarche MJ, Arimoto H (1999) Gram-scale synthesis of (+)-discodermolide. *Org Lett* 1:1823–1826; (c) Smith III AB, Kaufman MD, Beauchamp TJ, LaMarche MJ, Arimoto H (2000) Gram-scale synthesis of (+)-discodermolide. *Org Lett* 2:1983; (d) Smith III AB, Beauchamp TJ, LaMarche MJ, Kaufman MD, Qiu YP, Arimoto H, Jones DR, Kobayashi K (2000) Evolution of the gram-scale synthesis of discodermolide. *J Am Chem Soc* 122:8654–8664; (e) Smith III AB, Freeze BS, Brouard I, Hirose T (2003) A practical improvement, enhancing the large-scale synthesis of (+)-discodermolide: a third generation approach. *Org Lett* 5:4405–4408; (f) Smith III AB, Freeze BS, Xian M, Hirose T (2005) Total synthesis of discodermolide: a highly convergent fourth-generation approach. *Org Lett* 7:1825–1828
83. (a) Paterson I, Florence GJ, Gerlach K, Scott JP (2000) Total synthesis of the antimicrotubule agent (+)-discodermolide using boron-mediated aldol reaction of chiral ketones. *Angew Chem Int Ed* 39:377–380; (b) Paterson I, Florence GJ (2000) Synthesis of (+)-discodermolide and analogues by control of asymmetric induction in aldol reaction of γ -chiral (Z)-enals. *Tetrahedron Lett* 41:6935–6939; (c) Paterson I, Florence GJ, Gerlach K, Scott JP, Sereinig N (2001) A practical synthesis of (+)-discodermolide and analogues: fragment union by complex aldol reactions. *J Am Chem Soc* 123:9535–9544; (d) Paterson I, Delgado O, Florence GJ, Lyothier I, Scott JP, Sereinig N (2003) 1,6-Asymmetric induction in boron-mediated aldol reactions: Application to a practical total synthesis of (+)-discodermolide. *Org Lett* 5:35–38; (e) Paterson I, Delgado O, Florence GJ, Lyothier I, O'Brien M, Scott JP, Sereinig N (2005) A second generation total synthesis of (+)-discodermolide: the development of a practical route using solely substrate-based stereocontrol. *J Org Chem* 70:150–160; (f) Paterson I, Lyothier I (2004) Total synthesis of (+)-discodermolide: an improved endgame exploiting a Still-Genarri-type olefination with a C1-C8 β -ketophosphonate fragment. *Org Lett* 6:4933–4936; (g) Paterson I, Lyothier I (2005) Development of a third-generation total synthesis of (+)-discodermolide: an expedient Still-Gennari-type fragment coupling utilizing an advanced β -ketophosphonate. *J Org Chem* 70:5494–5507
84. (a) Harried SS, Yang G, Strawn MA, Myles DC (1997) Total synthesis of (-)-discodermolide: an application of a chelation-controlled alkylation reaction. *J Org Chem* 62:6098–6099; (b) Harried SS, Lee CP, Yang G, Lee TIH, Myles DC (2003) Total synthesis of the potent microtubule-stabilizing agent (+)-discodermolide. *J Org Chem* 68:6646–6660
85. (a) Marshall JA, Johns BA (1998) Total synthesis of (+)-discodermolide. *J Org Chem* 63:7885–7892; (b) Marshall JA, Lu ZH, Johns BA (1998) Synthesis of discodermolide subunits by S_N2' addition of nonracemic allenylstannanes to aldehydes. *J Org Chem* 63:817–823
86. Arefolov A, Panek JS (2005) Crotylsilane reagents in the synthesis of complex polyketide natural products: total synthesis of (+)-discodermolide. *J Am Chem Soc* 127:5596–5603
87. de Lemos E, Porée FH, Commercon A, Betzer JF, Pancrazi A, Ardisson J (2007) α -Oxygenated crotyltitanium and dyotropic rearrangement in the total synthesis of discodermolide. *Angew Chem Int Ed* 46:1917–1921
88. (a) Mickel SJ, Sedelmeier GH, Niederer D, Daeffler R, Osmani A, Schreiner K, Seeger-Weibel M, Berod B, Schaer K, Gamboni R, Chen S, Chen W, Jagoe CT, Kinder FR, Loo M, Prasad K, Repic O, Shieh W-C, Wang R-M, Waykole L, Xu DD, Xue S (2004) Large-scale synthesis of the anti-cancer marine natural product (+)-discodermolide. Part 1: synthetic strategy and preparation of a common precursor. *Org Process Res Dev* 8:92–100; (b) Mickel SJ, Sedelmeier GH, Niederer D, Schuerch F, Grimler D, Koch G, Daeffler R, Osmani A, Hirni A, Schaer K, Gamboni R, Bach A, Chaudhary A, Chen A, Chen W, Chen B, Hu B, Jagoe CT, Kim H-Y, Kinder FR, Liu Y, Lu Y, McKenna J, Prasad M, Ramsey TM, Repic O,

- Rogers L, Shieh W-C, Wang R-M, Waykole L (2004) Large-scale synthesis of the anti-cancer marine natural product (+)-discodermolide. Part 2: synthesis of fragment C1-6 and C9-14. *Org Process Res Dev* 8:101–106; (c) Mickel SJ, Sedelmeier GH, Niederer D, Schuerch F, Koch G, Kuesters E, Daeffler R, Osmani A, Seeger-Weibel M, Schmid E, Himi A, Schaer K, Gamboni R, Bach A, Chen S, Chen W, Geng P, Jagoe CT, Kinder FR, Lee GT, McKenna J, Ramsey TM, Repic O, Rogers L, Shieh W-C, Wang R-M, Waykole L (2004) Large-scale synthesis of the anti-cancer marine natural product (+)-discodermolide. Part 3: synthesis of the C15-21 fragment. *Org Process Res Dev* 8:107–112; (d) Mickel SJ, Sedelmeier GH, Niederer D, Schuerch F, Seger M, Schreiner K, Daeffler R, Osmani A, Bixel D, Loiseleur O, Cercus J, Stettler H, Schaer K, Gamboni R (2004) Large-scale synthesis of the anti-cancer marine natural product (+)-discodermolide. Part 4: preparation of the C7-24 fragment. *Org Process Res Dev* 8:113–121; (e) Mickel SJ, Niederer D, Daeffler R, Osmani A, Kuesters E, Schmid E, Schaer K, Gamboni R, Chen W, Loeser E, Kinder FR, Königsberger K, Prasad K, Ramsey TM, Repic O, Wang R-M, Florence G, Lyothier I, Paterson I (2004) Large-scale synthesis of the anti-cancer marine natural product (+)-discodermolide. Part 5: linkage of fragments C1-6 and C7-24 and finale. *Org Process Res Dev* 8:122–130; (f) Mickel SJ (2004) Toward a commercial synthesis of (+)-discodermolide. *Curr Opin Drug Dev* 7:869–881; (g) Mickel SJ, Fischer R, Marterer W (2004) Broad spectrum chemistry as practised by novartis process research. *Chimia* 58:640–648
89. Mita A, Lockhart C, Chen TL, Bocinski K, Curtright J, Cooper W, Hammond L, Rothenberg M, Rowinsky E, Sharma S (2004) A phase I pharmacokinetic (PK) trial of XAA296A (Discodermolide) administered every 3 wks to adult patients with advanced solid malignancies. In: ASCO annual meeting proceedings (Post-Meeting Edition) *J Clin Oncol* 22(14S) (July 15 Suppl). Abstract 2025
90. (a) Evans DA, Coleman PJ, Dias LC (1997) Enantioselective synthesis of althoyrtin C (spongistatin 2): synthesis of the AB- and CD- spiroketal subunits. *Angew Chem Int Ed* 36:2738–2741; (b) Evans D A, Trotter BW, Côté B, Coleman PJ (1997) Enantioselective synthesis of Alrohyrtin C (spongistatin 2): synthesis of the EF- bis(pyran) subunit. *Angew Chem Int Ed* 36:2741–2744; (c) Evans DA, Trotter BW, Côté B, Coleman PJ, Dias LC, Tyler AN (1997) Enantioselective synthesis of althoyrin C (spongistatin 2): fragment assembly and revision of the spongistatin 2 stereochemical assignment. *Angew Chem Int Ed* 36:2744–2747; (d) Evans DA, Trotter BW, Coleman PJ, Côté B, Dias LC, Rajapakse HA, Tyler AN (1999) Enantioselective total synthesis of althoyrtin C (spongistatin 2). *Tetrahedron* 55:8671–8726
91. (a) Guo J, Duffy KJ, Stevens KL, Dalko PI, Roth RM, Hayward MM, Kishi Y (1998) Total synthesis of althoyrtin A (spongistatin 1): part 1. *Angew Chem Int Ed* 37:187–190; (b) Hayward MM, Roth RM, Duffy KJ, Dalko PI, Stevens KL, Guo J, Kishi Y (1998) Total synthesis of althoyrtin A (spongistatin 1): part 2. *Angew Chem Int Ed* 37:192–196
92. (a) Smith III AB, Lin Q, Doughty VA, Zhuang L, McBriar MD, Kerns JK, Brook CS, Murase N, Nakayama K (2001) The spongistatins: architecturally complex natural products-Part one: a formal synthesis of (+)-spongistatin 1 by construction of an advanced ABCD fragment. *Angew Chem Int Ed* 40:196–199; (b) Smith III AB, Zhu W, Shirakami S, Sfougatakis C, Doughty VA, Bennett CS, Sakamoto Y (2003) Total synthesis of (+)-spongistatin 1. An effective second-generation construction of an advanced EF Wittig salt, fragment union, and final elaboration. *Org Lett* 5:761–764; (c) Smith III AB, Tomioka T, Risatti CA, Sperry JB, Sfougatakis C (2008) Gram-scale synthesis of (+)-spongistatin 1: Development of an improved, scalable synthesis of the F-ring subunit, fragment union and final elaboration. *Org Lett* 10:4359–4362
93. (a) Paterson I, Chen DY-K, Coster MJ, Acena JL, Bach J, Gibson KR, Keown LE, Oballa RM, Trieselmann T, Wallace DJ, Hodgson AP, Norcross RD (2001) Stereocontrolled total synthesis of (+)-althoyrtin A/spongistatin 1. *Angew Chem Int Ed* 40:4055–4060; (b) Paterson I, Chen DYK, Coster MJ, Acena JL, Bach J, Wallace DJ (2005) The stereocontrolled total synthesis of

- altohyrtin A/spongistatin 1: fragment couplings, completion of the synthesis, analogue generation and biological evaluation. *Org Biomol Chem* 3:2431–2440
94. Crimmins MT, Katz JD, Washburn DG, Allwein SP, McAtee LF (2002) Asymmetric total synthesis of spongistatins 1 and 2. *J Am Chem Soc* 124:5661–5663
95. Heathcock CH, McLaughlin M, Medina J, Hubbs JL, Wallace GA, Scott R, Claffey MM, Hayes CJ, Ott GR (2003) Multigram synthesis of the C29–C51 subunit and completion of the total synthesis of altohyrtin C (spongistatin 2). *J Am Chem Soc* 125:12844–12849
96. Ball M, Gaunt MJ, Hook DF, Jessiman AS, Kawahara S, Orsini P, Scolaro A, Talbot AC, Tanner HR, Yamanoi S, Ley SV (2005) Total synthesis of spongistatin 1: a synthetic strategy exploiting its latent pseudo-symmetry. *Angew Chem Int Ed* 44:5433–5438
97. (a) Newhouse T, Lewis CA, Baran PS (2009) Enantioselective total syntheses of kapakahines B and F. *J Am Chem Soc* 131:6360–6361; (b) Newhouse T, Lewis CA, Eastman KJ, Baran PS (2010) Scalable total syntheses of N-linked tryptamine dimers by direct indole-aniline coupling: Psychotrimine and kapakahines B and F. *J Am Chem Soc* 132:7119–7137
98. (a) Espejo VR, Rainier JD (2010) Total synthesis of kapakahine E and F. *Org Lett* 12:2154–2157; (b) Rainier JD, Espejo VR (2011) Total syntheses of kapakahines E and F. *Israel J Chem* 51:473–482
99. Fürstner A, Nevado C, Tremblay M, Chevrier C, Teplý F, Aïssa C, Waser M (2006) Total synthesis of ilejimalide B. *Angew Chem Int Ed* 45:5837–5842
100. (a) Rinehart KL, Holt TG, Fregeau NL, Stroh JG, Keifer PA, Sun F, Li LH, Martin D (1990) Ecteinascidins 729, 743, 745, 759A, 759B, and 770: potent antitumor agents from the Caribbean tunicate *Ecteinascidia turbinata*. *J Org Chem* 55:4512–4515; (b) Rinehart KL, Holt TG, Fregeau NL, Stroh JG, Keifer PA, Sun F, Li LH, Martin DG (1991) Ecteinascidins 729, 743, 745, 759A, 759B, and 770: potent antitumor agents from the Caribbean tunicate *Ecteinascidia turbinata* [erratum to document cited in CA113(9):75189d]. *J Org Chem* 56:1676
101. Cuevas C, Francesch A (2009) Development of Yondelis (trabectedin, ET-743). A semisynthetic process solves the supply problem. *Nat Prod Rep* 26:322–337
102. Corey EJ, Gin DY, Kania RS (1996) Enantioselective total synthesis of ecteinascidin 743. *J Am Chem Soc* 118:9202–9203
103. Martinez EJ, Corey EJ (2000) A new, more efficient, and effective process for the synthesis of a key pentacyclic intermediate for production of ecteinascidin and phthalascidin antitumor agents. *Org Lett* 2:993–996
104. Cuevas C, Pérez M, Martin MJ, Chicharro JL, Fernández-Rivas C, Flores M, Francesch A, Gallego P, Zarzuelo M, de la Calle F, Gracia J, Polanco C, Rodriguez I, Manzanares I (2000) Synthesis of ecteinascidin ET-743 and phthalascidin Pt-650 from cyanosafracin B. *Org Lett* 2:2545–2548
105. Endo A, Yanagisawa A, Abe M, Tohma S, Kan T, Fukuyama T (2002) Total synthesis of ecteinascidin 743. *J Am Chem Soc* 124:6552–6554
106. Chen J, Chen X, Bois-Choussy M, Zhu J (2006) Total synthesis of ecteinascidin 743. *J Am Chem Soc* 128:87–89
107. Zheng S, Chan C, Furuuchi T, Wright BJD, Zhou B, Guo J, Danishefsky SJ (2006) Stereo-specific formal total synthesis of Ecteinascidin 743. *Angew Chem Int Ed* 45:1754–1759
108. Fishlock D, Williams RM (2008) Synthetic studies on ET-743. Assembly of the pentacyclic core and a formal synthesis. *J Org Chem* 73:9594–9600
109. Kishi Y, Fang FG, Forsyth CJ, Scola PM, Yoon SK (1995) Halichondrins and related compounds. US Patent 5,338,865
110. Jackson KL, Henderson JA, Phillips AJ (2009) The Halichondrins and E7389. *Chem Rev* 109:3044–3079
111. (a) Horton PA, Koehn FE, Longley RE, McConnell OJ (1994) Lasonolide A, a new cytotoxin macrolide from the marine sponge *forcepia* sp. *J Am Chem Soc* 116:6015–6016. (b) Lee E, Song HY, Kang JW, Kim D-K, Jung C-K, Joo JM (2002) Lasonolide A: structural revision and synthesis of the unnatural (–)-enantiomer. *J Am Chem Soc* 124:384–385. (c) Lee E,

- Song, HY, Joo JM, Kang JW, Kim D-K, Jung C-K, Hong CY, Jeong SW, Jeon K (2002) Synthesis of (+)-lasonolide A: (–)-lasonolide A is the biologically active enantiomer. *Bioorg Med Chem Lett* 12:3519–3520. (d) Song HY, Joo JM, Kang JW, Kim D-S, Jung C-K, Kwak HS, Park JH, Lee E, Hong CY, Jeong SW, Jeon K, Park JH (2003) Lasonolide A: structural revision and total synthesis. *J Org Chem* 68:8080–8087
112. (a) Sharma P, Alam MJ (1988) Sclerophytins A and B. Isolation and structures of novel cytotoxic diterpenes from the marine coral *Sclerophyllum capitalis*. *J Chem Soc Perkin Trans 1*: 2537–2540. (b) Alam M, Sharma P, Zektzer AS, Martin GE, Ji X, van der Helm D (1989) Sclerophytin C-F: isolation and structures of four new diterpenes from the soft coral *Sclerophyllum capitalis*. *J Org Chem* 54: 1896–1900. (c) Paquette LA, Moradei OM, Bernardelli P, Lange T (2000) Synthesis of the alleged structure of Sclerophytin A. The setting of two oxygen bridges within the fused cyclodecanol B ring is not Nature's Way. *Org Lett* 2: 1875–1878. (d) Friedrich D, Dorskotch RW, Paquette LA (2000) Revised constitution of sclerophytins A and B. *Org Lett* 2:1879–1882. (e) Bernardelli P, Moradei OM, Friedrich D, Yang J, Gallou F, Dyck BP, Dorskotch RW, Lange T, Paquette LA (2001) Total asymmetric synthesis of the putative structure of the cytotoxic diterpenoid (–)-sclerophytin A and of the authentic natural sclerophytins A and B. *J Am Chem Soc* 123: 9021–9032. (f) Overman LE, Pennington LD (2000) Total synthesis of the supposed structure of (–)-sclerophytin A and an improved route to (–)-7-deacetoxyalcyonin acetate. *Org Lett* 2: 2683–2686. (g) MacMillan DWC, Overman LE, Pennington LD (2001) A general strategy for the synthesis of cladiellin diterpenes: enantioselective total syntheses of 6-acetoxycladiell-7(16),11-dien-3-ol (deacetoxyalcyonin acetate), cladiell-11-ene-3,6,7-triol, sclerophytin A, and the initially purported structure of sclerophytin A. *J Am Chem Soc* 123:9033–9044. (h) Gallou F, MacMillan DWC, Overman LE, Paquette LA, Pennington LD, Yang J (2001) Enantioselective syntheses of authentic sclerophytin A, sclerophytin B, and cladiell-11-ene-3,6,7-triol. *Org Lett* 3: 135–137
113. (a) Carroll AR, Coll JC, Bourne DJ, MacLeod JK, Zabriskie TM, Ireland CM, Bowden BF (1996) Patellins 1–6 and trunkamide A: Novel cyclic hexa-, hepta-, and octa- peptides from colonial ascidians, *lissoclinum* sp. *Aust J Chem* 49:659–667. (b) Wipf P, Uto Y (2000) Total synthesis and revision of stereochemistry of the marine metabolite trunkamide A. *J Org Chem* 65:1037–1049
114. (a) Degnan BM, Hawkins CJ, Lavin MF, McCaffrey EJ, Parry DL, Watters DJ (1989) Novel cytotoxin compounds from the ascidian *lissoclinum bistratum*. *J Med Chem* 32:1354–1359. (b) Statsuk AV, Liu D, Kozmin SA (2004) Synthesis of bistramide A. *J Am Chem Soc* 126:9546–9547
115. (a) Patil AD, Freyer AJ, Taylor PB, Carté B, Zuber G, Johnson RK, Faulkner DJ (1997) Batzelladines F-I, novel alkaloids from the sponge *batzella* sp.: Inducers of p56lck-CD4 dissociation. *J Org Chem* 62:1814. (b) Cohen F, Overman LE (2001) Enantioselective total synthesis of batzelladine F: structural revision and stereochemical definition. *J Am Chem Soc* 123:10782–10783
116. (a) Oettit GR, Cichacz ZA, Gao F, Boyd MR (1994) Isolation and structure of the cancer cell growth inhibitor dictyostatin 1. *J Chem Soc Chem Commun* 1111–1112. (b) Paterson I, Britton R, Delgado O, Meyer A, Poullennec KG (2004) Total synthesis and configurational assignment of (–)-dictyostatin, a microtubule-stabilizing macrolide of marine sponge origin. *Angew Chem Int Ed* 43:4629–4633. (c) Shin Y, Fournier J-H, Fukui Y, Brückner AM, Curran DP (2004) Total synthesis of (–)-dictyostatin: confirmation of relative and absolute configurations. *Angew Chem* 116:4734–4737
117. (a) Pettit GR, Herald CL, Kamano Y (1983) Antineoplastic agents. 93. Structure of the *bugular neritina* (marine bryozoa) antineoplastic component bryostatin 3. *J Org Chem* 48:5354–5356. (b) Ohmori K, Ogawa Y, Obitsu T, Ishikawa Y, Nishiyama S, Yamamura S (2000) Total synthesis of bryostatin 3. *Angew Chem Int Ed* 39:2290–2294

Part 3

Marine Natural Products and Chemical Ecology

Antipredatory Defensive Roles of Natural Products from Marine Invertebrates

12

Joseph R. Pawlik

Contents

12.1	Introduction and Scope	678
12.2	General and Theoretical Considerations	679
12.2.1	Predator–Prey Interactions, Generalists and Specialists	679
12.2.2	Palatability, Toxicity, Learning, and Aposematic Coloration	680
12.2.3	Resource Limitation and Metabolite Function	684
12.3	Techniques for Assessing Invertebrate Chemical Defenses Against Predators	685
12.3.1	Historical Development	685
12.3.2	Current Approach	686
12.3.3	Technical Problems	692
12.4	Additivity and Synergism	696
12.5	Optimization, Differential Allocation, Induction, and Activation	697
12.6	Resource Trade-Offs and the Cost of Chemical Defense	701
12.7	Structure-Activity Relationships and the Commonality of Chemical Defenses	702
12.8	Study Questions	703
	References	705

Abstract

This chapter provides a broad and critical evaluation of investigations of the antipredatory defenses of marine invertebrates with a target audience of graduate students in ecology or natural products chemistry. After considering important concepts and theoretical issues associated with the research topic, techniques for assessing invertebrate chemical defenses against predators are detailed, with a focus on potential methodological problems. In particular, the importance of determining concentrations of metabolites in invertebrate tissues using a volumetric rather than gravimetric method is explained. Relevant concepts from the recent literature are reviewed and discussed, including the cost of

J.R. Pawlik

Department of Biology and Marine Biology, Center for Marine Science, University of North Carolina Wilmington, Wilmington, NC, USA

e-mail: pawlikj@uncw.edu

chemical defenses, synergistic effects of defenses, optimization of defenses, and structure-activity relationships of deterrent metabolites. Comparisons are made between the life histories and evolutionary environments of terrestrial and marine invertebrates to argue that the highly optimized chemical defense mechanisms and complex systems of color mimicry described for some terrestrial insects are unlikely to be equaled among marine invertebrates.

12.1 Introduction and Scope

Marine chemical ecology is a young discipline, having emerged from the collaboration of natural products chemists and ecologists in the 1980s with the goal of examining the ecological functions of the unusual secondary metabolites that were being isolated from the tissues of marine organisms. The result has been a progression of experimental protocols that have increasingly refined the ecological relevance of the research; some would argue, to a greater extent than the much older discipline of terrestrial chemical ecology.

The topic of this chapter is restricted to antipredatory chemical defenses of marine invertebrates, although much of what will be discussed is more broadly applicable to other defensive roles (allelopathic, antifouling, antimicrobial) and to other organisms, plants, and animals, both marine and terrestrial. In point of fact, it is not the author's intention to survey the primary literature for references pertaining to the topic, but only to cite examples that illustrate concepts as they are discussed. This contribution serves as an opportunity to address the subject in a broader, more analytical manner, with special attention to methodological problems, unanswered questions, and new research directions. Moreover, this chapter has been written for a target audience of *beginning graduate students* in ecology, or better, in chemistry, who might be considering marine chemical ecology as their field of study. For more thorough literature reviews, readers are directed to one excellent review of bioassay techniques [1], general reviews of marine chemical ecology [2], and the chemical defenses of marine organisms [3–5].

The author has contributed to the literature on this chapter's topic for over 25 years, and will unabashedly cite the work that he is most familiar with: his own. This might be interpreted as laziness or pretension, but more is now understood about the antipredatory defenses of a larger number of species of Caribbean marine invertebrates, specifically sponges, gorgonian corals, and ascidians, than for invertebrate taxa from any other marine biogeographic region. The Caribbean reef community is dominated by gorgonians and sponges, the species composition is remarkably similar across the entire region, and trophic relationships are well described. Within this framework, research has advanced from autecological characterizations of the defensive metabolites of individual species to community-level investigations that test higher-order ecological theory. As such, studies of Caribbean marine invertebrates provide the best body of work from which to draw examples that illustrate the concepts considered herein.

12.2 General and Theoretical Considerations

A series of interrelated research questions provide the framework for this chapter's topic: Do secondary metabolites produced by marine invertebrates defend them from predators? If they do, why? Are they toxic, or do they simply taste bad? Do metabolites require specific structural components to be active as defenses? How do they affect the behavior or physiology of the predator? Do the same metabolites affect all possible predators? Is predation a driving force in the evolution of defensive metabolites? Are defensive metabolites costly to the source invertebrate? If the defended invertebrate has endosymbionts, which of the two makes the metabolites, and how does that affect the cost to the invertebrate? Why don't predators surmount chemical defenses? If a secondary metabolite does not deter predation, does it have some other function? Does it only act in concert with other metabolites to deter predation? Might a secondary metabolite have no function at all?

12.2.1 Predator–Prey Interactions, Generalists and Specialists

It is well known that predation is an important force in controlling populations of marine invertebrates and in shaping their evolution. But it is not the only selective force; indeed, a host of abiotic and biotic factors interact to different degrees and at different times in structuring the ecology and evolution of any species (Fig. 12.1) [6, 7]. Because predation is often a dominant factor, organisms have evolved a number of defensive strategies to deter predators, ranging from behavioral mechanisms (nocturnal activity, rapid escape), to physical (spines, armor) and chemical defenses. Some predators have evolved counterstrategies to lesser or greater degrees, and in some cases, an evolutionary “arms race” has resulted in highly specialized predators that are adapted to eat highly defended prey [8]. At its most extreme, specialization can result in specific pairings of predator and prey, as for some nudibranch slugs that eat particular sponges, but more common are diffuse specializations that allow a predator to exploit a range of prey species that have developed a shared defensive trait, such as the jaws and pharyngeal mills of parrot fishes that allow them to eat many species of stony corals as well as calcified algae and sponges [9, 10]. The evolution of specialization has been the subject of considerable theoretical interest [11].

A high degree of prey specialization is comparatively rare, however, and most predators in marine environments are generalists, meaning that they consume many different prey species. So, to cite the example of sponges on Caribbean coral reefs, Randall and Hartman [12] examined the gut contents of the dominant predatory group, fishes, and they found the vast majority were generalist predators that did not eat sponges, a small minority were sponge predators that ate some sponges as part of their diet, and very few species ate sponges as most of their diet. One species appears to eat mostly one sponge species, making it more highly specialized than the rest. As we will see, knowledge of the generalist and specialist predators of

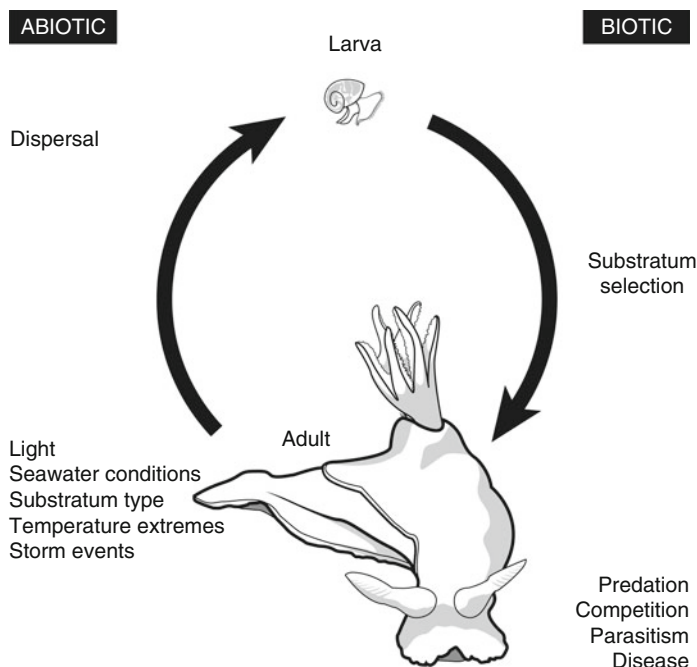


Fig. 12.1 Some of the abiotic and biotic factors that may affect the distribution and abundance of benthic marine invertebrates. For most species, the dispersive phase of the life cycle occurs during a planktonic (microscopic) larval stage, with the adult phase having limited mobility (the opposite situation is found for terrestrial insects). Note that predation is only one of the many factors that may impact the survival of a given species. Natural selection acts strongly on just a few characteristics of an organism at a time relative to the full range of factors that influence their survival; selective forces do not shape an “optimal” phenotype, nor does evolution permit only the best-adapted organisms to reproduce. Moreover, the focus of selection is likely to change over time as the relative influence of different abiotic and biotic factors change

a target invertebrate species within a community is a prerequisite for designing ecologically relevant experiments for assessing chemical defenses against potential predators. Few marine communities are characterized well enough that this level of understanding of trophic relationships exists [13, 14].

12.2.2 Palatability, Toxicity, Learning, and Aposematic Coloration

It is generally supposed that chemically defended prey produce metabolites that are unpalatable to predators (for the purpose of the discussion in this section, we will focus on fish predators, as they are the dominant predators in many marine ecosystems), and further, that this distastefulness is evidence of the toxicity of the metabolites. In the previous sentence, *toxicity* is understood to mean that a metabolite causes physiological damage to the predator that ingests it, while

unpalatability (distastefulness, deterrence) means that food offerings containing the metabolite are rejected by potential predators without any necessary subsequent harm to the predator. However, any linkage between palatability and toxicity is far from clear. There are certainly examples of defensive metabolites that are known to be toxic in pharmacological assays [15], but little evidence that other unpalatable metabolites are toxic, and some strongly toxic metabolites may be quite palatable. Indeed, in the limited number of studies that have brought data to bear on the question, no relationship could be found between palatability and toxicity [16, 17].

There are good reasons to believe that palatability, and not toxicity, is the important driving force in the evolution of chemical defenses in marine invertebrates, although a defensive metabolite could have both properties. Distasteful secondary metabolites elicit an immediate response by a potential predator that permits the predator to learn to avoid chemically defended prey through the recognition of visual or chemical cues [18]. In aquatic systems, distastefulness is not perceived by predators at a distance, but only when prey mucus or tissue comes in contact with chemosensory structures in or around the mouth of the predator. Because an attack on distasteful prey is not usually fatal for the prey (particularly for clonal marine invertebrates), the prey and others like it will benefit from subsequent avoidance by the predator. If, however, the prey contained toxic metabolites that were not distasteful and had no physiological effect on the predator for many minutes or hours after ingestion, the predator could not learn to avoid the prey, as there would be no direct association between subsequent illness (or death) and the moment of attack on the prey. Moreover, the prey would likely be killed by the predator in the absence of the immediate deterrent effect of distastefulness. So, death of the predator, while seemingly a good strategy for the prey, is not so if it also means the death of the prey.

Why not produce chemical defenses that are both distasteful and highly toxic? The most likely reason is that highly toxic metabolites often have broad-spectrum, negative effects on living cells. Any prey producing a potent toxin would also have to contain it to prevent autotoxicity, and this could come at a high metabolic cost. In addition, if distastefulness alone prevents predatory attack, and confers a survival advantage to the prey, there is no need to bother with the cost of dealing with potent toxicity. But in the absence of toxicity, what would prevent a predator from circumventing distastefulness? Generalist predators (i.e., most predators) have other prey species available to eat, so there is no strong selective pressure to circumvent the distastefulness of one or a few species, as they can simply move on to other prey species. If, however, prey availability is limited to chemically defended species, predators may evolve behavioral and physiological mechanisms to circumvent defenses. Under enhanced predatory pressure, greater toxicity of the chemical defenses of prey may arise, leading to the “arms race” described frequently in the terrestrial chemical ecology literature [19].

So what is the evidence regarding distastefulness, toxicity, and learning among marine invertebrates and their predators? There is abundant confirmation that fish predators, like avian predators in terrestrial systems, use visual cues to discriminate among undefended and defended prey and learn to avoid the latter [18, 20].

Moreover, immediate regurgitation is the usual mode by which naïve predators reject defended prey, although in some cases learning occurs despite a lack of rejection, suggesting that toxic effects may be perceived quickly enough that some predators can learn to avoid prey despite being unable to reject novel defenses at the time of initial consumption [18]. It is conceivable that mildly toxic chemical defenses could have more insidious, long-term effects that alter growth rates, lifespan, or fecundity of predators [21], but the selective pressures that would favor a more complex mechanism over the straight-forward path of distastefulness are harder to imagine.

With visually acute predatory fish dominating many marine systems, and with good evidence of learned recognition of chemically defended prey by these predators, one might expect clear evidence of warning coloration (aposematism) and mimicry similar to that described for frogs and butterflies in terrestrial systems. Many sessile benthic invertebrates are brilliantly colored (e.g., sponges), and a clear candidate for mimicry are nudibranch mollusks, brilliantly colored shell-less slugs with potent chemical defenses that they derive from their diet or manufacture themselves, depending on the species [22]. Yet the evidence for these phenomena among marine invertebrates is not nearly as strong as for their terrestrial counterparts (butterflies, beetles, frogs, etc.).

No relationship has been found between bright colors and chemical defenses for Caribbean sponges [16]. Sponge-eating predators, including angelfishes, parrot fishes and hawksbill turtles appear to rely on visual cues that transcend color alone, quickly finding and eating preferred sponge species, whether brightly colored or drab, among similarly colored defended species in experimental arrays [23]. It had been proposed that spongivorous fishes used a “smorgasbord” strategy of alternating colors of sponges in their diets to avoid the accumulation of toxic compounds present in any one species [12, 24], but subsequent experimental work did not support this hypothesis [13, 23]. Indeed, the bright color of sponges may owe more to bacterial symbionts or dietary pigments than to the selective forces of predation [14, 16].

Among opisthobranch mollusks, herbivorous sea hares are mostly cryptically colored, and yet they often bear potent chemical defenses [25–27], although these may be targeted primarily at crustacean predators that rely less on visual cues. Blue and yellow stripes are a common color scheme for chemically defended Caribbean and Mediterranean nudibranchs [28], a pattern that blends to green at a distance, often rendering these slugs cryptically colored, although it has been proposed that the color pattern is indicative of a mimetic circle of species [29]. The large and brightly colored Spanish dancer nudibranch is primarily nocturnal and cryptically concealed during the day, but it reveals dramatically contrasting mantle markings when disturbed or swimming [30]. This species has a mantle that is bright crimson red in shallow water, but it would appear brown or black to potential predators at the range of depths it is most commonly found. Similarly, the alga-eating sacoglossan mollusk *Cyerce nigricans* also strongly chemically defended [31], appears mostly black in contrast to the bright green alga on which it feeds. Two congeneric gastropod slug species share the same chemically defended host sponge, and both are

similarly unpalatable, but while one has a strongly contrasting pattern on its body, the other is highly cryptic [32]. Even if it is arguable that visual cues help to protect some opisthobranch species, the general level of aposematism among marine slugs does not rise to that found in terrestrial insects, nor does it seem to provide a strong foundation for mimicry [33].

Stronger evidence for aposematism exists for Indo-Pacific nudibranchs of the family Phyllidiidae, but rather than settle the case, it only raises more questions. Natural assemblages of reef fishes consumed less of foods associated with the contrasting color patterns modeled after two of five species of these brightly colored, diurnal nudibranchs, providing evidence of aposematic coloration to the authors of the study [34]. However, the crude organic extract of one of the two nudibranch species having an avoided color pattern was not deterrent at the site in which feeding experiments were conducted, while at least one species with a color pattern that was not avoided by fish predators yielded a deterrent extract. The most strongly contrasting color pattern tested in the study and modeled after *Phyllidia polkadotsa* had no effect on predation.

In a thorough review of aposematic coloration in nudibranchs, Edmunds found the direct evidence inconclusive [33]. As part of his analysis, he noted the absence of extensive examples among nudibranchs of Batesian or Mullerian mimics, both of which are common among butterflies. A similar argument could be made against aposematism in marine flatworms [35] and for polychaetes with brightly colored feeding appendages [36, 37], although some claims have been made for mimicry among flatworms [35, 38]. Overall, the fact that the evidence for aposematism is nowhere near as pervasive for marine invertebrates as it is for their terrestrial counterparts further supports the contention that the relative selective pressures of predation on visual cues related to chemical defenses are not as intense in marine systems and do not result in the levels of optimized defenses, or complex chains of mimicry, that are seen in terrestrial insects.

Why should aposematism and associated mimicry be common among tropical terrestrial invertebrates (particularly butterflies) but rare among their marine counterparts? One possibility is that predation is a much more important selective force on insects than on marine invertebrates (Fig. 12.1) [7]. Butterflies are adults during the dispersive phase of their life history during which time they share the open air with their avian predators and cannot rely on crypsis, while adult benthic marine invertebrates crawl or are sessile. Female butterflies directly deposit their eggs on appropriate food plants for the nondispersive larval stage of their life history, while most marine invertebrates have a pelagic larval stage associated with considerable larval wastage and a very low probability of finding an appropriate settlement substratum [39]; in fact, the prevailing view of marine ecologists is that recruitment processes are a dominant, if not the most important, factor in determining distributions and abundances of marine invertebrates [40]. Many species of butterflies go through multiple generations in a season, greatly accelerating the evolutionary process compared to most marine invertebrates, which have generation times measured in years. Many of these life history differences may also explain why host specialization is often intense for insects, but not so for marine invertebrates.

An intriguing possibility for the limited existence of aposematism and mimicry among some opisthobranch mollusks is that it is evidence of past selection. Predation may have been a much more important factor guiding the evolution of opisthobranch species living in the warmer and more extensive shallow seas of the geological past than it is today.

12.2.3 Resource Limitation and Metabolite Function

All organisms have a finite amount of metabolic energy to allocate to the biological functions of maintenance, movement, growth, reproduction, and defense. Greater investment in one of these categories must come at the expense of the others. A marine invertebrate may defend itself in many ways, and it is conceivable that it may not defend itself at all. Mobile animals can hide or flee, while sessile species may exhibit armor, spines, or pincers. While the foregoing defense mechanisms have fairly obvious metabolic costs to the animals that use them, the situation is more ambiguous for chemical defenses. The cost of a chemical defense may be substantial if the invertebrate must synthesize a complex compound from primary metabolic building blocks, move the compound from the site of synthesis to a location where it will be most effective, and then either store the compound or release it. But what if the compound is an effective chemical defense in very small quantities, or it can be stored for long periods of time? What if it is derived directly from the diet of the animal, as for some nudibranch mollusks [30]? What if it is synthesized entirely by symbiotic algae or bacteria living within the tissues of the animal, as may be true for some sponges [41]? It is conceivable that a chemical defense could come at little or no cost to the invertebrate that uses it.

Just as it is likely that a chemical defense comes with a cost to the organism that exhibits it, it also seems reasonable to expect that any complex secondary metabolite found in the tissues of a marine invertebrate must have some sort of function, whether as a chemical defense or some other purpose. Again, this may not be the case. Secondary metabolites may be “biochemical baggage,” in that they are produced as by-products of the synthesis of other metabolites, whether primary or secondary, or that they are waste products that accumulate in the tissues of an organism [42]. If selective forces are neutral to the presence of these metabolites, or if they change over time from positive to neutral, they will continue to be produced in the population of organisms that exhibit them.

Marine natural products chemists are familiar with the broad diversity of unusual secondary metabolites present in the tissues of many benthic marine invertebrates, particularly sponges, ascidians, and gorgonian corals [43]. Often a single animal is the source of many compounds. Of this enormous chemical diversity, we can only ascribe ecological function, based on relevant experiments, to a tiny fraction. Bioassay-guided isolation techniques invariably exclude secondary metabolites that are not active in that assay system. It is entirely possible that these excluded metabolites have other important functions, but it is also possible that no particular function exists for these metabolites [42].

One interesting possible example of “biochemical baggage” is prostaglandins in the Caribbean gorgonian coral *Plexaura homomalla* [44]. This common sea whip grows among ten or more other species of gorgonians, including at least one congener, and yet only *P. homomalla* has very high concentrations of prostaglandins in its tissues (1–8% of tissue wet mass, mostly the acetoxymethyl ester of prostaglandin A₂(PGA₂)). Experiments conducted with the hydroxy acids of PGA₂ indicated that these compounds were potent antipredatory defenses against fishes [45], but when experiments were performed on the naturally occurring acetoxymethyl esters, they were not deterrent to potential predators [44], even though the crude organic extract of *P. homomalla* deterred predatory fishes, indicating the presence of other defensive metabolites [46]. Experiments also discounted antifouling and allelopathic roles for prostaglandins in *P. homomalla* [47]. Although specialist predatory snails of gorgonians, *Cyphoma* spp., exhibited higher levels of enzymes associated with detoxification when collected from *P. homomalla* [48], these snails are just as likely to graze on *P. homomalla* as any of the other gorgonian species that lack prostaglandins. Why should one common species of gorgonian contain such high concentrations of PGA₂ when all of the other species around it, many equally abundant, do not? It appears that the presence of PGA₂ in the tissues of *P. homomalla* makes very little difference to the survival of sea whips of this species.

12.3 Techniques for Assessing Invertebrate Chemical Defenses Against Predators

12.3.1 Historical Development

The field of marine natural products chemistry experienced a “gold rush” in the 1970s and 1980s when organic chemists took advantage of two emerging technologies: SCUBA diving and rapidly advancing spectroscopic methods (mostly NMR). The result was a rapid increase in the number of publications describing novel metabolites from benthic marine invertebrates and algae. Relying upon the assumption that secondary metabolites must serve some purpose (see previous section), many of these publications ascribed ecologically important properties to new compounds without empirical evidence; in point of fact, whole reviews of “chemical ecology” from this period were compiled of references with little or no assay data to support an ecological function for secondary metabolites [49].

At about the same time, ecologists were also taking advantage of the advent of SCUBA diving and describing the distributions and abundances of benthic animals and plants previously known only from much less effective sampling methods, such as dredging. The assumption of these researchers was that anything sessile and soft-bodied must be chemically defended to avoid consumption by abundant and ever-present predators [12]. In an effort to introduce empiricism to what was otherwise descriptive work on species abundances, some ecologists began extrapolating chemical defenses from toxicity assays in which fish (usually goldfish or guppies)

were exposed to aqueous suspensions of crude organic extracts of invertebrate tissues [50]. Looking back, it is surprising that publications in prestigious journals used similar techniques having little or no ecological relevance [51, 52] and that these studies are still widely cited today!

Indeed, not only are past studies that purport to investigate marine invertebrate chemical defenses on the basis of toxicity data cited in the current literature, studies based on toxicity data continue to be published [53–55]. In fact, one of the most up-to-date citations in this chapter is a study that attempts to link greater conspicuousness of nudibranch coloration with chemical defense by drawing entirely on brine shrimp toxicity data [56]! This is not entirely surprising because data from toxicity assays, particularly brine shrimp, Microtox, and fish toxicity experiments, are very easy to generate relative to time-intensive feeding experiments conducted with ecologically relevant predators. But beyond possible (and rather limited) pharmacological significance, toxicity data have no ecological value because these assays have no bearing on the manner in which potential predators perceive prey under natural conditions. In point of fact, studies that have compared data from toxicity and feeding assay experiments have found no relationship between them [16, 17]. Simply put, marine chemical ecologists should dispense with toxicity assays, editors and reviewers should not allow toxicity data to be published in the ecological literature, and past studies consisting of toxicity assays should not be cited as evidence of ecologically meaningful information.

12.3.2 Current Approach

In brief, the approach for assessing the antipredatory activity of the tissues of a marine invertebrate can be summarized as follows, and is further detailed in the paragraphs below: (1) determine the appropriate generalist predators for feeding experiments, (2) collect target invertebrates and properly extract secondary metabolites, (3) use an appropriate assay, and (4) employ suitable experimental and statistical methods.

1. *Determine the appropriate generalist predators for experiments.* It seems obvious that an appropriate, co-occurring generalist predator should be chosen for feeding experiments, but many past studies have instead opted for a more convenient “model” predator, which, while certainly better than using toxicity assays (above), nevertheless reduces the ecological relevance of the study. Clearly, a generalist coral reef fish should not be used to investigate defenses of a target invertebrate from a Norwegian fjord; instead, the local population of potential predators, whether vertebrate or invertebrate, should be determined, either from past studies or as part of a survey of the habitat of the target invertebrate. Some examples: fishes are the primary predators of invertebrates on Caribbean coral reefs [12, 23], while sea stars are the primary predators of the Antarctic benthos in McMurdo Sound [14], and crabs and lobsters are the dominant predators on some temperate reefs [57]. Generalist predators, and not specialists, are chosen for feeding experiments because specialists may

have surmounted prey defenses, and the research question addresses defenses against the most common classes of predators for the habitat of the target invertebrate.

2. *Collect organisms and extract secondary metabolites properly.* Under the best of circumstances when collecting target invertebrates, several geographically distant collections of individual specimens are obtained so that independent feeding experiments can be performed on each, thereby revealing potential variability in chemical defenses at the species or population level [58]. However, this is not always practical because multiple collections are not possible, the organism is rare, or the organism is small, and insufficient organic extract is available from individual organisms for assays. Under any of these circumstances, it is better to extract a mass collection of the target invertebrate and assume that the extract reflects a composite mean level of defense for the population of organisms from that collection site [59].

In preparing crude organic extracts of a target invertebrate, it is best to extract freshly collected tissue to avoid any possibility of sample degradation. As an alternative, fresh collections are quickly frozen and maintained solidly frozen until processed. Some older studies were performed on air-dried invertebrate tissues [60], which necessitated re-evaluation of the experiments performed on extracts from these species with better techniques that resulted in some very different findings [46].

Prior to extraction, the total volume of the tissue must be determined. This is usually done by adding the tissue samples to a graduated cylinder partially filled with either water or the extraction solvent and recording the displaced volume. After tissue volume has been determined, the tissue may be further chopped or shredded to expedite the extraction process. Each step in the extraction process should use a volume of solvent about twice that of the tissue sample. The solvent mixture of choice for extracting wet tissue is a mixture of equal parts dichloromethane and methanol, which rapidly permeates tissue, solubilizing membranes and dehydrating cellular material. Separation of the dichloromethane phase from the resulting miscible mixture of methanol and water from the tissue occurs very quickly, so it is best to agitate the extraction containers to keep the semi-emulsified extraction liquid in contact with the whole tissue sample. After a minimum of 6 h, preferably under cold and dark conditions, the first extraction solvent mixture is poured off and the tissue squeezed before the same volume of methanol alone is used for the second extraction, which again is best done with agitation for a minimum of 6 h. A third extraction round, also with methanol, is necessary only when the tissue is particularly dense. Evaporation of the solvents should be done to minimize exposure of the extracts to heat and light; for example, the dichloromethane partition of the extract can easily be separated from the aqueous methanol partition in a separatory funnel and evaporated nearly to dryness on low heat by rotary evaporation. Rotary evaporation will also quickly remove solvent from the last methanol extract. The aqueous methanol partition is best evaporated using a vacuum evaporator system. When most of the solvent has been removed

from each, the partitions of the extract are combined into a single vial, completely dried by vacuum evaporation, and stored frozen under nitrogen, if not used immediately for feeding experiments.

3. *Use an appropriate assay.* Feeding experiments can be performed in the laboratory or in the field, with the advantage of the former in simplicity and speed, and of the latter in enhanced ecological relevance. Optimally, feeding experiments will begin in the laboratory and then be duplicated at some level in the field [61]. Feeding experiments are most often behavioral assays in which consumption or rejection of an artificial food that predators do not otherwise recognize is scored. Artificial foods are used because they allow precise control of the nutritional quality of the food as well as the concentration of crude organic extract or metabolites from the invertebrate under investigation. Additionally, the predatory subjects are unfamiliar with artificial foods, have neither learned to avoid nor prefer them, and tend to sample them carefully, resulting in a behavioral assay that is easier for the investigator to observe. For assays in which fish are the predatory subject, artificial foods made from a polysaccharide gelling agent such as agar, carrageen, or Phytigel are commonly employed. These gelling agents add little nutritional value to the artificial food and have the distinct advantage of solubilizing many lipid-soluble metabolites in suspension in the gel matrix, allowing a homogeneous presentation of secondary metabolites in the food. One minor disadvantage of these gelling agents is that they must be heated to boiling after being mixed in water in order for solidification to subsequently occur, and there is always some concern that heat-labile secondary metabolites may be degraded as they are mixed in the molten gel. However, it seems unlikely that wholesale degradation of otherwise stable natural metabolites would occur from such a brief exposure to heat, and the author knows of no example to support this concern. Nevertheless, as an alternative, the sodium salt of alginic acid can be mixed in much the same way as the previously cited gelling agents, but rather than requiring heat, alginic acid forms a solid gel when exposed to a solution of calcium chloride. Proper solidification requires a high surface-to-volume ratio, however, so use of this gelling agent is largely restricted to small volumes of artificial food that are extruded through a syringe housing and into the calcium chloride solution to form long noodles that are then cut to form food pellets [16]. When food pellets are prepared, the feeding assay scores consumption or rejection of individual pellets [16], but when larger food samples are prepared, changes in the mass of treated and control food samples are scored after exposure to predatory fishes [62].

Whatever the artificial food matrix used to volumetrically reconstitute the secondary metabolites from the tissues of the target invertebrate, the food should match the nutritional quality of the same tissues by addition of a nutritional substitute, such as fish meal, or squid mantle. This is important because it is likely that the same sensory processes that predators use to reject feeding deterrent metabolites also perceive the nutritional quality of foods. Foods with very low nutritional quality may be rejected by potential predators at much lower levels of chemical defense [63], and conversely, secondary metabolites may

only be deterrent at higher-than-natural concentrations if those metabolites are presented in an artificial food that is more nutritious than the tissue from which it was derived. Nutritional quality of tissues is determined using calorimetry (to assess total energy content) as well as specific assays for protein, lipid, and carbohydrate [46, 64]. Of these, it is generally agreed that matching the protein content of the invertebrate tissue in the artificial food is the most important. Powdered, freeze-dried squid mantle is a particularly useful nutritional substitute because it is readily available, easy to measure, and its nutritional characteristics have already been determined [64]. Avoid nutritional substitutes that are excessively oily (e.g., tuna packed in oil) or those that may have high levels of free amino acids (e.g., some commercial fish foods) as the stimulatory effects of these substances may act against potential feeding deterrent metabolites present in the tissues of the target invertebrate.

Feeding experiments involve potential predators making choices between foods treated with secondary metabolites from the target invertebrate and control foods, which lack the secondary metabolites, but may contain the solvents (often methanol) used to dissolve the metabolites for homogeneous addition to the food matrix. Because crude organic extracts of invertebrate tissues are often strongly pigmented while most control food mixtures are not, it may be necessary to color-match the treated and control food samples. This is done to prevent assay fish from learning to reject pigmented food samples when multiple assays of different target invertebrate species are being performed in succession with the same group of assay fish, as when doing a survey for chemical defenses [16]. Color-matching can be done by adding drops of food dye while preparing artificial foods, and it is easier to add dye to both treatment and control mixtures to give the same color (masking the natural pigment of the extract in the treatment mixture) rather than trying to match the color of the treatment mixture by adding dye solely to the control mixture.

Once artificial food has been prepared containing a natural volumetric concentration of secondary metabolites from the target invertebrate and having a nutritional quality that approximates the tissues of the target invertebrate, food samples can be presented to assay predators in laboratory or field assays. A single feeding experiment is made up of multiple replicate assays, each of which must be independently performed. For laboratory feeding experiments with fish, independent replication is achieved by splitting up the population of assay fish into separate cells so that no group of fish is assayed more than once with the same treatment. Independent replication can be more difficult for field assays because one or a few hungry fish may monopolize a SCUBA diver who exposes food samples to fishes in the field, and multiple samples eaten by the same predator would not constitute independent replicates. One way around this problem is to place paired treatment and control food strips at replicate feeding stations that are a sufficient distance apart so that the same fishes are not feeding from more than one station [44, 65]. Paired samples are then removed after predators have had a chance to consume some of the food, with feeding deterrence evident when more of the control has been eaten relative to the

treatment food, as determined by measuring the remaining food strips. The difficulty with this type of field assay is that it works well only with “nibbling” fish predators – those that grab the whole food sample and swim off, only to reject the sample after moving away from the feeding station, will render this field assay method useless.

This review has largely focused on fish feeding assays because fishes are often the dominant predators in marine habitats, but there are many examples of feeding assays that have been designed around invertebrate predators. Invertebrate feeding assays are of two types: those that measure consumed assay foods directly and those that score behavioral differences in response to assay foods. The latter category is often necessary because many invertebrate predators feed slowly, consume little, or feed in such a way that it is difficult to score loss of food material. There are examples of invertebrate assays performed in the laboratory with pelleted assay foods that parallel those described previously for fishes [66, 67]. But the most common method for direct measurement of assay food consumption by invertebrates is the “screen gel assay” adapted from sea urchin assays of algal metabolites [68] and adapted for use with crabs [69], sea stars [70], and other invertebrate predators [71]. For these assays, paired treatment and control gel-based foods (as previously described) are solidified onto fiberglass window screen as a thin coating, and the relative number of squares in the screen within the gel area that are consumed over a certain period of time are recorded. For invertebrates that consume larger amounts of material, cubes or strips of gel-based foods can be incorporated onto the screen and weighed before and after the feeding experiment [72]. An assay designed for the opposite situation, to test whether shrimp feed on small amounts of brightly colored control or treatment foods, scores the color change of the shrimp gut by observing it through its clear carapace [55].

Perhaps the best example of a behavioral assay performed with an invertebrate predator for the purpose of testing for chemical defense is the “tube-foot retraction” assay used to test the responses of sea stars, the dominant benthic predators of McMurdo Sound, Antarctica, to potential prey sponges and mollusks and to the organic extracts from these target invertebrates [73–75]. The assay consists of touching the tube feet along one arm of a replicate sea star with the experimental treatment and then measuring the time it takes for the retracted tube feet to extend again from the ambulacral groove. For assays of extracts or pure compounds, the control used is a glass rod coated with silicone grease, and this elicits a retraction time of about 25 s for tube feet of the sea star *Perknaster fuscus*; the response to grease with fish tissue extract is about 28 s, while the response to grease treated with metabolites from the chemically defended sponge *Latrunculia apicalis* is about twice that amount of time [76].

4. *Employ suitable experimental and statistical methods.* The importance of appropriate experimental methods has already been discussed to some extent in describing collection and assay techniques, particularly regarding replication of sampling and when performing feeding experiments. Additionally, if an

investigator wishes to compare the chemical defenses of one or a group of invertebrates relative to a previous study, it is imperative that the same methodology be used, or any comparative conclusions will be compromised by technical differences between the two studies.

One important concern when isolating the chemical defense of a target invertebrate is in the use of bioassay-guided fractionation. Once the presence of a chemical defense has been ascertained by assaying the crude organic extract of the tissues of the target invertebrate, the same assay is employed as the crude extract is chromatographically fractionated into smaller subsets of compounds that make up the mixture. Again, this should be done on a volumetric basis, using “mL equivalents” of tissue extract rather than mass equivalents. As the separation proceeds, fractions are best assayed as a serial dilution relative to the natural volumetric concentration: $4\times$, $2\times$, and $1\times$. This span of concentrations takes into account the likely reduction in deterrent activity that comes from splitting the active metabolites over two or more chromatographic fractions or from loss of active metabolites through decomposition, reaction, or attachment to chromatographic media. Once the active metabolites have been isolated by bioassay-guided fractionation, the investigator should endeavor to identify them using standard spectroscopic techniques and should also do the same for inactive fractions that may have secondary metabolites. For the reasons explained earlier in this chapter regarding their functional significance, it is equally important to know which secondary metabolites are active in ecologically relevant experiments as to know which metabolites are not.

Appropriate statistical analyses of data are as important for behavioral assays as for any other scientific research that involves determining the significance of differences in experimental outcomes. Fortunately, these analyses are usually simple and routine. The significance of most laboratory feeding experiments, in which consumption of control and treated foods is compared, is usually determined with some form of contingency table analysis of which Fisher’s exact test is commonly employed [16]. The assumption for these experiments is that all of the control food offerings will be consumed because the investigator would not be using experimental predators that were not feeding on control foods. In one example, a useful boundary in food pellet consumption was designated that separates palatable from defended treatment foods, based on Fisher’s exact test, in which a treatment is considered deterrent if six or less of ten food pellets are eaten [16].

To analyze data from field experiments, paired, nonparametric statistical tests are usually employed, such as the Wilcoxon paired-sample test [63]. Nonparametric, paired tests are necessary because the variance in the amount of food consumed between replicate pairs of samples positioned in different places in the field is often greater than the difference in consumption between the control and treatment food sample within a pair, a reflection of the “patchiness” of predators in field situations. These nonparametric tests analyze the directionality of the results rather than comparing the mean consumption of control and treated foods.

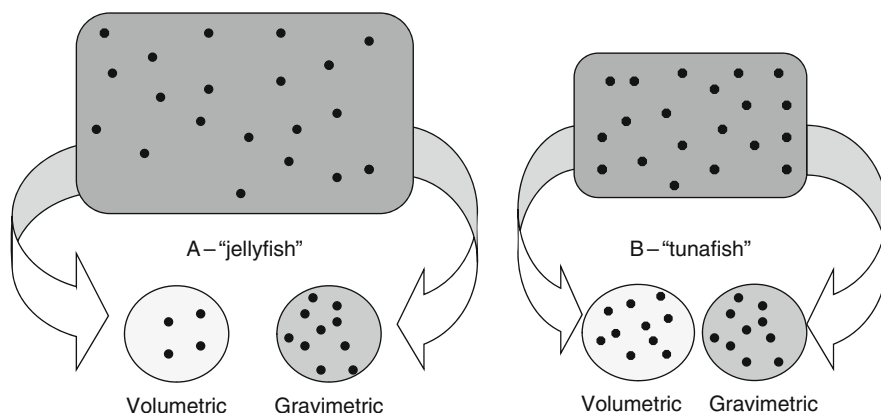


Fig. 12.2 Comparison of volumetric and gravimetric methods for reproducing the concentration of a defensive component in invertebrate tissues. In these diagrams, the *black dots* represent the components of interest (secondary metabolites, spicules, sclerites, etc.) that are assumed to be homogeneously dispersed in the freshly collected (wet) tissue. In example A, the components are sparsely distributed in highly hydrated tissue (jellyfish), while in B, the same amount of components are distributed in about half the volume (tuna fish). Any predator taking an equal volume bite out of A would experience the defensive components at half the concentration of the same bite of B. If the components are reconstituted in an artificial food matrix as a function of wet tissue volume (volumetric), the concentration of the components are identical to the original tissue concentration for both A and B, but if the components are reconstituted as a function of dry mass (gravimetric), they are likely to be more highly concentrated than the original tissue for A (depending on the dry mass of the artificial food used)

12.3.3 Technical Problems

Gravimetric vs. volumetric concentration determination. One long-standing technical problem plaguing the marine chemical ecology literature is with the determination of extract or metabolite concentration in an organism and duplication of the natural metabolite concentration in artificial assay foods. Natural products chemists are accustomed to reporting metabolite concentrations as a function of dry tissue mass, but predators eat wet tissue, and marine invertebrate tissues vary widely in the amount of water contained in their tissues. From the perspective of a predator, a bite of a jellyfish or sea anemone would contain substantially more water per unit dry mass than the same sized bite of a squid or sea slug. For highly hydrated tissues, the concentration of metabolite per unit dry mass would be much higher than per unit volume, but volume (bites) is the measure that is ecologically relevant (Fig. 12.2).

In addition to differences in water content, tissues of marine invertebrates may have very different densities because of skeletal inclusions. For example, some sponges have tissues that are perfused with glass spicules, which have a very high density, but are not part of the living organism (similarly dense limestone inclusions are found in soft corals and tunicates). Dry mass calculations of metabolite concentration would include the heavy mass of these spicules, which are not part of the

living tissue of the sponge, driving down the relative mass of any metabolite found in the tissue. Because the concentration of skeletal inclusions can vary greatly between organisms of the same species, and sometimes between parts of the same organism, perceived differences in metabolite concentration based on dry mass could be accountable entirely to differences in skeletal element concentrations.

The problem of gravimetric concentration determination particularly affects any study aimed at testing for differences in levels of defense between parts of the same organism or between individuals in a population. For example, investigators wishing to test for differential allocation of chemical defenses in one part of the body of a study organism are faced with potential differences in hydration or skeletal inclusions that could confound any differences in metabolite concentration on a dry mass basis. Similarly, investigations of seasonal cycles in metabolite concentration may be confounded by changes in hydration, tissue quality associated with changes in diet (e.g., presence of more lipids in well fed organisms), changes in skeletal inclusions due the changes in flow or wounding, or changes in the abundance or development of gametes.

Determination of metabolite concentration by volume solves both the problems of differences in tissue hydration and density variation from skeletal and tissue inclusions, and it is the most relevant measure from the standpoint of consumption of tissue by a potential predator. It requires that tissue volume be measured at the onset of an extraction protocol, by displacement of water or solvent in a graduated cylinder, and that the resulting extract be treated as a *volume-equivalent* (e.g., “mL equivalents”) throughout the bioassay-guided metabolite isolation process. Dry mass determinations should also be performed during the isolation process because these comparative data are necessary for the marine natural products literature should a novel metabolite be isolated and reported.

The importance of using volumetric methods for determination of metabolite concentration is illustrated in surveys of the chemical defenses of Caribbean gorgonian corals against the generalist predatory bluehead wrasse, *Thalassoma bifasciatum*. The initial survey of 1987, one of the earliest to systematically examine chemical defenses of a broad range of species from a biogeographic community, used a gravimetric approach to estimate natural concentrations of metabolites in experimental foods and documented considerable variability in chemical defenses among common Caribbean gorgonian corals [60]. Subsequent studies introduced the technical superiority of volumetric concentration determination [77]. The gorgonian survey was repeated 15 years later, using volumetric concentration determination and improved techniques for sample processing, and this time, all 32 gorgonian species yielded deterrent crude organic extracts [46]. As an example from the technically improved study, the dry masses and volumes of two tissue samples from the common Caribbean sea fan, *Gorgonia ventalina* were 19.72 g and 27 mL and 22.86 g and 57 mL, respectively (i.e., the mass of the second was 16% greater than that of the first but occupied 111% more volume). In a gravimetric assay, the extracts of these two samples would be applied to similar masses of food of unknown volume because the assay food is also measured and prepared on the basis of mass, not volume. In a volumetric assay, however,

the extract of the second sample would be applied to more than twice the volume of food as the first. The relative concentrations of each extract would be very different in the gravimetric and volumetric assays, as likely would be the feeding responses by the assay organisms.

As was also pointed out in the foregoing technically improved survey of Caribbean gorgonian chemical defenses [46], gravimetric feeding assays fail to control for the nutritional quality of the target organisms. Invertebrate tissues contain nutritionally valuable (e.g., protein) and inert components (e.g., mineralized skeletal elements). When assay foods are prepared gravimetrically, the mass of the nutritionally poor portion is replaced almost entirely by an equivalent mass of nutritionally valuable matrix. As a result, a gravimetrically prepared assay food cannot replicate the nutritional quality of tissue. When assay foods are prepared volumetrically, however, organic extract from a volume of tissue is added to a volume of assay food that can be modified to have a similar nutritional quality (more or less powdered freeze-dried squid mantle). The proportion of the nutritional components is controlled for in a volumetric assay. Thus, volumetric assays are more ecologically relevant than their gravimetric counterparts because the assay food more closely models hydrated tissue in both nutritional quality and extract concentration. A note of caution, however: the foregoing assumes that tissue constituents (secondary metabolites, skeletal elements, etc.) are homogeneously distributed in the tissue under investigation. If it is suspected that the tissue constituent of interest is, for example, concentrated in the surface of the target organism, then a more careful, separate extraction of inner and outer layers of tissue will be required.

Extraction protocol. Experiments designed to assess chemical defenses of marine invertebrates require that secondary metabolites be extracted and assayed separately from any structural defenses that may be present in their tissues. To this end, the full range of potential defensive metabolites, from nonpolar (e.g., terpenes) to polar (e.g., glycosides), must be extracted from tissues and recovered in nearly 100% yield with minimal degradation prior to reconstituting the metabolites in assay foods and performing feeding experiments with potential predators.

Very little comparative work has been published on extraction protocols, but the choice of wet or freeze-dried tissue and extraction solvent can substantially alter extraction efficiency [78]. Minor variations on the aforementioned extraction scheme are the norm for most studies of marine invertebrate chemical defenses [16, 46], particularly when natural products chemists are involved as collaborators. Substitution of one extraction solvent for another of the same polarity is unlikely to have much effect on the extraction outcome, particularly if the extract is prepared from freshly distilled solvents and processed quickly. Tissue extraction may be incomplete, however, if an inappropriate solvent is used. Extraction with methanol alone, for example, may not liberate all the nonpolar metabolites from the tissue. Freeze-drying tissue before extraction, which is often done to speed and simplify the process by removing water, may also be problematic because very polar metabolites may not be extracted from freeze-dried tissue with methanol unless the tissue is first rehydrated. Experience in the author's laboratory has

shown that yields of some metabolites from sponges are higher when using wet tissue than freeze-dried tissue, as has been determined for similar extractions of macroalgae [78].

A combination of the aforementioned technical pitfalls is illustrated in a recent set of studies that claims to demonstrate latitudinal variation in sponge chemical defenses as a function of relative predation pressure, comparing species that are found off the coast of the southeastern United States, where fish predators are scarce, and in the Caribbean, where predators are common [79, 80]. Sponge tissue samples were freeze-dried and then extracted only in a mixture of equal parts dichloromethane and methanol, a protocol that would likely not liberate the most polar secondary metabolites from the tissues of some sponge species. Data from feeding assays performed using sponge extracts prepared in this manner were compared to those done on wet-extracted tissue using the protocol described previously [16], and the authors found lower levels of chemical defense in the sponges from the coast of the southeastern US than had previously been documented from the Caribbean [79]. Unfortunately, incomplete extraction of sponge tissue is an alternative and more parsimonious explanation for the difference in feeding assay outcomes for the more recent study, and a less equivocal test of the latitudinal variation hypothesis will require complete and identical extraction protocols. Moreover, the preceding example provides a cautionary tale in support of using identical methodologies when seeking to compare data from two studies.

Nutritional quality of assay foods and the feeding state of assay predators. When conducting feeding experiments to determine whether organic extracts of marine invertebrates contain chemical defenses, it is important that other variables that affect assay food quality not confound or interact with the effects of the metabolites being tested. In particular, the nutritional quality of assay foods is important [63, 81]. Metabolites that are mildly deterrent are more likely to induce predators to reject them when they are incorporated into foods with little or no nutritional quality than when they are incorporated into high-quality foods. High food quality is usually linked with protein content, and many associated amino acids and peptides are strong feeding stimulants [82], which may interact with feeding deterrents. Indeed, the converse may also be true – assay foods with very high nutritional quality may mask the deterrent effects of minimally effective defensive metabolites.

It is incumbent on the investigator to match the nutritional quality of the artificial assay food with that of the marine invertebrate from which the crude organic extract or metabolites have been derived. Sometimes this is relatively simple; for example, the mantle tissue of a nudibranch and a squid are likely to be fairly similar in food value, so an artificial food prepared from the latter should be a good stand-in for the tissue of the former. But the tissues of sponges, ascidians, and soft corals may contain high concentrations of both water and skeletal elements that make their interspecific nutritional quality highly variable, particularly on a volumetric basis (see above, Fig. 12.2) [46, 64, 83]. Therefore, replicate tissue samples should minimally be subjected to a combination of bomb calorimetry for total caloric content and a suitable assay of soluble protein to determine reasonable nutritional

parameters for artificial assay foods [46]. Because the gelling agent used in most assay foods (agar, carrageenan, alginic acid, or similar) has little nutritional value, a nutritional component can be added to the gelling agent to approximate the food value of the invertebrate tissue. Performing the same analyses on the selected nutritional component, such as powdered, freeze-dried squid mantle or a commercial flake food for aquarium fish, will provide the comparative basis for determining the recipe to match the invertebrate tissue, which, again, should be calculated on a volumetric basis.

Along the same lines, the feeding state of the assay predator can have an important effect on the outcome of feeding experiments. Predators that have been starved are likely to consume artificial food offerings despite the presence of a chemical defense that would otherwise deter them. This problem is well known to experimentalists who regularly run feeding experiments, but few studies have quantified the importance of the feeding state of consumers [84]. It is likely that predators of marine invertebrates are well fed; observations of fishes on coral reefs certainly support this contention [10, 23]. Therefore, if experiments are to be performed in the laboratory, assay predators should be maintained on a healthy diet to observe normal feeding behavior. However, it is not uncommon to deny assay predators food for a short period of time prior to a feeding experiment in order to boost the speed at which a feeding choice is made.

12.4 Additivity and Synergism

Complicating any exploration of chemical defenses of marine invertebrates is the possibility that a single metabolite does not act in isolation but in association with other metabolites or in association with physical defenses. The interaction of the individual component defenses may be *additive*, that is, their combined deterrent effect is equal to the sum of their individual effects, or it may be *synergistic*, wherein their combined deterrent effect is greater than the sum of their individual effects. A third case, in which the interactive effect of components leads to a loss of activity, is termed *antagonistic* and is exemplified in the previously cited interaction between compounds that enhance feeding (e.g., amino acids) and chemical defenses.

Marine invertebrates are likely candidates for interactive effects of potential defenses. Many species of sponges, soft corals, and ascidians are known to contain in their tissues: (1) mixtures of secondary metabolites of the same structural class, (2) multiple secondary metabolites of different structural classes, and (3) skeletal elements, such as glass spicules (sponges) or calcitic inclusions (soft corals, ascidians). The possibilities for exploring the interactions among these components quickly become numerically astronomical, but what remains ecologically relevant is whether their sum is deterrent to potential predators, and this is an experimentally approachable question using the techniques already described. However, when components are separated and are no longer deterrent at natural concentrations, two questions arise: (1) Did degradation or loss of metabolites during isolation or

purification result in activity falling below some threshold level? (2) Did separation of multiple active components from each other result in activity falling below threshold? Additionally, the effectiveness of any combination of chemical or physical defenses may depend on the nutritional quality of the prey [85].

Experimental examinations of additivity or synergism are rare in chemical ecology [86], and the terms may be used improperly. The complexity of evaluating additive vs. synergistic effects is illustrated in an exchange of publications on the chemical and physical defenses of calcified marine algae against herbivorous fishes [68, 87, 88].

In only one case has a systematic statistical approach for identifying additivity or synergism been undertaken: Jones et al. [89] used an isobolographic analysis and logit model to examine the interaction between chemical defenses and spicules in the tissues of Caribbean sponges. For each sponge species examined, multiple assays of each defensive component (crude organic extract or isolated siliceous spicules) in artificial foods were performed using the bluehead wrasse fish as the experimental predator. Assays of serial dilutions of each defensive component were performed to determine the 50% effective dose (ED_{50}) of each, and then a series of combination assays were carried out at concentrations equal to or less than the ED_{50} of each component in isolation. Synergism between chemical and physical defenses at natural component concentrations was observed for three of seven sponge species that exhibited intermediate levels of chemical defenses, suggesting that spicules may synergistically enhance chemical defenses for some sponge species, but the authors suggested that this effect was more likely to be an exaptation of the primary function of spicules in sponges, which is to provide structural support to the organism. While Jones et al. [89] provided a novel analytical technique and an important proof of concept, their procedure has yet to be applied to defensive variability within a single species.

12.5 Optimization, Differential Allocation, Induction, and Activation

It is generally supposed that organisms are “optimized” in all respects for their environment by natural selection, but as discussed previously, this is certainly not true: The physical and biological environment changes through time, and evolution acts on the sum of the phenotypic characteristics that make up an individual organism – some will be more important at any one time, some less, some perhaps not at all. If defense is particularly important to the survival of an organism because predation is intense, and a coevolutionary “arms race” develops in which the prey must develop ever more sophisticated methods of combating predatory attack while somehow keeping the cost of those methods to a minimum, we might expect optimization of chemical defenses. In fact, optimization strategies have been described in the terrestrial chemical ecology literature, particularly for insects, and include mechanisms like differential allocation or induction of chemical defenses, as well as other protective measures, such as mimicry.

Chemical defenses that are *differentially allocated* are found at higher concentrations in the parts of an organism that are more susceptible to attack, thereby saving the organism the cost required to make and store defensive metabolites throughout its body. *Induction* describes the initiation of metabolite synthesis in response to tissue damage caused by predatory attack. An *induced chemical defense* is very economical because metabolites are produced only when needed, but the process would not provide immediate protection because metabolite synthesis would require some time. Another strategy often confused with induction is termed activation. An *activated chemical defense* is stored by the organism in a less bioactive form but is converted to a more potent form either when tissue is damaged or the defense is released in response to attack. The advantage of an activated defense to the prey is one of storage, in that it is potentially less costly to maintain relatively nontoxic precursor metabolites than to deal with autotoxicity from storing the product metabolite.

Evidence for optimized chemical defenses of marine invertebrates has been relatively scarce. This is interesting, because marine chemical ecologists often look for examples of optimized defenses in the system they are studying that parallel those described in terrestrial systems, not only to provide additional examples of the phenomena but also because they are intrinsically interesting, “just so” evolutionary narratives. When optimized defenses are found in a system, it is often interpreted that they can be generalized to other organisms, but when optimized defenses are not found, the research results are generally not published. Therefore, the paucity of reports of optimized chemical defenses among marine invertebrates more likely reflects scarceness rather than insufficient effort in uncovering the phenomena.

Differential allocation is certainly present in nudibranch mollusks, which have higher concentrations of deterrent metabolites in their dorsal surface and eggs [30], or associated with specialized glands on the dorsum and sides of the slugs [90]. For sessile benthic marine invertebrates, it has been claimed that some gorgonian corals invest higher levels of chemical defenses in their polyps than in the coenenchyme tissue that surrounds the axial skeleton of the coral [91], but the comparative data used to support this conclusion were based on gravimetric determinations of metabolite concentration (dry mass basis) rather than on a volumetric determination. Because the polyps of most gorgonians are free of calcitic sclerites, while the coenenchyme is infused with them to varying degrees, the high density of sclerites would result in much lower concentrations of metabolites on a dry mass basis in coenenchyme than on a volumetric basis, as explained previously [46]. Therefore, claims of differential allocation of chemical defenses in gorgonian corals await confirmation using a volumetric approach.

For sponges, differential allocation of defenses has been investigated for several species, with no evidence of the phenomenon in some [92] and some evidence in others [76, 93–95]. Here, the issue may be complicated by the method by which a predator feeds or whether the metabolite plays multiple roles. Fish predators of sponges take large bites of sponge tissue [23], which would make differential allocation ineffective [92]. But sea stars, the dominant invertebrate predators in

Antarctic benthic communities, feed by everting their guts on the surface of prey and appear to have driven the evolution of differential allocation of defenses to the surface tissues in some co-occurring sponge species [76]. The same may be true for sponges that are grazed by nudibranch mollusks [94] or have chemical defenses against fish predators that also serve as antifouling agents [93].

Differential allocation has been invoked for one species of morphologically distinct sponge from the Indo-Pacific, *Oceanapia* sp., which grows buried in the substratum but produces a stalk and cap structure that sticks up into the water column, where it is ostensibly subject to greater predatory attack [95]. As with the previous gorgonian example, the claim that the protruding structures contain higher concentrations of deterrent metabolites is confounded by the gravimetric (dry mass) method of determining metabolite concentration [95] because the concentration of glass spicules in the sponge tissue is highly variable, much greater in the sponge base and decreasing to the tip of the protruding structure. While the growth form of *Oceanapia* sp. certainly makes it a likely candidate for differential allocation of chemical defenses, volumetric measurements of metabolite concentrations will be needed to confirm this.

Induced defenses of marine invertebrates have been the subject of far fewer published studies than differential allocation of defenses, and in no case is there unequivocal evidence of the phenomenon. The chicken liver sponge *Chondrilla nucula* presents an excellent candidate for induced defenses: it has a high degree of intraspecific variability in chemical defense [16] and is abundant in a variety of habitats in the Caribbean, from reefs where fish predators are common to mangrove and grass bed habitats where they are rare. A more in-depth study of variation in chemical defenses of this species failed to resolve site-specific patterns in chemical defenses or induced increases in defense as a function of simulated predation [92].

Following up on preliminary data that suggested an induced defense [96], a transcriptome profiling approach was taken in a study of an Indo-Pacific soft coral *Sinularia polydactyla* that tracked changes in mRNA pool complexity as well as metabolite concentration for corals reciprocally transplanted to areas of high and low predation [97]. While there were clear differences in transcriptome complexity between transplanted corals, perhaps representing induced changes in metabolite production, the metabolite profiles in transplanted corals did not necessarily support induced defenses [97].

One of the more interesting and controversial areas of research into marine invertebrate antipredatory defenses has been that of activated defenses. It is important to remember that activated defenses are not optimized in the same way that differentially allocated or induced defenses are because these last two mechanisms reduce the overall expenditure of the organism on defensive metabolite production: They are cost-saving measures that optimize the use of defenses. An activated defense requires the synthesis of a full complement of precursor molecules, in addition to whatever enzyme or catalyst is required for conversion of the precursors into the defensive metabolite after the organism is attacked. As such, an activated defense could conceivably be *more expensive* to maintain than a constitutive defense. The potential advantage of an activated defense is one of

potency: A nonreactive precursor can be stored easily until attack, at which time tissue disruption and interaction of precursor and catalyst results in the nearly instantaneous formation of a highly deterrent (and possibly autotoxic) product metabolite. The foregoing is important because although it is easy to understand the evolution of resource-saving optimization schemes like differentially allocated or induced defenses (despite the paucity of evidence for their general existence among marine invertebrates), the evolution of activated defenses is more difficult to envision. After all, if the organism has to go to all the trouble of making the full complement of a chemical defense, why not make it constitutive?

An activated antipredatory defense was originally proposed for the Mediterranean sponge *Aplysina aerophoba* on the basis of laboratory experiments with freeze-dried sponge tissue [98]. Mechanistically, high molecular weight brominated tyrosine derivatives were thought to be rapidly converted by a putative enzyme to form smaller, more active chemical defenses after predatory damage to the sponge tissue. Because *Aplysina* spp. are found worldwide and all contain very similar secondary metabolites, it was proposed that this “biotransformation” was a common feature of the chemical defense of the genus. However, no evidence of activation was found in a combination of rigorous laboratory and field experiments with living specimens of two species of *Aplysina* in the Caribbean [99]. Without going into excessive detail, well over a decade after the initial report [98] and despite the rigorous field experiments performed in the Caribbean [99], there are now more than ten publications that directly relate to the putative activated defenses of *Aplysina* spp. [100]. The putative enzyme responsible for this activation defies isolation and characterization, and it is now suggested that the smaller brominated metabolites are important as antimicrobial agents that defend the wounded sponge tissue but not as antipredatory defenses [100, 101].

Another curious example of an activated defense has been described for the hydroid *Tridentata marginata*. Like most hydroids, *T. marginata* has stinging cells (cnides), but in addition it has a chemical defense against generalist fish predators that is effective even after the cnides have been discharged [102]. Further research suggested that the metabolites responsible for the chemical defense were stored in a nondeterrent form in the cnides, and that the crushing action associated with predation resulted in release and conversion to the deterrent metabolites, tridentatols A-C [103]. At one level, it is unclear why one species of hydroid should develop chemical defenses along with cnides while other co-occurring species have cnides alone, although the authors suggest that cnides offer a relatively ineffective physical defense in this species [102]. But in this example, the justification for activated defenses based on autotoxicity seems to be obviated by the isolation of the defensive precursors in cnide capsules.

The most recent example of an activation scheme has been proposed for the Indo-Pacific reef sponge *Aplysinella rhax*, a close relative of sponges of the genus *Aplysina* [104]. Maceration or wounding of the sponge tissue caused the rapid formation of psammaphin A from its sulfate salt, a reaction that was suggested to be enzyme catalyzed. The activated metabolite was claimed to be a more deterrent defense on the basis of feeding assays using fractions of extracts of the sponge, but

when the purified metabolite and the sulfate salt were assayed in the field, there was no difference in consumption of the two, casting doubt on the importance of the conversion as a requirement for an enhanced chemical defense. The authors of this study [104] suggest that evidence of activated chemical defenses have been underreported in the literature on marine chemical ecology, but an alternative explanation is that activated defenses are very rare (if they exist at all) for the simple reason that they do not provide an evolutionary advantage over constitutive defenses. Past observations of activated defenses in sponges may be attributable to differential tissue extraction efficiency, hydrolysis from less soluble precursors, or the heterogeneous distribution of metabolites in sponge tissue [99].

In summary, research to date warrants that claims of optimized or activated defenses among marine invertebrates be assessed with skepticism and with a higher standard of evidence. While the evolutionary narrative inspired by studies of terrestrial plants and insects is highly appealing, marine invertebrates in general have not been under the same selective predatory pressures that result in more complicated optimized defense strategies (Fig. 12.1). Comparing the basic aspects of the biology and ecology of marine invertebrates to terrestrial invertebrates (insects) may give us clues that explain why induction, differential allocation, and activation, as well as complex levels of aposematism and mimicry are common to the latter but not to the former: Marine invertebrates are fairly long-lived and exhibit indeterminate growth (some sponges may live thousands of years [105]), and while predation is an important part of their ecology, so too are other aspects, particularly recruitment. Terrestrial insects, on the other hand, may complete multiple generations in a single summer and exhibit determinate growth, and their populations are under intense and directed predatory pressure. Therefore, it is not surprising that many of the interesting phenomena found among butterflies and beetles are not evident among sponges, corals, and nudibranchs.

12.6 Resource Trade-Offs and the Cost of Chemical Defense

While terrestrial chemical ecologists have addressed costs in some systems [106–108], few studies in marine ecology have attempted to demonstrate that chemical defenses have a cost to the marine invertebrates that produce them. Perhaps the easiest way to address the cost of defense is to compare resource parameters within a species that has defended and undefended individuals, whether by constitutive (genotypic) or facultative (induced) means. As we have seen above, there are few examples of intraspecific variability in defenses among marine invertebrates, and none in which costs have been examined.

An alternative method for investigating the cost of chemical defenses is to quantify relative rates of growth or reproduction among co-occurring species that exhibit different levels of defense. Assuming that all life functions (respiration, growth, reproduction) have a cost, the production of chemical defenses should result in a trade-off, such that defended species exhibit lower rates of growth or reproduction than undefended species. Making this comparison can be difficult,

either because relative levels of defense among species in the community are unknown or because all the species in the community are similarly well defended, as in Caribbean gorgonian corals [46]. Moreover, different species may invest in mechanisms other than chemical defenses, which are also likely to have costs. Also, if endosymbionts of a chemically defended invertebrate (e.g., zooxanthellae in hard and soft corals) are responsible for the production of the chemical defense, it may come at little or no cost to the host invertebrate.

The Caribbean coral reef sponge community has provided an interesting system in which trade-offs between chemical defense and life functions have been evident. The most common sponges on Caribbean reefs are either chemically defended or undefended [16], and the latter group is consumed by a suite of sponge-eating fishes [10, 23]. When the rate of wound healing was compared between the two groups, undefended species were found to heal much faster than defended species [109]. More indicative of resource trade-offs between the two groups, however, were the results of surveys of an artificial reef shipwreck that provided new substratum for sponge recruitment and growth [110]. If undefended sponge species are able to divert metabolic resources to growth and reproduction, they would be expected to colonize new substrata faster than defended species that use their resources to synthesize and store chemical defenses. And in fact, undefended sponge species dominated an artificial reef shipwreck off the Florida Keys 4 years after it was sunk (96.0% of sponge cover was made up of undefended species vs. 15.2% on adjacent reefs), with initial recruits of defended species observed 18 months later [110], corroborating a resource trade-off between chemical defense and reproduction or growth.

12.7 Structure-Activity Relationships and the Commonality of Chemical Defenses

In pursuit of developing more effective insecticides, plant–insect chemical ecologists have systematically investigated the relationships between metabolite structure and feeding deterrent activity for many insect species [111]. Similar efforts have been rare in marine chemical ecology. When multiple pure compounds have been assayed together for feeding deterrent activity, it is not uncommon for comparisons to be made and preliminary conclusions drawn about relationships between structure and activity [59, 112], but these have not addressed the issue in a systematic way.

One study has examined the relationship between metabolite structure and feeding-deterrent activity for a series of analogs having minor modifications to determine the importance of metabolite size, shape, and functionality [113]. Using a fish feeding assay, 21 compounds, including pyrrole-imidazole alkaloids isolated from sponges of the genus *Agelas* and synthetic analogs, were tested at a range of concentrations. Additional observations of structure-activity relationships for metabolites from *Agelas* sp. were reported in a companion publication [114]. The pyrrole moiety was required for feeding deterrent activity, while the imidazole

group enhanced activity. Imidazole metabolites lacking the pyrrole were not active, while feeding-deterrent activity was enhanced by dimerization, increased polarity, or the addition of bromine.

Interestingly, there do not yet appear to be any common structural themes among secondary metabolites that have been isolated and identified as chemical defenses of marine invertebrates. Compounds of several classes and of very different polarities are represented among feeding deterrents, from nonpolar terpenoids [115] to polar glycosides [116]. This variability suggests that compound polarity, and therefore solubility in water, is not a critical factor in the evolution of marine invertebrate chemical defenses. Bad-smelling volatile compounds present in some sponges do not appear to act as chemical defenses [61]. While acidity is known to deter feeding, and is used by some ascidians as a chemical defense [83], this mechanism of defense is surprisingly uncommon, and many ascidians also have secondary metabolites as chemical defenses [59], perhaps suggesting that the metabolic demands of containing inorganic acids within invertebrate tissues are greater than their advantages relative to organic compounds as chemical defenses.

Recent technical developments in molecular genetics may permit structure-activity relationships to be addressed at the cellular level. Metabolites from the sponges *Ectyoplasia ferox* and *Erylus formosus* that had previously been identified as feeding deterrents using co-occurring fish predators [116, 117] also deterred feeding of the freshwater zebra fish [118]. Transcripts made from a zebra fish cDNA library were expressed in the oocytes of the frog *Xenopus laevis* and tested for chemoreceptor activation using electrophysiological techniques. Oocytes expressed gene sequences from the library and exhibited electrophysiological responses when exposed to the deterrent metabolites formoside and ectyoplasides A and B, indicating that the chemical defense-activated signaling pathway was reconstituted in *Xenopus* oocytes [118].

There is some evidence that chemical defenses may be broadly effective against predators, not only against different species (such as fishes) [79, 119], but also against different predatory taxa (crabs, seastars) [69, 70]. This commonality in response suggests that chemoreceptive responses of diverse taxa of predators are similar at the molecular level. In at least one case, for triterpenoid glycosides from two Caribbean sponges, multiple defensive roles have been proposed that extend beyond antipredatory effects to allelopathic and antifouling functions [93]. In terms of resource allocation, the advantages of multifunctional defenses are clear, and this is an area that is ripe for further investigation.

12.8 Study Questions

1. An eminent Ivy League bryozoan taxonomist finishes her survey of Indonesian coastal waters and sends 410 dried bryozoan samples representing 53 species ($N > 2$ for each) to her first-year graduate student, with instructions to investigate their chemical defenses. Following the advice of the elderly entomologist in the lab next-door, the graduate student decides to use diethyl ether as the sole

extraction solvent and to run Microtox toxicity assays on serial dilutions of each extract as a function of extract dry mass. He is delighted to discover very clear differences in toxicity between mangrove and coral reef species and runs a complex statistical analysis to support his conclusions. He submits their work on “The chemical defenses of Indonesian bryozoans” to a top-rated ecology journal.

Q1: What problems are reviewers of this manuscript likely to cite in recommending that it not be published?

Q2: What should the graduate student do after receiving the negative decision?

2. A graduate student in a natural products laboratory is studying the variability of secondary metabolites in a species of soft coral that produces a potential anti-cancer drug, xenopterolide. She determines that there is a significant difference in the mean concentration of xenopterolide, which is also a well-known fish feeding deterrent, in replicate samples ($N = 20$) from high-flow reef crest environments ($30 \mu\text{g}$ xenopterolide/mg dry tissue mass) vs. low-flow patch reef environments ($100 \mu\text{g}/\text{mg}$). She concludes that fish predation on this soft coral is more intense in patch reef environments.

Q3: What is an alternative explanation? Hint: Soft corals increase the density of their skeletal elements (limestone sclerites) as a function of increasing flow regime.

Q4: How would you re-design the methodology for this project?

3. A postdoctoral researcher is studying seasonal variation in secondary metabolite concentration in a species of sponge by removing a tissue sample from each of 20 sponges every month for a year (no sponge is sampled more than once). The sponge is hermaphroditic, producing sperm and eggs in the spring, brooding large numbers of large embryos throughout its tissue for several months, and then releasing them in late summer. The researcher determines metabolite concentrations as a function of both volume and mass.

Q5: What pattern of metabolite concentration might the researcher expect to see, on a gravimetric vs. volumetric basis, if the sponge tissue is full of glass spicules, but the embryos are free of spicules?

Q6: What if neither sponge nor embryos have spicules?

Q7: What if the sponge differentially provisions embryos with high levels of chemical defenses?

Q8: For a seasonal study like this, why might the investigator also want to measure the mass of the crude organic extract for each tissue sample?

4. An MS graduate student completes his 2-year dissertation research on the ecological functions of a suite of previously characterized secondary metabolites in a temperate colonial ascidian. He uses all the proper extraction and assay techniques to explore possible defenses against several co-occurring predators, as well as meticulously investigating antifouling, allelopathic, and antimicrobial functions. His data show no defensive effect of the metabolites in any of his assays. His advisor is sympathetic but tells him that his work is not publishable because “nobody should publish negative results” and that “all secondary

metabolites must have ecological functions, otherwise the organism wouldn't make or store them."

Q9: Why is the advisor wrong about each of the statements in quotes?

Acknowledgments The author thanks his graduate students for editorial comments on earlier drafts of this chapter. This work was supported by grants from the National Science Foundation's Biological Oceanography Program (OCE 0550468, 1029515).

References

1. Hay ME et al (1998) Bioassays with marine and freshwater macroorganisms. In: Haynes KF, Millar JG (eds) *Methods in chemical ecology*. Chapman and Hall, New York, pp 39–141
2. McClintock JB, Baker BJ (eds) (2001) *Marine chemical ecology*. CRC Press, Washington, DC, 610 p
3. Pawlik JR (1993) Marine invertebrate chemical defenses. *Chem Rev* 93:1911–1922
4. Paul VJ et al (2007) Chemical defenses: from compounds to communities. *Biol Bull* 213:226–251
5. Pohnert G (2004) Chemical defense strategies of marine organisms. *Top Curr Chem* 239:179–219
6. Chase JM et al (2002) The interaction between predation and competition: a review and synthesis. *Ecol Lett* 5:302–315
7. Rose MR, Mueller LD (2006) *Evolution and ecology of the organism*, 1st edn. Pearson, Upper Saddle River, 693 p
8. Whalen KE et al (2010) Biochemical warfare on the reef: the role of glutathione transferases in consumer tolerance of dietary prostaglandins. *PLoS One* 5(1):e8537
9. Mumby PJ (2009) Herbivory versus corallivory: are parrotfish good or bad for Caribbean coral reefs? *Coral Reefs* 28:683–690
10. Dunlap M, Pawlik JR (1998) Spongivory by parrotfish in Florida mangrove and reef habitats. *Mar Ecol* 19:325–337
11. Johnson KH (2000) Trophic-dynamic considerations in relating species diversity to ecosystem resilience. *Biol Rev Camb Philos Soc* 75:347–376
12. Randall JE, Hartman WD (1968) Sponge-feeding fishes of the West Indies. *Mar Biol* 1:216–225
13. Pawlik JR (1997) Fish predation on Caribbean reef sponges: an emerging perspective of chemical defenses. In: Lessios HA, Macintyre IG (eds) *Proceedings of the 8th international coral reef symposium, Panama, June 24–29, 1996, vol 2*. Smithsonian Tropical Research Institute, Balboa, pp 1255–1258
14. McClintock JB et al (2005) Ecology of Antarctic marine sponges: an overview. *Integr Comp Biol* 45:359–368
15. Albrizio S et al (1995) Amphitoxin, a new high molecular weight antifeedant pyridinium salt from the Caribbean sponge *Amphimedon compressa*. *J Nat Prod* 58:647–652
16. Pawlik JR et al (1995) Defenses of Caribbean sponges against predatory reef fish. I. Chemical deterrence. *Mar Ecol Prog Ser* 127:183–194
17. Schulte BA, Bakus GJ (1992) Predation deterrence in marine sponges – laboratory versus field studies. *Bull Mar Sci* 50:205–211
18. Long JD, Hay ME (2006) Fishes learn aversions to a nudibranch's chemical defense. *Mar Ecol Prog Ser* 307:199–208
19. Wheat CW et al (2007) The genetic basis of a plant-insect coevolutionary key innovation. *Proc Natl Acad Sci USA* 104:20427–20431
20. Warburton K (2003) Learning of foraging skills by fish. *Fish Fish* 4:203–215

21. Cruz-Rivera E, Hay ME (2003) Prey nutritional quality interacts with chemical defenses to affect consumer feeding and fitness. *Ecol Monogr* 73:483–506
22. Faulkner DJ, Ghiselin MT (1983) Chemical defense and evolutionary ecology of dorid nudibranchs and some other opisthobranch gastropods. *Mar Ecol Prog Ser* 13:295–301
23. Dunlap M, Pawlik JR (1996) Video monitored predation by Caribbean reef fishes on an array of mangrove and reef sponges. *Mar Biol* 126:117–123
24. Wulff JL (1994) Sponge feeding by Caribbean angelfishes, trunkfishes, and filefishes. In: van Soest RWM, van Kempen TMG, Braekman J-C (eds) *Sponges in time and space: biology, chemistry, paleontology*. A.A. Balkema, Rotterdam/Brookfield, pp 265–271
25. Derby CD et al (2007) Chemical composition of inks of diverse marine molluscs suggests convergent chemical defenses. *J Chem Ecol* 33:1105–1113
26. Nusbaum M, Derby CD (2010) Effects of sea hare ink secretion and its escapin-generated components on a variety of predatory fishes. *Biol Bull* 218:282–292
27. Kamio M et al (2010) The purple pigment aplysioviolin in sea hare ink deters predatory blue crabs through their chemical senses. *Anim Behav* 80:89–100
28. Grode SH, Cardellina JH (1984) Sesquiterpenes from the sponge *Dysidea etheria* and the nudibranch *Hypselodoris zebra*. *J Nat Prod* 47:76–83
29. Haber M et al (2010) Coloration and defense in the nudibranch gastropod *Hypselodoris fontandraui*. *Biol Bull* 218:181–188
30. Pawlik JR et al (1988) Defensive chemicals of the Spanish dancer nudibranch *Hexabranchus sanguineus* and its egg ribbons – macrolides derived from a sponge diet. *J Exp Mar Biol Ecol* 119:99–109
31. Roussis V et al (1990) Secondary metabolites of the chemically rich ascoglossan *Cyerce nigricans*. *Experientia* 46:327–329
32. Becerro MA, Starmer JA, Paul VJ (2006) Chemical defenses of cryptic and aposematic gastropod molluscs feeding on their host sponge *Dysidea granulosa*. *J Chem Ecol* 32:1491–1500
33. Edmunds M (1991) Does warning coloration occur in nudibranchs? *Malacologia* 32:241–255
34. Ritson-Williams R, Paul VJ (2007) Marine benthic invertebrates use multimodal cues for defense against reef fish. *Mar Ecol Prog Ser* 340:29–39
35. Ang HP, Newman LJ (1998) Warning colouration in pseudocerotid flatworms (Platyhelminthes, Polycladida). A preliminary study. *Hydrobiologia* 383:29–33
36. Kicklighter CE, Hay ME (2006) Integrating prey defensive traits: contrasts of marine worms from temperate and tropical habitats. *Ecol Monogr* 76:195–215
37. Meredith TL et al (2007) The polychaete *Cirriformia punctata* is chemically defended against generalist coral reef predators. *J Exp Mar Biol Ecol* 353:198–202
38. Newman LJ, Cannon LRG, Brunkhorst DJ (1994) A new flatworm (platyhelminthes, polycladida) which mimics a phyllidiid nudibranch (mollusca, nudibranchia). *Zool J Linn Soc* 110:19–25
39. Pawlik JR (1992) Chemical ecology of the settlement of benthic marine invertebrates. *Oceanogr Mar Biol* 30:273–335
40. Levin LA (2006) Recent progress in understanding larval dispersal: new directions and digressions. *Integr Comp Biol* 46:282–297
41. Unson MD, Holland ND, Faulkner DJ (1994) A brominated secondary metabolite synthesized by the cyanobacterial symbiont of a marine sponge and accumulation of the crystalline metabolite in the sponge tissue. *Mar Biol* 119:1–11
42. Haslam E (1986) Secondary metabolism – fact and fiction. *Nat Prod Rep* 3:217–249
43. Harper MK et al (2001) Introduction to the chemical ecology of marine natural products. In: McClintock JB, Baker BJ (eds) *Marine chemical ecology*, CRC marine science series. CRC Press, Boca Raton, pp 3–69
44. Pawlik JR, Fenical W (1989) A re-evaluation of the ichthyodeterrent role of prostaglandins in the Caribbean gorgonian coral *Plexaura homomalla*. *Mar Ecol Prog Ser* 52:95–98

45. Gerhart DJ (1984) Prostaglandin A2 – an agent of chemical defense in the Caribbean gorgonian *Plexaura homomalla*. *Mar Ecol Prog Ser* 19:181–187
46. O’Neal W, Pawlik JR (2002) A reappraisal of the chemical and physical defenses of Caribbean gorgonian corals against predatory fishes. *Mar Ecol Prog Ser* 240:117–126
47. Gerhart DJ (1986) Prostaglandin A2 in the Caribbean gorgonian *Plexaura homomalla* – evidence against allelopathic and antifouling roles. *Biochem Syst Ecol* 14:417–421
48. Vrolijk NH, Targett NM (1992) Biotransformation enzymes in *Cyphoma gibbosum* (gastropoda, ovulidae) – implications for detoxification of gorgonian allelochemicals. *Mar Ecol Prog Ser* 88:237–246
49. Karuso P (1987) Chemical ecology of the nudibranchs. In: Scheuer PJ (ed) *Biorganic marine chemistry*. Springer, Berlin, pp 32–60
50. Bakus GJ, Green G (1974) Toxicity in sponges and holothurians – geographic pattern. *Science* 185:951–953
51. Jackson JBC, Buss L (1975) Allelopathy and spatial competition among coral reef invertebrates. *Proc Natl Acad Sci USA* 72:5160–5163
52. Bakus GJ (1981) Chemical defense mechanisms on the great barrier reef, Australia. *Science* 211:497–499
53. Gemballa S, Schermutzki F (2004) Cytotoxic haplosclerid sponges preferred: a field study on the diet of the dotted sea slug *Peltodoris atromaculata* (doridoidea: nudibranchia). *Mar Biol* 144:1213–1222
54. de Voogd NJ, Cleary DFR (2007) Relating species traits to environmental variables in Indonesian coral reef sponge assemblages. *Mar Freshw Res* 58:240–249
55. Mollo E et al (2008) Factors promoting marine invasions: a chemolecological approach. *Proc Natl Acad Sci USA* 105:4582–4586
56. Cortesi F, Cheney KL (2010) Conspicuousness is correlated with toxicity in marine opisthobranchs. *J Evol Biol* 23:1509–1518
57. Siddon CE, Witman JD (2004) Behavioral indirect interactions: multiple predator effects and prey switching in the rocky subtidal. *Ecology* 85:2938–2945
58. Chanas B, Pawlik JR (1997) Variability in the chemical defense of the Caribbean reef sponge *Xestospongia muta*. In: Lessios HA, Macintyre IG (eds) *Proceedings of the 8th international coral reef symposium*, Panama, June 24–29, 1996. Smithsonian Tropical Research Institute, Balboa, pp 1363–1367
59. Vervoort HC, Pawlik JR, Fenical W (1998) Chemical defense of the Caribbean ascidian *Didemnum conchylitum*. *Mar Ecol Prog Ser* 164:221–228
60. Pawlik JR, Burch MT, Fenical W (1987) Patterns of chemical defense among Caribbean gorgonian corals – a preliminary survey. *J Exp Mar Biol Ecol* 108:55–66
61. Pawlik JR, McFall G, Zea S (2002) Does the odor from sponges of the genus *Ircinia* protect them from fish predators? *J Chem Ecol* 28:1103–1115
62. Slattery M et al (2008) Hybrid vigor in a tropical Pacific soft-coral community. *Ecol Monogr* 78:423–443
63. Chanas B, Pawlik JR (1996) Does the skeleton of a sponge provide a defense against predatory reef fish? *Oecologia* 107:225–231
64. Chanas B, Pawlik JR (1995) Defenses of Caribbean sponges against predatory reef fish. 2. Spicules, tissue toughness, and nutritional quality. *Mar Ecol Prog Ser* 127:195–211
65. Wilson DM et al (1999) Chemical defense of the Caribbean reef sponge *Axinella corrugata* against predatory fishes. *J Chem Ecol* 25:2811–2823
66. McClintock JB, Baker BJ (1997) Palatability and chemical defense of eggs, embryos and larvae of shallow-water Antarctic marine invertebrates. *Mar Ecol Prog Ser* 154:121–131
67. Lippert H et al (2004) Chemical defence against predators in a sub-Arctic fjord. *J Exp Mar Biol Ecol* 310:131–146
68. Hay ME, Kappel QE, Fenical W (1994) Synergisms in plant defenses against herbivores – interactions of chemistry, calcification and plant quality. *Ecology* 75:1714–1726

69. Waddell B, Pawlik JR (2000) Defenses of Caribbean sponges against invertebrate predators. I. Assays with hermit crabs. *Mar Ecol Prog Ser* 195:125–132
70. Waddell B, Pawlik JR (2000) Defenses of Caribbean sponges against invertebrate predators. II. Assays with sea stars. *Mar Ecol Prog Ser* 195:133–144
71. López-Legentil S, Turon X, Schupp P (2006) Chemical and physical defenses against predators in *Cystodytes* (ascidiacea). *J Exp Mar Biol Ecol* 332:27–36
72. Ferguson AM, Davis AR (2008) Heart of glass: spicule armament and physical defense in temperate reef sponges. *Mar Ecol Prog Ser* 372:77–86
73. McClintock JB et al (1994) Homarine as a feeding deterrent in the common shallow-water Antarctic lamellarian gastropod *Marseniopsis mollis* – a rare example of chemical defense in a marine prosobranch. *J Chem Ecol* 20:2539–2549
74. McClintock JB et al (1994) Chemotactic tube-foot responses of a spongivorous sea star *Perknaster fuscus* to organic extracts from Antarctic sponges. *J Chem Ecol* 20:859–870
75. McClintock JB et al (1994) Chemical defense of the common Antarctic shallow-water nudibranch *Tritoniella belli* Eliot (mollusca, tritonidae) and its prey, *Clavularia frankliniana* Roel (cnidaria octocorallia). *J Chem Ecol* 20:3361–3372
76. Furrow FB et al (2003) Surface sequestration of chemical feeding deterrents in the Antarctic sponge *Latrunculia apicalis* as an optimal defense against sea star spongivory. *Mar Biol* 143:443–449
77. Harvell CD, Fenical W, Greene CH (1988) Chemical and structural defenses of Caribbean gorgonians (*Pseudopterogorgia* spp.). I. Development of an in situ feeding assay. *Mar Ecol Prog Ser* 49:287–294
78. Cronin G et al (1995) Effects of storage and extraction procedures on yields of lipophilic metabolites from the brown seaweeds *Dictyota ciliolata* and *D. menstrualis*. *Mar Ecol Prog Ser* 119:265–273
79. Ruzicka R, Gleason DF (2008) Latitudinal variation in spongivorous fishes and the effectiveness of sponge chemical defenses. *Oecologia* 154:785–794
80. Ruzicka R, Gleason DF (2009) Sponge community structure and anti-predator defenses on temperate reefs of the South Atlantic Bight. *J Exp Mar Biol Ecol* 380:36–46
81. Pennings SC et al (1994) Effects of sponge secondary metabolites in different diets on feeding by three groups of consumers. *J Exp Mar Biol Ecol* 180:137–149
82. Refstie S, Olli JJ, Standal H (2004) Feed intake, growth, and protein utilisation by post-smolt Atlantic salmon (*Salmo salar*) in response to graded levels of fish protein hydrolysate in the diet. *Aquaculture* 239:331–349
83. Pisut DP, Pawlik JR (2002) Anti-predatory chemical defenses of ascidians: secondary metabolites or inorganic acids? *J Exp Mar Biol Ecol* 270:203–214
84. Cronin G, Hay ME (1996) Susceptibility to herbivores depends on recent history of both the plant and animal. *Ecology* 77:1531–1543
85. Duffy JE, Paul VJ (1992) Prey nutritional quality and the effectiveness of chemical defenses against tropical reef fishes. *Oecologia* 90:333–339
86. Berenbaum M, Neal JJ (1985) Synergism between myristicin and xanthotoxin, a naturally occurring plant toxicant. *J Chem Ecol* 11:1349–1358
87. Pennings SC (1996) Testing for synergisms between chemical and mineral defenses – a comment. *Ecology* 77:1948–1950
88. Hay ME (1996) Defensive synergisms? Reply. *Ecology* 77:1950–1952
89. Jones AC, Blum JE, Pawlik JR (2005) Testing for defensive synergy in Caribbean sponges: bad taste or glass spicules? *J Exp Mar Biol Ecol* 322:67–81
90. Avila C et al (1991) Defensive strategy of two *Hypselerodis* nudibranchs from Italian and Spanish coasts. *J Chem Ecol* 17:625–636
91. Harvell CD, Fenical W (1989) Chemical and structural defenses of Caribbean gorgonians (*Pseudopterogorgia* spp.) – intracolony localization of defense. *Limnol Oceanogr* 34:382–389

92. Swearingen DC, Pawlik JR (1998) Variability in the chemical defense of the sponge *Chondrilla nucula* against predatory reef fishes. *Mar Biol* 131:619–627
93. Kubanek J et al (2002) Multiple defensive roles for triterpene glycosides from two Caribbean sponges. *Oecologia* 131:125–136
94. Becerro MA, Paul VJ, Starmer J (1998) Intracolony variation in chemical defenses of the sponge *Cacospongia* sp. and its consequences on generalist fish predators and the specialist nudibranch predator *Glossodoris pallida*. *Mar Ecol Prog Ser* 168:187–196
95. Schupp P et al (1999) Distribution of secondary metabolites in the sponge *Oceanapia* sp. and its ecological implications. *Mar Biol* 135:573–580
96. Slattery M, Starmer J, Paul VJ (2001) Temporal and spatial variation in defensive metabolites of the tropical Pacific soft corals *Sinularia maxima* and *S. polydactyla*. *Mar Biol* 138:1183–1193
97. Hoover CA, Slattery M, Marsh AG (2007) Profiling transcriptome complexity and secondary metabolite synthesis in a benthic soft coral, *Sinularia polydactyla*. *Mar Biotechnol* 9:166–178
98. Teeyapant R, Proksch P (1993) Biotransformation of brominated compounds in the marine sponge *Verongia aerophoba* – evidence for an induced chemical defense. *Naturwissenschaften* 80:369–370
99. Puyana M, Fenical W, Pawlik JR (2003) Are there activated chemical defenses in sponges of the genus *Aplysina* from the Caribbean? *Mar Ecol Prog Ser* 246:127–135
100. Thoms C, Ebel R, Proksch P (2006) Activated chemical defense in *Aplysina* sponges revisited. *J Chem Ecol* 32:97–123
101. Thoms C et al (2004) Chemical defense of Mediterranean sponges *Aplysina cavernicola* and *Aplysina aerophoba*. *Z Naturforsch C* 59:113–122
102. Stachowicz JJ, Lindquist N (2000) Hydroid defenses against predators: the importance of secondary metabolites versus nematocysts. *Oecologia* 124:280–288
103. Lindquist N (2002) Tridentatols D-H, nematocyst metabolites and precursors of the activated chemical defense in the marine hydroid *Tridentata marginata* (Kirchenpauer 1864). *J Nat Prod* 65:681–684
104. Thoms C, Schupp PJ (2008) Activated chemical defense in marine sponges – a case study on *Aplysinella rhax*. *J Chem Ecol* 34:1242–1252
105. McMurray SE, Blum JE, Pawlik JR (2008) Redwood of the reef: growth and age of the giant barrel sponge *Xestospongia muta* in the Florida Keys. *Mar Biol* 155:159–171
106. Berenbaum MR, Zangerl AR (1994) Costs of inducible defense – protein limitation, growth and detoxification in parsnip webworms. *Ecology* 75:2311–2317
107. Zangerl AR, Arntz AM, Berenbaum MR (1997) Physiological price of an induced chemical defense: photosynthesis, respiration, biosynthesis, and growth. *Oecologia* 109:433–441
108. King DJ, Gleadow RM, Woodrow IE (2006) The accumulation of terpenoid oils does not incur a growth cost in *Eucalyptus polybractea* seedlings. *Funct Plant Biol* 33:497–505
109. Walters KD, Pawlik JR (2005) Is there a trade-off between wound-healing and chemical defenses among Caribbean reef sponges? *Integr Comp Biol* 45:352–358
110. Pawlik JR et al (2008) Patterns of sponge recruitment and growth on a shipwreck corroborate chemical defense resource trade-off. *Mar Ecol Prog Ser* 368:137–143
111. Messchendorp L, Gols GJZ, van Loon JJA (1998) Behavioral effects and sensory detection of drimane deterrents in *Myzus persicae* and *Aphis gossypii* nymphs. *J Chem Ecol* 24:1433–1446
112. Pawlik JR, Fenical W (1992) Chemical defense of *Pterogorgia anceps*, a Caribbean gorgonian coral. *Mar Ecol Prog Ser* 87:183–188
113. Lindel T et al (2000) Structure-activity relationship of inhibition of fish feeding by sponge-derived and synthetic pyrrole-imidazole alkaloids. *J Chem Ecol* 26:1477–1496
114. Assmann M et al (2000) Chemical defenses of the Caribbean sponges *Agelas wiedenmayeri* and *Agelas conifera*. *Mar Ecol Prog Ser* 207:255–262

115. Pawlik JR, Albizati KF, Faulkner DJ (1986) Evidence of a defensive role for limatulone, a novel triterpene from the intertidal limpet *Collisella limatula*. *Mar Ecol Prog Ser* 30:251–260
116. Kubanek J et al (2000) Triterpene glycosides defend the Caribbean reef sponge *Erylus formosus* from predatory fishes. *Mar Ecol Prog Ser* 207:69–77
117. Kubanek J, Fenical W, Pawlik JR (2001) New antifeedant triterpene glycosides from the Caribbean sponge *Erylus formosus*. *Nat Prod Lett* 15:275–285
118. Cohen SAP et al (2008) Reconstitution of a chemical defense signaling pathway in a heterologous system. *J Exp Biol* 211:599–605
119. Burns E et al (2003) Comparison of anti-predatory defenses of Red Sea and Caribbean sponges. I. Chemical defense. *Mar Ecol Prog Ser* 252:105–114

Antipredatory Defensive Role of Planktonic Marine Natural Products

13

Adrianna Ianora, Antonio Miralto, and Giovanna Romano

Contents

13.1	Introduction	712
13.2	Antiproliferative Compounds	713
13.2.1	Diatom Oxylipins	713
13.2.2	Dinoflagellate Antiproliferative Compounds	721
13.3	Feeding Deterrents	722
13.3.1	HAB Toxins	722
13.3.2	DMSP and DMS	729
13.3.3	Apo-fucoxanthinoids	731
13.4	Environmental Factors Affecting Toxin Production	731
13.5	Laboratory Protocols to Assess the Effects of Phytoplankton Metabolites	733
13.6	Concluding Remarks	738
13.7	Study Questions	740
	References	741

Abstract

This chapter deals with chemical ecology and the role of antipredatory metabolites in the plankton and how such plant–herbivore interactions structure communities in the pelagic zone of the oceans. The first section deals with antiproliferative compounds produced by unicellular diatoms that induce abortions or congenital defects in the offspring of zooplankton crustaceans such as copepods exposed to them during gestation. Such teratogenic compounds include numerous oxylipins, and polyunsaturated aldehydes (PUAs) in particular, that are very similar to those produced in higher terrestrial plants. Oxylipins are believed to play a pivotal role in plant defense because they act as chemical attractors (e.g., pheromones, pollinator attraction) or alarm signals against

A. Ianora (✉) • A. Miralto • G. Romano

Functional and Evolutionary Ecology, Laboratory Stazione Zoologica Anton Dohrn, Villa Comunale, Naples, Italy

e-mail: adrianna.ianora@szn.it, antonio.miralto@szn.it, romano@szn.it

herbivore attack (e.g., in tritrophic interactions) and as protective compounds (antibacterial, wound healing). The second section in this chapter deals with neurotoxic compounds (e.g., saxitoxins, brevetoxins, and others) produced mainly by dinoflagellates which induce severe pathologies (i.e., paralytic, neurotoxic, diarrhetic, and amnesic shellfish poisoning) in humans that consume shellfish containing high levels of these toxins and which are generally considered as feeding deterrents in the plankton. Strong physiological responses have also been reported in several copepod species after <24 h of feeding on these cells, such as elevated heart rates, regurgitation, loss of motor control, and twitching of the mouthparts, decreased feeding, decreased fecundity, delayed development, and direct mortality. Another important feeding deterrent in the plankton includes dimethylsulfoniopropionate (DMSP) found in numerous species of phytoplankton, but most prominently in the prymnesiophytes and dinoflagellates, which appears to act as a signal molecule or indicator of inferior prey rather than as a toxin. We discuss the environmental conditions which promote increased production of these metabolites and some of the classic bioassays to test their biological activity. We also discuss the multiple functions of antipredatory metabolites and the importance of chemical interactions in the plankton for shaping biodiversity and ecological functioning both at the community and cellular level.

13.1 Introduction

Plankton is the collective name for small or microscopic organisms that float or drift in large numbers, especially in the photic zone of the oceans. Plankton is of great importance because it serves as food for fish and larger organisms, and indirectly for humans whose fisheries depend on plankton. The plant-like component of the plankton is called phytoplankton and includes single-celled algal groups such as diatoms, dinoflagellates, coccolithophores, and other protists. The animal component is called zooplankton and is dominated mainly by crustaceans that subsist on phytoplankton and other small zooplankton. Copepods and other zooplankton crustaceans graze on large quantities of phytoplankton cells that must escape, deter, or tolerate herbivores in order to persist. Herbivory is therefore an important pressure for the evolution of defensive compounds in marine phytoplankton, as for terrestrial higher plants, and for shaping prey–predator relationships in the pelagic environment. These chemicals are secondary metabolites or natural products that are not directly involved in primary metabolism. They differ from the more prevalent macromolecules, such as proteins and nucleic acids that make up the basic machinery of life. Often, secondary metabolites constitute a very small fraction of the total biomass of an organism, and it is not always clear what the biological function of these compounds actually is. In recent years, it has become increasingly apparent that these metabolites have important ecological functions and may at times contribute as much as primary metabolites to the survival of the producing organism. The science that considers chemical interactions between

organisms and their environment is termed chemical ecology, considered one of the fastest growing and rapidly evolving environmental subdisciplines.

Research on chemically mediated interactions in the marine environment has historically focused on predator–prey interactions in the benthos, and there is now a considerable amount known about feeding preferences and deterrent molecules in macroalgae, sponges, mollusks, and corals (see ► [Chapter 12](#)). Much less is known on the chemical ecology of planktonic marine organisms. We also know very little as to why zooplankton avoid certain compounds, and few studies have assessed what happens when secondary metabolites are consumed. Studies on chemical interactions in the plankton are still in their infancy, but there is an increased awareness that natural products play fundamental roles as defenses against predators, competitors, and pathogens, and therefore drive ecosystem functionality in the plankton. In this chapter, we focus on some of the better studied antipredatory defenses in the plankton, and more specifically on where the specific compounds have been identified and tested in pure or semipurified form in manipulative experiments. The chapter does not attempt to provide a comprehensive overview on this subject, but rather to illustrate some examples of the diversity and importance of chemically mediated interactions involving planktonic organisms ([Fig. 13.1](#)), and some of the methodologies that have developed in this field in recent years. In the following sections, we focus on compounds that induce reproductive failure in grazers and those that induce feeding deterrence and mortality (summarized in [Table 13.1](#)). We then discuss the environmental conditions which promote increased production of these metabolites and some of the classic bioassays to test the biological activity of phytoplankton natural products on predatory copepods.

13.2 Antiproliferative Compounds

13.2.1 Diatom Oxylipins

The strongest evidence that phytoplankton use chemical defense to deter planktonic grazers comes from the work initiated over a decade ago on diatom oxylipins. Diatoms have traditionally been viewed as beneficial to the growth and survival of marine organisms and to the transfer of organic material through the food chain to top consumers and important fisheries. However, while diatoms may provide a source of energy for copepod larval growth, they often reduce fecundity and/or hatching success. These results constitute the paradox of diatom–copepod interactions in the pelagic food web [[12](#)]. This biological model is new and has no other equivalent in marine plant–herbivore systems, since most of the known negative plant–animal interactions are generally related to repellent or poisoning processes, but never to reproductive failure.

In terrestrial environments, there are many reports of compounds produced by plants that interfere with the reproductive capacity of grazing animals, and which act as a form of population control. These compounds are referred to as teratogens or substances that induce abortions or congenital malformations in the offspring of

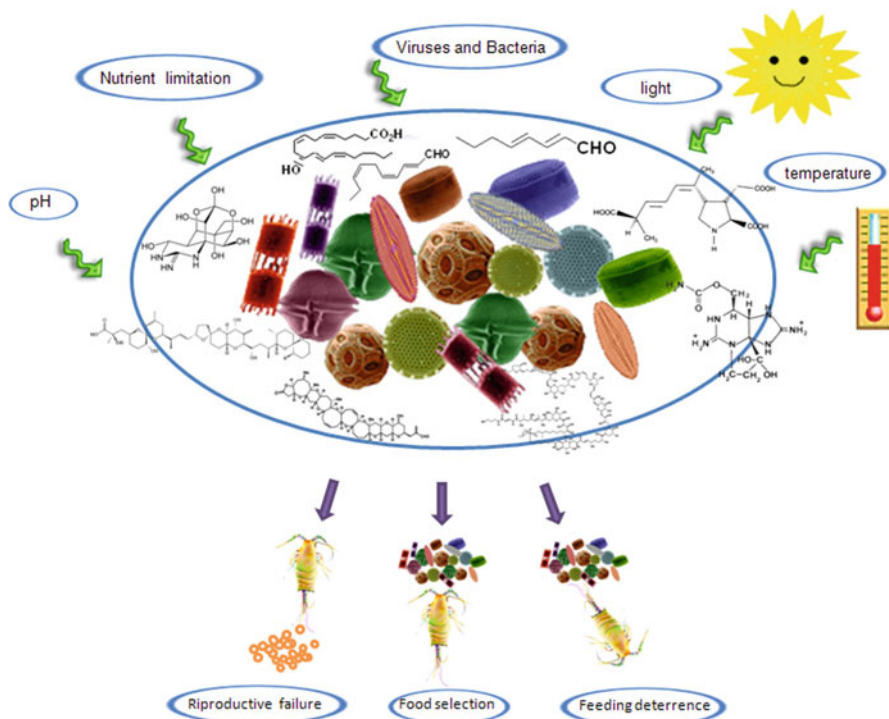


Fig. 13.1 Schematic representation of the environmental factors affecting the production of phytoplankton secondary metabolites (*green arrows*) and the effects of these metabolites on planktonic predatory copepods (*blue arrows*)

mothers exposed to them during gestation. Some classic examples of teratogens include caffeine, present in many plants processed for use as beverages and foods, and nicotine, the principal chemical present in tobacco. Nicotine has been shown to have possible teratogenic effects on fetal development in humans, and it is now widely accepted that pregnant woman should avoid smoking during their pregnancy. The same compound has been shown to have strong effects also in range animals that ingest tobacco plants, with newborns showing limb deformities and palate closure defects associated with the high content of nicotine in their tissues [13].

Nothing was known on the presence and effects of such compounds in the marine environment until the discovery of diatom oxylipins, including polyunsaturated aldehydes (PUAs), produced by diatom cells from precursor membrane-bound lipids [5, 14–16]. Diatom PUAs were first isolated by Miralto et al. [1] who showed, *in vitro*, that they reduced copepod hatching success, cleavage of sea urchin embryos, and proliferation of human adenocarcinoma cells. The same authors showed that diatoms also modified copepod hatching success in the field in February 1997 and 1998 during two major diatom blooms in the North Adriatic

Table 13.1 Effects of secondary metabolites produced by phytoplankton on predatory copepods. Only characterized compounds known to be produced by microalgae and for which the specific toxicity has been determined are reported (modified from Ianora et al. [152])

Compounds	Producer	Target organism	Effect	Mode of action	References
PUAs					
Decatrienal	<i>Thalassiosira rotula</i> and other <i>Thalassiosira</i> species	Copepods	Reduced hatching success, abnormal nauplii, growth inhibition	Antimitotic, apoptosis	[1, 2]
Octatrienal, octadienal, heptadienal	<i>Thalassiosira rotula</i> , <i>Skeletonema marinoi</i>	Copepods	Reduced hatching success, abnormal nauplii, growth inhibition	Antimitotic, apoptosis	[3, 4]
Hydroxy- and epoxy-fatty acid pool	<i>Thalassiosira rotula</i> , <i>Skeletonema marinoi</i> , <i>Pseudo-nitzschia delicatissima</i> , <i>Chaetoceros affinis</i> , <i>Chaetoceros socialis</i>	Copepods	Reduced hatching success, abnormal nauplii, growth inhibition	Antimitotic, apoptosis	[5, 6]
Fatty acid hydroperoxides	<i>Thalassiosira rotula</i> , <i>Skeletonema marinoi</i> , <i>Pseudo-nitzschia delicatissima</i> , <i>Chaetoceros affinis</i> , <i>Chaetoceros socialis</i>	Copepods	Reduced hatching success, abnormal nauplii, growth inhibition	Antimitotic, apoptosis	[5, 6]
Oxoacids	<i>Pseudo-nitzschia delicatissima</i>	Copepods	Reduced hatching success, abnormal nauplii, growth inhibition	Antimitotic, apoptosis	[7]
DMSP: acrylate, DMS	<i>Emiliana huxleyi</i>	Protistan, crustacean	Feeding deterrence, search behavior	Unknown	[8]
Apo-fucoxanthin	<i>Thalassiosira weissflogii</i> , <i>Phaeodactylum tricornutum</i>	Copepods	Feeding deterrence	Unknown	[9, 10]
PSP ^a	<i>Alexandrium</i> sp.	Copepods	Feeding deterrence	Unknown	[11]

^aPSP saxitoxin (STX), neo-STX, gonyautoxin (GTX), C-toxins

Sea. Egg viability in these periods was only 12% and 24%, respectively, of the total number of eggs produced compared to 90% after the bloom in June indicating that copepod recruitment was higher during postbloom conditions and not during the bloom as previously assumed.

Oxyplins, and PUAs in particular, have important biological and biochemical properties including the disruption of gametogenesis, gamete functionality,

fertilization, embryonic mitosis, and larval fitness and competence [17]. PUAs are also apoptogenic inducers through the activation of specific caspases that lead to the enzymatic breakdown of DNA [18, 19]. PUAs may be sequestered during oocyte development and be passed maternally to the embryo, or may act directly on embryos. By whichever route, the timing of reproduction in relation to toxic diatom abundance will have important consequences for invertebrate recruitment [20–22].

The PUA decadienal is the best-studied metabolite of this group and thus has become a model aldehyde for experimental studies on the effects of oxylipins on marine organisms. Numerous functions have been proposed for this highly reactive molecule, such as grazer defense [1, 23], allelopathy [24, 25], cell to cell signaling [26, 27], antibacterial activity [28], and bloom termination initiator [7, 29]. In terms of grazer defense, decadienal has been shown to negatively affect reproductive processes in planktonic copepods (reviewed by Ianora and Miralto [30]) and cladocerans [31], and benthic echinoderms [17, 18, 22], polychaetes [32], ascidians [33], mollusks [34], and benthic copepods [35] with widespread consequences on ecosystem functionality (Table 13.1).

The discovery of an enzyme cascade leading to the production of volatile biologically active oxylipins in marine phytoplankton is rather new [30] even though the oxidative cleavage of fatty acids to form similar defensive compounds is well known in higher terrestrial plants [36, 37] and freshwater microalgae [38]. Several papers have described the biochemical pathways leading to PUA production [6, 39]. Pohnert [40] described that the transformation of polyunsaturated fatty acids (PUFAs) such as C20 in the diatom *Thalassiosira rotula* was initiated by phospholipases, in particular phospholipase A2, that act immediately after cell damage. Liberated C20 PUFAs such as eicosapentaenoic (EPA) and arachidonic acids are then further converted by lipoxygenases and lyases to PUAs. Pohnert [40] suggested that in contrast to higher terrestrial plants that use lipases acting on galactolipids to release C18 linoleic fatty acids for the production of aldehydes, diatoms rely on phospholipids and the liberation of C20 EPA fatty acids by phospholipases to produce decadienal and decatrienal.

However, d'Ippolito et al. [15] described an alternative biochemical pathway from other complex lipids in the diatom *Skeletonema marinoi* which involves the hydrolysis of chloroplastic glycolipids and release of C20 EPA and C16 PUFAs such as hexadecatrienoic and hexadecadienoic acids. They showed that chloroplasts have a direct role in the production of PUAs in diatoms, similar to what occurs in higher terrestrial plants [36]. They proposed a biochemical pathway leading to the production of PUAs in diatoms whereby C20 and C16 PUFAs are liberated from chloroplast glycolipids and phospholipids by lipolytic acyl hydrolases. These PUFAs are then rapidly transformed into unstable hydroperoxides by either 9-lipoxygenase (LOX), 11-LOX, or 14-LOX enzymes. Hydroperoxides are, in turn, rapidly transformed to PUAs such as 2,4-heptadienal, 2,4-octadienal, and 2,4,7-decatrienal depending on the LOXs and other downstream enzymes present in the diatom cells.

The synthesis of PUAs begins immediately after cell wounding, thus implying that the proteins responsible for the oxidative metabolism of C16 and C20 fatty

acids are expressed constitutively in diatom cells. By studying the downstream enzymatic activity responsible for PUA synthesis, d'Ippolito et al. [41] demonstrated that the diatom *T. rotula* possesses an enzymatic arsenal capable of transforming C16 and C20 PUFAs to 2,4-octadienal or 2,4,7-decatrienal, whereas in the diatom *S. marinoi*, C16 and C20 PUFAs serve as specific substrates for the production of 2,4-heptadienal and 2,4-octadienal.

A mechanism for the production of PUAs only after cell lysis has been proposed so that toxins are released directly into the body of grazers [42], thereby avoiding intoxication to the diatom cells [24]. Fontana et al. [6] measured PUA production with time and showed that formation of PUAs begins soon after sonication of cells and increases steadily for several minutes thereafter, reaching concentrations of up to 50 fg cell⁻¹ in the diatom *T. rotula*. When PUAs are removed by keeping the cells under vacuum for 15 min, production is reinitiated immediately, giving rise to even higher levels (up to 100 fg cell⁻¹) 40 min later. More recently, Romano et al. [22] have shown that decadienal can be detected spectrophotometrically for up to 14 days in closed culture containers.

A major advancement in the study of the chemistry of diatoms was the discovery that they produce cytotoxic compounds other than PUAs (Fig. 13.2). Wichard et al. [2] had shown that only 36% of the investigated 51 species released PUAs upon cell damage, with PUA concentrations ranging from 0.01 to 9.8 fmol cell⁻¹ depending on the species or strain, thereby suggesting that many diatoms do not produce these compounds. But, at about the same time, d'Ippolito et al. [43] showed that the diatom *T. rotula* had an oxidizing potential capable of converting PUFAs to a variety of other unprecedented oxylipins, as later confirmed by Fontana et al. [5]. Fontana and coworkers compared the effects of the well-known PUA-producing diatom *S. marinoi* [1, 23] with two *Chaetoceros* (*C. similis* and *C. affinis*) species which did not produce PUAs, but which nonetheless impaired hatching success. They showed that when the *Chaetoceros* species were damaged, they produced fatty acid hydroperoxides and oxylipins such as hydroxyacids (HEPEs) and epoxyalcohols (HepETEs), as well as highly reactive oxygen species (ROS) of low acute toxicity to adult copepods but which depressed the viability of copepod gametes and offspring. Two of these compounds, 15S-HEPE and threo-13,14-HepETE, have now also been reported by d'Ippolito et al. [7] in the non-PUA-producing pennate diatom *Pseudo-nitzschia delicatissima* which produces large amounts of these metabolites in the late exponential and stationary phase of growth. d'Ippolito et al. also reported the presence of another metabolite, 15-oxo-5Z,9E,11E,13E-pentadecatetraenoic acid, which was only present in small amounts in the late stationary phase of the culture, demonstrating a precise timing in the production of these compounds during various stages of the cell cycle. Pohnert et al. [44] had already suggested the presence of aldehydic 9-oxo-nonadienoic and 12-oxo-dodecatienoic acids (12-ODTE) in the non-PUA-producing diatom *Phaeodactylum tricornutum* on the basis of the detection of high amounts of the C11-hydrocarbon hormosirene and the C8-hydrocarbon fucoserratene after wounding. Indeed, as reported by Pohnert and Boland [45], these hydrocarbons are released together with the aldehydic acids 9-ONDE and 12-ODTE by

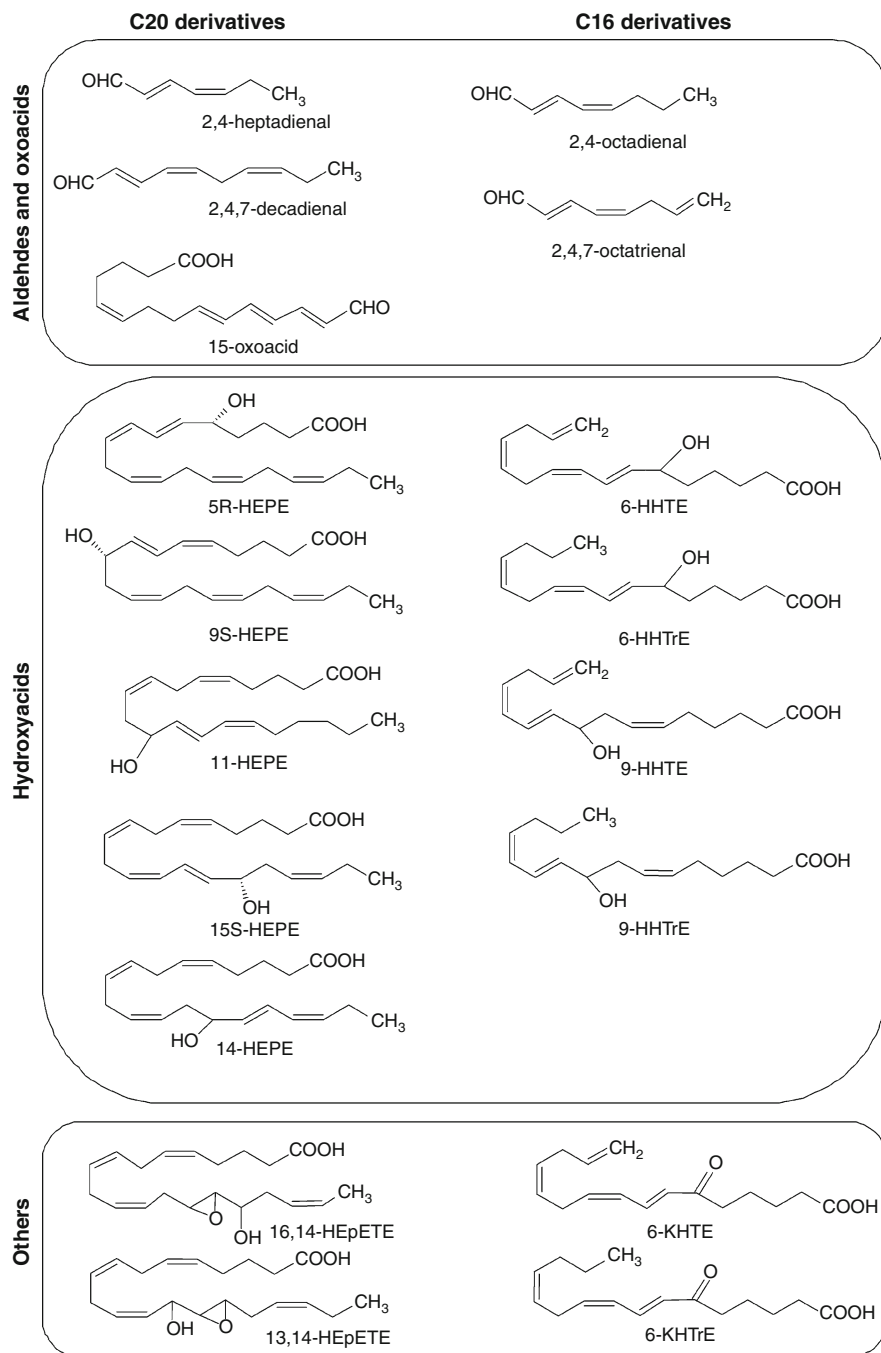


Fig. 13.2 (continued)

freshwater diatoms. These products are very similar to those produced by terrestrial plants [37], as shown in Fig. 13.3. A major difference, as in the case of PUAs, is in the precursor PUFAs, C16 and C20 fatty acids, used to synthesize these compounds in diatoms [39, 43] compared to the C18 fatty acids in terrestrial plants [36, 37]. Oxylipins formed in flowering plants include fatty acid hydroperoxides, hydroxyl- and keto-fatty acids, oxoacids, epoxyalcohols, divinyl ethers, PUAs, and the plant hormones 12-oxo-phytodienoic acid and jasmonic acid [46], several of which have not yet been found in diatoms (e.g., jasmonic acid). Oxylipins are believed to play a pivotal role in plant defense because they act as chemical attractors (e.g., pheromones, pollinator attraction), alarm signals against herbivore attack, and protective compounds (antibacterial, wound healing). Diatom oxylipins also show a high similarity to volatile organic carbons released from brown algae which are suggested to be involved in chemical signaling and pheromone attraction between gametes of different sex [46].

Testing the biological activity of oxylipins other than PUAs is quite recent. Pohnert et al. [44] reported that the lethal dose to induce 50% mortality (DL-50) in sea urchins with 12-ODTE was reached at concentrations around 9–10 μM which was in the range observed for decadienal (7.3 μM). Fontana et al. [5] found that a pool of oxylipins, other than PUAs from the diatom *S. marinoi*, blocked hatching success of the copepod *Calanus helgolandicus* at about 70 μM compared to a pool of aldehydes from the same diatom (32 μM) with induction of apoptosis and malformations in hatched nauplii for both pools of compounds. More recently, Ianora et al. [47] tested the hydroxyacid 15S-HEPE on newly spawned eggs of the copepod *Temora stylifera*, showing that this metabolite blocked hatching success at about 94 μM compared to heptadienal and decadienal (45 and 32 μM , respectively). All three compounds induced apoptosis and malformations in hatched nauplii. Taken together, these results indicate that PUAs are not the only class of molecules inducing reproductive failure in copepods. The “diatom effect” is therefore not due to a single class of compounds (i.e., PUAs), as previously believed, but rather to a blended mixture or bouquet of toxins which grazers are exposed to during feeding. Oxylipins such as 9S-hydroxyhexadecatrienoic (9S-HHTrE) and 9S-hydroxyhexadecatetraenoic (9S-HHTE) have also been found at sea, during a late spring bloom in the North Adriatic Sea of the non-PUA-producing diatom



Fig. 13.2 Diatom oxylipins characterized to date deriving from the oxidation of C16 and C20 fatty acids. Information on diatom species producing these compounds is given in Ianora and Miralto [30]. 5R-HEPE = 5R-hydroxy-(6,8,11,14,17)-eicosapentaenoic acid; 9 S-HEPE = 9 S-hydroxy-(5,7,11,14,17)-eicosapentaenoic acid; 11-HEPE = 11-hydroxy-(5,8,11,15,17)-eicosapentaenoic acid; 15 S-HEPE = 15 S-hydroxy-(5,8,11,13,17)-eicosapentaenoic acid; 14-HEPE = 14-hydroxy-(5,8,11,15,17)-eicosapentaenoic acid; 6-HHTE = 6-hydroxyhexadeca-(7,9,12,15)-tetraenoic acid; 6-HHTrE = 6-hydroxyhexadeca-(7,9,12)-trienoic acid; 9-HHTE = 9-hydroxyhexadeca-(6,10,12,15)-tetraenoic acid; 9-HHTrE = 9-hydroxyhexadeca-(6,10,12)-trienoic acid; 13,14-HEpETE = 13-hydroxy-(14,15)-epoxy-5,8,11,17-eicosatetraenoic acid; 16,14-HEpETE = 16-hydroxy-(14,15)-epoxy-5,8,11,17-eicosatetraenoic acid; 6-KHTE = 6-ketohehexadeca-(7,9,12,15)-tetraenoic acid; 6-KHTrE = 6-ketohehexadeca-(7,9,12)-trienoic acid

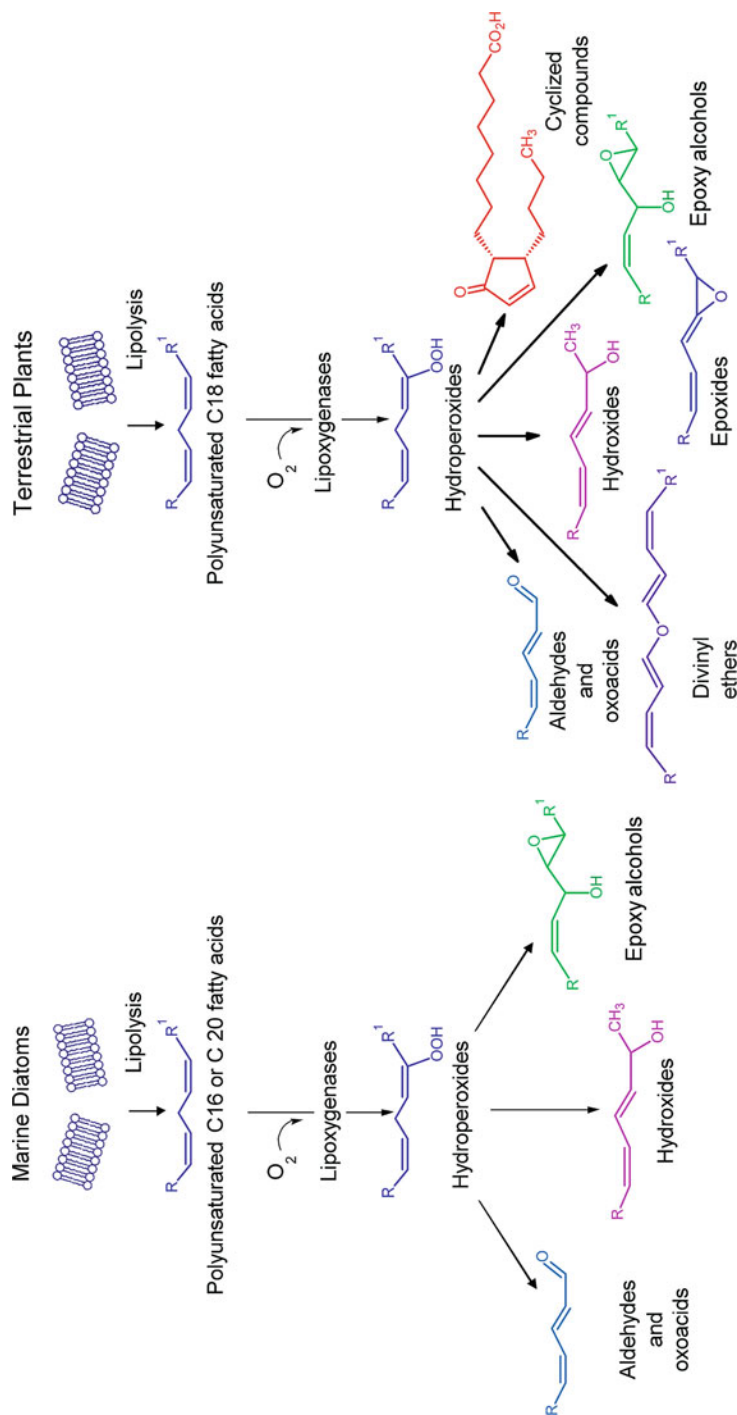


Fig. 13.3 Oxidative metabolism of fatty acids in (a) marine diatoms and (b) terrestrial plants. Starting mainly from eicosapentaenoic (C20) and exadecatetraenoic (C16) fatty acids in diatoms or from octadeca(e)noic (C18) fatty acids in plants, both oxidative pathways involve oxygenation of these fatty acids by oxygen addition through lipoxygenase activity to a *cis,cis*-1,4-pentadiene moiety

Cerataulina pelagica, the likely cause for reduced egg production and hatching success in *Acartia clausi*, *Calanus helgolandicus*, and *Temora longicornis* [48].

Diatoms are not the only class of marine phytoplankton to produce oxylipins. The bloom-forming phytoplankter *Phaeocystis pouchetii* (Prymnesiophyceae) has been shown to produce and release decadienal [19] even though it remains unclear as to what amounts are produced. In freshwater environments, PUAs are commonly released by diatoms and chrysophytes (see [49] and references therein) through cell lysis, independently from grazing, conferring rancid smells to source drinking water [50]. In this case, PUAs may not only serve to deter grazers [51] but may also function as intra- or interspecific signals, for example, to modulate population density or to signal the presence of pathogens or predators [52]. Their widespread occurrence in marine and freshwater photoautotrophs may be an indication of the great ecological importance of these compounds.

An alternative hypothesis for the ecological function of PUAs by diatoms was recently developed by Jüttner ([49] and references therein). Upon cell damage, diatom-dominated biofilms release small quantities of PUAs that are efficient repellents for herbivorous zooplankton. These substances probably function as “warning cues,” since upon cell damage, diatoms release high amounts of the polyunsaturated eicosapentaenoic acid (EPA) which is highly toxic for crustacean herbivores. Following cell wounding, a small fraction of the released EPA is further converted into PUAs which, in turn, can be detected by the grazers. Thus, grazers that initiate feeding on these diatoms cause the liberation of an activated warning cue that repels them, thereby protecting them from the toxic EPA and protecting the diatom from herbivores. A major challenge for the future will be to understand the ecological function of these metabolites and the physiological factors that lead to their production. We have just begun to understand the role of diatom oxylipins in the plankton, and there remains great scope for research into the effects of these toxins on gamete, embryonic, and larval development of herbivorous grazers.

13.2.2 Dinoflagellate Antiproliferative Compounds

Hatching failure in copepods can also depend on poor sperm quality. Interestingly, such effects have mainly been reported in copepods fed with dinoflagellate diets. For example, *Prorocentrum micans*, *Gymnodinium sanguineum* and *Gonyaulax polyedra* significantly modified spermatophore production and reduced the fertilization capacity of male sperm after 6–12 days of continuous feeding in the copepod *T. stylifera* [53]. A reduction in fertilization capacity was neither due to maternal effects nor to male age since hatching success returned to normal when males were substituted with freshly caught wild males or males conditioned with a good diet such as the dinoflagellate *Prorocentrum minimum* for the same length of time as couples fed with the poor diets. Microscope images of unhatched eggs colored with a nucleus-specific fluorescent dye showed that these eggs had not been fertilized.

Ianora et al. [54] later showed that extracts of a nontoxic strain of the dinoflagellate *Alexandrium tamarense* blocked fertilization but not cell divisions in sea

urchin embryos. Of the two organic extracts of *A. tamarense*, the one obtained in MeOH was the more active, and one of the fractions obtained by its separation on Sephadex LH-20 resin blocked fertilization of sea urchin oocytes at concentrations of $1 \mu\text{g mL}^{-1}$. The PUA decadienal, used as a control, had little or no effect on fertilization success at any of the concentrations tested. By contrast, the *A. tamarense* active fraction had little or no effect on sea urchin first cell cleavage as opposed to decadienal, which blocked cell cleavage at concentrations of $1 \mu\text{g mL}^{-1}$.

There are several examples of compounds isolated from marine dinoflagellates that block cell divisions in the classic sea urchin bioassay. These include goniodomin-A from *Goniodoma pseudogoniaulax* [55], amphidinolide-A from *Amphidinium* sp. [56], and okadaic acid and its derivative dinophysistoxin-1, which are common in some species of the genera *Prorocentrum* and *Dinophysis*, respectively [57]. Extracts of *A. tamarense* may also inhibit egg hatching and larval survival in the scallop *Chlamys farreri* [58]. In all of these studies, the molecules or extracts tested showed antimitotic activity with blockage of cell divisions in developing sea urchin embryos. In Ianora et al. [54], however, there was little or no adverse effect on cell cleavage, but very strong effects on fertilization success when oocytes were incubated for 30 min in *A. tamarense* extracts.

Clearly, these compounds were not feeding deterrents since both male and female *T. stylifera* copepods fed well on this *A. tamarense* strain, with fecal pellet production rates comparable to other dinoflagellate (*P. minimum*) diets [53]. Nonetheless, there were adverse effects on other life-history parameters such as fecundity, egg viability, and adult female survivorship.

Why do microalgae produce such compounds if they do not serve to deter feeding in their predators? According to chemical defense theory, there should be a selective survival advantage for species that can “protect” themselves from grazers, allowing such species to grow explosively, because the growth of the populations of their predators has been suppressed. This could occur through the production of chemicals that not only deter feeding activity but also reduce population growth. For example, diatom oxylipins reduce egg production and/or hatching success, thereby sabotaging copepod population growth and, consequently, predator grazing impact. In the case of *A. tamarense*, the defense machinery is potentially even more effective, because female longevity is reduced as well. The chemical structures of these compounds remain unknown.

13.3 Feeding Deterrents

13.3.1 HAB Toxins

Phytoplankton are among the most diverse organisms in the oceans, and due to the complexity of the habitat in which they live, these unicellular eukaryotes have evolved some of the most unique metabolites ever isolated in nature. Some of these are potent neurotoxins that can make their way up the marine food chain and are responsible for massive fish kills, both wild and farmed, as well as the deaths of

many aquatic birds and mammals, including whales and sea lions [59, 60]. There are a wide range of organisms that produce toxic compounds that are often referred to as harmful algal bloom (HAB) toxins. These include flagellates especially dinoflagellates, cyanobacteria, and some species of diatoms, silicoflagellates, prymnesiophytes, raphidophytes, and other phytoplankton. It is estimated that of the 300 species reported to be HABs, only 2% (60–80 species) actually produce toxins. The other HABs cause mortality of marine organisms after reaching high concentrations that may cause damage due to clogging or oxygen depletion. A detailed description of the different types of HAB toxins is beyond the scope of this chapter. Here, we consider only some examples of toxins which potentially serve as antipredatory defense compounds in the plankton (Table 13.1, Fig. 13.4).

Interestingly, the neurotoxic compounds produced by dinoflagellates which induce severe pathologies (i.e., paralytic, neurotoxic, diarrhetic, and amnesic shellfish poisoning) in humans that consume shellfish containing high levels of these toxins may have little or no effect on their direct zooplankton grazers. Several studies have demonstrated that some copepods show little or no behavioral effects of consuming toxic dinoflagellates (e.g., [61, 62]). On the other hand, there are other studies showing that certain dinoflagellates induce strong physiological responses in copepods after <24 h of feeding on these cells, such as elevated heart rates, regurgitation, loss of motor control, and twitching of the mouthparts [63], decreased feeding [64], decreased fecundity [65], delayed development [66], and direct mortality [61]. Furthermore, the copepods *Calanus finmarchicus* [67], *Eurytemora herdmanni*, and *Acartia tonsa* [68] have been shown to avoid feeding on paralytic shellfish toxin (PST)-containing prey when offered together with a nontoxic food option. Based on these findings and the negative effects that PST-containing phytoplankton have on some grazers, PSTs have been suggested to act as a protection against grazers [69], but direct demonstrations of paralytic shellfish toxins functioning as antigrazer defenses have not been demonstrated to date.

Most of these toxins are always present in the cells and are referred to as constitutive as compared to induced defenses that are produced only upon damage of the cells by predators (e.g., diatom oxylipins). If the primary function of these compounds is to protect the producers against grazers, the optimal defense theory predicts that cell-specific toxin content should correlate to the probability of attack [68]. Hence, their concentration in the cell should increase following contact with herbivore-specific chemicals [70]. This has, in fact, been shown for the marine copepod *A. tonsa* whereby waterborne chemicals produced by this copepod caused an increase in PST production in the harmful algal bloom-forming dinoflagellate *Alexandrium minutum* [11]. *A. minutum* contained up to 2.5 times more toxins than controls and was more resistant to further copepod grazing. Further investigations [71] showed that when *A. minutum* was grown under nitrate-rich conditions, but not in low-nitrate treatments, the presence of waterborne cues from grazers resulted in significantly increased cell-specific toxin content, implying that the magnitude of grazer-induced PST production is directly proportional to the degree of nitrogen availability. This response was also grazer-specific, with some species of copepods inducing a higher production of toxins (up to 20-fold increase in the presence of the

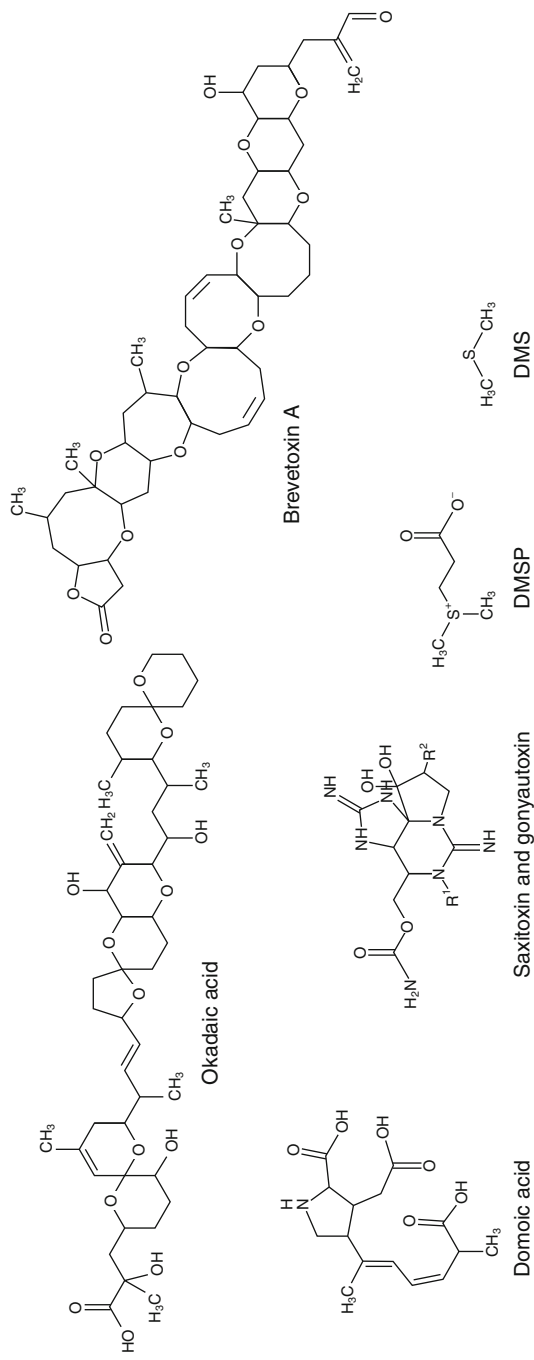


Fig. 13.4 (continued)

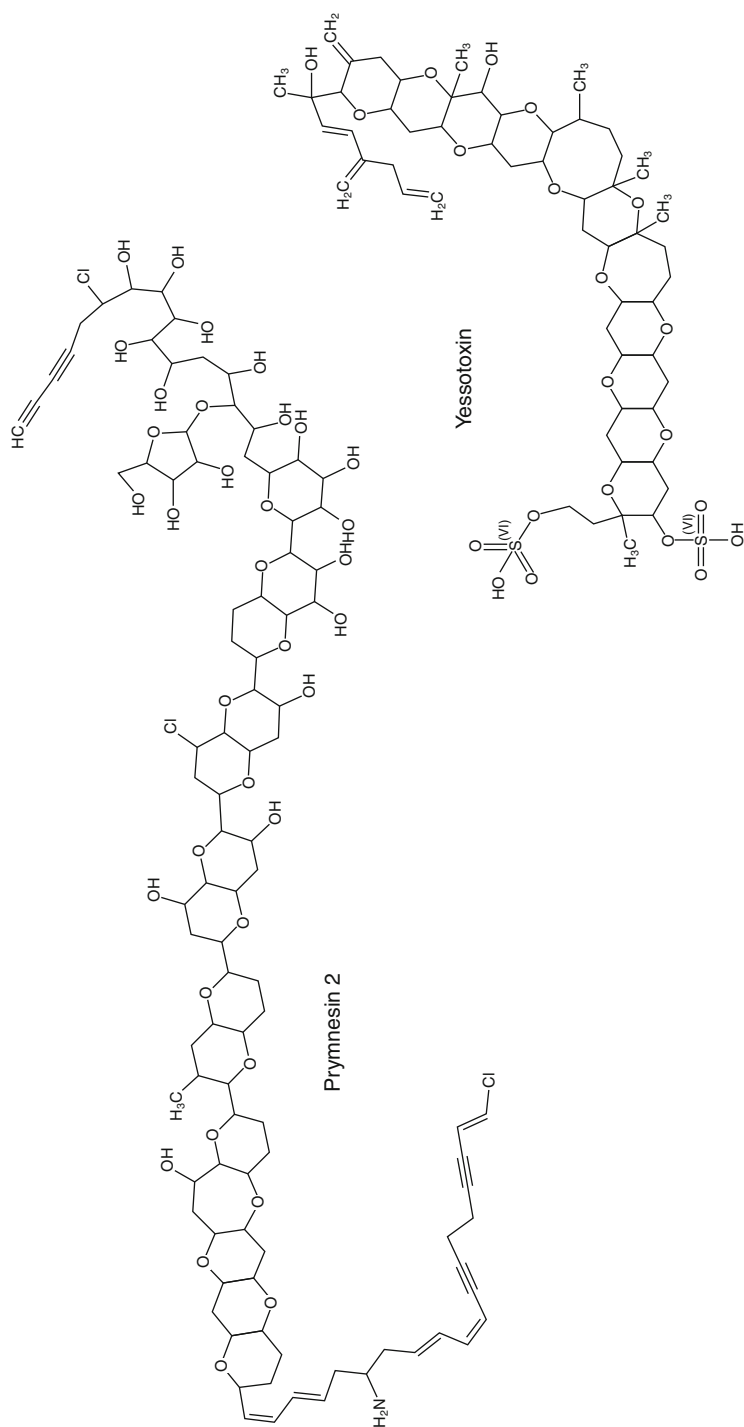


Fig. 13.4 Dinoflagellate and diatom neurotoxins suspected to have antifeeding and antireproductive activity on planktonic predatory copepods. Saxitoxin: $R^1 = H$, $R^2 = H$; Neosaxitoxin: $R^1 = OH$, $R^2 = H$; Gonyautoxin1: $R^1 = OH$, $R^2 = OSO_3^-$; Gonyautoxin2: $R^1 = H$, $R^2 = OSO_3^-$

copepod *Centropages typicus*) than others, which may induce no change at all (*Pseudocalanus* sp.). The ability of *A. minutum* to sense and respond to the presence of grazers by increased PST production, and the associated negative effect on grazers, is a strong evidence that these compounds are defensive metabolites, the purpose of which is not necessarily to intoxicate and kill the predator but to discourage further consumption.

The discovery and characterization of the molecules responsible for this biological activity are relatively recent (mainly 1980s). Okadaic acid was the first toxin isolated from a marine dinoflagellate even though it had previously been found in the sponge *Halichondria okadae*. The toxin was identified from a Tahitian strain of the dinoflagellate *Prorocentrum lima* and a derivative of this toxin, dinophysistoxin, was later isolated from temperate species of the dinoflagellate genus *Dinophysis*. Both okadaic acid and dinophysistoxin are associated with episodes of diarrhetic shellfish poisoning in humans (see [68, 72] for reviews on dinoflagellate toxins). Okadaic acid is a potent inhibitor of protein phosphorylase phosphatase 1 and 2A in the cytosol of mammalian cells that dephosphorylate serine and threonine. It is not only a potent tumor promoter but is also capable of reversing cell transformation in some oncogenes.

Other neurotoxins such as the brevetoxins are sodium channel activators causing repetitive depolarization of nerve membranes with an increase in the influx of sodium ions that ultimately deplete cellular reserves of acetylcholine at the synapses. The saxitoxins cause the opposite effect to the brevetoxins. They bind to the sodium channels and specifically block sodium permeability of the nerve membrane, ultimately causing paralysis and respiratory failure in humans. The differences in structure of the various saxitoxins alter the rates at which they bind to and depart from the binding site on the sodium channel. Yessotoxin, isolated from the dinoflagellate *Ptychodiscus brevis* (previously *Gymnodinium breve*), partially resembles the brevetoxins in structure and toxicity. Ciguatera poisoning produces various symptoms such as cardiovascular, gastrointestinal, sensory, and motor disturbances. No effective drug is currently known for therapy. The toxin is produced by a benthic dinoflagellate, *Gambierdiscus toxicus*, and is transmitted to fish along the marine food chain. *G. toxicus* also produces a more polar toxin, maitotoxin, which, together with ciguatoxin, is probably the most potent neurotoxin ever isolated from marine organisms.

There is high species-specific variability in the effects of these toxins on grazers, with effects ranging from severe physical incapacitation and death in some species [61] to no apparent physiological effects in others [73]. This variability may depend on the capability of some predators to detoxify or activate defense systems against these compounds. Recent studies [74] have shown that two days of feeding on a strong oxylipin-producing diatom (*Skeletonema marinoi*) is sufficient to inhibit a series of genes involved in aldehyde detoxification, apoptosis, cytoskeleton structure and stress response in the copepod *Calanus helgolandicus*. Of the 18 transcripts analyzed by RT-qPCR at least 50% were strongly downregulated (aldehyde dehydrogenase 9, 8 and 6, cellular apoptosis susceptibility and inhibitor of apoptosis IAP proteins, heat shock protein 40, alpha- and beta-tubulins) compared to animals fed

on a weak oxylipin-producing diet (*Chaetoceros socialis*) which showed no changes in gene expression profiles. These results provide molecular evidence of the toxic effects of strong oxylipin-producing diatoms on grazers showing that primary defense systems that should be activated to protect copepods against toxic algae can be inhibited. On the other hand other classical detoxification genes (glutathione S-transferase, superoxide dismutase, catalase, cytochrome P450) were not affected possibly due to short exposure times. At the same time, each herbivore species is likely to show unique features in detoxification/transport mechanisms as is the case for insect detoxification. Colin and Dam [62, 75] have shown that when two geographically distant populations of the copepod *Acartia hudsonica* were reared on the toxic dinoflagellate *Alexandrium fundyense*, the one that had not experienced recurrent blooms of the toxic algae had lower somatic growth, size at maturity, egg production, and survival, compared to the other population that showed no effects on these life-history parameters. Some copepod species also seem capable of concentrating toxins in their body tissues [76, 77], and such biotransformations typically yield the formation of more potent analogs of these toxins, as occurs in mollusks. Although there is no evidence that copepods are capable of long-term sequestration of such toxins, these predators provide not only a link for toxin flux in pelagic food webs but they may also act as a sink for toxins by metabolizing and removing them from the environment. Provided that they are not incapacitated by the toxin, in some cases, the accumulated toxin may even serve as a transient defense against more sensitive predators. Many benthic invertebrates are capable of sequestering compounds from the food they consume and using them as defensive molecules against predators [78]. There is no reason why this should not also occur in the plankton.

Some diatom species of the genus *Pseudo-nitzschia* produce the potent neurotoxin domoic acid which mimics the excitatory activity of the neurotransmitter L-glutamic acid, inducing destructive neuronal depolarization and successive degeneration of the hippocampus of the brain. In severe cases of this pathology, known as amnesic shellfish poisoning, victims show permanent loss of recent memory. Bioassays with pure compounds (<20 μ M domoic acid) induced 100% mortality after 24 h in the copepod *Tigriopus californicus* [79]. However, domoic acid has not been shown to induce negative effects on planktonic organisms that consume *Pseudo-nitzschia* species [80]. Olson et al. [81] found that copepod grazing impacts on field populations of *Pseudo-nitzschia* sp. were negligible, but this lack of grazing was not attributed to domoic acid. In a similar field-based study, Olson et al. [82] found no correlation between low grazing rates and particulate or dissolved domoic acid concentrations in field samples. On the other hand, Bargu et al. [83] found that krill exposed to abnormally high concentrations of dissolved domoic acid fed significantly less on a nontoxic food source than krill unexposed to domoic acid. However, due to the high concentrations and exposure methods used by these authors, little can be concluded about the putative antipredatory role of this toxin. If domoic acid is not a feeding deterrent to zooplankton grazing, zooplankton may facilitate vectorial transmission of the toxin which could have serious impacts on the marine ecosystem as well as on

the marine economy and human health. The genome sequence for *Pseudo-nitzschia multiseries* which will soon be available, should provide more insights into domoic acid biosynthesis, allowing researchers to profile production capabilities across different species, to better characterize their responses to environmental triggers, and to examine the molecular interactions between toxin-producing cells and their predators.

Blooms of the haptophyte *Prymnesium parvum* are well-known nuisances in brackish waters around the world that are usually accompanied by massive fish kills due to the production of prymnesins which exhibit potent cytotoxic, hemolytic, neurotoxic, and ichthyotoxic effects. These secondary metabolites are especially damaging to gill-breathing organisms, and they are believed to interact directly with plasma membranes, compromising integrity by permitting ion leakage. Several factors appear to function in the activation and potency of prymnesins including salinity, pH, ion availability, and growth phase [84]. Prymnesins may function as defense compounds to prevent herbivory, and some investigations suggest that they have allelopathic roles. Exposure to *P. parvum* can cause inactivity in the copepods *Eurytemora affinis* and *Acartia bifflora*, without the copepods actually consuming the toxic alga, resulting in reduced copepod reproductive success [85]. Sopanen et al. [86] found that cell-free filtrates of *P. parvum* also negatively impacted copepod survivorship. No studies are available testing the effects of pure compounds on grazers.

Karlodinium veneficum is a small athecate dinoflagellate commonly present in low levels in temperate, coastal waters. Occasionally, *K. veneficum* forms ichthyotoxic blooms due to the presence of cytotoxic, hemolytic compounds named karlotoxins. Exposure to a toxic strain of *K. veneficum* significantly lowered clearance and ingestion rates compared to a nontoxic strain and mixed diets dominated by the toxic strain, but did not induce mortality in the copepod *A. tonsa* [87]. These results support the hypothesis that karlotoxins in certain strains of *K. veneficum* deter grazing by potential predators and contribute to the formation and continuation of blooms. Another HAB dinoflagellate *Karenia brevis* produces brevetoxins, polyketide neurotoxins with acute toxic activity in waterborne or aerosol form against vertebrates [88]. However, according to Poulson et al. [89], negative effects of *K. brevis* on copepod egg production and survivability are not due to a chemical deterrent, but likely caused by the nutritional inadequacy of *K. brevis* as a food source. Again, there are no studies testing the effects of pure molecules on grazers.

There is also the possibility that compounds inducing negative effects on grazers are not only the PSP toxins produced by HABs but also other unknown allelopathic compounds that inhibit the growth, survival, and reproduction of competing algae [90, 91]. In *A. tamarense*, these compounds are presumably large molecules (>5 kDa), stable over broad temperature and pH ranges, and refractory to bacterial degradation [92]. *Alexandrium* allelochemicals have lytic activity targeting both competitors and grazers underlying the success of this species during blooms [93], suggesting that they are very important for structuring plankton communities.

13.3.2 DMSP and DMS

Dimethylsulfoniopropionate (DMSP) is found in numerous species of phytoplankton, but most prominently in the Prymnesiophyceae and Dinophyceae [94]. DMSP is cleaved during feeding by predators into the gas dimethyl sulfide (DMS) and acrylate which was originally hypothesized to act as a grazing deterrent (Table 13.1) via the accumulation of acrylate in grazer food vacuoles [95]. However, Strom et al. [96] showed that DMSP, not DMS or acrylate, acted as a chemical defense against protist grazers, causing a notable feeding rate reduction in several species.

DMSP released by phytoplankton into ambient seawater appears to act as a signal molecule or indicator of inferior prey rather than as a toxin. Fredrickson and Strom [97] have shown that adding DMSP (20 mM) to laboratory cultures of two ciliates (*Strombidinopsis acuminatum* and *Favella* sp.) and one dinoflagellate (*Noctiluca scintillans*) causes a 28–75% decrease in feeding rates and that these decreases were concentration-dependent with 20 nM as the lower threshold for an effect. Partial but not complete recovery of grazing rates occurred during long-term (24 h) exposure to dissolved DMSP, as long as concentrations remained above 12 mM.

There are other studies showing that DMSP-producing species of phytoplankton do not deter grazers, suggesting that some predators are less sensitive to or more capable of detoxifying this metabolite. The bloom-forming coccolithophore *Emiliania huxleyi* contains high intracellular levels of DMSP, yet some strains of *E. huxleyi* are a suitable food source for protist grazers [98–100]. Copepods also consume *E. huxleyi*, though not as a preferred food source [99]. Like *E. huxleyi*, the prymnesiophyte *Phaeocystis* is a suitable food source for some protist grazers even if it is a strong DMSP producer [101]. However, studies of copepod feeding upon *Phaeocystis* generally give varied results, many of which related to sizes of colonies, differences between copepod species and experimental techniques. Turner et al. [102] concluded that even though copepods may feed well upon *Phaeocystis*, resulting poor fecundity on this diet may inhibit copepod population increases during blooms, thereby contributing to the perpetuation of blooms. The high egg-hatching success on this diet argues against *Phaeocystis* containing chemical compounds that act as mitotic inhibitors reducing copepod egg viability, such as those found in diatoms and dinoflagellates.

Phaeocystis may also use morphological defenses to deter grazers. The life cycle of *Phaeocystis* includes solitary flagellated cells 3–8 μm in diameter, which are usually succeeded by blooms of colonial aggregations with hundreds of nonflagellated cells embedded in gelatinous colonies of up to 2 mm diameter ([102] and references therein). Gelatinous *Phaeocystis* colonies can form enormous nuisance blooms contributing to anoxia, beach fouling, and clogging of bivalve gills and fishing nets. Colony formation in *Phaeocystis* has been interpreted as a defense strategy against small grazers, because large colonies create a size-mismatch problem for small zooplankton ([70] references therein). *Phaeocystis* cells may therefore face a dilemma in a more complex food web context since colony formation will make the cells more vulnerable to larger grazers in the system

such as copepods. Long et al. [103] have shown that *Phaeocystis* colony formation was suppressed in the presence of a larger grazer (the copepod *A. tonsa*), but when small ciliate (*Euplotes* sp.) grazers attacked this alga, it shifted to the colonial form which was too large to be grazed by these ciliates. These results provide strong evidence that *Phaeocystis* cells not only sense that neighbors were being attacked but also that they “identified” the attacker and responded with opposing phenotypic shifts depending on the identity of the attacker [104]. The chemicals responsible for colony formation in this species have not yet been identified.

Not all induced morphological changes involve colony formation. For example, Pondaven et al. [105] reported grazing-induced changes in cell wall silicification in a marine diatom. Grazing-induced silicification may increase the mechanical resistance of the diatom’s frustule to copepod mandibles [106]. Pondaven et al. [105] compared changes in cell wall silicification of the marine diatom *Thalassiosira weissflogii* grown on three different preconditioned media which only differed by the fact that they had contained, either diatoms alone (control medium), nonfed copepods of the species *Calanus helgolandicus* (starved-copepods medium), or both diatoms and copepods (“diatoms and copepods” medium) before being used for culture experiments. Cells grown in preconditioned media that had contained both diatoms and herbivores were significantly more silicified than diatoms grown in media that contained diatoms alone or starved herbivores. These observations indicate that diatom cell wall silicification is not only a constitutive mechanical protection for the cell but also a phenotypically plastic trait modulated by grazing-related cues [70]. At present, it is still unknown which chemical compound(s) induces this defense.

DMS derived from the breakdown of DMSP also shows biological activity. A wide range of organisms seem to use DMS as a cue for food finding [107, 108]. It is possible that DMS odor plumes produced during zooplankton grazing are used by predators to detect, locate, and capture their prey. Plumes of DMS trigger a tail-flapping response in the copepod *Temora longicornis* which results in altered flow patterns and probably assists copepods in locating food [8]. The identification of the involved signal is important for general considerations about food finding by copepods. Since grazers are involved in the cell disintegration that triggers DMS production, this process could attract herbivores to patches with high food concentrations or assist predation on actively feeding herbivores. Carnivores can also benefit from the production of these infochemicals (information-conveying chemicals) which they sense and use to detect herbivores, thereby reducing the grazing pressure exerted by the herbivores on the plants [107]. Very little is known on such tritrophic (involving three trophic [feeding] levels) interactions in the plankton. A classic example of such complex feeding interactions in terrestrial ecosystems involves flies that sip nectar from flowers and are, in turn, eaten by spiders.

Despite the abundance and obvious presence in the plankton of these compounds, we still know little about the regulation of their production and their direct delivery to the interacting organisms. In phytoplankton cells, DMSP functions as a compatible solute, a cryoprotectant and, perhaps, an antioxidant [109–111]. Variation in phytoplankton intracellular DMSP concentration appears to facilitate

phytoplankton survival in a fluctuating environment. For example, increased DMSP production may occur under nutrient limitation [112] and when there is a decrease in temperature [113].

13.3.3 Apo-fucoanthinoids

Another class of feeding deterrents in the plankton is the apo-fucoanthinoids produced by the diatoms *Phaeodactylum tricornutum* and *Thalassiosira pseudonana* [9]. The compounds were identified as apo-10'-fucoxanthinal, apo-12'-fucoxanthinal, apo-12-fucoxanthinal, and apo-13'-fucoxanthinone. Feeding deterrent responses in the copepod *Tigriopus californicus* were observed at concentrations of 2–20 ppm which is about 1,000 times lower than the total apo-fucoanthinoid concentration in *P. tricornutum* [10]. Mortality occurred at concentrations ranging from 36.8 to 76.7 ppm. Thus, these compounds are present in concentrations which may have ecological significance in the control of bloom formation and grazing, even if *P. tricornutum* and *T. pseudonana* are not major blooming species.

The activity of these molecules was tested by dissolving them into the water in which copepods had been incubated, and fecal pellet production was used as an indication of feeding activity. A decrease in fecal pellet production after 24 h was interpreted as a result of feeding deterrence compared to control containers that had not been inoculated with these compounds. A reduction in fecal pellet production as an indication of feeding deterrence has also been inferred in other studies on copepod feeding behavior, although it remains unclear if negative effects on copepod fitness are due to reduced ingestion of cells, toxins interfering with digestive processes, or enhanced energy expenditure due to detoxification.

13.4 Environmental Factors Affecting Toxin Production

In general, changes in toxin content are associated with disturbed (unbalanced) physiology with the up-shock or down-shock of cells exiting or entering stationary phases (see [114] and references therein). Table 13.2 illustrates the importance of up/down-shock events in affecting toxicity for some of the toxin-producing species discussed until now. Phosphorus limitation often seems to enhance cellular toxin content. N limitation does so to a lesser extent, or may in the cases of domoic acid and PSPs do the opposite and lead to a fall in toxin content. Si-limited growth of *Pseudo-nitzschia* promotes synthesis of domoic acid [115]. The same occurs for PUA production in the diatom *S. marinoi* with a 7.5-fold increase ($27.5 \text{ fmol cell}^{-1}$) in Si-limited cells with respect to controls [116]. In most instances, toxin content is relatively low under nutrient-balanced conditions (N:P = 16:1). Physical factors can also affect toxin production. For example, low temperature decreased the growth rate of the PSP-producing dinoflagellates *Alexandrium catenella*,

Table 13.2 Toxic species and factors affecting toxin production

Toxic species	Factors increasing cell toxin	Toxin ^a	References
Toxins containing nitrogen			
<i>Alexandrium catenella</i> , <i>A. cohorticula</i>	Low temperature, low growth rate	PSP	[117]
<i>A. fundyense</i>	N- and P- limitation, temperature	PSP	[118–120]
<i>A. minutum</i>	P-limitation	PSP	[64]
<i>A. tamarense</i>	P-limitation, N-excess, organic matter	PSP	[117, 121–123]
<i>Pseudo-nitzschia australi</i> , <i>P. delicatissima</i> , <i>P. multiseriata</i> , <i>P. pungens</i> , <i>P. seriata</i>	P-/Si-limitation, N excess, growth phase, high light, high pH, high or low temperature, organic matter, Fe-limitation or Cu-stress	DA	[114, 124, 125]
Toxins with little or no nitrogen			
<i>Chrysochromulina leadbeateri</i> , <i>C. polylepis</i>	P-limitation, salinity, high pH, N or P-limitation	ICHT	[117, 126, 127]
<i>Dinophysis sp.</i> , <i>D. acuminata</i> , <i>D. acuta</i>	N-/or P-limitation, N-limitation; N-/P-sufficiency	OA, DTX, PTX	[117, 128]
<i>Fibrocapsa japonica</i>	Low salinity	PUFA	[129]
<i>Gymnodinium catenatum</i>	Low temperature, P-limitation	GYM	[117, 121, 130]
<i>Heterosigma akashiwo</i>	High temperature, Fe-limitation	ROS	[131]
<i>Karenia brevis</i>	Urea	Brevetoxin	[132]
<i>Ostreopsis ovata</i>	High temperature	Ostreocin	[133]
<i>Prymnesium parvum</i> , <i>P. patelliferum</i>	N-/or P-limitation	Prymnesin	[134, 135]
<i>Prorocentrum lima</i>	N-/or P-limitation, organic matter	OA, DTX	[117]
<i>Pseudo-nitzschia delicatissima</i>	Growth phase	15-HEPE, 15-oxoacid, 13,14- HepTE	[7]
<i>Skeletonema marinoi</i>	Growth phase, N- and P- limitation; Si- limitation	PUAs	[29, 115, 136]

Adapted from Graneli and Flynn [114]

GYM gymnodimine, ICHT ichthyotoxins, DA domoic acid, OA okadaic acid, DTX dinophysistoxin, PTX pectenotoxin, 15-HEPE 15-hydroxyeicosapentaenoic acid, 13,14- HepTE 13,14-hydroxy, epoxyeicosatetraenoic acid, PUAs polyunsaturated fatty aldehydes, ROS reactive oxygen species

^aPSP saxitoxin (STX), neo-STX, gonyautoxin (GTX), C-toxins

A. cohorticula, and *Gymnodinium catenatum*, whereas it increased toxin content per cell. In contrast, a low growth rate due to light inhibition did not cause an increase in toxin content, compared to cells growing at optimum illumination. In other studies, light seems to be essential for toxin production (e.g., *Prymnesium parvum*) with higher irradiance augmenting toxin production, but once the toxins were extracellular, they were rapidly inactivated by exposure to both visible light and UV radiation [117]. Briefly, there is wide variation in toxin production not only

between algal groups but also species and strains in response to different environmental conditions, and this will affect toxin production levels at sea in different years with cascading effects on predators.

13.5 Laboratory Protocols to Assess the Effects of Phytoplankton Metabolites

Marine chemical ecology is a young science, and the methodologies to study the effects of natural products on marine organisms are subject to rapid change. During the last two decades, bioassays have progressed from those that detected bioactivity without much concern for ecological relevance, to ecologically relevant tests to investigate possible functions of secondary metabolites in the phytoplankton. The problem is that often the natural concentrations of a compound, and therefore the concentrations that should be tested, are not known. Most feeding deterrents have been isolated and identified by natural products chemists looking for unusual secondary metabolites. Rarely have chemical studies provided information on the yield of these compounds after extraction. Hence, it is difficult for ecologists conducting bioassay experiments to know the natural concentrations of these metabolites to be tested. To further complicate matters, there are geographical variations in the concentration of secondary metabolites and within-region variation in some cases. Notwithstanding, much progress has been made in recent years in designing ecologically relevant bioassays with natural concentrations of a compound in many feeding trials. Here, we give a few examples of bioassay methods currently used to study chemical interactions in the plankton especially those involving antipredation and antigrowth activities.

The antiproliferative activity of phytoplankton metabolites on plankton predators has been tested mainly on zooplankton copepods ([30] and references therein) and cladocerans [31]. The majority of these studies have tested the effects of aqueous solutions containing toxic compounds by incubating embryos, larvae, or adults and studying the effects on fertilization, embryogenesis, and postembryonic development. Although the ecological relevance of these assays is questionable, because animals usually come into contact with these metabolites only through direct grazing and possibly during lysis of cells during the decay of a bloom, these assays are very useful for a preliminary screening of bioactive compounds in phytoplankton. They are also very useful for bioassay-guided separation of bioactive compounds or for testing the effects of pure compounds.

For example, Miralto et al. [1] tested the effects of PUAs which they had isolated for the first time from marine diatoms by incubating *T. stylifera* copepods in 5-mL tissue culture wells containing PUAs (2-*trans*-4-*cis*-7-*cis*-decatrienal, 2-*trans*-4-*trans*-7-*cis*-decatrienal, and 2-*trans*-4-*trans*-decadienal) at concentrations ranging from 0.5 to 5 $\mu\text{g mL}^{-1}$ (Fig. 13.5d). Fertilized eggs were freely spawned by females into containers, and the percentage of hatched eggs was determined 48 h later when

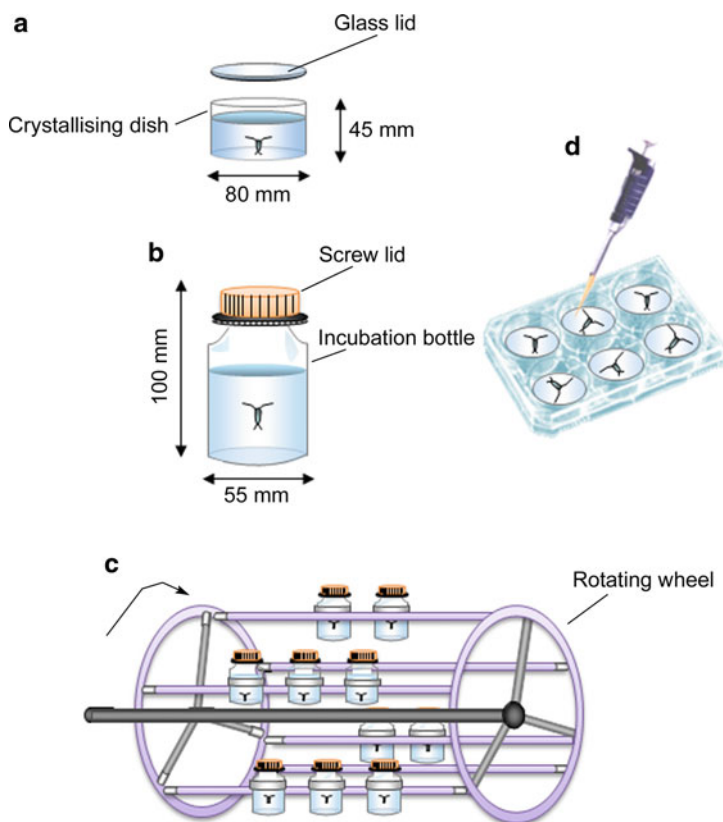


Fig. 13.5 Classic bioassays to test the biological activity of phytoplankton secondary metabolites on planktonic copepods. (a) 100-mL crystallizing dishes containing single females or male and female couples and natural food suspensions. (b): 1-L jars containing up to 20 copepods and food suspensions are placed on rotating wheel, as shown in (c). (d) 5-mL multitissue culture wells containing single copepods exposed to phytoplankton extracts or pure molecules. For explanation see text

control untreated eggs had hatched. Ianora et al. later used the same protocol to compare the effects of PUAs and 15S-HEPE on egg-hatching success of *T. stylifera*. Females were incubated individually in 5-mL tissue culture with known solutions of compounds and were removed when they had spawned to avoid cannibalization of eggs (Fig. 13.5d). Hatching was observed 48 h later.

More ecologically relevant studies on the antigrrowth activity of phytoplankton metabolites have been conducted using grazing experiments whereby copepods are fed microalgae that are known to produce toxic metabolites (e.g., diatom oxylipins) for several days (usually 15 days). Using these long-term feeding assays, Ceballos and Ianora [138] followed the effects of diatoms that produced toxic metabolites on reproductive success of adult copepod females (egg production and hatching viability of eggs), demonstrating that the microalgae tested arrested cell divisions

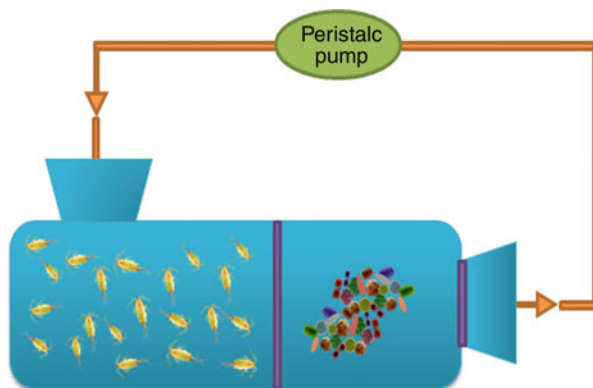
and embryonic development compared to control microalgae that did not produce these compounds. Feeding assays consisted in incubating females individually in 100-mL crystallizing dishes filled with 0.45- μm filtered seawater and a known quantity of toxic-producing and nontoxic-producing microalgae, at saturating food concentrations equivalent to about 1 $\mu\text{g C mL}^{-1}$ (Fig. 13.5a). Females were transferred to new containers with fresh algal suspensions daily for 15 days. A daily tally was kept of egg production and hatching success.

Feeding assays testing the effects of different algal diets have traditionally used larger experimental jars that are filled with food suspensions and then mounted on a rotating wheel (0.5 rpm), to keep the food suspended, in a controlled temperature room and on a fixed day–night light cycle (Fig. 13.5b). In this case, several copepods (5–10 in the case of 500 mL jars) are added to each of triplicate 500-mL experimental jars containing food suspension. A control jar with no copepods is treated in the same manner as the experimental jars, and an initial sample of food suspension is preserved at the beginning of each experiment. Experimental jars are filled and sealed, without air bubbles inside, and mounted on a rotating wheel (0.5 rpm), in a controlled temperature room at 20.5°C, on a 12:12 h L:D cycle for 24 h (Fig. 13.5c). After 24 h, copepods are removed from the experimental jars by pouring them into bowls to check for dead copepods. Food suspensions are then preserved with Lugol's solution, and phytoplankton cell numbers counted in Sedgwick-Rafter cells. At least 400 cells are counted in all cases to ensure $\pm 10\%$ precision. Ingestion rates are determined from differences in phytoplankton cell concentrations in initial, control, and triplicate experimental suspensions using the formulae of Frost [139]. Grazing rates for dead copepods are calculated assuming that they had fed for half of the experiment. Using these assays, Turner et al. [140] demonstrated that copepod egg-hatching success was strongly modified by some diatom diets, with hatching diminishing to 0% after 10 days of feeding on a diatom diet, and that this effect was diluted but not removed when the diatom was mixed with a dinoflagellate diet.

Bioassays have also been designed to test the antigrowth activity of metabolites on larval development to adulthood. Development assays consisted in incubating hatched copepod nauplii in experimental jars mounted on a rotating wheel with known quantities of algal food and following the development of nauplii to adulthood (Fig. 13.5b, c). Ianora et al. [23] sampled juveniles daily, counted and checked them under the microscope to determine the stage of development, and transferred them to new jars with fresh algal medium. A tally was kept of the most abundant larval stage and percentage of surviving individuals to calculate development and survival curves. Using this assay, Ianora et al. [23] showed that maternal diets affected offspring fitness. When mothers and their offspring were fed a diatom that produced unsaturated aldehydes, none of the larvae reached adulthood compared to control mothers and offspring that were fed a nondiatom diet. The effects on development were less severe when mothers received the control food and the offspring the treatment food.

A recent study has explored the possibility of using liposomes as a delivery system for copepods [141]. Giant liposomes were prepared and characterized in the

Fig. 13.6 Device to assess the effect of phytoplankton exudates on copepod activity. Phytoplankton and copepods are separated by a glass filter (see also Miralto et al. [143])



same size range of food ingested by copepods (mean diameter = 7 μm) and then encapsulated with the fluorescent dye fluorescein isothiocyanate (FITC) to verify copepod ingestion with fluorescence microscopy. Females of the calanoid copepod *T. stylifera* were fed with FITC-encapsulated liposomes alone or mixed with the dinoflagellate alga *P. minimum*. Control copepods were incubated with the *P. minimum* diet alone. When liposomes were supplied together with the algal diet, egg production rate, egg-hatching success, and fecal pellet production were as high as those observed for the control diet. On the contrary, egg production and hatching success was very low with a diet of liposomes alone, and fecal pellet production was similar to that recorded in starved females. This suggests that liposomes alone did not add any nutritive value to the diet, making them a good candidate as inert carriers to study the nutrient requirements or biological activity of different compounds.

In another study, Buttino et al. [142] used these giant liposomes to encapsulate decadienal in order to investigate the effect of PUAs on the reproductive biology of the copepods *T.* and *C. helgolandicus*. After 10 days of feeding, liposomes reduced egg-hatching success and female survival with a concomitant appearance of apoptosis in both copepod embryos and female tissues. Concentrations of decadienal-inducing blockage were one order of magnitude lower than those used in classical feeding experiments (e.g., Ianora et al. [23]), demonstrating that liposomes were a useful tool to quantitatively analyze the impact of toxins on copepods. This type of technology for the delivery of toxins and drugs in feeding trials has considerable potential as a means of delivering a known quantity of toxin under seminatural conditions, allowing the toxins ingested to be determined.

An experimental flow-through chamber was designed by Miralto et al. [143] to verify if copepod fertility was modified due to the release of chemical cues by other conspecifics. The apparatus (Fig. 13.6) was divided into two chambers, each of which had a 50-mL volume capacity. The chambers were separated by a glass fiber filter (20 μm pore size), and a peristaltic pump ensured diffusion of 0.45- μm filtered SW water at a flow rate of 8 mL min^{-1} . A similar chamber could be used to test if copepod exudates induce an increased production of defensive metabolites in

phytoplankton, as described by Selander et al. [72] who observed a 2.5-fold increase in PST production in the dinoflagellate *A. minutum* when exposed to waterborne cues from copepods.

The application of “omics” technologies (genomics, transcriptomics, proteomics, metabolomics, etc.) to studies of biosynthesis and regulation of bioactive secondary metabolites, and the concomitant effects on plankton population dynamics is an emerging but rapidly advancing field. Complete genome sequences have been reported for two diatoms, *Thalassiosira pseudonana* [144] and *Phaeodactylum tricornutum* [145], but others will soon be available for representative species of major groups (e.g., heterotrophic and photosynthetic bacteria, prasinophytes, diatoms, *Emiliana huxleyi*, *Phaeocystis*, and copepods). With access to these tools, chemical ecologists have an unprecedented opportunity to learn more about the biochemistry and ecological functioning of pelagic systems more quickly and comprehensively than ever. This is manifested by altered expression of superoxide dismutase and metacaspases, key components of stress and death pathways. Transgenic approaches for manipulating genes in key signaling and stress-related pathways in phytoplankton may provide the opportunity to gain further insights into trophic-level interactions.

Given the massive genome size and complexity characteristic of marine dinoflagellates, whole genome sequencing remains impractical. A functional genomics approach, involving generation of a cDNA library and sequencing of expressed sequence tags (ESTs), has proven useful in the search for putative biosynthetic genes for secondary metabolites, stress response genes, and those involved in growth regulation leading to bloom formation [146]. Particularly, when coupled with DNA microarrays, molecular approaches have the potential to reveal novel pathways that are up- or downregulated during certain stress situations and might reveal the biochemical and chemical basis for some observed species interactions that cannot be explained to date. One detailed study of intrapopulation diversity within the toxigenic dinoflagellate *A. tamarensis* [147] revealed that the abundant genetic diversity, determined by two independent molecular markers, was not directly correlated with the phenotypic variation in toxin spectrum and intracellular concentration.

Another powerful postgenomics tool, advanced metabolite profiling, also termed “metabolomics,” allows mapping of the chemical diversity and dynamic range of bioactive secondary metabolites of potential importance in ecological interactions. Thus, the response of phytoplankton cultures or communities to competing organisms, predators, and viruses can be monitored with limited bias toward a certain compound class. Statistical evaluation of the data provides insight into the metabolic changes within the cells as well as into the released metabolites that might represent the chemical language of the cells [148]. It is likely that knowledge of the complex patterns of chemicals released by microalgae and other plankton species will result in a paradigm shift revealing new mechanisms for processes such as community function, food location, or complex defensive and allelopathic interactions. The marriage of metabolomics and metagenomics has the potential to be a particularly powerful

combination in shedding light on planktonic and microbial interactions in marine ecosystems [149].

Another important tool in plankton chemical ecology studies will be the adoption of model organisms that will provide insight into the functioning of other organisms. This approach is widely used in the biomedical field to explore potential causes and treatments for human disease and is based on the concept of conservation of biochemical pathways and genetic material over the course of evolution. Models are chosen on the basis that they are suitable for experimental manipulation, have characteristics such as a short life cycle, are amenable for maintenance and breeding in the laboratory, and have nonspecialist living requirements. In terrestrial chemical ecology, the introduction of *Arabidopsis thaliana* as the first fully sequenced plant proved to be highly successful for the elucidation of rather general plant defensive pathways. Such an approach could also be useful in the plankton and would allow for the elucidation of fundamental biochemical mechanisms such as regulatory and metabolic pathways in producer organisms as well as the identification of the mechanisms of action in target organisms. Ideally, the models selected in plankton ecological studies would also be supported by genomic and postgenomic resources, databases, and infrastructure.

13.6 Concluding Remarks

In comparison to the large number of studies on the antipredatory compounds produced by terrestrial plants, those regarding marine phytoplankton are underrepresented. Most studies on the secondary metabolites of these microalgae have focused on bioactivity and structural elucidation, with a view toward potential pharmaceuticals or other commercial purposes. Nevertheless, the environmental and human health consequences of HABs have provided great impetus to conduct ecologically relevant studies on microalgae in the last decade (reviewed by Poulson et al. [89] and Sieg et al. [150]).

Marine chemical ecology is a young science that requires the collaborative effort of biologists, ecologists, and chemists. Identifying the compounds responsible for mediating feeding, reproduction, and behavioral interactions is only the first step in understanding the ecological relevance of a compound. These effects then need to be translated from laboratory assays to their natural context in order to provide the ultimate test and major challenge for field ecologists. An increased understanding of chemical defenses will be achieved when we know how ecologically realistic doses of these metabolites affect growth, reproduction, and survivorship of consumers. In the long run, such studies will lead to a better understanding of how these compounds can help regulate ecosystem functionality by underpinning the chemical and molecular processes that are crucial for the fitness and survival of the producing organisms.

A major challenge for the future will be to understand the multiple simultaneous functions of many of these secondary metabolites. For example, diatom PUAs may have an antipredatory function [14] and also act as allelopathic agents [135]. Furthermore, PUAs can affect growth of some bacterial strains [28] and possibly also

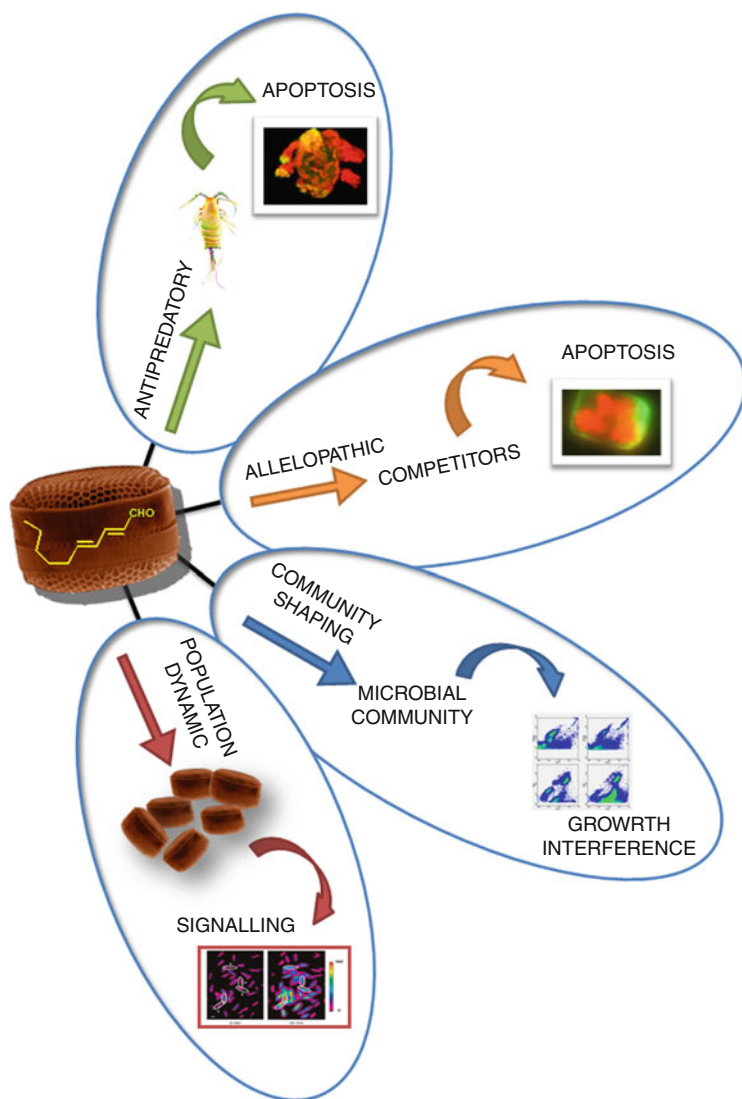


Fig. 13.7 Multiple effects of diatom polyunsaturated aldehydes (PUAs): From the top, Antiproliferative (teratogenic) effect on copepods. Abnormal *Calanus helgolandicus* copepod nauplius hatched from a mother fed with the PUA-producing diatom *Skeletonema marinoi*. Yellow parts indicate TUNEL-positive apoptotic tissues (from Ianora et al. [23]). Allelopathic effect on phytoplankton species in culture, *Skeletonema marinoi*, cell after incubation with decadienal. Red fluorescence indicates annexin positivity (apoptosis) (from Casotti et al. [24]). Growth interference of picoplankton. Flow cytograms represent a natural seawater sample from the Adriatic Sea; left panels are controls, right panels are picophytoplankton (top) and heterotrophic bacteria (bottom), after 24 h inoculation with a mixture of octadienal and heptadienal [28]). Signaling effect. Intracellular transmission of decadienal-derived signal induces NO in neighboring (from Vardi et al. [26]) influencing population dynamic

have a stress-signaling function [17], with potential consequences for food web structure and community composition (Fig. 13.7). Thus, the same secondary metabolites may act to deter different groups of organisms by different modes of action.

The chemical multifunctionality of secondary metabolites is well documented in higher terrestrial plants. For example, the anthraquinone emodin, identified in 17 plant families distributed worldwide, has numerous biological activities, some of which exhibit a wide spectrum of ecological impacts by mediating biotic or abiotic interactions of plants with their environment. In vegetative organs emodin may help protect plants against herbivores, pathogens, competitors and extrinsic abiotic factors (e.g., high light intensities). In unripe fruit pulp, emodin may facilitate seed dispersal by protecting the immature fruit against predispersal seed predation whereas in ripe pulp it may deter frugivores and thus reduce the chances that seeds will be defecated beneath the parent plant [151]. Natural selection should favor secondary metabolites with multiple functions because they protect the plants against a variety of unpredictable biotic and abiotic environments. Such metabolites also enhance plant defenses by using different molecular targets of specific enemies through a variety of mechanisms of action. As discussed in a recent paper [152] herbivores also vary profoundly in their tolerance to secondary metabolites, and future research should be directed to better understanding detoxification processes, or lack of such processes, in the plankton. The complexity of planktonic food webs allows a multitude of pathways for infochemicals that need to be better understood. The role of parasites and viruses, both in introducing toxins into the plankton, as well as removing them through detoxification or species-specific host–pathogen interactions is poorly known. Resulting trophic cascades may have important repercussions in plankton community structure with implications for higher trophic levels including important fisheries.

We have only barely begun to understand the importance of chemical interactions in the plankton and their role in shaping biodiversity and ecological functioning both at a community and cellular level. An increased understanding of the natural function of these compounds may lead to new strategies for the correct management and protection of these potentially important natural resources for the future and help find new biotechnological applications for these products in our day-to-day lives. Antifeedants have already been used to derive anticancer, antiviral, and antiaging products; toxins have been used to develop pain killers; and functional products have been obtained from the materials used by sessile organisms to colonize free surfaces. Knowledge of ecophysiological interactions may serve as a platform to facilitate the search for new biotechnological candidates, as well as to optimize culture conditions and achieve production of biomass for industrial applications.

13.7 Study Questions

1. What types of antipredator defensive strategies occur in the plankton and do these differ from those in benthic habitats?

2. How do antipredator defensive strategies in marine organisms compare to those in terrestrial habitats?
3. What is the function of oxylipins in diatoms?
4. Are dinoflagellate neurotoxins defensive metabolites against predators?
5. Are some classes of molecules more common as defensive metabolites than others?
6. How do toxin production levels vary in relation to environmental changes?

Acknowledgments We thank Flora Palumbo of the Functional and Evolutionary Ecology Laboratory of Stazione Zoologica Anton Dohrn for figures and drawings.

References

1. Miralto A, Barone G, Romano G, Poulet SA, Ianora A, Russo L, Buttino I, Mazzarella G, Laabir M, Cabrini M, Giacobbe MG (1999) The insidious effect of diatoms on copepod reproduction. *Nature* 402:173–176
2. Wichard T, Poulet SA, Halsband-Lenk C, Albaina A, Harris R, Liu D, Pohnert G (2005) Survey of the chemical defense potential of diatoms: screening of fifty-one species for a, b, c, d-unsaturated aldehydes. *J Chem Ecol* 31:949–958
3. d'Ippolito G, Romano G, Iadicicco O, Miralto A, Ianora A, Cimino G, Fontana A (2002) New birth-control aldehydes from the marine diatom *Skeletonema costatum*: characterization and biogenesis. *Tetrahedron Lett* 43:6133–6136
4. d'Ippolito G, Romano G, Iadicicco O, Fontana A (2002) Detection of short-chain aldehydes in marine organisms: the diatom *Thalassiosira rotula*. *Tetrahedron Lett* 43:6137–6140
5. Fontana A, d'Ippolito G, Cutignano A, Romano G, Lamari N, Massa Gallucci A, Cimino G, Miralto A, Ianora A (2007) A metabolic mechanism for the detrimental effect of marine diatoms on zooplankton grazers. *Chem Biochem* 8:1810–1818
6. Fontana A, d'Ippolito G, Cutignano A, Miralto A, Ianora A, Romano G, Cimino G (2007) Chemistry of oxylipin pathways in marine diatoms. *Pure Appl Chem* 79:475–484
7. d'Ippolito G, Lamari N, Montresor M, Romano G, Cutignano A, Gerech A, Cimino G, Fontana A (2009) 15 S-Lipoxygenase metabolism in the marine diatom *Pseudo-nitzschia delicatissima*. *New Phytol* 183:1064–1071
8. Steinke M, Stefels J, Stamhuis E (2006) Dimethyl sulfide triggers search behavior in copepods. *Limnol Oceanogr* 51:1925–1930
9. Shaw BA, Anderson RJ, Harrison PJ (1995) Feeding deterrence properties of apo-fucoanthinoids from marine diatoms. I. Chemical structures of apo-fucoanthinoids produced by *Phaeodactylum tricornutum*. *Mar Biol* 124:467–472
10. Shaw BA, Anderson RJ, Harrison PJ (1995) Feeding deterrence properties of apo-fucoanthinoids from marine diatoms. II. Physiology of production of apo-fucoanthinoids by the marine diatoms *Phaeodactylum tricornutum* and *Thalassiosira pseudonana*, and their feeding deterrent effects on the copepod *Tigriopus californicus*. *Mar Biol* 124:473–481
11. Selander E, Thor P, Toth G, Pavia H (2006) Copepods induce paralytic shellfish toxin production in marine dinoflagellates. *Proc R Soc Lond B Biol Sci* 273:1673–1680
12. Ban S, Burns C, Castel C, Christou E, Escribano R, Fonda Umani F, Gasparini S, Guerrero Ruiz F et al (1997) The paradox of diatom-copepod interactions. *Mar Ecol Prog Ser* 157:287–293
13. Knight AP, Walter RG (2004) Plants associated with congenital defects and reproductive failure. In: Knight AP, Walter RG (eds) *A guide to plant poisoning of animals in North America*. Teton NewMedia, Jackson

14. Pohnert G (2000) Wound-activated chemical defence in unicellular planktonic algae. *Angew Chem Int Ed* 39:4352–4354
15. d'Ippolito G, Tucci S, Cutignano A, Romano G, Cimino G, Miralto A, Fontana A (2004) The role of complex lipids in the synthesis of bioactive aldehydes of the marine diatom *Skeletonema costatum*. *Biochim Biophys Acta* 1686:100–107
16. Cutignano A, d'Ippolito G, Romano G, Cimino G, Febbraio F, Nucci R, Fontana A (2006) Chloroplastic galactolipids fuel the aldehyde biosynthesis in the marine diatom *Thalassiosira rotula*. *Chem BioChem* 7:450–456
17. Caldwell GS (2009) The influence of bioactive oxylipins from marine diatoms on invertebrate reproduction and development. *Mar Drugs* 7:367–400
18. Romano G, Russo GL, Buttino I, Ianora A, Miralto A (2003) A marine diatom-derived aldehyde induces apoptosis in copepod and sea urchin embryos. *J Exp Biol* 206:3487–3494
19. Hansen E, Ernsten A, Eilersten HC (2004) Isolation and characterization of cytotoxic polyunsaturated aldehyde from the marine phytoplankter *Phaeocystis pouchetii* (Hariot) Lagerheim. *Toxicology* 199:207–217
20. Ianora A, Poulet SA, Miralto A (2003) The effects of diatoms on copepod reproduction: a review. *Phycologia* 42:351–363
21. Caldwell GS, Watson SB, Bentley MG (2004) How to assess toxin ingestion and post-ingestion partitioning in zooplankton? *J Plankton Res* 26:1369–1377
22. Romano G, Miralto A, Ianora A (2010) Teratogenic effects of diatom metabolites on sea urchin *Paracentrotus lividus* embryos. *Mar Drugs* 8:950–967
23. Ianora A, Miralto A, Poulet SA, Carotenuto Y, Buttino I, Romano G, Casotti R, Pohnert G, Wichard T, Colucci-D'Amato L, Terrazzano G, Smetacek V (2004) Aldehyde suppression of copepod recruitment in blooms of a ubiquitous planktonic diatom. *Nature* 429:403–407
24. Casotti R, Mazza S, Brunet C, Vantrepotte V, Ianora A, Miralto A (2005) Growth inhibition and toxicity of the algal aldehyde 2-trans-2-cis decadienal on *Thalassiosira weissflogii* (Bacillariophyceae). *J Phycol* 41:7–20
25. Ribalet F, Berges JA, Ianora A, Casotti R (2007) Growth inhibition of cultured marine phytoplankton by algal-derived polyunsaturated aldehydes. *Aquat Toxicol* 85:219–227
26. Vardi A, Formiggini F, Casotti R, De Martino A, Ribalet F, Miralto A, Bowler C (2006) A stress surveillance system based on calcium and nitric oxide in marine diatoms. *PLoS Biol* 4:411–419
27. Vardi A, Bidle K, Kwityn C, Hirsh DJ, Thompson SM, Callow JA, Falkowski P, Bowler C (2008) A diatom gene regulating nitric oxide signaling and susceptibility to diatom-derived aldehydes. *Curr Biol* 18:895–899
28. Ribalet F, Intertaglia L, Lebaron F, Casotti R (2008) Differential effects of three polyunsaturated aldehydes on marine bacterial isolates. *Aquat Toxicol* 86:249–255
29. Vidoudez C, Pohnert G (2008) Growth phase-specific release of polyunsaturated aldehydes by the diatom *Skeletonema marinoi*. *J Plankton Res* 30:1305–1313
30. Ianora A, Miralto A (2010) Toxic effects of diatoms on grazers, phytoplankton and other microbes: a review. *Ecotoxicology* 19:493–511
31. Carotenuto Y, Wichard T, Pohnert G, Lampert W (2005) Life-history responses of *Daphnia pulex* to diets containing freshwater diatoms: effects of nutritional quality versus polyunsaturated aldehydes. *Limnol Oceanogr* 50:449–454
32. Caldwell GS, Bentley MG, Olive PJW (2002) Inhibition of embryonic development and fertilization in broadcast spawning marine invertebrates by water soluble diatom extracts and the diatom toxin 2-trans, 4-trans decadienal. *Aquat Toxicol* 60:123–137
33. Tosti E, Romano G, Buttino I, Cuomo A, Ianora A, Miralto A (2003) Bioactive aldehydes from diatoms block fertilization currents in ascidian oocytes. *Mol Reprod Dev* 66:72–80
34. Adolph S, Bach S, Blondel M, Cuffe A, Moreau M, Pohnert G, Poulet SA (2004) Cytotoxicity of diatom-derived oxylipins in organisms belonging to different phyla. *J Exp Biol* 207:2935–2946

35. Taylor RL, Caldwell GS, Dunstan HG, Bentley MG (2007) Short term impacts of polyunsaturated aldehyde-producing diatoms on the harpacticoid copepod, *Tisbe holothuriae*. J Exp Mar Biol Ecol 341:60–69
36. Blée E (1998) Phytooxylipins and plant defense reactions. Prog Lipid Res 37:33–72
37. Blée E (2002) Impact of phyto-oxylipins in plant defense. Trends Plant Sci 7:315–321
38. Jüttner F, Durst U (1997) High lipoxygenase activities in epilithic biofilms of diatoms. Archiv für Hydrobiologie 138:451–463
39. Pohnert G (2005) Diatom-Copepod interactions in plankton: the indirect chemical defense of unicellular algae. Chem Biochem 6:1–14
40. Pohnert G (2002) Phospholipase A2 activity triggers the wound-activated chemical defence in the diatom *Thalassiosira rotula*. Plant Physiol 129:103–111
41. d'Ippolito G, Cutignano A, Tucci S, Romano G, Cimino G, Fontana A (2006) Biosynthetic intermediates and stereochemical aspects of aldehyde biosynthesis in the marine diatom *Thalassiosira rotula*. Phytochemistry 67:314–322
42. Wichard T, Gerecht A, Boersma M, Poulet SA, Wiltshire K, Pohnert G (2007) Lipid and fatty acid composition of diatoms revisited: rapid wound-activated change of food quality parameters influences herbivorous copepod reproductive success. Chem BioChem 8:1146–1153
43. d'Ippolito G, Cutignano A, Briante R, Febbraio F, Cimino G, Fontana A (2005) New C16 fatty-acid-based oxylipin pathway in the marine diatom *Thalassiosira rotula*. Org Biomol Chem 3:4065–4070
44. Pohnert G, Lumineau O, Cueff A, Adolph S, Cordevan C, Lange M, Poulet S (2002) Are volatile unsaturated aldehydes from diatoms the main line of chemical defence against copepods? Mar Ecol Prog Ser 245:33–45
45. Pohnert G, Boland W (2002) The oxylipin chemistry of attraction and defense in brown algae and diatoms. Nat Prod Rep 19:108–122
46. Andreou A, Brodhun F, Feussner I (2009) Biosynthesis of oxylipins in non-mammals. Prog Lipid Res 48:148–170
47. Ianora A, Romano G, Carotenuto Y, Esposito F, Roncalli V, Buttino I, Miralto A (2011) Impact of the diatom oxylipin 15 S-HEPE on the reproductive success of the copepod *Temora stylifera*. Hydrobiologia. doi:10.1007/s10750-010-0420-7
48. Ianora A, Casotti R, Bastianini M, Brunet C, d'Ippolito G, Fontana A, Cutignano A, Turner JT, Miralto A (2008) Low reproductive success in copepod communities during a bloom of the diatom *Cerataulina pelagica* in the North Adriatic Sea. Mar Ecol 29:399–410
49. Jüttner F (2005) Evidence that polyunsaturated aldehydes of diatoms are repellent for pelagic crustacean grazers. Aquat Ecol 39:271–282
50. Watson SB, Satchwill T (2003) Chrysophyte odour production: resource-mediated changes at the cell population levels. Phycologia 42:393–405
51. Fink P (2007) Ecological functions of volatile organic compounds in aquatic systems. Mar Freshw Behav Phy 40:155–168
52. Watson SB (2003) Cyanobacterial and eukaryoticalgal odour compounds: signals or by-products? A review of their biological activity. Phycologia 42:332–350
53. Ianora A, Miralto A, Buttino I, Poulet SA, Romano G (1999) First evidence of some dinoflagellates reducing male copepod fertilization capacity. Limnol Oceanogr 44:147–153
54. Ianora A, Turner JT, Esposito F, d'Ippolito G, Romano G, Guisande C, Carotenuto Y, Miralto A (2004) Copepod egg hatching success is reduced by maternal diets of a non-neurotoxic strain of the dinoflagellate *Alexandrium tamarense*. Mar Ecol Prog Ser 280:199–210
55. Murakami M, Makabe K, Yamaguchi K, Konosu S (1988) Goniodomin A, a novel polyether macrolide from the dinoflagellate *Goniodoma pseudogoniaulax*. Tetrahedron Lett 29:1149–1152

56. Kobayashi J, Ishibashi M, Nakamura H, Ohizumi Y, Yamasu T, Sasaki T, Hirata Y (1986) Amphidinolide-A, a novel antineoplastic macrolide from the marine dinoflagellate *Amphidinium* sp. *Tetrahedron Lett* 27:5755–5758
57. Fujiki H, Suganuma M, Suguri H, Yoshizawa S et al (1988) Diarrhetic shellfish toxin, dinophysistoxin-1, is a potent tumor promoter on mouse skin. *Jpn J Cancer Res* 79: 1089–1093
58. Yan T, Mingjiang Z, Fu M, Wang Y, Yu R, Li J (2001) Inhibition of egg hatching success and larval survival of the scallop, *Chlamys farreri*, associated with exposure to cells and cell fragments of the dinoflagellate *Alexandrium tamarense*. *Toxicon* 39:1239–1244
59. Granéli E, Turner JT (2008) Ecology of harmful algae. Springer, Berlin/Heidelberg
60. Burkholder JM (2009) Harmful algal blooms. In: Likens GE (ed) *Encyclopedia of inland waters*. Elsevier, New York, pp 264–285
61. Turner JT, Tester PA (1997) Toxic marine phytoplankton, zooplankton grazers, and pelagic food webs. *Limnol Oceanogr* 42:1203–1214
62. Colin SP, Dam HG (2003) Effects of the toxic dinoflagellate *Alexandrium fundyense* on the copepod *Acartia hudsonica*: a test of the mechanisms that reduce ingestion rates. *Mar Ecol Prog Ser* 248:55–65
63. Sykes PF, Huntley MA (1987) Acute physiological reactions of *Calanus pacificus* to selected dinoflagellates: direct observations. *Mar Biol* 94:19–24
64. Teegarden GJ (1999) Copepod grazing selection and particle discrimination on the basis of PSP toxin content. *Mar Ecol Prog Ser* 181:163–176
65. Guisande C, Frangópulos M, Carotenuto Y, Maneiro I, Riveiro I, Vergara AR (2002) Fate of paralytic shellfish poisoning toxins ingested by the copepod *Acartia clausi*. *Mar Ecol Prog Ser* 240:105–115
66. Frangópulos M, Guisande C, Maneiro I, Riveiro I, Franco J (2000) Short-term and long-term effects of the toxic dinoflagellate *Alexandrium minutum* on the copepod *Acartia clausi*. *Mar Ecol Prog Ser* 203:161–169
67. Turriff N, Runge JA, Cembella AD (1995) Toxin accumulation and feeding behaviour of the planktonic copepod *Calanus finmarchicus* exposed to the red-tide dinoflagellate *Alexandrium excavatum*. *Mar Biol* 123:55–64
68. Cembella AD (2003) Chemical ecology of eukaryotic microalgae in marine ecosystems. *Phycologia* 42:420–447
69. Rhoades DF (1979) Evolution of plant chemical defense against herbivores. In: Rosenthal GA et al (eds) *Herbivores: their interaction with secondary plant metabolites*. Academic, New York
70. Van Donk E, Ianora A, Vos M (2011) Induced defenses in marine and freshwater phytoplankton: a review. *Hydrobiologia*. doi:10.1007/s10750-010-0395-4
71. Selander E, Cervin G, Pavia H (2008) Effects of nitrate and phosphate on grazer-induced toxin production in *Alexandrium minutum*. *Limnol Oceanogr* 53:523–530
72. Bhakuni DS, Rawat DS (2005) *Bioactive marine natural products*. Springer, New York and Anamaya Publishers, New Delhi, India
73. Teegarden GJ, Cembella AD (1996) Grazing of toxic dinoflagellates, *Alexandrium* spp., by adult copepods of coastal Maine: implications for the fate of paralytic shellfish toxins in marine food webs. *J Exp Mar Biol Ecol* 196:145–176
74. Lauritano C, Borra M, Carotenuto Y, Biffali E, Miralto A, Pracaccini G, Ianora A (2011) Molecular evidence of the toxic effects of diatom diets on gene expression patterns in copepods. *PLoS ONE* 6:e26850
75. Colin SP, Dam HG (2005) Testing for resistance of pelagic marine copepods to a toxic dinoflagellate. *Evol Ecol* 18:355–377
76. Tester PA, Turner JT, Shea D (2000) Vectorial transport of toxins the dinoflagellate *Gymnodinium breve* through copepods to fish. *J Plankton Res* 22:47–61
77. Doucette GJ, Turner JT, Powell CL, Keafer BA, Anderson DM, ECOHAB-Gulf of Maine (2005) Trophic accumulation of PSP toxins in zooplankton during *Alexandrium fundyense*

- blooms in Casco Bay, Gulf of Maine, April–June 1998. I. Toxin levels in *A. fundyense* and zooplankton size fractions. *Deep Sea Res II* 52:2764–2783
78. Cimino G, Ghiselin MT (2001) Marine natural products chemistry as an evolutionary narrative. In: McClintock JB, Baker BJ (eds) *Marine chemical ecology*. CRC Press, Boca Raton, pp 115–154
79. Shaw BA, Anderson RJ, Harrison PJ (1997) Feeding deterrent and toxicity effects of apofucocanthinoids and phycotoxins on a marine copepod (*Tigriopus californicus*). *Mar Biol* 128:273–280
80. Maneiro I, Iglesias P, Guisande C, Riveiro I, Barreiro A, Zervoudaki S, Granéli E (2005) Fate of domoic acid ingested by the copepod *Acartia clausi*. *Mar Biol* 148:123–130
81. Olson MB, Lessard EJ, Wong CHJ, Bernhardt MJ (2006) Copepod feeding selectivity on the microplankton, including the toxigenic diatom, *Pseudo-nitzschia* spp., in the coastal Pacific Northwest. *Mar Ecol Prog Ser* 326:207–220
82. Olson MB, Lessard EJ, Cochlan WP, Trainer VL (2008) Intrinsic growth and microzooplankton grazing on toxigenic *Pseudo-nitzschia* spp. diatoms from the coastal northeast Pacific. *Limnol Oceanogr* 53:1352–1368
83. Barga S, Lefebvre K, Silver MW (2006) Effect of dissolved domoic acid on the grazing rate of krill *Euphausia pacifica*. *Mar Ecol Prog Ser* 312:169–175
84. Manning SR, La Claire JW II (2010) Prymnesins: toxic metabolites of the golden alga, *Prymnesium parvum* Carter (Haptophyta). *Mar Drugs* 8:678–704
85. Sopanen S, Koski M, Kuuppo P, Uronen P, Legrand C, Tamminen T (2006) Toxic haptophyte *Prymnesium parvum* affects grazing, survival, egestion and egg production of the calanoid copepods *Eurytemora affinis* and *Acartia biflosa*. *Mar Ecol Prog Ser* 327:223–232
86. Sopanen S, Koski M, Uronen P, Kuuppo P, Lehtinen S, Legrand C, Tamminen T (2008) *Prymnesium parvum* exotoxins affect the grazing and viability of the calanoid copepod *Eurytemora affinis*. *Mar Ecol Prog Ser* 361:191–202
87. Waggett RJ, Tester PA, Place AR (2008) Anti-grazing properties of the toxic dinoflagellate *Karlodinium veneticum* during predator–prey interactions with the copepod *Acartia tonsa*. *Mar Ecol Prog Ser* 366:31–42
88. Baden DG (1989) Brevetoxins: unique polyether dinoflagellate toxins. *FASEB J* 3:1807–1817
89. Poulson KL, Sieg D, Kubanek J (2009) Chemical ecology of the plankton. *Nat Prod Rep* 26:729–745
90. Tillmann U, John U (2002) Toxic effects of *Alexandrium* spp. on heterotrophic dinoflagellates: an allelochemical defence mechanism independent of PSP-toxin content. *Mar Ecol Prog Ser* 230:47–58
91. Tillmann U, John U, Cembella A (2007) On the allelochemical potency of the marine dinoflagellate *Alexandrium ostenfeldii* against heterotrophic and autotrophic protists. *J Plankton Res* 29:527–543
92. Ma H, Krock B, Tillmann U, Cembella A (2009) Preliminary characterization of extracellular allelochemicals of the toxic marine dinoflagellate *Alexandrium tamarense* using a *Rhodomonas salina* assay. *Mar Drugs* 7:497–522
93. Tillmann U, Hansen PJ (2009) Allelopathic effects of *Alexandrium tamarense* on other algae: evidence from mixed growth experiments. *Aquat Microbial Ecol* 57:101–112
94. Keller MD, Bellows WK, Guillard RRL (1989) Dimethylsulfide production in marine phytoplankton. In: Saltzman ES, Cooper WJ (eds) *Biogenic sulfur in the environment*. American Chemical Society, Washington, DC, pp 167–183
95. Wolfe GV, Steinke M, Kirst GO (1997) Grazing-activated chemical defense in a unicellular marine alga. *Nature* 387:894–897
96. Strom SL, Wolfe GV, Slajer A et al (2003) Chemical defense in the microplankton II: inhibition of protist feeding by b-dimethylsulfoniopropionate. *Limnol Oceanogr* 48:230–237

97. Fredrickson KA, Strom SL (2009) The algal osmolyte DMSP as a microzooplankton grazing deterrent in laboratory and field studies. *J Plankton Res* 31:135–152
98. Wolfe GV, Sherr EB, Sherr BS (1994) Release and consumption of DMSP from *Emiliania huxleyi* during grazing by *Oxyrrhis marina*. *Mar Ecol Prog Ser* 111:111–119
99. Nejstgaard JC, Gismervik I, Solberg PT (1997) Feeding and reproduction by *Calanus finmarchicus* and microzooplankton grazing during mesocosm blooms of diatoms and the coccolithophore *Emiliania huxleyi*. *Mar Ecol Prog Ser* 147:197–217
100. Strom SL, Wolfe GV, Holmes J et al (2003) Chemical defense in the microplankton I: feeding and growth rates of heterotrophic protists on the DMS producing phytoplankter *Emiliania huxleyi*. *Limnol Oceanogr* 48:217–229
101. Tang KW, Jakobsen HH, Visser AW (2001) *Phaeocystis globosa* (Prymnesiophyceae) and the planktonic food web: feeding, growth and trophic interactions among grazers. *Limnol Oceanogr* 46:1860–1870
102. Turner JT, Ianora A, Esposito F, Carotenuto Y, Miralto A (2002) Zooplankton feeding ecology: does a diet of *Phaeocystis globosa* support good copepod survival, egg production and egg hatching success? *J Plankton Res* 24:1185–1195
103. Long JD, Smalley GW, Barsby T, Anderson JT, Hay ME (2007) Chemical cues induce consumer-specific defenses in a bloom-forming marine phytoplankton. *Proc Natl Acad Sci USA* 104:10512–10517
104. Hay ME (2009) Marine chemical ecology: chemical signals and cues structure marine populations, communities, and ecosystems. *Annu Rev Mar Sci* 1:193–212
105. Pondaven P, Gallinari M, Chollet S, Bucciarelli E, Sarthou G, Schultes S, Jean F (2007) Grazing-induced changes in cell wall silicification in a marine diatom. *Protist* 158:21–28
106. Hamm CE, Merkel R, Springer O, Jurkojc P, Maier C et al (2003) Diatom cells are mechanically protected by their strong, lightweight, silica shells. *Nature* 421:841–843
107. Steinke M, Malin G, Liss PS (2002) Tritrophic interactions in the sea: an ecological role for climate relevant volatiles. *J Phycol* 38:630–638
108. Pohnert G, Steinke M, Tollrian R (2007) Chemical cues, defence metabolites and the shaping of pelagic interspecific interactions. *Trends Ecol Evol* 22:198–204
109. Kirst GO (1989) Salinity tolerance of eukaryotic marine algae. *Annu Rev Plant Physiol Plant Mol Biol* 40:21–53
110. Kirst GO, Wolff CH, Nothnagel J et al (1991) Dimethyl-sulfonioisopropionate (DMSP) in ice algae and its possible biological role. *Mar Chem* 35:381–388
111. Sunda WG, Kieber DJ, Kiene RP et al (2002) An antioxidant function for DMSP and DMS in marine algae. *Nature* 418:317–320
112. Bucciarelli E, Sunda WG (2003) Influence of CO₂, nitrate, phosphate, and silicate limitation on intracellular dimethylsulfonioisopropionate in batch cultures of the coastal diatom *Thalassiosira pseudonana*. *Limnol Oceanogr* 48:2256–2265
113. van Rijssel M, Gieskes WWC (2002) Temperature, light, and the dimethylsulfonioisopropionate (DMSP) content of *Emiliania huxleyi* (Prymnesiophyceae). *J Sea Res* 48:17–27
114. Granéli E, Flynn K (2006) Chemical and physical factors influencing toxin content. In: Granéli E, Turner JT (eds) *Ecological studies*, vol 189, *Ecology of harmful algae*. Springer, Berlin/Heidelberg, pp 229–241
115. Bates SS (1998) Ecophysiology and metabolism of ASP toxin production. In: Anderson DM, Cembella AD, Hallegraeff GM (eds) *Physiological ecology of harmful algal blooms*, NATO ASI Series 41. Springer, Berlin/Heidelberg/New York, pp 405–426
116. Ribalet F, Vidoudez C, Cassin D, Pohnert G, Ianora A, Miralto A, Casotti R (2009) High plasticity in the production of diatom derived polyunsaturated aldehydes under nutrient limitation: physiological and ecological implications. *Protist* 160:444–451
117. Shilo M (1981) The toxic principles of *Prymnesium parvum*. In: Carmichael WW (ed) *The water environment: algal toxins and health*, vol 20. Plenum, New York, pp 37–47
118. Granéli E, Johansson N, Panosso R (1998) Cellular toxin contents in relation to nutrient conditions for different groups of phycotoxins. In: Reguera B, Blanco J, Fernandez ML,

- Wyatt T (eds) Harmful algae. Xunta de Galicia and Intergovern. Oceanographic Comm. of UNESCO, Paris, pp 321–324
119. Flynn KJ (2002) Toxin production in migrating dinoflagellates: a modelling study of PSP producing *Alexandrium*. Harmful Algae 1:147–155
120. Flynn KJ, Flynn K (1995) Dinoflagellate physiology, nutrient stress and toxicity. In: Lassus P, Arzul G, Le Denn EE, Gentien P, Marcaillou C (eds) Harmful marine algal blooms. Lavoisier Intercept, Paris, pp 541–550
121. John EH, Flynn KJ (2000) Growth dynamics and toxicity of *Alexandrium fundyense* (Dinophyceae): the effect of changing N:P supply ratios on internal toxin and nutrient levels. Eur J Phycol 35:11–23
122. Cembella AD (1998) Ecophysiology and metabolism of paralytic shellfish toxins in marine microalgae. In: Anderson DM, Cembella AD, Hallegraeff GM (eds) Physiological ecology of harmful algal blooms, NATO ASI Series 41. Springer, Berlin/Heidelberg/New York, pp 381–403
123. Flynn K, Franco JM, Fernández P, Reguera B, Zapata M, Wood G, Flynn KJ (1994) Changes in toxin content, biomass and pigments of the dinoflagellate *Alexandrium minutum* during nitrogen refeeding and growth into nitrogen and phosphorus stress. Mar Ecol Prog Ser 111:99–109
124. John EH, Flynn KJ (1999) Amino acid uptake by the toxic dinoflagellate *Alexandrium fundyense*. Mar Biol 133:11–20
125. Lundholm N, Hansen PJ, Kotaki Y (2004) Effect of pH on growth and domoic acid production by potentially toxic diatoms of the genera *Pseudo-nitzschia* and *Nitzschia*. Mar Ecol Prog Ser 273:1–15
126. Maldonado MT, Hughes MP, Rue EL, Wells ML (2002) The effect of Fe and Cu on growth and domoic acid production by *Pseudo-nitzschia multiseries* and *Pseudo-nitzschia australis*. Limnol Oceanogr 47:515–526
127. Anderson DM (1994) Red tides. Sci Am 271:52–58
128. Johansson N, Granéli E (1999) Cell density, chemical composition and toxicity of *Chrysochromulina polylepis* (Haptophyta) in relation to different N:P supply ratios. Mar Biol 135:209–217
129. Johansson N, Granéli E, Yasumoto T, Carlsson P, Legrand C (1996) Toxin production by *Dinophysis acuminata* and *D. acuta* cells grown under nutrient sufficient and deficient conditions. In: Yasumoto T, Oshima Y, Fukuyo Y (eds) Harmful and toxic algal blooms. IOC-UNESCO, Paris, pp 277–280
130. de Boer MK, Tyl MR, Vrieling EG, van Rijssel M (2004) Effects of salinity and nutrient conditions on growth and haemolytic activity of *Fibrocapsa japonica* (Raphidophyceae). Aquat Microb Ecol 37:171–181
131. Flynn KJ, Flynn K, John EH, Reguera B, Reyero MI, Franco JM (1996) Changes in toxins, intracellular and dissolved free amino acids of the toxic dinoflagellate *Gymnodinium catenatum* in response to changes in inorganic nutrients and salinity. J Plankton Res 18:2093–2111
132. Twiner MJ, Trick CG (2000) Possible physiological mechanisms for production of hydrogen peroxide by the ichthyotoxic flagellate *Heterosigma akashiwo*. J Plankton Res 22:1961–1975
133. Glibert PM, Terlizzi DE (1999) Co-occurrence of elevated urea levels and dinoflagellate blooms in temperature estuarine aquaculture ponds. Appl Environ Microbiol 65:5594–5596
134. Granéli E (2004) Toxic algae – a global problem. HavsUtsikt 2:12–13 (in Swedish)
135. Johansson N, Granéli E (1999) Influence of different nutrient conditions on cell density, chemical composition and toxicity of *Prymnesium parvum* (Haptophyta) in semicontinuous cultures. J Exp Mar Biol Ecol 239:243–258
136. Legrand C, Johansson N, Johnsen G, Borsheim KY, Granéli E (2001) Phagotrophy and toxicity variation in the mixotrophic *Prymnesium patelliferum* (Haptophyceae). Limnol Oceanogr 46:1208–1214

137. Ribalet F, Wichard T, Pohnert G, Ianora A, Miralto A, Casotti R (2007) Age and nutrient limitation enhance polyunsaturated aldehyde production in marine diatoms. *Phytochemistry* 68:2059–2067
138. Ceballos S, Ianora A (2003) Different diatoms induce contrasting effects in the copepod *Temora stylifera*. *J Exp Mar Biol Ecol* 294:189–202
139. Frost BW (1972) Effects of size and concentration of food particles on the feeding behavior of the marine planktonic copepod *Calanus pacificus*. *Limnol Oceanogr* 17:805–815
140. Turner JT, Ianora A, Miralto A, Laabir M, Esposito F (2001) Decoupling of copepod grazing rates, fecundity and egg hatching success on mixed and alternating diatom and dinoflagellate diets. *Mar Ecol Prog Ser* 220:187–199
141. Buttino I, De Rosa G, Carotenuto Y, Ianora A, Fontana A, Quaglia F, La Rotonda MI, Miralto A (2006) Giant liposomes as delivery system for ecophysiological studies in copepods. *J Exp Biol* 209:801–809
142. Buttino I, De Rosa G, Carotenuto Y, Mazzela M, Ianora A, Esposito F, Vitiello V, Quaglia F, La Rotonda MI, Miralto A (2008) Aldehyde-encapsulating liposomes impair marine grazer survivorship. *J Exp Biol* 211:1426–1433
143. Miralto A, Ianora A, Poulet SA, Romano G, Laabir M (1996) Is fertility modified by overcrowding in the copepod *Centropages typicus*? *J Plankton Res* 18:1033–1040
144. Armbrust EV, Berges JA, Bowler C, Green BR, Martinez D et al (2004) The genome of the diatom *Thalassiosira pseudonana*: ecology, evolution, and metabolism. *Science* 306(5693):79–86
145. Bowler C, Allen AE, Badger JH, Grimwood J, Jabbari K et al (2008) The *Phaeodactylum* genome reveals the evolutionary history of diatom genomes. *Nature* 456:239–244
146. Yang I, John U, Beszteri S, Glöckner G, Krock B, Goesmann A, Cembella AD (2010) Comparative gene expression in toxic versus non-toxic strains of the marine dinoflagellate *Alexandrium minutum*. *BMC Genomics* 11:248
147. Alpermann TJ, Tillmann U, Beszteri B, Cembella AD, John U (2010) Phenotypic variation and genotypic diversity in a planktonic population of the toxigenic marine dinoflagellate *Alexandrium tamarense* (Dinophyceae). *J Phycol* 46:18–32
148. Barofsky A, Vidoudez C, Pohnert G (2009) Metabolic profiling reveals growth stage variability in diatom exudates. *Limnol Oceanogr Methods* 7:382–390
149. Turnbaugh PJ, Gordon JI (2008) An invitation to the marriage of metagenomics and metabolomics. *Cell* 134:708–713
150. Sieg RD, Poulson-Ellestada KL, Kubanek J (2011) Chemical ecology of the marine plankton. *Nat Prod Rep*. doi:10.1039/c0np00051e
151. Izhaki I (2002) Emodin – a secondary metabolite with multiple ecological functions in higher plants. *New Phytologist* 155:205–217
152. Ianora A, Bentley MG, Caldwell GS, Casotti R, Cembella AD, Engström-Öst J, Halsband C, Sonnenschein E, Legrand C, Llewellyn CA, Paldavičienė A, Pilkaityte R, Pohnert G, Razinkovas A, Romano G, Tillmann U, Vaiciute D (2011) The relevance of marine chemical ecology to plankton and ecosystem function: an emerging field. *Mar Drugs* 9:1625–1648

Pei-Yuan Qian and Sharon Ying Xu

Contents

14.1	Introduction of Biofouling: Microfouling and Macrofouling	750
14.2	Methods of Assessment of Biofouling	754
14.3	Screening of Marine Natural Product as Antifoulants	755
14.3.1	General Strategies	755
14.3.2	Current Status	756
14.3.3	Selection of Marine Organisms for Chemical Extraction	759
14.3.4	General Extraction Procedures and Partition Methods	759
14.4	Methods for Screening Antimicrofouling Compounds	764
14.4.1	Antibacterial Assay	764
14.4.2	Antidiatom Assay	775
14.4.3	Antifungal Assays	778
14.4.4	Bacterial Challenge Culture	780
14.5	Antilarval Settlement and Antialgal Bioassay	781
14.5.1	Antialgal Assays	781
14.5.2	Antilarval Settlement Assays (Various Systems)	786
14.5.3	Antifouling Assays Using Larvae of Major Fouling Organisms	798
14.6	Methods of Antifouling Compounds Test	808
14.7	Mode-of-Action of Antifouling Compounds	808
14.7.1	Effects of Antifouling Compound on Gene Expression	809
14.7.2	Effects of Antifouling Compound on Protein Expression	811
14.8	Conclusions	815
14.9	Study Questions	816
References	816

P.-Y. Qian (✉) • S.Y. Xu

KAUST Global Collaborative Program, Division of Life Science, Hong Kong University of Science and Technology, Clear Water Bay, Hong Kong, China

e-mail: boqianpy@ust.hk

Abstract

With the global ban of application of organotin-based marine coatings by International Maritime Organization in 2008, there is a practical and urgent need of identifying environmentally friendly low-toxic and nontoxic antifouling compounds for marine industries. Marine natural products have been considered as one of the most promising sources of antifouling compounds in recent years. In antifouling compound screening processes, bioassay systems often play most critical/vital roles in screening efforts. To meet various needs, a variety of bioassay systems have been developed and/or adopted in both research and commercial laboratories. In this chapter, we provide a brief outline of common bioassay procedures for both antimicrofouling and antimacrofouling assays, which can serve as a general guideline for setting up bioassay systems in laboratories engaged in antifouling compound screening. Some bioassay procedures currently practiced in various laboratories are not included in this book chapter for various reasons. Individual laboratories should modify bioassay protocols based on their research interests or needs. Nevertheless, we highly recommend the research laboratories to adapt high-throughput assays as much as possible for preliminary screening assays, followed by more complex bioassay processes using multiple target species. We argue strongly for studies in mode-of-action of antifouling compounds against settling propagules, which shall lead to discovery of molecular biomarkers (genes, proteins, receptors, or receptor system) and will allow us to design more targeted bioassay systems.

14.1 Introduction of Biofouling: Microfouling and Macrofouling

Biofouling commonly refers to the undesirable accumulation of microorganisms, plants, algae, and animals on surfaces submerged in marine environments, particularly on the surface of ship hulls, fish cages and nets, and seawater intake systems. Although in natural environments, the biofouling process can also take place on innate surfaces, such as the surface of large marine organisms including sponges, corals, crabs, whales, and marine mammals, it is often termed as epibiosis. In fact, biofouling occurs on almost every exposed surface in natural environments other than marine, such as development of molds on walls, bacterial film on human teeth, microbial growth on membrane systems of bioreactors and desalinization systems. In general, we often classify the biofouling phenomena in aquatic systems into two types: microfouling and macrofouling.

Microfouling (Fig. 14.1) refers to the formation and development of biofilm on the surface. Biofilms are a conglomerate of organic molecules, bacteria, diatoms, fungi, and other microorganisms such as protozoans. Microfouling often begins with adsorption of dissolved organic matter to the surface within seconds of the initial exposure of a new surface to an aquatic system, which leads to formation of a very thin (about 100 nm) conditioning film – called molecular fouling [1].

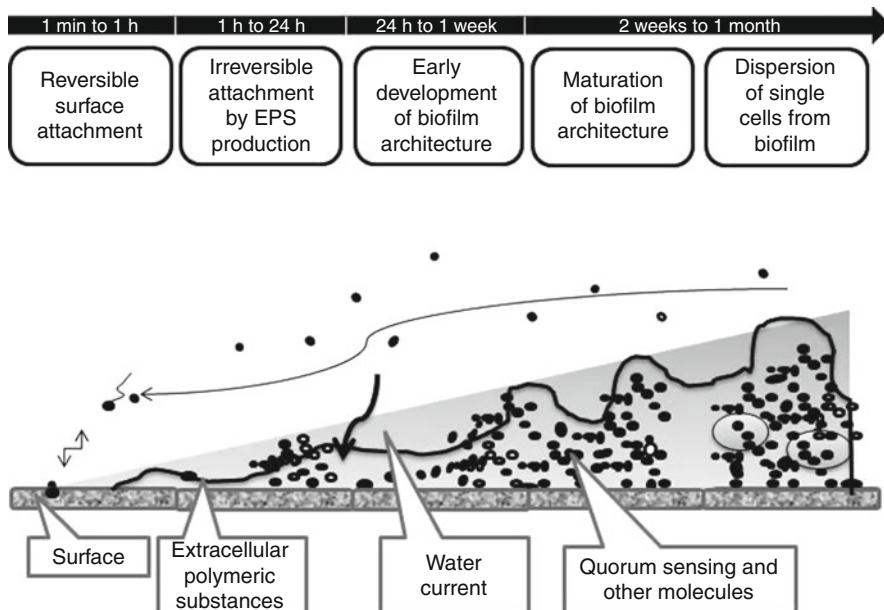


Fig. 14.1 The process of bacterial biofilm formation, showing attachment of bacteria, and extracellular polymeric substance (EPS) production. Quorum sensing and other molecules produced by bacteria are involved in the process. This figure is adapted from Fig. 3 on page 2 from Todar's Online Textbook of Bacteriology (Todar 2008), <http://textbookofbacteriology.net/normalflora2.html>

This thin film changes physical and chemical characteristics of the original surface [2], which, in turn, affects subsequent primary colonizers. Since bacteria often dominate the aquatic environment by number (besides viruses and macromolecules), they often attach to and interact with the conditioning film first. An early sequential model of biofilm development is thus primarily based on the relative abundance of each type of microfouling organisms in aquatic environment which follows the sequence of dissolved molecules > bacteria > fungi > diatom, protozoans, and algal spores. However, it is also apparent that physical and chemical characteristics of a new surface as well as behavior of settling microfoulers will also affect the early colonizers of the surface, which determines the development of a new biofilm [3].

Of course, the development of a biofilm is a continual process on any surface since microbial communities will go through continuous succession/evolution. Synergistic and/or competitive interactions among colonizers, together with the arrival of new recruits and/or loss of previous colonists, continuously shape the biofilm community [4]. Biofilm succession (development of microfouling) is influenced by physical and chemical conditions of the external environment as well as colonizers' physical and chemical conditions and behavior. The highly dynamic development and succession/changes of microbial communities in biofilms make it difficult for controlling microfouling processes in nature.

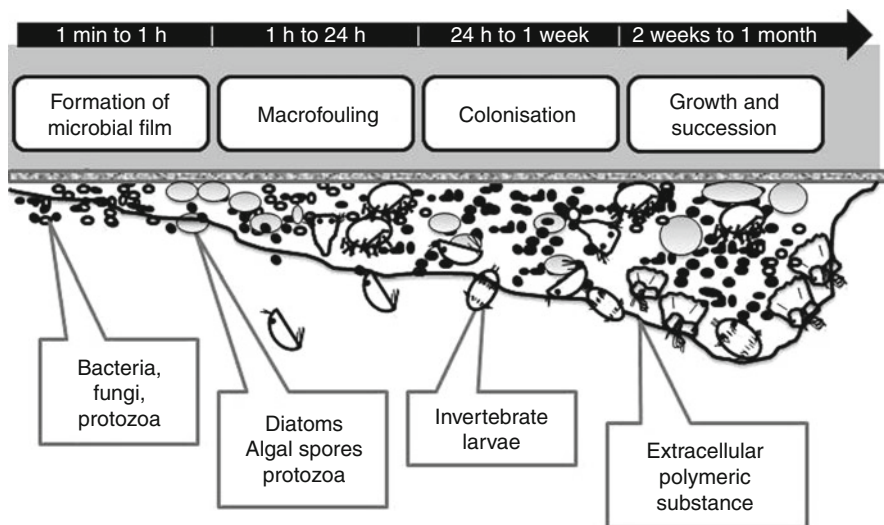


Fig. 14.2 The process of macrofouling, showing settlement and accumulation of primary settlers – bacteria, fungi, and protozoa followed by diatoms, spores of macroalgae, and larvae of marine sessile invertebrates. As with biofilm formation, EPS production is involved

Development of microfouling is also closely linked with marine corrosion since microbial metabolites released from the biofilm can corrode marine structures, which will not be discussed here as it is not the focus of this chapter.

Macrofouling refers to settlement of spores of macroalgae and larvae of marine sessile invertebrates and subsequent growth of these macroorganisms on marine surfaces. Accumulation of biomass of macroorganisms, such as seaweeds, mussels, oysters, calcareous tube-building polychaetes, clams, and barnacles that are often called as macrofoulers, is the real concerns of maritime industry and operation. In fact, some macrofouling species are small in size, but they can form enormous biomasses on ship hulls or in seawater intake systems that severely affect the performance of marine structure and system. Macrofouling often leads to substantial economic costs and operational challenges/difficulties in maritime industry, such as mariculture, shipping industry, naval vessels, power plants, and desalinization facilities. Therefore, how to control macrofouling has always been the top priority of the antifouling industry.

In summary, the development of biofouling community can be described as follows (Fig. 14.2).

Antifouling refers to the processes and means of controlling and/or preventing biofouling to take place or to clean up the biomass accumulation of fouling organisms, such as the control of biofilm development or preventing larvae or spores of macrofoulers from settlement on a new surface, and/or removal of biofilm and accumulated biomass of macrofoulers. For detailed information on pros and cons of different antifouling coatings, please see a nice review by Yebra et al. [5].

It is well known that larval or spore settlement of macrofoulers and their subsequent growth and development are affected by many factors, such as chemical and physical characteristics of marine surfaces, biophysical condition and behavior of settlers, hydrodynamics near the surface, physical, chemical, and biological environmental conditions. Due to complexity of interaction between macrofoulers and external environmental conditions, it is very difficult to stop the settlement process of settlers without using very destructive means (such as toxic antifouling compounds) in nature.

As biofouling has been a real challenge for as long as the history of human navigation at sea and in the rivers, antifouling technology was developed almost in parallel, which can be traced back to thousands of years. The ultimate goal of antifouling control is to stop the attachment of marine macrofoulers before they are allowed to grow on the ship hull surface. Before rapid industrialization era, raw materials, such as plant oil, tars, and brimstone, were commonly used as primary antifouling coating of ships and boats. In general, there were three major types: white antifouling coatings consisting of train oil, brimstone, and rosin; brown coatings consisting of tar, brimstone, and pitch; and black coatings consisting primarily of tar (giving the black color) and pitch. These coatings were proven to be very effective in protecting wooden structure from biofouling for a relatively long time. Of course, toxicity of these coatings was not the concern of navigation industry at that time (see Chapter 1 in [6]).

Metal-based antifouling coatings were proposed in the early seventeenth century when copper sheathing was suggested and finally applied to ship keels in the mid-seventeenth century. It was then discovered that copper-based antifouling coatings can effectively prevent the underwater structure from biofouling by seaweeds, worms, and mussels since copper can be oxidized and interact with chlorine in seawater to form toxic films that either deterred larval or spore settlement of macrofoulers or even killed the foulers coming close to ship hulls. Quickly, the British navy adopted copper-based coatings to their fleet, and the same or similar technology that was based on copper coatings was rapidly adopted by other industries. Since then, various types of metal-based coatings were developed and used until the discovery of tributyltin (TBT)-based coatings about half a century ago. TBT-based coatings were considered as the most cost-effective and non- or low-toxic antifouling coatings in the market for almost 40 years as it can effectively prevent attachment of macrofoulers at extremely low concentrations (at ng/L concentrations). Unfortunately, it was found in the 1980s that TBT can cause deformation of oyster shells at a concentration of 20 ng/L and imposex – development of male organs in female genitalia- in marine snails at 1 ng/L. TBT was also found to be accumulated through food chains and at high concentrations in marine mammals. These new discoveries led to the complete ban of organotin-based coatings by International Maritime Organization in September 2008 (although some countries still produce and apply them to marine structures at this point). Together with the ban of a number of toxic biocides, the marine coating industries are facing serious problems on what kind of coatings can be developed and marketed. At this point, many coating industries are forced to return to metal-based coating technology (with reduced metal concentrations) in combination with so-called booster biocides since

copper fails for some macroalgae. However, the environmental safety of most of those “booster biocides” has not been rigorously evaluated in the marine environment. These facts combine to demand for the discovery of nontoxic or low-toxic antifouling compounds. Developing alternative antifouling coating technology becomes an urgent but challenging issue, which calls for the rapid screening and discovery of marine natural products as non- or low-toxic antifouling compounds.

Besides chemical means of antifouling control, surface-polymer chemistry has recently been a major area of antifouling technology development, with the ultimate goal to create physical/chemical surfaces which weakens the strength of the attachment of settling spores, microbes, and larvae, so that these foulers will be washed away by the water flow (see reviews [5, 7]). The details will not be discussed here as it is not so relevant to the scope of this chapter.

As long as biofouling continues to develop on underwater structures, foulers need to be removed physically and the surfaces need to be repolished and repainted, which will not be discussed here either.

14.2 Methods of Assessment of Biofouling

Assessment of the biofouling condition of ship hulls, membrane filter systems (desalinization facilities), inside pipelines, and other underwater services is a very important step for developing antifouling control and maintenance strategies in maritime operations. Highly diverse methods and technologies have been developed to carry out biofouling monitoring, which vary based on practical needs. However, in general, the methods can be divided into two types based on the purpose of the assessment.

Methods of assessing microfouling which are commonly used to qualify and quantify biofilm development, particularly for bioreactor systems, membrane filter systems, and newly submerged surfaces [8] include (but do not exclude others that are not listed here):

- (a) Direct cell counting of bacteria, diatoms, algal spores, and other microscopic organisms under the microscope with or without staining methods
- (b) Counting the number of microbes (bacterial colonies) formed on agar plates with various culture media, and/or type of colonies and species
- (c) Determination of biomass, thickness, microbial density, and matrix of the biofilm under a confocal laser microscope
- (d) Determination of polymer matrix under atomic force microscope and 3-D structures of biofilms under scanning electronic microscope
- (e) Determination of biomass (wet weight, dry weight) or percentage of coverage of biofouling organisms within a given area
- (f) Determination of organic matter contents, proteins, lipids, hydrocarbons, ATP, or humic substances extracted from a harvested biofilm

As some of these methods are commonly used in antifouling bioassay systems, no details will be provided in this section, while others can be easily found in the literature.

Assessment of macrofouling involves routine monitoring of underwater marine installations, and most of these methods are relatively simple and easy to follow. They include:

- (a) Visual inspection of the seriousness of the fouling condition (either by naked eye, or video camera or camera imaging (which is particularly useful for pipeline inspection))
- (b) Determination of the percentage of coverage of surfaces
- (c) Determination of biomass and/or species composition (in terms of wet weight, dry weight, or numbers)
- (d) Determination of the thickness of fouling coverage
- (e) Determination of the attachment/adhesion strength of macrofouling organisms
- (f) Determination of the fouling rate, and so on

Again, these methods are not the real focus of this chapter and will not be reviewed extensively.

14.3 Screening of Marine Natural Product as Antifoulants

14.3.1 General Strategies

To screen marine natural products for effective antifouling compounds, the following general procedure is commonly practiced by different research groups, which can be divided into the following steps (Fig. 14.3):

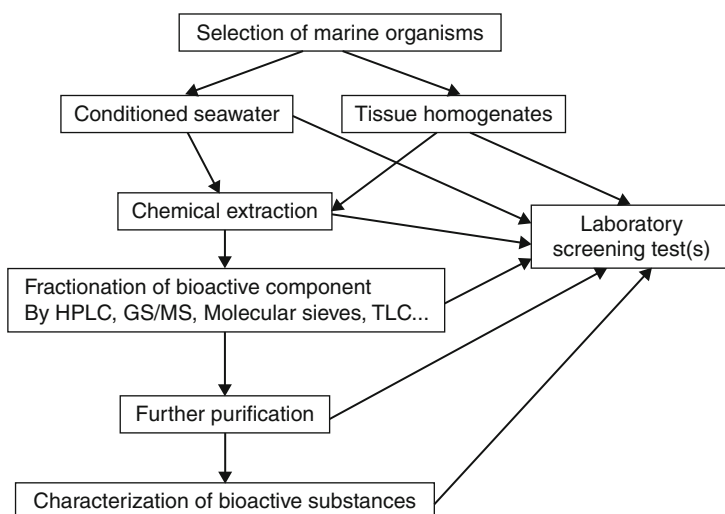


Fig. 14.3 General process for identification of natural antifouling compounds in marine natural products. Fractionation of bioactive components can be done through high-pressure liquid chromatography (HPLC), gas chromatography/mass spectrometry (GC/MS), molecular sieves, and thin layer chromatography (TLC)

1. Selecting marine organisms as a source of natural products
2. Obtaining sufficient raw biological materials through either fermentation (of microbes) or harvesting (of macroorganisms from either natural populations or marine farms)
3. Testing the antifouling potency of either conditioned seawater or homogenized tissues with screening bioassays
4. Extracting biomass with various solvents if the preliminary bioassay result is promising
5. Testing antifouling potency of various extracts with bioassay systems
6. Fractioning and partitioning extracts and identification of active fraction(s) based on bioassay results
7. Purifying bioactive compounds and testing their activities with bioassay systems
8. Characterizing chemical compounds using various instrumentation such as MS, NMR, X-ray, and so on
9. Confirming the bioactivity of the pure compound with further bioassays

14.3.2 Current Status

Screening of marine natural products for antifouling compounds has been a hot topic over the last few decades; many compounds isolated from marine invertebrates, seaweeds, and microbes showed promising activities, but so far, hardly any of those compounds have been commercialized as antifouling products due to various challenges (see reviews [9–11]). In total, about 200 compounds isolated from marine organisms have shown good antifouling activities against some major fouling organisms. These compounds are highly diverse in terms of molecular size, structure group, and solubility in seawater [9–11]. It is anticipated that more and more marine natural products will be patented as potential antifouling compounds each year as this area of research has been intensively carried out in recent years.

14.3.2.1 Natural Antifouling Compounds and their Synthetic Analogues

Over the last two decades, a considerable number of natural compounds have been reported to have antifouling activities from many marine organisms including sponges, algae, corals, as well as microorganisms. For some of these compounds, their structure–activity relationships have been extensively studied, and analogues with improved activity and reduced complexity of structure have been synthesized, which paves the way for future industrial application. Fusetani published a very nice book “*Antifouling Compounds*” in which many antifouling compounds isolated from marine sources were included. Herein, we will extract a few examples from that book about marine natural compounds and their synthetic analogues with pronounced antifouling activities. Please refer to the book for more in-depth reading as well as for the related references (Fig. 14.4).

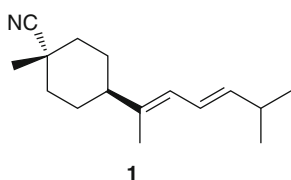
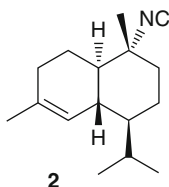
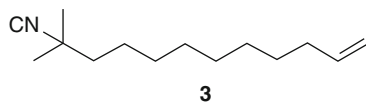
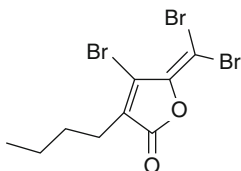
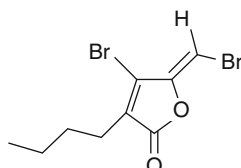
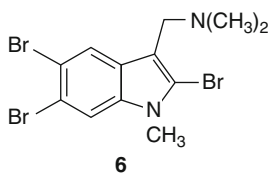
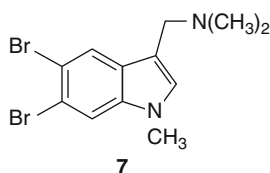
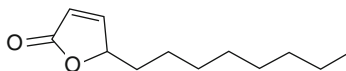

 $EC_{50} = 0.13 \mu\text{g mL}^{-1}$
 $LC_{50} > 100 \mu\text{g mL}^{-1}$

 $EC_{50} = 0.14 \mu\text{g mL}^{-1}$
 $LC_{50} > 100 \mu\text{g mL}^{-1}$

 $EC_{50} = 0.046 \mu\text{g mL}^{-1}$
 $LC_{50} > 30 \mu\text{g mL}^{-1}$

 $EC_{50} = 20 \text{ ng mL}^{-1}$

 $EC_{50} = 20 \text{ ng mL}^{-1}$

 $EC_{50} < 0.01 \mu\text{g mL}^{-1}$
 $LC_{50} > 1 \mu\text{g mL}^{-1}$

 $EC_{50} < 0.06 \mu\text{g mL}^{-1}$
 $LC_{50} > 0.6 \mu\text{g mL}^{-1}$

 $EC_{50} = 0.5 \mu\text{g mL}^{-1}$
 $LC_{50} > 50 \mu\text{g mL}^{-1}$

Fig. 14.4 Natural antifouling compounds and their synthetic analogues. EC_{50} values refer to their activity against barnacle cypris settlement. LC_{50} values refer to the half lethal concentration

A number of isocyano compounds (Fig. 14.4: 1–3) were isolated from the marine sponge *Acanthella cavernosa* and nudibranchs of the family Phillidiidae. These compounds show potent inhibitory activity against settlement of cypris of *Balanus amphitrite* without significant toxicity. Two compounds, 3-isocyanotheonellin and 10-isocyano-4-cadinene, have notable antifouling activity with EC_{50} values of 0.13 and 0.14 $\mu\text{g mL}^{-1}$, respectively, while their LC_{50} values are more than 100 $\mu\text{g mL}^{-1}$. Further structure–activity relationship studies and structural optimization led to the synthesis of a simple linear alkyl isocyanide whose EC_{50} was even lower than the original natural products. Field testing with this simple compound further proved its efficiency in controlling settlement of barnacles, ascidians, and bryozoans.

Halogenated furanones were isolated from red alga *Delisea pulchra*, and their ecological role and bioactivities were extensively investigated. These 2(5 *H*)-furanones showed excellent activities in preventing fouling of both macroorganisms and bacteria. In particular, they control bacterial fouling by interfering with the quorum sensing system in bacteria. Among these furanones, two compounds (Fig. 14.4: 4–5) can inhibit settlement of cypris of *Balanus amphitrite* with EC_{50} values around 20 ng mL^{-1} , which is 20 times more active than CuSO_4 . A large number of synthetic analogues of these furanones were screened for their bioactivity, and several of them are now in industrial uses for antimicrofouling and antimacrofouling purposes.

A heterocyclic compound, 2,5,6-tribromo-1-methylgramine (TBG) (Fig. 14.4: 6), was isolated from several marine bryozoans species. It showed remarkably strong antifouling activity with an EC_{99} of 0.03 $\mu\text{g mL}^{-1}$ against *B. amphitrite* cyprids. In subsequent studies, more than 150 gramines and related compounds were tested and compared for their antifouling compound, and 5,6-dichloro-1-methylgramine (DCMG) (Fig. 14.4: 7) was selected for further investigation because of its outstanding performance in antifouling assays. Field test and various toxicity tests were carried out for DCMG, and the results were quite satisfactory.

Other than marine macroorganisms, marine microorganisms are becoming a more important source for bioactive natural compounds. A group of simple butenolides were isolated from marine *Streptomyces*, and they showed moderate antifouling activity with EC_{50} values around 20 $\mu\text{g mL}^{-1}$. After localizing the functional group, Xu et al. had a simple alkyl butenolide (Fig. 14.4: 8) synthesized whose antifouling activity was greatly improved. In laboratory antisettlement assays, it could inhibit three major fouling organisms with EC_{50} values all less than 1 $\mu\text{g mL}^{-1}$, while its toxicity was quite low. In a field test carried out on a highly fouled fish farm, less than 5% of the compound (w/w) mixed with the basal paint could protect the surface from fouling for 3 months when compared to control surfaces which only had basal paint [99].

These examples give us confidence that it is promising to develop nontoxic antifouling compounds from marine-derived natural compounds. The marine environment, especially the microbes living in it, is an enormous untapped resource for us to find such treasures, and we shall be optimistic.

14.3.3 Selection of Marine Organisms for Chemical Extraction

The most important first step in antifouling studies is to select the right organisms as raw materials. Although there has not been a well-defined guideline for selecting marine organisms, for macroorganisms, we tend to select species that are:

1. Free of biofouling on their surfaces while their neighboring species are heavily fouled
2. Easy to be harvested in large biomass
3. Able to produce various chemical compounds as documented in the literature
4. Easy to be extracted with various chemical solvents (as some marine organisms that produce a large amount of mucous are very difficult to be extracted)
5. Not on the species list to be protected, and so on

For microorganisms, the species are often selected for further study after a preliminary screening bioassay. However, certain bacterial groups such as *Actinomyces* and microbes associated with sponges and corals are favorable targets.

14.3.4 General Extraction Procedures and Partition Methods

14.3.4.1 Extraction of Macroorganisms

Fresh marine macroorganisms are collected from the field (Figs. 14.5–14.7). The specimen is first washed with filtered seawater and then freeze-dried (alternatively, it can be dried in a fume hood). The dried specimen is homogenized and extracted by pure methanol for 24 h for three successive times. In addition, sonication can be included to assist the extraction of metabolites, but the temperature of the water bath must be controlled to avoid overheating the solvent. The combined methanol extract is evaporated under vacuum to generate the total organic extract (TOE). The TOE is subsequently extracted using distilled water (sample code W) and dichloromethane (sample code O as for organic). The W fraction is then partitioned using *n*-butanol (sample code WB). As butanol has a relatively high solubility in water, water-saturated butanol is preferred if a quantified extraction needs to be carried out. Inorganic salts are mostly present in the remaining water fraction (sample code WW), which is usually discarded. The dichloromethane, F fraction, is dissolved or sometimes suspended in 90% aqueous methanol and then partitioned using hexanes (sample code OH) to remove very lipophilic substances, such as lipids. The 90% aqueous methanol layer is then diluted to 50% aqueous methanol and partitioned using dichloromethane (sample code OD), and the remaining aqueous methanol is dried (sample code OM). This conventional lipid–lipid extraction and solvent partitioning is outlined in Fig. 14.5. Alternatively, some other routinely used partitioning schemes can be adopted, and a good example is the one described in [12].

In recent years, accelerated solvent extraction (ASE) has been occasionally adopted in extraction of marine macroorganisms and has proven to be an efficient

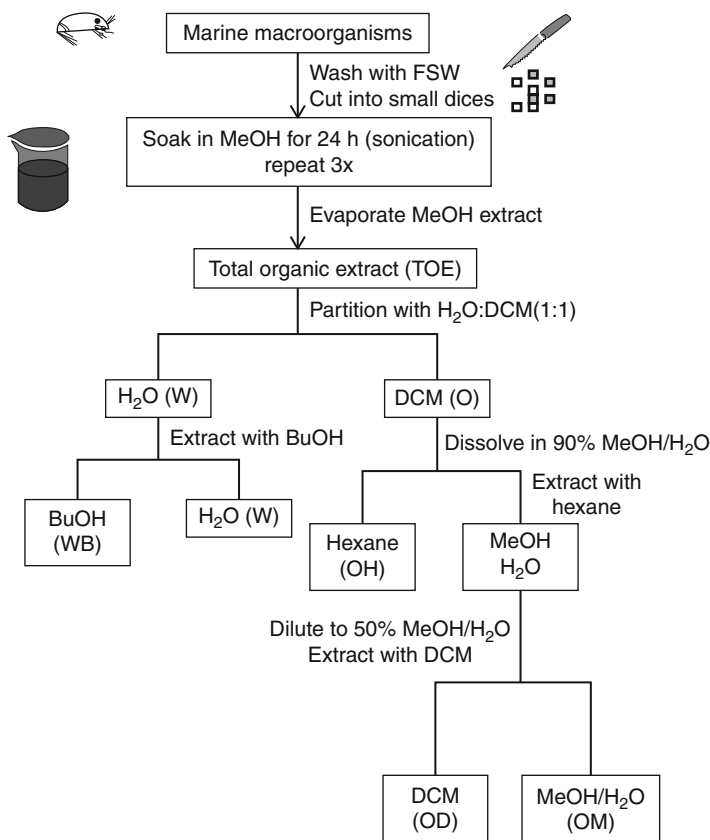


Fig. 14.5 Standard solvent partitioning of extracts of marine organisms, which is a conventional lipid–lipid extraction methodology. Abbreviations: *FSW* filtered seawater, *3x* three times, *MeOH* methanol, *DCM* dichloromethane, *BuOH* butanol

and environmentally friendly extraction method [13]. ASE employs higher pressure to keep the solvent at a temperature higher than its normal boiling point at atmospheric pressure. With higher temperature and reduced viscosity, the solvent is able to extract the specimen thoroughly in a very short period of time. Briefly, the specimen is loaded to an extraction cell in the ASE system and exposed to solvents at high temperature for a short period of time. Johnson et al. [13] first extracted 50 g of sponge sample using distilled H₂O to remove most of the inorganic salts. They then successively extracted the sponge sample with solvents that are routinely used in extraction, such as hexanes, dichloromethane, and methanol, which cover different levels of polarity. Moreover, at the end of each extraction, a purge with nitrogen dries the specimen so that less overlapping takes place between successive extractions. By using the ASE, Johnson et al. [13] demonstrated that the extraction efficiency of ASE is higher than conventional solvent extraction and partition.

Meanwhile, ASE requires much less time and labor. For example, grounding of the sample is unnecessary. However, researchers need to determine variables such as extraction temperature and time in order to optimize the extraction program and fulfill extra safety requirements. Nevertheless, ASE offers a new, efficient, and economically and environmentally friendly method.

14.3.4.2 Extraction of Microbial Cultures

Marine microorganisms – mainly bacteria and fungi – can be isolated from different marine habitats, such as seawater, sediments, surface and internal tissues of macroorganisms. Usually, a small-scale fermentation of isolated microorganisms is carried out and screened in specific antifouling bioassays. After the active strain is selected, a large-scale fermentation will be performed in order to isolate and characterize the pure compounds that exhibit the desirable antifouling activity. Most of the fermentation is carried out in liquid culture for a certain period of time, which is very critical for the production of the bioactive compounds. At the end of the fermentation, the first step is the separation of the microbial cells from culture medium, which is very important if one wants to know whether the bioactive compound is an extracellular or intracellular metabolite. This step usually can be done by either filtration or centrifugation depending on the nature of the microbial cells. For fungi, the easiest way is just to filter the whole liquid culture by several layers of cheesecloth. The filtrate is then extracted by liquid–liquid extraction using ethyl acetate or solid extraction using adsorbent resins such as Amberlite XAD-7 and Diaion HP20. The solid extraction method is preferred when dealing with a large-scale culture. The ethyl acetate extract or the eluent washed from the resin is then evaporated, and the obtained crude extract can then be processed using the standard solvent partition scheme described above. Metabolites associated with or inside the microbial cells are usually obtained by using methanol to extract the lyophilized mycelia or bacterial cells.

Sometimes, solid fermentation for microbes, especially for fungi, can be carried out. If the material is agar, then the agar plate/disk is usually cut into small pieces and extracted by 100% ethyl acetate or 80% ethyl acetate, 15% methanol, and 5% acetic acid. To achieve optimum extraction, the sliced agar and extraction solvent should be kept on a shaker for 24 h to increase extraction efficiency. The contents are then filtered and the filtrate is dried under vacuum on a rotary evaporator to obtain the crude extract for further separation and analysis. The work flow is described in Fig. 14.6.

14.3.4.3 Extraction of Volatile Metabolites

Volatile compounds are sometimes responsible for the chemical defense mechanisms of marine macroorganisms, such as sponges and algae. Volatile chemicals from bacteria or biofilms are involved in inducing or inhibiting larval settlement. To collect volatile chemicals, a simple closed-loop stripping apparatus (CLS) can be used according to Grob and Zürcher [14] and later modified by Harder et al. [15]. For macroorganisms, such as sponges, the sample will be first washed with filtered seawater and then submerged in filtered seawater in a clean

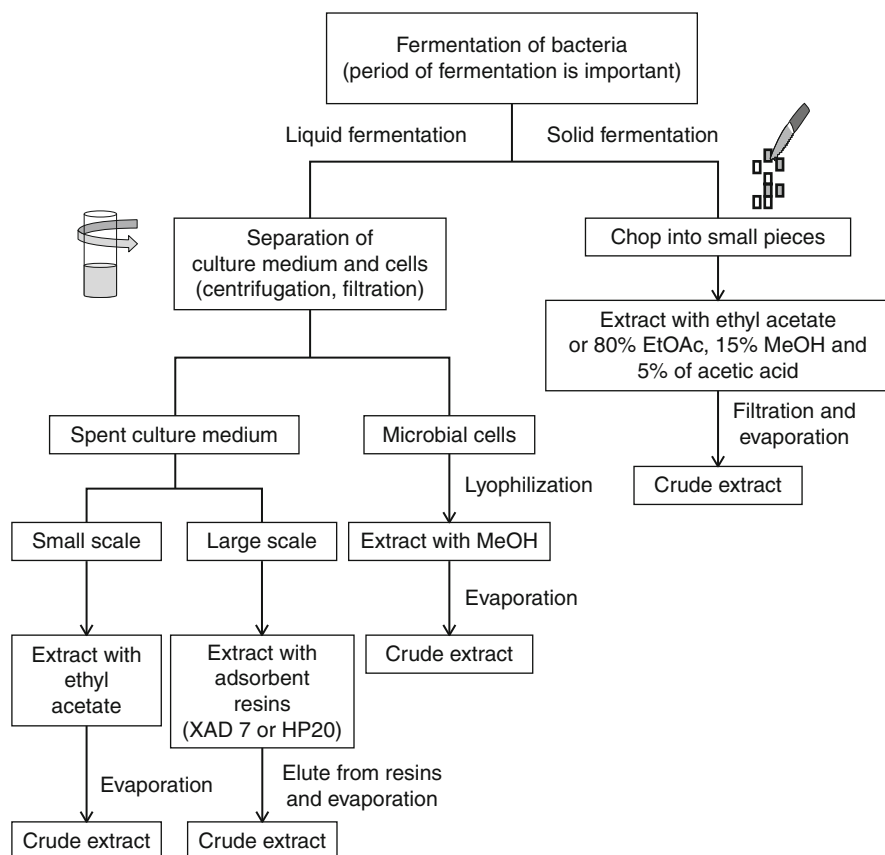
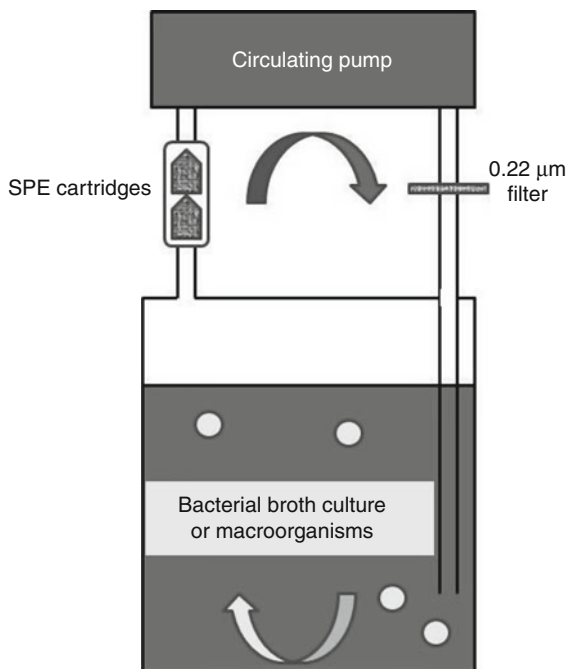


Fig. 14.6 Extraction workflow of marine microorganisms using fermentation to isolate and characterize pure compounds with antifouling activity

vessel. The closed loop will be formed by connecting the vessel to a pump generating air, a 0.22- μm membrane filter, and a solid extraction cartridge. A sketch of the apparatus is provided in Fig. 14.7. The air generated by the pump will pass through the membrane filter, enter the seawater which contains the macroorganism sample, and sweep volatile compounds out of the aqueous phase. The solid-phase extraction cartridge, which is commercially available in many forms, will absorb the volatile compounds. In addition, this system is also applicable for the extraction of volatile compounds from microorganisms. To do that, the seawater is replaced by sterile medium which is subsequently inoculated with microorganisms. In fact, the whole system becomes a mini-bioreactor with adequate aeration. After being absorbed, volatile compounds can be eluted from the cartridge using acetone, and then the constituents of the volatile compounds can be analyzed by GC-MS.

In recent years, a more advanced solid-phase extraction technique called Stir Bar Solid Extraction (SBSE) was developed by Baltussen et al. [16].

Fig. 14.7 Apparatus for extraction of volatile compounds. A closed loop is formed by connecting the vessel to a pump, a 0.22- μm membrane filter, and a solid-phase extraction (SPE) cartridge. This figure adapted from Harder et al. [15]



The main advantage of this technique is its high sensitivity, enabling identification of trace amounts of volatile compounds. Moreover, SBSE is a solvent-less, simple method which allows extraction and concentration in a single step. The principle of this method is to use a magnetic stir bar coated with a polydimethylsiloxane (PDMS) film. The PDMS-coated stir bar is firstly introduced into the sample (either gaseous or aqueous matrices), and a predetermined extraction method (extraction temperature, time and speed of stirring) is used to extract the compounds from the sample. Compounds are desorbed from the stir bar by thermal desorption using a commercial TDU (thermal desorption unit, Gerstel) with a programmed-temperature vaporization injector (Gerstel) and analyzed by GC-MS. The whole process can be done automatically, and high-throughput screening is therefore made possible. Many volatile compounds have been analyzed using this technique. Demyttenaere et al. [17] used SBSE coupled to GC-MS to analyze the organic volatile compounds produced by fungi and found that this technique is able to enrich compounds normally present in trace amounts. Therefore, this new technique could provide an alternative to traditional methods.

14.3.4.4 Extraction of Metabolites from Parts of Marine Macroorganisms (Also Applicable to Localization of Metabolites)

To isolate a natural antifouling compound, which really plays the same ecological role in protecting its host from biofouling (epibiosis), it is important to know where the metabolite is localized in the macroorganism. Many compounds with

antifouling activity have been isolated from sponges. However, to know if these compounds play a real antifouling role in nature will require more evidence, such as the localization of the compounds. Furthermore, as many marine invertebrates contain microbial symbionts, determining the origin of a secondary metabolite (from the host or the microbial symbionts) is also important in understanding its possible antifouling function in nature. Here we describe a method for extraction of a metabolite from different types of cells that is applicable to sponges, algae, and tunicates. The macroorganism sample is collected from the field and cleaned of debris, rinsed with calcium- and magnesium-free artificial seawater (CMF-ASW), pH 7.4 to replace the natural seawater. The tissue is then cut into small pieces using a razor blade and completely immersed in aerated CMF-ASW. After 2 h, the cloudy water which contains dissociated cells is filtered through a 100- μm nylon mesh using vacuum filtration to remove large spicules and cell aggregates. This step is repeated using a 50- μm mesh. The cells are then fixed in 3% glutaraldehyde in artificial seawater, pH 7.4, and left overnight at 4°C in the dark. The purpose of fixation is to protect dissociated cells from rupturing and to prevent aggregation of cells. Just prior to fractionation, the fixed cells are diluted with CMF-ASW, spun down at 600 g and 4°C for 5 min and then washed twice with fresh CMF-ASW to completely wash away the fixative. The fixed cell suspension is then fractionated according to density via centrifugation (600 g at ambient temperature) across discontinuous Percoll gradients, such as 20%, 40%, 60%, and 80% in CMF-ASW, or other gradients that have been predetermined. The bands of cells that accumulate at the density interfaces are then carefully collected by pipette and washed twice with CMF-ASW and centrifugation. The fractions can then be extracted by organic solvents such as dichloromethane and methanol and further separation and analysis of the extract can be done in the same way as described in previous sections. A flow chart is provided for reference in Fig. 14.8.

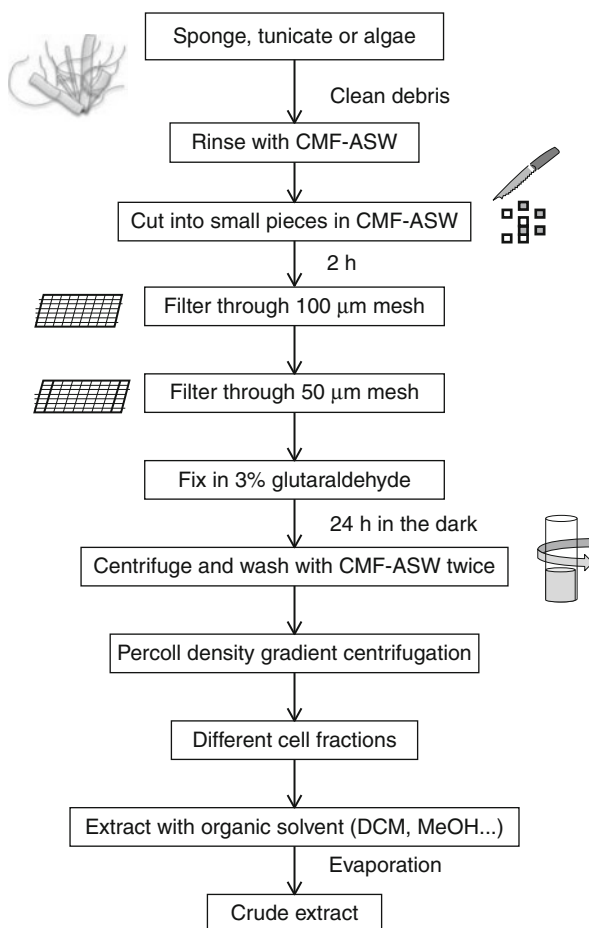
14.4 Methods for Screening Antimicrofouling Compounds

For microbial fouling on submerged surface, we need to control the attachment and growth of microbes, particularly bacteria (which are dominant components of biofilms), and biofilm formation and development. Therefore, antibacterial attachment and growth, antibiofilm formation, and quorum sensing bioassays are the most commonly used antimicrobial assays, while antifungal and antidiatom attachment and growth assays are often the secondary assays.

14.4.1 Antibacterial Assay

Antibacterial growth and attachment assays are the laboratory bioassays most commonly used for many decades and are primarily based on the performance of individual bacterial species/strains. Selection of bacterial species and strains is target-driven. For instance, pathogenic bacterial strains and species are commonly

Fig. 14.8 Extraction of metabolites from different types of cells in marine macroorganisms such as sponges, algae, and tunicates (also applicable to localization of metabolites). Abbreviations: *CMF-ASW* calcium- and magnesium-free artificial seawater



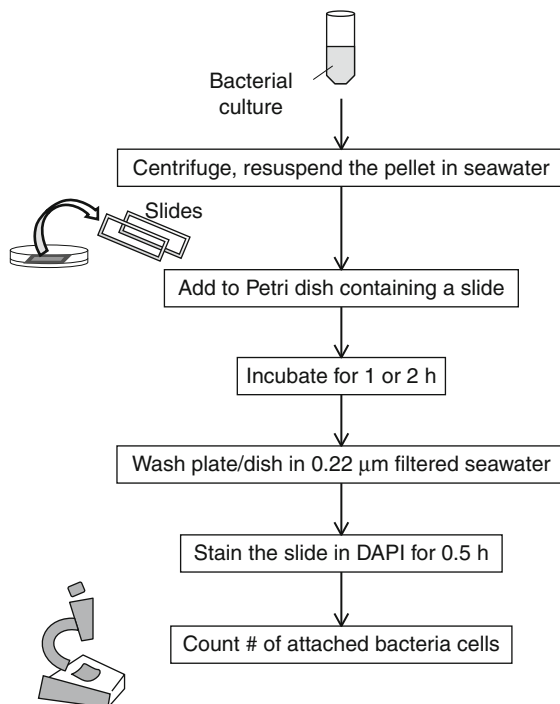
used in antibiotic screening (to be covered in other chapters). In general, for antimicrobial assay screening, the following characteristics can make bacterial species and strains ideal target organisms:

- Being the common and dominant ones in natural biofilms
- Having good motility
- Attaching quickly on an agar or exposed surface (such as glass or Petri dishes)
- Being stable under laboratory conditions (they do not mutate frequently)
- Being easy to grow and maintain in laboratory conditions
- Growing well on common bacterial culture media
- Forming a good biofilm
- Having the property either inducing algal spore attachment or larval settlement of marine invertebrates

Fig. 14.9 General antibacterial attachment assay. The treatment solution should contain the test solution of extract or compound, the negative controls should use a small amount of solvent used to dissolve the extract in the treatment, and the positive controls should use an antibiotic solution.

Abbreviations: *DAPI*

4',6-diamidino-2-phenylindole, a fluorescent stain that binds strongly to DNA



We have used the following species in our laboratory bioassays: *Loktanelia hongkongensis*, *Micrococcus luteus*, *Pseudoalteromonas* sp., *Rhodovulum* sp. (MB253), *Ruegeria* sp., *Staphylococcus haemolyticus*, *Vibrio fluvialis*, *Vibrio halioticoli*, *Vibrio* sp. (NAP-4), and 7 strains of common marine pathogens: *Moraxella phenylpyruvica*, *Pseudoalteromonas piscida*, *Shewanella algae*, *Vibrio alginolyticus*, *Vibrio furnissii*, *Vibrio harveyi*, and *Vibrio vulnificus*.

Stock culture of selected bacterial strains to be used for bioassays is obtained from either bacterial culture collections or from a research laboratory deposit and inoculated into sterile culture broth (with a suitable culture medium, which can be species specific in order to provide optimal growth, attachment, and performance of the test species) and grown at a defined temperature until the culture reaches its stationary phase. Suspended bacteria are harvested by centrifugation and diluted in autoclaved FSW to an optical density of 0.1 at a wavelength of around 600 nm or optimal density for the bioassays described in following sections.

14.4.1.1 Antibacterial Attachment

Various antibacterial attachment assays have been developed and applied. Here, we only introduce one protocol. Other methods such as bacterial attachment onto agar surfaces and Petri dish surfaces more or less follow the following steps (Fig. 14.9):

- Adding bacterial suspension into a Petri dish containing a acid-washed slide
- Incubating for a desired period of time

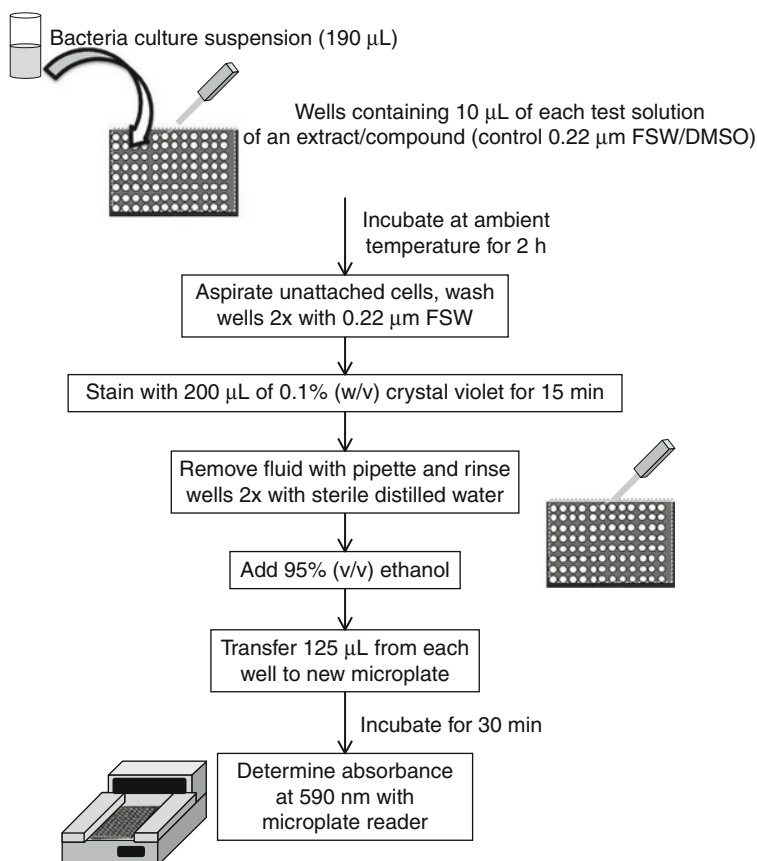


Fig. 14.10 Anti-adhesion/attachment assay in microplates for bacteria

- Washing the plate or dish in 0.22- μm filtered seawater
- Staining the slide in DAPI for 0.5 h
- Counting the number of attached bacterial cells in at least 10 fields of view under an epifluorescence microscope

In these assays, for treatment, the test solution of extract or compound is either incorporated into the agar plate or added directly into Petri dishes; for the negative controls, the small amount of solvent that is used to dissolve the extract is added instead; for the positive controls, antibiotic solution will be used.

Anti-adhesion/attachment assay in microplates (Fig. 14.10): Ten μL of DMSO or solution of dissolved extracts/compounds in seawater is placed into each well of a 96-well microplate containing 190 μL of diluted bacterial culture suspension and incubated at ambient temperature for 2 h. Unattached cells are then aspirated off, and wells are washed twice with sterile 0.22- μm filtered seawater. Attached bacterial cells are stained with 200 μL of 0.1% (w/v) crystal violet for 15 min at room temperature. The fluid in each well is removed with pipette, and the wells

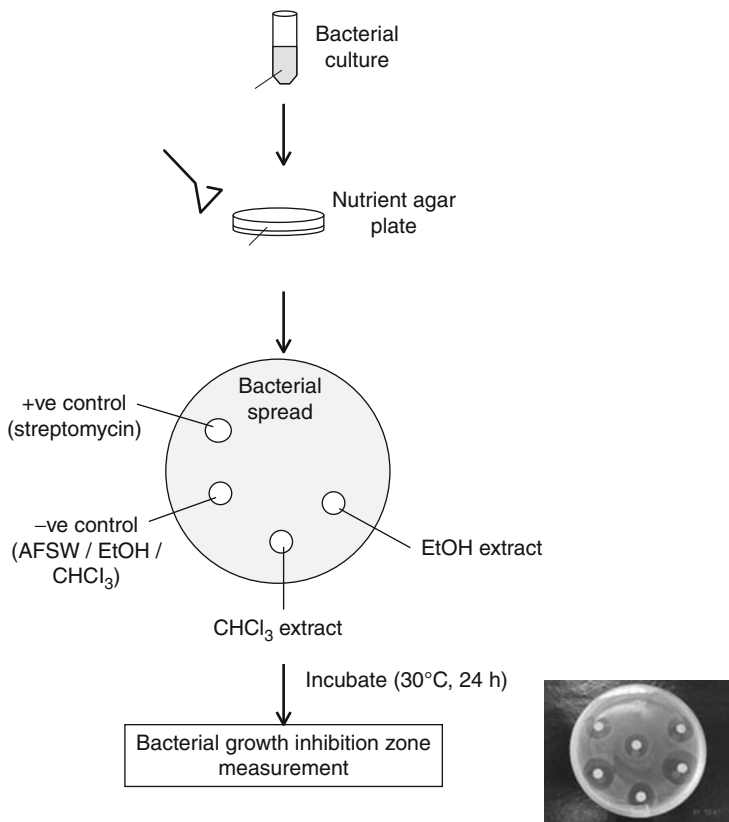


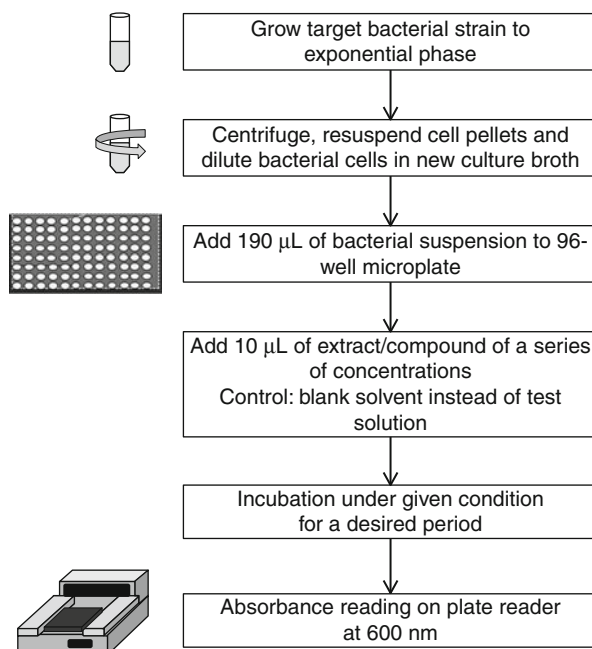
Fig. 14.11 Disk diffusion assay to test antibacterial property of chemical extract or compound against target bacterial strains. Abbreviations: +ve positive, -ve negative, *EtOH* ethanol, *CHCl₃* chloroform

are rinsed twice with sterile distilled water. A solution of 95% (v/v) ethanol is added to the wells and incubated for 30 min. The contents are briefly mixed, and 125 μL of the ethanol containing solubilized crystal violet is transferred to the wells of a new microplate. Afterward, the absorbances of the wells are read at 590 nm in a microplate reader. As a control for treatment, 10 μL of DMSO or sterile 0.22- μm filtered seawater can replace the test solution in the wells and incubated for 2 h. Wells are washed, stained, and read as above.

14.4.1.2 Antibacterial Growth

Disk Diffusion Assay (Fig. 14.11): A standard disk diffusion assay can be used to test the antibacterial property of a chemical extract or pure compound [18–20] using target bacterial strains. For antimicrofouling testing, we recommend using bacterial strains that can induce attachment of dispersing propagules of marine seaweeds or invertebrates or a dominant species in natural biofilms [3]. Each sterile

Fig. 14.12 Microtiter bioassay using bacteria, using a 96-well polystyrene cell culture plate with flat bottom, for screening for drugs and antibiotics



filter paper disk (Whatman No. 1; 6 mm in diameter with disk volume = 20 mm³) is prepared and loaded with a given volume (usually less than 20 µL for a disk with a diameter about 6 mm) of the test extract or compound dissolved in a solvent (such as acetone which can easily be evaporated and be able to dissolve the extract or compound); the amount loaded onto each disk is dependent on potency of the extract and compound. After evaporation of the solvent, the paper disk is placed onto agar plates (plastic Petri dishes) that have already been spread with a culture suspension of a test bacterium prepared, as described above. Again, agar medium is suitable for bacterial growth. Two disks, one containing streptomycin at a concentration of 10 µg disk⁻¹ and one pretreated with the same solvent, may serve as the positive and negative controls, respectively. There should be at least three replicates for each test concentration of the chemical extract or compound. The plates are incubated at a temperature suitable for the test bacterium to grow as a confluent film on the agar. The diameter of bacterial growth inhibition zones or halos (growth inhibition zones between the disk and the unaffected bacterial lawn) is recorded to the nearest 0.5 mm and compared.

Microplate reader assay [21] (Fig. 14.12): Microtiter plate bioassay (96-well polystyrene cell culture plate with flat bottom) for antibacterial growth is the common method for screening for drugs and antibiotics and has been covered in other chapters of this book; therefore, we will not give a very elaborate account on this method. Briefly, a bacterial culture suspension prepared above is further diluted in the broth medium to a concentration ranging from 0.5×10^3 to 2.5×10^3 CFU mL⁻¹.

Each well of the plate is filled with 175 μL of bacterial culture. To each well, 20 μL solution of the test extract or compound, or the appropriate solvent or antibiotic solution is added as the treatment or negative or positive controls, respectively. The plates are incubated for a desired period of time. The turbidity of each well is determined by running the entire plate through an automatic multiple plate reader. The relationship between turbidity and cell density of bacteria can be determined easily as the number of bacterial cells in a well can be counted with a Flow Cell Cytometer.

In fact, there are numerous types of antibacterial growth assays developed by various groups for various purposes, which can be modified for antimicrofouling compound screening. We have no intention to provide an exhaustive list of such assay protocols here.

14.4.1.3 Antibiofilm Formation

Biofilm development assessed by Laser Confocal Microscopy (Fig. 14.13): A pure bacterial culture at stationary phase of the test species or strain is centrifuged ($3,000\times g$, 10 min) first, and bacterial cell pellets are resuspended in autoclaved 0.22-mm filtered seawater (FSW) to achieve an optical density of 0.15 at 600 nm. Four mL of the suspension is then added to a polystyrene Petri dish (diameter, 50 mm; Falcon no. 1006) [22]. Each Petri dish contains an acid-washed glass slide. A small volume ($<40\ \mu\text{L}$) of a test solution (usually DMSO) of the extracts or compounds is then added to the Petri dish. After incubation at a suitable temperature for a desired period of time (bacterial species-dependent), biofilm biomasses are determined indirectly by quantification of acridine orange (Sigma, USA) which is used to stain the biofilm according to the method described by Genevaux et al. [23] with slight modifications. Briefly, the glass slides covered by biofilms are rinsed three times with AFSW, incubated in $50\ \mu\text{g mL}^{-1}$ acridine orange in the dark for 10 min, and then rinsed again by AFSW. Acridine orange from stained biofilms is then redissolved with 3-mL ethanol, and its fluorescence is measured spectrophotometrically at 430 nm.

Biofilms on the glass slides are stained with fluorescein isothiocyanate-conjugated (FITC) concanavalin A (Sigma, USA; concentration = $1\ \text{mg mL}^{-1}$) for 30 min in the dark. Then the biofilms are rinsed in AFSW before being viewed under a Nikon C1 Confocal Microscope (Japan). The argon laser line at 488 nm for scanning excitation and a 515–565 nm band-pass filter is used to detect green-fluorescence emission signals. The alignments of the laser and monitor setup are checked according to the manufacturer's instructions. Samples are observed under $40\times$ (dry: NA 0.75) and $100\times$ (oil immersion: NA 1.4) lens, with the latter used for image acquisition. EZ-C1 software is used to generate pictures and data through the biofilms. The threshold value is set manually and retained for all sections in the same plane. Biofilm biomass, cell density, and thickness are compared among treatments and the control.

Gel-based assay [24] (Figs. 14.14, 14.15): The immobilization of chemical extracts or compound under test in agar gel or phyto gel was originally developed for both laboratory and field assays for chemical defenses against

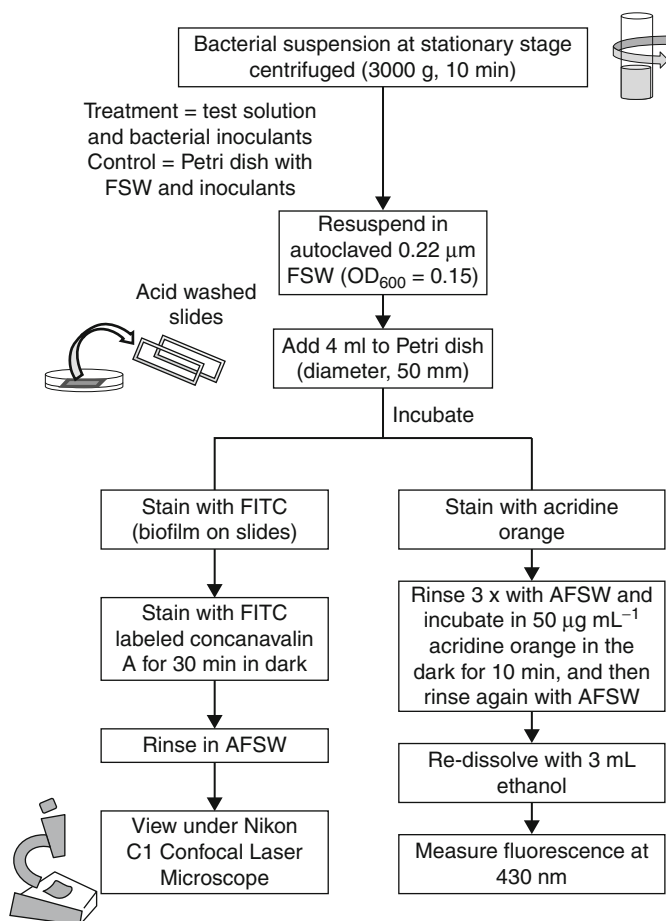
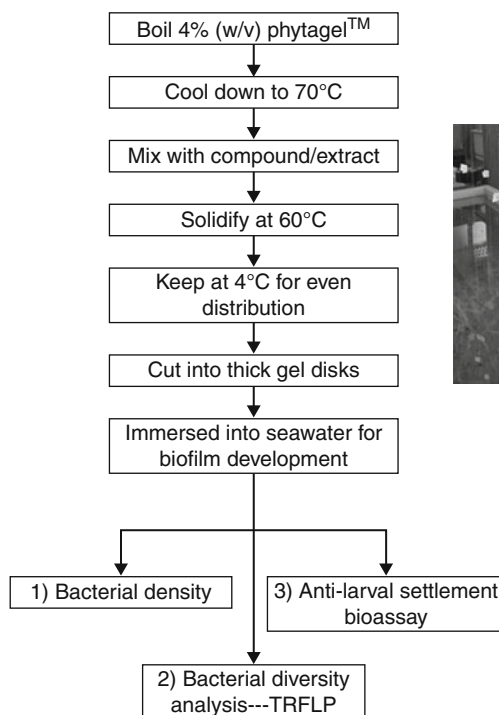


Fig. 14.13 Antibiofilm development assay, which can be assessed by Laser Confocal Microscopy. Abbreviations: *FITC* fluorescein isothiocyanate-conjugated concanavalin A

fish predation [25]. This method has at least the following advantages over the conventional antibacterial assays: (1) a culture-independent approach, i.e., there is no bias with respect to the choice of ecologically relevant test bacteria because the gels are exposed to a natural assemblage of microbial colonizers, (2) no restriction to particular modes of inhibitory microbial colonization, i.e., antibiotic and/or repellent, (3) extracts are incorporated into gels at presumably natural volumetric concentrations, (4) extracts within the gel matrix do not alter the physical characteristics of the settlement surface, (5) the ability to perform this assay under flow conditions, and (6) avoiding problems associated with laboratory assays such as unrealistic water flow and exposure to only one or a few species of test organisms. In addition, as assay gels contain a concentration of chemical extract or pure compound that decreases with time, this technique should provide conservative

Fig. 14.14 General procedure of assay using Phytogel to screen for antifouling activity, with microbial community structure and biomass of biofilm as end points. Abbreviations: *TRFLP* terminal restriction fragment length polymorphism



evidence of antifouling activity. As such, our research team developed a phytogel assay that can be used to screen for antifouling activity, using microbial community structure and the biomass of biofilm as end points.

The chemical extract/compound is dissolved in DMSO to test concentrations and transferred into sterile 50 mL Corning tubes. Gels are prepared by adding Phytogel™ (Sigma Chemical) into a stirred beaker of boiling distilled water to yield a 4% (w/v) gel concentration. After the gel solution is cooled to 70°C, the test solution in DMSO is vigorously mixed with the liquid gel solution in corning tubes to evenly distribute the extract/compound in the viscous hydrogel. Due to the high boiling point of DMSO (189°C), the extract volume will remain constant during this procedure. A control can be prepared accordingly with pure DMSO instead of test solution. The closed tubes are turned upside down and allowed to slowly solidify in a water bath at 60°C. After 5 min, the trapped air bubbles will migrate out of the solution yielding a transparent gel cylinder. The cylinders should be kept at 4°C overnight to allow for a homogenous diffusion of test solution through the gel. Subsequently, cylinders are removed and sliced into 5-mm-thick gel disks with a sterile razor blade. The gel disks are pierced with fishing line and anchored 10 cm below the water surface in individual 10 L aquaria that are continuously supplied with natural seawater from the same source at a flow rate of 60 Lh⁻¹. To avoid potential cross contamination of experiments by leached test solution, only the experimental gels of the same group are kept in the same

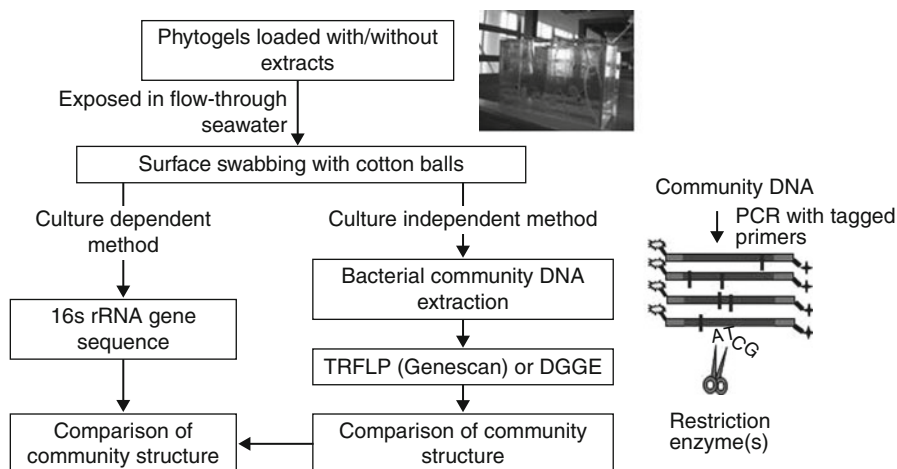


Fig. 14.15 Procedure to analyze community structure using Phytogel assay. Abbreviations: *PCR* polymerase chain reaction, *DGGE* denaturing gradient gel electrophoresis

aquarium. After a 48-h exposure to natural seawater, the phytogel disks are retrieved to determine bacterial and diatom density, and for microbial community structure analysis. For bacterial counts, phytogels (3 replicates per treatment or control) are fixed in 4% formaldehyde in seawater, and the bacterial density is determined under a microscope after DAPI staining. The surfaces (6 cm²) of each of the other three disks are swabbed with sterile cotton buds for the collection of epibiotic microbes. Swabs from each gel will be individually suspended in 0.8-mL extraction buffer (100 mM Tris-HCl, 100 mM EDTA, 100 mM sodium phosphate, 1.5 M sodium chloride, 1% CTAB; at pH 8) in 2-mL microcentrifuge tubes [26]. To lyse the cells, the samples are subjected to three cycles of freezing and thawing followed by 2 h incubation in 20% SDS at 65°C. Cotton buds are removed, and the total DNA is extracted with an equal volume of 24:1 chloroform:isoamylalcohol followed by precipitation in isopropanol at room temperature for 15 min. The precipitated DNA is washed with cold ethanol and resuspended in 50 µL of autoclaved double-distilled water and frozen until use.

PCR of 16 S rRNA genes (rDNA) in bacterial community DNA is performed according to method described in [26]. Fluorescently labeled PCR products are purified and analyzed using TRFLP or DGGE methods [26, 27]. Microbial community structures among the treatments and controls are compared accordingly [26, 27], for which the protocols and procedure are not discussed in details.

14.4.1.4 Antiquorum Sensing Bioassay

Quorum sensing (QS) molecules produced by marine bacteria are very important for development of bacterial films, and blocking production of QS molecules can lead to prevention of biofilm formation. Therefore, screening for quorum sensing blockers is a valuable way for controlling biofilm development. Over the last

30 years, several strategies with various QS blocker screening assays have been developed, and there is a very good review on this topic [28]. A general strategy is to expose a biosensor strain to test solution that may or may not cause a loss of signal response. Alternatively, a wild-type strain containing a QS-regulated phenotype can be used as a biosensor and grown in liquid media before being added into microtiter plate wells containing test solution of an extract or compounds. Changes in pigmentation of bacteria can be probed at a given time during or after incubation.

In a QS blocker screening assay, the most important first step is to select appropriate reporter strains. Although many species have been used for such a purpose [28], two bacterial species are commonly used: *Chromobacterium violaceum* [29] that produces purple violacein and pigmented *Pseudomonas aureofaciens* strain 30–84 that produces orange phenazine [29]. The QS blocking activity can be observed via a loss of their colorful pigmentation, which can be detected by eye and quantified by spectrophotometers.

Here, we will only introduce two basic methods.

Microplate assay (modified from [30–32]) (Fig. 14.16): *Chromobacterium violaceum* CV026, which is a mini-Tn5 mutant of the wild-type strain, is not able to produce the purple pigment violacein. Its violacein production is dependent on external addition of *N*-hexanoylhomoserine lactone (HHL). To screen for quorum sensing blockers, strain CV026 is grown to the stationary phase in culture medium containing 0.5% yeast extract and 1% tryptone. One hundred μL of bacterial culture is added into each well of 96-well microplates (with flat bottom). Then *N*-hexanoylhomoserine lactone (optimal concentration: 3.7×10^{-8} M for violacein induction) and 5 μL of DMSO containing an extract/compound is added into the well, respectively. The wells without test solution but with HHL and without HHL serve as the positive and negative controls. After exposure for 16 h at 27°C, the microplate is centrifuged at 13,000 *g* for 10 min to precipitate the insoluble violacein. The culture supernatant is then discarded, and 200 μL of DMSO is added to the pellet. The solution is then vortexed vigorously for 30 s to completely solubilize violacein and centrifuged at 13,000 *g* for 10 min to remove the cells. One hundred μL of the violacein-containing supernatants is then transferred to the wells of a new 96-well flat-bottomed microplate where the absorbance can be recorded with a microplate reader at a wavelength of 585 nm.

Agar overlay technique (Fig. 14.17): QSI indicator bacterial strains such as *Chromobacterium violaceum* 12472 and *Pseudoalteromonas aureofaciens* 30–84 are grown overnight in LB broth [29]. Following overnight growth, the test solution is placed onto an LB agar plate and then overlaid with LB soft agar containing the indicator organism. After incubation, the production of color around the bacterial colonies is observed.

In the case of screening for QS blocker producing bacteria, the test bacterial strains are streaked to the central part of LB agar plates and allowed to grow overnight. Alternatively, several test strains can be streaked onto one agar plate for high-throughput screening. After overnight growth, 5 μL of the organisms is vigorously mixed with 5 mL of molten LB soft agar of the indicator organisms

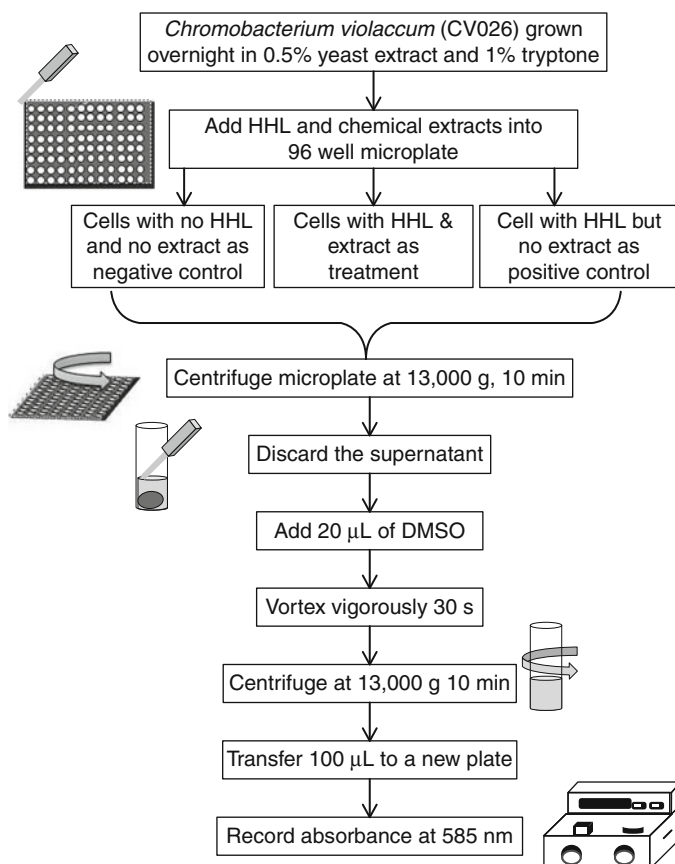


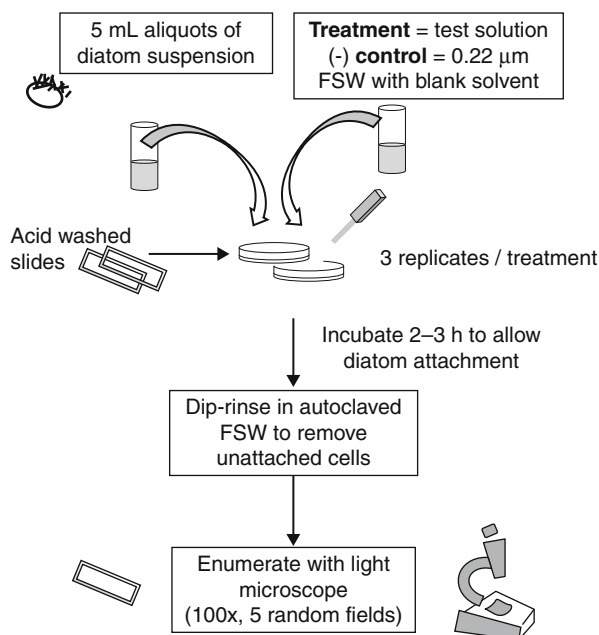
Fig. 14.16 Microplate assay for quorum sensing blockers using reporter bacterial strain *Chromobacterium violaceum* CV026. This strain is unable to produce the purple pigment violacein, so violacein production is dependent on an external addition of *N*-hexanoylhomoserine lactone (HHL). This figure is adapted from McLean et al. [28]

C. violaceum ATCC 12472 [29] or *P. aureofaciens* 30–84 and quickly overlaid onto the agar containing the testing bacterial strain. After incubation, a positive QSI result can be detected by the growth of living, but nonpigmented indicator organisms in the vicinity of the test organism.

14.4.2 Antidiatom Assay

Diatoms are common microfouling organisms and one of major component of marine biofilm [33]. The diatoms in biofilm can release inductive and/or inhibitive materials for spore and/or larval settlement of macrofouling organisms, in addition to causing microfouling problems. Therefore, controlling diatom

Fig. 14.18 Antidiatom attachment assay, with three replicates per treatment and 0.22- μm filtered seawater used in place of testing solution for negative control



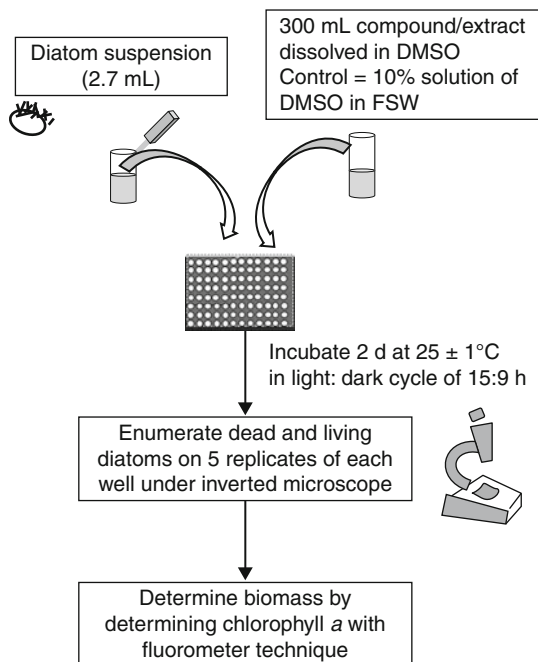
14.4.2.1 Antidiatom Attachment

Briefly, 5-mL aliquots of the suspensions are added into sterile Petri dishes each containing an acid-washed glass slide. In the negative control, only 0.22- μm filtered seawater is added while in the treatment, test solutions are added (Fig. 14.18). There should be at least three replicates per treatment. After incubation for 2–3 h (depending on species) to allow diatom cells to attach, filmed glass slides are dip-rinsed in autoclaved FSW to remove unattached cells. Diatom cells on glass slides are enumerated by light microscopy at a magnification of 100X in 5 randomly chosen fields of view (Zeiss Axiophot; $\lambda_{\text{Ex}} = 359 \text{ nm}$, $\lambda_{\text{Em}} = 441 \text{ nm}$) [35] or are counted using image analysis similar to that described for algal spore attachment in Sect. 5. The effect of the extract/compound on attachment of diatoms is determined by comparing the result of each treatment with that in the control. For cell detachment assays, slides are exposed to shear stress also according to the methods described for testing algal spore adhesion strength in Sect. 5. Percentage removal of diatom cells will be calculated accordingly [36].

14.4.2.2 Antidiatom Growth

Prior to the experiment, an extract or compound is dissolved in DMSO to a given concentration (Modified from [33]; Fig. 14.19). Three hundred μL of the test solution is added to each Petri dish or each well of a multiwell plate that contains 2.7 mL of diatom suspension (about $2 \times 10^5 \text{ cells mL}^{-1}$). A 10% (v/v) solution of

Fig. 14.19 Antidiatom growth assay. This figure is adapted from Dobretsov et al. [33]. Abbreviations: *DMSO* dimethylsulfoxide



DMSO in filtered (pore size 0.22 μm) seawater (FSW) is used as a control. The dishes or plates are incubated for 2 days at $25 \pm 1^\circ\text{C}$ at a light:dark cycle of 15:9 h. Then, the numbers of dead and living diatoms are counted on 5 replicates of each well or dish under an inverted microscope. Empty diatom shells are treated as dead diatoms and those with distinct chloroplasts are considered as live ones. In addition, the amount of *chl a* of each Petri dish or well can be determined by a fluorometer technique [37] as an indication of the diatom biomass.

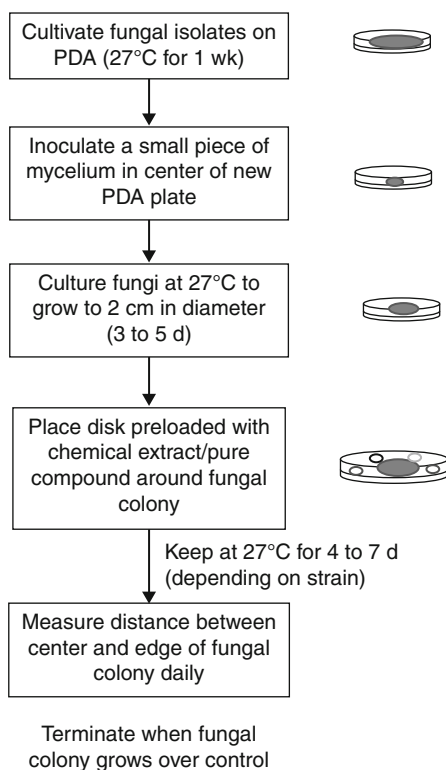
14.4.3 Antifungal Assays

Fungal strains/species isolated from marine biofilms are used as test organisms, and selection criteria are similar to those outlined for selection of bacteria species/strains in Sect. 4.1.

14.4.3.1 PDA Plating Assay

Prior to each assay, selected fungal isolates are cultivated on a PDA (potato dextrose agar, Sigma) plate at 27°C for 1 week or other culture media under a given culture condition, depending on species to be tested (Fig. 14.20). A small piece of mycelium is then inoculated in the center of a new PDA plate. The fungi is cultured at 27°C and allowed to grow to 2 cm in diameter (3 to 5 days). An autoclaved paper disk loaded with the test solution of a chemical extract or pure compound is then placed around the fungal colony (1 cm to the edge of the

Fig. 14.20 Antifungal assay using potato dextrose agar (PDA). This figure is adapted from Miao and Qian [20]



fungal colony) and kept at 27°C for 4 to 7 days, depending on the growth rate of the fungal strain. For the control, 5 μL of the blank solvent without extract/compound is used. For screening for bacteria with antifungal activity, bacteria strains can be directly inoculated near the fungal colony. The assay is terminated when the fungal colony grows over the control. The distance between the center and the edge of the fungal colony is measured daily. The inhibition of fungal growth is determined by comparing the radii of the fungal colony under the treatment and control conditions [20].

14.4.3.2 Microtiter Plate Assay

Prior to assay, fungal strains are cultured with a suitable culture medium under a given culture condition, and the commonly used culture medium often consists of yeast extract, soluble starch, and agar. After inoculation for several days, the conidia are collected by a sterile swab, suspended in filtered seawater, filtered to get rid of the mycelia, and adjusted to 1×10^4 to 5×10^4 CFU mL^{-1} of conidia by adding sterilized 0.22- μm filtered seawater. Two hundred μL of the conidia suspension is allocated to each well of a microplate. Ten μL of the extract/compound dissolved in DMSO is added to each well. A selected antibiotic chemical is used as positive control. The assay plates are incubated at 27°C until the shape of fungal growth can be observed and compared with the controls under an inverted microscope [38] (Fig. 14.21).

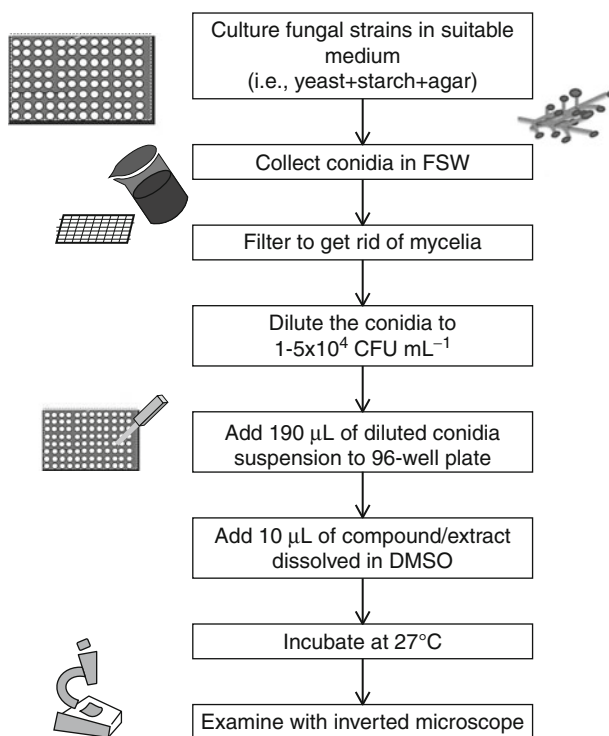


Fig. 14.21 Antifungal assay using a microtiter plate. This figure is adapted from Byun et al. [38]. Abbreviations: *CFU/mL* colony forming unit per milliliter

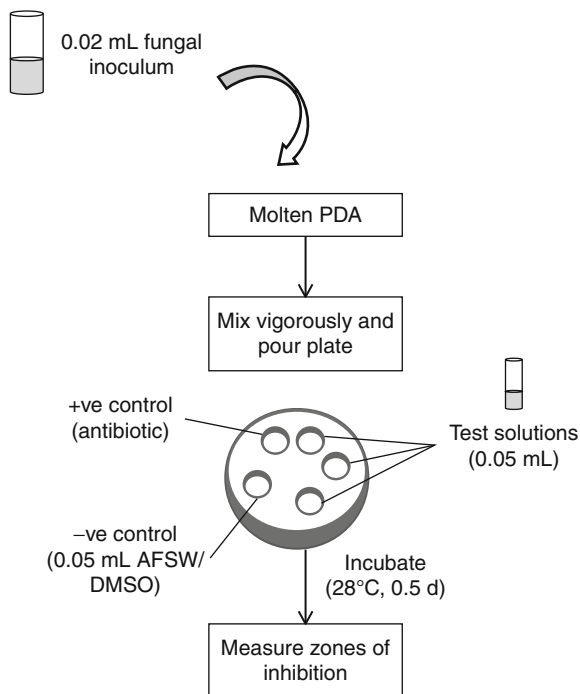
14.4.3.3 Agar Well Diffusion Assay

The agar well diffusion assay is also used for measuring antifungal activity. An aliquot (0.02 mL) of fungal inoculum is added to molten potato dextrose agar (PDA) and then poured into a Petri dish using sterile technique. After solidification, wells of 6.0 mm in diameter are drilled with a sterile cork borer on the agar plate. Then, 0.05 mL of test solution of a chemical extract or pure compound is added into each well. Similarly, 0.05 mL of either sterile filtered seawater or solvent is added into the wells that serve as the negative control, while antibiotic solution is added into the wells that serve as the positive control. The plates are incubated for 1 to 2 days at 28°C or until fungal growth can be observed in the negative control. The antifungal activity is evaluated by measuring zones of inhibition of fungal growth surrounding the wells in mm. There should be at least three replicates per treatment [39] (Fig. 14.22).

14.4.4 Bacterial Challenge Culture

Selected fungal strains are inoculated into appropriate culture medium and inoculated at 25°C for 5 days, while target bacterial strains are cultured in suitable

Fig. 14.22 Antifungal assay using agar well diffusion assay. In this assay, wells are created by drilling with a sterile cork borer after solidification of molten potato dextrose agar. Test or control solutions are poured into the wells. There should be at least three replicates per treatment. This figure is adapted from Matti et al. [39]



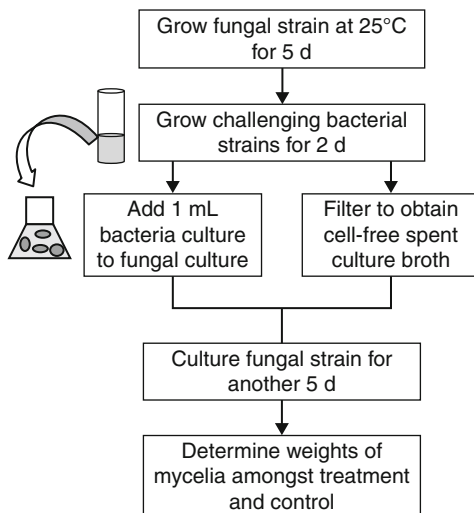
culture medium for 2 days. The bacterial cultures are then centrifuged at 5000 rpm for 15 min, and the cell pellets are resuspended in 5-mL fresh autoclaved culture medium. The resuspended bacterial cells are added into 5-day fungal cultures (3 replicates per sample). In case that bacterial extract or bacterial metabolites are tested, a given amount of the test solution is added into each fungal culture container. The treatments are cultured for another 5 days. The control set is added with 5-mL fresh autoclaved medium only. The fungal growth is determined according to the dry weights of mycelia and compared among the treatments and the controls [40] (Fig. 14.23).

14.5 Antilarval Settlement and Antialgal Bioassay

14.5.1 Antialgal Assays

Marine macroalgae (seaweeds) are common foulers on marine surfaces and often form dense mats that can clog seawater intakes, increase drag coefficients, or increase the weight of buoys. Therefore, controlling attachment and growth of macroalgae has been as challenging as controlling hard foulers such as barnacles and calcareous tubeworms. Here, we introduce antialgal bioassays that are commonly used in research laboratories.

Fig. 14.23 Competition assay, in which bacterial challenge strains are cultured against fungi. This figure is adapted from Miao et al. [40]

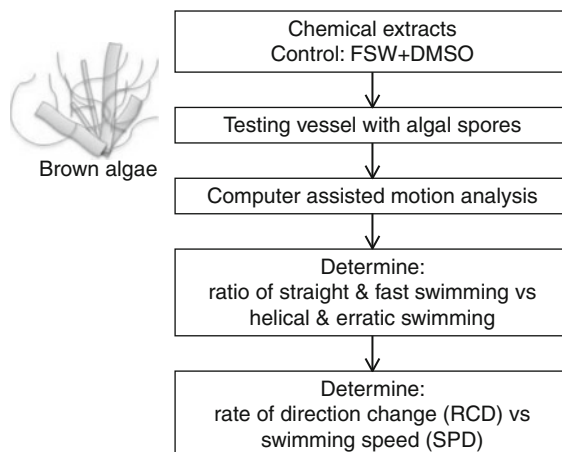


14.5.1.1 Preparation of Algal Spores

The most commonly used macroalgae are various green algal species of the genus *Ulva* since this group of seaweeds is not only common foulers on marine underwater surfaces but also on a wide distribution of organisms. The procedure to induce release of algal zoospores from *Ulva* spp. has been well developed [41–43] and is easy to follow. As described by Joint et al. [44], prior to permanent attachment onto a surface, free-swimming spores often undergo a behavior change from random swimming to a “searching” pattern of exploration close to the substratum [41]. Like some marine invertebrate larvae, during the searching process, the spores often spin downward using their flagella as propellers, and thus, their apical domes may come in close contact with the substratum. They may temporarily attach to the substratum and thus extrude a pad of elastic material that is left behind on the surface if they reject the surface and continue their search for a suitable place for permanent attachment. During the attachment process, the spores secrete an N-linked, polydisperse, self-aggregating glycoprotein that anchors them to the substratum and also makes the attachment irreversible. Therefore, surface texture, chemical characteristics, and microbial films all play important roles in spore attachment [41].

Briefly, fertile individuals of *Ulva* spp. are collected from the field and used immediately or kept in seawater tables with a flow-through seawater supply and illuminated with full spectrum light for as short a period of time as possible. To induce sporulation, each algal blade is rinsed with fresh seawater to remove loosely attached epibionts and mucous on the blade surface, and then placed in separate glass beakers containing sterile 0.22- μ m filtered fresh seawater. The beakers are placed directly near a pointed light source (but avoid overheating due to light energy). Newly released zoospores swim toward the light and thus can be easily collected with a pipette. Newly released spores are then transferred to a small beaker containing sterile 0.22- μ m filtered fresh seawater and are used immediately

Fig. 14.24 Antialgal spore swimming behavior assay, using computer-assisted motion analysis to determine swimming properties



for antismimming behavior, antisettlement, and adhesion strength experiments, as described below. Sometimes, in order to collect enough spores, the collected spores can be placed in a beaker on ice to prevent their settlement, and this procedure does not change the settling rate of the spores compared to freshly used spores in later experiments [41]. Similar procedures can be used to induce spore release in brown algae and red algae, however, with some minor modifications such as drying the algal blades in cold and dark conditions and then applying thermal shocks.

14.5.1.2 Zoospore Swimming Behavior Assay

This bioassay was developed by Callow et al. [42] and has been used in many of their studies. For a preliminary screening bioassay, this may be considered to be more challenging and may not be suitable for high-throughput purposes. However, it may be very useful for in-depth study of individual compounds (Fig. 14.24).

A slide is placed in each Petri dish (9 cm in diameter). Twenty-five mL of a spore suspension (2×10^6 spores mL^{-1}) together with the test extract/compound is added into the Petri dish that is placed on the stage of a Zeiss Universal microscope in a darkroom to prevent phototactic spore movements. Spore movement is filmed using a video camera. After 10 min, the microscope is focused on a plane just above the slide surface so that both swimming and settled spores can be observed. Time-lapse images are collected every 3 min for 60 min by using a timer controller. Single images are captured on the video camera. At the end of the filming, unsettled spores are washed off by rinsing slides gently with filtered seawater. The number of firmly attached spores to each sector is assessed by recording images of the slide. Finally, the slide is fixed and processed by using the standard cell counting procedure. Spores are counted using three consecutive video images representing each time point. The mean number of attached spores per square millimeter is calculated for each group of three images. Attached spores are counted by using the single video image after the slide is washed. Settled spores on the fixed slide are counted in 20 fields of view located at 100- μm intervals along the diagonal of each square, starting at the central corner. The mean number of attached spores mm^{-2} is calculated.

14.5.1.3 Algal Spore Settlement Assays

Different types of antialgal spore attachment assays have been used in previous studies [41, 42, 45], with some being more complicated than others. Here we introduce one of the simplest assays developed by an Australian research group [43]. One hundred μL (about 50 spores) of the algal spore suspension is added into each well of a 24-well culture plates containing 1 mL of 0.22- μm filtered seawater within which a testing extract/compound (treatment) or DMSO (the control) is preincluded. The plates are incubated in the dark for 2 h to allow for an even settlement of spores and then incubated at room temperature under natural light. After 24 h, the solution in each well is removed by pipette and 1 mL of 0.22- μm filtered seawater is added to each well. Algal spore settlement is assessed after 3 days using an inverted light microscope (Zeiss). Counts of germinated spores are conducted for ten fields of view under the microscope. All of the samples are tested in at least two to three replicate wells with spores pooled from at least three separate algal thalli. The results are compared to the controls (Fig. 14.25).

One may use 5-mL Petri dishes instead of 24-well culture plates in assays and also change incubation times for algal spore germination, depending on the germination speed of the individual species. In addition, the number of settled (attached and germinated) and unsettled (not in contact with the surface) spores can be determined under a microscope after 1 to 2 days (before unattached spores are washed out of the test vessel). In this situation, the percentage of settlement rather than the actual number of settled spores among treatments is determined and compared [43].

14.5.1.4 Settlement and Adhesion Assays

Prior to conducting a settlement and adhesion strength assay, glass microscope slides should be washed in a mixture of 50% methanol/50% concentrated HCl and then placed in 100% concentrated HCl for at least 2 h ([41, 42, 46], Fig. 14.26). Then, the slides are rinsed in double-distilled water to remove acid. One glass slide is placed in individual glass dishes. Ten mL of the zoospore suspension ($1\text{--}5 \times 10^6$ spores mL^{-1} in seawater (control) or in test solution (treatment)) is added into each dish. The dishes are placed in the dark at room temperature for at least 1 h to allow zoospores to settle evenly onto the glass slide (they will also settle on the dish, which is not used for assessment). The slides are then gently rinsed in sterilized 0.22- μm filtered natural seawater (or artificial seawater made of Instant Ocean in case natural seawater is unavailable); this removes unattached zoospores from the slides. At least three replicate slides are immediately fixed in 2% (v/v) glutaraldehyde in seawater for 10 min, washed carefully according to the method described in Callow et al. [41], and used as the “control” group, i.e., not exposed to the water jet. The remaining slides are incubated for various periods of time before exposing them to calibrated surface pressures in the water jet, followed by fixation. To ensure reproducible evaluation of short-term attachment strength on microscope slides, glass slides are mounted on a motorized holder with computer-controlled stepper motors that allow the bank of slides to be moved horizontally and vertically in a raster pattern across the path of the water jet, at speeds between

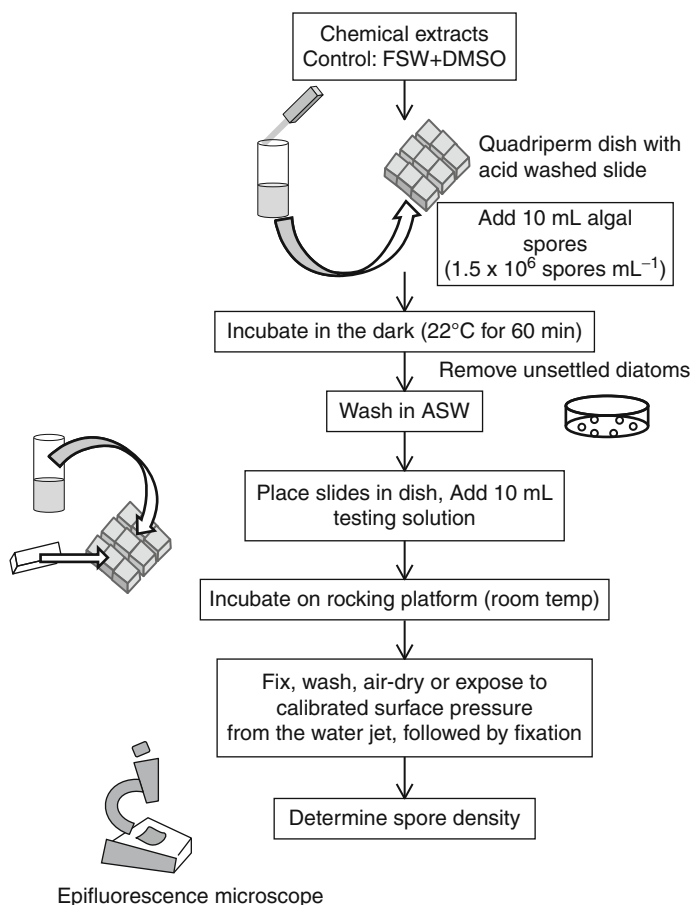


Fig. 14.25 Antialgal zoospore settlement assay. This figure is adapted from assay developed by Holmstrøm et al. [43]

2.5 and 12.5 mm s⁻¹. The pitch of movement in the vertical direction at the end of each horizontal traverse is set at 2 mm. The water jet nozzle with an internal exit diameter of 1.6 mm is mounted 25 mm from the bank of slides. The instrument is typically operated at a speed of 10 mm s⁻¹ for ten swathes to allow an area of 500 mm² in the mid-region of each slide to be exposed to water jet. The water supply is housed in a pressure resistant tank and pressurized using a compressed air supply from a conventional SCUBA tank as described by Swain and Schultz [47] who designed the original water jet apparatus for assessment of fouled panels in the field. The pressure of the water jet is increased until all attached spores are removed or until the maximum pressure of the apparatus is achieved.

Adhered zoospores are counted under epifluorescence microscope equipped with an image capture analysis system [42]. Counts are taken for 30 fields of view on each of 3 replicate slides. The number of spores that remain attached to

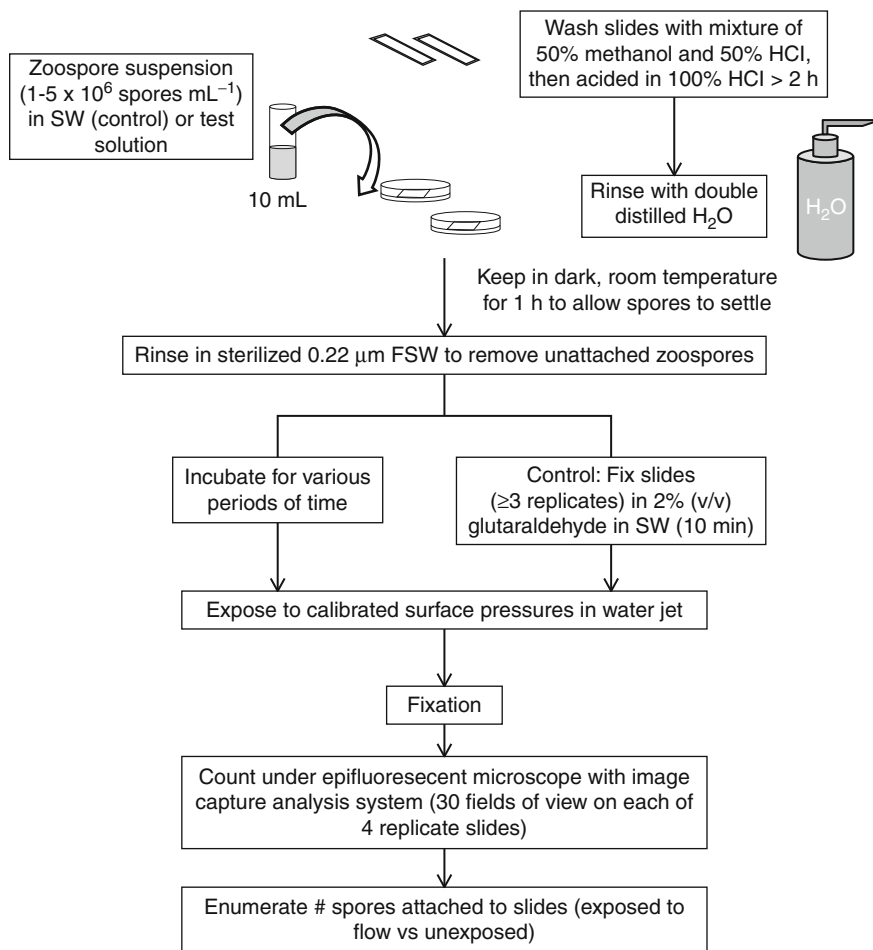


Fig. 14.26 Zoospore settlement and adhesion assay. This figure is adapted from method described by Callow et al. [41]

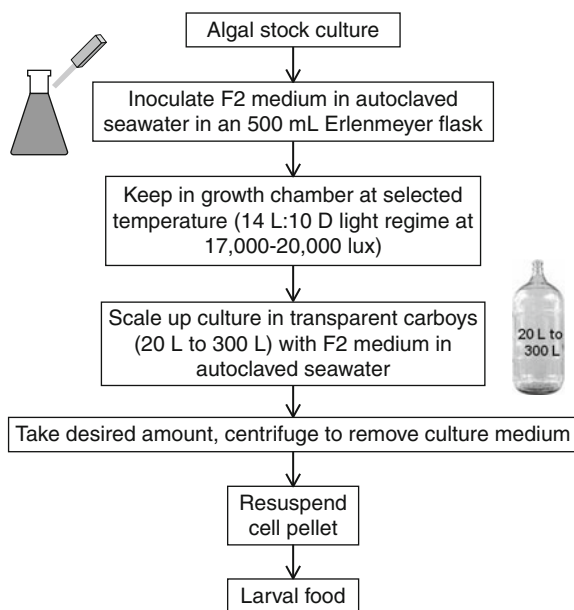
slides exposed to flow is determined and compared with unexposed controls. Since the level of settlement in each experiment may be different (because different spore batches may be used), data is presented in terms of percentage of spore removal in comparison with the controls.

14.5.2 Antilarval Settlement Assays (Various Systems)

14.5.2.1 Microalgal Culture as Feed of Invertebrate Larvae

Different invertebrate larvae prefer different algal foods, and different algal species also have different nutrient values that are also affected by culture condition of the algal species. Furthermore, it has also been proven that a mixture of algal species is

Fig. 14.27 Microalgal culture, to be used as feed for invertebrate larvae



often better than single algal species food. Therefore, it is very important to select the right algal species for individual larval species and also work out the optimal culture condition of individual algal species before developing large and routine larval culture for antifouling bioassays. Numerous studies have demonstrated that larval physiological conditions affect attachment and metamorphosis [48, 49], and these have a drastic impact on bioassay results and interpretation. Nevertheless, one can still follow the general protocol illustrated in Fig. 14.27 to get started with algal culture.

A review of literature on larval cultures of major fouling organisms that are routinely used in laboratory antifouling bioassay reveals the following tips as a general guideline:

1. *Isochrysis galbana*, *Chaetoceros gracilis*, *Thalassiosira pseudonana*, and *Skeletonema costatum* are common larvae food for barnacle larval culture. Energy reserves of larvae fed on different diatoms at a concentration of 1×10^6 cells mL^{-1} are ranked in the order: silicate-limited *C. gracilis* > *C. gracilis* > *T. pseudonana* > *S. costatum*. There is a significant linear relationship between the TAG content of the diet and cyprid energy reserves [49]. Clearly, although *Skeletonema costatum* has been recommended as larval food for barnacle larval culture decades ago [50], it is not a desirable algal species due to its poor nutrient concentration.
2. For barnacle larval culture, food concentrations should be maintained at least $> 10^3$ algal cells mL^{-1} . Nauplius II of *B. amphitrite* cannot survive through successive naupliar stage at *Skeletonema costatum* concentrations $\leq 10^3$ cells mL^{-1} [51] and failed to develop to cypris with a mixture of

- algae *Pavlova lutheri*, *Platymonas* sp., and *Thalassiosira pseudonana* at concentrations of $<1 \times 10^5$ cells mL^{-1} [52]. The recorded minimal algal concentration to support larval development of *Balanus amphitrite* was at <300 cells mL^{-1} [53], $<1,000$ cells mL^{-1} [54], and $<3.6 \times 10^3$ cells mL^{-1} .
3. For the tube-building polychaete *Hydroides elegans* larvae culture, *Isochrysis galbana* appears to be better algal feed than the others. At concentrations $<10^3$ cells mL^{-1} , $>35\%$ larvae survived through the 10-day experiment but lost their ability to become competent. The concentration of 10^5 cells mL^{-1} was the optimal for growth, development, and larval physiological condition for attachment and metamorphosis [55].
 4. A mixture of algal food often supports a better growth and development of performance of these test organisms.
 5. Temperature, salinity, and other culture variables have profound effects on larval growth and development, and competency to attach and metamorphose [49, 56].

14.5.2.2 Larval Culture

Acorn barnacles are common sessile intertidal organisms and also among the major hard foulers. As barnacles secrete glycoproteinous glue to cement themselves permanently onto hard substrates [57], they form surface structures that are very difficult to be removed. Accumulation of those structures can clog water intakes of nuclear power stations, desalination systems, and pipelines or create substantial drag in moving vessels. The damage caused by fouling barnacle has been documented for many centuries and is the major task of antifouling control. Therefore, larvae of barnacles have been logically used in antifouling bioassay for many decades.

As sessile barnacles can be found in almost all surfaces (both hard, such as rocky shore, and soft surfaces, such as the skin of sharks and whales, trunks of mangrove trees, and the floating algal blades and wooden boards), the adaptive power for living in diverse environments is very high in this group of organisms. Of course, there are also many barnacle species worldwide, providing diverse choice of barnacle species as test organisms [58, 59]. Nevertheless, the life cycle of most barnacle species is similar, and the most common barnacle species used in laboratory bioassay is *Balanus (Amphibalanus) amphitrite*. Therefore, in this chapter, we will use this species as a model organism to introduce larval development and culture methods.

Like other acorn barnacle species, *Balanus amphitrite* (Darwin) adults are hermaphroditic (meaning the same individual have both sexual organs) but can hardly carry out self-fertilization. Since they live in calcareous plates (there are six plates in general, but for some species, those plates may merge) cemented to the surface, adults can only cross-fertilize with their neighbors with their long penis (modified cirri). Fertilized eggs are developed inside the body in the base and hatch into nauplius I stage, which is characterized by one bright red eye but without a thorax or abdomen [60]. Nauplius I larvae are released from the adults into the water column and are nonfeeding organisms; they often molt into nauplius II larvae

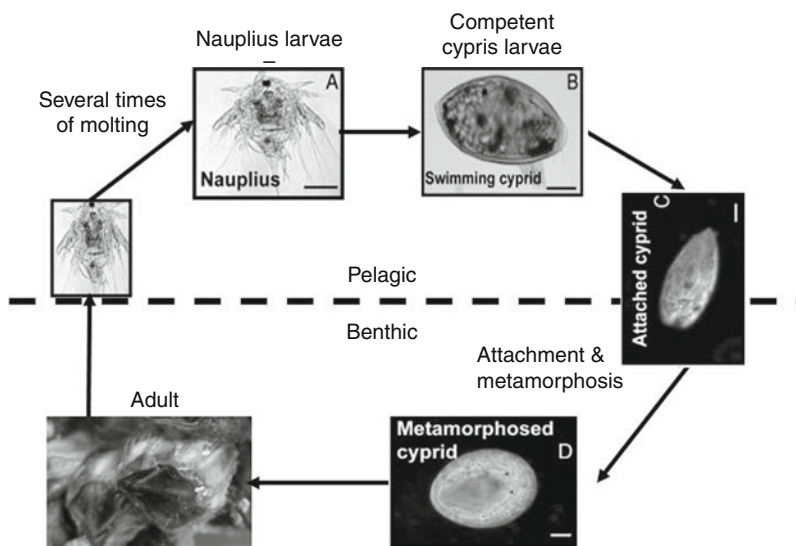


Fig. 14.28 Life cycle of *Balanus amphitrite*. Nauplius I larvae begin their life cycle by being released from adults into the water column. They molt into nauplius II a few hours later and feed on plankton. They continue to molt into nauplius III, IV, V, and VI larvae within 3–4 days. Cyprids actively search for a suitable place to settle with modified antennules. When they have found a suitable place, they attach and secrete a glue. Attached cyprids molt into young juvenile within a few hours

within a few hours and begin to feed on both phytoplankton and zooplankton right after completing the molting process. Nauplius II larvae molt into nauplius III, IV, V, and VI larvae within 3–4 days in *B. amphitrite* (Fig. 14.28), but may take weeks to months to complete those moltings in other barnacle species. The nauplius VI larvae molt into cyprid that are nonfeeding larvae again. Cypris stage may last hours and days, again depending on the species. Cyprids often actively search for a suitable place to settle with modified antennules. When they find a suitable place, they attach using their antennules and secrete a glycoprotein glue. Before the glue/cement hardens, the cyprids still have the ability to deattach themselves from the surface. However, as soon as the cement solidifies, attachment becomes irreversible. The attached cyprids molt into a young juvenile within a few hours. There is substantial evidence that young cyprids have a high discriminating power on assessing surface suitability based on texture [61], wettability [62], color, chemistry, the presence and absence of a natural profilum or the composition of the microbial community structure of the biofilm [63–68], chemical cues of conspecific species, and flow dynamics [50, 69, 70]. However, aged cyprids (naturally and artificially) often become less selective to settling sites and tend to settle on any available surface, and this is linked to an exhaustion of energy reserves in cyprids [48, 49, 56, 71–73].

To develop larval culture of *B. amphitrite*, adults collected from the field or kept in the laboratory but fed well with newly hatched *Artemia* sp. are used for

experiments. The brood stocks can be induced to release nauplius I larvae by changing the water and stimulating by light-shock. Alternatively, the egg lamellae of individual adults containing late stage developing embryos can be dissected and placed in 0.5 L of seawater. Nauplius I larvae are hatched during the 1-day incubation at room temperature. If they are healthy, they should be able to molt into nauplius II within 2–3 h. Please keep in mind that brood stock can be kept in aerated seawater at room temperature (ca. 24°C). If adults are well fed with newly hatched *Artemia* sp. larvae daily and, in some cases, supplemented with the diatom *Skeletonema costatum*, they shall be able to release nauplius I larvae every few days. This allows laboratories far from coastal areas to maintain reproductive barnacle populations for the antifouling bioassay.

Newly molted Nauplius II larvae are attracted to a point-source light and can be directed for collection with a pipette under a dissecting microscope. Planktotrophic nauplius II larvae are cultured at a density of 2 larvae mL⁻¹ in 0.22-μm-filtered natural seawater at 30 ppt salinity (FSW) using *Chaetoceros gracilis* Schutt as the ideal food source (although the diatom *Skeletonema costatum* has been used by many laboratories, it has been proven to be a relatively poor diet for barnacle larval culture) [56]. Nauplius II larvae develop through planktotrophic nauplius III, IV, V, VI and then molt to a nonfeeding cyprids in several days (depending on the rearing condition). During the rearing period, successive algal food is added to each culture beaker (ideally at least twice per day), and seawater in culture beakers is changed daily by filtration or siphoning. Crystamycin (22.5 mg mL⁻¹, Penicillin G, and 37.5 mg mL⁻¹ Streptomycin sulfate) shall be added to the culture beaker to inhibit bacterial growth. Previous studies indicated that addition of the above antibiotics in the culture medium has no adverse effect on barnacle larval development [74]. The culture is maintained at 24°C under a 12 L:12D photoperiod until all larvae became cyprids. The naupliar stages of *Balanus amphitrite* can be identified and described [75] under a compound microscope at 24-h intervals. Freshly molted cyprids or aged cyprids can be used for antifouling assays.

H. elegans (Fig. 14.29) is a gregarious calcarious tube-building polychaete that occurs in tropical and subtropical waters. This animal causes a serious biofouling problem in the Pearl Harbor, Sydney Harbor, and Southern parts of the Chinese coast (including Hong Kong) as juveniles and adults secrete calcified tubes that jam pipelines of the cooling systems of power stations, buildings, submarines, clog nets and cages of mariculture, forming a high biomass on submerged surfaces and on the surfaces of farmed animals such as abalones and pearl oysters. In Hong Kong, during the spring and summer months, fish farmers need to clean their nets and cages that are heavily fouled by *H. elegans* every other week. Unfortunately, it is always very difficult to remove calcified worm tubes on fish nets. Therefore, this species is considered one of major foulers in tropic and subtropical regions and has been used as an antifouling target in a number of research laboratories [76, 77]. *H. elegans* in fact is a small animal (only about 2 cm long of soft body in 2–6 cm long of calcified tube); however, it only takes about 1–2 weeks for a juvenile to develop into a sexually mature adult that can release several thousand small eggs (about 50–65 μm in diameter). The males and females release their gametes into the

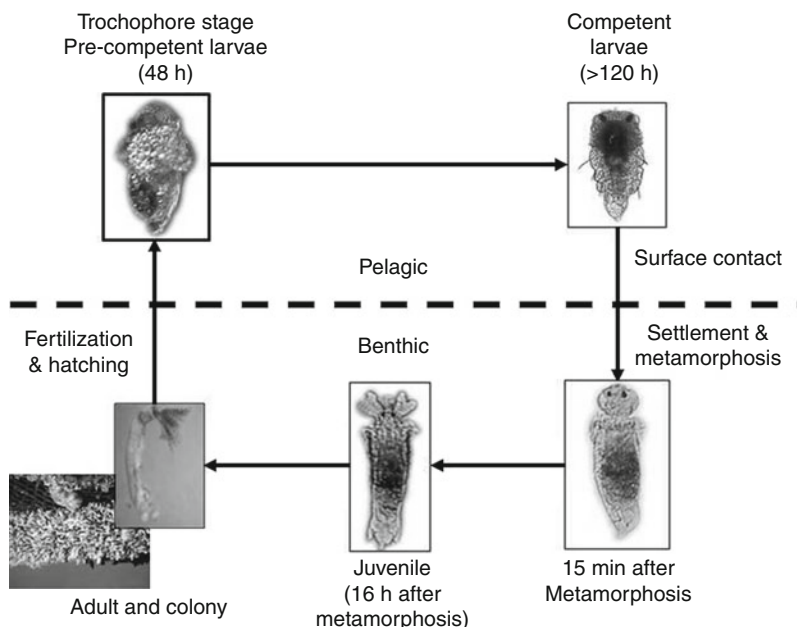


Fig. 14.29 Life cycle of *Hydroides elegans*. Gametes are released into the water column, and fertilized eggs can hatch into young trochophores within 24 h. Four to five days later, trochophores complete attachment and metamorphosis within a time span of 9–12 h

water column, and the fertilized eggs can hatch into young trochophores within 24 h. With sufficient food supply, trochophore can develop into competency to attach and metamorphose within 4–5 days. It takes settling larvae only 9–12 h to complete attachment and metamorphosis. The same adult can release mature gametes every 7–10 days with a life span of about 8–10 months. This animal has almost all the required characteristics for a laboratory test animal, such as short generation time, fast growth, high fecundity, repeat spawning ability, ability to reproduce all year round, and ease of culturing (for both larvae and adults) [55, 76–79].

The development of larval culture can follow the protocol outlined in Fig. 14.30. Freshly collected adults should be used immediately or be brought to the laboratory and kept in water tables supplied with filtered flow-through seawater (if possible) or in the aquarium filled with filtered seawater. Adult females and males are carefully isolated from their neighbors (could be *H. elegans* or *Bugula neritina*) under a dissecting microscope and placed in separate 5-mL Petri dishes. Individual adults are forced to release their gametes when their tubes are gently broken with a dissecting needle or fine forceps [55, 78, 80]. Female bodies are often orange in color (due to the presence of yolky eggs), while males are often milky white. Matured females release eggs of similar size and bright orange in color and spherical in shape. When females are not ready to spawn or not in good condition but forced to release their eggs, these are often pale in color and in different sizes and shapes, which should not be used for developing larval culture. High-quality

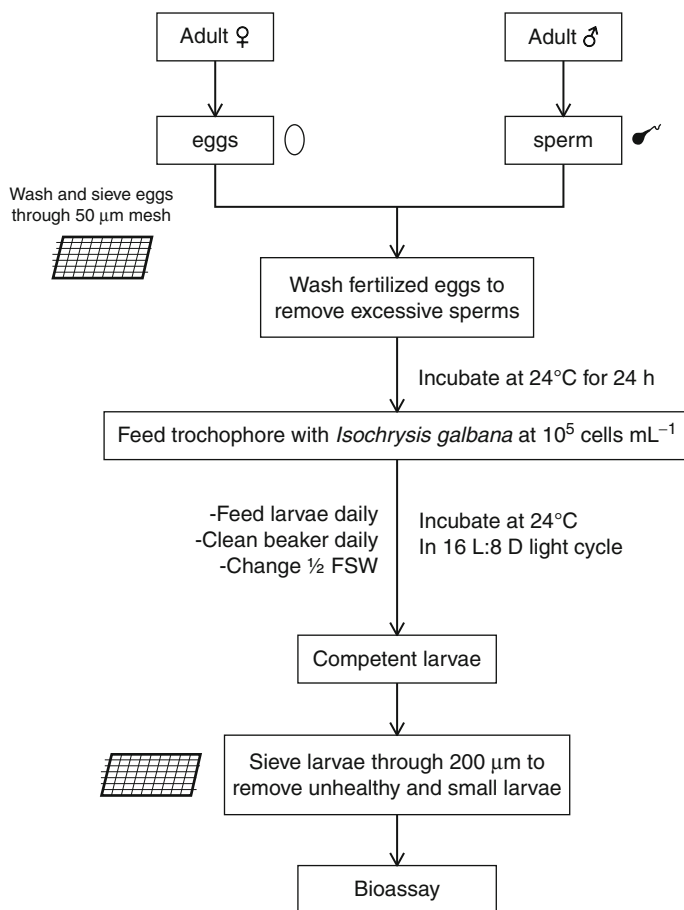


Fig. 14.30 Larval culture of *Hydroides elegans* for bioassay

eggs from several females are pooled together, sieved through a 35-µm mesh (to eliminate small eggs that are often unhealthy) using autoclaved 0.22-µm filtered seawater, and placed in 150-mL Erlenmeyer culture beaker. A few drops of highly concentrated sperm (from several males) are added into the beaker and well mixed with the egg suspension to allow fertilization to take place. As fertilization rate is near maximal in this species over a remarkably wide range of sperm concentrations (approximately 10⁵–10⁸ cells mL⁻¹ – even at 10³ sperm mL⁻¹ at least 60% of eggs are fertilized) [81], there is no real need to monitor sperm concentration. After a few minutes, the fertilized eggs are filtered through a 35-µm mesh submerged in autoclaved filtered seawater to decant excess sperm, and transferred to 1 liter culture beakers containing 0.22-µm filtered seawater. The culture beakers are kept at 25°C under a 12 L:12D photoperiod in a growth chamber. After 20 h, the hatched trochophore larvae are transferred to clean beakers containing 0.22-µm filtered seawater. Larvae are fed with the flagellate *Isochrysis galbana* (Tahitian

strain) at a concentration of $1-2 \times 10^5$ cells mL⁻¹ in batch culture. Before algal food is added to the culture, the algal culture is centrifuged to remove algal culture media and algal pellets are resuspended in 0.22- μ m filtered seawater. Larval culture is maintained under the same culture conditions for 3–4 days. The larval culture is transferred to a clean culture beaker and fed daily, by filtering or pipetting. When most of the larvae reach competency to attach and metamorphose, the culture is filtered through a 150- μ m mesh to eliminate small larvae before being used for the antifouling bioassay.

Larval competency to attach and metamorphose must be tested before larvae are used for antifouling bioassays since competency affects bioassay results drastically. Competence can be assessed by pipetting a 24 subsample of larvae into a solution of 10^{-4} M IBMX in seawater. Replicates consisting of 10–15 larvae are placed in six-cell tissue culture wells containing 5 mL of treatment solution and incubated at 22°C on a 15 h light:9 h dark photoperiod. The status of larvae in experimental dishes is determined using a dissecting microscope at 24 h after initiation of an assay. Larvae that can attach to the culture well, produce a tube, and grow tentacles are considered to have undergone normal metamorphosis, while unattached and swimming or crawling larvae are considered to be unmetamorphosed [80]. Once at least 90% of subsampled larvae become competent to metamorphose in response to IBMX, the remaining larvae can be used for antifouling bioassay.

Alternatively, larval competency can be tested by using well-developed natural biofilms as positive cues. However, due to variation in the bioactivity of natural biofilms developed under different conditions, reproducibility of a bioassay may not be as good as using IBMX as the inducer.

The cheilostome bryozoan *Bugula neritina* (Linne) (Fig. 14.31) is one of the most abundant fouling organisms [82]. It is widely distributed in subtropical and temperate marine waters [83], but its population peaks at different months in different locations. As this species releases larvae that are competent to attach and metamorphose within minutes without the need of an inducer [84], it has been widely used as a test organism in antifouling bioassays [85]. Laboratory cultures can be developed to provide a consistent supply of raw materials for drug screening.

To prepare larvae for bioassay (Fig. 14.32), fresh colonies are brought to the laboratory and transferred to plastic mesh cages submerged in fresh seawater tanks in the dark overnight with aeration. Colonies are placed in 4-L beakers containing filtered seawater in the early morning and placed directly under an artificial light source. Adults usually release brooded larvae in response to light shock; larvae are attracted to the beam of the supplementary light source and can be easily transferred to test vessels using a pipette. The metamorphosis can be divided into two phases [86, 87]. The first phase is drastic and quick; metamorphosis initiates when the swimming larvae attaches to the substratum, with concomitant morphogenetic movements including eversion of the internal sac, retraction of the apical disk and involution of the corona, and formation of the precursor to the cystid and polypide [86, 87]. The second phase of metamorphosis is more gradual, ranging in duration from 36 to 48 h, and includes complete degradation of larval tissues and substantial morphological reorganization.

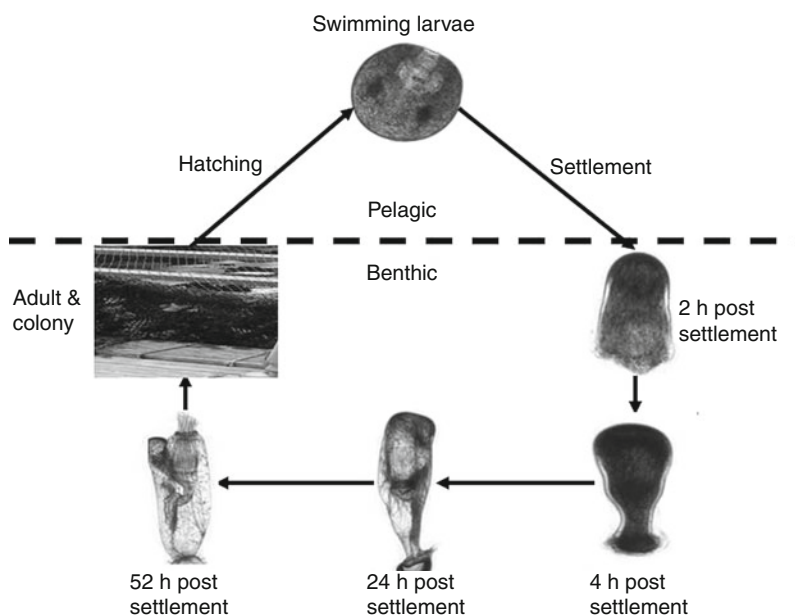


Fig. 14.31 Life cycle of *Bugula neritina*, consisting of a swimming larval stage and a sessile juvenile and adult stage

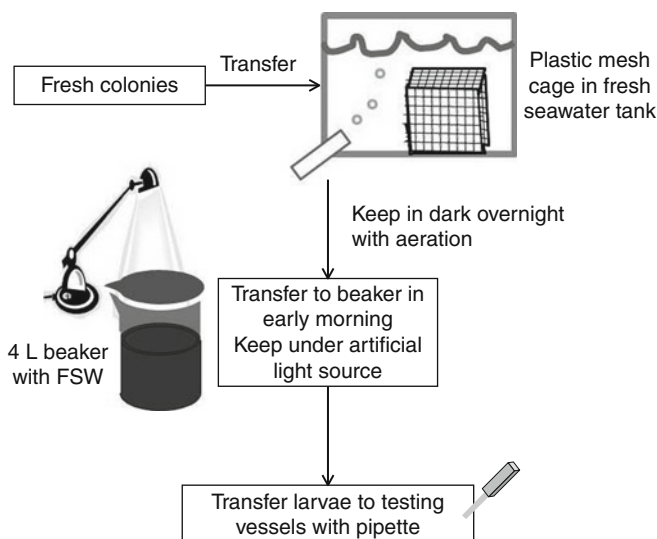
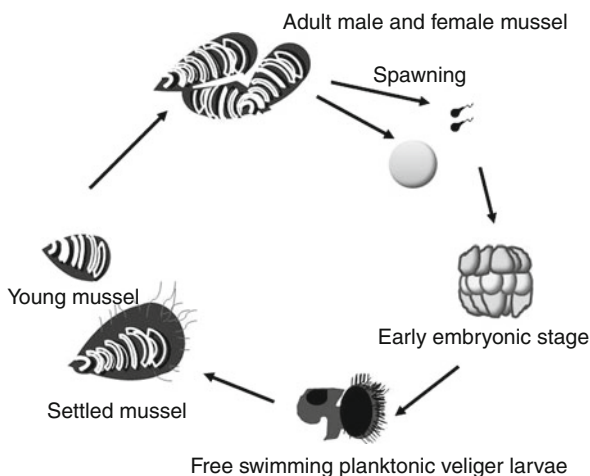


Fig. 14.32 Larval culture of *Bugula neritina*, which can be developed in the laboratory to provide a consistent supply

Fig. 14.33 Life cycle of the common mussels. Gametes are released and fertilized in seawater, and hatch into trochophore larvae that quickly develop into free-swimming planktonic veliger larvae in 1–2 days. Veliger larvae feed on plankton and develop into pediveliger larvae in 1–4 weeks before developing competency to attach and metamorphosis. This figure was adapted from Bord Iscaigh Mhara (1990) <http://www.piscestt.com/FileLibrary%5C12%5CMussel%20Culture.PDF>



Mussels are major foulers in aquatic environments. Small (0.63–3.8 cm long) freshwater zebra mussels (*Dreissena polymorpha*) (Fig. 14.33) fouling caused possibly the largest economic loss in Europe and North America in human history by a single fouling species (http://en.wikipedia.org/wiki/Zebra_mussel) as they clog water intakes of municipal water supplies and hydroelectric companies, and block pipelines in many freshwater environments such as the Great Lakes area. Meanwhile, marine mussels such as *Mytilus* spp. and *Perna* spp. are found all around the coasts in the world. The history of biofouling problems caused by these species is as long as that of harvesting them for human consumption or for fishing bait (for catching crabs, lobsters, and fishes). Mariculture industries of marine mussels have been developed [88] in almost all the coastal countries, and mussel farming can be traced back to thousands of years ago. These bivalves are often the dominant organisms on the shores of oceans and seas.

Mussels are dioecious bivalves and highly prolific bivalves. Individual females can produce millions of eggs a year. The matured female gonads are often reddish orange in color while the male yellowish cream or milky white. The major spawning season peaks in the spring or early summer, but for some mussel species, there may be a second spawning season in late fall (which is never as extensive as the spring one). During the spawning season, the males and females shed their gametes into the seawater where fertilization takes place. Spawning is often synchronized in a mussel population to maximize the fertilization rate and can be triggered by various factors. The fertilized eggs hatch into young trochophore larvae that quickly develop into free-swimming planktonic veliger larvae in a day or two. Veliger larvae remain in the water column, feed on phytoplankton, and develop into pediveliger larvae in 1–4 weeks, depending on species, water temperature, and availability of food until they reach competency to attach and metamorphose. Competent larvae become negatively phototactic and sink to the bottom and search and attach on a suitable surface by secreting byssus (proteinous substances).

During the metamorphosis process, the larval organs such as velum (swimming organs) are shed or adsorbed, meaning that animals are no longer able to swim with ciliated swimming organs. However, similar to other marine bivalves, determination of complete metamorphosis in the mussel is often difficult. Therefore, in most bioassays using mussel larvae as test organisms, we use larval attachment and loss of swimming organs as the end point. In addition, for mussel species, young juveniles may deattach themselves and ride on water currents by secreting mucous threads in order to relocate their site for permanent settlement. This ability/characteristic has also been used for antimussel attachment assays in antifouling screening.

Freshly collected adult mussels are brought to the research laboratory and carefully cleaned by removing all encrusting epifaunal organisms on individual shells. Large individuals with wider shells are selected and kept in flow-through seawater tables temporarily. Spawning is induced by injecting 2 mL 0.5 M KCl into the mantle cavity of each mussel and allowing them to stand out of water at room temperature for 1 h before immersion into 1- μ m-filtered, UV-light-irradiated seawater (FSW) in individual glass or plastic beakers at room temperature [89]. Spawning can also be induced by thermal shock (transferring mussels between temperatures of approximately 10°C and 25°C at hourly intervals [90]) or by air drying the mussel in cold and dark environmental chambers and then submerging in warm seawater at hourly intervals. If these methods do not induce spawning, both male and female gonads can be dissected from healthy mussels. After checking the eggs' size and shapes, as well as sperm swimming ability under a microscope, gametes can be used for larval culture (personal experience).

Freshly released/obtained eggs and sperm are mixed at 100 and 200 sperm egg⁻¹ ratio to allow fertilization to take place [91] in 1 L glass beakers containing 0.22- μ m filtered seawater. Fertilization success is checked by subsampling mixed gametes to check for polar bodies in the fertilized eggs under a microscope. Cultures with high fertilization rates and normal embryo development (>80%) are used. The fertilized eggs suspension is transferred to a small aquarium containing 0.22- μ m filtered seawater and held undisturbed until the formation of trochophore larvae (may take 24–72 h, depending on species and culture temperature). Trochophore larvae at a density of 100–200 larvae mL⁻¹ are transferred to a clean aquarium by either siphoning or filtering (to decant unfertilized eggs and unhealthy embryos), and the larval condition is monitored by examining subsamples of larvae under the microscope. If a high rate of abnormality is detected, the entire larval culture should be abandoned [92] (Fig. 14.34). Larvae are fed with either individual species or a mixture of microalgae *Isochrysis galbana*, *Chaetoceros* spp., or other available algal species at a concentration of 10⁵ cells mL⁻¹ [92, 93]. The larval feed is added, and at least 1/3 of the seawater in the culture container is replaced with fresh 0.22- μ m filtered seawater by siphoning daily. Debris and deposits on the bottom of the culture are also removed by siphoning. The larval culture is transferred to a clean culture container every 2–3 days (to avoid biofilm formation on the container walls) by siphoning the culture over a 45- μ m mesh sieve. Development and growth of larvae are inspected under the microscope to detect any abnormality every 2–3 days until all of the larvae reach competency to attach and metamorphose.

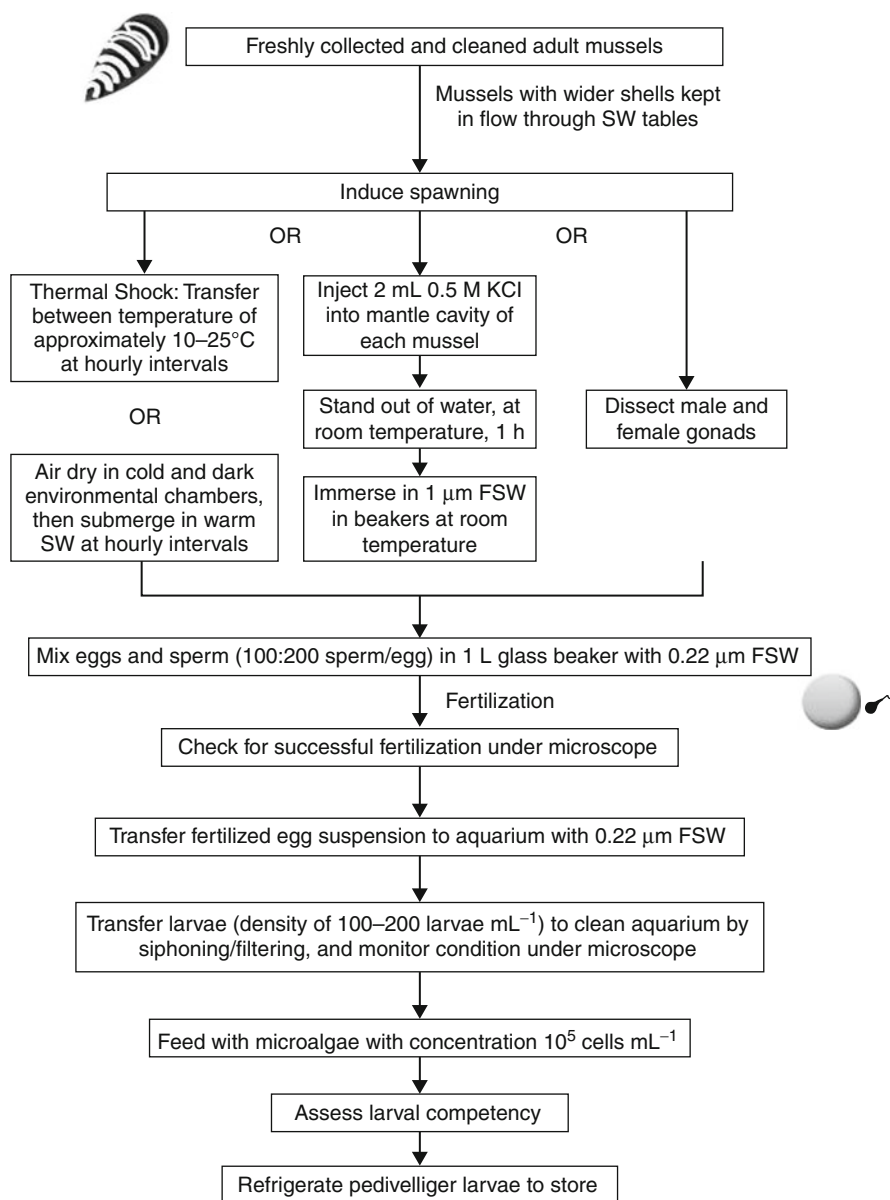


Fig. 14.34 Larval culture of mussels

Larval competency can be assessed by a slightly modified methodology from [94]. Briefly, after larvae reach pediveliger stage, 20–30 larvae are transferred in 5 mL to Petri dishes containing elevated KCl concentrations in seawater to assess metamorphic competence daily. The optimal concentration of excessive KCl

to induce mussel larvae to settle varies (10–50 mM above ambient) from species to species and needs to be determined carefully. There should be at least five to six replicate dishes. All individuals exposed to KC1 are checked to determine for the presence of gill filaments and shell brims.

Refrigeration of pediveliger larvae of the mussel for various periods has been examined and suggested to be a good way to store competent larvae for up to 1–3 months for antifouling bioassay purposes [95].

14.5.3 Antifouling Assays Using Larvae of Major Fouling Organisms

When using invertebrate larvae as test organisms in antifouling bioassays, various end points have been used, including swimming speed, swimming behavior (mode of locomotion and phototaxis, response to flow), survival, but most importantly, the attachment rate and metamorphosis rate. While in most cases, larval attachment and metamorphosis are treated as a single end point, that is, larval settlement, there have also been cases to treat larval attachment and metamorphosis as distinctive and distinguishable processes.

Regardless of what end points are recorded and what larval species are targeted, the following important quantitative indices are used: LC_{50} and EC_{50} , and the ratio of these two.

1. LC_{50} refers to the lethal compound concentration where 50% of the targeted organisms die within a given period of time, which can range from minutes to several days, depending on the bioassay protocol and test organisms.
2. EC_{50} refers to the concentration that leads to 50% inhibition of a particular biological activity, such as settlement in antisetlement screening assays.
3. A theoretical ratio of LC_{50} and EC_{50} data implies the possible relationship between toxicity and the inhibition of performances. When this ratio is small (close to 1.0 or below 1.0), it suggests that the compounds/extracts may act on test organisms through toxic mechanisms, while a large ratio (such as >15) indicates that the substance may act in a less or nontoxic manner. Therefore, this ratio is commonly used to guide the screening for antifouling compounds. A sensible strategy for screening for antifouling compounds looks for substances of low or negligible toxicity that inhibit larval settlement of major foulers, since these compounds may have a better chance to get through more rigid environmental regulation in the future.

Because larval settlement is not only affected by many exogenous factors such as substratum type, rugosity, light, surface films, host inductance but also by indigenous ones such as genetic differences, physiological conditions, and sensory perception between larval batches, it requires substantial background research before one species can be adopted for antifouling screening bioassays. This may well explain why only a few larval species have been routinely used over the last several decades, although many species have been tried or suggested for antifouling bioassay. Keeping this in mind, we will describe testing protocols only for the species introduced above.

14.5.3.1 Using Barnacle Larvae as Test Organisms

Range-finding assays (Fig. 14.34) [96]: To define a possible functional range (regardless of EC_{50} or LC_{50}), a preliminary bioassay on cyprid settlement can be carried out using 24-well polystyrene plates (Falcon, USA), although the results of this type of assay are hardly ever seen in publication. The pure compounds or chemical extracts are dissolved in dimethyl sulfoxide (DMSO) and added to autoclaved FSW to yield final concentrations ranging from very low (around $\mu\text{g mL}^{-1}$) to very high ($200 \mu\text{g mL}^{-1}$). Cyprids (10 ± 2 individuals) are added to each well with 1 mL of the test solution. In total, there are 8 test solutions of target compounds or extracts, plus wells containing FSW and wells containing FSW with DMSO serving as two types of negative controls. Each treatment should have two replicates. The plates are incubated at $28\text{--}30^\circ\text{C}$ for 24 h in an environment with a 15 h:9 h L:D photoperiod. After incubation, the wells are examined under a dissecting microscope. Cyprids that do not move with their appendages extended or do not respond when touched with a dissecting needle are counted as dead, while those unattached/swimming ones are counted as unsettled. The assay is terminated by adding two to three drops of 10% formalin to each well. All of the unattached larvae are washed away with deionized water, while attached juveniles are enumerated [59]. The percentage of larval

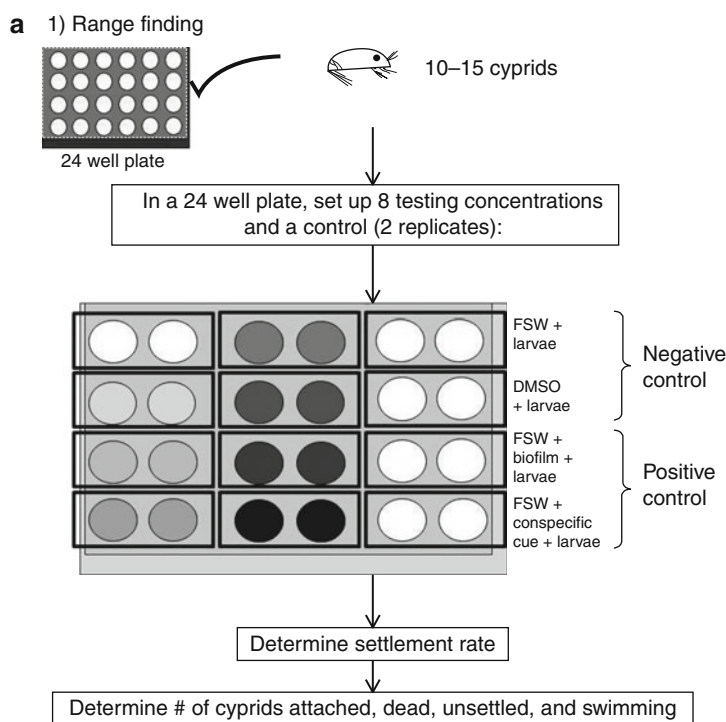


Fig. 14.35 (continued)

b 2) Narrow range for determination of EC_{50} and LC_{50} , 5-6 replicates

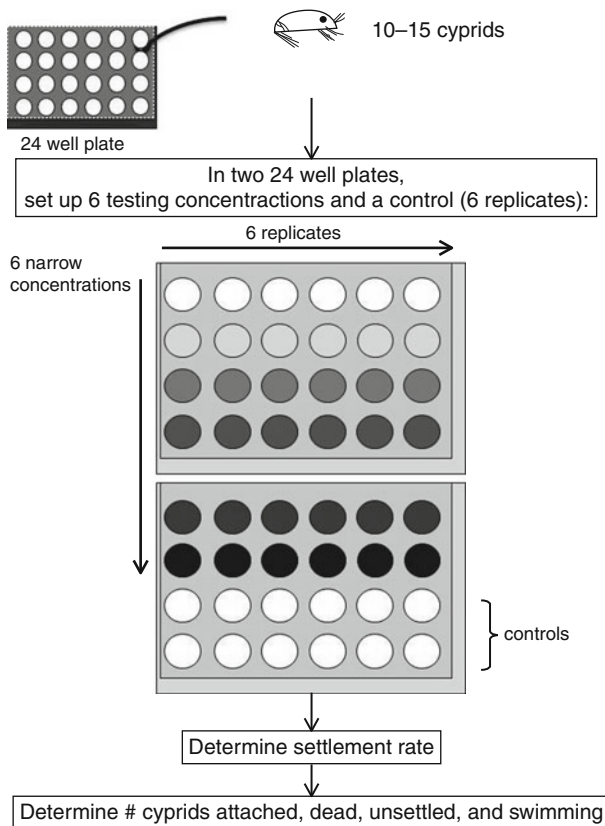


Fig. 14.35 Range finding assay for antifouling compounds, in order to define a possible functional range of cyprids. Abbreviations: LC_{50} lethal concentration (the concentration causing death of 50% of the group of test organisms), EC_{50} effective concentration (the concentration inducing an effect on half of a group of test organisms, and in this case, the effect would be settlement)

settlement is determined by counting the number of settled individuals under a dissecting microscope and expressed as a proportion of the total number of larvae in the well. The therapeutic ratio (a comparison of the amount of an antifouling compound/extract that inhibits 50% larval settlement to the amount that causes 50% larval death) (LC_{50}/EC_{50}) is roughly estimated (Fig. 14.35).

Following up range finding assays, the bioassay is repeated with six test concentrations within a relative narrow range. For each treatment, there should be at least five to six replicate wells. The therapeutic ratio is calculated in order to determine the effectivity of the antifouling compound against larval settlement. The EC_{50} (with 95% confidence interval) for settlement inhibition is estimated by probit analysis counts of a log dilution series of the test compound.

14.5.3.2 Using *Hydroides elegans* Competent Larvae as Testing Organisms

Fifteen competent larvae are placed into each of the experimental dishes. Experiments are conducted for 24 h at 24°C under continuous illumination, and then swimming and settled larvae are counted under the microscope. A larval bioassay is conducted with five to six replicates in multiwell polystyrene dishes (#3047, Falcon, USA). AFSW-filled dishes are used as the negative controls, while the phosphodiesterase inhibitor 3-isobutyl-1-methylxanthine (IBMX, Fluka Ltd.) is commonly used as an artificial stimulator (as the positive controls) for larval attachment at 10^{-4} M in AFSW [81]. Otherwise, dishes with well-developed natural marine biofilms are used as the positive controls (because larvae often settle well in response to well-developed natural biofilms). After this period of time, swimming, settled and dead larvae are counted under a dissecting microscope. LC_{50} and EC_{50} of the test compound or extract are determined according to the same method described in the barnacle larval settlement assays (Fig. 14.36).

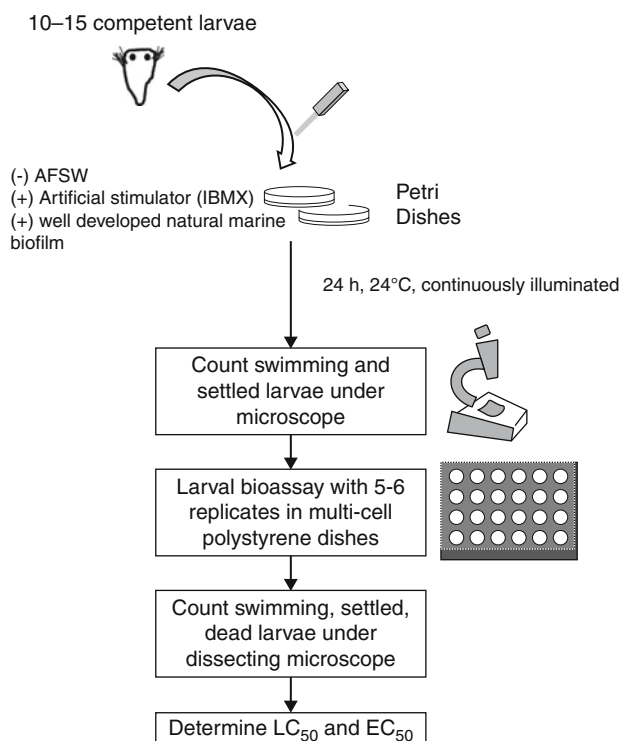


Fig. 14.36 *Hydroides elegans* as test organism for extracts or compounds. Abbreviations: (–), negative control; AFSW autoclaved filtered seawater, (+) positive control, IBMX 3-isobutyl-1-methylxanthine (a phosphodiesterase inhibitor that is used as an artificial stimulator for the positive control)

14.5.3.3 Using *Bugula neritina* Larvae as a Test Organism

Approximately 20 newly released larvae (i.e., within 15 min) can be sterilely added to each well of a 24-well polystyrene plate containing 1 mL of the test solution per well. Five replicates per treatment are used. Wells containing only filtered seawater with DMSO serve as the controls (Fig. 14.37). The plates are incubated at 27°C for 1–3 h, and the percentage of larval settlement is determined by counting the settled, live larvae under a dissecting microscope. Results are expressed as a proportion of the total number of larvae in the well. EC_{50} (inhibits 50% of settlement of larvae in comparison with the control) and LC_{50} (the concentration at which 50% of larvae were dead in comparison with the control) levels of pure compound or extract are calculated by using the Probit software [97–99].

14.5.3.4 Using Mussel Larvae and Juveniles as Test Organisms

Since larval culture of mussels is often time-consuming and challenging (in maintaining very healthy larval culture and assessing competency to attach and metamorphose as well as in determining the completion of metamorphosis), this larval settlement bioassay is becoming less popular. Instead, young juveniles collected from natural environments are more commonly used in antifouling bioassay.

Mussel larval settlement and metamorphosis assay [100, 101] (Fig. 14.38): Prior to the antifouling bioassay, 5-mL Falcon Petri dishes are allowed to develop natural biofilms in seawater tables supplied with flow-through seawater. Twenty competent pediveliger larvae of mussels are added into each 5-mL Petri dish (Falcon, USA) containing 5-mL FSW as the positive controls or 5 mL of test

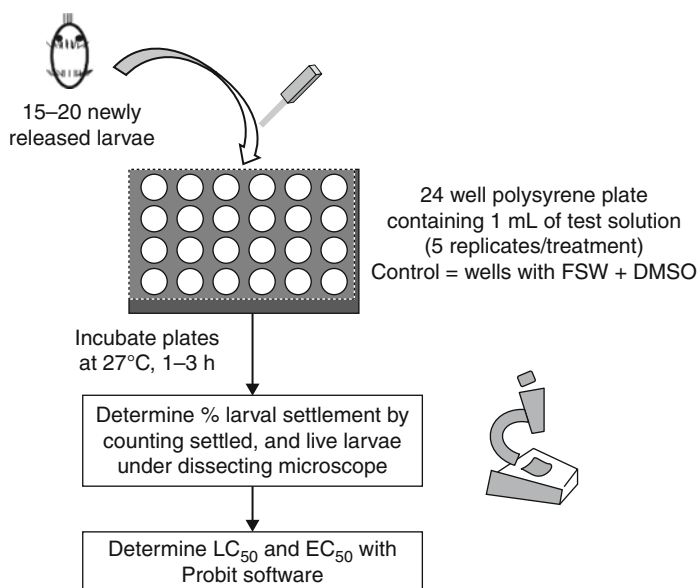


Fig. 14.37 Using *Bugula neritina* as test organisms

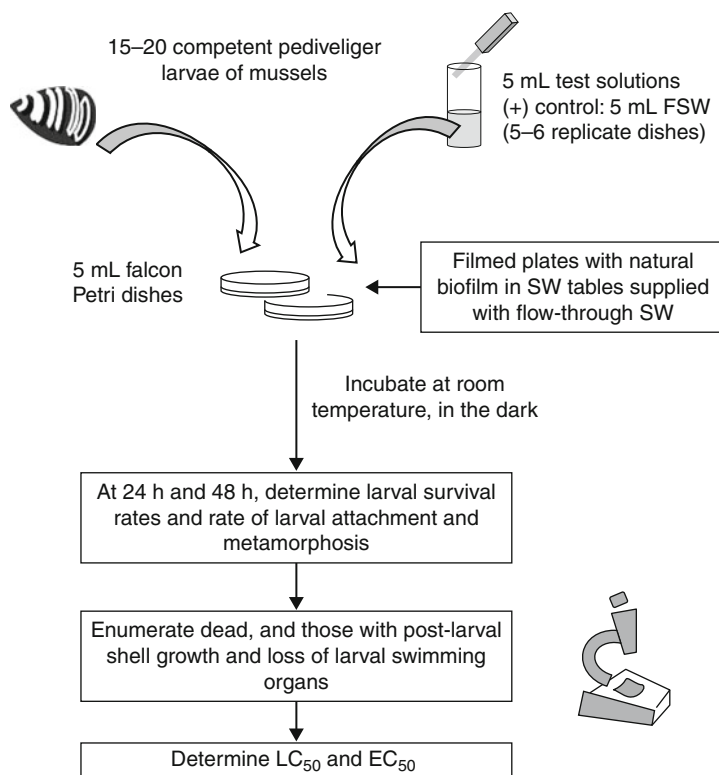
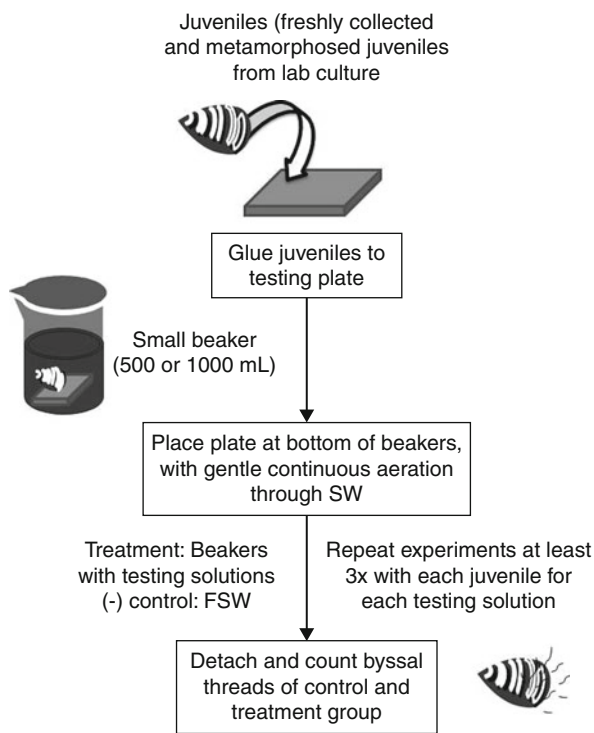


Fig. 14.38 Mussel larval settlement and metamorphosis assay. This figure is adapted from Dobretsov and Qian [100]; Bao et al. [101]

solutions as the treatment. In case that natural biofilm development becomes rather difficult or bioactivity of natural biofilms for inducing mussel larval settlement is unstable or too low, competent larvae are treated for 10–20 min with elevated KCl solution at an optimal concentration defined in the competency assay described in the larval rearing section, prior to being added into each Petri dish uncoated with natural biofilms. All of the Petri dishes are incubated at room temperature in the dark, and at least five to six replicate Petri dishes are used for each treatment. Larval survival rate, as well as the rate of larval attachment and metamorphosis, is determined under a microscope after 24 and 48 h from the commencement of the experiment by counting the number of dead individuals (mortality) and the number of individuals with postlarval shell growth and loss of larval swimming organs. LC₅₀ and EC₅₀ are calculated according to the methods described in the previous section.

Free single mussel assay A (modified from Etoh et al. [102]) (Fig. 14.39): Freshly collected from field and metamorphosed juveniles from laboratory culture are glued to the test plate using nontoxic ‘crazy glue’ (or other glues). The plate is placed at the bottom of a small beaker (500–1000 mL) containing seawater with continuous but gentle aeration and left for 4 h. Beakers containing test solution are used as treatment,

Fig. 14.39 Free single mussel assay. This figure is adapted from Etoh et al. [102]

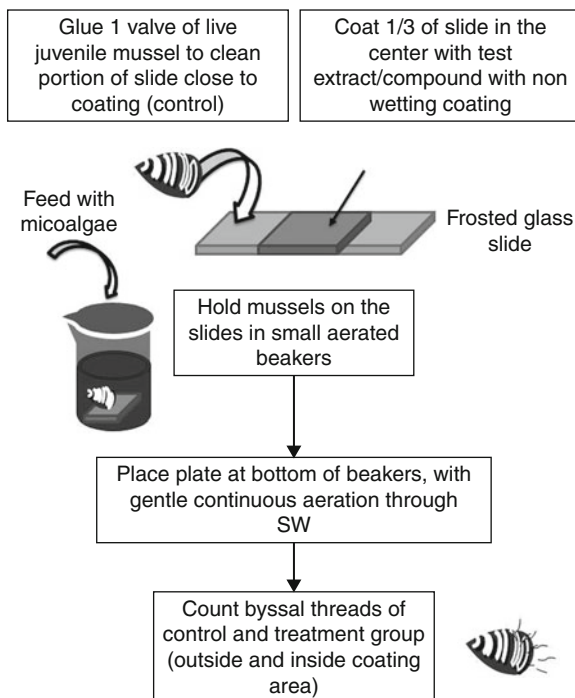


while ones with fresh filtered seawater serve as the negative controls. After 4 h, a number of byssal threads produced by each juvenile are counted by detaching threads one by one. The experiments are repeated at least three times with each juvenile for each test solution (to save juveniles and chemicals). The number of byssus produced by each mussel in both the treatment and controls is calculated and compared.

Juvenile byssus threads assays [103, 104] (Fig. 14.40): The byssal thread bioassay is developed and extensively used by Japanese scientists. In the laboratory bioassay, 1/3 of the center of clean frosted glass slides are coated with test extract or compound alone or extract/compound with nonwetting coating (EXTRUDETTM). One valve of a live juvenile mussel is glued to the clean portion of the slide close to the coating. Mussels on the slides are held in small aerated beakers for 1–10 days and fed with microalgae. The number of the byssal threads attached outside and inside the coating area of each mussel is counted at the end of experiment and is compared to that in the controls (area without extract or compound coating). A compound or extract would be considered as active (antifouling) if >90% of the byssal threads are found outside of the areas.

A similar system has been used for field antifouling bioassays in Japan [103]. A piece of cardboard (Webron, Tokusyu Seishi Co., Ltd., Japan) is trimmed into 50 × 1 cm strips, washed with methanol, and dried before use. The front side of the cardboard (40 cm²), except for both ends, which is used for attachment, is coated with a test compound or extract dissolved in 0.5 mL of organic solvent (mainly

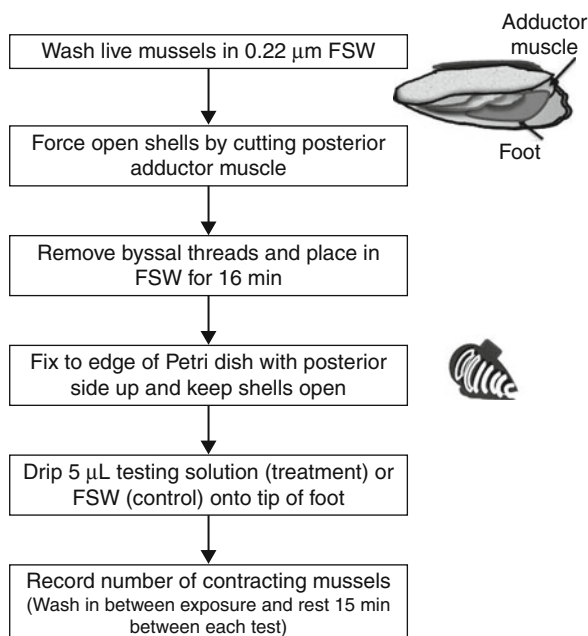
Fig. 14.40 Juvenile mussel byssal thread assay. This figure is adapted from Ina et al. [103], and Sera et al. [104]



MeOH), using an absorbent cotton ball. The blank plate is prepared by the same procedure described above. After the solvent is evaporated, both plates are arranged in a line fixed tightly on an exclusive stand without wrapping. Ten test mussels are fixed around each zone. Each plate is set at the bottom of an experimental aquarium with running seawater, which is covered to create dark conditions. After 3 h, the number of byssuses attached outside the coated zones and total number of byssuses of each mussel is determined. The number of inactive (dead) mussels is also recorded. Antifouling activity is determined as a percentage at each concentration of the test compound or extract as follows: number of byssuses \times 100 (%).

Mussel foot contraction assay [105] (Fig. 14.41): This type of bioassay is not commonly used as observation of behavior may not be as easy as counting settlement, metamorphosis, or byssal thread production. Yet, it provides an other means of bioassay screening. Briefly, live mussels are first washed in 0.22- μ m filtered seawater, and then mussel shells are forced open by cutting the posterior adductor muscle. After removal of byssus threads, the mussels are placed in filtered seawater for 15 min. Each mussel is then fixed to the edge of a Petri dish with the posterior side up by using a holder or glued while their shells are kept open to expose their foot. For the control, 5 μ L of FSW is dripped onto the tip of the foot gently (try not to physically stimulate the foot). Only mussels that do not respond to FSW drips should be used for follow-up experiments. To test antifouling compounds, 5 μ L of test solution (of compounds or extract) is gently dripped onto the mussel foot following the same method as in the controls. If the mussel contracts in a few

Fig. 14.41 Mussel foot contraction assay, as an alternative to observing settlement, metamorphosis, or byssal thread production. This figure is adapted from Hayashi and Miki [105]



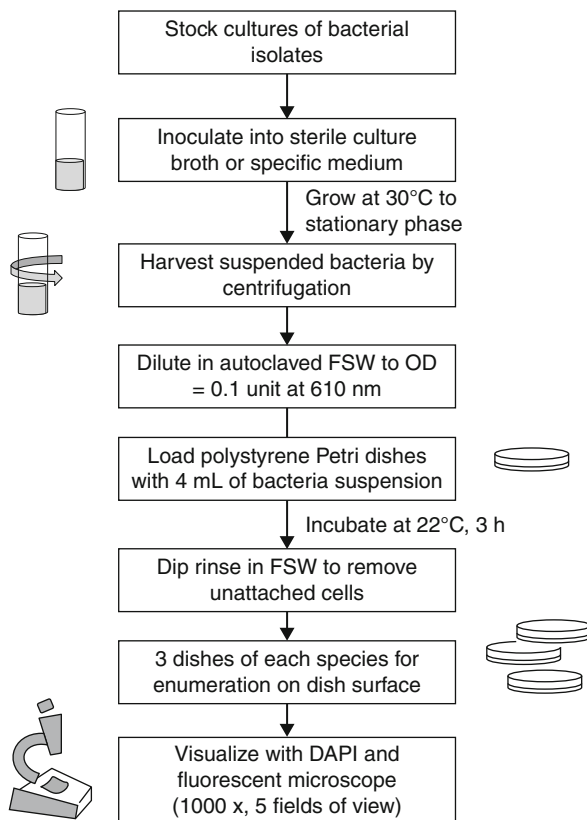
seconds, this is considered as a response. The number of responding mussels is recorded. In this type of assay, the same group of mussels can be reused. To do so, the mussel feet are gently washed with filtered seawater immediately after observation of their responses to chemical exposure. The animals should be allowed to rest in filtered seawater for at least 15 min before the next round of testing. The concentration of the test solution can be raised from the point of dripping the ASW as control until all the mussels show a reaction. The responses of the mussels are indicated by percentages at each concentration of test solution, calculated as number of reactive mussels/ (number of reactive mussels + unreactive mussels) \times 100 (%).

14.5.3.5 Antilarval Settlement of Bacterial and Diatom Films

Besides testing bioactivity of chemical extracts or pure compounds from marine macroorganisms and microbes, antilarval settlement of biofilms developed from monospecies of bacteria or multispecies of bacteria is often the first step in screening for bioactive bacteria and diatoms, which leads to subsequent isolation and purification of antifouling compounds from bioactive strains and species (methods described in early section). Therefore, here, we introduce the general protocol for antilarval settlement of bacterial and diatom films, using larvae of *B. amphitrite*, *H. elegans*, and *Bugula neritina* [85, 97, 106] (Fig. 14.42).

Development of bacterial film: Start with stock cultures of bacterial isolates from the Marine Bacteria Culture Collection. All bacteria are inoculated into sterile culture broth [0.5% (w/v) peptone, 0.3% (w/v) yeast extract in sterilized filtered (FSW)] or specific medium (for some unique species and grow at 30°C to the

Fig. 14.42 Development of biofilms, for subsequent screening of bacteria and diatoms for antifouling compounds. Abbreviations: OD optical density



stationary phase [106]. Suspended bacteria are then harvested by centrifugation and diluted in autoclaved FSW to an optical density of 0.1 unit at a wavelength of 610 nm (using a spectrophotometer of TechComp, China). Polystyrene Petri dishes (# 1006, Falcon, USA) are loaded with 4 mL of the bacterial suspension and incubated for 3 h at 22°C to allow bacteria to attach and form consolidated biofilms. Thereafter, the dishes are dip-rinsed in FSW to remove unattached cells before being used for larval settlement assays. For each bacterial species, three dishes are diverted for the enumeration of bacteria on the dish surface. Falcon dishes or glass slides (used as microscopic slides) ($n = 3$), are formalin-fixed (4% in FSW), rinsed with distilled water, and stained with the DNA-binding fluorochrome 4',6-diamidino-2-phenylindole (DAPI) (Fluka Chemie AG, Switzerland) [107] at $0.5 \mu\text{g mL}^{-1}$ for 5 min. Stained substrata are wet-mounted on a fluorescence microscope (Zeiss Axiophot, Germany), and bacterial cells are recorded at $1000\times$ magnification in five fields of view chosen randomly ($\lambda_{\text{Ex}} = 359 \text{ nm}$, $\lambda_{\text{Em}} = 441 \text{ nm}$). Data is given as means \pm SE of 5 replicates.

Development of diatom biofilms: Diatoms from the culture collection are cultivated in aerated 400-mL Erlenmeyer culture flasks according to the procedure of Harder et al. [15]. When visible diatom films have developed in the flask,

the monospecific diatom suspensions are transferred to experimental Petri dishes (Falcon, USA) and incubated for 24 h to allow diatoms to attach and develop films on the substrata. These prepared Petri dishes are then washed carefully in FSW. Three dishes are fixed with a 5% solution of formalin in seawater and used for diatom counts using the same methods for determining bacterial density.

Development of natural biofilms: Natural biofilms (NBF) are developed by exposing Falcon Petri dishes to surface sea waters for 5 days before using them for larval bioassays.

Larval settlement bioassays on filmed surfaces: Newly released *Bugula neritina* larvae (i.e., within 15 min) or newly molted barnacle cyprids (obtained as described in earlier session) are used in bioassays without any further treatment. For *Hydroides elegans* competent larvae, they are treated with IBMX according to methods described in the *H. elegans* larval settlement assay prior to be added to filmed Petri dishes. Ten to twenty larvae are added to each filmed Petri dish (either with bacterial film, diatom film, or natural biofilm) in 4 mL of sterile-filtered (0.22 μm) seawater (FSW). Petri dishes without biofilms and containing sterile filtered seawater are used as controls. There should be at least five replicate dishes per treatment. Bioassay conditions for each larval species should follow the protocols described in previous session. At the end of bioassay, the number of attached juveniles is recorded and bioactivity of the biofilm is determined by the settling rate in each treatment in comparison with that in the control.

14.6 Methods of Antifouling Compounds Test

After a potent antifouling compound is identified, the chemical needs to be incorporated into a marine coating (basic coating with or without other biocides) and tested in both laboratory and field assays. Both static panel immersion testing (D3623) and dynamic testing (ASTM D 4938 & 4939) are conducted according to the protocols detailed by the American Society for Testing Materials (ASTM 1998). As recommended, field testing must be conducted in a heavily fouled marine environment, typically a port area, and left for periods of time to determine the degree of resistance provided by the test coatings against attachment of hard (barnacles, oysters) and soft (algae, seaweeds, sponges, etc.) fouling. The details will not be discussed in this chapter.

14.7 Mode-of-Action of Antifouling Compounds

Up to now, very little has been done on the mode-of-action of antifouling compounds at the molecular level while the effects of compounds on behavior and physiology (often indicated by enzymatic activities) of settling propagules of macrofouler have been investigated sporadically. In comparison, more work on the effects of compounds on bacteria and biofilm formation has been carried out because more biological information (genomics, proteomics, transcriptomics, and metabolomics) on

microbes is available. Here we will discuss the general procedures on how to investigate the effects of antifouling compounds on gene and protein expression in settling larvae of marine invertebrate foulers. We hope more work in this area of research will shed light on the molecular mechanisms and targets of antifouling compounds, which will be important for designing biofouling control strategies.

14.7.1 Effects of Antifouling Compound on Gene Expression

To investigate the possible effects of antifouling compounds on settling larvae of marine invertebrate foulers at the gene level, *the first step* is to select target gene(s). The ideal candidate genes should be the ones with (1) known functions in other model organisms (since up to now, there is hardly any solid evidence on the function of any genes in larval settlement and metamorphosis of marine fouling organisms) and (2) full length of the gene sequence (well-matched and informative). However, if we know a given protein is involved in regulating larval settlement and metamorphosis, we can also design primers for the target genes even before we obtain full length sequences of the relevant genes (Figs. 14.43, 14.44).

The second step is to design primers for the candidate genes with Primer Express software (Version 1.0, PE Applied Biosystems, Foster City, CA) for real-time PCR. All primer sets should have a calculated annealing temperature of $\geq 58^{\circ}\text{C}$ (nearest neighbor method), and the PCR products can be easily amplified. Internal controls need to be selected for Quantitative Real-time PCR reaction, and we found that QuantumRNA™ 18s internal standards primers (Ambion Inc., Austin, TX) can serve as internal controls.

The third step is to challenge competent larvae (which are prepared according to methods described in previous sections) with an antifouling compound at a given

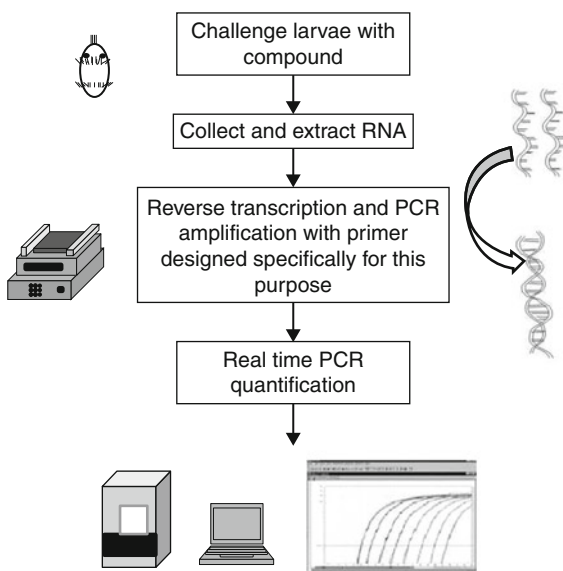


Fig. 14.43 Real-time PCR detection of gene expression

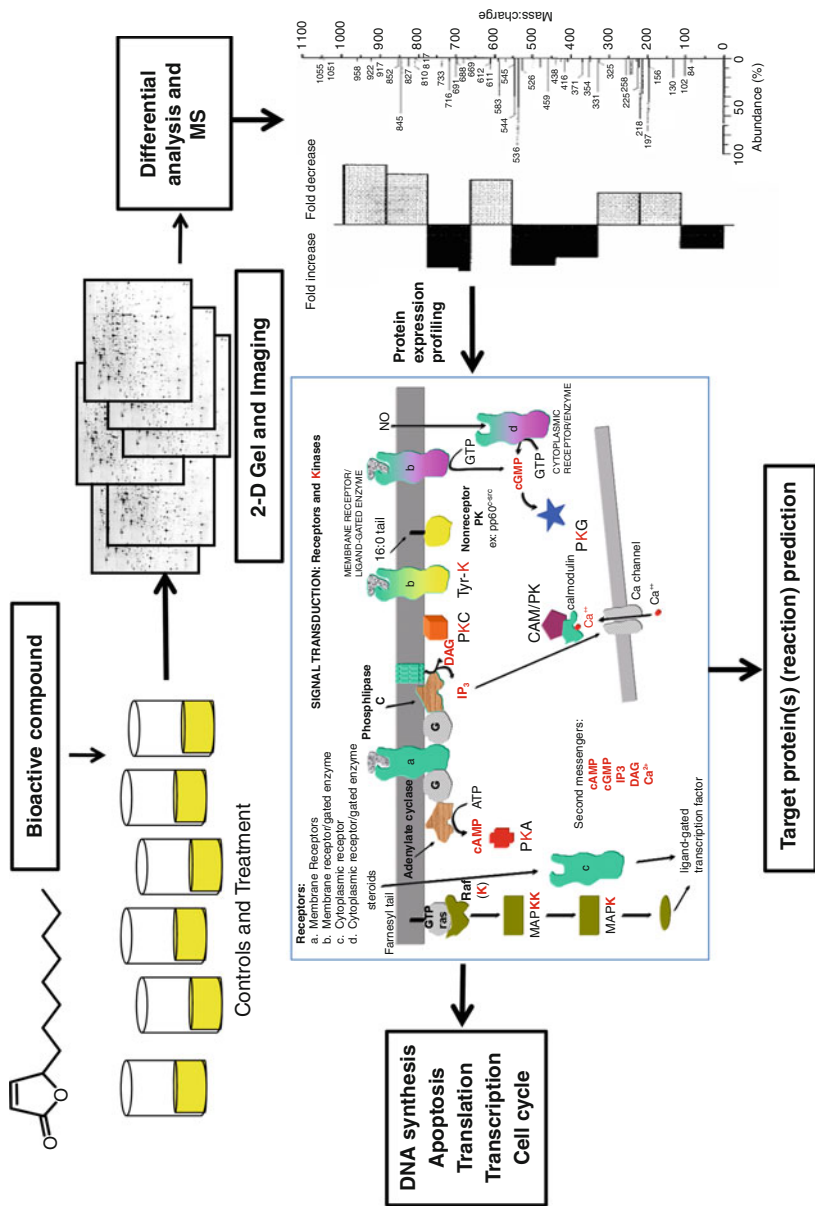


Fig. 14.44 Proteomics is a new technology used to study the mode of action of compounds. For example, signal transduction involves receptors and kinases, resulting in various processes in a cell such as DNA synthesis or translation

concentration and for a given duration (both need to be optimized). Competent larvae without being challenged with the antifouling compound are induced and/or allowed to settle normally and are used as the negative control.

The fourth step is to extract RNA from the control larvae and treated larvae. A sufficient number of larvae in both treatment and control groups are homogenized in TRIzol reagent. The total RNA of each sample is extracted according to the manufacturer's instructions and can be quantified with a GeneQuant Spectrophotometer. RNA samples are treated with RNase free DNase I to eliminate possible trace amounts of genomic DNA contamination immediately prior to proceeding with cDNA synthesis. First-strand complementary DNA can be synthesized from total RNA samples using M-MLV Reverse Transcriptase (USB Corporation, Cleveland, OH) with (N)₆ random primers (TaKaRa, Dalian, China). Briefly, N₆ random primer primed first-strand cDNA can thus be synthesized in a total volume of 20 μ L containing 2 μ g of total RNA [108].

The fifth step is to conduct qRT-PCR. The PCR reactions normally take place in 96-well microtiter plate wells in reaction volumes of 25 μ L with SYBR Green Master Mix at the optimal concentrations of specific primers, using an ABI Prism 7000 Sequence Detector or similar Real-time PCR. Reaction conditions should be predetermined and optimized for particular genes and then programmed in the PCR machine. For each bioassay, there should be at least three replicates, tested cDNA samples and the controls. Specificity of PCR amplification of each pair of primers is confirmed by analyzing PCR products through agarose gel electrophoresis and dissociation curve analysis. Differences in gene expression can then be calculated by the comparative Ct method that compares test samples to a calibrator sample and uses results obtained from a uniformly expressed control gene to correct for differences in the amount of RNA present in the two samples being compared to generate a Δ Ct value. The formula used for fold difference calculation often sets for $2^{-\Delta\Delta Ct}$, where the value of Δ Ct is the difference in Δ Ct values obtained with calibrator and test samples.

14.7.2 Effects of Antifouling Compound on Protein Expression

Studying the effects of antifouling compounds on protein expression is challenging since this requires technology and high-tech instrumentation for protein extraction, purification, separation, and identification. However, this area of research may provide us with a better success rate in identifying the targets of antifouling compounds, which can be very important in developing antifouling strategies. Here, we introduce 2-DE-based proteomic techniques for reference (gel-free proteomics requires substantial LC-MS/MS machine times) [109–111] (Figs. 14.45, 14.46).

The competent larvae are challenged with antifouling compounds at a given concentration and for a period of time (to be optimized for a particular species), and larvae without compound treatment serve as the negative controls [109–111]. After treatment, larvae are collected and placed in lysis buffer, frozen in liquid nitrogen for 5 min, and then stored at -70°C until use. In solution, IEF fractionation

followed by narrow-range 2-DE can substantially improve the proteome coverage. Briefly, the frozen larval samples are added with lysis buffer (7 M urea, 2 M thiourea, 4% CHAPS, 40 mM dithiothreitol (DTT)), homogenized, and then subject to sonication. Protein samples are centrifuged to remove insoluble materials, followed by acetone precipitation (5 volume of precooled acetone). Protein samples are pelleted and resuspended in 0.5-mL IEF fractionation buffer (7 M urea, 2 M thiourea, 4% CHAPS, 40 mM dithiothreitol (DTT), and 1% 3–10 ampholytes). An RC/DC protein assay is conducted, and around 2 mg per sample is taken and then adjusted to 3.25 mL using the IEF fractionation buffer. The electrophoresis of the protein sample solution is analyzed with a Zoom IEF fractionator at constant power (2 W) and limiting current (2 mA) using six isoelectric partition membranes. A 16- μ L aliquot of each fraction is checked for fractionation efficiency

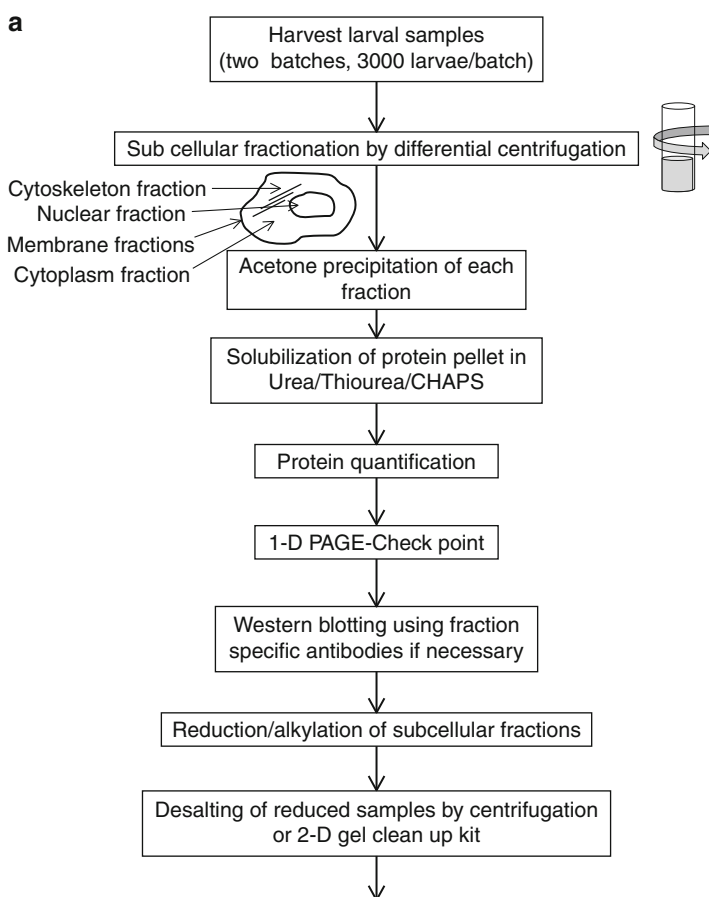


Fig. 14.45 (continued)

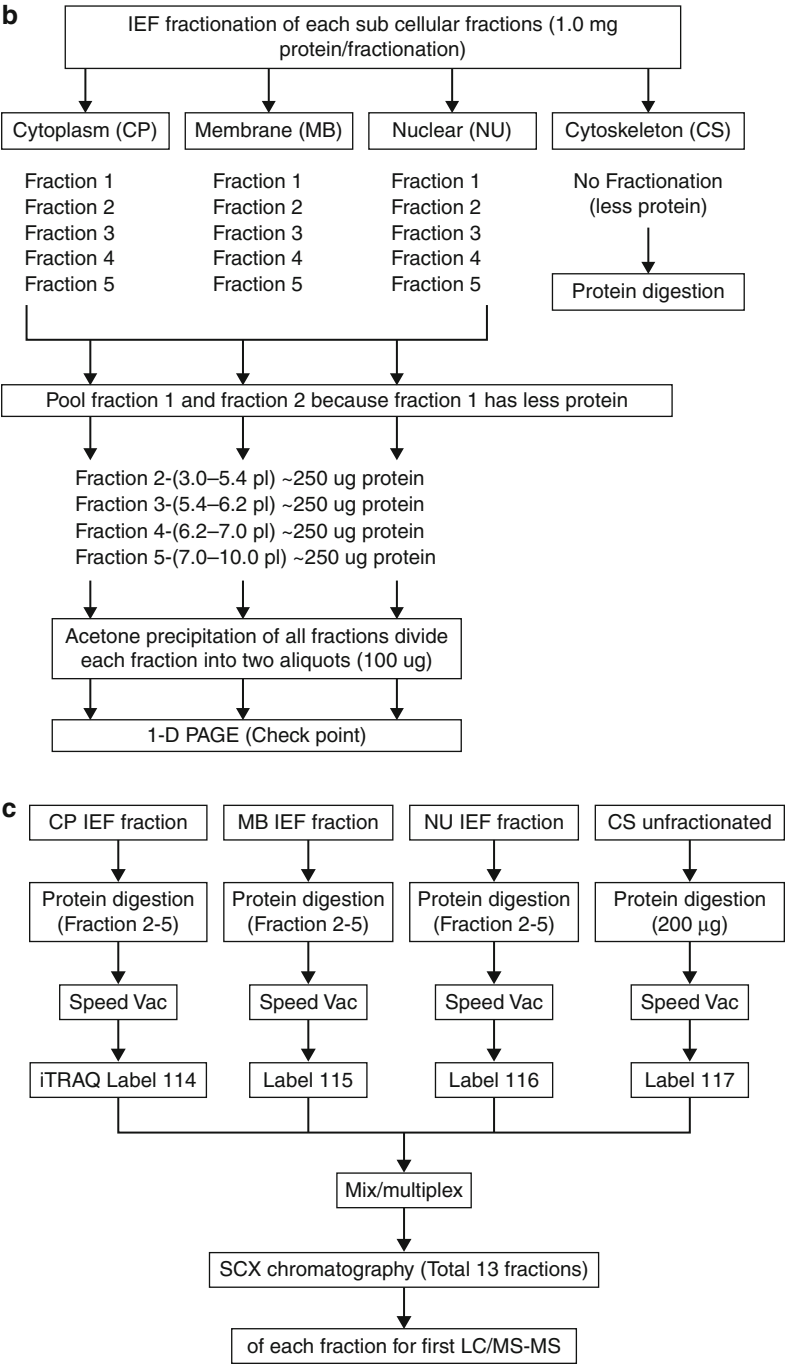
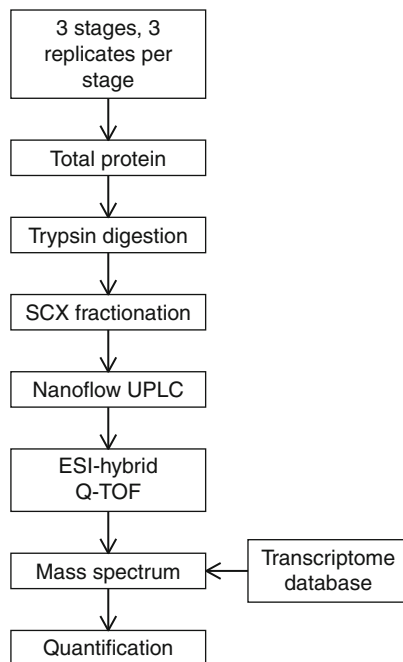


Fig. 14.45 (continued)

Fig. 14.46 Shotgun proteomic study of marine organisms. Abbreviations: *Nanoflow UPLC* nanoflow ultra performance liquid chromatography, *ESI-hybrid*, energy storage inverter, *Q-TOF* quadrupole-time of flight, *ESI-hybrid*



with SDS-PAGE. Zoom IEF fractions are precipitated in acetone and dissolved in 300- μ L rehydration buffer (7 M urea, 2 M thiourea, 4% CHAPS, 1% DTT, and 0.5% IPG buffer). The solution is sonicated for 10 min twice, incubated at room temperature for 1 h, and centrifuged at 12,000 rpm for 10 min. IPG strips (*e.g.*, *pH* 3.0–7.0) are rehydrated with sample solution overnight at 20°C with 50 mA current for 14 h and subjected to IEF using a Protean IEF Cell. IEF is performed under the following conditions: 250 V for 20 min, 1,000 V for 2 h, and with a gradient of 10,000 V for a total of 60,000 Vh. After IEF, the second dimension is performed at 20°C at a maximum of 24 mA per gel for approximately 8 h until the bromophenol blue reaches the bottom of the gel. All gels are fixed in 50% methanol and 10% acetic acid overnight, stained for phosphoproteins and total proteins, and imaged on a Typhoon trio imager. The scanned gels can be analyzed using the PDQuest software (version 8.0; Bio-Rad) according to the protocol provided by the developer. Spots on ProQ Diamond stained gels are matched to SYPRO Ruby

Fig. 14.45 Proteomic analysis of *Bugula neritina*. Abbreviations: *CHAPS* 3-[93-cholamidopropyl]-dimethylammonio-1-propanesulfonate, a detergent, *1-D PAGE* one-dimensional polyacrylamide gel electrophoresis, *SCX chromatography* strong cation exchange chromatography, *iTRAQ* isobaric tag for relative and absolute quantification, *CP IEF* cytoplasm isoelectric focusing, *MB IEF* membrane isoelectric focusing, *NU IEF* nuclear isoelectric focusing, *CS* cytoplasm, *LC/MS-MS* liquid chromatography–mass spectroscopy

image replicate groups. The quantitative detection of changes in phosphoprotein and total protein abundance are set at a threshold of more than 1.5-fold. The number of spots that are significantly different between the controls and treatments is identified and compared (Student's *t* test, $p < 0.05$).

2-DE is stained with Coomassie Blue G-250. Differentially expressed phosphoproteins and protein spots are excised, and the excised gel pieces are destained with 50% MeOH/50 mM NH_4HCO_3 , dehydrated with 50% acetonitrile (ACN) twice, and then 100% ACN. The gel pieces are dried by vacuum centrifugation for 30 min. The completely dried gel pieces are added with 20 μL of 12.5 ng μL^{-1} trypsin (Promega, USA) in 10 mM NH_4HCO_3 /10%ACN, and digestion proceeds at 37°C for 16 h. The peptides are extracted following the protocol described in Thiagarajan et al. [110] and analyzed using an MALDI-TOF/TOF or LC-MS-MS. MS and MS/MS data is combined through the MS BioTools program (Bruker-Daltonics) to search the NCBI database using Mascot software (Matrix Science, London, UK), and protein identification is conducted according to the method specified in Qian et al. [111].

14.8 Conclusions

Screening for low-toxic and nontoxic antifouling compounds from marine organisms will remain at the frontier of research for the coming decades until a suite of very effective and environmentally friendly marine natural products are identified, commercialized, and applied as routine antifouling agents, due to the practical needs and huge market potential. Bioassay systems will play most critical and vital roles in screening efforts and have to be taken as top priority in antifouling screening research. Ideally, a battery of screening bioassays shall consist of both antimicrofouling and antimacrofouling assays with multiple target species for each group. And certainly, target species shall include both hard foulers and soft foulers.

In reality, to reduce operational costs and save time, high-throughput assays using microtiter plates shall be used as much as possible, particularly for preliminary screening assays, followed by more complex bioassay processes. In the near future, it is expected that molecular biomarkers (genes, proteins, receptors, or receptor system) will provide a better means to design more targeted bioassay systems, which may not only speed up screening process but also save time needed to conduct an environmental safety and mode-of-action study of identified chemical compounds because the molecular target is already known.

However, to develop a targeted bioassay (using molecular markers), we need to gain a much better understanding of:

1. Molecular mechanisms of spore and larval attachment and metamorphosis
2. Mode-of-action of antifouling compounds against settling propagules (how they act, how long it takes for a compound to reach the target, what they target)
3. Behavior of chemical compounds (synergistic or antagonistic interactions), accumulation, transportation, and transformation

4. Effects of the physical and chemical environment on chemical function, such as water flow dynamics, surface matrix, and pH
5. Effect of biological factors on compound function and behavior, such as biofilm development, microbial interaction and metabolites; responses of fouling organisms to compounds, ontogenetic susceptibility shift, and so on

14.9 Study Questions

1. Why do we need to screen for antifouling compounds from marine organisms?
2. What kind of compound would be an ideal antifouling compound with market potential in the future, why?
3. What are the pros and cons of using marine microbes as the source of antifouling compounds?
4. What characteristics would make a species desirable for antifouling bioassays?
5. Why do we need to study the mode of action of antifouling compounds?

Acknowledgments The authors would like to thank Miss Cherry HT Kwan for her help in preparing flowcharts and commenting on the draft. This work was supported by the grant from the China Ocean Mineral Resources Research and Development Association (COMRRDA) and an award SA-C0040/UK-C0016 from the King Abdullah University of Science and Technology to P. Y. Qian.

References

1. Little BJ, Zsolnay ZA (1985) Chemical fingerprinting of adsorbed organic materials on metal surfaces. *J Coll Interface Sci* 104:79–86
2. Characklis WG, Cooksey KE (1983) Biofilm and microbial fouling. *Adv Appl Microbiol* 29:93–148
3. Lau SCK, Mak KKW, Chen F, Qian PY (2002) Bioactivity of bacterial strains isolated from marine biofilms in Hong Kong waters for the induction of larval settlement in the marine polychaete *Hydroides elegans*. *Mar Ecol Prog Ser* 226:301–310
4. Wimpenny J (1996) Ecological determinants of biofilm formation. *Biofouling* 10:43–63
5. Yebra DM, Kiil S, Dam-Johansen K (2004) Review: Antifouling technology – past, present and future steps towards efficient and environmentally friendly antifouling coatings. *Prog Organ Coatings* 50:75–104
6. Woods Hole Oceanographic Institute (1952) Marine fouling and its prevention. US Naval Institute/George Banta Publishing Co., Annapolis/Menasha
7. Chambers LD, Stokes KR, Walsh FC, Wood RJK (2006) Modern approaches to marine antifouling coatings. *Surf Coatings Technol* 201:3642–3652
8. Veza JM, Ortiz M, Sadhwani JJ, Gonzalez JE, Santana FJ (2008) Measurement of biofouling in seawater: some practical tests. *Desalination* 220:326–334
9. Fusetani N (2004) Biofouling and antifouling. *Nat Prod Rep* 21:94–104
10. Fusetani N, Clare A (2006) Antifouling compounds. Springer, Berlin/New York
11. Qian PY, Xu Y, Fusetani N (2010) Natural products as antifouling compounds: recent progress and future perspectives. *Biofouling* 26:223–234

12. Ebada SS, Edrada RA, Lin WH, Proksch P (2008) Methods for isolation, purification and structural elucidation of bioactive secondary metabolites from marine invertebrates. *Nat Protoc* 3:1820–1831
13. Johnson TA, Morgan MVC, Aratow NA, Estee SA, Sashidhara KV, Loveridge ST, Segraves NL, Crews P (2010) Assessing pressurized liquid extraction for the high-throughput extraction of marine-sponge-derived natural products. *J Nat Prod* 73:359–364
14. Grob K, Zürcher F (1976) Stripping of trace organic substances from water: equipment and procedure. *J Chromatogr* 117:285–294
15. Harder T, Lau SCK, Dahms HU, Qian PY (2002) Isolation of bacterial metabolites as natural inducers for larval settlement in the marine polychaete *Hydroides elegans* (Haswell). *J Chem Ecol* 28:2029–2043
16. Baltussen E, Sandra P, David F, Cramers C (1999) Stir Bar Sorptive Extraction (SBSE), a novel extraction technique for aqueous samples, theory and principles. *J Microcolumn Sep* 11:737–747
17. Demyttenaere JCR, Morina RM, Sandra P (2003) Monitoring and fast detection of mycotoxin-producing fungi based on headspace solid-phase microextraction and headspace sorptive extraction of the volatile metabolites. *J Chromatogr* 985:127–135
18. Acar JF (1980) The disc susceptibility test. In: Lorian V (ed) *Antibiotics in laboratory and Medicine*. Williams and Wilkins, Baltimore, pp 24–54
19. Dobretsov SV, Dahms HU, Qian PY (2004) Antilarval and antimicrobial activity of waterborne metabolites of the sponge *Calyspongia (Euplaccella) pulvinata*: evidence of allelopathy. *Mar Ecol Prog Ser* 271:133–146
20. Miao L, Qian PY (2005) Antagonistic antimicrobial activity of marine fungi and bacteria isolated from marine biofilm and seawater of Hong Kong waters. *Aquat Microb Ecol* 38:231–238
21. Marchetti O, Moreillon P, Glauser MP, Bille J, Sanglard D (2000) Potent synergism of the combination of fluconazole and cyclosporine in *Candida albicans*. *Antimicrob Agents Chemother* 44:2373–2381
22. Huang YL, Dobretsov SV, Xiong HR, Qian PY (2007) Effect of biofilm formation by *Pseudoalteromonas spongiae* on induction of larval settlement of the polychaete *Hydroides elegans*. *Applied Environ Microbiol* 73:6284–6288
23. Genevaux P, Muller S, Bauda PA (1996) rapid screening procedure to identify mini-Tn10 insertion mutants of *Escherichia coli* K-12 with altered adhesion properties. *FEMS Microbiol Lett* 142:27–30
24. Harder T, Lau SCK, Tam WY, Qian PY (2004) A bacterial culture-independent method to investigate chemically-mediated control of bacterial epibiosis in marine invertebrates by using TRFLP analysis and natural bacterial populations. *FEMS Microbiol Ecol* 47:93–99
25. Henrikson AA, Pawlik JR (1995) A new antifouling assay method: results from field experiments using extracts of four marine organisms. *J Exp Mar Biol Ecol* 194:157–165
26. Lee OO, Qian PY (2003) Chemical control of bacterial epibiosis and larval settlement of *Hydroides elegans* in the red sponge *Mycale adhaerens*. *Biofouling* 19:171–180
27. Lee OO, Chui PY, Wong YH, Pawlik JR, Qian PY (2009) Evidence for vertical transmission of bacterial symbionts from adult to embryo in the Caribbean sponge *Svenzea zeai*. *Appl Environ Microbiol* 75:6147–6156
28. McLean RJC, Bryant SA, Vattem DA, Givskov M, Rasmussen TB, Balaban N (2008) Detection in vitro of quorum-sensing molecules and their inhibitors, Chapter 2. In: Balaban N (ed) *The control of biofilm infections by signal manipulation*. Springer, Heidelberg, pp 39–70
29. McLean RJC, Pierson LS, Fuqua C (2004) A simple screening protocol for the identification of quorum signal antagonists. *J Microbiol Methods* 58:351–360
30. Martinelli D, Grossmann G, Sequin U, Brandl H, Bachofen R (2004) Effects of natural and chemically synthesized furanones on quorum sensing in *Chromobacterium violaceum*. *BMC Microbiol* 4:1–10

31. Blosser RS, Gray KM (2000) Extraction of violacein from *Chromobacterium violaceum* provides a new quantitative bioassay for N-acyl homoserine lactone autoinducers. *J Microbiol Methods* 40:47–55
32. Choo JH, Rukayadi Y, Hwang JK (2006) Inhibition of bacterial quorum sensing by vanilla extract. *Lett Appl Microbiol* 42:637–641
33. Dobretsov S, Dahms HU, Qian PY (2005) Antibacterial and anti-diatom activity of Hong Kong sponges. *Aquatic Microbial Ecol* 38:191–201
34. Guillard RRL, Ryther JH (1962) Studies of marine planktonic diatoms. I. *Cyclotella nana* Hustedt, and *Detonula confervacea* (cleve) Gran. *Can. J Microbiol* 8:229–239
35. Lam CKS, Harder T, Qian PY (2003) Induction of larval settlement in the polychaete *Hydroides elegans* by surface-associated settlement cues of marine benthic diatoms. *Mar Ecol Prog Ser* 263:83–92
36. Schilp S, Kueller A, Rosenhahn A, Grunze M, Pettitt ME, Callow ME, Callow JA (2007) Settlement and adhesion of algal cells to hexa(ethylene glycol)-containing self-assembled monolayers with systematically changed wetting properties. *Biointerphases* 2:143–150
37. Lorenzen CJ (1967) Determination of chlorophyll and phaeopigments: spectrophotometric equations. *Limnol Oceanogr* 12:343–346
38. Byun HG, Zhang H, Mochizuki M, Adachi K, Shizuri Y, Lee WJ, Kim SK (2003) Novel antifungal diketopiperazine from marine fungus. *J Antibiot (Tokyo)* 56:102–106
39. Matti KM, Savanurmath CJ, Hinchigeri SB (2010) A promising broad spectrum antimicrobial red fluorescent protein present in silkworm excreta. *Biol Pharm Bull* 33: 1143–1147
40. Miao L, Kwong TF, Qian PY (2006) Effect of culture conditions on mycelial growth, antibacterial activity, and metabolite profiles of the marine-derived fungus *Arthrinium c.f. saccharicola*. *Appl Microbiol Biotechnol* 72:1063–1073
41. Callow ME, Callow JA, Pickett-Heaps JD, Wetherbee R (1997) Primary adhesion of *Enteromorpha* (Chlorophyta, Ulvales) propagules: quantitative settlement studies and video microscopy. *J Phycol* 33:938–947
42. Callow ME, Callow JA, Ista LK, Coleman SE, Nolasco AC, Lopez GP (2000) Use of self-assembled monolayers of different wettabilities to study surface selection and primary adhesion processes of green algal (*Enteromorpha*) zoospores. *Appl Environ Microbiol* 66:3249–3254
43. Holmstrøm C, Egan S, Franks A, McCloy S, Kjelleberg S (2002) Antifouling activities expressed by marine surface associated *Pseudoalteromonas* species. *FEMS Microbiol Ecol* 41:47–58
44. Joint I, Callow ME, Callow JA, Clarke KR (2000) The attachment of *Enteromorpha* zoospores to a bacterial biofilm assemblage. *Biofouling* 16:151–158
45. Egan S, James S, Holmstrom C, Kjelleberg S (2001) Inhibition of algal spore germination by the marine bacterium *Pseudoalteromonas tunicata*. *FEMS Microbiol Ecol* 35:67–73
46. Finlay JA, Callow ME, Schultz MP, Swain GW, Callow JA (2002) Adhesion strength of settled spores of the green alga *Enteromorpha*. *Biofouling* 18:251–256
47. Swain GW, Schultz MP (1996) The testing and evaluation of non-toxic antifouling coatings. *Biofouling* 10:187–197
48. Thiagarajan V, Harder T, Qian PY (2002) Effect of the physiological condition of cyprids and laboratory-mimicked seasonal conditions on the metamorphic successes of *Balanus amphitrite* Darwin (Cirripedia :Thoracica). *J Exp Mar Biol Ecol* 274:65–74
49. Thiagarajan V, Harder T, Qian PY (2002) Relationship between cyprid energy reserves and metamorphosis in the barnacle *Balanus amphitrite* Darwin (Cirripedia: Thoracica). *J Exp Mar Biol Ecol* 280:79–93
50. Rittschof D, Branscomb ES, Costlow JD (1984) Settlement and behavior in relation to flow and surface in larval barnacles, *Balanus amphitrite* Darwin. *J Exp Mar Biol Ecol* 82:131–146

51. Qiu JW, Qian PY (1997) Effects of food availability, larval source and culture method on larval development of *Balanus amphitrite amphitrite* Darwin: implications for experimental design. *J Exp Mar Biol Ecol* 217:47–61
52. Moyses JA (1963) Comparison of the value of various flagellates and diatoms as food for barnacle larvae. *J Cons Int Explor Mer* 28:175–187
53. Cai BJ (1990) Planktonic larvae in Daya Bay. In: Third Institute of Oceanography (ed) Collections of papers on marine ecology in Daya Bay (II). Ocean Press, China, pp 232–236
54. Thompson GB (1986) The 1976/77 phytoplankton cycle in Aberdeen Harbor. *Hong Kong Asian Mar Biol* 3:33–45
55. Qiu JW, Qian PY (1997) Combined effects of salinity, temperature and food on early development of the polychaete *Hydroides elegans*. *Mar Ecol Prog Ser* 152:79–88
56. Thiagarajan V, Harder T, Qian PY (2003) Combined effects of temperature and salinity on larval development and attachment of the subtidal barnacle *Balanus trigonus* Darwin (Cirripedia: Thoracica). *J Exp Mar Biol Ecol* 287:223–236
57. Doyle P, Mather AE, Bennett MR, Bussell A (1997) Miocene barnacle assemblages from southern Spain and their palaeoenvironmental significance. *Lethaia* 29:267–274
58. Rittschof D, Clare AS, Gerhart DJ, Avelin Mary S, Bonaventura J (1992) Barnacle in vitro assays for biologically active substances: toxicity and settlement assays using mass cultured *Balanus amphitrite* Darwin. *Biofouling* 6:115–122
59. Rittschof D, Clare AS, Gerhart DJ, Bonaventura J, Smith C, Hadfield M (1992) Rapid field assessment of antifouling and foul-release coatings. *Biofouling* 6:181–192
60. Crustacean SAJ (1987) Issues 5: Barnacle biology. Balkema, A. A, Rotterdam, p 392
61. Rittschof D, Costlow JD (1989) Surface determination of macroinvertebrate larval settlement. In: Styczynsk-Jurewicz E (ed) Proceedings of the 21st European Marine Biology Symposium of the Polish Academy of Sciences, Institute of Oceanology, Gdansk, pp 155–163
62. Rittschof D, Costlow JD. Bryozoan and barnacle settlement in relation to initial surface wettability: a comparison of laboratory and field studies. (1989). In: Ros JD (ed) Topics in marine biology, Proceedings of the 22nd European Marine Biology Symposium of the Instituto de Ciencias del Mar, Barcelona, pp 411–416
63. Maki JS, Rittschof D, Costlow JD, Mitchell R (1988) Inhibition of attachment of larval barnacles *Balanus amphitrite* by bacterial surface films. *Mar Biol* 97:199–206
64. Maki JS, Rittschof D, Schmidt AR, Snyder AG, Mitchell R (1989) Factors controlling attachment of bryozoan larvae; a comparison of bacterial films and unfilmed surfaces. *Biol Bull* 177:295–302
65. Maki JS, Rittschof D, Samuelsson MO, Szwedzyk U, Yule AB, Kjelleberg B, Costlow JD, Mitchell R (1990) Effect of marine bacteria and their exopolymers on the attachment of barnacle cypris larvae. *Bull Mar Sci* 46:499–511
66. Maki JS, Rittschof D, Mitchell R (1992) Inhibition of larval barnacle attachment to bacterial films: an investigation of physical properties. *Microb Ecol* 23:97–106
67. Maki JS, Yule AB, Rittschof D, Mitchell R (1994) The effect of bacterial films on the temporary adhesion and permanent fixation of cypris larvae, *Balanus amphitrite* Darwin. *Biofouling* 8:121–131
68. Qian PY, Thiagarajan V, Lau SCK, Cheung S (2003) Relationship between microbial community and the attachment of acorn barnacle *Balanus amphitrite* Darwin. *Aquat Microb Ecol* 33:225–237
69. Qian PY, Rittschof D, Sreedhar B, Chia FS (1999) Macrofouling in unidirectional flow: miniature pipes as experimental models for studying the effects of hydrodynamics on invertebrate larval settlement. *Mar Ecol Prog Ser* 191:141–151
70. Qian PY, Rittschof D, Sreedhar B (2000) Macrofouling in unidirectional flow: miniature pipes as experimental models for studying the interaction of flow and surface characteristics on the attachment of barnacle, bryozoan and polychaete larvae. *Mar Ecol Prog Ser* 207:109–121

71. Satuito CG, Shimizu K, Natoyama K, Yamazaki M, Fusetani N (1996) Age-related success by cyprids of the barnacle *Balanus amphitrite*, with special reference to consumption of cyprid storage protein. *Mar Biol* 127:125–130
72. Harder T, Thiagarajan V, Qian PY (2001) Effect of cyprid age on the settlement of *Balanus amphitrite* Darwin in response to natural biofilms. *Biofouling* 17:211–219
73. Harder T, Thiagarajan V, Qian PY (2001) Combined effect of cyprid age and lipid content on larval attachment and metamorphosis of *Balanus amphitrite* Darwin in response to natural biofilms. *Biofouling* 17:257–262
74. Tighe-Ford DJ, Power MJD, Vaile DC (1970) Laboratory rearing of barnacle larvae for antifouling research. *Helgolander wiss Meeresunters* 20:393–405
75. Costlow JD, Bookhout CG (1958) Larval development of *Balanus amphitrite* var. *denticulata* Broch reared in the laboratory. *Biol Bull* 114:284–295
76. Hadfield MG, The D (1998) P Wilson lecture: Research on settlement and metamorphosis of marine invertebrate larvae: past, present and future. *Biofouling* 12:9–29
77. Qian PY (1999) Larval settlement of polychaetes. *Hydrobiologia* 402:239–253
78. Bryan PJ, Kreider JL, Qian PY (1998) Settlement of the serpulid polychaete *Hydroides elegans* (Haswell) on the arborescent bryozoan *Bugula neritina* (L.): evidence of a chemically mediated relationship. *J Exp Mar Bio Ecol* 220:171–190
79. Bryan PJ, Qian PY, Kreider JL, Chia FS (1997) Induction of larval settlement and metamorphosis by pharmacological and conspecific associated compounds in the serpulid polychaete *Hydroides elegans*. *Mar Ecol Prog Ser* 146:81–90
80. Qian PY, Pechenik JA (1998) Effects of larval starvation and delayed metamorphosis on juvenile survival and growth of the tube-dwelling polychaete *Hydroides elegans*. *J Exp Mar Biol Ecol* 227:169–185
81. Pechenik JA, Qian PY (1998) Onset and maintenance of metamorphic competence in the marine polychaete *Hydroides elegans* Haswell in response to three chemical cues. *J Exp Mar Biol Ecol* 226:51–74
82. Dahms HU, Dobretsov S, Qian PY (2004) The effect of bacterial and diatom biofilms on the settlement of the bryozoan *Bugula neritina*. *J Exp Mar Biol Ecol* 313:191–209
83. Ryland JS (1958) *Bugula simplex* Hincks, a newly recognized polyzoan from British waters. *Nature* 181:1148–1149
84. Wong YH, Arellano SM, Zhang H, Ravasi T, Qian PY (2010) Dependency on de novo protein synthesis and proteomic changes during metamorphosis of the marine bryozoan *Bugula neritina*. *Proteome Sci* 8:e25
85. Bryan PJ, Rittschof D, Qian PY (1997) Settlement inhibition of bryozoan larvae by bacterial films and aqueous leachates. *Bull Mal Sci* 61:849–857
86. Woollacott RM, Zimmer RL (1971) Attachment and metamorphosis of the cheilostenostome bryozoan *Bugula neritina* (Linne). *J Morphol* 134:351–382
87. Reed CG, Woollacott RM (1982) Mechanisms of rapid morphogenetic movements in the metamorphosis of the bryozoan *Bugula neritina* (Cheilostomata, Cellulariodea). I. Attachment to the substratum. *J Morphol* 172:335–348
88. Loosanoff VL, Davis HC (1963) Rearing of bivalve molluscs. In: Russell FS (ed) *Advances in marine biology*, vol 1. Academic, London, pp 1–136
89. Beaumont AR, Budd MD (1984) High mortality of the larvae of the common mussel at low concentrations of tributyltin. *Mar Pollut Bull* 15:402–405
90. Utting SD, Spencer BE (1991) The hatchery culture of bivalve mollusc larvae and juveniles. *Lab Leaflet*, 68. MAFF Fish Res, Lowestoft, p 31
91. Beaumont AR, Turner G, Wood AR, Skibinski DOF (2004) Hybridisations between *Mytilus edulis* and *Mytilus galloprovincialis* and performance of pure species and hybrid veliger larvae at different temperatures. *J Exp Mar Biol Ecol* 302:177–188
92. Galley TH, Batista FM, Braithwaite R, King J, Beaumont AR (2010) Optimisation of larval culture of the mussel *Mytilus edulis* (L.). *Aquac Int* 18:315–325

93. Pechenik JA, Eyster LS, Widdows J, Bayne BL (1990) The influence of food concentration and temperature on growth and morphological differentiation of blue mussel *Mytilus edulis* (L.) larvae. *Mar Biol* (Berl) 136:47–64
94. Zimmerman KM, Pechenik JA (1991) How do temperature and salinity affect relative rates of growth, morphological differentiation, and time to metamorphic competence in larvae of the marine gastropod *Crepidula plana*? *Biol Bull* 180:372–386
95. Satuito CG, Bao WY, Yang JL, Kitamura H (2005) Survival, growth, settlement and metamorphosis of refrigerated larvae of the mussel *Mytilus galloprovincialis* Lamarck and their use in settlement and antifouling bioassays. *Biofouling* 21:217–225
96. Branscomb ES, Rittschof D (1984) An investigation of low frequency sound waves as a means of inhibiting barnacle settlement. *J Exp Mar Biol Ecol* 79:149–154
97. Qi SH, Xu Y, Xiong HR, Qian PY, Zhang S (2009) Antifouling antibacterial compounds from a marine fungus *Cladosporium* sp. F14. *World J Microbiol Biotechnol* 25:399–406
98. Zhou XJ, Xu Y, Jin CL, Qian PY (2009) Reversible anti-settlement activity against (*Amphibalanus* (= *Balanus*) *amphitrite*, *Bugula neritina*, and *Hydroides elegans* by a nontoxic pharmaceutical compound, mizolastine. *Biofouling* 25:739–747
99. Xu Y, He HP, Schulz S, Liu X, Fusetani H, Xiong HR, Xiao X, Qian PY (2010) Potent antifouling compounds produced by marine *Streptomyces*. *Bioresour Technol* 101:1331–1336
100. Dobretsov SV, Qian PY (2003) Pharmacological induction of larval settlement and metamorphosis in the blue mussel *Mytilus edulis* L. *Biofouling* 19:57–63
101. Bao WY, Satuito CG, Yang JL, Kitamura H (2007) Larval settlement and metamorphosis of the mussel *Mytilus galloprovincialis* in response to biofilms. *Mar Biol* 150:565–574
102. Etoh H, Hageshita S, Ina K (1997) An improved assay for attachment-promoting substances of the blue mussel, *Mytilus edulis galloprovincialis*. *J Mar Biotechnol* 5:24–26
103. Ina K, Takasawa R, Yagi A, Yamashita N, Etoh H, Sakata K (1989) An improved assay for antifouling substances using the blue mussel, *Mytilus edulis*. *Agric Biol Chem* 53:3319–3321
104. Sera Y, Iida S, Adachi K, Shizuri Y (2000) Improved plate assay for antifouling substances using blue mussel *Mytilus edulis*. *Mar Biotechnol* 2:314–318
105. Hayashi Y, Miki W (1996) A newly developed bioassay system for antifouling substances using the blue mussel, *Mytilus edulis galloprovincialis*. *J Mar Biotechnol* 4:127–130
106. Lau SCK, Thiagarajan V, Qian PY (2003) The bioactivity of bacterial isolates in Hong Kong waters for the inhibition of barnacle (*Balanus amphitrite* Darwin) settlement. *J Exp Mar Biol Ecol* 282:43–60
107. Daley RJ, Hobbie JE (1975) Direct counts of aquatic bacteria by a modified epifluorescence technique. *Limnol Oceanogr* 20:875–882
108. Xu Y, Li HL, Li X, Xiao X, Qian PY (2009) Inhibitory effects of a branched-chain fatty acid on larval settlement of the polychaete *Hydroides elegans*. *Mar Biotech* 11:495–504
109. Thiagarajan V, Wong T, Qian PY (2009) 2D gel-based proteome and phosphoproteome analysis during larval metamorphosis in two major marine biofouling invertebrates. *J Proteome Res* 8:2708–2719
110. Thiagarajan V, Qian PY (2008) Proteome analysis of larvae during development, attachment and metamorphosis in the fouling barnacle *Balanus amphitrite*. *Proteomics* 8:3164–3172
111. Qian PY, Wong YH, Zhang Y (2010) Changes in the proteome and phosphoproteome expression in the bryozoan *Bugula neritina* larvae in response to the antifouling agent butenolide. *Proteomics* 10:3435–3446

Chemically Mediated Competition and Host–Pathogen Interactions Among Marine Organisms

15

Marc Slattery and Deborah J. Gochfeld

Contents

15.1	Competition	824
15.1.1	Algae	825
15.1.2	Sponges	828
15.1.3	Hard Corals	830
15.1.4	Soft Corals	831
15.1.5	Others	833
15.2	Pathogenesis	834
15.2.1	Coral Diseases	835
15.2.2	Algae/Seagrass Diseases	842
15.2.3	Sponge Diseases	844
15.2.4	Soft Coral/Gorgonian Diseases	848
15.2.5	Tunicate Diseases	849
15.3	Conclusions	849
	References	850

Abstract

Competition and pathogenesis are two important ecological processes in marine ecosystems. Competition defines interactions between individuals relative to the acquisition of limiting resources. This process includes the act of fouling, but for the purposes of this chapter, we will focus largely on competitive interactions between macroorganisms. Pathogenesis is the initiation and progression of

M. Slattery (✉)

Department of Pharmacognosy, The University of Mississippi, Oxford, MS, USA
and

National Center for Natural Products Research, The University of Mississippi, Oxford, MS, USA
e-mail: slattery@olemiss.edu

D.J. Gochfeld

National Center for Natural Products Research, The University of Mississippi, Oxford, MS, USA
e-mail: gochfeld@olemiss.edu

a disease in a host organism, and it has become recognized as an increasingly important process in marine ecosystems, particularly in the face of accelerating climate change and stress from anthropogenic stressors. There is fairly solid evidence that these processes can be mediated by allelochemicals and antimicrobials, respectively. Yet unequivocal proof that natural products are acting in an ecologically relevant manner, *in situ*, represents a major experimental challenge for marine ecologists. The goal of this chapter is to (1) provide an overview of these ecological processes, (2) single out particularly successful research techniques relative to these processes, and (3) distinguish marine natural products that have been identified as defenses against competitors and pathogens. This chapter will focus on sessile invertebrates and plants since their mechanisms for defending themselves against competition and pathogenesis are more likely to include the production of natural products. To date, there are several examples of extracts from marine plants and invertebrates that have demonstrated allelopathic and antimicrobial activity using a diversity of experimental methodologies. Highlighted are examples of metabolites shown to play a role in allelopathic interactions with algae, soft corals, and sponges, as well as compounds that display antimicrobial activity in algae, soft corals, and sponges.

15.1 Competition

Competition can be one of the most significant ecological processes in the structure and function of terrestrial and aquatic communities [1]. Competition is typically associated with the acquisition of limiting resources such as space, light, and/or food [2]. In marine communities, competition can be particularly intense between benthic organisms that are attached to the substrate, including algae, sponges, hard and soft corals, and tunicates. Competition has been further characterized as either occurring through contact with another organism (= “direct”) or as occurring across a distance (= “indirect”) [3]. In marine communities, indirect competition is often mediated through overgrowth/shading [4, 5], but it can also involve the use of toxic natural products [6]. Rice [7] first coined the term “allelopathy” to generically include any instance in which a natural product (= “allelochemical”) is released into the environment by an organism, where it either harms or aids another organism in the vicinity (i.e., a potential competitor). While this definition has been further refined with time, a persistent concern is proving whether allelopathy actually occurs in nature [8].

Allelopathic interactions in marine communities include the production of antifoulants that limit overgrowth and thus access to various resources, primarily by microorganisms; this is the subject of a separate chapter in this text (see ► [Chapter 14](#)). In addition, allelopathic interactions can occur between benthic macroorganisms via direct contact, when the allelochemicals are surface-bound, or via indirect interactions, when the compounds diffuse through the water column to a distant competitor. Despite reasonable field observations supporting potential allelopathic interactions,

there are few unequivocal experimental studies of chemically mediated competition in marine communities and even fewer that have characterized the natural products responsible. Here, we will provide an overview of those studies relative to several important sessile organisms and use the results to comment on the technical challenges of assessing allelopathic interactions in marine communities.

15.1.1 Algae

Macroalgae are important components of most marine ecosystems and are often effective competitors against other organisms. Phase shifts from coral- to algal-dominated communities throughout the Caribbean during the 1980s demonstrate the delicate competitive balance between these key constituents [9, 10]. For example, when the dynamics of space utilization by brown and red seaweeds and the coral *Oculina arbuscula* were examined at 12 reef habitats in North Carolina, across a 25-m-depth gradient, there was a strong negative correlation between algae and coral cover that appeared to be mediated by light preference of these taxa and by algal inhibition of coral recruitment [11]. Manipulative grazer exclusion/nutrient addition experiments further demonstrated that competition with seaweeds, through shading and scour, limits the distribution of corals on these temperate reefs. This study provides an excellent example of the subtle competitive interactions between algae and corals and the complexity of experimental design requisite to tease apart these factors.

Few studies have provided evidence for allelopathy in macroalgae; three important cases are reviewed here. Kuffner et al. [12] examined larval recruitment of the hard coral *Porites astreoides* and the gorgonian *Briareum asbestinum* in the presence of five species of algae and three species of cyanobacteria. The authors performed field surveys of three reefs in the Florida Keys to ascertain benthic cover of algae, cyanobacteria, sponges, corals, and suitable settlement substrata to assess potential competitors to larval coral recruits. They then constructed replicate larval recruitment chambers [12] that contained conditioned tiles (= control), tiles with an artificial aquarium plant (= mimic), or tiles with one of the algal or cyanobacterial species that were deployed in the field or in an aquarium. One hundred coral larvae were introduced to each chamber and allowed to settle for 4–9 days, at which point the percent survival, percent recruitment, and locations on the tiles were recorded. Their results demonstrated that all but one species of algae caused avoidance behavior or inhibition of recruitment by *P. astreoides* larvae and that *Lyngbya confervoides* and *Dictyota menstrualis* caused significant larval mortality. *Lyngbya majuscula* similarly reduced recruitment and survival of *B. asbestinum* larvae. Recent work has demonstrated that extracts of *D. pulchella* and *D. pinnatifida* affect larval survival of *P. astreoides* (V. Paul, personal communication 2009). While an actual allelochemical compound has not been isolated to date, given field data on the distributions of these algae and cyanobacteria, this research indicates that allelopathy may perpetuate current phase shift

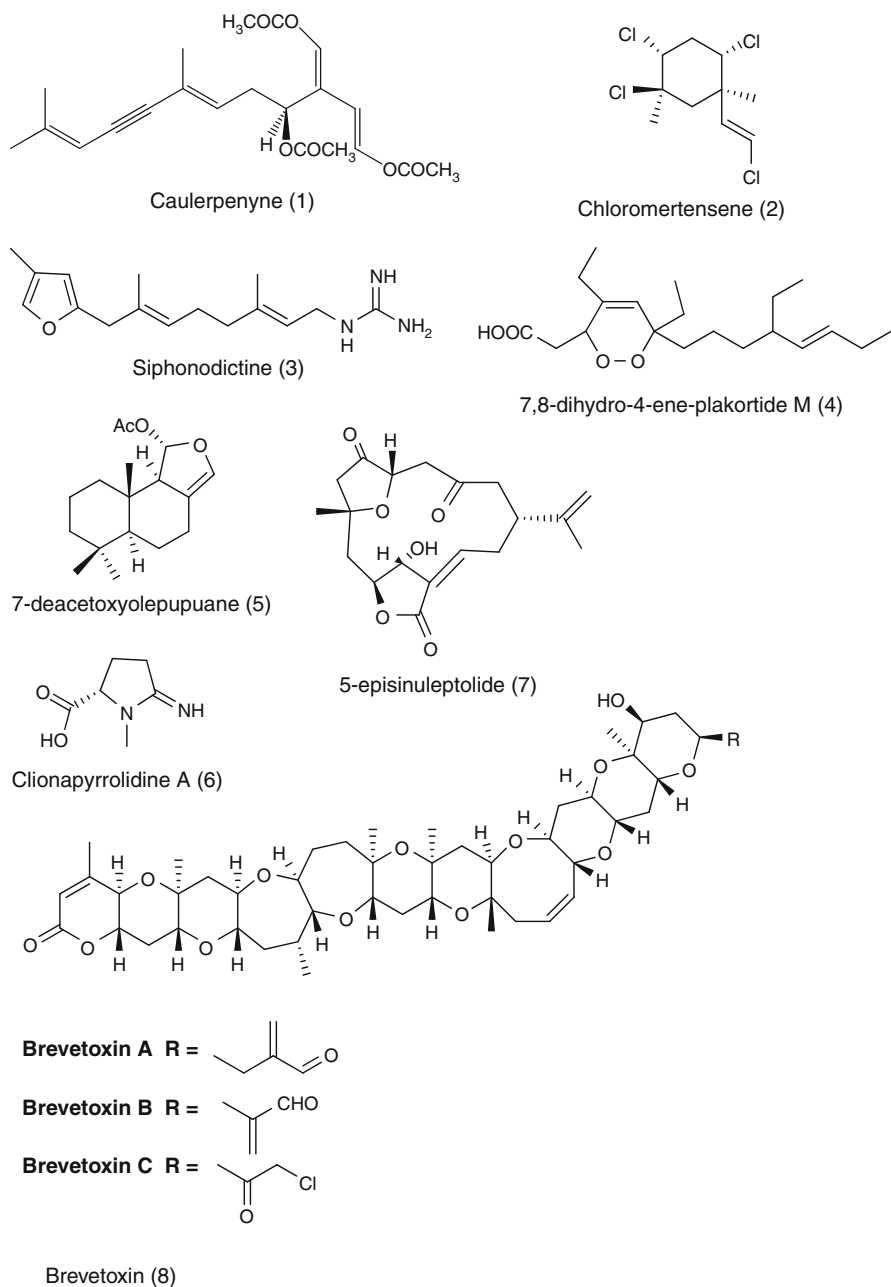


Fig. 15.1 Allelopathic natural products isolated from marine organisms

conditions on tropical reefs by inhibiting the ability of corals to settle and become established.

The Australian seaweed *Caulerpa racemosa* var. *cylindracea* has become invasive in the Mediterranean Sea where it has caused significant changes to the benthic communities [13] and physiological stress to the native seagrass *Cymodocea nodosa* [14]. Crude extracts of the invasive alga at 100 ppm and three known pure compounds at 10 and 1 ppm were exposed to leaf fragments of *C. nodosa* for 6 days under controlled laboratory conditions [15]. The leaf fragments were analyzed daily using pulse amplitude modulated (PAM) fluorometry to assess optimal quantum yield ($= F_v/F_m$), which can be considered a proxy for chlorophyll *a* content [16]. Only the crude extract and caulerpenyne (Fig. 15.1:1) at 10 ppm were found to significantly depress quantum yield and therefore photosystem function. While this study provides preliminary evidence for a *C. racemosa* allelochemical that inhibits the native seagrass *C. nodosa*, it suffers from many of the arguments used to criticize allelopathy [8]. Specifically, there is no supporting evidence from field manipulations to demonstrate that an allelochemical was responsible for the stress to *C. nodosa*, and if present, whether the metabolites were waterborne or surficial. There is also no analytical evidence to demonstrate that the compounds were tested at ecologically relevant concentrations; the activity at 10 ppm may be meaningless if caulerpenyne occurs at levels closer to the inactive 1 ppm. Finally, the absence of activity in two other compounds isolated from *C. racemosa*, and the lack of a bioassay-guided isolation approach, does not rule out additional additive and/or synergistic allelopathic compounds.

More compelling with respect to allelopathy in algae is the work of de Nys et al. [17]. They observed varying degrees of tissue necrosis in the sponge *Dictyoceratida* sp. the gorgonian *Isis* sp., and the soft corals *Sinularia cruciata*, *S. flexibilis*, *S. polydactyla*, and *Clavularia* sp. near the red alga *Plocamium hamatum* on the Great Barrier Reef, Australia. When in contact with the green alga *Chlorodesmis fastigata*, these species did not exhibit tissue necrosis. To assess potential allelopathic activity of this alga, the authors performed two manipulative field experiments. In the first experiment, they placed *P. hamatum* in contact and noncontact settings (5 and 30 cm distance) with the soft coral *S. cruciata*, and they tagged/monitored unmanipulated field “controls” to rule out handling effects; necrosis was assessed at 24 h, 48 h, and 14 days. The second experiment controlled for mechanical abrasion due to contact, by “painting” the algal metabolite chloromertensene (Fig. 15.1:2) onto artificial aquarium plants at a concentration of 2%, which is within the reported range of the metabolite in natural populations [18]. In both cases, contact with the metabolite resulted in tissue necrosis within 48 h, which provided strong evidence for allelopathic inhibition of the soft coral due to the algal monoterpene. However, the authors note that this response was not as extreme as when the soft corals were in contact with the algae, suggesting that there might be other important allelopathic compounds. In contrast to the study by Raniello et al. [15], this study was grounded in solid field observations and manipulative trials. However, the inclusion of a crude extract treatment would have been useful in this study.

15.1.2 Sponges

The functional roles of sponges on reefs, and their numerical dominance, make them some of the most important benthic taxa [19, 20]. In addition, sponges are one of the best-studied models in marine chemical ecology [21], producing a diversity of natural products [22]. Like algae, sponges must protect themselves from competition at the microscale (i.e., epibiosis) [23] and at the macroscale. Although there are more examples of allelopathy by sponges than by algae, many of the methodological challenges faced by phycologists exist for sponge researchers as well. There have been several field studies related to the distributions of marine invertebrates and sponges that demonstrate competitive dominance by chemically defended species [24, 25] or inhibition of settlement and/or metamorphosis near these species [26, 27]. One of the first attempts to address allelopathy on coral reefs focused on the sponge *Aka* (= *Siphonodictyon*) sp. from Palau [28]. This sponge burrows into coral heads leaving only an osculum, surrounded by dead coral tissue, to filter seawater for nutrients. The authors isolated the compound siphonodictine (Fig. 15.1:3) from the sponge and tested its effect at 10 ppm and 100 ppm in seawater in laboratory assays with the coral *Acropora formosa*. Within 30 min, they observed toxin-like effects of respiratory depression and tissue necrosis for the low and high doses, respectively. While these data are intriguing from the anecdotal point of view, this study suffers from methodological details. For example, the original field observations were made on the massive coral *Montipora* sp.; staghorn corals like *A. formosa* do not suffer from infestation by this burrowing sponge. Also, ecologically relevant concentrations of the metabolite were never tested, nor were concentrations within sponge mucus, which was identified as the likely “delivery system” of the compound. This is a model species that would benefit from a revised study using a more robust experimental design.

More recently, the crude extracts of 20 Caribbean sponges were tested against 3 species of Caribbean sponges that are fast overgrowers (*Tedania ignis*, *Lissodendoryx isodictialis*, and *Haliclona hogarthi*) and the extract of the North Carolina sponge *Aplysilla longispina* against the colonial tunicate *Diplosoma listerianum* [29]. The authors developed a novel assay approach that placed overgrowth species in the center of a 15 × 15 cm acrylic plate surrounded on opposing sides by either control or extract-treated Phytigel™ (see [29]). This provided the overgrowth sponges with the potential for lateral growth in any direction over a 3-week period, and it allowed the researchers to ascertain whether extract-treated gels were avoided (= allelopathic). Their results showed that only 7 of the 20 Caribbean sponge extracts inhibited overgrowth, while 3 sponges promoted overgrowth, and the rest had no effect. A separate test demonstrated that extracts of a subset of these sponges were stable in the gels for up to 3 weeks, so the authors concluded that their results indicate that allelopathy among sponges may not be widespread. Nonetheless, they do acknowledge that specifics of each of these extracts tested may account for false negatives in their dataset, and this study should be considered a conservative estimate of the degree of allelopathy in Caribbean sponges. This holistic project clearly demonstrates the potential

importance of allelochemical-mediated competition among sponges, and it should prove useful for testing hypotheses based on field observations and relative to the isolation of specific allelopathic compounds.

Porter and Targett [30] focused more specifically on a single species of Caribbean sponge, *Plakortis halichondroides*, and its interaction with the coral *Agaricia lamarcki*, in St. Croix, US Virgin Islands. Field surveys indicated that this sponge is common between 20 and 30 m depth, and when it occurs in contact with a coral, the coral exhibits signs of physiological stress about 40% of the time. Moreover, 14 species of coral, representing 8 of the 9 Caribbean coral families, were overgrown and killed by this sponge. The authors tested 11 hypotheses related to competition-mediated physiological stress as measured through changes in biomass and oxygen flux. They conducted manipulative field experiments including (1) noncontact scenarios, (2) contact with sponge exudate only, (3) direct contact with the sponge for 24 h, and (4) direct contact with the sponge for extended periods. The latter three treatments resulted in a significant depression of zooxanthellae density, chlorophyll *a* concentrations, and nitrogen mass, relative to controls. Likewise, oxygen flux, representative of net photosynthesis, was also depressed under “contact” conditions. This bleaching response approximated the observed responses of natural field interactions, and the fact that a physiological response could be generated by contact with the sponge exudate alone provided compelling evidence for an allelochemical. Interestingly, in a study of sponge-dominated marine caves in the Bahamas, *P. halichondroides* was separated from other species by clear substrate [31]. The water surrounding these sponges contained the metabolite 7,8-dihydro-4-ene-plakortide M (Fig. 15.1:4), and at ecologically relevant concentrations, this compound killed cells of a potential sponge competitor *Oscarella* sp. in the laboratory. *Plakortis* spp. produce many compounds of similar structure to 4, so it is possible that this or a related compound was responsible for coral tissue necrosis in the study by Porter and Targett [30].

To date, the strongest evidence for allelochemical interactions amongst sponges was generated on Guam, USA, where frequent overgrowth of the sponge *Cacospongia* sp., by the sponge *Dysidea* sp., was observed [32]. This overgrowth often resulted in *Cacospongia* sp. tissue necrosis but not reduction in the defensive metabolites of this species. The authors suspended natural concentrations of crude extracts from *Dysidea* sp. in agar solidified onto window screen and cable-tied these strips to branches of the *Cacospongia* colony in the field. Control strips were similarly prepared, but they contained the carrier solvent only, and these were attached to a neighboring branch of the same colony [32]. Approximately 80% of the tissue under the extract-treated agar strips was necrotic after 1 week, while necrosis under control strips was negligible. In a similar assay using the *Dysidea* metabolite 7-deacetoxyolepupane (Fig. 15.1:5) at ecologically relevant concentrations, they also observed a significant treatment response, but the tissue necrosis was only about half that of the crude extract, suggesting that there may be additive effects. The metabolite yields of *Dysidea* in contact with either *Cacospongia* or rock substrate did not differ, indicating that competition does not induce the production of the allelochemical. This study went on to assess the effects of

Cacospongia extracts on *Dysidea* metabolite production, but it found no significant differences between control and treatment groups. It also demonstrated that the allelochemical (Fig. 15.1:5) functions as a feeding deterrent compound against the predatory angelfish *Pomacanthus imperator*. This study is a solid model for future studies of allelopathy in marine systems; the use of field observations to generate testable hypotheses has produced a complete picture of the chemical interactions between two competitive species. The sole flaw of this study, the lack of a bioassay-guided approach to isolate additional allelopathic compounds, actually highlights a challenge faced by researchers studying competition in marine ecosystems. These processes tend to be quite slow, so viable bioassays might occur over temporal scales measured in weeks. To sequentially follow multiple chemical fractions, in a replicated manner, could literally take years of fieldwork. Thus, researchers often have to rely on a “best guess” based on the activity of related molecules and/or the concentration relative to the dry mass of the organism. Nonetheless, two recent papers have reduced the time needed to run an allelopathic assay. Sponge allelopathy against the coral *Diploria labyrinthiformis* was assessed using extracts incorporated into Phytigel™ molds [33]. Nine common bioactive Caribbean sponges were extracted, and volumetric equivalents were mixed into the gels and fixed to the surface of corals for 18 h. They used PAM fluorometry to assess impacts to symbiotic zooxanthellae photosystem function, which was indicative of stress. Although allelopathic metabolites were not identified, this process offers promise for future studies assuming the response to the allelochemicals is manifested in zooxanthellae productivity. A similar bioassay procedure was used to assess allelopathy by the burrowing sponge *Cliona tenuis* against the hard coral *Siderastrea siderea* [34]. They were able to follow a bioassay-guided approach to the bioactive compound clionapyrrolidine A (Fig. 15.1: 6) by limiting exposures to 24 h. While this paper lacked the field detail of the study by Thacker et al. [32], it demonstrates the apparent toxicity of their allelochemical and the potential implications for competition research.

15.1.3 Hard Corals

Scleractinian (= “hard”) corals are the primary reef-building components of tropical marine hard-bottom communities, and as such, they are often in contact and potentially in competition with other community constituents. Hard corals are known to utilize overgrowth, extracoelomic digestion, and/or “sweeper tentacles” to gain a competitive edge [4, 35], but at least two studies have addressed potential allelopathy in this group of benthic invertebrates. Competitive hierarchies between hard and soft corals were examined on the reefs of southern Taiwan [36]. The investigation was restricted to the study of natural interactions totaling 1,168 pairwise contacts characterized by either (1) the production of a dead margin, (2) overgrowth without tissue necrosis, or (3) stand-offs which lacked necrosis and overgrowth. Results of this broad field survey indicated that soft corals were typically subordinate to the scleractinians in this competitive network. Nonetheless,

the author noted at least eight interactions that appeared to represent allelopathy, and in all of these cases, soft corals were dominant to their hard-coral competitors. Allelopathic competition in the coral *Tubastraea faulkneri* was also studied on the Great Barrier Reef, Australia [37]. This laboratory-based study assessed the toxicity of *T. faulkneri* extracts against 12 species of scleractinian larvae at standard concentrations ranging from 10 to 500 $\mu\text{g ml}^{-1}$. These experimental concentrations were estimated to be 100–5,000 times lower than tissue levels. Larval mortality varied between the coral species, and there was no toxicity to conspecifics. Four indole alkaloids were isolated from *T. faulkneri*, but these were not assayed for allelopathic activity. Based on these data, the authors conclude that these compounds are released into the water column to prevent larval recruitment in the vicinity of *T. faulkneri*. While both these studies provide useful preliminary information, neither offers unequivocal proof that hard corals control competitors using allelochemical compounds.

15.1.4 Soft Corals

Like sponges, soft corals have also been the subjects of much interest relative to their chemical ecology, including studies regarding their competitive abilities [38]. Much of that work occurred on the Great Barrier Reef where soft corals are a spatial dominant of the benthic communities [39] and often interact with other soft and hard corals [5]. Some of the earlier experiments that addressed potential allelopathic effects of these soft corals were based on field observations of movement away from a competitor, stunted growth, tissue necrosis, and/or mortality. In some cases, there were responses in the absence of physical contact, suggesting that waterborne allelochemicals may have been involved [40]. However, field manipulations of soft corals into contact interactions suffered from poor experimental design. Specifically, the use of multiple contact treatments against individuals prevents attribution of the observed necrotic effects [41]. More recently, the role of local environmental factors on the competitive ability of two soft corals, *Clavularia inflata* and *Briareum stechei*, and a hard coral, *Acropora longicyathus*, was examined in all pairwise interactions [42]. These manipulative field experiments involved transplanting between an inshore and a midshelf reef, with appropriate back-transplant and nonhandled controls. Competitive endpoints included overgrowth, tissue bleaching and necrosis, and whole colony mortality. Their results at the inshore site gave a dominance pattern of *Briareum* > *Clavularia* > *Acropora*, while the midshelf site exhibited a reversal of dominance between *Clavularia* and *Acropora*. The authors hypothesized that nutrient enrichment, lower light, and predation at the inshore site may be responsible for the soft coral superiority there. While allelopathy was not specifically addressed in this well-designed field study, the responses observed argue for terpene-mediated competitive dominance and for future studies focused on this question. Later experiments by this group were designed to assess the mechanistic processes by which soft coral allelochemicals impact hard coral competitors. Toxic diterpenes were exuded into

the water column by the soft corals *Sinularia flexibilis* and *Lobophytum hedleyi* at concentrations of 5–20 ppm [43]. They found that at concentrations higher than 5 ppm, branchlets of the hard corals *Acropora formosa* and *Porites cylindrica* expelled their zooxanthellae and nematocysts. The authors concluded that these responses would reduce the corals' abilities to obtain nutrients and defend themselves, respectively, thus lowering their fitness in highly competitive environments. While the ecological relevance of the allelochemical concentrations might be questioned, this study nonetheless provides compelling insights into the mechanism of action of putative allelopathic metabolites.

Competition is not limited to interactions between disparate groups of organisms. Competitive dominance of the hybrid soft coral *Sinularia maxima* × *polydactyla* was observed over its parents *S. maxima* and *S. polydactyla* on the reefs of Guam [44]. A significant decline in the parent soft coral populations was noted over a period from 1994 to 2003, associated with an increase in the hybrid population. To determine whether contact-mediated competition might account for the differences in population dynamics, they assessed the outcome of 124 interactions between the hybrid and either parent in the field. After 3 weeks, 80% of these interactions resulted in tissue necrosis on the parent species (i.e., hybrid dominance), while 20% of the interactions were not resolved. A field assay, similar in technique to that described by Pawlik et al. [33], was conducted on these soft corals. However, tissue necrosis was used as an endpoint after 3 weeks of exposure to extract-containing gels. The parent soft corals and the hybrid all produced extracts that exhibited some degree of tissue necrosis to congeners, but not to conspecifics. Necrosis induced by the hybrids was on the order of 40–60% of the exposed tissue, while the parent extracts induced only 5–10% tissue necrosis. The length of this assay made it impractical to conduct a bioassay-guided isolation of the hybrid allelochemical. Nonetheless, recent assays with the isolated metabolite, 5-episinuleptolide (Fig. 15.1:7), indicate that this compound is partially responsible for the bioactivity attributed to the hybrid extract (Slattery, 2005).

Like tropical reefs, Antarctic benthic communities are also space limited and therefore highly competitive [45]. The soft coral *Alcyonium paessleri* appears to use contact-mediated allelopathy to compete with at least one space dominant sponge in McMurdo Sound [46]. Replicate soft corals and sponges were cemented individually into small flower pots and then moved to the field in contact and noncontact situations for 1 year. Tissue necrosis was not observed when *A. paessleri* was placed in contact with conspecifics, the soft coral *Clavularia frankliniana*, or four common sponges. However, a fifth sponge, *Mycale acerata*, exhibited significant tissue necrosis when in contact with *A. paessleri*. Interestingly, this sponge was a competitive dominant to the sponge *Kirkpatrickia variolosa* [45], which was a competitive equal to *A. paessleri* [46], suggestive of the competitive hierarchy feedback loops proposed by Jackson and Buss [6]. While a putative allelochemical from *A. paessleri* was not identified, it is possible that the cytotoxic metabolite 22-dehydro-7 β -hydroxy-cholesterol (which was a negative olfactory cue for soft-coral predators) might also have allelopathic properties. This compound, along with three other waterborne sterols, was collected in situ near *A. paessleri* colonies using

60 cc syringes [47]. A more elegant allelochemical collection device was developed and tested on soft coral exudates; this apparatus has the potential to further studies of allelopathic compounds released into the water column [48].

15.1.5 Others

Among the most obvious sessile invertebrates on tropical and temperate reefs are the colonial tunicates, and these individuals are often competitive dominants to other groups of benthic organisms [49]. Tunicates typically produce important natural products with defensive properties [22, 50], particularly related to the prevention of surficial fouling [51, 52]. However, most studies associated with tunicate-macroorganism competition seem to indicate that this process is mediated by overgrowth, not allelopathy [53, 54]. On Caribbean coral reefs, the zoanthid *Palythoa caribaeorum* is a dominant member of the benthic community. With some of the fastest growth rates (2.5–4.0 mm/day) recorded for anthozoans, this organism overgrows virtually every other benthic invertebrates, placing itself at the top of the competitive hierarchies in these communities [55]. This species also produces a diversity of natural products, including palytoxin; however, the use of these as allelochemicals has not been evaluated. In contrast, soft bottom communities are often dominated by infaunal worms, including the terebellid polychaete *Thelepus crispus*. This species produces brominated aromatic metabolites that deter the recruits of competitive nereid polychaetes *Nereis vexillosa* [56]. Moreover, these compounds are nonpolar and thus likely remain in the sediment around the polychaete burrows for long periods of time.

Two additional papers demonstrate the complexity of competitive interactions within marine ecosystems. Up to this point, all of the examples of interactions have focused on macroorganisms in benthic communities. While antibiotic-mediated competition between microbes is relatively well accepted [57], the question of competition between microbial and animal decomposers for benthic food falls represents a unique approach to studies of allelopathy [58]. The authors used traps baited with either fresh or microbe-laden (= 48 h colonization in flowing seawater) carrion to assess attractiveness to scavengers; the former bait was 2.6 times more attractive to scavengers. The stone crab preferred the frozen carrion 2.4 times more often than the microbe-laden carrion. In addition, organic extracts of microbe-laden carrion contained noxious extracts that repelled many of the scavengers in the system. While this paper failed to identify the specific metabolites produced by the microbes, this unique field and laboratory study demonstrated a previously underappreciated ecological interaction.

Allelochemical-mediated competition within planktonic communities has also been studied [59]. Specifically, the authors studied the dinoflagellate *Karenia brevis*, which is responsible for monospecific blooms that cause red tide conditions in the Gulf of Mexico. They compared the growth of *K. brevis* with 12 co-occurring phytoplankton species under monoculture and mixed culture laboratory conditions. In nine of the mixed culture conditions, *K. brevis* inhibited growth rates relative to

growth in monocultures, while *Rhodomonas lens* growth was enhanced, and two additional species were unaffected. In a follow-up experiment, the extracellular filtrates of *K. brevis* were collected, extracted, and introduced to monocultures of the competitive phytoplankton. Six of the nine species were inhibited by the filtrate and lipophilic extracts of *K. brevis*, supporting an allelopathic mechanism for bloom characteristics. In the final competition experiment, ecologically relevant concentrations of brevetoxin (Fig. 15.1:8) were introduced to monocultures of the competitive phytoplankton. This compound only caused weak inhibition in one species, *Skeletonema costatum*, although it did induce autoinhibition in *K. brevis*. This study demonstrated appropriate methodologies for dealing with allelopathy in planktonic organisms, and it provides compelling evidence for multiple allelochemicals within *K. brevis* that likely act somewhat selectively and/or in an additive manner.

15.2 Pathogenesis

In contrast to competition, the importance of pathogenesis as an ecological phenomenon within marine ecosystems has only recently received much attention. In recent decades, reports of diseases affecting populations of marine organisms have increased dramatically worldwide [60–63]. This is especially true for corals, but diseases also threaten algae, seagrasses, sponges, gorgonians, molluscs, crustaceans, sea urchins, fishes, and marine mammals [61, 64]. Not only is the rate at which emerging diseases are being discovered escalating but also the number of host species and geographic ranges of diseases has also been increasing. Diseases affecting natural populations threaten biodiversity, resilience, and the ecological balance of communities, as well as the ecological services they provide to humans [65].

Mass mortalities resulting from infectious disease outbreaks (epizootics) have resulted in major changes in community structure of marine ecosystems in recent years. For example, during the 1980s, a waterborne disease of the long-spined sea urchin *Diadema antillarum* spread rapidly throughout the Caribbean, reducing the abundance of this important herbivore by nearly 99% on most Caribbean reefs [66]. This keystone species served a major ecological role by removing macroalgae from Caribbean reefs, and in its absence, algae overgrew reef surfaces and inhibited the survival and settlement of corals, resulting in a phase shift from coral-dominated to algal-dominated reefs Caribbean-wide [9]. This alteration of community types has remained stable for nearly three decades. Unfortunately, at the time, our knowledge of marine diseases was relatively minimal and the pathogen was never identified, nor were appropriate samples collected and preserved for future analysis.

Why have diseases increased to such unprecedented levels? Increased anthropogenic stress in near-shore environments, overfishing, and environmental conditions associated with global climate change have all been implicated as contributing to increased disease levels [60, 61, 67–69]. It is unknown whether the emergence of these diseases is due to the introduction of novel pathogens [61, 70], changes in virulence or range of existing pathogens [71–73], or changes in host susceptibility

[60, 74]. Overall declines in coral reef communities may also play a role, as reduced species and genetic diversity due to declining population sizes may increase susceptibility to emerging infectious diseases [75]. Understanding diseases in marine ecosystems is increasingly important given that a large proportion of the world's population lives near the coast; this need is particularly acute where societies are closely tied to and depend upon coral reefs for their economic and social well-being.

15.2.1 Coral Diseases

Due to their high profile in the public eye, diseases of scleractinian corals are by far the best described in the marine environment, and new diseases are reported with increasing frequency in an expanding number of hosts on a global scale [63, 76, 77]. Coral disease has emerged as a serious threat to coral reefs worldwide and a major cause of reef deterioration [67, 78]. Although our understanding of coral diseases still lags far behind those of terrestrial wildlife, several lessons can be learned from research accomplishments to date, so we will use this important marine functional group as a case study for disease dynamics and resistance mechanisms.

15.2.1.1 Pathogenesis

Disease transmission, onset, and progression are the result of complex interactions between the host, environment, and pathogen, and all must interact in a precise way for disease to occur. For example, in *Vibrio*-induced coral bleaching, the mere presence of the *Vibrio* bacterium associated with the coral host is not sufficient to cause disease. Adhesion and ingress of the bacterium into the coral also requires elevated seawater temperatures [79]. Thus, understanding coral disease dynamics is difficult due to this complex interplay between both abiotic and biotic interactions. Moreover, just like in human host–pathogen transmission, additional species may act as vectors of disease in marine environments [80].

The frequent association of abundant *Vibrio* spp. with diseased coral tissues has led some researchers to question whether they act as primary pathogens for certain diseases or whether they are more opportunistic, colonizing previously compromised hosts [81, 82]. *Vibrio* spp. are abundant and relatively nonselective, so they could be opportunistic [83], but so far, no evidence directly supports this hypothesis, and there is no evidence from molecular screening studies that *Vibrio* spp. found associated with diseased tissues are pathogenic, or that only compromised hosts are infected.

15.2.1.2 Etiology

Nearly 30 coral diseases have been described from reefs across the world in recent years [77, 78], although only a handful of causes (etiologies) have been elucidated. To date, Koch's postulates have only been fulfilled for five coral diseases (see Table 15.1). Koch's postulates represent the gold standard for the verification of

Table 15.1 Etiology of coral diseases for which Koch's postulates have been fulfilled

Disease	Species affected	Geographic region	Pathogen	Vector	Bioactive extracts/ compounds tested
White band disease-II	<i>Acropora</i> spp.	Caribbean	<i>Vibrio charchariae</i> (= <i>V. harveyi</i>) [192, 200]	–	–
White plague-II	30+ hard coral	Caribbean	<i>Aurantimonas coralicida</i> [201]	–	Pathogen tested against extracts from 18 Caribbean corals ([202], Gochfeld, unpublished data 2009) and three Hawaiian corals [117]
White pox disease	<i>Acropora palmata</i>	Caribbean	<i>Serratia marcescens</i> * [94]	–	Pathogen tested against extracts from 18 Caribbean corals ([202], Gochfeld, unpublished data 2009) and three Hawaiian corals [117], mucus and bacteria from <i>Acropora palmata</i> [122]
Aspergillosis	10+ gorgonian	Caribbean	<i>Aspergillus sydowii</i> [70, 181]	African dust, or terrestrial runoff [182, 183]	Pathogen tested against extracts from Caribbean gorgonians [135, 136, 185, 188], mild activity against julieannafuran from <i>Gorgonia ventalina</i> [71]
Bacterial bleaching	<i>Oculina patagonica</i>	Mediterranean	<i>Vibrio shilonii</i> (= <i>V. shiloi</i>) [203, 204]	Fireworm <i>Hermodice carunculata</i> [205]	Pathogen tested against extracts from 18 Caribbean corals ([202], Gochfeld, unpublished data 2009) and three Hawaiian corals [117]
Bacterial bleaching	<i>Pocillopora damicornis</i>	Indo-Pacific	<i>Vibrio coralliilyticus</i> [109]	–	Pathogen tested against extracts from 18 Caribbean corals, ([202], Gochfeld, unpublished data 2009) and three Hawaiian corals [117]

(continued)

Table 15.1 (continued)

Disease	Species affected	Geographic region	Pathogen	Vector	Bioactive extracts/ compounds tested
White syndrome	20+ hard coral	Indo-Pacific	Two new <i>Vibrio coralliilyticus</i> strains + four other <i>Vibrio</i> spp.* (Note: different pathogens affected different coral species) [83]	—	—

*Tested at concentrations exceeding those likely to be found in the marine environment

Koch's postulates represent a procedure proposed by Robert Koch in the late 1800s [206] to verify that a presumed microbial pathogen is the actual cause of a particular disease. Under these rules:

- The putative pathogen must always be found associated with a particular disease.
- The putative pathogen must be isolated from the disease state and grown in pure culture under laboratory conditions.
- The pure culture of the putative pathogen must reproduce the disease when inoculated into or onto a healthy organism.
- The putative pathogen must be reisolated from the newly diseased organism and identified as the same putative pathogen.

Satisfaction of Koch's postulates is difficult under the best of circumstances, but particularly so when the host is a marine organism since (1) less than 1% of known marine microbes have been successfully cultured under laboratory conditions. For the most part, we do not understand the specific biotic and abiotic conditions to which these organisms are exposed, and these conditions have rarely been successfully duplicated in the laboratory. (2) For a particular microorganism to cause pathogenesis to a particular host, additional factors may be required, such as the presence of specific other microorganisms (e.g., as in the polymicrobial black band disease), aspects of seawater chemistry, temperature, light, or metabolites produced by the host, symbiont, or microbial associates. (3) In most cases, even those for which Koch's postulates have been performed, the natural mode of infection of a pathogen is not known; hence, exposing the intact healthy host to a slurry of bacteria in an aquarium may have little relevance to the real world. (4) Likewise, the concentration of pathogen used for inoculation in laboratory experiments may be far greater than a host would ever be exposed to in nature. (5) Pathogenesis may only occur when a host's immune system is already compromised by other pathogens or other types of environmental stressors, following predation or another type of injury, or when the host's physiological condition is more susceptible (e.g., during periods of rapid growth or reproduction). (6) Natural transmission of the pathogen may require an intermediate host or vector rather than through the water column. (7) Reisolation of the pathogen from the site of the new infection cannot necessarily prove whether the pathogen was not there prior to inoculation or occurred in the surrounding water. (8) Marine invertebrates, particularly sponges and corals, are relatively simple organisms. The signs or symptoms that can be seen (at least by the human eye) are relatively few but may in fact represent responses to many different types of conditions, pathogens, or other stressors. Therefore, even if a putative pathogen is identified using Koch's postulates, it does not mean that only that pathogen is responsible for a particular response. More than one pathogen may cause the same response in a given host. (9) Through host–environment interactions, it is highly likely that pathogens may cause different signs or symptoms in different individual hosts or in different species of hosts.

disease etiology; however, fulfilling Koch's postulates requires the ability to culture the pathogen in the laboratory, which may not be possible for many marine diseases [84]. Several other hurdles in the characterization of disease etiologies exist [85]. For example, corals can only exhibit a limited range of symptoms that a human observer can visually identify; therefore, it is likely that multiple types of etiologies may result in the same signs in a coral. The converse is also a problem; any given pathogen or abiotic stressor may cause multiple signs in corals. This could vary depending upon the coral host genotype, zooxanthellae clade, associated microbial community or interactions among any of these factors.

In the past five years, numerous new coral diseases have been described, particularly from the Indo-Pacific region, and our knowledge of their etiologies has advanced rapidly. Three new diseases were reported from the Great Barrier Reef, Australia [86]: skeletal eroding band caused by the protozoan, *Halofolliculina corallasia*; a ciliate disease called brown band disease; and white syndrome, a collective term for disease resulting in tissue loss. White syndrome infections in certain coral species in Palau, the Great Barrier Reef, and the Marshall Islands were found to be caused by six different strains of pathogenic *Vibrio* spp. [82]; these pathogens were shown to cause infection and were identified at the site of infection using molecular methods.

Other etiologies are more difficult to confirm. Dark spot syndrome (DSS) in corals from American Samoa and Hawaii was found to be associated with endolithic fungi [87]. This was also found to be the case for DSS in the Caribbean coral *Siderastrea siderea* but other unidentified endolithic organisms were found associated with DSS in *Agaricia* sp. [88]. Due to the endolithic nature of these fungi, fulfilling Koch's postulates is unlikely. A new bacterial strain *Thalassomonas loyaeana*, isolated from white plague in *Favia fava* from the Red Sea, was found to infect the coral in laboratory experiments, but only in the presence of a filterable factor in the water, and reisolation of the pathogen was not performed [89, 90]. Black band disease (BBD), the first coral disease reported, consists of a polymicrobial consortium, the components of which may vary with environmental conditions [91]; due to this variability, it will likely be impossible to fulfill Koch's postulates for all possible combinations.

15.2.1.3 Geographic Variability

In the Caribbean, coral disease has been implicated as a major factor contributing to the decline of coral reefs, resulting in apparent ecological phase shifts from coral- to algal-dominated ecosystems [9, 76]. An outbreak of white band disease in the 1980s killed acroporid corals throughout the Caribbean [92, 93], and an outbreak of white pox disease in the Florida Keys reduced the cover of the dominant *Acropora palmata* by over 70% between 1996 and 2002 [94]. Until recently, Indo-Pacific corals were believed to be relatively immune to disease; however, it is now apparent that coral diseases are major problems on Indo-Pacific reefs as well [77]. Although coral disease research in the Indo-Pacific is in its infancy, there are clear signs that diseases are emerging as a serious threat to these reefs. For example, a substantial increase in white syndrome has been observed on the Great

Barrier Reef [86]. Coral diseases have also been reported from Philippines [95], American Samoa [96], Marshall Islands [83], Marianas Islands [97], main Hawaiian Islands [98], and even from comparatively pristine areas such as the North-western Hawaiian Islands [99] and Palmyra Atoll [100].

15.2.1.4 Environmental Stressors

Natural and anthropogenic stressors have been implicated in the increased incidence and prevalence of marine diseases. Climate change, particularly elevated seawater temperature, may influence pathogenesis, either by reducing coral resistance or by increasing the growth and virulence of coral pathogens [60, 68, 72, 101]. For example, there is a significant relationship between the frequency of warm temperature anomalies and outbreaks of white syndrome on the Great Barrier Reef [102], and an outbreak of white plague following a thermally induced bleaching event on reefs in the US Virgin Islands caused an average of 51.5% loss in coral cover [103]. BBD also appears to be affected by water temperature, with distinct seasonal increases in disease prevalence on both Caribbean and Indo-Pacific reefs [104, 105]. Bacterial bleaching of *Oculina patagonica* is restricted to summer temperatures [106]. However, not all coral diseases are affected by thermal stress. For example, although there was seasonality in the prevalence of DSS in the Bahamas, this seasonality was not directly related to seawater temperature [107]. Nonetheless, the virulence of certain pathogens does increase at higher temperatures [72, 108, 109], and elevated temperature as expected with climate change predictions may facilitate the expansion of a pathogen's ecological niche [73].

Anthropogenic impacts on coastal areas are increasingly reducing the water quality on coral reefs, with evidence of direct negative impacts on coral health and of interacting effects with pathogens. Experimental studies have demonstrated that nutrient enrichment significantly increases coral mortality and the severity of yellow band disease [110], as well as the rate of progression of BBD [111], and addition of dissolved organic carbon caused coral pathologies similar to band diseases [112]. Correlative data suggest that disease prevalence increases with exposure to anthropogenic stressors, including nutrients [74, 113]. Both BBD and white plague type II were significantly more prevalent on reefs closest to sewage effluent in the Virgin Islands [114]. However, the high prevalence of coral diseases at relatively pristine sites [99, 100, 107, 115, 116] argues against a direct role of human disturbance in all diseases. In addition to nutrients, sediment from terrestrial runoff may serve as a potential reservoir for opportunistic pathogens of corals [77].

Sewage can also bring human enteric pathogens into the sea [94]. These organisms can survive in the ocean, have been isolated from the surfaces of corals, and should therefore be considered potential pathogens to marine organisms. Protection from these potential pathogens may be particularly important in near-shore habitats that might be more susceptible to leaching or spills. In assays testing the antibacterial activity of three Hawaiian corals, the highest levels of inhibitory activity were against the human enteric bacteria *Serratia marcescens*, *Clostridium perfringens*, and *Yersinia enterocolitica* [117]. *Clostridium perfringens* and

other enteric bacteria have been found within the surface mucus layers of several species of corals in the Florida Keys [118]. Since coral diseases have typically been reported more frequently from reefs with higher levels of human activities, these fecal pathogens may represent risk factors associated with coral disease.

15.2.1.5 Susceptibility

Differential susceptibility to disease has consistently been found among coral genera. In the Caribbean, the genus *Acropora* is selectively targeted by certain diseases [76], and in the Indo-Pacific, disease prevalence appears to be greatest among acroporids, poritids, and pocilloporids [86, 95, 99]. Intraspecific variability has also been observed, with diseased colonies found immediately adjacent to unaffected conspecifics [107, 117]. The fact that affected genera, species, or colonies (individuals) occur adjacent to unaffected ones indicates a high degree of variability in resistance to infection. Whether they originate from the host coral, zooxanthellae symbionts, or microbial associates, differences in levels of defenses within and between coral species and colonies and from different locations may help explain patterns of disease occurrence on reefs.

15.2.1.6 Resistance

Corals employ a suite of defense mechanisms to rid themselves of sediment, settling organisms, and potential pathogens, including mucus, phagocytic cells, enzymes and other proteins that are upregulated in response to various stressors, and antimicrobial chemical defenses [64, 76, 117, 119, 120]. Differences in types and levels of defense vary among genera, species, and even at the level of the individual colony [117]. These differences might enable particular populations, species, or genotypes to have an advantage over others in resisting invasion by pathogens [121]. To date, few studies have specifically examined mechanisms of defense against pathogens, yet an understanding of mechanisms of disease resistance in corals is essential to our understanding of patterns of disease prevalence and virulence.

It has been suggested that coral mucus-associated bacteria may act as a first line of defense in the protection of corals and may help prevent infection by occupying niches on the coral surface and tissues and/or by producing antimicrobial compounds, possibly as allelopathic defenses against potential competitors [120, 122–124]. These natural microbial communities preferentially utilize carbon sources in the mucus for their own metabolism [125]. Natural coral-associated bacterial communities have been shown to change in response to environmental stress, including pathogenesis. For example, there was a shift in the mucus-associated bacterial community on *Acropora palmata* following bleaching; there was a decline in the natural complement of bacteria, many of which exhibited antibacterial activity and an increase in *Vibrio* spp. [122]. It was concluded that this could indicate an environmentally induced shift away from beneficial bacteria in the healthy host, and that variability in the protective qualities of coral mucus could allow the emergence of disease. In addition, chemical compounds produced by corals or their microbial

associates can also function as attractants to certain bacteria [117], which may represent a mechanism by which pathogenesis is initiated or by which the natural coral-associated microbial community can be maintained.

Chemical defenses in sessile soft-bodied organisms provide protection from predators, competitors, pathogens, and fouling organisms [126–129] and are necessary for the survival of these species. Site-specific variability in chemical defenses may result from a variety of abiotic and biotic factors, including light [130, 131], temperature [132], predation pressure [133, 134], competition [125], or pathogens [71, 117, 135, 136]. By comparison with the soft-bodied invertebrates, there have been fewer investigations of chemical defenses in scleractinian corals. This is likely due to a combination of conservation concerns, since most corals are listed as threatened or endangered species in many countries, and the technical difficulties of working with scleractinian corals. The presence of antimicrobial chemical defenses has been proposed as a potential mechanism of disease resistance in scleractinian corals [76, 119], but few studies have tested this directly.

In one of the earliest studies on coral chemical defenses, antimicrobial activity was documented in aqueous extracts of at least one colony from 37 of 55 species of Australian corals [137]. In another study on Australian corals, extracts from 100 coral species inhibited the growth of a marine cyanobacterium, and extracts from eight species inhibited the growth of marine bacteria [138]. These studies used the standard disk diffusion assay to assess the presence of antimicrobial activity. In this assay, a lawn of the test microbe is grown on an agar plate, and extract is added to a paper disk, which is placed on the lawn. Antimicrobial activity is observed as a zone of inhibition surrounding the disk in which microbial growth was inhibited. Although still widely used, and one of the only assay options for extracts with limited solubility in aqueous growth media, this assay has limitations. First, it requires that the extract be able to diffuse out of the disk and into the growth media at a rate that is uniform and relevant to microbial growth. Second, assay duration needs to be carefully considered since initial inhibition may be masked by later growth. Third, the concentration of extract added to the disks likely has little relevance to the concentration found in the organisms themselves. These two studies also assessed antimicrobial activity using a single standard concentration of extract, but neither compared this to the concentration of extracts in the corals themselves.

Coral eggs have also been evaluated for the production of antimicrobial chemical defenses, but extracts of eggs from only one out of 11 coral species inhibited growth of only three out of 94 bacterial strains [139]. The Indo-Pacific coral, *Pocillopora damicornis*, rapidly (1 min) produced antibacterial activity in response to mechanical stress [140]. They added cultures of *Vibrio coralliilyticus*, the pathogen that causes bacterial bleaching in *P. damicornis*, to seawater in which a coral had been stressed, and the released antibacterial activity in the seawater killed the pathogen. Of the several bacterial strains tested, the greatest antibacterial activity was observed against this natural pathogen. The Caribbean coral *Siderastrea siderea* also exhibits antibacterial activity against ecologically relevant marine bacteria using the disk diffusion assay [107]. More recently, a liquid growth assay was used to demonstrate that aqueous extracts from several species of

Caribbean corals, and three species of Hawaiian corals exhibit antibacterial activity against a panel of bacteria including known coral pathogens, potential pathogens from human waste, and bacteria isolated from the surfaces of Hawaiian corals [117]. This assay was performed in 96-well plate format, and natural concentrations of extracts were added to wells of bacterial cultures to assess their ability to inhibit bacterial growth. To date, the only natural products isolated from hard corals known to have antibacterial activity to potential ecologically relevant bacteria (i.e., anthropogenic *Escherichia coli*) are montiporic acid A and B [141]. Interestingly, the former compound performs multiple ecological roles, also acting as a feeding attractant to the coral specialist mollusc *Drupella* sp. [142].

Selectivity is a hallmark of antimicrobial activity in corals [107, 117, 137, 140]. This selectivity may be adaptive if it facilitates the development or maintenance of the coral's natural microbial community. Instead, selection to inhibit only those organisms that might be detrimental to coral health should be favored. The presence of antimicrobial activity in various coral extracts suggests that corals may be able to regulate, to some extent, the microbial communities that are associated with their surfaces.

Antibacterial activity also varies by coral condition. Concentrations of specific chemical components in extracts from *Siderastrea siderea* vary with tissue condition (healthy colonies vs. healthy and diseased tissues on colonies with DSS), reflecting changes in levels of infection of individual colonies [107]. When healthy tissues on colonies of *Montipora capitata* affected by *Montipora* white syndrome (MWS) were compared to those from their nearest healthy neighbors (controls), control extracts exhibited significantly greater antibacterial activity against *Yersinia enterocolitica*, and there was a trend toward this pattern against six other bacterial strains, suggesting that higher levels of antibacterial activity in control corals may protect them from pathogens and may help explain why these colonies remain disease free on a reef with other infected colonies [117]. Within colonies affected by MWS, diseased tissues had significantly greater antibacterial activity against *Aurantimonas corallicida*, and there was a trend toward this pattern against five other bacterial strains. This could result from induced defenses in diseased tissues in response to pathogen challenge.

15.2.2 Algae/Seagrass Diseases

Seagrass pathogenesis causes dramatic and long-lasting effects within regional ecosystems. An outbreak of eelgrass wasting disease nearly eradicated populations of the eelgrass *Zostera marina* from North America and Europe in the 1930s, with periodic recurrences in the intervening decades [143]. The zoosporic fungus *Labyrinthula zosterae* was identified as the etiologic agent of this disease [144], and an unidentified congener has been attributed to the mortality of the seagrass *Thalassia testudinum* [145]. *Labyrinthula* spp. are ubiquitous in coastal marine habitats, but only periodically do they become pathogenic, and the reasons for this are not clear, but they may be associated with other environmental stressors reducing overall seagrass health, and therefore resistance.

Marine algae are also susceptible to disease. Red spot disease affecting the commercially important Japanese kelp *Laminaria japonica* is the result of a bacterial infection, although the identity of the pathogen remains in question [146]. The kelp *Nereocystis luetkeana* suffers from a bacterial infection known as white rot disease, caused by *Acinetobacter* sp. [147]. “Raisin disease” in *Sargassum* spp. is caused by a fungal infection of *Lindra thalassiae* [148], and other fungal infections have afflicted the commercially cultivated red algae *Porphyra* spp. in Japan [149]. Coralline algae are also susceptible to disease. The most common, coralline lethal orange disease, affects a diversity of crustose coralline algal species worldwide; to date, the bacterial pathogen has not been identified [150]. A coralline white band syndrome also affects coralline algae in the Caribbean, causing extensive mortality [151].

Antimicrobial activity is widespread in marine plants. Using a combination of disk diffusion assays and liquid growth assays to test extracts from 49 Caribbean marine algae and three seagrasses for antimicrobial effects against five ecologically relevant marine microbes, 90% of extracts were active against at least one microorganism, and 77% of extracts were active against two or more [152]. In the same assays, comparable levels of activity were observed among 54 species of Indo-Pacific marine algae and two species of seagrasses [153]. A more targeted assessment of antifungal activity in seagrasses from Florida demonstrated that four out of five species selectively inhibited the growth of fungi, including the seagrass pathogen *Lindra thalassiae* [154]. In addition to identifying antifungal activity in whole tissues and organic extracts, this study demonstrated that oxidative stress signaling pathways are also incorporated into the seagrasses’ defense against fungal infection [154].

Phenolic metabolites (including condensed tannins) represent the major group of secondary metabolites in seagrasses, and their proposed ecological activities include antipredator and antimicrobial defenses [155]. Infection by the pathogen *Labyrinthula zosterae* induces an increase in phenolic production in *Zostera marina*, even in areas distant from the site of infection, suggesting that the induced response is systemic [156]. In particular, caffeic acid (Fig. 15.2: 9) increases in response to infection with *L. zosterae* and exhibits antimicrobial activity against the pathogen [157]. Gallic acid (Fig. 15.2: 10) concentration increased by 250% following infection by *L. zosterae*, but its ability to inhibit the growth of the pathogen has not yet been established [156]. In the seagrass *Thalassia testudinum*, there is also evidence that phenolic levels increase in blades infected with the pathogen *Labyrinthula* sp.; however, this does not appear to be induced by the infection per se. Instead, this was considered pseudoinduction, a result of compounds accumulating in a localized region of the blade as the lesion inhibited the flow of resources within the blade [145]. Thus, unlike induced responses to pathogenesis, changes in levels of phenolics in *T. testudinum* in response to infection are unlikely to be adaptive [145]. In addition to phenolics, *T. testudinum* produces the flavone glycoside 7-O-beta-D-glucopyranosyl-2"-sulfate (Fig. 15.2:11), which provides antifungal protection [158].

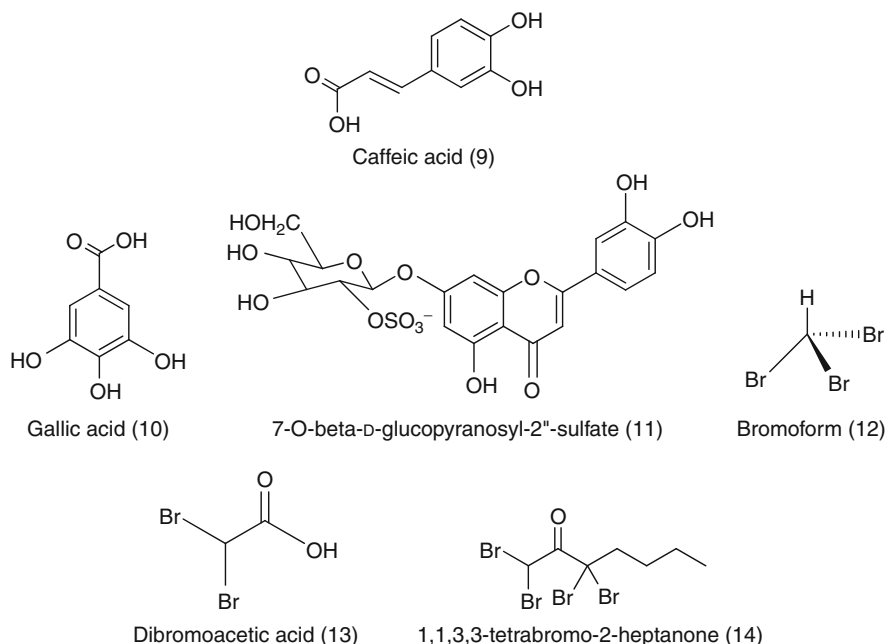


Fig. 15.2 Antimicrobial natural products isolated from marine algae and seagrasses

The red alga *Asparagopsis armata* exhibits antibacterial activity against ecologically relevant *Vibrio* spp. and biomedical bacteria [159]. In this species, the antibacterial compounds are bromoform (Fig. 15.2:12) and dibromoacetic acid (Fig. 15.2:13), both of which are released into the water column and may thereby interact with bacteria prior to settlement [159]. When *A. armata* is cultured in media without bromine, higher densities of epiphytic bacteria grew on algae that did not produce these brominated compounds. The low level of fouling observed on the Swedish red alga *Bonnemaisonia hamifera* is due to the antibacterial compound 1,1,3,3-tetrabromo-2-heptanone (Fig. 15.2: 14), a poly-halogenated 2-heptanone [160]. This compound was tested at natural surface concentrations against 18 bacteria isolated from red algae and exhibited selective antibacterial activity. In addition, when applied to gels and deployed in the sea, natural surface concentrations of this compound reduced overall bacterial growth relative to controls [160]. The red alga *Delisea pulchra* produces halogenated furanones, which, at natural concentrations, prevents surface bacterial colonization by inhibiting bacterial quorum sensing [161].

15.2.3 Sponge Diseases

In contrast to corals, diseases of sponges were documented as early as the 1930s, when disease outbreaks devastated the commercial bath sponge industry in the

Caribbean and later in the Mediterranean [162]. In the past few years, reports of sponge diseases have reemerged across the globe. In only a few cases have the etiologic agents been identified. Tissue necrosis in *Geodia papyracea* from Belize resulted from the sponge's own symbiotic cyanobacteria multiplying faster than the host could control their numbers under thermal stress [163]. A spongin-boring alpha-proteobacterium was identified as the etiologic agent of disease in *Rhopaloeides odorabile* from the Great Barrier Reef through the fulfillment of Koch's postulates [164]. Various other bacteria [165], including those that specifically attack structural spongin fibers [166], fungi [167], and cyanobacteria [168], have also been postulated as sponge pathogens, although these have not been confirmed. Recently, the disease *Aplysina* red band syndrome (ARBS) was described from the Bahamas, where it affected approximately 10% of *Aplysina* spp. rope sponges [168]. This disease manifests as a red band composed of filamentous cyanobacteria surrounding a necrotic lesion that becomes colonized with algae. ARBS is easily transmitted via sponge–sponge contact. ARBS reduces sponge growth and weakens the sponge skeleton, which often breaks at the site of the lesion.

Sponges produce a diversity of secondary metabolites that play important roles in their survival [32, 127, 169] and provide an impressive source of pharmacologically active molecules [170–172]. Some of these compounds are believed to be produced *de novo* by the sponges themselves, while others are now recognized to be products of microbial symbionts [173]. Sponges naturally host diverse microbial communities, consisting of symbionts, opportunists, and pathogens [174]. Most of the early studies on sponge antimicrobials used biomedical models (i.e., human pathogens) to assess potential antimicrobial activity of sponge extracts or metabolites, and numerous compounds with pharmaceutical interest have been identified. More recently, assays evaluating potential ecological roles have been developed, and these have used microorganisms isolated from marine sources, usually the sponge itself, the water column, or the surfaces of nearby biotic or abiotic substrata. Clearly, these assays have more relevance in terms of the efficacy of antimicrobial activity against potential pathogens to which the sponge would naturally be exposed. The greatest number of studies has assessed the antifouling effects of sponge metabolites (discussed in ► Chapter 14), but the prevention of microbial fouling of the sponge surface is of course relevant to the protection of the sponge from pathogenesis as well.

Antimicrobial activity of sponge extracts is widespread, both taxonomically and geographically [175]. Fewer studies have characterized individual metabolites that act to inhibit marine microbes specifically. Extracts and pure compounds from several species of Caribbean sponges were assessed for their ability to inhibit attachment of *Vibrio harveyi*, a ubiquitous marine bacterium, to agar blocks [176]. Since attachment is a primary step in settlement, this process is critical to both fouling and pathogenesis. Eighty-one percent of the sponges tested, and six compounds isolated from four different sponge species inhibited *V. harveyi* attachment at natural or lower concentrations [176]. Extracts from a subset of these sponge species were also tested for their effects on the growth and attachment of

24 marine bacterial isolates from the sponges' natural habitat [169]. Using the disk diffusion assay, only four of these extracts inhibited microbial growth. One isolate from the surface of the sponge *Agelas conifera* exhibited increased attachment but reduced growth when exposed to the extract from that sponge [169]. Using bioassay-guided isolation of the extract from *Aiolochoira crassa*, ianthellin (Fig. 15.3: 15) was identified as a metabolite that inhibited attachment, while a bromotyrosine derivative (Fig. 15.3: 16) inhibited bacterial swarming, a mechanism by which bacteria colonize a surface [169]. In a study of Red Sea sponges, the disk diffusion assay was used to characterize the effects of sponge extracts on the growth of several ecologically relevant bacteria [177]. Eight of the 11 sponge extracts inhibited bacterial growth, and bioassay-guided isolation of the active compounds from *Amphimedon viridis*, the sponge with the greatest activity, yielded a mixture of two pyridinium alkaloids, halitoxin (Fig. 15.3: 17) and amphitoxin (Fig. 15.3: 18). This mixture exhibited selective activity against seawater isolates, whereas isolates from the sponge itself were not inhibited. Interestingly, the surface of *A. viridis* appeared to be free of bacterial fouling, suggesting that bacteria in the water column are unable to colonize the surface of *A. viridis*, whereas bacteria associated with the sponge may be actively selected by the fact that they are immune to the sponge's chemical defenses. Following wounding, an activated defense in *Aplysina aerophoba* catalyzes the production of the antibacterial compounds aeroplysinin-1 (Fig. 15.3: 19) and dienone (Fig. 15.3: 20) to concentrations known to be active; this response might protect injured cells that may have an increased probability of penetration by potential pathogens [178].

The location of metabolites within the sponge may provide clues as to their potential utility as antimicrobial defenses under natural conditions, as well as to their biosynthetic origin. In one of the few studies to address these issues, a variety of techniques were used to demonstrate that oroidin (Fig. 15.3: 21) and sceptrin (Fig. 15.3: 22) were affiliated with sponge rather than bacterial cells in *Agelas conifera* and indicated that sponge spherulous cells were responsible for production of these metabolites [179]. Natural concentrations of extracts caused polyp retraction in the coral *Madracis mirabilis*, and the pure metabolites exhibited antimicrobial activity and feeding deterrence [179]. Tissue wounding increased the concentration of these metabolites, both of which were also found to be released into the water column. The antimicrobial brominated compounds aerothionin (Fig. 15.3: 23) and homoaerothionin (Fig. 15.3: 24) in *Aplysina fistularis* are also exuded into the water column and are believed to play a role in inhibiting surface fouling [180]. The ability of antimicrobial compounds to be released into the water column in the vicinity of the sponge surface, or at least to be bioavailable on the sponge surface, is likely crucial to their efficacy in preventing pathogenesis. Novel methods to measure these compounds, which likely occur in very dilute concentrations, are clearly needed. Solid-phase microextraction (SPME) fibers may provide one method to detect minute concentrations of specific types of metabolites over very fine spatial scales.

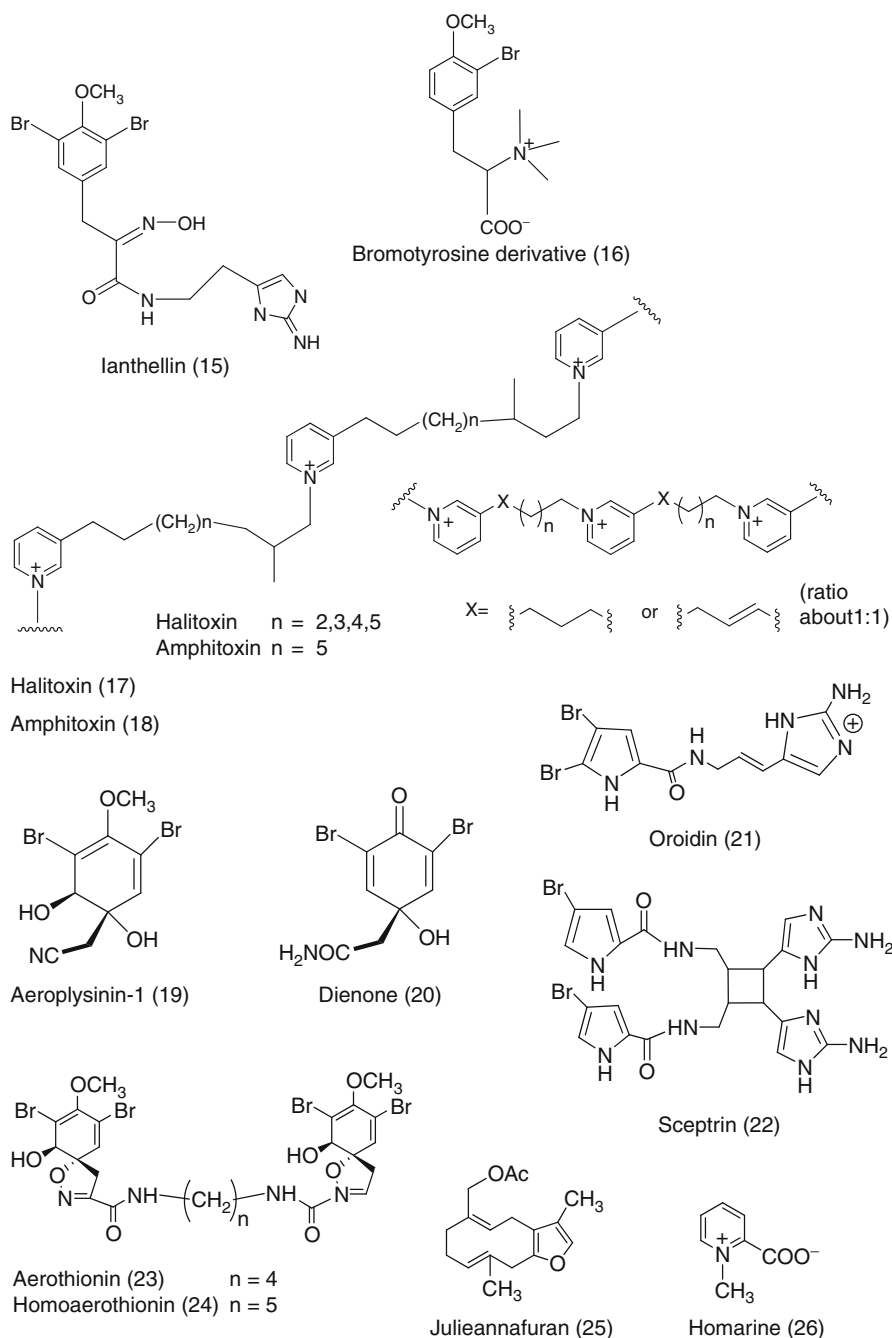


Fig. 15.3 Antimicrobial natural products isolated from marine invertebrates

15.2.4 Soft Coral/Gorgonian Diseases

One of the most extensively studied marine diseases is Aspergillosis, a disease affecting Caribbean gorgonian corals. Aspergillosis is caused by the terrestrial fungus *Aspergillus sydowii* [181], which finds its way onto Caribbean reefs via dust storms from the Sahara Desert and in sediment that runs off of land as a result of human activity [182, 183]. A Caribbean-wide outbreak of Aspergillosis resulted in extensive mortality of the sea fans *Gorgonia* spp. [183, 184]. Both waterborne and physical transmission of Aspergillosis have been demonstrated [183]. Secondary metabolite production by *A. sydowii* isolated from diseased sea fans may be associated with pathogenicity, but this has not yet been verified [183].

Temperature increases activation of certain host immune responses (e.g., oxidative enzymes and cellular immunity), suggesting that gorgonians may increase resistance to disease when faced with warming climatic conditions [68]. However, elevated temperature has been shown to reduce the efficacy of chemical defenses against the fungal pathogen *A. sydowii* [185], suggesting perhaps a trade-off in immune responses under different environmental conditions. Reduced variability in levels of disease resistance on reefs with higher levels of Aspergillosis suggests selection for disease resistance [136], and it has been proposed that resistance in the remaining population of sea fans following the Caribbean-wide Aspergillosis epidemic may explain the recent decline in prevalence of this disease [186].

Extracts from many Caribbean gorgonian species have antimicrobial activity [187], and several inhibit spore germination of *Aspergillus sydowii* [135, 188]. The immune system of the Caribbean Sea fan, *Gorgonia ventalina*, has been studied extensively, and antifungal compounds are one of several immune mechanisms employed in response to Aspergillosis infection. These antifungal compounds are found in higher concentrations in infected sea fans and may be induced by infections with Aspergillosis [135, 136, 189]. Differences in levels of antifungal chemical defenses have been linked to both interspecific [190] and intraspecific [191] variability in susceptibility to Aspergillosis. Intraspecific variability in antifungal activity occurs at the level of the individual sea fan, with elevated levels of antifungal activity in the vicinity of the lesion itself [135], as well as among reefs, which may explain some of the geographic variability observed in the prevalence of this disease [136, 191]. To date, there have not been any bioassay-guided attempts to identify antifungal compounds. In contrast with changes in antifungal activity, there was an indirect effect of pathogenesis on chemical defense: infected sea fans produced significantly reduced concentrations of the feeding-deterrent compound julieannafuran (Fig. 15.3: 25), thereby increasing the susceptibility of diseased corals to predation [71]. Bacteria isolated from the surfaces of gorgonians also produce antibacterial defenses [192] and could thereby be participating in the host's defense against pathogenesis.

Alcyonacean soft coral extracts from the Antarctic [193], Red Sea [194], and Indo-Pacific [195] also exhibit widespread antimicrobial activity. Some of this activity is associated with waterborne molecules released from the surface of the coral that inhibit bacterial attachment [47, 195]; one such molecule is the highly polar homarine

(Fig. 15.3:26; [47]). These studies used a variety of methods to obtain the waterborne molecules, including the use of syringes to sample water at different distances from soft corals in situ [47], and “conditioning” seawater in the laboratory by placing soft corals into individual containers and sampling the water therein [195].

15.2.5 Tunicate Diseases

Of the invertebrates, tunicates possess the most complex cell-based immune system, while still maintaining a cell-free immune response, which includes the production of antibacterial peptides and other antimicrobial secondary metabolites [64, 196]. Like other sessile marine organisms, the antifouling properties of tunicate extracts and secondary metabolites have been widely studied [51, 197]. With regards to antimicrobial activity that might aid in preventing pathogenesis, tunicate compounds have been evaluated predominantly against potential human pathogens, and a diversity of proteins and other metabolites has been considered as viable leads for pharmaceutical research (e.g., [172]). For example, when extracts from the tunicate *Ecteinascidia turbinata* were injected into the American eel, *Anguilla rostrata*, suffering from a bacterial infection, the extract increased antibody titers and survival [198], confirming a diversity of mechanisms of action for tunicate antibacterial defenses. In a rare example of ecological relevance, the chemical inhibition of bacterial settlement was compared with antibacterial toxicity in Mediterranean tunicates, and it was concluded that while these two processes were likely complementary, they were controlled by different metabolites [199].

15.3 Conclusions

Marine communities worldwide face unprecedented variation due, in part, to climate change and anthropogenic stressors. While the importance of predation to the structure and function of these communities has long been accepted, it is increasingly clear that competition and pathogenesis will play significant roles in the near future. Reduced biodiversity in marine communities will likely lead to greater competition for limiting resources; this should favor selection of species with allelopathic compounds. These compounds might act to prevent fouling organisms or macroorganisms from overgrowing surface tissues via contact-mediated (“direct”) processes. Alternatively, the more proactive (“indirect”) approach of releasing allelopathic compounds into the water column where they can act at a distance will also be beneficial. The significant impact of pathogenesis on marine communities has been recognized for at least three decades. In that time, more species have been affected, with increasing frequency, and over broader spatial scales. Antimicrobial compounds often represent the most targeted defense system of the organisms that produce them as they often exhibit selective activity against particular species. These disease resistance mechanisms exhibit similar variability among individuals within a population, as innate immunity does for human hosts exposed to pathogenic microbes.

To date, there is good evidence to support allelopathy and antimicrobial activity in marine algae and invertebrates. More challenging is the use of bioassay-guided isolation of the putative marine natural products involved in competitive and pathogenic interactions. Competitive processes are often characterized by interactions that occur over spatial scales of weeks to months, too long and costly for bioassay-guided procedures. However, recent elegant experimental designs with algae, sponges, and soft corals have led to the identification of allelopathic compounds of ecological relevance. In contrast, whereas pathogenic interactions might occur over a time span of several hours, many marine microbes are at present “unculturable,” and for those, performing ecologically relevant antimicrobial assays in a laboratory setting will be impossible. Nonetheless, the molecular biology revolution has provided important insights into putative pathogens and mechanisms of infectivity. There have also been some successes isolating bioactive antimicrobial natural products from seagrasses, algae, sponges, and soft corals. Future studies of competition and pathogenesis in marine communities should focus on the role of bioactive natural products and include the experimental lessons reviewed here.

Acknowledgments Thanks to S. Ankisetty and H.N. Kamel for the help with locating references and drawing structures for this chapter. Funding was provided by NOAA/NIUST and NSF to M. Slattery and D.J. Gochfeld. For this support, we are grateful.

References

1. Schoener TW (1983) Field experiments on interspecific competition. *Am Nat* 122:240–285
2. Dayton PK (1971) Competition, disturbance and community organization: The provision and subsequent utilization of space in a rocky intertidal community. *Ecol Monog* 41:351–389
3. Connell JH (1973) Population ecology of reef-building corals. In: Jones OA, Endean R (eds) *Biology and geology of coral reefs*. Academic, New York
4. Stimson J (1985) The effect of shading by the table coral *Acropora hyacinthus* on understory corals. *Ecology* 66:40–53
5. Griffith JK (1997) Occurrence of aggressive mechanisms during interactions between soft corals (Octocorallia: Alcyoniidae) and other corals on the Great Barrier Reef, Australia. *Mar Fresh Res* 48:129–135
6. Jackson JBC, Buss L (1975) Allelopathy and spatial competition among coral reef invertebrates. *Proc Nat Acad Sci USA* 72:5160–5163
7. Rice EL (1979) Allelopathy – an update. *Botan Rev* 45:15–109
8. Harper J (1975) Allelopathy. *Q Rev Biol* 50:493–495
9. Hughes TP (1994) Catastrophes, phase shifts, and large-scale degradation of a Caribbean coral reef. *Science* 265:1547–1551
10. McCook LJ, Jompa J, Diaz-Palido G (2001) Competition between corals and algae on coral reefs: a review of the evidence and mechanisms. *Coral Reefs* 19:400–417
11. Miller MW, Hay ME (1996) Coral-seaweed-grazer-nutrient interactions on temperate reefs. *Ecol Monogr* 66:323–344
12. Kuffner IB, Walters LJ, Becerro MA, Paul VJ, Ritson-Williams R, Beach KS (2006) Inhibition of coral recruitment by macroalgae and cyanobacteria. *Mar Ecol Prog Ser* 323:107–117

13. Piazzì L, Ceccherelli G, Cinelli F (2001) Threat to macroalgal diversity: effects of the introduced green alga *Caulerpa racemosa* in the Mediterranean. *Mar Ecol Prog Ser* 210:149–159
14. Ceccherelli G, Campo D (2002) Different effects of *Caulerpa racemosa* on two co-occurring seagrasses. *Bot Mar* 45:71–76
15. Raniello R, Mollo E, Lorenti M, Gavagnin M, Buia MC (2007) Phytotoxic activity of caulerpenyne from the Mediterranean invasive variety of *Caulerpa racemosa*: a potential allelochemical. *Bio Invasions* 9:361–368
16. Jones RJ, Kildea T, Hoegh-Guldberg O (1999) PAM chlorophyll fluorometry: a new *in situ* technique for stress assessment in scleractinian corals, used to examine the effects of cyanide from cyanide fishing. *Mar Poll Bull* 38:864–874
17. De Nys R, Coll JC, Price IR (1991) Chemically mediated interactions between the red alga *Plocamium hamatum* (Rhodophyta) and the octocoral *Simularia cruciata* (Alcyonacea). *Mar Biol* 108:315–320
18. Wright AD (1986) Chemical Investigations of Tropical Marine Algae. Ph.D. thesis. James Cook University of North Queensland
19. Diaz MC, Rützler K (2001) Sponges: an essential component of Caribbean coral reefs. *Bull Mar Sci* 69:535–546
20. Bell JJ (2008) The functional roles of marine sponges. *Est Coast Shelf Sci* 79:341–353
21. Pawlik JR (1997) Fish predation on Caribbean reef sponges: an emerging perspective on chemical defenses. Proceedings of the 8th international coral reef symposium, Panama, vol 2, pp 1255–1258
22. Harper MK, Bugni TS, Copp BR, James RD, Lindsay BS, Richardson AD, Schnabel PC, Tasdemir D, VanWagoner RM, Verbitski SM, Ireland CM (2001) Introduction to the chemical ecology of marine natural products. In: McClintock JB, Baker BJ (eds) *Marine chemical ecology*. CRC Press, Boca Raton
23. Wahl M (1989) Marine epibiosis. I. Fouling and antifouling: some basic aspects. *Mar Ecol Prog Ser* 58:175–189
24. Turon X, Becerro MA, Uriz MJ (1996) Seasonal patterns of toxicity in benthic invertebrates: the encrusting sponge *Crambe crambe* (Poecilosclerida). *Oikos* 75:33–40
25. Nishiyama GK, Bakus GJ (1999) Release of allelochemicals by three tropical sponges (Demospongiae) and their toxic effects on coral substrate competitors. *Mem Queensl Mus* 44:411–417
26. Bingham BL, Young CM (1991) Influence of sponges on invertebrate recruitment: a field test of allelopathy. *Mar Biol* 109:19–26
27. Green KM, Russell BD, Clark RJ, Jones MK, Garson MJ, Skilleter GA, Degnan BM (2002) A sponge allelochemical induces ascidian settlement but inhibits metamorphosis. *Mar Biol* 140:355–363
28. Sullivan B, Faulkner DJ, Webb L (1983) Siphonodictine, a metabolite of the burrowing sponge *Siphonodictyon* sp. that inhibits coral growth. *Science* 221:1175–1176
29. Engel S, Pawlik JR (2000) Allelopathic activities of sponge extracts. *Mar Ecol Prog Ser* 207:273–281
30. Porter JW, Targett NM (1988) Allelochemical interactions between sponges and corals. *Biol Bull* 175:230–239
31. Slattery M, Gochfeld DJ, Iliffe T, Kakuk B, Kelly M (2002) Biodiversity and competitive interactions of cave sponges in the Bahamas. *Boll Mus Ist Biol Univ Genova* 66–67:184
32. Thacker RW, Becerro MA, Lumbang WA, Paul VJ (1998) Allelopathic interactions between sponges on a tropical Pacific reef. *Ecology* 79:1740–1750
33. Pawlik JR, Steindler L, Henkel TP, Beer S, Ilan M (2007) Chemical warfare on coral reefs: Sponge metabolites differentially affect coral symbiosis. *Limnol Oceanogr* 52:907–911
34. Chaves-Fonnegra A, Castellanos L, Zea S, Duque C, Rodriguez J, Jimenez C (2008) Clionapyrrolidine A – a metabolite from the encrusting and excavating sponge *Cliona tenuis* that kills coral tissue upon contact. *J Chem Ecol* 34:1565–1574

35. Richardson CA, Dustan P, Lang JC (1979) Maintenance of living space by sweeper tentacles of *Montastrea cavernosa*, a Caribbean reef coral. *Mar Biol* 55:181–186
36. Dai CF (1990) Interspecific competition in Taiwanese corals with special reference to interactions between alcyonaceans and scleractinians. *Mar Ecol Prog Ser* 60:291–297
37. Koh EGL, Sweatman H (2000) Chemical warfare among scleractinians: bioactive natural products from *Tubastraea faulkneri* Wells kills larvae of potential competitors. *J Exp Mar Biol Ecol* 251:141–160
38. Sammarco PW, Coll JC (1992) Chemical adaptations in the Octocorallia: evolutionary considerations. *Mar Ecol Prog Ser* 88:93–104
39. Dinesen ZD (1983) Patterns in the distribution of soft corals across the Great Barrier Reef. *Coral Reefs* 1:229–236
40. Sammarco PW, Coll JC, La Barre S, Willis B (1983) Competitive strategies of soft corals (Coelenterata: Octocorallia): allelopathic effects on selected scleractinian corals. *Coral Reefs* 1:173–178
41. La Barre SC, Coll JC, Sammarco PW (1986) Competitive strategies of soft corals (Coelenterata: Octocorallia) III. Spacing and aggressive interactions between alcyonaceans. *Mar Ecol Prog Ser* 28:147–156
42. Alino PM, Sammarco PW, Coll JC (1992) Competitive strategies in soft corals (Coelenterata, Octocorallia). IV. Environmentally induced reversals in competitive superiority. *Mar Ecol Prog Ser* 81:129–145
43. Aceret TL, Sammarco PW, Coll JC (1995) Toxic effects of alcyonacean diterpenes on scleractinian corals. *J Exp Mar Biol Ecol* 188:63–78
44. Slattery M, Kamel HN, Ankisetty S, Gochfeld DJ, Hoover CA, Thacker RW (2008) Hybrid vigor in a tropical Pacific soft coral community. *Ecol Monogr* 78:423–443
45. Dayton PK, Robilliard GW, Paine RT, Dayton LB (1974) Biological accommodation in the benthic community at McMurdo Sound, Antarctica. *Ecol Monogr* 44:105–128
46. Slattery M, McClintock JB (1997) An overview of the population structure and chemical defenses of three species of Antarctic soft corals. In: Battaglia B, Valencia J, Walton DWH (eds) *Antarctic communities: species, structure and survival*. Cambridge University Press, England
47. Slattery M, Hamann MT, McClintock JB, Perry TP, Puglisi MP, Yoshida W (1997) Ecological roles for waterborne metabolites from Antarctic soft corals. *Mar Ecol Prog Ser* 161:133–144
48. Schulte BA, De Nys R, Bakus GJ, Crews P, Eid C, Naylor S, Manes LV (1991) A modified allomone collecting apparatus. *J Chem Ecol* 7:1327–1332
49. Nadakumar K, Tanaka M, Kikuchi T (1993) Interspecific competition among fouling organisms in Tomioka Bay, Japan. *Mar Ecol Prog Ser* 94:43–50
50. Lindquist N, Hay ME, Fenical W (1992) Defense of ascidians and their conspicuous larvae: adult vs. larval chemical defenses. *Ecol Monogr* 62:547–568
51. Davis AR (1991) Alkaloids and ascidian chemical defense: evidence for the ecological role of natural products from *Eudistoma olivaceum*. *Mar Biol* 111:375–379
52. Teo SLM, Ryland JS (1995) Potential antifouling mechanisms using toxic chemicals in some British ascidians. *J Exp Mar Biol Ecol* 188:49–62
53. Russ GR (1982) Overgrowth in a marine epifaunal community: competitive hierarchies and competitive networks. *Oecologia* 53:12–19
54. Schmidt GH, Warner GF (1986) Spatial competition between colonial ascidians: the importance of stand-off. *Mar Ecol Prog Ser* 31:101–104
55. Suchanek TH, Green DJ (1981) Interspecific competition between *Palythoa caribaeorum* and other sessile invertebrates on St. Croix reefs, US Virgin Islands. *Proceedings of the 4th international coral reef symposium, Manila, vol 2*, pp 679–684
56. Woodin SA, Marinelli RL, Lincoln DE (1993) Allelochemical inhibition of recruitment in a sedentary assemblage. *J Chem Ecol* 19:517–530

57. Slattery M, Rajbandhari I, Wesson KJ (2001) Competition-mediated antibiotic induction in the marine bacterium *Streptomyces tenjimariensis*. *Microb Ecol* 41:90–96
58. Burkepille DE, Parker JD, Woodson CB, Mills HJ, Kubanek J, Sobecky PA, Hay ME (2006) Chemically mediated competition between microbes and animals: microbes as consumers in food webs. *Ecol* 87:2821–2831
59. Kubanek J, Hicks MK, Naar J, Villareal TA (2005) Does the red tide dinoflagellate *Karenia brevis* use allelopathy to outcompete other phytoplankton? *Limnol Oceanogr* 50:883–895
60. Harvell CD, Kim K, Burkholder JM, Colwell RR, Epstein PR, Grimes DJ, Hofmann EE, Lipp EK, Osterhaus ADME, Overstreet RM, Porter JW, Smith GW, Vasta GR (1999) Emerging marine diseases – climate links and anthropogenic factors. *Science* 285:1505–1510
61. Lafferty KD, Porter JW, Ford SE (2004) Are diseases increasing in the ocean? *Ann Rev Ecol Evol Syst* 35:31–54
62. Ward JR, Lafferty KD (2004) The elusive baseline of marine disease: are diseases in ocean ecosystems increasing? *PLoS Biology* 2:0542–0547
63. Rosenberg E, Loya Y (eds) (2004) Coral health and disease. Springer, Berlin
64. Mydlarz LD, Jones LE, Harvell CD (2006) Innate immunity, environmental drivers, and disease ecology of marine and freshwater invertebrates. *Ann Rev Ecol Evol Syst* 37:251–288
65. Knowlton N (2001) The future of coral reefs. *Proc Nat Acad Sci USA* 98:5419–5425
66. Lessios H (1988) Mass mortality of *Diadema antillarum* in the Caribbean: What have we learned? *Ann Rev Ecol Syst* 19:371
67. Harvell CD, Jordan-Dahlgren E, Merkel S, Raymundo L, Rosenberg E, Smith G, Weil E, Willis B (2007) Coral disease, environmental drivers, and the balance between coral and microbial associates. *Oceanography* 20:172–195
68. Harvell D, Altizer S, Cattadori IM, Harrington L, Weil E (2009) Climate change and wildlife diseases: when does the host matter the most? *Ecology* 90:912–920
69. Sokolow S (2009) Effects of a changing climate on the dynamics of coral infectious disease: a review of the evidence. *Dis Aquat Org* 87:5–18
70. Smith GW, Ives LD, Nagelkerken IA, Ritchie KB (1996) Caribbean Sea-fan mortalities. *Nature* 383:487
71. Slattery M (1999) Fungal pathogenesis of the sea fan *Gorgonia ventalina*: direct and indirect consequences. *Chemoecol* 9:97–104
72. Rosenberg E, Ben-Haim Y (2002) Microbial diseases of corals and global warming. *Env Microbiol* 4:318–326
73. Remily ER, Richardson LL (2006) Ecological physiology of a coral pathogen and the coral reef environment. *Microb Ecol* 51:345–352
74. Green EP, Bruckner AW (2000) The significance of coral disease epizootiology for coral reef conservation. *Biol Conserv* 96:347–361
75. Altizer S, Harvell D, Friedle E (2003) Rapid evolutionary dynamics and disease threats to biodiversity. *Trends Ecol Evol* 18:589–596
76. Sutherland KP, Porter JW, Torres C (2004) Disease and immunity in Caribbean and Indo-Pacific zooxanthellate corals. *Mar Ecol Prog Ser* 266:273–302
77. Raymundo LJ, Couch CS, Bruckner AW, Harvell CD, Work TM, Weil E, Woodley CM, Jordan-Dahlgren E, Willis BL, Sato Y, Aeby GS (2008) Coral disease handbook: guidelines for assessment, monitoring and management. Coral Reef Targeted Research & Capacity Building for Management Program
78. Wilkinson CR (2004) Status of coral reefs of the world, (2004), Australian Institute of Marine Science. Cape Ferguson, Queensland
79. Toren A, Landau L, Kushmaro A, Loya Y, Rosenberg E (1998) Effect of temperature on adhesion of *Vibrio* strain AK-1 to *Oculina patagonica* and on coral bleaching. *Appl Env Microbiol* 64:1379–1384
80. Aeby GS, Santavy DL (2006) Factors affecting the susceptibility of the coral *Montastraea faveolata* to black-band disease. *Mar Ecol Prog Ser* 318:103–110

81. Lesser MP, Bythell JC, Gates RD, Johnstone RW, Hoegh-Guldberg O (2007) Are infectious diseases really killing corals? Alternative interpretations of the experimental and ecological data. *J Exp Mar Biol Ecol* 346:36–44
82. Sussman M, Mieog JC, Doyle J, Victor S, Willis BL, Bourne DG (2009) *Vibrio* zinc-metalloprotease causes photoinactivation of coral endosymbionts and coral tissue lesions. *PLoS ONE* 42:e4511
83. Sussman M, Willis BL, Victor S, Bourne DG (2008) Coral pathogens identified for White Syndrome (WS) epizootics in the Indo-Pacific. *PLoS ONE* 3:e2393
84. Ritchie KB, Polson SW, Smith GW (2001) Microbial disease causation in marine invertebrates: problems, practices, and future prospects. *Hydrobiology* 460:131–139
85. Work TM, Aeby GS (2006) Systematically describing gross lesions in corals. *Dis Aquat Org* 70:155–160
86. Willis B, Page C, Dinsdale E (2004) Coral disease on the Great Barrier Reef. In: Rosenberg E, Loya Y (eds) *Coral health and disease*. Springer, Berlin
87. Work TM, Aeby GS, Stanton FG, Fenner D (2008) Overgrowth of fungi (endolithic hypermycosis) associated with multifocal to diffuse distinct amorphous dark discoloration of corals in the Indo-Pacific. *Coral Reefs* 27:663
88. Renegar DA, Blackwelder PL, Miller JB, Gochfeld DJ, Moulding AL (2009) Ultrastructural and histological analysis of Dark Spot Syndrome in *Siderastrea siderea* and *Agaricia agaricites*. Proceedings of the 11th international coral reef symposium, Ft. Lauderdale, Florida, July 2008, pp 185–189
89. Barash Y, Sulam R, Loya Y, Rosenberg E (2005) Bacterial strain BA-3 and a filterable factor cause a white plague-like disease in corals from the Eilat coral reef. *Aquat Microbial Ecol* 40:183–189
90. Thompson FL, Barash Y, Sawabe T, Sharon G, Swings J, Rosenberg E (2006) *Thalassomonas loyana* sp. nov., a causative agent of the white plague-like disease of coral on the Eilat coral reef. *Int J Syst Evol Microbiol* 56:365–368
91. Richardson LL (2004) Black band disease. In: Rosenberg E, Loya Y (eds) *Coral health and disease*. Springer, Berlin
92. Gladfelter WB (1982) White-band disease in *Acropora palmata*: implications for the structure and growth of shallow reefs. *Bull Mar Sci* 32:639–643
93. Aronson RB, Precht WF (2001) White-band disease and the changing face of Caribbean coral reefs. *Hydrobiology* 460:25–38
94. Patterson KL, Porter JW, Ritchie KB, Polson SW, Mueller E, Peters EC, Santavy DL, Smith GW (2002) The etiology of white pox, a lethal disease of the Caribbean elkhorn coral, *Acropora palmata*. *Proc Natl Acad Sci USA* 99:8725–8730
95. Raymundo LJH, Rosell KB, Reboton CT, Kaczmarzky L (2005) Coral diseases on Philippine reefs: genus *Porites* is a dominant host. *Dis Aquat Org* 64:181–191
96. Aeby G, Work T, Fenner D, Didonato E (2009) Coral and crustose coralline algae disease on the reefs of American Samoa. Proceedings of the 11th international coral reef symposium, Ft. Lauderdale, Florida, pp 197–201
97. Starmer J, Asher J, Castro F, Gochfeld D, Gove J, Hall A, Houk P, Keenan E, Miller J, Moffit R, Nadon M, Schroeder R, Smith E, Trianni M, Vroom P, Wong K, Yuknavage K (2008) The state of coral reef ecosystems of the Commonwealth of the Northern Mariana Islands. In: Waddell JE, Clarke AM (eds) *The state of coral reef ecosystems of the United States and Pacific freely associated states: 2008*, vol 73, NOAA Technical Memorandum NOS NCCOS. NOAA/NCCOS Center for Coastal Monitoring and Assessment's Biogeography Team, Silver Spring
98. Williams GJ, Aeby GS, Cowie ROM, Davy SK (2010) Predictive modeling of coral disease distribution within a reef system. *PLoS ONE* 5:e9264
99. Aeby GS (2006) Baseline levels of coral disease in the Northwestern Hawaiian Islands. *Atoll Res Bull* 543:471–788

100. Williams GJ, Davy SK, Aeby GS (2008) Coral disease at Palmyra Atoll, a remote reef system in the Central Pacific. *Coral Reefs* 27:207
101. Harvell CD, Mitchell CE, Ward JR, Altizer S, Dobson AP, Ostfeld RS, Samuel MD (2002) Climate warming and disease risks for terrestrial and marine biota. *Science* 296:2158–2162
102. Bruno JF, Selig ER, Casey KS, Page CA, Willis BL, Harvell CD, Sweatman J, Melendy AM (2007) Thermal stress and coral cover as drivers of coral disease outbreaks. *PLoS Biol* 5:1–8
103. Miller J, Muller E, Rogers C, Waara R, Atkinson A, Whelan KRT, Patterson M, Witcher B (2009) Coral disease following massive bleaching in 2005 causes 60% decline in coral cover on reefs in the US Virgin Islands. *Coral Reefs* 28:925–937
104. Kuta KG, Richardson LL (1996) Black band disease and the fate of diseased coral colonies in the Florida Keys. *Proceedings of the 8th international coral reef symposium, Panama*, pp 575–578
105. Sato Y, Bourne DG, Willis BL (2009) Dynamics of seasonal outbreaks of black band disease in an assemblage of *Montipora* species at Pelorus Island (Great Barrier Reef, Australia). *Proc Roy Soc B* 276:2795–2803
106. Rosenberg E, Falkovitz L (2004) The *Vibrio shiloi/Oculina patagonica* model system of coral bleaching. *Ann Rev Microbiol* 58:143–159
107. Gochfeld DJ, Olson JB, Slaterry M (2006) Colony versus population variation in susceptibility and resistance to dark spot syndrome in the Caribbean coral *Siderastrea siderea*. *Dis Aquat Org* 69:53–65
108. Israely T, Banin E, Rosenberg E (2001) Growth, differentiation and death of *Vibrio shiloi* in coral tissue as a function of seawater temperature. *Aquat Microbial Ecol* 24:1–8
109. Ben-Haim Y, Thompson FL, Thompson CC, Cnockaert MC, Hoste B, Swings J, Rosenberg E (2003) *Vibrio coralliilyticus* sp. nov., a temperature-dependent pathogen of the coral *Pocillopora damicornis*. *Intl J Syst Evol Microbiol* 53:309–315
110. Bruno JF, Petes LE, Harvell CD, Hettinger A (2003) Nutrient enrichment can increase the severity of coral diseases. *Ecol Lett* 6:1056–1061
111. Voss JD, Richardson LL (2006) Nutrient enrichment enhances black band disease progression in corals. *Coral Reefs* 25:569–576
112. Kline DI, Kuntz NM, Breitbart M, Knowlton N, Rohwer F (2006) Role of elevated organic carbon levels and microbial activity in coral mortality. *Mar Ecol Prog Ser* 314:119–125
113. Kuta KG, Richardson LL (2002) Ecological aspects of black band disease of corals: relationships between disease incidence and environmental factors. *Coral Reefs* 21:393–398
114. Kaczmarek LT, Draud M, Williams EH (2005) Is there a relationship between proximity to sewage effluent and the prevalence of coral disease? *Carib J Sci* 41:124–137
115. Weil E, Urreiztieta I, Garzon-Ferreira J (2000) Geographic variability in the incidence of coral and octocoral diseases in the wider Caribbean. *Proceedings of the 9th international coral reef symposium, Bali, Indonesia, vol 2*, pp 1231–1237
116. Bruckner AW, Bruckner RJ (2006) Consequences of yellow band disease (YBD) on *Montastraea annularis* (species complex) populations on remote reefs off Mona Island, Puerto Rico. *Dis Aquat Org* 69:67–73
117. Gochfeld DJ, Aeby GS (2008) Antimicrobial chemical defenses in Hawaiian corals: possible protection from disease? *Mar Ecol Prog Ser* 362:119–128
118. Lipp EK, Jarrell JL, Griffin DW, Lukasik J, Jacukiewicz J, Rose JB (2002) Preliminary evidence for human fecal contamination in corals of the Florida Keys, USA. *Mar Pollut Bull* 44:666–670
119. Mullen KM, Peters EC, Harvell CD (2004) Coral resistance to disease. In: Rosenberg E, Loya Y (eds) *Coral health and disease*. Springer, Berlin
120. Brown BE, Bythell JC (2005) Perspectives on mucus secretion in reef corals. *Mar Ecol Prog Ser* 296:291–309
121. Vollmer SV, Kline DI (2008) Natural disease resistance in threatened staghorn corals. *PLoS ONE* 3:e3718

122. Ritchie KB (2006) Regulation of microbial populations by coral surface mucus and mucus-associated bacteria. *Mar Ecol Prog Ser* 322:1–14
123. Nissimov J, Rosenberg E, Munn CB (2009) Antimicrobial properties of resident coral mucus bacteria of *Oculina patagonica*. *FEMS Microbiol Lett* 292:210–215
124. Schnit-Orland M, Kushmaro A (2009) Coral mucus-associated bacteria: a possible first line of defense. *FEMS Microbiol Ecol* 67:371–380
125. Ritchie KB, Smith GW (1995) Preferential carbon utilization by surface bacterial communities from water mass, normal, and white-band diseased *Acropora cervicornis*. *Molec Mar Biol Biotech* 4:345–352
126. Paul VJ (ed) (1992) Ecological roles of marine natural products. Cornell University Press, Ithaca
127. Pawlik JR (1993) Marine invertebrate chemical defenses. *Chem Rev* 93:1911–1922
128. Hay ME (1996) Marine chemical ecology: what's known and what's next? *J Exp Mar Biol Ecol* 200:103–134
129. McClintock JB, Baker BJ (2001) Marine chemical ecology. CRC Press, Boca Raton
130. Cronin G, Hay ME (1996) Susceptibility to herbivores depends on recent history of both plant and animal. *Ecology* 77:1531–1543
131. Slattery M, Paul VJ (2008) Indirect effects of bleaching on predator deterrence in the tropical Pacific soft coral *Sinularia maxima*. *Mar Ecol Prog Ser* 354:169–179
132. Michalek-Wagner K, Bowden BF (2000) Effects of bleaching on secondary metabolite chemistry of alcyonacean soft corals. *J Chem Ecol* 26:1543–1562
133. Swearingen DC III, Pawlik JR (1998) Variability in the chemical defense of the sponge *Chondrilla nucula* against predatory reef fishes. *Mar Biol* 131:619–627
134. Slattery M, Starmer J, Paul VJ (2001) Temporal and spatial variation in defensive metabolites of the tropical Pacific soft corals *Sinularia maxima* and *S. polydactyla*. *Mar Biol* 138:1183–1193
135. Kim K, Harvell CD, Kim PD, Smith GW, Merkel SM (2000) Fungal disease resistance of Caribbean Sea fan corals (*Gorgonia* spp.). *Mar Biol* 136:259–267
136. Dube D, Kim K, Alker AP, Harvell CD (2002) Size structure and geographic variation in chemical resistance of sea fan corals *Gorgonia ventalina* to a fungal pathogen. *Mar Ecol Prog Ser* 231:139–150
137. Gunthorpe L, Cameron AM (1990) Widespread but variable toxicity in scleractinian corals. *Toxicon* 28:1199–1219
138. Koh EGL (1997) Do scleractinian corals engage in chemical warfare against microbes? *J Chem Ecol* 23:379–398
139. Marquis CP, Baird AH, de Nys R, Homstrom C, Koziuni N (2005) An evaluation of the antimicrobial properties of the eggs of 11 species of scleractinian corals. *Coral Reefs* 24:248–253
140. Geffen Y, Rosenberg E (2005) Stress-induced rapid release of antibacterials by scleractinian corals. *Mar Biol* 146:931–935
141. Fusetani N, Toyoda T, Asai N, Matsunaga S, Maruyama T (1996) Montiporic acids A and B, cytotoxic and antimicrobial polyacetylene carboxylic acids from eggs of the scleractinian coral *Montipora digitata*. *J Nat Prod* 59:796–797
142. Kita M, Kitamura M, Koyama T, Teruya T, Matsumoto H, Nakano Y, Uemura D (2005) Feeding attractants for the muricid gastropod *Drupella cornus*, a coral predator. *Tet Lett* 46:8583–8585
143. Short FT, Muehlstein LK, Porter D (1987) Eelgrass wasting disease: cause and recurrence of a marine epidemic. *Biol Bull* 173:557–562
144. Muehlstein LK, Porter D, Short FT (1991) *Labyrinthula zosterae* sp. nov., the causative agent of wasting disease of eelgrass, *Zostera marina*. *Mycologia* 83:180–191
145. Steele L, Caldwell M, Boettcher A, Arnold T (2005) Seagrass-pathogen interactions: 'pseudo-induction' of turtlegrass phenolics near wasting disease lesions. *Mar Ecol Prog Ser* 303:123–131

146. Sawabe T, Tanaka R, Iqbal MM, Tajima K, Ezura Y, Ivanova EP, Christen R (2000) Assignment of *Alteromonas elyakovii* KMM 162^T and five strains isolated from spot-wounded fronds of *Laminaria japonica* to *Pseudoalteromonas elyakovii* comb. nov. and the extended description of the species. *Intl J Syst Evol Microbiol* 50:265–271
147. Andrews JH (1977) Observations on the pathology of seaweeds in the Pacific Northwest. *Can J Bot* 55:1019–1027
148. Andrews JH (1976) The pathology of marine algae. *Biol Rev* 51:211–253
149. Kazama FY (1979) Pythium “red rot disease” of *Porphyra*. *Experientia* 35:443
150. Littler MM, Littler DS (1995) Impact of CLOD pathogen on Pacific coral reefs. *Science* 267:1356–1360
151. Ballantine DL, Weil E, Ruiz H (2005) Coralline white band syndrome, a coralline algal affliction in the tropical Atlantic. *Coral Reefs* 24:117
152. Engel S, Puglisi MP, Jensen PR, Fenical W (2006) Antimicrobial activities of extracts from tropical Atlantic marine plants against marine pathogens and saprophytes. *Mar Biol* 149:991–1002
153. Puglisi MP, Engel S, Jensen PR, Fenical W (2007) Antimicrobial activities of extracts from Indo-Pacific marine plants against marine pathogens and saprophytes. *Mar Biol* 150:531–540
154. Ross C, Puglisi MP, Paul VJ (2008) Antifungal defenses of seagrasses from the Indian River Lagoon, Florida. *Aquat Bot* 88:134–141
155. Arnold TM, Targett NM (2002) Marine tannins: the importance of a mechanistic framework for predicting ecological roles. *J Chem Ecol* 28:1919–1934
156. McKone KL, Tanner CE (2009) Role of salinity in the susceptibility of eelgrass *Zostera marina* to the wasting disease pathogen *Labyrinthula zosterae*. *Mar Ecol Prog Ser* 377:123–130
157. Vergeer LHT, Develi A (1997) Phenolic acids in healthy and infected leaves of *Zostera marina* and their growth-limiting properties towards *Labyrinthula zosterae*. *Aquat Bot* 58:65–72
158. Jensen PR, Jenkins KM, Porter D, Fenical W (1998) Evidence that a new antibiotic flavone glycoside chemically defends the sea grass *Thalassia testudinum* against zoospore fungi. *Appl Env Microbiol* 64:1490–1496
159. Paul NA, de Nys R, Steinberg PD (2006) Chemical defence against bacteria in the red alga *Asparagopsis armata*: linking structure with function. *Mar Ecol Prog Ser* 306:87–101
160. Nylund GM, Cervin G, Persson F, Hermansson M, Steinberg PD, Pavia H (2008) Seaweed defence against bacteria: a poly-brominated 2-heptanone from the red alga *Bonnemaisonia hamifera* inhibits bacterial colonization. *Mar Ecol Prog Ser* 369:39–50
161. Manefield M, Rasmussen TB, Henzter M, Anderson JB, Steinberg P, Kjelleberg S, Givskov M (2002) Halogenated furanones inhibit quorum sensing through accelerated LuxR turnover. *Microbiol* 148:1119–1127
162. Webster NS (2007) Sponge disease; a global threat? *Env Micro* 9:1363–1375
163. Rützler K (1988) Mangrove sponge disease induced by cyanobacterial symbionts: failure of a primitive immune system? *Dis Aquat Org* 5:143–149
164. Webster NS, Negri AP, Webb RI, Hill RT (2002) A spongin-boring α -proteobacterium is the etiological agent of disease in the Great Barrier Reef sponge *Rhopaloeides odorabile*. *Mar Ecol Prog Ser* 232:305–309
165. Cervino JM, Winiarski-Cervino K, Polson SW, Goreau T, Smith GW (2006) Identification of bacteria associated with a disease affecting the marine sponge *Ianthella basta* in New Britain, Papua New Guinea. *Mar Ecol Prog Ser* 324:139–150
166. Vacelet J, Vacelet E, Gaino E, Gallissian MF (1994) Bacterial attack of spongin skeleton during the 1986–1990 Mediterranean sponge disease. In: van Soest RWM, van Kempen TMG, Braekman JC (eds) *Sponges in time and space*. Balkema, Rotterdam
167. Galstoff PS (1942) Wasting disease causing mortality of sponges in the West Indies and Gulf of Mexico. *Proceedings of the 8th American science congress*, vol 3, pp 411–421

168. Olson J, Gochfeld D, Slattery M (2006) *Aplysina* red band syndrome: a new threat to Caribbean sponges. *Dis Aquat Org* 71:163–168
169. Kelly SR, Garo E, Jensen PR, Fenical W, Pawlik JR (2005) Effects of Caribbean sponge secondary metabolites on bacterial surface colonization. *Aquat Microbial Ecol* 40:191–203
170. Attaway DH, Zaborsky OR (1993) Marine biotechnology, vol 1, Pharmaceutical and bioactive natural products. Plenum, New York
171. Gochfeld DJ, El Sayed KA, Yousaf M, Hu J, Bartyzel P, Dunbar DC, Wilkins SP, Zjawiony JK, Schinazi RF, Wirtz SS, Tharnish PM, Hamann MT (2003) Anti-HIV activity of structurally diverse marine natural products: a review. *Mini Rev Med Chem* 3:401–424
172. Blunt JW, Copp BR, Hu WP, Munro MHG, Northcote PT, Prinsep MR (2008) Marine natural products. *Nat Prod Rep* 25:35–94
173. Becerro MA, Paul VJ (2004) Effects of depth and light on secondary metabolites and cyanobacterial symbionts of the sponge *Dysidea granulosa*. *Mar Ecol Prog Ser* 280:115–128
174. Taylor MW, Radax R, Steger D, Wagner M (2007) Sponge-associated microorganisms: evolution, ecology, and biotechnological potential. *Micro Molec Biol Rev* 71:295–347
175. Kelman D (2004) Antimicrobial activity of sponges and corals. In: Rosenberg E, Loya Y (eds) *Coral health and disease*. Springer, Berlin
176. Kelly SR, Jensen PR, Henkel TP, Fenical W, Pawlik JR (2003) Effects of Caribbean sponge extracts on bacterial attachment. *Aquat Microbial Ecol* 31:175–182
177. Kelman D, Kashman Y, Rosenberg E, Ilan M, Ifrach I, Loya Y (2001) Antimicrobial activity of the reef sponge *Amphimedon viridis* from the Red Sea: evidence for selective toxicity. *Aquat Micro Ecol* 24:9–16
178. Thoms C, Ebel R, Proksch P (2006) Activated chemical defense in *Aplysina* sponges revisited. *J Chem Ecol* 32:97–123
179. Richelle-Maurer E, De Kluijver MJ, Feio S, Gaudêncio S, Gaspar H, Gomez R, Tavares R, Van de Vyver G, Van Soest RWM (2003) Localization and ecological significance of oroidin and scep trin in the Caribbean sponge *Agelas conifera*. *Biochem Syst Ecol* 31:1073–1091
180. Walker RP, Thompson JE, Faulkner DJ (1985) Exudation of biologically-active metabolites in the sponge *Aplysina fistularis*. II. Chemical evidence. *Mar Biol* 88:27–32
181. Geiser DM, Taylor JW, Ritchie KB, Smith GW (1998) Cause of sea fan death in the West Indies. *Nature* 394:137–138
182. Shinn EA, Smith GW, Prospero JM, Betzer P, Hayes ML, Garrison VH, Barber RT (2000) African dust and the demise of Caribbean coral reefs. *Geol Res Lett* 27:3029–3032
183. Smith GW, Weil E (2004) Aspergillosis of gorgonians. In: Rosenberg E, Loya Y (eds) *Coral health and disease*. Springer, Berlin
184. Nagelkerken I, Buchan K, Smith GW, Bonair K, Bush P, Garzon-Ferreira J, Botero L, Gayle P, Harvell CD, Heberer C, Kim K, Petrovic C, Pors L, Yoshioka P (1997) Widespread disease in Caribbean Sea fans: II. Patterns of infection and tissue loss. *Mar Ecol Prog Ser* 160:255–263
185. Alker AP, Smith GW, Kim K (2001) Characterization of *Aspergillus sydowii* (Thom et Church), a fungal pathogen of Caribbean Sea fans. *Hydrobiology* 460:105–111
186. Kim K, Harvell CD (2004) The rise and fall of a six-year coral-fungal epizootic. *Am Nat* 164: S52–S63
187. Jensen PR, Harvell CD, Wirtz K, Fenical W (1996) Antimicrobial activity of extracts of Caribbean gorgonian corals. *Mar Biol* 125:411–419
188. Kim K, Kim PD, Alker AP, Harvell CD (2000) Chemical resistance of gorgonian corals against fungal infections. *Mar Biol* 137:393–401
189. Mydlarz LD, Harvell CD (2007) Peroxidase activity and inducibility in the sea fan coral exposed to a fungal pathogen. *Comp Biochem Physiol Part A* 146:54–62
190. Mullen KM, Harvell CD, Alker AP, Dube D, Jordan-Dahlgren E, Ward JR, Petes LE (2006) Host range and resistance to aspergillosis in three sea fan species from the Yucatan. *Mar Biol* 149:1355–1364

191. Couch CS, Mydlarz LD, Harvell CD, Douglas NL (2008) Variation in measures of immunocompetence of sea fan coral, *Gorgonia ventalina*, in the Florida Keys. *Mar Biol* 155:281–292
192. Gil-Agudelo DL, Myers C, Smith GW, Kim K (2006) Changes in the microbial communities associated with *Gorgonia ventalina* during aspergillosis infection. *Dis Aquat Org* 69:89–94
193. Slattery M, McClintock JB, Heine JN (1995) Chemical defenses in Antarctic soft corals: evidence for antifouling compounds. *J Exp Mar Biol Ecol* 190:61–77
194. Kelman D, Kashman Y, Rosenberg E, Kusmaro A, Loya Y (2006) Antimicrobial activity of Red Sea corals. *Mar Biol* 149:357–363
195. Harder T, Lau SCK, Dobretsov S, Fang TK, Qian PY (2003) A distinctive epibiotic bacterial community on the soft coral *Dendronephthya* sp. and antibacterial activity of coral tissue extracts suggest a chemical mechanism against bacterial epibiosis. *FEMS Microbiol Ecol* 43:337–347
196. Findlay C, Smith VJ (1995) Antimicrobial factors in solitary ascidians. *Fish Shellfish Immunol* 5:645–658
197. Raveendran TV, Limna Mol VP (2009) Natural product antifoulants. *Current Sci* 97:508–520
198. Davis JF, Hayasaka SS (1984) The enhancement of resistance of the American eel, *Anguilla rostrata* Le Sueur, to a pathogenic bacterium, *Aeromonas hydrophila*, by an extract of the tunicate, *Ecteinascidia turbinata*. *J Fish Dis* 7:311–316
199. Wahl M, Jensen PR, Fenical W (1994) Chemical control of bacterial epibiosis on ascidians. *Mar Ecol Prog Ser* 110:45–57
200. Sussman M, Loya Y, Fine M, Rosenberg E (2003) The marine fireworm *Hermodice carunculata* is a winter reservoir and spring–summer vector for the coral-bleaching pathogen *Vibrio shiloi*. *Env Microbiol* 5:250–255
201. Koch R (1884) Die Aetiologie der Tuberkulose. *Mitt Kaiser Gesundh* 2:1–88
202. Ritchie KB, Smith GW (1998) Type II white-band disease. *Rev Biol Trop* 46(Suppl 5):199–203
203. Richardson LL, Goldberg WM, Kuta KG, Aronson RB, Smith GW, Ritchie KB, Halas JC, Feingold JS, Miller SL (1998) Florida's mystery coral killer identified. *Nature* 392:557–558
204. Pappas KE (2010) Effect of bleaching and disease stress on antimicrobial chemical defenses in corals. Honors thesis, Sally McDonell Barksdale Honors College, University of Mississippi
205. Kushmaro A, Loya Y, Fine M, Rosenberg E (1996) Bacterial infection and coral bleaching. *Nature* 380:396
206. Kushmaro A, Banin E, Loya Y, Stackebrandt E, Rosenberg E (2001) *Vibrio shiloi* sp. nov., the causative agent of bleaching of the coral *Oculina patagonica*. *Intl J Syst Evol Microbiol* 51:1383–1388

Stephen H. Wright, Andrea Raab, Jörg Feldmann, Eva Krupp, and Marcel Jaspars

Contents

16.1	Introduction	862
16.2	Metal Surveys of Marine Invertebrates	865
16.3	Why Do Marine Invertebrates Concentrate Metals?	869
16.4	Marine Natural Products Isolated Containing Metals	873
16.5	Marine Natural Product Complexation Studies	876
16.6	Methods to Identify Metal Complexes from Marine Invertebrates	882
16.7	Conclusion – A Proposal for a Structured Search for Marine Natural Products Containing Metals	887
16.8	Study Questions	888
	References	889

Abstract

This chapter covers the unique ability of marine invertebrates to bioconcentrate transition metals by up to 8 orders of magnitude above background concentrations. A brief introduction deals with the bioinorganic principles of the subject matter and the natural concentrations of metals in the environment. Next, previous metal surveys of marine invertebrates and the potential reasons for hyperaccumulation are discussed, and this is followed by a section on previously

S.H. Wright (✉) • A. Raab • J. Feldmann

Marine Biodiscovery Centre, Department of Chemistry, University of Aberdeen, Old Aberdeen, Scotland, UK

e-mail: a.raab@abdn.ac.uk, j.feldmann@abdn.ac.uk

E. Krupp

Department of Chemistry, Marine Biodiscovery Centre, University of Aberdeen, Old Aberdeen, Scotland, UK

e-mail: e.krupp@abdn.ac.uk

M. Jaspars

Department of Chemistry, Marine Biodiscovery Centre, University of Aberdeen, Aberdeen, UK

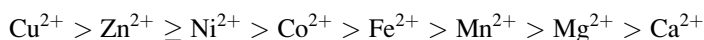
e-mail: m.jaspars@abdn.ac.uk

isolated marine natural product – transition metal complexes. Studies on marine natural product complexation using physical methods are described in the context of their binding specificity and affinity. Many of these studies were conducted to try and discover potential functions for the marine natural product – transition metal complexes. Methodological aspects to discover new complexes of this type are discussed, especially hyphenated techniques utilizing elemental and molecular mass spectrometric methods. A final section proposes a rational way to uncover new marine natural product – transition metal complexes and potential methods to determine their function in nature.

16.1 Introduction

A number of metal ions are essential to life. This includes the bulk ones such as sodium, potassium, magnesium, and calcium used for osmotic balance and in the formation of biomaterials. In addition, there are trace metal ions that are critical in metalloenzymes and cofactors in enzymes and proteins [1]. Most of these are found in the first transition period such as vanadium, manganese, iron, cobalt, nickel, copper, and zinc. It is recognized that certain transition metals usually fulfill certain roles in metalloenzymes, for instance, zinc is often involved in hydrolysis enzymes and copper in oxidation enzymes [1]. An important role for metals is in oxygen transport, which in many animals is carried out by hemoglobin, containing an iron-porphyrin cofactor, and in crustaceans by the copper-containing protein, hemocyanin. An imbalance in the metal concentrations in most organisms will lead to disease or failure to thrive, and therefore, maintenance of metal homeostasis is vital to an organism's survival. For this reason, all life has developed sophisticated mechanisms for the acquisition, storage, and utilization of metal ions as well as elegant methods to keep the concentrations within an acceptable and healthy range. Metal uptake is affected by a number of factors, including speciation, chelation, pH, temperature, salt concentration, and redox potential, as well as age, sex, and physiology of the organism, yet levels are exquisitely controlled in healthy organisms [2].

The main barrier to metal uptake is the hydrophobic cell membrane, and two key mechanisms exist for internalizing biologically important metal ions (Fig. 16.1) [3]. The first is via the use of an energy pump which actively transports M^{2+} into the cell. The second is of more relevance here and involves the use of a transport ligand, often known as an ionophore, or siderophore when it is iron specific (L_t in Fig. 16.1). The ligand L_t complexes to M^{2+} , which is either in a hydrated form or in equilibrium with an external ligand L_e . Thus, the stability constant of L_t must be greater than that of L_e for the transport ligand to be effective. It must be remembered that for divalent metal ions, the stability of complexation to flexible ligands is essentially independent of the ligand and follows the Irving–Williams series shown below and that this may affect which metal is bound by such an ionophore [1].



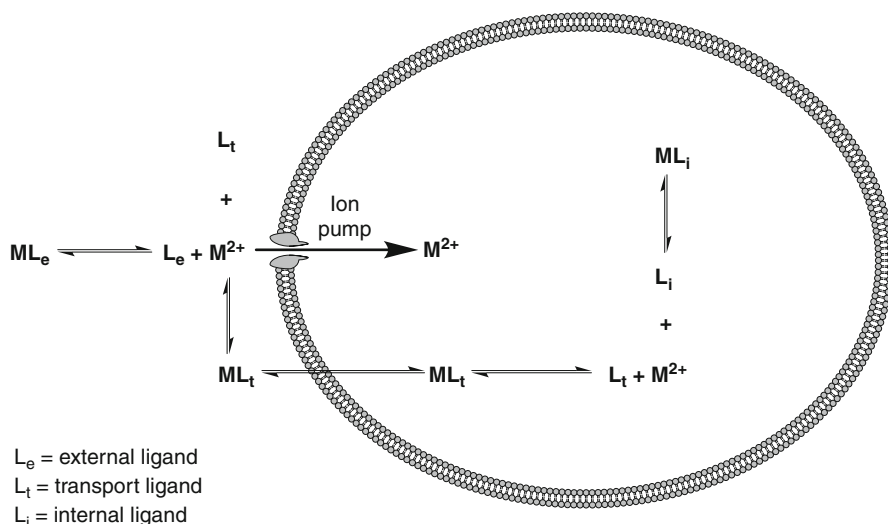


Fig. 16.1 Different routes by which a divalent metal can be taken up into a cell across the membrane [3]

The formation of an ionophore–metal complex generates a concentration gradient of the metal ions across the membrane despite the cell’s already high internal metal concentration. Once inside the cell, the metal ions are bound strongly to internal ligands (L_i in Fig. 16.1) which cannot diffuse out of the cell, thus forming a kinetic trap so that there is little transport of the metal out of the cell. This implies that the stability constant of L_i must be greater than that of L_t for this to occur. There are many examples of ionophores and siderophores which allow transmembrane transport of vital metal ions.

Measurements of the concentrations of these essential metal ions in the earth’s crust show that the bulk metal ions (Na, Mg, K, Ca) are present in high amounts, in the order of moles per kg (Fig. 16.2). The trace transition metal ions are present in much lower concentrations, ranging from 10^{-2} – 10^{-3} mol/kg, excepting Fe, which is present at about 1 mol/kg. The biological availability of these metals in the crust is much lower than these reported concentrations as they are often not in a form that is accessible to organisms that need them. In the marine environment, the situation is different with the bulk metal ions 1–3 orders of magnitude less concentrated in open-ocean seawater and the trace metal ions, present at 10^{-9} – 10^{-10} M concentrations, 7–10 orders of magnitude lower than in the earth’s crust [4]. On the continental shelf, these values are slightly higher due to the input from terrestrial runoff and rivers. In the open ocean, the major input of trace metal ions is dust deposition from the atmosphere with a minor contribution from hydrothermal vents. These low concentrations are worsened by the fact that these metal ions are not present in seawater as hydrated ions, but may be complexed to an organic ligand, or present inside an organism, with some studies reporting that greater than 99% of certain

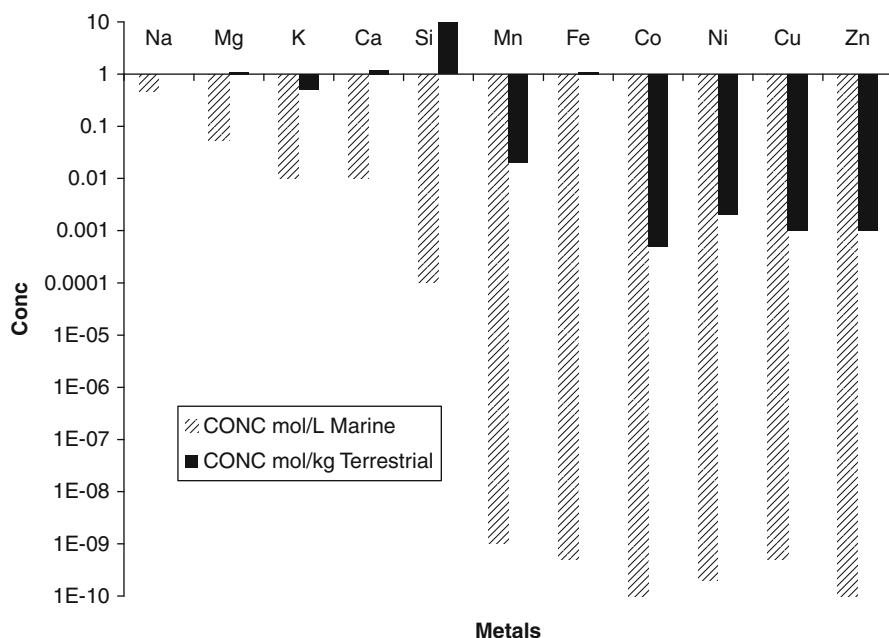


Fig. 16.2 Comparison of biologically important metal ions in marine and terrestrial environments (oceanic seawater and the earth's crust)

trace metal ions are complexed (e.g., Fe, Cu) [5]. Nutrient cycling for these metal ions is very fast compared to the bulk metal ions, exemplified by residence times of tens to hundreds of years compared to millions of years for the bulk ions. Essential nutrient ions also show a characteristic depth profile, with a very low concentration at the surface where it is heavily utilized by life in the photic zone, and then increasing to an asymptote at greater depth [4].

Given these high pressures for such vital, essential resources, marine organisms must have evolved unique mechanisms for acquisition, sequestration, and utilization of trace elements. Most research in this area has been carried out for open-ocean planktonic microorganisms which are responsible for most of the Earth's primary productivity (photosynthesis). It is known that in certain regions of the world's oceans, this productivity is limited by the scarcity of essential ions, particularly iron, and this may have an impact on the Earth's climate [6]. Iron acquisition by siderophores produced by marine microorganisms involves a number of very elegant mechanisms, and these compounds show some of the highest iron affinity constants ever recorded [7]. Very little is known about the way that marine macroorganisms, particularly invertebrates, carry out these essential functions, despite the fact that some marine invertebrates, such as sea squirts, hyperaccumulate certain metals. For this reason, this chapter will be limited to the

current understanding of the role of small molecule natural products in the complexation of metal ions in benthic, sessile marine invertebrates and will exclude the vast body of knowledge on marine microbial siderophores and ionophores.

16.2 Metal Surveys of Marine Invertebrates

For nearly a century, it has been known that there are extraordinary concentrations of vanadium in the blood cells of some ascidian species [8]. Only now are the processes becoming clearer by which this hyperaccumulation of vanadium is achieved by a factor of 10^7 over seawater [9]. The functional role of the vanadium to the ascidian is still undefined, and the necessity for the reported 0.35 M concentrations of vanadium in certain types of ascidian blood cells is unclear [9]. Speculation is rife with suggestions as to its true function from acting as an oxygen store [10] to playing a role in antifouling [11], but neither of these has been substantiated to date.

These findings spurred a great deal of research in the 1980s and 1990s on the possible mode of complexation of vanadium, which was proposed to be by the small molecule tunichromes (e.g., **1**), but cytochemical studies report that high concentrations of vanadium and the tunichromes do not appear in the same blood cell types [12]. Recent work shows that the vanadium is coordinated by amine nitrogen of the unusual 10.5 kDa peptide vanabins from *Ascidia sydneiensis samea*, which contain an unusual fold and nine disulfide bridges [9].

Besides vanadium, little has been reported on the complete metal complement of ascidians or other sessile marine invertebrates such as sponges, soft corals, or echinoderms. Studies reporting concentrations of other metals in sessile marine invertebrates are very limited, and many of these are collected for ascidians in Monniot's 1978 review [13]. This reports elevated concentrations of a number of transition metals in ascidian tissues, but often gives no exact concentrations or how these were measured. However, for iron, it gives a concentration of 5,100 ppm in *Pyura stolonifera*. Reports of lower iron concentrations are more common and often co-occur with elevated vanadium concentrations [8]. Some other metal concentrations that are provided in the Monniot review have been summarized in Table 16.1 [13]. For other metals that are not included in the table, either these are not significantly elevated (Sr, Zn, Sc, Eu, Th) or the concentrations are not provided explicitly (Co, Cu, Zr, Mo).

Our recent preliminary work on ascidians from the Great Barrier Reef using inductively coupled plasma mass spectrometry (ICP-MS) on $\text{HNO}_3/\text{H}_2\text{O}_2$ digests of the whole organism tissues shows a range of metals at concentrations significantly above the local seawater levels (Table 16.2). In particular, vanadium, iron, and arsenic were observed at high concentrations. Iron was observed at around 100 ppm or greater in 6 of the 11 organisms, while vanadium showed the highest concentrations of all the metals analyzed. The concentrations of iron ranged within $1\frac{1}{2}$ orders of magnitude, while the concentrations of vanadium were highly variable,

Table 16.1 Reported concentrations of metals in ascidians from Monniot et al. [13]

Organism	Metal	Concentration
<i>Ciona intestinalis</i>	Sn	$10^6 \times$ seawater conc.
<i>Microcosmus sulcatus</i>		
<i>Styela plicata</i>		
<i>Ciona</i> sp	Mn	120 ppm
<i>Eudistoma ritteri</i>	Ti	1,512 ppm
	Cr	144 ppm
<i>Pyura stolonifera</i>	Fe	5,100 ppm
<i>Molgula manhattensis</i>	Nb	25–98 ppm
<i>Styela plicata</i>	Nb	250 ppm
	Ta	540 ppm

ranging across 5 orders of magnitude from being almost absent (0.2 mg/kg) to reaching part-per-thousand levels (2,050 mg/kg). The variability did not seem to correlate with taxonomic groups, with two species of *Didemnum* accounting for the extremes of the observed vanadium concentrations and members of two families accounting for the highest concentrations. Comparing the measured concentrations with the reported oceanic concentrations (Table 16.2) [14] of a range of metals gives the indicative bioconcentration factors shown in Fig. 16.3. The range of bioconcentration factors ranges over 7 orders of magnitude with the highest values observed for Fe (1.6×10^7), Mn (2.2×10^6), and V (1.0×10^6). Biologically important metals are highly concentrated which suggests active acquisition is occurring, but also nonessential metals such as Cd and U are being concentrated by 3–4 order of magnitude. Clearly, much more work is required to fully appreciate the extent of metal concentration by ascidians, including the range of metals and the bioconcentration factors.

These surveys can mark the beginning of investigations into possible complexation of the accumulated metals by secondary metabolites. A total metals analysis of the organic extract of the organism can guide the search for chelating agents. For example, the high iron present in the organic ($\text{CH}_2\text{Cl}_2/\text{MeOH}$) extract of *Eudistoma gilboviride* (Fig. 16.4) led us to discover Fe^{II} chelates that comprised 0.4% w/w of the extract [15]. This study is described in more detail later in the chapter.

Apart from the Monniot review and our own work reported above, we have been unable to locate more recent broad studies encompassing other sessile marine invertebrate phyla reporting on the concentrations of a range of metals in environmentally noncontaminated environments. Filter-feeding invertebrates, mainly sponges, have been used as bioindicators for metal pollution; however, this represents the organisms' responses to high metal loads and not their native state. The Mediterranean sponge *Crambe crambe* was shown to accumulate Cu and Pb, and could be regarded as a useful bioindicator for these metals [16]. A 12-year longitudinal study on twelve metals in the Mediterranean sponge *Spongia officinalis* showed spatial and temporal variation in their concentrations indicating a significant reduction in heavy metals after a sewage plant came

Table 16.2 Preliminary investigation of metal concentrations in 11 ascidians from the Great Barrier Reef and oceanic concentrations [14] of those metals presented in ppm (mg of metal per kg of organism, dry weight or mg per kg of seawater). Values are measurements of single HNO₃/H₂O₂ digests of ground whole dry organism

Leptoclinides		Apidium		Didemnum		Didemnum		Didemnum		Polysyncraton		Didemnum		Polycarpa		Didemnum		Didemnum		Lissoclinum		Oceanic metals	
Species	sp	sp 1	sp 2	sp 3	sp	sp	sp 4	sp 5	sp 6	sp	sp	sp 4	sp 5	sp 6	sp	sp	sp 4	sp 5	sp 6	patella	concentrations		
Li	0.9	1.8	1.4	2.1	2.7	1.2	0.5	1.5	0.3	0.3	1.5	0.5	0.3	0.3	1.5	1.8 × 10 ⁻¹							
V	31	970	2,050	82	0.7	0.9	0.7	6.2	0.2	0.7	6.2	0.7	0.2	0.7	0.4	2.0 × 10 ⁻³							
Cr	0.7	9.0	4.2	1.7	1.4	2.8	7.4	5.4	1.0	1.2	5.4	7.4	1.0	1.2	0.8	2.1 × 10 ⁻⁴							
Mn	1.3	43	19	3.4	2.5	8.7	11	19	1.3	0.9	19	11	1.3	0.9	3.1	2.0 × 10 ⁻⁵							
Fe	52	480	270	220	29	160	97	100	14	14	100	97	14	14	43	3.0 × 10 ⁻⁵							
Co	0.3	0.8	0.3	0.3	0.2	0.3	0.2	0.3	0.1	0.2	0.3	0.2	0.1	0.2	0.1	1.2 × 10 ⁻⁶							
Ni	1.5	7.3	3.0	3.3	0.9	1.9	3.6	5.6	2.0	1.8	5.6	3.6	2.0	1.8	1.7	4.8 × 10 ⁻⁴							
Cu	5.9	4.7	5.2	7.1	0.8	3.2	1.5	1.5	1.5	1.6	1.5	1.5	1.5	1.6	4.1	1.5 × 10 ⁻⁴							
Zn	23	24	8.2	20	7.1	7.0	0.2	5.7	0.1	0.3	5.7	0.2	0.1	0.3	4.3	3.5 × 10 ⁻⁴							
As	8.9	9.5	11	120	1.6	8.7	4.6	15	6.0	4.5	15	4.6	6.0	4.5	6.7	1.2 × 10 ⁻³							
Se	1.0	1.8	1.6	4.9	0.2	1.1	1.0	2.1	0.3	0.2	2.1	1.0	0.3	0.2	0.7	1.6 × 10 ⁻⁴							
Rb	1.1	1.6	2.5	3.5	0.5	1.5	1.9	2.2	0.3	0.5	2.2	1.9	0.3	0.5	2.4	1.2 × 10 ⁻¹							
Mo	0.6	1.6	1.6	1.7	0.2	1.0	0.7	4.6	0.5	0.4	4.6	0.7	0.5	0.4	0.3	1.0 × 10 ⁻²							
Cd	0.2	0.2	0.7	1.6	0.2	1.1	0.5	0.2	0.0	0.2	0.2	0.5	0.0	0.2	0.5	7.0 × 10 ⁻⁵							
Ba	5.2	5.6	6.3	1.1	9.2	6.3	8.6	7.2	4.9	10	7.2	8.6	4.9	10	3.4	1.5 × 10 ⁻²							
U	3.4	1.6	2.5	1.5	0.2	3.1	1.8	0.9	2.9	3.9	0.9	1.8	2.9	3.9	1.8	3.2 × 10 ⁻³							

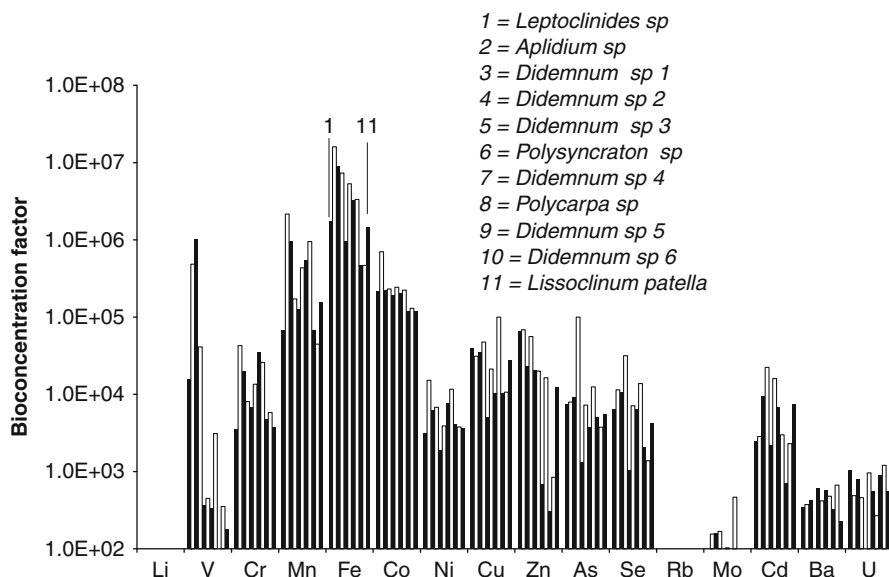


Fig. 16.3 Indicative bioconcentration factors for 11 ascidians from the Great Barrier Reef using information given in [Table 16.2](#)

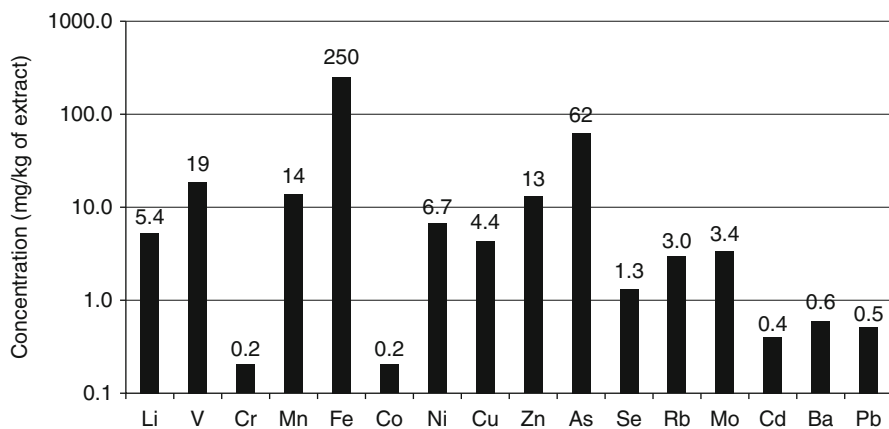


Fig. 16.4 Concentration (mg/kg) of a selected range of metals in the organic extract of the Great Barrier Reef ascidian *Eudistoma gilboviride*. Values are results of an $\text{HNO}_3/\text{H}_2\text{O}_2$ digest of a $\text{CH}_2\text{Cl}_2/\text{MeOH}$ extract of the dried organism. Metals that were analyzed but present at less than 0.05 mg/kg are not shown (Be, Ga, Ag, Te, Tl, Bi, and U) [15]

into operation [17]. One final report is worthy of note. The deepwater sponge *Tedania charcoti* collected in Prydz Bay, Antarctica, was shown by ICP-atomic emission spectroscopy to have extraordinary levels of Cd (15,000 ppm) and Zn (5,100 ppm) [18].

16.3 Why Do Marine Invertebrates Concentrate Metals?

Concentration of metals by up to 7 orders of magnitude from seawater by these invertebrates is a significant feat, and it is assumed that a number of specialized metal ligands and metal transport proteins are involved in this process, such as the vanabins mentioned previously. Internal transport proteins have been well defined in other organisms such as transferrin and ferritin for iron and the amino-terminal Cu and Ni binding motif in a number of Cu and Ni transport proteins [1]. The involvement of natural small molecule organic ligands has often been speculated (i.e., L_t in Fig. 16.1), but there is little concrete evidence that these are involved in the uptake and possible storage of nutrient metals for marine invertebrates, as has been shown for bacterial siderophores and ionophores [1]. A small number of marine natural products have been isolated complexed to transition metals, and a variety of roles have been speculated for the metal in these complexes [19].

The most obvious role of marine invertebrate compounds with the potential to complex metals is that they sequester metals for the organism's metabolism (i.e., L_t or L_i in Fig. 16.1). Some of the known compounds will be catalogued in the next section, but proof of their function as siderophores or ionophores in the producing organism is still lacking. An indication that marine siderophores differ from their terrestrial counterparts is exemplified by alterobactin (2), isolated from the open-ocean marine bacterium *Alteromonas luteoviolacea*, which has one of the highest stability constants ever reported [7]. This compound is secreted in response to low iron environments and complexes iron via the catecholate and β -hydroxyaspartate moieties.

It is possible that metal complexation is a way to imbue the natural product with biological activity and thus allow it to play a role in preventing predation and fouling, but this has not been shown conclusively so far. Some invertebrate marine natural products may complex a redox-active metal to confer reactivity to the ligand-metal complex. A terrestrial example is the anticancer agent bleomycin, derived from the microbe *Streptomyces verticillus*, which requires the presence of Fe(II) or Cu(I) and molecular oxygen to enable sequence-selective DNA binding and cleavage [20]. This hypothesis has been tested for very few marine natural products, the most significant of which is the copper-mediated nuclease activity of tambjamine E (3) isolated from the ascidian *Atapozoa* sp. [21]. It appears that a 2:2 complex of 3 with Cu(II) in the presence of oxygen, but in the absence of an external reducing agent, gives rise to stoichiometric DNA cleavage via a mechanism involving a reactive oxygen species. The pyridoacridine alkaloid ascididemnin (4) from the ascidian *Didemnum* sp. looks like a suitable candidate for binding to transition metals, especially Cu(II), and it was initially suggested that the mechanism by which it induced topoisomerase-II-mediated DNA cleavage involved a ascididemnin-Cu complex which was capable of generating reactive oxygen species [22]. However, the presence of Cu was shown not to be required and reactive oxygen species are produced by direct reduction of the iminoquinone moiety.

It is possible that the presence of a nonredox active metal in a complex with a marine natural product confers a preferred bioactive conformation to the complex. A protein example of this is the ubiquitous calmodulins, which change conformation upon binding to Ca, thus allowing the complex to bind to specific proteins and elicit a specific response [23]. A final suggestion is that the metal ions are necessary for templating the biosynthesis of macrocyclic ligands, but there has been no direct evidence for this hypothesis although there is some synthetic evidence that the presence of metal ions may assist such reactions [24].

The examples already discussed show that certain functional groups (e.g., hard/soft ligands) and molecular features (e.g., macrocycles, structural constraints) are often encountered in organic metal ligands. Learning from the metalloproteins, the presence of residues such as histidine, methionine, cysteine, tyrosine, aspartic and glutamic acid, and their derivatives in a natural product may suggest that the compound is involved in metal binding. Care needs to be taken that the coordination environment these represent is taken into consideration. Typical functional groupings found in siderophores and ionophores such as catecholates, hydroxamates, and β -hydroxyaspartates also imply a role of the compound in metal complexation. Complexation sites such as those present in heteroaromatics such as **3** and **4** are also very suggestive of a role in metal complexation. A number of moieties expected in metal-complexing natural products have been summarized in Fig. 16.5. More difficult to predict are conformations of macrocycles which present carbonyl, amide, or other functional groups in a coordination environment ideal for metal binding.

Based on such principles, a large number of marine metabolites are proposed to function as metal ligands; however, only very few cases have been substantiated. Most of the structural types that are suspected of being able to complex to metal ions have been catalogued in the influential review by Michael and Pattenden [19]. Rather than duplicating this information, we will give a brief survey of the structural classes which have proposed complexing abilities, followed in the next section by those in which either the metabolite was isolated as a metal complex or for which complexation studies have been carried out.

We have already seen examples in which obvious chelating functionalities are present such as the tunichrome **1** which contains three trihydroxyphenylalanine-derived substructures [8]. There is now evidence that these compounds are not involved in the complexation of vanadium, but it is possible that they are involved in the complexation of iron [12]. Similar moieties, in this case a dihydroxyphenol in addition to two β -hydroxyaspartates, are present in **2**, which has been shown to be a strong iron-complexing agent [7]. Tambjamine **3** has characteristic pyrrole functionality which predisposes it to bind to copper [21]. Ascididemin **4** has a bipyridyl “bay” region, which again makes it a likely candidate for complexing to transition metals, but the initial isolation study showed it did not complex iron(II) [25]. The eudistomins from *Eudistoma* sp. (e.g., **5**) have long been suspected of

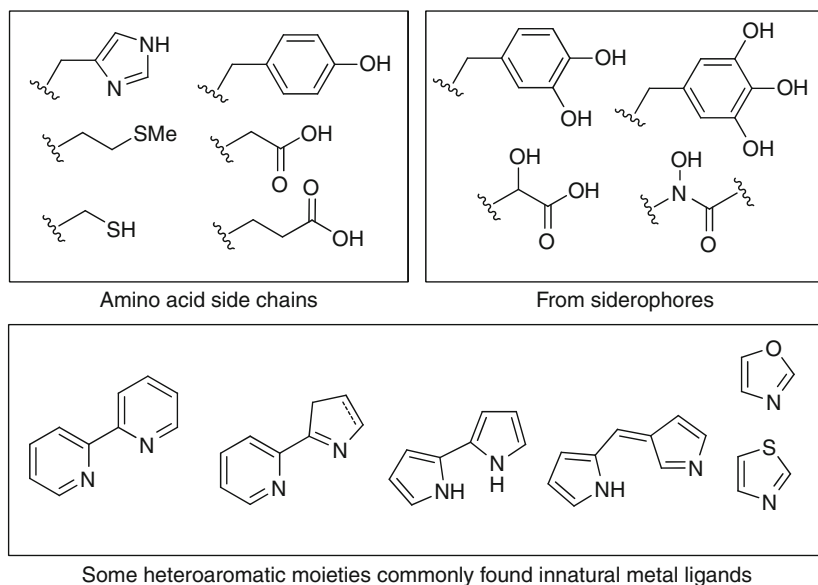
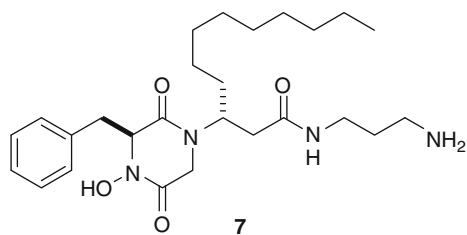
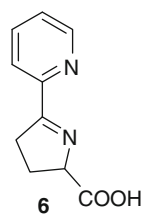
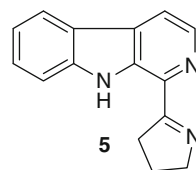
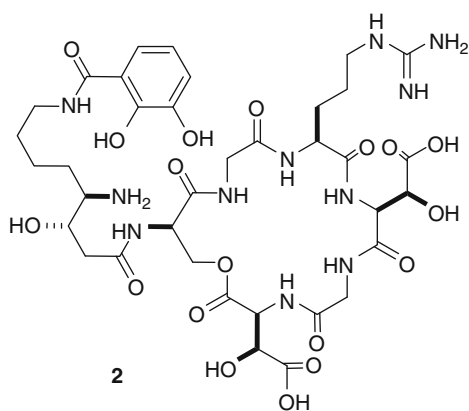
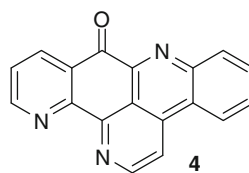
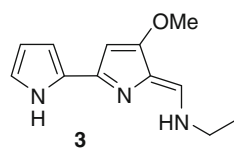
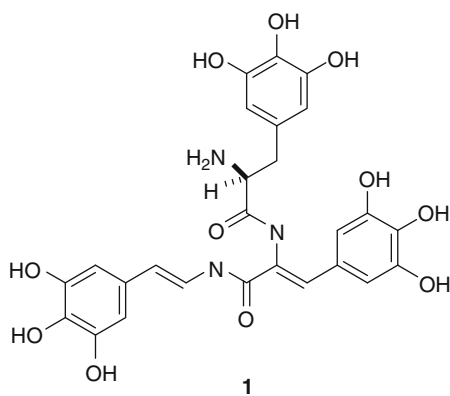
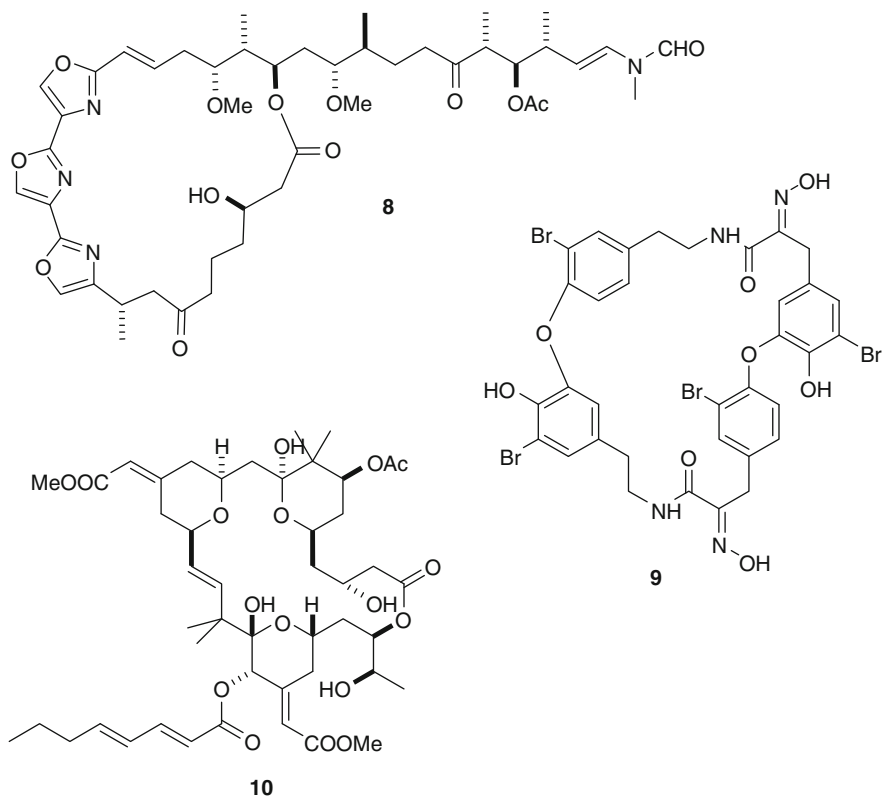


Fig. 16.5 Functional groups often encountered in natural metal ligands

being capable of chelating iron [26], due to their resemblance to the Fe(II) chelator pyrimine (**6**) isolated from a *Pseudomonas* sp. [27]. Etzionin (**7**) isolated from an unidentified Red Sea ascidian [28] contains a hydroxamate functionality as well as a terminal amine, and the combinations of these moieties are reminiscent of the potent siderophore deferrioxamine [29]. Compounds containing small heterocycles (e.g., oxazoles, oxazolines, thiazoles, thiazolines) are often suspected of being capable of chelating metals. One such example is ulapualide (**8**), isolated from the nudibranch *Hexabranchus sanguineus*, containing an array of three oxazoles. A molecular mechanics study was carried out with **8** complexed to a dummy metal ion and was used to predict its relative stereochemistry [30]. This structure also typifies the large macrocycles with a wealth of chelating functionality which make them appear ideal candidates for metal complexation. Other macrocycles such as the oxime-containing iodotyrosine-derived bastadins from the sponge *Ianthella basta* (e.g., **9**) [31] are also suspected of complexing metals, but there has been no definitive proof. Similarly, polyether macrolides such as the bryostatins derived from the bryozoan *Bugula neritina* (e.g., **10**) apparently display a perfect coordination environment for the binding of metals, but this has not been substantiated despite being suggested when its structure was first reported [32].





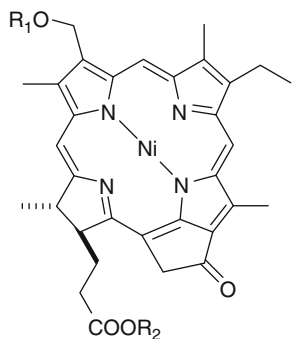
16.4 Marine Natural Products Isolated Containing Metals

A survey of the literature and databases reveals very few marine invertebrate natural products which have been isolated as metal complexes. Compared to the last comprehensive survey by Michael and Pattenden which highlighted compounds **11–13**, only a few more complexes have been reported (**14**, **16**) [19]. In addition to this, a few marine microorganism-derived metal complexes have been isolated, but these are beyond the scope of this review. Of the previously reviewed compounds, the nickel-containing porphyrin tunichlorin (**11a**) was originally isolated from the Caribbean ascidian *Trididemnum solidum* [33] and again later from the South Pacific Ocean sea hare *Dolabella auricularia* [34]. Subsequently, a large

number of acyl tunichlorin analogues (**11b**) were isolated from *Trididemnum solidum* where the acyl chains ranged from C_{14:0} to C_{22:6} [35]. Zinc complexes have been isolated from calcareous sponges; the first one was the clathridine–zinc complex (**12**) isolated from the Mediterranean sponge *Clathrina clathrus* [36]. A second zinc-complexing compound was isolated from a Fijian *Leucetta* sponge, the zinc complex of isonaamidine C (**13**) [37].

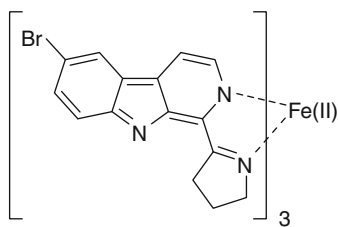
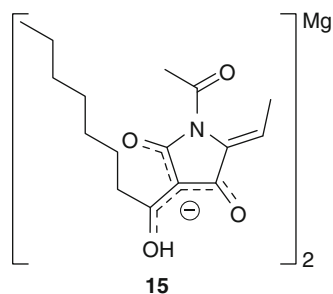
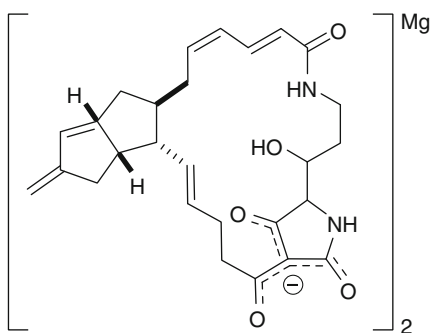
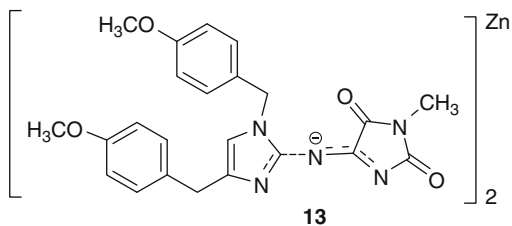
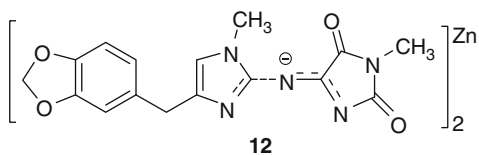
The unique geodin A, a macrocyclic polyketide lactam tetramic acid, was isolated as its magnesium complex (**14**) from the Australian sponge *Geodia* sp. [38]. The 2:1 complex was originally observed by mass spectrometric methods, and the stoichiometry was confirmed by atomic absorption spectroscopy. Geodin A is related to the tetramic acid magnesidin A (**15**) produced by the marine *Vibrio gazogenes*. Magnesidin A (**15**) was isolated as its magnesium complex but was found to be unstable to chromatographic methods using TFA [39]. This raises the point that although a marine natural product may exist as a metal complex in vivo, the extraction and isolation procedures may destroy the complex. The complexes reported above have all been stable to the work-up and chromatographic conditions, but it is likely that many others do not survive. Additional evidence for this comes from the existence of several zinc-free clathridines and naamidines from calcareous sponges, which may have been present as their zinc complexes in vivo but are destroyed during extraction and isolation procedures. To take this into account, we developed an isolation procedure using size exclusion chromatography which was mild enough to enable weak complexes to survive the purification process [15]. Application of this methodology, which is described in detail in Sect. 16.6, enabled the recovery of the 3:1 eudistomin–iron complex (**16**) from the Australian ascidian *Eudistoma gilboviride*, whose metal complement we had previously determined (Fig. 16.4). The methodology also enabled us to calculate that 0.4% of the organic extract of the organism was composed of the complex **16** and its analogues and that this represented 75% of the total lipophilic iron found in *E. gilboviride* and therefore a significant proportion of the organism's total iron content [15]. In addition, a reexamination of the crude extract by UV spectroscopy indicated that complex **16** was indeed present at this stage of the isolation procedure. It is possible that the formation of this complex is an artifact of sample preparation, but its concentration and presence in the original extract seem to suggest that it plays an important role in the organism's physiology as iron chelator. As mentioned previously, the eudistomin core structure (**5**) resembles the known iron chelator pyrimine (**6**) which also forms a 3:1 complex with iron(II) [27]. Further studies with pyrimine (**6**) showed that its complexes with Cu(II), Fe(II), and Mn(II) acted as efficient superoxide dismutase mimetics, with Cu(II) giving the best results [40]. It is possible, therefore, that the role of complex **16** in *E. gilboviride* is for the

removal of reactive oxygen species which may be generated in the high light environment it inhabits.



11a $R_1 = R_2 = H$

11b $R_1 = \text{acyl}, R_2 = H \text{ or Me}$



16.5 Marine Natural Product Complexation Studies

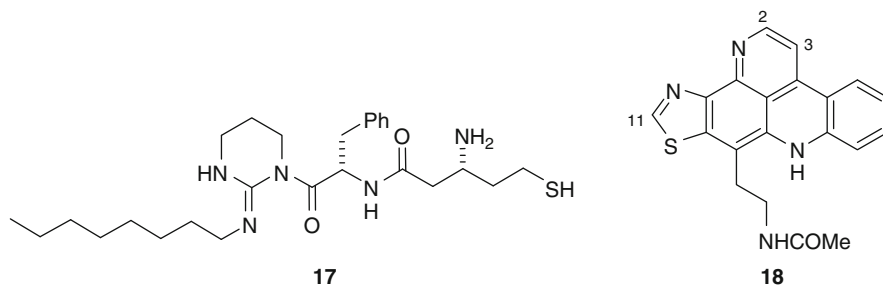
In the preceding sections, we have seen a limited number of authentic complexes isolated from marine invertebrates and some speculation based on the combined functionality and conformation of a molecule presenting a coordination environment suitable for complexing metals. The eventual aim of any studies based around determining metal chelation by marine natural products is to predict their function and hence their benefit to the producing organism. The nuclease activity determined for the copper complex of tambjamine (**3**), mentioned above, may indeed be its natural function, and it may thus act as a means of chemical defense. Similarly, the potential role of the eudistomin–iron complex **16** as a superoxide dismutase appears to make sense in its normal environment, yet neither of the assertions regarding these complexes' native function is easy to confirm.

As a first step toward understanding the function of marine metabolite–metal complexes, the basic structural and physicochemical parameters need to be determined. Several research groups have tried to confirm suspected complexation ability of marine natural products using spectroscopic and other methods. A useful parameter in such work is the binding selectivity for a particular metal ion, and then its binding affinity must also be measured. The ligand atoms involved in the complexation must also be determined so that the complete coordination environment and eventually the full three-dimensional structure of the complex in the solid or solution state should be solved. In this section, we will discuss illustrative examples of how combined physical, spectroscopic, and theoretical methods can be used to confirm the metal-complexing ability of some of the suspected ligands derived from marine invertebrates.

The simplest studies just involve one or two techniques to determine the metal complexation ability of a potential ligand, and this was the case for the highly unusual peptide caledonin (**17**), isolated from the New Caledonian ascidian, *Didemnum rodriguesi* [41]. The structural features of **17**, a penicillamine-like β -amino acid at one end and a hydrophobic chain at the other, made the investigators suspect that it was involved in metal ion transport across membranes. ^1H NMR titration studies of **17** with Zn(II) resulted in a 2:1 ligand to metal complex which was confirmed by mass spectrometric studies. Changes in the ^1H NMR spectrum on complexation to Zn(II) suggested that the terminal thiol and amino groups were involved in the binding.

Kuanoniamine D (**18**) contains a bipyridyl-type “bay” chelating functionality, and this was investigated in more detail using a variety of techniques and a range of metals which provided evidence for the formation of 2:1 ligand–metal complexes [42]. ^1H NMR titrations increasing the amount of ZnCl_2 showed line broadening of the signals at H2, H3, and H11 in **18** which sharpened and remained unchanged once a 2:1 ratio was attained. Kuanoniamine D fluoresces with λ_{ex} 350 nm and λ_{em} 524 nm, and the emission peak was greatly attenuated upon addition of excess Zn(II), Fe(II), and Cu(II) and was completely quenched on addition of Co(II). Fluorescence titrations could therefore be used to confirm the ligand to metal

ratio for Cu(II) and Co(II) in the complex and determine stability constants of $2.5 \times 10^{10} \text{ M}^{-2}$ for Co(II) and $1.3 \times 10^{10} \text{ M}^{-2}$ for Cu(II).



The original isolation paper of ascididemin (**4**) indicates that it does not bind to iron(II) [25]. The compound was subsequently reisolated from a *Lissoclinum* sp., measurements of the metal content in the ascidian extract showed elevated levels of several transition metals (Cu, Zn, Fe), and the mass spectrum showed an isotope pattern consistent with a **4**-CuOAc complex, which suggested that **4** might complex copper [43]. As ascididemin is fluorescent (λ_{ex} 219 nm, λ_{em} 295, 334 nm), a fluorescence quenching study was carried out (Fig. 16.6), and the fluorescence quenching mechanism and efficiency were evaluated. This showed that the fluorescence quenching efficiency is significantly greater for the Cu(II) complex than the Co(II) or Ni(II) ones.

An early complexation study was initiated by the realization that the cyclic depsipeptide jasplakinolide (Fig. 16.7a, **19**), isolated from the Fijian sponge, *Jaspis* sp., resembled several other depsipeptide ionophores such as the enniatins [44]. Consequently, Inman and coworkers conducted ^1H NMR titrations of a 200-mM solution of **19** in CD_3CN with Li^+ , Na^+ , and K^+ . Only Li^+ generated significant changes in the spectrum, which were used to calculate a binding constant of 60 M^{-1} for the 1:1 complex of **19** with Li^+ . Significant conformational changes were observed via the change in a number of coupling constants, implying changes in dihedral angles of **19**. A molecular mechanics study using explicit Li^+ revealed a conformation consistent with these dihedral angles that allowed the carbonyls at C1, C10, and C14 to bind to the Li^+ with reasonable Li–O bond lengths, and that Li–O distance was too long for the carbonyl at C17. A more recent study took a different approach and first determined the solution conformation of **19** in CD_3CN using NOE-restrained molecular dynamics calculations (Fig. 16.7b) [45]. This was followed by the determination of the solution structure of 16 mM **19** in CD_3CN in the presence of 1 equivalent of Li^+ which was modeled using NOE restraints without the use of an explicit Li^+ . Again, large changes in the conformation on formation of a 1:1 ligand to metal complex were evident, as is clear from the resulting minimum energy structure represented in Fig. 16.7c. This conformation appeared very different from that determined in the earlier study [44], perhaps as an effect of the much lower concentration employed in the more recent study [45].

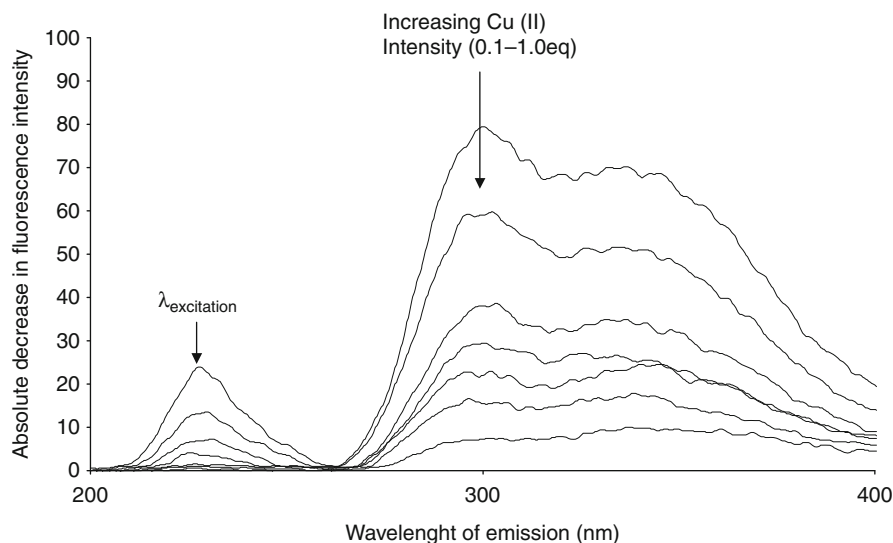


Fig. 16.6 Titration of ascididemin (**4**) with increasing amounts of Cu(II) monitored by fluorescence spectroscopy showing fluorescence quenching with increasing amounts of Cu(II). Excitation wavelength set at 219 nm and emission monitored at 295 and 334 nm

A full conformational search without NOE restraints in the presence of explicit Li^+ found a low-energy conformation that was similar to the solution conformation in Fig. 16.7c. An overlay of the calculated and experimentally determined chelating structures is shown in Fig. 16.7d. This then suggests that at this concentration, the Li^+ binds outside the macrocycle, involving the carbonyls at C14 and C17, and the π -electrons of the β -tyrosine. A comparison of these two studies thus casts light on another difficulty, that weak complexes such as this may display different modes of coordination depending on the concentration.

The cyanobactins, exemplified by the patellamides, **20**, and westiellamide, **21**, are posttranslationally modified ribosomal cyclic peptides containing azole moieties isolated from cyanobacteria. The patellamides, **20**, were originally isolated from the ascidian *Lissoclinum patella* but were subsequently shown to be produced by the symbiotic cyanobacterium *Prochloron didemni* [46, 47]. One study showed elevated levels of copper and zinc in the tissues of *Lissoclinum patella* [48], adding ecological significance to the previously observed crystal structure of ascidiacyclamide **23** with two equivalents of copper and a bridging carbonate (Fig. 16.8a, b) [49]. These authors studied these complexes by a number of techniques and found that in the solid state the $\text{Cu} \cdots \text{Cu}$ distance was 4.43 Å, whereas a separate study showed this to be 3.7 Å in solution using EPR measurements coupled with molecular simulations [50]. The key findings of many studies, by a number of authors using a range of techniques, including mass spectrometry,

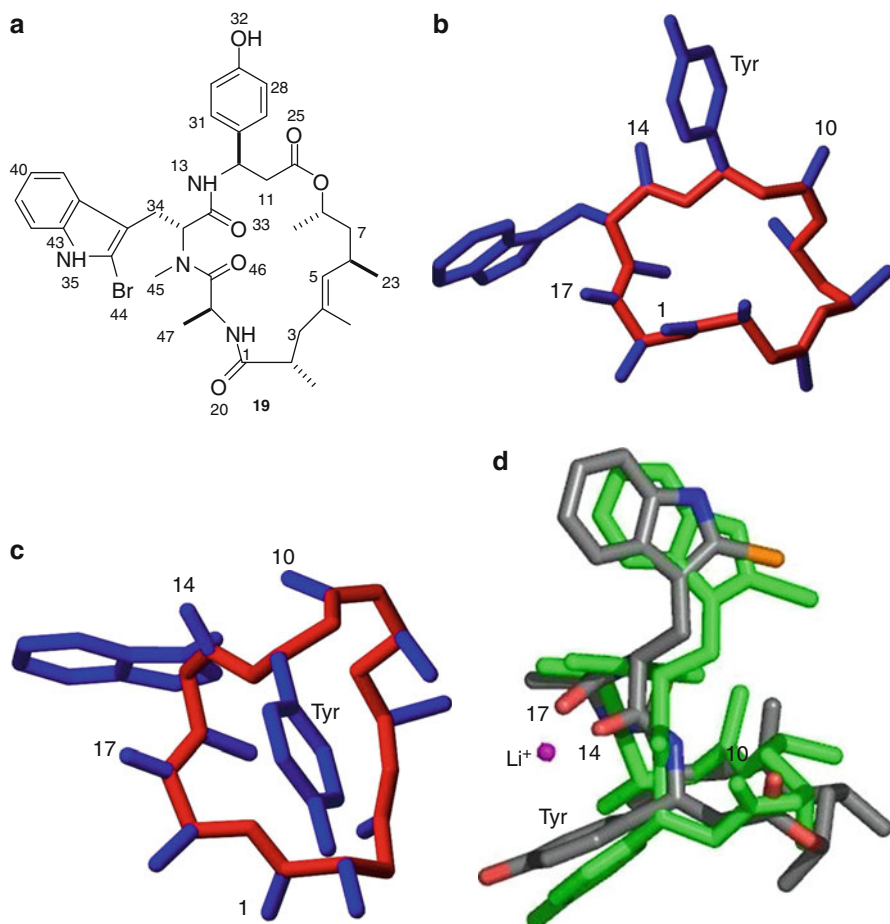
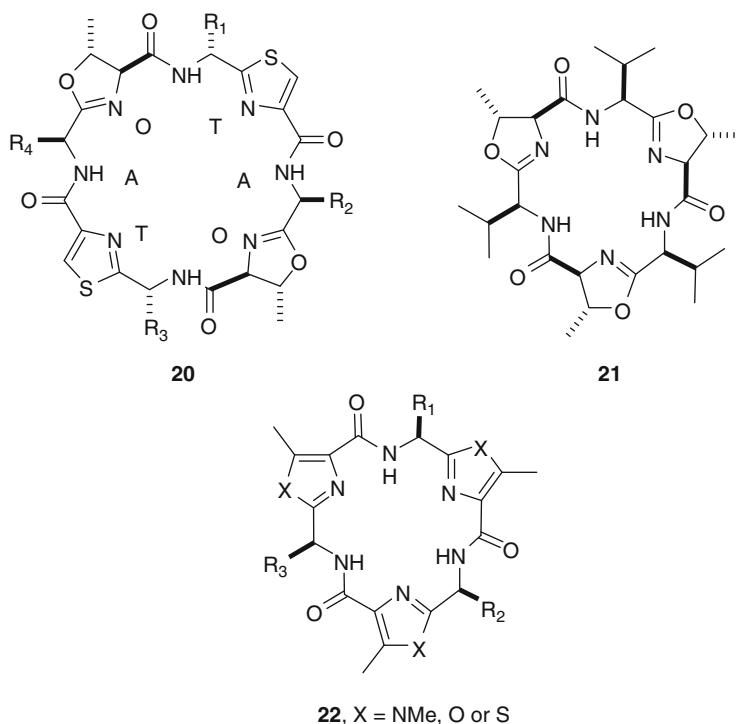


Fig. 16.7 (a) Structure of jaspakinolide; (b) NOE-restrained molecular dynamics structure of jaspakinolide in CD₃CN; (c) NOE-restrained molecular dynamics structure of jaspakinolide with 1 equivalent of Li⁺ in CD₃CN; (d) Overlay of the structure in (c) with a Li⁺ docked minimized jaspakinolide obtained by conformational searching

ultraviolet, circular dichroism, NOE-restrained molecular dynamics calculations, and magnetic susceptibility have been recently summarized [24]. This intensive research was prompted by Hawkins' original suggestion that the patellamides (20) could complex two equivalents of copper via the thiazole (T), amine (A), and oxazole (O) nitrogens, as later confirmed by many of these studies.[26] A cooperative binding mechanism was demonstrated in which the binding of one Cu(II) ion unfolded the patellamide molecule to present a second TAO-binding site ready to accept the second Cu(II) ion (Fig. 16.8c) [51]. The presence of elevated

levels of copper in *Lissoclinum patella* and the ideal coordination environment presented for the complexation of two Cu(II) ions suggested that this complex played an important role in the ecology of the organism, whereas the role of a Zn–patellamide complex was deemed less important due to the lower stability of the complexes formed [48, 51]. The distance between the two copper centers in the patellamide–dicopper complexes tantalizingly suggested that they might have a role in activating dioxygen, similar to the dicopper proteins, but this has not been verified to date [52].



The study of westiellamide (**21**) was initiated by the unusual sandwich complex generated with four Ag(I) ions (Fig. 16.8d) [53]. The near-planar structure of **21**, upon complexation with Ag, is modified by the rotation of the oxazoline rings perpendicular to the macrocycle, with the coordination environment for the fourth Ag(I) ion generated by the carbonyl groups pointing toward the center of the sandwich. A detailed study of these complexes of **21** and analogues **22** has been published recently, showing that the compounds are highly preorganized for Cu(II)

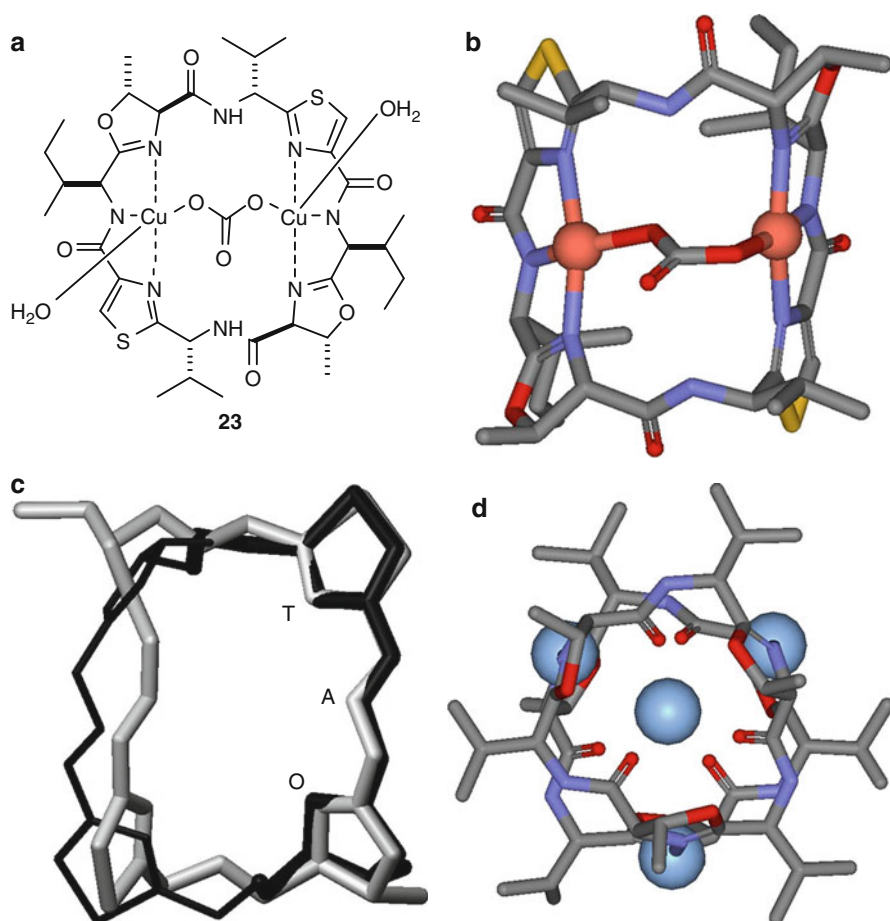
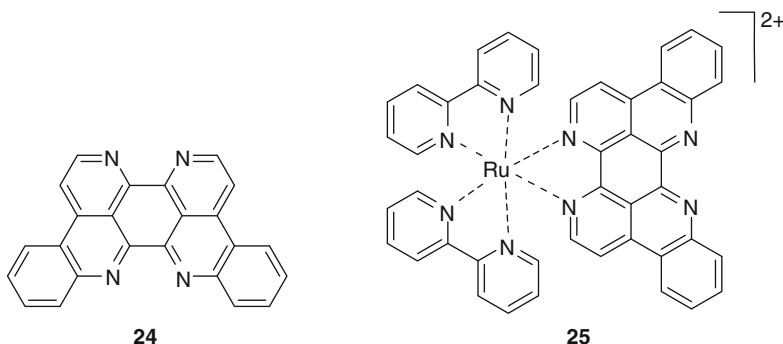


Fig. 16.8 (a) Asciadiacyclamide-Cu₂CO₃ structure. (b) Crystal structure of the asciadiacyclamide-Cu₂CO₃ complex, Cu depicted as spheres. (c) Overlay of the patellamide C-Cu NOE-restrained molecular dynamics structure (*black*) with the asciadiacyclamide crystal structure (*gray*) showing the TAO nitrogens in the correct configuration to accept the second Cu ion. (d) Sandwich complex of two westiellamide molecules with four Ag ions, Ag depicted as spheres

coordination [54]. These examples show that although some of these complexes may form with biologically relevant metals, in other cases, novel complexes can be formed using other metal ions. Such is the case for eilatin (24), isolated from the Red Sea ascidian *Eudistoma* sp. which forms complexes with ruthenium and two

bipyridyl units (**25**) [55]. These complexes have anti-HIV activity in vitro by binding to DNA and RNA.



16.6 Methods to Identify Metal Complexes from Marine Invertebrates

From the preceding discussion, it is clear that metal-complexing agents from marine invertebrates are underinvestigated. The complexes that have been studied, either isolated as complexes, or ligands studied in the presence of metals show excellent selectivity, high affinity, and some fascinating biological activities. For this reason, efficient methods for the recovery of intact complexes or potential ligands need to be developed. Much work has been done on developing rapid colorimetric methods for the discovery of iron ligands such as the chrome azurol S (CAS) assay [56], but there is a dearth of similar assays for other metals of interest in addition to which a more general method, able to cope with a range of metals, would be preferable.

The method of choice for the detection of trace elements in solution is ICP-MS (inductively coupled plasma mass spectrometry), an elemental mass spectrometric technique, which is able to detect most elements in solution below concentrations of 1 ng/mL (ppb). The method is not only sensitive but also has the ability to detect multiple elements simultaneously which enables the screening of extracts or acid-digested tissues for a series of elements of interest. These can be the classical transition elements: metalloids such as arsenic and selenium, and nonmetals such as bromine, iodine, phosphorus, and sulfur. Hence, the ICP-MS analysis of extracts from marine organisms can quickly establish which samples contain significant quantities of elements of interest.

ICP-MS uses a hard ionization source that completely destroys, atomizes, and ionizes every compound, so with this technique, it is intrinsically impossible to determine intact molecules. However, when chromatographic separation in the form of HPLC (high-performance liquid chromatography) is interfaced to ICP-MS, molecular information can be gained indirectly; different molecules

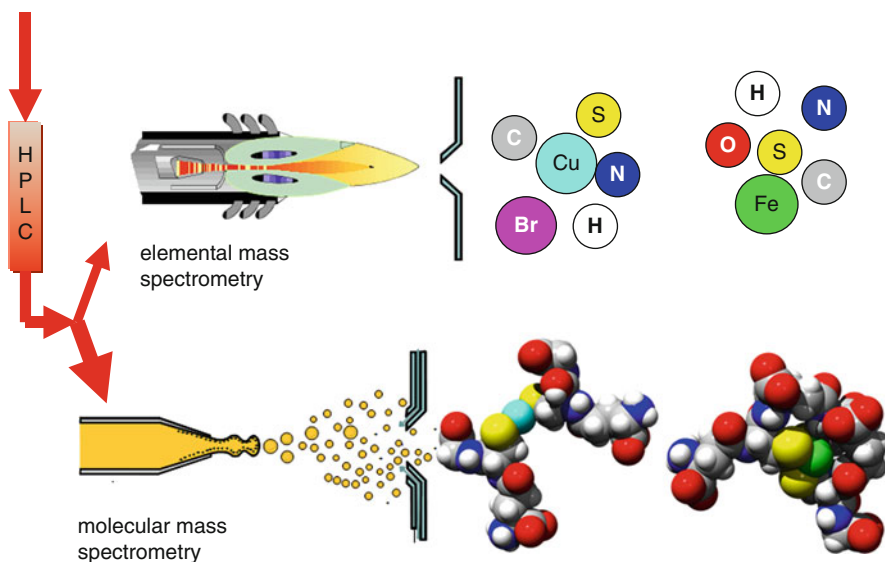


Fig. 16.9 HPLC hyphenated simultaneously to ICP-MS and ES-MS to identify and quantify metal complexes in extracts of biological marine specimens

containing trace elements are separated by HPLC, and element-specific detection is achieved with ICP-MS. The molecular identification relies on retention time comparison with standard compounds. This technique can also be used to screen for unknown compounds and can give information whether or not different compounds containing a certain element occur in a sample extract. However, HPLC-ICPMS alone cannot identify novel compounds where no standard compound is available. For molecular identification of unknown compounds in a sample extract, molecular mass spectrometric methods such as electrospray ionization mass spectrometry (ES-MS) are needed. Electrospray is a soft ionization technique that is able to ionize molecules, complexes, and even unstable compounds without fragmentation. When HPLC is interfaced to ES-MS, compounds can be separated and detected, but it is very difficult to identify the metal-containing species from an ES mass spectrum. Here, the combination of ICP-MS and ES-MS has proven ideal for the detection of labile metal compounds in complex extract matrices. The combination of both MS detectors capitalizes on their complementary analytical features, and recently HPLC has been coupled simultaneously to both detectors. Figure 16.9 illustrates this innovative arrangement of interfacing HPLC in parallel to ICP and ES mass spectrometers.

All metal compounds in an extract can be detected simultaneously, and elemental as well as molecular information can be collected. While the ICP-MS identifies the “needle in the haystack” by giving direct information about the retention time of the molecules containing the element of interest (which could be characteristic for the ligand such as bromine in **9** and **16** or for the complexed metal-like zinc in **12**

and **13** or iron in **16**), ES-MS provides molecular information in the same time window. This enables the identification of traces of metal complexes in a crude biological extract, without having a standard at hand. This system is especially useful for the identification of target species with unknown elemental composition and structure and which are potentially labile during chromatography. Since only one chromatographic system is used, the system can be tailored for the identification of certain complexes. This has been demonstrated for the identification of labile arsenic and mercury phytochelatin complexes, which were separated on a reverse-phase column in a methanol/formic acid mobile phase [57, 58].

However, the major disadvantage of all MS-based techniques is that they have to be linked to chromatography or capillary electrophoresis. Ion-exchange chromatography and capillary electrophoresis typically use buffers with high aqueous content, which are not generally suitable for natural products due to solubility issues. Reverse-phase HPLC is the most commonly used form of LC-MS for analysis of natural products, but it tends to result in dissociation of all but strong chelates. To enable LC-MS of even weak natural product chelates, we investigated size-exclusion chromatography (SEC) with a natural product friendly solvent system. Contrary to other forms of chromatography, SEC involves minimal interaction between the analytes and the stationary phase, which helps to prevent dissociation of metal complexes. We combined the use of a poly(methyl methacrylate) SEC-HPLC column with a methanolic buffer. However, analyte interactions with residual hydrophilic sites on the stationary phase resulted in chelate dissociation and excessive retention. Through much trial and error, we developed a buffer (50 mM trimethylamine carbonate, pH 8.8) that was able to prevent the dissociation of weak chelates [15]. Although some chelates were still strongly retained on the column, these could be eluted with 100 mM formic acid in methanol with minimal complex dissociation.

This SEC-HPLC method was coupled to both ICP-MS and ES-MS to investigate organic extracts of ascidians for chelates. As previously mentioned, cyclic peptides produced by the ascidian *Lissoclinum patella*, such as the patellamides (**20**), are able to chelate copper with stability constants in the region of 1×10^4 – 3×10^5 [48, 59, 60]. These copper complexes were successfully observed using SEC-HPLC-ICP/ES-MS in an extract of *L. patella* that had been spiked with copper. The unspiked extract of *L. patella* was also analyzed by this method, but no complexes were observed, which suggested that these cyclic peptides were not complexed to copper in the organism.

Many novel natural product chelates that exist undetected may be discovered by SEC-HPLC-ICP/ES-MS. A crude extract of *Eudistoma gilboviride*, in which we had discovered high levels of iron (Fig. 16.4), was analyzed using this method. Peaks in the ES mass spectrum were detected that coeluted with Fe peaks in the ICP-MS chromatogram (Fig. 16.10). Despite only using low resolution ES-MS, we were able to identify complexes of Fe(II) with eudistomin H (**16**) and its analogues. The incorporation of high-resolution ES-MS would enhance this method's potential for discovery of novel chelates manifold. While the presence of these novel Fe(II)–eudistomin chelates were identified in the organic extract, the question remains as

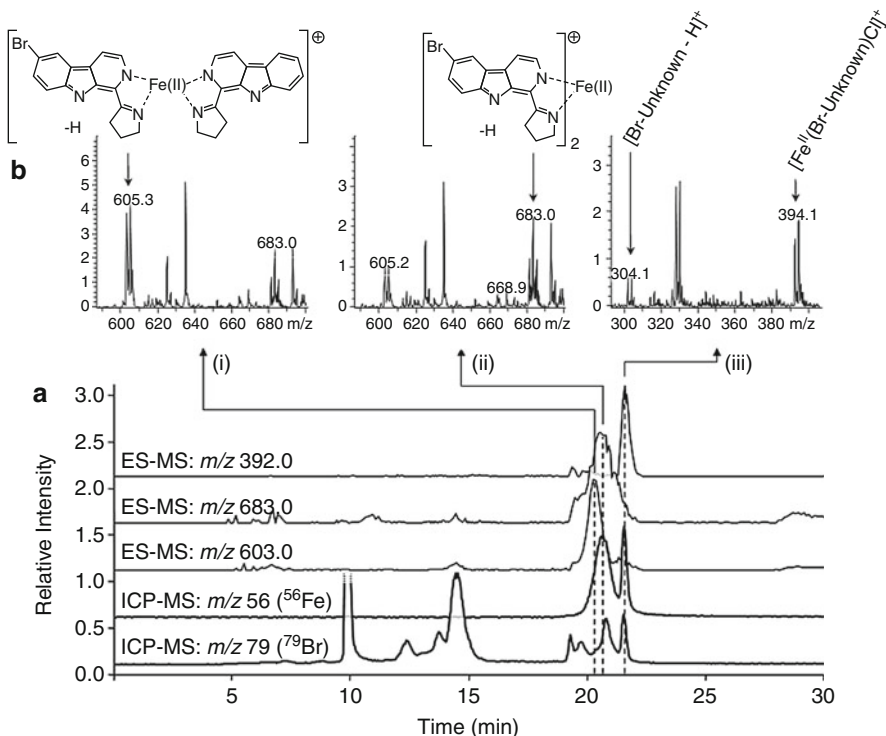


Fig. 16.10 Iron(II) complexes identified in a organic extract of the ascidian *Eudistoma gilboviride* by size exclusion chromatography coupled in parallel to ICP-MS and ES-MS. (a) Selected ICP-MS (Fe, Br) and ES-MS (603, 683, 392 m/z) extracted ion chromatograms. (b) Mass spectra and identifications for peaks at 20.5, 20.8, and 21.6 min [15]

to whether they were present in the organism itself or were formed during the extraction process.

If the metal complexes dissociate during chromatographic separation, other methodologies which do not rely on separation techniques have to be employed, such as electrochemical (EC) detection. These techniques are usually applied to aqueous solutions but have a potential to be used for nonaqueous extracts. EC techniques can thus detect complexes with different stability constants by tuning experimental parameters and can distinguish between free metal ions, labile metal complexes, and inert stable complexes. Although it cannot directly identify the molecular structure of the complex, it is possible to determine the conditional stability constant of the complex. So far, no study has been published which applied EC techniques for the identification of metal complexes in biological extracts. Although EC methods are well-established methods in oceanography, the reason why these are not widely used for the analysis of metal-containing natural products might be the severe matrix problems when they are used in nonaqueous solution.

In order to overcome this problem, and to guarantee the integrity of the metal complex during analysis, direct analytical methods need to be employed which do not rely on the extraction step in the first place, methods that can be used to determine whether a complex is actually present in the organism itself. These are elemental and molecular imaging methods. One type of analysis is based on the absorption of synchrotron radiation. In particular, X-rays generated by tuneable synchrotron radiation can be applied to the specimen, and the absorption is then recorded as a function of the energy. X-ray absorption near edge spectroscopy (XANES) and extended X-ray absorption fine structure (EXAFS) give information about the element and the redox state as well as the bond length to the ligands. For example, it is possible to identify whether arsenic is trivalent or pentavalent and whether it binds to ligands via oxygen or sulfur using the fresh specimen without any extraction steps. EXAFS analysis is often only used for the identification of the redox state of the metal. For example, the identification of the different redox ions in different ascidians (*Ascidia ceratodes* and *Ascidia nigra*) gave evidence of subgeneric differences and was the basis for further investigations to identify vanadium(IV)-binding proteins in ascidians [9, 61].

The drawback of these synchrotron radiation (SR)-based methods is that they cannot be used as routine analysis for screening analysis since beamtime at a synchrotron is limited and very expensive. SR methods can reveal whether any novel metal complexes are disintegrated or formed *de novo* during the sample preparation and the analysis. The complementary use of XANES/EXAFS methods compared to MS-based methods has never been applied to the identification of novel marine products, but was successfully employed for the identification of arsenic complexes in plants [62].

Another approach is to analyze marine organisms directly using elemental and molecular imaging techniques. Micro-XANES analysis makes it possible to record an element spectrum on a spot the size of 100 μm . Rastering the target in the laser beam enables the construction of an image which contains semiquantitative data of the element distribution in the organism with additional information of its redox state or binding ligands. This can be used to identify the organ in which the most interesting metal complexes are located. Where synchrotrons are not available, other laboratory-based techniques such as LA-ICP-MS (laser ablation ICPMS) can be used for generating elemental maps of the organism. For this analysis, it is necessary to produce thin sections, by microtoming, of the organism, and by interrogating it with a laser beam of variable energy, the material is ablated and transported into the ICP-MS. Multielement maps can be constructed on specimen size up to 10 cm^2 with a spatial resolution as low as 10 μm .

Although these techniques give vital information about the spatial distribution of metals and metalloids, no metal complexes can be identified. Hence, again molecular information is a necessary addition to the elemental mapping. In recent years, new surface molecular imaging methods have been developed which can assist to gain information on small molecules and metal chelates. After a surface application of a matrix of easily ionizable substances, soft ionization of the molecules can

easily transfer the charge to molecules to form molecular ions which can be transported into a mass spectrometer for analysis. This technique is called MALDI-TOF-MS (matrix-assisted laser desorption ionization time of flight mass spectrometry). This method has recently been used to identify secondary metabolites produced by marine cyanobacteria and sponges [63]. The newest development is the use of DESI (desorption electrospray ionization) MS for the localization of natural products directly on the marine organism without applying any matrix on the surface) [64].

If elemental and molecular imaging techniques are used with adjacent thin sections of one organism, metal and ligand maps can be matched and superimposed using image manipulation techniques. This has never been demonstrated with marine organisms, but its potential was demonstrated when it was successfully used to identify metal–protein complexes in a liver abscess [65].

In summary, a variety of analytical methodologies can be used for screening analysis of metal-containing natural products in extracts. To choose the best methodology, readers may refer to a recent review which critically appraises different methodologies for the determination of trace element compounds in biological samples [66].

16.7 Conclusion – A Proposal for a Structured Search for Marine Natural Products Containing Metals

Besides developing the tools to more efficiently discover complexes and ligands from marine invertebrates, it is also worth thinking carefully about how a constructive search for these might be structured. There are some structural features and general considerations which are important when looking for complexes and ligands from marine invertebrates, and these could form the search parameters for a directed search.

The first parameter to consider is the metal content of the invertebrate tissues and organic extracts. A high concentration of metals in the organic extract suggests that they are complexed by an organic ligand. Interest in the eudistomins (e.g., **5**) was aroused by the high content of Fe in the extract of *Eudistoma gilboviride* (Fig. 16.4), which led to the discovery of the eudistomin–iron complex **16** [15]. Therefore, the screening of the organisms to look for transition metals (e.g., Mn, Fe, Co, Ni, Cu, Zn, Mo) in organic extracts will be very productive, but as has been discussed before, few studies have addressed this.

In assessing compounds with potential metal-complexing properties, structural features of known compounds can be very suggestive of good metal ligands. Initially, this may include looking for hard/soft ligands, groups which are involved in metal binding in metalloproteins such as histidine, methionine, cysteine, tyrosine, aspartic and glutamic acid, as well as the coordination environment these present (Fig. 16.5). Additionally, we can look for typical functional groupings found in siderophores and ionophores such as catecholates, hydroxamates, and

β -hydroxyaspartates as well as those present in heteroaromatics (Fig. 16.5). If we are considering the functions of these complexes, such as the generation of reactive oxygen species by the tambjamine (**3**)–copper complex, then the metal center should be coordinatively unsaturated to allow a substrate to bind.

Cyclic compounds have a greatly reduced conformational space compared to acyclic compounds, often allowing them to present ideal coordination environments for metal complexation. This, together with constraining features such as azole rings and prolines, should be given priority as search parameters. Other features such as disulfide bridges also reduce the conformational space accessible.

If we are considering the potential biological functions of these metal complexes, we should look for groups with potential for involvement in redox processes. Some of the compounds have signatures implying the possibility of redox involvement such as disulfide bridges. Similarity to known metalloprotein active sites may also be considered an important search parameter to ascribe a function to a complex, such as the similarity of the patellamide dicopper complexes (Fig. 16.8a, b) to dicopper proteins. A similarity search according to substructures is likely to be less successful than a similarity search based on key coordinating atoms in the active site. One final feature to look out for is protection of the coordination environment by lipophilic groups which might be important for controlling substrate access.

These search parameters, when combined, may lead to the discovery of a number of exciting new complexes from marine invertebrates with associated biological functions and potential for medical or biotechnological applications.

16.8 Study Questions

1. Suggest reasons why marine invertebrates might hyperaccumulate metals. What evidence is there to support each theory?
2. Many marine natural products contain functionality that suggests an ability to complex transition metals. What functional groups and structural features might be important in complexing transition metals? From the marine natural product literature or databases, identify four such structures and propose which metals they might bind to and why.
3. Which physical methods might you use to determine the binding specificity and affinity of marine natural products for transition metals?
4. If you were presented with an organic invertebrate extract that was identified as containing high levels of zinc, what steps would you take to isolate and determine the structure of the zinc complexed to the marine natural product?
5. Draw a flowchart explaining the steps that need to be taken to carry out a structured search for marine natural product metal complexes. You should explain the choice of your steps and the methods to be used at each stage.

References

1. Kaim W, Schwederski B (1994) Bioinorganic chemistry: inorganic elements in the chemistry of life. Wiley, Chichester
2. Depledge M, Rainbow P (1990) Models of regulation and accumulation of trace metals in marine invertebrates. *Comp Biochem Physiol* 97C:1–7
3. Rainbow P (1997) Trace metal accumulation in marine invertebrates: marine biology or marine chemistry? *J Mar Biol Ass UK* 77:195–210
4. Butler A (1998) Acquisition and utilization of transition metal ions by marine organisms. *Science* 281:207–210
5. Rue E, Bruland K (1995) Complexation of iron (III) by natural organic ligands in the central north pacific as determined by a new competitive ligand equilibration/adsorptive cathodic stripping voltammetric method. *Marine Chem* 50:117–138
6. Jickells T, An Z, Andersen K, Baker A, Bergametti G, Brooks N, Cao J, Boyd P, Duce R, Hunter K, Kawahata H, Kubilay N, laRoche J, Liss P, Mahowald N, Prospero J, Ridgwell A, Tegen I, Torres R (2005) Global iron connections between desert dust, ocean biogeochemistry and climate. *Science* 308:67–71
7. Reid RT, Live DH, Faulkner DJ, Butler A (1993) A siderophore from a marine bacterium with an exceptional ferric ion affinity constant. *Nature* 366:455–458
8. Smith M, Kim D, Horenstein K, Nakanishi K, Kustin K (1991) Unravelling the chemistry of tunichrome. *Acc Chem Res* 24:117–124
9. Hamada T, Asanuma M, Ueki T, Hayashi F, Kobayashi N, Yokoyama S, Michibata H, Hirota H (2005) Solution structure of vanabin2, a vanadium(IV)-binding protein from the vanadium rich ascidian, *Ascidia sydneiensis samea*. *J Am Chem Soc* 127:4216–4222
10. Smith M (1989) Vanadium biochemistry: the unknown role of vanadium containing cells in ascidians (sea squirts). *Experientia* 45:452–457
11. Stoecker D (1980) Relationships between chemical defense and ecology in benthic ascidians. *Mar Ecol Prog Ser* 3:257–265
12. Martoja R, Gouzerh P, Monniot F (1994) Cytochemical studies of vanadium, tunichromes and related substances in ascidians, possible biological significance. *Oceanogr Mar Biol Annu Rev* 32:531–556
13. Monniot F (1978) Connaissances actuelles sur les ions métalliques chez les ascidies. *Actualites Biochim Mar*: 185–194.
14. Nozaki Y (1997) A fresh look at element distribution in the North Pacific Ocean. *Eos, Trans Am Geophys Union* 78:221
15. Wright S, Raab A, Tabudravu J, Feldmann J, Long P, Battershill C, Dunlap W, Milne B, Jaspars M (2008) Marine metabolites and metal ion chelation: intact recovery and identification of an iron(II) complex in the extract of the ascidian *Eudistoma gilboviride*. *Angew Chem Int Ed* 47:8090–8092
16. Cebrian E, Uriz M-J, Turon X (2005) Sponges as biomonitors of heavy metals in spatial and temporal surveys in Northwestern Mediterranean: multispecies comparison. *Environ Toxicol Chem* 26:2430–2439
17. Perez T, Longet D, Schembri T, Rebouillon P, Vacelet J (2005) Effect of 12 years' operation of a sewage treatment plant on trace metal occurrence within a Mediterranean commercial sponge (*Spongia officinalis*, Demospongiae). *Mar Pollut Bull* 50:301–309
18. Capon R, Elsbury K, Butler M, Lu C, Hooper J, Rostas J, O'Brien K, Mudge L-M, Sim A (1993) Extraordinary levels of cadmium and zinc in a marine sponge, *Tedania charcoti* Topsent: inorganic chemical defense agents. *Experientia* 49(3):263–264
19. Michael JP, Pattenden G (1993) Marine metabolites and metal ion chelation: the facts and the fantasies. *Angew Chem Int Ed Engl* 32:1–23
20. Hecht S (2000) Bleomycin: new perspectives on the mechanism of action. *J Nat Prod* 63:158–168

21. Borah S, Melvin M, Lindquist N, Manderville R (1998) Copper mediated nuclease activity of a tambjamine alkaloid. *J Am Chem Soc* 120:4557–4562
22. Matsumoto S, Biggs J, Copp B, Holden J, Barrows L (2003) Mechanism of ascididemin induced cytotoxicity. *Chem Res Toxicol* 16:113–122
23. Lodish H, Berk A, Kaiser C, Krieger M, Scott M, Bretscher A, Ploegh H, Matsudaira P (2007) *Molecular cell biology*. Scientific American Books, New York
24. Bertram A, Pattenden G (2007) Marine metabolites: metal binding and metal complexes ofazole-base cyclic peptides of marine origin. *Nat Prod Rep* 24:18–30
25. Kobayashi J, Cheng J, Nakamura H, Ohizumi Y, Hirata Y, Sasaki T, Ohta T, Nozoe S (1988) Ascididemin, a novel pentacyclic aromatic alkaloid with potent antileukemic activity from the Okinawan tunicate *Didemnum* sp. *Tetrahedron Lett* 29:1177–1180
26. Hawkins CJ (1988) Unusual chelates isolated from Ascidacea. *Pure Appl Chem* 60:1267–1270
27. Shiman R, Neilands JB (1965) Isolation, characterisation and synthesis of pyrimine, an iron (II) binding agent from *Pseudomonas* GH. *Biochemistry* 4:2233–2236
28. Vaz E, Fernandez-Suarez M, Munoz L (2003) Determination of the absolute stereochemistry of Etzionin. *Tetrahedron* 14:1935–1942
29. Ijima M, Someno T, Amemiya M, Sawa R, Naganawa H, Ishizuka M, Takeuchi T (1999) IC202A, a new siderophore with immunosuppressive activity produced by *Streptoalloteichus* sp. 1454–19. II. physico-chemical properties and structure elucidation. *J Antibiot* 52:25–28
30. Chattopadhyay S, Pattenden G (1998) Total synthesis of ulapualide A, a novel tris-oxazole containing macrolide from the marine nudibranch *Hexabranchus sanguineus*. *Tetrahedron Lett* 39:6095–6098
31. Jaspars M, Rali T, Laney M, Schatzman RC, Diaz MC, Schmitz FJ, Pordesimo EO, Crews P (1994) The search for inosine 5'-phosphate dehydrogenase (Impdh) inhibitors from marine sponges – evaluation of the bastadin alkaloids. *Tetrahedron* 50:7367–7374
32. Pettit G, Herald C, Doubek D, Herald E, Arnold J, Clardy J (1982) Isolation and structure of bryostatin-1. *J Am Chem Soc* 104:6846–6848
33. Rinehart K, Kishore V, Bible K, Sakai R, Sullins D, Li K-M (1988) Didemnins and tunichlorin: novel natural products from the marine tunicate *Tridemnum solidum*. *J Nat Prod* 51:1–21
34. Pettit G, Kantoci D, Doubek D, Tucker B, Pettit W, Schroll R (1993) Isolation of the nickel-chlorin chelate tunichlorin from the South Pacific Ocean sea hare *Dolabella auricularia*. *J Nat Prod* 56:1981–1984
35. Sings H, Bible K, Rinehart K (1998) Acyl tunichlorins: A new class of nickel chlorins isolated from the Caribbean tunicate *Tridemnum solidum*. *Proc Natl Acad Sci* 93:10560–10565
36. Ciminiello P, Fattorusso E, Mangoni A (1990) Structure of clathridine-Zn complex, a metabolite of the marine sponge *Clathrina clathrus*. *Tetrahedron* 46:4387–4392
37. Alvi K, Peters B, Hunter L, Crews P (1993) 2-Aminoimidazoles and their zinc complexes from Indo-Pacific Leucetta sponges and *Notodoris nudibranchs*. *Tetrahedron* 49:329–336
38. Capon R, Skene C, Lacey E, Gill J, Wadsworth D, Friedel T (1999) Geodin A magnesium salt, a novel nematocide from a Southern Australian marine sponge geodia. *J Nat Prod* 62:1256–1259
39. Imamura N, Adachi K, Sano H (1994) Magnesidin A, a component of the marine antibiotic magnesidin, produced by *Vibrio gazogenes* ATCC29988. *J Antibiot* 47:257–261
40. Itami C, Matsunaga H, Sawada T, Sakurai H, Kimura Y (1993) Superoxide dismutase mimetic activities of metal complexes of pyrimine. *Biochem Biophys Res Commun* 197:536–541
41. Vasquez M, Quinoa E, Riguera R, Ocampo A, Iglesias T, Debitus C (1995) Caledonin, a natural peptide bolaphile with Zn(II) and Cu(I) complexing properties from the tunicate *Didemnum rodriguesi*. *Tetrahedron Lett* 48:8853–8856
42. Gunawardana G, Koehn F, Lee A, Clardy J, He H, Faulkner DJ (1992) Pyridoacridine alkaloids from deep water marine sponges of the family Pachastrellidae: structure revision

- of dercitin and related compounds and correlation with the kuanoniamines. *J Org Chem* 57:1523–1526
43. Kyeremeh K (2006) in Chemistry. PhD Thesis, Aberdeen University
 44. Inman W, Crews P, McDowell R (1989) Novel marine sponge derived amino acids. 9. Lithium complexation of jaspakinolide. *J Org Chem* 54:2523–2526
 45. Tabudravu J, Morris L, Milne B, Jaspars M (2005) Conformational studies of free and Li^+ complexed jaspakinolide, a cyclic depsipeptide from the Fijian marine sponge *Jaspis splendens*. *Org Biomol Chem* 3:745–749
 46. Long P, Dunlap W, Battershill C, Jaspars M (2005) Heterologous expression of the patellamide nonribosomal peptide gene cluster for sustained metabolite production. *Chembiochem* 6:1760–1765
 47. Schmidt E, Nelson J, Rasko D, Sudek S, Eisen J, Haygood M, Ravel J (2005) Patellamide A and C biosynthesis by a microcin-like pathway in *Prochloron didemni*, the cyanobacterial symbiont of *Lissoclinum patella*. *Proc Natl Acad Sci USA* 102:7315–7320
 48. Morris LA, Jaspars M, Kettenes van den Bosch JJ, Versluis K, Heck AJR, Kelly SM, Price NC (2001) Metal binding of *Lissoclinum patella* metabolites: part 1, Patellamides A, C and Ulithiacyclamide. *Tetrahedron* 57:3185–3197
 49. van den Brenk A, Byriel K, Fairlie D, Gahan L, Hanson G, Hawkins C, Jones A, Kennard C, Moubaraki B, Murray K (1994) Crystal structure, electrospray ionization mass spectrometry, electron paramagnetic resonance, and magnetic susceptibility study of $[\text{Cu}_2(\text{ascidH}_2)(1,2\text{-}\mu\text{-CO}_3)(\text{H}_2\text{O})_2]\cdot 2\text{H}_2\text{O}$, the bis(copper(II)) complex of ascidiacyclamide(ascidH_4), a cyclic peptide isolated from the ascidian *Lissoclinum patella*. *Inorg Chem* 33:3549–3557
 50. Van den Brenk A, Fairlie D, Hanson G, Gahan L, Hawkins C, Jones A (1994) Binding of copper(II) to the cyclic octapeptide patellamide D. *Inorg Chem* 33:2280–2289
 51. Morris LA, Milne BF, Thompson GS, Jaspars M (2002) Conformational change in the thiazole and oxazoline containing cyclic octapeptides, the patellamides. Part I: Cu^{2+} and Zn^{2+} induced conformational change. *J Chem Soc Perkin Trans* 2:1072–1075
 52. Morris LA, Jaspars M (2000) A Cu^{2+} selective marine metabolite. In: Wrigley S, Hayes MA, Thomas R, Chrystal EJT, Nicholson N (eds) Biodiversity: a source of new leads for the pharmaceutical and agrochemical industries. Royal Society of Chemistry, London, pp 140–168
 53. Wipf P, Venkatraman S, Miller C, Geib S (1994) Metal complexes of marine peptide metabolites: a novel Ag_4 cluster. *Angew Chem Int Ed* 33:1516–1518
 54. Comba P, Gahan L, Habenbauer G, Hanson G, Noble C, Seibold B, van den Brenk A (2008) Copper (II) coordination chemistry of westiellamide and its imidazole, oxazole and thiazole analogues. *Chem Eur J* 14:4393–4403
 55. Leudtke NW, Hwang JS, Glazer EC, Gut D, Kol M, Tor Y (2002) Eilatin Ru(II) complexes display anti-HIV activity and enantiomeric diversity in the binding of RNA. *Chembiochem* 3:766–771
 56. Schwyn B, Neilands JB (1987) Universal chemical assay for the detection and determination of siderophores. *Anal Biochem* 160:47–56
 57. Bluemlein K, Raab A, Feldmann J (2009) Stability of arsenic peptides in plant extracts: off-line versus on-line parallel elemental and molecular mass spectrometric detection for liquid chromatographic separation. *Anal Bioanal Chem* 393:357–366
 58. Krupp EM, Mestrot A, Wielgus J, Meharg AA, Feldmann J (2009) The molecular form of mercury in biota: identification of novel mercury peptide complexes in plants. *Chem Commun* 28:4257–4259
 59. Freeman DJ, Pattenden G, Drake AF, Siligardi G (1998) Marine metabolites and metal ion chelation. CD studies of metal binding to *Lissoclinum* peptides. *J Chem Soc Perkin Trans* 2:129–135
 60. Morris LA, Milne BF, Jaspars M, Kettenes van den Bosch JJ, Versluis K, Heck AJR, Kelly SM, Price NC (2001) Metal binding of *Lissoclinum patella* metabolites: part 2, Lissoclinamides 9 and 10. *Tetrahedron* 57:3199–3207

61. Frank P, Hodgson KO, Kustin K, Robinson WE (1998) Vanadium K-edge x-ray absorption spectroscopy reveals species differences within the same ascidian genera – a comparison of whole blood from *ascidia nigra* and *ascidia ceratodes*. *J Biol Chem* 273:24498–24503
62. Bluemlein K, Raab A, Meharg AA, Charnock JM, Feldmann J (2008) Can we trust mass spectrometry for determination of arsenic peptides in plants: comparison of LC-ICP-MS and LC-ES-MS/ICP-MS with XANES/EXAFS in analysis of *thunbergia alata*. *Anal Bioanal Chem* 390:1739–1751
63. Esquenazi E, Coates C, Simmons L, Gonzalez D, Gerwick WH, Dorrestein PC (2008) Visualizing the spatial distribution of secondary metabolites produced by marine cyanobacteria and sponges via MALDI-TOF imaging. *Mol Biosyst* 4:562–570
64. Esquenazi E, Dorrestein PC, Gerwick WH (2009) Probing marine natural product defenses with DESI-imaging mass spectrometry. *Proc Natl Acad Sci USA* 106:7269–7270
65. Corbin BD, Seeley EH, Raab A, Feldmann J, Miller MR, Torres VJ, Anderson KL, Dattilo BM, Dunman PM, Gerads R, Caprioli RM, Nacken W, Chazin WJ, Skaar EP (2008) Metal chelation and inhibition of bacterial growth in tissue abscesses. *Science* 319:962–965
66. Feldmann J, Salaun P, Lombi E (2009) Critical review perspective: elemental speciation analysis methods in environmental chemistry – moving towards methodological integration. *Environ Chem* 6:275–289

Part 4

Biosynthesis of Marine Natural Products

Angelo Fontana, Emiliano Manzo, M. Letizia Ciavatta, Adele Cutignano, Margherita Gavagnin, and Guido Cimino

Contents

17.1	Introduction	896
17.2	Main Steps in the History of Feeding Biosynthetic Experiments in Marine Organisms	896
17.3	Main Steps on Selected Biosynthetic Topics	906
17.4	Recent Feeding Biosynthetic Studies	911
17.5	Feeding Experiments and Detection Techniques	921
17.6	Lipoxygenase Pathways in Marine Diatoms	925
17.7	Polypropionates in Sacoglossan Mollusks: When Biosynthesis and Function are Hand in Glove	930
17.8	Conclusions	936
17.9	Study Questions	936
	References	937

Abstract

This chapter deals with feeding experiments in biosynthetic studies of secondary metabolites from marine organisms. The evolution of the field is traced through a critical report of both review papers published from the 1980s and selected studies published in the latest years. The progress in the methodologies, from simple modification of advanced precursors, through incorporation of substrates with radioactive or stable isotopes, to recent extensive use of molecular genetic techniques, served as a main guideline for the preparation of this overview. Finally, after a section dedicated to the methodologies, the biosynthesis of

*The chapter is dedicated to the memory of Prof. Constantinos Vagias, valuable friend and talented scientist.

A. Fontana (✉) • E. Manzo • M.L. Ciavatta • A. Cutignano • M. Gavagnin • G. Cimino (✉)
Istituto di Chimica Biomolecolare – Consiglio Nazionale delle Ricerche, Via Campi Flegrei,
Pozzuoli (Naples), Italy

e-mail: afontana@icb.cnr.it, emiliano.manzo@icb.cnr.it, letizia.ciavatta@icb.cnr.it,
adele.cutignano@icb.cnr.it, margherita.gavagnin@icb.cnr.it, guido.cimino@icb.cnr.it

oxylipins from diatoms and propionates from Mediterranean sacoglossans, recently conducted in the authors' institute, will be discussed with more detail.

17.1 Introduction

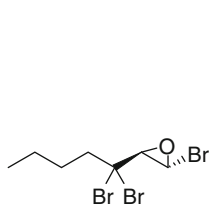
Biosynthesis (bios = life and synthesis = building up) concerns the biochemical process by which simple substrates (e.g., acetate) are converted to complex molecules in living organisms. The subject matter, which has historically occupied a key role in the Chemistry of Natural Products, deals with the biochemical transformations committed to production of a metabolite and also offers unique clues on the regulation of these processes and their relationships with the general metabolism in living organisms. Recently [1], the extensive use of molecular genetic methods opened new and surprising perspectives in this field. However, feeding experiments with labeled precursors continue to offer the basic information to construct a correct biosynthetic pathway. The history of the biosynthesis on marine natural products is quite recent. The first comprehensive review on this topic appeared only in 1983 [2]. It could be interesting to report some words used by the editor to introduce this chapter in the preface of the book: "Our scanty knowledge of living habits of marine organisms and to their adaptation to laboratory conditions has hampered biosynthetic research of marine metabolites. It is hoped that this chapter will stimulate others to venture in this *mare incognitum*." The suggestion was accepted by many scientists, and several overviews [3–9] have recorded the progressive growth from the infancy to the adult age of this research activity. A number of overviews deal with biosynthesis in selected organisms: mollusks [10], dinoflagellates [11], and opisthobranchs [12]; others are dedicated to the biosynthesis of selected classes of compounds: sterols [13], polypropionates [14], algal oxylipins [15], macrolides [16], and isocyanides [17].

In this chapter, we will try to delineate through a critical reading of these reviews the main biosynthetic route in marine natural products covered by using feeding experiments. Recent investigations completed in the last 4 years and some selected studies mainly carried out in the authors' institute will be described with more detail. Finally, for nonexpert readers, a short section, Sect. 17.5, is dedicated to technical issues related to administration and detection of labeled precursors in biosynthetic studies.

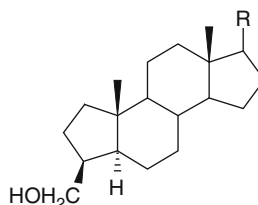
17.2 Main Steps in the History of Feeding Biosynthetic Experiments in Marine Organisms

The chapter by Barrow [2] reports the first biosynthetic experiments on marine organisms. Feeding experiments with a simple labeled precursor, [1-¹⁴C]acetate, indicated that in the sponge *Microciona prolifera* the unusual fatty acids with chain lengths of C₂₄ to C₂₈ are obtained by a chain elongation from C₁₆

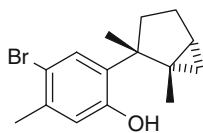
precursors [18]. A polyketide pathway was also detected in the red alga *Bonnemaisonia nootkana* [19] for *trans*-1,3,3-tribromo-1-heptene oxide (**1**). The majority of the feeding experiments reported by Barrow were realized with advanced precursors committed to transformations in the side chains and the polycyclic core of dietary sterols in sponges and also in the skeleton of halogenated sesquiterpenoids of the sea hare *Aplysia californica*. A selected example is the administration of [$4\text{-}^{14}\text{C}$]cholesterol to sponge *Axinella verrucosa* to prove the biosynthesis of the hydroxymethyl carbon of 3β -hydroxymethyl-A-norsteranes (**2**) from C-3 of cholesterol by contraction of the ring A followed by bond formation between C-2 and C-4 [20], whereas doubly labeled precursor with tritium at positions 3 and 4 proved the loss of 3α and 4β hydrogen atoms [21]. Feeding experiments with tritiated laurinterol (**3**) established the conversion of the algal metabolite **3** into aplysin (**4**) by the opisthobranch *A. californica* [22]. Barrow pointed out the necessity of avoiding conclusions supported only by preliminary evidence: "It seems unwise to speculate and postulate novel chemistry on the basis of feeding experiments," and concluded his chapter with the prophetic expectation for a larger use of stable isotopes in the coming years.



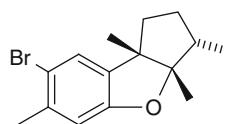
1 *trans*-1,3,3-tribromo-1-heptene oxide



2 3β -hydroxymethyl-A-norsteranes



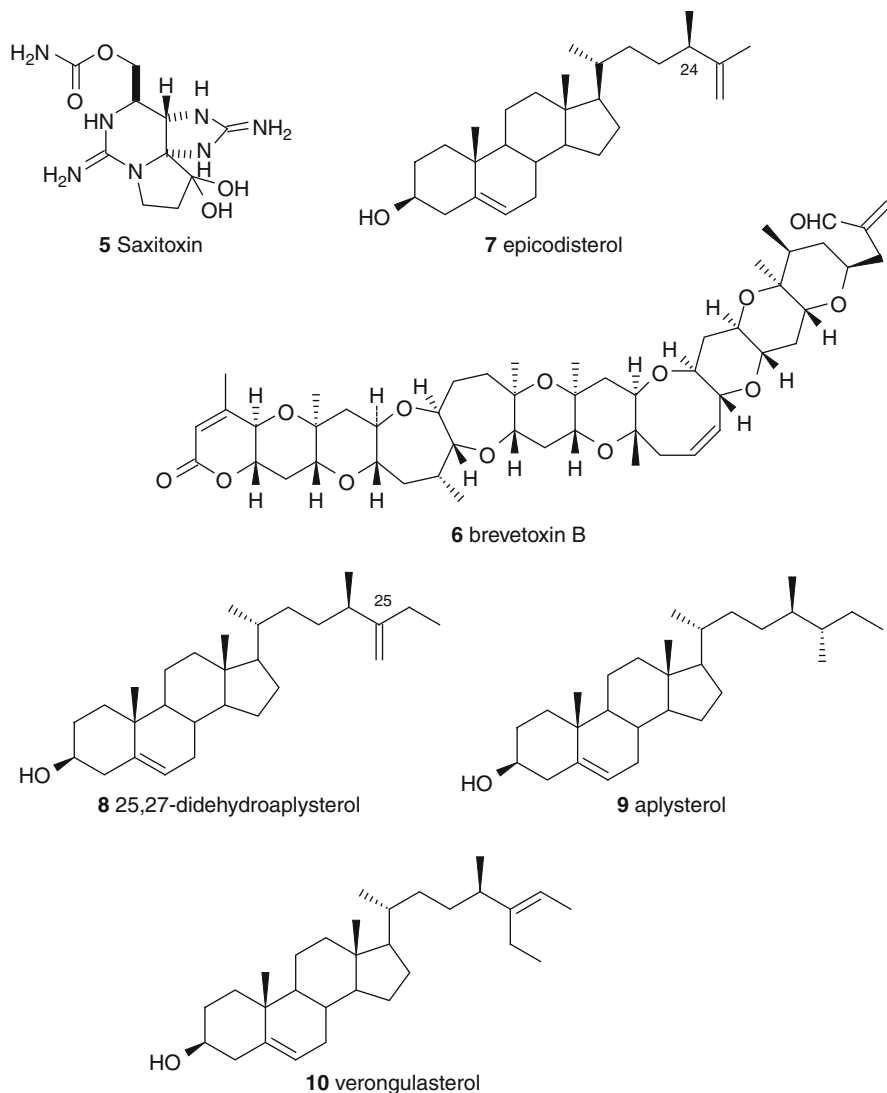
3 Laurinterol



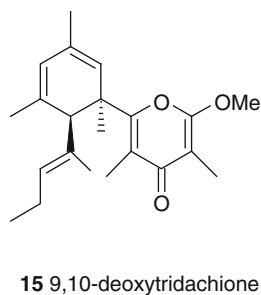
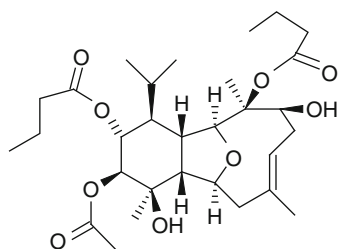
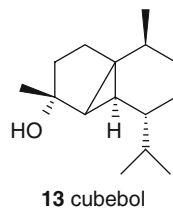
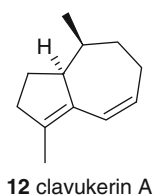
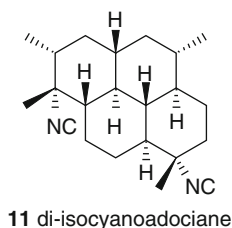
4 Aplysin

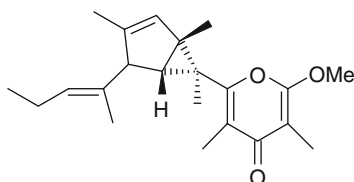
The subsequent reviews by Mary Garson [3, 4] underline the extraordinary development of biosynthetic studies in the late 1980s. These studies embraced the main marine phyla, although stable isotopes were seldom utilized. Most of the general comments reported in these articles are still relevant today. The authors' attention is especially focused on the technical difficulties in biosynthetic experiments with marine organisms, as well as on the potential role of symbiotic microorganisms as true producers of the investigated metabolites. The biosynthetic studies are envisaged as a very promising tool to overcome the uncontrolled harvest of bulk quantities of marine organisms according to a rightful respect of environmental and ecological arguments. The reviews mostly report studies on

microorganisms. Of particular interest is the discussion of the biosynthetic studies [23, 24] on the dinoflagellate toxins saxitoxin (**5**) in *Gonyaulax tamarens* and brevetoxins, e.g., brevetoxin B (**6**), in *Gymnodinium breve*. In line with Barrow, great relevance is given to Djerassi's investigation on the ability of sponges to modify dietary metabolites and, in particular, the side chain of sterols. In this frame, epicodisterol (**7**), but not its 24-epimer, was identified as precursor of 25,27-didehydroaplysterol (**8**), aplysterol (**9**), and verongulasterol (**10**) in *Aplysina fistularis* [25].

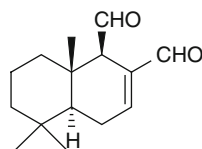


The first rigorous evidence of incorporation of cyanide into a diterpenoid skeleton was obtained studying an *Amphimedon* sponge [26, 27]. Some words on the methodology adopted during this experiment are necessary. The feeding experiments with sodium[^{14}C]cyanide started in small aquaria (6–10 dm³) then the sponge was transplanted to a fixed grid in the sea for almost 30 days. Clear incorporation was detected in both the isocyanide groups present in diisocyanoadociane (**11**). This research opened the way to relevant studies that will be successively discussed. Biosynthesis of terpenes from soft corals has been proven by feeding *Heteroxenia* sp. with [1- ^{14}C]acetate and [2- ^{14}C]mevalonate and detecting clear incorporation into the two terpenoids clavukerin A (**12**) and cubebol (**13**) [28]. The Kuhn–Roth degradation of the labeled mevalonate samples indicated isotopic scrambling due to acetate incorporation after degradation of mevalonate. In the same paper, feeding experiments with [2- ^{14}C]acetate led to radioactive enrichment of the diterpenoid **14** from *Alcyonium molle* due to labeling of the acyl substituents. The result underlines the technical constraint of feeding experiments with radioactive tracers, as well as the risks of putting forward hypotheses based only on this technique. Biosynthesis de novo of 9,10-deoxytridachione (**15**) and photodeoxytridachione (**16**) in the sacoglossan mollusk *Placobranchus ocellatus* was inferred by use of [^{14}C]bicarbonate [29]. In addition to historical value, this paper is a milestone that underlined for the first time the potential of opisthobranchs as candidates for biosynthetic studies. In confirmation of Ireland and Scheuer's insight, the biosynthesis of the terpene skeleton of the defensive allomone polygodial (**17**) was for the first time proved by direct injection of [2- ^{14}C]mevalonate in opisthobranchs of the genus *Dendrodoris* a few years later [30].



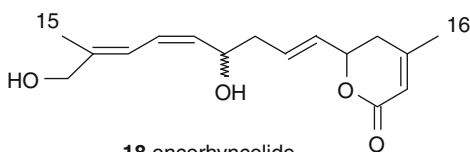


16 photodeoxytridachione

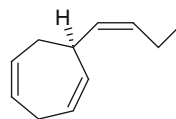


17 polygodial

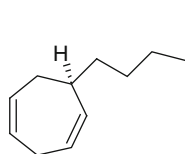
Garson's second review [4] reports the introduction of the use of stable isotopes in biosynthetic experiments with marine organisms. An outstanding example is the study of the bacterial metabolite oncorhyncolide (**18**) through incorporation of seven intact acetate units in the alkyl chain and labeling of carbons 15 and 16 from C-2 of two other acetate units [31]. Biosynthesis of cyanobacteria and dinoflagellate toxins was the subject of different investigations that generally improved the knowledge of these processes. Of particular interest was the study of the volatile pheromones, ectocarpene (**19**) and dictyotene B (**20**), involved in sexual reproduction of brown macrophytic algae (Phaeophyta). Fortuitously, the same metabolites are also produced in the terrestrial plant *Senecio isatideus* by cyclization and decarboxylation of (3Z, 6Z, 9Z)-dodeca-3,6,9-trienoic acid and (3Z, 6Z)-dodeca-3,6-dienoic acid, respectively, starting from natural C₁₈ [32]. By analogy, the same biochemical pathway was suggested for the algal pheromones. However, feeding experiments with deuterated substrates proved that arachidonic acid is the real precursor of dictyotene B (**20**) in the alga *Ectocarpus siliculosus*. The origin of the pheromones from eicosanoids in algae was confirmed by further studies [33]. The use of doubly labeled [¹³C, ¹⁵N] cyanide established the incorporation of intact C–N bond in the sponge metabolite 9-isocyanoneopupukeanane (**21**) [34]. On the basis of the large coupling constant ($J_{15\text{N}-13\text{C}}$ 13 Hz), hydrolysis of compound **21** to the corresponding formamide **22** was also suggested.



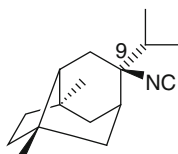
18 oncorhyncolide



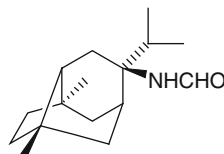
19 ectocarpene



20 dictyotene B



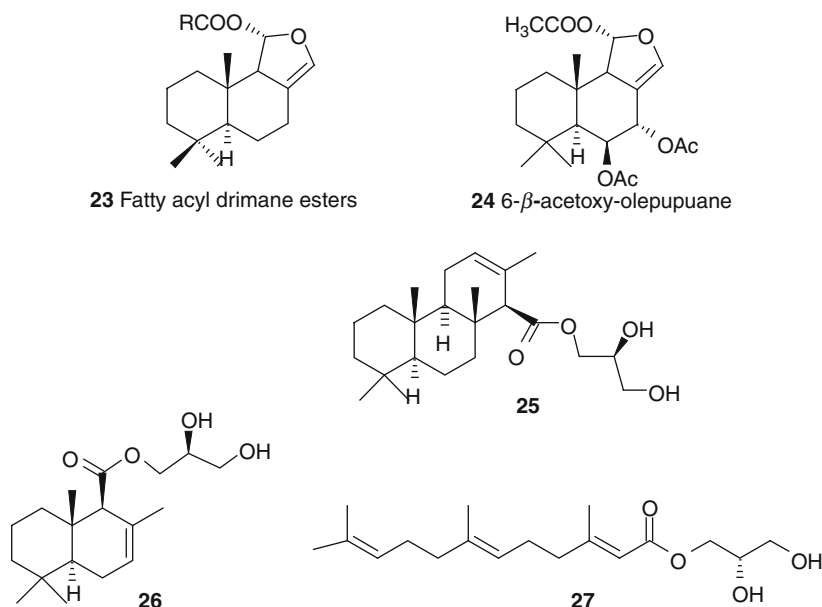
21 9-isocyanoneopupukeanane



22

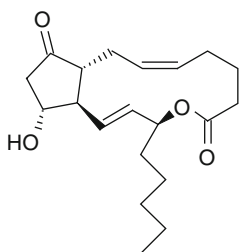
Structural analogies between products from microorganisms, coelenterate, and tunicates were discussed in support to the role of symbionts in the synthesis of the secondary metabolites isolated from the invertebrates. Nevertheless, most of these correlations appear to be only speculative and are not supported by following studies. Much attention

is dedicated to the biosynthesis in mollusks, especially nudibranchs. These invertebrates are apparently vulnerable, the mechanical protection of the shell being completely absent. The animals have replaced the physical protection with a complex defense strategy that also involves the use of chemicals mostly sequestered from the diet. However, in a few examples, the defensive allomones are produced *de novo* by the mollusks [35–37]. Feeding experiments with [2- ^{14}C]mevalonate proved biosynthesis of drimane sesquiterpenoids **17**, **23**, and **24** in the Mediterranean *Dendrodoris limbata* and *Dendrodoris grandiflora* [38–41], as well as of terpene part of glycerides **25–27** in the Canadian *Archidoris montereyensis* and *Archidoris odhneri* [42, 43].

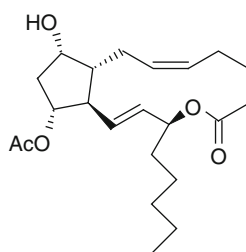


Feeding experiments established the origin of prostaglandin-1,15-lactones from arachidonic acid in the nudibranch *Tethys fimbria* [44–48]. This mollusk adopts a very effective defensive strategy known as autotomy. The nudibranch lives hidden in the sand and, when molested, detaches some dorsolateral appendages named cerata which continue to wriggle for many hours, distracting the predators. The key product is the defensive allomone PGE₂-1,15-lactone (**28**) that is found only in cerata and mucus. Synthesis of this molecule involves formation of PGF_{2α}-11-acetate-1,15-lactone (**29**) in the mantle. By transesterification, **29** is also the likely precursors of the corresponding 9- and 11-fatty acyl esters (e.g., **30**) in the reproductive glands. Compound **28** is transformed into the corresponding PGE₂ (**31**) that is suggested to induce the contractions of the detached cerata. Another interesting study reported by Garson is that on pulmonate mollusks of the genus *Siphonaria* [49, 50]. Feeding experiments with [1- ^{14}C]propionate led to establish the *de novo* synthesis of very unusual polypropionates: denticulatin A (**32**), denticulatin B (**33**), siphonarins A (**34**), and siphonarins B (**35**). The structural analogy with actinomycete metabolites raised the suspicion that the true producers of marine

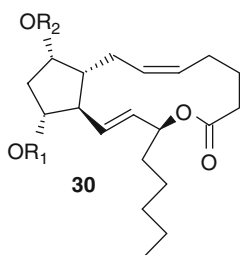
polypropionates could be bacterial symbionts. All these experiments were realized with intact organisms by direct injection of the precursor. This methodology displays a clear advantage from avoiding the dilution of the precursor in the seawater, although the complexity of mollusk physiology and the body barriers sometimes hamper the distribution of the metabolite into the mollusk organs.



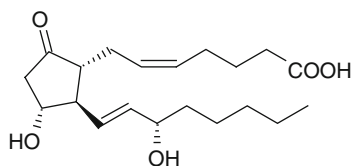
28 PGE₂-1,15 lactone



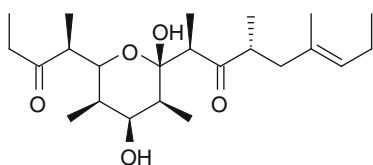
29 PGF_{2α}11-acetate-1,15 lactone



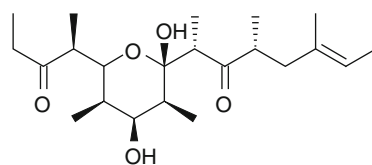
R1= H, R2=fatty acyl or
R1= fatty acyl, R2=H



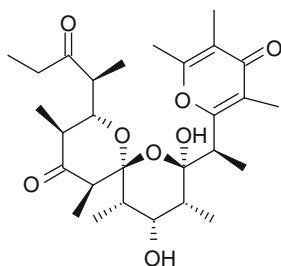
31 PGE₂



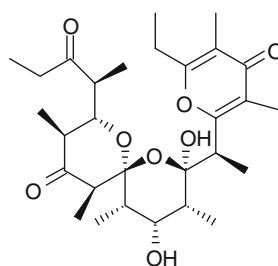
32 denticulatin A



33 denticulatin B

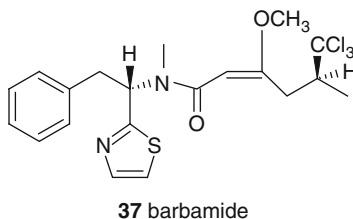
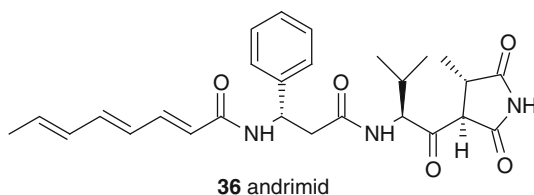


34 siphonarin A



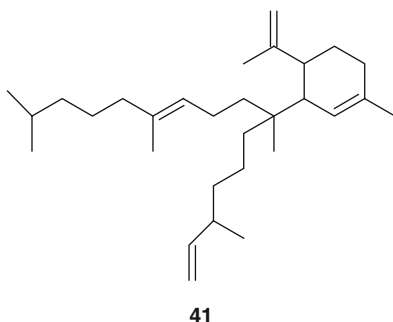
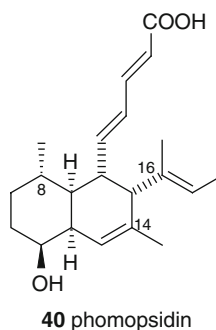
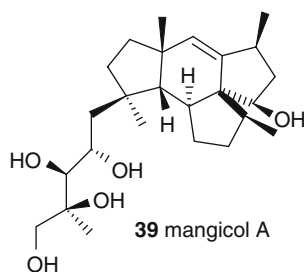
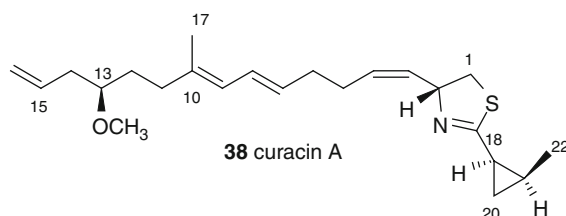
35 siphonarin B

Through three excellent chapters, Moore realized a comprehensive overview on marine biosynthesis covering the literature until the end of 2004 [5, 8, 9]. The first report takes into consideration 10 years (1989–1998) of studies on microorganisms and macroalgae. It proves the enormous development of the use of stable precursors fostered by the progress of NMR and MS instrumentations and the first application of molecular genetic techniques. Particularly active was Andersen's group, which, for example, investigated the biosynthesis of the antibiotic andrimid (**36**), a metabolite produced by the bacterium *Pseudomonas fluorescens* isolated from an unidentified Alaskan tunicate [51]. Experiments with C-13-labeled acetate gave incorporation of intact C₂ units in the acyl chain and in the unusual acylsuccinimide moiety. The experiment also proved the acetate origin of the methyl substituent on the heterocyclic ring, thus suggesting that the succinimide of andrimid derived from a mixed process with acetate and amino acid. Biosynthetic studies in cyanobacteria and dinoflagellates targeted complex polyethers, macrolides, and also small molecules like barbamide (**37**), a halogenated molluscicidal metabolite of *Lyngbya majuscula* [52]. Well-designed experiments with differently [¹³C]-labeled L-leucines proved that chlorination exclusively occurs at the *pro-S* methyl group of leucine. The issue of the true producers of marine natural products is an old one, but remains of current interest. In this review, more than 20 metabolites from sponges and tunicates are suggested to be microbial products on the basis of structural analogies.

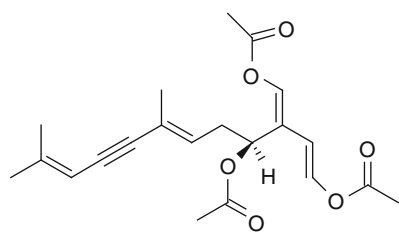
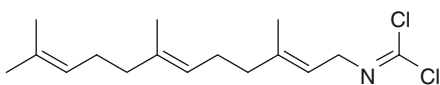
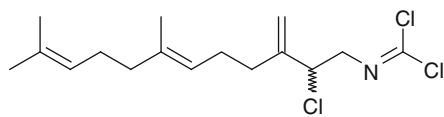
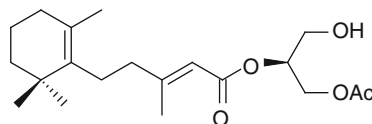
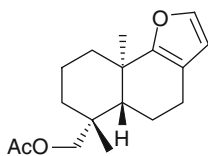
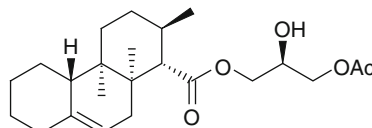


Moore's second review is dominated by the rise of the molecular techniques. This topic is treated with more detail in another chapter of this book. The majority of the overviewed studies are, according to the previous reports, on bacteria, cyanobacteria, and dinoflagellates. A good example is the biosynthesis of curacin A (**38**) [53]. Curacin A was isolated from a Curaçao strain of the marine cyanobacterium *Lyngbya majuscula* and is a potent antiproliferative and cytotoxic agent against many cancer-derived cell lines. Rigorous biosynthetic experiments demonstrated the incorporation of eight intact C₂ units (18/19, 21/22, 4/5, 6/7, 8/9, 10/11, 12/13, 14/15) and the origin of C-16 and C-20 from C-2 of two further acetate units. The methyl groups at C-10 and C-13 incorporated [methyl-¹³C]methionine, whereas the O-13 derived from the oxygen of an acetate unit. These results suggest that the polyketide pathway starts

from cysteine units, and then, after elongation with eight acetate units, a terminal dehydrative decarboxylation leads to the double bond at carbons 15, 16. Surprisingly, the origin of the terminal 5 carbons (from C-18 to C-22) is not isoprenic but is obtained by a Claisen acetyl acetate/acetate condensation. The first biosynthetic studies on marine fungi were also reviewed. Feeding experiments with [^{13}C]acetate proved a mevalonate pathway (MVA) for the sesterterpene mangicol A (**39**) [54] from a *Fusarium* marine fungus, whereas phomopsidin (**40**) from a marine-derived *Phomopsis* fungus incorporated nine intact acetate units and three methyls (at carbons 8, 14, and 16) from L-[S- ^{13}C]methionine [55]. The review also reports some biosynthetic studies on oxylipins and highly branched isoprenoids (HBIs) from diatoms. The first topic will be treated with more particular in one of the following sections of this chapter. Feeding experiments with [1- ^{13}C]acetate [56, 57] on the planktonic diatoms *Rhizosolenia setigera* and *Haslea ostrearia* provided evidence that the terpenoids (sesterterpenoids, sterols, and phytol) from the *H. ostrearia* were biosynthesized following the methylerythritol (MEP) pathway, whereas the branched triterpenoid (**41**) in *R. setigera* was obtained by the MVA pathway that leads first to geranyl pyrophosphate and geranylgeranyl pyrophosphate and then to their coupling.



The last review by Moore [9] deals with the biosynthesis of marine secondary metabolites in marine macroorganisms, especially on oxylipins and halogenated monoterpenes from macroalgae were reviewed. Administration of $[1-^{13}\text{C}]$ acetate and $[^{13}\text{C}]\text{CO}_2$ to the invasive alga *Caulerpa taxifolia* established synthesis of the sesquiterpene caulerpenyne (**42**) from the methylerythritol-4-phosphate (MEP) pathway [58]. The studies on sponges were mainly directed toward the metabolic relationships between sponges and their symbionts through the cellular localization of the secondary metabolites. Feeding experiments with $[^{14}\text{C}]$ -labeled cyanide and thiocyanate clarified the origin of the dichloroimine moiety of two metabolites, stylotellane A (**43**) and B (**44**), isolated from the tropical sponge *Stylotella aurantium* [59, 60]. A relevant part of this review considers again the biosynthesis of opisthobranch products by injection of precursors labeled with stable isotopes. The methodology introduced by Andersen's and Faulkner's groups [61] established the origin of the terpenoids **25**, **27**, and **45** through the mevalonate (MVA) pathway in *A. montereyensis*, *A. odhneri*, and *Sclerodoris tanya*. Analogously, feeding experiments [62] with $[6-^{13}\text{C}]$ glucose and $[^{13}\text{C}_2]$ acetate proved the MVA pathway for the drimane esters **23** and (–)-pallascensin A (**46**) present in *Doriopsilla areolata*, which confirmed the results previously obtained by radioactive precursors [63]. Interestingly, related sesquiterpenoids showing an enantiomeric ring junction of the decaline are also present in a *Dysidea* sponge which could be included in the diet of the mollusk [64]. Feeding experiments with $[6-^{13}\text{C}]$ and $[5-^{13}\text{C}]$ glucose yielded low but complementary labeling that strongly supported the MVA origin of the terpene part of verrucosin A (**47**), a toxic glyceride of the nudibranch *Doris verrucosa* [65].

**42** caulerpenyne**43** stylotellane A**44** stylotellane B**45****46** (–) pallascensin A**47** verrucosin A

This 30-year ride among the main biosynthetic studies on marine natural products reveals the outstanding and independent contribution of many groups from all over the world for the progress of the field. After the pioneering and stylish studies with radioisotopes, the introduction of stable isotopes has led to a tremendous advancement in the knowledge of biosynthetic mechanisms. As Moore suggested on the verge of the marine genomic era [8], the extensive application of the molecular methodologies is expected to have an even more important impact in deepening our understanding and appreciation for complex marine pathway.

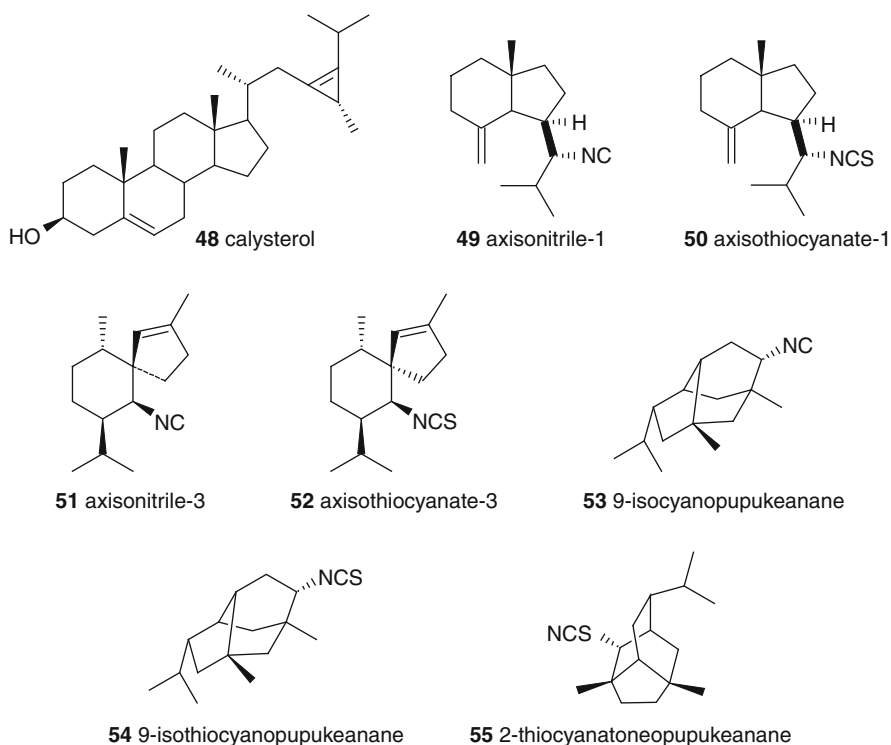
17.3 Main Steps on Selected Biosynthetic Topics

Reports of biosynthetic data on specific topics are extremely numerous. Our selection of the topics discussed in this chapter has been driven by the idea to provide a general view of the biosynthesis by feeding experiments in marine organism.

From the 1990s, a series of review papers have been focused on specific biosynthetic topics. The biosynthesis of marine sterol side chains was overviewed by Giner [66]. The chapter covers the studies on sterols from different organisms even if the major attention was paid to sponges. This primitive group of multicellular organisms displays the richest variety of unusual sterols. The first structural studies led to the characterization of sterols featured by unusual chains, e.g., aplysterol (**9**) [67] and calysterol (**48**) [68], and A-nor and 19-nor nuclei [69, 70]. After the first biosynthetic studies by Minale's group on these compounds [71], a development of the subject was mostly due to the impressive contribution of Carl Djerassi by use of radioisotopes [72]. These studies established the first elucidation of the chemical mechanisms responsible for dealkylation and methylation of the side chain, as well as for the construction of cyclopropyl and cyclopropenyl rings. Giner's overview reports a detailed presentation of the biosynthetic experiments that reveal the ability of sponges to modify dietary sterols but not to carry out *de novo* synthesis.

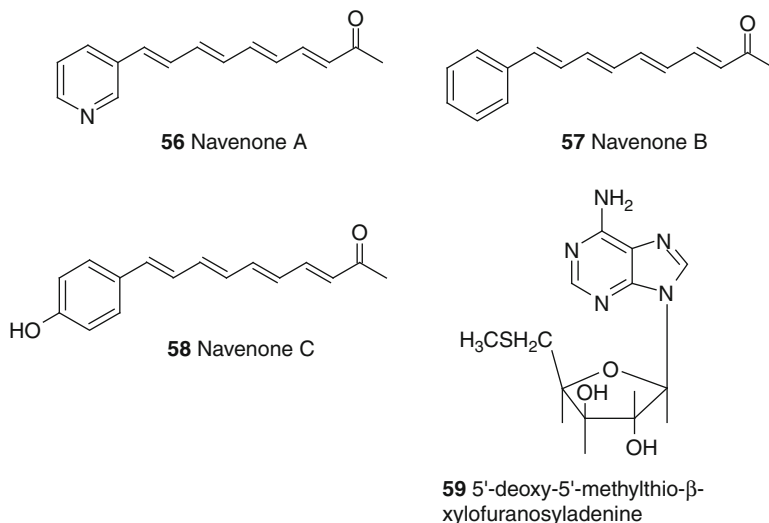
Biosynthesis of marine isocyanides and related natural products was recently reviewed [17], and the relevance of the topic suggests us to discuss the key points. In 1973, Fattorusso's group reported the finding of the first marine terpene isocyanides, axisonitrile-1 (**49**) and axisothiocyanate-1 (**50**), in the Mediterranean sponge *Axinella cannabina* [73]. These compounds exemplify a family of which members have been isolated from other sponges and invertebrates. Generally, isocyanides co-occur with the corresponding isothiocyanates, for example, axisonitrile-3 (**51**) and axisothiocyanate-3 (**52**) [74], and their biosynthetic origin has been for long time a challenging task. The first evidence that sponges are able to link inorganic cyanide to terpene skeletons was obtained by Garson [26]. Feeding experiments with [^{14}C]cyanide on the sponge *Amphimedon terpenensis* resulted into the incorporation of radioactivity in the diterpene diisocyanoadociane (**11**). Later, the same authors observed that compounds **51** and **52** incorporate both labeled thiocyanate and cyanide in *Acanthella cavernosa* [75]. The sponge was able to interconvert cyanide and isothiocyanate before or after the incorporation in the secondary metabolite. Analogous results were obtained studying the biosynthesis of 9-isocyanopopukeanane (**53**) and 9-isothiocyanopopukeanane (**54**) in

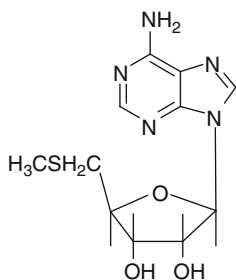
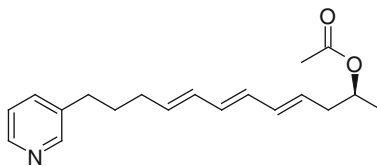
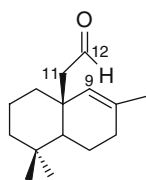
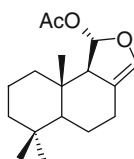
the sponge *Axinissa* n.sp. [76]. In another experiment, in addition to **53** and **54**, inorganic cyanide and isothiocyanate were incorporated into 2-thiocyanatoneopupukeanane (**55**), thus strongly supporting that the conversion precedes synthesis of the secondary metabolite. In the same paper, the authors reported experiments with advanced labeled precursors, [^{14}C]9-isocyanopupukeanane (**53**) and [^{14}C]9-isothiocyano-pupukeanane (**54**), that proved the interconversion of the two compounds and the role of inorganic thiocyanate as former precursor. Nudibranchs belonging to the Phyllidiidae family generally are protected by terpene isocyanides and related metabolites of dietary origin [77, 78]. When the nudibranch *Phyllidiella pustolosa* feeds upon *A. cavernosa* incubated with [^{14}C]cyanide and [^{14}C]thiocyanate, labeled axisonitrile-3 (**51**) and axisothiocyante-3 (**52**) were detected in the mollusk. In control experiments, no incorporation was found after injection of radioactive salts into the mollusk.



Opisthobranchs are another group of marine invertebrates that has been the subject of numerous biosynthetic studies [10, 12]. In addition to the elucidation of the biochemical pathways, distribution of the labeled metabolites among the different organs and tissues has been envisaged as a tool to investigate the physiology and ecology of these mollusks. Most of these studies concern successive development of the themes discussed in three milestone papers about the biosynthesis of navenones A–C (**56–58**) in cephalaspideans the biosynthesis of 9,10-deoxytridachione (**15**) and photodeoxytridachione (**16**) in sacoglossans [29], and biosynthesis of polygodial (**17**)

in nudibranchs [30]. Relevant exceptions were the above-reported biosynthetic studies on prostaglandin lactones from *Tethys fimbria* [47, 48] and the nucleotide **59** [80], the first naturally occurring analogue of MTA (5'-deoxy-5'-methylthioadenosine, **60**), from the Mediterranean *Doris verrucosa*. Use of stable isotopes has been a crucial factor in the latest investigations with opisthobranchs and has improved our understanding of secondary metabolism in marine invertebrates. Biosynthesis of the alkyl pyridine skeleton of haminols (**61**) clearly shows the potential of this approach. Haminol 2 (**61**) is the prototype of a family of compounds present in the cephalaspidean *Haminoea*. Its structure is closely related to that of navenone A (**56**) but also to the complex architecture of sponge 3-alkypyridines. Feeding experiments with d₄-nicotinic acid, [1-¹³C]acetate, and [1,2-¹³C₂]acetate proved that haminol 2 (**61**) is biosynthesized by the mollusk starting from nicotinic acid that is elongated with six acetate units with decarboxylation of the last C₂-unit [81, 82]. In another experiment with the dorid nudibranch *Acanthodoris nanaimoensis*, administration of [1,2-¹³C₂]acetate clarified that the aldehyde group at C-11 of isoacanthodorol (**62**) is obtained by shift of C-12 from C-9 to C-11 [83]. In fact, after the injection of the labeled precursor, all carbons of compound **62** exhibited clear incorporation according to a classic mevalonate pathway. Nevertheless, only five intact units were detected, whereas no coupling was observed for C-9 and C-12. The study with stable isotopes ([6-¹³C]glucose, [5-¹³C]glucose, [1-¹³C]acetate, [1,2-¹³C₂]acetate) of the biosynthesis of drimane sesquiterpenoids in porostome nudibranchs was also overviewed. These experiments confirmed the results previously obtained with radiolabeled precursors on compounds **17**, **23** and **24** [30, 38] and proved that all these metabolites are biosynthesized according to a classic mevalonate (MVA) pathway. In particular, the clear biosynthesis of 7-deacetoxyolepupane (**63**) in the nudibranch *Dendrodoris limbata* is of relevant interest [84]. In fact, compound **63** has also been found in a *Dysidea* sponge [85] that could be included among the preys of the mollusk, but its dietary origin was rigorously ruled out by the clear incorporation of ¹³C in all positions predicted according to a MVA pathway.



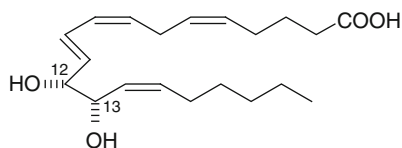
**60** 5'-deoxy-5'-methylthioadenosine**61** Haminol 2**62** Isoacanthodoral**63** 7-deacetoxyolepupane

Labeled propionates have been used in the biosynthesis of the sacoglossan metabolites. Polypropionates are very rare in nature. They are unknown in animals, with the surprising exception of some higher marine gastropods (opisthobranchs and pulmonates). Otherwise, their presence is restricted to terrestrial bacteria and fungi, where they are produced through different biosynthetic pathways from propionate or acetate-methionine, respectively. The topic was overviewed in excellent manner by Davies-Coleman and Garson [14] and will be treated with more detail in Sect. 17.7 of this chapter.

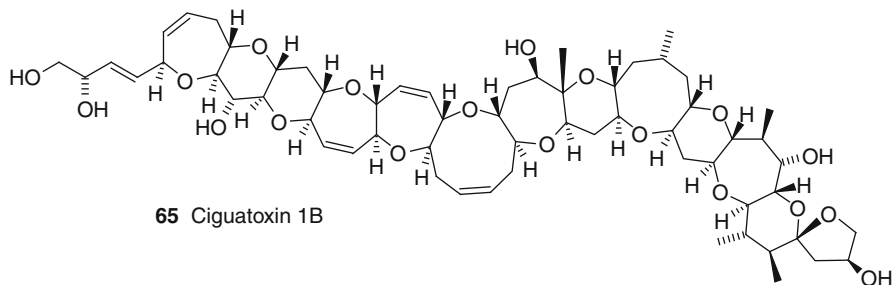
Feeding experiments were extensively applied in the study of oxylipin biosynthesis in algae. The matter was extensively reviewed by Gerwick [15]. The three major groups of macrophytic algae possess unique oxylipins. Generally, red algae (Rhodophyta) metabolize C_{20} acids by oxidation at C-12; green algae (Chlorophyta), C_{18} acids, by oxidation at carbons 9 and 13; and brown algae (Phaeophyceae), both C_{18} and C_{20} , by selective lipoxygenase that recognize (*n*-6) polyunsaturated fatty acids. Experiments led to the understanding of the biosynthesis of vicinal diols like 12*R*,13*S*-dihydroxyeicosatetraenoic acid (**64**) in the red alga *Glacilaria lemaneiformis*. Cell-free preparation of the alga was treated [86] with exogenous arachidonic acid under an atmosphere enriched in $^{18}O_2$. Compound **64** was recovered as methyl ester and exhibited incorporation of ^{18}O in both hydroxyl groups. Further experiments with advanced precursors [87] established that both oxygen atoms derive from a single molecule of oxygen, concluding that vicinal diols in *G. lemaneiformis* are biosynthesized by sequential action of an arachidonic acid 12*S*-lipoxygenase followed by a hydroperoxide isomerase.

Dinoflagellates possess potent toxins that display at least three different skeletons: polyether ladders (e.g., ciguatoxin 1B, **65**), linear polyethers (e.g., okadaic acid, **66**), and macrolides (e.g., amphinolide B, **67**). The marine dinoflagellates of

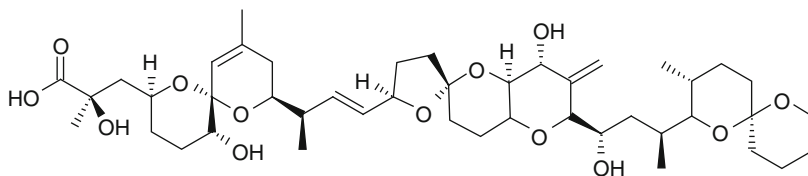
the genus *Amphidinium* produce an impressive series of macrolides, of which biosynthesis has been surveyed by Kobayashi and Tsuda [16]. The incorporation pattern after feeding experiments with $[1,2-^{13}\text{C}_2]$ acetate revealed the acetate origin for all carbons of the macrolides and, in particular, all carbons of the branched methyls were derived from C-2 of acetate and linked either to C-1 of intact acetate or to an isolated C-2 of acetate. The apparent anomaly that the polyketide chain is interrupted by isolated C-2 of acetate units has been justified through an oxidation of C-2 of an acetate unit to α -diketide followed by a Favorskii-like rearrangement that leads to C-1 deletion by elimination of carbon dioxide [88].



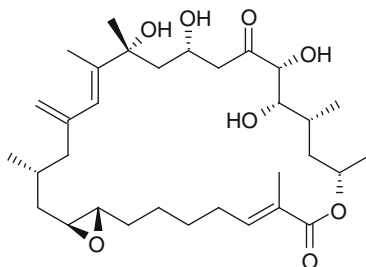
64 12*R*,13*S*-dihydroxyeicosatetraenoic acid



65 Ciguatoxin 1B



66 Okadaic acid



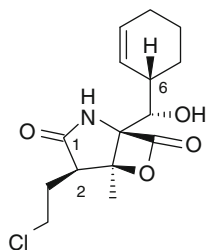
67 Amphidinolide B

17.4 Recent Feeding Biosynthetic Studies

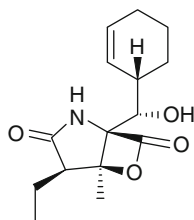
Lately, a variety of biosynthetic researches have been carried out especially in marine microorganisms, algae, and mollusks. Some of these studies are discussed with more detail in this section.

The biosynthesis of salinosporamide A (**68**) was established by Moore's group [89–91]. This work is an excellent example of the importance of rigorous feeding experiments to predict metabolite assembly in biological systems. Salinosporamides (**68–72**) are potent anticancer agents produced by the marine bacterium *Salinispora tropica* [92–94]. They are characterized by a densely functionalized γ -lactam- β -lactone bicycle displaying at C-2 an alkyl substituent sometimes halogenated in ω position. Recently, the salinosporamide family has been enlarged to embrace a related metabolite, cinnabaramide A (**73**), isolated from a terrestrial streptomycete [95]. In consideration of the structural features of salinosporamides A and B (**68** and **69**), coupling of acetate, butyrate, and a nonproteinogenic phenylalanine derivative was predicted as putative biogenesis of both bacterial polyketides. According to this hypothesis, feeding experiments with [1,2- $^{13}\text{C}_2$] acetate led to the incorporation of three intact acetate units in salinosporamide B (**69**) but, surprisingly, only one intact acetate unit in salinosporamide A (**68**). Administration of [U- $^{13}\text{C}_6$] glucose gave enrichment of all carbons of both compounds but showed an enrichment pattern in agreement with the results from the [1,2- $^{13}\text{C}_2$] acetate. The data indicated an apparent divergence in the biosynthesis of the four-carbon fragment bearing the chlorination site, which initially was interpreted as implying the use of tetrose for **68** or butyrate for **69**. Contribution of these building blocks could not be proven, whereas the authors reported the involvement of the unusual chloroethylmalonyl-CoA in **68** and ethylmalonyl-CoA in **69** [91]. Interestingly, these new PKS extender units arose from two different biochemical pathways that fully agreed with the labeling results. The role of ethylmalonyl-CoA as biosynthetic precursor had been previously reported by Kubanek and Andersen in the opisthobranchs *Triopha catalinae* and *Diaulula sandiegensis* (reviewed in ref. [9]). According to this hypothesis, feeding experiments with [1- ^{13}C]propionate in other salinosporamides led to clear incorporation at C-1 of salinosporamide D (**70**) but also at C-12 of salinosporamide E (**71**) [90]. Compound **71** could be obtained by using a pentanoate building block derived from acetate and propionate precursors. Good incorporation was also observed giving pentanoic acid, but better results were obtained with *trans*-2-pentenoic acid, suggesting that α,β -pentenoic carboxylic acids are an advanced intermediate in other salinosporamides. The feeding experiments also ruled out the anticipated function of phenylalanine. In fact, [1- ^{13}C] phenylalanine was not incorporated into **68**, whereas the origin of the aromatic residue from shikimate was verified; after that, C-1, but not C-7, of [1,7- $^{13}\text{C}_2$] shikimic acid (**74**) was assimilated at C-6 of **68** [89]. On this basis, a hybrid polyketide synthase-nonribosomal peptide synthetase (PKS-NRPS) pathway was suggested. This nice work is emblematic to testify the impressive progress in the biosynthesis of marine natural products but also to draw attention on the key role of the feeding experiments with stable isotopes. The information on the exact site of incorporation is extremely

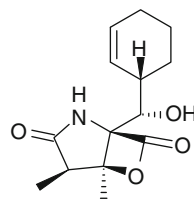
informative and allows the elucidation of the chemical mechanism also in unusual process, such as the rare case of PKS assembly based on pentyl building blocks.



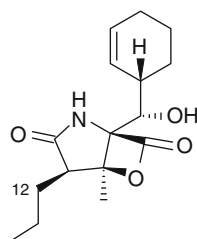
68 Salinosporamide A



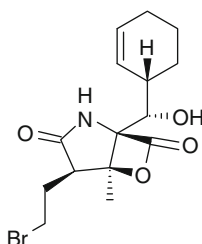
69 Salinosporamide B



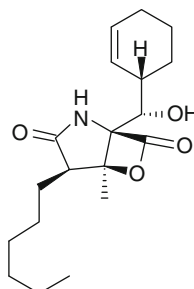
70 Salinosporamide D



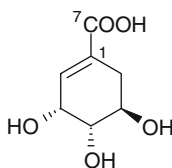
71 Salinosporamide E



72 Bromosalinosporamide



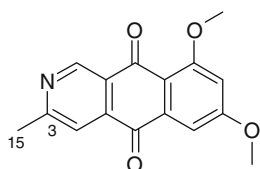
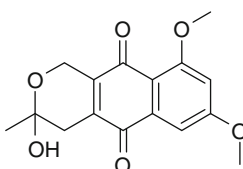
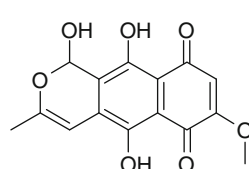
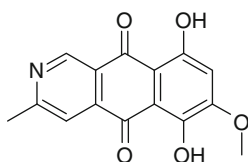
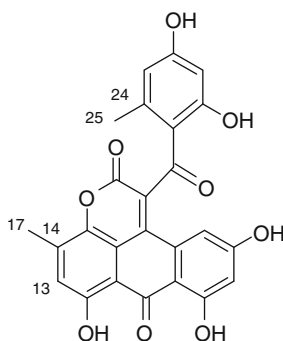
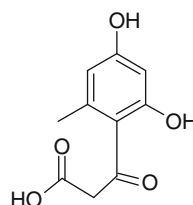
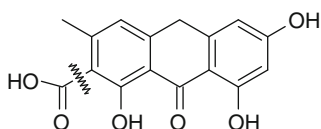
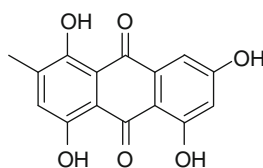
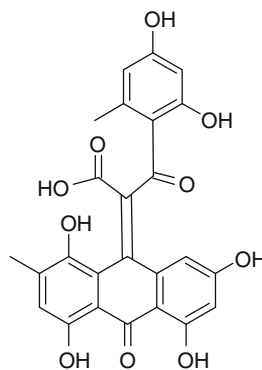
73 Cinnabaramide A



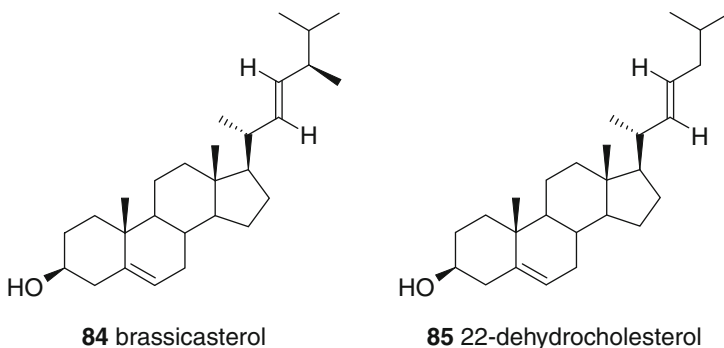
74 Shikimic acid

Biosynthesis in marine fungi is a recent topic in marine science, and a few successful investigations have been reported only in the latest years. Scorpinone (**75**) is a 2-aza-antraquinone present in the fungus *Amorosia littoralis* isolated from marine sediment [96, 97]. Two alternative biosynthetic pathways can be suggested. The first involves a polyketide structure containing seven linear acetate units with subsequent incorporation of a nitrogen atom, the second, six acetate units linked to alanine (N, C-3, C-15) with final decarboxylation. Feeding biosynthetic studies [98] with [2-¹³C]acetate and [1,2-¹³C₂]acetate confirmed the first hypothesis. In fact, seven intact acetate units were incorporated in scorpinone (**75**). The same incorporation was observed in herbarin (**76**), a related co-occurring metabolite previously isolated from the yeast *Torula herbarum* [99]. Herbarin displays a cyclic hemiketal structure where oxygen replaces nitrogen at position 2 of **75**. Herbarin could be the precursor of scorpinone. This hypothesis is well supported by the interconversion in benzene containing excess ammonia between two related metabolites, anhydrofusarubin lactol (**77**) and bostrycoidin (**78**), isolated from terrestrial fungi [100]. Aspergiolide A (**79**) is a novel

antitumor compound produced by the marine-derived filamentous fungus *Aspergillus glaucus* [101]. The clear polyketide pathway was recently investigated by a series of feeding experiments with $[1-^{13}\text{C}]$ acetate, $[2-^{13}\text{C}]$ acetate, and $[1,2-^{13}\text{C}_2]$ acetate [102]. All carbons of **79** displayed good incorporation. Twelve intact acetate units were detected, whereas the signal of C-13 showed a single enrichment deriving from C-2 of acetate. The ^{13}C labeling observed for all carbons of **79** excluded the possibility that the polyketide pathway starts from a single acetate unit with subsequent elongation with 12 C_2 extender units and decarboxylation of the last fragment. Actually, aspergiolide (**79**) is biosynthesized starting from two acetate units, C-25/C-24 and C-17/C-14, which are elongated with four and seven C_2 extender units, respectively, giving two intermediates, A (**80**) and B (**81**). Decarboxylation of **81** leads to catenarin (**82**), a polyketide previously isolated from *A. glaucus* [103]. Aldol condensation between intermediate A and catenarin gives the putative intermediate C (**83**), which after an intramolecular esterification forms aspergiolide (**79**).

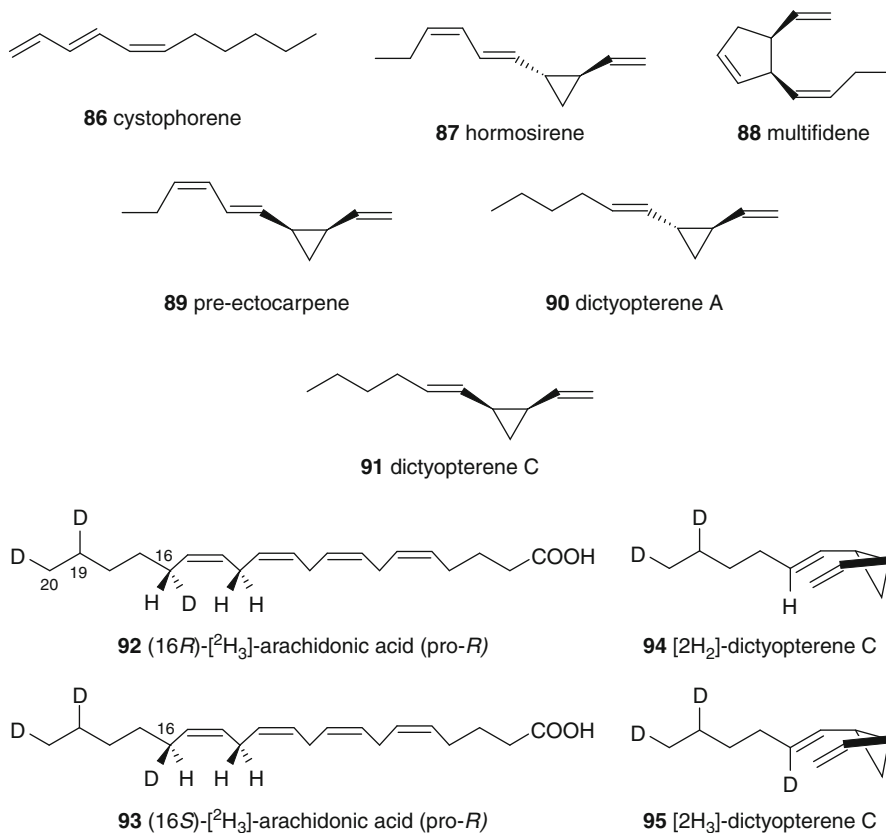
**75** scorpinone**76** Herbarin**77** anhydrosfusarubin lactol**78** bostrycoidin**79** aspergiolide A**80** intermediate A**81** intermediate B**82** catenarin**83** intermediate C

An interesting biosynthetic procedure was used by Chu's group for the inspection of two marine heterotrophic dinoflagellates species, *Oxyrrhis marina* and *Gyrodinium dominans* [104]. The authors proved that the two protists are not able to biosynthesize de novo the sterol core, but *G. dominans* can alkylate and desaturate dietary sterols, transforming cholesterol into brassicasterol (**84**) and 22-dehydrocholesterol (**85**). This result, which closely resembles Djerassi's conclusions with sponges, is of great importance for the innovative methodology employed in the work. Advanced precursors were sequestered by the two protists through the microalga *Perkinsus marinus* which is not able to biosynthesize sterols but accumulates them. The microalga was cultured in a medium with [3,4-¹³C]cholesterol and then was offered to the two protists. GC/MS analysis revealed in *P. marinus* the presence of cholesterol and **85**. The same mixture was detected in *O. marina* whereas the sterol pattern of *G. dominans* exhibited the enhancement of compound **85** together with brassicasterol (**84**) and other three unidentified C₂₈, C₂₉, and C₃₀ sterols. The authors also tried to deliver [¹³C]brassicasterol to *O. marina* and *G. dominans* by the same methodology in order to establish whether the two dinoflagellates are able to demethylate the sterol. C-13-labeled brassicasterol (**84**) was produced by the unicellular alga *Rhodomonas salina* cultured in f/2 medium enriched with [¹³C]CO₂. Assimilation of this product into *P. marinus* was unfortunately unsuccessful because of the inability of the microalga to grow in culture medium containing the labeled compound. Because of this, gelatin acacia microspheres (GAMs) containing labeled brassicasterol with dimensions similar to those of *P. marinus* were prepared and delivered to *O. marina* and *G. dominans*. Labeled [¹³C] carbons were detected only in brassicasterol (**84**). On the contrary, *G. dominans* displaying labeled C_{29:1} and C_{30:0} sterols confirmed its ability to alkylate dietary sterols. In this study, the incorporation of labeled substrates was detected only by mass spectroscopy. The feeding methodology is however of great interest, and, whenever associated with analysis by NMR spectroscopy, could be of general application in biosynthetic studies with marine protists.



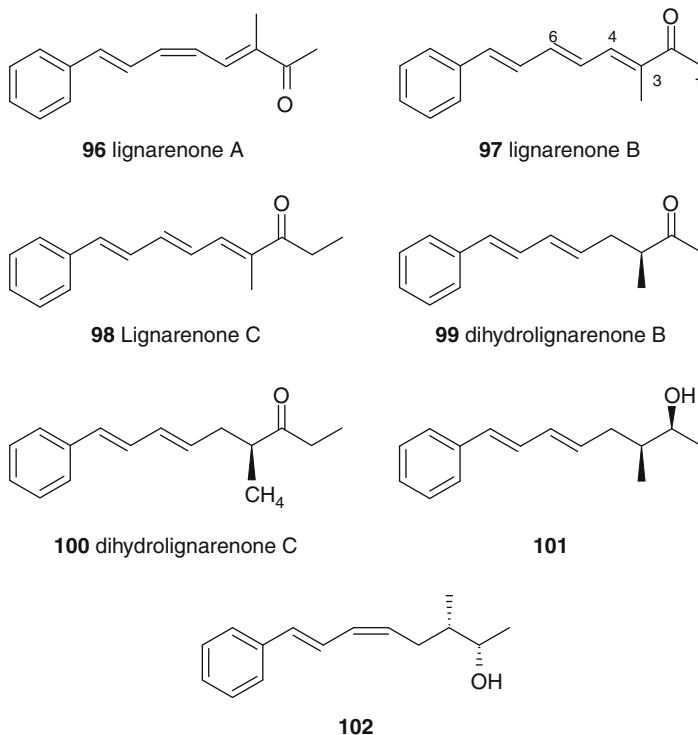
During sexual reproduction, female gametes of brown algae release C₁₁ hydrocarbons that attract their male partners [33]. These compounds show linear and monocyclic structures (**19**, **20**, **86–91**) that derive from the aliphatic terminus of polyunsaturated fatty acids, including arachidonic acid and eicosapentaenoic acid [105]. The mechanistic details of this process have been very recently addressed in the

brown alga *Ectocarpus siliculosus* by Rui and Boland [106]. Algal pheromone production in *E. siliculosus* is particularly interesting since the genuine lipoxygenase product pre-ectocarpene (**89**) is inactivated by a Cope rearrangement to ectocarpene (**19**) (2,000-fold less active than **89**) in a short time [107]. Administration of chirally labeled precursors, (16*R*)- and (16*S*)-[16,19,20- $^2\text{H}_3$]arachinoid acids (**92**, **93**), to the culture of the algal gametes gave [$^2\text{H}_2$]dictyoptere C (**94**) and [$^2\text{H}_3$]dictyoptere C (**95**), respectively, proving in a rigorous manner that cycle formation is associated to loss of the C(16)- H_R . The paper shows also an elegant synthesis of the deuterated substrates by Wittig reaction involving a chirally labeled hexanal.



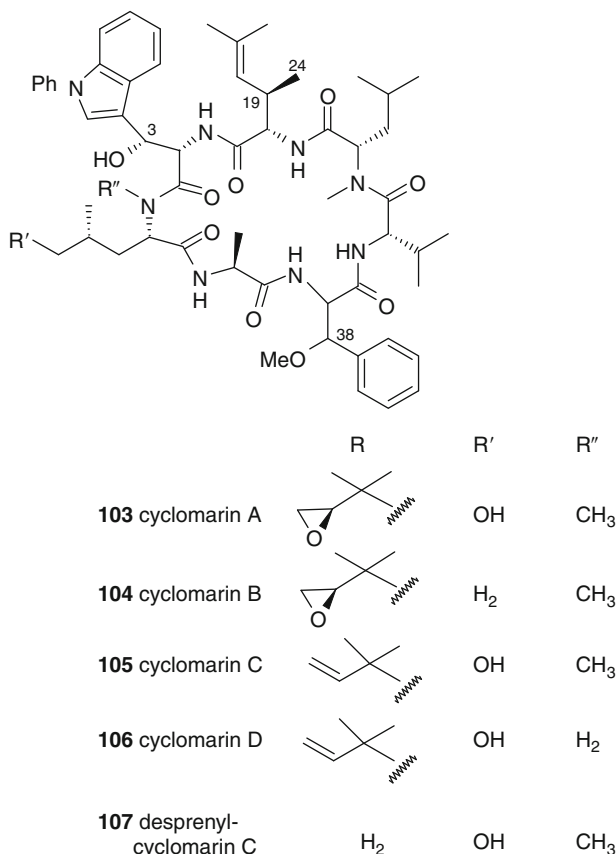
During the last few years, some biosynthetic experiments with stable isotopes were undertaken to study the polypropionate pathway in opisthobranch mollusks. Most of them will be discussed in the last section of this chapter. An apparent propionate unit is also present in lignarenones (**96–102**), aryl-alkenyl metabolites possessed by the cephalaspidean mollusk *Scaphander lignarius* [108, 109]. Feeding experiments with [$^2\text{H}_5$]phenylalanine [110] led to a strong incorporation in lignarenone B (**97**), then injecting [1,2- $^{13}\text{C}_2$]acetate, two intact acetate units were detected by ^{13}C -NMR at carbons 7/6 and 5/4, whereas a clear enhancement was

observed for C-1. No incorporation was recorded at carbons 2/3/8 that, apparently, could belong to a propionate unit. This hypothesis was recently confirmed in the authors' institute [111] by a feeding experiment with $[3-^2\text{H}_3]\text{propionate}$. In conclusion, benzoic acid is elongated by two extender acetate units, then one propionate unit, and, finally, another acetate unit to give the lignarenones **96** and **100**, whereas the loss of the last carbon leads to lignarenones **96**, **97**, **99**, **101**, and **102**. Probably, an analogue pathway could be suggested for navenone B (**57**) [79].



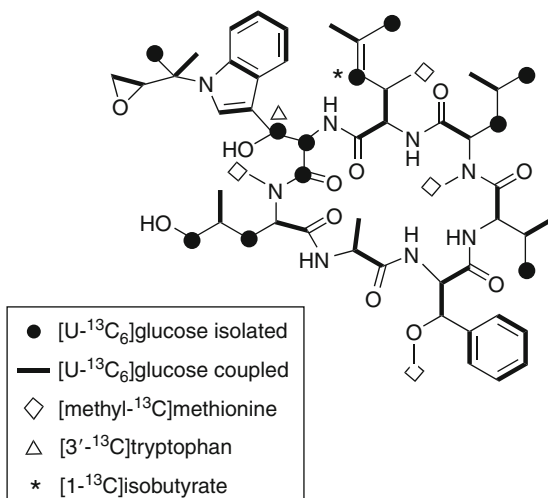
Feeding experiments with stable isotope-containing precursors is an extraordinary tool to investigate the complex mechanistic implications of natural product pathways. Also, as demonstrated by the biosynthesis of salinosporamides [89–91] described above, they represent an essential complement to molecular genomic techniques. In this view, an excellent paper that combines both approaches concerns the biosynthesis of cyclomarin A (**103**) [112]. Cyclomarins A–C (**103**–**105**) are potent anti-inflammatory marine natural products isolated from an estuarine streptomycete, strain CNB-982 [113]. Cyclomarins A and C were also found in another marine actinomycete, *Salinispora arenicola* CNS-205 from Palau, along with two truncated diketopiperazines, cyclomarinazine A and B, and other cyclomarin derivatives, cyclomarin D (**106**) and desprenyl cyclomarin C (**107**) [114–116]. Cyclomarin A (**103**) is a 21-membered cyclic heptapeptide with five modified nonproteinogenic amino acid residues. The fragments are (1) *N*-(1,1-dimethyl-2,3-epoxypropyl)- β -hydroxytryptophan,

(2) *N*-methyl- δ -hydroxyleucine, (3) alanine, (4) β -methoxyphenylalanine, (5) *N*-methylleucine, (6) valine, and (7) 2-amino-3,5-dimethyl-4-hexenoic acid (ADH).



Feeding experiments with stable isotopes on *Streptomyces* sp. CNB-982 are summarized in Fig. 17.1. Incorporations prove that the moieties 1, 2, and 5 derive from standard amino acids by simple modifications, including oxidation at C-3 and C-38, methylation of two amides and C-38 oxygen, and prenylation at the nitrogen atom of the pyrrol ring. Administration of [*U*-¹³C]glucose also established that the prenyl unit arises, prevalently from mevalonate pathway (MVA) with a minor contribution from the methylerythritol pathway (MEP). Despite incorporation at C-20 from [1-¹³C] isobutyrate, at C-24 by methylation from [methyl-¹³C]methionine, and, finally, at carbons 17–19 from [*U*-¹³C]glucose, the biosynthesis of the 2-amino-3,5-dimethyl-4-hexenoic acid (ADH) fragment was unresolved by the feeding experiments. On the contrary, molecular genetic methods suggested an origin of ADH from isobutyrate, pyruvate, and methionine precursors. In conclusion, this nice work establishes by complementary experiments that cyclomarins are biosynthesized through a nonribosomal peptide synthetase (NRPS) able to link nonproteinogenic amino acids in cyclic peptide products.

Fig. 17.1 Feeding experiments in cyclomarins A [113]



Biosynthesis and molecular genetics of marine natural products from dinoflagellates were also treated in a recent review [117]. Many feeding-based biosynthetic studies have been carried out on the potent paralytic shellfish poisoning (PSP) saxitoxin (**5**) and its analogues that are produced by *Gymnodinium catenatum* and by gonyaulacoid dinoflagellates of the genus *Alexandrium* and *Pyrodinium* [118]. A comprehensive overview of these studies was elaborated by Shimizu [119] which summarized the biosynthesis of saxitoxin (**5**) in eight steps that are summarized in Fig. 17.2: (1) Claisen-condensation between arginine and acetate; (2) a guanidine group is transferred from a second arginine unit to the free amino group of the intermediate B; (3) cyclization leads to the heterocycle D; (4) methylation by *S*-adenosyl methionine (SAM) and desaturation gives the intermediate E; (5) epoxidation; (6) opening of the epoxide to an aldehyde with subsequent reduction; (7) O-carbamoylation of the hydroxymethyl side-chain; finally (8) di-hydroxylation completes the biosynthesis. This well-consolidated biosynthetic pathway has been recently [120, 121] revised on the basis of molecular genetic studies. The new biosynthetic pathway is characterized by a different sequence where the SAM-methylation transforms acetate into propionate. Then, the biosynthesis proceeds including substantially the same previously reported biochemical reactions.

All the above-described results open extraordinary new perspectives in the chemistry of marine natural products. Of course, the structural elucidation continues to be the main focus. Then, establishing the structure with extreme rigor and studying its chemical reactivity, the basic biosynthetic steps can be clarified by interdisciplinary studies where the feeding experiments have to be integrated with complementary molecular genetic tools. This approach is also envisaged to boost the development of new drug candidates. However, until now, a crucial point remains undefined. Are symbiotic microorganisms the true producers of many metabolites found in marine macroorganisms? The topic has been treated in Piel's excellent review [122], which in part reanalyzes the remarkable structural analogies among metabolites from sponges and bacteria previously discussed

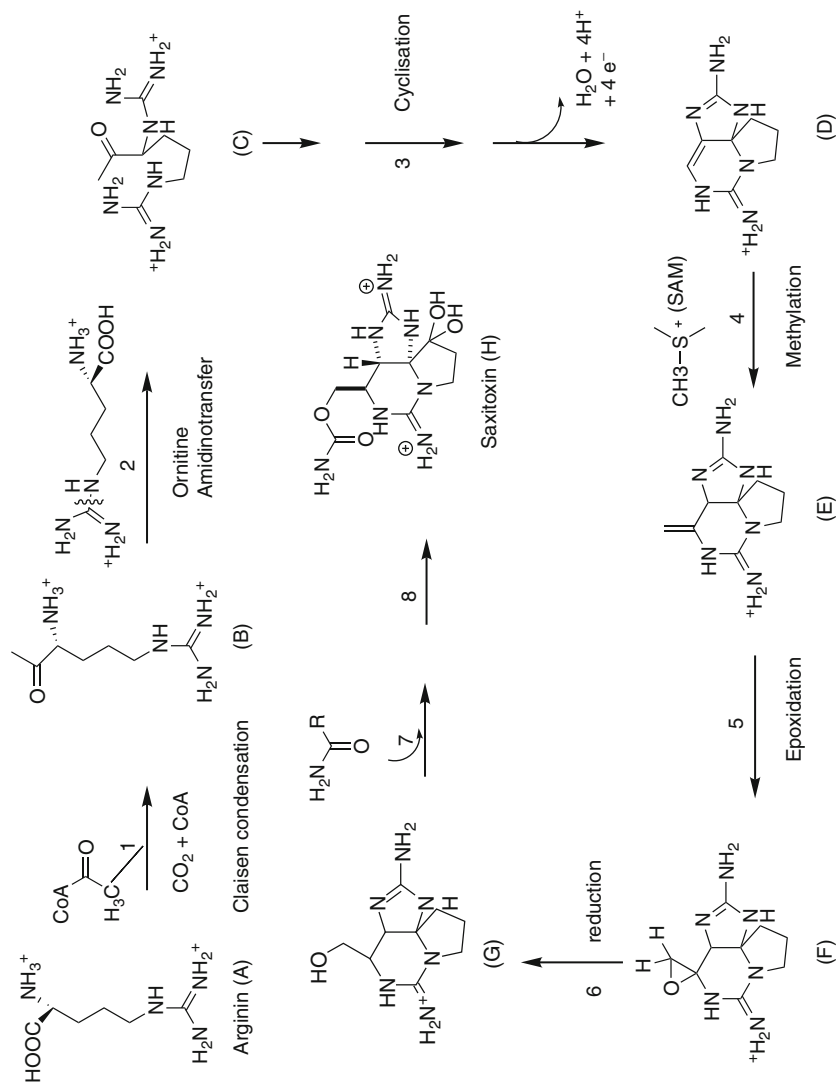
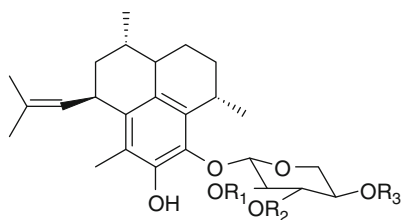


Fig. 17.2 Biosynthetic assembly of saxitoxin [119]

by other authors [5, 123]. Generally, these compounds are polyketides and nonribosomal peptides. Rarely, the isolated symbiotic bacteria preserve the metabolism of the host organism. Analogous conclusions were reported in Li's more recent overview [124] on marine microbial symbionts. These uncultured symbiotic microorganisms are extremely promising candidates for future studies that without disciplinary restriction could gain in importance for biomedical applications.

The recent work on the biosynthesis of pseudopterosins is a step toward this direction. Pseudopterosins are a family of anti-inflammatory and analgesic diterpene glycosides produced by the gorgonian *Pseudoptero-gorgia elisabethae* found in a few areas of the Caribbean. After the isolation of pseudopterosins A–D [125] (**108–111**), many other related metabolites were isolated, including the seco-pseudopterosins A–D (**112–115**) which display a serrulatane ring system [126]. Separation of the intracellular dinoflagellate symbiont *Symbiodinium* sp. [127] allowed the authors to obtain cultures that incubated with ^{14}C -labeled inorganic carbon and ^3H -GGPP gave radiolabeled **108–111**, thus supporting for the first time the symbiotic origin of pseudopterosins. Furthermore, feeding experiments with ^3H -GGPP on a cell-free extract of *P. elisabethae* led to radiolabeled pseudopterosins but also to the isolation of labeled elisabethatriene (**116**) [128]. Radiolabeled assay based on **116** was used to trace the diterpene cyclase activity and to isolate elisabethatriene synthase, a soluble protein that is responsible for the synthesis of serrulatane skeleton [129]. Recently, further mechanistic details with advanced precursors [130, 131] have further embellished this extremely interesting biosynthetic research [132].



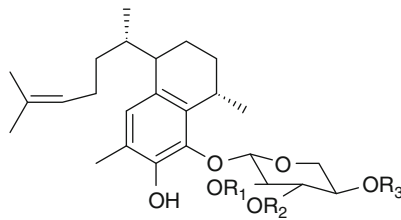
108 PsA R1=R2=R3= H

109 PsB R1=Ac, R2=R3= H

110 PsC R2=Ac, R1=R3= H

111 PsD R3=Ac, R1=R2= H

Pseudopterosins

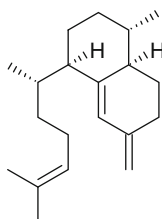


112 seco-PsA R1=R2=R3= H

113 seco-PsB R1=Ac, R2=R3= H

114 seco-PsC R2=Ac, R1=R3= H

115 seco-PsD R3=Ac, R1=R2= H



116 Elisabethatriene

17.5 Feeding Experiments and Detection Techniques

The experimental verification of a biosynthetic hypothesis requires establishment of the single steps involved in both construction and functionalization of the carbon skeleton. Until the purified enzyme for each biochemical step is available, biosynthetic studies can be carried out by administering a labeled precursor committed to the synthesis of the product of interest. Despite modest incorporations with complex organisms, feeding studies with stable isotopes have made a deep impact on biosynthetic studies in marine organisms, as much as with the terrestrial counterparts [8, 9]. As a matter of fact, since biosynthetic studies in marine organisms started much later than in terrestrial habitat, most of the experiments carried on in marine species have been made using stable precursors. There are a few but historically important exceptions to this assumption. Sponges are envisaged as the most prolific source of secondary metabolites in marine environments [133]. Nevertheless, the biosynthesis of most of these compounds is puzzling and, with the exception of the metagenomic methods [134–137] and exceptional reports of bacterial association [138, 139], their origin is not clearly understood even though many authors are inclined to consider associated or symbiotic microbes as the most likely producers [140, 141]. As reported in the previous paragraphs, sponge sterols have been the subject of numerous studies from Minale's and Djerassi's groups in the 1980s by employing both radioactive labeling and cell-free extracts (reviewed by Djerassi and Silva [72] and Giner [66]). In these studies, incorporation of ^{14}C -, ^3H -, or, less often, doubly ^3H -, ^{14}C -labeled precursors is followed by complicated analysis of the biosynthetic products by chemical degradation. Both carbon-14 and tritium are β -emitting nuclides that can be detected and accurately measured by a β -counter; after that, the weak radiation is converted into light by scintillation liquid. The procedure consists of dissolving the sample in the scintillation liquid and then measuring the level of emitted photons, which indicates the activity of radionuclides. It is usually possible to carry out quantification of samples containing two different isotopes, for example, ^{14}C and ^3H , and it is also feasible to perform analysis on line by intercepting the liquid coming from the chromatographic column of an HPLC instrument. Nevertheless, the technique is destructive, and the indirect measurement of radiation can be drastically reduced (quenching) by chemical and physical factors (e.g., chlorine compounds, colored samples, two-phase solution) that interfere with the counting process.

Simple incorporation of radioactive CO_2 , acetate, or mevalonate in the soluble form of DBED salt has been used to prove the *de novo* origin of polyketide and terpene carbon skeletons in marine organisms. The major impediments in these experiments arise from (1) the very low level of incorporation that follows administration of the labeling and (2) the difficulties of purifying the target compounds at homogeneity. To avoid this latter problem, products are transformed into derivatives of different polarity by simple and predictable chemical reactions. Although the level of radioactivity can be established for each carbon atom of the target

metabolite, this is not possible in most cases, and therefore, feeding experiments with radiolabel are usually little informative about the biochemical pathways leading to the final compound.

On the contrary, if stable-isotope-containing precursors are used, labeling position in target compounds can be detected by mass spectrometry (MS) and nuclear magnetic resonance (NMR). Both techniques are less sensitive than radioactivity-based methods, but allow unambiguous location of labeling without the requirement of degradation or chemical transformation. Furthermore, the astonishing improvements of these spectroscopic and spectrometric techniques in recent years have strongly lowered the limit of application, thus broadening the field of utilization of stable isotopes in biosynthetic studies.

In the past 20 years, single and doubly ^{13}C -labeled substrates have been employed to elucidate biosynthesis of secondary metabolites in algae, bacteria, fungi, and invertebrates from marine environments. In these studies, analysis of the labeled material is usually carried out by NMR [142]. Carbon-13 has a nuclear spin $I = \frac{1}{2}$ that allows the NMR identification of carbon atoms just as proton NMR identifies hydrogen atoms. In nature, the abundance of the isotope is only 1.1%, and therefore, only a few nuclei are observable by NMR in ordinary compounds. On the other hand, since carbon forms the backbones of organic molecules, the possibility of enriching a specific position and of locating the labeling directly is a powerful tool for elucidating the biochemical transformations leading to primary and secondary metabolites. ^{13}C -NMR spectroscopy has also other advantages deriving by the wide chemical shift range and spin-spin correlation due to coupling constant of vicinal or proximal active nuclides. Many common biogenetic precursors like acetate, propionate, mevalonate, glucose, and related compounds are commercially available with 99% ^{13}C enrichment in specific positions. Other precursors can be directly obtained by a number of standard procedures for synthesis of isotopically labeled substrates.

The precursors can be supplied in very imaginative ways that often depend on the organisms. The precursors are usually added to incubation media or aquarium water in feeding experiments with culturable organisms. They also can be administered by injection, using physiological buffer solution or sterile seawater, with macroorganisms. In this last case, a pulsed administration is used to improve the incorporation yields. The duration of the experiments varies from species to species, but usually, they last for 1–2 weeks. At the end of the feeding protocol, the treated organism is extracted and the target compound is purified by classical chromatographic methods. A cell-free system is a widely used tool for studying *in vitro* biological reactions without the complex interactions found in an intact cell. Cell-free systems are prepared after cellular lysis by using either the whole cell lysate or subcellular fractions. This methodology is often utilized when feeding experiments with the whole organism are not practicable or when information on specific biochemical transformations are sought after.

Isotopic incorporation is usually determined by acquisition of ^{13}C -NMR spectrum through comparison of labeled and natural sample of the compound of interest. Labeling is revealed by intensification of the signals due to those carbons

containing ^{13}C nuclide. The higher the enrichment is, the stronger the signal intensification. With precursors enriched at specific positions, the incorporation is restricted to specific carbons as an effect of the biosynthetic pathway. Individual examples are discussed in the paragraphs below, but probably the most clear application of feeding experiments with carbon-13 is given by the use of labeled glucose to elucidate the terpene biosynthesis from mevalonate or methylerythritol pathways [143, 144]. According to the biochemical reactions leading to the isoprene precursors isopentenyl pyrophosphate (IPP) and dimethylallyl pyrophosphate (DMAPP), C-1 of glucose is specifically placed at positions C-2, C-4, and C-5 of IPP and DMAPP by the mevalonate pathway, or at C-1 and C-4 of IPP and DMAPP by the methylerythritol pathway. Consequently, in experiments with $[1-^{13}\text{C}]\text{glucose}$, the backbones of terpenes derived from mevalonate pathway show NMR signals enriched at carbons 2, 4, and 5 of the isoprene units, whereas the enriched signals correspond to the positions 1 and 5 for those compounds produced by methylerythritol pathway (Fig. 17.3).

Biosynthetic studies of molecular backbones arising from rearrangements or cyclization of linear precursors are particularly well pursued by feeding experiments with substrates containing more than one ^{13}C nuclide. In these studies, information is directly deduced from the spin systems of adjacent carbon-13 atoms, which is revealed by splitting of the corresponding signals because of spin coupling. This phenomenon produces multiplets according to the role of multiplicity that also governs proton NMR. The shape of the resulting signals is diagnostic to determine the spin systems and thus to establish the connectivities between the carbons forming the molecular backbone. Although different types of compounds containing more than one carbon atoms have been used, $[1,2-^{13}\text{C}_2]\text{acetate}$ is the most common example of this family of substrates in feeding experiments with marine organisms. In ^{13}C -NMR spectra, the incorporation of intact C_2 -unit deriving from the doubly labeled acetate is revealed by two doublets flanking the central resonances of the natural carbons (Fig. 17.4). The distance from the two lines (coupling constant) is identical for both signals and is a function of stereoelectronic features of the molecule, thus being diagnostic to recognize the carbons even in the presence of other doublets. In a recent advance, ^{13}C - ^{13}C correlation spectroscopy (COSY) has been used to map the coupling carbons in secondary metabolite. Like the corresponding experiment based on ^1H detection, basic ^{13}C resonances appears on the diagonal, whereas interacting carbons are easily identified by cross-peaks symmetrical to the diagonal [110].

Nuclides other than carbon 13 have not been widely employed in feeding experiments with marine organisms. Deuterium-labeled substrates have been recently used in experiments with marine mollusks, bacteria, and microalgae. Detection of ^2H is usually achieved by MS or MS/MS techniques that also allow localization of the label by analysis of the daughter ions. Deuterium atoms, having nuclear spin $I = 1$, can be also detected by NMR, but the resulting spectra suffer of severe line broadening due to the quadrupole moment of the nucleus. Consequently, deuterium NMR has a range of chemical shift similar to proton NMR but with poor resolution that hampers the general application of this methodology. However, comparison with the

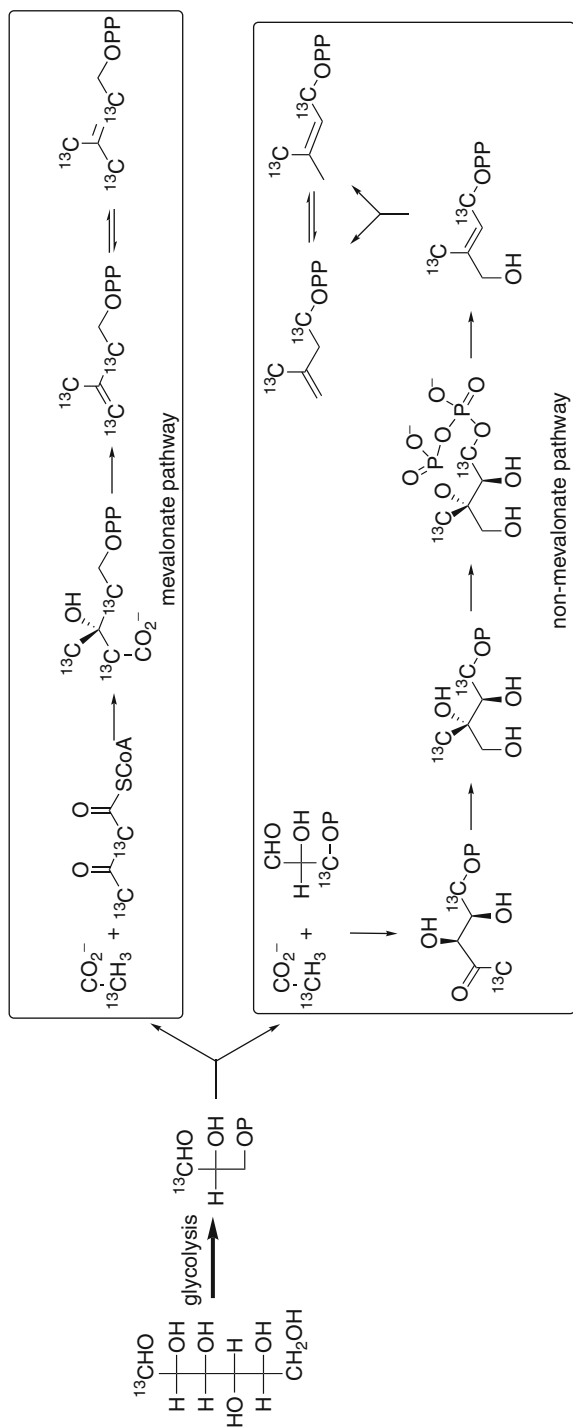


Fig. 17.3 Influence of metabolism due to mevalonate and nonmevalonate pathways on labeling in isoprene precursors, isopentenyl pyrophosphate, and dimethylallyl pyrophosphate. C-13 atoms are shown in the structures

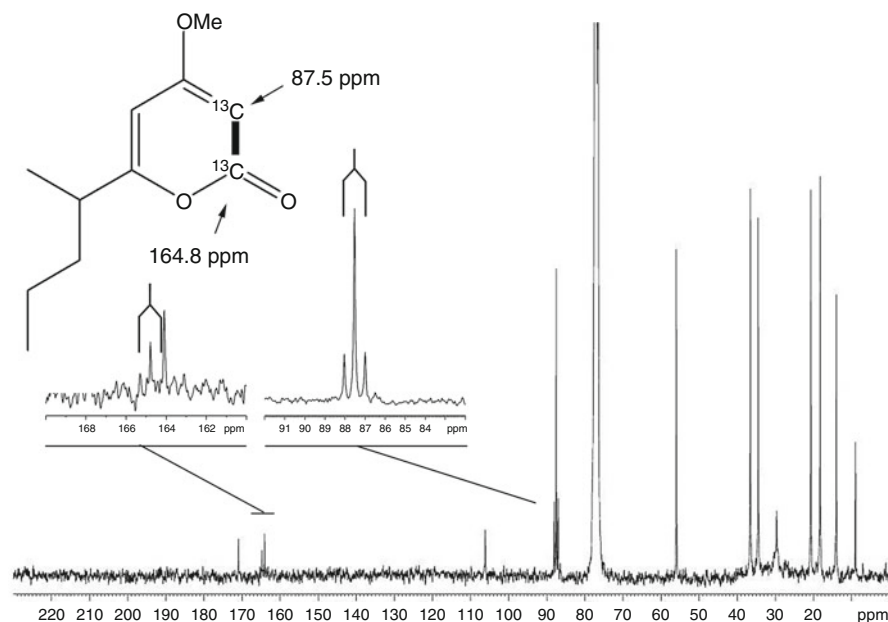


Fig. 17.4 ^{13}C -NMR spectrum of placidene E (**153**) after incorporation of $[1,2-^{13}\text{C}_2]$ acetate. The insert shows the doublet ($J = 78.1$ Hz) flanking the signals of the natural isotopomer

corresponding ^1H -NMR spectrum of the natural compound clearly is usually sufficient to establish which hydrogen has been replaced by deuterium, thus allowing one to determine the main steps of the biosynthetic pathway.

17.6 Lipxygenase Pathways in Marine Diatoms

Diatom oxylipins embrace a family of lipoxygenase (LOX)-derived fatty acid products reported by independent studies from freshwater and marine genera in the last few years [145–148]. The family consists of (1) breakdown metabolites, such as polyunsaturated aldehydes (PUAs) and ω -oxo-fatty acids, and (2) oxygenated compounds that conserve the original structure of the fatty acid precursor, i.e., hydroxy, keto, oxo, and epoxy derivatives (Fig. 17.5). These metabolites occur commonly and are widely distributed within the diatom lineage; they are characterized by an apparent species specificity that arise from the variability of the oxidation site, the structure of the fatty acids recognized as LOX substrates, and finally, the enzymatic transformations downstream to LOX oxidation [146–150].

Oxylipin pathways are likely encoded by the genome of nearly all photosynthetically active eukaryotes [151], and despite the chemical nature of the individual compounds, the signaling pattern and functional roles are much the same across

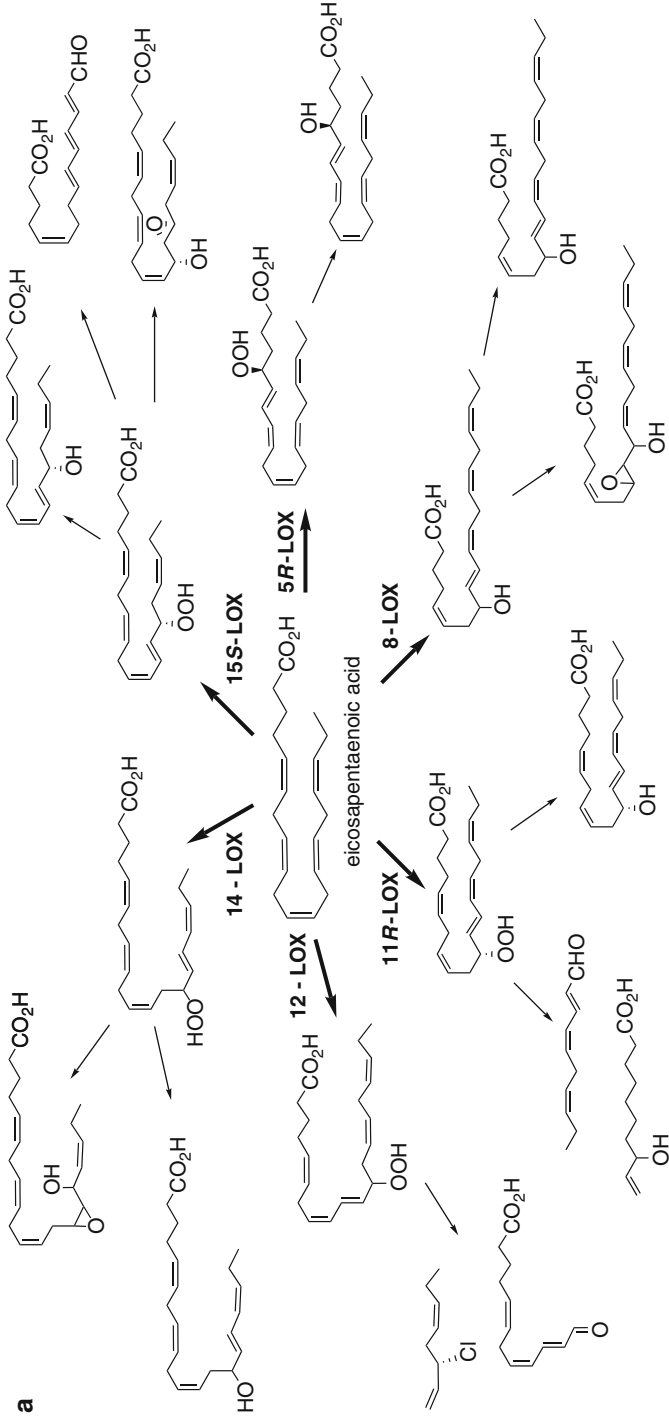


Fig. 17.5 (continued)

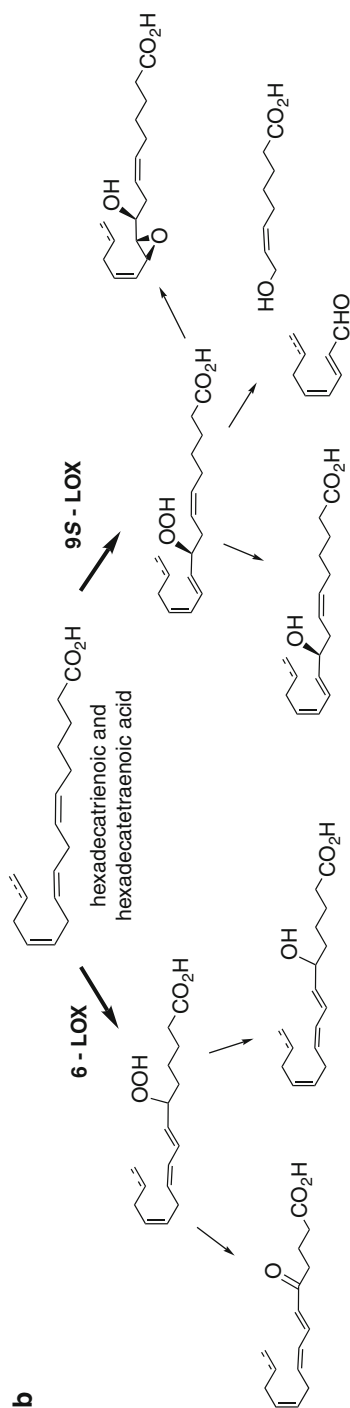
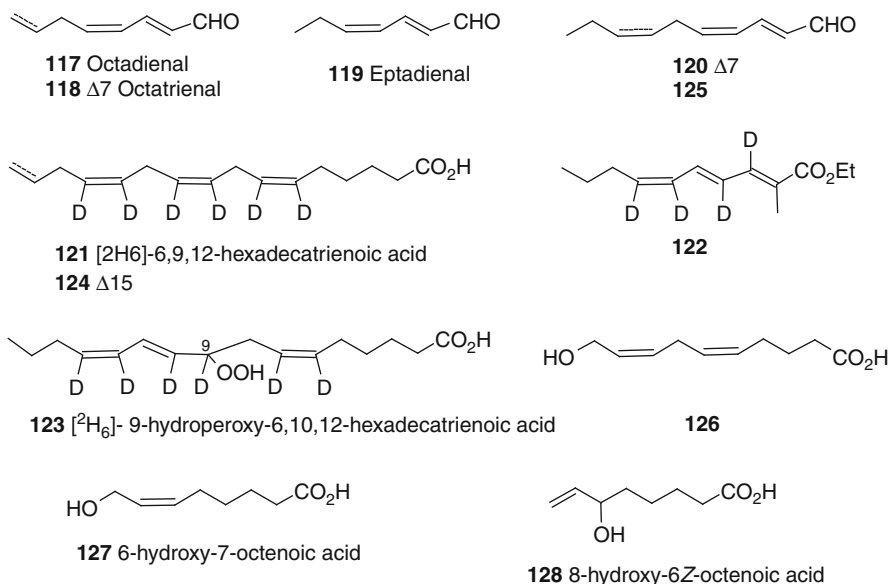


Fig. 17.5 Schematic view of lipoxygenase pathways in marine diatoms. (a) oxylipins from C20-fatty acids, (b) oxylipins from C16-fatty acids. For a discussion of the products, see main text

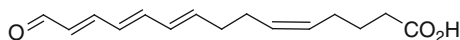
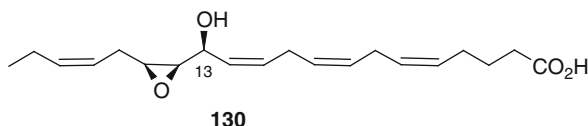
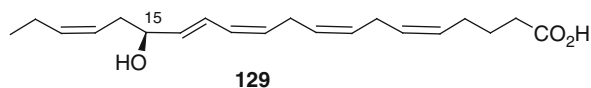
different lineages. In higher plants, where these molecules are mostly synthesized by lipoxygenase (LOX)-dependent oxidation at the 9 or 13 position of C₁₈ polyunsaturated fatty acids [152], oxylipins have played a crucial role in the defense and development [153, 154]. Algal oxylipins [151, 155–157] are mainly synthesized from C₂₀ PUFAs in response to stress conditions or perception of external stimuli as essential intermediates for innate immunity [158, 159]. In diatoms, circumstantial evidence suggests that these molecules are responsible for both the detrimental effects of this lineage on copepod grazers [161], and chemical communication between diatom cells [149, 160–162].

Lipoxygenase metabolism starts with peroxidation of the polyunsaturated fatty acid and formation of a 2,4-pentadienyl hydroperoxide moiety that undergoes spontaneous or enzymatic conversion [163]. Biosynthetic studies in diatoms rely mostly on incubation of labeled fatty acids in cell-free preparation or enzymatic fractions. This approach has been widely used to determine the origin of PUAs (117–120), as illustrated for the production of octadienal (117) from [6,7,9,10,12,13-²H₆]-6,9,12-hexadecatrienoic acid (121) in the planktonic diatom *Skeletonema costatum* (taxonomically reassigned as *Skeletonema marinoi*) [164]. The cells of this microalga were suspended in distilled water and incubated with the labeled acid prepared by deuteration of a polyalkyne intermediate deriving from coupling of propargyl bromide with terminal alkyne in the presence of cesium carbonate [164]. To recover the deuterated derivative of the volatile aldehyde 117, the rough extracts were derivatized with carbetoxyethylidene-triphenylphosphorane (CET-triphenylphosphorane) to give the stable polyunsaturated ester 122, which showed a significant M + 4 peaks (natural C₁₃H₂₀O₂⁺, *m/z* 208; labeled C₁₃H₁₆D₄O₂⁺, *m/z* 212) in GCMS. The labeling position of this isotopomer was established by ²H NMR spectroscopy that revealed the exchange of protons with deuterium at C-1 (δ 7.22), C-2 (δ 6.42), C-4 (δ 6.20), and C-5 (δ 5.91) in full agreement with a lyase-dependent breakage of the [6,7,9,10,12,13-²H₆]-9-hydroperoxy-6,10,12-hexadecatrienoic acid (123). The subsequent identification of this intermediate by ESI⁺ LC-MS in *Thalassiosira rotula* [146] and the finding of a similar mechanism for the synthesis of octatrienal (118) from [6,7,9,10,12,13,15,16-²H₈]-6,10,12,15-hexadecatetraenoic acid (124) [165] corroborated the origin of C₈ PUAs from C₁₆ PUFAs. A similar strategy with incubation of *T. rotula* cell free was also used to prove the synthesis of the ω-3 PUAs heptadienal (119) and decatrienal (120) from eicosapentaenoic acid (EPA) [166]. The enzymatic mechanisms leading to synthesis of 117–120 has been recently suggested as a unique transformation that does not rely to pathways known in other organisms [167]. In *T. rotula*, transformation of d₈-arachidonic acid to deuterated decadienal (125), an unnatural analogue of 120, was complemented by synthesis of [²H₄]-10-hydroxy-5,8-dacdienoic acid (126). In full agreement with this result, incorporation of 9,10-[²H₂]-6,10,12,15-hexadecatetraenoic acid led to octatrienal (118) together with the isomeric 6-hydroxy-7-octenoic acid (127) and 8-hydroxy-6Z-octenoic acid (128). Formation of hydroxy acid, such as 126–128, in lyase process is unusual and

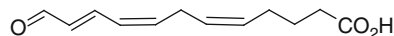
further investigation with [^{18}O]water proved that the alcoholic oxygen derives from the medium, as a result of a carbon-carbon breaking presumably assisted by water.



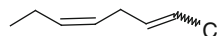
In homogenates of *Chaetoceros socialis*, *Chaetoceros affinis*, and *S. marinoi*, experiments with tritiated EPA also led to specific incorporation into hydroxy, hydroperoxy, and epoxy alcohol derivatives [147]. In *Pseudo-nitzschia delicatissima* (recently reassigned as *Pseudo-nitzschia arenysensis*), eicosapentaenoic acid-dependent 15S-lipoxygenase pathway was responsible for production of oxylipins (**129–131**) along the growth curve, with remarkable changes that are apparently dependent on cellular density. At least one of these compounds, namely (5Z, 9E, 11E, 13E)-15-oxo-5,9,11,13-pentadecatetraenoic acid (**131**), is formed only in the stationary phase immediately before the demise of the culture. Origin of this metabolite was proved by radioactive incorporation after administration of tritiated EPA. No information is hitherto available on the mechanism underlying the lyase activity in *P. delicatissima* [149], but the involvement of an unprecedented cleavage has been proposed for the biosynthesis of the related (5Z, 8Z, 10E)-12-oxo-5,9,11,13-dodecatrienoic acid (**132**) in the diatom *Stephanopyxis turris* [168]. Incubation of this microalga with deuterated arachidonic acid and tritiated 12-hydroperoxy-eicosatetraenoic acid gave incorporation of the labeling in **132** and C₈ chloroalkanes (e.g., **133**). The halogen atoms originate from seawater and are introduced at the same time of the cleavage of the fatty acid hydroperoxide, although it cannot be excluded that the two reactions proceed through two parallel pathways.



131 (5Z,9E,11E,13E)-15-oxo-5,9,11,13-pentadecatetraenoic acid



132 (5Z,8Z,10E)-12-oxo-5,9,11,13-dodecatrienoic acid



133

C₁₆-Fatty acids, such as those incorporated in the synthesis of C₈ PUAs **117** and **118**, are typically components of thylakoid membranes of chloroplasts. Experiments with radioactive tracers [169] and partially purified enzymes [170] suggest that these organelles are the primary source of LOX substrates in diatoms. The activation of the pathway is initiated with the release of free fatty acids by a lipolytic activity that is involved in the hydrolysis of both galactolipids (GLs) and phospholipids (PLs) [169]. The biochemical relationship between these lipidic pools and oxylipins was tested by incubation of ³H-PLs and ³H-GLs in *S. costatum*. Although the specific radioactivity was rather higher in PLs than in GLs, the percentage of radioactivity recovered in heptadienal (**119**) was three times higher after incubation of the sugar conjugates [169]. In a second set of experiments [170], the whole pool of PUAs in *T. rotula* (**117**–**120**) was obtained from GL incubated with an enzymatic preparation.

17.7 Polypropionates in Sacoglossan Mollusks: When Biosynthesis and Function are Hand in Glove

Polyketides are structurally diverse natural products sharing a common biosynthetic process that relies on a stepwise chain assembly through successive rounds of Claisen-type condensation between an activated malonic acid derivative and an acyl thioester [171]. The family embraces a large variety of bioactive compounds found in many different organisms, from prokaryotes to eukaryotes but seldom in animals. The processive biosynthesis is under control of multicatalytic enzymes, named polyketide synthases (PKS), which are roughly classified as type I, type II, and type III on the basis of the protein architecture.

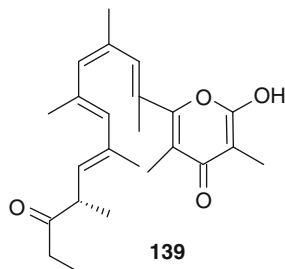
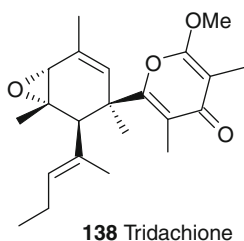
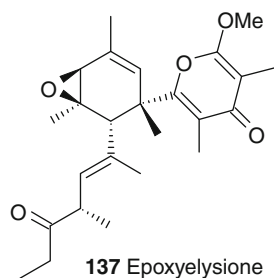
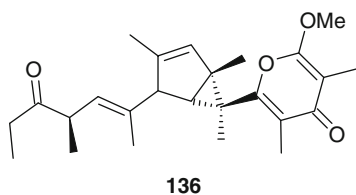
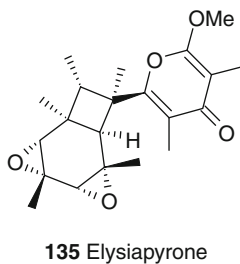
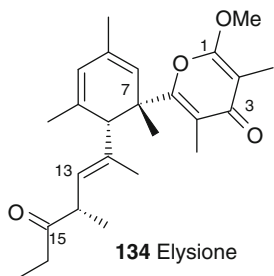
Some opisthobranch gastropods of the order Sacoglossa are able to produce a very specific and rare class of polyketides that, being based on repetition of C-3 units, are collectively named polypropionates. Sacoglossans have also

another unique ability. These marine mollusks derive photosynthetically viable chloroplasts from the algae upon which they feed. The photosynthetic products are transferred from these plastids to mollusk tissues and can sustain the slugs for several months in the absence of a food source [172, 173]. The symbiosis implies a unique exchange of genes between eukaryotic alga and animal [174]. The fixed carbon appears also in secondary metabolites of the mollusks, as first proved by Ireland and Scheuer [29] with incorporation of [^{14}C]bicarbonate into the polypropionates **15** and **16** of the Pacific sacoglossan *Placobranchus ocellatus*. Advanced precursors and chemical transformations involved in the biosynthesis of this family of compounds have been later established in the Mediterranean *Elysia viridis*. Administration of tritiated propionate to seawater gave a clear enrichment of radioactivity in elysione **134** (approximately 37,000 dpm/mg) [175]. To a further study with sodium [$1\text{-}^{13}\text{C}$]propionate, enrichment was in full agreement with incorporation of intact C_3 units in the skeleton of the mollusk metabolite [176]. As such, elysione is suggested to derive from a PKS process based on the repetitive addition of propionate units and final formation of the pyrone ring by spontaneous cyclization occurring after release of the polyketide chain from the thiotemplate [177].

Elysione (**134**) prototypes an impressive number of metabolites including a pyrone ring appended to a range of complex cyclic cores and side chains, which are usually formed by six to eight propionate units [178]. In consideration of the central core, the family embraces at least three structural types featured by cyclohexadiene (e.g., 9,10-deoxytridachione, **15**), bicyclo[3,1,0]hexane (e.g., photodeoxytridachione **16**), and bicyclo[4,2,0]octane (e.g., elysiapyrone **135**) [36, 179, 180]. Photochemical conversion of the propionate skeletons generates 9,10-deoxytridachione (**15**) from photodeoxytridachione (**16**), as well as compound **136** from elysione (**134**) both in vivo and in vitro [29, 176]. The chemical transformation has been extensively proved by synthetic methods, and it is nowadays accepted that the different polypropionate backbones are the result of rearrangement of a common precursor by photochemical or thermal stress [181–186]. On the contrary, exposure of living specimens of *E. viridis* to nonstressing levels of light ($350\ \mu\text{E m}^{-2}\ \text{s}^{-1}$) does not induce detectable rearrangement of the cyclohexadiene skeleton of **134** but decreases the levels of an epoxy derivative named epoxyelysione (**137**). The levels of these pairs of metabolites change in response to light, being the amount of **137** significantly dominant in the dark. The apparent equilibrium between elysione (**134**) and epoxyelysione (**137**) suggests a physiological regulation based on epoxidation or de-epoxidation of the polyketide. Although not tested, a similar process is likely to occur also for 9,10-deoxytridachione (**15**) and tridachione (**138**) of *P. ocellatus* [29] and *Tridachia diomedea* [187]. Since the skeleton rearrangement induced by light overexposure is impossible in absence of the conjugated double bond of the cyclohexadiene core, the reactions of epoxidation/de-epoxidation control the physiological pool of the molecules (i.e., elysione, **134**) in the animal tissue. Because elysione (**134**) and 9,10-deoxytridachione (**15**) are suggested to have a sunscreen role to protect the animals in photophilic environments, the

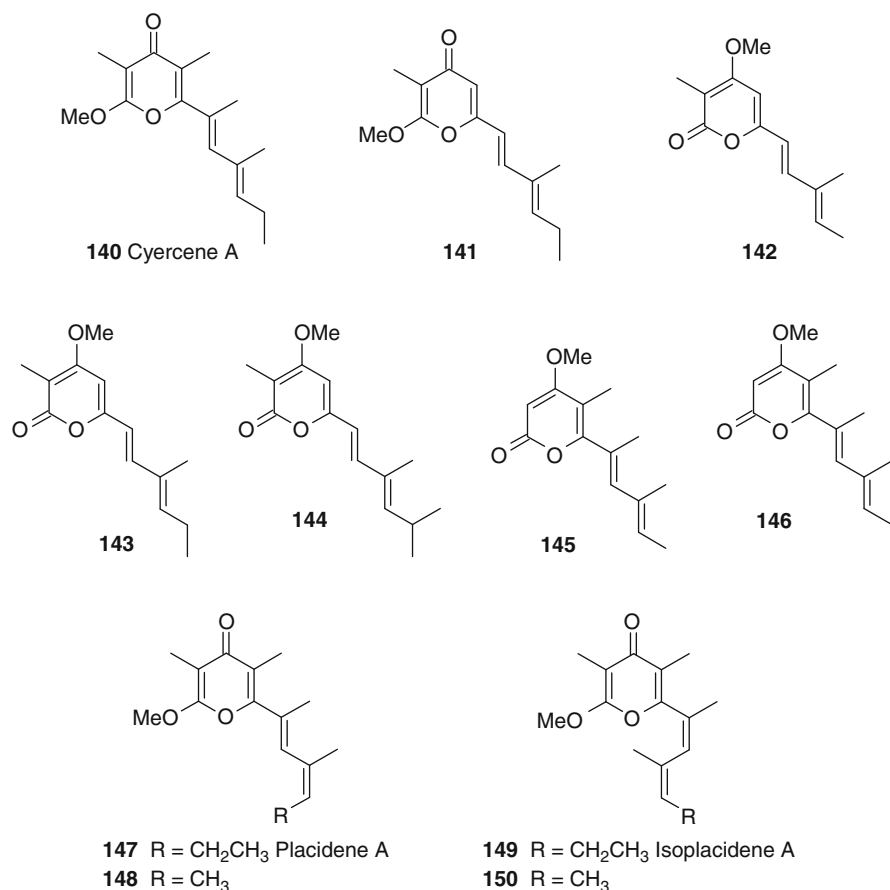
biochemical outcome is a photoprotective process reminiscent of the xanthophyll cycle in higher plants, Chlorophyta and Phaeophyceae [188].

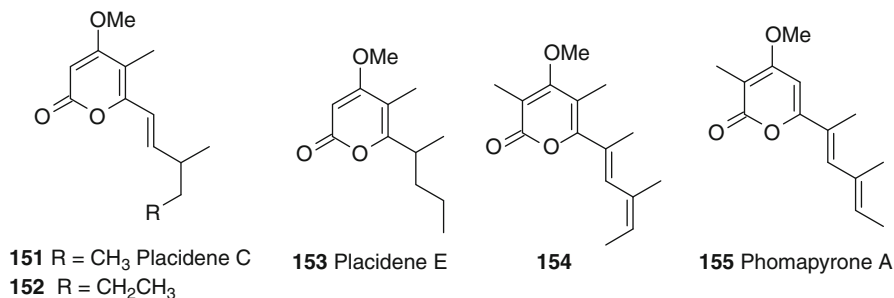
In specimens of *E. viridis* kept in the dark for a few days, a careful analysis led to the identification of a labile product that was not detectable in the animals collected from natural environments. The structural characteristics of this product agreed with a conjugated tetraene polypropionate (**139**) that is likely to represent the primary product of the polyketide biosynthesis in the mollusk [176]. As brilliantly demonstrated by biomimetic synthesis [181–185], the rearrangement of the unstable tetraene **139** followed by pericyclic processes gives access to the impressive molecular variability of mollusk propionates in response to environmental conditions. Since a similar mechanism is also likely to take place for the synthesis of chiral compounds, e.g., 9,10-deoxytridachione (**15**), the reaction of cyclization of the achiral tetraene is suggested to depend on enzymatic catalysis in vivo [176, 180].



Biosynthesis of pyrone propionates, closely related to elysione (**134**), has also been established in other sacoglossans. Injection of $[2-^{14}\text{C}]$ propionate to the Mediterranean molluscs *Cyerce cristallina* and *Ercolania funerea* [189–191] led to selective incorporation in cyercenes (**140–146**), members of a family of putative scavengers that includes also products of the sacoglossan *Placida dendritica* (**147–154**) [192, 193]. A possible interconversion of cyercenes and placidenes has been hypothesized by Zuidema and Jones [192, 193], who proved the biomimetic synthesis of placidene A (**147**) and isoplacidene A (**149**) from cyercene A (**140**) under photochemical conditions.

The structural motif of cyercenes has also been reported in a family of fungal metabolites, including infectopyrone from *Alternaria infectoria* [194], dihydroinfectopyrone and further congeners from *Petriella* sp. [195], nectriapyrone from *Gyrostroma missouriense* [196], stemphyropyrene from *Stemphylium globuliferum* [197], and phomapyrones D and E from *Leptosphaeria maculans* (asexual stage: *Phoma lingam*) [198].





Biosynthesis of polypropionates in fungi has been recently established on phomapyrone A (**155**) by administration of sodium [2-¹³C]acetate, sodium [1,2-¹³C]acetate, sodium [2-¹³C]malonate, [3,3,3-²H₃]propanoic acid, and L-[Me-²H₃]methionine to cultures of *L. maculans* [198] (Fig. 17.6a). The distribution of labeling indicated the lack of incorporation of propanoic acid and the assimilation of four methionine-derived methyl groups, in agreement with the origin of the polypropionate from methylation of a linear penta-acetate precursor. Similar experiments carried out by injection of sodium [1-¹³C]propionate, sodium [2-¹³C]acetate, and sodium [1,2-¹³C₂]acetate to 64 specimens of *P. dendritica* gave totally different results [199]. In fact, the analysis of the regular skeleton of placidene A (**147**) showed incorporation in carbons derived from C1 of labeled propionate. No carbon of **147** was enriched from labeled acetates that otherwise gave the enrichment of C2-C3, C6-C7, and C10-C11 units of placidene C (**151**) and E (**153**) (Fig. 17.6b) [199].

The experiments with *P. dendritica* proved that the sacoglossan polypropionates are the result of a peculiar biochemical combination of light-dependent reactions and mixed polyketide assembly. The de novo origin of **147** by sequential addition of intact C₃ units to the emerging polyketide underlines a biosynthetic pathway different from that described in fungi, thus implying that the same compound can derive from two different pathways in the two phyla [199]. This is a very important point that suggests a need for caution in speculations about the biogenesis of marine products. Our knowledge of the biochemical transformations in these systems is very inadequate. Frequently, metabolic pathways operating in marine organisms are discussed in relation to terrestrial processes, and assumptions about the origin of marine secondary metabolites, especially from invertebrates, are based on structural similarities to known metabolites of microbial source. The metabolic divergence between fungi and mollusks is in clear contradiction with this line of reasoning. As such, sacoglossan polypropionates represent a very special case that should be adequately considered before one hastily puts forward considerations about the biosynthesis of secondary metabolites especially if derived from marine organisms.

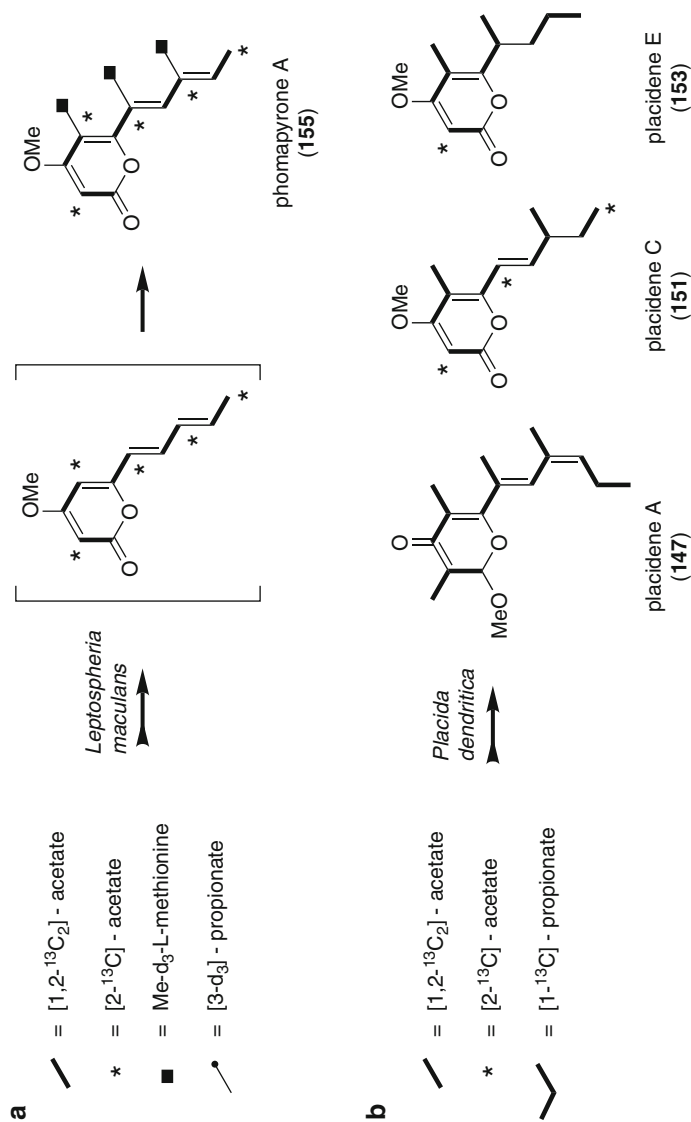


Fig. 17.6 Biosynthesis of polypropionate in the fungus *Leptosphaeria maculans* (a) and the mollusk *Placida dendritica*, (b) The structure in square bracket is a putative intermediate deriving from cyclization of a postulated linear petaketide. There is no evidence that supports the real occurrence of this intermediate

17.8 Conclusions

This chapter has covered feeding biosynthetic studies of the last four decades on marine organisms. The emerging scenario underlines the evolution of the field that has been constantly moving on from the pioneering studies with radioactive tracers to the modern molecular approaches through the use of techniques relying on stable isotopes and enzymatic transformations. Relevance of this research has hitherto concerned (1) the origin of the molecules in relation to the potential role of symbiotic association, (2) the chemistry of biosynthetic reactions as inspiration of synthetic methods in organic chemistry, and (3) the control of the biosynthetic pathways in view of the elucidation of the functional role of the natural products.

In the coming years, full application of molecular techniques to biosynthetic pathways is expected to give access to natural and artificial variants of bioactive products with an unpredictable impact on human medicine. Four decades of studies of marine organisms have led to an extremely rich arsenal of bioactive molecules [133] that, however, have seldom established a position in the drug market [200]. Limiting constraints are for the most part (a) the scarcity of the natural source that reduces the availability of the bioactive molecule and (b) the structural complexity of the bioactive molecules that often hampers their chemical synthesis.

Disclosure of genes coding for the synthesis of these molecules and subsequent engineering of these pathways by heterologous expression is envisaged as a promising way to overcome the present hurdles that limit biotech access to marine natural products and hence open a new era for the development of new drugs. The potentiality of this methodology is underlined by a series of recent papers reporting studies on many marine organisms, including cyanobacteria [201], dinoflagellates [202], marine bacteria [112], and gorgonian symbionts [132]. However, the success of this approach will also depend on the exact knowledge of the biogenesis of secondary metabolites and therefore cannot leave out those biosynthetic studies that are based on feeding experiments.

17.9 Study Questions

1. What is known about the biosynthesis of sponge sterols?
2. Describe the major differences of terpene biosynthesis by mevalonate and methylerythritol pathways.
3. Describe the incorporation of [1-¹³C]glucose into terpenes by mevalonate and methylerythritol pathways.
4. Describe the biosynthesis of pyrone-containing polypropionates in mollusks and fungi.
5. Describe the incorporation of acetate in macrolides of dinoflagellates of the genus *Amphidinium*.
6. How is the presence of β -emitting radionuclides detected in biosynthetic studies?

7. Describe the NMR spectra of molecules after incorporation of singly and doubly labeled ^{13}C -precursors.
8. Which are the arguments for and against the use of radioactive and stable isotopes in biosynthetic experiments?

References

1. Walsh CT, Fischbach MA (2010) Natural products version 2.0: connecting genes to molecules. *J Am Chem Soc* 132:2469–2493
2. Barrow KD (1983) Biosynthesis of marine metabolites. In: Scheuer PJ (ed) *Marine natural products: chemical and biological perspectives*, vol 5. Academic, New York
3. Garson MJ (1989) Biosynthetic studies on marine natural products. *Nat Prod Rep* 6:143–170
4. Garson MJ (1993) The biosynthesis of marine natural products. *Chem Rev* 93:1699–1733
5. Moore BS (1999) Biosynthesis of marine natural products: microorganisms and macroalgae. *Nat Prod Rep* 16:653–674
6. Kerr RG (2000) Biosynthesis of bioactive marine natural products. In: Raman A (ed) *Studies in natural product chemistry*, vol 21. Elsevier, Amsterdam
7. Bhakuni DS, Rawat DS (2005) Bioactive marine natural products – biosynthesis of bioactive metabolites of marine organisms. Anamaya, New Delhi
8. Moore BS (2005) Biosynthesis of marine natural products: microorganisms (part A). *Nat Prod Rep* 22:580–593
9. Moore BS (2006) Biosynthesis of marine natural products: macroorganisms (part B). *Nat Prod Rep* 23:615–629
10. Cimino G, Sodano G (1993) Biosynthesis of secondary metabolites in marine molluscs. In: Scheuer PJ (ed) *Topics in current chemistry*, vol 167. Springer, Berlin-Heidelberg
11. Rein KS, Snyder RV (2006) The biosynthesis of polyketide metabolites by dinoflagellates. In: Laskin A, Sariaslani S, Gadd G (eds) *Advances in applied microbiology*, vol 59. Elsevier (Academic Press), Amsterdam
12. Cimino G, Fontana A, Cutignano A, Gavagnin M (2004) Biosynthesis in opisthobranch molluscs: general outline in the light of recent use of stable isotopes. *Phytochem Rev* 3:285–307
13. Baker BJ, Kerr RG (1993) Biosynthesis of marine sterols. In: Scheuer PJ (ed) *Topics in current chemistry*, vol 167. Springer, Berlin-Heidelberg
14. Davies-Coleman MT, Garson MJ (1998) Marine polypropionates. *Nat Prod Rep* 15:477–493
15. Gerwick WH (1994) Structure and biosynthesis of marine algal oxylipins. *Biochim Biophys Acta* 1211:243–255
16. Kobayashi J, Tsuda M (2004) Amphidinolides, bioactive macrolides from symbiotic marine dinoflagellates. *Nat Prod Rep* 21:77–93
17. Garson MJ, Simpson JS (2004) Marine isocyanides and related natural products – structure, biosynthesis and ecology. *Nat Prod Rep* 21:164–179
18. Morales RW, Litchfield C (1977) Incorporation of $1\text{-}^{14}\text{C}$ -Acetate into C_{26} fatty acids of the marine sponge *Microciona prolifera*. *Lipids* 12:570–576
19. Young DN, McConnell OJ, Fenical W (1981) In vivo biosynthesis of tribromoheptene oxide in *Bonnemaisonia nootkana*. *Phytochemistry* 20:2335–2337
20. De Rosa M, Minale L, Sodano G (1976) Metabolism in Porifera VI. Role of the 5,6 double bond and the fate of the C-4 cholesterol during the conversion into 3β -hydroxymethyl-A-nor- 5α -steranes in the sponge *Axinella verrucosa*. *Experientia* 32:1112–1113
21. Bibolino L, Minale L, Sodano G (1978) Investigations on the ring contraction step in the biosynthesis of A-nor-stanols by the marine sponge *Axinella verrucosa*. *J Chem Soc Chem Commun* 13:524–525

22. Stallard MO, Faulkner DJ (1974) Chemical constituents of the digestive gland of the sea hare *Aplysia californica* II. Chemical transformations. *Comp Biochem Physiol B* 49:37–41
23. Hori A, Shimizu Y (1983) Biosynthetic ^{15}N -enrichment and ^{15}N n.m.r. spectra of neosaxitoxin and gonyautoxin-II: application to structure determination. *J Chem Soc Chem Commun* 790–792
24. Lee MS, Repeta DJ, Nakanishi K, Zagorski MG (1986) Biosynthetic origins and assignments of ^{13}C NMR peaks of brevetoxin B. *J Am Chem Soc* 108:7855–7856
25. Catalan CAN, Thompson JE, Kokke WCMC, Djerassi C (1985) Biosynthetic studies of marine lipids—3: experimental demonstration of the course of side chain extension in marine sterols. *Tetrahedron* 41:1073–1084
26. Garson MJ (1986) Biosynthesis of the novel diterpene isonitrile diisocyanoadociane by a marine sponge of the *Amphimedon* genus: incorporation studies with sodium [^{14}C]cyanide and sodium [2- ^{14}C]acetate. *J Chem Soc Chem Commun* 35–36
27. Fookes CJR, Garson MJ, MacLeod JK, Skelton BW, White AH (1988) Biosynthesis of diisocyanoadociane, a novel diterpene from the marine sponge *Amphimedon* sp. Crystal structure of a monoamide derivative. *J Chem Soc Perkin Trans 1*:1003–1011
28. Garson MJ (1986) Abstracts of 8th National organic meeting Royal Australian Chemical Institute, Adelaide; further published as: Dai MC, Garson MJ, Coll JC (1991) Biosynthetic processes in soft corals. I. A comparison of terpene biosynthesis in *Alcyonium molle* (Alcyoniidae) and *Heteroxenia* sp. (Xeniidae). *Comp Biochem Physiol B* 99:775–783
29. Ireland C, Scheuer PJ (1979) Photosynthetic marine mollusks: in vivo ^{14}C incorporation into metabolites of the sacoglossan *Placobranchius ocellatus*. *Science* 205:922–923
30. Cimino G, De Rosa S, De Stefano S, Sodano G, Villani G (1983) Dorid nudibranch elaborates its own chemical defense. *Science* 219:1237–1238
31. Needham J, Andersen RJ, Kelly MT (1992) Biosynthesis of oncorhyncholide, a metabolite of the seawater bacterial isolate MK 157. *J Chem Soc Chem Commun* 18:1367–1369
32. Boland W, Mertes K (1985) Biosynthesis of algal pheromones. A model study with the compositae *Senecio isatideus*. *Eur J Biochem* 147:83–91
33. Stratmann K, Boland W, Muller DG (1992) Pheromones of marine brown algae; a new branch of the eicosanoid metabolism. *Angew Chem Int Ed Engl* 31:1246–1248
34. Karuso P, Scheuer PJ (1989) Biosynthesis of isocyanoterpenes in sponges. *J Org Chem* 54:2092–2095
35. Cimino G, Ghiselin MT (2009) Chemical defense and the evolution of opisthobranch gastropods. California Academy of Sciences, San Francisco
36. Cimino G, Fontana A, Gavagnin M (1999) Marine opisthobranch molluscs: chemistry and ecology in sacoglossans and dorids. *Curr Org Chem* 3:327–372
37. Cimino G, Ciavatta ML, Fontana A, Gavagnin M (2001) Metabolites of marine opisthobranchs: chemistry and biological activity. In: Tringali C (ed) *Bioactive compounds from natural sources*. Taylor and Francis, London
38. Cimino G, De Rosa S, De Stefano S, Morrone R, Sodano G (1985) The chemical defense of nudibranch molluscs: structure, biosynthetic origin and defensive properties of terpenoids from the dorid nudibranch *Dendrodoris grandiflora*. *Tetrahedron* 41:1093–1100
39. Cimino G, De Rosa S, De Stefano S, Sodano G (1985) Observations on the toxicity and metabolic relationships of polygodial, the chemical defense of the nudibranch *Dendrodoris limbata*. *Experientia* 41:1335–1336
40. Cimino G, De Rosa S, De Stefano S, Sodano G (1986) Marine natural products: new results from Mediterranean invertebrates. *Pure Appl Chem* 58:375–386
41. Cimino G, Sodano G (1989) The chemical ecology of Mediterranean opisthobranchs. *Chem Scr* 29:389–394
42. Gustafson K, Andersen RJ, Chen MHM, Clardy J, Hochlowski JE (1984) Terpenoid acid glycerides from the dorid nudibranch *Archidoris montereyensis*. *Tetrahedron Lett* 25:11–14
43. Gustafson K, Andersen RJ (1985) Chemical studies of British Columbia nudibranchs. *Tetrahedron* 41:1101–1108

44. Cimino G, Spinella A, Sodano G (1989) Naturally occurring prostaglandin-1,15-lactones. *Tetrahedron Lett* 30:3589–3592
45. Cimino G, Crispino A, Di Marzo V, Spinella A, Sodano G (1991) Prostaglandin 1,15-lactones of the F series from the nudibranch mollusk *Tethys fimbria*. *J Org Chem* 56:2907–2911
46. Cimino G, Crispino A, Di Marzo V, Sodano G, Spinella A, Villani G (1991) A marine mollusc provides the first example of in vivo storage of prostaglandins: prostaglandin-1,15-lactones. *Experientia* 47:56–60
47. Di Marzo V, Cimino G, Crispino A, Minardi C, Sodano G, Spinella A (1991) A novel multifunctional metabolic pathway in a marine mollusc leads to unprecedented prostaglandin derivatives (prostaglandin-1,15-lactones). *Biochem J* 273:593–600
48. Di Marzo V, Minardi C, Vardaro RR, Mollo E, Cimino G (1992) Prostaglandin F-1,15-lactone fatty acyl esters: a prostaglandin lactone pathway branch developed during the reproduction and early larval stages of a marine mollusk. *Comp Biochem Physiol* 101B:99–104
49. Manker DC, Garson MJ, Faulkner DJ (1988) *De novo* biosynthesis of polypropionate metabolites in the marine pulmonate *Siphonaria denticulata*. *J Chem Soc Chem Commun* 1061–1062
50. Garson MJ, Small CJ, Skelton BW, Thinapong P, White AH (1990) Structural and stereochemical correlations of polypropionate metabolites from marine pulmonates: revision of the relative stereochemistry of pectinatone by X-ray structure analysis. *J Chem Soc Perkin Trans* 1:805–807
51. Needham J, Kelly MT, Ishige M, Andersen RJ (1994) Andrimid and moiramides A-C, metabolites produced in culture by a marine isolate of the bacterium *Pseudomonas fluorescens*: structure elucidation and biosynthesis. *J Org Chem* 59:2058–2063
52. Sitachitta N, Rossi J, Roberts MA, Gerwick WH, Fletcher MD, Willis CL (1998) Biosynthesis of the marine cyanobacterial metabolite barbamide. 1. Origin of the trichloromethyl group. *J Am Chem Soc* 120:7131–7132
53. Chang Z, Sitachitta N, Rossi JV, Roberts MA, Flatt PM, Jia J, Sherman DH, Gerwick WH (2004) Biosynthetic pathway and gene cluster analysis of curacin a, an antitubulin natural product from the tropical marine cyanobacterium *Lyngbya majuscula*. *J Nat Prod* 67:1356–1367
54. Renner MK, Jensen PR, Fenical W (2000) Mangicols: structures and biosynthesis of a new class of sesterterpene polyols from a marine fungus of the genus *Fusarium*. *J Org Chem* 65:4843–4852
55. Kobayashi H, Meguro S, Yoshimoto T, Namikoshi M (2003) Absolute structure, biosynthesis, and anti-microtubule activity of phomopsidin, isolated from a marine-derived fungus *Phomopsis* sp. *Tetrahedron* 59:455–459
56. Massé G, Belt ST, Rowland SJ, Rohmer M (2004) Isoprenoid biosynthesis in the diatoms *Rhizosolenia setigera* (Brightwell) and *Haslea ostrearia* (Simonsen). *Proc Natl Acad Sci USA* 101:4413–4418
57. Massé G, Belt ST, Rowland SJ (2004) Biosynthesis of unusual monocyclic alkenes by the diatom *Rhizosolenia setigera* (Brightwell). *Phytochemistry* 65:1101–1106
58. Pohnert G, Jung V (2003) Intracellular compartmentation in the biosynthesis of caulerpenyne: study on intact macroalgae using stable-isotope-labeled precursors. *Org Lett* 5:5091–5093
59. Brust A, Garson MJ (2003) Advanced precursors in marine biosynthetic study. Part 3: the biosynthesis of dichloroimines in the tropical marine sponge *Stylotella aurantium*. *Tetrahedron Lett* 44:327–330
60. Simpson JS, Brust A, Garson MJ (2004) Biosynthetic pathways to dichloroimines; precursor incorporation studies on terpene metabolites in the tropical marine sponge *Stylotella aurantium*. *Org Biomol Chem* 2:949–956
61. Graziani EI, Andersen RJ, Krug PJ, Faulkner DJ (1996) Stable isotope incorporation evidence for the *de novo* biosynthesis of terpenoid acid glycerides by dorid nudibranchs. *Tetrahedron* 52:6869–6878

62. Fontana A, Tramice A, Cutignano A, d'Ippolito G, Gavagnin M, Cimino G (2003) Terpene biosynthesis in the nudibranch *Doriopsilla areolata*. *J Org Chem* 68:2405–2409
63. Gavagnin M, Mollo E, Castelluccio F, Ghiselin MT, Calado G, Cimino G (2001) Can mollusks biosynthesize typical sponge metabolites? The case of the nudibranch *Doriopsilla areolata*. *Tetrahedron* 57:8913–8916
64. Butler MS, Capon RJ (1993) Beyond polygodial: new drimane sesquiterpene from a Southern marine sponge *Dysidea* sp. *Aust J Chem* 46:1255–1267
65. Fontana A, Tramice A, Cutignano A, d'Ippolito G, Cimino G (2003) Studies on the biogenesis of verrucosins, toxic diterpenoid glycerides of the Mediterranean mollusc *Doris verrucosa*. *Eur J Org Chem* 16:2104–2108
66. Giner JL (1993) Biosynthesis of marine sterol side chains. *Chem Rev* 93:1735–1752
67. De Luca P, De Rosa M, Minale L, Sodano G (1972) Marine sterols with a new pattern of side-chain alkylation from the sponge *Aplysina*(=*Verongia*) *aerophoba*. *J Chem Soc Perkin Trans 1*:2132–2135
68. Fattorusso E, Magno S, Mayol L, Santacroce C, Sica D (1975) Calysterol: a C₂₉ cyclopropene-containing marine sterol from the sponge *Calyx nicaensis*. *Tetrahedron* 31:1715–1716
69. Minale L, Sodano G (1974) Marine sterols: unique 3 β -hydroxymethyl-A-nor-5 α -steranes from the sponge *Axinella verrucosa*. *J Chem Soc Perkin Trans 1*:2380–2384
70. Minale L, Sodano G (1974) Marine sterols: 19-nor-stanol from the sponge *Axinella polypoides*. *J Chem Soc Perkin Trans 1*:1888–1892
71. De Rosa M, Minale L, Sodano G (1975) Metabolism in Porifera-V. Biosynthesis of 19-nor-stanols: conversion of cholesterol into 19-nor-cholestanols by the sponge *Axinella polypoides*. *Experientia* 31:758–759
72. Djerassi C, Silva CJ (1991) Biosynthetic studies of marine lipids. 41 Sponge sterols: origin and biosynthesis. *Acc Chem Res* 24:371–378
73. Cafieri F, Fattorusso E, Magno S, Santacroce C, Sica D (1973) Isolation and structure of axisonitrile-1 and axisothiocyane-1 two unusual sesquiterpenoids from the marine sponge *Axinella cannabina*. *Tetrahedron* 29:4259–4262
74. Di Blasio B, Fattorusso E, Magno S, Mayol L, Pedone C, Santacroce C, Sica D (1976) Axisonitrile-3, axisothiocyane-3 and axamide-3. Sesquiterpenes with a novel spiro[4,5] decane skeleton from the sponge *Axinella cannabina*. *Tetrahedron* 32:473–478
75. Dumdei J, Flowers AE, Garson MJ, Moore CJ (1997) The biosynthesis of sesquiterpene isocyanides and isothiocyantes in the marine sponge *Acanthella cavernosa* (Dendy); Evidence for dietary transfer to the dorid nudibranch *Phyllidiella pustulosa*. *Comp Biochem Physiol A Physiol* 118:1385–1392
76. Simpson JS, Garson MJ (2004) Biosynthetic pathways to isocyanides and isothiocyantes; precursor incorporation studies on terpene metabolites in the tropical marine sponges *Amphimedon terpenensis* and *Axinyssa* n.sp. *Org Biomol Chem* 2:939–948
77. Karuso P (1987) Chemical ecology of the nudibranchs. In: Scheuer PJ (ed) *Bioorganic marine chemistry*, vol 1. Springer, Berlin
78. Cimino G, Sodano G (1994) Transfer of sponge secondary metabolites to predators. In: Van Soest RWM, Van Kempen TMG, Braekman JC (eds) *Sponges in time and space: biology, chemistry, paleontology*. AA Balkema, Rotterdam
79. Fenical W, Sleeper HL, Paul VJ, Stallard MO, Sun HH (1979) Defensive chemistry of *Navanax* and related opisthobranch molluscs. *Pure Appl Chem* 51:1865–1874
80. Porcelli M, Cacciapuoti G, Zappia V, Cimino G, Gavagnin M, Sodano G (1989) Biosynthesis and metabolism of 9-[5'-deoxy-(methylthio)- β -D-xylofuranosyl] adenine, a novel natural analog of methylthioadenosine. *Biochem J* 263:635–640
81. Cutignano A, Tramice A, De Caro S, Villani G, Cimino G, Fontana A (2003) Biogenesis of 3-alkylpyridine alkaloids in the marine mollusc *Haminoea orbignyana*. *Angew Chem Int Ed* 42:2633–2636

82. Cutignano A, Cimino G, Giordano A, d'Ippolito G, Fontana A (2004) Polyketide origin of 3-alkylpyridines in the marine mollusc *Haminoea orbignyana*. *Tetrahedron Lett* 45:2627–2629
83. Graziani EI, Andersen RJ (1996) Investigations of sesquiterpenoid biosynthesis by the dorid nudibranch *Acanthodoris nanaimoensis*. *J Am Chem Soc* 118:4701–4702
84. Fontana A, Villani G, Cimino G (2000) Terpene biosynthesis in marine molluscs: incorporation of glucose in drimane esters of *Dendrodoris nudibranchs* via classical mevalonate pathway. *Tetrahedron Lett* 41:2429–2433
85. Garson MJ, Dexter AF, Lambert LK, Liokas V (1992) Isolation of the bioactive terpene 7-deacetoxyolepupane from the temperate marine sponge *Dysidea* sp. *J Nat Prod* 55:364–367
86. Moghaddam MF, Gerwick WH (1991) Cell-Free biosynthesis and source of hydroxyl groups in (12*R*,13*S*)-dihydroxy-(5*Z*,8*Z*,10*E*,14*Z*)-eicosatetraenoic acid, a novel eicosanoid from the marine alga *Gracilariopsis lemaneiformis*. *J Nat Prod* 54:1619–1624
87. Gerwick WH, Moghaddam MF, Hamberg M (1991) Oxylipin metabolism in the red alga *Gracilariopsis lemaneiformis*: mechanism of formation of vicinal dihydroxy fatty acids. *Arch Biochem Biophys* 290:436–444
88. Xiang L, Kalaitzis JA, Moore BS (2004) EncM, a versatile enterocin biosynthetic enzyme involved in Favorskii oxidative rearrangement, aldol condensation, and heterocycle-forming reactions. *Proc Natl Acad Sci USA* 101:15609–15614
89. Beer LL, Moore BS (2007) Biosynthetic convergence of salinosporamides a and B in the marine actinomycete *Salinispora tropica*. *Org Lett* 9:845–848
90. Liu Y, Hazzard C, Eustáquio AS, Reynolds KA, Moore BS (2009) Biosynthesis of salinosporamides from α , β -unsaturated fatty acids: implications for extending polyketide synthase diversity. *J Am Chem Soc* 131:10376–10377
91. Eustáquio AS, McGlinchey RP, Liu Y, Hazzard C, Beer LL, Florova G, Alhamadsheh MM, Lechner A, Kale AJ, Kobayashi Y, Reynolds KA, Moore BS (2009) Biosynthesis of the salinosporamide A polyketide synthase substrate chloroethylmalonyl-coenzyme A from S-adenosyl-L-methionine. *Proc Natl Acad Sci USA* 106:12295–12300
92. Feling RH, Buchanan GO, Mincer TJ, Kauffman CA, Jensen PR, Fenical W (2003) Salinosporamide a: a highly cytotoxic proteasome inhibitor from a novel microbial source, a marine bacterium of the new genus *Salinispora*. *Angew Chem Int Ed* 42:355–357
93. Williams PG, Buchanan GO, Feling RH, Kauffman CA, Jensen PR, Fenical W (2005) New cytotoxic salinosporamides from the marine actinomycete *Salinispora tropica*. *J Org Chem* 70:6196–6203
94. Reed KA, Manam RR, Mitchell SS, Xu J, Teisan S, Chao TH, Deyanat-Yazdi G, Neuteboom STC, Lam KS, Potts BCM (2007) Salinosporamides D–J from the marine actinomycete *Salinispora tropica*, bromosalinosporamide, and thioester derivatives are potent inhibitors of the 20S proteasome. *J Nat Prod* 70:269–276
95. Stadler M, Bitzer J, Mayer-Bartschmid A, Müller H, Benet-Buchholz J, Gantner F, Tichy HV, Reinemer P, Bacon KB (2007) Cinnabaramides a–G: analogues of lactacystin and salinosporamide from a terrestrial streptomycete. *J Nat Prod* 70:246–252
96. Miljkovic A, Mantle PG, Williams DJ, Rassing B (2001) Scorpionone: a new natural azaanthraquinone produced by a *Bispora*-like tropical fungus. *J Nat Prod* 64:1251–1253
97. Mantle PG, Hawksworth DL, Pazoutova S, Collinson LM, Rassing BR (2006) *Amorosia littoralis* gen. sp. nov., a new genus and species name for the scorpionone and caffeine-producing hyphomycete from the littoral zone in the Bahamas. *Mycol Res* 110:1371–1378
98. Van Wagoner RM, Mantle PG, Wright JLC (2008) Biosynthesis of scorpionone, a 2-azaanthraquinone from *Amorosia littoralis*, a fungus from marine sediment. *J Nat Prod* 71:426–430
99. Kadkol MV, Gopalkrishnan KS, Narasimhachari N (1971) Isolation and characterization of naphthaquinone pigments from *Torula herbarum* (pers.) herbarin and dehydroherbarin. *J Antibiot* 24:245–248

100. Parisot D, Devys M, Barbier M (1989) Conversion of anhydrofusarubin lactol into the antibiotic bostrycoidin. *J Antibiot* 42:1189–1190
101. Du L, Zhu T, Fang Y, Liu H, Gu Q, Zhu W (2007) Aspergiolide A, a novel anthraquinone derivative with naphtho[1,2,3-*de*]chromene-2,7-dione skeleton isolated from a marine-derived fungus *Aspergillus glaucus*. *Tetrahedron* 63:1085–1088
102. Tao K, Du L, Sun X, Cai M, Zhu T, Zhou X, Gu Q, Zhang Y (2009) Biosynthesis of aspergiolide A, a novel antitumor compound by a marine-derived fungus *Aspergillus glaucus* via the polyketide pathway. *Tetrahedron Lett* 50:1082–1085
103. Anke H, Kolthoum I, Zähler H, Laatsch H (1980) Metabolic products of microorganisms. 185. The anthraquinones of the *Aspergillus glaucus* group. 1. Occurrence, isolation, identification and antimicrobial activity. *Arch Microbiol* 126:223–230
104. Lund ED, Chu FLE, Littreal PR, Ruck KE, Harvey E (2009) An investigation of the mechanisms for sterol synthesis and dietary sterol bioconversion in the heterotrophic protists *Oxyrrhis marina* and *Gyrodinium dominans*. *J Exp Mar Biol Ecol* 374:150–159
105. Stratmann K, Boland W, Müller DG (1993) Biosynthesis of pheromones in female gametes of marine brown algae (phaeophyceae). *Tetrahedron* 49:3755–3766
106. Rui F, Boland W (2010) Algal pheromone biosynthesis: stereochemical analysis and mechanistic implications in gametes of *Ectocarpus siliculosus*. *J Org Chem* 75:3958–3964
107. Ponhert G, Boland W (1997) Pericyclic reactions in nature: synthesis and cope rearrangement of thermolabile bis-alkenylcyclopropanes from female gametes of marine brown algae (phaeophyceae). *Tetrahedron* 53:13681–13694
108. Cimino G, Spinella A, Sodano G (1989) Potential alarm pheromones from the Mediterranean opisthobranch *Scaphander lignarius*. *Tetrahedron Lett* 30:5003–5004
109. Della Sala G, Cutignano A, Fontana A, Spinella A, Calabrese G, Domenech-Coll A, d'Ippolito G, Della Monica C, Cimino G (2007) Towards the biosynthesis of the aromatic products of the Mediterranean mollusc *Scaphander lignarius*: isolation and synthesis of analogues of lignarenones. *Tetrahedron* 63:7256–7263
110. Cutignano A, Avila C, Domenech-Coll A, d'Ippolito G, Cimino G, Fontana A (2008) First biosynthetic evidence on the phenyl-containing polyketides of the marine mollusc *Scaphander lignarius*. *Org Lett* 10:2963–2966
111. Fontana A, unpublished data.
112. Schultz AW, Oh DC, Carney JR, Williamson RT, Udworthy DW, Jensen PR, Gould SJ, Fenical W, Moore BS (2008) Biosynthesis and structures of cyclomarins and cyclomarazines, prenylated cyclic peptides of marine actinobacterial origin. *J Am Chem Soc* 130:4507–4516
113. Renner MK, Shen YC, Cheng XC, Jensen PR, Frankmoelle W, Kauffman CA, Fenical W, Lobkovsky E, Clardy J (1999) Cyclomarins A – C, new antiinflammatory cyclic peptides produced by a marine bacterium (*Streptomyces* sp.). *J Am Chem Soc* 121:11273–11276
114. Jensen PR, Williams PG, Oh DC, Zeigler L, Fenical W (2007) Species-specific secondary metabolite production in marine actinomycetes of the genus *Salinispora*. *Appl Environ Microbiol* 73:1146–1152
115. Gontang EA, Fenical W, Jensen PR (2007) Phylogenetic diversity of Gram-positive bacteria cultured from marine sediments. *Appl Environ Microbiol* 73:3272–3282
116. Fenical W, Jensen PR (2006) Developing a new resource for drug discovery: marine actinomycete bacteria. *Nat Chem Biol* 2:666–673
117. Kellmann R, Stüken A, Orr RJS, Svendsen HM, Jakobsen KS (2010) Biosynthesis and molecular genetics of polyketides in marine dinoflagellates. *Mar Drugs* 8:1011–1048
118. Hallegraeff GM, Anderson DM, Cembella AD (2003) Manual on harmful marine microalgae, 2nd edn. UNESCO, Paris
119. Shimizu Y (1996) Microalgal metabolites: a new perspective. *Ann Rev Microbiol* 50:431–465
120. Kellmann R, Neilan BA (2007) Biochemical characterization of paralytic shellfish toxin biosynthesis in vitro. *J Phycol* 43:497–508

121. Kellmann R, Mihali TK, Jeon YJ, Pickford R, Pomati F, Neilan BA (2008) Biosynthetic intermediate analysis and functional homology reveal a saxitoxin gene cluster in cyanobacteria. *Appl Environ Microbiol* 74:4044–4053
122. Piel J (2004) Metabolites from symbiotic bacteria. *Nat Prod Rep* 21:519–538
123. Bewley CA, Faulkner DJ (1998) Lithistid sponges: star performers or hosts to the stars. *Angew Chem Int Ed* 37:2162–2178
124. Li Z (2009) Advances in marine microbial symbionts in the China Sea and related pharmaceutical metabolites. *Mar Drugs* 7:113–129
125. Look SA, Fenical W, Matsumoto GK, Clardy J (1986) The pseudopterosins: a new class of antiinflammatory and analgesic diterpene pentosides from the marine sea whip *Pseudoptergorgia elisabethae* (Octocorallia). *J Org Chem* 51:5140–5145
126. Look SA, Fenical W (1987) The seco-pseudopterosins, new anti-inflammatory diterpene-glycosides from a Caribbean gorgonian octocoral of the genus *Pseudoptergorgia*. *Tetrahedron* 43:3363–3370
127. Mydlarz LD, Jacobs RS, Boehnlein J, Kerr RG (2003) Pseudopterosin biosynthesis in *Symbiodinium* sp., the dinoflagellate symbiont of *Pseudoptergorgia elisabethae*. *Chem Biol* 10:1051–1056
128. Coleman AC, Kerr RG (2000) Radioactivity-guided isolation and characterization of the bicyclic pseudopterosin diterpene cyclase product from *Pseudoptergorgia elisabethae*. *Tetrahedron* 56:9569–9574
129. Kohl AC, Kerr RG (2004) Identification and characterization of the pseudopterosin diterpene cyclase, elisabethatriene synthase, from the marine gorgonian, *Pseudoptergorgia elisabethae*. *Arch Biochem Biophys* 424:97–104
130. Ferns TA, Kerr RG (2005) Oxidations of erogorgiaene in pseudopterosin biosynthesis. *Tetrahedron* 61:12358–12365
131. Ferns TA, Kerr RG (2005) Identification of amphilectosins as key intermediates in pseudopterosin biosynthesis. *J Org Chem* 70:6152–6157
132. Kerr RG, Kohl AC, Ferns TA (2006) Elucidation of the biosynthetic origin of the anti-inflammatory pseudopterosins. *J Ind Microbial Biotechnol* 33:532–538
133. Blunt JW, Copp BR, Hu WP, Munro MHG, Northcote PT, Prinsep MR (2011) Marine natural products. *Nat Prod Rep* 28:196–268
134. Piel J, Hui D, Wen G, Butzke D, Platzer M, Fusetani N, Matsunaga S (2004) Antitumor polyketide biosynthesis by an uncultivated bacterial symbiont of the marine sponge *Theonella swinhoei*. *Proc Natl Acad Sci USA* 101:16222–16227
135. Schirmer A, Gadkari R, Reeves CD, Ibrahim F, DeLong EF, Hutchinson CR (2005) Metagenomic analysis reveals diverse polyketide synthase gene clusters in microorganisms associated with the marine sponge *Discodermia dissoluta*. *Appl Environ Microbiol* 71:4840–4849
136. Kennedy J, Marchesi JR, Dobson ADW (2007) Metagenomic approaches to exploit the biotechnological potential of the microbial consortia of marine sponges. *Appl Microbiol Biotechnol* 75:11–20
137. Kennedy J, Flemer B, Jackson SA, Lejon DPH, Morrissey JP, O’Gara F, Dobson ADW (2010) Marine metagenomics: new tools for the study and exploitation of marine microbial metabolism. *Mar Drugs* 8:608–628
138. Hamann MT, Roggo S, Hill RT (2007) Marine natural products. Key advances to the practical application of this resource in drug development. *CHIMIA* 61:313–321
139. Kasanah NK, Rao KV, Yousaf M, Wedge DE, Hill RT, Hamann MT (2004) Biotransformation studies of the manzamine alkaloid. *Mar Biotechnol* 6:S268–S272
140. Thomas TRA, Kavlekar DP, LokaBharathi PA (2010) Marine drugs from sponge-microbe association – A review. *Mar Drugs* 8:1417–1468
141. Newman DJ, Hill RT (2006) New drugs from marine microbes: the tide is turning. *J Ind Microbiol Biotechnol* 33:539–5418

142. Simpson TJ (1998) Application of isotopic methods to secondary metabolic pathways. In: Leeper FJ, Vederas JC (eds) Biosynthesis. Polyketides and vitamins. Springer, Berlin
143. Rohmer M (1999) The discovery of a mevalonate-independent pathway for isoprenoid biosynthesis in bacteria, algae and higher plants. *Nat Prod Rep* 13:565–574
144. Dewick PM (2002) The biosynthesis of C₅-C₂₅ terpenoid compounds. *Nat Prod Rep* 16:97–130
145. Wendel T, Jüttner F (1996) LOX-mediated formation of hydrocarbons and unsaturated aldehydes in freshwater diatoms. *Phytochemistry* 41:1445–1449
146. d'Ippolito G, Cutignano A, Briante R, Febbraio F, Cimino G, Fontana A (2005) New C₁₆ fatty-acid-based oxylipin pathway in the marine diatom *Thalassiosira rotula*. *Org Biomol Chem* 3:4065–4070
147. Fontana A, d'Ippolito G, Cutignano A, Romano G, Lamari N, Massa Gallucci A, Cimino G, Miralto A, Ianora A (2007) LOX-induced lipid peroxidation as mechanism responsible for the detrimental effect of marine diatoms on zooplankton grazers. *Chembiochem* 8:1810–1818
148. Fontana A, d'Ippolito G, Cutignano A et al (2007) Oxylipin pathways in marine diatoms: a look at the chemical aspects. *Pur Appl Chem* 79:481–490
149. d'Ippolito G, Lamari L, Montresor M (2009) 15S-Lipoxygenase metabolism in the marine diatom *Pseudonitzschia delicatissima*. *New Phytol* 183:1064–1071
150. Wichard T, Poulet S, Pohnert G (2005) Determination and quantification of α , β , γ , δ -unsaturated aldehydes as pentafluorobenzyl-oxime derivatives in diatom cultures and natural phytoplankton populations: application in marine field studies. *J Chromatogr B* 814:155–161
151. Bouarab K, Adas F, Gaquerel E, Kloreg B, Salaün JP, Potin P (2004) The innate immunity of a marine red alga involves oxylipins from both the eicosanoid and octadecanoid pathways. *Plant Physiol* 135:1838–1848
152. Feussner I, Wasternack C (2002) The LOX pathway. *Annu Rev Plant Biol* 53:275–297
153. Blée E (2002) Impact of phyto-oxylipins in plant defense. *Trends Plant Sci* 7:315–321
154. Howe GA, Schilmiller AL (2002) Oxylipin metabolism in response to stress. *Curr Opin Plant Biol* 5:230–236
155. Gerwick WH, Roberts MA, Vulpanovici A (1999) Biogenesis and biological function of marine algal oxylipins. *Adv Exp Med Biol* 447:211–218
156. Pohnert G, Boland W (2002) The oxylipin chemistry of attraction and defense in brown algae and diatoms. *Nat Prod Rep* 19:108–122
157. Guschina IA, Harwood JL (2006) Lipids and lipid metabolism in eukaryotic algae. *Prog Lipid Res* 45:160–186
158. Potin P (2008) Oxidative burst and related responses in biotic interactions of algae. In: Amsler CD (ed) *Algal chemical ecology*. Springer, Berlin, pp 245–271
159. Weinberger F (2007) Pathogen-induced defense and innate immunity in macroalgae. *Biol Bull* 213:290–302
160. Ianora A, Miralto A (2010) Toxicogenic effects of diatoms on grazers, phytoplankton and other microbes: a review. *Ecotoxicol* 19:493–511
161. Bowler CP, Vardi A, Allen A (2009) Oceanographic and biogeochemical insights from diatom genomes. *Ann Rev Mar Sci* 2:333–365
162. Ribalet F, Wichard T, Pohnert G, Ianora A, Miralto A, Casotti R (2007) Age and nutrient limitation enhance polyunsaturated aldehyde production in marine diatoms. *Phytochemistry* 68:2059–2067
163. Andreou A, Brodhun F, Feussner I (2009) Biosynthesis of oxylipins in non-mammals. *Prog Lipid Res* 48:148–170
164. d'Ippolito G, Romano T, Caruso T, Spinella A, Cimino G, Fontana A (2003) Production of octadienal in the marine diatom *Skeletonema costatum*. *Org Lett* 5:885–887
165. Pohnert G, Adolph S, Wichard T (2004) Short synthesis of labeled and unlabeled 6Z,9Z,12Z,15-hexadecatetraenoic acid as metabolic probes for biosynthetic studies on diatoms. *Chem Phys Lipids* 131:159–166

166. d'Ippolito G, Cutignano A, Tucci S, Romano G, Cimino G, Fontana A (2006) Biosynthetic intermediates and stereochemical aspects of the aldehyde biosynthesis in the marine diatom *Thalassiosira rotula*. *Phytochemistry* 67:314–322
167. Barofsky A, Pohnert G (2007) Biosynthesis of polyunsaturated short chain aldehydes in the diatom *Thalassiosira rotula*. *Org Lett* 9:1017–1020
168. Wichard T, Pohnert G (2006) Formation of halogenated medium chain hydrocarbons by a lipooxygenase/hydroperoxide halolyase-mediated transformation in planktonic microalgae. *J Am Chem Soc* 128:7114–7115
169. d'Ippolito G, Cutignano A, Tucci S, Romano G, Cimino G, Miralto A, Fontana A (2004) The role of complex lipids in the synthesis of bioactive aldehydes of the marine diatom *Skeletonema costatum*. *Biochim Biophys Acta* 1686:100–107
170. Cutignano A, d'Ippolito G, Romano G, Lamari N, Cimino G, Febbraio F, Nucci R, Fontana A (2006) Chloroplastic galactolipids fuel the aldehyde biosynthesis in the marine diatom *Thalassiosira rotula*. *Chembiochem* 7:450–456
171. Staunton J, Weissman KJ (2001) Polyketide biosynthesis: a millennium review. *Nat Prod Rep* 18:380–416
172. Trench RK, Greene RW, Bystrom BG (1969) Chloroplasts as functional organelles in animal tissues. *J Cell Biol* 42:404–417
173. Green BJ, Li WY, Manhart JR, Fox TC, Summer EJ, Kennedy RA, Pierce SK, Rumpho ME (2000) Mollusc-algal chloroplast endosymbiosis. Photosynthesis, thylakoid protein maintenance, and chloroplast gene expression continue for many months in the absence of the algal nucleus. *Plant Physiol* 124:331–342
174. Pierce SK, Massey SE, Hanten JH, Curtis NE (2003) Horizontal transfer of functional nuclear genes between multicellular organisms. *Biol Bull* 204:237–240
175. Gavagnin M, Marin A, Mollo E, Crispino A, Villani G, Cimino G (1994) Secondary metabolites from Mediterranean Elysioidea: origin and biological role. *Comp Biochem Physiol* 108B:107–115
176. Cutignano A, Cimino G, Villani G, Fontana A (2009) Shaping the polypropionate biosynthesis in the solar powered mollusc *Elysia viridis*. *Chembiochem* 10:315–322
177. Muller M, He J, Hertweck C (2006) Dissection of the late steps in aureothin biosynthesis. *Chembiochem* 7:37–39
178. Fontana A (2006) Biogenetic proposals and biosynthetic studies on secondary metabolites of opisthobranch molluscs. In: Cimino G, Gavagnin M (eds) *Molluscs: from chemo-ecological study to biotechnological application*, vol 43, *Progress in molecular and subcellular biology*, subseries marine molecular biotechnology. Springer, Berlin
179. Manzo E, Ciavatta ML, Gavagnin M, Mollo E, Wahidulla S, Cimino G (2005) New gamma-pyrone propionates from the Indian ocean sacoglossan *Placobranchus ocellatus*. *Tetrahedron Lett* 46:465–468
180. Cueto M, D'Croz L, Matè JL, San-Martín A, Darias J (2005) Elysiapyrones from *Elysia diomedea*. Do such metabolites evidence an enzymatically assisted electrocyclization cascade for the biosynthesis of their bicyclo [18.2.0]octane core? *Org Lett* 7:415–418
181. Miller AK, Trauner D (2005) Mining the tetraene manifold: total synthesis of complex pyrones from *Placobranchus ocellatus*. *Angew Chem Int Ed* 44:4602–4606
182. Miller AK, Trauner D (2006) Mapping the chemistry of highly unsaturated pyrone polyketides. *Synlett* 14:2295–2316
183. Eade SJ, Walter MW, Byrne C, Odell B, Rodriguez R, Baldwin J, Adlington RM, Moses JE (2008) Biomimetic studies of pyrone-derived natural products: exploring chemical pathways from a unique polyketide precursor. *J Org Chem* 73(13):4830–4839
184. Brückner S, Baldwin JE, Moses J, Adlington RM, Cowley AR (2003) Mechanistic evidence supporting the biosynthesis of photodeoxytridachione. *Tetrahedron Lett* 44:7471–7473
185. Zuidema DR, Miller AK, Trauner D, Jones PB (2005) Photosynthesized conversion of 9,10-deoxytridachione to photodeoxytridachione. *Org Lett* 7:4959–4962

186. Diaz-Marrero A, Cueto M, D'Croz L, Darias J (2008) Validating an endoperoxide as a key intermediate in the biosynthesis of elysiapyrones. *Org Lett* 10:3057–3060
187. Ireland C, Faulkner DJ (1981) The metabolites of the marine molluscs *Tridachia diomedea* and *Tridachia crispata*. *Tetrahedron* 37:233–240
188. Demming-Adams B, Gilmore AM, Adams WW (1996) In vitro function of carotenoids in higher plants. *FASEB* 10:403–412
189. Di Marzo V, Vardaro RR, De Petrocellis L, Villani G, Minei R, Cimino G (1991) Cyercenes, novel pyrones from the sacoglossan mollusc *Cyerce cristallina*. Tissue distribution, biosynthesis and possible involvement in defense and regenerative processes. *Experientia* 47:1221–1227
190. Vardaro RR, Di Marzo V, Crispino A, Cimino G (1991) Cyercenes, novel polypropionates pyrones from the autotomizing Mediterranean mollusc *Cyerce cristallina*. *Tetrahedron* 47:5569–5576
191. Vardaro RR, Di Marzo V, Marin A, Cimino G (1992) α - and γ -Pyrone-polypropionates from the Mediterranean ascoglossan mollusc *Ercolania funerea*. *Tetrahedron* 48:9561–9566
192. Zuidema DR, Jones PB (2006) Triplet photosensitization in cyercene A and related pyrones. *J Photochem Photobiol B* 83:137–145
193. Zuidema DR, Jones PB (2005) Photochemical relationships in sacoglossan polypropionates. *J Nat Prod* 68:481–486
194. Larsen TO, Perry NB, Andersen B (2003) Infectopyrone, a potential mycotoxin from *Alternaria infectoria*. *Tetrahedron Lett* 44:4511–4513
195. Proksch P, Ebel R, Edrada RA, Riebe F, Liu H, Diesel A, Bayer M, Li X, Lin WH, Grebenyuk V, Mueller WEG, Draeger S, Zuccaro AA, Schulz B (2008) Sponge-associated fungi and their bioactive compounds: the *Suberites* case. *Bot Mar* 51:209–218
196. Nair MSR, Carey ST (1975) Metabolites of *Pyrenomyces*. II: nectriapyrone, an antibiotic monoterpenoid. *Tetrahedron Lett* 19:1655–1658
197. Debbab A, Aly AH, Edrada-Ebel R, Wray V, Müller WEG, Totzke F, Zirrgebel U, Schächtele C, Kubbutat MHG, Lin WH, Mosaddak M, Hakiki A, Proksch P, Ebel R (2009) Bioactive metabolites from the endophytic fungus *Stemphylium globuliferum* isolated from *Mentha pulegium*. *J Nat Prod* 72:626–631
198. Pedras MSC, Chumala PB (2005) Phomapyrones from blackleg causing phytopathogenic fungi: isolation, structure determination, biosyntheses and biological activity. *Phytochemistry* 66:81–87
199. Cutignano A, Cimino G, Villani G, Fontana A (2009) Origin of C₃-unit in placidenes: further insights into taxa divergence of polypropionate biosynthesis in marine molluscs and fungi. *Tetrahedron* 65:8161–8164
200. Molinski TF, Dalisay DF, Lievens SL, Saludes JP (2009) Drug development from marine natural products. *Nat Rev Drug Discov* 8:69–85
201. Jones AC, Gu L, Sorrels CM, Sherman DH, Gerwick WL (2009) New tricks from ancient algae: natural products biosynthesis in marine cyanobacteria. *Curr Opin Chem Biol* 13:216–223
202. Rein KS, Snyder RV (2006) The biosynthesis of polyketide metabolites by dinoflagellates. *Adv Appl Microbiol* 59:93–125

David H. Sherman, Christopher M. Rath, Jon Mortison,
Jamie B. Scaglione, and Jeffrey D. Kittendorf

Contents

18.1	Introduction	948
18.1.1	Function of Polyketide Synthases and Nonribosomal Peptide Synthetases ..	950
18.2	Examples	953
18.2.1	Curacin	953
18.2.2	Cryptophycin/Arenastatin	956
18.3	Trans AT Domain Pathways – A Rich Source of Unusual Biochemistry	958
18.3.1	Trans AT Hybrid PKS/NRPS Systems: An Introduction	958
18.3.2	Known Trans AT Hybrid PK/NRP Pathways	959
18.3.3	Biological Activity and Structure of Trans AT Hybrid PK/NRPs	961
18.3.4	In Vivo Analysis of <i>Trans</i> AT Hybrid PK/NRP Systems	961
18.3.5	In Vitro Characterization of Trans AT Hybrid PKS/NRPS Pathways	964
18.3.6	Evolution, Biology, and Symbiosis of Trans AT Hybrid PKS/NRPS Systems	964
18.3.7	Onnamide/Pederin	965
18.3.8	Evolution, Biology, and Symbiosis of Trans AT Hybrid PKS/NRPS Systems	967
18.4	Technologies	968
18.4.1	DNA Sequencing Strategies in Hybrid PK/NRP Systems	968
18.4.2	Mass Spectrometry in Hybrid PK/NRP Systems	969
18.4.3	Structural Biology in PKS/NRPS Systems	971
18.5	Summary	971
	References	972

Abstract

Marine natural products are emerging as important sources of new drugs for human health concerns. By understanding the fascinating enzymatic assembly

D.H. Sherman (✉) • C.M. Rath • J. Mortison •

J.B. Scaglione • J.D. Kittendorf

Life Sciences Institute and Department of Medicinal Chemistry, University of Michigan, 210

Washtenaw Ave, Ann Arbor, MI, USA

e-mail: davidhs@umich.edu

lines that generate these molecules, we gain deeper insight into the common mechanisms behind the diversity in structure and biological functions observed in these compounds. Indeed, a better understanding of these pathways could allow improved access to the drugs through heterologous expression or through the use of enzymes as biocatalysts. The mixed nonribosomal peptide synthase/polyketide synthase biosynthetic pathways for the natural products curacin and cryptophycin are explored as case studies in enzymatic diversity. The expanding class of atypical *trans* AT natural products is also discussed. Emerging tools for characterizing these enzymes are also explored.

18.1 Introduction

Natural products have proved to be an exceptionally rich source of small molecule ligands for discovery and analysis of diverse molecular targets relating to human disease. From 1940 to 2006, 47% of approved anticancer therapeutics were natural products or natural product-derived chemical entities [1]. Between 2005 and 2007, 13 natural product, natural product-derived, or semisynthetic drugs have been launched [2]. Natural products may well enjoy a resurgence in drug discovery and development efforts as recent advances such as the ability to engineer and heterologously express biosynthetic pathways may provide effective solutions to current challenges including adequate natural product supplies, improved cost of goods, and effective analogue development.

A significant number of marine natural products contain pharmacological activities that are beneficial to human health. Although there are many examples of terrestrial-derived natural product compounds that are in clinical use, including antibacterial penicillins, cephalosporins, immunosuppressive cyclosporin A, and the cholesterol-lowering HMG-CoA reductase inhibitors best known as the “statins” [3], secondary metabolites from the marine environment are just starting to reach the clinic. These molecules, which have achieved their (largely unknown) endogenous functions over the course of millions of years of evolution, offer chemical scaffolds for development of new analogues with improved or altered biological activity (Fig. 18.1). New bioactive analogues that contain novel structural elements may be generated by both semisynthesis and total synthesis efforts [4, 5].

Indeed, the synthases that produce nonribosomal peptide (NRP) and polyketide (PK) natural products are equally interesting in terms of their application in natural product fermentation and as biocatalysts. The number of natural products that function in biological systems is large but represents only a small fraction of the total possible number of small carbon-based compounds, indicating the importance of stereochemistry and functional groups in natural product functions [6]. Modern synthetic chemistry has encountered significant challenges in preparation of complex, high molecular weight natural products containing a great number of reactive groups and stereocenters for the generation of drug leads in the pharmaceutical industry. Incorporating the use of biocatalysts during natural product synthesis represents a promising strategy for the production of compounds that are a key

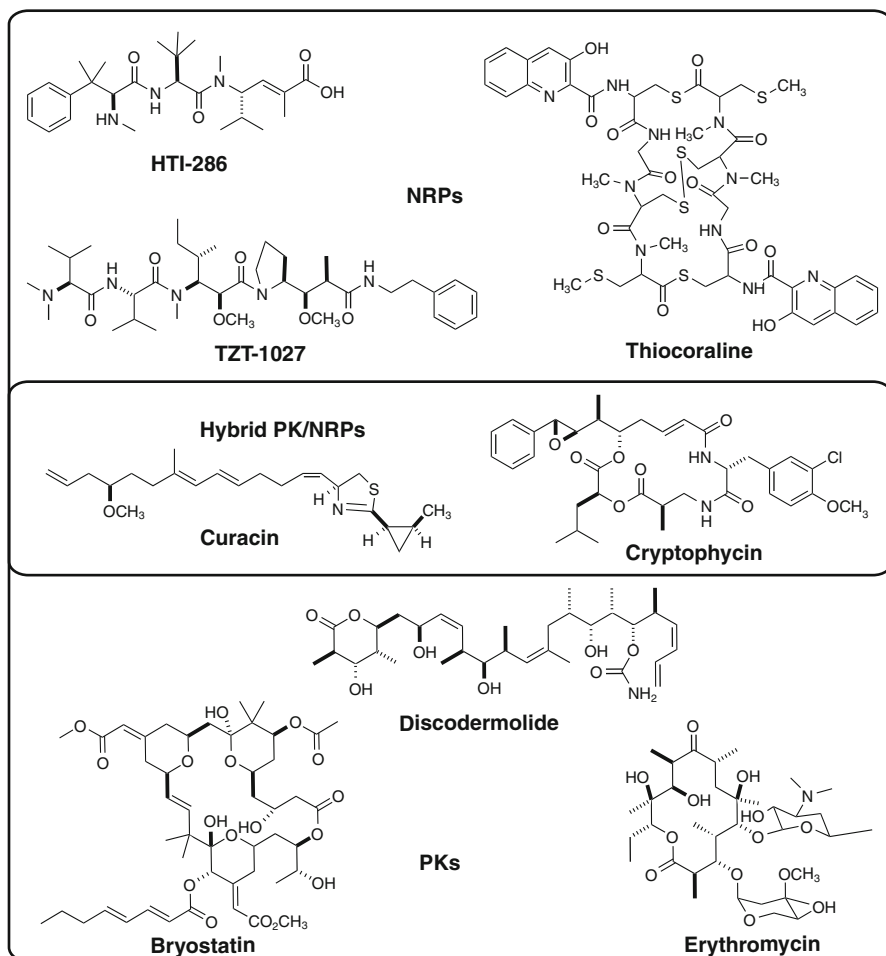


Fig. 18.1 Examples of nonribosomal peptide (NRP), polyketide (PK), and hybrid (PK/NRP) natural products

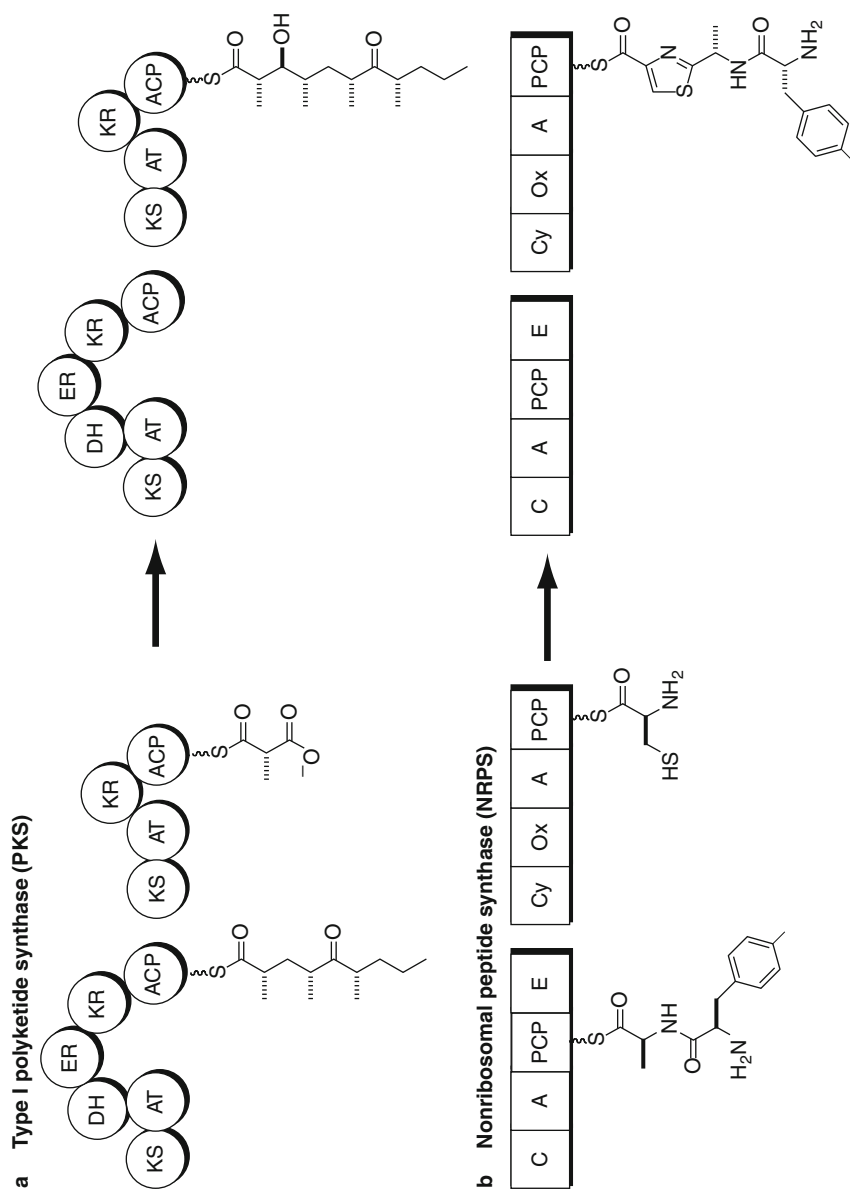
element in pharmaceutical discovery and development efforts [7, 8]. Although enzymes residing in living cells have been extensively used as biocatalysts in the food and beverage industry, isolated enzymes are playing increasingly critical roles in performing chemical transformations on organic compounds for pharmaceutical development [9–12]. Often, these remarkable catalysts are able to perform a wide array of reactions on structurally diverse compounds. Furthermore, enzymes can also selectively catalyze reactions with chiral (enantio-) and positional (regio-) selectivities [12]. With these advantages, enzymes are applied in organic synthesis to avoid tedious protection and deprotection steps commonly required for enantio- and regioselective synthesis. The inherent selectivity of enzymes generates few by-products and provides an environmentally friendly alternative to chemical

catalysts. Enzymes used in organic synthesis include acyl transferases (e.g., lipases, esterases, peptidases, amidases, and acylases), carbohydrate-processing enzymes (e.g., glycosidases, glycosyltransferases), hydrolytic enzymes (e.g., nitrilases, nitrile hydratases), reductases, oxidases and oxygenases, aldolases, and oxynitrilases [9].

18.1.1 Function of Polyketide Synthases and Nonribosomal Peptide Synthetases

Polyketides (PKs), nonribosomal peptides (NRPs), and PK/RP or NRP/PK hybrids represent three large subclasses of highly diverse natural products with various bioactivities [13]. These natural products are generated by large megaenzymes, polyketide synthases (PKSs), and nonribosomal peptide synthetases (NRPSs). Type I PKSs consist of multiple modules, with each module minimally containing three core domains: acyltransferase (AT) domain, ketosynthase (KS) domain, and thiolation (T) domain [also called acyl carrier protein (ACP) domain]. Typically, one type I PKS module catalyzes a single elongation cycle for PK production (Fig. 18.2). During elongation, the AT domain serves as the gatekeeper for specificity, responsible for selecting the appropriate acyl-CoA extender unit (e.g., malonyl-CoA, methylmalonyl-CoA) and transferring the extender unit to the sulfhydryl terminus of the phosphopantetheinyl arm on the T domain [14]. The KS domain catalyzes the decarboxylation of acyl-S-T to generate a carbanion that reacts with the PK intermediate linked to T domain generated in the previous elongation cycle. The resulting α -ketoacyl-S-T becomes the substrate for the next cycle of elongation catalyzed by the subsequent elongation module. In addition to type I PKSs, there are two other classes, type II PKSs and type III PKSs [15]. Unlike the type I class, type II PKSs consist of discrete enzymes that are organized as a multicomponent system [16]. The type III PKSs are distinguished from the others by lack of an AT and T domain. Type III PKS systems typically use CoA substrates (i.e., malonyl-CoA), but there is precedent for their ability to accept acyl-S-T substrates [15, 17].

Similar to the type I PKSs, NRPSs are comprised of multifunctional enzymes that are arranged into modules. Each NRPS module contains three core domains: adenylation (A), condensation (C), and thiolation (T) (also called peptidyl carrier protein [PCP] domain) [18] (Fig. 18.2). The A domain is responsible for selecting and activating the natural or modified amino acid monomer. The activated amino acid monomer is covalently attached via a thioester bond to the cysteamine group of a phosphopantetheinyl arm in the holo-T domain. The condensation (C) domain catalyzes formation of the peptide bond between the amino acid monomer and the peptidyl intermediate tethered to a T domain in an adjacent module. Similar to type I PKS modules, each NRPS module performs a single elongation step of the growing peptidyl chain. In both NRPSs and PKSs, there are several additional domains that contribute to natural product structural diversity. Ketoreductase (KR), dehydratase (DH), and enoyl reductase (ER), and methyltransferase (MT) domains are commonly found in PKS modules, while cyclization (Cy), *N*-MT, and epimerase (E) domains are sometimes embedded within NRPS modules. These additional

**Fig. 18.2** (continued)

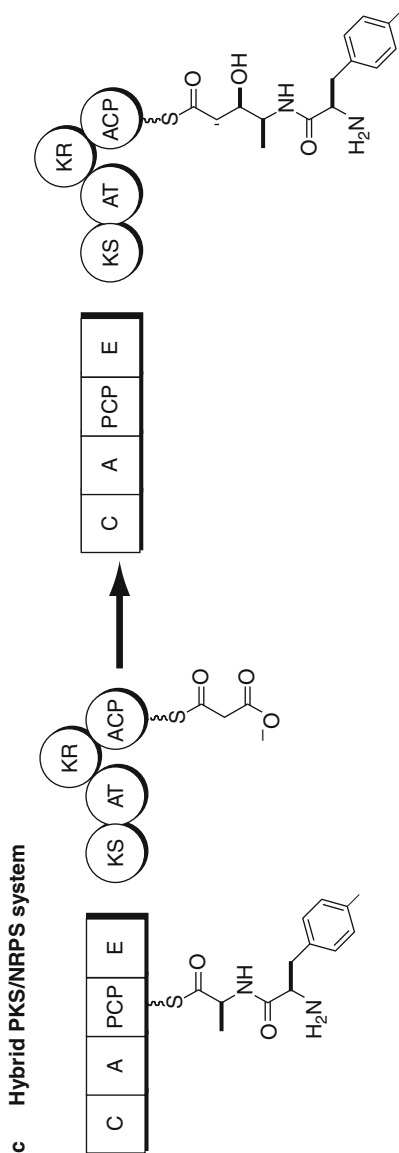


Fig. 18.2 Hypothetical examples of the modular organization in polyketide synthases (PKSs), nonribosomal peptide synthases (NRPs), and hybrid PKS/NRPSs. (a) Two consecutive PKS elongation modules from a hypothetical polyketide biosynthetic pathway that catalyze the elongation of the growing polyketide intermediate by two carbons (from methylmalonyl-CoA), and subsequent β -keto reduction; (b) two consecutive NRPS elongation modules from a hypothetical nonribosomal peptide biosynthetic pathway that catalyze peptide bond formation between the growing peptide intermediate and an activated cysteine residue with subsequent cyclization/oxidation of the incorporated cysteine residue to a thiazole; (c) consecutive NRPS and PKS elongation modules from a hypothetical hybrid nonribosomal peptide/polyketide biosynthetic pathway that catalyze the two-carbon extension (from malonyl-CoA) of the peptide intermediate and subsequent β -keto reduction

domains contribute significantly to the diversity and bioactivity of PKs and NRPs. Thioesterase (TE) domains, typically found at the C-terminus of the final elongation module in both PKs and NRPs, are responsible for terminating biosynthesis. In most cases, TE domains catalyze intramolecular macrocyclization or hydrolysis of the thioester bond between the final T domain and the PK or NRP intermediate [8]. The structures of the nascent PK and NRP products are often further modified through oxidation, glycosylation, acylation, alkylation, and halogenation reactions catalyzed by tailoring enzymes in natural product biosynthetic pathways [19, 20].

In the sections below, a series of marine natural product biosynthetic systems will be described that provide an in-depth overview of genetic and biochemical mechanisms involved in assembly and tailoring of many of these beautifully complex and biologically active molecules.

18.2 Examples

18.2.1 Curacin

18.2.1.1 Isolation and Biological Activity

Curacin A (Fig. 18.3) is a mixed PK/NRP natural product with potent antiproliferative and antimitotic activity against colon, renal, and breast cancer-derived cell lines [21]. The compound was originally isolated from strains of the tropical marine cyanobacterium *Lyngbya majuscula* discovered in Curaçao by Gerwick et al. [22] and found to possess unusual structural features, including a cyclopropane ring, thiazoline moiety, *cis*-alkenyl group, and terminal double bond. Curacin A has been shown to block cell cycle progression by interacting with the colchicine-binding site on tubulin and inhibiting microtubule polymerization [23]. The clinical development of curacin has been hindered by its high lipophilicity; however, structural analogues having improved water solubility and potency have been recently synthesized to enable continued preclinical studies [24, 25].

18.2.1.2 Gene Cloning, Sequence Analysis

The Gerwick and Sherman laboratories conducted a series of isotope-labeled precursor feeding and NMR studies that established the metabolic origin of all curacin A atoms and their order of assembly [26]. The studies indicated the compound is composed of one cysteine residue, ten acetate units, and two *S*-adenosyl methionine-derived methyl groups, thus suggesting that curacin A was of mixed PKS–NRPS origin. Through the creation and screening of a cosmid library from *L. majuscula* using a general PKS probe, a 64-kb gene cluster containing 14 ORFs was identified. As predicted by the precursor incorporation experiments, the curacin metabolic system (Fig. 18.3) was found to contain nine PKS modules and one NRPS module. Interestingly, this biosynthetic system is unique in that all PKS multifunctional proteins, with the exception of the CurF hybrid PKS/NRPS, are monomodular [26].

Curacin A biosynthesis is initiated by the unique CurA PKS. Bioinformatic analysis of the AT domain located at the amino-terminus of CurA indicated homology with the *N*-acetyltransferase (GNAT) domain, PedI, from the putative pederin gene cluster [26, 27]. Interestingly, a recent study established the role of an astonishing biochemical chain initiation strategy for the loading module of curacin A that involves an unusual tridomain found at the amino-terminus of CurA [28]. This tridomain is comprised of an adapter domain, a GNAT domain, and an ACP domain. In vitro biochemical studies of the isolated tridomain have shown that the GNAT has unprecedented bifunctional activity, as it is capable of first decarboxylating malonyl-CoA to acetyl-CoA and then directing the transfer from acetyl-CoA onto the ACP domain phosphopantetheine arm to produce the acetyl-ACP intermediate [28].

A series of three tandem ACP domains (ACP₃) reside at the C-terminus of the CurA polypeptide that together with four ORFs encoding CurB–CurE, as well as the first two domains of CurF, was predicted to direct formation of the unique cyclopropyl ring in curacin A. Indeed, recent biochemical and structural studies confirmed that the CurE/CurF ECH₁–ECH₂ enzyme pair catalyzes successive dehydration and decarboxylation of (*S*)-HMG-ACP to generate a 3-methylcrotonyl-ACP intermediate for subsequent formation of the cyclopropane ring [29, 30]. Moreover, the CurA ACP₃ domains have been shown to work synergistically, resulting in enhanced catalytic output of the early chain elongation intermediate bearing the cyclopropyl ring [31].

The remainder of the molecule is assembled by seven PKS monomodules, CurG–CurM, that catalyze seven successive rounds of condensation with malonyl-CoA extender units. Furthermore, embedded methyltransferase domains in CurJ and CurL are predicted to catalyze transfer of the C-17 and O-13 methyl groups, respectively. Of final interest is the atypical biosynthetic termination mechanism that is predicted to function in both product release and decarboxylative dehydration to form the unusual terminal alkene. Like the majority of other known PK/NRP biosynthetic pathways, the final elongation module of the curacin pathway, CurM, contains a terminal thioesterase domain that was predicted to play a direct role in formation of the terminal olefin. Bioinformatic analysis of the CurM PKS monomodule also predicted the presence of a sulfotransferase (ST) domain immediately preceding the TE. ST domains are typically responsible for transferring a sulfonate group from a donor molecule (such as 3'-phosphoadenosine-5'-phosphosulfate, PAPS) to a variety of acceptor carbohydrates, proteins, and other low molecular weight metabolites [32]. Although STs had been previously characterized from both eubacterial and eukaryotic organisms, the presence of an ST domain within a PKS system was unprecedented.

Recent work has revealed the precise functions of the ST and TE domains in terminal olefin formation during termination of curacin biosynthesis (Fig. 18.3). The first step involves ST domain-catalyzed transfer of a sulfonate group (donated by PAPS) to the 3(*R*)-hydroxyl group of the ACP-bound thioester chain, followed by hydrolytic termination of curacin A biosynthesis by the TE to produce the linear free acid bearing a 3(*R*)-sulfate leaving group. High-resolution X-ray crystal

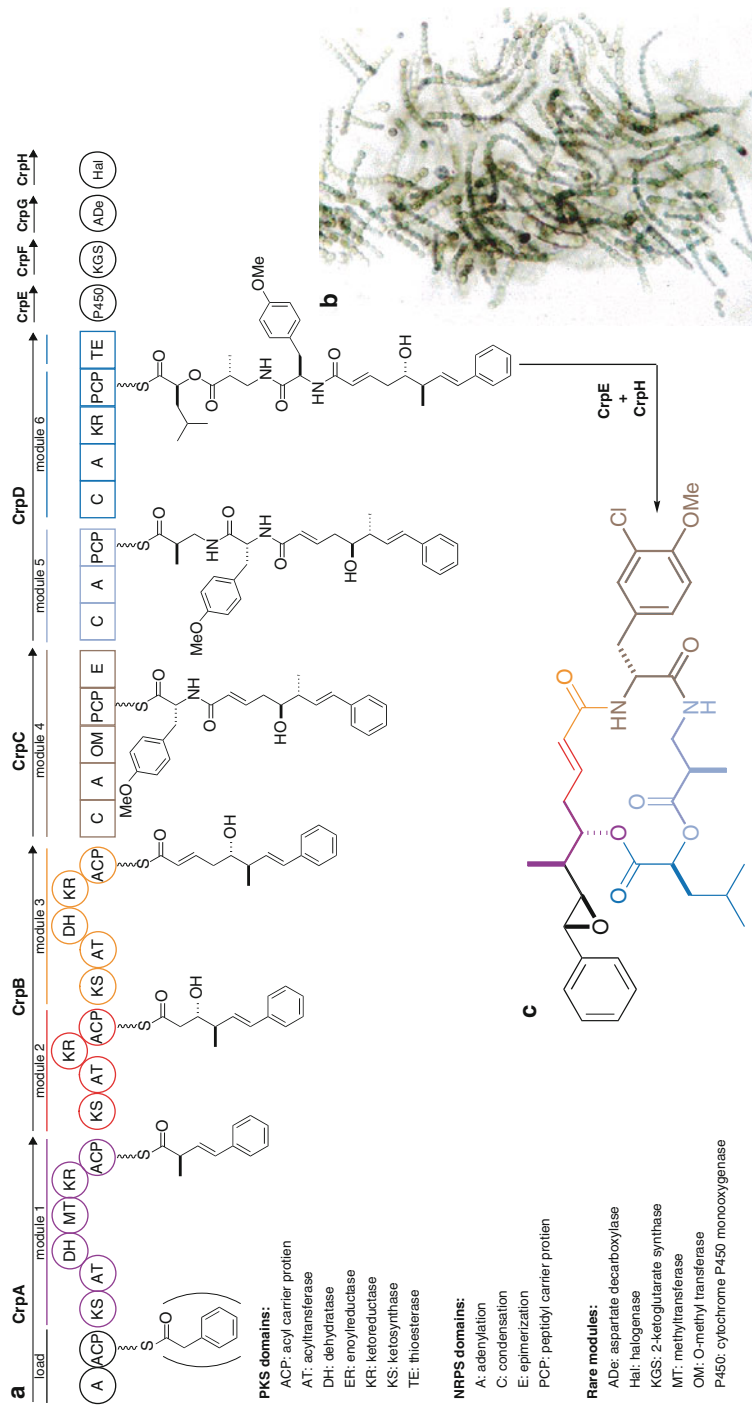
structure analysis of the CurM TE domain provides strong evidence that it catalyzes decarboxylation of the free acid, after which formation of the double bond would be energetically driven by elimination of the sulfate leaving group. Although it is conceivable that upon TE catalyzed hydrolysis, the decarboxylation reaction occurs spontaneously as a result of the presence of the sulfate leaving group at carbon 3, isolation of a substrate mimic bearing these two functional groups indicates that enzyme catalysis by the TE is required. Further efforts to develop this unique polyketide termination mechanism have important implications for facile conversion of fatty acid intermediates into valuable liquid fuels.

18.2.2 Cryptophycin/Arenastatin

18.2.2.1 Isolation and Biological Activity

Cryptophycins, a large class of peptolides, were originally isolated from the cyanobacteria *Nostoc* sp. ATCC 53789 by researchers at Merck as a potent fungicide. A gross structure was proposed, but Merck abandoned the project because the compounds were too toxic to be developed as antifungals [33]. Several years later, interest in the cryptophycins was renewed when a screen of the lipophilic extract of *Nostoc* sp. GSV 224 exhibited potent cytotoxic activity [34]. This activity was attributed to the cryptophycin natural products, which have since been found to have antimitotic activity and cytotoxicity toward tumor cells in culture, as well as anticancer activity against murine solid tumor models and human tumor xenografts [35–37]. While there are more than 25 naturally occurring analogues (in addition to the nearly structurally identical marine natural product arenastatin [38]), the major compound from both *Nostoc* sp. ATCC 53789 and *Nostoc* sp. GSV 224, cryptophycin 1 (Fig. 18.4), consists of four subunits: hydroxyphenyloctenoic acid (unit A), 3-chloro-*O*-methyl-D-tyrosine (unit B), methyl- β -alanine (unit C), and L-leucic acid (unit D) linked in a cyclic clockwise sequence [34, 39, 40]. Other naturally occurring cryptophycins are analogues that differ from cryptophycin 1 by one or two of these subunits.

Cryptophycin 1 is one of the most potent tubulin destabilizing agents ever discovered, resulting in cellular arrest at the G2/M phase via hyperphosphorylation of Bcl-2, thereby triggering the apoptotic cascade [41]. Cryptophycins are also attractive as chemotherapeutics because they are active against multidrug-resistant tumor cell lines and are not substrates for *p*-glycoprotein pumps [37]. A synthetic analogue, cryptophycin 52 (LY355703), was developed by Eli Lilly & Co. and ultimately reached phase II clinical trials; however, high production costs coupled with dose-limiting toxicity halted its development [42]. In spite of this, a subsequent phase II clinical trial involving patients with platinum-resistant advanced ovarian cancer concluded that the rate of disease stabilization in the absence of adverse events might justify further investigation of cryptophycin 52 [43]. A second generation of cryptophycin 1 analogues with improved solubility properties has been synthesized, and preclinical studies indicate a marked increase in efficacy against a variety of tumors [44].



18.2.2.2 Gene Cloning, Sequence Analysis

The Sherman and Moore laboratories worked collaboratively to isolate and characterize the cryptophycin gene cluster (Fig. 18.4) using a strategy that relied on comparative metabolomic analysis [45]. In this approach, the A and KS domain sequences of *Nostoc* sp. ATCC 53789 were compared to that of *Nostoc punctiforme* ATCC 29133, a strain that does not produce cryptophycin. This comparative method resulted in the identification of six A domain sequences that were present in *Nostoc* sp. ATCC 53789 but not in *Nostoc punctiforme*. Of these six, a single A domain appeared to be a candidate for the cryptophycin pathway. From this initial lead, the 40-kb cryptophycin biosynthetic gene cluster was identified by cosmid library screening [45].

The cryptophycin gene cluster consists of two modular PKS genes (*crpA* and *crpB*) and two modular NRPS genes (*crpC* and *crpD*). In total, these open reading frames encode seven elongation modules that contain the requisite catalytic domains for assembly of the cryptophycin macrocyclic core structure. In addition, a series of open reading frames, designated *crpE*–*crpH*, are located downstream of *crpA*–*D* and are predicted to encode enzymes that modify the nascent macrocycle to yield cryptophycin 1. These include a cytochrome P450 epoxidase (*crpE*), a putative 2-ketoglutarate-dependent enzyme (*crpF*), an aspartate decarboxylase (*crpG*), and a flavin-dependent halogenase (*crpH*). In addition to characterization of the gene cluster, the Sherman and Moore groups have produced novel cryptophycin analogues by precursor-directed biosynthesis [45]. In vitro biochemical work has also been performed to characterize the TE domain of CrpD [46, 47], the aspartate decarboxylase, CrpG [48], and the P450 epoxidase, CrpE [49]. These studies have unveiled the genetic blueprint of cryptophycin biosynthesis in *Nostoc* sp. ATCC 52789, thereby providing access to a set of catalytic tools for chemoenzymatic construction and modification of new cryptophycin analogues.

18.3 Trans AT Domain Pathways – A Rich Source of Unusual Biochemistry

18.3.1 Trans AT Hybrid PKS/NRPS Systems: An Introduction

One emerging subclass of hybrid PKS/NRPS pathways is the “*trans* AT” hybrid biosynthetic systems. Rather than containing embedded AT domains within their PKS modules, the *trans* AT systems feature a separately encoded, discrete AT domain that is responsible for loading ACP domains with the appropriate CoA substrate (Fig. 18.5). Interestingly, remnants of embedded ATs are found within *trans* AT hybrid pathways and have been proposed to act as “AT docking domains,” or recognition elements, thus providing evidence of an evolutionary link between the two types of pathways [50]. This subclass of natural product synthase serves as an example of the great diversity in pathway architecture represented by these systems.

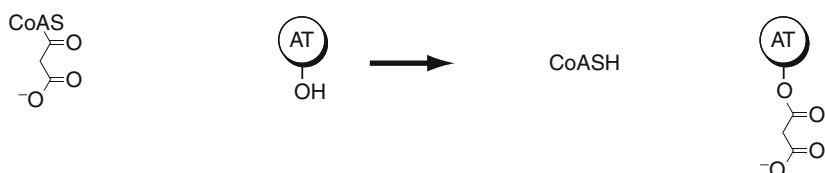
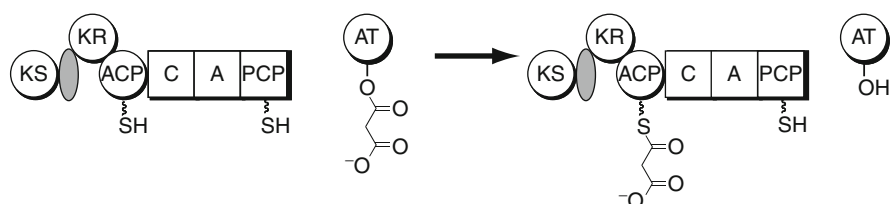
a Loading of *trans*-AT domain**b Transthioesterification of ACP domain**

Fig. 18.5 A schematic of a *trans* AT reaction scheme utilizing a hybrid PKR-NRPS biosynthetic module. (a) Loading of malonyl-CoA onto the AT active site serine; (b) transfer from *trans* AT to the phosphopantetheine arm of the PKS module ACP

Aspects of known NRPS/PKS *trans* AT hybrid biosynthetic pathways including products, pathway organization, in vitro and in vivo biochemistry, biological roles, and potential for future engineering efforts will be explored within this section. For further information, the reader is directed toward one of the many reviews that have been recently published on closely related topics. These include: hybrid NRPS/PKS pathways in general [14, 51], developing molecular tools to engineer these systems [52], compounds derived from marine invertebrates and bacteria [53], symbiotic bacteria-produced secondary metabolites [54, 55], and absence of colinearity including skipping and iteration [56].

18.3.2 Known *Trans* AT Hybrid PK/NRP Pathways

Over the past several years, *trans* AT hybrid biosynthetic pathways have been discovered in a wide range of bacterial species (summarized in Table 18.1, Fig. 18.6). Moreover, in several cases (e.g., onnamide, pederin, bryostatin, and rhizoxin), the bacterial species is engaged in important symbiotic relationships with multicellular hosts. These symbiotic relationships often complicate the identification of the species of origin of the hybrid PK/NRP natural product. With few exceptions, such as those involved in the biosynthesis of mycosubtilin and albicidin, the majority of *trans* AT hybrid pathways are predominantly composed of PKS elongation modules. In fact, it should be noted that *trans* AT pathways that are entirely comprised of PKS modules have been characterized: CpPKS1 [57], mupirocin [58], macrolactam [59], difficidin [60], and bryostatin [61, 62].

Table 18.1 Known hybrid PKS/NRPS *trans* AT pathways. The known hybrid *trans* AT PK/NRP products are listed above by bioactivity, with bacterial class and biometical. For symbiont products, the host organism is also designated. Protein and gene abbreviations are noted along with PKS and NRPS module composition

Name	Activity	Bacterial class	Producing bacteria	Host	Designation	PKS	NRPS
Albicidin	Cytotoxic	γ -Proteobacteria	<i>Xanthomonas albilineans</i>	N/A	Alb/ <i>alb</i>	3	7
Chivosazol	Cytotoxic	δ -Proteobacteria	<i>Sorangium cellulosum</i>	N/A	Chi/ <i>chi</i>	16	1
Disorazol	Cytotoxic	δ -Proteobacteria	<i>Sorangium cellulosum</i>	N/A	Dis/ <i>dis</i>	10	1
Leinamycin	Cytotoxic	Actinobacteria	<i>Streptomyces atroolivaceus</i>	N/A	Lnn/ <i>lnn</i>	7	2
Onnamide	Cytotoxic	Unknown		Sponge: <i>Theonella swinhoei</i>	Omn/ <i>onn</i>	?	?
Pederin	Cytotoxic	γ -Proteobacteria	<i>Pseudomonas aeruginosa</i>	Beetle: <i>Paederus</i> sp.	Ped/ <i>ped</i>	9	2
Rhizoxin	Cytotoxic	Betaproteobacteria	<i>Burkholderia rhizoxina</i>	Fungi: <i>Rhizopus microsporus</i>	Rhi/ <i>rhi</i>	11	1
Antibiotic TA	Antimicrobial	δ -Proteobacteria	<i>Myxococcus xanthus</i>	N/A	Ta/ <i>ta</i>	11	1
Bacillaene	Antimicrobial	Bacilli	<i>Bacillus subtilis</i>	N/A	Pks/ <i>pks</i>	13	2
Lankacidin	Antimicrobial	Actinobacteria	<i>Streptomyces rochei</i>	N/A	Lkc/ <i>lkc</i>	5	1
Mycosubtilin	Antimicrobial	Bacilli	<i>Bacillus subtilis</i>	N/A	Myc/ <i>myc</i>	1	7
Virginiamycin M	Antimicrobial	Actinobacteria	<i>Streptomyces virginiae</i>	N/A	Vir/ <i>vir</i>	8	2
Thailandamide A		Bacilli	<i>Bacillus thailandensis</i>	N/A		16	1

18.3.3 Biological Activity and Structure of *Trans* AT Hybrid PK/NRPs

PKS/NRPS-derived natural products that are assembled from *trans* AT biosynthetic pathways can be broadly classified as either antimicrobials or cytotoxic chemotherapeutics based on their biological activity (Table 18.1, Fig. 18.6). Certain antimicrobial compounds, such as albicidin and mycosubtilin, have well-defined activities while others, such as bacillaene, chivosazol, and lankacidin, have yet to be rigorously characterized in terms of biochemical targets. Given their ability to cause damage to rapidly growing cells, leinamycin, onnamide, and disorazol each has potential as an anticancer therapeutic. As discussed above, many hybrid PK/NRP natural products have demonstrated clinical utility; however, with the exception of antibiotic TA, none of the compounds are derived from *trans* AT hybrid PKS/NRPS pathways.

18.3.4 In Vivo Analysis of *Trans* AT Hybrid PK/NRP Systems

To date, at least 13 *trans* AT hybrid PK/NRP biosynthetic pathways have been described in the literature (Table 18.1, Fig. 18.6). Intriguingly, aside from the presence of the *trans* AT domain, each of these pathways displays multiple deviations from the typical PKS/NRPS modular organization and composition. In fact, only five of these pathways are colinear with genetic organization, as is typically observed in bacterial PKS or NRPS systems. Module splits, whereby the domains of a single module are divided among multiple polypeptides, are frequently observed within *trans* AT hybrid pathways. 3-Hydroxy-3-methylglutaryl synthase (HMGS) cassettes are also commonly found in these biosynthetic pathways. These cassettes are responsible for the insertion of β -branch points into the middle of the growing polyketide chain [63]. Repeated “tandem” domains and unusual or uncharacterized enzymatic domains are also often present in biosynthetic pathways that employ *trans* AT domains [56]. Additional nonstandard features, such as iteratively acting modules or inactive modules, can often be inferred from the chemical structure of the natural product.

Putative *trans* AT biosynthetic pathways can be linked to a specific natural product through comprehensive bioinformatic analysis which is used to determine domain compositions and predicted acyl [64] or peptidyl substrate [65] incorporation of AT or A domains, respectively [66]. However, in nonlinear pathways, or in pathways that skip or iterate elongation modules, these predictions are challenging and can be misleading. Pathway assignment is typically obtained through genetic disruption and complementation. For example, if the inactivation of a key biosynthetic gene results in a nonproducing phenotype, the pathway/product link is verified. However, this genetic approach is not a viable option for bacteria that are not culturable in the laboratory (often the case for symbionts) or for microorganisms that are not amenable to genetic manipulation. In such cases, the final proof may require complete pathway reconstitution in a heterologous host – a task not yet accomplished for any symbiont pathway. Alternatively, detailed biochemical

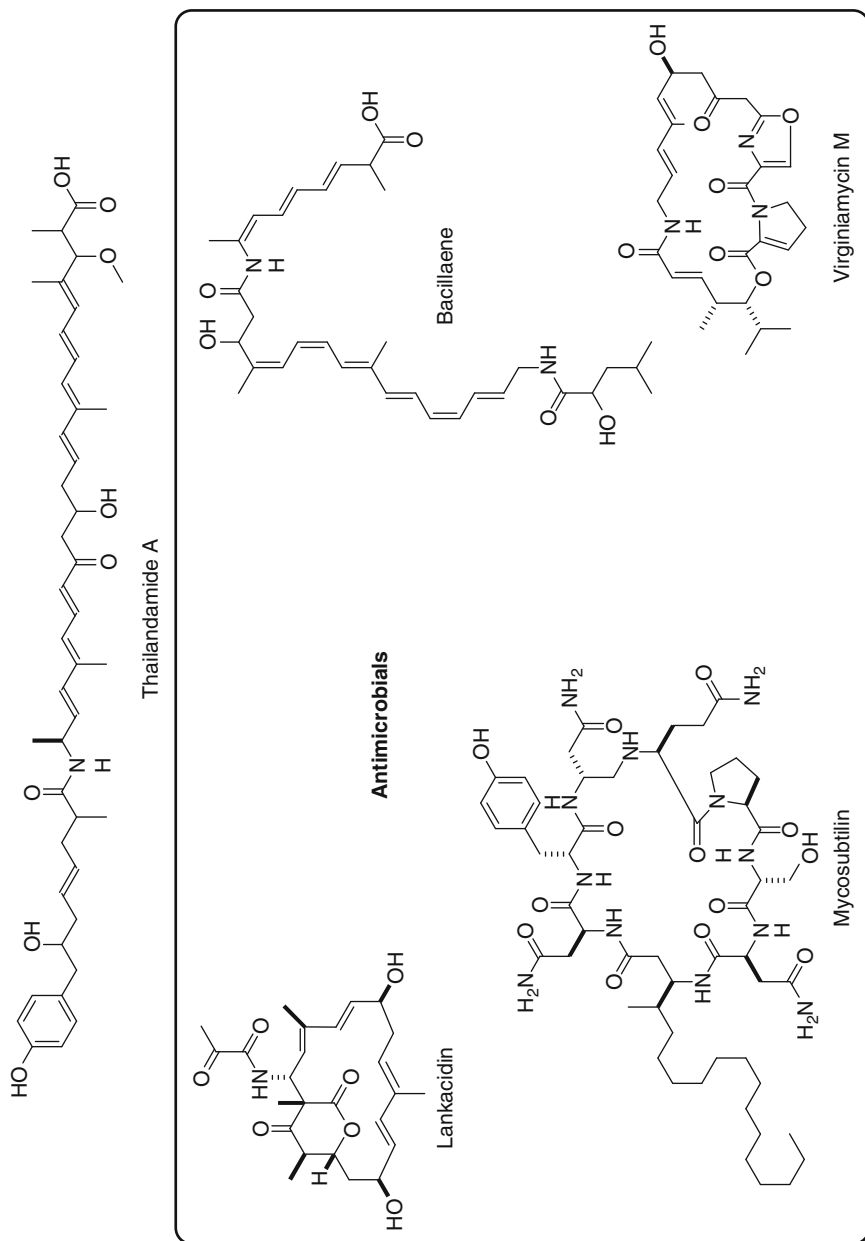


Fig. 18.6 (continued)

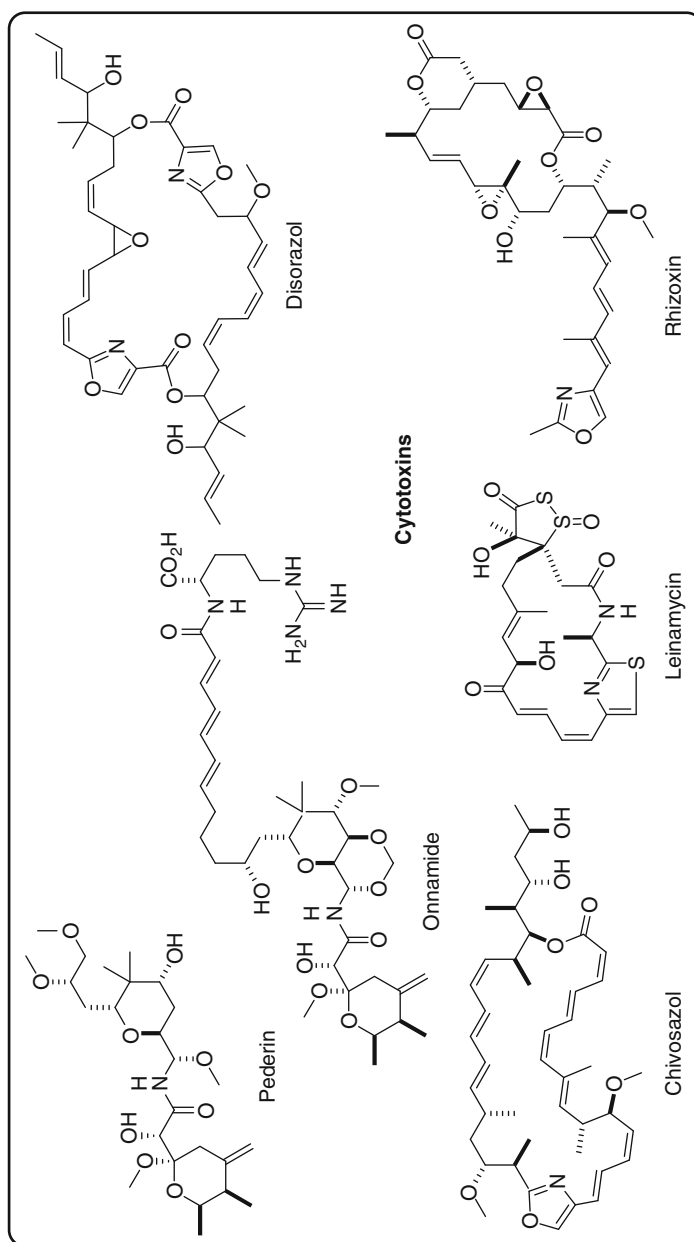


Fig. 18.6 *Trans* AT hybrid PKS/NRPS biosynthetic pathways grouped by bioactivity

studies that provide direct evidence for conversion of a specific natural product biosynthetic intermediate for its cognate enzyme offers key information to correlate pathways from unculturable marine microbial symbionts. Studies on the *trans* AT and β -branching pathways in the bryostatin biosynthetic pathway have offered unique insights into this important marine natural product with anticancer and neuroprotective activity [62, 67].

18.3.5 In Vitro Characterization of Trans AT Hybrid PKS/NRPS Pathways

Given the many unusual features of the *trans* AT hybrid PK/NRP biosynthetic pathways, the precise sequence of compound assembly and the exact role of specific domains cannot always be easily ascertained from either sequence analysis or in vivo biochemistry. A more direct approach toward understanding these issues is to perform detailed in vitro biochemical investigations employing recombinant enzymes. Using defined assay conditions, detailed enzymology studies can provide important details of these hybrid megasynthetases. Additionally, heterologous expression and purification of recombinant proteins enable the possibility of gaining key structural data and might eventually inform new avenues toward pathway reengineering in vitro. It is becoming increasingly apparent that rigorous in vitro examination of enzymes from a few select pathways has dramatically improved our understanding of the role of unusual domains and architecture in these pathways [63, 68–74].

18.3.6 Evolution, Biology, and Symbiosis of Trans AT Hybrid PKS/NRPS Systems

Elucidation of the biological roles of PKS, NRPS, and hybrid PK/NRP natural products that are produced by *trans* AT PKS/NRPS synthetases is a rapidly emerging field of research, particularly in relation to developing models of microbial symbiosis in natural product biosynthesis. Why do organisms expend so much energy and genome composition to generate these elaborate natural products? While the chemical ecology of some of these compounds has been explored, considerable work remains to understand the role these compounds serve for the producing organism [75]. Indeed, even the identity of the organism (host versus symbiont) that is responsible for natural product biosynthesis is an area of intense interest. Macroscopic eukaryotes including insects, plants, marine sponges, and tunicates have long been recognized as sources of diverse natural products. Yet time and time again, experimental evidence strongly suggests that associated microorganisms are responsible for many marine natural product biosyntheses, especially when similar compounds are isolated from taxonomically diverse producers. Cell separation experiments, as performed in the marine sponge *Theonella swinhoei*, have shown that the isolated fraction of bacteria colocalized with

secondary metabolite production [76]. The complexity of this problem becomes evident when it is recognized that up to 40% of the mass of a sponge may be composed of bacteria, fungi, and other microorganisms [77].

18.3.7 Onnamide/Pederin

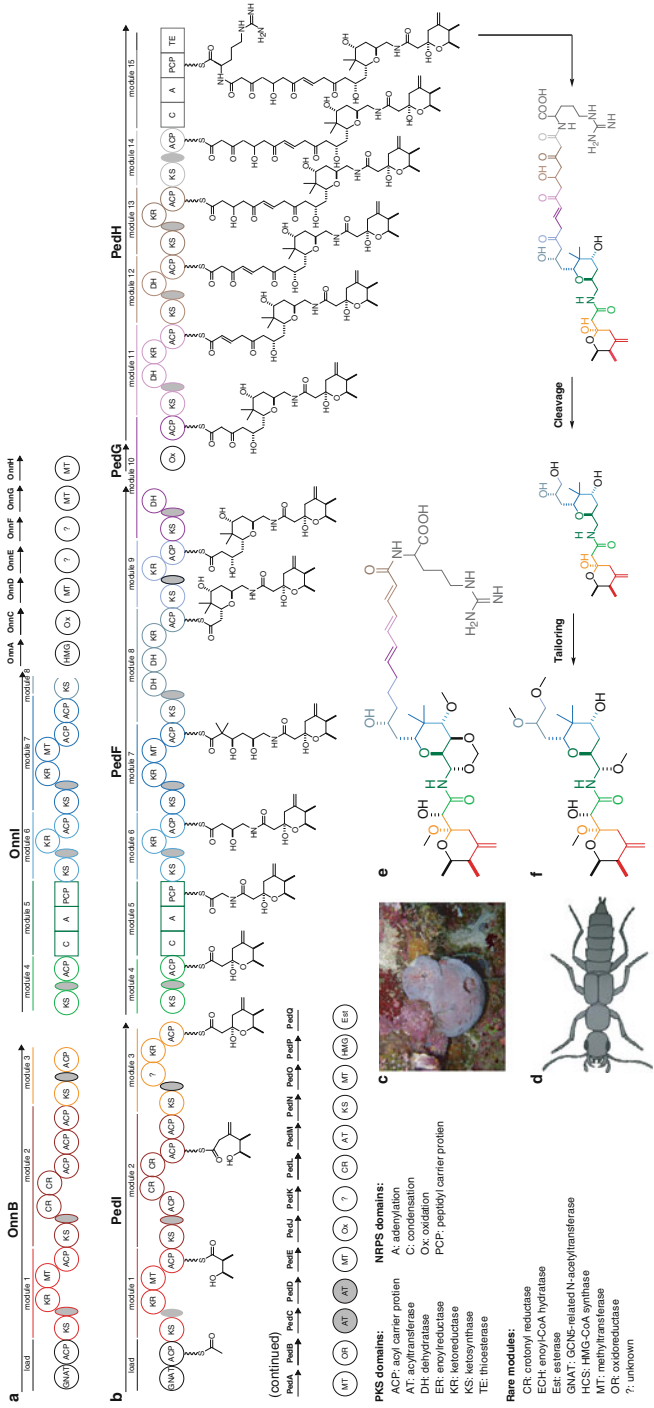
18.3.7.1 Biological Activity and Structure of Trans AT Hybrid PK/NRP

Both onnamide and theopederin, a close analogue of pederin (Fig. 18.7), are nanomolar inhibitors of protein synthesis, leading to induction of ribotoxic stress response, p38 kinase activity, and apoptosis. These activities were discovered during a screen for activators of transforming growth factor β (TGF- β) expression [78]. It has been hypothesized that these compounds may directly bind to the eukaryotic ribosome, thus resulting in downstream activation of apoptotic pathways [78].

Onnamide and pederin each contain a similar carbon backbone with two tetrahydropyran rings linked through an amide bond. Furthermore, each features an exocyclic double bond. Differences between the two natural product compounds include the presence of an additional hydroxyl group in onnamide that results in formation of a third six-membered ring. Onnamide also contains a longer, conjugated side chain that terminates in an arginine residue. The structural similarity shared between onnamide and pederin was proposed as evidence for the existence of a related symbiont producer in natural product biosynthesis [79, 80] well before Piel obtained the gene clusters from the producing organisms [81, 82].

18.3.7.2 In Vivo Biochemistry of Trans AT Hybrid PK/NRP

The biosynthesis of pederin and onnamide will be discussed together due to the close chemical and biosynthetic similarities that are shared between the compounds and pathways [81–83]. The role of these pathways (Fig. 18.7) in settling the long-standing debate over the source of natural products in marine invertebrates (e.g., sponges, tunicates) is discussed below. Both pederin and onnamide are initiated from a PKS elongation module (OnnB/PedI) that begins with a GNAT-loading domain. A similar initiation mechanism is found in the curacin biosynthetic pathway [28]. The domain composition and arrangement is identical for each pathway over the first 12 domains, encompassing two PKS elongation modules. Interestingly, 2 unusual domains exist within these first 12 domains and have been annotated as crotonyl-CoA reductases. Divergence in biosynthesis of the two molecules occurs beyond this point. The onnamide biosynthetic machinery proceeds with a tandem triple ACP, whereas pederin biosynthesis continues with a tandem di-ACP. In addition, the final PKS module of OnnB contains only KS and ACP domains, whereas the final module in PedB features a KS domain, a domain of unknown function, a KR domain, and finally an ACP domain. The subsequent polypeptides, OnnI or PedF, share a high degree of similarity, with the arrangement of the first 12 domains being identical. Briefly, each polypeptide begins with a PKS elongation module, followed by an NRPS module, and



a second PKS module. At this point in the biosynthetic pathways, divergence is observed. Here, OnnI terminates with tandem ACP domains, followed by a KS domain. It should be noted that the DNA sequence of onnamide biosynthetic pathway is presumably incomplete, and therefore OnnI does not likely represent the terminus of the metabolic system. This is because out of a 500,000-member clone library, only one cosmid containing the incomplete onnamide gene cluster was isolated [82]. In comparison, PedF continues with a single ACP domain that is followed by two additional PKS modules, the first of which contains a tandem DH didomain. At this point, two biosynthetic possibilities have been proposed. First, PedG catalyzed hydrolysis of the chain elongation intermediate from PedI and yields the pederin nascent intermediate (pretailored). Alternatively, chain extension continues through PedH, which results in a product having a very similar structure to onnamide. This “onnamide” type intermediate would then presumably be cleaved to give the beetle-derived product, pederin. The domain arrangement of PedH involves a presumed oxygenase, PedG, of the previous split module, PedF. PedH continues with four PKS elongation modules prior to the final arginine incorporating NRPS module that terminates with TE. Additional discrete proteins are also present in the pederin pathway. These include PedA/E/Q (methyltransferases), PedB (oxidoreductase), PedC/D/M (*trans* AT tridomain), PedJ (oxidase), PedK (unknown function), PedL (crotonyl-CoA reductase), PedN (KS), PedP (HMG-ACP synthase), and PedO (esterase). Several proteins with high sequence similarity are found in the onnamide pathway. These include OnnA (HMG-ACP synthase), OnnC (oxidase), OnnD/G/H (methyltransferases), and OnnE/F (unknown function) [81–83]. As a matter of caution, it is important to note that these pathway assignments are considered putative, as they have not been confirmed as the metabolite source through heterologous expression or through detailed biochemical analysis of corresponding purified proteins.

18.3.8 Evolution, Biology, and Symbiosis of *Trans* AT Hybrid PKS/NRPS Systems

One of the mysteries that have intrigued natural product chemists for years is how structurally similar natural products can be isolated from evolutionarily distinct hosts (e.g., marine sponges, myxobacteria). These discoveries have led to the hypothesis that microorganisms are the likely producers of many marine invertebrate-derived natural products. Support for this hypothesis was offered by Piel, who isolated, characterized, and comparatively analyzed the DNA encoding the biosynthetic pathways of pederin and onnamide from the rove beetle and a marine sponge, respectively. The isolation and subsequent screening of DNA from the gut bacteria of the pederin source (rove beetle) eventually lead to the identification of the pederin pathway that originated from an unculturable symbiont [81]. Subsequently, Piel hypothesized that a similar symbiotic relationship accounted for the existence of a homologous pathway for onnamide production in the marine sponge *Theonella swinhoei*. Screening of a *T. swinhoei* metagenomic DNA library led to

the identification of a biosynthetic pathway having a high similarity with that of pederin [82]. The relationship of pederin and onnamide represents a fascinating example in which similar natural product biosynthetic gene clusters are derived from unique, phylogenetically distinct strains from widely disparate macroorganisms. Extensive gene sequencing has identified that *Pseudomonas aeruginosa* is the beetle endosymbiont responsible for pederin production [84]. To date, the microbial symbiont of the sponge has yet to be determined, but the DNA appears to be of bacterial origin [83]. Further questions regarding evolution and divergence of the two pathways and host diversity remain to be fully explored.

Recent work to investigate the evolution of *trans* AT PKS systems, the main class of synthase isolated to date from marine microbial symbiotic organisms, may help frame the pertinent biological questions. Piel recently grouped known *trans* AT synthases and subjected them to multiple amino acid sequence alignments [66]. Interestingly, only the KS and MT domains showed conservation in all examined sequences. *Trans* AT KS specific clades formed in an intriguing manner. Domains did not cluster based on whether or not they were from the same gene cluster, as seen for *cis* ATs, but rather based on what final extension unit is generated. From this analysis, several insights are gained. First, it is possible to predict *trans* AT PKS product structure to a reasonable degree of accuracy, even in cases where pathways have reductive or β -branching domains acting in *trans*. Such a prediction was illustrated for thailandamide [66]. Secondly, and perhaps most importantly, Piel et al. revealed that *trans* AT systems have likely evolved through a very different mechanism compared to their *cis* AT PKS counterparts. In *trans* AT pathways, horizontal gene transfer and recombination appear to be the driving force, as opposed to recombination. This suggests that *trans* AT PKS pathways may be classified separately from their *cis* AT counterparts, much in the sense that PKS and NRPS pathways are to each other [66].

The rapidly growing number of complete genome sequences from free-living and symbiotic bacteria, as well as from environmental samples, is expected to lead to an increase in the number of characterized *trans* AT hybrid PKS/NRPS pathways [66]. Previous comparative studies made with significantly smaller amounts of sequence data began to show evidence of distinct clades forming between methylmalonyl-CoA *cis* ATs, malonyl-CoA *cis* ATs, and *trans* AT modular PKS domains [68]. Interestingly, it appears that *trans* AT PKS or PKS/NRPS systems may be underrepresented in current databases, as relatively larger numbers of *trans* AT PKS systems have been observed (relative to *cis* AT PKS systems) in random sequencing of bacterial strains [85].

18.4 Technologies

18.4.1 DNA Sequencing Strategies in Hybrid PK/NRP Systems

When searching for bioactive compounds in nature, or the genes that direct their biosynthesis, it is best to survey a relatively large pool of structural or genetic

diversity. However, given that 16 S rRNA gene sequence analysis suggests that less than 0.1% of bacterial species collected in a marine sample are amenable to traditional laboratory culturing techniques, alternative approaches become necessary [86]. One strategy involves the collection of whole environmental DNA (eDNA) and subsequent screening for biosynthetic gene clusters based on homology to known genes. The disadvantage of this approach is that it typically requires densely populated DNA libraries (e.g., pederin and onnamide). Even having access to large DNA libraries does not ensure successful identification of desired gene clusters, as was demonstrated in the recent search for the discodermolide biosynthetic pathway from the sponge *Discodermia dissoluta*. Screening of more than 150,000 cosmids produced over 4 GB of DNA sequence data but failed to identify the gene cluster [87]. Interestingly 90% of the DNA sequenced appeared to be bacterial in nature, thereby suggesting that the sponge does contain a diverse microbial community with high biosynthetic potential [87]. Because of this promise, investigators continue to pursue the development techniques to enable the efficient manipulation and screening of huge pools of DNA, such as clone pooling in semiliquid medium [88].

The rise of rapid and inexpensive whole genome DNA sequencing is also expected to have a profound impact on to the ability to access data from environmental samples of microbial consortia (Fig. 18.8). Early experiments have demonstrated that there are seven diverse biosynthetic pathways in a single strain of *Salinispora tropica* [89]. Genome mining has also been applied in the search for rhizoxin pathway homologs in other source strains [90]. In the near future the ready access to inexpensive, high-throughput DNA sequencing will undoubtedly enable direct targeting of PKS and NRPS pathways from diverse metagenomic samples [91].

18.4.2 Mass Spectrometry in Hybrid PK/NRP Systems

High-performance mass spectrometry, particularly FT-ICR MS experiments [92], have been conducted to characterize a wide variety of enzyme-bound intermediates in PKS, NRPS, and hybrid PKS/NRPS pathways. Application of this technology has greatly enabled analysis of enzyme kinetics using radiolabel-free approaches by identifying and characterizing intermediates with a high degree of sensitivity and selectivity [92]. FT-ICR MS has also been applied toward the screening of new pathways. This work has relied on a phage display to express protein segments encoding thiolation domains, which are then identified in a high-throughput manner using loss of the phosphopantetheine prosthetic group as a specific signal [93]. New hybrid MS approaches, developed further by the Dorrestein laboratory, are also highly innovative. By using MALDI imaging to localize marine natural products to a specific location, micromanipulation can be employed to simplify the environmental sample prior to whole genome sequencing [94]. Finally, the combination of multiple analytical techniques, such as enzyme

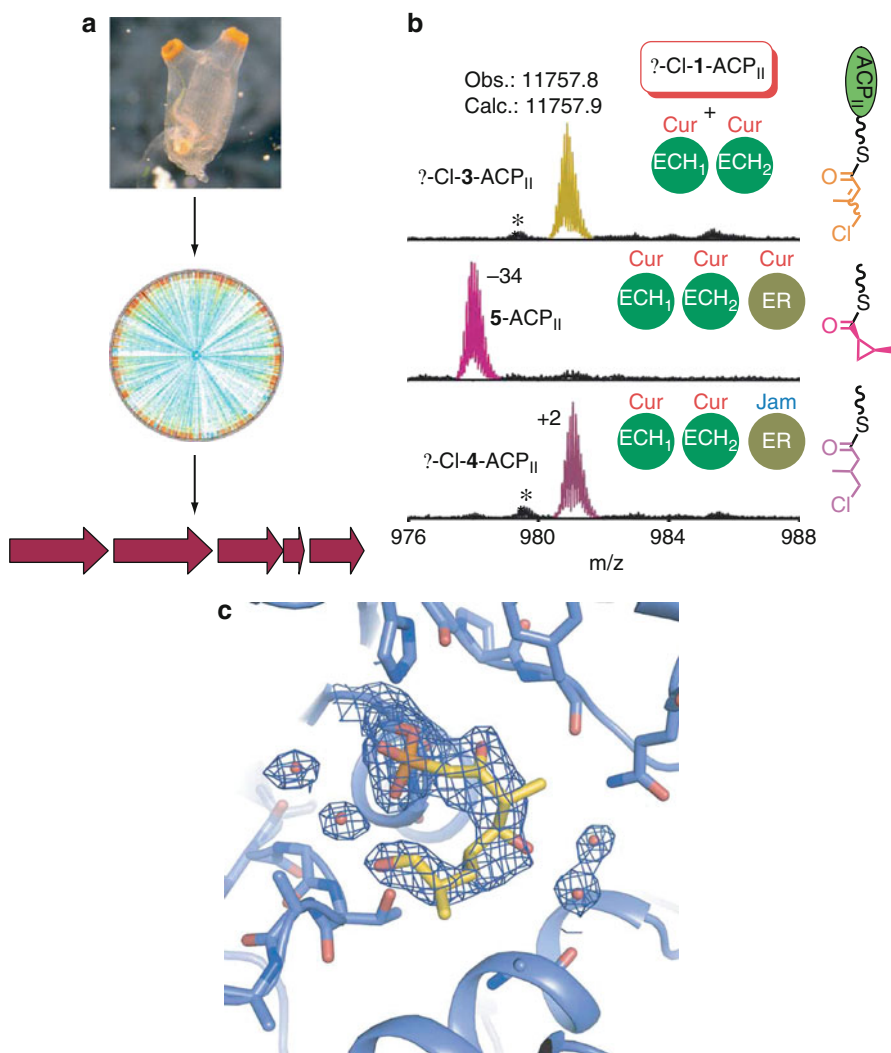


Fig. 18.8 Technology for improved analysis of natural product biosynthetic systems. (a) Metagenomic sequencing may be applied to symbiont–host systems to rapidly identify genes, which can then be probed *in silico* for biosynthetic genes. (b) Mass spectrometry allows for the direct interrogation of enzyme-bound intermediates in the curacin biosynthetic pathway. (c) Covalent probes and X-ray crystallography allow for active site specificity determining structures to be mapped in the pikromycin biosynthetic pathway

kinetics, FT-ICR mass spectrometry, and X-ray crystallography, enables the enzymology of diverse PKS/NRPS systems to be explored in remarkable detail, as was recently demonstrated in the curacin biosynthetic pathway β -branching cassette (Fig. 18.8) [28].

18.4.3 Structural Biology in PKS/NRPS Systems

X-ray crystallography and NMR-based structural analysis of biosynthetic enzymes can enhance our fundamental understanding of how these protein machines manufacture diverse natural products. The rate-limiting step for X-ray crystallography often resides in protein crystallization; however, high-throughput techniques to rapidly clone and express diverse gene constructs offer one viable strategy for overcoming this problem [95]. Fundamental questions, such as the nature of PKS/NRPS systems and whether they have a dimeric (PKS) or monomeric (NRPS) quaternary structure, can be addressed by structural analysis, as was demonstrated with recent crystallographic work in the type I iterative fatty acid synthase [96–101]. The most structurally well-characterized natural product biosynthetic system is the erythromycin (DEBS) modular PKS, which has been explored by X-ray crystallography through a series of excised catalytic domains and didomains [102]. One limiting factor in the complete structural determination of these megasynthases appears to be the overall flexibility of the ACP domains. Currently, structural information of ACPs has been derived by solution-phase NMR studies [103–105]. Emerging approaches for studying large protein complexes such as cryo-EM may also be integrated with high-resolution X-ray structural information as a step toward full understanding of these fascinating multicomponent biochemical machines.

18.5 Summary

By studying the coupled PKS and NRPS programming of PKS/NRPS pathways, a vast realm of biosynthetic space can be explored. Likewise, products of these pathways present a large pool of novel chemical entities that have been selected during evolution by providing an advantage to the producer/host. By leveraging these two pools of diversity, it is possible to access new tools to treat human health conditions within the sphere of cancer, immunomodulatory, infectious diseases, and other areas, as illustrated above. These clinically relevant marine-derived PK/NRP products represent a potent and expanding source of clinical leads. The coupling of this biosynthetic and chemical diversity is enabling us to take steps toward bypassing the traditional drawbacks of natural products research by providing facile access to metabolites through fermentation, and modification of existing products through pathway engineering.

Through further investigations of the unusual biosynthetic capabilities of the emerging class of noncanonical *trans* AT PKSs, we can hope to both expand our repertoire of capabilities while expanding our fundamental understanding of the flexibility of PK/NRP biosynthesis. Other developing topics such as the role of symbiosis in marine natural product biosynthesis seem to be uniquely located within these unusual *trans* AT systems. It is encouraging to look forward with the hope of applying modern techniques in molecular biology, biochemistry, and analytical chemistry to further dissect and manipulate the mixed PK/NRP natural products through rational design of their PKS/NRPS biosynthetic machinery.

NIH support for research on PKS/NRPS systems in the Sherman laboratory is gratefully acknowledged through grants GM076477, CA108874, and ICBG U01TW007404.

References

1. Newman DJ, Cragg GM (2007) Natural products as sources of new drugs over the last 25 years. *J Nat Prod* 70:461–477
2. Butler MS (2005) Natural products to drugs: natural product-derived compounds in clinical trials. *Nat Prod Rep* 25:162–195
3. Mozaffarian D, Nye R, Levy WC (2004) Statin therapy in congestive heart failure. *Am J Cardiol* 93:1124–1129
4. Nicolaou KC, Pfefferkorn JA, Roecker AJ, Cao GQ, Barluenga S, Mitchell HJ (2000) Natural product-like combinatorial libraries based on privileged structures. *J Am Chem Soc* 122:9939–9953
5. Wohlleben W, Pelzer S (2002) New compounds by combining “modern” genomics and “Old-fashioned” mutasynthesis. *Chem Biol* 9:1163–1164
6. Dobson CM (2004) Chemical space and biology. *Nature* 432:824–828
7. Hojati Z et al (2002) Structure, biosynthetic origin, and engineered biosynthesis of calcium-dependent antibiotics from *Streptomyces coelicolor*. *Chem Biol* 9:1175–1187
8. Kopp F, Marahiel M (2007) Where chemistry meets biology: the chemoenzymatic synthesis of nonribosomal peptides and polyketides. *Curr Opin Biotechnol* 18:513–520
9. Davis BG, Boyer V (2001) Biocatalysis and enzymes in organic synthesis. *Nat Prod Rep* 18:618–640
10. Gupta MN (1992) Enzyme function in organic solvents. *Eur J Biochem* 203:25–32
11. Wohlgemuth R (2007) Interfacing biocatalysis and organic synthesis. *J Chem Tech Biotech* 82:1055–1062
12. Schmid A et al (2001) Industrial biocatalysis today and tomorrow. *Nature* 409:258–268
13. Fischbach MA, Walsh CT (2006) Assembly-line enzymology for polyketide and nonribosomal peptide antibiotics: logic, machinery, and mechanisms. *Chem Rev* 106:3468–3496
14. Walsh CT (2004) Polyketide and nonribosomal peptide antibiotics: modularity and versatility. *Science* 303:1805–1810
15. Austin MB, Noel JP (2003) The chalcone synthase superfamily of type III polyketide synthases. *Nat Prod Rep* 20:79–110
16. Hopwood DA (1997) Genetic contributions to understanding polyketide synthases. *Chem Rev* 97:2465–2498
17. Gruschow S, Buchholz TB, Seufert W, Dordick JS, Sherman DH (2007) Substrate profile analysis and ACP-mediated acyl transfer in *Streptomyces coelicolor* type III polyketide synthases. *Chembiochem* 8:863–868
18. Marahiel MA, Stachelhaus T, Mootz HD (1997) Modular peptide synthetases involved in nonribosomal peptide synthesis. *Chem Rev* 97:2651–2674
19. Hicks LM, O'Connor SE, Mazur MT, Walsh CT, Kelleher NL (2004) Mass spectrometric interrogation of thioester-bound intermediates in the initial stages of epothilone biosynthesis. *Chem Biol* 11:327–335
20. Murphy CD (2006) Recent developments in enzymatic chlorination. *Nat Prod Rep* 23:147–152
21. Verdier-Pinard P et al (1998) Structure-activity analysis of the interaction of curacin A, the potent colchicine site antimitotic agent, with tubulin and effects of analogs on the growth of MCF-7 breast cancer cells. *Mol Pharmacol* 53:62–76

22. Gerwick WH et al (1994) Structure of Curacin-a, a novel antimitotic, antiproliferative, and brine shrimp toxic natural product from the marine cyanobacterium *Lyngbya majuscula*. *J Org Chem* 59:1243–1245
23. Blokhin AV et al (1995) Characterization of the interaction of the marine cyanobacterial natural product curacin A with the colchicine site of tubulin and initial structure-activity studies with analogues. *Mol Pharmacol* 48:523–531
24. Wipf P, Reeves JT, Balachandran R, Day BW (2002) Synthesis and biological evaluation of structurally highly modified analogues of the antimitotic natural product curacin A. *J Med Chem* 45:1901–1917
25. Wipf P, Reeves JT, Day BW (2004) Chemistry and biology of curacin A. *Curr Pharm Des* 10:1417–1437
26. Chang Z et al (2004) Biosynthetic pathway and gene cluster analysis of curacin A, an antitubulin natural product from the tropical marine cyanobacterium *Lyngbya majuscula*. *J Nat Prod* 67:1356–1367
27. Piel J, Wen G, Platzer M, Hui D (2004) Unprecedented diversity of catalytic domains in the first four modules of the putative pederin polyketide synthase. *Chembiochem* 5:93–98
28. Gu L et al (2007) GNAT-like strategy for polyketide chain initiation. *Science* 318:970–974
29. Gu L et al (2006) Metabolic coupling of dehydration and decarboxylation in the curacin a pathway: functional identification of a mechanistically diverse enzyme pair. *J Am Chem Soc* 128:9014–9015
30. Geders TW et al (2007) Crystal structure of the ECH2 catalytic domain of CurF from *lyngbya majuscula*. Insights into a decarboxylase involved in polyketide chain beta-branching. *J Biol Chem* 282:35954–35963
31. Gu L et al (2011) Tandem acyl carrier proteins in the curacin pathway promote consecutive multienzyme reactions with a synergistic effect. *Ange Chem Int Ed* 50(12):2795–2798
32. Negishi M et al (2001) Structure and function of sulfotransferases. *Arch Biochem Biophys* 390:149–157
33. Schwartz RE et al (1990) Pharmaceuticals from cultured algae. *J Ind Microbiol* 5:113–124
34. Trimurtulu G et al (1994) Total structures of cryptophycins, potent antitumor depsipeptides from the blue-green alga *Nostoc* sp. strain GSV224. *J Am Chem Soc* 116:4729–4737
35. Corbett TH et al (1996) Preclinical anticancer activity of cryptophycin-8. *J Exp Ther Oncol* 1:95–108
36. Panda D, Himes RH, Moore RE, Wilson L, Jordan MA (1997) Mechanism of action of the unusually potent microtubule inhibitor cryptophycin 1. *Biochemistry* 36:12948–12953
37. Smith CD, Zhang X, Mooberry SL, Patterson GM, Moore RE (1994) Cryptophycin: a new antimicrotubule agent active against drug-resistant cells. *Cancer Res* 54:3779–3784
38. Kobayashi M, Aoki S, Ohyabu N, Kurosu M, Wang W, Kitagawa I (1994) Arenastatin A, a potent cytotoxic depsipeptide from the Okinawan marine sponge *Dysidea arenaria*. *Tetrahedron Lett* 35:7969–7972
39. Subbaraju GV, Golakoti T, Patterson GM, Moore RE (1997) Three new cryptophycins from *Nostoc* sp. GSV 224. *J Nat Prod* 60:302–305
40. Chaganty S, Golakoti T, Heltzel C, Moore RE, Yoshida WY (2004) Isolation and structure determination of cryptophycins 38, 326, and 327 from the terrestrial cyanobacterium *Nostoc* sp. GSV 224. *J Nat Prod* 67:1403–1406
41. Lu K, Dempsey J, Schultz RM, Shih C, Teicher BA (2001) Cryptophycin-induced hyperphosphorylation of Bcl-2, cell cycle arrest and growth inhibition in human H460 NSCLC cells. *Cancer Chemother Pharmacol* 47:170–178
42. Edelman MJ et al (2003) Phase 2 study of cryptophycin 52 (LY355703) in patients previously treated with platinum based chemotherapy for advanced non-small cell lung cancer. *Lung Cancer* 39:197–199
43. D'Agostino G et al (2006) A multicenter phase II study of the cryptophycin analog LY355703 in patients with platinum-resistant ovarian cancer. *Int J Gynecol Cancer* 16:71–76

44. Liang J et al (2005) Cryptophycins-309, 249 and other cryptophycin analogs: preclinical efficacy studies with mouse and human tumors. *Invest New Drugs* 23:213–224
45. Magarvey NA et al (2006) Biosynthetic characterization and chemoenzymatic assembly of the cryptophycins. *ACS Chem Biol* 1:766–779
46. Seufert W, Beck ZQ, Sherman DH (2007) Enzymatic release and macrolactonization of cryptophycins from a safety-catch solid support. *Angew Chem Int Ed Engl* 46:9298–9300
47. Beck ZQ, Aldrich CC, Magarvey NA, Georg GI, Sherman DH (2005) Chemoenzymatic synthesis of cryptophycin/arenastatin natural products. *Biochemistry* 44:13457–13466
48. Beck ZQ, Burr DA, Sherman DH (2007) Characterization of the beta-methylaspartate-alpha-decarboxylase (CrpG) from the cryptophycin biosynthetic pathway. *Chembiochem* 8:1373–1375
49. Ding Y, Seufert WH, Beck ZQ, Sherman DH (2008) Analysis of the cryptophycin P450 epoxidase reveals substrate tolerance and cooperativity. *J Am Chem Soc* 130:5492–5498
50. Tang GL, Cheng YQ, Shen B (2004) Leinamycin biosynthesis revealing unprecedented architectural complexity for a hybrid polyketide synthase and nonribosomal peptide synthetase. *Chem Biol* 11:33–45
51. Du L, Shen B (2001) Biosynthesis of hybrid peptide-polyketide natural products. *Curr Opin Drug Discov Devel* 4:215–228
52. Kittendorf JD, Sherman DH (2006) Developing tools for engineering hybrid polyketide synthetic pathways. *Curr Opin Biotechnol* 17:597–605
53. Fortman JL, Sherman DH (2005) Utilizing the power of microbial genetics to bridge the gap between the promise and the application of marine natural products. *Chembiochem* 6:960–978
54. Piel J (2004) Metabolites from symbiotic bacteria. *Nat Prod Rep* 21:519–538
55. Schmidt EW (2008) Trading molecules and tracking targets in symbiotic interactions. *Nat Chem Biol* 4:466–473
56. Moss SJ, Martin CJ, Wilkinson B (2004) Loss of co-linearity by modular polyketide synthases: a mechanism for the evolution of chemical diversity. *Nat Prod Rep* 21:575–593
57. Zhu G et al (2002) *Cryptosporidium parvum*: the first protist known to encode a putative polyketide synthase. *Gene* 298:79–89
58. El-Sayed AK et al (2003) Characterization of the mupirocin biosynthesis gene cluster from *pseudomonas fluorescens* NCIMB 10586. *Chem Biol* 10:419–430
59. Ogasawara Y et al (2004) Cloning, sequencing, and functional analysis of the biosynthetic gene cluster of macrolactam antibiotic vicenistatin in *streptomyces halstedii*. *Chem Biol* 11:79–86
60. Chen X-H et al (2006) Structural and functional characterization of three polyketide synthase gene clusters in *bacillus amyloliquefaciens* FZB 42. *J Bacteriol* 188:4024–4036
61. Sudek S et al (2007) Identification of the putative bryostatin polyketide synthase gene cluster from “*candidatus endobugula sertula*,” the uncultivated microbial symbiont of the marine bryozoan *bugula neritina*. *J Nat Prod* 70:67–74
62. Lopanik NB et al (2008) In vivo and In vitro trans-acylation by BryP, the putative bryostatin pathway acyltransferase derived from an uncultured marine symbiont. *Chem Biol* 15:1175–1186
63. Calderone CT, Kowtoniuk WE, Kelleher NL, Walsh CT, Dorrestein PC (2006) Convergence of isoprene and polyketide biosynthetic machinery: isoprenyl-S-carrier proteins in the pksX pathway of *bacillus subtilis*. *Proc Natl Acad Sci USA* 103:8977–8982
64. Yadav G, Gokhale RS, Mohanty D (2003) Computational approach for prediction of domain organization and substrate specificity of modular polyketide synthases. *J Mol Biol* 328:335–363
65. von Dohren H, Dieckmann R, Pavela-Vranic M (1999) The nonribosomal code. *Chem Biol* 6:R273–R279
66. Nguyen T et al (2008) Exploiting the mosaic structure of trans-acyltransferase polyketide synthases for natural product discovery and pathway dissection. *Nat Biotechnol* 26:225–233

67. Buchholz TJ et al (2010) Polyketide β -branching in bryostatin biosynthesis: identification of surrogate acetyl-ACP donors for BryR, an HMG-ACP synthase. *Chem Biol* 17: 1092–1100
68. Cheng YQ, Tang GL, Shen B (2003) Type I polyketide synthase requiring a discrete acyltransferase for polyketide biosynthesis. *Proc Natl Acad Sci USA* 100:3149–3154
69. Tang GL, Cheng YQ, Shen B (2006) Polyketide chain skipping mechanism in the biosynthesis of the hybrid nonribosomal peptide-polyketide antitumor antibiotic leinamycin in *streptomyces atroolivaceus* S-140. *J Nat Prod* 69:387–393
70. Aron ZD, Dorrestein PC, Blackhall JR, Kelleher NL, Walsh CT (2005) Characterization of a new tailoring domain in polyketide biogenesis: the amine transferase domain of MycA in the mycosubtilin gene cluster. *J Am Chem Soc* 127:14986–14987
71. Reddick JJ, Antolak SA, Raner GM (2007) PksS from *bacillus subtilis* is a cytochrome P450 involved in bacillaene metabolism. *Biochem Biophys Res Commun* 358:363–367
72. Hansen DB, Bumpus SB, Aron ZD, Kelleher NL, Walsh CT (2007) The loading module of mycosubtilin: an adenylation domain with fatty acid selectivity. *J Am Chem Soc* 129:6366–6367
73. Aron ZD, Fortin PD, Calderone CT, Walsh CT (2007) FenF: servicing the mycosubtilin synthetase assembly line in trans. *Chembiochem* 8:613–616
74. Dorrestein PC et al (2006) Facile detection of acyl and peptidyl intermediates on thiotemplate carrier domains via phosphopantetheinyl elimination reactions during tandem mass spectrometry. *Biochem* 45:12756–12766
75. Fischbach MA, Walsh CT, Clardy J (2008) The evolution of gene collectives: how natural selection drives chemical innovation. *Proc Natl Acad Sci USA* 105:4601–4608
76. Bewley CA, Faulkner DJ (1998) Lithistid sponges: star performers or hosts to the stars. *Ange Chem Int Ed* 37:2162–2178
77. Haygood MG, Schmidt EW, Davidson SK, Faulkner DJ (1999) Microbial symbionts of marine invertebrates: opportunities for microbial biotechnology. *J Mol Microbiol Biotechnol* 1:33–43
78. Lee K-H et al (2005) Inhibition of protein synthesis and activation of stress-activated protein kinases by onnamide A and theopederin B, antitumor marine natural products. *Cancer Sci* 96:357–364
79. Perry NB, Blunt JW, Munro MHG, Pannel LK (1988) Mycalamide A, an antiviral compound from a New Zealand sponge of the genus *Mycale*. *J Am Chem Soc* 110:4850–4851
80. Sakemi S, Ichiba T, Kohmoto S, Saucy G, Higa T (1988) Isolation and structure elucidation of onnamide A, a new bioactive metabolite of a marine sponge, *Theonella* sp. *J Am Chem Soc* 110:4851–4853
81. Piel J (2002) A polyketide synthase-peptide synthetase gene cluster from an uncultured bacterial symbiont of *Paederus* beetles. *Proc Natl Acad Sci USA* 99:14002–14007
82. Piel J et al (2004) Antitumor polyketide biosynthesis by an uncultivated bacterial symbiont of the marine sponge *Theonella swinhoei*. *Proc Natl Acad Sci USA* 101:16222–16227
83. Piel J et al (2005) Exploring the chemistry of uncultivated bacterial symbionts: antitumor polyketides of the pederin family. *J Nat Prod* 68:472–479
84. Piel J, Hofer I, Hui D (2004) Evidence for a symbiosis island involved in horizontal acquisition of pederin biosynthetic capabilities by the bacterial symbiont of *paederus fuscipes* beetles. *J Bacteriol* 186:1280–1286
85. Li Z-F et al (2007) Evolutionary diversity of ketoacyl synthases in cellulolytic *myxobacterium sorangium*. *Syst Appl Microbiol* 30:189–196
86. Webster NS, Wilson KJ, Blackall LL, Hill RT (2001) Phylogenetic diversity of bacteria associated with the marine sponge *rhopaloeides odorabile*. *Appl Environ Microbiol* 67:434–444
87. Schirmer A et al (2005) Metagenomic analysis reveals diverse polyketide synthase gene clusters in microorganisms associated with the marine sponge *discodermia dissoluta*. *Appl Environ Microbiol* 71:4840–4849

88. Hrvatin S, Piel J (2007) Rapid isolation of rare clones from highly complex DNA libraries by PCR analysis of liquid gel pools. *J Microbiol Method* 68:434–436
89. Udvary DW et al (2007) Genome sequencing reveals complex secondary metabolome in the marine actinomycete *Salinispora tropica*. *Proc Natl Acad Sci USA* 104:10376–10381
90. Loper JE, Henkels MD, Shaffer BT, Valeriote FA, Gross H (2008) Isolation and identification of rhizoxin analogs from *Pseudomonas fluorescens* Pf-5 by using a genomic mining strategy. *Appl Environ Microbiol* 74:3085–3093
91. Piel J, Hui D, Fusetani N, Matsunaga S (2004) Targeting modular polyketide synthases with iteratively acting acyltransferases from metagenomes of uncultured bacterial consortia. *Environ Microbiol* 6:921–927
92. Dorrestein PC, Kelleher NL (2006) Dissecting non-ribosomal and polyketide biosynthetic machineries using electrospray ionization Fourier-Transform mass spectrometry. *Nat Prod Rep* 23:893–918
93. Yin J et al (2007) Genome-wide high-throughput mining of natural-product biosynthetic gene clusters by phage display. *Chem Biol* 14:303–312
94. Esquenazi E et al (2008) Visualizing the spatial distribution of secondary metabolites produced by marine cyanobacteria and sponges via MALDI-TOF imaging. *Mol Biosyst* 4:562–570
95. Dunlap WC et al (2006) New methods for medicinal chemistry—universal gene cloning and expression systems for production of marine bioactive metabolites. *Curr Med Chem* 13:697–710
96. Smith S (2002) Modular NRPSs are monomeric. *Chem Biol* 9:955–956
97. Maier T, Jenni S, Ban N (2006) Architecture of mammalian fatty acid synthase at 4.5 Å resolution. *Science* 311:1258–1262
98. Jenni S et al (2007) Structure of fungal fatty acid synthase and implications for iterative substrate shuttling. *Science* 316:254–261
99. Leibundgut M, Jenni S, Frick C, Ban N (2007) Structural basis for substrate delivery by acyl carrier protein in the yeast fatty acid synthase. *Science* 316:288–290
100. Smith S (2007) The type I fatty acid and polyketide synthases: a tale of two megasynthases. *Nat Prod Rep* 24:1041–1072
101. Maier T (2008) The crystal structure of a mammalian fatty acid synthase. *Science* 321:1315–1322
102. Khosla C, Tang Y, Chen AY, Schnarr NA, Cane DE (2007) Structure and mechanism of the 6-deoxyerythronolide B synthase. *Annu Rev Biochem* 76:195–221
103. Alekseyev VY, Liu CW, Cane DE, Puglisi JD, Khosla C (2007) Solution structure and proposed domain domain recognition interface of an acyl carrier protein domain from a modular polyketide synthase. *Protein Sci* 16:2093–2107
104. Mercer AC, Burkart MD (2007) The ubiquitous carrier protein—a window to metabolite biosynthesis. *Nat Prod Rep* 24:750–773
105. Zhou Z, Kai JR, Walsh CT (2007) Directed evolution of aryl carrier proteins in the enterobactin synthetase. *Proc Natl Acad Sci USA* 104:11621–11626

Claudia Wagner and Gabriele M. König

Contents

19.1	Introduction	978
19.1.1	Classification of Halogenating Enzymes According to their Mechanism	978
19.2	Haloperoxidases	979
19.3	Nonheme Fe ^{II} /α-Ketoglutarate/O ₂ -Dependent Halogenases	983
19.4	FADH ₂ -Dependent Halogenases	988
19.4.1	Sequence Specificities and Enzymatic Activity of FADH ₂ -Dependent Halogenases	999
19.4.2	Biotechnological Potential of FADH ₂ -Dependent Halogenases	1007
19.5	Halogenating Enzymes Utilizing S-Adenosyl-L-Methionine	1011
19.6	Concluding Remarks	1013
19.7	Study Questions	1013
19.7.1	Answer–Keywords	1014
	References	1015

Abstract

Chemical halogenation often requires harsh reaction conditions and results in unwanted by-product formation. It is thus of great interest to investigate the biosynthesis of halogenated natural products and the biotechnological potential of halogenating enzymes. Most of the biogenic organohalogens known today are marine-derived and often proposed to serve as antifeedant and antibacterial defense agents; however, knowledge on biological halogenation in marine organisms still is very limited. Today, mainly vanadate-depending haloperoxidases (Va-HPO) and nonheme Fe^{II}/α-ketoglutarate/O₂-dependent halogenases are described for secondary metabolite biosynthesis in marine

C. Wagner (✉) • G.M. König (✉)

Institute for Pharmaceutical Biology, University of Bonn, Nussallee 6, Bonn, Germany
e-mail: claudia.wagner@uni-bonn.de, g.koenig@uni-bonn.de

organisms. Beyond that, also enzymes utilizing *S*-adenosyl-L-methionine in halogen transfer are found in marine environments. This review aims to give a comprehensive overview on the different strategies used by nature to incorporate halogens into secondary metabolites.

19.1 Introduction

Approximately 4,500 compounds known to be produced by living organisms are organohalogens [1–4]. Structural classes range from simple phenolic or aliphatic compounds to complex polyketides and oligopeptides (Figs. 19.4, 19.6, 19.9, 19.10, 19.11, 19.12, 19.13). Biological activities are equally diverse, e.g., antibiotic and antitumor activity as known for chloramphenicol (Fig. 19.12), glycopeptide antibiotics, and cryptophycin (Fig. 19.9), or specific proteasome inhibition as found for salinosporamide A (Fig. 19.16). While from terrestrial organisms a variety of chlorinated metabolites are known, marine halogenated secondary metabolites are more commonly brominated. In general, fluorinated metabolites are extremely rare, mainly due to the high desolvation energy required to activate F^- in aqueous solution [5].

Overall, most of the biogenic organohalogens are marine-derived [1] and often proposed to serve as antifeedant and antibacterial defense agents. However, knowledge on biological halogenation in marine organisms still is very limited. Today, mainly vanadate-depending haloperoxidases (Va-HPO) and nonheme Fe^{II}/α -ketoglutarate/ O_2 -dependent halogenases are described for secondary metabolite biosynthesis in marine organisms. More recently, the unique *S*-adenosyl-L-methionine-requiring enzyme, SalL, has been identified to be involved in the salinosporamide A biosynthesis by the marine actinomycete *Salinispora tropica* [6]. Beyond that, to complete the picture, this review will also include the important group of $FADH_2$ -depending halogenases, even though such enzymes were not yet identified from marine organisms.

19.1.1 Classification of Halogenating Enzymes According to their Mechanism

Halogenating enzymes mainly can be grouped into two classes:

1. Less specific haloperoxidases (HPO), utilizing hydrogen peroxide and having heme or vanadate involved as cofactor.
2. Highly substrate-specific halogenases requiring dioxygen for enzymatic activity. In dioxygen-depending halogenases, either α -ketoglutarate, in nonheme Fe^{II}/α -ketoglutarate/ O_2 -dependent halogenases, or flavin, in $FADH_2$ -depending halogenases, is found to function as a cosubstrate.

Furthermore, methyltransferases are involved in the formation of the carbon–halogen bonds of CH_3Cl , CH_3Br , and CH_3I , and other enzymes requiring *S*-adenosyl-L-methionine as catalyst have been identified to be involved in fluorination and chlorination reactions [6, 7].

19.2 Haloperoxidases

Until the mid-1990s, the understanding of biological halogenation reactions was restricted to haloperoxidases (HPO). These enzymes generate hypohalous acid (HOX) or related halogenating intermediates, such as OX^- , X_3^- , and X^+ , by the reaction of a metal-bound hydroperoxy species with a halide ion (Fig. 19.1). In most cases, the halogenating species is then released from the enzyme to act on organic substrates that are susceptible to an attack by electrophiles. The enzymes are found to contain either heme or vanadate as cofactor in their active site [8–10]. In heme-containing HPOs, the formation of hypohalous acid is driven by a redox mechanism, whereas vanadate-containing HPOs do not change their oxidation state during the enzymatic cycle but rather function as Lewis acids. HPOs are further classified according to the halide ion which they are predominantly able to utilize for

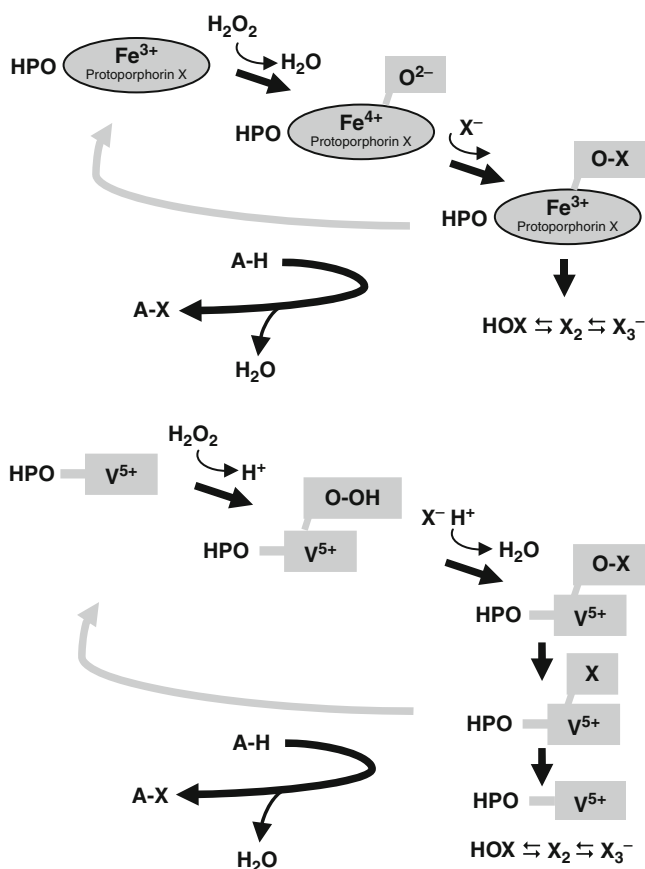


Fig. 19.1 Both heme- and vanadium-dependent HPOs are thought to generate bound hypohalite intermediates and hypohalous acid which react as X^+ equivalents with electron-rich substrates (X: halide, A: organic substrate)

halogenation [11]. Thus, the nomenclature is based on the most electronegative halide oxidized by the enzyme. Chloroperoxidases (CPOs) catalyze the oxidation of chloride, bromide, and iodide, while bromoperoxidases (BPOs) only catalyze the oxidation of bromide and iodide, and iodoperoxidases (IPOs) are specific for iodide oxidation [12]. However, hydrogen peroxide does not have the driving force to oxidize fluoride [8].

The first halogenating enzyme was described from the caldariomycin-producing fungus *Caldariomyces fumago* as a heme-containing HPO [13]. Hager and coworkers developed a spectrophotometric assay, using monochlorodimedone as a mimic of the natural precursor of caldariomycin, to monitor for HPO activity (Fig. 19.2). Based on this assay, several heme HPOs were subsequently discovered from diverse fungi, algae, and microorganisms [9, 10, 14]. The detected HPOs were shown to have a broad substrate specificity, accepting organic compounds, which are generally susceptible to electrophilic attack. Thus, regioselectivity was the same as that seen in chemical halogenations.

In addition to halogenating activity, ferric heme HPOs have been shown to share catalytic properties with at least three further classes of heme-containing oxidoreductases, namely, classical peroxidases, cytochrome P450 monooxygenases, and catalases [10]. Intensive studies on structural and functional aspects of the heme HPO have focused mainly on the initially described CPO from *C. fumago*. Under investigation was the chlorination activity of this enzyme, as well as its epoxidation and sulfoxidation activity in the absence of halide [10, 15–19]. A recent study on the chlorination mechanism confirmed that the final chlorine transfer to various substrates occurs outside the active site via a free diffusible species without any special mode of substrate recognition [20]. In contrast, epoxidation and sulfoxidation are performed regioselectively, providing *C. fumago* CPO as

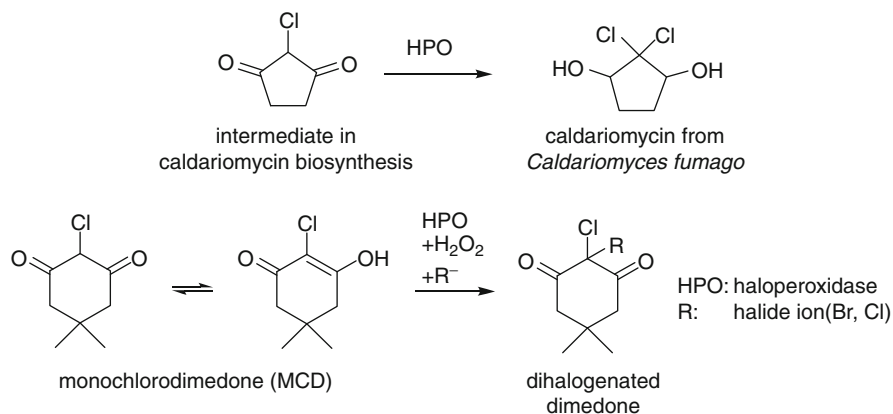


Fig. 19.2 2-Chloro-1,3-cyclopentanedione is a late intermediate in caldariomycin biosynthesis, the natural product from *Caldariomyces fumago*. Based on this reaction, the conversion of the synthetic analog monochlorodimedone is applied in HPO activity assays

a useful tool in synthetic applications. Further investigations were conducted towards the dehalogenation of trihalophenols and *p*-halophenols [21]. *C. fumago* CPO proved to be capable of catalyzing such degradation processes and was significantly more robust than other peroxidases. Thus, this CPO might be applicable in biodegradation of polychlorinated phenols and further noxious haloaromatic compounds, under reaction conditions often too harsh for other biocatalysts.

Vanadate ion-containing bromoperoxidases (Va-BPOs) have been isolated mainly from marine algae. This group of enzymes most likely seems to play a role in the formation of marine natural products, e.g., the halogenation and cyclization of terpenes [22]. Va-HPOs bind hydrogen peroxide and halides leading to a putative enzyme-bound or active site-trapped brominating moiety [23]. X-ray crystal structures of the Va-BPO from *Curvularia inaequalis* [24], *Ascophyllum nodosum* [25], and *Corallina officinalis* [26] displayed a channel leading to the vanadium binding site, which is proposed to influence substrate specificity [27]. Competitive kinetic studies, comparing the bromination of indole substrates by Va-HPO with enzyme-free preparations under aqueous conditions, showed that these reactions were not congruent, since Va-HPO preferably brominated indole derivatives even in the presence of other substrates, such as monochlorodimedone or phenol red [8, 28]. In the absence of a suitable substrate, however, HOBr is released from the enzyme and carries out unselective bromination as observed for aqueous bromine. The role of Va-BrPO in biosynthesis has been further established by the observation that the ratio of formed diastereomers was also found to differ between purely chemical and enzymatic reactions. Accordingly, asymmetric bromination and cyclization of the terpenoid precursor (*E*)-(+)-nerolidol could be demonstrated for Va-BPO, producing single diastereomers of the marine natural product β -snyderol as isolated from *Laurencia* sp. [27] (Fig. 19.3).

The first Va-BPO to be characterized was from the brown seaweed *Ascophyllum nodosum* [29]. However, with the isolation of a Va-BPO from the lichen *Xanthoria parietina*, it became obvious that this group of enzymes not only occurs in the marine environment but also can be found in terrestrial eukaryotic organisms [30]. Va-CPOs on the other hand have been mainly found in fungi even though, to date, halogenated natural products have not been identified from the corresponding strains [31]. The first indication of the potential involvement of a Va-CPO in the biosynthesis of a marine natural product has recently been discussed regarding the chlorination and cyclization of napyradiomycin (Fig. 19.12), a compound obtained from the marine sediment-derived *Streptomyces* sp. CNQ-525 [31, 32].

In contrast to the iron heme haloperoxidases, Va-HPOs do not catalyze the direct disproportion of hydrogen peroxide and, therefore, have no catalase activity [33]. However, their structural similarity to acid phosphatases is noticeable, particularly in the domains providing the vanadate and phosphate binding site. Therefore, a common evolutionary origin is proposed as being likely [23].

Recent studies aim to characterize the active site in Va-HPO more precisely, whereby the residues involved in the selection and binding of the specific halide are the main focus [31]. Heterologous expression and mutagenesis studies of Va-BPO

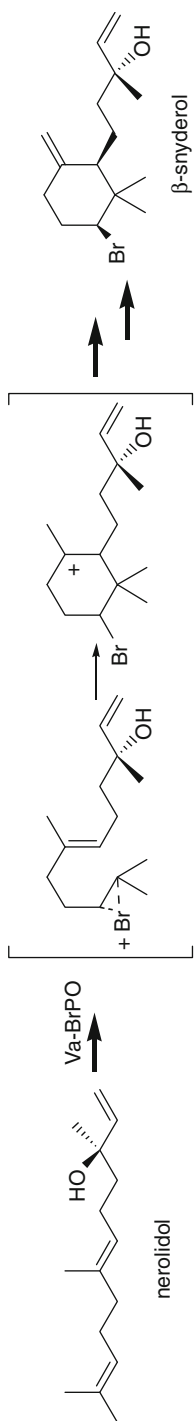


Fig. 19.3 Proposed mechanism of the stereospecific snyderol biosynthesis by Va-BrPO [27]

from *Curvularia inaequalis* and *Corallina officinalis* explore the potential of this type of enzymes in biotransformations [34, 35].

Hypohalous acid is a bactericidal agent, and many halogenated compounds have antimicrobial activity, illustrating the possible involvement of HPO systems in natural defense mechanisms. This might prevent biofouling by microorganisms on the surface of marine algae as well as act as an antifeeding system. Experiments with the marine alga *Laminaria digitata* demonstrated that natural HPO systems are also capable of mediating the deactivation of acylated homoserine lactones, which are important as cell-to-cell signaling molecules for biofilm formation [36]. This suggests that oxidized halogens may control biofouling not only via a bactericidal mechanism but also by possibly interfering with bacterial cell signaling systems. As described above, an involvement of HPOs in the biosynthesis of natural products has only been suggested in a very few cases [22, 27, 32]. The physiological function of CPOs in fungi is mainly proposed as being important for the degradation of plant cell walls. The hypohalous acid produced thus oxidizes lignocellulose and facilitates penetration of the fungal hyphen into a host [23]. Furthermore, Va-IPOs seem to play a role in iodine accumulation of brown algae as a main vector of the iodine biogeochemical cycle [37]. Species like *Laminaria digitata* are thereby able to take up an average content of 1% of their dry weight, representing approximately a 30,000-fold accumulation of iodine from seawater. Iodine efflux and the production of volatile halocarbons, then again, are proposed to be part of an early defense response to various biotic and abiotic stresses by these organisms. This assumption was strengthened, since the transcription of members of the Va-IPO gene family was demonstrated to be rapidly and highly induced as a defense response [38].

19.3 Nonheme Fe^{II}/α-Ketoglutarate/O₂-Dependent Halogenases

In the last years, evidence has accumulated that another class of halogenating enzymes, able to carry out chlorination of inactivated carbon centers, plays an important role in the biosynthesis of marine organohalogenes. Using α-ketoglutarate (α-KG) as cosubstrate, these halogenases are involved in the chlorination of terminal methyl groups of amino acids linked to peptidyl carrier proteins (Table 19.1).

Initial insight into their catalytic mechanism is derived from investigations on SyrB2, which chlorinates the γ-methyl group of L-threonine in syringomycin E (Fig. 19.4) biosynthesis in *Pseudomonas syringae* [39, 40]. Halogenation of L-threonine occurs only when bound to the peptidyl carrier protein SyrB1, while free L-threonine is not accepted as a substrate. Reactions performed with an excess of sodium bromide demonstrated that SyrB2 was also capable of incorporating bromine into the threonyl-S-protein [41], however, with a clear preference to chlorine over bromine. From crystallographic data [42], it was confirmed that Fe^{II} of the active site is complexed by two histidine residues. A halide ligand (chloride or bromide) together with α-KG and water coordinates the iron in the

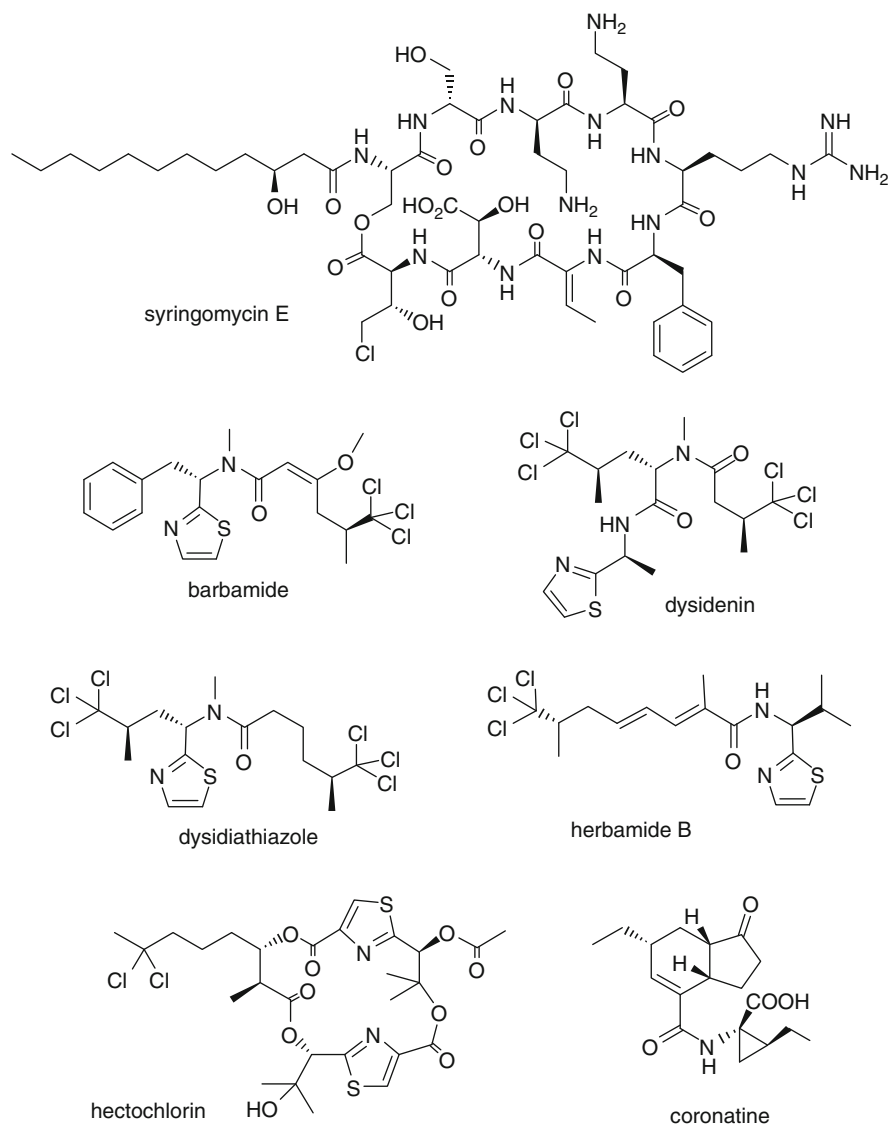
Table 19.1 Fe^{II}/α-ketoglutarate/O₂-dependent halogenases

Halogenases	Natural product <i>Organism</i>	Halogenated structural element	GenBank accession number [reference]
SyrB2	Syngomycin E <i>Pseudomonas syringae</i>	L-threonine ^a	U25130, AF047828 [40, 127, 128]
BarB1/BarB2	Barbamide <i>Lyngbya majuscula</i>	L-leucine ^b	AF516145 [48, 49, 129]
DysB1/DysB2	Dysidenin <i>Oscillatoria spongeliae</i> 35P1 ^c	N.S. ^d	AY628171 AY628172 [50]
CytC3	Armentomycin <i>Streptomyces</i> spp.	L-aminobutyrate ^e	n.d. ^f [55]
HctB	Hectochlorin <i>Lyngbya majuscula</i>	N.S. ^d	AY974560 [130]
CmaB ^g	Coronatine <i>Pseudomonas syringae</i>	L- <i>allo</i> -isoleucine	U14657 [57, 131]
KtzD ^h	Kutznerides <i>Kutzneria</i> sp. 744	N.S. ^d	EU074211 [132]
JamHal ⁱ	Jamaicamides <i>Lyngbya majuscula</i> JHB	N.S. ^d	AY522504 [51, 52]
CurHal ^j	Curacin A <i>Lyngbya majuscula</i> JHB	(s)-3-hydroxy-3-methylglutaryl	AY652953 [52, 133]

^aOnly when bound to the peptidyl carrier protein SyrB1^bThe triple chlorination is catalyzed by a tandem action of the two enzymes^c*Oscillatoria spongeliae* 39P1: AY628173, AY628174 [50]; *Oscillatoria spongeliae* AY648943 [134]^dNot specified^eBound to the peptidyl carrier protein CytC2^fNo sequence data available in GenBank^gMediates the formation of the cyclopropane ring^hHypothesized to be involved in the formation of the cyclopropane ringⁱEmbedded in the PKS module JamE^jEmbedded in the PKS module CurA

resting Fe^{II} state (Fig. 19.5). Dioxygen attack results in decarboxylation of α-KG, and a highly reactive iron-oxo species (Fe^{IV} = O) is formed as a general key feature of catalysis by these α-oxoacid-dependent dioxygenases [43]. The Fe^{IV} = O abstracts a hydrogen radical from an aliphatic carbon center of the actual substrate, which, in turn, abstracts the halide from the coordination sphere. It has been shown that in vitro SyrB2 was rapidly deactivated during catalysis and no more than about seven turnovers of the enzyme were possible [43]. Further mechanistic studies, especially focusing on the preference of halogenation over hydroxylation during the catalytic cycle, are still ongoing, e.g., as recently published by de Visser and Latifi [44], Wong et al. [45], Matthews et al. [46, 47], and Kulik et al. [4].

For several marine natural products that are halogenated at an unactivated carbon center, analogous halogenating enzymes were suggested to be involved in their biosynthesis, e.g., barbamide, dysidenin, dysideathiazole, jamaicamides, and

**Fig. 19.4** (continued)

herbamide B (Fig. 19.4) [41, 48–54]. Indeed, in the barbamide gene cluster of *Lyngbya majuscula*, two genes, i.e., *barB1* and *barB2*, homologous to *syrB2* could be identified. The initial biosynthetic step is the chlorination of L-leucine to a trichloroleucine derivative, followed by a subsequent conversion to a unique trichloroisovaleryl starter unit in a mixed nonribosomal peptide (NRPS)/polyketide

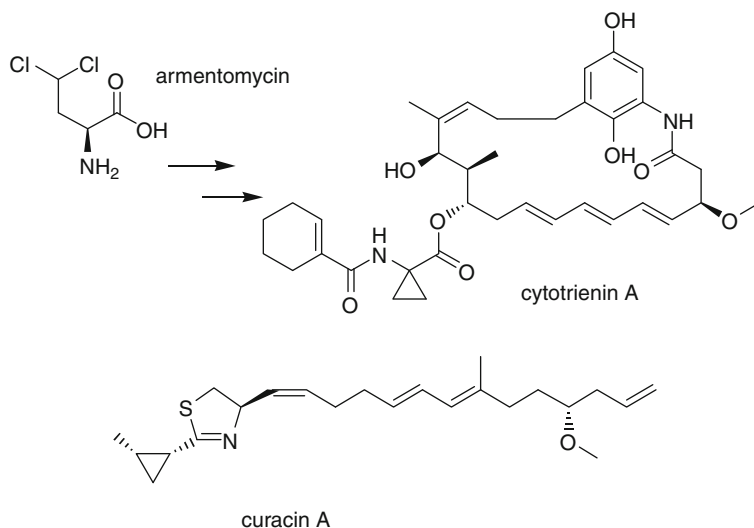


Fig. 19.4 Natural products to be halogenated by $\text{Fe}^{\text{II}}/\alpha$ -ketoglutarate/ O_2 -dependent halogenases. Cyclopropyl ring formation of coronatine is executed via a γ -chlorination of *L*-allo-isoleucine followed by intramolecular cyclization

(PKS) pathway [48, 49]. Regarding dysidenin production in dictyoceratid sponges, similar genes (*dysB1/dysB2*) were found and could be ascribed to the cyanobacterial symbiont *Oscillatoria spongeliae* [50].

A $\text{Fe}^{\text{II}}/\alpha$ -ketoglutarate/ O_2 -dependent halogenase homologous enzyme, CytC3, involved in the formation of the γ,γ -dichloroaminobutyrate armentomycin (Fig. 19.4) was identified from a soil *Streptomyces* sp. [55]. Interestingly, the γ,γ -dichloroaminobutyryl moiety is postulated to be further cyclized and to act as a precursor in cytotrienin A formation. CytC3 could be demonstrated to act on *L*-aminobutyrate bound to a peptidyl carrier protein, CytC2. Spectroscopic monitoring of the enzymatic reaction confirmed that the chlorination proceeds through an Fe^{IV} intermediate that cleaves the C–H bond of the amino acid substrate [56], as described above. By analogy, γ -chlorination of an *L*-allo-isoleucine by the $\text{Fe}^{\text{II}}/\alpha$ -ketoglutarate/ O_2 -dependent halogenase CmaB mediates the formation of the cyclopropane ring in coronatine (Fig. 19.4), which is produced by several *Pseudomonas syringae* strains [57]. The intermediate γ -chloroaminoacyl β -thioester is then converted to a γ -carbanion, which, in turn, is accessible to intramolecular cyclization [58]. Evidence for a very similar biosynthetic mechanism was observed for the marine secondary metabolite curacin A (Fig. 19.4). From the respective gene cluster of *Lyngbya majuscula*, it was deduced that the formation of the β -branched cyclopropane moiety is initiated by an analogous γ -chlorination step [52].

19.4 FADH₂-Dependent Halogenases

Even though not yet firmly linked to any biosynthetic pathway from organisms of the marine habitat, FADH₂-dependent halogenases form another very important class of halogenating enzymes and thus are included in this overview. This group of enzymes was first discovered when investigating pyrrolnitrin (Fig. 19.6) and chlorotetracycline (Fig. 19.9) biosynthesis [59, 60]. The four enzymes (PrnA, B, C, D) involved in pyrrolnitrin production have been identified from a 6.2-kb genomic DNA region of *Pseudomonas fluorescens* BL915 [59], and their function was proved by construction of deletion mutants for all four genes of the cluster [61]. PrnA (Table 19.2) and the PrnC (Table 19.4) were shown to act as highly substrate-specific halogenases, i.e., the tryptophan halogenase (PrnA) was not able to chlorinate the PrnC substrate monodechloramino-pyrrolnitrin and vice versa [62]. Both enzymes also perform the respective chlorination reaction highly regioselectively, and van Pée and coworkers demonstrated that PrnA is able to halogenate L-tryptophan in a site-specific manner to yield 7-chlorotryptophan [63]. Even though other indole derivatives were also accessible to halogenation by PrnA, they were chlorinated at different sites, i.e., at positions C-2 or C-3. Thus, for regioselectivity, the exact positioning of the specific biosynthetic intermediate at the active site of the halogenating enzyme seems to be of major importance and allows chlorination at a site of the molecule not accessible to chemical halogenation.

It was further shown that the enzymes, PrnA and PrnC ascribed to the two halogenating steps of pyrrolnitrin biosynthesis, require FADH₂ as cofactor [64, 65], which is produced from FAD and NADH by a flavin reductase. A direct contact between the halogenase and the flavin reductase is thereby not absolutely necessary since free diffusible FADH₂ can also be used. Even chemically reduced flavin, regenerated using organometallic complexes, can be utilized [66]. However, free FADH₂ is rapidly decomposed into FAD and H₂O₂ with molecular oxygen, which leads to a significant decrease in halogenase activity. Recent sequencing of the *Pseudomonas fluorescens* Pf-5 genome [67] has revealed that the complete gene clusters for pyrrolnitrin as well as pyoluteorin biosynthesis contain genes encoding for a flavin reductase. This gives rise to the assumption that a distinct flavin reductase specifically interacts with each halogenase to prevent loss of FADH₂ through autooxidation [68].

The mechanism for regioselective chlorination has been further characterized using a purified protein from a *P. fluorescens* BL915 PrnA overexpression system. Cocrystallization of the enzyme with tryptophan and FAD yielded yellow diamond-shaped crystals, indicating that FAD was bound to the protein [69]. From further investigations, it could be demonstrated that FAD and Cl⁻ are bound at the same site of the enzyme, while the tryptophan-binding module is located at a 10-Å distance [70]. FADH₂ reacts with O₂ and forms a peroxide-linked isoalloxazine ring, as generally known from flavin-dependent monooxygenases. Subsequently, HOCl is produced as chlorinating agent and channeled through an intraenzymatic tunnel to the substrate binding pocket. However, HOCl is not released from the enzyme to act in a freely diffusible form in solution. Dong et al.

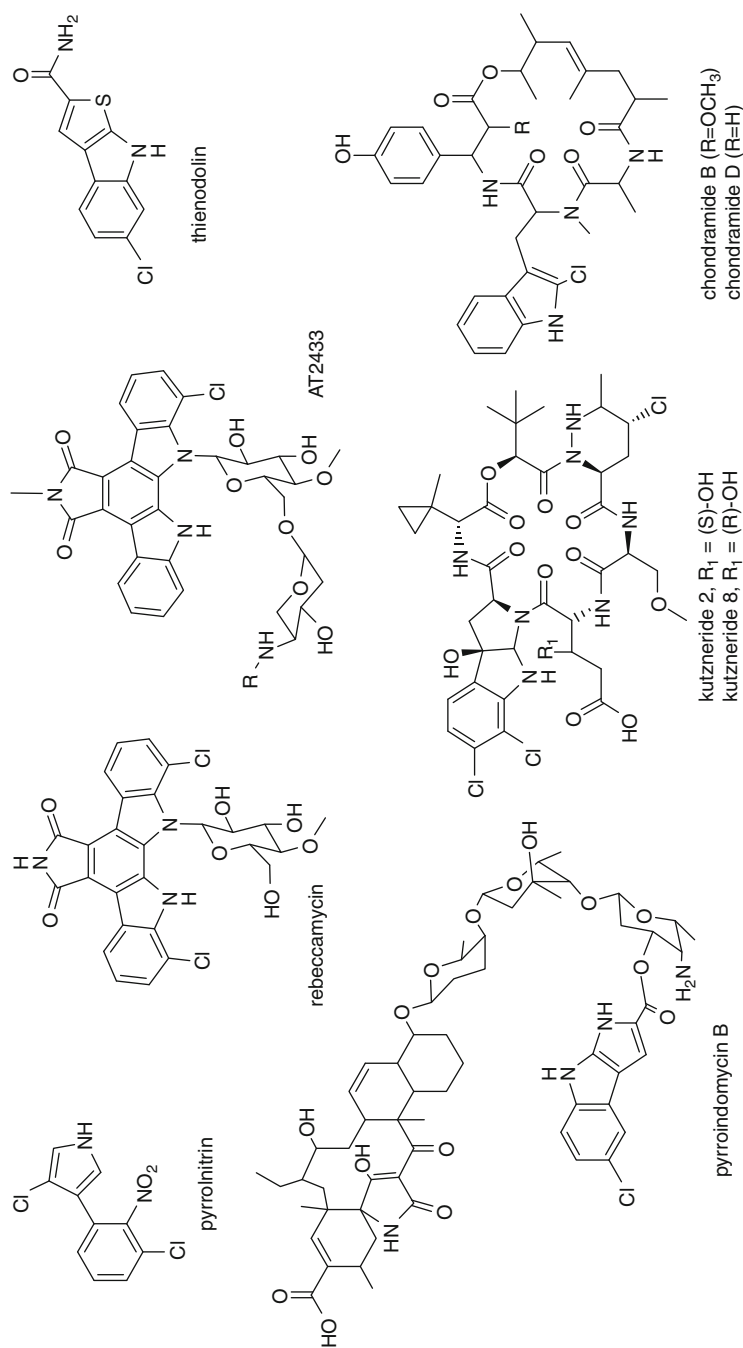


Fig. 19.6 Compounds with chlorinated indole moieties formed from tryptophan. In pyrrolnitrin, rebeccamycin, and AT2433 biosynthesis, a tryptophan-7-halogenase; in thienodolin biosynthesis, a tryptophan-6-halogenase; and in pyrroindomycin biosynthesis, a tryptophan-5-halogenase were identified to catalyze the initial biosynthetic step. In the kutznerides biosynthesis, a tryptophan-7-halogenase and a tryptophan-6-halogenase work in a tandem action to produce 6,7-dichloro-L-tryptophan. Only the tryptophan halogenation at position C-2 in chondramide B and D biosynthesis occurs during NRPS assembly

Table 19.2 FADH₂-dependent halogenases that halogenate tryptophan in the initial step of the respective natural product biosynthesis

Halogenases	Natural product <i>Organism</i>	Halogenated structural element	GenBank accession number [reference]
PmA	Pyrrolnitrin <i>Pseudomonas fluorescens</i> BL915	Tryptophan at position C-7	PFU74493 [59]
RebH	Rebeccamycin <i>Lechevalieria aerocolonigenes</i> ATCC 39243	Tryptophan at position C-7	AJ414559 [72]
PyrH	Pyroindomycin B <i>Streptomyces rugosporus</i> LL-42D005	Tryptophan at position C-5	AY623051 [77]
Thal	Thienodolin <i>Streptomyces albogriseolus</i>	Tryptophan at position C-6	EF095207 [71]
KtzQ ^a	Kutznerides <i>Kutzneria</i> sp. 744	Tryptophan at position C-7	EU074211[132]
KtzR ^a	Kutznerides <i>Kutzneria</i> sp. 744	7-Cl-tryptophan at position C-6 ^b	EU074211[132]
AtmH	AT2433 <i>Actinomadura melliaura</i>	Tryptophan at position C-7	DQ297453 [135]

^aWorking in a tandem action, first KtzQ on unmodified tryptophan followed by KtzR on 7-Cl-L-tryptophan to form 6,7-dichlorotryptophan [136]

^bWith an approximate 120-fold preference over unsubstituted tryptophan [136]

postulated that chlorine may be hydrogen-bound to the Lys-79 residue located at the end of the tunnel. In this manner, chlorine would be activated by increased electrophilicity, allowing it to react with tryptophan. In addition, the importance of Glu-346 to stabilize and then deprotonate the substrate intermediate during this process was confirmed by site-directed mutagenesis experiments. The basis for regioselective halogenation is thus the controlled presentation of the substrate to the bound Cl-species via particular amino acid residues in the substrate binding site (Fig. 19.7) [71].

RebH (Table 19.2) is another tryptophan-7-halogenase which has been identified within the rebeccamycin (Fig. 19.6) biosynthetic gene cluster of *Lechevalieria aerocolonigenes* ATCC39243 [72, 73]. RebH was shown to catalyze the initial step of rebeccamycin biosynthesis converting L-tryptophan to 7-chlorotryptophan [74]. RebF catalyzes the NADH-dependent reduction of FAD to provide FADH₂ and thus acts together with RebH in a robust two-component reductase/halogenase system. From spectroscopically performed kinetic analysis of RebH, a detailed reaction scheme was proposed (Fig. 19.8) [75]. Initially, FADH₂ is transferred to a FAD(C4a)-oxygenated species, and from this FAD(C4a)-OOH intermediate (observed as an increase in absorbance at 390 nm), an OH⁺ equivalent reacts with a chlorine ion yielding HOCl and FAD(C4a)-OH. Finally, an increase in absorbance at 450 nm indicated the dehydration of FAD(C4a)-OH to fully oxidize FAD. The actual chlorination of tryptophan thus occurs independently after the oxidative

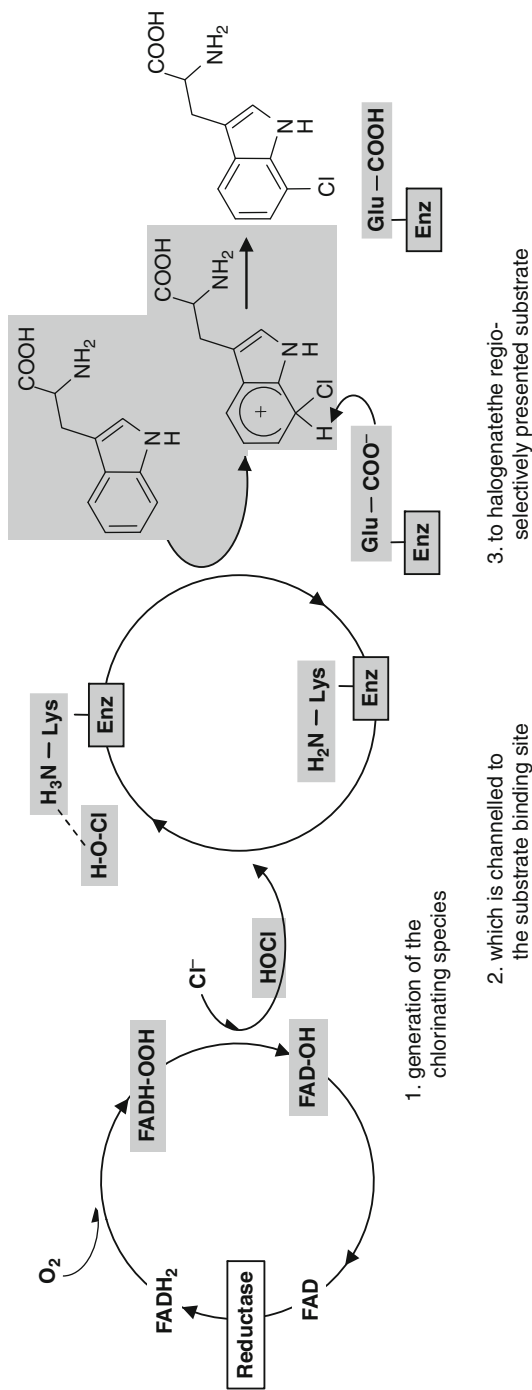


Fig. 19.7 Mechanism of the halogenation reaction of a FADH₂-dependent halogenase (gray-shaded are the processes that proceed within the halogenase enzyme)

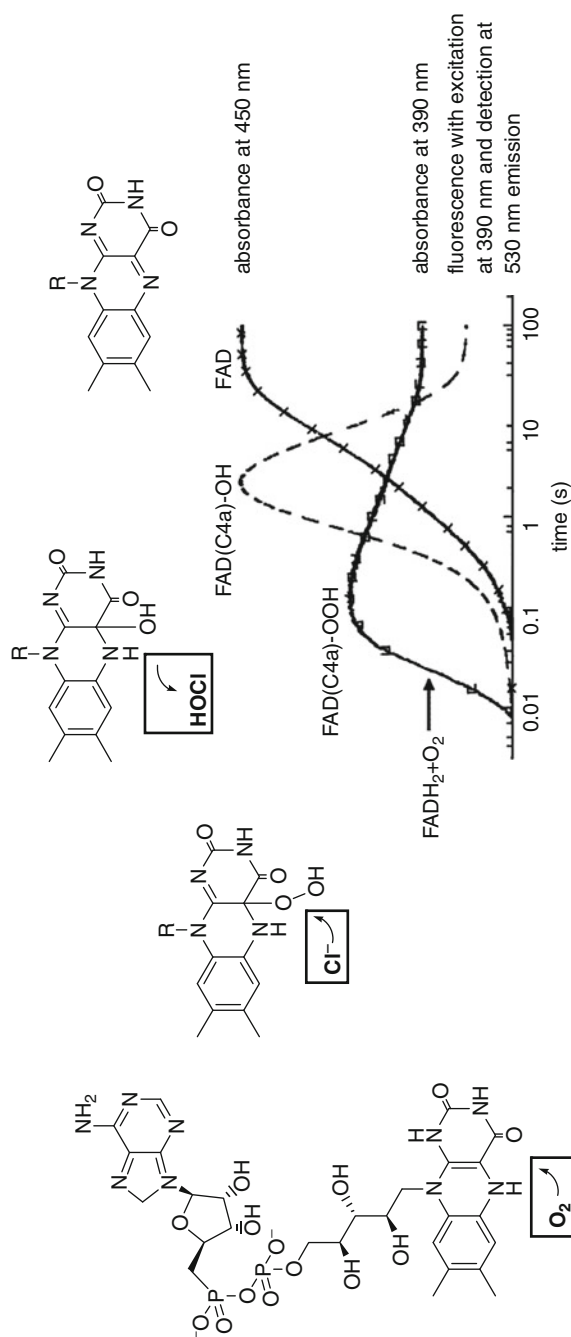


Fig. 19.8 Timing of flavin intermediates and product formation as spectroscopically monitored by Walsh and coworkers [75]

reaction of flavin is completed. Protein dynamics leading to conformational changes are assumed to shield the oxygenated FAD(C4a) intermediates from solvent, thereby preventing their rapid breakdown and providing a site for generating the chlorinating agent. Recently, it has been demonstrated that a stable long-living enzyme-bound chlorinating species ($t_{1/2}$ of 28 h at 25°C) is formed during the reaction of RebH with FADH₂, Cl⁻, and O₂, which remains on the active site even after removal of FAD until a substrate becomes available for reaction [76]. This chlorinating intermediate is proposed to be a covalently bound lysine chloramine (Lys79-εNH-Cl), located ideally to deliver a Cl⁺ equivalent for the electrophilic aromatic substitution of the tryptophan indole ring at C-7.

Further specific halogenases (Table 19.2) capable to chlorinate tryptophan at positions C-6 and C-5 were also found. A selective tryptophan-5-halogenase (PyrH) was shown to be involved in pyrroindomycin B (Fig. 19.6) biosynthesis of *Streptomyces rugosporus* LL-42D005 [77] as well as a tryptophan-6-halogenase (Thal) in the thienodolin (Fig. 19.6) production by *Streptomyces albogriseolus* [71], both ascribed to catalyze initial steps in the biosynthesis. From comparison of the crystal structure of the tryptophan-5-halogenase (PyrH) with that of the tryptophan-7-halogenases, significant differences in the tryptophan-binding module were observed. This, together with site-directed mutagenesis studies, further explained the regioselectively controlled chlorination of tryptophan, showing that the respective carbon atom to be halogenated is solely presented to the chlorine species, while other potential reactive sites are shielded [78].

In contrast to the above-mentioned halogenases, the tryptophan-2-halogenase, CmdE, which is associated with the formation of chondramides B and D (Fig. 19.6; Table 19.3) from the myxobacterium *Chondromyces crocatus* Cm c5, was demonstrated to be part of a biosynthetic assembly line [79]. Chondramides are of mixed NRPS/PKS origin, and, to date, CmdE is the only example of a tryptophan halogenase integrated in such a modular biosynthetic pathway. Consequently, it is not surprising that the highest homologies of CmdE can be found in halogenases like those involved in cryptophycin (CrpH), avilamycin A (AviH), and clorobiocin (Clo-Hal) biosynthesis (Table 19.3) rather than in the above-described typical tryptophan halogenases (Table 19.2), i.e., only 20% identity to PyrH, while no significant similarity to the tryptophan-7-halogenases, PmA and RebH, was found [79].

In general, FADH₂-dependent halogenases can be grouped into those accepting free small molecules as described above and those that act on carrier-bound substrates. Further examples of halogenases involved in multienzymatic NRPS/PKS assembly lines are summarized in Tables 19.3 and 19.4, subdivided into those suggested to chlorinate phenolic moieties (Table 19.3, Fig. 19.9) as in complestatin [80] and glycopeptide antibiotic formation [81], e.g., vancomycin, and those that halogenate peptidyl carrier-bound pyrrole moieties (Table 19.4; Fig. 19.10), e.g., PltA in pyoluteorin biosynthesis [82]. In the latter case, proline is bound as a thioester to the carrier protein PltL and enzymatically desaturated to a pyrrolyl-S-PltL intermediate. This is then chlorinated regiospecifically at position C-5 and subsequently at position C-4 of the heteroaromatic ring, as observed through temporal product formation. Both halogenations are catalyzed by the

Table 19.3 FADH₂-dependent halogenases that halogenate phenolic moieties as an integrated step in multienzymatic biosynthesis

Halogenases	Natural product <i>Organism</i>	Halogenated structural element	GenBank accession number [reference]
CmdE	Chondramides B/D <i>Chondromyces crocatus</i> Cm c5	Tryptophan at position C-2	AM179409 [79]
CTC-chl (=cts4)	Chlorotetracycline <i>Streptomyces aureofaciens</i> NRRL3203	4-Ketoanhydro-tetracycline ^a	D38214 [60, 122]
CrpH	Cryptophycin 1 <i>Nostoc</i> sp. ATCC 53789	Tyrosine	EF159954 [94]
ComH	Complestatin <i>Streptomyces lavendulae</i>	Hydroxyphenylglycine	AF386507 [80]
“Halogenase gene”	Vancomycin <i>Amycolatopsis orientalis</i>	N.S. ^b	AF486630 [137]
BhaA	Balhimycin <i>Amycolatopsis balhimycina</i> DMS5908	β-Hydroxy-tyrosine	Y16952 [81, 138]
Tcp21	Teicoplanin <i>Actinoplanes teichomyceticus</i> ATCC31131	Tyrosine and β-hydroxy-tyrosine	AJ605139 [139]
ORF10 (=dbv10)	A40926 <i>Nonomuraea</i> sp. ATCC39727	Dihydroxyphenylglycine and β-hydroxy-tyrosine	AJ561198 [140]
ApdC	Anabaenopeptilide 90B <i>Anabaena circinalis</i> 90	Tyrosine	AJ269505 [141]
McnD ^c	Cyanopeptolin-984 <i>Microcystis</i> sp. NIVA-CYA 172/5	Tyrosine	DQ075244 [142]
AerJ ^d	Aeruginosin peptides <i>Microcystis</i> sp. PCC 9812	3-(4-Hydroxyphenyl) lactic acid	AM773664 [143]
ChlB4	Chlorothricin <i>Streptomyces antibioticus</i> DSM 40725	6-Methylsalicylic acid	DQ116941 [144]
SgcC3	C-1027 <i>Streptomyces globisporus</i>	β-Tyrosine ^e	n.d. ^f [145]
CndH	Chondrochloren <i>Chondromyces crocatus</i> Cm c5	Tyrosine	AM988861 [88, 146]

^aIndicates that halogenation occurs while the elongating acyl chain is still tethered to carrier proteins during the PKS assembly line

^bNot specified

^cAlso identified from other *Microcystis* strains (AM773679, AM773678, AM773677, AM773676, AM773675, AM773674) [143]

^dAlso identified from other *Microcystis* strains (AM773663, AM773662, AM773661, AM773660, AM773659, AM773658, AM773657, AM773656, AM773655, AM773654 [143], PCC7806, NIES-98 [147])

^eIn vitro characterized to halogenate tyrosine tethered to a peptidyl carrier protein

^fNo sequence data available in GenBank

Table 19.4 FADH₂-dependent halogenases involved in the halogenation of pyrrole moieties

Halogenases	Natural product <i>Organism</i>	Halogenated structural element	GenBank accession number [reference]
PltA	Pyoluteorin <i>Pseudomonas fluorescens</i> Pf-5	Proline ^a	AF081920 [82]
HrmQ	Hormaomycin <i>Streptomyces griseoflavus</i> W-384	Pyrrole ^b	EU583477 [98]
PmC	Pyrrolnitrin <i>Pseudomonas fluorescens</i> BL915	Monodechloramino- pyrrolnitrin	PFU74493 [59]
HalB	Pentachloropseudilin <i>Actinoplanes</i> sp. ATCC33002	Pyrrole	AF450451 [148]
Pyr29 ^c	Pyrrolomycin A, B, C, D <i>Actinosporangium</i> <i>vitaminophilum</i> ATCC31673	Proline	EF140901 [149]

^aProline halogenation while bound to a peptidyl carrier protein

^bMost likely halogenation via a peptidyl carrier protein-bound proline
65% similarity to PltA

same enzyme, i.e., PltA. During this process, chlorination is specific for pyrrolyl-*S*-PltL, since prolyl-*S*-PltL or free pyrrole-2-carboxylate is not accepted as substrate for halogenation by PltA.

Even more halogenases involved in the chlorination of phenolic moieties, but not explicitly described to function as an integral part of enzymatic assembly lines, are shown in Table 19.5 (for structures, see Fig. 19.11).

Besides the FADH₂-dependent halogenases involved in halogenation of aromatic compounds, recognizing tryptophan/indole or phenol/pyrrole moieties, enzymes involved in the halogenation of aliphatic compounds are known (Table 19.6; Fig. 19.12). For example, for chloramphenicol biosynthesis in *Streptomyces venezuelae* ISP5230, the function of CmlS as a halogenating enzyme has been proved by gene disruption experiments, whereby corynecins were produced in place of chloramphenicol [83]. CmlS shows the highest homology to the FADH₂-dependent halogenase PltA (Table 19.4). It has been suggested that a substrate derived from glucose is halogenated and that dichloroacetyl-CoA is then attached to the amino group of the side chain of an enzyme-tethered *p*-aminophenylalanine [84]. For napyradiomycin (Fig. 19.12) from the marine sediment-derived *Streptomyces* sp. CNQ-525, not only Va-CPOs, as described above, are discussed to be involved in its biosynthesis but also a FADH₂-dependent halogenase, NapH2. The gene for the latter was found within the biosynthesis cluster. Thus, NapH2 is the first FADH₂-dependent halogenase described to be potentially involved in a halogenation reaction in a marine organism. Considering structural similarities between terrestrial and marine natural products, it may be conducted, however, that FADH₂-dependent halogenases very likely also contribute to the biosynthesis of many marine compounds (Fig. 19.13).

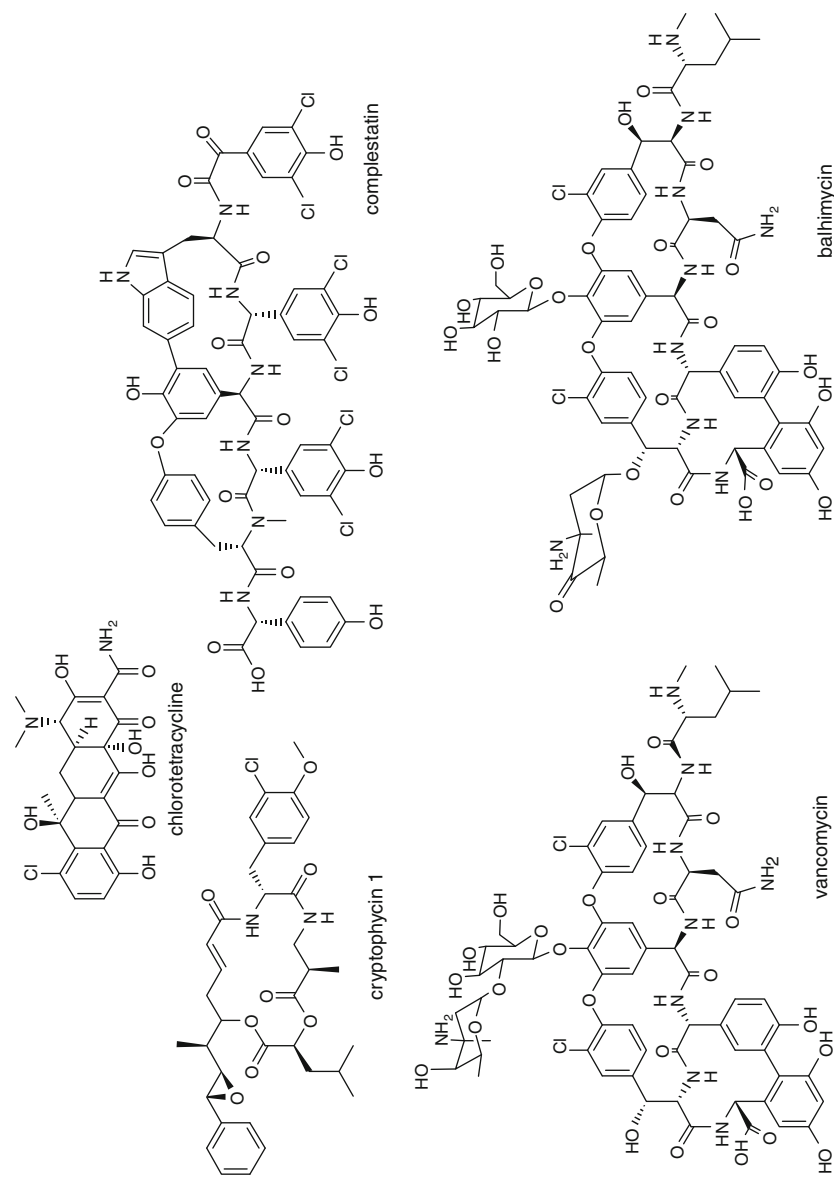
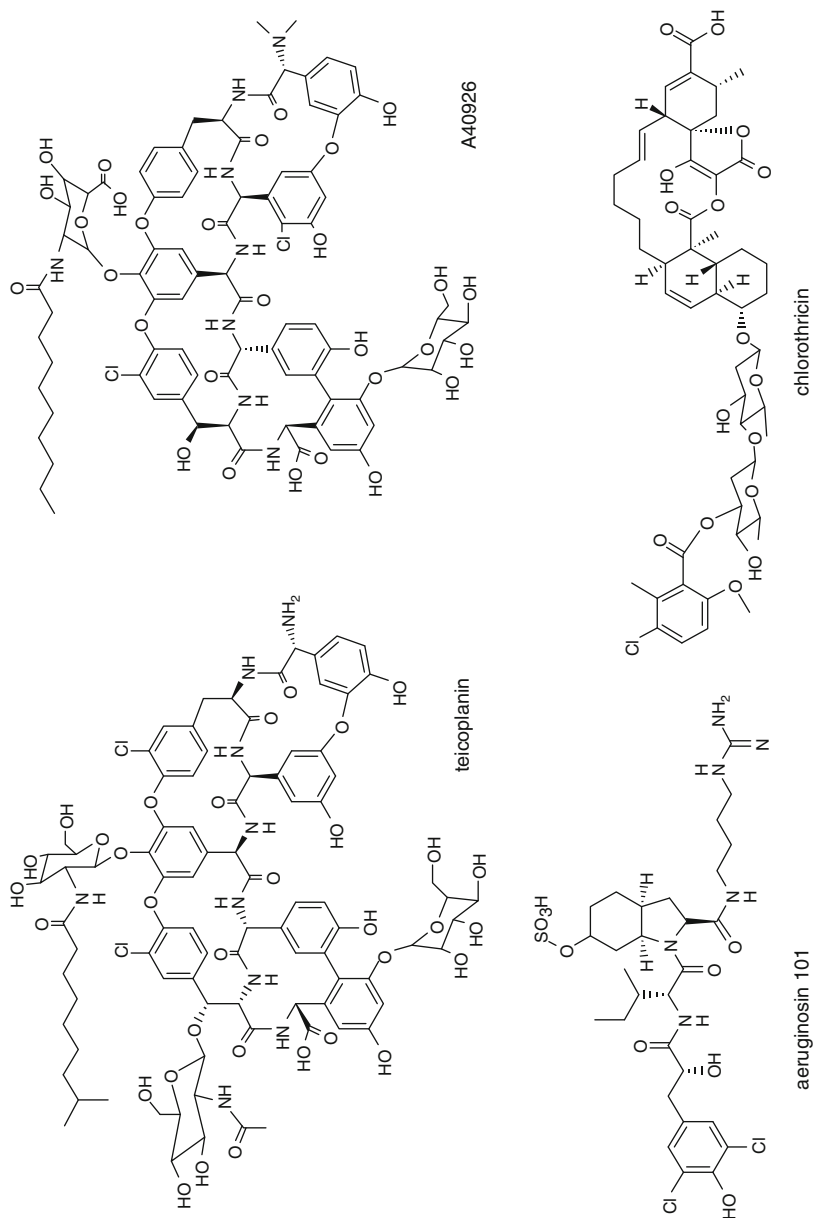


Fig. 19.9 (continued)

**Fig. 19.9** (continued)

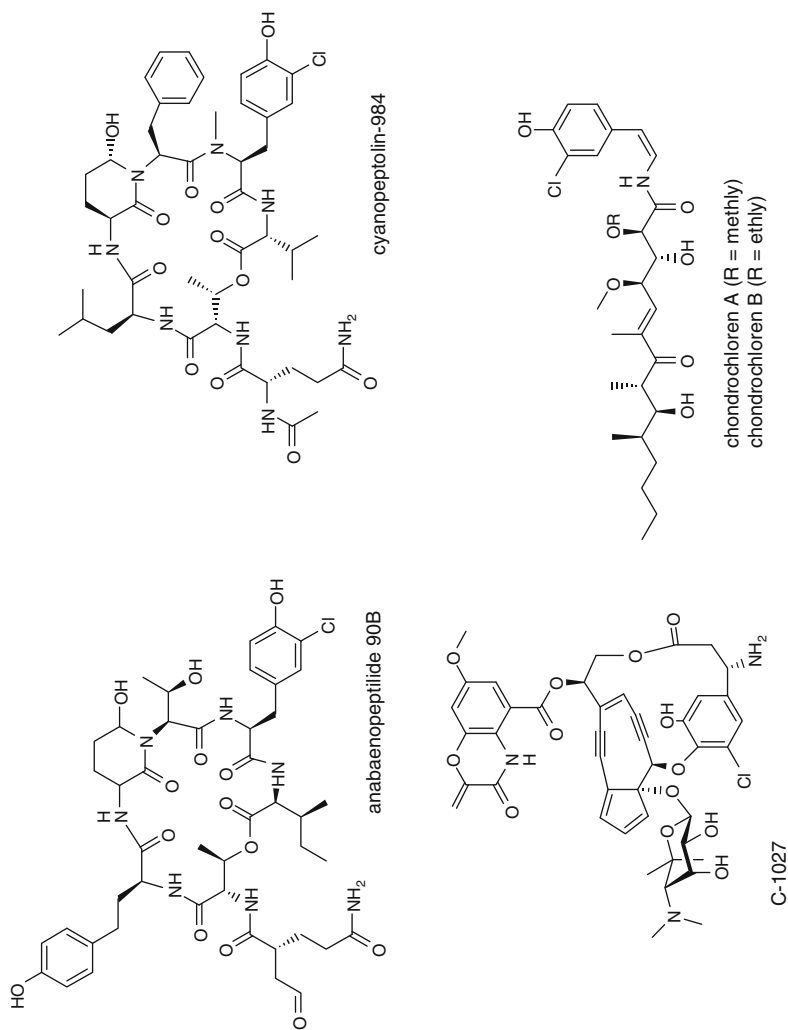


Fig. 19.9 Compounds with chlorinated phenolic structures where FADH₂-dependent halogenation most likely occurs within multienzymatic biosynthesis assembly lines (e.g., PKS/NRPS)

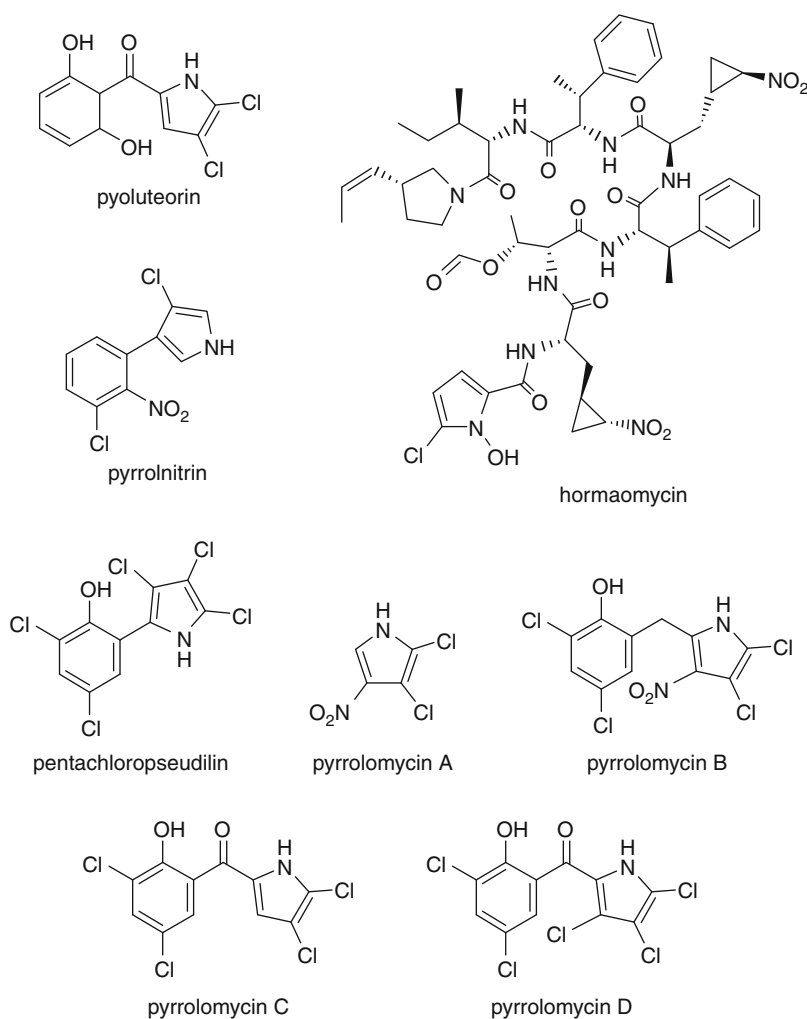


Fig. 19.10 Compounds with chlorinated pyrrole structural elements halogenated by FADH_2 -dependent halogenases

19.4.1 Sequence Specificities and Enzymatic Activity of FADH_2 -Dependent Halogenases

The *in vitro* enzymatic activity of halogenases has been investigated only in a very few cases until now, and the function of many biosynthetic genes as halogenases (Tables 19.2, 19.3, 19.4, 19.5, 19.6) was assigned only putatively. Nevertheless, halogenases are known to have an approximate size of 550 amino acids and thus to be encoded by a corresponding DNA consisting of 1,500–1,600 bp (Fig. 19.14).

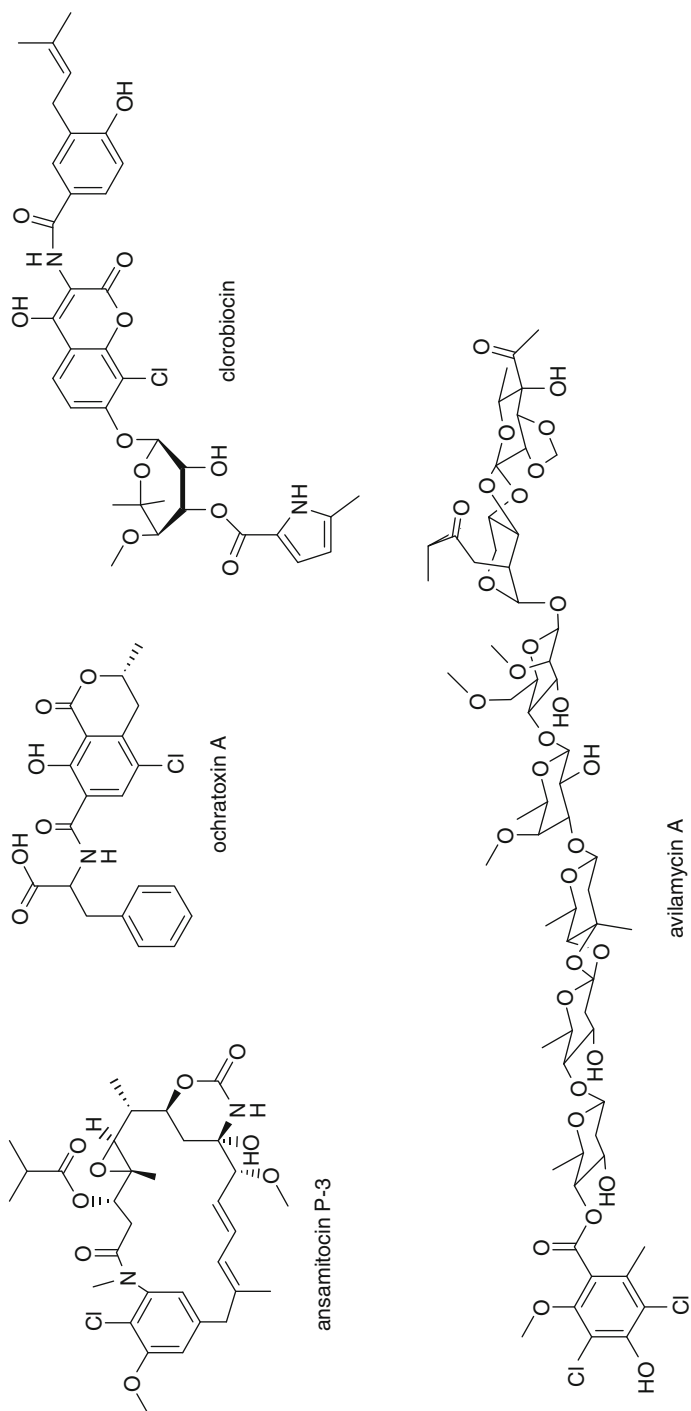
Table 19.5 FADH₂-dependent halogenases involved in the halogenation of phenolic moieties

Halogenases	Natural product <i>Organism</i>	Halogenated structural element	GenBank accession number [reference]
Pyr16/17	Pyrrolomycin A, B, C, D <i>Actinosporangium vitaminophilum</i> ATCC31673	Phenol ^a	EF140901 [149]
Asm12	Ansamitocin P-3 <i>Actinosynnema pretiosum</i> ATCC31565	Proansamitocin ^b	AF453501 [150, 151]
n.d. ^c	Ochratoxin A <i>Penicillium nordicum</i>	Mellein intermediate ^d	n.d. ^c [152]
Clo-Hal	Clorobiocin <i>Streptomyces roseochromogenes</i>	Aminocoumarin	AF329398 [95, 153]
AviH	Avilamycin A <i>Streptomyces viridochromogenes</i> Tü57	Orsellinic acid ^e	AF333038 [154]
CalO ₃	Calicheamicin γ 1 <i>Micromonospora echinospora</i> spp. <i>calichensis</i>	Orsellinic acid	AF497482 [155]
SimD4	Simocyclinone D8 <i>Streptomyces antibioticus</i> Tü6040	Aminocoumarin	AF324838 [156]
RadH ^f	Radiciol <i>Chaetomium chiversii</i>	Phenol ^a	EU980390 [157]
ChlA	DIF-1 (differentiation-inducing factor 1) <i>Dictyostelium</i> strain Ax2	Phenol ^a	DDB_G0290825 ^g [158]

^aPhenol moiety polyketide derived^bHalogenation of proansamitocin as first PKS-tailoring reaction^cNo sequence data available in GenBank^dPost-PKS^eDichloro-isoverninic acid attached to the preformed heptasaccharide^fAlso identified from *Pochonia chlamydosporia* (EU520419, termed Rdc2 [159])^gAt dictyBase, <http://dictybase.org/>

The flavin binding site is located at the amino terminal end and includes a GxGxxG motive, which is extremely conserved within this enzyme group [85]. Another conserved region, i.e., WxWxIP, is found in the middle of the sequence [85]. The tryptophan residues of the latter motif are assumed to prevent the enzyme from catalyzing monooxygenase-type reactions by sterically hampering substrate binding next to the isoalloxazine ring of FADH₂ [71].

Further insight in the mechanism how FADH₂-dependent halogenases can halogenate such a wide range of substrates derived from the crystal structure of CmlS [86, 87], the halogenase involved in the chloramphenicol biosynthesis, in comparison to those characterized for tryptophan halogenases (e.g., PrnA) and CndH, a tyrosyl chlorinating halogenase acting during chondrochloren

**Fig. 19.11** (continued)

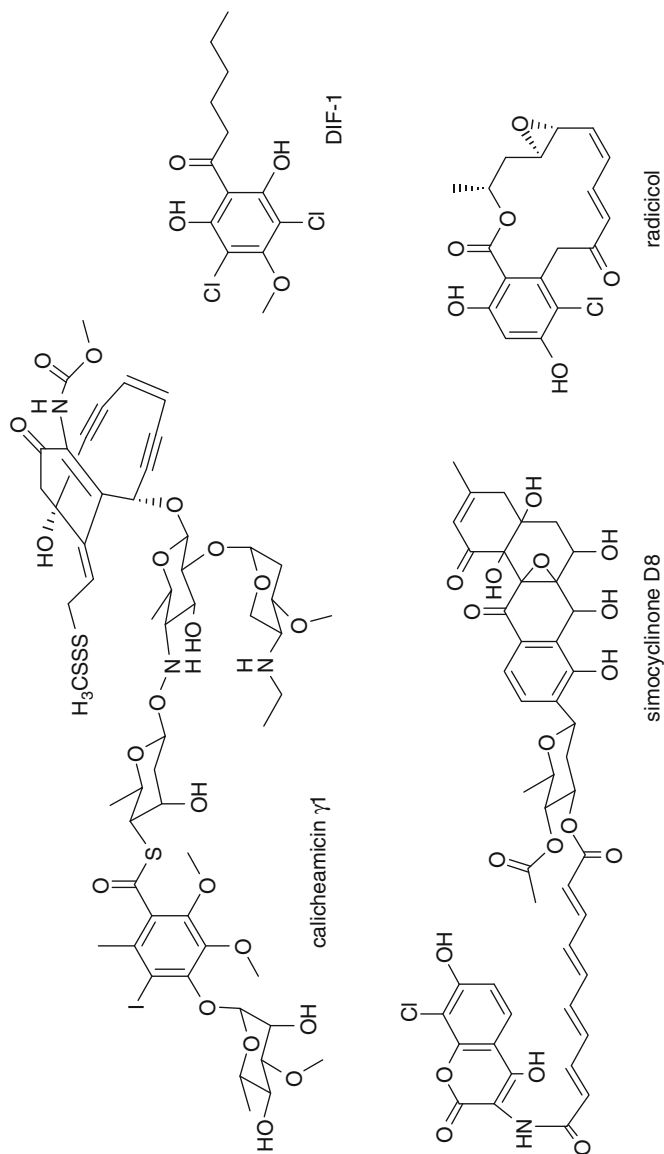
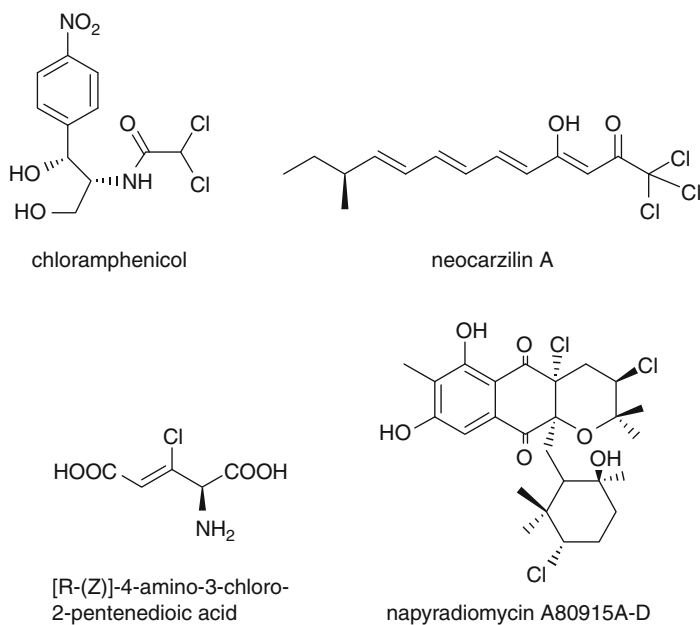


Fig. 19.11 Further compounds with halogenated aromatic substructures for which an involvement of $FADH_2$ -dependent halogenases is discussed

Table 19.6 FADH₂-dependent halogenases discussed to be involved in the chlorination of aliphatic structural elements

Halogenases	Natural product <i>Organism</i>	Halogenated structural element	GenBank accession number [reference]
CmlS	Chloramphenicol <i>Streptomyces venezuelae</i> ISP5230	Aliphatic moiety ^a	AY026946 [83]
ORF3 ^b	Neocarzilin A <i>Streptomyces carinostaticus</i>	Aliphatic moiety	AB097904 [160]
n.d. ^c	(<i>R</i> -(<i>Z</i>))-4-amino-3-chloro-2-pentenedioic acid <i>Streptomyces viridogenes</i> ATCC39387	Aliphatic moiety ^d	DQ782376 [161]
NapH2	Napyradiomycin A80915A-D <i>Streptomyces</i> sp. CNQ-525	Aliphatic moiety ^e	EF397638 [32]

^aLikely in an enzyme-bound assembly line (similarity to PltA)^bSimilarity to HalB^cOnly partial gene sequence^dHalogenation postulated via a pyrrole intermediate^eAlso Va-CPOs (NapH1,3,4) identified within the gene cluster**Fig. 19.12** Compounds with chlorinated aliphatic moieties for which an involvement of FADH₂-dependent halogenases is discussed

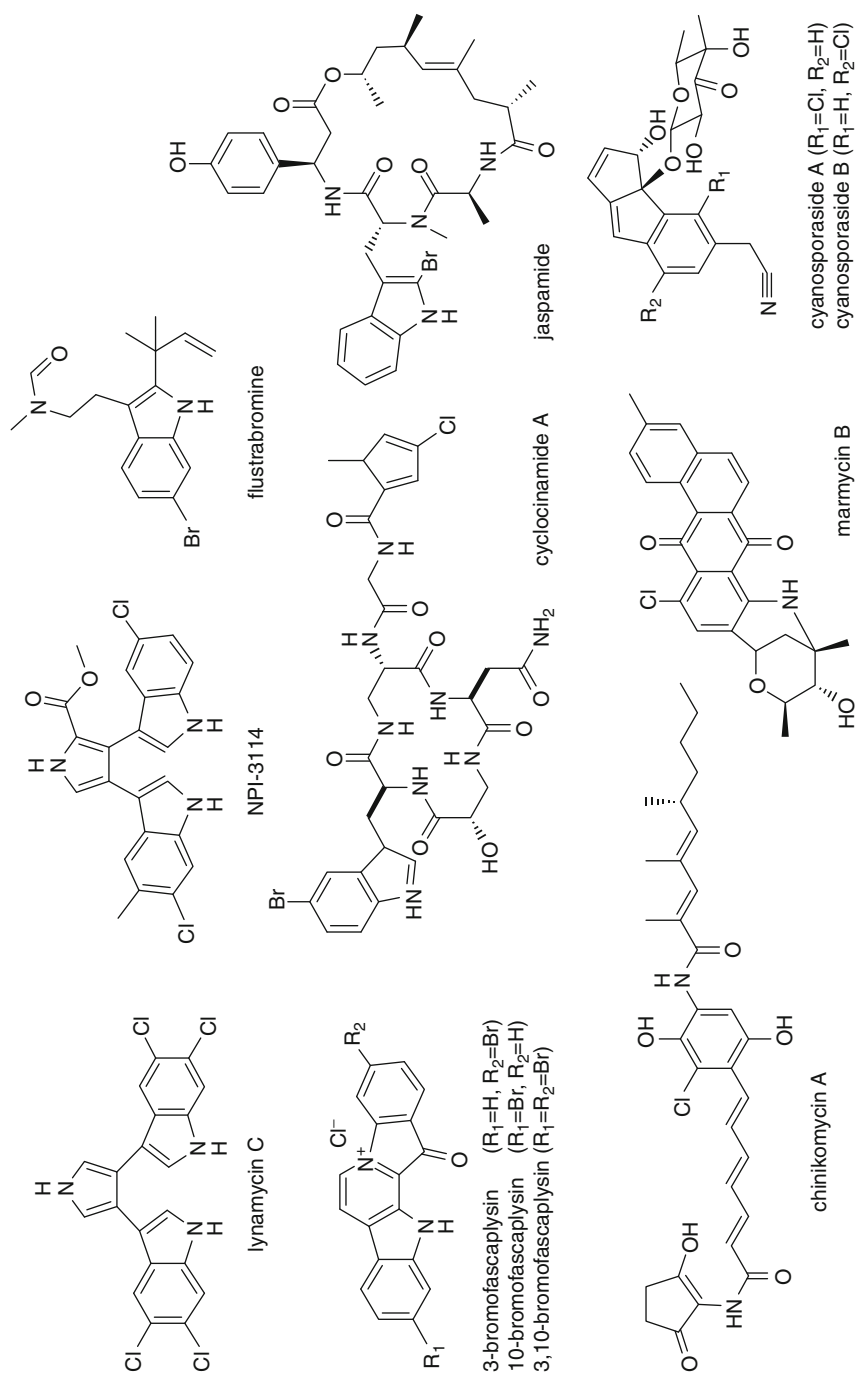


Fig. 19.13 (continued)

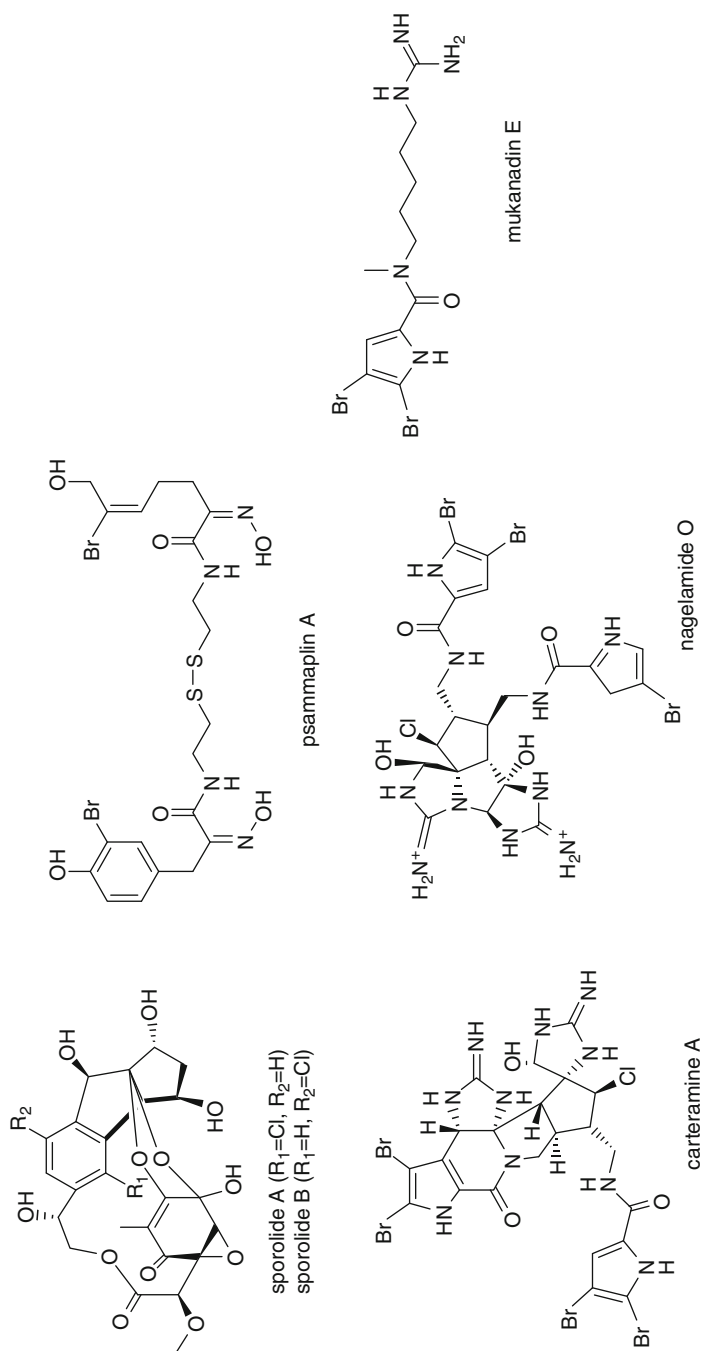


Fig. 19.13 Marine compounds potentially synthesized via corresponding $FADH_2$ -dependent halogenases, e.g., compounds with halogenated indole moieties as isolated from marine actinomycetes (dynamycins [162] and NPI 3114 [163]), algae (flustrabromine [164]), and sponges (bromofascaplysin [165], cyclocinamide A [166]), as well as the chondramide analog jaspamide [167]). Secondary metabolites with halogenated phenol and pyrrole moieties are also known from various marine actinomycete (e.g., chinikomycins [168], sporolides [169], cyanosporasides [170], and marmycins B [171]) and sponges (psammaplins A [172], carteramine A [173], nagelamides [174], and mukonanadins [174])



Fig. 19.14 General amino acid (aa) sequence assembly of FADH₂-depending halogenases, showing the conserved motives in all FADH₂-depending halogenases

biosynthesis [88]. Based on characteristic features of these crystal structures, two variants of FADH₂-dependent halogenase have been distinguished [88]. Variant A enzymes (e.g., PrnA), acting on free small molecules, enclose their substrate completely in the active halogenation site. Thereby, the C-terminus of the enzymes seems to cover the active halogenation site and to somehow form a tunnel into which the substrate must enter. In variant B enzymes (CndH), the active center remains open, giving access to a sterically much larger carrier-bound substrate. From simple primary structure alignment, CmlS would rather be classified as a variant B halogenase; however, due to the occurrence of a bulky C-terminal lobe, it seems more likely that a free small molecule enters the active halogenation site (variant A enzyme). The structural diversity observed in the C-termini of FADH₂-dependent halogenases appears to reflect the overall diversity of substrates that are halogenated, potentially by sterically restricted access to the active halogenation site. Together with this, specific features within the active halogenating site contribute to the substrate selectivity and regioselectivity. In the case of CmlS, an overall hydrophobic pocket with three phenylalanine residues (F87, F304, F357) is present in the active halogenation site [87], in contrast to a glutamic acid accompanied by two histidine residues (E346, H101, H395) in PrnA, which are thought to ensure tryptophan halogenation. From the crystal structure of the tryptophan-5-halogenase PryH, it became obvious that as a result of amino acid insertion and deletions, compared to PrnA, the substrate binding pocket is substantially rearranged. As a result, tryptophan is bound differently, exposing the respective C atom for chlorination to the key lysine and glutamate residues, while the other sites of potential reactivity will be protected by the enzyme structure [78]. Amino acid sequence alignment of Thal (tryptophan-6-halogenases) and PrnA showed only few differences lining the active halogenation site, i.e., I56/I82/T348 in PrnA and V56/V86/S364 in Thal, which are potentially involved in the directed substrate presentation for regioselective halogenation [71].

Early studies investigating the incorporation of bromine instead of chlorine in chloramphenicol, chlorotetracycline, and pyrrolnitrin resulted in the formation of the corresponding bromo analogs, giving the first indication that the involved enzymes are not exclusively specific for chloride [89–91]. Thus, the ability of FADH₂-dependent halogenases to alternatively incorporate bromide instead of chloride has been subjected to further detailed investigations [92–94]. For PryH (Table 19.2), it could be shown that in the presence of bromide, 5-bromotryptophan was obtained, although chlorination is favored. In any case, only the regioselective monohalogenation of tryptophan at the C-5 position occurred [77]. Similarly, Thal and RebH (Table 19.2) were demonstrated to catalyze monochlorination regioselectively, as well as monobromination of tryptophan in vitro resulting in

6- and 7-halotryptophan, respectively [71, 74]. Bromide ions were also able to compete with and replace chloride in the PltA (Table 19.4) reaction on pyrrolyl-*S*-PltL. However, the sterically larger bromide slowed down the halogenation reaction to 10–20% conversion in 1 h, as opposed to >90% when chloride was the only halide present [82].

19.4.2 Biotechnological Potential of FADH₂-Dependent Halogenases

The considerable progress made in understanding biological halogenation mediated through FADH₂-dependent halogenases gave rise to probing the biotechnological potential of these enzymes. The aim of such investigations was to allow halogenations at specific sites of substrates not accessible to direct chemical halogenation as well as to avoid the formation of unwanted by-products.

Combinatorial biosynthesis yielded new derivatives of the aminocoumarin antibiotics, novobiocin, clorobiocin, and coumermycin A1 (Fig. 19.15). Inactivation of the *clo-hal* gene in the clorobiocin biosynthetic gene cluster of *Streptomyces roseochromogenes* resulted in the formation of the hydrogen analog novclobiocin 101, and coexpression of the putative methyltransferase *novO* led to the production of novclobiocin 102, which is methylated at C-8 of the aminocoumarin ring [95]. More interestingly, coexpression of *clo-hal* in a *novO*[−] mutant resulted in the chlorinated novobiocin derivative novclobiocin 114 [96]. An attempt to functionally replace *clo-hal* by the balhimycin halogenase (Table 19.3) *bhaA* both in the *clo-hal*[−] and *novO*[−] mutant, did not yield in the respective chlorinated aminocoumarin derivatives (clorobiocin or novclobiocin 114), thus underlining the different substrate specificity of Clo-Hal and BhaA [96]. However, introduction of *clo-hal* into the cluster of coumermycin A1 again resulted in the formation of the respective mono- and dichlorinated derivatives [97]. In a study investigating the halogenating potential of the hormaomycin halogenase HrmQ (Table 19.4) in combinatorial biosynthesis, coexpression experiments of *hrmQ* in a *cloN6*[−] clorobiocin mutant strain were conducted [98]. The results confirmed that HrmQ specifically chlorinates pyrrole moieties at the C-5 position and thus yielded the new clorobiocin derivatives, novclobiocin 124 and 125.

As a result of their potential therapeutic applications as antitumor and neuroprotective agents [99, 100], great efforts have been made to generate derivatives of indolocarbazole alkaloids. Novel halogenated compounds were obtained by recombining genes found within the biosynthetic gene clusters of rebeccamycin and staurosporine with the halogenases RebH, PyrH, and Thal (Table 19.2). In this way, Salas and coworkers were able to generate “hybrid” indolocarbazoles by modifying the staurosporine aglycon using rebeccamycin chlorination, glycosylation, and sugar methylation activities. Besides nonhalogenated products, this approach yielded chloro- and dichloro-staurosporine derivatives [100]. The major bis-indole products obtained when coexpressing PyrH and Thal (Table 19.2) had a chloride substitution at positions C-5 and C-6 of the indole moiety, respectively.

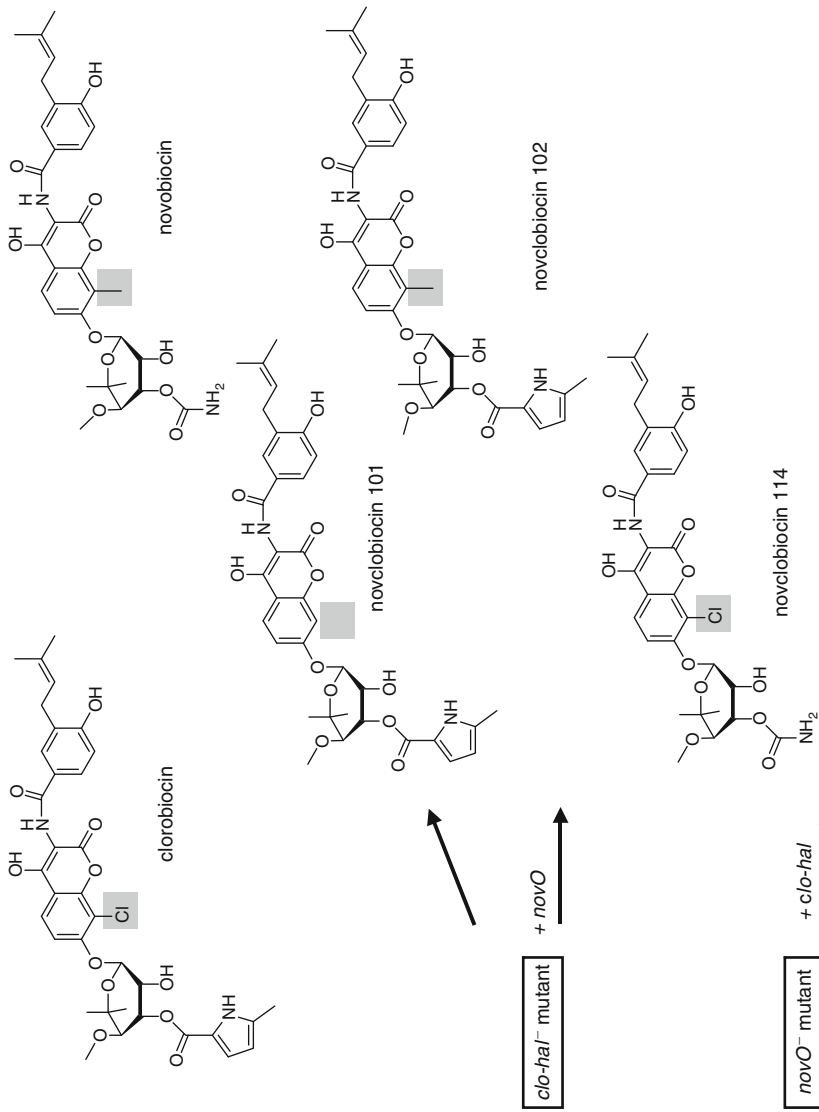


Fig. 19.15 (continued)

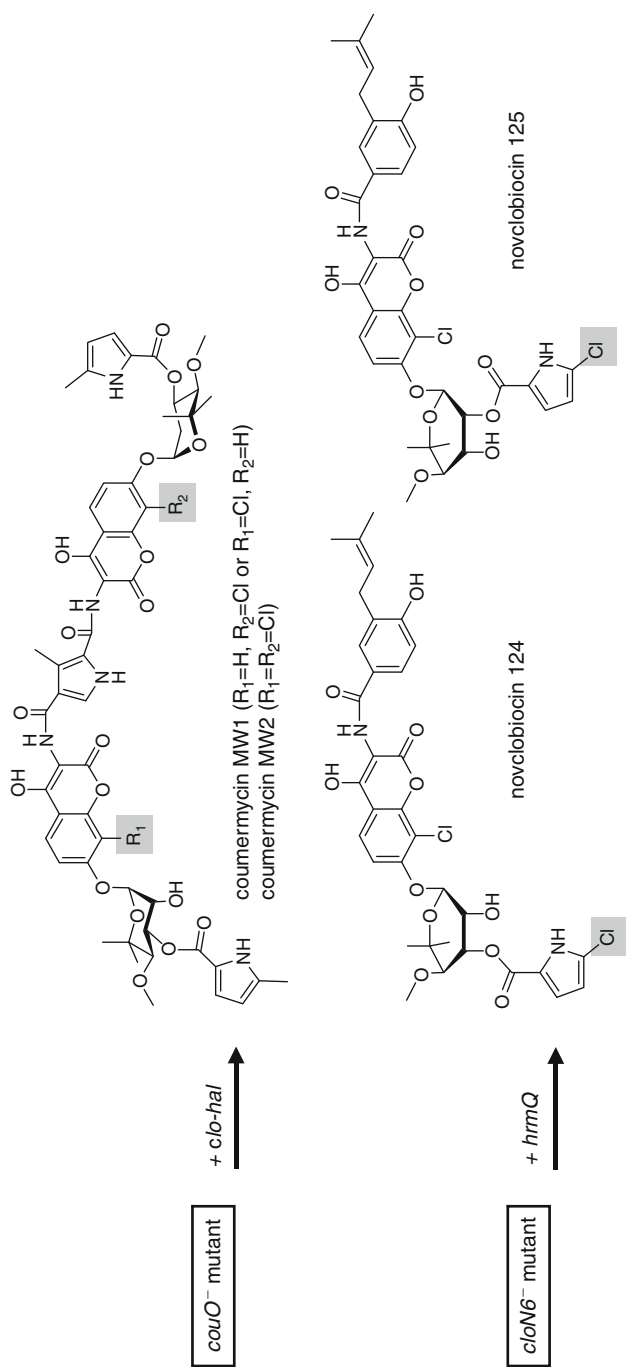


Fig. 19.15 Novel aminocoumarin derivatives derived by combinatorial biosynthesis

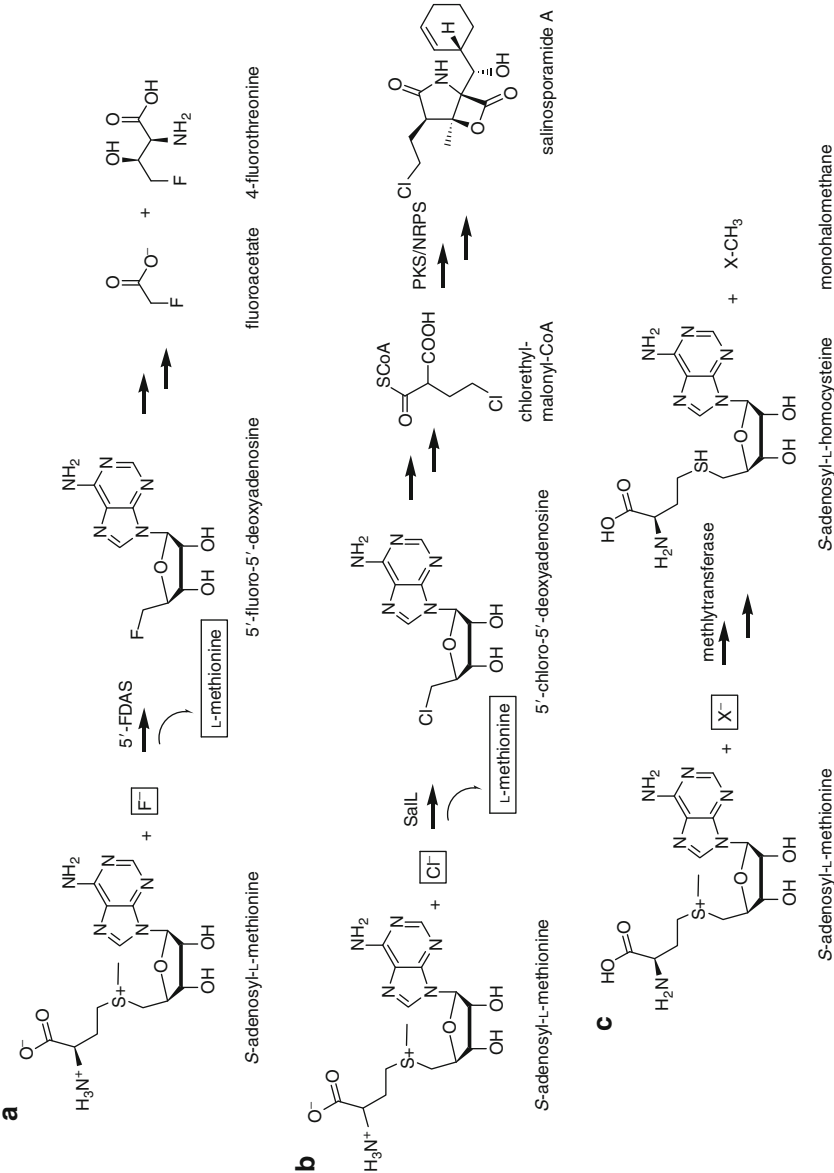


Fig. 19.16 (continued)

In another approach, *Thal* was investigated in a recombinant pyrrolnitrin producer strain [71]. Overexpression of *thal* yielded the new phenylpyrrole derivative, 3-(2'-amino-4'-chlorophenyl)pyrrole, but no pyrrolnitrin or aminopyrrolnitrin was detected. The authors concluded that the overproduction of *Thal* resulted in the chlorination of all the available tryptophan to 6-chlorotryptophan, which was then accepted by PrnB, the second enzyme in pyrrolnitrin biosynthesis catalyzing the subsequent ring rearrangement. However, the phenylpyrrole compound produced was not a substrate to PrnC for further halogenation reaction.

The use of tryptophan-5-halogenases (PyrH) (Table 19.2) in producing halogenated serotonin precursors has been the focus of further research [101]. The aim of these efforts was to obtain 5-bromotryptophan, which is regarded as a suitable intermediate for a subsequent nucleophilic hydroxylation to yield 5-hydroxytryptophan (oxitriptan). The latter is a component of many antidepressant drugs and, to date, commonly obtained by extraction of the seeds of the African plant *Griffonia simplicifolia*. The main limitation at this point is the low activity of the purified enzyme as well as the unsatisfactory production of the recombinant enzyme. Optimization of the reaction conditions, however, has already led to a nearly 20-fold improvement of the 5-bromotryptophan yield, and ongoing efforts aim to enhance the recombinant enzyme production [101]. The temperature sensitivity of the enzymes and the high NADH consumption to restore the cofactor FADH₂ for the halogenase reaction, however, hamper an economical application of these enzymes [102].

19.5 Halogenating Enzymes Utilizing S-Adenosyl-L-Methionine

Fluoride is the most nucleophilic halogen and does not allow any electrophilic or radical biological chemistry, as is known for Cl⁻, Br⁻, and I⁻. Even though, thermodynamically, the formation of carbon–fluoride bonds would be favorable, due to the extremely high desolvation energy required to activate F⁻ in aqueous solution, biological reactions with fluoride are rather rare [5]. Unique enzymes are needed to overcome this kinetic barrier, and, to date, the only one to be characterized is the 5'-fluoro-5'-deoxyadenosine synthetase (5'-FDAS). This enzyme was isolated from *Streptomyces cattleya* and utilizes S-adenosyl-L-methionine (SAM) as cosubstrate [7]. Fluoride is thereby thought to be placed in a hydrophobic pocket where desolvation is achieved as protein residues coordinate to water. In turn, a S_N2 substitution of methionine at SAM takes place [103]. In this way, 5'-fluoro-5'-deoxyadenosine is formed as an intermediate and subsequently converted to fluoroacetate and 4-fluorothreonine (Fig. 19.16a).



Fig. 19.16 SAM in biohalogenation processes. (a) Enzymatic conversion of inorganic fluoride to organic fluoride by 5'-fluoro-5'-deoxyadenosine synthetase. (b) The chlorinated moiety of salinosporamide A could be shown to derive from tetrose, and SalL was identified as a 5'-FDAS analog halogenating enzyme. The intermediate chloroethylmalonyl-CoA has been identified to act as an unusual starter unit for the subsequent PKS/NRPS biosynthesis part. (c) Methyltransferases mediate the transfer of a methyl group from SAM to a halide (X: halide ion)

For the biosynthesis of the potent proteasome inhibitor salinosporamide A (Fig. 19.16b) produced by the marine actinomycete *Salinispora tropica*, the deschloro analog, salinosporamide B, was initially presumed to be the direct precursor, and thus, the halogenation of the unactivated C-13 methyl group was suggested to be catalyzed by a nonheme iron halogenase. However, from feeding experiments, a different origin of the four-carbon moiety was demonstrated for these two molecules [104]. Thus, for salinosporamide B, a butyrate-derived ethylmalonyl-CoA was identified as a building block, whereas in salinosporamide A, an unprecedented PKS extender unit was shown to originate from a sugar precursor. The enzyme involved in the chlorination step (SalL) has been characterized as a 5'-FDAS similar enzyme, which converts SAM to 5'-chloro-5'-deoxyadenosine [6]. This sugar is subsequently converted to chloroethylmalonyl-CoA to further act as unique PKS extender unit [105]. The 5'-halo-5'-deoxyadenosine synthetase was shown to also be capable of utilizing bromide as well as iodide, but not fluoride.

Fluorine substitution is a prevalent strategy to enhance pharmacodynamic and pharmacokinetic properties of biologically active lead compounds; thus, the usefulness of the fluorinase 5'-FDAS to initiate C-F bonds in organohalogen synthesis has been further investigated. By genetic engineering, 5'-FDAS was successfully utilized in a *salL*-knockout mutant of *S. tropica* revealing fluorosalinosporamide [106]. Earlier studies, where this fluorometabolite was produced via chemical compensation of a *salL*-knockout mutant with synthetic 5'-fluoro-5'-deoxyadenosine, already showed that the proteasome inhibition activity of this salinosporamide derivative was slightly lower than that of the chlorinated natural product, however, also with reduced cytotoxicity [107]. This is thought to be due to a reversible binding of fluorosalinosporamide versus an irreversible binding of salinosporamide A. In further bioengineering approaches, the unique chloroethylmalonyl-CoA [105] and probably also analogous fluoroethylmalonyl-CoA [106] produced by salinosporamide A and respective genetically engineered biosynthetic systems may provide new opportunities in drug development. They may be used, e.g., as PKS extender units. Function of the fluorinase in isolated systems has already also been proven; thus, further application of this enzyme in *in vitro* biotransformation processes is conceivable [108].

SAM is also involved in the formation of monohalomethanes, albeit in a different way, namely, as methyl donor (Fig. 19.16c). At an early stage, Harper predicted that most likely other enzymes than haloperoxidases would be involved in the formation of halomethanes [109], and Wuosmaa and Hager were the first to detect and partially purify corresponding methyltransferases responsible for the methyl chloride production, e.g., from the red algae *Endocladia muricata* [110]. Several studies dealing with the emission of gaseous iodine and chlorine from the biosphere to the atmosphere resulted in the identification of respective enzymes in marine as well as terrestrial bacteria, macro- and microalgae, wood-rotting fungi, and terrestrial higher plants [111–113].

19.6 Concluding Remarks

In the last years, our understanding of biohalogenation processes has extended tremendously. Several groups of halogenating enzymes have been discovered and investigated on the biochemical and genetic level. Each group of these enzymes performs halogenation reactions on chemically distinct and different substructures, i.e., indole, phenol, pyrrole, and aliphatic moieties, using a specific reaction mechanism. The halogenation of marine natural products, however, is still not as well investigated as that of terrestrial metabolites.

A detailed insight to natural biological halogenation processes will not only further our understanding of natural biological halogenation processes but will also give rise to alternative methods for generating halogenated analogs of biologically active metabolites [10, 85, 114, 115]. By means of such enzymatic reactions, modified compounds may be generated with potentially improved biological properties [95, 116–118].

Investigations concerning the biotechnological potential of halogenating enzymes, however, are still in their infancy. Results obtained in the latter area so far prove that some halogenases can be expressed recombinantly and subsequently applied to directly halogenate suitable substrates, e.g., tryptophan halogenases [63, 71, 72, 100, 101]. Other halogenases only function in a multienzymatic biosynthetic environment, and combinatorial biosynthetic strategies need to be implemented to use their enzymatic capabilities.

For further details regarding biohalogenation beyond the scope of this book chapter, we recommend the comprehensive reviews based on the pioneering work of the research groups of van Pée and Walsh in the field of dioxygen-depending halogenases [64, 68, 85, 114, 118–123]. The recently published comparison of the halide-binding sites of different halogenating enzymes and their corresponding selectivities are discussed by Blasiak and Drennan [117]. Further insights concerning the mechanisms of enzymatic halogenation were described by Dolfing [124], Anderson and Chapman [2], and Murphy [115], as well as Naismith [5]. In addition, reviews focusing on haloperoxidases have recently been published by Hofrichter and Ullrich [10], Butler and Carter-Franklin [8], and Raugei and Carloni [125], as well as Bortolini and Conte [126] and Winter and Moore [31].

19.7 Study Questions

1. Name the different halogenating enzymes known for natural product biosynthesis.
2. What are the cofactors utilized within haloperoxidases?
3. Which is the actual halogenation agent of haloperoxidases?
4. How do chloroperoxidases, bromoperoxidases, and iodoperoxidases differ?
5. Where are iodoperoxidases mainly found?

6. What is the halogenation strategy within nonheme $\text{Fe}^{\text{II}}/\alpha$ -ketoglutarate/ O_2 -dependent halogenases?
7. Which are the structural elements halogenated by $\text{Fe}^{\text{II}}/\alpha$ -ketoglutarate/ O_2 -dependent halogenases?
8. Which is the actual halogenation agent within FADH_2 halogenases, and how is regioselective halogenation secured?
9. How are FADH_2 halogenases further classified?
10. What is the function of SAM within the respective halogenating enzymes?
11. Why are fluorinated metabolites so rare in nature?

19.7.1 Answer–Keywords

1. Haloperoxidases, halogenases, *S*-adenosyl-L-methionine-utilizing enzymes
2. Heme or vanadate as cofactors
3. Hypohalous acid (HOX , or related halogenating intermediates, such as OX^- , X^{3-} , and X^+):
 - In heme HPO, the final chlorine transfer to various substrates occurs outside the active site via a free diffusible species without any special mode of substrate recognition.
 - Va-HPOs bind hydrogen peroxide and halides leading to a putative enzyme-bound or active site-trapped brominating moiety. In the absence of a suitable substrate, however, HOBr is released from the enzyme and carries out unselective bromination as observed for aqueous bromine.
4. Nomenclature is based on the most electronegative halide oxidized by the enzyme.
5. Va-IPOs seem to play a role in iodine accumulation of brown algae as a main vector of the iodine biogeochemical cycle.
6. A highly reactive iron-oxo species ($\text{Fe}^{\text{IV}} = \text{O}$) is formed within the catalytic cycle. This abstracts a hydrogen radical from an aliphatic carbon center of the actual substrate, which, in turn, abstracts the halide from the coordination sphere of the enzyme.
7. $\text{Fe}^{\text{II}}/\alpha$ -ketoglutarate/ O_2 -dependent halogenase are involved in the chlorination of terminal methyl groups of amino acids linked to peptidyl carrier proteins and, occasionally, in the formation of cyclopropane moieties.
8. Enzyme-trapped HOCl is produced as chlorinating agent and channeled through an intraenzymatic tunnel to the substrate binding pocket. Here this chlorinating intermediate is proposed to be a covalently bound lysine chloramine ($\text{Lys79-}\epsilon\text{NH-Cl}$). Regioselective halogenation is thereby secured by controlled presentation of the substrate to the bound Cl -species via particular amino acid residues in the substrate binding site.
9. Halogenases can be grouped into:
 - Those accepting free small molecules and those that act on carrier-bound substrates, e.g., involved in multienzymatic NRPS/PKS assembly lines

- Subdivided by the moieties to be chlorinated, i.e., aromatic compounds, recognizing tryptophan/indole or phenol/pyrrole moieties and enzymes involved in the halogenation of aliphatic compounds
10. Enzymes utilizing *S*-adenosyl-L-methionine (SAM) as cosubstrate:
 - Classically act in methyltransferases and, in this manner, are involved in the production of monohalomethanes.
 - Furthermore, in the unique enzyme 5'-FDA synthetase, substitution of methionine at SAM by fluoride takes place, and in turn, 5'-fluoro-5'-deoxyadenosine is formed as an intermediate (which is subsequently converted to fluoroacetate and 4-fluorothreonine). The chloro analog enzyme SalL converts SAM to 5'-chloro-5'-deoxyadenosine, which is subsequently converted to chloroethylmalonyl-CoA to further act as unique PKS extender unit.
 11. Difficulties in the formation of fluorinated metabolites:
 - Extremely high desolvation energy required to activate F^- in aqueous solution makes biological reactions with fluoride rather rare.
 - Fluoride, as most nucleophilic halogens, does not allow any electrophilic or radical biological chemistry.
 - Unique enzymes are needed to overcome this kinetic barrier (e.g., hydrogen peroxide does not have the driving force to oxidize fluoride).

References

1. Gribble GW (2003) The diversity of naturally produced organohalogenes. *Chemosphere* 52:289–297
2. Anderson JLR, Chapman SK (2006) Molecular mechanisms of enzyme-catalysed halogenation. *Mol Biosyst* 2:350–357
3. Vetter W (2006) Marine halogenated natural products. *Rev Environ Contam Toxicol* 188:1–57
4. Kulik HJ, Blasiak LC, Marzari N, Drennan CL (2009) First-principles study of non-heme Fe (II) halogenase SyrB2 reactivity. *J Am Chem Soc* 131:14426–14433
5. Naismith JH (2006) Inferring the chemical mechanism from structures of enzymes. *Chem Soc Rev* 35:763–770
6. Eustáquio AS, Pojer F, Noel JP, Moore BS (2008) Discovery and characterization of a marine bacterial SAM-dependent chlorinase. *Nat Chem Biol* 4:69–74
7. Dong CJ, Deng H, Dorward M, Schaffrath C, O'Hagan D, Naismith JH (2003) Crystallization and X-ray diffraction of 5'-fluoro-5'-deoxyadenosine synthase, a fluorination enzyme from *Streptomyces cattleya*. *Acta Crystallogr D Biol Crystallogr* 59:2292–2293
8. Butler A, Carter-Franklin JN (2004) The role of vanadium bromoperoxidase in the biosynthesis of halogenated marine natural products. *Nat Prod Rep* 21:180–188
9. van Pée KH (1990) Bacterial haloperoxidases and their role in secondary metabolism. *Biotechnol Adv* 8:185–205
10. Hofrichter M, Ullrich R (2006) Heme-thiolate haloperoxidases: versatile biocatalysts with biotechnological and environmental significance. *Appl Microbiol Biotechnol* 71:276–288
11. Ballschmiter K (2003) Pattern and sources of naturally produced organohalogenes in the marine environment: biogenic formation of organohalogenes. *Chemosphere* 52:313–324

12. Colin C, Leblanc C, Wagner E, Delage L, Leize-Wagner E, Van Dorsselaer A, Kloareg B, Potin P (2003) The brown algal kelp *Laminaria digitata* features distinct bromoperoxidase and iodoperoxidase activities. *J Biol Chem* 278:23545–23552
13. Morris DR, Hager LP (1966) Chloroperoxidase. I. Isolation and properties of the crystalline glycoprotein. *J Biol Chem* 241:1763–1768
14. Butler A, Walker JV (1993) Marine haloperoxidases. *Chem Rev* 93:1937–1944
15. Sanfilippo C, D'Antona N, Nicolosi G (2004) Chloroperoxidase from *Caldariomyces fumago* is active in the presence of an ionic liquid as co-solvent. *Biotechnol Lett* 26:1815–1819
16. Spreti N, Germani R, Incani A, Savelli G (2004) Stabilization of chloroperoxidase by polyethylene glycols in aqueous media: kinetic studies and synthetic applications. *Biotechnol Prog* 20:96–101
17. Yi XW, Conesa A, Punt PJ, Hager LP (2003) Examining the role of glutamic acid 183 in chloroperoxidase catalysis. *J Biol Chem* 278:13855–13859
18. Baciocchi E, Fabbrini M, Lanzalunga O, Manduchi L, Pochetti G (2001) Prochiral selectivity in H(2)O(2)-promoted oxidation of arylalkanols catalysed by chloroperoxidase. The role of the interactions between the OH group and the amino-acid residues in the enzyme active site. *Eur J Biochem* 268:665–672
19. Sundaramoorthy M, Terner J, Poulos TL (1998) Stereochemistry of the chloroperoxidase active site: crystallographic and molecular-modeling studies. *Chem Biol* 5:461–473
20. Manoj KM (2006) Chlorinations catalyzed by chloroperoxidase occur via diffusible intermediate(s) and the reaction components play multiple roles in the overall process. *Biochim Biophys Acta, Proteins Proteomics* 1764:1325–1339
21. Osborne RL, Raner GM, Hager LP, Dawson JH (2006) *C. fumago* chloroperoxidase is also a dehaloperoxidase: oxidative dehalogenation of halophenols. *J Am Chem Soc* 128:1036–1037
22. Carter-Franklin JN, Parrish JD, Tschirret-Guth RA, Little RD, Butler A (2003) Vanadium haloperoxidase-catalyzed bromination and cyclization of terpenes. *J Am Chem Soc* 125:3688–3689
23. Wever R, Hemrika W (2001) Vanadium haloperoxidases. In: Messerschmidt A, Huber R, Wieghardt K, Poulos T (eds) *Handbook of metalloproteins*. Wiley, Chichester, pp 1417–1428
24. Messerschmidt A, Wever R (1996) X-ray structure of a vanadium-containing enzyme: chloroperoxidase from the fungus *Curvularia inaequalis*. *Proc Natl Acad Sci USA* 93:392–396
25. Weyand M, Hecht HJ, Kiess M, Liaud MF, Vilter H, Schomburg D (1999) X-ray structure determination of a vanadium-dependent haloperoxidase from *Ascophyllum nodosum* at 2.0 Å resolution. *J Mol Biol* 293:595–611
26. Isupov MN, Dalby AR, Brindley AA, Izumi Y, Tanabe T, Murshudov GN, Littlechild JA (2000) Crystal structure of dodecameric vanadium-dependent bromoperoxidase from the red algae *Corallina officinalis*. *J Mol Biol* 299:1035–1049
27. Carter-Franklin JN, Butler A (2004) Vanadium bromoperoxidase-catalyzed biosynthesis of halogenated marine natural products. *J Am Chem Soc* 126:15060–15066
28. Martinez JS, Carroll GL, Tschirret-Guth RA, Altenhoff G, Little RD, Butler A (2001) On the regiospecificity of vanadium bromoperoxidase. *J Am Chem Soc* 123:3289–3294
29. Vilter H (1984) Peroxidases from Phaeophyceae – a vanadium(V)-dependent peroxidase from *Ascophyllum nodosum*. *Phytochemistry* 23:1387–1390
30. Plat H, Krenn BE, Wever R (1987) The bromoperoxidase from the lichen *Xanthoria parietina* is a novel vanadium enzyme. *Biochem J* 248:277–279
31. Winter JM, Moore BS (2009) Exploring the chemistry and biology of vanadium-dependent haloperoxidases. *J Biol Chem* 284:18577–18581
32. Winter JM, Moffitt MC, Zazopoulos E, McAlpine JB, Dorrestein PC, Moore BS (2007) Molecular basis for chloronium-mediated meroterpenoid cyclization – cloning,

- sequencing, and heterologous expression of the napyradiomycin biosynthetic gene cluster. *J Biol Chem* 282:16362–16368
33. Soedjak HS, Butler A (1990) Characterization of vanadium bromoperoxidase from macrocystis and fucus – reactivity of vanadium bromoperoxidase toward acyl and alkyl peroxides and bromination of amines. *Biochemistry* 29:7974–7981
 34. Hasan Z, Renirie R, Kerkman R, Ruijsenaars HJ, Hartog AF, Wever R (2006) Laboratory-evolved vanadium chloroperoxidase exhibits 100-fold higher halogenating activity at alkaline pH: catalytic effects from first and second coordination sphere mutations. *J Biol Chem* 281:9738–9744
 35. Coupe EE, Smyth MG, Fosberry A, Hall RM, Littlechild JA (2007) The dodecameric vanadium-dependent haloperoxidase from the marine algae *Corallina officinalis*: cloning, expression, and refolding of the recombinant enzyme. *Protein Expr Purif* 52:265–272
 36. Borchardt SA, Allain EJ, Michels JJ, Stearns GW, Kelly RF, McCoy WF (2001) Reaction of acylated homoserine lactone bacterial signaling molecules with oxidized halogen antimicrobials. *Appl Environ Microbiol* 67:3174–3179
 37. Leblanc C, Colin C, Cosse A, Delage L, La Barre S, Morin P, Fievet B, Voiseux C, Ambroise Y, Verhaeghe E, Amouroux D, Donard O, Tessier E, Potin P (2006) Iodine transfers in the coastal marine environment: the key role of brown algae and of their vanadium-dependent haloperoxidases. *Biochimie* 88:1773–1785
 38. Cosse A, Potin P, Leblanc C (2009) Patterns of gene expression induced by oligoguluronates reveal conserved and environment-specific molecular defense responses in the brown alga *Laminaria digitata*. *New Phytol* 182:239–250
 39. Krebs C, Galonic FD, Walsh CT, Bollinger JM Jr (2007) Non-heme Fe(IV)-oxo intermediates. *Acc Chem Res* 40:484–492
 40. Vaillancourt FH, Yin J, Walsh CT (2005) SyrB2 in syringomycin E biosynthesis is a nonheme Fe-II α -ketoglutarate- and O₂-dependent halogenase. *Proc Natl Acad Sci USA* 102:10111–10116
 41. Vaillancourt FH, Vosburg DA, Walsh CT (2006) Dichlorination and bromination of a threonyl-S-carrier protein by the non-heme Fe(II) halogenase SyrB2. *Chembiochem* 7:748–752
 42. Blasiak LC, Vaillancourt FH, Walsh CT, Drennan CL (2006) Crystal structure of the non-haem iron halogenase SyrB2 in syringomycin biosynthesis. *Nature* 440:368–371
 43. Straganz GD, Nidetzky B (2006) Variations of the 2-His-1-carboxylate theme in mononuclear non-heme Fe-II oxygenases. *Chembiochem* 7:1536–1548
 44. de Visser SP, Latifi R (2009) Carbon dioxide: a waste product in the catalytic cycle of α -ketoglutarate dependent halogenases prevents the formation of hydroxylated by-products. *J Phys Chem B* 113:12–14
 45. Wong C, Fujimori DG, Walsh CT, Drennan CL (2009) Structural analysis of an open active site conformation of nonheme iron halogenase CytC3. *J Am Chem Soc* 131:4872–4879
 46. Matthews ML, Neumann CS, Miles LA, Grove TL, Booker SJ, Krebs C, Walsh CT, Bollinger JM Jr (2009) Substrate positioning controls the partition between halogenation and hydroxylation in the aliphatic halogenase, SyrB2. *Proc Natl Acad Sci USA* 106:17723–17728
 47. Matthews ML, Krest CM, Barr EW, Vaillancourt FH, Walsh CT, Green MT, Krebs C, Bollinger JM (2009) Substrate-triggered formation and remarkable stability of the C-H bond-cleaving chloroferryl intermediate in the aliphatic halogenase, SyrB2. *Biochemistry* 48:4331–4343
 48. Flatt PM, O'Connell SJ, McPhail KL, Zeller G, Willis CL, Sherman DH, Gerwick WH (2006) Characterization of the initial enzymatic steps of barbamide biosynthesis. *J Nat Prod* 69:938–944
 49. Chang Z, Flatt P, Gerwick WH, Nguyen VA, Willis CL, Sherman DH (2002) The barbamide biosynthetic gene cluster: a novel marine cyanobacterial system of mixed polyketide

- synthase (PKS)-non-ribosomal peptide synthetase (NRPS) origin involving an unusual trichloroleucyl starter unit. *Gene* 296:235–247
50. Ridley CP, Bergquist PR, Harper MK, Faulkner DJ, Hooper JNA, Haygood MG (2005) Speciation and biosynthetic variation in four dictyoceratid sponges and their cyanobacterial symbiont, *Oscillatoria spongeliae*. *Chem Biol* 12:397–406
 51. Edwards DJ, Marquez BL, Nogle LM, McPhail K, Goeger DE, Roberts MA, Gerwick WH (2004) Structure and biosynthesis of the jamaicamides, new mixed polyketide-peptide neurotoxins from the marine cyanobacterium *Lyngbya majuscula*. *Chem Biol* 11:817–833
 52. Gu L, Wang B, Kulkarni A, Geders TW, Grindberg RV, Gerwick L, Håkansson K, Wipf P, Smith JL, Gerwick WH, Sherman DH (2009) Metamorphic enzyme assembly in polyketide diversification. *Nature* 459:731–735
 53. Balunas MJ, Linington RG, Tidgewell K, Fenner AM, Urena LD, Togna GD, Kyle DE, Gerwick WH (2010) Dragonamide E, a modified linear lipopeptide from *Lyngbya majuscula* with antileishmanial activity. *J Nat Prod* 73:60–66
 54. Jimenez JI, Scheuer PJ (2001) New lipopeptides from the Caribbean cyanobacterium *Lyngbya majuscula*. *J Nat Prod* 64:200–203
 55. Ueki M, Galonic DP, Vaillancourt FH, Garneau-Tsodikova S, Yeh E, Vosburg DA, Schroeder FC, Osada H, Walsh CT (2006) Enzymatic generation of the antimetabolite γ , γ -dichloroaminobutyrate by NRPS and mononuclear iron halogenase action in a streptomycete. *Chem Biol* 13:1183–1191
 56. Galonic DP, Barr EW, Walsh CT, Bollinger JM Jr, Krebs C (2007) Two interconverting Fe (IV) intermediates in aliphatic chlorination by the halogenase CytC3. *Nat Chem Biol* 3:113–116
 57. Vaillancourt FH, Yeh E, Vosburg DA, O'Connor SE, Walsh CT (2005) Cryptic chlorination by a non-haem iron enzyme during cyclopropyl amino acid biosynthesis. *Nature* 436:1191–1194
 58. Kelly WL, Boyne MT, Yeh E, Vosburg DA, Galonic DP, Kelleher NL, Walsh CT (2007) Characterization of the aminocarboxycyclopropane-forming enzyme CmaC. *Biochemistry* 46:359–368
 59. Hammer PE, Hill DS, Lam ST, van Pée KH, Ligon JM (1997) Four genes from *Pseudomonas fluorescens* that encode the biosynthesis of pyrrolnitrin. *Appl Environ Microbiol* 63:2147–2154
 60. Dairi T, Nakano T, Aisaka K, Katsumata R, Hasegawa M (1995) Cloning and nucleotide sequence of the gene responsible for chlorination of tetracycline. *Biosci Biotechnol Biochem* 59:1099–1106
 61. Kirner S, Hammer PE, Hill DS, Altmann A, Fischer I, Weislo LJ, Lanahan M, van Pée KH, Ligon JM (1998) Functions encoded by pyrrolnitrin biosynthetic genes from *Pseudomonas fluorescens*. *J Bacteriol* 180:1939–1943
 62. Hohaus K, Altmann A, Burd W, Fischer I, Hammer PE, Hill DS, Ligon JM, van Pée KH (1997) NADH-abhängige Halogenasen sind wahrscheinlich eher an der Biosynthese von Halometaboliten beteiligt als Haloperoxidasen. *Angew Chem* 109:2102–2104
 63. Hölzer M, Burd W, Reißig H-U, van Pée KH (2001) Substrate specificity and regioselectivity of tryptophan 7-halogenase from *Pseudomonas fluorescens* BL915. *Adv Synth Catal* 343:591–595
 64. van Pée KH (2001) Microbial biosynthesis of halometabolites. *Arch Microbiol* 175:250–258
 65. Keller S, Wage T, Hohaus K, Hölzer M, Eichhorn E, van Pée KH (2000) Purification and partial characterization of tryptophan 7-halogenase (PrnA) from *Pseudomonas fluorescens*. *Angew Chem Int Ed Engl* 39:2300–2302
 66. Unversucht S, Hollmann F, Schmid A, van Pée KH (2005) FADH(2)-dependence of tryptophan 7-halogenase. *Adv Synth Catal* 347:1163–1167
 67. Paulsen IT, Press CM, Ravel J, Kobayashi DY, Myers GSA, Mavrodi DV, Deboy RT, Seshadri R, Ren QH, Madupu R, Dodson RJ, Durkin AS, Brinkac LM, Daugherty SC,

- Sullivan SA, Rosovitz MJ, Gwinn ML, Zhou LW, Schneider DJ, Cartinhour SW, Nelson WC, Weidman J, Watkins K, Tran K, Khouri H, Pierson EA, Pierson LS, Thomashow LS, Loper JE (2005) Complete genome sequence of the plant commensal *Pseudomonas fluorescens* Pf-5. *Nat Biotechnol* 23:873–878
68. van Pée KH, Dong CJ, Flecks S, Naismith J, Patallo EP, Wage T (2006) Biological halogenation has moved far beyond haloperoxidases. *Adv Appl Microbiol* 59:127–157
69. Dong C, Kotzsch A, Dorward M, van Pée KH, Naismith JH (2004) Crystallization and X-ray diffraction of a halogenating enzyme, tryptophan 7-halogenase, from *Pseudomonas fluorescens*. *Acta Crystallogr D Biol Crystallogr* 60:1438–1440
70. Dong CJ, Flecks S, Unversucht S, Haupt C, van Pée KH, Naismith JH (2005) Tryptophan 7-halogenase (PrnA) structure suggests a mechanism for regioselective chlorination. *Science* 309:2216–2219
71. Seibold C, Schnerr H, Rumpf J, Kunzendorf A, Hatscher C, Wage T, Ernyei AJ, Dong CJ, Naismith JH, van Pée KH (2006) A flavin-dependent tryptophan 6-halogenase and its use in modification of pyrrolnitrin biosynthesis. *Biocatal Biotransform* 24:401–408
72. Sánchez C, Butovich IA, Braña AF, Rohr J, Méndez C, Salas JA (2002) The biosynthetic gene cluster for the antitumor rebeccamycin: characterization and generation of indolocarbazole derivatives. *Chem Biol* 9:519–531
73. Onaka H, Taniguchi S, Igarashi Y, Furumai T (2003) Characterization of the biosynthetic gene cluster of rebeccamycin from *Lechevalieria aerocolonigenes* ATCC 39243. *Biosci Biotechnol Biochem* 67:127–138
74. Yeh E, Garneau S, Walsh CT (2005) Robust in vitro activity of RebF and RebH, a two-component reductase/halogenase, generating 7-chlorotryptophan during rebeccamycin biosynthesis. *Proc Natl Acad Sci USA* 102:3960–3965
75. Yeh E, Cole LJ, Barr EW, Bollinger JM, Ballou DP, Walsh CT (2006) Flavin redox chemistry precedes substrate chlorination during the reaction of the flavin-dependent halogenase RebH. *Biochemistry* 45:7904–7912
76. Yeh E, Blasiak LC, Koglin A, Drennan CL, Walsh CT (2007) Chlorination by a long-lived intermediate in the mechanism of flavin-dependent halogenases. *Biochemistry* 46:1284–1292
77. Zehner S, Kotzsch A, Bister B, Süssmuth RD, Méndez C, Salas JA, van Pée KH (2005) A regioselective tryptophan 5-halogenase is involved in pyrroindomycin biosynthesis in *Streptomyces rugosporus* LL-42D005. *Chem Biol* 12:445–452
78. Zhu XF, De Laurentis W, Leang K, Herrmann J, Lhiefeld K, van Pée KH, Naismith JH (2009) Structural insights into regioselectivity in the enzymatic chlorination of tryptophan. *J Mol Biol* 391:74–85
79. Rachid S, Krug D, Kunze B, Kochems I, Scharfe M, Zabriskie TM, Blöcker H, Müller R (2006) Molecular and biochemical studies of chondramide formation – highly cytotoxic natural products from *Chondromyces crocatus* Cm c5. *Chem Biol* 13:667–681
80. Chiu HT, Hubbard BK, Shah AN, Eide J, Fredenburg RA, Walsh CT, Khosla C (2001) Molecular cloning and sequence analysis of the complestatin biosynthetic gene cluster. *Proc Natl Acad Sci USA* 98:8548–8553
81. Puk O, Bischoff D, Kittel C, Pelzer S, Weist S, Stegmann E, Süssmuth RD, Wohlleben W (2004) Biosynthesis of chloro- β -hydroxytyrosine, a nonproteinogenic amino acid of the peptidic backbone of glycopeptide antibiotics. *J Bacteriol* 186:6093–6100
82. Dorrestein PC, Yeh E, Garneau-Tsodikova S, Kelleher NL, Walsh CT (2005) Dichlorination of a pyrrolyl-S-carrier protein by FADH₂-dependent halogenase PltA during pyoluteorin biosynthesis. *Proc Natl Acad Sci USA* 102:13843–13848
83. Pirae M, White RL, Vining LC (2004) Biosynthesis of the dichloroacetyl component of chloramphenicol in *Streptomyces venezuelae* ISP5230: genes required for halogenation. *Microbiology* 150:85–94
84. Pacholec M, Sello JK, Walsh CT, Thomas MG (2007) Formation of an aminoacyl-S-enzyme intermediate is a key step in the biosynthesis of chloramphenicol. *Org Biomol Chem* 5:1692–1694

85. Kling E, Schmid C, Unversucht S, Wage T, Zehner S, van Pée KH (2005) Enzymatic incorporation of halogen atoms into natural compounds. *Ernst Schering Res Found Workshop* 51:165–194
86. Latimer R, Podzelinska K, Soares A, Bhattacharya A, Vining LC, Jia ZC, Zechel DL (2009) Expression, purification and preliminary diffraction studies of CmlS. *Acta Crystallogr Sect F Struct Biol Cryst Commun* 65:260–263
87. Podzelinska K, Latimer R, Bhattacharya A, Vining LC, Zechel DL, Jia ZC (2010) Chloramphenicol biosynthesis: the structure of CmlS, a flavin-dependent halogenase showing a covalent flavin-aspartate bond. *J Mol Biol* 397:316–331
88. Buedenbender S, Rachid S, Müller R, Schulz GE (2009) Structure and action of the myxobacterial chondrochloren halogenase CndH: a new variant of FAD-dependent halogenases. *J Mol Biol* 385:520–530
89. van Pée KH, Salcher O, Fischer P, Bokel M, Lingens F (1983) The biosynthesis of brominated pyrrolnitrin derivatives by *Pseudomonas aureofaciens*. *J Antibiot* 36:1735–1742
90. Smith CG (1958) Effect of halogens on the chloramphenicol fermentation. *J Bacteriol* 75:577–583
91. Doerschuk AP, McCormick JRD, Goodman JJ, Szumski SA, Growich JA, Miller PA, Bitler BA, Jensen ER, Matrishin M, Petty MA, Phelps AS (1959) Biosynthesis of tetracyclines. I. The halide metabolism of *Streptomyces aureofaciens* mutants – The preparation and characterization of tetracycline, 7-chloro-36-tetracycline and 7-bromotetracycline. *J Am Chem Soc* 81:3069–3075
92. Bister B, Bischoff D, Nicholson GJ, Stockert S, Wink J, Brunati C, Donadio S, Pelzer S, Wohlleben W, Sussmuth RD (2003) Bromobalhimycin and chlorobromobalhimycins - Illuminating the potential of halogenases in glycopeptide antibiotic biosyntheses. *Chembiochem* 4:658–662
93. Stander MA, Steyn PS, Lübben A, Miljkovic A, Mantle PG, Marais GJ (2000) Influence of halogen salts on the production of the ochratoxins by *Aspergillus ochraceus* Wilh. *J Agric Food Chem* 48:1865–1871
94. Magarvey NA, Beck ZQ, Golakoti T, Ding YS, Huber U, Hemscheidt TK, Abelson D, Moore RE, Sherman DH (2006) Biosynthetic characterization and chemoenzymatic assembly of the cryptophycins. Potent anticancer agents from *Nostoc* cyanobionts. *ACS Chem Biol* 1:766–779
95. Eustáquio AS, Gust B, Luft T, Li SM, Chater KF, Heide L (2003) Clorobiocin biosynthesis in *Streptomyces*: identification of the halogenase and generation of structural analogs. *Chem Biol* 10:279–288
96. Eustáquio AS, Gust B, Li SM, Pelzer S, Wohlleben W, Chater KF, Heide L (2004) Production of 8'-halogenated and 8'-unsubstituted novobiocin derivatives in genetically engineered *Streptomyces coelicolor* strains. *Chem Biol* 11:1561–1572
97. Wolpert M, Heide L, Kammerer B, Gust B (2008) Assembly and heterologous expression of the coumermycin A1 gene cluster and production of new derivatives by genetic engineering. *Chembiochem* 9:603–612
98. Heide L, Westrich L, Anderle C, Gust B, Kammerer B, Piel J (2008) Use of a halogenase of hormaomycin biosynthesis for formation of new clorobiocin analogues with 5-chloropyrrole moieties. *Chembiochem* 9:1992–1999
99. Akinaga S, Sugiyama K, Akiyama T (2000) UCN-01 (7-hydroxystaurosporine) and other indolocarbazole compounds: a new generation of anti-cancer agents for the new century? *Anticancer Drug Des* 15:43–52
100. Sánchez C, Zhu LL, Braña AF, Salas AP, Rohr J, Méndez C, Salas JA (2005) Combinatorial biosynthesis of antitumor indolocarbazole compounds. *Proc Natl Acad Sci USA* 102:461–466
101. Muffler K, Retzlaff M, van Pée KH, Ulber R (2007) Optimisation of halogenase enzyme activity by application of a genetic algorithm. *J Biotechnol* 127:425–433

102. Muffler K, Ngnigha ARK, Ulber R (2010) Determination of kinetic parameters of the FADH (2)-dependent tryptophan-5-halogenases from *Streptomyces rugosporus*. *Chem Ing Tech* 82:121–127
103. Dong CJ, Huang FL, Deng H, Schaffrath C, Spencer JB, O'Hagan D, Naismith JH (2004) Crystal structure and mechanism of a bacterial fluorinating enzyme. *Nature* 427:561–565
104. Beer LL, Moore BS (2007) Biosynthetic convergence of salinosporamides A and B in the marine actinomycete *Salinispora tropica*. *Org Lett* 9:845–848
105. Eustáquio AS, McGlinchey RP, Liu Y, Hazzard C, Beer LL, Florova G, Alhamadsheh MM, Lechner A, Kale AJ, Kobayashi Y, Reynolds KA, Moore BS (2009) Biosynthesis of the salinosporamide A polyketide synthase substrate chloroethylmalonyl-coenzyme A from S-adenosyl-L-methionine. *Proc Natl Acad Sci USA* 106:12295–12300
106. Eustáquio AS, O'Hagan D, Moore BS (2010) Engineering fluorometabolite production: fluorinase expression in *Salinispora tropica* yields fluorosalinosporamide. *J Nat Prod* 73:378–382
107. Eustáquio AS, Moore BS (2008) Mutasynthesis of fluorosalinosporamide, a potent and reversible inhibitor of the proteasome. *Angew Chem Int Ed Engl* 47:3936–3938
108. Deng H, Cross SM, McGlinchey RP, Hamilton JT, O'Hagan D (2008) In vitro reconstituted biotransformation of 4-fluorothreonine from fluoride ion: application of the fluorinase. *Chem Biol* 15:1268–1276
109. Harper DB (1985) Halomethane from halide ion – A highly efficient fungal conversion of environmental significance. *Nature* 315:55–57
110. Wuosmaa AM, Hager LP (1990) Methyl chloride transferase – A carbocation route for biosynthesis of halometabolites. *Science* 249:160–162
111. Ohsawa N, Tsujita M, Morikawa S, Itoh N (2001) Purification and characterization of a monohalomethane-producing enzyme S-adenosyl-L-methionine: halide ion methyltransferase from a marine microalga, *Pavlova pinguis*. *Biosci Biotechnol Biochem* 65:2397–2404
112. Amachi S, Kamagata Y, Kanagawa T, Muramatsu Y (2001) Bacteria mediate methylation of iodine in marine and terrestrial environments. *Appl Environ Microbiol* 67:2718–2722
113. Saxena D, Aouad S, Attieh J, Saini HS (1998) Biochemical characterization of chloromethane emission from the wood-rotting fungus *Phellinus pomaceus*. *Appl Environ Microbiol* 64:2831–2835
114. van Pée KH (1996) Biosynthesis of halogenated metabolites by bacteria. *Annu Rev Microbiol* 50:375–399
115. Murphy CD (2006) Recent developments in enzymatic chlorination. *Nat Prod Rep* 23:147–152
116. Reed KA, Manam RR, Mitchell SS, Xu JL, Teisan S, Chao TH, Deyanat-Yazdi G, Neuteboom STC, Lam KS, Potts BCM (2007) Salinosporamides D-J from the marine actinomycete *Salinispora tropica*, bromosalinosporamide, and thioester derivatives are potent inhibitors of the 20S proteasome. *J Nat Prod* 70:269–276
117. Blasiak LC, Drennan CL (2009) Structural perspective on enzymatic halogenation. *Acc Chem Res* 42:147–155
118. Neumann CS, Fujimori DG, Walsh CT (2008) Halogenation strategies in natural product biosynthesis. *Chem Biol* 15:99–109
119. Chen X, van Pée KH (2008) Catalytic mechanisms, basic roles, and biotechnological and environmental significance of halogenating enzymes. *Acta Biochim Biophys Sin (Shanghai)* 40:183–193
120. van Pée KH, Patallo EP (2006) Flavin-dependent halogenases involved in secondary metabolism in bacteria. *Appl Microbiol Biotechnol* 70:631–641
121. van Pée KH, Hölzer M (1999) Specific enzymatic chlorination of tryptophan and tryptophan derivatives. *Adv Exp Med Biol* 467:603–609
122. Vaillancourt FH, Yeh E, Vosburg DA, Garneau-Tsodikova S, Walsh CT (2006) Nature's inventory of halogenation catalysts: oxidative strategies predominate. *Chem Rev* 106:3364–3378

123. Fujimori DG, Walsh CT (2007) What's new in enzymatic halogenations. *Curr Opin Chem Biol* 11:553–560
124. Dolfing J (1998) Halogenation of aromatic compounds: thermodynamic, mechanistic and ecological aspects. *FEMS Microbiol Lett* 167:271–274
125. Rauei S, Carloni P (2006) Structure and function of vanadium haloperoxidases. *J Phys Chem B* 110:3747–3758
126. Bortolini O, Conte V (2005) Vanadium (V) peroxocomplexes: structure, chemistry and biological implications. *J Inorg Biochem* 99:1549–1557
127. Guenzi E, Galli G, Grgurina I, Gross DC, Grandi G (1998) Characterization of the syringomycin synthetase gene cluster – A link between prokaryotic and eukaryotic peptide synthetases. *J Biol Chem* 273:32857–32863
128. Zhang JH, Quigley NB, Gross DC (1995) Analysis of the *syrB* and *syrC* genes of *Pseudomonas syringae* pv. *syringae* indicates that syringomycin is synthesized by a thiotemplate mechanism. *J Bacteriol* 177:4009–4020
129. Galonic DP, Vaillancourt FH, Walsh CT (2006) Halogenation of unactivated carbon centers in natural product biosynthesis: trichlorination of leucine during barbamide biosynthesis. *J Am Chem Soc* 128:3900–3901
130. Ramaswamy AV, Sorrels CM, Gerwick WH (2007) Cloning and biochemical characterization of the hectochlorin biosynthetic gene cluster from the marine cyanobacterium *Lyngbya majuscula*. *J Nat Prod* 70:1977–1986
131. Ullrich M, Guenzi AC, Mitchell RE, Bender CL (1994) Cloning and expression of genes required for coronamic acid (2-ethyl-1-aminocyclopropane 1-carboxylic acid), an intermediate in the biosynthesis of the phytotoxin coronatine. *Appl Environ Microbiol* 60:2890–2897
132. Fujimori DG, Hrvatin S, Neumann CS, Strieker M, Marahiel MA, Walsh CT (2007) Cloning and characterization of the biosynthetic gene cluster for kutznerides. *Proc Natl Acad Sci USA* 104:16498–16503
133. Chang Z, Sitachitta N, Rossi JV, Roberts MA, Flatt PM, Jia J, Sherman DH, Gerwick WH (2004) Biosynthetic pathway and gene cluster analysis of curacin A, an antitubulin natural product from the tropical marine cyanobacterium *Lyngbya majuscula*. *J Nat Prod* 67:1356–1367
134. Flatt P, Gautschi J, Thacker R, Musafija-Girt M, Crews P, Gerwick W (2005) Identification of the cellular site of polychlorinated peptide biosynthesis in the marine sponge *Dysidea (Lamellodysidea) herbacea* and symbiotic cyanobacterium *Oscillatoria spongeliae* by CARD-FISH analysis. *Mar Biol* 147:761–774
135. Gao Q, Zhang C, Blanchard S, Thorson JS (2006) Deciphering indolocarbazole and enediyne aminodideoxypentose biosynthesis through comparative genomics: insights from the AT2433 biosynthetic locus. *Chem Biol* 13:733–743
136. Heemstra JR Jr, Walsh CT (2008) Tandem action of the O₂- and FADH₂-dependent halogenases KtzQ and KtzR produce 6,7-dichlorotryptophan for kutzneride assembly. *J Am Chem Soc* 130:14024–14025
137. Zerbe K, Pylypenko O, Vitali F, Zhang W, Rouset S, Heck M, Vrijbloed JW, Bischoff D, Bister B, Süssmuth RD, Pelzer S, Wohlleben W, Robinson JA, Schlichting I (2002) Crystal structure of OxyB, a cytochrome P450 implicated in an oxidative phenol coupling reaction during vancomycin biosynthesis. *J Biol Chem* 277:47476–47485
138. Pelzer S, Süssmuth R, Heckmann D, Recktenwald J, Huber P, Jung G, Wohlleben W (1999) Identification and analysis of the balhimycin biosynthetic gene cluster and its use for manipulating glycopeptide biosynthesis in *Amycolatopsis mediterranei* DSM5908. *Antimicrob Agents Chemother* 43:1565–1573
139. Sosio M, Kloosterman H, Bianchi A, de Vreugd P, Dijkhuizen L, Donadio S (2004) Organization of the teicoplanin gene cluster in *Actinoplanes teichomyceticus*. *Microbiology* 150:95–102
140. Sosio M, Stinchi S, Beltrametti F, Lazzarini A, Donadio S (2003) The gene cluster for the biosynthesis of the glycopeptide antibiotic A40926 by *Nonomuraea* species. *Chem Biol* 10:541–549

141. Rouhiainen L, Paulin L, Suomalainen S, Hyytiäinen H, Buikema W, Haselkorn R, Sivonen K (2000) Genes encoding synthetases of cyclic depsipeptides, anabaenopeptilides, in *Anabaena* strain 90. *Mol Microbiol* 37:156–167
142. Tooming-Klunderud A, Rohrlack T, Shalchian-Tabrizi K, Kristensen T, Jakobsen KS (2007) Structural analysis of a non-ribosomal halogenated cyclic peptide and its putative operon from *Microcystis*: implications for evolution of cyanopeptolins. *Microbiology* 153:1382–1393
143. Cadel-Six S, Dauga C, Castets AM, Rippka R, Bouchier C, de Marsac NT, Welker M (2008) Halogenase genes in nonribosomal peptide synthetase gene clusters of *Microcystis* (cyanobacteria): sporadic distribution and evolution. *Mol Biol Evol* 25:2031–2041
144. Jia XY, Tian ZH, Shao L, Qu XD, Zhao QF, Tang J, Tang GL, Liu W (2006) Genetic characterization of the chlorothricin gene cluster as a model for spirotetronate antibiotic biosynthesis. *Chem Biol* 13:575–585
145. Lin S, Van Lanen SG, Shen B (2007) Regiospecific chlorination of (S)- β -tyrosyl-S-carrier protein catalyzed by SgcC3 in the biosynthesis of the enediyne antitumor antibiotic C-1027. *J Am Chem Soc* 129:12432–12438
146. Rachid S, Scharfe M, Blocker H, Weissman KJ, Müller R (2009) Unusual chemistry in the biosynthesis of the antibiotic chondrochlorens. *Chem Biol* 16:70–81
147. Ishida K, Welker M, Christiansen G, Cadel-Six S, Bouchier C, Dittmann E, Hertweck C, Tandeau DM (2009) Plasticity and evolution of aeruginosin biosynthesis in cyanobacteria. *Appl Environ Microbiol* 75:2017–2026
148. Wynands I, van Pée KH (2004) A novel halogenase gene from the pentachloropseudilin producer *Actinoplanes* sp ATCC 33002 and detection of in vitro halogenase activity. *FEMS Microbiol Lett* 237:363–367
149. Zhang X, Parry RJ (2007) Cloning and characterization of the pyrrolomycin biosynthetic gene clusters from *Actinosporangium vitaminophilum* ATCC 31673 and *Streptomyces* sp. strain UC 11065. *Antimicrob. Agents Chemother* 51:946–957
150. Yu TW, Bai LQ, Clade D, Hoffmann D, Toelzer S, Trinh KQ, Xu J, Moss SJ, Leistner E, Floss HG (2002) The biosynthetic gene cluster of the maytansinoid antitumor agent ansamitocin from *Actinosynnema pretiosum*. *Proc Natl Acad Sci USA* 99:7968–7973
151. Spiteller P, Bai LQ, Shang GD, Carroll BJ, Yu TW, Floss HG (2003) The post-polyketide synthase modification steps in the biosynthesis of the antitumor agent ansamitocin by *Actinosynnema pretiosum*. *J Am Chem Soc* 125:14236–14237
152. Färber P, Geisen R (2004) Analysis of differentially-expressed ochratoxin A biosynthesis genes of *Penicillium nordicum*. *Eur J Plant Pathol* 110:661–669
153. Li SM, Heide L (2006) The biosynthetic gene clusters of aminocoumarin antibiotics. *Planta Med* 72:1093–1099
154. Weinbauer G, Mühlenweg A, Trefzer A, Hoffmeister D, Süßmuth RD, Jung G, Welzel K, Vente A, Girreser U, Bechthold A (2001) Biosynthesis of the orthosomycin antibiotic avilamycin A: deductions from the molecular analysis of the *avi* biosynthetic gene cluster of *Streptomyces viridochromogenes* Tu57 and production of new antibiotics. *Chem Biol* 8:569–581
155. Ahlert J, Shepard E, Lomovskaya N, Zazopoulos E, Staffa A, Bachmann BO, Huang KX, Fonstein L, Czisny A, Whitwam RE, Farnet CM, Thorson JS (2002) The calicheamicin gene cluster and its iterative type I enediyne PKS. *Science* 297:1173–1176
156. Trefzer A, Pelzer S, Schimana J, Stockert S, Bihlmaier C, Fiedler HP, Welzel K, Vente A, Bechthold A (2002) Biosynthetic gene cluster of simocyclinone, a natural multihybrid antibiotic. *Antimicrob Agents Chemother* 46:1174–1182
157. Wang S, Xu Y, Maine EA, Wijeratne EM, Espinosa-Artiles P, Gunatilaka AA, Molnár I (2008) Functional characterization of the biosynthesis of radicicol, an Hsp90 inhibitor resorcylic acid lactone from *Chaetomium chiversii*. *Chem Biol* 15:1328–1338
158. Neumann CS, Walsh CT, Kay RR (2010) A flavin-dependent halogenase catalyzes the chlorination step in the biosynthesis of *Dictyostelium* differentiation-inducing factor 1. *Proc Natl Acad Sci USA* 107:5798–5803

159. Reeves CD, Hu Z, Reid R, Kealey JT (2008) Genes for the biosynthesis of the fungal polyketides hypothemycin from *Hypomyces subiculosus* and radicol from *Pochonia chlamydosporia*. *Appl Environ Microbiol* 74:5121–5129
160. Otsuka M, Ichinose K, Fujii I, Ebizuka Y (2004) Cloning, sequencing, and functional analysis of an iterative type I polyketide synthase gene cluster for biosynthesis of the antitumor chlorinated polyenone neocarzinil in “*Streptomyces carzinostaticus*”. *Antimicrob Agents Chemother* 48:3468–3476
161. Hutchinson RI, Grant RJ, Murphy CD (2006) Biosynthetic origin of [R-(Z)]-4-amino-3-chloro-2-pentenedioic acid in *Streptomyces viridogenes*. *Biosci Biotechnol Biochem* 70:3046–3049
162. McArthur KA, Mitchell SS, Tsueng G, Rheingold A, White DJ, Grodberg J, Lam KS, Potts BC (2008) Lynamycins A-E, chlorinated bisindole pyrrole antibiotics from a novel marine actinomycete. *J Nat Prod* 71:1732–1737
163. Gullo VP, McAlpine J, Lam KS, Baker D, Petersen F (2006) Drug discovery from natural products. *J Ind Microbiol Biotechnol* 33:523–531
164. Peters L, König GM, Terlau H, Wright AD (2002) Four new bromotryptamine derivatives from the marine bryozoan *Flustra foliacea*. *J Nat Prod* 65:1633–1637
165. Segraves NL, Robinson SJ, Garcia D, Said SA, Fu X, Schmitz FJ, Pietraszkiewicz H, Valeriote FA, Crews P (2004) Comparison of fascaplysin and related alkaloids: a study of structures, cytotoxicities, and sources. *J Nat Prod* 67:783–792
166. Clark WD, Corbett T, Valeriote F, Crews P (1997) Cyclocinamide A. An unusual cytotoxic halogenated hexapeptide from the marine sponge Psammocinia. *J Am Chem Soc* 119: 9285–9286
167. Zabriskie TM, Klocke JA, Ireland CM, Marcus AH, Molinski TF, Faulkner DJ, Xu CF, Clardy JC (1986) Jaspamide, a modified peptide from a *Jaspis* sponge, with insecticidal and antifungal activity. *J Am Chem Soc* 108:3123–3124
168. Li F, Maskey RP, Qin S, Sattler I, Fiebig HH, Maier A, Zeeck A, Laatsch H (2005) Chinikomycins A and B: isolation, structure elucidation, and biological activity of novel antibiotics from a marine *Streptomyces* sp. isolate M045. *J Nat Prod* 68:349–353
169. Buchanan GO, Williams PG, Feling RH, Kauffman CA, Jensen PR, Fenical W (2005) Sporolides A and B: structurally unprecedented halogenated macrolides from the marine actinomycete *Salinispora tropica*. *Org Lett* 7:2731–2734
170. Oh DC, Williams PG, Kauffman CA, Jensen PR, Fenical W (2006) Cyanosporasides A and B, chloro- and cyano-cyclopenta[a]indene glycosides from the marine actinomycete “*Salinispora pacifica*”. *Org Lett* 8:1021–1024
171. Martin GD, Tan LT, Jensen PR, Dimayuga RE, Fairchild CR, Raventos-Suarez C, Fenical W (2007) Marmycins A and B, cytotoxic pentacyclic C-glycosides from a marine sediment-derived actinomycete related to the genus *Streptomyces*. *J Nat Prod* 70:1406–1409
172. Quiñoà E, Crews P (1987) Phenolic constituents of *Psammoplysilla*. *Tetrahedron Lett* 28:3229–3232
173. Kobayashi H, Kitamura K, Nagai K, Nakao Y, Fusetani N, van Soest RWM, Matsunaga S (2007) Carteramine A, an inhibitor of neutrophil chemotaxis, from the marine sponge *Stylissa carteri*. *Tetrahedron Lett* 48:2127–2129
174. Yasuda T, Araki A, Kubota T, Ito J, Mikami Y, Fromont J, Kobayashi J (2009) Bromopyrrole alkaloids from marine sponges of the genus *Agelas*. *J Nat Prod* 72:488–491

Part 5

Biomedical Potential of Marine Natural Products

Raymond J. Andersen, Dehai Li, Matt Nodwell, Michel Roberge,
Wendy Strangman, and David E. Williams

Contents

20.1	Introduction	1028
20.2	Microtubules as an Anticancer Drug Target	1029
20.2.1	The Biological Role of Microtubules in Mitosis	1029
20.2.2	Drug Binding Sites on Tubulin	1032
20.2.3	Approaches to Discovering Antimitotic Marine Natural Products	1033
20.3	Microtubule-Depolymerizing Agents	1034
20.3.1	Polyketides	1034
20.3.2	Peptides and Mixed Polyketide/Peptide	1041
20.3.3	Meroterpenoids	1051
20.4	Microtubule-Stabilizing Agents	1052
20.4.1	Polyketides	1052
20.4.2	Alkaloids	1058
20.4.3	Glycolipids	1059
20.4.4	Terpenoid Glycosides	1060
20.5	Summary	1062
20.6	Study Questions	1064
	References	1064

R.J. Andersen (✉) • D. Li • M. Nodwell • W. Strangman • D.E. Williams
Departments of Chemistry and Earth & Ocean Sciences, University of British Columbia,
Vancouver, BC, Canada
e-mail: raymond.andersen@ubc.ca, dehaili@chem.ubc.ca, mnodwell@chem.ubc.ca,
strangman@uncw.edu, davewill@chem.ubc.ca

M. Roberge
Department of Biochemistry & Molecular Biology, University of British Columbia, Vancouver,
BC, Canada
e-mail: michelr@interchange.ubc.ca

Abstract

This chapter illustrates the large number and variety of microtubule-targeting natural product chemotypes that have been discovered from marine organisms. Microtubules are the biological target of many marine natural products, and antimetabolic agents are potent toxins making them highly effective chemical defenses for algae and sessile or slow-moving invertebrates. Marine sponges account for roughly half of the new chemotypes, with the remainder coming from ascidians, soft corals, mollusks, macroalgae, blue-green algae, bacteria, and fungi.

20.1 Introduction

The widespread use of the antimetabolic plant natural products vincristine, vinblastine, paclitaxel, and synthetic analogs of these compounds to treat cancer has provided unparalleled validation of microtubules as a high-value molecular target for the development of new anticancer drugs [1–6]. Organisms living in the world's oceans have turned out to be an extremely rich source of potentially cytotoxic and structurally complex natural products that target microtubules. These antimetabolic marine natural products provide inspiration for the development of new chemical classes of anticancer drugs, and, as such, they have received considerable attention from both academic and industrial researchers who are interested in their bioactivity and chemistry. One major impediment to the development of any antimetabolic natural product into a useful drug is the sustainable production of an adequate supply of the natural product or an analog for clinical use. The intellectual and experimental challenge posed by the complex structures of antimetabolic marine natural products and the need for practical ways to produce them have engaged the synthetic organic chemistry community, resulting in the development of many elegant routes to these valuable targets. A number of antimetabolic marine natural products or synthetic analogs have cleared the multiple hurdles of the drug development pathway to reach phase I and phase II clinical trials, and there is the real hope that one or more of these will become clinically useful drugs alongside the Vinca alkaloids and the taxanes.

The primary goals of this chapter will be (1) to provide some basic background about the role of microtubules in the process of mitosis in order to illustrate how disrupting microtubule dynamics leads to inhibition of cell proliferation and cell death and (2) to present a comprehensive review of the known marine natural products that target microtubules. Natural product structures are grouped first according to their ability to inhibit or promote tubulin polymerization *in vitro* and second according to their putative biogenetic origins.

Another group of very interesting marine natural products, including the protein phosphatase inhibitors okadaic acid, the calyculins, and the spirastrellolides, arrest cells in mitosis at nM concentrations by inhibiting cell-signaling enzymes.

Antimitotic compounds in this category that do not target microtubules will not be reviewed in this chapter. A review of the extensive literature describing synthetic approaches to microtubule-targeting marine natural products is beyond the scope of this chapter, and only selected references will be provided.

20.2 Microtubules as an Anticancer Drug Target

20.2.1 The Biological Role of Microtubules in Mitosis

Microtubules are highly dynamic polymeric protein fibers that have important cellular roles in mitosis, transport, positioning of organelles, and determination of shape [1, 2]. The building blocks of microtubules are heterodimers of the homologous 50-kDa proteins α - and β -tubulin. These heterodimers polymerize in a head-to-tail fashion to form protofilaments, and alignment of 13 protofilaments in a parallel fashion creates the circular walls of a microtubule (Fig. 20.1). One end of the microtubule, the “+” end, has β -tubulin exposed, and the other “−” end has α -tubulin exposed. The α -tubulin unit in the heterodimer has a bound GTP nucleotide that can only be removed by protein denaturation. A second guanine nucleotide that can be either GDP or GTP is bound to an exchangeable site on the β -tubulin unit. Microtubule assembly requires occupancy of the exchangeable site on β -tubulin by GTP, which is hydrolyzed to GDP during polymerization. Once formed, the GDP remains bound to the polymer as long as the β -tubulin unit that it is associated with is still part of the microtubule. The presence of a small cap of tubulin with a GTP bound at the exchangeable site stabilizes the microtubule and inhibits depolymerization.

The length of the microtubules involved in equal partitioning of the duplicate chromosomes synthesized during S phase into daughter cells during mitosis is highly dynamic [7, 8]. Microtubules undergo two types of polymerization/depolymerization behaviors known as “dynamic instability” and “treadmilling.” In dynamic instability, microtubule plus and minus ends randomly and independently switch between phases of growth and shortening. The plus end changes length more rapidly and to a greater extent than the minus end. Dynamic instability is characterized by the rates of growth and shortening and the frequencies of “catastrophe” and “rescue.” Catastrophe is defined as a change in microtubule polymerization from growth or pause to shortening, and rescue is defined as a change from shortening to pause or growth. Pause is a period where no change in microtubule length is detectable by light microscopy. During treadmilling, the growth at the plus microtubule end is exactly balanced by shortening at the minus end, resulting in a net flow of individual tubulin units from the plus to minus ends without a change in overall length. Treadmilling is particularly important in mitotic spindles.

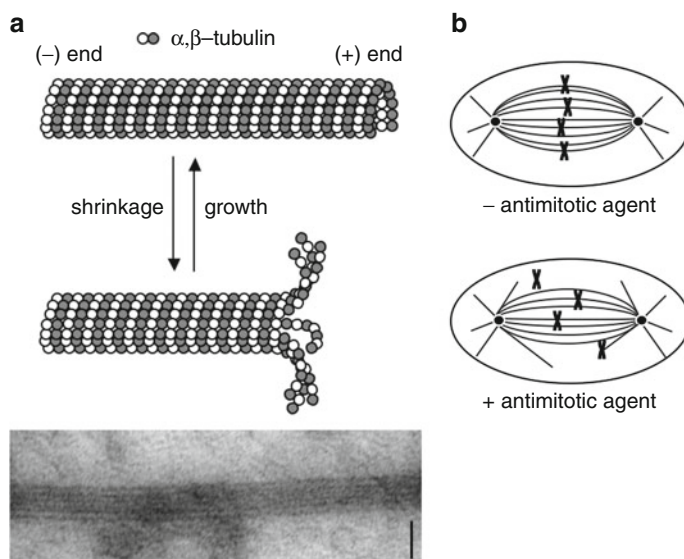


Fig. 20.1 Microtubules and the disruption of their mitotic function by antimetabolic agents. **(a)** Schematic representation of microtubules showing their growth and shrinkage cycle. The lower panel is an electron micrograph of a microtubule whose *in vitro* assembly from pure α - and β -tubulin was stimulated by ceratamine A (97). Scale bar, 30 nm. **(b)** Disruption of microtubule spindle dynamics leads to mitotic arrest. During a normal mitosis, the mitotic spindle aligns chromosomes at the metaphase plate before segregating them to the two daughter cells. Low concentrations of antimetabolic agents cause defects in microtubule dynamics that prevent the efficient capture and alignment of all chromosomes by spindle microtubules, leading to mitotic arrest

Disrupting microtubule dynamics during mitosis is the main effect of anticancer drugs that target microtubules [1, 2]. When cells enter mitosis, the interphase microtubule network disassembles and is replaced by a highly dynamic population of spindle microtubules. During prometaphase, a bipolar mitotic spindle forms. Microtubules radiating from microtubule-organizing centers (MTOC) make extensive growth and shortening excursions probing the cytoplasm until they become attached to chromosomes at their kinetochores. Once microtubules from one MTOC have become attached to a kinetochore, the growth and shortening of microtubules from a second MTOC has to be dynamic enough to allow them to become attached to the kinetochore of the sister chromatid, thereby creating a complete bipolar spindle. During metaphase, the attached chromosomes become aligned along the equatorial region of the spindle, and they are kept in alignment by tension caused by dynamic instability and treadmilling of the kinetochore microtubules (Fig. 20.2). During anaphase, the chromosomes are pulled apart and toward

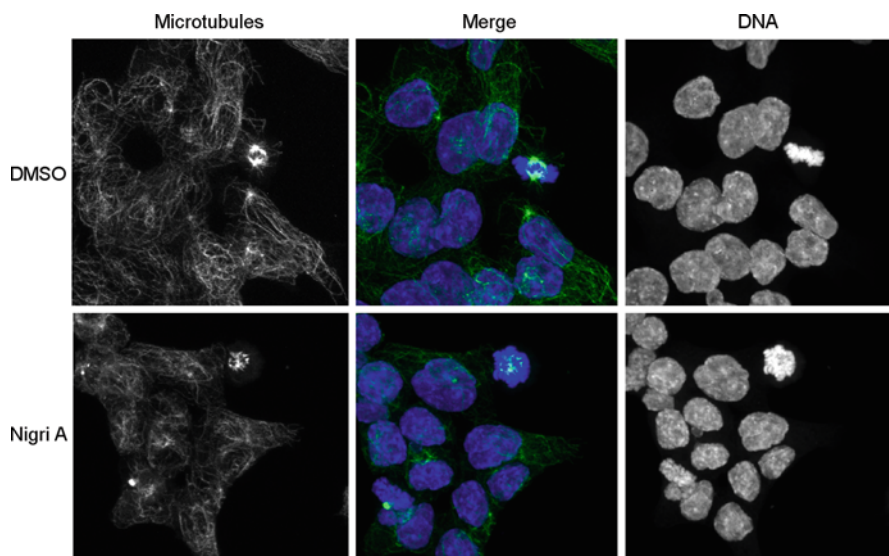


Fig. 20.2 Induction of mitotic arrest by the dimethyl ester of nigricanoside A (**101**). Microtubules were visualized by immunostaining (*left panels*) and chromosomes with the DNA dye Hoechst 33342 (*right panels*). The central panels show merged pictures with microtubules in green and chromosomes in blue. A normal metaphase cell with a bipolar mitotic spindle and aligned chromosomes is shown in control cells (*upper panels*). A cell arrested at mitosis with an abnormal spindle and misaligned chromosomes is seen in the dimethyl ester of nigricanoside A (**101**)-treated sample (*lower panel*)

the spindle poles by depolymerizing microtubules. In telophase, the cell begins to constrict to form two daughter cells, each having one complement of the chromosomes. A series of mitotic checkpoints monitor the progress of spindle formation and chromosome separation during mitosis, and if there are flaws in any of the steps, the cell cycle will be arrested in mitosis, leading to inhibition of cell proliferation and cell death.

Microtubule-targeting natural products are usually described as microtubule “stabilizers/polymerizers” or “destabilizers/depolymerizers” based on their ability to promote or inhibit the polymerization of pure tubulin *in vitro* [1, 2, 6] (Fig. 20.3). However, this classification is misleading because the effects on *in vitro* tubulin polymerization leading to changes in microtubule mass are usually observed only at micromolar concentrations, while the effects of the compounds on cell death are frequently observed at nanomolar concentrations. Evidence now indicates that it is the ability of microtubule-targeting drugs to modulate essential microtubule dynamics at low concentrations without necessarily altering microtubule mass that leads to mitotic arrest and cell death. Cancer cells are thought to be more

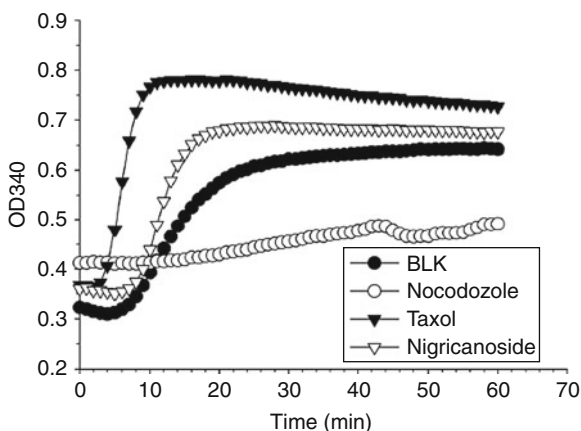


Fig. 20.3 In vitro microtubule polymerization assay. Tubulin spontaneously polymerizes into microtubules when incubated with GTP at 32°C. Microtubule formation may be monitored by turbidimetry at 340 nm. The graph shows that the microtubule depolymerizing agent nocodazole prevents microtubule formation while the microtubule-polymerizing agents taxol and the dimethyl ester of nigricanoside A (**101**) enhance the rate of microtubule assembly

susceptible to microtubule-targeting drugs than normal cells in part because they divide more rapidly, and therefore, they more frequently pass through mitosis where they are vulnerable to disruption of microtubule dynamics. Recent studies have shown that some microtubule-targeting agents are extremely effective at collapsing tumor vasculature in mouse models, leading to death of tumor cells due to lack of oxygen and nutrients [9, 10]. The antivascular effects are often observed at concentrations well below the cytotoxic concentrations of the drugs, raising the possibility of effective metronomic drug treatment regimes aimed at tumor vasculature with reduced cytotoxic side effects.

20.2.2 Drug Binding Sites on Tubulin

Most known microtubule-targeting antimitotic drugs bind to one of four well-described sites on tubulin, although several of the marine natural products presented below have revealed new binding sites [1, 6]. The first of the known sites is the taxane binding site, and it only has a high affinity for drugs when tubulin has polymerized into microtubules. Compounds that bind at the taxane site, such as paclitaxel, cause hyperassembly of microtubules with increased stability in the in vitro polymerization assay (Fig. 20.3). Cells arrested in mitosis with these microtubule “stabilizing” drugs show an increase in microtubule density, and their microtubules are much shorter than normal and aggregated into bundles.

Compounds that bind to the other three sites all inhibit tubulin polymerization into microtubules in vitro, and compound-arrested cells show a thinning or complete disappearance of microtubules along with subtle defects in spindle function. The first group of “destabilizing” antimitotic agents alkylate the thiol group of Cys-239 in tubulin, and some of these inhibit the ability of tubulin to bind colchicine. A second group of “destabilizing” compounds competitively inhibit colchicine binding to tubulin. The third group of destabilizers bind to a region of tubulin known as the “Vinca domain” because of their ability to interfere with the binding of vincristine and vinblastine to tubulin. Some of these compounds are competitive inhibitors of Vinca alkaloid binding, and others are noncompetitive inhibitors.

20.2.3 Approaches to Discovering Antimitotic Marine Natural Products

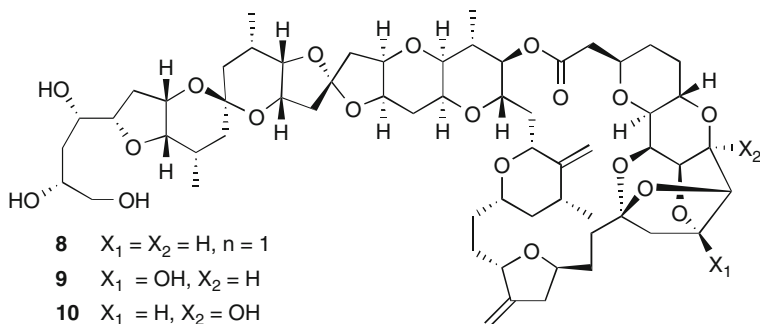
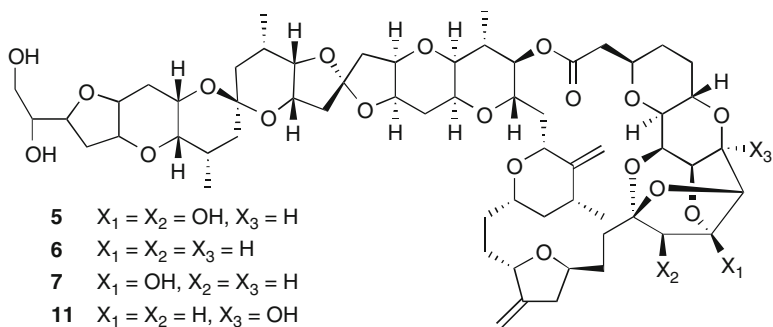
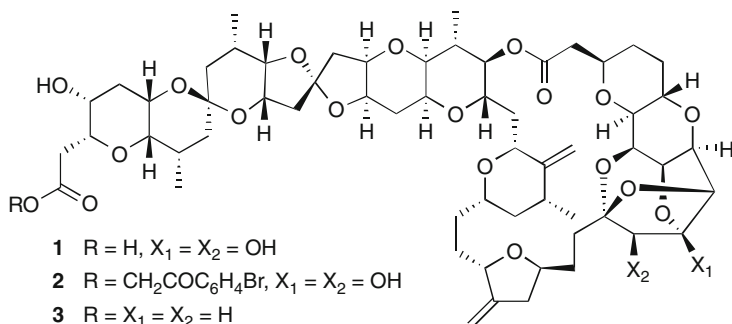
The majority of microtubule-targeting natural products, including the Vinca alkaloids and paclitaxel, were initially discovered because they were potentially cytotoxic, and it was only much later, when their mechanism of action was investigated in detail, that they were found to arrest cells in mitosis and modulate tubulin polymerization in vitro. Horwitz’s seminal discovery that paclitaxel stabilizes microtubules and the subsequent success of paclitaxel in the clinic stimulated a vigorous worldwide search for additional natural product chemotypes possessing this important biological activity [11]. As part of this search, several new assays that can directly detect antimitotic agents in crude extracts have been used to aid the discovery of microtubule-targeting marine natural products.

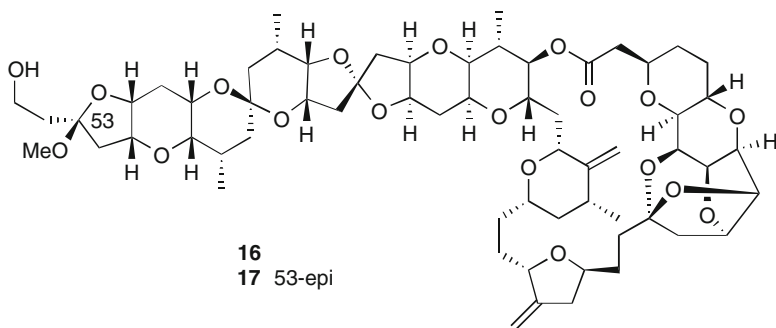
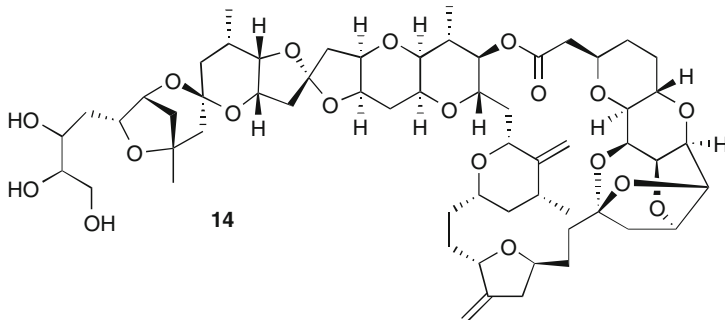
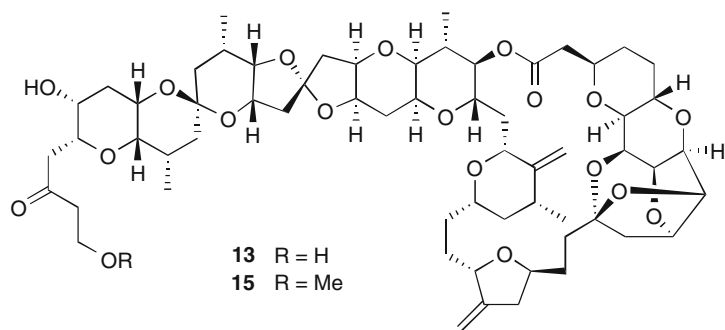
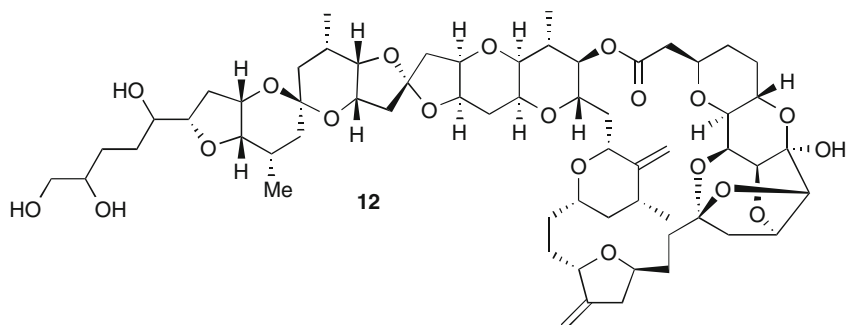
Roberge developed a robust and sensitive cell-based assay for antimitotic agents that uses the monoclonal antibody TG3 to detect a phosphoepitope on the nuclear protein nucleolin that is only present in mitosis [12]. Microscopic examination of tubulin in cells that have been arrested by a hit in the assay can often reveal if the active components are microtubule-depolymerizing or microtubule-stabilizing agents. In this way, the assay can be used as an effective direct screen for microtubule-stabilizing natural products. Barrows developed a cell-based assay that takes advantage of the ability of dibutyryl-cAMP to rapidly induce a spherical morphology in rat glioma cells [13]. The morphological change is due to tubulin polymerization, and therefore, microtubule “destabilizing” antimitotic natural products will inhibit the rounding up. Spherical cells can be selectively aspirated from 96-well plates leaving behind unresponsive cells resulting from treatment with a tubulin-depolymerizing agent, that are quantified by treatment with MTT and spectrophotometric detection of the formazan product. Namikoshi and coworkers have used a modification of the in vitro tubulin polymerization assay [14] and the deformation of mycelia germinated from conidia of the rice plant pathogenic fungus *Pyricularia oryzae* [15] to screen marine extracts for antimitotic agents.

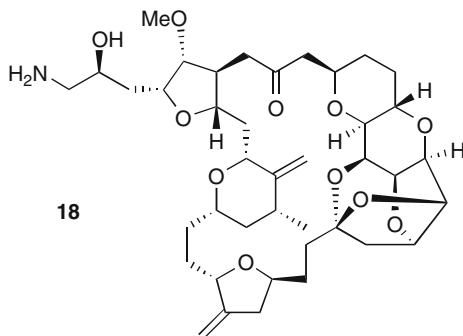
20.3 Microtubule-Depolymerizing Agents

20.3.1 Polyketides

20.3.1.1 Halichondrins and Halistatins







Uemura's group reported the isolation of the polyether macrolide norhalichondrin A (**1**) from the Japanese sponge *Halichondria okadai* Kadota in 1985 [16]. The structure of **1**, including the absolute configuration, was elucidated by single crystal X-ray diffraction analysis of the *p*-bromophenacyl ester derivative (**2**). The same sponge subsequently yielded norhalichondrins B (**3**) and C (**4**); homohalichondrins A (**5**), B (**6**), and C (**7**); and halichondrins B (**8**) and C (**9**) [17]. In 1993, Pettit and coworkers reported the isolation of halistatin 1 (**10**), an isomer of halichondrin C, from the sponge *Phakellia carteri* collected in the Republic of Comoros [18]. They later described the structure of halistatin 2 (**11**) [19], obtained from *Axinella* cf. *carteri* also collected in the Comoros, and halistatin 3 (**12**) obtained from a *Phakellia* sp. collected in the Federated State of Micronesia [20]. Blunt, Munro, and coworkers reported the isolation of isohomohalichondrin B (**13**) [21], neonorhalichondrin B (**14**), 55-methoxyisohomohalichondrin B (**15**), 53-methoxyneoisohomohalichondrin B (**16**), and 53-epi-53-methoxyneoisohomohalichondrin B (**17**) from specimens of the sponge *Lissodendoryx* sp. obtained by dredging in deep water (>100 m) off the Kaikoura Peninsula in New Zealand [22]. They also reported an analog neohomohalichondrin B that has the same constitution as halistatin 3 (**12**), but since no direct comparison was made between the two compounds and neither Pettit or Munro and Blunt assigned the configuration of the side chain chiral centers, it is not possible to say if the compounds are identical or not.

Halichondrin B (**8**) was reported by Uemura to be a potent in vitro cytotoxin (IC₅₀ vs. B-16 melanoma = 0.093 ng/mL), and it also showed impressive %T/C values (157–244) in vivo against the same cell line [17]. Hamel et al. evaluated halichondrin B (**8**) and homohalichondrin B (**6**) in the NCI 60 cell line panel and used the COMPARE analysis to show that it was an antimitotic agent [23]. Halichondrin B was found to inhibit the polymerization of purified tubulin in vitro (IC₅₀ 7.2 μM) and noncompetitively inhibit vinblastine binding. The promising anticancer activity of halichondrin B and the limited supply stimulated

its total synthesis by Kishi and coworkers [24]. As part of the synthetic efforts, scientists at Eisai Research Institute made more than 180 analogs, and they found that eribulin (E7389) (**18**), containing only the macrolide fragment of halichondrin B, was just as active as the natural product in vitro and in vivo [25–27].

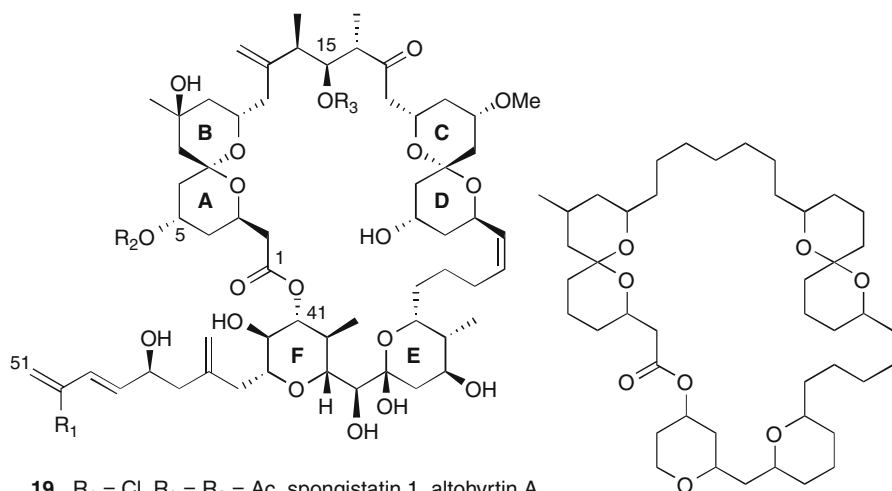
More detailed studies showed that unlike other antimitotic drugs such as vinblastine and paclitaxel that suppress both shortening and growth phases of microtubule dynamic instability, eribulin (**18**) did not affect shortening events nor the catastrophe or rescue frequencies, but it did significantly reduce the rate and extent of microtubule growth [28]. It also generated tubulin aggregates that are different from those created by other antimitotic drugs [29]. These results showed that eribulin (**18**) has a novel mechanism of action involving modulation of microtubule dynamics. Eribulin (**18**) has entered a series of phase I and phase II anticancer clinical trials [30, 31].

20.3.1.2 Spongistatins/Altohyrtins/Cinachyrolide

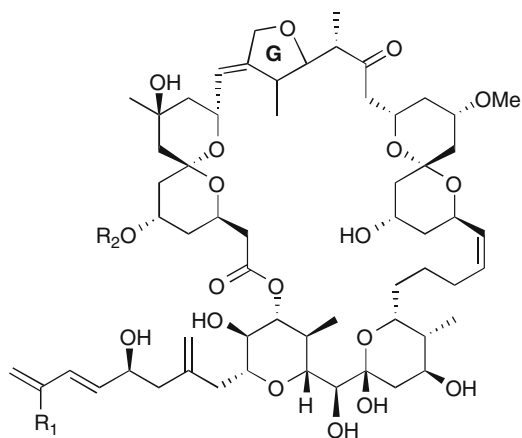
In 1993, the Pettit, Fusetani, and Kitigawa groups independently reported the isolation of members of a family of potentially cytotoxic macrolides from extracts of marine sponges. Spongistatin 1 (**19**) was isolated by Pettit's group from a *Spongia* sp. collected in the Republic of the Maldives in the Indian Ocean [32]. Approximately 14 mg of spongistatin 1 was obtained from 400-kg wet weight of the sponge ($3 \times 10^{-7}\%$ yield), and the paucity of material limited the initial structure elucidation to a determination of the molecule's constitution. Evaluation of spongistatin 1 (**19**) in the NCI 60 cell line panel showed potent broad-spectrum activity (GI_{50} s of 0.25–0.35 nM), and analysis of the pattern of cellular selectivity revealed that it was a microtubule-interactive antimitotic agent. Pettit proposed the name “spongipyran” for the macrocyclic skeleton (**20**) of spongistatin 1.

Fusetani et al. reported the isolation of cinachyrolide A (**21**), which differs from spongistatin 1 (**19**) only by the absence of an acetate ester at C-15, from extracts of a sponge in the genus *Cinachyra* collected off Hachijojima Island 300 km south of Tokyo [33]. They determined the relative configurations of each of the A/B, C/D, and E/F pairs of tetrahydropyran rings and their attached substituents by analysis of NOESY and scalar coupling constant data, but they were not able to relate the relative configurations of the pairs to each other (i.e., A/B to C/D or E/F). Fusetani reported that cinachyrolide A was cytotoxic in vitro against murine leukemia cells with an IC_{50} of <0.6 ng/mL.

Kitigawa and coworkers reported the isolation of altohyrtin A from extracts of the sponge *Hyrtios altum* collected in Okinawa [34]. They determined the constitution of the molecule and the relative configurations of each of the spiroketal and tetrahydropyran ring systems by analysis of NMR data. Altohyrtin A has the same constitution as that reported for spongistatin 1 (**19**). Kitigawa's group subsequently reported isolating altohyrtins B (**22**) and C (**23**) and 5-desacetyl altohyrtin A (**24**) from *H. altum* [35], and Pettit's group reported the isolation of spongistatins 2 (**23**) and 3 (**24**) from the *Spongia* sp. [36].



- 19** R₁ = Cl, R₂ = R₃ = Ac spongistatin 1, altohyrtin A
21 R₁ = Cl, R₂ = Ac, R₃ = H cinachyrolide A, spongistatin 4
22 R₁ = Br, R₂ = R₃ = Ac altohyrtin B
23 R₁ = H, R₂ = R₃ = Ac altohyrtin C, spongistatin 2
24 R₁ = Cl, R₂ = H, R₃ = Ac 5-desacetylaltohyrtin A, spongistatin 3
26 R₁ = H, R₂ = Ac, R₃ = H spongistatin 6



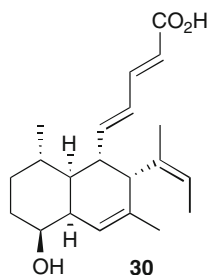
- 25** R₁ = Cl, R₂ = H spongistatin 5
27 R₁ = H, R₂ = H spongistatin 7
28 R₁ = H, R₂ = Ac spongistatin 8
29 R₁ = Cl, R₂ = Ac spongistatin 9

Kitigawa's group determined the complete absolute configuration of the altohyrtins (**19**, **22**, **23**, **24**) using a combination of the modified Mosher ester NMR approach and exciton chirality CD methodology [37, 38]. They also proposed

that the absolute configurations of the spongistatins and cinachyrolide A were identical to the altohyrtins, as shown in **19**, **22**, **23**, and **24**. Proof that altohyrtin A was identical to spongistatin 1 and altohyrtin C was identical to spongistatin 2, and that they had the absolute configurations shown in **19** and **23**, was provided by Kishi's total synthesis of **19** [39] and Evans' total synthesis of **23** [40]. Pettit et al. subsequently reported the isolation of spongistatin 4 (**21**), which is identical to cinachyrolide A, and spongistatins 5 (**25**), 6 (**26**), 7 (**27**), 8 (**28**), and 9 (**29**) from the sponge *Spirastrella spinispirulifera* collected along the Southeast Coast of Africa [41–43].

The spongistatins/altohyrtins/cinachyrolides contain a number of notable structural features including the two spiroketal systems (A/B and C/D rings) and the two tetrahydropyran rings (E and F) embedded in a 42-membered macrocycle and the vinyl chloride functionality in the side chain. Further studies of the interaction of spongistatin 1 with tubulin showed that it is a noncompetitive inhibitor of vinblastine and dolastatin 10 binding, leading to the proposal that the spongistatins bind to a site on β -tubulin that is close to but distinct from those where the Vinca alkaloids and peptide antimetabolic agents bind [44]. A lack of material has hindered the animal testing and preclinical evaluation/development of this family of compounds. One report, described as a personal communication, indicates that curative responses with no associated toxicities have been observed in human melanoma and ovarian carcinoma xenografts at doses of 25 $\mu\text{g/kg}$ of spongistatin 1 (**19**) [45]. Recent synthetic efforts have been focused on generating practical routes aimed at making grams of the spongistatins, which should facilitate further biological evaluation of this family of potent antimetabolic agents [46].

20.3.1.3 Phomopsidin

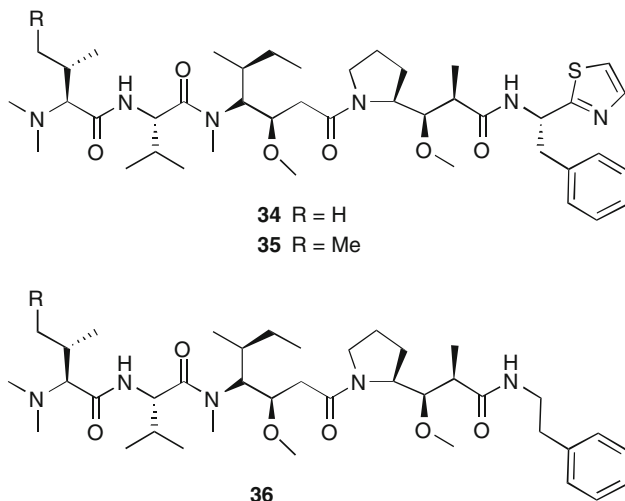


Namikoshi et al. isolated the polyketide phomopsidin (**30**) from cultures of the fungus *Phomopsis* (strain TUF 95 F47) obtained from a fallen mangrove branch collected on the bottom of a coral reef in Pohnpei [47, 48]. The antimetabolic activity of the culture extract was detected using a screening method that looks for deformations of mycelia germinated from conidia of the fungus *Pyricularia oryzae* [15]. Phomopsidin (**30**) inhibited the polymerization of purified bovine tubulin in vitro with an IC_{50} of 5.7 μM . Stable-isotope feeding studies have shown that phomopsidin is a linear nonaketide with the branching methyl groups coming from SAM.

endosymbiont in the genus *Burkholderia* that was actually responsible for producing the rhizoxins isolated from *Rhizopus* cultures [51]. Bacteria in the genera *Burkholderia* and *Pseudomonas* are closely related taxonomically. Rhizoxin (33) has been evaluated in phase II clinical trials [52].

20.3.2 Peptides and Mixed Polyketide/Peptide

20.3.2.1 Dolastatins, Symplostatin, and Belamide

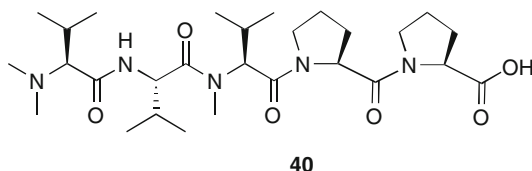
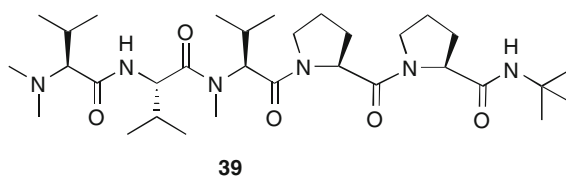
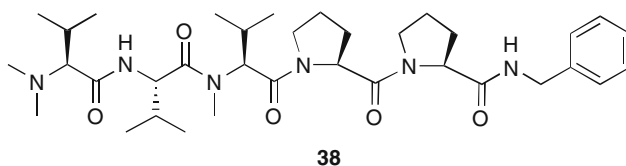
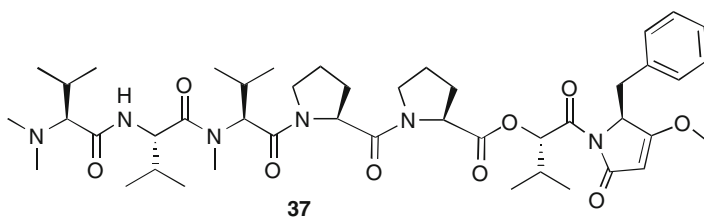


In 1987, Pettit's group reported the constitution of the potently cytotoxic linear peptide dolastatin 10 (34) isolated from extracts of the Indian Ocean sea hare *Dolabella auricularia* (in vitro ED₅₀ = 0.046 ng/mL vs. P388 murine leukemia) [53]. Dolastatin 10 (34) was present in the sea hare extracts in extremely small quantities (ca. \approx 1 mg in 100 kg), making the assay-guided isolation and structure elucidation exceptionally challenging. The report of its structure was the culmination of a 15-year sustained effort. Pettit's group subsequently reported the total synthesis of dolastatin 10 (34), which established its complete absolute configuration [54]. The four nonprotein amino acids dolavaline (Dov), dolaisoleucine (Dil), dolaproline (Dap), and dolaphenine (Doe) were first encountered in dolastatin 10. Two of these amino acids, dolaisoleucine and dolaproline, appear to be derived from isoleucine and proline residues that have been homologated with acetate units, a hallmark of cyanobacterial metabolism. Consistent with this biogenetic observation, dolastatin 10 (34) and the closely related analog symplostatatin 1 (35) have both been isolated from field samples of cyanobacteria in the genus *Symploca* collected in Palau and Guam [55].

Hamel and coworkers have shown that dolastatin 10 (34) inhibits tubulin polymerization and the associated GTP hydrolysis in vitro (IC₅₀ 1.2 μ M),

noncompetitively inhibits the binding of vinblastine to tubulin, interferes with nucleotide exchange, induces an intra- β -tubulin crosslink between Cys-12 and either Cys-201 or Cys-211, and induces the formation of nonmicrotubule polymers of tubulin plus microtubule-associated proteins (MAP) in the presence of GTP [56, 57]. Dolastatin 10 showed potent *in vivo* activity in a variety of mouse models of cancer [38], and it has been evaluated in several phase I and phase II anticancer clinical trials [58–61].

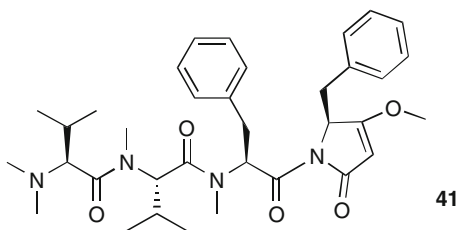
Miyazaki and coworkers synthesized a series of dolastatin 10 analogs and found that TZT-1027 (Soblidotin) (**36**) missing the thiazole ring also showed excellent antitumor activity in mouse models [62, 63]. Further studies on TZT-1027 revealed a selective antivascular effect on tumor vessels [64], and it was proposed that TZT-1027 kills tumors in mouse models by exerting a combination of indirect antivascular effects and direct cytotoxic effects [65]. TZT-1027 has been evaluated in both phase I and phase II clinical trials [66–68].



In 1989, Pettit's group reported the isolation of the cytostatic depsipeptide dolastatin 15 (**37**) from extracts of the same Indian Ocean sea hare *Dolabella*

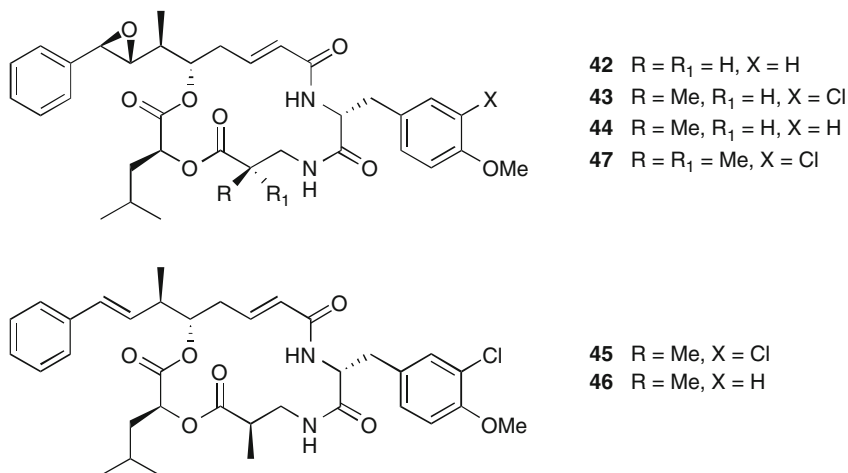
auricularia that was the source of dolastatin 10 (**34**) [69]. Dolastatin 15 (**37**) was also a trace component in the extract (6.2 mg from 1,600-kg wet weight of mollusc), and it too showed potent inhibition of the growth of the murine leukemia P388 cell line in vitro (ED_{50} 2.4 ng/mL). Pettit et al. established the absolute configuration of dolastatin 15 (**37**) via total synthesis [70]. The structure of dolastatin 15 (**37**) is similar to dolastatin 10 (**34**) in the dolavaline-valine sequence at the *N*-terminus and in the aromatic character of the *C*-terminus. After extensive investigations of the effects of dolastatin 15 (**37**) on P388 cells, Bai et al. concluded that the toxicity of the depsipeptide resulted from interference with mitosis [71]. However, they found that the interaction of dolastatin 15 (**37**) with purified tubulin was very weak and the most convincing evidence that it was an inhibitor of tubulin polymerization was the disappearance of microtubules in cells treated with relatively high concentrations of the drug. Further studies using Hummel-Dreyer chromatography provided evidence for weak binding of dolastatin 15 to the Vinca domain of tubulin [72].

A number of synthetic analogs of dolastatin 15 (**37**) have been tested for biological activity. These include cemadotin (LU103793) (**38**) [73] and tasidotin (ILX651) (**39**) [74]. Jordan et al. found that cemadotin strongly suppressed dynamic instability of microtubules [75]. It reduced the rate and extent of growth and shortening, increased the frequency of rescue, and increased the amount of time spent in a paused state. Cemadotin did not inhibit vinblastine binding to tubulin, so it was concluded that the cytotoxicity of cemadotin was caused by suppression of spindle microtubule dynamics as a result of binding at a novel site on tubulin. Tasidotin (**39**) was also shown to modulate spindle microtubule dynamics in a fashion similar to cemadotin, (**38**) and it was found that it is a prodrug for the much more potent *C*-terminus carboxylic acid metabolite **40** [76]. Cemadotin (**38**) [77, 78] and tasidotin (**39**) [79] have both been evaluated in clinical trials.



Belamide A (**41**), a truncated structural analog of the dolastatins, was reported by Gerwick and coworkers in 2006 [80]. This highly methylated linear tetrapeptide was isolated from the marine cyanobacterium *Symploca* sp., and it contains the *N*-terminal *N,N*-dimethylvaline and *C*-terminal benzyl methoxy pyrrolinone moieties characteristic of the dolastatins. Belamide A (**41**) has been shown to have moderate cytotoxicity (IC_{50} of 0.74 μ M against HCT-116 cells), and it disrupts microtubules at 20 μ M.

20.3.2.2 Cryptophycins and Arenastatin



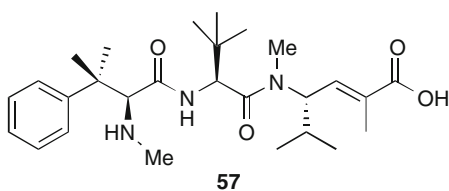
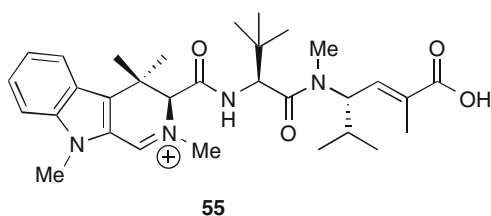
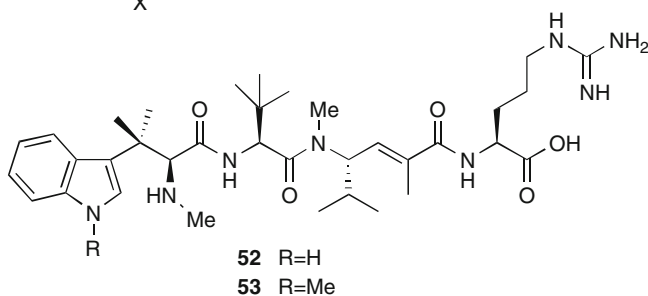
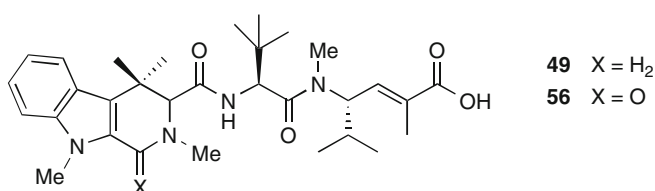
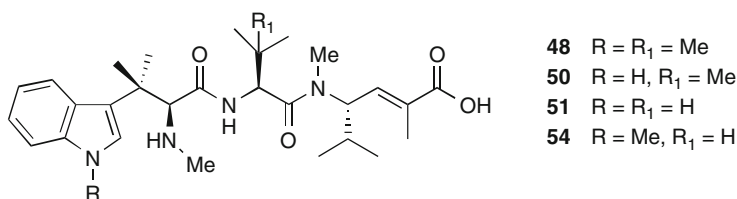
Kitagawa and coworkers reported in 1994 the isolation of the cyclic depsipeptide arenastatin A (**42**) from specimens of the sponge *Dysidea arenaria* collected in Okinawa [81]. Arenastatin A was cytotoxic to KB cells in vitro with an IC₅₀ of 5 pg/mL. The absolute configuration of arenastatin A (**42**) was determined by Kitagawa's group using NMR analysis and the chiral synthesis of a methanolysis degradation product [82]. Also in 1994, Moore's group reported the isolation of cryptophycins A (**43**) to D (**46**) from laboratory cultures of the freshwater cyanobacterium *Nostoc* sp. (GVS 224) [83]. Crude extracts from the *Nostoc* cultures had attracted Moore's attention because they showed significant tumor-selective cytotoxicity in the Corbett assay.

Total synthesis confirmed the assigned structures of **43** to **46** and led to a revision in the assignment of the configuration of the α -amino acid residues to D [84]. Both the Kitagawa and Moore groups noted that scientists at Merck had previously isolated an antifungal depsipeptide they named cryptophycin from extracts of a cultured *Nostoc* sp. [85]. The Merck group had not determined any of the relative or absolute configurations for their compound, which turned out to be identical to Moore's cryptophycin A (**43**). Moore's group went on to isolate a large number of additional cryptophycins from *Nostoc* sp. cultures, including cryptophycin 24 that turned out to be identical to Kitagawa's arenastatin (**42**) [86, 87]. The isolation of arenastatin (**42**) from a cyanobacterium culture confirmed the speculation that the material isolated from the Okinawan sponge *D. arenaria* was in fact a microbial natural product.

Cryptophycin A (**43**) inhibits tubulin polymerization in vitro, disassembles preformed microtubules, inhibits nucleotide exchange, causes tubulin to aggregate into small ring-shaped oligomers, and noncompetitively inhibits the binding of vinblastine but not colchicine to tubulin by binding to the Vinca domain [88, 89]. Cryptophycin A is 100 to 1,000 times more potent than vinblastine or paclitaxel as an antiproliferative agent. It is a powerful disrupter of microtubule dynamics, with

its major effects being to decrease the shortening rate and length of depolymerization during a shortening event and enhancing the number of rescue events [90]. It also inhibits the growth rate and length grown but less effectively than the shortening rate. Cryptophycin-52 (47), a synthetic analog of cryptophycin A (43), has been evaluated in phase I clinical trials [91, 92].

20.3.2.3 Hemiasterlins, Criamides, and Milnamides



Hemiasterlin (**48**) was first isolated by Kashman's group in 1994 from the sponge *Hemiasterella minor* (Kirkpatrick) collected in Sodwana Bay, South Africa [93]. At virtually the same time, Crews and coworkers reported the isolation of milnamide A (**49**) from the sponge *Auletta* cf. *constricta* collected in Milne Bay, Papua New Guinea [94]. Hemiasterlin (**48**) is a tripeptide comprised of the rare amino acid *tert*-leucine and the two novel amino acids 4-amino-2,5-dimethylhex-2-enoic acid and *N,N'*, β,β -tetramethyltryptophan. Milnamide A (**49**) has a β -carboline, formally derived from *N,N'*, β,β -tetramethyltryptophan via a Pictet-Spengler condensation with formaldehyde, in place of the *N,N'*, β,β -tetramethyltryptophan residue in hemiasterlin (**48**). The 4-amino-2,5-dimethylhex-2-enoic acid residue in **48** and **49** appears to have a biogenetic origin involving *N*-methylvaline and propionic acid building blocks. There were no relative or absolute configurations assigned to the amino acids in hemiasterlin (**48**) or milnamide A (**49**) in the original reports of their structures.

Andersen's group reported the isolation of hemiasterlin (**48**), hemiasterlins A (**50**) and B (**51**), and criamides A (**52**) and B (**53**) from the sponge *Cymbastela* sp. collected on reefs off of Madang, Papua New Guinea [95]. All three amino acids in hemiasterlin and the arginine residue in the criamides were shown to have the *L* configuration by a combination of Marfey's analysis on the natural product and single crystal X-ray diffraction analysis of hemiasterlin methyl ester [96]. Andersen et al. reported the first total synthesis of hemiasterlin (**48**), and they showed that the synthetic material had bioactivity identical to the natural samples [97].

Boyd and coworkers reported finding hemiasterlins in two sponges also collected in Papua New Guinea. An *Auletta* sp. yielded the known compounds hemiasterlin (**48**) and hemiasterlin A (**50**), along with the new tripeptide hemiasterlin C (**54**) [98]. Two *Siphonochalina* spp. were also found to contain the same hemiasterlin tripeptides **48**, **50**, and **54**. Ireland's group reported isolating hemiasterlin (**48**), milnamide A (**49**), and the new compound milnamide D (**55**) from specimens of *Cymbastela* sp. collected in Milne Bay, Papua New Guinea [99], and Crews' reinvestigation of *Auletta* sp. yielded milnamide C (**56**) [100]. An enantioselective total synthesis of milnamide A (**49**) and the observation that it undergoes facile autoxidation to milnamide D (**55**) confirmed that the absolute configurations of the milnamides were the same as the hemiasterlins and suggested that milnamide D (**55**) may have a nonbiogenic origin [101].

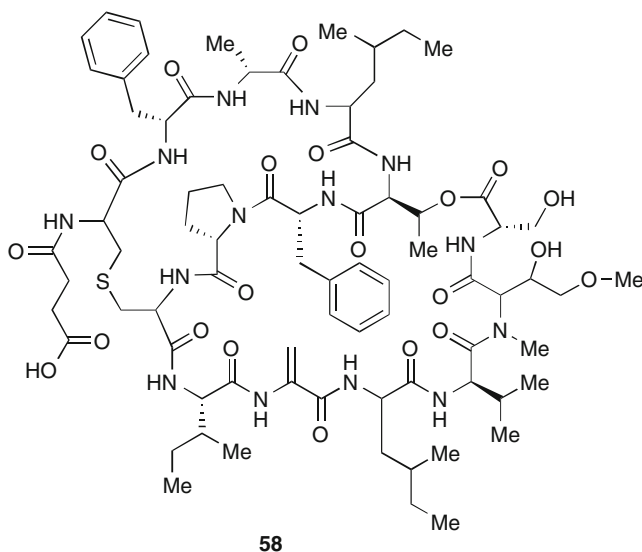
Kashman reported that hemiasterlin (**48**) showed in vitro cytotoxicity against murine leukemia P388 cells at a concentration of ≈ 19 nM [93]. Andersen and coworkers reported an IC_{50} of 87 pM versus P388 for hemiasterlin (**48**), over two orders of magnitude lower than Kashman's value [95], and potent activity was also observed against a small panel of human cancer cell lines. The milnamides are also cytotoxic but much less potent than the hemiasterlins [94, 98]. Roberge and coworkers examined the effects of hemiasterlins on cell cycle progression in human mammary carcinoma MCF-7 cells and found that hemiasterlins block cells in mitosis at the same concentrations that showed cytotoxicity [102]. Microscopic examination showed that hemiasterlins arrested cells at a metaphase-like

stage with effects on the morphology of the mitotic spindle that were similar to those caused by tubulin-targeting agents such as vinblastine. High concentrations of hemiasterlin caused complete microtubule depolymerization, and at low concentrations, cells displayed bipolar spindles with long astral microtubules or multiple asters. Chromosomes failed to align at metaphase and were unable to proceed through later stages of mitosis because of activation of the spindle checkpoint. Roberge concluded that hemiasterlins exert their cytotoxic effects by inhibiting spindle microtubule dynamics at mitosis.

Detailed studies of the interactions of hemiasterlin (**48**) with tubulin showed that it inhibited tubulin polymerization in vitro ($IC_{50} = 1 \mu M$), noncompetitively inhibits the binding of vinblastine, competitively inhibits the binding of dolastatin 10, inhibits nucleotide exchange on β -tubulin, and induces the formation of tubulin aggregates with a ring-like structure [103, 104]. Overall, these effects resembled, but were not identical to, those of dolastatin and cryptophycin A, which bind to the same site on tubulin.

Neiman et al. synthesized a small library of hemiasterlin analogs, including the phenylalanine analog HTI-286 (**57**) that has been evaluated in phase I and phase II clinical trials [105–108]. The tubulin-binding properties of HTI-286 [109] have been probed with STD-NMR [110], photoaffinity probes [111], and synthesis of numerous analogs [112, 113]. HTI-286 has also been shown to have promising activity in mouse models of prostate and bladder cancer [114, 115].

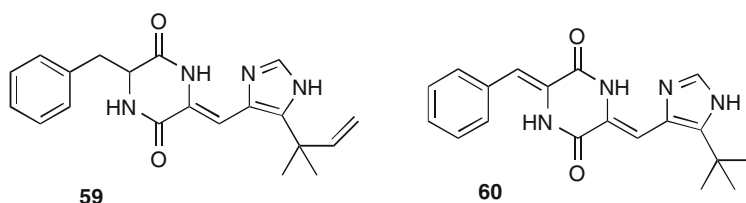
20.3.2.4 Vitilevuamide



In 1999, Ireland and coworkers reported the isolation of vitilevuamide (**58**) from the ascidian *Didemnum cuculiferum* collected in the Beqa lagoon in Fiji [116, 117].

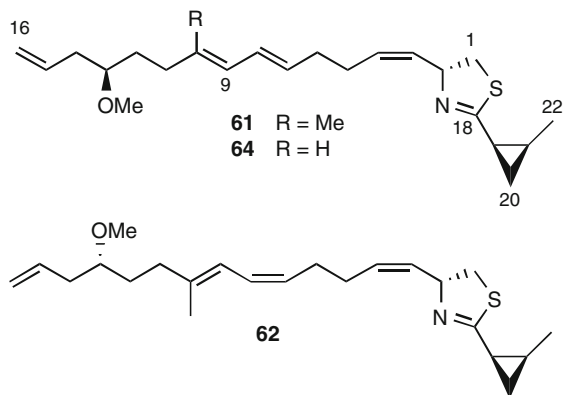
Vitilevuamide was also isolated from another acidian *Polysyncranton lithostrotum*, indicating that it may be produced by microbial symbionts. The structure of this bicyclic 13-membered peptide was determined by NMR and mass spectral analysis and shown to contain the unusual amino acids lanthionine, a monosulfide analog of cystine, and *N*-methyl methoxinine. In vitro studies showed that vitilevuamide (**58**) was an inhibitor of tubulin polymerization at 2 μ M, noncompetitively inhibited vinblastine binding, stabilized colchicine binding, and only affected dolastatin 10 binding at high concentrations, indicating that it likely has a unique binding site. Further in vivo studies determined that vitilevuamide (**58**) had an ILS of 70% at 30 μ g/kg against P388 murine leukemia.

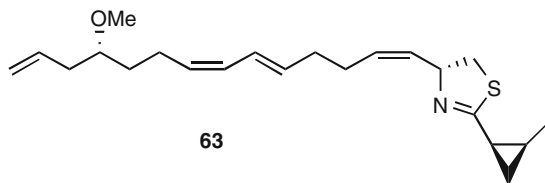
20.3.2.5 Halimide



In 2000, Fenical and coworkers reported the discovery of halimide (**59**) in a patent [118, 119]. The *S*-isomer of this prenylated cyclic dipeptide was isolated from an unidentified fungal strain collected from the surface of an alga in the genus *Halimeda*. Halimide is a tubulin-depolymerizing agent that binds to the colchicine-binding site on tubulin [119]. It showed no cross-resistance to multidrug-resistant cancer cell lines expressing a P-glycoprotein drug efflux pump and caused tumor regression in an in vivo model of Taxol-resistant breast cancer. SAR studies at Nereus Pharmaceuticals have resulted in the discovery of an analog (NPI-2358: Plinabulin) **60** that is currently in phase II clinical trials [119].

20.3.2.6 Curacins

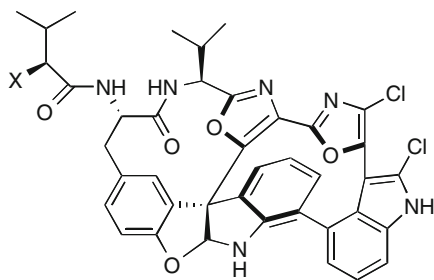




Curacin A (**61**) was isolated by Gerwick's group in 1994 from extracts of a field sample of the blue-green alga *Lyngbya majuscula* collected in Curaçao that showed potent brine shrimp toxicity and antiproliferative activity [120]. Further examination of the initial Curaçao collection of *L. majuscula* subsequently led to the isolation of the minor analogs curacins B (**62**) and C (**63**) [121], while a Virgin Islands collection yielded curacin D (**64**) [122]. The absolute configuration of curacin A (**61**) was established by comparison of degradation products obtained from the natural product with the same compounds prepared enantiospecifically via synthesis [123] and was confirmed by White's asymmetric total synthesis [124]. Stable-isotope feeding studies showed that the atoms in curacin A (**61**) come from one cysteine (S, N, and C-1 to C-3), ten acetate units (C-4 to C-16 and C-18 to C-22), and two units of S-adenosylmethionine (C-17 and OMe) [125]. Analysis of the biosynthetic genes showed that the metabolic pathway is comprised of a nonribosomal peptide synthase (NRPS) and multiple polyketide synthases (PKSs). Further studies of the curacin A (**61**) biosynthetic pathway have revealed that cryptic chlorination and sulfonation steps are involved in the formation of the cyclopropyl ring and the terminal alkene functionalities, respectively [126, 127].

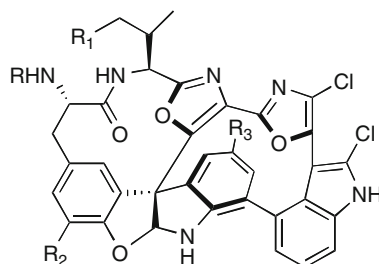
Evaluation of curacin A (**61**) in the NCI cell line panel and analysis of its differential cytotoxicity pattern using the COMPARE algorithm provided the first indication that the compound was a tubulin-binding agent [120]. Curacin A inhibited the polymerization of purified tubulin in vitro with an IC_{50} of 0.7 μ M, and it was found to strongly inhibit the binding of colchicine but not vinblastine to tubulin. More detailed studies showed that curacin A was a competitive inhibitor of colchicine binding and that its binding rate to tubulin is rapid and its dissociation rate from tubulin is extremely slow due to its extremely large association constant [128, 129]. It is a potent in vitro cytotoxin that inhibits the growth of cancer cells at low nM concentrations. Curacin A has conjugated diene and a thiazoline substructure that makes it sensitive to acid, base, and air oxidation, and it is extremely lipophilic. These instability and unfavorable solubility properties have prevented the preclinical evaluation and development of the natural product. Nevertheless, the promising biological activity of the curacins coupled with their novel structures have stimulated extensive synthetic efforts toward making analogs that might have more promising drug-like properties [130].

20.3.2.7 Diazonamides



65 X = OH

70 X = NH₂

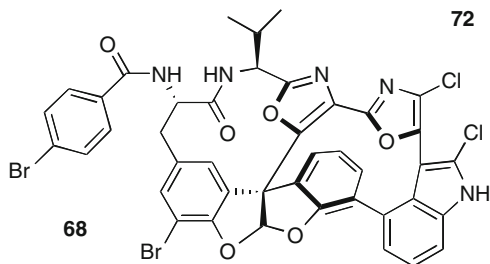


66 R = R₁ = R₃ = H, R₂ = Br

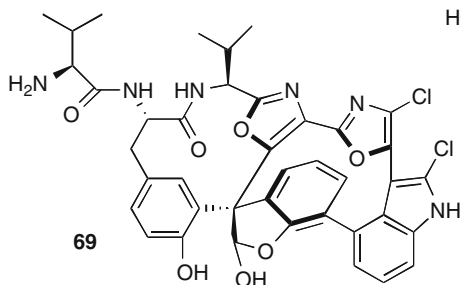
67 R₁ = R₃ = H, R₂ = Br, R = *p*-bromobenzoyl

71 R₁ = CH₃, R = R₂ = H, R₃ = Cl

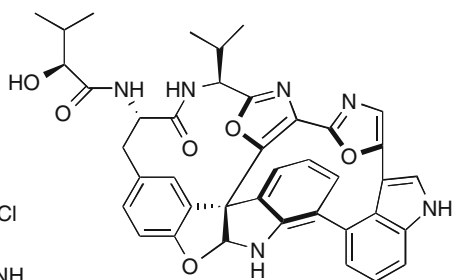
72 R₁ = CH₃, R = R₂ = R₃ = H



68



69



73

The potentially cytotoxic cyclic peptides diazonamides A (**65**) and B (**66**) (diazonamide A: IC₅₀ < 15 ng/mL vs. HCT-116 human colon carcinoma cell line) were isolated in 1991 by Fenical, Clardy, and coworkers from extracts of the colonial ascidian *Diazona chinensis* collected on the ceiling of a small cave along the coast of Siquijor Island in the Philippines [131]. The *p*-bromobenzoyl derivative of diazonamide B was initially assigned as structure **68** via analysis of single-crystal X-ray diffraction and mass spectrometry data. Working from structure **68** for diazonamide B and the NMR data for the closely related metabolite diazonamide A led to the assignment of structure **69** to diazoniamide A. It was assumed that a hemiketal in natural diazoniamide B, that was assigned to the same position in structure **69** proposed for diazoniamide A, had been converted to the

ketal observed in the X-ray analysis of *p*-bromobenzoyl derivative of diazonamide B during preparation of the *p*-bromobenzoyl ester.

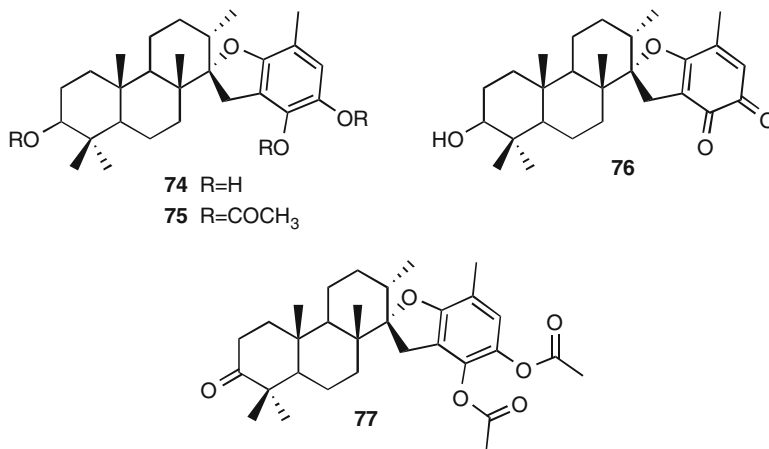
The extremely novel chemical structures of the diazonamides and their potent cytotoxic activity immediately captured the imagination of the synthetic chemistry community. Harran and coworkers completed a total synthesis of the structures **68** and **69** proposed for the *p*-bromobenzoyl derivative of diazonamide B and diazonamide A, respectively, and showed that neither of them corresponded to the natural materials [132]. They proposed the alternate structures **65** for diazonamide A and **67** for the *p*-bromobenzoyl derivative of diazonamide B [133], and these were confirmed by Nicolaou's total synthesis of the revised structure of diazonamide A [134].

A subsequent investigation of a *Diazonia* sp. collected in Indonesia yielded the additional diazonamides C (**70**), D (**71**), and E (**72**), which all displayed modest cytotoxicity [135].

Hamel and coworkers reported that diazonamide A (**65**) is a potent inhibitor of in vitro tubulin polymerization, strongly inhibits tubulin-dependent GTP hydrolysis, has little effect on nucleotide exchange from tubulin, shows no inhibition of the binding of radiolabeled vinblastine or dolastatin 10 to tubulin, and does not induce formation of stable tubulin aggregates [136]. This combination of properties suggested a unique mode of binding to tubulin. However, subsequent preclinical assessment of the diazonamide analog AB-5 (**73**) found that it does not bind directly to tubulin but instead induces mitotic arrest by interacting with a specifically proteolyzed form of ornithine δ -amino transferase involved in spindle formation [137]. AB-5 showed very promising in vivo activity against human tumor xenografts in mice with an absence of overt toxicity.

20.3.3 Meroterpenoids

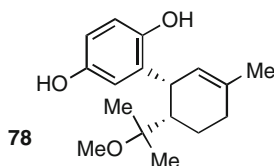
20.3.3.1 Stypodiolis



In 1979, Fenical, Clardy, and coworkers reported the discovery of stypotriol (**74**), stypotriacetate (**75**), and stypoldione (**76**) from the marine brown algae

Styopodium zonale and reported their toxic and anti-fish feeding activities [138]. Further biological investigations by Jacobs, Wilson, and coworkers in the 1980s revealed that these compounds showed micromolar microtubule-disruptive activities, inhibited cytokinesis, and arrested cells in the G2 stage of development [139, 140]. In 1998, Maccioni et al. reported the isolation of 14-keto-stypodiol diacetate (77) from the algae *Styopodium flabelliforme* collected off the coast of Easter Island, which they determined to have similar activity against microtubules [141].

20.3.3.2 Methoxyconidiol

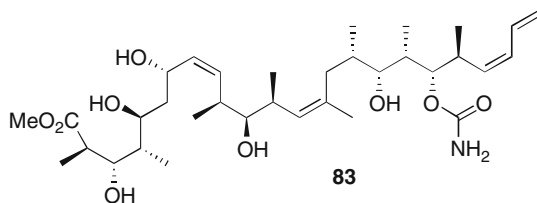
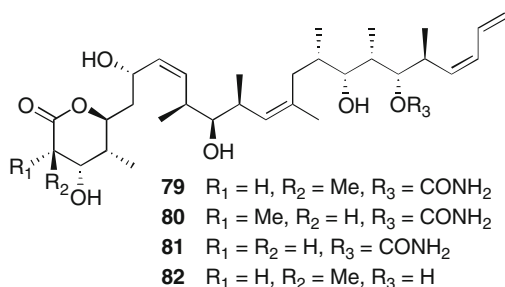


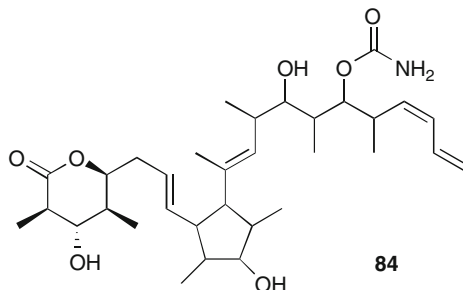
Methoxyconidiol (**78**) was isolated by Banaigs and coworkers in 2005 from the ascidian *Aplidium aff. densusum* collected off the coast of Masirah Island, Oman [142]. Initial biological investigations showed that it was moderately active against microbial proliferation and inactive at millimolar concentrations against mammalian tumor cell lines. Further investigation in sea urchin embryos revealed that methoxyconidiol arrests cells in M phase, completely blocks cytokinesis, and disrupts the establishment of the mitotic spindle at 10 μ M while having no effect on DNA replication [143].

20.4 Microtubule-Stabilizing Agents

20.4.1 Polyketides

20.4.1.1 Discodermolides



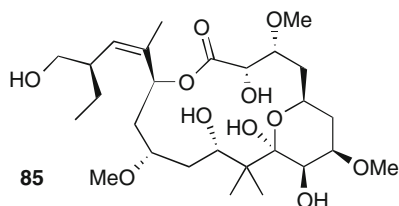


The polyketide lactone discodermolide (**79**) was isolated in 1990 by Gunasekera et al. from extracts of the sponge *Discodermia dissoluta* collected at Lucay on Grand Bahama Island [144]. X-ray diffraction analysis of a crystal of **79** confirmed the constitution assigned from the NMR data and established the relative configuration. Schreiber's group synthesized both (+) and (–) optical antipodes of **79**, which showed that the natural product was the (+) enantiomer [145, 146]. A dozen years after their first report, Gunasekera et al. reported the isolation of 2-*epi*-discodermolide (**80**), 2-*des*-methyldiscodermolide (**81**), 19-*des*-aminocarbonyldiscodermolide (**82**), 5-hydroxymethyldiscodermolate (**83**), and 9(13)-cyclodiscodermolide (**84**) from samples of sponges in the genus *Discodermia* collected in waters around the Bahamian archipelago [147].

Gunasekera et al. reported that discodermolide inhibited the in vitro proliferation of P388 murine leukemia cells with an IC_{50} of 0.5 $\mu\text{g/mL}$, inhibited the growth of *Candida albicans*, and suppressed the two-way mixed-lymphocyte response of both murine splenocytes and human peripheral blood lymphocytes at 0.5 and 5 $\mu\text{g/mL}$, respectively, with greater than 85% viability of the splenocyte cells [148]. ter Harr et al. showed that discodermolide was an antimetabolic agent that stabilizes microtubules in cells and in biochemical systems more potently than taxol and binds competitively to the taxoid site on β -tubulin [149, 150]. Kowalski et al. showed that discodermolide was not a substrate for the P-glycoprotein efflux pump and was potently cytotoxic toward paclitaxel-resistant cancer cell lines [151]. At the time of its discovery, discodermolide (**79**) joined taxol and the epothilones as only the third class of compounds, and the first marine natural product, known to stabilize microtubules. The analogs **80** to **83** showed in vitro cytotoxicity comparable to discodermolide, but the analog **84** having an additional ring was almost completely inactive [147].

The novel structure of discodermolide (**79**) combined with its ability to stabilize microtubules and inhibit the growth of paclitaxel-resistant cancer cell lines made it an extremely attractive candidate for clinical development. As with all drug candidates isolated from marine invertebrates, a limiting factor in the clinical evaluation of discodermolide was the availability of material. A landmark 36-step synthesis carried out by scientists at Novartis in collaboration with Paterson's group at Cambridge University generated 60 g of (+)-discodermolide, which enabled early phase clinical trials [150, 151]. Unfortunately, the trials had to be stopped when indications of toxicity surfaced [152, 153].

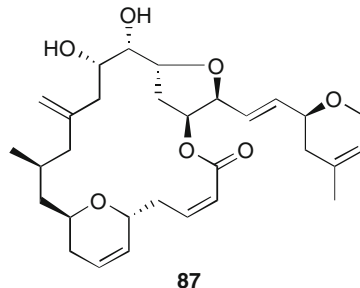
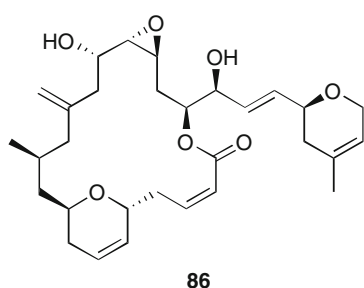
20.4.1.2 Peloruside A

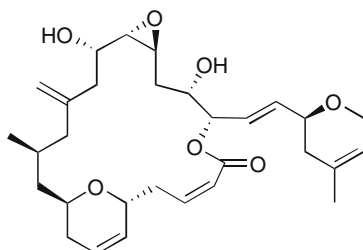


Peloruside A (**85**), a cytotoxic 16-membered macrolide, was isolated by Northcote's group in 2000 from extracts of the sponge *Mycale hentscheli* collected in Pelorus Sound on the north coast of the South Island, New Zealand [154]. The same sponge extract also yielded the previously known cytotoxins mycalamide A and pateamine. Detailed analysis of the NMR data obtained for peloruside A (**85**) led to the elucidation of the molecule's constitution and complete relative configuration. The absolute configuration was established by De Brabander's report of the total synthesis of (–)-peloruside A, which turned out to be the enantiomer of the natural product **85** [155].

Northcote et al. reported that peloruside A (**85**) was cytotoxic to murine leukemia P388 cells at 10 ng/mL [154]. A more detailed investigation showed that peloruside A (**85**) caused cancer cells to arrest in the G₂-M phase of the cell cycle and, like paclitaxel, induced tubulin to form long straight microtubules at 37°C [156]. The microtubules formed in the presence of peloruside A were stable at 0°C and in the presence of 5 mM CaCl₂. Subsequent studies found that peloruside A is not a good substrate for the P-glycoprotein efflux pump, was active against drug-resistant cell lines with point mutations in the paclitaxel binding site on β -tubulin, and was not able to displace the fluorescent paclitaxel derivative Flutax-2 from tubulin [157]. These data suggested that peloruside A (**85**) binds at a site that is different from the paclitaxel binding site. Positive synergistic effects on tubulin polymerization and in vitro cytotoxicity have been observed with peloruside A (**85**) and other microtubule-stabilizing agents that bind to the taxoid site [158, 159]. Aquaculture [160] and total synthesis [161] approaches are both being explored as avenues for the large-scale production of peloruside A (**85**) needed to support further preclinical evaluation of this interesting anticancer drug candidate.

20.4.1.3 Laulimalides (Fijianolides)



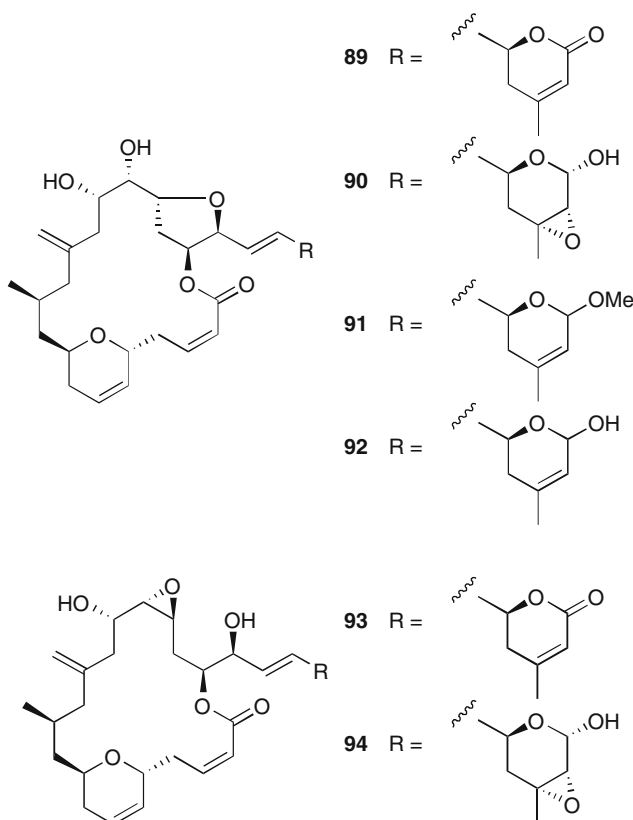


88

Crews' group at UCSC [162] and the Scheuer, Moore, and Paul groups jointly at Hawaii and Guam [163] reported the structures of the cytotoxic polyketide macrolides laulimalide (fijianolide B) (**86**) and isolaulimalide (fijianolide A) (**87**) in back-to-back papers published in 1988. The simultaneous reports from the two groups resulted in two initial sets of names for **86** and **87**, but most subsequent references to these macrolides have used the laulimalide designation, perhaps due to the slightly earlier submission date of the manuscript originating from the Hawaiian/Guam groups. Crews' group isolated **86** and **87** from specimens of the sponge *Spongia mycofijiensis*, and a nudibranch *Chromodoris lochi* found attached to the sponge, collected in Vanuatu. The Scheuer, Moore, and Paul groups isolated **86** and **87** from the Indonesian sponge *Hyatella* sp. and specimens of the nudibranch *C. lochi* grazing on the sponge. It was subsequently proposed that Crews' specimen of *S. mycofijiensis* should be reclassified as *Cacospongia mycofijiensis* [164]. Scheuer, Moore, and Paul named the compounds laulimalides after the Hawaiian term "laulima" used to describe "people working together" since the three groups cooperated in their discovery. The initial reports of **86** and **87** described constitutions and relative configurations for the laulimalides that were based on analysis of NMR data. A re-isolation of laulimalide (**86**) from the sponge *Fasciospongia rimosa* collected in Okinawa generated crystals that confirmed the structural features assigned from NMR data and facilitated an assignment of the absolute configuration via single-crystal X-ray diffraction analysis [165]. The same sponge yielded neolaulimalide (**88**) [166].

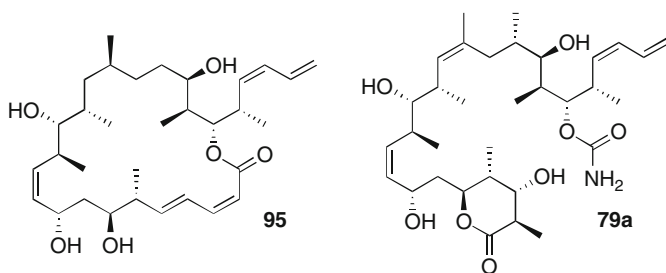
Crews reported modest cytotoxicities (IC_{50} s of 0.5–11 μ g/mL) for **86** and **87** versus HT-29 human colon tumor cells and P388 murine leukemia [162], while the Hawaiian/Guam groups reported more potent cytotoxic activity (IC_{50} 15 ng/mL) for laulimalide (**86**) and isolaulimalide (**87**) (IC_{50} > 200 ng/mL) against the KB cell line [163]. Interest in the laulimalides intensified after Mooberry, Davidson, and coworkers reported that **86** and **87** were microtubule-stabilizing agents that stimulated tubulin polymerization in vitro more effectively than paclitaxel and were poor substrates for the P-glycoprotein efflux pump [167]. Further investigations showed that laulimalide binds to a site on the tubulin polymer that is distinct from the taxoid site [168]. Consistent with this finding, microtubules formed in the presence of both laulimalide and paclitaxel contained near-equimolar quantities, relative to tubulin, of both drugs, and laulimalide and paclitaxel synergistically enhanced tubulin

polymerization in vitro [169]. It has been suggested that laulimalide (**86**) and peloruside (**85**) bind to the same or overlapping site(s) on microtubules [158].



A reinvestigation of *C. mycofijiensis* by Crews' group resulted in the isolation of sufficient quantities of laulimalide (**86**) for preliminary in vivo evaluation and also identified six new analogs named fijianolides D (**89**) to I (**94**) [170]. Laulimalide (**86**) was shown by Crews and coworkers to significantly inhibit the growth of HCT-116 tumor xenografts in SCID mice. There have been several total syntheses of laulimalide (**86**) aimed at providing material for further biological evaluation [171, 172]. Notable among these efforts was the synthesis of gram quantities of laulimalide (**86**) by scientists at Eisai Research Institute [173]. In contrast with Crews' report, the Eisai group found that synthetic laulimalide (**86**) exhibited only minimal tumor growth inhibition in vivo that was accompanied by severe toxicity and mortality, leading them to the conclusion that the unfavorable efficacy to toxicity ratio in vivo made it a poor candidate for clinical development.

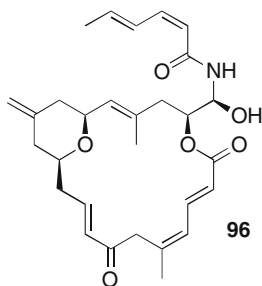
20.4.1.4 Dictyostatin-1



In 1994, Pettit and coworkers reported the isolation of the cytotoxic polyketide macrolide dictyostatin-1 (**95**) from extracts of an Indian Ocean marine sponge identified as a *Spongia* sp. (order: Dictyoceratida) that was collected in the Maldives [174]. The initial structure elucidation was based on analysis of the NMR data obtained from a very small sample (≈ 1.4 mg), and it only provided the constitution of the molecule and the configurations of the disubstituted alkenes. Even though no IC_{50} s were reported, dictyostatin-1 was described as being cytotoxic toward murine leukemia P388 cells in vitro. Almost a decade later, Wright's group isolated dictyostatin-1 from extracts of a sponge identified as a *Corallistidae* sp. that was collected by submersible at a depth of 442 m off the north coast of Jamaica in the Caribbean [175]. Paterson and Wright's groups determined the relative configuration of dictyostatin-1 (**95**) using J-based configurational analysis and molecular modeling [176]. The absolute configuration was established by Paterson's total synthesis of (–)-dictyostatin-1 [177].

Wright and coworkers found that dictyostatin-1 (**95**) induced the polymerization of tubulin in vitro to form microtubules that were stable at low temperatures and that it was highly potent as an in vitro cytotoxin against paclitaxel-resistant cancer cell lines expressing the P-glycoprotein efflux pump [175]. Further studies by Day and coworkers showed that dictyostatin-1 (**95**) strongly inhibited the binding of discodermolide (**79**) to microtubules and that both compounds had equivalent activity as inhibitors of the binding of radiolabeled epothilone B and paclitaxel to microtubules [178]. They concluded that the macrocyclic template of dictyostatin-1 (**95**) was likely a model for the bioactive conformation of discodermolide binding (**79a** above) to the taxoid site, as proposed by Paterson et al. [176].

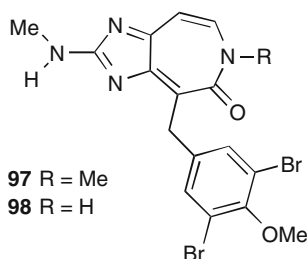
20.4.1.5 Zampanolide



Tanaka and Higa isolated the cytotoxic macrolide (–)-zampanolide (**96**) from extracts of the sponge *Fasciospongia rimosa* collected at Cape Zampa, Okinawa in 1996 [179]. Specimens of the same sponge collected at Shimoji Island, Okinawa, had previously yielded laulimalide (**86**) and neolaulimalide (**88**) [166]. The absolute configuration of (–)-zampanolide (**96**) was established by Smith et al.'s total synthesis of the enantiomer (+)-zampanolide [180]. Northcote, Miller, and coworkers re-isolated zampanolide (**96**) from a Tongan collection of *C. mycofijiensis* and showed that it is a microtubule-stabilizing agent with potent in vitro cytotoxicity ($IC_{50} \approx 7$ nM) against paclitaxel-resistant human ovarian cancer cells A2780 overexpressing the P-glycoprotein efflux pump [181].

20.4.2 Alkaloids

20.4.2.1 Ceratamines

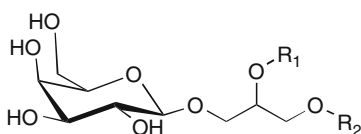


In 2003, the Roberge and Andersen groups reported the isolation of the novel heterocyclic alkaloids ceratamines A (**97**) and B (**98**) from extracts of the marine sponge *Pseudoceratina* sp. collected in Papua New Guinea that showed promising activity in Roberge's cell-based assay for antimitotic agents [12, 182]. At the time of discovery, the imidazo[4,5-*d*]azepine core heterocycle in the ceratamines had no precedent at any oxidation state among known natural products. Nodwell's synthesis of desbromoceratamine analogs provided confirmation of the natural product structure and illustrated the importance of the bromine atoms for full biological activity [183, 184]. Coleman and coworkers reported the first synthetic route to ceratamines A (**97**) and B (**98**) that has the potential to produce sufficient quantities of the natural products for preclinical evaluation [185].

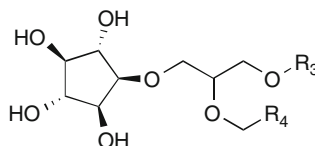
Roberge et al. showed that the ceratamines are microtubule-stabilizing agents that either do not bind to the paclitaxel site or bind with an affinity that is too low to displace radiolabeled paclitaxel from microtubules. The ceratamines generated an unusual mitotic arrest phenotype involving formation of pillar-like structures of tubulin that extended vertically from the basal surface of the cell-cycle-arrested cells [186].

20.4.3 Glycolipids

20.4.3.1



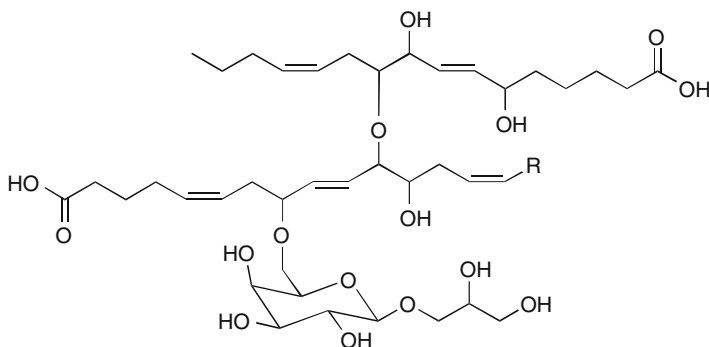
99 R_1 = fatty acyl, R_2 = fatty acyl



100 R_3 = fatty acyl, R_4 = alkyl

Namikoshi and coworkers reported in 2002 that mixtures of glycolipids of general structures **99** and **100** isolated from the Okinawan sponge *Pseudoceratina* sp. showed stimulation of microtubule assembly from purified tubulin in vitro at rather high concentrations [14]. There was no indication that glycolipids **99** or **100** were cytotoxic or could arrest cells at mitosis.

20.4.3.2 Nigricanosides



101 $R =$

102 $R =$

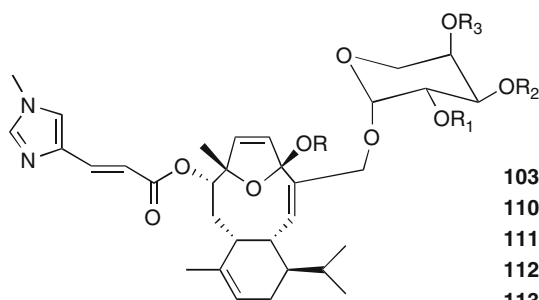
In 2007, the Andersen and Roberge groups reported the bioassay-guided isolation of the potentially cytotoxic glycolipids nigricanosides A (**101**) and B (**102**) from extracts of the green alga *Avrainvillea nigricans* collected in Dominica [187]. Crude extracts of *A. nigricans* attracted attention because they showed strong activity in Roberge's cell-based assay for antimitotic agents. However, the nigricanosides were present in the extract in trace quantities ($\approx 2 \times 10^{-6}\%$ wet wt.), and only repeated collections of the alga over an 8-year period produced sufficient material for structure elucidation. The methyl ester of nigricanoside A was found to stimulate the polymerization of pure tubulin in vitro at 10 μM ,

arrest human breast cancer MCF-7 cells in mitosis with an IC_{50} of 3 nM, and inhibit the proliferation of both MCF-7 and HCT-116 cancer cells with IC_{50} s of \approx 3 nM.

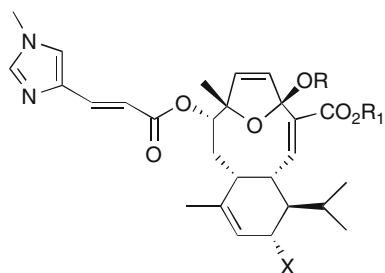
Although the nigricanosides contain the same structural components as the monogalactosyldiacylglycerols that are major membrane lipids in higher plants and blue-green algae, the oxidation of the fatty acids to oxylipins and the ether linkages connecting the oxylipins to each other and to the galactose residue in the nigricanosides are without precedent, making them the first examples of a new class of ether-linked glycoglycerolipids. The lack of information about the relative or absolute configurations of the stereogenic centers in the nigricanosides is a major impediment to the preparation of material for biological evaluation via total synthesis. MacMillan and coworkers have reported initial progress toward resolving the configurational details of the nigricanosides [188].

20.4.4 Terpenoid Glycosides

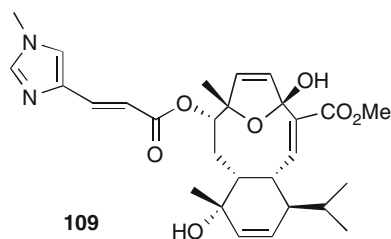
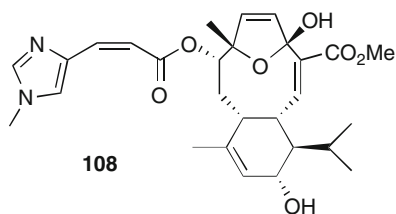
20.4.4.1 Eleuthosides/Sarcodictyins

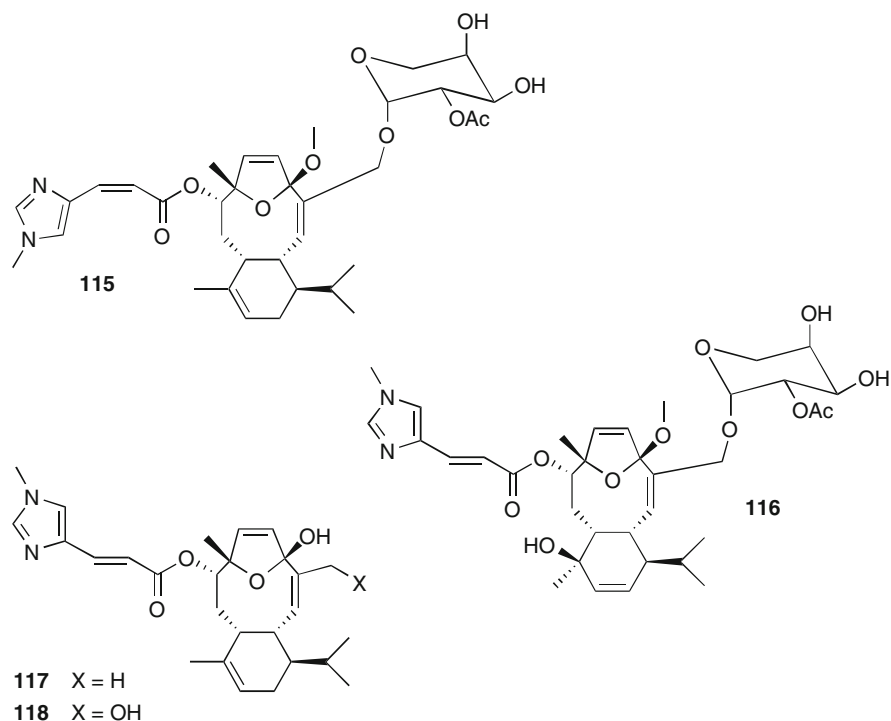


- 103** R = Me, R_1 = Ac, R_2 = R_3 = H
110 R = H, R_1 = R_2 = Ac, R_3 = H
111 R = H, R_1 = R_3 = Ac, R_2 = H
112 R = R_2 = R_3 = H, R_1 = Ac
113 R = Me, R_1 = R_2 = R_3 = H
114 R = Me, R = R_2 = R_3 = H, R_2 = Ac



- 104** R = X = H, R_1 = Me
105 R = X = H, R_1 = Et
106 R = H, X = OH, R_1 = Me
107 R = H, X = OAc, R_1 = Me





In 1997, Fenical's group reported the isolation of the potentially cytotoxic diterpene glycoside eleutherobin (**103**) ($IC_{50}s \approx 10\text{--}15$ nM against a panel of tumor tissue cell lines) from extracts of a rare soft coral identified as an *Eleutherobia* sp. that they had collected near Bennett's Shoal in Western Australia [189]. The same paper revealed that eleutherobin stabilized microtubules and was a competitive inhibitor of paclitaxel binding. Eleutherobin is related to the sarcodictyins A (**104**) to F (**109**) isolated by Pietra's group in 1987 [190] and 1988 [191] from the Mediterranean soft coral *Sarcodictyon roseum*, and to the eleuthosides A (**110**) and B (**111**) isolated by Kashman's group from the South African soft coral *Eleutherobia aurea* in 1996 [192].

The Andersen and Roberge groups reported in 2000 that they had discovered eleutherobin (**103**) in extracts of the abundant Caribbean octocoral *Erythropodium caribaeorum* using Roberge's cell-based antimitotic assay as a screening tool [193]. Extracts of *E. caribaeorum* showed strong mitotic arrest in the assay, and microscopic examination of cells arrested in mitosis revealed evidence of tubulin bundling similar to the effects caused by paclitaxel. In addition to eleutherobin, the *E. caribaeorum* extract also yielded the new analogs **112** to **118**, which all showed antimitotic activity in the cell-based assay [193, 194]. Cultured specimens of *E. caribaeorum*, several generations removed from the wild stock, continue to produce eleutherobin in roughly the same amounts as found in wild specimens, suggesting that mariculture could be a sustainable source of

the compound for drug use [195]. As part of the investigation of *E. caribaeorum*, it was shown that eleutherobin itself is an isolation artifact formed by reaction of the actual natural product desmethyleleutherobin (**112**) with methanol during the extraction and purification steps [194]. The fortuitous formation of a crystal of eleutherobin in an NMR sample dissolved in DMSO-*d*₆ led to the determination of its solid state and solution conformations via analysis of X-ray diffraction and solution NOE data [196].

Chemical transformations of natural eleutherobin revealed that the $\Delta^{2',3'}$ olefin in the *N*-methylurocanic ester moiety is essential for antimitotic activity [197]. Nicolaou's group reported the first total syntheses of sarcodictyin A (**104**) [198], eleutherobin (**103**) [199], and analogs for SAR [200], and Danishefsky's group reported the second total synthesis of eleutherobin a year later [201]. Ojima and Danishefsky incorporated the eleuthosides into one of the first proposals for a common pharmacophore for microtubule-stabilizing natural products [202].

Fenical, Fairchild, and coworkers [203] as well as Hamel's group at NIH [204] reported detailed evaluations of the cytotoxicity and tubulin interactions of eleutherobin (**103**) and sarcodictyins A (**104**) and B (**105**). These studies confirmed that eleutherobin is a potent in vitro cytotoxin against cancer cell lines, is a microtubule-stabilizing agent capable of inducing tubulin polymerization to form microtubules that are resistant to cold or Ca-ion-induced depolymerization, may be a substrate for the P-glycoprotein efflux pump, and binds to the taxoid site on tubulin.

20.5 Summary

This chapter illustrates the large number and variety of microtubule-targeting natural product chemotypes that have been discovered from marine organisms. Marine sponges account for roughly half of the new chemotypes, with the remainder coming from ascidians, soft corals, mollusks, macroalgae, blue-green algae, bacteria, and fungi. The histories of laulimalide, dictyostatin-1, and zampanolide show that there is frequently a significant period of time, often a decade or more, between the discovery of potent new cytotoxins and the recognition that they target microtubules. Therefore, it is likely that more microtubule-targeting agents remain to be identified among already known marine natural product cytotoxins.

It seems reasonable to ask why microtubules should be one of the favored biological targets of marine natural products. The answer may simply be that antimitotic agents are potent toxins making them highly effective chemical defenses for algae and sessile or slow-moving invertebrates. The amino acid sequence of tubulin is highly conserved in eukaryotes [205], enabling antimitotic agents to show broad-spectrum activity against varied eukaryotic organisms, a desirable trait for a chemical deterrent.

Some challenges for the simple view that antimitotic marine natural products are defensive agents include the fact that many of the compounds show significant

geographic variation in occurrence and are present in the source organisms in extremely low concentrations, perhaps too low to be effective deterrents, and the increasing circumstantial evidence suggesting that many natural products isolated from marine invertebrates are produced by symbiotic or dietary prokaryotes. It is possible that prokaryotes associated with invertebrates make antimetabolic agents specifically for their own benefit, perhaps to help establish or maintain their populations when they are free living or within the host, and that the compounds offer no particular advantage to the invertebrate source organisms.

Alternatively, establishing a complex symbiotic relationship for chemical deterrent production may offer some advantages to invertebrates. Bacterial cells do not use microtubules for chromosome segregation. Instead, they rely on a mechanism involving attachment of their duplicated chromosome to the plasma membrane. With the apparent exception of a single phylum (verrucomicrobia), bacteria do not have tubulin genes or microtubules [206]. The absence of the tubulin target in bacteria makes it easier for them to produce antimetabolic agents that specifically affect eukaryotes without affecting the producing prokaryote.

Unfortunately, although a great deal is known about the effects of antimetabolic marine natural products on cancer cells, almost nothing is known about their toxic or feeding deterrent effects on potential predators or competitors of the source organisms, or whether or not the source organisms are resistant to the antimetabolic agents extracted from their tissues. Future work on antimetabolic marine natural products would ideally extend beyond their medicinal potential to also address the important issues of what are the actual producing organisms, microbes, or invertebrates, and what are the ecological roles, if any, of these potent cytotoxins.

The wide acceptance of microtubules as a highly validated anticancer drug target has meant that almost all of the marine natural products that target microtubules have attracted significant interest as drug leads. This interest has resulted in the development of synthetic methodology suitable for the gram scale production of several of the antimetabolic natural products or simpler pharmacophore analogs required to support their preclinical development and ultimately clinical trials. To date, 11 microtubule-targeting marine natural products or synthetic analogs have been evaluated in phase I/phase II clinical trials. With the exception of discodermolide, all of the compounds that have been taken into clinical trials are depolymerizing agents. The evaluation of microtubule-stabilizing marine natural products has generally lagged behind, and most of these have not even been evaluated in animal models yet due to the limited supply of compound that has been available. None of the antimetabolic marine natural product clinical trial candidates have progressed beyond phase II trials, and many have been pulled from further trials due to toxicity or lack of sufficient efficacy. Therefore, even though widespread scientific interest in this class of marine natural products as drug leads remains, there are still no new drugs inspired by these lead compounds on the short-term horizon. This may change as more drug candidates based on microtubule-stabilizing marine natural products progress to clinical trials in the coming years.

20.6 Study Questions

1. Given that there are many extremely potent microtubule-targeting antimitotic natural product drug leads already known and in clinical development, is there any compelling need to identify new microtubule-targeting natural product chemotypes for anticancer drug development, or have we already gone as far as we can in terms of modulating microtubule dynamics with small molecules? Explain your answer in detail.
2. What attributes would one look for in new antimitotic drug candidates that would distinguish them from paclitaxel, the Vinca alkaloids, and the other marine natural products described in this review? How would you screen crude extracts and pure compounds for these properties?
3. Identify an unexplored environmental niche and group of source organisms that might be a rich source of new antimitotic marine natural products. Briefly rationalize your choice and explain how you would explore this niche for new natural product chemistry.
4. Which of the antimitotic marine natural products described in this review that have been isolated from extracts of marine macroorganisms such as algae, sponges, soft corals, or ascidians might actually be produced by associated microorganisms? Provide a rationale for each compound that you have identified as having a putative microbial source. Suggest some experiments that could be used to test the possibility of a microbial origin for the compounds.
5. Propose a biogenesis for spongistatin 1 (**19**).
6. Propose a biogenesis for diazonamide (**65**).
7. Propose a biogenesis for ceratamine A (**97**).
8. Propose biochemical mechanisms for (1) the addition of the oxygen atoms to the fatty acid chains, (2) the formation of the ether linkage between the two fatty acid chains, and (3) the formation of the ether linkage between the fatty acid and the galactose residues in nigricanoside A (**101**).

References

1. Jordan MA, Kamath K (2007) How do microtubule-targeted drugs work? An overview. *Curr Cancer Drug Targets* 7:730–742
2. Jordan MA, Wilson L (2004) Microtubules as a target for anticancer drugs. *Nat Rev Cancer* 4:253–265
3. Kingston DGI (2009) Tubulin-interactive natural products as anticancer agents. *J Nat Prod* 72:507–515
4. Altmann K-H (2001) Microtubule-stabilizing agents: a growing class of important anticancer drugs. *Curr Opin Chem Biol* 5:424–431
5. Altman KH, Gertsch J (2007) Anticancer drugs from nature - natural products as a unique source of new microtubule-stabilizing agents. *Nat Prod Rep* 24:327–357
6. Hamel E (1996) Antimitotic natural products and their interactions with tubulin. *Med Res Rev* 16:207–231
7. Kerssemakers JWJ, Munteanu EL, Laan L et al (2006) Assembly dynamics of microtubules at molecular resolution. *Nature* 442:709–712

8. Rodionov VI, Borisy GG (1997) Microtubule treadmilling in vivo. *Science* 275:215–218
9. Kerbel RS, Kamen BA (2004) The anti-angiogenic basis of metronomic chemotherapy. *Nat Rev Cancer* 4:423–436
10. Cristofanilli M, Charsangavej C, Hortobagyi GN et al (2002) Angiogenesis modulation in cancer research: novel clinical approaches. *Nat Rev Drug Discov* 1:415–426
11. Schiff PB, Fant J, Horwitz SB (1979) Promotion of microtubule assembly in vitro by taxol. *Nature* 277:665–667
12. Roberge M, Cinel B, Anderson HJ et al (2000) Cell-based screen for antimetabolic agents and identification of analogues of rhizoxin, eleutherobin, and paclitaxel in natural extracts. *Cancer Res* 60:5052–5058
13. Kokoshka JM, Ireland CM, Barrows LR (1996) Cell-based screen for identification of inhibitors of tubulin polymerization. *J Nat Prod* 59:1179–1182
14. Meguro S, Namikoshi M, Kobayashi H (2002) A new screening method for antimetabolic substances and isolation of glycolipids as stimulators of tubulin polymerization from okinawan sponge *Pseudoceratina* sp. *J Antibiot* 55:256–262
15. Kobayashi H, Namikoshi M, Yoshimoto T et al (1996) A screening method for antimetabolic and antifungal substances using conidia of *Pyricularia ovyzae*, modification and application to tropical marine fungi. *J Antibiot* 9:873–879
16. Uemura D, Takahashi K, Yamamoto T et al (1985) Norhalichondrin A: An antitumor polyether macrolide from a marine sponge. *J Am Chem Soc* 107:4796–4798
17. Hirata Y, Uemura D (1986) Halichondrins – antitumor polyether macrolides from a marine sponge. *Pure Appl Chem* 58:701–710
18. Pettit GR, Tan R, Gao F et al (1993) Isolation and structure of halistatin 1 from the eastern Indian Ocean marine sponge *Phakellia carteri*. *J Org Chem* 58:2538–2543
19. Pettit GR, Gao F et al (1993) Antineoplastic agents. CCLII. Isolation and structure of halistatin 2 from the Comoros marine sponge *Axinella carteri*. *Gazz Chim Ital* 123:371–377
20. Pettit GR, Ichihara Y, Wurzel G et al (1995) Isolation and structure of halistatin 3 from the Western Pacific (Chuuk) marine sponge *Phakellia* sp. *J Chem Soc Chem Commun* 26(27):383–385
21. Litaudon M, Hart JB, Blunt JW et al (1994) Isohomohalichondrin B, a new antitumor polyether macrolide from the New Zealand deep-water sponge *Lissodendoryx* sp. *Tetrahedron Lett* 35:9435–9438
22. Litaudon M, Hickford SJH, Lill RE et al (1997) Antitumor polyether macrolides: New and hemisynthetic halichondrins from the New Zealand deep-water sponge *Lissodendoryx* sp. *J Org Chem* 62:1868–1871
23. Bai RL, Paull KD, Herald CL et al (1991) Halichondrin B and homohalichondrin B, marine natural products binding in the vinca domain of tubulin. Discovery of tubulin-based mechanism of action by analysis of differential cytotoxicity data. *J Biol Chem* 266:15882–15889
24. Aicher TD, Buszek KR, Fang FG et al (1992) Total synthesis of halichondrin B and norhalichondrin B. *J Am Chem Soc* 114:3162–3164
25. Zheng W, Seletsky BM, Palme MH et al (2004) Macrocyclic ketone analogues of halichondrin B. *Bioorg Med Chem Lett* 14:5551–5554
26. Yu MJ, Kishi Y, Littlefield BA (2005) Discovery of E7389, a fully synthetic macrocyclic ketone analog of halichondrin B. In: Cragg GM, Kingston DGI, Newman DJ (eds) *Anticancer agents from natural products*. CRC Press, Boca Raton, FL, pp 241–265
27. Towle MJ, Salvato KA, Budrow J et al (2001) In vitro and in vivo anticancer activities of synthetic macrocyclic ketone analogues of halichondrin B. *Cancer Res* 61:1013–1021
28. Jordan MA, Kamath K, Manna T et al (2005) The primary antimetabolic mechanism of action of the synthetic halichondrin E7389 is suppression of microtubule growth. *Mol Cancer Ther* 4:1086–1095
29. Dabydeen DA, Burnett JC, Bai R et al (2006) Comparison of the activities of the truncated halichondrin B analog NSC 707389 (E7389) with those of the parent compound and a proposed binding site on tubulin. *Mol Pharmacol* 70:1866–1875

30. Blum JL, Pruitt B, Fabian CJ et al (2007) Phase II study of eribulin mesylate (E7389) halichondrin B analog in patients with refractory breast cancer. *J Clin Oncol* (Meeting Abstracts) 25(18):1034
31. Spira AI, Iannotti NO, Savin MA et al (2007) Phase II study of eribulin mesylate (E7389), a mechanistically novel inhibitor of microtubule dynamics, in patients with advanced non-small cell lung cancer (NSCLC). *J Clin Oncol* (ASCO Meeting Abstracts) 25(18):7546
32. Pettit GR, Cichacz ZA, Gao F et al (1993) Isolation and structure elucidation of spongistatin 1. *J Org Chem* 58:1302–1304
33. Fusetani N, Shinoda K, Matsunaga S (1993) Cinachryolide A: a potent cytotoxic macrolide possessing two spiro ketals from marine sponge *Cinachyra* sp. *J Am Chem Soc* 115:3977–3981
34. Kobayashi M, Aoki S, Sakai H et al (1993) Altohrytin A, a potent anti-tumor macrolide from the Okinawan marine sponge *Hyrtios altum*. *Tetrahedron Lett* 34:2795–2798
35. Kobayashi M, Aoki S, Sakai H et al (1993) Altohrytins B and C and 5-desacetylalttohrytin A, potent cytotoxic macrolide congeners of alttohrytin A, from the Okinawan marine sponge *Hyrtios altum*. *Chem Pharm Bull* 41:989–991
36. Pettit GR, Cichacz ZA, Gao F et al (1993) Isolation and structure of the remarkable human cancer cell growth inhibitors spongistatins 2 and 3 from an Eastern Indian Ocean *Spongia* sp. *J Chem Soc Chem Commun* 14:1166–1168
37. Kobayashi M, Aoki S, Kitagawa I (1994) Absolute stereostructures of alttohrytin A and its congeners, potent cytotoxic macrolides from the Okinawan marine sponge *Hyrtios altum*. *Tetrahedron Lett* 35:1234–1246
38. Kobayashi M, Aoki S, Gato K et al (1996) Marine natural products XXXVIII. Absolute stereostructures of alttohrytins A, B, C and 5-desacetylalttohrytin A, potent cytotoxic macrolides, from the Okinawan marine sponge *Hyrtios altum*. *Chem Pharm Bull* 44:2142–2149
39. Hayward MM, Roth RM, Duffy KJ (1998) Total synthesis of alttohrytin A (spongistatin 1): part 2. *Angew Chem Int Ed* 37:190–196
40. Evans DA, Trotter BW, Côté B et al (1997) Enantioselective synthesis of alttohrytin C (spongistatin 2): fragment assembly and revision of the spongistatin 2 stereochemical assignment. *Angew Chem Int Ed* 36:2744–2747
41. Pettit GR, Herald CL, Cichacz ZA et al (1993) Isolation and structure of the powerful human cancer cell growth inhibitors spongistatins 4 and 5 from an African *Spirastrella spinispirulifera* (porifera). *J Chem Soc Chem Commun* 58:1805–1807
42. Pettit GR, Herald CL, Cichacz ZA et al (1993) Antineoplastic agents. 293. The exceptional human cancer cell growth inhibitors spongistatins 6 and 7. *Nat Prod Lett* 3:239–244
43. Pettit GR, Cichacz ZA, Herald CL et al (1994) Antineoplastic agents 300. Isolation and structure of the rare human cancer inhibitory macrocyclic lactones spongistatins 8 and 9. *J Chem Soc Chem Commun* 1605–1606
44. Bai R, Taylor GF, Cichacz ZA et al (1995) The spongistatins, potentially cytotoxic inhibitors of tubulin polymerization, bind in a distinct region of the Vinca domain. *Biochemistry* 34:9714–9721
45. Pettit RK, McAllister SC, Pettit GR et al (1998) A broad spectrum antifungal from the marine sponge *Hyrtios erecta*. *Int J Antimicrob Agents* 9:147–152
46. Smith AB, Sfougataakis C, Risatti CA et al (2009) Spongipyran synthetic studies. Evolution of a scalable total synthesis of (+)-spongistatin 1. *Tetrahedron* 65:6489–6509
47. Namikoshi M, Kobayashi H, Yoshimoto T et al (1997) Phomopsidin, a new inhibitor of microtubule assembly produced by *Phomopsis* sp isolated from coral reef in Pohnpei. *J Antibiot* (Tokyo) 50:890–892
48. Kobayashi H, Meguro S, Yoshimoto T et al (2003) Absolute structure, biosynthesis, and anti-microtubule activity of phomopsidin, isolated from a marine-derived fungus *Phomopsis* sp. *Tetrahedron* 59:455–459

49. Sullivan AS, Prasad V, Roach MC et al (1990) Interaction of rhizoxin with bovine brain tubulin. *Cancer Res* 50:4277–4280
50. Scherlach K, Partida-Martinez LP, Dahse H-M et al (2006) Antimitotic rhizoxin derivatives from a cultured bacterial endosymbiont of the rice pathogenic fungus *Rhizopus microsporus*. *J Am Chem Soc* 128:11529–11536
51. Partida-Martinez LP, Hertweck C (2005) Pathogenic fungus harbours endosymbiotic bacteria for toxin production. *Nature* 437:884–888
52. McLeod HL, Murray LS, Wanders J et al (1996) Multicentre phase II pharmacological evaluation of rhizoxin. *Br J Cancer* 74:1944–1948
53. Pettit GR, Kamano Y, Herald CL et al (1987) The isolation and structure of a remarkable marine animal antineoplastic constituent: dolastatin 10. *J Am Chem Soc* 109:6883–6885
54. Pettit GR, Singh SB, Hogan F et al (1989) The absolute configuration and synthesis of natural (–)-dolastatin 10. *J Am Chem Soc* 111:5463–5465
55. Luesch H, Moore RE, Paul VJ et al (2001) Isolation of dolastatin 10 from the marine cyanobacterium *Symploca* species VP642 and total stereochemistry and biological evaluation of its analogue symplostatin 1. *J Nat Prod* 64:907–910
56. Bai R, Pettit GR, Hamel E (1990) Dolastatin 10, a powerful cytostatic peptide derived from a marine animal. *Biochem Pharmacol* 39:1941–1949
57. Bai R, Taylor GF, Schmidt JM et al (1995) Interaction of dolastatin 10 with tubulin: induction of aggregation and binding and dissociation reactions. *Mol Pharmacol* 47:965–976
58. Pitot HC, McElroy EA Jr et al (1999) Phase I trial of dolastatin-10 (NSC 376128) in patients with advanced solid tumors. *Clin Cancer Res* 5:525–531
59. Vaishampayan U, Glode M, Du W et al (2000) Phase II study of dolastatin-10 in patients with hormone-refractory metastatic prostate adenocarcinoma. *Clin Cancer Res* 6:4205–4208
60. Madden T, Tran HT, Beck D et al (2000) Novel marine-derived anticancer agents: A phase I clinical, pharmacological, and pharmacodynamic study of dolastatin 10 (NSC 37618) in patients with advanced solid tumors. *Clin Cancer Res* 6:1293–1301
61. Saad ED, Kraut EH, Hoff PM et al (2002) Phase II study of dolastatin-10 as first-line treatment for advanced colorectal cancer. *Am J Clin Oncol (CCT)* 25:451–453
62. Miyazaki K, Kobayashi M, Natsume T et al (1995) Synthesis and antitumor activity of novel dolastatin 10 analogs. *Chem Pharm Bull* 43:1706–1718
63. Kobayashi M, Natsume T, Tamaoki S et al (1997) Antitumor activity of TZT-1027, a novel dolastatin 10 derivative. *Jpn J Cancer Res* 88:316–327
64. Watanabe J, Natsume Kobayashi M (2006) Antivascular effects of TZT-1027 (Soblidotin) on murine colon26 adenocarcinoma. *Cancer Sci* 97:1410–1416
65. Otani M, Natsume T, Watanabe J et al (2000) TZT-1027, an antimicrotubule agent, attacks tumor vasculature and induces tumor cell death. *Jpn J Cancer Res* 91:837–844
66. Schöffski P, Thate B, Beutel G et al (2004) Phase I and pharmacokinetic study of TZT-1027, a novel synthetic dolastatin 10 derivatives, administered as a 1-hour intravenous infusion every 3 weeks in patients with advanced refractory cancer. *Ann Oncol* 15:671–679
67. JongeMJAd GA, Planting AST et al (2005) Phase I and pharmacokinetic study of the dolastatin 10 analogue TZT-1027, given on days 1 and 8 of a 3-week cycle in patients with advanced solid tumors. *Clin Cancer Res* 11:3806–3813
68. Patel S, Keohan ML, Saif MW et al (2006) Phase II study of intravenous TZT-1027 in patients with advanced or metastatic soft-tissue sarcomas with prior exposure to anthracycline-based chemotherapy. *Cancer* 107:2881–2887
69. Pettit GR, Kamano Y, Dufresne C et al (1989) Isolation and structure of the cytostatic linear depsipeptide dolastatin 15. *J Org Chem* 54:6005–6006
70. Pettit GR, Herald DL, Singh SB et al (1991) Antineoplastic agents. 220. Synthesis of natural (–)-dolastatin15. *J Am Chem Soc* 113:6692–6693
71. Bai R, Friedman S, Pettit GR et al (1992) Dolastatin 15, a potent antimitotic depsipeptide derived from *Dolabella auricularia*. *Biochem Pharmacol* 43:2637–2645

72. Cruz-Monserrate Z, Mullaney JT, Harran P et al (2003) Dolastatin 15 binds in the vinca domain of tubulin as demonstrated by Hummel-Dreyer chromatography. *Eur J Biochem* 270:3822–3828
73. Arruda MD, Cocchiario CA, Nelson CM et al (1995) LU103793 (NSC D-669356): a synthetic peptide that interacts with microtubules and inhibits mitosis. *Cancer Res* 55:3085–3092
74. Cunningham C, Appleman LJ, Kirvan-Visovatti M et al (2005) Phase I and pharmacokinetic study of the dolastatin-15 analogue tasidotin (ILX651) administered intravenously on days 1, 3, and 5 every 3 weeks in patients with advanced solid tumors. *Clin Cancer Res* 11:7825–7833
75. Jordan MA, Walker D, Arruda MD et al (1998) Suppression of microtubule dynamics by binding of cemadotin to tubulin: possible mechanism for its antitumor action. *Biochemistry* 37:17571–17578
76. Ray A, Okouneva T, Manna T et al (2007) Mechanism of action of the microtubule-targeted antimitotic depsipeptide tasidotin (formerly ILX651) and its major metabolite tasidotin C-carboxylate. *Cancer Res* 67:3767–3776
77. Marks RS, Graham DL, Sloan JA et al (2003) A phase II study of the dolastatin 15 analogue LU 103793 in the treatment of advanced non-small-cell lung cancer. *Am J Clin Oncol (CCT)* 26:336–337
78. Mross K, Berdel WE, Fiebig HH et al (1998) Clinical and pharmacologic phase I study of cemadotin-HCl (LU103793), a novel antimitotic peptide, given as 24-hour infusion in patients with advanced cancer. *Ann Oncol* 9:1323–1330
79. Mita AC, Hammond LA, Bonate PL et al (2006) Phase I and pharmacokinetic study of tasidotin hydrochloride (ILX651), a third-generation dolastatin-15 analogue, administered weekly for 3 weeks every 28 days, in patients with advanced solid tumors. *Clin Cancer Res* 11:5207–5215
80. Simmons TL, McPhail KL, Ortega-Barría E et al (2006) Belamide A, a new antimitotic tetrapeptide from a Panamanian marine cyanobacterium. *Tetrahedron Lett* 47:3387–3390
81. Kobayashi M, Aoki S, Ohayabu N et al (1994) Arenastatin A, a potent cytotoxic depsipeptide from the Okinawan marine sponge *Dysidea arenaria*. *Tetrahedron Lett* 35:7969–7972
82. Kobayashi M, Kurosu M, Ohayabu N et al (1994) The absolute stereostructure of arenastatin A, a potent cytotoxic depsipeptide from the Okinawan marine sponge *Dysidea arenaria*. *Chem Pharm Bull* 42:2196–2198
83. Golakoti T, Ohtani I, Patterson GML et al (1994) Total structures of cryptophycins. Potent antitumor depsipeptides from the blue-green alga *Nostoc* sp. strain GSV 224. *J Am Chem Soc* 116:4729–4737
84. Barrow RA, Hemscheidt T, Liang J et al (1995) Total synthesis of cryptophycins. revision of the structures of cryptophycins A and C. *J Am Chem Soc* 117:2479–2490
85. Schwartz RE, Hirsch CF, Sesin DF et al (1990) Pharmaceuticals from cultured algae. *J Ind Microbiol Biotechnol* 5:113–124
86. Golakoti T, Ogino J, Heltzel CE (1995) Structure determination, conformational analysis, chemical stability studies, and antitumor evaluation of the cryptophycins. Isolation of 18 new analogs from *Nostoc* sp. strain GSV 224. *J Am Chem Soc* 117:12030–12049
87. Chaganty S, Golakoti T, Heltzel C et al (2004) Isolation and structure determination of cryptophycins 38, 326, and 327 from the terrestrial cyanobacterium *Nostoc* sp. GSV 224. *J Nat Prod* 67:1403–1406
88. Kerkisiek K, Mejillano MR, Schwartz RE et al (1995) Interaction of cryptophycin 1 with tubulin and microtubules. *FEBS Lett* 377:59–61
89. Bai R, Schwartz RE, Kepler JA et al (1996) Characterization of the interaction of cryptophycin 1 with tubulin: Binding in the vinca domain, competitive inhibition of dolastatin 10 binding, and an unusual aggregation reaction. *Cancer Res* 56:4398–4406
90. Panda D, Himes RH, Moore RE et al (1997) Mechanism of action of the unusually potent microtubule inhibitor cryptophycin 1. *Biochemistry* 36:12948–12953

91. Stevenson JP, Sun W, Gallagher M (2002) Phase I trial of the cryptophycin analogue LY355703 administered as an intravenous infusion on a day 1 and 8 schedule every 21 days. *Clin Cancer Res* 8:2524–2529
92. Sessa C, Weigang-Kohler K, Pagani O et al (2002) Phase I and pharmacological studies of the cryptophycin analogue LY355703 administered on a single intermittent or weekly schedule. *Eur J Cancer* 38:2388–2396
93. Talpir R, Benayahu Y, Kashman Y (1994) Hemiasterlin and geodiamolide TA; Two new cytotoxic peptides from the marine sponge *Hemiasterella minor* (Kirkpatrick). *Tetrahedron Lett* 35:4453–4456
94. Crews P, Farias JJ, Emrich R et al (1994) Milnamide A, an unusual cytotoxic tripeptide from the marine sponge *Aulettacis constricta*. *J Org Chem* 59:2932–2934
95. Coleman JE, de Silva ED, Kong F et al (1995) Cytotoxic peptides from the marine sponge *Cymbastela* sp. *Tetrahedron* 51:10653–10662
96. Coleman JE, Patrick BO, Andersen RJ et al (1996) Hemiasterlin methyl ester. *Acta Crystallogr C* 52:1525–1527
97. Andersen RJ, Coleman JE, Piers E et al (1997) Total synthesis of (–)-hemiasterlin, a structurally novel tripeptide that exhibits potent cytotoxic activity. *Tetrahedron Lett* 38:317–320
98. Gamble WR, Durso NA, Fuller RW et al (1999) Cytotoxic and tubulin-interactive hemiasterlins from *Aulettacis* sp. and *Siphonochalina* spp. sponges. *Bioorg Med Chem* 7:1611–1615
99. Chevallier C, Richardson AD, Edler MC et al (2003) A new cytotoxic and tubulin-interactive milnamide derivative from a marine sponge *Cymbastela* sp. *Org Lett* 5:3737–3739
100. Sonnenschein RN, Farias JJ, Tenney K et al (2004) A further study of the cytotoxic constituents of a milnamide-producing sponge. *Org Lett* 6:779–782
101. Liu C, Masuno MN, Macmillan JB et al (2004) Enantioselective total synthesis of (+)-milnamide A and evidence of its autoxidation to (+)-milnamide D. *Angew Chem Int Ed Engl* 43:5951–5954
102. Anderson HJ, Coleman JE, Andersen RJ et al (1997) Cytotoxic peptides hemiasterlin, hemiasterlin A, and hemiasterlin B include mitotic arrest and abnormal spindle formation. *Cancer Chemother Pharmacol* 39:223–226
103. Bai R, Durso NA, Sackett DL et al (1999) Interactions of the sponge-derived antimitotic tripeptide hemiasterlin with tubulin: comparison with dolastatin 10 and cryptophycin 1. *Biochemistry* 38:14302–14310
104. Boukari H, Nossal R, Sackett DL (2003) Stability of drug-induced tubulin rings by fluorescence correlation spectroscopy. *Biochemistry* 42:1292–1300
105. Nieman JA, Coleman JE, Wallace DJ et al (2003) Synthesis and antimitotic/cytotoxic activity of hemiasterlin analogues. *J Nat Prod* 66:183–199
106. Ratain MJ et al (2003) Phase I and pharmacological study of HTI-286, a novel antimicrotubule agent: correlation of neutropenia with time above a threshold serum concentration. *Proc Am Soc Clin Oncol* 22:516
107. Andersen RJ, Roberge M (2005) HTI-286, a synthetic analogue of the antimitotic natural product hemiasterlin. In: Cragg GM, Kingston DGI, Newman DJ (eds) *Anticancer agents from natural products*. CRC Press, Boca Raton, pp 267–280
108. Loganzo F, Discafani CM, Annable T et al (2003) HTI-286, a synthetic analogue of the tripeptide hemiasterlin, is a potent antimicrotubule agent that circumvents P-glycoprotein-mediated resistance in vitro and in vivo. *Cancer Res* 63:1838–1845
109. Rav M, Zask A, Rush TS III (2005) Structure-based identification of the binding site for the hemiasterlin analogue HTI-286 on tubulin. *Biochemistry* 44:15871–15879
110. Milto MJ, Williamson RT, Koehn FE (2006) Mapping the bound conformation and protein interactions of microtubule destabilizing peptides by STD-NMR spectroscopy. *Bioorg Med Chem Lett* 16:4279–4282

111. Nunes M, Kaplan J, Wooters J et al (2005) Two photoaffinity analogues of the tripeptide, hemiasterlin, exclusively label α -tubulin. *Biochemistry* 44:6844–6857
112. Lo M-C, Aulabaugh A, Krishnamurthy G et al (2004) Probing the interaction of HTI-286 with tubulin using a stilbene analogue. *J Am Chem Soc* 126:9898–9899
113. Yamashita A, Norton EB, Kaplan JA et al (2004) Synthesis and activity of novel analogs of hemiasterlin as inhibitors of tubulin polymerization: modification of the A segment. *Bioorg Med Chem Lett* 14:5317–5322
114. Hadaschik BA, Ettinger S, Sowery RD et al (2008) Targeting prostate cancer with HTI-286, a synthetic analog of the marine sponge product hemiasterlin. *Int J Cancer* 122:2368–2376
115. Hadaschik BA, Adomat H, Fazli L et al (2008) Intravesical chemotherapy of high-grade bladder cancer with HTI-286, a synthetic analogue of the marine sponge product hemiasterlin. *Clin Cancer Res* 14:1510–1518
116. Fernandez AM, He H, McDonald LA et al (1998) Structural studies of marine pep tides. *Pure Appl Chem* 70:2130
117. Edler MC, Fernandez AM, Lassota P et al (2002) Inhibition of tubulin polymerization by vitilevuamide, a bicyclic marine peptide, at a site distinct from colchicine, the vinca alkaloids, and dolastatin 10. *Biochem Pharmacol* 63:707–715
118. Fenical W, Jensen PR, Cheng XC (1999) Halimide, a cytotoxic marine natural product, derivatives thereof, and therapeutic use in inhibition of proliferation. *PCT Int. Appl. WO* 9948889
119. Nicholson B, Lloyd GK, Miller BR et al (2006) NPI-2358 is a tubulin-depolymerizing agent: in vitro evidence for activity as a tumor vascular-disrupting agent. *Anti-Cancer Drugs* 17:25–31
120. Gerwick WH, Proteau PJ, Nagel DG et al (1994) Structure of curacin A, a novel antimitotic, antiproliferative, and brine shrimp toxic natural product from the marine cyanobacterium *Lyngbya majuscula*. *J Am Chem Soc* 59:1243–1245
121. Yoo H-D, Gerwick WH (1995) Curacins B and C, new antimitotic natural products from the marine cyanobacterium *Lyngbya majuscula*. *J Nat Prod* 58:1961–1965
122. Márquez B, Verdier-Pinard P, Hamel E et al (1998) Curacin D, an antimitotic agent from the marine cyanobacterium *Lyngbya majuscula*. *Phytochemistry* 49:2387–2389
123. Nagle DG, Geraldts RS, Yoo H-D et al (1995) Absolute configuration of curacin A, a novel antimitotic agent from the tropical marine cyanobacterium *Lyngbya majuscula*. *Tetrahedron Lett* 36:1189–1192
124. White JD, Kim TS, Nambu M (1995) Synthesis of curacin A: a powerful antimitotic from the cyanobacterium *Lyngbya majuscula*. *J Am Chem Soc* 117:5612–5613
125. Chang Z, Sitachitta N, Rossi JV et al (2004) Biosynthetic pathway and gene cluster analysis of curacin A, an antitubulin natural product from the tropical marine cyanobacterium *Lyngbya majuscula*. *J Nat Prod* 67:1356–1367
126. Gu L, Wang B, Kulkarni A et al (2009) Metamorphic enzyme assembly in polyketide diversification. *Nature* 459:731–735
127. Gu L, Wang B, Kulkarni A et al (2009) Polyketide decarboxylative chain termination preceded by O-sulfonation in curacin A biosynthesis. *J Am Chem Soc* 131:16033–16035
128. Ludueña RF, Prasad V, Roach MC et al (1997) Interaction of the cyanobacterial thiazoline-containing lipid curacin A with bovine brain tubulin. *Drug Develop Res* 40:223–229
129. Verdier_Pinard P, Lai J-Y, Yoo H-D et al (1997) Structure-activity analysis of the interaction of curacin A, the potent colchicine site antimitotic agent, with tubulin and effects of analogs on the growth of MCF-7 breast cancer cells. *Mol Pharmacol* 53:62–76
130. Wipf P, Reeves JT, Day BW (2004) Chemistry and biology of curacin A. *Curr Pharm Des* 10:1417–1437
131. Lindquist N, Fenical W, Van Duyne GD et al (1991) Isolation and structure elucidation of diazonamides A and B, unusual cytotoxic metabolites from the marine ascidian *Diazonia chinensis*. *J Am Chem Soc* 113:2303–2304

132. Li J, Jeong S, Esser L et al (2001) Total synthesis of nominal diazonamides – Part 1: Convergent preparation of the structure proposed for (–)-diazonamide A. *Angew Chem Int Ed Engl* 40:4765–4770
133. Li J, Burgett AWG, Esser L et al (2001) Total synthesis of nominal diazonamides – Part 2: On the true structure and origin of natural isolates. *Angew Chem Int Ed Engl* 40:4770–4773
134. Nicolaou KC, Chen DYK, Huang X et al (2004) Chemistry and biology of diazonamide A: first total synthesis and confirmation of the true structure. *J Am Chem Soc* 126:12888–12896
135. Fernández R, Martín MJ, Rodríguez-Acebes R et al (2008) Diazonamides C-E, new cytotoxic metabolites from the ascidian *Diazonina* sp. *Tetrahedron Lett* 49:2283–2285
136. Cruz-Monserate Z, Vervoort HC, Bai R et al (2003) Diazonamide A and a synthetic structural analog: disruptive effects on mitosis and cellular microtubules and analysis of their interactions with tubulin. *Mol Pharmacol* 63:1273–1280
137. Williams NS, Burgett AWG, Atkins AS et al (2007) Therapeutic anticancer efficacy of a synthetic diazonamide analog in the absence of overt toxicity. *Proc Natl Acad Sci* 104:2074–2079
138. Gerwick WH, Fenical W, Fritsch N et al (1979) Stypotriol and stypolidone; ichthyotoxins of mixed biosynthesis from the marine alga *Stypopodium zonale*. *Tetrahedron Lett* 20:145–148
139. White SJ, Jacobs RS (1983) Effect of stypoldione on cell cycle progression, DNA and protein synthesis, and cell division in cultured sea urchin embryos. *Mol Pharm* 24:500–508
140. O'Brien ET, Asai J, Jacobs RS, Wilson L (1988) Selective inhibition of cytokinesis in sea urchin embryos by low concentrations of stypoldione, a marine natural product that reacts with sulfhydryl groups. *Mol Pharm* 35:635–642
141. Depix MS, Martínez J, Santivañez F et al (1998) The compound 14-keto-stypodiol diacetate from the algae *Stypopodium flabelliforme* inhibits microtubules and cell proliferation in DU-145 human prostatic cells. *Mol Cell Biochem* 187:191–199
142. Simon-Levert A, Arrault A, Bontemps-Subielos N et al (2005) Meroterpenes from the ascidian *Aplidium aff. densum*. *J Nat Prod* 68:1412–1415
143. Simon-Levert A, Aze A, Bontemps-Subielos N et al (2007) Antimitotic activity of methoxyconidiol, a meroterpene isolated from an ascidian. *Chem Biol Interact* 168:106–116
144. Gunasekera SP, Gunasekera M, Longley RE (1990) Discodermolide: a new bioactive polyhydroxylated lactone from the marine sponge *Discodermia dissoluta*. *J Org Chem* 55: 4912–4915; *ibid* (1991) 56: 1346
145. Nerenberg JB, Hung DT, Somers PK et al (1993) Total synthesis of the immunosuppressive agent (–) discodermolide. *J Am Chem Soc* 115:12621–12622
146. Hung DT, Nerenberg JB, Schreiber SL (1994) Distinct binding and cellular properties of synthetic (+)- and (–)-discodermolides. *Chem Biol* 1:67–71
147. Gunasekera SP, Paul GK, Longley RE et al (2002) Five new discodermolide analogues from the marine sponge *Discodermia* species. *J Nat Prod* 65:1643–1648
148. ter Harr E, Kowalski RJ, Hamel E et al (1996) Discodermolide, a cytotoxic marine agent that stabilizes microtubules more potently than taxol. *Biochemistry* 35:243–250
149. Kowalski RJ, Giannakakou P, Gunasekera SP et al (1997) The microtubule-stabilizing agent discodermolide competitively inhibits the binding of paclitaxel (Taxol) to tubulin polymers, enhances tubulin nucleation reactions more potently than paclitaxel, and inhibits the growth of paclitaxel-resistant cells. *Mol Pharmacol* 52:613–622
150. Mickel SJ, Niederer D, Daeffler R et al (2004) Large scale synthesis of the anti-cancer marine natural product (+)-discodermolide. Part 5: linkage of fragments C₁₋₆ and C₇₋₂₄ and finale. *Org Proc Res Dev* 8:122–130
151. Mita A, Lockhart AC, Chen T-L et al (2004) A phase I pharmacokinetic (PK) trial of XAA296A (discodermolide) administered every 3 wks to adult patients with advanced solid malignancies. *J Clin Oncol* 22(14S):2025
152. Fan Y, Schreiber EM, Day BW (2009) Human liver microsomal metabolism of (+)-discodermolide. *J Nat Prod* 72:1748–1754

153. Shaw SS (2008) The structure activity relationship of discodermolide analogues. *Mini Rev Med Chem* 8:276–284
154. West LM, Northcote PT, Battershill CN (2000) Peloruside A: a potent cytotoxic macrolide isolated from the New Zealand marine sponge *Mycale* sp. *J Org Chem* 65:445–449
155. Liao X, Wu Y, De Brabander JK (2003) Total synthesis and absolute configuration of the novel microtubule-stabilizing agent peloruside A. *Angew Chem Int Ed* 42:1648–1652
156. Hood KA, West LM, Rouwé B et al (2002) Peloruside A, a novel antimitotic agent with paclitaxel-like microtubule-stabilizing activity. *Cancer Res* 62:3356–3360
157. Gaitanos TN, Buey RM, Díaz RM et al (2004) Peloruside A does not bind to the taxoid site on β -tubulin and retains its activity in multidrug-resistant cell lines. *Cancer Res* 64:5063–5067
158. Hamel E, Day BW, Miller JH et al (2006) Synergistic effects of peloruside and laulimalide with taxoid site drugs, but not each other, on tubulin assembly. *Mol Pharmacol* 70:1555–1564
159. Wilmes A, Bargh K, Kelly C et al (2007) Peloruside A synergizes with other microtubule stabilizing agents in cultured cancer cell lines. *Mol Pharm* 4:269–280
160. Page MJ, Northcote PT, Webb VL et al (2005) Aquaculture trials for the production of biologically active metabolites in the New Zealand sponge *Mycale hentscheli* (Demospongiae: Poecilosclerida). *Aquaculture* 250:256–269
161. Evans DA, Welch DS, Speed AWH et al (2009) An aldol-based synthesis of (+)-pleoruside A, a potent microtubule-stabilizing agent. *J Am Chem Soc* 131:3840–3841
162. Quinòa E, Kakou Y, Crews P (1988) Fijianolides, polyketide heterocycles from a marine sponge. *J Org Chem* 53:3642–3644
163. Corley DG, Herb R, Moore RE et al (1988) Laulimalides: new potent cytotoxic macrolides from a marine sponge and a nudibranch predator. *J Org Chem* 53:3644–3646
164. Sanders ML, van Soest RWM (1996) A raised classification of *Spongia mycofijiensis*. *Biologie* 66:117–122, Suppl
165. Jefford CW, Bernardinelli G, Tanaka J et al (1996) Structures and absolute configurations of the marine toxins, latrunculin A and laulimalide. *Tetrahedron Lett* 37:159–162
166. Tanaka J, Higa T, Bernardinelli G et al (1996) New cytotoxic macrolides from the sponge *Fasciospongia rimosa*. *Chem Lett* 25:255–256
167. Mooberry SL, Tuen G, Hernandez AH et al (1999) Laulimalide and isolaulimalide, new paclitaxel-like microtubule-stabilizing agents. *Cancer Res* 59:653–660
168. Pryor DE, O’Brate AO, Bilcer G et al (2002) The microtubule stabilizing agent laulimalide does not bind to the taxoid site, kills cells resistant to paclitaxel and epothilones, and may not require its epoxide moiety for activity. *Biochemistry* 41:9109–9115
169. Gapud EJ, Bai R, Ghosh AK et al (2004) Laulimalide and paclitaxel: comparison of their effects on tubulin assembly and their synergistic action when present simultaneously. *Mol Pharmacol* 66:113–121
170. Jphnson TA, Tenney K, Cichewicz RH et al (2007) Sponge-derived fijianolide class: further evaluation of their structural and cytotoxic properties. *J Med Chem* 50:3795–3803
171. Ghosh AK, Wang Y (2000) Total synthesis of (–) laulimalide. *J Am Chem Soc* 122:11027–11028
172. Paterson I, CeSavi C, Tudge M (2001) Total synthesis of the microtubule-stabilizing agent (–)-laulimalide. *Org Lett* 3:3149–3152
173. Liu J, Towle MJ, Cheng H et al (2007) In vitro and in vivo anticancer activities of synthetic (–)-laulimalide, a marine natural product microtubule stabilizing agent. *Anticancer Res* 27:1509–1518
174. Pettit GR, Cichacz ZA, Gao F et al (1994) Isolation and structure of the cancer cell growth inhibitor dictyostatin 1. *J Chem Soc Chem Commun* 9:1111–1112
175. Isbrucker RA, Cummins J, Pomponi SA et al (2003) Tubulin polymerizing activity of dictyostatin-1, a polyketide of marine origin. *Biochem Pharmacol* 66:75–82

176. Paterson I, Britton R, Delgado O et al (2004) Stereochemical determination of dictyostatin, a novel microtubule-stabilizing macrolide from the marine sponge *Corallistidae* sp. *Chem Commun* 6:632–633
177. Paterson I, Britton R, Delgado O et al (2004) Total synthesis and configurational assignment of (–)-dictyostatin, a microtubule-stabilizing macrolide of marine sponge origin. *Angew Chem Int Ed* 43:4629–4633
178. Madiraju C, Edler MC, Hamel E et al (2005) Tubulin assembly, taxoid site binding, and cellular effects of the microtubule-stabilizing agent dictyostatin. *Biochemistry* 44: 15053–15063
179. Tanaka J, Higa T (1996) Zampanolide, a new cytotoxic macrolide from a marine sponge. *Tetrahedron Lett* 37:5535–5538
180. Smith AB, Safonov IG, Corbett RM (2001) Total synthesis of (+)-zampanolide. *J Am Chem Soc* 123:12426–12427
181. Field JJ, Singh AJ, Kanakkanthara A et al (2009) Microtubule-stabilizing activity of zampanolide, a potent macrolide isolated from the Tongan marine sponge *Cacospongia mycofijiensis*. *J Med Chem* 52:7328–7332
182. Manzo E, van Soest R, Matainaho L et al (2003) Certamines A and B, antimitoic heterocyclic alkaloids isolated from the marine sponge *Pseudoceratina* sp. collected in Papua New Guinea. *Org Lett* 5:4591–4594
183. Nodwell M, Riffell JL, Roberge M et al (2008) Synthesis of antimitoic analogs of the microtubule stabilizing sponge alkaloid ceratamine A. *Org Lett* 10:1051–1054
184. Nodwell M, Pereira A, Riffell JL et al (2009) Synthetic approaches to the microtubule-stabilizing sponge alkaloid ceratamine A and desbromo analogues. *J Org Chem* 74:995–1006
185. Coleman RS, Campbell EL, Carper DJ (2009) A direct and efficient total synthesis of the tubulin-binding agents ceratamine A and B; use of IBX for a remarkable heterocyclic dehydrogenation. *Org Lett* 11:2133–2136
186. Karjala G, Chan Q, Manzo E et al (2005) Ceratamines, structurally simple microtubule-stabilizing antimitotic agents with unusual cellular effects. *Cancer Res* 65:3040–3043
187. Williams DE, Sturgeon CM, Roberge M et al (2007) Nigricanosides A and B, antimitoic glycolipids isolated from the green alga *Avrainvillea nigricans* collected in Dominica. *J Am Chem Soc* 129:5822–5823
188. Espindola APDM, Crouch R, DeBergh JR et al (2009) Deconvolution of complex NMR spectra in small molecules by multi frequency homonuclear decoupling (MDEC). *J Am Chem Soc* 131:15994–15995
189. Lindel T, Jensen PR, Fenical W et al (1997) Eleutherobin, a new cytotoxin that mimics paclitaxel (Taxol) by stabilizing microtubules. *J Am Chem Soc* 119:8744–8745
190. D'Ambrosio M, Guerriero A, Pietra F (1987) Sarcodictyin A and sarcodictyin B, novel diterpenoidic alcohols esterified by (E)-N(1)-methylurocanic acid. Isolation from the Mediterranean stolonifer *Sarcodictyon roseum*. *Helv Chim Acta* 70:2019–2027
191. D'Ambrosio M, Guerriero A, Pietra F (1988) Isolation from the Mediterranean stoloniferan coral *Sarcodictyon roseum* of sarcodictyin C, D, E, and F, novel diterpenoidic alcohols esterified by (E)- or (Z)-N(1)-methylurocanic acid. Failure of the carbon-skeleton type as a classification criterion. *Helv Chim Acta* 71:964–976
192. Ketzinel S, Rudi A, Schleyer M et al (1996) Sarcodictyin A and two novel diterpenoid glycosides, Eleuthosides A and B, from the soft coral *Eleutherobia aurea*. *J Nat Prod* 59:873–875
193. Cinel B, Roberge M, Behrisch H et al (2000) Antimitotic diterpenes from *Erythropodium caribaeorum* test pharmacophore models for microtubule stabilization. *Org Lett* 2:257–260
194. Britton R, Roberge M, Berisch H et al (2001) Antimitotic diterpenoids from *erythropodium caribaeorum*: isolation artifacts and putative biosynthetic intermediates. *Tetrahedron Lett* 42:2953–2956
195. Taglialatela-Scafati O, DeoJangra U, Campbell M et al (2002) Diterpenoids from cultured *Erythropodium caribaeorum*. *Org Lett* 4:4085–4088

196. Cinel B, Patrick BO, Roberge M et al (2000) Solid-state and solution conformations of eleutherobin obtained from X-ray diffraction analysis and solution NOE data. *Tetrahedron Lett* 41:2811–2815
197. Britton R, de Silva ED, Bigg CM et al (2001) Synthetic transformations of eleutherobin reveal new features of its microtubule-stabilizing pharmacophore. *J Am Chem Soc* 123:8632–8633
198. Nicolaou KC, Xu JY, Kim S et al (1997) Synthesis of the tricyclic core of eleutherobin and sarcodictyins and total synthesis of sarcodictyin A. *J Am Chem Soc* 119:11353–11354
199. Nicolaou KC, van Delft F, Ohshima T et al (1997) Total synthesis of eleutherobin. *Angew Chem Int Ed* 36:2520–2524
200. Nicolaou KC, Pfefferkorn J, Xu J et al (1999) Total synthesis and chemical biology of the sarcodictyins. *Chem Pharm Bull* 47:1199–1213
201. Chen XT, Zhou B, Bhattacharya SK et al (1998) The total synthesis of eleutherobin: a surprise ending. *Angew Chem Int Ed* 37:789–792
202. Ojima I, Chakravarty S, Inoue T et al (1999) A common pharmacophore for cytotoxic natural products that stabilize microtubules. *Proc Natl Acad Sci* 96:4256–4261
203. Long BH, Carboni JM, Wasserman AJ et al (1998) Eleutherobin, a novel cytotoxic agent that induces tubulin polymerization, is similar to paclitaxel. *Cancer Res* 58:1111–1115
204. Hamel E, Sackett DL, Vourloumis D et al (1999) The coral-derived natural products eleutherobin and sarcodictyins A and B: effects on the assembly of purified tubulin with and without microtubule-associated proteins and binding to the taxoid polymer site. *Biochemistry* 38:5490–5498
205. Doolittle RF (1992) Reconstructing history with amino acid sequences. *Protein Sci* 1:191–200
206. Li JY, Wu CF (2005) New symbiotic hypothesis on the origin of eukaryotic flagella. *Naturwiss* 92:305–309

Ernesto Fattorusso and Orazio Taglialatela-Scafati

Contents

21.1	Introduction	1076
21.2	Malaria	1078
21.2.1	Clinical Symptoms and Social Impact	1078
21.2.2	Endoperoxides	1081
21.2.3	Isonitrile-Containing Compounds	1087
21.2.4	Alkaloids and Peptides	1089
21.2.5	Quinones and Other Antimalarial Compounds	1092
21.3	Leishmania	1094
21.3.1	Clinical Symptoms and Social Impact	1094
21.3.2	Alkaloids and Peptides	1096
21.3.3	Terpenoids	1097
21.3.4	Endoperoxides	1099
21.4	Trypanosoma	1100
21.4.1	Clinical Symptoms and Social Impact	1100
21.4.2	Marine Antitrypanosomal Agents	1101
21.5	Concluding Remarks	1103
21.6	Study Questions	1104
	References	1105

Abstract

Protozoa are the causative agents of human diseases which affect more than one billion people and cause more than one million deaths per year, with a particular incidence in developing countries. The major contribution to these dramatic numbers is given by malaria, followed by leishmaniasis and trypanosomiasis (African trypanosomiasis and Chagas' disease).

E. Fattorusso (✉) • O. Taglialatela-Scafati (✉)
Dipartimento di Chimica delle Sostanze Naturali, Università di Napoli Federico II,
Via Montesano 49, Naples, Italy
e-mail: fattoru@unina.it, scatagli@unina.it

In this chapter we have provided an overview of the most significant contributions given by marine natural product chemistry to the field of antiprotozoan drug research. We have selected more than 70 marine secondary metabolites belonging to different chemical classes, which are active (commonly only in vitro data are available) against one or more protozoan strains. When available, details on structure–activity relationship studies and investigation of the mechanisms of action have been provided.

21.1 Introduction

Protozoa is a large family (including over 30,000 different genera) of microorganisms classified as unicellular eukaryotes. Protozoa were previously grouped in the kingdom of Protista, together with the plant-like algae and fungus-like slime molds, and frequently protozoa are referred to be the link between plants and animals. Protozoa usually range from 10 to 50 micron, but they can grow up to 1 mm and can be easily identified using a microscope. Protozoa have traditionally been divided on the basis of their means of locomotion into flagellates, amoeboids, sporozoans, and ciliates.

Protozoa exist throughout aqueous environments and soil, and they prey upon unicellular or filamentous algae, bacteria, and microfungi, and, therefore, they are believed to play a vital role in controlling bacterial populations and biomasses. All protozoa digest their food in stomach-like compartments called vacuoles. As components of the micro- and meiofauna, protozoa are an important food source for microinvertebrates. Thus, the ecological role of protozoa in the transfer of bacterial and algal production to successive trophic levels is important. Some protozoa have life stages alternating between proliferative stages (e.g., trophozoites) and dormant cysts. As cysts, protozoa can survive harsh conditions, such as exposure to extreme temperatures and harmful chemicals, or long periods without access to nutrients. The cyst form enables parasitic species to survive outside of the host, and allows their transmission from one host to another. When protozoa are in the form of trophozoites, they actively feed and grow.

Single-celled protozoal parasites are the causative agents of diseases which affect more than one billion people per year with a particular incidence in tropical countries. The major contribution to these dramatic numbers is given by malaria, caused by protozoans belonging to the genus *Plasmodium*, with *P. falciparum* being responsible for most severe forms of the disease and most fatal cases. The improvement of hygienic conditions, the massive use of insecticides, and the discovery of different drugs played a great role in the nearly complete extinction of malaria in developed countries. Unfortunately, malaria is still a common cause of death (approximately one million per year) in the tropical countries of Africa, Asia, and America, and most of the victims are children under the age of five: every 30 s a child dies of malaria [1]. The increase in the number of fatal cases registered in recent years is principally due to the spread of mosquitoes (vectors of *Plasmodium*

into humans) resistant to common insecticides and, more importantly, the emergence of multidrug-resistant strains of *Plasmodium*. The latter problem makes many of the available drugs useless, leaving some efficacy only to the artemisinin-based therapies.

The mortality of the remaining protozoal diseases is much less marked (nearly 100,000 deaths per year), but their morbidity is also extremely high, severely affecting the quality of life of the infected people. African trypanosomiasis (sleeping sickness) is caused by *Trypanosoma brucei* species, which invade the central nervous system, leading to behavioral changes, coma, and, if untreated, death [2]. Chagas' disease is caused by *T. cruzi* and transmitted by a blood-sucking insect (triatome), which bites the victim and contaminates the wound with infected feces. The disease, which is also known as South American trypanosomiasis, is one of the major health problems in Latin America. Leishmaniasis is caused by over twenty species of intracellular parasites belonging to the genus *Leishmania*, which are transmitted to humans by sand flies. This disease can give different clinical symptoms including cutaneous, mucosal, and visceral forms [3]. Both the cutaneous and mucosal forms can cause severe deformities to patients, including ulcerative skin lesions and the destruction of mucous membranes, in some cases leading to permanent disfigurement. The visceral form of the disease, caused principally by *L. donovani*, *L. infantum*, and *L. chagasi*, represents the greatest threat to human health, with symptoms ranging from fever and weight loss to hepatosplenomegaly, leading to death in untreated cases [4].

Other protozoa, causing less-dramatic human diseases, are *Toxoplasma gondii*, *Giardia lamblia*, and *Entamoeba histolytica*. *Toxoplasma gondii* infects most genera of warm-blooded animals, including humans, but the primary hosts are cats (more precisely, the felid family). Contact with raw meat or with feces of infected cats is the more significant source of human infections in many countries. During the first few weeks, the infection typically causes a mild flu-like illness with muscle ache, but, in healthy adults, there is no other following symptom. However, people with a weakened immune system, such as those infected with advanced HIV disease, those who have recently received an organ transplant, or those who are pregnant, may become seriously ill, and it can occasionally be fatal. The parasite can cause encephalitis and can affect the heart, liver, and eyes.

Giardia lamblia is a flagellated protozoan parasite that colonizes and reproduces in the small intestine, causing giardiasis, an affection which does not spread via the bloodstream and remains confined to the lumen of the small intestine. *Giardia* infection can occur through ingestion of dormant cysts in contaminated water, food, or by the fecal–oral route. Symptoms of infection include diarrhea, steatorrhea, epigastric pain, nausea, diminished interest in food, and vomiting, and the infection can be particularly severe and prolonged in patients who are immunocompromised, or who have decreased gastric acid secretion. Finally, *Entamoeba histolytica* is an anaerobic parasitic protozoan whose infection can lead to amoebic dysentery or amoebic liver abscess. Symptoms can include fulminating dysentery, bloody diarrhea, weight loss, abdominal pain, and amoeboma. The amoeba can

actually “bore” into the intestinal wall, causing lesions and intestinal symptoms, and it may reach the blood stream. From there, it can reach different vital organs of the human body, usually the liver, but sometimes the lungs, brain, spleen, etc. A common outcome of this invasion of tissues is a liver abscess, which can be fatal if untreated.

The chemotherapeutic options to control and treat these protozoal infections are dramatically limited to few classes of sometimes old drugs which, in many cases, are associated with severe toxicity and variable efficacy. In some cases (as for giardiasis and leishmaniasis), antibiotics are very effective, but in many cases, the costs of treatments are unaffordable (e.g., amphotericin B for treatment of leishmaniasis). These considerations, together with the emerging resistance against many drug classes, make discovery and development of new, safe, and effective antiprotozoan agents a pressing need.

In this chapter we will describe the contribution given by marine chemistry to the field of antiprotozoan drug research. Marine organisms constitute a universally recognized source of potentially bioactive molecules which have been enzymatically engineered and biologically validated. In particular, marine invertebrates are producers of a number of potent antibiotic agents and intense research efforts have been devoted in recent years to the discovery of potential antiprotozoan lead compounds. Following the lines of the most pressing needs and of the most significant research efforts, we have decided to focus our attention on three protozoan pathologies, namely, malaria, leishmaniasis, and trypanosomiasis. We will provide a picture of the most significant leads found in marine organisms against these diseases, describing them in separate paragraphs, although some of these leads are active against two or more different diseases. A number of periodic reviews of the literature can be consulted to gain updated information about the activity of marine compounds against protozoa [5]. Moreover, some detailed reviews focused on the most promising classes of marine antimalarial lead compounds [6] are present in the literature.

21.2 Malaria

21.2.1 Clinical Symptoms and Social Impact

Malaria is an infectious disease caused by *Plasmodium falciparum* and by several other protozoans belonging to the genus *Plasmodium*. The protozoan comes in contact with humans through the vector contribution of female *Anopheles* mosquitoes. Within 30 min after injection into the blood stream, the parasite (in the sporozoites form) infects hepatocytes, multiplying asexually and asymptotically for a period of 6–15 days. When the protozoans reach the merozoite stage, they are released from the liver and invade the erythrocytes, starting to feed on the hemoglobin. After proliferation, the rupture of the erythrocyte membrane and the consequent liberation of other merozoites that invade other erythrocytes cause

the massive infection and the symptoms. A small portion of merozoites develops into the sexual stage of gametocytes, a form that is able to restart the life cycle of the malaria parasite when a mosquito takes a blood meal from an infected person [7].

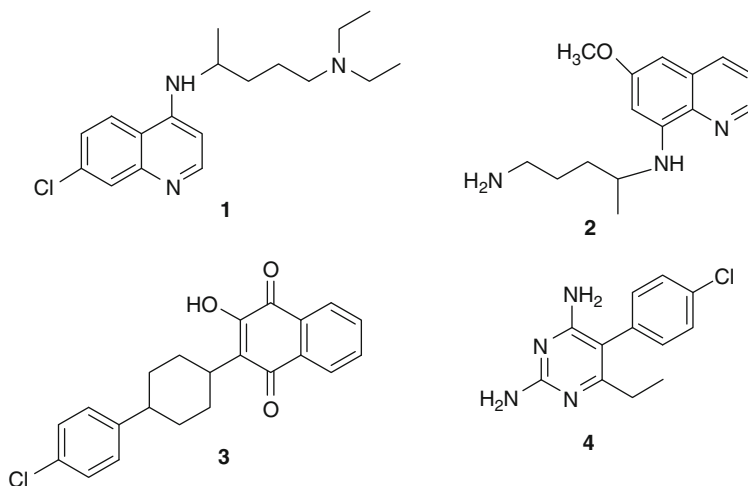
The clinical symptoms of malaria infections are almost exclusively attributable to parasites in the erythrocytic stage. The rupture of infected erythrocytes is associated with the release into the blood stream of cell debris responsible for the characteristic fever spike patterns by the induction of interleukin-1 and tumor necrosis factor. In the lethal cases, a specific protein produced by the protozoan is embedded into the cell membrane of the infected erythrocyte, and, as a consequence of this modification, the erythrocyte sticks to the walls of capillaries causing obstruction of vessels. When this mechanism operates at the level of brain vessels, the loss of consciousness is the first symptom, but if this form of cerebral malaria is not treated immediately, it is soon followed by death.

It is now widely accepted that the optimal strategy to combat against malaria infections should necessarily be multilateral and combine different approaches based both on prevention (mosquito nets, insect repellents, vaccines, prophylaxis) and treatment of infections (drugs). Both the number of different strains causing the pathology and their tendency to genetic mutations posed great obstacles to the development of the vaccine strategy. At the moment, RTS,S is heading phase III trials, and it appears to be the most promising malaria vaccine candidate [8]. This vaccine candidate is a recombinant protein that fuses a part of the *P. falciparum* sporozoite protein with the hepatitis B surface antigen molecule. Combined with a proprietary GSK adjuvant system, RTS,S induces the production of antibodies as well as of white blood cells that are believed to diminish the capacity of the malaria parasite to infect, survive, and develop in the human liver. In addition to inducing partial protection against malaria, the RTS,S vaccine candidate stimulates a protective immune response to hepatitis B, a common infection in developing countries.

The drug treatment of malaria infections holds an important place in the history of medicinal chemistry and of natural product chemistry. Indeed, the first specific treatment for malaria dates back to the seventeenth century when the bark of cinchona trees was used to face infections of malaria that was endemic not only in Africa and Asia but also in several parts of Europe and North America. Later, malaria was the first disease to be treated with an active principle isolated from a natural source, quinine, isolated from the cinchona bark in 1820, and, later again, the first human disease to be treated with a synthetic drug (methylene blue in 1891).

In the course of twentieth century, especially during World War II, a series of effective synthetic antimalarial drugs have been developed. Unfortunately, the available chemical weapons to treat malaria cases are largely based on these old molecules, as 4-aminoquinolines (e.g., chloroquine, **1**), 8-aminoquinolines (e.g., primaquine, **2**), naphthoquinones (e.g., atovaquone, **3**), or dihydrofolate reductase inhibitors (e.g., pyrimethamine, **4**). These molecules largely contributed to the

nearly complete eradication of malaria in developed countries; currently, their association with artemisinin analogues represents the most advanced malaria treatment.



Although the above remedies can give some good results, the therapeutic choices are evidently too limited. Indeed, in our days malaria still continues to be an extremely important threat to the health and economic prosperity of the human race, constituting a major cause of morbidity and mortality in tropical countries of Asia, Africa, and South America. The reality is probably worse than that commonly conceived: about 40% of the world population lives in countries where the disease is endemic; a recent analysis estimates between 700,000 and 2.0 million deaths each year from malaria (over 75% of them are African children) and between 400 and 900 million acute febrile episodes per year in African children under the age of 5 living in malaria-endemic regions where there is limited or inadequate access to formal healthcare [9]. In the eastern and southern African regions, an estimated 30% of all recorded deaths during pregnancy are attributed to malaria infection. Part of the reason for the failure to control malaria in these areas is the emergence and spread of resistance to first-line antimalarial drugs, cross-resistance between the members of the limited number of drug families available, and in some areas, multidrug resistance [10]. It has been estimated that in the last 30 years only four to five new drugs have been registered against malaria. This picture dramatically illustrates the unquestionable evidence that efforts of pharmaceutical companies are obviously not proportional to the number of deaths for a pathology but principally to the potential market of the developed drugs. Not surprisingly, funds invested in the malaria research by academic and nonprofit agencies (e.g., EU, MMV, and Gates foundation) overcome those invested by pharmaceutical companies.

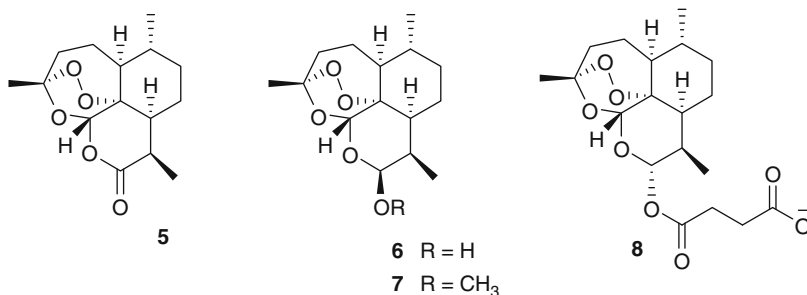
On the other hand, the sequencing of the entire genome of both the malarial parasite and its insect vector disclosed a number of potential pharmaceutical targets

to prevent and/or treat the disease [11]. Therefore, the pharmacological therapy will likely remain also in the near future an important strategy in the fight against malaria. However, it is now recognized that the next significant advancement in the field of antimalarial drugs will not be obtained through the discovery of a single potent compound but through the introduction of an innovative drug to be used in a combined therapy, preferably composed by molecules acting at different stages of the malaria parasite life cycle. For example, studies conducted with the rodent model *P. chabaudi* revealed that the stress conditions imposed by drug treatment determine an increase in the gametocyte production, and gametocytes have been shown to have a much longer lifespan than the asexual stages. These observations are important from a public health point of view, as they imply that the use of an antimalarial drug, although beneficial at the individual level, might be detrimental for the community, leading to an increase of malaria transmission, or, at least, guaranteeing the transmission of the parasites. The rationale for designing antimalarial combinations acting also on gametocytes and on sporogonic stages developing in the vector derives from these considerations.

In the following paragraphs, we will highlight the contribution of marine chemistry to the field of antimalarial research, with particular emphasis on recent discoveries. Marine antimalarials are divided into four different classes basing on their chemical structures: (1) endoperoxides, (2) isonitrile-containing derivatives, (3) alkaloids, and (4) quinones and other compounds.

21.2.2 Endoperoxides

The development of antimalarial endoperoxide-containing drugs started with the discovery of the potent activity exhibited by artemisinin (**5**), a low-nanomolar antimalarial active also against chloroquine-resistant strains of *Plasmodium* [12] and acting in the early form of the malarial blood stages. Artemisinin is a cadinane sesquiterpene lactone embedding a 1,2,4-trioxane moiety, isolated from leaves of the sweet wormwood, *Artemisia annua* (Compositae). In spite of the presence of adjacent peracetal, acetal, and lactone functionalities, artemisinin is a stable and easily crystallizable compound.



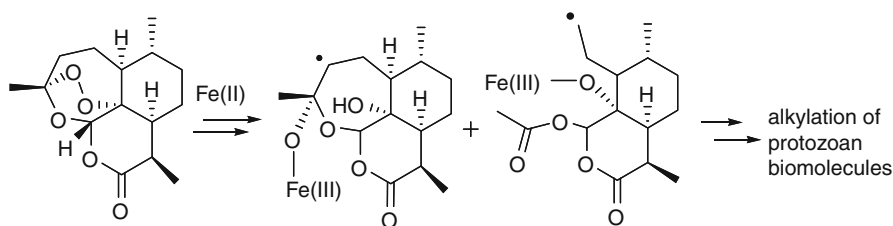


Fig. 21.1 The C-centered radical species postulated for the antimalarial activity of artemisinin

A number of semisynthetic artemisinin derivatives have been prepared, as dihydroartemisinin (**6**), the oil-soluble artemether (**7**), and the water-soluble artesunate (**8**). Although a total synthesis of artemisinin has also been reported [13], it is not a sustainable supply of this drug.

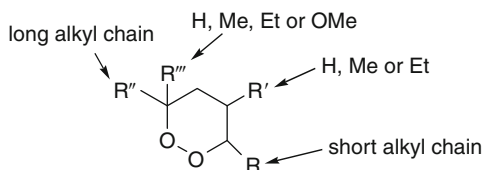
The endoperoxide linkage is essential for the antimalarial activity of artemisinin and of its derivatives, as proved by the inactivity of deoxyartemisinin, an artemisinin derivative lacking the endoperoxide bridge. The most widely accepted hypothesis on the mechanism of action of artemisinins postulates that the endoperoxide bond of these molecules, interacting with the iron(II) center of the heme unit, released in the food vacuole during the digestion of hemoglobin, gives rise to oxygen-centered radicals. As a result of an intramolecular rearrangement, these reactive species are converted into free C-centered radicals, toxic to the parasite through alkylation of macromolecular targets (Fig. 21.1). Most likely, artemisinin activity is not mediated by interaction with a single enzyme, also in the light of the scarce tendency of this compound (and its analogues) to develop resistance. It has been proposed that the Fe(II)-containing species interacting with the endoperoxide bond is not heme [14]; however, this hypothesis does not change the general lines of the delineated mechanism of action.

Endoperoxide-containing compounds of marine origin constitute a rather large group of secondary metabolites, some of which exhibit a quite potent *in vitro* antimalarial activity. In some cases, a number of semisynthetic or totally synthetic derivatives have been prepared. Unfortunately, only few of the isolated endoperoxide marine metabolites have been tested for their antimalarial activity, and, therefore, data available could have been even more rich and informative.

Commonly, these molecules possess a simple six-membered 1,2-dioxxygenated ring (1,2-dioxane) bearing two or three alkyl/aryl groups of different length and complexity (Fig. 21.2). A small number of molecules show some variations on this general structure: (1) 1,2-dioxolanes, (2) molecules showing a double bond between the two nonoxygenated carbons of the ring, and (3) molecules showing an additional ring fused to the dioxane ring.

An important feature of these compounds is the nature of the substituent R''' . Indeed, molecules linking H, methyl, and ethyl groups at that position are simple 1,2-dioxanes, while molecules linking a methoxy group are peroxyketal

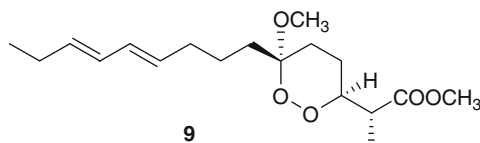
Fig. 21.2 General structure of dioxane antimalarials of marine origin



derivatives. In this chapter, marine endoperoxides have been divided in two categories according to this structural feature.

21.2.2.1 Peroxyketal Endoperoxides

The parent compounds in the class of 3-alkoxy-1,2-dioxane (peroxyketals) derivatives are peroxyplakoric acids and their methyl esters (e.g., peroxyplakoric acid B3 **9**), isolated from *Plakortis* sp. [15].



These marine derivatives showed a potent *in vitro* activity ($IC_{50} = 50$ ng/mL against *P. falciparum*) with a good selective toxicity index (about 200). The simple structures of these compounds made possible the total syntheses of the natural molecules and of several analogues [16]. A number of evidence pointed to the critical importance of the “long” alkyl side chain for the antimalarial activity within this class. For example, a synthetic analogue showing a methyl group in place of the nonadienyl group was almost completely devoid of activity, while a pentyl group proved to be well compatible with the antimalarial activity, retaining the *in vitro* potency of the natural analogues. When these compounds were examined *in vivo* against *P. berghei* infection, they showed little antimalarial potency because of the relative instability in mouse serum. This undesired finding was demonstrated to be due to the hydrolysis of the ester function to the much less active carboxylic acid derivative. In order to enhance the stability in physiological media, a number of semisynthetic analogues were prepared; the monoethyl amide analogues proved to be stable to hydrolysis in the serum and showed a good *in vivo* activity [17].

The reaction of peroxyplakoric ester analogues with Fe(II) species was explored to mimic the interaction with heme and gain further information on the structural requirements for the biological activity [18]. Analysis of the products obtained upon this reaction suggested the formulation of the mechanism of action illustrated in Fig. 21.3. Similarly to artemisinin, the peroxyketal derivative is believed to interact with the Fe(II) center of the heme residue with consequent homolytic cleavage of the O–O bond. In this case, the O-centered radical should be almost exclusively located at the oxygen attached to the methoxy-linking carbon. This

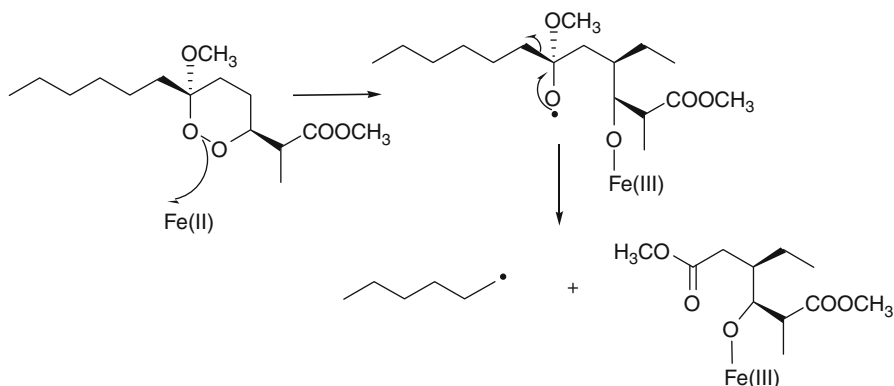
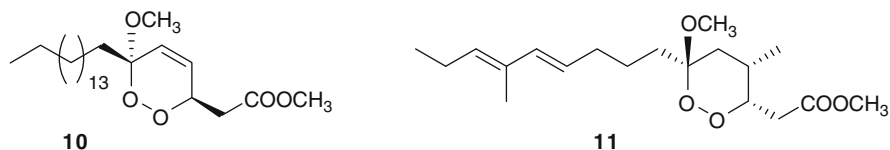


Fig. 21.3 The postulated mechanism of action of peroxyplakoric derivatives

radical would evolve through a regiospecific carbon–carbon cleavage producing a neutral methyl ester species and a very reactive primary carbon radical which should be the toxic species responsible for the death of the parasite. Although this model has the merit of providing a rationale for the observed importance of the alkyl side chain, it should also be noted that some synthetic compounds, potentially producing reactive carbon radicals, failed to show a significant activity.

The low antimalarial activity observed for chondrillin (**10**) [19], a marine endoperoxide strictly related to peroxyplakoric derivatives, indicated that the presence of a double bond within the 3-methoxy-1,2-dioxane skeleton is detrimental for the activity. However, a negative pharmacokinetic role played by the long C₁₆ saturated alkyl chain cannot be excluded.

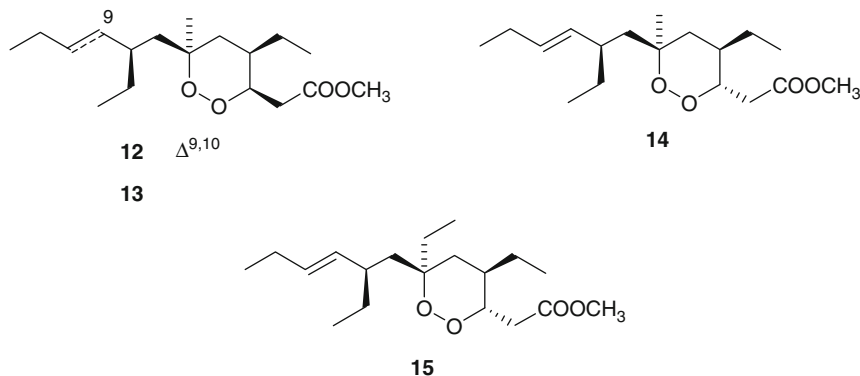


An Indonesian specimen of *Plakortis* sp. afforded some endoperoxide peroxyketals, named manadoperoxides (e.g., manadoperoxide B **11**) [20], whose structures are strictly reminiscent of those of peroxyplakoric derivatives (see **9**). They differ almost exclusively for the position of a methyl group, which is moved from the short alkyl chain to the dioxane ring. This corresponds to a difference in the last two steps of the hypothesized polyketide biogenesis: for peroxyplakoric derivatives the last two units are, most likely, acetate–propionate, while in the case of manadoperoxides, the sequence of the last two incorporated units should be reversed, i.e., propionate–acetate. Surprisingly, this minor structural change caused a dramatic decrease in the antimalarial activity (IC₅₀ of **11** = 3.70 μM).

A computational study revealed that, in the populated conformations for manadoperoxides, the endoperoxide linkage is either not accessible to heme iron or it cannot evolve to produce a toxic C-centered radical. This result evidences that also minor structural changes can have a deep impact on the antimalarial activity, when they affect the conformational behavior of the molecule, and, consequently, its ability to interact with heme and produce the toxic C-centered radical, responsible for the final activity.

21.2.2.2 Nonperoxyketal Endoperoxides

The parent compound of this class of marine antimalarials is plakortin (**12**), a simple 1,2-dioxane metabolite with a likely butyrate-based polyketide biosynthetic origin. This molecule was isolated more than 30 years ago from *Plakortis halichondrioides*, as a mild antibacterial agent [21], but it was later reisolated in remarkable amounts from the Caribbean sponge *Plakortis simplex*, and the absolute configuration at the four stereogenic carbons of plakortin was determined [22]. A number of related endoperoxide derivatives were isolated from the same source. These include dihydroplakortin (**13**) [22], 3-epiplakortin (**14**) [23], and plakortide Q (**15**) [23].



These compounds exhibited a quite good antimalarial activity, and, similarly to artemisinin, they were more potent on the W2 strain ($IC_{50} \approx 0.3 \mu M$) and devoid of cytotoxicity [24]. To further investigate the structure–activity relationships in the plakortin series, a number of semisynthetic derivatives were prepared [25]. Among them, the plakortin diol, obtained upon reduction with Zn/AcOH of the endoperoxide bond, proved to be completely inactive, thus providing an unambiguous evidence of the crucial role of the endoperoxide bond for the antimalarial activity. A multidisciplinary investigation, based on molecular dynamics/mechanics, ab initio calculations, and chemical reactions, provided interesting insights into the mechanism of the antimalarial action of plakortin derivatives [26]. These molecules, after interaction of the endoperoxide bond with Fe(II), should

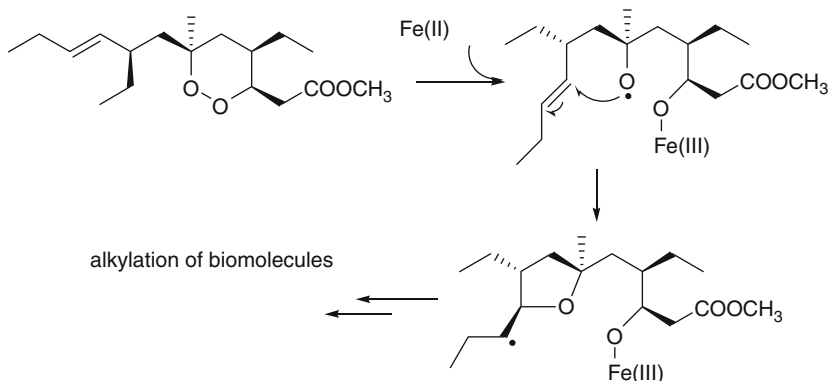
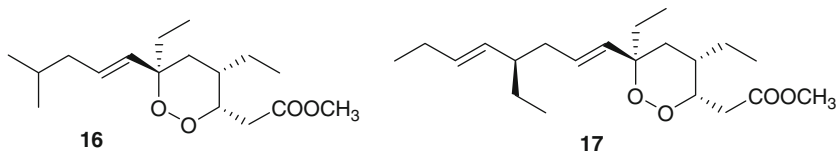


Fig. 21.4 The mechanism proposed for the antimalarial action of plakortin

give rise to the formation of an oxygen radical, followed by rearrangement to give a carbon radical centered on the “western” alkyl side chain, the toxic intermediates responsible for subsequent reactions leading to plasmodium death (Fig. 21.4). It is interesting to notice that in this case the cleavage mechanism, postulated for peroxyplakortin derivatives (see before), should not operate, being completely substituted by a rearrangement evolution of the oxygen radical.

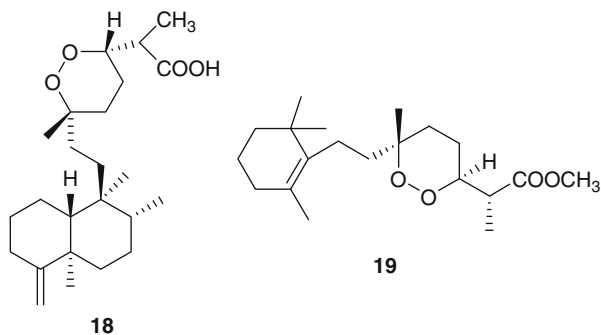
Following this mechanism, the very low *in vitro* antimalarial activity ($IC_{50} > 8 \mu\text{g/mL}$) of plakortides L (**16**) [27] and O (**17**) [28], in spite of their similarity with the plakortin scaffold, could be explained. Indeed, the side-chain double bond, directly attached at the dioxane ring, likely prevents the evolution of the oxygen radical to a side-chain carbon radical.



Strong evidence has been gathered about the plakortin production by the microbial population hosted by the sponge *Plakortis simplex* [29]. In the future, an approach based on identification, cloning, and expression of the gene cluster(s) for plakortin or related compounds, from the metagenome of the sponge, could allow the production of these molecules by low-cost bacterial fermentation, thus fulfilling one of the essential requirements for antimalarial drugs of the next generation.

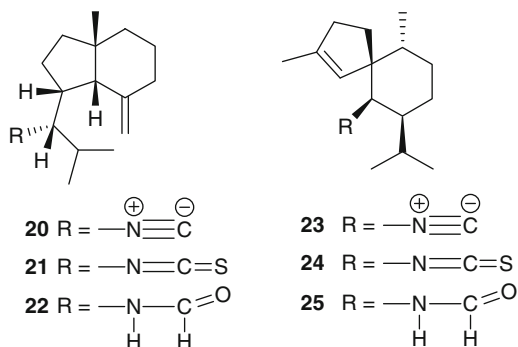
Compared to polyketide-based compounds, very few marine endoperoxide-containing terpenoids have been tested for their antimalarial activity, and none

of them showed an antimalarial activity comparable to that of molecules belonging to the plakortin family. Sigmosceptrellin A (**18**), a norsesterterpene derivative of spongal origin, showed a discrete activity against *P. falciparum* ($IC_{50} \approx 450$ ng/mL) [30], and, interestingly, its epimer, named sigmosceptrellin B, was four times less active [31]. Methyl-3-epinuapapuanate (**19**) is a norditerpene derivative isolated from the New Caledonian sponge *Diacarnus levii*, showing a moderate activity against chloroquine-resistant strains of *P. falciparum* [32].

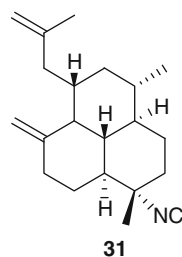
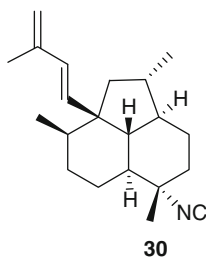
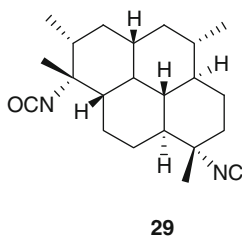
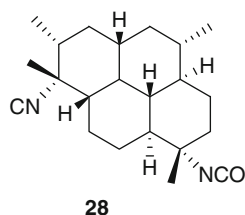
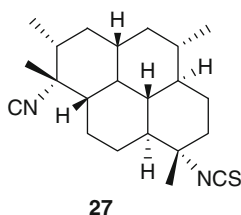
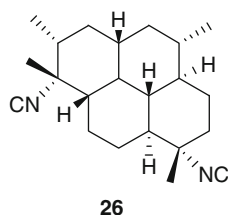


21.2.3 Isonitrile-Containing Compounds

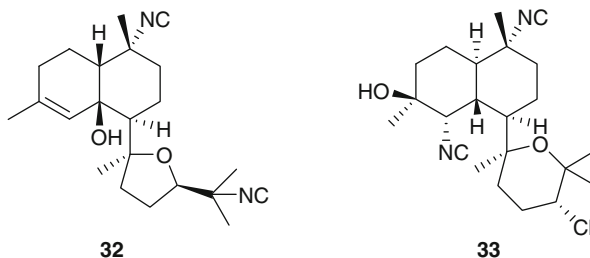
Isonitrile-containing terpenoids are typically marine secondary metabolites. The first isolated compound of this class is axisonitrile-1 (**20**), isolated in 1973 from the marine sponge *Axinella cannabina*, where it co-occurred with the strictly related axisothiocyante-1 (**21**) [33]. The same source successively proved to contain a number of related metabolites, as axamide-1 (**22**), [34] axisonitrile-3 (**23**), axisothiocyante-3 (**24**), and axamide-3 (**25**) [35].



More recently, axisonitrile-3 (**23**) has been reisolated from the sponge *Acanthella klethra* and found to possess a potent antimalarial activity both on chloroquine-sensitive (D6, 142 ng/mL) and chloroquine-resistant (W2, 17 ng/mL) *P. falciparum* strains [36]. The closely related axisothiocyanate-3 (**24**) was inactive, suggesting a crucial role for the isonitrile functional group. Following these remarkable findings, a number of isonitrile-containing secondary metabolites have been isolated from different marine sources, particularly marine sponges of the Axinellidae and Halicondridae families. The chemical analysis of *Cymbastela hooperi* (Axinellidae) afforded a series of diterpenes based on amphilectane, isocycloamphilectane, and neoamphilectane skeletons and bearing isonitrile, isothiocyante, and the rare isocyanate functionalities [37]. These molecules displayed a significant (low nM range) and selective in vitro antimalarial activity, and the co-occurrence of several strictly related analogues suggested some structure–activity relationships. Comparison among the activities exhibited by the closely related isocycloamphilectanes **26** (IC_{50} = about 4 ng/mL), **27** (IC_{50} = about 40 ng/mL), and **28** (IC_{50} = about 60 ng/mL) illustrated the relative potency of isonitrile, isothiocyante, and isocyanate groups, supporting the previous observation that the bioactivity is particularly associated to the presence of the isonitrile group. However, the location of functional groups also plays a role, as suggested by the comparison between the activities of compounds **28** and **29** (IC_{50} = about 3 ng/mL), where the positions of isocyanate and isonitrile groups are interchanged. Moreover, the activity of the neoamphilectane derivative **30** (IC_{50} on D6 = 90 ng/mL; on W2 = 30 ng/mL) is considerably higher than that of compound **31**, indicating that the carbon skeleton can modulate the antiplasmodial activity of isonitrile derivatives [38].



Kalihinols, further isonitrile-containing antimalarial derivatives, have been isolated from the Japanese sponge *Acanthella* sp. (e.g., **32–33**) [39]. These molecules, belonging to the class of the kalihinane diterpenoids, showed a potent antiplasmodial activity in the very low nanogram range [e.g., kalihinol A (**33**), $IC_{50} = 0.4$ ng/mL].



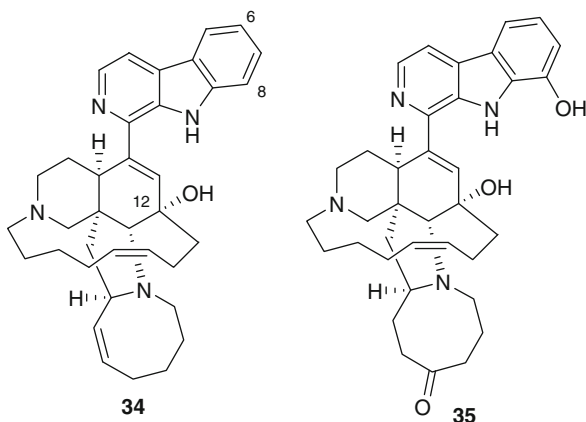
Isonitrile antimalarials have been proposed to interact with free heme by forming a coordination complex with the iron center, thus inhibiting the transformation of heme into β -hematin and then hemozoin, a polymer produced by *Plasmodium* in order to neutralize the toxic (detergent-like) free heme produced in the food vacuole. In addition, isonitriles were shown to prevent both the peroxidative and glutathione-mediated destruction of heme under conditions that mimic the environment within the malaria parasite [40]. The pharmacophore must possess an overall lipophilic rigid molecular core comprising at least a tricyclic framework carrying an isonitrile group and establishing further hydrophobic interactions above the ring plane.

21.2.4 Alkaloids and Peptides

This heterogeneous group of compounds includes some marine antimalarials with very different carbon frameworks, but with the common feature of the presence of one (or more) nitrogen atoms. In many cases, the biosynthetic origin of these compounds is not known as well as the mechanism of their antimalarial action.

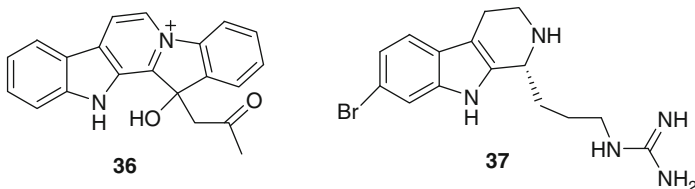
The most important members of this class are manzamines, very complex polycyclic (seven to eight rings or more) alkaloids characterized by an intricate heterocyclic system attached to a β -carboline moiety, first reported from an Okinawan sponge belonging to the genus *Haliclona* [41]. Since the first report of manzamine A (**34**), at least 60 additional manzamine-type alkaloids have been reported from taxonomically unrelated sponges belonging to different genera (e.g., *Xestospongia*, *Ircinia*, and *Amphimedon*) and different orders. These findings strengthen the hypothesis that manzamines are not true sponge metabolites but, more likely, they have a symbiotic origin. Accordingly, microbial community

analyses for one of the most common manzamine-producing sponges resulted in the identification of *Micronospora* as the bacterial strain producing manzamines [42]. A recent paper hypothesized a common biosynthetic route for cyclostelletamines, halicyclamines, and manzamines, thus highlighting the existence of “nature diversity-oriented syntheses” [43].



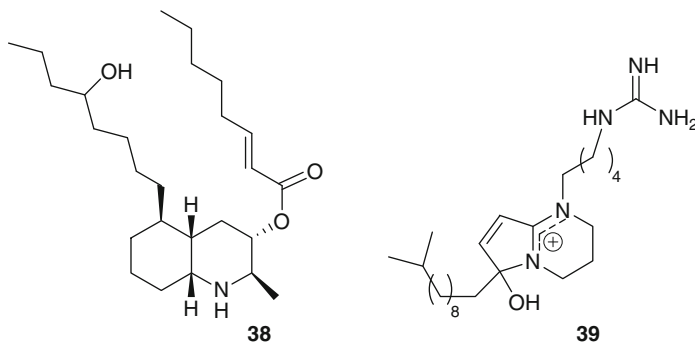
Hamann et al. disclosed the antimalarial potential of manzamine A and of its 8-hydroxy derivative [44]. These molecules were found to potently inhibit the growth of *Plasmodium falciparum* both in vitro ($IC_{50} \approx 5.0$ ng/mL) and in vivo. Unfortunately, the therapeutic index of these molecules is somewhat narrow (gastrointestinal distress), and further studies are needed to improve this value. Interestingly, a closely related derivative of manzamine A, manzamine F (35), was completely devoid of activity ($IC_{50} > 1,000$ ng/mL), thus evidencing the key role of the eight-membered ring. Similarly, the attachment of the hydroxyl group at position 6, in place of position 8, has a deleterious impact on the antimalarial activity, as indicated by the lower potency of 6-hydroxy-manzamine A [45]. The crucial role of a free hydroxy group at position 12 has also been highlighted by a recent study reporting that acetylation of this group significantly reduced the antimalarial activity [46].

Manzamines have also been reported to be antibacterial and antituberculosis agents and to exhibit activity against AIDS opportunistic pathogens as the protozoan *Toxoplasma gondii* [47] (see “Introduction” for a brief description of this parasite). More recently, manzamine A and derivatives have been shown to possess inhibitory activity against glycogen synthase kinase-3 (GSK-3) with potential application in Alzheimer’s disease [48].



The β -carboline group is also present in the structures of homofascaplysin A (**36**), isolated from the sponge *Hyrtios erecta* [49], and of bromotripargyne (**37**) from *Ancorina* sp. [50]. These alkaloids showed good activity against chloroquine-resistant *P. falciparum* strains, but in the first case a marked toxicity toward human cells was detected.

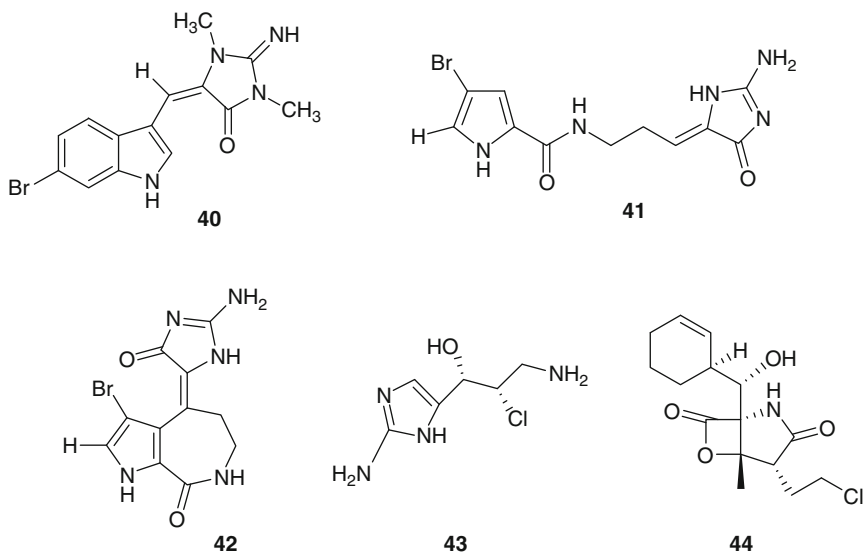
Lepadins are decahydroquinoline derivatives bearing a linear eight-carbon chain obtained from two tunicates of Australian origin, *Clavelina lepadiformis* [51] and *Didemnum* sp. [52]. Lepadin E (**38**) exhibited a significant antimalarial activity ($IC_{50} = 400$ ng/mL), while its analogues lacking the 2*E*-octenoic acid ester functionality were completely inactive. Authors have proposed that this conformationally mobile side chain could serve to stabilize nonbonding interactions with heme, or with any other “receptor” molecule. Phloeodictynes (e.g., **39**) are marine antimalarials, and similarly to lepadins they show a bicyclic nitrogen-containing ring system bearing a long alkyl chain. They have been isolated from sponges belonging to the genus *Oceanapia* [53, 54] as good antimalarial agents ($IC_{50} = 300$ ng/mL) against the chloroquine-resistant FGB1 strain of *P. falciparum*.



6-Bromoaplysinopsin (**40**) is a simple indole derivative first isolated in 1985 [55] and later reobtained from the sponge *Smenospongia aurea* [56], active against the D6 clone of *P. falciparum*. A recent study, aimed at evaluating the antiprotozoan potential of bromopyrrole alkaloids [57], identified dispacamide B (**41**) and spongiacidin B (**42**) as good antimalarial agents. Interestingly, both these compounds, similarly to bromoaplysinopsin, show the presence of an aminoimidazolone (alkylidene glycoyamidine) ring. Interestingly, a very simple 2-aminoimidazole derivative, girolline (**43**), extracted from *Cymbastela cantharella* [58], showed antiplasmodial activity in the IC_{50} range of 77.0–215.0 nM and was active in vivo at a dose of 1.0 mg/kg/day. The aminoimidazole moiety was necessary for the antimalarial activity since the synthetic analogues of two series, 5-deazathiogirolline and 4-deazathiogirolline, without the aminoimidazole moiety, were devoid of any activity.

Salinosporamide A (**44**), a γ -lactam alkaloid isolated from a marine bacterium of the new genus *Salinispora* [59], has been found to be a parasite proteasome inhibitor and to possess a significant antimalarial activity in vitro

($IC_{50} = 11.4$ nM) [60]. Salinosporamide was determined to act in the erythrocytic stage and maintained its potent activity in a malaria mouse model with inhibition of the parasite growth in treated mice at extremely low doses (130 μ g/kg).

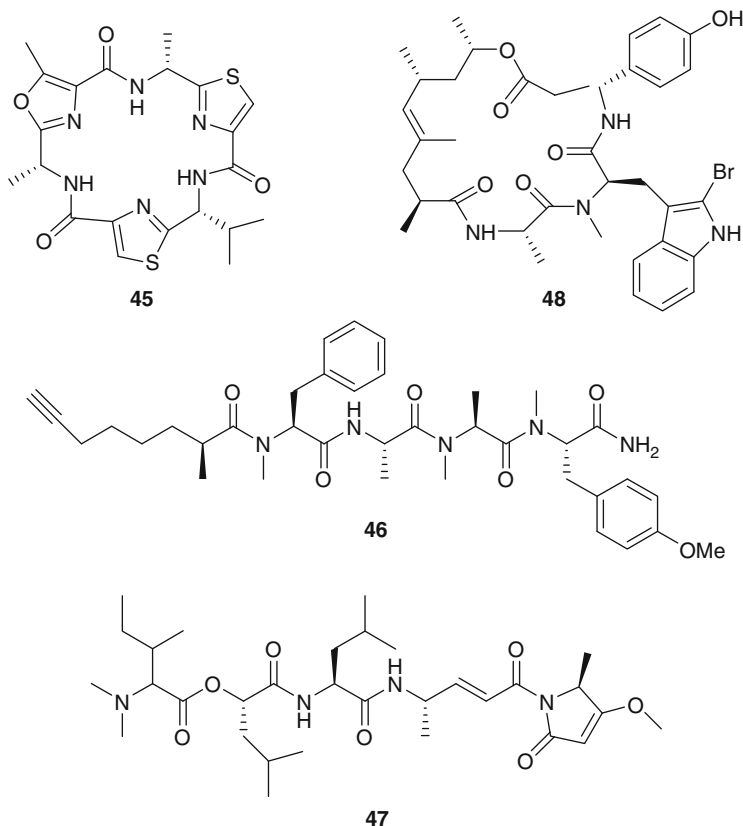


Two modified cyclic hexapeptides, venturamides (e.g., venturamide A, **45**), isolated from the marine cyanobacterium *Oscillatoria* sp., exhibited a moderate activity against *P. falciparum* ($IC_{50} \approx 6\text{--}7$ μ M) [61], with a good selectivity. A similar antimalarial profile was also exhibited by dragomabin (**46**), a linear alkynoic lipopeptide isolated from a Panamanian strain of the marine cyanobacterium *Lyngbya majuscula* [62]. Gallinamide A (**47**), isolated from *Schizothrix* species, containing an *N,N*-dimethyl isoleucine terminus, exhibited moderate in vitro antimalarial activity [63]. Jasplakinolide (**48**), a cyclic peptide isolated from the marine sponge *Jaspis* sp., markedly decreased parasitemia of *P. falciparum* by virtue of an apical protrusion that appears to interfere with the erythrocyte invasion by the merozoites and whose mechanism of formation is possibly related to an increase in F-actin content of the treated merozoites [64].

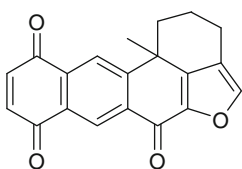
21.2.5 Quinones and Other Antimalarial Compounds

In the frame of a search for *Plasmodium* protein kinase inhibitors, the previously known xestoquinone (**49**) [65] proved to be a selective active inhibitor of Pfnek-1, a never-in-mitosis/*Aspergillus* (NIMA)-related protein kinase of *P. falciparum* [66]. However, the in vitro antiplasmodial activity of xestoquinone was moderate ($IC_{50} \approx 3$ μ M). A series of quinone derivatives, named alisiaquinones (e.g., **50**) structurally related to xestoquinone, have been isolated from an unidentified New Caledonian sponge [67].

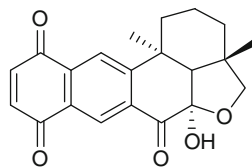
Not surprisingly they showed activity against Pfnek-1 and a micromolar antiplasmodial activity similar to those exhibited by xestoquinone. However, quite interestingly, alisiaquinone C (**51**), bearing an additional heterocycle formed by a taurine substituent, exhibited a submicromolar activity ($IC_{50} \approx 0.1 \mu M$) on *P. falciparum*. This higher activity of alisiaquinone C resulted to be unrelated to inhibition of Pfnek-1, but it was due to a significant inhibition of the plasmodial enzyme farnesyl transferase.



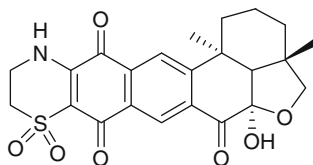
The polyether **52**, obtained from the marine *Streptomyces* sp. H668, exhibited a significant in vitro antimalarial activity ($IC_{50} \approx 150 \text{ ng/mL}$), with a good selectivity [68]. Similarly, to other polyethers of terrestrial origin, probably, this compound acts as ionophore on protozoan-infected cell membrane. Pycnidione (**52**), isolated from the marine fungus *Phoma* sp. [69], exhibited significant antiplasmodial activity against three strains of *P. falciparum* ($IC_{50} = 0.15\text{--}0.4 \mu M$). The structural similarities between pycnidione and the known antimalarial agent atovaquone, (Malarone[®]), widely used in the malaria prophylaxis, appear of particular interest.



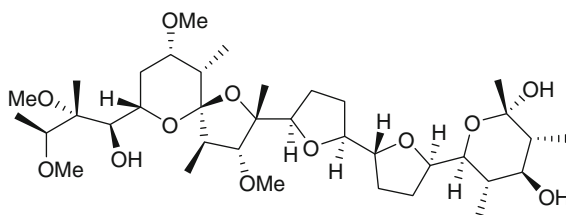
49



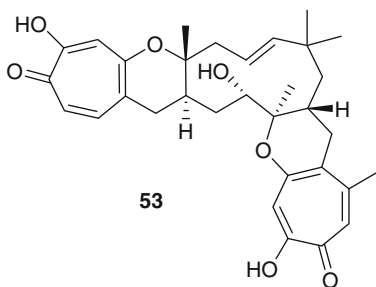
50



51



52



53

21.3 Leishmania

21.3.1 Clinical Symptoms and Social Impact

Leishmaniasis is an animal and human infection caused by over 20 different protozoan parasites belonging to the genus *Leishmania* (e.g., *L. donovani*, *L. infantum*, *L. chagasi*). It is transmitted by the bite of *Lutzomyia* and *Phlebotomus* sand flies (subfamily Phlebotominae). The sand flies inject the infective stage, metacyclic promastigotes, during blood meals. These are phagocytized by

macrophages and transform into amastigotes which are able to affect different tissues and cause the differing clinical manifestation, depending in part on which *Leishmania* species is involved and partly also on the immunological status of the infected individual. Some forms of the disease are transmissible to humans only from animals (zoonosis), but some other can be diffused between humans.

The most important types of human leishmaniasis are cutaneous leishmaniasis (characterized by skin sores, sometimes called Jericho button) and visceral leishmaniasis (also known as kala-azar), a severe and potentially fatal form in which the parasites have migrated to the vital organs with frequent damages to the spleen and liver [3]. The cutaneous leishmaniasis commences with a sore at the bite site but can progress in diffuse cutaneous leishmaniasis (with widespread skin lesions which resemble leprosy) and mucocutaneous leishmaniasis (extending to tissues of nose and mouth and can cause permanent disfigurement).

Leishmaniasis is diffused in tropical and subtropical countries with particular incidence in the Indian subcontinent, in Northeastern African (as Sudan), or Central and South American (as Brazil) countries. It affects as many as 12 million people worldwide, with 1.5–2 million new cases each year. The visceral form of leishmaniasis has an estimated incidence of 0.5 million new cases and about 50,000 deaths each year, and it appears that the incidence of fatal forms of human leishmaniasis is increasing. The World Health Organization has designated leishmaniasis as a category 1 disease, signifying that it is an emerging and uncontrolled global health problem.

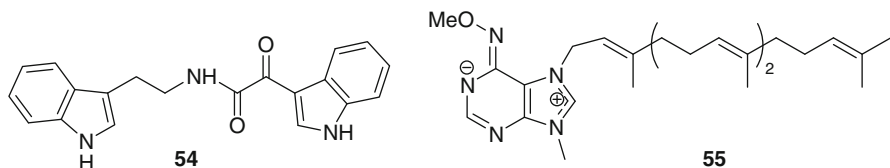
The treatment of leishmaniasis is made particularly difficult by the intramacrophagic location of the infectious form. Victims of this illness present an immune deficiency and are not able to eliminate the parasites through a natural mechanism of defense. Moreover, malnutrition is associated with certain cases of leishmaniasis. Parallel infection with diseases such as malaria and pneumonia increases the fatality of the illness if it is not diagnosed and treated in time. The problem of leishmaniasis has been worsened by the evolution of AIDS due to parallel infections in AIDS patients, as well as by the development of drug resistance by parasites. The traditional treatment for leishmaniasis is based on drugs containing antimony (pentavalent antimonials), e.g., meglumine antimoniate (Glucantime) and sodium stibogluconate (Pentostam). These are very old drugs and their introduction dates back to the 1940s. The resistance developed by parasites against these drugs [70] and the possibility of severe renal and cardiac side effects at the recommended doses strongly encourage the search of effective alternatives. Two potent antibiotics (amphotericin and paromomycin) and miltefosine are becoming frequently used to treat leishmaniasis, although their cost can be sometimes unaffordable for people with least socioeconomic ability. Miltefosine is a phosphocholine analogue originally developed as anticancer agent which is an effective drug for visceral and cutaneous leishmaniasis [71]; it appears to be well tolerated and has also the advantage of the oral formulation, but it is already facing instances of resistance in some areas. Interestingly, HIV protease inhibitors (nelfinavir and ritonavir) have been found to be active against *Leishmania* species and are currently investigated as possible therapeutic options for leishmaniasis [72]. Furthermore, the genomic sequencing of *Leishmania* is a stimulating result which could provide sources for vaccine candidates and potential targets for drug therapies.

The number of marine metabolites active against *Leishmania* parasites is significantly lower compared to those exhibiting antimalarial activity, but this is likely a consequence of the lower number of compounds tested. Some marine compounds exhibited both antimalarial and antileishmanial activities: those included in the following paragraphs have been tested exclusively against *Leishmania*, or, alternatively, their antileishmanial activity is more significant compared to the antimalarial one. For example, manzamines (see Sect. 21.2.4) showed also discrete antileishmanial activity; however, their antimalarial activity is surely more significant being comparable to that of the reference compound artemisinin. Noticeably, in very few cases, the mechanism of the antileishmanial action has been investigated.

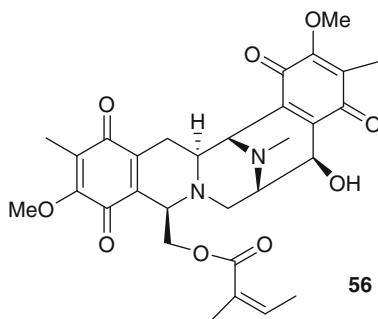
21.3.2 Alkaloids and Peptides

Dihydrocoscinamide (**54**), a synthetic analogue of the coscinamide indole alkaloids, obtained from the sponge *Coscinoderma* sp., exhibited a nearly complete inhibition against promastigotes and amastigotes of *Leishmania donovani* at 10 $\mu\text{g/mL}$ [73]. A series of synthetic analogues of **54** were also prepared, but only the compound showing methylation at both indole nitrogens proved to be equally active.

Agelasines are purino-terpene alkaloids isolated from sponges of the genus *Agelas* showing different pharmacological activities, including antibacterial, anti-fungal, and antifouling activities. Some synthetic analogues of agelasines have been prepared, and one of them (**55**) was found to potently inhibit the growth of *L. infantum* ($\text{IC}_{50} = 0.09 \mu\text{g/mL}$) with a good selectivity index [74].

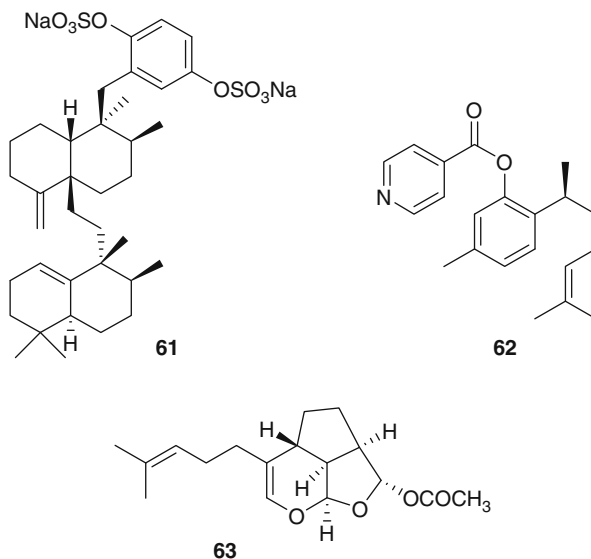


Renieramycin A (**56**) is a complex quinone-containing alkaloid isolated from the sponge *Neopetrosia* sp. which showed a dose-dependent inhibition of the growth of *Leishmania amazoensis* with an IC_{50} of 0.2 $\mu\text{g/mL}$ [75]. Some quinone derivatives also proved to be active against malaria protozoans (see Sect. 21.2.5).



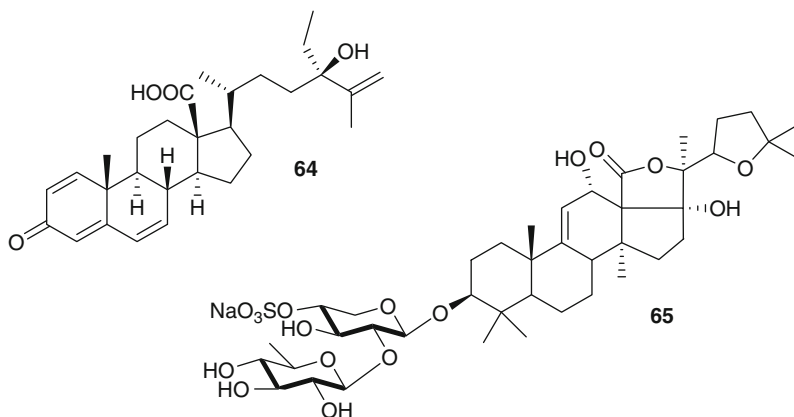
while parasites lack the de novo pathway, mammals have de novo and salvage purine synthesis pathways. Isoakaterpin is the first marine natural product to show inhibition of APRT; however, since its chemical structure is relatively similar to that of other marine meroterpenoids, further investigations of this class of compounds would be particularly interesting.

The phenol moiety is also present in the structure of the marine sesquiterpene (+)-curcuphenol isolated from sponges of the genera *Didiscus* and *Myrmekioderma* showing a moderate activity against *Leishmania* spp. ($IC_{50} = 11 \mu M$). A number of semisynthetic derivatives of (+)-curcuphenol showing esterification of the phenol group have been prepared and evaluated against protozoan parasites [79]. In particular, compound **62** showed a dramatic increase of the antileishmanial activity compared to the parent compound ($IC_{50} = 0.6 \mu M$). The basicity of the pyridine ring is likely to be important in this activity increase since analogues showing a phenyl or an indole in place of the pyridine proved to be less active.



Another sesquiterpene, euplotin C (**63**), isolated from the marine ciliate protist *Euplotes crassus*, showed a moderate activity ($IC_{50} = 4.6 \mu M$) against two *Leishmania* species [80]. The highly oxidized steroids norselic acids A–E (e.g., norselic acid A, **64**), isolated from the Antarctic sponge *Crella* sp., showed antileishmanial activity in the $2\text{-}\mu M$ range [81]. These compounds are reminiscent of the dimeric sterols crellastatins, and they could be conceived as their monomeric units. Interestingly, these monomers lack the potent cytotoxicity exhibited by the corresponding dimers.

The coral reef sea cucumber *Actinopyga lecanora* afforded the previously reported tetraglycosylated triterpene holoturin A and the diglycosylated holoturin B (**65**), which share the same aglycone moiety. Holoturin B displayed a good in vitro and moderate in vivo antileishmanial activity [82].

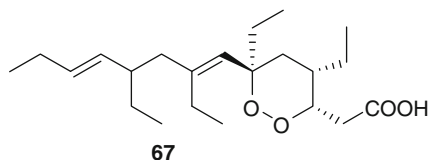
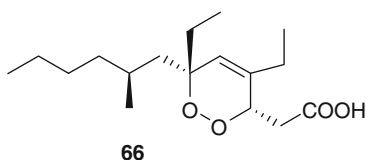


21.3.4 Endoperoxides

Endoperoxide polyketides from *Plakortis* sponges constitute a prominent class of marine antimalarials (see Sect. 21.2.2), but some of them have also been shown to exhibit a good antileishmanial activity, once again indicating the potential of this class of compounds for the treatment of parasitic diseases.

The Palauan sponge *Plakortis* aff. *angulospiculatus* afforded the two endoperoxide polyketide acids **66** and **67** which showed inhibition of growth of *Leishmania mexicana* with LD₅₀ = 0.29 µg/mL and 1.00 µg/mL, respectively [83]. The enantiomer of **67** was later isolated from a Korean specimen of *Plakortis* sp. [84] and found to exhibit exactly the same activity of **67**. This enantiomer was then coupled at the C1 position of ircinol A, and the ircinol-cyclic peroxide ester exhibited an increased antileishmanial activity with IC₅₀ = 0.7 µg/mL [85]. Furthermore, plakortide P, a diastereoisomer of **67**, showed leishmanicidal activity with IC₅₀ = 1.9 µg/mL [86]. In the same study, the mode of action of plakortide P was investigated, and it was evidenced that it eliminated efficiently intracellular amastigotes by other than NO upregulation, probably involved in the specific leishmanicidal activity. It is interesting to notice that all these results on the antileishmanial potential of marine endoperoxide have been obtained practically

with molecules sharing the single carbon framework of **67**. Likely, a thorough investigation of the antileishmanial potential of the many endoperoxides isolated to date would give interesting outcomes.



21.4 Trypanosoma

21.4.1 Clinical Symptoms and Social Impact

Trypanosoma infections in humans show different clinical symptoms according to the specific protozoan involved in the human infection. African trypanosomiasis (sleeping sickness) is caused by *Trypanosoma brucei gambiense* (representing more than 90% of reported cases) and *T. brucei rhodesiense* (found in Eastern and Southern Africa, it accounts for less than 10% of reported cases) [87]. These parasites are transmitted to humans by tsetse fly (*Glossina* genus) bites which have acquired their infection from human beings or from animals harboring the human pathogenic parasites. At first the trypanosomes multiply in subcutaneous tissues, blood, and lymph. Then, the parasites cross the blood-brain barrier and infect the central nervous system. The process can take years with *T. b. gambiense*. When the parasites invade the central nervous system, they lead to behavioral changes, coma, and ultimately, if untreated, death. Disturbance of the sleep cycle, which gives the disease its name, is an important feature of this second stage of the disease. Tsetse flies are found throughout sub-Saharan Africa in vegetation by rivers and lakes, in gallery forests, and in vast stretches of wooded savannah, and, thus, sleeping sickness threatens millions of people in 36 countries with an estimated number of cases between 50,000 and 70,000 per year. The rural populations living in regions where transmission occurs and which depend on agriculture, fishing, animal husbandry, or hunting are the most exposed to the bite of the tsetse fly and therefore to the disease.

Treatment of African trypanosomiasis is based on molecules which were introduced at the beginning of the twentieth century. For the treatment of the first stage, pentamidine and suramin are the preferred treatments, while to treat the second, cerebral stage, the arsenic derivative melarsoprol is practically the only therapeutic option [88]. Melarsoprol has many disadvantages: it can induce a reactive encephalopathy (encephalopathic syndrome) which can be fatal (3–10%); moreover, an increase of resistance to the drug has been observed in central Africa. In recent

years, only one compound, DB2897 (a synthetic analogue of pentamidine), received serious clinical evaluation against African trypanosomiasis, but further development was discontinued in 2008.

Chagas' disease (South American trypanosomiasis) is caused by *T. cruzi* with the vector contribution of a blood-sucking insect (triatome), which bites the victim and contaminates the wound with infected feces. Disease may also be spread through blood transfusion and organ transplantation, ingestion of food contaminated with parasites, and from a mother to her fetus.

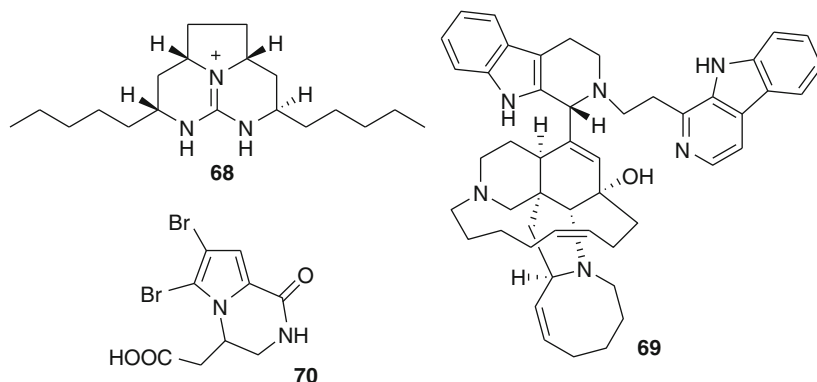
The symptoms of Chagas' disease vary over the course of an infection. In the early, acute stage, symptoms are mild, being restricted to local swelling at the site of infection. After 4–8 weeks, untreated individuals with still active infections enter the chronic phase of Chagas' disease. This is asymptomatic for 60–80% of chronically infected individuals, but 20–40% of them will develop life-threatening heart and digestive system disorders, including cardiomyopathy, which causes heart rhythm abnormalities and may result in sudden death. About one third of patients go on to develop digestive system damage, resulting in dilation of the digestive tract (megacolon and megaesophagus), accompanied by severe weight loss. It is estimated that as many as 8–11 million people in Mexico, Central America, and South America have Chagas' disease, some of whom do not know they are infected. There is no vaccine against Chagas' disease, and the currently available drug treatments are benznidazole (a 2-nitroimidazole) and nifurtimox (now no longer manufactured), which can cause side effects in many patients including skin disorders, brain toxicity, and digestive system irritation. Also in this case, the recent sequencing of *T. cruzi* genome promises to reveal new possible drug targets [89].

21.4.2 Marine Antitrypanosomal Agents

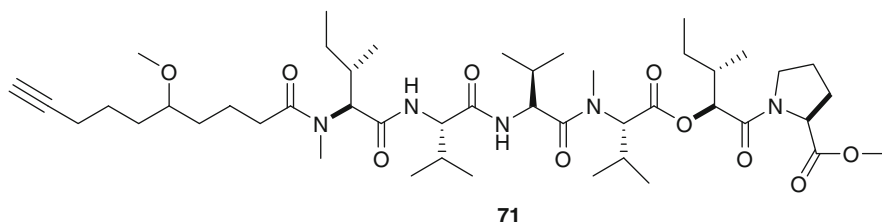
The number of marine natural products tested against trypanosomiasis is very limited, and less than ten molecules have shown encouraging results. These molecules, all grouped in this paragraph, belong to the classes of alkaloids, terpenes, and endoperoxide derivatives, thus closely paralleling the above-cited classes of antileishmanial compounds.

Merobatzelladine A (**68**) and its close analogue merobatzelladine B, tricyclic guanidine alkaloids with hexahydro-5,6,6a-triazaacenaphthalene ring system, isolated from the sponge *Monanchora* sp., inhibited *T. brucei* with $IC_{50} = 0.24 \mu\text{g/mL}$. The same molecules also exhibited a good antimalarial activity and antimicrobial activity against *Vibrio anguillarum* [90]. A new member of the manzamine family, zamamidine C (**69**), possessing a second β -carboline ring via an ethylene unit at N-2 of manzamine D, obtained from the sponge *Amphimedon* sp. [91], showed activity against *T. brucei* with an $IC_{50} = 0.24 \mu\text{g/mL}$, accompanied by antimalarial activity in the same concentration range. A recent investigation of the antiprotozoal activity of bromopyrrole alkaloids from Agelasida and Axinellida sponges [57] selected longamide B (**70**) as a promising agent against *T. brucei*

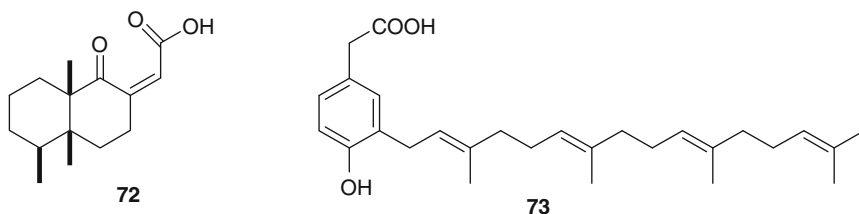
rhodesiense with $IC_{50} = 1.53 \mu\text{g/mL}$ and a selectivity index of 10. Since the related longamide A, showing a hydroxyl group in place of the $-\text{CH}_2\text{COOH}$, is inactive, this latter moiety should play a critical role for the bioactivity.



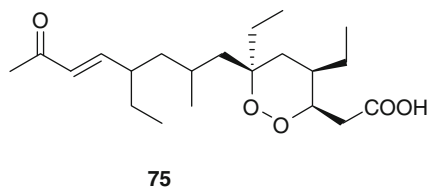
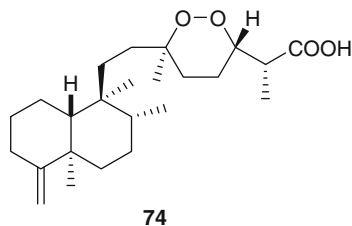
Viridamide A (**71**) is a lipopeptide from the cyanobacterium *Oscillatoria nigroviridis* which showed antitrypanosomal (against *T. cruzi*) activity with $IC_{50} = 1.1 \mu\text{g/mL}$ [92]. Viridamide A also exhibited significant activity against *Leishmania mexicana*.



A simple antitrypanosomal sesquiterpene, aignopsanoic acid A (**72**), has been recently obtained from the sponge *Cacospongia mycofijiensis* [93]. The activity of this compound against *T. brucei* was moderate ($IC_{50} = 6.0 \mu\text{g/mL}$), but, interestingly, the natural analogue showing isomerization of the carbon-carbon double bond geometry (*E* in place of *Z*) was about five times less active. The simple meroterpenoid **73** was found to be very active against *T. brucei rhodesiense* with $IC_{50} = 0.60 \mu\text{g/mL}$ [94].



Marine endoperoxy-containing derivatives proved to be active also against *Trypanosoma*, although a few studies have been carried out in this field. (–)-Sigmosceptrellin B (**74**), isolated together with new and known peroxyterpenes from the marine sponge *Diacarnus bismarckensis*, showed a very good activity ($IC_{50} = 0.20 \mu\text{g/mL}$) against *T. brucei* [95], and it constitutes an excellent starting point for SAR modifications. Sigmosceptrellin B had been evaluated also against *P. falciparum* but it showed only a moderate activity (see Sect. 21.2.2.2), lower than the antimalarial activity exhibited by its diastereomer sigmosceptrellin A. Fractionation of the crude extract obtained from the Australian marine sponge *Plakortis* sp. led to the isolation of the polyketide endoperoxide **75**, which showed an IC_{50} value of 49 nM against *Trypanosoma brucei brucei* [96], qualifying it as one of the most potent marine natural product against African trypanosomiasis. A related compound with modified side chain showing a carboxylic acid group in place of the conjugated ketone group exhibited a 20-fold reduction of activity. The structural similarity between compound **75** and compound **67**, active against *Leishmania* (see Sect. 21.3.4), is remarkable.



21.5 Concluding Remarks

Infectious diseases caused by protozoan parasites, including malaria, African trypanosomiasis, Chagas' disease, and leishmaniasis, are major public health threats in developing countries where, according to the figures of World Health Organization, they affect about one billion people and cause more than one million deaths per year. These pathologies are often called "tropical diseases" or "neglected diseases" to express the relatively scarce attention that pharma industry devote to the development of effective therapies to prevent and treat them. It has been estimated that only 16 of the nearly 1,400 new drugs marketed between 1975 and 1999 were developed for the treatment of neglected diseases [97].

In recent years the drug discovery programs launched by academia and public agencies have resulted in the identification of some lead compounds to hopefully develop effective alternatives to the old drugs used, whose efficacy is diminishing due to the multidrug resistance developed by parasites and to severe side effects, sometimes completely preventing their utilization.

The aim of this chapter was to provide an overview of the most significant contributions given by marine research in the field of antiprotozoal lead compounds. Although this chapter cannot be considered exhaustive, we have listed

which we believe are the most interesting compounds against tropical diseases. Other marine compounds showing a high degree of cell toxicity or a too low level of activity have not been considered. Thus, the chapter includes about 70 marine secondary metabolites belonging to different chemical classes. It is noteworthy that some alkaloids, linear peptides, and endoperoxides appear to possess a broad-spectrum antiprotozoan activity. Manzamines, isonitriles as kalihinols, salinosporamide, plakortin (for the antimalarial activity), almiramides, isoakaterpin (for the antileishmanial activity), merobatzelladine, sigmosceptrellin B, and the endoperoxide polyketide **75** (for the antitrypanosomal activity) are, in our opinion, the most promising molecules emerging from this survey. Unfortunately, with the exception of manzamines, in none of these cases, the investigation has significantly surpassed the initial stage of assessment of *in vitro* (in very few cases, *in vivo*) activity. It should be admitted that, especially in the cases of antileishmanial and antitrypanosomal agents, the evaluation of marine natural products as antiprotozoan agents is still in its infancy. It is significant that practically all the antitrypanosomal agents cited in [Sect. 21.4.2](#) have been discovered in the last 2 years. Detailed structure–activity relationship studies, investigation of the mechanisms of action, optimization of the chemical structures for pharmacokinetics and pharmacodynamics, and complete evaluation of the toxicity profiles are greatly expected in the near future for marine antiprotozoans. Then, the big issue of the low-cost production of the selected molecule(s) will be open.

21.6 Study Questions

1. The *Target Product Profile* (TPP), published by Medicine for Malaria Venture (MMV), is a list of requirements that a new molecule should satisfy in order to be evaluated as clinical candidate for antimalarial therapy. Among these requirements, oral activity and a cost treatment that should be not more than 1\$ for simple malaria and 5\$ for cerebral malaria are of particular relevance. Should an antimalarial agent from the sea ever follow these indications? What is the role that antimalarials from the sea could play? Explain your answers in detail.
2. Propose a list of realistic requirements for a marine compound exhibiting antimalarial activity.
3. Propose a biosynthetic pathway for the polyketide plakortin (see [Sect. 21.2.2.2](#)). The key step is the formation of the endoperoxide linkage. Some alternative possibilities can be proposed for this step.
4. (a) The isonitrile group, very uncommon in natural products, is present in a series of terpenes with potent antimalarial activity. Propose a biosynthetic origin for this group. (b) The isonitrile group resembles the structure of carbon monoxide, a known ligand of heme Fe(II). Could this observation be important for the mechanism of action of antimalarial isonitriles?
5. Discovering untapped natural sources of novel antiprotozoal compounds remains a major challenge. Discuss how combinatorial chemistry and genomics can complete and/or guide this investigation on marine organisms.

References

1. Data taken from Malaria Foundation International. <http://www.malaria.org> and linked sites. Accessed 3 May 2010
2. Brun R, Blum J, Chappuis F, Burri C (2010) Human African trypanosomiasis. *Lancet* 375:148–159
3. Bern C, Maguire JH, Alvar J (2008) Complexities of assessing the disease burden attributable to leishmaniasis. *PLoS Negl Trop Dis* 2:e313
4. Reithinger R (2008) Leishmaniasis' burden of disease: ways forward for getting from speculation to reality. *PLoS Negl Trop Dis* 2:e285
5. Mayer AM, Rodriguez AD, Berlinck RG, Hamann MT (2009) Marine pharmacology in 2005–6: marine compounds with anthelmintic, antibacterial, anticoagulant, antifungal, anti-inflammatory, antimalarial, antiprotozoal, antituberculosis, and antiviral activities; affecting the cardiovascular, immune, and nervous systems and other miscellaneous mechanisms of action. *Biochim Biophys Acta* 1790:283–308 and previous reviews of this series
6. Fattorusso E, Tagliatela-Scafati O (2009) Marine antimalarials. *Mar Drugs* 7:130–152 and other reviews cited herein
7. Casteel DA (1997) Antimalarial agents. In: Wolff ME (ed) *Burger's medicinal chemistry and drug discovery*. vol 5. Wiley, New York, pp 3–91
8. Collins WE, Barnwell JW (2008) A hopeful beginning for malaria vaccines. *N Engl J Med* 359:2599–2601
9. Breman JG, Egan A, Keusch G (2001) The intolerable burden of malaria: a new look at the numbers. *Am J Trop Med Hyg* 64:iv–vii
10. Olliaro P, Cattani J, Wirth D (1996) Malaria, the submerged disease. *JAMA* 275:230–233
11. Gardner MJ, Hall N et al (2002) Genome sequence of the human malaria parasite *Plasmodium falciparum*. *Nature* 419:498–511
12. Klayman DL, Lin AJ, Acton N et al (1984) Isolation of artemisinin (qinghaosu) from *Artemisia annua* growing in the United States. *J Nat Prod* 47:715–717
13. Avery MA, Chong WKM, Jennings-White C (1992) Stereoselective total synthesis of (+)-artemisinin, the antimalarial constituent of *Artemisia annua* L. *J Am Chem Soc* 114:974–979
14. Haynes RK, Ho W, Chan H (2004) Highly antimalaria-active artemisinin derivatives: biological activity does not correlate with chemical reactivity. *Angew Chem Int Ed* 43:1381–1385
15. Kobayashi M, Kondo K, Kitagawa I (1993) Antifungal peroxyketals from an Okinawan marine sponge of *Plakortis* sp. *Chem Pharm Bull* 41:1324–1326
16. Murakami N, Kawanishi M, Itagaki S et al (2002) New readily accessible peroxides with high antimalarial potency. *Bioorg Med Chem Lett* 12:69–72
17. Murakami N, Kawanishi M, Mostaqul HM et al (2003) New anti-malarial peroxides with in vivo potency derived from spongy metabolites. *Bioorg Med Chem Lett* 13:4081–4084
18. Kawanishi M, Kotoku N, Itagaki S et al (2004) Structure-activity relationship of anti-malarial spongy peroxides having a 3-methoxy-1,2-dioxane structure. *Bioorg Med Chem* 12:5297–5307
19. Quinoa E, Kho E, Manes LV, Crews P (1986) Heterocycles from the marine sponge *Xestospongia* sp. *J Org Chem* 51:4260–4264
20. Fattorusso C, Persico M, Calcinai B, Cerrano C, Parapini S, Taramelli D, Novellino E, Romano A, Scala F, Fattorusso E, Tagliatela-Scafati O (2010) Manadoperoxides A–D from the Indonesian sponge *Plakortis* cfr. *simplex*. Further insights on the structure–activity relationships of simple 1,2-dioxane antimalarials. *J Nat Prod* 73:1138–1145
21. Higgs MD, Faulkner DJ (1978) Plakortin, an antibiotic from *Plakortis halichondrioides*. *J Org Chem* 43:3454–3457
22. Cafieri F, Fattorusso E, Tagliatela-Scafati O, Ianaro A (1999) Metabolites from the sponge *Plakortis simplex*. Determination of absolute stereochemistry of plakortin. Isolation and stereostructure of three plakortin related compounds. *Tetrahedron* 55:7045–7056

23. Campagnuolo C, Fattorusso E, Romano A, Taglialatela-Scafati O, Basilico N, Parapini S, Taramelli D (2005) Antimalarial polyketide cycloperoxides from the marine sponge *Plakortis simplex*. *Eur J Org Chem* 2005:5077–5083
24. Fattorusso E, Parapini S, Campagnuolo C, Basilico N, Taglialatela-Scafati O, Taramelli D (2002) Activity against *Plasmodium falciparum* of cycloperoxide compounds obtained from the sponge *Plakortis simplex*. *J Antimicrob Chemother* 50:883–888
25. Fattorusso C, Campiani G, Catalanotti B, Persico M, Basilico N, Parapini S, Taramelli D, Campagnuolo C, Fattorusso E, Romano A, Taglialatela-Scafati O (2006) Endoperoxide derivatives from marine organisms: 1,2-dioxanes of the plakortin family as novel antimalarial agents. *J Med Chem* 49:7088–7094
26. Taglialatela-Scafati O, Fattorusso E, Romano A, Scala F, Barone V, Cimino P, Stendardo E, Catalanotti B, Persico M, Fattorusso C (2010) Insight into the mechanism of action of plakortins, simple 1,2-dioxane antimalarials. *Org Biomol Chem* 8:846–856
27. Hu J, Gao H, Kelly M et al (2001) Plakortides K–N, four new cyclic peroxides from an undescribed Jamaican sponge *Plakortis* sp. (Homosclerophorida, Plakinidae). *Tetrahedron* 57:9379–9383
28. Jimenez MS, Garzon SP, Rodriguez AD (2003) Plakortides M and N, bioactive polyketide endoperoxides from the Caribbean marine sponge *Plakortis halichondrioides*. *J Nat Prod* 66:655–661
29. Laroche M, Imperatore C, Grozdanov L et al (2006) Cellular localization of secondary metabolites isolated from the Caribbean sponge *Plakortis simplex*. *Marine Biol* 151:1365–1373
30. El Sayed KA, Dunbar DC, Goins DK et al (1996) The marine environment: a resource for prototype antimalarial agents. *J Nat Toxins* 5:261–285
31. El Sayed KA, Hamann MT, Hashish NE et al (2001) Antimalarial, antiviral, and antitoxo-plasmosis norsesesterterpene peroxide acids from the Red Sea sponge *Diacarnus erythraeanus*. *J Nat Prod* 64:522–524
32. D'Ambrosio M, Guerriero A, Deharo E et al (1998) New types of potentially antimalarial agents. Epidioxy-substituted norditerpene and norsesesterterpenes from the marine sponge *Diacarnus levii*. *Helv Chim Acta* 81:1285–1292
33. Cafieri F, Fattorusso E, Magno S, Santacroce C, Sica D (1973) Isolation and structure of axisonitrile 1 and axisothiocyante 1, two unusual sesquiterpenoids from the marine sponge *Axinella cannabina*. *Tetrahedron* 29:4259–4262
34. Fattorusso E, Magno S, Mayol L, Santacroce C, Sica D (1974) Isolation and structure of axisonitrile 2. New sesquiterpenoid isonitrile from the sponge *Axinella cannabina*. *Tetrahedron* 30:3911–3913
35. Di Blasio B, Fattorusso E, Magno S, Mayol L, Pedone C, Santacroce C, Sica D (1976) Axisonitrile-3, axisothiocyante-3 and axamide-3. Sesquiterpenes with a novel spiro[4,5] decane skeleton from the sponge *Axinella cannabina*. *Tetrahedron* 32:473–478
36. Angerhofer CK, Pezzuto JM, Koenig GM, Wright AD, Sticher O (1992) Antimalarial activity of sesquiterpenes from the marine sponge *Acanthella klethra*. *J Nat Prod* 55:1787–1789
37. Koenig GM, Wright AD, Angerhofer CK (1996) Novel potent antimalarial diterpene isocyanates, isothiocyantes, and isonitriles from the tropical marine sponge *Cymbastela hooperi*. *J Org Chem* 61:3259–3267
38. Wrigth AD, Lang-Unnasch N (2009) Diterpene formamides from the tropical marine sponge *Cymbastela hooperi* and their antimalarial activity in vitro. *J Nat Prod* 72:492–495
39. Miyaoka H, Shimomura M, Kimura H, Yamada Y, Kim HS, Wataya Y (1998) Antimalarial activity of kalihinol A and new relative diterpenoids from the Okinawan sponge, *Acanthella* sp. *Tetrahedron* 54:13467–13474
40. Wright AD, Wang H, Gurrath M, Koenig GM, Kocak G, Neumann G, Loria P, Foley M, Tilley L (2001) Inhibition of heme detoxification processes underlies the antimalarial activity of terpene isonitrile compounds from marine sponges. *J Med Chem* 44:873–885

41. Sakai R, Higa T, Jefford CW, Bernardinelli G (1986) Manzamine A, a novel antitumor alkaloid from a sponge. *J Am Chem Soc* 108:6404–6405
42. Yousaf M, El Sayed KA, Rao KV, Lim CW, Hu J, Kelly M, Franzblau SG, Zhang F, Peraud O, Hill RT, Hamann MT (2002) 12,34-Oxamanzamines, novel biocatalytic and natural products from manzamine producing Indo-Pacific sponges. *Tetrahedron* 58:7397–7402
43. Wypych JC, Nguyen TM, Nuhant P, Benechie M, Marazano C (2008) Further insight from model experiments into a possible scenario concerning the origin of manzamine alkaloids. *Angew Chem Int Ed* 47:5418–5421
44. Ang KKH, Holmes MJ, Higa T, Hamann MT, Kara UAK (2000) In vivo antimalarial activity of the β -carboline alkaloid manzamine A. *Antimicrob Agents Chemother* 44:1645–1649
45. Rao KV, Donia MS, Pen J, Garcia-Palomero E, Alonso D, Martinez A, Medina M, Franzblau SG, Tekwani BL, Khan SI, Wayhuono S, Willett KL, Hamann MT (2006) Manzamine B and E and ircinal A related alkaloids from an Indonesian *Acanthos-trongylophora* sponge and their activity against infectious, tropical Parasitic, and alzheimer's diseases. *J Nat Prod* 69:1034–1040
46. Shilabin AG, Kasanah N, Tekwani BL, Hamann MT (2008) Kinetic studies and bioactivity of potential manzamine prodrugs. *J Nat Prod* 71:1218–1221
47. Rao KV, Santarsiero BD, Mesecar AD, Schinazi RF, Tekwani BL, Hamann MT (2003) New manzamine alkaloids with activity against infectious and tropical parasitic diseases from an Indonesian sponge. *J Nat Prod* 66:823–828
48. Hamann MT, Alonso D, Martin-Aparicio E, Fuertes A, Perez-Puerto J, Castro A, Morales S, Navarro ML, del Monte-Millan M, Medina M, Pennaka H, Balaiah A, Peng J, Cook J, Wahyuono S, Martinez A (2007) Glycogen synthase kinase-3 (GSK-3) inhibitory activity and structure-activity relationship (SAR) studies of the manzamine alkaloids. Potential for Alzheimer's disease. *J Nat Prod* 70:1397–1405
49. Kirsch G, Koeng GM, Wright AD, Kaminsky R (2000) A new bioactive sesterterpene and antiplasmodial alkaloids from the marine sponge *Hyrtilos cf. erecta*. *J Nat Prod* 63:825–829
50. Davis RA, Duffy S, Avery VM, Camp D, Hooper JNA, Quinn RJ (2010) (+)-7-Bromotrypargine: an antimalarial β -carboline from the Australian marine sponge *Ancorina* sp. *Tetrahedron Lett* 51:583–585
51. Steffan B (1991) Lepadine A, a decahydroquinoline alkaloid from the tunicate *Clavelina lepadiformis*. *Tetrahedron* 42:8729–8732
52. Wright AD, Goclik E, Koenig GM, Kaminsky RJ (2002) Lepadins D–F: antiplasmodial and antitrypanosomal decahydroquinoline derivatives from the tropical marine tunicate *Didemnum* sp. *J Med Chem* 45:3067–3072
53. Kourany-Lefoll E, Pais M, Sevenet T, Guittet E, Montagnac A, Fontaine C, Guenard D, Adeline MT, Debitus C (1992) Phloeodictines A and B: new antibacterial and cytotoxic bicyclic amidinium salts from the new Caledonian sponge, *Phloeodictyon* sp. *J Org Chem* 57:3832–3835
54. Mancini I, Guella G, Sauvain M, Debitus C, Duigou A, Ausseil F, Menou J, Pietra F (2004) New 1,2,3,4-tetrahydropyrrolo[1,2-a]pyrimidinium alkaloids (phloeodictynes) from the New Caledonian shallow-water haplosclerid sponge *Oceanapia fistulosa*. Structural elucidation from mainly LC-tandem-MS-soft-ionization techniques and discovery of antiplasmodial activity. *Org Biomol Chem* 2:783–787
55. Tymiak AA, Rinehart KL (1985) Constituents of morphologically similar sponges. *Aplysina* and *smenospongia* species. *Tetrahedron* 41:1039–1047
56. Hu J, Schetz JA, Kelly M, Peng J, Ang KKH, Flotow H, Leong CY, Ng SB, Buss AD, Wilkins SP, Hamann MT (2002) New anti-infective and human 5-HT₂ receptor binding natural and semisynthetic compounds from the Jamaican sponge *Smenospongia aurea*. *J Nat Prod* 65:476–480
57. Scala F, Fattorusso E, Menna M, Tagliatela-Scafati O, Tierney M, Kaiser M, Tasdemir D (2010) Bromopyrrole alkaloids as lead compounds against protozoan parasites. *Mar Drugs* 8:2162–2174

58. Benoit-Vical F, Saléry M, Soh PN, Ahond A, Poupat C (2008) Girolline: a potential lead structure for antiplasmodial drug research. *Planta Med* 74:438–444
59. Feling RH, Buchanan GO, Mincer TJ, Kauffman CA, Jensen PR, Fenical W (2003) Salinosporamide A: a highly cytotoxic proteasome inhibitor from a novel microbial source, a marine bacterium of the new genus *Salinispora*. *Angew Chem Int Ed* 42:355–357
60. Prudhomme J, McDaniel E, Ponts N, Bertani S, Fenical W, Jensen P, Le Roch K (2008) Marine actinomycetes: a new source of compounds against the Human malaria parasite. *PLoS One* 3:e2335
61. Linington RG, Gonzalez J, Urena LD, Romero LI, Ortega-Barria E, Gerwick WH (2007) Venturamides A and B: antimalarial constituents of the panamanian marine cyanobacterium *Oscillatoria* sp. *J Nat Prod* 70:397–401
62. McPhail KL, Correa J, Linington RG, Gonzalez J, Ortega-Barria E, Capson TL, Gerwick WH (2007) Antimalarial linear lipopeptides from a panamanian strain of the marine cyanobacterium *Lyngbya majuscula*. *J Nat Prod* 70:984–988
63. Linington RG, Clark BR, Trimble EE, Almanza A, Urena LD, Kyle DE, Gerwick WH (2009) Antimalarial peptides from marine cyanobacteria: isolation and structural elucidation of gallinamide A. *J Nat Prod* 72:14–17
64. Mizuno Y, Makioka A, Kawazu S, Kano S, Kawai S, Akaki M, Aikawa M, Ohtomo H (2002) Effect of jasplakinolide on the growth, invasion, and actin cytoskeleton of *Plasmodium falciparum*. *Parasitol Res* 88:844–848
65. Nakamura H, Kobayashi J, Kobayashi M, Ohizumi Y, Hirata Y (1985) Physiologically active marine natural products from Porifera. VII. Xestokinone. A novel cardiotonic marine natural product isolated from the Okinawan sea sponge *Xestospongia sapra*. *Chem Lett* 6:713–716
66. Laurent D, Jullian V, Parenty A, Knibiehler M, Dorin D, Schmitt S, Lozach O, Lebouvier N, Frostin M, Alby F, Maurel S, Doerig C, Meijer L, Sauvain M (2006) Antimalarial potential of xestokinone, a protein kinase inhibitor isolated from a Vanuatu marine sponge *Xestospongia* sp. *Bioorg Med Chem* 14:4477–4482
67. Desoubzdanne D, Marcourt L, Raux R, Chevalley S, Dorin D, Doerig C, Valentin A, Ausseil F, Debitus C (2008) Alisiaquinones and alisiaquinol, dual inhibitors of *Plasmodium falciparum* enzyme targets from a New Caledonian deep water sponge. *J Nat Prod* 71:1189–1192
68. Na M, Meujo DAF, Kevin D, Hamann MT, Anderson M, Hill RT (2008) A new antimalarial polyether from a marine *Streptomyces* sp. H668. *Tetrahedron Lett* 49:6282–6285
69. Wright AD, Lang-Unnasch N (2005) Potential antimalarial lead structures from fungi of marine origin. *Planta Med* 71:964–966
70. Arevalo J, Ramirez L, Adaui V et al (2007) Influence of *Leishmania* (Viannia) species on the response to antimonial treatment in patients with American tegumentary leishmaniasis. *J Infect Dis* 195:1846–1851
71. Jha TK, Sundar S, Thakur CP et al (1999) Miltefosine, an oral agent, for the treatment of Indian visceral leishmaniasis. *New Engl J Med* 341:1795–1800
72. Trudel N et al (2008) Intracellular survival of *Leishmania* species that cause visceral leishmaniasis is significantly reduced by HIV-1 protease inhibitors. *J Infect Dis* 198:1292–1299
73. Gupta L, Talwar A, Nishi PS, Gupta S, Chauhan PMS (2007) Synthesis of marine alkaloid: 8,9-dihydrococcinamide B and its analogues as novel class of antileishmanial agents. *Bioorg Med Chem Lett* 17:4075–4079
74. Vik A, Prosenyak A, Vermeersch M, Cos P, Maes L, Gundersen L (2009) Screening of Agelasine D and Analogs for Inhibitory Activity against Pathogenic Protozoa; Identification of Hits for Visceral Leishmaniasis and Chagas Disease. *Molecules* 14:279–288
75. Nakao Y, Shiroya T, Murayama S, Matsunaga S, Goto Y, Matsumoto Y, Fusetani N (2004) Identification of renieramycin A as an antileishmanial substance in a marine sponge *Neopetrosia* sp. *Mar Drugs* 2:55–62

76. Balunas MJ, Linington RG, Tidgewell K, Fenner AM, Urena LD, Della Togna G, Kyle DE, Gerwick WH (2010) Dragonamide E, a modified linear lipopeptide from *Lyngbya majuscula* with antileishmanial activity. *J Nat Prod* 73:60–66
77. Sanchez LM, Lopez D, Vesely BA, Della Togna G, Gerwick WH, Kyle DE, Linington RG (2010) Almiramides A–C: discovery and development of a new class of leishmaniasis lead compounds. *J Med Chem* 53:4187–4197
78. Gray CA, de Nira SP, Silva L, Pimenta EF, Thiemann OH, Oliva G, Hajdu E, Andersen RJ, Berlinck RGS (2006) Sulfated meroterpenoids from the Brazilian sponge *Callyspongia* sp. Are inhibitors of the antileishmaniasis target adenosine phosphoribosyl transferase. *J Org Chem* 71:8685–8690
79. Gul W, Hammond NL, Yousaf M, Peng J, Holley A, Hamann MT (2007) Chemical transformation and biological studies of marine sesquiterpene (S)-(+)-curcuphenol and its analogs. *Biochim Biophys Acta* 1770:1513–1519
80. Savoia D, Avanzini C, Alice T, Callone E, Guella G, Dini F (2004) Antimicrobial activity of euplotin C, the sesquiterpene taxonomic marker from the marine ciliate *Euplotes crassus*. *Antimicrob Agents Chemother* 48:3828–3833
81. Ma WS, Mutka T, Vesley B, Amsler MO, McClintock JB, Amsler CD, Perman JA, Singh MP, Maiese WM, Zaworotko MJ, Kyle DE, Baker BJ (2009) Norselic acids A–E, highly oxidized anti-infective steroids that deter mesograzers, from the Antarctic Sponge *Crella* sp. *J Nat Prod* 72:1842–1846
82. Singh N, Kumar R, Gupta S, Dube A, Lakshmi V (2008) Antileishmanial activity in vitro and in vivo of constituents of sea cucumber *Actinopyga lecanora*. *Parasitol Res* 103:351–354
83. Compagnone RS, Pina IC, Rangel HR, Dagger F, Suarez AI, Reddy MVR, Faulkner DJ (1998) Antileishmanial cyclic peroxides from the Palauan sponge *Plakortis* aff. *angulospiculatus*. *Tetrahedron* 54:3057–3068
84. Lim CW, Lim Y, Youn HD, Park H (2006) Enantiomeric compounds with antileishmanial activities from a sponge, *Plakortis* sp. *Agric Chem Biotechnol* 49:21–23
85. Lim CW, Kim Y, Jang M, Park J, Park H (2006) Coupling of ent-cyclic peroxide and ircinol A, two biologically active natural marine products. *J Fish Sci Technol* 9:175–178
86. Kossuga MH, Nascimento AM, Reimão JQ, Tempone AG, Taniwaki NN, Veloso K, Ferreira AG, Cavalcanti BC, Pessoa C, Moraes MO, Mayer AMS, Hajdu E, Berlinck RGS (2008) Antiparasitic, antineuroinflammatory, and cytotoxic polyketides from the marine sponge *Plakortis angulospiculatus* collected in Brazil. *J Nat Prod* 71:334–339
87. Barrett MP, Burchmore RJ, Stich A et al (2003) The trypanosomiasis. *Lancet* 362:1469–1480
88. Burri C, Nkunku S, Merolle A, Smith T, Blum J, Brun R (2000) Efficacy of new, concise schedule for melarsoprol in treatment of sleeping sickness caused by *Trypanosoma brucei gambiense*: a randomised trial. *Lancet* 355:1419–1425
89. El-Sayed NM, Myler PJ, Bartholomeu DC (2005) The genome sequence of *Trypanosoma cruzi*, etiologic agent of Chagas disease. *Science* 309:409–415
90. Takishima S, Ishiyama A, Iwatsuki M, Otaguro K, Yamada H, Omura S, Kobayashi H, van Soest RWM, Matsunaga S (2009) Merobatzelladines A and B, anti-infective tricyclic guanidines from a marine sponge *Monanchora* sp. *Org Lett* 11:2655–2658
91. Yamada H, Takahashi Y, Kubota T, Fromont J, Ishiyama A, Otaguro K, Yamada H, Omura S, Kobayashi J (2009) Zamamidine C, 3,4-dihydro-6-hydroxy-10,11-epoxymanzamine A, and 3,4-dihydromanzamine J N-oxide, new manzamine alkaloids from sponge *Amphimedon* sp. *Tetrahedron* 65:2313–2317
92. Simmons TL, Engene N, Urena LD, Romero LI, Ortega-Barria E, Gerwick L, Gerwick WH (2008) Viridamides A and B, lipodepsipeptides with antiprotozoal activity from the marine cyanobacterium *Oscillatoria nigro-viridis*. *J Nat Prod* 71:1544–1550
93. Johnson TA, Amagata T, Sashidhara KV, Oliver AG, Tenney K, Matainaho T, Ang KKH, McKerrow JH, Crews P (2009) The aignopsanes, a new class of sesquiterpenes from selected chemotypes of the sponge *Cacospongia mycofijiensis*. *Org Lett* 11:1975–1978

94. Orhan I, Sener B, Kaiser M, Brun R, Tasdemir D (2010) Inhibitory activity of marine sponge-derived natural products against parasitic protozoa. *Mar Drugs* 8:47–58
95. Rubio BK, Tenney K, Ang KH, Abdulla M, Arkin M, McKerrow J, Crews P (2009) The marine sponge *Diacarnus bismarckensis* as a source of peroxiterpene inhibitors of *Trypanosoma brucei*, the causative agent of sleeping sickness. *J Nat Prod* 72:218–222
96. Feng Y, Davis RA, Sykes M, Avery VM, Camp D, Quinn RJ (2010) Antitrypanosomal cyclic polyketide peroxides from the Australian marine sponge *Plakortis* sp. *J Nat Prod* 73:716–719
97. Trouiller P, Olliaro P, Torreele E, Orbinski J, Laing R, Ford N (2002) Drug development for neglected diseases: a deficient market and a public-health policy failure. *Lancet* 359:2188–2194

Mechanism-based Screening for Cancer Therapeutics with Examples from the Discovery of Marine Natural Product-based HIF-1 Inhibitors

22

Dale G. Nagle and Yu-Dong Zhou

Contents

22.1	Introduction	1112
22.2	Bioassay Target Selection	1113
22.3	Molecular Target Validation	1116
22.4	Selection of Measurable Biochemical Processes Suitable for Bioassay Development	1119
22.5	Techniques Used to Acquire or Measure the Bioassay Data	1120
22.6	Design and Use of Proper Experimental Controls	1121
22.7	Bioassay Validation and the Application of Appropriate Statistical Methods	1123
22.8	Bioassay Method-Specific Experimental Artifacts	1126
22.9	Identification of Active Marine Natural Products	1127
22.10	Dereplication of Nuisance Compounds	1135
22.11	Concluding Remarks	1138
22.12	Study Questions	1139
	References	1140

Abstract

Recent advances in cancer genetics combined with an increasing number of new methods in molecular and cell biology provide exciting new antitumor drug targets and a wide array of means to design bioassay systems for the discovery of novel cancer chemotherapeutics. Marine natural products continue to play a vital role in molecular-targeted antitumor drug discovery. Although most recognize the critical and expanding role mechanism-based antitumor bioassays play in modern anticancer drug discovery, few natural products chemists have specific training in bioassay technology. Critical bioassay development factors are outlined and introduced at a level intended to provide a basic understanding to

D.G. Nagle (✉) • Y.-D. Zhou

Department of Pharmacognosy, School of Pharmacy, The University of Mississippi, Oxford, MS, USA

e-mail: dnagle@olemiss.edu, ydzhou@olemiss.edu

a general audience. These include molecular target identification, antitumor target validation, selection of assayable biochemical processes, data acquisition methods, experimental controls, bioassay validation and statistical methods, experimental artifacts, active compound identification, and the dereplication of nuisance compounds. Marine natural products have been identified that inhibit the activation of the anticancer drug target hypoxia-inducible factor-1 (HIF-1). Bioassay systems and recent results from marine HIF-1 inhibitor discovery programs are used to illustrate important factors that must be considered when using molecular-targeted antitumor bioassay methods.

22.1 Introduction

Marine natural products research is a dynamic and constantly changing field that has evolved and adapted new technologies with cutting-edge molecular and cell biology. Modern high-field multidimensional nuclear magnetic resonance (NMR) methods facilitate the rapid structure elucidation of minute quantities of pharmacologically active natural products. Advances in microbial sourcing have yielded exciting new biological diversity. This is especially true in the field of marine natural products, where marine bacteria and fungi have begun to eclipse sponges and other invertebrates as important sources of novel chemistry (see ► [Chap. 3](#)) [1–5].

The activation of oncogenes and/or the inactivation of tumor suppressor genes plays an important role in the etiology and progression of cancer, an assemblage of diseases that result from accumulated mutations. Our knowledge of cancer genetics has expanded rapidly during the past few decades. Since the initial discovery of oncogenes, the field of cancer biology has grown to include the elucidation of the molecular mechanisms that underlie tumorigenesis, tumor growth, progression, metastasis, tumor cell death, and treatment resistance. As a result, mechanism-based drug discovery efforts have prospered and molecular-targeted agents (i.e., trastuzumab) are in clinical use. By integrating critical technological advancements with a growing number of important molecular mechanism-based antitumor targets, marine natural products research currently plays a vital role in anticancer drug discovery [6, 7]. In addition, newly developed strategies aim to alter the genetic regulation of secondary metabolite biosynthesis. Taken together, these advances show great promise to increase the structural diversity of natural products for drug discovery.

While the face of natural products chemistry has dramatically changed, the therapeutic potential of compounds identified in anticancer marine natural product programs remains inexorably tied to the quality of the bioassay methods used to direct the discovery efforts. In this respect, there is a fundamental need for cutting-edge molecular and biomedical research to support nearly all aspects of contemporary antitumor drug discovery. Most natural products chemists recognize the importance of excellent bioassays to support their research efforts. Yet, few chemists are specifically trained to critically evaluate the cell biology that supports the

potential significance of anticancer targets or the molecular biology involved in the design of molecular-targeted antitumor bioassay methods. To ensure the quality of these efforts, the most successful programs usually depend on strong collaborative research efforts with molecular and tumor cell biologists, pharmacologists, and experts in the design of high-throughput bioassay systems.

Important factors that must be considered when using modern molecular-targeted antitumor bioassay methods comprise a relatively short list of drug target-associated, bioassay method-dependent, and test sample source-specific factors. These may include, but are not limited to, the following list of points that require careful consideration: (a) identification of a molecular target; (b) validation of the antitumor target; (c) selection of a measurable biochemical, chemical, or biological process for the assay; (d) methods used to acquire or measure the data; (e) use of experimental controls; (f) bioassay validation and the application of appropriate statistical methods; (g) possible experimental artifacts; (h) active compound identification; and (i) nuisance compounds and methods for chemical dereplication. It may not be feasible to expect all natural products chemists to become experts in bioassay systems. Nonetheless, a general appreciation for these important assay components is critical to the success of every molecular-targeted antitumor drug discovery process.

The transcription factor hypoxia-inducible factor-1 (HIF-1) has emerged as an important target for anticancer drug discovery [8–12]. Hypoxic conditions (decreased oxygen tension) that are present within actively growing tumor masses activate HIF-1. The heterodimeric protein complex known collectively as HIF-1 then regulates the transcriptional response to tumor hypoxia [13]. Numerous natural products have been identified that regulate HIF-1 activation and suppress tumor-related HIF-1 target genes [14–16]. Because of its current distinction in the drug discovery process, HIF-1 has been selected as a representative example to demonstrate the importance of the previously outlined points that must be considered in the design and implementation of molecular-targeted bioassays used in the discovery of antitumor natural products. Screening efforts have shown the marine invertebrate and algal extracts in the U.S. National Cancer Institute's Open Repository to be a valuable source of new regulators of HIF-1 signaling [14]. Compounds isolated from marine organisms appear to either inhibit or promote HIF-1 activation. In addition to its coverage of basic concepts in molecular-targeted antitumor drug discovery, this chapter highlights the emerging role of marine natural products as potential regulators of HIF-mediated hypoxic signaling.

22.2 Bioassay Target Selection

Perhaps, nowhere in natural product-based drug discovery is bioassay target selection more important than in the field of molecular-targeted antitumor drug discovery. Traditional antitumor drug discovery has relied heavily on tumor cell viability assays for the identification of new natural product-based anticancer compounds [17–19]. Assay target selection consisted mainly of a choice in tumor cell lines and/or in the design of specific assays to discriminate between agents that

produce either a cytostatic or cytotoxic effect. In these cases, the bioassay target can be considered the tumor class, which is equated to the tumor cell line tissue source. Although this strategy may currently be considered less fashionable, it continues to produce some of the most promising anticancer marine natural products (salinosporamide [20, 21] and Yondelis/ET-743/trabectedin [22, 23]). Marine natural products researchers have taken advantage of modern high-throughput bioassays to identify new compounds that function through an assorted array of antitumor molecular targets [14].

The definition of an antitumor molecular target is somewhat subjective. One investigator may consider an enzyme/enzymatic activity, protein-protein interaction, or protein-DNA interaction as the molecular target. Superficially, enzymes such as receptor protein kinases, cyclin-dependent kinases, checkpoint kinases, topoisomerases, DNA polymerases, and other proteins that mediate important reactions can be thought of in this way. In this case, an antitumor molecular target is something as conceptually straightforward as a specific protein or protein-mediated biochemical reaction. However, another drug discovery group may consider the disruption of a genetically controlled process as the molecular target, even though many individual steps may be involved in regulating the control of the overall process. In this case, the molecular target is viewed more as a complex set of biochemical and genetic events that may involve many proteins or other macromolecules. Under this broader definition, antitumor molecular targets include such occurrences as apoptosis-related cellular signaling, mammalian target of rapamycin (mTOR)-regulated protein expression, proteasome-mediated protein degradation, heat shock protein-dependent protein stability, etc. This broader view also includes the targeting of specific genes and the transcriptional or translational events involved in protein-mediated processes. According to this broader definition, drug discovery groups may employ assays that specifically examine the effects of small molecules on the multistep processes that regulate the expression or function of genes that are considered to be important in tumorigenesis, tumor progression, or metastasis. In this light, oncogenic gene transcription and the proteins involved in regulating tumor-associated gene transcription have emerged as major targets for anticancer drug discovery programs that focus on the regulation of specific tumor-specific gene function [24].

The distinctions between various molecular target definitions quickly blur when one considers the interactions between the systems involved in each class of antitumor molecular target. Enzymes may be considered biochemical targets, but enzymes can regulate the synthesis of proteins that control gene expression. Similarly, oncogenes may code for the production of enzymes or other proteins that play an important role in biochemical processes that enhance the growth and spread of tumors. Oncogenes may also code for transcription factors that regulate the expression of other genes involved in tumorigenesis. In such cases, each specific step in the process of DNA replication, transcription, translation, and protein function may represent a potentially druggable step within a single molecular target.

Hypoxia is one of the signature features of the tumor microenvironment. The rapid growth of tumor cells outstrips the capacity of tumor blood vessels to supply oxygen. Newly formed tumor blood vessels often fail to mature, and the tumor blood flow is sluggish and irregular [25]. The combination of increased oxygen demand and insufficient oxygen delivery yields hypoxic regions that are commonly found in solid tumors. Clinical studies indicate that the extent of tumor hypoxia correlates with advanced disease stages and poor prognosis. Unlike normal cells from the same tissue, tumor cells are often chronically hypoxic [26]. Since hypoxia can activate both survival and death programs, it serves as a form of physiological pressure that selects for the oncogenically transformed cells with diminished apoptotic potential [27]. The tumor cells that have adapted to a hypoxic environment are more aggressive [25, 26, 28]. Because of hypoxia-associated resistance to radiation treatment and chemotherapy, hypoxic tumor cells are considered an important contributor to malignant progression and disease relapse [25, 26]. Approaches such as breathing carbogen (95% O₂, 5% CO₂) have been employed to overcome tumor hypoxia by increasing tumor oxygenation. Most of the initial drug discovery efforts target the direct effects of hypoxia – lack of cellular oxygen – by either discovering chemical sensitizers that improve the outcome of radiation or developing hypoxic cytotoxins that selectively kill hypoxic cells [25, 26]. No hypoxic cytotoxin is currently approved, and there is only one bioreductive drug (tirapazamine) in clinical trials [29]. Although mixed results have been reported from clinical trials with tirapazamine, it is undeniable that drugs that target tumor hypoxia have significant therapeutic potential as part of a combination therapy [30]. Clearly, tumor hypoxia represents an important unmet therapeutic need, and molecular-targeted drug discovery efforts should be directed at this target.

Hypoxia-inducible factor-1 is an important molecular target for anticancer drug discovery that targets tumor hypoxia. First discovered as the transcriptional activator that binds to the promoter of human erythropoietin (*EPO*) gene and activates transcription under hypoxic conditions [31], HIF-1 was later shown to regulate the expression of genes that promote cellular adaptation and survival under hypoxic conditions [32, 33]. For example, Semenza and coworkers [32, 33] have generally classified the HIF-1 target genes that enhance the survival of hypoxic tumor cells into the following major functional groups: (1) those that increase oxygen delivery by promoting erythropoiesis [erythropoietin (*EPO*), transferrin, etc.], angiogenesis [vascular endothelial growth factor (*VEGF*), etc.], and vasodilatation (heme oxygenase, nitric oxide synthase II, etc.); (2) those that decrease oxygen consumption by switching to anaerobic metabolism (glucose transporter 1, glycolytic enzymes that include hexokinase 1, hexokinase 2, aldolase A, enolase 1, lactate dehydrogenase A, etc.); and (3) those that promote autocrine growth/survival (insulin-like growth factor II, etc.). Recent studies indicate that HIF-1 also regulates the expression of genes that are involved in processes ranging from tumor cell immortalization, genetic instability, dedifferentiation, invasion, metastasis, to treatment resistance [32–34]. These observations suggest that HIF-1 plays an important role in the etiology and malignant progression of cancers.

22.3 Molecular Target Validation

Molecular target validation is the process of establishing that a potential molecular target is essential for a disease process and that inhibition (or dysregulation) of that specific target can produce a potential therapeutic benefit. Screening efforts that use poorly validated antitumor molecular targets can be extremely expensive and time consuming in identifying active compounds that may fail to produce a significant antitumor effect in living cells. Demonstrating that a drug or other representative inhibitor of the molecular target produces the desired therapeutic outcome in patients may be the ultimate form of target validation. For example, the validation of antitumor targets such as tubulin/microtubules or topoisomerases may be considered solidly validated as druggable molecular targets by the therapeutic efficacy of the microtubule-targeted anticancer drugs vincristine and paclitaxel and by the topoisomerase inhibitors topotecan and etoposide, respectively. However, most innovative molecular-targeted marine natural product discovery programs aim to identify potential new agents that function through nontraditional mechanisms, rather than simply seek to isolate compounds that act in the same manner as clinically approved drugs. Under these conditions, molecular target validation can be considered the construction of an evidence-based case to support the essential nature and causative role of the target to a specific disease. Evidence to validate the target can come from clinical studies, but is most often derived from a combination of *in vitro* and preclinical animal-based experimental results.

Drugs often fail in clinical studies because they either do not produce the desired therapeutic effect or because they exhibit severe side effects, or toxicities, that render them unsafe for patient use [35]. Both reasons for the clinical failure of new drugs have been attributed to a lack of thorough target validation [35]. Therefore, it is essential to design a strategy for target validation that not only evaluates the therapeutic relevance of the target but that will also examine the specificity of the molecular target for the biochemical or physiological processes that contribute to the disease process. This is crucial in order to discriminate between disease-specific activity and off-target-related effects. While many *in vitro* cell-based methods (e.g., DNA-microarray or proteomic-based systems) are widely used in target validation, the most convincing data usually come from those models that more closely represent the disease condition in humans [36]. Various forms of gene/target knockout models are used to examine the physiological relationship between a specific gene, or gene product protein, and a particular disease phenotype. Traditional gene knockout methods (e.g., homologous recombination-based methods) and alternative gene knockdown or silencing methods (e.g., RNA interference) have proven invaluable as *in vivo* means to validate the critical role of a selected molecular target for a specific disease process [37]. Data from animal-based models that include physiological, genomic, or proteomic results from *in vivo* models are generally considered important for reliable target validation [35].

As a model for a validated antitumor drug target, multiple lines of evidence support the critical involvement of HIF-1 in the growth, progression, and metastatic spread of various forms of cancer [8–12]. In line with the laboratory findings, clinical studies indicate that overexpression of the oxygen-regulated HIF-1 α protein correlates with advanced disease stages, treatment resistance, and poor prognosis among patients with tumors derived from tissues that range from brain to breast [25, 26]. In general, the availability and activity of the oxygen-regulated HIF-1 α subunit determines the activity of HIF-1, a heterodimer of the bHLH-PAS (basic helix-loop-helix–PER–ARNT–SIMM) proteins HIF-1 α and HIF-1 β /ARNT (aryl hydrocarbon receptor nuclear translocator). Under normoxic conditions, HIF-1 α protein is degraded rapidly (protein half-life <5 min) while HIF-1 β protein is constitutively expressed. In many of the clinical specimens examined, the expression of HIF-1 α protein is directly linked to the extent of tumor hypoxia. The decrease in oxygen tension inhibits the hydroxylases that tag HIF-1 α protein for degradation and inactivation. The stabilized HIF-1 α protein then translocates into the nucleus, heterodimerizes with HIF-1 β protein, binds to the hypoxia response elements (HREs), and activates transcription of HIF-1 target genes (Fig. 22.1). In other cases such as renal clear cell carcinoma, HIF-1 α protein is expressed at high levels even under well-oxygenated conditions [38]. One of the molecular mechanisms for hypoxia-independent induction of HIF-1 α protein is the loss of function of the tumor suppressor von Hippel-Lindau gene (VHL). The VHL gene product pVHL mediates the degradation of HIF-1 α protein by proteasome. In the presence of oxygen and iron, HIF-1 α proteins are modified posttranslationally by prolyl hydroxylases [39–41]. The prolyl hydroxylated HIF-1 α proteins are then recognized by pVHL, polyubiquitinated by the pVHL-associated E3 ubiquitin ligase complex, and degraded by the proteasome. Inactivation of pVHL due to loss of function prevents the degradation of HIF-1 α protein. As a result, HIF-1 is activated under normoxic conditions and the HIF-1 regulated pathways such as angiogenic processes are highly active. In addition to the loss of function of VHL, other tumor-specific mechanisms that induce HIF-1 α protein and activate HIF-1 in a hypoxia-independent manner include the activation of oncogenes such as ras (rat sarcoma viral oncogene homolog), src (avian sarcoma viral oncogene), myc (avian myelocytomatosis viral oncogene homolog), and the loss of tumor suppressor genes such as PTEN (phosphatase and tensin homolog) [42, 43].

Results from numerous animal-based studies further support the notion that HIF-1 is an important molecular target for anticancer drug discovery [44, 45]. In general, overexpression of a gene product in tumor cells does not necessarily support the role of that particular gene as a molecular target for cancer therapeutics. It is anticipated that the inhibition of a true molecular target will suppress tumor progression, while the activation of a molecular target will promote tumor progression in animal-based models. Most of the animal-based studies that substantiate HIF-1 as a target for molecular-based therapeutics focus on the HIF-1A gene.

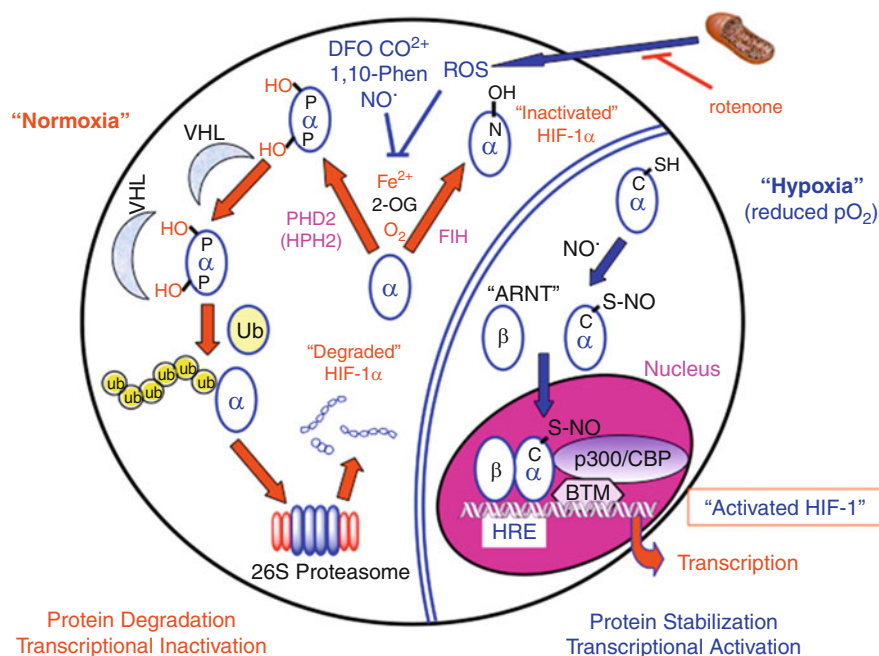


Fig. 22.1 Hypoxic regulation of hypoxia-inducible factor-1 (HIF-1). The transcription factor HIF-1 is a heterodimer composed of an HIF-1 α subunit that is regulated by cellular oxygen levels and an HIF-1 β subunit (also known as ARNT) that is constitutively expressed. Under normoxic conditions, HIF-1 α protein is hydroxylated at specific proline residues by Fe²⁺/2-oxoglutarate/O₂-dependent prolyl hydroxylase enzymes (e.g., PHD2). This prolyl-hydroxylation “tags” HIF-1 α protein for von Hippel-Lindau tumor suppressor protein (pVHL)-E3 ubiquitin ligase-mediated polyubiquitination. The “ubiquitin-tagged” HIF-1 α protein is then rapidly degraded by the 26S proteasome. Hydroxylation of an asparagine residue in the C-terminal transcriptional activation domain (CTD) contributes another level of oxygen-dependent regulation by inactivating HIF-1 α protein. Like PHD2, this asparaginyl hydroxylase [“factor inhibiting HIF” (FIH)] is also an Fe²⁺/2-oxoglutarate/O₂-dependent hydroxylase that modifies the asparagine residue in the CTD region of HIF-1 α protein. Once hydroxylated, the interaction between HIF-1 and the coactivator CBP/p300 is disrupted and transcriptional activation is blocked. Besides hypoxic conditions, HIF-1 α protein can be stabilized by addition of iron chelators, transition metals, nitric oxide radical (NO⁻), or inhibitors of PHDs [e.g., dimethylxaloylglycine (DMOG)]. Such inducing conditions inactivate the prolyl hydroxylases that tag HIF-1 α protein for ubiquitination and proteasomal degradation, and suppress the asparaginyl hydroxylase that normally inactivates the transcriptional activity of HIF-1. In addition, binding between HIF-1 and CBP/p300 can be enhanced by direct nitrosylation of a sulfhydryl moiety in HIF-1 α . When the level of O₂ decreases to a level below a certain threshold, reactive oxygen species (ROS) generated by hypoxic mitochondria inhibit PHD2 and FIH by oxidizing the Fe²⁺ in their catalytic sites. Natural products that inhibit the mitochondrial electron transport chain (e.g., rotenone) block HIF-1 activation by suppressing the hypoxia-induced increase in ROS production by mitochondria. This promotes the PHD2-mediated degradation and FIH-facilitated inactivation of the HIF-1 α subunit (Figure and caption reproduced with the permission of D.G. Nagle [© 2010] at the University of Mississippi)

22.4 Selection of Measurable Biochemical Processes Suitable for Bioassay Development

Since HIF-1 is a transcription factor, a cell-based reporter assay should be selected as the method to monitor the activity of HIF-1. Upon induction and activation, HIF-1 binds to the HRE present in the promoter region and activates transcription of the reporter gene [45, 46]. In general, the reporter gene may encode an enzyme such as luciferase, whose activity can be easily measured in a high-throughput format. The activity of the reporter (e.g., luciferase) correlates with the expression of the reporter gene that serves as an indicator of HIF-1 activity. It is anticipated that compounds/extracts that activate HIF-1 will increase the activity of the reporter, while HIF-1 inhibitory compounds/extracts will decrease the reporter activity. The advantage of such a cell-based reporter assay is that it will detect a wide range of chemicals with dissimilar mechanisms of action. The challenge is that it may take considerable effort to resolve the mechanism(s) of action once the active compounds are identified. In the event that the active compound(s) has been well characterized, the compound may serve as a molecular probe to further investigate the crosstalk between signaling pathways.

In contrast, assays that monitor one specific step within a signaling pathway will facilitate the discovery of active leads with a defined mechanism of action. For example, an assay measuring the activity of a particular kinase can be used to identify inhibitors of that particular kinase. Among the approaches used to discover HIF-1 inhibitors, one is to identify compounds that can disrupt the interaction between HIF-1 and the coactivator CBP/p300 [(cAMP-response element-binding protein)-binding protein/E1A-binding protein, 300 kD] [47]. In general, the activity of HIF-1 is determined by the availability and activity of the oxygen-regulated HIF-1 α subunit (Fig. 22.1). In the presence of oxygen and iron(II), the HIF-1 α subunits are hydroxylated by prolyl hydroxylases, and this posttranslational modification triggers pVHL-mediated proteasome degradation of HIF-1 α proteins [39–41]. Upon a reduction in cellular oxygen levels or in the presence of iron chelators, the hydroxylation reaction is inhibited and the stabilized HIF-1 α proteins translocate into the nucleus, heterodimerize with HIF-1 β subunits, and activate gene transcription. The interaction between HIF-1 and CBP/p300 enhances the formation of the transcriptional initiation complex and increases the transcription of target genes. Oxygen-dependent asparaginyl hydroxylation of HIF-1 α protein (Asn803) by factor inhibiting HIF (FIH) abrogates the interaction between HIF-1 and CBP/p300. To discover disruptors of HIF-1 α /p300 interaction, Kung and colleagues employed a time-resolved fluorescence high-throughput screening assay to detect the binding between a 41-amino-acid HIF-1 α -derived polypeptide representing the minimal p300/CBP binding domain and a glutathione-S-transferase (GST) fusion protein that contains the 122-amino-acid minimal HIF-1 α -binding domain from p300 (GST-CH1) [47]. The biotinylated HIF-1 α -derived polypeptide was immobilized onto streptavidin-coated plates. The interactions between the HIF-1 α polypeptide and the GST-CH1 fusion protein were examined using time-resolved fluorescence to monitor a europium-conjugated anti-GST

antibody probe. A library of >600,000 natural products and synthetic compounds was evaluated, and the dithiodiketopiperazine metabolite chetomin was identified as a submicromolar inhibitor of HIF-1 α /p300 interaction. The advantage of such a biochemical process-based assay is that it can be used to discover active compounds that selectively target a specific predetermined mechanism. However, some of the active compounds identified in this type of *in vitro* assays may not be further pursued if they fail to demonstrate efficacy in cell-based systems. In the case of chetomin, it exhibited anticancer efficacy *in vivo*. Since the CH1 domain is also required for CBP/p300 to serve as a coactivator to other transcriptional activators, the relative “nonspecificity” and subsequent toxicity prevented the further development of chetomin as a chemotherapeutic drug.

Small-molecule HIF-1 inhibitors have also been identified using other approaches such as an ELISA (enzyme-linked immunosorbent assay)-based assay that detects the interaction between the HIF-1 α and HIF-1 β PAS A domains [48]. As previously discussed, biochemical process-based *in vitro* assays may facilitate the discovery of HIF inhibitors that target one specific mechanism or process. For enzyme-based assays, the recombinant protein should retain the native and active conformation. Active compounds identified from the screening effort may have a higher possibility of being active in cell-based assays, if they can penetrate the host cells. In the case of *in vitro* assays that monitor protein interactions, the proteins used are often only polypeptides or otherwise truncated proteins that contain the domain(s) of interest. These “protein” reagents may not retain the native conformation that is required for proper binding. As such, a large percentage of the actives from the primary screening efforts with such biochemical assays may fall out of the “hit list” when evaluated in cell-based systems. In addition, further studies are still required to discern the specificity and the bioavailability of active compounds before the agent can be advanced to animal-based studies.

22.5 Techniques Used to Acquire or Measure the Bioassay Data

Following rapid advances in molecular techniques, most of the assay-related reagents are available from commercial sources. For screening purposes, it is important to select the method(s) that is suitable for a high-throughput format as well as cost effective. In the case of discovering small-molecule HIF-1 inhibitors, we have chosen a cell-based luciferase assay as the format for primary screening [49]. In this cell-based assay, the activity of HIF-1 correlates with the enzymatic activity of the luciferase reporter. The luciferase assay itself is straightforward, and the reagents are readily available from commercial sources. In addition, other accessories such as cell culture plates and plate readers are available in both 96- and 384-well format for the purpose of screening. Cell-based reporter assays require cellular uptake of the reporter constructs by either transient or stable transfection. The transient transfection method is relatively fast, but the cells need to be transfected every time the assay is performed. The stable transfection approach is relatively time consuming in regard to the initial effort to establish

a genetically modified cell line that has incorporated the reporter construct into its genome. However, once a stable cell line is established, the cells can be directly assayed without transfection.

Upon selecting a transient transfection approach for our HIF-1 inhibitor discovery efforts, the initial studies were directed at identifying the optimal model system for the cell-based reporter assay. A panel of human breast tumor cell lines that represent different disease stages and malignant progression were selected as *in vitro* models (early stage estrogen dependent: T47D and MCF-7; highly metastatic estrogen independent: MDA-MB-231). First, the conditions for transient transfection were optimized in each cell line using a control construct (pGL3-control, Promega) that expresses luciferase under the control of a constitutively active promoter. Second, a cell-based reporter assay for HIF-1 activity was performed in each cell line. The objective was to identify the cell line with the highest level of HIF activation. In order to improve screening efficiency, a robust assay with a high level of induction was sought to provide a low rate of background noise—associated false-positive experimental artifacts. The cells were transiently transfected with the pHRE3-TK-luc reporter to monitor HIF-1 activity and exposed to inducing conditions that activate HIF-1. The conditions that activate HIF-1 range from hypoxia (decreased oxygen tension), iron chelators, transition metals (Co^{2+} , Ni^{2+} , etc.), to oncogenic mutations (activation of oncogenes and/or inactivation of tumor suppressor genes). In solid tumors, hypoxia is a common pathophysiological condition and the extent of tumor hypoxia correlates with advanced disease stages and poor prognosis. Since HIF-1 is a key regulator of hypoxia-regulated gene expression that promotes tumor cell adaptation to hypoxia and overall treatment resistance, compounds that inhibit hypoxic activation of HIF-1 represent potential drug leads that selectively target tumor hypoxia. The focus of our discovery project was the identification of small molecules that inhibit HIF-1 activation by hypoxia. Among the cell lines examined (Fig. 22.2), T47D breast tumor cells exhibited the highest level of HIF-1 induction upon hypoxic exposure (1% O_2 /5% CO_2 /94% N_2 , 16 h). This T47D cell-based HIF-1 reporter assay produced the greatest signal to noise (background) ratio. The effectiveness of the cell-based reporter assay for detecting HIF-1 inhibitors was examined with a known HIF-1 inhibitor, MEK1 (meiosis-specific serine/threonine protein kinase) inhibitor PD98059. In MCF-7, MDA-MB-231, and T47D cells, PD98059 inhibited HIF-1 activation by hypoxia with comparable potencies (Fig. 22.3). Further cell viability studies in T47D cells excluded the possibility of false positives due to cytotoxicity.

22.6 Design and Use of Proper Experimental Controls

In an ideal situation, all molecular-targeted screening efforts should be conducted in a statistically significant way ($N \geq 3$) to achieve accuracy and reliability. However, it is time consuming and not feasible for many small academic laboratories with limited resources to examine tens of thousands of samples in triplicate. To meet this challenge, one approach is to include some element of replication and

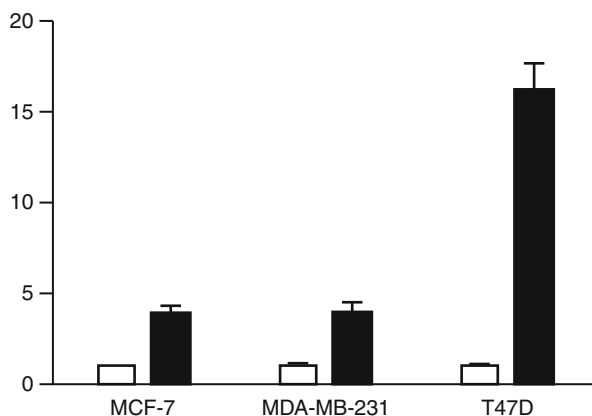


Fig. 22.2 Cell line-dependent hypoxic activation of HIF-1 determined in a cell-based reporter assay. Three human breast tumor cell lines (MCF-7, MDA-MB-231, and T47D) were transiently transfected with a pHRE-TK-Luc construct and exposed to hypoxic conditions (1% O₂/5% CO₂/94% N₂, 16 h). Control cells were incubated under normoxic conditions (95% air/5% CO₂, 16 h). The cells were lysed, and luciferase activity was determined and presented as relative luciferase activity to the control. Data shown are averages from one representative experiment performed in triplicate, and the error bars indicate one standard deviation

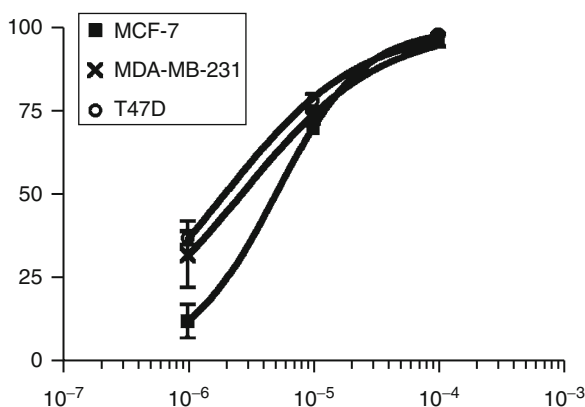
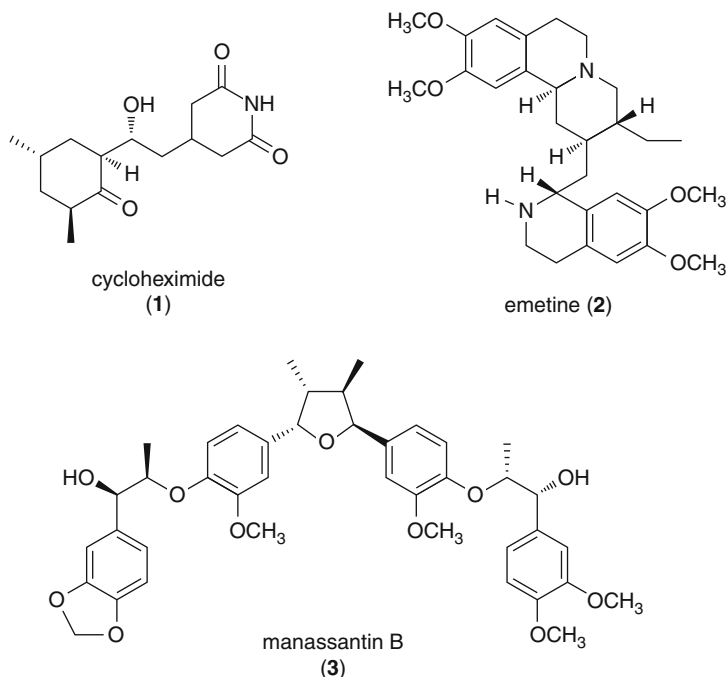


Fig. 22.3 PD98059 inhibits hypoxic activation of HIF-1 in a concentration-dependent manner. Human breast tumor cells (MCF-7, MDA-MB-231, and T47D) were transiently transfected with a pHRE-TK-Luc construct and exposed to hypoxic conditions (1% O₂/5% CO₂/94% N₂, 16 h) in the presence of PD98059 at the final concentrations of 1, 10, and 100 μM. The cells were lysed, and luciferase activity was determined and presented as percent inhibition of the solvent-treated control. Data shown are averages from one representative experiment performed in triplicate, and the error bars indicate one standard deviation

proper experimental controls to ensure the effectiveness of the bioassays. If an assay is deemed effective, then we can assume that the results obtained with the samples will have a higher probability of accuracy. In the T47D cell-based reporter assay for HIF-1 activity, the ratio of luciferase activity under hypoxic conditions

versus that under normoxic conditions serves as an indicator for the extent of HIF-1 activation. The inhibition of HIF-1 activity observed in the presence of an HIF-1 inhibitor (e.g., cycloheximide) (**1**) indicates the effectiveness of the assay for detecting HIF-1 inhibitors [50]. Other HIF-1 inhibitors have also been used as positive controls in HIF-1 bioassays. These positive controls include the nonselective alkaloid-based protein synthesis inhibitor emetine (**2**) [51–53] and *Saururus cernuus* dineolignan HIF-1 inhibitor manassantin B (**3**) [54].



Upon identification of the proper controls, another factor that impacts the screening outcome is the final concentration of the test sample. When the sample concentration is too high, nonspecific and/or less potent inhibitors will appear as positives in the assay, and this will lead to an unmanageably high hit rate. As shown in Fig. 22.4a, approximately 78% of the extracts on a 96-well sample plate inhibited HIF-1 activation by >50% when tested at the concentration of 50 $\mu\text{g/mL}$. In contrast, the hit rate in the primary assay was reduced to 2% when the same samples were examined at 5 $\mu\text{g/mL}$ (Fig. 22.4b).

22.7 Bioassay Validation and the Application of Appropriate Statistical Methods

The results of molecular-targeted antitumor assays can only be considered reliable if the experiments are properly controlled, the bioassay methods have been

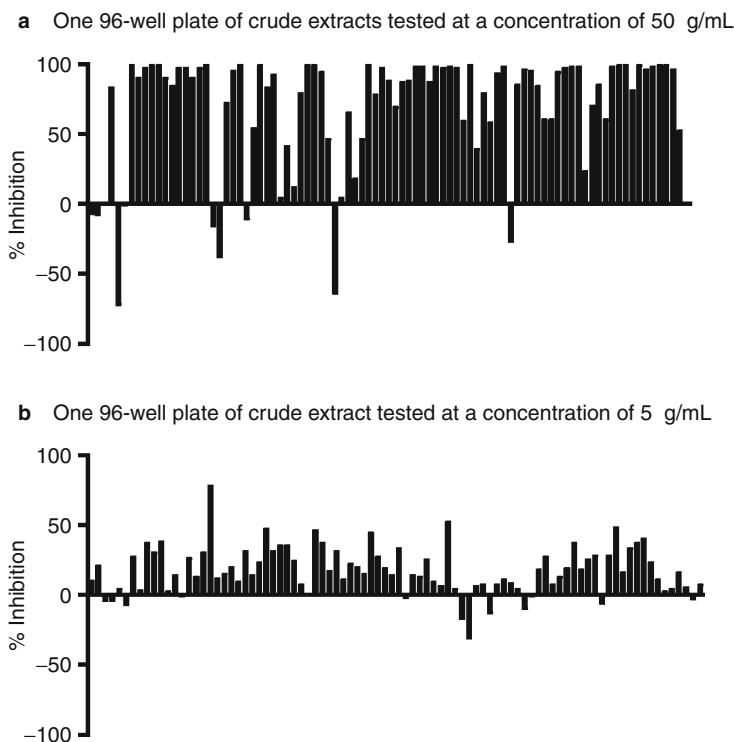


Fig. 22.4 Results for hypoxia-induced HIF-1 inhibitory effects observed for a representative 96-well plate of extracts evaluated at two different final concentrations. T47D human breast tumor cells were transiently transfected with a pHRE-TK-Luc construct and exposed to hypoxic conditions (1% O_2 /5% CO_2 /94% N_2 , 16 h) in the presence and absence of natural product-rich extracts. The cells were lysed, and luciferase activity was determined and presented as percent inhibition relative to a nontreated hypoxic control. **(a)** Approximately 78% of the extracts on a 96-well sample plate of chemically diverse plant extracts inhibited HIF-1 activation by $>50\%$ when tested at the concentration of 50 $\mu\text{g/mL}$. **(b)** When the identical 96-well plate of extracts was evaluated at a final concentration of 5 $\mu\text{g/mL}$, the corresponding hit rate in the primary assay was reduced to only 2%

rigorously validated, and the results are analyzed using suitable statistical methods for the particular bioassay design. Despite the fact that these criteria are necessary for the publication of manuscripts that specifically describe new bioassay methods, such standards are seldom given sufficient attention in publications that describe the biological activities associated with either marine or terrestrial natural products. It is relatively common to see publications that combine the isolation and structure elucidation, total synthesis, and other aspects of medicinal chemistry with biological testing results. All too often these reports focus on the natural products chemistry but fall short in respect to their standards for the bioassay acquisition methods and statistical data analysis. Experimental results are commonly reported

without including the data for positive or negative experimental controls, IC_{50} values are frequently reported without any indication of experimental replication, and structure-activity relationship studies are sometimes supported by tables of results that do not specify the magnitude of the observed experimental error or if the differences in bioactivity between structurally related compounds have statistical significance.

It is beyond the scope of this chapter to describe the statistical methods by which various molecular-targeted bioassays must be evaluated. However, recent articles, reviews, and texts provide a detailed perspective of statistical methods used to analyze and evaluate bioassay data [55–59].

In order to ensure the reliability of bioassays used to screen extracts, active chromatographic fractions, and purified natural products from marine organisms, these assays must be validated with respect to an array of assay parameters (robustness, linearity, accuracy, precision, sensitivity, and specificity). For our screening purposes, we define these bioassay validation terms in a similar manner to the “Guidelines for Industry” text on Validation of Analytical Procedures of the International Conference on Harmonisation (ICH) [60–62]:

- Assay “robustness” is a measure of an assay’s tendency to be susceptible to minor background variation in responses and is reflected by the magnitude of response (or signal) relative to background variation (or noise). Robust bioassays are generally more sensitive and require fewer replicates to observe statistical significance.
- Assay “linearity” is the ability of the assay to obtain test results that are uniformly proportional (within a specific range) to either the molecular/biochemical process evaluated or, in the case of analytical procedures, directly proportional to the concentration of sample.
- Assay “accuracy” is a measure of how close the results of the assay are relative to accepted reference or control values.
- Assay “precision” is the variation between multiple replicates and is generally expressed in terms of standard deviation, coefficient of variation, etc. Bioassay precision is a measure of experiment to experiment repeatability (intra-assay precision within a given laboratory), intermediate variation (between various equipment, personnel, etc.), and assay reproducibility between different laboratories. The sensitivity is a measure of the minimum detection limits of a bioassay method.
- Assay “specificity” is determined by the ability of the assay method to specifically respond to the desired molecular or biochemical process, relative to the bioassay’s susceptibility to false positives due to off-target effects produced by test substances.

Shen and colleagues took an siRNA (small interfering RNA)-based loss-of-function screening approach to identify potential druggable targets that control the HIF-1 pathway [63]. A non-small-cell lung carcinoma H1299 cell-derived stable HIF-1 reporter cell line (H1299_HRE) was established. Expression of this luciferase reporter was under the control of the HRE from the enolase promoter and hypoxic exposure increased luciferase activity by three- to fivefold. For assay

validation, H1299_HRE cells were transfected with an HIF-1A siRNA as a positive control and a scramble siRNA as a negative control. The transfected cells were exposed to hypoxic conditions and the luciferase activities determined. The assay used in this initial screening had Z-factor values that were greater than 0.5. This indicated that the H1299_HRE-based reporter assay was suitable for high-throughput screening. The Z-factor is a simple statistical parameter used to assess assay quality, defined as $Z\text{-factor} = 1 - [3 \times (\sigma_p + \sigma_n)]/|\mu_p - \mu_n|$ [64]. The four parameters are the means (μ) and the standard deviations (σ) of the controls [positive (p) and negative (n)]. An ideal assay will yield a Z-factor of 1, an excellent assay Z-factor between 0.5 and 1.0, a marginal assay Z-factor between 0 and 0.5, and a highly variable assay will produce a Z-factor less than 0.

Based on the Z-factor analysis, the H1299_HRE-based reporter assay was considered suitable for high-throughput screening (HTS) and was used to examine an siRNA library against approximately 4,000 druggable targets. However, confirmation studies revealed that the hits identified in the primary assay were caused by siRNA-mediated off-target gene silencing that nonspecifically inhibited HIF-1. The H1299_HRE cells were used to establish a 384-well-based reporter assay for HIF-1 activity. A library of 691,200 small molecules was examined in this assay (Z-factor 0.18), and this chemical genomics approach led to the identification of alkyliminophenylacetate compounds as potent HIF-1 inhibitors. The low Z-factor indicates that this latter HTS assay would have only marginal reliability.

22.8 Bioassay Method-Specific Experimental Artifacts

Every assay format has method-specific advantages and disadvantages. For the purpose of HTS screening, most bioassays employ colorimetric, fluorescent, or luminescent methods to measure the outcomes. In the case of marine organism extracts, many substances in the crude extracts can potentially interfere with fluorescence- or luminescence-based methods due to autofluorescence or quenching of the fluorescent and/or luminescent signals. To reduce the rate of false positives associated with method-related experimental artifacts, the active samples should be first evaluated in a secondary screening system that acts as a control for substances that particularly interfere with the selected bioassay method. For example, active extracts that inhibit HIF-1 activation in our previously described T47D cell-based reporter assay are then examined in T47D cells that are transfected with a control construct (pGL3-control) [49, 65]. The pGL3-control construct contains a simian virus 40 (SV40) promoter and enhancer sequences that strongly express a modified firefly luciferase reporter gene (luc+) in many mammalian cell lines. A false positive that inhibits the luciferase reaction and/or expression will also suppress luciferase activity in the tumor cells that have been transfected with the control construct. Similarly, active samples identified using a fluorescence-based method can be evaluated in a separate fluorescence-based assay for an unrelated target. In general, false positives associated with

a specific method will inhibit all similar assays that examine unrelated targets using the same assay method. In this respect, it is critical to establish a screening protocol that incorporates procedures that remove method-related experimental artifacts.

22.9 Identification of Active Marine Natural Products

Just as demonstrating clinical efficacy results is the most definitive form of target validation, the identification of therapeutically effective compounds that regulate the selected molecular target can be considered strong practical proof of bioassay validation. The subject of molecular-targeted anticancer marine natural product discovery has been reviewed with respect to antitumor compounds that were specifically identified through the use of molecular-targeted bioassays [6].

To date, only a relatively small number of marine natural products have been found to inhibit HIF-1 activation in various tumor cell lines (reviewed in 14). The University of Mississippi HIF discovery program identified most of these marine-derived HIF-1 inhibitors [66]. Over 10,560 lipid extracts of marine invertebrates and algae crude extracts have been evaluated in the primary T47D human breast tumor cell-based reporter assay for the ability to inhibit hypoxia-induced HIF-1 activation [49]. As previously described, the extracts were examined in the T47D cell-based reporter assay (5 $\mu\text{g/mL}$ = 5 ppm) and the threshold for actives was set at $\geq 70\%$ inhibition. Actives from the primary screen were subjected to a panel of additional bioassays designed to aid in the confirmation, prioritization, deselection, and dereplication process (Fig. 22.5).

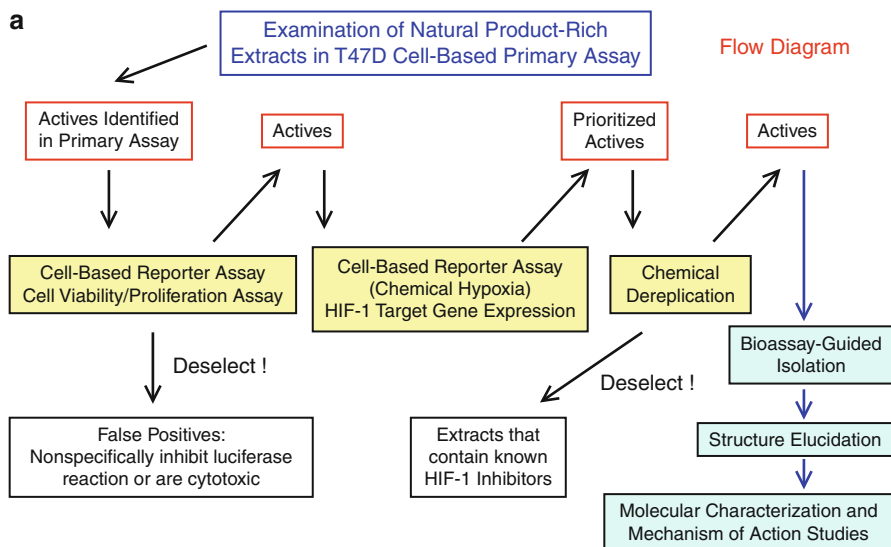


Fig. 22.5 (continued)

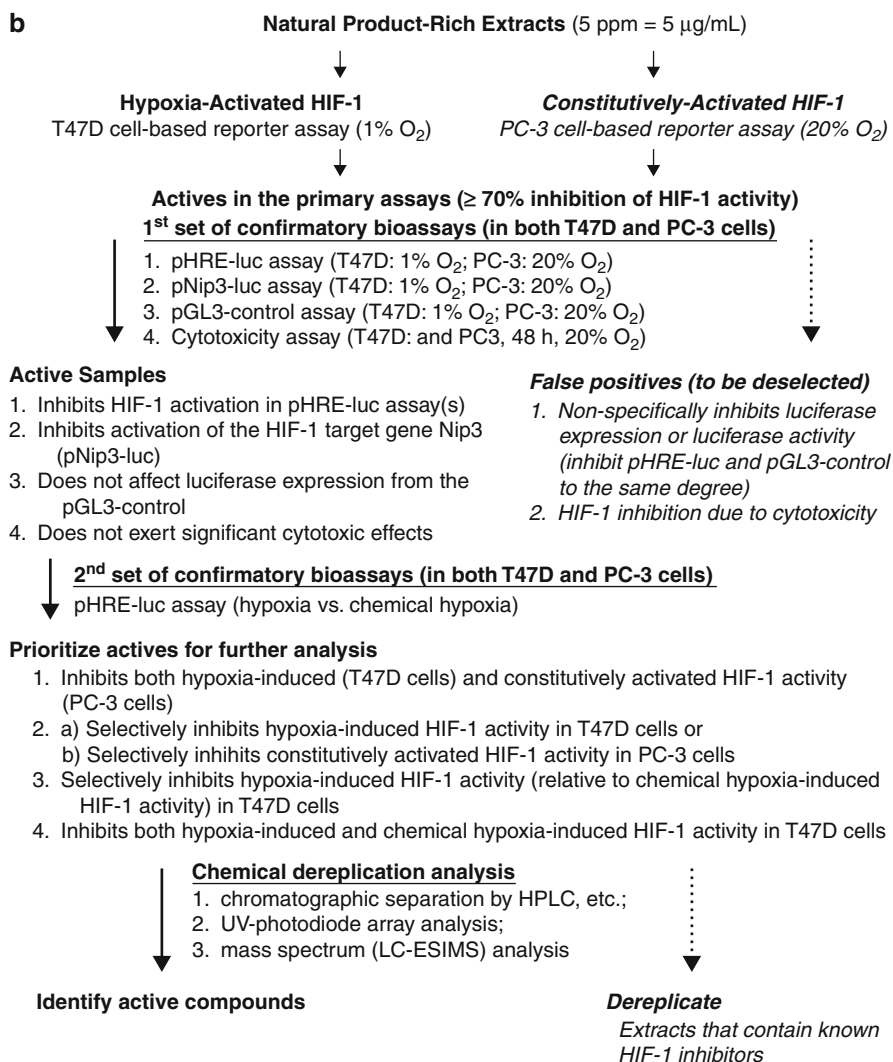


Fig. 22.5 Flow diagrams depicting representative bioassays used in HIF-1 inhibitor confirmation, prioritization, deselection, and dereplication process. **(a)** General flow diagram outlining HIF-1 bioassay evaluation system; **(b)** specific experimental protocols used to confirm, prioritize, deselect, and dereplicate extracts, fractions, and purified compounds detected in primary HIF-1 luciferase reporter assay system

Since the number of samples in the NCI Open Repository of marine invertebrate and algae extracts [67] was relatively large (10,560 lipid extracts), screening results from this large group of samples were analyzed and summarized in the following synopsis. A total of 109 active extracts (1% hit rate) were identified in the primary screen (Fig. 22.6a). Over one-half of the active samples were lipid extracts of marine sponges (57 out of 109). Although, a broad range of organisms were shown to have HIF-1 inhibitory activity (sea hares, algae, echinoderms, bryozoans, nudibranchs, and cnidarians). Active extracts were subjected to additional bioassays that include the following: (1) a pNip3-luc reporter assay for detecting substances that inhibit HIF-1 activation [68]; (2) a pGL3-control (Promega) reporter assay to deselect false positives that inhibit luciferase expression/activity [49, 65]; (3) a cell proliferation/viability assay to exclude cytotoxic extracts; and (4) a pHRE-TK-Luc reporter assay to confirm the initial results and discern the specificity toward the inhibition of low-oxygen (1% O₂) hypoxia-induced HIF-1 activation relative to the ability of chemical hypoxia [1,10-phenanthroline (10 μM)] to induce HIF-1 activation. Between 80% and 90% of the active extracts were confirmed upon retesting. Less than one-half of the samples suppressed tumor cell proliferation/viability by more than 50%. Over 50% of the active extracts showed selectivity for inhibiting hypoxia-induced HIF-1 activation over chemical hypoxia-induced HIF-1 activation. From the original 109 extracts that were active in the primary T47D cell-based reporter assay, 40 extracts (0.38% of the 10,560 extracts examined) withstood confirmatory secondary testing and were prioritized for further study (Fig. 22.6b). Samples from the NCI Open Repository are available on a first-come-first-serve basis, and the availability of many extracts is extremely limited. Supply-based prioritization suggested that only 33 extracts (out of the original 109 active extracts) were available from the NCI-Developmental Therapeutics Program (NCI-DTP) in sufficient quantity (typically 2–4 g) to guarantee any probability of successful bioassay-guided isolation and structure elucidation efforts, to ensure that the quantities of active pure compounds isolated would be adequate for in vitro mechanistic studies, and/or to evaluate for efficacy in vivo. Based on results from the biological confirmatory studies and the quantity of samples available, about one-third of the samples were assigned as “high-priority” for isolation efforts.

This synopsis exemplified several of the advantages of sourcing the NCI Open Repository – the large number of samples available for HTS assays, low-cost access to chemical diversity, logistical ease relative to investigator-initiated collection efforts and intellectual property negotiations, and the ability to identify new pharmacological activities even for “known” natural products. Efforts to source NCI samples are also associated with a number of disadvantages. These include limited sample availability due to previous use by other investigators and a lack of samples from microbial sources. Despite these possible disadvantages, a variety

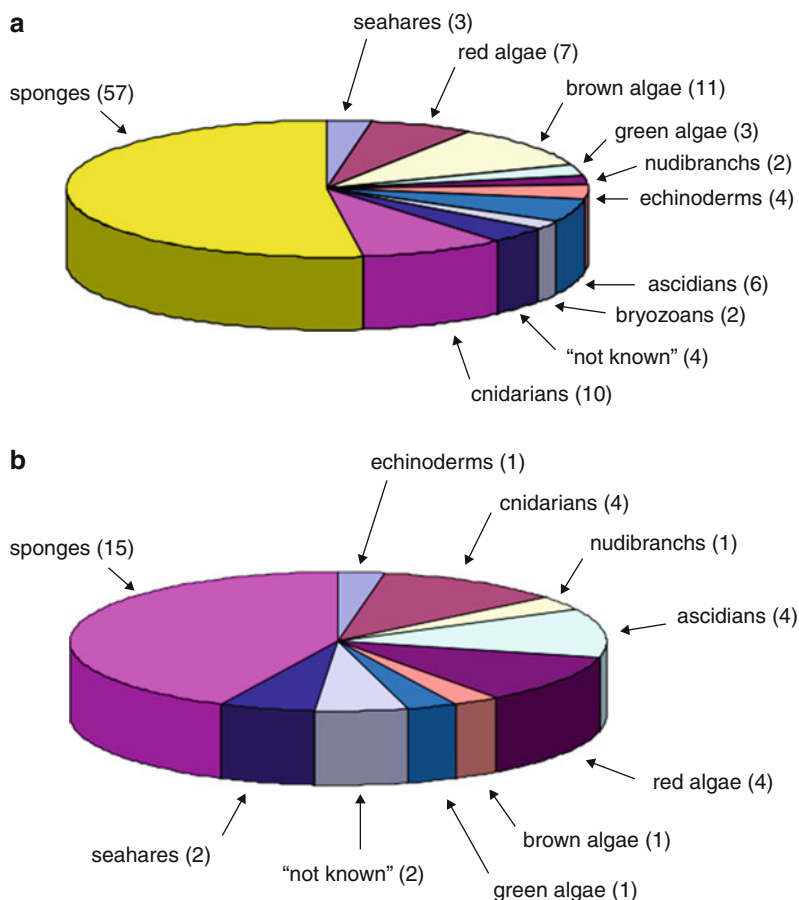


Fig. 22.6 Charts illustrating numbers and distribution of marine organism extracts found to inhibit HIF-1 activation in a cell-based reporter assay. Lipid extracts (10,560) from the NCI Open Repository of marine invertebrate and algae extracts were examined for the ability to inhibit hypoxia-induced HIF-1 activation in a T47D breast tumor cell line-based luciferase reporter assay. **(a)** Primary screening revealed 109 extracts strongly inhibited HIF-1 activation in the primary assay (a $\geq 70\%$ decrease in pTK-HRE3-Luc). **(b)** Only 40 extracts remained following secondary evaluation in assays designed to confirm and prioritize the samples that were shown to be active in the primary reporter assay. Extracts from a variety of marine organisms were found to contain substances that potentially inhibited hypoxic-induced HIF-1 activation (Figures and caption reproduced with the permission of D.G. Nagle [© 2010] at the University of Mississippi)

Table 22.1 Examples of marine natural products that inhibit HIF-1 activation

Compound name (no.)	Source	IC ₅₀ (μM) ^a	References
Laurenditerpenol (4)	<i>Laurencia intricata</i>	0.4	[70]
7-Hydroxyneolamellarin (5)	<i>Dendrilla nigra</i>	1.9	[53]
Furospongolide (6)	<i>Lendenfeldia</i> sp.	2.9	[72]
Sodwanone V (7)	<i>Axinella</i> sp.	15	[73]
9,9'-Oxybis-neocomantherin (8)	<i>Comantheria rotula</i>	0.8	[65]
Neocomantherin (9)	<i>C. rotula</i>	1.9	[65]
Comantherin (10)	<i>C. rotula</i>	2.7	[65]
5,8-Dihydroxy-6-methoxy-2-propyl-4 <i>H</i> -benzo[<i>g</i>]chromen-4-one (11)	<i>C. rotula</i>	0.6	[65]
8- <i>O</i> -Methylneocomantherin (12)	<i>C. rotula</i>	2.0	[65]
TMC-256A1 (13)	<i>C. rotula</i>	0.9	[65]
Comaparvin (14)	<i>C. rotula</i>	3.0	[65]
Mycalenitrile-6 (15)	<i>Mycale</i> sp.	7.8	[74]
Mycalenitrile-7 (16)	<i>Mycale</i> sp.	8.6	[74]
Caulerpin (17)	<i>Caulerpa</i> spp.	10	[75]
Strongylophorine 2 (18)	<i>Petrosia strongylata</i>	8 ^b	[76]
Strongylophorine 3 (19)	<i>P. strongylata</i>	13 ^b	[76]
Strongylophorine 8 (20)	<i>P. strongylata</i>	6 ^b	[76]
Latrunculin A (21)	<i>Negombata magnifica</i>	6.7	[52]

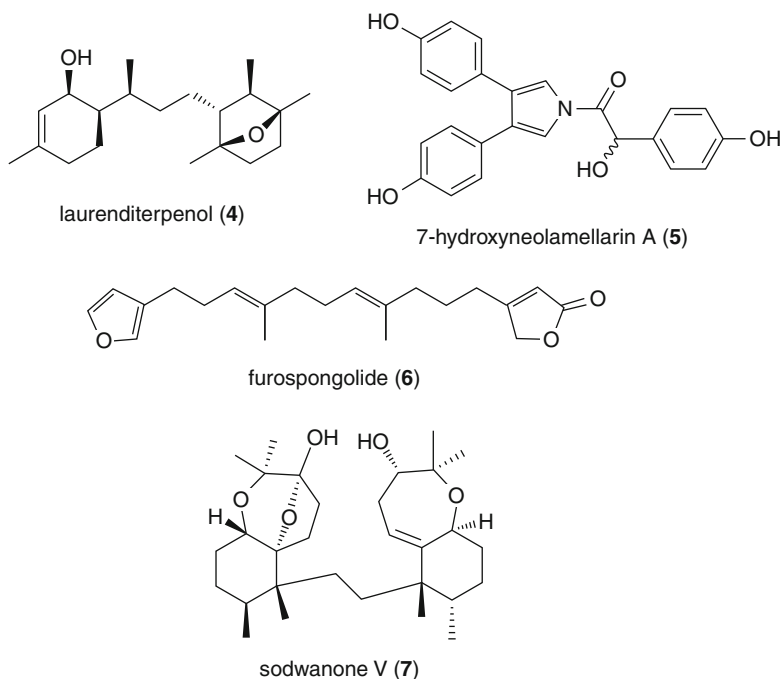
^a IC₅₀ values for hypoxia (1% O₂)-induced HIF-1 activation in a T47D cell-based reporter assay, unless otherwise noted

^b EC₅₀ values for hypoxia (1% O₂)-induced HIF-1 activation in a U251 cell-based reporter assay

of novel HIF-1 inhibitors were discovered from the available samples, and some of these were described in two recent reviews on natural product-derived inhibitors of HIF-1 (Table 22.1) [14, 69].

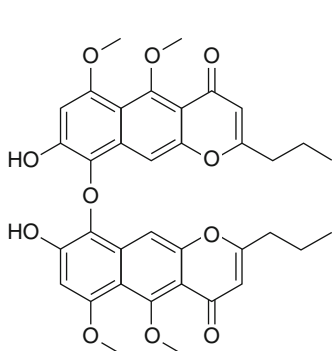
Once the active compounds were isolated, a combination of spectroscopic and spectrometric methods including multidimensional NMR spectroscopy and high-resolution mass spectrometry (HRMS) were employed to elucidate the structures of active compounds. This unique HIF-1 inhibitor discovery effort that combined the chemical diversity offered by natural products with effective and reliable bioassays has resulted in the identification of some of the most potent HIF-1 inhibitors known [16]. The first marine natural product found to inhibit hypoxia-induced HIF-1 activation in tumor cells was from the lipid extract of a Jamaican collection of the red alga *Laurencia intricata* Lamouroux (Rhodomelaceae). Laurenditerpenol (**4**), a novel bicyclic diterpene, was found to be the active constituent of the alga. Compound **4** inhibited hypoxia (1% O₂)-induced HIF-1 activation in T47D cells at submicromolar concentrations (Table 22.1) [70]. The absolute configuration of **4**

has recently been defined by total synthesis [71]. Total synthesis may also afford sufficient quantities of **4** and various related isomers for further biological evaluation and a study of structure-activity relationships (SARs).

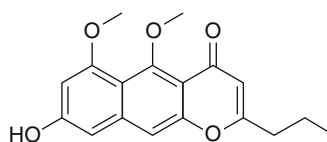


The NCI Open Repository of marine invertebrate and algae extracts has proven to be a valuable source of small-molecule inhibitors of HIF-1 activation. These marine natural product-based HIF-1 inhibitors include the sponge metabolites 7-hydroxyneolamellarin (**5**) [53], furospongolide (**6**) [72], and a series of sodwanone and yardenone triterpenoids [i.e., sodwanone V (**7**)] [73]. Similarly, benzo[*g*]chromen-4-one and benzo[*h*]chromen-4-one pigments (**8–14**) from a tropical marine crinoid (Comasteridae) were also found to inhibit hypoxia-induced activation of HIF-1 [65]. However, these benzochromenones were not further pursued because their ability to inhibit HIF-1 activation did not translate into a significant effect on the HIF-1 target genes examined (i.e., secreted VEGF) and, for all practical purposes, these crinoid pigments are now considered possible nuisance compounds. Recently, bioassay-guided fractionation of an active extract of a *Mycale* sp. sponge yielded 18 new and 8 previously reported lipophilic 2,5-disubstituted pyrroles, collectively known as mycalenitriles and mycalazals [e.g., mycalenitrile-6 (**15**) and mycalenitrile-7 (**16**)] [74]. The red pigment caulerpin (**17**) was first isolated from green algae of the genus *Caulerpa* [75].

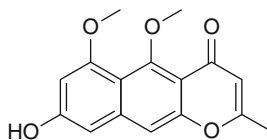
Caulerpin (**17**) inhibited hypoxia-induced and 1,10-phenanthroline-induced HIF-1 activation [51]. The angiogenic factor VEGF is regulated by HIF-1. Caulerpin (10 μ M) suppressed hypoxic induction of secreted VEGF protein and the ability of hypoxic T47D cell-conditioned media to promote tumor angiogenesis in vitro.



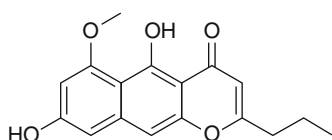
9,9'-oxybis-neocomantherin
(**8**)



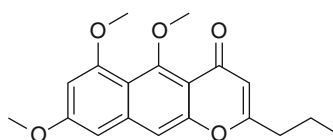
neocomantherin
(**9**)



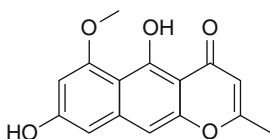
comantherin
(**10**)



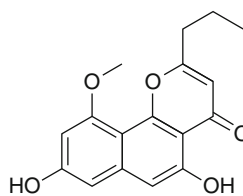
5,8-dihydroxy-6-methoxy-2-propyl-4H-benzo[chromen]-4-one
(**11**)



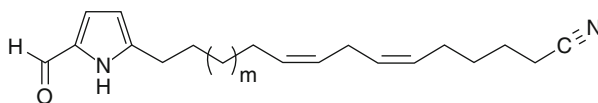
8-O-methylnocomantherin
(**12**)



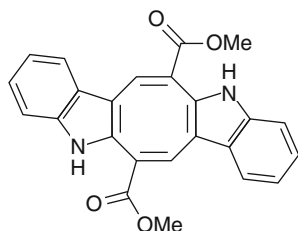
TMC-256A1
(**13**)



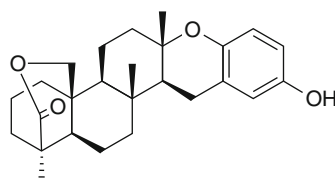
comaparvin
(**14**)



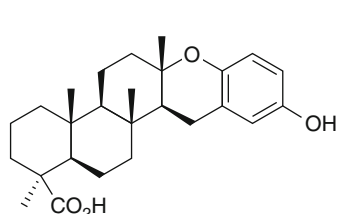
mycalenitrile-6 (**15**) $m=9$
mycalenitrile-7 (**16**) $m=11$



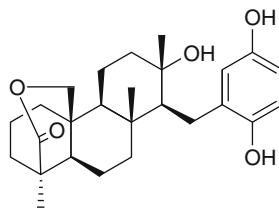
caulerpin (17)



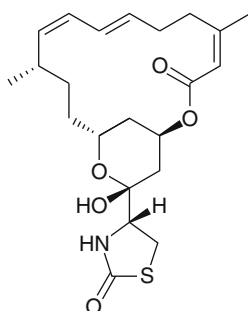
stronglylporine 2 (18)



stronglylporine 3 (19)



stronglylporine 8 (20)



latrunculin A (21)

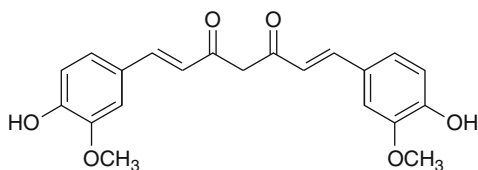
In addition to sourcing from the NCI Open Repository, several laboratories have reported the isolation and identification of HIF-1 inhibitors from their field collections of marine organism extracts. Ireland and coworkers recently found that an extract from a Papua New Guinea collection of the sponge *Petrosia* (*Strongylophora*) *strongylata* significantly inhibited HIF-1 activation at 1 μ g/mL [76]. Through a process of bioassay-guided isolation, three previously reported stronglylporine meroditerpenoids were identified to be responsible for the

observed HIF-1 inhibition. Strongylophorines 2 (**18**), 3 (**19**), and 8 (**20**) inhibited hypoxia-induced HIF-1 activation in a genetically engineered U251 human glioma cell-based luciferase reporter assay [76]. The Red Sea sponge macrolide latrunculin A (**21**) disrupts actin polymerization and inhibits microfilament formation by reversibly binding to actin monomers [77–79]. This sponge-derived actin inhibitor has recently been shown to inhibit hypoxia-induced HIF-1 activation in T47D cells [52]. Not only are these marine natural products inhibitors of HIF-1 activation in tumor cells, but many appear to function through mechanisms that have not yet been recognized to regulate HIF-1 activity. A summary of the marine-derived HIF-1 inhibitors discovered in this program is provided in [Table 22.1](#).

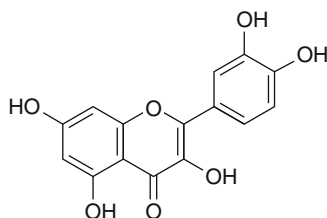
22.10 Dereplication of Nuisance Compounds

The concept of “nuisance” compounds is highly subjective and depends on the focus of the individual antitumor discovery group. In high-throughput screening, nonselective compounds that exert a variety of effects on various assay systems are typically considered nuisance compounds. Similarly, if the research program is solely interested in the discovery of novel chemical entities with a particular pharmacological activity, the researchers may consider all previously identified known compounds that show activity in other systems to be nuisance compounds. Each particular type of bioassay method is associated with assay-specific nuisance compounds. Chemically reactive compounds, including certain phenolic compounds, may nonselectively bind to proteins and inhibit enzyme-based assays [80, 81]. Pigments and other colored natural products can interfere with colorimetric assays. It is widely known that fluorescence-based assays may be susceptible to interference by fluorescent natural products [e.g., curcumin (**22**)] or compounds such as the flavonoid quercetin (**23**) that acts to quench the fluorescence [82]. Poorly controlled fluorescence-based bioassays have been used to support the premise that these natural products regulate a plethora of diverse molecular targets. Although less appreciated, pigmented and fluorescent natural products may also interfere with luciferase reporter gene assays that rely on fluorescent reagent formulations to enhance their light readouts. Cytotoxic natural products may be considered nuisance compounds when observed in cell-based bioassays that screen for inhibitors of a tumor cell selective molecular target. Similarly, compounds that do not penetrate cell membranes may be regarded as nuisance compounds in solution-based enzyme/protein-based *in vitro* assays. In such cases, whether or

not certain compounds are regarded as nuisance compounds depends on the particular objectives of the screening program.



curcumin (**22**)



quercetin (**23**)

Just as in other forms of natural product screening, molecular-targeted drug discovery programs that aim to identify marine natural product-derived anticancer agents must avoid the unnecessary replication of previously identified inhibitors (or activators) of the selected molecular target and common substances that exert nonselective effects on biological systems. One of the most powerful and inexpensive means to reduce the replication of chemical isolation and structure elucidation efforts in marine natural products is the use of chemotaxonomic literature related to the particular marine organism. Databases of marine natural products literature are readily accessible to most molecular-targeted drug discovery groups. These include general chemical (Chemical Abstracts Service (American Chemical Society)-SciFinder/SciFinder Scholar [83]) and biological (U.S. National Library of Medicine/National Institutes of Health-MEDLINE database accessible through PubMed [84]) databases. Highly specialized marine natural product databases (Marinlit [85]) that include searchable NMR and other spectroscopic data are also available and can greatly enhance chemical dereplication efforts. These databases can be used to identify known compounds and to distinguish previously reported redundant biological activities that may be associated with a particular marine natural product. Dereplication with chemotaxonomic data from chemical and biological literature databases is most efficient when examining well-characterized species of marine invertebrates and algae, but may be only of limited utility in screening programs that focus on poorly characterized new species of cultured marine microbes. One potential limitation of the use of chemotaxonomic literature for chemical dereplication efforts is that many species of marine organisms are

poorly characterized chemically as well as taxonomically [2, 86]. Since most marine natural products chemists are not in the habit of regularly reporting known compounds when they are found to occur in new species, estimates of the potential chemical diversity of many readily collectible species may be significantly underestimated. Chemical and biological dereplication for many of these species is often achievable by analysis of the chemotaxonomic and pharmacological literature related to other members of the same genera or taxonomic family. While practical limitations exist, the importance of chemical and biological databases in reducing the need for unnecessary marine natural product isolation and structure elucidation efforts cannot be overstated.

The subject of natural product dereplication has been the subject of recent reviews [87]. Compound dereplication strategies also commonly include various libraries of compound data sets that are used with a “hyphenated” technique that combines a purification method with a spectroscopic or spectrometric detection system. Sarker and Nahar have recently reviewed the field of hyphenated separation and spectroscopic/spectrometric techniques with respect to various classes of natural products [88]. Typical examples may include traditional methods such as high-performance liquid chromatography (HPLC) coupled with ultraviolet (UV) photodiode detection. Dereplication efforts have more recently come to rely on methods that combine liquid chromatography (LC) and mass spectrometry (MS) or nuclear magnetic resonance (NMR) spectroscopy. Tandem LC-MS and LC-MS-MS methods are among the most sensitive means to derePLICATE known compounds. While inherently less sensitive, coupled LC-NMR methods have the advantage that they can be simultaneously used for dereplication and the structure elucidation of new natural products. Hyphenated techniques and their use in the dereplication of natural products are further described in recent reviews [87].

The expenditure of unnecessary efforts due to the occurrence of natural products that act by relatively general means to produce numerous nonspecific effects in bioassay systems must also be reduced. The previously described methods of compound dereplication can be used to identify known compounds that exert nonselective effects on assay systems. Alternatively, experimental procedures with appropriate controls can be designed directly into the assay systems to dramatically cut the number of bioassay “hits” that result from active compounds with no selectivity for the molecular target. This strategy can readily deselect nuisance compounds without requiring any sample purification, chemical analysis, or other dereplication procedure. Examples of this type of bioassay design-based nuisance compound dereplication include the use of alternative isoforms of a particular enzyme in a parallel screening platform [89] and the concurrent measurement of cell viability with cell-based bioassays for a molecular target that should not produce a cytotoxic effect on certain cell types.

The need to derePLICATE known marine natural product HIF-1 inhibitors has only recently emerged as several groups have begun to identify marine invertebrate and

algae compounds that inhibit HIF-1 activation (reviewed in 14). The marine natural product-based HIF-1 inhibitors described in Table 22.1 include algal metabolites, crinoid benzochromenone pigments, latrunculin actin inhibitors, terpenes, and various lipids from marine sponges. In addition, various HIF-1 discovery groups have examined terrestrial natural products [15, 16] and synthetic pure compound libraries [63] and have reported that compounds that regulate certain central cellular biochemical processes may also suppress HIF-1 activation. Both academic and industrial HIF-1 screening efforts have found that mitochondrial electron transport chain (ETC) inhibitors suppress HIF-1 activation by hypoxia [63, 70], presumably by interfering with mitochondrial reactive oxygen species (ROS)-mediated signaling and destabilizing HIF-1 α protein under hypoxic conditions. The emerging role of mitochondrial reactive oxygen species (ROS) on the regulation of HIF-mediated hypoxic signaling is highlighted by a recent review by Hamanaka and Chandel [90]. New classes of unique ETC inhibitors have been identified that may prove to be pharmacological leads or valuable probes of HIF-1 signaling and mitochondrial function. However, at some point, these terrestrial and marine mitochondrial ETC inhibitors may be deemed biochemically active nuisance compounds, for the purpose of HIF-1 inhibitor drug discovery. Similarly, the expression of HIF-1 α protein and subsequent activation of HIF-1 can be strongly suppressed by pharmacologically active compounds that inhibit eukaryotic protein translation [15, 50, 91, 92]. While translation inhibitors have been found to inhibit HIF-1 signaling in tumor cells, the off-target effects associated with the generalized inhibition of protein synthesis may limit the therapeutic potential of these compounds and render such agents to be essentially nuisance compounds, at least for the purpose of bioassay dereplication.

22.11 Concluding Remarks

The field of antitumor marine natural products research has evolved over the years to incorporate an emphasis on molecular-targeted drug discovery. These changes have dramatically increased the appreciation among most natural products chemists for molecular and cell biology in natural product-based drug discovery. This shift in focus has also spurred a similar need for a general understanding of the factors that must be considered when using modern molecular-targeted antitumor bioassays. Researchers working in natural products must be acutely aware of the nature and validity of their selected molecular target, consider what particular methods their assays will use to measure the target processes, make sure appropriate controls are used, appreciate how the data will be analyzed, understand how the assay method will be validated, and establish suitable means for chemical dereplication. The scientific validity and clinical potential of any newly discovered antitumor natural product are only as solid as the reliability of the biological data that support its potential activity. This is true not only for the researchers involved in mechanism-based drug discovery; it is also true for those involved in the peer

review process. If manuscripts and grant proposals that involve molecular-targeted natural products research are not held to acceptable standards, the value of this discipline to the broader drug discovery community will be diminished. Therefore, an appreciation for all of these factors is essential for modern molecular-targeted antitumor drug discovery. Through mechanism-based drug discovery efforts, marine natural products have been identified that potently inhibit the hypoxia-induced activation of HIF-1 in tumor cells. As an important antitumor molecular target, the bioassay systems used in the identification of new HIF-1 inhibitors provide compelling examples to illustrate the various components of molecular-targeted bioassay design and analysis that are essential for the discovery of antitumor marine natural products.

22.12 Study Questions

1. Why is it important for natural products chemists (even those that do not perform their own bioassays) to have an understanding of the biological principles involved in bioassays and the important considerations used to evaluate assay quality?
2. Why are thoroughly validated and established molecular targets often less-exciting targets for novel drug discovery than newer, less fully validated, targets?
3. Why is the mere overexpression of a particular gene (or protein) in a disease condition insufficient to validate the gene (or protein) as a disease-specific molecular target?
4. What are the potential consequences of poor or inadequate molecular target validation in the drug discovery and development process?
5. What features of the transcription factor hypoxia-inducible factor-1 (HIF-1) make it a suitable representative molecular target to illustrate each of the principles involved in quality bioassay design and analysis?
6. What is the difference between bioassay validation and target validation?
7. Why is it critical for bioassay method validation to include both positive and negative control compounds?
8. Why is the definition of a bioassay “nuisance” compound in any particular bioassay considered to be subjective?
9. Why is compound dereplication so vital to a successful high-throughput screening assay-based drug discovery effort?
10. Chemical and biological literature databases are among the most economical sources of compound information regarding the production of specific natural products by any given species of organism. What are the practical limitations of literature databases in regard to the marine natural product dereplication efforts?

Acknowledgments Funding was provided in part by the NIH/NCI grant CA98787 (DGN/YDZ) and NOAA/NIUST grant NA16RU1496.

References

1. Newman DJ, Cragg GM (2006) Natural products from marine invertebrates and microbes as modulators of antitumor targets. *Curr Drug Targets* 7:279–304
2. Newman DJ, Hill RT (2006) New drugs from marine microbes: the tide is turning. *J Ind Microbiol Biotechnol* 33:539–544
3. König GM, Kehraus S, Seibert SF, Abdel-Lateff A, Müller D (2006) Natural products from marine organisms and their associated microbes. *Chembiochem* 7:229–238
4. Newman DJ, Cragg GM (2009) Microbial antitumor drugs: natural products of microbial origin as anticancer agents. *Curr Opin Investig Drugs* 10:1280–1296
5. Williams PG (2009) Panning for chemical gold: marine bacteria as a source of new therapeutics. *Trends Biotechnol* 27:45–52
6. Nagle DG, Zhou YD, Mora FD, Mohammed KA, Kim YP (2004) Mechanism targeted discovery of antitumor marine natural products. *Curr Med Chem* 11:1725–1756
7. Bailly C (2009) Ready for a comeback of natural products in oncology. *Biochem Pharmacol* 77:1447–1457
8. Poon E, Harris AL, Ashcroft M (2009) Targeting the hypoxia-inducible factor (HIF) pathway in cancer. *Expert Rev Mol Med* 11:e26
9. Onnis B, Rapisarda A, Melillo G (2009) Development of HIF-1 Inhibitors for Cancer Therapy. *J Cell Mol Med* 13:2780–2786
10. Milani M, Harris AL (2008) Targeting tumour hypoxia in breast cancer. *Eur J Cancer* 44:2766–2773
11. Semenza GL (2008) Hypoxia-inducible factor 1 and cancer pathogenesis. *IUBMB Life* 60:591–597
12. Semenza GL (2009) Defining the role of hypoxia-inducible factor 1 in cancer biology and therapeutics. *Oncogene* 29:625–634
13. Wang GL, Jiang BH, Rue EA, Semenza GL (1995) Hypoxia-inducible factor 1 is a basic-helix-loop-helix-PAS heterodimer regulated by cellular O₂ tension. *Proc Natl Acad Sci USA* 92:5510–5514
14. Nagle DG, Zhou Y-D (2009) Marine natural products as inhibitors of hypoxic signaling in tumors. *Phytochem Rev* 8:415–429
15. Liu Y, Veena CK, Morgan JB, Mohammed KA, Jekabsons MB, Nagle DG, Zhou YD (2009) Methylalpinumisoflavone inhibits hypoxia-inducible factor-1 (HIF-1) activation by simultaneously targeting multiple pathways. *J Biol Chem* 284:5859–5868
16. Nagle DG, Zhou YD (2006) Natural product-based inhibitors of hypoxia-inducible factor-1 (HIF-1). *Curr Drug Targets* 7:355–369
17. Shoemaker RH (2006) The NCI 60 human tumour cell line anticancer drug screen. *Nat Rev Cancer* 6:813–823
18. Suggitt M, Bibby MC (2005) 50 years of preclinical anticancer drug screening: empirical to target-driven approaches. *Clin Cancer Res* 11:971–981
19. Cragg GM, Newman DJ, Yang SS (2006) Natural product extracts of plant and marine origin having antileukemia potential – The NCI experience. *J Nat Prod* 69:488–498
20. Feling RH, Buchanan GO, Mincer TJ, Kauffman CA, Jensen PR, Fenical W (2003) Salinosporamide A: a highly cytotoxic proteasome inhibitor from a novel microbial source, a marine bacterium of the new genus *Salinospora*. *Angew Chem Int Ed Engl* 42:355–357
21. Fenical W, Jensen PR, Palladino MA, Lam KS, Lloyd GK, Potts BC (2009) Discovery and development of the anticancer agent salinosporamide A (NPI-0052). *Bioorg Med Chem* 17:2175–2180
22. Ganjoo KN, Patel SR (2009) Trabectedin: an anticancer drug from the sea. *Expert Opin Pharmacother* 10:2735–2743
23. Aune GJ, Furuta T, Pommier Y (2002) Ecteinascidin 743: a novel anticancer drug with a unique mechanism of action. *Anticancer Drugs* 13:545–555

24. Dong Z, Nör JE (2009) Transcriptional targeting of tumor endothelial cells for gene therapy. *Adv Drug Deliv Rev* 61:542–553
25. Brown JM, Wilson WR (2004) Exploiting tumour hypoxia in cancer treatment. *Nat Rev Cancer* 4:437–447
26. Tatum JL, Kelloff GJ, Gillies RJ et al (2006) Hypoxia: importance in tumor biology, noninvasive measurement by imaging, and value of its measurement in the management of cancer therapy. *Int J Radiat Biol* 82:699–757
27. Graeber TG, Osmanian C, Jacks T et al (1996) Hypoxia-mediated selection of cells with diminished apoptotic potential in solid tumours. *Nature* 379:88–91
28. Fang JS, Gillies RD, Gatenby RA (2008) Adaptation to hypoxia and acidosis in carcinogenesis and tumor progression. *Semin Cancer Biol* 18:330–337
29. Marcu L, Olver I (2006) Tirapazamine: from bench to clinical trials. *Curr Clin Pharmacol* 1:71–79
30. Covens A, Blessing J, Bender D et al (2006) A phase II evaluation of tirapazamine plus cisplatin in the treatment of recurrent platinum-sensitive ovarian or primary peritoneal cancer: a gynecologic oncology group study. *Gynecol Oncol* 100:586–590
31. Semenza GL, Wang GL (1992) A nuclear factor induced by hypoxia via de novo protein synthesis binds to the human erythropoietin gene enhancer at a site required for transcriptional activation. *Mol Cell Biol* 12:5447–5454
32. Semenza GL (2003) Targeting HIF-1 for cancer therapy. *Nat Rev Cancer* 3:721–732
33. Semenza GL (2007) Evaluation of HIF-1 inhibitors as anticancer agents. *Drug Discov Today* 12:853–859
34. Axelson H, Fredlund E, Ovenberger M et al (2005) Hypoxia-induced dedifferentiation of tumor cells—a mechanism behind heterogeneity and aggressiveness of solid tumors. *Semin Cell Dev Biol* 16:554–563
35. Smith C (2003) Drug target validation: hitting the target. *Nature* 422:341, 343, 345 passim
36. Benson JD, Chen YN, Cornell-Kennon SA, Dorsch M, Kim S, Leszczyniecka M, Sellers WR, Lengauer C (2006) Validating cancer drug targets. *Nature* 441:451–456
37. Zambrowicz BP, Holt KH, Walke DW, Kirkpatrick LL, Eberhart DE (2007) Generation of Transgenic Animals. In: Metcalf BW, Dillon S (eds) *Target validation in drug discovery*. Academic, New York
38. Maynard MA, Ohh M (2004) Von Hippel-Lindau tumor suppressor protein and hypoxia-inducible factor in kidney cancer. *Am J Nephrol* 24:1–13
39. Ivan M, Kondo K, Yang H, Kim W, Valiando J, Ohh M, Salic A, Asara JM, Lane WS, Kaelin WG Jr (2001) HIF α targeted for VHL-mediated destruction by proline hydroxylation: implications for O₂ sensing. *Science* 292:464–468
40. Jaakkola P, Mole DR, Tian YM, Wilson MI, Gielbert J, Gaskell SJ, Kriegsheim AV, Hebestreit HF, Mukherji M, Schofield CJ, Maxwell PH, Pugh CW, Ratcliffe PJ (2001) Targeting of HIF- α to the von Hippel-Lindau ubiquitylation complex by O₂-regulated prolyl hydroxylation. *Science* 292:468–472
41. Lando D, Peet DJ, Whelan DA, Gorman JJ, Whitelaw ML (2002) Asparagine hydroxylation of the HIF transactivation domain a hypoxic switch. *Science* 295:858–861
42. Isaacs JS, Jung YJ, Mimnaugh EG, Martinez A, Cuttitta F, Neckers LM (2002) Hsp90 regulates a von Hippel Lindau-independent hypoxia-inducible factor-1 α -degradative pathway. *J Biol Chem* 277:29936–29944
43. Liu YV, Baek JH, Zhang H, Diez R, Cole RN, Semenza GL (2007) RACK1 competes with HSP90 for binding to HIF-1 α and is required for O₂-independent and HSP90 inhibitor-induced degradation of HIF-1 α . *Mol Cell* 25:207–217
44. Ryan HE, Poloni M, McNulty W, Elson D, Gassmann M, Arbeit JM, Johnson RS (2000) Hypoxia-inducible factor-1 α is a positive factor in solid tumor growth. *Cancer Res* 60:4010–4015
45. Chau NM, Rogers P, Aherne W, Carroll V, Collins I, McDonald E, Workman P, Ashcroft M (2005) Identification of novel small molecule inhibitors of hypoxia-inducible factor-1 that

- differentially block hypoxia-inducible factor-1 activity and hypoxia-inducible factor-1 α induction in response to hypoxic stress and growth factors. *Cancer Res* 65:4918–4928
46. Rapisarda A, Uranchimeg B, Scudiero DA, Selby M, Sausville EA, Shoemaker RH, Melillo G (2002) Identification of small molecule inhibitors of hypoxia-inducible factor 1 transcriptional activation pathway. *Cancer Res* 62:4316–4324
 47. Kung AL, Zabudoff SD, France DS, Freedman SJ, Tanner EA, Vieira A, Cornell-Kennon S, Lee J, Wang B, Wang J, Memmert K, Naegeli HU, Petersen F, Eck MJ, Bair KW, Wood AW, Livingston DM (2004) Small molecule blockade of transcriptional coactivation of the hypoxia-inducible factor pathway. *Cancer Cell* 6:33–43
 48. Park EJ, Kong D, Fisher R, Cardellina J, Shoemaker RH, Melillo G (2006) Targeting the PAS-A domain of HIF-1 α for development of small molecule inhibitors of HIF-1. *Cell Cycle* 5:1847–1853
 49. Hodges TW, Hossain CF, Kim YP, Zhou YD, Nagle DG (2004) Molecular-targeted antitumor agents: the *Saururus cernuus* dineolignans manassantin B and 4-*O*-demethylmanassantin B are potent inhibitors of hypoxia-activated HIF-1. *J Nat Prod* 67:767–771
 50. Zhou YD, Kim YP, Mohammed KA, Jones DK, Muhammad I, Dunbar DC, Nagle DG (2005) Terpenoid tetrahydroisoquinoline alkaloids emetine, klugine, and isocephaline inhibit the activation of hypoxia-inducible factor-1 in breast tumor cells. *J Nat Prod* 68:947–950
 51. Liu Y, Morgan JB, Coothankandaswamy V, Liu R, Jekabsons MB, Mahdi F, Nagle DG, Zhou YD (2009) The *Caulerpa* pigment caulerpin inhibits HIF-1 activation and mitochondrial respiration. *J Nat Prod* 72:2104–2109
 52. Sayed KA, Khanfar MA, Shallal HM, Muralidharan A, Awate B, Youssef DT, Liu Y, Zhou YD, Nagle DG, Shah G (2008) Latrunculin A and its C-17-*O*-carbamates inhibit prostate tumor cell invasion and HIF-1 activation in breast tumor cells. *J Nat Prod* 71:396–402
 53. Liu R, Liu Y, Zhou YD, Nagle DG (2007) Molecular-targeted antitumor agents. 15. Neolamellarins from the marine sponge *Dendrilla nigra* inhibit hypoxia-inducible factor-1 activation and secreted vascular endothelial growth factor production in breast tumor cells. *J Nat Prod* 70:1741–1745
 54. Hossain CF, Kim YP, Baerson SR, Zhang L, Bruick RK, Mohammed KA, Agarwal AK, Nagle DG, Zhou YD (2005) *Saururus cernuus* lignans—potent small molecule inhibitors of hypoxia-inducible factor-1. *Biochem Biophys Res Commun* 333:1026–1033
 55. Coma I, Herranz J, Martin J (2009) Statistics and decision making in high-throughput screening. *Methods Mol Biol* 565:69–106
 56. Achyuthan KE, Whitten DG (2007) Design considerations for high-throughput screening and *in vitro* diagnostic assays. *Comb Chem High Throughput Screen* 10:399–412
 57. Govindarajulu Z (2001) Statistical techniques in bioassay, 2nd edn. S. Karger AG, Basel
 58. Buncher CR, Tsay J-Y (eds) (1994) Statistics in the pharmaceutical industry, 2nd edn. Marcel Dekker, New York
 59. Bohlin L, Bruhn JG (1999) Bioassay methods in natural product research and drug development. In: Proceedings of the Phytochemical Society of Europe. Kluwer Academic, Boston
 60. International Conference on Harmonisation of Technical Requirements for Registration of Pharmaceuticals for Human Use (1995) Center for Drug Evaluation and Research, Guideline for Industry: text on validation of analytical procedures. <http://www.fda.gov/downloads/Drugs/GuidanceComplianceRegulatoryInformation/Guidances/ucm073381.pdf>. Accessed 10 Dec 2009
 61. International Conference on Harmonisation of Technical Requirements for Registration of Pharmaceuticals for Human Use (1996) Center for Drug Evaluation and Research, Guideline for Industry: Q2B validation of analytical procedures: methodology. <http://www.fda.gov/downloads/Drugs/GuidanceComplianceRegulatoryInformation/Guidances/ucm073381.pdf>. Accessed 10 Dec 2009
 62. International Conference on Harmonisation of Technical Requirements for Registration of Pharmaceuticals for Human Use (2001) Center for Drug Evaluation and Research, Guidance

- for Industry: bioanalytical method validation. <http://www.fda.gov/downloads/Drugs/GuidanceComplianceRegulatoryInformation/Guidances/ucm073381.pdf>. Accessed 10 Dec 2009
63. Lin X, David CA, Donnelly JB, Michaelides M, Chandel NS, Huang X, Warrior U, Weinberg F, Tormos KV, Fesik SW, Shen Y (2008) A chemical genomics screen highlights the essential role of mitochondria in HIF-1 regulation. *Proc Natl Acad Sci USA* 105:174–179
 64. Zhang JH, Chung TD, Oldenburg KR (1999) A simple statistical parameter for use in evaluation and validation of high throughput screening assays. *J Biomol Screen* 4:67–73
 65. Dai J, Liu Y, Jia H, Zhou YD, Nagle DG (2007) Benzochromenones from the marine crinoid *Comantheria rotula* inhibit hypoxia-inducible factor-1 (HIF-1) in cell-based reporter assays and differentially suppress the growth of certain tumor cell lines. *J Nat Prod* 70:1462–1466
 66. Nagle DG, Zhou Y-D (2009) Research in progress. The biological-chemical interface: anti-cancer drug discovery projects at OleMiss. Department of Pharmacognosy, University of Mississippi. <http://www.pharmacy.olemiss.edu/pharmacognosy/Nagle/Nagleres.html>. Accessed 26 March 2010
 67. Natural Products Repository. Natural Products Branch, Developmental Therapeutics Program NCI/NIH (2011) <http://dtp.nci.nih.gov/branches/npb/repository.html>. Accessed 7 Nov 2011
 68. Bruick RK (2000) Expression of the gene encoding the proapoptotic Nip3 protein is induced by hypoxia. *Proc Natl Acad Sci USA* 97:9082–9087
 69. Manolescu B, Oprea E, Busu C, Cercasov C (2009) Natural compounds and the hypoxia-inducible factor (HIF) signalling pathway. *Biochimie* 91:1347–1358
 70. Mohammed KA, Hossain CF, Zhang L, Bruick RK, Zhou YD, Nagle DG (2004) Laurenditerpenol, a new diterpene from the tropical marine alga *Laurencia intricata* that potently inhibits HIF-1 mediated hypoxic signaling in breast tumor cells. *J Nat Prod* 67:2002–2007
 71. Chittiboyina AG, Kumar GM, Carvalho PB, Liu Y, Zhou YD, Nagle DG, Avery MA (2007) Total synthesis and absolute configuration of laurenditerpenol: a hypoxia inducible factor-1 activation inhibitor. *J Med Chem* 50:6299–6302
 72. Liu Y, Liu R, Mao SC, Morgan JB, Jekabsons MB, Zhou YD, Nagle DG (2008) Molecular-targeted antitumor agents. 19. Furospongolide from a marine *Lendenfeldia* sp. sponge inhibits hypoxia-inducible factor-1 activation in breast tumor cells. *J Nat Prod* 71:1854–1860
 73. Dai J, Fishback JA, Zhou YD, Nagle DG (2006) Sodwanone and yardenone triterpenes from a South African species of the marine sponge *Axinella* inhibit hypoxia-inducible factor-1 (HIF-1) activation in both breast and prostate tumor cells. *J Nat Prod* 69:1715–1720
 74. Mao SC, Liu Y, Morgan JB, Jekabsons MB, Zhou YD, Nagle DG (2009) Lipophilic 2,5-disubstituted pyrroles from the marine sponge *Mycale* sp. inhibit mitochondrial respiration and HIF-1 activation. *J Nat Prod* 72:1927–1936
 75. Aguilar-Santos G (1970) Caulerpin, a new red pigment from green algae of the genus *Caulerpa*. *J Chem Soc Perkin I*(6):842–843
 76. Mohammed KA, Jadulco RC, Bugni TS, Harper MK, Sturdy M, Ireland CM (2008) Strongylophorines: natural product inhibitors of hypoxia-inducible factor-1 transcriptional pathway. *J Med Chem* 51:1402–1405
 77. Kashman Y, Groweiss A, Shmueli U (1980) Latrunculin, a new 2-thiazolidinone macrolide from the marine sponge *Latrunculia magnifica*. *Tetrahedron Lett* 21:3629–3632
 78. Spector I, Shochet NR, Kashman Y, Groweiss A (1983) Latrunculins: novel marine toxins that disrupt microfilament organization in cultured cells. *Science* 219:493–495
 79. Spector I, Shochet NR, Blasberger D, Kashman Y (1989) Latrunculins—novel marine macrolides that disrupt microfilament organization and affect cell growth: I. Comparison with cytochalasin D. *Cell Motil Cytoskeleton* 13:127–144
 80. Haslam E (1996) Natural polyphenols (vegetable tannins) as drugs: possible modes of action. *J Nat Prod* 59:205–215
 81. Cardellina JH II, Munro MH, Fuller RW, Manfredi KP, McKee TC, Tischler M, Bokesch HR, Gustafson KR, Beutler JA, Boyd MR (1993) A chemical screening strategy for the

- dereplication and prioritization of HIV-inhibitory aqueous natural products extracts. *J Nat Prod* 56:1123–1129
82. Zou L, Harkey MR, Henderson GL (2002) Effects of intrinsic fluorescence and quenching on fluorescence-based screening of natural products. *Phytomedicine* 9:263–267
 83. SciFinder/SciFinder Scholar (2011) Chemical Abstracts Service – American Chemical Society. <http://www.cas.org/products/sfacad/index.html>. Accessed 7 Nov 2011
 84. PubMed Database (2011) U.S. National Library of Medicine/National Institutes of Health. <http://www.ncbi.nlm.nih.gov/pubmed>. Accessed 7 Nov 2011
 85. MarinLit Database (2011) Department of Chemistry, University of Canterbury. <http://www.chem.canterbury.ac.nz/marinlit/marinlit.shtml>. Accessed 7 Nov 2011
 86. Newman DJ, Cragg GM (2004) Marine natural products and related compounds in clinical and advanced preclinical trials. *J Nat Prod* 67:1216–1238
 87. Dinan L (2006) Dereplication and partial identification of compounds. In: Sarker SD, Latif Z, Gray AI (eds) *Methods in biotechnology*, vol 20. Natural products isolation, 2nd edn. Humana Press, Totowa
 88. Sarker SD, Nahar L (2006) Hyphenated techniques. In: Sarker SD, Latif Z, Gray AI (eds) *Methods in Biotechnology*, vol 20, Natural products isolation, 2nd edn. Humana Press, Totowa
 89. Bain J, Plater L, Elliott M, Shpiro N, Hastie CJ, McLauchlan H, Klevermic I, Arthur JS, Alessi DR, Cohen P (2007) The selectivity of protein kinase inhibitors: a further update. *Biochem J* 408:297–315
 90. Hamanaka RB, Chandel NS (2009) Mitochondrial reactive oxygen species regulate hypoxic signaling. *Curr Opin Cell Biol* 21:1–6
 91. Narita T, Yin S, Gelin CF, Moreno CS, Yepes M, Nicolaou KC, Van Meir EG (2009) Identification of a novel small molecule HIF-1 α translation inhibitor. *Clin Cancer Res* 15:6128–6136
 92. Tan C, de Noronha RG, Roecker AJ, Pyrzynska B, Khwaja F, Zhang Z, Zhang H, Teng Q, Nicholson AC, Giannakakou P, Zhou W, Olson JJ, Pereira MM, Nicolaou KC, Van Meir EG (2005) Identification of a novel small-molecule inhibitor of the hypoxia-inducible factor 1 pathway. *Cancer Res* 65:605–612

Yoichi Nakao and Nobuhiro Fusetani

Contents

23.1	Introduction	1146
23.2	Oxidoreductases (EC 1.-.-)	1147
23.2.1	Aldose Reductase (EC 1.1.1.21)	1147
23.2.2	Enoyl-ACP Reductase (EC 1.3.1.9)	1148
23.2.3	Lipoxygenases (EC 1.13.11.12)	1149
23.2.4	Indoleamine 2,3-Dioxygenases (EC 1.13.11.42)	1150
23.2.5	Neuronal Nitric Oxide Synthase (EC 1.14.13.39)	1151
23.3	Transferases (EC 2.-.-)	1152
23.3.1	1 α -1,3-Fucosyltransferases (EC 2.4.1.214)	1152
23.3.2	Adenosine Phosphoribosyltransferase (EC 2.4.2.7)	1153
23.3.3	Farnesyl Protein Transferase (EC 2.5.1.58)	1154
23.3.4	Geranylgeranyltransferase Type I (EC 2.5.1.59)	1156
23.3.5	HIV Reverse Transcriptase (EC 2.7.7.49)	1157
23.3.6	HIV Integrase (EC 2.7.7.-)	1158
23.3.7	Telomerase (EC 2.7.7.49)	1160
23.3.8	Epidermal Growth Factor Receptor Kinase (EC 2.7.10.1)	1162
23.3.9	Tyrosine Kinase pp60 ^{V-SRC} (EC 2.7.10.2)	1163
23.3.10	Other Tyrosine Protein Kinase	1164
23.3.11	MSK1 (EC 2.7.11.1) and MAPKAPK-2	1164
23.3.12	Raf/MEK1/MAPK	1164
23.3.13	Checkpoint Kinases (EC 2.7.11.1)	1164
23.3.14	Protein Kinase C (EC 2.7.11.13)	1166
23.3.15	Cyclin-Dependent Kinases (EC 2.7.11.22)	1170
23.3.16	Glycogen Synthase Kinase-3 (2.7.11.17)	1171
23.4	Hydrolases (EC 3.-.-)	1172
23.4.1	Phospholipase A ₂ (EC 3.1.1.4)	1172

Y. Nakao (✉)

School of Advanced Sciences and Technologies, Waseda University, 3-4-1, Okubo, Shinjuku-ku, Tokyo, Japan

N. Fusetani

Fisheries and Oceans Hakodate, Graduate School of Fisheries Sciences, Hokkaido University, 3-1-1, Minato-cho, Hakodate, Japan

23.4.2	Acetylcholinesterase (EC 3.1.1.7)	1177
23.4.3	Protein Phosphatases (EC 3.1.3.16)	1178
23.4.4	Protein Tyrosine Phosphatases (EC 3.1.3.48)	1183
23.4.5	Phospholipase C (EC 3.1.4.3)	1184
23.4.6	Phosphodiesterase (EC 3.1.4.-)	1185
23.4.7	Sialidase (EC 3.2.1.18)	1186
23.4.8	Chitinase (EC 3.2.1.14)	1188
23.4.9	α -Glucosidases (EC 3.2.1.20)	1189
23.4.10	S-Adenosylhomocysteine Hydrolase (EC 3.3.1.1)	1190
23.4.11	Serine Proteases (EC 3.4.21.-)	1191
23.4.12	Cysteine Proteases (EC 3.4.22.-)	1196
23.4.13	Aspartic Proteases (EC 3.4.23.-)	1198
23.4.14	Metalloproteases (EC 3.4.24.-)	1198
23.4.15	Histone Deacetylases (EC 3.23.-)	1200
23.4.16	ATPases (EC 3.6.1.3)	1202
23.5	Lyases (EC 4.-.-)	1208
23.5.1	ATP Citrate Lyase (EC 4.1.3.8)	1208
23.6	Isomerases (EC 5.-.-)	1209
23.6.1	Topoisomerase	1209
23.7	Conclusions	1213
23.8	Study Questions	1213
References	1214

Abstract

Marine invertebrates are the rich source of small molecules with unique chemical skeletons and potent bioactivities; however, the major biological activities tested for marine natural products have been mainly limited to the traditional phenotype-oriented bioactivities such as cytotoxicity or anti-microbial activities. Enzyme inhibition is the target-oriented bioactivity and small molecule inhibitors are quite useful for controlling biological processes and understanding complicated biological phenomena. Recently, it has been recognized that the natural products are superior source of small molecule probes useful for the chemical biology. Especially, marine-derived enzyme inhibitors still remain to be fully investigated in spite of their high potentials as a source of unique compounds. In this chapter, selected enzyme inhibitors from marine invertebrates are described.

23.1 Introduction

Enzymes are vital to living organisms, maintaining the homeostasis of their lives by mediating/regulating numerous biochemical events, including metabolism, catabolism, cellular signal transduction, cell cycles, and development. Dysfunction, overexpression, or hyperactivation of the enzymes are often associated with human diseases as evidenced from the molecular-based analysis of diseases. Umezawa's pioneering work on enzyme inhibitors resulted in the discovery of

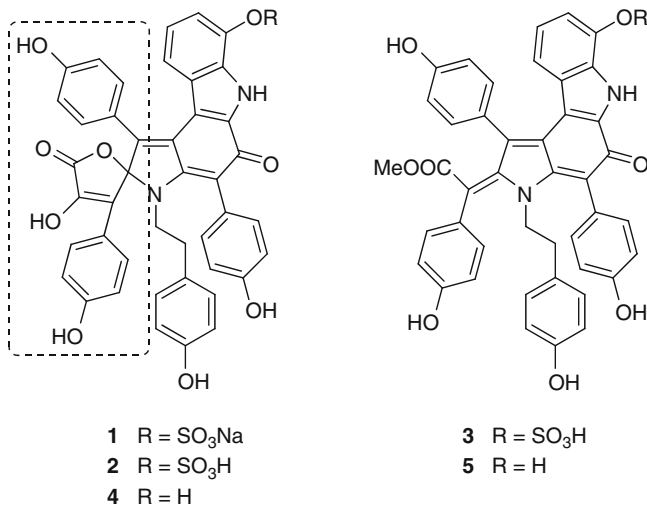
numbers of valuable compounds from terrestrial microorganisms [1]. Thereafter, search for small molecular enzyme inhibitors has been actively conducted in both academia and pharmaceutical industries, and a considerable number of enzyme inhibitors have been developed as drugs, including blockbusters such as statins. However, only recently, the majority of the marine natural products chemists started systematic programs for discovering enzyme inhibitors; the first systematic investigation was done by our group for H,K-ATPase inhibitors [2]. Although a large proportion of enzyme inhibitors reported from marine organisms were known compounds found to inhibit enzymes in the reevaluation of activities, these known compounds with new activities are important for the related research areas such as chemical biology. It may be predicted that the trends of marine natural products chemistry will move from finding merely “*new structures*” to finding “*new activities*” of known compounds. Recent reevaluation of natural products as a superior source of small molecule probes useful for studying biological phenomena is encouraging natural products chemists to investigate compounds with new activities.

In this chapter, we will describe the structures and activities of selected enzyme inhibitors isolated from marine invertebrates. Some inhibitors are not from marine invertebrates, but they are related to structures from microorganisms. Synthetic enzyme inhibitors based on the marine natural products are also described. Most of them were designed based on the crystal structures of enzyme–inhibitor complexes and gave a detailed insight into the modes of action. However, we excluded most of bromotyrosines, polyacetylenes, and highly sulfated steroids which are often termed “nuisance compounds,” because they show a variety of biological activities including inhibition of enzymes. Inhibitors are listed according to the classification of target enzymes (EC number).

23.2 Oxidoreductases (EC 1.-.-.)

23.2.1 Aldose Reductase (EC 1.1.1.21)

Aldose reductase catalyzes the reduction of glucose to sorbitol with concomitant conversion of NADPH to NADP⁺. The highly activated enzyme under hyperglycemic environment results in unusual accumulation of sorbitol in the eye lens or peripheral nerves that lead to retinopathy, cataract, neuropathy, nephropathy, or cardio-vascular diseases. Three polycyclic *bis*-indoles (**1**–**3**) from a marine sponge *Dictyodendrilla* sp. strongly inhibited bovine lens aldose reductase with IC₅₀ values of 49, 125, and 112 nM, respectively. Interestingly, the sulfate group in **1** and **2** did not influence the activity (**4**: IC₅₀ 102 nM), while the sulfate group in **3** potentiated the activity (**5**: IC₅₀ 567 nM) [3].

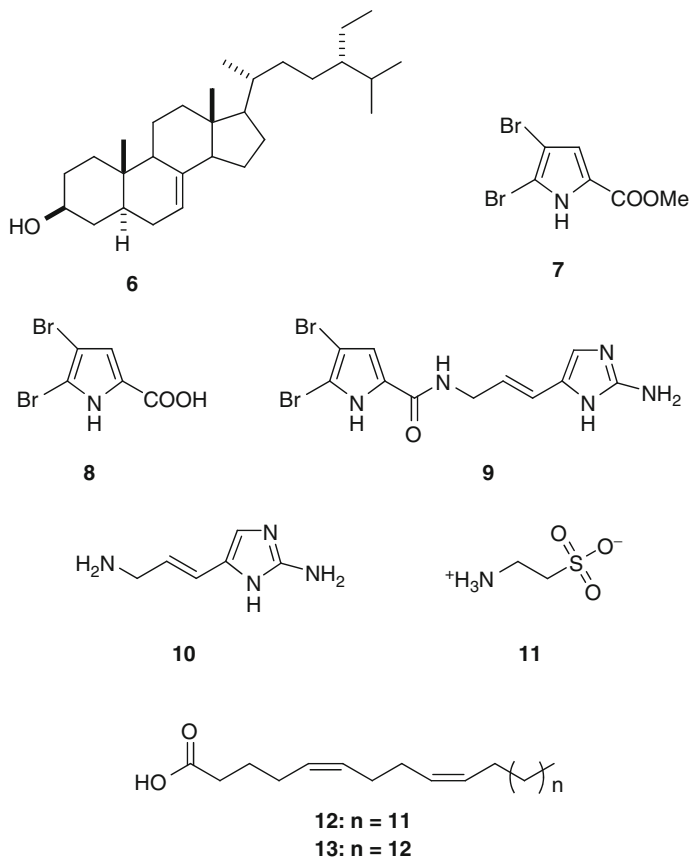


23.2.2 Enoyl-ACP Reductase (EC 1.3.1.9)

In mammals and other higher eukaryotes, all reactions in fatty acid synthesis are catalyzed by the type I fatty acid synthase (FAS-I), while bacteria, plants, and algae contain a type II system (FAS-II), in which each reaction is carried out by a monofunctional enzyme. The type II fatty acid biosynthetic pathway has recently been discovered in a number of Apicomplexan parasites, including the malaria parasite, *Plasmodium falciparum*. *Mycobacterium tuberculosis* employs both FAS-I and FAS-II systems. FAS-I is responsible for the synthesis of short-chain FAs, whereas the FAS-II system extends these FAs to very long-chain mycolic acids, important components of the mycobacterial cell wall. The central role of FA biosynthesis and the structural differences between the human and microbial FAS systems render FAS-II as an attractive target for antimicrobial drug discovery.

The FabI (enoyl-ACP reductase) is a crucial enzyme of all FAS-II systems, since it catalyzes the last NADH-dependent reduction step in each elongation cycle. Six known metabolites (**6–11**) and complex fatty acid mixtures (**FAMA-FAMG**) isolated from the Turkish marine sponge *Agelas oroides* were identified as active components in the target (*Pf* FabI)-based antimalarial screening. Compounds **6–11** showed inhibitory activity against *Pf* FabI with IC₅₀ values of >100, >100, 40, 0.30, 5.0, >100, and >100 µg/mL, respectively. Interestingly, TFA salt of **8** showed better inhibitory activity (IC₅₀ 40 µg/mL), while the activity of TFA salt of **9** became weaker (IC₅₀ 5.0 µg/mL). These enzyme inhibitory activities were well correlated with anti-plasmodial activities against *P. falciparum*, except that **10** showed better anti-protozoan activity (IC₅₀ 7.4 µg/mL) compared to its enzyme inhibitory activity.

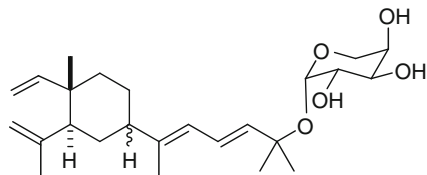
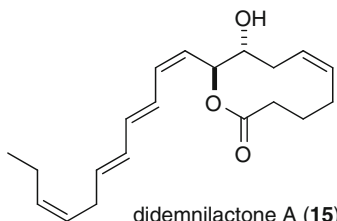
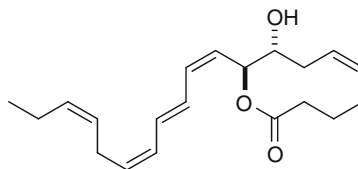
Mixtures of fatty acids showed *Pf* FabI inhibitory activity with IC_{50} s in the range of 0.35–20 $\mu\text{g/mL}$, while they showed anti-plasmodial activities against *P. falciparum* (IC_{50} s 3.4–40.9 $\mu\text{g/mL}$), *Trypanosoma brucei rhodesiense* (IC_{50} s 5.3–42.3 $\mu\text{g/mL}$), *Trypanosoma cruzi* (IC_{50} s 16 to > 30 $\mu\text{g/mL}$), *Leishmania donovani* (IC_{50} s 6.0–14.4 $\mu\text{g/mL}$), respectively. In addition, two mixtures (**FAMA** and **FAMD**) inhibited FabI of *Mycobacterium tuberculosis* (*Mt*FabI, IC_{50} s 9.4 and 8.2 $\mu\text{g/mL}$, respectively) and *Escherichia coli* (*Ec*FabI, IC_{50} s 0.5 and 0.07 $\mu\text{g/mL}$, respectively). FAMA was a mixture of 5,9-dienoic fatty acids of C_{23} (**12**) and C_{24} (**13**), while FAMD contained 10-methylhexadecanoic and palmitic acids as major lipids [4].



23.2.3 Lipoxygenases (EC 1.13.11.12)

Lipoxygenases (LO) mediate hydroperoxidation of polyunsaturated fatty acids (PUFAS), leading to formation of leukotrienes and lipoxins. Selective inhibitors of lipoxygenase isoforms can be useful for pharmacological agents, nutraceuticals,

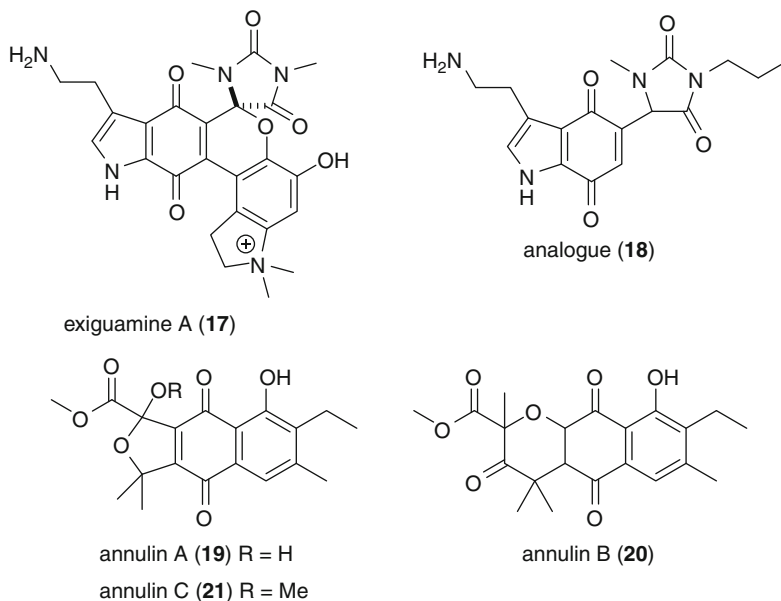
or molecular tools. Fucosides, originally isolated from the Caribbean gorgonian *Eunicea fusca* [5], selectively and irreversibly inhibited leukotriene (LT) formation in murine models of inflammation. Further pharmacological study indicated that fucoside B (**14**) inhibits conversion of arachidonic acid (AA) to leukotriene B₄ (LTB₄) by inhibition of 5-LO with an IC₅₀ of 18 μ M [6]. Similarly, didemnilactones A (**15**) and B (**16**) isolated from the tunicate *Didemnum moseleyi* showed inhibition against lipoxygenases of human polymorphonuclear leukocytes with IC₅₀ values of 9.4 and 8.5 μ M (**15** and **16**, respectively against 5-LO), and 41 μ M (**15** against 15-LO) [7].

fucoside B (**14**)didemnilactone A (**15**)didemnilactone B (**16**)

23.2.4 Indoleamine 2,3-Dioxygenases (EC 1.13.11.42)

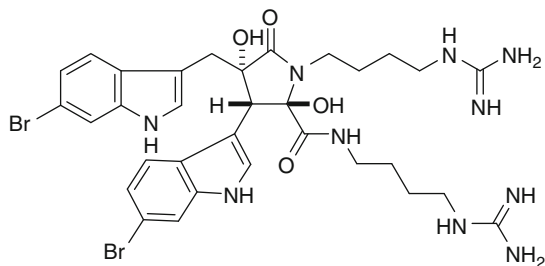
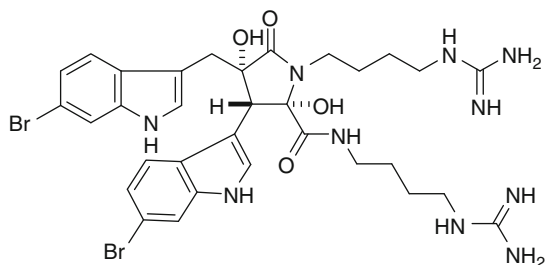
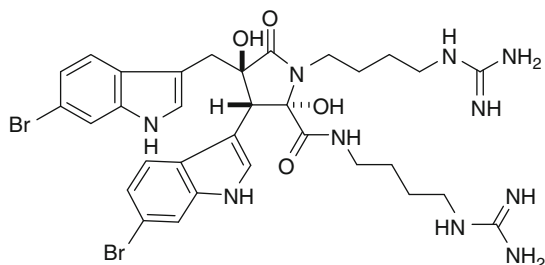
Indoleamine-2,3-dioxygenase (IDO) catalyzes the oxidation of tryptophan to *N*-formylkynurenine at the rate-limiting step in the metabolic degradation of tryptophan. Because T-cells are sensitive to tryptophan depletion, overexpression of IDO in most tumors is thought to cause apoptosis of T-cells and, as the results, leads to immune escape of solid tumors. Significant regression of tumors observed in a mouse model system treated by a combination of relatively poor IDO inhibitor such as 1-methyltryptophan and cytotoxic agents (e.g., paclitaxel) have provided proof of demonstration for the potential value of IDO inhibitors in cancer treatment. Exiguamine A (**17**) was isolated as an IDO inhibitor from the marine sponge *Neopetrosia exigua* collected at Papua New Guinea. The biogenesis of the unprecedented complex hexacyclic alkaloid skeleton of **17** was proposed to be starting from DOPA, tryptophan, and *N,N*-dimethylhydantoin. Exiguamine A has a *K_i* of 210 nM for inhibition of IDO in vitro [8]. Synthetic analogues of **17** were prepared and evaluated their inhibitory activity against IDO. Although all of the synthetic analogues turned out to be less active than **17** (*K_i* 41 nM in the modified

assay system), a simpler analogue **18** showed relatively potent noncompetitive inhibition against IDO (K_i 200 nM) [9]. Four new polyketides annulin C (**21**), 2-hydroxygarveatin, garveatin, and garvin C, as well as known annulins A (**19**) and B (**20**), garveatins A and C, and 2-hydroxy garvin A were isolated from the Northeastern Pacific hydroid *Garveia annulata*. Among these compounds, annulins A–C showed potent submicromolar IDO inhibition with K_i values of 0.14, 0.69, and 0.12 μ M, respectively [10].



23.2.5 Neuronal Nitric Oxide Synthase (EC 1.14.13.39)

Neuronal nitric oxide synthase (nNOS) represents an important therapeutic target for neuropathological disorders, such as stroke, Alzheimer's disease, Parkinson's disease, AIDS, and dementia, because NO plays an important multifunctional role in the modulation of many neurotransmitters in the brain and its overproduction has been associated with such diseases. Eusynstyelamides A–C (**22–24**) isolated from the Australian ascidian *Eusynstyela latericius* inhibited nNOS with IC_{50} values of 41.7, 4.3, and 5.8 μ M, respectively, while they were found to be nontoxic toward the three human tumor cell lines MCF-7 (breast), SF-268 (CNS), and H-460 (lung). Eusynstyelamides A and B were mildly antibacterial against *Staphylococcus aureus* (IC_{50} s 5.6 and 6.5 mM, respectively), and weakly inhibited the C4 plant regulatory enzyme pyruvate phosphate dikinase (PPDK) (IC_{50} values of 19 and 20 mM, respectively) [11].

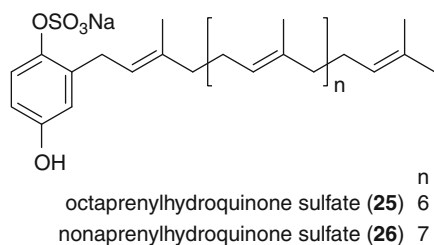
eusynstyelamide A (**22**)eusynstyelamide B (**23**)eusynstyelamide C (**24**)

23.3 Transferases (EC 2.-.-.)

23.3.1 1 α -1,3-Fucosyltransferases (EC 2.4.1.214)

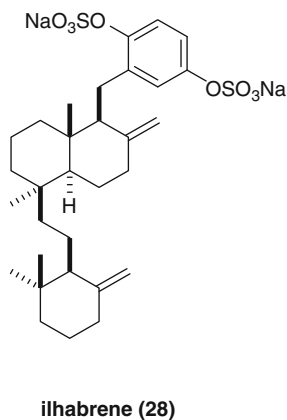
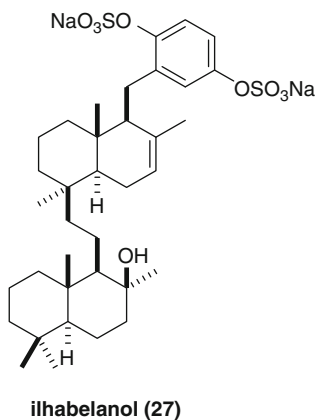
α -1,3-Fucosyltransferases (Fuc Ts, EC 2.4.1.214) which catalyze the transfer of L-fucopyranoside residues from guanosine diphosphate fucose (GDP-fucose) to glycoconjugate acceptors are known to be involved in the biosynthesis of sialyl Lewis X (SLe^X) present on the extracellular surfaces of leukocytes. The E-selectin-SLe^X interaction encourages leukocytes to move from the bloodstream into sites of injury or infection and to cause inflammation, thus indicating that inhibitors

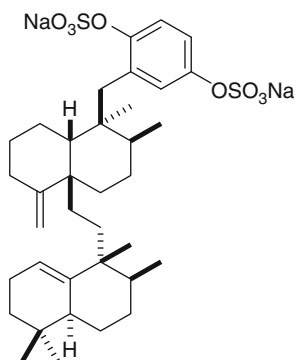
of α -1,3-fucosyltransferase are potential drugs for the treatment of inflammatory diseases [12]. Octa- and nonaprenylhydroquinone sulfates **25** and **26** isolated from an Australian marine sponge *Sarcotragus* sp. inhibited α -1,3-fucosyltransferase VII (Fuc TVII) with IC_{50} values of 3.9 and 2.4 μ g/mL, respectively, while they showed very weak activity against Fuc TVI [13].



23.3.2 Adenosine Phosphoribosyltransferase (EC 2.4.2.7)

Adenosine phosphoribosyltransferase (APRT) catalyzes the salvage pathway of purine nucleotides. In mammals, there are both *de novo* and salvage pathways for purine nucleotides synthesis, while kinetoplastid parasites such as *Leishmania* spp. lack the *de novo* pathway. Therefore, selective inhibitors of phosphoribosyl transferase should compromise the parasite metabolism selectively. Three new disulfated meroterpenoids, ilhabelanol (**27**), ilhabrene (**28**), and isoakaterpin (**29**) were isolated from a Brazilian sponge *Callyspongia* sp. as *L. tarentolae* adenosine phosphoribosyltransferase (L-APRT) inhibitors. Isoakaterpin (**29**) inhibited L-APRT with an IC_{50} of 1.05 μ M, while the accurate IC_{50} values for ilhabelanol (**27**) and ilhabrene (**28**) could not be obtained because of the too small amount of isolated compounds [14].



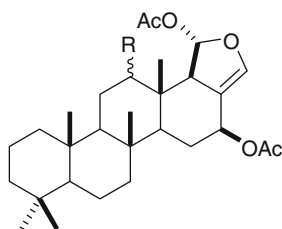
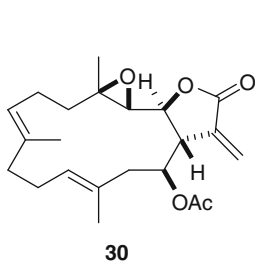


isoakaterpin (29)

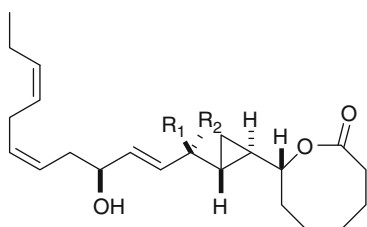
23.3.3 Farnesyl Protein Transferase (EC 2.5.1.58)

The Ras family of guanine nucleotide binding proteins plays important roles in signal transduction and regulation of cell differentiation and proliferation. The Ras protein requires posttranslational processing in order to associate with the plasma membrane and to function in signal transduction or cellular transformation. The first processing step is catalyzed by farnesyl protein transferase (FPT) which adds a farnesyl group to a cysteine residue near the carboxy terminus of the Ras protein. Inhibition of FPT is a potential therapeutic target for novel anticancer agents. A cembranolide diterpene **30** isolated from the soft coral *Lobophytum cristagalli* showed potent inhibitory activity against FPT at an IC_{50} of 0.15 μM [15]. The bioassay guided isolation of FPT inhibitors from the marine sponge *Hyrtios reticulate* yielded a known sesterterpene, heteronemin (**31**) as the active constituent which inhibited FPT with an IC_{50} value of 3 μM , while its 12-epimer (**32**) did not show any noticeable activity [16]. Solandelactones C (**33**), D (**34**), and G (**35**) were cyclopropyl oxylipins isolated from the hydroid *Solanderia secunda* and exhibited moderate inhibitory activity against FPT (69, 89, and 61% inhibition at 100 $\mu g/mL$, respectively) [17]. Spongolactams A–C (**36–38**) were FPT inhibitors isolated from an Okinawan marine sponge *Spongia* sp. by employing newly developed LC/MS-guided assay systems. To study their structure–activities relationships, spongolactams were semisynthesized from the known diterpene. The inhibitory activities of **36–38** against FPT were confirmed as IC_{50} values of 23, 130, and >260 μM , respectively [18]. Four new dual inhibitors, alisiaquinones A–C (**39–41**) and alisiaquinol (**42**), against FPT and plasmoidal kinase Pfnek-1 were isolated from an unidentified New Caledonian deepwater sponge. Compounds **39–42** showed FPT inhibition at IC_{50} values of 2.8, 2.7, 1.9, and 4.7 μM , respectively.

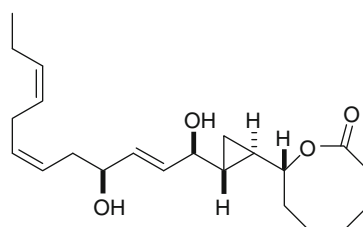
Moreover, alisiaquinone A and alisiaquinol strongly inhibited plasmoidal NIMA-like kinase Pfnek-1 at as low as 1 μM , whereas alisiaquinone C (**41**) showed almost no inhibition at this concentration. However, alisiaquinone C showed a much better inhibitory activity against *P. falciparum* in vitro. These results correlated with a better activity of alisiaquinone C on FPT, as was shown by the dramatic effects of FPT inhibitors on malaria parasites. The in vivo activity of alisiaquinones A and C was investigated on rodent malaria and was shown that they reduced by 50% the parasitemia at 5 mg/kg and displayed relatively high level of toxicity with 100% and 80% mortality, respectively at 20 mg/kg, which precluded further antimalarial development [19].



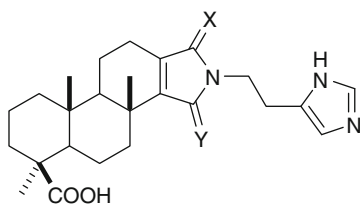
heteronemin (**31**) R = $\beta\text{-OH}$
12-epi-heteronemin (**32**) R = $\alpha\text{-OH}$



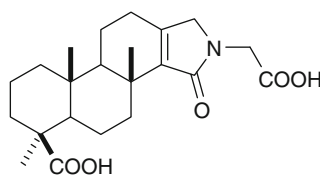
	R ₁	R ₂
solandelactone C (33)	OH	H
solandelactone D (34)	H	OH



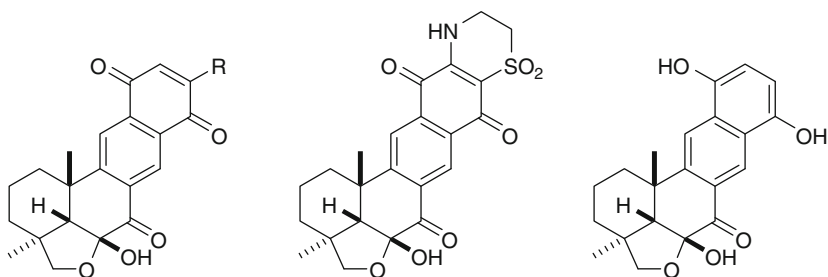
solandelactone G (**35**)



spongolactam A (**36**) X = H₂, Y = O
spongolactam B (**37**) X = O, Y = H₂



spongolactam C (**38**)



alisiaquinone A (39) R = H

alisiaquinone B (40) R = OMe

alisiaquinone C (41)

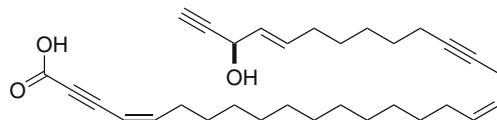
alisiaquinol (42)

23.3.4 Geranylgeranyltransferase Type I (EC 2.5.1.59)

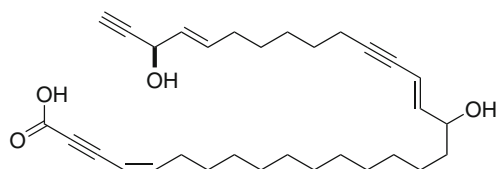
Geranylgeranyltransferase type I (GGTase I) catalyzes the posttranslational attachment of the geranylgeranyl unit on the carboxy terminal cysteine residues of proteins, to promote membrane interaction and biological activities of these proteins [20]. Rho1p, a regulatory subunit of 1,3- β -D-glucan synthesis and the key player in cell wall biosynthesis [21], is known as one of the targets of GGTase I and is essential for viability of *Saccharomyces cerevisiae*. Since there is only 30% sequence homology between the human and pathogenic fungus *Candida albicans* GGTase I [22], its inhibitors are expected to be selective antifungal agents.

Corticatic acids are the polyacetylenic GGTase I inhibitors isolated from the marine sponge *Petrosia corticata*. Corticatic acids A (43), D (44), and E (45) inhibited *C. albicans* GGTase I with IC_{50} values of 1.9, 3.3, and 7.3 μ M, respectively, while corticatic acid A (43) also inhibited the growth of *C. albicans* with an MIC value of 54 μ M [23].

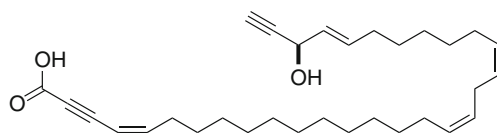
Massadine (46), a highly oxygenated alkaloid isolated from the marine sponge *Stylissa* aff. *massa* as an inhibitor of GGTase I from *C. albicans* inhibited GGTase I with an IC_{50} value of 3.9 μ M [24].



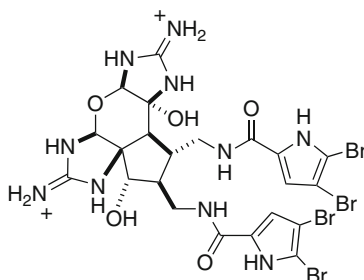
Corticatic acid A (43)



Corticatic acid D (44)



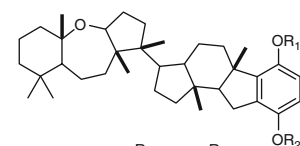
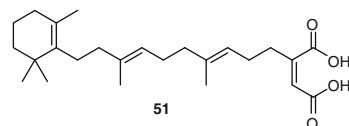
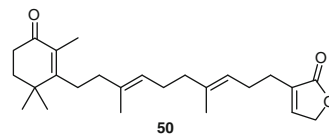
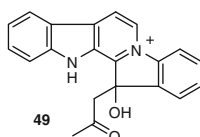
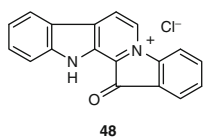
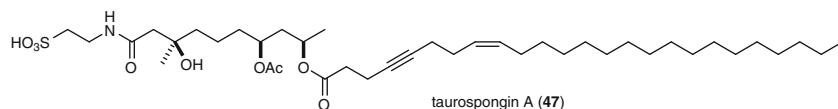
Corticatic acid E (45)



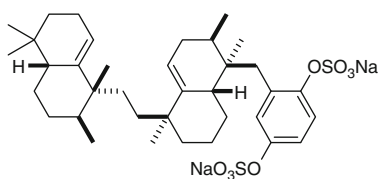
Massadine (46)

23.3.5 HIV Reverse Transcriptase (EC 2.7.7.49)

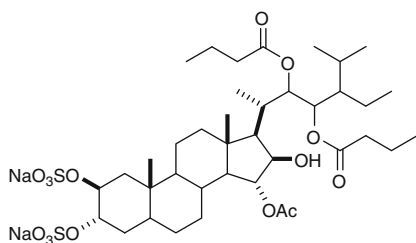
Reverse transcriptase (RT) is the key enzyme in the life cycle of human immunodeficiency virus (HIV). RT is a multifunctional enzyme responsible for the transcription of viral RNA into double-stranded DNA, and exhibits both RNA-dependent DNA polymerase (RDDP) and DNA-dependent DNA polymerase (DDDP) activities as well as an inherent ribonuclease H (RNase H) activity. All the catalytic functions of RT play a pivotal role in HIV replication. Taurospongins A (47), a metabolite of an Okinawan sponge *Hippospongia* sp., is another example of acetylenic compounds which possess HIV RT inhibitory activity (IC_{50} 6.5 μ M, K_i 1.3 μ M), along with inhibitory activity against DNA polymerase β (IC_{50} 7.0 μ M, K_i 1.7 μ M) and c-erbB-2 kinase (IC_{50} 28 μ g/mL), but no cytotoxicity (IC_{50} > 10 μ g/mL) against L1210 and KB cells [25]. Tryptophan-derived pigments 48 and 49 and accompanying sesterterpenes 50 and 51 isolated from the Fijian sponge *Fascaplysinopsis reticulata* showed weak inhibition against HIV RT [26]. Toxicols A–C (52–54) and toxiusol (55), triterpenes isolated from the Red Sea sponge *Toxiclona toxius*, were reported to be inhibitory against HIV RT, but no detailed bioactivities were available [27]. Clathsterol (56) isolated from a Red Sea sponge *Clathria* sp. showed anti-HIV-1 RT at 10 μ M [28]. Polycitane A (57), a general inhibitor of retroviral reverse transcriptases and cellular DNA polymerases, was isolated from an ascidian *Polycitor* sp. It inhibited RDDP and DDDP activity of HIV-1 RT with IC_{50} values of 245 and 470 nM, respectively, while it showed general inhibition against MuLV (murine leukemia virus) RT, MMTV (mouse mammary tumor virus) RT, calf-thymus pol α , human pol β , and KF (*E. coli* DNA polymerase I) with IC_{50} values ranging from 73 to 600 nM [29].



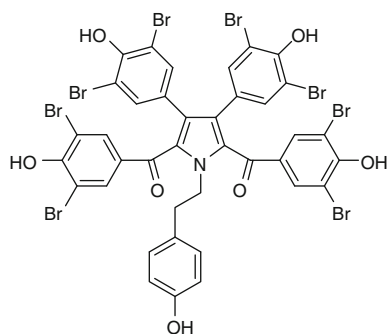
	R ₁	R ₂
toxicol A (52)	SO ₃ Na	SO ₃ Na
toxicol B (53)	H	H
toxicol C (54)	SO ₃ Na	H



toxiosol (55)



clathsterol (56)

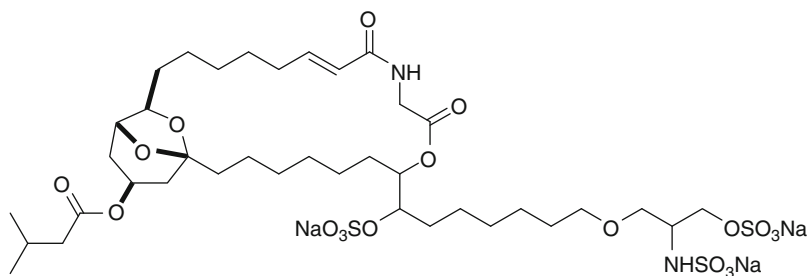
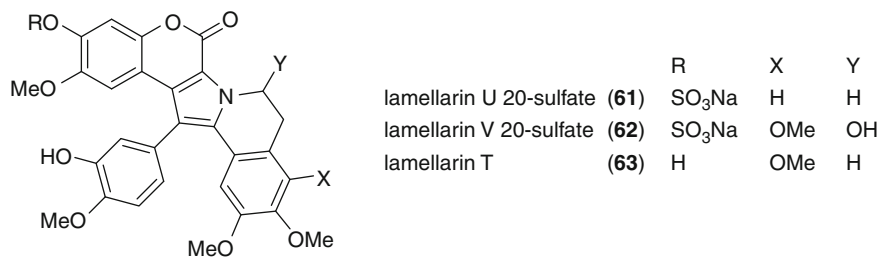


polycitron A (57)

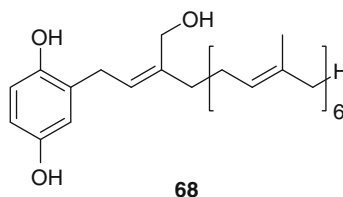
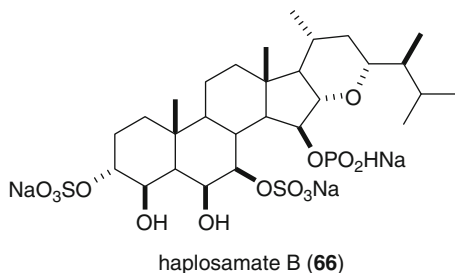
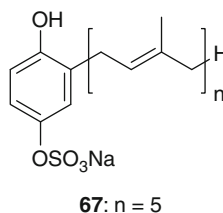
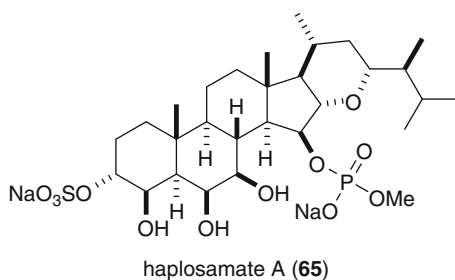
23.3.6 HIV Integrase (EC 2.7.7.-)

HIV integrase catalyzes the initial DNA-breaking and DNA-joining reactions responsible for the attachment of HIV cDNA to host DNA. Since there are no similar proteins known to be important for normal function of cells, HIV integrase

is a promising target for less toxic anti-HIV drugs. A series of ascidian alkaloids, the lamellarins (**58**)–(**63**) showed selective inhibition of HIV integrase with IC_{50} values of 16–73 μM for terminal cleavage and 14–51 μM for strand transfer activities, respectively; lamellarin α 20-sulfate (**58**) showed inhibition in the early steps of replication of HIV-1 in cell culture with an IC_{50} value of 8 μM [30]. Cyclodidemniserinol trisulfate (**64**) isolated from the Palauan ascidian *Didemnum guttatum* showed inhibition against HIV integrase at an IC_{50} of 60 $\mu g/mL$ [31]. Haplosamates A (**65**) and B (**66**) isolated from two haplosclerid sponges (*Xestospongia* sp. and unidentified sponge) inhibited HIV-1 integrase with IC_{50} values of 50 and 15 $\mu g/mL$, respectively [32]. Prenylhydroquinone sulfates **67** and **68** from a deepwater sponge *Ircinia* sp. showed HIV-1 integrase inhibition (65% inhibition at 1 $\mu g/mL$ and 45% inhibition at 5 $\mu g/mL$, respectively) [33].



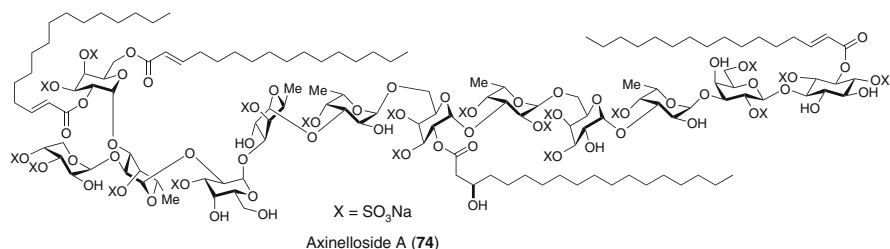
cyclodidemniserinol trisulfate (**64**)



23.3.7 Telomerase (EC 2.7.7.49)

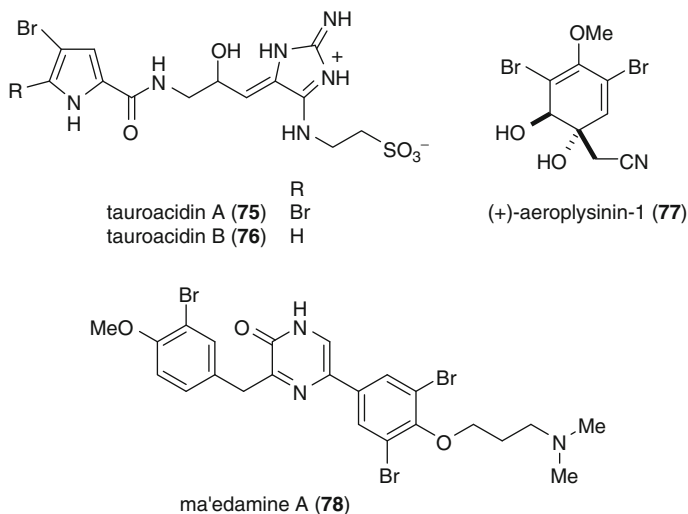
Telomerase is a ribonucleoprotein enzyme that adds repeats of the DNA sequence, TTAGGG, called telomere, onto the 3'-ends of chromosomes [34]. Telomerase activity is found in about 90% of human tumors, but not in normal cells [35]. Thus, inhibitors of telomerase are potential antitumor agents [36]. In fact, some synthetic inhibitors based on the function of telomerase have been successful in clinical trials [37]. From the marine sponge *Dictyodendrilla verongiformis* collected in southern Japan, five telomerase inhibitors, dictyodendrins A–E (**69**–**73**) were isolated along with the sodium salts of two known compounds (**2** and **3**) which were obtained as aldose reductase inhibitors from a marine sponge of the same genus [3]. All these seven compounds showed 100% inhibition of telomerase activity at the concentration of 50 $\mu\text{g/mL}$, while the desulfated analogue of dictyodendrins C (**71**) was not active at this concentration [38]. Recently, the total synthesis of dictyodendrins B (**70**), C (**71**), and E (**73**) was accomplished [39]. An unprecedented highly sulfated lipopolysaccharide, axinelloside A (**74**), isolated from the marine sponge *Axinella infundibula* showed a potent inhibition against human telomerase (IC_{50} 2.0 $\mu\text{g/mL}$) [40].





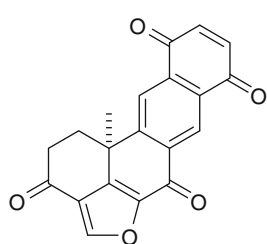
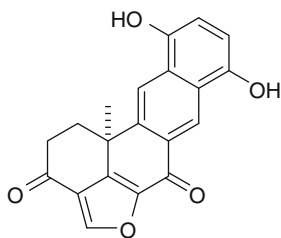
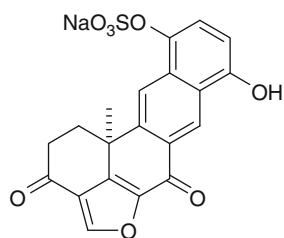
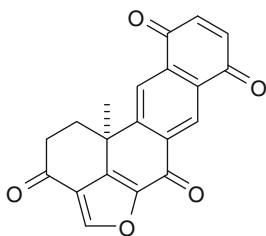
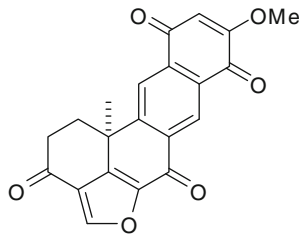
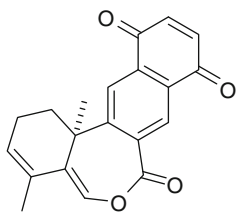
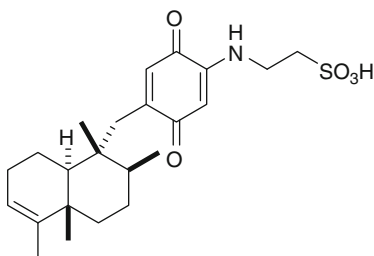
23.3.8 Epidermal Growth Factor Receptor Kinase (EC 2.7.10.1)

Protein tyrosine kinases comprise a large family of enzymes that regulate cell growth and intracellular signaling pathways; inhibitors of these enzymes may be potential anticancer drugs [41]. There are at least four members of the type 1 growth factor receptor gene family, including the epidermal growth factor receptors (EGFR), erbB-1, erbB-2, erbB-3, and erbB-4. Members of this tyrosine kinase receptor family have been implicated in the establishment or progression of human cancer, particularly breast cancer, and enormous amounts of effort have been made to identify specific small molecule inhibitors of EGFR tyrosine kinase [42]. Tauroacidins A (75) and B (76), bromopyrrole metabolites of an Okinawan sponge *Hymeniacidon* sp., exhibited inhibitory activity against c-erbB-2 kinase with an IC₅₀ of 20 µg/mL [43]. (+)-Aeropylsinin-1 (77) isolated from the marine sponge *Verongia aerophoba* inhibited EGF receptor kinase completely at 0.5 µM [44]. Ma'edamine A (78), a cytotoxic bromotyrosine alkaloid isolated from a marine sponge *Suberea* sp., inhibits c-erbB-2 kinase with an IC₅₀ value of 6.7 µg/mL [45].



23.3.9 Tyrosine Kinase pp60^{V-SRC} (EC 2.7.10.2)

A tyrosine kinase, pp60^{V-SRC} is the oncogenic protein encoded by Rous sarcoma virus. Halenaquinone (**79**), halenaquinol (**80**), halenaquinol sulfate (**81**), and xestoquinone (**82**) isolated from the Fijian sponge *Xestospongia* cf. *carbonaria* was found to inhibit the kinase activity of pp60^{V-SRC} with IC₅₀ values of 1.5, 60, 0.55, and 28 μ M, respectively [46]. Halenaquinone (**79**) also inhibited phosphatidylinositol 3-kinase with an IC₅₀ value of 3 μ M [47]. Two more pp60^{V-SRC} inhibitors, 14-methoxyhalenaquinone (**83**) and xestoquinolide A (**84**) were isolated from the same sponge (IC₅₀ values of 5 and 80 μ M, respectively) [48]. Melemeleone B (**85**), a sesquiterpene quinone isolated from two *Dysidea* sponges, showed inhibitory activity against pp60^{V-SRC} with an IC₅₀ value of 28 μ M [49].

halenaquinone (**79**)halenaquinol (**80**)halenaquinol sulfate (**81**)xestoquinone (**82**)14-methoxyhalenaquinone (**83**)xestoquinolide B (**84**)melemeleone B (**85**)

23.3.10 Other Tyrosine Protein Kinase

Four prenylhydroquinone sulfates **67–68** and **90–91** obtained from a deepwater sponge *Ircinia* sp. showed inhibitory activity of tyrosine phosphorylation by membrane fraction prepared from HER2 overexpressing 3T3 cells with IC_{50} values of 8, 4, 8, and 5.9 $\mu\text{g/mL}$, respectively. Compounds **67** and **68** were also reported to be HIV-1 integrase inhibitors [33].

23.3.11 MSK1 (EC 2.7.11.1) and MAPKAPK-2

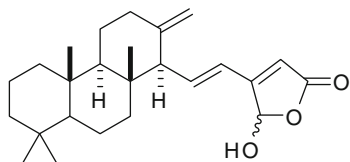
Mitogen- and stress-activated kinase 1 (MSK1) and mitogen-activated protein kinase-activated protein kinase 2 (MAPKAPK2) are two serine protein kinases involved in signal transduction. Both of these enzymes are located in the nucleus and are involved in the late stage of signal transduction pathway, therefore, selective inhibitors of these enzymes are most likely to exhibit highly specific cellular effects. Four cheilanthane sesterterpenoids **86–89** were isolated from a marine sponge *Ircinia* sp. as inhibitors of both MSK1 (IC_{50} s 4 μM for all compounds) and MAPKAPK-2 (IC_{50} 90 μM for all compounds) [50].

23.3.12 Raf/MEK1/MAPK

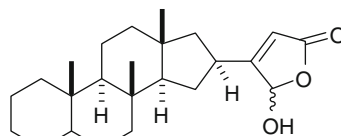
The Ras-MAPK-signaling cascade is found in all eukaryotic organisms and is involved in cellular signaling processes. Since the oncogenic form of Ras is associated with 30% of all cancers, Ras and the downstream kinases represent attractive targets for pharmacological intervention. The Raf/MEK-1/MAPK cascade inhibition assay-guided fractionation of the Philippine marine sponge *Stylissa massa* yielded eight known pyrrole alkaloids, aldisine (**92**), 2-bromoaldisine (**93**), 10Z-debromohymenialdisine (**94**), a 1:1 mixture of 10E- and 10Z-hymenialdisines (**95–96**), hymenin (**97**), oroidin (**98**), and 4,5-dibromopyrrole-2-carbonamide (**99**), among which **93–97** were active with IC_{50} s ranging from 3 to 1288 nM; the most active were **95** and **96** (IC_{50} s 3 and 6 nM, respectively). In addition, all compounds showed essentially identical IC_{50} values in the MEK-1 to MAPK assay, while none of them showed activity in the Raf to MEK-1 assay [51].

23.3.13 Checkpoint Kinases (EC 2.7.11.1)

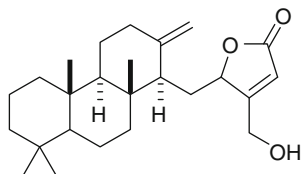
The synthetic 10Z-debromohymenialdisine (**94**) inhibited checkpoint kinases Chk1 and 2 with IC_{50} values of 3 and 3.5 μM , respectively [52]. Further investigation into its inhibitory activity toward kinases led to identification of 11 new targets including p90RSK, KDR, c-Kit, Fes, MAPK1, PAK2, PDK1, PKC θ , PKD2, Rsk1, and SGK for this class of alkaloids [53].



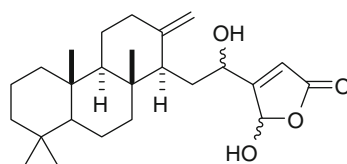
86



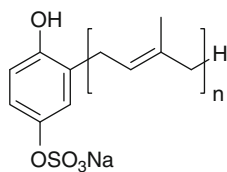
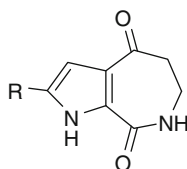
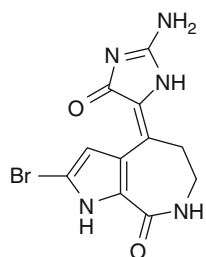
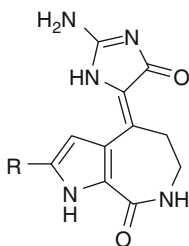
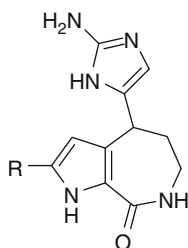
87



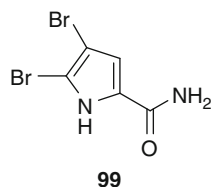
88



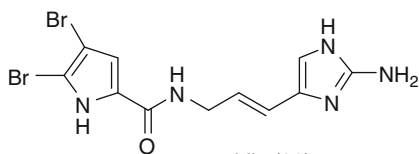
89

90: $n = 6$ 91: $n = 7$ aldisine (92) $R = H$ 2-bromoaldisine (93) $R = Br$ 10*E*-hymenialdisine (95)10*Z*-debromohymenialdisine (94) $R = H$ 10*Z*-hymenialdisine (96) $R = Br$ 

hymenin (97)



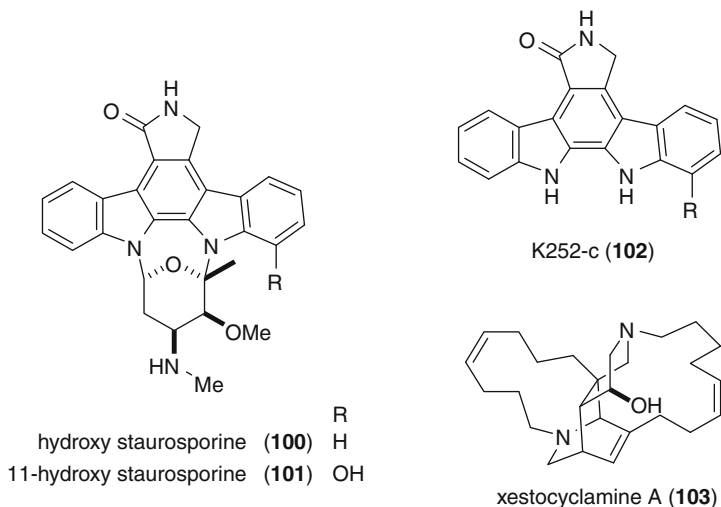
99

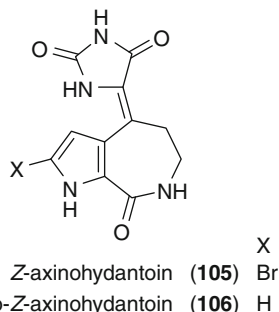
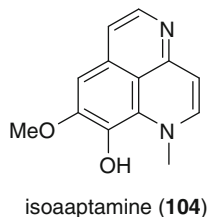


oroidin (98)

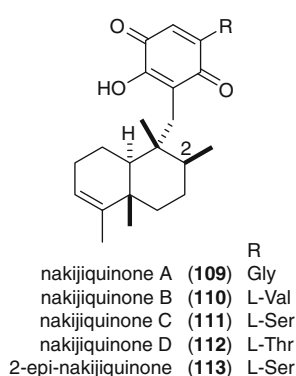
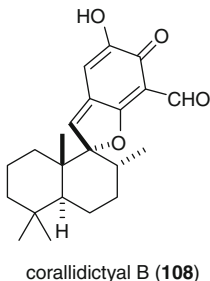
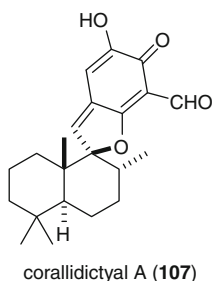
23.3.14 Protein Kinase C (EC 2.7.11.13)

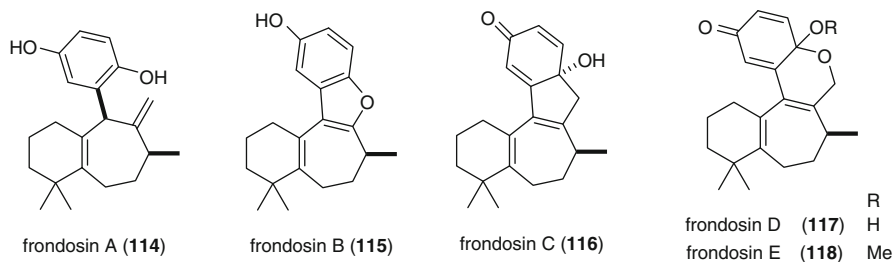
Protein kinase C (PKC), a phospholipid-dependent protein phosphorylating enzyme, is a key player of cellular signal transduction and is believed to be responsible for cancer, cardiovascular and renal disorders, and immunosuppression and autoimmune diseases, such as rheumatoid arthritis. Therefore, inhibitors of protein kinase C (PKC) can be potential drug leads for the treatment of such diseases. Staurosporine (**100**), isolated from *Streptomyces staurosporeus*, is the most famous natural product PKC inhibitor [54]. 11-Hydroxystaurosporine (**101**) isolated from a tunicate *Eudistoma* sp. collected in Pohnpei inhibited PKC with an IC_{50} value of 2.2 nM which is about 30% more active than staurosporine (**100**) [55]. Staurosporine aglycone K252-c (**102**) isolated from another *Eudistoma* sample inhibited eight cloned PKC isoenzymes α , β I, β II, δ , ϵ , η , γ , and ζ with IC_{50} values of 1.3, 0.6, 0.5, 1.2, 1.1, 0.8, 1.5, and >6.4 μ M, respectively [56]. Xestocyclamine A (**103**), bis-alkylpiperadines from a marine sponge *Xestospongia* sp., moderately inhibited PKC ϵ (IC_{50} 4 μ g/mL) [57]. Isoaaptamine (**104**), which was first reported from a suberitid sponge in 1988, was found to be a PKC inhibitor; recent evaluation of PKC inhibitory and antitumor activities for synthetic isoaaptamine and its derivatives disclosed that none of them met the criteria for further evaluation after the primary screen in the NCI tumor cell line panel [58]. Z-axinohydantoin (**105**) and debromo-Z-axinohydantoin (**106**) isolated from the marine sponge *Stylotella aurantium*, moderately inhibited PKC (IC_{50} s 9.0 and 22 μ M, respectively) [59].



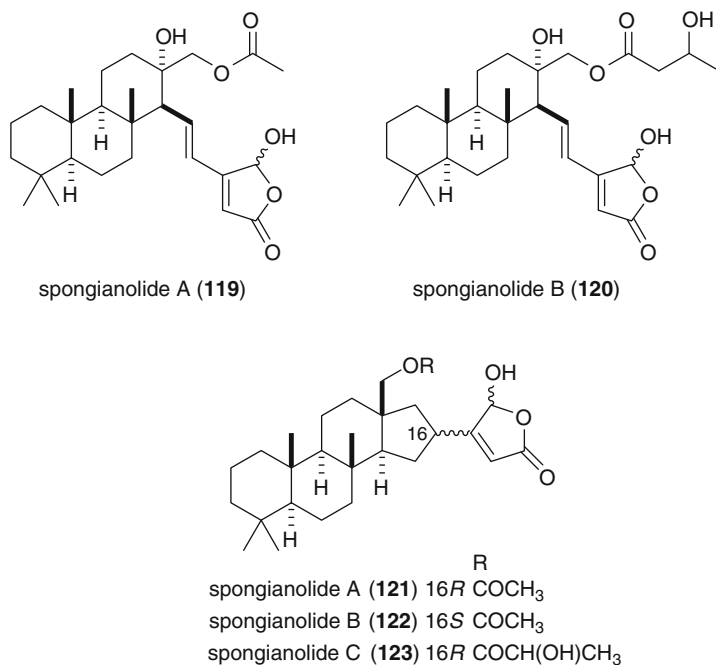


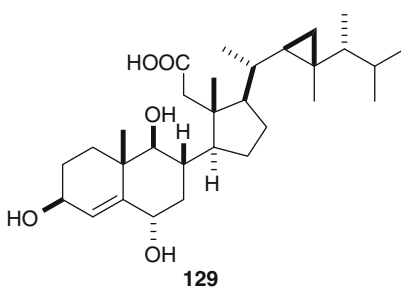
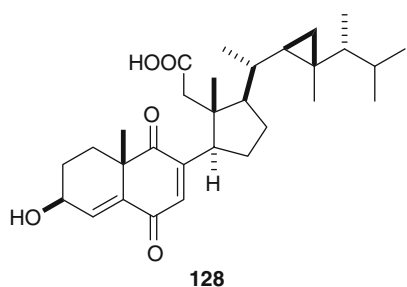
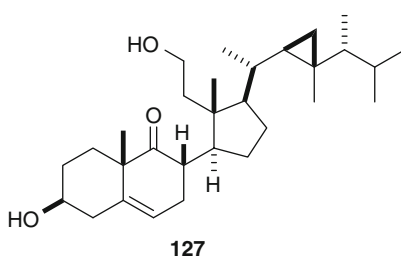
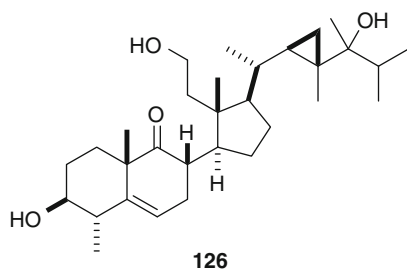
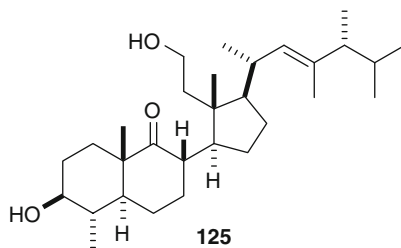
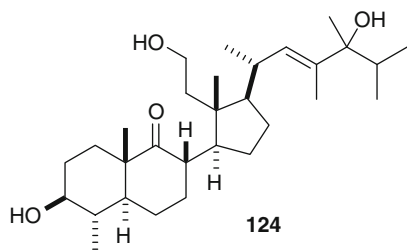
The mixture of corallidictyals A (**107**) and B (**108**), spirosesquiterpene aldehydes isolated from the marine sponge *Aka* (*Siphonodictyon*) *coralliphagum*, inhibited PKC with an IC_{50} value of 28 μ M. Interestingly, the corallidictyal mixture selectively inhibited PKC α with an IC_{50} value of 30 μ M (IC_{50} s 89, >300, and >300 μ M for ϵ , η , and ζ , respectively). In addition, the corallidictyal mixture inhibited the growth of cultured Vero (African green monkey kidney) cells with an IC_{50} value of 1 μ M after continuous exposure (72 h) [60]. Nakijiquinones A–D (**109**–**112**), sesquiterpene quinones isolated from an Okinawan marine sponge of the family Spongiidae, exhibited inhibitory activity against PKC with IC_{50} values of 270, 200, 23, and 220 μ M, respectively, whereas they were also active against EGF receptor kinases and c-erbB-2 kinase with IC_{50} values of >400, 250, 170, and >400 μ M, and 30, 95, 26, and 29 μ M, respectively [61]. Recently, enantioselective total synthesis of nakijiquinones and closely related analogues was reported [62]. The evaluation of their biological activities disclosed that C-2 epimer of nakijiquinone (**113**) was a potent and selective inhibitor of tyrosine kinase VEGFR2 (KDR) with an IC_{50} value of 21 μ M. Incidentally, VEGFR2 is a receptor for the vascular endothelial growth factor (VEGF) family and is responsible for endothelial cell proliferation and blood vessel permeability, therefore inhibitors of VEGFR2 are potential anti-angiogenic drugs [62]. Frondosines A–E (**114**–**118**), sesquiterpenoids from the sponge *Dysidea frondosa*, inhibited PKC with IC_{50} values of 1.8, 4.8, 20.9, 26, and 30.6 μ M, respectively [63].



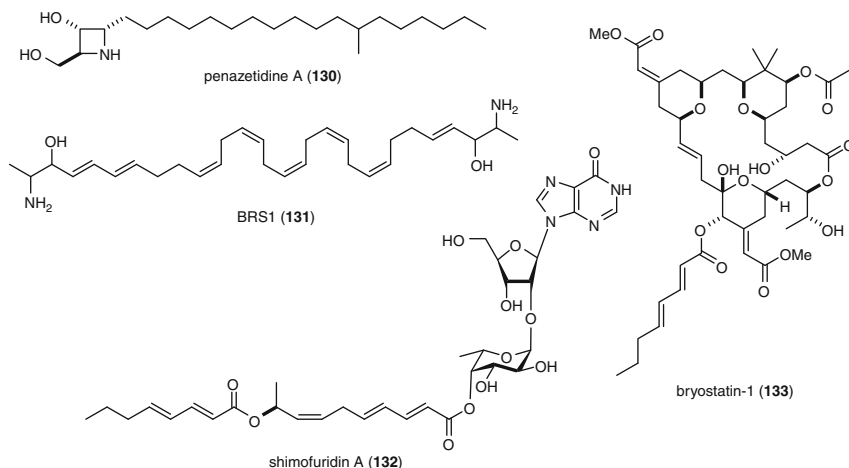


Spongianolides A–E (**119–123**), cytotoxic sesterterpenes isolated from a marine sponge *Spongia* sp., inhibited PKC at IC_{50} values of 20–30 μ M [64]. Three secosterols **124–126** isolated from a gorgonian *Pseudopterogorgia* sp. inhibited the human PKC α , β I, β II, γ , δ , ϵ , η , and ζ with IC_{50} values in the range of 12–50 μ M. The semisynthetic derivatives **127–129** also showed similar activity [42].



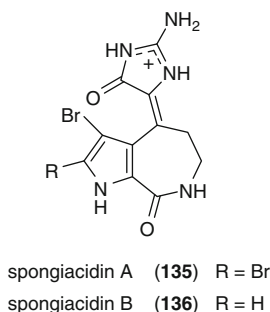
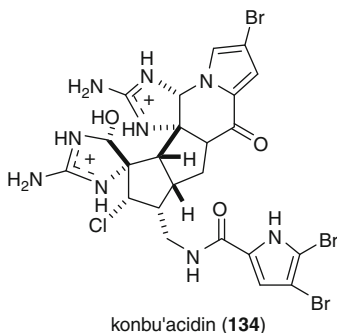


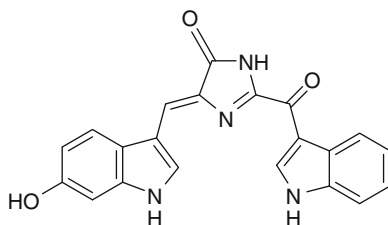
Penazetidine A (**130**), an azetidine isolated from the Indo-Pacific sponge *Penares sollasi*, inhibited PKC with an IC_{50} value of 1 μM [65]. BRS1 (**131**), a C_{30} *bis*-amino, *bis*-hydroxy polyunsaturated lipid from an unidentified Australian sponge of the class Calcarea, inhibited not only PKC (EC_{50} 98 μM) but also radiolabeled phorbol ester binding to the enzyme (EC_{50} 9.2 μM) [66]. Shimofuridin A (**132**) isolated from an Okinawan marine tunicate *Aplidium multiplicatum* inhibited PKC at an IC_{50} of 20.0 $\mu g/mL$ [67]. Bryostatin-1 (**133**) which was isolated from the bryozoa *Bugula neritina* as an anticancer agent [68], is known to bind the C1 domain of PKC and regulate its activity [69].



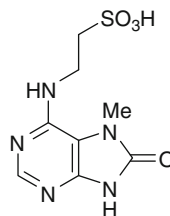
23.3.15 Cyclin-Dependent Kinases (EC 2.7.11.22)

Cyclin-dependent kinases (CDK) are also a family of protein tyrosine kinases, some of which are involved in cell cycles, and their inhibitors are expected to be potential anticancer drugs. Konbu'acidin A (**134**) is a bromopyrrole alkaloid possessing inhibitory activity against CDK4 (IC_{50} 20 $\mu\text{g/mL}$) isolated from a marine sponge *Hymeniacidon* sp. [70]. Spongiacidins A (**135**) and B (**136**) also isolated from the same sponge inhibited c-erbB-2 kinase (IC_{50} s 8.5 and 6.0 $\mu\text{g/mL}$, respectively) and cyclin-dependent kinase 4 (CDK4) (IC_{50} s 32 and 12 $\mu\text{g/mL}$, respectively) [71]. Rhopaladins A–D isolated from an Okinawan tunicate *Rhopalaea* sp. are the first example of *bis*-indole alkaloids possessing an imidazolinone moiety as tunicate metabolites; rhopaladin B (**137**) inhibited CDK4 and c-erbB-2 kinase with IC_{50} values of 12.5 and 7.4 $\mu\text{g/mL}$, respectively [72]. Microxine (**138**) from an Australian marine sponge *Microxina* sp. inhibited CDK1 (cdc2) kinase with an IC_{50} value of 13 μM [73].





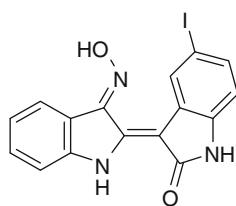
Rhopaladin B (137)



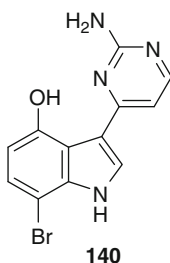
microxine (138)

23.3.16 Glycogen Synthase Kinase-3 (2.7.11.17)

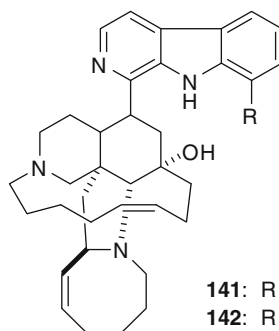
Glycogen synthase kinase-3 (GSK-3) is a serine-threonine kinase ubiquitously expressed and involved in the regulation of many cell functions. GSK-3 phosphorylates glycogen synthase or the microtubule-associated protein tau, being implicated in type-2 diabetes, Alzheimer's disease, or different tau pathologies such as Pick's disease. Hymenialdisine (96) [74], indirubine (139) [75], and meridianine (140) [76] are the known marine-derived GSK-3 inhibitors isolated from several species of marine sponges, the mollusk *Hexaplex trunculus*, and the ascidian *Aplidium meridianum*, respectively. Hymenialdisine (96) potently inhibited GSK-3 β (IC₅₀ 10 nM) and plant GSK-3 (ASK- γ) with an IC₅₀ value of 80 nM as well. It inhibited in vivo phosphorylation of specific neuronal proteins by GSK-3 β and CDK5 such as AD-characteristic phosphorylation of tau completely [74]. Indirubin inhibited GSK-3 α/β with an IC₅₀ value of 1.00 μ M [75]. Studies of structure-activity relationship (SAR) in the class of manzamine alkaloids revealed that manzamine A (141) inhibited GSK-3 β at an IC₅₀ value of 10.2 μ M; 8-hydroxymanzamine A (142) being the most potent analogue (IC₅₀ 4.8 μ M) [77].



139



140



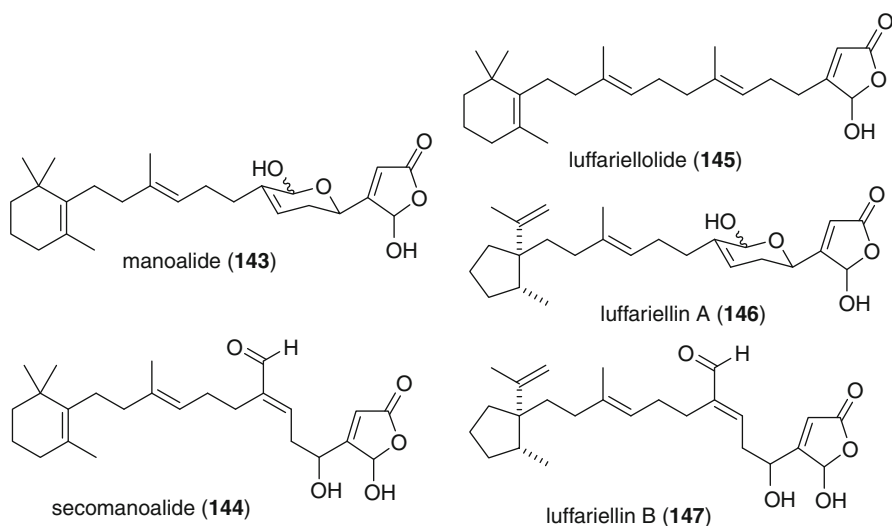
141: R = H

142: R = OH

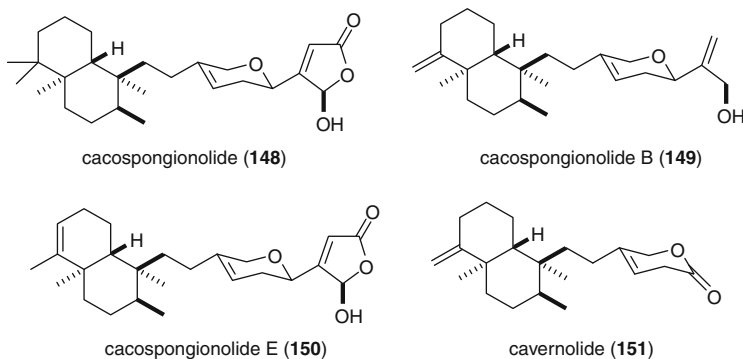
23.4 Hydrolases (EC 3.-.-.)

23.4.1 Phospholipase A₂ (EC 3.1.1.4)

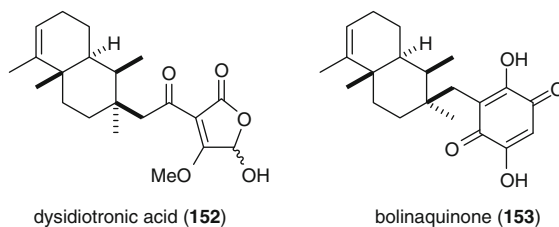
Phospholipase A₂ (PLA₂) cleaves the ester linkage of the β -position of phospholipids to release arachidonic acid which is metabolized to prostaglandins, leukotrienes, and other mediators of inflammation. Prostaglandins are implicated in various forms of pain and inflammation. In biogenesis of prostaglandins, arachidonic acid formation is the rate-determining step, thus, PLA₂ inhibitors are expected to be potential anti-inflammatory drugs. Manoalide (**143**), initially isolated as an antibacterial metabolite from the marine sponge *Luffariella variabilis* [78], was later found to be a potent inhibitor of PLA₂ with an IC₅₀ value of 1.7 μ M [79], which led to synthesis and anti-inflammatory evaluation of more than 100 analogues. Unfortunately, none of them was developed for drugs. Three congeners of manoalide were also obtained from the same sponge [80], of which secomanalide (**144**) is more potent against bovine pancreatic PLA₂ [81]. Luffariellolide (**145**) isolated from a Palauan sponge *Luffariella* sp. also inhibited the bee venom PLA₂ with an IC₅₀ of 0.23 μ M. The partially reversible and weaker inhibitory activity of **145** was suggesting that the γ -lactol group in **143** was responsible for the irreversible reaction of **143** with Lys residues on PLA₂ [82]. Luffariellins A (**146**) and B (**147**) isolated from *L. variabilis* are very potent against bee venom PLA₂ with IC₅₀ values of 56 and 62 nM, respectively [83]. These sesterterpenes are known to covalently and specifically modify PLA₂ by a Schiff base formation between Lys-56 residue of PLA₂ and the hemiacetal or aldehyde functionality of these terpenoids [84]. According to this mechanism, Katsumura and coworkers designed PLA₂ inhibitors, one of which potently and selectively inhibited bovine pancreas PLA₂ [85].

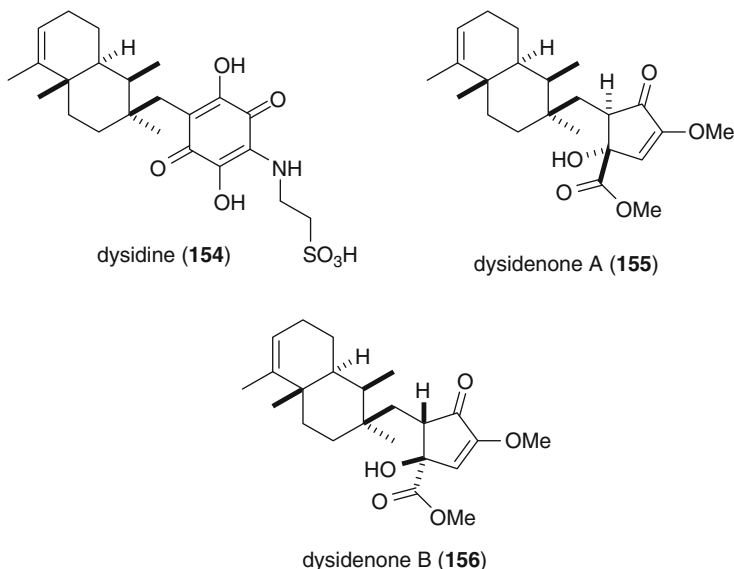


Cacospongionolides (**148–150**), originally isolated as antitumor compounds from the Mediterranean sponge *Fasciospongia cavernosa* [86], preferentially inhibited bee venom and human synovial PLA₂ among PLA₂s of various origins. Cacospongionolide B (**149**) exhibited specific inhibition against human PLA₂ [87], while cacospongionolide E (**150**) was the most potent inhibitor toward human synovial PLA₂ (IC₅₀ 1.4 μ M), showing higher potency than manoalide [88]. The structure–activity relationship study on synthetic analogues suggested that **149** has an enantiospecific interaction with the enzyme that is independent of the γ -hydroxybutenolide moiety [89]. Furthermore, cacospongionolide B (**149**) was reported to suppresses the expression of inflammatory enzymes including inducible nitric oxide synthase (iNOS) and cyclooxygenase-2 (COX-2) as well as to reduce tumor necrosis factor- α (TNF- α) [90]. Cavernolide (**151**) isolated from a marine sponge *Fasciospongia cavernosa* selectively inhibited human PLA₂ with an IC₅₀ value of 8.8 μ M [91].



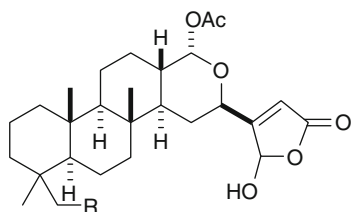
Dysidiotronic acid (**152**), a sesquiterpenoid from a Vanuatu sponge *Dysidea* sp., inhibited human synovial PLA₂ with an IC₅₀ value of 2.6 μ M [92], while bolinaquinone (**153**), dysidine (**154**), and a 1:1 mixture of dysideonones A (**155**) and B (**156**) significantly inhibited human synovial PLA₂, among which **153** showed the most potent activity with an IC₅₀ value of 0.2 μ M, but was not a selective inhibitor toward this enzyme. On the contrary, dysidine (**150**) showed selective inhibition against this enzyme with an IC₅₀ value of 2.0 μ M. However, **153–156** did not inhibit cPLA₂ [93].



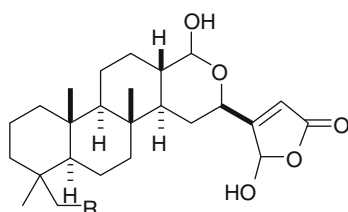


Petrosaspongiolides M–R (**157**–**161**), sesterterpens from the New Caledonian marine sponge *Petrosaspongia nigra* inhibited PLA₂; the most potent petrosaspongiolide M (**157**) inhibited human synovial and bee venom PLA₂ with IC₅₀ values of 1.6 and 0.6 μ M, respectively, while petrosaspongiolide P (**159**) inhibited human synovial PLA₂ (IC₅₀ 3.8 μ M) more selectively than bee venom PLA₂ (IC₅₀ >10 μ M). Other petrosaspongiolides N (**158**), Q (**160**), and R (**161**) showed only weak activity [94]. Petrosaspongiolide M was shown to form the covalent adduct between PLA₂ and γ -hydroxybutenolide which is essential for the activity [95]. Ironically, a mild non-covalent PLA₂ inhibitor, 25-acetyl-petrosaspongiolide M, was found to be hydrolyzed with PLA₂ to form the potent inhibitor, petrosaspongiolide M [96]. Interestingly, a full characterization of the *bv* PLA₂ adduct with petrosaspongiolide R (**161**), one of the least active and most structurally different among petrosaspongiolides, using LC-MS, MSⁿ, and computational methods, confirmed the same inhibition mechanism and covalent binding site already found for petrosaspongiolide M (**167**). The correct arrangement of the ligand in the active site, induced by non-covalent interactions, is of pivotal importance in the inactivation process [97]. The anti-inflammatory effects of petrosaspongiolide M was suggested to be mediated by inhibition of NF- κ B signaling pathway [98].

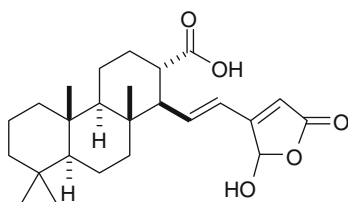
Aplyolide (**162**), a sesterterpene isolated from the marine sponge *Aplysinopsis elegans* inhibited human PLA₂ with an IC₅₀ value of 10.5 μ M [99], whereas the related terpenoid, luffolide (**163**) isolated from a Palauan *Luffariella* sp., completely inhibited bee venom PLA₂ at a concentration of 3.5 μ M [100].



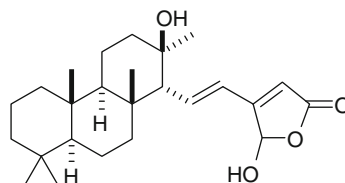
petrosaspongiolide M (**157**)
 R H
 N (**158**) OAc



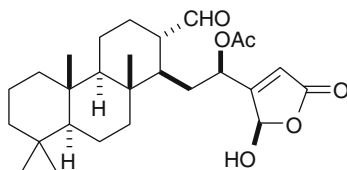
petrosaspongiolide P (**159**)
 R H
 Q (**160**) OAc



petrosaspongiolide R (**161**)

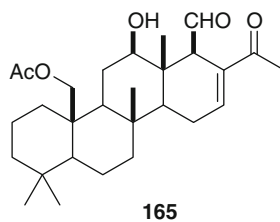
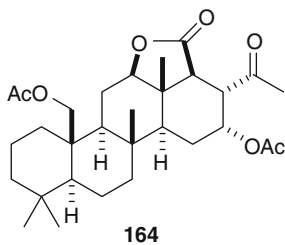


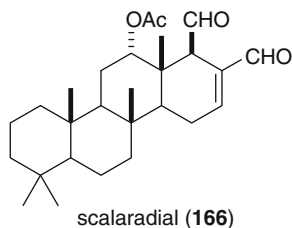
aplyolide A (**162**)



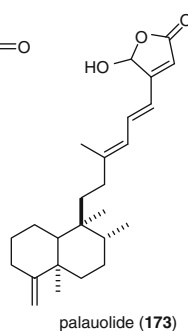
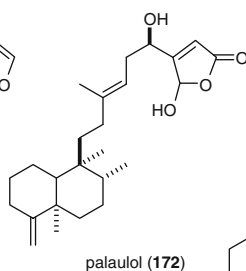
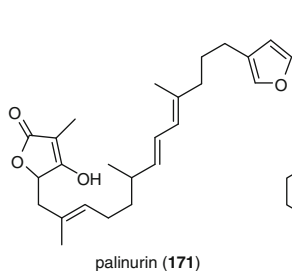
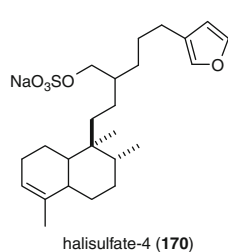
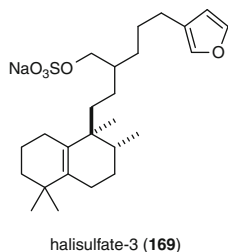
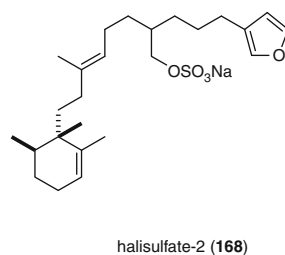
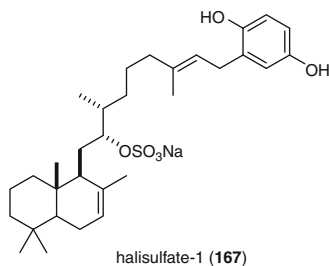
luffolide (**163**)

A homoscalarane sesterterpene (**164**) isolated from a marine sponge *Lendenfeldia frondosa* showed moderate PLA₂ inhibition (35% inhibition at 8 μ M) [101]. A sesterterpene, 12-deacetyl-23-acetoxy-20-methyl-12-epi-scalaradial (**165**), from the Pacific nudibranchs *Glossodoris sedan* and *G. dalli* inhibited mammalian cytosolic PLA₂ with an IC₅₀ value of 18.0 μ M [102]. The parent compound, scalaradial (**166**) is more potent (IC₅₀ 0.6 μ M) [84a, 103].

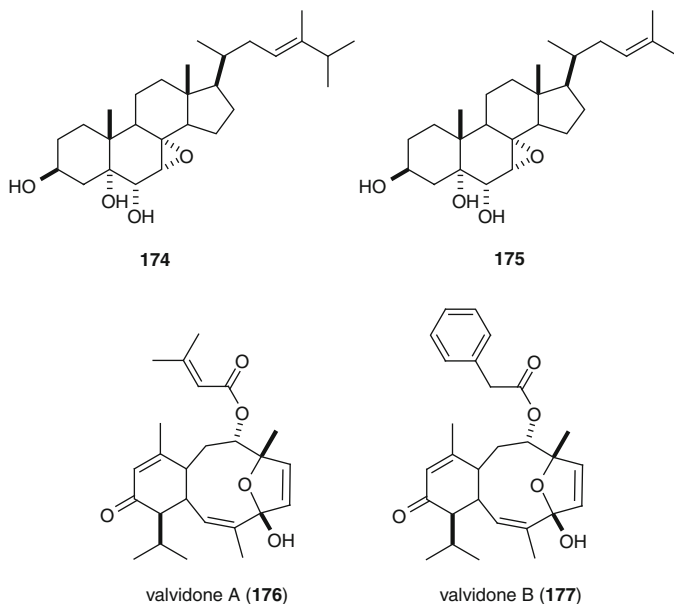




Halisulfate 1 (**167**) from a halichondrid sponge inhibited PLA₂ completely at 16 µg/mL, while a mixture of halisulfates 2–4 (**168–170**) inhibited PMA-induced inflammation in the mouse ear edema assay as well as PLA₂ (data not shown) [104]. Palinurin (**171**), originally isolated from the Mediterranean marine sponge *Ircinia variabilis* [105], was inhibitory against PLA₂ with an IC₅₀ value of 50 µM [2]. Two sesterterpenes, palauolol (**172**) and palauolide (**173**) isolated from a Palauan sponge *Fascaplysinopsis* sp. inhibit bee venom PLA₂ (85% and 82% inhibition at 0.8 µg/mL, respectively) [106].

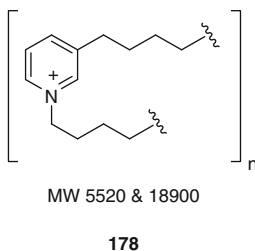


Two polyhydroxy sterols **174** and **175** from the Korean gorgonian *Acabaria undulata* inhibited PLA₂ with IC₅₀ values of 13.8 and 21.5 μ M, respectively [107]. Valdivones A (**176**) and B (**177**), diterpenoids isolated from the South African soft coral *Alcyonium valdivae*, strongly inhibited chemically induced inflammation in the mouse ear assay (93% and 72% inhibition at 50 μ g/ear, respectively), but their activity against bee venom PLA₂ was not potent (43% inhibition at 16 μ g/mL for both) [108].



23.4.2 Acetylcholinesterase (EC 3.1.1.7)

3-Alkylpyridinium polymers **178** from a marine sponge *Reniera sarai* showed potent inhibitory activity against electric eel acetylcholinesterase (AChE), human erythrocyte AChE, insect recombinant AChE, and horse serum butylcholinesterase (BuChE) with IC₅₀ values of 0.06, 0.08, 0.57, and 0.14 μ g/mL, respectively, while it did not inhibit trypsin or alkaline phosphatase [109].

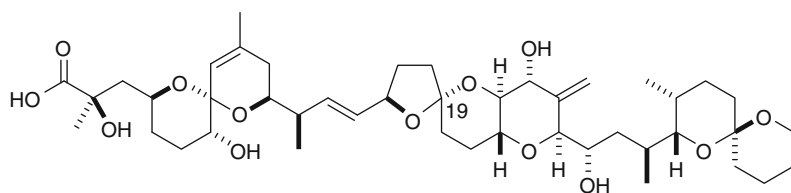


23.4.3 Protein Phosphatases (EC 3.1.3.16)

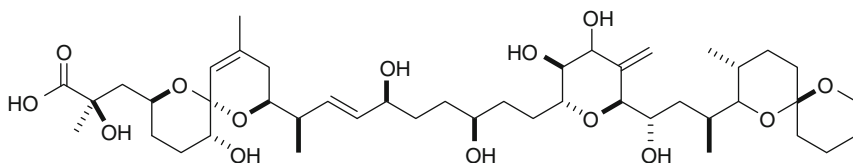
Reversible protein serine/threonine phosphorylation regulates numerous cellular functions, including muscle contraction, neurotransmission, cell proliferation, carcinogenesis, and apoptosis. Although a large number of protein kinases have been well investigated for several decades, it is quite recent that our understanding of protein phosphatases (PPs), namely PP1, PP2A, PP2B, and PP2C, has been considerably deepened by the discovery of natural product inhibitors.

23.4.3.1 PP1 and PP2

Okadaic acid (**179**), the first natural product inhibitor of PP1 and PP2A, is a polyether polyketide isolated as a cytotoxic substance from two sponges, Japanese *Halichondria okadai* and Caribbean *H. melanodocia* [110]. It was succeedingly identified as a causative agent of the diarrhetic shellfish poisoning. Later, **179** was found to show a potent tumor promoting activity caused by potent inhibition of PP1 and PP2A with IC_{50} values of 3 and 0.2–1 nM, respectively, whereas it showed only weak or no inhibition against PP2B or PP2C [111]. It has become a powerful tool for the study of biological processes mediated by protein phosphorylation. The crystal structure of PP1 γ -okadaic acid complex was elucidated in 1995 [112]. A remarkable reduction of inhibitory activity against PP1 (IC_{50} 465 nM) was observed for 19-*epi*-okadaic acid isolated from dinoflagellate *Prorocentrum belizeanum*, whereas the inhibitory activity against PP2A remained as the same level (IC_{50} 0.47 nM) for **179**. It was suggested that the stereochemistry at C19 is crucial for the selectivity between PP1 and PP2A [113]. A new okadaic acid class compound, belizeanic acid (**180**) with an unusual skeleton was isolated from the dinoflagellate *Prorocentrum belizeanum*. Despite its opening of C/D rings, it still retains the potent inhibitory activity against PP1 (IC_{50} 318 nM), slightly reduced potency compared to okadaic acid (IC_{50} 62 nM in the same assay system) [114].

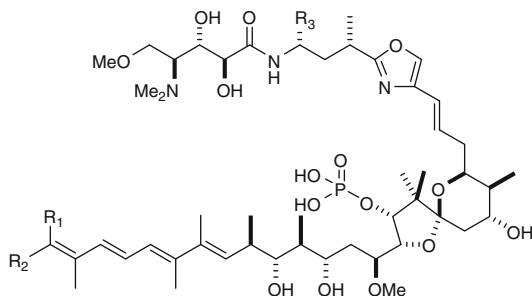


okadaic acid (**179**)

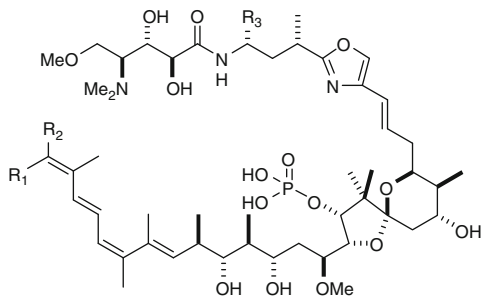


(**180**)

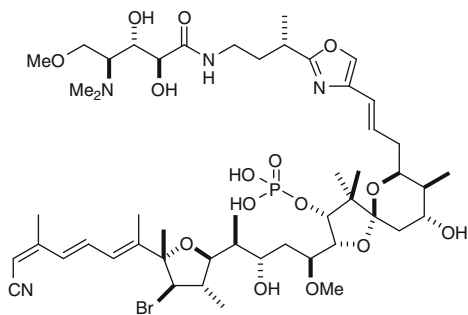
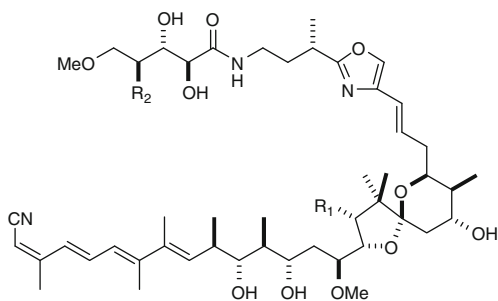
Calyculin A (**181**) was isolated from the Japanese marine sponge *Discodermia calyx* as a potent antitumor agent [115]. Like okadaic acid, it was found to be a potent tumor promoter and to inhibit PP1 and PP2A with IC_{50} values of 1.4 and 2.6 nM, respectively, while it showed weak inhibition against PP2B [116]. Calyculins B–H (**182**–**188**), geometrical isomers of **181**, or their 32-methyl derivatives which were succeedingly isolated from the same sponge, were originally reported to have similar inhibitory activity against PP2A (IC_{50} 1.0–6.0 nM) [117], but this was later found to be not correct; the geometry of the tetraene portion affects the enzyme inhibition significantly [119]. Furthermore, calyculin J (**189**), calyculinamides A (**190**) and F (**191**), des-*N*-methylcalyculin A (**192**) and dephosphonocalyculin A (**193**) were isolated as PP2A inhibitors from *D. calyx* [118]. Later, isolation of hemicalyculin A (**194**) from *D. calyx* and structure-activity relationship studies were reported [119]. Hemicalyculin A (**194**) was equipotent as calyculin A (**181**) against PP1 γ and PP2A with IC_{50} values of 14 and 1.0 nM, respectively. Interestingly, **194** showed cytotoxicity over 2000 times less than that of **181**. More recently, the crystal structure of the calyculin A-PP1 γ complex was solved by X-ray crystallography [120], which showed that the hydrophobic tail, phosphate, and 13-OH moieties are essential for binding to PP1 γ . These features are the cases of the PP1c/microcystin LR [121] and PP1c/okadaic acid complexes [112]. Clavosines A–C (**195**–**197**), glycosylated derivatives of C21-*epi*-calyculinamide C, were isolated from the marine sponge *Myriastra clavosa*. Clavosines A (**195**) and B (**197**) inhibited PP1 γ (IC_{50} s 0.5 and 13 nM, respectively), native PP1c (IC_{50} s 0.25 and 1.0 nM, respectively), and PP2Ac (IC_{50} s 0.6 and 1.2 nM, respectively) [122].



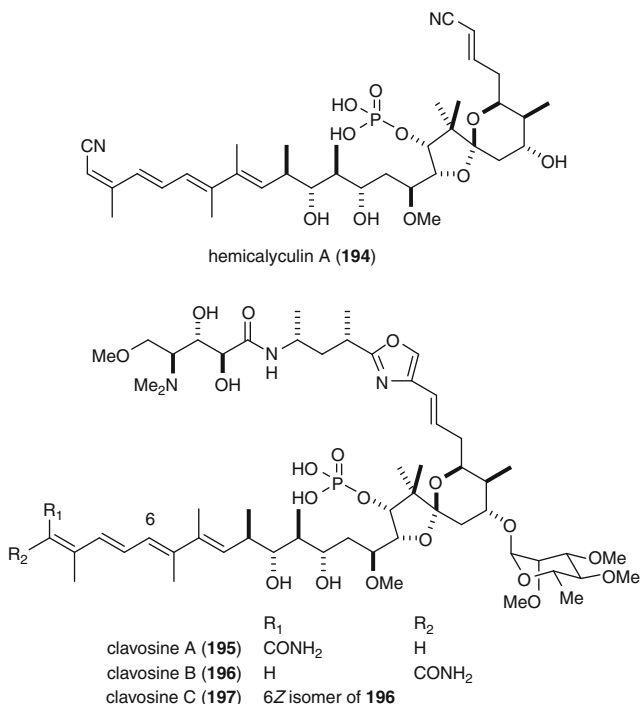
	R ₁	R ₂	R ₃
calyculin A (181)	CN	H	H
calyculin B (182)	H	CN	H
calyculin C (183)	CN	H	Me
calyculin D (184)	H	CN	Me
calyculinamide A (190)	CONH	H	H



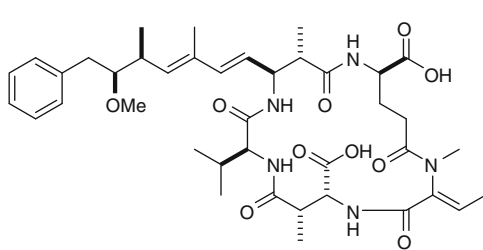
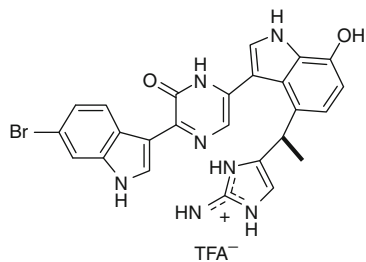
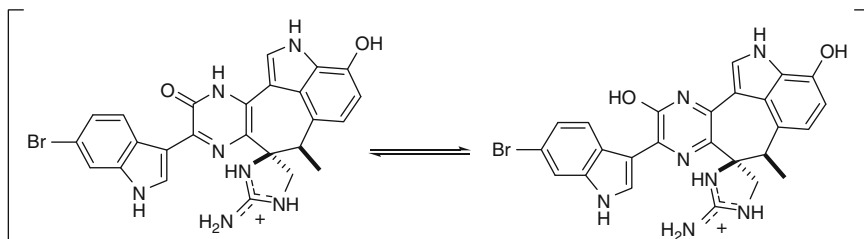
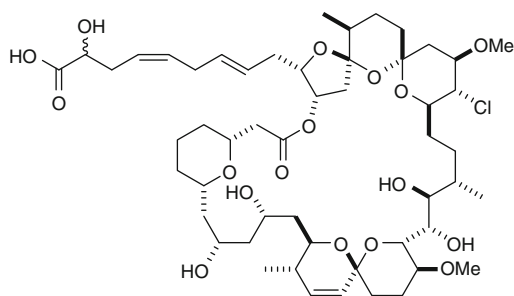
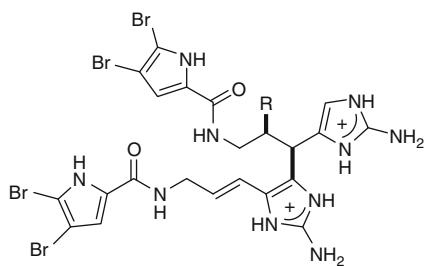
	R ₁	R ₂	R ₃
calyculin E (185)	CN	H	H
calyculin F (186)	H	CN	H
calyculin G (187)	CN	H	Me
calyculin H (188)	H	CN	Me
calyculinamide F (191)	H	CONH	H

calyculin J (**189**)

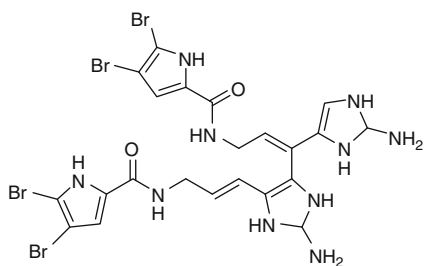
	R ₁	R ₂
des- <i>N</i> -methylcalyculin A (192)	OPO ₃ H ₂	NHMe
dephosphonocalyculin A (193)	OH	NMe ₂

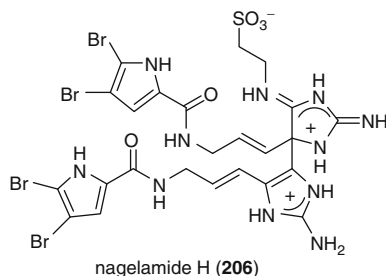
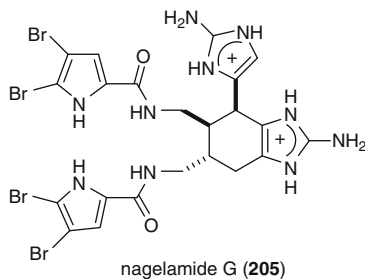


Motuporin A (**198**), one of the most potent PP1 inhibitors known, isolated from the Papua New Guinea sponge *Theonella swinhoei* inhibited PP1 at <1 nM [123]. Dragmacidins D (**199**) and E (**200**) isolated from a southern Australian deepwater sponge *Spongisorites* sp. are potent serine-threonine protein phosphatase inhibitors; **199** selectively inhibited PP1, while **200** inhibited both PP1 and PP2A in the preliminary test (data not shown). Dragmacidin E (**200**) seemed to exist in tautomeric equilibrium between pyrazine and pyrazinone forms [124]. Spirastrellolide A (**201**) was a novel macrolide isolated from the marine sponge *Spirastrella coccinea* as an antimitotic agent [125]. Recently, its revised structure and selective inhibitory activity against PP2A (IC₅₀ 1 nM) were reported [126]. Nagelamides are dimeric bromopyrrole alkaloids isolated from a marine sponge *Agelas* sp., among which nagelamides A–C (**202–204**), G (**205**), and H (**206**) were shown to inhibit PP2A (IC₅₀ 13 to >50 μ M) [127].

motuporin A (**198**)dragmacidin D (**199**)dragmacidin E (**200**)spirastrellolide A (**201**)

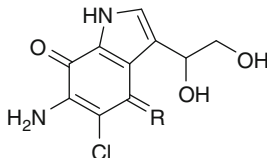
nagelamide A (**202**) R = H
 B (**203**) R = OH

nagelamide C (**204**)



23.4.3.2 Calcineurin (PP2B)

Calcineurin (CaN), a serine-threonine protein phosphatase (PP2B) involved in signal transduction, is recognized as one of the principal signaling molecules that regulates the immune response [128]. Immunosuppressants such as FK506 and cyclosporin A have been shown to exert their effect through inhibition of CaN following their association with binding proteins [129]. Thus, inhibitors of CaN may be useful as immunosuppressants. Secobatzellines A (**207**) and B (**208**) isolated from a Caribbean deepwater sponge *Batzella* sp. inhibited CaN with IC_{50} values of 0.55 and 2.21 $\mu\text{g/mL}$, respectively. Secobatzelline A (**207**) also inhibited peptidase activity of CPP32 (IC_{50} 0.02 $\mu\text{g/mL}$), a cysteine protease known as caspase-3 which play a major role in the programmed cell death known as apoptosis [130].



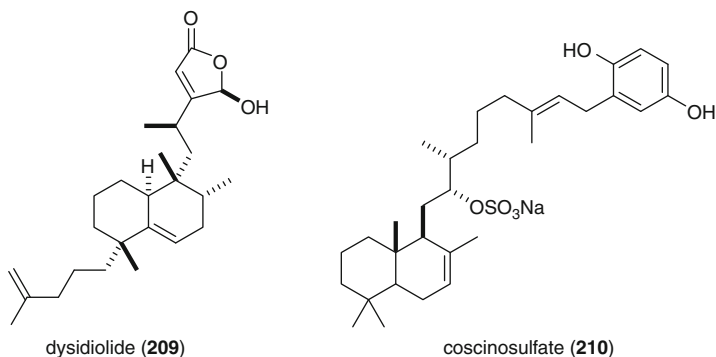
secobatzelline A (**207**) R = NH

secobatzelline B (**208**) R = O

23.4.4 Protein Tyrosine Phosphatases (EC 3.1.3.48)

Cdc25 is a dual-specificity protein tyrosine phosphatase which regulates activation of CDKs (cyclin-dependent kinases) through the dephosphorylations of a threonine and a tyrosine residues of CDKs. Due to their unique substrate selectivity and their essential functions in cell cycle control, cdc25 phosphatases are attractive screening target to identify new antimitotic compounds. Dysidiolide (**209**) is the first natural product inhibitor of cdc25A isolated from the Caribbean sponge *Dysidea etheria*. It inhibited the dephosphorylation of *p*-nitrophenol phosphate by cdc25A phosphatase with an IC_{50} of 9.4 μM [131].

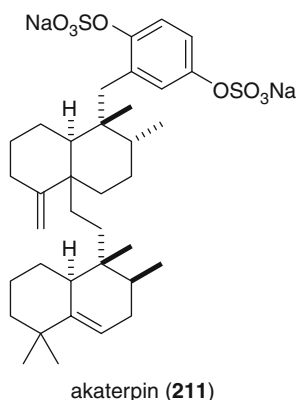
Because of its unusual structure and interesting biological activity, a number of synthetic chemists entered the race of total synthesis of dysidiolide, from which some important structure-activity relationships were provided [132]. Coscinosulfate (**210**), a sesquiterpene sulfate isolated from the New Caledonian sponge *Coscinoderma mathewsi* exhibited selective inhibition against cdc25A phosphatase with an IC_{50} of 3 μ M [133].



23.4.5 Phospholipase C (EC 3.1.4.3)

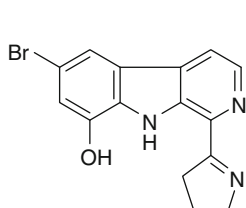
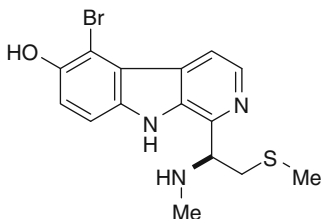
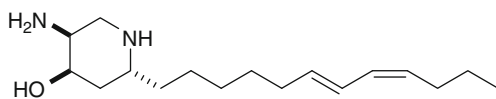
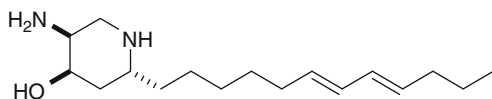
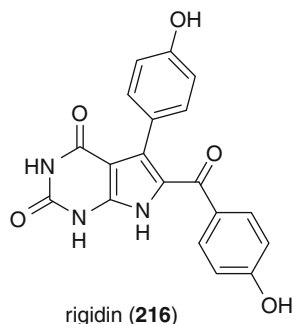
Phosphatidylinositol-specific phospholipase C (PI-PLC) is the rate-limiting enzyme in the phosphatidylinositol turnover. PI-PLC hydrolyzes the phosphate-glycerol linkage of phosphatidylinositol to produce two second messengers, inositol triphosphate and diacylglycerol which play key roles in cellular signal transduction induced by growth factors and hormones [134].

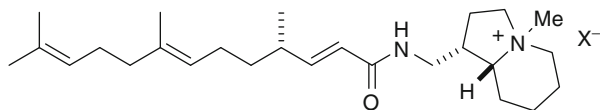
Akaterpin (**211**) isolated from an Okinawan marine sponge *Callyspongia* sp. showed potent inhibition against PI-PLC (IC_{50} 0.5 μ g/mL) as well as weak inhibition against neutral sphingomyelinase with an IC_{50} value of 30 μ g/mL [135].



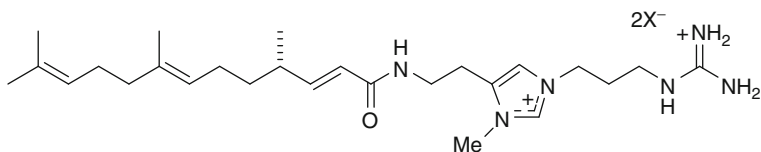
23.4.6 Phosphodiesterase (EC 3.1.4.-)

The Ca^{2+} -calmodulin system plays an important role in the control of cellular proliferation and tumor formation. A calmodulin antagonist, W-7, has been found to inhibit proliferation of Chinese hamster cells and formation of mouse skin tumors. Eudistomin A (**212**), a β -carboline alkaloid isolated from the Okinawan tunicate *Eudistoma glaucus*, inhibited calmodulin-activated brain phosphodiesterase with an IC_{50} value of 20 μM [136], while eudistomin C (**213**) exhibited calmodulin antagonistic activity (IC_{50} 30 μM) [137]. Pseudodistomins A (**214**) and B (**215**), unusual alkylpiperazines of the Okinawan tunicate *Pseudodistoma kanoko*, inhibited calmodulin-activated brain phosphodiesterase at the same concentration (IC_{50} 30 μM), which is about three times more potent than W-7 [138]. Rigidin (**216**) isolated from an Okinawan tunicate *Eudistoma* cf. *rigida* inhibited calmodulin-activated brain phosphodiesterase with an IC_{50} value of 50 μM [139]. Stelletamide A (**217**), an unusual indolizidine alkaloid originally isolated from a marine sponge *Stelletta* sp. as an antifungal and cytotoxic compound [140], was found to inhibit Ca^{2+} /calmodulin-dependent phosphodiesterase and $(\text{Ca}^{2+}\text{-Mg}^{2+})\text{-ATPase}$ with IC_{50} values of 52 and 100 μM , respectively [141]. Related alkaloids, stelletazole A (**218**) [142], bistellettadines A (**219**), and B (**220**) [143], from the same sponge showed moderate inhibitory activity against Ca^{2+} /calmodulin-dependent phosphodiesterase (**218**: 45% inhibition at 100 μM , **219** and **220**: 40% inhibition at 100 μM).

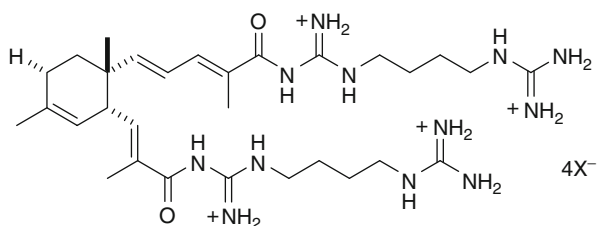
eudistomin A (**212**)eudistomin C (**213**)pseudodistomin A (**214**)pseudodistomin B (**215**)rigidin (**216**)



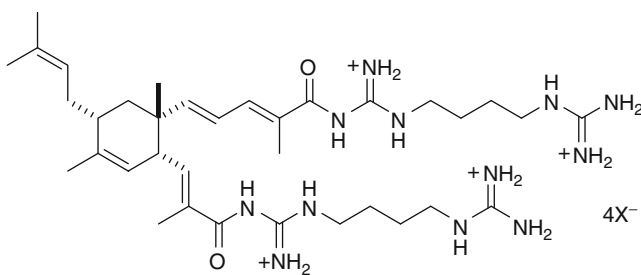
stellettamide A (217)



stellettazole A (218)



bistellettadine A (219)

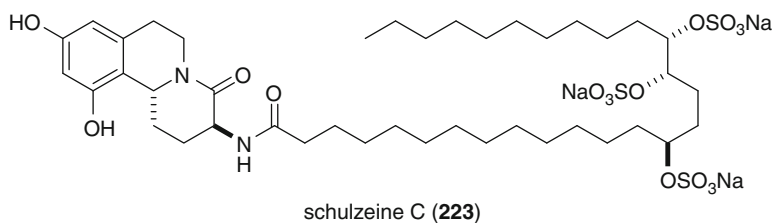
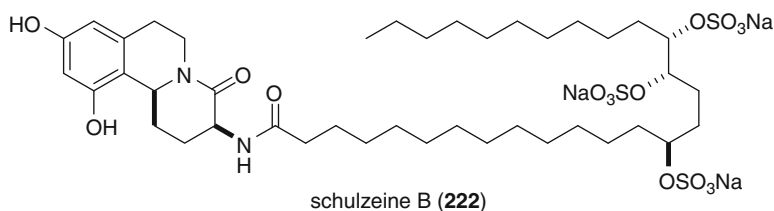
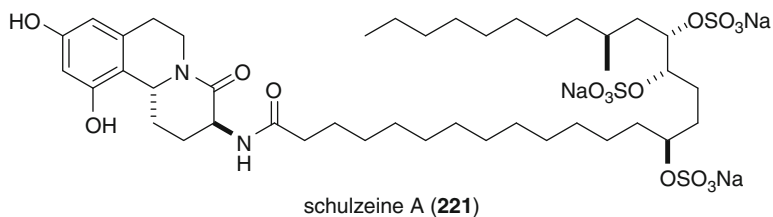


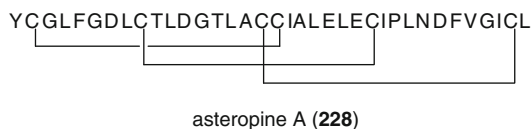
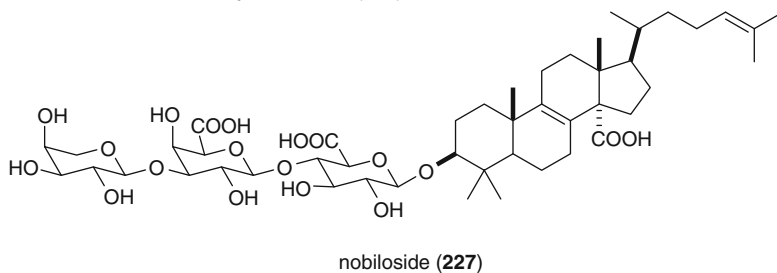
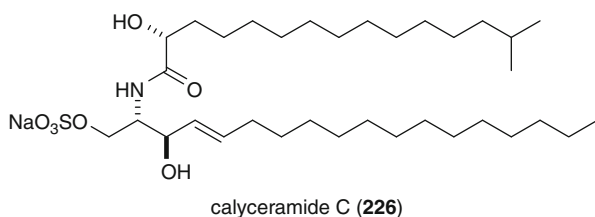
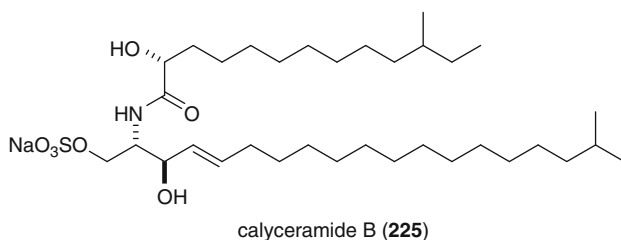
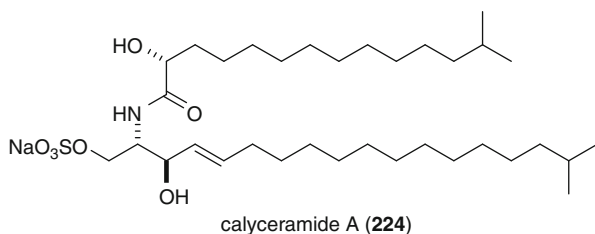
220

23.4.7 Sialidase (EC 3.2.1.18)

Sialidase cleaves an α -linked terminal *N*-acetylneuraminic acid from glycoproteins, glycolipids, and oligosaccharides. In several viral and bacterial infections, neuraminidases play important roles; influenza virus employs this enzyme to detach itself from the infected cell in the budding stage, thus indicating requirement of neuraminidase for replication of the virus. Therefore, selective inhibitors

of sialidase are potential therapeutic agents against influenza. The α -glucosidase inhibitors, schulzeines A–C (**221–223**), were also inhibitory against viral neuraminidase with IC_{50} values of 60 μ M. Calyceramides A–C (**224–226**), sulfated ceramides isolated from the marine sponge *Discodermia calyx*, inhibited sialidase from *Clostridium perfringens* with IC_{50} values of 0.4, 0.2, and 0.8 μ g/mL, respectively [144]. Another example of a marine sialidase inhibitor is nobiloside (**227**), a triterpenoid saponin of the marine sponge *Erylus nobilis*, which inhibited *Clostridium perfringens* sialidase with an IC_{50} value of 0.46 μ g/mL [145]. Asteropine A (**228**) is the first cystine knot of sponge origin isolated from *Asteropus simplex*. Asteropine A showed potent and competitive inhibition against bacterial sialidases (from *Clostridium perfringens*, *Vibrio choleae*, and *Salmonella typhimurium*) with K_i values of 36.7, 340, and 350 nM, respectively [146].

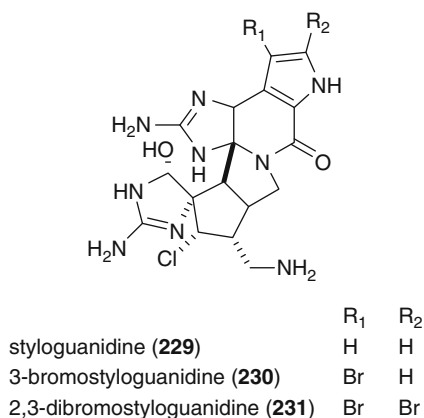




23.4.8 Chitinase (EC 3.2.1.14)

Chitinase plays crucial roles in a wide variety of organisms ranging from nutrition to defence and control of ecdysis in arthropods, thus indicating their potential for antifungal and insecticidal agents. Styloguanidines (**229–231**) isolated from the

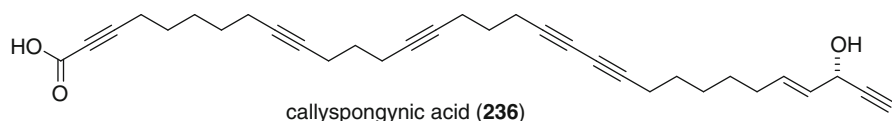
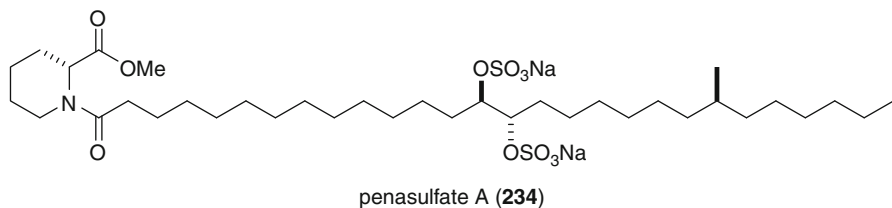
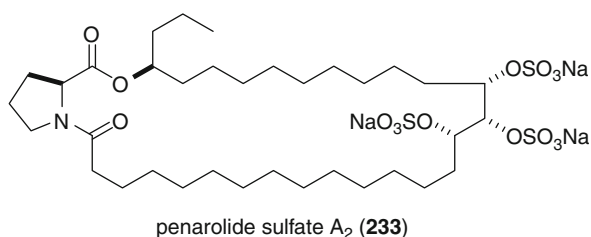
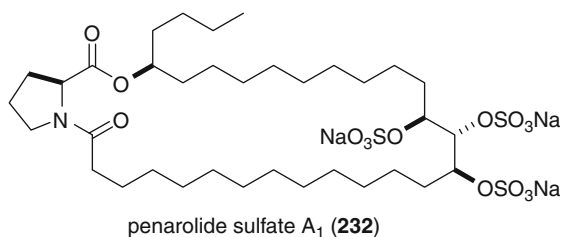
sponge *Stylotella aurantium* collected off Yap showed inhibitory activity against chitinase from a bacterium *Schwanella* sp. at the dose of 2.5 µg/disc by using the “squid chitin agar plate method.”[147].



23.4.9 α-Glucosidases (EC 3.2.1.20)

α-Glucosidases are involved in glycoprotein processing and glycogenolysis and, therefore, their inhibitors can be applied for treatment of diabetes, obesity, viral infections, and cancer. Penarolide sulfates A₁(**232**) and A₂(**233**), L-proline containing macrolide trisulfates isolated from a marine sponge *Penares* sp., inhibited α-glucosidase of yeast origin with IC₅₀ values of 1.2 and 1.5 µg/mL, respectively, while they showed only weak or no inhibition against β-glucosidase or β-galactosidase. Penarolide sulfates also inhibited thrombin with IC₅₀ values of 3.7–4.2 µg/mL. Perhaps, the three sulfate groups are responsible for the activity [148]. A linear type congener, penasulfate A (**234**), in which L-proline was replaced by D-pipecolic acid, was isolated from the same sponge. Penasulfate A (**234**) showed about ten times as potent inhibition (IC₅₀ 0.14 µg/mL) as penarolides against the same enzyme, while the inhibitory activity against the enzyme from the different source remained the same level [149]. The known 1,4-dideoxy-1,4-imino-D-arabinitol (**235**) was isolated as an α-glucosidase inhibitor from a marine sponge *Haliclona* sp. collected in Western Australia. Iminopentitol (**235**) strongly inhibited yeast α-glucosidase at an IC₅₀ value of 0.16 µg/mL [150]. Callyspongynic acid (**236**), a polyacetylenic acid was isolated from the Japanese marine sponge *Callyspongia truncata*. Callyspongynic acid (**236**) inhibited α-glucosidase with an IC₅₀ value of 0.25 µg/mL, but was inactive against β-glucosidase, β-galactosidase, thrombin, and trypsin at 100 µg/mL. Both the carboxylic acid and the allylic alcohol linked to an acetylene are thought to be important for the activity [151]. The Japanese marine sponge *Penares schulzei* afforded three new α-glucosidase inhibitors, schulzeines A–C (**221–223**), which showed potent inhibitory

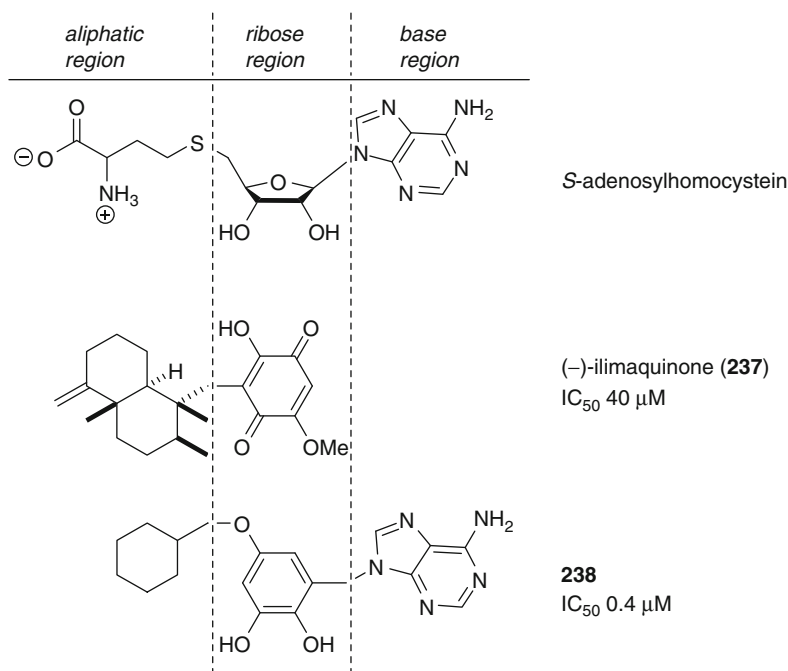
activity against α -glucosidase with IC_{50} values of 48–170 nM. It should be noted that desulfated schulzeines A and B still retained activity (IC_{50} s 2.5 and 1.1 μ M, respectively) [152]. Recently, the stereochemistry at C-20 of **221** was revised on the basis of total chemical synthesis [153].



23.4.10 S-Adenosylhomocysteine Hydrolase (EC 3.3.1.1)

S-adenosylhomocysteine hydrolase that reversibly hydrolyzes S-adenosylhomocysteine to homocysteine and adenosine has been considered an attractive target for the design of antiviral, antiparasitic, antiarthritic and immunosuppressive agents. Ilimaquinone (**237**) has been reported to possess antiviral,

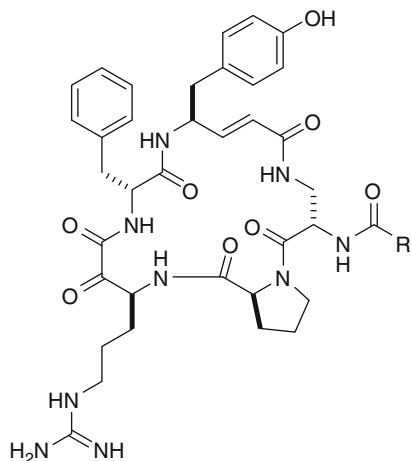
antimitotic, antimicrobial, and anti-HIV activities. It was also shown to vesiculate the Golgi apparatus as well as to protect cells against the toxic effects of ricin and diphtheria. Whole-cell and cytosolic photoaffinity labeling and affinity chromatography studies with chemical probes prepared from **237** converged on *S*-adenosylhomocysteine hydrolase as a cellular target of **237**. Subsequent studies with isolated enzyme indicated that ilimaquinone is a competitive inhibitor of *S*-adenosylhomocysteine hydrolase (IC_{50} 40 μ M). On the basis of SAR studies, pharmacophore modeling, and computer docking studies have allowed for the design and preparation of a simplified structural variant (**238**) possessing a 100-fold greater inhibitory activity than that of natural (–)-ilimaquinone (**237**) [154].



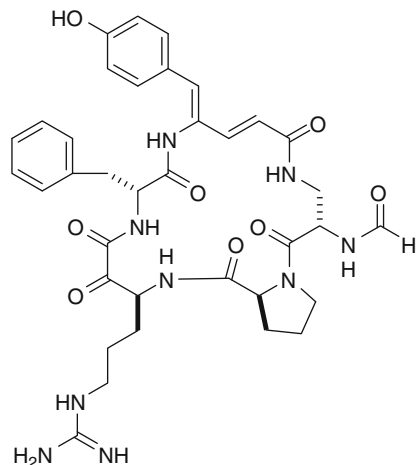
23.4.11 Serine Proteases (EC 3.4.21.-)

Proteolytic enzymes are classified into serine proteases, cysteine proteases, aspartic proteases, and metalloproteases on the basis of their catalytic centers. Trypsin-like enzymes, a group of serine proteases, are associated with many disease states. The hyperproteolytic activities of this homologous family of enzymes are attractive chemotherapeutic targets in pathways of blood coagulation, fibrinolysis, kinin formation, complement activation, digestion, reproduction, and phagocytosis. Thus,

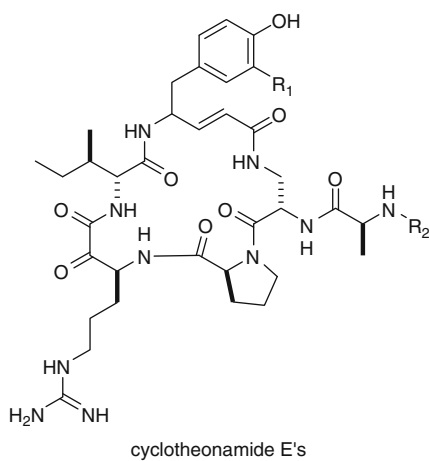
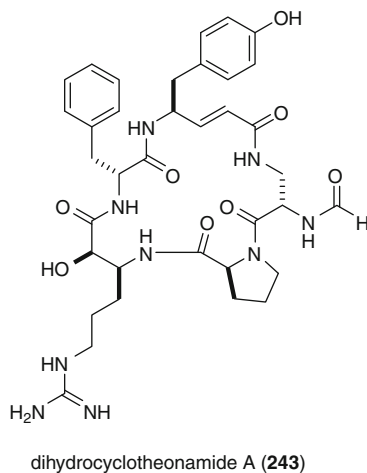
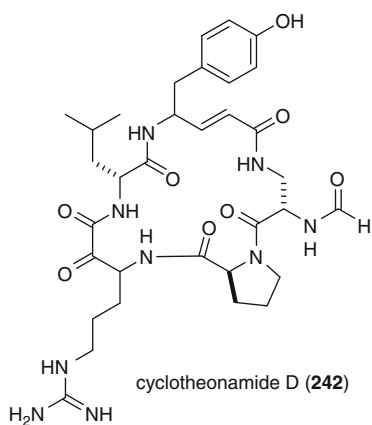
inhibitors of specific serine proteases can be potential drug-leads for many disease status [155]. Cyclotheonamides A (**239**) and B (**240**) from a marine sponge *Theonella* sp. (now known to be *T. swinhoei*) inhibited thrombin, trypsin and plasmin with IC_{50} values of 0.076, 0.2, and 0.3 $\mu\text{g/mL}$, respectively [156]. Further investigation of *T. swinhoei* yielded cyclotheonamides C (**241**) and D (**242**) [157]. Cyclotheonamides E series (**244–248**) were not found from this sponge, but from the other type of *T. swinhoei* whose interior part is white (E1–E3) [158] and from an Okinawan sponge *Ircinia* sp. (E4–E5) [159]. Cyclotheonamides C (**241**), D (**142**), and E1–E5 (**244–248**) showed potent inhibition against thrombin and trypsin with IC_{50} values of 2.9–68 nM and 7.4–55 nM, respectively. Cyclotheonamide E1 (**244**), E4 (**247**), and E5 (**248**) strongly inhibited both mouse and human tryptases (IC_{50} s 6.9, 23, and 84.7 nM for human tryptase, and 17.0, 6.5, and 54.1 nM for mouse tryptase, respectively) [159]. Dihydrocyclotheonamide A (**243**), pseudotheonamides A₁ (**249**), A₂ (**250**), B₂ (**251**), C (**252**), and D (**253**) from *T. swinhoei*, in which α -ketohomoarginine (k-Arg) residues are cyclized, showed only moderate activity against these enzymes with IC_{50} values ranging from 0.19 to 3.0 μM (thrombin) and 3.8 μM (trypsin) [160]. Complexes between cyclotheonamide A and human α -thrombin and between cyclotheonamide A and trypsin were successfully crystalized and their crystal structures were solved, disclosing that cyclotheonamide A binds to the catalytic center of these enzyme; particularly k-Arg which forms the hemiacetal linkage with Ser195 of one of a catalytic triad is important for the binding to the enzyme [161]. From the same *T. swinhoei*, was isolated a thrombin inhibitory linear peptide, nazumamide A (**254**) which inhibited thrombin with an IC_{50} value of 2.8 $\mu\text{g/mL}$, but not trypsin at 100 $\mu\text{g/mL}$ [162]. Retro-binding mode of nazumamide A to human thrombin was demonstrated by X-ray crystallography of the nazumamide A/thrombin complex [163].



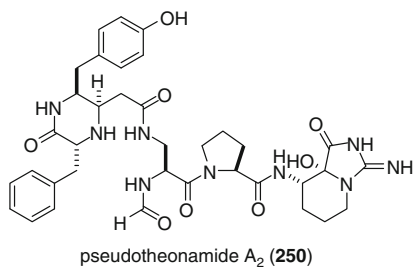
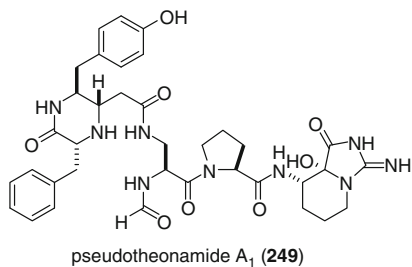
cyclotheonamide A (**239**) R = H
cyclotheonamide B (**240**) R = Ac

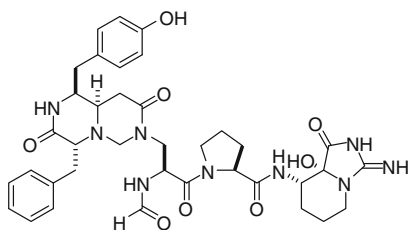
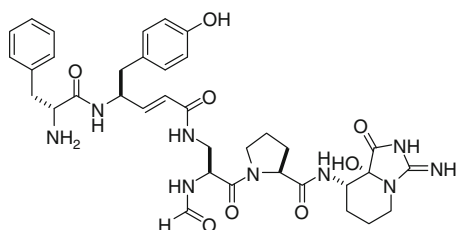
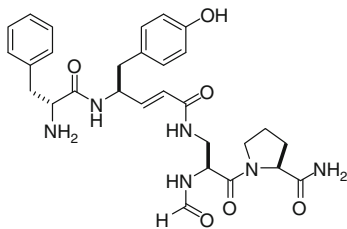
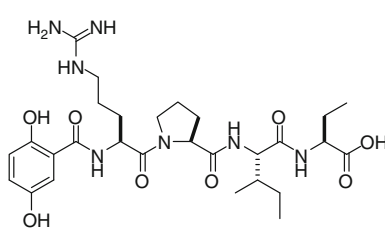


cyclotheonamide C (**241**)

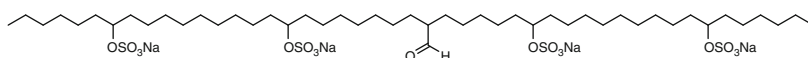
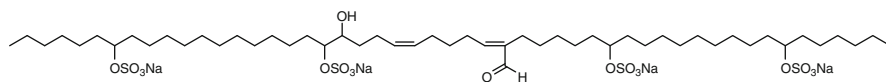
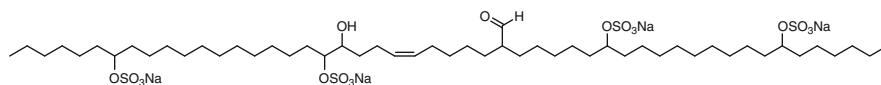
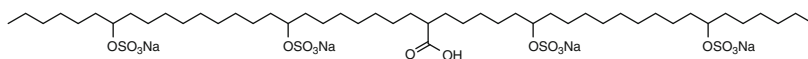


	R ₁	R ₂
E1 (244)	H	
E2 (245)	H	
E3 (246)	H	
E4 (247)	H	
E5 (248)	OH	



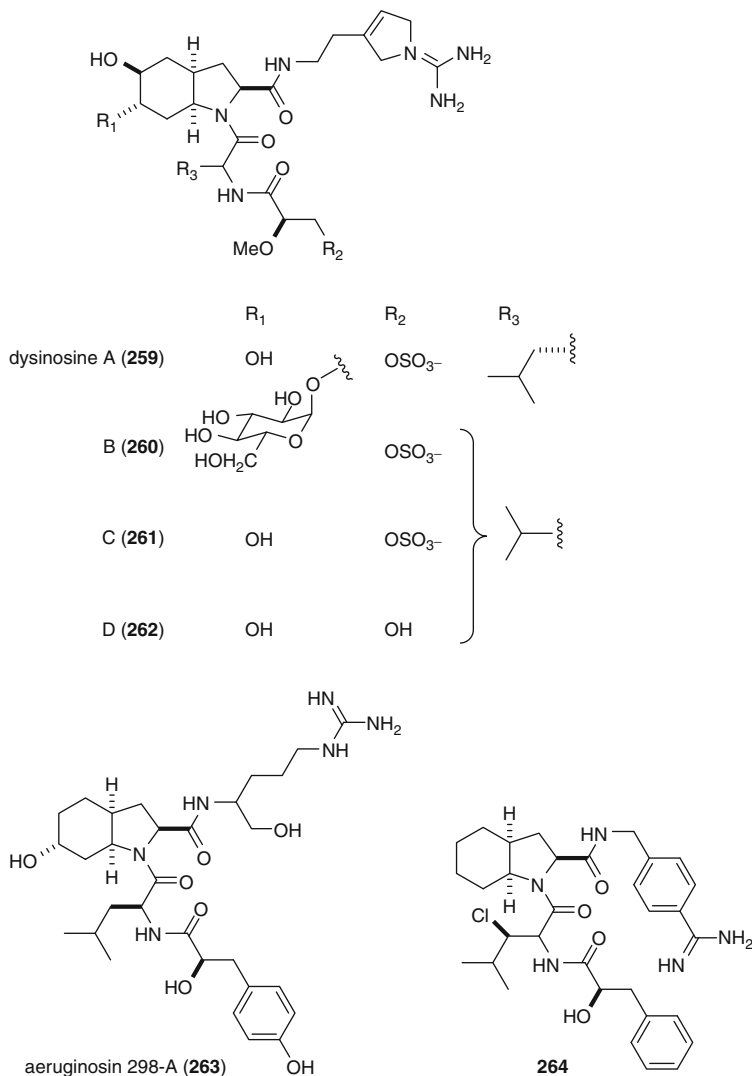
pseudotheonamide B₂ (**251**)pseudotheonamide C (**252**)pseudotheonamide D (**253**)nazumamide A (**254**)

Toxadocials A–C (**255–257**) and toxadocic acid A (**258**) isolated from a marine sponge *Toxadocia* sp., are alkyl sulfate thrombin inhibitors with IC₅₀s of 6.5, 4.6, 3.2, and 2.7 µg/mL, respectively [164]. The mode of enzyme inhibition of toxadocials is not known.

Toxadocial A (**255**)Toxadocial B (**256**)Toxadocial C (**257**)Toxadocic acid A (**258**)

Dysinosins A–D (**259–262**) are inhibitors of factor VIIa and thrombin isolated from the Australian sponge *Lamelloydysidea chlorea*. Dysinosins showed potent inhibitory activity against factor VIIa and thrombin with K_i values of 0.090 to 1.32

and 0.17 to $> 23 \mu\text{M}$, respectively [165]. The structural similarity of dysinosins to that of aeruginosins (**263**) which were the serine protease inhibitors isolated from the cyanobacteria *Microcystis aeruginosa* [166] and *Oscillatoria agardhii* [167] implied that they were biosynthesized by symbiotic microbes. Based on X-ray crystallographic data of complexes of chlorodysynsin A with thrombin, a series of analogues were synthesized varying the nature of the P_1 , P_2 , and P_3 pharmacophoric sites and the central octahydroindole carboxamide core. Introduction of a hydrophobic substituent on the D-Leu amide dramatically improved the inhibitory activity against thrombin (**264**: IC_{50} 1.6 nM) [168].

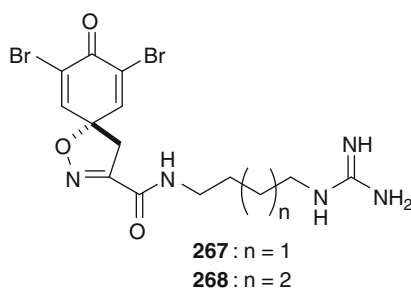
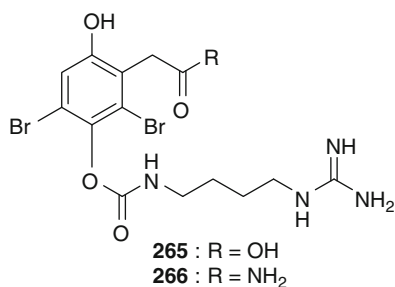


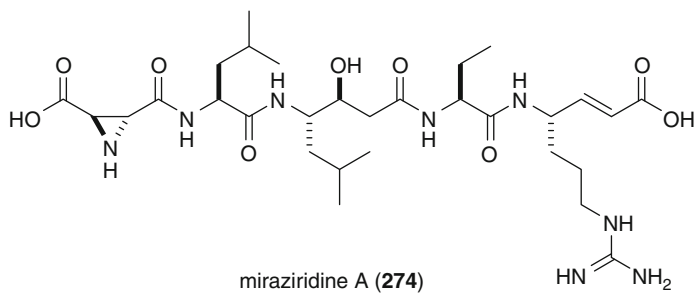
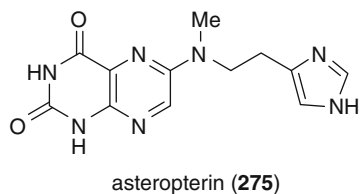
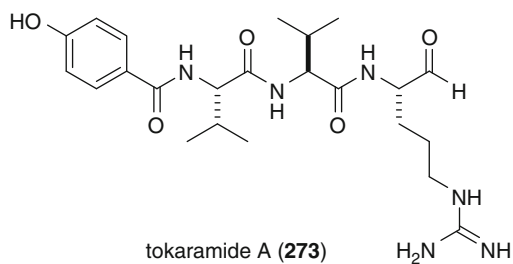
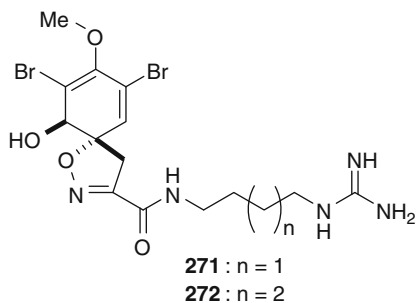
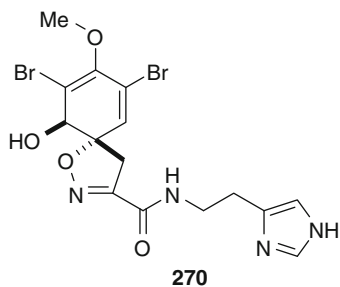
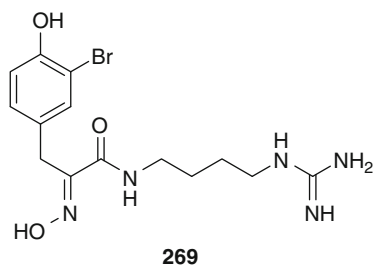
Factor XIa (FXIa) is a trypsin-like serine protease that plays a major role in the amplification phase of the coagulation cascade and in maintaining clot integrity. It is a unique target where specific inhibitors of FXIa might inhibit thrombosis without completely interrupting the function of normal hemostasis and might prevent or minimize the risk of hemostasis complication. Clavatadines A–E (**265**–**269**) were isolated as FXIa inhibitors from the Australian sponge *Suberea clavata* along with known aerophobin 1 (**270**), purealdin L (**271**), and aplysinamisine II (**272**). Compounds **265** and **266** inhibited FXIa with IC_{50} values of 1.3 and 27 μ M, respectively, whereas they did not inhibit FIXa ($< 5\%$ inhibition at 222 μ M). The crystal structure obtained by soaking of compound **265** into a single crystal of FXIa showed only the carbamate side chain of **265** covalently bonded to the active site serine residue (Ser 195) [169]. Compounds **267**–**272** were shown to be weaker inhibitors (12–59% inhibition at 222 μ M) [170].

23.4.12 Cysteine Proteases (EC 3.4.22.-)

23.4.12.1 Cathepsin B (EC 3.4.22.1)

Cysteine proteases which have cysteine and histidine as the catalytic center are involved in cytosolic protein metabolisms. Cathepsin B, a cysteine protease, is known to be involved in various disease states, such as inflammation, trauma, muscular dystrophy, and tumors. In particular, its possible roles in cancer metastasis are of major concern in cancer chemotherapy. Two peptidic inhibitors, tokaramide A (**273**) [171] and miraziridine A (**274**) [172] with IC_{50} values of 29 and 1,400 ng/mL were isolated from the marine sponge *Theonella* aff. *mirabilis*. Miraziridine A (**274**) contains three unusual amino acid residues; particularly unusual are vinyllogous arginine and aziridine-2,3-dicarboxylic acid. Secobatzelline A (**207**) isolated from a sponge *Batzella* sp. showed inhibition against peptidase activity of CPP32, a member of caspases which are cysteine proteases playing a major role in the programmed cell death mechanism known as apoptosis, with an IC_{50} value of 0.02 μ g/mL as well [130]. Asteropterin (**275**), a unique molecule with a combination of lumazine and *N*-methyl histamine isolated from the marine sponge *Asteropus simplex*, inhibited cathepsin B with an IC_{50} value of 1.4 μ g/mL [173].



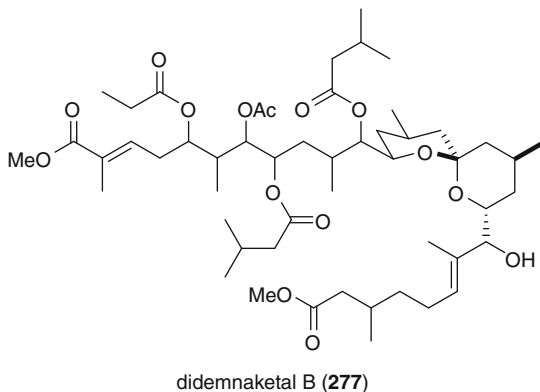
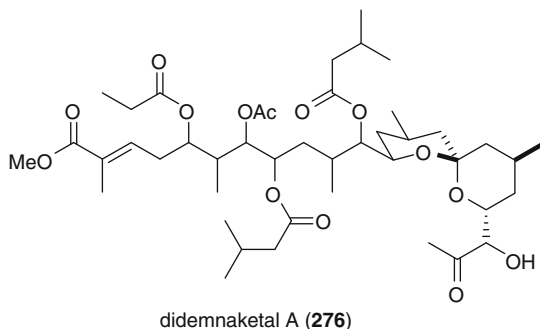


23.4.13 Aspartic Proteases (EC 3.4.23.-)

23.4.13.1 HIV Protease (EC 3.4.23.47)

Replication of HIV involves the expression of several viral polypeptides that requires the presence of a virus-specific protease for their maturation. Inhibition of this enzyme results in immature viral particles; therefore, HIV-1 protease is an ideal target for AIDS chemotherapeutics.

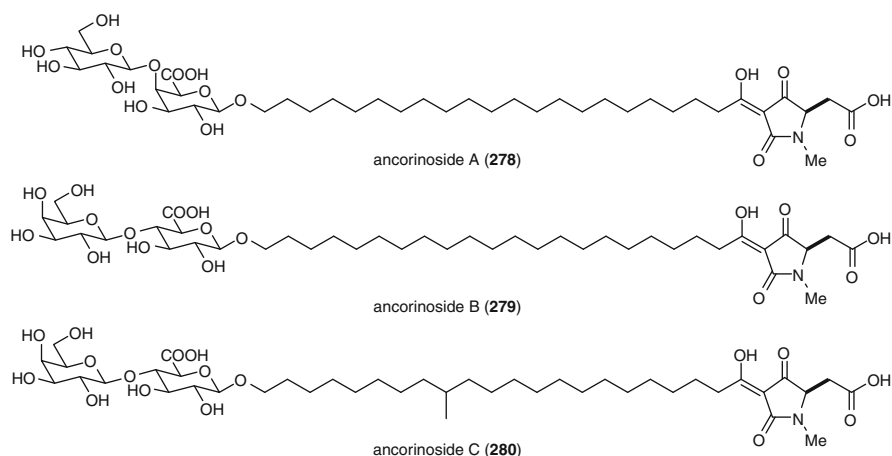
Didemnaketals A (**276**) and B (**277**), isolated from a Palauan ascidian *Didemnum* sp., inhibited HIV-1 protease with IC_{50} values of 2 and 10 μ M, respectively [174]. The unusual structures and potent activity of didemnaketals indicated their possibility as attractive synthetic targets [175]. Recently, simplified analogues lacking the spiroketal portion were synthesized, some of which were as potent as didemnaketals A. It was also proposed that didemnaketals inhibit dimerization of HIV-1 protease monomers [176].

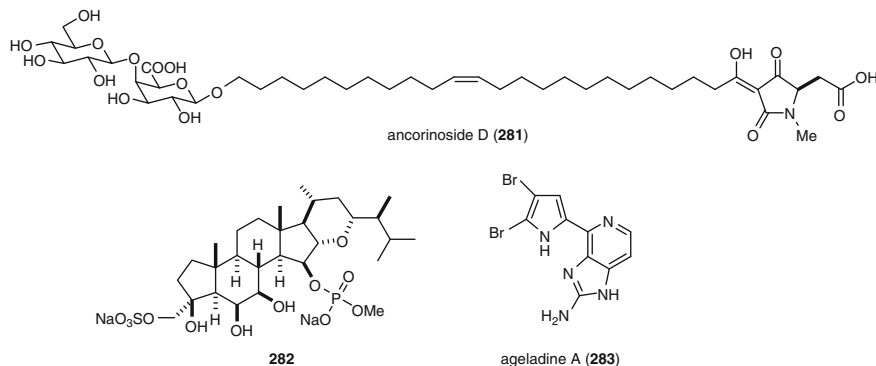


23.4.14 Metalloproteases (EC 3.4.24.-)

Metalloproteases contain metal ions such as Zn^{2+} , Co^{2+} , Mn^{2+} , etc., in their catalytic centers. The matrix metalloproteinases (MMPs), members of a large

subfamily of proteases which contains a catalytic zinc-binding domain, play important roles in the remodeling and degradation of extracellular matrix (ECM). They are linked to a range of physiological and pathological processes, including wound healing, bone remodeling, angiogenesis, inflammation, and tumor progression and metastasis. The membrane-type matrix metalloproteinases (MT-MMPs) are known as key enzymes in tumor metastasis. They activate progelatinase A to the fully matured form which in turn degrades type IV collagen, the major component of the basal membrane which prevents tumor progression. Thus, inhibitors of MT-MMPs are believed to be potential anticancer drugs. Ancorinosides B–D (**279–281**) [177] were isolated as MT1-MMP inhibitors from the marine sponge *Penares sollasi* along with known ancorinoside A (**278**) [178] which was originally isolated as an inhibitor of blastulation of starfish embryos from a marine sponge *Ancorina* sp. Ancorinosides A–D (**278–281**) inhibited MT1-MMP with IC₅₀ values of 440, 500, 370, and 180 µg/mL, respectively. Ancorinoside B (**279**) also inhibited gelatinase A (MMP2) with an IC₅₀ value of 22 µg/mL. Haplosamate A (**65**) and its congener (**282**) were isolated from a Japanese marine sponge *Cribrochalina* sp. as MT1-MMP inhibitors with IC₅₀ values of 150 and 160 µg/mL, respectively; [179] **65** was originally isolated as an HIV integrase inhibitor from Philippine haplosclerid sponges [32]. Ageladine A (**283**) is a fluorescent alkaloid isolated from the marine sponge *Agelas nakamurai*. The IC₅₀ values of **283** against MMPs 1, 2, 8, 9, 12, and 13 were 1.2, 2.0, 0.39, 0.79, 0.33, and 0.47 µg/mL, respectively, while its *N*-methylated derivatives did not inhibit MMP2. Unlike other MMP inhibitors, ageladine A (**283**) was not capable to chelate Zn²⁺ and not a competitive inhibitor against MMP2 [180]. With such interesting aspects of inhibition mode, as well as its anti-angiogenic activity, ageladine A became a target of total synthesis [181].

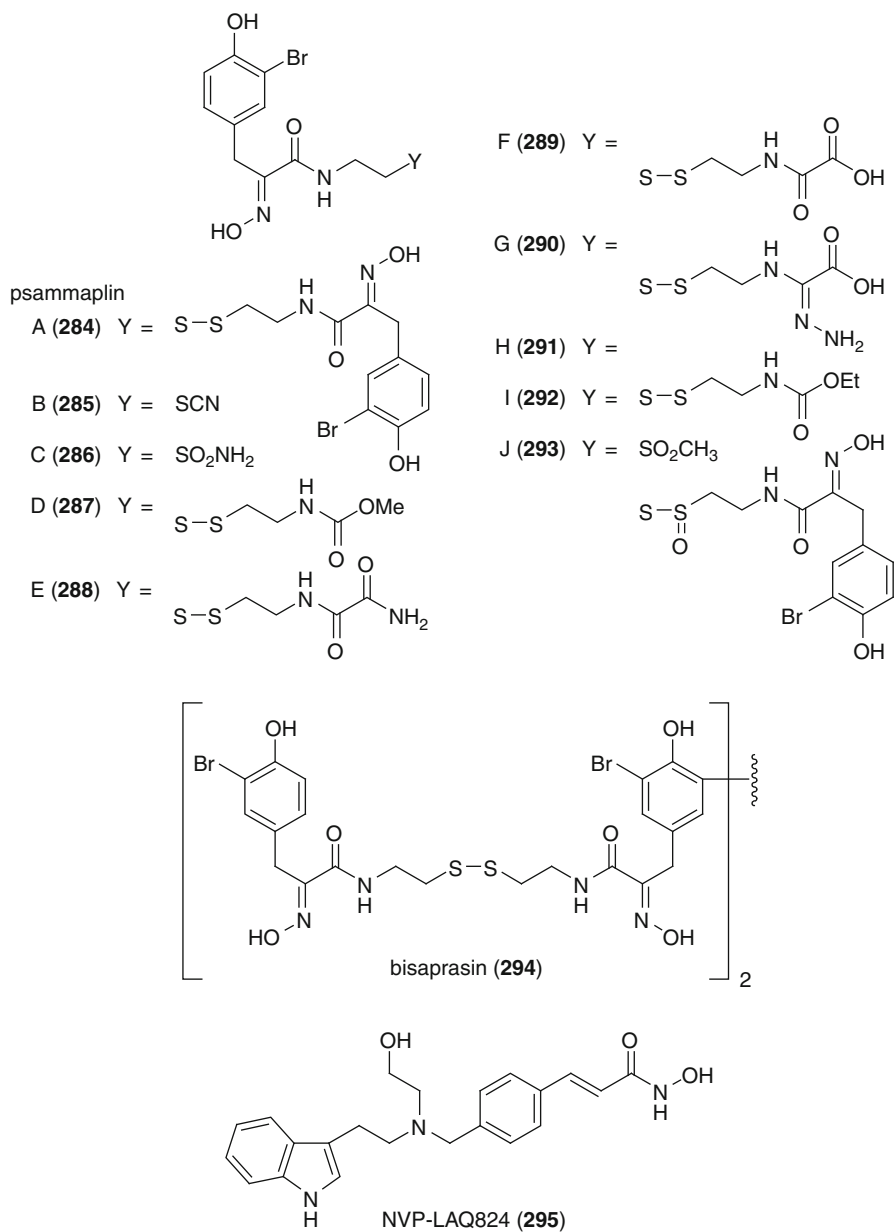


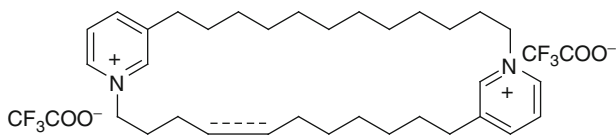


23.4.15 Histone Deacetylases (EC 3.23.-)

Histone acetylation and deacetylation are catalyzed by histone acetyltransferases (HATs) and histone deacetylases (HDACs), respectively, which play important roles in transcriptional regulation [182]. Inhibitors of these enzymes are known to induce cell cycle arrest [183], p53-independent induction of the cyclin dependent kinase inhibitor p21 [184], tumor-selective apoptosis [185], and differentiation of normal and malignant cells [186]. HDAC inhibitors were also demonstrated to exert anti-angiogenic effects through the alteration of vascular endothelial growth factor (VEGF) signaling [187]. These direct and indirect effects on tumor growth and metastasis indicate that HDAC inhibitors are potential anti-cancer agents. Six new psammaplins E–J (**288–293**) were isolated from the marine sponge *Pseudoceratina purpurea* collected in Papua New Guinea along with known psammaplins A–D (**284–287**), and bisaprasin (**294**). These compounds showed potent inhibitory activity against HDAC (IC_{50} s 2.1–327 nM) and cell-based p21 promoter activity (IC_{50} s 0.7–15 μ M), in addition to inhibitory activity against DNA methyltransferase (DNMT) [188]. NVP-LAQ824 (**295**) which was developed on the basis of structures of HDAC inhibitors including psammaplins [189] entered phase I clinical trials in patients with solid tumors or leukemia [190]. Three new cyclostelletamines, cyclostelletamine G (**297**), dehydrocyclostelletamines D (**298**) and E (**299**), were isolated together with the known cyclostelletamine A (**296**) from a marine sponge of the genus *Xestospongia*. These compounds inhibited HDAC with IC_{50} values of 17–80 μ M [191]. Five new cyclic tetrapeptides, azumamides A–E (**300–304**) were isolated from the marine sponge *Mycale izuensis*. Azumamides showed inhibitory activity against human HDAC at IC_{50} values of 0.045–1.3 μ M. In the cell-based assay using K562 cells, azumamide A (**300**) inhibited deacetylation of Ac-H3 (Lys9 and Lys 14) and Ac-H4 (Lys 8) in a dose-dependent manner

(0.19–19 μM). Furthermore, azumamide A inhibited angiogenesis in the in vitro vascular organization model using mouse ES cells [192].



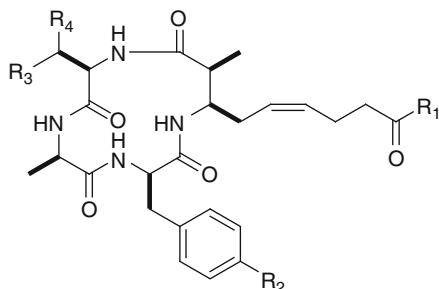


cyclostelletamine A (**296**) : $m = 1, n = 2$

G (**297**) : $m = 1, n = 1$

dehydrocyclostelletamine D (**298**) : $m = 1, n = 4, \Delta^{13}$

E (**299**) : $m = 2, n = 4, \Delta^{13}$



	R ₁	R ₂	R ₃ = R ₄
azumamide A (300)	NH ₂	H	Me
B (301)	NH ₂	OH	Me
C (302)	OH	OH	Me
D (303)	NH ₂	H	H
E (304)	OH	H	Me

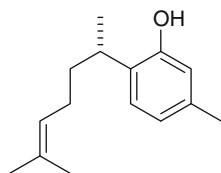
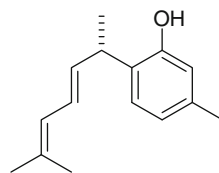
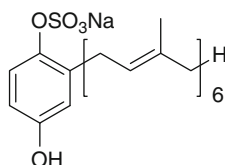
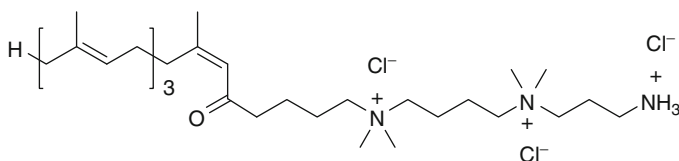
23.4.16 ATPases (EC 3.6.1.3)

23.4.16.1 H,K-ATPase

H,K-ATPase mediates acid secretion from gastric wall cells. Thus, excess activation of this enzyme leads to hyperacidity, causing gastric ulcer. In order to discover potential antiulcer leads, a number of Japanese marine invertebrates have been screened for inhibition of porcine H,K-ATPase which resulted in isolation of several inhibitors.

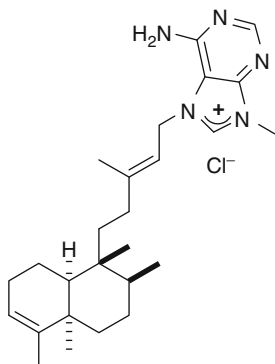
S-(+)-curcuphenol (**305**) and dehydrocurcuphenol (**306**), isolated from a Japanese marine sponge *Epipolasis* sp., inhibited porcine H,K-ATPase with IC₅₀s of 8.3 and 23 μM, respectively, while hydroxycurcuphenol was inactive [193]. It should be noted that the *R*-(-)-curcuphenol had already been reported from the Caribbean gorgonian *Pseudopterogorgia rigida* [194]. Hexaprenylhydroquinone sulfate (**307**) obtained from a marine sponge *Dysidea* sp. inhibited

H,K-ATPase with an IC_{50} of $4.6 \mu M$ [195]. Since **307** showed promising activity, a number of its analogues were synthesized and evaluated for inhibition of acid secretion and antiulcer activity, however, the results were disappointing [2]. Sinulamide (**308**) derived from a soft coral *Sinularia* sp. inhibited the enzyme activity with an IC_{50} of $5.5 \mu M$ [2]. The structure of **308** was recently refined by synthetic approach [196].

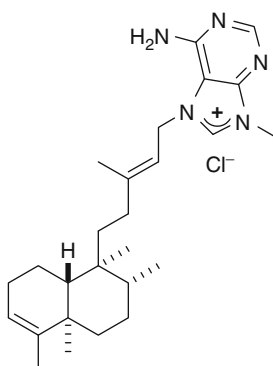
S-(+)-curcuphenol (**305**)dehydrocurcuphenol (**306**)hexaprenylhydroquinone sulafte (**307**)sinulamide (**308**)

23.4.16.2 Na,K-ATPase

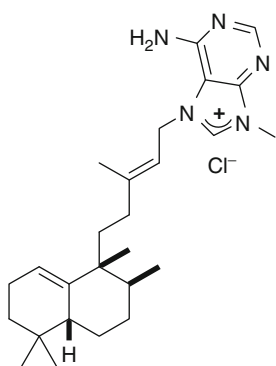
Na,K-ATPase regulates Na^+ transport through cell membranes and is directly related to contraction and relaxation of smooth muscles, thus indicating that inhibitors of the enzyme are potential drug leads for cardiovascular diseases. Agelasines A–F (**309–314**), 9-methyladenine derivatives of diterpenes, isolated from the Okinawan marine sponge *Agelas nakamurai*, were reported to inhibit Na,K-ATPase, though their detailed activity is not available [197]. Two hypotaurocyamine derivatives of diterpene, agelasidines B (**315**) and C (**316**) from the same sponge inhibited not only Na,K-ATPase with IC_{50} values of $10–50 \mu M$, but also contraction of smooth muscle [198].



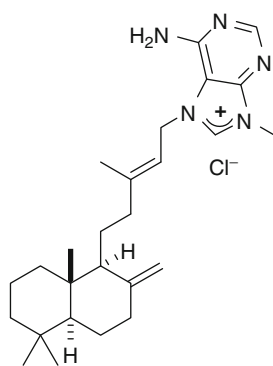
agelasin A (309)



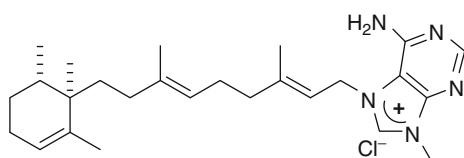
agelasin B (310)



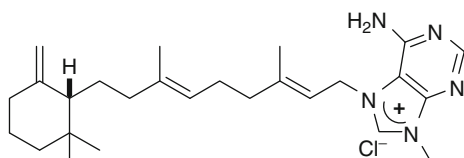
agelasin C (311)



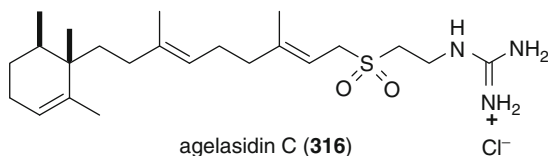
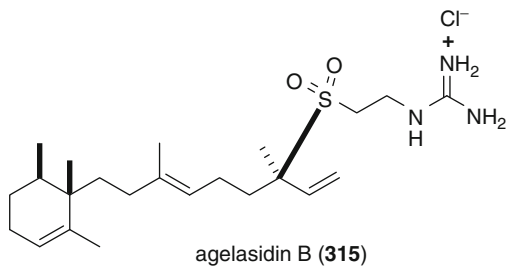
agelasin D (312)



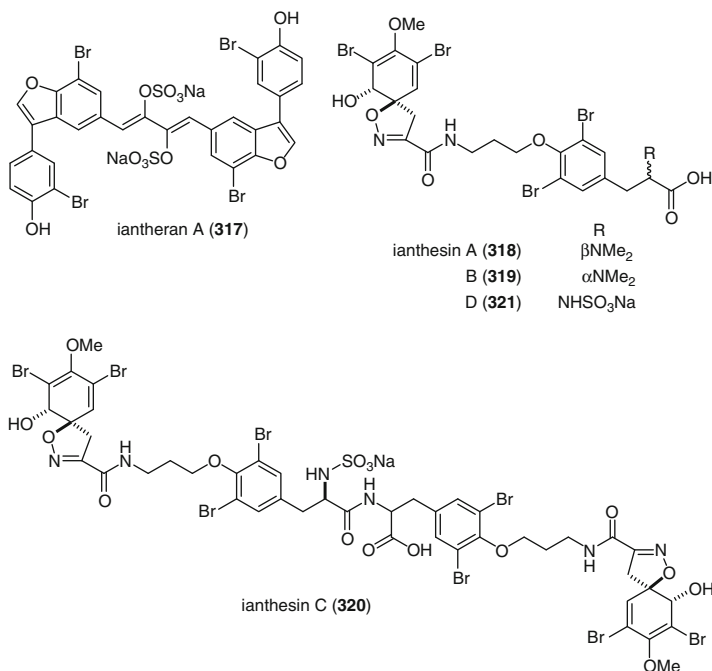
agelasin E (313)



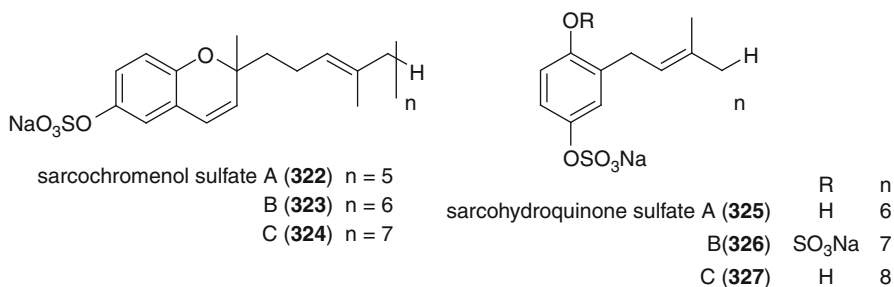
agelasin F (314)



Iantheran A (**317**), its diacetate, and α -hydroxy enone derivatives, isolated from an Australian marine sponge *Ianthella* sp. showed moderate inhibitory activity against Na,K-ATPase with IC_{50} values of 2.5, 5.0, and 10 μ M, respectively [199]. This sponge also yielded ianthesins A–D (**318–321**), of which ianthesins B–C inhibited dog kidney Na,K-ATPase with IC_{50} values of 440, 50, and 280 μ M, respectively [200].



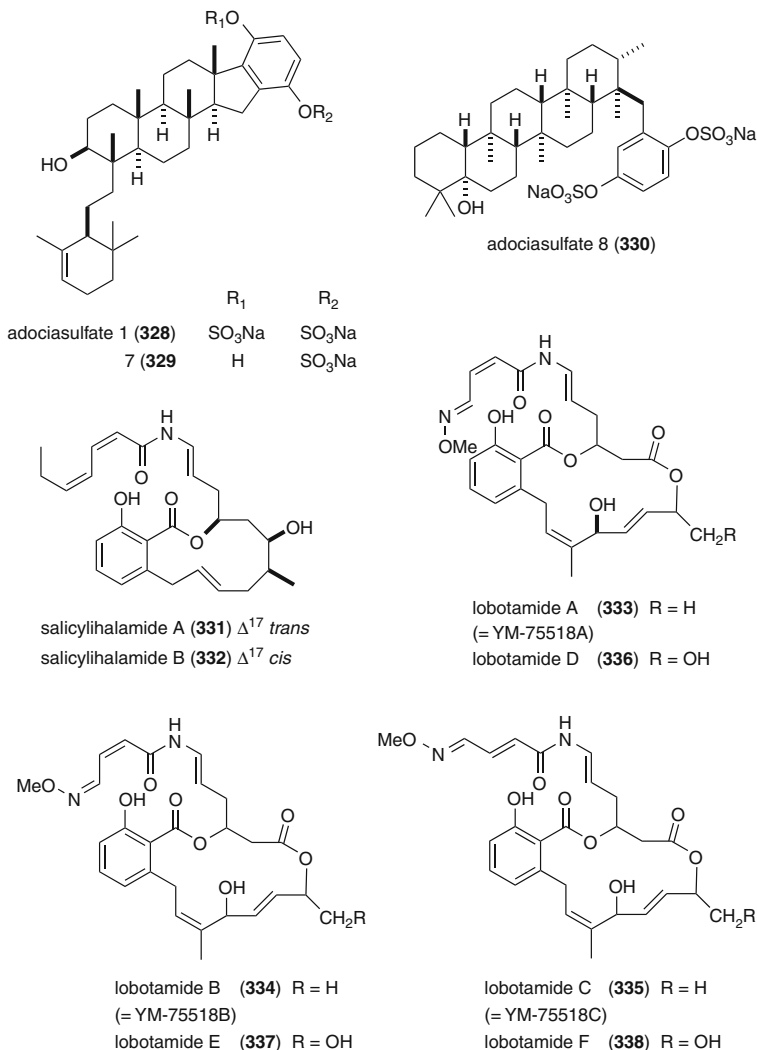
Xestoquinone (**82**), a polycyclic quinone, which was isolated together with the known antimicrobial substance halenaquinone (**79**) [201], from the Okinawan marine sponge *Xestospongia sapra*, inhibited Na,K-ATPase. Xestoquinone was the first example of marine natural products having parallelism between the inotropic action and Na,K-ATPase inhibition. Halenaquinol (**80**) [202], a natural cardioactive pentacyclic hydroquinone, from the marine sponge *Petrosia seriata*, was found to be a powerful inhibitor of the rat brain stem and cortex Na,K-ATPases and the rabbit muscle sarcoplasmic reticulum Ca^{2+} -ATPase with IC_{50} values of 0.70, 1.3, and 2.5 μM , respectively [203]. Sarcochromenol sulfate A (**322**) and sarcohydroquinone sulfates A–C (**325**–**327**) isolated from the New Zealand sponge *Sarcotragus spinulosus* inhibited the rat brain Na,K-ATPase with IC_{50} values of 1.6, 1.6, 1.4, and 1.3 μM , respectively, while sarcochromenol sulfates B (**323**) and C (**324**) were inactive [204].

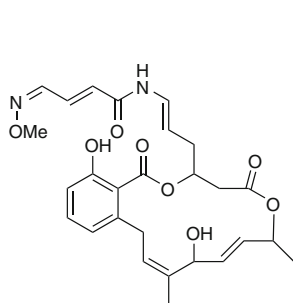
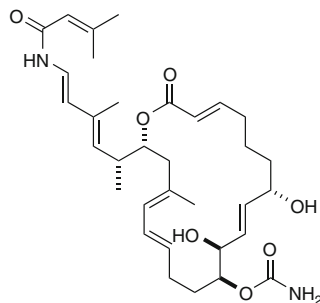


23.4.16.3 Vacuolar ATPases

Vacuolar H^+ -ATPases, a class of proton pumps present in all eukariotic cells, are responsible for proton transport in bone-derived membrane vesicles, and the process of osteoclast-mediated bone resorption is directly dependent on H^+ -translocating ATPases. Inhibition of osteoclast vascular H^+ -ATPase may be effective for reducing the rate of bone resorption in pathological conditions such as osteoporosis. Adociasulfate 1 (**328**), a sesterterpenoid isolated from an Australian marine sponge *Adocia* sp., reduced proton pump activity in hen bone-derived membrane vesicles with an IC_{50} value of 3.6 μM and proton pumping in brain-derived vesicles with an IC_{50} value of 4.69 μM , while adociasulfates 7 (**329**) and 8 (**330**) were less active (IC_{50} 30 μM and 55% inhibition at 100 μM , respectively) [205]. Recently, antitumor polyketides, salicylihalamides A (**331**) and B (**332**) isolated from a marine sponge *Haliclona* sp. [206] and lobotamides A–F (**333**–**338**) from the tunicate *Aplidium lobatum* [207], both of which share the core structure with YM-75518 (**339**), an antifungal metabolite of *Pseudomonas* sp. Q38009 [208], were found to be a potent and selective inhibitors of mammalian V-ATPases (IC_{50} s 0.40–14.0 nM) [209]. Palmerolide A (**340**) isolated from the Antarctic tunicate *Synoicum adareanum* is a cytotoxic macrolide. It showed 3 orders of magnitude greater sensitivity (LC_{50} 18 nM) against melanoma relative to other cell lines tested in the NCI 60 cell line panel.

Palmerolide A displayed a 60-cell-line activity profile which correlated, using the NCI COMPARE algorithm, to several vacuolar ATPase inhibitors. Indeed, it inhibited V-ATPase with an IC_{50} of 2 nM and to be active in NCI's hollow-fiber assay [210]. Following study on its stereochemistry by degradation [211] or total synthesis [212] revised its stereochemistry at C7, C10, and C11. The SAR study of palmerolides using synthetic analogues showed that a phenyl substitution on side chain and removal of the C7 hydroxy group enhanced the potency, while the selectivity against melanoma of **340** was not reproduced [213].

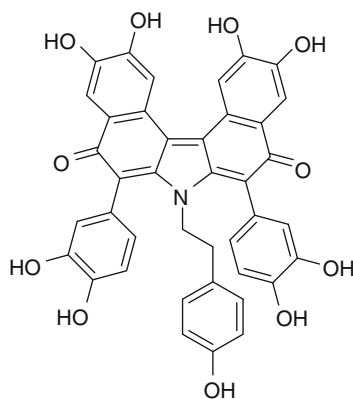


YM-75518D (**339**)palmerolide A (**340**)

23.5 Lyases (EC 4.-.-.)

23.5.1 ATP Citrate Lyase (EC 4.1.3.8)

Since the very-low-density lipoproteins (VLDL) are metabolic precursors of low-density lipoproteins (LDL) which play a key role in hypercholesterolemia, intervention of VLDL synthesis has provided a strategic target for hypercholesterolemia therapy. Inhibitors of ATP-citrate lyase (ACL) are anticipated to reduce the production of acetyl CoA and can affect both lipogenesis and cholesterologenesis, and as a result, expected to reduce VLDL synthesis. Purpurone (**341**), a poly catecholic pyrrole isolated from a marine sponge *Iotrochota* sp., inhibits ATP-citrate lyase in a dose-dependent manner with an IC_{50} value of 7 μ M [214].

purpurone (**341**)

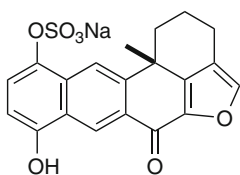
23.6 Isomerases (EC 5.-.-.)

23.6.1 Topoisomerase

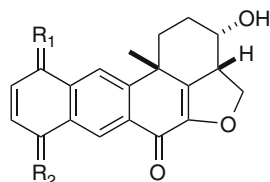
DNA topoisomerases are nuclear enzymes that catalyze DNA breaking and unwinding during cellular replication and RNA transcription. In eukaryotic cells, DNA topoisomerases I (topo I) and II (topo II) play distinct roles in DNA unwinding. Topo I catalyzes single-strand “nicking” to allow supercoiled DNA to unwind, whereas topo II facilitates chromosomal duplication by relaxing and unwinding the DNA duplex. Thus, inhibitors of topo I and topo II are expected to control cancer cell proliferation and thought to be important targets for cancer chemotherapy.

23.6.1.1 Topoisomerase I (EC 5.99.1.2)

Xestoquinol sulfate (**342**) and xestosaprols A (**343**) and B (**344**), as well as a known compound **345** and halenaquinol sulfate (**81**), were isolated as topo I inhibitors from the Okinawan sponge *Xestospongia sapra*; **342**–**344** inhibited DNA topo I with MICs of 10, 12.5, and 12.5 $\mu\text{g/mL}$, respectively, while **345**, xestoquinone (**82**), and halenaquinone (**79**) were more potent with MICs of 2.5, 2, and 0.4 $\mu\text{g/mL}$, respectively [215]. Interestingly, halenaquinol sulfate (**81**) was not active in this assay. Makaluvamine G (**346**), a cytotoxic pigment which was isolated from an Indonesian sponge *Histodermella* sp., inhibited topo I with an IC_{50} value of 3.0 μM [216]. Two ceramide 1-sulfates **347** and **348** from the Japanese bryozoa *Watersipora cucullata* inhibited human topo I with IC_{50} s of 0.4 and 0.2 μM , respectively [217]. Similarly, amphimic acids A (**349**) and related long-chain fatty acids from an Australian sponge *Amphimedon* sp. showed topo I inhibition with IC_{50} s ranging from 0.47 to 6.7 μM [218].



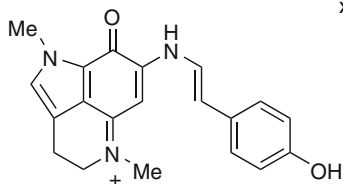
xestoquinol sulfate (**342**)



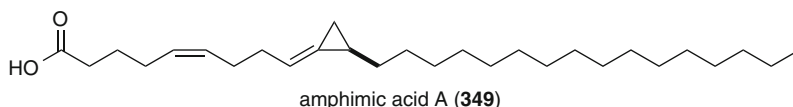
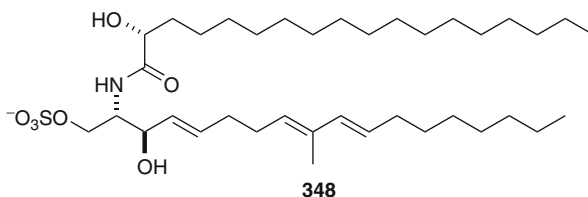
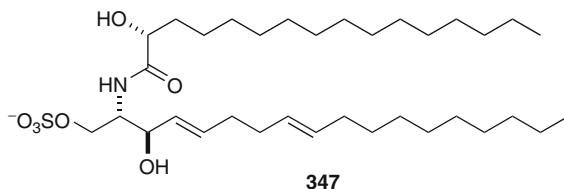
xestosaprol A (**343**) $\text{R}_1 = \text{H}, \text{OH}; \text{R}_2 = \text{O}$

xestosaprol B (**344**) $\text{R}_1 = \text{R}_2 = \text{H}, \text{OH}$

(**345**) $\text{R}_1 = \text{O}; \text{R}_2 = \text{H}, \text{OH}$

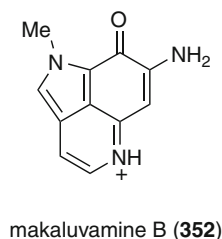
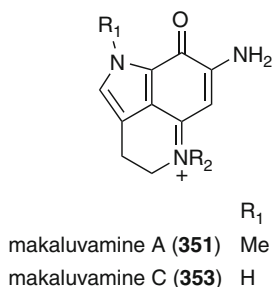
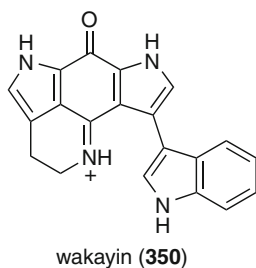


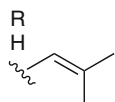
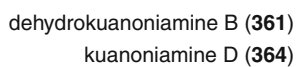
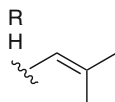
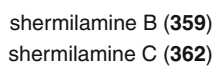
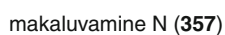
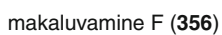
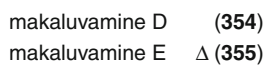
makaluvamine G (**346**)



23.6.1.2 Topoisomerase II (EC 5.99.1.3)

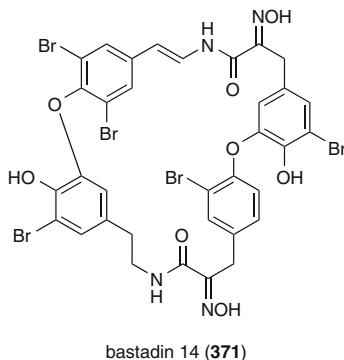
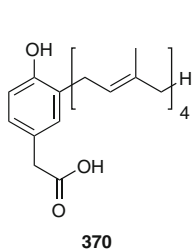
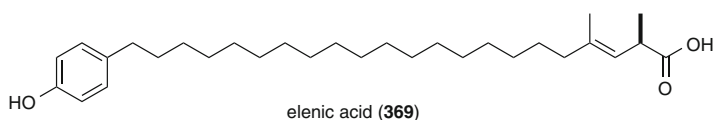
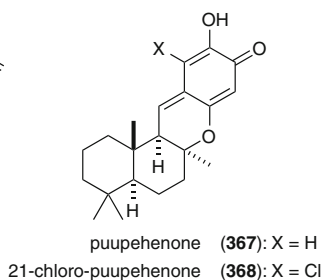
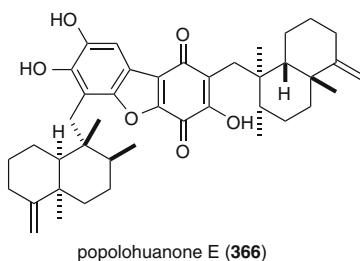
Wakayin (**350**), a cytotoxic pyrroloiminoquinone alkaloid, isolated from the ascidian *Clavelina* sp., inhibited topo II at 250 μ M [219]. Pyrroloiminoquinones, makaluvamines A–F (**351**–**356**) which were isolated from Fijian sponges of the genus *Zyzzya*, showed topo II inhibition with IC_{50} s of 41, >500, 420, 320, 310, and 25 μ M, respectively, while related makaluvone and damirone B were not active. The makaluvamines showed differential toxicity toward the topo II-sensitive CHO cell line xrs-6; makaluvamines A (**351**) and C (**353**) exhibited in vivo antitumor activity against the human ovarian carcinoma Ovar3 implanted in athymic mice [220]. Similarly, makaluvamine N (**357**) isolated from the Philippine sponge *Zyzzya fuliginosa* exhibited greater than 90% inhibition of topo II at 5 μ g/mL [221]. Other makaluvamines G–H did not show inhibitory activity against topo II [222], whereas only makaluvamine G showed moderate inhibition against topo I [189]. Bengacarboline (**358**), a β -carboline alkaloid isolated from a marine ascidian *Didemnum* sp., inhibited topo II at 32 μ M [223].

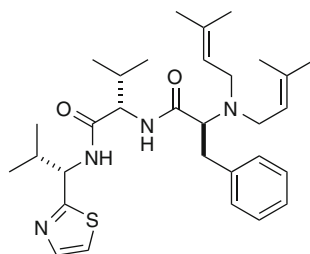




Two aromatic alkaloids, shermilamine B (**359**) [224] and ascididemin (**360**) [225] were reported to inhibit topo II at 30 and 75 μM , respectively [226]. Similarly, dehydrokuanoamine B (**361**), shermilamine C (**362**), cystodytin (**363**), kuanoniamine D (**364**), and diplamine (**365**) from an ascidian *Diplosoma* sp., inhibited topo II with IC_{50} values of 115, 138, 8.4, 127, and 9.2 μM , respectively [227]

Popolohuanone E (**366**), an oxidatively dimerized arenarol derivative isolated from a Pohnpei sponge *Dysidea* sp., was reported to be inhibitory against topo II with an IC_{50} of 400 nM and selectively cytotoxic against the A549 non-small-cell human lung cancer cell line (IC_{50} 2.5 $\mu\text{g/mL}$) [228]. Puupehenone (**367**) and 21-chloro-puupehenone (**368**), sesquiterpene hydroquinones isolated from a verongid sponge, were tested for a wide variety of biological activities including inhibitory activity against topo II, adenosine deaminase (ADA), glutathione reductase (GR), dihydrofolate reductase (DHFR), and thymidylate synthetase (TS), which disclosed that **367** inhibited topo II with an IC_{50} value of 1 $\mu\text{g/mL}$, in addition that **367** and **368** inhibited ADA at IC_{50}s >25 and > 25 $\mu\text{g/mL}$, respectively, GR with an IC_{50} of 6 $\mu\text{g/mL}$ for **368**, DHFR with IC_{50}s of 5 and 5 $\mu\text{g/mL}$, respectively, and TS with IC_{50}s of 8 and 3 $\mu\text{g/mL}$, respectively [229].



virenamide A (**372**)

3. Which should we attach more importance, to new structures or to new activities?
4. What is the status of our understanding on the mechanisms of action for marine natural products?
5. How can marine natural products chemistry contribute to the upcoming trend of life sciences?

References

1. Umezawa H (1982) Low-molecular-weight enzyme-inhibitors of microbial origin. *Annu Rev Microbiol* 36:75–99
2. Fusetani N (1990) Research toward drugs from the sea. *New J Chem* 14:721–728
3. (a) Sato A, Morishita T, Shiraki T, Yoshioka S, Horikoshi H, Kuwano H, Hanzawa H, Hata T (1993) Aldose reductase inhibitors from a marine sponge *Dictyodendrilla* sp. *J Org Chem* 58:7632–7634; (b) Wang Z, Ling B, Zhang R, Suo Y, Liu Y, Yu Z, Liu C (2009) Docking and molecular dynamics studies toward the binding of new natural phenolic marine inhibitors and aldose reductase. *J Mol Graph Model* 28:162–169
4. Tasdemir D, Topaloglu B, Perozzo R, Brun R, O'Neill R, Carballeira NM, Zhang X, Tonge PJ, Linden A, Rüedi P (2007) Marine natural products from the Turkish sponge *Agelas oroides* that inhibit the enoyl reductases from *Plasmodium falciparum*, *Mycobacterium tuberculosis* and *Escherichia coli*. *Bioorg Med Chem* 15:6834–6845
5. Shin J, Fenical W (1991) Fucosides A-D: antiinflammatory diterpenoid glycosides of new structural classes from the Caribbean gorgonian *Eunicea fusca*. *J Org Chem* 56:3153–3158
6. (a) Jacobson PB, Jacobs RS (1992) Fucoside – an antiinflammatory marine natural product which selectively inhibits 5-lipoxygenase. 1. Physiological and biochemical studies in murine inflammatory models. *J Pharmacol Exp Ther* 262:866–873; (b) Jacobson PB, Jacobs RS (1992) Fucoside – an antiinflammatory marine natural product which selectively inhibits 5-lipoxygenase. 2. Biochemical studies in the human neutrophil. *J Pharmacol Exp Ther* 262:874–882
7. Niwa H, Watanabe M, Inagaki H, Yamada K (1994) Didemnilactones A and B and neodidemnilactone, 3 new fatty-acid metabolites isolated from the tunicate *Didemnum moseleyi* (Herdman). *Tetrahedron* 50:7385–7400
8. Brastianos HC, Vottero E, Patrick BO, van Soest R, Matainaho T, Mauk AG, Andersen RJ (2006) Exiguamine A, an indoleamine-2,3-dioxygenase (IDO) inhibitor isolated from the marine sponge *Neopetrosia exigua*. *J Am Chem Soc* 128:16046–16047
9. Carr G, Chung MKW, Mauk AG, Andersen RJ (2008) Synthesis of indoleamine 2,3-dioxygenase inhibitory analogues of the sponge alkaloid exiguamine A. *J Med Chem* 51:2634–2637
10. Pereira A, Vottero E, Roberge M, Mauk AG, Andersen RJ (2006) Indoleamine 2,3-dioxygenase inhibitors from the Northeastern Pacific marine hydroid *Garveia annulata*. *J Nat Prod* 69:1496–1499
11. Tapiolas DM, Bowden BF, Abou-Mansour E, Willis RH, Doyle JR, Muirhead AN, Liptrot C, Llewellyn LE, Wolff CWW, Wright AD, Motti CA (2009) Eusynstyelamides A, B, and C, nNOS inhibitors, from the ascidian *Eusynstyela latericius*. *J Nat Prod* 72:1115–1120
12. Shinoda K, Morishita Y, Sasaki K, Matsuda Y, Takahashi I, Nishi T (1997) Enzymatic characterization of human alpha 1,3-fucosyltransferase Fuc-TVII synthesized in a B cell lymphoma cell lines. *J Biol Chem* 272:31992–31997
13. Wakimoto T, Maruyama A, Matsunaga S, Fusetani N, Shinoda K, Murphy PT (1999) Octa- and nonaprenylhydroquinone sulfates, inhibitors of alpha 1,3-fucosyltransferase VII, from an Australian marine sponge *Sarcotragus* sp. *Bioorg Med Chem Lett* 9:727–730
14. Gray CA, de Lira SP, Silva M, Pimenta EF, Thiemann OH, Oliva G, Hajdu E, Andersen RJ, Berlinck RGS (2006) Sulfated meroterpenoids from the Brazilian sponge *Callyspongia* sp.

- are inhibitors of the antileishmaniasis target adenosine phosphoribosyl transferase. *J Org Chem* 71:8685–8690
15. Coval SJ, Patton RW, Petrin JM, James L, Rothofsky ML, Lin SL, Patel M, Reed JK, McPhail AT, Bishop WR (1996) A cembranolide diterpene farnesyl protein transferase inhibitor from the marine soft coral *Lobophytum cristagalli*. *Bioorg Med Chem Lett* 6:909–912
 16. Ledroit V, Debitus C, Ausseil F, Raux R, Menou JL, Hill BT (2004) Heteronemin as a protein farnesyl transferase inhibitor. *Pharm Biol* 42:454–456
 17. Mori D, Kimura Y, Kitamura S, Sakagami Y, Yoshioka Y, Shintani T, Okamoto T, Ojika M (2007) Spongolactams, farnesyl transferase inhibitors from a marine sponge: isolation through an LC/MS-guided assay, structures, and semisyntheses. *J Org Chem* 72: 7190–7198
 18. Desoubzdanne D, Marcourt L, Raux R, Chevalley S, Dorin D, Doerig C, Valentin A, Ausseil F, Debitus C (2008) Alisiaquinones and alisiaquinol, dual inhibitors of *Plasmodium falciparum* enzyme targets from a New Caledonian deep water sponge. *J Nat Prod* 71:1189–1192
 19. Seo Y, Cho KW, Rho JR, Shin J, Kwon BM, Bok SH, Song JI (1996) Solandelactones A-I, lactonized cyclopropyl oxylipins isolated from the hydroid *Solanderia secunda*. *Tetrahedron* 52:10583–10596
 20. Casey PJ, Thissen JA, Moomaw JF (1991) Enzymatic modification of proteins with a geranylgeranyl isoprenoid. *Proc Natl Acad Sci USA* 88:8631–8635
 21. Kondoh O, Tachibana Y, Ohya Y, Arisawa M, Watanabe T (1997) Cloning of the RHO1 gene from *Candida albicans* and its regulation of beta-1,3-glucan synthesis. *J Bacteriol* 179:7734–7741
 22. Drgonová J, Drgon T, Tanaka K, Kollár R, Chen GC, Ford RA, Chan CSM, Takai Y, Cabib E (1996) Rho1 p, a yeast protein at the interface between cell polarization and morphogenesis. *Science* 272:277–279
 23. (a) Li HY, Matsunaga S, Fusetani N (1994) Corticaticacids A-C, antifungal acetylenic acids from the marine sponge, *Petrosia corticata*. *J Nat Prod* 57:1464–1467; (b) Nishimura S, Matsunaga S, Shibazaki M, Suzuki K, Harada N, Naoki H, Fusetani N (2002) Corticatic acids D and E, polyacetylenic geranylgeranyltransferase type I inhibitors, from the marine sponge *Petrosia corticata*. *J Nat Prod* 65:1353–1356
 24. Nishimura S, Matsunaga S, Shibazaki M, Suzuki K, van Furihata K, Soest RWM, Fusetani N (2003) Massadine, a novel geranylgeranyltransferase type I inhibitor from the marine sponge *Stylissa aff. massa*. *Org Lett* 5:2255–2257
 25. Ishiyama H, Ishibashi M, Ogawa A, Yoshida S, Kobayashi J (1997) Taurospongins A, a novel acetylenic fatty acid derivative inhibiting DNA polymerase beta and HIV reverse transcriptase from sponge *Hippospongia* sp. *J Org Chem* 62:3831–3836
 26. Jiménez C, Quiñoà E, Adamczeski M, Hunter LM, Crews P (1991) Novel sponge-derived amino acids. 12. Tryptophan-derived pigments and accompanying sesterterpenes from *Fascaplysinopsis reticulata*. *J Org Chem* 56:3403–3410
 27. Isaacs S, Hizi A, Kashman Y (1993) Toxicols A-C and toxiusol – new bioactive hexaprenoid hydroquinones from *Toxiclona toxius*. *Tetrahedron* 49:4275–4282
 28. Rudi A, Yosief T, Loya S, Hizi A, Schleyer M, Kashman Y (2001) Clathsterol, a novel anti-HIV-1 RT sulfated sterol from the sponge *Clathria* species. *J Nat Prod* 64:1451–1453
 29. Loya S, Rudi A, Kashman Y, Hizi A (1999) Polycitene A, a novel and potent general inhibitor of retroviral reverse transcriptases and cellular DNA polymerases. *Biochem J* 344:85–92
 30. (a) Reddy MVR, Rao MR, Rhodes D, Hansen MST, Rubins K, Bushman FD, Venkateswarlu Y, Faulkner DJ (1999) Lamellarin α 20-sulfate, an inhibitor of HIV-1 integrase active against HTV-1 virus in cell culture. *J Med Chem* 42:1901–1907; (b) Yamaguchi T, Fukuda T, Ishibashi F, Iwao M (2006) The first total synthesis of lamellarin α 20-sulfate, a selective inhibitor of HIV-1 integrase. *Tetrahedron Lett* 47:3755–3757
 31. Mitchell SS, Rhodes D, Bushman FD, Faulkner DJ (2000) Cyclodidemniserinol trisulfate, a sulfated serinolipid from the Palauan ascidian *Didemnum guttatum* that inhibits HIV-1 integrase. *Org Lett* 2:1605–1607

32. Qureshi A, Faulkner DJ (1999) Haplosamates A and B: new steroidal sulfamate esters from two haplosclerid sponges. *Tetrahedron* 55:8323–8330
33. Bifulco G, Bruno I, Minale L, Riccio R, Debitus C, Bourdy G, Vassas A, Lavayre J (1995) Bioactive prenylhydroquinone sulfates and a novel C₃₁ furanoterpene alcohol sulfate from the marine sponge, *Ircinia* sp. *J Nat Prod* 58:1444–1449
34. (a) Blackburn EH (2001) Switching and signaling at the telomere. *Cell* 106:661–673; (b) Cech TR (2000) Life at the end of the chromosome: telomeres and telomerase. *Angew Chem Int Ed* 39:34–43; (c) Maser RS, DePinho RA (2002) Connecting chromosomes, crisis, and cancer. *Science* 297:565–569
35. Lavelle F, Riou JF, Laoui A, Mailliet P (2000) Telomerase: a therapeutic target for the third millennium? *Crit Rev Oncol Hematol* 34:111–126
36. (a) White LK, Wright WE, Shay JW (2001) Telomerase inhibitors. *Trends Biotechnol* 19:114–120; (b) Neidle S, Parkinson G (2002) Telomere maintenance as a target for anticancer drug discovery. *Nat Rev Drug Discov* 1:383–393; (c) Helder MN, Wisman GBA, van der Zee AGJ (2002) Telomerase and telomeres: from basic biology to cancer treatment. *Cancer Invest* 20:82–101
37. Gowan SM, Harrison JR, Patteson L, Valenti M, Read MA, Neidle S, Kelland LR (2002) A G-quadruplex-interactive potent small-molecule inhibitor of telomerase exhibiting in vitro and in vivo antitumor activity. *Mol Pharmacol* 61:1154–1162
38. Warabi K, Matsunaga S, van Soest RWM, Fusetani N (2003) Dictyodendrins A-E, the first telomerase-inhibitory marine natural products from the sponge *Dictyodendrilla verongiformis*. *J Org Chem* 68:2765–2770
39. Fürstner A, Domostoj MM, Scheiper B (2006) Total syntheses of the telomerase inhibitors dictyodendrin B, C, and E. *J Am Chem Soc* 128:8087–8094
40. Warabi K, Hamada T, Nakao Y, Matsunaga S, Hirota H, van Soest RWM, Fusetani N (2005) Axinelloside A, an unprecedented highly sulfated lipopolysaccharide inhibiting telomerase, from the marine sponge, *Axinella infundibula*. *J Am Chem Soc* 127:13262–13270
41. (a) Frampton JE, Easthope SE (2004) Gefitinib – A review of its use in the management of advanced non-small-cell lung cancer. *Drugs* 64:2475–2492; (b) Ciardiello F (2000) Epidermal growth factor receptor tyrosine kinase inhibitors as anticancer agents. *Drugs* 60 (Suppl 1):25–32; (c) Baselga J, Averbuch SD (2000) ZD1839 ('Iressa')(1,2) as an anticancer agent. *Drugs* 60 (Suppl 1):33–40
42. He H, Kulanthaivel P, Baker BJ, Kalter K, Darges J, Cofield D, Wolff L, Adams L (1995) New antiproliferative and antiinflammatory 9,11-secosterols from the gorgonian *Pseudopterogorgia* sp. *Tetrahedron* 51:51–58
43. Kobayashi J, Inaba K, Tsuda M (1997) Tauroacidins A and B, new bromopyrrole alkaloids possessing a taurine residue from *Hymeniacidon* sponge. *Tetrahedron* 53:16679–16682
44. Kreuter MH, Leake RE, Rinaldi F, Müller-Klieser W, Maidhof A, Müller WEG, Schröder HC (1990) Inhibition of intrinsic protein tyrosine kinase-activity of EGF-receptor kinase complex from human breast cancer cells by the marine sponge metabolite (+)-aeropysinin-1. *Comp Biochem Physiol* 97B:151–158
45. Hirano K, Kubota T, Tsuda M, Watanabe K, Fromont J, Kobayashi J (2000) Ma'edamines A and B, cytotoxic bromotyrosine alkaloids with a unique 2(1H)pyrazinone ring from sponge *Suberea* sp. *Tetrahedron* 56:8107–8110
46. Lee RH, Slate DL, Moretti R, Alvi KA, Crews P (1992) Marine sponge polyketide inhibitors of protein tyrosine kinase. *Biochem Biophys Res Commun* 184:765–772
47. Fujiwara H, Matsunaga K, Saito M, Hagiya S, Furukawa K, Nakamura H, Ohizumi Y (2001) Halenaquinone, a novel phosphatidylinositol 3-kinase inhibitor from a marine sponge, induces apoptosis in PC12 cells. *Eur J Pharmacol* 413:37–45
48. Alvi KA, Rodríguez J, Diaz MC, Moretti R, Wilhelm RS, Lee RH, Slate DL, Crews P (1993) Protein-tyrosine kinase inhibitory properties of planar polycyclics obtained from the marine sponge *Xestospongia* cf *carbonaria* and from total synthesis. *J Org Chem* 58:4871–4880

49. Alvi KA, Diaz MC, Crews P, Slate DL, Lee RH, Moretti R (1992) Evaluation of new sesquiterpene quinones from two *Dysidea* sponge species as inhibitors of protein tyrosine kinase. *J Org Chem* 57:6604–6607
50. Buchanan MS, Edser A, King G, Whitmore J, Quinn RJ (2001) Cheilanthane sesterterpenes, protein kinase inhibitors, from a marine sponge of the genus *Ircinia*. *J Nat Prod* 64:300–303
51. Tasdemir D, Mallon R, Greenstein M, Feldberg LR, Kim SC, Collins K, Wojciechowski D, Mangalindan GC, Concepción GP, Harper MK, Ireland CM (2002) Aldisine alkaloids from the Philippine sponge *Stylissa massa* are potent inhibitors of mitogen-activated protein kinase kinase-1 (MEK-1). *J Med Chem* 45:529–532
52. (a) Curman D, Cinel B, Williams DE, Rundle N, Block WD, Goodarzi AA, Hutchins JR, Clarke PR, Zhou BB, Lees-Miller SP, Andersen RJ, Roberge M (2001) Inhibition of the G(2) DNA damage checkpoint and of protein kinases Chk1 and Chk2 by the marine sponge alkaloid debromohymenialdisine. *J Biol Chem* 276:17914–17919; (b) Meijer L, Thunnissen AMWH, White AW, Garnier M, Nikolic M, Tsai LH, Walter J, Cleverley KE, Salinas PC, Wu YZ, Mandelkow EM, Kim SH, Pettit GR (2000) Inhibition of cyclin-dependent kinases, GSK-3 beta and CK1 by hymenialdisine, a marine sponge constituent. *Chem Biol* 7:51–63; (c) Annoura H, Tatsuoka T (1995) Total synthesis of hymenialdisine and debromohymenialdisine – stereospecific construction of the 2-amino-4-oxo-2-imidazolin-5(Z)-disubstituted ylidene ring-system. *Tetrahedron Lett* 36:413–416; (d) Xu YZ, Yakushijin K, Horne DA (1997) Synthesis of C11N5 marine sponge alkaloids: (+/–)-hymenin, stevensine, hymenialdisine, and debromohymenialdisine. *J Org Chem* 62:456–464; (e) Sosa ACB, Yakushijin K, Horne DA (2000) A practical synthesis of (Z)-debromohymenialdisine. *J Org Chem* 65:610–611; (f) Prager RH, Tsopelas C (1992) Knoevenagel reactions of 6,7-dihydropyrrolo [2,3-c]azepine-4,8(1H, 5H)-dione: an approach to the synthesis of pyrrolic marine natural products. *Aust J Chem* 45:1771–1777; (g) Cho H, Matsuki S, Mizuno A, Annoura H, Tatsuoka T (1997) Synthesis of pyrroloazepines. Facile synthesis of 2-substituted pyrrole derivatives by the phosgene method. *J Heterocycl Chem* 34:87–91; (h) Portevin B, Golsteyn RM, Pierré A, De Nanteuil G (2003) An expeditious multigram preparation of the marine protein kinase inhibitor debromohymenialdisine. *Tetrahedron Lett* 44:9263–9265
53. Wan YQ, Hur WY, Cho CY, Liu Y, Adrian FJ, Lozach O, Bach S, Mayer T, Fabbro D, Meijer L, Gray NS (2004) Synthesis and target identification of hymenialdisine analogs. *Chem Biol* 11:247–259
54. (a) Takahashi I, Saitoh Y, Yoshida M, Sano H, Nakano H, Morimoto M, Takamori T (1989) UCN-01 and UCN-02, new selective inhibitors of protein kinase C. II. Purification, physicochemical properties, structural determination and biological activities. *J Antibiot* 42:571–576; (b) Koshino H, Osada H, Isono K (1992) A new inhibitor of protein kinase C, RK-1409 (7-oxostaurosporine). II. Fermentation, isolation, physicochemical properties and structure. *J Antibiot* 45:195–198
55. Kinnel RB, Scheuer PJ (1992) 11-Hydroxystaurosporine: a highly cytotoxic, powerful protein kinase C inhibitor from a tunicate. *J Org Chem* 57:6327–6329
56. Horton PA, Longley RE, McConnell OJ, Ballas LM (1994) Staurosporine aglycone (K252-C) and scryflavin-A from the marine ascidian, *Eudistoma*. *Experientia* 50:843–845
57. (a) Rodríguez J, Peters BM, Kurz L, Schatzman RC, McCarley D, Lou L, Crews P (1993) An alkaloid protein kinase C inhibitor, xestocyclamine A, from the marine sponge *Xestospongia* sp. *J Am Chem Soc* 115:10436–10437; (b) Rodríguez J, Crews P (1994) Novel marine sponge alkaloids acids. 7. Revised structure of xestocyclamine A and description of a new analogue. *Tetrahedron Lett* 35:4719–4722
58. Walz AJ, Sundberg RJ (2000) Synthesis of 8-methoxy-1-methyl-1H-benzo[de][1,6]naphthyridin-9-ol (isoaptamine) and analogues. *J Org Chem* 65:8001–8010 and references cited therein
59. Patil AD, Freyer AJ, Killmer L, Hofmann G, Johnson RK (1997) Z-axinohydantoin and debromo-Z-axinohydantoin from the sponge *Stylotella aurantium*: inhibitors of protein kinase C. *Nat Prod Lett* 9:201–207

60. Chan JA, Freyer AJ, Carté BK, Hemling ME, Hofmann GA, Mattern MR, Mentzer MA, Westley JW (1994) Protein kinase C inhibitors: novel spirosesquiterpene aldehydes from a marine sponge *Aka* (= *Siphonodictyon*) *coralliphagum*. *J Nat Prod* 57:1543–1548
61. (a) Shigemori H, Madono T, Sasaki T, Mikami Y, Kobayashi J (1994) Nakijiquinone A and B, new antifungal sesquiterpenoid quinones with an amino acid residue from an Okinawan marine sponge. *Tetrahedron* 50:8347–8354; (b) Kobayashi J, Madono T, Shigemori H (1995) Nakijiquinone C and D, new sesquiterpenoid quinones with a hydroxy amino-acid residue from a marine sponge inhibiting c-erbB-2 kinase. *Tetrahedron* 51:10861–10874
62. (a) Stahl P, Kissau L, Mazitschek R, Huwe A, Furet P, Giannis A, Waldmann H (2001) Total synthesis and biological evaluation of the nakijiquinones. *J Am Chem Soc* 123:11586–11593; (b) Stahl P, Kissau L, Mazitschek R, Giannis A, Waldmann H (2002) Natural product derived receptor tyrosine kinase inhibitors: identification of IGF1R, Tie-2, and VEGFR-3 inhibitors. *Angew Chem Int Ed* 41:1174–1178
63. Patil AD, Freyer AJ, Killmer L, Offen P, Carte B, Jurewicz AJ, Johnson RK (1997) Frondosins, five new sesquiterpene hydroquinone derivatives with novel skeletons from the sponge *Dysidea frondosa*: inhibitors of interleukin-8 receptors. *Tetrahedron* 53:5047–5060
64. He HY, Kulanthaival P, Baker BJ (1994) New cytotoxic sesterterpenes from the marine sponge *Spongia* sp. *Tetrahedron Lett* 35:7189–7192
65. Alvi KA, Jaspars M, Crews P, Strulovici B, Oto E (1994) Penazetidine A, an alkaloid inhibitor of protein kinase C. *Bioorg Med Chem Lett* 4:2447–2450
66. Willis RH, DeVries DJ (1997) BRS1, a C30 bis-amino, bis-hydroxy polyunsaturated lipid from an Australian calcareous sponge that inhibits protein kinase C. *Toxicon* 35:1125–1129
67. Kobayashi J, Doi Y, Ishibashi M (1994) Shimofuridin A, a nucleoside derivative embracing an acylfucopyranoside unit isolated from the Okinawan marine tunicate *Aplidium multiplicatum*. *J Org Chem* 59:255–257
68. (a) Pettit GR, Herald CL, Doubek DL, Herald DL (1982) Anti-neoplastic agents. 86. Isolation and structure of bryostatin 1. *J Am Chem Soc* 104:6846–6848; (b) Pettit GR (1996) Progress in the discovery of biosynthetic anticancer drugs. *J Nat Prod* 59:812–821
69. (a) Kortmansky J, Schwartz GK (2003) Bryostatin-1: a novel PKC inhibitor in clinical development. *Cancer Invest* 21:924–936; (b) Etcheberrigaray R, Tan M, Dewachter I, Kuipéri C, Van der Auwera I, Wera S, Qiao L, Bank B, Nelson TJ, Kozikowski AP, Van Leuven F, Alkon DL (2004) Therapeutic effects of PKC activators in Alzheimer's disease transgenic mice. *Proc Natl Acad Sci USA* 101:11141–11146; (c) Wender PA, Verma VA (2006) Design, synthesis, and biological evaluation of a potent, PKC selective, B-ring analog of bryostatin. *Org Lett* 8:1893–1896
70. Kobayashi J, Suzuki M, Tsuda M (1997) Konbu'acidin A, a new bromopyrrole alkaloid with cdk4 inhibitory activity from *Hymeniacidon* sponge. *Tetrahedron* 53:15681–15684
71. Inaba K, Sato H, Tsuda M, Kobayashi J (1998) Spongiacidins A-D, new bromopyrrole alkaloids from *Hymeniacidon* sponge. *J Nat Prod* 61:693–695
72. Sato H, Tsuda M, Watanabe K, Kobayashi J (1998) Rhopaladins A ~ D, new indole alkaloids from marine tunicate *Rhopalaea* sp. *Tetrahedron* 54:8687–8690
73. Killday KB, Yarwood D, Sills MA, Murphy PT, Hooper JNA, Wright AE (2001) Microxine, a new cdc2 kinase inhibitor from the Australian marine sponge *Microxina* species. *J Nat Prod* 64:525–526
74. Meijer L, Thunnissen AMWH, White AW, Garnier M, Nikolic M, Tsai LH, Walter J, Cleverley KE, Salinas PC, Wu YZ, Biernat J, Mandelkow EM, Kim SH, Pettit GR (2000) Inhibition of cyclin-dependent kinases, GSK-3 β and CK1 by hymenialdisine, a marine sponge constituent. *Chem Biol* 7:51–63
75. Meijer L, Skaltsounis AL, Magiatis P, Polychronopoulos P, Knockaert M, Leost M, Ryan XP, Vonica CA, Brivanlou A, Dajani R, Crovace C, Tarricone C, Musacchio A, Roe SM, Peart L, Greengard P (2003) GSK-3-selective inhibitors derived from Tyrian purple indirubins. *Chem Biol* 10:1255–1266

76. Gompel M, Leost M, Joffe EBK, Puricelli L, Franco LH, Palermo J, Meijer L (2004) Meridianins, a new family of protein kinase inhibitors isolated from the ascidian *Aplidium meridianum*. *Bioorg Med Chem Lett* 14:1703–1707
77. Hamann M, Alonso D, Martín-Aparicio E, Fuertes A, Pérez-Puerto MJ, Castro A, Morales S, Navarro ML, del Monte-Millán M, Medina M, Pennaka H, Balaiah A, Peng J, Cook J, Wahyuono S, Martínez A (2007) Glycogen synthase kinase-3 (GSK-3) inhibitory activity and structure-activity relationship (SAR) studies of the manzamine alkaloids. Potential for Alzheimer's disease. *J Nat Prod* 70:1397–1405
78. de Silva ED, Scheuer PJ (1980) Manoalide, an antibiotic sesterterpenoid from the marine sponge *Luffariella variabilis* (Polejaff). *Tetrahedron Lett* 21:1611–1614
79. (a) de Freitas JC, Blankemeier LA, Jacobs RS (1984) In vitro inactivation of the neurotoxic action of β -bungarotoxin by the marine natural product, manoalide. *Experientia* 40:864–865; (b) Lombardo D, Dennis EA (1985) Cobra venom phospholipase A_2 inhibition by manoalide – a novel type of phospholipase inhibitor. *J Biol Chem* 260:7234–7240
80. de Silva ED, Scheuer PJ (1981) Three new sesterterpenoid antibiotics from the marine sponge *Luffariella variabilis* (Polejaff.). *Tetrahedron Lett* 22:3147–3150
81. Katsumura S, Han Q, Kadono H, Fujiwara S, Isoe S, Fujii S, Nishimura H, Ikeda K (1992) Phospholipase A_2 inhibition by manoalide: development of simple analogs and necessary functional groups for inhibition. *Bioorg Med Chem Lett* 2:1263–1266
82. Albizzati KF, Holman T, Faulkner DJ, Glaser KB, Jacobs RS (1987) Luffariellolide, an antiinflammatory sesterterpene from the marine sponge *Luffariella* sp. *Experientia* 43:949–950
83. Kernan MR, Faulkner DJ, Jacobs RS (1987) The luffariellins, novel antiinflammatory sesterterpenes of chemotaxonomic importance from the marine sponge *Luffariella variabilis*. *J Org Chem* 52:3081–3083
84. (a) Potts BCM, Faulkner DJ, de Carvalho MS, Jacobs RS (1992) Chemical mechanism of inactivation of bee venom phospholipase A_2 by the marine natural-products manoalide, luffariellolide, and scalaradial. *J Am Chem Soc* 114:5093–5100; (b) Fujii S, Tahara Y, Toyomoto M, Hada S, Nishimura H, Inoue S, Ikeda K, Inagaki Y, Katsumura S, Samejima Y, Omori-Satoh T, Takasaki C, Hayashi K (1995) Chemical modification and inactivation of phospholipases A_2 by a manoalide analog. *Biochem J* 308:297–304
85. Tanaka K, Kamatani M, Mori H, Fujii S, Ikeda K, Hisada M, Itagaki Y, Katsumura S (1999) The inhibitory mechanism of bovine pancreatic phospholipase A_2 by aldehyde terpenoids. *Tetrahedron* 55:1657–1686
86. (a) De Rosa S, De Stefano S (1988) Cacospongionolide: a new antitumoral sesterterpene, from the marine sponge *Cacospongia mollior*. *J Org Chem* 53:5020–5023; (b) Puliti R, De Rosa S, Mattia CA, Mazzarella L (1990) Structure and stereochemistry of an acetate derivative of cacospongionolide, a new antitumoral sesterterpenoid from marine sponge *Cacospongia mollior*. *Acta Cryst C* 46:1533–1536; (c) De Rosa S, Crispino A, De Giulio A, Iodice C, Pronzato R, Zavodnik N (1995) Cacospongionolide B, a new sesterterpene from the sponge *Fasciospongia cavernosa*. *J Nat Prod* 58:1776–1780; (d) Soriente A, Crispino A, De Rosa M, De Rosa S, Scettri A, Scognamiglio G, Villano R, Sodano G (2000) Stereochemistry of antiinflammatory marine sesterterpenes. *Eur J Org Chem*:947–953
87. Pastor PG, De Rosa S, De Giulio A, Payá M, Alcaraz MJ (1999) Modulation of acute and chronic inflammatory processes by cacospongionolide B, a novel inhibitor of human synovial phospholipase A_2 . *Brit J Pharmacol* 126:301–311
88. De Rosa S, Crispino A, De Giulio A, Iodice C, Benrezzouk R, Terencio MC, Ferrándiz ML, Alcaraz MJ, Payá M (1998) A new cacospongionolide inhibitor of human secretory phospholipase A_2 from the Tyrrhenian sponge *Fasciospongia cavernosa* and absolute configuration of cacospongionolides. *J Nat Prod* 61:931–935
89. Cheung AK, Snapper ML (2002) Total syntheses of (+)- and (–)-cacospongionolide B: new insight into structural requirements for phospholipase A_2 inhibition. *J Am Chem Soc* 124:11584–11585

90. Posadas I, De Rosa S, Terencio MC, Payá M, Alcaraz MJ (2003) Cacospongionolide B suppresses the expression of inflammatory enzymes and tumour necrosis factor- α by inhibiting nuclear factor- κ B activation. *Brit J Pharm* 138:1571–1579
91. Posadas I, Terencio MC, De Rosa S, Payá M (2000) Cavernolide: a new inhibitor of human sPLA₂ sharing unusual chemical features. *Life Sci* 67:3007–3014
92. Giannini C, Debitus C, Posadas I, Payá M, D'auria MV (2000) Dysidotronic acid, a new and selective human phospholipase A₂ inhibitor from the sponge *Dysidea* sp. *Tetrahedron Lett* 41:3257–3260
93. Giannini C, Debitus C, Lucas R, Ubeda A, Payá M, Hooper JNA, D'Auria MV (2001) New sesquiterpene derivatives from the sponge *Dysidea* species with a selective inhibitor profile against human phospholipase A₂ and other leukocyte functions. *J Nat Prod* 64:612–615
94. Randazzo A, Debitus C, Minale L, Pastor PG, Alcaraz MJ, Payá M, Gomez-Paloma L (1998) Petrosaspongiolides M-R: new potent and selective phospholipase A₂ inhibitors from the New Caledonian marine sponge *Petrosaspongia nigra*. *J Nat Prod* 61:571–575
95. (a) Dal Piaz F, Casapullo A, Randazzo A, Riccio R, Pucci P, Marino G, Gomez-Paloma L (2002) Molecular basis of phospholipase A₂ inhibition by petrosaspongiolide M. *ChemBioChem* 3:664–671; (b) Monti MC, Casapullo A, Riccio R, Gomez-Paloma L (2004) Further insights on the structural aspects of PLA₂ inhibition by γ -hydroxybutenolide-containing natural products: a comparative study on petrosaspongiolides M-R. *Bioorg Med Chem* 12:1467–1474
96. Monti MC, Casapullo A, Riccio R, Gomez-Paloma L (2004) PLA₂-mediated catalytic activation of its inhibitor 25-acetyl-petrosaspongiolide M: serendipitous identification of a new PLA₂ suicide inhibitor. *FEBS Lett* 578:269–274
97. Monti MC, Riccio R, Casapullo A (2009) Effects of petrosaspongiolide R on the surface topology of bee venom PLA₂: a limited proteolysis and mass spectrometry analysis. *Bioorg Chem* 37:6–10
98. Posadas I, Terencio MC, Randazzo A, Gomez-Paloma L, Payá M, Alcaraz MJ (2003) Inhibition of the NF- κ B signaling pathway mediates the anti-inflammatory effects of petrosaspongiolide M. *Biochem Pharmacol* 65:887–895
99. Crews P, Jiménez C, O'Neil-Johnson M (1991) Using spectroscopic and database strategies to unravel structures of polycyclic bioactive marine sponge sesterterpenes. *Tetrahedron* 47:3585–3600
100. Kernan MR, Faulkner DJ, Parkanyi L, Clardy J, de Carvalho MS, Jacobs RS (1989) Luffolide, a novel anti-inflammatory terpene from the sponge *Luffariella* sp. *Experientia* 45:388–390
101. Alvi KA, Crews P (1992) Homoscalarane sesterterpenes from *Lendenfeldia frondosa*. *J Nat Prod* 55:859–865
102. Fontana A, Mollo E, Ortea J, Gavagnin M, Cimino G (2000) Scalarane and homoscalarane compounds from the nudibranchs *Glossodoris sedna* and *Glossodoris dalli*: chemical and biological properties. *J Nat Prod* 63:527–530
103. Cimino G, DeStefano S, Minale L (1974) Scalaradial, a sesterterpene with the tetracarboxylic skeleton of scalarin, from the sponge *Cacospongia mollior*. *Experientia* 30:846–847
104. Kernan MR, Faulkner DJ (1988) Sesterterpene sulfates from a sponge of the family Halichondriidae. *J Org Chem* 53:4574–4578
105. Alfano G, Cimino G, DeStefano S (1979) Palinurin, a new linear sesterterpene from a marine sponge. *Experientia* 35:1136–1137
106. Schmidt EW, Faulkner DJ (1996) Palauolol, a new anti-inflammatory sesterterpene from the sponge *Fascaplysinopsis* sp. from Palau. *Tetrahedron Lett* 37:3951–3954
107. Shin JH, Seo YW, Rho JR, Cho KW (1996) Isolation of polyhydroxysteroids from the gorgonian *Acabaria undulata*. *J Nat Prod* 59:679–682
108. Seo Y, Cho KW, Chung H, Lee HS, Shin J (1998) New secosteroids from a gorgonian of the genus *Muricella*. *J Nat Prod* 61:1441–1443

109. Sepcic K, Guella G, Mancini I, Pietra F, Serra MD, Menestrina G, Tubbs K, Macek P, Turk T (1997) Characterization of anticholinesterase-active 3-alkylpyridinium polymers from the marine sponge *Reniera sarai* in aqueous solutions. *J Nat Prod* 60:991–996
110. Tachibana K, Scheuer PJ, Tsukitani Y, Kikuchi H, Engen VD, Clardy J, Gopichand Y, Schmitz FJ (1981) Okadaic acid, a cytotoxic polyether from two marine sponges of the genus *Halichondria*. *J Am Chem Soc* 103:2469–2471
111. Takai A, Murata M, Torigoe K, Isobe M, Mieskes G, Yasumoto Y (1992) Inhibitory effect of okadaic acid derivatives on protein phosphatases: A study on structure-affinity relationship. *Biochem J* 284:539–544
112. Maynes JT, Bateman KS, Chemey MM, Das AK, Luu HA, Holmes CF, James MN (2001) Crystal structure of the tumor-promoter okadaic acid bound to protein phosphatase-1. *J Biol Chem* 276:44078–44082
113. Cruz PG, Daranas AH, Fernández JJ, Norte M (2007) 19-*epi*-Okadaic acid, a novel protein phosphatase inhibitor with enhanced selectivity. *Org Lett* 9:3045–3048
114. Cruz PG, Fernández JJ, Norte M, Daranas AH (2008) Belizeanic acid: a potent protein phosphatase 1 inhibitor belonging to the okadaic acid class, with an unusual skeleton. *Chem Eur J* 14:6948–6956
115. Kato Y, Fusetani N, Matsunaga S, Hashimoto K (1986) The bioactive marine metabolites. 16. Calyculin A, a novel antitumor metabolite from the marine sponge *Discodermia calyx*. *J Am Chem Soc* 108:2780–2781
116. Ishihara H, Martin BL, Brautigan DL, Karaki H, Ozaki H, Kato Y, Fusetani N, Watabe S, Hashimoto K, Uemura D, Hartshorne DJ (1989) Calyculin A and okadaic acid: inhibitors of protein phosphatase activity. *Biochem Biophys Res Commun* 159:871–877
117. (a) Kato Y, Fusetani N, Matsunaga S, Hashimoto K (1988) Isolation and structure elucidation of calyculin B, C, and D, novel antitumor metabolites, from the marine sponge *Discodermia calyx*. *J Org Chem* 53:3930–3932; (b) Matsunaga S, Fujiki H, Sakata D, Fusetani N (1991) Calyculins E, F, G, and H, additional inhibitors of protein phosphatase 1 and 2A, from the marine sponge *Discodermia calyx*. *Tetrahedron* 47:2999–3006
118. (a) Matsunaga S, Wakimoto T, Fusetani N (1997) Bioactive marine metabolites. 78. Isolation of four new calyculins from the marine sponge *Discodermia calyx*. *J Org Chem* 62:2640–2642; (b) Matsunaga S, Wakimoto T, Fusetani N, Suganuma M (1997) Isolation of dephosphonocalyculin A from the marine sponge, *Discodermia calyx*. *Tetrahedron Lett* 38:3763–3764
119. Wakimoto T, Matsunaga S, Takai A, Fusetani N (2002) Insight into binding of calyculin A to protein phosphatase 1: isolation of hemicalyculin A and chemical transformation of calyculin A. *Chem Biol* 9:309–319
120. Kita A, Matsunaga S, Takai A, Kataiwa H, Wakimoto T, Fusetani N, Isobe M, Miki K (2002) Crystal structure of the complex between calyculin A and the catalytic subunit of protein phosphatase 1. *Structure* 10:715–724 & 1149
121. (a) Goldberg J, Huang HB, Kwon YG, Greengard P, Naim AC, Kuriyan J (1995) Three-dimensional structure of the catalytic subunit of protein serine/threonine phosphatase-1. *Nature* 376:745–753; (b) Egloff MP, Cohen PTW, Reinemer P, Barford D (1995) Crystal-structure of the catalytic subunit of human protein phosphatase-1 and its complex with tungstate. *J Mol Biol* 254:942–959
122. Fu X, Schmitz FJ, Kelly-Borges M, McCreedy TL, Holmes CFB (1998) Clavosines A-C from the marine sponge *Myriastra clavosa*: potent cytotoxins and inhibitors of protein phosphatases 1 and 2A. *J Org Chem* 63:7957–7963
123. de Silva ED, Williams DE, Andersen RJ, Klix H, Holmes CFB, Allen TM (1992) Motuporin, a potent protein phosphatase inhibitor isolated from the Papua New Guinea sponge *Theonella swinhoei* Gray. *Tetrahedron Lett* 33:1561–1564
124. Capon RJ, Rooney F, Murray LM, Collins E, Sim ATR, Rostas JAP, Butler MS, Carroll AR (1998) Dragmacidins: new protein phosphatase inhibitors from a southern Australian deep-water marine sponge, *Spongosorites* sp. *J Nat Prod* 61:660–662

125. Williams DE, Roberge M, Van Soest R, Andersen RJ (2003) Spirastrellolide A, an antimicrobial macrolide isolated from the Caribbean marine sponge *Spirastrella coccinea*. *J Am Chem Soc* 125:5296–5297
126. Williams DE, Lapawa M, Feng XD, Tarling T, Roberge M, Andersen RJ (2004) Spirastrellolide A: revised structure, progress toward the relative configuration, and inhibition of protein phosphatase 2A. *Org Lett* 6:2607–2610
127. Endo T, Tsuda M, Okada T, Mitsuhashi S, Shima H, Kikuchi K, Mikami Y, Fromont J, Kobayashi J (2004) Nagelamides A–H, new dimeric bromopyrrole alkaloids from marine sponge *Agelas* species. *J Nat Prod* 67:1262–1267
128. Guerini D (1997) Calcineurin: not just a simple protein phosphatase. *Biochem Biophys Res Comm* 235:271–275
129. Liu J, Farmer JD, Lane WS, Friedman J, Weissman I, Schreiber SL (1991) Calcineurin is a common target of cyclophilin-cyclosporine A and FKBP-FK506 complex. *Cell* 66:807–815
130. Gunasekera SP, McCarthy PJ, Longley RE, Pomponi SA, Wright AE (1999) Secobatzellines A and B, two new enzyme inhibitors from a deep-water Caribbean sponge of the genus *Batzella*. *J Nat Prod* 62:1208–1211
131. Gunasekera SP, McCarthy PJ, Kelly-Borges M, Lobkovsky E, Clardy J (1996) Dysidiolide: a novel protein phosphatase inhibitor from the Caribbean sponge *Dysidea etheria* de Laubenfels. *J Am Chem Soc* 118:8759–8760
132. (a) Corey EJ, Roberts BE (1997) Total synthesis of dysidiolide. *J Am Chem Soc* 119:12425–12431; (b) Boukouvalas J, Cheng YX, Robichaud J (1998) Total synthesis of (+)-dysidiolide. *J Org Chem* 63:228–229; (c) Magnuson SR, Sepp-Lorenzino L, Rosen N, Danishefsky SJ (1998) A concise total synthesis of dysidiolide through application of a dioxolenium-mediated Diels-Alder reaction. *J Am Chem Soc* 120:1615–1616; (d) Takahashi M, Dodo K, Sugimoto Y, Aoyagi Y, Yamada Y, Hashimoto Y, Shirai R (2000) Synthesis of the novel analogues of dysidiolide and their structure-activity relationship. *Bioorg Med Chem Lett* 10:2571–2574; (e) Demeke D, Forsyth CJ (2000) Novel total synthesis of the anticancer natural product dysidiolide. *Org Lett* 2:3177–3179; (f) Brohm D, Metzger S, Bhargava A, Müller O, Lieb F, Waldmann H (2002) Natural products are biologically validated starting points in structural space for compound library development: solid-phase synthesis of dysidiolide-derived phosphatase inhibitors. *Angew Chem Int Ed* 41:307–311
133. (a) Loukaci A, Le Saout I, Samadi M, Leclerc S, Damiens E, Meijer L, Debitus C, Guyot M (2001) Coscinosulfate, a CDC25 phosphatase inhibitor from the sponge *Coscinotheca mathewsi*. *Bioorg Med Chem* 9:3049–3054; (b) Poigny S, Nouri S, Chiaroni A, Guyot M, Samadi M (2001) Total synthesis and determination of the absolute configuration of coscinosulfate. A new selective inhibitor of Cdc25 protein phosphatase. *J Org Chem* 66:7263–7269
134. Berridge MJ (1987) Inositol trisphosphate as a 2nd messenger in signal transduction. *Annu Rev Biochem* 56:159–193
135. Fukami A, Ikeda Y, Kondo S, Naganawa H, Takeuchi T, Furuya S, Hirabayashi Y, Shimoike K, Hosaka S, Watanabe Y, Umezawa K (1997) Akaterpin, a novel bioactive triterpene from the marine sponge *Callyspongia* sp. *Tetrahedron Lett* 38:1201–1202
136. Kobayashi J, Nakamura H, Ohizumi Y, Hirata Y (1986) Eudistomidin A, a novel calmodulin antagonist from the Okinawan tunicate *Eudistoma glaucus*. *Tetrahedron Lett* 27:1191–1194
137. Kobayashi J, Cheng JF, Ohta T, Nozoe S, Ohizumi Y, Sasaki T (1990) Eudistomidins B, C, and D: novel antileukemic alkaloids from the Okinawan marine tunicate *Eudistoma glaucus*. *J Org Chem* 55:3666–3670
138. (a) Ishibashi M, Ohizumi Y, Sasaki T, Nakamura H, Hirata Y, Kobayashi J (1987) Pseudodistomins A and B, novel antineoplastic piperidine alkaloids with calmodulin antagonistic activity from the Okinawan tunicate *Pseudodistoma kanoko*. *J Org Chem* 52:450–453; (b) Knapp S, Hale JJ (1993) Synthesis of (+)-tetrahydropseudodistomin. *J Org Chem* 58:2650–2651

139. Kobayashi J, Cheng JF, Kikuchi Y, Ishibashi M, Yamamura S, Ohizumi Y, Ohta T, Nozoe S (1990) Rigidin, a novel alkaloid with calmodulin antagonistic activity from the Okinawan marine tunicate *Eudistoma cf rigida*. *Tetrahedron Lett* 31:4617–4620
140. Hirota H, Matsunaga S, Fusetani N (1990) Bioactive marine metabolites. 32. Stelletamide A, an antifungal alkaloid from a marine sponge of the genus *Stelletta*. *Tetrahedron Lett* 31:4163–4164
141. Abe Y, Saito S, Hori M, Ozaki H, Fusetani N, Karaki H (1997) Stelletamide-A, a novel inhibitor of calmodulin, isolated from a marine sponge. *Brit J Pharmacol* 121:1309–1314
142. Tsukamoto S, Yamashita T, Matsunaga S, Fusetani N (1999) Bioactive marine metabolites – Part 89 – Stelletazole A: an antibacterial guanidinoimidazole alkaloid from a marine sponge *Stelletta* sp. *Tetrahedron Lett* 40:737–738
143. Tsukamoto S, Yamashita T, Matsunaga S, Fusetani N (1999) Bistellettadines A and B: two bioactive dimeric stellettadines from a marine sponge *Stelletta* sp. *J Org Chem* 64:3794–3795
144. Nakao Y, Takada K, Matsunaga S, Fusetani N (2001) Calyceramides A-C: neuraminidase inhibitory sulfated ceramides from the marine sponge *Discodermia calyx*. *Tetrahedron* 57:3013–3017
145. Takada K, Nakao Y, Matsunaga S, van Soest RWM, Fusetani N (2002) Nobiloside, a new neuraminidase inhibitory triterpenoidal saponin from the marine sponge *Erylus nobilis*. *J Nat Prod* 65:411–413
146. Takada K, Hamada T, Hirota H, Nakao Y, Matsunaga S, van Soest RWM, Fusetani N (2006) Asteropine A, a sialidase-inhibiting conotoxin-like peptide from the marine sponge *Asteropus simplex*. *Chem Biol* 13:569–574
147. Kato T, Shizuri Y, Izumida H, Yokoyama A, Endo M (1995) Styloguanidines, new chitinase inhibitors from the marine sponge *Stylorella aurantium*. *Tetrahedron Lett* 36:2133–2136
148. Nakao Y, Maki T, Matsunaga S, van Soest RWM, Fusetani N (2000) Penarolide sulfates A₁ and A₂, new α -glucosidase inhibitors from a marine sponge *Penares* sp. *Tetrahedron* 56:8977–8987
149. Nakao Y, Maki T, Matsunaga S, van Soest RWM, Fusetani N (2004) Penasulfate A, a new α -glucosidase inhibitor from a marine sponge *Penares* sp. *J Nat Prod* 67:1346–1350
150. Saludes JP, Lievens SC, Molinski TF (2007) Occurrence of the α -glucosidase inhibitor 1,4-dideoxy-1,4-imino-D-arabinitol and related iminopentitols in marine sponges. *J Nat Prod* 70:436–438
151. Nakao Y, Uehara T, Matsunaga S, Fusetani N, van Soest RWM (2007) Callyspongynic acid, a polyacetylenic acid which inhibits α -glucosidase, from the marine sponge *Callyspongia truncata*. *J Nat Prod* 65:922–924
152. Takada K, Uehara T, Nakao Y, Matsunaga S, van Soest RWM, Fusetani N (2004) Schulzeines A-C, new α -glucosidase inhibitors from the marine sponge *Penares schulzei*. *J Am Chem Soc* 126:187–193
153. Bowen EG, Wardrop DJ (2009) Total synthesis of the α -glucosidase inhibitors schulzeine A, B, and C and a structural revision of schulzeine A. *J Am Chem Soc* 131:6062–6063
154. Kim BG, Chun TG, Lee HY, Snapper ML (2009) A new structural class of S-adenosylhomocysteine hydrolase inhibitors. *Bioorg Med Chem* 17:6707–6714
155. Bertrand JA, Oleksyszyn J, Kam CM, Boduszek B, Presnell S, Plaskon RR, Suddath FL, Powers JC, Williams LD (1996) Inhibition of trypsin and thrombin by amino(4-amidinophenyl)methanephosphonate diphenyl ester derivatives: X-ray structures and molecular models. *Biochemistry* 35:3147–3155
156. Fusetani N, Matsunaga S, Matsumoto H, Takebayashi Y (1990) Bioactive marine metabolites. 33. Cyclotheonamides, potent thrombin inhibitors, from a marine sponge *Theonella* sp. *J Am Chem Soc* 112:7053–7054
157. Nakao Y, Matsunaga S, Fusetani N (1995) Three more cyclotheonamides C, D, and E, potent thrombin inhibitors from the marine sponge *Theonella swinhoei*. *Bioorg Med Chem* 3:1115–1122

158. Nakao Y, Oku N, Matsunaga S, Fusetani N (1998) Cyclotheonamides E2 and E3, new potent serine protease inhibitors from the marine sponge of the genus *Theonella*. *J Nat Prod* 61: 667–670
159. Murakami Y, Takei M, Shindo K, Kitazume C, Tanaka J, Higa T, Fukamachi H (2002) Cyclotheonamide E4 and E5, new potent tryptase inhibitors from an *Ircinia* species of sponge. *J Nat Prod* 65:259–261
160. Nakao Y, Masuda A, Matsunaga S, Fusetani N (1999) Pseudotheonamides, serine protease inhibitors from the marine sponge *Theonella swinhoei*. *J Am Chem Soc* 121:2425–2431
161. (a) Lee AY, Hagihara M, Karmacharya R, Albers MW, Schreiber SL, Clardy J (1993) Atomic structure of the trypsin cyclotheonamide A complex: lessons for the design of serine protease inhibitors. *J Am Chem Soc* 115:12619–12620; (b) Maryanoff BE, Qiu XY, Padmanabhan KP, Tulinsky A, Almond Jr HR, Andrade-Gordon P, Greco MN, Kauffman JA, Nicolaou KC, Liu A, Brungs PH, Fusetani N (1993) Molecular basis for the inhibition of human α -thrombin by the macrocyclic peptide cyclotheonamide-A. *Proc Natl Acad Sci USA* 90:8048–8052; (c) Greco MN, Maryanoff BE (1997) In: Abell A (ed) *Advances in Amino Acid Mimetics and Peptidomimetics*, vol. 1, JAI Press, Greenwich; (d) Ganesh V, Lee AY, Clardy J, Tulinsky A (1996) Comparison of the structures of the cyclotheonamide A complexes of human α -thrombin and bovine β -trypsin. *Protein Sci* 5:825–835
162. (a) Fusetani N, Nakao Y, Matsunaga S (1991) Bioactive marine metabolites. 39. Nazumamide A, a thrombin-inhibitory Tetrapeptide, from a marine sponge, *Theonella* sp. *Tetrahedron Lett* 32:7073–7074; (b) Hayashi K, Hamada Y, Shioiri T (1992) Synthesis of nazumamide A, a thrombin-inhibitory linear tetrapeptide, from a marine sponge, *Theonella* sp. *Tetrahedron Lett* 33:5075–5076
163. Nienaber VL, Amparo EC (1996) A noncleavable retro-binding peptide that spans the substrate binding cleft of serine proteases. Atomic structure of nazumamide A: human thrombin. *J Am Chem Soc* 118:6807–6810
164. (a) Nakao Y, Matsunaga S, Fusetani N (1993) Toxadocial A: a novel thrombin inhibitor from the marine sponge *Toxadocia cylindrica*. *Tetrahedron Lett* 34:1511–1514; (b) Nakao Y, Matsunaga S, Fusetani N (1993) Toxadocial B, toxadocial C and toxadocial acid A: thrombin-inhibitory aliphatic tetrasulfates from the marine sponge, *Toxadocia cylindrica*. *Tetrahedron* 49:11183–11188
165. (a) Carroll AR, Pierens GK, Fechner G, Leone P, Ngo A, Simpson M, Hyde E, Hooper JNA, Bostrom SL, Musil D, Quinn RJ (2002) Dysinosin A: a novel inhibitor of factor VIIa and thrombin from a new genus and species of Australian sponge of the family Dysideidae. *J Am Chem Soc* 124:13340–13341; (b) Carroll AR, Buchanan MS, Edser A, Hyde E, Simpson M, Quinn RJ (2004) Dysinosins B-D, inhibitors of factor VIIa and thrombin from the Australian sponge *Lamellodysidea chlorea*. *J Nat Prod* 67:1291–1294
166. (a) Murakami M, Ishida K, Okino T, Okita Y, Matsuda H, Yamaguchi K (1995) Aeruginosins 98-A and 98-B, trypsin inhibitors from the blue-green alga *Microcystis aeruginosa* (NIES-98). *Tetrahedron Lett* 36:2785–2788; (b) Matsuda H, Okino T, Murakami M, Yamaguchi K, (1996) Aeruginosins 102-A and B, new thrombin inhibitors from the cyanobacterium *Microcystis viridis* (NIES-102). *Tetrahedron* 46:14501–14506; (c) Ishida K, Okita Y, Matsuda H, Okino T, Murakami M (1999) Aeruginosins, protease inhibitors from the cyanobacterium *Microcystis aeruginosa*. *Tetrahedron* 55:10971–10988
167. Shin HJ, Matsuda H, Murakami M, Yamaguchi K (1997) Aeruginosins 205A and -B, serine protease inhibitory glycopeptides from the cyanobacterium *Oscillatoria agardhii* (NIES-205). *J Org Chem* 62:1810–1813
168. (a) Hanessian S, Ersmark K, Wang X, Valle JRD, Blomberg N, Xue Y, Fjellström O (2007) Structure-based organic synthesis of unusual aeruginosin hybrids as potent inhibitors of thrombin. *Bioorg Med Chem Lett* 17:3480–3485; (b) Ersmark K, Valle JRD, Hanessian S (2008) Chemistry and biology of the aeruginosin family of serine protease inhibitors. *Angew Chem Int Ed* 47:1202–1223

169. Buchanan MS, Carroll AR, Wassling D, Jobling M, Avery VM, Davis RA, Feng Y, Xue Y, Öster L, Fex T, Deinum J, Hooper JNA, Quinn RJ (2008) Clavatadine A, a natural products with selective recognition and irreversible inhibition of factor X_{II}. *J Med Chem* 51: 3583–3587
170. Buchanan MS, Carroll AR, Wassling D, Jobling M, Avery VM, Davis RA, Feng Y, Hooper JNA, Quinn RJ (2009) Clavatadines C-E, guanidine alkaloids from the Australian sponge *Suberea clavata*. *J Nat Prod* 72:973–975
171. Fusetani N, Fujita M, Nakao Y, Matsunaga S (1999) Tokaramide A, a new cathepsin B inhibitor from the marine sponge *Theonella* aff. *mirabilis*. *Bioorg Med Chem Lett* 9:3397–3402
172. (a) Nakao Y, Fujita M, Warabi K, Matsunaga S, Fusetani N (2000) Bioactive marine metabolites. Part 104. Miraziridine A, a novel cysteine protease inhibitor from the marine sponge *Theonella* aff. *mirabilis*. *J Am Chem Soc* 122:10462–10463; (b) Konno H, Kubo K, Makabe H, Toshiro E, Hinoda N, Nosaka K, Akaji K (2007) Total synthesis of miraziridine A and identification of its major reaction site for cathepsin B. *Tetrahedron* 63:9502–9513
173. Murayama S, Nakao Y, Matsunaga S (2008) Asteroperin, an inhibitor of cathepsin B, from the marine sponge *Asteropus simplex*. *Tetrahedron Lett* 49:4186–4188
174. (a) Potts BCM, Faulkner DJ, Chan JA, Simolike GC, Offen P, Hemling ME, Francis TA (1991) Didemnaketals A and B, HIV-1 protease inhibitors from the ascidian *Didemnum* sp. *J Am Chem Soc* 113:6321–6322; (b) Salomon CE, Williams DH, Lobkovsky E, Clardy JC, Faulkner DJ (2002) Relative and absolute stereochemistry of the didemnaketals, metabolites of a Palauan ascidian, *Didemnum* sp. *Org Lett* 4:1699–1702
175. (a) Wang PZ, Tu YQ, Yang L, Dong CZ, Kitching W (1998) Synthetic studies of didemnaketals analogue – construction of the (+)- and (–)-5,6-dihydroxy-3,7-dimethyloctanal intermediates. *Tetrahedron Asymmetry* 9:3789–3795; (b) Jia YX, Wu B, Li X, Ren SK, Tu YQ, Chan ASC, Kitching W (2001) Synthetic studies of the HIV-1 protease inhibitive didemnaketals: stereocontrolled synthetic approach to the key mother spiroketals. *Org Lett* 3:847–849; (c) Jia YX, Li X, Wang PZ, Wu B, Zhao X, Tu Y (2002) Convergent synthesis of the spiroketal core of the HIV-1 protease inhibitors the didemnaketals. *J Chem Soc Perkin Trans 1* 565–570; (d) Jia YX, Li X, Wu B, Zhao XZ, Tu YQ (2002) A convergent synthesis of the spiroketal moiety of the HIV-1 protease inhibitors didemnaketals. *Tetrahedron* 58:1697–1708; (e) Zhao XZ, Tu YQ, Peng L, Li XQ, Jia YX (2004) Synthetic studies of the HIV-1 protease inhibitive didemnaketals: stereocontrolled synthesis of an ester side chain. *Tetrahedron Lett* 45:3713–3716; (f) Zhao XZ, Peng L, Tang M, Tu YQ, Gao SH (2005) Synthetic studies of the HIV-1 protease inhibitive didemnaketals: precise and stereocontrolled synthesis of the key mother spiroketal. *Tetrahedron Lett* 46:6941–6944
176. Fan X, Flentke GR, Rich DH (1998) Inhibition of HIV-1 protease by a subunit of didemnaketals A. *J Am Chem Soc* 120:8893–8894
177. Fujita M, Nakao Y, Matsunaga S, Seiki M, Itoh Y, van Soest RWM, Fusetani N (2001) Ancorinosides B-D, inhibitors of membrane type 1 matrix metalloproteinase (MT1-MMP), from the marine sponge *Penares sollasi* Thiele. *Tetrahedron* 57:1229–1234
178. Ohta S, Ohta M, Ikegami S (1997) Ancorinoside A: a novel tetramic acid glycoside from the marine sponge. *Ancorina* sp. which specifically inhibits blastulation of starfish embryos. *J Org Chem* 62:6452–6453
179. Fujita M, Nakao Y, Matsunaga S, Seiki M, Itoh Y, van Soest RWM, Heubes M, Faulkner DJ, Fusetani N (2001) Isolation and structure elucidation of two phosphorylated sterol sulfates, MT1-MMP inhibitors from a marine sponge *Cribrochalina* sp.: revision of the structures of haplosamates A and B. *Tetrahedron* 57:3885–3890
180. Fujita M, Nakao Y, Matsunaga S, Seiki M, Itoh Y, Yamashita J, van Soest RWM, Fusetani N (2003) Bioactive marine metabolites, Part 124. Ageladine A: an antiangiogenic matrix-metalloproteinase inhibitor from the marine sponge *Agelas nakamurai*. *J Am Chem Soc* 125:15700–15701

181. (a) Meketa ML, Weinreb SM (2006) Total synthesis of ageladine A, an angiogenesis inhibitor from the marine sponge *Agelas nakamurai*. *Org Lett* 8:1443–1446; (b) Shengule SR, Karuso P (2006) Concise total synthesis of the marine natural product ageladine A. *Org Lett* 8:4083–4084; (c) Ando N, Terashima S (2007) Synthesis and matrix metalloproteinase (MMP)-12 inhibitory activity of ageladine A and its analogs. *Bioorg Med Chem Lett* 17:4495–4499; (d) Ando N, Terashima S (2009) Synthesis of novel ageladine A analogs showing more potent matrix metalloproteinase (MMP)-12 inhibitory activity than the natural product. *Bioorg Med Chem Lett* 19:5461–5463
182. Bayle JH, Crabtree GR (1997) Protein acetylation: more than chromatin modification to regulate transcription. *Chem Biol* 4:885–888
183. (a) Sambucetti LC, Fischer DD, Zabludoff S, Kwon PO, Chamberlin H, Trogani N, Xu H, Cohen D (1999) Histone deacetylase inhibition selectively alters the activity and expression of cell cycle proteins leading to specific chromatin acetylation and antiproliferative effects. *J Biol Chem* 274:34940–34947; (b) Sato N, Ohta T, Kitagawa H, Kayahara M, Ninomiya I, Fushida S, Fujimura T, Nishimura G, Shimizu K, Miwa K (2004) FR901228, a novel histone deacetylase inhibitor, induces cell cycle arrest and subsequent apoptosis in refractory human pancreatic cancer cells. *Int J Oncol* 24:679–685
184. (a) Minucci S, Pelicci PG (2006) Histone deacetylase inhibitors and the promise of epigenetic (and more) treatments for cancer. *Nat Rev Cancer* 6:38–51; (b) Han JW, Ahn SH, Park SH, Wang SY, Bae GU, Seo DW, Kwon HK, Hong S, Lee HY, Lee YW, Lee HW (2000) Apicidin, a histone deacetylase inhibitor, inhibits proliferation of tumor cells via induction of p21(WAF1/Cip1) and gelsolin. *Cancer Res* 60:6068–6074; (c) Ju R, Muller MT (2003) Histone deacetylase inhibitors activate p21(WAF1) expression via ATM. *Cancer Res* 63:2891–2897
185. (a) Insinga A, Monestiroli S, Ronzoni S, Gelmetti V, Marchesi F, Viale A, Altucci L, Nervi C, Minucci S, Pelicci PG (2005) Inhibitors of histone deacetylases induce tumor-selective apoptosis through activation of the death receptor pathway. *Nat Med* 11:71–76; (b) Nebbioso A, Clarke N, Voltz E, Germain E, Ambrosino C, Bontempo P, Alvarez R, Sch-avone EM, Ferrara F, Bresciani F, Weisz A, de Lera AR, Gronemeyer H, Altucci L (2005) Tumor-selective action of HDAC inhibitors involves TRAIL induction in acute myeloid leukemia cells. *Nat Med* 11:77–84
186. (a) Munster PN, Troso-Sandoval T, Rosen N, Rifkind R, Marks PA, Richon VM (2001) The histone deacetylase inhibitor suberoylanilide hydroxamic acid induces differentiation of human breast cancer cells. *Cancer Res* 61:8492–8497; (b) Jung M, Brosch G, Kölle D, Scherf H, Gerhäuser C, Loidl P (1999) Amide analogues of trichostatin A as inhibitors of histone deacetylase and inducers of terminal cell differentiation. *J Med Chem* 42:4669–4679
187. Deroanne CF, Bonjean K, Servotte S, Devy L, Colige A, Clausse N, Blacher S, Verdin E, Foidart JM, Nussgens BV, Castronovo V (2002) Histone deacetylases inhibitors as anti-angiogenic agents altering vascular endothelial growth factor signaling. *Oncogene* 21:427–436
188. (a) Piña IC, Gautschi JT, Wang GYS, Sanders ML, Schmitz FJ, France D, Cornell-Kennon S, Sambucetti LC, Remiszewski SW, Perez LB, Bair KW, Crews P (2003) Psammaplins from the sponge *Pseudoceratina purpurea*: inhibition of both histone deacetylase and DNA methyltransferase. *J Org Chem* 68:3866–3873; (b) Godert AM, Angelino N, Woloszynska-Read A, Morey SR, James SR, Karpf AR, Sufrin JR (2006) An improved synthesis of psammaplin A. *Bioorg Med Chem Lett* 16:3330–3333
189. Remiszewski SW, Sambucetti LC, Bair KW, Bontempo J, Cesarz D, Chandramouli N, Chen R, Cheung M, Cornell-Kennon S, Dean K, Diamantidis G, France D, Green MA, Howell KL, Kashi R, Kwon P, Lassota P, Martin MS, Mou Y, Perez LB, Sharma S, Smith T, Sorensen E, Taplin F, Trogani N, Versace R, Walker H, Weltchek-Engler S, Wood A, Wu A, Atadja P (2003) *N*-hydroxy-3-phenyl-2-propenamides as novel inhibitors of human histone deacetylase with in vivo antitumor activity: discovery of (2*E*)-*N*-hydroxy-3-[4-[(2-hydroxyethyl)[2-(1*H*-indol-3-yl)ethyl]amino]methyl]-phenyl]-2-propenamide (NVP-LAQ824). *J Med Chem* 46:4609–4624

190. Simmons TL, Andrianasolo E, Mcphail K, Flatt P, Gerwick W (2005) Marine natural products as anticancer drugs. *Mol Cancer Ther* 4:333–342
191. Oku N, Nagai K, Terada Y, van Soest RWM, Matsunaga S, Fusetani N (2004) Three new cyclostellletamines, which inhibit histone deacetylase, from a marine sponge of the genus *Xestospongia*. *Bioorg Med Chem Lett* 14:2617–2620
192. (a) Nakao Y, Yoshida S, Matsunaga S, Shindoh N, Terada Y, Nagai K, Yamashita JK, Ganesan A, van Soest RWM, Fusetani N (2006) Azumamides A-E: histone deacetylase inhibitory cyclic tetrapeptides from the marine sponge *Mycale izuensis*. *Angew Chem Int Ed* 45:7553–7557; (b) Izzo I, Maulucci N, Bifulco G, De Riccardis F (2006) Total synthesis of azumamides A and E. *Angew Chem Int Ed* 45:7557–7560
193. Fusetani N, Sugano M, Matsunaga S, Hashimoto K (1987) (+)-Curcuphenol and dehydrocurcuphenol, novel sesquiterpenes which inhibit H,K-ATPase, from a marine sponge *Epipolasis* sp. *Experientia* 43:1234–1235
194. McEnroe FJ, Fenical W (1978) Structures and synthesis of some new antibacterial sesquiterpenoids from gorgonian coral *Pseudopterogorgia rigida*. *Tetrahedron* 34:1661–1664
195. Fusetani N, Sugano M, Matsunaga S, Hashimoto K, Shikama H, Ohta A, Nagano H (1987) Isolation of a hexaprenylhydroquinone sulfate from the marine sponge *Dysidea* sp. as an H, K-ATPase inhibitor. *Experientia* 43:1233–1234
196. Sata NU, Sugano M, Matsunaga S, Fusetani N (1999) Bioactive marine metabolites – Part 88 – Sinulamide: an H,K-ATPase inhibitor from a soft coral *Sinularia* sp. *Tetrahedron Lett* 40:719–722
197. (a) Nakamura H, Wu H, Ohizumi Y, Hirata Y (1984) Agelasines A, B, C and D, novel bicyclic diterpenoids with a 9-methyladeninium unit possessing inhibitory effects on Na,K-ATPase from the Okinawan sea sponge *Agelas* sp. *Tetrahedron Lett* 25:2989–2992; (b) Wu H, Nakamura H, Kobayashi J, Ohizumi Y, Hirata Y (1984) Agelasines E and F, novel monocyclic diterpenoids with a 9-methyladeninium unit possessing inhibitory effects on Na, K-ATPase isolated from the Okinawan sea sponge *Agelas nakamurai* Hoshino. *Tetrahedron Lett* 25:3719–3722; (c) Wu H, Nakamura H, Kobayashi J, Kobayashi M, Ohizumi Y, Hirata Y, (1986) Physiologically active marine natural products from porifera. 12. Structures of agelasines, diterpenes having a 9-methyladeninium chromophore isolated from the Okinawan marine sponge *Agelas nakamurai* Hoshino. *Bull Chem Soc Jpn* 59:2495–2504
198. Nakamura H, Wu H, Kobayashi J, Kobayashi M, Ohizumi Y, Hirata Y (1985) Agelasidines – novel hypotaurocyamine derivatives from the Okinawan sea sponge *Agelas nakamurai* Hoshino. *J Org Chem* 50:2494–2497
199. Okamoto Y, Ojika M, Sakagami Y (1999) Iantheran A, a dimeric polybrominated benzofuran as a Na,K-ATPase inhibitor from a marine sponge, *Ianthella* sp. *Tetrahedron Lett* 40:507–510
200. Okamoto Y, Ojika M, Kato S, Sakagami Y (2000) Ianthesines A-D, four novel dibromotyrosine-derived metabolites from a marine sponge, *Ianthella* sp. *Tetrahedron* 56:5813–5818
201. Nakamura H, Kobayashi J, Kobayashi M, Ohizumi Y, Hirata Y (1985) Physiologically active marine natural product from Porifera.7. Xestoquinone: a novel cardiotonic marine natural product isolated from the Okinawan sea sponge *Xestospongia sapra*. *Chem. Lett* 713–716
202. (a) Kobayashi M, Shimizu N, Kyogoku Y, Kitagawa I (1985) Halenaquinol and halenaquinol sulfate, pentacyclic hydroquinones from the Okinawan marine sponge *Xestospongia sapra*. *Chem Pharm Bull* 33:1305–1308; (b) Kobayashi M, Shimizu N, Kitagawa I, Kyogoku Y, Harada N, Uda H (1985) Absolute stereostructures of halenaquinol and halenaquinol sulfate, pentacyclic hydroquinones from the Okinawan marine sponge *Xestospongia sapra*, as determined by theoretical calculation of CD spectra. *Tetrahedron Lett* 26:3833–3836
203. Gorshkova IA, Gorshkov BA, Fedoreev SA, Shestak OP, Novikov VL, Stonik VA (1999) Inhibition of membrane transport ATPases by halenaquinol, a natural cardioactive pentacyclic hydroquinone from the sponge *Petrosia seriata*. *Comp Biochem Physiol* C 122:93–99

204. Stonik VA, Makarieva TN, Dmitrenok AS (1992) Sarcochromenol sulfate A, sarcochromenol sulfate B, sarcochromenol sulfate C, and sarcohydroquinone sulfate A, sarcohydroquinone sulfate B, sarcohydroquinone sulfate C, new natural products from the sponge *Sarcotragus spinulosus*. *J Nat Prod* 55:1256–1260
205. Kalaitzis JA, Leone PD, Harris L, Butler MS, Ngo A, Hooper JNA, Quinn RJ (1999) Adociasulfates 1, 7, and 8: new bioactive hexaprenoid hydroquinones from the marine sponge *Adocia* sp. *J Org Chem* 64:5571–5574
206. (a) Erickson KL, Beutler JA, Cardellina II JH, Boyd MR (1997) Salicylihalamides A and B, novel cytotoxic macrolides from the marine sponge *Haliclona* sp. *J Org Chem* 62:8188–8192; (b) Erickson KL, Beutler JA, Cardellina II JH, Boyd MR (2001) Salicylihalamides A and B, novel cytotoxic macrolides from the marine sponge *Haliclona* sp. *J Org Chem* 66:1532–1532
207. (a) Galinis DL, McKee TC, Pannell LK, Cardellina II JH, Boyd MR (1997) Lobatamides A and B, novel cytotoxic macrolides from the tunicate *Aplidium lobatum*. *J Org Chem* 62:8968–8969; (b) McKee TC, Galinis DL, Pannell LK, Cardellina II JH, Laakso J, Ireland CM, Murray L, Capon RJ, Boyd MR (1998) The lobatamides, novel cytotoxic macrolides from southwestern Pacific tunicates. *J Org Chem* 63:7805–7810
208. Suzumura K, Takahashi I, Matsumoto H, Nagai K, Setiawan B, Rantiatmodjo RM, Suzuki K, Nagano N (1997) Structural elucidation of YM-75518, a novel antifungal antibiotic isolated from *Pseudomonas* sp. Q38009. *Tetrahedron Lett* 38:7573–7576
209. (a) Boyd MR, Farina C, Belfiore P, Gagliardi S, Kim JW, Hayakawa Y, Beutler JA, McKee TC, Bowman BJ, Bowman EJ (2001) Discovery of a novel antitumor benzolactone enamide class that selectively inhibits mammalian vacuolar-type (H⁺)-ATPases. *J Pharmacol Exp Ther* 297:114–120; (b) Wu Y, Liao X, Wang R, Xie XS, De Brabander JK (2002) Total synthesis and initial structure-function analysis of the potent V-ATPase inhibitors salicylihalamide A and related compounds. *J Am Chem Soc* 124:3245–3253; (c) Shen RC, Lin CT, Bowman EJ, Bowman BJ, Porco Jr. JA (2003) Lobatamide C: total synthesis, stereochemical assignment, preparation of simplified analogues, and V-ATPase inhibition studies. *J Am Chem Soc* 125:7889–7901
210. Diyabalanage T, Amsler CD, McClintock JB, Baker BJ (2006) Palmerolide A, a cytotoxic macrolide from the Antarctic tunicate *Synicum adareanum*. *J Am Chem Soc* 128:5630–5631
211. Lebar MD, Baker BJ (2007) On the stereochemistry of palmerolide A. *Tetrahedron Lett* 48:8009–8010
212. (a) Nicolaou KC, Guduru R, Sun YP, Banerji B, Chen DYK (2007) Total synthesis of the originally proposed and revised structures of palmerolide A. *Angew Chem Int Ed* 46:5896–5900; (b) Nicolaou KC, Sun YP, Guduru R, Banerji B, Chen DYK (2007) Total synthesis of the originally proposed and revised structures of palmerolide A and isomers thereof. *J Am Chem Soc* 130:3633–3644
213. Nicolaou KC, Leung GYC, Dethe DH, Guduru R, Sun YP, Lim CS, Chen DYK (2007) Chemical synthesis and biological evaluation of palmerolide A analogues. *J Am Chem Soc* 130:10019–10023
214. Chan GW, Francis T, Thureen DR, Offen PH, Pierce NJ, Westley JW, Johnson RK, Faulkner DJ (1993) Purpurone, an inhibitor of ATO citrate lyase: a novel alkaloid from the marine sponge *Iotrochota* sp. *J Org Chem* 58:2544–2546
215. Kobayashi J, Hirase T, Shigemori H, Ishibashi M, Bae MA, Tsuji T, Sasaki T (1992) New pentacyclic compounds from the Okinawan marine sponge *Xestospongia sapra*. *J Nat Prod* 55:994–998
216. Carney JR, Scheuer PJ, Kelly-Borges M (1993) Makaluvamine B, a cytotoxic pigment from an Indonesian sponge *Histodermella* sp. *Tetrahedron* 49:8483–8486
217. Ojika M, Yoshino G, Sakagami Y (1997) Novel ceramide 1-sulfates, potent DNA topoisomerase I inhibitors isolated from the Bryozoa *Watersipora cucullata*. *Tetrahedron Lett* 38:4235–4238

218. (a) Nemoto T, Ojika M, Sakagami Y (1997) Amphimic acids, novel unsaturated C28 fatty acids as DNA topoisomerase I inhibitors from an Australian sponge *Amphimedon* sp. *Tetrahedron Lett* 38:5667–5670; (b) Nemoto T, Yoshino G, Ojika M, Sakagami Y (1997) Amphimic acids and related long-chain fatty acids as DNA topoisomerase I inhibitors from an Australian sponge, *Amphimedon* sp: isolation, structure, synthesis, and biological evaluation. *Tetrahedron* 53:16699–16710
219. Copp BR, Ireland CM (1991) Wakayin: a novel cytotoxic pyrroloiminoquinone alkaloid from the ascidian *Clavelina* species. *J Org Chem* 56:4596–4597
220. Radisky DC, Radisky ES, Barrows LR, Copp BR, Kramer RA, Ireland CM (1993) Novel cytotoxic topoisomerase II inhibiting pyrroloiminoquinones from Fijian sponges of the genus *Zyzzya*. *J Am Chem Soc* 115:1632–1638
221. Venables DA, Concepción GP, Matsumoto SS, Barrow LR, Ireland CM (1997) Makaluvamine N: a new pyrroloiminoquinone from *Zyzzya fuliginosa*. *J Nat Prod* 60:408–410
222. Schmidt EW, Harper MK, Faulkner DJ (1995) Makaluvamines H-M and damirone C from the Pohnpei sponge *Zyzzya fuliginosa*. *J Nat Prod* 58:1861–1867
223. Foderaro TA, Barrows LR, Lassota P, Ireland CM (1997) Bengacarboline, a new beta-carboline from a marine ascidian *Didemnum* sp. *J Org Chem* 62:6064–6065
224. (a) Cooray NM, Scheuer PJ, Parkanyi I, Clardy J (1988) Shermilamine A: a pentacyclic alkaloid from a tunicate. *J Org Chem* 53:4619–4620; (b) Carroll AR, Cooray NM, Pointer A, Scheuer PJ (1989) A second shermilamine alkaloid from a tunicate *Trididemnum* sp. *J Org Chem* 54:4231–4232
225. Kobayashi J, Cheng J, Nakamura H, Ohizumi Y, Hirata Y, Sasaki T, Ohta T, Nozoe S (1988) Ascididemin, a novel pentacyclic aromatic alkaloid with potent antileukemic activity from the Okinawan tunicate *Didemnum* sp. *Tetrahedron Lett* 29:1177–1180
226. Schmitz FJ, DeGuzman FS, Hossain MB, van der Helm D (1991) Cytotoxic aromatic alkaloids from the ascidian *Amphicarpa meridiana* and *Leptoclinides* sp.: Meridine and 11-hydroxyascididemin. *J Org Chem* 56:804–808
227. McDonald LA, Eldredge GS, Barrows LR, Ireland CM (1994) Inhibition of topoisomerase II catalytic activity by pyridoacridine alkaloids from a *Cystodytes* sp. ascidian: a mechanism for the apparent intercalator-induced inhibition of topoisomerase II. *J Med Chem* 37:3819–3827
228. Carney JR, Scheuer PJ (1993) Popolohuanone E, a topoisomerase II inhibitor with selective lung tumor cytotoxicity from the pohnpei sponge *Dysidea* sp. *Tetrahedron Lett* 34:3727–3730
229. Hamann MT, Scheuer PJ, Kelly-Borges M (1993) Biogenetically diverse, bioactive constituents of a sponge, order Verongida: bromotyramines and sesquiterpene-shikimate derived metabolites. *J Org Chem* 58:6565–6569
230. Juagdan EG, Kalidindi RS, Scheuer PJ, Kelly-Borges M (1995) Elenic acid, an inhibitor of topoisomerase II, from a sponge, *Plakinastrella* sp. *Tetrahedron Lett* 36:2905–2908
231. Baz JP, Cañedo LM, Tapiolas D (1996) A new tetraprenylhydroquinone derivative with an acetic acid unit from the marine sponge *Ircinia muscarum*. *J Nat Prod* 59:960–961
232. Carney JR, Scheuer PJ (1993) A new bastadin from the sponge *Psammaphysilla purpurea*. *J Nat Prod* 56:153–157
233. Carroll AR, Feng YJ, Bowden BF, Coll JC (1996) Studies of Australian ascidians. 5. Virenarnides A-C, new cytotoxic linear peptides from the colonial didemnid ascidian *Diplosoma virens*. *J Org Chem* 61:4059–4061

Fluorescent Proteins from the Oceans: Marine Macromolecules as Advanced Imaging Tools for Biomedical Research

24

Edward G. Smith, Cecilia D'Angelo, Franz Oswald,
G. Ulrich Nienhaus, and J. Wiedenmann

Contents

24.1	Introduction	1232
24.2	Sources of GFP-like Proteins	1233
24.3	Structural Aspects of GFP-like Proteins	1235
24.3.1	The Three-Dimensional Structure	1235
24.3.2	Chromophore Structures	1236
24.4	Isolation of Novel GFP-like Proteins	1239
24.5	Applications of Fluorescent Proteins from Marine Invertebrates	1242
24.5.1	Gene Expression	1243
24.5.2	Labeling of Proteins and Subcellular Compartments	1243
24.5.3	Protein–Protein Interactions	1246
24.5.4	Sensors	1246
24.6	Photoactivatable GFP-like Proteins (PAFPs)	1247
24.6.1	Pulse-Chase Experiments	1248
24.6.2	Super-Resolution Microscopy	1248

E.G. Smith • C. D'Angelo • J. Wiedenmann (✉)

National Oceanography Centre Southampton, University of Southampton, European Way,
Southampton, UK

e-mail: e.smith@soton.ac.uk, C.D'angelo@soton.ac.uk, joerg.wiedenmann@noc.soton.ac.uk

F. Oswald

Department of Internal Medicine I, University of Ulm, Albert-Einstein-Allee 23, Ulm, Germany

e-mail: franz.oswald@uni-ulm.de

G.U. Nienhaus

Center for Functional Nanostructures, Karlsruhe Institute of Technology, Wolfgang-Gaede-Str. 1 a,
Karlsruhe, Germany

and

Department of Physics, University of Illinois at Urbana-Champaign, 1110 West Green Street,
Urbana, IL, USA

e-mail: uli@uiuc.edu

E. Fattorusso, W. H. Gerwick, O. Taglialatela-Scafati (eds.),

Handbook of Marine Natural Products, DOI 10.1007/978-90-481-3834-0_24,

© Springer Science+Business Media B.V. 2012

1231

24.7 Conclusion 1251

24.8 Study Questions 1252

References 1252

Abstract

Fluorescent proteins (FPs) of the green fluorescent protein (GFP)-like protein family are not only responsible for the spectacular colors of some reef corals, but they can be also found in several other marine invertebrate taxa. The chromophore of these proteins resides in the center of an 11-stranded β -barrel and is formed by autocatalytic reactions in the presence of oxygen. In some proteins, photochemical reactions are involved in the maturation of the chromophore. The variability of the chromophore structures and the interactions with the surrounding protein scaffold are responsible for the diverse emission colors, ranging from cyan to green and yellow to red. FPs develop their fluorescence also upon expression in recombinant cells which allows their use as genetically encoded markers. Application examples include the labeling of cells, cellular compartment or proteins, studies of gene activity, and sensor studies. Recently, photoactivatable FPs enabled live-cell imaging with a resolution beyond the diffraction barrier of optical microscopy. Nevertheless, before their potential as advanced markers can be fully exploited, FPs often need to undergo extensive protein engineering to alter some detrimental properties such as the tendency to form stable multimers.

24.1 Introduction

Fluorescent proteins have become an indispensable component of the biomedical imaging toolbox [15, 51, 103]. The first representative of this protein family, the green fluorescent protein (GFP), emerged from a study of bioluminescence in the hydrozoan *Aequorea victoria* by Osamu Shimomura and colleagues [77]. Further studies of bioluminescent cnidarians identified more GFPs from marine bioluminescent organisms such as the seapen *Renilla* and hydrozoan polyp *Obelia* [52, 53]. In bioluminescent cnidarians, GFP acts as secondary emitter in the bioluminescence reaction during which the chromophore of GFP is excited as result of a radiationless energy transfer from the photoprotein aequorin [52, 54]. Shimomura and colleagues were the first to propose the structure of the GFP chromophore [13, 76].

It took about 30 years from the discovery of GFP until the potential of this protein as a genetically encoded fluorescence marker was fully realized. The first important step towards its application as an imaging tool was the cloning of GFP-encoding DNA by Prasher et al. [66]. Subsequently, Chalfie and coworkers succeeded in expressing the protein functionally in the nematode worm *Caenorhabditis elegans* [9]. These groundbreaking studies transformed GFP from a scientifically interesting marine pigment to a fluorescence marker with enormous application and commercial potential. Studies soon thereafter began to focus on engineering of the GFP to provide new colors and to render the protein more suitable

for cellular imaging applications, for instance, by enhancing its brightness or by producing blue, cyan, and yellow variants [86]. The tremendous impact of GFP technology on life science research was recognized by the award of the 2008 Nobel Prize for Chemistry to Osamu Shimomura, Martin Chalfie, and Roger Tsien [15, 55].

Despite extensive efforts to create novel color variants of GFP, red fluorescent proteins (RFPs) appeared elusive during the early years of GFP research [47]. These longer wavelength markers are particularly desirable for imaging applications because of reduced cellular autofluorescence in this spectral region, reduced phototoxicity of the excitation light, and the better penetration of long wavelength light in tissue [103]. Furthermore, RFPs were in demand for novel fluorescence resonance energy transfer (FRET) applications [17, 32].

Ultimately, it was nature that provided the first sources of RFPs. The search for natural FPs had originally focused on bioluminescent organisms as the discovery of GFPs in these animals suggested a strict coupling of FPs to bioluminescence reaction. Contrary to this common notion, Wiedenmann [96] proposed the existence of red-emitting GFP-like proteins and nonfluorescent homologues in the sea anemone *Anemonia sulcata* and other cnidarians [96]. Subsequent studies confirmed the presence of GFP-like proteins in numerous nonbioluminescent anthozoans [18, 43, 99, 100] while uncovering the RFPs DsRed and eqFP611; the latter being the natural RFP with the most red-shifted emission [43, 100]. These studies revealed nonbioluminescent anthozoans as a rich source of natural FPs, giving access to a broad palette of emission colors [56]. In particular, the diversity of RFPs among anthozoans was exploited to create advanced marker proteins with optimized biochemical and spectral properties [8, 32, 36, 72].

Interestingly, anthozoans, especially reef corals, harbor a variety of photoactivatable FPs (PAFPs) [3, 4, 37, 40, 61, 101]. While the basic chromophore forms in an autocatalytic reaction as in GFP from *Aequorea victoria*, the final emission color is determined by the exposure to distinct light quantities and qualities [56]. The chromoprotein asulCP (synonym asFP595), for instance, combines reversible “on”/“off” switching of red fluorescence in response to alternating irradiation with low intensities of green and blue light with an irreversible “on” switching under high levels of green light [5]. In contrast, photoconvertible FPs such as Kaede and EosFP first develop a green fluorescent chromophore that is irreversibly converted into a red fluorescent state under illumination with violet light [57]. PAFP have a high application potential as markers in pulse-chase experiments, whereby the fate of a certain subset of labeled cells or cellular components can be monitored independently by selective excitation after targeted photoactivation [97]. Moreover, photoactivatable proteins were key tools in the realization of imaging concepts that enable light microscopy with a resolution beyond the diffraction barrier [6, 28].

24.2 Sources of GFP-like Proteins

The first GFP was found in the bioluminescent hydromedusa *A. victoria* [77]; subsequent studies discovered GFPs also in other bioluminescent organisms

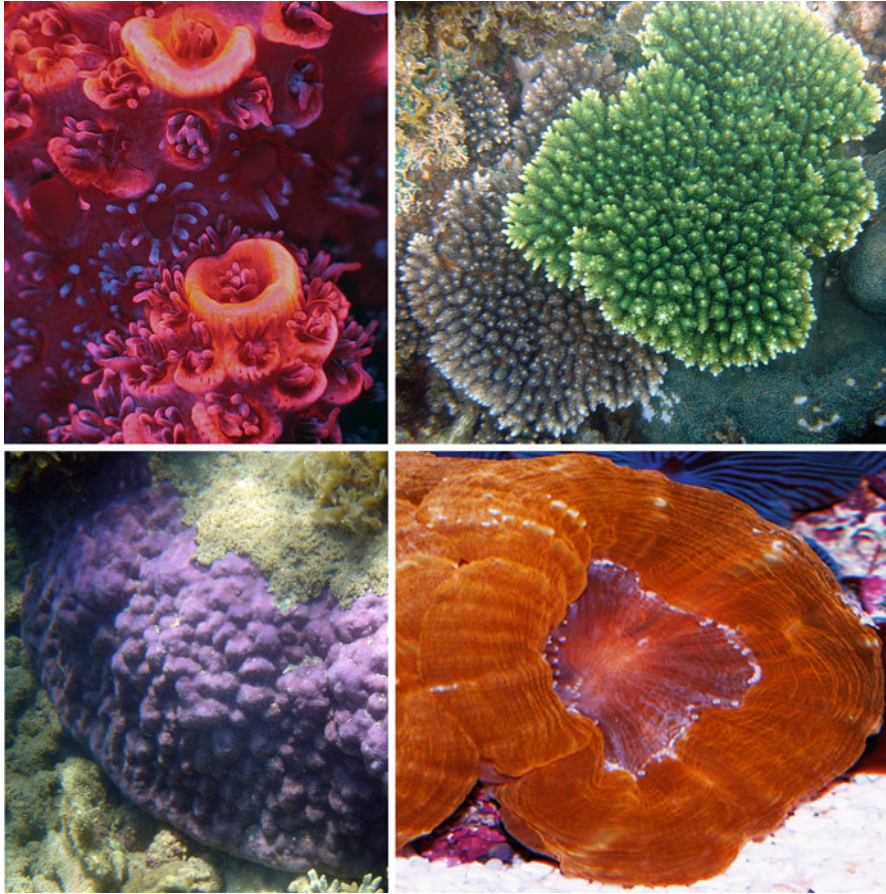


Fig. 24.1 Sources of GFP-like proteins. Anthozoa, particularly scleractinian corals, harbor a huge variety of GFP-like proteins. *Left panel:* Localization of red and cyan fluorescent proteins in the tissue of *Acropora millepora*. Fluorescence was excited under the microscope and photographed through a dual bandpass filter. The emission of cyan fluorescent protein appears blue under these conditions. *Upper right panel:* Color polymorphism among *Acropora* sp. GFPs lend the green color to the upper colony, whereas the dominant brown tones of the lower colony are caused by the photosynthetic pigments of symbiotic alga (zooxanthellae). *Lower left panel:* The purple color of the *Porites* sp. colony is due to high-level expression of a nonfluorescent, GFP-like chromoprotein. *Lower right panel:* The orange colour of *Lobophyllia hemprichii* is produced by a green-to-red photoconvertible protein

including *Renilla* and *Obelia* [52, 53]. The studies of FPs in anthozoans showed that FPs are expressed throughout all major taxa of the anthozoans including sea anemones, corals, ceriantharians, octocorals, and disk anemones (Fig. 24.1). The GFP-like pigments in these organisms show emission colors ranging from cyan green over yellow to red [56]. Some individuals also contain chromoproteins (CPs), yet another subpopulation within the family of GFP-like proteins which are intensely colored but essentially nonfluorescent [40, 67]. In fact, several

anthozoans, particularly corals, express more than five different GFP-like proteins within a single individual [14, 99]. Different expression levels of both FPs and CPs are primarily responsible for the color polymorphism that can be frequently observed among reef-building corals (scleractinia) and sea anemones (Actiniaria) [38, 61, 98]. Fluorescent proteins are often present in the tentacles and in other light-exposed body parts of corals and sea anemones [38, 98]. This can be partially explained by the finding that numerous FP- or CP-encoding genes are upregulated in response to elevated light intensities in their habitat. In this context, D'Angelo et al. found that blue light is most effective in regulating the tissue content of GFP-like proteins [14]. However, several species of sea anemones and corals show a constitutive high-level expression of CPs or FPs that is only minimally or not at all regulated by the environmental light [33, 61]. Taxonomic variability is also found concerning the tissue in which the proteins are expressed. In *Anemonia sulcata*, expression is limited to ectodermal cells, whereas both *Lobophyllia hemprichii* and *Montastrea cavernosa* express FPs in ectodermal and gastrodermal cells [38, 99]. GFP-like proteins may contribute up to 14% of the total soluble protein content in the tissue [37]. However, the slow turnover of these proteins facilitates the maintenance of such high tissue concentration [37].

GFP-like proteins are not only confined to the taxon Cnidaria, but have also been identified in other phyla such as Ctenophora, Crustacea, and even Chordata [16, 25, 71]. Interestingly, a non-fluorescent, colorless structural homologue of GFP, the G2 domain of the extracellular matrix protein nidogen, is present even in mammals [29].

While FPs have been found in a range of organisms other than anthozoans, this animal group remains the most promising source for novel marker proteins due to the vast diversification that the GFP homologues experienced in the course of the evolution of this taxon.

24.3 Structural Aspects of GFP-like Proteins

24.3.1 The Three-Dimensional Structure

GFP-like proteins have a distinct structure comprising of an 11-stranded β -barrel with a helix running along the central axis of the protein [56, 105]. Close to the geometric center of the molecule, the central helix is interrupted by the chromophore (Fig. 24.2). The chromophore is formed from a tripeptide sequence in an autocatalytic reaction in the presence of molecular oxygen [27]. The chromophore is primarily responsible for the spectral characteristics of the GFP-like proteins, with the wavelength of absorption and emission increasing with the number of the conjugated π bonds [69]. Interactions with adjacent amino acids, however, can shift the absorbance and emission spectra by up to 20 nm [69].

GFP exists in a predominantly monomeric form at concentrations below 1 mg/mL [95]. In contrast, GFP from *Renilla* exists as a stable dimer [95]. Most anthozoan FPs form tight tetrameric assemblages, although a number of dimeric variants have also been described in corals and sea anemones [57, 59, 60] (Fig. 24.2).

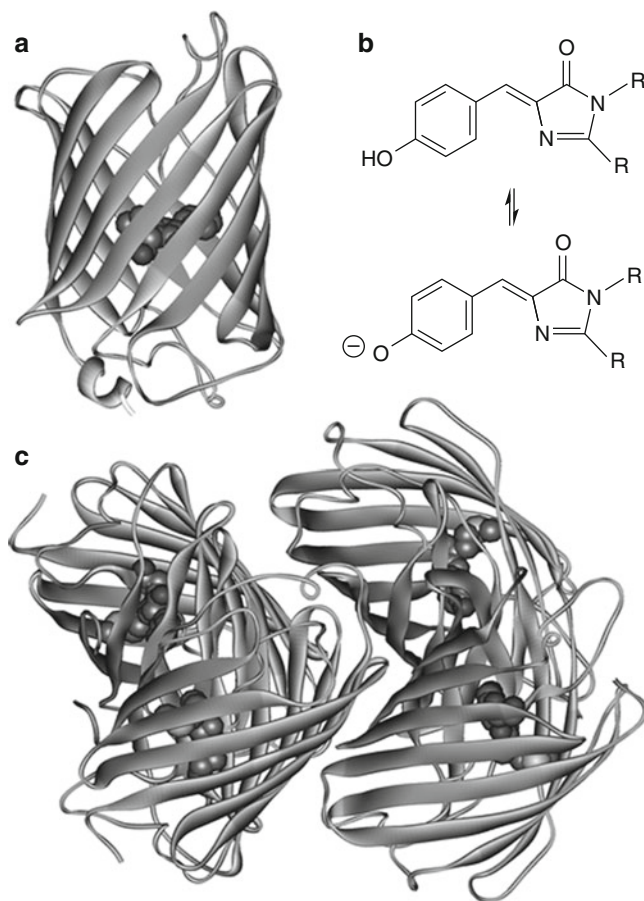


Fig. 24.2 Structural aspects of GFP-like proteins. (a) Ribbon diagram of GFP exhibiting the arrangement of the 11 β -sheets around the central helix. The position of the chromophore in the center of the molecule is represented by Van der Waals spheres. (b) The p-HBI chromophore of GFP in its neutral (maximal absorption at 395 nm; *upper structure*) and deprotonated state (maximal absorption at 475 nm; *lower structure*). (c) Typical assembly of protomers in a tetramer of an anthozoan FP as “dimers of dimers.” The β -can fold of GFP is highly conserved

24.3.2 Chromophore Structures

The amino acid triad that forms the GFP chromophore, Ser65-Tyr66-Gly67, undergoes a three-step process of cyclization, dehydration, and oxidation to form the functional chromophore [78]. Firstly, the amide of Gly67 attacks the carbonyl of Ser65 to form imidazole. Dehydration converts the imidazole to imidazolinone and subsequent oxidation of the $C\alpha$ - $C\beta$ bond of Tyr66 extends the conjugated π electron system from the imidazolinone to the aromatic group of Tyr66 to yield the final 4-(p-hydroxybenzylidene)-5-imidazolinone (p-HBI) chromophore [78].

The GFP chromophore features two states depending on the protonation of the hydroxybenzyl group (Fig. 24.2). The neutral (protonated) chromophore absorbs maximally at 395 nm, whereas the anionic (deprotonated) form is excited best by blue light at 475 nm [86]. The interesting phenomenon that both states emit mostly green fluorescence can be explained by an excited-state proton transfer that occurs upon excitation of the neutral chromophore [10].

The color diversity of natural FPs is derived from modifications of the green fluorescent p-HBI chromophore (Fig. 24.3), which is considered to be the ancestral form [2]. In the following paragraphs, an overview of the chromophore types responsible for the different photophysical properties of GFP-like proteins will be presented.

24.3.2.1 Cyan/Green Emission

Cyan/green emission of GFP-like proteins results from p-HBI chromophores [59, 60]. Emission maxima of cyan/green FPs have been recorded in the range from 470 to 520 nm [2]. The cyan FPs (CFPs) are characterized by wider excitation/emission bands and larger Stokes shifts compared to the green FPs [2]. The chromophore environment plays an important role in the spectral properties of these proteins. For example, it is responsible for the blue shift in the CFP emission relative to GFP. Fluorescence of both the anionic and the neutral forms of the chromophore are observed in some members of this group, for instance, in asFP499 [60] (Fig. 24.3).

24.3.2.2 Yellow Emission

To date, only two naturally occurring yellow FPs have been discovered, phiYFP [71] and zFP538 [43] (Fig. 24.3). These two proteins have an emission maxima of 537 and 538 nm and excitation maxima of 525 and 528 nm, respectively. They achieve yellow fluorescence through different modifications of the p-HBI chromophore. The yellow fluorescence of zFP538 results from a three-ringed chromophore, whereas phiYFP's fluorescence results from π -stacking interactions of the tyrosyl moiety of p-HBI with the chromophore environment [65].

24.3.2.3 Red Emission

Numerous natural orange/red FPs have been identified, and many more engineered, with emission wavelengths up to 611 nm (Table 24.1) [56, 100]. There are two classes of red fluorescent proteins, distinguished by the pathway in which the red fluorescent chromophore is achieved. Each class is named after the protein for which the type of chromophore was described: DsRed-type chromophores and Kaede/EosFP-type chromophores.

Maturation of the DsRed-type chromophore begins with the formation of the neutral chromophore. At this point, the chromophore can follow one of two possible pathways. There have been different pathways proposed for the formation of the mature red chromophore but both acknowledge that it is a result of the formation of a double bond between the C(α) and the amide N of Gln66 [82, 89]. DsRed-type chromophores usually adopt a *cis* conformation [106] (Fig. 24.3). An exception is eqFP611 in which the red-shifted natural emission is produced by a DsRed-type chromophore in *trans* conformation [64] (Fig. 24.3).

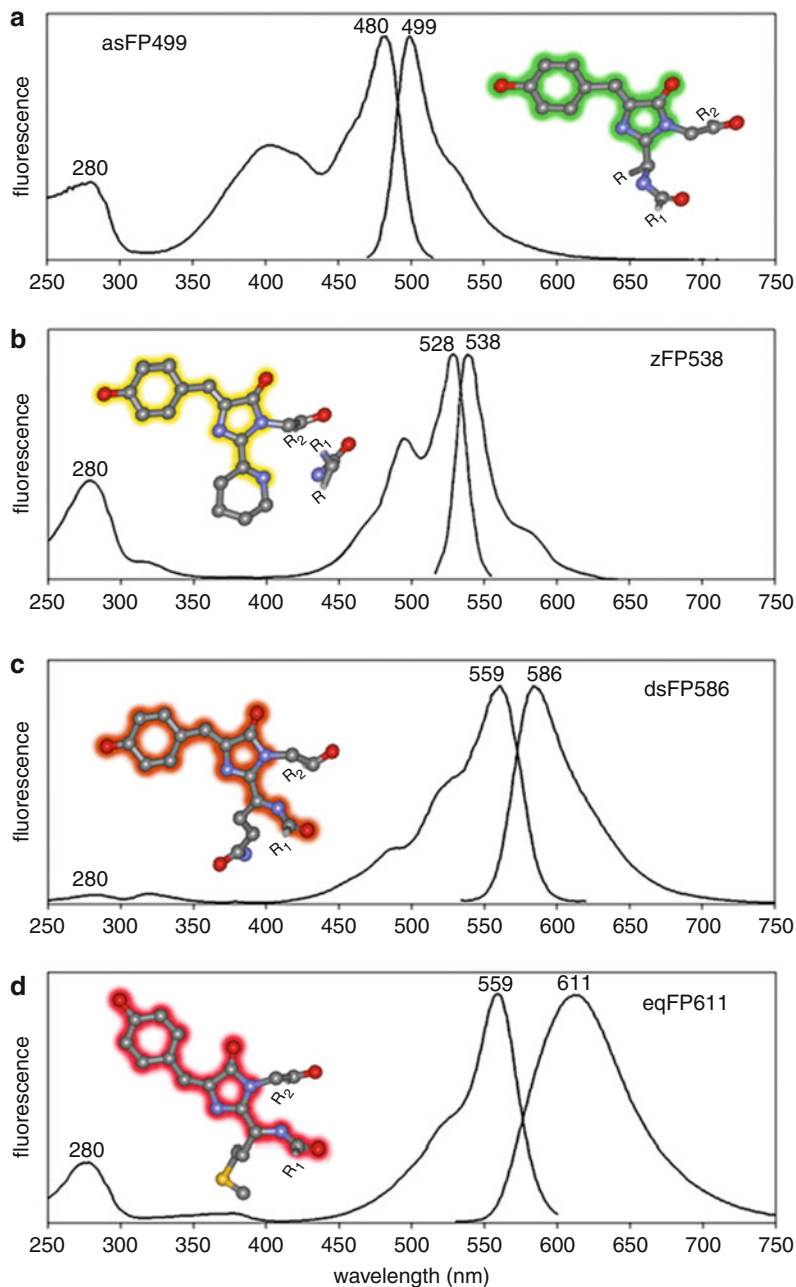


Fig. 24.3 Chromophore structures of major FP color classes. Excitation and emission spectra are shown with the position of the peak maxima in (nm) indicated above the peaks. Structural models of the different chromophore types were constructed using representative GFP-like proteins (protein data bank code A: 1W7S, B: 2OGR, C: 1GGX, D: 3E5T). The extension of the conjugated

Once expressed in cells, both Kaede, EosFP, and related proteins form a green fluorescent p-HBI chromophore that exists predominantly in the deprotonated state [57, 101]. However, illumination of the neutral p-HBI chromophore with violet light (~ 390 nm) causes cleavage of the peptide backbone at the $N\alpha$ – $C\alpha$ bond of the first chromophore-forming residue, which is always a histidine in these photoconvertible proteins [3, 61, 101]. The red emission arises from the extension of the conjugated π -electron system into the imidazole group of the histidine [50].

24.3.2.4 Chromoproteins

Nonfluorescent chromoproteins absorb between ~ 550 and ~ 600 nm and are characterized by purple, lilac, and blue hues [14]. Emission is virtually absent from the chromoproteins. However, a chromoprotein from the sea anemone *Anemonia sulcata* becomes brightly fluorescent upon intense green-light irradiation [40]. The absence of fluorescence in chromoproteins is attributed to the nonplanarity and *trans* conformation of the DsRed-type chromophore [67, 68].

24.4 Isolation of Novel GFP-like Proteins

Anthozoans are currently considered to be the most promising source of novel marker proteins because of the vast diversification of these proteins within this taxon [2]. This notion is supported by the numerous anthozoan proteins that have been already rendered into valuable imaging tools [103]. The wide taxonomic distribution of GFP-like proteins, however, suggests that pigment proteins can be discovered from virtually any taxonomic group. Therefore, broad screening might yield further variants with new properties. The spectral properties of the organism can be used to guide the choice for subsequent analysis. It is important to note, though, that many variants are expressed at very low levels and might be difficult to detect, especially in the presence of high levels of GFP-like protein with different spectral properties. The discovery of eqFP611 is an example for which an analysis of the whole complement of pigments in a heterologous system helped identify underrepresented variants with interesting properties [100]. As exemplified by EosFP, the proteins can exist in a mature state in the source organism, and the photochemical reactions that make them interesting as marker proteins may not be easily detected [101]. Prior to the selection of an organism, tests on the tissue extract with organic solvents can help prevent nonprotein pigments becoming the subject of unsuccessful cloning attempts [102].

The cloning of the gene coding for a protein of interest begins with the creation of a cDNA library. The library can subsequently be probed for the presence of the



Fig. 24.3 (continued) π -bond system is marked by colors symbolizing the emission color. (a) asFP499: The secondary excitation maximum at ~ 400 nm of the cyan-green FP results from the neutral p-HBI chromophore undergoing excited-state proton transfer. (b) The chromophore of the yellow fluorescent zFP538 features a 3-ring structure. (c) The DsRed-type chromophore of dsFP586 is extended along the peptide backbone. (d) The red-shifted emission of eqFP611 is associated with a DsRed-type chromophore adopting a *cis* conformation

Table 24.1 Properties of engineered orange-red-emitting FPs derived from cnidarian pigments

FP variant	Source organism	Oligomerization degree (# protomers)	Excitation maximum (nm)	Emission maximum (nm)	Stokes shift	QY	E_{mol} ($M^{-1} cm^{-1}$)	Relative brightness ^a (% of EGFP)
EGFP [63]	<i>Aequorea victoria</i>	1	488	507	19	0.6	53,000 ^b	100
mKO2 [70]	<i>Funaria concinna</i>	1	551	565	14	0.62	63,800 ^b	124
td-Tomato [72]	<i>Discosoma</i> sp.	2	554	581	27	0.69	69,000	150
mOrange2 [73]	<i>Discosoma</i> sp.	1	549	565	16	0.60	58,000 ^c	109
TurboRFP [45]	<i>Entacmaea quadricolor</i>	2	553	574	21	0.67	92000 ^c	194
TagRFP-T [73]	<i>Entacmaea quadricolor</i>	1	555	584	29	0.41	81,000 ^c	104
mRuby [36]	<i>Entacmaea quadricolor</i>	1	558	605	47	0.35	Not applicable ^c	123
DsRed-Express2 [81]	<i>Discosoma</i> sp.	4	554	591	37	0.42	35,600	47
eqFP611 [100]	<i>Entacmaea quadricolor</i>	4	559	611	52	0.45	116,000 ^c	164 ^c
mCherry [72]	<i>Discosoma</i> sp.	1	587	615	28	0.22	72,000 ^c	50
mKeima [34]	<i>Montipora</i> sp.	1	440	620	180	0.24	14,400 ^b	11
mRaspberry [94]	<i>Discosoma</i> sp.	1	598	625	27	0.15	86,000 ^c	41

RFP630 [35]	<i>Entacmaea quadricolor</i>	4	583	630	47	0.35	50,000 ^e	55
mKate2 [75]	<i>Entacmaea quadricolor</i>	1	588	635	47	0.4	62,500 ^e	79
Kaushka [74]	<i>Entacmaea quadricolor</i>	2	588	635	47	0.34	65,000 ^e	70
RFP637 [35]	<i>Entacmaea quadricolor</i>	4	587	637	50	0.23	72,000 ^e	52 ^c
							141,300 ^d	102 ^d
RFP639 [35]	<i>Entacmaea quadricolor</i>	4	588	639	51	0.18	69,000 ^e	39 ^c
							110,400 ^d	63 ^d
hcRed [23]	<i>Heteractis crispa</i>	2	594	645	51	0.05	70,000 ^e	11
mPlum [94]	<i>Discosoma</i> sp.	1	590	649	59	0.1	41,000 ^e	13 ^c
							143,400 ^{d,f}	45 ^d
AQ14(52)	<i>Actinia equina</i>	4	595	663	68	–	–	–

^aProduct of QY and E_{mol} of purified proteins compared to the brightness of EGFP (53,000 M⁻¹ cm⁻¹ × 0.60)

^bConcentration of the red chromophore deduced from the protein concentration as determined by colorimetric methods

^cConcentration of the red chromophore determined by the alkaline denaturation method [22]

^dConcentration of the red chromophore determined by the *dynamic difference method* [35]

^eDetermined from expression in HEK293 cells

^fValues from Ref. [35]

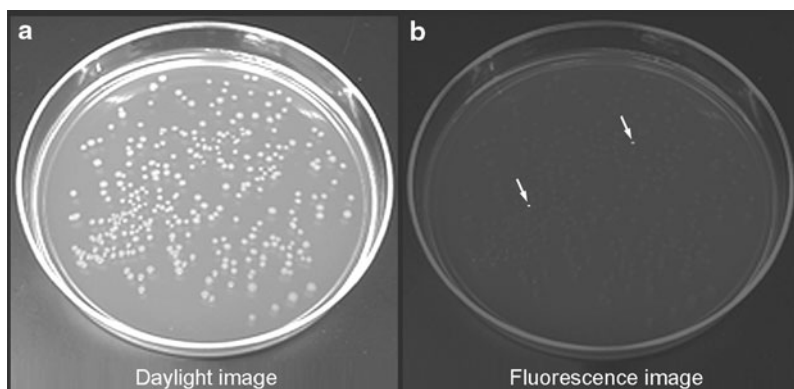


Fig. 24.4 Isolation of novel GFP-like proteins. (a) *Escherichia coli* was transformed with expression plasmids containing a cDNA library from the fluorescent tentacles of the sea anemone *Entacmaea quadricolor* and spread on agar plates. After growth of the bacterial colonies, the plates were incubated at 4°C for several days to allow maturation and accumulation of the expressed proteins. (b) When viewing the plates under UVA (~366 nm) or blue light (~450 nm) through suitable green or red long pass filters, colonies containing potential proteins of interest (arrows) can be identified by their fluorescence

GFP-coding genes by using one of two methods. The choice of method depends on a multitude of factors including knowledge of the target protein, availability of homologous sequences, and quality of the cDNA.

The first method involves PCR amplification of cDNA fragments using degenerate primers based on conserved regions of the GFP-like protein genes. The main advantages of this method are: its sensitivity, which allows isolation cDNAs expressed at low transcript levels; the applicability to cDNA samples of limited quality; and the relative speed of the process [2]. However, the method hinges on the performance of the degenerate primers which can become a major limitation when screening for novel FPs in taxonomic groups only remotely related to the source organisms that provided the templates for primer design. An alternative method to the direct PCR amplification is the functional expression of the cDNA library in recombinant systems such as bacteria [100]. Subsequently, bacterial colonies can be screened quickly and efficiently by their color or fluorescence on agar plates for the presence of interesting candidate proteins (Fig. 24.4). Toxicity of the FP may compromise the success of the method; however, the method is ideally suited for the search of GFP-like proteins in new taxonomic groups as it is not constrained by the primer design.

24.5 Applications of Fluorescent Proteins from Marine Invertebrates

GFP-like proteins have revolutionized the field of cellular imaging over the past two decades [15, 103]. The autocatalytic formation of the functional chromophore

without the requirement for cofactors, their diverse spectral characteristics, and the *in vivo* stability of the chromophore over a range of physiological conditions has resulted in their widespread popularity as live-cell markers. As the chromophore can be expressed, matured, and maintained *in vivo*, FPs represent unrivaled tools with which, for instance, complex biochemical pathways can be studied within the living cell. Fluorescent proteins belonging to the GFP-like family have been used for various studies including gene expression, protein localization, protein–protein interactions, and monitoring of intracellular biochemistry [15, 103]. In addition, photoactivatable proteins have enabled super-resolution optical imaging beyond the diffraction limit through techniques such as photoactivated localization microscopy (PALM) or reversible saturable optical fluorescence transitions (RESOLFT) [6, 28]. This section aims to provide an overview of the applications of fluorescent protein technology.

24.5.1 Gene Expression

The suite of genes expressed by a particular cell is a fundamental aspect of cell differentiation. Interpreting the patterns of gene expression, both spatially and temporally, is therefore key to understanding the functioning of different cells, under different stimuli and different stages of development. FPs offer the opportunity to monitor gene expression in living organisms [9]. For this purpose, the FP of choice is expressed in the cells of interest under the control of the target promoter. An adequate stimulation of the experimental promoter can be detected by the increase in cellular fluorescence (Fig. 24.5). Although the *in vitro* maturation of many FPs is fairly swift, it often takes several hours until significant amounts of the reporter have accumulated in the cells. Protein engineering helped accelerate the maturation times of several FPs, but there is presently still further demand for natural or engineered variants with faster maturation rates [7]. Monitoring of the downregulation of a gene is often complicated by the long half-decay time of FPs [37]. The long persistence in the cell can be attributed to the stability of the β -can fold. Biotechnological manipulation such as the introduction of PEST sequences can be used to create variants with faster turnover rates that can be used to determine the time when genes are switched off [42]. Fluorescent timer proteins were created from anthozoan FPs by mutagenesis [84, 85]. In these variants, the ratio of blue-, green-, and red-emitting states of DsRed-type chromophores changes over time and can be used to backtrack the onset of gene expression. The oligomerization degree (monomeric vs. tetrameric) of the protein is less important for the successful application as long as the FPs do not form unspecific aggregates [103].

24.5.2 Labeling of Proteins and Subcellular Compartments

Proteins are involved in essentially all processes in a living organism, and the knowledge of their location within the cell is an important part of understanding their function. FPs provide an invaluable tool with which to tag proteins within

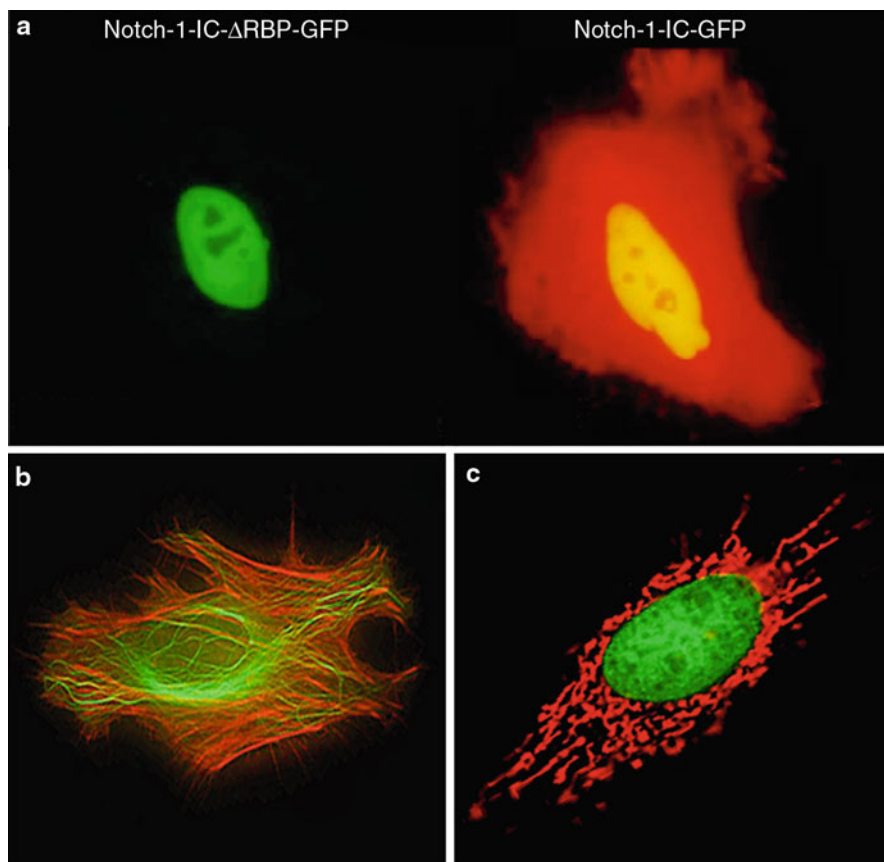


Fig. 24.5 Applications of fluorescent proteins from marine invertebrates. (a) Combined application of FPs as markers of subcellular compartments and gene expression. A Notch1-responsive promoter element was cloned upstream of the cDNA encoding mRuby, the monomeric variant of eqFP611. Cells were cotransfected with this reporter construct and expression vectors encoding truncated forms of the Notch1 receptor fused to GFP. The presence of the receptor is indicated by the green fluorescence of the nucleus (appearing yellow in the right cell due to the overlay with red fluorescence). Truncated Notch1 forms lacking the binding site for the recombination signal-binding protein (Notch1-IC-ΔRBP-GFP) fail to stimulate the expression of the reporter protein (*left cell*). The red fluorescence of the right cells indicates activity of the reporter gene and therefore the presence of a functional RBP binding site – the construct encoding the complete intercellular domain of Notch1 (Notch1-IC-GFP). (b) Dual color labeling of the cytoskeleton. Tubulin fibers are stained green by the tubulin-binding protein RITA expression in fusion with GFP. Actin fibers are labeled red by the fluorescence of mRuby fused to the actin-binding peptide Lifeact. (c) The mitochondrial network of a HeLa cell is highlighted in red by mRuby fused to a mitochondrial targeting signal from subunit VIII of cytochrome c oxidase. The nucleus is stained green by the presence of histone 2B expressed in fusion with GFP

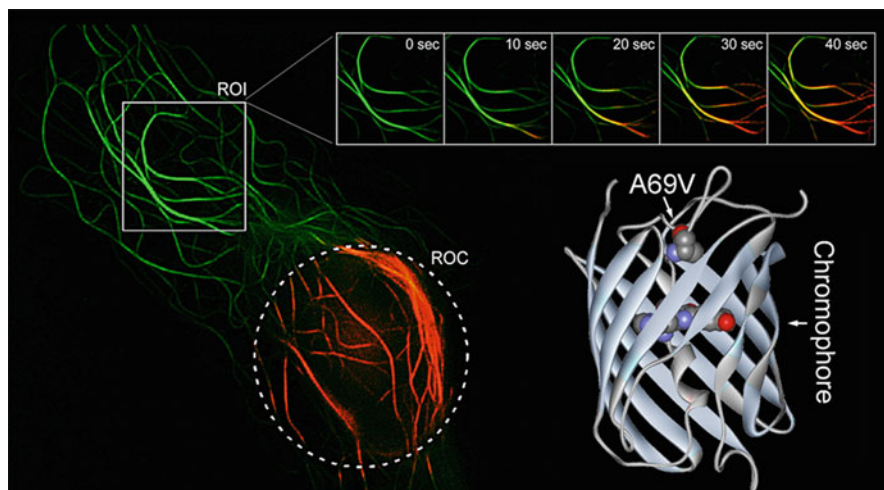


Fig. 24.6 Pulse-chase experiments using green-to-red photoconvertible mEosFPthermo. The ribbon diagram on the *right side* shows the localization of the amino acid A69 exchanged for a valine (represented by Van der Waals spheres) that improves functional expression of the protein at 37°C. The *background image* shows the tubulin skeleton of a HeLa cell highlighted by the green fluorescence of mEosFPthermo fused to the tubulin-binding protein RITA. Local photoconversion was induced by illumination of the region of conversion (ROC) with violet light. Subsequently, the movement of mEosFPthermo-RITA along the tubulin fibers can be followed by the red fluorescence in the region of interest (ROI)

cells [15]. The FP-encoding DNA can be coupled with another fragment coding for the protein of interest, but it is important to remove any stop codon that might be present between the two DNAs. Consequently, the FP is expressed in the cells in tandem together with the protein of interest. In most cases, FPs behave neutral in terms of their cellular localization as long as no unspecific aggregates are formed [103]. The location of the fluorescent tandem will be dominated by the protein of interest, allowing insights in its whereabouts in the cell at distinct time points (Fig. 24.5). The correct localization of fusion proteins can be impaired by an existing oligomerization tendency of the FP. For instance, the correct localization of the tubulin-binding protein RITA is strongly promoted by the monomeric character of the label. Here, the monomeric RFP mRuby and the thermostable monomeric EosFP variant, mEosFPthermo, were used to visualize the close association of RITA with tubulin fibers [92] (Figs. 24.5 and 24.6). Therefore, considerable efforts have been invested to created monomeric versions of multimeric anthozoan proteins [8, 31, 36, 45, 72].

The oligomerization tendency of the label is usually not of concern if they are used to label whole cells or cellular organelles (Fig. 24.5). The short-signaling peptides required for correct targeting in a distinct subcellular compartment are usually not affected in their functionality. The aforementioned applications may use multiple FPs to monitor different targets at the same time.

24.5.3 Protein–Protein Interactions

Studies of protein–protein interactions are very important to assess the function of certain proteins and understand the pathways that these proteins are involved in. A co-localization of two proteins as determined by dual-color labeling techniques using standard fluorescence microscopy does not prove their interaction at the molecular level.

Fluorescence resonance energy transfer (FRET), the radiationless transfer of energy from one chromophore to the other is only possible at distances that are usually provided by molecular interactions [48]. Hence, FRET can be used to determine whether or not two colocalized proteins are indeed interacting. FRET applications require two differently colored FPs, where the emission spectrum of the donor FP needs to overlap with the excitation spectrum of the acceptor FP [20, 32]. These markers are used to label the two proteins under study. Only if the target proteins bring the FPs close enough to be indicative of molecular interactions, FRET will occur and an excitation of the donor will result in an increased emission of the acceptor FP [88].

24.5.4 Sensors

The exact knowledge of molecular changes, post-transcriptional modifications, and the resulting structural changes within the target molecules is an important prerequisite for the development of reliable biosensors.

Fluorescent protein-based sensors have been designed to allow visualization of changes in intracellular conditions (Fig. 24.5). The FRET-based sensors of intracellular calcium levels were among the first sensors based on fluorescent proteins [48, 49]. These so-called chameleons represent a fusion between two FPs that are connected by a linker comprising of calmodulin (CaM) and a 26-residue CaM-binding peptide, called M13, from the myosin light-chain kinase. Upon binding to calcium ions, the linker induces a conformation change in the fusion, bringing the two FPs close enough together for FRET to occur. Consequently, fluctuations of the intracellular calcium levels can be inferred from changes in the ratio of donor and acceptor fluorescence [49]. In another FRET-based sensor for kinase activity, the linker between the donor and acceptor FPs is composed of the SH2 domain of c-Src kinase, a flexible linker region, and an Src substrate peptide from p130cas. Upon phosphorylation, the substrate peptide interacts strongly with the SH2 domain and induces a conformational change within the sensor. In contrast to the above-mentioned chameleons, FRET efficiency decreases in response to increases of the analyte concentrations [93].

Another approach to visualize the presence of analytes is based on monitoring changes in the subcellular localization of FP fusions as a consequence of cellular signal transduction processes. G-protein-coupled receptor (GPCR) signaling leads to cAMP production and subsequent release of intracellular Ca^{2+} . High Ca^{2+} in turn activates the Ca^{2+} /calmodulin-dependent phosphatase calcineurin.

Dephosphorylation of the transcription factor NFAT (nuclear factor of activated T-cells) by calcineurin induces its nuclear translocation and activation of NFAT target genes. Therefore, the rapid migration of an NFAT–FP fusion protein from the cytoplasm to the nucleus can also be used as a calcium sensor in living cells [104].

In addition, FP sensors that report the presence of analytes/ligands by fluorescence changes induced by interactions with the target molecules are available. The fluorescence emission of sensors for transition metal ions and chloride, for instance, anions, are altered by the structural impact of binding in proximity to the chromophore. The anion-sensitive GFP-based YFP-H148Q is an example of an FP whose emission characteristics are altered by interaction with a target molecule of interest, i.e., chloride. The fluorescence of the protein decreases with increasing chloride concentration due to a halide-binding site near the chromophore resulting in a promising tool for high-throughput drug screening for cystic fibrosis [30, 41]. Changes in pH of FP solution can result in changes of the absorption and emission properties of the dye molecules. Some pH-sensible FPs were successfully applied as probes to measure for instance the pH of different compartments in living cells [26, 39, 46].

A fluorescence-based endoplasmic reticulum (ER) stress sensor exploits the activity of a specific ribonuclease. Upon accumulation of misfolded proteins in the endoplasmic reticulum, the so-called *unfolded protein response* (UPR) leads to the activation of the ER transmembrane protein IRE-1. Active IRE-1 targets the mRNA of a transcription factor called XBP-1 and excises exactly 26 nucleotides in a particular cytoplasmic splicing reaction. The excision produces a reading frame shift within the XBP-1 mRNA and a different, now highly active XBP-1 transcription factor variant is produced to activate the transcription of UPR proteins (for example heat shock proteins, HSPs) [107]. An engineered XBP-1–FP fusion construct was developed which becomes fluorescent when the splicing reaction and the resulting frame shift occurs during ER stress [108].

An elegant tension sensor was constructed by linking to FPs suitable to form a FRET couple via an elastic part of the spider silk protein flagelliform [21]. The FRET efficiency decreases gradually under tension and recovers upon relaxation, enabling measurements of forces in the piconewton range.

24.6 Photoactivatable GFP-like Proteins (PAFPs)

PAFPs allow the willful manipulation of their fluorescence by controlled illumination with light of specific quantities and qualities. Subsequently, the optically marked fraction can be independently monitored among the whole population of the marker molecules. Three major responses of PAFPs can be distinguished: reversible on/off switching, irreversible activation, and irreversible conversion from one emission color to another. A few natural FPs including asulCP and cerFP505 show pronounced photoactivation responses [40, 90]. In contrast, a number of FPs such as Kaede and EosFP feature green-to-red photoconversion as part of the chromophore maturation [97]. Protein engineering succeeded in

creating numerous variants in which reversible on/off switching or irreversible on switching was strongly enhanced (Table 24.2). Monomeric derivatives were also created to satisfy the demand for PAFPs useful for protein labeling (Table 24.2). IrisFP and its monomeric form are markers that join reversible switching responses with irreversible photoconversion of the chromophore [1, 19]. The two major application fields of PAFPs, pulse-chase experiments, and super-resolution microscopy are described in the following paragraphs.

24.6.1 Pulse-Chase Experiments

Once the markers are expressed and matured, a small subsample of the population is activated with a light pulse. Subsequently, the movement of the activated target proteins can be tracked in real time [97] (Fig. 24.6). Photoconvertible proteins such as Kaede, EosFP, and their derivatives have been proven particularly useful for pulse-chase imaging due to the exceptionally high optical contrast that is generated between the activated and the nonactivated form. Moreover, the use of spectrally well-separated light colors for activation and detection of the markers largely reduces the risk of undesired activation during the tracking phase of the experiment: blue and green light is used for detection, whereas violet light is used to induce photoconversion. Pulse-chase experiments can be performed at the level of cells or tissue, for instance, to monitor the fate of cells during embryonic development [91]. When targeted to subcellular compartments, PAFPs allow the tracking of movement and fusion or fission processes of organelles [97]. In these applications, the oligomerization degree of the marker proteins is usually not an issue as long as no unspecific aggregates are formed. Consequently, the excellent optical properties of tetrameric proteins such as EosFP can be exploited. In contrast, protein-tracking studies might be impaired by the size of the label, so the use of tandem dimer or monomeric variants is often advisable [44, 58] (Fig. 24.6).

24.6.2 Super-Resolution Microscopy

PAFP have also enabled the realization of imaging concepts that achieve resolutions beyond the diffraction barrier of standard optical microscopy. This allows the visualization of structures which are separated less than 200 nm from each other [6, 28]. Here, the photoactivated localization microscopy (PALM) shall be explained in greater detail. Firstly, proteins are labeled with the PAFP of choice. Secondly, the sample is illuminated briefly at low intensity with light that induces activation. Consequently, only a few molecules are activated that are far enough apart for their blurred images to be captured with a conventional microscope. The center of the blurred spots is determined for each molecule, and all loci of the molecules are recorded. Subsequently, the activated molecules are either switched off or photobleached to erase the screen for a new round of activation and localization. Over numerous cycles, a large number of marker molecules are registered until enough data are accumulated to allow reconstruction of an image from the

Table 24.2 Properties of engineered photoactivatable FPs derived from cnidarian pigments

FP variant	Source organism	Oligomerization degree (# protomers)	Type of fluorescence activation	Wavelengths (nm)		Emission maximum (nm)	Molar extinction coefficient	Quantum yield	Relative brightness ^a (% of EGFP)
				required for fluorescence activation	Excitation maximum (nm)				
PA-GFP [62]	<i>Aequorea victoria</i>	1	Off-On	488	504	517	17,400	0.79	43
PS-CFP [11]	<i>Aequorea coerulescens</i>	1	Cyan-green conversion	405	402/490	468/511	34,000/27,000	0.16/0.19	17/16
Kaede [3]	<i>Trachyphyllia geoffroyi</i>	4	Green-red conversion	~400	508/572	518/580	98,800/60,400	0.88/0.33	273/63
KikGR [87]	<i>Favia favius</i>	4	Green-red conversion	~400	507/583	517/593	53,700/35,100	0.70/0.65	118/72
EosFP [101]	<i>Lobophyllia hemprichii</i>	4	Green-red conversion	~400	506/571	516/581	72,000/41,000	0.70/0.62	159/80
Dendra2 [12]	<i>Dendronephthya</i> sp.	1	Green-red conversion	~400	490/553	507/573	45,000/35,000	0.50/0.55	71/61
mKikGR [24]	<i>Favia favius</i>	1	Green-red conversion	~400	505/580	515/591	49,000/28,000	0.69/0.63	106/56
tdEosFP [58]	<i>Lobophyllia hemprichii</i>	1	Green-red conversion	~400	506/569	516/581	84,000/33,000	0.66/0.60	174/62
mEosFP [101]	<i>Lobophyllia hemprichii</i>	1	Green-red conversion	~400	505/569	516/581	67,200/37,000	0.64/0.62	135/72
mEosFP2 [44]	<i>Lobophyllia hemprichii</i>	1 ^b	Green-red conversion	~400	506/573	519/584	56,000/46,000	0.84/0.66	148/96
Dronpa [4]	<i>Pectiniid coral</i>	1	Reversible on/off switching	~400/~488	503	518	95,000	0.85	254
rsFastLime [79]	<i>Pectiniid coral</i>	1	Reversible on/off switching	~400/~488	496	518	39,000	0.77	94

(continued)

Table 24.2 (continued)

FP variant	Source organism	Oligomerization degree (# protomers)	Type of fluorescence activation	Wavelengths (nm) required for fluorescence activation	Excitation maximum (nm)	Emission maximum (nm)	Molar extinction coefficient	Quantum yield	Relative brightness ^a (% of EGFP)
rsCherry [80]	<i>Discosoma</i> sp.	1	Reversible on/off switching	~450/~550	572	610	80,000 ^c	0.005 ^c	5.
rsCherryRev [80]	<i>Discosoma</i> sp.	1	Reversible on/off switching	~450/~550	572	608	84,000 ^c	0.02 ^c	1.3
PAmCherry [83]	<i>Discosoma</i> sp.	1	Reversible on/off switching	390–440/570	570	596	18,000	0.46	26
IrisFP [1]	<i>Lobophyllia hemprichii</i>	4	Green–red conversion, rev. on/off switching	405 (conversion) ~400/~488 (green) ~440/532 (red)	488/551	516/580	52,200/35,400	0.43/0.47	71/52
mIrisFP [19]	<i>Lobophyllia hemprichii</i>	1	Green–red conversion, rev. on/off switching	405 (conversion) ~400/~488 (green) ~440/532 (red)	486/546	516/578	47,000/33,000	0.54/0.59	80/62

^aDetermined for purified proteins

^bDimerization tendency [44]

^cData from Ref. [80]

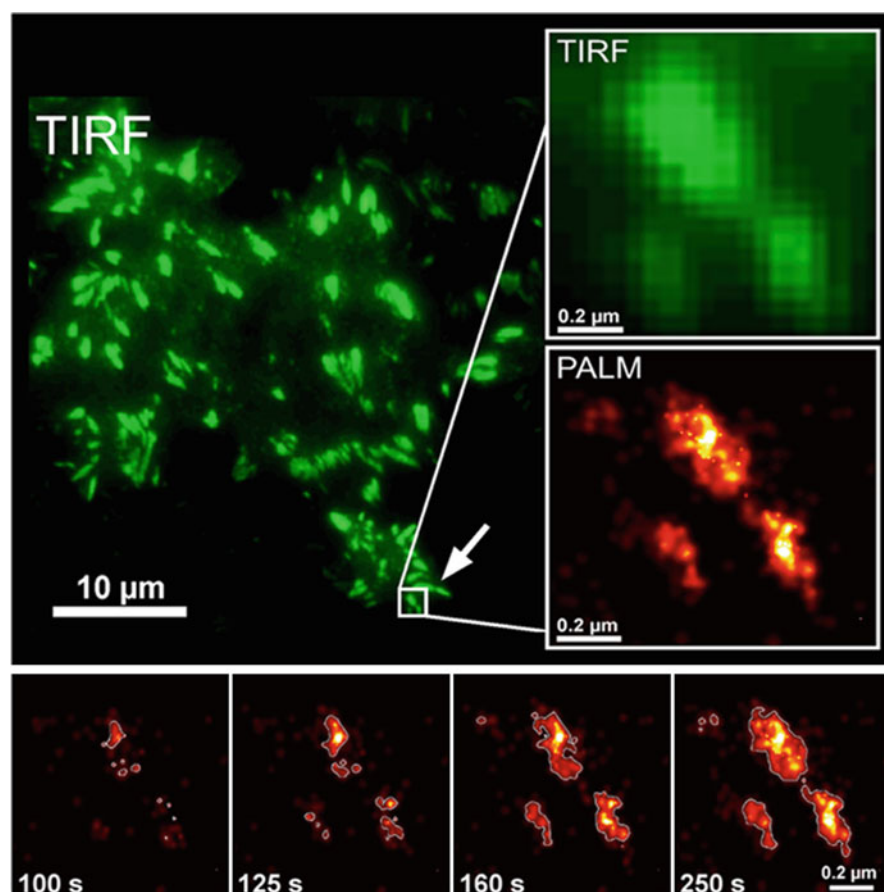


Fig. 24.7 Applications of PAFPs for PALM imaging. mIrisFP was expressed in fusion with paxillin in a HeLa cell. *Upper panel:* The green fluorescent mIrisFP-paxillin accumulates predominantly in focal adhesions. Insets: exploiting the reversible photoswitching of mIrisFP for PALM, images can be constructed with a significantly higher resolution compared to those obtained by conventional TIRF microscopy. *Lower panels:* Pulse-chase experiments with super-resolution. mIrisFP-paxillin was photoconverted by illumination with violet light. PALM images were acquired by photoswitching of the red form of mIrisFP in intervals of 0–100, 0–125, 0–160, and 0–250 s. The increase of molecules over time indicates the growth of the focal adhesions

individual loci. Resolutions between 30 and 100 nm can be regularly achieved by this method. With the recent advent of mIrisFP, it is now also possible to perform pulse-chase experiments at super-resolution [19] (Fig. 24.7).

24.7 Conclusion

Fluorescent proteins from marine organisms revolutionized biomedical research by enabling completely new approaches to study live cells. The vast majority of

fluorescent proteins that can be found in the oceans are yet unstudied. Hence, the combination of “gene hunting” in the marine realm and “protein engineering” in the laboratory will certainly lead to exciting discoveries also in the future. In summary, fluorescent proteins hold a great promise to meet the increasing demand for optical research tools.

24.8 Study Questions

1. In which taxa of marine invertebrates can fluorescent proteins be found?
2. What is the tertiary structure shared by all FPs?
3. How can the diversity of emission colors be explained?
4. Which property of FPs enables their use as genetically encoded markers?
5. What are major applications of FPs and how are they related to their biochemical and photophysical properties?
6. Which properties of FPs can hamper the application as markers?
7. How can the properties of FPs be altered?

Acknowledgment J.W. acknowledges funding by the Deutsche Forschungsgemeinschaft (DFG) (Grant Wi1990/2-1); the Network Fluorescence Applications in Biotechnology and Life Sciences, FABLs, Australia; the Landesstiftung Baden-Württemberg (Elite Postdoctoral Program); the Natural Environment Research Council, UK (*NE/G009643/1*; *NE/I01683X/1*); and the University of Southampton. G.U.N. was supported by the DFG and the State of Baden-Württemberg through the Center for Functional Nanostructures, by DFG grant NI 291/9 and by the Baden-Württemberg Stiftung. E.G.S is funded by a NERC-studentship.

References

1. Adam V, Lelimosin M, Boehme S, Desfonds G, Nienhaus K et al (2008) Structural characterization of IrisFP, an optical highlighter undergoing multiple photo-induced transformations. *Proc Natl Acad Sci USA* 105:18343–18348
2. Alieva NO, Konzen KA, Field SF, Meleshkevitch EA, Hunt ME et al (2008) Diversity and evolution of coral fluorescent proteins. *PLoS One* 3:e2680
3. Ando R, Hama H, Yamamoto-Hino M, Mizuno H, Miyawaki A (2002) An optical marker based on the UV-induced green-to-red photoconversion of a fluorescent protein. *Proc Natl Acad Sci USA* 99:12651–12656
4. Ando R, Mizuno H, Miyawaki A (2004) Regulated fast nucleocytoplasmic shuttling observed by reversible protein highlighting. *Science* 306:1370–1373
5. Andresen M, Wahl MC, Stiel AC, Gräter F, Schaefer LV et al (2005) Structure and mechanism of the reversible photoswitch of a fluorescent protein. *Proc Natl Acad Sci USA* 102:13070–13074
6. Betzig E, Patterson GH, Sougrat R, Lindwasser OW, Olenych S et al (2006) Imaging intracellular fluorescent proteins at nanometer resolution. *Science* 313:1642–1645
7. Bevis BJ, Glick BS (2002) Rapidly maturing variants of the Discosoma red fluorescent protein (DsRed). *Nat Biotechnol* 20:83–87
8. Campbell RE, Tour O, Palmer AE, Steinbach PA, Baird GS et al (2002) A monomeric red fluorescent protein. *Proc Natl Acad Sci USA* 99:7877–7882

9. Chalfie M, Tu Y, Euskirchen G, Ward WW, Prasher DC (1994) Green fluorescent protein as a marker for gene expression. *Science* 263:802–805
10. Chatteraj M, King BA, Bublitz GU, Boxer SG (1996) Ultra-fast excited state dynamics in green fluorescent protein: multiple states and proton transfer. *Proc Natl Acad Sci USA* 93:8362–8367
11. Chudakov DM, Lukyanov S, Lukyanov KA (2007) Tracking intracellular protein movements using photoswitchable fluorescent proteins PS-CFP2 and Dendra2. *Nat Protoc* 2:2024–2032
12. Chudakov DM, Lukyanov S, Lukyanov KA (2007) Using photoactivatable fluorescent protein Dendra2 to track protein movement. *Biotechniques* 42:553, 555, 557 passim
13. Cody CW, Prasher DC, Westler WM, Prendergast FG, Ward WW (1993) Chemical structure of the hexapeptide chromophore of the *Aequorea* green-fluorescent protein. *Biochemistry* 32:1212–1218
14. D'Angelo C, Denzel A, Vogt A, Matz MV, Oswald F et al (2008) Blue light regulation of host pigment in reef-building corals. *Mar Ecol Prog Ser* 364:97–106
15. Day RN, Davidson MW (2009) The fluorescent protein palette: tools for cellular imaging. *Chem Soc Rev* 38:2887–2921
16. Deheyn DD, Kubokawa K, McCarthy JK, Murakami A, Porrachia M et al (2007) Endogenous green fluorescent protein (GFP) in amphioxus. *Biol Bull* 213:95–100
17. Erickson MG, Moon DL, Yue DT (2003) DsRed as a potential FRET partner with CFP and GFP. *Biophys J* 85:599–611
18. Fradkov AF, Chen Y, Ding L, Barsova EV, Matz MV et al (2000) Novel fluorescent protein from *Discosoma* coral and its mutants possesses a unique far-red fluorescence. *FEBS Lett* 479:127–130
19. Fuchs J, Bohme S, Oswald F, Hedde PN, Krause M et al (2010) A photoactivatable marker protein for pulse-chase imaging with superresolution. *Nat Methods* 7:627–630
20. Goedhart J, Vermeer JE, Adjobo-Hermans MJ, van Weeren L, Gadella TW (2007) Sensitive detection of p65 homodimers using red-shifted and fluorescent protein-based FRET couples. *PLoS One* 2:e1011
21. Grashoff C, Hoffman BD, Brenner MD, Zhou R, Parsons M et al (2010) Measuring mechanical tension across vinculin reveals regulation of focal adhesion dynamics. *Nature* 466:263–266
22. Gross LA, Baird GS, Hoffman RC, Baldrige KK, Tsien RY (2000) The structure of the chromophore within DsRed, a red fluorescent protein from coral. *Proc Natl Acad Sci USA* 97:11990–11995
23. Gurskaya NG, Fradkov AF, Tersikh A, Matz MV, Labas YA et al (2001) GFP-like chromoproteins as a source of far-red fluorescent proteins. *FEBS Lett* 507:16–20
24. Habuchi S, Tsutsui H, Kochaniak AB, Miyawaki A, van Oijen AM (2008) mKikGR, a monomeric photoswitchable fluorescent protein. *PLoS One* 3:e3944
25. Haddock SH, Mastroianni N, Christianson LM (2010) A photoactivatable green-fluorescent protein from the phylum Ctenophora. *Proc R Soc Lond B: Biol Sci* 277:1155–1160
26. Hanson GT, McAnaney TB, Park ES, Rendell ME, Yarbrough DK et al (2002) Green fluorescent protein variants as ratiometric dual emission pH sensors. 1. Structural characterization and preliminary application. *Biochemistry* 41:15477–15488
27. Heim R, Prasher DC, Tsien RY (1994) Wavelength mutations and posttranslational autoxidation of green fluorescent protein. *Proc Natl Acad Sci USA* 91:12501–12504
28. Hofmann M, Eggeling C, Jakobs S, Hell SW (2005) Breaking the diffraction barrier in fluorescence microscopy at low light intensities by using reversibly photoswitchable proteins. *Proc Natl Acad Sci USA* 102:17565–17569
29. Hopf M, Gohring W, Ries A, Timpl R, Hohenester E (2001) Crystal structure and mutational analysis of a perlecan-binding fragment of nidogen-1. *Nat Struct Mol Biol* 8:634–640
30. Jayaraman S, Haggie P, Wachter RM, Remington SJ, Verkman AS (2000) Mechanism and cellular applications of a green fluorescent protein-based halide sensor. *J Biol Chem* 275:6047–6050

31. Karasawa S, Araki T, Yamamoto-Hino M, Miyawaki A (2003) A green-emitting fluorescent protein from Galaxiidae coral and its monomeric version for use in fluorescent labeling. *J Biol Chem* 278:34167–34171
32. Karasawa S, Araki T, Nagai T, Mizuno H, Miyawaki A (2004) Cyan-emitting and orange-emitting fluorescent proteins as a donor/acceptor pair for fluorescence resonance energy transfer. *Biochem J* 381:307–312
33. Kelmanson IV, Matz MV (2003) Molecular basis and evolutionary origins of color diversity in great star coral *Montastraea cavernosa* (Scleractinia: Faviida). *Mol Biol Evol* 20:1125–1133
34. Kogure T, Karasawa S, Araki T, Saito K, Kinjo M et al (2006) A fluorescent variant of a protein from the stony coral *Montipora* facilitates dual-color single-laser fluorescence cross-correlation spectroscopy. *Nat Biotechnol* 24:577–581
35. Kredel S, Nienhaus K, Oswald F, Wolff M, Ivanchenko S et al (2008) Optimized and far-red-emitting variants of fluorescent protein eqFP611. *Chem Biol* 15:224–233
36. Kredel S, Oswald F, Nienhaus K, Deuschle K, Roecker C et al (2009) mRuby, a bright monomeric red fluorescent protein for labeling of subcellular structures. *PLoS One* 4:e4391
37. Leutenegger A, D'Angelo C, Matz MV, Denzel A, Oswald F et al (2007) It's cheap to be colorful. Anthozoans show a slow turnover of GFP-like proteins. *FEBS J* 274:2496–2505
38. Leutenegger A, Kredel S, Gundel S, D'Angelo C, Salih A et al (2007) Analysis of fluorescent and non-fluorescent sea anemones from the Mediterranean Sea during a bleaching event. *J Exp Mar Biol Ecol* 353:221–234
39. Llopis J, McCaffery JM, Miyawaki A, Farquhar MG, Tsien RY (1998) Measurement of cytosolic, mitochondrial, and Golgi pH in single living cells with green fluorescent proteins. *Proc Natl Acad Sci USA* 95:6803–6808
40. Lukyanov KA, Fradkov AF, Gurskaya NG, Matz MV, Labas YA et al (2000) Natural animal coloration can be determined by a nonfluorescent green fluorescent protein homolog. *J Biol Chem* 275:25879–25882
41. Ma T, Vetrivel L, Yang H, Pedemonte N, Zegarra-Moran O et al (2002) High-affinity activators of cystic fibrosis transmembrane conductance regulator (CFTR) chloride conductance identified by high-throughput screening. *J Biol Chem* 277:37235–37241
42. Mateus C, Avery SV (2000) Destabilized green fluorescent protein for monitoring dynamic changes in yeast gene expression with flow cytometry. *Yeast* 16:1313–1323
43. Matz MV, Fradkov AF, Labas YA, Savitsky AP, Zaraisky AG et al (1999) Fluorescent proteins from nonbioluminescent Anthozoa species. *Nat Biotechnol* 17:969–973
44. McKinney SA, Murphy CS, Hazelwood KL, Davidson MW, Looger LL (2009) A bright and photostable photoconvertible fluorescent protein. *Nat Methods* 6:131–133
45. Merzlyak EM, Goedhart J, Shcherbo D, Bulina ME, Shcheglov AS et al (2007) Bright monomeric red fluorescent protein with an extended fluorescence lifetime. *Nat Methods* 4:555–557
46. Miesenbock G, De Angelis DA, Rothman JE (1998) Visualizing secretion and synaptic transmission with pH-sensitive green fluorescent proteins. *Nature* 394:192–195
47. Mishin AS, Subach FV, Yampolsky IV, King W, Lukyanov KA et al (2008) The first mutant of the *Aequorea victoria* green fluorescent protein that forms a red chromophore. *Biochemistry* 47:4666–4673
48. Miyawaki A, Llopis J, Heim R, McCaffery JM, Adams JA et al (1997) Fluorescent indicators for Ca^{2+} based on green fluorescent proteins and calmodulin. *Nature* 388:882–887
49. Miyawaki A, Griesbeck O, Heim R, Tsien RY (1999) Dynamic and quantitative Ca^{2+} measurements using improved cameleons. *Proc Natl Acad Sci USA* 96:2135–2140
50. Mizuno H, Mal TK, Tong KI, Ando R, Furuta T et al (2003) Photo-induced peptide cleavage in the green-to-red conversion of a fluorescent protein. *Mol Cell* 12:1051–1058
51. Mocz G (2007) Fluorescent proteins and their use in marine biosciences, biotechnology, and proteomics. *Mar Biotechnol* 9:305–328

52. Morin JG (1974) Coelenterate bioluminescence. In: Muscatine L, Lenhoff HM (eds) Coelenterate biology reviews and new perspectives. Academic, New York, pp 397–448
53. Morin JG, Hastings JW (1971) Biochemistry of the bioluminescence of colonial hydroids and other coelenterates. *J Cell Physiol* 77:305–312
54. Morin JG, Hastings JW (1971) Energy transfer in a bioluminescent system. *J Cell Physiol* 77:313–318
55. Nienhaus GU (2008) The green fluorescent protein: a key tool to study chemical processes in living cells. *Angew Chem Int Ed* 47:8992–8994
56. Nienhaus GU, Wiedenmann J (2009) Structure, dynamics and optical properties of fluorescent proteins: perspectives for marker development. *Chemphyschem* 10:1369–1379
57. Nienhaus K, Nienhaus GU, Wiedenmann J, Nar H (2005) Structural basis for photo-induced protein cleavage and green-to-red conversion of fluorescent protein EosFP. *Proc Natl Acad Sci USA* 102:9156–9159
58. Nienhaus GU, Nienhaus K, Holzle A, Ivanchenko S, Red F et al (2006) Photoconvertible fluorescent protein EosFP: biophysical properties and cell biology applications. *Photochem Photobiol* 82:351–358
59. Nienhaus K, Renzi F, Vallone B, Wiedenmann J, Nienhaus GU (2006) Exploring chromophore-protein interactions in fluorescent protein cmFP512 from *Cerianthus membranaceus*: X-ray structure analysis and optical spectroscopy. *Biochemistry* 45:12942–12953
60. Nienhaus K, Renzi F, Vallone B, Wiedenmann J, Nienhaus GU (2006) Chromophore-protein interactions in the anthozoan green fluorescent protein asFP499. *Biophys J* 91:4210–4220
61. Oswald F, Schmitt F, Leutenegger A, Ivanchenko S, D'Angelo C et al (2007) Contributions of host and symbiont pigments to the coloration of reef corals. *FEBS J* 274:1102–1109
62. Patterson GH, Lippincott-Schwartz J (2004) Selective photolabeling of proteins using photoactivatable GFP. *Methods* 32:445–450
63. Patterson GH, Knobel SM, Sharif WD, Kain SR, Piston DW (1997) Use of the green fluorescent protein and its mutants in quantitative fluorescence microscopy. *Biophys J* 73:2782–2790
64. Petersen J, Wilmann PG, Beddoe T, Oakley AJ, Devenish RJ et al (2003) The 2.0-angstrom crystal structure of eqFP611, a far red fluorescent protein from the sea anemone *Entacmaea quadricolor*. *J Biol Chem* 278:44626–44631
65. Pletneva NV, Pletnev SV, Chudakov DM, Tikhonova TV, Popov VO et al (2007) Three-dimensional structure of yellow fluorescent protein zYFP538 from *Zoanthus* sp. at the resolution 1.8 angstrom. *Bioorg Khim* 33:421–430
66. Prasher DC, Eckenrode VK, Ward WW, Prendergast FG, Cormier MJ (1992) Primary structure of the *Aequorea victoria* green-fluorescent protein. *Gene* 111:229–233
67. Prescott M, Ling M, Beddoe T, Oakley AJ, Dove S et al (2003) The 2.2 Å crystal structure of a pocilloporin pigment reveals a nonplanar chromophore conformation. *Structure* 11:275–284
68. Quillin ML, Anstrom DM, Shu X, O'Leary S, Kallio K et al (2005) Kindling fluorescent protein from *Anemonia sulcata*: dark-state structure at 1.38 Å resolution. *Biochemistry* 44:5774–5787
69. Remington SJ (2006) Fluorescent proteins: maturation, photochemistry and photophysics. *Curr Opin Struct Biol* 16:714–721
70. Sakaue-Sawano A, Kurokawa H, Morimura T, Hanyu A, Hama H et al (2008) Visualizing spatiotemporal dynamics of multicellular cell-cycle progression. *Cell* 132:487–498
71. Shagin DA, Barsova EV, Yanushevich YG, Fradkov AF, Lukyanov KA et al (2004) GFP-like proteins as ubiquitous metazoan superfamily: evolution of functional features and structural complexity. *Mol Biol Evol* 21:841–850
72. Shaner NC, Campbell RE, Steinbach PA, Giepmans BN, Palmer AE et al (2004) Improved monomeric red, orange and yellow fluorescent proteins derived from *Discosoma* sp. red fluorescent protein. *Nat Biotechnol* 22:1567–1572

73. Shaner NC, Lin MZ, McKeown MR, Steinbach PA, Hazelwood KL et al (2008) Improving the photostability of bright monomeric orange and red fluorescent proteins. *Nat Methods* 5:545–551
74. Shcherbo D, Merzlyak EM, Chepurnykh TV, Fradkov AF, Ermakova GV et al (2007) Bright far-red fluorescent protein for whole-body imaging. *Nat Methods* 4:741–746
75. Shcherbo D, Murphy CS, Ermakova GV, Solovieva EA, Chepurnykh TV et al (2009) Far-red fluorescent tags for protein imaging in living tissues. *Biochem J* 418:567–574
76. Shimomura O (1995) A short story of Aequorin. *Biol Bull* 189:1–5
77. Shimomura O, Johnson FH, Saiga Y (1962) Extraction, purification and properties of aequorin, a bioluminescent protein from the luminous hydromedusan, *Aequorea*. *J Cell Comp Physiol* 59:223–239
78. Sniegowski JA, Lappe JW, Patel HN, Huffman HA, Wachter RM (2005) Base catalysis of chromophore formation in Arg96 and Glu222 variants of green fluorescent protein. *J Biol Chem* 280:26248–26255
79. Stiel AC, Trowitzsch S, Weber G, Andresen M, Eggeling C et al (2007) 1.8 Å bright-state structure of the reversibly switchable fluorescent protein Dronpa guides the generation of fast switching variants. *Biochem J* 402:35–42
80. Stiel AC, Andresen M, Bock H, Hilbert M, Schilde J et al (2008) Generation of monomeric reversibly switchable red fluorescent proteins for far-field fluorescence nanoscopy. *Biophys J* 95:2989–2997
81. Strack RL, Strongin DE, Bhattacharyya D, Tao W, Berman A et al (2008) A noncytotoxic DsRed variant for whole-cell labeling. *Nat Methods* 5:955–957
82. Strack RL, Strongin DE, Mets L, Glick BS, Keenan RJ (2010) Chromophore formation in DsRed occurs by a branched pathway. *J Am Chem Soc* 132:8496–8505
83. Subach FV, Patterson GH, Manley S, Gillette JM, Lippincott-Schwartz J et al (2009) Photoactivatable mCherry for high-resolution two-color fluorescence microscopy. *Nat Methods* 6:311
84. Subach FV, Subach OM, Gundorov IS, Morozova KS, Piatkevich KD et al (2009) Monomeric fluorescent timers that change color from blue to red report on cellular trafficking. *Nature Chem Biol* 5:118–126
85. Terskikh A, Fradkov A, Ermakova G, Zarsisky A, Tan P et al (2000) “Fluorescent timer”: protein that changes color with time. *Science* 290:1585–1588
86. Tsien RY (1998) The green fluorescent protein. *Annu Rev Biochem* 67:509–544
87. Tsutsui H, Karasawa S, Shimizu H, Nukina N, Miyawaki A (2005) Semi-rational engineering of a coral fluorescent protein into an efficient highlighter. *EMBO Rep* 6:233–238
88. van Roessel P, Brand AH (2002) Imaging into the future: visualizing gene expression and protein interactions with fluorescent proteins. *Nat Cell Biol* 4:E15–E20
89. Verkhusha VV, Chudakov DM, Gurskaya NG, Lukyanov S, Lukyanov KA (2004) Common pathway for the red chromophore formation in fluorescent proteins and chromoproteins. *Chem Biol* 11:845–854
90. Vogt A, D’Angelo C, Oswald F, Denzel A, Mazel CH et al (2008) A green fluorescent protein with photoswitchable emission from the deep sea. *PLoS One* 3:e3766
91. Wacker SA, Oswald F, Wiedenmann J, Knochel W (2007) A green to red photoconvertible protein as an analyzing tool for early vertebrate development. *Dev Dyn* 236:473–480
92. Wacker SA, Alvarado C, von Wichert G, Knippschild U, Wiedenmann J et al (2011) RITA, a novel modulator of Notch signalling, acts via nuclear export of RBP-J. *EMBO J* 30:43–56
93. Wang Y, Chien S (2007) Analysis of integrin signaling by fluorescence resonance energy transfer. *Methods Enzymol* 426:177–201
94. Wang L, Jackson WC, Steinbach PA, Tsien RY (2004) Evolution of new nonantibody proteins via iterative somatic hypermutation. *Proc Natl Acad Sci USA* 101:16745–16749
95. Ward WW (2005) Biochemical and physical properties of green fluorescent protein. In: Chalfie M, Kain SR (eds) *Green fluorescent protein: properties, applications and protocols*, 2nd edn. Wiley, Hoboken, pp 39–65

96. Wiedenmann J (1997) The application of an orange fluorescent protein and further colored proteins and the corresponding genes from the species group *Anemonia* sp. (*sulcata*) Pennant, (Cnidaria, Anthozoa, Actinaria) in gene technology and molecular biology. Patent DE 197 18 640. Deutsches Patent und Markenamt, Deutschland, pp 1–18
97. Wiedenmann J, Nienhaus GU (2006) Live-cell imaging with EosFP and other photoactivatable marker proteins of the GFP family. *Expert Rev Proteomics* 3:361–374
98. Wiedenmann J, Röcker C, Funke W (1999) The morphs of *Anemonia* aff. *sulcata* (Cnidaria, Anthozoa) in particular consideration of the ectodermal pigments. *Verh Ges Ökol* 29:497–503
99. Wiedenmann J, Elke C, Spindler KD, Funke W (2000) Cracks in the beta-can: fluorescent proteins from *Anemonia sulcata* (Anthozoa, Actinaria). *Proc Natl Acad Sci USA* 97:14091–14096
100. Wiedenmann J, Schenk A, Rocker C, Girod A, Spindler KD et al (2002) A far-red fluorescent protein with fast maturation and reduced oligomerization tendency from *Entacmaea quadricolor* (Anthozoa, Actinaria). *Proc Natl Acad Sci USA* 99:11646–11651
101. Wiedenmann J, Ivanchenko S, Oswald F, Schmitt F, Rocker C et al (2004) EosFP, a fluorescent marker protein with UV-inducible green-to-red fluorescence conversion. *Proc Natl Acad Sci USA* 101:15905–15910
102. Wiedenmann J, Ivanchenko S, Oswald F, Nienhaus GU (2004) Identification of GFP-like proteins in nonbioluminescent, azooxanthellate anthozoa opens new perspectives for bioprospecting. *Mar Biotechnol* 6:270–277
103. Wiedenmann J, Oswald F, Nienhaus GU (2009) Fluorescent proteins for live cell imaging: opportunities, limitations, and challenges. *IUBMB Life* 61:1029–1042
104. Wolff M, Kredel S, Haasen D, Wiedenmann J, Nienhaus GU et al (2010) High content screening of CXCR2-dependent signalling pathways. *Comb Chem High Throughput Screen* 13:3–15
105. Yang F, Moss LG, Phillips GN Jr (1996) The molecular structure of green fluorescent protein. *Nat Biotechnol* 14:1246–1251
106. Yarbrough D, Wachter RM, Kallio K, Matz MV, Remington SJ (2001) Refined crystal structure of DsRed, a red fluorescent protein from coral, at 2.0-Å resolution. *Proc Natl Acad Sci USA* 98:462–467
107. Yoshida H, Matsui T, Yamamoto A, Okada T, Mori K (2001) XBP1 mRNA is induced by ATF6 and spliced by IRE1 in response to ER stress to produce a highly active transcription factor. *Cell* 107:881–891
108. Yuan L, Cao Y, Oswald F, Knochel W (2008) IRE1beta is required for mesoderm formation in *Xenopus* embryos. *Mech Dev* 125:207–222

From Biosilica of Sponges (Demospongiae and Hexactinellida) to Fabricated Biomedical Materials

25

Xiaohong Wang, Heinz C. Schröder, Matthias Wiens, Lu Gan, Wolfgang Tremel, and Werner E. G. Müller

Contents

25.1	Introduction: Sponges	1260
25.2	The Power of “Nature as Model” in Bioinorganic Material Science: Shift of a Paradigm	1261
25.3	Levels of Biomineralization	1263
25.4	Spicule Network in Siliceous Sponges: A Unique Skeleton	1265
25.4.1	Spicule Diversity: Case Study Hexactinellid <i>Monorhaphis</i>	1268
25.4.2	Giant Basal Spicules from <i>Monorhaphis</i> : The Largest Bio-Silica Structure on Earth	1268
25.4.3	Chemical Composition	1271
25.4.4	Giant Basal Spicules – Protein Scaffold	1272
25.4.5	Biochemical Properties and Intracellular Localization of Silicatein	1272
25.4.6	Cloning of the Hexactinellid Silicatein cDNA	1273
25.5	Modeling of the Morphology of the Spicules	1274
25.5.1	Phases of Silica Deposition During Spicule Formation	1276
25.5.2	Giant Basal Spicules – Mechanical Properties	1277

X. Wang

National Research Center for Geoanalysis, 26 Baiwanzhuang Dajie, Beijing, China
and

Institute for Physiological Chemistry, Medical Center of the Johannes Gutenberg University,
Duesbergweg 6, Mainz, Germany

e-mail: wxh0408@hotmail.com

H.C. Schröder • M. Wiens • W.E.G. Müller (✉)

Institute for Physiological Chemistry, Medical Center of the Johannes Gutenberg University,
Duesbergweg 6, Mainz, Germany

e-mail: wmueller@uni-mainz.de

L. Gan

National Research Center for Geoanalysis, 26 Baiwanzhuang Dajie, Beijing, China

W. Tremel

Institute for Chemistry, Johannes Gutenberg University Mainz, Duesbergweg 10-14, Mainz,
Germany

E. Fattorusso, W. H. Gerwick, O. Tagliapietra-Scafati (eds.),

Handbook of Marine Natural Products, DOI 10.1007/978-90-481-3834-0_25,

© Springer Science+Business Media B.V. 2012

1259

25.5.3 Giant Basal Spicules – Optophysical Properties	1279
25.6 Biomimetic Approaches	1281
References	1282

Abstract

Only 13 years after realizing, during a repair of a telegraph cable pulled out from the deep sea, that the bottom of the ocean is plentifully populated with a highly diverse fauna and flora, the Challenger expedition (1873–1876) treasured up a rich collection of vitreous sponges (Hexactinellida). They have been described by Schulze and represent the phylogenetically oldest class of siliceous sponges (phylum Porifera); they are eye-catching because of their distinct body plan, which relies on a filigree skeleton. It is constructed by an array of morphologically determined elements, the spicules. During the German Deep Sea Expedition “Valdivia” (1898–1899), Schulze could describe the largest siliceous hexactinellid sponge on Earth, the up to 3 m high *Monorhaphis chuni*, which likewise forms the largest biosilica structure, the giant basal spicule. Using such spicules as a model, basic knowledge on the morphology, formation, and development of the skeletal elements could be acquired. They are formed by a proteinaceous scaffold (composed of a 27-kDa protein), which mediates the formation of siliceous lamellae that encase the protein. The 27-kDa protein represents an enzyme that forms polysilicate from silicic acid monomers. The silica matrix is composed of almost pure silicon and oxygen, providing it with unusual optophysical properties that are superior to those of man-made waveguides. Experiments suggest that the spicules function in vivo as a nonocular photoreception system. In addition, the spicules are provided with exceptional mechanical properties, combining mechanical stability with strength and stiffness. These basic insights, obtained from the spicule formation in sponges, will surely contribute to a further applied utilization and exploration of silica in biomaterial/biomedical science.

25.1 Introduction: Sponges

The sponges (phylum Porifera) have occupied – since Aristotle (384–322 BC) – a distinguished position among the animals because of their biomedical potential, their beauty, and their enigmatic evolutionary origin. Difficulties in their systematic positioning and in the elucidation of their relationship to other multicellular organisms have resulted in their designation as “zoophytes” or “plant-animals” (a taxon placed between plants and animals) until they were finally recognized as genuine metazoans, which diverged first from the animal ancestor, the urmetazoan [1]. By then it became clear that sponges are not “simple blobs of cells” but contain and express a variety of metazoan-like transcription factors and in turn form sophisticated tissue assemblies [2]. After the discovery/appreciation of the glass sponges [3], the sponges have been grouped into three classes: Demospongiae, Hexactinellida (both have a siliceous skeleton), and Calcarea (calcareous skeleton) [4].

Figure 25.1 gives examples of hexactinellids (*Hyalonema sieboldi*, Fig. 25.1A; *Monorhaphis chuni*, Fig. 25.1F) and one example of demosponge (*Suberites domuncula*, Fig. 25.1G). Sponges were united to the phylum Porifera due to the characteristic and distinct pores on the surface of the animals. They represent the evolutionary oldest, still extant taxon which testifies the developmental level of animals living in the Neoproterozoic Eon (1,000–520 million years ago [MYA]); hence they can be termed “living fossils” [5].

The Hexactinellida are the oldest group of sponges in fossil records of the Sansha section in Hunan (Early Cambrian; China), where more or less completely preserved sponge fossils, like *Solactiniella plumata* (Fig. 25.1B), have been found [6]. This fossil is noteworthy since it shows, besides an unusual body preservation, also very intact siliceous spicules (skeletal elements). The approximately 40-mm-large specimen comprises 0.5–5-mm-long spicules with a diameter of 0.1 mm (Fig. 25.1C); some of them are broken and present the open axial canals. It should be mentioned that high-resolution scanning electron microscopic (HR-SEM) analyses (Fig. 25.1C), coupled with energy-dispersive X-ray, identified those spicules of *S. plumata* as to be composed of the original amorphous silica. In contrast, the characteristic fossil hexactin spicules from hexactinellids found in the Xinjiang Province from the Tarim basin, and dated back to the Ordovician (510–445 MYA), have not conserved their silica state but have been diagenetically converted to calcite microcrystals (Fig. 25.1D, E).

The siliceous sponges disclosed – after application of modern molecular biological and cell biological techniques – a hitherto unknown biochemical reaction, the synthesis of a polymeric inorganic molecule (silica) via an organic molecule, an enzyme (reviewed in [7–9]). Such an activity/reaction was not known before. A thorough elucidation of this process resulted in a paradigm shift which might contribute also to new directions in biomaterial sciences.

25.2 The Power of “Nature as Model” in Bioinorganic Material Science: Shift of a Paradigm

In 1828 Wöhler [10] succeeded to copy nature by producing an organic compound from inorganic reactants. He synthesized urea from the inorganic ammonium cyanate, establishing the first rules in organic chemistry. However, to copy organic (bio)synthetic reactions comprehensively, the existence of enzymes had to be discovered, an important step which dates back to Pasteur [11]. He found that lactic acid is a fermentation product, and thus proved the basis for the discipline biochemistry. In fact, already in 1784 Spallanzani [12] described that gastric juice, soaked into a horny sponge that he had swallowed and subsequently removed from his own stomach, had the potency to digest meat. This experiment can be taken as a first demonstration of (enzymatic) reactions inside living organisms. The causal-analytical understanding of organic reactions in biological systems became possible after the deciphering of the genetic code and the subsequent elucidation and application of molecular biological, recombinant techniques.

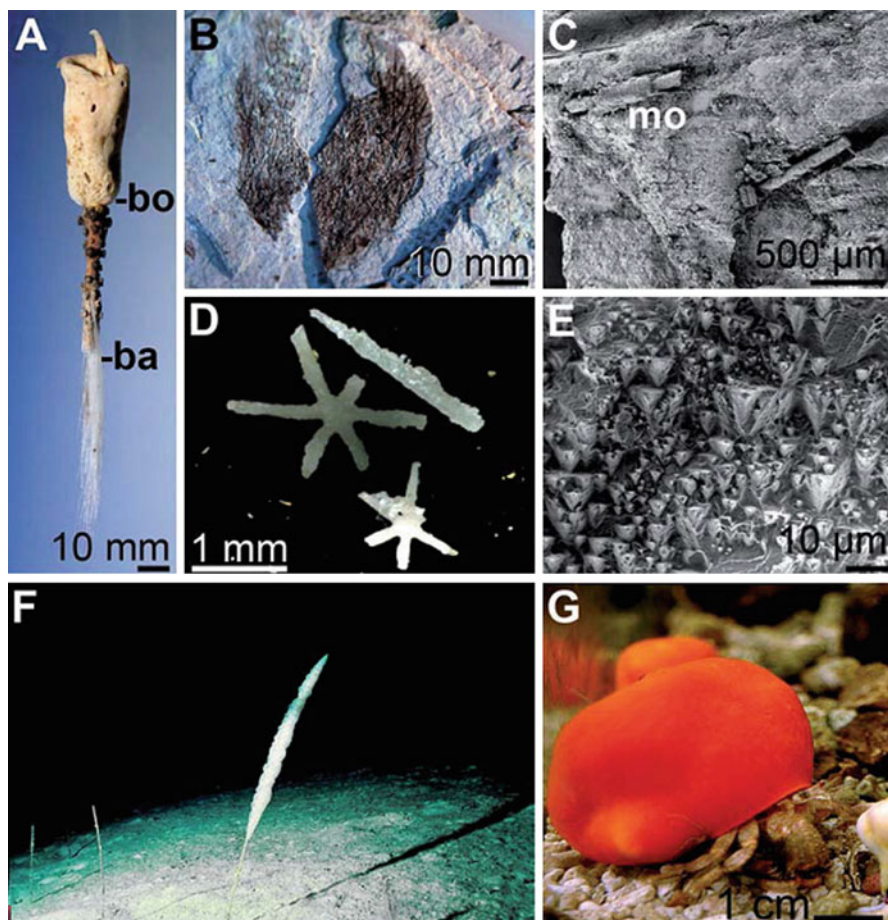


Fig. 25.1 Fossil and present-day siliceous sponges. (A) Hexactinellida: *Hyalonema sieboldi*. Lateral view of a specimen showing the body and the stalk (size 500 mm). Specimens of this hexactinellid can be morphologically divided into the cylindrical upper body (bo) which is attached to 30-cm-long basal stalk spicules, also termed basalia (ba), that fix the specimens to the substratum. (B) Earliest sponge in body preservation, *Solactiniella plumata* (Lowermost Cambrian Sansha section [Hunan, China]) (size 40 mm). (C) High-resolution scanning electron microscope (HR-SEM) analysis was performed to visualize the monaxial spicules (mo) from *S. plumata*. (D) Characteristic fossil hexactin spicules from a hexactinellid, found in the Tarim basin (Xinjiang Province, China); Ordovician (510–445 million years). (E) The silica material in these spicules had been diagenetically converted to calcite microcrystals; HR-SEM. (F) *Monorhaphis* in its natural soft bottom habitat of bathyal slopes off New Caledonia (Photograph taken by Michel Roux, University of Reims; reproduced with permission). (G) Demospongiae: example *Suberites domuncula*. This specimen lives on the hermit crab *Paguristes oculatus* which resides in shells of the mollusk *Trunculariopsis trunculus*; size 30 mm

However, only recently first strategies could be formulated and experimentally proven, to outline the biosynthesis of inorganic structures formed in uni- and multicellular organisms. At present, in a self-accelerating progress, the matrices (templates), e.g., collagen, and the organic catalysts (enzymes, e.g., silicatein) required for the synthesis of such inorganic structures and skeletal elements have been illuminated with the help of inorganic/organic chemists, biochemists, molecular biologists, and material scientists. These interacting and cooperating activities established the discipline of “bioinorganic material science.” The first opportunities have been touched in biomedicine and electronics, providing us with a first indication about the power and potential of this new technology [13–16].

25.3 Levels of Biomineralization

Biomineralization describes processes by which living organisms produce minerals. These widely discovered reactions include also the formation of silica (biosilica) in algae, plants, and invertebrates or of calcium phosphates and carbonates in vertebrates [17–20]. The biologically mediated reactions result in the formation of sea shells or the bones in mammals and birds. Less frequently than silicon- and calcium-based skeleton formation occurs the biomineral formation using copper, iron, and gold deposits. It is one current challenging task to mimic the natural ways of producing minerals/“inorganic polymers” (biomimetics). While related man-made processes, performed by chemical reactions only, require elevated temperatures and strong chemicals, the organisms are able to lay down and form mineral structures at ambient temperatures. Most frequently, those mineralization processes in biological systems allow the formation of composites which comprise, in addition to the inorganic polymer, an organic part, often proteins, which controls those reactions (biomineralization; [19, 20]).

It is the achievement of Lowenstam and Weiner [17] to have systematized processes of biomineralization into the following two categories: the biologically induced mineralization and the biologically controlled mineralization. These two groups are distinguished by the properties of the guiding functions of the organic components. In biologically induced mineralization processes, organic surfaces act as nucleation for the biomineralization. The processes are driven either by the chemical and/or physical properties of organic surfaces only (Fig. 25.2, left), or involve also biochemical reactions (Fig. 25.2, middle). An example for biomineralization processes, occurring on organic surfaces and mediated by their chemical and/or physical properties, is the formation of ferromanganese crusts on marine basaltic seamounts. The deposition of the minerals is facilitated by the pH and redox environment in the vicinity of the coccolith/coccolithophore algae. The formation of manganese nodule involves a biochemical reaction which is based on exoenzymes. Those enzymes facilitate the oxidation of manganese and iron under formation of insoluble reaction products. Finally, the biologically

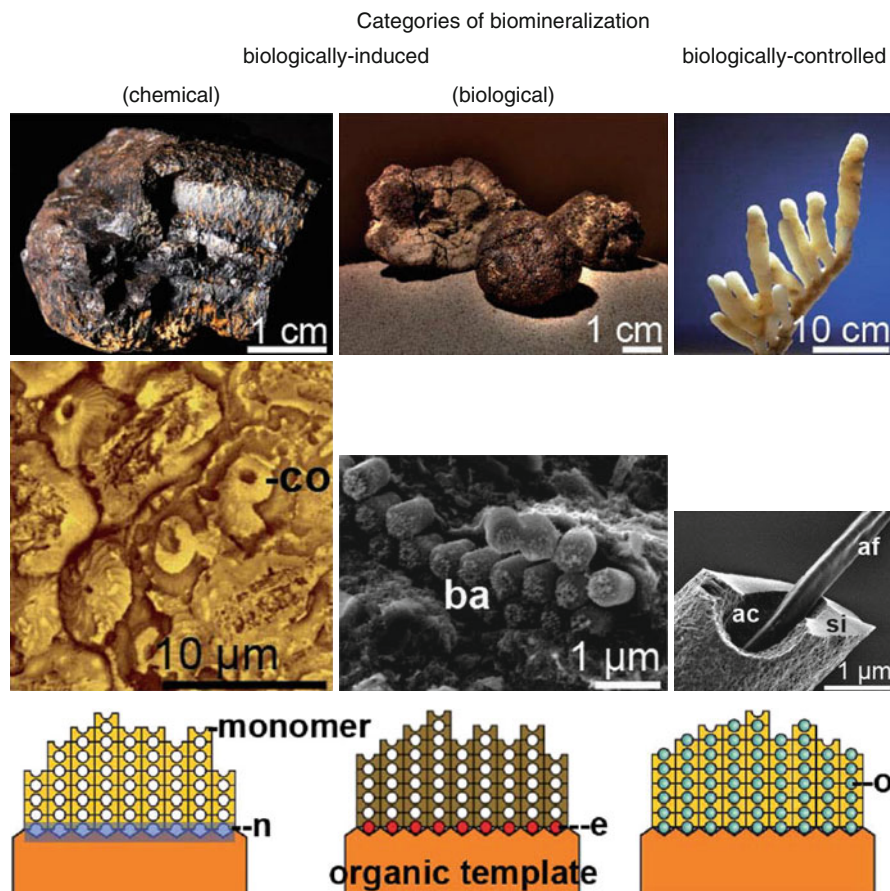


Fig. 25.2 Categories of biomineralization. *Left*: Biologically induced mineralization (based on chemical and physical properties of organic surfaces). Those processes had been elucidated in ferromanganese crusts, formed on basaltic seamounts in the deep sea (*top*). The formation of those mineral deposits is (passively) initiated by the surfaces of calcareous algae, the coccoliths/coccolithophores (co) (*middle*). These organisms act with their surfaces in the initial stage of mineral formation, the induction phase of nucleation (n). The inorganic monomers are deposited, after the nucleation phase, without help of an organic component (*bottom*). *Middle*: Biologically induced mineralization (based on biochemical reactions, which proceed on organic surfaces). In manganese nodules (as likely examples), exoenzymes (e) mediate oxidation of Mn(II) to Mn(IV) and/or Fe(II) to Fe(III) (*top*). The insoluble reaction products precipitate onto organic surfaces. Those oxidation reactions occur on S-layers of bacteria (ba) (*middle*). The further growth of the mineral is independent of organic components (*bottom*). *Right*: Biologically controlled mineralization (the deposition of the minerals is guided by an organic scaffold). This type of mineralization is controlled by an organic matrix and results in the formation of a composite biomineral. The organic component (o) is intimately involved in the formation of polymeric inorganic molecules (*bottom*). Prominent examples for an enzymatically, biologically controlled mineralization are the siliceous skeletons from sponges (*top*) with an example of *Lubomirskia baicalensis*. The enzymatic/proteinaceous matrix is composed of silicatein, which forms the axial filament (af), that resides in the axial canal (ac) and mediates the formation of the silica layers (si) of the spicules (*middle*)

controlled mineralization (the deposition of the minerals guided by an organic scaffold) must be highlighted since in this category the morphology of the inorganic deposition is controlled by an organic matrix. Hence those biominerals represent a composite, formed from the inorganic polymer and an organic component (protein, polysaccharide, glycoprotein). The associations of inorganic monomers are linked together by organic polymers (Fig. 25.2, right). A prominent/unique example of this category is represented by the siliceous sponges. In these organisms the skeletal siliceous elements is enzymatically formed by association of the silicic acid monomers to amorphous biosilica (Fig. 25.2, bottom right).

25.4 Spicule Network in Siliceous Sponges: A Unique Skeleton

In living organisms four major groups of biominerals exist: (1) iron compounds, which are restricted primarily to Prokaryota; (2) calcium phosphates, found in Metazoa; (3) calcium carbonates, used by Prokaryota, Protozoa, Plantae, Fungi, and Metazoa; and (4) silica (opal), present in sponges and diatoms [21]. The formation of the skeleton is a multifaceted process and can be explained in an exemplary way for the siliceous sponges. Even though these animals comprise the simplest body plan, their biomineral structure formation is already highly complex and by far not completely understood. Like the skeletons in triploblasts, the skeleton formation in the diploblastic Porifera also is intimately connected with morphogenesis [8, 22]).

The formation of siliceous spicules in sponges is a genetically controlled process that initiates the morphogenesis phase. Data demonstrated that suitable silicate concentrations induce genes, e.g., those encoding collagen, silicatein, or myotrophin [23]. A major step to elucidate the formation of the siliceous spicules on molecular level was the finding that the “axial organic filament” of siliceous spicules is in reality an enzyme [24–26], silicatein, which mediates the apposition of amorphous silica and hence the formation of spicules.

The skeletal framework of the sponges is highly ordered. In the examples of the demosponge *Suberites domuncula* (Fig. 25.1G) and the hexactinellid *Monorhaphis chuni* (Figs. 25.1F and 25.3A, B), as well as the freshwater sponge *Lubomirskia baicalensis* (Fig. 25.2, upper right), it can strikingly be seen that the growth of the sponges proceeds in a highly organized architecture, mostly in a radiate accretive manner. Most siliceous sponges comprise larger megascleres (>100 μm long) (Fig. 25.3F), and smaller microscleres (<100 μm) (Fig. 25.3D). Some microscleres have bizarre shapes (Figs. 25.3B and 25.4G), while the megascleres usually have a long central rod (Fig. 25.3A). Importantly, the spicules (Fig. 25.4) contain, both in the central hole and within the outer concentric silica layers, the enzyme silicatein. The silica shell of the spicules is synthesized in the initial stage by the silicatein fiber which exists in the central hole, the axial canal. Around this canal a >3- μm -thick siliceous hollow fiber is finally formed (Fig. 25.4B, C, H) [27, 28].

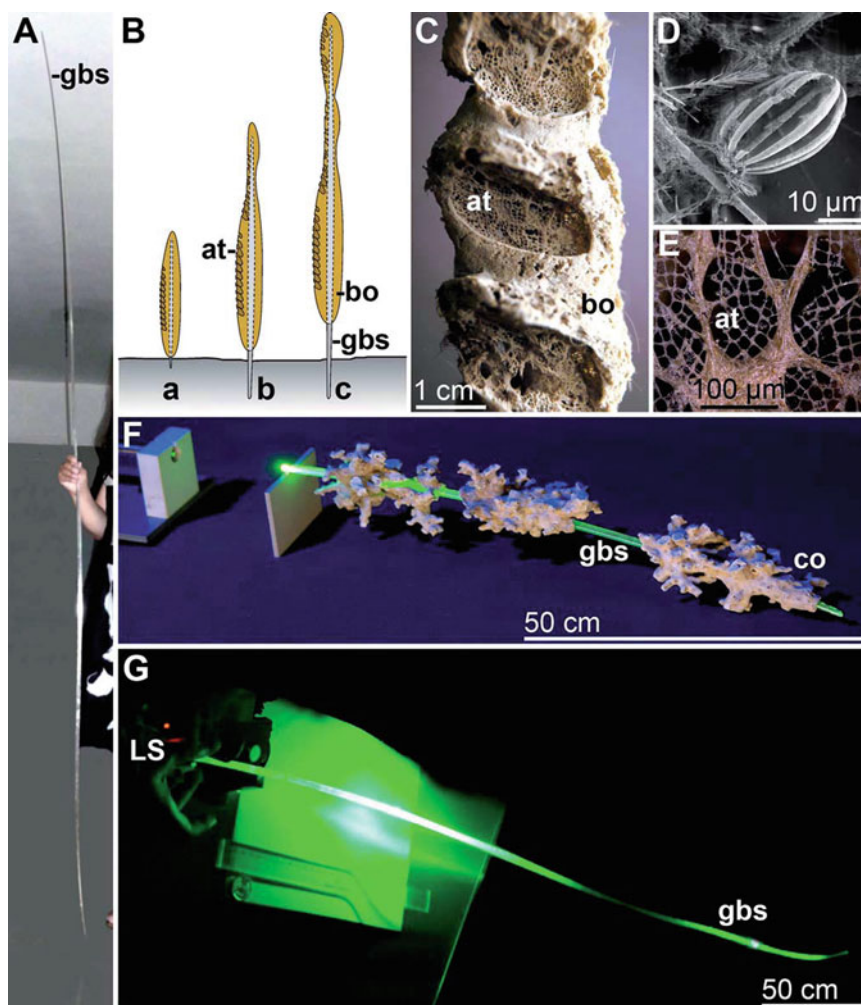


Fig. 25.3 Extreme size and morphology of the spicules in the hexactinellid sponge *Monorhaphis*. (A) A 270-cm-long giant basal spicule (gbs) having a diameter of up to 11 mm. (B) Schematic representation of the growth phases of the sessile animals with their giant basal spicule (gbs) which anchors them to the substratum and holds their surrounding soft body (bo). The characteristic habitus displays linearly arranged large atrial openings (at) of approximately 2 cm in diameter. With growth the soft body dies off in the basal region and exposes the bare giant basal spicule (a–c). (C) Part of the body (bo) with its atrial openings (at). The body surface is interspersed with ingestion openings allowing a continuous water flow through canals in the interior which open into oscules that are centralized in atrial openings, the sieve plates. (D) An ornate mesamphidisk. (E) Grilles forming the atrial openings (at) are composed of different types of spicules, tauactines, framing of lattices, on which the pentactines are arranged in a phalanx. (F) Giant basal spicule (80 cm long), collected 1898/1899 at a depth of 1,079 m off the coast of Somalia (06°18.800'N–049°32.500'E) (Museum für Naturkunde Berlin, Germany; ZMB Por 12700). The spicule (gbs) is surrounded by stony corals (co). (G) The 270-cm-long giant basal spicule was used as an optical waveguide; green light was used as a light source (LS)

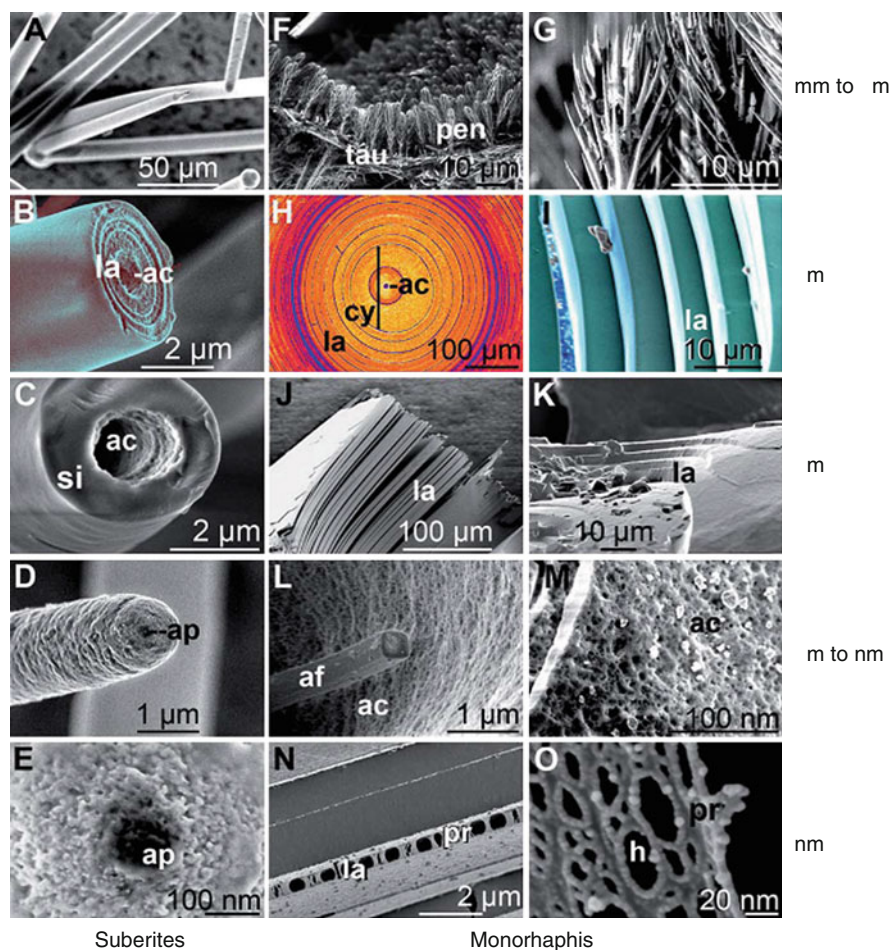


Fig. 25.4 Morphology of the spicules from *S. domuncula* (A–E) and *Monorhaphis* (F–O), as analyzed by their top-down hierarchical organizations. Sequentially, images from the cm to μm level, then around the μm range, proceeding from the μm to nm scale and finally from the nm level are given. *Organization of the S. domuncula tylostyles* ($\leq 400\ \mu\text{m}$): (A) nest of some tylostyles. (B and C) Cross breaks through tylostyles. In (B) a lamellar organization (la) of the silica spicule becomes visible after etching with hydrofluoric acid (HF) vapor. This zonation of the siliceous mantle (si) is absent in those spicules which remained native (C). In both samples the axial canal (ac) is seen. (D) Young tylostyle, approximately $20\ \mu\text{m}$ in length, displays an open aperture (ap) which runs into the axial canal. (E) Higher magnification of the apical aperture (ap). *Monorhaphis spicules*: (F) HR-SEM image of the lattice of a grille. The pentactines (pen) are oriented toward the exterior of the body thus forming a mechanical and relative sealing of the atrial opening. The strutting columns are formed from tauactines (tau). (G) Tip of a dermal pentactine pinnule. (H and I) Structural arrangement of the lamellae in the giant basal spicules; cross sections. In the center of the spicule, the axial canal (ac) is surrounded by the axial cylinder (cy), a region formed from electron-dense homogeneous silica. The third and major part of the spicules is composed of the outer 300–800 concentrically arranged lamellae (la) (H). (I) Higher magnification of the image in (H), taken from the lamellar region. (J and K) Cross breaks through a spicule, showing the piled

25.4.1 Spicule Diversity: Case Study Hexactinellid *Monorhaphis*

The sponge *Monorhaphis chuni* is distributed in the Indo-West Pacific region and is found in depths between 516 and 1,920 m. For most of the studies, specimens dredged from 800 m in the Okinawa Trough and from 1,000 m in the South China Sea have been used. *Monorhaphis* inhabits muddy substrata and is fixed there by a single giant basal spicule. Photographs taken from the natural environment by Roux et al. [29] are available (Fig. 25.1F). Young specimens have been imagined to comprise a continuous body; one giant basal spicule anchors the specimen to the substratum and carries the cylindrical body (Fig. 25.3B). The body is interspersed with many atrial openings which are located along one side (Fig. 25.3B, C, E). Special dermal pinnular pentactine spicules exist (Fig. 25.4F, G) that are aligned along tauactines that frame the atrial openings, the sieve plates (Figs. 25.3E and 25.4F). These tauactines form the grille of the atrial openings and are armed by pentactines, allowing a mechanical sealing of the body toward the aqueous environment. The size of a mesamphidisk (microsclere) is approximately 100 μm (Fig. 25.3D). The diameter of the body reaches in larger specimens 8 cm. During growth the specimens elongate together with an extension of their giant basal spicules (Fig. 25.3B). Older specimens apparently lose the basal portions of their soft body and expose the bare giant basal spicule. While recently giant basal spicules of a size of 1.7 m in maximum have been discovered, now giant spicules with a length of 2.7 m have been collected that are used by the author for the studies. The maximum diameter of that spicule is at its middle 12 mm and at its base 3 mm [27, 30].

25.4.2 Giant Basal Spicules from *Monorhaphis*: The Largest Bio-Silica Structure on Earth

The spicules consist of an organic scaffold and an inorganic silica layer/mantel. The silica mantel is formed from individual lamellae. These lamellae had been analyzed mainly by SEM. The morphological description here proceeds from the millimeter to the nanometer scale. Initial studies on the morphology of siliceous spicules were performed with the spicules from *S. domuncula* [26]. This demosponge comprises only one type of spicules, the tylostyles. They reach in the outer layer of the animals a size of $200 \times 5 \mu\text{m}$ and in the center of the specimens $300\text{--}500 \times 5\text{--}8 \mu\text{m}$ (Fig. 25.4A). All spicules have a $0.3\text{--}1.6\text{-}\mu\text{m}$ -wide axial canal in their center. As shown in SEM images (Fig. 25.4B, C), the central canal is surrounded by lamellated

←

Fig. 25.4 (continued) lamellae (la) (J). (K) A tangential view to a cross break of a giant basal spicule displaying the stepwise layering of the silica lamellae. (L and M) In the axial canal (ac) the square axial filament (af) is seen (L). (M) Higher magnification of the wall of the axial canal toward the center of the spicule. (N and O). Appearance of the proteinaceous palisade-like scaffold (pr) within one lamella (la) after exposure of the spicule to HF vapor. The fibrous structures are interrupted by holes (N). (O) The proteinaceous palisade-like scaffold protein (pr) is composed of fibers that are interconnected and leave open holes (h) whose rims are reinforced

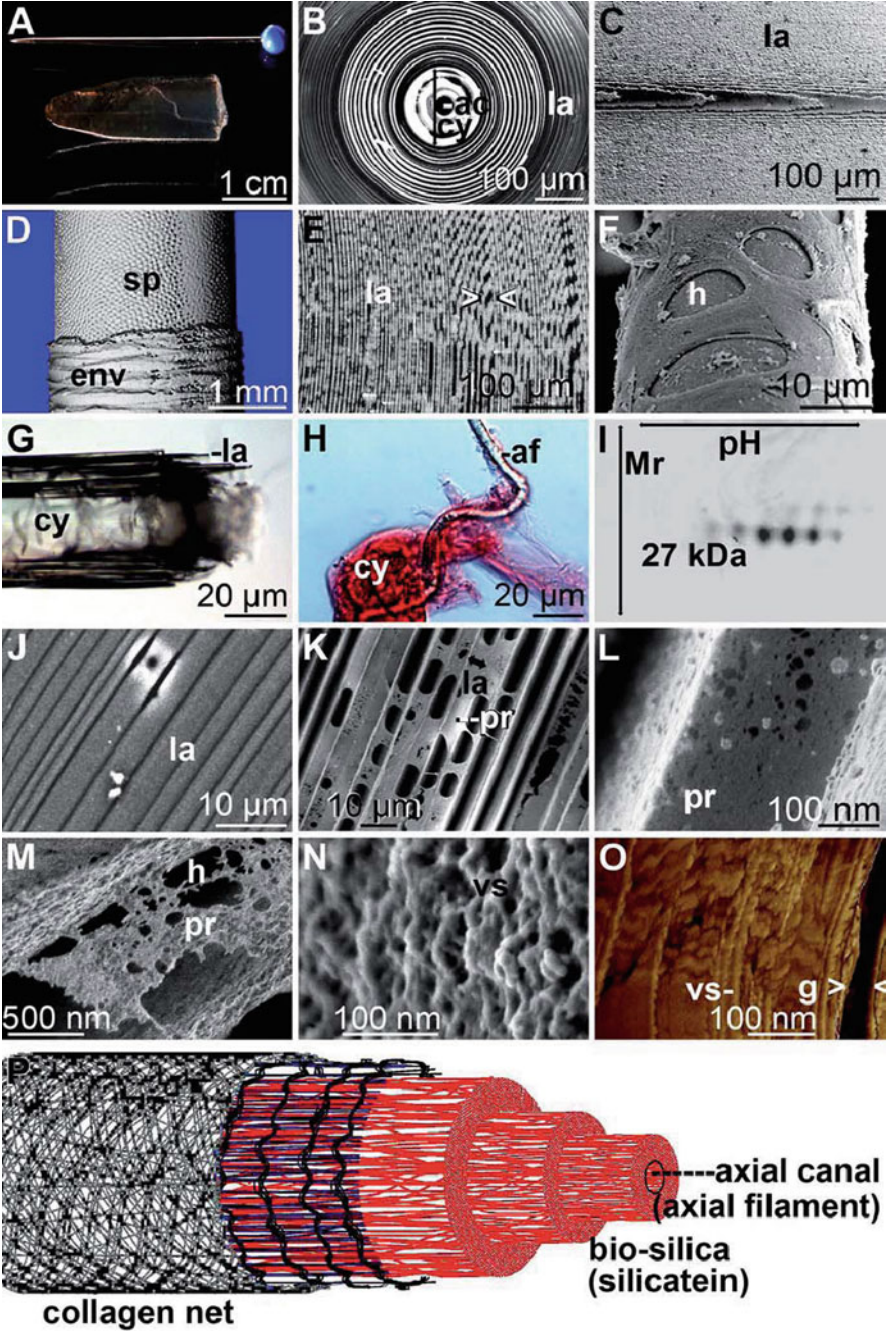


Fig. 25.5 Composite characteristics of the giant basal spicule (*Monorhaphis*). (A) Comparison between the tip of a giant basal spicule (diameter of 7 mm) and a pin/needle. (B) Polished cross

silica layers (Fig. 25.4B). In young, just growing spicules, their tips are open and display an aperture of a size of 100 nm (Fig. 25.4D, E). Based on these exploratory studies, a detailed analysis of the giant basal spicules from *Monorhaphis* became possible [27, 30, 31].

A view of a broken giant basal spicule from *Monorhaphis*, with a large diameter of up to 12 mm (Fig. 25.5A), discloses at the fracture surface the lamellar-wise organization of the silica mantel. A cut through a giant basal spicule shows that the lamellae are arranged in perfect concentric rings around the central axial cylinder (Fig. 25.4H, I).

Millimeter to micrometer scale: Studies were performed by high-resolution scanning electron microscopy (HR-SEM), allowing a resolution of the morphology of the giant basal spicules. A diagonal SEM analysis of a polished cross section of a spicule shows the structural division of the spicule into three zones (Fig. 25.4H). In the center of the spicules lies the axial canal which is surrounded by a region of electron-dense homogeneous silica constituting the axial cylinder of a diameter of 100–150 μm (Fig. 25.4H). The major part of the spicules is composed of 300–800 regularly and concentrically arranged lamellae (each 3–10 μm thick; Fig. 25.4H, I, as well as Fig. 25.5B, C, E). Cross breaks of those spicules show piles of lamellae that open like pages of a book (Fig. 25.4J). A lateral view opens the stepwise arrangement of the layers, reminiscent of the



Fig. 25.5 (continued) section through a giant basal spicule, displaying its three parts, the axial canal (ac), the axial cylinder (cy), and the lamellar region (la). (C) A longitudinal cut through the spicule shows the foliate, lamellar (la) piling of the layers within a spicule. (D) MicroCT analysis of a giant basal spicule. 3D reconstruction of the spicule close to the tip. There, the spicule (sp) is surrounded by an organic envelope (env). The surface of the lamellae shows that protrusions are regularly arranged on the spicule. (E) Polished cross section through a spicule pointing to the discontinued gaps between the lamellae (la). It appears that the connections between the lamellae have an ordered arrangement. One of those connections is marked (> <). (F) A collagen net, perforated with holes (h), surrounds the spicules. (G) During the process of stepwise dissolution of the silica shell around the axial filament (by HF), the lamellar zone (la) starts already after 1–3 min to dissolve. (H) In a later phase the proteins in the axial cylinder (cy) are released that surrounds the axial filament (af); stained with Sirius red. (I) Analysis of the proteins in total extract of the spicules by two-dimensional gel electrophoresis (first isoelectric focusing and then size separation). The gel has been stained with Coomassie brilliant blue. A set of ≈ 27 kDa proteins are stained reflecting their different phosphorylation status. (J–L) Stepwise release of the protein matrix within the lamellae (la), giving rise to the palisade-like proteinaceous scaffold (pr); exposure to HF for 1 min (J), 30 min (K), or 180 min (L). (M) Higher magnification of the fibrous structure from the lamellae, the palisade-like scaffold (pr), disclosing holes (h). (N) A slightly etched cross section through a spicule. Vermicular structures (vs) within the lamellae are disclosed. (O) Analysis of those spicular surfaces by atomic force microscope (AFM), displaying the vermicular structures (vs) as concentric arranged cables. In addition, one gap between two lamellae is visible (g). (P) Scheme summarizing the morphological zones of the giant basal spicules, outlining their composite property. The axial canal harbors the organic axial filament. This structure is surrounded by the silica mantel which comprises within its lamellae the protein/enzyme, silicatein. This silica mantel is surrounded by a collagen net

seat rows in an amphitheater (Fig. 25.4K). The interlamellar space of the spicules does surprisingly not constitute a continuous open slit. The slit is in average 0.1–0.2 μm wide and is composed of alternating fusion zones and open gaps; apparently the fusion zones allow a continuum between silica lamellae (Fig. 25.5E). The axial canal harbors the organic axial filament which has a characteristic rectangular shape (Fig. 25.4L). The wall of the axial canal is not completely smooth but displays a fine-structured network, composed of 20–40-nm-large silica granules (Fig. 25.4M).

Nanometer scale: Studies, to obtain an insight into the structural organization of the spicules at the nm scale, have been performed after mild, partial, and limited dissolution of the silica material by hydrofluoric acid (HF). Under such conditions the organic matrix is released from the interior of the lamellae (Fig. 25.4N, O). In light microscopic studies it could be shown that the dissolution kinetics (caused by HF) is different in the region of the axial cylinder and the lamellar region. The dissolution starts from cracks in the spicule, primarily following the gaps between the lamellae (Fig. 25.5G). During this process the lamellar zone can be distinguished from the axial cylinder by the protruding ends of dissolving individual lamellae (Fig. 25.5G). The dissolution of the axial cylinder proceeds from the periphery without revealing individual lamellae (Fig. 25.5H). Application of different dyes allows a differential visualization of the proteinaceous components. While Coomassie brilliant blue stains the released protein from the lamellae and the axial cylinder, the polypeptides released from the axial cylinder react selectively with Sirius red (Fig. 25.5H).

Next the HR-SEM technique was applied to detect/identify the proteinaceous scaffold that is released after HF treatment (Fig. 25.5J–L). In the transition phase, until a complete dissolution by HF is reached, the siliceous surfaces of the lamellae remain visible (Figs. 25.4N and 25.5K); they are held up by palisade-like pillar structures composed of proteinaceous material. The individual pillars have a diameter of 0.1–0.2 μm and a length of 5–10 μm (Figs. 25.4O and 25.5M). The proteinaceous material obtained was characterized biochemically as one distinct protein with an apparent size of ~ 27 kDa. Slightly etched spicules show on the surfaces vermicular structures of diameters of 20–30 nm (Fig. 25.5N), likely to represent the proteinaceous matrix. The different mechanical properties of these vermicular structures within a lamella can be visualized by atomic force microscope (AFM) analysis (Fig. 25.5O); these structures follow the concentric arrangement/orientation of the lamellae [8].

25.4.3 Chemical Composition

The gross chemical composition of sponge spicules has been described both for Demospongiae and for Hexactinellida. Already Schulze [32] determined that besides Si (silicon) and O (oxygen) (96%), only trace amounts of Na and K contribute to the inorganic material. Hence the silica (opal) of the spicules possesses quartz glass quality [33].

25.4.4 Giant Basal Spicules – Protein Scaffold

Surprisingly it was found that the siliceous lamellae, composing the spicules from *Monorhaphis*, contain also a proteinaceous scaffold. The proteinaceous material obtained was characterized by NaDodSO₄-PAGE and found to represent one distinct protein with an apparent size of ≈ 27 kDa (Fig. 25.5I) [31, 34, 35]. If such a protein sample is subjected to two-dimensional gel electrophoresis, the proteins are separated into acidic and alkaline sets of protein (Fig. 25.5I). Work had been focused especially on the identification of the function of the ≈ 27 -kDa protein. By applying biochemical and immunobiochemical techniques, it could be established that this ≈ 27 -kDa protein represents the silica-forming enzyme, silicatein. This molecule constitutes the axial filament as well as the matrix of the silica lamellae. Hence, the “inorganic” silica material of the spicules represents a composite, formed of protein and silica (Fig. 25.5P).

Collagen is surely, also in sponges, an important component in the morphogenesis of the spicules. These fiber polypeptides surround the spicules as a fibrous sheath. By application of the SEM technique, the collagen net was found to be regularly interrupted by circular holes (7–10 μm ; Fig. 25.5F). Microtomography (MicroCT) analysis revealed that this organic envelope (collagen fibrils) surrounds the inorganic spicule (Fig. 25.5D). In addition, it could be visualized that the surface of the silica spicule is not even but has a serrated relief structure. The protrusions are arranged in an organized pattern, an almost regular helical succession of small projections (Fig. 25.5D, P) [36].

25.4.5 Biochemical Properties and Intracellular Localization of Silicatein

The kinetic parameters for silicatein follow those of usual enzymes; the Michaelis constant (K_m) for silicatein was determined to be 22.7 μM , and the corresponding V_{max} (maximal velocity) was 9.6 nM/min [9].

The spicules are formed in the first stage intracellularly and are completed extracellularly. Silicic acid is taken up intracellularly via a $\text{Na}^+/\text{HCO}_3^-$ [$\text{Si}(\text{OH})_4$]-cotransporter system [37]. There silicic acid is accumulating in special organelles, the silicasomes (Fig. 25.6). Within this compartment, the first immature spicules are formed from silicic acid under formation of polysilica around the silicatein/axial filament (Fig. 25.6A). Subsequently those immature spicules are extruded into the extracellular space where the spicules are completed by the (also) extracellularly existing silicatein. This biomineralization pathway, enzymatic formation of intracellular polysilica structures and subsequent extracellular completion of the spicules by silicatein, is unique and found only in sponges (Fig. 25.6A).

These data, first the selective uptake of silicic acid by membrane-associated transporters and then formation of polysilica structures by the enzyme silicatein, allows also a biochemical explanation of the ability of sponges to form high-quality

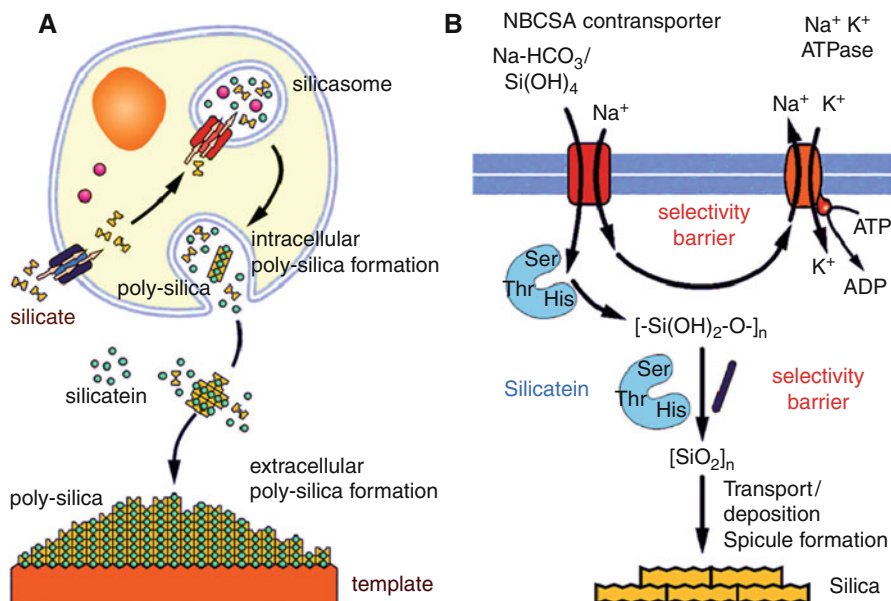


Fig. 25.6 Schematic outline of the enzymatic synthesis of polysilica structures (biosilica) and of the transport of silicic acid into sponge cells. **(A)** Orthosilicate (silicic acid) is taken up by a membrane-associated transporter. From there the silicic acid monomers are transported into the silicasomes and undergo association with the silicatein enzyme. After formation of the first silica structures, the immature spicules are released from the cells and completed extracellularly by the existing silicatein molecules and silicic acid. **(B)** Scheme outlining the two selectivity barriers that control the synthesis of the pure biosilica product. The Na⁺-bicarbonate⁻/silicic acid cotransporter mediates the uptake of silicate, allowing a strong selective enrichment of silicate in the cells and in the tissue of the sponges (first selectivity control). Na⁺ is pumped out via the Na⁺/K⁺ ATPase transporter under the consumption of ATP. The second selectivity control is on the level of silicatein, which will accept – substrate specifically – only silicate under formation of biosilica

quartz glass spicules. This high purity is the result of a selective uptake [Si(OH)₄-cotransporter system] and selective deposition of polysilica (silicatein) (Fig. 25.6B).

25.4.6 Cloning of the Hexactinellid Silicatein cDNA

Only sponges are provided with the polysilica-forming enzyme, silicatein. After cloning of the silicateins from demosponges, it became obvious that silicatein belongs to the class of cathepsins, with cathepsin L as the most prominent member [23, 25]. This lysosomal enzyme belongs to the family of papain-like peptidases that are characterized by the catalytic triad of cysteine (Cys), histidine (His), and asparagine (Asn). The silicateins are distinguished from the cathepsins by the exchange of the first amino acid (aa) residue in the catalytic triad, Cys by Ser. In addition, the silicateins are distinguished from the cathepsins by the presence of

a Ser stretch that precedes the second aa in the catalytic triad, His. Like demosponges (Fig. 25.7), also hexactinellids contain the silicatein enzyme. Recently, also the gene encoding this enzyme in Hexactinellida has been isolated from *Crateromorpha meyeri* [34].

25.5 Modeling of the Morphology of the Spicules

The determination of the spicule morphology remains one of the most enigmatic processes in sponges. Surely, the sizes and forms of the spicules are under species-specific control. However, only little information is presently known to define those control systems, governing the growth and form processes. The basis of the spicule formation is defined by the axial filament that elongates by a controlled interaction of silicatein molecules. Silicatein, especially if it is extracted from the spicules under mild, nonharsh conditions, readily forms dimers through noncovalent linkages. Subsequently, filaments/aggregates are formatted from monomeric silicatein, suggesting a reassembly through fractal-like structures [28, 38, 39]. Those native protein samples reveal after NaDodSO₄-PAGE (one-dimensional separation) analysis only one band of a size of 27 kDa (Fig. 25.8A-a). If the sample is subjected to two-dimensional gel electrophoresis, the proteins are separated into a series of isoenzymes, due to different phosphorylation states. The number of silicatein spots on the gel is considerably larger if extracts obtained by mild (short) HF dissolution (Fig. 25.8A-b) are analyzed, than with extracts obtained after extensive (>24 h) HF dissolution (Fig. 25.8A-c). This finding reflects the fact that during HF treatment, phosphate groups are split off from the protein.

We ascribe to the axial filament a major role as a form factor for the determination of the morphology of the spicules. From the *S. domuncula* silicatein it is known that the enzyme exists in at least two isoforms, transcribed from two different genes, silicatein- α and silicatein- β [28, 38, 39]. These proteins readily form dimers, tetramers, as well as hexamers. Furthermore, it could be worked out that the two isoforms associate in a defined stoichiometric ratio: four molecules of silicatein- α with one molecule of silicatein- β . It has been suggested that the four silicatein- α molecules form a platform with serine clusters directed to the center. These serines of the coaxially arranged silicateins interact with silicatein- β . In order to attribute a function to the obviously crucial phosphate units linked to the silicatein, it is proposed that the orientation of the 4:1 silicatein assembly undergoes alterations driven by different phosphorylation levels of the enzyme (Fig. 25.8C). The first support came from studies with the different silicatein molecules isolated from the demosponge *Geodia cydonium*. This species comprises two types of spicules, sterrasters (which are microscleres) and anatriaenes (megascleres) (Fig. 25.8D, E). It could be shown that these spicules comprise not only a different set of silicateins but also silicateins with a distinct and different phosphorylation pattern. We propose that cells adjacent to the spicules secrete both silicatein and collagen that forms a well-controlled proteinaceous tube into which the axial cylinder and the lamellar zone are imbedded.

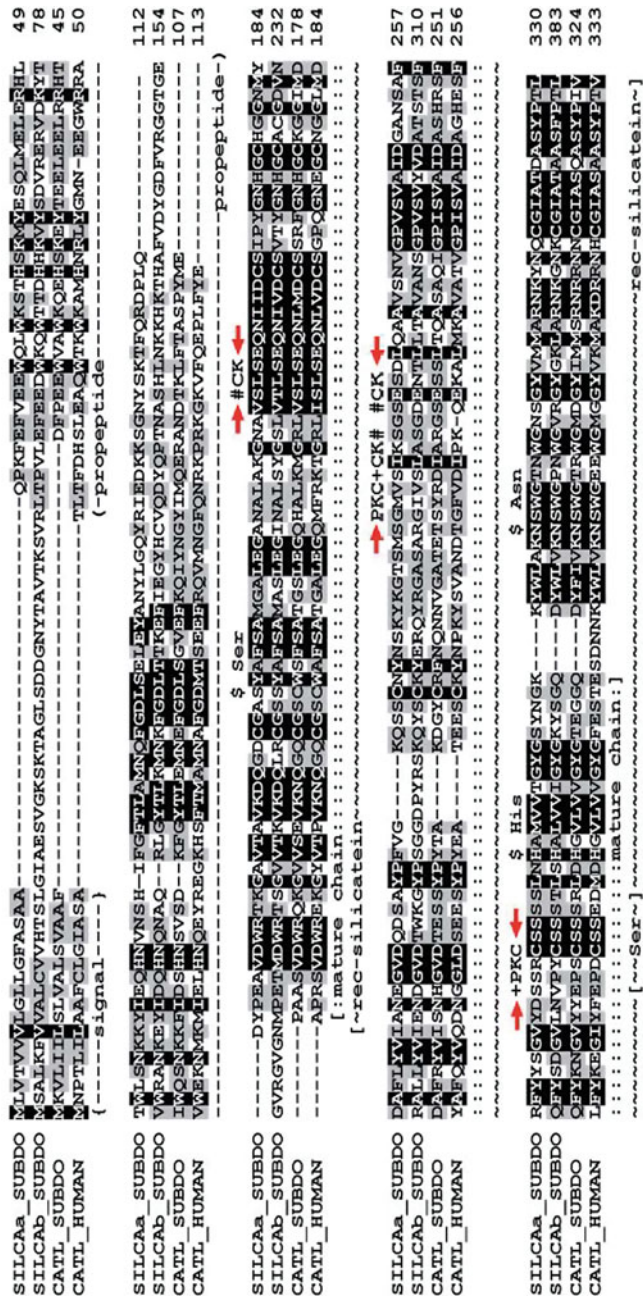


Fig. 25.7 Silicae:in: sequence. The silicae protein from the hexactinellid *C. meyeri* was deduced from the isolated cDNA and aligned with silicae- α from *S. domuncula* (SILCAa, SUBDO) and silicae- β from *S. domuncula* (SILCAB, SUBDO) and one isoform of silicae- α from *L. baicalensis* (α -3) (SILCAa3, LUBAI) as well as with the cathepsin L sequences from *S. domuncula* (CATL, SUBDO) and human (CATL_HUMAN). Residues conserved (similar or related with respect to their physicochemical properties) in all sequences are shown in white on black, and those in at least four sequences in black on gray. The characteristic sites in the sequences are marked; the catalytic triad (CT) amino acids, Ser in silicae and Cys in cathepsin, and His and Asn. The borders within the mature silicae (mature peptide), the signal peptide as well as the propeptide are given. The stretch of the enzymatically active silicae molecule has been used for the preparation of recombinant, active silicae. The “conventional” serine cluster (Ser) is marked. Finally the potential phosphorylation sites within the sequences are listed above the alignment

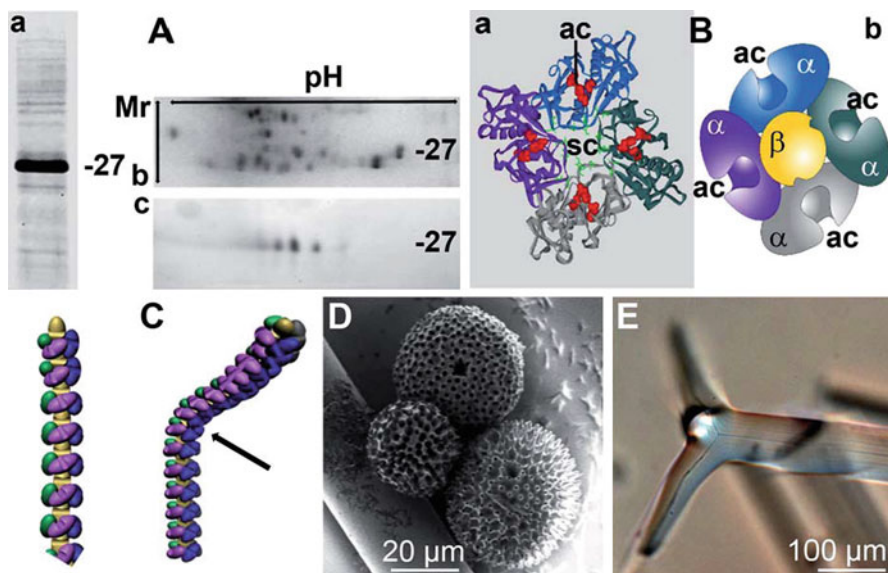


Fig. 25.8 Silicatein protein, space model and backbone for the synthesis of the diverse silica structures, giving rise to the spicules. (**A-a**) Analysis of the total spicule extract by one-dimensional gel electrophoresis. The line marks the position of the 27 kDa protein. The gel was stained with Coomassie brilliant blue. (**A-b** and **A-c**) Analysis of a total spicule extract by two-dimensional gel electrophoresis (first isoelectric focusing and then size separation). Protein extract was collected after mild (short) (**A-b**) or extensive (>24 h) (**A-c**) HF-dissolution. The lines mark the positions of the 27-kDa polypeptides. (**B**) Schematic representation of planar-oriented silicatein- α tetramer (α ; green-gray-blue-pink) with one silicatein- β (β) in the center (yellow). The amino acids involved in the active centers (ac) of the silicateins are marked. In this orientation the Ser-rich clusters (sc) are directed toward the center of tetramer (**B-a**). (**B-b**) Graphical model of the silicatein- α tetramer with the silicatein- β in the center. (**C**) Working model proposing that the orientation of the 4:1 silicatein assembly is changed by an alteration of the level of phosphorylation state of the enzyme molecules (arrow). (**D**) Sterrasters (microscleres) from the demosponge *Geodia cydonium*. (**E**) The tip of a megasclere (anatriaene)

25.5.1 Phases of Silica Deposition During Spicule Formation

The process of spicule formation can be divided into the following phases: the initial intracellular steps and the extracellular final and shaping phase.

The intracellular phase in the sclerocytes: In the first steps silicatein is synthesized as a proenzyme and processed via the 34.7-kDa form (propeptide-mature enzyme) to the 23-kDa mature enzyme [26, 27]. Very likely during the transport through the endoplasmic reticulum and the Golgi complex, silicatein undergoes phosphorylation and is transported into silicasomes where it forms rods, the axial filaments (Fig. 25.6A). After assembly to filaments the first layer(s) of silica is (are) formed. Silica deposition occurs in two directions: first from the axial canal to the surface (centrifugal orientation) and second from the mesohyl to the surface of the

spicule (centripetal). Finally the spicules are released into the extracellular space where they grow in length and diameter by appositional growth.

Extracellular phase (appositional growth): Silicatein is present also in the extracellular space. It came surprising that also there the silicatein molecules are organized to larger entities. The immunogold electron microscopical analysis showed that the silicatein molecules are arranged along strings, which are organized in parallel to the surfaces of the spicules. In the presence of Ca^{2+} , silicatein associates with galectin and allows the appositional growth of the spicules (Fig. 25.9). Since the surface of a new siliceous spicule is also covered with silicatein, the appositional growth/thickening of a spicule hence proceeds from two directions (centrifugal and centripetal). In the next step, the galectin-containing strings are organized by collagen fibers to net-like structures. It is very likely that collagen, which is released by the specialized cells the collencytes, provides the organized platform for the morphogenesis of the spicules. The longitudinal growth of the spicules can be explained by the assumption that at the tips of the spicules, the galectin/silicatein complexes are incorporated into deposited biosilica under formation and elongation of the axial canal [39].

25.5.2 Giant Basal Spicules – Mechanical Properties

Inspired by studies with *Monorhaphis*, a new concept of natural composite material in rigid biological systems was born and fundamentally outlined by Mayer [40]. The organic phase controls energy dissipation especially in systems that are interspersed by very thin organic layers. In continuation of this topic, it had been proposed from their load–displacement studies that breakage of hexactinellid spicules follows a telescope-like pattern [30, 31].

Images from a typical load–displacement experiment with spicules from *Monorhaphis* are given in Fig. 25.10. The pattern of fractures within the spicule was correlated with the organization of the lamellar zone and the axial cylinder, since both areas are characterized by different bioorganic/inorganic hybrid compositions (Fig. 25.10A–D). With increasing load, a sequential breakage of the lamellae occurred. At first the outer, concentrically arranged silica layers burst, followed by the more inwardly located layers. If a sample from an unbroken, nontreated spicule was subjected to the classical bend test, the resulting load–displacement curve showed at first a linear increase reflecting the elastic response of the outer lamellar layers of the spicule. The following deflection does not drop to zero but is fixed according to the viscoelastic view by the more central lamellar layers.

The stepwise breakage of an untreated giant spicule (from the hexactinellid *Hyalonema sieboldi*; diameter of 0.8 mm) is shown in Fig. 25.10E–L. The spicule was inserted into a traction device between two moving rubber wheels, and continuous pulling was achieved by a motor. If the breaking process is recorded with a high-speed camera, the first crack of the outer lamellae is not visible even if the spicule has been completely bent by one circumvolution, leaving a diameter of the circular, wrapped-around spicule of 4.5 cm (Fig. 25.10E). However, after

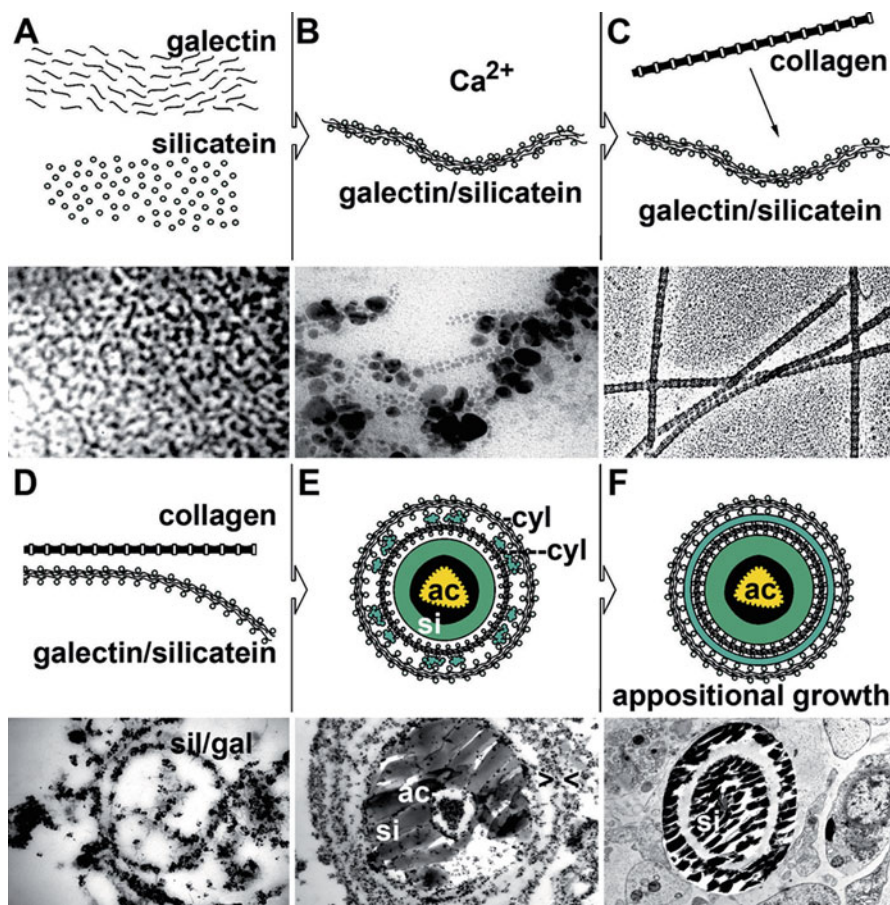


Fig. 25.9 Schematic outline of the appositional spicule formation in sponge (example *S. domuncula*). The process of the appositional growth of the spicules occurs in the extracellular space (mesohyl). (**A** and **B**) There, galectin molecules associate in the presence of Ca^{2+} to strings (nets) that allow binding of silicatein molecules. (**C**) Collagen fibers orient the silicatein-galectin strings concentrically round the growing spicules. (**D–F**) In the last steps, the silicatein-galectin strings oriented by collagen fibers circle and allow biosilica deposition within the formed cylinder (> <). After completion of one biosilica lamella (si), the next biosilica lamella starts in the same manner by apposition onto the previous lamella (**E**). The initial biosilica layer is formed around the silicatein rod (axial filament), existing in the axial canal (ac) of the spicules. Below the graphs the corresponding electron microscopic images are given

pulling the circle down to 4 cm, the first set of the outer lamellae blasts off (Fig. 25.10F). Then another period of flexible bending proceeds until the second breakage point is reached (Fig. 25.10H). Again, a further flexible bending phase takes place until a third spalling of the lamellae occurs, followed by a final fracture of the spicule (Fig. 25.10K). In comparison, the breakage of a quartz glass fiber of

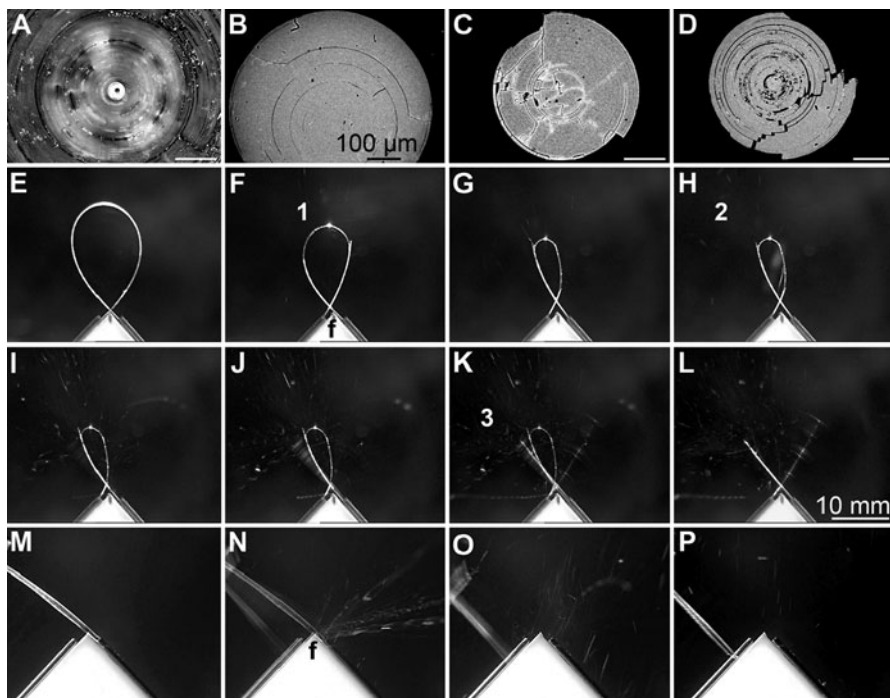


Fig. 25.10 Force displacement relationship of a giant basal spicule, as measured in a 3-point bending assay. (A) SEM analysis of a partially noncracked spicule. (B–D) After increased loading, the silica layers crack starting from the surface of the spicules. (E–L) Flexible breakage of a giant spicule (from *H. sieboldi*), (M–P) in comparison to quartz glass fibers. The diameter of both fibers was about 0.8 mm. The fibers were inserted into a traction device between two moving rubber wheels and were continuously pulled toward the fixation point (F) using a motor. The breakage was recorded with a high-speed camera. The spicule had been completely bent by one circumvolution; the diameter of the circular, wrapped-around spicule was initially 4.5 cm. After proceeding traction, three stepwise breaking steps can be recorded (F, H, and K) which are interrupted by phases of flexible bending. In contrast, an abrupt and total fracture of a quartz glass fiber is recorded. Even before a complete circle could be wound, the fiber blasted

a similar diameter has been recorded (Fig. 25.10M–P). As expected, the glass fiber cannot even be bent to a large circle but cracks almost immediately after an inflection of about 30°.

25.5.3 Giant Basal Spicules – Optophysical Properties

Sponges can react fast to physical stimulation from the environment with contraction or expansion. These observations could imply that the coordinate reactions are governed by a nerve system. However, until now no nerve fibers or synapses could be identified in sponges. Nevertheless, our previous studies showed that the siliceous demosponges *S. domuncula* and *G. cydonium* contain and express genes coding for neuronal molecules, e.g., a metabotropic glutamate/GABA

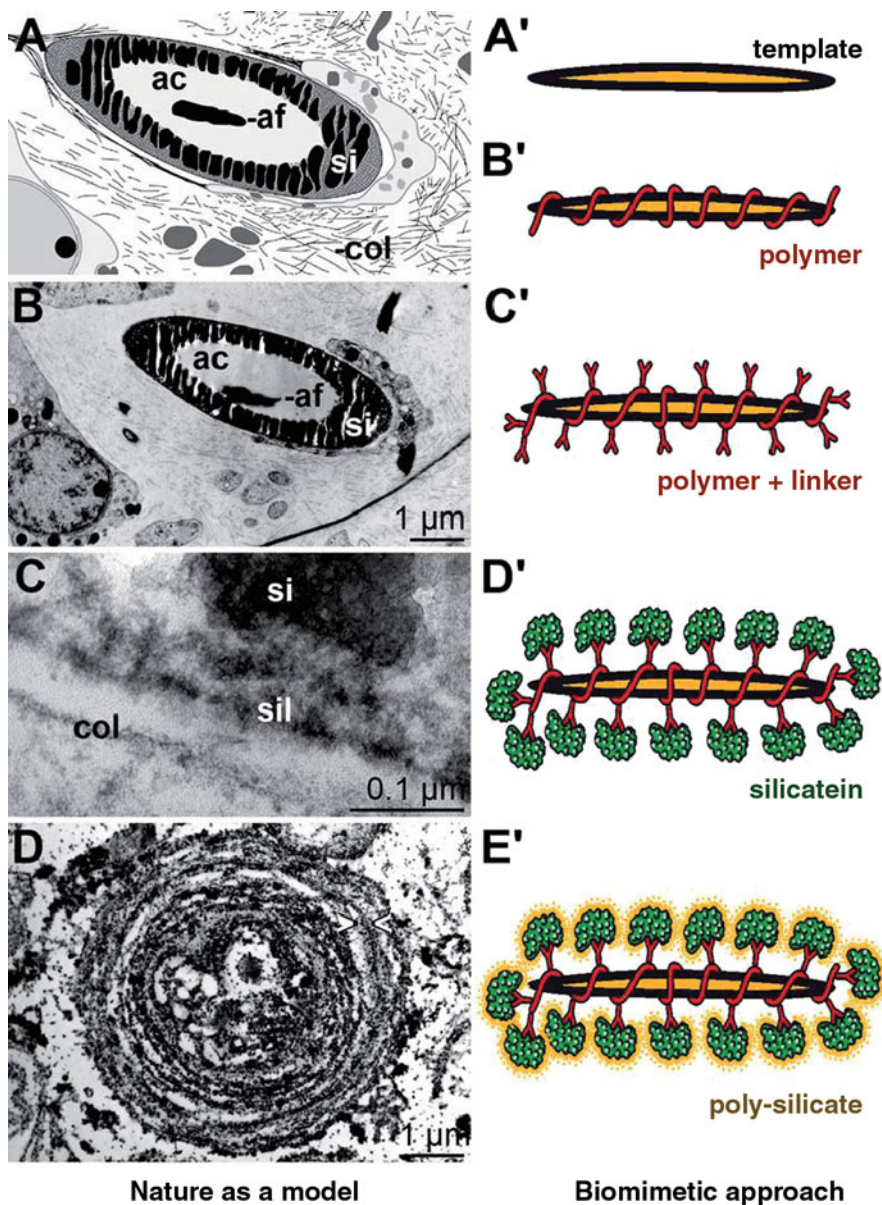


Fig. 25.11 “Nature as a Model” – a biomimetic approach. (Left panel: A–D) Synthesis of spicules in the extracellular space. (A) Scheme; cross section through a growing spicule with the silica mantle (si) which surrounds the axial canal (ac) that harbors the axial filament (af). In the extracellular space collagen (col), fibers are indicated. (B and C) SEM images showing the respective sections; silicatein molecules are marked (sil). (D) Immunogold labeling with antibodies raised against silicatein to visualize the organic cylinders which guide and mediate the synthesis of the silica layers in an appositional manner (marked > <). (Right panel: A'–E') The

(γ -aminobutyric acid)-like receptor. Furthermore, it is well established that sponge embryos and adult sponges react to light. So far all attempts to identify photosensory cells in sponges failed. Therefore, the question was raised, if noncellular structures, like spicules, might function as biological receiver for light energy. The first prerequisite was already discovered to a great extent by the findings that spicules from sponges can transmit light. In these elegant studies, the hexactinellids *Rossella racovitzae* and *E. aspergillum*, *H. sieboldi*, and *Monorhaphis* (Fig. 25.3G) were used. It could be demonstrated that these large spicules transmit light with high efficiency. The blue light with a wavelength between 400 and 600 nm is filtered out. Based on this finding, it has been suggested that the spicules from hexactinellids act as an optical absorbent in a novel photo-reception. This assumption has been supported by the recent finding that sponges possess the luciferase enzyme [41].

25.6 Biomimetic Approaches

Electron microscopy studies revealed that spicule formation occurs by appositional layering. In the extracellular space, the spicules grow through apposition of lamellar silica layers up to their final size of 450 μm (Demospongiae) or 2.5 m (Hexactinellida). Based on the experimental studies on the extracellular growth of the spicules, the natural principle (“Nature as a Model”) was applied in a biomimetic way. As mentioned, growth of the spicules is guided by an organic cylinder formed from silicatein and galectin that results in the formation of biosilica lamellae (Fig. 25.11; left panel) [15, 16].

This concept from the elucidation of the different phases of spiculogenesis and the molecules involved in it allows a wide application of silicatein in the field of nanobiotechnology. This principle has been utilized by the group of Tremel to synthesize on an “inert” surface (matrix), biosilica from monomeric precursors [42–44]. The matrix used had been activated by cysteamine to allow binding to a reactive polymer; in turn this polymer is able to chemisorb the nitrilotriacetic acid ligand. Finally, this architecture allowed the binding of recombinant histidine-tagged silicatein (Fig. 25.11, right panel). Surprisingly enough, silicatein immobilized onto this matrix has the capacity to catalyze biosilica and even biotitania and biozirconia from the monomeric precursors. This is a further striking example to show that nature can be used as a biological blueprint for nanobiotechnological applications. In addition, this technology introduces a new concept, the synthesis of inorganic polymers by an organic molecule (silicatein). Just in opposite, in 1828, Wöhler succeeded with his epochal experiments on the synthesis of



Fig. 25.11 (continued) biomimetic approach. (A' and B') The template is functionalized with a reactive ester polymer and (C') then with the NTA linker. (D') The recombinant silicatein is bound via the His-tagged to the NTA polymer. (E') The recombinant silicatein mediates polysilica formation and forms a silica lamella like nature does in sponge spicules

urea, an organic compound, from inorganic basic materials (“die künstliche Erzeugung eines organischen, und zwar animalischen, Stoffes aus unorganischen Stoffen”).

Acknowledgments W.E.G.M. is holder of an ERC Advanced Investigator Grant (No. 268476 – BIOSILICA). This work was supported by grants from the German Bundesministerium für Bildung und Forschung (Project “Center of Excellence *BIOTECmarin*”), the Deutsche Forschungsgemeinschaft (Schr 277/10-1), the International Human Frontier Science Program, the European Commission (Grant No. 031541-BIO-LITHO [biomineralization for lithography and microelectronics]), the consortium BiomaTiCS at the Universitätsmedizin of the Johannes Gutenberg-Universität Mainz, and the Public Welfare Project of Ministry of Land and Resources of the People’s Republic of China (Grant No. 201011005–06).

References

1. Müller WEG (2001) How was the metazoan threshold crossed? The hypothetical Urmetazoa. *Comp Biochem Physiol A* 129:433–460
2. Müller WEG, Wiens M, Adell T, Gamulin V, Schröder HC, Müller IM (2004) Bauplan of urmetazoa: basis for genetic complexity of metazoa. *Int Rev Cytol* 235:53–92
3. Schulze FE (1887) Report on the Hexactinellida collected by H.M.S. Challenger during the Years 1873–76. In: Sir. C. Wyville Thomson, Knt., F.R.S., & C. Regius (ZOOLOGY Part LIII), Murray J (eds) Report of the scientific results of the voyage of H.M.S., London
4. Hooper JNA (1997) Sponge guide to sponge collection and identification. Internet: <http://www.qmuseum.qld.gov.au/nature/explorenature/sponge.can> and <http://xa.yimg.com/kq/groups/21368769/1183738468/name/Guide+to+sponge+identification.pdf>
5. Müller WEG, Li J, Schröder HC, Qiao L, Wang XH (2007) The unique skeleton of siliceous sponges (Porifera; Hexactinellida and Demospongiae) that evolved first from the Urmetazoa during the Proterozoic: a review. *Biogeosciences* 4:219–232
6. Wang XH, Hu S, Gan L, Wiens M, Müller WEG (2010) Sponges (Porifera) as living metazoan witnesses from the Neoproterozoic: biomineralization and the concept of their evolutionary success. *Terra Nova* 22:1–11
7. Morse DE (1999) Silicon biotechnology: harnessing biological silica production to construct new materials. *Trends Biotechnol* 17:230–232
8. Müller WEG, Wang XH, Belikov SI, Tremel W, Schloßmacher U, Natoli A, Brandt D, Boreiko A, Tahir MN, Müller IM, Schröder HC (2007) Formation of siliceous spicules in demosponges: example *Suberites domuncula*. In: Bäuerlein E (ed) Handbook of biomineralization, vol 1, The biology of biominerals structure formation. Wiley-VCH, Weinheim, pp 59–82
9. Müller WEG, Schloßmacher U, Wang XH, Boreiko A, Brandt D, Wolf SE, Tremel W, Schröder HC (2008) Poly(silicate)-metabolizing silicatein in siliceous spicules and silicasomes of demosponges comprises dual enzymatic activities (silica-polymerase and silica-esterase). *FEBS J* 275:362–370
10. Wöhler F (1828) Ueber künstliche Bildung des Harnstoffs. *Annalen Physik Chemie* 12:253–256
11. Pasteur L (1857) Mémoire sur la fermentation appelée lactique. *Mém Soc Sci Agric et Arts* 5:13–26
12. Müller WEG, Batel R, Schröder HC, Müller IM (2004) Traditional and modern biomedical prospecting: I. The history. Sustainable exploitation of biodiversity (sponges and invertebrates) in the adriatic sea at Rovinj (Croatia). *Evid Based Complement Altern Med* 1:71–82

13. Aizenberg J, Sundar VC, Yablon AD, Weaver JC, Chen G (2004) Biological glass fibers: correlation between optical and structural properties. *Proc Natl Acad Sci USA* 101:3358–3363
14. Aizenberg J, Weaver JC, Thanawala MS, Sundar VC, Morse DE, Fratzel P (2005) Skeleton of *Euplectella* sp.: structural hierarchy from nanoscale to the macroscale. *Science* 309:275–278
15. Schröder HC, Brandt D, Schloßmacher U, Wang XH, Tahir MN, Tremel W, Belikov SI, Müller WEG (2007) Enzymatic production of biosilica-glass using enzymes from sponges: basic aspects and application in nanobiotechnology (material sciences and medicine). *Naturwissenschaften* 94:339–359
16. Schröder HC, Wang XH, Tremel W, Ushijima H, Müller WEG (2008) Biofabrication of biosilica-glass by living organisms. *Nat Prod Rep* 25:455–474
17. Lowenstam HA, Weiner S (1989) On biomineralization. Oxford University Press, Oxford
18. Weiner S, Dove PM (2003) An overview of biomineralization processes and the problem of the vital effect. *Rev Mineral Geochem* 54:1–29
19. Wang XH, Müller WEG (2009) Marine biominerals: perspectives and challenges for polymetallic nodules and crusts. *Trends Biotechnol* 27:375–383
20. Wang XH, Gan L, Müller WEG (2009) Contribution of biomineralization during growth of polymetallic nodules and ferromanganese crusts from the Pacific Ocean. *Front Mater Sci China* 3:109–123
21. Perry CC (2003) Silicification: the process by which organisms capture and mineralize silica. *Rev Miner Geochem* 54:291–327
22. Müller WEG (2005) Spatial and temporal expression patterns in animals. In: Meyers RA (ed) *Encyclopedia of molecular cell biology and molecular medicine*, vol 13. Wiley-VCH, Weinheim, pp 269–309
23. Krasko A, Batel R, Schröder HC, Müller IM, Müller WEG (2000) Expression of silicatein and collagen genes in the marine sponge *Suberites domuncula* is controlled by silicate and myotrophin. *Eur J Biochem* 267:4878–4887
24. Shimizu K, Cha J, Stucky GD, Morse DE (1998) Silicatein alpha: cathepsin L-like protein in sponge biosilica. *Proc Natl Acad Sci USA* 95:6234–6238
25. Cha JN, Shimizu K, Zhou Y, Christiansen SC, Chmelka BF, Stucky GD, Morse DE (1999) Silicatein filaments and subunits from a marine sponge direct the polymerization of silica and silicenes in vitro. *Proc Natl Acad Sci USA* 96:361–365
26. Müller WEG, Rothenberger M, Boreiko A, Tremel W, Reiber A, Schröder HC (2005) Formation of siliceous spicules in the marine demosponge *Suberites domuncula*. *Cell Tissue Res* 321:285–297
27. Müller WEG, Belikov SI, Tremel W, Perry CC, Gieskes WWC, Boreiko A, Schröder HC (2006) Siliceous spicules in marine demosponges (example *Suberites domuncula*). *Micron* 37:107–120
28. Müller WEG, Boreiko A, Schloßmacher U, Wang XH, Tahir MN, Tremel W, Brandt D, Kaandorp JA, Schröder HC (2007) Fractal-related assembly of the axial filament in the demosponge *Suberites domuncula*: relevance to biomineralization and the formation of biogenic silica. *Biomaterials* 28:4501–4511
29. Roux M, Bouchet P, Bourseau JP, Gaillard C, Grandperrin R, Guille A, Laurin B, Monniot C, Richer de Forges B, Rio M, Segonzac M, Vacelet J, Zibrowius H (1991) L'environnement bathyal au large de la Nouvelle-Calédonie: résultats préliminaires de la campagne CALSUB et conséquences paléocéologiques. *Bull Soc Geol France* 162:675–685
30. Wang XH, Schröder HC, Müller WEG (2009) Giant siliceous spicules from the deep-sea glass sponge *Monorhaphis chuni*: morphology, biochemistry, and molecular biology. *Int Rev Cell Mol Biol* 273:69–115
31. Müller WEG, Wang XH, Kropf K, Ushijima H, Geurtsen W, Eckert C, Tahir MN, Tremel W, Boreiko A, Schloßmacher U, Li J, Schröder HC (2008) Bioorganic/inorganic hybrid composition of sponge spicules: matrix of the giant spicules and of the comitalia of the deep sea hexactinellid *Monorhaphis*. *J Struct Biol* 161:188–203

32. Schulze FE (1904) Hexactinellida. In: Chun C (ed) Wissenschaftliche Ergebnisse der Deutschen Tiefsee-Expedition auf dem Dampfer "Valdivia" 1898–1899. Gustav Fischer, Jena
33. Müller WEG, Jochum K, Stoll B, Wang XH (2008) Formation of giant spicule from quartz glass by the deep sea sponge *Monorhaphis*. Chem Mater 20:4703–4711
34. Müller WEG, Wang XH, Kropf K, Boreiko A, Schloßmacher U, Brandt D, Schröder HC, Wiens M (2008) Silicatein expression in the hexactinellid *Crateromorpha meyeri*: the lead marker gene restricted to siliceous sponges. Cell Tissue Res 333:339–351
35. Müller WEG, Boreiko A, Schloßmacher U, Wang XH, Eckert C, Kropf K, Li J, Schröder HC (2008) Identification of a silicatein(–related) protease in the giant spicules of the deep sea hexactinellid *Monorhaphis chuni*. J Exp Biol 211:300–309
36. Müller WEG, Eckert C, Kropf K, Wang XH, Schloßmacher U, Seckert C, Wolf SE, Tremel W, Schröder HC (2007) Formation of the giant spicules of the deep sea hexactinellid *Monorhaphis chuni* (Schulze 1904): electron microscopical and biochemical studies. Cell Tissue Res 329:363–378
37. Schröder H-C, Perović-Ottstadt S, Rothenberger M, Wiens M, Schwertner H, Batel R, Korzhev M, Müller IM, Müller WEG (2004) Silica transport in the demosponge *Suberites domuncula*: fluorescence emission analysis using the PDMPO probe and cloning of a potential transporter. Biochem J 381:665–673
38. Murr MM, Morse DE (2005) Fractal intermediates in the self-assembly of silicatein filaments. Proc Natl Acad Sci USA 102:11657–11662
39. Schröder HC, Boreiko A, Korzhev M, Tahir MN, Tremel W, Eckert C, Ushijima H, Müller IM, Müller WEG (2006) Co-expression and functional interaction of silicatein with galectin: matrix-guided formation of siliceous spicules in the marine demosponge *Suberites domuncula*. J Biol Chem 281:12001–12009
40. Mayer G (2005) Rigid biological systems as models for synthetic composites. Science 310:1144–1147
41. Müller WEG, Kasueske M, Wang XH, Schröder HC, Wang Y, Pisignano D, Wiens M (2009) Luciferase a light source for the silica-based optical waveguides (spicules) in the demosponge *Suberites domuncula*. Cell Mol Life Sci 66:537–552
42. Tahir MN, Théato P, Müller WEG, Schröder HC, Janshoff A, Zhang J, Huth J, Tremel W (2004) Monitoring the formation of biosilica catalysed by histidin-tagged silicatein. Chem Commun 24:2848–2849
43. Tahir MN, Théato P, Müller WEG, Schröder HC, Borejko A, Faiss S, Janshoff A, Huth J, Tremel W (2005) Formation of layered titania and zirconia catalysed by surface-bound silicatein. Chem Commun (Camb) 44:5533–5535
44. Tahir MN, Eberhardt M, Théato P, Faiss S, Janshoff A, Gorelik T, Kolb U, Tremel W (2006) Reactive polymers: a versatile toolbox for the immobilization of functional molecules on TiO₂ nanoparticles. Angew Chem Int Ed 45:908–912

David J. Newman and Gordon M. Cragg

Contents

26.1	Introduction	1286
26.2	Case Study 1: Didemnin B and Dehydrodidemnin B (Aplidine)	1287
26.2.1	Didemnin B	1287
26.2.2	Dehydrodidemnin B (Aplidine)	1289
26.2.3	Lessons from Case Study 1	1290
26.3	Case Study 2: Bryostatin 1 and Derivatives	1291
26.3.1	Bryostatin 1 from Natural Sources (Wild Collections and Aquaculture) ...	1291
26.3.2	Bryostatins by Chemical Synthesis	1292
26.3.3	Bryostatin Analogues/Mimics by Chemical Synthesis	1293
26.3.4	Putative Microbial Source(s) of Bryostatins	1293
26.3.5	Lessons from Case Study 2	1294
26.4	Case Study 3: Dolastatin 10 and Derivatives	1295
26.4.1	Dolastatin 10, Original Source and Syntheses	1295
26.4.2	Auristatin PE/TZT-1027; Dolastatin 10 Derivatives	1295
26.4.3	Actual Source(s) of the Dolastatins	1296
26.4.4	Lessons from Case Study 3	1296
26.5	Case Study 4: Halichondrin B and Eribulin	1297
26.5.1	Halichondrin B from Natural Sources (Wild Collections and Aquaculture)	1297
26.5.2	Synthetic Production of Halichondrin B and Derivatives	1299
26.5.3	Lessons from Case Study 4	1300
26.6	Case Study 5: Ecteinascidin 743 (Yondelis®)	1301
26.6.1	Ecteinascidin 743 from Natural Sources (Wild Collections and Aquaculture)	1301
26.6.2	Ecteinascidin 743 from Chemical Synthesis	1302
26.6.3	Lessons from Case Study 5	1302
26.7	Case Study 6: Salinosporamide A	1303
26.7.1	Discovery of Salinosporamide A	1303

D.J. Newman (✉) • G.M. Cragg
Natural Products Branch, Developmental Therapeutics Program, National Cancer Institute,
NCI-Frederick, Frederick, MD, USA
e-mail: newmand@mail.nih.gov, gmcragg@verizon.net

26.7.2	Large-Scale Fermentation/Isolation of cGMP Product	1303
26.7.3	Synthetic Processes	1304
26.7.4	Genomic Methods	1304
26.7.5	Lessons from Case Study 6	1305
26.8	In Conclusion	1305
26.9	Study Questions	1306
References		1306

Abstract

Perhaps the major perception both in the general medical and scientific communities, and also to some extent in the natural products community, is that marine natural products are of interest but not directly feasible for further development. This perception was fundamentally correct up through roughly the early 1990s, due to major physical difficulties in obtaining enough raw materials from which to isolate the compound of interest. In this chapter, we will show how application of novel techniques in growth and isolation processes, increased knowledge of genomics, and major advances in chemical synthesis have made observers alter their perceptions to the extent that, nowadays, production of marine natural product molecules is a combination of many techniques, each adding their quota of experience. We will use a case study mechanism to demonstrate how these methods evolved and have now enabled marine natural products to be serious contenders as drug candidates.

26.1 Introduction

Marine natural products with significant activities in many pharmacologic areas have been well documented over the years, particularly in the extensive reviews initiated by the late Dr. John Faulkner and now continued by the New Zealand marine group [1]. However, there was a perception, based on reality prior to the middle to late 1990s, that the development of marine-based compounds would require immense efforts from the aspect of recovery and processing of large amounts of biomass in order to obtain even enough material for initial *in vivo* screening. Added to this was that very large amounts would be necessary for further drug development processes, where requirements might well be in the hundreds of grams to multikilogram levels of pure compound produced under current good manufacturing practices (cGMP).

These perceptions were not aided by the fact that most of the agents reported from marine sources were exquisitely potent, often with IC_{50} values in the nanomolar range and present at very low levels in the invertebrate. For example, when reports indicated that 18 g of bryostatin 1 was isolated from over 13 metric tons of *Bugula neritina* or 300 mg of halichondrin B from 1 metric ton of a deep water *Lyssodendoryx* sp., it did not help sell the concept of “drugs from the sea” to pharmaceutical houses. Although these figures were true at the time of publication, nowadays thanks to advances in biology and chemistry over the last 10 plus years the situation has undergone a “sea change,” with combination methods and routes

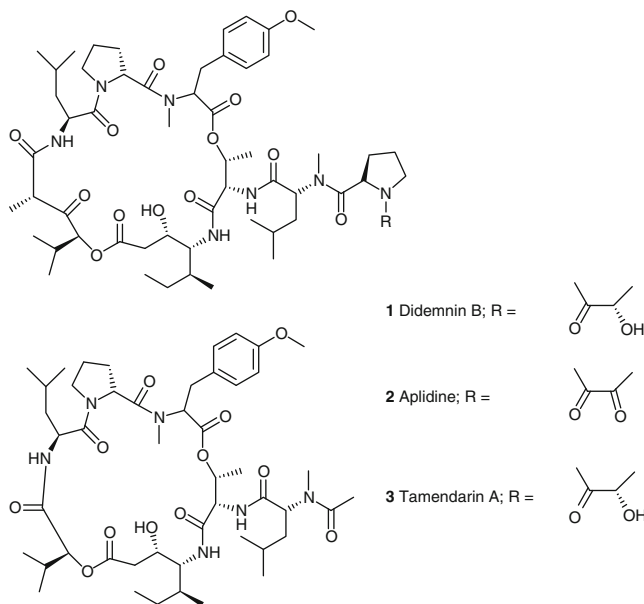
such as microbial biosynthesis, aquaculture (in sea or on land) coupled to potential chemical syntheses, now being considered as part and parcel of the initial discovery/development process.

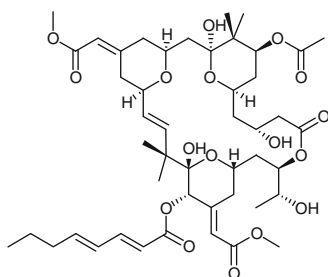
In order to put the recent advances in perspective, we will discuss a series of marine-sourced agents being evaluated in anticancer therapies, mainly due to the initial funding coming from the National Cancer Institute (NCI) or its European equivalents. These case studies in general have been chosen in order to demonstrate how the initial large-scale harvesting methods, necessary in some cases due to the time frame of the initial discovery, have been transformed as knowledge from many sources were applied to the situations as time progressed.

26.2 Case Study 1: Didemnin B and Dehydrodidemnin B (Aplidine)

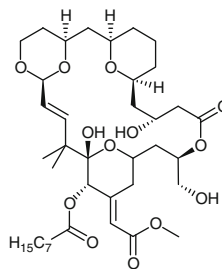
26.2.1 Didemnin B

The first compound entered into human clinical trials directly from a marine source was the cyclic depsipeptide, didemnin B (**1**), isolated by the Rinehart group from the encrusting tunicate *Trididemnum solidum* [2, 3]. This was one of a number of very similar compounds isolated from the same organism and included a very close analogue differing by only two hydrogens, dehydrodidemnin B (DDB) now known as aplidine (**2**). This compound subsequently followed DB into human clinical trials [4] approximately 15 years later.

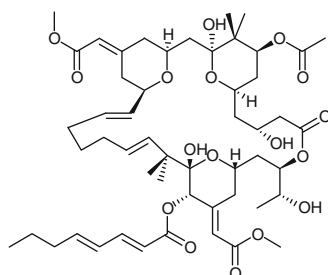




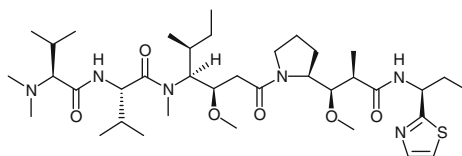
4 Bryostatin 1



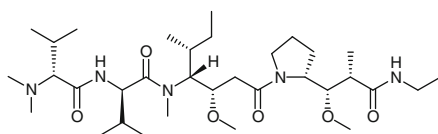
5 Wender's Bryolog



6 Ring Expanded Bryostatin 1



7 Dolastatin 10



8 TZT-1027

Due to the paucity of the producing organism, the level of didemnin B and the multiple derivatives coproduced by the invertebrate, plus the requirement for the production of materials for clinical trials under “current good manufacturing practice (cGMP)” for human trials, synthetic methods were the only viable route at that time for production of compound. In 1987, the Rinehart group published a synthetic method to three of the didemnins, A, B, and C [5] followed the same year with a publication from the Joullie group demonstrating how to synthesize further derivatives of the unusual amino acid “statine” found in the didemnins [6].

In 1991, the Jouin group in France reported on synthesized derivatives that had the linear lipophilic peptide side chain modified. They showed that except for a derivative where palmitic acid was substituted for the lactyl group of didemnin B, the biological activities both in vitro and in vivo were not significantly changed when compared with the natural product [7]. However, the palmityl derivative lost effectively all cytotoxic activity, though no immunosuppressive assays were reported as didemnin B and other congeners exhibited significant immunosuppressive activities [8].

Seven further syntheses by the Schmidt, Shioiri, Joullie, and Jou groups were later discussed in detail in a 2002 review by Vera and Joullie [9]. These, together with the 1996 paper from the Rinehart group referred to above [8], yielded a very significant number of enantiomerically pure analogues together with the required didemnin B. As an example of what can be done, using modern techniques once the materials are available in purity is the report in 2004 by Marco et al., where the probable target for cytotoxicity of the didemnins was shown to be elongation factor eLF1A [10].

Didemnin B was placed into a significant number of clinical trials by the NCI working through a variety of groups but was taken off trials in the middle 1990s due to (cardiac) toxicities [11], with the last published example being the report from a phase II trial in brain carcinomas by Mittelman et al. in 1999 [12]. What is of potential significance, however, were the retrospective comments made by Vera and Joullie (2002) on the methods of delivery used in these early trials – a single bolus dose at close to the maximum tolerated dose (MTD). From later work with aplidine [4], the use of different dosing schedules and a modicum of other supportive medications avoided the significant toxicities seen previously with didemnin B.

26.2.2 Dehydrodidemnin B (Aplidine)

This compound was reported as being isolated from the Mediterranean tunicate *Aplidium album* in a review on the 1990 USA-Japan Seminar on Bioorganic Marine Chemistry by Schmitz and Yasumoto [13], and it was also reported in a US patent in 1994 [14] and in a citation to an application for a UK patent in 1989 in the synthetic paper by Sakai et al. [8] with the initial report of formal activity of dehydrodidemnin B (DDB or aplidine) in animals being the paper in 1996 by Urdiales et al. [15].

Just as in the case of its very close analogue, didemnin B, the amounts required for both initial preclinical studies and then for any future studies precluded the use of wild collections; thus total synthesis was the only viable route to production of this agent, even though there had been reports in some of the very early papers on these agents implying production by a symbiotic interaction between the blue-green alga *Synechocystis trididemni* and the invertebrate [7, 16, 17].

The method used for the production of aplidine was a route based upon the liquid phase peptide synthesis described in 1997 by Jou et al. [18] in which synthetic didemnin A was coupled with the side chain “pyruvate-proline-OH” to give DDB.

Two routes to produce a protected didemnin A were investigated by Jou et al. The first used macrocyclization of a linear seven-membered peptide containing the first extracyclic amino acid of the didemnin side chain. This gave an overall yield of 4% of the protected didemnin A. The other approach, initial formation of the basic didemnin macrocycle followed by coupling of the first extracyclic amino acid, used a six-membered linear peptide that led to the didemnin macrocycle on cyclization. Following addition of the first amino acid of the side chain, the overall yield of the protected didemnin A was 27%. Irrespective of the methods used to derive didemnin A, the subsequent coupling step to yield DDB proceeded with a 62% yield.

These methods will have been further optimized in order to produce materials under cGMP conditions for the clinical development of the agent but as is usual, the information that is given in the chemical and manufacturing controls (CMC) section for an investigational new drug application (INDA) for the FDA, or its equivalent section in any submission to the EMEA in the European Union, is not available for public dissemination nor have any publications with such information been published as far as can be determined to date.

Aplidine (DDB or plitidepsin) is currently in phase I/II clinical trials predominately in blood-based carcinomas, including multiple myeloma where a phase II trial (NCT00229203) has just completed and a phase II trial (NCT00884286) has just commenced studying its activity in non-Hodgkin's lymphoma, with a new phase III trial (NCT01102426) beginning to recruit patients for a comparison of aplidine plus dexamethasone versus dexamethasone in relapsed/refractory myeloma (ADMYRE trial). In addition, over the years, it has been in trials against a variety of cancers in the EU, Canada, and the USA with a significant number of publications listed through the middle of 2005 [4, 11], and eight more reports from phase I/II shown in a current search of the Scopus database from late 2005 to date.

26.2.3 Lessons from Case Study 1

As a result of the very low yields of material from the natural sources (encrusting didemnin invertebrates), though the possibility of a symbiotic production from a cyanobacterium (blue-green alga) of metabolites was suggested as early as 1979 [16], the only viable method of production was total chemical synthesis. The initial work of the Rinehart group led to the very successful application of liquid-phase methods by the Jou group, leading to the current clinical trials of DDB.

The lessons learned from these compounds were aptly demonstrated by two other investigators involved in the didemnin story, and led to a report in 2007 of variations in the synthetic approaches to the didemnin analogues, the tamandarins (3) [19]. These synthetic variations compared to those originally reported [20, 21]

led to significantly increased synthetic yields and production of analogues with in vitro antitumor activity, thus, extending the structure activity relationships in this very active series.

26.3 Case Study 2: Bryostatin 1 and Derivatives

26.3.1 Bryostatin 1 from Natural Sources (Wild Collections and Aquaculture)

After didemnin B, the next “direct from the sea” compound to go into clinical trials was bryostatin 1 (**4**); currently it has been in over 80 clinical trials, with six phase I/II trials in cancer still being listed in the NIH clinical trials database, of which five are still active but not recruiting further patients, and the remaining one is a phase I trial involving bryostatin 1 in concert with temsirolimus. In addition, a phase II trial in Alzheimer’s is listed but not yet recruiting patients.

That this compound ever made it from a biological discovery to human clinical trials can be ascribed to the determination of G. Robert (Bob) Pettit, who first reported this class of compounds in 1970 [22]. The subsequent work, leading to the identification of 19 variations on the same basic structure, mainly as a result of Pettit’s group at Arizona State University (ASU) and collaborators in multiple other institutions has been reported in a large number of papers and reviews [23, 24]. The latest “variation” on the basic structure from a natural source was the new bryostatin derivative (bryostatin 20) reported from an Atlantic *Bugula neritina* by Lopanik et al. in 2004 [25], and on comparison with the known 19 earlier molecules, its structure is effectively the ring-closed version of bryostatin 10.

As a result of the initial preclinical and clinical (phase I) responses to bryostatin 1 [26, 27], it was necessary to produce gram quantities of the compound for initial trials. No synthetic method was available so the NCI contracted a small California company, Marinus Inc., in Long Beach to collect close to 13 metric tonnes of wet *Bugula neritina* from depths between 3 and 30 m off the coast of Southern California. Since this particular animal is a large-scale fouling organism and is ubiquitous in the waters off California, no significant effect on the environment was anticipated.

Following shipment of the 40,000 L of wet organism in isopropanol to NCI-Frederick, the US Government contractor who ran the NCI-Frederick Cancer Research Center, then Program Resources Incorporated together with scientists from NCI and Bristol Myers Squibb (who had licensed the bryostatin patent from ASU), produced 18 g of cGMP quality bryostatin 1 in 10 months of work [28]. A later small-scale rework of the process using supercritical fluid extraction rather than conventional liquid–liquid extraction, followed by large-scale chromatography reduced the processing time from 10 months to under a month assuming scaling would be relatively linear [29].

From the raw material supply problems that arose in the case of Taxol® [30, 31], NCI decided in the early 1990s to “plan for success” when natural product-sourced

compounds entered preclinical/clinical trials. Therefore, as a result of the volumes of wild-collected material that would be involved if bryostatin 1 was successful as an antitumor drug, a very large amount of raw material would be required in order to produce enough of the compound for clinical use, NCI funded a competitive SBIR phase I and a subsequent phase II contract with the small California biotechnology company, CalBioMarine.

The aim of this initial contract (phase I), and its subsequent extension (phase II), was to grow *Bugula neritina* using both in-sea and on-land aquaculture in order to avoid the problems of seasonal variation in both levels of this bryozoan and, as learned later, in the levels of bryostatin in the animal. The goals of the contract were successfully met, demonstrating that the organism could be produced by either in-tank aquaculture or via seeded screens suspended in the Pacific Ocean off La Jolla, California. The levels of bryostatin were high enough to obtain a useful supply of the compound, though significant optimization of feeding protocols and recovery methods would have been necessary. The work involved was subsequently described by one of the CalBioMarine principals, Dominick Mendola [32].

26.3.2 Bryostatins by Chemical Synthesis

From the initial reports on the structures of the bryostatins, chemists recognized the base molecule as a challenge for their synthetic skills. A significant number of syntheses of parts of the bryostatin 1 molecule and total syntheses of various members of the complex were reported, with the first being the enantiomeric synthesis of bryostatin 7 in 1990 by Masamune's group [33], followed by papers from the Evans' group giving details of an enantiomeric synthesis of bryostatin 2 in the 1998–1999 time frame [34, 35]. The third in the initial series was the synthesis of bryostatin 3 by Nishiyama and Yamamura in 2000 [36]. These earlier syntheses together with partial syntheses of other bryostatins were reviewed in detail through 2002 by Hale et al. [37]. Following a break of 8 years, in 2008, Trost and Dong published [38] their relatively simple and quite elegant synthesis of bryostatin 16 involving some novel metal-linked catalysis steps [39], including a ruthenium tandem alkyne-enone coupling and then a palladium catalyzed alkyne-ynoate macrocyclization to give the cyclized precursor of bryostatin 16.

In spite of all of these elegant methods, to date, no de novo synthesis of bryostatin 1 has been published, though in the early days of studying the bryostatins, Pettit et al. demonstrated that bryostatin 2 could be converted to bryostatin 1 and bryostatin 12 [40]. Thus, one could argue that a formal synthesis of bryostatin 1 has been achieved by using the Evans et al. bryostatin 2 asymmetric synthesis [34, 35] and then applying the Pettit conversion method. Very recently, an excellent review of the synthetic chemistry surrounding the bryostatins was published by Hale and Manaviazar [41], which should be consulted by those interested in the specific methodological differences between the various syntheses.

26.3.3 Bryostatin Analogues/Mimics by Chemical Synthesis

From the early days of the bryostatins, Wender's group postulated that if one could synthesize a simpler analogue with comparable activity, then chemical production of such an agent might well be a viable option. Over the years, Wender and his colleagues have successfully synthesized a significant number of what they have named "bryologs"; nominally simpler molecules that have pharmacologic characteristics similar to bryostatin 1. These were originally designed by modeling bryostatin 1 on to the binding site of the phorbol esters on protein kinase C and over the years, a significant number have been published with the latest variations being those reported in 2008 [42, 43], with a representative molecule being shown in (5). Other synthetic groups have also produced synthetic modifications that are different from the Wender bryologs, but still have significant biological activities. One example is the ring-expanded molecule (6) where five extra carbon atoms have been inserted between the C₁₆ and C₁₇ carbon atoms of bryostatin 1 [44] while maintaining bryostatin-like activity. However, other more subtle modifications where only four changes were made on the periphery of the bryostatin 1 molecule, converted the bryostatin 1 structure to a molecule that had biological activities that mimicked those of the phorbol ester tumor promoters rather than those of the parent molecule [45]. Thus, one has to be very careful in assessing the actual activities of what appear to be small modifications to the base molecule.

26.3.4 Putative Microbial Source(s) of Bryostatins

One of the discoveries made from the collections made by Calbiomarine of wild *Bugula neritina* when they were collaborating with the Haygood group at the Scripps Institution of Oceanography was that there appeared to be two potential subspecies, one from deep (below ~10 m) and one from shallow (above ~7 m). However, the bacterial symbionts of the invertebrate were investigated [46], and suggested that the actual producer of the bryostatins was a previously unrecognized and, as yet, noncultured bacterium.

Over the next 10 plus years, in conjunction with experts in gene identification and cloning, Haygood and her collaborators have been able to identify and clone, but not yet express in a heterologous host, the putative biosynthetic cluster that should produce what they are calling bryostatin 0, that would then be further elaborated by as yet unidentified tailoring enzymes. Thus, Haygood and her collaborators investigated the potential sources of bryostatins in both the adult animal and in the larvae. In a series of excellent investigations, they demonstrated that within the larvae of bryostatin-producing animals there were as yet uncultured bacteria (given the name of *Candidatus Endobugula sertula*) in the first report by Davidson and Haygood in 1999 [47] and extended in 2001 [48].

A series of later papers included a review of the possibilities of identification and expression of genes from symbionts [49], the identification of different symbionts from other *Bugula* species that produced bryostatins and contained similar gene constructs [50], together with the identification of a putative *bryA* cluster [51]. Further work by Lopanik et al. on Atlantic-sourced, rather than Pacific or Gulf Coast-sourced *Bugula neritina*, has confirmed the presence of *bryA*-like fragments from this geographic area's organisms as well [52].

It should be emphasized that in none of the cases described does the identification of the *bryA* cluster in these organisms prove the absolute production of bryostatins by the symbiont, but the evidence is highly suggestive. Currently the complete putative genomic sequence has been identified and sequenced but not yet expressed [53] including the recognition of an unusual transacylase [54]. Finally, in addition to the genomic work related to the biosynthesis in a variety of *Bugula* species and locations, work from an ecological perspective has also been reported by Haygood and collaborators, demonstrating that bryostatins are important molecules from an ecological as well as a pharmacological perspective [54, 55].

26.3.5 Lessons from Case Study 2

Just as in the case of didemnin B, bryostatin 1 was present in vanishingly small amounts in what was thought to be the producing organism, the encrusting and fouling bryozoan, *Bugula neritina*. Unlike didemnin B, due to the massive amounts of organism available off the California coast, it proved ecologically feasible to isolate 18 g of cGMP quality material from 13 metric tonnes of wet organism, and methods were also developed on a small scale for a much faster isolation process using supercritical fluid extraction.

Due to the obvious problems of very low levels and massive collection programs if bryostatin became a potential drug, NCI, who had learned their lesson from the problems of sourcing enough *Taxus* bark for clinical trials of Taxol[®], commissioned aquacultural methods and directly and indirectly through the NIH grants programs, aided in funding synthetic approaches to both bryostatins and their "simpler" modifications, the "bryologs."

Basic ecological studies coupled to the massive advances in the study of biosynthetic gene processes led to the recognition that an as yet uncultured symbiotic microbe may be a potential source of bryostatin precursors; these may be modified by either chemistry or genomic methods to produce the desired chemical skeletons for further development.

Finally, although bryostatin is not a particularly viable antitumor agent at the present time, it may well have utility in Alzheimer's disease as shown in the work by researchers at the University of West Virginia [56–58] and the approval from the FDA for a phase II clinical trial of bryostatin 1 in patients with Alzheimer's under the ClinicalTrials.gov identifier number NCT00606164.

26.4 Case Study 3: Dolastatin 10 and Derivatives

26.4.1 Dolastatin 10, Original Source and Syntheses

In the same time frame as the bryostatins, the Pettit group also reported on the dolastatins, a series of cytotoxic linear and cyclic peptides that were originally isolated in very low yield from the Indian Ocean gastropod mollusk *Dolabella auricularia*. The history and work-up of the dolastatins, in particular the tubulin interactive linear peptide dolastatin 10 (**7**) through early 2005, were reported in detail by Flahive and Srirangam in a 2005 book chapter [59].

Similarly to the case of didemnin B, the original discoverers realized from the beginning that only total chemical synthesis would yield the necessary amounts of material to even pursue advanced preclinical and hopefully clinical studies. Thus, the Pettit group devised synthetic methods for the large-scale enantiomeric syntheses of the unusual γ -amino- β -methoxy-acid residues dolaproline and dolaisoleucine, each of which contained three chiral centers, and the novel C-terminal residue, dolaphenine, which contains a thiazole and is derived from phenylalanine. Their approach was described in a paper in 1989 [60] and fuller details of this and other syntheses were reported in an excellent review by Pettit in 1997 [61].

Due to the potency, at the time it was the most potent agent tested by the NCI, and mechanism of action as a tubulin-interactive agent binding close to the *Vinca* domain [62–64], dolastatin 10 entered phase I clinical trials in the 1990s under the auspices of the NCI. It progressed through to phase II trials as a single agent, but although tolerated at the doses used, which were high enough to give the expected levels in vivo to inhibit cell growth, it did not demonstrate significant antitumor activity in a phase II trial against prostate cancer [65], nor in metastatic melanoma [66].

26.4.2 Auristatin PE/TZT-1027; Dolastatin 10 Derivatives

Although the natural products did not succeed in demonstrating activity in humans, the syntheses described by Pettit and others led the way to a series of other molecules based upon the natural product but with modifications to the base linear peptide. Numbers of these have been discussed in the literature including a compound simultaneously synthesized by both the Pettit group under the name of auristatin PE [67] and a group from the Japanese company Teikoku Hormone (**8**) under the name TZT-1027 [68]. This compound under the names, TZT-1027, auristatin PE, and soblidotin, depending on the particular organization sponsoring the compound, went into phase I/II trials with mixed results and is not currently listed as being in active trials in the NIH clinical trials site.

However, demonstrating how compounds that exhibit interesting activities can be further optimized by clever chemistry and biology, the compound with a small linker was used as a warhead by Seattle Genetics. Two variations differing in the

antibody and the specific linker are currently in phase II (glembatumumab vedotin) and phase III (brentuximab vedotin) with another (anti-CD19-vcMMAE) in preclinical trials. Using the auristatin PE derivative, auristatin F (where the C-terminal amino acid is now phenylalanine), a third monoclonal antibody-warhead combination (1 F6-MMAF) is currently in phase I clinical trials and unlike the other two, it does not have a cleavable linker. Up-to-date discussions of the rationale behind the use of such methods with both cleavable and noncleavable linkers are presented by Senter's group from Seattle Genetics [69, 70] and by Teicher from Genzyme [71].

In addition to the linked molecules referred to above, auristatin PE itself was shown to be a vascular disruption agent with three relatively recent papers discussing the possibilities of such agents as antitumor treatments as they cause the internal vasculature of the tumor to collapse [72–74]

26.4.3 Actual Source(s) of the Dolastatins

Similarly to the situation with the bryostatins and the didemnins, there was always a potential question with the dolastatins as to whether or not they were microbial in origin, as peptides with unusual amino acids have been well documented in the literature as coming from the Cyanobacteria. In the last few years, this supposition has been shown to be a fact. Thus, in 1998, workers at the Universities of Guam and Hawaii reported the isolation and purification of simplostatins 1 [75] from the marine cyanobacterium *Simploca hynoides*. This molecule differed from dolastatin 10 by the addition of a methyl group on the first *N*, *N*-dimethylated amino acid. Subsequently, in 2001, the same groups reported the direct isolation of dolastatin 10 from another marine cyanobacterium that was known to be grazed on by *D. auricularia* [76]. Dolastatin 10 was in fact isolated from the opisthobranch following feeding of the cyanobacterium, thus confirming the original hypothesis (Paul 2006, #145).

26.4.4 Lessons from Case Study 3

As with didemnin B, recognition that collections of the raw material source was not a feasible method led to the derivation by Pettit's group of synthetic methods on a large scale (for an academic institution) for the intermediates. These individual syntheses then allowed the synthesis of dolastatin 10 with its multiple chiral centers and three very unusual amino acids in its short peptide structure. From these initial studies came the capability to produce novel molecules such as auristatin PE. Modifications around that structure combined with clever utilization of monoclonal antibody technologies have led to currently active agents in phases I to III clinical trials.

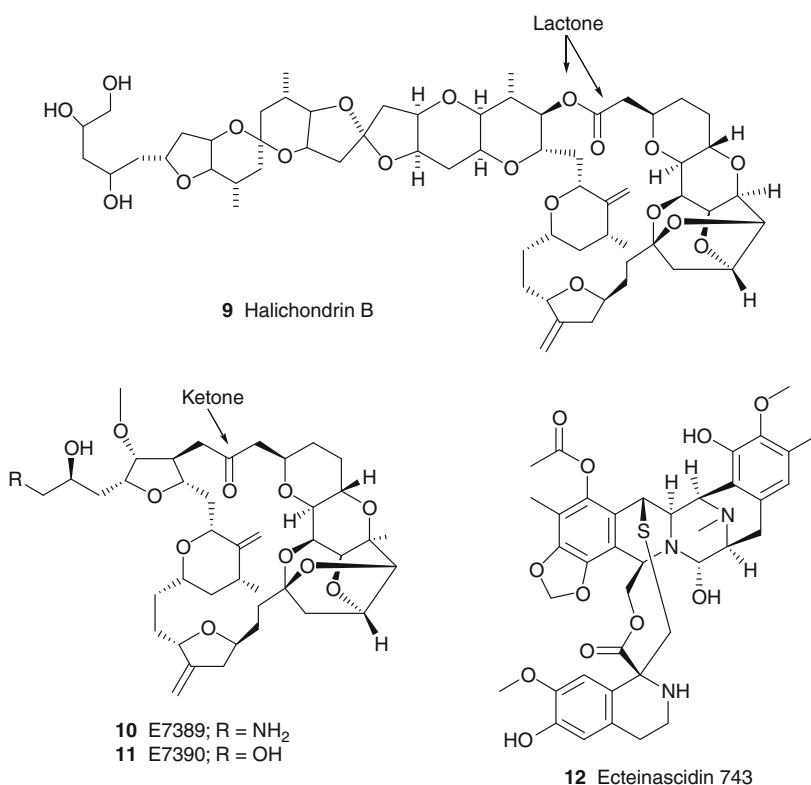
The work in the late 1990s by the Hawaii and Guam groups demonstrating that, as suspected for many years, the agents were linked to cyanobacterial diets of the opisthobranchs, leads to the possibility that in due course the biosynthetic gene

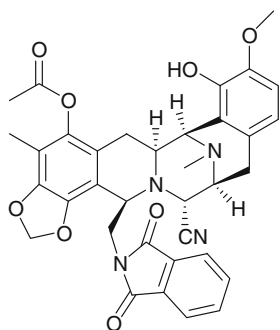
clusters may be identified. If this can be done, then there is the possibility that the metabolites might be expressed in a heterologous host. Examples of this technique were reported simultaneously by two groups with *Prochloron* peptide metabolites using the heterologous host *E. coli*. One used shotgun cloning of the gene clusters [77] and the other identification of the cluster(s) followed by cloning and subsequent expression [78].

26.5 Case Study 4: Halichondrin B and Eribulin

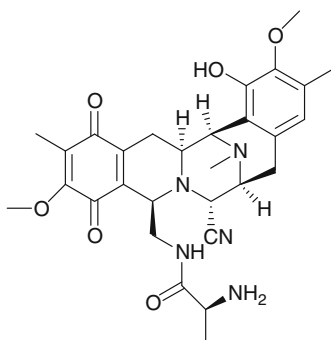
26.5.1 Halichondrin B from Natural Sources (Wild Collections and Aquaculture)

Halichondrin B (**9**) was first reported from the Japanese sponge *Halichondria oakdai* by Uemura's group in 1985 [79] and 1986 [80], and, subsequently, halichondrin B or congeners were reported over the next few years from a variety of other sponge sources. These initial reports were then followed by two papers that made this series of agents very interesting for development as antitumor agents.

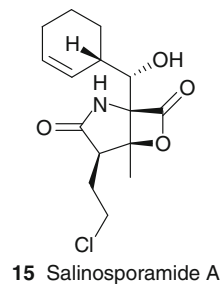




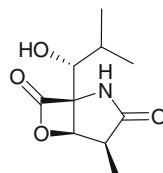
13 Phthalascidin



14 Cyanosafracin B



15 Salinosporamide A



16 Omuralide

The first, in 1991, showed that halichondrin B acted as a tubulin interactive agent (TIA) potentially binding close to the *Vinca* site [81]. The other, in 1992 from Kishi's group at Harvard (funded by NCI), presented a synthetic route to halichondrin B [82]. As a result of the first of these reports and other work at NCI, the NCI's Decision Network Committee decided in early 1992 to recommend further preclinical development of halichondrin B.

Although recommended for development, there was no natural source of the material reported to that time that had the potential to provide enough material for even initial preclinical studies. Thus, the NCI's Natural Products Branch (NPB) put out a general request to the natural products worldwide community asking for potential sources. The New Zealand groups at the University of Canterbury (Munro and Blunt) and the New Zealand Government's National Institute of Water and Atmospheric Research (Battershill) responded with information that had not been published on the presence of halichondrins in a deepwater sponge identified as a species of *Lissodendoryx* that had been collected by dredging off the Kaikoura peninsula at a depth of ~100 m.

The NCI first funded an environmental assessment of the extent of the sponge field and using this data, were able to obtain a permit from the New Zealand government that permitted up to 1 tonnes of sponge to be dredged, extracted, and processed in a joint operation between the New Zealand collaborators and the NCI. Direct funding was provided by the NCI with (predominately) payment in kind by the New Zealand operations. The raw materials were harvested over the next 4 years and processed in New Zealand to yield 300 mg of 98% pure halichondrin B.

Contemporaneously, NCI financed a series of significant in-sea aquaculture experiments in New Zealand waters that demonstrated for the first time that

a deepwater sponge could be cultured in shallow water and still produce a significant amount of the desired secondary metabolite. The initial reports were given in abstract format, covering the experiments in mussel farms in South Island, New Zealand at depths up to 30 m and also in waters as shallow as 10 m in Wellington harbor. These results were then used as the basis for a larger series of experiments, and the results were published as a case study by the New Zealand scientists who were directly involved [83].

By the end of 1997, NCI had samples from a very significant supply of pure halichondrin B and used it to compare activities of the pure halichondrin B versus materials that had only been isolated in very small amounts (3–5 mg) from other sources. These were reported in abstract format at the American Association for Cancer Research (AACR). Thus, the stage was set to use the sponge-derived materials to perform early preclinical studies and optimistically, to be able to produce material via in-sea aquaculture in order to provide material for later development [83].

26.5.2 Synthetic Production of Halichondrin B and Derivatives

In 1992, at the same time as the decision by NCI to develop halichondrin B, Kishi's group at Harvard reported the total synthesis of halichondrin B [82], a study funded via an NCI grant. Because of the relationship between the Eisai Research Institute (ERI) in the USA and Professor Kishi, this organization investigated the potential of the Kishi synthesis, having licensed the essential patent from Harvard [84].

Kishi's group had shown, in patent form, that the required portion of the molecule for maintenance of bioactivity was the macrolide ring, whereas other groups had been modifying the "tail" part of the molecule. The Eisai chemical group realized that they could convert the macrolide ring into a ketone by changing the oxygen to a methylene group while still maintaining the basic activity. In addition, truncation of the "tail" and changes to the oxygen heterocycle next to the macrocyclic ring led to two very similar compounds E7389 and E7390.

Fortuitously, the head of ERI's oncology group happened to see the work that NCI's Developmental Therapeutics Program (DTP) scientists reported in abstract form on the *in vitro* activity of pure halichondrin B at the 1998 AACR meeting. This led to a collaborative project between ERI/Kishi and DTP, comparing the NCI's pure halichondrin B with two truncated, fully synthetic molecules that they had made, E7389 (**10**) and E7390 (**11**). This preliminary work demonstrated that E7389 was more active *in vivo* and with a better therapeutic index than either halichondrin B or its chemical precursor, E7390. ERI then provided sufficient E7389 synthesized under cGMP conditions that permitted NCI to perform preclinical studies including IND-directed toxicology and led to approval in 2001 by the then NCI Decision Network Committee for human clinical trials.

The compound was approved by the NCI for clinical development in 2001, entered clinical trials soon thereafter and as of January 2010, was in phase III clinical trials against refractory breast carcinoma under the Eisai Metastatic Breast

Cancer Study Assessing Physician's Choice versus E-7389 (the EMBRACE studies, ClinicalTrials.gov Identifier NCT00388726). In addition to the global studies under the EMBRACE consortium, eribulin is in other trials at the phase II level in different carcinomas. Applications were made to both Switzerland and Singapore for marketing approval in 2009 on the preliminary results from the global studies and were followed in early 2010 by simultaneous submissions to the US FDA, the EU's EMEA, and the Japanese Ministry of Health, Labor and Welfare (MHLW) for approval for the treatment of inoperable or recurrent breast cancer. As of mid 2010, the FDA and the MHLW have given priority review status to these submissions.

A short paper presenting the basic chemistry was published by the ERI group in 2004 [85], whereas a thorough discussion of the details of the synthetic and base biological information was published by the leaders of the studies at ERI in 2005 [86]. In 2007, a short article covering the basic details but with later clinical citations was published by Wang [87], and recently Kishi's group have published novel and simpler routes to the macrocyclic ring of halichondrin and eribulin [88, 89].

The molecule, like its parent, is a tubulin-interactive agent with very potent activity at the nanomolar level in *in vitro* studies [90] and binding at or close to the *Vinca* site from modeling studies [91]. In a recent paper from Jordan's group, the mechanism of action is defined as: "The strong correlation between suppression of kinetochore-microtubule dynamics and mitotic arrest indicates that the primary mechanism by which eribulin blocks mitosis is suppression of spindle microtubule dynamics" [92].

26.5.3 Lessons from Case Study 4

This is an example of where the base molecule was the initial active agent, and a source had to be identified with the political agreements necessary for collections of the deepwater sponge negotiated at government to government levels. Once permission had been obtained, then large-scale collection and extraction processes had to be developed. At the same time, methods of large-scale production had to be considered, even before the first large-scale deepwater collection had been made, because if the compound was successful, multiple grams of material would be required. Thus, aquaculture methods ran in concert with the large-scale recovery and purification.

NCI had funded, via a competitive grant mechanism quite distinct from the NPB-directed work, a total synthesis of the base halichondrin B molecule which was reported at the same time as the initial decision to go forward with the compound in preclinical studies at NCI. The synthesis was not judged by DTP to be feasible under their restricted chemical synthetic capabilities as a substitute for the natural product. What was not known by DTP/NCI at the time was the relationship between Professor Kishi and the ERI. ERI licensed the Harvard patents that demonstrated the viability of the truncated halichondrins (realized from biological assays of the intermediates in the synthesis at ERI).

Once DTP reported their *in vitro* work with the pure halichondrin B at the 1998 AACR meeting, discussions were held between the ERI scientists, Prof. Kishi, and

DTP in the late summer of 1998, at which time the two compounds ultimately known as E7389 and E7390 were tested by DTP biologists against a series of cell lines *in vitro* and *in vivo*. The compounds tested were the last samples that ERI had as their synthetic tour de force (over 200 variations had been synthesized at ERI) was winding down. When the DTP data was reported to ERI, they began a synthesis of the most active compound with the highest therapeutic index and produced enough cGMP grade E7389 by total synthesis for NCI to proceed with the necessary pre-IND directed studies in toxicology, culminating in the entry into phase I clinical trials in early 2002, 10 years after the Decision Network Committee had approved further development of the natural product.

Thus, this particular example demonstrates how modern synthetic chemistry can build extremely complex molecules that have clinical potential, based upon the natural product structure, and in quantities sufficient for clinical use. However, it must not be forgotten that eribulin or its congeners would not have entered clinical trials in the absence of the massive effort across the globe to obtain enough of the natural product to use as both a standard and as a comparator. Another beneficial spin-off was the knowledge gained in how to aquaculture deepwater sponges in shallow water and maintain metabolite production.

26.6 Case Study 5: Ecteinascidin 743 (Yondelis®)

26.6.1 Ecteinascidin 743 from Natural Sources (Wild Collections and Aquaculture)

The antitumor activity of extracts of *Ecteinascidia turbinata* was first reported in 1969 [93], and the isolation and structure of ET743 was independently reported by the groups of Wright [94] and Rinehart [95] in back to back papers in 1990. Evaluation of the structures showed that they contained the essential aspects of the saframycins, known terrestrial microbial tetrahydroisoquinoline antitumor antibiotics, and that there were other marine natural products of a similar basic structure in the literature. For further information on this general class of molecules, the 2002 review by Scott and Williams should be consulted [96].

ET743 (12) was licensed in the very early 1990s to PharmaMar for development, and over the next 10 or so years, a whole variety of methods were utilized in order to obtain enough biomass to isolate the compound of interest. These included wild collections in the Caribbean where three production periods were usually seen [97], and the Mediterranean sea where temporal variation due to temperature meant that only in the summer could the Mediterranean stocks be sampled [98, 99], as well as in-sea and lake-based aquaculture [100]. Using multiple sites in addition to major operations in the Spanish Balearic island Formentera and surrounding areas, PharmaMar in the years between 1998 and 2004 produced approximately 100 tonnes of biomass, from which enough material was purified to carry preclinical and clinical trials to phase II [101]. The overall approximate yield to purification was $\leq 1.0 \mu\text{g} \cdot \text{g}^{-1}$, or 100 g from 100 metric tonnes.

26.6.2 Ecteinascidin 743 from Chemical Synthesis

In order to provide enough material for advanced clinical trials and then commercial production, it became apparent that none of the then-current methods would suffice. Although Corey et al. had reported an enantioselective synthesis inspired by the proposed biosynthesis [102] of the natural product in 1996 [103], it was not amenable to large-scale production. Martinez and Corey then published a revised synthetic method that was designed to increase yields significantly, but it was still not adequate for industrial-scale production [104]. However, it did demonstrate a method of production of a simpler analogue named phthalascidin (**13**) that had similar activity to ET-743 [105].

Since these methods were not satisfactory for multigram production under cGMP conditions, the PharmaMar group published [106] a semisynthetic method starting with a microbial product, cyanosafracin B (**14**), produced by large-scale fermentation of *Pseudomonas fluorescens* [107, 108]. The capabilities of this particular method were demonstrated by the preparation of a large number of natural ecteinascidins [109], together with a process that also permitted production of “unnatural” analogues [101]. A more detailed discussion of the developments through early 2005 was reported by Henriquez et al. in 2005 [4] and extended recently by Cuevas and Francesch in an excellent review in 2009 [101].

Et743 was approved by the EMEA in September 2007 for treatment of sarcoma and was launched in Sweden, Germany, and the UK by the end of 2007, thus becoming the first marine natural product used as an antitumor drug. Currently, mid-2010, there are 25 clinical trials listed in the NIH clinical trials database, with three recruiting at the phase III level, and recently it was approved in the EU for ovarian carcinoma treatment in conjunction with liposomal doxorubicin.

26.6.3 Lessons from Case Study 5

Just as in the case of bryostatin, enough material was obtained from a combination of wild collections and very extensive aquaculture in a number of in-sea and on-land operations to produce enough material for preclinical and clinical trials up through some early phase II trials. Although academic groups had produced enantiomeric syntheses of both the natural product and an active derivative that was similar in concept to the bryologs, it was realized that these were not amenable to the large-scale production necessary for further clinical trials and hoped for commercialization.

PharmaMar then decided to use a semisynthetic method based upon modification of a known microbial metabolite, cyanosafracin B, which could be obtained by fermentation on a very large scale, and thus a low overall yield could be tolerated [110]. This method was optimized and modified permitting the synthesis of unnatural derivatives by a relatively simple modification of one of the synthetic steps [101]. Thus, the methods developed were designed to increase the number of potential derivatives to “expand the franchise” where or when necessary.

26.7 Case Study 6: Salinosporamide A

In this particular case, the paradigm is quite different, in that rather than wild collections, syntheses and other methods of large-scale production, including identification of the actual rather than the potential producer, the producing organism was known at the beginning of the work as a prokaryote, in this case a marine-sourced actinomycete. Though we will use the same format in the previous five case studies, this one will be a simpler story as it has taken only 3–4 years from recognition of the molecule and its potential mechanism of action (MOA) to a first use in human phase I clinical trial.

26.7.1 Discovery of Salinosporamide A

In the late 1980s, Fenical and Jensen at Scripps Institution of Oceanography began their systematic investigation of the microbial diversity of marine habitats and its potential relationship to marine natural products. In late 1989, the SIO group investigated the distribution of actinomycetes in near-shore sediments in the Bahamas and discovered a number of organisms that required seawater for growth, and that the majority of such organisms were possibly new genera within the family *Micromonosporaceae* [111]. Although some cursory inspection of the secondary metabolites was performed at that time, no further work was done with these samples until in 1999, a reassessment of their phylogeny at the molecular level suggested that these were a new genus, originally named *Salinospira* within the *Micromonosporaceae* [112]. Further work confirmed this postulate and the genus was renamed *Salinispora* [113].

A reinvestigation of the secondary metabolite profile of these organisms led rapidly to an organism known as CNB-440, which when fermented on a 20-L scale, yielded a very potent cytotoxin named as salinosporamide A (**15**), whose structure was reminiscent of omuralide (**16**) but with significant variations, including a chlorine substituent that was required for the activity [114]. The final confirmation of the structure and proof of its MOA as a proteasome inhibitor was obtained via X-ray crystallographic techniques as described in detail by Groll et al. [115].

26.7.2 Large-Scale Fermentation/Isolation of cGMP Product

Salinosporamide A and other variants were licensed to San Diego Nereus Pharmaceuticals for further development as a cytotoxin. Nereus scientists, in concert with the now defunct fermentation group at Industrial Research Limited (IRL) in Lower Hutt, North Island, New Zealand, were able to produce the necessary cGMP product for clinical trials by fermentation in a saline environment, the first time that this task had been successfully performed on any significant (1,000 L) scale with a marine-sourced microbe. This work included the proof required for the production of a Drug Master

File (DMF), that such fermentation processes could be performed in a saline/alkali metal ion environment. The reason for concern was that such media would “pit” stainless steel fermentation vessels and, therefore, would need quite different cleaning/validation techniques in order to maintain the FDA requirements for cGMP production of the active pharmaceutical intermediates (APIs). This was successful, and the material obtained was satisfactory for advanced toxicology and then clinical trials in man. A series of reports on the fermentation media and on some of the other metabolites produced during the large scale isolation processes have begun to appear in print in the last few years [116–120], and fermentation modifications demonstrating that differing formulations with lower sodium ion concentration [121] or substitution by sodium sulfate can still maintain production but reduce corrosiveness of the medium [122], and in a later paper the same year, the same authors demonstrated that the ionic strength is a major determinant in growth and production [123]. In addition, an excellent discussion of the entire salinosporamide A story was published by Fenical et al. in 2009 [124].

26.7.3 Synthetic Processes

Even though the supply of material for clinical trials is from fermentation (a replacement for IRL was identified by Nereus in Eastern Canada so the supply of material was assured), chemists rose to the challenge and a number of groups including Nereus chemists have published total syntheses of salinosporamide A and analogues [125–134], thus demonstrating if one has a novel structure, chemists will devise syntheses for it as rapidly as possible. As mentioned earlier, the method of production is fermentation for the clinical candidate, but it is possible that derivative production may utilize some form of semisynthesis via the chemistries described above in due course.

26.7.4 Genomic Methods

Although some of the possibilities for genomic modifications/production were alluded to in the discussions on bryostatin (Sect. 26.3, Case 2) and dolastatin (Sect. 26.4, Case 3) where the producing microbe has been “identified,” salinosporamide, in addition to all of its other “firsts,” is the first antitumor agent whose biosynthetic pathway has been described and worked on contemporaneously with the late preclinical and early clinical studies. The genomic sequence of the producing actinomycete was investigated and 17 (plus) genomic clusters, one of which was the salinosporamide cluster, were reported by the SIO group of Moore in collaboration with the Fenical/Jensen group in 2007 [135]. The impact of this information from just the biosynthetic control of salinosporamide microbial synthesis can be seen by the papers that have been published using this basic information in the last 2 or so years. Thus, the biosynthetic route to the very unusual chlorinase that is essential for salinosporamide A’s activity has been reported [136]

together with methods of extending the polyketide synthons to give “unnatural derivatives” [137, 138] and a discussion on more general aspects of bioengineering from the organism itself [139, 140].

26.7.5 Lessons from Case Study 6

This example is quite different from the previous five in that the time frame has been very significantly compressed, from 18 to 20 plus years to less than 3 from realization that the microbes were a new marine-sourced genus, to identification of the metabolites and their potential. Thus, there was no large-scale method necessary except for development of fermentation processes to proceed with this compound. It should also be realized that the fermentation of marine-based microbes had never been attempted in regular fermentation systems prior to this work, let alone produce cGMP quality materials from such a process.

What also needs to be borne in mind is that there have been massive advances in genomic analyses in the last 5 plus years with the first actinomycete genomic sequence being published in 2002. The rapid development of recognition methods by earlier workers for defining the biosynthetic potential of gene clusters enabled the SIO discoverers and their collaborators in Nereus Pharma and SIO, in particular Moore’s group, to be able to use chemistry, knowledge of biosynthetic processes and the fermentation capabilities of Nereus to explore the producing microbe(s) extremely rapidly.

It is obvious from this example that the essential factors, aside from timing, are the dramatic interplay of scientists from many areas of chemistry and biology. Thus, a true multidisciplinary effort is absolutely essential for success.

26.8 In Conclusion

The examples used here for teaching purposes were chosen to show how scientists had to adapt to what was feasible rather than what might make sense using the knowledge of today. Thus, except for case study 6, a wide variety of collection and production methods were used as the time and funds permitted with recognition that at times, chemical synthesis was the only feasible route. Thus, the dolastatins were the product of total synthesis, as was aplidine. Initially, PharmaMar had developed a series of productive aquacultural methods that were used to produce Yondelis[®] for some of the earlier clinical trials and then moved to semisynthesis from a microbial secondary metabolite for large-scale clinical production.

With eribulin, Eisai used a modification of the natural product, halichondrin B, that relied upon an academic exercise in total synthesis of the natural product, during which the active pharmacophore was identified, although published only in a patent. It required a head-to-head comparison with the wild-collected natural product by NCI before Eisai was willing to commit to full scale synthetic production.

In case study 6, we have shown how the dramatic scientific advances in genomics and the influence of these techniques coalesced around a marine microbial metabolite that is currently the fastest natural product agent (and maybe even the fastest compound irrespective source) to go from discovery to clinical trials in under 4 years.

Thus, in the second decade of the twenty-first century, once an “active” agent has been identified as a potential drug lead, all methods for obtaining large-scale production are “on the table” for discussion and if/when the necessity arises for the production of significant amounts, the examples given above show what is currently available and investigators will mix and match as necessary, now that the pioneering work has been performed and evaluated. However, one can predict that new, currently unimagined technologies will come into being, and assist in the ever problematic issue of “meeting the supply needs of marine natural products.”

26.9 Study Questions

1. You have discovered a novel agent from a mixture of marine invertebrates. How would you determine if it was the product of an individual invertebrate? If it is, what are your next obvious steps? If it is not, what could be your best options?
2. You think that you have a small peptide as your active agent. What could be the various methodologies that could be used to produce larger quantities of the material in question, and why?
3. You have an active but quite toxic agent that you want to consider as a potential drug. How might you deliver this agent and why might one method be superior to another?
4. You have a very potent but complex structure as your discovery. What possible method(s) could you use to optimize the discovery for investigation as a potential drug?
5. You think that you have the producing microbe identified. How would you utilize current knowledge to prove that this is the case?

Acknowledgments The opinions expressed in this chapter are those of the authors, not necessarily those of the US Government.

References

1. Blunt JW, Copp BR, Munro MHG et al (2010) Marine natural products. *Nat Prod Rep* 27:165–237
2. Rinehart KL Jr, Gloer JB, Hughes RG Jr et al (1981) Didemnins: antiviral and antitumor depsipeptides from a Caribbean tunicate. *Science* 212:933–935
3. Rinehart KL Jr, Shaw PD, Shield LS et al (1981) Marine natural products as sources of antiviral, antimicrobial, and antineoplastic agents. *Pure Appl Chem* 53:795–817

4. Henriquez R, Faircloth G, Cuevas C (2005) Ecteinascidin 743 (ET-743TM; YondelisTM), aplidin, and kahalalide F. In: Cragg GM, Kingston DGI, Newman DJ (eds) Anticancer agents from natural products. Taylor and Francis, Boca Raton, pp 215–240
5. Rinehart KL Jr, Kishore V, Nagarajan S et al (1987) Total synthesis of Didemnin-A, Didemnin-B, and Didemnin-C. *J Am Chem Soc* 109:6846–6848
6. Harris BD, Bhat KL, Joullie MM (1987) Synthetic studies of didemnins. II. Approaches to statine diastereomers. *Tetrahedron Lett* 28:2837–2840
7. Jouin P, Poncet J, Dufour M-N et al (1991) Antineoplastic activity of didemnin congeners: nordidemnin and modified chain analogues. *J Med Chem* 34:486–491
8. Sakai R, Rinehart KL Jr, Kishore V et al (1996) Structure-activity relationships of the didemnins. *J Med Chem* 39:2819–2834
9. Vera MD, Joullie MM (2002) Natural products as probes of cell biology: 20 years of didemnin research. *Med Res Rev* 22:102–145
10. Marco E, Martín-Santamaría S, Cuevas C et al (2004) Structural basis for the binding of didemnins to human elongation factor eEF1A and rationale for the potent antitumor activity of these marine natural products. *J Med Chem* 47:4439–4452
11. Yao L (2003) Aplidin PharmaMar. *IDrugs* 6:246–250
12. Mittelman A, Chun HG, Puccio C et al (1999) Phase II clinical trial of didemnin B in patients with recurrent or refractory anaplastic astrocytoma or glioblastoma multiforme (NSC 325319). *Invest New Drugs* 17:179–182
13. Schmitz FJ, Yasumoto T (1991) The 1990 United States-Japan seminar on bioorganic marine chemistry, meeting report. *J Nat Prod* 54:1469–1490
14. Rinehart KL Jr (1994) Pharmaceutical compositions containing didemnins. US Patent 5,294,603
15. Urdiales JL, Morata P, Núñez De Castro I et al (1996) Antiproliferative effect of dehydroididemnin B (DDB), a depsipeptide isolated from Mediterranean tunicates. *Cancer Lett* 102:31–37
16. LaFargue F, Duclaux G (1979) Premier exemple en Atlantique tropical d'une association symbiotique entre une ascidie didemnidae et une cyanophyceae chroococcale: *Trididemnum cyanophorum* nov sp et *Synechocystis trididemni* nov sp. *Ann Inst Oceanogr Paris* 55:163–184
17. Sings HL, Rinehart KL Jr (1996) Compounds produced from potential tunicate-blue-green algal symbiosis: a review. *J Ind Microbiol* 17:395–396
18. Jou G, Gonzalez I, Albericio F et al (1997) Total synthesis of dehydroididemnin B. Use of uronium and phosphonium salt coupling reagents in peptide synthesis in solution. *J Org Chem* 62:354–366
19. Adrio J, Cuevas C, Manzanares I et al (2007) Total synthesis and biological evaluation of tamandarin B analogues. *J Org Chem* 72:5129–5138
20. Joullie MM, Portonovo P, Liang B et al (2000) Total synthesis of (–)-tamandarin B. *Tetrahedron Lett* 41:9373–9376
21. Gutiérrez-Rodríguez M, Martín-Martínez M, García-López MT et al (2004) Synthesis, conformational analysis, and cytotoxicity of conformationally constrained aplidine and tamandarin A analogues incorporating a spirolactam β -turn mimetic. *J Med Chem* 47: 5700–5712
22. Pettit GR, Day JF, Hartwell JL et al (1970) Antineoplastic components of marine animals. *Nature* 227:962–963
23. Pettit GR, Herald CL, Hogan F (2002) Biosynthetic products for anticancer drug design and treatment. In: Baguley BC, Kerr DJ (eds) Anticancer drug development. Academic, San Diego, pp 673–683
24. Newman DJ (2005) The bryostatins. In: Cragg GM, Kingston DGI, Newman DJ (eds) Anticancer agents from natural products. Taylor and Francis, Boca Raton, pp 137–150
25. Lopanik N, Gustafson KR, Lindquist N (2004) Structure of Bryostatin 20: a symbiont-produced chemical defense for larvae of the host bryozoan, *Bugula neritina*. *J Nat Prod* 67:1412–1414

26. Philip PA, Rea D, Thavasu P et al (1993) Phase I study of Bryostatin 1: assessment of interleukin 6 and tumor necrosis factor a induction in vivo. *J Natl Cancer Inst* 85: 1812–1818
27. Prendiville J, Crowther D, Thatcher N et al (1993) A phase I study of intravenous bryostatin 1 in patients with advanced cancer. *Br J Cancer* 68:418–424
28. Schaufelberger DE, Koleck MP, Beutler JA et al (1991) The large-scale isolation of Bryostatin 1 from *Bugula neritina* following current good manufacturing practices. *J Nat Prod* 54:1265–1270
29. Newman DJ (1996) Bryostatin – from bryozan to cancer drug. In: Gordon DP, Smith AM, Grant-Mackie JA (eds) *Bryozoans in space and time*. NIWA, Wellington, pp 9–17
30. Cragg GM, Schepartz SA, Suffness M et al (1993) The Taxol supply crisis. New NCI policies for handling the large-scale production of novel natural product anticancer and anti-HIV agents. *J Nat Prod* 56:1657–1668
31. Cragg GM (1998) Paclitaxel (Taxol®): a success story with valuable lessons for natural product drug discovery and development. *Med Res Rev* 18:315–331
32. Mendola D (2003) Aquaculture of three phyla of marine invertebrates to yield bioactive metabolites: process developments and economics. *Biomol Eng* 20:441–458
33. Kageyama M, Tamura T, Nantz MH et al (1990) Synthesis of bryostatin 7. *J Am Chem Soc* 112:7407–7408
34. Evans DA, Carter PH, Carreira EM et al (1998) Asymmetric synthesis of bryostatin 2. *Angew Chem Int Ed* 37:2354–2359
35. Evans DA, Carter PH, Carreira EM et al (1999) Total synthesis of bryostatin 2. *J Am Chem Soc* 121:7540–7552
36. Ohmori K, Ogawa Y, Obitsu T et al (2000) Total synthesis of bryostatin 3. *Angew Chem Int Ed* 39:2290–2294
37. Hale KJ, Hummersone MG, Manaviazar S et al (2002) The chemistry and biology of the bryostatin antitumour macrolides. *Nat Prod Rep* 19:413–453
38. Trost BM, Dong G (2008) Total synthesis of bryostatin 16 using atom-economical and chemoselective approaches. *Nature* 456:485–488
39. Miller AK (2009) Catalysis in the total synthesis of bryostatin 16. *Angew Chem Int Ed* 48:3221–3223
40. Pettit GR, Sengupta D, Herald CL et al (1991) Synthetic conversion of Bryostatin-2 to Bryostatin-1 and related bryopyrans. *Can J Chem* 69:856–860
41. Hale KJ, Manaviazar S (2010) New approaches to the total synthesis of the bryostatin antitumor macrolides. *Chem, – Asian J* 5:704–754
42. Wender PA, DeChristopher BA, Schrier AJ (2008) Efficient synthetic access to a new family of highly potent bryostatin analogues via a Prins-driven macrocyclization strategy. *J Am Chem Soc* 130:6658–6659
43. Wender PA, Verma VA (2008) The design, synthesis, and evaluation of C7 diversified bryostatin analogs reveals a hot spot for PKC affinity. *Org Lett* 10:3331–3334
44. Trost BM, Yang H, Thiel OR et al (2007) Synthesis of a ring-expanded bryostatin analogue. *J Am Chem Soc* 129:2206–2207
45. Keck GE, Kraft MB, Truong AP et al (2008) Convergent assembly of highly potent analogues of bryostatin 1 via pyran annulation: bryostatin look-alikes that mimic phorbol ester function. *J Am Chem Soc* 130:6660–6661
46. Haygood MG, Davidson SK (1997) Small-subunit rRNA genes and *in situ* hybridization with oligonucleotides specific for the bacterial symbionts in the larvae of the bryozoan *Bugula neritina* and proposal of “*Candidatus endobugula sertula*”. *Appl Environ Microbiol* 63:4612–4616
47. Davidson SK, Haygood MG (1999) Identification of sibling species of the bryozoan *Bugula neritina* that produce different anticancer bryostatins and harbor distinct strains of the bacterial symbiont “*Candidatus Endobugula sertula*”. *Biol Bull* 196:273–280

48. Davidson SK, Allen SW, Lim GE et al (2001) Evidence for the biosynthesis of bryostatins by the bacterial symbiont "*Candidatus Endobugula sertula*" of the Bryozoan *Bugula neritina*. Appl Environ Microbiol 67:4531–4537
49. Hildebrand M, Waggoner LE, Lim GE et al (2004) Approaches to identify, clone, and express symbiont bioactive metabolite genes. Nat Prod Rep 21:122–142
50. Lim GE, Haygood MG (2004) "*Candidatus Endobugula glebosa*," a specific bacterial symbiont of the marine bryozoan *Bugula simplex*. Appl Environ Microbiol 70:4921–4929
51. Hildebrand M, Waggoner LE, Liu H et al (2004) *bryA*: an unusual modular polyketide synthase gene from the uncultivated bacterial symbiont of the marine bryozoan *Bugula neritina*. Chem Biol 11:1543–1552
52. Lopanik N, Targett NM, Lindquist N (2006) Isolation of two polyketide synthase gene fragments from the uncultured microbial symbiont of the marine bryozoan *Bugula neritina*. Appl Environ Microbiol 72:7941–7944
53. Sudek S, Lopanik NB, Waggoner LE et al (2007) Identification of the putative bryostatin polyketide synthase gene cluster from "*Candidatus Endobugula sertula*", the uncultivated microbial symbiont of the marine bryozoan *Bugula neritina*. J Nat Prod 70:67–74
54. Lopanik NB, Shields JA, Buchholz TJ et al (2008) *In vivo* and *in vitro* trans-acylation by *bryP*, the putative bryostatin pathway acyltransferase derived from an uncultured marine symbiont. Chem Biol 15:1175–1186
55. Lim-Fong GE, Regali LA, Haygood MG et al (2008) Evolutionary relationships of "*Candidatus endobugula*" bacterial symbionts and their *Bugula* bryozoan hosts. Appl Environ Microbiol 74:3605–3609
56. Etcheberrigaray R, Tan M, Dewachtert I et al (2004) Therapeutic effects of PKC activators in Alzheimer's disease transgenic mice. Proc Natl Acad Sci, USA 101:11141–11146
57. Sun M-K, Alkon DL (2006) Bryostatin-1: pharmacology and therapeutic potential as a CNS drug. CNS Drug Rev 12:1–8
58. Wang D, Darwish DS, Schreurs BG et al (2008) Analysis of long-term cognitive-enhancing effects of bryostatin-1 on the rabbit (*Oryctolagus cuniculus*) nictitating membrane response. Behav Pharmacol 19:245–256
59. Flahive E, Srirangam J (2005) The dolastatins: novel antitumor agents from *Dolabella auricularia*. In: Cragg GM, Kingston DGI, Newman DJ (eds) Anticancer agents from natural products. Taylor and Francis, Boca Raton, pp 191–213
60. Pettit GR, Singh SB, Hogan F et al (1989) Antineoplastic agents. Part 189. The absolute configuration and synthesis of natural (–)-dolastatin 10. J Am Chem Soc 111:5463–5465
61. Pettit GR (1997) The dolastatins. Fortschr Chem Org Naturst 70:1–79
62. Bai R, Pettit GR, Hamel E (1990) Dolastatin 10, a powerful cytostatic peptide derived from a marine animal: inhibition of tubulin polymerization mediated through the vinca alkaloid binding domain. Biochem Pharmacol 39:1941–1949
63. Bai R, Pettit GR, Hamel E (1990) Binding of dolastatin 10 to tubulin at a distinct site for peptide antimitotic agents near the exchangeable nucleotide and vinca alkaloid sites. J Biol Chem 265:17141–17149
64. Bai R, Friedman SJ, Pettit GR et al (1992) Dolastatin 15, a potent antimitotic depsipeptide derived from *Dolabella auricularia*: interactions with tubulin and effects on cellular microtubules. Biochem Pharmacol 43:2637–2645
65. Vaishampayan H, Glode M, Du W et al (2000) Phase II study of dolastatin-10 in patients with hormone-refractory metastatic prostate adenocarcinoma. Clin Cancer Res 6:4205–4208
66. Margolin K, Longmate J, Synold TW et al (2001) Dolastatin-10 in metastatic melanoma: a phase II and pharmacokinetic trial of the California Cancer Consortium. Invest New Drugs 19:335–340
67. Pettit GR, Srirangam JK, Barkoczy J et al (1995) Antineoplastic agents 337. Synthesis of dolastatin 10 structural modifications. Anticancer Drug Des 10:529–544

68. Miyazaki K, Kobayashi M, Natsume T et al (1995) Synthesis and antitumor activity of novel dolastatin 10 analogs. *Chem Pharm Bull* 43:1706–1718
69. Carter PJ, Senter PD (2008) Antibody-drug conjugates for cancer therapy. *Cancer J* 14: 154–169
70. Alley SC, Zhang X, Okeley NM et al (2009) The pharmacologic basis for antibody-auristatin conjugate activity. *J Pharmacol Exp Ther* 330:932–938
71. Teicher BA (2009) Antibody-drug conjugate targets. *Curr Can Drug Targets* 9:982–1004
72. Akashi Y, Okamoto I, Suzuki M et al (2007) The novel microtubule-interfering agent TZT-1027 enhances the anticancer effect of radiation *in vitro* and *in vivo*. *Br J Cancer* 96: 1532–1539
73. Lippert JW III (2007) Vascular disrupting agents. *Bioorg Med Chem* 15:605–615
74. Watanabe J, Natsume T, Kobayashi M (2007) Comparison of the antivascular and cytotoxic activities of TZT-1027 (Soblidotin) with those of other anticancer agents. *Anti-Cancer Drugs* 18:905–911
75. Harrigan GG, Luesch H, Yoshida WY et al (1998) Symplostatin 1: a dolastatin 10 analogue from the marine cyanobacterium *Symploca hynoides*. *J Nat Prod* 61:1075–1077
76. Luesch H, Moore RE, Paul VJ et al (2001) Isolation of dolastatin 10 from the marine cyanobacterium *Symploca* species VP642 and total stereochemistry and biological evaluation of its analogue symplostatin 1. *J Nat Prod* 64:907–910
77. Long PF, Dunlap WC, Battershill CN et al (2005) Shotgun cloning and heterologous expression of the Patellamide gene cluster as a strategy to achieving sustained metabolite production. *Chembiochem* 6:1760–1765
78. Schmidt EW, Nelson JT, Rasko DA et al (2005) Patellamide A and C biosynthesis by a microcin-like pathway in *Prochloron didemni*, the cyanobacterial symbiont of *Lissoclinum patella*. *Proc Natl Acad Sci, USA* 102:7315–7320
79. Uemura D, Takahashi K, Yamamoto T et al (1985) Norhalichondrin A: an antitumor polyether macrolide from a marine sponge. *J Am Chem Soc* 107:4796–4798
80. Hirata Y, Uemura D (1986) Halichondrins: antitumor polyether macrolides from a marine sponge. *Pure Appl Chem* 58:701–710
81. Bai R, Paull KD, Herald CL et al (1991) Halichondrin B and homohalichondrin B, marine natural products binding in the vinca domain of tubulin: discovery of tubulin-based mechanism of action by analysis of differential cytotoxicity data. *J Biol Chem* 266:15882–15889
82. Aicher TD, Buszek KR, Fang FG et al (1992) Total synthesis of halichondrin B and norhalichondrin B. *J Am Chem Soc* 114:3162–3164
83. Munro MHG, Blunt JW, Dumdei EJ et al (1999) The discovery and development of marine compounds with pharmaceutical potential. *J Biotech* 70:15–25
84. Kishi Y, Fang F, Forsyth CJ et al (1993) Halichondrins and related compounds. *WO* 93/17690
85. Zheng W, Seletsky BM, Palme MH et al (2004) Macrocyclic ketone analogues of halichondrin B. *Bioorg Med Chem Lett* 14:5551–5554
86. Yu MJ, Kishi Y, Littlefield BA (2005) Discovery of E7389, a fully synthetic macrocyclic ketone analog of halichondrin B. In: Cragg GM, Kingston DGI, Newman DJ (eds) *Anticancer agents from natural products*. Taylor and Francis, Boca Raton, pp 241–265
87. Wang Y, Serradell N, Bolos J et al (2007) Eribulin mesilate. *Drugs Future* 32:681–698
88. Kim D-S, Dong C-G, Kim JT et al (2009) New syntheses of E7389 C14-C35 and halichondrin C14-C38 building blocks: double-inversion approach. *J Am Chem Soc* 131:15636–15641
89. Dong C-G, Henderson JA, Kaburagi Y et al (2009) New syntheses of E7389 C14-C35 and halichondrin C14-C38 building blocks: reductive cyclization and oxy-Michael cyclization approaches. *J Am Chem Soc* 131:15642–15646
90. Jordan MA, Kamath K, Manna T et al (2005) The primary antimetabolic mechanism of action of the synthetic halichondrin E7389 is suppression of microtubule growth. *Mol Cancer Ther* 4:1086–1095

91. Dabydeen DA, Burnett JC, Bai R et al (2006) Comparison of the activities of the truncated halichondrin B analog NSC 707389 (E7389) with those of the parent compound and a proposed binding site on tubulin. *Mol Pharmacol* 70:1866–1875
92. Okouneva T, Azarenko O, Wilson L et al (2008) Inhibition of centromere dynamics by eribulin (E7389) during mitotic metaphase. *Mol Cancer Ther* 7:2003–2011
93. Sigel MM, Wellham LL, Lichter W et al (1969) Anticellular and antitumor activity of extracts from tropical marine invertebrates. In: Youngen HW Jr (ed) *Food-drugs from the sea proceedings*. Marine Technology Society, Washington, DC, pp 218–294
94. Wright AE, Forleo DA, Gunawardana GP et al (1990) Antitumor tetrahydroisoquinoline alkaloids from the colonila ascidian *Ecteinascidia turbinata*. *J Org Chem* 55:4508–4512
95. Rinehart KL Jr, Holt TG, Fregeau NL et al (1990) Ecteinascidins 729, 743, 745, 759A, 759B and 770: potent antitumor agents from the Caribbean tunicate *Ecteinascidia turbinata*. *J Org Chem* 55:4512–4515
96. Scott JD, Williams RM (2002) Chemistry and biology of the tetrahydroisoquinoline antitumor antibiotics. *Chem Rev* 102:1669–1730
97. Morgan TO (1979) Reproduction, growth, and longevity of three species of West Indian colonial ascidians. In: *Proceedings of the association of island marine laboratories of the Caribbean*, vol 12, Caribbean, Marine Biological Institute, Curacao, pp 1–44
98. Carballo JL, Hernandez-Zanuy A, Naranjo S et al (1999) Recovery of *Ecteinascidia turbinata* Herman 1880 (Ascidacea: Perophoridae) populations after different levels of harvesting on a sustainable basis. *Bull Mar Sci* 65:755–760
99. Carballo JL (2000) Larval ecology of an ascidian tropical population in a Mediterranean enclosed ecosystem. *Mar Ecol Prog Ser* 195:159–167
100. Carballo JL, Naranjo S, Kukurtzı B et al (2000) Production of *Ecteinascidia turbinata* (Ascidacea: Perophoridae) for obtaining anticancer compounds. *J World Aquac Soc* 31:481–490
101. Cuevas C, Francesch A (2009) Development of Yondelis^(R) (trabectedin, ET-743). A semisynthetic process solves the supply problem. *Nat Prod Rep* 26:322–337
102. Kerr RG, Miranda NF (1995) Biosynthetic studies of ecteinascidins in the marine tunicate *Ecteinascidia turbinata*. *J Nat Prod* 58:1618–1621
103. Corey EJ, Gin DY, Kania RS (1996) Enantioselective total synthesis of ecteinascidin 743. *J Am Chem Soc* 118:9202–9203
104. Martinez EJ, Corey EJ (2000) A new, more efficient, and effective process for the synthesis of a key pentacyclic intermediate for production of ecteinascidin and phthalascidin antitumor agents. *Org Lett* 2:993–996
105. Martinez EJ, Owa T, Schreiber SL et al (1999) Phthalascidin, a synthetic antitumor agent with potency and mode of action comparable to ecteinascidin 743. *Proc Nat Acad Sci USA* 96:3496–3501
106. Cuevas C, Perez M, Martin MJ et al (2000) Synthesis of Ecteinascidin ET-743 and Phthalascidin Pt-650 from Cyanosafracin B. *Org Lett* 2:2545–2548
107. Ikeda Y, Idemoto H, Hirayama F et al (1983) Safracins, new antitumor antibiotics. I. Producing organism, fermentation and isolation. *J Antibiot* 36:1279–1283
108. Ikeda Y, Matsuki H, Ogawa T et al (1983) Safracins, new antitumor antibiotics. II. Physicochemical properties and chemical structures. *J Antibiot* 36:1284–1289
109. Menchaca R, Martínez V, Rodríguez A et al (2003) Synthesis of natural ecteinascidins (ET-729, ET-745, ET-759B, ET-736, ET-637, ET-594) from cyanosafracin B. *J Org Chem* 68:8859–8866
110. Fernandez-Puentes JM (2002) Personal communication
111. Jensen PR, Dwight R, Fenical W (1991) Distribution of actinomycetes in near-shore tropical marine sediments. *Appl Environ Microbiol* 57:1102–1108
112. Mincer TJ, Jensen PR, Kauffman CA et al (2002) Widespread and persistent populations of a major new marine actinomycete taxon in ocean sediments. *Appl Environ Microbiol* 68:5005–5011

113. Maldonado LA, Fenical W, Jensen PR et al (2005) *Salinispora arenicola* gen. nov., sp. nov. and *Salinispora tropica* sp. nov., obligate marine actinomycetes belonging to the family *Micromonosporaceae*. Int J Syst Evol Microbiol 55:1759–1766
114. Feling RH, Buchanan GO, Mincer TJ et al (2003) Salinosporamide A: a highly cytotoxic proteasome inhibitor from a novel microbial source, a marine bacterium of the new genus *Salinispora*. Angew Chem Int Ed 42:355–357
115. Groll M, Huber R, Potts BCM (2006) Crystal structures of salinosporamide A (NPI-0052) and B (NPI-0047) in complex with the 20 S proteasome reveal important consequences of b-lactone ring opening and a mechanism for irreversible binding. J Am Chem Soc 128: 5136–5141
116. Jensen PR, Williams PG, Oh D-C et al (2007) Species-specific secondary metabolite production in marine actinomycetes of the genus *Salinispora*. App Environ Microbiol 73:1146–1152
117. Lam KS, Tsung G, McArthur KA et al (2007) Effects of halogens on the production of salinosporamides by the obligate marine actinomycete *Salinispora tropica*. J Antibiot 60:13–19
118. Reed KA, Manam RR, Mitchell SS et al (2007) Salinosporamides D-J from the marine actinomycete *Salinispora tropica*, Bromosalinosporamide, and thioester derivatives are potent inhibitors of the 20 S proteasome. J Nat Prod 70:269–276
119. Tsung G, Lam KS (2007) Stabilization effect of resin on the production of potent proteasome inhibitor NPI-0052 during submerged fermentation of *Salinispora tropica*. J Antibiot 60:469–472
120. Tsung G, McArthur KA, Potts BCM et al (2007) Unique butyric acid incorporation patterns for salinosporamides A and B reveal distinct biosynthetic origins. Appl Microbiol Biotechnol 75:999–1005
121. Tsung G, Lam KS (2008) A low-sodium-salt formulation for the fermentation of salinosporamides by *Salinispora tropica* strain NPS21184. Appl Microbiol Biotechnol 78:821–826
122. Tsung G, Teisan S, Lam KS (2008) Defined salt formulations for the growth of *Salinispora tropica* strain NPS21184 and the production of Salinosporamide A (NPI-0052) and related analogs. Appl Microbiol Biotechnol 78:827–832
123. Tsung G, Lam KS (2008) Growth of *Salinispora tropica* strains CNB440, CNB476, and NPS21184 in nonsaline, low-sodium media. Appl Microbiol Biotechnol 80:873–880
124. Fenical W, Jensen PR, Palladino MA et al (2009) Discovery and development of the anticancer agent salinosporamide A (NPI-0052). Bioorg Med Chem 17:2175–2180
125. Reddy LR, Saravanan P, Corey EJ (2004) A simple stereocontrolled synthesis of salinosporamide A. J Am Chem Soc 126:6230–6231
126. Endo A, Danishefsky SJ (2005) Total synthesis of salinosporamide A. J Am Chem Soc 127:8298–8299
127. Macherla VR, Mitchell SS, Manam RR et al (2005) Structure-activity relationship studies of salinosporamide A (NPI-0052), a novel marine derived proteasome inhibitor. J Med Chem 48:3684–3687
128. Shibasaki M, Kanai M, Fukuda N (2007) Total synthesis of lactacystin and salinosporamide A. Chem Asian J 2:20–38
129. Gil M, Henry N, Romo D (2007) Concise total synthesis of (±)-salinosporamide A, (±)-cinnabaramide A, and derivatives via a bis-cyclization process: implications for a biosynthetic pathway? Org Lett 9:2143–2146
130. Ling T, Macherla VR, Manam RR et al (2007) Enantioselective total synthesis of (–)-salinosporamide A (NPI-0052). Org Lett 9:2289–2292
131. Mulholland NP, Pattenden G, Walters IAS (2008) A concise and straightforward total synthesis of (±)-salinosporamide A, based on a biosynthesis model. Org Biomol Chem 6:2782–2789

132. Villanueva MI, Rupnicki L, Lam HW (2008) Formal synthesis of salinosporamide A using a nickel-catalyzed reductive aldol cyclization-lactonization as a key step. *Tetrahedron* 64:7896–7901
133. Fukuda T, Sugiyama K, Arima S et al (2008) Total synthesis of salinosporamide A. *Org Lett* 10:4239–4242
134. Momose T, Kaiya Y, Hasegawa J-I et al (2009) Formal synthesis of salinosporamide A starting from D-glucose. *Synthesis* 17:2983–2991
135. Udworthy DW, Zeigler L, Asolkar RN et al (2007) Genome sequencing reveals complex secondary metabolome in the marine actinomycete *Salinispora tropica*. *Proc Nat Acad Sci USA* 104:10376–10381
136. Eustáquio AS, McGlinchey RP, Liu Y et al (2009) Biosynthesis of the salinosporamide A polyketide synthase substrate chloroethylmalonyl-coenzyme A from S-adenosyl-L-methionine. *Proc Nat Acad Sci USA* 106:12295–12300
137. Liu Y, Hazzard C, Eustáquio AS et al (2009) Biosynthesis of salinosporamides from α , β -unsaturated fatty acids: implications for extending polyketide synthase diversity. *J Am Chem Soc* 131:10376–10377
138. Nett M, Gulder TAM, Kale AJ et al (2009) Function-oriented biosynthesis of β -lactone proteasome inhibitors in *Salinispora tropica*. *J Med Chem* 52:6163–6167
139. Nett M, Moore BS (2009) Exploration and engineering of biosynthetic pathways in the marine actinomycete *Salinispora tropica*. *Pure Appl Chem* 81:1075–1084
140. Nett M, Ikeda H, Moore BS (2009) Genomic basis for natural product biosynthetic diversity in the actinomycetes. *Nat Prod Rep* 26:1362–1384

Gordon M. Cragg, Flora Katz, David J. Newman, and Joshua Rosenthal

Contents

27.1	Introduction	1316
27.2	The NCI Experience	1319
27.2.1	Achievements: 1955–1982	1319
27.2.2	Contract Collections: 1986–Present. The NCI Letter of Collection	1320
27.2.3	Source Country Collaboration	1321
27.2.4	Direct Collaboration with Source Country Organizations. The NCI Memorandum of Understanding	1322
27.2.5	Case Study. The Calanolides	1323
27.3	The International Cooperative Biodiversity Groups (ICBG) Program	1325
27.3.1	Agreements Governing Collaborative Research and Nature of Benefits ...	1327
27.3.2	Achievements	1331
27.3.3	Case Studies	1332
27.4	Conclusions and Recommendations	1335
27.4.1	Commercial Drug – A Rarity!	1335
27.4.2	Drug Development Costs and Time Frame	1336
27.4.3	Recommended Collaborative Process	1337
27.5	Study Questions	1339
	References	1340

G.M. Cragg (✉) • D.J. Newman

Natural Products Branch, Developmental Therapeutics Program, National Cancer Institute,
NCI-Frederick, Frederick, MD, USA

e-mail: gmccragg@verizon.net, newmand@mail.nih.gov

F. Katz • J. Rosenthal

John E. Fogarty International Center, National Institutes of Health, 31 Center Drive, MSC 2220,
Bethesda, MD, USA

e-mail: katzf@mail.nih.gov, Joshua_Rosenthal@nih.gov

E. Fattorusso, W. H. Gerwick, O. Taglialatela-Scafati (eds.),

Handbook of Marine Natural Products, DOI 10.1007/978-90-481-3834-0_27,

© Springer Science+Business Media B.V. 2012

1315

Abstract

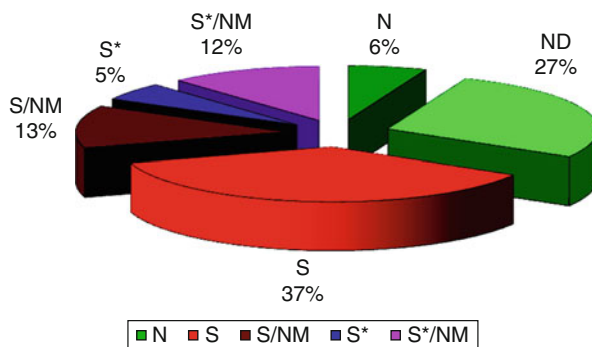
The discovery and development of novel, biologically active agents from natural sources, whether they be drugs, agrochemicals, or other bioactive entities, involve a high level of interdisciplinary as well as international collaboration. Such collaboration, particularly at the international level, requires the careful negotiation of collaborative agreements protecting the rights of all parties, with special attention being paid to the rights of host (source) country governments, communities, and scientific organizations. While many biodiversity-rich source countries currently might not have the necessary resources for in-country drug discovery and advanced development, they provide valuable opportunities for collaboration in this endeavor with research organizations from more developed nations. This chapter discusses the experiences of the US National Cancer Institute and the US government-sponsored International Cooperative Biodiversity Groups program in the establishment of international agreements promoting fair and equitable collaboration with source countries in the investigation of their rich biological resources, and includes recommendations for achieving such collaboration.

27.1 Introduction

Natural products have made, and continue to make, an indispensable contribution to the discovery and development of effective drugs for the treatment of many of the diseases afflicting humankind. A recent review [1] summarizes all approved agents during the past 25½ years from January 1981 to June 2006 for all diseases worldwide (Fig. 27.1).

In the analysis, new drugs were classified as N (an unmodified natural product), ND (a modified natural product), S (a synthetic compound with no natural product conception), S/NM (a synthetic compound showing competitive inhibition of the natural product substrate), S* (a synthetic compound with a natural product pharmacophore), and S*/NM (a synthetic compound with a natural product pharmacophore showing competitive inhibition of the natural product substrate). While 66% of the 974 small-molecule new chemical entities (NCEs) are formally synthetic, the analysis indicated that 17% correspond to synthetic molecules containing pharmacophores derived directly from natural products (classified as S* and S*/NM). Furthermore, 12% were considered to actually model a natural product inhibitor of the molecular target of interest or mimic (i.e., competitively inhibit) the endogenous substrate of the active site, such as ATP (S/NM). Thus, only 37% of the 974 NCEs were considered as truly synthetic (i.e., devoid of natural inspiration) in origin (S). In considering disease categories, close to 70% of anti-infectives (antibacterial, antifungal, antiparasitic, and antiviral) were classified as naturally derived or inspired (N, ND, S*, S*/NM, S/NM), while in the cancer treatment area, 77.8% were in this category, with the figure being 63% if the S/NM category is excluded.

Fig. 27.1 Small-molecule new chemical entities. January 1981–June 2006, by source (N = 974)



The importance of marine-derived secondary metabolites in chemical ecology, and as a source of leads for the development of potential new drugs or agrochemicals, is amply illustrated in the discussions contained in many of the chapters of this book. Indeed, in the area of cancer treatment, an impressive number of marine-derived agents have advanced into clinical development [2, 3].

While natural products are a proven source of novel, bioactive molecules, the actual compound isolated from the natural source often is not suitable for development into an effective drug or agrochemical product, but may, however, be regarded as a lead molecule which can form the basis for further chemical or biochemical modification. The discovery of promising bioactive molecules always involves close collaboration with biologists in the provision of suitable disease-oriented screens, while the optimization of the lead molecule often requires significant input from medicinal and synthetic chemists. The preclinical development of an agent always requires close collaboration with pharmacologists and toxicologists in the determination of the optimal pharmacodynamic and toxicological parameters suitable for advancement of the agent into clinical trials with human patients.

As discussed above, effective discovery and development of novel drugs require multidisciplinary collaboration. In the area of natural product bioactive lead discovery, close international collaboration is an additional, important requirement. Much of the world's biological diversity resides in low- and middle-income countries located in tropical and subtropical regions. The United Nations Law of the Sea (LOS) Treaty allows for open access in international waters or the high seas (<http://www.un.org/Depts/los/index.htm>). However, most accessible marine biodiversity and the vast majority of marine natural product collections come from territorial waters or those that fall under the exclusive economic zones of countries. As such, marine collections of biodiversity for natural products fall under the United Nations Convention on Biological Diversity (CBD); (<http://www.biodiv.org/convention/articles.asp>). The CBD has established a general framework for "access and benefit-sharing" that is being negotiated in more detail and may eventually become binding international law. The objectives as stated in the CBD are "the conservation of biological diversity, the sustainable use of its components and the fair and

equitable sharing of the benefits arising out of the utilization of genetic resources, including by appropriate access to genetic resources and by appropriate transfer of relevant technologies, taking into account all rights over those resources and to technologies, and by appropriate funding.” Irrespective of the legal trajectory of this central component of the CBD, dozens of countries have already implemented the objectives in national laws or policies, and the general expectation today in the international community is that productive interaction between these biodiversity-rich source countries and the more “science and technology-rich” countries is guided by the CBD principles and strives to conduct itself in a fair and equitable framework including access and benefit-sharing. Many of the naturally derived bioactive leads are isolated from organisms located and collected in these biodiversity-rich source countries, and it is incumbent on scientists involved in the biodiscovery process (often called bioprospecting) to establish collaborative agreements meeting the requirements of the CBD with the scientific communities and government agencies in these countries before proceeding with such programs.

Over the past 20 years, a number of international organizations have issued declarations or resolutions urging greater international collaboration and coordination in efforts to promote the conservation of biological and cultural diversity worldwide. Among these have been the Goteborg Resolution [4], and guidelines issued by the American Society of Pharmacognosy [5, 6] and the International Union of Pure and Applied Chemistry [7]. In addition, several books dealing with the commercial and legal aspects have been written [8–12]. The central theme of these publications is the fact that the source countries (mainly low- and middle-income) and their indigenous peoples are the custodians of the majority of the world’s genetic resources and that conservation of these resources requires fair and equitable collaboration and compensation in the development of their resources, as well as just recognition of the inventive and intellectual contributions of the indigenous peoples to the knowledge of the use of these resources. Emphasis is given to training, the exchange of ideas, results and technology, the promotion of traditional health care systems, and the completion of species and traditional knowledge inventories, with the dissemination of this information to all interested parties, including where possible in native languages.

It is clear that, without suitable economic, intellectual, and technological incentives for sustainable development, the genetically rich source countries and their communities will be unable to preserve these valuable resources for research into their beneficial uses for humankind. Although the focus to date has been on the depletion of plant resources, similar arguments apply equally well to the conservation of other organisms, such as those of marine origin.

In order to illustrate the application of the principles of the CBD to the collection and study of genetic resources, the following sections will discuss the experiences of the US National Cancer Institute (NCI) and the International Cooperative Biodiversity Groups (ICBG) program coordinated and administered by the Fogarty International Center (FIC) of the US National Institutes of Health (NIH).

27.2 The NCI Experience

The NCI has been involved in drug discovery and development for close to 50 years and has made significant contributions to the development of many of the anticancer drugs currently used clinically. The success of much of this effort has depended on close collaboration with organizations worldwide, and international collaboration continues to be an important feature of the NCI programs [13].

27.2.1 Achievements: 1955–1982

The NCI (<http://www.nci.nih.gov>) was established in 1937, its mission being “to provide for, foster and aid in coordinating research related to cancer.” In 1955, NCI set up the Cancer Chemotherapy National Service Center (CCNSC) to coordinate a national voluntary cooperative cancer chemotherapy program, involving the procurement of drugs, screening, preclinical studies, and clinical evaluation of new agents. The responsibility for drug discovery and preclinical development at NCI now rests with the Developmental Therapeutics Program (DTP; <http://dtp.nci.nih.gov>), a major component of the Division of Cancer Treatment and Diagnosis (DCTD). Thus, NCI has for the past 50 years provided a resource for the preclinical screening of compounds and materials submitted by scientists and institutions, public and private, worldwide, and has played a major role in the discovery and/or development of many of the available commercial and investigational anticancer agents. During this period, more than 500,000 chemicals, both synthetic and natural, have been screened for antitumor activity.

Initially, most of the materials screened were pure compounds of synthetic origin, but the program also recognized that natural products were an excellent source of complex chemical structures with a wide variety of biological activities. The original plant collections from 1960 to 1982 were performed by the US Department of Agriculture (USDA) through an interagency agreement with NCI and involved the random collection of over 35,000 plant samples, mainly from temperate regions. These collections led to the discovery of paclitaxel (Taxol[®]) and camptothecin which formed the basis for the semisynthesis of several clinically effective drugs. Marine invertebrates were generally collected by academic investigators, mainly funded through grants from the NCI, while microbial samples were obtained from pharmaceutical companies and research institutes, such as the Institute of Microbial Chemistry in Japan, some of which were funded through contracts with the NCI. From 1960 to 1982, over 180,000 microbial-derived, some 16,000 marine organism-derived, and over 114,000 plant-derived extracts were screened for antitumor activity, mainly by the NCI, and as mentioned above, a number of clinically effective chemotherapeutic agents have been developed [14].

27.2.2 Contract Collections: 1986–Present. The NCI Letter of Collection

The systematic collection of marine invertebrates and terrestrial plants was initiated in 1986 and is coordinated by the DTP Natural Products Branch (NPB; <http://dtp.nci.nih.gov/branches/npb/index.html>). Marine organism collections originally focused in the Caribbean and Australasia but, in 1992, were expanded to the Central and Southern Pacific and to the Indian Ocean (off East and Southern Africa) through a contract with the Coral Reef Research Foundation, which is based in Palau in Micronesia. With the renewal of the contract in 2002, collections are now performed worldwide. Terrestrial plant collections have been carried out in over 25 countries in tropical and subtropical regions worldwide through contracts with the Missouri Botanical Garden (Africa and Madagascar), the New York Botanical Garden (1986–1996; Central and South America), the University of Illinois at Chicago (Southeast Asia), the Morton Arboretum, and World Botanical Associates (USA mainland and territories).

The NCI collection contractors are required to obtain all of the necessary permits, including visas and collecting shipping and export permits, from the appropriate source country agencies or departments. The NCI provides the contractors with the NCI Letter of Collection (LOC; <http://ttc.nci.nih.gov/forms/>) [15] for transmission to the appropriate source country authorities and scientific organizations. The LOC states NCI's willingness to collaborate with local scientists and/or authorities in the discovery and development of novel drugs from organisms (plants, marine invertebrates, microbes) collected in their countries and/or territorial waters, and if requested, the NCI will enter into formal agreements based on the LOC with the relevant source country government agency or organization. Fourteen such agreements have been signed (Table 27.1); there are also 24 countries which have not, as yet, signed formal agreements with the NCI (Table 27.2). These countries, however, are fully aware of the terms of the LOC and granted the necessary permits for NCI contractor activities without requiring a formal agreement. In this respect, the NCI is totally committed to the terms of the LOC irrespective of whether or not a formal agreement has been signed [16]. Marine collections have been performed in the territorial waters of Australia, Federated States of Micronesia, Indonesia, Maldives, Marshall Islands, Mauritius, Palau, Papua New Guinea, Tanzania, and Thailand.

This absence of formal agreements has not been due to lack of effort on the part of the NCI contractors and/or NCI staff to solicit formal agreements from the source countries involved. Indeed, NPB staff has interacted with source country government representatives and scientists, both in their countries, or more frequently during NCI-sponsored visits to NCI and contractor US-based home facilities. The purpose of these visits is to provide opportunities for source country officials and scientists to observe the NCI drug discovery facilities and the processes to which their raw materials are subjected, and to discuss collaboration in the drug discovery process. During the past 20 years, over 65 source country officials and scientists have visited NCI, either to discuss participation in NCI contract collections or to discuss direct collaboration in the drug discovery process.

Table 27.1 Source countries with which NCI has collaborated in the collection of plants and marine organisms. Collaborating countries with which NCI had a Letter of Collection agreement

Source country	Source country organization	Year of agreement
Australia	Museum of the Northern Territories	2002
Bangladesh	Bangladesh National Herbarium, Dhaka	1994
Cambodia	Forest and Wildlife Research Institute, Department of Forestry and Wildlife, Phnom Penh	2000
Ecuador	The AWA Peoples Federation	1993
Gabon	Centre National de la Recherche Scientifique et Technologique (CENAREST), Libreville	1993
Ghana	University of Ghana, Legon	1993
Laos	Research Institute of Medicinal Plants, Ministry of Public Health, Vientiane	1998
Madagascar	Centre National D'Applications des Recherches Pharmaceutiques, Antananarivo	1990
Palau	Government of Palau	2002
Papua New Guinea	University of Papua New Guinea, Port Moresby	2001
Philippines	Philippines National Museum, Manila	1992
Sarawak, Malaysia	State Government of Sarawak: State Department of Forests	1994
Sarawak, Malaysia	Sarawak Biodiversity Council (marine collections)	2002
Tanzania	Traditional Medicine Research Institute, Muhumbili University College of Health Sciences, University of Dar Es Salaam	1991
Vietnam	Institute of Ecology and Biological Resources, National Center for Natural Science and Technology, Hanoi	1997

Table 27.2 Collaborating countries with no Letter of Collection agreement with NCI^a

Bahrain	Dominican Republic	Maldives	St. Lucia
Belize	Federated States of Micronesia (e.g., Chuuk, Yap)	Marshall Islands	Thailand
Bolivia	Guatemala	Martinique	Tonga
Cameroon	Guyana	Mauritius	—
Central African Republic	Honduras	Nepal	—
Colombia	Indonesia	Paraguay	—
Dominica	Malaysia	Peru	—

^aNCI is totally committed to LOC terms irrespective of whether or not an official agreement has been signed

27.2.3 Source Country Collaboration

In carrying out collections, the NCI contractors work closely with qualified organizations in each of the source countries. Botanists and marine biologists from source country organizations (SCOs) collaborate in field collection activities and taxonomic identifications, and their knowledge of local species and conditions is indispensable to the success of the NCI collection operations. SCOs provide

facilities for the preparation, packaging, and shipment of the samples to the NCI's Natural Products Repository (NPR) in Frederick, Maryland. The collaboration between the SCOs and the NCI collection contractors, in turn, provides support for expanded research activities by source country biologists, and the deposition of a voucher specimen of each species collected in the national herbarium or repository is expanding source country holdings of their biota. NCI contractors also provide training opportunities for local personnel through conducting workshops and presentation of lectures, both in-country and at the contractor's US facilities.

In addition, through its Letter of Collection and agreements based upon it, the NCI: (1) sponsors visits by scientists nominated by SCOs to its facilities, and/or equivalent facilities in other approved US or local organizations, for 1–12 months to participate in collaborative natural products research involving disciplines pertaining to drug discovery, such as the screening and bioassay-directed fractionation of extracts (over 20 such visits have been sponsored), and (2) dictates arrangements for benefit-sharing and use of source country resources in the event of the licensing and development of a promising drug candidate. Successful licensees of patented agents discovered from NCI contract collections are required to negotiate agreements with the relevant source country government agencies or organizations dictating terms of collaboration and compensation. The terms apply irrespective of whether the potential drug is the actual natural isolate or a product structurally based upon the isolate, a synthetic material for which the natural product material provided a key development lead, or a method of synthesis or use of any aforementioned isolate, product, or material. The terms (e.g., percentage of royalties) negotiated as payment, however, might vary depending upon the relationship of the marketed drug to the originally isolated product.

The formulation of the NCI policies for collaboration and compensation embodied in the Letter of Collection predated the drafting of the United Nations Convention on Biological Diversity signed in Rio de Janeiro by some 4 years. It must be stressed that the NCI abides by the terms of the LOC even if the collaborating source country has not signed a formal agreement. In addition, the NCI and the ICBG US-based collaborating organizations respect the terms of the CBD even though the US has not ratified the treaty, as yet in 2010.

27.2.4 Direct Collaboration with Source Country Organizations. The NCI Memorandum of Understanding

As discussed above, the collections of plants and marine organisms have been carried out in over 25 countries through contracts with qualified botanical and marine biological organizations working in close collaboration with qualified SCOs, and all collections are performed subject to the terms of the NCI Letter of Collection. Particularly in the area of plant-related studies, source country scientists and governments are becoming increasingly committed to performing more of the drug discovery operations in-country, as opposed to the export of raw materials. The NCI has recognized this fact for several years, and contract collections of plants have been

de-emphasized in favor of establishing direct collaborations with qualified organizations in the source countries where the necessary expertise and infrastructure exist.

The NCI has established collaborative agreements [Memoranda of Understanding (MOUs); <http://ttc.nci.nih.gov/forms/>] with over 20 SCO's suitably qualified to perform in-country processing (Table 27.3).

In establishing these agreements, the NCI undertakes to abide by the same policies of collaboration and compensation as specified in the LOC. NCI also assists the SCO's to establish their own drug discovery programs through training in techniques of antitumor screening and natural product isolation. NCI has sponsored long-term visitors from 18 countries for purposes of such collaboration and training. Where suitable infrastructure is available at source country institutions, the NCI will provide human cancer cell lines, as well as the appropriate cell line and virus (genetically modified to be noninfectious) for a cell-based anti-HIV screen, at minimal cost to those institutions to enable them to set up screens for their own in-house drug discovery programs.

It is anticipated that the discovery of novel anticancer drugs will be performed by the SCO at its own expense, with assistance from the NCI in terms of free secondary in vitro and in vivo testing. All results from such secondary testing are considered the sole intellectual property of the SCO (NCI regards such testing as a routine service to the scientific community) and can be used by the SCO in the application for patents covering sufficiently promising inventions. The NCI will devote its resources to collaborating with the SCO in the preclinical and clinical development of any SCO-discovered drug which meets the NCI selection criteria and will make a sincere effort to transfer any knowledge, expertise, and technology developed during such collaboration to the SCO, subject to the provision of mutually acceptable guarantees for the protection of intellectual property associated with any patented technology.

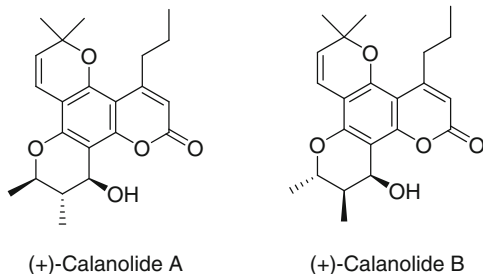
Through this mechanism, collaborations in the collection and study of marine organisms have been established with organizations in Australia, Brazil, Fiji, New Zealand, Papua New Guinea, and South Africa.

27.2.5 Case Study. The Calanolides

An extract of the leaves and twigs of the tree, *C. lanigerum*, collected in Sarawak, Malaysia, in 1987, yielded (+)-calanolide A (Fig. 27.2) which showed significant anti-HIV activity [17]. Efforts to relocate the original tree failed, and collections of other specimens of the same species gave only trace amounts of calanolide A. A detailed survey of *C. lanigerum* and related species discovered that latex of *C. teysmanii* yielded extracts with significant anti-HIV activity. The active constituent was found to be an isomer, (–)-calanolide B (Fig. 27.2), which was isolated in yields of 20–30%. While (–)-calanolide B is slightly less active than (+)-calanolide A, it has the advantage of being readily available from the latex which is tapped in a sustainable manner by making small slash wounds in the bark of mature trees without causing any harm to the trees. The calanolides were licensed by NCI/NIH

Table 27.3 MOUs between NCI and source country organizations: direct collaborations

Source country	Source country organization	Year of agreement
Australia	Australian Institute of Marine Sciences, Townsville, Queensland	1999
Bangladesh	The University of Dhaka	1998
Brazil	Fundacao Oswaldo Cruz – FIOCRUZ, Rio de Janeiro	1999
	South American Organization for Anticancer Drug Development, Canoas	1995
	Universidade do Paulista, Sao Paulo	1997
	Universidade Federal do Parana	1998
China	Universidade Federal do Ceara, Fortaleza	2001
	Hong Kong University of Science and Technology	1998
	Kunming Institute of Botany, Yunnan	1995
	Peking University and State Key Laboratory, Beijing	2001
Costa Rica	Instituto Nacional de Biodiversidad (INBio)	1994
Fiji	University of the South Pacific, Suva	1999
Iceland	The University of Iceland, Reykjavik	1998
Republic of Korea	Korean Research Institute of Chemical Technology (KRICT)	1995
Mexico	Instituto de Quimica, Universidad Nacional Autonoma de Mexico, Mexico City	1995
New Zealand	National Institute of Water and Atmospheric Research (NIWA), Wellington	1996
Nicaragua	Universidad Nacional Autonoma de Nicaragua, Leon	1999
Pakistan	HEJ Research Institute of Chemistry, University of Karachi	1994
Papua New Guinea	University of Papua New Guinea, Port Moresby	2001
Panama	University of Panama	1996
South Africa	Council for Scientific and Industrial Research (CSIR), Division of Food, Biological and Chemical Technologies (BIO/CHEMTEK), Pretoria	1996
	Rhodes University, Grahamstown	1998
Zimbabwe	Zimbabwe National Traditional Healers Association (ZINATHA)	1994

**Fig. 27.2** Potential anti-HIV agents. Calanolides A and B

to Medichem Research, Inc., (now Advanced Life Sciences) which, as required by the NCI LOC [15], negotiated an agreement with the Sarawak State Government. The drugs were initially being developed by Sarawak Medichem Pharmaceuticals, a joint venture company formed between the Sarawak State Government and Medichem Research, Inc., but the lead role in the development is now being undertaken by Craun Research Sendirian Berhad, a company incorporated in Sarawak. Medichem Research had synthesized (+)-calanolide A, and it is currently headed for Phase II clinical trials, while (–)-calanolide B is in preclinical development. The earlier development of the calanolides has been reviewed as a “Benefit-Sharing Case Study” for the Executive Secretary of the CBD by staff of the Royal Botanic Gardens, Kew, UK [18]. It is interesting that subsequent to the discovery of the calanolides, Sarawak established the Sarawak Biodiversity Center (<http://www.sbc.org.my/>) which performs an in-country bioprospecting program as well as other biodiversity-related activities.

27.3 The International Cooperative Biodiversity Groups (ICBG) Program

The International Cooperative Biodiversity Groups (ICBG) Program, in its original conception, adopted several key elements of the NCI experience described above, but is a much broader effort with multiple goals. Initiated in 1993 as a US Government (USG) interagency initiative led by the Fogarty International Center of the NIH, the ICBG program aims to discover new bioactive molecules from nature while providing incentives for sustainable biodiversity conservation. It is based on the premise that biodiscovery, scientific capacity building, and biodiversity conservation are fundamentally interdependent and can yield synergistic benefits from an integrated program that returns economic and scientific benefits to the host countries.

At a basic level, the ICBG program, like that of the NCI programs, is one of international collaboration that pays particular attention to benefit-sharing. However, the ICBGs differ in structure and scope in that they are a competitive grants program through which international research consortia assemble in response to a solicitation to build partnerships between at least one US academic research institution and at least one non-US host organization in biodiversity-rich, low- and middle-income countries (http://www.fic.nih.gov/programs/research_grants/icbg/index.htm; <http://www.icbg.org/>). Because of the multiple goals of the program, consortia typically include between three and ten organizations with different missions and expertise, all collaborating toward joint, interdependent goals.

The first round of the program was jointly sponsored by components of the National Institutes of Health, the National Science Foundation, and the Agency for International Development. The initial focus of the ICBG program was on the identification of compounds and extracts that might lead to the development of new drugs or botanicals in a wide variety of therapeutic areas. With the addition of

Table 27.4 Cosponsors of the ICBG program

USG Agency	Period of participation	Program interest
<i>National Institutes of Health</i>		
Fogarty International Center	1993–present Administrative lead, financial support	Global health, international collaborations, scientific capacity building
National Cancer Institute	1993–present Technical and financial support	Anticancer agents
National Heart, Lung, and Blood Institute	1993–2002	Cardiovascular agents
National Institute of Mental Health	1993–present Technical and financial support	Agents for psychiatric disorders
National Institute of Allergy and Infectious Diseases	1993–2008 Technical and financial support	Anti-infective agents
National Center for Complementary and Alternative Medicine	2003–present Technical and financial support	Ethnomedical remedies
Office of Dietary Supplements	2003–present Technical and financial support	Botanical analysis
National Institute on Drug Abuse	1997–2008 Technical and financial support	Anti-addiction agents
National Institute of General Medical Sciences	2003–present Technical and financial support	Novel bioactive molecules and new chemistry
<i>National Science Foundation</i>		
Directorate of Biological Sciences	1993–present Technical and financial support	Biodiversity inventory and conservation; microbial diversity
Directorate of Geosciences	2003–present Technical and financial support	Marine Biology
<i>US Agency for International Development</i>		
	1993–1996 Technical and financial support	Biodiversity conservation and economic development
<i>US Department of Agriculture</i>		
Foreign Agriculture Service	1997–2003 Technical and financial support	Sustainable use of biodiversity, crop protection
Forest Service	1997–2003 Technical support	Sustainable use of biodiversity, conservation
Cooperative State Research, Extension and Education Service (Current name: National Institute of Food and Agriculture)	2008–present Technical and financial support	Sustainable use of biodiversity, crop protection and animal health
<i>Department of Energy</i>		
Office of Biological and Environmental Research	2008–present Technical and financial support	Biological sources of energy conversion and CO ₂ assimilation

(continued)

Table 27.4 (continued)

USG Agency	Period of participation	Program interest
<i>National Oceanic and Atmospheric Administration</i>		
Oceans and Human Health Initiative	2009–present Technical and financial support	Health products from the ocean; training in marine biotechnology for health; healthy oceans and marine conservation

the US Department of Agriculture (USDA) in 1997 and the Department of Energy (DOE) in 2008, this mandate has expanded further to include discovery of leads for agrochemicals, animal health agents, bioenergy agents, and biofuels. Increased focus on marine research has brought the National Oceanographic and Atmospheric Administration into the partnership. Currently, the program is jointly sponsored by five USG agencies, including six components of the NIH. [Table 27.4](#) outlines the history of USG agency participation and the interest of each component in the program.

Over the history of the program, there have been 7 planning grants and 14 ICBGs, several of which have been competitively renewed for multiple 5-year cycles. In total, these latter have involved multiyear collaborative efforts in 20 countries. While the emphasis in the earlier ICBGs was largely on tropical plants, the projects were encouraged to expand efforts to involve marine and microorganisms in 2003 (NIH Guide: RFA TW-03-004, [19]) and in subsequent competitions. There are currently eight funded ICBGs operating, of which six include significant marine collections. These six are outlined in [Table 27.5](#).

27.3.1 Agreements Governing Collaborative Research and Nature of Benefits

The ICBGs have negotiated viable agreements for collections, research, and the sharing of benefits with organizations in 20 collaborating countries. The collaborating countries include Suriname, Peru, Chile, Argentina, Mexico, Costa Rica, Panama, Vietnam, Laos, Papua New Guinea, Philippines, Indonesia, Fiji, Madagascar, Cameroon, Nigeria, Uzbekistan, the Kyrgyz Republic, Tajikistan, and Kazakhstan. In each of these countries, the projects vetted the agreements with national authorities and local authorities and obtained permission to proceed under the prevailing access-and benefit-sharing policies available at the time. As mentioned above, until recently, most of these have been terrestrial projects. For projects that have had multiple cycles, these agreements and associated permits have evolved and been renewed with the project multiple times.

ICBG marine collections have largely been confined to internal and territorial waters, or fall within the exclusive economic zones of the participating nations and are subject to the same national laws regulating terrestrial collections, as outlined in

Table 27.5 ICBG projects that include marine collections and research

Project (principal investigator: project period)	Organismal focus	Principal participating institutions (current and former)
Biodiversity Conservation and Drug Discovery in <i>Madagascar</i> (David G. I. Kingston: 1993–present)	Tropical plants, microbes, and marine organisms	Virginia Polytechnic Institute and State University Missouri Botanical Garden; Conservation International; Madagascar National Centers for Pharmaceutical, Environmental and Oceanographic Research; University of Maryland Biotechnology Institute; Eisai Research Institute; Dow AgroSciences
ICBG: Training, Conservation and Drug Discovery using <i>Panamanian</i> Microorganisms (Phyllis Coley: 1998–2002; William H. Gerwick: 2003–present)	Tropical plants; endophytic fungi; marine algae, microbes, and marine invertebrates	Smithsonian Tropical Research Institute University of California San Diego; University of Panama Santa Cruz; Oregon State University; University of Panama; National Secretariat for Science, Technology and Innovation (Panama); Novartis Institutes for Biomedical Research; Dow AgroSciences; Eisai Research Institute
Conservation and Sustainable Use of Biodiversity in <i>Papua New Guinea</i> (Louis R. Barrows: 2003–present)	Tropical and medicinal plants, marine and terrestrial microbes, marine invertebrates	University of Utah Smithsonian Institution; University of Minnesota; University of Papua New Guinea; Natural History Museum, London; National Forest Research Institute (PNG); PNGBioNET; Wyeth Research Laboratories
Discovery of Natural Product-based Drugs from <i>Costa Rican</i> Biota (Jon Clardy: 2004–2007; David H. Sherman: 2008–present)	Endophytic fungi, lichens, marine actinomycetes and cyanobacteria, marine invertebrates, insect microbial endosymbionts	University of Michigan Harvard Medical School Instituto Nacional de Biodiversidad (INBio, Costa Rica), Broad Institute of Harvard and MIT, Novartis Institutes for BioMedical Research
Exploration, Conservation, and Development of Marine Biodiversity in <i>Fiji</i> (Mark E. Hay: 2004–present)	Coral reef organisms and marine microbes	Georgia Institute of Technology Scripps Institution of Oceanography; University of the South Pacific (Fiji); Bristol-Myers Squibb
Diverse drug lead compounds from bacterial symbionts in tropical marine mollusks (<i>Philippines</i>) (Margo Haygood: 2008–present)	Marine mollusks and their bacterial symbionts	Oregon Health & Science University University of Utah; University of the Philippines (Quezon City, Philippines); Academy of Natural Sciences of Philadelphia; Ocean Genome Legacy Foundation

the Convention on Biodiversity. Beyond these limits, collections would fall under the United Nations Law of the Sea Treaty (<http://www.un.org/Depts/los/index.htm>).

ICBG projects are governed by legal agreements that must be negotiated individually by the participants in each Group, sometimes including participants from three or more countries. The ICBG Request for Applications lays out a set of

“Principles for accessing genetic resources, the treatment of intellectual property and the sharing of benefits” including requirements to develop fair and equitable agreements that include sharing of diverse and substantial benefits with host country (equivalent to “source country” used in the discussions of NCI programs) partners and to obtain legal access permits, before proceeding (<http://grants.nih.gov/grants/guide/rfa-files/RFA-TW-08-010.html>). These principles or guidelines are very similar to those that have emerged in the CBD process over the past decade and have been modified slightly to accommodate evolution in that arena.

The original ICBG Guidelines drew heavily on the NCI experience with their Letter of Collection program, and the NCI programs have been influenced by ICBG experiences. However, because the programs are operationally distinct and the goals are different in scope, there are a few important differences in how agreements have been developed. The root of these differences derives from the fact that in the ICBGs, the funding agencies are not party to the access and benefit-sharing agreements. Beyond requiring that the project agreements address the general guidelines mentioned above, the agencies do not specify the form or specific terms the agreements should take. Rather, each consortium must develop agreements that meet the needs of its partners and respond to the guiding principles of the program. These agreements and associated host country permits are then submitted to the Fogarty International Center for review and approval in order to receive continued funding past the first year and before any collections can take place or materials can be sent outside the host country.

Consequently, the ICBG agreements have followed a variety of models. The legal documents involved include permits to make collections, community prior informed consent from the owners of the biodiversity, material transfer agreements, benefit-sharing agreements, trust funds, license option agreements, and memoranda of understanding that govern the general conduct of the research and general terms for commercialization of any products discovered by the consortium [20–22]. Often, a partnership involves several of these components in separate but linked documents. The agreements that structure an ICBG are typically organized as a series of bilateral agreements between partner organizations, sometimes in a hub and spoke arrangement around the prime grantee, or a consortium agreement in which three or more of the organizations are parties to one jointly negotiated contract [20]. Most often, an ICBG entails some combination of consortium and bilateral agreements. ICBG agreements are generally among institutional partners, including academic, governmental, and industrial organizations; some include community organizations, especially where traditional knowledge is involved or collections involve land or coastal waters controlled by the communities [20, 23].

Although agreements commonly take 1 year or longer to negotiate, the core criteria developed and benefits sought have many common features. The agreements typically outline the responsibilities of all the parties, establish the principle of full and equal collaboration, limit third-party transfer of materials without written consent of all relevant parties, establish terms of confidentiality and publication of results, and address near-term benefits that accrue to the host country for

access to materials. These benefits most importantly include training of host country scientists in the various disciplines needed to carry out a biodiversity program (field biology, taxonomy, chemistry, bioassays, and others) and access to technology. When industrial partners are included in the consortium, there is sometimes an agreement to provide additional up-front funds from the industrial partner to host country institutions or a local trust fund to further enhance laboratory capability or support community conservation and development efforts beyond the terms of the grant.

Longer-term benefits associated with commercialization of a discovery, such as milestone or royalty payments, may be included as contingent benefits, with discussions of who gets what in a variety of scenarios based on relative contributions to the discovery or other metrics. Negotiating these scenarios was more common in the early years of the ICBG program. However, given the rarity of commercial development and the added transaction costs of these more difficult negotiations, this practice is less common today than a “two-stage” approach. The two-stage approach is generally to negotiate the initial agreements in the context of academic research, with a stipulation that further agreements must be negotiated should discoveries move into a commercialization pathway. This two-phase approach often incorporates a commercial agreement trigger, and tends to ease the burden and speed up negotiation at the outset, and, very importantly, creates more flexibility for the scientists to carry out basic research and training (see [Sect. 27.4.3](#) below).

An increasing emphasis on microbial collections in the last 5 years has created additional challenges in negotiating agreements. Several countries, for example Madagascar and the Philippines, have laws or policies that prohibit export of self-replicating organisms because their provenance may be hard to trace and commercial development may not materially require recollection in the original host country. Consequently, some ICBG agreements specify that all microbes must first be isolated and identified in the host country before they can be tested in bioassays, and only chemical extracts or isolated compounds can leave the country. In other agreements, a host country scientist is required to accompany the microbes and participate in the research if they do need to leave the country to move the research forward. Not infrequently, the authorization for transfer of culturable microbial samples is feasible after a project has had a year or two of collaborative work and an opportunity to develop more trust among partners and host country authorities.

One positive result of microbial transfer restrictions may be the development of microbial technology and expertise in the host country, a benefit in keeping with the goals of the ICBG program. But ultimately, it is often necessary to engage more sophisticated analyses than are possible in a relatively small- or low-resource country even with additions of state-of-the-art equipment. Furthermore, as molecular systematics, molecular diversity analysis, and molecular taxonomy become increasingly common for microbial collections, export of DNA for genomic, metagenomic, and PCR sequencing has recently become an issue. Government officials that oversee biodiversity permits and agreements in many low- and

middle-income countries may be only familiar with the general concept of DNA and anxious about the traceability issues mentioned above. However, because of the increasingly fundamental role of these techniques in modern academic microbiology, this is changing rapidly. Our experience is that clear presentations of the science by the researchers involved to local government officials, especially when it occurs in the context of a project based on equitable partnerships and transparency, are often an effective means of addressing this problem.

Despite the most painstakingly negotiated agreements, there are unique challenges to projects working in low- and middle-income countries that each ICBG must navigate. Countries are implementing access and benefit-sharing policies in diverse ways depending on their preexisting legal environment. Many still have none in place. Even clear regulations can shift with the changing political landscape. In the past 17 years, the ICBGs have been faced with coup d'états (Madagascar, Fiji, Kyrgyz Republic), changes of governments and associated policy changes that temporarily paralyzed parts of the research program (Suriname, Panama), changes in political relations with the USA that forced suspension of international projects (Uzbekistan), and traditional knowledge disputes that temporarily halted one project (Peru) and shut down another (Chiapas, Mexico). Despite these disruptions, with the exception of the Chiapas project and the Uzbekistan component of the Central Asia project, the ICBGs have generally managed to adjust and continue their research, conservation, and capacity building activities.

27.3.2 Achievements

Despite the challenges of negotiating and maintaining these complex research partnerships, the ICBGs have been successful in producing exciting new science and providing benefits both locally and nationally to host countries. From 1993–2009, the ICBGs screened over 83,000 extracts (1.3 million primary screening events) from approximately 10,630 uniquely identified species (of which about 10% were of marine origin) and 50,000 isolated microbial strains in over 78 therapeutic and agrochemical assay areas. These materials, collected specifically for biodiscovery, were largely derived from plant sources during the first 10 years of the program, but since 2003 have increasingly included terrestrial and marine microbes, endophytic fungi, and marine invertebrates and their microbial symbionts (see [Table 27.5](#)). Over 1,400 unique bioactive molecules have been isolated, many of which are new to science. Approximately 20 molecules are currently considered active leads for potential new therapeutics or agrochemicals. Overall, the achievements of the program have been described in over 600 publications, mostly by the investigators themselves.

In addition to biodiscovery, the ICBGs have made significant contributions to building research capacity in host countries. Most critically, over 4,000 individuals have been trained in biodiversity and biodiscovery sciences. These included 350 long-term (1 year or longer) training opportunities, resulting in 135 Masters and

PhD degrees. Approximately 70% of long-term trainees are from host countries. ICBGs have also helped to upgrade collaborating laboratories in host countries through provision of chemistry- and bioassay-related equipment, such as liquid chromatography devices, nuclear magnetic resonance (NMR) technology, spectrometers, microscopes, and PCR machines, computers, and others. The projects have helped to modernize local laboratory, culture, and museum facilities and in some countries have contributed to the creation of national laboratories for chemistry and biological screening.

Biodiversity conservation contributions have been substantial. The scientific basis for conservation has been enhanced by developing or enhancing publicly available bioinventory records for all ICBGs. In addition, bioinventory activities have resulted in the publication in print or on the web of national and regional taxonomy and identification guides, such as the Atlas of Seed Plants of Cuc Phuong National Park (<http://fm2.fieldmuseum.org/plantatlas/>), descriptions of medicinal plants in the public domain [24], and deposition of voucher specimens in national and international repositories. At least two dozen new species and genera of plants have been identified, as well as hundreds of microbes and fungi. ICBG efforts have led to the creation of new protected areas in Panama (see below), Laos, Suriname, and Madagascar and have strengthened existing reserves in many other countries. These contributions have formed a basis for local and regional collaborations and new economic activities in most of these countries.

Finally, the ICBGs have informed policy in many of the countries in which they have worked. As an on-the-ground test of the CBD goal of providing equitable benefits to host countries in return for access to genetic resources, their challenges and lessons learned have been closely observed and extensively documented in academic and policy literature and in multiple CBD forums. For instance, a search on ICBG in the CBD website (<http://www.cbd.int/>) turns up 116 documents including numerous case studies and third-party reports written or translated in multiple languages.

27.3.3 Case Studies

The ICBG Requests for Application that have structured the program require that every Group develop a proposal to address the three major goals of biodiscovery, biodiversity conservation, and return of benefits in the form of scientific capacity and/or economic development, preferably by undertaking activities that integrate these goals and allow them to be mutually reinforcing. Examples of how these goals have been integrated in two projects that currently focus on marine collections are described below.

27.3.3.1 The Panama ICBG

The Panama ICBG (see [Table 27.5](#)), first awarded in 1998, originally focused on plant collections throughout Panama. In 2003, however, in the second cycle of their ICBG, they expanded to include marine collections and began to focus many of their activities around Coiba Island off the Pacific coast of Panama in the Gulf of

Chiriqui. Due to the historical presence of a penal colony on the island since 1919, the vegetation and surrounding waters were exceptionally well conserved. However, when the Panama ICBG began working there in 2003, the penal colony was closing down, and the future of the island was a topic of national debate.

The ICBG project supported extensive bioinventory and drug discovery collections on and around Coiba Island. From both terrestrial and marine species, some of which are endemic to the island, the team has isolated promising bioactive molecules in therapeutic areas important to the population of Panama including novel compounds active against parasitic diseases [25] and cancer [26].

Based in part on this scientific evidence, the Panamanian parliament gave the area National Park protection in 2004 [27]. Working together with the government and other interested parties, the Park and a surrounding special zone of marine protection was proposed to UNESCO as a World Heritage Site, a status that was granted in 2005 (<http://whc.unesco.org/en/list/1138>). This is likely to serve as a basis for expanded tourism and economic revenue for Panama for years to come and creates a clear valuation for national biodiversity conservation, a major goal of the CBD. Conservation of the island and surrounding waters also allows for continued research in relatively pristine areas that would otherwise be rapidly transformed by commercial development and exploitation.

A key feature of the Panama ICBG has been the investment in Panamanian researchers as major collaborators. The philosophy of the project has been that by doing as much of the work as possible in Panama with Panamanian scientists, they are most likely to leave a sustainable research base in the country. The scientific and conservation activities outlined above and many others were used to train University of Panama students in field and marine biology, drug discovery, and chemistry. Some of the Panamanian students were subsequently selected by the Panamanian government for scholarships to undertake MSc and PhD studies abroad and are now returning to Panama to join the project as investigators. Meanwhile, Panamanian scientists working in Spain and the USA have been attracted back to work on the ICBG as investigators at the University of Panama or its Institute for Advanced Studies. Because much of the scientific research of the ICBG has been concentrated in Panamanian institutions throughout the project period, the ICBG has built significant laboratory infrastructure and human capacity for research in biodiversity and biodiscovery sciences [28, 29]. They have also developed bioassays suitable for working in low-resource countries [30, 31].

Together, these capabilities should contribute to the ability of Panama to continue to explore and reap the benefits of its biodiversity in the years ahead.

27.3.3.2 The Fiji ICBG

The goals of the Fiji ICBG (see Table 27.5) include the discovery of pharmaceutical and bioenergy leads from coral reef organisms and marine microbes, promotion of marine biodiversity conservation through understanding the ecological processes that result in reef degradation and by working with local communities to help protect community reefs, and development of scientific capacity at the University of the South Pacific.

A memorandum of understanding and material transfer agreements were negotiated, and national collection permits were obtained. However, the coral reefs in Fiji are effectively owned by local communities [32]. Consequently, beginning with a planning grant in 2002, the team developed a partnership with a local community to determine appropriate benefits that would accrue to the community in return for access to their coral reefs to conduct scientific research. The negotiations with the village chief in their first intensive collection site were greatly facilitated by the long-term village relationships built by team members from the University of the South Pacific.

Degradation of the reefs and declining fish catch were major concerns of the community. While many factors are involved, both of these problems are exacerbated by the commercial harvesting and sale of living coral (live rock) for the international aquarium trade. Fiji is one of the few countries in the world where this practice is legal, and tons of coral are harvested annually, making Fiji one of the largest suppliers of live rock in the world.

The Fiji ICBG began a pilot arrangement that allowed the community to produce “cultured live rock,” an artificial coral, while they suspended any live rock collections. The scientific expertise of the ICBG team helped optimize culture conditions. An international company agreed to purchase this rock from the community in place of live rock. The newly opened Georgia Aquarium in Atlanta agreed to purchase the cultured material and use it in their displays, and the community was able to collect and sell several harvests of this product to the aquarium [33] and the company. Other communities have shown an interest in engaging in similar projects on their reefs, and the national government has discussed banning all sale of live rock in Fiji should this approach be successful and scalable. This local alternative enterprise is now being expanded, and new versions of the cultured rock are being explored for broader markets by the project with new cycles of funding.

In parallel, the discovery research of the Group has discovered new bioactivities from organisms collected on these community reefs [34–37], in part using ecologically guided techniques involving antifeedant behavior in fish. Based partly on results from experiments originally conducted elsewhere [38], the team worked with the community leaders to alter fish catching practices to optimize both increases in fish yield and enhanced coral conservation on their reefs. These methods have become part of a newly initiated and rapidly growing network of Fijian local marine management areas. The project established a small trust charity, Adopt a Reef (<http://adopt-a-reef-fiji.org/>), to attract charitable donations to support careful management and conservation at the community level, including the marine management areas.

Finally, in the conduct of the research, they have made significant investments in enhanced scientific infrastructure and training of local scientists to build the capability of the University of the South Pacific to conduct independent and collaborative natural products research.

This integrated strategy has produced new science, enhanced protection of the biodiversity on which both new discoveries and the livelihood of the local communities are based, and has laid the groundwork for future biodiscovery by Fijians in Fiji.

27.4 Conclusions and Recommendations

27.4.1 Commercial Drug – A Rarity!

With the signing of the treaty on the Convention on Biological Diversity, there was a surge of optimistic anticipation that the rich biodiversity located in many source countries, particularly in tropical and subtropical regions, would yield a host of new miracle drugs which would rapidly generate considerable wealth for many source (mainly developing) countries (so-called green gold). An oft-quoted estimate is that 1 in 10,000 biologically active leads will lead to the development of a commercial, conventional drug, but with natural products, this ignores the initial phase of isolating and identifying the active lead compound from the original active crude extract. Thus, unfortunately, the realities of natural product drug discovery and development are in direct contradiction to the “green gold” expectations.

In their chapter on natural products and the pharmaceutical industry, ten Kate and Laird [10] estimate that the primary screening of five million “compounds,” presumably crude extracts, will yield 1,000 “hits” (a “hit rate” of 1/5,000), which, after bioassay-guided fractionation and purification, dereplication, structural elucidation, and secondary screening, will yield ten bioactive novel leads. Subsequent optimization of the lead candidate, involving yield improvement, analog synthesis, formulation and bioavailability studies, and enhancement of the therapeutic index (the ratio of the activity versus toxicity ratio), narrows the field to five drug candidates which enter advanced preclinical development and, after approval by the regulatory authorities, enter clinical trials. After Phase III clinical trials, one of these candidates is finally approved for registration and marketing. Their numerical estimates probably apply best to the discovery of new antibiotics from microbial broths produced by the fermentation of many microbial cultures under multiple different fermentation conditions. Comparable probability estimates for collection-based natural products research range widely in both directions from those above, but the essential truth here is that the probability of discovering a novel commercial drug is extremely low.

Possibly a more relevant example is the NCI experience in the early years of its natural product drug discovery and development program. From 1960 to 1982, some 35,000 plant samples (representing about 12,000–13,000 species) were processed to yield 114,000 extracts. Despite the discovery of a significant number of interesting active chemotypes, only two pure compounds advanced to the stage of development into commercial products. These were Taxol[®] (e.g., paclitaxel and its analog, docetaxel) and camptothecin, which, though it proved to be too toxic in clinical trials to become a commercial drug, has yielded commercial analogs, such as topotecan (Hycamptine[®]) and irinotecan (Camptosar[®]). One other product, homoharringtonine, has advanced through clinical trials for the treatment of several refractory leukemias, though it is limited to investigational clinical use. Thus, 114,000 extracts derived from approximately 12,000 species, thus far, have given only two compounds currently yielding products of commercial value (further derivatives and analogs of Taxol and camptothecin are being developed which

will probably become commercial products), with homoharringtonine being another likely product. Another discovery from the early NCI program was maytansine which has been conjugated to suitable carrier molecules such as monoclonal antibodies that target specific tumors. These products are in various stages of clinical development, and it is possible that one or more may advance to commercial use. Thus, new developments aimed at the targeting of toxic products to tumors through conjugation to suitable carrier molecules, such as monoclonal antibodies, may well improve the success rate.

Irrespective of which scenario is used, the message is clear – the chances of discovering a product that will eventually become a commercial drug are extremely small! Having made this observation, it is also clear that exposure of the initial natural product extracts to as many screens as possible enhances the chances of discovering a useful commercial drug. Thus, host (source) countries can optimize the potential value of their resources through expanding their collaborations with suitable screening organizations, subject to the negotiation of agreements protecting the rights of all the parties. Projects such as the ICBGs in which samples from a given project are exposed to screens in multiple end use areas, including potentially three or four therapeutic targets as well as agricultural or energy targets, would logically enhance probabilities of success. However, to date, this younger program has yet to yield a commercial product, despite many successes in other areas.

27.4.2 Drug Development Costs and Time Frame

Numerous estimates of costs and times of drug development have been proposed. In 1991, the estimated cost of “bringing a new medicine to the market” was US\$231 million [39], and current estimates range from over US\$800 million to US\$1.7 billion [40] (although see Angell [41] on how these calculations are made). In considering costs, allowance must be made for the considerable costs of research and development devoted to the many potential leads and candidates which eventually fail to become commercial products, as well as the substantial costs of “borrowing money” to finance these very expensive enterprises.

The time frames for drug discovery and development also vary considerably. ten Kate and Laird [10] provide estimates ranging from 7 to 18 years. In the case of Taxol[®], 30 years elapsed from initial collection of the source plant material (1962) to final approval of paclitaxel (1992). Another valuable case study is that of the discovery and development of the cholesterol-lowering drug, lovastatin, where some 30 years elapsed between the discovery of HMG-CoA as the major rate-limiting step in cholesterol biosynthesis to the final approval of lovastatin as a drug [39]. With the discovery and development processes constantly being streamlined, the time frame for “bringing a new medicine to the market” should be greatly reduced; nevertheless, it remains an extremely costly and time-consuming operation.

The time frames for development of an agrochemical, herbal drug, or dietary supplement may be somewhat shorter than for conventional drugs, but there remain

considerable challenges involved in their development. Safety and toxicity studies are still necessary for these products, while there are substantial issues related to achieving acceptable quality control of herbal drugs and dietary supplements [10].

27.4.3 Recommended Collaborative Process

It is clear from the above discussions that the preclinical and clinical drug development processes are costly and lengthy undertakings which require considerable international and multidisciplinary collaboration. The same principle applies to the development of other bioactive entities, such as agrochemicals, which have to meet strict regulatory requirements, although the total costs are significantly less than those for drugs. The discovery and development processes must be carried out with prior informed consent and the necessary collection and export permits from the relevant source country government and stakeholders, and working in close collaboration with source country organizations. Appropriate agreements must be negotiated encompassing the terms of training and technology transfer, protection of the environment and sustainable development, and plans for benefit-sharing. Mechanisms for establishing such agreements have been discussed above, and based on the NCI and ICBG experience, a “two-phase approach” to the exploration of source country genetic resources as a source of potential novel drugs and other bioactive agents may often be the best approach.

A two-phase approach is favored, both to shorten the time required to negotiate an agreement where the probability of commercialization is low, and facilitate development decisions for nonblockbuster products since the terms of the second phase, the Phase II Commercial Development Agreement (CDA; Sect. 27.4.3.2), could vary considerably depending on the nature of the drug (or other agent) being advanced into preclinical and clinical development. If the drug has been selected for treatment of a rare disease with a small patient population, or for a tropical disease with no developed country market, the returns on commercialization and sales are likely to be far smaller than if the candidate is being developed for treatment of a common disease having a large patient population and potentially large sales. If a drug has the potential for large sales, and hence large revenues for the company involved in its development, the percentage of royalties or other possible benefits which could accrue to the source country could be substantially higher.

This approach has been widely embraced by the research and policy communities, including in the Nagoya Protocol on Access and Benefit-Sharing (<http://www.cbd.int/abs/>), a supplementary agreement to the Convention on Biological Diversity adopted by the Conference of the Parties to the CBD at its tenth meeting held on October 2010 in Nagoya, Japan.

27.4.3.1 Phase I. Basic Research Agreement

Phase I of the process can involve negotiation of a *Basic Research Agreement* between a research organization in a “developed” country and another research organization or relevant government department or agency in the source or host

country. The significant involvement of a suitably qualified local organization is an ethical standard today even where not legislated. It is also important to enable transparency of the project, to maximize understanding of the legal environment, to facilitate logistical feasibility, and to minimize the likelihood that follow-up of an exciting outcome is not blocked by regulatory bodies or political turmoil. The Basic Research Agreement should incorporate terms of collaboration covering exchange of data, joint publication, training, and technology transfer. In addition, there should be requirements for adequate protection of the environment and endangered species.

Obtaining the prior informed consent of relevant local stakeholders (e.g., indigenous peoples, local communities, and healers, where appropriate) ideally should be the responsibility of the local collaborating organization, or if an appropriate collaborator is not identified, the relevant local government agency can often assist in this process. If a pharmaceutical or other company is involved as a partner with the research organization in negotiating the agreement, the possibility of establishing a trust fund to support local source country stakeholders in small community projects may be considered. Most importantly, the Basic Research Agreement should clearly require the negotiation of separate agreements (Phase II agreements) covering any agents which are subsequently selected for preclinical or equivalent advanced development.

An important but less commonly articulated benefit that can accrue to host country organizations in low- and middle-income countries is the development of long-term collaborative relationships with international scientists. Such things are not generally included in agreements. However, these relationships are especially important to a host country after a project is completed, and are an important avenue for future collaborative support for research and training and for access to scientific literature and modern technological innovations. ICBGs often have career-changing effects for participating scientists from both countries and can be transformative for smaller developing country organizations. But maintaining those collaborations in some form after a project terminates is often more important for the developing country partners than for US or European scientists and merits some forethought.

Selection of an agent for advanced (e.g., preclinical) development will probably trigger submission of an application for patent coverage, but it is important to emphasize that issue of a patent is far removed from the possibility of commercialization. In fact, very few patented agents ever reach the stage of commercialization. Generally, from available data we estimate that less than 4% of patented pharmaceutical drug candidates actually become commercial drugs [42].

27.4.3.2 Phase II. Commercial Development Agreement (CDA)

Selection of a drug lead candidate for preclinical or equivalent development should trigger negotiations of a new Phase II Commercial Development Agreement (CDA) covering the specific issues related to the development and possible commercialization of the candidate. Local scientists and communities should be involved in these negotiations or at the least kept abreast of their nature, trajectory, and terms, depending on the terms of the Phase I agreement and the nature of the collaboration.

The CDA should address terms of collaboration in the large-scale procurement of supplies of raw material for production of sufficient quantities of the drug candidate for preclinical and possible clinical development in the case of pharmaceutical agents. Such terms should address environmental impact studies, the possibility of sustainable harvest, and the possible need for cultivation of the source organism. The CDA should also include terms of collaboration in the production of the development candidate (extraction, isolation, analysis, etc.) depending on the facilities and expertise available in the source country, and training and technology transfer where appropriate, as well as training in the preclinical development aspects of a drug candidate (e.g., formulation, pharmacology). In the above two points, it must be noted that conditions of current Good Manufacturing Practice (cGMP) (e.g., approved facilities) have to be met to satisfy the requirements of the US Food and Drug Administration (FDA) and equivalent regulatory bodies in other countries. These are extremely expensive conditions to fulfill, and generally, these processes will be best performed by the collaborating research organization.

Finally, terms should be included covering milestone payments when certain stages of development are achieved (e.g., FDA approval for entry into Phase I clinical trials, completion of Phase I trials), and payment of a percentage of royalties on the sales of the drug, should it become commercialized. An attractive alternative or complement to royalties that may be considered by a source country may be the provision of supplies of the drug free or at highly discounted cost for treatment of the local population, and/or provision of other drugs more useful to the source country, or the granting of a royalty-free license for production of the drug for use in the source country only.

Given the very low success rate in actually developing a product to the stage of commercial use, it is strongly recommended that agreements should focus on short-term and accessible benefits such as training, technology transfer, and milestone payments, rather than attempting to maximize royalty payments which, in all likelihood, will never materialize. There are decided advantages to maximizing short-term benefits in terms of improving the capacity of host country organizations and personnel to perform the drug discovery and early development steps in-country, thereby optimizing the value of their resources. In addition, discovery of promising drug leads entirely in-country creates the opportunity for source country organizations to gain complete control of their inventions through application for appropriate sole source country inventorship patent coverage (composition of matter patents in the case of novel chemical entities or use patents in the case of novel uses for known chemical entities).

27.5 Study Questions

1. What are the prime objectives of the UN Convention on Biological Diversity? When first introduced, the CBD led to some unrealistic expectations. What were these expectations, and how would you address these issues when negotiating an agreement for initiating a joint biodiscovery exploration program with host

- country stakeholders, including government officials, institutional collaborators, and local communities?
2. In exploring the possibility of initiating biodiscovery programs in biodiversity-rich nations, research groups have often encountered obstacles on issues, such as identifying the correct points of contact for obtaining the necessary approvals, permits, etc. Elaborate on how you think the recently published Nagoya Protocol (April 2011) has addressed some of these problems.
 3. “A ‘two-phase approach’ to the exploration of host/source country genetic resources as a source of potential novel drugs and other bioactive agents may often be the best approach to initiating a biodiscovery program.” Discuss this statement, and identify the possible advantages and disadvantages of such an approach.
 4. You wish to carry out a biodiscovery project in country X in collaboration with country X institution and a local community. On the basis of the information and experiences recorded in this chapter, discuss the factors you would consider in conducting negotiations for entering into an agreement with the authorities in country X for initiation of the project.
 5. During the course of studying sponges collected in country X coastal waters as a source of novel bioactive compounds, you discover that the likely sources of some of the bioactive compounds are microbial symbionts. Microbial sources were not included in your original agreements with country X government authorities, nor with the local collaborating institution. Discuss what measures you would take in negotiating amendments of the agreements to include microbes as sources of bioactive compounds.
 6. Discuss the impact of biodiscovery programs on the conservation and sustainable development of biological resources in host/source countries.

References

1. Newman DJ, Cragg GM (2007) Natural products as sources of new drugs over the last 25 years. *J Nat Prod* 70:461–477
2. Newman DJ, Cragg GM (2004) Marine natural products and related compounds in clinical and advanced preclinical trials. *J Nat Prod* 67:1216–1238
3. Newman DJ, Cragg GM (2009) Recent progress of natural marine products as anticancer drugs. In: Chabner B (ed) *Marine anticancer compounds in the era of targeted therapies*. P Permanyer SL, Barcelona
4. Eisner T, Meinwald J (1990) The Goteborg resolution. *Chem Ecol* 1:38
5. Baker JT, Borris RP, Carte B, Cordell GA, Soejarto DD, Cragg GM, Gupta MP, Iwu MM, Madulid DR, Tyler VE (1995) Natural product drug discovery and development: new perspectives on international collaboration. *J Nat Prod* 58:1325–1357
6. Cragg GM, Baker JT, Borris RP, Carte B, Cordell GA, Soejarto DD, Gupta MP, Iwu MM, Madulid DR, Tyler VE (1997) Interactions with source countries. Guidelines for members of the American society of pharmacognosy. *J Nat Prod* 60:650–655
7. Fischli AE, Pandit UK, St C, Black D (2002) Molecular basis of biodiversity, conservation, and sustained innovative utilization (IUPAC technical report). *Pure Appl Chem* 74:697–702

8. Reid WV, Laird SA, Meyer CA, Gamez R, Sittenfeld A, Janzen DH, Gollin MA, Juma C (1993) Biodiversity prospecting. World Resources Institute, Baltimore
9. Grifo F, Rosenthal J (eds) (1997) Biodiversity and human health. Island Press, Washington, DC
10. ten Kate K, Laird SA (1999) The commercial use of biodiversity. Earthscan, London
11. Svarstad H, Dhillon SS (2000) Responding to bioprospecting. Spartacus Forlag AS, Oslo
12. Sampath PG (2005) Regulating bioprospecting. United Nations University Press, Tokyo/New York/Paris
13. Cragg GM, Grothaus PG, Newman DJ (2009) Impact of natural products on developing new anti-cancer agents. *Chem Rev* 109:3012–3043
14. Newman DJ, Cragg GM (2005) The discovery of anticancer drugs from natural sources. In: Zhang L, Fleming GA, Demain AL (eds) Natural products: drug discovery, therapeutics, and preventative medicine. Dekker, New York, pp 129–168
15. Mays TD, Mazan KD, Cragg GM, Boyd MR (1997) Triangular privity—a working paradigm for the equitable sharing of benefits from biodiversity research and development. In: Hoagland KE, Rossman AY (eds) Global genetic resources: access, ownership and intellectual property rights. Association of Systematics Collections, Washington, DC, pp 279–298
16. Kaufman D (1993) Botany 2000. *ASIA Newsl* 2:6
17. Kashman Y, Gustafson KR, Fuller RW, Cardellina JH II, McMahon JB, Cragg GM, Boyd MR (1992) The calanolides, a novel HIV-inhibitory class of coumarins derivatives from the tropical rainforest tree, *Calophyllum lanigerum*. *J Med Chem* 35:2735–2743
18. ten Kate K, Wells A (1998) Benefit-sharing case study: access and benefit-sharing policies of the United States National Cancer Institute: a comparative account of the discovery and development of the drugs Calanolide and Topotecan. Executive Secretary of the Convention on Biological Diversity. <http://www.cbd.int/doc/case-studies/abs/cs-abs-nci.pdf>. Accessed 2 Nov 2011
19. Rosenthal JP, Katz F (2003) Natural products research partnerships with multiple objectives in global biodiversity hotspots: nine years of the ICBG program. In: Bull A (ed) Microbial diversity and bioprospecting. ASM Press, Washington, DC
20. Rosenthal JP (1997) Equitable sharing of biodiversity benefits: agreements on genetic resources. In: Investing in biological diversity – proceedings of the international conference on biodiversity incentive measures. OECD Press, Paris
21. Rosenthal JP, Beck D, Bhat A, Biswas J, Brady L, Bridbord K, Collins S, Cragg G, Edwards J, Fairfield A, Gottlieb M, Gschwind L, Hallock Y, Hawks R, Hegyeli R, Johnson G, Keusch G, Lyons E, Miller R, Rodman J, Roskoski J, Siegel-Causey D (2000) Combining high-risk science with ambitious social and economic goals. *Pharm Biol* 37(Suppl):6–21
22. Soejarto DD, Gyllenhaal C, Fong HHS, Xuan LT, Hiep NT, Hung NV, Bich TQ, Southavong B, Sydara K, Pezzuto JM (2004) The UIC ICBG (University of Illinois at Chicago International Cooperative Biodiversity Group) memorandum of agreement: a model of benefit-sharing arrangement in natural products drug discovery and development. *J Nat Prod* 67:294–299
23. Rosenthal JP (2007) Politics, culture and governance in the development of prior informed consent and negotiated agreements with indigenous communities. In: McManis C (ed) Biodiversity, biotechnology and traditional knowledge. Earthscan, London
24. Eisenman E, Zaurov D, Struwe L (eds) (2010) Medicinal plants of central Asia: Kyrgyzstan and Uzbekistan. The New York Botanical Garden Press, New York (in press)
25. Gutiérrez M, Tidgewell K, Capson TL, Engene N, Almanza A, Schemies J, Jung M, Gerwick WH (2010) Malyngolide dimer, a bioactive symmetric cyclodepside from the Panamanian marine cyanobacterium *Lyngbya majuscula*. *J Nat Prod* 73(4):709–711
26. Medina RA, Goeger DE, Hills P, Mooberry SL, Huang N, Romero LI, Ortega-Barria E, Gerwick WH, McPhail KL (2008) Coibamide A, a potent antiproliferative cyclic depsipeptide from the Panamanian marine cyanobacterium *Leptolyngbya* sp. *J Am Chem Soc* 130:6324–6325
27. Capson TL (2006) Panama's Coiba National Park: a jewel of the tropical eastern Pacific. *World Herit* 42:24–29

28. Kursar TA, Caballero-George CG, Capson TL, Cubilla-Rios L, Gerwick WH, Gupta MP, Ibanez A, Linington RG, McPhail KL, Ortega-Barria E, Romero LI, Solis PN, Coley PD (2006) Securing economic benefits and promoting conservation through bioprospecting. *Bioscience* 56:1005–1012
29. Kursar TA, Caballero-George CC, Capson TL, Cubilla-Rios L, Gerwick WH, Heller MV, Ibanez A, Linington RG, McPhail KL, Ortega-Barria E, Romero LI, Coley PD (2007) Linking bioprospecting with sustainable development and conservation: the Panama case. *Biodivers Conserv* 16:2789–2800
30. Williams C, Espinosa OA, Montenegro H, Cubilla L, Capson TL, Ortega-Barria E, Romero L (2003) Hydrosoluble formazan XTT: its application to natural products drug discovery for *Leishmania*. *J Microbiol Meth* 55:813–8161
31. Corbett Y, Herrera L, Gonzalez J, Cubilla-Rios L, Capson TL, Coley PD, Kursar TA, Romero LI, Ortega-Barria E (2004) A novel DNA-based microfluorimetric method to evaluate anti-malarial drug activity. *Am J Trop Med Hyg* 70:119–124
32. Aalbersberg B, Tawake A, Parras T (2005) Village by village: recovering Fiji's coastal fisheries. In: *The wealth of the poor: managing ecosystems to fight poverty*. World Resources Institute, Washington, DC, pp 144–151
33. Sanders JM (2005) Reefing the benefits. *Res Horiz* 23:6–11
34. Kubanek J, Prusak AC, Snell TW, Giese RA, Hardcastle KI, Fairchild CR, Aalbersberg W, Raventos-suarez C, Hay ME (2005) Anti-neoplastic diterpene- benzoate macrolides from the Fijian red alga *Callophycus serratus*. *Org Lett* 7(5261):5264
35. Kubanek J, Prusak AC, Snell TW, Giese RA, Fairchild CR, Aalbersberg W, Hay ME (2006) Bromophycolides C-I from the Fijian red alga *Callophycus serratus*. *J Nat Prod* 69:731–735
36. Lane AL, Stout EP, Hay ME, Prusak AC, Hardcastle K, Fairchild CR, Franzblau SG, Le Roch K, Prudhomme J, Aalbersberg W, Kubanek J (2007) Callophycoic acids and callophycols from the Fijian red alga *Callophycus serratus*. *J Org Chem* 72:7343–7351
37. Stout EP, Hassemeyer AP, Lane AL, Davenport TM, Engel S, Hay ME, Fairchild CR, Prudhomme J, Le Roch K, Aalbersberg W, Kubanek J (2009) Antibacterial Neurymenolides from the Fijian red alga *Neurymenia fraxinifolia*. *Org Lett* 11:225–228
38. Burkepille DE, Hay ME (2008) Herbivore species richness and feeding complementarity affect community structure and function on a coral reef. *Proc Natl Acad Sci USA* 105:16201–16206
39. Vagelos PR (1991) Are prescription drug prices high? *Science* 252:1080–1084
40. Mullin R (2003) Drug development cost about \$1.7 billion. *Chem Eng News* 81(50):8–9
41. Angell M (2004) *The truth about the drug companies*. Random House, New York, 305 p
42. Adams S (1999) SmithKline Beecham: analysis of patenting 1995–1998. *Expert Opin Ther Pat* 9:1173–1183

Part 6

Marine Toxins: A Problem for Public Health and Seafood Resources

Patrizia Ciminiello, Martino Forino, and Carmela Dell'Aversano

Contents

28.1	Introduction	1346
28.2	Azaspiracids: A Recent Class of Toxins Targeting the Human Gastrointestinal Tract	1353
28.3	Brevetoxins: Typical Aerosolized Red-Tide Neurotoxins	1354
28.4	Ciguatera: A Fitting Example of How Chemical Structure of Marine Biotoxins Is Investigated	1357
28.5	Cyclic Imine Toxins: A Category of Miscellaneous Emerging Toxic Compounds	1361
28.6	Domoic Acids: The Only Marine Biotoxins Produced by Diatoms	1363
28.7	Okadaic Acids: The Subtle Threat of Potent Tumor Promoters	1366
28.8	Palytoxins: Potent Tropical Toxins Now Rife Across the Mediterranean Basin ...	1368
28.9	Pectenotoxins: Potent Cytotoxic Compounds with Still Unknown Potential Implications to Public Health in the Long Term	1371
28.10	Saxitoxins: The First News We Have About Seafood Toxin-Related Human Poisoning	1373
28.11	Yessotoxins: Potent Toxic Compounds with Controversial Impact on Public Health	1375
	References	1378

Abstract

Once believed to affect only scattered areas of the world, nowadays, harmful algal blooms (HAB) plague virtually any coastal area of the planet. Usually caused by a pool of microalgae, HAB-related outbreaks not only harm human health but wreak havoc on maritime economy. Over the past decades, following the steadily increase of human poisonings, an ever-growing number of countries have been forced to set appropriate measures in order to cope with the sanitary

P. Ciminiello (✉) • M. Forino • C. Dell'Aversano
Dipartimento di Chimica delle Sostanze Naturali, Università degli Studi di Napoli "Federico II",
Via D. Montesano, 49, Naples, Italy
e-mail: ciminiel@unina.it, forino@unina.it, dellaver@unina.it

and economic predicaments brought about by HABs. Out of the thousand microalgae reported this far, only a limited number of them have been proven to produce marine biotoxins. Such molecules, once assumed by seafood, easily find their way up to the table of unaware consumers. Moreover, particular phytoplankton blooms can directly affect humans through contaminated marine aerosol. Depending on the symptoms shown by patients, the major human illnesses caused by toxin-contaminated seafood are commonly referred to as paralytic, neurotoxic, amnesic, diarrhetic shellfish, and ciguatera fish poisonings (PSP, NSP, ASP, DSP, and CFP, respectively). In this chapter, a wide-ranging and multifaceted overview of the main marine biotoxin classes is presented.

28.1 Introduction

As healthy a food for humans as it may be, occasionally, fish and shellfish can cause serious harm to consumers by accumulating high levels of natural marine biotoxins produced by noxious algae. Every year, some 50,000–500,000 human intoxications following exposure to marine biotoxins are reported worldwide with an alarming mortality rate on a global basis [1]. Until a few decades ago, only scattered locations seemed to be plagued by harmful algal blooms (HABs), while nowadays, every coastal State is virtually exposed to toxic outbreaks, often induced by more than just one toxic algal species. Out of the thousands of microscopic algal species, only several dozens have been this far individuated as producers of potent marine biotoxins [2, 3], frequently occurring in seawater in such small amounts as to not pose any hazard to human health and environment as well. Nevertheless, when toxic algal species happen to proliferate abundantly in seawater, they can be accumulated by filter-feeding shellfish, zooplankton, fishes, crabs, and tunicates, among others [4–6]. As a result, algal toxins find their way up through the food chain, landing onto the table of unaware seafood consumers.

The major illnesses following assumption of toxin-contaminated shellfish are commonly referred to as paralytic, neurotoxic, amnesic, diarrhetic shellfish, and ciguatera fish poisonings (PSP, NSP, ASP, DSP, and CFP, respectively), according to the symptoms shown by patients [6, 7]. Beyond these well-known classic intoxications, also other toxin-related poisoning syndromes have been described after exposure to azaspiracid toxins, yessotoxins, cyclic imines toxins, and palytoxins [6, 7]. ASP aside – which are caused by diatoms – all of the other major intoxications are basically due to blooming in the phytoplankton of dinoflagellates – microscopic, often unicellular, flagellated algae.

The HAB impact on public health grows even more alarming if it is considered that particular phytoplankton blooms can directly affect humans either accidentally swimming in infested waters or breathing contaminated marine aerosol.

Even though HABs often take place as massive “red tides” or blooms capable of discoloring seawater, sometimes, high concentrations of noxious cells get noticed only because of the harm they provoke by means of their potent biotoxins, which

rank among the most potent toxic compounds in the world, with some of them lethal to humans even at doses in the range of few micrograms per kilogram [8].

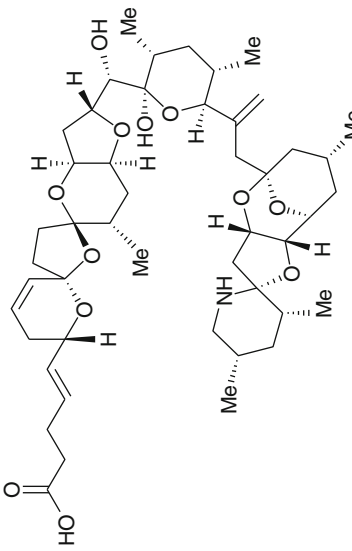
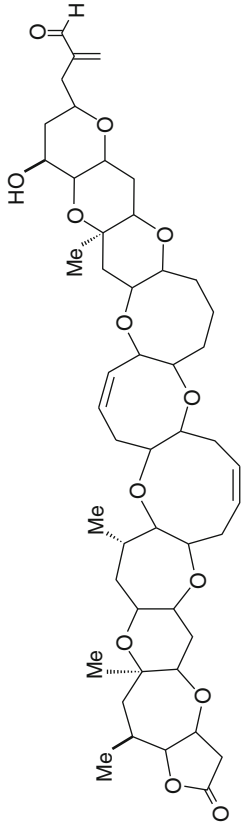
The role toxins play in the internal economy of their producers has not yet been totally understood. In this regard, toxins are likely used as tool for competing for space, for fighting predation, or even for warding off possible overgrowth of other organisms [9].

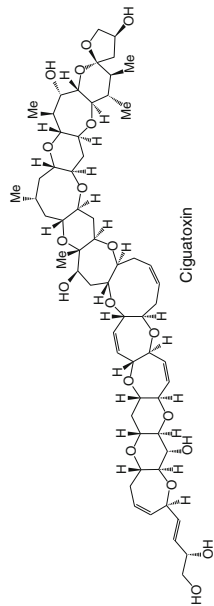
Unfortunately, toxin-contaminated seafood neither looks nor tastes any different from safe seafood, and no culinary treatment can guarantee inactivation of marine biotoxins. As a consequence, fish and shellfish farms have to run costly monitoring programs in order to check constantly the quality of their products before putting them on the market. At the moment, there are several chemical, functional, and biological methods able to check the occurrence of algal toxins in seafood, each with its own shortcomings. Considering that the only common feature of all of the known marine toxins is toxicity, it is little wonder that live-animal bioassay, such as the mouse bioassay, is still the most widely used detection method in any regulatory setting [10]. It is generally carried out by intraperitoneally injecting a given sample extract into a 20-g mouse kept under observation over a certain stretch of time, with the purpose of determining the onset of specific symptoms and eventually the time-to-death. Both symptoms and time-to-death are correlated to the kind as well as to the amount of a toxin possibly occurring in the injected extract. Toxicity is reported in terms of “mouse units,” which refer to the amount of toxin(s) capable of killing a mouse in a given stretch of time. Nonetheless, the mouse bioassay, even though suitable to the analysis of nearly every class of biotoxins, is quite controversial. In fact, it lacks specificity as it does not allow any differentiation between the various components within each class of toxins, and in addition, it requires both specialized animal facilities and proficiency without mentioning that many countries across the world have been dealing with both ethical and scientific issues regarding the employment of live-animal assay in their regulatory settings.

Besides their noxious impacts on human health, some marine toxins also induce severe ecological disruption through occasional widespread killing of fish, shellfish, marine mammals, seabirds, and any other living organism linked to the marine food web [4, 5]. Furthermore, the steady increase of HABs across the world has become a global concern also for the havoc they wreak on the economy. In fact, in coincidence with toxic algal proliferations, shellfish production areas as well as aquacultures are forced to stay closed for weeks, sometimes for months. From this predicament, fishery and tourism do not emerge unscathed either, since in the presence of HABs, governmental and competent institutions responsible for public safety have to shut down large stretches of coast to any fishing and/or recreational activity.

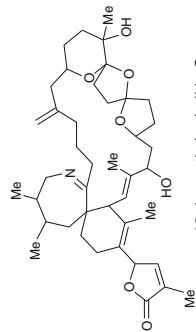
Causes of the worldwide expansion of HABs are still a long way off from being completely ascertained, but explosive growth of toxic plankton seems to be strictly intertwined with continuous changes in weather conditions. Also, other factors, such as variations in upwelling, temperature, transparency, turbulence, or salinity of seawater alongside concentration of dissolved nutrients, wind, and surface illumination, are likely playing a crucial role [9].

Table 28.1 Algal toxins: most common classes of marine biotoxins

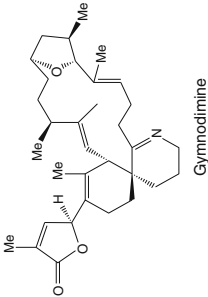
Toxin class	Main algal sources	Toxicity	Structure of a representative
Azaspiracids	<i>Protoperidinium crassipes</i>	Neurotoxic	<div><p>A complex polycyclic molecule with multiple fused rings, including a decalin system, a cyclohexane ring, and a cyclopentane ring. It features several hydroxyl groups, methyl groups, and a carboxylic acid group. The structure is labeled 'Azaspiracid'.</p></div>
Brevetoxins	<i>Karenia brevis</i>	Neurotoxic	<div><p>A complex polycyclic molecule with multiple fused rings, including a decalin system, a cyclohexane ring, and a cyclopentane ring. It features several hydroxyl groups, methyl groups, and a carboxylic acid group. The structure is labeled 'Brevetoxin-1'.</p></div>



Ciguatoxins *Gambierdiscus toxicus* Ciguatera



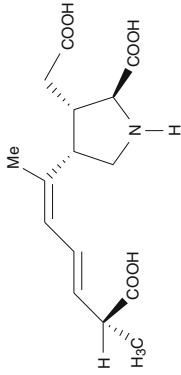
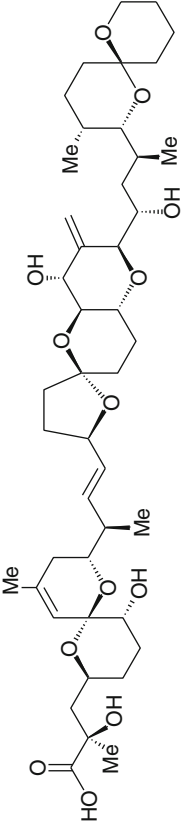
Cyclic imines *Alexandrium ostenfeldii*
(spirolides)



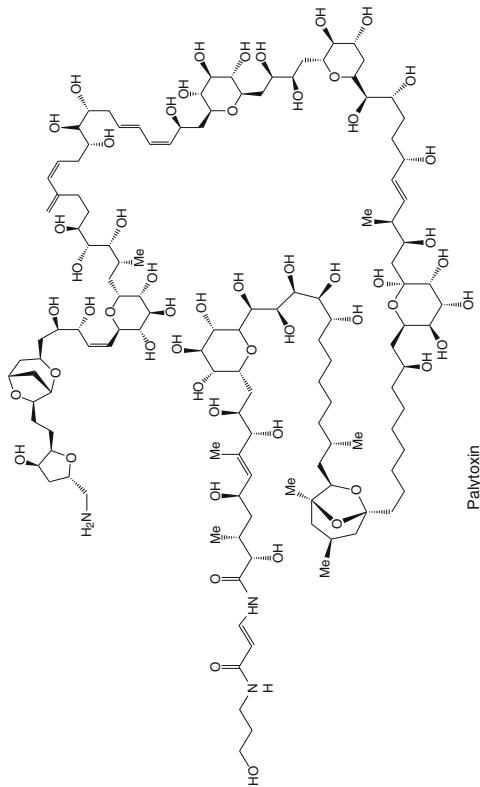
Karenia selliformis
(gymnodimines)

(continued)

Table 28.1 (continued)

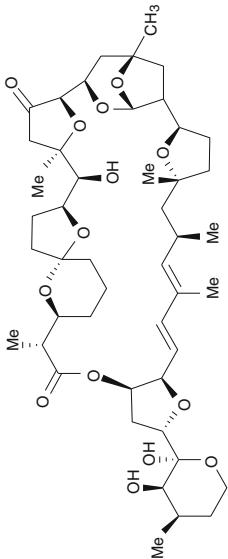
Toxin class	Main algal sources	Toxicity	Structure of a representative
Domoic acids	<i>Pseudo-nitzschia</i> species	Annesic	<div><p>Domoic acid</p></div>
Okadaic acids	<i>Dynophysis</i> species <i>Prorocentrum lima</i>	Diarrhetic tumor promoter	<div><p>Okadaic acid</p></div>

Palytoxins *Ostreopsis* species Neurotoxic tumor promoter



Palytoxin

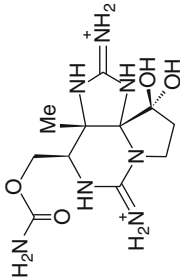
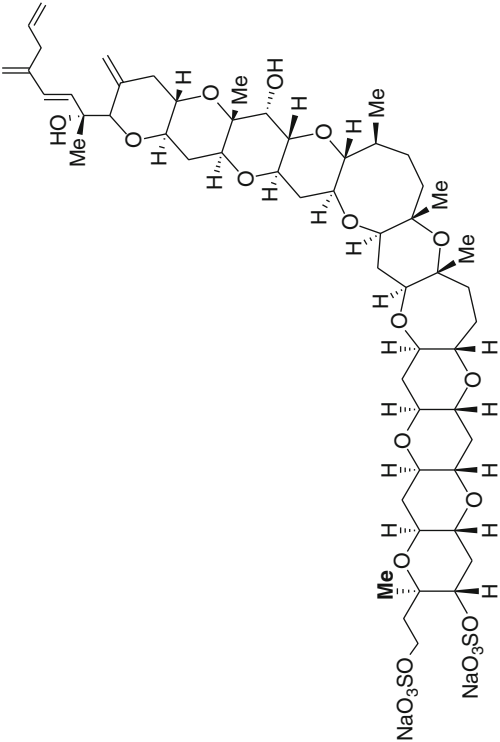
Pectenotoxins *Dinophysis* species Diarrhetic



Pectenotoxin-2

(continued)

Table 28.1 (continued)

Toxin class	Main algal sources	Toxicity	Structure of a representative
Saxitoxins	<i>Alexandrium</i> species	Paralytic	<div><p>The chemical structure of Saxitoxin is a complex pentacyclic molecule. It features a central five-membered ring with a nitrogen atom. Attached to this ring are various functional groups, including a guanidinium group (NH₂⁺), a hydroxyl group (OH), and a side chain containing an amide group (NH-C(=O)-NH₂) and a methoxy group (OCH₃). The structure is labeled "Saxitoxin" below it.</p></div>
Yessotoxins	<i>Protoceratium reticulatum</i>		<div><p>The chemical structure of Yessotoxin is a long, complex polyether molecule. It consists of a long chain of interconnected rings, including several tetrahydrofuran and tetrahydropyran rings. The molecule is highly branched and contains multiple oxygen atoms. It is labeled "Yessotoxin" below it.</p></div>

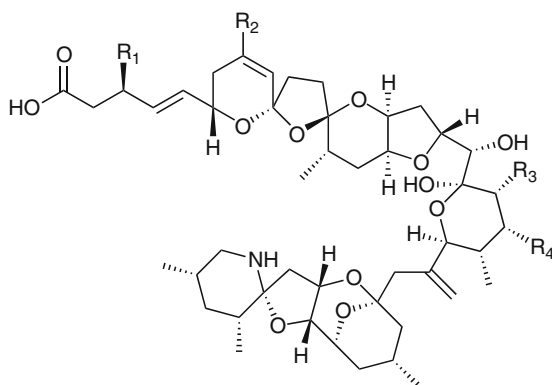
Chemically, marine toxins are often large molecules and only available in small quantities (Table 28.1). So, investigation of marine biotoxins structure usually requires employment of sensitive NMR- and mass spectrometry-based techniques along with HPLC analysis and sometimes combination of chemical degradation and partial or total synthesis as well.

Etiological studies are also a challenging goal since they call for in-depth knowledge in marine ecology and analytical chemistry alike. In this frame, once a candidate organism is thought to be the producer of a given toxin, it needs to be cultured with the purpose of confirming its toxigenicity. Still, some species are difficult or totally unable to be cultured, without mentioning that not all of the clones produce toxins in quantities sufficient for a chemical analysis.

28.2 Azaspiracids: A Recent Class of Toxins Targeting the Human Gastrointestinal Tract

The recently discovered azaspiracids (AZAs) are toxins structurally characterized by a polyether backbone and some unique structural features: a trispiro ring assembly, an azaspiro ring fused with a 2,9-dioxabicyclo[3.3.1]nonane, and a terminal carboxylic acid group (Fig. 28.1).

The first incident due to azaspiracids occurred in the Netherlands in 1995 following consumption of Irish mussels (*Mytilus edulis*) [11]. The symptoms of intoxication closely resembled those associated with DSP including vomiting,



	R ₁	R ₂	R ₃	R ₄
Azaspiracid-1 (AZA1)	H	H	Me	H
Azaspiracid-2 (AZA2)	H	Me	Me	H
Azaspiracid-3 (AZA3)	H	H	H	H
Azaspiracid-4 (AZA4)	OH	H	H	H
Azaspiracid-5 (AZA5)	H	H	H	OH

Fig. 28.1 Structures of principal azaspiracids (AZAs)

severe diarrhea, stomach cramps, and headache. AZA1 was identified as the causative toxin of the outbreak [12]. Later on, the methyl and desmethyl analogues of AZA1, namely AZA2 and AZA3, respectively, were identified in Irish mussels responsible for a second human intoxication [13]. Hydroxylated derivatives of azaspiracids have also been identified in shellfish and structurally determined [14, 15]. Up to now, approximately 20 analogues have been reported to occur naturally in shellfish [16]. However, only two of these, AZA1 and AZA2, have been reported to be produced by the previously unknown dinoflagellate *Azadinium spinosum* [17]. Following development of liquid chromatography–mass spectrometry (LC–MS) methods for determination of azaspiracids, a wide geographical distribution of such toxins across Europe was established, including Norway, the eastern coasts of England, Denmark, Northern France, and northwestern coasts of Spain [18].

Mice-based toxicological studies demonstrated that the major target of azaspiracids is the gastrointestinal tract, where an extensive necrotic atrophy of lamina propria of the villi was observed [19]. Multiple organ damages were also observed mainly in the liver (fatty changes and single cell necrosis) and in T and B lymphocytes in the thymus and spleen [20]. Repeated administrations of the toxins were shown to induce lung tumors [21]. However, the limited availability of pure azaspiracids limited the statistical value of the *in vivo* studies.

The mechanism of action of azaspiracids has been studied using *in vitro* systems. Roman et al. indicated the cytoskeleton as an important cellular target for AZA1 and that it does not induce apoptosis [22]. In addition, AZA1 did not alter membrane potential in excitable neuroblastoma cells, suggesting that it does not produce neurotoxic effects. In human lymphocytes, AZA1 increased cytosolic calcium and cAMP levels and did not affect cytosolic pH. The effect of AZA2 and AZA3 on intracellular cAMP, cytosolic calcium, and pH has also been evaluated, and the obtained results highlighted a structure–activity relationship (SAR) among the different azaspiracids on intracellular pH and calcium levels [23]. Risk assessment individuated a safe level of 0.16 mg/kg of azaspiracids in shellfish. This was adopted by the food safety authority of Ireland and proposed to the European Food Safety Authority and Codex Alimentarius.

28.3 Brevetoxins: Typical Aerosolized Red-Tide Neurotoxins

Brevetoxins are neurotoxic polyether toxins produced by *Karenia brevis* (formerly known as *Gymnodinium breve* and *Ptychodiscus brevis*). This toxic microalga has a long history of extensive blooms in the Gulf of Mexico that initiated offshore and subsequently carried inshore by wind and current conditions [24, 25]. These blooms have caused massive fish kills and respiratory irritation in humans [26]. It was later realized that the toxins in these blooms could also be passed on to humans via shellfish to cause a syndrome named neurotoxic shellfish poisoning (NSP). In the early 1990s, outbreaks of neurotoxic shellfish toxicity were also reported in New Zealand and Australia and resulted in the identification of additional *Gymnodinium* species producing NSP-like toxins [27]. This dinoflagellate species produces two

types of lipid-soluble toxins: hemolytic and neurotoxic compounds [28] causing massive fish kills, bird deaths, and marine mammal mortalities [29, 30].

Recently, neurotoxins have also been found in other fish-killing flagellate species, *Chatonella marina*, *C. antiqua*, *Fibrocapsa japonica* and *Heterosigma akashiwo* [31–33].

It was only in the 1960s, nearly two decades after the toxic episodes in Florida caused by *K. brevis*, that a toxic fraction causing a neurological poisoning was isolated from this dinoflagellate and contaminated shellfish [34]. Over the next years, substantial efforts were dedicated to purifying brevetoxins. However, it was not until 1979, with the introduction of high-pressure liquid chromatography, that the primary congeners of brevetoxins were isolated [35], and within the next 5 years, their long cyclic polyether structures were elucidated by X-ray crystallography and NMR [36, 37].

Like many of the known marine toxins, brevetoxins are tasteless, odorless, and heat (up to 300°C) and acid stable.

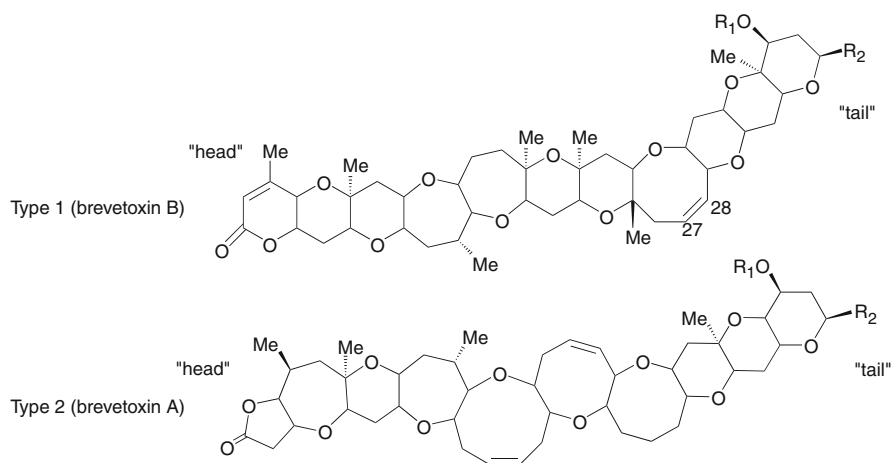
Structurally, brevetoxin congeners fall into two types based on their backbone structure (Fig. 28.2): brevetoxin B backbone (type 1) and brevetoxin A backbone (type 2) [38, 39]. The B-type backbone consists of 11 fused cyclic ether rings, while the A-type backbone is formed by ten fused cyclic ether rings, including a unique nine-membered ring in the E-position connecting the A-D and F-J moieties, thus inducing greater flexibility than that found in the B backbone. Type 1 and type 2 toxins share a lactone in the A ring (“head” of the molecule) and a conserved structure on the “tail” ring, comprising three six-membered fused cyclic ether rings with conserved R-ring substitutions. Both ends are required for the toxicity of brevetoxins. Proximal to the three six-membered rings, there is an eight-membered ring that gives the molecule flexibility to form a boat-chair or crown conformation.

Among brevetoxins, PbTx-2 T is the major brevetoxin produced by *K. brevis* [39]. This alga also produces shorter ring structures (Fig. 28.3) with only four-fused cyclic ether rings (7, 7, 6, 6), named hemibrevetoxins [40]. Two five-fused cyclic ether rings (6, 7, 6, 7, 7) have also been described and named brevenals [41, 42].

Brevetoxins are depolarizing substances that open voltage-gated sodium (Na^+) ion channels in cell walls interacting with neurotoxin binding site 5 on the α -subunit of the channel in a 1:1 stoichiometry [43]. This alters the membrane properties of excitable cell types in ways that enhance the inward flow of Na^+ into the cell, resulting in inappropriate opening of the channel under conditions in which it is normally closed, and it also inhibits channel inactivation. The increased membrane permeability to sodium initially determines excitatory cellular response (including release of neurotransmitters at some synapses), then followed by loss of cell excitability, leading to paralysis [44].

The mouse LD50 is 170 $\mu\text{g}/\text{kg}$ body weight (0.15–0.27) intraperitoneally, 94 $\mu\text{g}/\text{kg}$ body weight intravenously, and 520 $\mu\text{g}/\text{kg}$ body weight orally [45]. Pathogenic dose for humans is in the order of 42–72 mouse units.

In humans, the symptoms of NSP intoxication may occur after either inhaling aerosol containing the toxins or as a consequence of eating contaminated seafood. In the former case, symptoms include primarily respiratory distress, as well as eye and nasal membrane irritation, caused principally by exposure to sea-spray aerosols



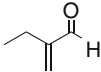
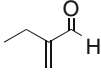
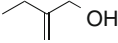
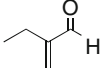
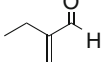
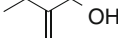
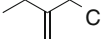
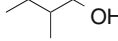
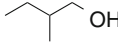
Toxin	Type	R ₁	R ₂
PbTx-1	2	H	
PbTx-2	1	H	
PbTx-3	1	H	
PbTx-5	1	COCH ₃	
PbTx-6	1	H	 27,28 epoxide
PbTx-7	2	H	
PbTx-8	1	H	
PbTx-9	1	H	
PbTx-10	2	H	

Fig. 28.2 Structure of brevetoxins (PbTxs)

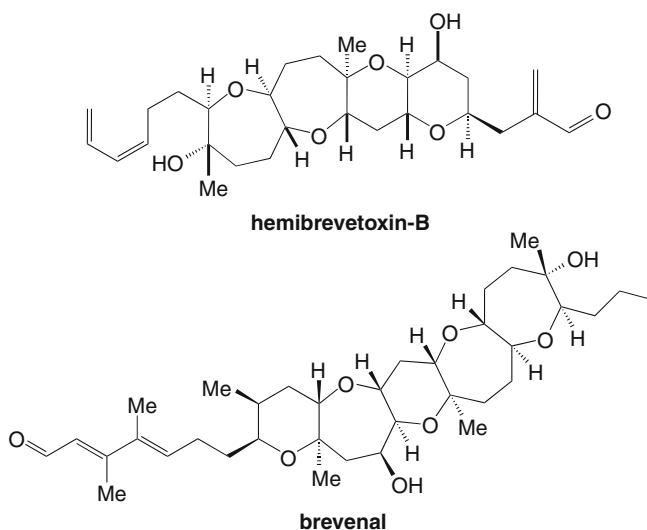


Fig. 28.3 Structure of hemibrevetoxin B and brevenal

and by direct contact with toxic blooms while swimming [46]. When intoxication is through contaminated shellfish, the symptoms are more severe than those found when contaminated aerosol is involved and include nausea, tingling and numbness of the perioral area, loss of motor control, and severe muscular pain [47]. There have been no reported fatalities from NSP, although the toxin kills test mammals when administered by various routes, including the oral one.

To date, brevetoxin-group toxins have not been reported in shellfish or fish from Europe. However, the discovery of new algae producing brevetoxins and the apparent trend toward expansion of algal bloom distribution suggest that this group of toxins could also emerge in Europe. Currently, there are no regulatory limits for these toxins in shellfish or fish in Europe.

28.4 Ciguatera: A Fitting Example of How Chemical Structure of Marine Biotoxins Is Investigated

In subtropical and tropical regions, consumption of contaminated coral reef fishes may cause a syndrome referred to as ciguatera, so called after the Caribbean word “cigua” indicating small marine snails whose ingestion had long induced human poisonings [48]. Every year, some 25,000 people are affected by ciguatera fish poisoning (CFP) that for such a reason has long been regarded as a world health problem [49]. The exogenous origin of the causative agent of ciguatera has been easily ascertained because fish toxicity entwined with this poisoning has all along fluctuated individually, seasonally, regionally, and even annually. In the late 1960s, a Hawaiian research group isolated from moray eels a toxin – named ciguatoxin (CTX) – that was proposed to be accumulated in fish by the food chain [50].

To the aim of tracking the real producer of CTX down through the food chain, Yasumoto et al. chose to investigate the guts of a small surgeonfish, *Ctenochaetus striatus*, on the basis of the following considerations: (1) the fish was clearly intertwined with many ciguatera outbreaks in Tahiti, (2) the fish grazes on a limited variety of microalgae and other microorganisms, and (3) it is a favorite prey for carnivores thus being a clear link with larger fishes in the food chain. The outcome of Yasumoto's studies was the identification in the guts of the analyzed fish of a lipophilic toxin chromatographically identical with CTX [48]. In the late 1970s, in the digestive contents from *C. striatus* was detected the occurrence of a dinoflagellate successively classified as *Gambierdiscus toxicus* that is now well known to be the producer of ciguatera toxins [51]. This confirmed the hypothesis that surgeon fishes obtain CTX from their diet and transfer it to carnivores through the food chain.

Ciguatoxins are a class of more than 20 heat-stable, lipid-soluble, cyclic polyether molecules whose chemical architecture is strictly reminiscent of that of brevetoxins [52–57] (Fig. 28.4). The planar structure of ciguatoxin was achieved by Yasumoto et al. who had to work on less than 1 mg of pure compound isolated from 124 kg of viscera deriving from 4 t of contaminated moray eels [52]. Despite the very small amount of pure compound, Yasumoto succeeded in elucidating the structure of CTX by extensive NMR analysis. Successive studies on both wild and cultured *G. toxicus* allowed the isolation and structure determination of further CTXs, such as gambierol [58], and a potent antifungal compound named gambieric acid [59]. Yasumoto could also establish the stereochemistry of the isolated CTXs by resorting to a combination of chiral fluorescent HPLC reagents or anisotropic NMR reagents with chemical degradation and synthesis of partial structures [60].

With regard to their biological activity, CTXs give rise to a wide array of symptoms remarkably varying depending on the geographic region that can be classified in four main categories: gastrointestinal, neurological, cardiovascular, and general symptoms [61]. If injected intraperitoneally into a mouse, ciguatoxin shows a DL_{50} of 0.45 $\mu\text{g/kg}$, while oral intake of 0.1 μg of toxin can cause illness in humans. As previously pointed out, CTXs chemically resemble brevetoxins, of which they exert also the same mechanism of action. In fact, CTXs activate the voltage-sensitive Na^+ channel at nM to pM concentrations thus being around 30-fold more affine than brevetoxins [62]. CTXs are particularly active on sodium channels located along peripheral nerves (nodes of Ranvier) thus inducing a massive influx of Na^+ with cell depolarization and the onset of spontaneous action potentials in excitable cells [63]. As a result, plasma membranes are no longer able to preserve the internal environment and the volume of cells with a consequent alteration of bioenergetic mechanisms. Concerning the cardiovascular impact of CTXs, it must be underlined that once these toxins make Na^+ move intracellularly, cells start extruding sodium and taking up calcium, which is a known intracellular trigger for muscle contraction. Indeed, an increased force of cardiac muscle contraction is a common symptom associated to CFP. Likewise, surge of calcium concentrations in intestinal epithelial cells induced by CTXs

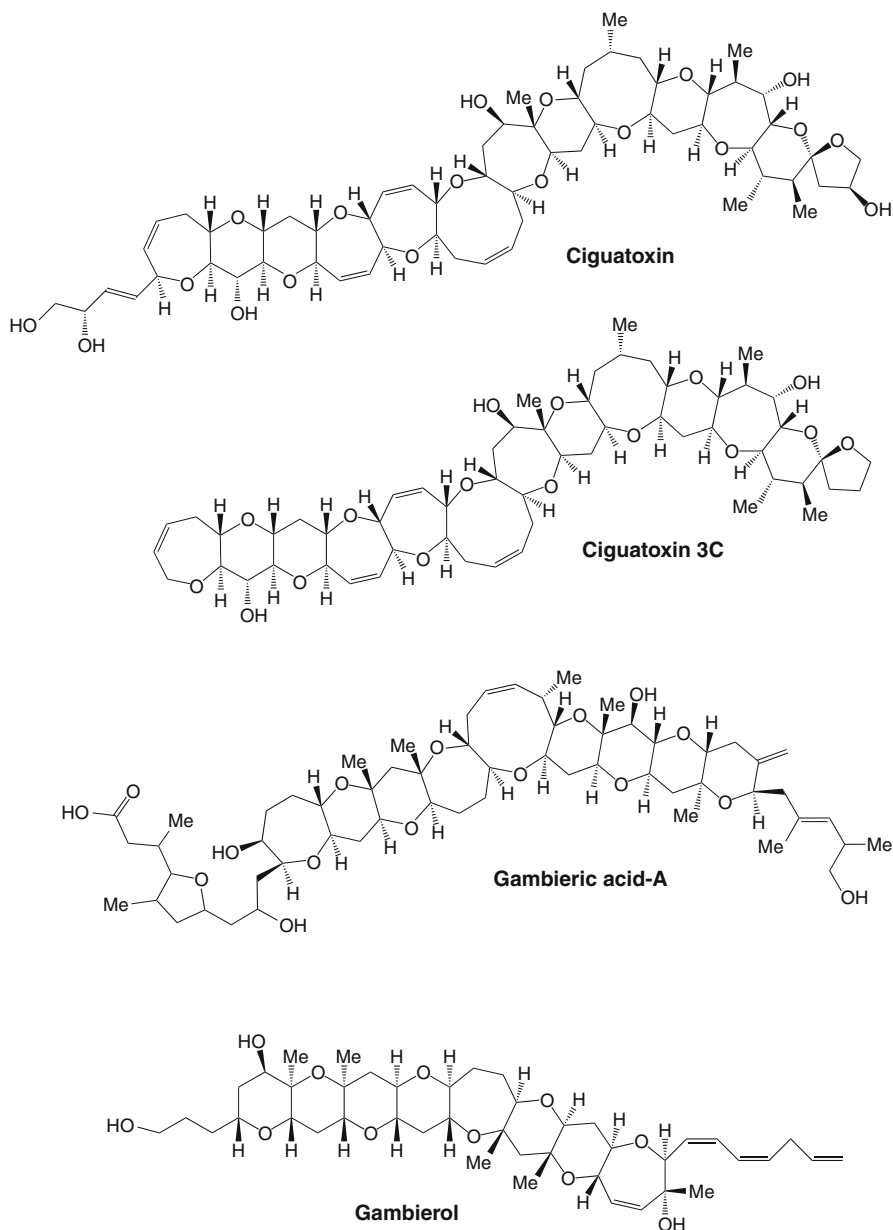
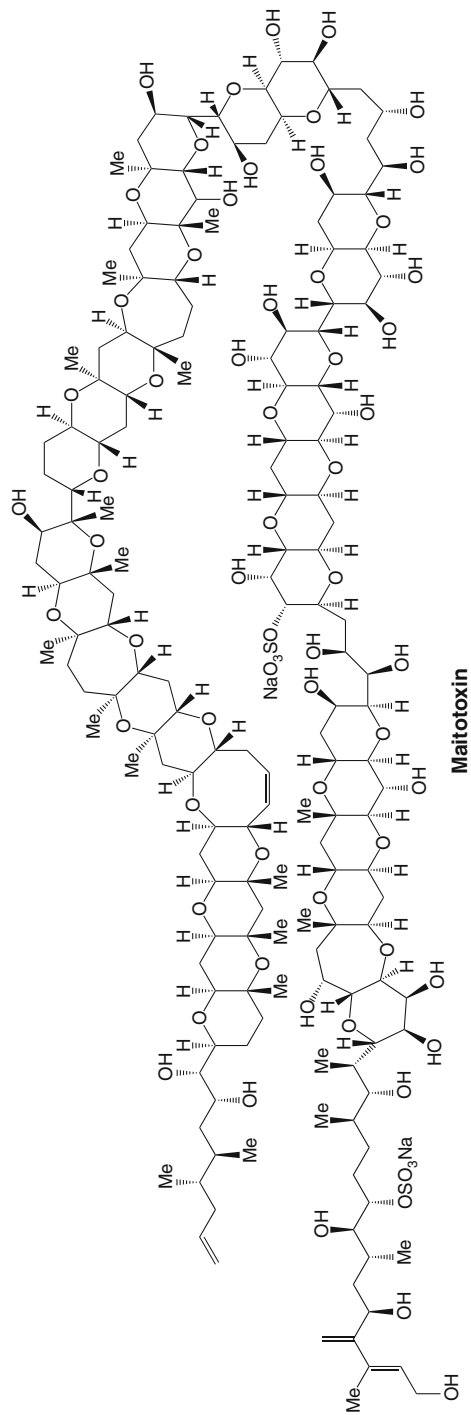


Fig. 28.4 Structure of principal ciguatera-related toxins

affects important cellular ion-exchange systems thus triggering fluid secretion and diarrhea [64].

Another important neurotoxin involved in CFP is maitotoxin (MTX, Fig. 28.5). So far, three further analogues of MTX have been identified from *G. toxicus* [65].

**Fig. 28.5** Structure of maitotoxin

With a molecular weight of 3,422, maitotoxin is by far the largest nonpolymeric natural product of all, and apart from some proteic bacterial toxins, it is also one of the most toxic compounds. From a chemical point of view, MTX is a ladder-shaped polycyclic highly hydroxylated molecule. Pharmacological studies have proven MTX a potent activator of voltage-gated calcium channels [66]. At the moment, though, its primary target remains undefined and the molecular mechanism of action still presents many blind spots.

28.5 Cyclic Imine Toxins: A Category of Miscellaneous Emerging Toxic Compounds

Cyclic imine toxins constitute a heterogeneous class of marine biotoxins all featuring a macrocyclic structure with a typical imine moiety apparently being the bioactive pharmacophore. Quite a number of toxic compounds currently belong to this class of toxins:

- Gymnodimines [67]
- Pinnatoxins [68]
- Prorocentrolides [69]
- Pteriatoxins [70]
- Spirolides [71]
- Spiro-prorocentrimine [72]

In Fig. 28.6, representatives of each class of cyclic imines are reported. All of these compounds are referred to as a class of emerging toxins as in-depth knowledge about them is still lacking. First and foremost, it would be necessary assessing their real impact on human health. Cyclic imine toxins are indeed usually classified as fast-acting toxins since they induce death within minutes from their intraperitoneal injection into mice and show an acute threshold response in mammalian bioassays. Beyond this, though, the real toxicity of this class of toxins is still a long way off from being clearly elucidated. This is surely due to their relatively recent discovery – dated back to about two decades ago – with a concurrent lack of standards, reference, or purified material, which has so far hampered thorough toxicological evaluations. In addition, regulatory authorities have been all along reluctant to undertake studies on the effect of such a class of compounds in the absence of ascertained cyclic imine-related human intoxications. As a result, no regulatory limits have been set for any of the above cyclic imines, which are at the moment relegated to a category of compounds supposed safe for consumers until proven otherwise [73].

All of the cyclic imine toxins with the exception of spirolides – that have been detected worldwide – have been individuated only in scattered locations and in taxonomically restricted group of vectors. Nonetheless, their geographical distribution is reasonably bound to spread as monitoring programs increase and sensitivity in analytical methods improves.

Unlike pinnatoxins and pteriatoxins that have been detected exclusively in shellfish even though thought to represent a dietary incorporation in bivalves, all

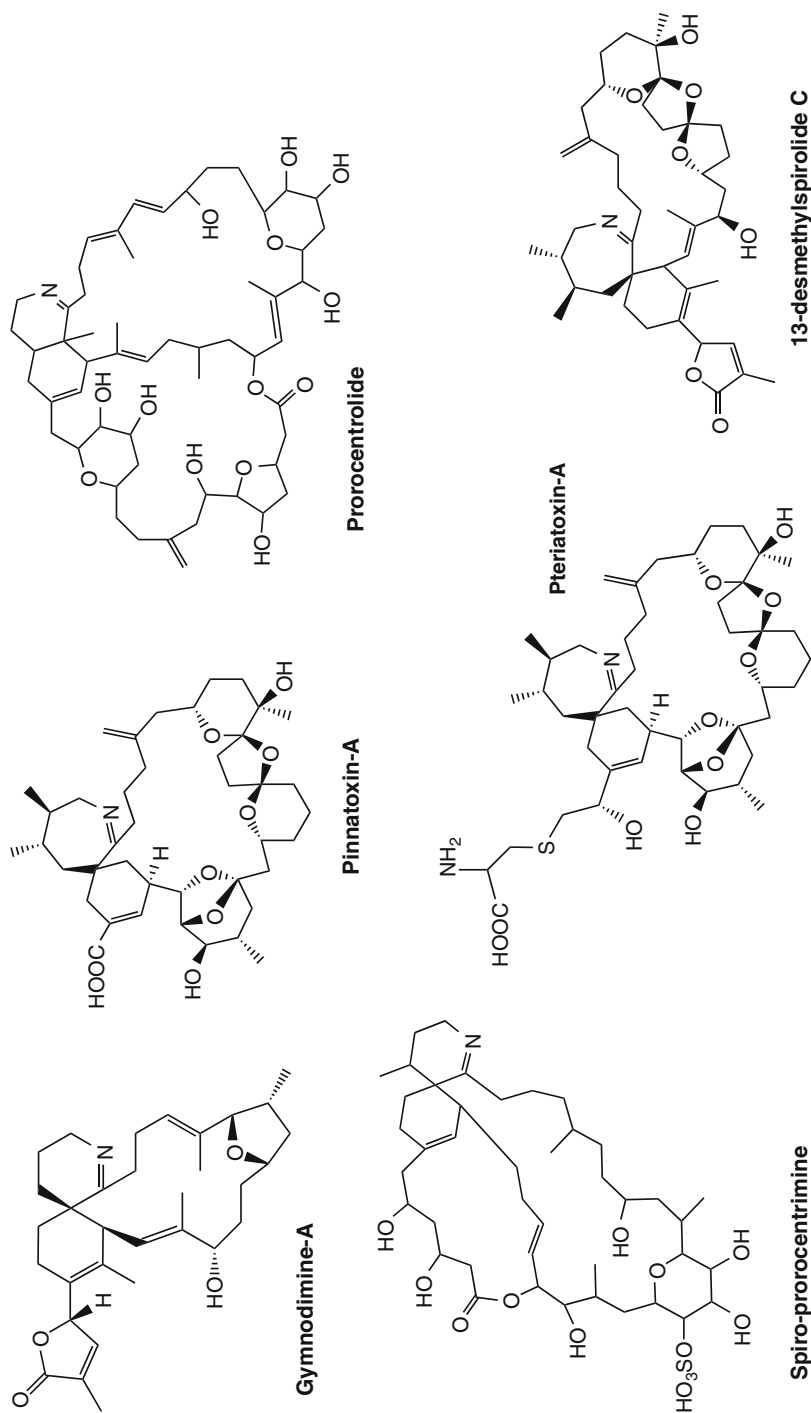


Fig. 28.6 Structure of representatives of cyclic imine toxins classes

of the other cyclic imines are strongly believed to be synthesized by either benthic or pelagic marine dinoflagellates on account of their chemical features apparently deriving from polyketide biosynthetic pathways common to other polyether biotoxins [74].

Gymnodinium sp. was first regarded as culprit species of gymnodimine toxicity [67], but successive taxonomic studies individuated the marine dinoflagellate *Karenia selliformis* as the most likely producer of this group of toxins [75].

Benthic or epiphytic *Prorocentrum* species are the microorganisms producing prorocentrolides [69] and spiro-prorocentrimine [72], clearly termed after their producers.

Regarding the biological origin of spirolides, the marine dinoflagellate *Alexandrium ostenfeldii* has been described as their primary, if not exclusive, producer [76]. It is worthwhile highlighting that such a dinoflagellate is reported to produce different kinds of toxins depending on its geographical provenance. In fact, while Canadian [77] and Adriatic [78] strains of *A. ostenfeldii* were proven to produce high levels of a number of spirolides, New Zealand strains only produced PSP toxins [79]. Even more complex was the toxin profile of certain *A. ostenfeldii* populations from Scandinavia that were shown to produce both spirolides and PSP toxins [76].

As already described above, biological activity and mechanism of action of cyclic imine toxins are not comprehensively understood. What seems quite plain is that the intact imine group plays a crucial role in their toxicity as pointed out by a dramatic decrease in biological activity upon its hydrolysis. Indeed, spirolide E and F originating from keto amine hydrolysis are both basically inactive [80]. On account of the similar symptomatology shown by cyclic imine toxins, a common mode of action for all of them can be presumed. More in detail, spirolides seem to affect calcium ions [80], while gymnodimine activates sodium channels even in a far weaker way than other classic ion channel effectors, namely brevetoxins, tetrodotoxin, or even saxitoxin [67]. Moreover, both transcriptional and histological analyses of brain tissues revealed that muscarinic and nicotinic subreceptors were upregulated following exposure to spirolides. Consequently, such receptors could represent the spirolides' biological target [81].

Effort should be expended to extend the knowledge on cyclic imine toxins toxicology well beyond what is currently accessible, with the purpose of resolving their oral toxicity and assessing the real risks they pose to human health.

28.6 Domoic Acids: The Only Marine Biotoxins Produced by Diatoms

One morning in the summer of 1961, hundreds of crazed birds attacked the seaside town of Capitola, California. The birds “cried like babies” as they dove into streetlamps, crashed through glass windows, and attacked people on the ground. Most of the birds were sooty shearwaters, a normally nonaggressive species that feeds on small fish and comes ashore only to breed. The incident fascinated Alfred

Hitchcock, who was vacationing nearby and likely inspired one of his most famous movie, *The Birds*, which appeared in cinemas 2 years later.

In the winter of 1987, the agent that is now believed to be responsible for the Capitola incident struck on the opposite shore of the continent. This time, it struck higher on the food chain. Over a hundred people became extremely ill within hours after dining on cultured blue mussels in restaurants around Prince Edward Island in Canada [82]. It quickly became apparent that this was no ordinary outbreak of food poisoning. Vomiting, cramps, diarrhea, and incapacitating headaches were followed by confusion, loss of memory, disorientation, and (in severe cases) seizures and coma. A few exhibited emotional volatility, with uncontrolled crying or aggressiveness. Three elderly victims died in the hospital and one 3 months later [83].

The causative agent of this deadly syndrome, now known as amnesic shellfish poisoning (ASP), was identified as domoic acid [84, 85], a nonproteic amino acid with antihelminthic activity originally isolated in 1959 from a red marine macroalga, *Chondria armata* [86].

The chain-forming diatom *Pseudo-nitzschia multiseries* (formerly known as *Nitzschia pungens*) was recognized as the causative agent of that toxic event [87, 88]. Several further species of *Pseudo-nitzschia* (*P. australis*, *P. pseudo-delicatissima*, *P. galaxiae*, *P. multistriata*, *P. pungens*, *P. seriata*, *P. turgidula*, *P. fraudulenta*, *P. delicatissima*, *P. calliantha*) have successively been found to produce domoic acid, although some species are not always toxic and there is a considerable variability in toxicity [89–91]. These diatom species are distributed worldwide. Consequently, accumulation of domoic acid in bivalves has also been reported from various parts of the world [92–94]. On the other hand, domoic acid is reported to accumulate in sea birds and marine mammals by a food-web transfer, which can result in mass mortality of these animals [95]. Scholin et al. [96] suggested that the origin of the domoic acid causing the deaths of sea lions on the California coast is *Pseudo-nitzschia australis*. Such findings show that domoic acid occurs widely in marine ecosystems. However, knowledge of the distribution of domoic acid in various organisms is limited to those in temperate waters. Little is known about accumulation of domoic acid in tropical marine organisms. It is worthwhile emphasizing that ASP is the only shellfish poisoning produced by a diatom.

Structurally, domoic acid (DA) is a water-soluble excitatory tricarboxylic amino acid (Fig. 28.7), belonging to the kainoid class of compounds, structurally resembling the excitatory neurotransmitter glutamic acid. Its molecular structure was determined in the late 1950s [86, 97–99] and then confirmed following total synthesis [100].

Several congeners of domoic acid have been identified so far, of which three geometrical isomers, isodomoic acids D, E, and F, and the C5'-diastereomer were found in small amounts in both the diatom and shellfish tissue (Fig. 28.7) [101, 102].

The biological mode of action of domoic acid results in neuronal depolarization; the resultant short-term memory loss is symptomatic of domoic acid poisoning

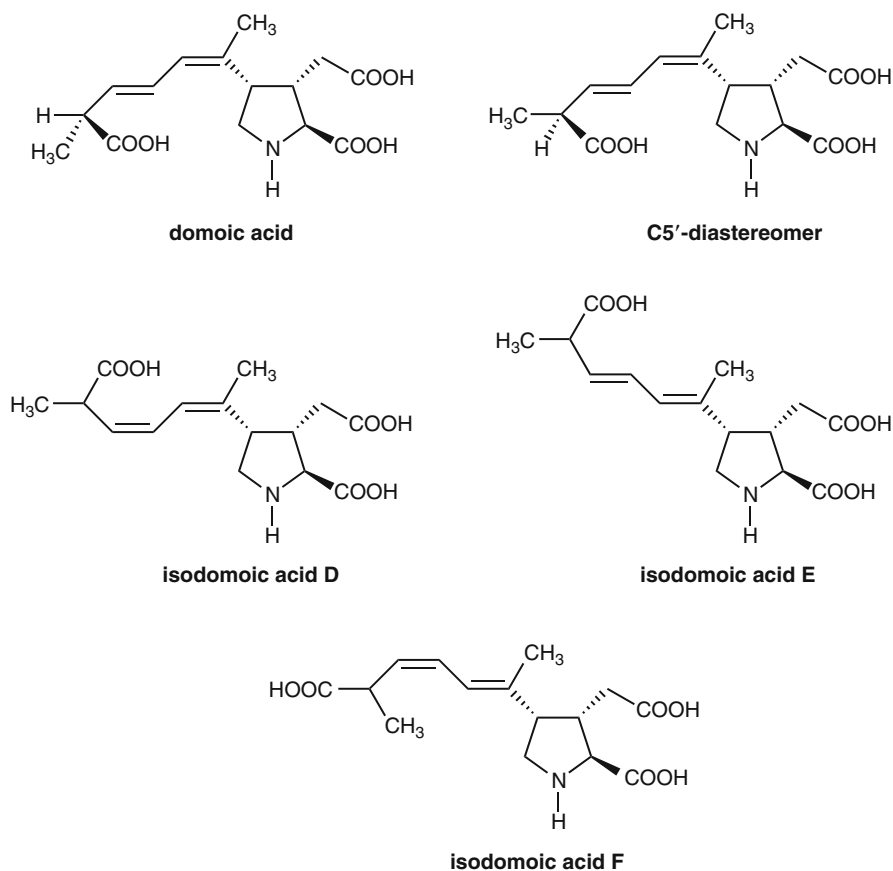


Fig. 28.7 Structure of principal domoic acids (DAs)

(reported by 25% of those affected by the Canadian amnesic shellfish poisoning outbreak). The mechanism of DA toxicity is explained by its structural similarity with the excitatory neurotransmitter glutamic acid but with a much stronger receptor affinity. Domoic acid binds predominantly to both kainate and AMPA subtypes of glutamate receptor [103], resulting in depolarization of neurons. Subsequently, the permeability to calcium ions increases [104]. This induces lesions in areas of the brain where glutaminergic pathways are heavily concentrated, particularly in the CA1 and CA3 regions of the hippocampus, areas responsible for learning and memory processing [105]. The loss of memory in patients intoxicated with mussel toxin appears to be similar to patient with Alzheimer's disease. However, the loss of memory in mussel-intoxicated patients was not affected by the age of patients, whereas symptoms of Alzheimer's disease intensify with aging and are generally noted in older people. Further, the findings that intellect and higher cortical functions are not influenced by DA intoxication distinguish the mussel-induced intoxication from Alzheimer's disease.

Other clinical symptoms of ASP include abdominal cramps, vomiting, diarrhea, incapacitating headaches, and disorientation. In the most severe case of poisoning, patients are victims of seizures, coma, profuse respiratory secretions, unstable blood pressure, and even death.

28.7 Okadaic Acids: The Subtle Threat of Potent Tumor Promoters

The syndrome diarrhetic shellfish poisoning (DSP) was first discovered in the 1970s following the occurrence of a mussel intoxication in northeastern Japan [106]. Ever since, DSP has known a steady spreading across the globe. It is essentially associated with seafood consumption such as mussels, clams, and scallops, which can accumulate dinoflagellate toxins in their digestive glands by seawater filtering process. The major toxin responsible for most DSP in humans is okadaic acid (OA) alongside a number of analogues termed dinophysistoxin-1 (DTX1) and dinophysistoxin-2 (DTX2), among others (Fig. 28.8) [107]. A number of further congeners are also involved in DSP syndrome, but all of them are believed to be either precursors or shellfish-modified metabolites of the active toxins [108].

OA was primarily isolated from the marine sponges *Halichondria okadai* and *Halichondria melanodocia*, and subsequently proven to be produced by dinoflagellates belonging to the genera *Dinophysis* and *Prorocentrum* [109, 110]. With regard to this latter, the benthic species *Prorocentrum lima* is worth being mentioned [111, 112], while among the *Dinophysis* species, *D. acuta*, *D. fortii*, *D. acuminata*, *D. norvegica*, *D. mitra* and *D. caudata* must be listed [113].

Chemically, OA is a polyether compound characterized by a carboxylic acid group and three spiro-keto ring assemblies, one of which connects a five with a six-membered ring.

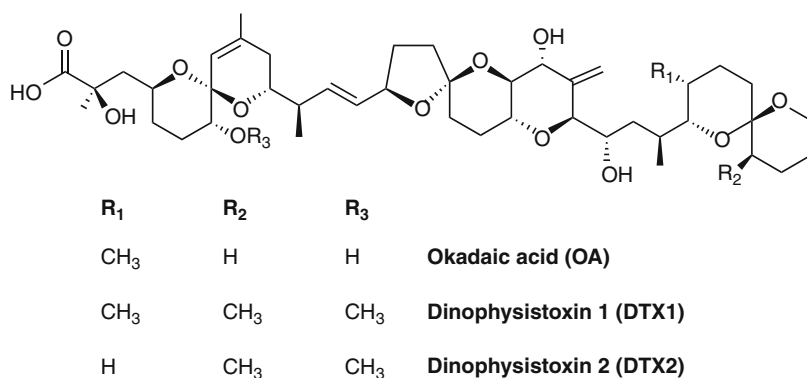


Fig. 28.8 Structure of principal okadaic acids (OAs)

Oral assumption of okadaic acid-contaminated seafood leads to the typical DSP symptoms usually within 30 min from ingestion. Symptoms shown by intoxicated patients are mainly gastrointestinal-like. Diarrhea, nausea, vomiting, and abdominal cramps are among the most common disturbances suffered by humans. No DSP-related casualty has been reported so far, but sometimes remarkable morbidity has required hospitalization. The treatment, if necessary, includes fluid replacement and electrolyte reintegration.

OA has long been known as a potent inhibitor of Ser/Thr protein phosphatases that represent an array of enzymes catalyzing dephosphorylation of phosphoserine or phosphothreonine residues in eukaryotes [114]. Ser/Thr protein phosphatases are involved in an extraordinary number of physiological processes in mammals ranging from glycogen metabolism to coordination of cell cycle and even gene expression. It follows that DSP toxins impact on Ser/Thr protein phosphatases can be devastating for living organisms. More in detail, of the four major groups of Ser/Thr protein phosphatases, OA inhibits PP2Ac at the lowest concentration ($IC_{50} = 0.2$ nM) and PP1c at the next lowest concentration ($IC_{50} = 20$ nM) as opposed to PP2B – which is slightly affected by the toxin – and to PP2C on which no effect is detectable [115]. Inhibition of Ser/Thr protein phosphatases by OA is known to provoke all of the gastrointestinal disorders in humans as soon as the toxin reaches the digestive tract.

Besides, there is another far more harmful threat posed by okadaic acids (OAs) to unaware contaminated seafood consumers: their potent tumor-promoting activity. Indeed, OA and DTX1 are classified as non-12-*O*-tetradecanoylphorbol-13-acetate (TPA)-type tumor promoters [116]. Unlike phorbol esters which activate protein kinase C, these two DSP toxins neither bind to phorbol ester receptors in cell membranes nor activate protein kinase C in in vitro studies [116]. OA and DTX1 have shown a potent tumor promotion activity on mouse skin. It appears that by inhibiting PP2A, OA causes a general decrease of cell adhesion and cytoskeletal reorganization resulting in an increased cell motility and invasiveness alike [114].

Considering the alarming harmfulness of OAs to consumers, it is apparent that a strict monitoring program needs to be run on seafood aimed at preventing possible human intoxications. With regard to this, it needs to be emphasized that the European Community has been recently forced to modify the official extraction procedure for analyzing seafood. In fact, by applying the old extraction method, yessotoxins – which in many toxic outbreaks have occurred together with DSP toxins – and OAs were recovered in the same organic layer [106]. Therefore, the mouse bioassay – the reference method in Europe to detect toxicity in seafood – could not lead to any confident assessment of the toxin(s) involved. So, as these two classes of toxins show a remarkably different toxicity on humans with, accordingly, very different official allowance levels in shellfish (16 µg of OA and 100 µg of yessotoxin in 100 g of mollusk, respectively), a new extraction method capable of separating yessotoxin in an aqueous layer and OAs in a lipophilic one was set up [117].

28.8 Palytoxins: Potent Tropical Toxins Now Rife Across the Mediterranean Basin

The lethal potency of palytoxin was well known to ancient Hawaiians who used to smear a moss containing such toxin on their spearpoints to make them fatal. According to an old legend, the lethal moss – known to native Hawaiians as limu-make-o-Hana – started lining the walls of a tide pool near the harbor of Hana after the ashes of an evil Shark God killed by some fishermen had been thrown into it [118]. In the early 1960s, thanks to some local informers, P. Helfrich and J. Shupe from the Hawaii Institute of Marine Biology succeeded in individuating the tide pool, from which they collected some samples of the toxic moss. Fascinated by the legend and propelled by his profound interest in marine toxins, Professor P. Scheuer from the University of Hawaii, a pioneer of the chemistry of marine metabolites, in collaboration with P. Helfrich and R. Moore, investigated the toxic samples collected from the legendary tide pool [119]. It was then assessed that the limu-make-o-Hana was not a seaweed but an animal belonging to the phylum Coelenterata – possibly a new species – assigned to the genus *Palythoa* [120] after which the molecule responsible for its high toxicity was named palytoxin. After its isolation in 1971 and the preliminary structural insights offered by Scheuer [119], it took nearly 11 years before the correct chemical structure of palytoxin (Fig. 28.8) was disclosed [121, 122]. It is a complex polyhydroxylated water-soluble compound, containing both lipophilic and hydrophilic part structures. In 1982, the complete stereochemistry of palytoxin – encompassing as many as 64 stereogenic centers in addition to eight double bonds – was disclosed [123], and a few years later confirmed by its total synthesis [124].

Following the first report on palytoxin in 1971, many research groups from across the world have undertaken scientific studies with the purpose of investigating this fascinating molecule. Efforts carried out by proficient chemists have significantly contributed to identify quite a number of palytoxin analogues (Fig. 28.9).

The real biological origin of this class of toxins remains controversial. In fact, even though several palytoxin-like compounds have been isolated from zoanthids belonging to the genus *Palythoa* – such as homopalytoxin, bishomopalytoxin, neopalytoxin, deoxypalytoxin [125], and 42-hydroxypalytoxin [126] – of late many have defended the assumption that palytoxins are indeed produced by microorganisms. In particular, dinoflagellates belonging to the genus *Ostreopsis* seem to be the most probable biogenetic originators of palytoxins [127, 128]. In 1995, in fact, Yasumoto isolated and structurally characterized some palytoxin analogues, named ostreocins, from extracts of the dinoflagellate *O. siamensis*. The major constituent of the isolated ostreocins, accounting for 70% of the total toxicity, resulted to be ostreocin D, whose chemical structure was assigned as 42-hydroxy-3,26-didemethyl-19,44-dideoxypalytoxin by detailed 2D NMR analyses of both the intact compound and its ozonolysis products [129, 130].

Successively, further palytoxin-like compounds, termed mascarenotoxins, were extracted from *O. mascarenensis* [131]. These toxins were confirmed as palytoxin analogues on the basis of their mass spectrum profile and fragmentation pattern obtained by nano-electrospray ionization quadrupole time-of-flight MS.

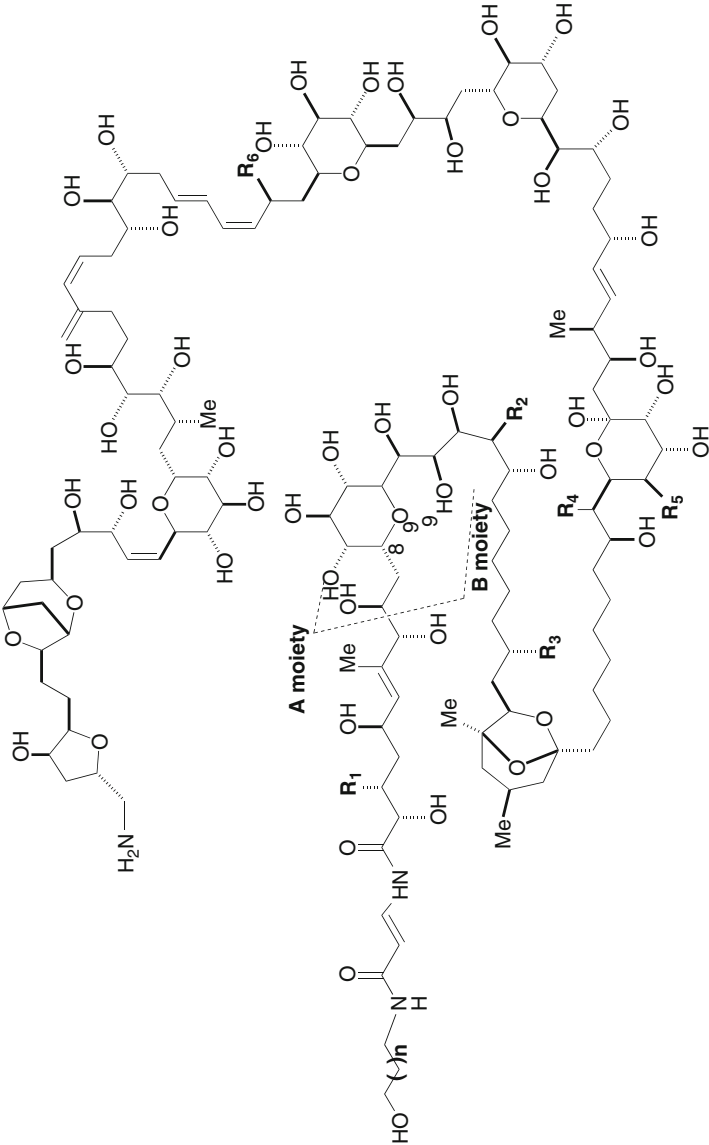
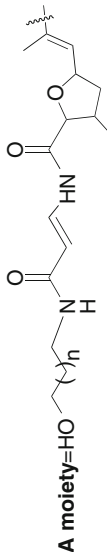


Fig. 28.9 (continued)

	n	R ₁	R ₂	R ₃	R ₄	R ₅	R ₆
Palytoxin	1	Me	OH	Me	H	OH	OH
Ostreocin-D	1	H	H	H	OH	H	OH
Homopalytoxin	2	Me	OH	Me	H	OH	OH
Bishomopalytoxin	3	Me	OH	Me	H	OH	OH
Neopalytoxin	1	-	OH	Me	H	OH	OH
Deoxypalytoxin	1	Me	OH	Me	H	OH	H
42-Hydroxy-palytoxin	1	Me	OH	Me	OH	OH	OH



A moiety=HO

Fig. 28.9 Structure of palytoxin and some of its analogues

Recently, palytoxin and some of its analogues, named ovatoxins, have been detected in the Mediterranean *O. ovata* [132–134]. Ovatoxins have been identified by high-resolution LC–MS/MS and present molecular formulae similar to palytoxin's, with elemental composition differences residing either in the A or B moiety of palytoxin molecule [133, 134].

More in detail, by accurately interpreting complex HRMS/MS spectra, it was ascertained that (1) ovatoxin-a presents two oxygen atoms less than palytoxin and the same A moiety; (2) ovatoxin-b presents C_2H_4O more than ovatoxin-a, the structural difference between the two molecules residing in the A moiety whereas part structure B is identical; (3) ovatoxin-c presents the same A moiety as ovatoxin-b and an additional oxygen atom in the B moiety; and (4) ovatoxin-d and ovatoxin-e are isobaric compounds that present one oxygen atom more than ovatoxin-a, located either in the B moiety (ovatoxin-d) or in the A moiety (ovatoxin-e).

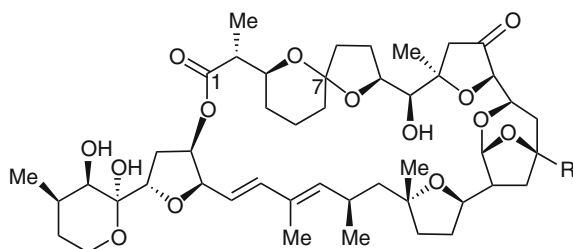
Palytoxins constitute a class of extremely potent nonproteic marine biotoxins, whose main biological target is the Na^+/K^+ -ATPase, membrane pumps maintaining ionic gradients critical to cell function [135]. The effect of palytoxins is basically a conversion of these ion-specific pumps into nonselective cationic pores, thus triggering several biological effects, some of which even life threatening.

Due to their high potency, palytoxins harm human health through diverse routes of exposure ranging from ingestion of contaminated seafood to dermal contacts, or inhalation of marine aerosol [136, 137]. Some fatal human poisonings attributed to palytoxin have been reported worldwide [138, 139]; the toxin has been suggested as the possible cause of clupeotoxism, a poorly understood syndrome caused by ingestion of edible fish [140]. Symptoms of intoxication include vasoconstriction, hemorrhage, ataxia, muscle weakness, ventricular fibrillation, pulmonary hypertension, ischemia, and death. Toxicity strongly depends on the route of administration. As way of example, palytoxin exhibits high toxicity in mammals when intravenously administered (LD₅₀ ranging between 25 and 450 ng/kg) [141], while intragastric administration in rats shows a significantly lower toxicity (LD₅₀ > 40 µg/kg) [141, 142].

In the late 1980s, palytoxin was also identified as a skin tumor promoter [143, 144]. In contrast to TPA (12-O-tetradecanoylphorbol-13-acetate), palytoxin induces neither ornithine decarboxylase in mouse skin nor HL-60 cell adhesion. Furthermore, palytoxin neither binds to protein kinase C in vitro nor increases ornithine decarboxylase activity in mouse skin. On the basis of such evidence, palytoxin is classified as a non-TPA-type tumor promoter [145].

28.9 Pectenotoxins: Potent Cytotoxic Compounds with Still Unknown Potential Implications to Public Health in the Long Term

Pectenotoxins (PTXs) are lipophilic macrocyclic polyethers, whose chemical structures resemble okadaic acid in having cyclic ethers and a carboxyl group in the molecule. Unlike okadaic acid, in many PTXs, the carboxyl moiety is engaged in a macrocyclic lactone (Fig. 28.10). To date, 15 different PTXs have been isolated



R	C-7	C-7
CH ₂ OH	<i>R</i> Pectenotoxin 1 (PTX1)	<i>R</i> Pectenotoxin 2 seco acid (PTX2SA)
CH ₃	<i>R</i> Pectenotoxin 2 (PTX2)	<i>S</i> 7- <i>epi</i> -Pectenotoxin 2 seco acid (PTX2SA)
CHO	<i>R</i> Pectenotoxin 3 (PTX3)	
CH ₂ OH	<i>S</i> Pectenotoxin 4 (PTX4)	
COOH	<i>R</i> Pectenotoxin 6 (PTX6)	
COOH	<i>S</i> Pectenotoxin 7 (PTX7)	

Fig. 28.10 Structures of principal pectenotoxins (PTXs)

and characterized from a range of source organisms [146]. PTXs in filter-feeding organisms originate from dietary microalgae. Up to now, only the genus *Dinophysis* (e.g., *D. acuta*, *D. fortii*, *D. acuminata*, and *D. caudata*) has been implicated in contamination of shellfish with PTXs [146]. However, only PTX-2 and the seco acids of PTX-2 (PTX-2SA and *epi*-PTX-2SA) have been isolated from phytoplankton, while the other compounds have been detected only in shellfish samples. Therefore, it has been supposed that an oxidation occurs in the hepatopancreas of shellfish, and that many PTXs are products of shellfish metabolism after ingestion of PTX-producing microalgae [146, 147].

Pectenotoxins in shellfish are always accompanied by okadaic acids and/or yessotoxins and are co-extracted with them. So, initially, pectenotoxins have been grouped together with okadaic acids and yessotoxins in the DSP class. However, animal studies have indicated that pectenotoxins do not induce diarrhea and they are much less toxic than okadaic acid by oral administration [148]. In addition, unlike many DSPs which are potent phosphatase inhibitors, PTX-1 and PTX-6 are inactive against PP-1 and PP2A [149]. Thus, PTXs are currently considered as a separate group of toxins.

Since PTXs often co-occur with other phycotoxins in shellfish, no toxic episodes in humans can be unequivocally related to them, and therefore, there is no information about their toxicity to humans. It has been shown that PTXs are potently cytotoxic [150] and cause necrosis to hepatocytes [151]. Nothing is known of the chronic toxicology of PTXs or the potential implications to public health in the long term.

28.10 Saxitoxins: The First News We Have About Seafood Toxin-Related Human Poisoning

One of the first recorded fatal cases of human poisoning after eating shellfish contaminated with dinoflagellate toxins happened in 1793, when Captain George Vancouver and his crew landed in British Columbia in an area now known as Poison Cove [152]. He noted that for local Indian tribes, it was taboo to eat shellfish when seawater became phosphorescent due to dinoflagellate blooms. However, the link between toxic shellfish and dinoflagellates was only ascertained right before World War II, when Sommer et al. studied toxic outbreaks that occurred in the San Francisco Bay between 1920 and 1937 [153, 154].

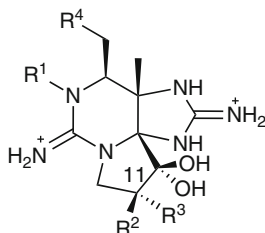
The causative toxins of these events are alkaloids, referred to as paralytic shellfish poisoning (PSP) toxins.

Historically, PSP incidents are associated with dinoflagellates, such as *Alexandrium* [155] – the first to be identified as PSP toxin producers – *Pyrodinium* and *Gymnodinium* species [156]. Besides, with developments in technology and research on marine algae, more species and classes of microorganism have been found to produce these toxins. Marine bacteria such as *Moraxella* [157] and *Alteromonas tetraodonis* [158] and freshwater cyanobacteria such as *Aphanizomenon flos-aquae*, *Anabaena circinalis*, *Lyngbya wollei*, *Cylindrospermopsis raciborskii* and *Protogonyaulax* [159] have all been found to produce or influence the production of these toxins in algae. Infection of *Ostreopsis lenticularis* by *Pseudomonas* species was also found to affect the production of toxins [160].

The parent compound of this class of toxins is saxitoxin (STX), of which over 29 congeners are currently known [161]. Chemically, they are tetrahydropurine derivatives whose structures vary by different combination of hydroxyl and sulfate substitutions at four sites on the molecule. Based on substitutions at R4, the saxitoxins can be subdivided into four groups: (1) the neurotoxic and highly potent carbamate toxins which include the nonsulfated saxitoxins (STX) and neosaxitoxin (NEO), and gonyautoxins (GTX1–GTX4) which are singly sulfated and more lethal than the nonsulfated carbamate toxins; (2) weakly toxic N-sulfocarbamoyl toxins (B1, B2, C1–C4) which are the least toxic to mammals of all the PSP toxins; (3) decarbamoyl (dc-) analogues which are thought to arise from the metabolism of dinoflagellate toxins within the shellfish; and (4) deoxydecarbamoyl (do-) toxins that have been detected until now only in Australian populations of *G. catenatum* [162] (Fig. 28.11).

Recently, the use of hydrophilic interaction liquid chromatography–mass spectrometry (HILIC–MS) followed by in-depth NMR investigation allowed to elucidate the structure of new analogues: 11 β -hydroxy-N-sulfocarbamoyl saxitoxin and the unusual 11,11-dihydroxy saxitoxin and 11,11-dihydroxy-N-sulfocarbamoyl saxitoxin [163, 164].

Saxitoxins are classified as fast-acting neurotoxins as PSP symptoms develop fairly rapidly, within 0.5–2 h after ingestion of contaminated shellfish, depending on the amount of toxin consumed [165]. In humans, the peripheral nervous system



STX = saxitoxin

NEO = neosaxitoxin

GTX = gonyautoxin

<u>R¹</u>	<u>R²</u>	<u>R³</u>	<u>R⁴</u>	Carbamate toxins —O—C(=O)—NH_2	N-Sulfocarbamoyl toxins $\text{—O—C(=O)—NH—SO}_3^-$	Decarbamoyl toxins —OH	Deoxydecarbamoyl toxins —H
H	H	H		STX	GTX5, B1	dcSTX	doSTX
OH	H	H		NEO	GTX6, B2	dcNEO	
H	H	OSO ₃ [−]		GTX2	C1	dcGTX2	doGTX2
H	OSO ₃ [−]	H		GTX3	C2	dcGTX3	doGTX3
OH	H	OSO ₃ [−]		GTX1	C3	dcGTX1	
OH	OSO ₃ [−]	H		GTX4	C4	dcGTX4	
H	H	OH		11αOH-STX		11αOH-dcSTX	
H	OH	H		11βOH-STX		11βOH-dcSTX	
OH	H	OH		11αOH-NEO		11αOH-dcNEO	
OH	OH	H		11βOH-NEO		11βOH-dcNEO	

Fig. 28.11 Structures of principal paralytic shellfish poisoning (PSP) toxins

is affected, with symptoms ranging from tingling of the tongue and lips, followed by a numbness spreading toward the extremities, to vomiting, pain, diarrhea, loss of coordination, and breathing difficulty. In severe cases, ataxia, muscle weakness, and respiratory paralysis can occur. Symptoms can turn into coma or death, but recovery is generally complete, with no lasting side effects, when respiratory support is provided within 12 h of exposure. In unusual cases, because of the weak hypotensive action of the toxins, death may occur from cardiovascular collapse despite respiratory support.

Saxitoxins are potent, reversible blockers of voltage-activated sodium channels on excitable cells [166], but, due to the differences in charge state and substitution groups to the basic STX structure, they bind with different affinities to site 1 of sodium channels, resulting in different toxicities [167]. Thus, health risks can be reliably assessed just if the level of each toxin is individually determined.

28.11 Yessotoxins: Potent Toxic Compounds with Controversial Impact on Public Health

Yessotoxins (YTXs) represent a class of lipophilic polyether compounds, including a number of analogues that have been detected in shellfish and/or phytoplankton.

The parent compound of this class of toxins is yessotoxin (YTX), isolated for the first time in 1986 from the scallops *Patinopecten yessoensis* that were implicated in a diarrhetic shellfish poisoning episode in Japan [168]. The first unicellular organism identified as a producer of YTX was the dinoflagellate *Protoceratium reticulatum* (Claparède and Lachmann) Bütschli 1885 [169]. Subsequently, YTX has been found in cells of *P. reticulatum* from different places in Japan [170–172]; in the Adriatic Sea in Italy [173]; in Nova Scotia, Canada [174]; in Norway [175]; and in Spain [176, 177]. Other confirmed producers of YTXs are the dinoflagellates *Lingulodinium polyedrum* (Stein) Dodge [177, 178], and *Gonyaulax spinifera* Dodge [179]. Some authors suggested that the real producers of YTXs are bacteria associated with the dinoflagellates; however, to our knowledge, there is no solid evidence for this [180].

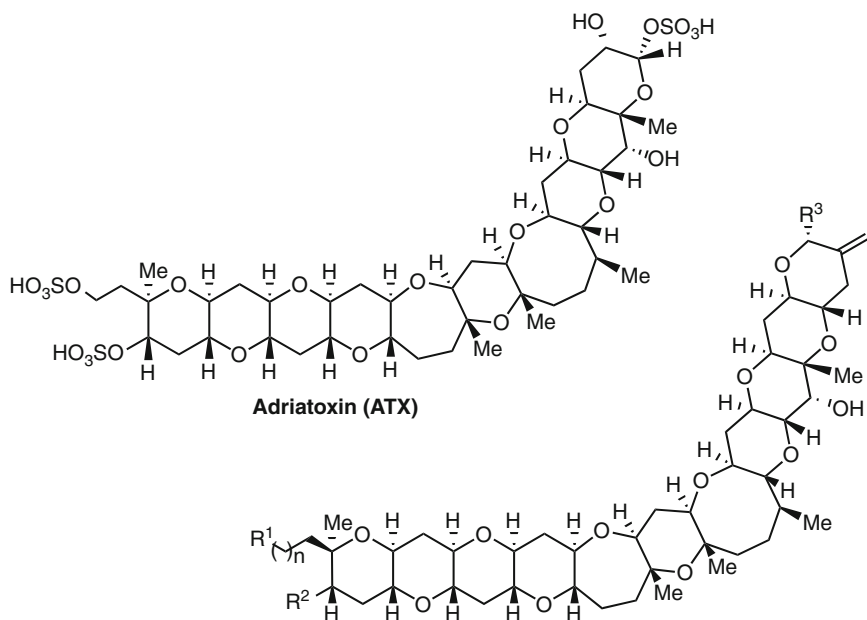
YTX production within and among dinoflagellate species tested to date is highly variable. As for the YTXs profile in the producing organisms, the data on the relative amounts are not so numerous, and all refer to cultures of *P. reticulatum*. The data reported in the literature concur that YTX is by far the major toxin produced by *P. reticulatum*. HomoYTX and a great number of other YTX analogues were sometimes shown to be present in the cultures, but in much lesser quantities [181]. There are, however, two reports in which the major toxin of *P. reticulatum* cultures is homoYTX [182, 183]. About the other two microalgae which were reported to produce YTXs, cultures of *Lingulodinium polyedrum* were shown to contain YTX [177], while *Gonyaulax spinifera* cultures were reported to produce unspecified YTXs identified by ELISA analyses [179].

Going to the contaminated shellfish, the YTX profile dramatically changes. YTX (or homoYTX) is no more the dominant toxin, but other analogues, such as hydroxylated and carboxylated derivatives, originating from metabolic oxidation within the mollusk, take the scene [181].

Chemically, yessotoxins are polycyclic ether compounds, structurally closely related to brevetoxins and ciguatoxins (Fig. 28.12).

The structure of YTX was established first [168, 184] and gave the basic framework to elucidate the structures of the other YTXs. It is a disulfated polyether, with a characteristic ladder shape formed by 11 adjacent ether rings of different sizes and a terminal acyclic unsaturated side chain consisting of nine carbons and two sulfate esters.

Since the initial discovery of YTX from Japanese scallops, a significant number of analogues, including the homoyessotoxins (homoYTXs), have been identified in toxic shellfish and/or algal cultures from different countries, suggesting the spread of this toxin worldwide [181]. Although the structure of some of them are still unknown [185], for many of them, full structure determination was carried out by NMR and/or liquid chromatography coupled with mass spectrometry (LC–MS).



	R ¹	R ²	R ³	n
Yessotoxin (YTX)	OSO ₃ H	OSO ₃ H		1
45-Hydroxyyessotoxin (45-hydroxyYTX)	OSO ₃ H	OSO ₃ H		1
45,46,47-Trinoryessotoxin (NorYTX)	OSO ₃ H	OSO ₃ H		1
Homoyessotoxin (homoYTX)	OSO ₃ H	OSO ₃ H		2
45-Hydroxyhomoyessotoxin (45-OHhomoYTX)	OSO ₃ H	OSO ₃ H		2
1-Desulfoyessotoxin (1-dsYTX)	OH	OSO ₃ H		1
Carboxyessotoxin (carboxyYTX)	OSO ₃ H	OSO ₃ H		1
Carboxyhomoyessotoxin(carboxyhomoYTX)	OSO ₃ H	OSO ₃ H		2

Fig. 28.12 (continued)

Noroxohomoyessotoxin (NoroxohomoYTX)	OSO ₃ H	OSO ₃ H		2
Noroxoyessotoxin (NoroxoYTX)	OSO ₃ H	OSO ₃ H		2
44,55-Dihydroxyessotoxin	OSO ₃ H	OSO ₃ H		1
1-Desulfocarboxyhomoyessotoxin	OH	OSO ₃ H		2
4-Desulfocarboxyhomoyessotoxin	OSO ₃ H	OH		2
45-Hydroxycarboxyessotoxin	OSO ₃ H	OSO ₃ H		1

Fig. 28.12 Structures of principal yessotoxins (YTXs)

There is evidence that some YTX analogues identified, such as hydroxylated and carboxylated derivatives, largely result from metabolism of yessotoxin in the shellfish after ingestion [186].

Yessotoxin and its analogues were at beginning included within the diarrhetic shellfish poisoning (DSP) group mainly because, following the standard procedure of mouse bioassay, they are extracted together with the DSP toxins okadaic acid (OA) and dinophysistoxins (DTXs), when they co-occur in contaminated shellfish. However, their toxic activities are significantly different; in fact, YTX and its analogues do not induce diarrhea and, compared to OA, show a much lower (four orders of magnitude) potency for the inhibition of protein phosphatase 2A [187]. On the contrary, their cardiotoxic effects have been demonstrated in mice after intra-peritoneal (i.p.) and oral exposure of very high doses of YTX [188]. For these reasons, YTXs are not anymore included in the list of DSP toxins.

The toxicological studies carried out on YTX revealed that it is more toxic than any DSP toxin, when intraperitoneally injected, since the dose inducing 50% of mice lethality is very low (100 µg/kg) [188]; on the contrary, its oral toxicity is weaker, as deduced by considering that the oral dose of 1 mg/kg – which is ten times the lethal dose by intraperitoneal injection – does not kill the mice [187, 189]. Thus, on account of their diverse relative harmfulness, the European Food Safety Authorities have established an allowance level for yessotoxin in shellfish which is almost tenfold as high as that set for DSP toxins (16 µg of okadaic acid and 100 µg of yessotoxin in 100 g of mollusk, respectively) [117]. Accordingly, the EU set up a new protocol of extraction capable of separating OAs and YTXs in lipophilic and hydrophilic layer, respectively [117], as already described in the okadaic acids section of this chapter. Nevertheless, the recent finding of desulfocarboxy-homoYTXs in Adriatic mussels [190] raises some additional concerns, due to the fact that these two new desulfoyessotoxins are unexpectedly recovered together

with OAs in the lipophilic layer, so that the purpose of the European new protocol fails. Hence, a further overhaul of the EU control procedure would be urgently needed.

The chemical structure of YTX resembles that of brevetoxins, which are known to interfere with the voltage-sensitive sodium channel [191]; this finding suggested a possible interaction between YTX and cellular ion channels. Recently, however, it has been observed that YTX does not interact with sodium channels nor induces any competitive displacement of brevetoxins from site 5 of sodium channels [192]. It has been proposed that YTX may interact with calcium channels inducing an uptake of calcium in human lymphocytes [193, 194].

Another molecular effect elicited by YTX is the disruption of the E-cadherin system in epithelial cells [195, 196]. Finally, studies on immune cells point to phosphodiesterases as an intracellular target for YTX [197].

Although no human intoxication is known to have been caused by consumption of shellfish contaminated by YTXs, the widespread occurrence of these compounds in shellfish, sometimes at high levels, arouses an increasing interest in studying YTX toxicity. Unfortunately, data on the toxicity by oral ingestion for most YTX analogues are lacking; this appears particularly critical for some compounds, such as desulfoYTXs, where the lack of a sulfate group decreases their hydrophilicity in comparison to YTXs. So the biomembranes permeability and, consequently, the toxicity level by oral ingestion could be greatly affected. An additional issue related to the presence of desulfoYTXs in contaminated shellfish comes from two toxicological studies. In 1990, Terao et al. [187] found that totally desulfated YTX, differently from YTX, did not affect the heart but caused severe fatty degeneration and intracellular necrosis in the liver and pancreas. Finally, a recent report [198] provided evidence that desulfated YTX interacts with transmembrane helix domains.

References

1. Hallegraeff GM (2005) Harmful algal blooms: a Global review. In: Hallegraeff GM, Anderson DM, Cembella AD (eds) Manual on harmful marine microalgae. UNESCO, Landais, pp 25–49
2. Van Dolah FM (2000) Diversity of marine and freshwater algal toxins. In: Botana LM (ed) Seafood and freshwater toxins – pharmacology, physiology, and detection. Marcel Dekker, New York, pp 19–43
3. Tibbetts J (1998) Toxic tides. *Environ Health Perspect* 106:A326–A331
4. Shumway SE (1990) A review of the effects of algal blooms on shellfish and aquaculture. *J World Aquacult Soc* 21:65–104
5. Ahmed FE (1991) Naturally occurring seafood toxins. *J Toxicol Toxin Rev* 10:263–287
6. Egmond HP, Van Apeldoorn ME, Speijers GJ (2004) Marine biotoxins. FAO Food and Nutrition Paper 80, Food and Agricultural Organization of the United Nations, Rome
7. FAO/IOC/WHO (2004) Report on the Joint FAO/IOC/WHO ad hoc expert consultation on biotoxins in bivalve molluscs, Oslo, 26–30 Sept 2004. <http://www.who.int/foodsafety/chem/meetings/biotoxin/en/index.html>

8. Aune T (2008) Risk assessment of marine toxins. In: Botana LM (ed) *Seafood and freshwater toxins – pharmacology, physiology, and detection*, 2nd edn. CRC Press/Taylor & Francis, Boca Raton, pp 3–20
9. Botana LM, Rodriguez-Vieytes M, Alfonso A et al (1996) Phycotoxins: paralytic shellfish poisoning and diarrhetic shellfish poisoning. In: Nolle LML (ed) *Handbook of food analysis – residues and other food component analysis*, vol 2. Marcel Dekker, New York, pp 1147–1169
10. Japanese Ministry of Health and Welfare (1981) Method of testing for diarrhetic shellfish toxin. *Food Sanit Res* 7:60–65
11. McMahon T, Silke J (1995) Winter toxicity of unknown aetiology in mussels. *Harmful Algae News* 14:2
12. Satake M, Ofuji K, Naoki H et al (1998) Azaspiracid, a new marine toxin having unique spiro ring assemblies isolated from Irish mussels *Mytilus edulis*. *J Am Chem Soc* 120:9967–9968
13. Ofuji K, Satake M, McMahon T et al (1999) Two analogs of azaspiracid isolated from mussels, *Mytilus edulis*, involved in human intoxication in Ireland. *Nat Toxins* 7:99–102
14. James KJ, Diaz Sierra M, Lehane M et al (2003) Detection of five new hydroxyl analogues of azaspiracids in shellfish using multiple tandem mass spectrometry. *Toxicon* 41:277–283
15. Rehmann N, Hess P, Quilliam MA (2008) Discovery of new analogs of the marine biotoxin azaspiracid in blue mussels (*Mytilus edulis*) by ultra-performance liquid chromatography/tandem mass spectrometry. *Rapid Commun Mass Spectrom* 22:549–558
16. Krock B, Tillmann U, John U et al (2009) Characterization of azaspiracids in plankton size-fractions and isolation of an azaspiracid-producing dinoflagellate from the North Sea. *Harmful Algae* 8:254–263
17. Tillmann U, Elbrachter M, Krock B et al (2009) *Azadinium spinosum* gen. et sp. nov (Dinophyceae) identified as a primary producer of azaspiracid toxins. *Eur J Phycol* 44:63–79
18. James KJ, Furey A, Lehane M et al (2002) First evidence of an extensive northern European distribution of azaspiracid poisoning (AZP) toxins in shellfish. *Toxicon* 40:909–915
19. Ito E (2008) Toxicology of azaspiracid-1: acute and chronic poisoning, tumorigenicity, and chemical structure relationship to toxicity in a mouse model. In: Botana LM (ed) *Seafood and freshwater toxins – pharmacology, physiology, and detection*, 2nd edn. CRC Press/Taylor & Francis, Boca Raton, pp 775–784
20. Ito E, Satake M, Ofuji K et al (2000) Multiple organ damage caused by a new toxin azaspiracid, isolated from mussels produced in Ireland. *Toxicon* 38:917–930
21. Ito E, Satake M, Ofuji K et al (2001) Chronic effects in mice caused by oral administration of sublethal doses of azaspiracid, a new marine toxin isolated from mussels. *Toxicon* 40:193–203
22. Roman Y, Alfonso A, Louzao MC et al (2002) Azaspiracid –1, a potent, nonapoptotic new phycotoxin with several cell targets. *Cell Signal* 14:703–716
23. Roman Y, Alfonso A, Vieytes MR et al (2004) Effects of azaspiracids 2 and 3 on intracellular cAMP, $[Ca^{2+}]$, and pH. *Chem Res Toxicol* 17:1338–1349
24. Davis C (1948) *Gymnodinium breve*: a cause of discoloured water and animal mortality in the Gulf of Mexico. *Bot Gaz* 109:358–360
25. Woodstock A (1948) Note concerning human respiratory irritation associated with high concentrations of plankton and mass mortality of marine organisms. *Mar Res* 7:56–62
26. Steidinger KA, Vargo GA, Tester PA et al (1998) Bloom dynamics and physiology of *Gymnodinium breve* with emphasis on the Gulf of Mexico. In: Anderson DM, Cembella AD, Hallegraeff GM (eds) *Physiological ecology of harmful algal blooms*, NATO-advanced study institute series. Springer, Berlin, pp 133–154
27. Haywood A, MacKenzie L, Garthwaite I et al (1996) *Gymnodinium breve* “look-alikes”: three *gymnodinium* isolates from New Zealand. In: Yasumoto T, Oshima Y, Fukuyo Y (eds) *Harmful and toxic algal blooms*. International Oceanographic Committee of UNESCO, Paris, pp 227–230

28. Baden DG, Mende TJ (1982) Toxicity of two toxins from the Florida red tide marine dinoflagellate, *Gymnodinium breve*. *Toxicon* 20:457–461
29. Poli M, Mende TJ, Baden DG (1986) Brevetoxins, unique activators of voltage-sensitive sodium channels bind to specific sites in rat brain synaptosomes. *Mol Pharmacol* 30:129–135
30. Baden D, Fleming LE, Bean JA (1995) Marine toxins. In: de Wolf FA (ed) *Handbook of clinical neurology: intoxications of the nervous system part H. Natural toxins and drugs*. Elsevier, Amsterdam, pp 141–175
31. Sagir Ahmed MD, Arakawa O, Onoue Y (1995) Toxicity of cultured *Chatonella marina*. In: Lassus P, Arzul G, Erhard E, Gentien P, Marcaillou C (eds) *Harmful marine algal blooms*. Lavoisier, Paris, pp 499–504
32. Khan S, Arakawa O, Onoue Y (1997) Neurotoxins in a toxic red tide of *Heterosigma akashiwo* (Raphidophyceae) in Kagoshima Bay. *Jpn Aquacul Res* 28:9–14
33. Hallegraeff GM, Munday BL, Baden DG et al (1998) *Chatonella marina* raphidophyte bloom associated with mortality of cultured bluefin tuna (*Thunnus maccoyii*) in South Australia. In: Reguera B, Blanco J, Ferandz ML, Wyatt T (eds) *Harmful algae*. Xunta de Galicia and IOC, Santiago de Compostela, Spain, pp 93–96
34. McFarren EF, Tanabe H, Silva FJ et al (1965) The occurrence of a ciguatera-like poison in oysters, clams, and *Gymnodinium breve* cultures. *Toxicon* 3:111–123
35. Risk M, Lin YY, Sadagopa Ramanujam VM et al (1979) High pressure liquid chromatographic separation of two major toxic compounds from *Gymnodinium breve* Davis. *J Chromatogr Sci* 17:400–405
36. Lin YY, Risk M, Ray SM et al (1981) Isolation and structure of brevetoxin B from the “red tide” dinoflagellate *Ptychodiscus brevis* (*Gymnodinium breve*). *J Am Chem Soc* 103:6773–6775
37. Shimizu Y, Chou HN, Bando H (1986) Structure of brevetoxin A (GB-1 toxin), the most potent toxin in the Florida red tide organism *Gymnodinium breve* (*Ptychodiscus brevis*). *J Am Chem Soc* 108:514–515
38. Baden DG (1989) Brevetoxins: unique polyether dinoflagellate toxins. *FASEB J* 3:1807–1819
39. Baden DG, Bourdelais AJ, Jacocks H et al (2005) Natural and derivative brevetoxins: historical background, multiplicity, and effects. *Environ Health Persp* 113:621–625
40. Prasad AVK, Shimizu Y (1989) The structure of hemibrevetoxin-B: a new type of toxin in the Gulf of Mexico red tide organism. *J Am Chem Soc* 111:6476–6477
41. Bourdelais AJ, Jacocks HM, Wright JL et al (2005) A new polyether ladder compound produced by the dinoflagellate *Karenia brevis*. *J Nat Prod* 68:2–6
42. Fuwa H, Ebine M, Bourdelais AJ et al (2006) Total synthesis, structure revision, and absolute configuration of (–)- brevenal. *J Am Chem Soc* 128:16989–16999
43. Rein KS, Baden DG, Gawley RE (1994) Conformational analysis of the sodium channel modulator, brevetoxin A, comparison with brevetoxin B conformations, and a hypothesis about the common pharmacophore of the “site” toxins. *J Org Chem* 59:2101–2106
44. Baden DG, Adams DJ (2000) Brevetoxins: chemistry, mechanism of action and methods of detection. In: Botana LM (ed) *Seafood and freshwater toxins – pharmacology, physiology, and detection*. Marcel Dekker, New York, pp 505–532
45. Kirkpatrick B, Fleming LE, Squicciarini D et al (2004) Literature review of Florida red tide: implications for human health effects. *Harmful algae* 3:99–115
46. Fleming LE, Backer LC, Baden DG (2005) Overview of aerolized Florida red tide toxins: exposures and effects. *Environ Health Persp* 113:618–620
47. Gessner BD, McLaughlin JB (2008) Epidemiologic impact of toxin episodes: neurotoxic toxins. In: Botana LM (ed) *Seafood and freshwater toxins – pharmacology, physiology, and detection*. Marcel Dekker, New York, pp 449–472
48. Yasumoto T (2005) Chemistry, etiology, and food chain dynamics of marine toxins. *Proc Japan Acad Ser B* 81:43–51

49. Lewis RJ (2006) Ciguatera: Australian perspectives on a global problem. *Toxicon* 48:799–809
50. Scheuer PJ, Takahashi W, Tsutsumi J et al (1967) Ciguatoxin: isolation and chemical nature. *Science* 155:1267–1268
51. Adachi R, Fukuyo Y (1978) The thecal structure of a marine toxic dinoflagellate *Gambierdiscus toxicus* gen. et sp. nov. collected in a ciguatera endemic area. *Bull Japan Soc Sci Fish* 45:67–71
52. Murata M, Legrand AM, Ishibashi Y et al (1989) Structures of ciguatoxin and its congener. *J Am Chem Soc* 111:8929–8931
53. Murata M, Legrand AM, Ishibashi Y et al (1990) Structures and configurations of ciguatoxin from the moray eel *Gymnothorax javanicus* and its likely precursor from the dinoflagellate *Gambierdiscus toxicus*. *J Am Chem Soc* 112:4380–4386
54. Satake M, Ishibashi Y, Legrand AM et al (1997) Isolation and structure of ciguatoxin-4A, a new ciguatoxin precursor, from cultures of dinoflagellate *Gambierdiscus toxicus* and parrotfish *Scarus gibbus*. *Biosci Biotechnol Biochem* 60:2103–2105
55. Vernoux JP, Lewis RJ (1997) Isolation and characterisation of Caribbean ciguatoxins from the horse-eye jack (*Caranx latus*). *Toxicon* 35:889–900
56. Lehane L (2000) Ciguatera update. *Med J Aust* 172:176–179
57. Lehane L, Lewis RJ (2000) Review ciguatera: recent advances but the risk remains. *Int J Food Microbiol* 61:91–125
58. Satake M, Murata M, Yasumoto T (1993) Gambierol: a new toxic polyether compound isolated from the marine dinoflagellate *Gambierdiscus toxicus*. *J Am Chem Soc* 115:361–362
59. Nagai H, Torigoe K, Satake M et al (1992) Gambieric acids: unprecedented potent antifungal substances isolated from cultures of a marine dinoflagellate *Gambierdiscus toxicus*. *J Am Chem Soc* 114:1102–1103
60. Satake M, Morohashi M, Oguri H et al (1997) The absolute configuration of ciguatoxin. *J Am Chem Soc* 119:11325–11326
61. Dickey RW (2008) Ciguatera toxins: chemistry, toxicology and detection. In: Botana LM (ed) *Seafood and freshwater toxins – pharmacology, physiology, and detection*, 2nd edn. CRC Press/Taylor & Francis, Boca Raton, pp 479–500
62. Lewis RJ, Molgo J, Adams DJ (2000) Pharmacology of toxins involved in ciguatera and related fish poisonings. In: Botana LM (ed) *Seafood and freshwater toxins – pharmacology, physiology, and detection*. Marcel Dekker, New York, pp 419–447
63. Mattei C, Dechraoui MY, Molgó J et al (1999) Neurotoxins targeting receptor site 5 of voltage-dependent sodium channels increase the nodal volume of myelinated axons. *J Neurosci Res* 55:666–673
64. Allsop JL, Martini L, Lebris H et al (1986) Neurologic manifestations of ciguatera. 3 cases with a neurophysiologic study and examination of one nerve biopsy. *Rev Neurol* 142:590–597
65. Holmes MJ, Lewis RJ (1994) Purification characterization of large and small maitotoxins from cultured *Gambierdiscus toxicus*. *Nat Toxins* 2:64–72
66. Estacion M (2000) Ciguatera toxins: mechanism of action and pharmacology of maitotoxin. In: Botana LM (ed) *Seafood and freshwater toxins – pharmacology, physiology, and detection*. Marcel Dekker, New York, pp 473–504
67. Seki T, Satake M, Mackenzie L et al (1995) Gymnodimine, a new marine toxin of unprecedented structure isolated from New Zealand oysters and the dinoflagellate *Gymnodinium* sp. *Tetrahedron Lett* 36:7093–7096
68. Uemura D, Chou T, Haino T et al (1995) Pinnatoxin A: a toxic amphoteric macrocycle from the Okinawan bivalve *Pinna muricata*. *J Am Chem Soc* 117:1155–1156
69. Torigoe K, Murata M, Yasumoto T et al (1988) Prorocentrolide, a toxic nitrogenous macrocycle from a marine dinoflagellate, *Prorocentrum lima*. *J Am Chem Soc* 110:7876–7877

70. Takada N, Umemura N, Suenaga K et al (2001) Structural determination of pteriatoxins A, B and C, extremely potent toxins from the bivalve *Pteria penguin*. *Tetrahedron Lett* 42:3495–3497
71. Hu T, Curtis JM, Oshima Y et al (1995) Spirolides B and D, two novel macrocycles isolated from the digestive glands of shellfish. *J Chem Soc Chem Commun* 20:2159–2161
72. Lu CK, Lee GH, Huang R et al (2000) Spiro-prorocentrimine, a novel macrocyclic lactone from a benthic *Prorocentrum* spp. of Taiwan. *Tetrahedron Lett* 42:1713–1716
73. Cembella A, Krock B (2008) Cyclic imine toxins: chemistry, biogeography, biosynthesis, and pharmacology. In: Botana LM (ed) *Seafood and freshwater toxins – pharmacology, physiology, and detection*, 2nd edn. CRC Press/Taylor & Francis, Boca Raton, pp 561–580
74. MacKinnon SL, Cembella AD, Burton IW et al (2006) Biosynthesis of 13-desmethyl spirolide C by the dinoflagellate *Alexandrium ostenfeldii*. *J Org Chem* 71:8724–8731
75. Miles CO, Wilkins AL, Stirling DJ et al (2003) Gymnodimine C, an isomer of gymnodimine B, from *Karenia selliformis*. *J Agric Food Chem* 51:4838–4840
76. Cembella AD, Lewis NI, Quilliam MA (2000) The marine dinoflagellate *Alexandrium ostenfeldii* (Dinophyceae) as the causative organism of spirolide shellfish toxins. *Phycologia* 39:67–74
77. Cembella AD, Lewis NI, Quilliam MA (1999) Spirolide composition of micro-extracted pooled cells isolated from natural plankton assemblages and from cultures of the dinoflagellate *Alexandrium ostenfeldii*. *Nat Toxins* 7:197–206
78. Ciminiello P, Dell'Aversano C, Fattorusso E et al (2007) Spirolide toxin profile of Adriatic *Alexandrium ostenfeldii* and structure elucidation of 27-hydroxy-13,19-didesmethyl spirolide C. *J Nat Prod* 70:1878–1883
79. Mackenzie L, White D, Oshima Y, Kapa J (1996) The resting cyst of *Alexandrium ostenfeldii* (Dinophyceae) in New Zealand. *Phycologia* 35:148–155
80. Hu T, Curtis JM, Walter JA et al (1996) Characterization of biologically inactive spirolides E and F: identification of the spirolide pharmacophore. *Tetrahedron Lett* 37:7671–7674
81. Gill S, Murphy M, Clausen J et al (2003) Neural injury biomarkers of novel shellfish toxins. Spirolides: a pilot study using immunochemical and transcriptional analysis. *Neurotoxicology* 24:593–604
82. Perl TM, Bedard L, Remis RS et al (1987) Intoxication following mussel ingestion in Montreal. *Can Dis Weekly Rep* 13–49:224–225
83. Teitelbaum JS, Zatorre RJ, Carpenter S et al (1990) Neurologic sequelae of domoic acid intoxication due to the ingestion of contaminated mussels. *N Engl J med* 322:1781–1787
84. Wright JLC, Boyd RK, DeFreitas ASW et al (1989) Identification of domoic acid, a neuroexcitatory amino acid, in toxic mussels from eastern Prince Edward Island. *Can J Chem* 67:481–490
85. Perl TM, Bedard L, Kosatsky T et al (1990) An outbreak of toxic encephalopathy caused by eating mussels contaminated with domoic acid. *N Engl J Med* 322:1775–1780
86. Takemoto T, Daigo K (1958) Constituents of *Chondria armata*. *Chem Pharm Bull* 6:578–580
87. Subba Rao DV, Quilliam MA, Pocklington R (1988) Domoic acid – a neurotoxic amino acid produced by the marine diatom *Nitzschia pungens* in culture. *Can J Fish Aquat Sci* 45:2076–2079
88. Bates SS, Bird CJ, deFreitas ASW et al (1989) Pennate diatom *nitzschia pungens* as the primary source of domoic acid, a toxin in shellfish from eastern prince Edward island, Canada. *Can J Fish Aquat Sci* 46:1203–1215
89. Garrison DL, Conrad SM, Eilers PP et al (1992) Confirmation of domoic acid production by *pseudo-nitzschia australis* (bacillariophyceae) cultures. *J Phycol* 28:604–607
90. Martin JL, Haya K, Burrige LE et al (1990) *Nitzschia pseudodelicatissima* – a source of domoic acid in the Bay of Fundy, eastern Canada. *Marine Ecol Progr Ser* 67:177–182
91. Cerino F, Orsini L, Sarno D et al (2005) The alternation of different morphotypes in the seasonal cycle of the toxic diatom *pseudo-nitzschia galaxiae*. *Harmful Algae* 4:33–48

92. Wekell J, Gauglitz EJ, Barnett H et al (1994) Occurrence of domoic acid in Washington state razor clams (*siliqua patula*) during 1991–1993. *Nat Toxins* 2:197–205
93. Vale P, Sampayo MAM (2001) Domoic acid in Portuguese shellfish and fish. *Toxicon* 39:893–904
94. James KJ, Gillman M, Amandi MF et al (2005) Amnesic shellfish poisoning toxins in bivalve molluscs in Ireland. *Toxicon* 46:852–858
95. Bates SS, Trainer VL (2006) The ecology of harmful diatoms. In: Graneli E, Turner JT (eds) *Ecology of harmful algae, ecological studies*, vol 189. Springer, Berlin, pp 81–94
96. Scholin CA, Gulland F, Doucette GJ et al (2000) Mortality of sea lions along the central California coast linked to a toxic diatom bloom. *Nature* 403:80–84
97. Takemoto T, Diago K (1958) Constituents of *chondria armata*. *Chem Pharm Bull* 6:578–580
98. Daigo K (1959) Studies on the constituents of *chondria armata*. II: detection of the anthelmintic constituents & II: isolation of an anthelmintic constituent. *Yakugaku Zasshi (J Pharm Soc Japan)* 79:350–356
99. Takemoto T, Daigo K, Kondo Y, Kondo K (1966) Studies on the constituents of *chondria armata*: on the structure of domoic acid. *Yakugaku Zasshi* 86:874–877
100. Ohfuné Y, Tomita M (1982) Total synthesis of (–)-domoic acid – a revision of the original structure. *J Am Chem Soc* 104:3511–3513
101. Wright JLC, Falk M, McInnes AG et al (1990) Identification of isodomoic acid D and two new geometrical isomers of domoic acid in toxic mussels. *Can J Chem* 68:22–25
102. Walter JA, Falk M, Wright JLC (1994) Chemistry of the shellfish toxin domoic acid: characterization of related compounds. *Can J Chem* 72:430–436
103. Hampson DR, Huang X, Wells JW et al (1992) Interaction of domoic acid and several derivatives with kainic acid and AMPA binding sites in rat brain. *Eur J Pharmacol* 218:1–8
104. Xi D, Ramsdell JS (1996) Glutamate receptors and calcium entry mechanisms for domoic acid in hippocampal neurons. *Neuroreport* 7:1115–1120
105. Peng YG, Ramsdell JS (1996) Brain fos induction is a sensitive biomarker for the lowest observed neuroexcitatory effects of domoic acid. *Fundam Appl Toxicol* 31:162–168
106. Yasumoto T, Oshima Y, Yamaguchi M (1978) Occurrence of a new type of shellfish poisoning in the Tohoku district. *Nippon Suisan Gakkaishi* 44:1249–1255
107. Yasumoto T, Murata M (1993) Marine toxins. *Chem Rev* 93:1897–1909
108. Hu T, Doyle J, Jackson D et al (1992) Isolation of a new diarrhetic shellfish poison from Irish mussels. *J Chem Soc Chem Commun* 30:39–41
109. Cembella A (1989) Occurrence of okadaic acid, a major diarrhetic shellfish toxin, in natural populations of *dinophysis* spp. From the eastern coast of north America. *J Appl Phycol* 1:307–310
110. Dickey RW, Bobzin SC, Faulkner DJ et al (1990) Identification of okadaic acid from a Caribbean dinoflagellate, *prorocentrum concavum*. *Toxicon* 28:371–377
111. Rhodes LL, Syhre M (1995) Okadaic acid production by a New Zealand *prorocentrum lima* isolate. *New Zealand J Mar Freshwat Res* 29:367–370
112. Bravo I, Fernandez ML, Ramilo I et al (2001) Toxin composition of the toxic dinoflagellate *prorocentrum lima* isolated from different locations along the Galician coast (NW Spain). *Toxicon* 39:1537–1545
113. Lee JS, Igarashi T, Fraga S et al (1989) Determination of diarrhetic shellfish toxins in various dinoflagellate species. *J Appl Phycol* 1:147–152
114. Vale C, Botana LM (2008) Marine toxins and the cytoskeleton: okadaic acid and dinophysistoxins. *FEBS J* 275:6060–6066
115. Cohen P, Holmes CFB, Tsukitani Y (1990) Okadaic acid: a new probe for the study of cellular regulation. *Trends Biochem Sci* 15:98–102
116. Suganuma M, Fujiki H, Suguri H et al (1988) Okadaic acid – an additional non-phorbol-12-tetradecanoate-13-acetate-type tumor promoter. *Proc Natl Acad Sci USA* 85:1768–1771
117. Directive of the European Commission 2002/225/EC and “decreto del Ministero della Salute-16/05/2002

118. Malo D (1951) Hawaiian antiquities, 2nd edn. Bishop Museum, Honolulu, pp 201–226
119. Moore RE, Scheuer PJ (1971) Palytoxin: a new marine toxin from a coelenterate. *Science* 172:495–498
120. Walsh GE, Bowers RE (1971) A review of Hawaiian zoanthids with description of three new species. *Zool J Linn Soc* 50:161–180
121. Moore RE, Bartolini G (1981) Structure of palytoxin. *J Am Chem Soc* 103:2491–2494
122. Uemura D, Ueda K, Hirata Y et al (1981) Further studies on palytoxin. II. Structure of palytoxin. *Tetrahedron Lett* 22:2781–2784
123. Cha JK, Christ WJ, Finan JM et al (1982) Stereochemistry of palytoxin. Part 4. Complete structure. *J Am Chem Soc* 104:7369–7371
124. Armstrong RW, Beau JM, Cheon SH et al (1989) Total synthesis of palytoxin carboxylic acid and palytoxin amide. *J Am Chem Soc* 111:7530–7533
125. Uemura D, Hirata Y, Iwashita T et al (1985) Studies on palytoxins. *Tetrahedron* 41:1007–1017
126. Ciminiello P, Dell'Aversano C, Dello Iacovo E et al (2009) Stereostructure and biological activity of 42-hydroxy-palytoxin: a new palytoxin analogue from Hawaiian *palythoa* subspecies. *Chem Res Toxicol* 22:1851–1859
127. Usami M, Satake M, Ishida S et al (1995) Palytoxin analogs from the dinoflagellate *ostreopsis siamensis*. *J Am Chem Soc* 117:5389–5390
128. Taniyama S, Osamu A, Masamitsu T, Sachio N, Tomohiro T, Yahia M, Tamao N (2003) *Ostreopsis* sp., a possible origin of palytoxin (PTX) in parrotfish *scarus oviifrons*. *Toxicon* 42:29–33
129. Ukena T, Satake M, Usami M et al (2001) Structure elucidation of ostreocin D, a palytoxin analog isolated from the dinoflagellate *ostreopsis siamensis*. *Biosci Biotechnol Biochem* 65:2585–2588
130. Ukena T, Satake M, Usami M et al (2002) Structural confirmation of ostreocin-D by application of negative-ion fast-atom bombardment collision-induced dissociation tandem mass spectrometric methods. *Rapid Commun Mass Spectrom* 16:2387–2393
131. Lenoir S, Ten-Hage L, Turquet J et al (2004) First evidence of palytoxin analogues from an *ostreopsis mascarenensis* (dinophyceae) benthic bloom in southwestern Indian ocean. *J Phycol* 40:1042–1051
132. Ciminiello P, Dell'Aversano C, Fattorusso E et al (2006) The Genoa 2005 outbreak. Determination of putative palytoxin in Mediterranean *Ostreopsis ovata* by a new liquid chromatography tandem mass spectrometry method. *Anal Chem* 78:6153–6159
133. Ciminiello P, Dell'Aversano C, Fattorusso E et al (2008) Putative palytoxin and its new analogue, ovatoxin-a, in *ostreopsis ovata* collected along the ligurian coasts during the 2006 toxic outbreak. *J Am Soc Mass Spectrom* 19:111–120
134. Ciminiello P, Dell'Aversano C, Dello Iacovo E et al (2010) Complex palytoxin-like profile of *ostreopsis ovata*. Identification of four new ovatoxins by high resolution LC-MS. *Rapid Commun Mass Spectrom* 24:2735–2744
135. Vale C (2008) Palytoxins: pharmacology and biological detection methods. In: Botana LM (ed) *Seafood and freshwater toxins – pharmacology, physiology, and detection*, 2nd edn. CRC Press/Taylor and Francis, Boca Raton, pp 675–691
136. Deeds JR, Schwartz MD (2010) Human risk associated with palytoxin exposure. *Toxicon* 56:150–162
137. Aligizaki K, Katikou P, Milandri A et al (2010) Occurrence of palytoxin-group toxins in seafood and future strategies to complement the present state of art. *Toxicon*. doi:10.1016/j.toxicon.2010.11.014
138. Alcalá AC, Alcalá LC, Garth JS et al (1988) Human fatality due to ingestion of the crab *demania reynaudii* that contained a palytoxin-like toxin. *Toxicon* 26:105–107
139. Noguchi T, Hwang DF, Arakawa G et al (1987) Palytoxin as the causative agent in the parrotfish poisoning. In: Gopalakrishnakone P, Tan CK (eds) *Progress in venom and toxin research*. National University, Singapore, pp 325–335

140. Onuma Y, Satake M, Ukena T et al (1999) Identification of putative palytoxin as the cause of clupeotoxism. *Toxicon* 37:55–65
141. Wiles JS, Vick JA, Christensen MK (1974) Toxicological evaluation of palytoxin in several animal species. *Toxicon* 12:427–433
142. Vick JA, Wiles JS (1975) The mechanism of action and treatment of palytoxin poisoning. *Toxicol Appl Pharmacol* 34:214–223
143. Wattemberg EV (2007) Palytoxin: exploiting a novel skin tumor promoter to explore signal transduction and carcinogenesis. *Am J Physiol Cell Physiol* 292:C24–C32
144. Wattemberg EV, Uemura D, Byron KL et al (1989) Structure-activity studies of the norphorbol tumor promoter palytoxin in carcinogenesis. *Cancer Res* 49:5837–5842
145. Fujiki H, Suganuma M, Nakayasu M et al (1986) Palytoxin is a non-12-O-tetradecanoylphorbol-13-acetate type tumor promoter in two-stage mouse skin carcinogenesis. *Carcinogenesis* 7:707–710
146. Suzuki T (2008) Chemistry, metabolism and chemical detection methods of pectenotoxins. In: Botana LM (ed) *Seafood and freshwater toxins – pharmacology, physiology, and detection*, 2nd edn. CRC Press/Taylor and Francis, Boca Raton, pp 343–359
147. Yasumoto T, Murata M, Lee JS et al (1989) Polyether toxins produced by dinoflagellates. In: Natori S, Hashimoto K, Ueno Y (eds) *Mycotoxins and phycotoxins*. Elsevier, Amsterdam, pp 375–382
148. Gonzalez JC, Leira F, Fontal OI et al (2002) Inter-laboratory validation of the fluorescent protein phosphatase inhibition assay to determine diarrhetic shellfish toxins: intercomparison with liquid chromatography and mouse bioassay. *Anal Chim Acta* 466:233–246
149. Lun HA, Chen DZ, Magoon J et al (1993) Quantification of diarrhetic shellfish toxins by identification of novel protein phosphatase inhibitors in marine phytoplankton and mussels. *Toxicon* 31:75–83
150. Jung JH, Sim CJ, Lee CO (1995) Cytotoxic compounds from a two-sponge association. *J Nat Prod* 58:1722–1726
151. Ishige M, Satoh N, Yasumoto T (1988) Pathological studies on the mice administered with the causative agent of diarrhetic shellfish poisoning (okadaic acid and pectenotoxin-2). *Bull Hokkaido Inst Public Health* 38:15–19
152. Dale B, Yentsch CM (1978) Red tide and paralytic shellfish poisoning. *Oceans* 21:41–49
153. Sommer H, Meyer KF (1937) Paralytic shellfish poisoning. *AMA Arch Pathol* 24:560–598
154. Sommer H, Whedon WF, Kofoed A et al (1937) Relation of paralytic shellfish poison to certain plankton organisms of the genus *Gonyaulax*. *AMA Arch Pathol* 24:537–559
155. Schantz EJ (1986) Chemistry and biology of saxitoxins and related toxins. *Ann NY Acad Sci* 479:15–23
156. Kodama M (2000) Ecobiology, classification and origin. In: Botana LM (ed) *Seafood and freshwater toxins – pharmacology, physiology, and detection*. Marcel Dekker, New York, pp 125–149
157. Kodama M (1990) Possible link between bacteria and toxin production in algal blooms. In: Graneli E, Sundstrom B, Edler L et al (eds) *Toxic marine phytoplankton*. Elsevier, Amsterdam, pp 52–62
158. Gallacher S, Birkbeck TH (1995) Isolation of marine bacteria producing sodium channel blocking toxins and the seasonal variation in their frequency in sea water. In: *Harmful marine algal blooms*. Intercept, Nantes
159. Sivonen K (2000) Freshwater cyanobacterial neurotoxins: ecobiology, chemistry, and detection. In: Botana LM (ed) *Seafood and freshwater toxins – pharmacology, physiology, and detection*. Marcel Dekker, New York, pp 567–581
160. Gonzalez L, Tosteson CG, Hensley V et al (1995) Associated bacteria and toxicity development in cultured *Ostreopsis lenticularis*. In: Lassus P, Arzul G, Denn EE et al (eds) *Harmful marine algal blooms, proceedings of the sixth international conference on toxic marine phytoplankton*, October 1993, Nantes. Lavoisier, Intercept, Paris, pp 415–456

161. Shimizu Y (2000) Chemistry and mechanism of action. In: Botana LM (ed) Seafood and freshwater toxins – pharmacology, physiology, and detection. Marcel Dekker, New York, pp 151–172
162. Oshima Y, Itakura H, Lee KC et al (1993) Toxin production by the dinoflagellate *gymnodinium catenatum*. Develop Marine Biol 3:907–912
163. Dell'Aversano C, Hess P, Quilliam MA (2005) Hydrophilic interaction liquid chromatography-mass spectrometry for the analysis of paralytic shellfish poisoning toxins. J Chromatogr A 1081:190–201
164. Dell'Aversano C, Walter JA, Burton IW et al (2008) Isolation and structure elucidation of new and unusual saxitoxin analogues from mussels. J Nat Prod 71:1518–1523
165. Hall S, Strichartz G, Moczydowski E et al (1990) The saxitoxins: sources, chemistry, and pharmacology. In: Hall S, Strichartz G (eds) Marine toxins: origin, structure and molecular pharmacology. American Chemical Society, Washington, DC, pp 29–65
166. Narahashi T (1972) Mechanism of action of tetrodotoxin and saxitoxin on excitable membranes. Fed Proc 31:1124–1132
167. Genenah AA, Shimizu Y (1981) Specific toxicity of paralytic shellfish poisons. J Agric Food Chem 29:1289–1291
168. Murata M, Kumagai M, Lee JS et al (1987) Isolation and structure of yessotoxin, a novel polyether compound implicated in diarrhetic shellfish poisoning. Tetrahedron Lett 28:5869–5872
169. Satake M, MacKenzie L, Yasumoto T (1997) Identification of *protoceratium reticulatum* as the biogenetic origin of yessotoxin. Nat Toxins 5:164–167
170. Eiki K, Satake M, Koike K et al (2005) Confirmation of yessotoxin production by the dinoflagellate *protoceratium reticulatum* in Mutsu Bay. Fish Sci 71:633–638
171. Suzuki T, Satake M, Yoshimatsu S et al (2007) Yessotoxin analogues in several strains of *protoceratium reticulatum* in Japan determined by liquid chromatography-hybrid triple quadrupole/linear ion trap mass spectrometry. J Chromatogr A 1142:172–177
172. Satake M, Ichimura T, Sekiguchi K et al (1999) Confirmation of yessotoxin and 45,46,47-trinoryessotoxin production by *protoceratium reticulatum* collected in Japan. Nat Toxins 7:147–150
173. Ciminiello P, Dell'Aversano C, Fattorusso E et al (2003) Complex yessotoxins profile in *protoceratium reticulatum* from northwestern Adriatic sea revealed by LC–MS analysis. Toxicon 42:7–14
174. Stobo LA, Lewis J, Quilliam MA et al (2003) Detection of yessotoxin in UK and Canadian isolates of phytoplankton and optimization and validation of LC-MS methods. In: Bates S (ed) Eighth Canadian workshop on harmful marine algae. Gulf Fisheries Centre, Moncton, New Brunswick, pp 8–14
175. Samdal IA, Naustvoll LJ, Olseng CD et al (2004) Use of ELISA to identify *protoceratium reticulatum* as a source of yessotoxin in Norway. Toxicon 44:75–82
176. Paz B, Riobó P, Ramilo I, Franco JM (2007) Yessotoxins profile in strains of *protoceratium reticulatum* from Spain and USA. Toxicon 50:1–17
177. Paz B, Riobó P, Fernandez ML et al (2004) Production and release of yessotoxins by the dinoflagellates *protoceratium reticulatum* and *lingulodinium polyedrum* in culture. Toxicon 44:251–258
178. Tubaro A, Sidari L, Della Loggia R et al (1998) Occurrence of homoyessotoxin in phytoplankton and mussels from northern Adriatic Sea. In: Reguera B, Blanco J, Fernandez ML, Wyatt T (eds) Harmful algae. Xunta de Galicia and Intergovernmental Oceanographic Commission of UNESCO, Grafisant, Santiago de Compostela, pp 470–472
179. Rhodes L, McNabb P, deSalas M et al (2006) Yessotoxin production by *gonyaulax spinifera*. Harmful Algae 5:148–155
180. Paz B, Daranas AH, Norte M, Riobó P, Franco JM, Fernández JJ (2008) Yessotoxins, a group of marine polyether toxins: an overview. Mar Drugs 6:73–102

181. Ciminiello P, Fattorusso E (2008) Yessotoxins: chemistry, metabolism and chemical analysis. In: Botana LM (ed) *Seafood and freshwater toxins – pharmacology, physiology, and detection*, 2nd edn. CRC Press/Taylor and Francis, Boca Raton, pp 287–314
182. Konishi M, Yang X, Li B et al (2004) Highly cytotoxic metabolites from the culture supernatant of the temperate dinoflagellate *protoceratium* cf. *Reticulatum*. *J Nat Prod* 67:1309–1313
183. Suzuki T, Horie Y, Koike K et al (2007) Yessotoxin analogues in several strains of *protoceratium reticulatum* in Japan determined by liquid chromatography-hybrid triple quadrupole/linear ion trap mass spectrometry. *J Chromatogr A* 1142:172–177
184. Takahashi H, Kusumi T, Kan Y (1996) Determination of the relative and absolute configuration of yessotoxin, a polyether compound implicated in diarrhetic shellfish poisoning, and its analogs. In: Tennen Yuki Kagobutsu Toronkai Koen Yoshishu, Faculty of Agriculture, Tohoku University, Tohoku, 38, 475–480
185. Miles CO, Samdal IA, Aasen JAG et al (2005) Evidence of numerous analogs of yessotoxin in *protoceratium reticulatum*. *Harmful Algae* 4:1075–1091
186. Aasen J, Samdal IA, Miles CO et al (2005) Yessotoxins in Norwegian blue mussels (*mytilus edulis*): uptake from *protoceratium reticulatum*, metabolism and depuration. *Toxicon* 45:265–272
187. Terao K, Ito E, Oarada M et al (1990) Histopathological studies on experimental marine toxin poisoning: 5. The effects in mice of yessotoxin isolated from *Patinopecten yessoensis* and of a desulfated derivative. *Toxicon* 28:1095–1104
188. van Egmond HP, Aune T, Lassus P et al (1993) Paralytic and diarrhetic shellfish poisons: occurrence in Europe, toxicity, analysis and regulation. *J Nat Toxins* 2:41–83
189. Ogino H, Kumagai M, Yasumoto T (1997) Toxicologic evaluation of yessotoxin. *Nat Toxins* 5:255–259
190. Ciminiello P, Dell'Aversano C, Fattorusso E et al (2007) Novel desulfoyessotoxins from Adriatic mussels. A new problem for the seafood safety control. *Chem Res Toxicol* 20:95–98
191. Huang JM, Wu CH, Baden DG (1984) Depolarizing action of a red-tide dinoflagellate brevetoxin on axonal membranes. *J Pharmacol Exp Ther* 229:615–621
192. Inoue M, Dirama M, Satake M et al (2003) Inhibition of brevetoxins binding to voltage-gated sodium channel by gambierol and gambieric acid-A. *Toxicon* 41:469–474
193. de la Rosa LA, Alfonso A, Vilarino N et al (2001) Modulation of cytosolic calcium levels of human lymphocytes by yessotoxin, a novel marine phycotoxin. *Biochem Pharmacol* 61:827–833
194. de la Rosa LA, Alfonso A, Vilarino N et al (2001) Maitotoxin-induced calcium entry in human lymphocytes: modulation by yessotoxin, Ca^{2+} channel blockers and kinases. *Cell Signal* 13:711–716
195. Ronzitti G, Callegari F, Malaguti C et al (2004) Selective disruption of the E-cadherin-catenin system by an algal toxin. *Br J Cancer* 90:1100–1107
196. Callegari F, Rossini GP (2008) Yessotoxin inhibits the complete degradation of E-cadherin. *Toxicology* 244:133–144
197. Alfonso A, de la Rosa LA, Vieytes MR et al (2003) Yessotoxin a novel phycotoxin, activates phosphodiesterases activity. Effect of yessotoxin on cAMP levels in human lymphocytes. *Biochem Pharmacol* 65:193–208
198. Mori M, Oishi T, Matsuoka S et al (2005) Ladder-shaped polyether compound, desulfated yessotoxin, interacts with membrane-integral α -helix peptides. *Bioorg Med Chem* 13:5099–5103

Hiroshi Nagai

Contents

29.1	Introduction	1390
29.2	Protein Toxins of Fish	1391
29.3	Protein Toxins of Jellyfish	1395
29.4	Protein Toxins of Sea Anemones	1401
29.5	Protein Toxins of Fire Coral	1406
29.6	Protein Toxins of Hydra	1407
29.7	Protein Toxins of Starfish	1409
29.8	Protein Toxins of Sea Urchin	1412
29.9	Protein Toxin of Cephalopods	1412
29.10	Concluding Remarks	1413
29.11	Study Questions	1413
	References	1414

Abstract

Many marine animals produce protein toxins that are used for both predation and protection from predators. It is known that venomous stings by specific fish and jellyfish are sometimes fatal. For many years, detailed characterization of the causative toxins has been hampered by their instability. In recent years, various protein toxins have been successfully isolated and characterized from marine venomous animals. These studies have revealed that marine protein toxins exhibit unique structures and biological activities. A novel protein toxin family from the box jellyfish, the membrane-attack complex/perforin (MACPF) protein toxins isolated from the sea anemone, DNase II toxins from the starfish, and

H. Nagai

Department of Ocean Science, Tokyo University of Marine Science and Technology, 4-5-7

Konan, Minato-ku, Tokyo, Japan

e-mail: nagai@kaiyodai.ac.jp

a dermatopontin family toxin from fire coral are representatives of some of these unique toxins. In this chapter, the most current studies on protein toxins isolated from marine venomous animals are discussed.

29.1 Introduction

Numerous marine animals produce protein toxins that are used for both predation and protection from predators. Toxic proteins that cause severe illness or injury to humans by accidental contact are produced by marine venomous animals. Many species of fish, sea urchins, starfish, sea anemones, and jellyfish are often categorized as venomous marine animals. For example, the stonefish, Portuguese man-of-war, and *Chironex* jellyfish are famous for their painful stinging ability that may even result in human fatality.

Protein toxins produced by venomous marine animals have been extensively investigated for over 100 years. For example, Richet first examined the proteinaceous venom produced by the sea anemone *Anemonia sulcata*. In this study, dogs were intravenously injected with a small amount of venom before receiving a second dose 2–3 weeks later. The dogs immediately developed intense vomiting, pruritus, respiration difficulties, foaming at the mouth, bloody diarrhea, and died within a few hours. This hypersensitivity phenomenon was termed anaphylaxis [1]. Richet was later awarded a Nobel Prize for his investigations into anaphylaxis and its symptoms. Many studies of the protein toxins produced by jellyfish and sea anemones have subsequently been conducted. However, the precise characterization of these protein toxins remains incomplete. Interestingly, the vast majority of proteinaceous toxins synthesized by marine venomous animals are quite unstable, and thus, the isolation of these toxins in their active forms is often very difficult. In fact, this instability is the major reason why most proteinaceous marine toxins have not been precisely characterized to date.

Peptides and proteins are often categorized together as polypeptides. However, in this chapter, we have divided the overall polypeptide group into a peptide group that includes small polypeptides with a molecular weight (MW) of less than 10,000 and a protein group comprised of large polypeptides with a MW of greater than 10,000. Peptide toxins produced by venomous marine animals have been investigated since the 1970s. These smaller peptide toxins are generally more stable than protein toxins to purification, thus making them more accessible than protein toxins. Given this increased stability, a number of peptide toxins synthesized by sea anemones and cone shells have been isolated and characterized with high precision. For the interested reader, several published reviews provide a more detailed description of the peptide toxins of marine venomous animals [2, 3].

Recently, several protein toxins have been successfully isolated and characterized from venomous marine animals. These studies have revealed that protein toxins exhibit a unique structure and mode of action. In this chapter, some of the most current studies on protein toxins isolated from venomous marine animals will be discussed.

29.2 Protein Toxins of Fish

A number of fish species including stonefish, scorpion fish, striped eel catfish, weever fish, rabbitfish, and the stingray are known to generate proteinaceous toxins. All of these fish species use their protein toxins as defensive tools against predators. The venom apparatus of venomous fishes are generally located along either their spines or fins. Among the venomous fish described to date, stonefish are commonly regarded as the most dangerous fish worldwide. Stonefish are distributed throughout the tropical and subtropical oceans of the world. A sting from the spine of a stonefish causes excruciating pain, massive local edema, and necrosis of affected tissues. Such a sting is often fatal to humans [4]. The stonefish toxin was isolated and characterized by a research group in Singapore in 1996 [5]. However, from the initial report on the stonefish toxin in 1965 [6], three decades passed before it was fully characterized. The toxin, stonustoxin (SNTX, 148 kDa), was isolated from the stonefish species *Synanceia horrida* and is comprised of two subunits termed α (71 kDa, 702 amino acid residues) and β (79 kDa, 699 amino acid residues) (Fig. 29.1) [5]. The cDNA clone encoding SNTX was isolated and sequenced from a venom gland cDNA library and was shown to contain a B30.2 domain in the molecule. The B30.2 domain is thought to function as a protein–protein interacting module [7]. Thus, the molecular target of SNTX may be a specific protein encoded by a victim stung by *S. horrida*. The amino acid sequences of the α -subunit and β -subunit of SNTX revealed 50% homology with each other. SNTX is lethal to mice ($LD_{50} = 17 \mu\text{g/kg}$) when injected intravenously. SNTX also possesses edema-inducing, vascular permeability-increasing, hemolytic, and hypotensive activity. Many of the symptoms experienced by those injected with the venom of *S. horrida* are in accordance with SNTX activity, and therefore, SNTX most likely represents the major active toxin in *S. horrida* venom. Using cDNA cloning experiments, a French research group subsequently elucidated the complete amino acid sequence of the β -subunit (79 kDa, 708 amino acid residues) of verrucotoxin (VTX) isolated from the venom of *Synanceia verrucosa* originating from Kenya (Fig. 29.1) [8]. The amino acid sequence of the VTX β -subunit demonstrated 86% identity with the SNTX β -subunit. Information regarding the amino acid sequence of the α -subunit of VTX has not been reported to date. VTX is known to comprise the major component of the venom released by *S. verrucosa*. It has also been reported that VTX exhibits similar activity to SNTX [9].

Neoverrucotoxin (neoVTX) has also been isolated and was subsequently characterized from the venom of *S. verrucosa* (Fig. 29.2) originating from Okinawa, Japan [10]. NeoVTX was lethal to mice (LD_{50} of $47 \mu\text{g/kg}$) and demonstrated potent hemolytic activity. NeoVTX was found to be a dimeric 166-kDa protein composed of an α -subunit (702 amino acid residues) and β -subunit (699 amino acid residues) (Fig. 29.1). Alignment of the amino acid sequences revealed that the neoVTX α - and β -subunits shared 87% and 95% identity with the SNTX α - and β -subunits, respectively. In addition, the sequence of the neoVTX β -subunit revealed 90% identity with the VTX β -subunit. Thus, it appears that the major toxins isolated from stonefish (*S. horrida*, Kenyan *S. verrucosa*, and Japanese *S. verrucosa*) form a new family of

SNTX-alpha	VVLKMQRAQTFC	DHVNDFE	KSRNVG	FFITALE	NGKFOG	ASIIYYKE	GSLATQ	DTFPR	MPVQGY	KKRS	DLLWY	ACDLT	FD	RNTINN	WI	539	
neoVTX-alpha	VVLKMQRAQTFC	DHVNDFE	KSRNVG	FFITALE	NGKFOG	ASIIYYKE	GSLATQ	DTFPR	MPVQGY	KKRS	DLLWY	ACDLT	FD	RNTINN	WI	539	
SNTX-beta	I	PETMREK	AYLFR	NI	LAKEM--	NNRCV	HFFVT	AI	HNPKQ	EGAGI	HY	RESIQ	II	DEFT	PYP	MGVES	536
neoVTX-beta	I	PETMREK	AYLFR	NI	LAKEM--	NNRCV	HFFVT	AI	HNPKQ	EGAGI	HY	RESIQ	II	DEFT	PYP	MGVES	536
VTX-beta	I	PETMREK	AYLFR	NI	LAKEM--	NNRCV	HFFVT	AI	HNPKQ	EGAGI	HY	RESIQ	II	DEFT	PYP	MGVES	536
	...	*	*	*	*	*	*	*	*
SNTX-alpha	SLSDNDTFA	ASEHGK	RQNP	KHP	ERFV	SFNQ	VLCNE	GLMK	HW	EV	WNGY	ID	VGIA	YIS	IRKE	IDF	629
neoVTX-alpha	SLSDNDTFA	ASEHGK	RQNP	KHP	ERFV	SFNQ	VLCNE	GLMK	HW	EV	WNGY	ID	VGIA	YIS	IRKE	IDF	629
SNTX-beta	TLSEGNK--	KAVSGN	TKSPT	DH	LEKFS	HQV	QVMCT	KGL	SGR	HY	WE	LSG	WY	KG	AG	VTYK	624
neoVTX-beta	TLSEGNK--	KAVSGN	TKSPT	DH	LEKFS	HQV	QVMCT	KGL	SGR	HY	WE	LSG	WY	KG	AG	VTYK	624
VTX-beta	TLSEGNK--	RQCRG	VRVTR	RR	SLRE--	FSHF	QQVM	CHQ	GA	EWTP	LLG	VR	VAG	HVS	AG	VTYK	623
	*****	*	*	*	*	*	*	*	*
SNTX-alpha	ERHKKREYN	VRAPN	PGFK	RLG	LFLD	WRYS	ISFY	AVSS	DE	VH	HLHT	FKTK	FT	EP	VP	PA	702
neoVTX-alpha	ERYNQRQY	YVTV	PT	PG	KQLG	VLN	WPD	GS	LSFY	AVSS	DE	VH	HLHT	FKTK	FT	EP	702
SNTX-beta	QIHNSKKT	RTVTS	TSTG	FK	LLGV	LDW	PAGT	LSFY	MV	NKAW	VT	HLHT	FT	TK	FNE	AV	699
neoVTX-beta	QIHNGKNAR	TVSS	IG	FK	Q	LV	LDW	PAGT	LSFY	MV	NKAW	VT	HLHT	FT	TK	FNE	699
VTX-beta	QIHNGKNAR	TVSS	IG	FK	Q	LV	LDW	PAGT	LSFY	IG	QQ	SL	GS	PHL	PHQ	IL	695
	*	*	*	*	*	*	*	*

Fig. 29.1 Sequence comparison of the stonefish toxins. The alignment of stonustoxin (SNTX) alpha-subunit (GenBank, protein, AAC60022), NTX beta-subunit (GenBank, protein, AAC60021), verrucotoxin (VTX) beta-subunit (GenBank, protein, CAA69254), neoverucotoxin (neoVTX) alpha-subunit (GenBank, protein, BAF41221), and neo VTX beta-subunit (GenBank, protein, BAF41222) is shown by the single letter amino acid code. Identical residues are marked by asterisks. Conserved residues are marked by dots



Fig. 29.2 The stonefish *Synanceia verrucosa* from Okinawa

highly bioactive proteins. It has been reported that neoVTX was soluble only in buffers with high ionic strength and that this unique property permitted purification of unstable neoVTX from *S. verrucosa* venom using a simple procedure [10]. It was hypothesized that this purification method may also be applicable to the isolation of the major protein toxins from other stonefish species.

Among the stonefish toxins isolated to date, SNTX is the only toxin that has been subjected to pharmacological investigations. These studies demonstrated that the primary lethal action of SNTX was due to its potent hypotensive effects. It was shown in studies using rat aortic strips that SNTX mediated its vasorelaxant activity via the L-arginine-nitric oxide (NO) synthase pathway [11]. It was also shown that hydrogen sulfide (H_2S) and NO acted synergistically in mediating SNTX-induced vasorelaxation [12]. Furthermore, it was revealed that SNTX occupied substance P receptors located on endothelial cells or induced substance P activity. This cascade of events subsequently results in the activation of potassium channels and leads to vasorelaxation in rat aortic rings [13]. In experiments using monoclonal antibodies directed against SNTX, it was suggested that different domains are responsible for the lethal and hemolytic activities [14]. Nevertheless, these studies on SNTX [5] represent the first reports of the characterization of an unstable protein toxin synthesized by a venomous marine animal.

Weever fish are the most famous venomous fish located in Europe. Dracotoxin (105 kDa) was isolated as the major proteinaceous toxin obtained from the venom of the greater weever fish species *Trachinus draco*. Dracotoxin was found to cause hemolysis of rabbit erythrocytes with an EC_{50} of 3 ng/mL. However, a precise characterization of dracotoxin has not yet been reported [15].

It has been reported that the major toxin produced by stingrays is also a proteinaceous toxin [16, 17]. However, no protein toxins have been characterized from this source to date. A 10-kDa vasoconstrictor peptide was isolated and subsequently characterized from the venom of the Brazilian stingray *Potamotrygon*

gr. *orbignyi* [18]. Envenomation caused by the stingray results in immediate, local, and intense pain and edema. Necrosis was also demonstrated in the skin of a number of victims. Given these symptoms, it is uncertain if the vasoconstrictor peptide is responsible for the major effects of stingray envenomation. Numerous other protein toxins have also been purified from venomous fish species, including the lesser weever fish *Trachinus vipera* [19], Indian catfish *Plotosus canius* [20], scorpion fish *Scorpaena guttata* [21], *Notesthes robusta* [22], and *Thalassophryne nattereri* [23]. However, among the protein toxins of fish, only the three toxins from the scorpion fish (*S. horrida*, Kenyan *S. verrucosa*, Japanese *S. verrucosa*) described above have been formerly characterized to date.

29.3 Protein Toxins of Jellyfish

A vast number of jellyfish stings to humans occur in all of the world's oceans, especially in nearshore environments. Given the severe stinging ability of some species of jellyfish, a number have been categorized as venomous animals. Jellyfish are classified into the cnidarians, a group that consists of almost 10,000 species of related animals including jellyfish, sea anemones, hydra, and soft and hard corals. All cnidarians are armed with nematocysts, explosive capsule organs used for stinging (Fig. 29.3). The nematocysts vary from 5 to 100 μM in size and consist of an inverted compactly coiled tubule (needle) and venom surrounded by a strong outer wall. The role of the nematocyst is to capture prey and to guard against predation. Thus, all cnidarians generate venom to some extent.

Perhaps the best known venomous jellyfish is *Chironex fleckeri* (one of the box jellyfish) which has caused a large number of fatalities along the Australian coast. The Portuguese man-of-war *Physalia physalis* is also notorious given its severe sting that may occasionally result in death. Because of their importance to public health, jellyfish toxins have been extensively examined and were revealed to be mostly comprised of proteinaceous toxins. However, the precise chemical nature of jellyfish toxins has not been successfully determined, as the chemical instability of these toxins has hampered further studies [24, 25]. Among the many jellyfish species that have been identified as venomous, the box jellyfish (Cubozoan jellyfish) is recognized as an especially hazardous marine animal. *C. fleckeri*, *Chiropsalmus quadrigatus* (Fig. 29.4, recently renamed *Chironex yamaguchii* [26]), *Carukia barnesi*, and *Carybdea* spp. [27, 28] are genera and species generally known as venomous box jellyfish.

The box jellyfish *Carybdea rastoni* (Fig. 29.5) is one of the most hazardous marine organisms for swimmers and bathers along the Japanese seashore. A sting from *C. rastoni* may cause cutaneous pain and inflammation in humans. Given the frequency of stings by this jellyfish, and the symptoms that these stings cause, *C. rastoni* was chosen as the first target of investigation in our laboratory. During our studies on *C. rastoni*, we found that the toxicity of the proteinaceous toxins was markedly decreased during the process of purification, storage, and sample concentration. Thus, determining the optimal conditions for the purification and storage

Fig. 29.3 (a) The isolated intact nematocysts of the jellyfish *Chiropsalmus quadrigatus*. (b) The discharge nematocyst of *C. quadrigatus*

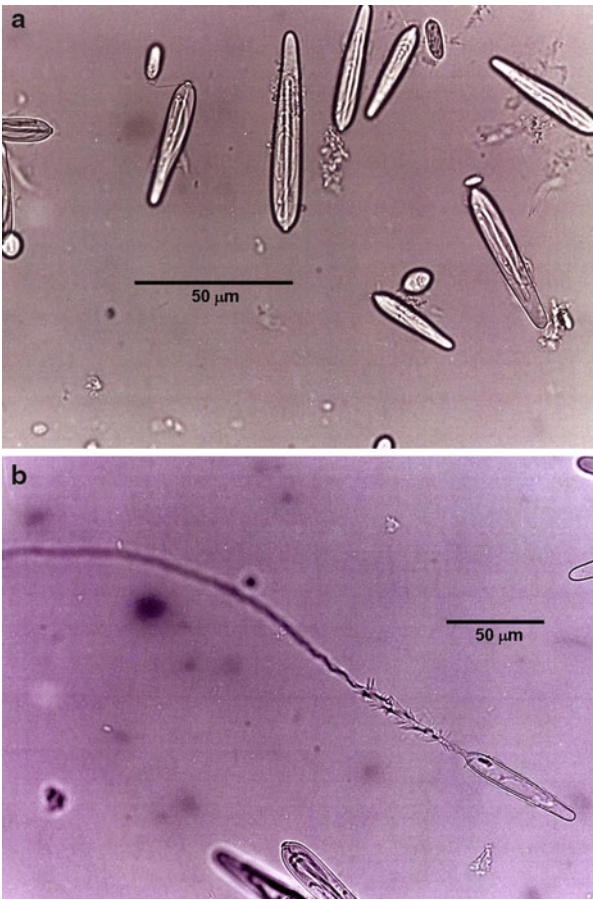


Fig. 29.4 The box jellyfish *Chiropsalmus quadrigatus*

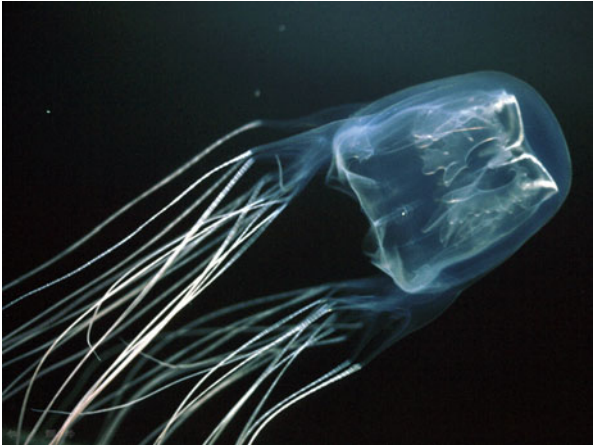
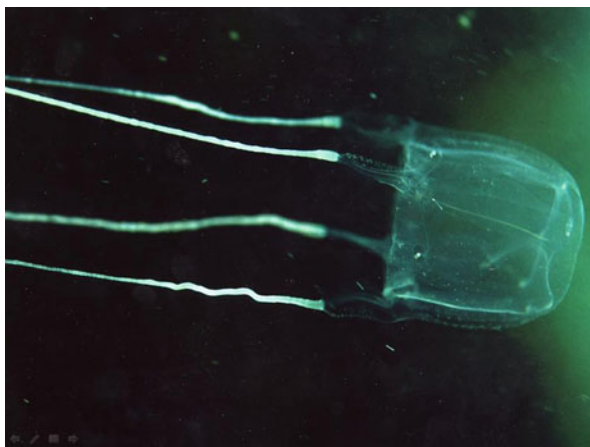


Fig. 29.5 The box jellyfish
Carybdea rastoni



of these toxins was a key step in their characterization. We demonstrated that ion-exchange chromatography rather than ultrafiltration was suitable for concentration of the toxins. We also found that storage of the purified samples in a high-salt-concentration solution was required and that the samples should not be frozen or freeze-dried. Thus, purified toxins were stored in a high-salt solution such as 0.8 M sodium chloride containing 10 mM phosphate buffer (pH 6.0) at 4°C. Under these conditions, 90% of the hemolytic activity of the *C. rastoni* toxin could be retained for more than 6 months of storage [29].

Using these methods, we were able to isolate the active forms of two proteinaceous toxins, *Carybdea rastoni* toxins A and B (CrTX-A, 43 kDa and CrTX-B, 46 kDa), from the tentacles of the box jellyfish species *C. rastoni*. We also determined the full-length cDNA (1600 bp) that encoded both CrTX-A and CrTX-B (Fig. 29.6) [29]. Histopathologic studies showed that CrTX-A (0.1 µg/injection) caused inflammation of the affected area, an effect that was comparable to the symptoms observed in humans after a *C. rastoni* sting. CrTX-A was found to be the main toxin housed in the nematocyst. Thus, the results of the pathologic study revealed that CrTX-A was responsible for the cutaneous inflammation observed in humans following a *C. rastoni* sting. CrTX-A was the first toxin isolated and shown to be the causative agent of cutaneous inflammation following jellyfish stings [29].

The sea wasp species *Carybdea alata*, also in the box jellyfish family, is another type of stinging jellyfish. A *C. alata* sting results in cutaneous pain and inflammation in humans, symptoms that are similar to those caused by *C. rastoni*. *C. alata* is widely distributed in the tropical zones of the Atlantic, Pacific, and Indian Oceans. On the southern shores of Oahu, Hawaii (Waikiki Beach), massive invasion by this species occurs every 9th or 10th day following a full moon [30]. The *Carybdea alata* toxins A and B (CaTX-A, 43 kDa and CaTX-B, 45 kDa) were successfully isolated using the toxin isolation procedure developed for *C. rastoni* [31]. Interestingly, it was found that CaTX-A, but not CaTX-B, was present in *C. alata*

nematocysts. The full-length cDNA (2000 bp) that encoded a 463–amino acid protein (CaTX-A) was also determined (Fig. 29.6).

The Okinawan sea wasp *Chiropsalmus quadrigatus* (synonym *Chironex yamaguchii*) is widely distributed in the tropical Indo-Pacific region. A sting from *C. quadrigatus* is sometimes so severe that it proves fatal to humans. In Okinawa, a tropical region of Japan, three fatal stings from *C. quadrigatus* have been officially reported to date. Death was caused by cardiac arrest in systole or respiratory failure with acute pulmonary edema. Children are particularly susceptible to stings from *C. quadrigatus*. *Chiropsalmus quadrigatus* toxin A (CqTX-A, 44 kDa) was isolated using the isolation procedure developed for the characterization of the *C. rastoni* toxin. However, the procedure for CqTX-A was modified in that cleanly isolated nematocysts were used as the starting material. Using these methods, a full-length cDNA (1938 bp) was defined that encoded a 462–amino acid proteinaceous toxin (CqTX-A) (Fig. 29.6) [32]. Alignment of the amino acid sequences for CrTX-A and CrTX-B, CaTX-A, and CqTX-A revealed 20–45% identity between the toxins [31, 32], suggesting that these box jellyfish toxins form another novel family of protein toxins.

The LD₅₀ values for the injection of CqTX-A, CrTX-A, and CaTX-A into crayfish (*Procambarus clarkii*) were 80, 5, and 5–25 µg/kg, respectively [29, 31, 32]. CqTX-A, CrTX-A, and CaTX-A were also found to result in 50% hemolysis in 0.8% sheep red blood cells at a concentration of 160, 2, and 70 ng/ml, respectively [29, 31, 32]. These findings generally indicated that CqTX-A was less toxic than CrTX-A and CaTX-A. The number of tentacles present on *C. quadrigatus* is known to be several times greater than that of *C. alata* and *C. rastoni*. Furthermore, the overall length of the tentacles of *C. quadrigatus* is at least three times that of *C. alata* and *C. rastoni*. Therefore, for human stings, the total amount of toxin injected into the victim from *C. quadrigatus* is likely much greater than the total amount injected by *C. alata* or *C. rastoni*. This is one reason why *C. quadrigatus* is considered more dangerous than *C. rastoni* or *C. alata*. Indeed, massive regional stings were observed at autopsy after fatal *C. quadrigatus* incidents. CqTX-A was the major toxin located in the nematocysts, and thus, CqTX-A is most likely the causative toxin in fatal *C. quadrigatus* sting cases.

Australian research groups have subsequently isolated two of the most abundant proteins in their non-active form from the nematocysts of the most deadly box jellyfish species, *Chironex fleckeri*. These proteins have been termed *C. fleckeri* toxin-1 (CfTX-1, 43 kDa) and toxin-2 (CfTX-2, 45 kDa). The amino acid sequences of the mature CfTX-1 and CfTX-2 have been shown to share homology with the CrTXs, CaTX-A, and CqTX-A (Fig. 29.6). Secondary structural analysis of these toxins predicted the presence of amphiphilic α -helices in the *N*-terminus region. It has been suggested that amphiphilic structures present in some cytolytic protein toxins promote the formation of pores in cell membranes [33, 34]. This activity of the amphiphilic structures present in the box jellyfish toxins may explain some aspects of their potent hemolytic activity. Indeed, further studies on the mode of action of these toxins may aid in the development of effective and specific treatments for box jellyfish stings.

A protein toxin termed CARTOX (102–107 kDa) has also been isolated in its active form from the nematocysts of *Carybdea marsupialis* that reside in the

CrTXs	MILKH-LPW-LFIVL--AITS-AKHG--KRSDVNSLITKVFETALKE-AS-GSNEAAL-EALEGLKEIQTKP-DRVQOATKILGSVGSAL	79
CaTX-A	MSRGYSLHLVFLVLSTAFPSPQARLSRYRRSAADAVSTDIDIGIQNDLGDPTKRLKEALQGVQAVKKEPPATTIAKVSTIVSGVGGSL	90
CqTX-A	-----WANMLYFSLALLFWMTGIA-SEGTISSGLASLAKAKIDAK-RPSGKQLFDKVVANMQKQIEEFKFSNDDERAKVMGAI-GSLSTAV	80
CfTX-1	-----MYKMLFFAFLPILFWMTGIA-AESTISSGLNSLTKIDAK-MPSGKQLFDKVVEMQKQIDAKFSDNDDERAKVMGAI-GSLSTAV	80
CfTX-2	-----MILVSLPILFWMTGIA-SESTISSGLASLAKAKIDIK-KPTGKQLFDKVKVMEQALENKFSDDDERAKVMGAI-GSLGTAI	77
 * * * *	
CrTXs	GKLN SGDATKIIISGCLDIVAGIATTFGGFVGMGIGAVASFVSSILSLFTGSSAKNSVAVIDRALSKHRDEAIQRHAAAGAKRDFAESAF	169
CaTX-A	SKFKSGDPFDVAGCLDIIASVATTFGGPYGIAIGAVASLISSILSLFSGNSMGSAIKQVIDDFAKKYRDQELEDNVKGAKRTFNNAVITF	180
CqTX-A	GKFGSGDPAKIASGCLDIIIVGISSVLKD-FA-KFSPIFSILSMVWGLFSGTKAEESSGVSVKVKVQEQSDQELQEAALYGVKREYAVSKAF	168
CfTX-1	GKFGSGDPAKIASGCLDIIIVGISSVLKD-FA-KFSPIFSILSLWGLFSGTKAEESSGVSVKVKAVQEQSDQELQEAALYGVKREYAVSKAF	168
CfTX-2	GKFGSGDPASIASGCLDIIIVGISSVLKD-FA-KFSPVFSILSLWGLFSGTKAEESSVSVVTKAIQEQSDQELQEAALYGVKREFAVSKAF	165
	*****.*****. * * * *	
CrTXs	-IQVMKQOSNLTDSDLSIIAANVPVYKFSNFIGQLESRIISQGAATTSLSDAKRAVDIFILYQQLVVMRETLVLVDLAILYRK-GNA-EHVA	256
CaTX-A	-VNSVSKTENLITEVHLDSDVRDAVRVDAFTNMLGVLESKRINRGSVSTDNNEAMRTINFIPLYQLSVMRETLTQVILLYKRAGGAYDELA	269
CqTX-A	LDGVRNETSDLSPTSEVSALGANVPVYQGVRFIAMVQRIKNNRKPRTSEI-KRVLSMLELFTDLCILRDLILLDLYLQVLATPFGHSPNIAS	257
CfTX-1	LDGVRNETSDLSPTSEVSALAANVPIYQGVRFIAMVQRIKIKPKTSEI-KRMLTMLELFTDLCILRDLILLDLYLQVLATPFGHSPNIAS	257
CfTX-2	LDGVRNEESDLRPTSEVSALAANIPVYQGVRFIAMVQRIKIKPKTSEI-KRMLTMLELFTDLCILRDLILLDLHLQLIATPFGHSPNIAS	254
	*****.*****. * * * *	
CrTXs	SAVENANRVNKELAADTLDFLHKLIPEQALIGAVYHPISASETSKALINITYKFGVPDVPR-PIGNRRYKFTN-SYWNITYSICSEAYMGN	344
CaTX-A	LSLSLTSDQNKEATRETVTFLHQMETKYSLCGSYYYPIDHSKAAIGILKLTKFYFGVPDPARTFDGLIYRQN-RAWNRYSICKESYAGN	358
CqTX-A	GIREVSNLGREEYKKVFEDLLKTNDKETYLFLSYLYPRENEQSQKIFKFFDLMKVYDDRLKQDLTGIGIYFSSLHWPNYFLC---SSKD	344
CfTX-1	GIREVSNLGREEYKKVFEDLLKNDDKETYLFLSYLYPREKNEQSRIKFNFFDLMKVYDDRLKQDLTGIVKTFNSNVHWPNYFMC---SSND	344
CfTX-2	GIREVTSNLGREEYQVRFEDLLKTDDDEETFLFSYLYPREKNEQSRIKIFKFFDIEVKYDDRFKLDLSGGQALSTLQWPNYYLC---PHND	341
	*****.*****. * * * *	

Fig. 29.6 (continued)

Northern Adriatic Sea [35]. CARTOX was shown to possess potent hemolytic activity; however, the precise features of CARTOX giving rise to this activity have not been reported to date. A proteinaceous neurotoxin was also isolated from a Caribbean *C. marsupialis*, and the existence of some cytolyisin was demonstrated [36]. However, once again, a precise characterization of Caribbean *C. marsupialis* toxin has not been reported to date. While CfTX-1 and CfTX-2 were suggested to be the main proteinaceous toxins of the box jellyfish *Chironex fleckeri* [37], the existence of two additional hemolytic protein toxins (39 and 41 kDa) in the nematocyst of *C. fleckeri* have been reported [38]. These toxin profiles were shown to differ from those of CfTX-1 and CfTX-2 by immunoblotting using rabbit polyclonal antibodies raised against CfTX-1 and CfTX-2 [38]. Nevertheless, a precise characterization of these new toxins has not yet been established. The existence of plural protein toxins was reported by Burnett's group [39] and indicated that numerous box jellyfish species contain both major and minor protein toxins. Thus, the severe symptoms resulting from a box jellyfish sting may be the result of multiple effects caused by different protein toxin types.

Scyphozoa jellyfish are of typical shape and size and include the moon jellyfish species *Aurelia aurita*. Another scyphozoan, *Chrysaora quinquecirrha*, is present in the Chesapeake Bay and is commonly known as the "sea nettle." Comprehensive studies on the venom of *C. quinquecirrha* have been conducted by Burnett's group [40, 41] who reported the presence of various protein toxins. From the scyphozoan *Rhizostoma pulmo* residing in the Bay of Naples, rhizolysin (260 kDa) was obtained and shown to function as a hemolytic protein [42]. However, rhizolysin did not exhibit any phospholipase A₂ activity. A protein toxin termed T-Ar (182 kDa) was isolated from the scyphozoan *Acromitus rabanchatu* located in the Bay of Bengal [43]. Pharmacological studies on T-Ar suggested that this toxin possessed a direct paralyzing effect on muscle membranes [43].

With the exception of the toxin isolated from the Mediterranean scyphozoan *Rhopilema nomadica*, none of the scyphozoan jellyfish protein toxins mentioned above have been precisely characterized to date. The polypeptide toxin (17 kDa) isolated in its active form from the tentacles of *R. nomadica* was found to be lethal to fish [44]. The N-terminal amino acid sequence of the *R. nomadica* toxin revealed homology with phospholipase A₂ toxins isolated from the lizard [45] and honeybee [46].

The Portuguese man-of-war *Physalia physalis* is one of the most famous venomous jellyfish and belongs to the hydrozoan jellyfish. While a hemolytic protein (240 kDa) that is lethal to mice has been isolated from the nematocyst of *P. physalis* [47], this toxin has also not been fully characterized.

29.4 Protein Toxins of Sea Anemones

Sea anemone toxins have been extensively studied, especially in regards to peptide toxins that have a molecular weight of less than 10 kDa. The most extensively studied group of these peptide toxins have been mainly categorized as either sodium

channel toxins or potassium channel toxins [2]. A number of these toxins have been used as valuable tools for the study of the structure and function of ion channels. Here, we describe protein toxins (molecular weight of more than 10 kDa) isolated from the sea anemone.

Among the protein toxins synthesized by sea anemones, only the actinoporin family of toxins has been subjected to extensive research (Fig. 29.7). Actinoporins are 20-kDa pore-forming cytolytins [48] and, as a family, are considerably more stable than other marine protein toxins investigated to date. Actinoporins create 2-nm pores in eukaryotic lipid membranes via the self-association of four monomers [49]. Sphingomyelin located in the outer leaflet of the plasma membrane has been shown to be the binding target of actinoporins [50]. The actinoporin family has been mainly isolated and characterized from Actiniidae and Stichodactylidae sea anemones [48], with more than ten actinoporin protein toxins isolated and characterized so far. The crystal structures of equinatoxin II isolated from *Actinia equina* and sticholysin II isolated from *Stichodactyla helianthus* revealed a tightly folded sandwich of ten β -strands that were embedded with two α -helices [51, 52].

It has also been shown that echotoxin 2 from the salivary gland of the marine gastropod *Monoplex echo* belongs to the actinoporin family [53]. Echotoxin 2 represents the first example of an actinoporin that was not isolated from a sea anemone. The cytolytic and lethal activity of echotoxins 1, 2, and 3 are known to be specifically inhibited by gangliosides [54]. When compared to this inhibition by gangliosides, sphingomyelin was shown to be almost 100 times weaker [54]. Thus, the mode of echotoxin action may differ from the usual actinoporins. The existence of an actinoporin-like protein (Dr1) was also found in the zebrafish *Danio rerio* genomic database [55]. This report represented the first characterization of an actinoporin in a vertebrate species. Dr1 has been subsequently cloned and expressed in *Escherichia coli*. The expressed Dr1 protein displayed membrane-binding behavior, but did not exhibit any permeabilizing activity or sphingomyelin specificity, two properties that are typical of actinoporins [55].

In the subtropical and tropical coasts, venomous sea anemones such as *Phyllodiscus semoni* (Fig. 29.8) and *ActinERIA villosa* (Fig. 29.9) (both Aliciidae) are widely distributed. Envenomation by these species results in a painful fulminant dermatitis. The protein toxins comprising the venom of these sea anemones have been studied from the Japanese Okinawan coast. It was shown that *Phyllodiscus semoni* toxins 60A and 60B (PsTX-60A and PsTX-60B) [56, 57] and *ActinERIA villosa* toxin 60A (AvTX-60A) [58] were the major protein toxins present in the nematocyst venom of these anemones, respectively. Each of these toxins possessed a molecular weight of 60 kDa, and the cDNA of the three protein toxins was cloned and sequenced (Fig. 29.10) [56–58]. The results of protein domain analysis by Pfam [59] and SMART [60] revealed that PsTX-60A, PsTX-60B, and AvTX-60A were novel members of the membrane-attack complex/perforin (MACPF) domain family (Fig. 29.10). The MACPF domain consists of approximately 200 amino acid residues, and the MACPF family of proteins was originally described as pore-forming factors used in the mammalian host defense immune system [61, 62]. These sea anemone toxins represented the first MACPF proteins isolated from

Fig. 29.8 The sea anemone
Phyllodiscus semoni



Fig. 29.9 The sea anemone
ActinERIA villosa



nonmammalian species as actual proteins. Furthermore, these reports were the first studies to describe the use of MACPF proteins as a venom in animals. These new sea anemone toxins also showed potent hemolytic activity. Thus, the mode of action of these MACPF toxins may be explained by their pore-forming activity, in a manner similar to the way in which MACPF proteins function in the mammalian immune system. Actinoporins PsTX-20A [63] and Avt-I [64] have also been isolated as minor toxic components from the nematocyst venom of *P. semoni* and *A. villosa*, respectively. On rare occasions, a sting by *P. semoni* may cause acute renal failure in humans [65]. A 115-kDa protein toxin called PsTX-115 was subsequently isolated as the nephrotoxic component of the venom. Crude venom isolated from the nematocysts of *P. semoni* as well as purified PsTX-115 was found to be highly nephrotoxic. These toxic effects were due to the induction of complement activation [66]. These findings suggest that the MACPF domain toxins may

also be involved in acute renal failure due to their complement-like activity. However, a precise characterization of PsTX-115 has not yet been reported.

An 80-kDa cytolytic protein—designated metridiolysin has also been purified from the tissues of *Metridium senile* residing in the North Atlantic Ocean. Metridiolysin has an isoelectric point at a pH of approximately 5.0 and is composed of two unequal sized subunits. The hemolytic activity of metridiolysin was specifically inhibited by cholesterol [67]. The amino acid sequence of metridiolysin has not yet been determined. Thus, to date, only the protein toxins belonging to the actinoporins and MACPF-type toxins have been chemically characterized from the sea anemone.

29.5 Protein Toxins of Fire Coral

While the vast majority of hermatypic corals belong to the class Anthozoa, fire corals are members of the class Hydrozoa. Fire corals consist of only one genus known as *Millepora*. Branching and blade fire corals are most commonly encountered on coral reefs. Direct contact with fire coral causes a severe burning sensation but is usually not life threatening. Envenomation is caused by nematocysts, similar to other cnidarians such as jellyfish and sea anemones. Recent studies have revealed difficulties associated with the taxonomy and distinction among various *Millepora* species [68].

In the early 1970s, the venom of *Millepora alcicornis* from Florida and *Millepora tenera* (initially termed *M. dichotoma*) and *Millepora dichotoma* from the Marshall Islands were extensively studied [69–71]. In these investigations, it was shown that branching *Millepora* spp. produce unstable hemolytic and lethal protein toxins. In the late 1980s, an attempt was made to isolate the protein toxins from the venom of the branching fire coral *M. dichotoma* and the blade fire coral *Millepora platyphylla* from Okinawa [72]. While the protein from *M. dichotoma* was too unstable to isolate, a 31.5-kDa protein was isolated from *M. platyphylla*. At least one additional toxic component was located in the venom of *M. platyphylla* and subsequently reported [72]. In 2004, it was shown that a hemolytic protein—designated milleporin-1 (ca. 32 kDa) could be isolated from *M. platyphylla* collected from the Red Sea. Milleporin-1 was also shown to exhibit phospholipase A₂ activity [73]; however, no further information regarding the chemical structure of this protein has been published.

An 18-kDa protein toxin has subsequently been isolated and characterized from Okinawan *M. dichotoma* var. *tenera* (Fig. 29.11) [74]. This toxin was designated as *Millepora* cytotoxin 1 (MCTx-1) and was found to be unstable during purification. MCTx-1 was potently cytotoxic ($EC_{50} = 79$ ng/mL) towards L1210 mouse leukemia cells, was able to hemagglutinate a 0.8% suspension of sheep erythrocytes (0.2 µg protein/mL), and was lethal to crayfish (LD_{50} , 106 µg/kg). The MCTx-1 toxin did not show any hemolytic or phospholipase A₂ activity. Therefore, it was suggested that MCTx-1 represented a different protein toxin to the formerly reported protein toxins isolated from *Millepora* spp. According to the BLAST database, MCTx-1 belongs to the dermatopontin family of proteins (Fig. 29.12).

Fig. 29.11 The fire coral *Millepora dichotoma* var. *tenera*



Dermatopontin was initially isolated from bovine dermal extracts as an extracellular matrix protein [75]. Thereafter, dermatopontins were isolated from human, pig, rat, and mouse as extracellular matrix proteins [76–78] and from invertebrates including the horseshoe crab, sponge, and snail [79–81]. However, MCTx-1 was the first toxic dermatopontin to be discovered. MCTx-1 exhibited highest homology (36%) with the hemagglutinin/amebocyte aggregation factor from the horseshoe crab *Limulus polyphemus* [79]. Of the reported dermatopontins, only MCTx-1 and the *Limulus* aggregation factor have demonstrated hemagglutination activity. Bovine dermatopontin does not have hemagglutinating activity [82], whereas *Limulus* aggregation factor has phospholipase A₂ activity [83] and MCTx-1 does not. Various proteins originating from snake and spider venom have also been shown to have hemagglutinating activity [84–86]. Galactoside-specific lectin (BJcuL) isolated from the venom of the snake *Bothrops jararacussu* [87] also has hemagglutinating activity and significant cytotoxicity [88]. Injection of BJcuL into the paws of mice results in a dose-dependent edema and vascular permeability [89]. Thus, BJcuL has been shown to participate in edema formation induced by snake bite. MCTx-1 also exhibits hemagglutination activity and potent cytotoxicity similar to BJcuL. Thus, MCTx-1 may be at least partially responsible for the edema associated with *Millepora* stings.

29.6 Protein Toxins of Hydra

Hydra are freshwater animals that belong to the phylum Cnidaria, and thus, they also synthesize proteinaceous toxins. A limited number of studies have investigated their toxic components. We have chosen to review the toxins synthesized by Hydra, even though these toxins do not originate from a marine animal, because of their relationships to other marine life forms.

It has been reported previously that two protein toxins exist in the isolated nematocysts of *Hydra attenuata* [90]. One of these toxins demonstrated hemolytic

MCTx-1	MVTLYLHVPILLVITARAAKPKDTHNPFDELSSVA-EKQDLHYGDRSRKDPFIAQNDVG-N-NFRDGTQENLTKVRSKVNQYDQPF	87
Limulus	M-NSPAIVII-FSTLTF-SEAW---NDWDGALNFOQLKDSIKTSSIHSHHEDRRWNFGCERTLRD-PS-CYFTNYVNDWDKLLHF	82
Snail	M-SQSLYLAI-LMTVA--SAAYV---NDWDQPFNFCPDGQVSVYSSVHDNRDRRWEFLC--RTARQTHS-CTDSGYVNDFDGPLVY	81
Sponge	MKMFVNATVGLFVLIVLALHAAAFQYQNDYDKPLHVECPDKQALIYYQSIHSNRHEDRRFENCKHAANKKWSHCFTWTHLNNYDGLNY	90
	* * * *	
MCTx-1	KCPLETIKSIGSIHDNHYEDRQWDIDCKPAGYTMGISTWSPYANDYDGSNFECSVVTGMSIHDNYYEDRRYQLMCSYLNWKR	177
Limulus	TCKSGEATAGFNSYHDNRDRRWKIYC---C-KDNKCTDY-RTCAWT-GYVNSWDGDLHYTPKDYLTGVI SEHDNHREDRRWK	165
Snail	TCFGNKVMVGVHSYHNNRDRRFGFYC---C--DVQGSTP--RDCYTT-DYVNDWDGKLT LAVPEGRAVKAAFSHHNNRDRRWQ	162
Sponge	QCPNNLMTGVKSEHSNHEDRRWSFKC---C-KANGYHT---KSCIMT-GYINSYDNPMHAAAHYNNHFFAGAYSVHSNHEDRIWK	171
	* * * *	
MCTx-1	SCAWTSYTTYDASFVELTPTGKFLVGMKSQHNNYYEDRKFKMLYC	222
Limulus	HCRL-KNC-----	172
Snail	ICAL-----	166
Sponge	ECKYSKIYT-E-SLT-----	184
	*	

Fig. 29.12 Sequence comparison of invertebrate dermatopontin homologs and MCTx-1. The alignment of MCTx-1 from the fire coral (GenBank, nucleotide, AB299385), dermatopontin homologs from the horseshoe crab *Limulus polyphemus* (GenBank, protein, Q01528), from the snail *Biomphalaria glabrata* (GenBank, protein, Q3YU8), and from the sponge *Suberites domuncula* (GenBank, protein, Q966Y2) is shown by the single-letter amino acid code. Identical residues are marked by asterisks. Conserved residues are marked by dots

activity and caused initial spasmodic contractions in larval and adult *Drosophila*. The second protein toxin caused long-lasting paralysis that caused death in the tested *Drosophila*. However, both toxins failed to exhibit any phospholipase activity. While the toxin molecular weights remain unclear, the hemolytic toxin was clearly larger than the lethal toxin when assessed by gel permeation chromatography [90].

An Israeli research group also isolated a paralytic and cytolytic 27-kDa protein, termed hydralysin, from the body of the green hydra *Chlorohydra viridissima* [91]. The cDNA of hydralysin was subsequently cloned and sequenced. The deduced amino acid sequence of hydralysin revealed homology with pore-forming protein toxins isolated from bacteria and fungi [91]. Recombinant hydralysin also demonstrated dose-dependent cytotoxic effects on insect sf9 cells. It is also noteworthy that hydralysin is located within the hydra body, but not the nematocyst. Thus, the function of hydralysin in *C. viridissima* was speculated as follows [91]. Firstly, hydralysin may function as a defensive allomone that acts in combination with stinging cells to deter possible predators. The second possibility is that hydralysin acts as an allomone by prolonging the paralysis of the prey following ingestion. The same research group also reported the presence of hydralysin isoforms in *C. viridissima* [92]. Functional characterization of the hydralysin isoforms revealed that the soluble monomers were rich in β -structure, as shown by far UV circular dichroism and computational analysis [92]. A large-scale expressed sequence tag (EST) database for *Hydra magnipapillata* has recently been accumulated. Search within this database revealed that *H. magnipapillata* expressed orthologs of phospholipase A₂ as well as cytolytins belonging to the actinoporin family [93].

29.7 Protein Toxins of Starfish

Starfish are echinoderms that belong to the class Asteroidea. Among the approximately 2,000 starfish species, it is only the crown-of-thorns starfish *Acanthaster planci* (Fig. 29.13) that is known to produce a venomous sting within their spines. *A. planci* is covered with spines which each secrete a venom. This starfish is widely distributed throughout tropical and subtropical coral reef areas. Feeding almost exclusively on living coral polyps, *A. planci* prefers preys such as branching and plate corals. Indeed, massive proliferation of *A. planci* populations can be fatal to coral reefs. Thus, volunteer divers are currently attempting to collect and control the numbers of *A. planci* from coral reefs around Okinawa. During these collections, divers are often accidentally stung by *A. planci*. Envenomation by *A. planci* results in severe local pain associated with immediate and intense swelling, redness, and numbness at the site of envenomation. Severe sting cases may also cause necrosis at the sting site.

Protein toxins have been isolated from the spines of *A. planci* and were termed plancitoxins I and II for the major and minor toxins, respectively [94]. Both toxins demonstrated an LD₅₀ value of 140 μ g/kg when intravenously injected into mice. Injection of a sublethal dose of plancitoxin I or II into mice also significantly elevated serum levels of glutamic oxaloacetic transaminase and glutamic pyruvic

Fig. 29.13 The crown-of-thorns starfish *Acanthaster planci*



transaminase. This finding demonstrated that both toxins were potently hepatotoxic. SDS-PAGE analysis revealed that both of the plancitoxins were composed of two subunits termed the α -subunit (10 kDa) and the β -subunit (27 kDa) that were bridged by a disulfide bond. Based on the determined N-terminal amino acid sequences of the α - and β -subunits, the full-length cDNA (1,820 bp) encoding plancitoxin I was cloned. The α -subunit (92 amino acid residues) and β -subunit (240 residues) were coded in this order by the same cDNA. Interestingly, the deduced amino acid sequence of plancitoxin I revealed 40–42% homology with mammalian deoxyribonuclease II (DNase II) (Fig. 29.14). In addition, plancitoxin I exhibited DNA-degrading activity at a pH of 7.2. Plancitoxin I represents the first example of a toxic DNase II whose structure has been elucidated [94], and is the first DNase II to be reported from a marine invertebrate species. Intriguingly, plancitoxin I induced apoptosis in rat liver cells, an event that was found to be independent of the caspase-3 cascade, the signaling complex that is generally accepted to regulate apoptotic processes [95].

It is well established that phospholipase A_2 enzymes hydrolyze glycerophospholipids at the *sn*-2 position of the glycerol backbone to release lysophospholipids and fatty acids. Phospholipase A_2 occurs ubiquitously in nature in both intracellular and extracellular forms. Mammalian phospholipase A_2 enzymes generally play a nontoxic and important role in their host. In contrast, snake venom phospholipase A_2 demonstrates a variety of pharmacological effects such as hemorrhage induction and myonecrotic and neurotoxic activities [96]. Among marine animals, the first phospholipase A_2 -type toxin reported was isolated from the scyphozoan jellyfish *Rhopilema nomadica* [44]. Subsequently, two toxic phospholipase A_2 proteins termed AP-PLA $_2$ -I and AP-PLA $_2$ -II were isolated from the spines of *A. planci* [97]. AP-PLA $_2$ -I and AP-PLA $_2$ -II exhibited hemorrhagic and capillary permeability-increasing activity. The full-length cDNAs encoding AP-PLA $_2$ -I and -II were then individually cloned. In common with both of the

AP-PLA₂ forms, the precursor protein was composed of a signal peptide, a propeptide, and a mature protein (136 and 135 residues for AP-PLA₂-I and -II, respectively) [98]. These two proteins were the first specifically characterized toxic phospholipase A₂ enzymes to be described from a marine animal.

29.8 Protein Toxins of Sea Urchin

Sea urchins belong to the phylum Echinodermata, and several species such as *Diadema setosum*, *Toxopneustes pileolus*, *Tripneustes gratilla*, and *Asthenosoma ijimai* are known to be venomous. Envenomation has been shown to be caused by stings from either the pedicellariae or spines. It has been reported that the main toxins produced by sea urchins are proteinaceous [99, 100]. Only three isolated lectins, contractin A (18 kDa), SUL-I (32 kDa), and SUL-II (23 kDa), from the pedicellariae of *T. pileolus* have been partially characterized to date [101, 102]. Contractin A was shown to cause contraction of the tracheal smooth muscle [101]. Interestingly, the N-terminal amino acid sequences of contractin A and SUL-II showed similarities with secretory phospholipase A₂ [102]. However, the N-terminal amino acid sequence of SUL-I did not show homology with any known proteins. It has also been reported that SUL-I induces dendritic cell maturation from human monocytes in vitro [103]. However, the involvement of these lectins in envenomation remains vague.

29.9 Protein Toxin of Cephalopods

Cephalopods include cuttlefish, squid, and octopus. Cephalopods are largely predatory and carnivorous animals that feed on Crustacea, bivalves, and, on occasion, fish. It is well established that cephalopods utilize venom excreted from the salivary gland for hunting and capturing prey. Their venomous bites either prevent prey movement or kill the prey directly. However, deadly envenomation in humans has only been reported for the blue-ringed octopus *Hapalochlaena maculosa*. Tetrodotoxin, also known as puffer fish toxin, is the toxic compound present in the venom of *H. maculosa* [104]. Tetrodotoxin is a small-molecular-weight alkaloid with potent neurotoxic properties. With the exception of the *H. maculosa* toxin, it has been reported that proteinaceous toxins form the major toxic component of cephalopod venom.

Cephalotoxin is the cephalopod protein toxin that causes paralysis and eventual death in crabs. It is synthesized by the posterior salivary gland of the cuttlefish *Sepia officinalis* and the octopus species *Octopus vulgaris* and *O. macropus* [105, 106]. A cephalotoxin has also been purified from the octopus *Eledone cirrhosa* [107] and the salivary gland of *Octopus dofleini* [108]. Two additional paralysis-inducing proteins termed α -cephalotoxin (91 kDa) and β -cephalotoxin (34 kDa) have been isolated from the salivary gland of *O. vulgaris* [109]. However, detailed descriptions of the properties and primary structures of these cephalotoxins have not yet been reported.

The first detailed characterization of a cephalotoxin was conducted on SE-cephalotoxin isolated from the salivary gland of the cuttlefish *Sepia esculenta* [110]. SE-cephalotoxin was shown to be a 100-kDa monomeric glycoprotein with an LD₅₀ of 2 µg/kg (towards crabs). A full-length cDNA (3,402 bp) encoding SE-cephalotoxin was subsequently cloned and the deduced amino acid sequence of the mature SE-cephalotoxin (1,023 amino acid residues) determined. SE-cephalotoxin did not share homology with any proteins in the database search. The mode of SE-cephalotoxin action remains to be solved.

29.10 Concluding Remarks

This chapter describes the studies published to date on protein toxins isolated from venomous marine animals. For many years, detailed characterization of these toxins has been hampered by their instability and the difficulty in obtaining sufficient quantities of animal samples. Only recently has the precise characterization of a few of these protein toxins been reported. However, with the exception of the actinoporin family, the number of characterized toxins remains small. It has been revealed that protein toxins synthesized by marine venomous animals are quite unique in both their structure and biological activities. MACPF protein toxins isolated from the sea anemone, a novel protein toxin family from the box jellyfish, DNase II toxins from the starfish, and a dermatopontin family toxin from fire coral are representatives of some of these unique toxins.

At present, sting cases caused by venomous marine animals are only treated symptomatically. If the precise structure and mode of action of the proteinaceous toxins produced by venomous marine animals were better characterized, specific and effective remedies to treat these cases could be developed. Furthermore, protein toxins that exhibit unique bioactivities may be utilized as molecular pharmacological probes in the medical and biochemical fields. The study of protein toxins produced by venomous marine animals has the potential to generate many interesting discoveries in the future.

29.11 Study Questions

1. Which is the most dangerous one among venomous marine animals that utilize protein toxins?
2. Do cnidarians generally recognized as nonvenomous, for example, a moon jelly, also have the toxin?
3. From the marine animals, many famous nonpolypeptide toxins such as tetrodotoxin, palytoxin, and ciguatoxin have been reported. Why do most of the marine venomous animals use the protein (polypeptide) toxins instead of the nonpolypeptide toxins?
4. Why are most of protein toxins from marine venomous animals so unstable?
5. How do the marine venomous animals protect themselves from their own venom?

Acknowledgments The author thanks Okinawa Prefectural Institute of Health and Environment for the courtesy of the photographs.

References

1. Halstead BW (1988) Hydroids, jellyfishes, sea anemones, corals. Poisonous and venomous marine animals of the world. Darwin Press, Princeton, pp 99–186
2. Honma T, Shiomi K (2006) Peptide toxins in sea anemones: structural and functional aspects. *Mar Biotechnol* 8:1–10
3. Halai R, Craik DJ (2009) Conotoxins: natural product drug leads. *Nat Prod Rep* 26:526–536
4. Halstead BW (1988) Venomous scorpionfishes. Poisonous and venomous marine animals of the world. Darwin Press, Princeton, pp 839–906
5. Ghadessy FJ, Chen D, Kini M, Chung MCM, Jeyaseelan K, Khoo HE, Yuen R (1996) Stonustoxin is a novel lethal factor from stonefish (*Synanceja horrida*) venom - cDNA cloning and characterization. *J Biol Chem* 271:25575–25581
6. Austin L, Gills RG, Youatt G (1965) Stonefish venom: some biochemical and chemical observations. *Aust J Exp Biol Med Sci* 43:79–90
7. Woo JS, Imm JH, Min CK, Kim KJ, Cha SS, Oh BH (2006) Structural and functional insights into the B30.2/SPRY domain. *EMBO J* 25:1353–1363
8. Garnier P, Ducancel F, Ogawa T, Boulain JC, Goudey-Perrière F, Perrière C, Ménez A (1997) Complete amino-acid sequence of the beta-subunit of VTX from venom of the stonefish (*Synanceia verrucosa*) as identified from cDNA cloning experiments. *Biochem Biophys Acta* 1337:1–5
9. Garnier P, Goudey-Perrière F, Breton P, Dewulf C, Petek F, Perrière C (1995) Enzymatic properties of the stonefish (*Synanceia verrucosa* Bloch and Schneider, 1801) venom and purification of a lethal, hypotensive and cytolytic factor. *Toxicon* 33:143–155
10. Ueda A, Suzuki M, Honma T, Nagai H, Nagashima Y, Shiomi K (2006) Purification, properties and cDNA cloning of neoverrucotoxin (neoVTX), a hemolytic lethal factor from the stonefish *Synanceia verrucosa* venom. *Biochim Biophys Acta* 1760:1713–1722
11. Low KS, Gwee MC, Yuen R, Gopalakrishnakone P, Khoo HE (1993) Stonustoxin: a highly potent endothelium-dependent vasorelaxant in the rat. *Toxicon* 31:1471–1478
12. Liew HC, Khoo HE, Moore PK, Bhatia M, Lu J, Moolchhala SM (2007) Synergism between hydrogen sulfide (H₂S) and nitric oxide (NO) in vasorelaxation induced by stonustoxin (SNTX), a lethal and hypotensive protein factor isolated from stonefish *Synanceja horrida* venom. *Life Sci* 80:1664–1668
13. Sung JML, Low KS, Khoo HE (2002) Characterization of the mechanism underlying stonustoxin-mediated relaxant response in the rat aorta in vitro. *Biochem Pharmacol* 63:1113–1118
14. Yuen R, Cai B, Khoo HE (1995) Production and characterization of monoclonal antibodies against stonustoxin from *Synanceja horrida*. *Toxicon* 33:1557–1564
15. Chaatwal I, Dreyer F (1992) Isolation and characterization of dracotoxin from the venom of the greater weever fish *Trachinus draco*. *Toxicon* 30:87–93
16. Russel FE, Fairchild MD, Michaelson J (1958) Some properties of the venom of the stingray. *Med Arts Sci* 12:78–86
17. Magalhães KW, Lima C, Piran-Soares AA, Marques EE, Hiruma-Lima CA, Lopes-Ferreira M (2006) Biological and biochemical properties of the Brazilian Potamotrygon stingrays: *Potamotrygon* cf. *scobina* and *Potamotrygon* gr. *orbignyi*. *Toxicon* 47:575–583
18. Conceição K, Konno K, Melo RL, Marques EE, Hiruma-Lima CA, Lima C, Richardson M, Pimenta DC, Lopes-Ferreira M (2006) Orpotrin: a novel vasoconstrictor peptide from the venom of the Brazilian stingray *Potamotrygon* gr. *orbignyi*. *Peptides* 27:3039–3046

19. Perriere C, Goudey-Perriere F (1989) Origin and function of supporting cells in the venom glands of the lesser weeverfish (*Trachinus vipera*). *Toxicon* 27:287–295
20. Auddy B, Gomes A (1996) Indian catfish (*Plotosus canius*, Hamilton) venom. Occurrence of lethal protein toxin (toxin-PC). *Adv Exp Med Biol* 391:225–229
21. Schaeffer RC Jr, Carlson RW, Russell FE (1971) Some chemical properties of the venom of the scorpionfish *Scorpaena guttata*. *Toxicon* 9:69–78
22. Hahn ST, O'Connor JM (2000) An investigation of the biological activity of bullrout (*Notesthes robusta*) venom. *Toxicon* 38:79–89
23. Lopes-Ferreira M, Barbaro KC, Cardoso DF, Moura-Da-Silva AM, Mota I (1998) *Thalassophryne nattereri* fish venom: biological and biochemical characterization and serum neutralization of its toxic activities. *Toxicon* 36:405–410
24. Williamson J, Burnett J (1995) Clinical toxicology of marine coelenterate injuries. In: Meiter J, White J (eds) *Clinical toxicology of animal venoms and poisons*. CRC Press, Boca Raton, pp 89–116
25. Walker MJA (1988) Coelenterate and Echinoderm toxins: mechanisms and actions. In: Tu AT (ed) *Handbook of natural toxins*, vol 3. Marcel Dekker, New York, pp 279–325
26. Lewis C, Bentlage B (2009) Evolution of box jellyfish (Cnidaria: Cubozoa), a group of highly toxic invertebrates. *Zootaxa* 2030:59–65
27. Fenner PJ, Williamson JA (1996) Worldwide deaths and severe envenomation from jellyfish stings. *Med J Australia* 165:658–661
28. Fenner PJ, Harrison SL (2000) Irukandji and Chironex fleckeri jellyfish envenomation in tropical Australia. *Wilderness Environ Med* 11:233–240
29. Nagai H, Takuwa K, Nakao M, Ito E, Miyake M, Noda M, Nakajima T (2000) Novel proteinaceous toxins from the box jellyfish (sea wasp) *Carybdea rastoni*. *Biochem Biophys Res Commun* 275:582–588
30. Thomas CS, Scott SA, Galanis DJ, Goto RS (2001) Box jellyfish (*Carybdea alata*) in Waikiki: Their influx cycle plus the analgesic effect of hot and cold packs on their stings to swimmers at the beach: a randomized, placebo-controlled, clinical trial. *Hawaii Med J* 60:100–107
31. Nagai H, Takuwa K, Nakao M, Sakamoto B, Crow GL, Nakajima T (2000) Isolation and characterization of a novel protein toxin from the Hawaiian box jellyfish (sea wasp) *Carybdea alata*. *Biochem Biophys Res Commun* 275:589–594
32. Nagai H, Takuwa-Kuroda K, Nakao M, Oshiro N, Iwanaga S, Nakajima T (2002) A novel protein toxin from the deadly box jellyfish (Sea Wasp, Habu-kurage) *Chiropsalmus quadrigatus*. *Biosci Biotech Biochem* 66:97–102
33. Kini RM, Evans HJ (1989) A common cytolytic region in myotoxins, hemolysins, cardiotoxins and antibacterial peptides. *Int J Peptide Protein Res* 34:277–286
34. Belmonte G, Menestrina G, Pederzoli C, Krizaj I, Gubensek F, Turk T, Macek P (1994) Primary and secondary structure of a pore-forming toxin from the sea anemone, *Actinia equina* L., and its association with lipid vesicles. *Biochem Biophys Acta* 1192:197–204
35. Rottini G, Gusmani L, Parovel E, Avian M, Patriarca P (1995) Purification and properties of a cytolytic toxin in venom of the jellyfish *Carybdea marsupialis*. *Toxicon* 33:315–326
36. Sánchez-Rodríguez J, Torrens E, Segura-Puertas L (2006) Partial purification and characterization of a novel neurotoxin and three cytotoxins from box jellyfish (*Carybdea marsupialis*) nematocyst venom. *Arch Toxicol* 80:163–168
37. Brinkman D, Burnell J (2007) Identification, cloning and sequencing of two major venom proteins from the box jellyfish, *Chironex fleckeri*. *Toxicon* 50:850–860
38. Brinkman D, Burnell J (2008) Partial purification of cytolytic venom proteins from the box jellyfish, *Chironex fleckeri*. *Toxicon* 51:853–863
39. Othman I, Burnett JW (1990) Techniques applicable for purifying *Chironex fleckeri* (box-jellyfish) venom. *Toxicon* 28:821–835

40. Burnett JW, Bloom DA, Imafuku S, Houck H, Vanucci S, Aurelian L, Morris SC (1996) Coelenterate venom research 1991–1995: clinical, chemical and immunological aspects. *Toxicon* 34:1377–1383
41. Ishikawa T, Vucenik I, Shamsuddin A, Niculescu F, Burnett JW (2004) Two new actions of sea nettle (*Chrysaora quinquecirrha*) nematocyst venom: studies on the mechanism of actions on complement activation and on the central nervous system. *Toxicon* 44:895–899
42. Cariello L, Romano G, Spagnuolo A, Zanetti L (1988) Isolation and partial characterization of rhizolysin, a high molecular weight protein with hemolytic activity, from the jellyfish *Rhizostoma pulmo*. *Toxicon* 26:1057–1065
43. Ghosh TK, Gomes A, Chaudhuri AK (1993) Isolation of a toxin from jellyfish *Acromitus rabanchatu* and its effect on skeletal muscle. *Toxicon* 31:873–880
44. Lotan A, Fishman L, Zlotkin E (1996) Toxin compartmentation and delivery in the Cnidaria: the nematocyst's tubule as a multiheaded poisonous arrow. *J Exp Zool* 275:444–451
45. Sosa BP, Alagón AC, Martin BM, Possani LD (1986) Biochemical characterization of the phospholipase A2 purified from the venom of the Mexican beaded lizard (*Heloderma horridum horridum* Wiegmann). *Biochemistry* 25:2927–2933
46. Shipolini RA, Doonan S, Vernon CA (1974) The disulphide bridges of phospholipase A2 from bee venom. *Eur J Biochem* 48:477–483
47. Tamkun MM, Hessinger DA (1981) Isolation and partial characterization of a hemolytic and toxic protein from the nematocyst venom of the Portuguese Man-of-War, *Physalia physalis*. *Biochim Biophys Acta* 667:87–98
48. Anderluh G, Macek P (2002) Cytolytic peptide and protein toxins from sea anemones (Anthozoa: Actiniaria). *Toxicon* 40:111–124
49. Kristan K, Podlessek Z, Hojnik V, Gutiérrez-Aguirre I, Guncar G, Turk D, González-Mañas JM, Lakey JH, Macek P, Anderluh G (2004) Pore formation by equinatoxin, a eukaryotic pore-forming toxin, requires a flexible N-terminal region and a stable beta-sandwich. *J Biol Chem* 279:46509–46517
50. Bakrac B, Gutiérrez-Aguirre I, Podlessek Z, Sonnen AF, Gilbert RJ, Macek P, Lakey JH, Anderluh G (2008) Molecular determinants of sphingomyelin specificity of a eukaryotic pore-forming toxin. *J Biol Chem* 283:18665–18677
51. Athanasiadis A, Anderluh G, Macek P, Turk D (2001) Crystal structure of the soluble form of equinatoxin II, a pore-forming toxin from the sea anemone *Actinia equina*. *Structure* 9:341–346
52. Mancheño JM, Martín-Benito J, Martínez-Ripoll M, Gavilanes JG, Hermoso JA (2003) Crystal and electron microscopy structures of sticholysin II actinoporin reveal insights into the mechanism of membrane pore formation. *Structure* 11:1319–1328
53. Kawashima Y, Nagai H, Ishida M, Nagashima Y, Shiomi K (2003) Primary structure of echotoxin 2, an actinoporin-like hemolytic toxin from the salivary gland of the marine gastropod *Monoplex echo*. *Toxicon* 42:491–497
54. Shiomi K, Kawashima Y, Mizukami M, Nagashima Y (2002) Properties of proteinaceous toxins in the salivary gland of the marine gastropod (*Monoplex echo*). *Toxicon* 40:563–571
55. Gutiérrez-Aguirre I, Trontelj P, Macek P, Lakey JH, Anderluh G (2006) Membrane binding of zebrafish actinoporin-like protein: AF domains, a novel superfamily of cell membrane binding domains. *Biochem J* 398:381–392
56. Nagai H, Oshiro N, Takuwa-Kuroda K, Iwanaga S, Nozaki M, Nakajima T (2002) Novel proteinaceous toxins from the nematocyst venom of the Okinawan sea anemone *Phyllodiscus semoni* Kwietniewski. *Biochem Biophys Res Commun* 294:760–763
57. Satoh H, Oshiro N, Iwanaga S, Namikoshi M, Nagai H (2007) Characterization of PsTX-60B, a new membrane-attack complex/perforin (MACPF) family toxin, from the venomous sea anemone *Phyllodiscus semoni*. *Toxicon* 49:1208–1210
58. Oshiro N, Kobayashi C, Iwanaga S, Nozaki M, Namikoshi M, Spring J, Nagai H (2004) A new membrane-attack complex/perforin (MACPF) domain lethal toxin from the nematocyst venom of the Okinawan sea anemone *Actinaria villosa*. *Toxicon* 43:225–228

59. Bateman A, Coin L, Durbin R, Finn RD, Hollich V, Griffiths-Jones S, Khanna A, Marshall M, Moxon S, Sonnhammer EL, Studholme DJ, Yeats C, Eddy SR (2004) The Pfam protein families database. *Nucleic Acids Res* 32:D138–D141
60. Letunic I, Goodstadt L, Dickens NJ, Doerks T, Schultz J, Mott R, Ciccarelli F, Copley RR, Ponting CP, Bork P (2002) Recent improvements to the SMART domain-based sequence annotation resource. *Nucleic Acids Res* 30:242–244
61. Müller-Eberhard HJ (1986) The membrane attack complex of complement. *Annu Rev Immunol* 4:503–528
62. Liu CC, Walsh CM, Young JD (1995) Perforin: structure and function. *Immunol Today* 16:194–201
63. Nagai H, Oshiro N, Takuwa-Kuroda K, Iwanaga S, Nozaki M, Nakajima T (2002) A new polypeptide toxin from the nematocyst venom of an Okinawan sea anemone *Phyllodiscus semoni* (Japanese name “unbachi-isoginchaku”). *Biosci Biotechnol Biochem* 66:2621–2625
64. Uechi G, Toma H, Arakawa T, Sato Y (2005) Molecular cloning and functional expression of hemolysin from the sea anemone *ActinERIA villosa*. *Protein Expr Purif* 40:379–384
65. Mizuno M, Nishikawa K, Yuzawa Y, Kanie T, Mori H, Araki Y, Hotta N, Matsuo S (2000) Acute renal failure after a sea anemone sting. *Am J Kidney Dis* 36:E10
66. Mizuno M, Nozaki M, Morine N, Suzuki N, Nishikawa K, Morgan BP, Matsuo S (2007) A protein toxin from the sea anemone *Phyllodiscus semoni* targets the kidney and causes a severe renal injury with predominant glomerular endothelial damage. *Am J Pathol* 171:402–414
67. Bernheimer AW, Avigad LS (1978) A cholesterol-inhibitable cytolytic protein from the sea anemone *Metridium senile*. *Biochim Biophys Acta* 541:96–106
68. Lewis JW (2006) Biology and ecology of the hydrocoral millepora on coral reefs. *Adv Mar Biol* 50:1–55
69. Wittle LW, Middlebrook RE, Lane CE (1971) Isolation and partial purification of a toxin from *Millepora alcornis*. *Toxicon* 9:327–331
70. Middlebrook RE, Wittle LW, Scura ED, Lane CE (1971) Isolation and purification of a toxin from *Millepora dichotoma*. *Toxicon* 9:333–336
71. Wittle LW, TScura ED, Middlebrook RE (1974) Stinging coral (*Millepora tenera*) toxin: a comparison of crude extracts with isolated nematocyst extracts. *Toxicon* 12:481–486
72. Shiomi K, Hosaka M, Yanaike N, Yamanaka H, Kikuchi T (1989) Partial characterization of venoms from two species of fire corals *Millepora platyphylla* and *Millepora dichotoma*. *Nippon Suisan Gakkaishi* 55:357–362
73. Radwan FF, Aboul-Dahab HM (2004) Milleporin-1, a new phospholipase A2 active protein from the fire coral *Millepora platyphylla* nematocysts. *Comp Biochem Physiol C* 139:267–272
74. Iguchi A, Iwanaga S, Nagai H (2008) Isolation and characterization of a novel protein toxin from fire coral. *Biochem Biophys Res Commun* 365:107–112
75. Neame PJ, Choi HU, Rosenberg LC (1989) The isolation and primary structure of a 22-kDa extracellular matrix protein from bovine skin. *J Biol Chem* 264:5474–5479
76. Superti-Furga A, Rocchi M, Schafer BW, Gitzelmann R (1993) Complementary DNA sequence and chromosomal mapping of a human proteoglycan-binding cell-adhesion protein (dermatopontin). *Genomics* 17:463–467
77. Cronshaw AD, MacBeath JR, Shackleton DR, Collins JF, Fothergill-Gilmore LA, Hulmes DJ (1993) TRAMP (tyrosine rich acidic matrix protein), a protein that co-purifies with lysyl oxidase from porcine skin. Identification of TRAMP as the dermatan sulphate proteoglycan-associated 22K extracellular matrix protein. *Matrix* 13:255–266
78. Tzen CY, Huang YW (2004) Cloning of murine early quiescence-1 gene: the murine counterpart of dermatopontin gene can induce and be induced by cell quiescence. *Exp Cell Res* 294:30–38
79. Fujii N, Minetti CA, Nakhasi HL, Chen SW, Barbehenn E, Nunes PH, Nguyen NY (1992) Isolation, cDNA cloning, and characterization of an 18-kDa hemagglutinin and amebocyte aggregation factor from *Limulus polyphemus*. *J Biol Chem* 267:22452–22459

80. Schütze J, Skorokhod A, Müller IM, Müller WE (2001) Molecular evolution of the metazoan extracellular matrix: cloning and expression of structural proteins from the demosponges *Suberites domuncula* and *Geodia cydonium*. *J Mol Evol* 53:402–415
81. Marxen JC, Nimtz M, Becker W, Mann K (2003) The major soluble 19.6 kDa protein of the organic shell matrix of the freshwater snail *Biomphalaria glabrata* is an N-glycosylated dermatopontin. *Biochim Biophys Acta* 1650:92–98
82. Okamoto O, Fujiwara S (2006) Dermatopontin, a novel player in the biology of the extracellular matrix. *Connect Tissue Res* 47:177–189
83. MacPherson JC, Jacobs RS (2000) An 18.5 kDa protein from the amebocyte of *Limulus polyphemus*, homologous to the previously described amebocyte aggregation factor, expresses alternative phospholipase A2 activity. *Comp Biochem Physiol B* 127:31–44
84. Lomonte B, Rojas G, Gutierrez JM, Ramirez G (1990) Isolation of a galactose-binding lectin from the venom of the snake *Bothrops godmani* (Godmann's pit viper). *Toxicon* 28:75–81
85. Liang SP, Pan X (1995) A lectin-like peptide isolated from the venom of the Chinese bird spider *Selenocosmia huwena*. *Toxicon* 33:875–882
86. Aragon-Ortiz F, Brenes-Brenes JR, Gubensek F (1989) Characterization of a lectin-like protein isolated from *Lachesis muta* snake venom. *Rev Biol Trop* 37:79–83
87. Carvalho DD, Marangoni S, Oliveira B, Novello JC (1998) Isolation and characterization of a new lectin from the venom of the snake *Bothrops jararacussu*. *Biochem Mol Biol Int* 44:933–938
88. de Carvalho DD, Schmitmeier S, Novello JC, Markland FS (2001) Effect of BJcuL (a lectin from the venom of the snake *Bothrops jararacussu*) on adhesion and growth of tumor and endothelial cells. *Toxicon* 39:1471–1476
89. Panunto PC, da Silva MA, Linardi A, Buzin MP, Melo SESFC, Mello SM, Prado-Franceschi J, Hyslop S (2006) Biological activities of a lectin from *Bothrops jararacussu* snake venom. *Toxicon* 47:21–31
90. Klug M, Weber J, Tardent P (1989) Hemolytic and toxic properties of *Hydra attenuata* nematocysts. *Toxicon* 27:325–339
91. Zhang M, Fishman Y, Sher D, Zlotkin E (2003) Hydralysin, a novel animal group-selective paralytic and cytolytic protein from a noncnidocystic origin in hydra. *Biochemistry* 42:8939–8944
92. Sher D, Fishman Y, Zhang M, Lebendiker M, Gaathon A, Mancheño JM, Zlotkin E (2005) Hydralysins, a new category of beta-pore-forming toxins in cnidaria. *J Biol Chem* 280:22847–22855
93. Sher D, Knebel A, Bsor T, Neshet N, Tal T, Morgenstern D, Cohen E, Fishman Y, Zlotkin E (2005) Toxic polypeptides of the hydra—a bioinformatic approach to cnidarian allomones. *Toxicon* 45:865–879
94. Shiomi K, Midorikawa S, Ishida M, Nagashima Y, Nagai H (2004) Plancitoxins, lethal factors from the crown-of-thorns starfish *Acanthaster planci*, are deoxyribonucleases II. *Toxicon* 44:499–506
95. Ota E, Nagashima Y, Shiomi K, Sakurai T, Kojima C, Waalkes MP, Himeno S (2006) Caspase-independent apoptosis induced in rat liver cells by plancitoxin I, the major lethal factor from the crown-of-thorns starfish *Acanthaster planci* venom. *Toxicon* 48:1002–1010
96. Kini RM (2003) Excitement ahead: structure, function and mechanism of snake venom phospholipase A2 enzymes. *Toxicon* 42:827–840
97. Shiomi K, Kazama A, Shimakura K, Nagashima Y (1998) Purification and properties of phospholipases A2 from the crown-of-thorns starfish (*Acanthaster planci*) venom. *Toxicon* 36:589–599
98. Ota E, Nagai H, Nagashima Y, Shiomi K (2006) Molecular cloning of two toxic phospholipases A2 from the crown-of-thorns starfish *Acanthaster planci* venom. *Comp Biochem Physiol B* 143:54–60
99. Alender CB, Feigen GA, Tomita JT (1965) Isolation and characterization of sea urchin toxin. *Toxicon* 3:9–17
100. Mebs D (1984) A toxin from the sea urchin *Tripneustes gratilla*. *Toxicon* 22:306–307

101. Nakagawa H, Tu AT, Kimura A (1991) Purification and characterization of Contractin A from the pedicellarial venom of sea urchin, *Toxopneustes pileolus*. Arch Biochem Biophys 284:279–284
102. Nakagawa H, Tanigawa T, Tomita K, Tomihara Y, Araki Y, Tachikawa E (2003) Recent studies on the pathological effects of purified sea urchin toxins. J Toxicol Toxin Rev 22:633–649
103. Takei M, Nakagawa H (2006) A sea urchin lectin, SUL-1, from the Toxopneustid sea urchin induces DC maturation from human monocyte and drives Th1 polarization in vitro. Toxicol Appl Pharmacol 213:27–36
104. Sheumack DD, Howden ME, Spence I, Quinn RJ (1978) Maculotoxin: a neurotoxin from the venom glands of the octopus *Hapalochlaena maculosa* identified as tetrodotoxin. Science 199:188–189
105. Ghiretti F (1959) Cephalotoxin: the Crab-paralysing Agent of the Posterior Salivary Glands of Cephalopods. Nature 183:1192–1193
106. Ghiretti F (1960) Toxicity of octopus saliva against crustaceans. Ann N Y Acad Sci 90:726–741
107. MacDonald NM, Cottrell GA (1970) Purification and mode of action of toxin from *Eledone cirrhosa*. Toxicon 8:142
108. Songdahl JH, Shapiro BJ (1974) Purification and composition of a toxin from the posterior salivary gland of *Octopus dofleini*. Toxicon 12:109–115
109. Cariello L, Zanetti L (1977) Alpha- and beta-cephalotoxin: two paralysing proteins from posterior salivary glands of *Octopus vulgaris*. Comp Biochem Physiol C 57:169–173
110. Ueda A, Nagai H, Ishida M, Nagashima Y, Shiomi K (2008) Purification and molecular cloning of SE-cephalotoxin, a novel proteinaceous toxin from the posterior salivary gland of cuttlefish *Sepia esculenta*. Toxicon 52:574–581

William H. Gerwick

Contents

30.1 Summary Perceptions on the Utility of Marine Natural Products 1421

30.2 A Futurist View on Marine Natural Products Research 1424

30.3 Study Questions 1427

References 1427

Abstract

This chapter provides a general conclusion to this textbook on marine natural products science by discussing a few outstanding achievements in the field, and then identifies several areas for future investigation that may be fertile. New technological advances will allow researchers to investigate issues of the production, utility, and function of marine natural products in highly insightful ways. Prospects for the field of marine natural products appear very bright because the field has embraced the involvement of many disciplines and technologies, thus ensuring high levels of innovation and vitality.

30.1 Summary Perceptions on the Utility of Marine Natural Products

This volume, intended as a textbook for students as well as a handbook for practitioners of the marine natural products sciences, has broadly surveyed a majority of the disciplines which make up this field. From overview chapters on

W.H. Gerwick
Scripps Institution of Oceanography, Skaggs School of Pharmacy and Pharmaceutical Sciences,
University of California, San Diego, CA, USA
e-mail: wgerwick@ucsd.edu

the distribution and chemical trends associated with different life forms to the methods used to study the intricate structures of their unique compounds, from the biosynthetic origin in the producing species to the chemical ecology, toxicology, and pharmacology, it is this complement of subjects from which the field derives such vitality and widespread interest. The confluence of multidisciplinary research, as experienced in marine natural products, is inherently rich in opportunities for innovation and creativity.

However, another factor helps to explain the passion of those learning and studying this area – curiosity! It is nearly universal for people to wonder how it is that sea creatures adapt to their underwater world, from their unusual shapes, colors, and sizes, to here an exploration of their adaptations at a chemical, biochemical, and genetic level. How do soft-bodied creatures avoid being eaten in shallow-water tropical ecosystems? How do creatures constantly bathed in microorganism-laden seawater resist microbial and viral infections? How do various shrimp, worms, and bacteria cope with the intense pressure and temperature of deep-sea vents or the sub-0°C temperatures under meters of continuous arctic sea ice? While in some cases, the answers or partial answers to these questions are known, many marine phenomena and habitats remain incompletely examined for their unique inhabitants and interesting life histories, even now in the early twenty-first century.

The field of marine natural products research has made important and widely recognized contributions in several arenas. Perhaps most notably visible have been the spectacular discoveries of marine natural products with utility to the biomedical disciplines. As chronicled in various chapters of this volume, new antineoplastic agents have been discovered from various marine life forms, and several are now approved to treat specific human cancers, including Halaven and Trabectedin [1]. Other useful agents have been developed from marine organisms to treat chronic pain (Prialt), whereas still others have commercially useful anti-inflammatory properties (pseudopterosin A) [2, 3]. Various unique protein-based adaptations of marine life have been studied and yielded such important products as Taq polymerase for amplifying DNA and green fluorescent protein for visualizing cellular and physiological events [4, 5]. And many promising agents in diverse therapeutic areas lie nearby on the development horizon!

However, on the converse side of useful biomedical products from the sea has been the characterization of numerous poisons and toxins created by marine life which negatively impact human health. Some of these are experienced as venoms from contacting these life forms directly, such as scorpion fish, sea snakes, or fish-hunting mollusks. Others enter our food chain through their accumulation in fish, shellfish, and other edible creatures from their ultimate microbial or microalgal sources, and characterization of their chemistry and pharmacology is a critical step in the process of detecting, avoiding, and treating such encounters. Ultimately, these toxins are potent agents that have the capacity to teach us new vistas of receptor and ion-channel pharmacology and, in a few cases, to offer leads toward drug development [6].

In this latter regard, biotechnological approaches are rapidly emerging as effective and ultimately affordable methods by which to develop some of these medical leads from the sea. Already, the protein products described above are produced by (and in some cases enable!) industrial-scale biotechnological manufacture. On the other hand, new genetic and biochemical understanding of the biosynthetic processes used to produce small molecules is being employed to create novel analog structures that allow structure-activity relationships to be examined, even in extraordinarily complex molecular classes. This is complemented by tremendous advances in synthetic organic chemistry that permit the industrial scale chemical synthesis of such elaborate and complicated structures as erubulin and discodermolide [7, 8]. These are indeed outstanding human achievements of the early twenty-first century!

In 1960, Professor David Keeling at the Scripps Institution of Oceanography published the now-iconic graph which recorded the yearly increase and seasonal variation in atmospheric carbon dioxide at Mauna Loa, Hawaii [9]. This marked the beginning of the current era of appreciation that human impacts on the earth can occur on a global scale. Consequences of this increased input of fossil fuel-derived CO₂ on various oceanic and atmospheric processes are under broad examination, and one of the most alarming is the measurable increase of ocean acidity resulting from CO₂ absorption into seawater and the resulting production of carbonic acid [10]. Various pH-dependent physiological processes, such as the aggregation of CaCO₃ to form the shells of mollusks and exoskeletons of corals, are impacted and place these marine life forms under increased stress. This global change in ocean pH will certainly hasten the extinction of many species as well as potentially lead to physical changes in the nearshore environment (e.g., coral reefs). In one sense, it is a race against time to more thoroughly understand and appreciate the capacity of marine organisms to produce small molecules of biomedical utility before they disappear! In this regard, the extraordinary developments in genome sequencing speed and capacity may at least allow a “genetic record” to be preserved of some of those species greatest at risk.

Remarkably, one group of ocean organisms, the microalgae, may hold a solution to our broad need for a sustainable source of liquid fuel [11]. Microalgae have many desirable characteristics, including their capacity to grow quickly, produce an abundance of oil that can be used as biodiesel, and use salt or brackish waters with nutrients derived from wastewater. Additionally, their culture does not compete with food-producing land (e.g., desert land may be ideal for microalgal pond cultures). It is important to recognize that burning of algal oil for energy production is carbon neutral in that it derives from the fixation of atmospheric CO₂ (as versus fossil fuels which add more carbon to the planetary biosphere). Moreover, the non-oil constituents and nutrients of algae can be recycled in an algal production facility or be used in other product streams such as a rich protein source for animal feed or pigments with diverse biotechnological applications. However, there are numerous technological, engineering, and scientific challenges before this vision might be realized, and this will require the passion, ingenuity, and persistent efforts of many talented people in the future.

30.2 A Futurist View on Marine Natural Products Research

From a futurist perspective, what can we look forward to in the development of the marine natural products sciences? As detailed throughout the chapters of this volume, there are many exciting frontiers in the field of marine natural products chemistry. While some of the basics are now in place, such as which organisms elaborate which types of natural products, and most recent estimates indicate some 22,000 different molecules have been isolated and chemically defined from marine life, these discoveries actually catalyze the emergence of even more questions for the future. This area of science, as so many are, has been strongly driven by technological capability, and the thoughts below are largely based on predictions of how technological advances will change the nature of the questions we will likely be asking in the future.

Inherent to the finding that a given molecule has an interesting biological activity is the question of biological target. With which specific protein or other macromolecule does this new substance interact? What is the nature of the interaction at a molecular level and at an atomic level? It is when understanding develops to this very specific level that true understanding of mechanism and rational drug design can take place. Related to this, a frontier not well developed in marine natural products chemistry is the use of modern structural biology coupled with computational science to understand the specific interactions between proteins and small molecules. A rich interface exists between drug action, structural biology, and computational chemistry; however, to date, there has been relatively little integration of computational chemistry into the field of natural products, and this will certainly change as these fields “discover one another.”

In a sense related to the foregoing discussion, there is an enormous opportunity to refine and extend the field of chemical ecology to a molecular level of understanding. With a desire to deepen understanding of the evolution of defensive secondary metabolites, it becomes of interest to again know the specific target of the defensive compound and the nature of the interaction. Clearly, to appreciate coevolution of these chemical and biochemical systems, it is critical to know of them and to know the nature of the interactions at a very specific and precise level.

Several chapters have specifically dealt with biosynthesis of marine natural products, and others have alluded to the pathways leading to assembly of their exotic and oftentimes complicated molecular structures. Some of the biosynthetic principals have been defined in a few groups of marine organisms, but for the most part, this is an area ripe for more exploration and innovation. One ultimate vision is that by study of the biosynthetic pathways at the genetic, protein, and mechanistic biochemical level, we will enable the capture and harness of these capacities so as to have efficient production systems of natural products and their analogs. However, the field of marine biosynthesis needs to demonstrate its relevance to biomedical research, the major funder of this type of research, through the creation of actual molecular entities that can be evaluated in biological systems. Unfortunately, this goal and vision has been difficult to realize largely because the pathways are

exceedingly complex and a number of spatial and geometrical constraints appear to govern their catalytic efficiency. For those pathways involving modular polyketide synthases (PKSs) and nonribosomal peptide synthetases (NRPSs), such as the curacin A pathway from the marine cyanobacterium *Lyngbya majuscula* [12], the construction of the molecular scaffold occurs as a result of numerous consecutive passages of product from one enzyme to become substrate of the next. In effect, it is like running a relay race with passage of the baton between 40 participants as they traverse a complex maze! But there have been a few successes in these regards, such as production of cryptophycin analogs by provision of advanced precursors to unique catalytic machinery captured from the biosynthetic pathway [13], or the formation of unique salinosporamide analogs through production of blocked mutants followed by provision of alternate substrates [14]. Other successes from developing knowledge of biosynthetic pathways include the prediction, functional expression, and biological evaluation of the products of so-called cryptic gene clusters (gene clusters for which the encoded metabolite has not yet been found or described) [15]. With so many developments in other aspects of genetic engineering and molecular biology, this general area remains a prime opportunity for creative and innovative research.

As detailed in several of the chapters of this textbook, marine microorganisms are increasingly being revealed as responsible for the production of diverse marine natural products. Of importance to this observation, which will certainly become better defined with further study, is the increasingly deep knowledge of the evolutionary relationships of marine microorganisms to one another. The last few years have seen a welcome shift to the broad use of the 16S rRNA gene by which to define microorganisms under study. This will continue to evolve as technological advances enable ever-increasing speed and efficiency of DNA sequencing, predicted to be just \$1 per megabase in a few years' time. With such ready access to genomic information, we will analyze relationships of microorganisms at the whole genome level; our current efforts using one or a few genes to define relationships will be viewed in a few years as primitive and lacking in power.

In the area of structural analysis, technologies are already emerging wherein we can directly see organic molecules by atomic force microscopy [16], and this will certainly improve to the point where this approach to structure determination will be commonplace. Gone will be indirect methods of structural analysis, such as NMR spectroscopy or X-ray crystallography, at least so within a laboratory environment. Rather, high-field benchtop NMR spectrometers and handheld mass spectrometers may soon be available and will allow for the direct analysis of plant and microbial samples in the field. Similarly, methods for genetic analysis will become miniaturized and perhaps provide real-time phylogenetic information in the field through wireless connection with gene databases. Possession of such powerful chemical and genetic information will allow the focused collection of organisms for further study. By coupling this detailed knowledge of structure to complete metabolomic, proteomic, transcriptomic, and genomic analyses, we will understand the relationships of genetics, epigenetics, and splice variations to individual differences and their responses to the environment.

Marine-derived macromolecules already constitute an important class of useful material, including such substances as microorganism-derived fluorescent proteins and temperature-stable DNA polymerases to algal polysaccharides with useful emulsifying or gelling properties. The many and highly diverse small-molecule natural products of marine life are the result of an even greater diversity of biosynthetic enzymes with unique reactivities and substrate specificities. At present, these enzymes largely represent a “conceptual toolbox” of useful catalysts; in the future, we will see their application to the production of novel substances with pharmaceutical or biotechnological utility. The biosynthesis of polysaccharides and other macromolecular classes will become even better understood, and it can be envisioned that we will be able to control their molecular assembly to produce polymeric materials with specifically desired properties.

The problem of “supply” has long plagued natural products drug development [17], and with smaller and smaller sample sizes succumbing to structure elucidation, this will only intensify (indeed, the theoretical lower limit is the single molecule, a limit already reached by atomic force microscopy!). However, one of the goals of chemical biology and biosynthetic investigations is to learn how to harness this genetic and biochemical machinery to produce compounds of interest and in the quantities necessary for meaningful biological evaluation. Such clever technological developments will also enable methods to express and study the products of “cryptic” gene clusters wherein the encoded product is not yet known due to either low or nil expression under normal culture conditions. While the quantities of a natural product needed for 1534-well plate assays are relatively easily achieved, to translate “screening hits” into meaningful lead compounds requires multiple milligrams for mechanism of action and *in vivo* evaluations. This need will continue to be a strong driver of chemical biology and innovative microbiological research well into the future.

Drug screening of natural product mixtures is certain to advance in ways that make the process more efficient and effective. This may involve innovative preselection of molecular classes for “desirable” pharmaceutical properties. Alternatively, transcriptomic and proteomic profiling to first assess mechanisms or pathways being modulated in advance of disease-specific biological assays may be a powerful new approach. Informatics analysis of data from screening of agents to a panel of targets or disease-causing organisms can also be efficient in identifying new agents that work by novel mechanisms of action. Clearly, much creativity and innovation is possible in the biological screening arena, and equally apparent, much is needed so as to have this process identify better drug candidates ever more efficiently.

The above thoughts represent a sampling of predictions that can be made at the present time, mainly through envisioning of specific technological advances, such as increased analytical power, DNA sequencing capability, or heterologous expression systems. What is not predicted, however, are the game-changing advances, the paradigm shifters, and the new technologies which will allow completely new approaches to be used and questions to be investigated. In composite, marine natural products science continues to be a vital and frontier field of investigation largely because it has embraced new technological advances and multidisciplinary approaches, and the future looks equally exciting!

30.3 Study Questions

1. Describe a technological advance other than those suggested above that will impact the field of marine natural products science.
2. Can you think of a paradigm-shifting advance in the field of marine natural products science? What knowledge or technological advances would be needed to realize your vision?

References

1. Mayer AMS, Glaser KB, Cuevas C, Jacobs RS, Kem W, Little RD, McIntosh JM, Newman DJ, Potts BC, Shuster DE (2010) The odyssey of marine pharmaceuticals: a current pipeline perspective. *Trends Pharmacol Sci* 31:255–265
2. Teichart RW, Olivera BM (2010) Natural products and ion channel pharmacology. *Future Med Chem* 2:731–744
3. Casapullo A, Monti MC, Riccio R (2008) Results and perspectives on anti-inflammatory marine natural products. In: Susan H (ed) *Natural products as future medicinal agents*. Transworld Research Network, Kerala, pp 165–194. ISBN 978-81-7895-394-6
4. Brownstein MJ (2004) PCR (polymerase chain reaction). *Encycl Biol Chem* 3:208–210
5. Tsien RY (2009) Constructing and exploiting the fluorescent protein paintbox (Nobel Lecture). *Angew Chem Int Ed* 48:5612–5626
6. Watters MR (2008) Marine neurotoxins as a starting point to drugs. In: Botana LM (ed) *Seafood and freshwater toxins: pharmacology, physiology, and detection*, 2nd edn. Taylor and Francis/CRC Press, Boca Raton, pp 889–897
7. Dalby SM, Paterson I (2010) Synthesis of polyketide natural products and analogs as promising anticancer agents. *Curr Opin Drug Discov Develop* 13:777–794
8. Mickel SJ (2007) Total synthesis of the marine natural product (+)- discodermolide in multigram quantities. *Pure Appl Chem* 79:685–700
9. Keeling CD (1960) The concentration and isotopic abundances of carbon dioxide in the atmosphere. *Tellus* 12:200–203
10. Feely RA, Orr J, Fabry VJ, Kleypas JA, Sabine CL, Langdon C (2009) Present and future changes in seawater chemistry due to ocean acidification. *Geophysical Monogr* 183:175–188
11. Huesemann M, Roesjadi G, Benemann J, Metting FB (2010) Biofuels from microalgae and seaweeds. In: *Biomass to Biofuels*. Wiley, New York, pp 165–184
12. Chang Z, Sitachitta N, Rossi JV, Roberts MA, Flatt PM, Jia J, Sherman DH, Gerwick WH (2004) Biosynthetic pathway and gene cluster analysis of Curacin A, an antitubulin natural product from the tropical marine cyanobacterium *lyngbya majuscula*. *J Nat Prod* 67:1356–1367
13. Rohr J (2006) Cryptophycin anticancer drugs revisited. *ACS Chem Biol* 1:747–750
14. Gulder TAM, Moore BS (2010) Salinosporamide natural products: potent 20 S proteasome inhibitors as promising cancer chemotherapeutics. *Angew Chem Int Ed* 49:9346–9367
15. Bergmann S, Schuermann J, Scherlach K, Lange C, Brakhage A, Hertweck C (2007) Genomics-driven discovery of PKS-NRPS hybrid metabolites from *Aspergillus nidulans*. *Nature Chem Biol* 3:213–217
16. Gross L, Mohn F, Moll N, Liljeroth P, Meyer G (2009) The chemical structure of a molecule resolved by atomic force microscopy. *Science* 325:1110–1114
17. Proksch P, Edrada-Ebel R, Ebel R (2003) Drugs from the sea – opportunities and obstacles. *Mar Drugs* 1:5–17

Index

A

- Abyssomicin C, 178
Acanthamides, 205
Acanthaster planci, 1409, 1410
Acanthella cavernosa, 758
Acantholides, 243
Acartia
 A. clausi, 721
 A. hudsonica, 727
 A. tonsa, 723
 A. bifflosa, 728
Accelerated solvent extraction (ASE), 759
ACD/ChemSketch, 574
Acetylcholinesterase inhibitors, 1177
Acinetobacter sp., 843
Acromitus rabanchatu, 1401
Acropora, 840
 A. formosa, 828, 832, 838
 A. longicyathus, 831
 A. palmata, 836, 840
Acroporids, 840
Acrosiphonia coalita, 103
Acrylate, 715
Actineria villosa, 1402, 1404
Actinia equina, 1402
Actinomyces, 759
Actinoporins, 1402, 1409
Adenosine phosphoribosyltransferase
 inhibitors, 1153–1154
Adhesion assay, 786
Aburatubolactam A, 169
Adociasulfates, 1206
Aequorin, 1232
Aerophobin 1, 1196
Aeroplysin–1, 208–210, 846,
 847, 1162
Aerothionin, 846, 847
Aeruginosins, 224, 1195
AFM. *See* Atomic force microscope (AFM)
Agaricia lamarcki, 829
Agaricia sp., 838
Agar overlay technique, 774
Agar well diffusion assay, 780
Ageladine A, 1199
Agelas, 702
 A. clathrodes, 198, 199, 535, 539
 A. conifera, 206, 846
 A. dispar, 199, 204
 A. longissima, 199, 204
 A. mauritiana, 199, 200
 A. nakamurai, 199, 200, 204
 A. oroides, 196, 200, 204
 A. sceptrum, 205
Agelasidines, 1203
Agelasines, 1096, 1203
Agelastatins, 204
Ageliferins, 198, 206, 217
Agrochelin A, 156
AI–2. *See* Autoinducer–2 (AI–2)
Aignopsanoic acid, 1102
Aiolochoira crassa, 846
Aka (= *Siphonodictyon*), 828
Akaterpin, 1184
Albicidin, 959, 961
Alboinon, 308
Alcyonacean soft coral, 848
Alcyonium paessleri, 832
Aldisines, 204, 1164
Aldose reductase inhibitors, 1147
Alexandrium, 715
 A. catenella, 81, 731
 A. fundyense, 727
 A. hiranoi, 85
 A. minutum, 723
 A. ostenfeldii, 1363
 A. tamarense, 721
Algal disease
 Porphyra spp., 843
 raisin disease, 843
 white rot disease, 843

- Algal spore settlement assays, 784
 Alisiaquinones, 1092, 1093, 1154, 1155
 Allelochemicals, 824
 Allelopathic effect, 739
 Allelopathy, 716, 824, 850
 Almiramides, 1097
 Altemicidin, 169
 Alterobactin, 869
Alteromonas
 A. luteoviolacea, 869
 A. tetraodonis, 1373
 Altohyrtins, 1038, 1039
 Amaminols, 326
 Amikacin, 480, 482
 Ammonificin B, 163
 Ammosamide A, 175
 Amnesic shellfish poisoning (ASP), 727, 1346, 1364, 1366
Amphicarpa meridiana, 299
 Amphiceramide B, 529
Amphidinium operculatum, 85
Amphidinium sp., 722
 Amphidinol-1, 86
 Amphidinolide-A, 722
 Amphidinolide A1, 637–640
 Amphidinolide N, 84
 Amphidinolides, 14, 909
 Amphidinols, 13
Amphimedon, 1089, 1101
 A. viridis, 846
 Amphimic acids, 1209
 Amphitoxin, 846, 847
Anabaena circinalis, 1373
 Ancorinosides, 1199
 Andrimid, 903
Anemonia sulcata, 1390
Anguilla rostrata, 849
 Anisotropic effects, 551
 Annulins, 1151
 Ansamitocin, 1000
 Anthozoans, 1233, 1234, 1239
 Anti-adhesion/attachment assay, 767
 Antialgal assays, 781–786
 Antibacterial assay, 764–775
 Antibacterial attachment assays, 766
 Antibiofilm formation, 770–773
 Antidiatom assay, 776
 attachment, 777
 growth, 777–778
 Antifoulants, 824
 Antifouling
 assays, 798–808
 bioassay, 802
 compounds, 755
 Antifungal assays, 778–780
 Antilarval settlement, 786–798
 Antillatoxin, 74, 75
 Antipredatory, 678
Aphanizomenon flos-aquae, 1373
Aphanocapsa feldmanni, 40
 Apicidins, 240
 Aplidiasphingosine, 326
 Aplidine, 41
 Aplidinones, 343, 344
Aplidium sp., 867, 868
 A. albicans, 338
 A. conicum, 308, 342, 343
 A. cyaneum, 310
 A. glabrum, 341
 A. haouarianum, 315
 A. lobatum, 349
 A. longithorax, 345
 A. meridianum, 309
 A. orthyum, 313
 A. pantherinum, 298
 A. pliciferum, 314
 A. uouo, 321
 Aplyolides, 27, 1174
Aplysia
 A. caissara, 208
 A. californica, 897
 Aplysiatoxins, 26, 27, 63
Aplysilla longispina, 828
Aplysina
 A. aerophoba, 700, 846
 A. fistularis, 846
 A. gerardogreeni, 214
 A. laevis, 208
 Aplysina red band syndrome (ARBS), 845
Aplysinella rhax, 210, 211, 790
 Aplysinones, 214
 Aplysinopsin, 24
 Aplysiol B, 595
 Aplysterol, 898, 906
 Apo-fucoanthin, 715
 Apo-fucoanthinoids, 731
 Apoptogenic inducers, 716
 Aposematism, 682
 AP-PLA2-I, 1410
 AP-PLA2-II, 1410
 Apratoxins, 41, 73, 74
 Aqabamycin E, 157
 Aquaculture, 1287, 1291, 1292, 1294, 1297–1302
Arabidopsis thaliana, 738

- Arachidonic acids, 716
Arborescines, 305
Arenamide A, 177
Arenastatin, 192, 223, 956, 1044–1045
Arenicolide A, 177
Arenimycin, 177
Ariakemicin A, 160
Armentomycin, 984
Arnoamines, 300
Arsenic, 865, 884, 886
Artemether, 1082
Artemisinin, 1077, 1080–1083, 1085, 1096
Artesunate, 1082
Arthropoda, 30
Ascidia
 A. ceratodes, 886
 A. mentula, 362
 A. nigra, 328, 886
 A. sydneyensis samea, 865
Ascidiacyclamide, 330, 878, 881
Ascididemin, 41, 299, 300, 869, 870, 877, 878, 1212
ASE. *See* Accelerated solvent extraction (ASE)
ASP. *See* Amnesic shellfish poisoning (ASP)
Asparagopsis armata, 844
Aspergillus, 414–415
 A. sydowii, 836, 848
Asteropine, 1187
Asteropterin, 1196
Asteropus sarasinum, 265
Asthenosoma iijimai, 1412
Astrosclera willeyana, 206
Atapozoa sp., 869
Atomaric acid, 125
Atomic force microscope (AFM), 1270, 1271, 1425, 1426
Atovaquone, 1079, 1093
Atrialum robustum, 361
Aurantimonas coralicida, 842
Aurelia aurita, 1401
Aureoverticillactam, 169
Auripyrone, 26, 28
Auristatin PE, 1295, 1296
Aurorals, 256, 257
Autoinducer-2 (AI-2), 158
Autotomy, 901
Autotoxicity, 681
Avilamycin A, 993, 1000
Avrainvillea
 A. longicaulis, 102
 A. nigricans, 102
 A. rawsonii, 102
Avrainvilleol, 102
Avt-I, 1404
AvTX-60A, 1402
Axinella
 A. carteri, 200, 204
 A. damicornis, 204
 A. verrucosa, 199, 200, 205, 897
Axinelloside, 1160
Axinohydantoins, 201
(Z)-Axinohydantoins, 202
Axisonitriles, 906, 907, 1087, 1088
Axisothiocyanates, 1087, 1088
Azadinium spinosum, 1354
Azamerone, 174
Azaspiracids (AZAs), 83, 84, 607–619, 622, 632–637, 1353, 1354
Azumamides, 239, 240, 1200

B
Bacillaene, 962
Bacillariolides, 90
Bacillistatin 1, 165
Bacillus amyloliquefaciens, 165
Bacilosarcin A, 165
Bacterial film, 806
Bahamamide A, 164
Balanus amphitrite, 758, 788–790
Barbamide, 903, 984
Barnacle cypris settlement, 757
Barnacle larvae, 799–800
Bastadins, 216, 217, 871
Batesian, 683
Batzelladine, 626
Belamide, 1041, 1043
Belizean acid, 1178
Bengacarboline, 305, 1210
Bengamide, 41
Benthic copepods, 716
Bifurcarenone, 125
Bifurcaria galapagensis, 125
Biodiesel, 1423
Biofilms, 750, 751, 754, 770
Bioluminescence, 1232, 1233
Biomineralization, 1264
 biologically controlled, 1263
 biologically induced, 1263
Biosensors, 1246
 fluorescent protein-based, 1246, 1247
Bioxalomycin α 1, 169
Bisaprasin A, 211, 1200
Biselides, 350
Bishomopalytoxin, 1368
Bispsammaplin A, 211

- Bistramides, 352, 353, 626
 Bistratamides, 333
 BJcuL, 1407
 Black band disease, 837
 Bleomycin, 869
 Bloom termination initiator, 716
 Bogorol A, 165
 Boltzmann distribution, 573, 582, 587
Bonannia graeca, 571, 573
 Bonannione B, 571, 573, 581, 589
 Bonannione B (1), 584
Bonellia viridis, 24
 Bonellin, 25
Bonnemaïsonia hamifera, 844
 Booster biocides, 754
 Born–Oppenheimer approximation, 583
Bothrops jararacussu, 1407
 Botryllamides, 313
 Botryllazines, 315
Botryllus leachi, 315
 Brassicasterol, 914
 Brevetoxins, 13, 74, 77, 79, 500, 622, 647, 726, 728, 834, 898, 1348, 1354, 1355, 1357
Briareum
 B. asbestinum, 825
 B. stechei, 831
 Bromoaldisine, 1164
 Bromoalterochromide A', 159
 Bromoaplysinopsin, 1091
 Bromoform, 844
 6-Bromoindole–3-carbaldehyde, 307
 Bromophycolide A, 114
 6-Bromotryptamine, 308
 Bryostatins, 1, 16, 25, 26, 41, 626, 641, 871, 949, 959, 964, 1169, 1286, 1291–1294, 1296, 1304
 bryA cluster, 1294
 bryologs, 1293
Bugula neritina, 791, 793, 794, 802, 806, 808, 814, 871, 1291–1293
 Butenolides, 758
 Byssal threads, 804
 Byssus, 795

C
 Caboxamycin, 169
Cacospongia sp., 829
 Cacospongionolides, 246, 1173
 CAD. *See* Collisionally activated decomposition (CAD)
 Caffeic acid, 843
 Caffeine, 714
 Calanolides, 1323–1325
Calanus
 C. funmarchicus, 723
 C. helgolandicus, 721, 726, 730, 739
 Caledonin, 876
Callipelta, 571, 589
 Callipeltins, 237, 238, 571, 589, 590, 592
Callista chione, 426
Callophycus serratus, 114, 115
 Callyspongynic acid, 1189
 Calmodulins, 870
 Calyceramides, 1187
 Calyculinamides, 404, 1179
 Calyculins, 403, 404, 1028, 1179
 Calysterol, 906, 907
 Camptothecin, 1319, 1335
 Capisterones, 98, 99
 CAplus, 392
Capnella lacertiliensis, 417
Carex pumila, 534
Caribdea rastoni, 1398
 Caribenolide I, 85
 Carmabins, 69
 Carteramine, 1005
 Cartilaginal, 469–471
 CARTOX, 1398, 1401
Carukia barnesi, 1395
Carybdea
 C. alata, 1397
 C. marsupialis, 1398, 1401
 C. rastoni, 1395, 1397
 Caspases, 716
 CAS REGISTRY, 392
 Catalases, 727, 980
 Cathepsin B, 1196–1197
 CaTX-A, 1397, 1398
 CaTX-B, 1397
Caulerpa
 C. racemosa, 827
 C. taxifolia, 905
 Caulerpenyne, 17, 18, 827, 905
 Caulerpin, 100, 101, 1131, 1132
 Cavernolide, 1173
 CBD. *See* Convention on biological diversity (CBD)
 CD. *See* Circular dichroism (CD)
 cDNA library, 737
 Cebulactam A1, 182
 Celebesides, 232, 233
Centropages typicus, 726
Cephalodiscus gilchristi, 31
 Cephalostatins, 31
 Cephalotoxin, 1413

- Ceratamines, 1058
Cerataulina, 721
CFP, 1346, 1357, 1359
CfTX-1, 1398, 1401
CfTX-2, 1398, 1401
Chaetoceros, 715, 717, 796
 C. gracilis, 787, 790
 C. socialis, 727
Chartellamides, 25
Chartellines, 25
Chattonella
 C. antiqua, 1355
 C. antique, 77
 C. marina, 77, 1355
CHCA. *See* α -Cyano-4-hydroxy-cinnamic acid (CHCA)
Chelynosus semperi, 300
ChemDraw, 574
Chemical abstracts service, 1136
Chemical deterrence
 activated chemical defense, 698
 additive, 696
 antagonistic, 696
 calcitic sclerites, 698
 induction, 698
 isobolographic analysis, 697
 logit model, 697
 synergistic, 696
Chemical ecology, 1422
Chetomin, 1120
Chinikomycin A, 169
 α -Chiral carboxylic acids, 555
Chironex
 C. fleckeri, 1395, 1398, 1401
 C. yamaguchii, 1395
Chiropsalmus quadrigatus, 1395, 1398
Chivosazol, 963
Chlamys farreri, 722
Chloramphenicol, 978, 995, 1000, 1003, 1006
Chlorodesmis fastigata, 827
Chlorohydra viridissima, 1409
Chloromertensene, 827
Chlorophyll *a*, 829
Chloroplastic glycolipids, 716
Chloroquine, 1079
Chlorotetracycline, 988, 1006
Chondramides, 222, 989, 993, 994, 1005
Chondria
 C. californica, 19
 C. crispus, 81
Chondrilla nucula, 699
Chondrillin, 1084
Chondrocoles, 468
Chondromyces crocatus, 222
Chromobacterium violaceum, 774
Chromobacterium violaceum CV026, 774
Chromodoris funerea, 244
Chromophore, 1236–1239
 p-HBI, 1236, 1237, 1239, 1243
Chromoproteins, 1233, 1239
Chrysaibol, 418
Chrysaora quinquecirrha, 1401
Chrysolaminarin, 16
Chrysopaentins, 93–95
Chrysophaeum taylori, 93
CID. *See* Collision-induced dissociation (CID)
Ciguatera, 726
Ciguatoxins, 79, 647, 909, 1349, 1357, 1358
Cinachyrolide, 1038, 1039
Cinchona bark, 1079
Ciona sp., 866
 C. intestinalis, 363, 866
 C. savignyi, 363
Circular dichroism (CD), 431, 498
 cotton effect, 498
 Davydov splitting, 500
 exciton chirality, 500
 octant rule, 500
Citorellamine, 308
Cladocerans, 716
Clarhamnoside peracetate, 539
Clathrina clathrus, 874
Clathrocin, 198
Clathroside B, 535, 536
Clathsterol, 1157
Clavaminols, 324
Clavatadines, 215, 1196
Clavelina
 C. cylindrica, 323
 C. lepadiformis, 323
 C. moluccensis, 323
 C. oblonga, 324
 C. phlegraea, 324
 C. picta, 322
Clavepictines, 322
Clavosines, 1179
Clavukerin, 899
Clavularia sp., 827
 C. frankliniana, 832
 C. inflata, 831
Clionapyrrolidine A, 830
Cliona tenuis, 830
Clorobiocin, 993, 1000, 1001
Clostridium perfringens, 839
Clupeotoxism, 1371
Coalital, 104

- Coccolith/coccolithophore algae, 1263
 Coibamide A, 41
 Collisionally activated decomposition (CAD), 451
 Collision-induced dissociation (CID), 451
 Comantherins, 1131
 Comaparvin, 1131
 Commercial databases, 392
 Community structure, 773
 Comoramides, 335
 COMPARE algorithm, 1049
 Conductor-like screening model (COSMO), 594
 Conicamin, 308
 Conicaquinones, 343
 Conicol, 342
 Conidione, 342
 Conitriol, 342
 ω -Conotoxin MVIIA, 39
 Constanolactones, 117
Constantinea simplex, 117
 Contractin A, 1412
Conus magus, 39
 Convention on biological diversity (CBD), 1317, 1318
 Copper-based antifouling coatings, 753
 Coral diseases, 835–842
 aspergillosis, 836
 bacterial bleaching, 836
 black band disease (BBD), 838
 brown band disease, 838
 dark spot syndrome (DSS), 838
 montipora white syndrome (MWS), 842
 resistance, 840–842
 susceptibility, 840
 white band disease-II, 836
 white plague-II, 836
 white pox disease, 836
 white syndrome, 837, 838
 Corallidictyals, 1167
 Coralline algae, 843
 Coralline white band syndrome, 843
 Coronatine, 984
 Corticatic acids, 1156
 Coscinamides, 1096
 Coscinosulfate, 1184
 COSMO. *See* Conductor-like screening model (COSMO)
 CqTX-A, 1398
 Crabtree's catalyst, 635
Crambe crambe, 866
 Crasserides, 20, 22
 Crellastatins, 1098
 Criamides, 1045, 1046
Cribrochalina olemda, 219, 227
 CrTX-A, 1397
 CrTX-B, 1397, 1398
 Crucigasterins, 324
 Cryptic gene clusters, 1425
 Cryptophycin(s), 41, 949, 978, 993, 994, 1044–1045, 1047, 1425
 biosynthesis, 957, 958
 Cryptophycin/Arenastatin, 956–958
Cryptotethia crypta, 9
 Crystamycin, 790
Ctenochaetus striatus, 1358
 Cubebol, 899
 Curacin(s), 41, 69, 72, 903, 904, 949, 953–956, 984, 986, 1048–1049, 1425
 biosynthesis, 949, 953–956
 Curcumin, 1135
 Curcuphenol, 1098, 1202
 Curtius rearrangement, 608, 643
 Cyanobacteria, 723
 metabolic and anatomical features, 58
 molecular weights of metabolites, 59
 symbiotic relationships, 58
 taxonomy, 57
 Cyanobactins, 64, 65, 67, 878
 α -Cyano-4-hydroxy-cinnamic acid (CHCA), 442
 Cyanopeptolins, 64, 65
 Cyanosafracin B, 658, 1302
 Cyanosporaside, 178, 1004
 Cyanthiwigin U, 643, 664
 Cyclin-dependent kinase inhibitors, 1170–1171
 Cyclodidemniserinol trisulfate, 351
 Cycloheximide, 1123
 Cyclomarins, 177, 916
 cyclomarine, 916
 feeding experiments, 918
 Cyclooroidin, 204
 Cyclopentyne, 427
 Cyclosporine, 488, 489
 Cyclostelletamines, 1090, 1200
 Cyclotheonamides, 228, 229, 1192
 Cyercenes, 933
Cyerce nigricans, 682
 Cylindricines, 323
Cylindrospermopsis raciborskii, 1373
 Cylodidemnamide, 331
Cymodocea nodosa, 827
Cymopolia barbata, 99
 Cymopols, 99–100
Cyphoma, 685
Cypridina hilgendorffii, 603

Cystodites dellechiaiei, 300

Cystodytes dellechiaiei, 298

Cystodytins, 298, 1212

D

DAD. *See* Diode array detector (DAD)

Danicalipin A, 92

Danio rerio, 1402

Daryamide A, 169

Dasycladus vermicularis, 102

Databases, 407

ACD/LABS, 391, 396

ACS SciFinder, 432

ANTIBASE, 391, 394, 400, 407, 419

ANTIMARIN, 391, 395, 399–401, 407,
408, 414, 416, 419

CA PLUS, 393

CASREACT, 393

CAS REGISTRY, 391, 393, 400, 401

CHEMCATS, 393

CHEMLIST, 393

CHEMnetBASE, 394

CHEMSPIDER, 391, 400, 401, 419, 432

CHEM SPIDERLS, 398

CSLS, 391, 397, 400, 401, 419

DICTIONARY OF MARINE NATURAL
PRODUCTS, 391, 393–394, 400,
401, 419

DICTIONARY OF NATURAL
PRODUCTS, 391, 393–394, 400,
401, 419

Dictionary of organic compounds, 432

HSQC/DEPT, 399

MARINLIT, 391, 394–395, 399–401, 407,
410, 413, 416, 419, 432

MARPAT, 393

MEDLINE, 393

Merck Index, 432

NAPRALERT, 391, 399, 400, 419

NAPROC–13, 391, 407

NMRSHIFTDB, 391, 407

PUBCHEM, 391, 397, 400, 419

REAXYS, 391, 393, 400, 419

SCI FINDER, 393, 419

SDBS, 391, 407

SPECINFO, 391, 396, 407

STN easy, 392

STN express, 392

SUPERNATURAL, 391, 407

Dauben oxidative transposition, 643

DCMG. *See* 5,6-dichloro–1-methylgramine
(DCMG)

7-Deacetoxyolepupane, 829

Debromoeudistomin K, 305

Debromohamigeran E, 409

Debromohymenialdisine, 200, 202, 1164

Decadial, 716, 722, 736

Decatrienal, 715

2,4,7-decatrienal, 717

Deferoxamine, 871

22-Dehydro–7 β -hydroxy-cholesterol, 832

Delisea pulchra, 758, 844

Dendrillia cactus, 216, 318

Dendrodoa grossularia, 307, 308

Dendrodoris limbata, 901, 908

Dendronephthya griffini, 92

Density functional theory (DFT), 498, 503, 584

Density functional theory, time-dependent
DFT (TDDFT), 498

Denticulatin, 901, 902

Deoxyartemisinin, 1082

5'-deoxyguanosine monophosphate, 441

Deoxypalytoxin, 1368

Dereplication, 390, 398–410, 432, 1127,
1135–1138

Dermatopontins, 1407

DESI (desorption electrospray ionization)
MS, 887

6-Desmethoxyhormothamnione, 93

Dess–Martin periodinane, 637

DFT. *See* Density functional theory (DFT)

6,7-Diacetoxy–4-methylcoumarin, 455

Diadema

D. antillarum, 834

D. setosum, 1412

Diaion HP20, 761

Diamagnetic anisotropy, 548

Diamagnetic spin-orbit (DSO), 590

Diarrhetic shellfish poisoning (DSP), 726,
1346, 1353, 1366, 1367, 1377

Diatom biofilms, 807

Diatoms, 713, 723, 775, 904, 925–930,
928, 930

Diazepinomicin, 178

Diazona, 611

D. angulata, 336

Diazonamides, 41, 336, 607–622, 664,
1050–1051

Dibromoagelospongin, 203

6,6'-dibromindigotin, 28

5,6-Dichloro–1-methylgramine (DCMG), 758

Dictyoceratida sp., 827

Dictyodendrins, 41, 1160

Dictyodial, 123

Dictyodioid, 123

- Dictyolactone, 123
 Dictyostatin, 41, 626, 1057
Dictyota
 D. crenulata, 123
 D. menstrualis, 825
 Dictyotenes, 121, 900
 Didemnaketals, 352, 354, 1198
 Didemnilactones, 1150
 Didemnimides, 311
 Didemnins, 29, 32, 41, 337, 338, 1287–1291, 1296
 aplidine, 1287–1291
 Didemniserinolipids, 326, 352
 Didemnolines, 304
Didemnum sp., 866–869
 D. candidum, 308
 D. conchyliatum, 311
 D. granulosum, 311
 D. guttatum, 351
 D. molle, 331, 333, 364
 D. rodriguezi, 340, 876
 D. ternatanum, 313
 Dideoxyverticillin A, 632
Didiscus oleata, 199
 Didmolamides, 333
 Dieckmann condensation, 643
 Diels–Alder reactions, 630, 631, 635
 Diethanolamine, 441
 Difficidin, 959
Digenia simplex, 56, 89
 Dihydroartemisinin, 1082
 7,8-Dihydro-4-ene-plakortide M, 829
 2,5-Dihydroxybenzoic acid, 442
 6,14-Dihydroxy-7-drimen-12,11-olide, 20
 Diisocyanoadociane, 899, 906
 Dimethylarsinoyl-ribosides, 26, 28
 Dimethyl sulfide (DMS), 715, 729
 Dimethylsulfoniopropionate (DMSP), 715, 729
Dinophysis, 722, 726
 D. acuminata, 1366, 1372
 D. acuta, 1366, 1372
 D. caudata, 1366, 1372
 D. fortii, 1366, 1372
 D. mitra, 1366
 D. norvegica, 1366
 Dinophysistoxin-1, 722, 1366
 Dinophysistoxins, 726, 1377
 Diode array detector (DAD), 402
 1,2-Dioxanes, 1082, 1084–1086
 Diplamines A, 298
Diploria labyrinthiformis, 830
Diplosoma
 D. listerianum, 828
 D. virens, 340
 Dipolycopenedioic acid xylosylester A, 163
 Discobahamins, 219, 220
Discodermia, 653
 Discodermmins, 219, 220
 Discodermolides, 41, 192, 653, 949, 969, 1052–1053, 1423
 Disk diffusion assay, 768
 Disorazol, 963
 Dispacamides, 199, 1091
 Diversolic acids, 504
 Divinyl ethers, 719
 DMS. *See* Dimethyl sulfide (DMS)
 DMSP. *See* Dimethylsulfoniopropionate (DMSP)
 DNA microarrays, 737, 1116
Dolabella auricularia, 72, 113, 873, 1295
 Dolastatins, 10, 41, 42, 72, 1041–1043, 1047, 1048, 1051, 1295–1297, 1304
 cemadotin, 1043
 dolaisoleucine, 1295
 dolaproline, 1295
 tasidotin, 1043
 Domoic acid, 16, 17, 88–90, 727, 731, 1350, 1364, 1365
 Dr1, 1402
 Dracotoxin, 1394
 Dragmacidins, 1181
 Dragomabin, 1092
 Dragonamides, 1097
Dreissena polymorpha, 795
Drupella sp., 842
 DSO. *See* Diamagnetic spin-orbit (DSO)
 DSP. *See* Diarrhetic shellfish poisoning (DSP)
Dysidea sp., 829
 D. arenaria, 223
 D. herbacea, 424
 Dysidenamide, 424
 Dysidenin, 984
 Dysideonones, 1173
 Dysidine, 1173
 Dysidiolide, 41, 1183
 Dysidiotronic acid, 1173
 Dysinosins, 224, 1194

E
 Echinodermata, 28–30
 Echinoderms, 716
 Echotoxin II, 1402
 Ecklonialactones, 126, 130

- Ecklonia stolonifera*, 126
Eckols, 121
Ecteinascidia
 E. turbinata, 39, 319, 655, 849, 1301
Ecteinascidins, 319, 321, 743, 1301, 1302
 phthalascidin, 1302
Ectocarpene, 120, 900, 915
Ectocarpus siliculosus, 120
Ectoine, 505
Ectyoplasia ferox, 261, 266, 703
Ectyoplasides, 261, 266, 267
Eggregiachlorides, 126
Eggregia menziesii, 126
Eicosapentaenoic acid (EPA), 716
Eilatin, 301, 881
EIMS. *See* Electronic impact mass spectrometry (EIMS)
Elatol, 113
Electronic impact mass spectrometry (EIMS), 445
Elenic acid, 1213
Eleutherobin, 41, 1061, 1062
Eleuthosides/Sarcodictyins, 1060–1062
ELISA. *See* Enzyme-linked immunosorbent assay (ELISA)
Elysione, 931, 933
Emetine, 1123
Emiliana huxleyi, 715, 729, 737
Emodin, 740
Endolithic fungi, 838
Endoperoxides, 1081, 1085, 1099–1100, 1104
Energy-dispersive X-ray, 1261
Enigmazole A, 552, 553, 555
Enniatins, 877
Enoyl-ACP Reductase inhibitors, 1148–1149
Entamoeba histolytica, 1077
Enzyme-linked immunosorbent assay (ELISA), 1120
EPA. *See* Eicosapentaenoic acid (EPA)
Epibiosis, 750
Epicodisterol, 898
Epigenetics, 1425
5-Episinuleptolide, 832
Epistypodiol, 125
Epothilones, 1053
Epoxyalcohols, 717, 719
Eribulin, 658, 1037, 1297, 1300, 1301, 1423
Erylosides, 261–263
Erylus,
 E. formosus, 261, 263, 703
 E. goffrilleri, 261, 262
 E. lendenfeldi, 261–263
 E. nobilis, 261, 263
 E. placenta, 263, 264
Erythromycin, 949, 971
Escherichia coli, 842
Essramycin, 168
ESTs. *See* Expressed sequence tags (ESTs)
ET–743, 655
Etoposide, 1116
Etzionin, 314, 871
Eudisroma olivaceum, 302
Eudistalbins, 302
Eudistoma sp., 870, 881
 E. gilboviride, 866, 868, 874, 884, 885, 887
 E. Ritteri, 866
Eudistomides, 336
Eudistomidins, 302–306
Eudistomins, 302, 305, 306, 870, 874, 884, 887, 1185
Eudistomin-iron, 876
Eudistones, 301
Euplotes, 730
Euplotins, 1098
Euryjanicins, 227
Eurytemora
 E. affinis, 728
 E. herdmanni, 723
Eusynstyela
 E. latericius, 298
 E. misakiensis, 341
Eusynstyelamides, 341, 1151
Evans-Saksena reduction, 655
EXAFS. *See* Extended X-ray absorption fine structure (EXAFS)
Exciton coupling, 500
Exiguamine, 1150
Expressed sequence tags (ESTs), 737
Extended X-ray absorption fine structure (EXAFS), 886
- F**
Farnesyl protein transferase inhibitors, 1154–1156
Fascaplysin, 312
Fascaplysinopsis, 312
Fasciospongia cavernosa, 244, 246
Fascicularin, 323
Fasmerianamines, 359
Favella, 729
Favia fava, 838
FC. *See* Fermi contact (FC)

- Feeding experiments, 896, 897, 899–901, 904–906, 908–911, 913, 915–917, 920, 922, 923
- Feeding stimulants, 695
- Fermi contact (FC), 590
- Feroxosides, 261, 266, 267
- Ferritin, 869
- Fibrocapsa japonica*, 77, 1355
- Fimbrilides, 110
- Finavarrene, 121
- Fisher's exact test, 691
- Flabellinol, 126
- Flabellinone, 126
- Flatworms, 683
- Floresolides, 347
- Fluorescence resonance energy transfer (FRET), 1246
- Flustra foliacea*, 25
- Food web, 713
- Formosides, 261, 263
- Friedel–Crafts alkylation, 613
- Friedel–Crafts reaction, 617
- Frondecaside, 29
- Frondosines, 1167
- FTMS, 448
- Fucols, 121
- Fucophlorethols, 121
- Fucoserratene, 120, 717
- Fucosides, 1150
- Fucosyltransferase inhibitors, 1152–1153
- Fucus serratus*, 20, 120
- Fuhalols, 121
- Furanosides, 540
- Furoplocamiods, 445
- Furospongolide, 1131, 1132
- G**
- Gabriel–Robinson cyclodehydration, 613
- Galactolipids, 716
- Galectin, 1277, 1278, 1281
- Gallinamide, 1092
- Gambierdiscus toxicus*, 79, 726, 1349, 1358, 1359
- Gametogenesis, 715
- Garcinia scortechinii*, 414
- Garveatin, 1151
- Gas chromatography (GC), 450
- Gauge including atomic orbitals (GIAO), 572, 585
- Gaussian 03, 585
- GBSA. *See* Generalized born surface area (GBSA)
- GC. *See* Gas chromatography (GC)
- GC–MS, 450
- Gel-based assay, 770
- Gel electrophoresis, 1270, 1272, 1274, 1276
- Generalist predators, 679
- Generalized born surface area (GBSA), 594
- Geodiamolides, 220, 222
- Geodia* sp., 874
- G. cydonium*, 1274, 1276, 1279
- G. globostellata*, 253
- G. japonica*, 255
- G. papyracea*, 845
- Geodin A, 874
- Geoditins, 255, 256
- Geranylhydroquinone, 296, 341
- GIAO. *See* Gauge including atomic orbitals (GIAO)
- Giardia lamblia*, 1077
- Gifthornelone A, 178
- Girolline, 1091
- Glabruquinones, 341
- Glaciapyrrole A, 169
- Globostellatic acids, 250, 254
- Glucosidases inhibitors, 1189–1190
- Glutathione S-transferase, 727
- Goniodoma pseudogoniaulax*, 85, 722
- Goniodomin A, 85, 722
- Gonyaulax*
- G. polyedra*, 721
- G. spinifera*, 1375
- Gonyautoxins, 715, 725
- Gorgonia* sp., 693, 848
- Gracilin L, 506
- Granulatimide, 311
- Grazer defense, 716
- Green fluorescent protein (GFP), 1232, 1233, 1422
- photoactivatable GFP-like Proteins, 1247–1251
- Griseofulvin, 405
- Grossularines, 307
- Grubbs' catalyst, 611, 631
- Grubbs–Hoveyda catalyst, 645
- Grubbs' second-generation catalyst, 630
- Gutingimycin, 168
- Gymnochrome A, 29
- Gymnochromes, 29
- Gymnocin A, 647
- Gymnodimines, 84, 1349, 1361, 1363
- Gymnodinium*
- G. breve*, 77, 726
- G. catenatum*, 732, 1373

G. sanguineum, 721
G. selliforme, 84
Gymnothrax javanicus, 79

H

Halaven, 664, 1422
Halawanone A, 169
Halenaquinol, 1163, 1206, 1209
Halenaquinone, 1163, 1209
Haliangicin, 156
Halichomycin, 169
Halichondria
 H. melanodocia, 1366
 H. oakdai, 1297
 H. okadai, 77, 726, 1366
Halichondrins, 41, 192, 658, 1034, 1036, 1286,
 1297–1300, 1305
 norhalichondrins, 1036
Haliclona
 H. hogarhi, 828
 H. nigra, 227
Halicyclamines, 1090
Halicyclindramides, 219, 220
Halogramides, 227
Halimedatrial, 17, 18
Halimide, 1048
Halipeptins, 227, 234
Halistatins, 1034, 1036
Halisulfate, 1176
Halitoxin, 846, 847
Halocyanines, 329
Halocynthia
 H. papillosa, 362
 H. roretzi, 329, 362
Halofolliculina corallasia, 838
Halogenases, 978, 983–1000, 1002, 1003,
 1005–1012
Haloperoxidases, 978–983, 1013
 bromoperoxidases, 980, 981
 chloroperoxidases, 980
 iodoperoxidases, 980
Hamigera taragensis, 409
Hamiltonian, 583
Hamiltonian operator, 583
Haminols, 908
Haouamines, 315
Hapalochlaena maculosa, 1412
Haplosamates, 1159, 1199
Hartree, 585
Hartree–Fock, 583
Haterumalides, 350, 352
Heck reaction, 613
Hectochlorin, 984
Hemiassterella minor, 220, 222
Hemiassterlins, 41, 192, 222, 223, 1045–1047
Hemibrevetoxin B, 622–630
Heptadienal, 715
2,4-Heptadienal, 717
Herbarin, 912
Hermodice carunculata, 836
Heteronemin, 1154
Heterosigma akashiwo, 77, 1355
Hexabranchus sanguineus, 871
N-Hexanoylhomoserine lactone (HHL), 774
¹H–¹H COSY, 430
HHL. *See* *N*-hexanoylhomoserine lactone
 (HHL)
9S-HHTE. *See* 9S-hydroxyhexadecatetraenoic
 (9S-HHTE)
9S-HHTrE. *See* 9S-hydroxyhexadecatrienoic
 (9S-HHTrE)
HIF-1. *See* Hypoxia-inducible factor-1
 (HIF-1)
High-pressure liquid chromatography
 (LC), 450
High-resolution mass spectrometry
 (HRMS), 447
High-resolution scanning electron microscopy
 (HR-SEM), 1261, 1262, 1267,
 1270, 1271
High-throughput bioassays, 1113, 1114, 1119,
 1126, 1135
Histone deacetylase inhibitors, 1200–1202
HIV integrase inhibitors, 1158–1160
HIV protease inhibitors, 1198
H,K-ATPase inhibitors, 1202–1203
HMBC, 430
Holoturins, 1099
Homarine, 19, 847, 849
Homoaerotherionin, 846, 847
Homoazulene, 427
Homoceruleide, 165
Homopolytoxin, 1368
Homophymines, 238, 239
Hopanoids, 22
Hopeaphenol, 535
Hormosirene, 121, 717
Hormothamnione, 93, 94
HPPD-1, 160
HRMS. *See* High-resolution mass spectrometry
 (HRMS)
HSQC, 430
HTI-286, 426
Hybridalactone, 117
Hydra attenuata, 1407

- Hydralysin, 1409
Hydroides elegans, 788, 791, 792, 801, 808
 Hydroperoxides, 719
 Hydroxyacids (HEPEs), 717
 9S-hydroxyhexadecatetraenoic (9S-HHTE), 719
 9S-hydroxyhexadecatrienoic (9S-HHTrE), 719
 7-Hydroxyneolamellarin, 1131, 1132
 42-Hydroxypalytoxin, 1368
Hymeniacidon aldis, 204
 Hymenialdisine, 200–202, 1171
 Hymenidin, 198, 217
 Hymenin, 202, 203, 1164
 Hypoxia-inducible factor-1 (HIF-1), 1113, 1115, 1117, 1119–1121, 1127, 1138
- I**
- Ianthella*
I. ardis, 208
I. basta, 216, 217, 871
I. quadrangulata, 216
 Ianthellin, 847
 Iantheran A, 1205
 Ianthesins, 1205
 IBMX. *See* 3-Isobutyl-1-methylxanthine (IBMX)
 ICBG. *See* International cooperative biodiversity groups (ICBG)
 ICP-MS. *See* Inductively coupled plasma mass spectrometry (ICP-MS)
 Iejimalides, 348, 352, 655
 Iheyamines, 312
 Ilhabelanol, 1153
 Ilhabrene, 1153
 Ilimaquinone, 1190, 1191
 IM. *See* Ion mobility (IM)
 Indirubins, 41, 1171
 Indoleamine dioxygenase inhibitors, 1150–1151
 Inductively coupled plasma mass spectrometry (ICP-MS), 865, 882
 Infochemicals, 730
 Infrared spectroscopy, 424, 430, 431, 492, 495
 International cooperative biodiversity groups (ICBG), 1318
 Ion analyzers, 447–449
 Ion mobility (IM), 449
 Ionophore, 862
 IR. *See* Infrared (IR)
 Ircinals A, 195
Ircinia, 1089
 Ircinols, 195, 1099
 Irinotecan, 1335
 Isatin, 159
Isis, 827
 ISISDraw, 574
 Isoaaptamine, 1166
 Isoakaterpin, 1097, 1098, 1153
 3-Isobutyl-1-methylxanthine (IBMX), 801
Isochrysis galbana, 787, 788, 792, 796
 10-Isocyano-4-cadinene, 758
 3-Isocyantheonellin, 758
 Isodomoic acids, 1364
 Isoepitaondiol, 126
 Isoeudistomin U, 306
 Isofistularin-3, 217
 Isofuhalols, 121
 Isogranulatimide, 311
 Isonaamidine C, 874
 Isonitriles, 1081, 1087–1089, 1104
 Isophakellins, 203
 Isopulegol, 471–473
 Isorawsonol, 102
 Isotopic abundances, 445
 Isotopic patterns, 443
 Iynamycin C, 1004
- J**
- Jamaicamides, 984
 Jasmonic acid, 719
 Jaspamides, 41, 220–222, 1004
 Jaspiferals, 256, 257
Jaspis sp., 877
J. splendens, 221
J. stellifera, 251, 253, 256
J. wondoensis, 267
 Jasplakinolide, 877, 879, 1092
 Jaspolides, 257, 261
 J-based configurational analysis, 1057
 JBIR-34, 169
 Julieannafuran, 836, 847, 848
- K**
- Kahakamide A, 180
 Kahalalide F, 17, 41
 Kahalalides, 18, 28
 Kainic acid, 19, 56, 89
 Kakelokelose, 31, 364
 Kalihinols, 1089, 1104
 Kapakahines, 219, 227, 655
Karenia
K. brevis, 77, 728, 833, 1348, 1354, 1355

- K. mikimotoi*, 647
K. selliformis, 84, 1363
Karlodinium veneficum, 728
Karlotoxins, 728
Kassina senegalensis, 305
Keramamides, 235
Keramaphidin B, 195
Kirkpatrickia variolosa, 832
Kita's conditions, 639
Koch's postulates, 837
Kohn–Sham orbitals, 584
Konbu'acidin, 1170
Koshikamides, 234
Kottamides, 310
Krill, 727
K-sulfoxide, 305
Kuanoniamines, 300, 876
Kutznerides, 984, 990
- L**
Labyrinthula zosterae, 842, 843
Lajollamycin, 169
Lamellarins, 26, 28, 32, 316, 317, 1159
Lamelldysidea chlorea, 224
Lamelomorpha strongylata, 403
Laminaria japonica, 843
Lankacidin, 962
Lanosol, 107, 108
Lanthionine, 1048
Laplacian operator, 583
Largazole, 41, 74
Laser ablation ICPMS, 886
Laser confocal microscopy, 770
Lasonolide, 626
Latrunculia, 571, 589, 690
Latrunculin, 1131, 1135
Laulimalides, 41, 1054–1056
Laurencia, 505
 L. elata, 113
 L. hybrida, 117
 L. okamurai, 111
 L. spectabilis, 110, 116
Laurencin, 19
Laurencione, 110
Laurenditerpenol, 1131
Laurinterol, 897
Leinamycin, 963
Leishmania, 1094–1100
Leishmaniasis, 1077
 cutaneous, 1095
 visceral, 1095
Lenthionine, 19
Leonard–Jones equation, 580
Lepadiformines, 323
Lepadins, 1091
Leptoclinides sp., 867, 868
Leucascandrolide, 502
Leucetta, 874
L-iduronic acid, 31
Lignarenones, 915, 916
Limulus polyphemus, 1407
Lindra thallasiae, 98, 843
Linear ion traps (LITs), 448
Lingulodinium polyedrum, 1375
Liposomes, 735
Lipoxazolidinone A, 175
Lipoxygenase inhibitors, 1149–1150
Lipoxygenases, 716, 909, 925, 927–929
Lissoclibadins, 359
Lissoclinamides, 330, 331
Lissoclinidines, 300
Lissoclinotoxins, 357–359
Lissoclins, 298, 305
Lissoclinum sp., 867, 877
 L. bistratum, 333–335, 353
 L. japonicum, 357
 L. notti, 298
 L. patella, 42, 67, 332, 334, 348, 868, 878, 880, 884
 L. perforatum, 357
 L. vareau, 298, 357
 L. voeltzkowi, 352
Lissodendoryx isodictialis, 828
Lissoketal, 352, 621
LITs. *See* Linear ion traps (LITs)
Lobatamides, 349, 350, 352
Lobophytum hedleyi, 832
Lodopyridone, 182
Loihichelin A, 160
Loktanella hongkongensis, 766
Lomaiviticins A, 178, 534, 535
Longamides, 204, 1101, 1102
Longithorols, 345
Longithorones, 345, 630–632, 664
Low-resolution mass spectrometry (LRMS), 447
Lucentamycin A, 180
Luciferase assay, 1119, 1120, 1122, 1126
Luciferin, 602
Luffariella
 L. geometrica, 244
 L. variabilis, 241, 244
Luffariellins, 244, 1172
Luffariellolide, 242, 243, 1172

- Luffarins, 244, 245
 Luffariolides, 243
 Luffolide, 1174
 Lukianols, 318
 Lyases, 716
 Lynamycin A, 175
Lyngbya
 L. bouillonii, 60, 73
 L. confervoides, 825
 L. majuscula, 60–63, 69, 74, 825, 953,
 984–986, 1425
 L. majuscula, 903
 L. wollei, 1373
 Lyngbyalioside, 60
 Lyngbyatoxin A, 61, 62
- M**
- MACPF, 1402, 1404
 Macroalgae, 825
 Macrofouling, 752, 755
 Macrolactam, 959
 Macrolactin A, 165
Madracis mirabilis, 846
 Ma'edamine A, 1162
 Ma'eganedin A, 196
 Magnesidin A, 157, 874
 Maitotoxin, 726, 1359, 1361
 Makaluvamines, 1209, 1210
 Malaria, 1078–1094
 cerebral, 1079
 resistance, 1080
 MALDI-TOF-MS (matrix-assisted laser
 desorption ionization time of flight mass
 spectrometry), 887
 Malhamensilipin A, 92
 Malynamide, 60
 Manadomanzamines, 196
 Manadoperoxides, 1084, 1085
 Manassantin, 1123
 Mangicol A, 904
 Manoalide, 241, 242, 1172
 Mansouramycin D, 169
 Manzamines, 192, 193, 195, 196, 437, 438,
 1089, 1090, 1096, 1101, 1104, 1171
 Marineosin A, 169
 Marine phyla distribution, 8
 Marinisporolide A, 175
 MarinLit, 607–622, 1136
 Marinomycin A, 175
 Marinomycins, 41
 Marinopyrrole B, 171
 Marmycin B, 168
- Mass accuracy, 447–449
 Massadine, 1156
 Mass defect, 450
 Mass spectrometry (MS), 424, 430, 431,
 433–454
 atmospheric pressure ionization, 439–440
 chemical ionization (CI), 435–436
 direct analysis in real time (DART), 440
 electron impact, 433–435
 electrospray, 433, 436
 fast atom bombardment (FAB), 440–442
 magic bullet, 441
 matrix-assisted laser desorption ionization
 (MALDI), 442
 photospray, 436
 secondary ion (SIMS), 440–442
 thermospray, 436
 Mass sufficiency, 450
 Mass-to-charge ratio, 433
 Mauritamide A, 200
 Mayotamides, 334
 Maytansine, 1336
 MCMM. *See* Monte Carlo multiple minimum
 methods (MCMM)
 MCTx–1, 1406, 1407
 MD. *See* Molecular dynamics (MD)
 Mechercharmycin A, 166
 MEDLINE, 1136
 Melemeleone, 1163
Melophlus
 M. isis, 261, 265
 M. sarassinorum, 261, 265
 Meridianins, 41, 309, 310, 1171
 Meridine, 299
 Merobatzelladines, 1101, 1104
 Metabolomics, 737
 Metacaspases, 737
 Metagenomics, 737
 Metalloenzymes, 862
 Metalloprotease inhibitors, 1198–1200
 Metalloproteins, 870
 Metamorphosis, 791
 α -Methoxy- α -trifluoromethylphenylacetic acid
 (MTPA), 548–549
 Methoxyconidiol, 342, 1052
 Methoxyphenylacetic acid (MPA), 552
 12-Methylbacteriohopanetetrol, 532
 12-Methylhopanetetrol, 533
 Methyl sarcophytoate, 630–632
 Metridiolysin, 1406
Metridium senile, 1406
 MF. *See* Molecular formula (MF)
Micrococcus luteus, 766

- Microcosmus vulgaris*, 362
Microcystis aeruginosa, 224
Microfoulers, 751
Microfouling, 750, 754
Micromonospora loiawitiensis, 534
Microcosmus sulcatus, 866
Microplate assay, 769, 774
Microsclerodermins, 234
Microtiter plate assay, 779–780
Microtomography, 1272
Microtubules, 1028–1032, 1056, 1062, 1116
 α - and β -tubulin, 1029
 β -tubulin, 1039, 1042, 1047, 1053, 1054
 microtubule-organizing centers (MTOC), 1030
 polymerization, 1033
 tubulin, 1032–1033, 1036, 1062
 tubulin polymerization, 1044, 1051, 1054
Micro-XANES, 886
Microxine, 1170
Millepora
 M. alcicornis, 1406
 M. dichotoma, 1406
 M. platyphylla, 1406
 M. tenera, 1406
Milleporin-1, 1406
Milnamides, 1045, 1046
Miltefosine, 1095
Mimicry, 682
Minabea, 410
Minabeolide-8, 411
Minalemines, 340
Mirabamides, 231, 232, 238
Miraziridine A, 1196
MKN-349A, 180
Molecular dynamics (MD), 572, 579
Molecular formula (MF), 432–454
Molecular mechanics, 582
Molecular modeling
 AM1, 582
 AMBER, 580
 discover, 576
 Gaussian, 584
 Gromacs, 576
 HyperChem, 584
 insight package, 576
 Jaguar, 584
 macromodel, 576
 MacroModel, 581
 MM2, 580
 MM3, 580
 OPLS, 580
 PM3, 582
 Spartan, 576, 584
Molgula manhattensis, 329, 866
Mollamides, 335
Møller-Plesset, 584
Mollusks, 716
Monooxygenases, 980
Monorhaphis chuni, 1260–1262, 1265, 1266, 1268, 1270, 1277, 1281
Monte Carlo method, 578
Monte Carlo multiple minimum methods (MCMM), 572–573
Montipora capitata, 842
Montipora sp., 828
Montiporic acid A, 842
Moraxella phenylpyruvica, 766
Mosher's method, 573
Motuporin, 1181
MPA. *See* Methoxyphenylacetic acid (MPA)
MS. *See* Mass Spectrometry (MS)
MS-MS. *See* Tandem mass spectrometry (MS-MS)
Muironolide A, 449
Mukaiyama aldol addition, 635, 637
Mukanadin A, 199, 204
Mukanadin E, 1005
Mullerian, 683
Multifidene, 121
Mupirocin, 959
Murata's method, 490
Mussel larvae, 802
Mussels, 795
Mycale
 M. acerata, 832
 M. izuensis, 239
 M. laxissima, 261, 265
Mycalcnitriles, 1131, 1132
Mycalcosides, 261, 265, 266
Mycosubtilin, 959, 961, 962
Myoglobin, 438, 439
Mytilus, 795
M. edulis, 1353
M. galloprovincialis, 92

N
Nagelamides, 198, 206–208, 1181
Nairaiamides A, 335
Nakadomarin A, 196
Na,K-ATPase inhibitors, 1203–1206
Nakijiquinones, 41, 1167
Nannocystis exedens, 156
Nanobiotechnology, 1281

- Napyradiomycin, 980, 995, 1003
Naseazoline A, 171
National Cancer Institute (NCI), 1318
Natural biofilms, 808
Natural products databases, 390–392
Nauplii, 719
Nauplius II, 787
Navenones, 907, 908, 916
Nazumamide, 1192
NBA. *See* 3-Nitrobenzyl alcohol (NBA)
NCI. *See* National Cancer Institute (NCI)
Negishi coupling, 628
Negishi cross-coupling, 653, 655
Neocarzin A, 1003
neo-kaulamine, 196
(E)-Neomanoalide, 241
(Z)-Neomanoalide, 241
Neopalytoxin, 1368
(+)-Neopeltolide, 502, 503
Neosaxitoxin, 725
Neosiphoniamolide A, 222
Neosiphonia superstes, 222
Neoverrucotoxin, 1391
Nephtes fascicularis, 323
Nereistoxin, 25
Nereis vexillosa, 833
Nereocystis luetkeana, 843
Nerolidol, 980
Neurotoxic shellfish poisoning (NSP), 1346, 1354, 1355, 1357
Newton–Raphson method, 580, 581
Nicotine, 714
Nicotinic acid, 442
Nigricanosides, 102, 103, 1032, 1059–1060
Ningalins, 318, 643, 664
Nitric oxide synthase inhibitors, 1151
9-Nitroanthracene, 442
3-Nitrobenzyl alcohol (NBA), 441
Nitrogen rule, 446
Nitzschia pungens, 90
N limitation, 731
NMR. *See* Nuclear magnetic resonance (NMR)
Nobiloside, 261, 263, 1187
Noctiluca scintillans, 729
NOE. *See* Nuclear Overhauser enhancement (NOE)
Nominal mass, 447
Nonparametric, paired tests, 691
Non ribosomal peptide synthase (NRPS), 948, 950–953, 1049, 1425
 hybrid PK/NRP pathways, 959
 hybrid PKS/NRPS system, 950, 952
 hybrids, 950, 958–959, 961, 964, 967–970
Norhalichondrin B, 647
Nor-segoline, 298
Norselic acids, 1098
Noteshes robusta, 1395
Novobiocin, 1008
Nozaki–Hiyama–Kishi coupling, 658
Nozaki–Hiyama–Kishi macrocyclization, 664
Nozaki–Kishi coupling, 653
NRP. *See* Non ribosomal peptide synthase (NRPS)
NSP. *See* Neurotoxic shellfish poisoning (NSP)
Nuclear magnetic resonance (NMR), 424, 430, 454–492
 ACCORDION, 490
 ACCORD-ADEQUATE, 530
 1,1-ADEQUATE, 490, 530
 advanced Mosher’s method, 549
 Altona equation, 468
 anisochronous, 460
 carbon chemical shifts, 459
 CASE, 493
 ¹³C-coupled HSQC, 528, 538
 chemical shifts, 456–457
 chiral anisotropic reagents, 548
 computer-assisted structure elucidation (CASE), 492
 COSY, 485, 520, 521
 COSY–90, 521
 coupling constants, 461, 466
 density functional theory, 565
 DEPT, 478
 diamagnetic shielding, 552
 diastereotopic, 460
 diastereotopic methylene protons, 561
 dipole-dipole relaxation, 476
 1D NOE, 480
 1D NOESY, 563
 DQF-COSY, 521, 522, 563
 1D ROESY, 563
 1D TOCSY, 536, 563
 1D-TOCSY, 480, 482
 E-COSY, 521, 563
 edited HSQC, 489
 enantiotopic, 460
 false HSQC, 534
 first-order spectra, 463–464
 four bond Js, 467
 H2BC, 530
 heteronuclear couplings, 559
 heterotopic, 460
 HETLOC, 491, 530, 563
 ¹H–¹H COSY, 477, 479, 483
 ¹H–¹H NOESY, 480

- ^1H - ^1H ROESY, 480
 ^1H - ^1H TOCSY, 479
HMBC, 479, 483–485, 520, 528
HMQC, 479, 483, 484, 527–528
HMQC-TOCSY, 490
HOHAHA, 490
homonuclear couplings, 559
homotopic, 460
HSQC, 483–485, 520, 527–528
HSQC-INADEQUATE, 530
HSQC-TOCSY, 490
HSQMBC, 490, 530, 563
INADEQUATE, 480, 485, 531
isochronous, 460
J-based configurational analysis, 556
J-HMBC, 490, 491, 563
Karplus equation, 465, 468, 521, 538
Larmor frequency, 487
long-range COSY, 521
modified Mosher's method, 551
Mosher's method, 567
MTPA ester, 550
multiplicity-edited HSQC, 528
Murata *J*-based method, 473–475
Murata method, 530, 556
NMR-SIM, 537
NOESY, 477, 483, 487–489, 525–527
n+1 rule, 463–464
NOE, 430, 454, 475–477, 521, 526, 585
one bond Js, 467
PANACEA, 542
proton chemical shifts, 458
ROE, 521
ROESY, 487–489, 525–527, 593
rotational axis, 457
scalar coupling, 461–463
Spin Works, 537
three bond Js, 467
TOCSY, 490, 523–525
T-ROESY, 526
two bond Js, 467
zNOESY, 527
zTOCSY, 523
Nucleolin, 1033
- O**
7-O-beta-D-glucopyranosyl-2''-sulfate, 843
Obscuraminols, 324
Obtusenyne, 19
Oceanapia, 699, 1091
Ochratoxin, 1000, 1001
Ochromonas danica, 92, 93
Ochtodene, 112, 113
Ochtodes osmundaceae, 112
Octadienal, 715, 717
Octatrienal, 715
Oculina
 O. arbuscula, 825
 O. patagonica, 836, 839
Odonthalia dentata, 107
12-ODTE. *See* 12-Oxo-dodecatienoic acids (12-ODTE)
Okadaic acid, 14, 77, 192, 722, 726, 909, 1028, 1178, 1350, 1366, 1367, 1377
Okamuralene, 111
Omuralide, 1303
Oncogenes, 1112, 1114, 1117, 1121
 myc, 1117
 ras, 1117
 src, 1117
Oncorhyncolide, 900
9-ONDE, 717
Onnamide, 959, 963, 965, 968
 biosynthesis, 965–967
Ophidianoside F, 424
Optical activity, molar rotations, 498
Optical rotatory dispersion (ORD), 431, 498
Optical rotatory dispersion-circular dichroism (ORD-CD), 430
Optical spectroscopic methods, 431
Orange disease, 843
Orbitrap, 449
ORD. *See* Optical rotatory dispersion (ORD)
ORD-CD. *See* Optical rotatory dispersion-circular dichroism (ORD-CD)
Oroidin, 196, 198, 200, 203, 846, 847, 1164
Oscarella sp., 829
Oscillatoria spongeliae, 424
Oscillatoxins, 63
Ostreocin D, 1368
Ostreopsis
 O. lenticularis, 1373
 O. mascarenensis, 1368
 O. ovata, 81, 1371
 O. siamensis, 81, 1368
Ovatoxins, 1371
Oxathiazepino-eudistomins, 306
Oxoacids, 719
12-Oxo-dodecatienoic acids (12-ODTE), 717
9-Oxo-nonadienoic, 717
12-Oxo-phytodienoic acid, 719
15-Oxo-5Z,9E,11E,13E-pentadecatetraenoic acid, 717
Oxylipins, 713, 719
Oxysceptrin, 198

P

- Pachastrelloside A, 261, 267, 268
 Pachydictyol A, 123
Pachydictyon coriaceum, 123
 Paclitaxel, 1319, 1335, 1336
 Palau'amine, 203, 607–623, 664
 Palauolide, 245, 246, 1176
 Palauolol, 246, 1176
 Palinurin, 1176
 Palmerolide A, 351, 607–622, 1206, 1207
Palythoa
 P. caribaeorum, 833
 P. toxica, 81
 Palytoxin, 81, 425, 602, 647, 833, 1351, 1368, 1371
 Pantherinine, 298
Pantoneura plocamioides, 445
 Papuamides, 231, 232, 238
 Paralytic shellfish poisoning (PSP), 1346, 1363, 1373
 saxitoxin, 715
 Paralytic shellfish toxin (PST), 723
 Paramagnetic spin-orbit (PSO), 590
 Parazoanthoxanthin A, 23
 Parguerene, 18, 19
 Patellamides, 42, 67, 329–331, 878, 879, 881, 884
 Patellazoles, 348
 Patellins, 334, 335
Patinopecten yessoensis, 1375
Pavlova lutheri, 788
 PCM. *See* Polarized continuum model (PCM)
 PCR amplification, 1242
 PDA. *See* Potato dextrose agar (PDA)
 Pectenotoxins, 1351, 1371, 1372
 Pederin, 959, 963, 965, 968
 biosynthesis, 965, 966
 Pediveliger, 797
 Peloruside, 41, 1054, 1056
 Penarolide sulfates, 1189
 Penasterol, 261
 Penasulfate, 1189
 Penazetidine, 453, 1169
 Penicillin G, 790
Penicillus capitatus, 98
 Pennate diatom *Pseudo-nitzschia*, 717
 Pentabromopseudilin, 159
 Pentalene, 427
 Perknaster, 690
Perna spp., 795
Perophora viridis, 361
 Peroxidases, 980
 Peroxyacarnic methyl ester, 426
 Peroxyplakoric acids, 1083, 1084, 1086
 Perthamides, 233, 234
Petrosaspongia nigra, 247
 Petrosaspongiolides, 247–249, 1174
 P-glycoprotein, 1048, 1053, 1054, 1057, 1058, 1062
 PGME. *See* Phenylglycine methyl ester (PGME)
Phaeocystis, 729, 737
Phaeocystis pouchetii, 721
 Phaeodactylum, 715, 717
Phaeodactylum tricornutum, 731, 737
Phakellia mauritiana, 203
 Phakellins, 203
 Phakellistatins, 203, 225
Phallusia mamillata, 329
 Phenazine, 774
 Phenylethylamine, 313
 Phenylglycine methyl ester (PGME), 552
 Phenylmannolone A, 156
 Pheromone, 719
 Phillidiidae, 758
 Phloeodictynes, 1091
 Phlorethols, 121
 Phomapyrones, 933–935
 Phomopsidin, 904, 1039
Phorbas, 449
 Phorboxazole, 41, 647
 Phosphodiesterase inhibitors, 1185–1186
 Phospholipase A2, 716
 Phospholipase C inhibitors, 1184
 Phospholipase inhibitors, 1172–1177
 Phospholipids, 716
 Phosphorus limitation, 731
 Photoactivated localization microscopy (PALM), 1243, 1248
Phyllidia, 683
Phyllodiscus semoni, 1402, 1404
 Phylogenetic tree of life, 6
Physalia physalis, 1395, 1401
 Phytogel, 772, 828, 830
 Phytogel assay, 773
 Phytoplankton, 713
 Piclavines, 322
 Pictamine, 322
 Pictet–Spengler condensation, 658
 Pinacol rearrangement, 613
 Pinane–1,2-diol, 481
 Pinnatoxins, 14, 28, 1361
 Piperazimycin A, 174
 Piperitone, 443

- PKS. *See* Polyketide synthase (PKS)
- Placidene, 934, 935
- Plakortides, 1086, 1099
- Plakortin, 1085–1087, 1104
- Plakortis* spp., 829, 1085, 1099, 1103
- P. halichondroides*, 829
- Plancitoxins, 1409, 1410
- Plankton, 713
- Platymonas, 788
- Plexaura homomalla*, 685
- Plocamium hamatum*, 827
- Plotosus canius*, 1395
- Pocillopora damicornis*, 836, 841
- Pocilloporids, 840
- Poecillastra wondoensis*, 267
- Polak–Ribier conjugate gradient algorithm, 581
- Polarized continuum model (PCM), 594
- Policitor adriaticus*, 362
- Polyandrocarpa* sp., 413
- Polyandrocarpamides, 308
- Polyandrocarpamines, 314, 413
- Polycarpa* sp., 867, 868
- P. aurata*, 313, 361
- P. clavata*, 361
- Polycarpamines, 361
- Polycarpaurines, 361
- Polycarpine, 361
- Polychaetes, 683, 716
- Polycitones, 318, 1157
- Polycitor africanus*, 318
- Polycitorella mariae*, 308
- Polycitorols, 323
- Polycitrins, 318
- Polydiscamides, 219, 220
- Polyethylene glycol, 441
- Polygodial, 899, 900, 907
- Polyketide synthase (PKS), 930, 948, 950, 951, 1049, 1425
- hybrid PK/NRP pathways, 959
- hybrid PKS/NRPS system, 950, 952
- hybrids, 950, 958–959, 961, 964, 967–970
- Poly- L-alanine peptide, 576
- Polysiphenol, 538
- Polysiphonia*
- P. ferulacea*, 108
- P. lanosa*, 107
- Polysyncraton* sp., 867, 868
- Polytheonamides, 228
- Polyunsaturated aldehydes (PUAs), 714, 719, 925, 928, 930
- Pomacanthus*
- P. imperator*, 830
- P. coeruleus*, 98
- Popolohuanone, 427, 1212
- Porites*
- P. astreoides*, 825
- P. cylindrica*, 832
- Poritids, 840
- Potato dextrose agar (PDA), 779
- Poterioochromonas malhamensis*, 92
- Prialt, 39, 41, 1422
- Primaquine, 1079
- Procambarus clarkii*, 1398
- Prochloron didemni*, 42, 878
- Product-ion scan, 451
- 6-Propionyllumazine, 25
- Prorocentrolides, 1361, 1363
- Prorocentrum*, 722
- P. lima*, 726, 1366
- P. micans*, 721
- Prostaglandins, 685
- Prosuberites laughlini*, 227
- Protein kinase C inhibitors, 1166–1170
- Protein–protein Interactions, 1246
- Protoceratium reticulatum*, 1375
- Protoberidinium crassipes*, 84
- Protozoa, 1076–1078
- cysts, 1076, 1077
- Proximicin A, 178
- Prunolides, 352–354
- Prymnesins, 96, 728
- Prymnesiophyceae, 721, 729
- Prymnesiophytes, 723
- Prymnesium parvum*, 96, 728, 732
- Psammaplins, 210, 211, 217, 239, 700, 1005, 1200
- Psammaplysenes, 213
- Psammaplysilla*
- P. purea*, 212
- P. purpurea*, 208, 210, 213, 216
- Pseudaxynissa cantharella*, 202, 203
- Pseudoalteromonas* sp., 766
- P. piscida*, 766
- Pseudocalanus* sp., 726
- Pseudoceratina purpurea*, 210, 211, 239
- Pseudodistoma*
- P. crucigaster*, 324
- P. kanoko*, 321
- P. obscurum*, 324
- Pseudodistomins, 303, 321
- Pseudomonas* sp., 871
- P. aureofaciens*, 774
- P. bromoutilis*, 159
- P. fluorescens*, 658
- Pseudo-nitzschia*, 715, 727, 731
- P. australis*, 1364

Pseudo-nitzschia (cont.)

- P. calliantha*, 1364
- P. delicatissima*, 1364
- P. fraudulenta*, 1364
- P. galaxiae*, 1364
- P. multiseriata*, 1364
- P. multistriata*, 1364
- P. pseudo-delicatissima*, 1364
- P. pungens*, 1364
- P. seriata*, 1364
- P. turgidula*, 1364

Pseudopterogorgia elisabethae, 920

Pseudopterossins, 41, 920, 1422

Pseudotheonamides, 229

Pseudozoanthoxanthin A, 23, 24

PSO. *See* Paramagnetic spin-orbit (PSO)PSP. *See* Paralytic shellfish poisoning (PSP)PST. *See* Paralytic shellfish toxin (PST)

PsTX-115, 1404, 1406

PsTX-20A, 1404

PsTX-60A, 1402

PsTX-60B, 1402

Pteriatoxins, 1361

Ptychodiscus brevis, 77, 726, 1354PUAs. *See* Polyunsaturated aldehydes (PUAs)

Purealidins, 212, 213

Purpurone, 1208

Puuphenone, 1212

Pycnidione, 1093

Pycnoclavella kottae, 310

Pyrimethamine, 1079

Pyrimine, 874

Pyroindomycin, 989

Pyroindomycin B, 990, 993, 1000

Pyrrolnitrin, 988–990, 995, 999, 1006, 1011

*Pyura**P. saciformis*, 307*P. stolonifera*, 865, 866**Q**QIT. *See* Quadrupole ion trap (QIT)

qRT-PCR, 811

QS. *See* Quorum sensing (QS)

Quadrupole ion trap (QIT), 448

Quantum mechanical ¹³C chemical shift calculations, 572

Quantum mechanical (QM) methods, 574, 582, 585

Quercetin, 1135

Quinones, 1081, 1092–1094

Quorum sensing (QS), 773

Quorum sensing blockers, 776

R

Ramachandran plot, 576, 578

Raphidophytes, 723

Rawsonol, 102

Reactive oxygen species (ROS), 717

Rebeccamycin, 990

Red fluorescent proteins, 1233, 1237

Red spot disease, 843

Reflectron mode, 448

Resolving power, 447

Reverse transcriptase inhibitors, 1157–1158

Reversible saturable optical fluorescence transitions (RESOLFT), 1243

Rhabdastrella globostellata, 251, 254, 256, 261

Rhabdastrellic acid–A, 251, 253

Rhabdastrellins, 252, 253

Rhizolysin, 1401

Rhizostoma pulmo, 1401

Rhizoxin analogs, 1040–1041

Rhizoxins, 959, 963, 1041

Rhodomela confervoides, 107*Rhodomonas lens*, 834*Rhodophyllis membranacea*, 19*Rhodovulum* sp., 766

Rhopaladins, 312, 1170

Rhopilema nomadica, 1401, 1410

Rigidins, 315, 1185

Ritterazines, 31

ROS. *See* Reactive oxygen species (ROS)

Rossinones, 345

Rubritalea squalenifaciens, 163

Rubrolides, 354

Ruegeria, 766

Rule of 13, 446

Ruthenium, 881

S

SAAF, 363

Saframycins, 1301

Sagittamides, 326

Salicylilhalamide A, 41

Salicylilhalamides, 350, 352, 1206

Salinamide A, 169

Saliniketal, 177

Saliniketal A/B, 41

Salinipyrone A, 177

Salinispora tropica, 911, 969, 978, 1012*Salinosporamide*, 41, 175, 176, 911, 916, 978, 1010, 1012, 1091, 1092, 1104, 1114, 1303–1305, 1425

cinnabaramide A, 911

- fluorosalinosporamide, 1012
Salinispora, 1303
Sarasinosides, 261, 265
Sarcochromenol sulfates, 1206
Sarcodictyins, 3, 23, 24
Sargassum spp, 843
Saxidomus giganteus, 81
Saxitoxin, 14, 725, 898
 biosynthesis, 918
Saxitoxins (STX), 81–83, 1352, 1373–1374
SBSE. *See* Stir bar solid extraction (SBSE)
Scalaradial, 1175
Scalemic, 430, 431
Sceptrin, 198, 205, 217, 846, 847
Schrödinger equation, 582, 583
Schulzeins, 1187, 1189, 1190
SciFinder, 1136
Scleractinian corals, 835, 841
Sclerophytin A, 626
Scorpaena guttata, 1395
Scorpinone, 912
Scripps Institution of Oceanography, 1423
SD. *See* Spin-dipole (SD)
Seagrass pathogenesis, 842
Sea star, 424
Sebastianines, 300
SEC. *See* Size-exclusion chromatography (SEC)
Secobatzelline A, 1196
Secobatzellines, 1183
Secomanoalide, 241
Securamines, 25
Segolines, 301
Selenohomocysteine, 165
Sepedonium chrysospermum, 418
Serine protease inhibitors, 1191–1196
Serratia marcescens, 836, 839
15S-HEPE, 717, 719
Shermilamines, 299, 1212
Shewanella algae, 766
Shimofuridin, 1169
Shishididemniols, 326
Shishijimicins, 304
Sialidase inhibitors, 1186–1188
Siderastrea siderea, 830, 838, 841
Siderophore, 862
Sidnyum turbinatum, 362
Sigmosceptrellins, 1087, 1103, 1104
Silicasomes, 1272, 1273, 1276
Silicatein, 1263–1265, 1272–1277, 1280, 1281
Silicoflagellates, 723
Si-limited, 731
Siliquariaspongia mirabilis, 231, 232
Simulated annealing, 579
Sinulamide, 1203
Sinularia
 S. cruciata, 827
 S. flexibilis, 832
 S. maxima * *polydactyla*, 832
 S. polydactyla, 699
Siphonarins, 901, 902
Siphonazole, 163
Siphonodictine, 828
Size-exclusion chromatography (SEC), 884
Skeletonema, 715, 716
 S. costatum, 787, 790, 834
 S. marinoi, 726, 739
Slagenins, 200
β-Snyderol, 981
Sodwanone, 1131
Sodwanone V, 1132
Sokodosides, 261, 263, 264
Solandelactones, 1154
Somamide A, 65
Spanish dancer nudibranch, 682
Specific rotation, 498
Spectrometric methods, 429
Spermatophore production, 721
Spheciospongia, 523
Spin-dipole (SD), 590
Spirastrellolides, 501, 503, 1028, 1181
Spirolides, 1349, 1361, 1363
Spiro-prorocentrimine, 1361, 1363
Spisulosine, 41
Splenosin A, 169
Sponge disease, 844–847
 alpha-proteobacterium, 845
 cyanobacteria, 845
Spongiacidins, 1091, 1170
Spongianolides, 1168
Spongia officinalis, 866
Spongidines, 248, 249
Spongistatins, 655, 1038, 1039
Spongistatins/altohyrtins/cinachyrolide, 1037–1038
Spongolactams, 1154
Spongothymidine, 9
Spongouridine, 9
Sporolide, 177, 1005
Squalamine, 32, 41
16S rRNA gene, 1425
SS–228Y, 169
Staphylococcus haemolyticus, 766
Statistical methods, 1125
 Z-factor, 1126
Staurosporines, 307, 1007, 1166

- Stelletins, 250–254
Stelletta
 S. globostellata, 253, 254
 S. tenuis, 251, 261
Stellettamide, 1185
Stelletazole A, 1185
Stelliferins, 250, 253, 254
Stevensine, 202
Stichodactyla helianthus, 1402
Stilbenes, 539
Stille cross-coupling, 611
Stille-type reaction, 621
Still–Gennari olefination, 653
Stir bar solid extraction (SBSE), 762
STN, 392
Stolonic acids, 355, 356
Stolonica socialis, 356
Stolonoxides, 355, 356
Stone crab, 833
Stonustoxin, 1391, 1394
Streptochlorin, 174
Streptokordin, 169
Streptomyces verticillus, 869
Streptomycin sulfate, 790
Strobilactone, 426
Strombidinopsis acuminatum, 729
Strongylophorines, 1131, 1134, 1135
STX. *See* Saxitoxin (STX)
Stylissa
 S. caribica, 227
 S. carteri, 202
 S. flabelliformis, 204
 S. plicata, 329, 866
Stylocheilus longicauda, 63, 113
Styloguanidines, 203, 1188
Stylotella
 S. agminata, 203
 S. aurantium, 203, 225, 227
Stylotellane, 905
Stypodiol, 125, 1051–1052
Stypohydroperoxide, 126
Stypolactone, 125
Stypoldione, 125
Stypopodium flabelliforme, 126
Stypotriol, 125
Stypotriolaldehyde, 126
Suberea clavata, 215
Suberites, 412–414
Suberites domuncula, 1261, 1265, 1279
SUL-I, 1412
SUL-II, 1412
Superoxide dismutase, 727, 737
Super-resolution microscopy, 1248–1251
Suzuki coupling, 617, 643
Suzuki cross-coupling, 608, 655
Suzuki–Miyaura coupling, 647
Sventrin, 198
Swern conditions, 637
Swimmer’s itch, 61, 63
Swinholide A, 40
Symbiodinolide, 86
Symplocamide A, 65
Symplostatin, 41, 1041
Synanceia
 S. horrida, 1391
 S. verrucosa, 1391
Synoicum, 608
 S. adareanum, 351
 S. prunum, 354
Syringomycin E, 983–985
- T**
Tamandarins, 339, 1290
Tambjamines, 869, 870, 876, 888
Tandem mass spectrometry (MS–MS), 448, 451–454
 multiple reaction monitoring (MRM), 453
 neutral-loss scan, 452
 precursor-ion scan, 452
 selected reaction monitoring (SRM), 452
Tanikolide, 63, 64
Taq polymerase, 1422
T-Ar, 1401
Target validation, 1116
Tauroacidins, 200, 1162
Taurodispacamide, 200
Tawicyclamides, 334
Taxanes, 1028
 binding sit, 1032
 paclitaxel, 1116
TBG. *See* 2,5,6-Tribromo-1-methylgramine (TBG)
TBT. *See* Tributyltin (TBT)
Tebbe’s reagent, 637
Tedania
 T. charcoti, 868
 T. ignis, 537, 828
Tedanol, 537
Teleocidin A₁, 169
Telomerase inhibitors, 1160–1162
Temora
 T. longicornis, 721, 730
 T. stylifera, 719
Terebellid polychaete, 833

- Tethys fimbria*, 28
 1,1,3,3-Tetrabromoheptanone, 108, 110
 1,1,3,3-Tetrabromo-2-heptanone, 844
 Tetramethylmethane, 456
 Tetramethylsilane, 456
 Tetrodotoxin, 32, 603, 664, 1412
 Thailandamide, 962, 968
Thalassia testudinum, 842, 843
Thalassiosira, 715
 T. pseudonana, 731, 737, 787, 788
 T. weissflogii, 730
Thalassoma bifasciatum, 693
Thalassophryne nattereri, 1395
Thalassomonas loyaeana, 838
Thelopus crispus, 833
Theonella
 T. mirabilis, 231
 T. swinhoei, 40, 228–233
 Theonellamides, 228
 Theonellaeptolides, 230
 Theopapuamides, 232, 233, 238
Thermovibrio ammonificans, 163
 Thiaplidiaquinones, 343
 Thienodolin, 990
 Thiocoraline, 41, 178, 949
 Thiomarinol B, 159
 Thorectandrols, 245, 246
Thorectopsamma xana, 210
 Threo-13,14-HepETE, 717
 Thyrsiferol, 18, 19, 116
Tigriopus californicus, 727, 731
 Time-of-flight (TOF), 448
 Time-resolved fluorescence, 1119
 Tirandamycin C, 171
 Tirapazamine, 1115
 Tiruchanduramine, 304
 Tobacco, 714
 TOF. *See* Time-of-flight (TOF)
 Tokaramide A, 1196
 Topoisomerase-II, 427, 869
 Topoisomerase inhibitors, 1209
 Topotecan, 1116, 1335
 Toxadocials, 1194
 Toxicols, 1157
 toxiusol, 1157
Toxoplasma gondii, 1077, 1090
Toxopneustes pileolus, 1412
 Trabectedin, 655, 1114, 1422
Trachinus
 T. draco, 1394
 T. vipera, 1395
 Transferrin, 869
 Trapoxins, 240
 2,5,6-Tribromo-1-methylgramine
 (TBG), 758
 Tributyltin (TBT), 753
Tridacna maxima, 28
Tridentata marginata, 700
 Tridentatols A-C, 700
Trididemnum
 T. cyanophorum, 337, 338
 T. cyclops, 353
 T. solidum, 337, 873, 874
 Triethanolamine, 441
 3,6,7-Trihydroxycoumarin, 102
Tripneustes gratilla, 1412
 Trisindoline, 157
 Trochophore larvae, 796
 Trochophores, 791
 Tropical diseases, 1103
 Trunkamide, 626
 Trunkamide A, 334, 335
Trypanosoma, 1100–1103
 Trypanosomiasis, 1077
 African, 1100
 South American, 1101
 Trypargimine, 306
 Tsuji decarboxylative allylation, 645
Tubastraea faulkneri, 831
 Tubastrine, 313
 Tulearin A, 506
 Tunicate diseases, 849
 Tunichlorin, 873, 874
 Tunichromes, 296, 327–329,
 865, 870
 Turbinamide, 362
 Tylostyles, 1267, 1268
 Tyrosol, 164
 TZT-1027, 72
- U**
Udotea flabellum, 98
 Udoteal, 98
 Udoteatrial, 98
 Ulapualide, 871
 Ulithiacyclamides, 331
 Ultraviolet (UV), 496
 chromophores, 497
 vacuum, 496
 Ultraviolet-visible (UV-VIS), 424, 430, 431
Ulva, 782
 UN. *See* Unsaturation number (UN)
 Unnarmicin A, 157
 Unpalatability, 681
 Unsaturation number (UN), 432–454

Uoamines, 321
 Urmetazoan, 1260
 UV. *See* Ultraviolet (UV)
 UV-VIS. *See* Ultraviolet-visible (UV-VIS)

V

Valdivones, 1177
 Vanabins, 865, 869
 Vanadium(IV), 886
 Vannusals, 505
 Varacin, 357
 Variolin, 41
 Variolin B, 401, 402
 Veliger larvae, 795
 Venturamides, 1092
 Verapliquinones, 341
Verongia aerophoba, 208
 Verongulasterol, 898
 Verrucosin, 905
 Verrucotoxin, 1391
 Vesparioside B, 523, 540, 542
 Vibrindole A, 157
Vibrio sp., 766, 835, 838, 844
 V. alginolyticus, 766
 V. coralliilyticus, 836, 837, 841
 V. fluvialis, 766
 V. furnissii, 766
 V. gazogenes, 157, 874
 V. halioticoli, 766
 V. harveyi, 158, 766, 845
 V. shilonii, 836
 V. vulnificus, 766
Vidalia obtusiloba, 108
 Vidalols, 108
 Vinca alkaloids, 1028, 1033, 1039
 Vinca domain, 1033, 1043, 1044
 Violacein, 774
 Virenamides, 340, 1213
 Virginiamycin, 962
 Viridamide, 1102
 Viridiol, 501
 Vitilevuamide, 41, 1047–1048

W

Wacker oxidation, 637
 Wadsworth–Emmons macrocyclization, 608

Wakayin, 311, 1210
Westiallopsis prolifica, 334
 Westiellamide, 878, 880
 Wilcoxon paired-sample test, 691
 Witkop reaction, 613, 664
 Wondosterols, 267, 268
 Woodinine, 302, 305

X

XANES. *See* X-ray absorption near edge spectroscopy (XANES)
Xenopus laevis, 703
 Xestocyclamine A, 1166
 Xestoquinol sulfate, 1209
 Xestoquinone, 1092, 1163, 1206, 1209
 Xestosaprols, 1209
Xestospongia, 1089
 X-ray absorption near edge spectroscopy (XANES), 886
 X-ray crystallography, 424, 430, 431

Y

Yamaguchi conditions, 608, 611
 Yanuthones, 347
 Yellow band disease, 839
Yersinia enterocolitica, 839, 842
 Yessotoxins, 726, 1346, 1352, 1367, 1372, 1375, 1377, 1378
 YM-266183, 165
 Yondelis (ET-743), 41, 39, 319, 655, 664

Z

Zamamidines, 196
 Zampanolide, 1057–1058
 Z-axinohydantoin, 1166
 Zebra mussels, 795
 Zooplankton, 713
 Zoospore settlement, 786
 Zoospore swimming behavior assay, 783
 Zooxanthellae, 829, 838
 Zooxanthellatoxin A, 86
Zostera marina, 843